

EFFECTS OF DIFFERENT MIXED PLANTING PATTERNS OF CHINESE FIR (*CUNNINGHAMIA LANCEOLATA*) ON CHEMICAL FORMS OF ALUMINUM IN SOIL

ZHANG, J.^{1*} – LIU, B.² – CUI, P.¹ – LIN, S.^{2*}

¹College of Life Science, Fujian Agriculture and Forestry University, Fuzhou 350002, China

²College of Forestry, Fujian Agriculture and Forestry University, Fuzhou 350002, China

*Corresponding authors

e-mail: jbzhangfj@163.com; szlin53@126.com

(Received 8th Aug 2018; accepted 2nd Jan 2019)

Abstract. Aluminum (Al) toxicity is an important cause of forest degradation. Al phytotoxicity is closely related to its chemical forms in soils. In this study, the effects of different mixed planting patterns of Chinese fir (*Cunninghamia lanceolata*) on four chemical forms of Al in soils were examined. One-year-old seedlings of *C. lanceolata*, *Michelia macclurei* and *Schima superba* were used. The results showed that the content of exchangeable Al and monomer hydroxy Al decreased by 2.3–8.1% and 2.6–14.2% in soil of mixed plantation of *C. lanceolata* with *M. macclurei*, whereas they decreased by 6.6–6.9% and 7.2–7.3% in bulk soil of *C. lanceolata* mixed with *S. superba*. The content of acid-soluble inorganic Al in soil of mixed plantation of *C. lanceolata* also indicated a decreasing tendency, whereas the content of humic acid Al indicated an increasing tendency. Meanwhile, soil pH indicated an increasing tendency and had a negative correlation with all chemical forms of Al in soil. These results indicated that mixed planting patterns of *C. lanceolata* could reduce active Al in soil and would be an alternative alleviation method to control the harmful effects of Al on *C. lanceolata* forest.

Keywords: *Cunninghamia lanceolata*, exchangeable Al, monomer hydroxy Al, acid-soluble inorganic Al, humic acid Al

Introduction

Aluminum (Al) in soil is one of the toxic metals to plants, especially for plants growth in acid soil (Kochian et al., 2015). Al can be absorbed by plants, although it is not a nutrient element (Arunakumara et al., 2013). Al in plant cells would be combined with cell pectin, membrane components, proteins, and nucleic acids (Matsumoto, 1988; Jones and Kochian, 1997; Tabuchi et al., 2001; Arunakumara et al., 2013; Shahnawaz et al., 2016), and thus it can influence the growth, cell membrane integrity, photosynthesis, nitrogen metabolism, nutrient uptake, and deoxyribonucleic acid (DNA) fragmentation (Prabagar et al., 2011; Ribeiro et al., 2013; Cruz et al., 2014; Yang et al., 2015; Anjum et al., 2016; Vardar et al., 2016; Awasthi et al., 2017). The potential toxicity of active Al in the terrestrial ecosystem was a major factor leading to the forest degradation overspreading across Central Europe in the 1970s (Ulrich et al., 1980).

However, phytotoxicity of soil Al does not depend on the total content of Al in soil but on its chemical forms (Shahnawaz et al., 2016). In fact, Al is the most abundant metal present in the Earth's crust (Arunakumara et al., 2013). It exists in many different forms in soil such as Al^{3+} , $Al(OH)^{2+}$, $Al(OH)_2^+$, $Al(OH)_3$, Al-OH polymer, Al-F complex, Al-SO₄ complex, phosphate, organic species, carbonate species, and oxide species (Wang et al., 2007; Zhou et al., 2011; Shahnawaz et al., 2016). Al toxicity to plants varies according to different chemical forms. Al in insoluble form is nonphytotoxic whereas Al^{3+} , $Al(OH)^{2+}$, and $Al(OH)_2^+$ are considered as the most toxic forms in soil and named

active Al (Zhou et al., 2011; Shahnawaz et al., 2016). The distribution of Al forms in the soil can be influenced by many factors including soil pH, soil types, predominant clay mineral, organic matter, organic acid, and plant species (Xu and Zhang, 2017). Therefore, many alleviating methods for Al toxicity are associated with the above-mentioned factors. Controlling soil acidity is one of the most common methods to alleviate Al toxicity, because Al forms are found to be dependent on soil pH. Under acidic conditions, Al can be solubilized into more toxic forms. The addition of alkali materials such as calcium carbonate, magnesium limestone, and calcium silicate could increase soil pH and reduce the stress effects of Al on plants (Cristancho et al., 2011; Elisa et al., 2016). Addition of organic materials and mineral ions are also alternative options (Muhrizal et al., 2003; Yang et al., 2009; Iqbal, 2014; Liu et al., 2014). For forest plants, a mixed species plantation might be an effective ecological method to alleviate Al toxicity. However, only a few cases have been reported until now (Li et al., 2008; Lei et al., 2014).

Chinese fir (*Cunninghamia lanceolata*) is one of the most important timber tree species in Southern China where the soil is acidic and ferrallitic. Increasing soil acidification caused by acid rain and the continuous planting of *C. lanceolata* will inevitably lead to Al toxicity in *C. lanceolata* (Liu et al., 2014), which may be closely related to its chemical forms in soil. A mixed plantation of *C. lanceolata* with other forest species has been confirmed to have promoting effects on phosphorus nutrition, microbial community, chemical properties, and carbon storages in soil (Zou et al., 1995; Liu et al., 2010; Richards et al., 2010; Wang et al., 2010). However, little is known about the changes in Al chemical forms. The aim of this study is to examine the effects of different mixed planting patterns of *C. lanceolata* on the chemical forms of Al in soils including exchangeable Al, monomer hydroxy Al, acid-soluble inorganic Al, and humic acid Al in both the rhizosphere and bulk soils. One-year-old seedlings of *C. lanceolata* were used, and the mixed plantation of *C. lanceolata* with both *Michelia macclurei* and *Schima superba* in high planting density was carried out.

Materials and methods

Study area

The experiment was performed in the Experimental Station of Forest located at a hillside of the campus of Fujian Agriculture and Forestry University, in Fujian Province, China (119°14' N and 26°05' E) where has subtropical monsoon climate with an annual average temperature of 15-20°C and an average annual rainfall of 900-2100 mm. The experiment started on May 8, 2014 when it was spring.

Soil for this study was a kind of acid red soil (based on Chinese Soil Taxonomy). The clay mineral composition was characterized by kaolinite with gibbsite and ferric oxide. The soil was taken from the same site of the Experimental Station of Forest. There were no trees except some natural herbs in this chosen area. Only the soil down to a depth of 1-2 m was collected in order to avoid any previous plant residues. Soil properties were examined before the onset of our experiment. The results are presented in *Table 1*.

Table 1. Properties of the soil used in this experiment

pH	Total N (%)	Total P (%)	Total K (%)	Available N (mg/kg ⁻¹)	Available P (mg/kg ⁻¹)	Available K (mg/kg ⁻¹)	Organic matter (%)
4.29	0.048	0.017	1.48	58.9	1.45	42.3	0.7

Mixed plantation

One-year-old seedlings of *C. lanceolata*, *M. Macclurei*, and *S. superba* were used as plant materials. Seedlings were planted in pots (length \times width \times height = 1 m \times 1 m \times 0.8 m) (Fig. 1). The pots were made of concrete and filled with soils mentioned in the above "Soil" section. Five different planting patterns including pure *C. lanceolata*, pure *M. macclurei*, pure *S. superba*, *C. lanceolata* in mixture with *M. macclurei* (1:1) and *C. lanceolata* in mixture with *S. superba* (1:1) were compared. For each planting patterns, there were four replicates (one pot per replicate). For each replicate, there were 16 seedlings for pure planting patterns and 8:8 seedlings for mixed planting patterns, respectively (Table 2). Seedling to seedling distance was 20 cm. All seedlings was watered regularly using tap water to avoid the pot soil too dry. The watering requency differed in different seasons (once per day in spring and autumn, once two days in winter, twice per day in summer). Four seedlings (2:2 for mixed planting patterns) were uprooted together with surrounding soil to the depth of 50 cm by using a plastic tube (15 cm in diameter for 6 months seedlings or 20 cm in diameter for 18 months seedlings) with sharp edge after 6 and 18 months, respectively. The uprooted soils were separated into rhizosphere and bulk soil. The rhizosphere soil was collected by gently shaking the plant roots and carefully removing the soil adhering to them. The rest soil was considered as bulk soil. Both rhizosphere and bulk soils were air-dried, passed through 2-mm sieve after removing visible plant material for further analyses.



Figure 1. Soil culture experiment

Table 2. Design of experiment

No	Planting patterns	Plants/pot		
		<i>C. lanceolata</i>	<i>M. macclurei</i>	<i>S. superba</i>
1	Pure <i>C. lanceolata</i>	16		
2	Pure <i>M. macclurei</i>		16	
3	Pure <i>S. superba</i>			16
4	<i>C. lanceolata</i> / <i>M. macclurei</i>	8	8	
5	<i>C. lanceolata</i> / <i>S. superba</i>	8		8

Determination of Al chemical forms and pH in soil

Chemical forms of Al in soils were extracted using continuous extraction methods (Huang and Qu, 1996; Zhou et al., 2011). Al in each fraction was determined by an auto discrete analyzer (SmartChem 200, WestCo Scientific Instruments Inc., and Italy).

Exchangeable Al: 1 mol L⁻¹ KCl was used to extract exchangeable Al (mainly Al³⁺).

Monomer hydroxy Al: 1 mol L⁻¹ CH₃COONH₄ was used to extract monomer hydroxy Al (mainly Al(OH)²⁺ and Al(OH)₂⁺).

Acid-soluble inorganic Al: 1 mol L⁻¹ HCl was used to extract acid-soluble inorganic Al (mainly Al(OH)₃).

Humic acid Al: 0.5 mol L⁻¹ NaOH was used to extract humic acid Al (mainly humic acid bound Al).

Soil pH was measured in 1 mol L⁻¹ KCl (1:2.5, w:v) using an PHS—3C pH meter (Shanghai INESA Scientific Instrument Co., Ltd, China).

Statistical analysis

Initial data were analyzed using Microsoft Excel. Values were represented as the means of four replicates (Mean ± SD) for each treatment. The relationship between soil pH and chemical forms of Al in soil was also analyzed using linear regression in Microsoft Excel. Differences between different treatments were statistically calculated using method of Tukey for analysis of variance (ANOVA) in SPSS 13.0. The data were considered to be significantly different at *P* < 0.05.

Results

Content of exchangeable Al

As presented in Fig. 2, the content of exchangeable Al decreased by 2.3–3.0% in rhizosphere soil and 7.3–8.1% (*P* < 0.01 for 6 months and *P* < 0.05 for 18 months) in bulk soil of mixed plantation of *C. lanceolata* with *M. macclurei* when compared to that of pure *C. lanceolata* plantation. The content of exchangeable Al increased by 2.1–5.4% in rhizosphere soil whereas it decreased by 6.6–6.9% (*P* < 0.01 for 6 months) in bulk soil of mixed plantation of *C. lanceolata* with *S. superba*.

As showed in Table 3, the content of exchangeable Al increased in rhizosphere soil but decreased in bulk soils of *M. macclurei* after mixed plantation. The soil exchangeable Al reduced in both rhizosphere and bulk soils of *S. superba*, and the changes were significant for the 6-month treatment.

Table 3. Changes in content of exchangeable Al in soils of *M. macclurei* and *S. superba* after mixed plantation with *C. lanceolata* (Mean + SD, *n* = 4 for all the treatments)

Planting patterns	Rhizosphere soil (mg/kg)		Bulk soil (mg/kg)	
	6 months	18 months	6 months	18 months
<i>M. macclurei</i>	190.9±22.3a	194.4±9.2b	224.3±14.6a	221.9±12.1a
<i>C. lanceolata/M. macclurei</i>	209.5±19.5a	215.9±10.7a	220.4±3.6a	219.9±8.5a
<i>S. superba</i>	189.5±5.1a	197.1±7.8a	238.1±3.0a	226.7±9.1a
<i>C. lanceolata/S. superba</i>	179.7±4.4a	191.1±6.6a	224.1±3.4b	217.8±4.37a

Different letters indicate significant differences at *P* < 0.05 between pure plantation and its mixed plantation as determined by the method of Tukey test

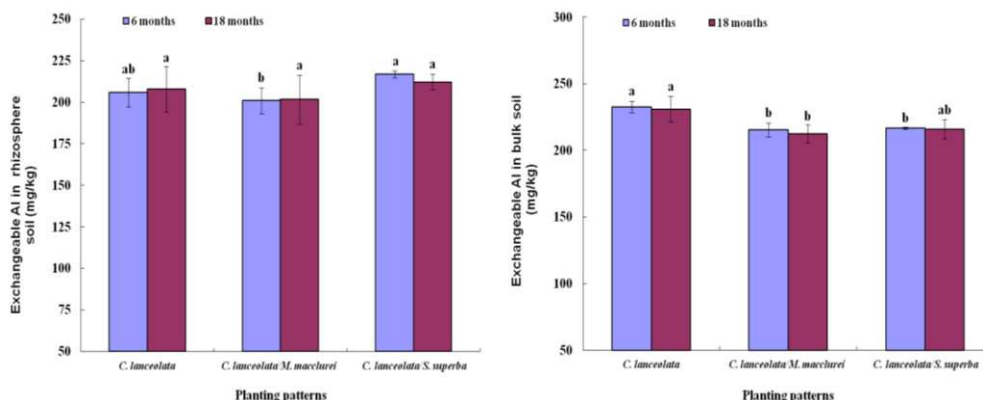


Figure 2. Effect of the mixed plantation of *C. lanceolata* on the content of exchangeable Al in both rhizosphere and bulk soils. Error bars are standard errors of the mean ($n = 4$ for all the treatments). Significant differences ($P < 0.05$) between pure *C. lanceolata* and its mixed plantation are marked by different letters

Content of monomer hydroxy Al

Content of monomer hydroxy Al (Fig. 3) in rhizosphere soil of mixed plantation of *C. lanceolata* with *M. macclurei* was 13.1–14.2% ($p < 0.01$ for 18 months) less than that of pure *C. lanceolata* plantation whereas the value in bulk soil was 2.6–12.4% ($P < 0.01$ for 18 months). The content of monomer hydroxy Al in bulk soil of mixed plantation of *C. lanceolata* with *S. superba* was 7.2–7.3% ($P < 0.05$ for 18 months) less than that of pure *C. lanceolata* plantation whereas its changing trend in the rhizosphere soil was inconsistent between 6 and 18 months treatments.

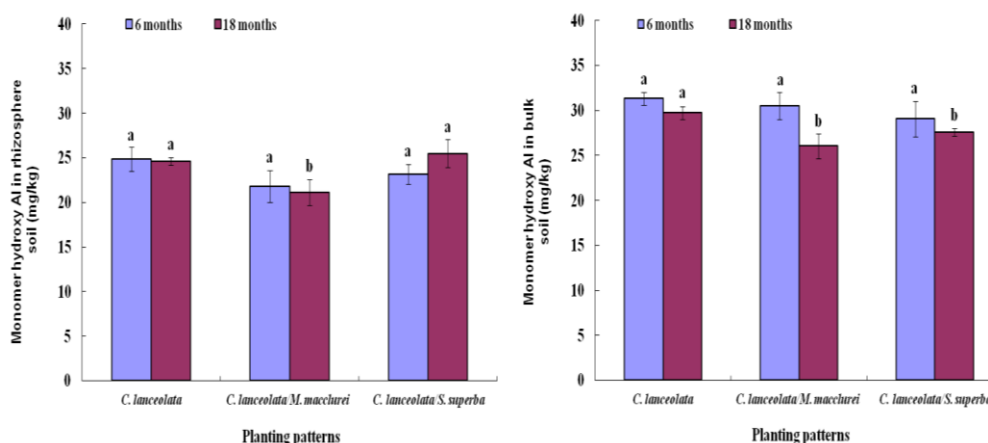


Figure 3. Effect of the mixed plantation on the content of monomer hydroxy Al in both rhizosphere and bulk soils. Error bars are standard errors of the mean ($n = 4$ for all the treatments). Significant differences between pure *C. lanceolata* and its mixed plantation are marked by different letters

The data of the effects of mixed plantation on *M. macclurei* and *S. superba* soils showed that the content of monomer hydroxy Al in both rhizosphere and bulk soils (Table 4) of *M. macclurei* in mixture with *C. lanceolata* and *S. superba* in mixture with

C. lanceolata was less than that of their pure plantations. The difference in monomer hydroxy Al content in bulk soil between mixed plantation and pure plantation was significant after a 6-month mixed plantation treatment of both species, and a 18-month mixed plantation treatment of *S. superba*.

Table 4. Changes in content of monomer hydroxy Al in soils of *M. macclurei* and *S. superba* after mixed plantation with *C. lanceolata* (Mean + SD, n = 4 for all the treatments)

Planting patterns	Rhizosphere soil (mg/kg)		Bulk soil (mg/kg)	
	6 months	18 months	6 months	18 months
<i>M. macclurei</i>	22.6±4.5a	30.5±2.7a	36.2±5.3a	32.7±3.5a
<i>C. lanceolata</i> / <i>M. macclurei</i>	21.3±1.6a	29.5±0.4a	28.7±2.3b	30.1±1.6b
<i>S. superba</i>	28.2±4.4a	31.2±2.2a	30.6±0.7a	29.8±0.2a
<i>C. lanceolata</i> / <i>S. superba</i>	23.8±3.1a	30.2±1.6a	26.4±1.7b	28.5±2.0a

Different letters indicate significant differences at $P < 0.05$ between pure plantation and its mixed plantation as determined by the method of Tukey test

Content of acid-soluble inorganic Al

Content of acid-soluble inorganic Al (Fig. 4) in rhizosphere soil of mixed plantation of *C. lanceolata* with *M. macclurei* was 6.5–9.9% less than that of pure *C. lanceolata* plantation whereas it increased slightly in the bulk soil. The content of acid-soluble inorganic Al in rhizosphere soil of mixed plantation of *C. lanceolata* with *S. superba* was 6.2–9.6% less than that of pure *C. lanceolata* plantation whereas the value in bulk soil was 2.5–7.0%. The statistic analysis did not show that all of the above changes in the content of acid-soluble inorganic Al after mixed plantation were significant.

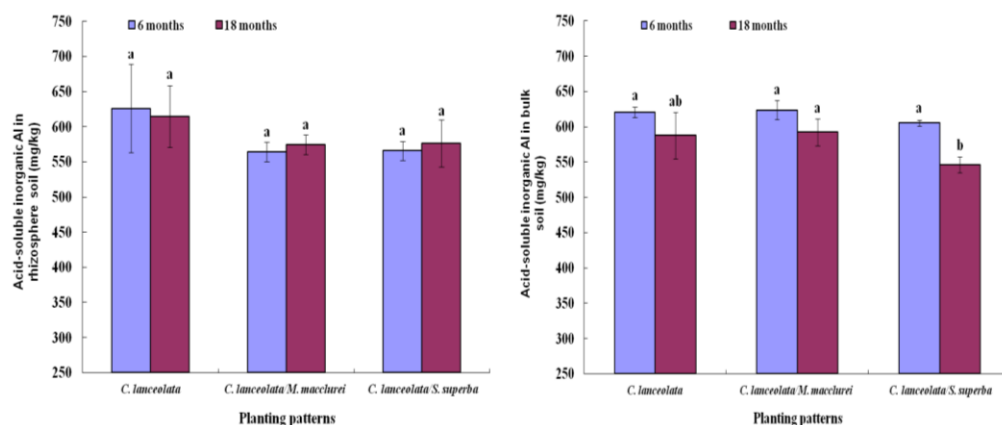


Figure 4. Effect of the mixed plantation on the content of acid-soluble inorganic Al in both rhizosphere and bulk soils. Error bars were standard errors of the mean (n = 4 for all the treatments). Significant differences between pure *C. lanceolata* and its mixed plantation are marked by different letters

Content of acid-soluble inorganic Al in rhizosphere soil of both *M. macclurei* and *S. superba* increased after mixed plantation (Table 5). But the changes were not significant. In contrast, the content of acid-soluble inorganic Al in bulk soil was significantly reduced after a 6-month treatment.

Table 5. Changes in content of acid-soluble inorganic Al in soils of *M. macclurei* and *S. superba* after mixed plantation with *C. lanceolata* (Mean + SD, n = 4 for all the treatments)

Planting patterns	Rhizosphere soil (mg/kg)		Bulk soil (mg/kg)	
	6 months	18 months	6 months	18 months
<i>M. macclurei</i>	598.6±30.7a	613.6±36.1a	619.7±18.9a	591.6±57.2a
<i>C. lanceolata</i> / <i>M. macclurei</i>	607.1±10.6a	628.2±10.3a	588.6±9.3b	583.2±13.8a
<i>S. superba</i>	635.2±15.5a	645.0±32.2a	624.4±11.7a	596.9±17.1a
<i>C. lanceolata</i> / <i>S. superba</i>	656.8±12.2a	667.9±7.3a	592.9±13.7b	631.9±29.6a

Different letters indicate significant differences at $P < 0.05$ between pure plantation and its mixed plantation as determined by the method of Tukey test

Content of humic acid Al

Content of humic acid Al (Fig. 5) in rhizosphere and bulk soils of mixed plantation of *C. lanceolata* with *S. superba* increased by 5.4–9.9% and 5.4–6.2% ($P < 0.01$ for bulk soil after 6 months) when compared to that of pure *C. lanceolata* plantation. For mixed plantation of *C. lanceolata* with *M. macclurei*, the content of humic acid Al had an increase of 0.8–3.4% in rhizosphere soil and a decrease of 0.7–3.5% in bulk soil, but the above changes were not significant.

For both *M. macclurei* and *S. superba*, the content of humic acid Al increased after mixed plantation (Table 6). The changes were significant in rhizosphere soil except 18 month treatment of *M. macclurei*.

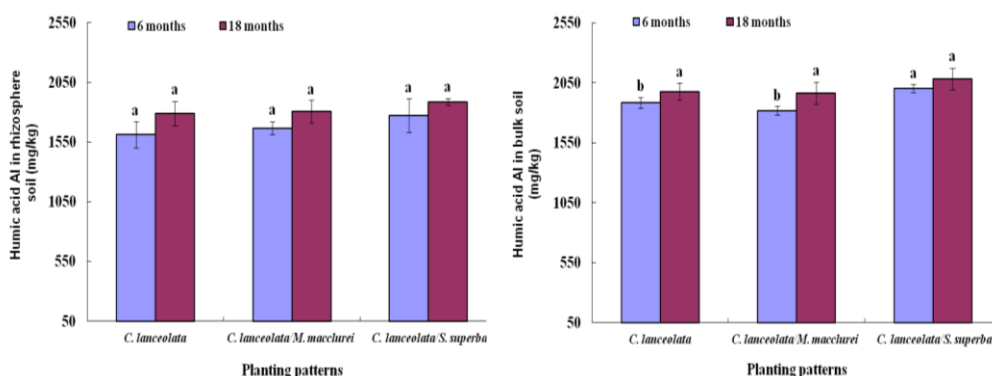


Figure 5. Effect of the mixed plantation on the content of humic acid Al in both rhizosphere and bulk soils. Error bars are standard errors of the mean (n = 4 for all the treatments). Significant differences between pure *C. lanceolata* and its mixed plantation are marked by different letters

Table 6. Changes in content of humic acid Al in soils of *M. macclurei* and *S. superba* after mixed plantation with *C. lanceolata* (Mean + SD, n = 4 for all the treatments)

Planting patterns	Rhizosphere soil (mg/kg)		Bulk soil (mg/kg)	
	6 months	18 months	6 months	18 months
<i>M. macclurei</i>	1856.1±223.1b	1874.4±232.7a	2084.4±280.6a	2060.5±271.2a
<i>C. lanceolata</i> / <i>M. macclurei</i>	2051.3±101.7a	1983.4±81.5a	2145.6±52.5a	2073.0±117.9a
<i>S. superba</i>	1907.0±20.7b	1925.9±38.8b	2055.0±42.8b	2076.9±93.2a
<i>C. lanceolata</i> / <i>S. superba</i>	2197.1±145.9a	2160.4±95.8a	2135.9±17.9a	2130.1±96.1a

Different letters indicate significant differences at $P < 0.05$ between pure plantation and its mixed plantation as determined by the method of Tukey test

Soil pH

The changed in soil pH was also observed after mixed plantation (Fig. 6). There was an increase in pH in both rhizosphere ($P < 0.05$) and bulk soils ($P < 0.05$ after 6 months) of the mixed plantation of *C. lanceolata* with *M. macclurei* when compared to that of pure *C. lanceolata* plantation. For mixed plantation of *C. lanceolata* with *S. superba*, only bulk soil pH showed a significant increase ($P < 0.05$). Table 7 shows the relationship between soil pH and four chemical forms of Al in soil of *C. lanceolata*. We found that soil pH had a negative correlation with exchangeable Al and monomer hydroxy Al, but the correlation was not significant. There was also a negative correlation between soil pH and both exchangeable Al and humic acid Al in soils of *M. macclurei* and *S. superba* plantation which were used as mixed species with *C. lanceolata* (Table 8). The the correlation between soil pH and exchangeable Al in soil was significant at 0.01 level.

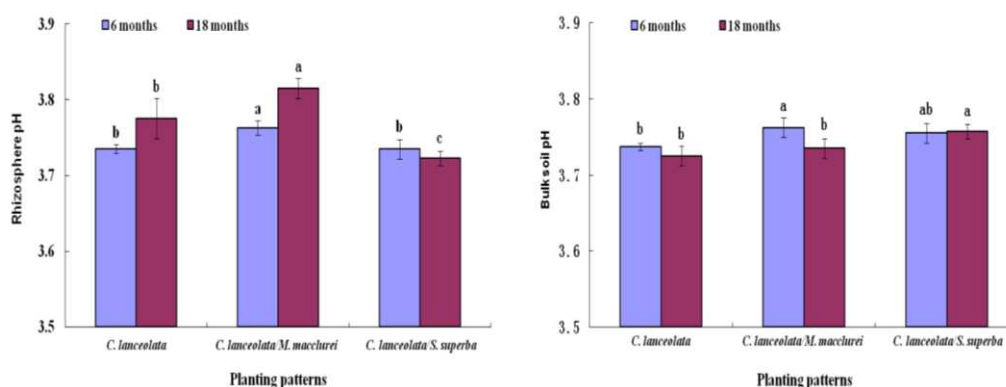


Figure 6. Effect of different mixed planting patterns of *C. lanceolata* on soil pH. (a) Rhizosphere soil; (b) Bulk soil. Error bars were standard errors of the mean ($n = 4$ for all the treatments). Significant differences between pure *C. lanceolata* and its mixed plantation are marked by different letters

Table 7. Relationship between soil pH and chemical forms of Al in soil of *C. lanceolata* ($n=12$)

	Chemical forms	Correlation coefficient
Soil pH	Exchangeable Al	-0.5562
	monomer hydroxy Al	-0.4238
	Acid-soluble inorganic Al	-0.0960
	Humic acid Al	-0.1589

Table 8. Relationship between soil pH and chemical forms of Al in soil of *M. macclurei* and *S. superba* ($n=16$)

	Chemical forms	Correlation coefficient
Soil pH	Exchangeable Al	-0.6955**
	monomer hydroxy Al	0.0173
	Acid-soluble inorganic Al	0.5411*
	Humic acid Al	-0.4577

* $P < 0.05$, ** $P < 0.01$

Discussion

Our results indicated that there were differences in chemical forms of soil Al between mixed and pure plantations of *C. lanceolata*. The mixed plantation of *C. lanceolata* with both *M. macclurei* and *S. superba* could reduce the exchangeable Al and monomer hydroxy Al content in all soils except in the rhizosphere soil of mixed plantation of *C. lanceolata* with *S. superba* (Figs. 2 and 3). This decreasing tendency was consistent with the result of Li et al. (2010) on the mixed plantation of *Pinus massoniana* with *Cinnamomum camphora*. Our finding could be explained through some research results related to mixed plantation in the literatures. It has been documented that mixed plantation could increase plant biomass, soil pH, organic carbon, organic matter, phosphorus nutrition, soil N availability, and microbial biomass, as well as an improvement in microbial community diversities and enzyme activities (Li et al., 2010; Richards et al., 2010; Singh et al., 2012; Forrester et al., 2013; Dutta and Hossain, 2017; Tchichelle et al., 2017). Then such changes may be attributed to the changes in Al chemical forms because the distribution of Al chemical forms in soil could be affected by some of the above-mentioned factors such as soil pH, organic carbon, organic matter and phosphorus nutrition (Godsey et al., 2007; Fang et al., 2014; Hagvall et al., 2015). In our experiment, *C. lanceolata* is an important coniferous species whereas *M. macclurei* and *S. superba* are broadleaved tree species. Broadleaf litter generally has higher nutrient concentrations and lower lignin and polyphenol concentrations than needle litter and has faster litter decomposition rate (Prescott et al., 2004). Moreover, coniferous species may create more acid soils (Götmark et al., 2005). Therefore, introducing broadleaved species in *C. lanceolata* plantation would be very useful for the improvement of soil properties. Our results showed that the soil pH in *C. lanceolata* had an increasing tendency after mixed plantation. This results is in accordance with Cremer et al. (2017), who reported that a mixed plantation of Douglas fir (*Pseudotsuga menziesii*) and European beech (*Fagus sylvatica*) had a higher forest floor and mineral soil pH than pure conifer stands. Similar report came from Berger et al. (2004), who documented that soil pHs under mixed species were higher than soil pHs under pure spruce. Statistic analysis further showed that there was a negative correlation between soil pH in *C. lanceolata* and Al chemical forms in soil, indicating that the change in soil pH may be one of the reasons for the changes in Al chemical forms after mixed plantation. However, further studies on the effects of the mixed plantation of *C. lanceolata* with both species on other soil properties and their relationships with Al chemical forms are needed in the future.

Our results also showed that the content of acid-soluble inorganic Al in soils of *C. lanceolata* decreased after mixed plantation except that in the rhizosphere soil of mixed *C. lanceolata* and *M. macclurei* plantation (Fig. 4), whereas content of humic acid Al increased in all soils except in the rhizosphere soil of mixed *C. lanceolata* and *M. macclurei* plantation (Fig. 5). Yang had found that there was a significant increase in humic acid in a the mixed forest of *C. lanceolata* when compared to its pure stand (Yang et al., 2002). Therefore, the increase of humic acid Al in soil in our experiment may be because of the increase of humic acid after mixed plantation of *C. lanceolata*. As mentioned in the introduction section, different Al forms in soil differed in their phytotoxicity (Zhou et al., 2011; Shah Nawaz et al., 2016). The toxicity potential was ranked in decreasing order as exchangeable Al, monomer hydroxy Al, acid-soluble inorganic Al, and humic acid Al. Therefore, the decrease in exchangeable Al, monomer hydroxy Al, and acid-soluble inorganic Al contents and the increase in humic acid Al

content indicated that such a mixed plantation could decrease the toxic Al forms, and consequently, Al phytotoxicity would be reduced.

We observed that chemical forms of Al in soil of *M. macclurei* and *S. superba* plantation also changed to different extent after mixed plantation with *C. lanceolata*. The exchangeable Al and monomer hydroxy Al content showed a decreasing trend as that of *C. lanceolata*. These results suggested that the mixed plantation is not only useful for *C. lanceolata*, but is also good for the two mixed species as for soil aluminum toxicity.

Conclusions

The experimental results indicated that mixed plantation of *C. lanceolata* could change the distribution of Al speciation in the soil. However, the changes varied among different chemical forms. There was a decreasing tendency in exchangeable Al in both mixed planting patterns. Similar results were also observed in the content of monomer hydroxy Al and acid-soluble inorganic Al. These results indicated that there was a general decrease tendency in the content of chemical forms with higher phytotoxicity including two most active chemical forms of Al in soils (i.e., exchangeable Al and monomer hydroxy Al). Therefore, we suggested that mixed planting patterns could be an alternative alleviation method to control the harmful Al effects on *C. lanceolata* forest although further studies are still needed.

Acknowledgements. We thank Rongmei Zhang for her great assistance in the entire soil culture and sampling. We are also grateful to Yu Chen for his professional advice in this study, Guangqiu Cao for his help with getting the plant material, Bifei Hang for her help with the analysis of Al content. We would also like to thank the National Natural Science Foundation of China (grant number 31370609) for providing the funding for this research.

REFERENCES

- [1] Anjum, S. A., Ashraf, U., Khan, I., Tanveer, M., Saleem, M. F., Wang, L. C. (2016): Aluminum and chromium toxicity in maize: implications for agronomic attributes, net photosynthesis, physio-biochemical oscillations, and metal accumulation in different plant parts. – *Water, Air, Soil Pollution* 227: 326. doi: 10.1007/s11270-016-3013-x.
- [2] Arunakumara, K. K. I. U., Walpola, B. C., Yoon, M. H. (2013): Aluminum toxicity and tolerance mechanism in cereals and legumes - a review. – *Journal of the Korean Society for Applied Biological Chemistry* 56: 1-9.
- [3] Awasthi, J. P., Saha, B., Regon, P., Sahoo, S., Chowra, U., Pradhan, A., Roy, A., Panda, S. K. (2017): Morpho-physiological analysis of tolerance to aluminum toxicity in rice varieties of North East India. – *PLoS ONE* 12(4): e0176357. doi:10.1371/journal.pone.0176357.
- [4] Berger, T. W., Köllensperger, G., Wimmer, R. (2004): Plant-soil feedback in spruce (*Picea abies*) and mixed spruce-beech (*Fagus sylvatica*) stands as indicated by dendrochemistry. – *Plant and Soil* 264: 69-83.
- [5] Cremer, M., Prietzel, J. (2017): Soil acidity and exchangeable base cation stocks under pure and mixed stands of European beech, Douglas fir and Norway spruce. – *Plant and Soil* 415(1-2): 393-405.

- [6] Cristancho, J. A. R., Hanafi, M. M., Omar, S. R. S., Rafii, Y. M., Martinez, F. M., Campos, C. E. C. (2011): Alleviation of aluminum in acidic soils and its effect on the growth of hybrid and clonal oil palm seedlings. – *Journal of Plant Nutrition* 34: 387-401.
- [7] Cruz, F. J. R., de Almeida, H. J., dos Santos, D. M. M. (2014): Growth, nutritional status and nitrogen metabolism in *Vigna unguiculata* (L.) Walp is affected by aluminum. – *Australian Journal of Crop Science* 8: 1132-1139.
- [8] Dutta, S., Hossain, M. K. (2017): Effects of mixed plantation on growth and biomass yield of two common plantation trees of Bangladesh. – *Journal of Forest Environment Science* 33: 22-32.
- [9] Elisa, A. A., Ninomiya, S., Shamshuddin, J., Roslan, I. (2016): Alleviating aluminum toxicity in an acid sulfate soil from Peninsular Malaysia by calcium silicate application. – *Solid Earth* 7: 367-374.
- [10] Fang, X. M., Chen, F. S., Hu, X. F., Yuan, P. C., Li, J., Chen, X. (2014): Aluminum and nutrient interplay across an age-chronosequence of tea plantations within a hilly red soil farm of subtropical China. – *Soil Science and Plant Nutrition* 60: 448-459.
- [11] Forrester, D. I., Pares, A., O'Hara, C., Khanna, P. K., Bauhus, J. (2013): Soil organic carbon is increased in mixed-species plantations of eucalyptus and nitrogen-fixing acacia. – *Ecosystems* 16: 123-132.
- [12] Godsey, C. B., Pierzynski, G. M., Mengel, D. B., Lamond, R. E. (2007): Changes in soil pH, organic carbon, and extractable aluminum from crop rotation and tillage. – *Soil Science Society of America Journal* 71: 1038-1044.
- [13] Götmark, F., Fridman, J., Kempe, G., Norden, B. (2005): Broadleaved tree species in conifer-dominated forestry: Regeneration and limitation of saplings in southern Sweden. – *Forest Ecology and Management* 214: 142-157.
- [14] Hagvall, K., Persson, P., Karlsson, T. (2015): Speciation of aluminum in soils and stream waters: The importance of organic matter. – *Chemical Geology* 417: 32-43.
- [15] Huang, Y. C., Qu, M. L. (1996): Dissolution of aluminum forms in soil. – *Environmental Science* 17: 57-59.
- [16] Iqbal, M. T. (2014): Phosphorus alleviates aluminum toxicity in aluminum -sensitive wheat seedlings. – *Communications in Soil Science and Plant Analysis* 45: 437-450.
- [17] Jones, D. L., Kochian, L. V. (1997): Aluminum interaction with plasma membrane lipids and enzyme metal binding sites and its potential role in aluminum cytotoxicity. – *FEBS Letters* 400: 51-57.
- [18] Kochian, L. V., Pineros, M. A., Liu, J. P., Magalhaes, J. V. (2015): Plant adaptation to acid soils: the molecular basis for crop aluminum resistance. – *Annual Review of Plant Biology* 66: 571-598.
- [19] Lei, B., Liu, B., Luo, C. D., Zhang, J., Xue, Y. J., Liu, L. (2014): Catabatic effect from artificial mixed plantation of *Cunninghamia lanceolata* on soil aluminum toxicity. – *Acta Ecologica Sinica* 34: 2884-2891.
- [20] Li, J. L., Tu, P. F., Chen, N., Tang, J. C., Wang, X. R., Nian, H., Liao, H., Yan, X. L. (2008): Effects of tea intercropping with soybean. – *Scientia Agricultura Sinica* 41: 2040-2047.
- [21] Li, Z. Y., Wang, Y. H., Yu, P. T., Zhang, Z. J., Du, S. C., He, P. W., Xiang, D. J., Li, Z. H. (2010): Soil chemical properties and growth characteristics of mixed plantation of *Pinus massoniana* and *Cinnamomum camphora* in the acid rain region of Chongqing China. – *Journal of Plant Ecology* 34: 387-395.
- [22] Liu, L., Duan, Z. H., Xu, M. K., Hu, J. C., Wang, S. L., Hu, Z. G., Zhang, Q. R., Wang, S. J. (2010): Effect of monospecific and mixed *Cunninghamia lanceolata* plantations on microbial community and two functional genes involved in nitrogen cycling. – *Plant and Soil* 327: 413-428.
- [23] Liu, B., Luo, C. D., Li, X. W., Gray, L., Zhang, F., Liu, M., Ju, J. L., Lei, B. (2014): Research on the threshold of aluminum toxicity and the alleviation effects of exogenous

- calcium, phosphorus, and nitrogen on the growth of Chinese fir seedlings under aluminum stress. – *Communications in Soil Science and Plant Analysis* 45: 126-139.
- [24] Matsumoto, H. (1988): Changes of the structure of pea chromatin by aluminum. – *Plant Cell Physiology* 29: 281-287.
- [25] Muhrizal, S., Shamshuddin, J., Husni, M. H. A., Fauziah, I. (2003): Alleviation of aluminum toxicity in an acid sulfate soil in Malaysia using organic materials. – *Communications in Soil Science and Plant Analysis* 34(19): 2993-3011.
- [26] Prabagar, S., Hodson, M., Evans, E. (2011): Silicon amelioration of aluminium toxicity and cell death in suspension cultures of Norway spruce (*Picea abies* (L.) Karst). – *Environmental and Experimental Botany* 70: 266-276.
- [27] Prescott, C. E., Blevins, L. L., Staley, C. (2004): Litter decomposition in British Columbia forests: Controlling factors and influences of forestry activities. – *BC Journal of Ecosystems and Management* 5: 44-57.
- [28] Ribeiro, M. A. Q., Almeida, A. A. F., Mielke, M. S., Gomes, F. P., Pires, M. V., Baligar, V. C. (2013): Aluminum effects on growth, photosynthesis and mineral nutrition of cacao genotypes. – *Plant Sciences* 36: 1161-1179.
- [29] Richards, A. E., Forrester, D. I., Bauhus, J., Scherer-Lorenzen, M. (2010): The influence of mixed tree plantations on the nutrition of individual species: a review. – *Tree Physiology* 30: 1192-1208.
- [30] Shahnawaz, M., Chauhan, R., Sanadhya, D. (2016): Aluminum (Al) toxicity in plants and resistance mechanism: a review. – *Journal of Plant Science Research* 32: 73-86.
- [31] Singh, K., Singh, B., Singh, R. R. (2012): Changes in physico-chemical, microbial and enzymatic activities during the restoration of degraded sodic land: Ecological suitability of mixed forest over monoculture plantation. – *Catena* 96: 57-67.
- [32] Tabuchi, A., Matsumoto, H., Tabuchi, A., Matsumoto, H. (2001): Changes in cell-wall properties of wheat (*Triticum aestivum*) roots during aluminum induced growth inhibition. – *Physiologia Plantarum* 112: 353-358.
- [33] Tchichelle, S. V., Epron, D., Mialoundama, F., Koutika, L. S., Harmand, J. M., Bouillet, J. P., Mareschal, L. (2017): Differences in nitrogen cycling and soil mineralisation between a eucalypt plantation and a mixed eucalypt and *Acacia mangium* plantation on a sandy tropical soil. – *South Forests* 79: 1-8.
- [34] Ulrich, B., Mayer, R., Khanna, P. K. (1980): Chemical changes due to acid precipitation in a loess derived soil in central Europe. – *Soil Science* 130: 193-199.
- [35] Vardar, F., Cabuk, E., Ayturk, O., Aydin, Y. (2016): Determination of aluminum induced programmed cell death characterized by DNA fragmentation in Gramineae species. – *Caryologia* 69: 111-115.
- [36] Wang, P., Bi, S. P., Zhou, Y. P., Tao, Q. S., Gan, W. X., Xu, Y., Hong, Z., Cai, W. S. (2007): Study of aluminum distribution and speciation in atmospheric particles of different diameters in Nanjing, China. – *Atmospheric Environment* 41: 5788-5796.
- [37] Wang, S. L., Zhang, W. D., Sanchez, F. (2010): Relating net primary productivity to soil organic matter decomposition rates in pure and mixed Chinese fir plantations. – *Plant and Soil* 334: 501-510.
- [38] Xu, X. L., Zhang, J. B. (2017): Research progress on aluminum toxicity and its control in forest soil-plant system. – *Chinese Journal of Ecology* 36: 1106-1116.
- [39] Yang, Y. S., Guo, J. F., Liu, Y. L., Lin R. Y. Chen, G. S. (2002): Composition and properties of soil humus in a mixed forest of *Cunninghamia lanceolata* and *Tsoongiodendron odorum*. – *Journal of Forestry Research* 13(1): 33-36.
- [40] Yang, S. Y., Zou, Y. B., Liu, X. H. (2009): Alleviation of soil aluminum phytotoxicity in a typical paddy soil in southern China by using weak organic acids. – *Journal of Plant Nutrition* 32: 893-906.
- [41] Yang, M., Tan, L., Xu, Y. Y., Zhao, Y. H., Cheng, F., Ye, S. M., Jiang, W. X. (2015): Effect of low pH and aluminum toxicity on the photosynthetic characteristics of different

- fast-growing eucalyptus vegetatively propagated clones. – PLoS ONE 10(6): e0130963. doi: 10.1371/journal.pone.0130963.
- [42] Zhou, N., Liu, P., Wang, Z. Y., Xu, G. D. (2011): The effects of rapeseed root exudates on the forms of aluminum in aluminum stressed rhizosphere soil. – Crop Protection 30: 631-636.
- [43] Zou, X., Binkley, D., Caldwell, B. A. (1995): Effects of dinitrogen-fixing trees on phosphorus biogeochemical cycling in contrasting forests. – Soil Science Society of America Journal 59: 1452-1458.

ISOLATION OF MAGNETOTACTIC BACTERIA FROM ENVIRONMENTAL SAMPLES AND OPTIMIZATION AND CHARACTERIZATION OF EXTRACTED MAGNETOSOMES

SALAM, M. A.¹ – KHAN, A.¹ – RAFIQ, M.² – SHAH, A. A.¹ – HASAN, F.^{1*}

¹*Department of Microbiology, Quaid-i-Azam University, Islamabad 44000, Pakistan*

²*Bristol Glaciology Centre, School of Geographical Sciences, University of Bristol
Bristol BS8 1SS, United Kingdom*

**Corresponding author*

e-mail: farihasan@yahoo.com; phone: +92-51-9064-3065

(Received 17th Oct 2018; accepted 2nd Jan 2019)

Abstract. Magnetotactic bacteria (MTB) have ability to accumulate biominerals intracellularly as iron nanoparticles in the form of ferric oxide (Magnetite) and ferric sulphide (Greigite), known as magnetosomes. Most of them belong to the α -proteobacteria, β -proteobacteria and γ -proteobacteria class. In Pakistan, the magnetotactic bacterial strains are not yet isolated. In current study, the Magnetotactic bacterial strains are isolated from different environmental samples and a modified specific growth medium was used to culture the isolated MTB strains. The technique used for accumulation of bacteria in water samples was the magnetic enrichment technique. The isolation of magnetotactic bacteria is difficult and identified number of strains of magnetotactic bacteria is less than a hundred. So, there is a need to focus more on the identification and classification of MTB. The selected strains were cultured on scale up production and extraction of magnetosomes were carried out by Boiling method. The extracted magnetosomes were characterized by Scanning electron microscopy (SEM), Fourier Transform Infrared (FTIR) spectroscopy and X-ray powder diffraction (XRD).

Keywords: *magnetosomes, scanning electron microscopy, X-ray powder diffraction, Fourier transform infrared spectroscopy*

Introduction

Many organisms can sense the geomagnetic field and this behaviour of organisms is known as “magneto-reception” (Kirschvink et al., 2001). The well-understood example of magneto-reception is present in prokaryotic organisms that can sense and align themselves along with the geomagnetic field lines (Lefèvre et al., 2011b). Those prokaryotes are known as Magnetotactic bacteria (MTB). The evolutionary history of magnetotaxis of MTB might be complex as magnetotaxis in the domain Bacteria is an ancient physiological trait (Lin et al., 2018). Magnetotactic bacteria are a diverse and fascinating group of micro-organisms that shared the ability of orientation towards the geomagnetic fields. The presence of iron oxide and sulphide molecules in bacterial cell makes them little compasses that have ability to direct themselves to the magnetic field lines (Bazylinski and Frankel, 2004). This attribute of MTB is due to the intracellular biomineralization of iron nanoparticles of ferric oxide (magnetite) and ferric sulfide (greigite), known as magnetosomes, which are responsible for magnetotaxis in MTB (Lefèvre and Bazylinski, 2013; Bazylinski et al., 2000). Magnetosomes are individually enclosed by a thin organic covering that confers high and constant dispersion in aqueous solutions as compared with artificial magnetite and this attribute make them ideal for use in biotechnological purpose (Arakaki et al., 2008). These magnetosomes are enclosed within a bilayer membrane that is thought to be an invagination of cytoplasmic

membrane, known as magnetosome membrane. The bacterial cells use the iron that accumulated in cell by the process of biomineralization. Different types of mechanism are used for assimilation and utilization of iron present in the cell (Tanaka et al., 2010). According to Li et al. (2017), extreme environment could provide the knowledge regarding to the evolution of magnetotaxis and biomineralization in MTB. Although magnetotactic bacteria (MTB) are present in various aquatic environments but the majorities of them are still uncultivable (Flies et al., 2005).

MTB are heterogeneous group of microorganisms, which are numerous in aquatic habitats. MTB are commonly resided in Oxic-Anoxic Interface (OAI) of chemically stratified zone where oxygen is present in low concentrations (Simmons et al., 2004). Magnetite-producing MTB are present in fresh water as well as marine water, while greigite-producing reside marine sediments (Bazylinski and Frankel, 2004). All identified MTB are gram negative as well as positive and microaerophilic in nature. The detection of MTB is easy as they move towards the magnetic field but the cultivation process is difficult (Shivangi and Sinha, 2017). According to Loghin et al. (2017), the magnetic gradient can be used to detect the MTB and can control their movements. MTB include various morphological forms as cocci, bacilli, vibrio, ovoids, spirilla and multicellular aggregates (Schuler et al., 1999).

The current study is about the isolation of magnetotactic bacteria from Pakistan fresh water samples. The magnetotactic bacteria were then optimized and were grown in broth medium. The magnetosomes were extracted and characterized by using analytical techniques, i.e. Scanning Electron Microscopy (SEM), Fourier-transform infrared spectroscopy (FTIR) and X-ray powder diffraction (XRD).

Material and methodology

Collection of water sample and magnetic enrichment technique

The water samples were collected from Tatta Pani (31.2488° N, 77.0895° E, Kashmir) and Attabad Lake (36.19° N, 4.48° E, Hunza) in May, 2017 from Pakistan (Fig. 1). The collection of water samples were done in Nalgene sample bottles with magnet inside the bottle. The collection was done about 2-3 feet below the water surface where the oxygen concentration was low and settled down the bottle for 30 min. Then the bottle was carefully closed tightly. The magnetic enrichment technique was used to accumulate the magnetotactic bacteria in water samples by placing bar magnets to the outer wall of sampling jars at room temperature. After 15 days water sample was collected from immediate vicinity of attached magnet so that the chance of isolation of magnetotactic bacteria might be increased (Flies et al., 2005b; Jogler et al., 2010).

Medium composition

The specific growth culturing medium was used for the magnetotactic bacterial growth, named. The composition of the medium was 5 g.L⁻¹ of tryptone, 3 g.L⁻¹ of beef extract, 5 g.L⁻¹ of sodium chloride, 20 ml.L⁻¹ of ferric quinate solution (Sharma and Chandrajit, 2011).

Isolation and detection of magnetotactic bacteria

About 0.5 ml of magnetically enriched water sample was spread on specific growth medium. The colonies were then detected on glass slides by movement of magnetotactic

bacteria as the magnet was placed near the glass slide under compound microscope. The movement of the culture was observed, and the obtained cultures were further confirmed by hanging drop method. Sulphate Indole Medium was used to check the motility of the bacterial strains (Waghmare et al., 2018).



Figure 1. A map indicating the location of sampling sites: Attabad Lake and Tatta Pani

Molecular identification through 16S rRNA gene sequencing

The total genomic DNA of selected bacterial strains was extracted by using Phenol/chloroform DNA extraction protocol. DNA was partially sequenced for 16S rRNA gene by Macrogen, Inc., Seoul, South Korea. Sequences were further analysed for the similar strains in NCBI using BLAST software (<http://blast.ncbi.nlm.nih.gov/Blast.cgi>). Phylogenetic trees were constructed by using MEGA 6 software, which determined the relationship of our isolates with the closely related strains.

Optimization of physiological properties of magnetotactic bacteria

The isolated strains were optimized on different temperatures (17, 27, 37 °C) and pH (6, 7, 8).

Extraction of magnetotactic bacteria

About 500 ml of specific growth medium was inoculated with the isolated bacterial strains and placed the flask in shaking incubator at 27 °C for 15-20 days. The colour of

the medium changes from light brown to dark brown that indicate the production of iron in the medium.

Boiling technique was used for the extraction of magnetosomes from magnetotactic bacteria. The growth medium was centrifuged at 8000 rpm for 15 min at 4 °C. The pellet was shifted to test tubes and washed with distilled water two times and then suspended in 5N NaOH solution for 20 min. Then the suspension was boiled by placing the test tubes in water bath for 2 h or until the suspension was turned into dark brown in colour. Then cool down the suspension and again centrifuge the suspension and collected the pellet in Eppendorf tubes (Frankel RB et al., 1983).

Characterization of magnetosomes

Different techniques will be used for the physico-chemical characterization of purified magnetosomes.

Scanning electron microscopy (SEM)

The surface topology of extracted magnetosomes was examined by scanning electron microscopy (JSM5910, JEOL, Japan) to find structure of magnetosomes after extraction. Magnetosomes were thoroughly washed with sterilized distilled water and mounted on copper stubs with gold paint. Gold plating was done in vacuum to increase the conductivity of the samples.

Fourier-transform infrared spectroscopy (FTIR)

In this study, the ATR-FTIR (Parkin Elmer spectrum 65 FTIR) spectrometer is used for the structural analysis of extracted magnetosomes. The sample was placed on the sample holder. The spectrum was recorded using an attenuated reflectance technique involving diamond crystal. The samples were then scanned from 4000-400 cm⁻¹ with resolution of 6.0 cm⁻¹ and were averaged over 200 scans.

X-ray powder diffraction (XRD)

X-ray powder diffraction (Xpert Pro. PANalytical) used for phase identification of a crystalline material and provide information on unit cell dimensions. The phase and purity of extracted magnetosomes were examined by X-ray diffraction (XRD) with 2 θ range of 5°-65°.

Statistical analysis

Optimization of temperature and pH were performed in duplicate. All the data with repeated measurements were statistically analysed with T-test.

Results

The water samples from Tatta Pani lake and Attabad lake were magnetically enriched by placing magnet and two isolates were selected after doing serial dilutions, Gram staining, inoculation in Sulphate Indole Medium to check the motility assessment and conversion of broth colour from light brown to dark brown by broth activity of inoculum. The colour change in broth showed the production of iron in the broth.

Molecular identification through 16S rRNA gene sequencing

The 16S rRNA sequences of strains were obtained by Macrogen, Inc., Seoul, Korea. The gene sequences were compared with other sequences in the GenBank databases, using the NCBI BLAST software. The bacterial strains CT-K1 and TP6-4 showed 87% and 100% resemblance with *Iron sulfide magnetotactic bacteria* and *Bacillus cereus* species of magnetotactic bacteria respectively (Fig. 2). The aligned sequences were then used to construct a phylogenetic tree by neighbour joining method using MEGA6 software. The accession numbers obtained of these strains are MK053797 for CT-K1 and MK053798 for TP6-4.

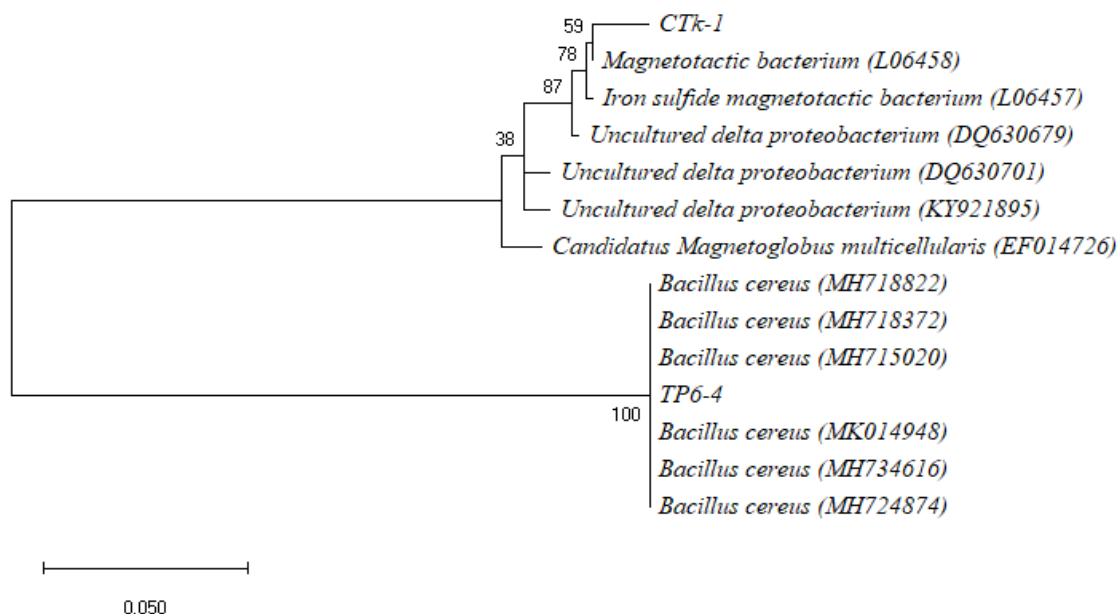


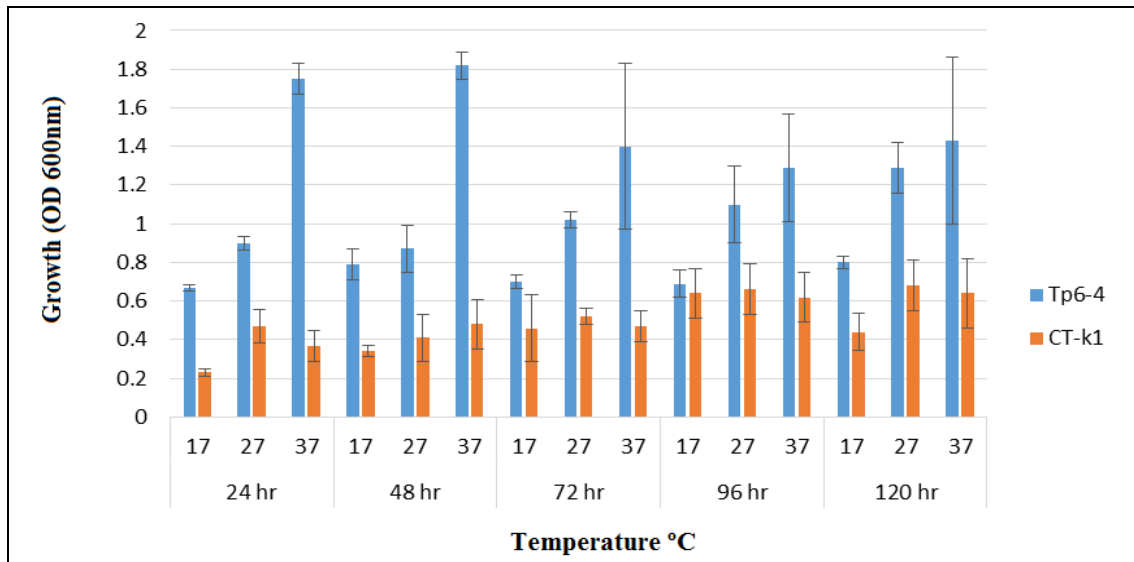
Figure 2. Phylogenetic trees of magnetotactic bacterial strains CT-K1 and TP6-4

Effect of temperature and pH on growth of magnetotactic bacteria

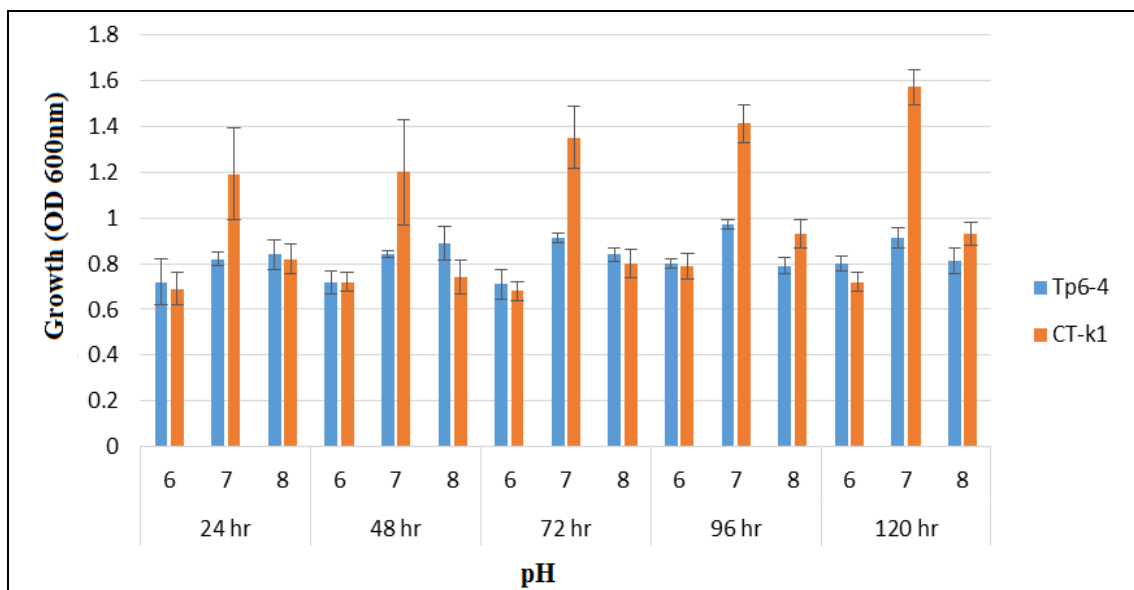
Optimization of physical parameters is of vital importance for obtaining a maximum growth of MTB. The bacterial growth was checked at different temperature after every 24 h. The strain TP6-4 showed high growth at 37 °C while the growth is low at 17 and 27 °C. The other bacterial strain CT-K1 also showed the same growth pattern, maximum growth at 27 °C (Fig. 3). The growth of Strain TP6-4 was better than the growth of CT-K1 to produce magnetosomes. The bacterial growth was checked at different pH after every 24 h. Both the bacterial strains showed maximum growth at 7 pH (Fig. 3). The graphical explanation of optimization of temperature and pH were shown in Figure 3.

Magnetosomes extraction

The bacterial strains TP6-4 and CT-K1 were extracted with boiling technique. The extracted product was brown in colour showed the property of iron. The extracted form of magnetosomes was showed in Figure 4. The brown coloured pallet were magnetosomes and these extracted magnetosomes were then characterized by different techniques.



a



b

Figure 3. Effect of (a) temperature and (b) pH on the growth of strains TP6-4 and CT-K1 ($p < 0.05$, error bars represented the standard error)



Figure 4. Collections of magnetosomes pellet after extraction

Characterization of magnetosomes

Scanning electron microscopy (SEM)

The scanning electron Microscopy showed the structure of magnetosomes that were cleared in the figures (Fig. 5). The bacterial strain TP6-4 showed cuboidal shape of magnetosomes and CT-K1 showed hexahedral shape of magnetosomes. The sizes of the magnetosomes extracted by TP6-4 and CT-K1 were 100 nm and 120 nm respectively.

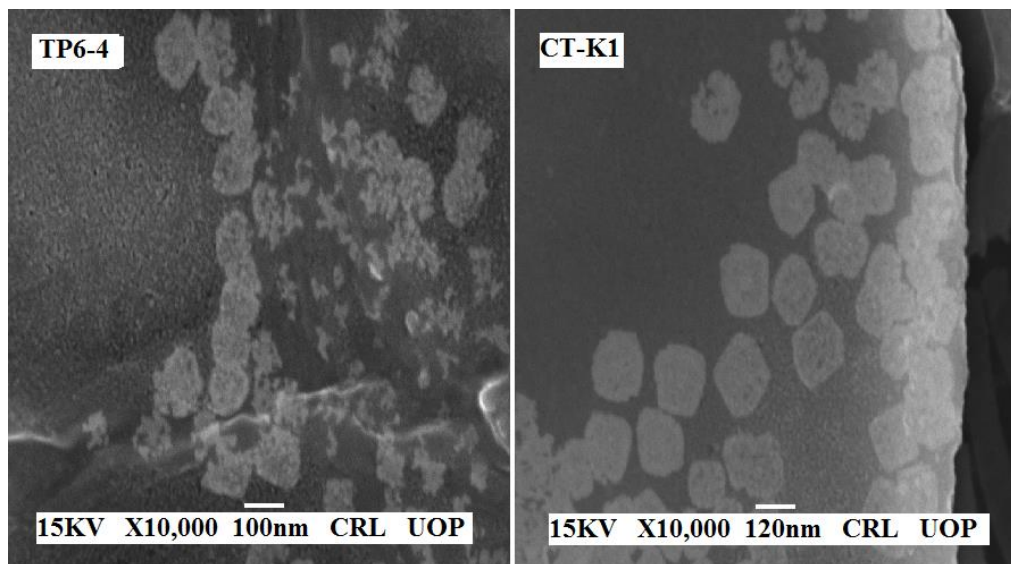


Figure 5. Scanning electron micrographs of biologically produced magnetosomes from CT-K1 and TP6-4

Fourier-transform infrared spectroscopy (FTIR)

The magnetosomes extracted from the bacteria were dried out and FTIR analysis done for the samples. The peaks at 631 and 629 cm^{-1} showed the Fe-O presence in the samples. The peaks appeared at 3460, 3422, 2957, 2916, 1725, 1646, 1650, 1469 and 1468 represented the NH bending, CH stretching, C = O and C = C stretching modes (Fig. 6).

X-ray powder diffraction (XRD)

The diffraction pattern in Figure 7 showed all the diffraction index of magnetite, the strong peaks at 101 at 19 and 311 at 25 representing the magnetite (Fe_2O_3) presence in the sample. The presence of intense and broad peaks confirmed the crystalline structure present in the samples.

Discussion

Magnetotactic bacteria are a diverse group of bacteria and are found in a complex environment of oxic-anoxic transition zone of water sediment. Therefore, the isolation of these bacteria is a difficult process and required more attention for their cultivation. These bacteria accumulate the magnetite and greigite depending upon the type of environment they are present. The medium used for the cultivation of these bacteria is

specific iron containing growth medium. This medium contained tryptone and peptone that is carbon source, ferric quinate solution that is used as an iron source for the bacterial uptake for the production of magnetosomes, NaCl for ion source and beef extract or meat extract for the nitrogen source (Calugay et al., 2004). Bacteria responded to the extreme intricacy of Fe^{3+} by discharging high similarity Fe^{3+} specific legends named as siderophore (Andrews et al., 2003). The molecular biology and microscopy of MTB cells discovered many new species that referred the significant phylogenetic diversity of MTB (Li et al., 2017).

The selected strains of MTB were motile and have flagella for the movement towards magnetic field lines. These bacteria may be monotrichous, peritrichous and amphitrichous according to the type of genus (Bazyliński et al., 1995; Bazyliński and Blakemore, 1983). Both the bacterial strains CT-K1 and TP6-4 are monotrichous in nature. A chemically defined medium known as sulphide indole medium was used to check the motility of the bacterial strains.

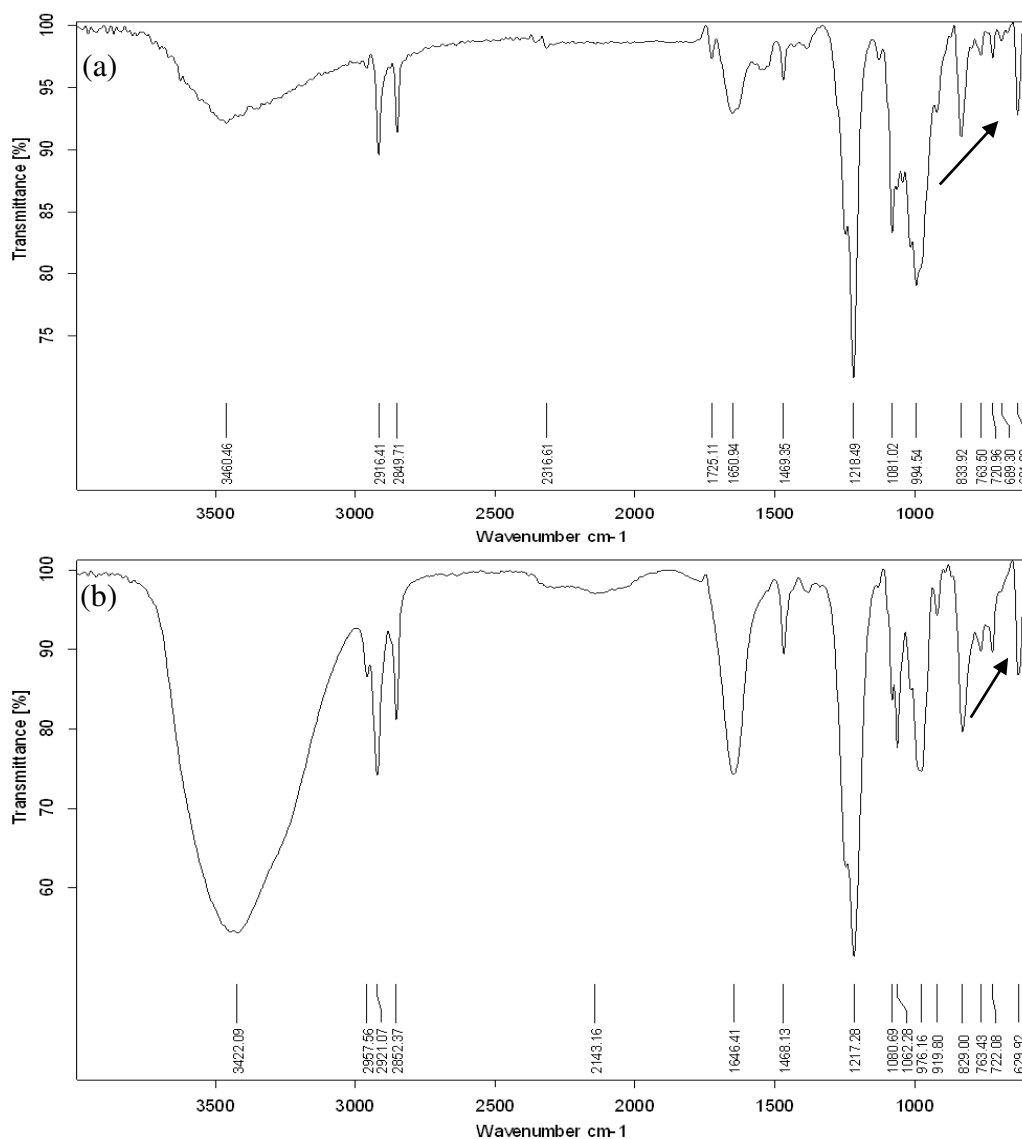


Figure 6. Fourier transform infrared spectrum of magnetosomes produced in iron specific medium extracted from (a) CT-K1 and (b) TP6-4

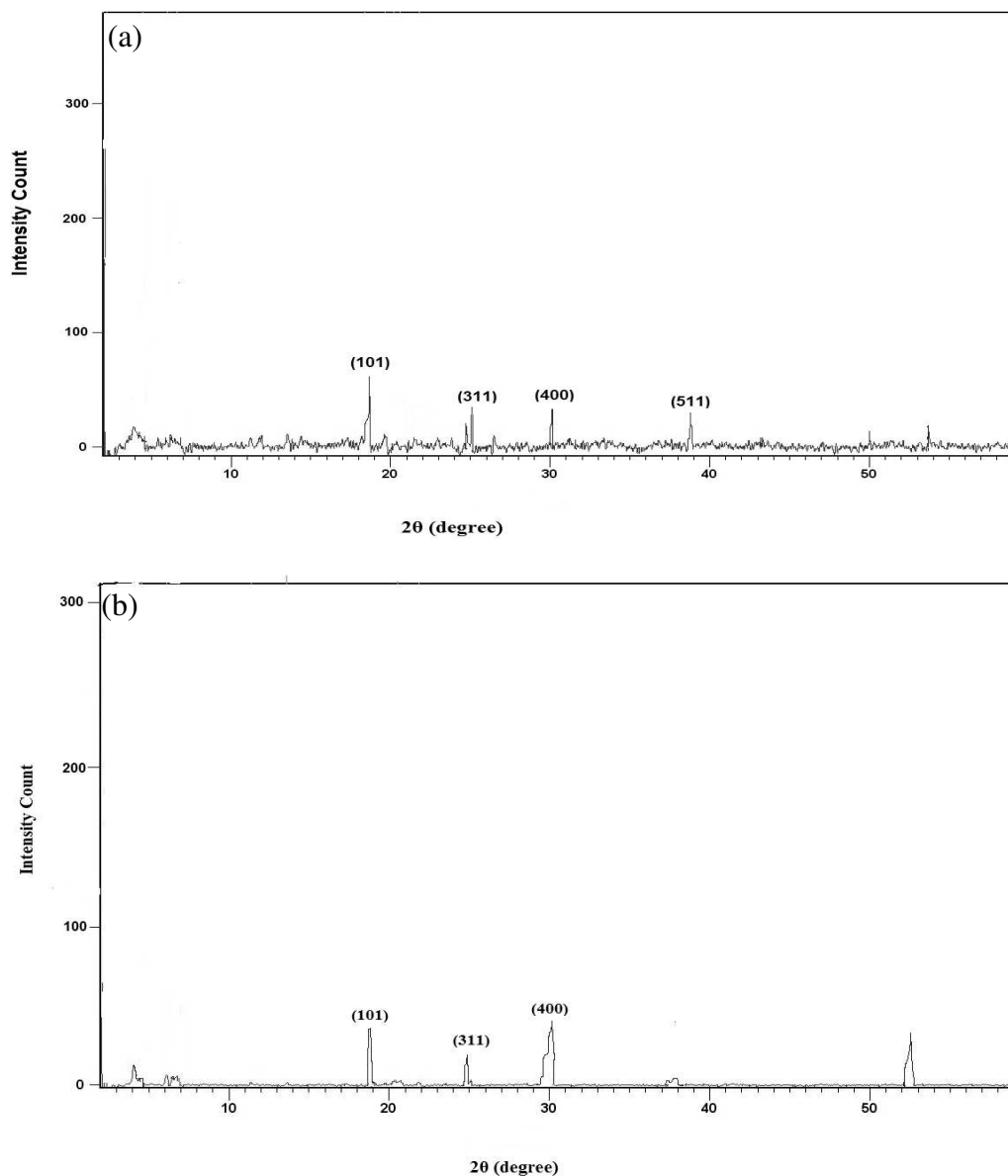


Figure 7. X-ray powder diffraction patterns of extracted magnetosomes from (a) CT-K1 and (b) TP6-4

Magnetotactic bacteria that contained chains of magnetosomes may be differentiated or identified from non-magnetotactic bacteria by magnetic assessment technique. In current study different assessment techniques were used for the isolation of bacteria containing magnetosomes. In the first technique the specific growth medium was prepared with 1% nutrient agar and strains were inoculated on medium with a magnet placed aside. After 4-5 days the movement of bacteria was clearly observed towards the magnet. This was the indication that these bacterial strains contained iron particles inside their cell. In another method the inoculation of the strains was carried out on semi solid medium. These bacterial strains showed movement towards the magnet. According to Comensoli et al. (2017), the change of colour of the medium was due to the precipitation of iron oxide and iron sulphate in the medium. The change in the colour also occurs due to sulphur reduction in the medium. In this study the bacteria that

showed a clear movement towards the magnet were inoculated in the broth medium. After 10 days the colour of the medium changed to dark brown colour that indicated the bacteria consumed the iron present in the medium and produced magnetosomes. Most cultivated and uncultivated magnetotactic bacteria are related with *alpha*, *gemma*, *delta*-*proteobacteria* classes of *Proteobacteria phylum* and *Nitrospira phylum*. Freshwater MTB biomineralize magnetite (Fe_3O_4) and MTB reside in marine settings, can biomineralize greigite (Fe_3S_4) have found in marine water (Frankel et al., 1979).

The DNA of the strains CT-K1 and TP6-4 were extracted through phenol-chloroform method (McOrist et al., 2002). The DNA was suspended in TE buffer for further process. The bacterial strain CT-K1 showed 87% resemblance with the *Iron sulfide magnetotactic bacteria* and the TP6-4 showed 100% resemblance with *Bacillus cereus*. Both the strains were examined to produce magnetosomes. In MTB, the magnetosome biomineralization process is under genetic and biochemical control. Specific genes are involved in the biomineralization and production of the magnetosome crystals (Werckmann et al., 2017).

The MTB bacterial strains have a wide range of temperatures for their growth. Most of the reported magnetotactic bacteria have an optimum growth temperature range from 25-37 °C (Schuler et al., 1999). The temperature optimization was done on 17, 27 and 37 °C for CT-K1 and TP6-4. The TP6-4 strain grew well at 37 °C while the strain CT-K1 grew well at 27 °C. The bacterial cultures showed a mesophilic nature of habitat growing best at mesophilic temperature. The basic purpose of the optimization study of parameters was to produce and extract the magnetosomes and characterized them by using analytical techniques.

In the current study, the scanning electron microscopy showed magnetosomes produced by TP6-4 were cuboidal in shape while magnetosomes produced by CT-K1 were hexahedral in shape and the size of magnetosomes were 100 nm (CT-K1) and 120 nm (TP6-4). According to the Devouard et al. (1998), the size range of the magnetosomes lied between 30 to 120 nm. According to Keutner et al. (2014), the SEM image of single magnetosomes chain in magnetotactic bacterial cell and also individual magnetosomes. They did the SEM analysis on four magnetotactic bacterial strains of *MS-1* on gold grid. The cryo-SEM and TEM was used to see the individual magnetosomes in bacterial cell and several rosette-like magnetosome bundles in *Candidatus Magnetobacterium bavaricum* from the deep branching *Nitrospira* phylum (Jogler et al., 2011). According to Revathy et al. (2017), the SEM and HRTEM micrograph clearly showed the cubo-octahedral shape of the magnetosome present in magnetotactic bacterial strain *Magnetospirillum gryphiswaldense (MSR1)*.

The Fortier Transform Infrared Spectroscopy is a significant tool for the identification of function groups in a compound. The exclusive assortment of absorption bands to confirm the identity of pure compounds or detection of existence of debris. The FTIR analysis was performed for the identification of presence of iron oxide in the extracted compound. According to the FTIR analysis of iron oxide the wavelength for this is between the range of 400-650 cm^{-1} (Revathy et al., 2017). The wavelength for the detection of iron oxide in the analysis was at 629 and 631 cm^{-1} for CT-K1 and TP6-4 respectively. FTIR spectra of iron oxide was well recognized. It was being observed that the immersion band at high wavelength region was due to the OH enlarging and the minor wavelength because of Fe-O matrix trembling. According to the Revathy et al., the FTIR spectrum showed two peaks, in 418 and 522 cm^{-1} that are due to the stretching vibration mode associated with the metal and oxygen absorption band that is Fe-O

bonds in the crystalline lattice of Fe_3O_4 . According to Xiang et al. in (2007), the FTIR analysis of purified magnetosomes showed peaks at 3273, 2921, 1735, 1531 and 1645 cm^{-1} . The peaks appeared at 3273 and 2921 cm^{-1} were representing the NH bending and CH stretching modes. These carbon and nitrogen bonding were representing the lipid bilayer and protein in the magnetosomes membrane. C = O and C = C stretching modes peaks were appeared at 1735, 1645 and 1531 cm^{-1} . FTIR analysis can also be used for the purity examination of magnetosomes. In the current study, the peaks appeared at 3460 and 2916 cm^{-1} in the sample of CT-K1 and peaks appeared at 3422 and 2957 cm^{-1} in the sample of TP6-4. The C = O and C = C stretching modes peaks were appeared at 1725 and 1650 cm^{-1} in the sample of CT-K1 and peaks appeared at 1646 and 1468 cm^{-1} in the sample of TP6-4. This study showed significant results for the characterization of magnetosomes.

The X-rays diffraction analysis showed presence of inverse spinel structure of iron oxide. The 2θ corresponded to the scattering angle of the crystal, the more the sharp edge of the sample the clearer will be the peak. The peaks of 101 and 311 showed the presence of iron oxide in sample and the broad spectrum is due to the crystallinity of the iron oxide. According to Bini et al. (2012), the peaks at wavelength 311 showed the iron oxide crystallinity. While according to Revathy et al. (2017) Magnetospirillum gryphiswaldense (MSR-1) produced magnetosomes and the peaks appeared at 27.05, 30.30, 35.71, 43.31, 55, corresponds to the Fe_3O_4 . In the current study, the peaks showed resemblance to the 27 (311), 30 (400) and 38.5 (511). These results revealed that the XRD analysis showed the presence of Fe_3O_4 in sample. These results of characterization of magnetosomes produced from *Iron sulfide magnetotactic bacteria* were given good evidences to use then in future studies.

Conclusion

Conclusively, the current study helped in finding the newest class of bacteria from the fresh water samples of Pakistan. This has been the tremendous and improved development in the field of microbiology to isolate the class of magnetite producing bacteria. This current study extensively investigated the new ways to isolate these magnetosomes producing bacteria from fresh water bodies. The diversity and ecology of intracellular bio-mineralizing bacteria and their molecular mechanisms of intracellular biomineralization are needed to be studied. The optimised bacterial strain helped in the maximum production of magnetosomes that would be used in many applications. The extracted magnetosomes shape was characterised by scanning electron microscopy so that significant potential use of magnetosomes in different application and ensuring high yield, increased reliability and stability in optimized conditions.

REFERENCES

- [1] Andrews, S. C., Robinson, A. K., Rodriguez-Quinones, F. (2003): Bacterial iron homeostasis. – FEMS Microbiol Rev 27: 215-237.
- [2] Arakaki, A., Nakazawa, H., Nemoto, M., Mori, T., Matsunaga, T. (2008): Formation of magnetite by bacteria and its application. – J Roy Soc Interface 5: 977-99.
- [3] Bazylinski, D. A., Blakemore, R. P. (1983): Denitrification and assimilatory nitrate reduction in *Aquaspirillum magnetotacticum*. – Appl Environ Microbiol 46: 1118-1124.

- [4] Bazylinski, D. A., Frankel, R. B. (2004): Magnetosome formation in prokaryotes. – *Nat Rev Microbiol* 2: 217-230.
- [5] Bazylinski, D. A., Frankel, R. B., Heywood, B. R., Mann, S., King, J. W., Donaghay, P. L., Hanson, A. K. (1995): Controlled biomineralization of magnetite (Fe₃O₄) and greigite (Fe₃S₄) in a magnetotactic bacterium. – *Appl Environ Microbiol* 61(9): 3232-3239.
- [6] Bazylinski, D. A., Dean, A. J., Schüler, D., Phillips, E. J., Lovley, D. R. (2000): N₂-dependent growth and nitrogenase activity in the *metal-metabolizing bacteria*, *Geobacter* and *Magnetospirillum* species. – *Environ Microbiol* 2: 266-273.
- [7] Bini, R. A., Marques, R. F. C., Santos, J. F., Chaker, A. J., Jafelicci, J. M. (2012): Synthesis and functionalization of magnetite nanoparticles with different amino-functional alkoxysilanes. – *J Magnetism Magnetic Mater* 324: 534-539.
- [8] Calugay, R. J., Okamura, Y., Wahyudi, A. T., Takeyama, H., Matsunaga, T. (2004): Siderophore production of a periplasmic transport binding protein kinase gene defective mutant of *Magnetospirillum magneticum* AMB-1. – *Biochem Biophys Res Commun* 323(3): 852-867.
- [9] Comensoli, L., Maillard, J., Albini, M., Sandoz, F., Junier, P., Joseph, E. (2017): Use of bacteria to stabilize archaeological iron. – *Appl Environ Microbiol* 17: 83(9).
- [10] Devouard, B., Posfai, M., Hua, X., Bazylinski, D. A., Frankel, R. B., Buseck, P. R. (1998): Magnetite from magnetotactic bacteria; size distributions and twinning. – *Am Mineral* 83: 1387-1398.
- [11] Flies, C. B., Peplies, J., Schüler, D. (2005a): Combined approach for characterization of uncultivated magnetotactic bacteria from various aquatic environments. – *Appl Environ Microbiol* 71: 2723-2731.
- [12] Flies, C. B., Jonkers, H. M., de Beer, D., Bosselmann, K., Böttcher, M. E., Schüler, D. (2005b): Diversity and vertical distribution of magnetotactic bacteria along chemical gradients in freshwater microcosms. – *FEMS Microbiol Ecol* 52: 185-195.
- [13] Frankel, R. B., Blakemore, R. P., Wolfe, R. S. (1979): Magnetite in freshwater magnetotactic bacteria. – *Science* 203: 1355-1356.
- [14] Jogler, C., Wannera, G., Kolinkoa, S., Nieblera, M., Amannb, R., Petersena, N., Kubec, M., Reinhard, R., Schülera, D. (2011): Conservation of proteobacterial magnetosome genes and structures in an uncultivated member of the deep-branching *Nitrospira phylum*. – *PNAS* 108(3): 1134-1139.
- [15] Jogler, C., Niebler, M., Lin, W., Kube, M., Wanner, G., Kolinko, S. (2010): Cultivation-independent characterization of '*Candidatus Magnetobacterium bavaricum*' via ultrastructural, geochemical, ecological and metagenomic methods. – *Environ Microbiol* 12: 2466-2478.
- [16] Keutner, C., Bohlen, A., Berges, U., Espeter, P., Schneider, C. M., Westphal, C. (2014): Photoemission electron microscopy and scanning electron microscopy of *Magnetospirillum magnetotacticum*'s magnetosome chains. – *Anal Chem* 86: 9590-9594.
- [17] Kirschvink, J. L., Walker, M. M., Diebel, C. E. (2001): Magnetite-based magnetoreception. – *Curr Opin Neurobiol* 11: 462-467.
- [18] Lefevre, C. T., Bazylinski, D. A. (2013): Ecology, diversity, and evolution of magnetotactic bacteria. – *Microbiol Mol Biol Rev* 77(3): 497-526.
- [19] Lefèvre, C., Frankel, R., Pósfai, M., Prozorov, T., Bazylinski, D. A. (2011): Isolation of obligately alkaliphilic magnetotactic bacteria from extremely alkaline environments. – *Environ Microbiol* 13(8): 2342-50.
- [20] Li, J., Zhang, H., Menguy, N., Benzerara, K., Wang, F., Lin, X., Chen, Z., Pan, Y. (2017): Single-cell resolution study of uncultured magnetotactic bacteria via fluorescence-coupled electron microscopy. – *Appl Environ Microbiol* 83(12).
- [21] Lin, W., Zhang, W., Zhao, X., Roberts, A. P., Paterson, G. A., Bazylinski, D. A., Pan, Y. (2018): Genomic expansion of magnetotactic bacteria reveals an early common origin of magnetotaxis with lineage-specific evolution. – *ISME J* 12(6): 1508-1519.

- [22] Loghin, D., Tremblay, C., Mohammadi, M., Martel, S. (2017): Exploiting the responses of magnetotactic bacteria robotic agents to enhance displacement control and swarm formation for drug delivery platforms. – *Int J Robotics Res* 36(11): 1195-1210.
- [23] Revathy, T., Jayasri, M. A, Suthindhiran, K. (2017): Toxicity assessment of magnetosomes in different models. – *3 Biotech* 7: 126.
- [24] Schuler, D., Spring, S., Bazylinski, D. A. (1999): Improved technique for the isolation of magnetotactic spirilla from freshwater sediment and their phylogenetic characterization. – *Syst Appl Microbiol* 22: 466-471.
- [25] Sharma, G. P., Chandrajit, B. (2011): Preliminary isolation report of aerobic magnetotactic bacteria in a modified nutrient medium. – *Recent Res Sci Technol* 3(11): 71-75.
- [26] Shivangi, U., Sinha, A. (2011): Magnetotactic bacteria and their application in environmental clean-up: A review. – *Int. Res. J. Environment Sci* 6(7): 63-68.
- [27] Simmons, S. L., Sievert, S. M., Frankel, R. B., Bazylinski, D. A., Edwards, K. J. (2004): Spatiotemporal distribution of marine magnetotactic bacteria in a seasonally stratified coastal salt pond. – *Appl Environ Microbiol* 70: 6230-6239.
- [28] Tanaka, M., Arakaki, A., Staniland, S. S., Matsunaga, T. (2010): Simultaneously discrete biomineralization of magnetite and tellurium nanocrystals in magnetotactic bacteria. – *Applied and Environmental Microbiology* 76(16): 5526-5532.
- [29] Waghmare, V., Kale, S., Pawar, K., Metri, A. (2018): Isolation, identification of magnetotactic bacteria and their magnetosomes from lonar lake. – *Int J Current Res Life Sci* 7(4): 1858-1862.
- [30] Werckmann, J., Cypriano, J., Lefèvre, C. T., Dembelé, K., Ersen, O., Bazylinski, D. A., Lins, U., Farina, M. (2017): Localized iron accumulation precedes nucleation and growth of magnetite crystals in magnetotactic bacteria. – *Scientific Reports* 7(1): 8291.
- [31] Xiang, L., Wei, J., Jianbo, S., Guili, W., Feng, G., Ying, L. (2007): Purified and sterilized magnetosomes from *Magnetospirillum gryphiswaldense* MSR-1 were not toxic to mouse fibroblasts in vitro. – *Letters Appl Microbiol* 45: 75-81.

GENETIC DIVERSITY AND RELATIONSHIPS AMONG 15 SPECIES OF *IRIS* BASED ON AMPLIFIED FRAGMENT LENGTH POLYMORPHISM MARKERS

XU, Y. F.¹ – HUSSAIN, K.² – YAN, X. F.³ – CHEN, X. H.¹ – SHAO, M. N.¹ – GUAN, P.¹ – QU, B.^{1*}

¹*College of Bioscience and Biotechnology, Shenyang Agricultural University
NO. 120 Dongling Street, Shenyang, Liaoning, China*

²*Department of Botany, University of Gujrat HH Campus, Gujrat, Pakistan*

²*Shuwen Biotech CO., LTD, NO. 139-1 Wenhua Road, Shenyang, Liaoning, China*

**Corresponding author
e-mail: syau_qb@163.com*

(Received 18th Oct 2018; accepted 2nd Jan 2019)

Abstract. Irises are among the most well-known ornamental flowers in the world. There are probably over 60 species of *Iris* in China, accounting for approximately one-fifth of the world's wild resources; however, there is little information available on the genetic diversity and relationships among these species. We accordingly studied the genetic diversity and relationships among 15 species of *Iris* collected in China using amplified fragment length polymorphism (AFLP) markers in conjunction with a combination of *EcoRI/MseI* restriction enzymes. A total of 378 clear and stable bands with sizes ranging from 50 to 800 bp were obtained using 9 pairs of primers screened from 64 primer combinations; the percentage of polymorphic bands was 99.74%. Some species – *I. setosa*, *I. uniflora*, *I. dichotoma*, *I. typhifolia*, *I. ventricosa*, and *I. japonica* – were differentiated by just a single specific band, and these band patterns were used for identification. An assessment of genetic diversity parameters using AFLP markers showed that *Iris* has high genetic diversity at the species level. Clustering analysis and principal coordinate analysis showed that the 15 species of *Iris* were genetically similar, and thus related. When the genetic similarity coefficient was 0.55, the 15 species could be divided into five distinct groups. The aforementioned results will verify, replenish, and consummate the classical taxonomy and systematology of *Iris*, and also provide references for the conservation, management, classification, identification, and breeding of *Iris* resources.

Keywords: *Iris*, AFLP, genetic diversity, relatedness, conservation

Introduction

The genus *Iris*, belonging to the family Iridaceae, includes more than 300 species of perennial and herbaceous plants. They are distributed mainly in northern temperate zones such as Asia, Europe, and North America. Among the 300 plus species, there are 60 species, 13 varieties, and 5 variants that are native to China, and these are principally distributed in the northwest, southwest, and northeast of China (Zhao, 1985; Waddick, 1992). The elegant flowers of *Iris* can be found in a breathtaking array of colors, ranging from white, yellow, and orange, through every tone of blue, purple, pink, and brown, to black. *Iris* species also produce beautiful linear foliage (Claire, 1957; Bailly, 2001). These perfect characteristics make irises one of the most favored ornamental plants. Because of their simple cultivation, extensive management, and low maintenance costs, species of *Iris* are widely utilized in landscaping. Additionally, because of their high resistance to cold, drought, disease, and salinity, some species, such as *Iris lactea*, *Iris sanguinea*, and *Iris halophila*, can be applied for improving coast and saline-alkaline land (Bai et al., 2008). In addition, *Iris tectorum*,

Belamcanda sinensis, *Iris germanica*, and a few other species have medicinal value, containing flavonoids with good detoxification effects (Agarwal et al., 1984; Burcu et al., 2014). Understanding the genetic diversity and relationships among plant species and varieties is very important for breeding and intellectual property rights (IPR) (Tay et al., 2006; Wanjala et al., 2013). *Iris* breeding began very early in Europe. Further, by crossbreeding, many new cultivars with desirable traits have been bred by using the extensive collections of wild species and varieties. Embryo culture, somatic hybridization, and transgenic breeding are a few other successful methods used for *Iris* breeding (Shimizu et al., 1999). Up until 2009, there were more than 30 000 *Iris* cultivars in the world, as catalogued by the American Iris Association (Zhang, 2010). In China, wild *Iris* resources with many good genes are abundant, and these may be used to improve, innovate, and preserve the *Iris* germplasm. However, *Iris* breeding started late and developed relatively slowly in China. Only a small part of the *Iris* resource is utilized directly without any modification, probably due to the lack of systematic research. Further, each year many new cultivars are being introduced, which represents a considerable annual expense. In breeding programs, breeders typically select parents with good performance and a wide hereditary basis, according to their genetic diversity and relatedness to parental germplasm, which are very important criteria for crossbreeding (Hesham et al., 2010; Matus et al., 2002). The classification of the genus *Iris* has been controversial, because of the focus on botany and horticulture. In recent years, the classification system of the American Iris Society, which is based on traditional morphological characteristics, has become popular (Lin et al., 2010). However, morphological classification has certain disadvantages, which often leads to an incorrect evaluation. The morphological characteristics of plants may be expressed differently in different environments, and can only sometimes be appraised correctly in adult plants, which could result in a waste of resources for plant growth and increase the difficulty of evaluation (Poppendieck, 1983; Vieira et al., 2007). Thus, the classification of *Iris* is vague and often invalid in practice. Consequently, it is not surprising to find different cultivars with the same name or to find the same plant referred to by different names (Zhang et al., 2008).

Because of the various species and relatively similar traits, confusion and misuse of *Iris* resources can easily occur. Therefore, it is important that a scientific and reliable identification method be established. With the continuous development of molecular biology techniques, several studies of *Iris* have been conducted at the molecular level. Over the past few decades, DNA-based markers have proven to be very successful in classifying plants (Vos et al., 1995; Qiao, 2007), and in assessing the intraspecific and interspecific genetic diversity of plants (Morales et al., 2013). Although some studies have been conducted on the genetic relationships and population genetic diversity among species or cultivars of *Iris* (Tang et al., 2010; Chung et al., 2014), because of the diversity of natural geographical distribution, only a few species have been studied, and the phylogenetic relationships of many other species in this genus is still currently unclear or disputed and needs to be further clarified.

Amplified fragment length polymorphism studies have been used extensively to examine genetic population structure and provide guidance for conservation efforts. AFLP is a molecular marker technology with high-integrated utility, which combines the advantages of RFLP and RAPD. Due to the characteristics of the required trace levels of DNA, high polymorphism levels, good reproducibility, high stability, ease of standardization, genome-wide marker distribution, and no prior sequence knowledge,

the AFLP method is considered to be a better tool for evaluating the genetic diversity (Jianab et al., 2009; Garrido et al., 2012) and genetic structure (Breinholt et al., 2009) of plants, and for plant genotyping (Allen et al., 2008) and DNA fingerprinting (Tatikonda et al., 2009) analyses. In addition, AFLP analysis is credibly applied to assessing the genetic diversity of intraspecies and interspecies (Umezuruike et al., 2010; Isaza et al., 2012; Hong et al., 2013).

In this study, using AFLP markers, we objectively evaluated the genetic diversity and genetic relationships of 15 wild *Iris* samples collected in northern China. The objectives of this study were to (1) verify, replenish, and consummate the classical taxonomy and systematology of *Iris*, and (2) provide references for the conservation, management, classification, identification, and breeding of *Iris* resources.

Materials and Methods

Sampling of species

In this study, 15 species of *Iris* were collected and analyzed (*Table 1 and Fig. 1*). The field studies did not involve endangered or protected species, and no specific permissions were required for the locations collected from. All plants were wild species and mainly obtained from northern China. Leaves of each species were taken outdoors, dried with silica gel, and stored in ziplock bags at room temperature for DNA extraction.

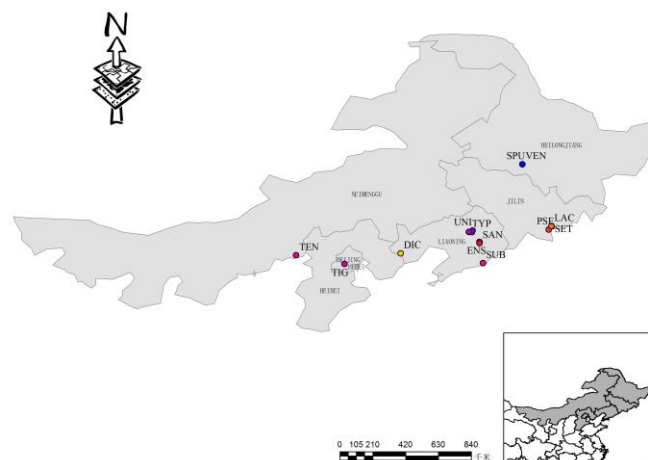


Figure 1. Locations of sampling sites of 15 species of *Iris* in North China

AFLP analysis

Genomic DNA was extracted from dried leaves using the CTAB method described by Wang et al. with some modifications (Wang et al., 2013). PVP was added when DNA extracted because there was more phenolics and flavonoids in leaves of *Iris*, and DNA extraction numbers were increased. The samples were initially ground with a pestle and mortar, and then with magnetic particles, without liquid nitrogen. The concentration and purity of genomic DNA were determined by agarose gel electrophoresis (1%) and UV spectrophotometry. Finally, the genomic DNA was diluted to a concentration of 50 ng/ μ l and stored at -20°C for AFLP analysis.

The AFLP reactions and procedures were performed according to the methods of Vos et al. (1995) and Chen et al. (2009) with some modifications. Genomic DNA was digested using an enzyme combination of *EcoRI* (Fermentas) and *MseI* (Sangon). Three species of *Iris* were selected randomly from the 15 *Iris* accessions for primer screening, namely *I. setosa* (Jilin), *I. lactea* var. *chinensis* (Liaoning), and *I. ventricosa* (Heilongjiang). Nine primer combinations and 64 AFLP primer pairs could amplify clear and reproducible polymorphic bands. AFLP-PCR products were separated by 6% denaturing polyacrylamide gel electrophoresis, with constant power of 55 W for approximately 2 h, and then the DNA bands were visualized by silver staining and imaged using a scanner.

Table 1. List of species of *Iris* included in the study

Name	Species code	Sample size	Location	Habitats
<i>Iris setosa</i> Pall. ex Link	SET	20	Changbaishan, Jilin, 128.193479,42.190904	marshland
<i>I. lactea</i> Pall. var. <i>chinensis</i> (Fisch.)Koidz.	LACV	22	Tianzhushan, Shenyang, Liaoning, 123.606614,41.84861	waste land
<i>I. pseudacorus</i> L.	PSE	22	Changbaishan, Jilin, 128.021804,42.004753	waterside
<i>I. spuria</i> L.	SPU	20	Haerbin, Heilongjiang 126.50726,45.79324	patana
<i>I. tenuifolia</i> Pall.	TEN	25	Bayintu,Fengzhen, Inner Mongolia, 113.505159,40.505955	Sandy meadow
<i>I. ensata</i> Thunb.	ENS	24	Benxi, Liaoning, 124.045916,41.280213	marshland
<i>I. uniflora</i> Pall. ex Link	UNI	20	Qipanshan, Shenyang, Liaoning, 123.642905,41.943596	patana
<i>I. dichotoma</i> Pall.	DIC	20	Jianchang, Huludao, Liaoning, 119.513145,40.61749	patana
<i>I. sanguinea</i> Donn ex Horn.	SAN	22	Benxi,Liaoning 124.047784,41.21838	marshland
<i>I. typhifolia</i> Kitagawa	TYP	22	Beiling Garden,Shenyang, Liaoning, 123.43881,41.860968	waterside
<i>I. ventricosa</i> Pall.	VEN	20	Haerbin, Heilongjiang 126.504816,45.792134	Sandy meadow
<i>I. lactea</i> Pall.	LAC	20	Changbaishan, Jilin 128.171363,42.195006	patana
<i>I. japonica</i> Thunb.	JAP	23	Wanshoushan,Beijing 116.281049,40.006067	forest edge
<i>I. tigridia</i> Bunge	TIG	25	Qianshan,Anshan,Liaoning 116.281049,40.006067	patana
<i>I. subdichotoma</i> Y. T. Zhao	SUB	24	Dandong ,Liaoning 124.246351,40.05011	patana

Data analysis

Amplified AFLP bands were scored as present (1) or absent (0) by visual inspection. Data entry in Excel created a 0/1 binary matrix, based on which we could calculate the number and percentage of polymorphic bands (PPB). Clustering analysis and principal component analysis (PCA) were then performed using NTSYS-pc (version 2.10e) software (Rohlf, 2000). The parameters of the differential degree and the genetic diversity among species of *Iris* were calculated using popgene32 (version 1.32) software (Yeh, 1997), including genetic similarity coefficient, genetic distance, the observed number of alleles (Na), the effective number of alleles (Ne), Nei's genetic diversity index (H), and Shannon's information index of diversity (I). All of the aforementioned calculations were performed based on the assumption that these species were in Hardy-Weinberg equilibrium.

Results

Polymorphism of amplified fragments

An AFLP amplification map was obtained using 9 pairs of primers for 15 species of *Iris*. A total of 378 generated bands were clear and stable, ranging in size from 50 to 800 bp, of which 377 bands (99.74%) were polymorphic (Table 2). The number of bands amplified per primer combination ranged from 34 to 53, with an average of 42, and the average number of polymorphic bands per primer pair was 41.89. The polymorphic percentage of bands per primer combination was close to 100%, showing that the 15 species of *Iris* have rich genetic diversity.

Furthermore, genetic diversity parameters (Table 3) demonstrated that the genus *Iris* has considerable genetic diversity at the species level. Because of the lack of gene flow among species, not only can these species be used as good breeding materials, but they should also be protected as wildlife resources.

Table 2. Amplified fragment length polymorphism (AFLP) detected using nine primer pairs for 15 species of *Iris*

Primer pairs	Total amplified bands	Number of polymorphic bands	Percentage of polymorphic bands (PPB %)
E-AAG/M-CTA	34	34	100.00
E-AAC/M-CAG	38	38	100.00
E-AAC/M-CAA	36	36	100.00
E-AAC/M-CAT	40	39	97.50
E-AGG/M-CTG	45	45	100.00
E-AGC/M-CTA	47	47	100.00
E-ACT/M-CAT	53	53	100.00
E-ACT/M-CAC	46	46	100.00
E-ACT/M-CTG	39	39	100.00
Sum	378	377	99.74
Mean	42	41.89	99.74

Table 3. Amplified fragment length polymorphism (AFLP) genetic diversity parameters of 15 species of *Iris*

Parameters	Na ^a	Ne ^b	H ^c	I ^d
Mean	1.9974	1.7950	0.4319	0.6193
SD	0.0514	0.2257	0.0890	0.1033

^aObserved number of alleles; ^bEffective number of alleles; ^cNei's gene diversity; ^dShannon's information index

Many specific bands were displayed by 0/1 binary matrix analysis (Table 4). For example, among the amplification products of primer combination E-AAG/M-CTA, the first band was absent from *I. japonica*, and among the amplification products of primer pair E-AAC/M-CAG, the 26th band was present in *I. dichotoma*.

Table 4. Specific bands and identification methods of 15 species of *Iris*

Sample	Primers								
	E-AAG /M-CTA	E-AAC /M-CAG	E-AAC /M-CAA	E-AAC /M-CAT	E-AGG /M-CTG	E-AGC /M-CTA	E-ACT /M-CAT	E-ACT /M-CAC	E-ACT /M-CTG
SET		8(1), 31(1)			21(0)		44(0)		
LACV		1(1),2(1),4(1),38(1)							
PSE				29(0)				26(1)	
SPU									38(0)
TEN			26(1)				37(1)		
ENS			18(1)				37(1)		
UNI	9(1),10(1)	2(1),8(1)	28(1)	24(0)					
DIC		5(1),7(1), 26(1) ,38(1)							31(0) ,39(0)
SAN	9(1),10(1)	1(1)					47(1)		
TYP		16(1)	36(1)	15(0)				26(1)	
VEN		3(1) ,4(1),16(1)			21(0)		11(0)		
LAC					21(0)				
JAP	1(0)					42(1)	11(0),47(1)		38(0),39(0)
TIG		5(1),7(1)		15(0)					
SUB				29(0)					

The bold numbers indicate a specific band per species that can be distinguished using only this band. A (B) means that the A band is present (1) or absent (0) in decreasing molecular weight (50–800 bp) of a primer amplification product. B has only two values—0 and 1. E.g., 9(1)^a under the primer pair E-AAG/M-CTA means that the band of *Iris sanguinea* appears in E-AAG/M-CTA amplified products at the ninth position by decreasing molecular weight

Moreover, different species of *Iris* can be distinguished by these specific bands. Some species—*I. setosa*, *I. uniflora*, *I. dichotoma*, *I. typhifolia*, *I. ventricosa*, and *I. japonica*—were differentiated by just a single specific band. Nevertheless, some species were differentiated by more than one specific band. In *I. pseudacorus* for instance, the 29th band was absent in the amplification products of primer combination E-AAC/M-CAT, but the 26th band was present among the amplification products of primer combination E-ACT/M-CAC.

Genetic similarity coefficient analysis

In taxonomy, the genetic similarity coefficient or Nei's genetic identity refers to a similarity index between two taxonomic units and is sometimes replaced by genetic distance, which is a complement parameter of the genetic similarity coefficient. The genetic similarity coefficient generally lies between 0 and 1 (Li et al., 2011). For *Iris*, the genetic similarity coefficient ranged from 0.4392 to 0.6296 (Table 5), and that between *I. tenuifolia* and *I. uniflora* (approx. 0.4392) was the smallest. The genetic similarity coefficient between *I. setosa* and *I. tenuifolia* (approx. 0.6296) was the largest. The genetic distance reflects the degree of genetic differentiation between species. The genetic distance in *Iris* ranged from 0.4626 to 0.8229, with the genetic distance between *I. setosa* and *I. tenuifolia* (approx. 0.4626) being the smallest, and that between *I. tenuifolia* and *I. uniflora* being the largest (approx. 0.8229). All other genetic distances indicated that the genus *Iris* has substantial genetic differentiation at the species level.

Table 5. Nei's genetic identity (above diagonal) and genetic distance (below diagonal)

	SET	LACV	PSE	SPU	TEN	ENS	UNI	DIC	SAN	TYP	VEN	LAC	JAP	TIG	SUB
SET	****	0.5741	0.5397	0.5132	0.6296	0.5185	0.4497	0.5608	0.5476	0.4550	0.5026	0.5661	0.4894	0.57360.4921	
LACV	0.5550	****	0.5476	0.5688	0.6058	0.5582	0.4683	0.5106	0.5291	0.5053	0.5688	0.6111	0.5344	0.57140.5582	
PSE	0.6168	0.6022	****	0.5767	0.6190	0.6085	0.4868	0.4974	0.4524	0.5238	0.4762	0.5238	0.5423	0.58990.5767	
SPU	0.6670	0.5643	0.5504	****	0.5820	0.5926	0.5556	0.5926	0.5265	0.5503	0.5450	0.5608	0.5688	0.62170.4921	
TEN	0.4626	0.5012	0.4796	0.5413	****	0.5873	0.4392	0.5132	0.5159	0.4974	0.5132	0.5926	0.5529	0.61110.5397	
ENS	0.6568	0.5830	0.4968	0.5232	0.5322	****	0.5026	0.5503	0.5106	0.5820	0.5026	0.5291	0.5688	0.55290.5503	
UNI	0.7991	0.7587	0.7200	0.5878	0.8229	0.6879	****	0.4921	0.5265	0.5291	0.5291	0.5132	0.5317	0.54230.4868	
DIC	0.5783	0.6722	0.6985	0.5232	0.6670	0.5974	0.7091	****	0.5212	0.5397	0.5450	0.4974	0.4788	0.53170.5714	
SAN	0.6022	0.6366	0.7932	0.6416	0.6619	0.6722	0.6416	0.6517	****	0.5582	0.5794	0.5423	0.5026	0.52380.5265	
TYP	0.7874	0.6826	0.6466	0.5974	0.6985	0.5413	0.6366	0.6168	0.5830	****	0.5556	0.5397	0.5317	0.52120.5238	
VEN	0.6879	0.5643	0.7419	0.6070	0.6670	0.6879	0.6366	0.6070	0.5458	0.5878	****	0.5344	0.5106	0.53170.5132	
LAC	0.5689	0.4925	0.6466	0.5783	0.5232	0.6366	0.6670	0.6985	0.6119	0.6168	0.6266	****	0.4788	0.52120.5820	
JAP	0.7145	0.6266	0.6119	0.5643	0.5926	0.5643	0.6316	0.7364	0.6879	0.6316	0.6722	0.7364	****	0.57670.5000	
TIG	0.5736	0.5596	0.5277	0.4753	0.4925	0.5926	0.6119	0.6316	0.6466	0.6517	0.6316	0.6517	0.5504	**** 0.5106	
SUB	0.7091	0.5830	0.5504	0.7091	0.6168	0.5974	0.7200	0.5596	0.6416	0.6466	0.6670	0.5413	0.6931	0.6722 ****	

Clustering analysis and principal component analysis

Based on the genetic similarity coefficient, genetic relationships among the 15 species of *Iris* were examined by clustering analysis using the UPGMA method (Fig. 2). When the genetic similarity coefficient was 0.55, the species could be divided into five groups: the first group: *I. dichotoma* and *I. subdichotoma*, belonging to Subgen. *Pardanthopsis*; the second group: *I. pseudacorus* (Subgen. *Limniris* Sect. *Limniris*), *I. ensata* (Subgen. *Limniris* Sect. *Limniris*), *I. spuria* (Subgen. *Xyridion*), *I. tigridia* (Subgen. *Iris* Sect. *Hexapogon*), and *I. japonica* (Subgen. *Crossiris* Sect. *Crossris*); the third group: *I. tenuifolia*, *I. setosa*, *I. lactea* var. *chinensis*, and *I. lactea*, all belonging to Subgen. *Limniris* Sect. *Limniris*; the fourth group: *I. sanguinea*, *I. ventricosa*, *I. typhifolia*, all belonging to Subgen. *Limniris* Sect. *Limniris*; and the fifth group: *I. uniflora* (Subgen. *Limniris* Sect. *Loniris*).

In addition, a further partition was noted when considering the genetic similarity coefficient of 0.59. The first group had two sub-groups: *I. dichotoma* and *I. subdichotoma*. The second group could be divided into three sub-groups: *I. pseudacorus*; *I. ensata*, *I. spuria*, and *I. tigridia*; and *I. japonica*. The third group had two sub-groups: *I. tenuifolia* and *I. setosa*; and *I. lactea* var. *chinensis* and *I. lactea*. The fourth group had three sub-groups: *I. sanguinea*, *I. ventricosa*, and *I. typhifolia*.

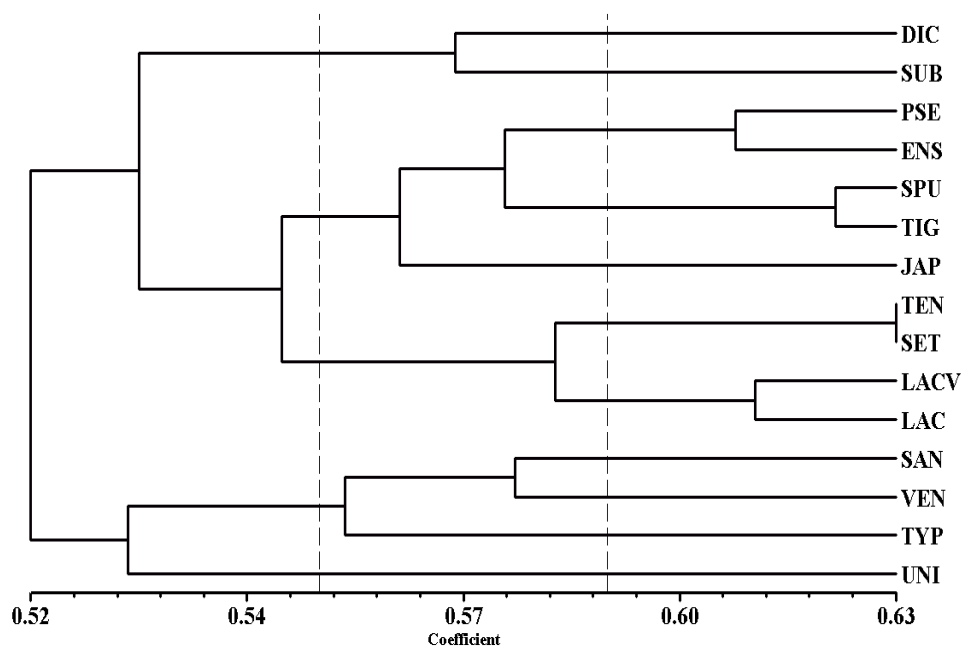


Figure 2. Phylogenetic analysis of 15 species of *Iris* based on AFLP markers

PCA of the 15 species of *Iris* based on the genetic similarity coefficient using NTsys2.10e software (Fig. 3) gave an important insight into their genetic relationships. The relationships among species showed a positive correlation with the genetic distance, and species close to each other on the shadow (Fig. 3a) were classified together (Fig. 3b), showing that the PCA and clustering analysis provided similar results when analyzing relationships. Therefore, PCA could be used to explain and verify the clustering results, which were similar to those reported by Huang et al. (2009).

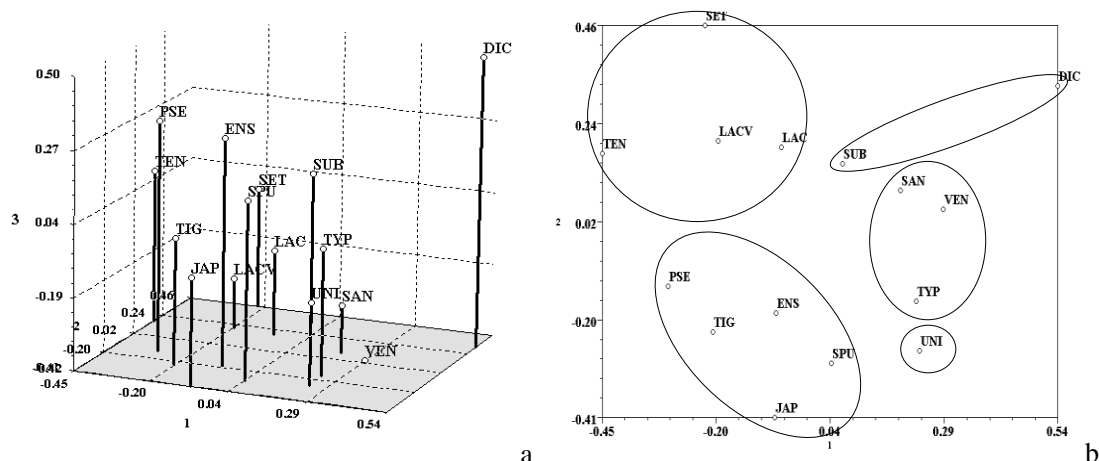


Figure 3. Principal coordinates analysis (PCA) of 15 species of *Iris* by AFLP markers. Fig. 3a is a 3D-plot, of which Fig. 3b is a 2D-plot with dimension 1 and dimension 2

Discussion

At present, the genetic diversity of many plants has been studied using molecular markers, including AFLP, SRAP, RAPD, ISSR, and SSR (Duffy et al., 2009; Bertoni et al., 2010; Talebi et al., 2011). Here, a total of 378 bands were obtained from 15 species of *Iris* using AFLP markers with 9 pairs of primers. The percentage of polymorphic bands was 99.74%, and the length of amplified fragment was approximately 50–800 bp. A combined analysis of genetic diversity parameters (Na, Ne, H, I) and genetic distance with the polymorphism of amplified fragments showed that the genus *Iris* has a rich genetic diversity and that there is relatively large genetic differentiation at the species level. Thus, it is important to use *Iris* wildlife resources for crossbreeding, as well as for ornamental and medicinal purposes. In addition, our results can assist in making effective decisions for the conservation of the germplasm of this species. The samples used in this study were all wild species, which may be one reason for the high genetic differentiation.

We found that different species of *Iris* had some specific bands, which can be reasonably used for identification. The morphological method and molecular marker method can be used together to accurately identify the species of *Iris*. In addition, the specific alleles will aid the assessment of stability and purity of genotypes in breeding and seed reproduction programs. Further, members of the genus *Iris* lacked mutual bands and there was a high specificity among species.

On the basis of soil and water requirements, *Iris* is divided into three categories (Liu et al., 2009): the first category includes species that prefer weakly alkaline, calcareous, damp, fertile, and well-drained soil, such as *Iris tectorum* Maxim. and *I. germanica*; the second category includes species that thrive in acidic and wet soil, such as *I. japonica* and *I. pseudacorus*; the third category includes species that adapt to any type of soil-poor, dry, or wet-such as *I. lactea* var. *chinensis*. In our study, *I. spuria* and *I. tigridia* in the second group belong to two different subgenera in the morphological classifications Subgen. *Xyridion* and Subgen. *Iris*, respectively. They grow in any soil and have strong adaptability, which contributes to explaining why *I. spuria* and *I. tigridia* clustered together.

On the basis of morphological systematics, the genus *Iris* is divided into six subgenera as recorded in the “*Flora of China*”: *Limniris*, *Xyridion*, *Nepalensis*, *Pardanthopsis*, *Crossiris*, and *Iris* (Zhao, 1985). The results obtained in this study are somewhat inconsistent with the classification mentioned above. For example, *Limniris* species occur in the second, third, fourth, and fifth groups. Therefore, Subgen. *Limniris* is a very unnatural group, and should be divided into several groups or subgenera, which would be more reasonable from the tree diagram analysis and is consistent with the viewpoint of Mou et al. (2011).

The principal components analysis (PCA) revealed some aspects of relationships that were not recognizable by clustering analysis (Marak et al., 2010). We also applied PCA for better presentation of the relationships among the species of *Iris*. *I. dichotoma* was distant from the others, and therefore it seems unreasonable that *I. dichotoma* and *I. subdichotoma* are clustered together. Since *I. uniflora* is clustered close to *I. typhifolia*, it should not be classified into the fifth group by itself.

In the *Iris* relationship analysis based on AFLP, we found that there were inconsistencies between the molecular marker method and the traditional method of classification, and sometimes there was no correspondence between the methods. Perhaps because the polymorphism of AFLP markers reflects differences in complex genomic DNA at the molecular level, whereas morphological traits are the results of certain functional gene expressions mediated by external environmental effects. Differences in DNA content may not be reflected in morphology, since some genes may remain unexpressed. Therefore, the genetic relationship and classification of *Iris* species should be assessed correctly and reasonably using the morphological method combined with the molecular marker method.

An understanding of the levels and patterns of genetic diversity is important for designing better conservation and improved management strategies for threatened and endangered species. Although the *Iris* samples collected in this work have a rich genetic diversity, considerable exploitation of the wild resources together with habitat destruction have led to a loss of *Iris* germplasm genetic diversity. Some wild *Iris* are difficult to collect because they have become rare. In order to actively protect wild plants of the *Iris* genus, wild plant germplasm nurseries have been established in many botany garden, which will provide the necessary genetic basis for breeding new species. The study on genetic diversity among 15 species of *Iris* based on AFLP marker will further identify relationships among species in molecular level. This results combined with morphological systematic, will be useful to breeders in selecting the best parental combinations for *Iris* breeding program in China.

Conclusion

In conclusion, AFLP markers were shown to be a good tool for assessing genetic diversity, genetic relationships, and identifications in *Iris*. The high percentage (99.74%) of polymorphic bands, genetic diversity parameters (Na, Ne, H, I), and genetic distances showed that the genus *Iris* has a rich genetic diversity and relatively large genetic differentiation at the species level. The 15 *Iris* species analyzed in this study can be divided into five groups and separated from each other by a few primer combinations. These results will be useful for the conservation, management, classification, identification, and breeding of *Iris* resources.

Acknowledgements. This study was supported by national public welfare industry (agriculture) research special funds and the Shenyang Science and Technology Bureau.

REFERENCES

- [1] Agarwal, V. K., Thappa, R. K., Agarwal, S. G. (1984): Isoflavones of two *Iris* species. – *Phytochemistry* 23: 2703-2704.
- [2] Allen, G., Williams, A., Rabinowicz, P. D. (2008): Worldwide genotyping of castor bean germplasm (*Ricinus communis* L.) using AFLPs and SSRs. – *Genet Res Crop Evol.* 55: 365-378.
- [3] Bai, W. B., Li, P. F., Li, B. G. (2008): Some physiological responses of Chinese *Iris* to salt stress. – *Pedosphere* 18: 454-463.
- [4] Bailly, C., Corbineau, F., Van Doorn, W. G. (2001): Free radical scavenging and senescence in *Iris* tepals. – *Plant Physiol Biochem.* 39: 649-656.
- [5] Bertoni, B. W., de C Telles, M. P., Malosso, M. G. (2010): Genetic diversity in natural populations of *Jacaranda decurrens* Cham. determined using RAPD and AFLP markers. – *Genet Mol Biol* 33: 532-538.
- [6] Breinholt, J. W., Van Buren, R., Kopp, O. R. (2009): Population genetic structure of an endangered Utah endemic, *Astragalus ampullarioides* (Fabaceae). – *Am J Bot.* 96: 661-667.
- [7] Burcu, B., Aysel, U., Nurdan, S. (2014): Antimicrobial, antioxidant, antimutagenic activities, and phenolic compounds of *Iris germanica*. – *Ind Crops Prod* 61: 526-530.
- [8] Chen, X. H., Gao, Y. B., Zhao, N. X. (2009): An AFLP analysis of genetic diversity and structure of *Caragana microphylla* populations in Inner Mongolia steppe, China. – *Biochem Syst Ecol.* 37: 395-401.
- [9] Chung, M. Y., López-Pujol, J., Lee, Y. M., Chung, M. G. (2014): Clonal and genetic structure of *Iris odaesanensis* and *Iris rossii* (Iridaceae): insights of the Baekdudaegan Mountains as a glacial refugium for boreal and temperate plants. – *Plant Syst Evol.* 02 Nov., online first.
- [10] Claire, A. (1957): *Irises: a gardener's encyclopedia*. – Portland: Timber Press, pp. 11-13.
- [11] Duffy, K. J., Scopece, G., Cozzolino, S. (2009): Ecology and genetic diversity of the dense-flowered orchid, *Neotinea maculata*, at the centre and edge of its range. – *Ann Bot.* 104: 507-516.
- [12] Garrido, J. L., Fenu, G., Mattana, E. (2012): *Bacchetta* G. Spatial genetic structure of *Aquilegia* taxa endemic to the island of Sardinia. – *Ann Bot.* 109: 953-964.
- [13] Hesham, A. A., Yan, W. G. (2010): Genetic diversity and relatedness of rice cultivars resistant to straighthead disorder. – *Plant Breed* 129: 304-312.
- [14] Hong, Z., Jin, L., Yi-ping, X. (2013): Determination of genetic relationships between evergreen azalea cultivars in China using AFLP markers. – *Zhejiang Univ.-Sci. B (Biomed & Biotechnol)* 14: 299-308.
- [15] Huang, C. Q., Zhang, Y. F., Liu, G. D. (2012): Genetic diversity of *Cynodon radiatus* assessed by sequence-related amplified polymorphism markers. – *Biochem Syst Ecol* 40: 56-61.

- [16] Isaza, L., Marulanda, M. L., López, A. M. (2012): Genetic diversity and molecular characterization of several *Heliconia* species in Colombia. – *Genet Mol Res* 11: 4552-4563.
- [17] Jianab, S., Shib, S. (2009): Genetic variation in *Heritiera littoralis* (Malvaceae) from east and south Asia revealed by AFLP markers. – *Plant Bios* 143: S56-S62.
- [18] Lin, H., Tao, Q. L., Zhang, J. J. (2010): *Iris* introduction of the latest international classification. – *Garden Technol* 118: 1-3.
- [19] Liu, W. J. (2009): The introduction of *Iris* classification. – *Chinese Flower Rep* 8: 1.
- [20] Marak, C. K., Laskar, M. A. (2010): Analysis of phenetic relationship between *Citrus Indica* Tanaka and a few commercially important citrus species by ISSR markers. – *Sci Hortic* 124: 345-348.
- [21] Matus, I. A., Hayes, P. M. (2002): Genetic diversity in three groups of barley germplasm assessed by simple sequence repeats. – *Genome* 45: 1095-1106.
- [22] Morales, R. G. F., Resende, J. T. V., Resende, F. V. (2013): Genetic divergence among Brazilian garlic cultivars based on morphological characters and AFLP markers. – *Genet Mol Res* 12: 270-281.
- [23] Mou, S. H., Peng, Z. H., Qie, G. F. (2011): Genetic diversity of *Iris* determined by AFLP markers. – *J North East Forest Univ.* 39: 124-126.
- [24] Poppendieck, H. H. (1983): Evolution and Classification of Seed Plants. – *Prog Bot* 45: 242-297.
- [25] Qiao, L. X., Liu, H. Y., Guo, B. T. (2007): Molecular identification of 16 *Porphyra* lines using sequence-related amplified polymorphism markers. – *Aquat Bot* 87: 203-208.
- [26] Rohlf, F. J. (2000): NYSYS-pc: numerical taxonomy and multivariate analysis system, version 2.1. – Exeter publications, Setauket.
- [27] Shimizu, K., Miyabe, Y., Nagaike, H. (1999): Production of somatic hybrid plants between *Iris ensata* Thunb. and *I. germanica*. – *Euphytica* 107: 105-113.
- [28] Talebi, M., Hajiahmadi, Z., Rahimmalek, M. (2011): Genetic diversity and population structure of four Iranian alfalfa populations revealed by sequence-related amplified polymorphism (SRAP) markers. – *J Crop Sci Biotech* 14: 173-178.
- [29] Tang, S., Okashah, R. A., Knapp, S. J. (2010): Transmission ratio distortion results in asymmetric introgression in Louisiana *Iris*. – *BMC Plant Biol* 10: 48.
- [30] Tatikonda, L., Wani, S. P., Kannan, S. (2009): AFLP-based molecular characterization of an elite germplasm collection of *Jatropha curcas* L., a biofuel plant. – *Plant Sci.* 76: 505-513.
- [31] Tay, D. (2006): Herbaceous Ornamental Plant Germplasm Conservation and Use. – In: Anderson, N.O. (ed.) *Flower Breeding and Genetics*. Netherlands: Springer, pp. 113-175.
- [32] Umezuruike, L. O., Dan, J., Nadiya, A. A. S. (2010): Analysis of genetic diversity in banana cultivars (*Musa* cvs.) from the South of Oman using AFLP markers and classification by phylogenetic, hierarchical clustering and principal component analyses. – *Zhejiang Univ.-Sci. B (Biomed & Biotechnol)* 11: 332-341.
- [33] Vieira, R. L., Nodari, R. O. (2007): Diversidade genética de cultivares de alho avaliada por marcadores RAPD. – *Ciênc Rural* 37: 51-57.

- [34] Vos, P., Hogers, R., Bleeker, M. (1995): AFLP: a new technique for DNA fingerprinting. – *Nucl Acids Res* 23: 4407-4414.
- [35] Waddick, J. W., Zhao, Y. T. (1992): *Iris of China*. – Portland (USA): Timber Press.
- [36] Wang, X. Z., Zhai, Q., Ling, X. Z. (2013): Effects of method and tissue on genomic DNA extraction of *Ambrosia trifida*. – *Hubei Agricul Sci*. 52: 1447-1449.
- [37] Wanjala, B. W., Obonyo, M., Wachira, F. N. (2013): Genetic diversity in Napier grass (*Pennisetum purpureum*) cultivars: implications for breeding and conservation. – *AOB Plants* 5: 1-10.
- [38] Yeh, F. C., Boyle, T. J. B. (1997): Population genetic analysis of co-dominant and dominant markers and quantitative traits. – *Belg. J. Bot.* 129:157.
- [39] Zhang, M., Huang, S. Z. (2008): Analysis of *Iris L.* germplasm based on ISSR markers. – *Journal of Nanjing Agricultural University* 31: 43-48.
- [40] Zhang, L. (2010): The *Iris* application in American garden. – *Garden* 8: 38-41. (in Chinese).
- [41] Zhao, Y. T. (1985): *Flora of China*. – Beijing: Science Press 16: 133-197. (in Chinese).

ECO-FRIENDLY AGRICULTURAL PRACTICES AND THEIR ASSENT BY FARMERS IN HARYANA STATE OF INDIA

ROHILA, A. K.^{1*} – KUMAR, A.¹ – GHANGHAS, B. S.² – MAHALLE, S. L.¹ – NIMBRAYAN, P. K.³ –
MAAN, D. S.⁴ – KUMAR, R.⁵

¹NAHEP - Indian Council of Agricultural Research, New Delhi-110 012, India

²Department of Extension Education, CCSHAU, Hisar-125 004, India

³Department of Agricultural Economics, CCSHAU, Hisar-125 004, India

⁴Faculty of Agriculture, Tanta University, Sri Ganganagar-335 001, India

⁵Department of Agriculture and Farmers Welfare, Rewari-123 401, Haryana, India

*Corresponding author

e-mail: rohillaextension@gmail.com

(Received 25th Oct 2018; accepted 29th Mar 2019)

Abstract. Intensive agricultural practices coupled with better input services has resulted in exponential growth in crop production in India, particularly in northern region states of the country like Haryana. Though self-sufficiency has been achieved, it was accompanied by negative environmental effects such as serious non-target agricultural pollution. Implementation of eco-friendly smart agricultural practices can effectively overcome such pollution. However, the major constraints in assent and adoption of these practices are not limited only to associate risks and potential benefits, but farmers' attitudes towards knowledge of scientifically validated practices too came into picture. In the presented study, opinions of 180 respondents were explored in personal interviews using a three-point continuum scale for the major constraints (very serious, serious and not so serious) and scores were given as 3, 2 and 1, respectively. Weighted mean score (WMS), rank orders, standard deviation, correlation and regression were computed for the better understanding. Results concluded that major constraints for smart agricultural practices in their assent were non-familiarization with improved practices (WMS = 2.46), procedure of registration for weather forecasting (2.37), conservation agriculture is more labour intensive (2.24), lack of training to access e-information (2.39), Climate change effects the seasonal temperature and rainfall (2.76), Slow result of eco- friendly practices (2.54), high initial cost of protected structure (2.52), and lack of proper training for agro-processing and value addition practices (2.42). The results also indicated that 11 independent variables which were included in the study jointly contributed 37.00% variations in the constraints faced by the farmers in adoption of smart agricultural practices.

Keywords: agriculture, adoption, climate, constraints, management and production

Introduction

The major challenge of Indian agriculture is to produce sufficient food grains as it has long been a priority of the country to achieve food security, as it one of the major challenges posed by shrinking landholdings and the over increasing population. About two-third population of Indian population is directly or indirectly depends on related activities for their livelihoods and this sector occupies almost 43% of India's total geographical area (Arjun, 2013). About, 85 percent farmer comes under the category of small and marginal landholding. Demands are continuously increasing on agricultural land for food, fibre, and fuel is predicted to increase exponentially in coming decades with continued population growth (Bommarco et al., 2013). Population growth and dietary changes will drive the global food demand to extraordinary levels in the coming

decades. To keep pace, food production will have to increase 60% by 2050 (FAO, 2013). Thus, population growth rate of 1.58%, India is predicted to have more than 1.7 billion people by the end of 2050.

India, with a total of 160 m ha of cultivated land comprises of only 39 million hectare irrigated by ground water and 22 million hectare by canals whereas about two third of cultivation in India is still depending on monsoon (Dhawan, 2017) and now there is a well-established fact and figures that natural resources such as land, water, forests, livestock, fisheries are deteriorating and degrading at a very fast rate which may be attributed to unmindful agricultural intensification, imbalanced use of fertilizers, overuse and inefficient use of irrigation water and deforestation.

While, other constraints like inadequate marketing channels and infrastructure, long intermediation, lack of accurate and timely market information system etc. are major challenges to the agricultural marketing system in the country. To prevent agricultural non-target pollution, ameliorate its effects and protect the environment in India, while maintaining or increasing crop yields, traditional practices are being re-evaluated and new eco-friendly agricultural practices are being intensively researched and developed (Shen and Du, 2009).

Therefore, there is immense need of adoption of smart agricultural practices (SAPs) to enhance the production and productivity to feed the continuous increasing population through sustainable use of natural resources along with to reduce the input cost, increase the net profit, and generate employment. SAPs, further, takes into consideration the diversity of social, economic and environmental contexts including agro-ecological zones/farming systems where it is to be applied. Implementation herein requires identification of integrated package of climate resilient technologies and practices for management of water, energy, land, crops, livestock, aquaculture etc. at the farm level while considering the linkage between agricultural production and ecosystems services at the landscape level. However, the real picture of overall sustainability and adoption of smart agricultural practices seems to be continued to face many challenges. Keeping in view the above concerns, study was conducted with objective to assess the constraints in adoption of smart agricultural practices.

Materials and methods

The study was conducted in Haryana state of India during 2017 (*Fig. 1*). Data were collected from From Hisar and Kaithal because main campus and sub campus of the university is situated in these districts. All respondents were recruited randomly from two districts viz. Hisar from South-West zone and Kaithal from North-East zone and three villages were selected from each district i.e. *Ladwa*, *Shahrwa* and *Rawalwas Khurd* villages from Hisar, whereas, *Kaul*, *Rasina* and *Bhana* villages were selected from Kaithal. Thirty farmers from each selected village were selected randomly. A well-structured and pre-tested questionnaire (see *Appendix*) was designed and used to survey opinions of a stratified sample of 180 farmers which were engaged in small-scale production. The data was analysed by Statistical Package for the Social Sciences (SPSS). Weighted mean score, rank orders, standard deviation, correlation and regression were computed for the better understanding. The responses of farmers' were obtained on three-point continuum scale in case of constraints (very serious, serious and not so serious) and scores were given as 3, 2 and 1, respectively. After that frequency was multiplied with the score (3, 2 or 1) and total weighted score was obtained and total

weighted score was divided by total respondents (180) for obtaining weighted mean score (WMS) and according to weighted mean score rank order were given.

$$\text{Weighted Mean Score (WMS)} = \frac{w_1 * x_1 + w_2 * x_2 + w_3 * x_3}{n}$$

where

w = number of respondents

x = value of seriousness i.e. Very Serious (x₁)-3, Serious (x₂)-2 and Not so serious (x₃)-1

n = total number of respondents

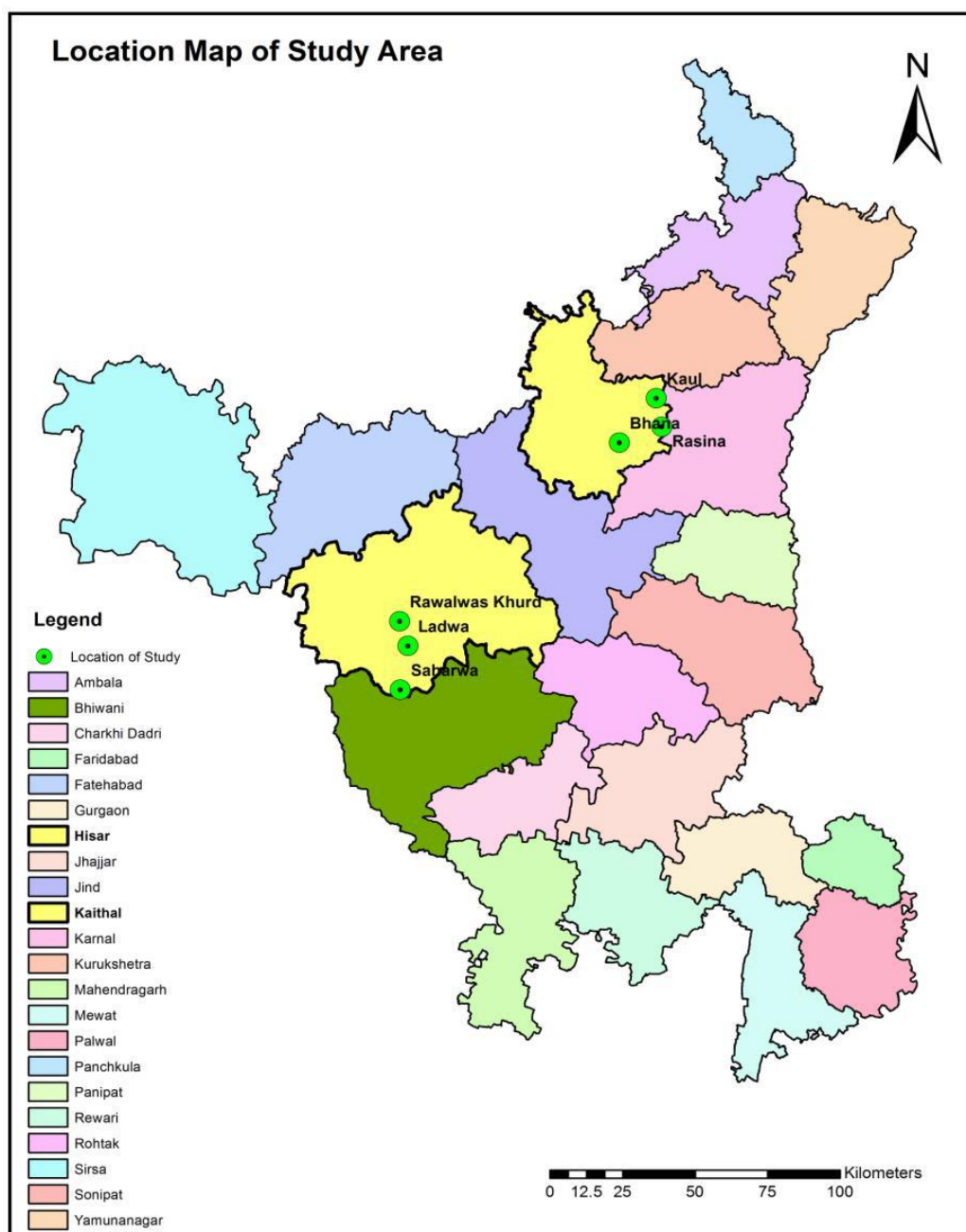


Figure 1. Map of Haryana showing the locale of study

Results and discussion

Profile of respondents

Results pertaining to the personal profile of the farmers indicated in *Table 1*. It was found that vast majority of the farmers (78.34%) belonged to productive age group i.e. young to middle. The age-wise distribution of the respondents is quite natural and expected that working farmers usually come from young and middle aged group. More than 85% farmers were found to literate from primary to post graduate. Educational status is important and plays a key role in enhancing the knowledge, encouraging and motivating them towards adopting the innovative technologies and their applications. It is generally presumed that higher the educational status higher will be the adoption level. Majority of the farmers had land holding up to 5 acres, followed by 6-10 acre (36.67%).

Table 1. Profile of respondents (n = 180)

Category	Frequency	Percentage
Age		
Young (21-39 Years)	75	41.67
Middle (39-57 Years)	66	36.67
Old (57-76 Years)	39	21.66
Education		
Illiterate	21	11.67
Primary	13	7.22
Middle	19	10.56
Metric	63	35.00
Higher secondary	29	16.11
Graduate	27	15.00
Postgraduate	8	4.44
Land holding		
Less than one acre	15	08.33
Up to 5 acres	83	46.11
6 to 10 acres	66	36.67
11 to 15 acres	9	5.00
16 to 20 acres	1	0.56
More than 20 acres	6	3.33

n = 180 represents the total number of respondents

Constraints in adoption of sustainable farming

The examination of the data presented in *Table 2* indicated the constraints in adoption of sustainable farming viz., ‘not familiar with improved practices’ as overall major and serious constraint (52.78%) and ranked 1st with highest weighted mean score (WMS) 2.46, followed by ‘small and fragmented land holding’, ‘not aware about training for sustainable farming’, ‘lack of skill to adopt sustainable farming’ and ‘lack of finance to adopt improved practices’ ranked 2nd, 3rd, 4th and 5th with WMS 2.41, 2.29, 2.24 and 2.21, respectively. The major constraint comes in adoption of smart

agricultural practices is that farmers are not familiar with improved practices and it might be possible due to the fact that clearly farmers develop and use cultural practices they are comfortable with and therefore minimize production risk associated with crop failure or yield reductions. Most farmers perceive these practices to be too costly. While Dsouza et al. (1993) concluded that adoption of sustainable agricultural practices is affected most by the environmental characteristic. Ikerd (1990) states that economic considerations and incentives are needed to encourage change to a different system. Secondly lack of awareness, training and skills about these practices are another factor. So, it is important to organize continuous awareness programs and provide the skill oriented training at local level in farming community. These results are in confirmation with those reported by Kumari (2012).

Table 2. Constraints in adoption of sustainable farming (n = 180)

S. No.	Sustainable constraints	Constraints			Total weighted score	Weighted mean score	Rank order
		Very serious (%)	Serious (%)	Not so serious (%)			
1	Small and fragmented land holding	95 (52.78)	63 (35.00)	22 (12.22)	433	2.41	II
2	Lack of skill to adopt sustainable farming	57 (31.67)	110 (61.11)	13 (7.22)	404	2.24	IV
3	Lack of finance to adopt improved practices	50 (27.78)	118 (65.56)	12 (6.66)	398	2.21	V
4	Not aware about training for sustainable farming	63 (35.00)	107 (59.44)	10 (5.56)	413	2.29	III
5	Not familiar with improved practices	95 (52.78)	72 (40.00)	13 (7.22)	442	2.46	I

n = 180 represents the total number of respondents

Constraints in adoption of weather forecasting

A perusal of data presented in *Table 3* indicated the weather forecasting viz., ‘not aware about the procedure of registration’ ranked 1st with highest weighted mean score (WMS) 2.37, followed by ‘irregularity in message’ ranked 2nd with WMS 2.23. ‘Information is useful only for until crop production’, ‘lack of resources and internet etc.’ and ‘not proper language of message’ ranked 3rd, 4th and 5th with WMS 2.22, 2.19 and 2.12, respectively. Farmers were not aware about the procedure of registration was ranked top and this may be possibly due to the region that extension personnel do not regularly interact with farmers to discuss climate forecasts. These constraints can be trimmed by providing proper guidance from the experts to the farmers with the help of literature, awareness campaign and mass media about weather forecasting advisory services to the farmers. Oyekale (2015) also reported that infrastructure and human capacities that are needed for attaining such efficiency were acutely lacking. This has also been reported by Murthy (2008) with respect to weather forecasts in Andhra Pradesh. Agricultural extension agents, working with farmers and forecasters could help forecasters to focus on the climate variables and spatial resolutions that matter to farmers and provide feedback from farmers to the forecasters about the performance and utility of the forecasts. They could assist farmers to interpret and apply forecasts for

making decisions such as the time of planting, choice of crops and crop varieties, application of fertilizers, herbicides, pesticides and irrigation water. These constraints can be overcome by frequent visits by extension personnel along with use of different teaching materials and methods, as extension personnel, rarely interact with farmers as well as the use of different teaching materials like display boards, bulletins (Feleke, 2015) and methods like personal contacts, informal discussion (Rajesh et al., 2016) on changing weather conditions were not given the deserved attention. Weather forecasting advisory services to the farmers and Climate Field Schools are discussed in this context by Stigter (2008).

Table 3. Constraints in adoption of weather forecasting (n = 180)

S. No.	Weather forecasting constraints	Constraints			Total weighted score	Weighted mean score	Rank order
		Very serious (%)	Serious (%)	Not so serious (%)			
1	Not aware about the procedure of registration	95 (52.78)	56 (31.11)	29 (16.11)	426	2.37	I
2	Irregularity in message	57 (31.67)	108 (60.00)	15 (8.33)	402	2.23	II
3	Not proper language of message	49 (27.22)	104 (57.78)	27 (15.00)	382	2.12	V
4	Lack of resources and internet etc.	50 (27.78)	114 (63.33)	16 (8.89)	394	2.19	IV
5	Information is useful only for until crop production	47 (26.11)	126 (70.00)	7 (3.89)	400	2.22	III

n = 180 represents the total number of respondents

Constraints in adoption of conservation agriculture (CA)

Data presented in Table 4 indicated the conservation agriculture (CA) constraints viz., ‘conservation agriculture is more labour intensive’ ranked 1st and major constraints with weighted mean score (WMS) 2.24, followed by ‘increasing weed infestation’, ‘poor soil quality’ and ‘fragmented land holding’ ranked 2nd, 3rd and 4th with WMS 2.21, 2.18 and 1.43, respectively. The conservation agriculture (CA) constraints viz., conservation agriculture is more labour intensive as well as prominent among farmers because full implementation of the principles of conservation agriculture involves a drastic change in many farm operations. So, there is immense need of proper training programs and policy about CA promotions (Grabowski, 2011; Kudi et al., 2011). A new knowledge base is needed by farmers to establish crops, manage weeds, manage crop residues, respond to newly emerging diseases and insect pests, and manage diverse crops that make the conservation agriculture more labour intensive (Pieri et al., 2002). Moreover, it cannot be reduced to a simple standard technology and thus pioneers and early adopters’ face many hurdles before the benefits of conservation agriculture can be revealed (Derpsch, 2008). Also, it is appeared that conservation agriculture is as yet a relatively unknown concept (Kassam et al., 2009). Indeed, conservation agriculture is not an easily transferable single component technology; the appropriateness of conservation agriculture depends on both biophysical and socioeconomic factors and their interactions.

Table 4. Constraints in adoption of conservation agriculture (CA) (n = 180)

S. No.	Conservation agriculture constraints	Constraints			Total weighted score	Weighted mean score	Rank order
		Very serious (%)	Serious (%)	Not so serious (%)			
1	Fragmented land holding	22 (12.22)	34 (18.89)	124 (68.89)	258	1.43	IV
2	Poor soil quality	47 (26.11)	119 (66.11)	14 (7.78)	393	2.18	III
3	Increasing weed infestation	45 (25.00)	128 (71.11)	7 (3.89)	398	2.21	II
4	Conservation agriculture is more labour intensive	53 (29.44)	118 (65.56)	9 (5.00)	404	2.24	I

n = 180 represents the total number of respondents

Constraints in adoption of information and communication technologies (ICTs)

Table 5 described the constraints in adoption of ICTs viz., ‘lack of training to access e-information’ ranked 1st with highest weighted mean score (WMS) 2.39, followed by ‘low internet access and electricity’, ‘inadequate infrastructural facilities’, ‘lack of resources and tools’, and ‘fear that ICTs provides irrelevant content’ ranked 2nd, 3rd, 4th and 5th with WMS 2.30, 2.25, 2.22 and 2.18, respectively. The first rank was ascribed to the statement that there is lack of training to access e-information and this could be possibly due to the reason that regulatory frameworks for ICTs are not necessarily conducive to widespread scale up of ICT in rural areas. Processes take several years and require many regular visits to monitor and encourage progress, without assurance of success. This can be achieved through information and training campaigns, suitable legislations and policy along with regulatory frameworks, research and development, incentive and credit programs (Friedrich and Kassam, 2009). Therefore, training programs should be organized to overcome the constraints along with to provide infrastructure facilities, resources, tools and internet (Albert, 2014). While Rohila et al. (2017) suggested that low cost ICT tools such as mobile phones etc. should be promoted to provide agricultural information.

Table 5. Constraints in adoption of ICTs (n = 180)

S. No.	ICTs constraints	Constraints			Total weighted score	Weighted mean score	Rank order
		Very serious (%)	Serious (%)	Not so serious (%)			
1	Inadequate infrastructural facilities	55 (30.56)	115 (63.89)	10 (5.55)	405	2.25	III
2	Lack of resources and tools	51 (28.33)	118 (65.56)	11 (6.11)	400	2.22	IV
3	Low internet access and electricity	64 (35.56)	106 (58.89)	10 (5.55)	414	2.30	II
4	Fear that ICTs provides irrelevant content	52 (28.89)	108 (60.00)	20 (11.11)	392	2.18	V
5	Lack of training to access e-information	79 (43.89)	92 (51.11)	9 (5.00)	430	2.39	I

n = 180 represents the total number of respondents

Constraints related to climate change

Table 6 narrated that climate change constraints viz., ‘climate change effects the seasonal temperature and rainfall’ ranked 1st with highest weighted mean score (WMS) 2.76, followed by ‘rapid change in weather conditions’ ranked 2nd with WMS 2.49. Whereas, ‘deterioration in the quality of crop produce’, ‘environmental degradation’, ‘effect on plant population and yield’, and ‘probability of droughts and floods’ ranked 3rd, 4th, 5th and 6th with WMS 2.47, 2.35, 2.28 and 2.22, respectively. The statement climate change effects the seasonal temperature and rainfall was ranked 1st with highest weighted mean score by the respondents and this might be due to the reason that climate change is arguably one of the most important challenge which is faced by farmers, largely due to their geographic exposure, low income, greater reliance on climate-sensitive sectors such as agriculture, and weak capacity to adapt to the changing climate. Farmers are adversely affected by climatic variability and change because of their dependency on rain-fed agriculture, with variability in rainfall and temperature directly affecting crop and livestock yields. Empirical results show that climate variability has significant economic costs as a result of periodic floods and droughts, which lead to major macro-economic costs and reductions in economic growth. This increased complexity requires a degree of experience and knowledge, which has to be acquired and learned. For early adopters this learning process and experiential knowledge has therefore involved a lot of trial and error until sufficient local experience and knowledge is accumulated to make the adoption easier (FAO, 2010; Mahato, 2014).

Table 6. Constraints related to climate change (n = 180)

S. No.	Climate change constraints	Constraints			Total weighted score	Weighted mean score	Rank order
		Very serious (%)	Serious (%)	Not so serious (%)			
1	Rapid change in weather conditions	92 (51.11)	85 (47.22)	3 (1.67)	449	2.49	II
2	Environmental degradation	68 (37.78)	107 (59.44)	5 (2.78)	423	2.35	IV
3	Climate change effects the seasonal temperature and rainfall	137 (76.11)	42 (23.33)	1 (0.56)	496	2.76	I
4	Deterioration in the quality of crop produce	93 (51.67)	79 (43.89)	8 (4.44)	445	2.47	III
5	Effect on plant population and yield	54 (30.00)	123 (68.33)	3 (1.67)	411	2.28	V
6	Probability of droughts and floods	52 (28.89)	115 (63.89)	13 (7.22)	399	2.22	VI

n = 180 represents the total number of respondents

Constraints in adoption of greenhouse gas mitigation practices

The data in Table 7 depicted the greenhouse gas mitigation constraints viz., ‘slow result of eco-friendly practices’ ranked 1st with highest weighted mean score (WMS) 2.54, followed by ‘ignorance about the bed effect of chemical hazardous on health’ ranked 2nd with WMS 2.45. While, ‘no reward for adoption of environmental measures’, ‘non-

availability of package of practices' and 'mostly farmers burn crop residue in the fields' ranked 3rd, 4th and 5th with WMS 2.38, 2.22 and 1.88, respectively. The statement slow result of eco-friendly practices ranked 1st may be because of the reason that eco-friendly practices contradicts the knowledge a farmer which he have learned from his experience and been told that the benefits offered by these practices are not obvious in the beginning. However, once the step-wise adoption begins, an eco-friendly practice improves its performance over time (Tebrugge and Bohrsen, 2000). From the results of the study, it is clear that farmers will more readily adopt sequestration of GHGs if the agricultural extension services, planning and strategies could be improved. These findings are in line with findings of Mukteshwar and Seharawat (2016).

Table 7. Constraints in adoption of greenhouse gas mitigation practices (n = 180)

S. No.	Greenhouse gas mitigation constraints	Constraints			Total weighted score	Weighted mean score	Rank order
		Very serious (%)	Serious (%)	Not so serious (%)			
1	Non-availability of package of practices	47 (26.11)	126 (70.00)	7 (3.89)	400	2.22	IV
2	No reward for adoption of environmental measures	86 (47.78)	76 (42.22)	18 (10.00)	428	2.38	III
3	Ignorance about the bed effect of chemical hazardous on health	84 (46.67)	93 (51.67)	3 (1.66)	441	2.45	II
4	Slow result of eco- friendly practices	105 (58.33)	68 (37.78)	7 (3.89)	458	2.54	I
5	Mostly farmers burn crop residue in the fields	52 (28.89)	55 (30.56)	73 (40.55)	339	1.88	V

n = 180 represents the total number of respondents

Constraints in adoption of protected cultivation

The data contained in *Table 8* showed the protected cultivation constraints viz., 'high initial cost' ranked 1st as major constraint with highest weighted mean score (WMS) 2.52, followed by 'poor quality of material' ranked 2nd with WMS 2.41. While, 'frequent occurrence of wind storms, hailstorms, rain etc.' and 'problem of nematodes and diseases' ranked 3rd and 4th with WMS 2.23 and 2.04, respectively. The statement high initial cost ranked 1st might be possibly due to the reason that polyhouse cultivation requires quality planting material, inputs, etc. which adds economic burden to the farmers. Singh and Sirohi (2006) also reported that the basic cost of fabrication and the operational cost of the climate-controlled greenhouses are very high, which are not suitable to the growers in India. Therefore, high initial investment, lack of availability of quality planting materials and inputs, poor post-harvest infrastructure and absence of price policy have led to very limited adoption of this technology by few farmers in certain pockets of the country. Above constraints can be countered to enhance farmers' adoption level with the help of manufacturing and financial sector support. It can be increased through capacity building of farmers, research and development coupled with adequate marketing system. Present study got support from the past research study of Ghanghas et al. (2015).

Table 8. Constraints in adoption of protected cultivation (n = 180)

S. No.	Protected cultivation constraints	Constraints			Total weighted score	Weighted mean score	Rank order
		Very serious (%)	Serious (%)	Not so serious (%)			
1	High initial cost	99 (55.00)	76 (42.22)	5 (2.78)	454	2.52	I
2	Poor quality of material	78 (43.33)	97 (53.89)	5 (2.78)	433	2.41	II
3	Frequent occurrence of wind storms, hailstorms, rain etc.	46 (25.56)	129 (71.67)	5 (2.77)	401	2.23	III
4	Problem of nematodes and diseases	25 (13.89)	137 (76.11)	18 (10.00)	367	2.04	IV

n = 180 represents the total number of respondents

Constraints in adoption agro-processing and value addition practices

Table 9 elaborated the agro-processing and value addition constraints viz., ‘lack of proper training’ ranked 1st as major constraint, followed by ‘lack of agro-processing unit’ ranked 2nd with WMS 2.38. Whereas, ‘lack of procurement policy’ and ‘lack of proper facilities’ ranked 3rd and 4th with WMS 2.25 and 2.23, respectively. However, ‘lack of consumption of agro processed food’ ranked 5th with lowest WMS 2.13. Lack of proper training among the farmers was encountered as major constraints possibly due to the number of notable factors like socio-economic, contact with extension workers, provision of infrastructure and other institutional factors, which influenced the adoption. Other factors are also reported including society membership, education (Lapar and Pandey, 1999; Weir and Knight, 2000) and household income (Lapar and Simeon, 2004), education levels (Irungu et al., 1998; Lapar and Simeon, 2004) that contribute in adoption of new agricultural technologies. However, these constraints can be adequately addressed through extension agencies by formation of SHGs and by adopting bottom-up approach. While considering these facts, the need-based and skill oriented training awareness campaign including credit support, market-driven and decentralized extension system of the agro-processors to upgrade their knowledge and skills in modern post-harvest technology is strongly recommended. Moreover, provision of credit facilities could change the perceived constraints into enabling factors for adoption of modern post-harvest technology enterprises (Meena et al., 2009; Musebe et al., 2013).

Correlation and regression coefficients of farmers’ personality traits with constraints encountered in adoption of smart agricultural practices

Table 10 narrated that correlation coefficient between the farmers’ personality traits like education, land holding, cropping system, farming system, mass media exposure, extension contact, risk orientation, economic motivation and innovation proneness had positive and significant correlation. However, remaining traits namely age and irrigation facilities did not show any significant association at 0.05 level of probability. While in case of the partial regression coefficient, the farmers’ education and mass media exposure were found significant, whereas, age, land holding, cropping system, farming system, irrigation facilities, extension contact, risk orientation, economic motivation and

innovation proneness did not show significantly contribution. These finding were found to partially support by the reports of Rajashekar et al. (2017). Further, it is revealed that all the eleven independent variables included in the study jointly contributed 37.00% variation in the constraints of the respondents regarding in adoption of smart agricultural practices when other factors were kept constant. This means that only 37.00% of the variation in the dependent variable was due to these variables and remaining 63.00% variations is due to other variables.

Table 9. Constraints in adoption agro processing and value addition practices (n = 180)

S. No.	Agro processing and value addition constraints	Constraints			Total weighted score	Weighted mean score	Rank order
		Very serious (%)	Serious (%)	Not so serious (%)			
1	Lack of proper facilities	46 (25.56)	130 (72.22)	4 (2.22)	402	2.23	IV
2	Lack of procurement policy	53 (29.44)	119 (66.11)	8 (4.44)	405	2.25	III
3	Lack of agro-processing unit	75 (41.67)	98 (54.44)	7 (3.89)	428	2.38	II
4	Lack of proper training	82 (45.56)	92 (51.11)	6 (3.33)	436	2.42	I
5	Lack of consumption of agro processed food	38 (21.11)	90 (50.00)	52 (28.89)	384	2.13	V

Table 10. Correlation and regression coefficients of farmers' personality traits with constraints encountered in adoption of smart agricultural practices

S. No.	Variables	S.D	Correlation coefficient	Regression coefficient	't' values
1	Age	0.772	0.082 ^{NS}	0.207	0.154 ^{NS}
2	Education	1.619	-0.356*	-2.182	-3.198*
3	Land holding	0.977	-0.366*	-1.459	-1.291 ^{NS}
4	Cropping system	0.787	-0.145 ^{NS}	-2.705	-2.2 ^{NS}
5	Farming system	0.508	-0.349*	-3.544	-1.409 ^{NS}
6	Irrigation facilities	0.524	-0.042 ^{NS}	1.269	0.727 ^{NS}
7	Mass media exposure	1.819	-0.447*	-1.948	-3.092*
8	Extension contacts	0.914	-0.356*	-1.51	-1.054 ^{NS}
9	Risk orientation	2.782	-0.110 ^{NS}	0.524	1.53 ^{NS}
10	Economic motivation	3.998	-0.246*	-0.478	-1.899 ^{NS}
11	Innovation proneness	1.028	-0.344*	-0.723	-0.667 ^{NS}

Dependent variable-constraints

*Significant at 0.05 levels

R² = 0.37, Constant value = 132.78

Conclusion

The results of this study showed that many factors can affect the decisions of farmers to accept and adopt the smart agricultural practices (SAPs), but cost is the most

important, followed by risks. Therefore, government should emphasize on the problems faced by farmers in adoption of smart agricultural practices (SAPs). Moreover, the action plans which may be more efficient and effective must be formulated and implemented at ground level by the government.

Acknowledgements. Author is highly thankful to CCS Haryana Agricultural University, Hisar (Haryana) India for successful completion of Ph.D. degree.

REFERENCES

- [1] Albert, C. O. (2014): Constraints to effective use of ICT among extension professionals and farmers in extension delivery in rivers state, Nigeria. – *Singaporean J. Business Econ. Manag. St.* 2(11): 135-142.
- [2] Arjun, K. M. (2013): Indian agriculture: status, importance and role in Indian economy. – *Int. J. of Agri. and Food Sci. Tech.* 4(4): 343-346.
- [3] Bommarco, R., Kleijn, D., Potts, S. G. (2013): Ecological intensification: harnessing ecosystem services for food security. – *Tree* 28: 230-238.
- [4] Derpsch, R. (2008): Critical Steps in No-Till Adoption. – *World Association of Soil and Water Conservation (WASWC), Bangkok*, pp. 479-495.
- [5] Dhawan, V. (2017): Water and Agriculture in India. – *Background Paper for the South Asia Expert Panel during the Global Forum for Food and Agriculture (GFFA)*.
- [6] Dsouza, G., Cyphers, D., Phipps, T. (1993): Factors affecting the adoption of sustainable agricultural practices. – *Agricultural and Resource Economics Review* 22(2): 159-165.
- [7] FAO (2010): *Climate-Smart Agriculture: Policies, Practices and Financing for Food Security, Adaptation and Mitigation*. – FAO, Rome.
- [8] FAO (2013): *The State of Food and Agriculture*. – FAO, Rome.
- [9] Feleke, H. G. (2015): Assessing weather forecasting needs of smallholder farmers for climate change adaptation in the central rift valley of Ethiopia. – *J. Earth Sci. Climate Change* 6(10): 1-8.
- [10] Friedrich, T., Kassam, A. (2009): Adoption of conservation agriculture technologies: constraints and opportunities. – *IVth World Congress on Conservation Agriculture, New Delhi, February 2009*.
- [11] Ghanghas, B. S., Mukteshwar, R., Shehrawat, P. S. (2015): Protected cultivation (polyhouse) in Haryana: Problems and prospects. – *Ind. J. of Applied Res.* 5(8): 684-685.
- [12] Grabowski, P. P. (2011): Constraints to adoption of conservation agriculture in the Angonia highlands of Mozambique: perspectives from smallholder hand-hoe farmers. – *M.Sc. Thesis, Michigan State University, East Lansing, MI*.
- [13] Ikerd, J. E. (1990): Agriculture's search for sustainability and profitability. – *J. Soil Water Cons.* 45: 18-23.
- [14] Irungu, P., Mbogo, S., Thorpe, W., Njubi, D. (1998): Factors influencing adoption of Napier grass in smallholder dairying in the highlands of Kenya. – *Food, Lands and Livelihoods: Setting Research Agendas for Animal Science, KARI Conference Center, Nairobi, Kenya, 27-30 January*.
- [15] Kassam A, Friedrich T, Shaxson F, Pretty J. (2009): The spread of conservation agriculture: justification, sustainability and uptake. – *Int. J. of Agri. Sust.* 7: 292-320.
- [16] Kudi, T. M., Bolaji, M., Akinola M. O., Nasa, D. H. (2011): Analysis of adoption of improved maize varieties among farmers in Kwara State, Nigeria. – *Int. J. Peace Dev. Stud.* 1(3): 8-12.
- [17] Kumari, G. (2012): Constraints in adoption of integrated pest management (IPM) practices by rice growing farmers of Jammu division. – *Ind. Res. J. Ext. Edu.* 2: 15-17.

- [18] Lapar, M. L. A., Pandey, S. (1999): Adoption of soil conservation: the case of the Philippines uplands. – *Agri. Econ.* 21: 241-256.
- [19] Lapar, M. L. A., Simeon, K. E. (2004): Factors affecting adoption of dual-purpose forages in the Philippine uplands. – *Agri. Sys.* 81(2): 95-114.
- [20] Mahato, A. (2014): Climate change and its impact on agriculture. – *Int. J. Sci. Res. Publ.* 4(4): 1-6.
- [21] Meena, M. S., Prasad, M., Singh, R. (2009): Constraints perceived by rural agro-processors in adopting modern post-harvest technologies. – *Ind. Res. J. of Ext. Edu.* 9(1): 1-5.
- [22] Mukteshwar, R., Seharawat, P. S. (2016): Constraints analysis in adoption of best farm practices towards sequestration of greenhouse gases. – *J. Applied Nat. Sci.* 8(1): 88-92.
- [23] Murthy, V. R. K. (2008): Seminars on Weather, Climate and Farmers. – INSAM, <http://www.agrometeorology.org/files-folder/repository/MurthyWCFFINAL.pdf> (accessed 19 February 2008).
- [24] Musebe, R., Adur, S., Phiri, N., Miiro, M., Mogga, M., Asea, G., Otim, M., Kimenyi, L. (2013): Upscaling new rice for Africa adoption in northern Uganda and south Sudan: socio-economic and technical prerequisites. – 11th African Crop Science Proceedings, Sowing Innovations for Sustainable Food and Nutrition Security in Africa Entebbe, Uganda, 14-17 October, pp. 577-583.
- [25] Oyekale, A. S. (2015): Access to risk mitigating weather forecasts and changes in farming operations in East and West Africa: evidence from a Baseline Survey. – *Sustainability* 7: 14599-14617.
- [26] Pieri, C., Evers, G., Landers, J., O'Connell, P., Terry, E. (2002): No-till farming for sustainable rural development. – In: *Agriculture and Rural Development*. Working Paper, FAO, Rome.
- [27] Rajashekar, B., Sudharani, V., Parveen, S. K. N., Shivacharan, G. (2017): Knowledge of farmers about integrated weed management (IWM) practices in major crops. – *Int. J. of Farm Sci.* 7(1): 33-36.
- [28] Rajesh, Godara, A. K., Autade, C. D., Mehta, S. K. (2016): Constraints associated with the use of weather forecasting service. – *Asian Sci.* 11(2): 125-128.
- [29] Rohila, A. K., Yadav, K., Ghanghas, B. S. (2017): Role of information and communication technology (ICT) in agriculture and extension. – *J. of App. and Nat. Sci.* 9(2): 1097-1100.
- [30] Shen, Y. D., Du, Z. Q. (2009): The constraints of environment-friendly agricultural technology development and its countermeasures. – *Ecol. Econ.* 9: 9-16.
- [31] Singh, B., Sirohi, N. P. S. (2006): Protected cultivation of vegetables in India: problems and future prospects. – *International Symposium on Greenhouses, Environmental Controls and Inhouse Mechanization for Crop Production in the Tropics and Sub-Tropics*. Acta Hort. 710.
- [32] Stigter, C. J. (2008): Agrometeorology from science to extension: assessment of needs and provision of services. Invited lecture at the 50th anniversary of the Chinese Academy of Agricultural Sciences, Beijing. – *Agriculture, Ecosystems and Environment* 126: 153-157.
- [33] Tebrugge, F., Bohrsen, A. (2000): Direktsaat - Beurteilung durch Landwirte und Experten in der EU und Nebraska. – *Landtechnik* 55(1): 17-19.
- [34] Weir, H., Knight, J. (2000): Adoption and Diffusion of Agricultural Innovations in Ethiopia: The Role of Education. – *CSAE Working Paper Series 2000-05*, Centre for the Study of African Economies, University of Oxford.

APPENDIX

DEPARTMENT OF EXTENSION EDUCATION CCS HARYANA AGRICULTURAL UNIVERSITY, HISAR-125004

The Investigator:

Anil Kumar Rohila

Admission No: 2014A21D

Appendix 1

Sr. No. __

Mobile N. _____

1. Name of Respondent: _____ 2. Father's Name: _____
3. Village: _____ 4. Block: _____
5. District: _____ 6. Age: _____

7. Education

S. No.	Qualification	
1	Illiterate	
2	Primary	
3	Middle	
4	Metric	
5	Higher Secondary	
6	Graduate	

8. Land Holding

S. No.	Particular	
1	Landless	
2	Less than one acre	
3	Up to 5 acres	
4	6 to 10 acres	
5	11 to 15 acres	
6	16 to 20 acres	
7	More than 20 acres	

9. Cropping System

S. No.	Particulars	Yes	No
1	Rice-Wheat		
2	Cotton-Wheat		
3	Sugarcane Based		
4	Rice-Other crops		
5	Other crops-Wheat		
6	Cotton-Other crops		

7	Bajra/Jwar/Gwar-Wheat		
8	Bajra/Jwar/Gwar-Fallow		
9	Fallow-Wheat		
10	Bajra/Fallow-Mustard		
11	Bajra/Fallow-Pulses		
12	Other Rotation		

10. Farming System

S. No.	Particulars	Yes	No
1	Livestock		
2	Poultry		
3	Fisheries		
4	Forestry		
5	Agro-forestry		
6	Mushroom cultivation		
7	Bee keeping		
8	Organic farming		
9	Floriculture		
10	Poly house nursery		
11	Poly house vegetable production		

11. Irrigation Facilities

S. No	Particulars	Yes	No
1	Submersible Pump		
2	Tube well		
3	Canal		
4	Others		

12. Farm Power

S. No	Particulars	
1	No draft animal	
2	1-2 draft animal	
3	3-4 draft animal	
4	one or more prestige animal	
5	Tractor	

13. Mass Media Exposure

S. No	Particulars	
1	Do you listen radio?	Yes/No
2	If yes. How frequently?	Daily/often/sometimes
3	Do you watch agriculture related T.V. programmes?	Yes/No
4	If yes. How frequently?	Daily/often/sometimes

5	Do you read newspaper?	Yes/No
6	If yes. How often?	Daily/often/sometimes
7	Do you read farm magazines?	Yes/No
8	Do you call Kisan Sewa Kendra for queries?	Yes/No
9	Do you search online solution for your problems?	Yes/No

14. Extension Contact

S. No.	Extension Official	Frequency of Contact				
		Weekly	Fortnightly	Monthly	Whenever needed	None
1	ADOs					
2	SDAO/SMS					
3	Scientists					
4	Progressive farmer					
5	NGO					
6	Others					
	Total					

15. Economic Motivation

S. No.	Statements	SA	A	N	D	SD
1	A farmer should work toward larger yields and economic profit					
2	The most successful farmer is one, who makes the most profit					
3	A farmer should try any new farming idea which may earn him more money					
4	A farmer should grow cash crops to increase monetary profits in comparison to growing of food crops for home consumption					
5	It is difficult for the farmers' children to make good start, unless he provides them with economic assistance					
6	A farmer must earn his living but the most important thing in life cannot be defined in economic terms					

16. Innovation proneness

S. No	Statements	Most Like	Least like
(A)1	I try to keep myself up to date with information of any improved farm practice, but that does not mean that I try out all the new methods on my farm.		
2	I fell restless, till I try out the improved farm practice, I heard about.		
3	They talk of many improved farm practices these days but who knows if they are better than the old one.		
(B)1	I am cautious about trying a new practice.		
2	After all our forefathers were wise about their farm practices and I don't see any reason for changing the old methods		
3	Often improved farm practices are not successful. However, they are promising I would surely like to accept them.		

(C)1	From time to time, I have heard from several improved farm practices and I have tried out most them in last few years,		
2	I usually wait to see what results my neighbours obtain before I try out the improved farm practices.		
3	Somehow, I believe that the traditional ways of farming are the best.		

Appendix 2

Constraints in adoption of sustainable farming

S. No.	Sustainable constraints	Constraints		
		Very serious	Serious	Not so serious
1	Small and fragmented land holding			
2	Lack of skill to adopt sustainable farming			
3	Lack of finance to adopt improved practices			
4	Not aware about training for sustainable farming			
5	Not familiar with improved practices			

Constraints in adoption of weather forecasting

S. No.	Weather forecasting constraints	Constraints		
		Very serious	Serious	Not so serious
1	Not aware about the procedure of registration			
2	Irregularity in message			
3	Not proper language of message			
4	Lack of resources and internet etc.			
5	Information is useful only for until crop production			

Constraints in adoption of conservation agriculture (CA)

S. No.	Conservation agriculture constraints	Constraints		
		Very serious	Serious	Not so serious
1	Fragmented land holding			
2	Poor soil quality			
3	Increasing weed infestation			
4	Conservation agriculture is more labour intensive			

Constraints in adoption of ICTs

S. No.	ICTs constraints	Constraints		
		Very serious	Serious	Not so serious
1	Inadequate infrastructural facilities			
2	Lack of resources and tools			
3	Low internet access and electricity			

4	Fear that ICTs provides irrelevant content			
5	Lack of training to access e-information			

Constraints related to climate change

S. No.	Climate change constraints	Constraints		
		Very serious	Serious	Not so serious
1	Rapid change in weather conditions			
2	Environmental degradation			
3	Climate change effects the seasonal temperature and rainfall			
4	Deterioration in the quality of crop produce			
5	Effect on plant population and yield			
6	Probability of droughts and floods			

Constraints in adoption of greenhouse gas mitigation practices

S. No.	Greenhouse gas mitigation constraints	Constraints		
		Very serious	Serious	Not so serious
1	Non-availability of package of practices			
2	No reward for adoption of environmental measures			
3	Ignorance about the bad effect of chemical hazardous on health			
4	Slow result of eco- friendly practices			
5	Mostly farmers burn crop residue in the fields			

Constraints in adoption of protected cultivation

		Very serious	Serious	Not so serious
1	High initial cost			
2	Poor quality of material			
3	Frequent occurrence of wind storms, hailstorms, rain etc.			
4	Problem of nematodes and diseases			

Constraints in adoption agro processing and value addition practices

S. No.	Agro processing and value addition constraints	Constraints		
		Very serious	Serious	Not so serious
1	Lack of proper facilities			
2	Lack of procurement policy			
3	Lack of agro-processing unit			
4	Lack of proper training			
5	Lack of consumption of agro processed food			

ISOLATION, MOLECULAR CHARACTERIZATION AND PATHOGENICITY OF *METARHIZIUM ANISOPLIAE* (METSCH.) SOROKIN (HYPOCREALES: CLAVICIPITACEAE) FROM SOIL IN ERZINCAN PROVINCE, TURKEY

KILIÇ, E.^{1*} – YAZICI, A.^{2,3} – ÖRTÜCÜ, S.^{2,3}

¹*Department of Basic Pharmaceutical Science, Faculty of Pharmacy
Erzincan University, Erzincan, Turkey*

²*Department of Molecular Biology and Genetics, Faculty of Science
Erzurum Technical University, Erzurum, Turkey*

³*High Technology Research Center
Erzurum Technical University, Erzurum, Turkey*

**Corresponding author
e-mail: enginfk@gmail.com; ORCID: 0000-0002-6838-5977*

(Received 2nd Nov 2018; accepted 28th Feb 2019)

Abstract. Developing good microbial pesticides depends on isolating and knowing their pathogenicity. For this purpose, entomopathogenic *Metarhizium anisopliae* fungi were isolated from soils in Erzincan province and Galleria bait method was used. Molecular identification of the isolates was performed by using ITS rDNA analysis. As a test organism, *Galleria mellonella* and *Tenebrio molitor* larvae were used and suspensions of 2×10^7 conidia ml⁻¹ were prepared adding Tween 80®. Bioassays were performed by dipping technique and mortality was recorded daily for 12 days. Each assay consisted of 3 replicates with 10 insects larvae. Ten fungal isolates were obtained from the bait method. Based on classical and molecular methods, all fungal isolates were identified as *M. anisopliae* and deposited into GenBank database with MH104853 - MH104862 accession numbers. All isolates of *M. anisopliae* were pathogenic to *G. mellonella* and *T. molitor* with a mortality rate of $63.3 \pm 3.3\%$ - $83.3 \pm 3.3\%$ and $30 \pm 5.8\%$ - $66.7 \pm 3.3\%$, respectively 12 days after application. As a result, MaEMR1a and MaEO3 isolates can be applied as good biological control agents for pest insects.

Keywords: *biological control, Metarhizium anisopliae, G. mellonella, T. molitor*

Introduction

Entomopathogenic fungi (EPF) have an increasing prevalence in microbial control (Kılıç, E., 2009-Kılıç, E., 2014). EPF unlike other entomopathogenic microorganism (bacteria and viruses) which have to be ingested to cause diseases, typically infect insects by direct penetration of the cuticle followed by multiplication in the hemocoel (St. Leger et al., 2011). It is reported that EPF causes approximately, 60% of insect diseases (Faria and Wraight, 2007). EPF can be an alternative to chemical pesticides and are considered as non-harmful biological control agents in terms of human and environmental health (Faria and Wraight, 2007). *M. anisopliae* has a global distribution as a member of the soil flora (Zimmermann, 1992). This species has been reported in soils from widely differing climatic zones (Gillespie, 1988; McCoy et al., 1988; Kılıç, 2017). Some researcher pointed out that many isolates of *M. anisopliae* have entomopathogenic activity against a range of arthropod pests (Gillespie, 1988; McCoy et al., 1988). Many scientists reported that *M. anisopliae* has been effective in controlling more than 200 species of insect pests (Pu and Li, 1996; Sabbour, 2002;

Brooks and Wall, 2005; Quesada-Moraga et al., 2008; Shanley et al., 2009; Dimbi et al., 2009; Dickson et al., 2010; Marius et al., 2011; Niassy et al., 2011).

In this paper, we isolated and characterized pathogenic fungi *M. anisopliae* for possible use as microbial control agent of *G. mellonella* and *T. molitor* and its pathogenicity was determined. Both insect species caused economic losses at storage.

Material And Methods

Insect culture

Galleria mellonella Linnaeus (Lepidoptera: Pyralidae) was collected from different beekeeping in 2014 in Erzincan province. At the same time *T. molitor* (Coleoptera: Tenebrionidae) was collected from flour factories in Erzurum and storages in Erzincan province. *G. mellonella* and *T. molitor* were grown under laboratory conditions [(25°C±2 and 70%±10 R.H.) (16: 8 h (L:D))] (Zimmermann, 1986).

Isolation and identification of entomopathogenic fungi

Insect-associated fungi were isolated from soil samples by using ‘Galleria bait method’ (Zimmermann, 1986). The wax moth larvae, *G. mellonella* were reared continuously in constant darkness at 26°C. The third or fourth instar larvae (approximately 30 days after hatching) were used as baits. Ten larvae were placed on the soil samples in each boxes and covered with a lid and incubated at 25±2°C for two weeks. The larvae were examined on days 7 and 14 after inoculation. Surface of dead larvae were sterilized by 3% sodium hypochlorite for 3 min and then rinsed twice with sterile distilled water. After removing free water of the larvae surface, they were placed onto PDA plates. The fungi were identified using morphological characteristics of reproductive structures with the aid of relevant taxonomic literature (de Hoog, 1972; Samson et al., 1988; Tzean et al., 1997; Domsch et al., 1980; Humber, R., 1997; Humber, R., et al., 2012) (Table 1).

Table 1. Fungal material and their geographical origin (2014-2016)

<i>Fungus Species</i>	Isolate Code	Substrate (Soil)	Geographical Origin of Isolates
<i>Metarhizium anisopliae</i>	MaEMR1a	Vegetable Field	ERZİNCAN, Turkey
	MaEMR2b	Vegetable Field	ERZİNCAN-Üzümlü, Turkey
	MaEK1a	Vegetable Field	ERZİNCAN-Kemah, Turkey
	MaEİ3	Field (Barly-Weat)	ERZİNCAN-İliç, Turkey
	MaEKLY1a	Fruit Garden	ERZİNCAN-Kemaliye, Turkey
	MaER3	Field (Barly-Weat)	ERZİNCAN-Refahiye, Turkey
	MaEM1	Vegetable Field	ERZİNCAN-Mercan, Turkey
	MaET3	Field (Barly-Weat)	ERZİNCAN-Tercan, Turkey
	MaEÇ3	Field (Barly-Weat)	ERZİNCAN-Çayırılı, Turkey
	MaEO3	Field (Barly-Weat)	ERZİNCAN-Otlukbeli, Turkey

The identification of the isolated entomopathogenic fungi were performed using ITS. For this purpose, ITS1 (TCCGTAGGTGAACCTGCGG) and ITS4 (TCCTCCGCTTATTGATATGC) primers were used for the PCR (White et al., 1990). Genomic DNA was isolated from fungal biomass following the protocols of the *EcoSpin*. Genomic DNA isolation kit (EcoTec Biotechnology, Turkey). The PCR cycling conditions were: 2 min at 95 °C, followed by 30 cycles at 95° C for 45 s, 55° C for 60 s, 72° C for 60 s with a final extension step of 72° C for 10 min. PCR products were analyzed in 1 % (w/v) agarose gels visualized by UV after staining with EtBr. The products were purified by following the protocols of the EcoSpin PCR Purification Kit (EcoTec Biotechnology, Turkey). After purification, ITS rDNA were sequenced in both directions with 4 same primers at OLIGOMER Biotechnology, Turkey. Sequences chromatograms were assembled into one complete sequence using Bioedit Program (Hall, 1999) and the sequences were compared to all known sequences by the use of BLASTN 2.2.26+ program (Zhang et al. 2000) and deposited into GenBank (Table 2).

Preparation of conidial suspension

M. anisopliae isolates conidia were harvested by scraping the surface of 3-week-old sporulating cultures grown on potato dextrose agar (PDA) in petri dishes in an incubation at 25°C±2 for three weeks from sowing. Fungus spores were harvested after three weeks by pouring a suspension that was prepared by adding 0.01% Tween 80 in sterilised and distilled water in a sterilized glass Erlenmeyer flask, into the Petri dish developed by *M. anisopliae*. Liquid mixture with fungi was drained into the sterilised glass Erlenmeyer flasks from cheese cloth. Then it was rinsed on a rinsing device for five minutes. After that, the spores were counted in the suspensions using a haemocytometer to 2x10⁷ spores/ml (Klingen et al., 2002a; Klingen et al., 2002b; Klingen et al., 2002c; Vänninen et al., 1999).

Incubation of fungal spores and its treatment on G. mellonella and T. molitor

Dipping technique was used and the fungus isolate was dipped in the tested spore suspensions for 10 second, then left to dry at room temperature. Every petri dish included 10 larvae for the experiments. For control treatment, the same process was followed but 3ml of sterilized and distilled water with 0.01% of Tween 80 was used instead of fungus isolate for the dipping. After all of the application petri dishes were stored in the incubator (25°C±2) (Butt et al., 1994; Butt, 2002; Safavi et al., 2010). Mortality was assessed daily for 12 days by direct inspection for any signs of mortality. The experiment was replicated three times.

Statistical analysis

The experimental design was a randomized complete block with three replicates, and each replicate consisted of 10 larvae. The collected data were analyzed by one-way ANOVA test using SPSS 15.0 and means were compared by Duncan test.

Results

All fungal isolates were pathogenic to *G. mellonella* and *T. molitor* with a mortality rate between 63.3±3.3% - 83.3±3.3% and 30±5.8% - 66.7±3.3%, respectively after 12 days from application. Microscopic investigations confirmed mycosis and fungi were reisolated from all dead individuals.

In this study, a total of 10 different isolates belonging to the genera *Metarhizium* were obtained. Based on classical and molecular methods, all fungal isolates were identified as *M. anisopliae* and deposited in the GenBank database under the accession numbers MH104853 - MH104862 as seen in *Table 2*.

Table 2. Fungal material and their geographical origin (2014-2016)

Species	Isolate Code	GenBank Accession Numbers
<i>Metarhizium anisopliae</i>	MaEMR1a	MH104853
	MaEMR2b	MH104854
	MaEK1a	MH104855
	MaEİ3	MH104856
	MaEKLY1a	MH104857
	MaER3	MH104858
	MaEM1	MH104859
	MaET3	MH104860
	MaEÇ3	MH104861
	MaEO3	MH104862

Isolates of MaEMR1a, MaEM1 and MaEO3 caused mortality in more than 80% of *G. mellonella* larvae. There was no significant difference between these isolates ($p < 0.05$). However, isolate MaEM1 led to earlier mortality than the others. Mortality was found to increase with time. The mortality percentages of isolates against *G. mellonella* are depicted in *Table 3*.

The most virulent isolates against *T. molitor* were MaEO3, MaET3, MaEKLY1a and MaEMR1a, which caused 60, 63.3, 66.7 and 63.3% mortality, respectively after 12 days from application. As seen in *Table 4*, *M. anisopliae* isolate MaEMR1a was consistently more virulent than other isolates because mortality caused by this isolate was found to be significantly different ($p < 0.05$) on the 10th day.

It is observed that the death rates have increased as time progressed. As the entomopathogenic fungi feed in the host and complete their development, secondary metabolites secreted to kill the host are exposed and the host is dying more rapidly. At the same time, the fungus develops inside the host and breaks down the integument of the intestine and hyphae appear on the host body surface.

Table 3. Mortality of *M. anisopliae* isolates against *G. mellonella* larvae (%)

Isolates	3.day	4.day	5.day	6.day	7.day	8.day	9.day	10.day	11.day	12.day
MaEMR1a	0 ^a	16.7 ^{±6.7ab}	23.3 ^{±6.7a}	40 ^{±0ab}	43.3 ^{±3.3c}	46.7 ^{±3.3cd}	60 ^{±0bcd}	63.3 ^{±3.3bc}	70 ^{±0ab}	83.3 ^{±3.3a}
MaEMR2b	0 ^a	16.7 ^{±3.3ab}	30 ^{±0a}	40 ^{±0ab}	46.7 ^{±3.3bc}	56.7 ^{±3.3abc}	63.3 ^{±3.3abc}	66.7 ^{±3.3bc}	73.3 ^{±3.3ab}	76.7 ^{±3.3ab}
MaEK1a	0 ^a	13.3 ^{±3.3abc}	23.3 ^{±3.3a}	33.3 ^{±8.9b}	40 ^{±5.8c}	40 ^{±5.8d}	50 ^{±0d}	63.3 ^{±3.3bc}	63.3 ^{±3.3bc}	76.7 ^{±3.3ab}
MaEİ3	0 ^a	10 ^{±0bc}	23.3 ^{±3.3a}	33.3 ^{±3.3b}	40 ^{±5.8c}	46.7 ^{±3.3cd}	56.7 ^{±3.3cd}	63.3 ^{±3.3bc}	73.3 ^{±3.3ab}	76.7 ^{±3.3ab}
MaEKLY1a	0 ^a	13.3 ^{±3.3abc}	30 ^{±5.8a}	36.7 ^{±6.7b}	40 ^{±5.8c}	53.3 ^{±3.3bc}	60 ^{±0bcd}	60 ^{±5.8c}	60 ^{±5.8c}	63.3 ^{±3.3c}
MaER3	3.3 ^{±3.3a}	20 ^{±5.8ab}	36.7 ^{±3.3a}	46.7 ^{±6.8ab}	50 ^{±5.8bc}	56.7 ^{±3.3abc}	63.3 ^{±3.3abc}	73.3 ^{±3.3ab}	73.3 ^{±3.3ab}	73.3 ^{±3.3ab}
MaEM1	0 ^a	20 ^{±5.8ab}	26.7 ^{±3.3a}	43.3 ^{±3.3ab}	53.3 ^{±3.3bc}	63.3 ^{±3.3ab}	70 ^{±0ab}	80 ^{±0a}	80 ^{±0a}	83.3 ^{±3.3a}
MaET3	3.3 ^{±3.3a}	16.7 ^{±3.3ab}	30 ^{±5.8a}	46.7 ^{±3.3ab}	53.3 ^{±3.3bc}	56.7 ^{±3.3abc}	63.3 ^{±3.3abc}	63.3 ^{±3.3bc}	70 ^{±0ab}	70 ^{±0bc}
MaEÇ3	0 ^a	10 ^{±5.8bc}	26.7 ^{±3.3a}	43.3 ^{±3.3ab}	66.7 ^{±3.3a}	66.7 ^{±3.3a}	66.7 ^{±3.3abc}	70 ^{±0abc}	73.3 ^{±3.3ab}	76.7 ^{±3.3ab}
MaEO3	3.3 ^{±3.3a}	26.7 ^{±3.3a}	36.7 ^{±3.3a}	53.3 ^{±3.3a}	60 ^{±0ab}	66.7 ^{±3.3a}	73.3 ^{±3.3a}	73.3 ^{±3.3ab}	76.7 ^{±3.3a}	83.3 ^{±3.3a}
Control	0 ^a	0 ^c	0 ^b	0 ^c	0 ^d	0 ^e	0 ^e	0 ^d	0 ^d	3.3 ^{±3.3d}

*All values are mean ± standard error of three determinations (n=3). Same alphabet letters in the same column are not significantly different at p<0.05.

Table 4. Mortality of *M. anisopliae* isolates against *Tenebrio molitor* larvae (%)

Isolates	3.day	4.day	5.day	6.day	7.day	8.day	9.day	10.day	11.day	12.day
MaEMR1a	0	10 ^{±5.8ab}	16.7 ^{±3.3bcd}	20 ^{±5.8cde}	20 ^{±5.8cd}	36.7 ^{±3.3bcd}	40 ^{±5.8bcd}	53.3 ^{±3.3abc}	56.7 ^{±3.3ab}	63.3 ^{±3.3a}
MaEMR2b	0	6.7 ^{±3.3ab}	13.3 ^{±8.9cde}	20 ^{±5.8cde}	26.7 ^{±12bcd}	30 ^{±11.5cde}	43.3 ^{±8.9abc}	43.3 ^{±8.9cd}	43.3 ^{±8.9bc}	53.3 ^{±8.9abc}
MaEK1a	0	10 ^{±5.8ab}	20 ^{±5.8abcd}	26.7 ^{±3.3abc}	30 ^{±5.8abc}	43.3 ^{±3.3abc}	53.3 ^{±3.3ab}	56.7 ^{±3.3abc}	56.7 ^{±3.3ab}	56.7 ^{±3.3ab}
MaEİ3	0	6.7 ^{±3.3ab}	13.3 ^{±3.3cde}	13.3 ^{±3.3}	23.3 ^{±3.3cd}	26.7 ^{±3.3de}	26.7 ^{±3.3de}	33.3 ^{±3.3de}	33.3 ^{±3.3c}	40 ^{±5.8cd}
MaEKLY1a	0	20 ^{±5.8a}	30 ^{±5.8ab}	36.7 ^{±3.3a}	36.7 ^{±3.3abc}	53.3 ^{±3.3a}	53.3 ^{±3.3ab}	63.3 ^{±3.3a}	63.3 ^{±3.3a}	66.7 ^{±3.3a}
MaER3	0	3.3 ^{±3.3b}	10 ^{±5.8de}	10 ^{±5.8ef}	10 ^{±5.8de}	20 ^{±5.8e}	20 ^{±5.8e}	23.3 ^{±3.3e}	30 ^{±5.8c}	30 ^{±5.8d}
MaEM1	0	20 ^{±5.8a}	26.7 ^{±3.3abc}	30 ^{±0abc}	33.3 ^{±3.3abc}	43.3 ^{±3.3abc}	46.7 ^{±3.3abc}	46.7 ^{±3.3bcd}	50 ^{±5.8ab}	53.3 ^{±3.3abc}
MaET3	0	10 ^{±5.8ab}	23.3 ^{±3.3abcd}	23.3 ^{±3.3bcd}	43.3 ^{±3.3ab}	43.3 ^{±3.3abc}	46.7 ^{±3.3abc}	60 ^{±5.8ab}	63.3 ^{±3.3a}	63.3 ^{±3.3a}
MaEÇ3	0	10 ^{±0ab}	13.3 ^{±3.3cde}	13.3 ^{±3.3}	20 ^{±5.8cd}	30 ^{±5.8cde}	36.7 ^{±3.3cd}	43.3 ^{±3.3cd}	43.3 ^{±3.3bc}	43.3 ^{±3.3bcd}
MaEO3	0	13.3 ^{±3.3ab}	33.3 ^{±3.3a}	33.3 ^{±3.3ab}	46.7 ^{±3.3a}	50 ^{±0ab}	56.7 ^{±6.7a}	60 ^{±5.8ab}	60 ^{±5.8a}	60 ^{±5.8a}
Control	0	0 ^b	0 ^e	0 ^f	0 ^e	0 ^f	0 ^f	0 ^f	0 ^d	0 ^e

*All values are mean ± standard error of three determinations (n=3). Same alphabet letters in the same column are not significantly different at p<0.05.

Discussion

Entomopathogenic fungi are used in the control of harmful insects and especially in the Integrated pest management system (IPM) and they are used successfully nowadays. It is important to know the virulence of the newly developed mycoinsecticides, the killing rates, the molecular characterization of these fungi and their genetic structure as soon as possible.

According to this study, MaEMR1a, MaEM1 and MaEO3 isolates of *M. anisopliae* have been determined to have potential to suppress *G. mellonella* larvae; MaEO3, MaET3, MaEKLY1a and MaEMR1a isolates have potential to suppress *T. molitor* larvae. Among them these isolates, MaEMR1a and MaEO3 isolates possessed a good potential against both *G. mellonella* and *T. molitor* larvae. Our results overlap with other pathogenicity tests on *T. molitor* and *G. mellonella* larvae (Pajar et al., 2013; Mora, E.A.M., 2016). Our results indicated that these two isolates (MaEMR1a and MaEO3) have a broad host range and can be used as biocontrol agents for *G. mellonella* and *T. molitor* and also they can be used as storages of biological control agents.

Acknowledgements. The EPF isolation part of this study was supported by the Erzinçan University Research Foundation (FEN-A-300614-0104).

REFERENCES

- [1] Alves, S. B., Lopes, R. B. (2008): Controle microbiano de pragas na América Latina: avanços e desafios. – Piracicaba: FEALQ: 414.
- [2] Bischoff, J. F., Rehner, S. A., Humber, R. A. (2009): A multilocus phylogeny of the *Metarhizium anisopliae* lineage. – *Mycologia* 101: 512–530.
- [3] Brooks, A., Wall, R. (2005): Horizontal transmission of fungal infection by *Metarhizium anisopliae* in parasitic Psoroptes mites (Acari: Psoroptidae). – *Biol Control* 34(1): 58-65.
- [4] But, T. M., Ibrahim, L., Ball, B. V., Clark, S. J. (1994): Pathogenicity of the entomogenous fungi *Metarhizium anisopliae* and *Beauveria bassiana* against crucifer pests and the honey bee. – *Biocont Sci Technol* 4: 207-214.
- [5] Butt, T. M. (2002): Use of Entomogenous Fungi for the Control of Insect Pests: 111–134. – In: Kempken, F. (ed.) *Agricultural Applications*, Springer Berlin Heidelberg, Berlin, 388.
- [6] Dickson, W. L., Robert, D. S., Edith, P. M., Deogratus, R. K., Ladslaus, L. M., Tanya, L. R., Fredros, O. O. (2010): An extra-domiciliary method of delivering entomopathogenic fungus, *Metarhizium anisopliae* IP 46 for controlling adult populations of the malaria vector, *Anopheles arabiensis*. – *Parasite Vector* 3(18): 1-6.
- [7] Dimbi, S., Maniana, N. K., Ekesi, S. (2009): Effect of *Metarhizium anisopliae* inoculation on the mating behavior of three species of African Tephritid fruit flies, *Ceratitis capitata*, *Ceratitis cosyra* and *Ceratitis fasciventris*. – *Biol Control* 50(2): 111-116.
- [8] Domsch, K. H., Games, W., Anderson, T. H. (1980): *Compendium of Soil Fungi* – Academic press. London.
- [9] Faria, M. R., Wraight, S. P. (2007): Mycoinsecticides and mycoacaricides: A comprehensive list with worldwide coverage and international classification of formulation types. – *Biological Control* 43: 237-256.

- [10] Gillespie, A. T. (1988): Use of fungi to control pest of agricultural importance. – In: Burge, M. N. (ed.) Fungi in biological control systems: 37-60, Manchester University Press.
- [11] Hall, T. A. (1999): BioEdit: a user-friendly biological sequence alignment editor and analysis program for Windows 95/98/NT. – Nucleic Acids Symp Ser 41: 95–98.
- [12] De Hoog, G. S. (1972): The genera Beauveria, Isaria, Tritirachium and Acrodontium gen.nov – Study Mycol 1:1-41.
- [13] Humber, R. (1997): Entomopathogenic Fungal Identification: 153-185 – In: Lacey, L. A. (ed.) Manual of Techniques In Insect Pathology San Diego.
- [14] Humber, R., Gryganskyi, A. P., Vilgalys, R. (2012): Phylogenetic reclassification raises new respect—and a new phylum!– for Entomophthorales. – Mol Phylogenet Evol 65(2): 682-94.
- [15] Kılıç, E. (2014): Biopesticides marked and Turkey. – International Conference on Biopesticides 7. Side Antalya, Turkey.
- [16] Kılıç, E. (2017): Isolation entomopathogenic fungi from Erzincan province. – 6th Entomopathogens and Microbial Control Congress. Tokat, Turkey.
- [17] Kılıç, E., Yıldırım, E., İskender, N. A., Algur, Ö. F. (2009): Pathogenicity of *Beauveria bassiana* (balsomo) Villenium 1826 (Deuteromycotina: Hypomycetes) isolates to various development stages of *Bemisia tabaci* (Homoptera: aleyrodiade) – Bio-Science research Bulletin 25: 17-28.
- [18] Klingen, I., Eilenberg, J., Meadow, R. (2002a): Efects of farming system, Weld margins and bait insect on the occurrence of insect pathogenic fungi in soils. – Agric Ecosyst Environ 91: 191–198.
- [19] Klingen, I., Hajek, A., Meadow, R., Renwick, J. A. A. (2002b): Efect of brassicaceous plants on the survival and infectivity of insect pathogenic fungi. – BioControl 47: 411–425.
- [20] Klingen, I., Meadow, R., Aandal, T. (2002c): Mortality of *Delia Xoralis*, *Galleria mellonella* and *Mamestra brassicae* treated with insect pathogenic hyphomycetous fungi. – J Appl Entomol 126: 231–237.
- [21] Marius, H., Godwin, P. K., Michael, S., Galina, G., Itamar, G. (2011): Pathogenicity of the entomopathogenic fungus *Metarhizium anisopliae* to the red-legged tick, *Rhipicephalus evertsi*. – Afr J Biotechnol 3(7): 68-72.
- [22] McCoy, C. W., Samson, R. A., Boucias, D. G. (1988): Entomogenous fungi. – In: Ignoffo, C. M., Mandava, N. B. (eds.) Handbook of natural pesticides. Boca, Ra-ton, Mr ic, Fla: Mr ic press. Microbial insectides 5, part A. Entomogenous protozoa and Fungi.
- [23] Mora, A. E. M., Chaco-Orozco, J. G., Harakava, R., Rouws, J. R. C., Fraga, M. E. (2016): Molecular characterization and virulence of *Beauveria bassiana* and *Metarhizium anisopliae* against *Galleria mellonella* (Lepidoptera: Pyralidae) and *Tenebrio molitor* (Coleoptera: Tenebrionidae) larvae. – African Journal of Microbiology Research 10(9): 662-668.
- [24] Niassy, S., Diarra, K., Ndiaye, S., Niassy, A. (2011): Pathogenicity of local *Metarhizium anisopliae* var. *acidum* strains on *Locusta migratoria migratorioides* Reiche and *Farmaire* and *Zonocerus variegatus* Linnaeus in Senegal. – Afr J Biotechnol 10(1): 28-33.
- [25] Pajar, J. A. L., Cabahug, D. V., Sumaya, N. H. N., Martinez, J. G. T., Madamba, R. S. B., Rivero, H. I. (2013): Virulence of Local *Metarhizium* spp. Isolates Against *Tenebrio Molitor* (Linn): An Initial Comparison with Non-Native and Commercially Available Strains. – International Journal of the Computer, the Internet and Management 21(1): 48-52.
- [26] Pu, Z. N., Li, Z. Z. (eds.) (1996): Insect Mycology – Anhui Publishing House of Science and Technology, Hefei, China (in Chinese).

- [27] Quesada-Moraga, E., Martin-Carballo, I., Garrido-Jurado, I., Santiago-Álvarez, C. (2008): Horizontal transmission of *Metarhizium anisopliae* among laboratory populations of *Ceratitis capitata* (Wiedemann) (Diptera: Tephritidae). – *Biol Control* 47(6): 115-124
- [28] Sabbour, M. M. (2002): The role of chemical additives in enhancing the efficacy of *Beauveria bassiana* and *Metarhizium anisopliae* against the potato tuber moth *Phthorimaea operculella* (Zeller) (Lepidoptera: Gelechiidae). – *Pak J Biol Sci* 5(11): 1155-1159.
- [29] Safavi, S. A., Kharrazi, A., Rasouljan, G. R., Bandani, A. R. (2010): Virulence of some isolates of entomopathogenic fungus, *Beauveria bassiana* on *Ostrinia nubilalis* (Lepidoptera: Pyralidae) larvae. – *Journal of Agricultural Science and Technology* 12(1): 13–21.
- [30] Samson, R. A., Evans, H. C., Latge, J. P. (1988): *Atlas of Entomopathogenic Fungi*. – Springer-Verlag, New York: 187.
- [31] Shanley, R. P., Keena, M., Wheeler, M. M., Leland, J., Hajek, A. E. (2009): Evaluating the virulence and longevity of non-woven fiber bands impregnated with *Metarhizium anisopliae* against the Asian long horned beetle, *Anoplophora glabripennis* (Coleoptera: Cerambycidae). – *Biol Control* 50(4): 94-102.
- [32] St. Leger, R. J., Wang, C., Fang, W. (2011): New Perspectives On Insect Pathogens. – *Fungal Biology Reviews* 25: 84-88.
- [33] White, T. J., Bruns, T., Lee S., Taylor, J. (1990): Amplification and direct sequencing of fungal ribosomal RNA genes for phylogenetics. – In: Innis, M. A., Gelfand, D. H., Sninsky, J. J., White, T. J. (eds.) *PCR Protocols: a guide to methods and applications*. Academic Press, New York: 315-322.
- [34] Tzean, S. S., Hsieh, L. S., Wu, W. J. (1997): *Atlas of Entomopathogenic Fungi from Taiwan*. – Council of Agriculture, Taiwan, R.O.C.: 214.
- [35] Vänninen, I., Hokkanen, H., Tyni-Juslin, J. (1999): Attempts to control cabbage root Xies, *Delia radicum* (L.) and *Delia Xoralis* (Fall.) (Dipt., Anthomyiidae), with entomopathogenic fungi: laboratory and greenhouse tests. – *J Appl Entomol* 123: 107-113.
- [36] Zhang, Z., Schwartz, S., Wagner, L., Miller, W. (2000): A greedy algorithm for aligning DNA sequences. – *Journal of Computational Biology* 7: 203-214.
- [37] Zimmermann, G. (1986): The *Galleria* bait method for detection of entomopathogenic fungi in soil. – *J Appl Entomol* 102: 213–215.
- [38] Zimmermann, G. (1992): *Pflanzenschutz-Nachr.* – Bayer 45: 113–128.

EFFECTS OF DIFFERENT HUMIC ACID AND SALINITY LEVELS ON SOME TRAITS OF KHUZESTANI SAVORY (*SATUREJA KHUZISTANICA* JAMZAD)

ZAREMANESH, H.¹ – EISVAND, H. R.^{1*} – AKBARI, N.¹ – ISMAILI, A.¹ – FEIZIAN, M.²

¹*Department of Agronomy and Plant Breeding, Faculty of Agriculture, Lorestan University, Khorramabad, Iran*

²*Department of Soil Science, Faculty of Agriculture, Lorestan University, Khorramabad, Iran*

**Corresponding author
e-mail: eisvand.hr@lu.ac.ir*

(Received 29th Nov 2018; accepted 28th Feb 2019)

Abstract. In order to study the impact of humic acid on some morphological, physiological and biochemical traits of Khuzestani savory under salinity stress condition, the present study was conducted in the greenhouse of the agricultural faculty of Lorestan University as a factorial experiment (combination of humic acid and salinity) in the form of randomized complete blocks design (RCBD) in 2017. Factors of the experiment included salinity in five levels (0, 25, 50, 75 and 100 mM of NaCl) and humic acid also in five levels (0, 10, 20, 30 and 40 mg/Kg of soil), which were applied as a pot experiment. Results revealed that in terms of morphological traits including stem length, root length, leaf length, leaf width and leaf area, the highest salinity (S5) and “without humic acid” (H1) (S5H1) produced the lowest values; whereas “without salinity” (S1) and highest humic acid (H5) (S1H5) produced the highest values for these traits. Moreover, S1H5 treatment produced the highest photosynthesis and transpiration rates of 24.04 $\mu\text{mol CO}_2 \text{ m}^{-2} \text{ s}^{-1}$ and 2.85 $\text{mmol H}_2\text{O}_2 \text{ m}^{-2} \text{ s}^{-1}$, respectively; whereas, lowest values for the traits were produced in S5H1 treatment to be 5.67 $\mu\text{mol CO}_2 \text{ m}^{-2} \text{ s}^{-1}$ and 0.65 $\text{mmol H}_2\text{O}_2 \text{ m}^{-2} \text{ s}^{-1}$, respectively. Furthermore, S1H5 treatment produced the highest (0.280 $\text{mol CO}_2 \text{ m}^{-2} \text{ s}^{-1}$) stomatal conductance rate and lowest substomatal CO_2 (85 ppm); whereas, S5H1 treatment produced the lowest (0.013 $\text{mol CO}_2 \text{ m}^{-2} \text{ s}^{-1}$) stomatal conductance rate and highest (406 ppm) substomatal CO_2 . The highest organic matter content (89.69% on average) was found in S2H3 treatment, whereas it reached to its lowest value (69.46% on average) in S4H5 treatment. Moreover, S5H2 treatment produced the highest (24.37% on average) and S1H5 treatment the lowest (10.35% on average) ash percentage trait. As for relative water content (RWC) of leaf, the highest (93.01% on average) and lowest (70.94%) values were produced in S1H5 and S5H1 treatments, respectively. S5H1 had the highest (0.334 mg/g of fresh weight) proline content and S5H5 had the highest (2.098 mg/g of dry matter) soluble sugar content; whereas, the lowest proline content (0.155 mg/g of fresh weight) and soluble sugar content (0.808 mg/g of dry matter) were produced in S1H5 and S1H1 (control) treatments, respectively.

Keywords: *salt stress, organic fertilizer, morphology, physiology, biochemistry*

Introduction

Plant growth and its resulting yield are influenced by numerous environmental factors. Worldwide, normal plant growth is challenged by a great number of environmental factors particularly drought, salinity, nutrient imbalance, toxicity and critical temperatures (Ashraf, 1994). Although, secondary plant metabolites are characterized by their importance in plant tolerance against environmental stresses, mechanism of their response to the environmental stresses keeps boggling the minds. Although, there is numerous evidence that the environmental stresses have an increasing effect on the secondary metabolites content of plants; this effect is limited and in some cases even happens in reverse. Furthermore, quality of these substances is

influenced by the environmental stresses as well. It is known that plant species mainly use the mechanism of growth reduction and change in constituents of the secondary metabolites to survive in the environmental stresses. Environmental stresses, both biotic and abiotic, are serious and unforgiving threats for the crops. Drought, salinity, extreme cold and warm temperatures are the most notable abiotic stresses that reduce yield and increase economical costs at the global level (Nakabayashi and Saito, 2015).

One of the globally most infamous environmental factors is salinity, which is known for its negative impact on growth and yield of plants all over the world (Sevengor et al., 2011; Amirjani et al., 2010; Zhani et al., 2012). More specifically, impacts of salinity stress on the plants include ionic toxicity, osmotic stress, mineral deficiency, physiological and biochemical disorders and a combination of them (Saleh, 2013; Rajaravindran, 2012).

Curiously, salinity inhibits plant growth mainly through decreasing water potential in root zone, salinity-induced accumulation of ions and compromised nourishment balance; which finally lead to physiological, morphological as well as metabolic changes (Parvin et al., 2012). Interestingly, the most important monitoring parameters of effects of environmental stresses, particularly salinity and drought stresses are stem length and root length. This is because roots are in direct contact with the soil and the water and nutrients it absorbs from the soil are transported by the stem to other parts of the plant; thus, changes in the lengths of stem and root can best represent the response of plants to the salinity stress (Jamil, 2005).

Although limited plant growth under salinity stress may not simply be attributed to a change in the specific physiological processes, photosynthesis is known to be the dominant physiological process limiting plant growth (Sudhir and Murthy, 2004). Salinity reduces plant growth and yield by compromising its physiological processes particularly photosynthesis; while intensity of the effect depends on the degree and duration of the salinity stress (Chaves et al., 2009). Reports suggest that lower water potential of leaf causes the stomata to close, compromises CO₂ supply of the plant and finally decreases the rate of photosynthesis. Closing of the stomata is probably the first line of defense against the loss of water and the most important factor affecting the rate of carbon fixation (Da Silva et al., 2008).

Furthermore, salinity stress decreases osmotic potential that leads to decreased water absorption followed by decreased transpiration, which if continued long enough can cause plants to die (Sivritepe et al., 2010). Moreover, proline accumulation is one of the key physiological parameters used to assess plant tolerance and plays an important part in its adaptation to stress. Generally, proline accumulation occurs in plants that are exposed to extreme conditions of drought and salinity. Probably, proline synthesis in a plant is the result of its nonspecific response to low water potential. Moreover, proline may play a part in osmoregulation and maintaining the enzymatic activity of plants. In addition to the part it plays in osmotic modification, this amino acid contributes to fixation of cellular parts, absorption of free radicals, buffering state of cell oxidation potential, and other various processes against stresses (Ashraf and Foolad, 2007).

Under salinity stress, the insoluble sugars (starch) are broken down to soluble ones and this enables the cell to maintain osmotic potential and avoid dehydration. In addition, decreased sugar consumption due to decreased photosynthesis during the salinity stress causes further increase in the intracellular concentration of soluble sugars (Parvaiz and Satyawati, 2008). The salinity induced damages to plants occur through osmotic effect, ion toxicity, and compromised nutrient absorption. Humic acid is a

constituent of humus and is dark brown in color. As a compound it contains sulfur, nitrogen, phosphorus in various percentages and some of the metals such as calcium, magnesium, copper, zinc etc. Soil salinity can be reduced by using new methods such as application of microorganisms, humic acid and folic acid, algae and herbal extracts to the soil (Bashan et al., 2014; Calvo et al., 2014).

Biochemically, humic acid is the active ingredient of humus (Nasouti Miandoab et al., 2011). Humic acid can have direct and positive impacts on plant growth by stimulating the growth of both shoot and root systems. Its impact on root is more predominant, while it can increase root volume which in turn improves efficiency of the root system. Humic acid can also increase the uptake of nitrogen, potassium, calcium, magnesium and phosphorus by the plant (Soltani, 2002). Possibly, humic acid contributes the growth traits through interaction with mineral ions, conversion to enzymes found in the plant, improving transpiration and photosynthesis and triggering hormonal activities (El-Sherbeny et al., 2012).

Owing to its characteristic composition, humic acid is capable of reducing the salt content of soil and negating its effect. Presence of humic acid in the soil can improve photosynthesis as well as tolerance against the biotic and abiotic stresses including diseases. Moreover, it boosts plant defense system by adding natural antioxidants and phenolic acid. Humic acid delays chlorosis through improving the uptake of magnesium and iron (Nasouti Miandoab et al., 2011).

Based on the above discussion and the increasing interest on medicinal plants, particularly in the technologically advanced communities, the importance of their preservation and propagation by using new cost-effective methods and create jobs and sustainable income can never be overemphasized. Khuzestani savory is one of the important medicinal plants in Iranian as well as global traditional medicine (*Fig. 1*). Khuzestani savory (*Satureja khuzistanica* Jamzad) is an aromatic perennial plant exclusively native to climatically arid southeastern region of Iran where it grows in limy-stony soils (Hadian et al., 2010). Geographical distribution of Khuzestani savory (*Fig. 2*) is in between Andimeshk and Pol Dokhtar towns in Palan village, Lorestan Province; and 72 km far from Andimeshk towards Khorramabad and 5 km after Tang Bridge on the clefts of limestone rocks in Sahara-Sindhi area at 474-520 m elevation (Jamzad, 2009). Savory belongs to Lamiaceae family and is among the species with remarkable antioxidant properties. For a long time, savory is being used as condiment and flavoring ingredient in canned food, soft drinks and manufacturing a variety of meat products and sausages. The essential oil content of above ground parts of savory varies in terms of the climatic condition under which the plant has grown and ranges between 1 and 2%. The most important compounds found in the essential oil of the plant include carvacrol (24.5%), thymol (23.12%), Gamma Terpinene (20.72%) and p-cymene (6.30%) (Kamkar et al., 2013).

More than 800 million hectares of the land area in the world, accounting for six percent of the total, is affected by salinity (Seckin et al., 2010). Salinity is a pervasive problem in Iran and limits sustainable agricultural production. Large parts of the arid and semi-arid regions in the country (especially in the Central Iranian Plateau, the southern coastal plains and the Khuzestan Plain) suffer from salinity (FAO, 1972; Naghizadeh et al., 2014).

Since wild Khuzestani savory (*Satureja khuzestanica*) grows in stony calcareous areas, this research was conducted to determine to what extent it could tolerate salinity and to prepare the ground for planting it on saline soils. Soil salinity plays a deciding

role in plant growth and development. Most plants are sensitive to salinity, but a small group of them can somewhat tolerate soil salinity. The quantity of active ingredients in medicinal plants is influenced by soil salinity. Therefore, determination of soil salinity level has an effective role in production of medicinal plants. Naturally, yield of Khuzestani savory also decreases under the harmful influence of salinity.



Figure 1. *Satureja khuzistanica*



Figure 2. *Satureja khuzestanica* habitat in Lorestan Province (Mohebbi et al., 2016)

This plant is wild-growing and found in sunny, stony, and calcareous areas of Lorestan and Khuzestan Provinces of Iran. Its cultivation is not common at present and most studies on it were conducted in greenhouses. Therefore, it is harvested in nature for medicinal purposes, which can be accompanied by the risk of its extinction. Nowadays, *Satureja hortensis* is widely planted. A summary of the method of cultivation this crop is as follows:

Like other annual plants, Khuzestani savory can be planted in rotation with most other crops. The desirable temperature for seed germination is 20-22 °C. Since this plant is sensitive to cold, the most suitable time for planting it is spring (from late April to late May). Seeds are planted in rows in the field in spring. Row spacing differs

depending on the planting method. In small-scale planting by hand, the suitable row spacing is 25-30 cm. If seeds are machine-planted, the 45-50 cm row spacing will be more appropriate. The suitable number of seeds is 120-140 per meter of row. Planting depth in different soils varies from 0.5 to 1.5 cm. 4-8 kg of seeds is required per hectare. It is recommended that the land is properly rolled after planting. This operation results in compaction of the surface soil layer and favorably influences uniform seed germination. The field must be irrigated after planting.

If planting density is high, thinning is carried out. The 4-6 leaf stage is suitable for this operation. Weed control is necessary during the growing season. Inter-row weed control by using a cultivator, especially after the first harvest, plays a major role in increasing yield. Plants have their highest essential oil content during the flowering stage. Therefore, harvesting the vegetative part is done at this stage. If plants are suitably looked after with respect to irrigation, soil, and contents of nutrients in soil that are necessary for satisfactory plant growth, it will be possible to harvest the crop 2 or even 3 times per year. The first harvest is carried out at the start of the flowering stage and the second in late September. All aerial organs of the plants are harvested by machine or manually using a scythe. Fruit usually matures 140-160 days after seed germination. Late August, when seeds gradually turn brown, is the suitable time for collecting seeds. Delays in collecting seeds should be avoided as completely mature seeds are scattered by the faintest blows inflicted on the plants.

The present study focused on effect of humic acid on some of the morphological, physiological and biochemical traits of the medicinal plant Khuzestani savory (*Satureja khuzistanica* Jamzad) under salinity stress. Hopefully, results from this study can pave the way for prospective studies in the field and help to promote cultivation of the medicinal plants.

Materials and methods

The present study was conducted as a greenhouse experiment in 2017 at Lorestan University, Iran. The experiment was conducted as factorial based on a randomized complete block design (RCBD) with four replications. The first factor included humic acid in five levels (zero, 10, 20, 30 and 40 mg/Kg soil) that was applied before planting. The second factor was salinity stress in five levels (zero, 25, 50, 75 and 100 mM NaCl) which was applied after sprouting and establishment of the plants during the fourth leaf stage. Levels of the factors being studied are shown in *Table 1*.

The humic acid was applied to the soil in the pots before the plantation of seeds. Pots used in the experiment were plastic pots made of polyethylene, each 280 g in weight 15.5 cm in diameter and 18 cm in height. Volume of each pot was 4 Kg and they were filled with soil-gravel-sheep manure in 2:1:0.5 ratio. Prior to plantation, savory seeds (*Satureja Khuzistanica* Jamzad) were disinfected by sodium hypochlorite 10% solution for 3 min and as many as 15 seeds were planted in each pot at a depth of 1-2 cm. After sprouting and during the fourth leaf stage the planting density was thinned to 8 plants. Cultivation included weeding, irrigation and application of salinity after fourth leaf stage to the treatments.

In order to study the morphological parameters, 5 plants were selected randomly from each experimental unit and average values were calculated in mm for traits such as stem length, root length, leaf length and leaf width by using a ruler.

Finally, analysis of variance of data was done using SAS9.4 software. Also, for post-hoc analysis, the comparing the means of combination of treatment was done using Duncan's multiple range test at 5% probability level.

Table 1. Different levels of salinity and humic acid applied in the experiment

Humic acid (mg/kg soil)		Salinity (NaCl mM)	
Level of treatment	Abbreviation	Level of treatment	Abbreviation
0	H1	0	S1
10	H2	25	S2
20	H3	50	S3
30	H4	75	S4
40	H5	100	S5

Leaf relative water content (RWC)

In order to measure the RWC of leaf, samples were taken from the reference leaf (last developed leaf) in the experimental units and immediately put into ice; then their wet weight was measured (in 0.0001 accuracy) in the lab. The samples were put into distilled water and kept in Cold Room under 4 °C for 24 h. Then, saturated weight of the leafs was measured before putting them in an oven under 70 °C for another 24 h and measuring their dry weight. The obtained values and the following equation were used to calculate the RWC (Ritchie et al., 1990):

$$RWC = (Fw - Dw / Sw - Dw) \times 100$$

where Fw is the wet weight of leaf immediately after sampling, Dw is the dry weight of leaf after taken out of oven, Sw is the saturated weight of leaf after removed from distilled water.

Measurement of leaf area

Leaf area were obtained using the leaf area measuring instrument (LI-3000A, USA) by putting leafs on the instrument.

Measurement of soluble sugars

Firstly, the sample leafs were dried out by putting into the oven under 110 °C for 48 h and digital scale was used to take 0.1 g of each sample. Then, as much as 10 mL 70% alcohol was added to each sample in polyethylene containers and kept in refrigerator for one week. During this process, the soluble sugars were solved in ethanol and accumulated at the top layer, from which 1 mL was taken and added to a mixture containing 1 mL 5% phenol and 5 mL concentrated sulfuric acid. The obtained solution was initially yellow in color, which changed over time. The solution was kept in the ambient temperature of laboratory to cool down for half an hour to obtain its final color. Finally, optical absorbance of the solution in 485 nm was obtained by using spectrophotometer. In order to calculate the density of soluble sugars for the samples (C), solutions with glucose 0, 10, 20, 50, 100, 200 and 300 mg/L were prepared as control sugar by using the standard curve and all the procedures were repeated on 2 mL

of each solution. Sugar value was obtained for the plant samples in mg/g (Kochert, 1978).

Extraction and measurement of proline

In the present study proline content was measured by using method of Bates et al. (1973). The measurement process involved pulverizing 0.5 g of wet plant material inside a porcelain mortar while gradually adding 10 mL 3% sulfosalicylic acid. Then, the obtained solution was centrifuged inside a test tube at 3000 round/min for 15 min to become homogenous. The solution was filtered and 2 mL of it was taken and after adding 2 mL ninhydrin as reagent and 2 mL pure acetic acid was put in bain-marie under 100 °C for 1 hour before being put into ice bath. After adding 4 mL toluene in each tube, two phases were formed. The upper phase containing colored complex, was used to measure the proline content. Absorbance of the upper phase was read at 520 nm wavelength by using spectrophotometer, while proline content was obtained by using the standard diagram.

Measurement of ash and organic matter

As much as 1 g of dried shoot and leaf of the savory was pulverized using a mortar and weighed in porcelain containers. Then, the samples were burned on the heater for 2 h and put into an oven under 550 °C for 6 h. The residual grey colored matter in the container was ash. The porcelain containers were reweighed in order to obtain the ash percentage. Following equation was used to determine the ash percentage (AOAC, 1990).

$$\text{Ash\%} = (M_3 - M_2 / M_1) \times 100$$

where M_3 was weight of porcelain container containing ash; M_2 was weight of porcelain container; and M_1 was weight of sample.

Furthermore, organic matter was measured using the following equation:

$$\text{Organic matter percentage} = 100 - \text{ash percentage}$$

Measurement of photosynthesis, transpiration, stomatal conductance and substomatal CO₂ concentration

Traits associated with gas exchanges were measured based on method developed by Sudhakar et al. (2016). Gas exchange analyzer (LCA4, ADC, England) was used to measure stomatal conductance ($\text{molCO}_2\cdot\text{m}^{-2}\cdot\text{s}^{-1}$), transpiration rate ($\text{mmol H}_2\text{O}\cdot\text{m}^{-2}\cdot\text{s}^{-1}$), photosynthesis rate ($\mu\text{molCO}_2\cdot\text{m}^{-2}\cdot\text{s}^{-1}$) and substomatal CO₂ concentration (ppm). All the measurements and note-takings concerning gas exchange values were carried out during morning hours (almost 8-10 PM).

Results

Length of stem and root

ANOVA results on the stem and root length traits (*Table 2*) and results obtained from comparing the means of interactive effects (*Table 3*) indicated that the S1H5

treatment composition produced the longest stems (28.4 cm) although there were no significant differences between them and those of the treatment composition S2H5. The shortest stems (14.5 cm) belonged to the treatment composition S5H1, but there were no significant differences between them and those of the treatment composition S5H2.

Table 2. Analysis of variance (mean squares) on morphological traits of Khuzestani savory under effects of salinity and humic acid

	df	Leaf area	Leaf width	Leaf length	Root length	Stem length
Rep	3	32.49	1.92	0.79	5.08	5.92
Salinity (S)	4	291.5**	4.85**	1.80**	16.02**	274**
Humic acid (H)	4	486**	4.26**	3.81**	30.25**	83.4**
S × H	16	1 ^{ns}	0.0098 ^{ns}	0.0054 ^{ns}	0.035 ^{ns}	0.61 ^{ns}
Error	72	7.82	0.19	0.13	1.26	0.97
CV%		3.96	13.64	11.41	7.10	4.62

ns, * and ** stand for non-significant, significant at 5 and 1% probability levels, respectively

Table 3. Mean comparison on interaction effects of salinity levels and humic acid on morphological traits of Khuzestani savory

	Leaf area (mm ²)		Leaf width (mm)		Leaf length (cm)		Root length (cm)		Stem length (cm)	
S1H1	69.5	fgh	3.34	defg	3.04	efghi	15.5	efghi	22.3	gh
S1H2	71.5	ef	3.54	cdef	3.24	cdefgh	16.3	cdefg	23.7	ef
S1H3	74.5	cde	4.07	abc	3.57	bcd	17.2	abcd	25.1	cd
S1H4	78.5	ab	4.36	ab	3.73	abc	17.9	ab	26.5	bc
S1H5	81.5	a	4.64	a	4.17	a	18.5	a	28.4	a
S2H1	67.5	ghi	2.78	hijk	2.79	ghijk	14.7	hijk	21.6	hi
S2H2	69.5	fgh	2.98	fghij	2.99	efghij	15.5	efghi	22.7	fgh
S2H3	72.5	def	3.31	defg	3.32	cdef	16.5	bcdef	24.2	de
S2H4	76.5	bc	3.62	cde	3.63	bcd	17.2	abcd	26.2	c
S2H5	80.5	a	3.85	bcd	3.86	ab	17.8	abc	27.7	ab
S3H1	65	ijk	2.58	ijkl	2.65	ijkl	14.05	ijkl	19.6	jk
S3H2	67	hi	2.78	ghijk	2.85	fghijk	14.8	ghijk	20.8	ij
S3H3	70	fgh	3.11	efghi	3.12	defghi	15.8	defgh	22.02	ghi
S3H4	74	cde	3.42	def	3.39	bcde	16.5	bcdef	23.22	efg
S3H5	76	bcd	3.65	cde	3.72	abc	16.9	bcde	24.5	de
S4H1	63	jkl	2.45	jkl	2.52	jkl	13.7	kl	16.7	nm
S4H2	65	ijk	2.65	hijkl	2.72	ijkl	14.5	hijkl	17.4	lm
S4H3	67	hi	2.98	fghij	3.05	efghi	15.3	fghij	18.3	kl
S4H4	71	efg	3.32	defg	3.36	bcde	16	defgh	19.5	jk
S4H5	74	cde	3.52	cdef	3.59	bcd	16.6	bcdef	20.8	ij
S5H1	59	l	2.15	l	2.22	l	13.1	l	14.5	o
S5H2	61.5	kl	2.35	kl	2.42	kl	13.9	jkl	15.5	no
S5H3	65.5	ij	2.68	hijkl	2.75	hijk	15.1	fghijk	16.7	nm
S5H4	69.5	fgh	2.99	fghij	3.06	efghi	15.8	defgh	17.6	lm
S5H5	72.5	def	3.22	efgh	3.29	cdefg	16.4	bcdefg	19.1	k

Means with at least one common alphabet have not significant differences based on Duncan's multiple range test at 5% probability level

The S1H5 treatment composition also had the longest roots (18.5 cm), but they were not significantly different from those of the S2H4, S1H3, S1H4, and S2H5 treatment compositions. The shortest roots (13.1 cm) were also observed in the S5H1 treatment composition, but they were not significantly different from those in the S4H2, S5H2, S4H1, and S3H1 treatment compositions.

Leaf length, leaf width and leaf area

ANOVA results on leaf length, leaf width and leaf area index, are presented in *Table 2*. Results obtained from comparing the means of the interactive effects (*Table 3*) revealed that the S1H5 treatment composition had the largest leaf area index (81.5 mm²), which was not significantly different from those of the S2H5 and S1H4 treatments. The smallest leaf area index (59 mm²) belonged to the S5H1 treatment composition, which was not significantly different from those of the S5H2 and S4H1 treatment compositions.

The largest leaf width (4.64 mm) was found in the S1H5 treatment composition, but it was not significantly different from those of the S1H4 and S1H3 treatment compositions. The smallest leaf width (2.15 mm) was observed in the S5H1 treatment compositions, but it was not significantly different from those of the S3H1, S4H1, S4H2, S5H2, S5H3 treatment compositions.

The treatment composition S1H5 enjoyed the longest leaves (4.17 cm), which was not significantly different from those in the S2H5, S1H4, and S3H5 treatment compositions. The shortest leaves (2.22 cm) were that of the S5H1 treatment composition, but they were not significantly different from those of the S4H1, S4H2, S5H2, and S3H1 treatment compositions.

Photosynthesis and transpiration

Significant interaction was observed in terms of the traits being studied, at 1% probability level (*Table 4*). Based on the results the highest rate of photosynthesis (24.04 $\mu\text{molCO}_2 \text{ m}^{-2} \text{ s}^{-1}$) and of transpiration (2.85 $\text{mmol H}_2\text{O}_2 \text{ m}^{-2} \text{ s}^{-1}$) were produced in S1H5 treatment; whereas the lowest values produced in S5H1 treatments and were as low as 5.67 $\mu\text{molCO}_2 \text{ m}^{-2} \text{ s}^{-1}$ and 0.65 $\text{mmol H}_2\text{O}_2 \text{ m}^{-2} \text{ s}^{-1}$, respectively (*Figs. 3 and 4*).

Stomatal conductance and substomatal cavity CO₂ concentration

Results from analysis of variance on these traits are shown in *Table 4*. There was a significant interaction between the salinity and humic acid factors in terms of the traits. Among the treatment levels, S1H5 produced the highest (0.280 $\text{molCO}_2 \text{ m}^{-2} \text{ s}^{-1}$) stomatal conductance and lowest (85 ppm) substomatal cavity CO₂ concentration. In contrast, S5H1 produced the lowest (0.013 $\text{molCO}_2 \text{ m}^{-2} \text{ s}^{-1}$) stomatal conductance and highest (406 ppm) substomatal cavity CO₂ concentration (*Figs. 5 and 6*).

Organic matter percentage

There was a significant interaction between the factors in terms of the organic matter percentage, at 1% probability level (*Table 5*). The highest (89.69% on average) and lowest (69.46% on average) organic matter percentage were produced in S2H3 and S4H5 treatments, respectively (*Fig. 7*).

Table 4. Analysis of variance (mean squares) on Photosynthesis traits of Khuzestani savory under effects of salinity and humic acid

	df	Substomatal CO ₂ (ppm)	Stomatal conductance (mol CO ₂ m ⁻² s ⁻¹)	Transpiration (mmol H ₂ O m ⁻² s ⁻¹)	Photosynthesis (μmol CO ₂ m ⁻² s ⁻¹)
Rep	3	216	0.00006	0.003	0.007
Salinity (S)	4	237077**	0.10**	5.41*	555.7**
Humic acid (H)	4	4967**	0.015**	1.52**	39**
S × H	16	555**	0.0002**	0.04**	0.64**
Error	72	130	0.00006	0.001	0.003
CV%		4.18	0.85	2.15	0.41

ns, * and ** stand for non-significant, significant at 5 and 1% probability levels, respectively

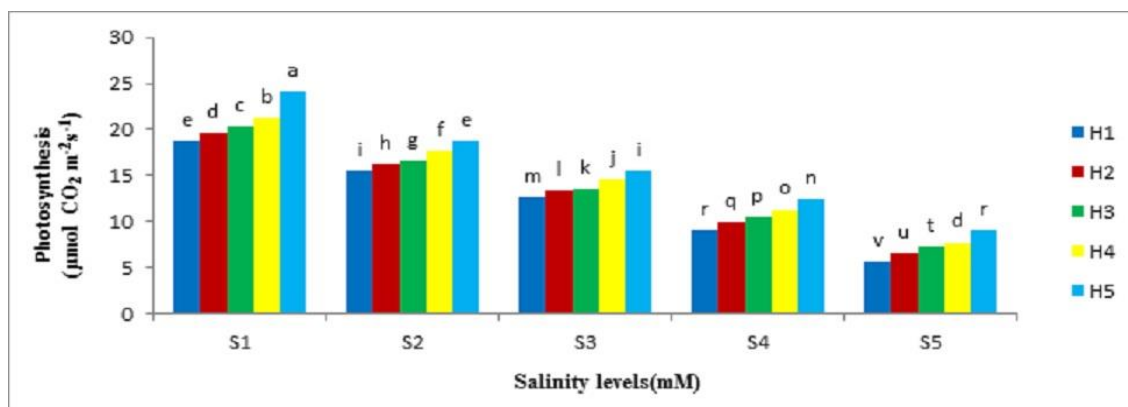


Figure 3. Interaction of salinity and humic acid on photosynthesis rate of Khuzestani savory (salinity (S) levels including 0, 25, 50, 75 and 100 mM of NaCl and humic acid (H) levels including 0 (hydropriming), 10, 20, 30 and 40 mg/kg soil, as explained in Table 1). Means with at least one common alphabet have not significant differences based on Duncan's multiple range test at 5% probability level

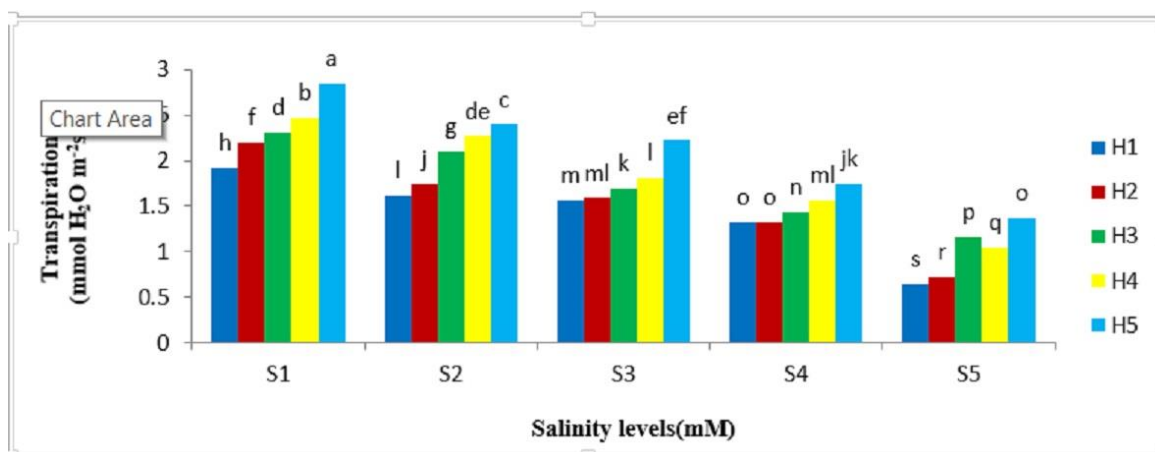


Figure 4. Interaction of salinity and humic acid on transpiration rate (salinity (S) levels including 0, 25, 50, 75 and 100 mM NaCl and humic acid (H) levels including 0 (hydropriming), 10, 20, 30 and 40 mg/kg soil, as explained in Table 1). Means with at least one common alphabet have not significant differences based on Duncan's multiple range test at 5% probability level

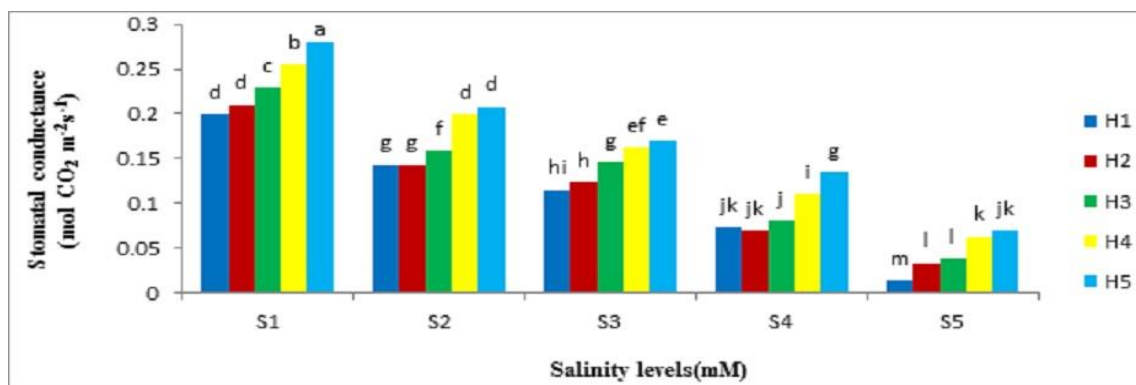


Figure 5. Interaction of salinity and humic acid on stomatal conductance (salinity (S) levels including 0, 25, 50, 75 and 100 mM of NaCl and humic acid (H) levels including 0 (hydropriming), 10, 20, 30 and 40 mg/kg soil, as explained in Table 1). Means with at least one common alphabet have not significant differences based on Duncan's multiple range test at 5% probability level

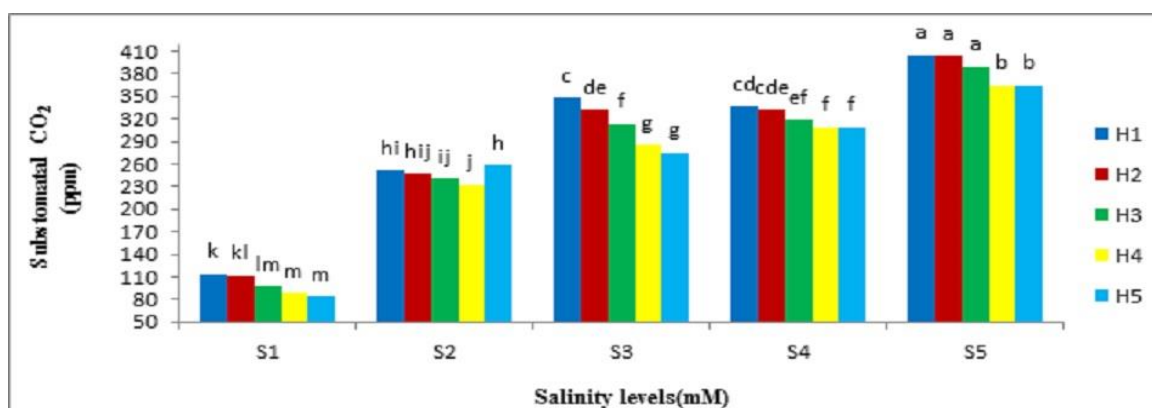


Figure 6. Interaction of salinity and humic acid on substomatal CO₂ (salinity (S) levels including 0, 25, 50, 75 and 100 mM of NaCl and humic acid (H) levels including 0 (hydropriming), 10, 20, 30 and 40 mg/kg soil, as explained in Table 1). Means with at least one common alphabet have not significant differences based on Duncan's multiple range test at 5% probability level

Table 5. Analysis of variance (mean squares) of traits such as RWC of leaf, organic matter percentage and ash percentage of Khuzestani savory under the effects of salinity and humic acid

	df	RWC of leaf) % (Organic matter percentage	Ash percentage
Rep.	3	0.514	0.96	0.23
Salinity (S)	4	479.15**	208**	137.2**
Humic acid (H)	4	51.04**	7.9**	28.4**
S × H	16	10.60**	86.6**	39.5**
Error	72	0.46	1.66	0.50
CV%		0.79	1.55	4.61

ns, * and ** stand for non-significant, significant at 5 and 1% probability levels, respectively

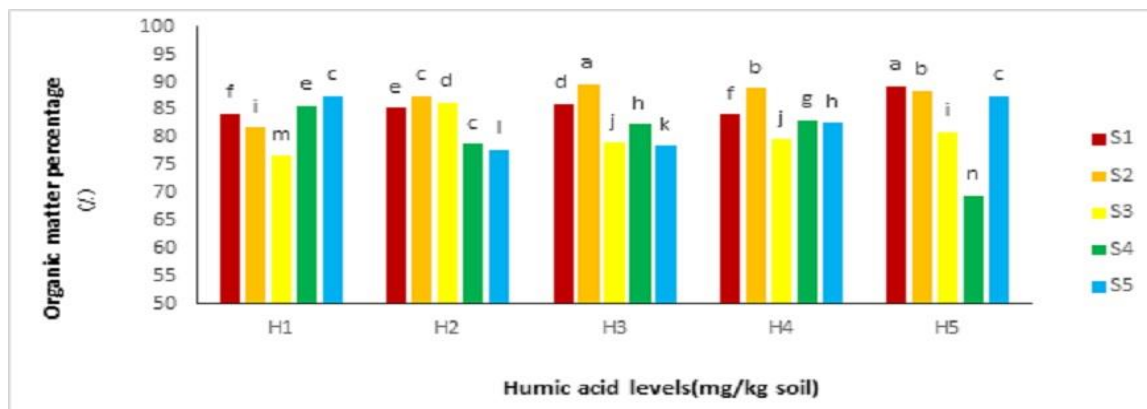


Figure 7. Interaction of salinity and humic acid on organic matter percentage (salinity (S) levels including 0, 25, 50, 75 and 100 mM NaCl and humic acid (H) levels including 0 (hydropriming), 10, 20, 30 and 40 mg/kg soil, as explained in Table 1). Means with at least one common alphabet have not significant differences based on Duncan's multiple range test at 5% probability level

Ash percentage

Results from analysis of variance revealed that there was a significant interaction between the salinity and humic acid factors, at 1% probability level (Table 5). The highest (24.37% on average) and lowest (10.35% on average) ash percentages were produced in S5H2 and S1H5 treatments, respectively (Fig. 8).

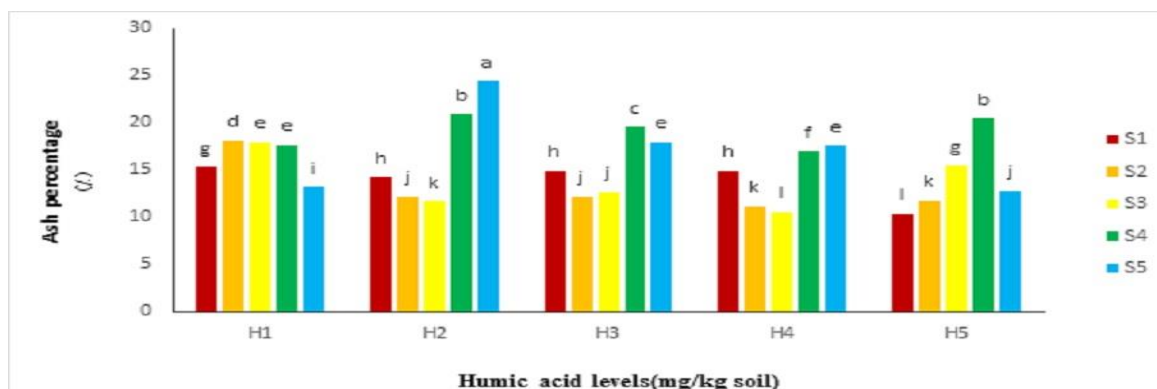


Figure 8. Interaction of salinity and humic acid on ash percentage (salinity (S) levels including 0, 25, 50, 75 and 100 mM NaCl and humic acid (H) levels including 0 (hydropriming), 10, 20, 30 and 40 mg/kg soil, as explained in Table 1). Means with at least one common alphabet have not significant differences based on Duncan's multiple range test at 5% probability level

Relative water content (RWC) of leaf

Results revealed that there was a significant interaction between the salinity and humic acid factors, at 1% probability level (Table 5). Based on the results, S1H5 treatment produced the highest (93.01% on average), whereas S5H1 treatment the lowest (70.94% on average) RWC of leaf; representing a reduction as much as 24% (Fig. 9).

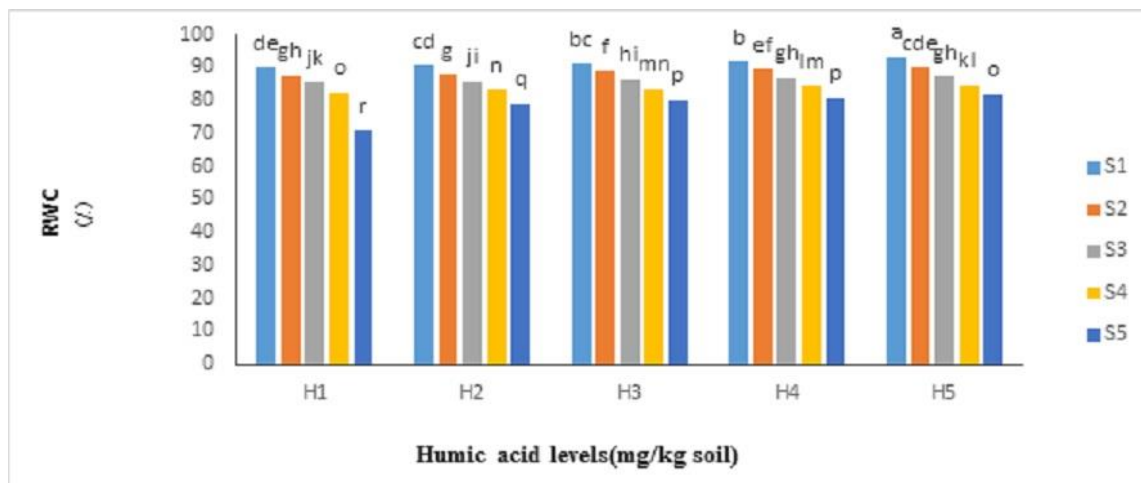


Figure 9. Interaction of salinity and humic acid on RWC (salinity (S) levels including 0, 25, 50, 75 and 100 mM NaCl and humic acid (H) levels including 0 (hydropriming), 10, 20, 30 and 40 mg/kg soil, as explained in Table 1). Means with at least one common alphabet have not significant differences based on Duncan's multiple range test at 5% probability level

Proline and soluble sugar

Significant interaction was found between the salinity and humic acid factors in terms of proline and soluble sugar traits, at 1% probability level (Table 6). Results showed that S5H1 and S5H5 treatments produced the highest proline content (0.334 mg/g in fresh weight) and highest soluble sugar content (2.098 mg/g in dry matter), respectively. Whereas, S1H5 and S1H1 (control) treatments produced the lowest (0.155 mg/g in fresh weight) and lowest soluble sugar content (0.808 mg/g in dry matter), respectively (Figs. 10 and 11).

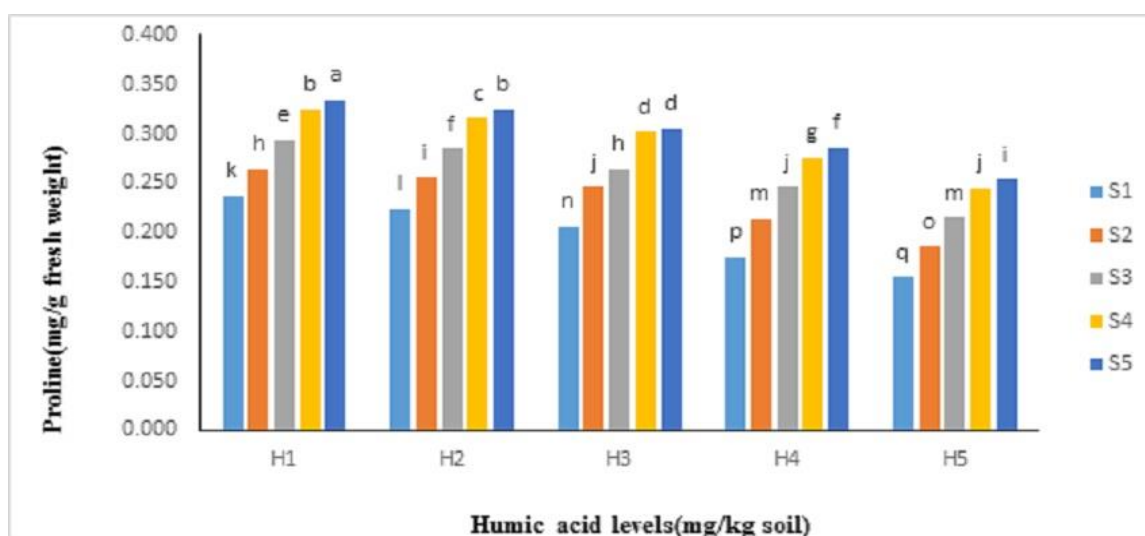


Figure 10. Interaction of salinity and humic acid on proline content (salinity (S) levels including 0, 25, 50, 75 and 100 mM NaCl and humic acid (H) levels including 0 (hydropriming), 10, 20, 30 and 40 mg/kg soil, as explained in Table 1). Means with at least one common alphabet have not significant differences based on Duncan's multiple range test at 5% probability level

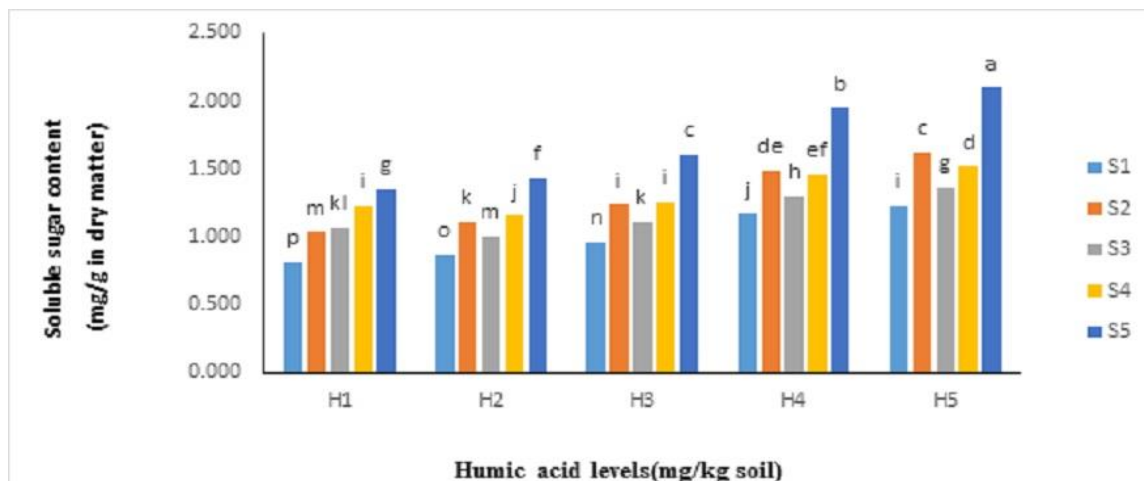


Figure 11. Interaction of salinity and humic acid on soluble sugar content (salinity (S) levels including 0, 25, 50, 75 and 100 mM NaCl and humic acid (H) levels including 0 (hydropriming), 10, 20, 30 and 40 mg/kg soil, as explained in Table 1). Means with at least one common alphabet have not significant differences based on Duncan's multiple range test at 5% probability level

Table 6. Analysis of variance (Mean Squares) on biochemical traits (proline and soluble sugar contents) of Khuzestani savory under the effects of salinity and humic acid

	df	Proline (mg/g of fresh weight)	Soluble sugar (mg/g in dry matter)
Rep.	3	0.000024	0.0006
Salinity (S)	4	0.035**	1.27**
Humic acid (H)	4	0.020**	0.90**
S × H	16	0.0003**	0.02**
Error	72	0.00009	0.0009
CV%		1.20	2.39

ns, * and ** represent non-significant, and significant at 5% and 1% probability levels

Discussion

Length of stem and root

Plant growth and height invariably depends on the environmental conditions in which it grows. One of these conditions is the availability of sufficient water to the plant. Otherwise, decreased height can be resulted by decreased turgor pressure of the cells that leads to decreased length of each individual cell. The osmotic stress resulted from salinity stress during the early stages leads to decreased water content of the cells caused by compromised water uptake. If salt accumulation continued to the next stages and its concentration in plant tissues reached to a toxic level, premature aging of leaves and decreased photosynthesizing area of leaf may ensue, which in turn leads to decreased growth and lengthening of the cells (Munnz et al., 2006).

Amiraa and Abdul (2011) stated that although increased salinity stress led to a severe decrease in root and stem lengths, it increased the protein content of the samples. Application of humic acid leads to increased height in plant by enabling it to uptake

micronutrients more efficiently. Acid humic can be used as a growth regulator, because it has an increasing effect on auxins, gibberellins and cytokinins, higher amounts of which cause lengthening of stems and improve plant growth. Results from the present study are consistent with those of study by Jariene et al. (2007) on pumpkin and of study by Ebrahimi and Miri Karbasak (2016) on Spaghetti.

Moreover, humic acid is characterized by its chelating effect on various nutrients such as sodium, potassium, magnesium, zinc, calcium, iron, copper, among others, that ensures sufficient nutrient supply to the plant and cause increased length and weight of primary root and formation of new lateral roots (Abedi and Pakniat, 2010). Humic acid application to pepper seedlings (*Capsicum annum* cv Derme) grown in pots and under salinity stress showed that in 1000 and 2000 mg/Kg dosages it increased traits such as stem and root lengths and wet and dry weights (Gulser et al., 2010).

Study on effects of irrigation regimes and humic acid spraying on some of the morphological and physiological traits of savory revealed that plants sprayed with 300 mg/L dosage of humic acid had the highest growth indices. More specifically, the highest values for plant height, dry and wet weights, leaf length and carbohydrate content were obtained in “100% irrigation + 300 mg/L humic acid” treatment (Sabouri et al., 2017). Humic acid increases plant growth and height through hormonal effects, boosting cellular metabolisms of plants, and improving uptake of nutrients by acting as a chelating agent (Salimon et al., 2012). Jumat et al. (2012) in their research into the impact of humic and folic acids on wheat reported that effect of humic acid fertilizer on the plant height was significant ($P < 0.01$).

Leaf length, leaf width and leaf area

Decreased leaf area may be due to the direct effect of salt on the cell division rate or to the shortened cell formation period. Seemingly, in glycophytes salt transport rate from root to shoot is higher than salt capacity of leaves; this slows down leaf growth and finally causes it to die (Parihar et al., 2015). There are three possible reasons for the decreased leaf area including decreased number of single-leaves, decreased production in young leaves and falling off of old leaves (Fahad et al., 2015).

Study on impacts of salinity from sodium chloride on savory has revealed that increased salinity stress has a decreasing effect on the growth parameters of the plant including leaf area; leaf water content; dry weight of root, stem and leaf; and chlorophyll and carotenoid contents. In contrast, it had an increasing effect on the proline and soluble sugar contents of the samples (Najafi et al., 2010). Root is the first plant organ affected by salinity stress and most of the times plays an important part in preventing salinity to reach the leaves. Leaf size depends on the number and size of its individual cells. Early leaf development stages are not sensitive to drought and salinity stresses; however leaf expansion is heavily influenced by salinity. Under salinity conditions leaf cellular swelling is decreased heavily, through which the stress can negatively affect leaf expansion (Razavizadeh and Rostami, 2003).

Based on the results from a study on myrtle plant (*Myrthus communis*) there was a significant difference between the salinity treatments in terms of most of the traits including plant height, leaf length and leaf width ($P < 0.01$). More specifically, the highest (1.69 cm) mean value of leaf length belonged to control treatment; whereas the lowest (1.28 cm) value for the trait was produced at the highest stress level of 6 dS/m). Furthermore, leaf width decreased as the salinity stress level and its application period increased (Vafadar et al., 2018).

In a research, savory sprayed with 300 mg/L of humic acid produced the highest growth indices. More specifically, the highest values for traits such as plant height, wet and dry weights, leaf length and carbohydrate content were produced in “100% irrigation level + 300 mg/L humic acid spraying” treatment (Sabouri et al., 2017). High salinity can decrease leaf area through decreased water uptake. In addition to decreasing leaf area, salinity stress decreases dry weight of the plant, which is responsible for decreased photosynthetic area and hormonal imbalance of the plant. Salinity stress increases CO₂ concentration of substomatal cavity through decreased stomatal conductance and diminishes dry weight of plant by preventing biochemical activities and sucrose synthesis (Salimi et al., 2014).

Based on the results from a study on Moldavian dragonhead plant, leaf length increased significantly with the increasing salinity stress, while the highest (5.66 cm) value for the trait was produced in “without salinity stress + 200 mM humic acid” treatment. Application of 200 mM humic acid and 100 mM ascorbic acid improved this trait at 50 and 100 mM salinity levels, respectively (Narimani et al., 2018).

Photosynthesis and transpiration

The reason for decreased photosynthetic activity under salinity stress is twofold: dehydration of cell membrane that reduces its CO₂ permeability and the reduced CO₂ absorption of leaf that causes stomata to close. Furthermore, salt toxicity increases the salinity-induced sensitivity; consequently, activity of the induced enzymes changes due to the structural changes in cytoplasm. At the end, the negative feedback of reduced SINK activity and reduced water potential have also been reported as the photosynthesis-decreasing factors (Negrao et al., 2017).

Reduced photosynthetic activity depends on two other aspects of salinity including the final salt concentration and availability of the other ions. High salinity concentration of soil and water leads to increased osmotic potential, consequently Na⁺ ions permeate into cytosol and inactivate electron transport in photosynthesis and transpiration. Moreover, there has been report that under high salinity condition the high concentration of sodium and reduced concentration of potassium lead to inhibition of photosystem II and reduced Rubisco carboxylation, dilation of thylakoid membranes, reduced number and depth of grana and finally reduced number of mesophyll cells (Parihar et al., 2015).

A great number of physiological studies suggest that salinity impedes plant growth through decreasing photosynthesis. It is known that decreased photosynthesis due to salinity stress involves numerous intervening factors such as cell dehydration and subsequently its reduced permeability to CO₂, toxicity caused by accumulation of sodium and chloride elements, decreased CO₂ concentration due to stomatal closure, accelerated aging process due to salt accumulation (leaf fall), changed activity of the enzymes due to structural changes in cytoplasm, and plant failure to utilize assimilates due to reduced growth (Negrao et al., 2017).

However, owing to the numerous parts it can play in improvement of plant growth, humic acid could diminish the effect of salinity stress on the photosynthetic activity of savory. It has been reported that humic acid increased photosynthetic activity of plant through the increased activity of RuBisCO enzyme. Moreover, humic acid improves longevity of the photosynthetic tissues and increases grain yield. Humic acid increases nutrient content of crops through improved synthesis of carbohydrate, protein and vitamin in the plant and its positive effect on the photosynthetic aspects (Sharif, 2002). There are

also numerous reports concerning the impacts of humic acid on decreasing transpiration rate under the stressed condition.

Under salinity stress condition, excessive diffusion of Na⁺ ions into the cell inactivates photosynthetic electron transport systems; this in turn leads to decreased photosynthetic activity of the plant (Allahverdiev et al., 1998). In addition, under the salinity stress Na⁺ ion competes with other ions, particularly potassium, which leads to decreased absorption of potassium by the plant as well as decreased cellular potassium/sodium ratio; this will negatively influence photosynthesis and development of the plant (Parida and Das, 2005). Salinity stress leads to nutrient imbalance, destruction of cellular organelles and compromised photosynthesis and transpiration in the plants (Aroca et al., 2013).

In a study conducted by Khalvandi et al. (2018), salinity stress led to a significant decrease in transpiration rate of peppermint. More specifically, an increase from 0 to 9 dS/m in salinity level decreased the transpiration rate by 56.49%. This means that in response to salinity stress, in order to minimize its impacts and maintain water balance of its leaves, the plant closed its stomata and prevented water loss through transpiration (Khalvandi et al., 2018).

Humic compounds influence plant growth and development both directly and indirectly. As for their indirect impacts, humic compounds improve soil fertility through by increasing beneficial microorganisms of soil, improving soil structure, increasing cationic exchange capacity and soil buffering capacity; whereas, their direct impacts are through increased photosynthesis, transpiration, and synthesis of proteins etc. (Saruhan et al., 2011). Molecules of humic acid prevent evaporation by binding to water molecules. Furthermore, molecules of folic acid (sub molecular part of humic acid) contribute to maintaining tissue hydration of plants as they penetrate into plant tissues and decrease transpiration by binding to water molecules (Bronick and Lay, 2005). Researchers demonstrated that humic substances contribute to uptake of nutrients, particularly nitrogen, which in high amount can increase chlorophyll content and photosynthesis of plants and accelerate their growth (Khayyat et al., 2007). In sour tea, humic acid spraying caused improved mobility and efficiency of nutrients, increased zinc and iron content of leaf and consequently increased photosynthesis and synthesis of carbohydrate and protein (Minai and Heidari, 2013). Humic acid contributes to photosynthetic activity through increasing the activity of RuBisCO (Chamani et al., 2012).

Stomatal conductance and substomatal cavity CO₂ concentration

It appears stomatal blockage under intensive stressed conditions contribute to reduction in stomatal conductance. Moreover, results have shown that decreased matter synthesis is mainly caused by reduced stomatal conductance; however, impacts of high salt concentrations on carboxylation efficiency should not be ignored (Ashraf and Harris, 2013). Reduced stomatal conductance under stressed conditions can be associated with low number and concentration of stomata. Researchers have argued that mesophyll cells in the plants subjected to salinity stress were smaller and more compact than those in control and even attributed the decreased CO₂ distribution to this physiological and anatomical change. Reduced stomatal conductance is the main pathway of leaf dehydration under stressed condition and is accompanied by reduced CO₂ absorption into the leaves and subsequently reduced photosynthesis. Another factor that can limit CO₂ distribution to its fixation site (chloroplasts) is mesophyll conductance, which is reduced under the stressed conditions particularly in response to salinity stress; and when CO₂

fails to make it to the sites of carbon fixation sites, reduced photosynthesis and stomatal conductance can ensue (Negrao et al., 2017).

Results from the present study concerning the substomatal CO₂ revealed that increased NaCl concentration led to decreased stomatal conductance. However, substomatal CO₂ rates exhibited an increasing trend, while there was a negatively significant correlation between them. Thus, it is expectable that in addition to reduced stomatal conductance, some other non-stomatal restrictions such as a potential damage to optical systems are influencing salinity-induced photosynthesis reduction.

Based on the results from a study on Moldavian dragonhead plant, stomatal conductance differed significantly at different levels of salinity stress in the absence of the stress relievers. Whereas, presence of humic acid and ascorbic acid led to a significant increase in this trait at all stressed levels, as compared to the control (absence of stress reliever) (Narimani et al., 2018).

Decreased water uptake induced by high salinity can result in decreased leaf area. In addition, salinity stress can cause a decrease in dry weight of plant; this in turn can cause decreased photosynthetic area as well as compromised hormonal balance inside the plant. Salinity stress leads to increased intrastomatal CO₂ concentration through decreased stomatal conductance, and to diminished dry weight of plant by preventing biochemical activities and sucrose synthesis (Salimi et al., 2014).

Organic matter percentage

Researches in the field have shown that soil salinity leads to decreased growth and subsequently decreased plant biomass through primary and secondary impacts; curiously, plant organs such as root, stem and offshoot respond differently to salinity stress as they differ in terms of sensitivity to it (Setia et al., 2013). Under the stressed conditions, application of compounds such as humic acid can influence plant growth through changing physiology of the plant and improving the physical, chemical and biological properties of the soil. Furthermore, humic acid can directly influence plant growth by stimulating growth of both shoot and root systems of plant. Impact of humic acid is more prominent on root system, as it can improve its efficiency through increasing its volume. Lastly yet importantly, humic acid can increase uptake of nitrogen, potassium, calcium, magnesium and phosphorus by the plant (Balakunbahan and Rajamani, 2010).

Ash percentage

Ash percentage is indicative of minerals content of plant tissues; while uptake of minerals by root is increased under salinity stress conditions. Humic acid improves root growth and increases uptake of nutrients and their transport into the organs, while has a decreasing effect on charging of the ionic salts (Shaaban et al., 2009).

Product of burning the organic plants is nonorganic ash (minerals) and the lesser is the residual ash the higher is the plant's quality. Some medicinal plants vary relatively highly in terms of ash percentage, which is very helpful in plant quality assessment (Omidbaigi, 2004). Thus, it can be seen that application of humic acid led to decreased ash percentage, which represents high quality of the treatments.

Relative water content (RWC) of leaf

Environmental stresses, particularly salinity stress, lead to reduction of available interstitial moisture through creating physiological drought so that plant water relations

are compromised and water imbalance ensues. However, positive effect of humic acid fertilizers on enlargement of plant root and subsequently on its ability to uptake water and nutrients, make them a desirable tool to improve plant water status. This is consistent with the result of the present study, as humic acid led to the increase of RWC of leaf. Sinclair and Ludlow (1985) reported the normal range of RWC to be 85-95%; in which, they believe water uptake by root and water loss through transpiration are in balance, so that the plant can maintain its natural functioning. Results from a study on peppermint revealed that increased salinity led to a significant decrease in RWC of all the treatments. This decrease is mainly associated with the decrease in stomatal conductance rate that leads to stomatal closing and decreased transpiration, and finally to decreased water uptake by the roots (Khalvandi et al., 2018).

Based on results of study by Beheshti and Tadayyon (2017) humic acid had a significant effect on RWC of leaf. More specifically, the highest RWC (83.6%) was obtained in 6 L/ha application of humic acid. Based on results from another study on Moldavian dragonhead plant the highest RWC (81%) was produced at both 100 mg/L and 200 mg/L humic acid levels under without stress condition. Furthermore, as the stress level increased the value of trait decreased and reached to its lowest value (56%) at 150 mmolar salinity stress in the absence of humic and ascorbic acids. However, in the same salinity stress level, application of 100 and 200 mg/L of humic acid and 200 mg/L of ascorbic acid is capable of improving the trait (Narimani et al., 2017).

Proline and soluble sugar

Proline is one of the active amino acids involved in osmoregulation. Accumulation of proline triggered by increased salinity and increased intracellular osmotic pressure is one of the mechanisms of salinity tolerance in plants. Since in plants proline is accumulated in response to salt and drought stresses, proline synthesis in plants may be the result of non-specific response to low water potential. Moreover, appropriation of more carbons to synthesize organic substances effective on osmoregulation such as proline, also can reduce plant growth (Ashraf and Foolad, 2007). Thus, increased synthesis of proline by the savory triggered by increased salinity may be one of the growth-reducing factors under the same condition. It has been reported that humic acid is capable of reducing the synthesis and accumulation of compounds compatible with cytoplasm such as proline.

Soluble sugars act as the osmoregulators, stabilizer of cell membrane and maintainer of cell turgidity. Actually, plants capable of accumulating higher amount of sugars under the stressed condition exhibit higher tolerance against the stress (Slama et al., 2007). Plants use various physiological mechanisms to deal with salinity stress such as storing sodium in vacuoles in order to reduce its toxic effects and producing osmolytes including glycine betaine, proline, soluble sugars, phenolic compounds etc. (Jouyban, 2012).

When under stress conditions, plants use proline as the source of energy, carbon and nitrogen to regenerate the damaged tissue (Najafi et al., 2010). As salinity level increases so does the amount of osmoregulators such as proline, which enable the plant to tolerate the environmental stresses. Proline is synthesized from glutamate and ornithine. Increased synthesis of proline is a type of osmoregulation strategy that may lead to reduced plant growth (Mirza Masoumzadeh et al., 2012). Reduced consumption of proline for protein synthesis under stressed condition may be another reason for proline accumulation (Mudgal et al., 2009).

Study on effects of salinity stress of sodium chloride on savory revealed that increased salinity stress caused a severe decrease in growth parameters including leaf area; leaf water content; dry weights of root, stem and leaf; and in chlorophyll and carotenoid content of leaf. Whereas, increased salinity caused increase in proline and soluble sugar content of the samples (Najafi et al., 2010). In their study on savory grown under salinity stress Vojodi Mehrabani et al. (2017) concluded that savory is capable of tolerating salinity up the level as high as 50 mmolar without suffering a considerable decrease in its dry weight. Furthermore, as salinity stress increases so does the proline content of the samples. More specifically, in their study the highest proline contents of the samples were found at 100 mmolar and 150 mmolar concentrations of NaCl; whereas control treatment produced the lowest proline content; which is consistent with the results of study by Akbari et al. (2013) concerning the proline content of savory samples under salinity stress. Furthermore, the highest soluble sugar content was produced at 100 and 150 mmolar NaCl concentrations.

Moreover, study by Najafi et al. (2010) on savory revealed that increased salt concentration led to increased soluble sugar content of the plant. Curiously, soluble sugars contribute to osmoregulation, and maintain membrane integrity and stability of the intracellular proteins.

Nouri et al. (2013) demonstrated that increased salinity led to increased proline content of stem in Shirazi chamomile, while the highest proline content was produced in 9.5 dS/m salinity treatment and the lowest value in control. Kafi et al. (2012) reported that increased content of soluble sugars under salinity stress condition may reveal that transport from above ground organs to the root of soluble carbohydrates has been compromised.

Conclusion

Salinity is one of the main environmental stresses in most parts of the globe that affect plant traits negatively. Based on the results from the present study, humic acid can alleviate the negative effects of salinity stress, while increasing concentrations of humic acid under salinity stress led to a significant increase in growth traits as compared with control. In conclusion, as water is becoming increasingly scarce and agricultural lands in arid and low rainfall areas are becoming increasingly saline, the importance of humic acid fertilizer as a tool to alleviate the harmful impacts of these agricultural and environmental challenges can never be overemphasized.

Suggestions

- Since Khuzestani savory is a wild species and its overexploitation may be accompanied by the danger of its extinction, it is necessary to conduct more experiments on expanding its cultivation. This will reduce its illegal harvest in nature and prevent its extinction.
- It is suggested that similar studies be carried out at higher salinity levels.
- The present research was conducted in a greenhouse. Therefore, it is suggested that studies be carried out at field level.
- It seems that long-term experiments are needed for more accurate studies on effects humic acid and salinity have on Khuzestani savory.

- It is suggested that effects of other organic fertilizers and environmental stresses, and also their interactive effects, on this plant be determined, and also effects of organic and chemical fertilizers on it be compared.
- Since this is a native plant of Lorestan and Khuzestan Provinces, it is suggested similar studies should be conducted in other regions and climates to determine its adaptability to different conditions.

REFERENCES

- [1] Abedi, T., Pakniyat, H. (2010): Antioxidant enzyme changes in response to drought stress in ten cultivars of oilseed rape (*Brassica napus* L.). – Czech Journal of Genetics and Plant Breeding 46(1): 27-34.
- [2] Akbari, S., Kordi, S., Fatahi, S., Ghanbari, F. (2013): Physiological responses of Summer Savory under salinity stress. – International Journal of Agriculture and Crop Science 5: 1702-1708.
- [3] Allahverdiev, S. R., Mavituna, M., Ganieva, R., Nafisi, S. (1998): Effects of salt stress and synthetic hormone polystimuline K on photosynthetic activity of *Trianea bogotensis* Karst. – Turkish Journal of Botany 22: 19-23.
- [4] Amiraa, M. S., Abdul, Q. (2011): Effect of salt stress on plant growth and metabolism of bean plant *Vicia faba* (L.). – Journal of the Saudi Society of Agricultural Sciences 10: 7-15.
- [5] Amirjani, M. R. (2010): Effect of NaCl on some physiological parameters of rice. – EJBS 3(1): 6-16.
- [6] Aroca, R., Ruiz-Lozano, J. M., Zamarreno, A. M., Paz, J. A., Garcia-Mina, J. M., Pozo, M. J., Lopez-Raez, J. A. (2013): Arbuscular mycorrhizal symbiosis influences strigolactone production under salinity and alleviates salt stress in lettuce plants. – Journal of Plant Physiology 170: 47-55.
- [7] Ashraf, M. (1994): Breeding for salinity tolerance in plants. – Critical Review in Plant Science 13: 17-42.
- [8] Ashraf, M., Foolad, M. R. (2007): Roles of glycine betaine and proline in improving plant abiotic stress resistance. – Environmental and Experimental Botany 59(2): 206-216.
- [9] Ashraf, M. H. P. J. C., Harris, P. J. C. (2013): Photosynthesis under stressful environments: an overview. – Photosynthetica 51(2): 163-190.
- [10] AOAC (1990): Official Methods of Analysis. 15th Ed. – Association of Official Analytical Chemists, Arlington, USA.
- [11] Balakumbahan, R., Rajamani, K. (2010): Effect of biostimulants on growth and yield of Senna (*Cassia angustifoliavar* KKM.1). – Journal of Horticultural Science & Ornamental Plants 2(1): 16-8.
- [12] Bashan, Y., de-Bashan, L. E., Prabhu, S. R., Hernandez, J.-P. (2014): Advances in plant growth-promoting bacterial inoculant technology: formulations and practical perspectives (1998–2013). – Plant Soil 378: 1-33.
- [13] Bates, L., Waldren, R., Teare, I. (1973): Rapid determination of free proline for water-stress studies. – Plant and Soil 39(1): 205-207.
- [14] Bronick, E. J., Lai, R. (2005): Soil structure and management. A review. – Geoderma 124: 3-22.
- [15] Calvo, P., Nelson, L., Kloepper, J. W., (2014): Agricultural uses of plant biostimulants. – Plant Soil 383: 3-41.
- [16] Chamani, F., Khodabandeh, N., Habibi, D., Asgharzadeh, D. F. (2012): Effect of salinity stress on yield and yield components in wheat, inoculated with growth promoting bacteria (*Azotobacter chroocum*, *Azospirillio lipophorum*, *Pseudomonas putida*) and humic acid. – Agronomy and Plant Breeding. 8(1): 37-25.

- [17] Chaves, M. M., Flexas, J., Pinheiro, C. (2009): Photosynthesis under drought and salt stress: regulation mechanisms from whole plant to cell. – *Annals of Botany* 103: 551-560.
- [18] Da Silva, E. C., Nogueira, R. J. M. C., De Araujo, F. P., De Melo, N. F., Neto, A. D. A. (2008): Physiological responses to salt stress in young umbu plants. – *Environmental and Experimental Botany* 63: 147-157.
- [19] Ebrahimi, M., Miri Karbasak, E., (2016): Investigation effect of humic acid on germination, seedling growth and photosynthesis pigments of medicinal plant Isabgol (*Plantago ovata* Forssk). – *Iranian Journal of Seed Science and Research* 3(3): 35-46 (in Persian).
- [20] El-Sherbeny, S. E., Hendawy, S. F., Youssef, A. A., Naguib, N. Y., Hussein, M. S. (2012): Response of turnip (*Brassica rapa*) plants to minerals or organic fertilizers treatments. – *Journal of Applied Sciences Research* 8(2): 628-634.
- [21] Fahad, S., Hussain, S., Matloob, A., Khan, F. A., Khaliq, A., Saud, et al. (2015): Phytohormones and plant responses to salinity stress: a review. – *Plant Growth Regulation* 75(2): 391-404.
- [22] FAO (1972): Soil Institute and Associated Pilot Development Project: Water Management and Soil Reclamation. – Technical Report 3. FAO, Rome.
- [23] Gulser, F., Sonmez, F., Boysan, S. (2010): Effects of calcium nitrate and humic acid on pepper seedling growth under saline condition. – *Journal of Environmental Biology* 31(5): 873-876.
- [24] Hadian, J., Azizi, A., Tabatabaei, M. F., Naghavi, M. R., Jamzad, Z., Friedt, W. (2010): Analysis of the genetic diversity and affinities of different Iranian *Satureja* species based on SAMPL markers. – *Planta Medica (Journal of Medicinal Plant and Natural Product Research)* 76: 1927-1933.
- [25] Jamil, M., Lee, C. C., Rehman, S. U., Lee, D. B., Ashraf, M., Rha, E. S. (2005): Salinity (NaCl) tolerance of Brassica species at germination and early seedling growth. – *Journal of Environ. Agric. Food Chem* 4: 970-976.
- [26] Jamzad, Z. (2009): Iranian Thyme and *Satureja*. – Research Institute of Forests and Rangelands of Iran, Tehran, pp. 171-172.
- [27] Jariene, E., Danilcenko, H., Kulaitiene, J., Gajewski, M. (2007): Effect of fertilizers on oil pumpkin seeds crude fat, fibre and protein quality. – *Journal of Agronomy Research* 5(1): 43-49.
- [28] Jouyban, Z. (2012): The effects of salt stress on plant growth. – *Technical Journal of Engineering and Applied Sciences* 2(1): 7-10.
- [29] Jumat, S., Nadia, S., Yousif, E. (2012): Synthesis and characterization of esters derived from ricinoleic acid and evaluation of their low temperature property. – *Sains Malaysiana* 41: 1239-1244.
- [30] Kafi, M., Borzouei, A., Salehi, M., Kamandi, A., Masoumi, A., Nabati, J. (2012): Environmental Stresses Physiology in Plants. – Mashhad Jihad Daneshgahi Publications, Mashhad (in Persian).
- [31] Kamkar, A., Tooryan, F., Akhondzadeh Basti, A. (2013): Chemical composition of summer savory (*Satureja hortensis* L.) essential oil and comparison of antioxidant activity with aqueous and alcoholic extracts. – *Iran J Vet Res* 68(2): 183-90.
- [32] Khalvandi, M., Amerian, M. R., Pirdashti, H.; Baradaran, M., Gholami, A. (2018): Effects of methyl jasmonate on some photosynthetic parameters of peppermint (*Mentha piperita*) in saline conditions. – *Journal of Plant Process and Function* 7(23): 233-24 (in Persian).
- [33] Khayyat, M., Tafazoli, E., Eshghi, S., Rajaei, S. (2007): Effect of nitrogen, boron, potassium and zinc spary on yield and fruit quality of date palm. – *American-Eurasian Journal of Agriculture and Environment Science* 2(3): 289-296.
- [34] Kochert, G. (1978): Carbohydrate determination by the phenol-sulfuric acid method. – *Handbook of Phycological Methods* 2: 95-97.
- [35] Mohebbi, J., Jamzad, Z., Bakhshi Khaniki, G. H. (2016): The conservation status of six endemic *Satureja* species in Iran. – *Journal of Iran Nature* 1(1): 74-79.

- [36] Munns, R., James, R. A., Lauchli, A. (2006): Approaches to increasing the salt tolerance of wheat and other cereals. – *Journal of Experimental Botany* 57: 1025-1043.
- [37] Minai, A., Heidari, M. (2013): The impact of drought and humic acid on performance and concentration of macro elements in the herb boage flowers (*Borago officinalis* L.). – *Journal of Plant Production* 21(1): 167-182 (in Persian).
- [38] Mirza Masoumzadeh, B., Imani, A. A., Khayamaim, S. (2012): Salinity stress effect on proline and chlorophyll rate in four beet cultivars. – *Scholars Res. Library* 3(12): 5453-5456.
- [39] Mudgal, V., Madaan, N., Mudgal, A., Mishra, S. (2009): Changes in growth and metabolic profile of chickpea under salt stress. – *Journal of Applied Biosciences* 23: 1436-1446.
- [40] Naghizadeh, M., Gholami Shabestari, M., Shamsaddin Saied, M. (2014): The study of some physiological responses of three Iranian saffron (*Crocus sativus* L.) landraces to salinity stress. – *Journal of Saffron Agronomy and Technology* 2(2): 127-144.
- [41] Najafi, F., Khanvari-Nejad, R. A., Siah Ali, M. (2010): The effect of salt stress on certain physiological parameters in summer savory (*Satureja hortensis*) plant. – *Journal of Stress Physiology and Biochemistry* 6: 13-21.
- [42] Nakabayashi, R., Saito, K. (2015): Integrated metabolomics for abiotic stress responses in plants. – *Current Opinion in Plant Biology* 24: 6-10.
- [43] Narimani, R., Moghaddam, M., Gasemi Pirbalouti, A., Nemati, S. H. (2018): Effect of humic acid and ascorbate on growth and biochemical traits of Moldavian balm (*Dracocephalum moldavica* L.) under salinity stress. – *Journal of Plant Process and Function* 7(23): 297-313 (in Persian).
- [44] Nasouti Miandoab, R., Samawat, S., Tehrani, M. M. (2011): The properties of humic acid fertilizer in soil and plant. – *Monthly Journal of Agriculture and Food* 101: 53-55 (in Persian).
- [45] Negrão, S., Schmöckel, S. M., Tester, M. (2017): Evaluating physiological responses of plants to salinity stress. – *Annals of Botany* 119(1): 1-11.
- [46] Noreen, Z., Ashraf, M. (2009): Changes in antioxidant enzymes and some key metabolites in some genetically diverse cultivars of radish (*Raphanus sativus* L.). – *Environ. Exp. Bot.* 67(2): 395-402.
- [47] Nouri, K., Omidi, H., Naghdi badi, H. A., Torabi, H., Fotokian, M. H. (2013): Effects of soil and water salinity on flower yield, soluble compounds, content of saline elements and essential oil quality of German chamomile (Shirazian Babooneh, *Matricaria recutita* L.). – *J. Water Res. Agri.* 26(4): 367-379.
- [48] Omidbaigi, R., (2004): Production and Processing of Medicinal Plants. – Astan Qods Razavi, Mashhad (in Persian).
- [49] Parida, A. K., Das, A. B. (2005): Salt tolerance and salinity effects on plants: a review. – *Ecotoxicology and Environmental Safety* 60(3): 324-349.
- [50] Parihar, P., Singh, S., Singh, R., Singh, V. P., Prasad, S. M. (2015): Effect of salinity stress on plants and its tolerance strategies: a review. – *Environmental Science and Pollution Research* 22(6): 4056-4075.
- [51] Parvaiz, A., Satyawati, S. (2008): Salt stress and phyto-biochemical responses of plants— a review. – *Plant, Soil and Environment* 54: 88-99.
- [52] Parvin, S., Lee, O. R., Sathiyaraj, G., Khoralragchaa, A., Kim, Y. J., Miah, M. J., Yang, D. C., (2012): Modulation of polyamine levels in ginseng hairy root cultures subjected to salt stress. – *Russian Journal of Plant Physiology* 59(6): 757-765.
- [53] Salimi, F.; Shekari, F., Hamzei, J. (2014): Effect of salinity stress and foliar application of methyl jasmonate on photosynthetic rate, stomatal conductance, water use efficiency and yield of German chamomile. – *Iranian Journal of Field Crops Research* 12(2): 328-334 (in Persian).
- [54] Sabouri, F., Sirousmehr, A., Gorgini Shabankareh, H. (2017): Effect of irrigation regimes and application of humic acid on some morphological and physiological characteristics of

- Savory (*Satureja hortensis* L.). – Iranian Journal of Plant Biology 9(34): 13-24 (in Persian).
- [55] Seckin, B., Turkan, I., Sekmen, A. H., Ozfidan, C. (2010): The role of antioxidant defence systems at differential salt tolerance of *Hordeum marinum* Huds. (sea barleygrass) and *Hordeum vulgare* L. (cultivated barley). – Environmental and Experimental Botany 69: 76-85.
- [56] Setia, R., Gottschalk, P., Smith, P., Marschner, P., Baldock, J., Setia, D., Smith, J. (2013): Soil salinity decreases global soil organic carbon stocks. – Science of the Total Environment 465: 267-272.
- [57] Soltani, A., Galeshi, S. (2002): Importance of rapid canopy closure for wheat production in a temperate sub-humid environment: experimentation and simulation. – Field Crops Research 77: 17-30.
- [58] Rajaravindran, M., Natarajan, S. (2012): Effects of salinity stress on growth and antioxidant enzymes of the halophyte *Sesuvium portulacastrum*. – International Journal of Research in Plant Science; 2(1): 23-28.
- [59] Razavizadeh, R., Rostami, F. (2013): Changes in growth and antioxidant capacity of canola by salinity and salicylic acid under in vitro. – International Research Journal of Applied and Basic Sciences 5(2): 192-200.
- [60] Ritchie, S. W., Nguyen, H. T. (1990): Leaf water content and gas exchange parameters of two wheat genotypes differing in drought resistance. – Crop Science 30: 105-111.
- [61] Saleh, B. (2013): Water status and protein pattern changes towards salt stress in cotton. – Journal of Stress Physiology & Biochemistry 9(1): 113-123.
- [62] Salimon, J., Salih, N., Yousif, E. (2012): Biolubricant basestocks from chemically modified ricinoleic acid. – Journal of King Saudi University 24: 11-17.
- [63] Saruhan, V., Kusvuran, A., Babat, S. (2011): The effect of different humic acid fertilization on yield and yield components performances of common millet (*Panicum miliaceum* L.). – Scientific Research and Essays 6(3): 663-669.
- [64] Sevengor, S., Yasar, F., Kusvuran, S., Ellialtioglu, S. (2011): The effect of salt stress on growth, chlorophyll content, lipid peroxidation and antioxidative enzymes of pumpkin seedling. – African Journal of Agricultural Research 6(21): 4920-4924.
- [65] Shaaban, S. H. A., Manal, F. M., Afifi, M. H. M. (2009): Humic acid foliar application to minimize soil applied fertilization of surface-irrigated Wheat. – World Journal of Agriculture Science 5(2): 207-210.
- [66] Shariff, M. (2002): Effect of lignitic coal derived HA on growth and yield of wheat and maize in alkaline soil. – Ph. D Dissertation, NWFP Agriculture University Peshawar, Pakistan.
- [67] Sinclair, I. R., Ludlow, M. M. (1985): Who taught plants thermodynamics? The unfulfilled potential of plant water potential. – Aus. J. Plantphysiol. 12: 213-217.
- [68] Sivritepe, N., Sivritepe, O., Celik, H., Katkat, V. (2010): Salinity responses of grafted grapevines: effects of scion and rootstock genotypes. – Not. Bot. Hort. Agrobot. Cluj. 38(3): 193-201.
- [69] Slama, I., Ghnaya, T., Hessini, K., Messedi, D., Savoure, A., Abdely, C. (2007): Comparative study of the effects of mannitol and PEG osmotic stress on growth and solute accumulation in *Sesuvium portulacastrum*. – Environmental and Experimental Botany 61: 10-17.
- [70] Sudhakar, P., Latha, P., Reddy, P. V. (2016): Phenotyping Crop Plants for Physiological and Biochemical Traits. – Academic Press, Cambridge, MA.
- [71] Sudhir, P., Murthy, S. D. S. (2004): Effects of salt stress on basic processes of photosynthesis. – Photosynthetica 42: 481-486.
- [72] Vafadar, Z., Rahimmalek, M., Sabzalian, M. R., Nikbakht, A. (2018): Effect of salt stress and harvesting time on morphological and physiological characteristics of Myrtle (*Myrtus communis*). – Journal of Plant Process and Function 7(23): 33-47 (in Persian).

- [73] Vojodi Mehrabani, L., Hassanpour Aghdam, M. B., Valizadeh Kamran, R. (2017): Growth and some physiological characteristics of savory (*Satureja hortensis* L.) as affected by salinity stress. – Journal of Crop Ecophysiology 11(1): 99-110 (in Persian).
- [74] Zhani, K., Mariem, B. F., Fardaous, M., Cherif, H. (2012): Impact of Salt stress (NaCl) on growth, chlorophyll content and fluorescence of Tunisian cultivars of chilli pepper (*Capsicum frutescens* L.). – Journal of Stress Physiology & Biochemistry 8(4): 236-252.

CHARACTERIZATION AND EVALUATION OF HEAVY METAL POLLUTION IN SOIL-WHEAT SYSTEM AROUND COAL MINES IN PINGDINGSHAN, CHINA

ZHANG, W. P.¹ – QIAN, J.¹ – XU, G. J.¹ – ZHANG, D. M.¹ – KANG, C.¹ – FENG, D. X.¹ – SHI, L.¹ – ZHANG, C. L.^{1,2*} – GUO, Z. Y.^{1*} – MA, J. H.^{1,2} – ZHANG, C. S.¹

¹*College of Environment and Planning, Henan University, Kaifeng 475001, China*

²*Institute of Natural Resources and Environment, Henan University, Kaifeng 475001, China*

³*School of Geography and Archaeology, National University of Ireland, Galway, Ireland*

**Corresponding author*

e-mail: zhangcl@henu.edu.cn, guozy9888@163.com; phone: +86-371-2388-1850; fax: +86-378-2388-1850

(Received 6th Dec 2018; accepted 4th Feb 2019)

Abstract. Indoor experiments were conducted to fully understand soil metal contamination around coal mines in Pingdingshan, Henan province, China. Forty-three paired soil and wheat product samples were collected from three main mining areas in Pingdingshan. Soil Cd, Zn and Pb were assessed using the diffusive gradients in thin films (DGT) and pentetic acid or diethylene triamine penlaacetic acid (DTPA). The pollution levels were evaluated. The Nemeru comprehensive pollution index shows the soil heavy metal pollution is slight; the single coefficient of potential ecological hazard indicates the soil pollution degree of heavy metals ranks as Cd > Pb > Zn, which is the most serious pollution. Cd is close to medium ecological hazard, and other heavy metals are minor ecological hazards.

Keywords: *coal mines, wheat, DGT, DTPA, potential ecological risk*

Introduction

Mineral resources are the basic source of human production and life, and an important material basis for socioeconomic development. As the demand for energy has increased since the industrial revolution, the human society has increasingly exploited fossil energy such as coal. The development of mineral resources plays an important role in promoting the national economy growth, but has also brought some environmental pollution problems. During the mining process, heavy metals in coal and coal gangue can enter the soil around mining areas through leaching, infiltration, migration and other ways. Heavy metal pollution in the soil affects the soil microbial activity and thus the structure and function of the soil ecosystem. Heavy metals in the soil enter the food chain through food and vegetables, causing health risks to humans.

Various heavy metal environmental pollutants have received much attention in recent years because of their persistent bioaccumulation and high toxicity.

Some heavy metals such as Zn and Cu above the safe concentration can be toxic, while other heavy metals can be harmful even at low concentrations. As reported, the farmland soil around a coal mine in north Bangladesh was severely contaminated by heavy metals such as Mn, Zn, As, Pb and Ti (Bhuiyan et al., 2010). Behaddya et al. used GIS to characterize the spatial distribution of heavy metal pollution in the surface soil of a coal mine area in Algeria (Behaddya and Hadjel, 2014). However, the effective assessment of health risks to residents is of very insufficient. In this research, The

objective of this study is used diffusive gradients in thin-films (DGT) to assess the heavy metal contents around the mining areas in Pingdingshan and to evaluate the heavy metal pollution levels and environmental risks.

Materials and methods

Sampling and sample pretreatment

Pingdingshan (33°08'-34°20' N, 112°14'-113°45' E) in Henan Province is known as the coal bunker of middle China. It is also an important base of the energy and raw material industry. In this study, 42 paired samples of soil and wheat were collected from mining areas of Pingdingshan in June 2017. The sampling sites were chosen near three local mines (Hugou-RA, Zaoyuan-RB, Bishan mines-RC). The sample number and GPS coordinates of Pingdingshan area are shown in *Table 1*. The soil samples were air-dried and then passed through < 2 mm, < 0.25 mm and < 0.15 mm sieves. The wheat samples were washed with deionized water, separated into roots and straws, and dried at 75 °C until constant weight.

Table 1. Sample number and GPS coordinates in Pingdingshan area

Sample name	GPS coordinates	Sample name	GPS coordinates
RA-1	33.7576929013,113.3456307421	RB-7	33.7772575173,113.3553975642
RA-2	33.754610741,113.3564701998	RB-8	33.7720293931,113.3683628691
RA-3	33.7498132802,113.3494517421	RB-9	33.757254742,113.3572521998
RA-4	33.754610741,113.3564701998	RB-10	33.7669667372,113.3614036575
RA-5	33.7498132801,113.3494517422	RB-11	33.755858741,113.3606531998
RA-6	33.7498132802,113.3494517421	RB-12	33.7672397372,113.3615656575
RA-7	33.7528111219,113.3536091998	RB-13	33.7772575173,113.3553975642
RA-8	33.7525591219,113.3533481998	RB-14	33.757254741,113.3572521998
RA-9	43.2086443635,116.6611639959	RB-15	33.7772575173,113.3553975642
RA-10	33.767433359,113.3566805642	RC-01	33.7501588052,113.3748027507
RA-11	33.7621259603,113.3745851151	RC-02	33.7503669635,113.3684036575
RA-12	33.7672397372,113.3615656575	RC-03	33.7503669635,113.3684036575
RA-13	33.7672397372,113.3615656575	RC-04	33.7580789603,113.3724291151
RA-14	33.7731903931,113.3681138691	RC-05	33.7580789603,113.3724291151
RA-15	33.7772575173,113.3553975642	RC-06	33.7580789603,113.3724291151
RB-1	33.757254741,113.3572521998	RC-07	33.7503669635,113.3684036575
RB-2	33.7660787372,113.3618146575	RC-08	33.755858741,113.3606531998
RB-3	33.757254741,113.3572521998	RC-09	33.7549999603,113.3749691151
RB-4	33.757254741,113.3572521998	RC-10	33.7550169603,113.3749571151
RB-5	33.766244359,113.3566705642	RC-11	33.7549549603,113.374636112
RB-6	33.757254741,113.3572521998	RC-12	33.7551279603,113.3750131151

Soil physicochemical analyses

Soil pH was measured by a pH detector in a 1:2.5 soil/water suspension (w/v). SOM (soil organic matter) was determined using the potassium dichromate volumetric method. Particle size was analyzed using a Mastersizer 3000 device (Cai et al., 2015).

Soil available Cd

Since it is available Cd rather than total Cd that matters in Cd toxicity, here available Cd was focused. Cd extracted by passive sampling methods such as diethylene triamine pentaacetic acid (DTPA) and DGT can be considered as available Cd in this work.

DGT deployment

DGT developed in 1994 by British scientists Davison and Zhang Hao is a contaminant in-situ research technique based on Fick's first law of diffusion. With DGT, the bioavailability of heavy metals can be studied by simulating the heavy metal absorption by plants or other organisms, and the results reflect both static processes (soil particles and soil solutions) and dynamic processes (Luo et al., 2011).

Compared with other traditional morphological analysis techniques, DGT can more efficiently measure the biological effective states of heavy metals in the nature and better reflect the heavy metals absorbed by organisms.

The DGT device consists of an innermost adsorption layer, a diffusion layer covered with specific thickness, and protective filter membranes (Wei et al., 2018).

As the adsorbent in the adsorption film has strong binding capacity with specific phosphorus and metals (metalloid), the target substance (analyte) in the solution can be rapidly and irreversibly fixed on the binding phase and consumed through the diffusion membrane.

Based on Fick's first law (Zhou et al., 2011), the diffusion flux F of the analyte is:

$$F = D\partial C / \partial x \quad (\text{Eq.1})$$

where D is the diffusion coefficient of the tested substance in the diffusion membrane; C is the concentration of the test substance in the solution.

The time-averaged concentration of the target substance measured by DGT can be calculated as follows:

$$C_{\text{DGT}} = M\Delta g / DA t \quad (\text{Eq.2})$$

where M is the amount of the target substance in the adsorbent, Δg is the thickness of the diffusive layer, A is the area of the DGT device window, and t is the adsorption time.

Soil and heavy metal determination

Air-dried soil samples over a 2-mm nylon sieve were weighed (20 g) and placed into 250-mL plastic containers (Fan et al., 2010).

Then deionized water with the maximum field water holding capacity of 70% was added under full stirring. The plastic wrap was covered to prevent moisture and evaporation, followed by equilibration at 25 °C constantly for 48 h.

After that, a small amount of the treated soil (about 3 g) was placed with a clean plastic spoon into the round hole of the DGT device and gently shaken parallel on the table surface, making the soil fully contact with the filter surface. Soil was further added until the inner cavity was filled.

The loaded DGT device was transferred to a ziplock bag added with a small amount of deionized water in advance, and the bag mouth was semi-closed (Xu et al., 2004).

After placement at a constant temperature for 24 h, the soil was removed and the DGT device was rinsed with deionized water. Then the fixed membrane was removed into the ziplock bag, and minor deionized water was dripped to wet it. After sealing, it was stored at 4 °C for analysis.

Single and comprehensive pollution indices

The soil pollution degree of each metal was measured using the single pollution index (P_i), which is the ratio of the heavy metal concentration in the contaminated soil to that in the reference soil. P_i was calculated as follows (Cai et al., 2015; Yang et al., 2012):

$$P_i = \frac{C_i}{C_o} \quad (\text{Eq.3})$$

where C_i and C_o are the heavy metal concentrations in the contaminated soil and the reference soil, respectively. The soil comprehensive pollution status for all the heavy metals was calculated as the Nemeru comprehensive pollution index P_c . The result not only considers the average pollution level of various heavy metals, but also indicates the most serious pollution in the soil contributed by single heavy metals. P_c was calculated as follows (Zhou et al., 2011; Chen et al., 2014; Gil-Sotres et al., 2004):

$$P_c = \sqrt{\frac{(\overline{P_i})^2 + \max(P_i)^2}{2}} \quad (\text{Eq.4})$$

Potential ecological hazard index

The potential ecological hazard index is based on the characteristics, environmental migration and sedimentation of heavy metals and evaluates heavy metals in soil or sediments from the perspective of sedimentology. This index considers the soil contents of heavy metals and combines ecology, environmental science and biotoxicology (Fan et al., 2003; Li et al., 2014). It comprehensively analyzes the heavy metal migration and transformation in soils and sediments and evaluates the sensitivity of geographical regions to heavy metals and the differences in background values of geographical regions. The degree of potential ecological hazard eliminates the influence of geographical differences (Xiong et al., 2017; Wang et al., 2017), reflects the relative contribution of biological effectiveness and spatial differences, and uncovers the potential impact of heavy metals on the environment. It is suitable for largescale comparison of sediments and soils (Xu et al., 2004). Relevant formulas are:

$$RI = \sum_{i=1}^n E_r^i \quad (\text{Eq.5})$$

$$E_r^i = T_r^i \times C_f^i \quad (\text{Eq.6})$$

$$C_f^i = \frac{C_s^i}{C_n^i} \quad (\text{Eq.7})$$

where E_r^i is a potential ecological hazard individual coefficient; T_r^i is the toxicity response coefficient of a certain metal based on Hakanson's standardized heavy metal toxicity coefficient (Cd = 30, Pb = 5, Zn = 1); C_r^i is the single pollution coefficient; C_s^i is the measured heavy metal content in surface soil; C_n^i is the reference value (from National Secondary Standard for Soil Environmental Quality).

Results and discussion

Soil properties and contents of metals

The general characteristics of the soils are shown in Table 2. Soil pH ranges from 5.2 to 8.3. In RA, the soils are weakly alkaline, with pH between 7.5 and 8.3. In RB, the majority of the soils are acidic, with pH between 5.2 and 6.6. As for RC, the pH is mainly in the neutral range, with the mean of 7.3. The soil organic carbon (OC) in the research areas ranges between 1.9% and 9.2%, which indicates the difference in soil fertilization degree. The Cd content ranges between 0.13 and 0.4 mg·kg⁻¹, with only one sample from RB exceeding farmland soil pollution risk screening value (GB 15618-2008). The Zn content ranges between 50.7 and 125.1 mg·kg⁻¹, while the Pb content ranges between 15.5 and 38.2 mg·kg⁻¹.

Table 2. General characteristics of soils collected from the study area

Sites		pH	OC (%)	Total concentration (mg·kg ⁻¹)			
				Cd	Zn	Pb	
RA	Mean	7.8	5.1	0.16	69.8	34.8	
	Range	7.5 - 8.3	2.6 - 9.2	0.15 - 0.19	61.9 - 79.8	30.8 - 38.2	
RB	Mean	5.8	4.1	0.18	67.9	22.6	
	Range	5.2 - 6.6	1.9 - 6.6	0.13 - 0.4	50.7 - 125.1	15.5 - 35.5	
RC	Mean	7.3	5.4	0.15	66.9	26.6	
	Range	6.7 - 8.3	2.9 - 7.3	0.1 - 0.3	57.4 - 94.9	17.7 - 35.7	
Standard limit	Soil background value of Henan Province ¹				0.064	62.5	21.8
	Environmental quality standard for soils ²				0.25 ^a	150 ^a	80 ^a
					0.30 ^b	200 ^b	80 ^b
					0.45 ^c	250 ^c	80 ^c
				0.80 ^d	300 ^d	80 ^d	

¹The soil background value of Henan province is derived from literature (Shao et al., 1998)

²The standard value of soil environmental quality originates from the secondary standard of soil environmental quality standard (GB15618-2008), a is soil pH < 5.50, b is pH between 5.50 and 6.50, c is soil pH between 6.50 and 7.50, and d is the corresponding quality standard when soil pH > 7.50

Table 3 shows the metal contents measured by DTPA and DGT. The ranges of Cd, Zn and Pb are 2.5-11.1, 85.3-520.2 and 0.65-4.88 µg·kg⁻¹ respectively (DTPA), and 2.3-5.5, 57.1-491.3 and 1.1-9.4 µg·kg⁻¹ respectively (DGT). DTPA has higher extraction capacity than DGT, which may be related to the different chemical properties of the extractants. DTPA is an efficient chelating agent with strong extraction ability and can extract water-soluble, exchange, mineral-bound and organic complex heavy metals in soil.

Table 3. Contents of metals measured using DTPA (C_{DTPA}) and DGT technique (C_{DGT})

Sites		C_{DTPA} ($\mu\text{g}\cdot\text{kg}^{-1}$)			C_{DGT} ($\mu\text{g}\cdot\text{kg}^{-1}$)		
		Cd	Zn	Pb	Cd	Zn	Pb
RA	Mean	4.0	190.0	3.8	3.3	176.3	4.0
	Range	3.5 - 6.1	85.3 - 300.1	2.7 - 4.9	2.3 - 5.5	88.8 - 491.3	1.9 - 8.2
RB	Mean	5.1	171.1	3.04	2.5	76.5	2.5
	Range	3.1-11.1	61.7 - 412.3	0.7 - 3.8	3.5 - 5.5	76.5 - 242.0	1.9 - 5.50
RC	Mean	5.0	337	3.4	3.0	115.7	4.5
	Range	2.5 - 6.8	41.5 - 520.2	0.8 - 4.5	2.4 - 4.3	57.1 - 178.3	1.1 - 9.4

Tables 4 and 5 show the bioavailable concentrations of Zn, Cd, Pb in the DGT resin eluent and the concentrations of heavy metals measured by DTPA. DTPA extractable heavy metals fraction, as a form of heavy metals with high biological effectiveness, can be used as an effective index of heavy metal pollution in similar soil by its rapid and convenient leaching (Yang et al., 2012; Lu and Zhao, 2017). DTPA can extract water-soluble, exchangeable, adsorptive, organic stationary and partially-oxidized heavy metals from soil, which is considered to be a highly bioactive form related to its total amount. The available heavy metals measured by DGT include the free state of soil solution and the unstable organic and inorganic complex state released from the surface of soil particles (Chen et al., 2012; Bernalte et al., 2013). The average extraction rates (i.e. the percentage of extracted heavy metal content in the total amount of this heavy metal) of Zn, Cd and Pb are 3.18%, 30.46% and 13.03%, respectively in DTPA, and 0.21%, 2.01% and 0.02%, respectively in DGT.

Table 4. C_{DGT} and C_{DTPA} of Zn, Cd and Pb

Sites	C_{DGT}			C_{DTPA}		
	Zn	Cd	Pb	Zn	Cd	Pb
1	117.25	2.27	8.25	2.39	0.04	4.00
2	126.16	3.68	3.38	2.49	0.04	4.88
3	491.39	3.60	2.09	1.70	0.04	3.02
4	316.63	5.52	2.89	3.01	0.04	4.65
5	153.30	2.87	4.98	2.11	0.04	4.49
6	120.56	2.94	2.39	1.25	0.04	2.93
7	123.72	2.82	2.68	1.63	0.04	4.09
8	163.01	3.71	5.13	2.14	0.04	4.47
9	116.85	2.79	1.94	2.52	0.04	3.84
10	161.59	2.50	3.97	0.97	0.05	2.99
11	136.34	2.79	4.97	0.85	0.05	2.67
12	88.76	4.44	5.48	1.70	0.06	3.48
13	136.10	3.22	3.85	1.39	0.05	3.19
14	97.44	2.75	4.49	0.61	0.03	0.65
15	177.21	3.28	5.49	1.55	0.04	2.30
16	132.24	2.48	4.95	1.29	0.05	2.85
17	184.63	12.01	5.03	1.69	0.07	3.10
18	162.93	2.65	3.62	1.09	0.05	2.30
19	124.35	2.82	3.59	0.89	0.05	3.18
20	101.86	2.85	3.86	0.98	0.05	3.77

Continue table 4. C_{DGT} and C_{DTPA} of Zn, Cd and Pb

21	187.55	4.11	4.45	1.56	0.03	3.39
22	139.18	3.15	5.24	1.41	0.05	3.58
23	130.74	2.63	5.13	1.40	0.06	3.79
24	76.51	3.25	4.97	4.37	0.05	2.59
25	128.21	2.72	2.49	1.48	0.06	3.10
26	153.62	3.17	5.54	1.82	0.05	3.37
27	98.63	3.02	2.55	4.72	0.11	3.54
28	159.61	5.57	3.53	1.23	0.05	3.52
29	76.29	3.54	2.54	2.40	0.05	3.53
30	116.06	2.44	9.41	3.67	0.05	3.51
31	57.08	2.52	1.15	5.20	0.06	3.66
32	116.30	2.80	5.36	2.37	0.05	3.43
33	140.60	2.56	3.97	2.15	0.05	3.34
34	150.31	2.45	7.24	1.71	0.04	2.63
35	143.91	2.74	5.81	2.79	0.05	3.09
36	166.08	3.75	4.42	0.41	0.02	0.83
37	108.88	4.34	3.52	4.74	0.06	3.67
38	70.18	3.31	2.26	3.84	0.06	3.99
39	96.73	2.77	4.12	4.84	0.07	3.93
40	178.31	2.73	6.15	4.69	0.05	4.50

Table 5. Statistical parameter of C_{DGT} and C_{DTPA} of Zn, Cd and Pb

Statistic	C_{DGT}			C_{DTPA}		
	Zn	Cd	Pb	Zn	Cd	Pb
Maximum	491.39	12.01	9.41	5.20	0.11	4.88
Minimum	57.08	2.27	1.15	0.41	0.02	0.65
Average	143.18	3.39	4.32	2.23	0.05	3.35
Standard deviation	70.41	1.57	1.67	1.29	0.01	0.85
Coefficient of variation	0.49	0.46	0.39	0.58	0.29	0.25

Table 6 presents the soil particle concentration (P_c) in each sampling point, the R_{diff} calculated using the 2D DIFS model, and the effective concentration (CE) calculated as the ratio between C_{DGT} and R_{diff} . In general, soil P_c in the same area is approximately the same, with the lowest SA. The CE ranks as Zn > Pb > Cd, while the heavy metal content extracted by DTPA ranks as Pb > Zn > Cd.

The relationships between Cd, Zn, Pb in the roots, straws and that extracted by DGT and DTPA are shown in Figure 1 and Table 7. Although the C_{DGT} of Cd, Zn and Pb in the soil is one to two orders-of-magnitude lower than those extracted by DTPA, C_{DGT} extraction is closer to wheat availability than DTPA extraction, and DTPA extraction may overestimate the concentration of available states, and some of the extracted metals may not be absorbed by wheat. More studies also show DGT better reflects plant uptake than chemical extraction. For example, PUEYO M used DGT to assess the influence factors on cadmium accumulation in rice grains from paddy soils of three parent materials and found that cadmium bioavailability could well be assessed by DGT (Pueyo et al., 2008). Bernd Nowack et al. used DGT to test undisturbed field soils and suggested that DGT can be successfully used under undisturbed field conditions to study the kinetics of metal resupply.

Table 6. R_{diff} and C_E of metals

Sample sites	$P_c \text{ g} \cdot \text{cm}^{-3}$	R_{diff}			$C_E (\mu\text{g} \cdot \text{L}^{-1})$		
		Cd	Zn	Pb	Cd	Zn	Pb
1	20.9	0.28	14.86	1.37	2.2652	117.2454	8.2474
2	17.4	0.455	15.99	0.562	3.68095	126.1611	3.38324
3	12.9	0.445	62.28	0.348	3.60005	491.3892	2.09496
4	23.4	0.682	40.13	0.48	5.51738	316.6257	2.8896
5	18.2	0.355	19.43	0.828	2.87195	153.3027	4.98456
6	24.9	0.363	15.28	0.397	2.93667	120.5592	2.38994
7	13.3	0.349	15.68	0.445	2.82341	123.7152	2.6789
8	26.1	0.459	20.66	0.852	3.71331	163.0074	5.12904
9	19.4	0.345	14.81	0.322	2.79105	116.8509	1.93844
10	16	0.309	20.48	0.659	2.49981	161.5872	3.96718
11	20.4	0.345	17.28	0.826	2.79105	136.3392	4.97252
12	15.63	0.549	11.25	0.91	4.44141	88.7625	5.4782
13	22.9	0.398	17.25	0.639	3.21982	136.1025	3.84678
14	28.3	0.34	12.35	0.746	2.7506	97.4415	4.49092
15	29.2	0.406	22.46	0.912	3.28454	177.2094	5.49024
16	32.1	0.306	16.76	0.822	2.47554	132.2364	4.94844
17	20.1	1.484	23.4	0.836	12.00556	184.626	5.03272
18	20.4	0.328	20.65	0.602	2.65352	162.9285	3.62404
19	35.7	0.348	15.76	0.596	2.81532	124.3464	3.58792
20	31.8	0.352	12.91	0.641	2.84768	101.8599	3.85882
21	28.2	0.508	23.77	0.739	4.10972	187.5453	4.44878
22	21.4	0.389	17.64	0.87	3.14701	139.1796	5.2374
23	22.2	0.325	16.57	0.852	2.62925	130.7373	5.12904
24	22.65	0.402	9.697	0.826	3.25218	76.50933	4.97252
25	22	0.336	16.25	0.414	2.71824	128.2125	2.49228
26	27.7	0.409	30.71	0.878	3.30881	242.3019	5.28556
27	13.2	0.373	12.5	0.423	3.01757	98.625	2.54646
28	24.2	0.688	20.23	0.587	5.56592	159.6147	3.53374
29	25.8	0.437	9.669	0.422	3.53533	76.28841	2.54044
30	24.6	0.301	14.71	1.563	2.43509	116.0619	9.40926
31	23.3	0.311	7.234	0.191	2.51599	57.07626	1.14982
32	21.6	0.346	14.74	0.89	2.79914	116.2986	5.3578
33	24	0.316	17.82	0.66	2.55644	140.5998	3.9732
34	25.7	78.033	872	1.202	631.287	6880.08	7.23604
35	26.4	0.339	18.24	0.965	2.74251	143.9136	5.8093
36	24.5	0.464	21.05	0.735	3.75376	166.0845	4.4247
37	18.7	0.536	13.8	0.584	4.33624	108.882	3.51568
38	27	0.409	8.895	0.376	3.30881	70.18155	2.26352
39	33.8	0.342	12.26	0.685	2.76678	96.7314	4.1237
40	21.7	0.337	22.6	1.022	2.72633	178.314	6.15244

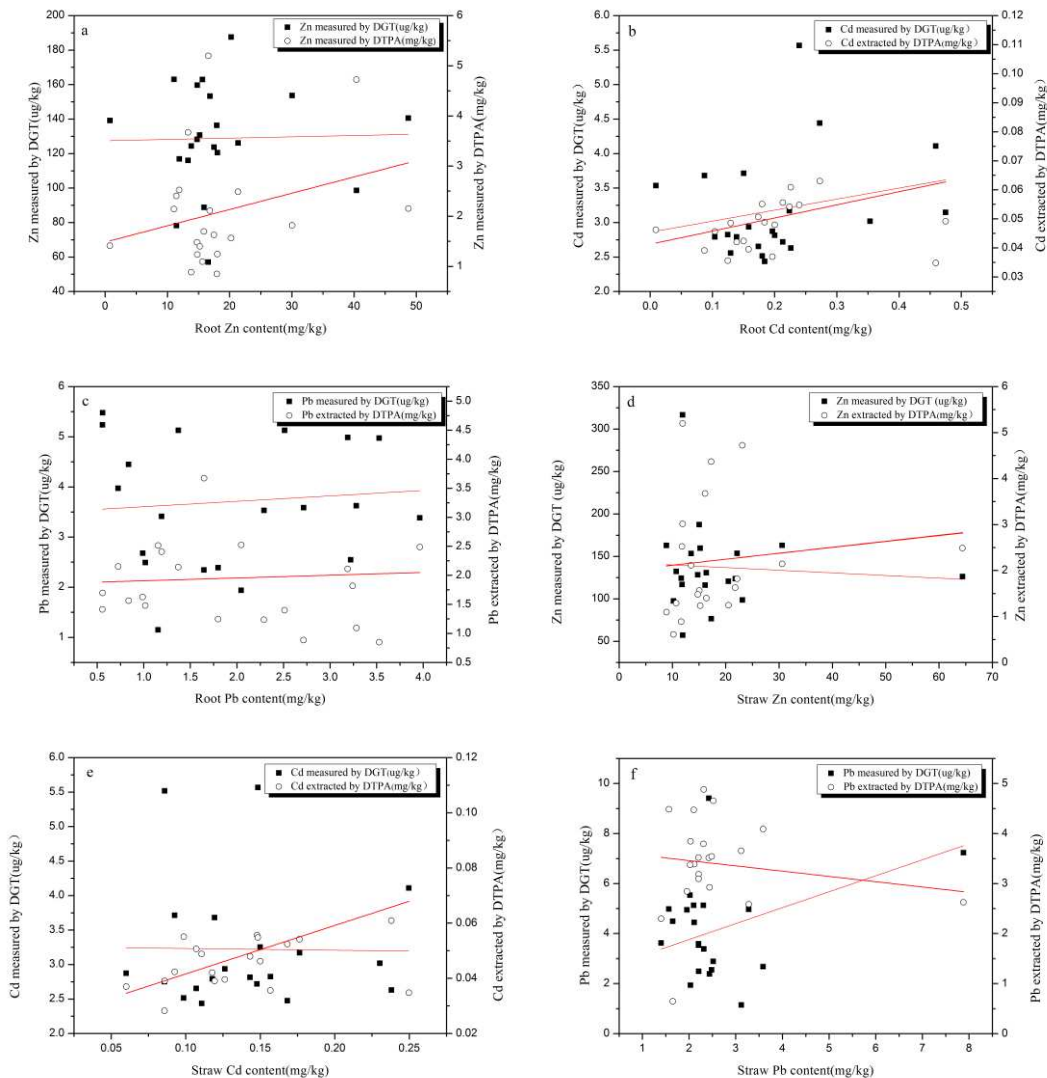


Figure 1. Relationship between heavy metals extracted by DGT and DTPA: relationship between the contents of (a) Zn, (b) Cd, (c) Pb in roots and from DGT and DTPA; relationship between the contents of (d) Zn, (e) Cd and (f) Pb in straw and from DGT and DTPA

Environment evaluation

Single and comprehensive pollution indices

The results of heavy metal pollution index are shown in Table 8. In terms of Zn, more than half of the samples are at light pollution, while others are still at clean level. In terms of Cd, most of the samples are in mild pollution (Liu et al., 2017; Shi et al., 2013), and only 9.76% of them are in moderate pollution. Noticeably, 3 samples are in severe pollution, which indicates high risks. As for Pb, 53.69 of the samples are in moderate pollution and others are in mild pollution. The Nemeru comprehensive pollution index of 43 samples ranges from 1.22 to 3.36 with a mean of $1.7 < 2$, indicating the soil is at slight pollution, and Cd is under the severest pollution.

The E_r^i and RI were calculated by Equations 3, 4 and 5 (Table 9). The single coefficient of potential ecological hazard and other elements belong to minor ecological hazards. Chu Chunjie et al. pointed out that Cu, Zn, Ni and Pb induced chronic non-

carcinogenic health risks (Chen et al., 2017; Bhuiyan et al., 2010), while Cr had a clear risk of cancer in the soil of hilly slopes around mining areas in Pingdingshan. The results indicate Zn and Pb in the soil around the mining areas of Pingdingshan exceed the standard, which is a non-carcinogenic health risk (Yenilmez et al., 2011).

Table 7. Relationship between heavy metals extracted by different extractants and that in wheat

		Linear equation	r	p
Root	Zn _{DGT}	y = 0.6694 x + 114.59	0.19	<0.01
	Zn _{DTPA}	y = 0.0013 x + 1.9466	0.01	<0.01
	Cd _{DGT}	y = 2.9972 x + 2.6501	0.34	<0.01
	Cd _{DTPA}	y = 0.0109 x + 0.0455	0.12	<0.01
	Pb _{DGT}	y = 0.371 x + 2.801	0.32	<0.01
	Pb _{DTPA}	y = 0.0231 x + 1.9169	0.03	<0.01
Straw	Zn _{DGT}	y = 0.1744 x + 92.806	0.33	<0.01
	Zn _{DTPA}	y = 0.0585 x + 1.1555	0.27	<0.01
	Cd _{DGT}	y = 3.7437 x + 2.3191	0.51	<0.01
	Cd _{DTPA}	y = 0.1624 x + 0.0259	0.49	<0.01
	Pb _{DGT}	y = 0.3985 x + 2.8309	0.61	<0.01
	Pb _{DTPA}	y = 0.0187 x + 3.0632	0.19	<0.01

Table 8. Heavy metal pollution index evaluation results

Heavy metal element	Zn	Cd	Pb
Clean (a)	0	0	0
Clean (%)	0	0	0
Still clean (a)	15	0	0
Still clean (%)	36.59	0	0
Mild pollution (a)	26	34	19
Mild pollution (%)	63.41	82.93	46.34
Moderate pollution (a)	0	4	22
Moderate pollution (%)	0	9.76	53.69
Severe pollution (a)	0	3	0
Severe pollution (%)	0	7.32	0

Table 9. Farmland soil E_r^i , RI in Pingdingshan mining area

E_r^{Cd}	E_r^{Cr}	E_r^{Ni}	E_r^{Cu}	E_r^{Zn}	E_r^{Pb}	RI
37.8	0.5	0.5	1.6	0.3	4.5	45.2

General situation of heavy metal pollution in soil

The results showed that the average pH values of wheat fields in the study area were 7.8, 5.8 and 7.3, respectively, in which RA and RC were at the alkaline level and RB was at the acidic level. According to the statistical results in Table 2, the average content of heavy metal elements in the wheat fields in the three mining areas all

exceeded the background value of soil elements in Henan province. The average values of Cd, Zn and Pb in the wheat fields in RA mining area were 2.50, 2.81 and 2.34 times of the background value, respectively. The average values of Cd, Zn and Pb in the wheat field in the RB mining area were 1.12, 1.09 and 1.07 times of the background values, respectively. The average values of Cd, Zn and Pb in wheat field in RC mining area were 1.60, 1.04 and 1.22 times of the background values, respectively. According to the grade ii standard of soil environmental quality standard (GB15618-2008), the average values of Cd, Zn and Pb in wheat fields in RA mining area were 0.20, 0.23 and 0.44 times of the standard values, respectively. The average values of Cd, Zn and Pb in the wheat field in the RB mining area were 0.60, 0.34 and 0.28 times of the standard values, respectively. RC mining area of wheat to Cd, Zn and Pb respectively, the average standard value of 0.33, 0.27, and 0.33 times. The soil heavy metal pollution degree of RB > RC > RA, and by a single heavy metal pollution degree, Cd > Pb > Zn, along with the exploitation of coal mine, the content of soil heavy metal levels in gradually rise, which is consistent with the research results of Chen et al. (2017).

Conclusions

In this paper, three typical coal mines in Pingdingshan were investigated to study the heavy metal pollution in the surrounding soil and wheat using the diffusive gradients in thin films (DGT) and pentetic acid or diethylene triamine penlaacetic acid (DTPA), and to explore its potential ecological risks. The results show that the soil heavy metal pollution around the main mining areas of Pingdingshan is under different levels. The average soil contents of Zn, Cd and Pb are 68.64, 0.68 and 26.96 mg·L⁻¹, respectively. According to the extraction effect of different extractants. DTPA has higher extraction capacity than DGT, which may be related to the different chemical properties of the extractants. From the average extraction efficiency of different extraction methods for the same heavy metal. The average extraction rates (i.e. the percentage of extracted heavy metal content in the total amount of this heavy metal) of Zn, Cd and Pb are 3.18%, 30.46% and 13.03%, respectively in DTPA, and 0.21%, 2.01% and 0.02%, respectively in DGT. The Nemeru comprehensive pollution index shows the soil pollution of heavy metals is slight. The single ecological coefficient of potential ecological hazard indicates the soil pollution degrees of various heavy metals rank as Cd > Pb > Zn, and the most serious pollution is Cd, which is close to medium ecohazards, while other heavy metals are under minor ecological hazards.

Acknowledgements. We sincerely appreciate the laboratory and diving assistance by the Science & Technology Innovation Team in Universities of Henan Province (19IRTSTHN029). This work was supported by the National Science Foundation for Young Scholars of China under Grant [41601522], China Postdoctoral Science Foundation under Grant [2017M612387], and Henan Postdoctoral Science Foundation under Grant [001701033].

REFERENCES

- [1] Behaddya, M. L., Hadjel, M. (2014): Spatial distribution and contamination assessment of heavy metals in surface soils of Hassi Messaoud, Algeria. – *Environmental Earth Sciences* 71(3): 1473-1486.

- [2] Bernalte, E., Marn, S. C., Pinilla, G. E. (2013): High-Throughput mercury monitoring in indoor dust microsamples by bath ultrasonic extraction and anodic stripping voltammetry on gold nanoparticles-modified screen-printed electrodes. – *Electroanalysis* 25(1): 289-294.
- [3] Bhuiyan, M. A., Parvez, L., Isiam, M. A. et al. (2010): Heavy metal pollution of coal mine-affected agricultural soils in the northern part of Bangladesh. – *Journal of Hazardous Materials* 173(1-3): 384-392.
- [4] Cai, L. M., Xu, Z. C., Qi, J. Y., Feng, Z. Z., Xiang, T. S. (2015): Assessment of exposure to heavy metals and health risks among residents near Tonglushan mine in Hubei, China. – *Chemosphere* 127: 127-135.
- [5] Chen, F., Dong, Z. Q., Wang, C. C. et al. (2017): Heavy metal contamination of soils and crows near a zinc smelter. – *Environmental Science* 38(10): 4360-4369.
- [6] Chen, J., Sun, Q., Yao, Y. et al. (2014): Comparison of DGT technique with traditional methods for evaluating cadmium bioavailability in soils with combined pollution. – *Research of Environmental Sciences* 27(10): 1172-1179.
- [7] Fan, S. X., Gan, Z. T., Li, M. J. (2010): Progress in evaluation methods of heavy metal pollution in soil. – *China's Agronomy Bulletin* 26(17): 310-315.
- [8] Fan, Y. H., Lu, Z. H., Cheng, J. L. et al. (2003): Major ecological and environmental problems and the ecological reconstruction technologies of the coal mining areas in China. – *Acta Ecologica Sinica* 23(10): 2144-2152.
- [9] Gil-Sotres, F., Trasar-Cepeda, C., Leirós, M. C., Seoane, S. (2004): Different approaches to evaluating soil quality using biochemical properties. – *Soil Biology and Biochemistry* 37(5): 877-887.
- [10] Li, B. J., Wang, L. C., Long, M. Z. et al. (2014): Evaluation of coal mining wasteland polluted by heavy metal of Huaxi District in Guiyang City. – *Guizhou Agricultural Sciences* 42(4): 130-135.
- [11] Liu, D., Zhao, Y. H., Zhou, D. et al. (2017): Ecological risk assessment of heavy metals pollution in a tungsten mine soil in south of Jiangxi Province. – *Environmental Chemistry* 36(7): 1556-1566.
- [12] Lu, J., Zhao, X. Q. (2017): Characteristics and ecological risk assessment of polluted soil by heavy metals in Shizishan, Tongling. – *Environmental Chemistry* 36(9): 1958-1967.
- [13] Luo, J., Wang, X. et al. (2011): Theory and application of diffusive gradients in thin films in soils. – *Journal of Agro-Environment Science* 30(2): 205-213.
- [14] Pueyo, M., Mateu, J., Rigol, A. et al. (2008): Use of the modified BCR three-step sequential extraction procedure for the study of trace element dynamics in contaminated soils. – *Environmental Pollution* 152(2): 330-341.
- [15] Shao, F., Zhou, H. (1998): Soil environmental background value of main elements in Henan province. – *Henan agriculture* (10): 29.
- [16] Shi, Z. F., Wang, L. (2013): Contents of soil heavy metals and evaluation on the potential pollution risk in Shenmu mining area. – *Journal of Agro-Environment Science* 32(6): 1150-1158.
- [17] Wang, Y. Q., Bai, Y. R., Wang, J. Y. (2016): Distribution of urban soil heavy metal and pollution evaluation in different functional zones of Yinchuan City. – *Environmental Science* 37(2): 710-716.
- [18] Wei, T., Guan, D., Fang, W. et al. (2018): Theory and application of diffusive gradients in thin-films (DGT) in the environment III: theoretical basis and application potential in phytoavailability assessment. – *Journal of Agro-Environment Science* 7(5): 841-849.
- [19] Xiong, S., Gui, H. R., Peng, W. H. (2017): Accumulation and health risk assessment of heavy metals in soil-maize system from coal mining area. – *Science Technology and Engineering* 17(8): 80-86.
- [20] Xu, Z. Q., Ni, J. S., Zhang, C. J. (2004): Assessment of heavy metals in sediments of Jinshajiang River in Panzhihua area by pollution load index method. – *Sichuan Environment* 23(3): 64-67.

- [21] Yang, S., Yuan, Z. et al. (2012): Heavy Metal contamination and bioavailability in Huayuan manganese and lead/zinc mineland, Xiangxi. – *Environmental Sciences* 33(5): 1718-1724.
- [22] Yenilmez, F., Kuter, N., Emil, M. K. et al. (2011): Evaluation of pollution levels at an abandoned coal mine site in Turkey with the aid of GIS. – *International Journal of Coal Geology* 86(1): 12-19.
- [23] Zhou, S. L., Li, R. H., Wu, S. H. (2011): *Study on Relations Between the Economic Development and the Spatial and Temporal Variation of Heavy Metals in Agricultural Land*. – China Land Press, Beijing.

LAND COVER CHANGE MAPPING USING A COMBINATION OF SENTINEL-1 DATA AND MULTISPECTRAL SATELLITE IMAGERY: A CASE STUDY OF SANANDAJ COUNTY, KURDISTAN, IRAN

TIEN BUI, D.^{1,2} – SHAHABI, H.^{3*} – MOHAMMADI, A.⁴ – BIN AHMAD, B.⁴ – BIN JAMAL, M. H.⁵ – NOOR MOHAMED, R. B.⁵ – AHMADI, M.⁶ – SHIRZADI, A.⁷ – RAHMANI, H.⁸ – PHAM, B. T.⁹ – AHMAD, A.⁴

¹*Geographic Information Science Research Group, Ton Duc Thang University, Ho Chi Minh City, Vietnam*

²*Faculty of Environment and Labour Safety, Ton Duc Thang University, Ho Chi Minh City, Vietnam
(e-mail: buitiendieu@tdt.edu.vn)*

³*Department of Geomorphology, Faculty of Natural Resources, University of Kurdistan, Sanandaj, Iran*

⁴*Faculty of Built Environment and Surveying, Universiti Teknologi Malaysia (UTM), 81310 Johor Bahru, Malaysia
(e-mail: ayubmohammadi1990@gmail.com, baharinahmad@utm.my, anuarahmad@utm.my)*

⁵*School Civil Engineering, Faculty of Engineering, Universiti Teknologi Malaysia (UTM), 81310 Johor Bahru, Malaysia
(e-mail: mhidayat@utm.my, roslli@utm.my)*

⁶*Department of Geomorphology, Faculty of Geography and Planning, University of Tabriz, Tabriz, Iran
(e-mail: mehdi.ahmadi2009@gmail.com)*

⁷*Department of Rangeland and Watershed Management, Faculty of Natural Resources, University of Kurdistan, Sanandaj, Iran
(e-mail: a.shirzadi@uok.ac.ir)*

⁸*Department of Computer Science, Engineering and IT, School of Electrical and Computer Engineering, Shiraz University, Shiraz, Iran
(e-mail: hosein.rhm@gmail.com)*

⁹*Institute of Research and Development, Duy Tan University, 550000 Da Nang, Vietnam
(e-mail: phambinhgtvt@gmail.com)*

**Corresponding author
e-mail: h.shahabi@uok.ac.ir; phone: +98-918-665-8739*

(Received 7th Dec 2018; accepted 28th Feb 2019)

Abstract. Land Cover Maps (LCMs) represent the integrated information about general status of a specific region, which are widely used as a baseline for many related purposes. This study aims to extract the land covers of Sanandaj County, Kurdistan, Iran, along with to highlight the occurred changes compared with an old map prepared by the Iranian Institute of Water and Soil in 2010. The combination model of Sentinel-1 and Landsat-8 satellite imageries was used for the dates 10/05/2017 and 11/05/2017, respectively. It is noted that based on the location of the study area we acquired Sentinel-1 data (S1A, IW,

and GRD) and a pair of Landsat-8 images. Using Sentinel Application Platform (SNAP) and Environment for Visualizing Image (ENVI) softwares all images were corrected, co-registered and stacked. The combination of RADAR, NDVI and thermal bands was utilized as the best combination for the visual interpretation, with which all land covers can be easily differentiated. However, with help of the Google Earth images the land covers (polygon by polygon) were checked and digitized. Results indicate that the visual interpretation of the combination model with the assist of Google Earth is a robust way to extract land covers, provided that the researchers have enough knowledge on the land covers of the study area. This study can be applicable for decision makers of Sanandaj City.

Keywords: *Landsat, land use, remote sensing, Google Earth, GIS, Sanandaj*

Introduction

Land Cover (LC) is one of the most important factors that reflects the impacts of human on the environment (Belal and Moghanm, 2011; Lausch and Herzog, 2002), which it is constantly changing due to human activities (Chen et al., 2003). The importance of identifying, quantifying and supervising LCMs and their changes have widely been considered by the global and the regional studies (Jin et al., 2013; Kumar et al., 2016; Xian et al., 2009; Zhu and Woodcock, 2014). LC is a key factor, which affects the function and the condition of an ecosystem (El-Kawy et al., 2011; Hansen and Loveland, 2012; Lunetta et al., 2006). As a matter of fact, satellite based remote data have been widely employed as a robust and fast way to provide LC coverage in a large geographic scope (Grecchi et al., 2014; Li et al., 2017; Liu and Yang, 2015; Lunetta, et al., 2006; Myint et al., 2011). LCM studies and their monitoring using the combination of a few satellite imageries is greatly associated with the appropriate satellite images to evaluate the LC map (Liu and Yang, 2015; Lunetta, et al., 2006).

Understanding and identifying the human activities and LC changes' patterns are essential for the proper land management and sustainable development (Rawat et al., 2013; Rawat and Kumar, 2015). Regarding its impact on a natural ecosystem, the LCM is one of the main concerns of the conservationists, the environmentalists and the land cover planners (Halmy et al., 2015). Development of an appropriate analytical procedure and the techniques to map all the land covers in an area, is one of the main problems in LCMs (Hansen and Loveland, 2012; Xian, et al., 2009). Extracting land covers by using a combination of satellite images is normally faced a number of challenges, including acquisition of two or more satellite imageries at the regional or the national scales.

LCM provides the valuable information for a better understanding of the changes' mechanism on the environment (Boori et al., 2015; Xian and Crane, 2005; Xian, et al., 2009). Continuous, precise and up-to-date LC information is essential for the natural resources and the environmental management (Homer et al., 2004; Loveland et al., 2002; Rawat and Kumar, 2015; Xian, et al., 2009). Another significance of this study is the availability of both satellite imageries of RADAR (Sentinel-1) and multispectral (Landsat-8).

Many researches have been conducted with the LCM studies using a variety of techniques and imageries, including Markov-chain analysis (López et al., 2001), multiple regression analysis (Theobald and Hobbs, 1998), logistic regression (Wu and Yeh, 1997), artificial neural networks (ANNs) (Li and Yeh, 2002), cellular automata (CA) (Batty and Xie, 1994, 1997; Clarke and Gaydos, 1998; White and Engelen, 1997; Yeh and Li, 2001), multi-agent systems (Brown et al., 2005; Sanders et al., 1997), updating LC automatically based on change detection using satellite images (Chen et al., 2012; Huang et al., 2017; Jin, et al., 2013; Xian, et al., 2009), multi-temporal remote

sensed imagery (Butt et al., 2015; Fichera et al., 2012; Islam et al., 2018; Nutini et al., 2013), and multispectral airborne laser scanner data (Matikainen et al., 2017). On the other hand, a combination model of RADAR imagery of Sentinel-1 and multispectral imagery of Landsat-8 Operational Land Imager (OLI) has not been performed by other researchers for extracting land covers.

The main objective of this study was to update land cover map using the Google Earth images and the visual interpretation of a combined imagery of RADAR (Sentinel-1) and multispectral (Landsat-8) in Sanandaj County, Kurdistan Province, Iran.

Materials and methods

Description of the study area

Sanandaj County was selected as the study area for this research. The city of Sanandaj, with a population of 432,330, is the most important and the biggest city in Kurdistan Province, Iran. Besides, this scope is located in the Longitudes $46^{\circ} 24' 00''$ E to $47^{\circ} 19' 00''$ E and Latitudes $35^{\circ} 3' 00''$ N to $35^{\circ} 39' 00''$ N (Fig. 1).

Moreover, it lies on the border area of Marivan, Divandarreh, Bijar, Dehgolan and Kamyaran Counties. Sanandaj County has a total area of about 3024 km². Furthermore, the elevation of the scope ranges from 1450 to 1538 m above the sea level. According to the meteorological department of Iran, the county has the cold and semi-arid climate, but the moderate weather during spring and summer seasons. On the other hand, the maximum and the minimum temperature are about 44 °C and -13.5 °C, in order. While, the average temperature in the spring, summer, autumn and winter are 15.20 °C, 25.20 °C, 10.40 °C and 1.60 °C, respectively (Table 1) (Hosseini et al., 2015; Izady, 2015).

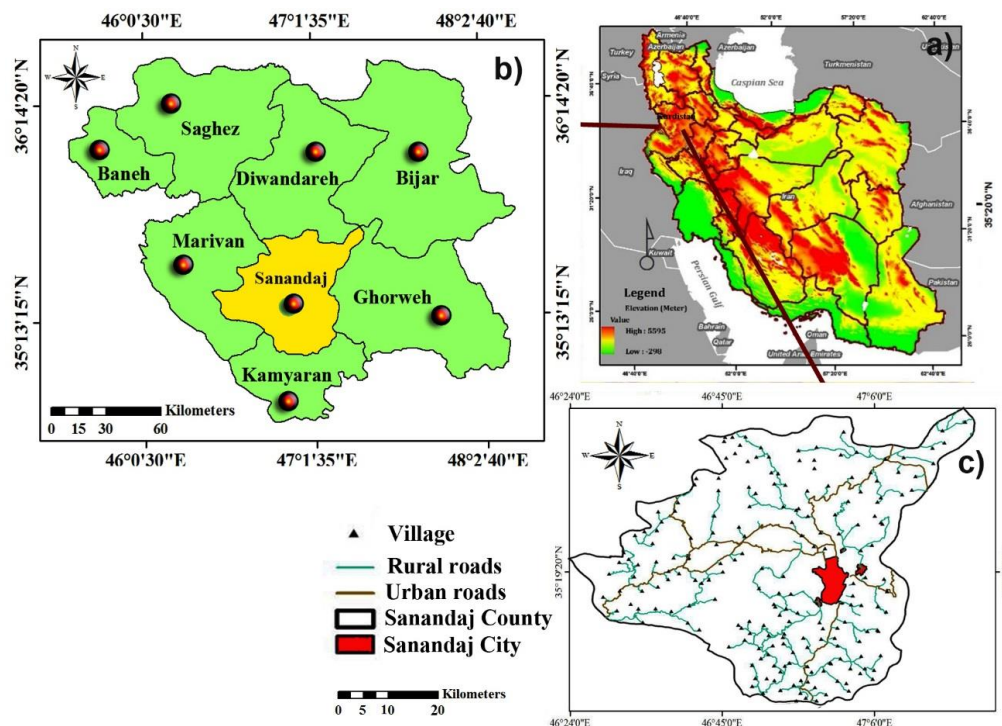


Figure 1. Geographical location of the study area in a) Northwest of Iran, b) Kurdistan Province, c) Sanandaj County

Table 1. Meteorological data applied for the study area

	Jan	Feb	Mar	Apr	May	Jun	Jul	Aug	Sep	Oct	Nov	Dec	Annual average
Average temperature (°C)	-0.5	0.7	6.4	12.1	16.3	22	26.8	26	20.6	14.7	8	2.3	13
Maximum temperature (°C)	4.8	6.6	13	20	25.3	32.6	44	36.2	32.1	24.3	15.4	8	21.3
Minimum temperature (°C)	-13.5	-5.2	-0.2	4.3	7.4	11.2	16.4	15.6	9.2	5.1	0.6	-3.4	4.6
Monthly average of precipitation (mm)	60.5	65.2	31.4	1	0.7	0.6	1.8	42.8	59.1	91.3	74.5	62.1	491

Image enhancement and visual interpretation

Visual interpretation is highly associated with the knowledge of an applicant about the land covers of an area. Its advantage compared to the automated classification methods is recognizing the dynamic changes more precisely (Kibret et al., 2016; Zhang et al., 2014). The automated classification methods, usually concentrate on the technological approaches, while the visual interpretation is applied for the practical usage (Zhang, et al., 2014).

One of the most important techniques to enhance image's spatial resolution and information is the co-registration and the combination with higher spatial resolution satellite imagery, which improve the visual interpretability of the imagery. However, the enhanced images are normally used for the visual analyses, while the original images are utilized for the automated one (Eastman, 1999; Lillesand et al., 2014).

In the most of remote sensing studies, pre-processing of satellite imageries is undeniable (Belward and Skøien, 2015; Ma et al., 2017). Data pre-processing was applied to provide a radiometrically, atmospherically, spectrally and geometrically corrected imageries. However, based on the study area we acquired 2 Landsat-8 imagery of two different rows of 35 and 36, but the same path of 167, which they were mosaicked and clipped as extend of the study area. Moreover, Sentinel-1 data was acquired for the combination with Landsat-8.

Improvement of the Landsat-8 spatial resolution from 15 m (after pan-sharpening with the 15 m panchromatic band) to 10 m as well as using for the combination model, are among positive points of Sentinel-1 satellite imagery in this study. Using ENVI software, multispectral bands of Landsat-8 imageries of the two rows were pre-

processed and mosaicked. Besides, the thermal band of Landsat-8 and created Normalized Difference Vegetation Index (NDVI) were stacked with the multispectral bands. Furthermore, using SNAP software, Sentinel-1 imagery was pre-processed and clipped as the study area. Moreover, using ENVI software the stacked imagery of multispectral, NDVI and thermal bands (as the slave imagery) was co-registered and stacked with the Sentinel-1 imagery (as the master image). However, the combination of NDVI, RADAR and thermal bands was used for the visual interpretation. At the same time, after extracting the land covers using the Google Earth images with the help of the visual interpretation, the topological errors was fixed in ArcGIS (Fig. 2).

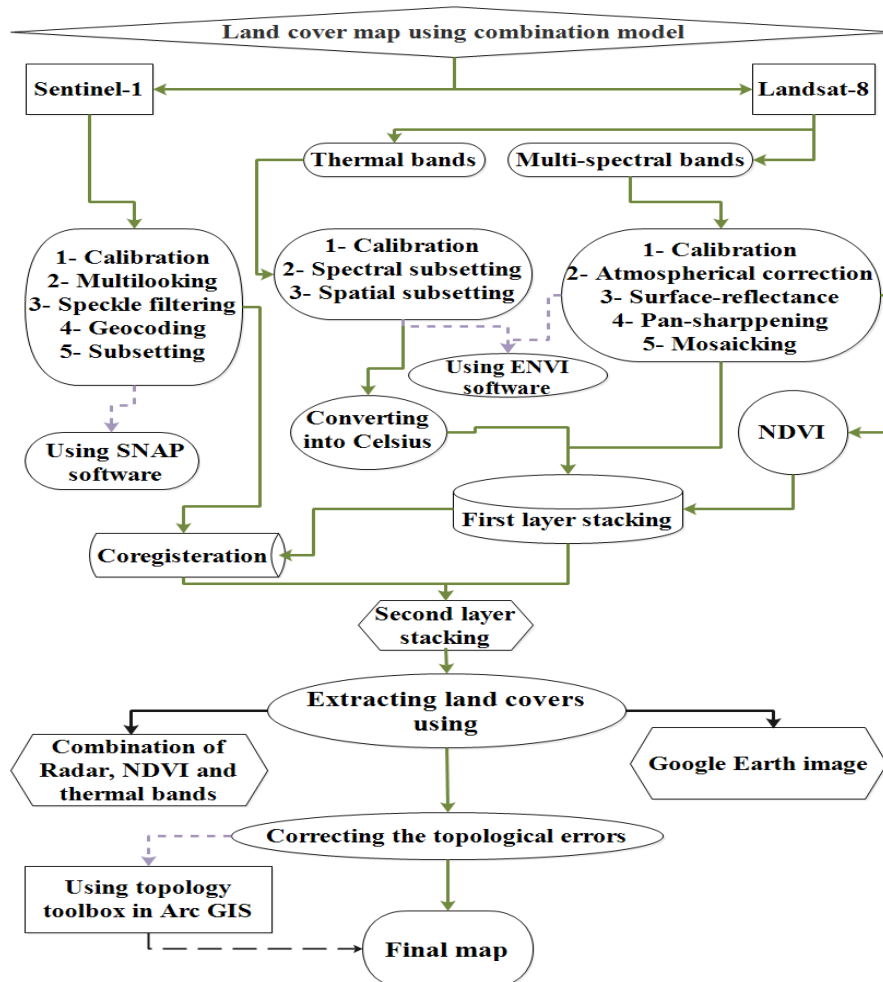


Figure 2. Methodology of the study

RADAR, NDVI and thermal bands as a clear combination were interpreted visually, by which the land covers can be differentiated easily. The contrast and brightness level panels were used to adjust the image view to an appropriate level. Figure 3 illustrates the differences among the land covers by the combined imagery.

Because of the distinguishing in the shape and color, the delineation of the land covers was clear from the combined image's visual interpretation. LCM of the study area was produced from the visual interpretation and digitization using the Google Earth image of the same date in Geographic Information System (GIS).

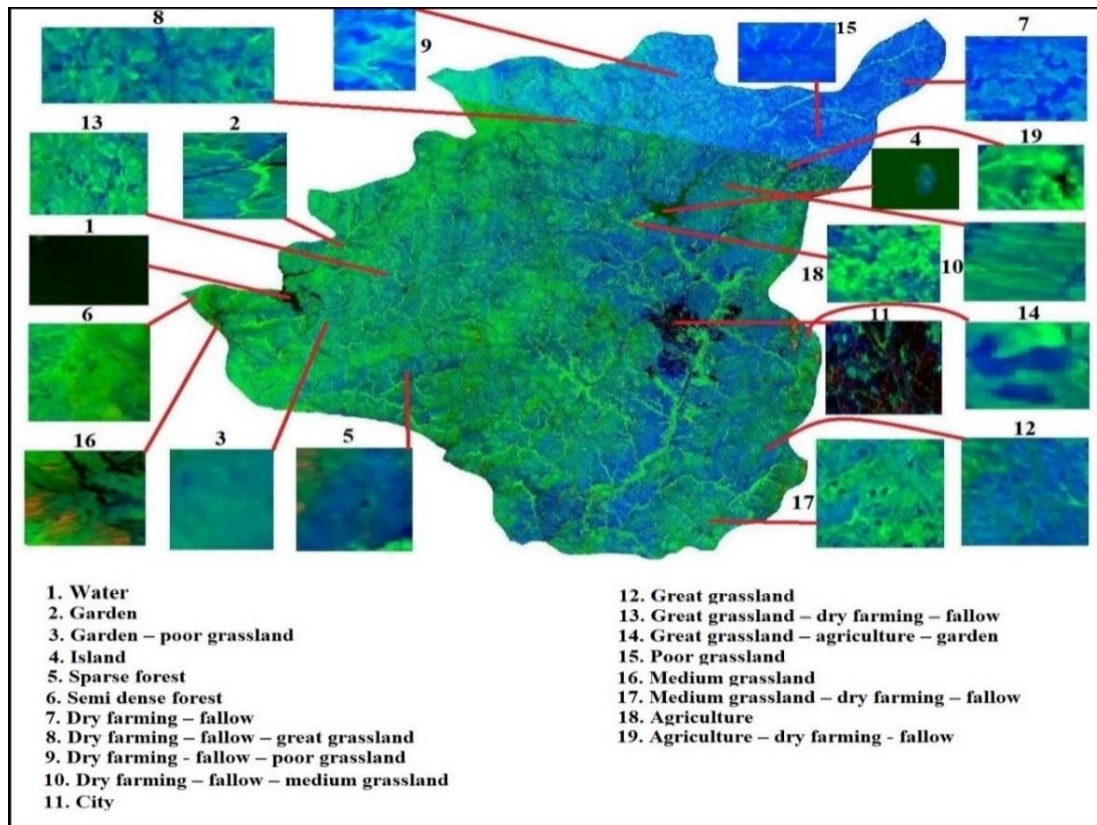


Figure 3. The combination image of RADAR (Sentinel-1), NDVI (Landsat-8) and thermal bands (Landsat-8)

Dataset

A pair of Landsat-8 satellite imageries of a same path but two different rows (167-35 and 167-36) were acquired for the study area through <https://libra.developmentseed.org> website. However, these datasets through ENVI software, were corrected and finalized to be co-registered with Sentinel-1 (Fig. 4).

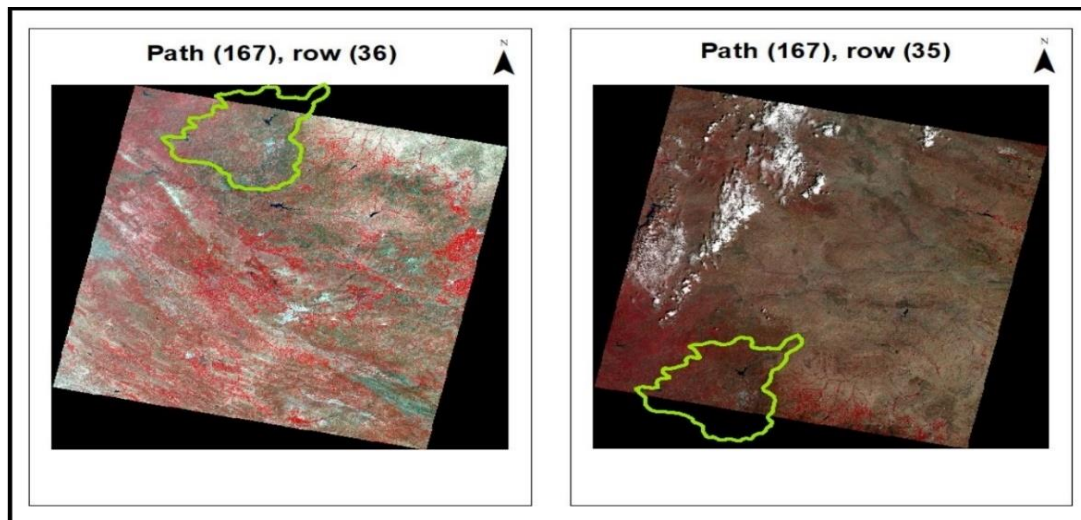


Figure 4. Landsat-8 images of scope of the study

Concerned with the Sentinel-1 satellite imagery, based on the study area a scene was downloaded online for free through www.scihub.copernicus.eu website. Using SNAP software, it was prepared for the co-registration process. *Table 2* and *Figure 5* illustrate the technical attributes of the satellite imageries of Sentinel-1 and Landsat-8 and the geographical position of Sentinel-1 data on the study area, respectively.

Table 2. *Technical attributes of the satellite data used in this study*

Characteristics	Sentinel-1	Landsat-8
Type of sensor	SAR	OLI
Spatial resolution	10 m	30 m (multispectral) 15 m (panchromatic)
Temporal resolution	12 days	16 days
Spectral resolution	Single band (C)	9 bands
Date	10/05/2017	11/05/2017
Sensor mode and product type	Interferometry Wide swath (IW) Ground Range Detected (GRD)	

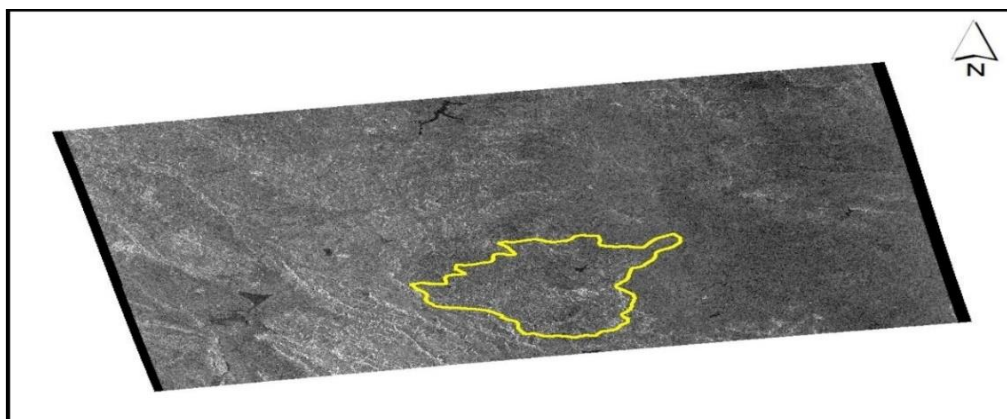


Figure 5. *Sentinel-1 image of scope of the study*

Accuracy assessment

In general, accuracy assessment illustrates the quality of information extracted from remotely sensed data (Alqurashi and Kumar, 2014; Congalton and Green, 2008). The used method for the accuracy assessment in this study was through applying the Google Earth images of the same date. However, it must be considered that using this method only applicable when the researchers have a complete knowledge about the land covers of the study area. For this reason, first the land covers through the visual interpretation of the combined imagery were identified, then all the land covers (polygon by polygon) were digitized and validated through the Google Earth images of the same date.

Results and discussion

The selection of a suitable combination among different bands of satellite imagery is an essential process for the visual interpretation. In order to make a better image visual interpretation, the enhancement technique was fulfilled. In this study, the band

combination of RADAR, NDVI and thermal, was selected as the best combination. An old map was prepared by the Iranian Institute of Water and Soil in 11/05/2010 using Landsat 7 images, ETM⁺ sensor with resolution 30 m (multispectral), with row 35 and path 167, which they were mosaicked and clipped as extend of the study area. The extracted images unbalanced machine support model and supervised classification (Fig. 6). Because of the big area of Sanandaj County and difficulties in preparation of a new map, this map has been the only available source for citation since 2010.

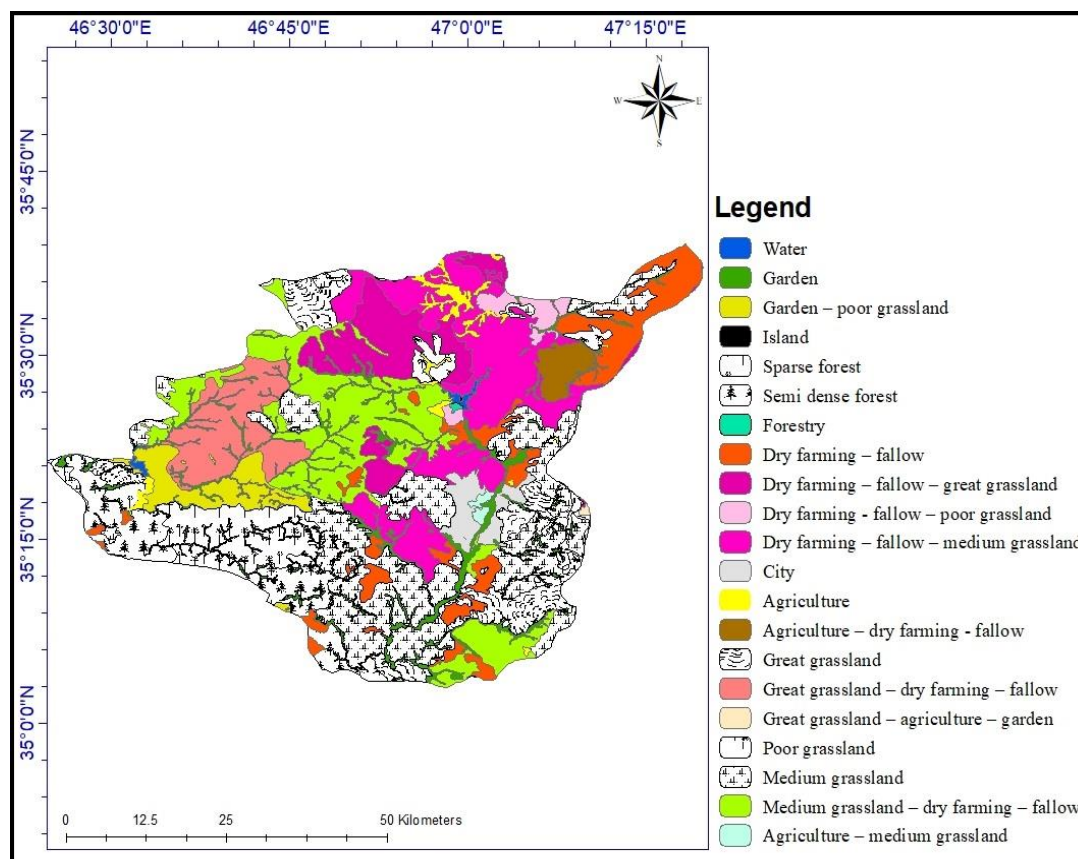


Figure 6. The land cover map of the study area in the year 2010

In this study a total number of 19 different land covers ranging from the small to big scales were extracted. However, medium grassland and medium grassland–dry farming–fallow have the biggest area of 497.5818 km² and 409.6083 km², respectively. Dry farming fallow is the third biggest area with 360.1108 km². Moreover, Dry farming–fallow–medium grassland with 259.4949 km² is one of the biggest land covers in Sanandaj County. Dry farming–fallow–great grassland, garden and great grassland–dry farming–fallow with 226.3668 km², 200.3053 km² and 187.1039 km², respectively are amongst the substantial land covers of the region. The minimum area of land cover belongs to the island with only 0.119052 km². Furthermore, great grassland–agriculture–garden with 1.370851 km² is the second smallest area in the study area. The land covers are highlighted in Figure 7 from the biggest to the smallest.

The final LCM was topologically corrected through the topology toolbox in ArcGIS. However, regardless the applicant patience in digitizing, new digitized layers will be faced with the small topologically errors, which can only be recognized and fixed using

the topology toolbox. Furthermore, in this study, after digitizing a total number of 146 small overlaps and 56 small gaps were identified and corrected one by one through the abovementioned toolbox. *Figure 8* and *Table 3* show the extracted land covers of the study area in the year 2017 and the occurred changes compared with the year of 2010, respectively.

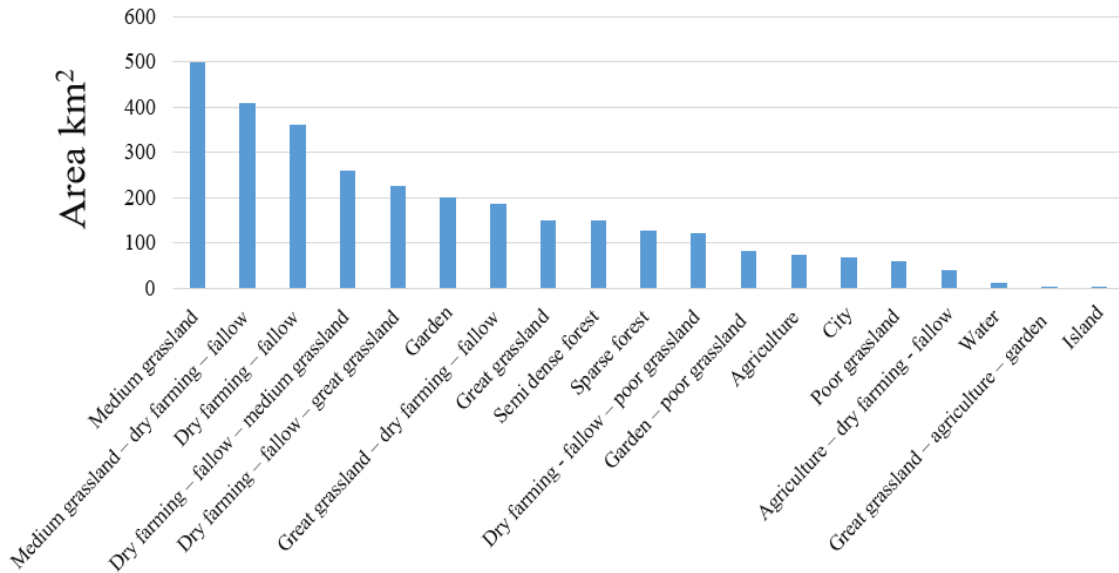


Figure 7. The land covers and area (km²) for the study area

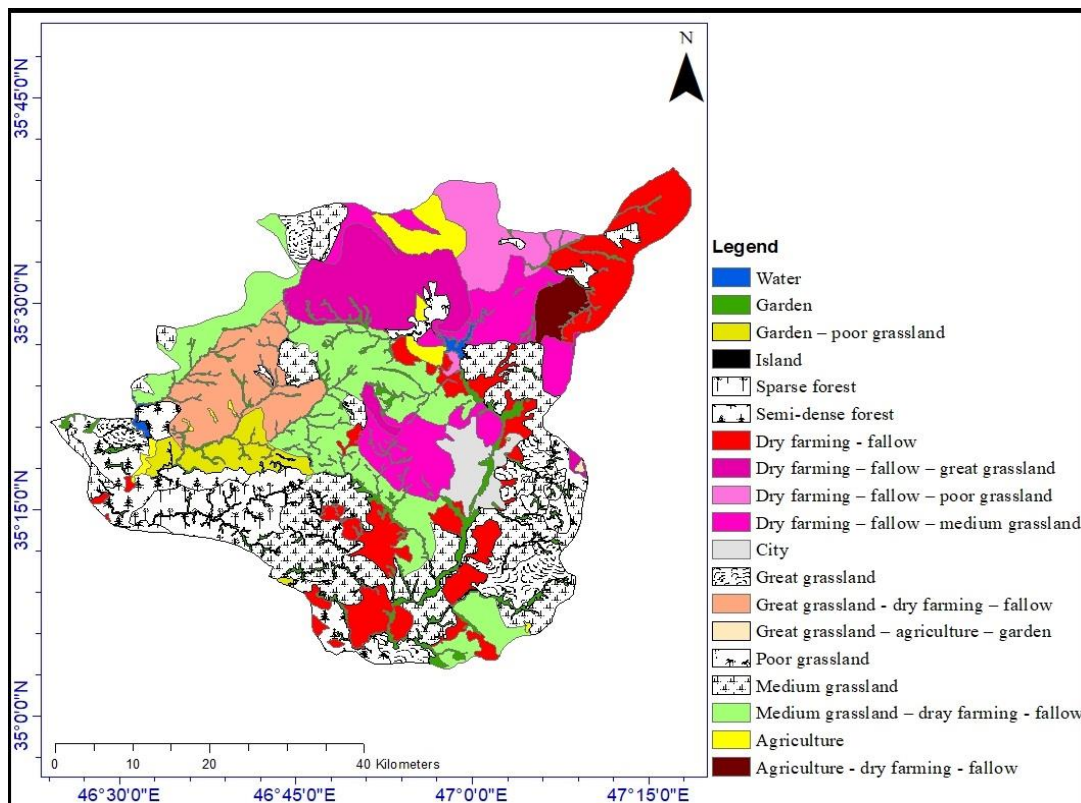


Figure 8. The land cover map of the study area in the year 2017

Table 3. The land cover types and area of each category for the years 2010 and 2017

No.	Land covers	Area (km ²) 2010	Area (km ²) 2017
1	Garden	196.561	200.3053
2	water	10.0364	11.61852
3	Garden-poor grassland	101.792	80.78231
4	island	0.238093	0.119052
5	Sparse forest	171.598	128.0167
6	Semi dense forest	171.892	149.8309
7	Forestry	1.4632	Replaced by the dry farming-fallow-poor grassland
8	Dry farming-fallow	230.546	360.1108
9	Dry farming-fallow-great grassland	210.06	226.3668
10	Dry farming-fallow-poor grassland	39.0384	122.2905
11	Dry farming-fallow-medium grassland	378.942	259.4949
12	City	58.6013	67.36704
13	Agriculture	40.9321	73.53178
14	Agriculture-dry farming-fallow	44.0775	39.24857
15	Agriculture-medium grassland	7.68398	Replaced by the city area
16	Great grassland	190.396	150.6862
17	Great grassland-dry farming-fallow	184.367	187.1039
18	Great grassland-agriculture-garden	1.58959	1.370851
19	Poor grassland	41.978	58.51491
20	Medium grassland	543.059	497.5818
21	Medium grassland-dry farming-fallow	399.51	409.6083

Comparing the results of the current study with the results of the research conducted with the Iranian soil and water organization (2010) showed that all the land covers have been faced changes of the small to the large scales. In the year 2017, dry farming-fallow has seen the most considerable changes, where 129.5648 km² has been added to its area in comparison with the year 2010. Dry farming-fallow-medium grassland has lost about 119.4471 km² of its area by the year 2017. However, because of rising in the water level, the island area decreased to 0.119052 km² by 2017 from 0.238093 km² in 2010. It is worth indicating that the forestry by the dry farming-fallow-poor grassland and the agriculture-medium grassland by the city area have been replaced.

Extracting land covers using the visual interpretation and the Google Earth is highly associated with the basic knowledge about the study area. However, this technique is very time consuming, but precise and reliable. For example, the water body was recognized from the visual interpretation and digitized through the Google earth image in full zoom, then using ArcGIS converted to the layer format and digitized through the editor toolbox. The obtained results of current study is similar with several previous published studies that investigate land use changes using satellite data in which some will be referred to in this part of the work. Sunar (1998) used five techniques, including: adding, subtracting, dividing, principle component (PCI), and post classification analysis to detect land cover changes in Aykitali, Turkey. He found out that the technique of adding and subtracting images was the most simple among these

techniques, while PCI and post classification analyses showed better results in change detection. Xian et al. (2009) applied Landsat imagery change detection methods for updating the 2001 National Land Cover Database land cover classification to 2006 in several metropolitan areas including Seattle, Washington; San Diego, California; Sioux Falls, South Dakota; Jackson, Mississippi; and Manchester. Results from the five study areas showed that the vast majority of land cover change was captured and updated with overall land cover classification accuracies of 78.32%, 87.5%, 88.57%, 78.36%, and 83.33% for these areas. Shahabi et al. (2012) investigated that green space destruction in urban area using three remote sensing techniques including NDVI, PCA, and post classification methods. To carry out these techniques, Thematic Mapper (TM) and Enhanced Thematic Mapper Plus (ETM+) LANDSAT data within the year 1989 to 2009 were used to recognize land use changes, especially the physical development of the area and its devastating effects on the green space. The result showed that green space has been reduced from 530 ha in 1989 to 198.3 ha in 2009. Butt et al. (2015) applied supervised classification-maximum likelihood algorithm in ERDAS imagine to detection of land cover/land use changes observed in Simly watershed, Pakistan using multispectral satellite data obtained from Landsat 5 and SPOT 5 for the years 1992 and 2012 respectively. The accrued results showed that land cover/land use practices in the study area have altered significantly in 20 years. The land cover/land use shift in the watershed area was evident by the decline in the area of vegetation and water class (38.2% and 74.3% respectively) and augmentation of area covered by classes of settlements (80.1%), Agriculture (163.7%) and barren land (63.3%). Islam et al. (2018) evaluated land use changes of Chunati wildlife sanctuary, Bangladesh from 2005 to 2015 using Landsat TM and Landsat 8 OLI/TIRS images. In the present study Maximum likelihood classification algorithm was used in order to derive supervised land use classification. The obtained results showed that about 256 ha of degraded forest area had been increased within 10 years (2005–2015) and the annual rate of change was 25.56%. Another 159 ha of naturally forested land had been changed to other land uses having an (-) annual rate of change of 15.88%.

Conclusion

In this study, in order to extract the land covers, the satellite imageries of RADAR with multispectral data were combined. The study area lies on an area about 3024 km². For this goal, we acquired satellite imageries of Sentinel-1 and Landsat-8 (OLI) for the dates 10/05/2017 and 11/05/2017, respectively (when vegetation coverage is in its best situation). Because of the scope of the study, two Landsat-8 imageries of two different rows (35 and 36) but the same path (167) were downloaded. Moreover, after correcting either Landsat imageries through ENVI Software they were mosaicked as a single image. Sentinel-1 data was corrected using SNAP Software, then as the master image co-registered and stacked with Landsat-8 as the slave image. Besides, RADAR, NDVI and thermal bands were used for the visual interpretation.

Through visual interpretation of the combined imagery with assist of the Google Earth image of the same date, all the land covers were extracted and the topological errors through the topology toolbox in ArcGIS were recognized and corrected. For accuracy assessment the Google Earth image was used, which is a robust way to validate land cover map provided that the researchers have a complete knowledge on the study area. Results illustrate that a total number of 19 different land covers were

recognized and mapped. However, medium grassland, medium grassland–dry farming–fallow and dry farming fallow have the biggest area of 497.5818 km², 409.6083 km² and 360.1108 km², respectively. The smallest area belongs to the island with only 0.119052 km², followed by the great grassland–agriculture–garden with 1.370851 km². The forestry by the dry farming–fallow–poor grassland and the agriculture–medium grassland by the city area have been replaced.

In this study RADAR imagery of Sentinel-1 (10-m pixel size) was combined with the multispectral data of Landsat-8 (15-m pixel size after pan-sharpening with its panchromatic band), to map the land covers of the study area; however, the combination of the Radar imagery of Sentinel-1 with the multispectral imagery of Sentinel-2 (10-m and 20-m pixel sizes) is highly recommended for such studies in the future.

Acknowledgements. The authors wish to express their sincere thanks to Universiti Teknologi Malaysia (UTM) based on Research University Grant (Q.J130000.2527.17H84) for their financial supports.

REFERENCES

- [1] Alqurashi, A. F., Kumar, L. (2014): Land use and land cover change detection in the Saudi Arabian desert cities of Makkah and Al-Taif using satellite data. – *Advances in Remote Sensing* 3: 106.
- [2] Batty, M., Xie, Y. (1994): From cells to cities. – *Environment and Planning B: Planning and Design* 21: S31-S48.
- [3] Batty, M., Xie, Y. (1997): Possible urban automata. – *Environment and Planning B: Planning and Design* 24: 175-192.
- [4] Belal, A., Moghanm, F. (2011): Detecting urban growth using remote sensing and GIS techniques in Al Gharbiya governorate, Egypt. – *The Egyptian Journal of Remote Sensing and Space Science* 14: 73-79.
- [5] Belward, A. S., Skøien, J. O. (2015): Who launched what, when and why: trends in global land-cover observation capacity from civilian earth observation satellites. – *ISPRS Journal of Photogrammetry and Remote Sensing* 103: 115-128.
- [6] Boori, M. S., Voženilek, V., Choudhary, K. (2015): Land use/cover disturbance due to tourism in Jeseníky Mountain, Czech Republic: a remote sensing and GIS based approach. – *The Egyptian Journal of Remote Sensing and Space Science* 18: 17-26.
- [7] Brown, D. G., Page, S., Riolo, R., Zellner, M., Rand, W. (2005): Path dependence and the validation of agent-based spatial models of land use. – *International Journal of Geographical Information Science* 19: 153-174.
- [8] Butt, A., Shabbir, R., Ahmad, S. S., Aziz, N. (2015): Land use change mapping and analysis using Remote Sensing and GIS: A case study of Simly watershed, Islamabad, Pakistan. – *The Egyptian Journal of Remote Sensing and Space Science* 18: 251-259.
- [9] Chen, G. P., He, C., Pu, R., Shi, P. (2003): Land-use/land-cover change detection using improved change-vector analysis. – *Photogrammetric Engineering & Remote Sensing* 69: 369-379.
- [10] Chen, X., Chen, J., Shi, Y., Yamaguchi, Y. (2012): An automated approach for updating land cover maps based on integrated change detection and classification methods. – *ISPRS Journal of Photogrammetry and Remote Sensing* 71: 86-95.
- [11] Clarke, K. C., Gaydos, L. J. (1998): Loose-coupling a cellular automaton model and GIS: long-term urban growth prediction for San Francisco and Washington/Baltimore. – *International Journal of Geographical Information Science* 12: 699-714.
- [12] Congalton, R. G., Green, K. (2008): *Assessing the Accuracy of Remotely Sensed Data: Principles and Practices*. – CRC, Boca Raton, FL.

- [13] Eastman, J. R. (1999): Guide to GIS and Image Processing (Vol. 1). – Clark Labs, Clark University, USA.
- [14] El-Kawy, O. A., Rød, J., Ismail, H., Suliman, A. (2011): Land use and land cover change detection in the western Nile delta of Egypt using remote sensing data. – *Applied Geography* 31: 483-494.
- [15] Fichera, C. R., Modica, G., Pollino, M. (2012): Land cover classification and change-detection analysis using multi-temporal remote sensed imagery and landscape metrics. – *European Journal of Remote Sensing* 45: 1-18.
- [16] Grecchi, R. C., Gwyn, Q. H. J., Bénié, G. B., Formaggio, A. R., Fahl, F. C. (2014): Land use and land cover changes in the Brazilian Cerrado: A multidisciplinary approach to assess the impacts of agricultural expansion. – *Applied Geography* 55: 300-312.
- [17] Halmy, M. W. A., Gessler, P. E., Hicke, J. A., Salem, B. B. (2015): Land use/land cover change detection and prediction in the north-western coastal desert of Egypt using Markov-CA. – *Applied Geography* 63: 101-112.
- [18] Hansen, M. C., Loveland, T. R. (2012): A review of large area monitoring of land cover change using Landsat data. – *Remote Sensing of Environment* 122: 66-74.
- [19] Homer, C., Huang, C., Yang, L., Wylie, B., Coan, M. (2004): Development of a 2001 national land-cover database for the United States. – *Photogrammetric Engineering & Remote Sensing* 70: 829-840.
- [20] Hosseini, G., Teymouri, P., Shahmoradi, B., Maleki, A. (2015): Determination of the concentration and composition of PM10 during the Middle Eastern dust storms in Sanandaj, Iran. – *Journal of Research in Health Sciences* 15: 182-188.
- [21] Huang, S., Ramirez, C., Kennedy, K., Mallory, J., Wang, J., Chu, C. (2017): Updating land cover automatically based on change detection using satellite images: case study of national forests in Southern California. – *GIScience & Remote Sensing* 54: 495-514.
- [22] Islam, K., Jashimuddin, M., Nath, B., Nath, T. K. (2018): Land use classification and change detection by using multi-temporal remotely sensed imagery: the case of Chhunati wildlife sanctuary, Bangladesh. – *The Egyptian Journal of Remote Sensing and Space Science* 21: 37-47.
- [23] Izady, M. (2015): *The Kurds: A Concise History and Fact Book*. – Taylor & Francis, New York.
- [24] Jin, S., Yang, L., Danielson, P., Homer, C., Fry, J., Xian, G. (2013): A comprehensive change detection method for updating the National Land Cover Database to circa 2011. – *Remote Sensing of Environment* 132: 159-175.
- [25] Kibret, K. S., Marohn, C., Cadisch, G. (2016): Assessment of land use and land cover change in South Central Ethiopia during four decades based on integrated analysis of multi-temporal images and geospatial vector data. – *Remote Sensing Applications: Society and Environment* 3: 1-19.
- [26] Kumar, K., Kumar, V., Kumar, D. (2016): Land use and land cover change detection in gagas river valley watershed using remote sensing and GIS. – *International Journal of Research in Engineering and Applied Sciences* 6: 31-37.
- [27] Lausch, A., Herzog, F. (2002): Applicability of landscape metrics for the monitoring of landscape change: issues of scale, resolution and interpretability. – *Ecological Indicators* 2: 3-15.
- [28] Li, X., Yeh, A. G.-O. (2002): Neural-network-based cellular automata for simulating multiple land use changes using GIS. – *International Journal of Geographical Information Science* 16: 323-343.
- [29] Li, Y., Cao, Z., Long, H., Liu, Y., Li, W. (2017): Dynamic analysis of ecological environment combined with land cover and NDVI changes and implications for sustainable urban–rural development: the case of Mu Us Sandy Land, China. – *Journal of Cleaner Production* 142: 697-715.
- [30] Lillesand, T., Kiefer, R. W., Chipman, J. (2014): *Remote Sensing and Image Interpretation*. – John Wiley & Sons, Hoboken.

- [31] Liu, T., Yang, X. (2015): Monitoring land changes in an urban area using satellite imagery, GIS and landscape metrics. – *Applied Geography* 56: 42-54.
- [32] López, E., Bocco, G., Mendoza, M., Duhau, E. (2001): Predicting land-cover and land-use change in the urban fringe: a case in Morelia city, Mexico. – *Landscape and Urban Planning* 55: 271-285.
- [33] Loveland, T., Sohl, T., Stehman, S., Gallant, A., Sayler, K., Napton, D. (2002): A strategy for estimating the rates of recent United States land-cover changes. – *Photogrammetric Engineering & Remote Sensing* 68: 1091-1099.
- [34] Lunetta, R. S., Knight, J. F., Ediriwickrema, J., Lyon, J. G., Worthy, L. D. (2006): Land-cover change detection using multi-temporal MODIS NDVI data. – *Remote Sensing of Environment* 105: 142-154.
- [35] Ma, L., Li, M., Ma, X., Cheng, L., Du, P., Liu, Y. (2017): A review of supervised object-based land-cover image classification. – *ISPRS Journal of Photogrammetry and Remote Sensing* 130: 277-293.
- [36] Matikainen, L., Karila, K., Hyypä, J., Litkey, P., Puttonen, E., Ahokas, E. (2017): Object-based analysis of multispectral airborne laser scanner data for land cover classification and map updating. – *ISPRS Journal of Photogrammetry and Remote Sensing* 128: 298-313.
- [37] Myint, S. W., Gober, P., Brazel, A., Grossman-Clarke, S., Weng, Q. (2011): Per-pixel vs. object-based classification of urban land cover extraction using high spatial resolution imagery. – *Remote Sensing of Environment* 115: 1145-1161.
- [38] Nutini, F., Boschetti, M., Brivio, P., Bocchi, S., Antoninetti, M. (2013): Land-use and land-cover change detection in a semi-arid area of Niger using multi-temporal analysis of Landsat images. – *International journal of remote sensing* 34: 4769-4790.
- [39] Rawat, J., Kumar, M. (2015): Monitoring land use/cover change using remote sensing and GIS techniques: a case study of Hawalbagh block, district Almora, Uttarakhand, India. – *The Egyptian Journal of Remote Sensing and Space Science* 18: 77-84.
- [40] Rawat, J., Biswas, V., Kumar, M. (2013): Changes in land use/cover using geospatial techniques: a case study of Ramnagar town area, district Nainital, Uttarakhand, India. – *The Egyptian Journal of Remote Sensing and Space Science* 16: 111-117.
- [41] Sanders, L., Pumain, D., Mathian, H., Guérin-Pace, F., Bura, S. (1997): SIMPOP: a multiagent system for the study of urbanism. – *Environment and Planning B: Planning and Design* 24: 287-305.
- [42] Shahabi, H., Ahmad, B. B., Mokhtari, M. H., Zadeh, M. A. (2012): Detection of urban irregular development and green space destruction using normalized difference vegetation index (NDVI), principal component analysis (PCA) and post classification methods: a case study of Saqqez City. – *International Journal of Physical Sciences* 7: 2587-2595.
- [43] Sunar, F. (1998): An analysis of changes in a multi-date data set: a case study in the Ikitelli area, Istanbul, Turkey. – *International Journal of Remote Sensing* 19: 225-235.
- [44] Theobald, D. M., Hobbs, N. T. (1998): Forecasting rural land-use change: a comparison of regression-and spatial transition-based models. – *Geographical and Environmental Modelling* 2: 65-82.
- [45] White, R., Engelen, G. (1997): Cellular automata as the basis of integrated dynamic regional modelling. – *Environment and Planning B: Planning and Design* 24: 235-246.
- [46] Wu, F., Yeh, A. G.-O. (1997): Changing spatial distribution and determinants of land development in Chinese cities in the transition from a centrally planned economy to a socialist market economy: a case study of Guangzhou. – *Urban Studies* 34: 1851-1879.
- [47] Xian, G., Crane, M. (2005): Assessments of urban growth in the Tampa Bay watershed using remote sensing data. – *Remote Sensing of Environment* 97: 203-215.
- [48] Xian, G., Homer, C., Fry, J. (2009): Updating the 2001 National Land Cover Database land cover classification to 2006 by using Landsat imagery change detection methods. – *Remote Sensing of Environment* 113: 1133-1147.

- [49] Yeh, A. G.-O., Li, X. (2001): A constrained CA model for the simulation and planning of sustainable urban forms by using GIS. – *Environment and Planning B: Planning and Design* 28: 733-753.
- [50] Zhang, Z., Wang, X., Zhao, X., Liu, B., Yi, L., Zuo, L., Hu, S. (2014): A 2010 update of National Land Use/Cover Database of China at 1: 100000 scale using medium spatial resolution satellite images. – *Remote Sensing of Environment* 149: 142-154.
- [51] Zhu, Z., Woodcock, C. E. (2014): Continuous change detection and classification of land cover using all available Landsat data. – *Remote Sensing of Environment* 144: 152-171.

POTENTIAL RESISTANCE OF OKRA LEAF Bt COTTON AGAINST INSECT PESTS

NAZIR, M. S.^{1*} – MALIK, T. A.¹ – SHAKEEL, A.¹ – AHMAD, J. N.²

¹*Department of Plant Breeding and Genetics, University of Agriculture, Faisalabad, Punjab, Pakistan*

²*Department of Entomology, University of Agriculture Faisalabad Punjab, Pakistan*

**Corresponding author
e-mail: 2008ag2267@uaf.edu.pk*

(Received 9th Dec 2018; accepted 28th Feb 2019)

Abstract. Cotton with Bt gene is only resistant against bollworms. Sucking insect pests also cause huge losses to cotton crop. It is reported that okra leaf cotton genotypes are resistant to sucking insect pests. The objective of this research was to explore the potential of okra leaf Bt cotton for resistance against bollworms and sucking insect pests. Okra leaf Bt cotton recombinant lines were developed by hybridization and selection process for use in this study. Comparative insect pest buildup/infestation was studied on non Bt normal leaf, normal leaf Bt, non Bt okra leaf and okra leaf Bt genotypes/cultivars/recombinant lines under field conditions using randomized complete block design with three replications. The genotypes/cultivars/recombinant lines were separated by nets to confine the insect population buildup within the genotype. Significantly lower buildup of sucking insect pests was found on okra leaf cotton compared to normal leaf cotton and significantly lower buildup/infestation of sucking insects as well bollworms was found on okra leaf recombinant lines with Bt gene. Development of Bt cultivars with okra leaf is recommended which would be resistant against bollworms as well as sucking insect pests attacks.

Keywords: *sucking insects, bollworms, okra leaf, normal leaf, Bt cotton*

Introduction

Pakistan is the 4th largest producer of cotton in the world. Cotton crop is severely damaged by many sucking insects (Jassid, whitefly, aphid, thrips) and bollworms (American bollworm, Spotted bollworm and Pink bollworm). Genetically modified Bt cotton is only resistant to bollworms but is not resistant to sucking insect pests (Din et al., 2016). Huge quantity of insecticide is applied to protect Bt cotton from sucking insect pests which increases production cost of cotton crop and pollute the environment. So, Bt cotton cultivars which may be resistant to sucking insect pests as well may be developed.

It has been reported that population buildup of sucking insect pests on cotton with okra leaf trait is comparatively low due to its open canopy (Chu et al., 2000; Soomro et al., 2000; Ahmad et al., 2005; Din et al., 2016). The objective of present research was to explore the potential of Bt cotton with okra leaf trait for resistance against sucking insect pests and bollworms.

Assessment of cotton against insect pests by scoring insect pest population buildup on genotype under field conditions is tedious work as the experimental plots of the genotypes have to be separated by nets to confine the insect population within the genotype. Thus, only a small number of such studies are found in the literature. The present study was conducted to assess the comparative insect pest buildup/infestation on okra leaf (non Bt and Bt) and normal leaf (non Bt and Bt) cotton under field condition.

Material and methods

The study was conducted in the field area of the University of Agriculture Faisalabad (Latitude = 31° 26' N, Longitude = 73° 06' E, Altitude = 184.4 m), Pakistan, during the year 2014 to 2016. Faisalabad possess the arid climate. It can touch both extremes, with a summer with maximum temperature 50 °C and winter temperature of -2 °C.

Development of okra leaf Bt cotton recombinant lines

In year 2014 crosses were made and F₁ generation was developed ((MNH-886 × Gumbo Okra), (CRS-456×Gumbo Okra) and (PB-38×Gumbo Okra)), in season 2015 F₁ were sown and F₂ was raised into the field. Recombinant okra leaf Bt cotton lines were selected from the F₂ populations of the cross of Gumbo okra (okra leaf) with normal leaf genotypes/cultivars. Recombinant plants from F₂ were selected on the basis of okra leaves with high yielding traits and Bt proteins test by using ELISA (Quali-Plate™ Kit for Cry1Ab/Cry1Ac by Enviro-Logics). The Enviro-Logix QualiPlate Kit is a “sandwich Enzyme-Linked Immuno Sorbent Assay” (ELISA). List of cotton genotypes/cultivars/recombinant lines used in the study is given in *Table 1*.

To assess the comparative insect pest buildup/infestation, Eight *G. hirsutum* genotypes/cultivars/recombinant lines were sown at the 27th of March (2016) under normal soil and irrigation conditions in randomized complete block design with three replications. Standard agronomic practices of growing cotton crop were used in the experiment. There were 24 rows, each 300 cm in length (10 plant in each row) in each replication (three rows for each genotype/cultivar/ recombinant line) by keeping the plant to plant distance of 30 cm and row to row distance of 75 cm.

Table 1. List of cotton genotypes/cultivars/recombinant lines evaluated for resistance against different insect pests under field condition

Sr. No.	Genotype/cultivar	Description
1.	PB-38	Cultivar with Normal leaf trait
2.	MNH-886	Cultivar with Normal leaf trait + Cry1Ac
3.	FH-142	Cultivar with Normal leaf trait + Cry1Ac
4.	FH-lalazar	Cultivar with Normal leaf trait + Cry1Ac
5.	Gumbo Okra	Genotype with Okra leaf trait
6.	RP ₁ (MNH-886 × Gumbo Okra)	Recombinant population with Okra leaf + Cry1Ac
7.	RP ₂ (CRS-456 × Gumbo Okra)	Recombinant population with Okra leaf + Cry1Ac
8.	RP ₃ (PB-38 × Gumbo Okra)	Recombinant population with Okra leaf trait

The data were taken at ten-day intervals beginning from 15th of May 2016 to 15th of November 2016 from ten healthy plants randomly selected from each genotype/cultivar/recombinant line. For sucking insects (thrips, jassid, aphid, whitefly and mites), from each plant three leaves were selected (one each from top, middle and bottom) and examined for both adult and nymph, using magnifying glass. The population of bollworms (Pink bollworm, Spotted bollworm, and American bollworm) were assessed by counting infested bolls, squares and flowers on per plant basis. Analysis of variance of insect pest's data was conducted and means were separated by LSD test as in Steel et al. (1997).

Results

The population means of insect pest buildup/infestation (Pink bollworm, American bollworm, thrips, jassid, whitefly, mites, aphid) on different genotypes/cultivars/recombinant lines are given in *Table 2*. The analysis of variance showed significant variation for insect pest population built up on different genotypes/cultivars/recombinant lines. Comparison of means of insect pests buildup/infestation of (Pink bollworm, American bollworm, thrips, jassid, whitefly, mites, aphid) on different genotypes/cultivars/ recombinant lines by using LSD test is also given in *Table 2*. The results showed that *Gossypium hirsutum* genotypes/cultivars with normal leaf trait had significantly higher thrips population buildup comparatively to the okra leaf genotypes/recombinant lines. Maximum infestation was found on FH-lalazar which is a normal leaf variety while minimum infestation was found on okra leaf line RP₂. Maximum number of Jassid population was found on FH-lalazar followed by other normal leaf cultivars while minimum number of infestations was found on okra leaf line RP₂. Results showed that comparative population built up of whitefly was significantly higher on normal leaf genotypes/cultivars as compared to okra leaf genotype/cultivar/ line.

Table 2. Mean population buildup/infestation of insect pests on cotton genotypes/cultivars/recombinant lines

Insects Genotypes	Thrip	Jassid	Whitefly	Aphid	Mites	Spotted bollworm	Pink bollworm	American bollworm
PB-38	5.273 b	4.410 c	8.420 b	8.333 a	7.563 b	10.037 a	9.553 a	11.070 a
MNH-886	5.204 b	4.589 c	8.306 b	9.016 a	8.261 a	0.291cd	1.078 cd	0.411 d
FH-142	5.728 a	5.076 b	8.816 a	8.551 a	8.116 a	0.744 c	202 c	0.869 d
FH-lalazar	5.941 a	5.559 a	7.309 c	8.861 a	7.414 b	0.478 cd	1.154 cd	0.620 d
Gumbo Okra	4.498 c	2.411 d	3.287 d	4.431 bc	5.187 e	4.096 b	6.341 b	4.341 b
RP ₁	3.519 d	2.485 de	2.780 e	3.764 cd	6.094 c	0.044 d	0.026 d	0.298 e
RP ₂	3.413 d	1.887 e	3.022 de	3.570 d	5.568 d	0.119 cd	0.053 cd	0.199 e
RP ₃	4.728 c	2.693 d	3.254 d	4.707 b	5.922 c	4.641 b	5.294 b	3.84 c
MS for genotype	2.661**	6.022**	23.131**	18.413**	4.374**	44.356**	65.528**	77.423**
LSD value	0.399	0.342	0.340	0.780	0.242	0.638	0.399	0.486

**Highly significant ($p < 0.01$)

*Significant ($p < 0.05$)

Genotypes/cultivars/recombinant lines not sharing the same letter are significantly different

Maximum number of whiteflies was found on normal leaf cultivar FH-142 followed by other normal leaf genotype/cultivar PB-38 and MNH-886. Minimum number of whiteflies were found on okra leaf line RP₁. Results showed that comparative population built up of whitefly was significantly higher on normal leaf genotypes/cultivars as compared to okra leaf genotype/cultivar/ recombinant line. Maximum number of whiteflies was found on normal leaf cultivar FH-142 followed by other normal leaf genotype/cultivar PB-38 and MNH-886. Minimum number of whiteflies was found on okra leaf line RP₁. Comparatively high infestation of mites was found on normal leaf genotypes/cultivars as compared to okra leaf genotypes/cultivars/recombinant lines. Maximum number of mites population was found on MNH-886 and FH-142 while minimum number of infestation was found at Gumbo okra followed by other okra leaf genotype/ recombinant lines. Overall results showed that normal leaf cotton (PB-38, MNH-886, FH-142 and FH-lalazar) had high buildup of sucking insect

pests compared to okra leaf cotton (Gumbo Okra, RP₁, RP₂ and RP₃). Significantly higher infestation of bollworms was found on non Bt cotton (PB-38, Gumbo Okra, and RP₃) compared to Bt cotton (MNH-886, FH-142, FH-lalazar RP₁ and RP₂). Non Bt okra leaf Cotton (Gumbo Okra, and RP₃) had lower infestation compared to normal leaf non Bt cotton (PB-38).

Discussion

Okra leaf trait is characterized by narrowly lobbed and deeply cleft leaves with less per leaf surface area compared to normal leaf cotton. It has been reported that okra leaf cotton is resistant to sucking insect pests and also relatively resistant to bollworms compared to normal leaf cotton. In the present study and in earlier reports lower buildup of sucking insect on okra leaf cotton compared to normal leaf cotton was due to its reduced leaf surface area and open canopy (Kular and Butter, 1999; Arif et al., 2006; Din et al., 2016). In a study of eight cotton cultivars from USA and six from Australia, Chu et al. (1999) observed that okra leaf cotton cultivars had lower attack of whitefly compared to normal leaf cotton cultivars. It was suggested that okra leaf trait had great potential for breeding upland cotton resistant to whitefly. Kanher et al. (2016) reported positive correlation of leaf area and aphid population on cotton. So, development of okra leaf cultivars has been suggested to control sucking insect pests (Wilson, 1994; Soomro et al., 2000; Chu et al., 2002; Ahmad et al., 2005; Din et al., 2016; Kanher et al., 2016). Wilson (1889) observed that okra leaf cotton required 33% less insecticide and had less damage by insect pests but yield was as much as normal leaf cultivars. Smith (2001) also compared okra leaf cotton with normal leaf cotton and found that okra leaf cotton was equal in fiber length, fiber strength and fiber fineness as well as yield. Wilson and George (1982) found that okra leaf cultivars were resistant to bollworms compared to the normal leaf cultivars. They concluded that okra leaf cultivars had smaller leaf area and open plant canopy leading to better light penetration and more air circulation which made these cultivars resistant to bollworms. Din et al. (2016) also found in a field study that okra leaf cotton was resistant to bollworms.

Okra leaf trait in cotton is controlled by single gene. Its locus has been reported on chromosome 15 on D genome (Andres et al., 2016). Okra leaf trait is monogenic in inheritance so, breeding cultivars with okra leaf trait may not be difficult. Results of present study and earlier findings suggest that okra leaf cotton Bt cultivars should be tailored to control sucking insect pests and bollworms.

Conclusion

Findings of this study revealed significantly lower buildup/infestation of bollworms (pink bollworm, American bollworm, spotted bollworm) and sucking insects (Aphid, Jassid, Whitefly, thrips and whitefly) on okra leaf Bt cotton compared to normal leaf Bt cotton. So, Bt cotton cultivars with okra leaf trait should be engineered which would be resistant to bollworms as well as sucking insect pests.

REFERENCES

- [1] Abro, G. H., Syed, T. S., Dayo. Z. A. (2003): Varietal resistance of cotton against *Earias* Spp. – Pakistan Journal of Biological Sciences 6: 1837-1839.

- [2] Ahmad, G., Arif, M. J., Ramzan, M., Sanpal, Z. (2005): Population fluctuation of jassid (*Amrasca devastans*) in cotton through morphological plant traits. – Caderno de pesquisa. Série Biologia 17: 71-79.
- [3] Andres, R. J., Coneva, V., Frank, M. H., Tuttle, J. R., Samayoa, L. F., Han, S. W., Kaur, B., Zhu, L., Fang, H., Bowman, D. T., Rojas-Pierce, M. (2016): Modifications to a LATE MERISTEM IDENTITY1 gene are responsible for the major leaf shapes of Upland cotton (*Gossypium hirsutum* L.). – Proceedings of the National Academy of Sciences 114: 57-66.
- [4] Arif, M. J., Gogi, M. D., Ahmad, G. (2006): Role of morpho-physical plant factors imparting resistance in cotton against thrips. – Arab Journal of Plant Protection 24: 57-60.
- [5] Chu, C. C., Cohen, A. C., Natwick, E. T., Simmons, G. S., Henneberry, T. J. (1999): *Bemisia tabaci* (Hemiptera: Aleyrodidae) biotype B colonization and leaf morphology relationships in upland cotton cultivars. – Australian Journal of Entomology 38: 127-131.
- [6] Chu, C. C., Natwick, E. T., Henneberry, T. J., Duggar, P., Richter, R. (2000): Susceptibility of normal leaf and okra leaf shape cotton to silver leaf whitefly and relationships to trichome densities. – Proceedings, Beltwide Cotton Conferences, 4-8 January, San Antonica, USA.
- [7] Chu, C. C., Natwick, E. T., Hennerberry, T. J. (2002): *Bemisia tabaci* biotype B colonization on okra and normal leaf upland cotton strains and cultivars. – Journal of Economic Entomology 95: 733-738.
- [8] Din, Z. M., Malik, T. A., Azhar, F. M., Ashraf, M. (2016): Natural resistance against insect pests in cotton. – Journal of Animal and Plant Science 25: 1346-1353.
- [9] Kanher, F. M., Syed, T. S., Abro, G. H., Jahangir, T. M. (2016): Effect of cotton leaf morphological characters on incidence of *Amrasca Devastans*. – Sindh University Research Journal 48: 271-280.
- [10] Kular, J. S., Butter, N. S. 1999. Influence of some morphological trait of cotton genotypes on resistance to whitefly, *Bemisia tabaci*. – Journal of Insect Science 12: 81-83.
- [11] Smith, C. W. (2001): Registration of three morphological variant upland cotton germplasm lines. – Crop Science 41: 1371-1372.
- [12] Soomro, A. R., Soomro, A. W., Mallah, G. H., Memon, A. M., Soomro, A. H. (2000): Okra leaf cotton, its commercial utilization in Sindh. – Pakistan Journal of Biological Sciences 3: 188-190.
- [13] Steel, R. G. D., Torrie, J. H., Dickey, D. A. (1997): Principles and Procedures of Statistics: A Biometrical Approach. 3rd. Ed. – McGraw Hill Book Co. Inc, New York, pp. 400-428.
- [14] Wilson, F. D. (1989): Yeild, earliness and fiber properties cotton carrying combined traits for pink bollworm resistance. – Crop Science 29: 7-12.
- [15] Wilson, F. D., George, B. W. (1982): Effects of okra leaf, frego bract, and smooth leaf mutants on pink boll worm damage and agronomic properties of cotton. – Crop Science 22: 798-801.
- [16] Wilson, L. J. (1994): Resistance of okra leaf cotton to two spotted spider mites. – Journal of Economic Entomology 87: 1726-1735.

META-ANALYSIS OF THE GLOBAL DIVERSITY AND SPATIAL PATTERNS OF APHID-ANT MUTUALISTIC RELATIONSHIPS

SIDDIQUI, J. A.^{1,2} – LI, J.^{1,2} – ZOU, X.^{1,2} – BODLAH, I.³ – HUANG, X.^{1,2*}

¹*State Key Laboratory of Ecological Pest Control for Fujian and Taiwan Crops, College of Plant Protection, Fujian Agriculture and Forestry University, Fuzhou 350002, China*

²*Fujian Provincial Key Laboratory of Insect Ecology, Fujian Agriculture and Forestry University, Fuzhou 350002, China*

³*Laboratory of Biosystematics, Department of Entomology, Pir Mehr Ali Shah Arid Agriculture University, Rawalpindi, Pakistan*

**Corresponding author*

e-mail: huangxl@fafu.edu.cn; phone: +86-591-8370-5205

(Received 10th Dec 2018; accepted 21st Mar 2019)

Abstract. Mutualism is a fundamental relationship that can shape species communities through co-evolutionary adaptations and also has great ability to change ecosystem functions. Aphids and ants are common insect groups which are distributed widely across the world. The mutualistic relationships between them have gained much attention in history. However, very few studies have been carried out on the diversity of associated aphid and ant species pairs. In this study, we tried to gather available published data about the diversity of species pairs of aphids and ants to find out potential ecological and geographical patterns. The results showed that 284 species of aphids belonging to 83 genera and 9 subfamilies were mutualistically associated with 193 species of ants belonging to 38 genera and 4 subfamilies. In this report we elucidated a total of 972 aphid-ant interactions and 915 ant-aphid interactions (one aphid species may associate with many ant species and vice versa). Among these relationships, a highest number of ant species were associated with the aphid genus *Aphis*, while a highest number of aphids were associated with the ant genus *Formica*. Besides, an obvious geographical pattern was indicated that the subtropical region may have a higher diversity of aphid-ant associations. This global analysis of current knowledge about diversity and patterns of aphid-ant mutualistic relationships also indicates that more taxonomic and ecological studies are needed to enrich our understanding of these associations.

Keywords: *multispecies interaction, symbiosis, myrmecophiles, Hymenoptera, Formicidae*

Introduction

Reciprocally beneficial associations (e.g. mutualism) support and promote biodiversity (Herre et al., 1999; Bascompte and Jordano, 2007; Ito and Gobin, 2009). These interactions are common and conspicuous in terrestrial communities from tropical to temperate regions (Buckley, 1987; Hölldobler and Wilson, 1990; Delabie, 2001; Styrsky and Eubanks, 2007). These associations trigger the dynamics of ecological communities by influencing the environmental variables, species evolution and survival rate (Bronstein, 2009; Hosseini et al., 2017). One classic example of mutualistic relationship are the interactions between aphids and ants (Darwin, 1859; Stadler and Dixon, 2005).

The aphids (Hemiptera: Aphididae) are a group with 24 subfamilies and more than 5000 species all over the world (Favret, 2018). The diversity of aphid species is far higher in the northern hemisphere temperate regions than anywhere else (Dixon et al., 1987; Heie, 1994; Huang et al., 2012). Some aphid species are destructive pests and voracious feeder of various crops, and also vectors of various plants diseases (Mittler, 1958;

Blackman and Eastop, 1984; Buruchara et al., 2010). The ants (Hymenoptera: Formicidae) are one of the most common insect group on the Earth, which is divided into 21 subfamilies with 497 genera and more than 26700 species (Ward, 2013). Ants usually are very diverse and economically important social insects mostly dominant in the tropical regions (Hölldobler and Wilson, 1990; Philpott and Armbrecht, 2006). Ants fulfill their dietary requirements by performing various roles like decomposers, pollinators, scavengers, predators, and herbivores (Blackman and Eastop, 1984). Ants also feed on honeydew secretions of hemipterans such as aphids, and have a symbiotic association among them (Jahn and Beardsley, 1996; Styrsky and Eubanks, 2007).

Mutualism is a fundamental element in aphid-ant communities and behavior through co-evolutionary adaptation (Herre et al., 1999; Carabalí-Banguero et al., 2013). These relationships can abundantly be found within various aphid-ant groups (Styrsky and Eubanks, 2007) and can shape the species richness, abundance, and distribution. There are two main groups of aphids; myrmecophilous (tended by ants) and non-myrmecophilous (untended by ants) (Novgorodova, 2002, 2005). Myrmecophilous aphids and ants share their habitats and build a strong bond by providing food and security. Ants collect honeydew produced by aphids, and in return they protect them from their predators, parasitoids, and adverse climatic conditions (Hölldobler and Wilson, 1990; Stadler and Dixon, 2005; Novgorodova and Ryabinin, 2017). Moreover, ants provide aphids protection from the sooty mold infestation by sanitation, which propagates in the presences of honeydew accumulation (Way, 1963; Hölldobler and Wilson, 1990; Stadler and Dixon, 2005; Novgorodova and Ryabinin, 2017). For example, the population of associated aphids increased due to these relationships, and they can damage host plants and reduce yield. Honeydew-producing hemipterans tended by ants have a wide range of host plants, including trees, shrubs, vines (Floate and Whitham, 1994; Rico-Gray and Castro, 1996; Styrsky and Eubanks, 2007), fobs and grasses (Moya-Ragoza and Nault, 2000). Besides, the degree of such protection was observed to differ among aphids attending by ants (Addicott, 1978; Katayama and Suzuki, 2003; Novgorodova and Gavrilyuk, 2012) and also depend on the aggressiveness of ants and honeydew collection approaches, in particular degree of specialty among foragers (Novgorodova and Gavrilyuk, 2012; Novgorodova, 2015). Due to the close aphid-ant interactions, complex networks of mutualistic interactions are formed between these insect groups of multispecies communities. The reason for their successful interaction is that they exist in a wide range of natural habitats (Buckley, 1987; Way and Khoo, 1992). However, ethological and ecological mechanisms of mutualism are still poorly understood.

The majority of previous studies have mainly focused on one or few pairs of aphid-ant species, while the general information of trophobiotic interactions among aphids and ants in most of regions are still limited. Besides, many review papers demonstrated the mutualistic ecology, cost and constraints, positive or negative mutualistic interactions of aphids and ants (Boucher et al., 1982; Buckley, 1987; Bronstein, 1994; Stadler and Dixon, 1998; Hoeksema and Bruna, 2000; Bronstein and Barbosa, 2002; Stadler and Dixon, 2005). However, there is a lack of the knowledge of diversity of aphid-ant species pairs which can provide complete information about their relationships in different ecological zones and can elaborate the patterns of these associations. A reason for this gap may be due to the lack of integration and meta-analysis of dispersed information on aphid-ant interactions in previous literature.

This study will generate an interest in quantifying the importance of aphid-ant interactions for global diversity patterns, distribution of species pairs and will also help

the examination of the interactions of aphid-ant species across different ecological zones. Furthermore, data on species pairs along with geographical information can be used to study aphid-ant interactions at regional and global scale. Therefore, there is a need to investigate the current state of knowledge about the diversity of aphid-ant species associations. Based on data from published literature, this paper aimed to depict the current state of the taxonomic diversity of aphid-ant species pairs as well as the spatial patterns of their interactions (Tylianakis et al., 2008; Gilman et al., 2010).

Materials and methods

Data collection of aphid-ant species pairs

We collected species and distribution data from the available previously published researches (1906 to 2016) on species pairs of mutualistic aphids and ants (*Table A1* in the *Appendix*). Literature searching was done by using tools including Web of Science, Google Scholar and Goolge. The data such as names of subfamilies, tribes, genera, and species as well as locations of aphids and associated ants were extracted from published researches. Many articles contained only species names and location, so for getting more details about their higher taxa the databases of Aphid Species File (<http://aphid.speciesfile.org>) and AntWeb (<https://www.antweb.org>) were used. These databases provide the complete taxonomic hierarchy of aphids and ants. The validation of species names was also rechecked based on these taxonomic databases. The Aphid Species File contained comprehensive information about aphids from all over the world and provided the taxonomic keys, taxa hierarchy, bibliographic data of aphids from all parts of the world. The AntWeb provides taxonomic keys, taxa hierarchy, specimen records, and natural history information and distribution maps on ants. Up till now, all types of biodiversity data of almost all species has been updated on these databases. The data in these two databases are freely accessible. Other information was fetched from the available published researches in different journals. Distribution localities for available species pairs along with geographical coordinates were compiled and arranged into a database (Microsoft Excel). Species localities were identified from the descriptions of previous literature. The accurate locality data points were collected according to the literature description, google earth and by using the website (www.findlatitudeandlongitude.com).

Geographical patterns of species associations

Latitudes and longitudes of species pairs were plotted on the outline of the World map with the help of Arc Map 10.2 (Geographical Information System, GIS) software. The ecological zones were selected by using the coordinates of temperate (35-66.5°), subtropical (23.5-35°) and tropical (0-23.5°) zones. The coordinates of temperate, subtropical and tropical regions were separated from primary data set. Separated data was plotted according to the coordinates of temperate, tropical and subtropical regions to find out the diversity of aphid-ant interactions in different regions.

Data analysis

Data analysis was conducted by using correlation test. For percentage of ant-associated aphids, non-parametric Spearman's test (two-tail) was used while for percentage of aphid-associated ants parametric Pearson test (two-tail) was used. To calculate the percentages

of genera and their species, the genera and species of each subfamily was divided by the total genera and species in all subfamilies. The fundamental statistical analysis has been applied to find out the diversity of species pairs in different regions of the world. The bar graphs were developed in Microsoft Excel by using extracted data.

Results

Taxonomic diversity

Aphid-associated ants

The percentage of all species numbers failed the normality test, so the non-parametric Spearman's test was used (two-tailed $P < 0.01$) for aphid associated ants. The results showed a positive correlation between the number of aphid species in relation with ant species ($t = 0.983$, $df = 8$, $P < 0.001$). Their patterns can be seen in (Table 1). Subfamily Aphidinae with about 59.85% of total aphid species was found associated with four subfamilies of ants (Table 1). Out of total 83 genera, the genus *Aphis* of subfamily Aphidinae was chiefly associated with 70.5% of ant species (Table 1).

Out of nine genera of subfamily Calaphidinae, genus *Symydobius* were associated with maximum number of ant species from four genera. Among the four genera of subfamily Chaitophorinae, about 81.25% species of the genus *Chaitophorus* were associated with 16 genera of ants. Out of 10 genera of the subfamily Eriosomatinae, the genus *Pemphigus* (only one species) was found supremely associated with 11 genera of ants. Among the eight genera of subfamily Lachninae, about 74.57% species of ants were interacting with the genus *Cinara*. In subfamily Drepanosiphinae the genus *Drepanaphis* having more interactions with ants. Genus *Thelaxes* received more ants than other genera under the subfamily Thelaxinae. For subfamilies Anoeciinae and Saltusaphidinae, only one genus from each was associated with ants (Table 1). Except subfamilies Thelaxinae and Saltusaphidinae, all genera from the other 7 subfamilies were mainly associated with species of ant genus *Formica*.

Table 1. The diversity of ant-associated aphids, with the numbers and percentages of aphid genera and species in each subfamily. The information of associated ants for each aphid group are also provided

Subfamily name	Aphid				Aphid-associated ant		
	Genus	Genus %	Species	Species %	Subfamily	Genus	Species
Anoeciinae	1	1.204	1	0.352	1	1	2
Aphidinae	46	55.421	170	59.859	4	37	161
Calaphidinae	9	10.843	12	4.225	2	6	15
Chaitophorinae	4	4.819	29	10.211	3	16	53
Drepanosiphinae	2	2.409	3	1.0563	2	3	6
Eriosomatinae	10	12.048	11	3.873	3	11	23
Lachninae	8	9.638	53	18.661	3	14	59
Thelaxinae	2	2.409	4	1.408	3	7	13
Saltusaphidinae	1	1.204	1	0.352	2	2	2
Total	83		284				

Ant-associated aphids

The data was found normal through the normality test, so the parametric Pearman's test was applied (two-tailed $P < 0.01$) for ant-associated aphids. The results showed a positive correlation between the numbers of aphid species and that of ant species ($t = 0.983$, $df = 3$, $P = 0.009$). The data presented graphically in *Table 2*. Out of four ant subfamilies, the Formicinae had maximum associations (66.84% of all) with all nine aphid subfamilies. The genus *Formica* was found highly associated with a maximum number of aphid species. Subfamily Myrmicinae contributes 29.53% of all associations with aphids, and out of the 16 genera associated with aphids, genus *Myrmica* tended maximum aphid species. Genus *Tapinoma* of subfamily Dolichoderinae found higher associations with aphids out of 6 other genera. Only genus *Tetraponera* of subfamily Pseudomyrmecinae interacted with only one species of ant (*Table 2*). Genus *Aphis* was found highly associated with almost all genera of all ant subfamilies.

Geographical diversity

Geographical diversity of species pairs varies in different geographical zones. *Figure 1* showed that the maximum aphid-ant species pairs were in the subtropical region. The ratios of species numbers of aphid to ant in these geographical zones were measured as 1.9:1 in the temperate, 1:2.8 in tropical while nearly equal associations with the ratio 1.1:1 in the subtropical region. In the temperate zone, eight subfamilies of aphids and three subfamilies of ants were associated. Only two aphid subfamilies and three ant subfamilies were associated in the tropical area. Higher associations were found in the subtropical region with eight aphid subfamilies and four ant subfamilies (*Table 3*). All collected information was extracted from 21 countries and the aphid-ant species pairs in each country were measured. In the current database, the USA contained a maximum number of species pairs in both temperate and subtropical zones. The second highest number of species pairs was recorded in Turkey (*Fig. 2*). However, equally associated species pairs were documented from subtropical areas of the world. Overall the patterns of aphid-ant interactions in different ecological zones can be seen in the *Figure 3*.

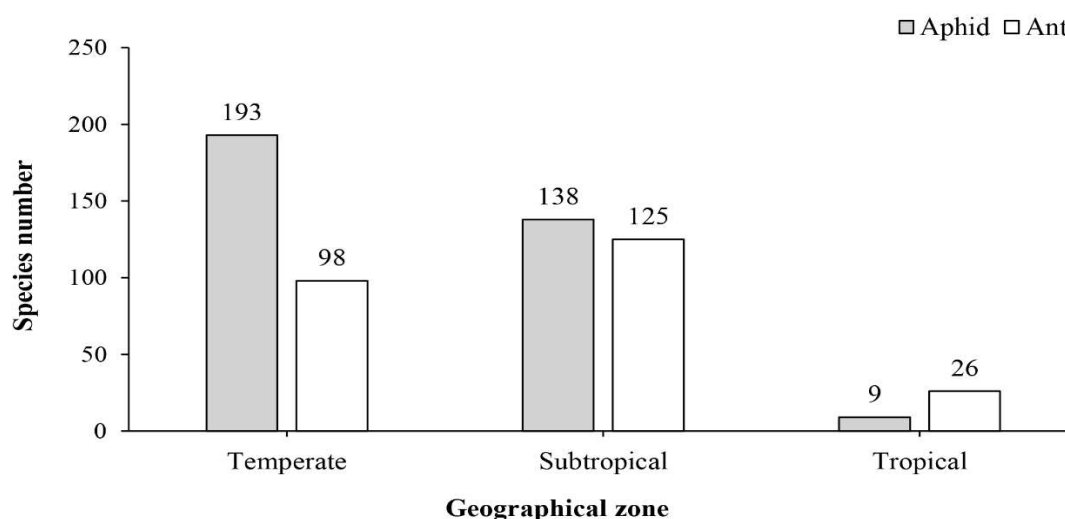


Figure 1. Aphid-ant species pairs in different geographical zones, with the values above bars indicating species numbers of each partner

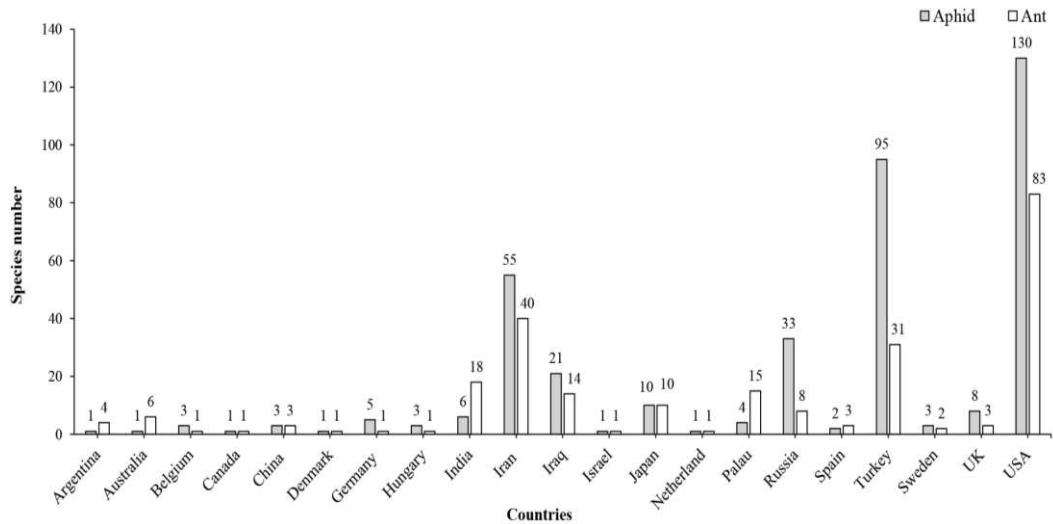


Figure 2. Aphid-ant species pairs in different countries, with the numbers above bars indicating species numbers

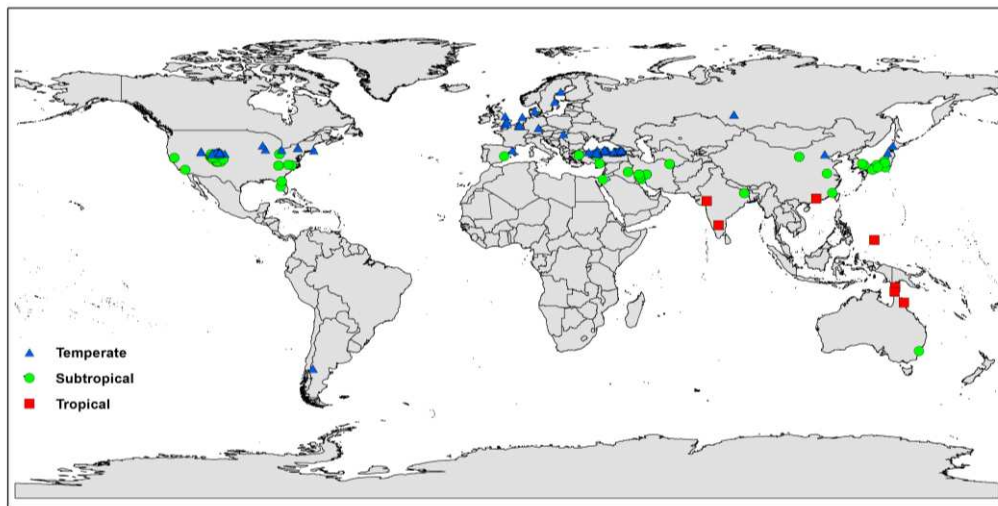


Figure 3. Distribution map of reported aphid-ant associations. The red square, green circle, and blue triangle indicate associations in the tropical, subtropical and temperate regions, respectively

Table 2. The diversity of aphid-associated ants, with the numbers and percentages of ant genera and species in each subfamily. The information of associated aphids for each ant group are also provided

Subfamily name	Ant				Ant-associated aphid		
	Genus	Genus %	Species	Species %	Subfamily	Genus	Species
Dolichoderinae	6	15.789	15	7.772	5	23	50
Formicinae	15	39.473	122	63.212	9	76	261
Myrmicinae	16	42.105	55	28.497	8	30	84
Pseudomyrmecinae	1	2.631	1	0.518	1	1	1
Total	38		193				

Table 3. Associated aphid and ant subfamilies in different geographical zones

Tropical		Subtropical		Temperate	
Aphid subfamily	Ant subfamily	Aphid subfamily	Ant subfamily	Aphid subfamily	Ant subfamily
Aphidinae	Dolichoderinae	Aphidinae	Dolichoderinae	Anoeciinae	Dolichoderinae
Eriosomatinae	Formicinae	Calaphidinae	Formicinae	Aphidinae	Formicinae
	Myrmicinae	Chaitophorinae	Myrmicinae	Calaphidinae	Myrmicinae
		Drepanosiphinae	Pseudomyrmecinae	Chaitophorinae	
		Eriosomatinae		Drepanosiphinae	
		Lachninae		Eriosomatinae	
		Saltusaphidinae		Lachninae	
		Theanaxinae		Theanaxinae	

Discussion

Our data showed that among the 24 subfamilies of Aphididae (Favret, 2018), only nine are myrmecophilous (Table 1). The aphid subfamily Aphidinae has maximum number of associations with ant species, which corresponds well to the total species diversity of this aphid subfamily. Their maximum associations might be due to some ecological traits and population dynamics (Stadler and Dixon, 2005). A large variety of biological components have been projected to account for population-level variance in aphid-ant interactions including local species abundance and composition of aphids (Horvitz and Schemske, 1984). There are total 23 subfamilies of ants, but only six of them are associated with hemipteran insects (Styrsky and Eubanks, 2007). According to previous statistics, only the subfamilies Dolichoderinae, Formicinae and Myrmicinae harvest honeydew from aphids (Nixon, 1951; Stadler and Dixon, 2005). According to this study, four ant subfamilies, Dolichoderinae, Formicinae, Myrmicinae, and Pseudomyrmecinae (Table 2), are involved in aphid-ant interactions. Styrsky and Eubank (2007) indicated that 89% of ants from Formicinae and Myrmicinae involved in ant-hemipteran relationships. In the data we compiled, it is observed that about 92% species of ants from Formicinae and Myrmicinae are associated with aphids. According to the Novgorodova and Gavrilyuk (2012) these subfamilies also have maximum trophobiotic interactions with aphids that have a significant effect on aphido-fauna. However, according to the results of this study few species of subfamilies Dolichoderinae and Pseudomyrmecinae were associated in trophobiotic relationships with aphid. The diversity of the mutualistic interaction of subfamily Formicinae might be due to their abundance and ecological dominance. Some subfamilies were less associated with aphids that might be due to less attention paid on these genera of ants.

Diversity and richness of aphid species was higher than ants in the temperate zone (Dixon et al., 1987; Clua et al., 2004), an aphid-ant species ratio of 1.2:1 indicated their abundance in this region (Figure 1). In the temperate region, one aphid species tended by many ant species such as the Novgorodova and Ryabinin (2017) documented that the aphid species *Symydobius oblongus*, *Chaitophorus populeti*, *Glyphina betulae*, *Aphis fabae*, *A. farinosa*, *A. urticata*, *Rhopalosiphum padi* were associated with 7 to 18 species of ants from temperate areas of Russia. In contrast, ants are exclusively abundant in the tropical zone (Hölldobler and Wilson, 1990; Sarnat et al., 2015). According to current study the aphid-ant species ratios in tropical areas were 1:2.8,

which indicated that the ants are more than half of the aphid species in these regions. For example, a tropical aphid *Cerataphis fransseni* attended by various species of ants (Stadler and Dixon, 2005) indicated the dominance of ants in the tropical region. On the other hand, the aphid-ant species ratio was 1.1:1 in subtropical region, which shows that the diversity of species pairs relatively higher in subtropical than the temperate and tropical regions (*Figure 1*). Most likely the aphids and ants might interact more in subtropical regions which have more favorable conditions for both groups.

The subtropical region consists of a typical warm humid climate with diverse vegetations (e.g. semi-evergreen or semi-deciduous forests, savannah, hardwood forests, pastures, warm temperate moist forests, semi-desert and nemoral deciduous forests) (Prentice et al., 1992; Webb, 2015), which supports the insect and plant biodiversity. Considering aphids are abundant in the temperate zone while ants are most diverse in the tropical, it is suggested that there should be more diverse aphid-ant associations because both groups can interact more in the subtropical zone located between temperate and tropical zones. Geographical species distribution patterns found linear on the borders of temperate and subtropics (*Figure 3*). There might be two possibilities, 1) the diversity of species pairs higher than other regions, and 2) the studies recorded aphid-ant interactions vastly carried out in these regions. However, the current data may also indicate the research on diversity of aphid-ant interactions is still inadequate, which causes an imbalance of information. Therefore, we suggest more future studies should be undertaken to record more associated species of aphids and ants and then we can understand more about their mutualistic relationships.

Conclusion

Based on a meta-analysis of currently available records of aphid-ant interactions, this study reports that 284 species belonging to the 83 genera of eight aphid subfamilies have mutualistic association with 193 species belonging to 38 genera of four subfamilies of ants. These species support a total of 972 aphid-ant interactions and 915 ant-aphid interactions (one aphid species may associate with many ant species and vice versa). The aphid genus *Aphis* has a highest number of associations with ant species while highest number of aphids are associated with the ant genus *Formica*. Geographically, maximum aphid-ant species pairs were found in subtropical areas of the world. Our results provide a base for identifying general patterns of aphid-ant species pairs in different ecological zones. Besides, more taxonomic and ecological studies are needed to enrich our understanding of the aphid-ant associations.

Acknowledgements. We would like to thank help from Dr. Jun Deng, Taimoor Hassan Farooq, Waqar Ahmed during this work. This work was supported by National Key R&D Program of China (2016YFE0203100) and Open Fund of Fujian Provincial Key Laboratory of Insect Ecology, Fujian Agriculture and Forestry University.

Author contribution. J.A.S., X. H. conceived and designed the study. J.A.S. performed all the formal analysis. J.L. performed the distribution mapping. J.A.S. and X.Z. collected and compiled the data. X.H. and I.B. reviewed and edited the manuscript.

Conflict of interests. Authors declared that there is no conflict of interests.

REFERENCES

- [1] Addicott, J. F. (1978): Competition for mutualists: aphids and ants. – *Canadian Journal of Zoology* 56(10): 2093–2096.
- [2] Bascompte, J., Jordano, P. (2007): Plant-animal mutualistic networks: the architecture of biodiversity. – *Annu. Rev. Ecol. Evol. Syst.* 38: 567–593.
- [3] Blackman, R. L., Eastop, V. F. (1984): *Aphids on the World's Crops*. – Wiley, Chichester, UK.
- [4] Boucher, D. H., James, S., Keeler, K. H. (1982): The ecology of mutualism. – *Annual Review of Ecology and Systematics* 13(1): 315–347.
- [5] Bronstein, J. L. (1994): Conditional outcomes in mutualistic interactions. – *Trends in Ecology & Evolution* 9(6): 214–217.
- [6] Bronstein, J. L. (2009): The evolution of facilitation and mutualism. – *Journal of Ecology* 97(6): 1160–1170.
- [7] Bronstein, J. L., Barbosa, P. (2002): *Multitrophic/Multispecies Mutualistic, Multitrophic Level Interactions*. – Cambridge University Press, New York.
- [8] Buckley, R. (1987): Ant-plant-homopteran interactions. – *Advances in Ecological Research* 16: 53–85.
- [9] Buruchara, R., Mukaruziga, C., Ampofo, K. O. (2010): *Bean Disease and Pest Identification and Management*. – Centro Internacional de Agricultura Tropical (CIAT), PABRA, Kampala, Uganda, pp. 1–79.
- [10] Carabalí-Banguero, D. J., Wyckhuys, K. A. G., Montoya-Lerma, J., Kondo, T., Lundgren, J. G. (2013): Do additional sugar sources affect the degree of attendance of *D ysmicoccus brevipis* by the fire ant *S olenopsis geminata*? – *Entomologia Experimentalis et Applicata* 148(1): 65–73.
- [11] Clua, A., Castro, A. M., Ramos, S., Gimenez, D. O., Vasicek, A., Chidichimo, H. O., Dixon, A. F. G. (2004): The biological characteristics and distribution of the greenbug, *Schizaphis graminum*, and Russian wheat aphid, *Diuraphis noxia* (Hemiptera: Aphididae), in Argentina and Chile. – *European Journal of Entomology* 101(1): 193–198.
- [12] Darwin, C. (1859): *On the Origin of Species by Means of Natural Selection*. – D. Appleton and Company, New York, pp. 83–85.
- [13] Delabie, J. H. C. (2001): Trophobiosis between Formicidae and Hemiptera (Sternorrhyncha and Auchenorrhyncha): an overview. – *Neotropical Entomology* 30(4): 501–516.
- [14] Dixon, A. F. G., Kindlmann, P., Leps, J., Holman, J. (1987): Why there are so few species of aphids, especially in the tropics. – *The American Naturalist* 129(4): 580–592.
- [15] Favret, C. (2018): *Aphid Species File Ver. 5.0*. – <<http://Aphid.SpeciesFile.org>> (accessed September 15, 2018).
- [16] Floate, K. D., Whitham, T. G. (1994): Aphid-ant interaction reduces chrysomelid herbivory in a cottonwood hybrid zone. – *Oecologia* 97(2): 215–221.
- [17] Gilman, S. E., Urban, M. C., Tewksbury, J., Gilchrist, G. W., Holt, R. D. (2010): A framework for community interactions under climate change. – *Trends in Ecology & Evolution* 25(6): 325–331.
- [18] Heie, O. E. (1994): Why are there so few aphid species in the temperate areas of the southern hemisphere? – *European Journal of Entomology* 91(1): 127–133.
- [19] Herre, E. A., Knowlton, N., Mueller, U. G., Rehner, S. A. (1999): The evolution of mutualisms: exploring the paths between conflict and cooperation. – *Trends in Ecology & Evolution* 14(2): 49–53.
- [20] Hoeksema, J. D., Bruna, E. M. (2000): Pursuing the big questions about interspecific mutualism: a review of theoretical approaches. – *Oecologia* 125(3): 321–330.
- [21] Hölldobler, B., Wilson, E. O. (1990): *The Ants*. – Belknap Press of Harvard University Press, Cambridge, MA.

- [22] Horvitz, C. C., Schemske, D. W. (1984), Effects of ants and an ant-tended herbivore on seed production of a neotropical herb. – *Ecology* 65(5): 1369–1378.
- [23] Hosseini, A., Hosseini, M., Katayama, N., Mehrparvar, M. (2017): Effect of ant attendance on aphid population growth and above ground biomass of the aphid's host plant. – *European Journal of Entomology* 114: 106–112.
- [24] Huang, X.-L., Xiang-Yu, J.-G., Ren, S.-S., Zhang, R.-L., Zhang, Y.-P., Qiao, G.-X. (2012): Molecular phylogeny and divergence times of Hormaphidinae (Hemiptera: Aphididae) indicate Late Cretaceous tribal diversification. – *Zoological Journal of the Linnean Society* 165(1): 73–87.
- [25] Ito, F., Gobin, B. (2009): Colony composition and behaviour of a queen and workers in the oriental ectatommine ant *Gnamptogenys cribrata* (Emery) 1900 in West Java, Indonesia. – *Asian Myrmecology* 2(1): 103–107.
- [26] Jahn, G. C., Beardsley, J. W. (1996): Effects of *Pheidole megacephala* (Hymenoptera: Formicidae) on survival and dispersal of *Dysmicoccus neobrevipes* (Homoptera: Pseudococcidae). – *Journal of Economic Entomology* 89(5): 1124–1129.
- [27] Katayama, N., Suzuki, N. (2003): Changes in the use of extrafloral nectaries of *Vicia faba* (Leguminosae) and honeydew of aphids by ants with increasing aphid density. – *Annals of the Entomological Society of America*, *BioOne* 96(4): 579–584.
- [28] Mittler, T. E. (1958): The excretion of honey-dew by *Tuberolachnus salignus* (Gmelin) (Homoptera: Aphididae). – *Proceedings of the Royal Entomological Society of London. Series A, General Entomology* 33: 49–55.
- [29] Moya-Ragoza, G., Nault, L. R. (2000): Obligatory mutualism between *Dalbulus quinquevittatus* (Homoptera: Cicadellidae) and attendant ants. – *Annals of the Entomological Society of America* 93(4): 929–940.
- [30] Nixon, G. E. J. (1951): *The Association of Ants with Aphids and Coccids*. – *Commonw. Inst. Ent.*, London.
- [31] Novgorodova, T. A. (2002): Study of adaptations of aphids (Homoptera, Aphidinea) to ants: comparative analysis of myrmecophilous and nonmyrmecophilous species. – *Entomological Review* 82(5): 569–576.
- [32] Novgorodova, T. A. (2005): Ant-aphid interactions in multispecies ant communities: Some ecological and ethological aspects. – *European Journal of Entomology* 102(3): 495–501.
- [33] Novgorodova, T. A. (2015): Organization of honeydew collection by foragers of different species of ants (Hymenoptera: Formicidae): effect of colony size and species specificity. – *European Journal of Entomology* 112(4): 688.
- [34] Novgorodova, T. A., Gavriljuk, A. V. (2012): The degree of protection different ants (Hymenoptera: Formicidae) provide aphids (Hemiptera: Aphididae) against aphidophages. – *European Journal of Entomology* 109(2): 187–196.
- [35] Novgorodova, T. A., Ryabinin, A. S. (2017): Ant-aphid relations in the south of western Siberia (Hymenoptera: Formicidae; Hemiptera: Aphididae). – *Arthropod-Plant Interactions*. DOI: 10.1007/s11829-017-9584-7.
- [36] Philpott, S. M., Armbrrecht, I. (2006): Biodiversity in tropical agroforests and the ecological role of ants and ant diversity in predatory function. – *Ecological Entomology* 31(4): 369–377.
- [37] Prentice, I. C., Cramer, W., Harrison, S. P., Leemans, R., Monserud, R. A., Solomon, A. M. (1992): Special paper: a global biome model based on plant physiology and dominance, soil properties and climate. – *Journal of Biogeography* 19(2): 117.
- [38] Rico-Gray, V., Castro, G. (1996): Effect of an ant-aphid interaction on the reproductive fitness of *Paullinia fuscescens* (Sapindaceae). – *The Southwestern Naturalist* 41: 434–440.
- [39] Sarnat, E. M., Fischer, G., Guénard, B., Economo, E. P. (2015): Introduced pheidole of the world: taxonomy, biology and distribution. – *ZooKeys* 2015(543): 1–109.
- [40] Stadler, B., Dixon, A. F. G. (1998): Costs of ant attendance for aphids. – *Journal of Animal Ecology* 67(3): 454–459.

- [41] Stadler, B., Dixon, A. F. G. (2005): Ecology and evolution of aphid-ant interactions. – Annual Review of Ecology, Evolution, and Systematics 36(1): 345–372.
- [42] Styrsky, J. D., Eubanks, M. D. (2007): Ecological consequences of interactions between ants and honeydew-producing insects. Proceedings. – Biological Sciences/The Royal Society 274(1607): 151–64.
- [43] Tylianakis, J. M., Didham, R. K., Bascompte, J., Wardle, D. A. (2008): Global change and species interactions in terrestrial ecosystems. – Ecology Letters 11(12): 1351–1363.
- [44] Ward, P. S. (ed.) (2013): AntWeb: Ants of California. – <http://www.AntWeb.org/california.jsp> (accessed 15 October 2018).
- [45] Way, M. J. (1963): Mutualism between ants and honeydew-producing Homoptera. – Annual Review of Entomology 8(1): 307–344.
- [46] Way, M. J., Khoo, K. C. (1992): Role of ants in pest management. – Annual Review of Entomology 37(1): 479–503.
- [47] Webb, L. J. (2015): Environmental relationships of the structural types of Australian rain forest vegetation. – Ecology 49(2): 296–311.

APPENDIX

Table A1. Species pairs of mutualistic aphids and ants

Aphid	Associated ant	Reference
Subfamily Aphidinae		
Tribe Aphidini		
<i>Aphis acetosae</i>	<i>Formica cunicularia</i>	Mortazavi et al. (2015)
<i>Aphis aiddletonii</i>	<i>Formica argentea</i>	Jones (1927)
<i>Aphis asclepiadis</i>	<i>Camponotus vicinus</i>	Jones (1927)
	<i>Formica argentea</i>	Jones (1927)
	<i>Formica aserva</i>	Addicott (1979a)
	<i>Formica canadensis</i>	Jones (1927)
	<i>Formica cinerea</i>	Jones (1927), Addicott (1979a)
	<i>Formica fusca</i>	Jones (1927), Addicott (1979a)
	<i>Formica integroides</i>	Addicott (1979a)
	<i>Formica lasioides</i>	Addicott (1979a)
	<i>Formica lepida</i>	Jones (1927)
	<i>Formica montana</i>	Jones (1927)
	<i>Formica neorufibarbis</i>	Addicott (1979a)
	<i>Formica obscuripes</i>	Addicott (1979a)
	<i>Formica opaciventris</i>	Jones (1927)
	<i>Formica podzolica</i>	Mooney and Agrawal (2008), Nielsen et al. (2009), Nielsen et al. (2009), Abdala-Roberts et al. (2012)
	<i>Myrmica incompleta</i>	Jones (1927)
	<i>Myrmica scabrinodis</i>	Jones (1927)
<i>Myrmica whymperi</i>	Jones (1927)	
<i>Pheidole bicarinata</i>	Jones (1927)	
<i>Tapinoma sessile</i>	Jones (1927), Addicott (1979a)	
<i>Aphis aurantii</i>	<i>Formica cinereofusca</i>	Akyildirim et al. (2014)

	<i>Lasius alienus</i>	Akyildirim et al. (2014)
	<i>Lasius turcicus</i>	Akyildirim et al. (2014)
	<i>Plagiolepis taurica</i>	Akyildirim et al. (2014)
<i>Aphis brassicae</i>	<i>Pheidole sp.</i>	Kataria and Kumar (2013)
	<i>Camponotus saxatilis</i>	Novgorodova (2005)
<i>Aphis brohmeri</i>	<i>Formica aquilonia</i>	Novgorodova (2005)
	<i>Formica polyctena</i>	Novgorodova (2005)
	<i>Camponotus aethiops</i>	Özdemir et al. (2008)
<i>Aphis brotericola</i>	<i>Camponotus piceus</i>	Özdemir et al. (2008)
	<i>Formica cunicularia</i>	Akyürek et al. (2016)
<i>Aphis brunellae</i>	<i>Lasius turcicus</i>	Akyürek et al. (2016)
<i>Aphis chloris</i>	<i>Camponotus piceus</i>	Özdemir et al. (2008)
<i>Aphis cinara</i>	<i>Formica lugubris</i>	Sudd (1983)
	<i>Camponotus vitreus</i>	Carver et al. (2003)
	<i>Iridomyrmex hartmeyeri</i>	Carver et al. (2003)
<i>Aphis clerodendri</i>	<i>Notoncus capitatus</i>	Carver et al. (2003)
	<i>Paratrechina vaga</i>	Carver et al. (2003)
	<i>Technomyrmex albipes</i>	Carver et al. (2003)
	<i>Crematogaster lineolata</i>	Favret et al. (2010)
	<i>Formica subsericea</i>	Favret et al. (2010)
<i>Aphis coreopsidis</i>	<i>Linepithema humile</i>	Altfeld and Stiling (2009)
	<i>Paratrechina longicornis</i>	Favret et al. (2010)
	<i>Paratrechina parvula</i>	Favret et al. (2010)
<i>Aphis cornifoliae</i>	<i>Prenolepis imparis</i>	Favret et al. (2010)
<i>Aphis cracca</i>	<i>Lasius niger</i>	Novgorodova (2005)
	<i>Camponotus compressus</i>	Kataria and Kumar (2013), Rakhshan and Ahmad (2015)
	<i>Camponotus invidus</i>	Rakhshan and Ahmad (2015)
	<i>Camponotus kurdistanicus</i>	Sary (1969)
	<i>Camponotus libanicus</i>	Shiran et al. (2013)
	<i>Camponotus oasisium</i>	Shiran et al. (2013)
	<i>Camponotus piceus</i>	Özdemir et al. (2008)
	<i>Cataglyphis aenescens</i>	Özdemir et al. (2008)
	<i>Crematogaster antaris</i>	Shiran et al. (2013)
	<i>Crematogaster inermis</i>	Mortazavi et al. (2015)
<i>Aphis craccivora</i>	<i>Crematogaster schmidti</i>	Mortazavi et al. (2015)
	<i>Crematogaster subdentata</i>	Mortazavi et al. (2015)
	<i>Formica aquilonia</i>	Novgorodova (2005)
	<i>Formica cinereofusca</i>	Akyildirim et al. (2014)
	<i>Formica cunicularia</i>	Özdemir et al. (2008), Mortazavi et al. (2015)
	<i>Formica fusca</i>	Akyürek et al. (2016)
	<i>Formica glauca</i>	Özdemir et al. (2008)
	<i>Formica polyctena</i>	Novgorodova (2005)
	<i>Formica pratensis</i>	Novgorodova (2005)
	<i>Lasius brunneus</i>	Akyürek et al. (2016)

	<i>Lasius japonicus</i>	Suzuki (2004), Katayama et al. (2013)
	<i>Lasius niger</i>	Novgorodova (2005), Kataria and Kumar (2013)
	<i>Lasius paralienus</i>	Özdemir et al. (2008), Shiran et al. (2013)
	<i>Lasius turcicus</i>	Akyildirim et al. (2014), Mortazavi et al. (2015)
	<i>Lepisiota bipartite</i>	Shiran et al. (2013)
	<i>Lepisiota frauenfeldi</i>	Rakhshan and Ahmad (2015)
	<i>Meranoplus bicolor</i>	Rakhshan and Ahmad (2015)
	<i>Monomorium destructor</i>	Shiran et al. (2013)
	<i>Monomorium latinode</i>	Rakhshan and Ahmad (2015)
	<i>Monomorium mayri</i>	Shiran et al. (2013)
	<i>Monomorium minimum</i>	Kataria and Kumar (2013)
	<i>Monomorium nitidiventre</i>	Mortazavi et al. (2015)
	<i>Monomorium pharaonis</i>	Rakhshan and Ahmad (2015)
	<i>Nylanderia fulva</i>	Sharma and Buss (2013)
	<i>Paratrechina longicornis</i>	Shiran et al. (2013), Rakhshan and Ahmad (2015)
	<i>Pheidole teneriffana</i>	Shiran et al. (2013)
	<i>Plagiolepis pallelescens</i>	Özdemir et al. (2008), Shiran et al. (2013)
	<i>Plagiolepis pygmaea</i>	Mortazavi et al. (2015)
	<i>Polyrhachis hauxwelli</i>	Rakhshan and Ahmad (2015)
	<i>Polyrhachis lacteipennis</i>	Shiran et al. (2013)
	<i>Pristomyrmex punctatus</i>	Katayama et al. (2013)
	<i>Tapinoma erraticum</i>	Mortazavi et al. (2015)
	<i>Tapinoma simrothi</i>	Sztybel (1969), Shiran et al. (2013)
	<i>Tetramorium chefteki</i>	Özdemir et al. (2008), Mortazavi et al. (2015)
	<i>Tetramorium forte</i>	Özdemir et al. (2008)
	<i>Tetramorium tsushimae</i>	Suzuki (2004), Katayama et al. (2013), Hayashi et al. (2015), Hayashi et al. (2016)
	<i>Tetraoponera rufonigra</i>	Rakhshan and Ahmad (2015)
<i>Aphis davletshinae</i>	<i>Pheidole pallidula</i>	Shiran et al. (2013)
	<i>Tapinoma simrothi</i>	Shiran et al. (2013)
<i>Aphis esulae</i>	<i>Formica fusca</i>	Akyürek et al. (2016)
<i>Aphis euphorbiae</i>	<i>Camponotus piceus</i>	Özdemir et al. (2008)
<i>Aphis evonymi</i>	<i>Formica aquilonia</i>	Novgorodova (2005)
	<i>Formica polyctena</i>	Novgorodova (2005)
<i>Aphis fabae</i>	<i>Camponotus aethiops</i>	Akyürek et al. (2016)
	<i>Camponotus compressus</i>	Kataria and Kumar (2013)
	<i>Camponotus piceus</i>	Özdemir et al. (2008)
	<i>Camponotus saxatilis</i>	Novgorodova (2005)
	<i>Cataglyphis lividus</i>	Shiran et al. (2013)
	<i>Cremastogaster scutellaris</i>	Akyürek et al. (2016)
	<i>Crematogaster lineolata</i>	Favret et al. (2010)
	<i>Formica aquilonia</i>	Novgorodova (2005)
	<i>Formica cinereofusca</i>	Akyildirim et al. (2014)

	<i>Formica cunicularia</i>	Akyürek et al. (2016)
	<i>Formica fusca</i>	Akyildirim et al. (2014)
	<i>Formica polyctena</i>	Novgorodova (2005)
	<i>Lasius alienus</i>	Akyildirim et al. (2014), Akyürek et al. (2016)
	<i>Lasius brunneus</i>	Akyürek et al. (2016)
	<i>Lasius emarginatus</i>	Akyildirim et al. (2014)
	<i>Lasius niger</i>	Liepert and Dettner (1993), Volkl et al. (1999), Offenberg (2001), Woodring et al. (2004), Fischer et al. (2005), Detrain et al. (2010), Sanders et al. (2010), Tegelaar et al. (2012), Tegelaar et al. (2013), Fischer et al. (2015), Tegelaar (2015), Vantaux et al. (2015)
	<i>Lasius paralienus</i>	Özdemir et al. (2008), Shiran et al. (2013)
	<i>Lasius turcicus</i>	Akyildirim et al. (2014), Akyürek et al. (2016)
	<i>Lepisiota bipartite</i>	Shiran et al. (2013)
	<i>Lepisiota nigra</i>	Mortazavi et al. (2015)
	<i>Monomorium libanicum</i>	Shiran et al. (2013)
	<i>Monomorium mayri</i>	Shiran et al. (2013)
	<i>Monomorium minimum</i>	Kataria and Kumar (2013)
	<i>Monomorium qarahe</i>	Shiran et al. (2013)
	<i>Myrmica ruginodis</i>	Akyildirim et al. (2014)
	<i>Plagiolepis pallescens</i>	Shiran et al. (2013)
	<i>Plagiolepis pygmaea</i>	Akyürek et al. (2016)
	<i>Prenolepis imparis</i>	Favret et al. (2010)
	<i>Tapinoma erraticum</i>	Mortazavi et al. (2015)
	<i>Tapinoma simrothi</i>	Sary (1969), Shiran et al. (2013)
	<i>Tetramorium caespitum</i>	Shiran et al. (2013), Akyildirim et al. (2014)
	<i>Tetramorium tsushimae</i>	Hayashi et al. (2015)
	<i>Formica glauca</i>	Özdemir et al. (2008)
<i>Aphis farinosa</i>	<i>Crematogaster antaris</i>	Shiran et al. (2013)
	<i>Formica cinereofusca</i>	Akyildirim et al. (2014)
	<i>Formica fusca</i>	Jones (1927)
	<i>Formica gagates</i>	Akyildirim et al. (2014)
	<i>Formica integroides</i>	Addicott (1978)
	<i>Lasius turcicus</i>	Akyildirim et al. (2014)
	<i>Myrmica whymperi</i>	Jones (1927)
	<i>Tetramorium caespitum</i>	Akyildirim et al. (2014)
<i>Aphis forbesi</i>	<i>Formica cinerea</i>	Jones (1927)
	<i>Myrmecina graminicola</i>	Jones (1927)
	<i>Myrmica scabrinodis</i>	Jones (1927)
<i>Aphis frangulae</i>	<i>Camponotus oasisium</i>	Shiran et al. (2013)
	<i>Cataglyphis nodus</i>	Shiran et al. (2013)
	<i>Crematogaster antaris</i>	Shiran et al. (2013)
	<i>Lasius paralienus</i>	Shiran et al. (2013)
	<i>Lepisiota bipartite</i>	Shiran et al. (2013)
	<i>Monomorium destructor</i>	Shiran et al. (2013)

	<i>Monomorium libanicum</i>	Shiran et al. (2013)
	<i>Monomorium mayri</i>	Shiran et al. (2013)
	<i>Monomorium qarahe</i>	Shiran et al. (2013)
	<i>Pheidole pallidula</i>	Shiran et al. (2013)
	<i>Plagiolepis pallescens</i>	Shiran et al. (2013)
	<i>Polyrhachis lacteipennis</i>	Shiran et al. (2013)
	<i>Tapinoma simrothi</i>	Shiran et al. (2013)
<i>Aphis galliiscabri</i>	<i>Formica glauca</i>	Özdemir et al. (2008)
	<i>Lasius alienus</i>	Özdemir et al. (2008)
	<i>Lasius paralienus</i>	Özdemir et al. (2008)
<i>Aphis gerardianae</i>	<i>Plagiolepis pygmaea</i>	Akyürek et al. (2016)
<i>Aphis gossypii</i>	<i>Anoplolepis gracilipes</i>	Idechiil et al. (2007)
	<i>Camponotus compressus</i>	Vergheze and Tandon (1987), Kataria and Kumar (2013), Lokeshwari et al. (2015)
	<i>Camponotus parius</i>	Lokeshwari et al. (2015)
	<i>Camponotus reticulatus</i>	Idechiil et al. (2007)
	<i>Cataglyphis nodus</i>	Sztybel (1969)
	<i>Crematogaster inermis</i>	Mortazavi et al. (2015)
	<i>Crematogaster lineolata</i>	Favret et al. (2010)
	<i>Formica argentea</i>	Jones (1927)
	<i>Formica cinerea</i>	Jones (1927)
	<i>Formica cinereofusca</i>	Akyildirim et al. (2014)
	<i>Formica fusca</i>	Jones (1927)
	<i>Iridomyrmex anceps</i>	Idechiil et al. (2007)
	<i>Lasius alienus</i>	Akyildirim et al. (2014), Akyürek et al. (2016)
	<i>Lasius emarginatus</i>	Akyildirim et al. (2014)
	<i>Lasius niger</i>	Kaneko (2003)
	<i>Lasius paralienus</i>	Özdemir et al. (2008)
	<i>Lasius turcicus</i>	Akyildirim et al. (2014), Akyürek et al. (2016)
	<i>Lepisiota nigra</i>	Mortazavi et al. (2015)
	<i>Linepithema humile</i>	Powell and Silverman (2010), Tena et al. (2013), LeVan and Holway (2015)
	<i>Lophomyrmex quadrispinosus</i>	Lokeshwari et al. (2015)
	<i>Monomorium floricola</i>	Idechiil et al. (2007)
	<i>Monomorium minimum</i>	Kataria and Kumar (2013)
	<i>Monomorium monomorium</i>	Idechiil et al. (2007)
	<i>Myrmica incompleta</i>	Jones (1927)
	<i>Myrmecaria brunnea</i>	Lokeshwari et al. (2015)
	<i>Paratrechina bourbonica</i>	Idechiil et al. (2007)
	<i>Paratrechina longicornis</i>	Idechiil et al. (2007), Lokeshwari et al. (2015)
	<i>Pheidole fervens</i>	Idechiil et al. (2007)
	<i>Plagiolepis pygmaea</i>	Akyürek et al. (2016)
	<i>Pristomyrmex pungens</i>	Kaneko (2003)
	<i>Solenopsis geminata</i>	Idechiil et al. (2007), Lokeshwari et al. (2015)
<i>Tapinoma erraticum</i>	Mortazavi et al. (2015)	

	<i>Tapinoma indicum</i>	Lokeshwari et al. (2015)
	<i>Tapinoma melanocephalum</i>	Idechiil et al. (2007), Lokeshwari et al. (2015)
	<i>Tapinoma sessile</i>	Powell and Silverman (2010)
	<i>Tapinoma simrothi</i>	Stary (1969)
	<i>Technomyrmex albipes</i>	Idechiil et al. (2007), Lokeshwari et al. (2015)
	<i>Tetramorium bicarinatum</i>	Idechiil et al. (2007)
	<i>Tetramorium caespitum</i>	Akyildirim et al. (2014)
<i>Aphis helianthi</i>	<i>Formica fusca</i>	Mooney et al. (2015)
	<i>Formica rufa</i>	Mooney et al. (2015)
	<i>Tapinoma sessile</i>	Mooney et al. (2015)
<i>Aphis hermistonii</i>	<i>Formica fusca</i>	Jones (1927)
<i>Aphis hillerislambersi</i>	<i>Lasius brunneus</i>	Akyürek et al. (2016)
<i>Aphis idaei</i>	<i>Lasius alienus</i>	Stary (1969)
	<i>Lasius niger</i>	Novgorodova (2005)
<i>Aphis illinoisensis</i>	<i>Myrmica punctiventris</i>	Favret et al. (2010)
<i>Aphis impatientis</i>	<i>Lasius emarginatus</i>	Akyildirim et al. (2014)
<i>Aphis jacobaeae</i>	<i>Formica aquilonia</i>	Novgorodova (2005)
	<i>Formica polyctena</i>	Novgorodova (2005)
	<i>Lasius niger</i>	Vrieling et al. (1991), Müller and Godfray (1999)
	<i>Myrmica ruginodis</i>	Müller and Godfray (1999)
<i>Aphis longituba</i>	<i>Lasius emarginatus</i>	Akyildirim et al. (2014)
<i>Aphis lugentis</i>	<i>Camponotus herculeanus</i>	Jones (1927)
	<i>Camponotus modoc</i>	Jones (1927)
	<i>Dorymyrmex pyramicus</i>	Jones (1927)
	<i>Formica argentea</i>	Jones (1927)
	<i>Formica canadensis</i>	Jones (1927)
	<i>Formica efiniventris</i>	Jones (1927)
	<i>Formica fusca</i>	Jones (1927)
	<i>Myrmica punctiventris</i>	Favret et al. (2010)
	<i>Tapinoma sessile</i>	Favret et al. (2010)
<i>Aphis maculatae</i>	<i>Formica fusca</i>	Jones (1927)
<i>Aphis maidiradicis</i>	<i>Lasius alienus</i>	Forbes (1906)
<i>Aphis medicaginis</i>	<i>Formica argentea</i>	Jones (1927)
	<i>Formica canadensis</i>	Jones (1927)
	<i>Formica cinerea</i>	Jones (1927)
	<i>Formica fusca</i>	Jones (1927)
	<i>Formica opaciventris</i>	Jones (1927)
	<i>Formica rufa</i>	Jones (1927)
	<i>Myrmica incompleta</i>	Jones (1927)
<i>Aphis middletonii</i>	<i>Lasius brunneus</i>	Akyürek et al. (2016)
<i>Aphis molluginis</i>	<i>Lasius alienus</i>	Akyildirim et al. (2014)
<i>Aphis nasturtii</i>	<i>Formica cinereofusca</i>	Akyildirim et al. (2014)
	<i>Formica cunicularia</i>	Akyürek et al. (2016)
	<i>Lasius alienus</i>	Özdemir et al. (2008)

	<i>Lasius brunneus</i>	Akyürek et al. (2016)
	<i>Lasius emarginatus</i>	Akyildirim et al. (2014)
	<i>Lepisiota bipartite</i>	Shiran et al. (2013)
	<i>Tapinoma simrothi</i>	Shiran et al. (2013)
<i>Aphis nerii</i>	<i>Camponotus compressus</i>	Kataria and Kumar (2013)
	<i>Iridomyrmex humilis</i>	Bristow (1991)
	<i>Lepisiota bipartite</i>	Shiran et al. (2013)
	<i>Linepithema humile</i>	Pringle et al. (2014)
	<i>Monomorium gracillimum</i>	Sary (1969)
	<i>Monomorium mayri</i>	Shiran et al. (2013)
	<i>Monomorium minimum</i>	Kataria and Kumar (2013)
	<i>Pheidole pallidula</i>	Sary (1969)
	<i>Tapinoma simrothi</i>	Shiran et al. (2013)
<i>Aphis oenotherae</i>	<i>Formica fusca</i>	Jones (1927)
	<i>Myrmica whymperei</i>	Jones (1927)
<i>Aphis oregonensis</i>	<i>Formica montana</i>	Jones (1927)
<i>Aphis parietariae</i>	<i>Lepisiota bipartite</i>	Shiran et al. (2013)
<i>Aphis polygonata</i>	<i>Monomorium mayri</i>	Shiran et al. (2013)
<i>Aphis pomi</i>	<i>Cremastogaster scutellaris</i>	Akyürek et al. (2016)
	<i>Formica aquilonia</i>	Novgorodova (2005)
	<i>Formica canadensis</i>	Jones (1927)
	<i>Formica cinerea</i>	Jones (1927)
	<i>Formica cunicularia</i>	Novgorodova (2005)
	<i>Formica fusca</i>	Jones (1927)
	<i>Formica polyctena</i>	Novgorodova (2005)
	<i>Formica rufibarbis</i>	Akyildirim et al. (2014)
	<i>Lasius alienus</i>	Akyürek et al. (2016)
	<i>Lasius brunneus</i>	Akyürek et al. (2016)
	<i>Lasius niger</i>	Novgorodova (2005)
	<i>Lasius turcicus</i>	Akyürek et al. (2016)
	<i>Myrmica incompleta</i>	Jones (1927)
	<i>Tapinoma erraticum</i>	Mortazavi et al. (2015)
	<i>Tapinoma simrothi</i>	Sary (1969)
<i>Aphis populicola</i>	<i>Myrmica incompleta</i>	Jones (1927)
<i>Aphis pseudocardui</i>	<i>Crematogaster inermis</i>	Mortazavi et al. (2015)
	<i>Crematogaster schmidtii</i>	Mortazavi et al. (2015)
	<i>Lasius alienus</i>	Akyürek et al. (2016)
<i>Aphis punicae</i>	<i>Lepisiota bipartite</i>	Shiran et al. (2013)
	<i>Tapinoma simrothi</i>	Sary (1969)
<i>Aphis rumicis</i>	<i>Lasius paralienus</i>	Özdemir et al. (2008)
	<i>Tetramorium chefteki</i>	Özdemir et al. (2008)
	<i>Tetramorium forte</i>	Özdemir et al. (2008)
	<i>Myrmica incompleta</i>	Jones (1927)
	<i>Myrmica whymperei</i>	Jones (1927)
	<i>Tapinoma simrothi</i>	Shiran et al. (2013)

<i>Aphis salicariae</i>	<i>Camponotus herculeanus</i>	Addicott (1979a)
	<i>Formica aserva</i>	Addicott (1979a)
	<i>Formica cinerea</i>	Addicott (1979a)
	<i>Formica fusca</i>	Addicott (1979a), Mooney et al. (2015)
	<i>Formica integroides</i>	Addicott (1979a)
	<i>Formica lasioides</i>	Addicott (1979a)
	<i>Formica neorufibarbis</i>	Addicott (1979a)
	<i>Formica obscuripes</i>	Addicott (1979a)
	<i>Formica puberula</i>	Addicott (1979a)
	<i>Formica rufa</i>	Mooney et al. (2015)
	<i>Tapinoma erraticum</i>	Mortazavi et al. (2015)
	<i>Tapinoma sessile</i>	Addicott (1979a), Mooney et al. (2015)
<i>Aphis salviae</i>	<i>Camponotus aethiops</i>	Özdemir et al. (2008)
	<i>Camponotus piceus</i>	Özdemir et al. (2008)
	<i>Tetramorium caespitum</i>	Akyürek et al. (2016)
<i>Aphis sambuci</i>	<i>Formica cinereofusca</i>	Akyildirim et al. (2014)
	<i>Lasius turcicus</i>	Akyildirim et al. (2014)
<i>Aphis sambucifolii</i>	<i>Formica argentea</i>	Jones (1927)
<i>Aphis serpylli</i>	<i>Formica cinereofusca</i>	Akyildirim et al. (2014)
<i>Aphis solanella</i>	<i>Formica cunicularia</i>	Akyürek et al. (2016)
	<i>Lasius alienus</i>	Akyürek et al. (2016)
<i>Aphis spiraecola</i>	<i>Camponotus lateralis</i>	Akyürek et al. (2016)
	<i>Cremastogaster scutellaris</i>	Akyürek et al. (2016)
	<i>Formica cinereofusca</i>	Akyildirim et al. (2014)
	<i>Formica cunicularia</i>	Akyürek et al. (2016)
	<i>Formica rufibarbis</i>	Akyürek et al. (2016)
	<i>Lasius brunneus</i>	Akyürek et al. (2016)
	<i>Lasius emarginatus</i>	Akyildirim et al. (2014)
	<i>Lasius turcicus</i>	Akyildirim et al. (2014), Akyürek et al. (2016)
	<i>Linepithema humile</i>	Tena et al. (2013)
	<i>Plagiolepis pygmaea</i>	Akyürek et al. (2016)
	<i>Plagiolepis taurica</i>	Akyildirim et al. (2014)
	<i>Tetramorium caespitum</i>	Akyürek et al. (2016)
<i>Aphis subnitidae</i>	<i>Formica aquilonia</i>	Novgorodova (2005)
	<i>Formica polyctena</i>	Novgorodova (2005)
<i>Aphis ulmariae</i>	<i>Formica argentea</i>	Jones (1927)
<i>Aphis umbrella</i>	<i>Lasius paralienus</i>	Shiran et al. (2013)
	<i>Lepisiota bipartite</i>	Shiran et al. (2013)
	<i>Pheidole pallidula</i>	Shiran et al. (2013)
	<i>Pheidole teneriffana</i>	Shiran et al. (2013)
	<i>Tapinoma simrothi</i>	Shiran et al. (2013)
<i>Aphis urticata</i>	<i>Lasius alienus</i>	Akyürek et al. (2016)
<i>Aphis valerianae</i>	<i>Camponotus herculeanus</i>	Jones (1927)
	<i>Camponotus vicinus</i>	Jones (1927)
	<i>Formica canadensis</i>	Jones (1927)

	<i>Formica podzolica</i>	Petry et al. (2012)
	<i>Formica rufa</i>	Jones (1927)
<i>Aphis vandergooti</i>	<i>Lasius niger</i>	Woodring et al. (2004)
<i>Aphis varians</i>	<i>Camponotus herculeanus</i>	Addicott (1979a)
	<i>Formica aserva</i>	Addicott (1979a)
	<i>Formica cinerea</i>	Addicott (1978), Addicott (1979a), Breton and Addicott (1992)
	<i>Formica fusca</i>	Addicott (1978), Addicott (1979a), Mooney et al. (2015)
	<i>Formica integroides</i>	Addicott (1978), Addicott (1979a)
	<i>Formica lasioides</i>	Addicott (1978), Addicott (1979a)
	<i>Formica neorufibarbis</i>	Addicott (1979a)
	<i>Formica obscuripes</i>	Addicott (1978), Addicott (1979a)
	<i>Formica puberula</i>	Addicott (1979a)
	<i>Formica rufa</i>	Mooney et al. (2015)
	<i>Tapinoma sessile</i>	Addicott (1979a), Mooney et al. (2015)
<i>Aphis verbasci</i>	<i>Formica cinereofusca</i>	Akyildirim et al. (2014)
	<i>Lasius alienus</i>	Özdemir et al. (2008), Akyürek et al. (2016)
<i>Aphis vernoniae</i>	<i>Nylanderia fulva</i>	Sharma and Buss (2013)
<i>Aphis viburni</i>	<i>Formica aquilonia</i>	Novgorodova (2005)
	<i>Lasius niger</i>	Novgorodova (2005)
<i>Brachyonguis harmalae</i>	<i>Tapinoma simrothi</i>	Shiran et al. (2013)
<i>Brachyonguis tamaricophilus</i>	<i>Tapinoma simrothi</i>	Shiran et al. (2013)
<i>Brachyunguis tamaricis</i>	<i>Formica cinereofusca</i>	Akyildirim et al. (2014)
<i>Brachyunguis tetrapteris</i>	<i>Formica fusca</i>	Jones (1927)
<i>Braggia eriogoni</i>	<i>Formica argentea</i>	Jones (1927)
	<i>Formica fusca</i>	Jones (1927)
<i>Hyalopterus amygdali</i>	<i>Lepisiota nigra</i>	Mortazavi et al. (2015)
	<i>Monomorium mayri</i>	Shiran et al. (2013)
	<i>Plagiolepis pallelescens</i>	Shiran et al. (2013)
<i>Hyalopterus pruni</i>	<i>Lasius brunneus</i>	Akyürek et al. (2016)
	<i>Lasius paralienus</i>	Shiran et al. (2013)
	<i>Lepisiota bipartite</i>	Shiran et al. (2013)
	<i>Pogonomyrmex occidentalis</i>	Jones (1927)
	<i>Tapinoma simrothi</i>	Stary (1969)
<i>Hysteroneura setariae</i>	<i>Camponotus navigator</i>	Idechiil et al. (2007)
	<i>Tapinoma melanocephalum</i>	Idechiil et al. (2007)
	<i>Technomyrmex albipes</i>	Idechiil et al. (2007)
<i>Protaphis middletonii</i>	<i>Camponotus vicinus</i>	Jones (1927)
	<i>Formica cinerea</i>	Jones (1927)
	<i>Formica fusca</i>	Jones (1927)
	<i>Myrmica incompleta</i>	Jones (1927)
<i>Protaphis terricola</i>	<i>Lasius turcicus</i>	Özdemir et al. (2008)
<i>Rhopalosiphum cerasifoliae</i>	<i>Lasius alienus</i>	Favret et al. (2010)
<i>Rhopalosiphum maidis</i>	<i>Formica cinerea</i>	Jones (1927)

	<i>Formica fusca</i>	Jones (1927)
	<i>Lasius alienus</i>	Barton and Ives (2014)
	<i>Lepisiota bipartite</i>	Shiran et al. (2013)
	<i>Monomorium mayri</i>	Shiran et al. (2013)
	<i>Monomorium qarahe</i>	Shiran et al. (2013)
	<i>Myrmica incompleta</i>	Jones (1927)
	<i>Polyrhachis lacteipennis</i>	Shiran et al. (2013)
	<i>Prenolepis imparis</i>	Barton and Ives (2014)
	<i>Tapinoma simrothi</i>	Stary (1969)
<i>Rhopalosiphum nymphaeae</i>	<i>Formica argentea</i>	Jones (1927)
	<i>Formica aserva</i>	Jones (1927)
	<i>Formica bradleyi</i>	Jones (1927)
	<i>Formica coloradensis</i>	Jones (1927)
	<i>Formica gnava</i>	Jones (1927)
	<i>Formica incerta</i>	Jones (1927)
	<i>Formica integroides</i>	Jones (1927)
	<i>Formica lasioides</i>	Jones (1927)
	<i>Formica lepida</i>	Jones (1927)
	<i>Formica limata</i>	Jones (1927)
	<i>Formica munda</i>	Jones (1927)
	<i>Formica neoclara</i>	Jones (1927)
	<i>Formica neogagates</i>	Jones (1927)
	<i>Formica neorufibarbis</i>	Jones (1927)
	<i>Formica obscuripes</i>	Jones (1927)
	<i>Formica oreas</i>	Jones (1927)
	<i>Formica puberula</i>	Jones (1927)
	<i>Formica ravidia</i>	Jones (1927)
	<i>Formica rubicunda</i>	Jones (1927)
	<i>Formica rufa</i>	Jones (1927)
	<i>Formica sanguinea</i>	Jones (1927)
	<i>Formica subaenescens</i>	Jones (1927)
	<i>Formica subintegra</i>	Jones (1927)
	<i>Formica subsericea</i>	Jones (1927)
	<i>Formica ulkei</i>	Jones (1927)
	<i>Lasius alienus</i>	Jones (1927)
	<i>Lasius claviger</i>	Jones (1927)
	<i>Lasius latipes</i>	Jones (1927)
	<i>Lasius nearcticus</i>	Jones (1927)
	<i>Lasius neoniger</i>	Jones (1927)
	<i>Lasius pallitarsis</i>	Jones (1927)
	<i>Leptothorax muscorum</i>	Jones (1927)
<i>Liometopum luctuosum</i>	Jones (1927)	
<i>Liometopum occidentale</i>	Jones (1927)	
<i>Monomorium minimum</i>	Jones (1927)	
<i>Rhopalosiphum padi</i>	<i>Formica aquilonia</i>	Novgorodova (2005)

	<i>Formica polyctena</i>	Novgorodova (2005)
	<i>Lepisiota bipartite</i>	Shiran et al. (2013)
	<i>Tapinoma simrothi</i>	Shiran et al. (2013)
<i>Sanbornia juniperi</i>	<i>Nylanderia fulva</i>	Sharma and Buss (2013)
<i>Schizaphis gramina</i>	<i>Formica aquilonia</i>	Novgorodova (2005)
	<i>Formica polyctena</i>	Novgorodova (2005)
<i>Schizaphis graminum</i>	<i>Camponotus herculeanus</i>	Jones (1927)
<i>Schizaphis miscanthi</i>	<i>Formica cinereofusca</i>	Akyildirim et al. (2014)
<i>Schizaphis nigerrima</i>	<i>Lepisiota nigra</i>	Mortazavi et al. (2015)
<i>Schizaphis pyri</i>	<i>Formica aquilonia</i>	Novgorodova (2005)
	<i>Formica polyctena</i>	Novgorodova (2005)
	<i>Lasius brunneus</i>	Akyürek et al. (2016)
Tribe Macrosiphini		
<i>Acyrtosiphon gossypii</i>	<i>Crematogaster inermis</i>	Mortazavi et al. (2015)
	<i>Lasius turcicus</i>	Mortazavi et al. (2015)
<i>Acyrtosiphon pisum</i>	<i>Crematogaster inermis</i>	Mortazavi et al. (2015)
	<i>Formica cunicularia</i>	Mortazavi et al. (2015)
	<i>Lasius turcicus</i>	Akyildirim et al. (2014), Akyürek et al. (2016)
	<i>Lepisiota dolabellae</i>	Mortazavi et al. (2015)
	<i>Plagiolepis pallelescens</i>	Mortazavi et al. (2015)
<i>Acyrtosiphon rubi</i>	<i>Formica cunicularia</i>	Mortazavi et al. (2015)
<i>Anuraphis subterranea</i>	<i>Formica argentea</i>	Jones (1927)
	<i>Formica fusca</i>	Jones (1927)
<i>Aphthargelia symphoricarpi</i>	<i>Formica cinerea</i>	Addicott (1978)
<i>Artemisaphis artemisicola</i>	<i>Formica fusca</i>	Jones (1927)
	<i>Myrmica incompleta</i>	Jones (1927)
<i>Aulacorthum solani</i>	<i>Formica subsericea</i>	Favret et al. (2010)
<i>Bipersona torticauda</i>	<i>Camponotus vicinus</i>	Jones (1927)
	<i>Formica altipetens</i>	Jones (1927)
	<i>Formica argentea</i>	Jones (1927)
	<i>Formica cinerea</i>	Jones (1927)
	<i>Formica fusca</i>	Jones (1927)
	<i>Tapinoma sessile</i>	Jones (1927)
<i>Brachcaudus helicrysi</i>	<i>Camponotus aethiops</i>	Özdemir et al. (2008)
<i>Brachycaudus amygdalinus</i>	<i>Lasius turcicus</i>	Mortazavi et al. (2015)
	<i>Proformica pilosiscapa</i>	Mortazavi et al. (2015)
	<i>Tapinoma erraticum</i>	Mortazavi et al. (2015)
<i>Brachycaudus cardui</i>	<i>Brachymyrmex patagonica</i>	Lescano et al. (2015)
	<i>Camponotus aethiops</i>	Özdemir et al. (2008), Akyürek et al. (2016)
	<i>Crematogaster sordidula</i>	Özdemir et al. (2008), Mortazavi et al. (2015)
	<i>Dorymyrmex tener</i>	Lescano et al. (2015)
	<i>Dorymyrmex wolffuegeli</i>	Lescano et al. (2015)
	<i>Formica cinereofusca</i>	Akyildirim et al. (2014)
	<i>Formica fusca</i>	Jones (1927), Akyildirim et al. (2014)

	<i>Formica glauca</i>	Özdemir et al. (2008)
	<i>Formica rufa</i>	Jones (1927)
	<i>Lasius alienus</i>	Akyürek et al. (2016)
	<i>Lasius brunneus</i>	Akyürek et al. (2016)
	<i>Lasius emarginatus</i>	Akyildirim et al. (2014)
	<i>Lasius niger</i>	Volkl et al. (1999), Müller and Godfray (1999), Woodring et al. (2004)
	<i>Lasius paralienus</i>	Özdemir et al. (2008)
	<i>Lasius turcicus</i>	Akyildirim et al. (2014), Akyürek et al. (2016)
	<i>Myrmica incompleta</i>	Jones (1927)
	<i>Myrmica ruginodis</i>	Müller and Godfray (1999), Akyildirim et al. (2014)
	<i>Plagiolepis pygmaea</i>	Akyürek et al. (2016)
	<i>Solenopsis richteri</i>	Lescano et al. (2015)
	<i>Tapinoma sessile</i>	Jones (1927)
	<i>Tapinoma simrothi</i>	Stary (1969)
	<i>Tetramorium caespitum</i>	Akyürek et al. (2016)
	<i>Tetramorium forte</i>	Akyildirim et al. (2014)
<i>Brachycaudus helichrysi</i>	<i>Aphaenogaster kurdica</i>	Mortazavi et al. (2015)
	<i>Formica cinerea</i>	Jones (1927)
	<i>Formica cinereofusca</i>	Akyildirim et al. (2014)
	<i>Lasius turcicus</i>	Akyürek et al. (2016)
	<i>Lepisiota nigra</i>	Mortazavi et al. (2015)
	<i>Myrmica scabrinodis</i>	Akyildirim et al. (2014)
	<i>Tapinoma simrothi</i>	Shiran et al. (2013)
<i>Brachycaudus lychnidis</i>	<i>Formica cinereofusca</i>	Akyildirim et al. (2014)
<i>Brachycaudus persicae</i>	<i>Formica fusca</i>	Jones (1927)
	<i>Myrmica scabrinodis</i>	Jones (1927)
<i>Brachycaudus prunicola</i>	<i>Myrmica incompleta</i>	Jones (1927)
<i>Brachycaudus schwartzi</i>	<i>Lasius emarginatus</i>	Akyildirim et al. (2014)
	<i>Crematogaster inermis</i>	Mortazavi et al. (2015)
	<i>Formica cunicularia</i>	Mortazavi et al. (2015)
	<i>Lepisiota dolabellae</i>	Mortazavi et al. (2015)
	<i>Lepisiota nigra</i>	Mortazavi et al. (2015)
	<i>Plagiolepis pallelescens</i>	Mortazavi et al. (2015)
	<i>Tapinoma erraticum</i>	Mortazavi et al. (2015)
	<i>Formica glauca</i>	Özdemir et al. (2008)
<i>Capitophorus elaeagni</i>	<i>Crematogaster lineolata</i>	Favret et al. (2010)
	<i>Prenolepis imparis</i>	Favret et al. (2010)
<i>Capitophorus hippophaes</i>	<i>Lasius alienus</i>	Özdemir et al. (2008)
<i>Capitophorus inulae</i>	<i>Tapinoma simrothi</i>	Shiran et al. (2013)
<i>Ceruraphis viburnicola</i>	<i>Formica fusca</i>	Jones (1927)
<i>Chaetosiphon tetraerhodum</i>	<i>Lasius turcicus</i>	Akyildirim et al. (2014)
<i>Colorado absinthiella</i>	<i>Tapinoma simrothi</i>	Shiran et al. (2013)

<i>Cryptomyzus ribis</i>	<i>Formica argentea</i>	Jones (1927)
	<i>Formica fusca</i>	Jones (1927)
	<i>Myrmica scabrinodis</i>	Jones (1927)
<i>Diuraphis calamagrostis</i>	<i>Formica cinerea</i>	Jones (1927)
<i>Dysaphis devectora</i>	<i>Formica rufibarbis</i>	Akyürek et al. (2016)
<i>Dysaphis foeniculus</i>	<i>Lasius alienus</i>	Akyürek et al. (2016)
<i>Dysaphis plantaginea</i>	<i>Lasius brunneus</i>	Akyürek et al. (2016)
	<i>Lasius niger</i>	Nagy et al. (2015)
<i>Dysaphis pyri</i>	<i>Lasius alienus</i>	Akyildirim et al. (2014)
<i>Dysaphis sorbi</i>	<i>Formica fusca</i>	Jones (1927)
	<i>Tapinoma sessile</i>	Jones (1927)
<i>Hyadaphis foeniculi</i>	<i>Lasius paralienus</i>	Özdemir et al. (2008)
<i>Hyadaphis hofmanni</i>	<i>Camponotus piceus</i>	Özdemir et al. (2008)
<i>Hyperomyzus lactucae</i>	<i>Formica argentea</i>	Jones (1927)
<i>Hyperomyzus nabali</i>	<i>Formica subsericea</i>	Favret et al. (2010)
<i>Macrosiphon rosae</i>	<i>Lepisiota nigra</i>	Mortazavi et al. (2015)
<i>Macrosiphoniella pulvera</i>	<i>Formica cunicularia</i>	Novgorodova (2005)
	<i>Formica polyctena</i>	Novgorodova (2005)
<i>Macrosiphoniella sanborni</i>	<i>Tetramorium caespitum</i>	Akyildirim et al. (2014)
<i>Macrosiphum chrysothamni</i>	<i>Camponotus vicinus</i>	Jones (1927)
	<i>Formica fusca</i>	Jones (1927)
	<i>Formica montana</i>	Jones (1927)
<i>Macrosiphum euphorbiae</i>	<i>Cataglyphis aenescens</i>	Mortazavi et al. (2015)
	<i>Formica argentea</i>	Jones (1927)
<i>Macrosiphum rosae</i>	<i>Formica cunicularia</i>	Akyürek et al. (2016)
<i>Macrosiphum valerianae</i>	<i>Camponotus vicinus</i>	Jones (1927)
<i>Metopeurum fuscoviride</i>	<i>Lasius niger</i>	Volkl et al. (1999), Fischer et al. (2002), Woodring et al. (2004)
<i>Microsiphoniella artemisiae</i>	<i>Formica sp.</i>	Jones (1927)
<i>Myzaphis rosarum</i>	<i>Formica argentea</i>	Jones (1927)
	<i>Formica fusca</i>	Jones (1927)
<i>Myzus cerasi</i>	<i>Lasius alienus</i>	Akyürek et al. (2016)
	<i>Lasius emarginatus</i>	Akyildirim et al. (2014)
	<i>Lasius turcicus</i>	Akyildirim et al. (2014), Akyürek et al. (2016)
	<i>Proformica kobachidzei</i>	Akyildirim et al. (2014)
	<i>Formica fusca</i>	Jones (1927)
<i>Myzus lythri</i>	<i>Formica cinereofusca</i>	Akyildirim et al. (2014)
	<i>Lasius emarginatus</i>	Akyildirim et al. (2014)
	<i>Lasius turcicus</i>	Akyildirim et al. (2014)
	<i>Tetramorium caespitum</i>	Akyürek et al. (2016)
<i>Myzus oenotherae</i>	<i>Formica fusca</i>	Jones (1927)
<i>Myzus ornatus</i>	<i>Formica rufibarbis</i>	Akyürek et al. (2016)
<i>Myzus padellus</i>	<i>Formica rufibarbis</i>	Akyürek et al. (2016)
<i>Myzus persicae</i>	<i>Camponotus compressus</i>	Kataria and Kumar (2013)

	<i>Cataglyphis cinnamomeus</i>	Shiran et al. (2013)
	<i>Crematogaster antaris</i>	Shiran et al. (2013)
	<i>Formica argentea</i>	Jones (1927)
	<i>Lasius paralienus</i>	Shiran et al. (2013)
	<i>Lepisiota bipartite</i>	Shiran et al. (2013)
	<i>Linepithema humile</i>	Powell and Silverman (2010)
	<i>Monomorium mayri</i>	Shiran et al. (2013)
	<i>Pheidole pallidula</i>	Shiran et al. (2013)
	<i>Pogonomyrmex occidentalis</i>	Jones (1927)
	<i>Solenopsis invicta</i>	Zhou (2014), Zhou (2012)
	<i>Tapinoma melanocephalum</i>	Zhou et al. (2015)
	<i>Tapinoma sessile</i>	Powell and Silverman (2010)
	<i>Tapinoma simrothi</i>	Shiran et al. (2013)
<i>Myzus varians</i>	<i>Lasius turcicus</i>	Akyürek et al. (2016)
<i>Nasonovia houghtonensis</i>	<i>Formica fusca</i>	Jones (1927)
<i>Nearctaphis bakeri</i>	<i>Formica cinereofusca</i>	Akyildirim et al. (2014)
	<i>Formica rufa</i>	Jones (1927)
	<i>Prenolepis imparis</i>	Favret et al. (2010)
	<i>Tapinoma simrothi</i>	Shiran et al. (2013)
<i>Neomyzus circumflexum</i>	<i>Formica subsericea</i>	Favret et al. (2010)
<i>Obtusicauda frigidae</i>	<i>Camponotus herculeanus</i>	Jones (1927)
	<i>Formica efiniventris</i>	Jones (1927)
	<i>Formica fusca</i>	Jones (1927)
<i>Ovatus crataegarius</i>	<i>Formica sp.</i>	Jones (1927)
<i>Pleotrichophorus glandulosus</i>	<i>Formica montana</i>	Jones (1927)
	<i>Formica cinerea</i>	Addicott (1978)
<i>Pleotrichophorus utensis</i>	<i>Formica obscuripes</i>	Billick et al. (2007)
<i>Pseudoepameibaphis tridentatae</i>	<i>Formica montana</i>	Jones (1927)
<i>Pterocomma bicolor</i>	<i>Formica fusca</i>	Jones (1927)
	<i>Myrmica incompleta</i>	Jones (1927)
<i>Pterocomma pilosum</i>	<i>Lasius fuliginosus</i>	Molnar et al. (2000)
<i>Pterocomma populeum</i>	<i>Camponotus herculeanus</i>	Jones (1927)
	<i>Lasius brunneus</i>	Akyürek et al. (2016)
	<i>Lasius turcicus</i>	Akyürek et al. (2016)
<i>Pterocomma rufipes</i>	<i>Cremastogaster scutellaris</i>	Akyürek et al. (2016)
	<i>Lasius fuliginosus</i>	Molnar et al. (2000)
<i>Pterocomma salicis</i>	<i>Formica fusca</i>	Jones (1927)
	<i>Myrmica incompleta</i>	Jones (1927)
<i>Pterocomma smithiae</i>	<i>Formica argentea</i>	Jones (1927)
<i>Sitobion fragariae</i>	<i>Lasius brunneus</i>	Akyürek et al. (2016)
<i>Staegeriella necopinata</i>	<i>Camponotus piceus</i>	Özdemir et al. (2008)
	<i>Plagiolepis vindobonensis</i>	Özdemir et al. (2008)
<i>Uroleucon ambrosiae ambrosiae</i>	<i>Formica argentea</i>	Jones (1927)
	<i>Formica canadensis</i>	Jones (1927)

	<i>Formica cinerea</i>	Jones (1927)
	<i>Formica fusca</i>	Jones (1927)
	<i>Myrmica incompleta</i>	Jones (1927)
<i>Uroleucon Dactynotus</i>	<i>Monomorium gracillimum</i>	Stary (1969)
	<i>Formica argentea</i>	Jones (1927)
<i>Uroleucon erigeronense</i>	<i>Formica cinerea</i>	Jones (1927)
	<i>Formica fusca</i>	Jones (1927)
<i>Uroleucon escalantii</i>	<i>Formica obscuripes</i>	Billick et al. (2007)
<i>Uroleucon kashmiricum</i>	<i>Lasius brunneus</i>	Akyürek et al. (2016)
<i>Uroleucon kikioense</i>	<i>Formica fusca</i>	Akyildirim et al. (2014)
<i>Uroleucon nigrotuberculatum</i>	<i>Formica japonica</i>	Ando and Ohgushi (2008)
<i>Uroleucon pieloui</i>	<i>Formica subsericea</i>	Favret et al. (2010)
<i>Uroleucon solidaginis</i>	<i>Formica argentea</i>	Jones (1927)
<i>Uroleucon sonchellum</i>	<i>Prenolepis imparis</i>	Favret et al. (2010)
<i>Uroleucon sonchi</i>	<i>Tetramorium forte</i>	Akyürek et al. (2016)
<i>Uroleucon taraxaci</i>	<i>Formica argentea</i>	Jones (1927)
<i>Wahlgreniella nervata</i>	<i>Myrmica incompleta</i>	Jones (1927)
Subfamily Calaphidinae		
Tribe Calaphidini		
	<i>Camponotus saxatilis</i>	Novgorodova (2005)
<i>Callipterinella tuberculata</i>	<i>Formica aquilonia</i>	Novgorodova (2005)
	<i>Formica polyctena</i>	Novgorodova (2005)
	<i>Lasius niger</i>	Novgorodova (2005)
<i>Neobetulaphis pusilla</i>	<i>Lasius alienus</i>	Akyildirim et al. (2014)
	<i>Lasius turcicus</i>	Akyildirim et al. (2014)
	<i>Camponotus saxatilis</i>	Novgorodova (2005)
	<i>Formica aquilonia</i>	Novgorodova (2005)
<i>Symydobius oblongus</i>	<i>Formica cinereofusca</i>	Akyildirim et al. (2014)
	<i>Formica polyctena</i>	Novgorodova (2005)
	<i>Formica pratensis</i>	Novgorodova (2005)
	<i>Lasius fuliginosus</i>	Novgorodova (2005)
	<i>Lasius niger</i>	Novgorodova (2005)
Tribe Panaphidini		
<i>Chromaphis obiensis</i>	<i>Lasius niger</i>	Novgorodova (2005)
<i>Myzocallis discolor</i>	<i>Formica argentea</i>	Jones (1927)
	<i>Formica fusca</i>	Jones (1927)
<i>Myzocallis kuricola</i>	<i>Lasius niger</i>	Sakata (1995)
<i>Shivaphis celti</i>	<i>Nylanderia fulva</i>	Sharma and Buss (2013)
<i>Pterocallis albidus</i>	<i>Formica cinereofusca</i>	Akyildirim et al. (2014)
<i>Pterocallis alni</i>	<i>Formica cinereofusca</i>	Akyildirim et al. (2014)
<i>Tinocallis platani</i>	<i>Plagiolepis pallelescens</i>	Shiran et al. (2013)
<i>Tuberculatus quercicola</i>	<i>Formica yessensis</i>	Yao and Akimoto (2001), Yao and Akimoto (2009), Yao and Akimoto (2009)
<i>Tuberculatus maximus</i>	<i>Crematogaster subdentata</i>	Mortazavi et al. (2015)

Subfamily Chaitophorinae		
Tribe Chaitophorini		
<i>Chaitophorous populialbae</i>	<i>Polyrhachis simplex</i>	Degen et al. (1986)
<i>Chaitophorus albitorosus</i>	<i>Formica aquilonia</i>	Novgorodova (2005)
	<i>Formica polyctena</i>	Novgorodova (2005)
<i>Chaitophorus albus</i>	<i>Camponotus saxatilis</i>	Novgorodova (2005)
	<i>Formica aquilonia</i>	Novgorodova (2005)
	<i>Formica cunicularia</i>	Novgorodova (2005)
	<i>Formica polyctena</i>	Novgorodova (2005)
	<i>Lasius niger</i>	Novgorodova (2005)
<i>Chaitophorus euphraticus</i>	<i>Lepisiota bipartite</i>	Shiran et al. (2013)
	<i>Monomorium destructor</i>	Shiran et al. (2013)
	<i>Monomorium mayri</i>	Shiran et al. (2013)
<i>Chaitophorus hillerislambersi</i>	<i>Lasius turcicus</i>	Mortazavi et al. (2015)
<i>Chaitophorus israeliticus</i>	<i>Crematogaster inermis</i>	Mortazavi et al. (2015)
	<i>Crematogaster schmidtii</i>	Mortazavi et al. (2015)
	<i>Lepisiota nigra</i>	Mortazavi et al. (2015)
	<i>Messor orientalis</i>	Mortazavi et al. (2015)
	<i>Tapinoma erraticum</i>	Mortazavi et al. (2015)
<i>Chaitophorus kapuri</i>	<i>Lasius alienus</i>	Akyildirim et al. (2014)
<i>Chaitophorus longisetosus</i>	<i>Formica cinereofusca</i>	Akyildirim et al. (2014)
	<i>Lasius emarginatus</i>	Akyildirim et al. (2014)
	<i>Lasius paralienus</i>	Akyildirim et al. (2014)
<i>Chaitophorus macrostachyae</i>	<i>Formica fusca</i>	Jones (1927)
	<i>Myrmica incompleta</i>	Jones (1927)
<i>Chaitophorus melanosiphon</i>	<i>Crematogaster scutellaris</i>	Akyürek et al. (2016)
<i>Chaitophorus nassonowi</i>	<i>Formica pratensis</i>	Novgorodova (2005)
<i>Chaitophorus nigrae</i>	<i>Camponotus novaeboracensis</i>	Jones (1927)
	<i>Formica argentea</i>	Jones (1927)
<i>Chaitophorus populeti</i>	<i>Camponotus saxatilis</i>	Novgorodova (2005)
	<i>Formica aquilonia</i>	Novgorodova (2005)
	<i>Formica cunicularia</i>	Novgorodova (2005)
	<i>Formica fusca</i>	Novgorodova (2005)
	<i>Formica polyctena</i>	Novgorodova (2005)
	<i>Formica pratensis</i>	Novgorodova (2005)
	<i>Formica sanguinea</i>	Akyürek et al. (2016)
	<i>Lasius fuliginosus</i>	Novgorodova (2005)
	<i>Lasius niger</i>	Fischer and Shingleton (2001), Novgorodova (2005)
<i>Lasius paralienus</i>	Shiran et al. (2013)	
<i>Chaitophorus populialbae</i>	<i>Camponotus saxatilis</i>	Novgorodova (2005)
	<i>Formica aquilonia</i>	Novgorodova (2005)

	<i>Formica cunicularia</i>	Novgorodova (2005)
	<i>Formica fusca</i>	Novgorodova (2005)
	<i>Formica polyctena</i>	Novgorodova (2005)
	<i>Lasius niger</i>	Fischer and Shingleton (2001), Novgorodova (2005)
	<i>Lasius paralienus</i>	Shiran et al. (2013)
<i>Chaitophorus populicola</i>	<i>Camponotus herculeanus</i>	Jones (1927)
	<i>Camponotus pennsylvanicus</i>	Jones (1927)
	<i>Formica argentea</i>	Jones (1927)
	<i>Formica dakotensis</i>	Jones (1927)
	<i>Formica montana</i>	Jones (1927)
	<i>Formica propinqua</i>	Wimp and Whitham (2001)
	<i>Linepithema humile</i>	Mondor and Addicott (2007)
	<i>Myrmica incompleta</i>	Jones (1927)
	<i>Tapinoma sessile</i>	Jones (1927)
<i>Chaitophorus populifolii</i>	<i>Camponotus herculeanus</i>	Jones (1927)
	<i>Camponotus vicinus</i>	Jones (1927)
	<i>Formica argentea</i>	Jones (1927)
	<i>Formica aterrima</i>	Jones (1927)
	<i>Formica canadensis</i>	Jones (1927)
	<i>Formica fusca</i>	Jones (1927)
	<i>Formica rufa</i>	Jones (1927)
	<i>Tapinoma sessile</i>	Jones (1927)
<i>Chaitophorus remaudierei</i>	<i>Lasius paralienus</i>	Shiran et al. (2013)
<i>Chaitophorus salicti</i>	<i>Formica aquilonia</i>	Novgorodova (2005)
	<i>Formica polyctena</i>	Novgorodova (2005)
	<i>Lasius turcicus</i>	Akyildirim et al. (2014)
<i>Chaitophorus saliniger</i>	<i>Camponotus japonicus</i>	Hembry et al. (2006)
	<i>Formica japonica</i>	Hembry et al. (2006)
	<i>Lasius japonicus</i>	Hembry et al. (2006)
<i>Chaitophorus tremulae</i>	<i>Camponotus saxatilis</i>	Novgorodova (2005)
	<i>Lasius niger</i>	Novgorodova (2005)
<i>Chaitophorus truncates</i>	<i>Crematogaster antaris</i>	Shiran et al. (2013)
	<i>Lasius paralienus</i>	Shiran et al. (2013)
	<i>Lepisiota bipartite</i>	Shiran et al. (2013)
<i>Chaitophorus viminalis</i>	<i>Camponotus vicinus</i>	Jones (1927)
	<i>Formica argentea</i>	Jones (1927)
	<i>Formica fusca</i>	Jones (1927)
	<i>Myrmecina graminicola</i>	Jones (1927)
	<i>Myrmica whymperi</i>	Jones (1927)
	<i>Tapinoma sessile</i>	Jones (1927)
<i>Chaitophorus viminicola</i>	<i>Crematogaster lineolata</i>	Favret et al. (2010)
	<i>Nylanderia fulva</i>	Sharma and Buss (2013)
<i>Chaitophorus vitellinae</i>	<i>Lasius fuliginosus</i>	Molnar et al. (2000)
<i>Periphyllus aceris</i>	<i>Formica cinereofusca</i>	Akyildirim et al. (2014)

	<i>Lasius brunneus</i>	Akyürek et al. (2016)
	<i>Lasius emarginatus</i>	Akyildirim et al. (2014)
<i>Periphyllus bulgaricus</i>	<i>Crematogaster subdentata</i>	Mortazavi et al. (2015)
	<i>Lasius alienus</i>	Mortazavi et al. (2015)
	<i>Lepisiota nigra</i>	Mortazavi et al. (2015)
<i>Periphyllus negundinis</i>	<i>Dorymyrmex pyramicus</i>	Jones (1927)
	<i>Formica argentea</i>	Jones (1927)
	<i>Formica fusca</i>	Jones (1927)
Tribe Siphini		
<i>Sipha maydis</i>	<i>Formica cinereofusca</i>	Akyildirim et al. (2014)
	<i>Formica cunicularia</i>	Akyürek et al. (2016)
	<i>Lasius alienus</i>	Akyürek et al. (2016)
Subfamily Drepanosiphinae		
<i>Drepanaphis acerifoliae</i>	<i>Formica argentea</i>	Jones (1927)
	<i>Formica canadensis</i>	Jones (1927)
	<i>Myrmica scabrinodis</i>	Jones (1927)
<i>Drepanaphis nigricans</i>	<i>Camponotus subbarbatus</i>	Favret et al. (2010)
	<i>Myrmica punctiventris</i>	Favret et al. (2010)
<i>Drepanosiphum braggii</i>	<i>Formica canadensis</i>	Jones (1927)
	<i>Formica fusca</i>	Jones (1927)
Subfamily Eriosomatinae		
Tribe Eriosomatini		
<i>Eriosoma americanum</i>	<i>Formica cinerea</i>	Jones (1927)
<i>Eriosoma crataegi</i>	<i>Myrmica incompleta</i>	Jones (1927)
<i>Tetraneura sp.</i>	<i>Technomyrmex albipes</i>	Idechiil et al. (2007)
Tribe Fordini		
<i>Forda marginata</i>	<i>Lasius americanus</i>	Cockerell (1903)
	<i>Lasius claviger</i>	Cockerell (1903)
	<i>Lasius flavus</i>	Cockerell (1903)
<i>Geoica sp.</i>	<i>Formica fusca</i>	Jones (1927)
<i>Paracletus cimiciformis</i>	<i>Tetramorium semilaeve</i>	Salazar et al. (2015)
Tribe Pemphigini		
<i>Pachypappa sacculi</i>	<i>Formica sp.</i>	Jones (1927)
<i>Pemphigus lasii</i>	<i>Lasius americanus</i>	Cockerell (1903), Palmer (1952)
<i>Pemphigus populiramulorum</i>	<i>Pheidole pilifera</i>	Jones (1927)
<i>Pentalonia nigronevosa</i>	<i>Anoplolepis gracilipes</i>	Idechiil et al. (2007)
	<i>Camponotus reticulatus</i>	Idechiil et al. (2007)
	<i>Cardiocondyla emeryi</i>	Idechiil et al. (2007)
	<i>Cardiocondyla wroughtonii</i>	Idechiil et al. (2007)
	<i>Paratrechina bourbonica</i>	Idechiil et al. (2007)
	<i>Tapinoma melanocephalum</i>	Idechiil et al. (2007)
	<i>Technomyrmex albipes</i>	Idechiil et al. (2007)
	<i>Tetramorium bicarinatum</i>	Idechiil et al. (2007)

<i>Prociphilus fraxinifolii</i>	<i>Formica argentea</i>	Jones (1927)
	<i>Formica cinerea</i>	Jones (1927)
<i>Thecabius populimonilis</i>	<i>Camponotus sansabeanus</i>	Jones (1927)
	<i>Camponotus vicinus</i>	Jones (1927)
	<i>Pheidole bicarinata</i>	Jones (1927)
Subfamily Lachninae		
Tribe Eulachnini		
<i>Cinara acutirostris</i>	<i>Formica cinereofusca</i>	Akyildirim et al. (2014)
<i>Cinara apini</i>	<i>Camponotus herculeanus</i>	Jones (1927)
	<i>Camponotus maculatus</i>	Jones (1927)
	<i>Formica argentea</i>	Jones (1927)
	<i>Formica comata</i>	Jones (1927)
	<i>Formica dakotensis</i>	Jones (1927)
	<i>Myrmica rubra</i>	Jones (1927)
<i>Cinara atlantica</i>	<i>Formica subsericea</i>	Favret et al. (2010)
	<i>Lasius alienus</i>	Favret et al. (2010)
	<i>Tapinoma sessile</i>	Favret et al. (2010)
<i>Cinara boernerii</i>	<i>Formica aquilonia</i>	Novgorodova (2005)
	<i>Formica cunicularia</i>	Novgorodova (2005)
	<i>Formica fusca</i>	Novgorodova (2005)
	<i>Formica polycтена</i>	Novgorodova (2005)
	<i>Formica pratensis</i>	Novgorodova (2005)
	<i>Lasius fuliginosus</i>	Novgorodova (2005)
<i>Cinara brevispinosa</i>	<i>Formica fusca</i>	Jones (1927)
	<i>Myrmica scabrinodis</i>	Jones (1927)
<i>Cinara cedri</i>	<i>Lasius brunneus</i>	Akyürek et al. (2016)
	<i>Tapinoma simrothi</i>	Shiran et al. (2013)
<i>Cinara coloradensis</i>	<i>Camponotus pennsylvanicus</i>	Jones (1927)
	<i>Formica cinerea</i>	Jones (1927)
<i>Cinara cupressi</i>	<i>Formica cinerea</i>	Jones (1927)
	<i>Lasius brunneus</i>	Akyürek et al. (2016)
	<i>Lasius turcicus</i>	Akyürek et al. (2016)
<i>Cinara edulis</i>	<i>Camponotus vicinus</i>	Jones (1927)
	<i>Creumatogaster lineolata</i>	Jones (1927)
	<i>Formica fusca</i>	Jones (1927)
<i>Cinara flexilis</i>	<i>Camponotus pennsylvanicus</i>	Jones (1927)
<i>Cinara hottesi</i>	<i>Camponotus herculeanus</i>	Jones (1927)
	<i>Formica cinerea</i>	Jones (1927)
<i>Cinara indica</i>	<i>Formica rufibarbis</i>	Akyürek et al. (2016)
<i>Cinara juniperivora</i>	<i>Nylanderia fulva</i>	Sharma and Buss (2013)
<i>Cinara laricis</i>	<i>Formica aquilonia</i>	Novgorodova (2005)
	<i>Formica fusca</i>	Novgorodova (2005)
	<i>Formica polycтена</i>	Novgorodova (2005)
	<i>Formica pratensis</i>	Novgorodova (2005)
	<i>Lasius fuliginosus</i>	Novgorodova (2005)

<i>Cinara maritimae</i>	<i>Formica cinereofusca</i>	Akyildirim et al. (2014)
<i>Cinara medispinosa</i>	<i>Formica montana</i>	Jones (1927)
<i>Cinara murrayanae</i>	<i>Crematogaster lineolata</i>	Jones (1927)
<i>Cinara occidentalis</i>	<i>Formica rufibarbis</i>	Akyürek et al. (2016)
<i>Cinara oregonensis</i>	<i>Camponotus vicinus</i>	Jones (1927)
	<i>Myrmica incompleta</i>	Jones (1927)
<i>Cinara palaestinensis</i>	<i>Lasius paralienus</i>	Shiran et al. (2013)
<i>Cinara palaestinesis</i>	<i>Cataglyphis emeryi</i>	LATIBARI et al. (2016)
	<i>Formica cunicularia</i>	LATIBARI et al. (2016)
	<i>Lasius alienus</i>	LATIBARI et al. (2016)
	<i>Lasius paralienus</i>	LATIBARI et al. (2016)
	<i>Pheidole pallidula</i>	LATIBARI et al. (2016)
<i>Cinara piceae</i>	<i>Formica aquilonia</i>	Novgorodova (2005), Gibb and Johansson (2010)
	<i>Formica polyctena</i>	Novgorodova (2005)
<i>Cinara piceicola</i>	<i>Formica aquilonia</i>	Gibb and Johansson (2010)
<i>Cinara pilicornis</i>	<i>Formica cinereofusca</i>	Akyildirim et al. (2014)
	<i>Formica fusca</i>	Akyildirim et al. (2014)
	<i>Lasius turcicus</i>	Akyildirim et al. (2014)
	<i>Tetramorium forte</i>	Akyildirim et al. (2014)
<i>Cinara pinea</i>	<i>Formica aquilonia</i>	Novgorodova (2005)
	<i>Formica fusca</i>	Novgorodova (2005)
	<i>Formica polyctena</i>	Novgorodova (2005)
	<i>Formica pratensis</i>	Novgorodova (2005)
	<i>Lasius fuliginosus</i>	Novgorodova (2005)
<i>Cinara pineti</i>	<i>Tapinoma sessile</i>	Jones (1927)
<i>Cinara pini</i>	<i>Camponotus saxatilis</i>	Novgorodova (2005)
	<i>Cardiocondyla shalbergi</i>	LATIBARI et al. (2016)
	<i>Cataglyphis aenescens</i>	LATIBARI et al. (2016)
	<i>Cataglyphis emeryi</i>	LATIBARI et al. (2016)
	<i>Cataglyphis nodus</i>	LATIBARI et al. (2016)
	<i>Crematogaster subdentata</i>	LATIBARI et al. (2016)
	<i>Formica aquilonia</i>	Novgorodova (2005)
	<i>Formica cunicularia</i>	Novgorodova (2005)
	<i>Formica fusca</i>	Novgorodova (2005)
	<i>Formica polyctena</i>	Novgorodova (2005)
	<i>Formica pratensis</i>	Novgorodova (2005)
	<i>Lasius alienus</i>	LATIBARI et al. (2016)
	<i>Lasius emarginatus</i>	Akyildirim et al. (2014)
	<i>Lasius niger</i>	Novgorodova (2005)
	<i>Lasius paralienus</i>	LATIBARI et al. (2016)
	<i>Lasius turcicus</i>	Akyildirim et al. (2014)
	<i>Lepisiota nigra</i>	LATIBARI et al. (2016)
<i>Tapinoma erraticum</i>	LATIBARI et al. (2016)	
<i>Cinara pinihabitans</i>	<i>Camponotus saxatilis</i>	Novgorodova (2005)

<i>Cinara pinivora</i>	<i>Formica subsericea</i>	Favret et al. (2010)
<i>Cinara ponderosae</i>	<i>Camponotus vicinus</i>	Jones (1927)
	<i>Crematogaster laeviuscula</i>	Jones (1927)
	<i>Formica argentea</i>	Jones (1927)
	<i>Tapinoma sessile</i>	Jones (1927)
<i>Cinara pruinosa</i>	<i>Formica cinereofusca</i>	Akyildirim et al. (2014)
<i>Cinara pseudotsugae</i>	<i>Camponotus herculeanus</i>	Jones (1927)
	<i>Camponotus vicinus</i>	Jones (1927)
	<i>Formica canadensis</i>	Jones (1927)
	<i>Formica cinerea</i>	Jones (1927)
	<i>Formica fusca</i>	Jones (1927)
	<i>Formica montana</i>	Jones (1927)
<i>Cinara schwarzii</i>	<i>Camponotus novaeboracensis</i>	Jones (1927)
	<i>Camponotus vicinus</i>	Jones (1927)
	<i>Crematogaster lineolata</i>	Jones (1927)
	<i>Formica comata</i>	Jones (1927)
<i>Cinara sibiricae</i>	<i>Camponotus vicinus</i>	Jones (1927)
<i>Cinara splendens</i>	<i>Camponotus herculeanus</i>	Jones (1927)
	<i>Formica comata</i>	Jones (1927)
<i>Cinara strobi</i>	<i>Camponotus pennsylvanicus</i>	Favret et al. (2010)
<i>Cinara tujaefilina</i>	<i>Lasius brunneus</i>	Akyürek et al. (2016)
	<i>Lasius turcicus</i>	Akyürek et al. (2016)
<i>Cinara vandykei</i>	<i>Camponotus herculeanus</i>	Jones (1927)
<i>Eulachnus tuberculostemmatum</i>	<i>Camponotus turkestanicus</i>	Mortazavi et al. (2015)
<i>Eulachnus tuberculostommata</i>	<i>Tapinoma simrothi</i>	Shiran et al. (2013)
<i>Schizolachnus pineti</i>	<i>Formica cinereofusca</i>	Akyildirim et al. (2014)
Tribe Lachnini		
<i>Lachnus ater</i>	<i>Crematogaster lineolata</i>	Jones (1927)
<i>Lachnus glaber</i>	<i>Formica argentea</i>	Jones (1927)
<i>Lachnus roboris</i>	<i>Camponotus aethiops</i>	Akyürek et al. (2016)
	<i>Lasius brunneus</i>	Akyürek et al. (2016)
	<i>Lasius grandis</i>	Paris and Espadaler (2009)
	<i>Lasius neglectus</i>	Paris and Espadaler (2009)
	<i>Proformica kobachidzei</i>	Akyildirim et al. (2014)
<i>Lachnus solitarius</i>	<i>Camponotus novaeboracensis</i>	Jones (1927)
	<i>Camponotus vicinus</i>	Jones (1927)
<i>Lachnus tropicalis</i>	<i>Lasius fuliginosus</i>	Zhang et al. (2015)
	<i>Lasius niger</i>	Sakata (1995)
<i>Pterochloroides persicae</i>	<i>Cataglyphis aenescens</i>	Mortazavi et al. (2015)
	<i>Cataglyphis nodus</i>	Mortazavi et al. (2015)
	<i>Lasius paralienus</i>	Shiran et al. (2013)
	<i>Lasius turcicus</i>	Akyildirim et al. (2014)

	<i>Lepisiota bipartite</i>	Shiran et al. (2013)
	<i>Lepisiota frauenfeldi</i>	Mortazavi et al. (2015)
	<i>Lepisiota nigra</i>	Mortazavi et al. (2015)
	<i>Tapinoma simrothi</i>	Sary (1969)
<i>Stomaphis hirukawai</i>	<i>Lasius productus</i>	Matsuura and Yashiro (2006)
<i>Stomaphis japonica</i>	<i>Lasius fuliginosus</i>	Zhang et al. (2015)
<i>Stomaphis quercus</i>	<i>Lasius fuliginosus</i>	Novgorodova (2005)
<i>Stomaphis yanonis</i>	<i>Lasius fuji</i>	Endo and Itino (2013)
Tribe Tramini		
<i>Trama troglodytes</i>	<i>Lasius niger</i>	Woodring et al. (2004)
Tribe Tuberolachnini		
<i>Tuberolachnus salignus</i>	<i>Formica canadensis</i>	Jones (1927)
	<i>Formica fusca</i>	Jones (1927)
	<i>Formica rufibarbis</i>	Akyürek et al. (2016)
Subfamily Thelaxinae		
Tribe Thelaxini		
<i>Glyphina betulae</i>	<i>Camponotus saxatilis</i>	Novgorodova (2005)
	<i>Formica aquilonia</i>	Novgorodova (2005)
	<i>Formica polycтена</i>	Novgorodova (2005)
<i>Thelaxes californica</i>	<i>Crematogaster schmidtii</i>	Akyildirim et al. (2014)
	<i>Lasius emarginatus</i>	Akyildirim et al. (2014)
<i>Thelaxes suberi</i>	<i>Camponotus aethiops</i>	Akyürek et al. (2016)
	<i>Lasius brunneus</i>	Akyürek et al. (2016)
<i>Thelaxes suberis</i>	<i>Camponotus gestroi</i>	Sary (1969)
	<i>Camponotus kurdistanicus</i>	Sary (1969)
	<i>Crematogaster auberti</i>	Sary (1969)
	<i>Crematogaster sordidula</i>	Sary (1969)
	<i>Pheidole pallidula</i>	Sary (1969)
	<i>Tapinoma simrothi</i>	Sary (1969)
Subfamily Saltusaphidinae		
Tribe Thripsaphidini		
<i>Callaphis juglandis</i>	<i>Crematogaster inermis</i>	Mortazavi et al. (2015)
	<i>Plagiolepis pallescens</i>	Mortazavi et al. (2015)

Table A2. Species interactions of aphid-associated ants

Ants	Associated aphids	Reference
Subfamily Dolichoderinae		
Tribe Leptomyrmecini		
<i>Dorymyrmex pyramicus</i>	<i>Aphis lugentis</i>	Jones (1927)
	<i>Periphyllus negundinis</i>	Jones (1927)
<i>Dorymyrmex tener</i>	<i>Brachycaudus cardui</i>	Lescano et al. (2015)
<i>Dorymyrmex wolffuegeli</i>	<i>Brachycaudus cardui</i>	Lescano et al. (2015)
<i>Iridomyrmex anceps</i>	<i>Aphis gossypii</i>	Idechiil et al. (2007)

<i>Iridomyrmex humilis</i>	<i>Aphis nerii</i>	Bristow (1991)
<i>Iridomyrmex hartmeyeri</i>	<i>Aphis clerodendri</i>	Carver et al. (2003)
<i>Linepithema humile</i>	<i>Aphis coreopsidis</i>	Altfeld and Stiling (2009)
	<i>Aphis gossypii</i>	Powell and Silverman (2010), Tena et al. (2013), LeVan and Holway (2015)
	<i>Aphis nerii</i>	Pringle et al. (2014)
	<i>Aphis spiraeicola</i>	Tena et al. (2013)
	<i>Chaitophorus populicola</i>	Mondor and Addicott (2007)
	<i>Myzus persicae</i>	Powell and Silverman (2010)
Tribe Tapinomini		
<i>Liometopum luctuosum</i>	<i>Rhopalosiphum nymphaeae</i>	Jones (1927)
<i>Liometopum occidentale</i>	<i>Rhopalosiphum nymphaeae</i>	Jones (1927)
<i>Tapinoma erraticum</i>	<i>Aphis craccivora</i>	Mortazavi et al. (2015)
	<i>Aphis fabae</i>	Mortazavi et al. (2015)
	<i>Aphis gossypii</i>	Mortazavi et al. (2015)
	<i>Aphis pomi</i>	Mortazavi et al. (2015)
	<i>Aphis salicariae</i>	Mortazavi et al. (2015)
	<i>Brachycaudus amygdalinus</i>	Mortazavi et al. (2015)
	<i>Brachycaudus tragopogonis</i>	Mortazavi et al. (2015)
	<i>Chaitophorus israeliticus</i>	Mortazavi et al. (2015)
	<i>Cinara pini</i>	LATIBARI et al. (2016)
<i>Tapinoma indicum</i>	<i>Aphis gossypii</i>	Lokeshwari et al. (2015)
<i>Tapinoma melanocephalum</i>	<i>Aphis gossypii</i>	Idechiil et al. (2007), Lokeshwari et al. (2015)
	<i>Hysteroneura setariae</i>	Idechiil et al. (2007)
	<i>Myzus persicae</i>	Zhou et al. (2015)
	<i>Pentalonia nigronervosa</i>	Idechiil et al. (2007)
<i>Tapinoma sessile</i>	<i>Aphis asclepiadis</i>	Addicott (1979a), Jones (1927)
	<i>Aphis gossypii</i>	Powell and Silverman (2010)
	<i>Aphis helianthi</i>	Mooney et al. (2015)
	<i>Aphis lugentis</i>	Favret et al. (2010)
	<i>Aphis salicariae</i>	Addicott (1979a), Mooney et al. (2015)
	<i>Aphis varians</i>	Addicott (1979a), Mooney et al. (2015)
	<i>Bipersona torticauda</i>	Jones (1927)
	<i>Brachycaudus cardui</i>	Jones (1927)
	<i>Chaitophorus populicola</i>	Jones (1927)
	<i>Chaitophorus populifolii</i>	Jones (1927)
	<i>Chaitophorus viminalis</i>	Jones (1927)
	<i>Cinara atlantica</i>	Favret et al. (2010)
	<i>Cinara pineti</i>	Jones (1927)
	<i>Cinara ponderosae</i>	Jones (1927)
	<i>Dysaphis sorbi</i>	Jones (1927)
	<i>Myzus persicae</i>	Powell and Silverman (2010)
<i>Tapinoma simrothi</i>	<i>Aphis craccivora</i>	Stary (1969), Shiran et al. (2013)
	<i>Aphis davletshinae</i>	Shiran et al. (2013)

	<i>Aphis fabae</i>	Sтары (1969), Shiran et al. (2013)
	<i>Aphis frangulae</i>	Shiran et al. (2013)
	<i>Aphis gossypii</i>	Sтары (1969)
	<i>Aphis nasturtii</i>	Shiran et al. (2013)
	<i>Aphis nerii</i>	Shiran et al. (2013)
	<i>Aphis pomi</i>	Sтары (1969)
	<i>Aphis punicae</i>	Sтары (1969)
	<i>Aphis rumicis</i>	Shiran et al. (2013)
	<i>Aphis umbrella</i>	Shiran et al. (2013)
	<i>Brachycaudus cardui</i>	Sтары (1969)
	<i>Brachycaudus helichrysi</i>	Shiran et al. (2013)
	<i>Brachyonguis harmalae</i>	Shiran et al. (2013)
	<i>Brachyonguis tamaricophilus</i>	Shiran et al. (2013)
	<i>Capitophorus inulae</i>	Shiran et al. (2013)
	<i>Cinara cedri</i>	Shiran et al. (2013)
	<i>Colorado absinthiella</i>	Shiran et al. (2013)
	<i>Eulachnus tuberculostommata</i>	Shiran et al. (2013)
	<i>Hyalopterus pruni</i>	Sтары (1969)
	<i>Myzus persicae</i>	Shiran et al. (2013)
	<i>Nearctaphis bakeri</i>	Shiran et al. (2013)
	<i>Pterochloroides persicae</i>	Sтары (1969)
	<i>Rhopalosiphum maidis</i>	Sтары (1969)
	<i>Rhopalosiphum padi</i>	Shiran et al. (2013)
	<i>Thelaxes suberis</i>	Sтары (1969)
<i>Technomyrmex albipes</i>	<i>Aphis clerodendri</i>	Carver et al. (2003)
	<i>Aphis gossypii</i>	Idechiil et al. (2007), Lokeshwari et al. (2015)
	<i>Hysteroneura setariae</i>	Idechiil et al. (2007)
	<i>Pentalonia nigronervosa</i>	Idechiil et al. (2007)
Subfamily Formicinae		
Tribe Camponotini		
<i>Camponotus aethiops</i>	<i>Aphis brotericola</i>	Özdemir et al. (2008)
	<i>Aphis fabae</i>	Akyürek et al. (2016)
	<i>Aphis salviae</i>	Özdemir et al. (2008)
	<i>Brachcaudus helicyrsi</i>	Özdemir et al. (2008)
	<i>Brachycaudus cardui</i>	Özdemir et al. (2008), Akyürek et al. (2016)
	<i>Lachnus roboris</i>	Akyürek et al. (2016)
	<i>Thelaxes suberi</i>	Akyürek et al. (2016)
<i>Camponotus compressus</i>	<i>Aphis craccivora</i>	Kataria and Kumar (2013), Rakhshan and Ahmad (2015)
	<i>Aphis fabae</i>	Kataria and Kumar (2013)
	<i>Aphis gossypii</i>	Vergheese and Tandon (1987), Kataria and Kumar (2013), Lokeshwari et al. (2015)
	<i>Aphis nerii</i>	Kataria and Kumar (2013)

	<i>Myzus persicae</i>	Kataria and Kumar (2013)
<i>Camponotus gestroi</i>	<i>Thelaxes suberis</i>	Sary (1969)
<i>Camponotus herculeanus</i>	<i>Aphis lugentis</i>	Jones (1927)
	<i>Aphis salicariae</i>	Addicott (1979a)
	<i>Aphis valerianae</i>	Jones (1927)
	<i>Aphis varians</i>	Addicott (1979a)
	<i>Chaitophorus populicola</i>	Jones (1927)
	<i>Chaitophorus populifolii</i>	Jones (1927)
	<i>Cinara apini</i>	Jones (1927)
	<i>Cinara hottesi</i>	Jones (1927)
	<i>Cinara pseudotsugae</i>	Jones (1927)
	<i>Cinara splendens</i>	Jones (1927)
	<i>Cinara vandykei</i>	Jones (1927)
	<i>Obtusicauda frigidae</i>	Jones (1927)
	<i>Pterocomma populeum</i>	Jones (1927)
	<i>Schizaphis graminum</i>	Jones (1927)
<i>Camponotus invidus</i>	<i>Aphis craccivora</i>	Rakhshan and Ahmad (2015)
<i>Camponotus japonicus</i>	<i>Chaitophorus saliniger</i>	Hembry et al. (2006)
<i>Camponotus kurdistanicus</i>	<i>Thelaxes suberis</i>	Sary (1969)
	<i>Aphis craccivora</i>	Sary (1969)
<i>Camponotus lateralis</i>	<i>Aphis spiraecola</i>	Akyürek et al. (2016)
<i>Camponotus libanicus</i>	<i>Aphis craccivora</i>	Shiran et al. (2013)
<i>Camponotus maculatus</i>	<i>Cinara apini</i>	Jones (1927)
<i>Camponotus modoc</i>	<i>Aphis lugentis</i>	Jones (1927)
<i>Camponotus navigator</i>	<i>Hysteroneura setariae</i>	Idechiil et al. (2007)
<i>Camponotus novaeboracensis</i>	<i>Chaitophorus nigrae</i>	Jones (1927)
	<i>Cinara schwarzii</i>	Jones (1927)
	<i>Lachnus solitarius</i>	Jones (1927)
<i>Camponotus oasisium</i>	<i>Aphis craccivora</i>	Shiran et al. (2013)
	<i>Aphis frangulae</i>	Shiran et al. (2013)
<i>Camponotus parius</i>	<i>Aphis gossypii</i>	Lokeshwari et al. (2015)
<i>Camponotus pennsylvanicus</i>	<i>Chaitophorus populicola</i>	Jones (1927)
	<i>Cinara coloradensis</i>	Jones (1927)
	<i>Cinara flexilis</i>	Jones (1927)
	<i>Cinara strobi</i>	Favret et al. (2010)
<i>Camponotus piceus</i>	<i>Aphis brotericola</i>	Özdemir et al. (2008)
	<i>Aphis chloris</i>	Özdemir et al. (2008)
	<i>Aphis craccivora</i>	Özdemir et al. (2008)
	<i>Aphis euphorbiae</i>	Özdemir et al. (2008)
	<i>Aphis fabae</i>	Özdemir et al. (2008)
	<i>Aphis salviae</i>	Özdemir et al. (2008)
	<i>Hyadaphis hofmanni</i>	Özdemir et al. (2008)
	<i>Staegeriella necopinata</i>	Özdemir et al. (2008)
<i>Camponotus reticulatus</i>	<i>Aphis gossypii</i>	Idechiil et al. (2007)
	<i>Pentalonia nigronervosa</i>	Idechiil et al. (2007)

<i>Camponotus sansabeanus</i>	<i>Thecabius populimonilis</i>	Jones (1927)
<i>Camponotus saxatilis</i>	<i>Aphis brohmeri</i>	Novgorodova (2005)
	<i>Aphis fabae</i>	Novgorodova (2005)
	<i>Callipterinella tuberculata</i>	Novgorodova (2005)
	<i>Chaitophorus albus</i>	Novgorodova (2005)
	<i>Chaitophorus populeti</i>	Novgorodova (2005)
	<i>Chaitophorus populialbae</i>	Novgorodova (2005)
	<i>Chaitophorus tremulae</i>	Novgorodova (2005)
	<i>Cinara pini</i>	Novgorodova (2005)
	<i>Cinara pinihabitans</i>	Novgorodova (2005)
	<i>Glyphina betulae</i>	Novgorodova (2005)
	<i>Symydobius oblongus</i>	Novgorodova (2005)
<i>Camponotus subbarbatus</i>	<i>Drepanaphis nigricans</i>	Favret et al. (2010)
<i>Camponotus turkestanicus</i>	<i>Eulachnus tuberculostemmatum</i>	Mortazavi et al. (2015)
<i>Camponotus vicinus</i>	<i>Aphis asclepiadis</i>	Jones (1927)
	<i>Aphis valeriana</i>	Jones (1927)
	<i>Bipersona torticauda</i>	Jones (1927)
	<i>Chaitophorus populifolii</i>	Jones (1927)
	<i>Chaitophorus viminalis</i>	Jones (1927)
	<i>Cinara edulis</i>	Jones (1927)
	<i>Cinara oregonensis</i>	Jones (1927)
	<i>Cinara ponderosae</i>	Jones (1927)
	<i>Cinara pseudotsugae</i>	Jones (1927)
	<i>Cinara schwarzii</i>	Jones (1927)
	<i>Cinara sibiricae</i>	Jones (1927)
	<i>Lachnus solitarius</i>	Jones (1927)
	<i>Macrosiphum chrysothamni</i>	Jones (1927)
	<i>Macrosiphum valeriana</i>	Jones (1927)
	<i>Protaphis middletonii</i>	Jones (1927)
	<i>Thecabius populimonilis</i>	Jones (1927)
	<i>Aphis clerodendri</i>	Carver et al. (2003)
<i>Polyrhachis hauxwelli</i>	<i>Aphis craccivora</i>	Rakhshan and Ahmad (2015)
<i>Polyrhachis lacteipennis</i>	<i>Aphis craccivora</i>	Shiran et al. (2013)
	<i>Aphis frangulae</i>	Shiran et al. (2013)
	<i>Rhopalosiphum maidis</i>	Shiran et al. (2013)
<i>Polyrhachis simplex</i>	<i>Chaitophorous populialbae</i>	Degen et al. (1986)
<i>Prenolepis imparis</i>	<i>Aphis cornifoliae</i>	Favret et al. (2010)
	<i>Aphis fabae</i>	Favret et al. (2010)
	<i>Capitophorus elaeagni</i>	Favret et al. (2010)
	<i>Nearctaphis bakeri</i>	Favret et al. (2010)
	<i>Rhopalosiphum maidis</i>	Barton and Ives (2014)
<i>Uroleucon sonchellum</i>	Favret et al. (2010)	
Tribe Formicini		
<i>Cataglyphis aenescens</i>	<i>Aphis craccivora</i>	Özdemir et al. (2008)

	<i>Cinara pini</i>	LATIBARI et al. (2016)
	<i>Macrosiphum euphorbiae</i>	Mortazavi et al. (2015)
	<i>Pterochloroides persicae</i>	Mortazavi et al. (2015)
<i>Cataglyphis cinnamomeus</i>	<i>Myzus persicae</i>	Shiran et al. (2013)
<i>Cataglyphis emeryi</i>	<i>Cinara palaestinesis</i>	LATIBARI et al. (2016)
	<i>Cinara pini</i>	LATIBARI et al. (2016)
<i>Cataglyphis livida</i>	<i>Subcryptosiphon sp.</i>	Sary (1969)
<i>Cataglyphis lividus</i>	<i>Aphis fabae</i>	Shiran et al. (2013)
<i>Cataglyphis nodus</i>	<i>Aphis frangulae</i>	Shiran et al. (2013)
	<i>Aphis gossypii</i>	Sary (1969)
	<i>Chaitophorus sp.</i>	Sary (1969)
	<i>Cinara pini</i>	LATIBARI et al. (2016)
	<i>Pterochloroides persicae</i>	Mortazavi et al. (2015)
<i>Cataglyphis protuberata</i>	<i>Lachnus sp.</i>	Sary (1969)
<i>Formica altipetens</i>	<i>Bipersona torticauda</i>	Jones (1927)
<i>Formica aquilonia</i>	<i>Aphis brohmeri</i>	Novgorodova (2005)
	<i>Aphis craccivora</i>	Novgorodova (2005)
	<i>Aphis evonymi</i>	Novgorodova (2005)
	<i>Aphis fabae</i>	Novgorodova (2005)
	<i>Aphis jacobaeae</i>	Novgorodova (2005)
	<i>Aphis pomi</i>	Novgorodova (2005)
	<i>Aphis subnitidae</i>	Novgorodova (2005)
	<i>Aphis viburni</i>	Novgorodova (2005)
	<i>Callipterinella tuberculata</i>	Novgorodova (2005)
	<i>Chaitophorus albitorosus</i>	Novgorodova (2005)
	<i>Chaitophorus albus</i>	Novgorodova (2005)
	<i>Chaitophorus populeti</i>	Novgorodova (2005)
	<i>Chaitophorus populialbae</i>	Novgorodova (2005)
	<i>Chaitophorus salicti</i>	Novgorodova (2005)
	<i>Cinara boernerii</i>	Novgorodova (2005)
	<i>Cinara laticis</i>	Novgorodova (2005)
	<i>Cinara piceae</i>	Novgorodova (2005), Gibb and Johansson (2010)
	<i>Cinara piceicola</i>	Gibb and Johansson (2010)
	<i>Cinara pinea</i>	Novgorodova (2005)
	<i>Cinara pini</i>	Novgorodova (2005)
	<i>Glyphina betulae</i>	Novgorodova (2005)
	<i>Rhopalosiphum padi</i>	Novgorodova (2005)
<i>Schizaphis gramina</i>	Novgorodova (2005)	
<i>Schizaphis pyri</i>	Novgorodova (2005)	
<i>Symydobius oblongus</i>	Novgorodova (2005)	
<i>Formica argentea</i>	<i>Anuraphis subterranea</i>	Jones (1927)
	<i>Aphis aiddletonii</i>	Jones (1927)
	<i>Aphis asclepiadis</i>	Jones (1927)
	<i>Aphis gossypii</i>	Jones (1927)

	<i>Aphis lugentis</i>	Jones (1927)
	<i>Aphis medicaginis</i>	Jones (1927)
	<i>Aphis sambucifolii</i>	Jones (1927)
	<i>Aphis ulmariae</i>	Jones (1927)
	<i>Bipersona torticauda</i>	Jones (1927)
	<i>Braggia eriogoni</i>	Jones (1927)
	<i>Chaitophorus nigrae</i>	Jones (1927)
	<i>Chaitophorus populicola</i>	Jones (1927)
	<i>Chaitophorus populifolii</i>	Jones (1927)
	<i>Chaitophorus viminalis</i>	Jones (1927)
	<i>Cinara apini</i>	Jones (1927)
	<i>Cinara ponderosae</i>	Jones (1927)
	<i>Cryptomyzus ribis</i>	Jones (1927)
	<i>Drepanaphis acerifoliae</i>	Jones (1927)
	<i>Hyperomyzus lactucae</i>	Jones (1927)
	<i>Lachnus glaber</i>	Jones (1927)
	<i>Macrosiphum euphorbiae</i>	Jones (1927)
	<i>Myzaphis rosarum</i>	Jones (1927)
	<i>Myzocallis discolor</i>	Jones (1927)
	<i>Myzus persicae</i>	Jones (1927)
	<i>Periphyllus negundinis</i>	Jones (1927)
	<i>Prociphilus fraxinifolii</i>	Jones (1927)
	<i>Pterocomma smithiae</i>	Jones (1927)
	<i>Rhopalosiphum nymphaeae</i>	Jones (1927)
	<i>Uroleucon ambrosiae</i>	Jones (1927)
	<i>Uroleucon erigeronense</i>	Jones (1927)
	<i>Uroleucon solidaginis</i>	Jones (1927)
	<i>Uroleucon taraxaci</i>	Jones (1927)
<i>Formica aserva</i>	<i>Aphis asclepiadis</i>	Addicott (1979a)
	<i>Aphis salicariae</i>	Addicott (1979a)
	<i>Aphis varians</i>	Addicott (1979a)
	<i>Rhopalosiphum nymphaeae</i>	Jones (1927)
<i>Formica aterrima</i>	<i>Chaitophorus populifolii</i>	Jones (1927)
<i>Formica bradleyi</i>	<i>Rhopalosiphum nymphaeae</i>	Jones (1927)
<i>Formica canadensis</i>	<i>Aphis asclepiadis</i>	Jones (1927)
	<i>Aphis lugentis</i>	Jones (1927)
	<i>Aphis medicaginis</i>	Jones (1927)
	<i>Aphis pomi</i>	Jones (1927)
	<i>Aphis valerianae</i>	Jones (1927)
	<i>Chaitophorus populifolii</i>	Jones (1927)
	<i>Cinara pseudotsugae</i>	Jones (1927)
	<i>Drepanaphis acerifoliae</i>	Jones (1927)
	<i>Drepanosiphum braggii</i>	Jones (1927)
	<i>Tuberolachnus salignus</i>	Jones (1927)
	<i>Uroleucon ambrosiae</i>	Jones (1927)

<i>Formica cinerea</i>	<i>Aphis asclepiadis</i>	Jones (1927)
	<i>Aphis forbesi</i>	Jones (1927)
	<i>Aphis gossypii</i>	Jones (1927)
	<i>Aphis medicaginis</i>	Jones (1927)
	<i>Aphis pomi</i>	Jones (1927)
	<i>Aphis varians</i>	Addicott (1978), Breton and Addicott (1992)
	<i>Aphthargelia symphoricarpi</i>	Addicott (1978)
	<i>Bipersona torticauda</i>	Jones (1927)
	<i>Brachycaudus helichrysi</i>	Jones (1927)
	<i>Cinara coloradensis</i>	Jones (1927)
	<i>Cinara cupressi</i>	Jones (1927)
	<i>Cinara hottesi</i>	Jones (1927)
	<i>Cinara pseudotsugae</i>	Jones (1927)
	<i>Diuraphis calamagrostis</i>	Jones (1927)
	<i>Eriosoma americanum</i>	Jones (1927)
	<i>Pleotrichophorus quadritrichus</i>	Addicott (1978)
	<i>Prociphilus fraxinifolii</i>	Jones (1927)
	<i>Protaphis middletonii</i>	Jones (1927)
	<i>Rhopalosiphum maidis</i>	Jones (1927)
<i>Uroleucon ambrosiae</i>	Jones (1927)	
<i>Uroleucon erigeronense</i>	Jones (1927)	
<i>Formica cinerea lepida</i>	<i>Aphis asclepiadis</i>	Addicott (1979a)
	<i>Aphis salicariae</i>	Addicott (1979a)
	<i>Aphis varians</i>	Addicott (1979a)
<i>Formica cinereofusca</i>	<i>Aphis craccivora</i>	Akyildirim et al. (2014)
	<i>Aphis fabae</i>	Akyildirim et al. (2014)
	<i>Aphis farinosa</i>	Akyildirim et al. (2014)
	<i>Aphis gossypii</i>	Akyildirim et al. (2014)
	<i>Aphis nasturtii</i>	Akyildirim et al. (2014)
	<i>Aphis sambuci</i>	Akyildirim et al. (2014)
	<i>Aphis serpylli</i>	Akyildirim et al. (2014)
	<i>Aphis spiraeicola</i>	Akyildirim et al. (2014)
	<i>Aphis verbasci</i>	Akyildirim et al. (2014)
	<i>Brachycaudus cardui</i>	Akyildirim et al. (2014)
	<i>Brachycaudus helichrysi</i>	Akyildirim et al. (2014)
	<i>Brachycaudus lychnidis</i>	Akyildirim et al. (2014)
	<i>Brachyunguis tamaricis</i>	Akyildirim et al. (2014)
	<i>Chaitophorus longisetosus</i>	Akyildirim et al. (2014)
	<i>Cinara acutirostris</i>	Akyildirim et al. (2014)
	<i>Cinara maritimae</i>	Akyildirim et al. (2014)
	<i>Cinara pilicornis</i>	Akyildirim et al. (2014)
	<i>Cinara pruinosa</i>	Akyildirim et al. (2014)
	<i>Myzus lythri</i>	Akyildirim et al. (2014)
<i>Nearctaphis bakeri</i>	Akyildirim et al. (2014)	

	<i>Periphyllus aceris</i>	Akyildirim et al. (2014)
	<i>Pterocallis albidus</i>	Akyildirim et al. (2014)
	<i>Pterocallis alni</i>	Akyildirim et al. (2014)
	<i>Schizaphis miscanthi</i>	Akyildirim et al. (2014)
	<i>Schizolachnus pineti</i>	Akyildirim et al. (2014)
	<i>Sipha maydis</i>	Akyildirim et al. (2014)
	<i>Symydobius oblongus</i>	Akyildirim et al. (2014)
	<i>Toxoptera aurantii</i>	Akyildirim et al. (2014)
<i>Formica coloradensis</i>	<i>Rhopalosiphum nymphaeae</i>	Jones (1927)
<i>Formica comata</i>	<i>Cinara apini</i>	Jones (1927)
	<i>Cinara schwarzii</i>	Jones (1927)
	<i>Cinara splendens</i>	Jones (1927)
<i>Formica cunicularia</i>	<i>Aphis pomi</i>	Novgorodova (2005)
	<i>Chaitophorus albus</i>	Novgorodova (2005)
	<i>Chaitophorus populeti</i>	Novgorodova (2005)
	<i>Chaitophorus populialbae</i>	Novgorodova (2005)
	<i>Cinara boernerii</i>	Novgorodova (2005)
	<i>Cinara pini</i>	Novgorodova (2005)
	<i>Macrosiphoniella pulvera</i>	Novgorodova (2005)
<i>Formica cunicularia</i>	<i>Acyrtosiphon pisum</i>	Mortazavi et al. (2015)
	<i>Acyrtosiphon rubi</i>	Mortazavi et al. (2015)
	<i>Aphis acetosae</i>	Mortazavi et al. (2015)
	<i>Aphis brotericola</i>	Akyürek et al. (2016)
	<i>Aphis craccivora</i>	Özdemir et al. (2008), Mortazavi et al. (2015)
	<i>Aphis fabae</i>	Akyürek et al. (2016)
	<i>Aphis nasturtii</i>	Akyürek et al. (2016)
	<i>Aphis solanella</i>	Akyürek et al. (2016)
	<i>Aphis spiraeicola</i>	Akyürek et al. (2016)
	<i>Brachycaudus tragopogonis</i>	Mortazavi et al. (2015)
	<i>Cinara palaestinesis</i>	LATIBARI et al. (2016)
	<i>Macrosiphum rosae</i>	Akyürek et al. (2016)
	<i>Sipha maydis</i>	Akyürek et al. (2016)
<i>Formica dakotensis</i>	<i>Chaitophorus populicola</i>	Jones (1927)
	<i>Cinara apini</i>	Jones (1927)
<i>Formica efiniventris</i>	<i>Aphis lugentis</i>	Jones (1927)
	<i>Obtusicauda frigidae</i>	Jones (1927)
<i>Formica fusca</i>	<i>Anuraphis subterranea</i>	Jones (1927)
	<i>Aphis asclepiadis</i>	Jones (1927), Addicott (1979a)
	<i>Aphis craccivora</i>	Akyürek et al. (2016)
	<i>Aphis esulae</i>	Akyürek et al. (2016)
	<i>Aphis fabae</i>	Akyildirim et al. (2014)
	<i>Aphis farinosa</i>	Jones (1927)
	<i>Aphis gossypii</i>	Jones (1927)
<i>Aphis helianthi</i>	Mooney et al. (2015)	

<i>Aphis hermistonii</i>	Jones (1927)
<i>Aphis lugentis</i>	Jones (1927)
<i>Aphis maculatae</i>	Jones (1927)
<i>Aphis medicaginis</i>	Jones (1927)
<i>Aphis oenotherae</i>	Jones (1927)
<i>Aphis pomi</i>	Jones (1927)
<i>Aphis salicariae</i>	Addicott (1979a), Mooney et al. (2015)
<i>Aphis varians</i>	Addicott (1978), Addicott (1979a), Mooney et al. (2015)
<i>Artemisaphis artemisicola</i>	Jones (1927)
<i>Bipersona torticauda</i>	Jones (1927)
<i>Brachycaudus cardui</i>	Jones (1927), Akyildirim et al. (2014)
<i>Brachycaudus persicae</i>	Jones (1927)
<i>Brachyunguis tetrapteralis</i>	Jones (1927)
<i>Braggia eriogoni</i>	Jones (1927)
<i>Ceruraphis viburnicola</i>	Jones (1927)
<i>Chaitophorus macrostachyae</i>	Jones (1927)
<i>Chaitophorus populeti</i>	Novgorodova (2005)
<i>Chaitophorus populialbae</i>	Novgorodova (2005)
<i>Chaitophorus populifolii</i>	Jones (1927)
<i>Chaitophorus viminalis</i>	Jones (1927)
<i>Cinara boernerii</i>	Novgorodova (2005)
<i>Cinara brevispinosa</i>	Jones (1927)
<i>Cinara edulis</i>	Jones (1927)
<i>Cinara loricis</i>	Novgorodova (2005)
<i>Cinara pilicornis</i>	Akyildirim et al. (2014)
<i>Cinara pinea</i>	Novgorodova (2005)
<i>Cinara pini</i>	Novgorodova (2005)
<i>Cinara pseudotsugae</i>	Jones (1927)
<i>Cryptomyzus ribis</i>	Jones (1927)
<i>Drepanosiphum braggii</i>	Jones (1927)
<i>Dysaphis sorbi</i>	Jones (1927)
<i>Macrosiphum chrysothamni</i>	Jones (1927)
<i>Myzaphis rosarum</i>	Jones (1927)
<i>Myzocallis discolor</i>	Jones (1927)
<i>Myzus cerasi</i>	Jones (1927)
<i>Myzus oenotherae</i>	Jones (1927)
<i>Nasonovia houghtonensis</i>	Jones (1927)
<i>Obtusicauda frigidae</i>	Jones (1927)
<i>Periphyllus negundinis</i>	Jones (1927)
<i>Protaphis middletonii</i>	Jones (1927)
<i>Pterocomma bicolor</i>	Jones (1927)
<i>Pterocomma salicis</i>	Jones (1927)
<i>Rhopalosiphum maidis</i>	Jones (1927)

	<i>Tuberolachnus salignus</i>	Jones (1927)
	<i>Uroleucon ambrosiae</i>	Jones (1927)
	<i>Uroleucon erigeronense</i>	Jones (1927)
	<i>Uroleucon kikioense</i>	Akyildirim et al. (2014)
<i>Formica gagates</i>	<i>Aphis farinosa</i>	Akyildirim et al. (2014)
<i>Formica glauca</i>	<i>Aphis craccivora</i>	Özdemir et al. (2008)
	<i>Aphis fabae</i>	Özdemir et al. (2008)
	<i>Aphis galliiscabri</i>	Özdemir et al. (2008)
	<i>Brachycaudus (Appelia) tragopogonis</i>	Özdemir et al. (2008)
	<i>Brachycaudus cardui</i>	Özdemir et al. (2008)
<i>Formica gnava</i>	<i>Rhopalosiphum nymphaeae</i>	Jones (1927)
<i>Formica incerta</i>	<i>Rhopalosiphum nymphaeae</i>	Jones (1927)
<i>Formica integroides</i>	<i>Aphis farinosa</i>	Addicott (1978)
	<i>Rhopalosiphum nymphaeae</i>	Jones (1927)
	<i>Aphis asclepiadis</i>	Addicott (1979a)
	<i>Aphis salicariae</i>	Addicott (1979a)
	<i>Aphis varians</i>	Addicott (1978), Addicott (1979a)
<i>Formica japonica</i>	<i>Chaitophorus saliniger</i>	Hembry et al. (2006)
	<i>Uroleucon nigrotuberculatum</i>	Ando and Ohgushi (2008)
<i>Formica lasioides</i>	<i>Aphis asclepiadis</i>	Addicott (1979a)
	<i>Aphis salicariae</i>	Addicott (1979a)
	<i>Aphis varians</i>	Addicott (1978), Addicott (1979a)
	<i>Rhopalosiphum nymphaeae</i>	Jones (1927)
<i>Formica lepida</i>	<i>Aphis asclepiadis</i>	Jones (1927)
	<i>Rhopalosiphum nymphaeae</i>	Jones (1927)
<i>Formica limata</i>	<i>Rhopalosiphum nymphaeae</i>	Jones (1927)
<i>Formica lugubris</i>	<i>Cinara pini</i>	Sudd (1983)
<i>Formica montana</i>	<i>Aphis asclepiadis</i>	Jones (1927)
	<i>Aphis oregonensis</i>	Jones (1927)
	<i>Chaitophorus populicola</i>	Jones (1927)
	<i>Cinara medispinosa</i>	Jones (1927)
	<i>Cinara pseudotsugae</i>	Jones (1927)
	<i>Macrosiphum chrysothamni</i>	Jones (1927)
	<i>Pleotrichophorus glandulosus</i>	Jones (1927)
	<i>Pseudoepameibaphis tridentatae</i>	Jones (1927)
<i>Formica munda</i>	<i>Rhopalosiphum nymphaeae</i>	Jones (1927)
<i>Formica neoclara</i>	<i>Rhopalosiphum nymphaeae</i>	Jones (1927)
<i>Formica neogagates</i>	<i>Rhopalosiphum nymphaeae</i>	Jones (1927)
<i>Formica neorufibarbis</i>	<i>Rhopalosiphum nymphaeae</i>	Jones (1927)
<i>Formica neorufibarbis gelida</i>	<i>Aphis asclepiadis</i>	Addicott (1979a)
	<i>Aphis salicariae</i>	Addicott (1979a)
	<i>Aphis varians</i>	Addicott (1979a)

<i>Formica obscuripes</i>	<i>Aphis asclepiadis</i>	Addicott (1979a)
	<i>Aphis salicariae</i>	Addicott (1979a)
	<i>Aphis varians</i>	Addicott (1978), Addicott (1979a)
	<i>Pleotrichophorus utensis</i>	Billick et al. (2007)
	<i>Rhopalosiphum nymphaeae</i>	Jones (1927)
	<i>Uroleucon escalantii</i>	Billick et al. (2007)
<i>Formica opaciventris</i>	<i>Aphis asclepiadis</i>	Jones (1927)
	<i>Aphis medicaginis</i>	Jones (1927)
<i>Formica oreas</i>	<i>Rhopalosiphum nymphaeae</i>	Jones (1927)
<i>Formica podzolica</i>	<i>Aphis asclepiadis</i>	Mooney et al. (2008), Nielsen et al. (2009), Abdala-Roberts et al. (2012)
	<i>Aphis valerianae</i>	Petry et al. (2012)
<i>Formica polyctena</i>	<i>Aphis brohmeri</i>	Novgorodova (2005)
	<i>Aphis craccivora</i>	Novgorodova (2005)
	<i>Aphis evonymi</i>	Novgorodova (2005)
	<i>Aphis fabae</i>	Novgorodova (2005)
	<i>Aphis jacobaeae</i>	Novgorodova (2005)
	<i>Aphis pomi</i>	Novgorodova (2005)
	<i>Aphis subnitidae</i>	Novgorodova (2005)
	<i>Callipterinella tuberculata</i>	Novgorodova (2005)
	<i>Chaitophorus albitorosus</i>	Novgorodova (2005)
	<i>Chaitophorus albus</i>	Novgorodova (2005)
	<i>Chaitophorus populeti</i>	Novgorodova (2005)
	<i>Chaitophorus populialbae</i>	Novgorodova (2005)
	<i>Chaitophorus salicti</i>	Novgorodova (2005)
	<i>Cinara boernerii</i>	Novgorodova (2005)
	<i>Cinara laricis</i>	Novgorodova (2005)
	<i>Cinara piceae</i>	Novgorodova (2005)
	<i>Cinara pinea</i>	Novgorodova (2005)
	<i>Cinara pini</i>	Novgorodova (2005)
	<i>Glyphina betulae</i>	Novgorodova (2005)
	<i>Macrosiphoniella pulvera</i>	Novgorodova (2005)
<i>Rhopalosiphum padi</i>	Novgorodova (2005)	
<i>Schizaphis gramina</i>	Novgorodova (2005)	
<i>Schizaphis pyri</i>	Novgorodova (2005)	
<i>Symydobius oblongus</i>	Novgorodova (2005)	
<i>Formica pratensis</i>	<i>Aphis craccivora</i>	Novgorodova (2005)
	<i>Chaitophorus nassonowi</i>	Novgorodova (2005)
	<i>Chaitophorus populeti</i>	Novgorodova (2005)
	<i>Cinara boernerii</i>	Novgorodova (2005)
	<i>Cinara laricis</i>	Novgorodova (2005)
	<i>Cinara pinea</i>	Novgorodova (2005)
	<i>Cinara pini</i>	Novgorodova (2005)
<i>Symydobius oblongus</i>	Novgorodova (2005)	
<i>Formica propinqua</i>	<i>Chaitophorus populicola</i>	Wimp and Whitham (2001)

<i>Formica puberula</i>	<i>Aphis salicariae</i>	Addicott (1979a)
	<i>Aphis varians</i>	Addicott (1979a)
	<i>Rhopalosiphum nymphaeae</i>	Jones (1927)
<i>Formica ravidata</i>	<i>Rhopalosiphum nymphaeae</i>	Jones (1927)
<i>Formica rubicunda</i>	<i>Rhopalosiphum nymphaeae</i>	Jones (1927)
<i>Formica rufa</i>	<i>Aphis helianthi</i>	Mooney et al. (2015)
	<i>Aphis medicaginis</i>	Jones (1927)
	<i>Aphis salicariae</i>	Mooney et al. (2015)
	<i>Aphis valerianae</i>	Jones (1927)
	<i>Aphis varians</i>	Mooney et al. (2015)
	<i>Brachycaudus cardui</i>	Jones (1927)
	<i>Chaitophorus populifolii</i>	Jones (1927)
	<i>Nearctaphis bakeri</i>	Jones (1927)
	<i>Rhopalosiphum nymphaeae</i>	Jones (1927)
<i>Formica rufibarbis</i>	<i>Aphis pomi</i>	Akyildirim et al. (2014)
	<i>Aphis spiraecola</i>	Akyürek et al. (2016)
	<i>Cinara indica</i>	Akyürek et al. (2016)
	<i>Cinara occidentalis</i>	Akyürek et al. (2016)
	<i>Dysaphis devectora</i>	Akyürek et al. (2016)
	<i>Myzus ornatus</i>	Akyürek et al. (2016)
	<i>Myzus padellus</i>	Akyürek et al. (2016)
	<i>Tuberolachnus salignus</i>	Akyürek et al. (2016)
<i>Formica sanguinea</i>	<i>Chaitophorus populeti</i>	Akyürek et al. (2016)
	<i>Rhopalosiphum nymphaeae</i>	Jones (1927)
<i>Formica subaenescens</i>	<i>Rhopalosiphum nymphaeae</i>	Jones (1927)
<i>Formica subintegra</i>	<i>Rhopalosiphum nymphaeae</i>	Jones (1927)
<i>Formica subsericea</i>	<i>Aphis coreopsidis</i>	Favret et al. (2010)
	<i>Aulacorthum solani</i>	Favret et al. (2010)
	<i>Cinara atlantica</i>	Favret et al. (2010)
	<i>Cinara pinivora</i>	Favret et al. (2010)
	<i>Hyperomyzus nabali</i>	Favret et al. (2010)
	<i>Neomyzus circumflexum</i>	Favret et al. (2010)
	<i>Rhopalosiphum nymphaeae</i>	Jones (1927)
	<i>Uroleucon pieloui</i>	Favret et al. (2010)
<i>Formica ulkei</i>	<i>Rhopalosiphum nymphaeae</i>	Jones (1927)
<i>Formica yessensis</i>	<i>Tuberculatus quercicola</i>	Yao and Akimoto (2001), Yao and Akimoto (2009)
<i>Proformica kobachidzei</i>	<i>Lachnus roboris</i>	Akyildirim et al. (2014)
	<i>Myzus cerasi</i>	Akyildirim et al. (2014)
<i>Proformica piloscapa</i>	<i>Brachycaudus amygdalinus</i>	Mortazavi et al. (2015)
Tribe Lasiini		
<i>Lasius alienus</i>	<i>Aphis fabae</i>	Akyildirim et al. (2014), Akyürek et al. (2016)
	<i>Aphis galliiscabri</i>	Özdemir et al. (2008)
	<i>Aphis gossypii</i>	Akyildirim et al. (2014), Akyürek et al. (2016)

	<i>Aphis idaei</i>	Sary (1969)
	<i>Aphis maidi-radicis</i>	Forbes (1906)
	<i>Aphis molluginis</i>	Akyildirim et al. (2014)
	<i>Aphis nasturtii</i>	Özdemir et al. (2008)
	<i>Aphis pomi</i>	Akyürek et al. (2016)
	<i>Aphis pseudocardui</i>	Akyürek et al. (2016)
	<i>Aphis solanella</i>	Akyürek et al. (2016)
	<i>Aphis urticata</i>	Akyürek et al. (2016)
	<i>Aphis verbasci</i>	Özdemir et al. (2008), Akyürek et al. (2016)
	<i>Brachycaudus (Appelia) tragopogonis</i>	Özdemir et al. (2008)
	<i>Brachycaudus cardui</i>	Akyürek et al. (2016)
	<i>Capitophorus hippophaes</i>	Özdemir et al. (2008)
	<i>Chaitophorus kapuri</i>	Akyildirim et al. (2014)
	<i>Cinara atlantica</i>	Favret et al. (2010)
	<i>Cinara palaestinesis</i>	LATIBARI et al. (2016)
	<i>Cinara pini</i>	LATIBARI et al. (2016)
	<i>Dysaphis foeniculus</i>	Akyürek et al. (2016)
	<i>Dysaphis pyri</i>	Akyildirim et al. (2014)
	<i>Myzus cerasi</i>	Akyürek et al. (2016)
	<i>Neobetulaphis pusilla</i>	Akyildirim et al. (2014)
	<i>Periphyllus bulgaricus</i>	Mortazavi et al. (2015)
	<i>Rhopalosiphum cerasifoliae</i>	Favret et al. (2010)
	<i>Rhopalosiphum maidis</i>	Barton and Ives (2014)
	<i>Rhopalosiphum nymphaeae</i>	Jones (1927)
	<i>Sipha maydis</i>	Akyürek et al. (2016)
	<i>Toxoptera aurantii</i>	Akyildirim et al. (2014)
<i>Lasius americanus</i>	<i>Pemphigus lasii</i>	Palmer (1952), Cockerell (1903)
	<i>Forda marginata</i>	Cockerell (1903)
<i>Lasius brunneus</i>	<i>Aphis craccivora</i>	Akyürek et al. (2016)
	<i>Aphis fabae</i>	Akyürek et al. (2016)
	<i>Aphis hillerislambersi</i>	Akyürek et al. (2016)
	<i>Aphis middletonii</i>	Akyürek et al. (2016)
	<i>Aphis nasturtii</i>	Akyürek et al. (2016)
	<i>Aphis pomi</i>	Akyürek et al. (2016)
	<i>Aphis spiraecola</i>	Akyürek et al. (2016)
	<i>Brachycaudus cardui</i>	Akyürek et al. (2016)
	<i>Cinara cedri</i>	Akyürek et al. (2016)
	<i>Cinara cupressi</i>	Akyürek et al. (2016)
	<i>Cinara tujafilina</i>	Akyürek et al. (2016)
	<i>Dysaphis plantaginea</i>	Akyürek et al. (2016)
	<i>Hyalopterus pruni</i>	Akyürek et al. (2016)
	<i>Lachnus roboris</i>	Akyürek et al. (2016)
	<i>Periphyllus aceris</i>	Akyürek et al. (2016)
	<i>Pterocomma populeum</i>	Akyürek et al. (2016)

	<i>Schizaphis pyri</i>	Akyürek et al. (2016)
	<i>Sitobion fragariae</i>	Akyürek et al. (2016)
	<i>Thelexes suberi</i>	Akyürek et al. (2016)
	<i>Uroleucon kashmiricum</i>	Akyürek et al. (2016)
<i>Lasius claviger</i>	<i>Forda marginata</i>	Cockerell (1903)
	<i>Rhopalosiphum nymphaeae</i>	Jones (1927)
<i>Lasius emarginatus</i>	<i>Anoecia corni</i>	Akyildirim et al. (2014)
	<i>Aphis fabae</i>	Akyildirim et al. (2014)
	<i>Aphis gossypii</i>	Akyildirim et al. (2014)
	<i>Aphis impatientis</i>	Akyildirim et al. (2014)
	<i>Aphis longituba</i>	Akyildirim et al. (2014)
	<i>Aphis nasturtii</i>	Akyildirim et al. (2014)
	<i>Aphis spiraecola</i>	Akyildirim et al. (2014)
	<i>Brachycaudus cardui</i>	Akyildirim et al. (2014)
	<i>Brachycaudus schwartzi</i>	Akyildirim et al. (2014)
	<i>Chaitophorus longisetosus</i>	Akyildirim et al. (2014)
	<i>Cinara pini</i>	Akyildirim et al. (2014)
	<i>Myzus cerasi</i>	Akyildirim et al. (2014)
	<i>Myzus lythri</i>	Akyildirim et al. (2014)
	<i>Periphyllus aceris</i>	Akyildirim et al. (2014)
<i>Thelexes californica</i>	Akyildirim et al. (2014)	
<i>Lasius flavus</i>	<i>Forda marginata</i>	Cockerell (1903)
<i>Lasius fuji</i>	<i>Stomaphis yanonis</i>	Endo and Itino (2013)
<i>Lasius fuliginosus</i>	<i>Chaitophorus populeti</i>	Novgorodova (2005)
	<i>Chaitophorus vitellinae</i>	Molnar et al. (2000)
	<i>Cinara boernerii</i>	Novgorodova (2005)
	<i>Cinara laticis</i>	Novgorodova (2005)
	<i>Cinara pinea</i>	Novgorodova (2005)
	<i>Lachnus tropicalis</i>	Zhang et al. (2015)
	<i>Pterocomma pilosum</i>	Molnar et al. (2000)
	<i>Pterocomma rufipes</i>	Molnar et al. (2000)
	<i>Stomaphis japonica</i>	Zhang et al. (2015)
	<i>Stomaphis quercus</i>	Novgorodova (2005)
<i>Symydobius oblongus</i>	Novgorodova (2005)	
<i>Lasius grandis</i>	<i>Lachnus roboris</i>	Paris and Espadaler (2009)
<i>Lasius japonicus</i>	<i>Aphis craccivora</i>	Suzuki et al. (2004), Katayama et al. (2013)
	<i>Chaitophorus saliniger</i>	Hembry et al. (2006)
<i>Lasius latipes</i>	<i>Rhopalosiphum nymphaeae</i>	Jones (1927)
<i>Lasius nearcticus</i>	<i>Rhopalosiphum nymphaeae</i>	Jones (1927)
	<i>Lachnus roboris</i>	Paris and Espadaler (2009)
<i>Lasius neoniger</i>	<i>Rhopalosiphum nymphaeae</i>	Jones (1927)
<i>Lasius niger</i>	<i>Aphis cracciae</i>	Novgorodova (2005)
	<i>Aphis craccivora</i>	Novgorodova (2005), Kataria and Kumar (2013)
	<i>Aphis fabae</i>	Liepert and Dettner (1993), Volkl et al.

		(1999), Offenberg (2001), Woodring et al. (2004), Fischer et al. (2005), Detrain et al. (2010), Sanders and Frank (2010), Tegelaar et al. (2012), Tegelaar et al. (2013), Fischer et al. (2015), Tegelaar (2015), Vantaux et al. (2015),
	<i>Aphis gossypii</i>	Kaneko (2003)
	<i>Aphis idaei</i>	Novgorodova (2005)
	<i>Aphis jacobaeae</i>	Vrieling et al. (1991), Müller and Godfray (1999)
	<i>Aphis pomi</i>	Novgorodova (2005)
	<i>Aphis vanderghooti</i>	Woodring et al. (2004)
	<i>Aphis viburni</i>	Novgorodova (2005)
	<i>Brachycaudus cardui</i>	Volkl et al. (1999), Müller and Godfray (1999), Woodring et al. (2004)
	<i>Callipterinella tuberculata</i>	Novgorodova (2005)
	<i>Chaitophorus albus</i>	Novgorodova (2005)
	<i>Chaitophorus populeti</i>	Fischer and Shingleton (2001), Novgorodova (2005)
	<i>Chaitophorus populialbae</i>	Fischer and Shingleton (2001), Novgorodova (2005)
	<i>Chaitophorus tremulae</i>	Novgorodova (2005)
	<i>Chromaphis obiensis</i>	Novgorodova (2005)
	<i>Cinara pini</i>	Novgorodova (2005)
	<i>Dysaphis plantaginea</i>	Nagy et al. (2015)
	<i>Lachnus tropicalis</i>	Sakata (1995)
	<i>Metopeurum fuscoviride</i>	Volkl et al. (1999), Fischer et al. (2002), Woodring et al. (2004)
	<i>Myzocallis kuricola</i>	Sakata (1995)
	<i>Symydobius oblongus</i>	Novgorodova (2005)
	<i>Trama troglodytes</i>	Woodring et al. (2004)
<i>Lasius pallitarsis</i>	<i>Rhopalosiphum nymphaeae</i>	Jones (1927)
<i>Lasius paralienus</i>	<i>Aphis craccivora</i>	Özdemir et al. (2008), Shiran et al. (2013)
	<i>Aphis fabae</i>	Özdemir et al. (2008), Shiran et al. (2013)
	<i>Aphis frangulae</i>	Shiran et al. (2013)
	<i>Aphis galliiscabri</i>	Özdemir et al. (2008)
	<i>Aphis gossypii</i>	Özdemir et al. (2008)
	<i>Aphis rumicis</i>	Özdemir et al. (2008)
	<i>Aphis umbrella</i>	Shiran et al. (2013)
	<i>Brachycaudus cardui</i>	Özdemir et al. (2008)
	<i>Chaitophorus longisetosus</i>	Akyildirim et al. (2014)
	<i>Chaitophorus populeti</i>	Shiran et al. (2013)
	<i>Chaitophorus populialbae</i>	Shiran et al. (2013)
	<i>Chaitophorus remaudierei</i>	Shiran et al. (2013)
	<i>Chaitophorus truncates</i>	Shiran et al. (2013)
	<i>Cinara palaestinesis</i>	Shiran et al. (2013)
	<i>Cinara palaestinesis</i>	LATIBARI et al. (2016)

	<i>Cinara pini</i>	LATIBARI et al. (2016)
	<i>Hyadaphis foeniculi</i>	Özdemir et al. (2008)
	<i>Hyalopterus pruni</i>	Shiran et al. (2013)
	<i>Myzus persicae</i>	Shiran et al. (2013)
	<i>Pterochloroides persicae</i>	Shiran et al. (2013)
<i>Lasius productus</i>	<i>Stomaphis hirukawai</i>	Matsuura and Yashiro (2006)
	<i>Acyrtosiphon gossypii</i>	Mortazavi et al. (2015)
	<i>Acyrtosiphon pisum</i>	Akyildirim et al. (2014), Akyürek et al. (2016)
	<i>Anoecia corni</i>	Akyildirim et al. (2014)
	<i>Aphis brunellae</i>	Akyürek et al. (2016)
	<i>Aphis craccivora</i>	Özdemir et al. (2008), Mortazavi et al. (2015)
	<i>Aphis fabae</i>	Akyildirim et al. (2014) , Akyürek et al. (2016)
	<i>Aphis farinosa</i>	Akyildirim et al. (2014)
	<i>Aphis gossypii</i>	Akyildirim et al. (2014), Akyürek et al. (2016)
	<i>Aphis pomi</i>	Akyürek et al. (2016)
	<i>Aphis sambuci</i>	Akyildirim et al. (2014)
	<i>Aphis spiraeicola</i>	Akyildirim et al. (2014) , Akyürek et al. (2016)
	<i>Brachycaudus amygdalinus</i>	Mortazavi et al. (2015)
	<i>Brachycaudus cardui</i>	Akyildirim et al. (2014), Akyürek et al. (2016)
<i>Lasius turcicus</i>	<i>Brachycaudus helichrysi</i>	Akyürek et al. (2016)
	<i>Chaetosiphon tetraerhodum</i>	Akyildirim et al. (2014)
	<i>Chaitophorus hillerislamberti</i>	Mortazavi et al. (2015)
	<i>Chaitophorus salicti</i>	Akyildirim et al. (2014)
	<i>Cinara cupressi</i>	Akyürek et al. (2016)
	<i>Cinara pilicornis</i>	Akyildirim et al. (2014)
	<i>Cinara pini</i>	Akyildirim et al. (2014)
	<i>Cinara tujafilina</i>	Akyürek et al. (2016)
	<i>Myzus cerasi</i>	Akyildirim et al. (2014) , Akyürek et al. (2016)
	<i>Myzus lythri</i>	Akyildirim et al. (2014)
	<i>Myzus varians</i>	Akyürek et al. (2016)
	<i>Neobetulaphis pusilla</i>	Akyildirim et al. (2014)
	<i>Phleomyzus passerini</i>	Akyildirim et al. (2014)
	<i>Protaphis terricola</i>	Özdemir et al. (2008)
	<i>Pterochloroides persicae</i>	Akyildirim et al. (2014)
	<i>Pterocomma populeum</i>	Akyürek et al. (2016)
	<i>Toxoptera aurantii</i>	Akyildirim et al. (2014)
<i>Nylanderia fulva</i>	<i>Aphis craccivora</i>	Sharma et al. (2013)
	<i>Aphis vernoniae</i>	Sharma et al. (2013)
	<i>Chaitophorus viminicola</i>	Sharma et al. (2013)

	<i>Cinara juniperivora</i>	Sharma et al. (2013)
	<i>Sanbornia juniperi</i>	Sharma et al. (2013)
	<i>Shivaphis celti</i>	Sharma et al. (2013)
<i>Paratrechina bourbonica</i>	<i>Aphis gossypii</i>	Idechiil et al. (2007)
	<i>Pentalonia nigronervosa</i>	Idechiil et al. (2007)
<i>Paratrechina longicornis</i>	<i>Aphis coreopsidis</i>	Favret et al. (2010)
	<i>Aphis craccivora</i>	Shiran et al. (2013), Rakhshan and Ahmad (2015)
	<i>Aphis gossypii</i>	Idechiil et al. (2007), Lokeshwari et al. (2015)
<i>Paratrechina parvula</i>	<i>Aphis coreopsidis</i>	Favret et al. (2010)
<i>Paratrechina vaga</i>	<i>Aphis clerodendri</i>	Carver et al. (2003)
Tribe Melophorini		
<i>Notoncus capitatus</i>	<i>Aphis clerodendri</i>	Carver et al. (2003)
Tribe Myrmelachistini		
<i>Brachymyrmex patagonica</i>	<i>Brachycaudus cardui</i>	Lescano et al. (2015)
Tribe Plagiolepidini		
<i>Acantholepis sp.</i>	<i>Aphis nerii</i>	Sary (1969)
	<i>Chaitophorus sp.</i>	Sary (1969)
	<i>Lachnus sp.</i>	Sary (1969)
	<i>Thelaxes suberis</i>	Sary (1969)
<i>Anoplolepis gracilipes</i>	<i>Aphis gossypii</i>	Idechiil et al. (2007)
	<i>Pentalonia nigronervosa</i>	Idechiil et al. (2007)
<i>Lepisiota bipartite</i>	<i>Aphis craccivora</i>	Shiran et al. (2013)
	<i>Aphis fabae</i>	Shiran et al. (2013)
	<i>Aphis frangulae</i>	Shiran et al. (2013)
	<i>Aphis nasturtii</i>	Shiran et al. (2013)
	<i>Aphis nerii</i>	Shiran et al. (2013)
	<i>Aphis parietariae</i>	Shiran et al. (2013)
	<i>Aphis punicae</i>	Shiran et al. (2013)
	<i>Aphis umbrella</i>	Shiran et al. (2013)
	<i>Chaitophorus euphraticus</i>	Shiran et al. (2013)
	<i>Chaitophorus truncates</i>	Shiran et al. (2013)
	<i>Hyalopterus pruni</i>	Shiran et al. (2013)
	<i>Myzus persicae</i>	Shiran et al. (2013)
	<i>Pterochloroides persicae</i>	Shiran et al. (2013)
	<i>Rhopalosiphum maidis</i>	Shiran et al. (2013)
<i>Rhopalosiphum padi</i>	Shiran et al. (2013)	
<i>Lepisiota dolabellae</i>	<i>Acyrtosiphon pisum</i>	Mortazavi et al. (2015)
	<i>Brachycaudus tragopogonis</i>	Mortazavi et al. (2015)
<i>Lepisiota frauenfeldi</i>	<i>Aphis craccivora</i>	Rakhshan and Ahmad (2015)
	<i>Pterochloroides persicae</i>	Mortazavi et al. (2015)
<i>Lepisiota nigra</i>	<i>Aphis fabae</i>	Mortazavi et al. (2015)
	<i>Aphis gossypii</i>	Mortazavi et al. (2015)
	<i>Brachycaudus helichrysi</i>	Mortazavi et al. (2015)

	<i>Brachycaudus tragopogonis</i>	Mortazavi et al. (2015)
	<i>Chaitophorus israeliticus</i>	Mortazavi et al. (2015)
	<i>Cinara pini</i>	LATIBARI et al. (2016)
	<i>Hyalopterus amygdali</i>	Mortazavi et al. (2015)
	<i>Macrosiphon rosae</i>	Mortazavi et al. (2015)
	<i>Periphyllus bulgaricus</i>	Mortazavi et al. (2015)
	<i>Pterochloroides persicae</i>	Mortazavi et al. (2015)
	<i>Schizaphis nigerrima</i>	Mortazavi et al. (2015)
	<i>Acyrtosiphon pisum</i>	Mortazavi et al. (2015)
<i>Plagiolepis pallescens</i>	<i>Aphis craccivora</i>	Özdemir et al. (2008), Shiran et al. (2013)
	<i>Aphis fabae</i>	Shiran et al. (2013)
	<i>Aphis frangulae</i>	Shiran et al. (2013)
	<i>Brachycaudus (Appelia) tragopogonis</i>	Özdemir et al. (2008)
	<i>Brachycaudus tragopogonis</i>	Mortazavi et al. (2015)
	<i>Callaphis juglandis</i>	Mortazavi et al. (2015)
	<i>Hyalopterus amygdali</i>	Shiran et al. (2013)
	<i>Tinocallis platani</i>	Shiran et al. (2013)
<i>Plagiolepis pygmaea</i>	<i>Aphis craccivora</i>	Mortazavi et al. (2015)
	<i>Aphis fabae</i>	Akyürek et al. (2016)
	<i>Aphis gerardianae</i>	Akyürek et al. (2016)
	<i>Aphis gossypii</i>	Akyürek et al. (2016)
	<i>Aphis spiraecola</i>	Akyürek et al. (2016)
	<i>Brachycaudus cardui</i>	Akyürek et al. (2016)
<i>Plagiolepis taurica</i>	<i>Aphis spiraecola</i>	Akyildirim et al. (2014)
	<i>Toxoptera aurantii</i>	Akyildirim et al. (2014)
<i>Plagiolepis vindobonensis</i>	<i>Staegeriella necopinata</i>	Özdemir et al. (2008)
Subfamily Myrmicinae		
Tribe Attini		
<i>Pheidole bicarinata</i>	<i>Aphis asclepiadis</i>	Jones (1927)
	<i>Thecabius populimonilis</i>	Jones (1927)
<i>Pheidole fervens</i>	<i>Aphis gossypii</i>	Idechiil et al. (2007)
<i>Pheidole pallidula</i>	<i>Aphis davletshinae</i>	Shiran et al. (2013)
	<i>Aphis frangulae</i>	Shiran et al. (2013)
	<i>Aphis umbrella</i>	Shiran et al. (2013)
	<i>Cinara palaestinesis</i>	LATIBARI et al. (2016)
	<i>Myzus persicae</i>	Shiran et al. (2013)
	<i>Aphis nerii</i>	Sary (1969)
	<i>Thelaxes suberis</i>	Sary (1969)
<i>Pheidole pilifera</i>	<i>Pemphigus populiramulorum</i>	Jones (1927)
<i>Pheidole teneriffana</i>	<i>Aphis craccivora</i>	Shiran et al. (2013)
	<i>Aphis umbrella</i>	Shiran et al. (2013)
Tribe Crematogastrini		
<i>Cardiocondyla emeryi</i>	<i>Pentalonia nigronervosa</i>	Idechiil et al. (2007)

<i>Cardiocondyla shalbergi</i>	<i>Cinara pini</i>	LATIBARI et al. (2016)
<i>Cardiocondyla wroughtonii</i>	<i>Pentalonia nigronervosa</i>	Idechiil et al. (2007)
<i>Crematogaster scutellaris</i>	<i>Aphis fabae</i>	Akyürek et al. (2016)
	<i>Aphis pomi</i>	Akyürek et al. (2016)
	<i>Aphis spiraeicola</i>	Akyürek et al. (2016)
	<i>Pterocomma rufipes</i>	Akyürek et al. (2016)
<i>Crematogaster antaris</i>	<i>Aphis craccivora</i>	Shiran et al. (2013)
	<i>Aphis farinosa</i>	Shiran et al. (2013)
	<i>Aphis frangulae</i>	Shiran et al. (2013)
	<i>Chaitophorus truncates</i>	Shiran et al. (2013)
	<i>Myzus persicae</i>	Shiran et al. (2013)
<i>Crematogaster auberti</i>	<i>Thelaxes suberis</i>	Sary (1969)
<i>Crematogaster inermis</i>	<i>Acyrtosiphon gossypii</i>	Mortazavi et al. (2015)
	<i>Acyrtosiphon pisum</i>	Mortazavi et al. (2015)
	<i>Aphis craccivora</i>	Mortazavi et al. (2015)
	<i>Aphis gossypii</i>	Mortazavi et al. (2015)
	<i>Aphis pseudocardui</i>	Mortazavi et al. (2015)
	<i>Brachycaudus tragopogonis</i>	Mortazavi et al. (2015)
	<i>Callaphis juglandis</i>	Mortazavi et al. (2015)
<i>Chaitophorus israeliticus</i>	Mortazavi et al. (2015)	
<i>Crematogaster laeviuscula</i>	<i>Cinara ponderosae</i>	Jones (1927)
<i>Crematogaster lineolata</i>	<i>Aphis coreopsidis</i>	Favret et al. (2010)
	<i>Aphis fabae</i>	Favret et al. (2010)
	<i>Aphis gossypii</i>	Favret et al. (2010)
	<i>Capitophorus elaeagni</i>	Favret et al. (2010)
	<i>Chaitophorus viminicola</i>	Favret et al. (2010)
	<i>Cinara edulis</i>	Jones (1927)
	<i>Cinara murrayanae</i>	Jones (1927)
	<i>Cinara schwarzii</i>	Jones (1927)
<i>Lachnus ater</i>	Jones (1927)	
<i>Crematogaster schmidti</i>	<i>Aphis craccivora</i>	Mortazavi et al. (2015)
	<i>Aphis pseudocardui</i>	Mortazavi et al. (2015)
	<i>Chaitophorus israeliticus</i>	Mortazavi et al. (2015)
	<i>Thelaxes californica</i>	Akyildirim et al. (2014)
<i>Crematogaster scutellaris</i>	<i>Chaitophorus melanosiphon</i>	Akyürek et al. (2016)
<i>Crematogaster sordidula</i>	<i>Brachycaudus cardui</i>	Özdemir et al. (2008), Mortazavi et al. (2015)
	<i>Thelaxes suberis</i>	Sary (1969)
<i>Crematogaster subdentata</i>	<i>Aphis craccivora</i>	Mortazavi et al. (2015)
	<i>Cinara pini</i>	LATIBARI et al. (2016)
	<i>Periphyllus bulgaricus</i>	Mortazavi et al. (2015)
	<i>Tuberculatus maximus</i>	Mortazavi et al. (2015)
<i>Crematogaster warburgi</i>	<i>Chaitophorus sp.</i>	Sary (1969)
<i>Leptothorax muscorum</i>	<i>Rhopalosiphum nymphaeae</i>	Jones (1927)
<i>Lophomyrmex</i>	<i>Aphis gossypii</i>	Lokeshwari et al. (2015)

<i>quadrispinosus</i>		
<i>Meranoplus bicolor</i>	<i>Aphis craccivora</i>	Rakhshan and Ahmad (2015)
<i>Myrmecina graminicola</i>	<i>Aphis forbesi</i>	Jones (1927)
	<i>Chaitophorus viminalis</i>	Jones (1927)
<i>Pristomyrmex punctatus</i>	<i>Aphis craccivora</i>	Katayama et al. (2013)
<i>Pristomyrmex pungens</i>	<i>Aphis gossypii</i>	Kaneko (2003)
<i>Tetramorium bicarinatum</i>	<i>Aphis gossypii</i>	Idechiil et al. (2007)
	<i>Pentalonia nigronervosa</i>	Idechiil et al. (2007)
<i>Tetramorium caespitum</i>	<i>Aphis fabae</i>	Shiran et al. (2013), Akyildirim et al. (2014)
	<i>Aphis farinosa</i>	Akyildirim et al. (2014)
	<i>Aphis gossypii</i>	Akyildirim et al. (2014)
	<i>Aphis salviae</i>	Akyürek et al. (2016)
	<i>Aphis spiraecola</i>	Akyürek et al. (2016)
	<i>Brachycaudus cardui</i>	Akyürek et al. (2016)
	<i>Macrosiphoniella sanborni</i>	Akyildirim et al. (2014)
<i>Tetramorium chefteki</i>	<i>Myzus lythri</i>	Akyürek et al. (2016)
	<i>Aphis craccivora</i>	Özdemir et al. (2008), Mortazavi et al. (2015)
<i>Tetramorium forte</i>	<i>Aphis rumicis</i>	Özdemir et al. (2008)
	<i>Aphis craccivora</i>	Özdemir et al. (2008)
	<i>Aphis rumicis</i>	Özdemir et al. (2008)
	<i>Brachycaudus cardui</i>	Akyildirim et al. (2014)
	<i>Cinara pilicornis</i>	Akyildirim et al. (2014)
<i>Tetramorium semilaeve</i>	<i>Uroleucon sonchi</i>	Akyürek et al. (2016)
<i>Tetramorium tsushimae</i>	<i>Paraclsetus cimiciformis</i>	Salazar et al. (2015)
<i>Tetramorium tsushimae</i>	<i>Aphis craccivora</i>	Suzuki et al. (2004), Katayama et al. (2013), Hayashi et al. (2015), Hayashi et al. (2016)
	<i>Aphis fabae</i>	Hayashi et al. (2015)
Tribe Myrmicini		
<i>Myrmica incompleta</i>	<i>Aphis asclepiadis</i>	Jones (1927)
	<i>Aphis gossypii</i>	Jones (1927)
	<i>Aphis medicaginis</i>	Jones (1927)
	<i>Aphis pomi</i>	Jones (1927)
	<i>Aphis populicola</i>	Jones (1927)
	<i>Aphis rumicis</i>	Jones (1927)
	<i>Artemisaphis artemisicola</i>	Jones (1927)
	<i>Brachycaudus cardui</i>	Jones (1927)
	<i>Brachycaudus prunicola</i>	Jones (1927)
	<i>Chaitophorus macrostachyae</i>	Jones (1927)
	<i>Chaitophorus populicola</i>	Jones (1927)
	<i>Cinara oregonensis</i>	Jones (1927)
	<i>Eriosoma crataegi</i>	Jones (1927)
	<i>Protaphis middletonii</i>	Jones (1927)
	<i>Pterocomma bicolor</i>	Jones (1927)
<i>Pterocomma salicis</i>	Jones (1927)	

	<i>Rhopalosiphum maidis</i>	Jones (1927)
	<i>Uroleucon ambrosiae</i>	Jones (1927)
	<i>Wahlgreniella nervata</i>	Jones (1927)
<i>Myrmica punctiventris</i>	<i>Aphis illinoisensis</i>	Favret et al. (2010)
	<i>Aphis lugentis</i>	Favret et al. (2010)
	<i>Drepanaphis nigricans</i>	Favret et al. (2010)
<i>Myrmica rubra</i>	<i>Cinara apini</i>	Jones (1927)
<i>Myrmica ruginodis</i>	<i>Aphis fabae</i>	Akyildirim et al. (2014)
	<i>Aphis jacobaeae</i>	Müller and Godfray (1999)
	<i>Brachycaudus cardui</i>	Müller and Godfray (1999), Akyildirim et al. (2014)
<i>Myrmica scabrinodis</i>	<i>Aphis asclepiadis</i>	Jones (1927)
	<i>Aphis forbesi</i>	Jones (1927)
	<i>Brachycaudus helichrysi</i>	Akyildirim et al. (2014)
	<i>Brachycaudus persicae</i>	Jones (1927)
	<i>Cinara brevispinosa</i>	Jones (1927)
	<i>Cryptomyzus ribis</i>	Jones (1927)
<i>Myrmica whymperei</i>	<i>Drepanaphis acerifoliae</i>	Jones (1927)
	<i>Aphis asclepiadis</i>	Jones (1927)
	<i>Aphis farinosa</i>	Jones (1927)
	<i>Aphis oenotherae</i>	Jones (1927)
	<i>Aphis rumicis</i>	Jones (1927)
<i>Pogonomyrmex occidentalis</i>	<i>Chaitophorus viminalis</i>	Jones (1927)
	<i>Hyalopterus pruni</i>	Jones (1927)
	<i>Myzus persicae</i>	Jones (1927)
Tribe Solenopsidini		
<i>Monomorium destructor</i>	<i>Aphis craccivora</i>	Shiran et al. (2013)
	<i>Aphis frangulae</i>	Shiran et al. (2013)
	<i>Chaitophorus euphraticus</i>	Shiran et al. (2013)
<i>Monomorium floricola</i>	<i>Aphis gossypii</i>	Idechiil et al. (2007)
<i>Monomorium gracillimum</i>	<i>Aphis nerii</i>	Sary (1969)
	<i>Uroleucon Dactynotus</i>	Sary (1969)
<i>Monomorium latinode</i>	<i>Aphis craccivora</i>	Rakhshan and Ahmad (2015)
<i>Monomorium libanicum</i>	<i>Aphis fabae</i>	Shiran et al. (2013)
	<i>Aphis frangulae</i>	Shiran et al. (2013)
<i>Monomorium mayri</i>	<i>Aphis craccivora</i>	Shiran et al. (2013)
	<i>Aphis fabae</i>	Shiran et al. (2013)
	<i>Aphis frangulae</i>	Shiran et al. (2013)
	<i>Aphis nerii</i>	Shiran et al. (2013)
	<i>Aphis polygonata</i>	Shiran et al. (2013)
	<i>Chaitophorus euphraticus</i>	Shiran et al. (2013)
	<i>Hyalopterus amygdali</i>	Shiran et al. (2013)
	<i>Myzus persicae</i>	Shiran et al. (2013)
<i>Rhopalosiphum maidis</i>	Shiran et al. (2013)	
<i>Monomorium minimum</i>	<i>Aphis craccivora</i>	Kataria and Kumar (2013)

	<i>Aphis fabae</i>	Kataria and Kumar (2013)
	<i>Aphis gossypii</i>	Kataria and Kumar (2013)
	<i>Aphis nerii</i>	Kataria and Kumar (2013)
	<i>Rhopalosiphum nymphaeae</i>	Jones (1927)
<i>Monomorium monomorium</i>	<i>Aphis gossypii</i>	Idechiil et al. (2007)
<i>Monomorium nitidiventre</i>	<i>Aphis craccivora</i>	Mortazavi et al. (2015)
<i>Monomorium pharaonis</i>	<i>Aphis craccivora</i>	Rakhshan and Ahmad (2015)
<i>Monomorium qarahe</i>	<i>Aphis fabae</i>	Shiran et al. (2013)
	<i>Aphis frangulae</i>	Shiran et al. (2013)
	<i>Rhopalosiphum maidis</i>	Shiran et al. (2013)
<i>Solenopsis geminata</i>	<i>Aphis gossypii</i>	Idechiil et al. (2007), Lokeshwari et al. (2015)
<i>Solenopsis invicta</i>	<i>Myzus persicae</i>	Zhou (2012), Zhou (2014)
<i>Solenopsis richteri</i>	<i>Brachycaudus cardui</i>	Lescano et al. (2015)
<i>Messor orientalis</i>	<i>Chaitophorus israeliticus</i>	Mortazavi et al. (2015)
<i>Myrmicaria brunnea</i>	<i>Aphis gossypii</i>	Lokeshwari et al. (2015)
Tribe Stenammini		
<i>Aphaenogaster kurdica</i>	<i>Brachycaudus helichrysi</i>	Mortazavi et al. (2015)
Subfamily Pseudomyrmecinae		
<i>Tetraponera rufonigra</i>	<i>Aphis craccivora</i>	Rakhshan and Ahmad (2015)

BODY COLOR REGULATION OF *LEPTOBOTIA TAENIOPS* THROUGH TYROSINASE GENE EXPRESSION

JIANG, H.^{1,2,3*} – LIU, S.^{1,2,3} – XIAO, T. Y.^{1,2,3*} – XIE, M.⁴

¹*College of Animal Science and Technology, Hunan Agricultural University
Changsha 410128, China*

²*Hunan Engineering Technology Research Center of Featured Aquatic Resources Utilization
Hunan Agricultural University, Changsha 410128, China*

³*Collaborative Innovation Center for Efficient and Health Production of Fisheries in Hunan
Province, Changde 415000, China*

⁴*Hunan Fisheries Science Institute, Changsha 410153, China*

*Corresponding authors

e-mail: 1176139630@qq.com (H. Jiang), tyxiao1128@163.com (T. Xiao)

(Received 11th Dec 2018; accepted 26th Feb 2019)

Abstract. Body color plays important roles in various behaviors of fish. *Leptobotia taeniops* exhibits two body color phenotypes at the same habitat. However, the mechanism is unclear. Tyrosinase plays a significant role in regulating synthesis of melanin. Therefore, we inferred that expression differences of tyrosinase gene was the primary reason for the different body colors of *L. taeniops*. To verify our inference, we firstly cloned and sequenced the whole-length cDNA sequence of *L. taeniops* tyrosinase gene through the rapid-amplification of cDNA ends cloning technology, and compared the expressions of the tyrosinase gene at different tissues between light and dark phenotypes using real-time quantitative reverse transcription PCR. The results showed the cDNA sequence was very similar to those from Cyprinidae fish. The expressions of tyrosinase gene in eyeball, dorsal fin, skin, muscle, liver and gill of the light phenotype were significantly lower than these in the dark phenotype. These results implied the expression of tyrosinase gene played an important role in regulating the body color of *L. taeniops*. The results provided important reference information to further elaborate the molecular mechanism of *L. taeniops* to adapt to their surrounding environment through changing color, protect wild *L. taeniops* resource, and cultivate new ornamental fish varieties.

Keywords: *Leptobotia taeniops*, tyrosinase, melanin, tissue differential expression, rapid-amplification of cDNA ends

Introduction

Body color plays important roles in various behaviors of fish, such as competition, courtship, avoiding predators and warning (Moretz and Morris, 2003; Hubbard et al., 2010; Culumber, 2013). Changes of body color is considered an adaptive response to environment changes. The way that the mechanism of body color changing works is a fundamental question in conservation ecology.

Leptobotia taeniops (Cypriniformes: Cobitidae) is an indigenous species in China, which mainly distributes in the Yangtze River and its tributary (Chen, 1980). There are two body color phenotypes of *L. taeniops* at the same freshwater habitat. The light phenotype of *L. taeniops* is near golden color. There are small black stripes and splashes on their body. The dark phenotype of *L. taeniops* is yellowish-brown. There are massive black stripes and splashes on their body. No obvious genetic differentiation is detected

between the light and the dark phenotypes (Meng, 2011). So far, the mechanism that regulated the body color phenotypes is still unclear.

Body color of fish is controlled by types, proportion and distribution of pigment cells in epidermis. The pigment cells mainly include melanocytes, xanthophore, erythrophore, iridophore and leucophore (Schartl et al., 2016). Melanocytes contain melanin and are widely distributed in skin, hair, retina and bone of vertebrates. Melanin plays important roles in preventing damage to DNA and proteins from ultraviolet rays (Slominski et al., 2015), enhancing antioxidant capacity (Tu et al., 2009), maintaining intracellular calcium homeostasis (Parekh, 2016), and regulating immunization of organisms through NF- κ B signaling pathway (Zhou et al., 2013). It is synthesized through tyrosine-tyrosinase reaction system and tyrosinase (TYR, EC 1.14.18.1) catalyzes tyrosine to the L-dihydroxyphenylalanine through hydroxylation and then converts to the dopaquinone. Therefore, tyrosinase is an iconic enzyme to melanin synthesis (Sánchez-Ferrer et al., 1995; Chen et al., 2015).

Therefore, we inferred that synthetic amount of melanin controlled the body colors of *L. taeniops* that living in the same freshwater habitat. To verify the inference, we firstly cloned and sequenced the whole-length cDNA sequence of tyrosinase gene through the rapid-amplification of cDNA ends (RACE) cloning technology. Then we compared the expression differences of the tyrosinase gene at different tissues between light and dark sub-populations of *L. taeniops* using real-time quantitative reverse transcription PCR (qRT-PCR). The results provided important reference information to further elaborate the molecular mechanism of *L. taeniops* to adapt to their surrounding environment through body color, protect wild *L. taeniops* resource, as well as cultivate new ornamental fish variety.

Materials and Methods

Sample collection

Total of 40 *L. taeniops* specimens (20 light phenotypic specimens and 20 dark phenotypic specimens) were collected from the Yueyang section of the Yangtze River during July to September, 2017. The specimens were transported to the Aquaculture Laboratory of Hunan Agricultural University, and temporary cultured 7 days in a culture system with circulating water at $25 \pm 1^\circ\text{C}$ before anaesthetized. The specimens were starved during the temporary cultured period. To eliminate the effect of healthy status on gene expression, each 6 specimens of light and dark phenotypes were chosen to further analyze according to their healthy status and exercise ability. The specimens were anaesthetized using MS-222, taken pictures, and measured their body lengths and body weights before dissected. After dissected, their sex was identified through sex gland. Their eyeball, skin at dorsal fin base, muscle, dorsal fin, gill, brain, liver and fish blubber were collected into freezing tubes and stored at -80°C for further analysis.

RNA extraction and sequencing cDNA of tyrosinase gene

The RNA used to synthesize cDNA of *L. taeniops* tyrosinase gene were extracted from 50-80 mg of skin using E.Z.N.A. Total RNA I kit (OMEGA, China) according to the manufacturer's introduction. The concentration and purity of RNA were measured using a nucleic acid and protein detector (Eppendorf, Germany). The degradation was assessed by 1.5% agarose gel electrophoresis with 120 V. The first strand of cDNA was

synthesized using a RevertAid™ First Strand cDNA Synthesis kit (Fermentas, USA) according to the manufacturer's introduction.

The intermediate primers, TYR-F and TYR-R, were designed according to the sequences of Cyprinidae tyrosinase genes in GenBank database using primer 6.0 software. Then the intermediate sequence was amplified using the primers and the first strand of cDNA as a template. The PCR product was purified using a Gel Extraction kit (Omega, China) and bound to pTOPO-T vectors (Aidlab, China) and cloned as a previous report (Ni et al., 2017). Five positive clones were screened and bidirectional sequenced to obtain the intermediate sequence of *L. taeniops* tyrosinase gene using ABI 3730 system at Wuhan Aokedingsheng Bio-Science, Ltd., China.

According to the sequences of Cyprinidae tyrosinase genes and the intermediate sequence of *L. taeniops* tyrosinase gene, the 5' and 3' bilateral primers TYR5'-outer and TYR3'-outer and 5' and 3' medial primers TYR5'-inner and TYR3'-inner for RACE amplifying were designed using Oligo 7.0 software (Table 1). The 5' RACE cDNA and 3' RACE cDNA were synthesized using the primers and approximately 2 µg RNA as the template according to the user manual of the SMARTer RACE 5'/3' kit (Clontech, USA). Subsequently, the 3' RACE and 5' RACE of *L. taeniops* tyrosinase gene were amplified using the 3' RACE cDNA and 5' RACE cDNA as the template. The PCR product was purified and sequenced as described above.

Table 1. The primer sequences used in the present study. RACE, rapid-amplification of cDNA ends; TYR, tyrosinase

Primers name*	Primer sequence (5'-3')	Utilization
TYR-F	GTCCTCGGTGTTCTCCTCTCT	Amplifying the intermediate sequence of TYR gene
TYR-R	CCTCCTCTTCACTGCTGTTCA	
TYR3'-outer	TTCTGCATCACGCCTTTATTGACA	Amplifying 3' RACE
TYR3'-inner	GAAACGGAGATTATTTCTGTCCAC	Amplifying 5' RACE
TYR5'-outer	GGGAGGCTGGTGTCTCCGTAGCCACT	
TYR5'-inner	TCCAGAGCGTTGCGGAAGCTCATGTTGG	RACE universal primers
Universal primer (UPM)	CTAATACGACTCACTATAGGGCAAGCAGTGGTATCAACGCAGAGT	
Short universal primer	CTAATACGAC TCACTATAGGGC	Primers for qRT-PCR
qRT-TYR-F	ATGCCTATTTGCTGGACCCC	
qRT-TYR-R	TATGCCGACATCTCCTGCG	Primers for qRT-PCR
β-Actin-F	CTGGACTTGGCTGGTCGTG	
β-Actin-R	CTCGAAGTCAAGGGCAACAT	

* F: forward primer; R: reverse primer

The sequences were merged to whole-length cDNA sequence of *L. taeniops* tyrosinase using SeqMan 5.01 module of DNASTar software. The amino acid sequence of *L. taeniops* tyrosinase was predicted based on the cDNA sequence using DNAMAN 7.0 software. The similar amino acid sequences of *L. taeniops* tyrosinase were retrieved from GenBank database using BLAST (<http://www.ncbi.nlm.nih.gov/blast>). The amino acid sequences of tyrosinase from koi carp (*Cyprinus carpio*, ANN11899.1), zebrafish

(*Danio rerio*, NP_571088.3), goldfish (*Carassius auratus*, ABI93943.1), Atlantic salmon (*Salmo salar*, ABD73809.1), finless eel (*Monopterus albus*, XP_020475631.1), midas cichlid (*Amphilophus citrinellus*, ANE23829.1), snakehead (*Channa argus*, AMQ24769.1), rainbow trout (*Oncorhynchus mykiss*, NP_001117694.1), medaka (*Oryzias latipes*, BAA31348.1), fugu rubripes (*Takifugu rubripes*, AAK13523.1), swordtail fish (*Xiphophorus maculatus*, XP_023207866.1), red crucian carp (*Carassius auratus auratus*, BAH03534.1), channel catfish (*Ictalurus punctatus*, AAF20161.1), sea pineapple (*Halocynthia roretzi*, BAC76424.1), lancelet (*Branchiostoma japonicum*, AFS33098.1), black-spotted pond frog (*Pelophylax nigromaculatus*, BAA02077.1), soft-shell turtle (*Pelodiscus sinensis japonicas*, BAB79632.1), egret (*Egretta garzetta*, KFP18390.1), chicken (*Gallus gallus*, AAB36375.1), horse (*Equus caballus*, XP_001492610.4), sheep (*Ovis aries*, NP_001123499.1), mouse (*Mus musculus*, NP_035791.1), and human being (*Homo sapiens*, NP_000363.1) were chose as reference sequences to construct phylogenetic tree. The sequences as well as that from *L. taeniops* were aligned using Clustal X2.1 and neighbor-joining phylogenetic tree with 1000 times of bootstrap was constructed using MEGA 6.0. Expasy (<http://www.expasy.org/>) and SMART (<http://smart.embl-heidelberg.de>) were used to analyze the amino acid sequences of *L. taeniops* tyrosinase and predict functional domains of the protein.

The whole-length cDNA sequence has been submitted to the GenBank database with accession number MG870259.

Expression analysis of tyrosinase gene in different tissues of L. taeniops

Total RNA in eyeball, skin, muscle, dorsal fin, eyeball, gill, brain, liver and fish blubber of light and dark *L. taeniops* phenotypes were extracted using an E.Z.N.A. Total RNA I kit (OMEGA, China). The first strand of cDNA was synthesized using a RevertAid™ First Strand cDNA Synthesis kit (Fermentas, USA) with Oligo(dT)₁₈ primer. Primers qRT-TYR-F and qRT-TYR-R were designed according to the coding sequence (CDS) of the tyrosinase gene for real-time qRT-PCR (Table 1). Primers β-Actin-F and β-Actin-R (Table 1) were designed according to the sequence of β-Actin gene for endogenous reference to detect the amplification efficiencies (*E*%) and the correlation coefficients (*R*²).

Real-time qRT-PCR was conducted on a CFX96 Touch™ real-time PCR detection system (Bio-Rad, USA) as a previous report (Ni et al., 2018) with minor modification. Briefly, each 25 µl reaction mixture consisted of 1 × SYBR Green II PCR master mix (TaKaRa, China) containing 200 nM each primer and 20 ng of cDNA. The reactions were performed by incubation for 10 min at 95°C, following by 10 s at 95°C, 10 s at 60°C and 15 s at 72°C for 35 cycles. The program of melt curve was increased 0.5°C each 5 s from 65°C to 95°C. The relative expressions of tyrosinase gene in different tissues were calculated by the comparative Ct (2^{-ΔΔC_t}) method (Li et al., 2012; Spivak et al., 2012).

Statistical analysis

One-way analysis of variance (ANOVA) for comparing the expressions of tyrosinase gene among different issues and Duncan's multiple range test for post-hoc test was conducted using R version 3.5.1. Independent *t*-test was conducted using R version 3.5.1 for comparing the body weights, the body lengths, and the expressions of

tyrosinase gene in specific issue between the light and the dark phenotypes. Binomial test for comparing the sex ratio between the light and the dark phenotypes was also conducted using R version 3.5.1. Results for each parameter are presented as means \pm standard deviation (SD) for each group. P-values < 0.05 were considered statistically significant.

Results

Physical characteristics of L. taeniops

The background color of *L. taeniops* was yellowish-brown. A lot of sparse black spots were on back of the light phenotype. Only very small gray spots were on their body sides (Fig. 1A). However, there were massive black stripes and splashes on the back and body sides of the dark phenotype (Fig. 1B). Body lengths of the light phenotype were 10.30 ± 0.60 cm, and these of the dark phenotype were 10.27 ± 0.95 cm (Fig. 1). Body weights of the light phenotype were 14.85 ± 2.30 g, and these of the dark phenotype were 15.33 ± 4.32 g. Neither the body length nor the body weight was detected significant difference between the light and dark phenotypes in the body length (independent *t*-test, $t = -0.073$, $p = 0.94$) and the body weight (independent *t*-test, $t = 0.24$, $p = 0.82$). Sex ratio between the light and dark phenotypes was also no significant difference ($\text{♀} : \text{♂}$ was 1 : 5 for the light phenotype; $\text{♀} : \text{♂}$ was 2 : 4 for the dark phenotype; Binomial test, $p = 0.263$).



Figure 1. Light (A) and dark (B) phenotypes of *Leptobotia taeniops*

cDNA and amino acid sequences of tyrosinase of L. taeniops

The whole-length cDNA sequence of *L. taeniops* tyrosinase was 2643 bp, which was comprised by a 1617 bp of open reading frame, a 22 bp of untranslated region (UTR) at upstream of 5' end, and a 1004 bp of UTR at downstream of 3' end. The cDNA sequence contained the typically polyadenylation signal (AATAAA) and Poly(A)-tail of vertebrates (Appendix 1). The complete CDS of *L. taeniops* tyrosinase gene was approximately 90% of similarity to those of Cyprinidae fishes, such as *Cryprinus carpiod*, *C. auratis* and *D. rerio*. Putative amino acid sequence was 538 amino-acid residues and was constituted by 4 conserved domains, i.e. signal peptide, epithelial growth factor-like domain (EGF-like domain), tyrosinase domain, and transmembrane region. Tyrosinase domain included two copper binding sites (CuA and CuB; Appendix 2). The structure of the CuA was (H-x(4,5)-F-[LIVMFTP]-x-[FW]-H-R-x(2)-[LVMT]-x(3)-E), which corresponding amino acid sequence was HESAAFLPWHRVYLLFWE. The structure of the CuB was (D-P-x-F-[LIVMFYW]-x(2)-x(3)-D), which corresponding amino acid sequence was DPIFLLHHAFID. The

structures of the CuA and CuB were highly conserved among vertebrate species. The structures of CuA and CuB of *L. taeniops* were completely identical with Cyprinidae *Cyprinus carpio*, *C. auratus* and *D. rerio* (Appendix 3). The molecular weight of *L. taeniops* tyrosinase was 60.81 kD. Theoretical isoelectric point of *L. taeniops* tyrosinase was 6.13. The predictive chemical structure formula was $C_{2718}H_{4105}N_{749}O_{788}S_{29}$. The instability coefficient was 56.16, which indicated that the protein was unstable. The prediction atlas of hydrophobicity showed that the tyrosinase of *L. taeniops* contained more hydrophilic regions than hydrophobic regions. Therefore, the tyrosinase was hydrophilic protein (Appendix 4). There were 13 cysteines in the tyrosinase of *L. taeniops*. Nine of 13 cysteines were at N-terminal, and other 4 cysteines were in the middle between CuA and CuB (Appendix 1).

Neighbor-Joining tree showed that all amino acid sequences of fish tyrosinase were clustered together, and those of amphibians, reptiles, birds and mammals were clustered to another cluster. *H. roretzi* of Urochordata and *B. japonicum* of Cephalochorda was clustered to two separate branches. *L. taeniops* was clustered together to Cyprinidae fishes (Fig. 2).

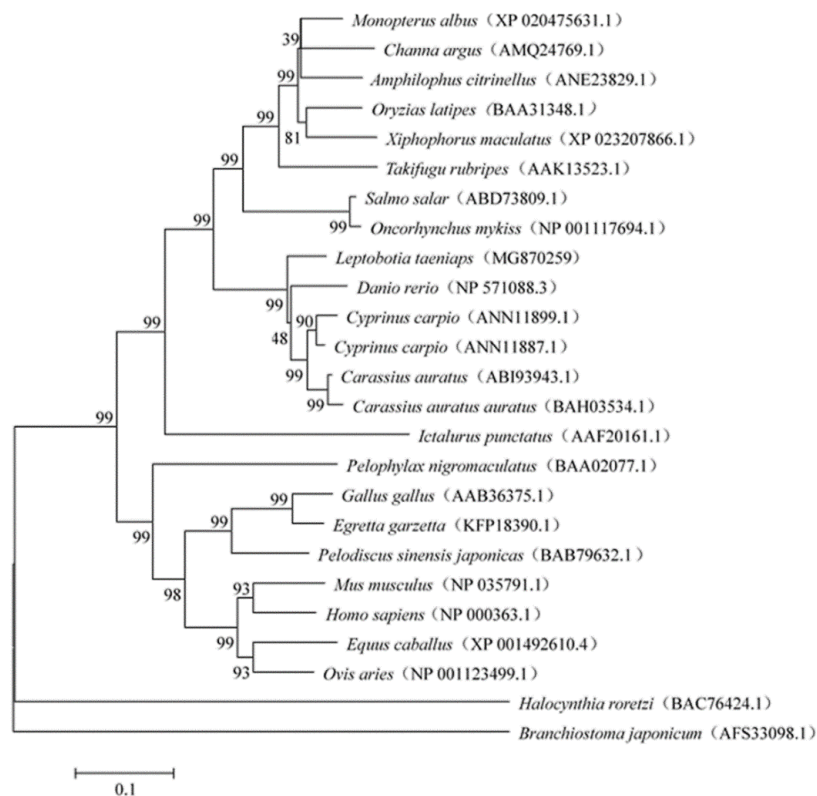


Figure 2. Phylogenetic relationships of *Leptobotia taeniops* and other representative vertebrates constructed based on amino acid sequences of tyrosinase

Expression of tyrosinase gene in different tissues and organs of *L. taeniops*

The amplification efficiencies ($E\%$) and the correlation coefficients (R^2) showed that the primer pairs qRT-TYR-F/R ($E\% = 104.8\%$, $R^2=0.991$) and β -Actin-F/R ($E\% = 104.7\%$, $R^2 = 0.998$) were in sufficient to the requirements of real-time qRT-PCR

(90% < $E\%$ < 105%, and $R^2 > 0.98$). The expressional trend of tyrosinase gene in skin, muscle, dorsal fin, eyeball, gill, brain, liver, and fish blubber was concordant between the light and dark phenotypes of *L. taeniops*. It was highest expressed in eyeball, and significantly different to other tissues (One-way ANOVA, $p < 0.01$), followed by dorsal fin, skin, muscle and brain. The expressions of tyrosinase gene in gill, liver and fish blubber of *L. taeniops* were very low, and no significant difference was detected among the three tissues (One-way ANOVA, $p > 0.05$; Fig. 3). The expressions of tyrosinase gene in eyeball (independent t -test, $t = 34.88$, $p < 0.01$), dorsal fin (independent t -test, $t = 19.85$, $p < 0.01$), skin (independent t -test, $t = 25.60$, $p < 0.01$), muscle (independent t -test, $t = 15.53$, $p < 0.01$), liver (independent t -test, $t = 5.77$, $p < 0.01$) and gill (independent t -test, $t = 7.35$, $p < 0.01$) of the light phenotype were significantly lower than these in the dark phenotype. No significant difference of the expressions in brain (independent t -test, $t = 1.07$, $p = 0.31$) and fish blubber (independent t -test, $t = 0$, $p = 1.00$) was found between the light and the dark phenotypes of *L. taeniops* (Fig. 3).

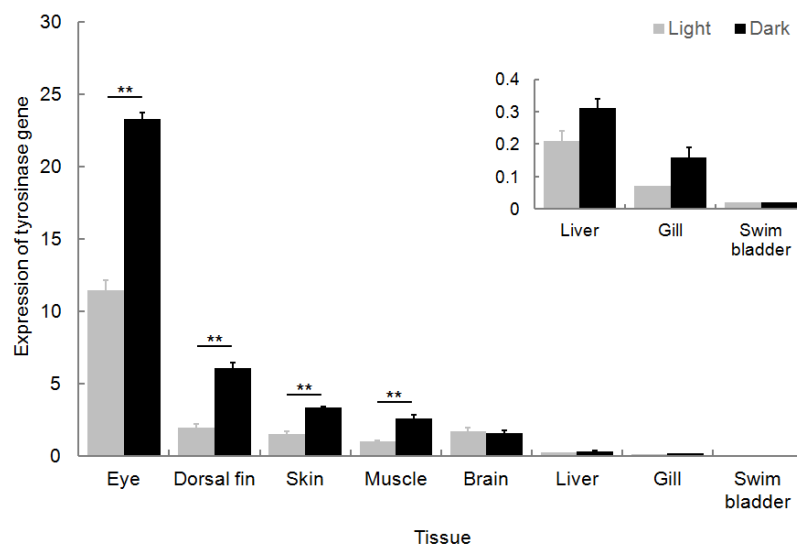


Figure 3. Expressions of tyrosinase gene in eight tissues of *Leptobotia taeniops*. The asterisks indicating differences between light and dark phenotypes. Independent t -test was used to compare the expressions of tyrosinase gene between the light and dark phenotypes of *L. taeniops*. *, $p < 0.05$; **, $p < 0.01$

Discussion

Tyrosinase is a key enzyme to synthesize melanin. The expression of tyrosinase gene controls the speed and production of melanin. The higher expression of tyrosinase gene promotes the intracellular synthesis of melanin (Gutiérrez-Gil et al., 2007). The expressions of tyrosinase gene in the peoples with dark skin are higher than those in the peoples with pale skin (Huang et al., 2008). The expressions of tyrosinase gene in skin are differences among different varieties of *Cryprinus carpiod*, and the expression is the highest in dark *C. carpiod* (Wang et al., 2012). The expressions of tyrosinase gene in scale, skin and tail fin of dark *A. citrinellus* are significantly higher than those of bright yellow ones (Jiang, 2016). Our results showed that the expressions of tyrosinase gene in eyeball (independent t -test, $t = 34.88$, $p < 0.01$), dorsal fin (independent t -test, $t = 19.85$, $p < 0.01$), skin (independent t -test, $t = 25.60$, $p < 0.01$), muscle (independent t -test,

$t = 15.53$, $p < 0.01$), liver (independent t -test, $t = 5.77$, $p < 0.01$) and gill (independent t -test, $t = 7.35$, $p < 0.01$) of the light phenotype were significantly lower than these in the dark phenotype. The result implied that the expressional differences of tyrosinase gene was the major reason that caused the differentiation of *L. taeniops* body color.

Expressional patterns of tyrosinase gene are different among fishes. The gene was expressed in eyeballs and skins of *D. rerio* (Chiu, 2003) and *O. latipes* (Zou et al., 2006), while it is not expressed in their livers. Our results showed that the expression of tyrosinase gene in eyeball of *L. taeniops* was the highest, followed by dorsal fin, skin, muscle and brain. The expressions of tyrosinase gene in gill, liver and fish blubber of *L. taeniops* were the lowest, coincident with the results in *C. auratus* (Chiu, 2003) and *C. carpiod* (Wang et al., 2012).

Melanin participates in many physiological processes of organisms. And tyrosinase is the essential enzyme to synthesize melanin. Therefore, the tyrosinase gene is expressed in various tissues of *L. taeniops*. There are lots of melanocytes in retinal pigment epithelium (RPE). As an antioxidant, the melanin protects RPE and nerve cells from oxidative damage (Zhang et al., 2011). Therefore, tyrosinase gene was highly expressed in eyeball. Nerve cells produce melanin during their development, and brain is the tissue in which nerve cells are concentrated. Therefore, tyrosinase gene was also expressed in brain (Sulzer et al., 2000). In addition, the expressions of tyrosinase gene in heart, fish blubber and liver implied that the tyrosinase probably did not only participate in the synthesizing melanin, but also regulating other physiological activities (Wang et al., 2012).

Although melanin plays important roles in preventing damage to DNA and proteins from ultraviolet rays (Slominski et al., 2015), enhancing antioxidant capacity (Tu et al., 2009), maintaining intracellular calcium homeostasis (Parekh, 2016), and regulating immunization of organisms through NF- κ B signaling pathway (Zhou et al., 2013), the reason caused the differentiation of *L. taeniops* body color are still needed to further study. Sex and development phase are two major factors that influence body color of fish (Bjerkeng et al., 2000; Suqimoto, 2002; Li et al., 2014). However, no significant difference in sex and development phase (it was indicated by the body length and the body weight) were detected between the light and the dark phenotypes in our study. Therefore, externally special stimulation was probably the reason that caused the expressional differences of tyrosinase gene between the light and dark phenotypes of *L. taeniops* and the differentiation of their body colors. It should be further studied which environmental factors regulate the expression of *L. taeniops* tyrosinase gene.

Our results showed the structure of *L. taeniops* tyrosinase was accordance with other vertebrates (Jagirdar et al., 2014; Ming et al., 2016; Yu et al., 2017). A signal peptide comprised 20 amino-acid residues (MRPSSISPLLFFIQLGLSL) was in tyrosinase gene of *L. taeniops*, which was the requisite structure to lead the newly synthesized protein to enter the endoplasmic reticulum to complete its modification (Wang et al., 2005). It can influence expression of the protein (Güler-Gane et al., 2016), and control location of the protein (Wei et al., 2006). Compared with amphibians, reptiles, birds and mammals, the tyrosinase gene sequence of *L. taeniops* was highly similar to the tyrosinase gene sequences from other fishes, especially Cyprinidae fishes. There were 13 cysteines in the tyrosinase of *L. taeniops*. Nine of 13 cysteines were at N-terminal, and other 4 cysteines were in the middle between CuA and CuB, in accordance with *C. carpiod* (Wang et al., 2012). This result verified that the amino acid sequence of tyrosinase was highly conservative in fishes, as showed by the phylogenetic tree

(Figure 2). The cysteine in protein promotes the active sites of tyrosinase to bind copper ion during its process (Bijelic et al., 2015; Lai et al., 2018). The EGF-like domain (CQCAGNYMGFDC) was rich in cysteines, which coded protein activating EGF signal pathway and was connected with the multienzyme complex that induces expression of the tyrosinase-related proteins (Jackson et al., 1990, 1992; Dunning et al., 2015). Tyrosinase was type III copper oxidase. Its tyrosinase domain included two domains of histidine residues (HESAAFLPWHRVYLLFWE and DPIFLLHHAFID) that bind to copper ion (Pretzler and Rompel, 2018). Binding by metal ion commonly changes the stability and function of protein. Copper ion endows the redox properties to tyrosinase (Solano, 2018), and plays important role in synthesizing melanin.

In conclusion, we firstly cloned and sequenced the whole-length cDNA sequence of *L. taeniops* tyrosinase gene, and compared the expressions of tyrosinase gene in different tissues between the light and dark phenotypes of *L. taeniops*. Tyrosinase gene was mainly expressed in eyeball, skin, dorsal fin, muscle and brain of both the light and dark phenotypes of *L. taeniops*. The expressions of tyrosinase gene in eyeball, dorsal fin, skin and muscle of the light phenotype were significantly lower than these in the dark phenotype ($p < 0.01$). These results implied that the expression of tyrosinase gene played important role in regulating the synthesis of melanin and the body color of *L. taeniops*. Our results provided important reference information to further elaborate the molecular mechanism of *L. taeniops* to adapt to their surrounding environment through body color, protect wild *L. taeniops* resource, as well as cultivate new ornamental fish variety. However, how external and intrinsic factors influence the expression of tyrosinase gene and which genes participate in regulation of the expression of tyrosinase gene should be further studied in the future.

Acknowledgements. This work was funded by the Earmarked Funds for China Agriculture Research System (CARS-45-48). The authors thank anonymous technicians at Guangdong Meilikang Bio-Science for assistance with data re-analysis and figure preparation.

REFERENCES

- [1] Bijelic, A., Pretzler, M., Molitor, C., Zekiri, F., Rompel, A. (2015): The structure of a plant tyrosinase from walnut leaves reveals the importance of “substrate-guiding-residues” for enzymatic specificity. – *Angewandte Chemie International Edition* 54(49): 14677-14860.
- [2] Bjerkgeng, B., Hatlen, B., Jobling, M. (2000): Astaxanthin and its metabolites idoxanthin and crustaxanthin in flesh, skin, and gonads of sexually imature and maturing Arctic charr (*Salvelinus alpinus* L.). – *Comparative Biochemistry and Physiology Part B* 125: 395-404.
- [3] Chen, J. (1980): A study on the classification of the botoid fishes of China. – *Zoological Research* 1(1): 3-26.
- [4] Chen, C., Lin, L., Yang, W., Bordon, J., Wang, H. D. (2015): An updated organic classification of tyrosinase inhibitors on melanin biosynthesis. – *Current Organic Chemistry* 19: 4-18.
- [5] Chiu, C. (2003): Molecular cloning of tyrosinase gene of goldfish and its impacts on the pigmentation of two ornamental fish (*Carassius auratus* and *Danio rerio*). – National Taiwan Ocean University, Taipei.
- [6] Culumber, Z. W. (2013): Pigmentation in *Xiphophorus*: An emerging system in ecological and evolutionary genetics. – *Zebrafish* 11(1): 57-70.

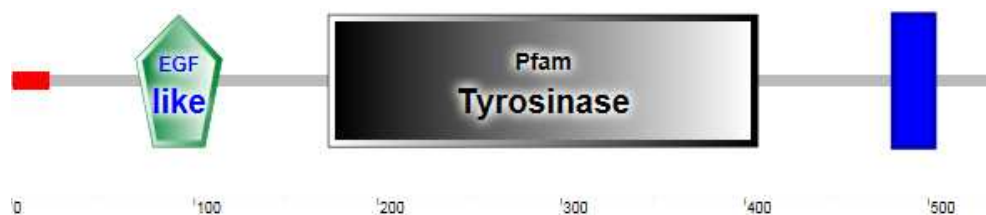
- [7] Dunning, K. R., Watson, L. N., Zhang, V. J., Brown, H. M., Kaczmarek, A. K., Robker, R. L., Russell, D. L. (2015): Activation of mouse cumulus-oocyte complex maturation *in vitro* through EGF-like activity of versican. – *Biology of Reproduction* 92(5): 116.
- [8] Gutiérrez-Gil, B., Wiener, P., Williams, J. L. (2007): Genetic effects on coat colour in cattle: dilution of eumelanin and pheomelanin pigments in an F2-Backcross Charolais × Holstein population. – *BMC Genetics* 8: 56.
- [9] Güler-Gane, G., Kidd, S., Sridharan, S., Vaughan, T. J., Wilkinson, T. C. I., Tigue, N. J. (2016): Overcoming the refractory expression of secreted recombinant proteins in mammalian cells through modification of the signal peptide and adjacent amino acids. – *PLoS One* 11(5): e155340.
- [10] Huang, Y. H., Lee, T. H., Chan, K. J., Hsu, F. L., Wu, Y. C., Lee, M. H. (2008): Anemonin is a natural bioactive compound that can regulate tyrosinase-related proteins and mRNA in human melanocytes. – *Journal of Dermatological Science* 49(2): 115-123.
- [11] Hubbard, J. K., Uy, J. A., Hauber, M. E., Hoekstra, H. E., Safran, R. J. (2010): Vertebrate pigmentation: from underlying genes to adaptive function. – *Trends in Genetics* 26(5): 231-239.
- [12] Jackson, I. J., Chambers, D., Rinchik, E. M., Bennett, D. C. (1990): Characterization of TRP-1 mRNA levels in dominant and recessive mutations at the Mouse *brown (b)* locus. – *Genetics* 126(2): 451-459.
- [13] Jackson, I., Chambers, D. M., Tsukamoto, K., Copeland, N. G., Gilbert, D. J., Jenkins, N. A., Hearing, V. (1992): A second tyrosinase-related protein, TRP-2, maps to and is mutated at the mouse slaty locus. – *EMBO Journal* 11(2): 527-535.
- [14] Jagirdar, K., Smit, D. J., Ainger, S. A., Lee, K. J., Brown, D. L., Chapman, B., Zhen, Z. Z., Montgomery, G. W., Martin, N. G., Stow, J. L., Duffy, D. L., Sturm, R. A. (2014): Molecular analysis of common polymorphisms within the human *Tyrosinase* locus and genetic association with pigmentation traits. – *Pigment Cell & Melanoma Research* 27(4): 552-564.
- [15] Jiang, Y. (2016): Body color variation and cloning, expression analysis of TYR gene in *Amphilophus citrinellus*. – Shanghai Ocean University, Shanghai.
- [16] Lai, X., Wichers, H. J., Soler-Lopez, M., Dijkstra, B. W. (2018): Structure and function of human tyrosinase and tyrosinase-related proteins. – *Chemistry* 24(1): 47-55.
- [17] Li, Q., Li, Y., Li, C., Yu, X. (2012): Enhanced ascorbic acid accumulation through overexpression of dehydroascorbate reductase confers tolerance to methyl viologen and salt stresses in tomato. – *Czech Journal of Genetics and Plant Breeding* 48(2): 74-86.
- [18] Li, H., Sang, W., Duan, Q. (2014): Advance of fish color mechanism and its regulation. – *Marine Sciences* 38(8): 109-115.
- [19] Meng, Y. (2011): Research on karyotype and genetic diversity of *Leptobotia taeniops*. – Anhui Agricultural University, Hefei.
- [20] Ming, L., Yi, L., Sa, R., Ji, R., Ha, S. (2016): Polymorphisms of the tyrosinase (TYR) gene in bactrian camel (*Camelus bactrianus*) with different coat colour. – *Journal of Camel Practice and Research* 23(1): 47-51.
- [21] Moretz, J. A., Morris, M. R. (2003): Evolutionarily labile responses to a signal of aggressive intent. – *Proceedings: Biological Sciences* 270(1530): 2271-2277.
- [22] Ni, J. J., Yan, Q. Y., Yu, Y. H., Wu, H. H., Chen, F. (2017): Dispersal patterns of endogenous bacteria among grass carp (*Ctenopharyngodon idellus*) guts. – *Iranian Journal of Fisheries Sciences* 16(2): 605-618.
- [23] Ni, J. J., Li, X. J., Chen, F., Wu, H. H., Xu, M. Y. (2018): Community structure and potential nitrogen metabolisms of subtropical aquaculture pond microbiota. – *Applied Ecology and Environmental Research* 16(6): 7687-7697.
- [24] Parekh, A. B. (2016): Advances in intracellular Ca²⁺ signalling. – *Journal of Physiology* 594(11): 2811-2812.
- [25] Pretzler, M., Rompel, A. (2018): What causes the different functionality in type-III-copper enzymes? A state of the art perspective. – *Inorganica Chimica Acta* 481(1): 25-31.

- [26] Sánchez-Ferrer, Á., Rodríguez-López, J. N., García-Cánovas, F., García-Carmona, F. (1995): Tyrosinase: a comprehensive review of its mechanism. – *Biochimica et Biophysica Acta (BBA) – Protein Structure and Molecular Enzymology* 1247(1): 1-11.
- [27] Schartl, M., Larue, L., Goda, M., Bosenberg, M. W., Hashimoto, H., Kelsh, R. N. (2016): What is a vertebrate pigment cell? – *Pigment Cell & Melanoma Research* 29(1): 8-14.
- [28] Slominski, R. M., Zmijewski, M. A., Slominski, A. T. (2015): The role of melanin pigment in melanoma. – *Experimental Dermatology* 24(4): 258-259.
- [29] Solano, F. (2018): On the metal cofactor in the tyrosinase family. – *International Journal of Molecular Sciences* 19(2): 633.
- [30] Spivak, C. E., Kim, W., Liu, Q. R., Lupica, C. R., Doyle, M. E. (2012): Blockade of β -cell K_{ATP} channels by the endocannabinoid, 2-arachidonoylglycerol. – *Biochemical and Biophysical Research Communications* 423: 13-18.
- [31] Sulzer, D., Bogulavsky, J., Larsen, K. E., Behr, G., Karatekin, E., Kleinman, M. H., Turro, N., Krantz, D., Edwards, R. H., Greene, L. A., Zecca, L. (2000): Neuromelanin biosynthesis is driven by excess cytosolic catecholamines not accumulated by synaptic vesicles. – *Proceedings of the National Academy of Sciences of the United States of America* 97(22): 11869-11874.
- [32] Suqimoto, M. (2002): Morphological color changes in fish: Regulation of pigment cell density and morphology. – *Microscopy Research & Technique* 58: 496-503.
- [33] Tu, Y., Xie, M., Sun, Y., Tyan, Y. (2009): Structural characterization of melanin from Black-bone silky fowl (*Gallus gallus domesticus* Brisson). – *Pigment Cell & Melanoma Research* 22(1): 134-136.
- [34] Wang, N., Daniels, R., Hebert, D. N. (2005): The cotranslational maturation of the type I membrane glycoprotein tyrosinase: The heat shock protein 70 system hands off to the lectin-based chaperone system. – *Molecular Biology of the Cell* 16(8): 3740-3752.
- [35] Wang, W., Hu, H., Sun, X., Niu, C. (2012): Analysis of tyrosinase gene and tissue expression in five different strains of Koi carp (*Cyprinus carpio* Koi). – *Journal of Fisheries of China* 36(11): 1658-1666.
- [36] Wei, X., Wang, D., Liu, S. (2006): Signal sequence and its application to protein expression. – *Biotechnology Bulletin* (6): 38-42.
- [37] Yu, S., Liao, J., Tang, M., Wang, Y., Wei, X., Mao, L., Zeng, C. (2017): A functional single nucleotide polymorphism in the tyrosinase gene promoter affects skin color and transcription activity in the black-boned chicken. – *Poultry Science* 96(11): 4061-4067.
- [38] Zhang, X., Zhang, H. F., Puliafito, C. A., Jiao, S. (2011): Simultaneous *in vivo* imaging of melanin and lipofuscin in the retina with photoacoustic ophthalmoscopy and autofluorescence imaging. – *Journal of Biomedical Optics* 16(8): 80504-1-80504-3.
- [39] Zhou, J., Shang, J., Song, J., Ping, F. (2013): Interleukin-18 augments growth ability of primary human melanocytes by PTEN inactivation through the AKT/NF- κ B pathway. – *International Journal of Biochemistry & Cell Biology* 45(2): 308-316.
- [40] Zou, J., Beermann, F., Wang, J., Kawakami, K., Wei, X. (2006): The Fugu *tyrp1* promoter directs specific GFP expression in zebrafish: tools to study the RPE and the neural crest-derived melanophores. – *Pigment Cell Research* 19(6): 615-627.

APPENDICES

1 ACATGGGGGTGCTGATGTAACAT**AGAGGCCTTCGTCCATCTCTCCGTTCTTCTTTCATTACAGTACCTGGGTCTCTC**
1 M R P S S I S P L L F F I Q Y L G L S
79 CCTCCAACAGTTTCCTCGACCCTGCACCCTCGGAGGTCTCCAAGCAAGCAGTGCTGCCCGGTCTGGCCGGGGA
20 L Q Q F P R P C T T P E V L Q S K Q C C P V W P G D
157 CCGTCTGGTGTGCGGGTCTTTCCGGTTCGAGGGTCTGCCGGACGTACGGTCTCGGACCTCCCAACCGGGCCGA
46 G S V C G V L S G R G F C R D V T V S D L P N G P Q
235 GTACCCTCACTCCGGCTGGATGATCGAGAGCGGTGGCTCTGGTGTCTACAACCGAACCTGCCAATGCGCCGTAA
72 Y P H S G V D D R E R W P L V F Y N R T C Q C A G N
313 CTACATGGGGTTCGACTGCGGTGAGTGAAGTTCGGTACTTCCGGCCCACTCGGGGAGAGCCGAGAATCCGTGCG
98 Y M G F D C G E C K F G Y F G P N C G E R R E S V R
391 CAGGGACATCTCCAGCTGTCCGTGGCGGAGACAGCGGTTGTCTCGTACCTGAATCTCGCAAGACCACCACAG
124 R D I F Q L S V A E R Q R F V S Y L N L A K T T T S
469 CCGCGTTACATGATCGTGACGGGCAGTACGGCAGATGAACGACGGCGCGACCCCATGTTCCGCAACGTGACGGT
150 P G Y M I V T G T Y A Q M N D G A T P M F A N V S V
547 GTATGACCTGTTCGTGGATGCACTACTACGTGCCGTGACGGCTGCTGGGGGCCCCGGGAACGTGTTGGCCGA
176 Y D L F V W M H Y Y V S R D A L L G G P G N V W A D
625 CATCGACTTTCGCGACGAGTCCGGCGCTTTCTGCCCTGGCACCGCGTGTATCTGTTGTTCTGGGAGCATGAGATCCG
202 I D F A H E S A A F L P W H R V Y L L F W E H E I R
703 GAAGCTGACCGGTACTTAACTTACCATCCCGTACTGGGACTGGCGGACGCGCGGACTGTACAGTGTGCACGGA
228 K L T G D F N F T I P Y W D W R D A A D C Q V C T D
781 TGAGCTGATGGGGCGCGACCCACTGAACCAACCTCATCAGCCCGTCTCGGTGTCTCTCTCTGGAAGTGGT
254 E L M G A R S P L N P N L I S P S S V F S S W K V V
859 GTGTTCCCAACCGAAGACTACAACAATCGGGAGGCTCTGTGTGACGGGTCTCTGAGGGCCGTTACTCCGTAACCC
280 C S Q P E D Y N N R E A L C D G S P E G P L L R N P
937 TGGTAACACGACCGCGTGTACGGCGCTGCCACCTCTGCAGACGTGGAATCTGTCGAGCCTCACAGGTA
306 G N H D R T R V R R L P T S A D V E S V L S L T E Y
1015 CGAGACGGGTCCATGGACCGGGCCCAACATGAGCTTCCGCAACGCTCTGGAAGGTTTTCGAGTCCAGAACGGG
332 E T G S M D R R A N M S F R N A L E G F A S P E T G
1093 ATTGGAATAACGGGTGACAGTCTGATGCACAACCTCTACACGTCTTCATGAATGGATCCATGTCTCAGTACAGGG
358 L A I T G Q S L M H N S L H V F M N G S M S S V Q G
1171 CTGGCCCAACGACCCATTTCTCTGATCAGCCCTTATTGACAGCATCTTTGAGCAGTGGTACCGGAGACCA
384 S A N D P I F L L H H A F I D S I F E Q W L R R H Q
1249 GCCTCCCGCACACATTACCCGACGCCAACGCTCCGATCGGACACAACGACGGCTATTTTCATGGTTCCTTACCCC
410 P P R T H Y P T A N A P I G H N D G Y F M V P F I P
1327 TCTGTACAGAAAACGGAGATTATTTCTGTCCACCAAGCTCTGGGATATGAATATGCCTATTTGCTGGACCCAGCCA
436 L Y R N G D Y F L S T K A L G Y E Y A Y L L D P S Q
1405 GCGTTCGTGACGAGGTTTTGACGCCGTACTAGGCAAGCTCAGCAGATCTGGCGTGGCGTGGCCGGGAAT
462 R F V Q E F L T P Y L E Q A Q Q I W R W L G A A G I
1483 CTTGGTGGCTCGTGGCGGAATCGTCGAGGATAATCGCCGTGGCGTTCGCGAGAAGGCAAAAGCGCAGGAAGAT
488 L G A L V A G I V A G I I A V A C R R R Q K R R K M
1561 GTCCGCATACGGGGAGAGACGCCGCTCTGAACAGCAGTGAAGAGGAGGGCTCAACTTCATATCAGACAACGCTG**TG**
514 **S A Y G E R Q P L L N S S E E E G S T S Y Q T T L ***
1639 AATCAAAACACACACACACACACTACAGGCAGGTGTCAGCGAGGACAGATACACTGTACCAACGGGAAAGACA
1717 CAACAGCCAGTTAACATGTGACAAATGAAGCAAGGCCCTACTCCTGAGCTCAGGTACAGTATGAGCCCTCGCACCCC
1795 TGTTCCAGTCATGAGACCAGGCTGTTCGGAACAGAAATACCACCATATTAATCTCACCCATGACAGTATAGAGGGGTT
1873 TTCACCCTTATTATATATCTTTTTTATAAAAACCTTGGATTATAATTGCAAAATAACAAAATAGTTGTTTACGA
1951 TGATAATGGGCTGAATTAATGCAGGTCAATTAACAGATTGAAACATGAAACACGCATCGGGACGGTTCGCCGTC
2029 AGGGCTTAAGTTAGTCCAGACTGAAATGCATGTTGAGGTCTTAAATGAAAGAGCTTACTGACGTATCTTAACA
2107 TACATCAGTGCCATTGATCTGCTTGAGATGCACATCAGTCATGTTTTGGTGAGGTATGTTGTATAAAAACACTATT
2185 TACTGATTGAATTAAGACTTCTGTTTAACTGAGGCCGTCTGGGAAACCGCCCATTTGTGTTTTGTTTACT
2263 TACTACTTAAAATAGTCCCGTTTTTATTACAAAGTACCCAGTGGTTAGTATCCGTTCCCAACAGGGTGTGCGCCT
2341 GAATTCAGCCAACCGTGAATAATGGTGCTTATGTCGCAATGTGGCACATGCGTACTGTATGTTAGGGCATAAAA
2419 CATATCCAATGAAATATAAACGGATGTTTTAAGAGGAATGAAGTGTGAAACAGAGATGATATGAAATTTTGCCA
2497 GTGTTTATAAAAATACATCCAGTCCATGTTGACATTTACATGGCCAACAATGTTAATGCTTTATCTTTGTTCAATA
2575 CCAATAGGAATAATAACAATACGTTCAAAA**ATAA**ACCAACCCCTCAACAAAAAAAAAAAAAAAAAAAA

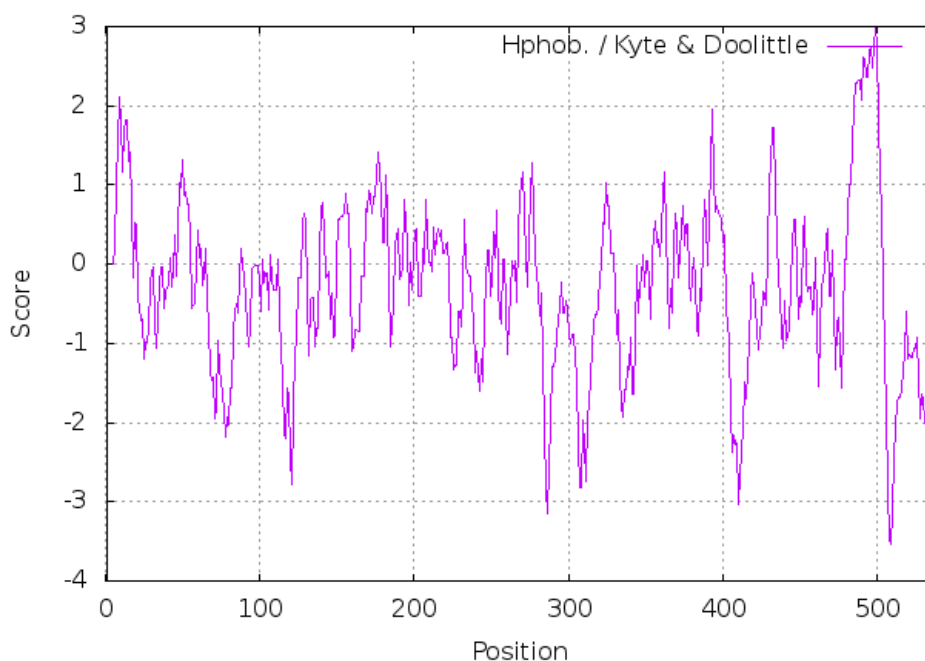
Appendix 1. Nucleotide sequence and deduced amino acid sequence of the tyrosinase cDNA. The start codon (ATG), the stop codon (TGA) and poly(A) signals(AATAAA) were marked with black bold font, The putative amino acid sequence of Signal Peptides domain (1-21 AA), EGF-like structure domain (AA), 68-115, Tyrosinase domain (173-407 AA) and Transmembrane region (481-503 AA) were underlined, CuA domain (206-223 AA) and CuB domain (387-398 AA) were shaded; Black dots represent Cys



Appendix 2. The structural features of the *Leptobotia taeniops* tyrosinase predicted by SMART

Appendix 3. Differences of tyrosinase among different species

Species	Amount of amino acid residues	Molecular weight	Theoretical pI
<i>Homo sapiens</i>	529	60.39 kD	5.71
<i>Mus musculus</i>	533	60.60 kD	5.67
<i>Equus caballus</i>	534	61.00 kD	6.07
<i>Danio rerio</i>	535	60.73 kD	6.07
<i>Oryzias latipes</i>	540	61.25 kD	5.99
<i>Cyprinus carpio</i>	535	60.63 kD	6.07
<i>Carassius auratus</i>	535	60.83 kD	5.71
<i>Leptobotia taeniops</i>	538	60.81 kD	6.13



Appendix 4. The hydrophobicity prediction atlas of *Leptobotia taeniops* tyrosinase. The horizontal coordinate is the amino acid position, and the ordinate is the scale value of the hydrophobicity (Hphob. / Kyte & Doolittle scale > 0 values indicates hydrophobicity, < 0 values indicates hydrophilicity)

REGIONAL AGRICULTURAL WATER FOOTPRINT AND CROP WATER CONSUMPTION STUDY IN YELLOW RIVER BASIN, CHINA

YIN, J.^{1,2*} – LU, Y.³ – OU, Z.²

¹*Research Center for China Western Modernization, Guizhou University of Finance and Economics, University City, Huaxi District, Guiyang 550025, China*

²*School of Water Conservancy and Civil Engineering, Northeast Agricultural University, No. 59, MuCai Rd., Xiangfang Dist., Harbin 150030, China*

³*GuoYuan Securities Co., Ltd, 18 Meishan Road, Shushan District, Hefei 230031, China*

**Corresponding author
e-mail: yinjianbnu@163.com*

(Received 16th Dec 2018; accepted 21st Mar 2019)

Abstract. The 12 main crops in the Yellow River Basin were selected as the research objects. Based on crop water consumption and effective precipitation, the regional crop water consumption and agricultural water footprint of the Yellow River Basin are studied. The results showed that the distribution of crop water consumption in the Yellow River Basin was similar to that of the annual average precipitation. Irrigation affected the data distribution in some areas. The areas with high crop water consumption value were mainly concentrated in the irrigation areas along the Yellow River. Rain-fed agriculture was dominant in other areas, and crop water consumption was relatively small. The total crop water consumption in the Yellow River Basin was 84.25 billion m³ in 2017, 66% of which is in Henan and Shandong provinces and 60% is for wheat and maize. The proportion of green water to crop water consumption in the Yellow River Basin was 78.7%. The spatial distribution of green water consumption in crops was basically the same as that of crop water consumption. The agricultural water footprint of the Yellow River Basin is 49.45 billion m³, accounting for 58.7% of the crop water consumption. The proportion of green water consumption to total water consumption of most crops is more than 80%, and the lowest is 58% for wheat. 56% of blue water in the river basin is used for wheat. Crop water consumption coefficient reflects the level of water use in production. The average crop water consumption coefficient in the Yellow River Basin is about 0.622 m³/kg.

Keywords: *water consumption coefficient distribution, annual average precipitation, reference evapotranspiration, green water, blue water*

Introduction

Humanity's direct need of fresh water is mainly due to food production, among which green water has a function that cannot be ignored on food production (Veetil and Mishra, 2016). The green water is a water resource that comes from precipitation, is stored in soil and consumed by evaporation of vegetation (Zuo et al., 2015). Green water has made outstanding contributions to crop production (Hoff et al., 2010). Thus the need to consider this resource in water availability and water scarcity studies (Fader et al., 2011). Water for agricultural irrigation in the Yellow River Basin, China is mainly originated from precipitation, and the role of green water is more prominent (Zhang et al., 2014). Defining the characteristics of human need for agricultural water helps to find a way of increasing agricultural production and reducing agricultural water consumption (Feng et al., 2012). In the Yellow River Basin, water is less efficiently consumed for agricultural irrigation. Less than half of irrigation water resource

consumed by agriculture is consumed by humans. In the Yellow River Basin in which the situation of agricultural water is grim, water is wasted in large quantities (Xiang et al., 2017). Coupled with imperfect water conservancy facilities, unreasonable water-saving irrigation system and unreasonable planting structure, the water consumption efficiency is very low in the basin (Gonçalves et al., 2007; Bai et al., 2017). Therefore, improving efficiency of irrigating water and giving full play to green water in the Yellow River Basin is an important way to improve efficiency of agricultural water, develop water-saving high-efficiency agriculture and alleviate the lack of water resource in the basin (Zhuo et al., 2014). A systematic analysis of the agricultural water footprint and crop water consumption in the basin provides the necessary scientific support for regional water resources safety and eco-economic system.

Crop water consumption, as a key indicator of analyzing the agricultural water footprint, is generally represented by the (evapotranspiration, ET) and subject to the calculation method of ET at the regional scale (González-Dugo et al., 2013; Yin et al., 2017; Wang et al., 2018). The difference is that when the ET at the regional scale is estimated, ET values of only a plant are selected at several moments (Serrano-Coronel et al., 2018). However, as there are multiple agricultural crops planted, calculation of agricultural water consumption should be subject to the amount of water consumed by all crops in their growth duration (Zhang et al., 2010). In addition, when the spatial distribution of water consumption of crops in growth duration is calculated, the existing research generally measures the amount of water that the crop takes up from the soil according to the water balance of the crops in the grid at the beginning and end of the growth duration to reduce the computational work. However, there are many factors affecting soil water content during the growth duration, beside crop water consumption (Mo et al., 2009; Li et al., 2016). Thus, subdividing the growth duration can approximate to the real facts. In order to improve the computational accuracy, inclusion of major crops in the study area, subdivision of the growth duration and use of high spatial resolution data is also a development direction (Barbagallo et al., 2004; Wei et al., 2016). In addition, advancement of remote sensing technique also provides the necessary conditions for monitoring crop water consumption in a real-time manner (Calera et al., 2017).

The 12 major crops in eight provinces of the Yellow River Basin are selected to analyze the spatial distribution of agricultural water consumption and green water consumption. Additionally, water consumption and primary industry water footprint are used as a basis to further study the agricultural water footprint. In order to provide support for formulating appropriate agricultural water-saving measures and ensuring the efficient and rational utilization of regional agricultural water resources.

Materials

The study area

The Yellow River originates from the Qinghai-Tibet Plateau and flows into the Bohai Sea. It flows through nine provinces (regions) including Qinghai, Sichuan, Gansu, Ningxia, Inner Mongolia, Shanxi, Shaanxi, Henan and Shandong, with 795,000 km² drainage area and 5464 km total length of the main river channel (*Fig. 1*). Of the Yellow River Basin, the terrain is rugged violently, descending in three steps from west to east. During 1956 to 2017, the average temperature of the basin is 8.6 °C; the average annual precipitation is 466 mm, decreasing from the southeast to the

northwest (Fig. 2); the annual sunshine hours fall between 1400 and 3300 h. The climate difference is distinct. The west is arid and the east is humid; The basin is divided by water condition into semi-humid region, semi-arid region and arid region from west to east, and by temperature condition into warm temperate zone, the middle temperate zone and the plateau climate zone.

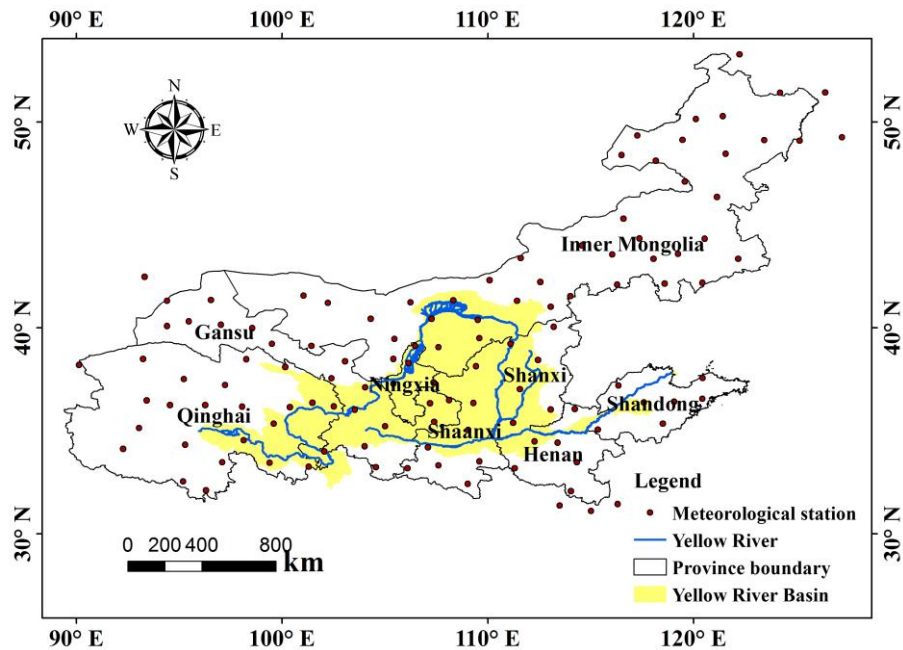


Figure 1. The map of the Yellow River Basin and the related nine provinces

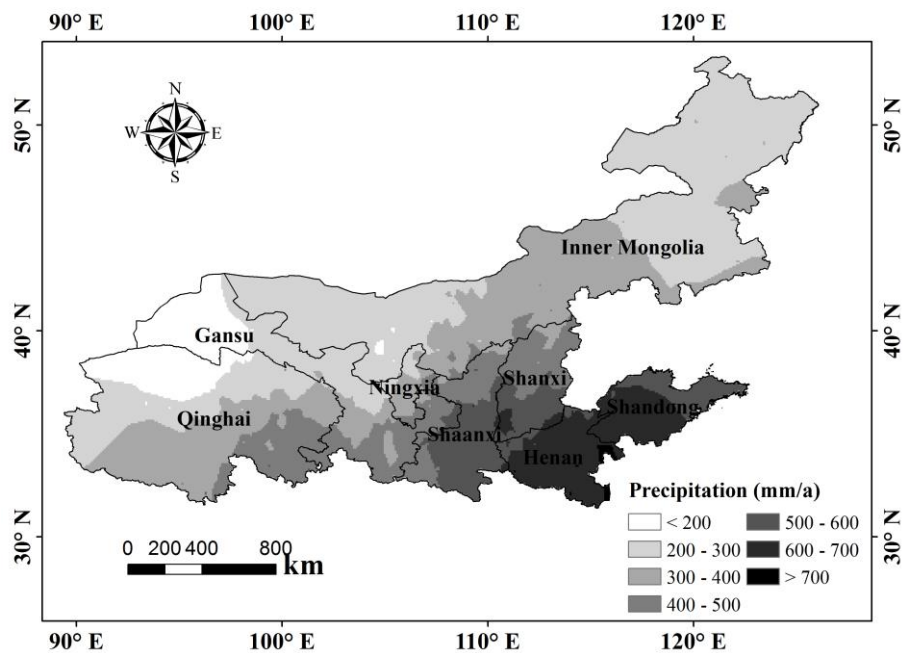


Figure 2. Spatial distribution of annual average precipitation in the Yellow River Basin (1956-2017)

Data

The planting area and yield data of the crop are obtained from the global major crop distribution map and yield distribution map formulated by You et al. (2014). The former gives a percentage of the harvest area of each crop in grid area, while the latter lists the average yield (t/ha) of each crop in the grid. In this study, 12 crops are selected, basically covering the varieties in the Yellow River Basin. Among them, wheat and corn have a large planting area, accounting for 4.3% and 2.9% of the total area of eight provinces, respectively. The meteorological data are collected from the 121 meteorological stations of Chinese National Meteorological Bureau (Fig. 1). They are mainly used as input terms of CROPWAT software, including maximum and minimum temperature, wind speed, daylight hours, relative humidity and precipitation. The above kinds of data are based on the statistical information of 2017.

The irrigation area distribution map (Fig. 3) is obtained from the website of FAO (<http://www.fao.org/nr/water/aquastat/irrigationmap/index.stm>). Irrigation facilities are concentrated in Shandong and Henan, between which irrigation facilities appear in more than 80% of Shandong (except central and southern region), and in more than 60% of Henan (except western region). The irrigated farmlands appear in a decentralized manner in Ningxia, Shanxi, Shaanxi and Gansu, and there are irrigated farmlands in the Yellow River irrigation area and Tongliao district in Inner Mongolia. Irrigated farmlands are scattered across the north side of the Yellow River Valley in eastern Qinghai. Regions with an irrigation ratio exceeding 70% include Ningmeng irrigation area, Central Shaanxi Plain, Jinzhong, lower reach of Yellow River (Henan section) and areas in Shandong along Yellow River, which are commonly characterized by border on Yellow River, convenience for water intaking, superior agricultural natural conditions and development of irrigated agriculture. The ArcGIS 10.3 was employed to realize data calculation and visualization.

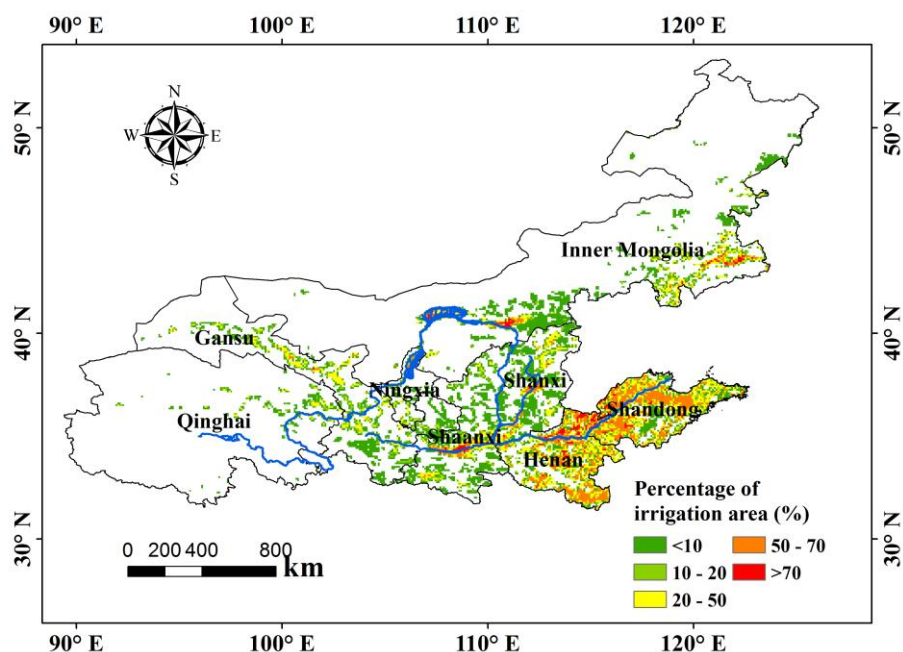


Figure 3. The percentage of irrigation area of the total agricultural land in 2017

Methodology

Crop water consumption

The calculation steps of regional crop water consumption are as *Equations 1–5*:

$$CWU = \sum_{c=1}^{12} CWU(c) \quad (\text{Eq.1})$$

where c is the crop type, $CWU(c)$ is the regional water consumption of the c -th crop, with the unit of m^3 .

$$CWU(c) = ET(c) \quad (\text{Eq.2})$$

The actual regional ET of the c -th crop $ET(c)$ is calculated by *Equation 3*.

$$ET(c) = ET_g(c) + ET_b(c) \quad (\text{Eq.3})$$

where $ET(c)_g$ and $ET(c)_b$ are respectively represent the green and blue water consumption of the c -th crop in the region. The blue water is the water resources of surface runoff and underground runoff. Then, the contribution rate of green water to the c -th crop's water consumption is:

$$GW(c) = \frac{ET_g(c)}{CWU(c)} \quad (\text{Eq.4})$$

Contribution rate of green water in the region is calculated as:

$$GW = \frac{\sum_{c=1}^{12} ET_g(c)}{\sum_{c=1}^{12} CWU(c)} \quad (\text{Eq.5})$$

Green water consumption

Crop evapotranspiration depends on crop water demand and soil water supply which comes from effective precipitation and irrigation. Here, a 5-arc minute resolution distribution map of irrigated farmland is selected. For Rain-fed Agricultural areas, effective precipitation is the only source of water available in soil, and evapotranspiration of crops is completely composed of green water. For irrigated areas, due to the lack of irrigation system data, it is assumed that irrigation water can meet crop water demand. Therefore, the transpiration of crops is the water demand of crops, in which the green water is supplied by effective precipitation and the blue water is supplied by irrigation water.

Crop water demand

When the blue and green water consumption of each crop in an area is analyzed, the crop water demand is first calculated at the observatory; then, Kriging interpolation is adopted to

determine the crop water demand in each grid of this area; Later, according to the agricultural crop sown area distribution map and the irrigated area distribution map, the blue and green water consumption in each grid is obtained and then separately accumulated to finally get the blue and green water consumption of the crop in this area.

The crop water demand for a certain growth period t is represented by $ET_c(c, t)$ which is calculated by Equation 6:

$$ET_c(c, t) = K_c(c, t) \times ET_0(c, t) \quad (\text{Eq.6})$$

where $K_c(c, t)$ and $ET_0(c, t)$ are respectively represent the crop coefficient and the reference ET.

CROPWAT 8.0 is used to calculated crop water demand, effective precipitation and irrigation water demand. In CROPWAT, the ET_0 was calculated by Penman-Monteith formula (Allen et al., 1998). K_c varies with crop growth stages, the K_c values refer to <http://www.fao.org/docrep/X0490E/x0490e0b.htm>.

Effective precipitation

Effective precipitation is defined depending on different professional fields. Without a clear definition in agricultural production field, effective precipitation usually refers to part of precipitation that can meet the need for crop evapotranspiration, excluding surface runoff and deep seepage (Sikorska et al., 2018). In the CROPWAT software, there are four methods to calculate effective precipitation, namely the fixed ratio method, precipitation-based method, empirical formula method and USDA SCS method. Among them, the SCS method is the most widely used for agricultural water resources management. The SCS method is an empirical formula as Equation 7, which is deduced by analyzing precipitation data at 22 test stations for 50 years, and has been simplified to calculate the effective precipitation (Mishra and Singh, 2007).

$$P_e = \begin{cases} P_t \times \frac{125 - 0.2P_t}{125}, & P_t < 250\text{mm} \\ 125 + 0.1 \times P_t, & P_t \geq 250\text{mm} \end{cases} \quad (\text{Eq.7})$$

where P_e is effective precipitation, mm; P_t is monthly precipitation, mm.

Green water consumption in grids

Taking 10 days as the calculation period, the green water consumption $ET_g(c, i, t)$ of the c -th crop in the No. i grid is determined by the crop water requirement $ET_c(c, i, t)$ and effective precipitation $P_e(c, i, t)$ in the period t , through Equation 8:

$$ET_g(c, i, t) = \min[ET_c(c, i, t), P_e(c, i, t)] \quad (\text{Eq.8})$$

Irrigation water requirement $IRR(c, i, t)$ during period t is calculated by Equation 9:

$$IRR(c, i, t) = ET_c(c, i, t) - ET_g(c, i, t) \quad (\text{Eq.9})$$

That is the amount of blue water is by (Eq. 10):

$$ET_b(c, i, t) = IRR(c, i, t) \quad (\text{Eq.10})$$

During the whole growth period, the amount of green water for the c -th crop on the i -th grid is:

$$ET_g(c, i) = \sum_t ET_g(c, i, t) \quad (\text{Eq.11})$$

During the whole growth period, the amount of blue water for the c -th crop on the i -th grid is:

$$ET_{b_g}(c, i) = \sum_t ET_b(c, i, t) \quad (\text{Eq.12})$$

Regional green water consumption

The regional green water consumption of the c -th crop $ET_g(c)$ is calculated by Equation 13:

$$ET_g(c) = \sum_i [ET_g(c, i) \times A(c, i)] \quad (\text{Eq.13})$$

where the $A(c, i)$ is the planting area percentage of the c -th crop on the i -th grid.

The regional blue water consumption of the c -th crop $ET_b(c)$ is obtained through Equation 14:

$$ET_b(c) = \sum_i [ET_b(c, i) \times A(c, i) \times I(c, i)] \quad (\text{Eq.14})$$

where the $I(c, i)$ is the irrigation area percentage of the c -th crop on the i -th grid.

Agricultural water footprint

The agricultural water footprint includes blue water and green water. The primary industry water footprint refers only to blue water. Some water consumed by crops flows out of the area, and some is used by local residents. The rest is the agricultural water footprint. Thus, calculation of agricultural water footprint is based on the primary industry water footprint and crop water consumption, and the total water consumed by the primary industry is composed of the water footprint of the primary industry and the primary industry net output virtual water. Considering that the Yellow River Basin is an important agricultural base, it is assumed that the net output virtual water of agriculture does not flow in but flow out. Then, the crop water consumption is equal to the amount of the agricultural water footprint and the net output. Thus, the proportion of the agricultural water footprint to the crop water consumption is equal to the proportion of the primary industry water footprint to the primary industry water. The agricultural water footprint can be calculated as shown in Equation 15:

$$WFP_{agr} = CWU \times \frac{WFP_{fir}}{WFP_{fir} - EWFP_{fir}} \quad (\text{Eq.15})$$

where WFP_{agr} is agricultural water footprint, m^3 ; WFP_{fir} is water footprint of primary industry, m^3 ; $EWFP_{fir}$ is external water footprint of primary industry, m^3 . WFP_{fir} and $EWFP_{fir}$ are calculated by input-output method according to the reference (Yin et al., 2016).

Crop water consumption coefficient

The crop water consumption coefficient refers to the water consumed per unit of yield, which is the ratio of crop water consumption to the yield. It is an important indicator to measure the water consumption efficiency in crop production. Here, the crop water consumption of each grid is obtained with the above method, and the yield data adopts a crop yield distribution map with 50-arc resolution. The water consumption coefficient calculation processes are *Equations 16-18*:

$$WCC(c, i) = ET(c, i) / Y(c, i) \quad (\text{Eq.16})$$

where $WCC(c, i)$ is the water consumption coefficient of the c -th crop on the i -th grid, and $Y(c, i)$ is the yield of the c -th crop on the i -th grid.

$$WCC(c) = \sum_i [ET(c, i)] / \sum_i [Y(c, i)] \quad (\text{Eq.17})$$

where $WCC(c)$ is the water consumption coefficient of the c -th crop in the area.

$$WCC = \frac{\sum_{c=1}^{12} \sum_i ET(c, i)}{\sum_{c=1}^{12} \sum_i Y(c, i)} \quad (\text{Eq.18})$$

where WCC is the agricultural water consumption coefficient in the area.

Results

Distribution of crop water consumption

We can see from *Figure 4* that similar to the precipitation contour, crop water consumption in the Yellow River Basin roughly tends to descend to zero from southeast to northwest, and local areas are affected by irrigation. Areas with high water consumption are closely related to irrigation facilities. The irrigation areas account for a large proportion in total irrigation districts along Yellow River, and the crop water consumption per unit area is also large. Crop water consumption has the maximum value in the areas with an irrigation area exceeding 70%, in which the crop water demand can be fully met and the multiple index and the planting density of crops are

high. Especially in Shandong and central and eastern Henan, the water consumption in the grid basically exceeds more than 10 million m^3 per year.

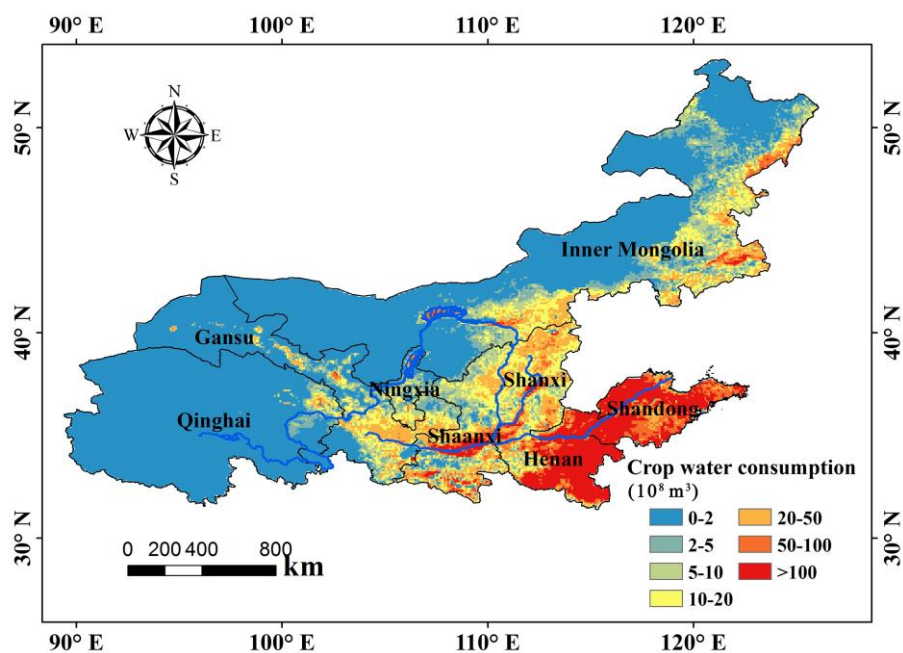


Figure 4. Spatial distribution of crop water consumption in 5 arc-minutes grid ($10^5 m^3/a$)

The entire range of Ningxia, Shanxi and Shaanxi, most part of Gansu and southeastern Inner Mongolia are basically covered by crop water consumption, as the proportion of irrigation areas in those regions are low and the agriculture is mostly rainfed. Except for the irrigated regions along Yellow River, the water consumption per unit area keeps basically less than 5 million m^3 per year in those regions, followed by regions along the northwest of which the water consumption per unit area is less than 1 million m^3 (roughly $150 m^3/ha$). The eastern valley in Qinghai Province is the area with small water consumption per unit area.

As far as crop water consumption is concerned (Fig. 5), corn and wheat are major crops that consume 31% and 29% of total crop water consumption, followed by cotton and soybeans, which both consume 9% of total water.

It can be seen from Table 1, the crop water consumption in the Yellow River Basin in 2017 was 84.25 billion m^3 . Henan and Shandong are at the top (36.1% and 30.0% respectively). Consistent with the above, the crop planting area is large in both provinces, and the water consumed per unit area is large. Inner Mongolia and Shaanxi are the next (respectively 11.1% and 10.1%), followed by Qinghai and Ningxia (0.5% and 1.1% respectively).

Agricultural water footprint

The agricultural water footprint of the Yellow River Basin amounts to 49.45 billion m^3 (Table 2), which is mainly caused by food production and is greatly related to the population. Henan tops the water footprint of the Yellow River Basin by 29.93 billion m^3 and Qinghai is at the bottom at 480 million m^3 . The proportion of

agricultural water footprint to crop water consumption explains the proportion of local food water consumption to the local water consumption, compared to 0.587 in the basin. Henan and Gansu are among the largest to 0.985 and 0.980 respectively. The food produced in these two provinces is basically self-consumed.

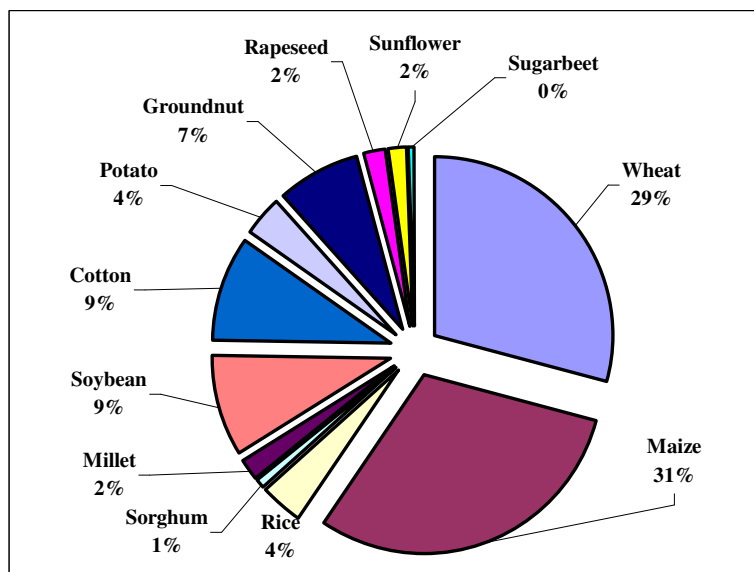


Figure 5. Percentage of crop water consumption per crop

Table 1. Crop water consumption and composition of provinces and autonomous regions in the Yellow River Basin

Province	Crop water consumption (10 ⁸ m ³)			Percentage of green water (%)	Percentage of crop water consumption in each province (%)
	Green water	Blue water	Total		
Qinghai	4.1	0.4	4.5	90.3	0.5
Gansu	26.7	5.3	32.0	83.5	3.8
Ningxia	5.0	4.2	9.2	54.5	1.1
Inner Mongolia	77.7	15.1	92.8	83.7	11.0
Shaanxi	69.8	14.9	84.7	82.4	10.1
Shanxi	52.0	10.8	62.8	82.7	7.5
Henan	240.6	63.4	303.9	79.1	36.1
Shandong	186.9	65.6	252.5	74.0	30.0
Total	662.7	179.7	842.5	78.7	100.0

The primary industry water footprint is all blue water. Difference with the agricultural blue water footprint lies that: firstly, the blue water footprint is the crop water consumption, while the primary industry water footprint contains irrigation losses; secondly, the blue water footprint is direct water consumption, but the primary industry water footprint contains indirect water consumption; thirdly, agriculture, forestry, animal husbandry and fishery industries are involved in the primary industry water footprint.

Table 2. Water footprint of provinces and areas in the Yellow River Basin

Province	Ratio of agricultural water footprint to crop water consumption	Water footprint (10 ⁸ m ³)			
		Agricultural water footprint	Green water footprint	Blue water footprint	Primary industry water footprint
Qinghai	1.068	4.8	4.3	0.5	36.7
Gansu	0.980	31.3	26.2	5.2	66.4
Ningxia	0.644	5.9	3.2	2.7	31.9
Inner Mongolia	0.106	9.8	8.2	1.6	26.2
Shaanxi	0.673	57.0	47.0	10.0	14.6
Shanxi	1.020	64.0	53.0	11.0	51.4
Henan	0.985	299.3	236.9	62.4	98.9
Shandong	0.697	176.1	130.3	45.8	72.4
Total	0.587	494.5	389.0	105.5	398.4

Green water consumption

As shown in *Table 1*, the green water consumption accounted for 78.7% of the crop water consumption in the Yellow River Basin, falling within the world average 75% ~ 81% caused by different research methods. Among 8 provinces, Qinghai consumes the most water with a percentage of 90.3%, followed by Inner Mongolia, Gansu, Shanxi and Shaanxi, of which the green water consumption percentage is close and measured between 82 and 84%. The third are Henan and Shandong with a percentage of 79.1% and 74.0%, respectively. The bottom one is Ningxia with a percentage of 54.5%. Obviously, in areas with more developed irrigated agriculture and high blue water utilization volume, the utilization rate of green water consumption is relatively low. Ningxia especially falls behind the other provinces in green water utilization rate, probably because of backward irrigation practice and the low water consumption efficiency. In addition, when the green water can meet the growth demand, unnecessary irrigation results in unnecessary wastage of water resources, and a decrease in the proportion of green water consumption.

Consistent with the distribution of water consumption (as shown in *Fig. 6*), the spatial distribution green water consumption in the Yellow River Basin tends to descent from southeast to northwest, partially affected by irrigation. In other words, the utilization volume of green water is related to the agricultural development intensity. In areas with developed agriculture, planting more corps lead to higher green water consumption. Relatively speaking, as the southeast is a natural and suitable area for agriculture owing to abundant precipitation, the agricultural is relatively highly developed. In the Ningmeng Irrigation Region in the northwest, Central Shaanxi Plain and Jinzhong, it is easy to draw the Yellow River water for agricultural irrigation purpose, although there is no abundant precipitation. The green water consumption in the above areas is correspondingly large.

The proportion of green water to crop water consumption reflects the extent to which natural water resources are used in agriculture. As shown in *Figure 7*, the percentage of green water consumption is mostly greater than 95% in the Yellow River Basin, dominated by rainfed agriculture. Except for several regions, the proportion of Ningmeng Irrigation Region, Central Shaanxi Plain, Jinzhong and East Inner Mongolia

Irrigation Region and the western Gansu are among the lowest in green water consumption to below 50%, followed by the northwest of Shanxi and the north of Henan at 50% to 70%. Among these areas, except for the western Gansu, the irrigation density is high in other areas; the proportion of green water consumption in western Gansu is smaller because of scarce precipitation and strong evaporation, and less effective precipitation available to crops.

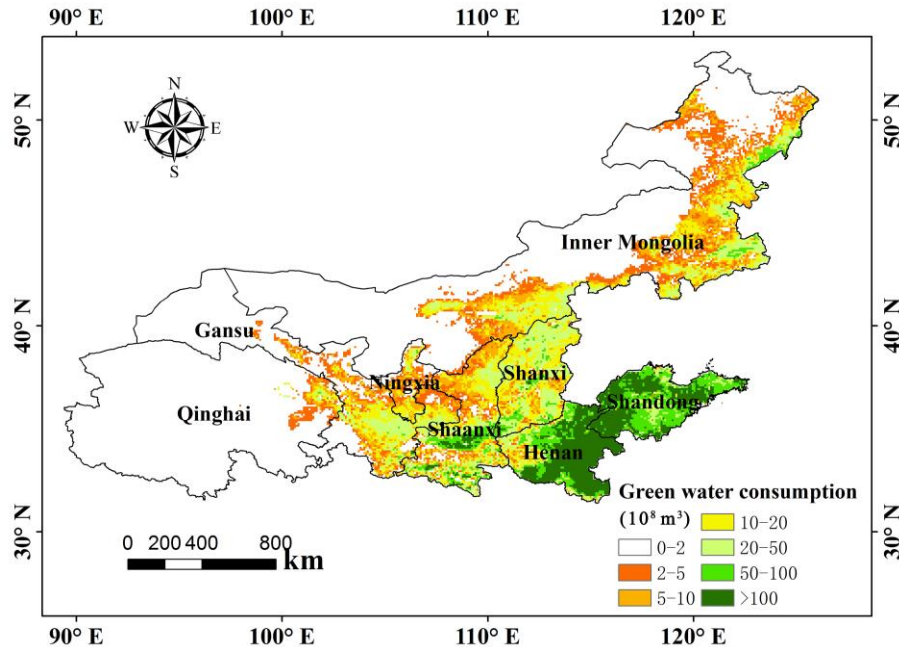


Figure 6. Spatial distribution of crop green water consumption in arc-minutes grid (10^5 m^3)

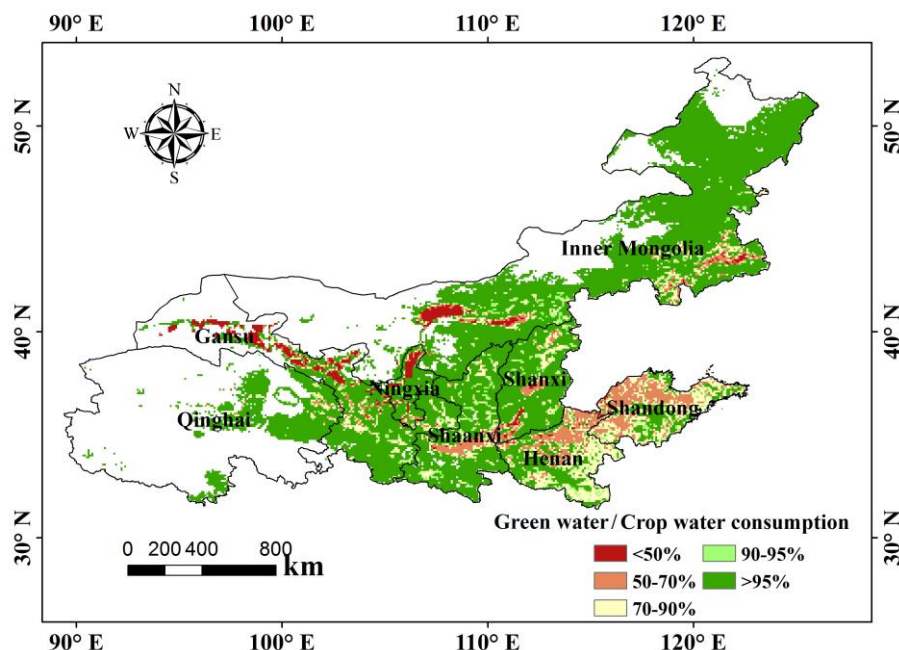


Figure 7. The percentage of green water consumption to crop water consumption

As shown in *Figure 8*, among the 12 crops, the rapeseed consume the most water with a percentage of 98%, and wheat and sugar beet consume the least water with a percentage of 58% and 66% respectively. The other crops account for 80 to 95% of water consumption. Wheat and corn are two crops with the largest planting area and water consumption in the Yellow River Basin, between which corn generally grows in rainy and hot season and its demand for water can be basically met by natural precipitation. On the contrary, in the critical growth period of wheat, the irrigation practice is required due to less precipitation. The wheat accounts for 29% of the total water consumption in the basin. According to the 74.1% percentage of green water consumption to crop water consumption in the basin, it can be concluded that the wheat accounts for 56% of the blue water consumption of the basin.

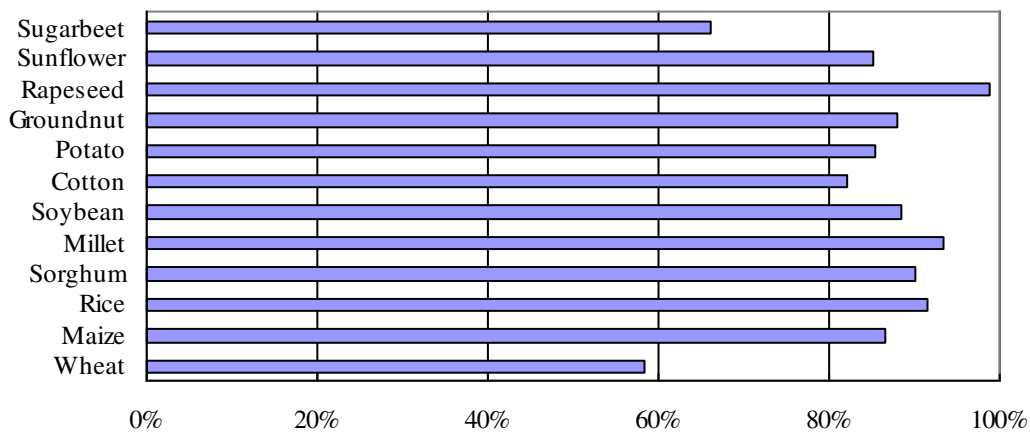


Figure 8. The percentage of green water in crop water

Crop water consumption coefficient

The crop water consumption coefficient refers to the water consumption per specific yield. Similar to the total water input coefficient defined in the water footprint (water consumption per specific yield), this coefficient can denote the crop water efficiency. The difference is that the total water input coefficient targets at withdrawals of blue water, including blue water consumption and recovery amount; however, the crop water consumption coefficient includes the portion of blue water that is consumed by the crops and the green water. As shown in *Figure 9*, the water consumption coefficient lies between 0.4-1.0 m³/kg for most areas. The water consumption coefficient is high in the southern part of the basin, and is low in western Gansu, northern Ningxia (excluding the Yellow River irrigation area), and central and southern Shandong. The low coefficient of western Gansu is caused by the low water consumption. This region has sufficient sunshine, which is conducive to crop growth, and keeps up certain production even if the water demand cannot be met. The central part of Shandong is a mountainous area with relatively underdeveloped irrigation facilities. Irrigation is to achieve output at the cost of water resources, and cannot significantly increase the crop water consumption coefficient.

The crop water consumption coefficient of the basin is 0.622 m³/kg, as shown in *Figure 10*. Those eight provinces can be divided by the crop water consumption coefficient into three levels: Ningxia, Gansu and Qinghai are at the bottom (less than 0.5 m³/kg) at 0.400 m³/kg, 0.427 m³/kg and 0.430 m³/kg, respectively, followed by

Inner Mongolia, Shandong and Shanxi (basically 0.5 - 0.6 m³/kg) measured 0.536 m³/kg and 0.562 m³/kg respectively. Shaanxi and Henan are at the top at 0.754 m³/kg and 0.748 m³/kg, respectively. For the entire basin, the level of agricultural production is highest in Henan and Shandong and lowest in Qinghai. Therefore, the current crop water consumption coefficient of the Yellow River Basin has no obvious relationship with the agricultural production level.

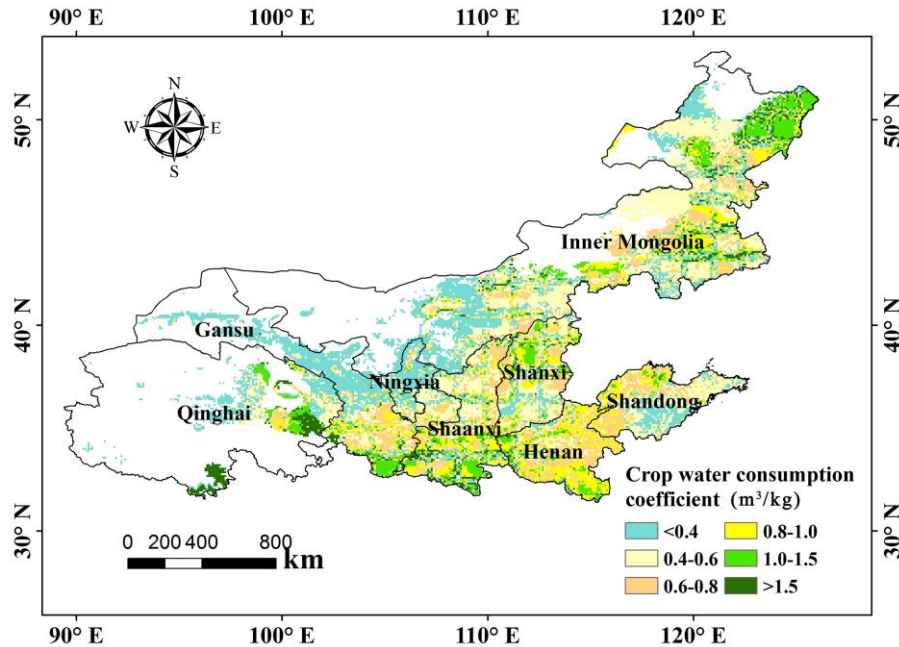


Figure 9. The spatial distribution of crop water consumption coefficient

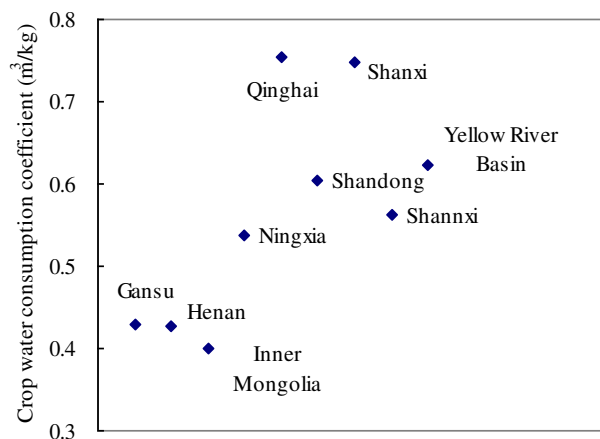


Figure 10. Crop water consumption coefficient in each province

For different crops, the water consumption coefficient is mainly related to crop characteristics. In the basin, sugar beet and potato consume the least water with a coefficient measured 0.118 m³/kg and 0.150 m³/kg, respectively. Cotton consumes the most water with a coefficient of 1.846 m³/kg (as shown in Fig. 11). Sugar beet and

potato have a high density of harvested products because tubers are harvested, while the cotton is low-density in the harvested product because fiber is harvested. The water consumption coefficient is almost the same among cereals, wheat, corn, sorghum and rice, close to oil crops. The water consumption coefficient of broomcorn millet is large mainly because of low yield of these two crops.

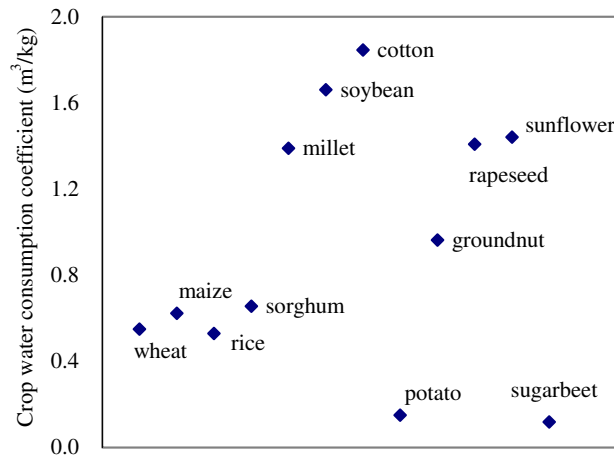


Figure 11. Crop water consumption coefficient for different crop types

Distribution of wheat's water consumption

Wheat is the crop in the Yellow River Basin (*Table 3*) with the largest planting area. As described earlier, the blue water consumed accounts for 56% of the total water consumption in the basin, mainly for wheat production. Understanding the water consumption characteristics of wheat, especially distribution of blue water, helps to propose measures of improving the wheat's water consumption efficiency and will have a significant effect on reducing agricultural water consumption throughout the basin.

Firstly, by analyzing wheat's overall water consumption and yield in all provinces/regions of the basin, we can see that the characteristic is obvious that wheat's water consumption is mainly confined to Henan and Shandong, as shown in *Table 3*. Henan is at the top, with 10.13 billion m³ of wheat's water consumption, followed by Shandong with 7.70 billion m³. Both provinces take up 72.8% of the total water consumed in the basin. Henan and Shandong also consume most of blue water, respectively 4.06 billion m³ and 3.86 billion m³, accounting for 39.8% and 37.9% of the total blue water consumption in the basin. Both provinces are equal in wheat yield and are the largest contributors in the basin for wheat, both accounting for 36.4% of the total wheat yield in the basin.

For the wheat's water consumption coefficient, Qinghai is at the lowest point to 0.350 m³/kg, mainly because there are few irrigation facilities in the province featured with basically rainfed agriculture and the small water consumption. It is similar with Gansu to this point. For other provinces, the water consumption coefficient depends mainly on the agricultural water productivity. Shaanxi is at the top to 0.704 m³/kg, and the agricultural water productivity is low. The water consumption coefficient of Henan is above the average, and its agricultural water productivity is also low. The water consumption coefficient of Shandong is under the average.

Table 3. Water consumption of wheat in provinces of the Yellow River Basin

Province	Water consumption (10 ⁸ m ³)			Yield (10 ⁹ kg)	Water consumption coefficient (m ³ /kg)	Green water/total (%)	Blue water consumption proportion (%)
	Green water	Blue water	Total value				
Qinghai	1.6	0.3	1.9	0.5	0.350	84.2	0.3
Gansu	9.8	2.7	12.5	2.7	0.462	78.4	2.6
Ningxia	1.3	1.5	2.8	0.6	0.466	46.4	1.4
Inner Mongolia	11.0	4.2	15.2	2.7	0.557	72.4	4.1
Shaanxi	13.2	9.2	22.4	3.2	0.704	58.9	9.0
Shanxi	6.8	4.8	11.6	2.4	0.488	58.6	4.8
Henan	60.7	40.6	101.3	16.2	0.625	59.9	39.8
Shandong	38.4	38.6	77.0	16.2	0.476	49.9	37.9
Total	142.8	101.9	244.7	44.55	0.549	58.4	100.0

By comparing the proportion of green and blue water consumption in wheat's water consumption (Fig. 12), the spatial distribution of wheat's water consumption in each province of the basin is analyzed.

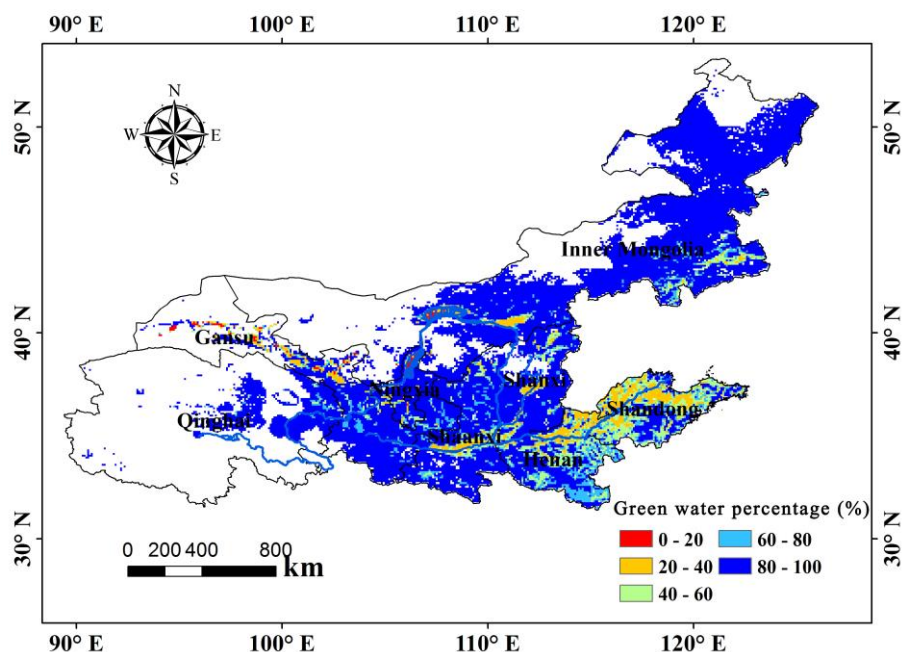


Figure 12. The percentage of green water to total water consumption in wheat

Wheat is widely cultivated in the basin, and the distribution of blue water consumption is consistent with that of irrigation facilities. As the largest blue water consumption per unit area is primarily centered on most areas of Henan and Shandong, and Central Shaanxi Plain, the wheat's irrigating water consumption in these three provinces is relatively large. Correspondingly, a bigger green water consumption corresponds to a smaller green water consumption. The spatial distribution of proportion of wheat's

green water consumption in wheat water consumption is similar to population distribution of all crops in the basin (Fig. 13). The proportion is bigger than 80% for most of planting areas, compared to 20% of Ningmeng irrigation region which is at the bottom one. From this point, it can also be proved that wheat is the main water-consuming crop in the basin, and its distribution has a greater impact on the population distribution of water consumption in the basin. Correspondingly, in Shandong, Henan, Central Shaanxi Plain, Ningmeng irrigation region, etc., according to the law of crop water demand, making full use of green water can effectively reduce the amount of irrigating water consumed, when guaranteeing the yield.

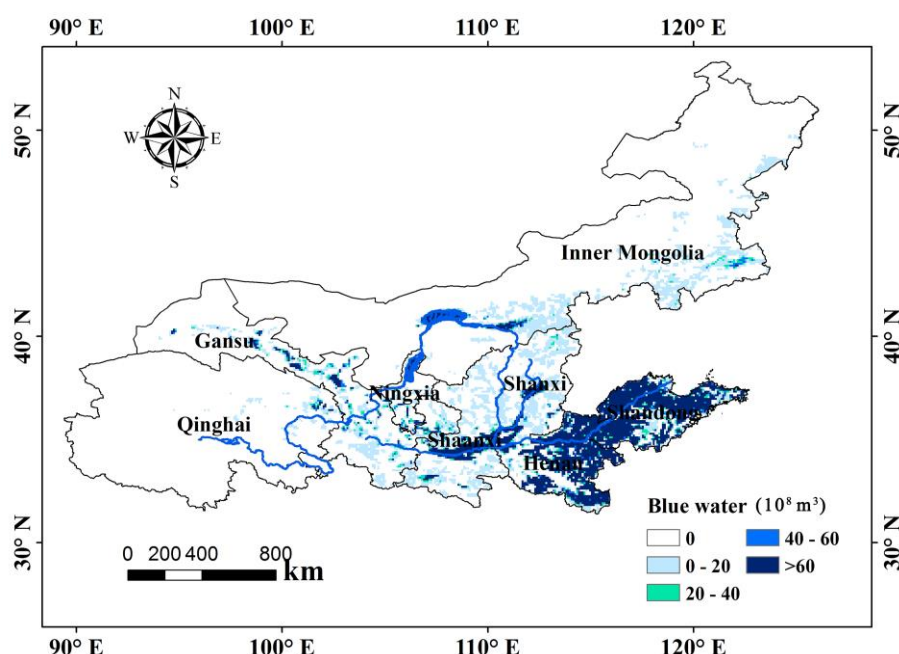


Figure 13. The spatial distribution of wheat blue water consumption in the 5 arc-minutes grid (10^5 m^3)

Conclusions and discussion

In this study, rainfed and irrigated farmlands are divided according to the irrigation area distribution map, and 12 major crops in the basin are selected as objects. According to crop water demand and effective precipitation, the method of calculating regional crop water consumption and agricultural water footprint is proposed to study the situation of the Yellow River Basin. The main conclusions are as follows:

(1) Similar to precipitation contour, distribution of crop water consumption in the Yellow River Basin tends to descend from southeast to northwest. Local areas are affected by irrigation. High value areas are mainly irrigation regions along the Yellow River and the others have small water consumption due to rainfed agriculture. In the Yellow River Basin, the agricultural water consumption in 2017 was 84.25 billion m^3 . Henan and Shandong take up 66% of the total water consumption, and the wheat and corn take up 60% of the total water consumption.

(2) The proportion of green water consumed in the Yellow River Basin is 78.7%, which is around the global average. The spatial distribution of crop green water

consumption generally conforms to the water consumption distribution. In areas with high water consumption, the amount of green water consumed increases because the agriculture is developed and there are more crops planted. As for most of rainfed agriculture-based areas in Yellow River Basin, green water consumption accounts for 95+% of crop water consumption. The lower values are in areas with well-developed irrigated agriculture, and in western Gansu due to less precipitation, strong evaporation, and less available effective precipitation for crops. In the irrigation areas, unnecessary irrigation can reduce the green water consumption.

(3) The agricultural water footprint is 52 billion m³ in the Yellow River Basin, in which Henan is at the top at 29.93 billion m³ and Qinghai is at the bottom at 480 million m³. The largest in Henan is m³, and the minimum in s 480 million m³. Agricultural water footprint accounts for 0.587 of crop water consumption. Henan and Gansu are at the top respectively at 0.985 and 0.980, indicating that the grain produced by these two provinces is basically used for themselves.

(4) The proportion of green water consumption is mostly higher than 80%. Wheat is required for water irrigation because the rain season does not move in line with high-temperature season during its growth duration. Its green water consumption accounts for 58% of the total water consumed during the growth period. In addition, wheat consumes 56% of the total blue water consumed by crops in the basin.

(5) The crop water consumption coefficient reflects the water utilization level. The average water consumption coefficient is 0.622 m³/kg for the Yellow River Basin, in which most of areas fall between 0.4-1.0 m³/kg. Ningxia, Gansu and Qinghai have the low water consumption coefficient, among which western Gansu, northern Ningxia (excluding the irrigation areas along Yellow River) and central and southern Shandong are among the lowest. The crop water consumption coefficient of the Yellow River Basin has no obvious relationship with the agricultural production level, and the irrigation cannot enhance the coefficient. For different crops, the water consumption coefficient is mainly related to the crop characteristics, and the water consumption coefficient of the tuberiferous crops is the largest.

In Rain-fed Agricultural areas, green water absorptivity is closely related to crop yield. Raising the utilization rate of green water in irrigated agricultural areas can reduce irrigation water use. The reason lies not in the low precipitation, but in the uneven distribution of precipitation, which is not consistent with the period of crop water demand. The total amount of water for crops is sufficient, but not at the right time.

Making full use of green water can start from two aspects. One is to increase the storage of green water through various measures, including deep tillage, mulching and other field management means to promote precipitation infiltration, reduce soil evaporation; and terraces in mountainous areas, rainwater collection and other facilities. Secondly, in view of irrigated agriculture, we should understand the distribution law of precipitation, the dynamics of soil moisture and the law of crop water demand, and supplement irrigation under the premise of insufficient green water.

Proportion of green water consumption to water consumption depends mainly on the volume of irrigating water. The green water consumption is negatively related to the irrigation amount. Ningxia is at the bottom, followed by Shandong. Both provinces rely too much on irrigating water and do not make full use of green water.

Irrigated area is one of the main factors of water footprint growth, so it is imperative to restrict the development of irrigation area. This refers to the traditional irrigated

farmland. Irrigation is an important guarantee for grain production in the basin. The effect of water saving irrigation on increasing income has been widely recognized and still needs to be vigorously implemented. In addition, improving the effective utilization rate of irrigation water are mainly aimed at the existing problems. Firstly, the irrigation facilities should be renovated to reduce the waste of water resources; secondly, the traditional surface irrigation methods should be changed and furrow irrigation should be adopted to improve the utilization rate of irrigation water; thirdly, a reasonable irrigation system should be established to improve the water use efficiency of crops by determining irrigation time and irrigation quota according to the critical period of crop water demand; thirdly, the crop planting structure should be adjusted according to the rainy season. Reasonable arrangement of crop distribution, such as crop water demand characteristics, can make full use of precipitation and alleviate the contradiction between irrigation and water use.

In the study, a comprehensive calculation method for the total water consumption of various crops was established, and the main crop such as wheat was selected for detailed analysis. The crop growth period was divided into smaller periods to improve the calculation accuracy. According to the export-oriented characteristics of agriculture in the Yellow River Basin, the calculation method of agricultural water footprint in the Yellow River Basin is put forward. Zhuo et al. (2016) studied the changes of water footprint and blue-green water of some crops in the Yellow River basin from 1961 to 2009. The spatial distribution of the results is relatively stable. The spatial distribution of agricultural water footprint and blue and green water in this study have the similar spatial correlation with the results of Zhuo et al.'s study.

The calculation of water consumption is mainly based on the empirical formula of reference crop ET and crop coefficient provided by FAO. The adaptability of this method to the study area needs further study. At present, there are many actual ET products available, such as (MODIS Global Evapotranspiration Project, MOD16), which can provide 8-day ET data. It is worth studying to compare the results based on the MOD16 or other ET products with the results of this study. At the same time, the spatial resolution of 5 arc-minutes is adopted, which may not be applicable to some smaller irrigation areas. Therefore, it is very important to study crop distribution on higher spatial resolution scale, which involves near-surface remote sensing, field mapping, high-resolution image data, and the collection of corresponding agricultural sector data. The above research will be launched in the near future to achieve in-depth study of regional agricultural water footprint and green water.

Acknowledgements. This work was partially supported by the MOE (Ministry of Education in China) Liberal arts and Social Sciences Foundation (Grant No. 19YJCZH228), and the Heilongjiang Natural Science Foundation Project (Grant No. E2018006), the National Natural Science Foundation of China (Grant No. 41401042), and 2018 Guizhou University of Finance and economics talent recruitment project (Grant No. 2018YJ27).

REFERENCES

- [1] Allen, R. G., Pereira, L. S., Raes, D., Smith, M. (1998): Crop Evapotranspiration—Guidelines for Computing Crop Water Requirements—FAO Irrigation and Drainage Paper No. 56. – FAO, Rome, Italy.

- [2] Bai, L., Cai, J., Liu, Y., Chen, H., Zhang, B., Huang, L. (2017): Responses of field evapotranspiration to the changes of cropping pattern and groundwater depth in large irrigation district of yellow river basin. – *Agricultural Water Management* 188: 1–11.
- [3] Barbagallo, S., Consoli, S., D’Urso, G., Gaggia, R. G., Toscano, A. (2004): Remote sensing of crop water requirements in orange orchards using high-spatial-resolution sensors. – *Proceedings of SPIE - The International Society for Optical Engineering* 5232(3): 119–127.
- [4] Calera, A., Campos, I., Osann, A., D’Urso, G., Menenti, M. (2017): Remote sensing for crop water management: from et modelling to services for the end users. – *Sensors* 17(5): 1104.
- [5] Fader, M., Gerten, D., Thammer, M., Heinke, J., Lotzcampen, H., Lucht, W., Cramer, W. (2011): Internal and external green-blue agricultural water footprints of nations, and related water and land savings through trade. – *Hydrology & Earth System Sciences* 15: 1641–1660.
- [6] Feng, K., Siu, Y. L., Guan, D., Hubacek, K. (2012): Assessing regional virtual water flows and water footprints in the Yellow River Basin, China: a consumption based approach. – *Applied Geography* 32(2): 691–701.
- [7] Gonçalves, J. M., Pereira, L. S., Fang, S. X., Dong, B. (2007): Modelling and multicriteria analysis of water saving scenarios for an irrigation district in the upper yellow river basin. – *Agricultural Water Management* 94(1–3): 93–108.
- [8] González-Dugo, M. P., Escuin, S., Cano, F., Cifuentes, V., Padilla, F. L. M., Tirado, J. L., Oyonarte, N., Fernández, P., Mateosd, L. (2013): Monitoring evapotranspiration of irrigated crops using crop coefficients derived from time series of satellite images. ii. application on basin scale. – *Agricultural Water Management* 125: 92–104.
- [9] Hoff, H., Falkenmark, M., Gerten, D., Gordon, L., Karlberg, L., Rockstrom, J. (2010): Greening the global water system. – *Journal of Hydrology* 384(3–4): 177–186.
- [10] Li, J., Zhu, T., Mao, X., Adeloje, A. J. (2016): Modeling crop water consumption and water productivity in the middle reaches of Heihe River basin. – *Computers and Electronics in Agriculture* 123: 242–255.
- [11] Mishra, S. K., Singh, V. P. (2007): Soil conservation service curve number (SCS-CN) methodology. – *Water Science & Technology Library* 22(3): 355–362.
- [12] Mo, X. G., Liu, S. X., Lin, Z. H., Guo, R. P. (2009): Regional crop yield, water consumption and water use efficiency and their responses to climate change in the north china plain. – *Agriculture Ecosystems & Environment* 134(1): 67–78.
- [13] Serrano-Coronel, G., Chipana-Rivera, R., Moreno-Pérez, M. F., Roldán-Cañas, J. (2018): Study of vertical water flows contribution to the crop water consumption in suka kollus, using a mixed drainage system. – *Agricultural Water Management* 206: 86–94.
- [14] Sikorska, A. E., Viviroli, D., Seibert, J. (2018): Effective precipitation duration for runoff peaks based on catchment modelling. – *Journal of Hydrology* 556: 510–522.
- [15] Veettil, A. V., Mishra, A. K. (2016): Water security assessment using blue and green water footprint concepts. – *Journal of Hydrology* 542: 589–602.
- [16] Wang, X., Huo, Z., Guan, H., Guo, P., Qu, Z. (2018): Drip irrigation enhances shallow groundwater contribution to crop water consumption in an arid area. – *Hydrological Processes* 32(6): 747–758.
- [17] Wei, Y., Tang, D., Ding, Y., Agoramoorthy, G. (2016): Incorporating water consumption into crop water footprint: a case study of China’s south-north water diversion project. – *Science of the Total Environment* 545–546: 601–608.
- [18] Xiang, X., Svensson, J., Jia, S. (2017): Will the energy industry drain the water used for agricultural irrigation in the yellow river basin? – *International Journal of Water Resources Development* 33(1): 69–80.
- [19] Yin, J., Wang, H., Cai, Y. (2016): Water footprint calculation on the basis of input–output analysis and a biproportional algorithm: a case study for the Yellow River Basin, China. – *Water* 8(9): 363.

- [20] Yin, J., Fu, Q., Xing, Z., Lu, Y., Ou, Z. (2017): Agricultural water-saving potential for Guanzhong irrigation areas under different guaranteed rates of precipitation. – *Applied Ecology and Environmental Research* 15(4): 1255–1274.
- [21] You, L., Wood, S., Wood-Sichra, U., Wu, W., Liu, Z., Li, Z., Zhou, Q., Tang, H. (2014): Generating global crop distribution maps: from census to grid. – *Agricultural Systems* 127: 53–60.
- [22] Zhang, B. Z., Kang, S. Z., Zhang, L., Du, T. S., Li, S. E., Yang, X. Y. (2010): Estimation of seasonal crop water consumption in a vineyard using Bowen ratio-energy balance method. – *Hydrological Processes* 21(26): 3635–3641.
- [23] Zhang, W., Zha, X., Li, J., Wei, L., Ma, Y., Fan, D., Li, S. (2014): Spatiotemporal change of blue water and green water resources in the headwater of Yellow River Basin, China. – *Water Resources Management* 28(13): 4715–4732.
- [24] Zhuo, L., Mekonnen, M. M., Hoekstra, A. Y. (2014): Sensitivity and uncertainty in crop water footprint accounting: a case study for the Yellow River basin. – *Hydrology and Earth System Sciences* 18(6): 2219–2234.
- [25] Zhuo, L., Mekonnen, M. M., Hoekstra, A. Y., Wada, Y. (2016): Inter- and intra-annual variation of water footprint of crops and blue water scarcity in the yellow river basin (1961-2009). – *Advances in Water Resources* 87: 29–41.
- [26] Zuo, D., Xu, Z., Peng, D., Song, J., Cheng, L., Wei, S., Abbaspour, K. C., Yang, H. (2015): Simulating spatiotemporal variability of blue and green water resources availability with uncertainty analysis. – *Hydrological Processes* 29(8): 1942–1955.

EVALUATION OF HERBICIDE TREATMENTS FOR CONTROL OF WILD GLADIOLUS (*GLADIOLUS SEGETUM*) IN WHEAT

MAJD, R.¹ – CHAMANABAD, H. R. M.¹ – ZAND, E.² – MOHEBODINI, M.³ – KHIAVI, H. K.⁴ –
ALEBRAHIM, M. T.^{1*} – TSENG, T. M.⁵

¹*Department of Agronomy and Plant Breeding, Faculty of Agriculture and Natural Resources
University of Mohaghegh Ardabili, Ardabil, Iran (phone: +98-9123501493)*

²*Department of Weed Research, Iranian Institute of Plant Protection, Tehran, Iran*

³*Department of Horticulture, Faculty of Agriculture and Natural Resource
University of Mohaghegh Ardabili, Ardabil, Iran*

⁴*Department of Plant Protection Research, Ardabil Agriculture and Natural Resources
Research and Education center, Ardabil, Iran*

⁵*Department of Plant and Soil Sciences, Mississippi State University
Mississippi State, Mississippi, USA (phone: +1-662-325-4725; fax: +1-662-325-8742)*

*Corresponding author

email: m_brahim@uma.ac.ir; phone: +98-9123501493

(Received 18th Dec 2018; accepted 28th Feb 2019)

Abstract. Wild gladiolus (*Gladiolus segetum*) is a problematic weed in dry land winter wheat fields of northwest and west provinces in Iran, and accounts for about 23% of yield losses in winter wheat. Greenhouse studies were conducted from 2014 to 2015 to evaluate different herbicide treatments to control of the noxious weed, *Gladiolus segetum*, commonly found in northwest of Iran. The objective was to evaluate potential control possibilities with commercial herbicides containing sulfosulfuron (Apirus®), mesosulfuron+ idosulfuron (Atlantis®), mesosulfuron-methyl + Iodosulfuron-methyl-sodium + Diflufenican (Othello®), metsulfuron-methyl + sulfosulfuron (Total®), clodinafop-propargyl (Topik®), and glyphosate. Herbicides were applied to fully developed stems (10 cm), at the 2-3 leaf stage of the weed which coincides with the tillering stage in wheat. Similar to sulfosulfuron and mesosulfuron + idosulfuron, higher rates of glyphosate resulted in higher biomass reduction of *G. segetum* in both years. But the application rates of glyphosate were remarkably higher compared to sulfosulfuron and mesosulfuron + idosulfuron. The ED₅₀ values of glyphosate were 1751.99 and 1919.93 g ai ha⁻¹, and the ED₉₀ values were 6349.96 and 7031.84 g ai ha⁻¹, in 2014 and 2015, respectively.

Keywords: dose response, dry weight, effective dose, noxious weed, weed management

Introduction

Gladiolus spp. from the Iridaceae family (subfamily of Crocoideae) is distributed in Africa, the Mediterranean basin, and Western Asia. It is a large genus that includes approximately 300 species (Goldblatt et al., 2001). *Gladiolus segetum* Ker Gawl and *G. italicus* Mill. are important weeds in dry land winter wheat fields of the Ardabil province in Iran (Ebadi et al., 2004-2007). The species can be identified by a set of characteristics such as narrow leaves, parallel venation, lowest leaf reduced to a subterranean sheathing cataphyll, and tubular or funnel-shaped perianth with synsepalous sepals (Davis, 1984; Dahlgren, 1985). Wild gladiolus (*Gladiolus segetum*) is a native weed in Greece, Turkey, Iraq, and Iran. They invade disturbed fields in the northern and western parts of Iran, particularly wheat, legume and other dryland fields (Rashed Mohassel et al., 2001; Majd et al., 2017). It is a major

constraint to wheat production in Iran, accounting for about 23% of yield losses (Khalaghani, 2008); and weed control in winter wheat relies almost exclusively on herbicides (Deihim-Fard and Zand, 2006).

Since wild gladiolus has high vigor and emerges simultaneously with winter wheat, it can become dominant and has the potential to cause heavy yield losses in infested wheat fields. It is thus necessary to identify strategies to effectively manage this problematic weed as like as others which can be nonchemical including fertilizer management had beneficial effect against Velvetleaf (Aghaie et al., 2013), physical (Majd et al., 2017) or chemical by applying new herbicides or using alternative herbicide to delay resistance (Alebrahim et al., 2017; Tahmasebi et al., 2018). Additionally, since wheat fields in different regions of Iran have variable climatic conditions, there is a need to tailor weed control strategies specific to each region. Finding an effective weed control strategy will greatly depend on the use of herbicides at effective doses; therefore, selecting an appropriate herbicide and dose is most important. Ebadi et al. (2015) reported that biomass of wild gladiolus was reduced by incorporating cultural strategies with herbicide mixtures such as clodinafop-propargyl, difenzoquat + 2,4-D, Topik + 2,4-D, clodinafop-propargyl + tribenuron-methyl, and glyphosate + fallow. The above mentioned mixtures had no differences in their effect on wild gladiolus. The highest and lowest percentage of biomass reduction was obtained by hand weeding and spraying with 2,4-D, respectively. In addition, their results revealed that clodinafop-propargyl controlled wild gladiolus and other weeds results in an increase in crop yield.

Herbicide dose response curves help determine the selectivity and efficacy of herbicides and in some situations help unravel the dose-range for effective weed control and minimal crop damage. Relationships of dose response depends on the weed species, range of doses used, herbicide type, and various environmental conditions, such as temperature, humidity, wind velocity, CO₂ and O₂ levels, and geographical altitude (Streibig et al., 1993). In our current study we selected several herbicides that belong to three mode-of-action groups: acetolactate synthase (ALS) inhibitors (including mesosulfuron-methyl + idosulfuron-methyl-sodium + diflufenican, mesosulfuron + idosulfuron, metsulfuron-methyl + sulfosulfuron, and sulfosulfuron), inhibitors of aromatic amino acid biosynthesis (including glyphosate), and acetyl-CoA carboxylase inhibitors (including clodinafop-propargyl). Herbicides such as the pyrimidinyl salicylates (Shimizu et al., 1994), triazolopyrimidine sulfonamide (Subramanian and Gerwick, 1989), imidazolinone (Shaner et al., 1984), and sulfonylurea (LaRossa and Schloss, 1984; Ray, 1984) herbicides has ALS as their primary target site of action. The ALS enzyme catalyzes the biosynthetic pathway for the production of three branched-chain amino acids such as valine, leucine and isoleucine. Exposure of plants to ALS-inhibitors therefore inhibits production of the three branched-chain amino acids.

Glyphosate [N-(phosphonomethyl)glycine], is a nonselective, broad spectrum herbicide discovered in 1971 (Baird et al., 1971), and was introduced in 1974 (Franz et al., 1997). Glyphosate was one of the first commercially important herbicide whose site of action was characterized as a single target enzyme in plants, and is the only herbicide known to inhibit 5-enolpyruvylshikimate 3-phosphate synthase (EPSPS). EPSPS catalyzes the penultimate reaction of the shikimate (Shk) pathway (Gruys and Sikorski, 1999) in certain bacteria and plants.

The cyclohexanediones (CHD) and aryloxyphenoxypropanoates (AOPP) inhibits the plastidic enzyme acetyl-CoA carboxylase (ACCase). CHD and AOPP herbicides are used to control a wide selection of grass weeds in both monocot and dicot crops. The basis of

selectivity differs between dicot and grasses: in dicots, tolerance is based on the inherent insensitivity of the ACCase to these herbicides, whereas in certain cereal crops, selectivity is based on higher rates of herbicide detoxification in the crop species (Devine and Shimabukuro, 1994).

The goal of our study was to compare the efficacy of different herbicides treatments, sulfosulfuron (Apirus®), mesosulfuron + idosulfuron (Atlantis®), mesosulfuron methyl + iodosulfuron-methyl-sodium + diflufenican (Othello®), metsulfuron-methyl + sulfosulfuron (Total®), clodinafop-propargyl (Topik®), and glyphosate (Roundup®), on the dry weight of wild gladiolus populations. These herbicides were selected because they are primarily used for weed control in wheat in Iran.

Materials and Methods

Study sites

Experiments were carried out from May 20, 2014 to August 22, 2014 and from May 20, 2015 to August 22, 2015 in the research greenhouse located in the College of Agriculture and Natural Resources, University of Mohaghegh Ardabili (longitude 48°17.600' 20.72" E, latitude 38°12.607' 29.51" N, and 1,386 m altitude), Ardabil, Iran.

Experimental design and treatments

The experiment was a completely randomized design (CRD) with 4 replications, and were independently repeated in time. Six herbicides with a range of doses were applied and the dry weight of gladiolus measured (*Table 1*). In April 2014, mature corms of wild gladiolus were collected from several fields of north-western part of Iran, from Germe city; located near Ardabil at longitude 48° 9' 24.46" E, latitude 39° 6' 36.20" N, and 1,350 m altitude. The rate per hectare was calculated based on the surface area of the pot (942 cm²). Herbicides were applied using a CO₂-pressurized backpack sprayer fitted with 8002 VS flat fan nozzles, MATABI model, calibrated to a deliver 250 L ha⁻¹ at 276 KPa, while maintaining the constant speed of 4.8 KPH. Herbicides were applied to fully developed stems (10 cm), at the two-to-three leaf stage of the weed and coincided with the tillering stage of wheat. Irrigation was performed every week from the beginning to end of experiments. Temperature was 19-25°C. Fertigation by using NPK (20:20:20) was done during experiments.

Table 1. List of herbicides used in the study

Herbicide	Rate (g ai ha ⁻¹)	Recommended Rate for Wheat in Iran (g ai ha ⁻¹) (Zand et al., 2017)
Sulfosulfuron (Apirus®)	0, 3.75, 7.5, 15, 22.5, 30	20
Mesosulfuron + Idosulfuron (Atlantis®)	0, 6, 18, 24, 30, 36	24
Mesosulfuron-methyl + Iodosulfuron-methyl-sodium + Diflufenican (Othello®)	0, 33, 66, 82.5, 99, 132	96
Metsulfuron-methyl + sulfosulfuron (Total®)	0, 22.5, 27, 31.5, 36, 40.5, 45	33
Clodinafop-propargyl (Topik®)	0, 0.032, 0.064, 0.080, 0.096, 0.128	60
Glyphosate®	0, 1025, 1230, 1435, 1640, 1845	1600

Sampling procedure

Shoots of weeds were collected from the soil surface in each pot, four weeks after herbicide treatment application. After drying in an oven at 70°C (for 72 h) dry weights were measured.

Statistical analysis

The dry weight per pot, y , was estimated using a log-logistic dose-response model with dose x in ai/haby R software:

$$y = \frac{d}{1 + \exp(b \cdot [\log(x) - \log(ED_{50})])} \quad (\text{Eq.1})$$

where, b denotes the relative slope around ED_{50} (Effective Dose), which is the dose required to produce one-half of the dry-weight relative to the upper limit, d . The dose-response curve takes a snapshot of the dry matter production at the time of harvesting the biomass (Ritz et al., 2006).

Results

The analysis of residuals and test for lack of fit ($p < 0.05$) confirmed the assumption that the data had constant variance, were normally distributed, and the dose-response curves described the variation in data. The efficacy of the herbicides were compared based on the ED_{50} and ED_{90} levels (Tables 2, 3, 4 and 5). As noted in Figs. 1 and 2, the doses were concentrated around the middle of the dose-response curve in order to obtain a precise ED_{50} .

Table 2. The nonlinear log-logistic regression fit of dry weight in the first year. Standard errors in parenthesis, and with upper 95% confidence interval of ED_{50} (g ai ha⁻¹)

Herbicide	Upper limit	Slope	ED ₅₀
Sulfosulfuron	0.36(0.01)	0.87(0.10)	20.6(2.72)
Mesosulfuron + Idosulfuron	0.33(0.02)	3.80(2.80)	44.03(4.48)
Glyphosate	1.24(0.03)	1.70(0.18)	1751(74.77)
Mesosulfuron-methyl + Iodosulfuron-methyl-sodium + Diflufenican	0.43(0.01)	0.64(0.13)	102.7(18.48)
Clodinafop-propargyl	0.35(0.01)	1.33(0.31)	193.8(27.55)
Metsulfuron-methyl + sulfosulfuron	0.33(0.01)	1.84(0.31)	61.24(4.55)

Table 3. The nonlinear log-logistic regression fit of dry weight in the second year. Standard errors in parenthesis, and with upper 95% confidence interval of ED_{50} (g ai ha⁻¹)

Herbicide	Upper limit	Slope	ED ₅₀
Sulfosulfuron	0.42 (0.01)	0.67(0.08)	20.8(3.43)
Mesosulfuron + Idosulfuron	0.42(0.02)	3.02(0.92)	38.29(2.12)
Glyphosate	1.20(0.02)	1.69(0.13)	1919(59.59)
Mesosulfuron-methyl + Iodosulfuron-methyl-sodium + Diflufenican	0.39(0.01)	0.74(0.13)	161.2(23.29)
Clodinafop-propargyl	0.31(0.01)	1.12(0.16)	92.57(9.58)
Metsulfuron-methyl + sulfosulfuron	0.37(0.01)	0.85(0.29)	71.05(16.31)

Table 4. ED_{90} ($g\ ai\ ha^{-1}$) levels of the first experiment with 95% confidence intervals for the first year

Herbicide	Estimate ED_{90}	Upper limit ED_{90}
Sulfosulfuron	255	392
Mesosulfuron + Idosulfuron	78	160.28
Glyphosate	6349	8217.82
Mesosulfuron-methyl + Iodosulfuron-methyl-sodium + Diflufenican	3077	7477.74
Clodinafop-propargyl	1005	1991.63
Metsulfuron-methyl + sulfosulfuron	201	302.19

Table 5. ED_{90} ($g\ ai\ ha^{-1}$) levels of the second experiment with 95% confidence intervals for the second year

Herbicide	Estimate ED_{90}	Upper limit ED_{90}
Sulfosulfuron	541	985.38
Mesosulfuron + Idosulfuron	79	117.13
Glyphosate	7031	8601.46
Mesosulfuron-methyl + Iodosulfuron-methyl-sodium + Diflufenican	3053	6581.38
Clodinafop-propargyl	651	1045.21
Metsulfuron-methyl + sulfosulfuron	918	2908.76

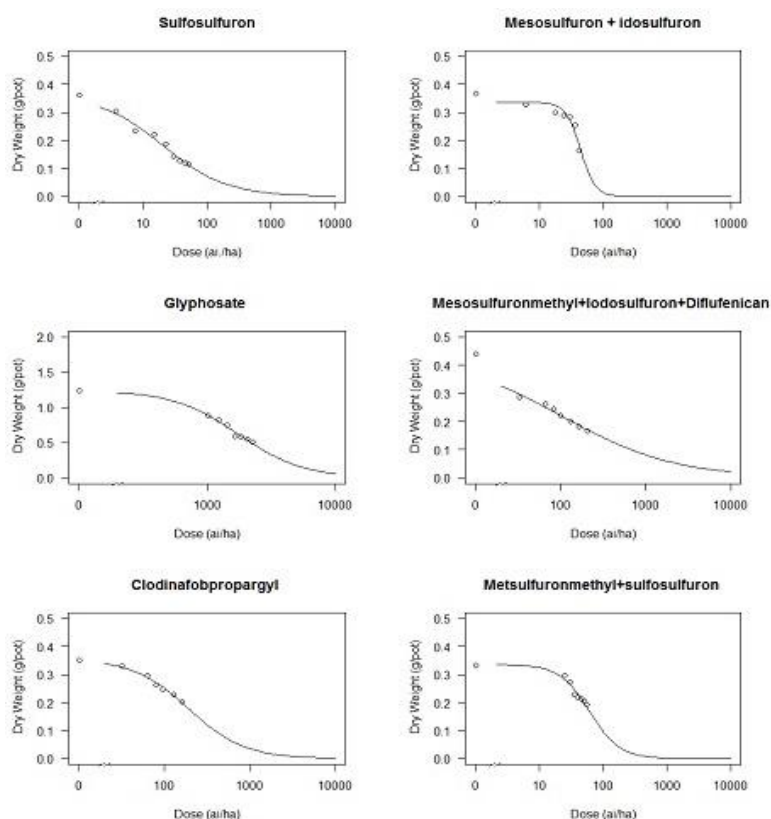


Figure 1. Estimated dose response curves of wild gladiolus to six herbicide treatments. Data shown as dry weight in the first year

Sulfosulfuron

The application rates of sulfosulfuron required to reduce wild gladiolus dry matter by 50% in 2014 and 2015, was 20.6 and 20.8 g ai ha⁻¹, respectively (Tables 2 and 3). Moreover, the application rates of sulfosulfuron required to achieve 90% wild gladiolus control in 2014 and 2015, were 255 and 541 g ai ha⁻¹, respectively (Tables 4 and 5). In both instances, the ED₉₀ was significantly different from zero even though there were not many observations at the lower part the curve, which is reflected in the precision of ED₉₀. The recommended rate for this herbicide in wheat is around 20 g ai ha⁻¹ (Table 1). Some studies have shown that the height of weed species and weed biomass at the time of post herbicide applications is an important factor in determining the level of control achieved (Craigmyle et al., 2013; Chahal et al., 2014).

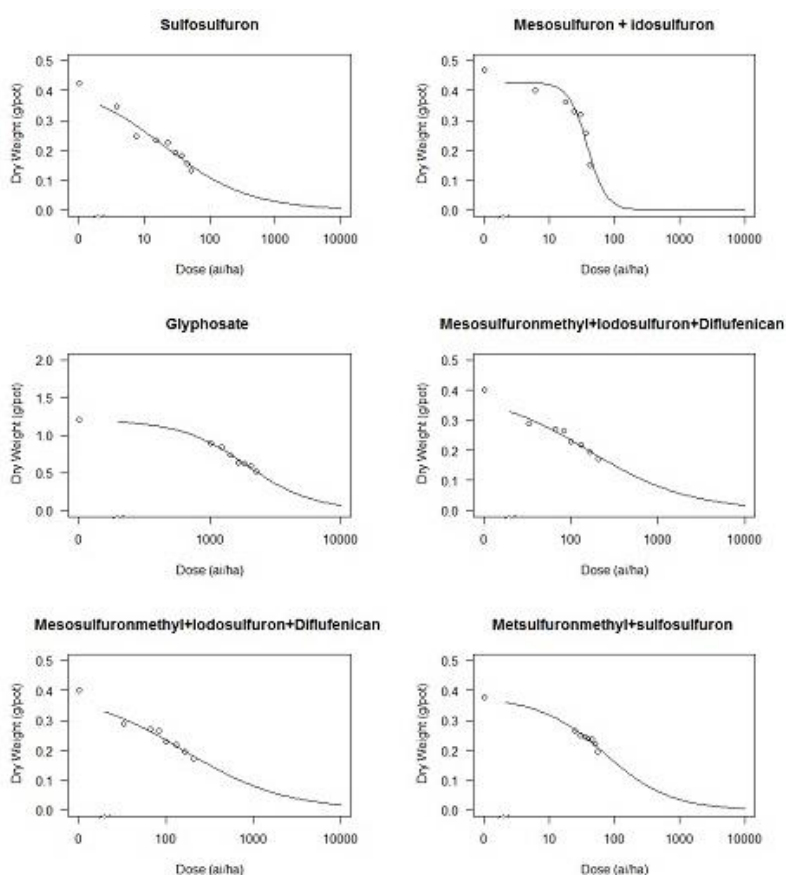


Figure 2. Estimated dose response curves of wild gladiolus to six herbicide treatments. Data shown as dry weight in the second year

Mesosulfuron+idosulfuron

In the case of mesosulfuron + idosulfuron application, the ED₅₀ increased almost 50% compared to the Sulfosulfuron (Figs. 1 and 2; and Tables 2 and 3). However, the mixtures had a much steeper dose-response curve than the sulfosulfuron, and thus, the ED₉₀ was much smaller for sulfosulfuron in 2014 and 2015, and were 78 and 79 g ai ha⁻¹, respectively (Tables 4 and 5). The recommended rate for this herbicide in wheat is around 24 g ai ha⁻¹ (Table 1). Kaiser and Gerhards (2015) reported different levels of ED₅₀ for several

multiple-resistant blackgrass (*Alopecurus myosuroides*). There was sufficient control of population ALOMY-S with an ED₅₀ of 2.42 g ai ha⁻¹. ED₅₀ values of 21.36 and 9.19 g ai ha⁻¹, were obtained for ALOMY-R1 and ALOMY-R2, respectively. Why you provide explanation on why you think so?

Glyphosate

Although the ED₅₀ was rather similar for both sulfosulfuron and mesosulfuron + idosulfuron, it is obvious that glyphosate will require much larger rates to attain ED₅₀ in both years (*Figs. 1 and 2; Tables 2 and 3*). The relative slopes of the glyphosate response curves were around 1 and were therefore comparatively flat in nature (*Figs. 1 and 2*). The ED₅₀ of glyphosate was 1751 and 1919 g ai ha⁻¹, in 2014 and 2015, respectively (*Tables 2 and 3*). In 2014 and 2015, the ED₉₀ values of glyphosate were 6349 and 7031 g ai ha⁻¹, respectively (*Tables 4 and 5*). It shows that although effective control of wild gladiolus can be achieved using glyphosate, a rather high dose is required; the recommended rate for this herbicide in wheat is around 1600 g ai ha⁻¹ (*Table 1*). Chahal et al. (2015) showed that the shoot biomass curve indicated a 50 and 90% reduction at 227 and 3704 g ai ha⁻¹, respectively, in 10-cm tall kochia; whereas, the ED₅₀ and ED₉₀ were 612 and 5885 g ai ha⁻¹, respectively for a 20-cm tall kochia.

Mesosulfuron-methyl + Iodosulfuron-methyl-sodium + Diflufenican

Results show that the ED₅₀ for this mixture of compounds had higher efficacy of weed control than glyphosate alone (*Figs. 1 and 2; Tables 2 and 3*). An up to 50% biomass reduction of wild gladiolus was observed at 102.75 and 161.20 g ai ha⁻¹, in the first and second year of experiment, respectively. The application rates of Mesosulfuron-methyl + Iodosulfuron-methyl-sodium + Diflufenican required for 90% reduction in wild gladiolus biomass in 2014 and 2015 were 3077 and 3053 g ai ha⁻¹, respectively. In this case, ED₉₀ values in two experimental years were similar, but was not significantly different from zero (*Tables 4 and 5*); the recommended rate for this herbicide in wheat is around 96 g ai ha⁻¹ (*Table 1*).

Clodinafop-propargyl

The ED₅₀ values of clodinafop-propargyl were 193.84 and 92.57 g ai ha⁻¹ in 2014 and 2015, respectively, with the ED₅₀ in 2014 being two times higher than in 2015. However, the ED₅₀ variation between the two years cancelled out, because the rates were not significantly different from zero (*Tables 2 and 3*). The ED₉₀ values in 2014 and 2015, were 1005 and 651 g ai ha⁻¹, respectively, and the difference is not dramatic considering the precision of the 95% confidence intervals. The relative slope of the dose-response curves in *Figs. 1 and 2* suggest that the herbicide had a similar slope as glyphosate; the recommended rate for this herbicide in wheat is around 60 g ai ha⁻¹ (*Table 1*). Stagnari et al. (2006) conducted a two years experiment to determine the ED₉₀ of clodinafop-propargyl for several weed species. The amount of ED₉₀ for *Lolium multiflorum*, *Avena ludoviciana*, and *Phalaris minor* were 60, 32 and 33.6 g ai ha⁻¹ in the first year, respectively. In the second year of experiment, the amount of ED₉₀ for *Avena ludoviciana* and *Phalaris minor* were 64.5 and 99.8 g ai ha⁻¹, respectively. It indicated that wild gladiolus can tolerate clodinafop-propargyl better than the grasses.

Metsulfuron-methyl + sulfosulfuron

Based on the results in *Figs. 1 and 2*, and *Tables 2 and 3*, the differences in ED₅₀ was not that dramatic between the first and second experimental years; ED₅₀ was 61.24 and 71.05 g ai ha⁻¹, respectively. ED₉₀ was 201.35 and 918.36 g ai ha⁻¹ in 2014 and 2015, respectively. There was vast difference in ED₉₀ between the two years, however, the ED₉₀ values were not different from zero (*Tables 4 and 5*). This poor precision of the ED₉₀ could be due to lack of observations to support the lower part of the curve and the much lower relative slope of 0.85 (*Table 3*). The recommended rate for this herbicide in wheat is 33 g ai ha⁻¹ (*Table 1*). Izadi-Darbandi and Aliverdi (2015) reported that the amount of ED₅₀ and ED₉₀ of sulfosulfuron+metsulfuron-methyl to control wild barley in wheat field were 26.64 and 41.95 g ai ha⁻¹, respectively.

Discussion

In our study, results revealed that the highest weed dry weight was associated with glyphosate treatment (*Tables 2 and 3*). This suggests that even after exposure to glyphosate, the weed is able to grow before the herbicide is distributed throughout whole plant and begin exerting its action. Atlantis, a mixture of mesosulfuron+idosulfuron, resulted in the next highest weed dry weight, while sulfosulfuron produced the lowest weed dry weight, thus indicating high efficacy of sulfosulfuron on the weed compared to other herbicides (*Tables 2 and 3*). The relative steepness of the dose-response curves for ED₅₀ were different; for example, a sharp decrease in wild gladiolus dry weight was observed after application of sulfosulfuron. Mesosulfuron+idosulfuron curve declined after a steady phase while other herbicide curves dropped slowly (*Tables 2 and 3; Figs. 1 and 2*). We observed that better control of wild gladiolus was obtained in the second year at the highest dose for all herbicides (*Fig. 2*). It is important to note that optimum efficacy is influenced by weed size, so that when the size of the weed is bigger, the control will be lower (Everitt and Keeling, 2007; Robinson et al., 2012).

Generally, among all herbicides tested, sulfosulfuron had the lowest ED₅₀ in both years, 2014 (20.6 g ai ha⁻¹) and 2015 (20.8 g ai ha⁻¹) (*Tables 2 and 3*); while glyphosate had the highest ED₅₀ in 2014 (1751.99 g ai ha⁻¹) and 2015 (1919.93 g ai ha⁻¹) (*Tables 2 and 3*). This suggests that sulfosulfuron and glyphosate were the highest and lowest performing herbicides with respect to wild gladiolus control. In the case of ED₉₀, mesosulfuron+idosulfuron and glyphosate had the highest and lowest influence on the control of wild gladiolus. The ED₉₀ values of mesosulfuron+idosulfuron were 78 and 79 g ai ha⁻¹ in 2014 and 2015, respectively (*Tables 4 and 5*). Also, the ED₉₀ values of glyphosate were 6349 and 7031g ai ha⁻¹ in 2014 and 2015, respectively (*Tables 4 and 5*).

Conclusion

The greenhouse experiment with six different herbicide treatments identified sulfosulfuron to be the most effective in controlling wild gladiolus. Although a few herbicides were identified to be most effective, it is crucial that we use incorporate the use of different herbicides with various modes of action to prevent or manage herbicide resistance in wild gladiolus. This will encourage herbicide rotation and tank mixing herbicides with different modes of action for effective and sustainable weed control. Further research on studying the effects of natural environmental conditions on the

efficacy of herbicides used in this study with regards to wild gladiolus control is under evaluation.

Acknowledgements. The authors would like to thank Dr. Jens Carl Streibig for his assistance with statistical analysis, and Dr. Rouzbeh Zangouejad for his support in formatting the manuscript.

Disclosure Statement. The authors declare no conflict of interests.

REFERENCES

- [1] Alebrahim, M. T., Zangouejad, R., Tseng, T. M. (2017): Biochemical and Molecular Knowledge about Developing Herbicide-Resistant Weeds. Chapter 5. – In: Pacanoski, Z. (eds.). Herbicide resistance in Weeds and Crops. – Intechopen, Zagreb, Croatia. 101-132.
- [2] Aghaie, P., Kazemini, S. A., Majd, R., Alebrahim, M. T. (2013): Role of Phosphorus in Maize (*Zea mays* L.) Competitiveness against Velvetleaf (*Abutilon theophrasti*). – International J. Agron. Plant Produc. 4(9): 2323-2329.
- [3] Baird, D. D., Upchurch, R. P., Homesley, W. B., Franz, J. E. (1971): Introduction of a new broad-spectrum post-emergence herbicide class with utility for herbaceous perennial weed control. – Proc North Cent Weed Control Conf. 26: 64-68.
- [4] Chahal, P. S., Kruger, G., Blanco-Canqui, H., Jhala, A. J. (2014): Efficacy of pre-emergence and post-emergence soybean herbicides for control of glufosinate-, glyphosate-, and imidazolinone-resistant volunteer corn. – J. Agri. Sci. 6: 131-140.
- [5] Chahal, P. S., Aulakh, J. S., Rosenbaum, K., Jhala, A. J. (2015): Growth Stage Affects Dose Response of Selected Glyphosate-Resistant Weeds to Premix of 2,4-D Choline and Glyphosate (Enlist Duo™ Herbicide*). – J Agric Sci. 7: 1-10.
- [6] Craigmyle, B. D., Ellis, J. M., Bradley, K. W. (2013): Influence of weed height and glufosinate and 2,4-D combinations on weed control in soybean with resistance to 2,4-D. – Weed Technol. 27: 271-280.
- [7] Dahlgren, R. M. T. (1985): The Families of the Monocotyledons. – Springer Verlag, Berlin, Heidelberg.
- [8] Davis, P. H. (1984): Flora of Turkey and the East Aegean Islands. – Vol. 8. Edinburgh University Press, UK, 441-450.
- [9] Deihimfard, R., Zand, E. (2005): Evaluating environmental impacts of herbicides on wheat agroecosystems in the provinces of Iran using EIQ model. – Environmental Science. 6: 1-9.
- [10] Devine, M. D., Shimabukuro, R. H. (1994): Resistance to acetyl coenzyme A carboxylase inhibiting herbicides. – In: Powles, S. B., Holtum, J. A. M. (eds.) Herbicide resistance in plants: biology and biochemistry. Lewis, Boca Raton 141-169.
- [11] Ebadi, A., Razmjoo, J., Ghanji, M., Sajed, K., Shahbazi, K., Davari, M. (2004-2007): Investigating the Control of Weed Control of Wild Gladiolus sp. and Sophoraalopecuriodes in Wheat and Cereal Cultivated Fields in Germe, Bile savar (Moghan) and Khalkhal (Ardabil). – Organization of Management and Planning of Ardebil Province.
- [12] Ebadi, A., Parmoon, G., Samadi Calkhoran, E., Sajed, K. (2015): Evaluation of the effect of mixture of herbicides on weeds control in rainfed bread wheat (*Triticum aestivum* L.) in Ardabil. – Iranian Journal of Crop Sciences 17(3): 179-192. (In Persian).
- [13] Everitt, J. D., Keeling, J. W. (2007): Weed control and cotton (*Gossypium Hirsutum*) response to preplant applications of dicamba, 2,4-D, and diflufenzopyr plus dicamba. – Weed Technol. 21: 506-510.
- [14] Franz, J. E., Mao, M. K., Sikorski, J. A. (1997): Glyphosate: a unique global herbicide. – ACS Monograph 189, American Chemical Society, Washington, DC.

- [15] Goldblatt, P., Manning, J. C., Bernhardt, P. (2001): Radiation of pollination systems in *Gladiolus* (Iridaceae: Ixioideae) in southern Africa. – *Annals of the Missouri Botanical Gardens*. 97: 317-344.
- [16] Gruys, K. J., Sikorski, J. A. (1999): Inhibitors of tryptophan, phenylalanine, and tyrosine biosynthesis as herbicides. – In: Singh, B. K. (ed.) *Plant amino acids: biochemistry and biotechnology*. Marcel Dekker, New York 357-384.
- [17] Izadi-Darbandi, E., Aliverdi, A. (2015): Optimizing Sulfosulfuron and Sulfosulfuron Plus Metsulfuron-methyl Activity when Tank-Mixed with Vegetable Oil to Control Wild Barley (*Hordeum spontaneum* Koch.). – *J. Agr. Sci. Tech*. 17: 1769-1780.
- [18] Kaiser, Y. I., Gerhards, R. (2015): Degradation and Metabolism of Fenoxaprop and Mesosulfuron + Iodosulfuron in Multiple Resistant Blackgrass (*Alopecurus myosuroides*). – *Gesunde Pflanzen*. 67: 109-117.
- [19] Khalaghani, J. (2008): Advanced study for estimation of yield loss due to weeds in wheat fields. – Final report of project, Iranian Research Institute of Plant Protec. 76.
- [20] LaRossa, R. A., Schloss, J. V. (1984): The sulfonylurea herbicide sulfometuron methyl is an extremely potent and selective inhibitor of acetolactate synthase in *Salmonella typhimurium*. – *J Bio Chem*. 25: 8753-8757.
- [21] Majd, R., Mohammaddust chamanabad, H. R., Zand, E., Mohebodini, M., Karbalaei Khiavi, H., Alebrahim, M. (2017): Evaluation of some ecophysiological factors for sustainable management of Wild Gladiolous (*Gladiolus segetum*). – *J. Agroecol*. 7(1): 172-185. (In Persian).
- [22] Rashed Mohassel, H., Najafi, H., Akbarzadeh, M. (2001): *Biology and Weed Control*. – Ferdowsi University Press, Mashhad. 350.
- [23] Ray, T. B. (1984): Site of action of chlorsulfuron: inhibition of valine and isoleucine biosynthesis in plants. – *Plant Physiol*. 75: 827-831.
- [24] Ritz, C., Cedergreen, N., Jensen, J. E., Streibig, J. C. (2006): Relative potency in nonsimilar dose–response curves. – *Weed Sci*. 54: 407-412.
- [25] Robinson, A. P., Simpson, D. M., Johnson, W. G. (2012): Summer annual weed control with 2,4-D and glyphosate. – *Weed Technol*. 26: 657-660.
- [26] Shaner, D. L., Anderson, P. C., Stidham, M. A. (1984): Potent inhibitors of acetohydroxyacid synthase. – *Plant Physiol*. 76: 545-546.
- [27] Shimizu, T., Nakayama, I., Nakao, T., Nezu, Y., Abe, H. (1994): Inhibition of plant acetolactate synthase by herbicides, pyrimidinylsalicylic acids. – *J Pestic Sci*. 19: 59-67.
- [28] Stagnari, F., Onofri, A., Covarelli, G. (2006): Influence of vegetable and mineral oils on the efficacy of some post-emergence herbicides for grass weed control in wheat. – *J. Pestic. Sci*. 31: 339-343.
- [29] Streibig, J. C., Rudemo, M., Jensen, J. E. (1993): Dose-response curves and statistical models. Chapter 3. – In: Streibig, J. C., Kudsk, P. (eds.) *Herbicide Bioassays*. CRC Press, Boca Raton, Florida, USA. 29-55.
- [30] Subramanian, M. V., Gerwick, B. C. (1989): Inhibition of acetolactate synthase by triazolopyrimidines. – *ACS Symp Ser* 389, Washington, DC. 277-288.
- [31] Tahmasebi, B. K., Alebrahim, M. T., Roldán-Gómez, R. A., Martins da Silveira, H., Bianco de Carvalho, L., Alcántara-de la Cruz, R., De Prado, R. (2018): Effectiveness of alternative herbicides on three *Conyza* species from Europe with and without glyphosate resistance. *Crop Protec*. 112: 350-355.
- [32] Zand, E., Baghestani, M. A., Nezamabadi, N., Shimi, P., Mousavi, S. K. (2017): A guide to chemical control of weeds in Iran. – J.D.M press, Iran, Mashhad.

EVALUATION OF HERBAGE YIELD AND NUTRITIVE VALUE OF EIGHT FORAGE CROP SPECIES

AKDENİZ, H.¹ – HOSAFLIOĞLU, I.² – KOÇ, A.³ – HOSSAIN, A.⁴ – ISLAM, M.S.⁵ – IQBAL, M. A.⁶ –
IMTIAZ, H.⁷ – GHARIB, H.⁸ – EL SABAGH, A.^{8*}

¹*Department of Field Crops, Faculty of Agriculture, Iğdır University, 7600 Iğdır, Turkey*

²*Department of Landscape Architecture, Faculty of Agriculture, Iğdır University,
76000 Iğdır, Turkey*

³*General Directorate of Agricultural Affairs, Ankara, Turkey*

⁴*Bangladesh Wheat and Maize Research Institute, 5200 Dinajpur, Bangladesh*

⁵*Department of Agronomy, Hajee Mohammad Danesh Science and Technology University,
Basherhat, Bangladesh*

⁶*Department of Agronomy, University of The Poonch, Rawalakot (AJK), Pakistan*

⁷*Department of Food Science and Technology, University of The Poonch, Rawalakot (AJK),
Pakistan*

⁸*Department of Agronomy, Faculty of Agriculture, Kafrelsheikh University,
33516 Kafr El Sheikh, Egypt*

**Corresponding author*

e-mail: ayman.elsabagh@agr.kfs.edu.eg

(Received 20th Dec 2018; accepted 19th Feb 2019)

Abstract. Determining nutritional quality of indigenous forage species constitutes prerequisite to improve the productivity of ruminants. This research was carried out at the research field of the Agricultural Research and Application Center of Iğdır University, Turkey in consecutive two years (2015 & 2016) to evaluate the herbage yield and nutritive value of eight forage species having diverse genetic make-up. Eight forage species such as Kentucky bluegrass (*Poa pratensis* var. Geromino), Perennial rye-grass (*Lolium perenne* var. Ovation), Red rescue (*Festuca rubra* rubra var. Corail), Slender creeping red fescue (*Festuca rubra* trichphylla var. Pinafore), Sheep fescue (*Festuca ovina* var. Ridu), Tall fescue (*Festuca arundinaceae* var. Jaguar 4G), Chewings fescue (*Festuca comutata* var. Longfellow II) and Colonial bentgrass (*Agrostis tenuis* var. Aristata) were used as plant materials and the experiment was arranged in a randomized complete design with three replications. Data on biomass yield, crude ash, crude protein, crude oil, crude cellulose, net digestible fiber (NDF), acid detergent fiber (ADF), dry matter intake (DMI), digestible dry matter (DDM) and relative feed value (RFV) were recorded during the investigation. Results of the present study indicated that species ‘Tall fescue’ (*Festuca arundinaceae* var. Jaguar 4G) yielded the highest herbage yield, followed by cultivar ‘Perennial rye-grass’ (*Lolium perenne* var. Ovation). While, ‘Kentucky bluegrass’ (*Poa pratensis* var. Geromino) was found to be inferior to all other forage species in the studied years. When nutritional quality was observed, the species ‘Colonial bentgrass’ (*Agrostis tenuis* var. Aristata) had the maximum crude protein and RFV, while cultivar ‘Perennial rye-grass’ had significantly higher RFV, DMI, DMD and the minimum fiber content, which indicated its superior quality for milch animals.

Keywords: *forage species, Iğdır-Turkey environmental, nutritional quality, yield.*

Abbreviations: ADF: acid detergent fiber; DDM: digestible dry matter; DMI: dry matter intake; NDF: net digestible fiber; RFV: relative feed value

Introduction

To meet the food demand of increasing population, crop intensification and a sustainability should be continued globally (Jiang and Huang, 2001, Iqbal et al., 2019). The efficient use of farm resources, such as organic manure and home-grown forage, is the key to a sustainable and successful farm operation for the grassland farmers, while to improve the quality of home-grown forage from meadows and pastures, different strategies have been developed (Iqbal et al., 2018). For example, establishment and renovation of grassland by over seeding with high-quality seed mixtures are the most importance task to meet the fodder demand (Poetsch et al., 2016).

Turkey is bestowed with a great number of animals; however, animals' productivity in terms of milk and meat production is very low as compared to their potential. One of the main reasons for this under-performance of animals is owing to deficiency of good quality forages. The most important feed sources are pastures for grazing and those are composed of forage crops such as alfalfa, vetch and sainfoin grown as field crops (Iqbal et al., 2017). Cultivation of forage crops as field crops is rather low in Turkey and areas under forage crop are continuously declining due to increasing demand for food crops. Therefore, it is necessary to expand the forage crops growing area, along with investigating intercropping and crop rotation, as well as developing improved high yielding forage crop species. Although there are some species of vetch and alfalfa, but most of these forage species are perennial grasses; as a result, the number of improved varieties is far beyond the demand (Özpinar et al., 2014).

Among the forage species, 'Kentucky bluegrass' is a common turf species used on golf courses, sports fields, municipal parks, sod farms, road banks, as well as residential and school yards. 'Turfgrass' productivity is largely influenced by fertilization, particularly nitrogen. However, a greater N use efficiency is observed in the soils with low N levels (Below, 1995; Muir et al., 2001; Wims et al., 2013). 'Turfgrass' plants need sufficient soil moisture to maintain normal growth and development. The ornamental value and quality of 'Turfgrass' is severely affected by drought (Kanapeckas et al., 2008). However, the most cool-season 'Turfgrass' species are particularly susceptible to salinity stress during seed germination, with the possible exception of 'perennial ryegrass' (*Lolium perenne* L.). 'Ryegrass' is one of the most important and valuable forage plants in grasslands and constitutes an indispensable component of seed mixtures for meadows, pastures, ley farming, and re-seeding measures (Poetsch et al., 2016). Grazed perennial ryegrass is one of the most important forages for dairy cows in temperate regions due to its high forage yield and nutritive value (van Wijk et al., 1993; Lemus et al., 2008; Kering et al., 2012; Kumar et al., 2016), and hence, provides a cheaper feed than silage or concentrates. Traditionally, perennial ryegrass species were mainly bred for high forage production. Many studies indicated that environmental stresses affected physiological changes, especially antioxidant responses, in many cool-season 'Turfgrass' species (Xu et al., 2006; Senthil-Kumar et al., 2007). The ability for avoiding oxidative stress is a very important factor in determining the environmental stress tolerance of turf-grasses (Wang et al., 2012). Creeping bent-grass (*Agrostis stolonifera* L.) establishment and management practices are well understood for this turf-grass, hence its popularity is widespread (Beard, 2002).

'Red fescue' (*Festuca rubra*), 'Sheep fescue' (*F. ovina*), and 'meadow fescue' (*F. pratensis*) are the subjects of intensive research. All are valued for both forage production and special purposes, ranging from the preparation of sport grounds, parks,

and house gardens, to preventing the erosion of soil from embankments and railroads (Stanisavljević et al., 2012). ‘Tall fescue’ has been considered one of the best-adapted cool-season grasses for hot and dry conditions (Turgeon, 1980; Smit et al., 2005a, b).

It is well-established that forage grasses require less intensive management and inputs that impart them superiority over conventional turf blends by reducing the need for fertilization, pest control, irrigation and mowing. The quality of a low maintenance turf is usually not so high, since minimal inputs cannot be expected to produce high quality forage (Prendes and Palencia, 2015). Up-till now, there are a very few studies which provide concrete and conclusive results pertaining to the variability of yield and seed quality including viability of these forage species. It is hypothesized that some of the forage species may outperform others in terms of herbage yield and nutritional quality under Mediterranean environment. Thus, considering the burning issue, the aim of this study was to assess the herbage yield and nutritive value for some forage crop species grown in Mediterranean conditions to meet the quality feed demand for increasing number of cattle.

Materials and methods

Locations and soil properties

This research was carried out at the research field of the Agricultural Research and Application Center, Iğdır University, Turkey during consecutive two years (2015 & 2016). Soil of the research site was characterized as clay-loamy texture, highly alkaline (pH: 8.6), lightly salted (EC: 1.37 dS/m), low organic matter content (1.20%) and rich in lime (CaCO₃: 22.27%). Beside these, available phosphorus (P) and potassium (K) contents in the soil were found to be 51.7 ppm and 852.4 ppm (Erdogan, 2013).

Treatments and experimental design and using materials

Selected eight forage species such as Kentucky bluegrass (*Poa pratensis* var. Geromino), Perennial rye-grass (*Lolium perenne* var. Ovation), Red rescue (*Festuca rubra* rubra var. Corail), Slender creeping red fescue (*Festuca rubra* tricphylla var. Pinafore), Sheep fescue (*Festuca ovina* var. Ridu), Tall fescue (*Festuca arundinaceae* var. Jaguar 4G), Chewings fescue (*Festuca comutata* var. Longfellow II) and Colonial bentgrass (*Agrostis tenuis* var. Aristata) were arranged in a randomized complete design with three replications. Each experimental plot had the net area of 12 m² (3 × 4 m). The list of the forage crops under investigation are described in *Table 1*.

Table 1. Forage crops used in the experiment

SL No.	English name	Latin name
1.	Kentucky bluegrass	<i>Poa pratensis</i> var. Geromino
2.	Perennial rye-grass	<i>Lolium perenne</i> var. Ovation
3.	Red rescue	<i>Festuca rubra</i> rubra var. Corail
4.	Slender creeping red fescue	<i>Festuca rubra</i> tricphylla var. Pinafore
5.	Sheep fescue	<i>Festuca ovina</i> var. Ridu
6.	Tall fescue	<i>Festuca arundinaceae</i> var. Jaguar 4G
7.	Chewings fescue	<i>Festuca comutata</i> var. Longfellow II
8.	Colonial bentgrass	<i>Agrostis tenuis</i> var. Aristata

Experimental procedure

In the first year, 5 kg nitrogen (N) and 8 kg phosphorus da^{-1} were applied in all plots during the final land preparation. In the second year, 15 kg da^{-1} nitrogen was applied to all plots, while half of the nitrogen was applied during April and May each year. During first year, seeds of all forage species were sown on 15 March 2014 and no yield could be recorded in this year. Therefore, the data obtained in the first year of the establishing were not taken into consideration and only the second and third year data were evaluated. Irrigation was applied as per field capacity. Cutting time was June 15, 2015 in the second year and June 20, 2016 the third year. After leaving 0.5 m from the sides of each plots 1, the rest of the plots (6 m^2) were cut with a machine called 'Figaro' and were weighed immediately using spring balance. Since the first year is the establishing year, the second and third year data are taken into consideration and subsequently analyzed statistically.

Chemical analyses

Chemical analyses regarding crude protein (CP) and ash concentration were performed as per procedures outlined by AOAC (2000). Neutral detergent fiber (NDF), acid detergent fiber (ADF), cellulose and lignin were determined by following Van Soest et al. (1991) using Fiber Tech analyzer (FibraPlus FES 6, Pelican, Chennai, India). Heat-labile α -amylase and sodium sulphite were used in NDF solution. Lignin (sa) was determined by dissolving cellulose with sulfuric acid in the ADF residue (Van Soest et al., 1991). Cellulose was estimated as the difference between ADF and lignin (sa) in the sequential analysis and hemicellulose was calculated as difference between NDF and ADF concentrations. Dry matter intake (DMI), digestible of dry matter (DDM), relative feed value (RFV) for different animal functions was determined as described by Undersander et al. (1993).

Statistical analysis

The obtained data were statistically analyzed, separately and combined, using "SAS" statistical package program. Variable means were compared at the significance level of $P < 0.05$. Correlation coefficients between different yield attributes were done by using the same statistical software (Snedecor and Cochran, 1994).

Results and discussion

Dry hay yield of different forage species

It was revealed that 'tall fescue' performed the best over other forage species under study in terms of dry matter yield, this result is in agreement with the finding of Campbell and Xia (2002). Forage cultivars 'Perennial rye-grass' and 'slender creeping red fescue' followed 'tall fescue' in terms of herbage yield in both years. 'Kentucky bluegrass' and 'colonial bentgrass' yielded the minimum hay (*Fig. 1; Table 2*). The significantly higher herbage yield contributed by 'tall fescue' might be attributed to significantly higher plant height and fast regrowth rate after cutting. In addition to this, early and strong spring growth could have positive effect on it (Özpinar et al., 2014, Campbell and Xia, 2002). To achieve appropriate yield and quality herbage and change

greatly depending on cultural practice, the species, variety and environment (Barutcular et al., 2017; Akdeniz et al., 2018a).

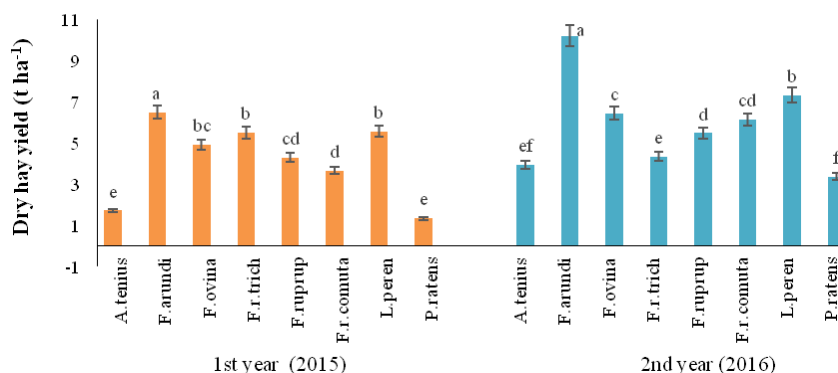


Figure 1. Dry hay yield ($t\ ha^{-1}$) of different forage species grown under the Mediterranean environment of Turkey during 2015 and 2016. Bar with same letter indicates that does not differ significantly, while with dissimilar letters indicates that differ significantly. Mean ($\pm SE$) was calculated from three replicates for each forage cultivars. Error bars represent significant difference at $p \leq 0.01$ (LSD test)

Table 2. Dry biomass yield and nutritional quality of hay of different forage species grown under Mediterranean environment during 2015 and 2016

Forage species	Dry hay yield ($t\ ha^{-1}$)	Crude ash (%)	Crude protein (%)	Crude oil (%)	Crude cellulose (%)	NDF (%)	ADF (%)	DMI	DDM	RFV
First year										
A. tenuis	1.71e	17.12b	21.06a	1.67abc	39.94bc	52.45bc	35.33de	2.29ab	61.38	109.06ab
F. arundi	6.50a	22.17a	15.84c	1.07cd	61.25a	62.89a	39.10cd	1.91c	58.44	86.45cd
F. ovina	4.93bc	10.43cd	13.59de	1.56bc	36.59cd	61.33a	43.19ab	1.96c	55.23	84.28d
F. r. trich	5.50b	17.99b	14.143cde	0.74d	65.81a	64.00a	45.78a	1.88c	50.64	73.67d
F. ruprup	4.30cd	18.06b	15.60c	0.75d	38.26bcd	63.71a	39.76bc	1.89c	57.93	84.72d
F. r. comuta	3.66d	11.09c	13.30e	0.74d	42.48b	64.28a	40.62bc	1.87c	57.26	82.99d
L. peren	5.57b	19.00b	17.92b	2.29a	33.59d	49.33c	32.88e	2.43a	63.28	119.41a
P. ratens	1.33e	8.39d	15.25cd	1.91ab	42.70b	55.79b	37.27cd	2.15b	59.87	99.94bc
LSD (0.05)	0.65	2.44	1.77	0.70	5.36	4.29	4.07	0.15	ns	14.32
Second year										
A. tenuis	3.94ef	7.51c	10.45b	1.60	36.77e	41.17d	24.93c	4.82a	56.83b	212.09b
F. arundi	10.23a	9.54a	9.86bc	1.15	44.85a	64.05c	47.64a	1.87bc	51.79d	75.22cd
F. ovina	6.46c	5.57d	5.80e	1.41	44.06ab	68.33b	45.58ab	1.76cd	53.39cd	72.71d
F. r. trich	4.337e	8.49b	8.85bcd	1.44	43.612abc	69.25b	44.26b	1.73cd	54.42c	73.11d
F. ruprup	5.48d	6.98c	7.91d	0.96	41.47cd	70.29b	46.31ab	1.71d	52.83cd	69.91d
F. r. comuta	6.13cd	5.44d	8.52cd	1.02	41.61bcd	83.25a	45.21ab	1.44e	53.68cd	59.99e
L. peren	7.33b	9.13ab	12.75a	1.52	36.33e	35.51e	24.82c	4.84a	61.24a	229.76a
P. ratens	3.36f	8.73ab	9.74bc	1.53	40.77d	62.63c	43.97b	1.92b	54.65c	81.19c
LSD (0.05)	0.72	0.81	1.63	ns	2.49	2.20	2.49	0.15	1.99	7.38

NDF: neutral detergent fiber; ADF: acid detergent fiber; DMI: intake, digestibility to calculate DM intake; DDM: digestible dry matter; RFV: relative feed value

Crude protein, crude ash, oil content, NDF, ADF and cellulose

Ash, oil content, NDF, ADF and cellulose were found to be varying among the species under investigation (Figs. 2 and 3; Table 2). However, ‘Colonial bentgrass’

proved to be superior to all in terms of crude protein content and it was followed by ‘perennial rye-grass’. The minimum crude protein content was recorded by ‘sheep fescue’ followed by ‘chewings fescue’. On the other hand, ‘tall fescue’ had the maximum ash and was closely followed by ‘perennial rye-grass’, ‘slender creeping red fescue’, ‘red rescue. Chewings fescue’ recorded the lowest crude oil content while ‘perennial rye-grass’ had quite high oil concentration. ‘Perennial rye-grass’ remained outstanding by recording the lowest cellulose and NDF as well as ADF contents (Fig. 3; Table 2).

Cereal stover and straws are usually low in crude protein and rich in fiber concentrations, and thus unable to meet the minimum crude protein requirements (7%) for maintenance of animals and rumen microbes (Minson, 1990). There is a dire need to supplement this stover with protein rich leguminous forage or non-protein nitrogen or protein sources in order to obtain sustainable supplies of milk from dairy animals. It was observed significant differences among the crops and their interaction with environment regarding yield and quality properties. However, variations have been also observed in different agronomic and quality were also noted by Barutcular et al. (2016a, b, c; Akdeniz et al., 2018b; Yıldırım et al., 2018). The variability in NDF, ADF, cellulose and lignin concentrations of sorghum stover in different species has been reported earlier (Hamed et al., 2015) and it is reported that forage with high NDF levels had higher concentrations of the CB2 fraction, which is more slowly degraded in the rumen, impacting microbial synthesis and animal performance (Ribeiro et al., 2001). Carvalho et al. (2007) reported that NDF concentration influences carbohydrate fraction CB2 and forages high in NDF concentration usually have higher values of CB2.

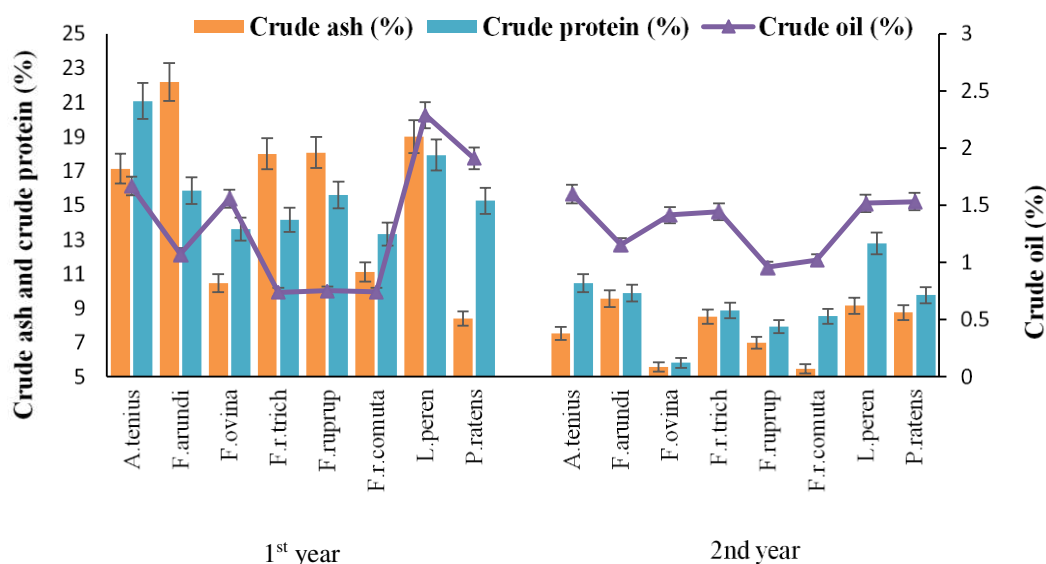


Figure 2. Crude ash, crude protein and crude oil of hay/forage as influenced by different forage species grown under Mediterranean environment

Intake, digestibility and relative feed value

The calculated values of DMI, DDM and RFV for different forage crops varied significantly during both years of study (Fig. 4). ‘Perennial rye-grass’ proved its superiority to other forage species by recording the highest DMI, DMD and RFV, while

it was followed by ‘colonial bentgras’. It was also revealed that ‘kentucky bluegrass’ was better than ‘slender creeping red fescue’, ‘red rescue’ and ‘chewings fescue’, but remained inferior to ‘perennial rye-grass’ and ‘Colonial bentgras’. Dietary fiber concentration, its digestibility and rate of degradation in the rumen are the most important forage characteristics that determine DMI (Roche et al., 2008). We attributed the lower RFV of stover in the present study to its lower quality relative to the whole plants examined at the younger age which is agreement with Bean et al. (2011), who noted that higher NDF and ADF concentrations influence the intake and digestibility of a fodder.

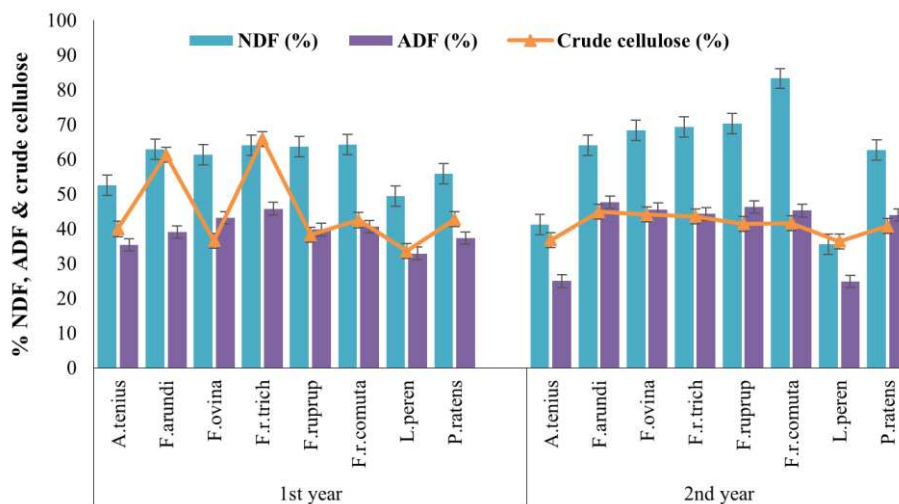


Figure 3. Acid detergent fiber (ADF), neutral detergent fiber (NDF) and crude cellulose of hay/forage as influenced by different forage species grown under Mediterranean environment

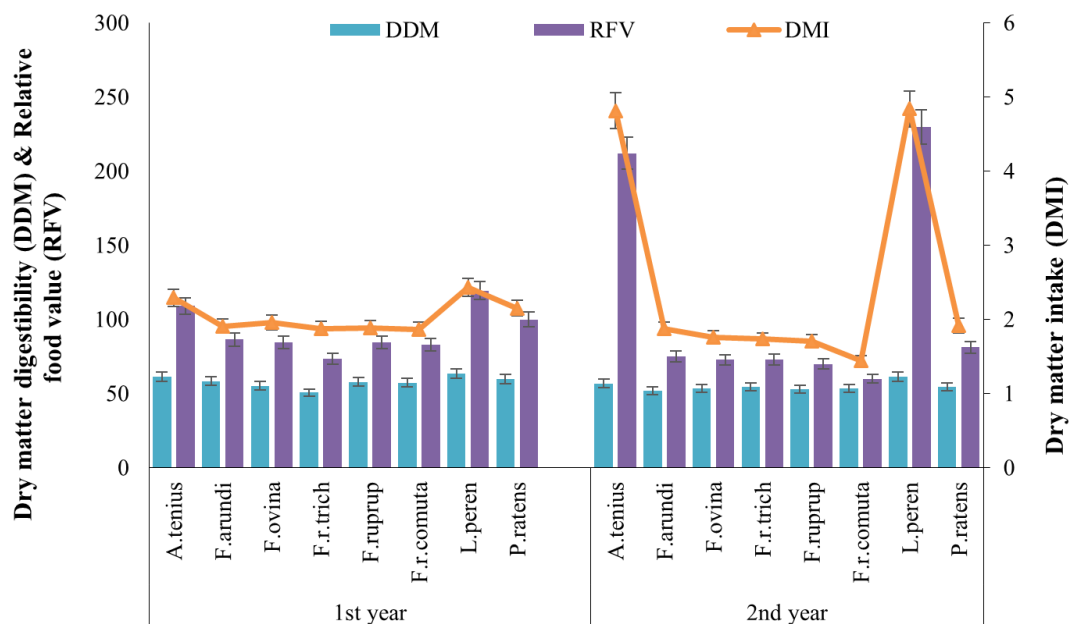


Figure 4. Intake, digestibility and relative value of dry hay/forage as influenced by different forage species grown under Mediterranean environment

Correlation coefficients among the different variables

Correlation coefficients among the variables under study were found to be significant (Table 3). In the present study, dry yield was positively correlated with ADF and NDF, while ADF remained positively correlated with NDF. The findings are in confirmation with those of Badrzadeh (2008), who reported ADF direct relationship with NDF. On the other hand, the NDF was negatively correlated with the DDM and RFV. The ADF was negative correlated with DMI, DDM and RFV. Genotypic differences in terms of all quality parameters were found significant, while ADF ratio was non-significant, our results are in accordance with the findings of (Yılmaz and Erol, 2015). Bani et al. (2007) recorded an inverse relationship between forage fiber fractions and DM digestibility.

Table 3. Correlation coefficients between different studied parameters

Study parameters	Dry yield (t ha ⁻¹)	Crude ash (%)	Crude protein (%)	Crude oil (%)	Crude cellulose (%)	NDF (%)	ADF (%)	Crude ash yield (t ha ⁻¹)	Protein yield (t ha ⁻¹)	Crude oil (t ha ⁻¹)	NDF (t ha ⁻¹)	ADF (t ha ⁻¹)	Dry matter intake	Digestible dry matter
1st year														
Crude ash, %	0.608													
Crude protein, %	-0.328	0.427												
Crude oil, %	-0.273	-0.169	0.513											
Crude cellulose, %	0.407	0.406	-0.268	-0.544										
NDF, %	0.354	-0.032	-0.762*	-0.917**	0.520									
ADF, %	0.317	-0.169	-0.751*	-0.724*	0.555	0.847**								
Crude ash yield, t/ha	0.913**	0.840**	-0.047	-0.220	0.519	0.207	0.091							
Protein yield, t/ha	0.959**	0.744*	-0.075	-0.089	0.308	0.115	0.055	0.954**						
Crude oil, yield/ha	0.636	0.352	0.117	0.543	-0.208	-0.431	-0.336	0.565	0.748*					
NDF, t/ha	0.973**	0.562	-0.443	-0.463	0.524	0.550	0.487	0.877**	0.884**	0.451				
ADF, t/ha	0.965**	0.515	-0.465	-0.438	0.535	0.534	0.550	0.840**	0.863**	0.462	0.989**			
Dry matter intake	-0.318	0.061	0.760*	0.906**	-0.522	-0.998**	-0.851**	-0.175	-0.077	0.460	-0.520	-0.504		
Digestible dry matter	-0.332	0.093	0.688	0.699	-0.629	-0.783*	-0.983**	-0.138	-0.088	0.313	-0.487	-0.562	0.783*	
Relative feed value	-0.328	0.084	0.773*	0.875**	-0.589	-0.972**	-0.945**	-0.161	-0.073	0.440	-0.525	-0.542	0.974**	0.903**
2nd year														
Crude ash, %	0.210													
Crude protein, %	0.100	0.720*												
Crude oil, %	-0.411	0.357	0.386											
Crude cellulose, %	0.334	-0.146	-0.705	-0.459										
NDF, %	0.016	-0.523	-0.747*	-0.693	0.779*									
ADF, %	0.174	-0.240	-0.717*	-0.624	0.919**	0.905**								
Crude ash yield, t/ha	0.906**	0.601	0.396	-0.192	0.201	-0.218	0.029							
Protein yield, t/ha	0.864**	0.541	0.585	-0.146	-0.074	-0.355	-0.209	0.939**						
Crude oil, yield/ha	0.867**	0.378	0.327	0.081	0.068	-0.373	-0.186	0.862**	0.871**					
NDF, t/ha	0.808*	-0.161	-0.375	-0.728*	0.720*	0.587	0.654	0.592	0.468	0.466				
ADF, t/ha	0.872**	0.043	-0.283	-0.617	0.716*	0.441	0.610	0.732*	0.566	0.583	0.967**			
Dry matter intake	-0.070	0.321	0.737*	0.610	-0.883**	-0.950**	-0.987**	0.093	0.302	0.283	-0.590	-0.514		
Digestible dry matter	-0.154	0.298	0.748*	0.613	-0.862**	-0.822*	-0.898**	-0.008	0.259	0.236	-0.645	-0.610	0.863**	
Relative feed value	-0.060	0.327	0.753*	0.607	-0.890**	-0.949**	-0.989**	0.101	0.320	0.299	-0.590	-0.517	0.998**	0.893**

Conclusion

The results from this study revealed that significant variability exists among forage species under study in terms of their potential for herbage yield and nutritive value under Mediterranean environment. This indicates that there is a considerable potential for selecting appropriate forage species, which have the adequate nutritional quality to improve forage supply for as well as to meeting ruminant dietary requirements. It is clear that the potentiality of *Festuca* species as forage and pasture plants under prevalent agro-climatic conditions is very high due to specific nutritional characteristics. *F. arundinacea* can also be promoted as forage and pasture specie due to higher potential to yield dry matter while using *F. rubra* as a pasture plants to improve natural grassland seems to be more suitable.

REFERENCES

- [1] AOAC (Association of Official Analytical Chemists) (2000): Official Methods of Analysis. – AOAC, Arlington, VA.
- [2] Akdeniz, H., Koc, A., Islam, M. S., EL Sabagh, A. (2018a): Performances of hairy vetch varieties under different locations of Mediterranean environment. – Fresenius Environmental Bulletin 27(6): 4263-4269.
- [3] Akdeniz, H., Koc, A., Hossain, A., El Sabagh, A. (2018b): Nutritional values of four hairy vetch (*Vicia villosa* Roth) varieties grown under Mediterranean environment. – Fresenius Environmental Bulletin 27(8): 5385-5390.
- [4] Badrzadeh, M., Zaragarzadeh, F., Esmailpour, B. (2008): Chemical composition of some forage *Vicia* spp. in Iran. – J. Food, Agric. Env. 6(2): 178-180.
- [5] Bani, P., Minuti, A., Obonyo, L., Ligabue, M., Ruozi, F. (2007): Genetic and environmental influences on in vitro digestibility of alfalfa. – Italian Journal of Animal Science 6: 251-253.
- [6] Barutcular, C., Dizlek, H., EL Sabagh, A., Sahin, T., M., Islam, M. S. (2016a): Nutritional quality of maize in response to drought stress during grain-filling stages in mediterranean climate condition. – J. Exp. Biol. Agric. Sci. 4: 644-652.
- [7] Barutcular, C., EL Sabagh, A., Konuskan, O., Saneoka, H. (2016b): Evaluation of maize hybrids to terminal drought stress tolerance by defining drought indices. – J. Exp. Biol. Agric. Sci. 4: 610-616.
- [8] Barutcular, C., Yildirim, M., Koc, M., Akıncı, C., Tanrıku, A., El Sabagh, A., Saneoka, H., Ueda, A., Islam, M. S., Toptas, I., Albayrak, O. (2016c): Quality traits performance of bread wheat genotypes under drought and heat stress conditions. – Fresen Environ Bull 25(12a): 6159-6165.
- [9] Barutcular, C., EL Sabagh, A., Koç, M., Ratnasekera, D. (2017): Relationships between grain yield and physiological traits of durum wheat varieties under drought and high temperature stress in Mediterranean conditions. – Fresen Environ Bull 26(4): 4282-4291.
- [10] Bean, B., Becker, J., Robinson, J., Pietsch, D. (2011): Limited Irrigated Texas Panhandle Sorghum Hay Trial. – Agri Life Extension Texas A&M System, Amarillo, TX.
- [11] Beard, J. B. (2002): Turf Management for Golf Courses. – Ann Arbor Press, Chelsea, Michigan.
- [12] Below, F. E. (1995): Nitrogen Metabolism and Crop Productivity. – In: Pessarakli, M. (ed.) Handbook of Plant and Crop Physiology. Marcel Dekker Inc., New York, pp. 275-301.
- [13] Carvalho, G. G. P., Garcia, R., Pires, A. J. V., Pereira, O. G., Fernandes, F. E. P., Obeid, J. A., Carvalho, B. M. A. (2007): Fracionamento de carboidratos de silagem de capim-

- elefante emurhecido ou com farelo de cacau. – Revista Brasileira de Zootecnia 36: 1000-1005.
- [14] Erdogan, H.E. (2013): Soil Definition Guide. ISBN: 978-605-4672-20-2.
- [15] Hamed, A. H. M., Abbas, S. O., Ali, K. A., Elimam, M. E. (2015): Stover yield and chemical composition in some sorghum varieties in Gadarif state, Sudan. – Animal Review 2: 68-75. DOI: 10.18488/journal.ar/2015.2.3/101.3.68.75.
- [16] Iqbal, M. A., Abdul, H., Imtiaz, H., Muzammil, H. S., Tanveer, A., Abdul, K., Zahoor, A. (2019): Competitive indices in cereal and legume mixtures in a South Asian environment. – Agronomy Journal 111: 242-249.
- [17] Iqbal, M. A., Asif, I., Rana, N. A. (2018): Spatio-temporal reconciliation to lessen losses in yield and quality of forage soybean (*Glycine max* L.) in soybean-sorghum intercropping systems. – Bragantia 77: 283-291.
- [18] Iqbal, M. A., Brandon, J. B., Asif, I., Rana, N. A., Zubair, A., Haroon, Z. K., Bilal, A. (2017): Agro-botanical response of forage sorghum-soybean intercropping systems under atypical spatio-temporal patterns. – Pakistan Journal of Botany 49: 987-994.
- [19] Jiang, Y., Huang, B. (2001): Physiological responses to heat stress alone or in combination with drought: A comparison between tall fescue and perennial ryegrass. – HortScience 36: 682-686.
- [20] Kanapeckas, J., Lemeziene N., Stukonis V., Tarakanovas P. (2008): Drought tolerance of turfgrass genetic resources. – Biologja 54: 121-124.
- [21] Kering, M. K., Butler, T. J., Biermacher, J. T., Guretzky, J. A. (2012): Biomass yield and nutrient removal rates of perennial grasses under nitrogen fertilization. – BioEnergy Research 5(1): 61-70.
- [22] Kumar, R., Singh, M., Tomar, S. K., Meena, B. S., Rathore, D. K. (2016): Productivity and nutritive parameters of fodder maize under varying plant density and fertility levels for improved animal productivity. – Indian J. Animal Resch 50: 199-202.
- [23] Lemus, R., Brummer, E. C., Burras, C. L., Moore, K. J., Barker, M. F., Molstad, N. E. (2008): Effects of nitrogen fertilization on biomass yield and quality in large fields of established switchgrass in southern Iowa, USA. – Biomass and Bioenergy 32(12): 1187-1194.
- [24] Minson, D. J. (1990): Forage in Ruminant Nutrition. – Academic Press, New York. DOI: 10.1016/B978-0-12-498310-6.50025-0.
- [25] Muir, J. P., Sanderson, M. A., Ocumpaugh, W. R., Jones, R. M., Reed, R. L. (2001): Biomass production of 'Alamo' switchgrass in response to nitrogen, phosphorus, and row spacing. – Agronomy Journal 93(4): 896-901.
- [26] Özpınar, H., Olcayto C. Sabancı, Alptekin A. (2014): Evaluation of fescue (*Festuca arundinacea* Schreb. and *Festuca rubra* L.) populations grown under Aegean region conditions. – ANADOLU, J. of AARI 24(2): 32-40.
- [27] Poetsch, E. M., Resch, R., Krautzer, B. (2016): Variability of yield and forage quality between three heading groups of english ryegrass (*Lolium perenne* L.) during the first growth / Variabilität von Ertrag und Futterqualität zwischen drei Reifegruppen von Englischem Raygras (*Lolium perenne* L.) im Verlauf des ersten Aufwuchses. – Die Bodenkultur: Journal of Land Management, Food and Environment 67(2): 69-75.
- [28] Prendes, J. A. O., Palencia, P. (2015): Morphological characterization and turf performance of Paula hard fescue and Casero colonial bentgrass selections under low maintenance conditions. – Czech J. Genet. Plant Breed. 51(3): 117-22.
- [29] Ribeiro, K. G., Pereira, O. G., Valadares Filho, S. C., Garcia, R., Cabral, L. S. (2001): Caracterização das frações que constituem as proteínas e os carboidratos e respectivas taxas de digestão, do feno de capim-tifton 85 de diferentes idades de rebrota. – Revista Brasileira de Zootecnia 30: 589-595.
- [30] Roche, J. R., Blache, D., Kay, J. K., Miller, D. R., Sheahan, A. J., Miller, D. W. (2008): Neuroendocrine and physiological regulation of intake with particular reference to domesticated ruminant animals. – Nutrition Research Reviews 21: 207-234.

- [31] Senthil-Kumar, M., Kumar, G., Srikanthbabu, V., Udayakumar, M. (2007): Assessment of variability in acquired thermotolerance: potential option to study genotypic response and the relevance of stress genes. – *Journal of Plant Physiology* 164(2): 111-125.
- [32] Smit, H. J., Tas, B. M., Taweel, H. Z., Tamminga, S., Elgersma, A. (2005a): Effects of perennial ryegrass (*Lolium perenne* L.) cultivars on herbage production, nutritional quality and herbage intake of grazing dairy cows. – *Grass and Forage Science* 60(3): 297-309.
- [33] Smit, H. J., Tas, B. M., Taweel, H. Z., Tamminga, S., Elgersma, A. (2005b): Sward characteristics important for intake in six *Lolium perenne* varieties. – *Grass and Forage Science* 60: 128-135.
- [34] Snedecor, G. W., Cochran, W. G. (1994): *Statistical Methods*. 8th Ed. – Oxford and IBH Publishing Company, Calcutta, India.
- [35] Stanislavljević, R. S., Vučković S. M., Simić A. S., Marković J. P., Lakić Z. P., Terzić D. V., Đokić D. J. (2012): Acid and temperature treatments result in increased germination of seeds of three fescue species. – *Not. Bot. Hort. Agrobot. Cluj* 40: 220–226.
- [36] Tilley, J. M. A., Terry, R. A. (1963): A two-stage technique for the in vitro digestion of forage crops. – *Journal of British Grassland Society* 18: 104-111. DOI: 10.1111/j.1365-2494.1963.
- [37] Turgeon, A. J. (1980): *Turfgrass Management*. – Reston Pub., Reston, VA.
- [38] Undersander, D., Mertens, D. W., Theix, N. (1993): *Forage Analysis Procedures*. – National Forage Testing Association, Omaha, NE.
- [39] Van Soest, P. J., Robertson, J. B., Lewis, B. A. (1991): Method for dietary fibre, neutral detergent fibre and non-starch polysaccharides in relation to animal nutrition. – *Journal of Dairy Science* 74: 3588-3597.
- [40] van Vuuren, A. M., van der Koelen, C. J., Valk, H., de Visser, H. (1993): Effects of partial replacement of ryegrass by low-protein feeds on rumen fermentation and nitrogen loss by dairy cows. – *Journal of Dairy Science* 76: 2982-2993.
- [41] van Wijk, A. J. P., Boonman, J. G., Rumball, W. (1993): Achievements and perspectives in the breeding of forage grasses and legumes. – In: Baker, M. J. (ed.) XVIIth International Grassland Congress, Wellington, New Zealand, pp. 379-384.
- [42] Wang, K., Zhang, X., Ervin, E. (2012): Antioxidative responses in roots and shoots of creeping bentgrass under high temperature: effects of nitrogen and cytokinin. – *Journal of Plant Physiology* 169(5): 492-500.
- [43] Wims, C. M., Mcevoy, M., Delaby, L., Boland, T. M., O'Donovan, M. (2013): Effect of perennial ryegrass (*Lolium perenne* L.) cultivars on the milk yield of grazing dairy cows. – *Animal* 7(3): 410-421.
- [44] Xu, S., Li, J., Zhang, X., Wei, H., Cui, L. (2006): Effects of heat acclimation pretreatment on changes of membrane lipid peroxidation, antioxidant metabolites, and ultrastructure of chloroplasts in two cool-season turfgrass species under heat stress. – *Environmental and Experimental Botany* 56(3): 274-285.
- [45] Yılmaz, M. F., Erol, A. (2015): Determination of forage yields and quality characteristics of some common vetch (*Vicia sativa* L.) genotypes. – *Türk Tarım ve Doğa Bilimleri Dergisi* 2(2): 142-151.
- [46] Yıldırım, M., Barutcular, C., Hossain, A., Koç, M., Dizlek, H., Akinci, C., Toptaş, I., Basdemir, F., Islam, M.S., EL Sabagh, A. (2018): Assessment of the grain quality of wheat genotypes grown under multiple environments using GGE Biplot analysis. – *Fresen Environ Bull* 27(7): 4830-4837.

URBAN SPRAWL ASSESSMENT USING TIME-SERIES LULC AND NDVI VARIATION: A CASE STUDY OF SEPANG, MALAYSIA

YASIN, M. Y. * – YUSOF, M. M. – NOOR, N. M.

*Department of Geography, Faculty of Arts and Social Sciences, University of Malaya
50603 Kuala Lumpur, Malaysia*

**Corresponding author
e-mail: yazrinyasin@gmail.com*

(Received 26th Dec 2018; accepted 6th Mar 2019)

Abstract. Rapid urbanization that caused urban sprawl is a major worldwide concern. In this study an assessment of urban sprawl was carried out based on Land Use Land Cover (LULC), Normalized Difference Vegetation Index (NDVI) and Normalized Difference Built-up Index (NDBI) variation in Sepang, Malaysia. The land cover classification consisted of Built-up Area (BUA), Vegetation Area (VA), Open Space Area (OSA), and Water Bodies (WB) from 1990 to 2018. Supervised classification based on maximum likelihood techniques were used to identify the land use classes. Based on the analysis of LULC, the majority of VA (i.e. forest field) was transformed into OSA and gradually the land was converted into BUA. Observation within 25 years, supported by NDVI and NDBI has discovered a consistent increase of BUA while contrastingly a decline of VA, while WB and OSA are suspected to have inconsistently varying highs and lows. This study has demonstrated that urban sprawl caused by rapid urbanization has not favour the population. Without proper planning and growth control, urban sprawl in Sepang would have undesirable consequences to the quality of life and the environment. Therefore, comprehensive land use and progressive environmental change can serve as prognostic measures to mitigate urban sprawl, and to achieve sustainable urbanization and to carry out effective planning and decision making.

Keywords: *urban sprawl, land use land cover, normalized difference vegetation index, normalized difference built-up index*

Introduction

Urban sprawl occurs on a micro basis in almost every major cities in the world in response to increased wealth and growing dependence on private transportation (Burchell et al., 2002). Population, resources and productive activity are highly and increasingly concentrated in cities, thus require comprehensive understanding especially in the context of demographic, geographic and economic. In regard to urban sprawl, it is a global phenomenon but it is always viewed in different ways on how and why it was resulted (Barnes et al., 2002). In Eastern Europe, urban sprawl was considered as an outcome of post-socialist of autocratic transformation into liberalization of economic and social well-being (Bussauw, 2012; Nuissl and Rink, 2005). In the USA, early spatial form of sprawl occurred after World War II because of the perception that the new suburbs are safer, more desirable and cheaper than urban alternatives (Peiser, 2001). In Asia, most recently China and India are experiencing the largest and most rapid urban sprawl because of their enormous economic transformation which affecting agricultural productivities (Yue, 2011). Generally, majority scholars admit that urban sprawl had indirectly provide negative impacts especially towards the social segregation and environmental degradation (Squires, 2002; Burchell et al., 2002). Strong supported by Hua and Ping (2018), Hua (2018, 2017a), Noor and Rosni (2013) as well as Abdullahs (2012) view that the problems caused by urban sprawl are exceeded the

expected of benefits due to increasing of population growth that live based on their own desires. Nevertheless, many academicians are invited to provide the ideas on urban sprawl for effectively containment, especially focuses about the sustainability development (Hua and Ping, 2018).

Since urbanization process taking place worldwide and are considered a universal phenomenon, therefore population growth, economy and infrastructure could be responsible to the increasing of this bewildering phenomenon. Specifically, any development of an urban area with no ability to visualize the growth through planning, policies and decision making process could resulted the sprawl. Therefore, urban sprawl is likely to be considered as the development of a city due to unplanned, uncontrolled, and uncoordinated growth, it could impact the wildlife habitat, encroachment of natural resources and farmland, increased environmental degradation, as well as social and economy deprivation (Hua, 2018, 2017b; Tehrany et al., 2013). Malaysia already going towards an over urbanized nation with 75% of the population is expected to live in urban areas in 2020 (Abdullah, 2012). His study also indicated, urban sprawl in Malaysia will continuously become part of the landscape of metropolitan and other major cities with the expansion of regional economic corridors. Greater Kuala Lumpur, an area surrounded by 10 municipalities surrounding Kuala Lumpur are considered far reaching the socio-economic and cultural conditions. These cities are having desire to compete among each other, and this had caused the economic activities to concentrated in the urban area and leaving the rural areas far behind in term of development. Since Greater Kuala Lumpur had a greater growth in the area and this trend had cause greater number of populations to reside in suburban areas rather than city.

Sepang is considered very significant in term of suburban living and sprawl. The study area was mainly selected based on the rapid urbanization and sudden increase in population especially in 1997-2007. This is probably due to government's decision on the relocation of the administrative of Putrajaya in 1995. Putrajaya is the biggest integrated development with a total land area of 4581.1 ha, conveniently located within the district of Sepang but with separated autonomy. Another integrated development located within Sepang is Cyberjaya, the IT-themed city aspired as Malaysia's Silicon Valley. Cyberjaya is part of Multimedia Super Corridor, a special economic corridor and high technology business district, Federal Government's knowledge based initiative. Sepang also houses KLIA and F1 Sepang circuit, both generated many chain of businesses and employment. This study examined the conceptualization and measurement of sprawl whereby its equates with non-urban e.g. farmland, cropland and open space that change into urban land e.g. building, infrastructures. Therefore, urban sprawl must be considered as the rate of increase relative to physical urban growth or land use change in a space-time context. Consequently the main objective of this study is to assess the land use change from 1990 to 2018 through detection techniques using Land Use Land Cover (LULC) and Normalized Differences Vegetation Index (NDVI). Both methods are considered accurate, common, and effective in change detection for mapping of urban sprawl (Lu et al., 2004).

The review on theoretical for measured urban sprawl

Another definition by pattern of growth is brought by Ewing and Hamidi (2008), refers urban sprawl as undesirable land use patterns whether scattered, leapfrog, ribbon or continuous low density development and at the same time has poor accessibility and lack of functional open spaces. The growth patterns are usually determined by the

availability of adjacent land and variations of terrain. Accessibility has direct correlation with the extent of scattered-ness of the pattern. The more scattered the pattern, the lower their accessibility. Ewing also included any urban growth pattern that have poor accessibility and lack of functional open space.

Combination rather than individually separated on the application techniques of remote sensing and GIS in the study for urban sprawl are better especially in monitoring nor simulation for the physical, social and economic data (Mohd Noor et al., 2012). Majority researchers are tends to use remote sensing and GIS to monitor and measure the urban sprawl (Hua, 2018; Noor and Rosni, 2013; Mohd Noor et al., 2012). Nevertheless, having strong definition on sprawl term with focus towards the problematic and undesirable development characteristic which majority stakeholders are debate on. Therefore, the advantageous of using remote sensing is the capability of producing consistent spatial dataset with coverage of larger areas assisted with its high spatial and temporal resolution. In other words, remote sensing can be considered as “unique view” on the spatial temporal change of the urban growth process and land use change (Herold et al., 2003). Another advantageous of using satellite remote sensing are land cover monitoring and detection at various scales to provide useful results (Wilson et al., 2003; Stefanov et al., 2001).

The present technology enable the integration of remote sensing and Geographical Information System (GIS) with Global Positioning System (GPS) allowing land use change detection and assessment become more effective (Muller and Zeller, 2002; Weng, 2002). The technique of mapping urban areas as source of data for modelling and urban growth analysis as well as dynamic change detection in land use land cover was proven as very beneficial (Wilson et al., 2003; Herold et al., 2003; Stefanov et al., 2001).

Materials and methods

Study area

The study area is Sepang, Selangor, Malaysia located at 2°45'38"N and 101°44'15"E with a total coverage of 56150 km² and the main land use are: built-up areas, vegetation and open spaces (*Fig. 1a* and *b*). The population within 20 years from 1995 is approximately 90,000 and the number is rising up to 190,000 in 2015 (Statistical Department of Malaysia, 2015). Geographically it is in the southern part of Selangor, neighboring to the district of Hulu Langat in the northeast, district of Kuala Langat in the west, and Petaling in the north and also neighboring to District of Nilai, Negeri Sembilan and surrounding the federal territory and administrative capital of Putrajaya. The municipal administration office originally located in pekan Sepang, a very small town consists of not more than 3 shop houses at that time. When the Kuala Lumpur International Airport (KLIA) was officially inaugurated in 1998, the office was moved to Salak Tinggi. For a second time, after Putrajaya was established and become the new administrative capital of Malaysia, the municipal was moved to Cyberjaya in 2008.

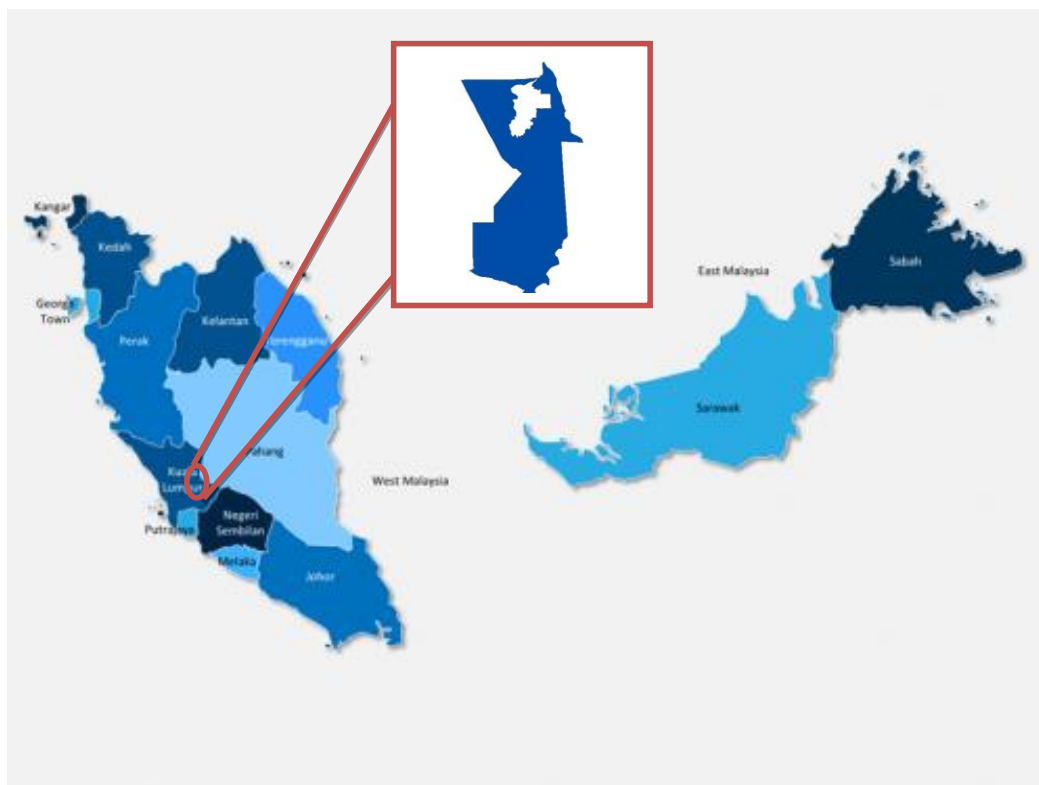
Primary data sources of Landsat thematic mapper (TM) and operational land imager (OLI) and thermal infrared sensor (TIRS)

Remotely sensed data was acquired from the United State Geological Survey (USGS) Earth Explorer for Landsat data of Thematic Mapper (TM) as well as

Operational Land Imager (OLI) and Thermal Infrared Sensor (TIRS). Supported by Landsat data, the boundary of Sepang district, Malaysia is based on the Department of Survey and Mapping Malaysia (JUPEM), which is important for abstracting process on the raw map using Area of Interest (AOI) technique in mapping procedures. The details on primary satellite data can be shown in *Table 1*.

Table 1. Primary satellite data of Landsat TM and OLI/TIRS

Sensors	Month/day	Year	Spatial resolution (m)	Time	Path/row	Band combination
Landsat TM	12/27	1990	30	10.30am	127/58	1,2,3,4,7
	11/25	1992	30	11.15am	127/58	
	11/28	1994	30	10.27am	127/58	
	06/26	1996	30	10.47am	127/58	
	02/08	1998	30	10.39am	127/58	
	03/17	2000	30	11.06am	127/58	
	05/02	2002	30	10.18am	127/58	
	12/23	2004	30	10.48am	127/58	
	03/02	2006	30	11.49am	127/58	
	07/29	2008	30	10.42am	127/58	
	01/02	2010	30	10.25am	127/58	
	06/04	2012	30	10.29am	127/58	
Landsat OLI/TIRS	03/24	2014	30	10.18am	127/58	2,3,4,5,7
	03/29	2016	30	11.13am	127/58	
	04/04	2018	30	10.30am	127/58	



a

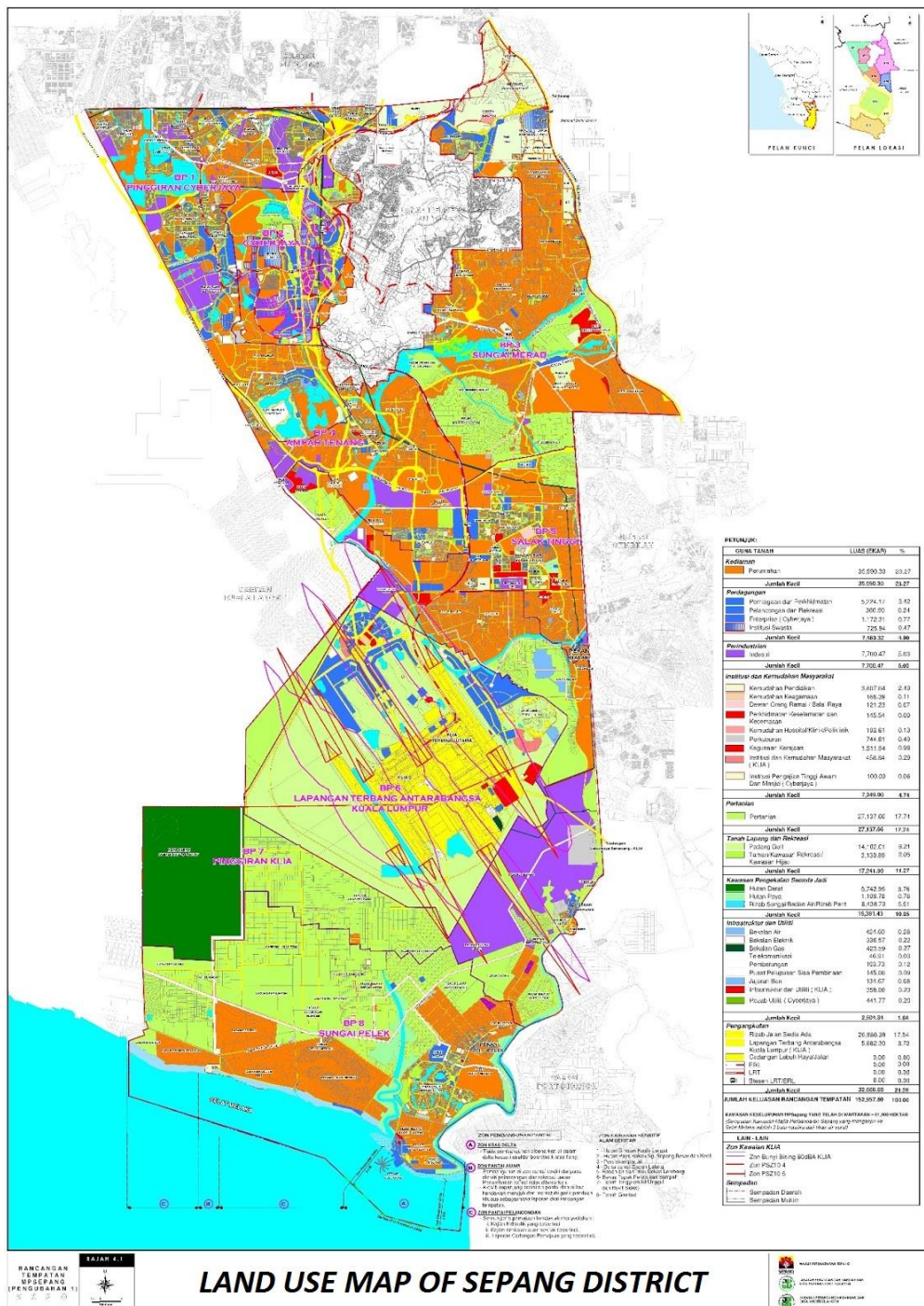


Figure 1. a Sepang district as study area in the research study. **b** The spatial distribution of Sepang District (Source: Sepang Municipal Council 2016)

Data preprocessing and land use/land cover classification

It is essential for a newly obtained time series of remotely sensed data to be preprocessed before any analytical process are made. First, using ArcGIS Ver. 10.1, the images have to go through pre-processing for geo-referencing, mosaicking, and sub

setting where only then, the specific area can be selected through Area of Interest (AOI) technique (Behera et al., 2012).

The main purposes to conduct preprocessing are to correct the sensor- and platform-specific radiometric and geometric distortions of data. This correction technique on the radiometric is required because of the variation in scene illumination and viewing geometry, atmospheric conditions, and sensor noise and responses. Fortunately, all satellite images obtained is cloud free or <10% cloud coverage (Tan et al., 2010). To avoid error and imprecise interpretation, the images for Landsat TM and OLI/TIRS were in original resolution of 30 m (*Table 1*).

Next, further processing for band combination of 3-2-1 in Landsat TM and 4-3-2 in Landsat OLI/TIRS are carried out in ArcGIS 10. Then classification of land use is conducted in ENVI Version 4.0. Classification was performed using Maximum Likelihood supervised using selected regions and Regions of Interest (ROI), which based on delineated classes of built-up area, vegetation area, water bodies, and open space area (*Table 2*). The built-up areas classes consists of residential, industrial, commercial, administration, cemetery and transportation, and sewage treatment plant. The vegetation classes consists of all forest and agricultural land, as well as open space whereby it include barren land. The final class is the water bodies which consists of rivers, lakes, stream, canals and reservoirs.

Table 2. Land use classification based on maximum likelihood supervised techniques

Land use class	Definition
Built up area	Includes all residential, industrial, commercial, administration, cemetery and transportation, and sewage treatment plant
Vegetation area	Includes all forest field and agricultural lands
Water bodies	Includes all water bodies (river, lakes, gravels, stream, canals, and reservoirs)
Open space area	Includes all land area that are in soil and barren area due to the human activities

Accuracy assessment

It is compulsory to conduct accuracy assessment of classified images from 1990 to 2018 (i.e. 15 images) to ensure accuracy, integrity and quality. Kappa tests are used to measure the accuracy of classification which have capability to test all confusion matrix of elements based on minimum requirement (Halmy et al., 2015). The Kappa tests can be measured based on the producer and user rating of assignment, which can be interpreted in formula as *Equation 1*:

$$K = \frac{P(A) - P(E)}{1 - P(E)} \quad (\text{Eq.1})$$

where, $P(A)$ is the total of k raters agree, and $P(E)$ is the total of k raters which expected to agree by chance (El-Kawy et al., 2011; Pontius and Millones, 2011). The accuracy of user can be explained as probability defined the pixel on image to represent a class on ground, while accuracy of producer is the probability pixel is correctly classified and usually it determine how good for particular area can be classified (Pontius and Millones, 2011). Therefore, four (4) classes had been set up earlier, whereby the delineated should be 50 points and above for each category to enhance the accuracy

assessment percentage (El-Kawy et al., 2011; Pontius and Malanson, 2005). So, the accuracy assessment for 1990, 1992, 1994, 1996, 1998, 2000, 2002, 2004, 2006, 2008, 2010, 2012, 2014, 2016, and 2018 are having the kappa value of 0.87, 0.84, 0.82, 0.83, 0.86, 0.88, 0.91, 0.80, 0.82, 0.82, 0.90, 0.86, 0.85, 0.84, and 0.91, respectively (Table 3a-o). Identified categories of LULC in accuracy assessment are considered achieved the required minimum, which is need to be at least 80% (Weng, 2010). Hence, the data can be exported into ENVI 4.0 for further analysis.

Table 3. a The accuracy assessment for 1990 of Sepang district

Class name (1990)	Reference total	Classified total	Number correct	Producers accuracy (%)	User accuracy (%)
Built up area	18	14	11	61.11	78.57
Vegetation area	558	560	557	99.82	99.46
Water bodies	0	4	0	0.00	0.00
Open space area	22	20	20	90.91	100.00

Overall classification accuracy = 98.33%; Kappa coefficient = 0.8654

Table 3. b The accuracy assessment for 1992 of Sepang district

Class name (1992)	Reference total	Classified total	Number correct	Producers accuracy (%)	User accuracy (%)
Built up area	245	148	120	48.98	81.08
Vegetation area	4182	4181	4179	99.93	99.95
Water bodies	50	63	38	76.00	60.32
Open space area	83	168	70	84.34	41.67

Overall classification accuracy = 96.64%; Kappa coefficient = 0.8357

Table 3. c The accuracy assessment for 1994 of Sepang district

Class name (1994)	Reference total	Classified total	Number correct	Producers accuracy (%)	User accuracy (%)
Built up area	277	183	126	45.49	68.85
Vegetation area	3717	3703	3667	98.65	99.03
Water bodies	90	89	89	98.89	100.00
Open space area	163	272	156	95.71	57.35

Overall classification accuracy = 95.08%; Kappa coefficient = 0.8217

Table 3. d The accuracy assessment for 1996 of Sepang district

Class name (1996)	Reference total	Classified total	Number correct	Producers accuracy (%)	User accuracy (%)
Built up area	778	927	497	63.88	53.61
Vegetation area	10102	9387	9383	92.88	99.96
Water bodies	162	603	158	97.53	26.20
Open space area	721	846	703	97.50	83.10

Overall classification accuracy = 94.31%; Kappa coefficient = 0.8279

Table 3. e The accuracy assessment for 1998 of Sepang district

Class name (1998)	Reference total	Classified total	Number correct	Producers accuracy (%)	User accuracy (%)
Built up area	3265	2702	2330	71.36	66.12
Vegetation area	8638	8329	8328	96.41	99.99
Water bodies	211	290	141	95.52	48.62
Open space area	199	992	152	94.38	80.82

Overall classification accuracy = 97.94%; Kappa coefficient = 0.8624

Table 3. f The accuracy assessment for 2000 of Sepang district

Class name (2000)	Reference total	Classified total	Number correct	Producers accuracy (%)	User accuracy (%)
Built up area	1581	1203	1059	91.98	88.03
Vegetation area	7541	7488	7484	99.24	99.95
Water bodies	104	437	100	96.15	88.22
Open space area	136	234	51	37.50	21.79

Overall classification accuracy = 95.86%; Kappa coefficient = 0.8758

Table 3. g The accuracy assessment for 2002 of Sepang district

Class name (2002)	Reference total	Classified total	Number correct	Producers accuracy (%)	User accuracy (%)
Built up area	1654	1646	1594	96.37	96.84
Vegetation area	5776	5675	5630	97.47	99.21
Water bodies	215	275	137	63.72	49.82
Open space area	115	164	107	93.04	65.24

Overall classification accuracy = 96.24%; Kappa coefficient = 0.9080

Table 3. h The accuracy assessment for 2004 of Sepang district

Class name (2004)	Reference total	Classified total	Number correct	Producers accuracy (%)	User accuracy (%)
Built up area	1982	1701	1581	79.77	92.95
Vegetation area	6654	6642	6533	98.18	98.36
Water bodies	207	54	11	5.31	20.37
Open space area	79	525	63	79.75	12.00

Overall classification accuracy = 92.77%; Kappa coefficient = 0.8025

Table 3. i The accuracy assessment for 2006 of Sepang district

Class name (2006)	Reference total	Classified total	Number correct	Producers accuracy (%)	User accuracy (%)
Built up area	1489	1072	1072	71.99	80.60
Vegetation area	4914	4725	4725	96.15	100.00
Water bodies	116	477	97	83.62	20.34
Open space area	303	290	187	61.72	64.48

Overall classification accuracy = 93.14%; Kappa coefficient = 0.8156

Table 3. j The accuracy assessment for 2008 of Sepang district

Class name (2008)	Reference total	Classified total	Number correct	Producers accuracy (%)	User accuracy (%)
Built up area	2149	1813	1517	70.59	83.67
Vegetation area	6312	6045	5975	94.66	90.84
Water bodies	241	245	111	46.06	45.31
Open space area	113	712	105	92.92	88.81

Overall classification accuracy = 90.44%; Kappa coefficient = 0.8225

Table 3. k The accuracy assessment for 2010 of Sepang district

Class name (2010)	Reference total	Classified total	Number correct	Producers accuracy (%)	User accuracy (%)
Built up area	3073	2926	2835	92.26	96.89
Vegetation area	5169	5096	5044	97.58	98.98
Water bodies	145	124	97	66.90	78.23
Open space area	65	306	64	98.46	80.92

Overall classification accuracy = 95.13%; Kappa coefficient = 0.9034

Table 3. l The accuracy assessment for 2012 of Sepang district

Class name (2012)	Reference total	Classified total	Number correct	Producers accuracy (%)	User accuracy (%)
Built up area	2743	2473	2379	86.73	96.20
Vegetation area	5228	5134	5075	97.07	98.85
Water bodies	145	243	135	93.10	55.65
Open space area	135	401	97	71.85	24.19

Overall classification accuracy = 93.15%; Kappa coefficient = 0.8643

Table 3. m The accuracy assessment for 2014 of Sepang district

Class name (2014)	Reference total	Classified total	Number correct	Producers accuracy (%)	User accuracy (%)
Built up area	3829	3172	2943	76.86	92.78
Vegetation area	3156	2995	2934	92.97	97.96
Water bodies	155	289	152	98.06	52.60
Open space area	318	1002	311	97.80	31.04

Overall classification accuracy = 95.01%; Kappa coefficient = 0.8523

Table 3. n The accuracy assessment for 2016 of Sepang district

Class name (2016)	Reference total	Classified total	Number correct	Producers accuracy (%)	User accuracy (%)
Built up area	4095	3635	3464	84.59	95.30
Vegetation area	5672	5445	5442	95.94	99.94
Water bodies	229	355	226	98.69	87.66
Open space area	150	711	107	71.33	50.05

Overall classification accuracy = 91.06%; Kappa coefficient = 0.8385

Table 3. o The accuracy assessment for 2018 of Sepang district

Class name (2018)	Reference total	Classified total	Number correct	Producers accuracy (%)	User accuracy (%)
Built up area	2158	2155	1992	92.31	92.44
Vegetation area	4978	4885	4851	97.45	99.30
Water bodies	108	120	108	100.00	90.00
Open space area	337	421	299	88.72	71.02

Overall classification accuracy = 95.63%; Kappa coefficient = 0.9115

Analysis of change detection in land use land cover

In LULC change detection, post-classification detection technique is proposed in this study using ENVI 4.0, where two classified images were compared to provide the information of changes on the pixel basis. In other words, these two images were interpreted to produce the changes “from- to” information. A 30 × 30 m to ground resolution of Landsat TM and Landsat OLI/TIRS were resampled and geo-rectified based on WGS84 UTM with RMSE less than 0.5 pixels were projected. Then, classified images based on two comparisons of data sets using cross-tabulation to determine the qualitative and quantitative changes for the periods from 1990 to 2018. The frequency and percentage of changes can be calculated according to simple formula as *Equations 2* and *3*:

$$K = F - I \quad (\text{Eq.2})$$

$$A = \frac{(F-I)}{I} \times 100 \quad (\text{Eq.3})$$

where, K is the magnitude of changes, A is the percentage of changes, F is the first data, and I is the references data (Mahmud and Achide, 2012). This research study uses LULC methods to map the urban sprawl by determine the differences of land use changes and to explain the percentages changes within the period of time.

Normalized difference vegetation index (NDVI)

Normalized difference vegetation index (NDVI) is measuring the vegetation through quantifies between near-infrared of differences (which refer to the stronger reflected light by vegetation) and red light (which refer to the light that absorbs by vegetation). The NDVI value is ranges from -1 to 1, but it is no exact boundary line between each type of land cover. For instance, when the value is negatives, which showing the pixel are in water coverage; meanwhile the value that close to +1, then the result are having high possibility of green leaves surrounding the area. Nevertheless, when the value of NDVI is close to zero, then the land use indicates no green leaves and probably showing an urbanized area. The NDVI can be interpreted into formula as *Equation 4*:

$$NDVI = \frac{(NIR-RED)}{(NIR+RED)} \quad (\text{Eq.4})$$

where, NIR - RED and NIR + RED indicate the surface reflectance averaged over ranges of wavelengths in the visible of red ($\lambda \sim 0.6 \mu\text{m}$) and near infrared, IR ($\lambda \sim 0.8 \mu\text{m}$),

respectively. In other words, NDVI is a standardized way to measure the healthy vegetation. When the NDVI value is higher, then the healthier is the vegetation at the study area.

Normalized difference built-up index (NDBI)

Having similar with NDVI, the normalized difference built-up index (NDBI) is used to measured the build-up area through quantifies between differences of short-wave infrared (SWIR) and near-infrared (NIR). The NDBI value is ranges from -1 to 1, whereby the negative value showing the pixel are non-built-up coverage area; meanwhile the positive value are having high possibility of built-up area surrounding the environment. The NDBI can be expressed into formula as *Equation 5*:

$$NDBI = \frac{(SWIR - NIR)}{(SWIR + NIR)} \tag{Eq.5}$$

where, SWIR – NIR and SWIR + NIR can be defined as surface reflectance averaged over ranges of wavelengths in the short infrared ($\lambda \sim 0.7 \mu\text{m}$) and near infrared ($\lambda \sim 0.8 \mu\text{m}$). When the NDBI value is higher, this circumstances indicate the study area is clustered with highly built-up activities within surrounding area.

Results and discussion

According to *Table 4*, the result indicated the density of LULC changes from 1990 to 2018 with four classes: built-up area, vegetation area, water bodies, and open space area (*Fig. 2*). Except in year 1992, the built-up area (BUA) class is observed to have continuously increase for 25 years. The percentage of increment is about 25.4% from 1990 to 2018. The study concluded that BUA classes are considered having the most increment due to rapid urbanization and population growth. It is followed by OSA class from 1990 to 2004 with an increment of 4.75% in average but beginning to decrease by 18.5% in the next 13 years. In other words, majority OSA class has gain benefit from the vegetation area (VA), and the most open space is suspected to change into BUA and/or other classes. Vegetation Area (VA) class consistently decreasing from 1990 to 2018 (*Fig. 3*) by 64.33%. This amount to 36123.07 ha of land. Except for waterbodies which has not seen any significant change, this uppermost land use changes is due to high demand in BOA to cater with population need and demand for residential-industrial-commercial activities as well as transportation facilities.

Table 4. Change of the LULC density classes from 1990 to 2018

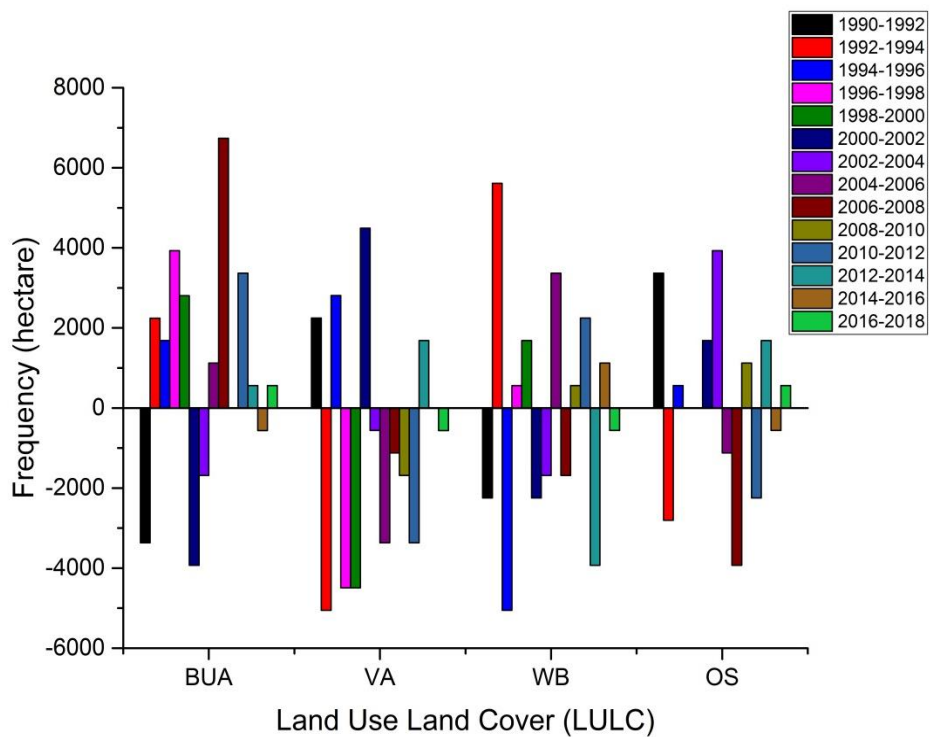
LULC density classes	1990		1992		1994		1996		1998		2000		2002		2004	
	Ha	%	Ha	%	Ha	%	Ha	%	Ha	%	Ha	%	Ha	%	Ha	%
BUA	8423	15	5054	9	7299	13	8984	16	12915	23	15722	28	11792	21	10107	18
VA	43235	77	45481	81	40428	72	43236	77	38743	69	34251	61	38743	69	38182	68
WB	3931	7	1685	3	7299	13	2246	4	2808	5	4492	8	2246	4	562	1
OSA	561	1	3930	7	1124	2	1684	3	1684	3	1685	3	3369	6	7299	13

	2006		2008		2010		2012		2014		2016		2018		
	Ha	%	Ha	%	Ha	%	Ha	%	Ha	%	Ha	%	Ha	%	
BUA	11230	20	17968	32	17968	32	21337	38	21899	39	21337	38	21898	39	
VA	34813	62	33690	60	32006	57	28637	51	30321	54	30321	54	29759	53	
WB	3931	7	2246	4	2807	5	5053	9	1123	2	2246	4	1685	3	
OSA	6176	11	2246	4	3369	6	1123	2	2807	5	2246	4	2808	5	





Figure 2. The LULC change from 1990 to 2018 in Sepang district



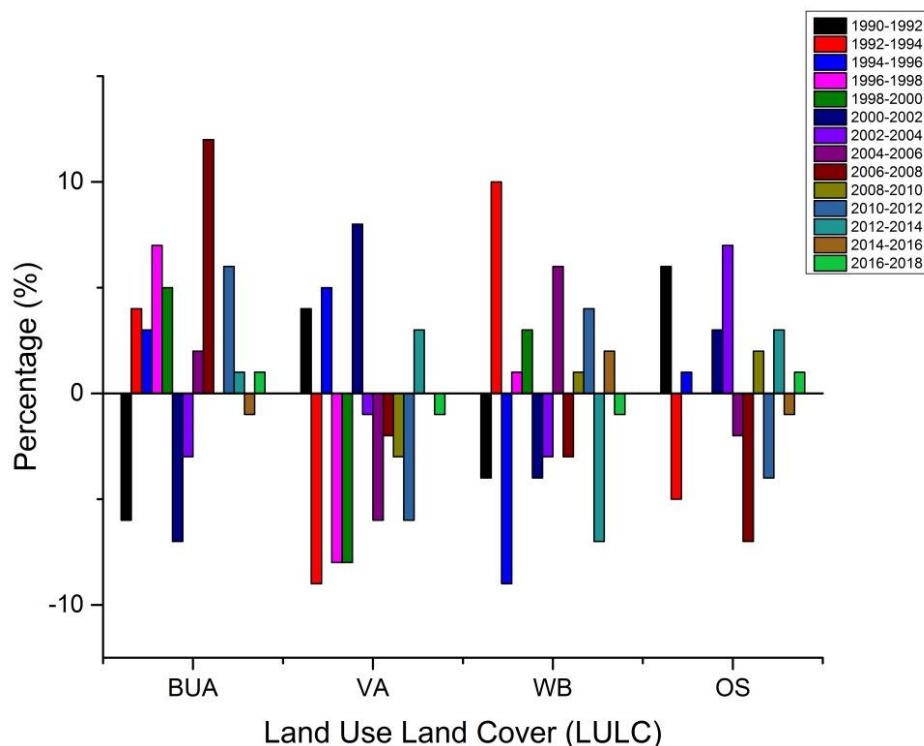


Figure 3. The comparison of areas and rate of changes in LULC classes between each two years from 1990 to 2018

Combining LULC change with Normalized Difference Vegetation Index (NDVI) and Normalized Difference Built-up Index (NDBI) techniques is considered recent and novelty. An NDVI is an equation that takes into account the amount of infrared reflected by plants. In classification process, supervised classification method based maximum likelihood algorithm was employed for NDVI, which is based on a set of user-defined classes and training areas through creating appropriate spectral signatures from Landsat TM and OLI/ TIRS. The result of changes of NDVI density classes for 25 years indicated that the vegetation index gradually reduced about 27.91% from year 1990 to year 2010, but the value sustained about 28.75% for the next 8 years from 2010 onwards (see Table 5).

Table 5. Change of the NDVI density classes from 1990 to 2018

NDVI density classes	1990		1992		1994		1996		1998		2000		2002		2004	
	Ha	%	Ha	%	Ha	%	Ha	%	Ha	%	Ha	%	Ha	%	Ha	%
H	17407	31	13476	24	16845	30	15161	27	17968	32	15161	27	16284	29	12353	22
M	22460	40	29198	52	36498	65	26390	47	37621	67	30321	54	13476	24	23583	42
L	16283	29	13476	24	2807	5	14599	26	561	1	10668	19	26390	47	20214	36
	2006		2008		2010		2012		2014		2016		2018			
	Ha	%	Ha	%	Ha	%	Ha	%	Ha	%	Ha	%	Ha	%		
H	11792	21	11230	20	15161	27	15722	28	12915	23	11230	20	14599	26		
M	29759	53	28637	51	23021	41	23583	42	29198	52	16845	30	25829	46		
L	14599	26	16283	29	17968	32	16845	30	14037	25	28075	50	15722	28		

In other words, the higher the value of index, indicated the healthier the vegetation would be. Therefore, the value constantly changing due to the majority of vegetation classes are subjected to transform to open space and built-up classes. The pattern of vegetation classes derived from NDVI density (see Fig. 4) were predominantly the main land use class in year 1990 to 1994. Beginning 1996 onwards, patches of other classes spread across Sepang starting to gradually increase year by year. This was interpreted as an encroachment and an environmental degradation of forest, farm and cropland and further reducing agricultural productive land. The encroachment of these land uses, the environmental degradation and reduced in agricultural productivities are among the characteristic of urban sprawl defined earlier in this study.



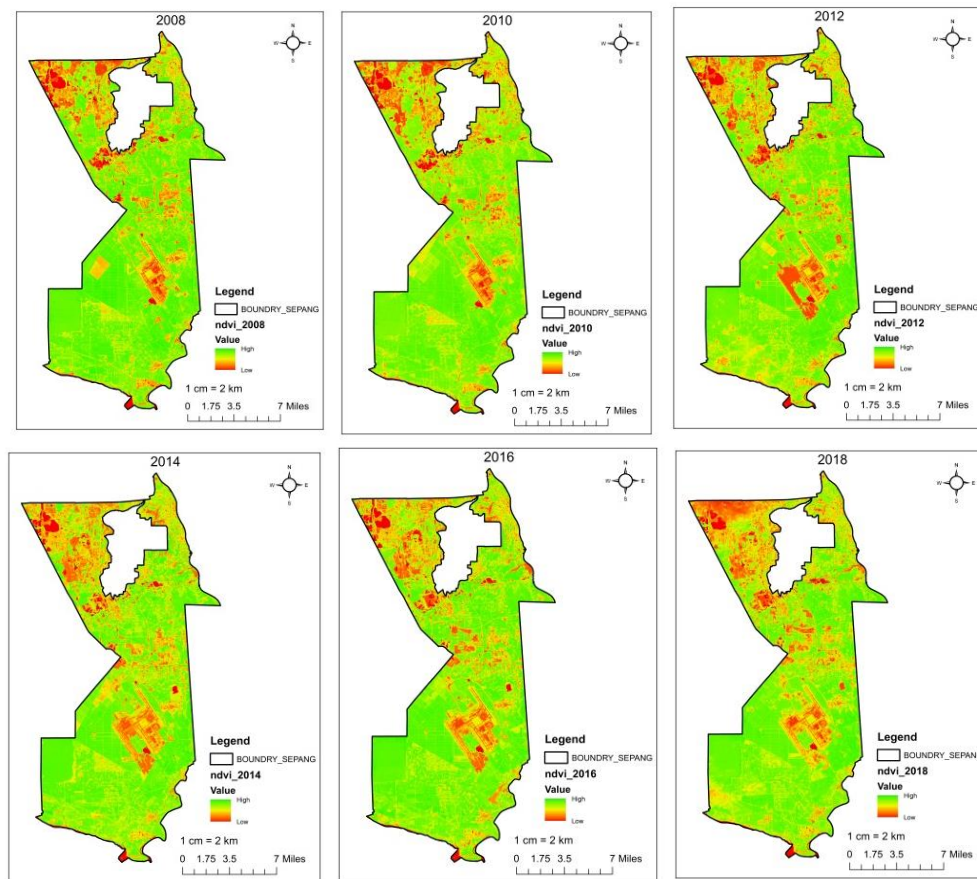


Figure 4. The NDVI density from 1990 to 2018 in Sepang district

A Normalized Difference Built-up Index (NDBI) is an arithmetic manipulation of NDVI except it is used for mapping built-up areas. The result of changes of index of very-high and high of NDBI density classes for 25 years indicated inconsistent of ups and downs of built-up classes. In contrarily, the result of changes of index of medium-and-low of NDBI indicated a consistent decreased throughout the longitudinal study. This is due to the fact that the highly demand for development on land use purposes will eventually cause an increasing in building index and reducing in vegetation index (Ewing and Hamidi, 2014). The pattern of built-up classes derived from NDBI density (see Fig. 5) was not the primary land use in early years. However, as early as the beginning of the longitudinal study, the built-up classes were already shown a sign of leapfrog, low density and scattered with polycentric development. Increased in built-up classes are necessary result in increase of impervious surface which effect water quality and increased of runoff water. By interpretation, Sepang has no specific urban growth boundary. Sepang was also part of Greater Kuala Lumpur with greater number of populations to reside in suburban areas. To add to the scenario, Putrajaya was rapidly growing at beginning of mid-1990s and continuously to do so, while Cyberjaya which also located within Sepang was the special economic corridor. Thus, Sepang was critically sprawled; backed with all the sprawl pattern – leapfrog, low density and scattered development; without any urban growth boundary; formed an urban environmental degradation, become the overpopulated suburban living for Putrajaya and Cyberjaya; and houses mass population for Greater Kuala Lumpur.



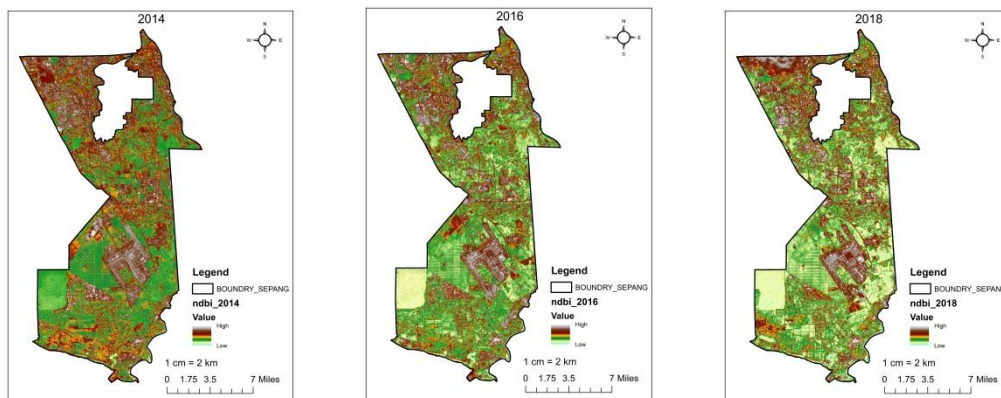


Figure 5. The NDBI density from 1990 to 2018 in Sepang district

Conclusion

Urbanization and rapid population growth are a major cause of land use changes and land conversions. It is essential in change detection to determine what type of land classes has change and the rate of change. Analyzing the spatial change with temporal aspects of urban growth can contribute to an effective planning and mitigate urban sprawl. Through this study, the urban expansion of Sepang over different period using time-series LULC and NDVI variation was achieved. The classification was able to clearly distinguished built-up area, vegetation area, water bodies, and open space. Land use land cover change detection showed an increased percentage of built-up area and open space, while reduce vegetation area. Only waterbodies had not shown any significant change. An NDVI quantified a steady declined of vegetation classes. The pattern of vegetation derived from NDVI density showed an encroachment and an environmental degradation of forest, farm and cropland and further reducing agricultural productive land. This is urban sprawl by definition. On the contrary, NDBI indicated inconsistent of ups and downs of built-up classes. However, the pattern of vegetation derived from NDBI density indicated urban sprawl patterns, urban sprawl characteristics and are associated with urban sprawl causes. Thus, the study proved urbanization and rapid population growth has caused urban sprawl to Sepang.

REFERENCES

- [1] Abdullah, J. (2012): City competitiveness and urban sprawl: their implications to socioeconomic and cultural life in Malaysian cities. – *Procedia-Social and Behavioral Sciences* 50: 20-29.
- [2] Barnes, K. B., Morgan III, J. M., Roberge, M. C., Lowe, S. (2001): *Sprawl Development. Its Patterns, Consequences and Measurement. A white paper.* – Towson University, Maryland.
- [3] Behera, D. M., Borate, S. N., Panda, S. N., Behera, P. R., Roy, P. S. (2012): Modelling and analyzing the watershed dynamics using Cellular Automata (CA)–Markov model–A geo-information based approach. – *Journal of Earth System Science* 121(4): 1011-1024.
- [4] Burchell, R. W., Lowenstein, G., Dolphin, W. R., Galley, C. C., Downs, A., Seskin, S., Gray Still, K., Moore, T. (2002): *Costs of Sprawl-2000. Transportation Cooperative Research Program, Report 74.* – National Academic Press, Washington, DC.

- [5] Bussauw, K. (2012): Challenges, threats and opportunities in post-conflict urbandevelopment in Kosovo. – *Habitat International* 36: 143-151.
- [6] El Garouani, A., Mulla, D. J., El Garouani, S., Knight, J. (2017): Analysis of urban growth and sprawl from remote sensing data: Case of Fez, Morocco. – *International Journal of Sustainable Built Environment* 6(1): 160-169.
- [7] El-Kawy, O. A., Rød, J. K., Ismail, H. A., Suliman, A. S. (2011): Land use and land cover change detection in the western Nile delta of Egypt using remote sensing data. – *Applied Geography* 31(2): 483-494.
- [8] Ewing, R., Hamidi, S. (2014): Measuring urban sprawl and validating sprawl measures. Technical Report Prepared for the National Cancer Institute, National Institutes of Health, the Ford Foundation, and Smart Growth America. – Smart Growth America, Washington, DC.
- [9] Halmy, M. W. A., Gessler, P. E., Hicke, J. A., Salem, B. B. (2015): Land use/land cover change detection and prediction in the north-western coastal desert of Egypt using Markov-CA. – *Applied Geography* 63: 101-112.
- [10] Herold, M., Goldstein, N. C., Clarke, K. C. (2003): The spatiotemporal form of urban growth: measurement, analysis and modeling. – *Remote Sensing of Environment* 86(3): 286-302.
- [11] Hua, A. K., Ping, O. W. (2018): The influence of land-use/land-cover changes on land surface temperature: a case study of Kuala Lumpur metropolitan city. – *European Journal of Remote Sensing* 51(1): 1049-1069.
- [12] Hua, A. K. (2017a): Application of Ca-Markov model and land use/land cover changes in Malacca River Watershed, Malaysia. – *Applied Ecology and Environmental Research* 15(4): 605-622.
- [13] Hua, A. K. (2017b): Land use land cover changes in detection of water quality: a study based on remote sensing and multivariate statistics. – *Journal of Environmental and Public Health*. <https://doi.org/10.1155/2017/7515130>.
- [14] Hua, A. K. (2018): SPATIAL-temporal analysis of pattern changes and prediction in Penang Island, Malaysia using LULC and CA-Markov model. – *Applied Ecology and Environmental Research* 16(4): 4619-4635.
- [15] Lu, D., Mausel, P., Brondizio, E., Moran, E. (2004): Change detection techniques. – *International Journal of Remote Sensing* 25(12): 2365-2401.
- [16] Mahmud, A., Achide, A. S. (2012): Analysis of land use/land cover changes to monitor urban sprawl in Keffi-Nigeria. – *Environmental Research Journal* 6(2): 129-134.
- [17] Mohd Noor, N., Alias, A., Mazlan, H., Zainora, M. A. (2012): Managing Urban Land In Developing Countries Using GIS And Remote Sensing: Towards Resilient Cities. – Department of Urban and Regional Planning, IIUM, Gombak, Malaysia.
- [18] Muller, D., Zeller, M. (2002): Land use dynamics in the central highlands of Vietnam: a spatial model combining village survey data with satellite imagery interpretation. – *Agricultural Economics* 27(3): 333-354.
- [19] Noor, N. M., Rosni, N. A. (2013): Determination of spatial factors in measuring urban sprawl in Kuantan using remote sensing and GIS. – *Procedia-Social and Behavioral Sciences* 85: 502-512.
- [20] Nuissl, H., Rink, D. (2005): The “Production” of urban sprawl in Eastern Germany as a phenomenon of post-socialist transformation. – *Cities* 22: 123-134.
- [21] Peiser, R. B. (2001): Decomposing urban sprawl. – *Town Planning Review* 72(3): 275-298.
- [22] Pontius, G. R., Malanson, J. (2005): Comparison of the structure and accuracy of two land change models. – *International Journal of Geographical Information Science* 19(2): 243-265.
- [23] Pontius Jr, R. G., Millones, M. (2011): Death to Kappa: birth of quantity disagreement and allocation disagreement for accuracy assessment. – *International Journal of Remote Sensing* 32(15): 4407-4429.

- [24] Squires, G. D. (Ed.) (2002): *Urban Sprawl: Causes, Consequences and Policy Responses*. – The Urban Institute Press, Washington, DC.
- [25] Statistical Department of Malaysia (2015): *Population and Housing Census 2015*. – Department of Statistic Malaysia, Putrajaya.
- [26] Sepang Municipal Council (2016). *Sepang Local Plan 2020 (Amendment 1)*. Retrieved from <http://www.mpsepang.gov.my/en/main>
- [27] Statistical Department of Malaysia (1992): *Population and Housing Census 1991*. – Department of Statistic Malaysia, Putrajaya.
- [28] Stefanov, W. L., Ramsey, M. S., Christensen, P. R. (2001): *Monitoring urban land cover change: An expert system approach to land cover classification of semiarid to arid urban centers*. – *Remote Sensing of Environment* 77(2): 173-185.
- [29] Tan, K. C., San Lim, H., MatJafri, M. Z., Abdullah, K. (2010): *Landsat data to evaluate urban expansion and determine land use/land cover changes in Penang Island, Malaysia*. – *Environmental Earth Sciences* 60(7): 1509-1521.
- [30] Tehrany, M. S., Pradhan, B., Jebur, M. N. (2013): *Remote sensing data reveals eco-environmental changes in urban areas of Klang Valley, Malaysia: contribution from object based analysis*. – *Journal of the Indian Society of Remote Sensing* 41(4): 981-991.
- [31] Weng, Q. (2002): *Land use change analysis in the Zhujiang Delta of China using satellite remote sensing, GIS and stochastic modelling*. – *Journal of Environmental Management* 64(3): 273-284.
- [32] Weng, Q. H. (2010): *Remote Sensing and GIS Integration*. – McGraw-Hill, New York.
- [33] Wilson, E. H., Hurd, J. D., Civco, D. L., Prisloe, M. P., Arnold, C. (2003): *Development of a geospatial model to quantify, describe and map urban growth*. – *Remote Sensing of Environment* 86(3): 275-285.
- [34] Yue, M.-Y. (2011): *Rethinking Asian cities and urbanization: four transformations in four decades*. – *Asian Geographer* 28(1): 65-83.

REMOVING ARSENIC, COPPER AND IRON FROM SEWAGE SLUDGE WITH REED (*Phragmites australis*)

CORTÉS-TORRES, C.¹ – BARRIENTOS-LOZANO, L.¹ – ALMAGUER-SIERRA, P.¹ – ROSAS-MEJÍA, M.² – ROCANDIO-RODRÍGUEZ, M.² – ALARCÓN, A.^{3*} – MORA-RAVELO, S. G.^{2*}

¹*División de Estudios de Posgrado e Investigación, Tecnológico Nacional de México-Instituto Tecnológico de Cd. Victoria, Blvd. Emilio Portes Gil No. 1301, 87010 Cd. Victoria, Tamaulipas, México*

²*Universidad Autónoma de Tamaulipas, Instituto de Ecología Aplicada, Av. División del Golfo núm. 356, Col. Libertad, 87019 Cd. Victoria, Tamaulipas, México*

³*Colegio de Postgraduados, Carretera México-Texcoco km.36.5, Montecillo, Texcoco 56230, Edo de México, México*

*Corresponding authors

e-mail: sgmora@docentes.uat.edu.mx; alexala@colpos.mx

(Received 2nd Jan 2019; accepted 28th Feb 2019)

Abstract. Agriculture can use the sewage sludge resulting from wastewater treatment. In order to use sewage sludge, it is necessary to eliminate the content of toxic pollutants, including heavy metals through phytoremediation. The purpose of this research work was to assess the capacity of *Phragmites australis* to remove As, Cu and Fe in wastewater sludge of the municipal treatment plant in Cd. Victoria, Tamaulipas. We established four treatments: T1 = sewage sludge + soil + *Phragmites australis*; T2 = sewage sludge + soil; T3 = Sludge + *Phragmites australis*; T4 = Check test. Each treatment had six replicates. The phytoremediation process lasted eight months. We took monthly samples from the substrate and samples of *P. australis* every four months to determine the contents of As, Fe and Cu. The sludge + soil + *P. australis* treatment was able to remove higher percentages of Fe (96.63%) and Cu (47.67%); while sludge + *P. australis* was able to remove higher percentage of arsenic (81.18%), with a bio-concentration factor of 7.76. The amount of metals removed from the substrates from highest to lowest were: Fe > Cu > As. Furthermore, the final concentration of Fe, Cu and Arsenic in the sludge was below the allowable limit established by NOM-004- SEMARNAT-2002 Standard.

Keywords: *bio-concentration factor, heavy metals, Phytoremediation, translocation factor*

Introduction

Wastewater treatment is a worldwide strategy to recover water contaminated by residential and industrial use. The process does not only produce treated water, but also suspended solids known as sewage sludge or bio-sludge (Jing et al., 2017). Sewage sludge is treated and biologically stabilized to avoid harming living creatures and the environment. Once stabilized, sewage sludge turns into bio-solids used in fertilization, crop enhancement, forest remediation, composting and power generation (Castañeda et al., 2011; CRA, 2000).

Like other countries, Mexico has implemented wastewater treatment programs since 2008, including PROTAR (Wastewater Treatment Program), aiming to increase the volume of treated water and improve existing treatment processes. Thanks to these projects, the number of operating wastewater treatment plants in the country increased to 2447 by December 2015, representing an installed capacity of 177973.58 L s⁻¹. Nevertheless, those plants treat only 120902.20 L s⁻¹ of wastewater, leaving behind 2911234 t year⁻¹ of bio-solids (CONAGUA 2015). CONAGUA (2011) reported that

37% of the treated wastewater streams produce 640,000 to 10 million t year⁻¹ of bio-solids. This difference is because sometimes the quantity is reported in terms of dry weight and in other cases the moisture content is not even mentioned; so in fact, there is no official data regarding sewage sludge and bio-solids production, and therefore, the percentage of treated bio-sludge is very low.

Sewage sludge obtained from wastewater treatment does not only have a high level of nutrients, but also several pollutants, such as heavy metals. The presence of trace elements transforms sewage sludge in a source of environmental pollution. The gases released when the sludge breaks down produce a fetid odor coming from a large number of fecal coliforms, including some pathogens like *Salmonella spp.*, and elements that are toxic in high concentrations. It is therefore important to treat sewage sludge and eliminate, reduce or form compounds that will not harm living organisms and the environment (Rojas and Mendoza 2012).

Stabilizing sewage sludge from wastewater plants implies very high operating costs. Phytoremediation is a solution to this problem, offering an effective, low-cost *in situ* solution. Wetlands retain trace elements in a natural way, in particular *Typha latifolia* L. and *P. australis* Cav. Trin. (Salema et al., 2014).

The cost of conventional stabilization and reuse of sewage sludge is unaffordable at Cd. Victoria, Tamaulipas' wastewater treatment plant. Therefore, untreated sludge is disposed inside the plant facilities, becoming a source of environmental pollution. This research work is aiming to determine *Phragmites australis*' capacity to remove arsenic, copper and iron from sewage sludge produced by Ciudad Victoria, Tamaulipas' wastewater treatment plant.

Materials and methods

The experiment was conducted from May 2015 to January 2016 at the hydroponic module of Ciudad Victoria's Technology Institute (ITCV).

500 kg of untreated sewage sludge were collected at Cd. Victoria, Tamaulipas' wastewater treatment plant and taken to ITVC facilities to fill 19 kg-pots which were used as individual experimental units, using a 5-cm gravel bed for planting and propagating *P. australis*. We established four treatments, each one with six replicates; 24 experimental units in total (Table 1).

We collected *P. australis* spikes from San Marcos River banks, Cd. Victoria, Tamaulipas. We selected the thicker spikes with the largest number of nodes for propagation. We made diagonal cuts every three nodes, in order to propagate the cuttings in every experimental unit. We organized the experimental units at random and we planted three cuttings in each experimental unit, watering them with drinking water. The experiment lasted eight months under uncontrolled conditions at an average temperature of 26 °C. We took monthly samples of the substrate (30 g) close to the roots and we selected one plant per treatment every four months, to determine the concentration of As, Cu and Fe on the substrate and on *P. australis*. (The first sampling was in September).

Substrate characteristics

Table 1 shows the soil and sludge initial characteristics. The initial pH of soil and the sewage sludge was slightly acidic and had a small increase after mixing both substrates. As and Cu concentrations were lower than the maximum allowable limits of 41-

75 mg kg⁻¹ and 1500-4300 mg kg⁻¹ respectively in dry weight, according to NOM-004-SEMARNAT-2002 standard.

Table 1. Initial characteristics of the waste sludge, soil and the mixture of both substrates

Parameter	Sludge	Soil	Sludge + soil
As (mg kg ⁻¹)	1.61	0.283	1.893*
Cu (mg kg ⁻¹)	12.411	1.29	13.701*
Fe (mg kg ⁻¹)	656.365	5.839	662.204*
pH	6.780	6.750	6.990
CE (dS m ⁻¹)	4.360	1.855	1.030
PR (mV)	-50.2	-45.9	-39.7
MO (%)	5.414	1.083	1.963
Nt (%)	1.072	0.142	0.389
P (mg kg ⁻¹)	33.161	1.005	15.576
K (cmol ₍₊₎ kg ⁻¹)	0.189	0.492	0.082

CE = Electrical conductivity, Nt = total nitrogen, ORP = redox potential

*For the case of the mixture, the concentrations of As, Cu and Fe were not determined, so the value presented here is an approximation, based on the initial concentration of the metals in the waste sludge and the soil

Heavy metals' determination: We analyzed the substrate and *P. australis* samples to determine the content of metals using inductively coupled plasma atomic emission spectroscopy (ICP-OES Varian model 725-ES, Agilent, Mulgrave, Australia).

Data analysis

The bio-concentration factor (BFC) (Chandra, 2013), was calculated using Equation 1:

$$BFC = \frac{C_p}{C_i} \quad (\text{Eq.1})$$

where: C_i = initial metal concentration in the substrate, and C_p = metal concentration in the plant.

The translocation factor (TF) (Chandra, 2013) was determined by Equation 2:

$$TF = \frac{C_a}{C_r} \quad (\text{Eq.2})$$

where: C_a = metal concentration in aerial plant parts and C_r = metal concentration in plant roots.

pH and reduction-oxidation potential (PR) results were analyzed by linear regression, to determine their dependency. Metal concentrations in the substrates were submitted to repeated measures analysis of variance and Fisher's LSD test ($p < 0.05$). We analyzed metal concentrations, BCF and TF of the plants by discrimination functions, in order to determine the difference among these variables. Finally, we applied a canonical correlation to find the relation between metal concentrations in the plant and the

substrates. We conducted the statistical analysis of the variables with PROC REG, MIXED, DISCRIM and CANCORR procedures, using SAS software (2002) and Statistica, version 7.

Results

The high temperatures in Cd. Victoria 18.5–31 °C dehydrated the substrates, reducing their initial volume. We had to add 12 kg more of sewage sludge to the experimental units in June and September in order to maintain the ratios that were originally proposed for each treatment (we determined the concentration of As, Cu and Fe in the sludge before the addition). The sewage sludge added during those months had lower concentrations of the three metals, than the initial concentrations of As, Cu and Fe found in the original substrates used for the experimental units (*Table 2*).

Table 2. Concentration of As, Cu and Fe in waste sludge and irrigation water

Sample	As (mg kg ⁻¹)	Cu (mg kg ⁻¹)	Fe (mg kg ⁻¹)
Sludge initial	1.61	12.411	656.365
Sludge july	0.000001	1.01	318.032
Sludge september	0.000001	1.143	270.181
Water sample irrigation	0.034	0.088	0.021

Only two, out of three plants that we planted in the experimental units survived. During the eight months that the experiment lasted, the plants showed phenotypic differences. Plants with sludge + *P. australis* had more foliage in the aerial parts; while plants growing on the sludge and soil + *P. australis* mix were taller.

We measured the pH and the reduction-oxidation potential (PR) in the samples of each substrate, four months after planting. The pH increased from 6.7 to 8.3, and significant differences were found in the correlation of pH with time ($R^2 = 0.307$ and $p < 0.05$) and PR ($R^2 = 0.312$ and $p < 0.05$). This parameter changed from -39.7 to 101.4 (*Fig. 1*).

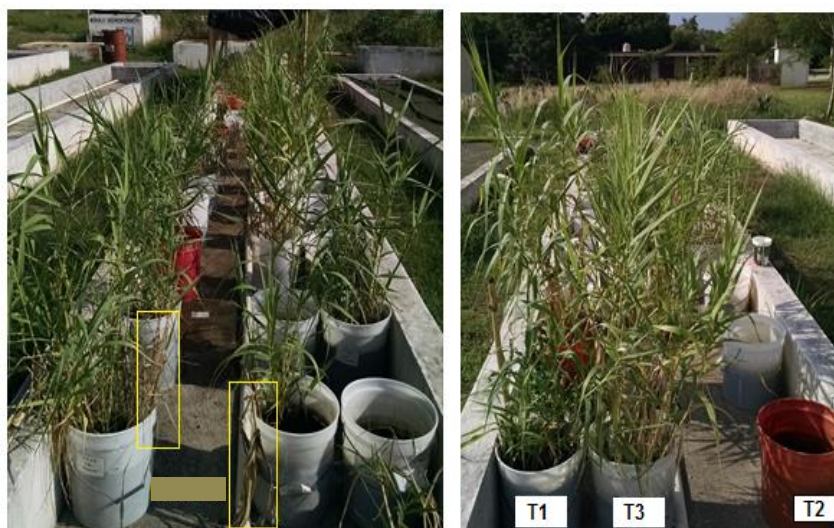


Figure 1. Plants of *P. australis* three months after sowing in the pots. T1 = sewage + soil + *P. australis*, T2 = sewage + soil, T3 = sewage + *P. australis*

We found significant differences in Arsenic concentration in the substrates throughout the eight months ($F = 2.43$ and $p < 0.05$). The higher concentration was in May, with 1.61 mg kg^{-1} and the lowest concentration was in November ($0.08 \pm 0.06 \text{ mg kg}^{-1}$). There were significant time differences among treatments ($F = 2.74$ and $p < 0.05$). In the second month (June) the sludge and soil + *P. australis* treatment had the highest concentration ($0.86 \pm 0.51 \text{ mg kg}^{-1}$), while the lowest concentration was found in October ($0.10 \pm 0.24 \text{ mg kg}^{-1}$). The sludge + soil treatment had the highest concentration in July ($0.44 \pm 0.38 \text{ mg kg}^{-1}$) and the lowest in November ($0.11 \pm 0.06 \text{ mg kg}^{-1}$). The sludge + *P. australis* treatment had the highest concentration in September ($0.56 \pm 0.46 \text{ mg kg}^{-1}$) and the lowest in November ($0.11 \pm 0.10 \text{ mg kg}^{-1}$). The check test (Sludge) had the highest concentration in August ($1.04 \pm 0.72 \text{ mg kg}^{-1}$) and the lowest in November ($0.08 \pm 0.05 \text{ mg kg}^{-1}$) (Fig. 2a). The sludge and soil + *P. australis* treatments, as well as the check test showed significant differences ($t = 0.74$ and $p = 0.0449$).

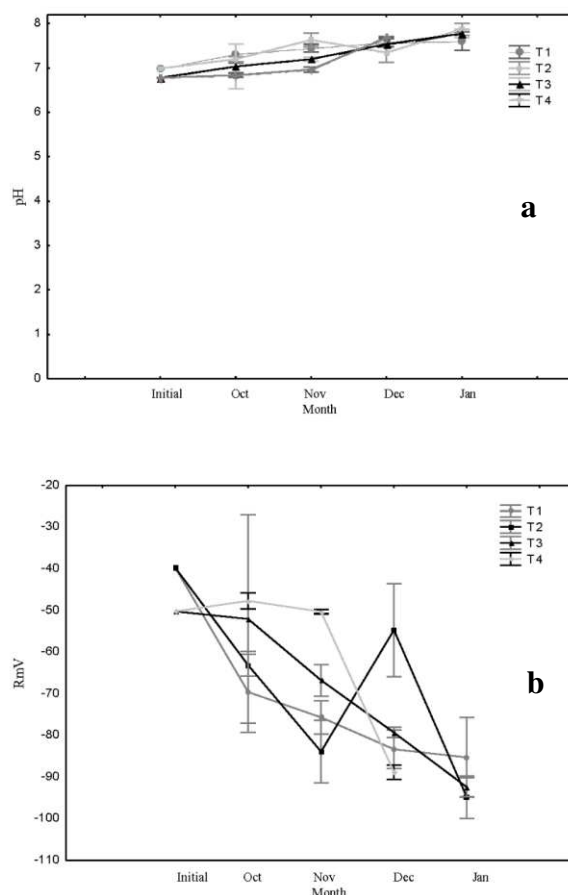


Figure 2. Average values of a) pH and b) PR with SD bars, during the last four months of the phytoremediation process, for the treatments, T1 = sewage + soil + *P. australis*, T2 = sewage + soil, T3 = sewage + *P. australis* and T4 = sewage, ($n = 6$) with confidence interval of ± 0.95

Cu concentration in all treatments had significant differences throughout the months ($F = 7.09$ and $p < 0.05$). The highest concentration was in May 12.41 mg kg^{-1} and the lowest was in December ($3.42 \pm 2.34 \text{ mg kg}^{-1}$). The treatments had significant time differences ($F = 3.06$ and $p < 0.05$), (Fig. 2b). LSD analysis showed that there are

significant differences in the sludge and soil + *P. australis* mix, and the check test ($t = 2.92$ and $p < 0.05$); as well as between the sludge + soil and the mix sludge and soil + *P. australis* ($t = 4.06$ and $p < 0.05$).

The mg kg^{-1} of Fe showed significant differences throughout the months ($F = 44.98$ and $p < 0.05$), with lower concentrations switching from one month to another, until reaching a final concentration (14.19 mg kg^{-1}) lower than the initial concentration ($656.36 \text{ mg kg}^{-1}$). There were also differences among treatments and among the months ($F = 13.25$ and $p < 0.05$), (Fig. 2c). LSD analysis proved that there were significant differences among the four treatments with $p < 0.05$.

The percentage of Arsenic removal from the substrates did not show significant differences among the months and the treatments ($F = 0.89$ and $F = 0.61$ respectively; $p \geq 0.05$). We defined a range of 73-83% in the eight months and in the four treatments. We found significant differences among the months for Cu removal percentage; however, there were no differences among the treatments ($F = 2.72$, $p < 0.05$; $F = 2.07$, $p \geq 0.05$). The treatments did not show significant differences on Fe removal percentage ($F = 3.38$, $p < 0.05$; $F = 2.98$, $p \geq 0.05$). We determined the overall removal percentage during the eight months in the four treatments, showing a higher value for Arsenic in the sludge + *P. australis* treatment, as well as for Cu and Fe in the mix of sludge and soil + *P. australis* (Table 3).

Table 3. Summary of the analysis of discriminant functions

% Removal	Treatment							
	SSP		SS		SP		S	
As	80.18	±3.74	80.78	±3.09	83.67	±9.08	73.67	±6.75
Cu	47.67	±10.41	31.08	±6.47	42.30	±11.75	23.11	±11.09
Fe	96.63	±2.32	87.15	±3.05	83.88	±4.64	76.48	±2.48

Accumulation of As, Cu and Fe in *P. australis*

Metal concentration in *P. australis* organs was the following: As: 0.07- 1.96, Cu: 0.92-28.7 and Fe: 121.13-10224.01 mg kg^{-1} in dry weight. The discrimination analysis found significant differences among the plant parts, regarding the accumulation of heavy metals [$F = 6.2994$, Wilks' Lambda = 0.00019, $p < 0.05$] (Table 4). We found differences in Arsenic concentration in the stem, and Cu concentration differences in the leaves (Fig. 3). There was a significant difference of $p = 0.1129$ at different times, in the sludge and soil + *P. australis* and sludge + *P. australis* mix treatments.

Estimated BCF values for Cu and Fe in the sludge and soil + *P. australis* and the sludge + *P. australis* mix treatments on September and January were greater than 1; while for As, the values were greater than 1 in September, and they were lower than 1 in January. TF for As was greater than 1 in the two samplings, on the sludge and soil + *P. australis* and sludge + *P. australis* mix treatments; while TF was below 1 for Cu and Fe (Table 5). BCF value was higher in Fe accumulation and lower in As with *P. australis*. The opposite happened with TF value, which was higher in Arsenic and lower in Fe (Fig. 4). Results of the discrimination function analysis showed that there were no significant differences among the months and the treatments regarding the BCF values for Cu and Fe ($F = 1.4780$, Wilks' Lambda = 0.15692, $p = 0.1697$). The only significant difference for BCF was Arsenic ($p < 0.001$) (Fig. 5).

Table 4. Summary of the analysis of discriminant functions

	Wilks'	Partial	F-remove	p-level
Root				
Cu	0.000726	0.261807	469.935	0.064384
Stem				
As	0.002895	0.065653	2.371.949	0.002196
Cu	0.000377	0.504194	163.894	0.293155
Fe	0.000456	0.417124	232.895	0.191443
Sheet				
As	0.000323	0.587784	116.884	0.408722
Cu	0.000598	0.317606	358.093	0.101736
Fe	0.000614	0.309561	371.730	0.095775

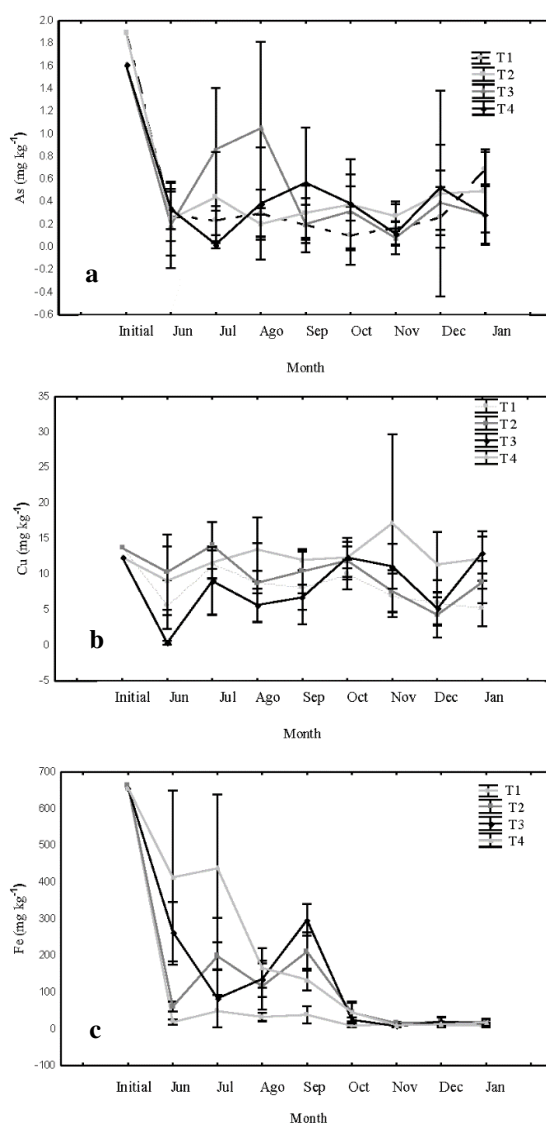


Figure 3. Variation in the concentrations of a) As, b) Cu and c) Fe, during the eight months of treatment. T1 = waste sludge + soil + *P. australis*, T2 = waste sludge + soil, T3 = waste sludge + *P. australis* and T4 = waste sludge, (n = 6), with a confidence interval of ± 0.95

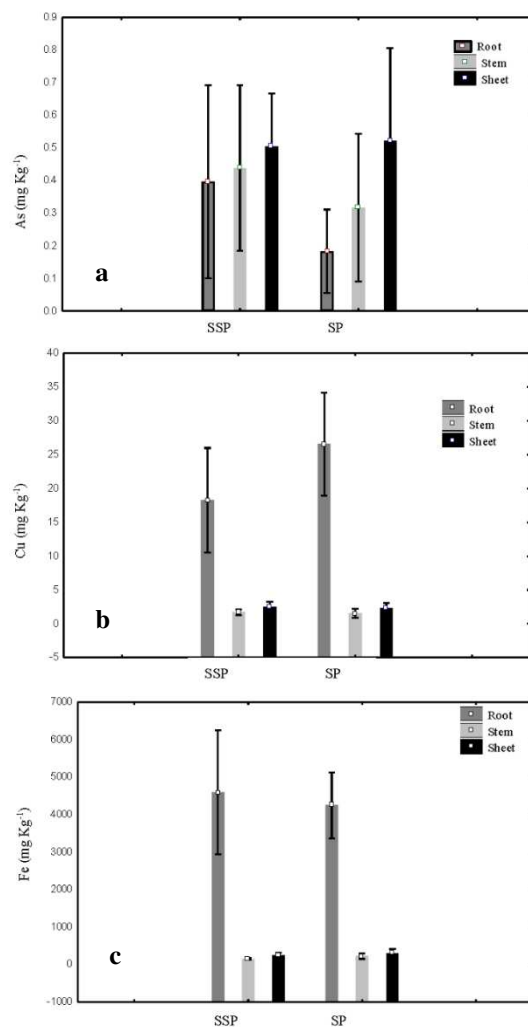


Figure 4. Concentration of the metals studied (mg kg^{-1}) in root, stem and leaf of *P. australis*, a) As, b) Cu and c) Fe. Bars represent the means \pm SD ($n = 6$).

Table 5. Mean values of the bioconcentration factor and the translocation factor for the SSP and SP treatments between months

Month	T	BCF						BF					
		As		Cu		Fe		As		Cu		Fe	
Sep	SSP	1.04	$\pm 0.33^{**}$	1.87	± 1.23	7.77	± 4.28	2.50	± 1.80	0.32	± 0.30	0.30	± 0.53
Sep	SP	1.07	$\pm 0.46^{**}$	2.32	± 0.42	6.93	± 1.69	5.25	± 2.46	0.22	± 0.10	0.15	± 0.06
Jan	SSP	0.34	$\pm 0.18^{**}$	1.41	± 0.44	7.31	± 3.95	9.15	± 2.09	0.28	± 0.15	0.11	± 0.06
Jan	SP	0.35	$\pm 0.11^{**}$	2.55	± 1.10	7.53	± 2.09	6.17	± 3.38	0.13	± 0.09	0.12	± 0.06

** $p < 0.001$

Canonical correlation among plants and substrates

Canonical correlation analysis was significant when we compared metal concentrations in plants versus metal concentration in the substrates ($R = 0.9659$,

$\chi^2 = 23.806$, $p = 0.4727$). Results showed a low correlation between metal concentrations in the plants versus the substrates (Table 6).

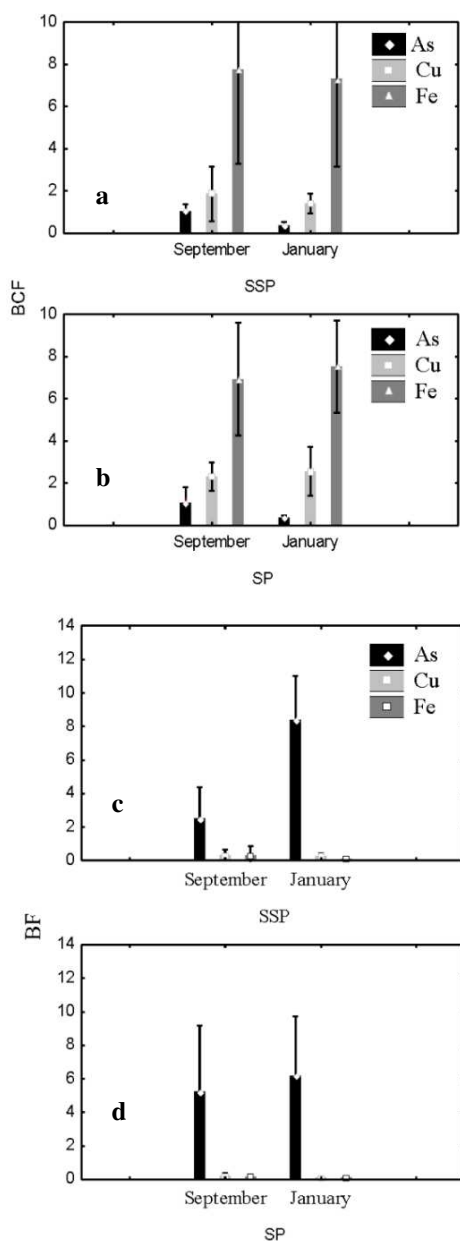


Figure 5. Bioconcentration factor of the metals studied for September and January a) SSP treatment; b) SP treatment Translocation factor of metals in aerial part/roots of the plant per month, c) SSP treatment and d) SP treatment Average ($n = 6$)

Table 6. Correlations between metals for plant and substrate

Plants	Substrates		
	As	Cu	Fe
As	0.378599	-0.218674	-0.358279
Cu	-0.632306	0.482277	0.547177
Fe	-0.240246	-0.224118	-0.408420

Discussion

General characteristics of plants during the phytoremediation process using P. australis

The optimal temperature range for *P. australis* plants is between 12–33 °C, according to Cooper (1996). However, in this essay, the plants were exposed to ambient temperature of 03–42 °C; exceeding by 8 °C the maximum value of said temperature. The temperature had an impact on the oldest leaves, which turned yellowish before wilting, a potential sign of heat stress (Yepes and Buckeridge, 2011). Although plants received consistent watering, the high temperatures affected the structure of substrates, leading to dehydration, compaction and low water availability (Paradelo, 2013).

Substrate characterization

pH was slightly acidic in every treatment, allowing the mobility and retention of As, Cu and Fe, since most metals have better availability at acidic pH (As, Ni, Cu, Fe, Pb) (Wilson et al., 2010; Bolan et al., 2014). Ansari et al. (2014) indicate that Cu solubility increases at pH = 5.5. In this case, the initial and final pH of substrates led to low solubility of Cu and Fe. Plants therefore showed a lower uptake of these metals (Pha et al., 2014); while As mobility increased at alkaline pH, as shown by the pH increase in the substrates, from 6.75 to 8.36 (Bolan et al., 2011). pH increases in this essay did not show significant differences among treatments. This pH increase was due to organic matter (MO) breakdown, the content of N in the sewage sludge, and the rainfall events where water leached some cations, afterwards replaced by acidic elements, such as iron (Valentín-Vargas et al., 2014).

PR is another property affecting metal bioavailability by changing the state of ions. PR value in this essay was low, allowing As, Fe and Cu to be available in the soil, at more soluble forms (Wilson et al., 2010; Bolan et al., 2014).

Heavy metal concentrations in initial substrates (As = 1.61, Cu = 12.411 and Fe = 656.365 mg kg⁻¹) did not exceed the values established by NOM-004-SEMARNAT-2002 (As = 41 and Cu = 1500 mg kg⁻¹). Nevertheless, it is important to minimize the metal content in sewage sludge, since metals have high capacity of bioaccumulation and biomagnification that increase their toxicity in trophic chains (Sabir et al., 2015; David et al., 2012).

Initial concentration of Arsenic in sewage sludge decreased from 1.61 to 0.345 mg kg⁻¹, which is equal to 79.57% removal. Sludge + *P. australis* treatment had the highest removal percentage (83.67%). Among the treatments of sludge and soil + *P. australis*; sludge and soil and sludge + *P. australis* there were no significant differences, indicating that *P. australis*, is not the only factor leading to Arsenic reduction in these treatments. These results were confirmed by the correlation analysis among plants and substrates, where we found a low correlation between the concentration of Arsenic in the substrate and Arsenic concentration in the plant (R = 0.37). However, we found significant differences between the treatment of sludge and soil + *P. australis* mix, and the Sludge treatment. Therefore, the type of substrate and the presence/absence of *P. australis* allowed us to determine that Arsenic removal was impacted by the reduction-oxidation potential; leaching during rainfall events and the mobility of Arsenic at the bottom of pots. The release of Arsenic particles depends on the formation of strong bonds between As particles and soil particles due to PR. In our case, soil aeration produced at low PR, led to a depletion of electron acceptors and the development of

anoxic conditions forming iron oxides and oxygen hydroxides requiring reduction and dissolution, minimizing the uptake of arsenic from the sludge solution where it can be leached (Elekes, 2014; Punshon et al., 2017).

Initial Cu concentration in sewage sludge decreased from 12.411 to 9.437 mg kg⁻¹, corresponding to an average removal percentage of 79.57%. The treatment of sludge and soil + *P. australis* mix showed a higher removal percentage of 47.67%. We observed significant differences among treatments, due to the type of substrate and the presence of *P. australis*. This is because alkaline pH affects trace elements like Cu, in terms of solubility and bioavailability of the element, besides transportation at soil level (Avci and Deveci, 2013). These results coincide with the reports of Torres et al. (2010), who used similar treatments to remove Cr with vetiver, finding that the most effective treatment was the plant + sewage sludge + organic manure. Canonical correlation was R = 0.482 when comparing Cu present in the substrates versus Cu present in the plants. This result explains the low removal percentage of Cu.

Likewise, in case of Fe, initial concentration of the sewage sludge decreased from 656.36 to 91.90 mg kg⁻¹, corresponding to an average removal percentage of 86.35%. Sludge and soil + *P. australis* mix treatment achieved the largest percentage of Fe removal (96.63%). We found significant differences among the four treatments, showing that in the case of Fe, the variables of plant and type of substrate (only sewage sludge or sludge and soil mix) had an impact on Fe removal. Canonical correlation indicated a low negative relation, when Fe decreased in the substrate, Fe increased in the plant (R = -0.408). However, the percentage of removal in substrates was high, maybe due to the leaching of Arsenic and the affinity to form iron sulfide under reduction conditions, such as the conditions found at test substrates. Other reasons might be a pH close to 7 and MO content, leading to low Fe solubility in the soil (Willscher et al., 2017).

Accumulation of As, Cu, Fe in P. australis

The test results showed significant differences among treatments (sludge and soil + *P. australis* mix and Sludge + *P. australis*) regarding Arsenic concentration in the stems and Cu concentration in the leaves. These results may imply that the type of substrate, pH, MO and PR can have an impact on the affinity of these elements towards specific plant organs (Willscher et al. 2017). We found significant differences in metal concentrations along the time, for the sludge and soil + *P. australis* mix (As = 1.96 to 0.65 mg kg⁻¹, Cu = 25.56 to 14.47 mg kg⁻¹ and Fe = 5142.22 to 722.23). The decrease in metal accumulation by the plants from September to January was due to the metals availability, depending on the different physical/chemical properties of substrates (Willscher et al., 2017; Avci and Deveci, 2013), and the variability of such properties, (pH, PR, MO) as a consequence of the sludge addition before the first sampling in September. This addition modified As, Cu and Fe concentrations, as well as the substrate characteristics (like it happened when mixing sewage sludge and soil), enabling better uptake of the three metals. The treatment sludge + *P. australis*, did not have any significant differences along the sampling months. We attributed this to the reports by Torres et al. (2010), indicating that the addition of the same substrate, in this case sewage sludge, does not imply a higher rate of metal uptake by the plants.

Plant tolerance to heavy metals like As, Cu and Fe is due to the fact that these metals are transition metals with oxidizing capacity, as well as with an the capacity to reduce different biomolecules (Choppala et al., 2014). Therefore, these effects in the reduction-

oxidation state of the cells enhanced due to the bonding reaction of these metals with biomolecules. This capacity can explain that the average concentration of As, Cu and Fe in the organs of *P. australis* in dry weight. These elements, (As: 0.61, Cu: 11.56 and Fe: 1420.99 mg kg⁻¹) were found within the typical ranges in plants reported by Larcher (2003) = Cu: 4 – 20 but not typical for Fe: 2 – 700 mg kg⁻¹. Although Cu is within the typical value range, it exceeds the value required by plants, just like Fe (1 – 5 mg kg⁻¹ Cu and 100 mg kg⁻¹ Fe).

As, Cu and Fe accumulation was found in certain plant organs. We found accumulated arsenic in the leaves (0.497 mg kg⁻¹). These results do not coincide with literature reports. *P. australis* belongs to the Poaceae family, characterized for having a great deal of roots promoting the accumulation of trace elements like As (Desjardins et al., 2018). According to Zhang et al. (2009) reports, there was an increase of As the roots of *Phragmites communis* (Trin., 1763).

Metals accumulated in the following order: root > stem > leaf. Higher concentration in the roots is due to the uptake of elements from the substrate, whereas the low concentration found in the stems may be due to their function as carriers of nutrients and minerals from the soil to aerial parts (Avci and Deveci, 2013).

BCF was determined in order to assess the accumulation efficiency of As, Cu and Fe by *P. australis*. For Fe and Cu the values were greater than one, in sludge and soil + *P. australis* and Sludge + *P. australis* treatments, during the two sampling months. These data indicates that *P. australis* is a hyper-accumulating species of these two metals, following the criterion established by Baker and Brooks (1989). The discrimination analysis showed that there were no significant differences in the BCF of Cu among the sampling months. However, the Sludge + *P. australis* treatment had a slightly higher value, indicating that Cu uptake efficiency is better in soilless substrates. The reason is the changes in the substrate characteristics, such as the pH increase and the bonding affinity of metal particles to the substrate (Avci and Deveci, 2013). In the case of arsenic, BFC value changed along the time and the treatments. We observed significant differences in this metal among different months and treatments, which can be attributed to leaching, and may be also to the chemical similarity between P and As contents in the substrate, as mentioned by Yan et al. (2017); Escutia-Lara and Lindig-Cisneros (2012). The roots were not able to uptake arsenic and the presence of other metals reduced the accumulation capacity of arsenic, coinciding with the reports of Desjardins et al. (2016).

BCF value for Cu (2.03) in *P. australis* was higher, compared to the reports from other species, including *Malva parviflora* (0.85), *Datura stramonium* L. (0.79), *Citrullus colocynthis* L. (0.84), *Lycium shawii* (Roem and Schult., 1990) (0.94) (Ibrahim et al., 2013). BCF value in Fe (7.38) was higher in *Elodea canadensis* (Michx.) (3.93), but it was lower, compared to *Polytrichum commune* (Hedw.) (0.9) and *Spirogyra* sp. (Link.) (10.25) (Busuioc et al., 2012). In both cases, Cu vales depended on the species, type of substrate, pH, PR and metal bioavailability (Desjardins et al., 2018; Ezeudo, 2014).

The translocation factor determining the capacity of metals to move from the roots to aerial parts was higher for arsenic (5.76 > 1), showing that Arsenic has great capacity to move into the leaves. This capacity can be the result of physiological factors of the species. *P. australis* has an extensive root system that can favor Arsenic permeability. Furthermore, this plant has the capacity to accumulate and transfer Arsenic from the roots to aerial parts (Yan et al., 2017). With regards to Cu (0.23) and Fe (0.17) TF

values were smaller than one, indicating that these metals are not easily taken to *P. australis* aerial parts. According to Padmavathamma and Li (2009), immobilization may be due to metal scavenging by the vacuoles or by the cell wall in the roots, inhibiting the interaction with high molecular weight compounds of the cytoplasm.

Conclusions and recommendations

-The order of heavy metals removal by *P. australis* was the following: Fe > Cu > As

-pH, PR and MO affected the mobility and availability of As, Cu and Fe.

-*P. australis* is a tolerant species capable of accumulating large concentrations of Fe and Cu in its organs, according to the following order: root > stem > leaf.

-The values of high BCF and low TF indicate that *P. australis* is a plant species that can be used to phytostabilize substrates polluted with Fe and Cu.

In the process of phytoremediation metal removal was observed not attributed to the plants so it may be appropriate to carry out leaching tests such as the Tessier scheme, in the waste sludge, soil and mixture in order to identify if it is because of these processes that decrease the concentration of metals in the waste sludge.

REFERENCES

- [1] Ansari, A, Singh, S., Gill, R., Lanza, G. Newman, L. (2014): Phytoremediation Management of Environmental Contaminants. – Springer, Berlin.
- [2] Avci, H., Deveci, T. (2013): Assessment of trace element concentrations in soil and plants from cropland irrigated with wastewater. – *Ecotoxicol. Environ. Saf.* 98: 283-291.
- [3] Bake, A. J. M., Brooks, R. R. (1989): Terrestrial higher plants which hyperaccumulate metallic. – *Biorecovery* 1: 81-126.
- [4] Bolan, N., Park, J. H., Robinson, B., Naidu, R., Huh, K. Y. (2011): Phytostabilization. A green approach to contaminant containment. – *Adv. Agron.* 112: 145-204.
- [5] Bolan, N. S., Kunhikrishnan, A., Thangarajan, R., Kumpiene, J., Park, J., Makino, T., Kirkham, M. B., Scheckel, K. (2014): Remediation of heavy metal(loid)s contaminated soils – To mobilize or to immobilize? – *J. Hazard. Mater.* 266: 141-166.
- [6] Busuioc, G., David, I., Mihaela, S., Iliescu, N. (2012): Evaluation of capacity for bioaccumulation of some heavy metals in three aquatic plants species. – *Water Resources and Wetlands* 14: 220-223.
- [7] Castañeda, A., Flore, H., Velazco, R., Martínez, M. (2011): Efectos de la aplicación de lodos orgánicos o biosólidos generados en el tratamiento de las aguas residuales domésticas sobre el suelo y la productividad de maíz forrajero en los Altos de Jalisco, México. – In: Spring, U., Sánchez, C., Miranda, M., Pérez, R., Domínguez, A., Garatuzza, J., Watts, C. (eds.) *Retos de la investigación del agua en México*. UNAM, México, D. F., pp. 227-237.
- [8] Chandra, P. V. (2013): Suitability of *Ricinus communis* L. cultivation for phytoremediation of fly ash disposal sites. – *Ecol Eng.* 57: 336-341.
- [9] Choppala, G., Saifullah., Bolan, N., Bibi, S., Iqbal, M., Rengel, Z., Kunhikrishnan, A., Nanjappa, A., Sik, O. (2014): Cellular mechanisms in higher plants governing tolerance to cadmium toxicity. *Crit. Rev. – Plant Sci.* 33: 374-391.
- [10] CONAGUA, Comisión Nacional de Agua (2011): Inventario Nacional de plantas municipales de potabilización y de tratamiento de aguas residuales en operación, diciembre 2013. – SEMARNAT, México.

- [11] CONAGUA, Comisión Nacional de Agua (2015): Inventario Nacional de plantas municipales de potabilización y de tratamiento de aguas residuales en operación, diciembre 2015. – SEMARNAT, México.
- [12] Cooper, P. (1996): Reed Beds and Constructed Wetlands for Wastewater Treatment. WRc, Severn Trent Water. – Marlow, Bucks, UK.
- [13] CRA, Comisión de Regulación de Agua Potable y Saneamiento Básico. (2000): Reglamento técnico del sector de agua potable y saneamiento básico RAS – 2000 Sección II, Título E, Tratamiento de aguas residuales. – Bogotá, D. C. Colombia.
- [14] David, L., Matache, M., Tudorache, A., Chisamera, G., Rozyłowicz, L., Lucian, G. (2012): Food chain biomagnification of heavy metals in samples from the lower prut foodplain natural park. *Environ. – Eng. Manag. J.* 11(1): 69-73.
- [15] Desjardins, D., Pitre, F. E. E., Nissim, W. G. G., Labrecque, M. (2016): Differential uptake of silver, copper and zinc suggests complementary species-specific phytoextraction potential. – *Int. J. Phytorem.* 18: 598-604.
- [16] Desjardins, D., Brereton, J. B. N., Marchand, L., Brisson, J., Pitre, E. F., Labrecque, M. (2018): Complementarity of three distinctive phytoremediation crops for multiple-trace element contaminated soil. – *Science of the Total Environment.* 610-611: 1428-1438.
- [17] Elekes, C. (2014): Eco-Technological Solutions for the Remediation of Polluted Soil and Heavy Metal Recovery. – In: Hernandez, M. (ed.) *Environmental Risk Assessment of Soil Contamination.* InTech, London.
- [18] Escutia-Lara, Y. y Lindig-Cisneros, R. (2012): Dinámica de *Phragmites australis* y *Schoenoplectus americanus* en respuesta a la adición de fósforo y nitrógeno. – *New Phytol* 181: 777-794.
- [19] Ezeudo, V. C. (2014): Mobility of heavy metals from the University of Nigeria sewage sludge disposal site to the surrounding soils and plants. – Dissertation, University of Nigeria.
- [20] Ibrahim, M., Alsahli, A., El-Gaaly, G. (2013): Evaluation of phytoremediation potential of six wild plants for metal in a site polluted by industrial wastes: a field study in Riyadh, Saudi Arabia. – *Pak J. Bot.* 42(2): 571-576.
- [21] Jing, X., Guojun, Y., Donghui, L., Yiran, L., Mai, L., Zhiqiang, Z., Peng, W. (2017): Effects of wastewater irrigation and sewage sludge application on soil residues of chiral fungicide benalaxyl. – *Environ. Pollut.* 224: 1-6.
- [22] Larcher, W. (2003): *Physiological Plant Ecology: Ecophysiology and Stress Physiology of Functional Groups.* 4th Ed. – Springer, Berlin.
- [23] Norma Oficial Mexicana NOM-004-SEMARNAT (2002): Secretaría del Medio Ambiente y Recursos Naturales. Protección ambiental. Lodos y Biosólidos - Especificaciones y límites máximos permisibles de contaminantes para su aprovechamiento y disposición final. – Viernes 15 de agosto de 2003.
- [24] Padmavathiamma, P., Li, L. (2009): Phytoremediation of metal – contaminated soil in temperature humid regions of British Columbia, Canada. – *Int. J. Phytoremediation* 11: 575-590.
- [25] Paradelo, R. (2013): Utilización de materiales compostados en la rehabilitación potencial de espacios afectados por residuos mineros y suelos de mina. – *Boletín Geológico y Minero.* 124(3): 405-419.
- [26] Pha, T., Minh, D., Xuan, D., Duc, L. (2014): Growth and absorbance of heavy metals of reed plants (*Phragmites australis*) in soil after mineral mining in Thai Nguyen Province of Vietnam. – *Res. J. Agric. & Biol. Sci.* 9(8): 1990-6145.
- [27] Punshon, T., Jackson, P. B., Meharg, A. A., Warczack, T., Scheckel, K., Guerinot, M. L. (2017): Understanding arsenic dynamics in agronomic systems to predict and prevent uptake by crop plants. – *Sci. Total Environ.* 581-582: 209-220.
- [28] Rojas, R., Mendoza, L. (2012): Utilización de biosólidos para la recuperación energética en México. – *Producción + limpia* 7: 74-94.

- [29] Sabir, M., Waraich, E. A., Hakeem, K. R., Öztürk, M., Ahmad, H. R., Shahid, M. (2015): Phytoremediation, Soil Remediation and Plants. – Elsevier Inc., Amsterdam.
- [30] Salema, B., Laffraya, X., Ashoour, A., Ayadib, H., and Aleyaa, L. (2014): Metal accumulation and distribution in the organs of Reeds and Cattails in a constructed treatment wetland (Etueffont, France). – Ecol. Eng. 64: 1-17.
- [31] SAS Institute. (2002): SAS System for Windows, Release 9.0. – SAS Institute, Cary, NC.
- [32] Torres, D., Cumana, A., Torrealba, O., Posada, D. (2010): Uso del vetiver para la fitorremediación de cromo en lodos residuales de una tenería. – REMEXCA 11(21): 175-188.
- [33] Valentín-Vargas, A., Root, R. A., Neilson, J. W., Chorover, J., Maier, R. M. (2014): Environmental factors influencing the structural dynamics of soil microbial communities during assisted phytostabilization of acid-generating mine tailings: a mesocosm experiment. – Sci. Total Environ. 500: 314-324.
- [34] Wilson, S. C., Lockwood, P. V., Ashley, P. M., Tighe, M. (2010): The chemistry and behaviour of antimony in the soil environment with comparisons to arsenic: a critical review. – Environ. Pollut. 158: 1169-1181.
- [35] Willscher, S., Jablonski, L., Fona, Z., Rahmi, R., Wittig, J. (2017): Phytoremediation experiments with *Helianthus tuberosus* under different pH and heavy metal soil concentrations. – Hydrometallurgy 168: 153-158.
- [36] Yan, X., Liu, Q., Wang, J., Liao, X. (2017): A combined process coupling phytoremediation and in situ flushing for removal of arsenic in contaminated soil. – J. of Environl. Sci. 57: 104-109.
- [37] Yepes, A., Buckeridg, M. (2011): Respuestas de las plantas ante los factores ambientales del cambio climático global - revisión. – Colombia Forestal. 14(2): 213-232.
- [38] Zhang, M., Cui, L., Sheng, L., Wang, Y. (2009): Distribution and enrichment of heavy metals among sediments, water body and plants in Hengshuihu Wetland of Northern China. – Ecol. Eng. 35: 563-569.

MORPHOLOGICAL AND REPRODUCTIVE TRAIT-VARIABILITY OF A FOOD DECEPTIVE ORCHID, *CEPHALANTHERA RUBRA* ALONG DIFFERENT ALTITUDES

GILIÁN, L. D.^{1*} – ENDRÉDI, A.² – ZSINKA, B.³ – NEMÉNYI, A.⁴ – NAGY, J. GY.¹

¹*Doctoral School of Biological Sciences, Institute of Botany and Ecophysiology, Szent István University, H-2100 Gödöllő, Páter Károly utca 1., Hungary
(phone: +36-28-522-000; fax: +36-28-410-804)*

²*Danube Research Institute, MTA Centre for Ecological Research, H-1113 Budapest, Karolina út 29.
(phone: +36-87-448-244; fax: +36-87-448-006)*

³*University of Veterinary Medicine, H-1078 Budapest, István u. 2.
(phone: +36-1-478-4100)*

⁴*Institute of Horticulture, Szent István University, H-2100 Gödöllő, Páter Károly utca 1., Hungary
(phone: +36-28-522-000; fax: +36-28-410-804)*

**Corresponding author
e-mail: lilla.gilian@gmail.com*

(Received 4th Jan 2019; accepted 27th Feb 2019)

Abstract. As climate change is forcing plant species to migrate northward and upward, it is important to know how species' vegetative traits and reproductive success vary along different climatic conditions. We aimed to examine the impact of elevation on the morphological and reproductive characteristics of *Cephalanthera rubra* in four different altitudes in Hungary: in a lowland oak forest (103 m), and in the beech forests of the Bükk-mountains (361 m, 533 m, 657 m). We counted the number of leaves, flowers, and fruits, and measured the height of each plant with the length and width of all leaves. Linear, negative binomial, and quasipoisson regressions were used to compare the populations. Our study has shown that the lowland and mountain populations of *C. rubra* are sharply different regarding their life history strategy and reproductive success, and altitudinal effects can be found only in the mountain populations. The number of flowers depends strongly on the vegetative production (height and leaf area) of the plants, but at the same time, the area that facilitates greater vegetative production - possibly because it also facilitates species with better competitiveness, and it is less favorable to its mimicked partners - were less beneficial in terms of fruit production.

Keywords: *Orchidaceae, elevation, Hungary, height, leaf size, floral display, pollination success*

Introduction

Extreme weather phenomena are becoming more and more frequent all over the world (WMO, 2011; Rahmstorf and Coumou, 2011; Coumou and Rahmstorf, 2012), which suggests that climate change is not just a future threat but is also an accelerating process in the present. The impacts of climate change can be detectable at different levels (e.g., community (Woodward et al., 1998) in species (Johnston and Schmitz, 1997), in population (Cochrane et al., 2014)) and they have already been examined on various aspects (mainly distribution (Parmesan and Yohe, 2003; Thuiller et al., 2005; Molnár V. et al., 2011) but also in survival, phenology (Fitter and Fitter, 2002; Morellato et al., 2016) or reproductive success (Ackermann, 1989; Aizen et al., 2002))

of many different species or communities (Parmesan and Handley, 2015; Molnár, 2015). Understanding the species' answer to this changing environment is extremely important in the case of plants, as their primary productive role is one of the essential components of almost all ecosystems on the Earth. In the context of this, the phenological or reproductive changes in the vegetation or populations may be the primary mediators for these effects on fauna and humankind (Parmesan and Hanley, 2015).

Orchidaceae is the largest family of flowering plants, incorporating almost 10% of all flowering plants, approximately 880 genera (Chase et al., 2015) and 20-30.000 species (Chase et al., 2003; Pillon and Chase, 2007). Simultaneously, it is one of the most vulnerable plant groups (Pridgeon, 1996; Scotland and Wortley, 2003; Clemente, 2009).

In general, global warming compels plants to migrate to higher latitudes and altitudes, searching for new, suitable habitats (Lenoir et al., 2008; Engler et al., 2011; Chen et al., 2011), which makes boreal and alpine vegetation and populations extremely vulnerable (Thuiller et al., 2005). Orchid populations showed a similar behaviour: in the planar region, they moved upward or poleward during the warming period (Jackson et al., 1987), while species in the mountain area with mild slopes, migrated upward along the elevation gradient (Thompson, 1990).

Availability of light and moisture is also affected by the changing climate. Orchids are known to be very sensitive to the change in the environmental factors (Fitter and Fitter, 2002; Seaton et al., 2010), and although they can tolerate slight variations in temperature and light, climate change of the last decade have forced them to migrate to more suitable places (Barman and Devadas, 2013).

During the last ca. 30 years, an increasing number of European terrestrial orchid species have experienced habitat loss (Barman and Devadas, 2013), population reduction and increased risk of extinction, thus they cannot keep pace with the climate change (Root et al., 2003; Thomas et al., 2004).

On the other hand, extreme rainfall can accelerate erosion (Selby, 1976), and an increased degree and frequency of erosion may negatively affect also the populations of orchids which live on hills (Barman and Devadas, 2013).

However, considering the life strategy components (individual survival and reproductive success) and their responses and vulnerability to biotic and abiotic environmental conditions, maintaining the highest fertilization rate is the most crucial factor for the species' survival, which highly depends on the pollinators (Tremblay et al., 2005). The flowering of orchid species and the temporal harmonization with their pollinators are the result of fine coevolution processes, leading to a high variety of flower structure and adaptation to pollination in this family, which are often in the focus of researchers (Darwin, 1984; Tremblay et al., 2005). This harmonization, as well, as directly the survival or flower/fruit production of the plants can be harmed due to climate change (Hegland et al., 2009), based on the fluctuation and change in temperature (Barman and Devadas, 2013) which is one of the main drivers of insect and plant phenology (Forest and Thompson, 2011), but we do not have enough information yet to predict the magnitude and direction of this.

To examine the potential response of morphological and phenological traits of orchids to climate change, in our study we focused on the morphological variability of a *Cephalanthera* (Orchidaceae) species between four Hungarian populations living on different altitudes. One characteristic of this group is that various breeding and reproductive strategies are present in it (Scacchi et al., 1991). In the genus, there are 15

food deceptive species, most of them are generalized food deceptive (Jersáková et al., 2006; Renner, 2006), but there are some species (e.g., *C. rubra* and *C. longifolia*, which also live in Hungary), which specifically imitate a special nectar producing group with Batesian mimicry. *C. longifolia* imitates *Cistus spp.* (Dafni and Ivri, 1981a,b) and *C. rubra* imitates *Campanula spp.* (Nilsson, 1983a). Deceptive species are strongly pollinator-limited, so that their fruit set is usually lower, than in the case of the nectar producing species (Tremblay et al., 2005). To increase the odds of the pollination, the flowering period of the generalized food deceptive species starts earlier, so that they could lure the naive pollinators (Pellissier et al., 2010a). According to Sonkoly et al. (2016), however the fruit number is low, they contain more seeds in general, as a compensation, and the gene flow is also found to be stronger within the populations than in the case of their nectar-producing relatives (Cozzolino and Widmer, 2005).

In Hungary, three species of the genus can be found: *C. damasonium* (Mill.) Druce, *C. longifolia* (L.) Fritsch, and *C. rubra* (L.) Rich (Tutin et al., 1980; Molnár, 2011). Although they frequently share the same habitat (beech forest), they show different morphological characters, as well as some differences in the flowering period (*C. rubra* flowers approximately 20-30 days later than the other two) (Scacchi et al., 1991). All of them are rhizomatous, perennial plants, but while *C. longifolia* is a typically outbreeding species, and *C. damasonium* is generally considered as an inbreeder (Summerhayes, 1985). *C. rubra* is an outbreeder which frequently reproduces vegetatively. In this latter case, a reduced ratio of plants germinated from seeds has been observed, while the number of plants originated from adventitious buds on the primary roots can be considerable (Ziegenspeck, 1936).

Considering this interesting variability in breeding systems and success, we chose *Cephalanthera rubra* to examine the impact of elevation (indirectly the temperature and precipitation) on the population's morphological characteristics, fecundity and reproduction strategy to predict the effects of the increasing temperature on this rare, endangered species.

C. rubra is a rhizomatous, perennial plant. The 4-10 pink flowers appear on a flexible flowering stalk, between June and at the beginning of July. *Chelostoma campanularum* and *Ch. fuliginosum* (Megachilidae) were reported as the main pollinators of the species (Nilsson, 1983b; Szlachetko and Skakuj, 1996; Newman et al., 2007).

The above-mentioned, relatively unrefined mechanism and the method of attracting pollinators by deception can explain, why most *Cephalanthera* species produce few ripe capsules and it gives the hypothesis that the populations are probably maintained and propagated mostly vegetatively (Delforge, 2006).

However, in the case of *C. rubra*, studies focusing on the reproduction strategy are ambivalent: on the one hand, the reproduction from seeds is considered to be dominant and vegetative propagation is sporadic (Kaźmierczakowa and Zarzycki, 2001), but in Italy a study showed that plants germinated from seeds were rare (Scacchi et al., 1991). According to Scacchi et al. (1991), *C. rubra* is an outbreeder, but at the same time, some results are showing that this species can frequently reproduce vegetatively.

As for the habitat, *Cephalanthera rubra* lives in 0-2000 m altitude, typically in scrubby grasslands, woodland margins, warmer calcareous beech forests, and oak forests. It prefers to grow in calcareous or slightly acidic soils in shaded or semi-shaded light conditions (Delforge, 1995; Vakhrameeva et al., 2008).

The distribution area of *Cephalanthera rubra* extends from Northern Europe to Iran and North-Africa (Fig. 1a). The northernmost localities were found in southern Finland, where according to Tuulik (1998), the plant is infrequent and flowers very rarely. In Poland, the middle of the European distribution area of this species is known from approximately 300 localities, but only half of them have been confirmed (Kaźmierczakowa and Zarzycki, 2001). In the European Region, the populations are found throughout the temperate regions and in parts of the Mediterranean, extending from the Atlantic to the Caspian Sea. It lives in every altitude in Hungary, from planar to mountain regions. Most of the populations are found in the Transdanubian Mountains, Mecsek, North Hungarian Mountains and in the Danube-Tisza interfluvial region (Molnár, 2011) (Fig. 1b).

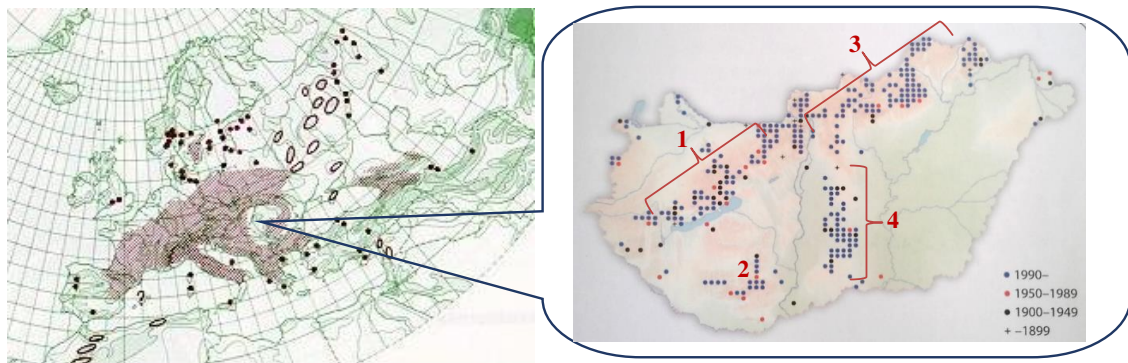


Figure 1. a Distribution of *C. Rubra* (http1) and **b** in Hungary (Molnár, 2011). 1: Transdanubian Mountains; 2: Mecsek; 3 North Hungarian Mountains; 4: Danube-Tisza interfluvial region

Although the species is widespread and often abundant, its distribution appears in small, isolated and severely fragmented populations and becomes rare in the margins of its distribution. The populations usually comprise 1-20, very occasionally more than 100 plants (Brzosko and Wróblewska, 2003). The size of the population is suspected to be declining, and many sites have already been lost (Delforge, 1995; Lang, 2004; Newman et al., 2007; Vakhrameeva et al., 2008; Harrap and Harrap, 2009).

The IUCN degree of threat of this species on the Red List of the Vascular Flora of Hungary is Least Concern (Király, 2007). Many populations have been lost and declined due to inappropriate site management, lack of pollination, forest fires, deforestation for building and construction work purposes as well as plant collection. In addition, populations may be genetically depauperate as this species can form clonal populations (Micheneau et al., 2010). However, the species occurs in numerous European countries with less threat in some; therefore, the risk of extinction at the European level is low, and *Cephalanthera rubra* is assessed as Least Concern (Rankou, 2011).

Jakubská et al. (2014) have investigated the extinction of the *Cephalanthera* species in Poland during the last 120 years, and conclude that their decline cannot be attributed to global change (climate warming or nitrogen deposition) as the shift took place in the first half of the 20th century. They suggest that the species decline should rather be explained by changes in land use, including alteration of deciduous forests into coniferous monocultures, as well as by intensification of agriculture.

In Hungary, the declining degree of the species is 22% (Molnár, 2011.) Some of the main reasons behind the disappearance of the species are those processes which are leading to increased shading of the forest floor (Brzosko and Wróblewska, 2003).

Regarding the predicted future changes, the Pannonian region is highly vulnerable: according to Thuiller et al. (2005), the expected species turnover in this area is about 66% which means a substantial species loss (migration to north) but also a huge species gain from the eastern Mediterranean region. Based on this, it is essential to examine the opportunities and behaviour of the Hungarian populations.

Materials and methods

Study sites

In this study, we examined four Hungarian populations in different altitudes (*Fig. 2*): One in the planar region (Jászfényszaru (J), 103 m), and three from different elevations of the Bükk-mountains: Kis-Oltár (KO, 361 m), Bikk-bérc (BB, 533 m), and Pongorlyuk peak (PP, 657 m).

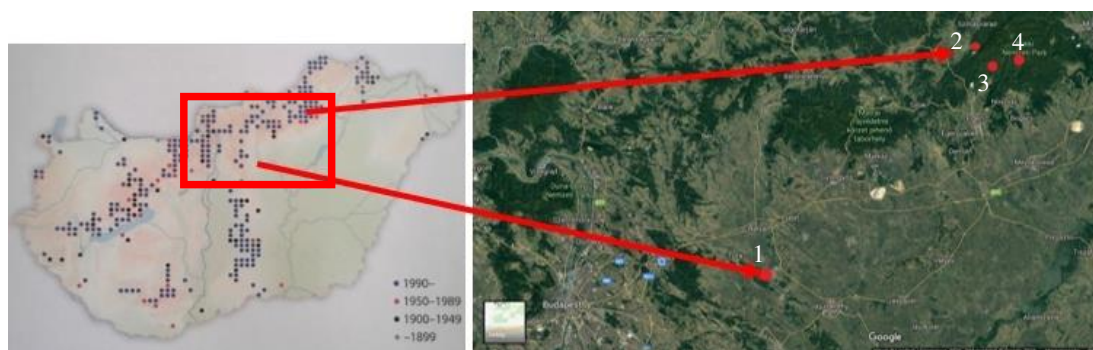


Figure 2. Habitats of the examined populations in Hungary (Molnár, 2011; GoogleEarth, 2018). 1: Jászfényszaru; 2: Kis-Oltár; 3: Bikk-bérc; 4: Pongorlyuk peak

Populations on the Bükk-mountain

The Bükk-mountain is located in the North Hungarian Mountains. We examined three populations living here, at different elevations. The soil of the study sites are brown forest soil on limestone bedrock. The annual average temperature is about 2 °C below the national average, only 7-8 °C, while on the highest part of the Bükk plateau it is even lower, only 6 °C.

Because of the continental effect, winter is cold (average temperature in January is -4 °C), the number of snowy days are the highest in the country. Summer is warm, frequently rainy at the beginning of July and the end of August. The distribution of annual precipitation is also affected by continentality. There are two precipitation maximums, one in the early summer and one in the autumn. The annual rainfall is 600-700 mm, and 800 mm on the Beech plateau. Based on data of MetNet (<http2>), the Walter-Lieth climate diagram (*Fig. 3*) represents the average climate of the study areas in the Bükk-mountain in 2018.

It is noticeable that there were three wet periods: at the end of the winter, at the end of February and at beginning of March, when the snow melts; also in June and in September.

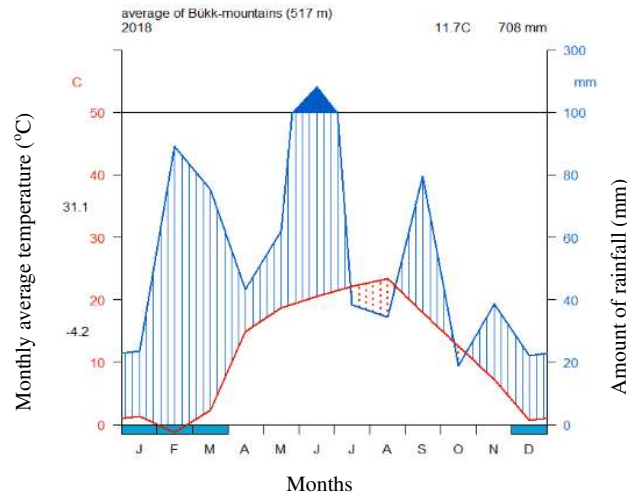


Figure 3. Walter-Lieth climate diagram of the Bükk mountain in average for 2018

Our three examined populations situated in Medio-European limestone beech forests of the *Cephalanthero-Fagion* (Natura 2000 habitat category is 9150). All their habitats can be found in light-spotted, mostly flat, bit rocky places. The shrub layer (because of the forestry activity) and the herbaceous layer are not dense, so that the amount of light, which reaches the surface is quite a lot.

The habitat of the Jászfényszaru population

The town of Jászfényszaru is located in the Great Plain, on the sub-region called Hatvani Plane. Its climate is moderately warm and dry, the dominant soil type is pise and chernozem brown forest soil on calcareous sand at the study site.

The annual average temperature is about 11 °C. The number of sunny hours is high.

Due to the characteristics of the continental climate, distribution of precipitation shows extremities within, and also between years (MNDI, 2010). The Walter-Lieth climate diagram (Fig. 4) represents the climate of the study area in Jászfényszaru in 2018. It was made from the online data through MetNet and were drawn in RStudio program by us. As it can be seen, there were two humid periods: in February and in the middle of June.

The examined population is situated in Euro-Siberian steppic woods with *Quercus robur* (Natura 2000 habitat category is 9110). It is found in the pedunculate oak forests, with high density of herbaceous- and shrub layers. The terrain is flat, as it is typical in the Great Plain.

Data collection

In our study, we examined the four populations two times in 2018. First, in the flowering period, in May-June we counted and marked all (J: 100, KO: 22, BB: 85, PP: 27) individuals by recording their GPS coordinates and we counted the number of

flowers, the number of the leaves, and measured the height of each plant and the length and width of all leaves. On the second occasion, in July-August, we counted the fruits of the same plants in the cases of three populations, but in the PP population (on the highest altitude), we did not have fruit data from 10/27 plants, partly because they had not started the fruiting period yet or the fruiting stems were consumed by animals.

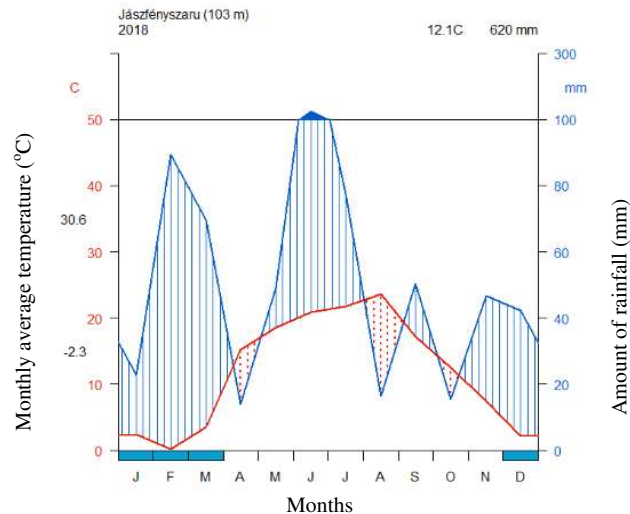


Figure 4. Walter-Lieth climate diagram of Jászfényszaru for 2018

Data analysis

Statistical analysis was made in R statistical software (R Core Team, 2017). The boxplots, scatterplots, and histograms which were used to visualize our data were made with the ggpubr package (Kassambara, 2017).

One-way analysis of variance (ANOVA, on the log-transformed height and leaf size data, lm function (R Core Team, 2017)), negative binomial regression (on the number of flowers and fruits, glm.nb function of the MASS package (Venables and Ripley, 2002)), and quasipoisson regression (on the number of leaves, glm function (R Core Team, 2017)) were used to compare the populations. Differences between the populations were tested with post-hoc analyses based on Tukey all-pair multiple comparisons, using the glht function of the multcomp package (Hothorn et al., 2008).

Results

Growth-related traits

Height

The average height of the plants was 29.44 centimeters, the highest individual (71 cm) was found in the lowest altitude (J), while the shortest individual (5.8 cm) was found at the highest altitude (PP) (Fig. 5). The average heights showed the same pattern: while the mountain populations looked similar, the average height of the plants in the Jászfényszaru population was (almost two times) greater (Fig. 5b).

This difference was found to be significant ($p < 2.2e-16$; Table A1 and Fig. A1 in the Appendix): according to the pair-wise comparisons, at the lowest altitude (J), the

expected average height of the plants is 2.125 (95% CI: [1.8; 2.5]) times higher than in the BB population, and even 1.79 (95% CI: [1.4; 2.3]) and 1.86 (95% CI: [1.5; 2.3]) times higher than in the KO and PP populations. The three mountain populations did not differ from each other (*Table A1*).

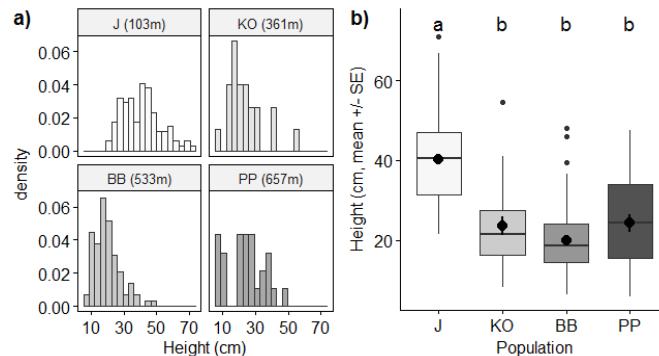


Figure 5. Histogram (a) and bloxpot (b) based on the height in the examined populations. Significant differences are indicated by different letters

Leaves

The average number of the leaves was 4.7, the most leaves (10 pcs) were found on an individual in J population, while the less (2 pcs) were found in the BB population. The number of leaves per individual showed a similar pattern (*Fig. 6*) as the heights of the plants (*Fig. 5*): individuals living at the lowest (J) altitudes had more leaves (*Fig. 6b*), however, in this case, only the J-BB, J-KO and PP-BB population pairs differed significantly ($p < 0.001$; *Table A2*) from each other.

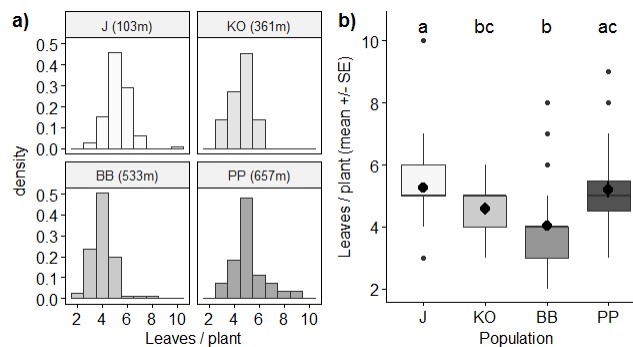


Figure 6. Histogram (a) and bloxpot (b) based on the leaves/plants in the examined populations. Significant differences are indicated by different letters

Regarding the estimated leaf size index (sum of the all leaf's lengths \times leaf widths per individual), our populations looked more similar (*Figs. 7* and *A1*). Again, only the J population showed a significantly higher average value than the others ($p < 0.001$; *Table A3*), which were not different from each other.

Summarizing the results regarding the growth-related traits of our populations, we can state that at a lower altitude (J population) the plants showed significantly longer stems, bigger- (*Fig. 5*) and a higher number (*Fig. 6*) of leaves. The three mountain

populations looked more similar, but because in some cases the BB population showed less production, the KO-PP population pair is considered to be the most similar regarding the growth-related traits.

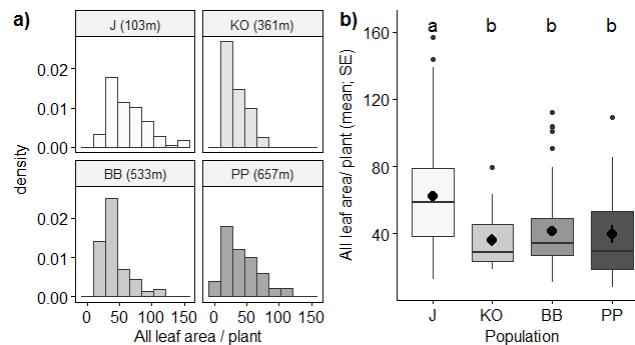


Figure 7. Histogram (a) and boxplot (b) based on the all leaf area/plants in the examined populations. Significant differences are indicated by different letters

Reproduction-related traits

Flowers

The average number of the flowers was 4.5, most of the flowers (20 pcs) were found on an individual in J population, while the fewest (0 pcs) were found in the PP and BB populations. According to the average number of flowers per individual, we did not find huge differences between the four habitats (Figs. 8 and A1), but the pattern is similar to that regarding the number of leaves (Fig. 6). The negative binomial regression showed significantly fewer flowers at the BB populations than in the J and the PP populations ($p < 0.001$; Table A4): The expected average flower number/individual is 1.84 times (95% CI: [1-38; 2.44]) and 2 times (95% CI: [1.35; 3,01]) times higher in the J and the PP populations than in the BB population.

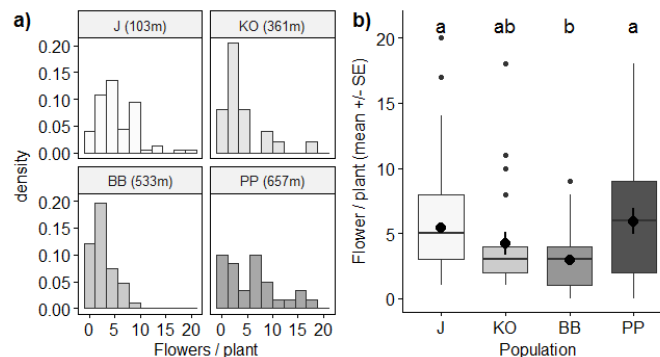


Figure 8. Histogram (a) and boxplot (b) based on the flowers/plants in the examined populations. Significant differences are indicated by different letters

Fruits

The average number of the fruits was 1.15, the most fruits (18 pcs) were found on an individual in KO population, while individuals with no fruits were found in all of the

four examined populations. Although we found a little bit more flowers per individual in the J and PP populations (*Fig. 8*), these two populations showed the least amount of fruits (in average) because there were plenty of plants in these habitats which had no fruit at all (*Fig. 9*). On the other hand, in the KO population, there was a plant which had an extremely high amount (18) of fruits compared to the others. Due to this outlier, the fine differences between the populations cannot be visible on the figures (*Fig. A2*), thus for the better visibility, we eliminated the outlier from *Figure 9* (but not from the model).

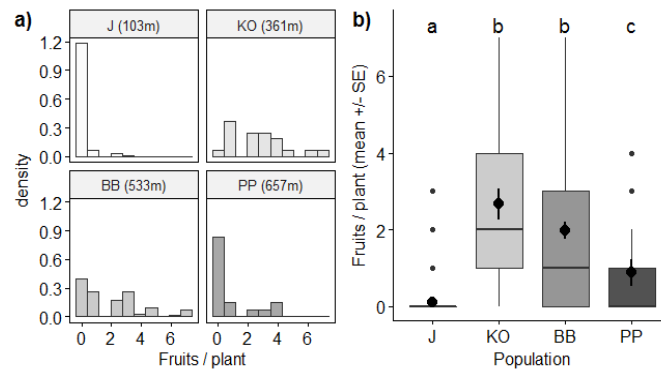


Figure 9. Histogram (a) and boxplot (b) based on the fruits/plants in the examined populations. Significant differences are indicated by different letters

According to the model and the pair-wise comparisons, except the KO-BB population pair ($p = 0.177$; *Table A5*), all population-pairs were different considering the average number of fruits/individuals ($p < 0.002$; *Table A5*). It is visible from these results and the figure (*Fig. 9*) that the population in Pongorlyuk-peak also had a significantly higher average fruit/individuals number than the Jászfényszaru population.

Based on the reproduction-related traits, the J-PP population pair seems to be the most similar, but the KO-BB population pair also behaves similarly (*Fig. 10*).

Correlations

From the results mentioned above, it is easy to see that the growth-related traits (height, leaf size, and leaf number) should be highly correlated with the number of flowers: the populations with higher plants (*Fig. 5*) and bigger leaf surface (*Fig. 7*) had a little bit more flowers (*Fig. 8*), but this does not increase the expected number of fruits (*Fig. 9*).

On the other hand, we checked the relationship between the growth-related traits and the number of flowers within the populations, too. In this case, both the heights (*Fig. 11a*) and the size of the leaves (*Fig. 11b*) showed a good correlation with the number of flowers, but there are some differences between the populations: the height of the plant shows a stronger relationship with the number of flowers in the cases of the KO and BB populations.

Considering the impact of the flower number on the number of fruits, *Fig. 11c* shows that in the cases of the mountain populations, the size of the inflorescence does not have impact on the number of the fruits. Although, in the J population, only individuals with

more than 10 flowers succeeded to produce any fruits and above this threshold, the number of fruits is highly dependent from the number of flowers.

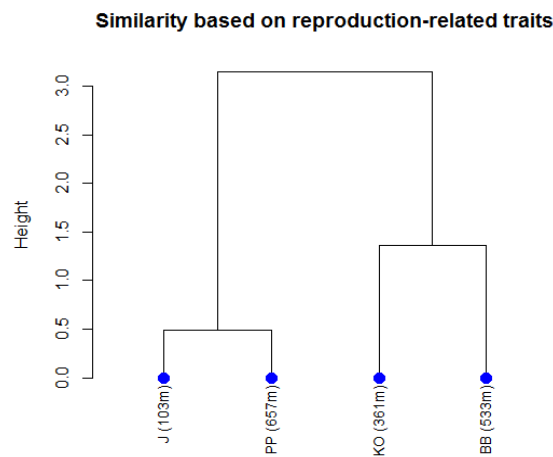


Figure 10. Similarity based on reproduction-related traits

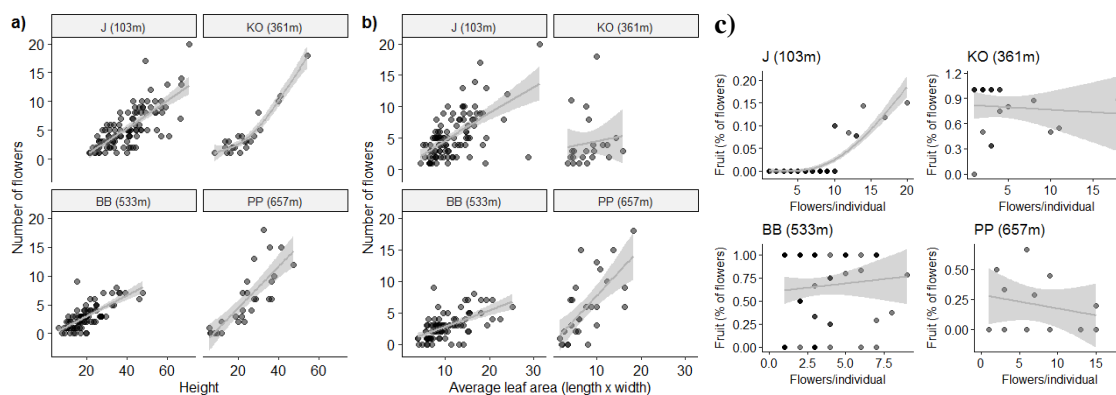


Figure 11. Relationship between the growth-related traits and the number of flowers (a-b) and the impact of flower number on the fruit/flower ratio (c) within the different populations

Discussion

Latitudinal and altitudinal range shifts have been already reported for many plant species, as the borders of the vegetation zones are moving to the north and increasing in the mountain regions due to climate change (e.g., Chen et al., 2011) or other factors like land use change (e.g., Bodin et al., 2013; Jakubská-Busse et al., 2014). Recently, it is a central challenge to predict future changes in the environment, the communities and the way how different species will adapt or not to the new environmental conditions of the future.

Examining populations of the same, widespread species or a given community in different latitude or altitude can give us valuable data about the species' requirements and adaptation capability; thus future tendencies can be predicted better. E.g., recent studies have shown, that individuals of a species usually become shorter with increasing altitude due to the decrease in temperature (Bjorkman et al., 2018), vegetative reproduction can become more important on higher altitudes (Young et al., 2002) and,

however, most montane plant species will profit from the increasing temperature (e.g., general food-deceptive orchids (Pellissier et al., 2010b)), high-elevation, cold-adapted plants are more vulnerable (Rumpf et al., 2018).

In our study, we chose *Cephalanthera rubra*, a widespread terrestrial orchid to see how its vegetative and reproductive traits change with altitude. The species inhabits semi-shade forests up to 2.000 m (Delforge, 2006), and although we do not have too much information about its altitudinal shift, Jakubska-Busse et al. (2014) found that in Poland the plant's populations moved upwards in the first half of the previous century, most probably due to land-use change. A bigger problem is that the number and size of the populations are usually small and continuously decreasing (Brzosko and Wróblewska, 2013, 2003; Scacchi et al., 1991), and the reproduction success is low (Brzosko and Wróblewska, 2013; Vakhrameeva et al., 2008), as it is in the case of every food-deceptive terrestrial orchid (Tremblay et al., 2005), which leads to low genetic diversity (Brzosko and Wróblewska, 2013; Scacchi et al., 1991), so a higher vulnerability of the populations.

In this study, we examined four populations at different altitudes. As the temperature is decreasing with increasing altitude, we expected a decrease also in height, flowering and fruit production on higher altitudes.

Although a continuous decrease in height could not be visible in our data, at the lowland (Jászfényszaru) habitat, the plants had significantly higher stems and bigger leaves than the individuals living in the Bükk-mountains, which were similar in height. On the other hand, the ratio of the flowering individuals decreased with the altitude: at the lowland habitat and the lowest mountain habitat, 100% of the examined specimens had flowers, while the flowering decreased to 90% and then to 81.5% at the highest altitudes. The decreasing temperature with increasing altitude can partially explain the flowering pattern, but light conditions can also have an impact on it. While at the lowland habitat, the canopy coverage was about 75-90%, at the mountain habitats it was above 90%, except a fifth of the lowest mountain habitat, where due to some tree-cutting, the light conditions were temporarily better than at the other two.

It is known that the species' populations and reproduction show high sensitivity to increased shading (Vakhrameeva et al., 2008; Fay and Taylor, 2015), however, the plants can get about 26% (SD = 11%) of their carbon needs from their mycorrhizal partner (Bidartondo et al., 2004), which make them moderately tolerate to shady conditions. In contrast, open habitats provide more light, - thus energy - to grow and flower, but also an increased competition which is also suspected to be disadvantageous to the plant (Fay and Taylor, 2015). It also must be noted that although the height and leaf area are considered to be a good proxy for condition and flowering capability, in the case of rhizomatous or tuberous orchids, these vegetative traits can affect more the flowering of the next year than the given year (Jersáková and Kindlman, 2002). E.g., Janečková et al. (2006) found that in the case of another nectarless orchid, *Dactylorhiza majalis*, the leaf area of the previous year was the best predictor of the flowering of the plants in the current year. Furthermore, although the leaf area in the given year was correlated with the height of the plant, it was affected mainly by the leaf area of the previous year (via carbohydrates stored in the tubers), while the stalk's heights could be explained more by the temperature and precipitation.

Based on these literature data, it seems that at the two lowest examined populations, the temperature and light were enough previously to all plants to produce flowers, while the more shady habitat of the highest mountain populations probably could not provide

enough energy to make all plants flower. However, it must be noted that these decreased flowerings are still extremely high compared to the literature data which implies that the plants of these populations were in good condition in this year.

Considering the number of flowers, although there was a similar - but not significant - decreasing pattern at the three lowest habitats with the altitude, the population of the highest altitude showed more flower per individual than the expected. The ratio of fruiting individuals also showed a decrease with the altitude in the case of the mountain habitats, but was much less at the lowland habitat, and the fruit number showed a reverse pattern compared to the flower number: the lowest and highest populations – which had the most flowers on average - had the least fruits per individual in general.

Deceptive orchids are strongly pollinator- and pollen-limited and their reproductive success is generally low (Tremblay et al., 2005). *C. rubra* is a mimicking food-deceptive orchid which mimics the flowers of the *Campanula* spp. (Nilsson, 1983b; Szlachetko and Skakuj, 1996; Newman et al., 2007), and although the species is completely self-compatible, spontaneous autogamy has not been observed yet (Tałałaj et al., 2017), thus reproductive success highly depends on the presence and abundance of its pollinator and mimicked species too. The observed pollinators (*Chelostoma fuliginosum* (Claessens et al., 2015; Newman et al., 2007), *Ch. campanularum* (Nilsson, 1983b, but see Newman et al., 2007), and *Miarus campanulae* (Claessens et al., 2015)) are highly related to *Campanula* spp. Furthermore, *Chelostoma* species also need standing dead trunks as a nesting place.

The habitat of our lowland population has a more open canopy, which could lead to a higher irradiance but also a higher herb competition which can decrease the visibility, thus the probability of the pollination. In a habitat like this, being taller and having more flowers can be a good strategy, especially because the abundance of the mimicking species is low at the neighborhood; thus pollinator abundance should also be low. Competition for the small number of pollinators can explain, why only the striking, high, and multi-flowered individuals showed remarkable pollination success (Kindlmann and Jersáková, 2006; Suetsugu et al., 2015) and it can lead to a more frequent vegetative reproduction as well. A higher frequency of vegetative reproduction may also be suggested by the fact, that this population contained much more individuals than the other examined populations.

The mountain populations had a higher abundance of *Campanula persicifolia* and *Campanula trachelium* nearby. The *Cephalanthera rubra* specimens showed shorter stems than in the lowland population, and also a decrease in flowering and fruiting individuals with the altitude. The reproduction success of the two lowest mountain populations was extremely high (83-85% of the flowers turned into fruits), while the Pongorlyuk-peak population, on the highest altitude, had a little bit more flowers but significantly fewer fruits (about 40% of the flowers turned into fruits). These results suggest that these areas are more suitable for the species, except at the highest altitude, where possibly the temperature or the irradiance is not enough to mature the fruits. On the other hand, it is worth mentioning, that the low number of fruits here does not necessarily mean low pollination success. It is also possible that the low number of fruits/individuals is attributable to the stronger herbivory pressure or some infections, as it is suggested by the fact that we have found several damaged shoots in the area.

Conclusions

Our study has shown that the lowland and mountain population of *C. rubra* are sharply different regarding their life history strategy and reproductive success, and altitudinal effects can be found only in the mountain populations.

The number of flowers of *C. rubra* depends strongly on the vegetative production (height and leaf area) of the plants, but at the same time the area that facilitated greater vegetative reproduction - possibly because they also facilitate species with better competitiveness and less favorable to its mimicked partners - were less beneficial in terms of fruit production.

To predict the expected population dynamics, trait distributions and vulnerability of the species it is important to continue the monitoring of the examined populations and combine the results with genetic examinations.

Acknowledgements. This research was supported by the ÚNKP-18. New National Excellence Program of the Ministry of Human Capacities, Hungary. Thank you so much for this opportunity. The publication was supported by the EFOP-3.6.3-VEKOP-16-2017-00008 project. The project is co-financed by the European Union and the European Social Fund. Many thanks in the field work to Nikolett Csukás, Bernadett Hetesi, Tímea Keszthelyi, Luca Hergott, Adrián Molnár and Gábor Kadosa. Thanks for help in statistics to Zsolt Lang.

REFERENCES

- [1] Ackermann, J. D. (1989): Limitations of sexual reproduction in *Encyclia krugii* (Orchidaceae). – Systematic Botany 14: 101-09.
- [2] Aizen, M. A., Ashworth, L., Galetto, L. (2002): Reproductive success in fragmented habitats: do compatibility systems and pollination specialization matter? – Journal of Vegetation Science 13: 885-92.
- [3] Barman, D., Devadas, R. (2013): Climate change on orchid population and conservation strategies: a review. – Journal of Crop and Weed 9: 1-12.
- [4] Bidartondo, M. I., Burghardt, B., Gebauer, G., Bruns, T. D., Read, D. J. (2004): Changing partners in the dark: isotopic and molecular evidence of ectomycorrhizal liaisons between forest orchids and trees. – Proc. R. Soc. London. Ser. B Biol. Sci. 271: 1799-1806. DOI: 10.1098/rspb.2004.2807.
- [5] Bjorkman, A. D., Myers-Smith, I. H., Elmendorf, S. C., Normand, S., Nadja, R., Beck, P. S. A., ..., Weiher, E. (2018): Plant functional trait change across a warming tundra biome. – Nature 562: 57-62.
- [6] Bodin, J., Badeau, V., Bruno, E., Cluzeau, C., Moisselin, J. M., Walther, G. R., Dupouey, J. L. (2013): Shifts of forest species along an elevational gradient in Southeast France: climate change or stand maturation? – J. Veg. Sci. 24: 269-283. DOI: 10.1111/j.1654-1103.2012.01456.x.
- [7] Brzosko, E., Wróblewska, A. (2003): Genetic variation and clonal diversity in island *Cephalanthera rubra* populations from the Biebrza National Park, Poland. – Botanical Journal of the Linnean Society 143: 99-108. DOI: 10.1046/j.1095-8339.2003.00201.x.
- [8] Brzosko, E., Wróblewska, A. (2013): Genetic diversity of nectar-rewarding *Platanthera chlorantha* and nectarless *Cephalanthera rubra*. – Botanical Journal of the Linnean Society 171(4): 751-763.
- [9] Chase, M. W., Cameron, K. M., Barrett, L. R., Freudenstein, J. V. (2003): DNA Data and Orchidaceae Systematics: A New Phylogenetic Classification. – In: Dixon, K. W., Kell, S. P., Barrett, R. L., P. J. Cribb (eds.) Orchid Conservation. Natural History Publications, Kota Kinabalu, Sabah, Malaysia, pp. 69-89.

- [10] Chase, M. W., Cameron, K. M., Freudenstein, J. V., Salazar, G., Van den Berg, C., Schuiteman, A. (2015): An updated classification of Orchidaceae. – Botanical Journal of the Linnean Society 177: 151-74.
- [11] Chen, I. C., Hill, J. K., Ohlemuller, R., Roy, D. B., Thomas, C. D. (2011): Rapid range shifts of species associated with high levels of climate warming. – Science 333: 1024-26. DOI: 10.1126/science.1206432.
- [12] Claessens, J., Beentjes, K. K., Heijerman, T., Miller, J., Gravendeel, B. (2015): Beobachtungen von *Miarus campanulae* als Bestäuber von *Cephalanthera rubra*. – J. Eur. Orchid. 47: 77-87.
- [13] Clemente, M. (2009): Orchid Conservation and Trade: Are These Concepts Incompatible? – In: Pridgeon, A. M., Suarez, J. P. (eds.) Proceedings of the Second Scientific Conference on Andean Orchids. Universidad Técnica Particular de Loja, Loja, Ecuador, pp. 46-55.
- [14] Cochrane, A., Yates, C. J., Hoyle, G. L., Nicotra, A. B. (2014): Will among-population variation in seed traits improve the chance of species persistence under climate change? – Glob. Ecol. Biogeogr. 24: 12-24.
- [15] Coumou, D., Rahmstorf, S. (2012): A decade of weather extremes. – Nature Climate Change 2: 491-96.
- [16] Cozzolino, S., Widmer, A. (2005): Orchid diversity: an evolutionary consequence of deception? – Trends Ecol Evol 20(9): 487-494. <https://doi.org/10.1016/j.tree.2005.06.004>.
- [17] Dafni, A., Ivri, Y. (1981a): The flower biology of *Cephalanthera longifolia* (Orchidaceae) - pollen imitation and facultative floral mimicry. – Plant Syst Evol 137: 229-240.
- [18] Dafni, A., Ivri, Y. (1981b): Floral mimicry between *Orchis israelitica* Baumann and *Dafni* (Orchidaceae) and *Bellevalia flexuosa* Boiss. (Liliaceae). – Oecologia 49: 229-232. <https://doi.org/10.1007/BF00349193>.
- [19] Darwin, C. (1984): The Various Contrivances by Which Orchids Are Fertilized by Insects. – University of Chicago Press, Chicago (first published: 1877).
- [20] Delforge, P. (2006): Orchids of Europe, North Africa and the Middle East. – Timber Press, Portland, OR.
- [21] Delforge, P. (1995): Orchids of Britain and Europe. – Delachaux et Niestlé Sa, Lausanne.
- [22] Engler, R., Randin, C. F., Thuiller, W., Dullinger, S., Zimmermann, N. E., Araújo, M. B., ... , Guisan, A. (2011): 21st century climate change threatens mountain flora unequally across Europe. – Glob. Change Biol. 17: 2330-2341.
- [23] Fay, M. F., Taylor, I. (2015): 807. *Cephalanthera Rubra*. – Curtis's Bot. Mag. 32: 82-90. DOI: 10.1111/curt.12095.
- [24] Fitter, A. H., Fitter, R. S. R. (2002): Rapid changes in flowering time in British plants. – Science 296: 1689-91.
- [25] Forrest, J., Thomson, J. (2011): An examination of synchrony between insect emergence and flowering in Rocky Mountain meadows. – Ecological Monographs 81: 469-491.
- [26] Harrap, A., Harrap, S. (2009): Orchids of Britain and Ireland - A Field and Site Guide. – A&C Black Publishers Ltd., London.
- [27] Hegland, S. J., Nielsen, A., Lázaro, A., Bjerknes, A. L., Totland, O. (2009): How does climate warming affect plant-pollinator interactions? – Ecology Letters 12.2: 184-195.
- [28] Hothorn, T., Bretz, F., Westfall, P. (2008): Simultaneous inference in general parametric models. – Biometrical Journal 50(3): 346-363.
- [29] [http 1: http://linnaeus.nrm.se/flora/mono/orchida/cepha/cephrubv.jpg](http://linnaeus.nrm.se/flora/mono/orchida/cepha/cephrubv.jpg).
- [30] [http 2: https://www.bnpi.hu/hu/reszletek/a-bukk-hegyseg-eghajlata-es-novenyzeti-kepe](https://www.bnpi.hu/hu/reszletek/a-bukk-hegyseg-eghajlata-es-novenyzeti-kepe).
- [31] Jackson, G., Webb III, T., Grimm, E. C., Ruddiman, W. F., Wright Jr, H. F. (1987): North America and adjacent oceans during the last deglaciation. – Geological Soc. Amer. 3: 277-88.
- [32] Jakubska-Busse, A., Pielech, R., Szcześniak, E. (2014): The extinction of terrestrial orchids in Europe: does disappearance of *Cephalanthera* Rich., 1817 (Orchidaceae,

- Neottieae) species show pattern consistent with the elevation gradient? – Life Sciences Journal 11(4): 140-144.
- [33] Janečková, P., Wotavová, K., Schödelbauerová, I., Jersáková, J., Kindlmann, P. (2006): Relative effects of management and environmental conditions on performance and survival of populations of a terrestrial orchid, *Dactylorhiza majalis*. – Biol. Conserv. 129: 40-49. DOI: 10.1016/j.biocon.2005.09.045.
- [34] Jersáková, J., Kindlmann, P., Stnkesky, M. (2002): Population Dynamics of *Orchis morio* in the Czech Republic under Human Influence. – In: Kindlmann, P., Willems, J. H., Whigham, D. F. (eds.) Trends and Fluctuations and Underlying Mechanisms in Terrestrial Orchid Populations. Backhuys, Leiden, pp. 209-224.
- [35] Jersáková, J., Johnson, S. D., Kindlmann, P. (2006): Mechanisms and evolution of deceptive pollination in orchids. – Biol. Rev. 81: 219-235.
- [36] Johnston, K. M., Schmitz, O. J. (1997): Wildlife and climate change: assessing the sensitivity of selected species to simulated doubling of atmospheric CO₂. – Glob. Change Biol. 3: 531-44.
- [37] Kassambara, A. (2017): ggpubr: 'ggplot2' Based Publication Ready Plots. R Package Version 0.1.6.999. – <http://www.sthda.com/english/rpkgs/ggpubr>.
- [38] Kaźmierczakowa, R., Zarzycki, K. (2001): Red Data Book of Poland (in Polish: Polska Czerwona Księga Roślin). – Instytut Botaniki im. Władysława Szafera. Polish Academy of Sciences, Kraków.
- [39] Kindlmann, P., Jersáková, J. (2006): Effect of floral display on reproductive success in terrestrial orchids. – Folia Geobot. 41: 47-60. DOI: 10.1007/BF02805261.
- [40] Király, G. (2007): Red List of the Vascular Flora of Hungary (in Hungarian: Vörös Lista: A Magyarországi Edényes Flóra Veszélyeztetett Fajai). – Saját Kiadás, Sopron.
- [41] Lang, D. (2004): Britain's Orchids. – Wildguides Ltd., Old Basing.
- [42] Lenoir, J., Grégout, J. C., Marquet, P. A., de Ruffray, P., Brisse, H. (2008): A significant upward shift in plant species optimum elevation during the 20th century. – Science 320(5884): 1768-1771.
- [43] Micheneau, C., Duffy, K. J., Smith, R. J., Stevens, L. J., Stout, J. C., Civeyrel, L., Cowan, R. S., Fay, M. F. (2010): Plastid microsatellites for the study of genetic variability in the widespread *Cephalanthera longifolia*, *C. damasonium* and *C. rubra* (Neottieae, Orchidaceae), and cross-amplification in other *Cephalanthera* species. – Botanical Journal of the Linnean Society 163: 181-93.
- [44] Ministry of National Development and Economy (MNDI) (2010): Integrated Urban Development Strategy. Urban Development Handbook. – MNDI, Jászfényszaru, Hungary.
- [45] Molnár, V. A. (2011): Atlas of Orchids in Hungary (in Hungarian). – Kossuth Kiadó, Budapest pp. 375-76 (Kossuth Természettár).
- [46] Molnár, V. A. (2015): Climate change and orchids (in Hungarian: Klímaváltozás és orchideák). – Természettudományi Közlöny 146: 1.
- [47] Molnár, V. A., Máté, A., Sramkó, G. (2011): An unexpected new record of the Mediterranean orchid, *Ophrys bertolonii* (Orchidaceae) in Central Europe. – Biologia 66(5): 778-82.
- [48] Morellato, L. P. C., Alberton, B., Alvarado, S. T., Borges, B., Buisson, E., Camargo, M. G. G., ... Peres, C. A. (2016): Linking plant phenology to conservation biology. – Biol. Conserv. 195: 60-72.
- [49] Newman, R. D., Showler, A. J., Harvey, M. C., Showler, D. A. (2007): Hand pollination to increase seed-set of red helleborine *Cephalanthera rubra* in the Chiltern Hills, Buckinghamshire, England. – Conservation Evidence 4: 88-93.
- [50] Nilsson, L. A. (1983a): Mimesis of bellflower (*Campanula*) by the red helleborine orchid *Cephalanthera rubra*. – Nature 305.5937: 799.

- [51] Nilsson, L. A. (1983b): Processes of isolation and introgressive interplay between *Platanthera bifolia* (L.) Rich and *P. chlorantha* (Custer) Reichb. (Orchidaceae). – *Botanical Journal of the Linnean Society* 87: 325-350.
- [52] Parmesan, C., Hanley, M. E. (2015): Plants and climate change: complexities and surprises. – *Annals of Botany* 116(6): 849-864. DOI: <https://doi.org/10.1093/aob/mcv169>.
- [53] Parmesan, C., Yohe, G. (2003): A globally coherent fingerprint of climate change impacts across natural systems. – *Nature* 421(6918): 37-42.
- [54] Pellissier, L., Pottier, J., Vittoz, P., Dubuis, A., Guisan, A. (2010a): Spatial pattern of floral morphology: possible insight into the effects of pollinators on plant distributions. – *Synthesising Ecology* 119(11): 1805-1813. <https://doi.org/10.1111/j.1600-0706.2010.18560.x>.
- [55] Pellissier, L., Vittoz, P., Internicola, A. I., Gigord, L. D. B. (2010b): Generalized food-deceptive orchid species flower earlier and occur at lower altitudes than rewarding ones. – *J. Plant Ecol.* 3: 243-250. DOI: 10.1093/jpe/rtq012.
- [56] Pillon, Y., Chase, M. (2007): Taxonomic exaggeration and its effects on orchid conservation. – *Conserv. Biol.* 21(1): 263-265.
- [57] Pridgeon, A. (1996): *Orchids: Status Survey and Conservation. Action Plan.* – IUCN, Gland.
- [58] R Core Team (2017): *R: A Language and Environment for Statistical Computing.* – R Foundation for Statistical Computing, Vienna, Austria. <https://www.R-project.org/>.
- [59] Rahmstorf, S., Coumou, D. (2011): Increase of extreme events in a warming world. – *Proc. Natl. Acad. Sci. USA* 108: 17905-09.
- [60] Rankou, H. (2011): *Cephalanthera rubra*. The IUCN Red List of Threatened Species 2011. – IUCN, Gland.
- [61] Renner, S. S. (2006): Rewardless Flowers in the Angiosperms and the Role of Insect Cognition in Their Evolution. – In: Waser, N. M., Ollerton, J. (eds.) *Plant-Pollinator Interactions: from Specialization to Generalization.* The University of Chicago Press, Chicago, IL, pp. 123-44.
- [62] Root, T. L., Price, J. L., Hall, K. R., Schneider, S. H., Rosenzweig, C., Pounds, J. A. (2003): Fingerprints of global warming on wild animals and plants. – *Nature* 421: 57-60.
- [63] Rumpf, S. B., Hülber, K., Klöner, G., Moser, D., Schütz, M., Wessely, J., Willner, W., Zimmermann, N. E., Dullinger, S. (2018): Range dynamics of mountain plants decrease with elevation. – *Proc. Natl. Acad. Sci.* 115: 1848-1853. DOI: 10.1073/pnas.1713936115.
- [64] Scacchi, R., De Angelis, G., Corbo, R. M. (1991): Effect of the breeding system on the genetic structure in three *Cephalanthera spp.* (Orchidaceae). – *Plant Syst. Evol.* 176: 53-61. DOI: 10.1007/BF00937945.
- [65] Scotland, R. W., Wortley, A. H. (2003): How many species of seed plants are there? – *Taxon* 52: 101-04.
- [66] Seaton, P. T., Hu, H., Perner, H., Pritchard, H. W. (2010): Ex situ conservation of orchids in a warming world. – *The Botanical Review* 76: 193-203.
- [67] Selby, M. J. (1976): Slope erosion due to extreme rainfall: a case study from New Zealand. – *Geografiska Annaler. Series A, Physical Geography* 58: 131-38.
- [68] Sonkoly, J., Vojtkó, A. E., Tökölyi, J., Török, P., Sramkó, G., Illyés, Z., Molnár, V. A. (2016): Higher seed number compensates for lower fruit set in deceptive orchids. – *Journal of Ecology* 104(2): 343-351. <https://doi.org/10.1111/1365-2745.12511>.
- [69] Suetsugu, K., Naito, R. S., Fukushima, S., Kawakita, A., Kato, M. (2015): Pollination system and the effect of inflorescence size on fruit set in the deceptive orchid *Cephalanthera falcata*. – *J. Plant Res.* 128: 585-594. DOI: 10.1007/s10265-015-0716-9.
- [70] Summerhayes, V. S. (1985): *Wild Orchids of Britain.* – Collins, London.
- [71] Szlachetko, D., Skakuj, M. (1996): *Orchids of Poland (in Polish: Storzycyki Polski).* – Sorus, Poznań.

- [72] Tałałaj, I., Ostrowiecka, B., Włostowska, E., Rutkowska, A., Brzosko, E. (2017): The ability of spontaneous autogamy in four orchid species: *Cephalanthera rubra*, *Neottia ovata*, *Gymnadenia conopsea*, and *Platanthera bifolia*. – Acta Biol. Cracoviensia s. Bot. 59: 51-61. DOI: 10.1515/abcsb-2017-0006.
- [73] Thomas, C. D., Cameron, A., Green, R. E., Bakkene, M. B., Beaumont, L. J., Collingham, Y. C., Erasmus, B. F., De Siqueira, M. F., Gringer, A., Hannah, L., Huges, L., Huntley, B., Van Jarrsveld, A. S., Midgley, G. F., Miles, L., Ortega-Hueta, M. L., Petersen, A. T., Phillips, O. L., Williams, S. E. (2004): Extinction risk from climate change. – Nature 427: 145-48.
- [74] Thompson, R. S. (1990): Late Quaternary Vegetation and Climate in the Great Basin. – In: Betancourt, J. L., Van Devender, T. R., Martin, P. S. (eds.) Packrat Middens: The Last 40000 Years of Biotic Change. The University of Arizona Press, Tucson, Arizona, pp. 200-239.
- [75] Thuiller, W., Lavorel, S., Araújo, M. B., Sykes, M. T., Prentice, I. C. (2005): Climate change threats to plant diversity in Europe. – Proceedings of the National Academy of Sciences 102: 8245-50.
- [76] Tremblay, R. L., Ackerman, J. D., Zimmerman, J. K., Calvo, R. N. (2005): Variation in sexual reproduction in orchids and its evolutionary consequences: a spasmodic journey to diversification. – Biological Journal of the Linnean Society 84: 1-54. DOI: 10.1111/j.1095-8312.2004.00400.x.
- [77] Tutin, T. G., Heywood, V. H., Burges, N. A., Moore, D. M., Valentine, D. H., Walters, S. M., Webb, D. A. (1980): Flora Europaea. 5. – Cambridge University Press, Cambridge.
- [78] Tuulik, T. (1998): Orchids of Hiiumaa (in Estonian: Hiiumaa orhideed). – Pirrujaak 5 Biosfääri Kaitseala Hiiumaa Keskus, Hiiumaa.
- [79] Vakhrameeva, M. G., Tatarenko, I. V., Varlygina, G. K., Zagulskii, M. N. (2008): Orchids of Russia and Adjacent Countries (Within the Borders of the Former USSR). – A. R. G. Gantner Verlag, Ruggell, Liechtenstein.
- [80] Venables, W. N., Ripley, B. D. (2002): Modern Applied Statistics with S. Fourth Ed. – Springer, New York.
- [81] WMO, World Meteorological Organization (2011): Weather Extremes in a Changing Climate: Hindsight on Foresight. – WMO, Geneva.
- [82] Woodward, F. I., Lomas, M. R., Betts, R. A. (1998): Vegetation-climate feedback in a greenhouse world. – Phil. Trans. R. Soc. Lond. B 353: 29-39.
- [83] Young, A. G., Hill, J. H., Murray, B. G., Peakall, R. (2002): Breeding system, genetic diversity and clonal structure in the sub-alpine forb *Rutidosia leiolepis* F. Muell. (Asteraceae). – Biol. Conserv. 106: 71-78. DOI: 10.1016/S0006-3207(01)00230-0.
- [84] Ziegenspeck, H. (1936): Orchidaceae. – In: Inkirchner, O., Loew, E., Schroeter, C. (eds.) Lebensgeschichte der Blütenpflanzen Mitteleuropas. Band. 1, Abt. 4. Enke, Stuttgart.

APPENDIX

Table A1. The results of the pair-wise comparisons according to the degree of the deviation in the **height** of the individuals. The significant differences between the habitats are bold and marked with stars

Population pair	Estimate	95% confidence interval		Adjusted p-value
		Lower	Upper	
J - BB	2.125	1.83	2.467	<1e-04 ***
J - KO	1.79	1.418	2.28	<1e-04 ***
J - PP	1.86	1.497	2.32	<1e-04 ***
KO - BB	1.181	1.09	5.86	0.281
PP - BB	1.14	0.912	1.425	0.424
PP - KO	0.965	0.722	1.29	0.989

Table A2. The results of the pair-wise comparisons according to the degree of the deviation in the **number of leaves**. The significant differences between the habitats are marked with three stars

Population pair	Estimate	95% confidence interval		adjusted p-value
		Lower	Upper	
J - BB	1.300	1.200	1.417	< 0.001***
J - KO	1.140	1.005	1.300	0.0390 *
J - PP	1.012	1.106	1.134	0.9920
KO - BB	1.140	1.000	1.306	0.0579
PP - BB	1.288	1.143	1.452	< 0.001***
PP - KO	1.129	0.966	1.320	0.1820

Table A3. The results of the pair-wise comparisons according to the degree of the deviation in the **leaf area**. The significant differences between the habitats are bold and marked with stars

Population pair	Estimate	95% confidence interval		Adjusted p-value
		Lower	Upper	
BB - J	-0.429	-0.627	-0.232	< 1e-04 ***
KO - J	-0.518	-0.832	-0.204	<0.001 ***
PP - J	-0.580	-0.869	-0.290	< 1e-04 ***
BB - KO	0.089	-0.231	0.409	0.8875
PP - BB	-0.150	-0.445	0.145	0.5493
PP - KO	-0.061	-0.444	0.322	0.9755

Table A4. The results of the pair-wise comparisons according to the degree of the deviation in the number of flowers/individuals. The significant differences between the habitats are bold and marked with stars

Population pair	Estimate	95% confidence interval		Adjusted p-value
		Lower	Upper	
J - BB	1.839	1.385	2.441	<0.001***
J - KO	1.280	0.828	1.980	0.460
J - PP	0.913	0.625	1.335	0.925
KO - BB	1.437	0.912	2.265	0.169
PP - BB	2.014	1.348	3.010	<0.001***
PP - KO	1.400	0.833	2.358	0.337

Table A5. The results of the pair-wise comparisons according to the degree of the deviation in the number of fruits/individuals. The significant differences between the habitats are marked with three stars

Population pair	Estimate	95% confidence interval		Adjusted p-value
		Lower	Upper	
BB - J	16.66	7.240	38.46	< 0.001***
KO - J	27.27	10.58	70.24	< 0.001***
PP - J	4.63	1.550	13.83	0.0019**
KO - BB	1.646	0.874	3.10	0.1767
BB - PP	3.58	1.547	8.28	< 0.001***
KO - PP	5.89	2.260	15.33	< 0.001***

Figure A1. The distribution of the different traits in the different populations

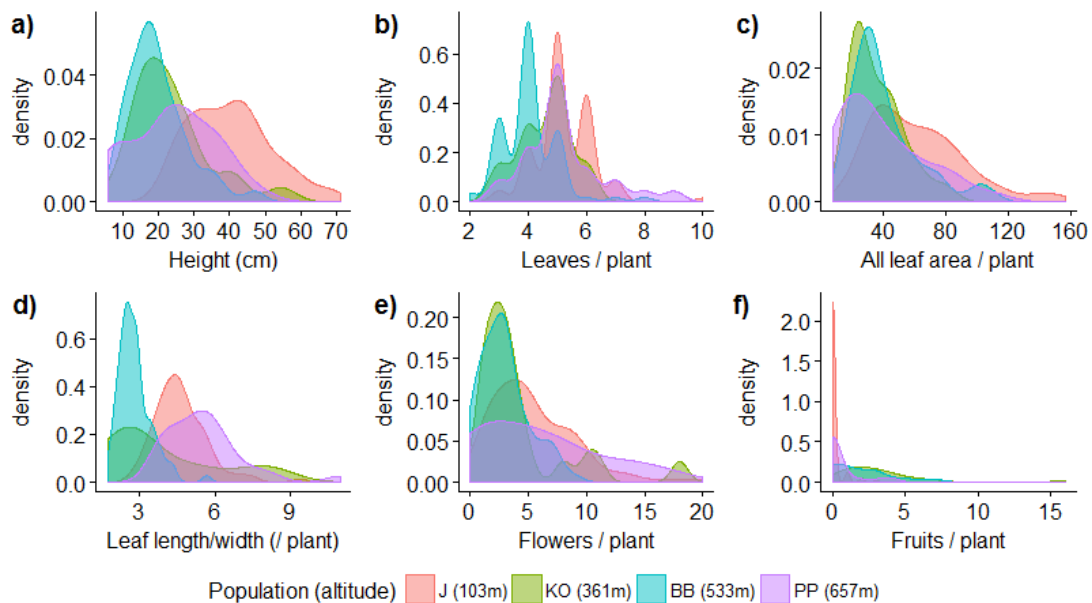
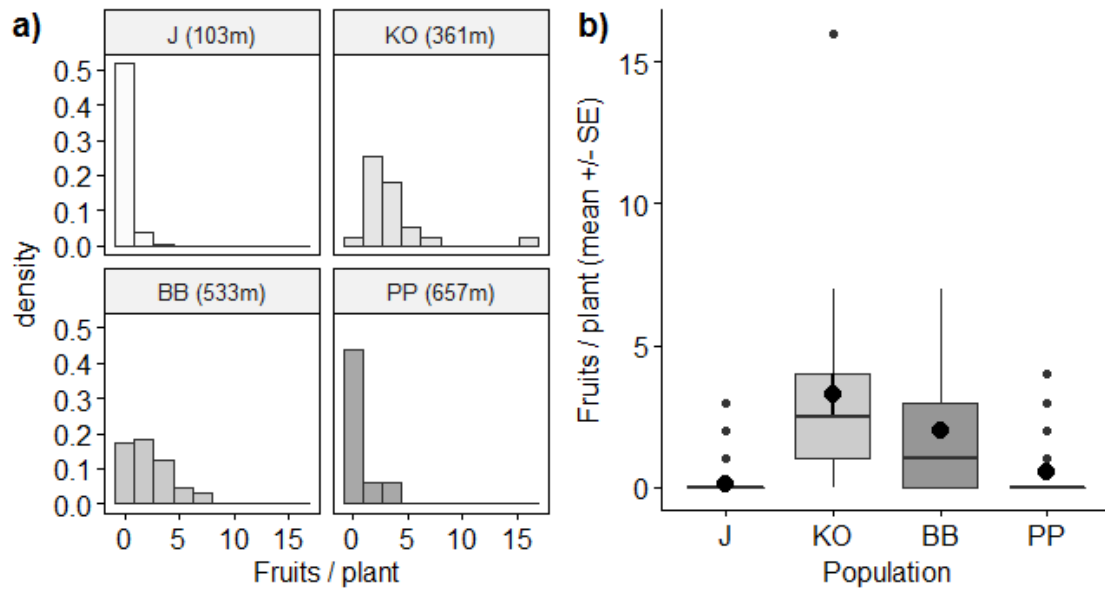


Figure A2. Number of fruits/individual in the different populations. In the KO population there was one plant which had an extremely high number of fruits, which makes difficult to see the slight differences between the populations



EFFECT OF NUTRIENT SOLUTIONS AND DIFFERENT PLANTING BED ON SOME GROWTH CHARACTERISTICS OF STEVIA REBAUDIANA IN INOCULUM CONDITIONS WITH MYCORRHIZAL FUNGUS

SEYEDMOHAMMADI, N. S.¹ – BARMAKI, M.^{1*} – DAVARI, M.² – HASHEMI MAJD, K.³

¹*Department of Agronomy and Plant Breeding, Faculty of Agriculture, University of Mohaghegh Ardabili, Ardabil, Iran*

²*Department of Plant Protection, Faculty of Agriculture, University of Mohaghegh Ardabili, Ardabil, Iran*

³*Department of Soil Science, Faculty of Agriculture, University of Mohaghegh Ardabili, Ardabil, Iran*

**Corresponding author
e-mail: barmakimorteza@gmail.com*

(Received 4th Jan 2019; accepted 12th Feb 2019)

Abstract. *Stevia* is a perennial plant and is well-known for its high content of steviol glycoside in dryleaf matter that is responsible for providing the non-caloric value sweet taste. *Stevia rebaudiana* leaves contain diterpen glycosides, which are about 250 to 300 times more sweetened than sucrose, and their sweeteners are widely used today in the food and pharmaceutical industries. In order to study the effect of mycorrhiza fungi on some growth characteristics of the stevia herb in inoculum conditions with mycorrhizal fungus, a factorial experiment based on randomized complete block design with four replications was conducted in greenhouse of Mohaghegh Ardabili University in 2016. The first factor was Imma & Angel and Novella nutrient solutions, the second factor was planting bed including leaf composts, vermicompost and biolan (peat & perlite) and third factor Inoculation with mycorrhiza and control fungi showed that the highest fresh and dry weight of leaves and number of number of leaves to the Imma & Angel nutrient solution in vermicompost planting bed under inoculation with mycorrhiza. The highest plant height was related to the Imma & Angel nutrient solution in leaf composts planting bed was observed under inoculum with mycorrhiza and the highest chlorophyll content was observed for Novella nutrient solution in vermicompost planting bed under inoculation conditions with mycorrhiza.

Keywords: *Stevia, biofertilizers, hydroponic, mycorrhiza*

Introduction

Stevia rebaudiana Bertoni (Asteracea family) is a herbaceous, perennial and indigenous herbaceous plant in Paraguay and Brazil and its leaf is used as a calorie-free natural sweetener for diabetic patients and for the prevention of obesity (Garana et al., 2010). *Stevia* has high nutrient requirements, especially N, P and K, and the lack of these elements has a major constraint on the quantity and quality of biomass of this plant (Pramanik and Singh, 2003). A proposal to prevent the effects of chemical fertilizers on the plant, which may overwhelm the good properties of the plant, is to examine the impact of bio-fertilizers that are present in mycorrhizal fungi or bacteria on the growth of this plant. Growth stimulating microorganisms include mycorrhizal fungi and a group of bacteria, and the most important glomus mycorrhizal fungi can be mentioned (Cocking, 2003). In hydroponic system, all essential elements should be given as soluble salts to the plant. A proper nutritional solution is a solution that

contains all the nutrients in certain concentrations, and the experts, based on the research components and the conditions of cultivation and plant species studied, have changed from standard solutions or different concentrations of it (Tabatabaei et al., 2006). Proper media, in addition to the desired physical, chemical and biological properties, should be accessible, sustainable and economically feasible (Davidson et al., 1998). The planting bed used in this qualification were listed (*Table 1*).

Table 1. Concentration of nutrient solution elements (mg / l)

Elements	Imma & Angel (2006)	Novella et al. (2008)
KNO ₃	40.4	505
Ca(NO ₃) ₂	254.2	656
NH ₄ NO ₃	352	47
KH ₂ PO ₄	598.4	240
MgSO ₄	96	180
Na ₂ MoO ₄	0.033	0/055
H ₃ BO ₃	2.21	1.56
CuSO ₄	0.481	0.912
ZnSO ₄	0.645	1.07
MnSO ₄	5.15	8.5
Fe-EDDHA	13.25	4

Vermicompost has substances such as plant growth hormones and enzymes that increase the microbial population of the soil and preserve the nutrients for longer periods without negative effects on the environment (Padmavathiamma et al., 2008). Perlite has a slight weight, is chemically neutral and has a high porosity and water holding capacity. Vermiculite also has a high cation exchange capacity and is chemically active (Malakouti et al., 2005). Perlites are often used alone or in combination with vermiculite 1: 1 volumes alone (Malakouti et al., 2008). This material provides suitable conditions for plant growth, such as ventilation, drainage and access to nutrients, especially in combination with other substrates (Martinez and Abad, 1992). Peat Moss is a degraded particle that is produced in humid and cold areas. The type of composition and its constituent varies in different types (Rafiei and Akbarzadeh, 2007).

Peat Moss is a plant material that breaks down slightly in mossy soils, as well as anaerobic conditions such as swamps and marshes, and has acidic pH. The cation exchange capacity of this substance is very high and the EC has a low (about ds.m 0.5) (Samiei et al., 2004). Mycorrhizal fungi in direct ways such as improving plant nutrition by increasing the absorption of water and nutrients, in particular, low-mobility elements such as phosphorus (Smith and Read, 1997), as well as the production of hormones such as auxin, cytokinin and abscisic acid in stimulating plant growth (Awotoye et al., 2009) and indirectly, such as reduction of biological stresses of plant diseases (Calvet et al., 1995) and non-toxic (salinity, drought, heavy metals, etc.) increase growth and yield Plants are hosted (Raiesi and Ghollarata, 2006). Research has shown that bio-fertilizers significantly provide plant nutrients such as nitrogen, phosphorus and potassium, and The other side protects the plant against various environmental stresses and increases plant resistance under stress conditions (Smith and Read, 1997).

The purpose of this study was to investigate the effect of nutrient solutions and planting bed (Peat moss and Perlite, leaf compost and vermicompost) simultaneously on *Glomus mosseae* mycorrhiza inoculum on some growth characteristics of stevia herb.

Methods and materials

In order to investigate the effect of Nutrient solutions and different planting bed on some growth characteristics of *Stevia rebaudiana* under inoculation with mycorrhizal fungus, a factorial design based on randomized complete block design with 4 replications in greenhouse of Mohaghegh Ardebili University in 2016 was conducted. The first factor was two levels: two different Nutrient solution solutions including Imma & Angel and Novella et al. (*Table 1*), the second factor was planting bed including Peat Moss and Perlite (Biolan), Vermicompost and Leaf composts in three levels and the third factor were inoculated with mycorrhizal fungus from *Glomus mosseae* and control treatment at two levels. After planting seedlings in pots, they were fed continuously with drops in nutrient solutions. Height of plant with ruler, number of leaves with counting, vegetation rate with cost meter (chlorophyll meter) Konica Minolta 502 according to SPAD index, fresh and dry weight of leaf was measured by digital scale. The analysis of data variance was done using SAS 9.2 software and the mean values were compared at the probability level of 1% and 5% using LSD Test.

Results and discussion

Leaf fresh weight

The results of analysis of variance of trait weight of leaf in stevia were significantly affected by the treatments at 1% level (*Table 2*). The results of analysis of variance of interaction between Nutrient solution solutions, different planting bed and inoculation with mycorrhizal fungus showed a significant difference. Mean comparison showed that the Imma & Angel solution in the planting bed of vermicompost under the conditions of mycorrhizal fungus (666.8 g) had the highest leaf fresh weight (*Table 3*).

Table 2. Analysis of variance of the effects of treatments on Leaf fresh weight, Leaf dry weight, Number of leaves, Plant height and Chlorophyll

Source of variances	Mean squares					
	df	Leaf fresh weight	Leaf dry weight	Number of leaves	Plant height	Chlorophyll
Repetition	3	6341/66	458/33	631637/5	712/423	18/57
Nutrient solution	1	88648/83**	732/57**	2643285/33**	1656/75*	147/17*
Planting bed	2	124957/51**	7237/26**	7710277**	347/078 ^{ns}	38/52 ^{ns}
Inoculation	1	46800/03**	2215/17**	99372**	2976/75**	0/574 ^{ns}
Planting bed×nutrient solution	2	78939/07**	727/6**	640164/33**	316/797 ^{ns}	31/48 ^{ns}
Nutrient solution×Inoculation	1	79283/76**	430/08**	2033633/33**	500/52 ^{ns}	30/16 ^{ns}
Planting bed×Inoculation	2	144228/91**	9578/57**	10889749**	1773/109*	116/122*
Planting bed×nutrient solution×Inoculation	2	11865/36**	1929/62**	4705210/33**	602/036 ^{ns}	182/967**
Error	33	520/04	19/17	4705210/33	386/62	24
%CV	-	14	10	9/5	20/23	12/88

**and * were significant at level of probability of 1% and 5% and without significant differences

Table 3. Comparison of the average effect of different treatments on Leaf fresh weight, Leaf dry weight, Number of leaves, Plant height and Chlorophyll

Treatments			Mean				
			Leaf fresh weight	Leaf dry weight	Number of leaves	Plant height	Chlorophyll
Novella	Leaf composts	Mycorrhiza inoculation	145b	46/8c	2332b	99/75abcd	36/45bc
		Control	81/5de	18/2g	993h	65/63d	41/838ab
	Vermicompost	Mycorrhiza inoculation	142/5b	77/5b	2080c	78/5de	45/513a
		Control	140/8b	38/6de	1736d	102/5abcd	37/2bc
	Peat moss & Perlite	Mycorrhiza inoculation	151/7b	39/7de	1480ef	109/63abc	39/388ab
		Control	84/7de	26/1f	687i	91/88bcde	38/213bc
Imma & Angel	Leaf composts	Mycorrhiza inoculation	150/3b	43/6cd	1646de	123a	36/225bc
		Control	123/6bc	35/2e	1060gh	81/5cde	41/538ab
	Vermicompost	Mycorrhiza inoculation	666/8a	128/1a	4653a	112ab	31/4cd
		Control	105/1cd	27/18f	1012h	96/25abcd	41/113ab
	Peat moss & Perlite	Mycorrhiza inoculation	96/7cde	26f	1270fg	107/5abc	38/463b
		Control	65/2e	18/3g	550i	98/13abcd	28/85d

Similar letters to the averages in each column indicate no significant difference at the 5% level (LSD test)

Leaf dry weight

The results of this experiment showed that this trait was affected by different nutrient solutions, different planting bed and inoculation with mycorrhizal fungus at a one percent significance level (Table 2). The results of analysis of variance of interaction between Nutrient solution solutions, different planting bed and inoculation with mycorrhizal fungus showed a significant difference. Mean comparison showed that the Imma & Angel nutrient solution in the planting bed of vermicompost had the highest leaf dry weight under inoculation with mycorrhizal fungus (128.1 g) (Table 3).

Research by Silveira et al. (2006) showed that the symbiosis of plants with mycorrhizal fungi improves plant growth characteristics, including the development of vegetative parts and the increase of fresh and dry weight of plant tissues. (Hawkesford et al., 2012) stated that phosphorus deficiency impairs plant growth and affects its various aspects of metabolism. Deficiency of phosphorus disrupts the transfer of water through the root, and because of the lack of adequate water for expansion of the cells, the leaves remain small and the growth of the air organs is prevented, thus, in the present experiment, Mycorrhiza fungus, with the availability of more phosphorus for the plant, increased the growth of the plant's airways. Also, vermicompost planting bed caused more vegetative growth because of the presence of more amounts of precipitated elements.

The trait of leaf number in *Stevia* plant was affected by the treatments at 1% level (Table 2). The results of analysis of variance of interaction between Nutrient solution solutions, different planting bed and inoculation with mycorrhizal fungus showed a significant difference. The mean comparison showed that the Imma & Angel diet in the planting bed of vermicompost had the highest number of leaves in inoculation with mycorrhizal fungus (4653) (Table 3). The growth of Imma & Angel, due to providing more suitable conditions for vegetative growth, resulted in more leaves. Vermicompost

has a positive effect on the amount of photosynthesis and production of biomass of stevia, by increasing the water absorption capacity and the optimum access to high-consumption and low nutrient elements, resulting in more plant growth and increased leaf number. Also, according to Yousefi Shayade et al. (2015), the planting bed containing vermicompost increased the number of leaves in the stevia. (Bachman and Metzger, 2008) reported that adding vermicompost to soil increases leaf number, leaf area. The amount of photosynthesis in the French spring rose. Today it is known that direct mycorrhizal fungi increase plant growth by direct methods such as improving plant nutrition through absorption of nutrients, as well as increasing plant and inbound water absorption, such as decreasing biological stresses (Tahat and Sijam, 2012). The increase in the number of leaves in plants was reported by inoculation with mycorrhizal fungus in comparison with non-inoculated plants in tomato (Khalied and Elkhider, 1993) and Citrus tangering seedlings (Wu and Xia, 2006). An increase in the number and level of leaf associated with mycorrhizal fungi has also been reported by Copetta et al. (2006) in Basil, which is consistent with the results of this experiment.

Plant height

The height of plant was affected by different nutrient solutions at 5% level, and the highest number of leaves belonged to Imma & Angel (91.313 cm). Inoculation with mycorrhizal fungus (105.063 cm) also showed a significant difference in the level of one percent (*Table 2*). The results of analysis of variance of interaction between different substrates of culture and inoculation with mycorrhizal fungi showed a significant difference at 1% level. The highest plant height was related to the culture of leaf soil culture under inoculation with mycorrhizal fungus with 111.375 (cm). The comparison of the mean showed that the Imma & Angel nutrient solution in the soil planting bed under inoculum conditions with mycorrhizae (123 cm) had the highest plant height (*Table 3*). Utumi et al. (1999) conducted a stevia test The effect of nitrogen nutrient deficiency on the absorption of high-energy elements by the plant was that they said that the deficiency of this nutrient component would reduce the absorption of high-energy nutrients in this plant and decrease the plant's height. Studies by Sheelavanta (1993) showed that with increasing nitrogen fertilization, the length of safflower stem increased. Principally, the cause of increasing altitude due to the use of urea can be attributed to the effect of nitrogen escalation on vegetative growth and cell division in the plant, especially the stem, and more photosynthetic extraction is expected to be produced by the plant, which is a good condition Provides for elongation of the stem (Nourmohammadi et al., 2001). Saberhamishiegi et al. (2012) reported a study on the effects of nitrogen and potassium on the *Stevia* plant. The highest stem length (altitude) was observed in 60 kg / ha treatment and the least nitrogen application was obtained. Due to the fact that the percentage of nitrogen in the Imma & Angel sugars is higher, it can be attributed to the effect of nitrogen on the height of plants treated with this solution. According to the results, arbuscular mycorrhizal fungi had a positive effect on growth traits (plant height and branch number), which was consistent with the results of Piedra et al. (2005) and Soriano et al. (2009).

Chlorophyll

The results of analysis of variance of interaction between Nutrient solution solutions, different planting bed and inoculation with mycorrhizal fungus showed significant differences. Comparison of the mean showed that Novella nutrient solution in

vermicompost was inoculated with mycorrhizal fungus at 45.513 (Table 3). With the presence of nitrogen in the chlorophyll components, it can be expected that with increasing nitrogen levels, it will have a significant effect on the chlorophyll content of leaves. The presence of chlorophyll as a source of light absorption and the synthesis of essential elements for the growth of plants associated with this element is critical (Saberhamishi et al., 2014). Sedeghi Moghadam and Mirzaie (2008) reported that adding vermicompost to soil causes nitrogen absorption by the roots, increasing vegetative growth and producing more leaves, which in turn increases the level of absorption of light, the level of photosynthesis, the creation and b, a hydrocarbon substances in leaves and total chlorophyll content increase.

Increasing chlorophyll content of leaves due to mycorrhizal coexistence can be due to increased phosphorus absorption from the soil by these fungi. Demir (2004) showed that mycorrhizal coexistence increases the concentration of chlorophyll in pepper plant leaves. According to the results of Hoseini et al. (2015), mycorrhizal inoculated plants contain more vegetation than control. Also, Tang et al. (2009) observed in their study of maize that insemination with the *G.mossea* mushroom improved the chlorophyll synthesis in the plant and increased the photosynthesis of the plant. They attributed this to increasing nitrogen absorption by mycorrhizal plants.

REFERENCES

- [1] Awotoye, O. O., Adewole, M. B., Salami, A. O., Ohiembor, M. O. (2009): Arbuscular mycorrhiza contribution to the growth performance and heavy metal uptake of *Helianthus annuus* LINN in pot culture. – *African Journal of environmental Science and Technology* 3: 157-163.
- [2] Bachman, C. R., Metzger, J. D. (2008): Growth of bedding plants in commercial potting substrate amended with vermicompost. – *Bioresour. Technol.* 99: 3155-3161.
- [3] Calvet, C., Pinochet, J., Hernandez-Dorrego, A., Estan, V., Camprubi, A. (2001): Field microplot performance of the peach-almond hybrid GF-677 after inoculation with arbuscular mycorrhizal fungi in a replant soil infested with root-knot nematodes. – *Mycorrhiza* 10: 295-300.
- [4] Cocking, E. C. (2003): Endophytic colonization of plant roots by nitrogen fixing bacteria. – *Plant Soil* 252: 169-175.
- [5] Copetta, A., Lingua, G., Bert, G. (2006): Effect of three AM fungi on growth, distribution of glandular facilitation of plant phosphate acquisition by arbuscular mycorrhiza from enriched soil patches roots and hyphae exploiting the same soil volume. – *New Phytol.* 133(3): 453-460.
- [6] Davidson, H., Mecklenburg, R., Peaterson, C. (1998): Nursery management: administration and culture. – Inc. New Jersey: 173.
- [7] Demir, S. (2004): Influence of arbuscular mycorrhiza on some physiological growth parameters of pepper. – *Turk. J. Biol.* 28: 85-90.
- [8] Gardana, C., Scaglianti, M., Simonetti, P. (2010): Evaluation of steviol and its glycosides in *Stevia rebaudiana* leaves and commercial sweetener by ultra-high-performance liquid chromatography-mass spectrometry. – *J. Chromatography A* 1217(9): 1463-1470.
- [9] Hawkesford, M., Horst, W., Kichey, T., Lambers, H., Schjoerring, J., Skrumsager Moller, I., White, P. (2012): Functions of macronutrients. – In: Marschner, P. (ed.) *Marschner's Mineral Nutrition of Higher Plants*. Oxford, UK. pp. 135-190.
- [10] Hoseini, R. Z., Goltapeh, E. M., Kalatejari, S., Dehghani Mashkani, M. R. (2015): Effect of vermicompost and inoculation of fungi on growth characteristics and steviosidicity of leafy herb (*Stevia rebaudiana* Betroni). – *Journal of Medicinal Plants* 4(56): 179-188.

- [11] Imma, F., Angel, M. (2006): Potato minituber production using aeroponics: Effect of plant density and harvesting intervals. – American Journal of Potato Research 83: 47-53.
- [12] Khalied, A. S., Elkhider, R. A. (1993): Vesicular-arbuscular mycorrhizas and soil salinity. – Mycorrhiza 4: 45-57.
- [13] Malakouti, M. J., Tabatabaei, J., Kafi, M. (2005): New methods for timely supply of nutrients in plants. – Senate Press, Tehran: 388.
- [14] Martinez, P. F., Abad, M. (1992): Soilless culture of tomato in different mineral substrates. – Acta Hort. 323: 251-259.
- [15] Nourmohammadi, G., Siyadat, S., Kashani, A. (2001): Agriculture (Vol. I-Grains). – Third edition, Shahid Chamran University Press. p. 446.
- [16] Novella, M. B., Andriolo, J. L., Bisognin, D. A., Melo, C. C., Guerra, B. M. (2008). Concentration of nutrient solution in the hydroponic production of potato minitubers. – Ciencia Rural, Santa Maria 38(6): 1529-1533.
- [17] Padmavathiamma, P. K., Li, L. Y., Kumari, U. R. (2008): An experimental study of vermi-biowaste composting for agricultural soil improvement. – Bio resource Technology 99: 1672-1681.
- [18] Paul, L. C., Metzger, J. D. (2005): Impact of vermicompost on vegetable transplant quality. – Hort. Sci. 40(7): 2020-2023.
- [19] Piedra, A., Sorianomartin, M., Sorriano, A., Fernandez, G. (2005): Influence of *Arbuscular mycorrhizas* on the growth rate of mist propagated olive plantlets. – Spanish journal of agricultural research 3(1): 98-105.
- [20] Pramanik, K., Singh, R. K. (2003): Effect of levels and mode of phosphorus application with and without biofertilizer on yield and nutrient uptake by chickpea (*Cicer arietinum*). – Ann. Agric. Res. New Sciences 24(4): 768.
- [21] Raiesi, F., Ghollarata, M. (2006): Interactions between phosphorus availability and an AM fungus (*Glomus intraradices*) and their effects on soil microbial respiration, biomass and enzyme activities in a calcareous soil. – Pedobiologia 50: 413-425.
- [22] Saberhameshagi, F., Torang, A. S. R., Mobalege, M., Dehpour, A. S. (2014): Effect of different levels of nitrogen and potassium on morphological and chemical characteristics of the *Stevia* plant. – The findings of modern agriculture 7(2): 128-135.
- [23] Sedghi Moghadam, M., Mirzaei, M. (2008): The Effect of Urban Waste Compost on the Quantitative and Qualitative Characteristics of Pumpkin (*Cucurbita Moschata* Duch. Ex Poir.). – Third National Recycling Congress and the Use of Renewable Organic Resources in Agriculture, Islamic Azad University, Khorasgan Branch, Isfahan, pp. 1-7.
- [24] Sheelavanta, M. N. (1993): Response of safflower (*Carthamus tinctorius* L.) varieties tonitrogen levels under rainfed condition. – M. Sc. (Agri.) Thesis, University of Agricultural Sciences Bangalore.
- [25] Silveira, S. A., Lorscheiter, R., Barrow, I. B. I., Schwarz, S. F., Souza, P. W. D. (2006): *Mentha piperata* as a multiplyin host of AM fungi. – [HYPERLINK "http://cassi.cas.org/publication.jsp?P=eCQtRPJo9AQyz133K_1l3zLPXfcr-WXfJIIAZaSqDc1O_ar-dDnYnTLPXfcr-WXfimSBIkq8XcUjhmk0WtYxnmzLPXfcr-WXfJNYTTBrP9cniVlhZUZVmng"](http://cassi.cas.org/publication.jsp?P=eCQtRPJo9AQyz133K_1l3zLPXfcr-WXfJIIAZaSqDc1O_ar-dDnYnTLPXfcr-WXfimSBIkq8XcUjhmk0WtYxnmzLPXfcr-WXfJNYTTBrP9cniVlhZUZVmng) Revista Brasileira. Pl. Med 8: 91-7.
- [26] Smith, S. E., Read, D. J. (1997): Mycorrhizal Symbiosis. – 2nd ed. Academic Press, San Diego, CA.
- [27] Soriano, A., Martin, M., Piedra, A., Azcon, R. (2009): *Arbuscular micorrhizal fungi* increased growth, nutrient uptake and tolerance to salinity in olive trees under nursery conditions. – Journal of Plant Physiology 166: 1350-1359.
- [28] Tabatabaei, J., Nazariju, R., Rostami, F., Azarmi, F., Pahnæi, S. (2006): Evaluation of nitrate concentration of leafy vegetables, germs and mites in Tabriz city. – Fourth Congress of Iranian Horticultural Sciences, Ferdowsi University of Mashhad.
- [29] Tahat, M. M., Sijam, K. (2012): Mycorrhizal fungi and abiotic environmental conditions relationship. – Res. J. Environ. Sci. 6: 125-133.

- [30] Tang, M., Chen, H., Huang, J. C., Tian, Z. Q. (2009): Arbuscular mycorrhiza fungi effects on the growth and physiology of (*Zea mays* L.) seedlings under diesel stress. – *Soil Biology Biochemistry* 41: 936-940.
- [31] Utumi, M. M., Monnerat, P. H., Pereira, P. R. G., Fontes, P. C. R., Godinho, V. D. P. C. (1999): Macronutrient deficiencies in *Stevia*: Visual symptoms and effects on growth, chemical composition, and stevioside production. – *Pesquisa Agropecuária Brasileira* 34(6): 1038-1043.
- [32] Wu, Q. S., Xia, R. X. (2006): Arbuscular mycorrhizal fungi influence growth, osmotic adjustment and photosynthesis of citrus under well-watered and water stress conditions. – *J. Plant Physiol.* 163: 417-425.
- [33] Yousefi Shayadeh, S. M., Chalavi, V., Zangi, S. (2015). Effect of different levels of vermicompost and duration of luminosity in greenhouse production of medicinal plant. – *Science and technology of greenhouse crops* 21(6): 31-38.

EFFECTS OF SHORT-TERM NITROGEN AND PHOSPHORUS ADDITION ON ROOT BIOMASS AND MORPHOLOGICAL CHARACTERISTICS OF *LIGUSTRUM LUCIDUM AIT* IN NEW RECLAMATION COASTAL FIELD

WANG, Z.^{1,2} – LIU, X.² – ZHANG, L.^{1,2} – JIANG, H.⁴ – DU, H.⁵ – YANG, D.^{6,7} – WU, H.³ – LIANG, J.^{3**} – CAI, Y.^{1,2*}

¹*Shanghai Key Lab for Urban Ecological Processes and Eco-Restoration
Shanghai 200241, China*

²*School of Ecological and Environmental Sciences, East China Normal University
Shanghai 200241, China*

³*Shanghai Academy of Landscape Architecture Science and Planning, Shanghai 200232, China*

⁴*Ecological Engineering College, Guizhou University of Engineering Science
Bijie 551700, Guizhou, China*

⁵*Shanghai Academy of Social sciences, Shanghai 200020, China*

⁶*School of Geographic Sciences, East China Normal University, Shanghai 200241, China*

⁷*Henan Key Laboratory of Integrative Air Pollution Prevention and Ecological Security,
College of Environment and Planning, Henan University, Kaifeng 475004, China*

**Corresponding authors
e-mail: ylcai@geo.ecnu.edu.cn*

(Received 9th Jan 2019; accepted 6th Mar 2019)

Abstract. Root system plays an important role in plant's nutrient acquisition and ecosystem carbon cycle. Nitrogen (N) and phosphorus (P) work significantly in promoting root system growth. To reveal the influence of N and P application on landscaping plants' root morphology characteristics, Ingrowth soil core fertilization method was applied in the coastal reclaimed soil (196.25 cm³) where *Ligustrum lucidum ait* grew from June to August in 2018. We set 11 processing gradients, including 0, 1, 3, 5, 7, 9, 11, 13, 15, 17, 20 g, and explored the influence of different N and P addition types on *Ligustrum lucidum ait* root morphology, biomass and other indicators. The results showed that compared with the control group, 3 g N application increased length of root by 62.39%, surface area by 120.87%, volume by 169.97%, biomass by 102.75%, root length density by 59.19% and root surface area density by 106.99%. 3 g P application increased those indexes by 77.37%, 111.15%, 147.50%, 98.05%, 73.87%, and 97.88%. The study indicated that compared with the control group, the application of 3 g N and P into 196.25 cm³ soil made significant differences on total length, diameter, surface area, volume, biomass, root length density, and root surface area density ($P < 0.05$).

Keywords: *root system, plant's nutrient acquisition, biomass, root morphology, Ligustrum lucidum ait*

Introduction

Most of the new coastal reclamation areas are the new land which forms through the sediment's being dredging from the seabed into the coastal tidal flat. After many years of natural desalination, salt washing and land abandonment for soil salinity reducing, they have gradually got suitable for the growth of green vegetation. However, this type of soil

is extremely deficient in nutrients, such as nitrogen and phosphorus, which is the key factor that restricts the growth of plants. The lack of nitrogen and phosphorus in soil will slow the growth of vegetation, which will affect the artificial afforestation and ecological restoration in the reclamation area. The problem of artificial afforestation and ecological restoration in the new coastal reclamation area is urgent to be solved.

The survival of artificial afforestation is determined by plant roots. Root system is the interface between plants and soil, and is an important organ that absorbs nutrients and water. Nutrient content in soil directly affects plant growth. The addition of nitrogen and phosphorus to soil can change the influence of soil environment, and then affect the characteristics of plant root system. Roots often adapt to the environmental changes by adjusting the characteristics of root system, such as morphology, surface area, volume and biomass, showing high plasticity (Pregitzer et al., 1993; Eissenstat and Yanai, 1997; Eissenstat et al., 2000; Robinson, 2010; Wurzbürger and Wright, 2016). Studies have shown that, under the condition of poor soil nutrients, the application of nutrient elements can help the root system grow rapidly enough to adapt to the changes in the environment (Schiefelbein and Benfey, 1991; Pregitzer et al., 1993; Bates and Lynch, 1996; Pregitzer et al., 1997, 2002; Wells et al., 2010; Robinson, 2010). For example, increased availability of soil nitrogen can lead to an increased fine root length, higher biomass and coarser diameters (Lynch, 1995; Messier, 2002; Pregitzer et al., 2002). It has also been found that N application increases root surface area and total length (King et al., 1997). It can also significantly affect the diameter, root length and specific root length of lower root order (Fitter and Stickland, 1991). Root plasticity has the same response to phosphorus (Fitter et al., 2010). For example, with the increase of soil phosphorus availability, *Larix gmelinii* increased root length to enhance the absorption of P, leading to the significant differences in root volume and lateral root tillers of *Pinus massoniana* in different species (Lynch, 1995).

However, most previous studies focused on the good soil environment and indoor experiments. The researches on phosphorus content in the wild arid field are very few. Then, the soil's nitrogen and phosphorus adding referred to be the surface spraying method, which was easily affected by weather (rain, snow), thus causing errors in the experiment results. Meanwhile, the way of adding nitrogen and phosphorus to soil was to apply fertilizer to the existing roots. The sampled roots included both old roots and new roots which grew right after the nutrient adding, so it's impossible to determine its specific influence on the characteristics of old roots or new roots. Ingrowth soil core avoids the above problems and can help master the growth characteristics of new root under different treatment conditions. And it can also contribute to clarifying the relationship between new root characteristics and soil nutrients (Peterjohn et al., 1999; Mcgrath et al., 2001).

Therefore, this study chose *Ligustrum lucidum ait* which grew on Shanghai coastal reclaimed soil with poor nitrogen and phosphorus content as the research object, applied ingrowth soil core to carry out short-term experiment of nitrogen and phosphorus adding to investigate the response of *Ligustrum lucidum ait* root morphology, biomass and other characteristics to soil's short-term nitrogen and phosphorus addition, so as to provide basic reference materials for the study on the relationship between root morphology and soil resource effectiveness as well as the construction and ecological restoration of artificial forests.

Materials and methods

Study area

The field site (30 ° 52 '54" N, 121 ° 54 '24 "E) was located in Lingang new Urban area in Shanghai (Fig. 1). It was damp, windy, warm, humid with abundant rainfall as well as with abundant sunshine in the region with four distinct seasons. And the annual average temperature in 2018 was 15°C to 15.8°C, with the lowest temperature (3.3°C) in January, the highest temperature in August (38°C). The annual total sunshine was 2000-2200 h, the annual precipitation was 900-1050 mm and the monthly average evaporation is 91.9 mm, which was a typical subtropical maritime climate. Soil was that of saline and alkaline sandy soil. Soil with a pH value greater than 8.5 took up 97.5%, and the organic matter content was less than 20 g/kg. The groundwater level was between 0.5 and 2.5 m. In order to solve the problem of barren soil vegetation, different vegetation planting experiments were carried out. Vegetation planting began in February 2010 and was completed in April 2010. The test site was 1200 m long, 20 m wide and 24000 m² for total area. All the plants in the site were native species. Representative plant *Ligustrum lucidum ait* was selected as the experimental sample.

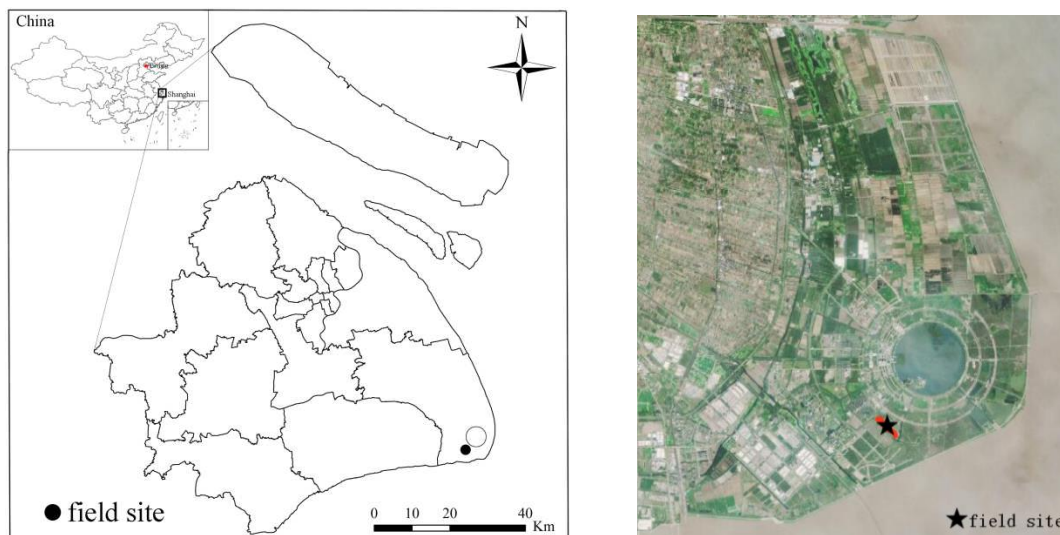


Figure 1. Map of the study area

Plot design

In the privet plantation (8 years old), a fixed standard plots of 20×30 m were set, and the privet with the same chest diameter, crown width and tree height were selected as samples in the sample plot (Table 1). The field within 1 m from the tree trunk was fertilized. A total of three groups were designed. I for nitrogen treatment, ten fertilizing gradients were set as: 1, 3, 5, 7, 9, 11, 13, 15, 17, 20 g; II for phosphorus processing, the gradients were set the same as those of nitrogen; III no treatment was done as a control.

Plant root sampler (l=10 cm, φ=5 cm, h=10 cm) was used. Most root system evenly distributed in surface area (Wang, 2004; Jiang, 2016), and the sampling depth was 10 cm. Then with the trunk as the center, 1 m from the center of trunk as the radius for sampling, 9 soil column samples were taken at the same distance around each tree, and 3 privet samples were taken as a treatment (Fig. 2). There was a total of 63 samples of *Ligustrum*

lucidum ait, and a total of 567 sample points were set. All roots were removed from soil cores with a sieve with a diameter of 3 mm. The soil was kept without roots, and then N, P was added to the soil. 270 soil cores of 30 privet samples were dealt with N of the 10 gradients, while another 270 soil cores of 30 privet samples were dealt with P of the 10 gradients, and 27 sampling points of three privet samples were not done with any fertilizer processing thus as a control.

Table 1. Tree and Soil characteristics properties

Tree characteristics		Soil characteristics	
Tree height (m)	4.37±0.31	pH	8.79±0.09
DBH (cm)	10.01±0.27	EC (ms/cm)	0.42±0.06
Crown width (m)	2.31±0.25	Organic matter (g/kg)	3.60±0.63
Plant distance (m)	3×3	Total salt content (g/kg)	0.78±0.03
Planting age (years)	8	Bulk density (g/cm ³)	1.37±0.02
		Soil Moisture (%)	29.23±2.92
		Total N (g·kg ⁻¹)	0.82 ± 0.04
		Total P (g·kg ⁻¹)	0.27 ± 0.02
		Total K (g·kg ⁻¹)	11.85 ± 0.73
		Texture	Sand loam

Data are provided in the form of mean ± standard deviation (SD). *DBH* diameter at breast height or basal

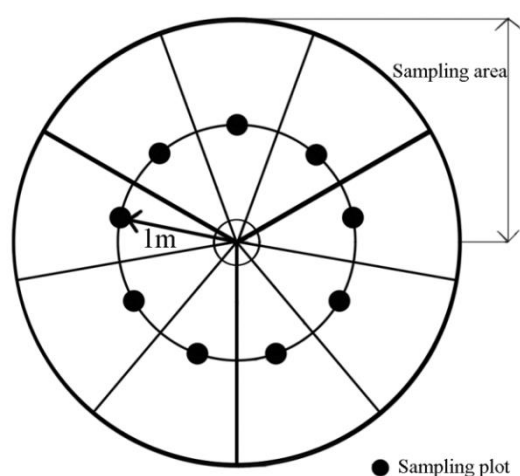


Figure 2. Sample points for soil N and P addition

Urea (CON₂H₄, 43% nitrogen content) was chosen as N fertilizer and calcium superphosphate (P₂O₅, 13% phosphorus content) as P fertilizer. Then the treated soil was put into nylon mesh bags with a pore size of 2 mm (l=10 cm, w=6cm), then the nylon mesh bags were placed in the cavities made through the core drilling. Then the soil inside the cores was gently patted, making its bulk density to a certain extent consistent with the surrounding soil bulk density. Then PVC tubes were put in the core positions (φ=5 cm, h=1 cm). The PVC pipes were covered with thin soil, in case that soil erosion caused by rainfall should affect the experiment results. The soil cores were set from June 16th, 2018 to June 18th, 2018 when it's the peak growth season for privet root system as well as the

most demanding season of privet for nitrogen and phosphorus fertilizer to blossom. During the study period in 2018, the average temperature was 18~28°C. The average precipitation was 134 mm. The average soil moisture content was 19.09%, and the average soil temperature was 21.34°C. The average temperature in July was 21~30°C, the average precipitation was 156 mm, the average moisture content of soil was 27.58, and the average temperature of soil was 28.41°C. In August, the average temperature was 20~30°C, the average precipitation was 140 mm, the average moisture content of the soil was 23.79 and the average temperature of the soil was 26.51°C.

Root sampling

The fine roots of *Ligustrum lucidum ait* grew slowly after August, so the soil cores was removed again (Wang, 2004; Jiang, 2016) after 60 days of root removal (in mid-August). The roots between nylon mesh and soil were cut off with a sharp soil knife. The soil cores were cut with a soil knife at the bottom and the excavated cores were taken out. Then, they were put into plastic bags and brought back to the laboratory in time.

Root determination

After the soil core being fully rinsed in water, the roots in nylon bags were sifted out with a soil sieve with a 2 mm diameter and the root surface were dried with absorbent paper. The prepared root samples were placed in a transparent scanner tray for the roots' full stretching. The root samples were scanned with a digital scanner Epson scanner. The root scan & analysis system of Win-RHIZO 2005C (Regent Instruments Inc., Quebec, Canada) was used to scan the root image and the length, diameter, surface area and other data of the root system were obtained then. Afterwards, root samples were placed in 80°C oven for drying for 48 h to a constant weight, and then the dry weight was weighed (accuracy: 0.0001 g). According to the root length and dry weight of each sample point, we calculated the biomass and specific root length, and then calculated root length density, specific surface area and surface area density according to the root length, surface area and the volume of soil cores. Finally, we calculated the average value of the samples in 27 soil cores in each treated soil layer and converted the average values into root biomass, root length density, specific root length, specific surface area, and root surface area density per unit volume. Root biomass, root length density, specific root length, specific surface area, and root surface area density were calculated as follows:

$$\text{Root biomass (g/m}^2\text{)} = g \times A \quad (\text{Eq.1})$$

$$\text{Root length density (m/m}^3\text{)} = L/V \quad (\text{Eq.2})$$

$$\text{Specific root length (m/g)} = m/g \quad (\text{Eq.3})$$

$$\text{Specific surface area (cm}^2\text{/g)} = a/g \quad (\text{Eq.4})$$

$$\text{Root surface area density (m}^2\text{/ m}^3\text{)} = a/V \quad (\text{Eq.5})$$

where, a is Root surface area; A is the area of soil; g is fine root dry weight; L is total length of fine root; m is the length of dry fine root in each Sample point; V is the volume of soil.

Statistical analysis

The average value of each processed sample was calculated and was ready for statistical analysis. Univariate anova and LSD multiple comparisons ($\alpha = 0.05$) were used to test the significant differences in the effects of different nitrogen and phosphorus addition treatments on the total length, average diameter, surface area, volume, biomass, specific root length, root length density, specific surface area, and root surface area density of the great privet root system. All statistical analyses were performed with SPSS 20.0 (IBM SPSS, Chicago, USA) software. Excel 2010 software was used to draw pictures.

Results

Effects of N and P addition on root morphology

As is seen in Fig. 3a, the total length of the root-system of *Ligustrum lucidum ait* appeared to increase first and decrease later under different N treatments. When 1 and 3 g were added, compared with the control group, the total length of root significantly increased by 57.62% and 62.39% ($P < 0.05$), when 5-11 g nitrogen were respectively applied, the total length of root system decreased gradually. No root growth was observed when 13 g N was applied. Under different P treatments, when 1 and 3 g were added, the root total length increased by 9.50% and 77.37% ($P < 0.05$). With 5-20 g applied, the total length of the root system gradually decreased, but no non-root-growth was found (Fig. 3a).

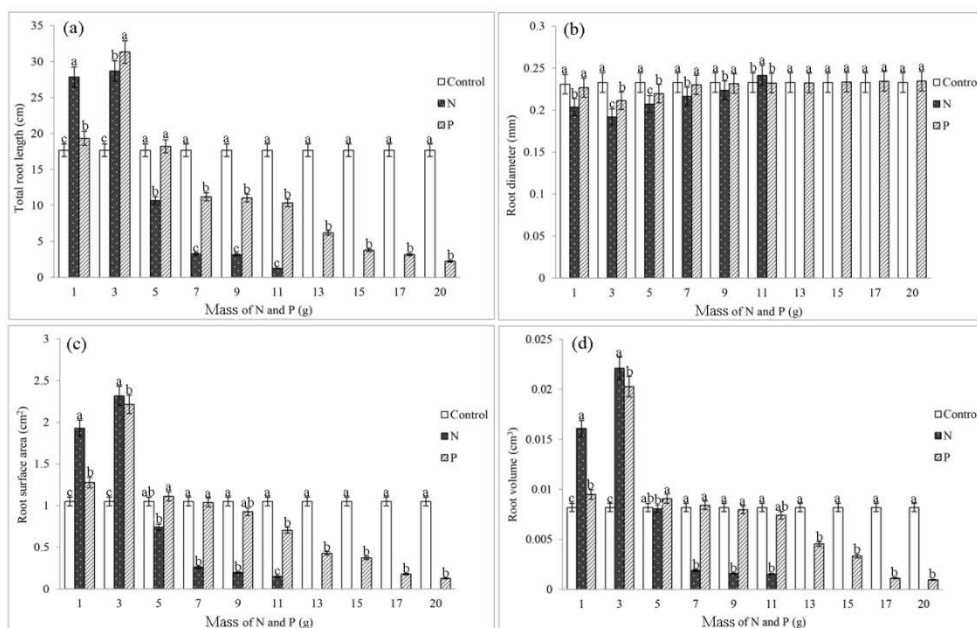


Figure 3. Effects of fertilization on the morphology of the root system of *Ligustrum lucidum ait*. (a) total root length, (b) root diameter, (c) root surface area, (d) root volume

The average diameter of root showed a tendency of thinning first and thickening then under different nitrogen and phosphorus treatments (Fig. 3b). Compared with the control group, the average diameter of the privet roots was thinned and significant difference was

found when 1 and 3 g N were applied ($P < 0.05$). When 3 g N was applied, the average diameter of root system reduced to the minimum, 0.19 mm. The average diameter of root system gradually increased when 5-11 g nitrogen were applied, and the maximum diameter 0.24 mm appeared at 11 g. When 1-20 g P were applied, the average diameter of roots showed a trend of thickening after thinning. When 3 g P was applied, the average diameter of the root system reduced to the minimum and the significant difference was achieved ($P < 0.05$). When 20 g P was applied, the maximum diameter was 0.23 mm.

When 1, 3 g N and P were applied, the average surface area and volume of root system gradually increased and the significant difference occurred, compared with the control group ($P < 0.05$) (Fig. 3c,d). The root surface area increased by 45.61% and 120.87%, and root volume increased by 96.34% and 169.97% when 1 and 3 g nitrogen were applied. With 5-11 g N, root surface area and volume gradually decreased. When 1 and 3 g P were applied, the root surface area increased by 21.79%, 111.15%, and the volume 15.96%, 147.50%. And the difference was significant ($P < 0.05$). When 11-20 g P were applied, compared with the control, no significant difference was found about the root diameter ($P > 0.05$) (Fig. 3b).

Effects of N and P addition on root biomass, root length density and specific root length

As is seen in Fig. 4a, with the increase of nitrogen and phosphate application, root biomass showed a trend of increasing first and decreasing then. Compared with the control group, the biomass and root length density of privet root increased and significant differences were found when 3 g N and P were applied ($P < 0.05$).

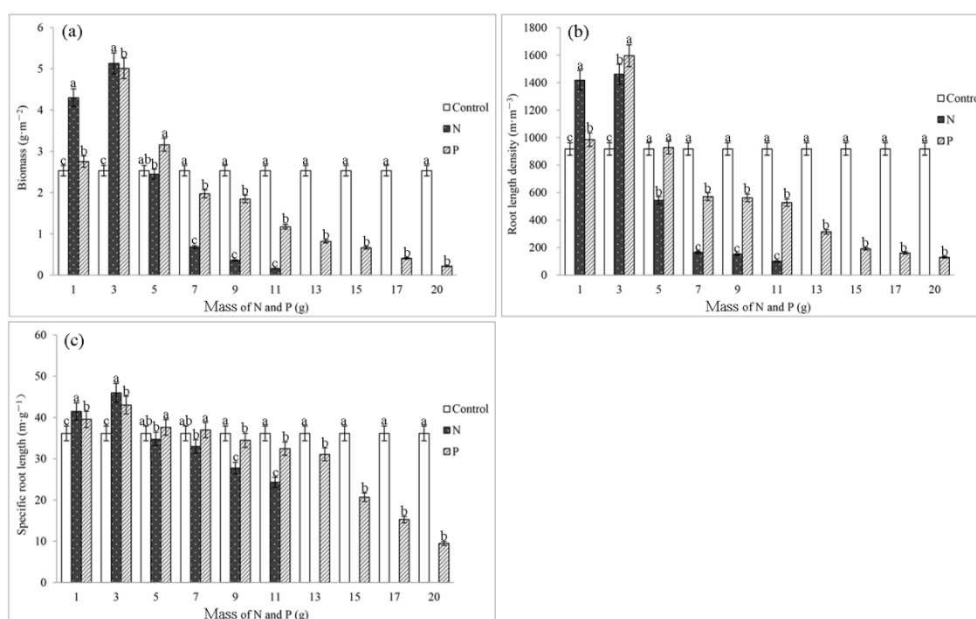


Figure 4. Effects of fertilization on root biomass (a), root length density (b), and specific root length (c) of *Ligustrum lucidum ait*

The application of 1 and 3 g N increased the biomass by 69.85% and 102.75%, respectively 4.30 g·m⁻² and 5.13 g·m⁻², and it also increased the root length density by 54.51% and 59.19%, respectively 1417.99 m·m⁻³ and 1460.90 m·m⁻³. The application of 3 g P increased the biomass by 98.05% and the root length density by 73.87%, respectively 5.01 g·m⁻² and 1595.62 g·m⁻² (Fig. 4a,b).

With the increase of N application, specific root length increased first and decreased then. When 1 and 3 g N and P were applied, the specific root length significantly increased compared with the control ($P < 0.05$) (Fig. 4c). The maximum specific root length reached $45.96 \text{ m}\cdot\text{g}^{-1}$ and $43.01 \text{ m}\cdot\text{g}^{-1}$ when nitrogen and phosphorus were applied to the roots respectively. The effect of nitrogen on specific root length was more significant compared with phosphate. When 5-11 g nitrogen were applied, the specific root length gradually reduced. The root stopped growing at 13 g. When 5-20 g phosphate fertilizer were applied, the specific root length gradually reduced.

Effects of N and P on specific surface area and surface area density

As is seen in Fig. 5a, with the increase of N and P application, the specific surface area of root showed a trend of increasing first and decreasing then. Compared with the control group, the root specific surface area reached the maximum and significant difference was found ($P < 0.05$) when 7 g N and P were applied ($350.20 \text{ cm}^2\cdot\text{g}^{-1}$ and $279.02 \text{ cm}^2\cdot\text{g}^{-1}$). With the increase of N and P application, the surface area density increased first and decreased then (Fig. 5b). Compared with the control group, the root surface area density had a significant difference ($P < 0.05$) when 1 and 3 g N and P were applied. The root surface area density was also the largest, increasing by 106.99% and 97.88%, respectively, which were $1.18 \text{ m}^2\cdot\text{m}^{-3}$ and $1.13 \text{ m}^2\cdot\text{m}^{-3}$ when 3 g N and 3 g P were added (Fig. 5b).

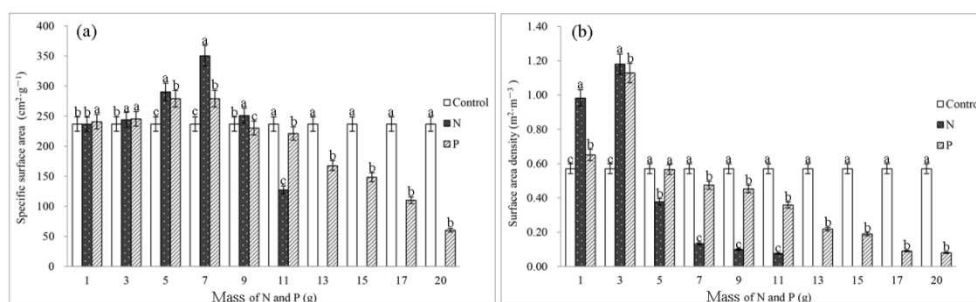


Figure 5. Effects of fertilization on specific surface area (a) and surface area density (b) of the root system of *Ligustrum lucidum ait*

Discussion

Effects of N and P addition on root morphology

Studies have shown that plant roots are highly plastic and can respond to the availability of different soil N and P contents. That is to say, when nutrients are limited, the ability to obtain nutrients can be improved by increasing the total length, surface area and volume of roots (Cuevas et al., 1991; Schmid and Kazda, 2002; Yang et al., 2003).

Increasing root length is an effective strategy for plants' nutrient and water obtaining. Under the treatments of 3 g N and 3 g P, the total length of root system increased by 62.39% and 77.37%, Wang et al. (2005) got this result too. Different nitrogen and phosphorus treatments had different effects on the total length of the root system of privet (Fig. 3a,b). Among those, 1 g, 3 g N and P significantly increased the total length of root system. 5-11 g N applications significantly decreased the total length of root system. No root growth was observed when 13-20 g N were applied. The total length of root system

significantly decreased when 5-20 g P were applied and no root growth was found. The reason was that the application of 1 g, 3 g N and P can change the ways of root system to obtain nutrient resources, promote the growth of the root system, and reflect the effects of N and P on the promotion (positive feedback) of the root system. Secondly, the lignification degree of the newly formed root system was low, which was easily affected by the soil environment and was very sensitive to the changes of soil resources. To obtain more nutrients, the root system grew rapidly. The applications of 5-20 g N and P inhibited the root growth to some extent, especially the death of plant roots was found after 13g addition of N.

Root diameter is an important parameter reflecting root structure and function (Robinson, 2010). Under different nitrogen and phosphorus treatments, the average diameter of root showed the phenomenon of first thinning and then thickening (Fig. 3b). N application of 1 g, 3 g and 5 g had a significant impact on the average diameter of root system, under which the average diameter became thinner. The average diameter under P application of 5-20 g gradually increased. The reason why the diameter first decreased and then increased under different fertilization treatments was that under the condition of low addition of N and P, the extension of root cells made the root diameter decrease for the root system to obtain more nutrient resources. With the high addition of N and P, N relatively inhibited the growth of the root system. To survive, the root system changed its survival strategies, appearing to be the increase of the root diameter and the prolonging of the root life to obtain nutrients and maintain its survival. For example, Wells et al. (2002) proved the relationship between root life and diameter of *Amygdalus persica l.* And it testified to a significant positive correlation between root life and diameter (Wells et al., 2002). Kern (2004)'s research showed that fertilization could significantly increase the root diameter of a poplar and shorten the root turnover time (Kern et al., 2004). According to the characteristics of root plasticity and the "cost-benefit" theory, the growth strategy of the root system always tends to choose the method with the minimum cost and the maximum benefit for survival (Eissenstat and Yanai, 1997; Bardgett et al., 2014).

Different N and P treatments can significantly affect root surface area and volume (Fig. 3c,d). Compared with the control group, application of 1 g, 3 g N and P increased root surface area by 45.61%, 120.87%, root volume by 96.34% and 169.97%. The increase of root surface area and volume is a way for the root system to have greater absorption surface area and maximally obtain soil nutrient resources.

Effects of N and P addition on root biomass, root length density, specific root length and surface area density

Addition of N and P significantly affected root biomass and root length density (Fig. 4a,b). At present, the effects of increased soil nitrogen availability on root biomass and production appear to be reduction and increase (Cotrufo and Gorissen, 1997; Kou et al., 2015). For example, the application of N can increase the fine root biomass of *Populus deltoides* by 21% (Kern et al., 2004) and the fine root biomass of *Picea abies* by 92% (Majdi, 2001). For example, the application of N can reduce the fine root biomass of *Larix kaempferi* by 15% and that of *Pseudotsuga menziesii* by 40% (Son and Wang, 2010). The response of root biomass to N addition may be related to the climate and soil nutrient conditions in the study area. And the effect of N addition on root biomass is also related to the genetic characteristics, phenological characteristics, N addition amount and treatment time of different roots.

In this study, compared with the control group, the biomass of root significantly increased after 1 and 3 g N application (69.85% and 102.75%, respectively) (Fig. 4a). Root biomass significantly decreased after 5-11 g N applications ($P < 0.05$). When 13 g N application was applied, no root growth was observed, and high nitrogen directly caused little root growth, reflecting the negative feedback effect of N on root. The increase of root biomass may be attributed to the increase in the effectiveness of soil N following the fertilization, which met the demand for N of the root system. Plant roots adopted the strategy of "rapid investment - income" to increase the carbon distribution to the root system and promote the growth of the root system. High nitrogen inhibits the growth or non-growth of the root system, leading to the reduction of root biomass. With respect to phosphorus addition, the biomass of root significantly increased after the 3 g phosphate fertilizer application (an increase of 98.05%). The reason may be that the phosphorus elements were involved in the composition of nucleic acids, nucleotides, and phospholipids, which was also the main component of cytoplasm and nuclei, so under a reasonable phosphorus add, the elongation of root cells can be increased. The total root length and root length density increased, leading to the increase of biomass. Under the treatment of high phosphorus, the root cell elongation decreased, root length decreased, and the biomass showed a trend of gradual decreasing. Root biomass gradually reduced when 5-20 g phosphate fertilizers were applied.

Specific root length refers to the total root length of unit mass root system, and it is an important indicator of root morphology and physiological function (Eissenstat, 1992; Pregitzer et al., 2002). Studies have shown that the value of specific root length is associated with the effectiveness of soil resources (Burton et al., 2000; Gordon and Jackson, 2000). It is generally believed that a root with a larger length has relatively higher nutrient and water absorption efficiency, and the value of specific root length can indicate the physiological activity of the root (Pregitzer et al., 2002).

The effects on specific root length are manifested in: under low N/P addition, compared with the control, the specific root length significantly increased ($P < 0.05$), and the high addition of N/P (5-20 g) significantly inhibited the increase of root length (Fig. 4c). The main reason was that the newly formed long roots had low lignification degree and high plasticity, and were easily affected by the soil environment, leading to the root system's length adjustment to satisfy its absorption of nutrients from soil (Guo et al., 2004). Different N and P addition's influence on root length density and surface area density was consistent with that of root biomass (Fig. 4b,5b). Among those, under the application of 5 g nitrogen and phosphorus, the root length density under phosphorus treatment was 9.22% higher than that under nitrogen treatment. The reason may be that under reasonable fertilization, phosphate fertilizer can increase the number of root tillers and stem tillers, leading to the increase of underground biomass and root length density.

In general, in the case of 1 g, 3 g N and P, N had a significant effect on total length, surface area, volume, biomass, and root length density of the root system, whose reason may be related to the mobility of N and P elements in soil. Phosphate roots in soil are usually affected by the obligate adsorption of iron oxide and aluminum oxide in soil. In the soil, N has a stronger mobility than P, mainly because nitrate nitrogen mobility is very strong. Under the condition of good ventilation, ammonia nitrogen can be converted into nitrate nitrogen through the action of nitrifying bacteria. The nitrate nitrogen which has a good mobility can easily spread to the root surface, realizing the rapid absorption of N elements and promoting the changes of root morphology and the biomass increase (Wang, 2004).

Scientific fertilization of artificial forests in new reclamation areas

N and P are the most demanding limiting nutrients for plant root growth. According to the cost-benefit theory, root growth depends on a large amount of nitrogen and phosphorus input (Eissenstat and Yanai, 1997; Nadelhoffer, 2000; Norby and Jackson, 2000). For example, Jackson et al. (1997) found that for every unit of nitrogen absorbed by the root system, 41 units of carbon were consumed (Jackson et al., 1997). Statistics also showed that when the first fruit of tomato grew to 4 cm in length, the amount of phosphorus absorbed from soil accounted for about 90% of that in the whole growth period. Therefore, the effectiveness of soil N and P significantly affected root growth. Hendrick and Pregitzer (1996) believed that root biomass may be positively correlated with soil nutrient availability or negatively correlated, depending on the plant species and the spatial heterogeneity of available nutrients distributed in soil (Hendrick and Pregitzer, 1996). In this study, it was found that the total length, surface area, volume, biomass, root length density and surface area density of the roots significantly increased when 1 g, 3 g N and P were applied, among which the effect of 3 g N and P was the best, showing that N and P promoted (positive feedback) the root system. When 5-20 g N and P were applied, the total length, surface area, volume, biomass, root length density and surface area density of the root significantly reduced, reflecting the inhibition (negative feedback) of N and P on the root system. Among those, no root growth was found in the soil core when 11 g N was applied, seriously hindering the growth of the root system. Although the soil's N and P content in coastal salt land is very low for the growth of vegetation, it is not better to apply more N and P but better to master the threshold of N and P required by plants. In this way a scientific and reasonable fertilization can be achieved.

Plant root growth, death and turnover is a dynamic process. The time of experiment design makes a great difference to the results of the experiment. In different months, root growth, death and turnover laws are constantly changing (Pregitzer et al., 1993). The effect of fertilization on the annual and monthly dynamics of root system needs to be further studied in the future. In this experiment, root systems were not classified. In different N and P treatment cases, the differences between all levels of N and P content within the root sequences and the different treatments are not clear. From the research of root physiological processes of carbon - nitrogen - phosphorus, it's more helpful for knowing the root better, and more helpful for knowing soil's N and P availability and reaction mechanism of spatial heterogeneity better, all of which needs to be discussed further.

Conclusions

The results showed that reasonable addition of N and P could significantly change the morphology and biomass of root system. Reasonable N and P add (3 g) can make the root total length, surface area, volume, biomass, root length density and root surface area density increase significantly, reflecting the promotion of root system (positive feedback) of N and P. More of that than the threshold will reduce these indexes gradually, reflecting the nitrogen and phosphorus's inhibition to the root system (negative feedback). With the treatments of different N and P gradients, the root diameter showed a tendency of first thinning and then coarsening, and the specific root length and specific surface area showed a trend of first increasing and then decreasing. The main reason for the occurrence was that the mobility of the two elements in soil was related to the absorption strategy of the root system. The study showed that the application of 3 g N and P into the soil filled

with 196.25 cm³ significantly promoted the growth of the root system, and more of that than the threshold will lead in the inhibition of N and P on the root. Short-term N and P addition had significant effects on total length, diameter, surface area, volume, biomass, root length density, specific root length, specific surface area and root surface area density of the privet root system ($P < 0.05$).

Acknowledgments. This project was supported by Science and Technology Commission of Shanghai Municipality (17DZ1202801). The soil research institute, planning research institute and ecological research institute of Shanghai Academy of Landscape Architecture Science and Planning also gave strong support to the research.

REFERENCES

- [1] Bardgett, R. D., Mommer, L., DeVries, F. T. (2014): Going underground: root traits as drivers of ecosystem processes. – *Trends in Ecology & Evolution* 29(12): 692-699.
- [2] Bates, T. R., Lynch, J. P. (1996): Stimulation of root hair elongation in *Arabidopsis thaliana* by low phosphorus availability. – *Plant Cell and Environment* 19: 529-538.
- [3] Burton, A. J., Pregitzer, K. S., Hendrick, R. L. (2000): Relationships between fine root dynamics and nitrogen availability in Michigan northern hardwood forests. – *Oecologia* 125(3): 389-399.
- [4] Cotrufo, M. F., Gorissen, A. (1997): Elevated CO₂ enhances below-ground C allocation in three perennial grass species at different levels of N availability. – *New Phytologist* 137(3): 421-431.
- [5] Cuevas, E., Brown, S., Lugo, A. E. (1991): Above- and belowground organic matter storage and production in a tropical pine plantation and a paired broadleaf secondary forest. – *Plant Soil* 135(2): 257-268.
- [6] Eissenstat, D. (1992): Costs and benefits of constructing roots of small diameter I. – *Journal of Plant Nutrition* 15(6-7): 763-782.
- [7] Eissenstat, D. M., Yanai, R. D. (1997): The Ecology of Root Lifespan. – *Advances in Ecological Research* 27: 1-60.
- [8] Eissenstat, D. M., Wells, C. E., Yanai, R. D., Whitbeck, J. L. (2000): Building roots in a changing environment: implications for root longevity. – *New Phytologist* 147(1): 33-42.
- [9] Fitter, A. H., Stickland, T. R. (1991): Architectural Analysis of Plant Root Systems. 2. Influence of Nutrient Supply on Architecture in Contrasting Plant Species. – *New Phytologist* 118(3): 383-389.
- [10] Fitter, A. H., Stickland, T. R., Harvey, M. L., Wilson, G. W. (2010): Architectural analysis of plant root systems. Architectural correlates of exploitation efficiency. – *New Phytologist* 121(2): 243-248.
- [11] Gordon, W. S., Jackson, R. B. (2000): Nutrient Concentrations in Fine Roots. – *Ecology* 81(1): 275-280.
- [12] Guo, D. L., Mitchell, R. J., Hendricks, J. J. (2004): Fine root branch orders respond differentially to carbon source-sink manipulations in a longleaf pine forest. – *Oecologia* 140(3): 450-457.
- [13] Hendrick, R. L., Pregitzer, K. S. (1996): Applications of minirhizotrons to understand root function in forests and other natural ecosystems. – *Plant Soil* 185(2): 293-304.
- [14] Jackson, R. B., Mooney, H. A., Schulze, E. D. (1997): A global budget for fine root biomass, surface area, and nutrient contents. – *Proc Natl Acad Sci USA* 94(14): 7362-7366.
- [15] Jiang, H. (2016): Space and temporal distribution of fine root and its influencing factors research in plantation of coastal salt land. – East China Normal University. (in Chinese).
- [16] Kern, C. C., Friend, A. L., Johnson, J. M. F., Coleman, M. D. (2004): Fine root dynamics in a developing *Populus deltoides* plantation. – *New Phytologist* 24(6): 651.

- [17] King, J. S., Thomas, R. B., Strain, B. R. (1997): Morphology and tissue quality of seedling root systems of *Pinus taeda* and *Pinus ponderosa* as affected by varying CO₂, temperature, and nitrogen. – *Plant Soil* 195(1): 107-119.
- [18] Kou, L., Guo, D., Yang, H., Gao, W., Li, S. (2015): Growth, morphological traits and mycorrhizal colonization of fine roots respond differently to nitrogen addition in a slash pine plantation in subtropical China. – *Plant Soil* 391(1-2): 207-218.
- [19] Lynch, J. (1995): Root Architecture and Plant Productivity. – *Plant Physiology* 109(1): 7-13.
- [20] Majdi, H. (2001): Changes in fine root production and longevity in relation to water and nutrient availability in a Norway spruce stand in northern Sweden. – *Tree Physiology* 21(14): 1057.
- [21] Mcgrath, D. A., Duryea, M. L., Cropper, W. P. (2001): Soil phosphorus availability and fine root proliferation in Amazonian agroforests 6 years following forest conversion. – *Agriculture Ecosystems & Environment* 83(3): 271-284.
- [22] Messier, C. (2002): Does soil heterogeneity and compaction in ingrowth-cores affect growth and morphology of black spruce fine-roots? – *Commun Soil Sci Plant* 33(7-8): 1027-1037.
- [23] Nadelhoffer, K. J. (2000): The potential effects of nitrogen deposition on fine-root production in forest ecosystems. – *New Phytologist* 147(1): 131-139.
- [24] Norby, R. J., Jackson, R. B. (2000): Research Review: Root Dynamics and Global Change: Seeking an Ecosystem Perspective. – *New Phytologist* 147(1): 3-12.
- [25] Peterjohn, W. T., Foster, C. J., Christ, M. J., Adams, M. B. (1999): Patterns of nitrogen availability within a forested watershed exhibiting symptoms of nitrogen saturation. – *Forest Ecology and Management* 119(1-3): 247-257.
- [26] Pregitzer, K. S., Hendrick, R. L., Fogel, R. (1993): The Demography of Fine Roots in Response to Patches of Water and Nitrogen. – *New Phytologist* 125(3): 575-580.
- [27] Pregitzer, K. S., Kubiske, M. E., Yu, C. K., Hendrick, R. L. (1997): Relationships among root branch order, carbon, and nitrogen in four temperate species. – *Oecologia* 111(3): 302-308.
- [28] Pregitzer, K. S., Deforest, J. L., Burton, A. J., Allen, M. F., Ruess, R. W., Hendrick, R. L. (2002): Fine Root Architecture of Nine North American Trees. – *Ecological Monographs* 72(2): 293-309.
- [29] Robinson, D. (2010): The responses of plants to non-uniform supplies of nutrients. – *New Phytologist* 127(4): 635-674.
- [30] Schiefelbein, J. W., Benfey, P. N. (1991): The development of plant roots: new approaches to underground problems. – *Plant Cell* 3(11): 1147.
- [31] Schmid, I., Kazda, M. (2002): Root distribution of Norway spruce in monospecific and mixed stands on different soils. – *Forest Ecology and Management* 159(1): 37-47.
- [32] Son, Y., Wang, J. H. (2010): Fine root biomass, production and turnover in a fertilized *Larix leptolepis* plantation in central Korea. – *Ecology Research* 18(3): 339-346.
- [33] Wang, Q. C. (2004): Fine roots responses of manchurian ash and korean larch to soil nutrients heterogeneity. – Northeast Forestry University. (in Chinese).
- [34] Wang, X. R., Wang, Z. Q., Han, Y. Z., Gu, J. C., Guo, D. L., Mei, L. (2005): Variations of fine root diameter with root order in manchurian ash and dahurian larch plantations. – *Acta Phytotaxonomica Sinica* 26: 871-877. (in Chinese).
- [35] Wells, C. E., Glenn, D. M., Eissenstat, D. M. (2002): Changes in the risk of fine-root mortality with age: a case study in peach, *Prunus persica* (Rosaceae). – *American Journal of Botany* 89(1): 79-87.
- [36] Wells, C. E., Glenn, D. M., Eissenstat, D. M. (2010): Soil insects alter fine root demography in peach (*Prunus persica*). – *Plant Cell Environment* 25(3): 431-439.
- [37] Wurzburger, N., Wright, S. J. (2016): Fine root responses to fertilization reveal multiple nutrient limitation in a lowland tropical forest. – *Ecology* 96(8): 2137-2146.

- [38] Yang, Y., Chen, G., Lin, P., Huang, R., Chen, Y., He, Z. (2003): Fine root distribution, seasonal pattern and production in a native forest and monoculture plantations in subtropical China. – *Acta Ecologica Sinica* 23(9): 1719-1730. (in Chinese).

MINERAL NITROGEN CONTENT IN SOILS DEPENDING ON LAND USE AND AGRONOMIC CATEGORY

WATROS, A.¹ – TKACZYK, P.² – LIPIŃSKA, H.³ – LIPIŃSKI, W.⁴ – KRZYSZCZAK, J.^{5*} –
BARANOWSKI, P.⁵ – BRODOWSKA, M. S.²

¹*New Chemical Synthesis Institute
Al. Tysiąclecia Państwa Polskiego 13 A, 24-110 Puławy, Poland*

²*Department of Agricultural and Environmental Chemistry, University of Life Sciences in
Lublin, ul. Akademicka 15, 20-950 Lublin, Poland*

³*Department of Grassland Science and Landscaping, University of Life Sciences in Lublin
ul. Akademicka 15, 20-950 Lublin, Poland*

⁴*State School of Higher Education in Chełm, ul. Pocztowa 54, 22-100 Chełm, Poland*

⁵*Institute of Agrophysics Polish Academy of Sciences
ul. Doświadczalna 4, 20-290 Lublin, Poland
(phone: +48 (81) 744 50 61; fax: +48 (81) 744 50 67)*

**Corresponding author
e-mail: jkrzyszczyk@ipan.lublin.pl; phone: (81) 744 50 61; fax: (81) 744 50 67*

(Received 9th Jan 2019; accepted 6th Mar 2019)

Abstract. Evaluation of mineral nitrogen content (N_{\min}) was performed for the 60-90 cm layer of grassland soils relative to other selected agricultural fodder crops. Soil samples were collected two times per year, in spring and autumn, over the period 2010-2012 from fixed locations scattered across whole Poland territory. Additionally, particle-size distribution was assessed in the tested soil samples, which allowed to assign soil agronomic categories to them and assess the relationship between N_{\min} content and assigned categories. Regardless of sampling date and land use, agronomic category had a significant effect on N_{\min} content. Generally the relationships between the percentage of particles with dimensions below 0.02 mm and N_{\min} content were characterized by a negative correlations, but in maize crops they were found to be positively correlated. Based on the obtained correlations, linear regression equations were developed. Calculated relations were less pronounced in spring, before fertilization, than in the autumn, after harvest. These equations can be very important from the practical point of view, as they may be used by farmer to plan a rational and sustainable fertilization based on forecasting of losses of mineral nitrogen content in the soil depending on the percentage of fine particles (agronomic category) of cultivated soil.

Keywords: *mineral soils, organic soils, maize, mixed cereals, regression equations*

Introduction

Nitrogen is one of the most important macronutrients, playing crucial role in crop growth process. The management of mineral nitrogen to ensure optimal level for plants is strongly dependent on physico-chemical properties of cultivated soil, such as particle-size distribution, bulk density, porosity or pH, crop management practices, as well as climatic conditions, which not only are a subject of constant changes, but also experienced a sudden shift related to climate change resulting in temperature increase (Swanson and Tsonis, 2009) and variation in precipitation structure. Increasing global food demand and gradually diminishing arable land area put new challenges for crop

production, which can be fulfilled by precision agriculture and sustainable soil management. For example, in Poland arable land as a share of land area fell gradually from 45.6 % in 2000 to 35.6 % in 2015 (The World Bank, 2015), but yields per hectare are increasing, which is related to the intensification of plant production. Usually it involves the use of higher doses of fertilizers, what results in the stronger impact of agriculture on the environment, as about 40 to 70% of nitrogen applied as normal fertilizer is either chemically bound in the soil and becomes unavailable to plants or is lost to the environment due to leaching (Jarosiewicz and Tomaszewska, 2003). In terms of sustainable agriculture, intensification should be strongly connected with optimization of efficiency of fertilizers use by modifications leading to graduation of their release time and biochemical activity. Also, the application of fertilizers for specific location should take into account soil bio-physico-chemical status, expressed through particle size distribution, mineralogical composition, soil pH, water retention properties and hydraulic conductivity, organic matter content or soil microbial community composition, activity of which can depend not only on N fertilization (Gleń-Karolczyk et al., 2018; Walkiewicz et al., 2018), but also on contamination (Walkiewicz et al., 2016; Wnuk et al., 2017). Poland is a region characterized by a significant diversification of soils and thus, the agricultural production conditions. Therefore, regular monitoring of soil properties and analysis of their relations with macro and micronutrients status (Tkaczyk et al., 2017; 2018a; 2018b) that is taking into account the diversity of soils is necessary for appropriate distribution and application of NPK fertilizers and their sustainable management (Tunbare et al., 2005; Watros et al., 2018). This can be done by precise prediction of soil properties variations in space and time using physical-mathematical modelling (Lamorski et al., 2013), which consider spatio-temporal variations of soil and climate conditions. To consider crop production in the conditions of a changing climate, various approaches can be applied. They capture projections of future climate from climatic models, which take into account various climate change scenarios, by either modification of amplitudes of partial density functions of measured time series to be in accordance with predicted climate change (Pirttioja et al., 2015; Fronzek et al., 2018) and consider adaptation measures (Ruiz-Ramos et al., 2018; Rodríguez et al., 2019), or take into account various statistical models (Murat et al., 2018) to forecast hourly or daily courses of future time series. It was shown that modifications of the weather time series structure (either by changing amplitudes or by an spatio-temporal aggregation) interfere with their inherent properties, such as long distance power-law correlations (Baranowski et al., 2015; Hoffmann et al., 2017; Krzyszczak et al., 2017a; 2017b; Krzyszczak et al., 2018) and therefore should be done with appropriate caution, as it may highly influence the results of modelling.

The most general form of presenting soil properties and analyzing their impact on crop production is the use of agronomic category. The studies on impact of agronomic category on mineral nitrogen in soil makes it possible for farmers to easily evaluate fertilization needs for a specific soil type. Up to this moment there are not many studies regarding the relation agronomic category on soil mineral nitrogen performed in large scale covering whole country area, which consider sampling date and land use. For example, it was already shown that, in general, soil mineral nitrogen content is affected by soil agronomic category (Paz and Ramos, 2004). Differences in soil mineral nitrogen content in spring and autumn sampling dates, as well as the assessment of percentage of nitrate and ammonium nitrogen in mineral nitrogen content were assessed by Fotyma

and Pietruch (2000) and Pietrzak (2014). Fotyma and Pietruch (2000) showed that in the 0-60 cm layer, the greatest variations in this respect were found in very light and light soils, whereas in the 60-90 cm layer heavy soils exhibited the largest differences. In medium and heavy soils, the percentage of ammonium nitrogen is about 30% of the total amount of mineral nitrogen, while in light soils this percentage is substantially higher, standing at 50%. It can be explained by greater denitrification intensity in heavy soils (Mosier et al., 2002). Pietrzak (2014) stated that in the topsoil (0-30cm) the highest content of mineral nitrogen are found in meadow soils with high permeability, i.e. light and very light soils, and that the amount of mineral nitrogen in meadow soils generally increases during growing season and decreases in the off-season.

Mineral nitrogen located in the 0-30 cm layer can migrate to deeper layers of the soil profile due to leaching (Powelson, 1988; Coyne and Frye, 2005). In the Soon et al. (2001) opinion, nitrogen losses in agriculture caused by nitrogen leaching are of significant importance for economic, production and environmental reasons. A direct consequence of mineral nitrogen leaching is pollution of ground and surface waters (Fotyma et al., 2010). In Poland monitoring of soil mineral nitrogen has been conducted for many years (Fotyma and Pietruch, 2000; Regulation, 2002; Jadczyzyn et al., 2010; Pietrzak, 2014). Based on this monitoring, the impact of soil N_{min} content on water quality can be predicted. This study attempted to identify factors determining nitrogen content in the 60-90 cm soil layer from which nitrogen can migrate to waters. As soil mineral nitrogen content is expected to be highly varied in time (Yu et al., 2003), with higher content during the spring and lower at the turn of August and September, which is a result of changes in the intensity of nitrification and enhanced nitrogen uptake by plants (Łoginow et al., 1987), therefore the analysis was carried out for two sampling dates – spring and autumn.

The study hypothesis is that, depending on selected soil properties, land use and sampling dates, significant differences exist in the content of mineral nitrogen in the soil layer beneath 60 cm, which is beyond the reach of the main root mass of crop plants in grassland soils (Mezhunts et al., 2005; Bonin et al., 2013) and in arable soils (Fan et al., 2016). The aim of this study was to evaluate mineral nitrogen content in grassland soils relative to other selected agricultural fodder crops in 60-90 cm layer depending on soil agronomic category.

Material and methods

Sampling sites

The results of environmental investigations conducted by the Regional Chemical and Agricultural Stations in agricultural farms across Poland over the period 2010-2012 were used to evaluate soil mineral nitrogen content for Polish soils under different land uses. The number of analyzed soil samples with the specified land use is presented in *Table 1*. Soil sampling sites, scattered over whole Poland territory, were identified by their geographical coordinates using GPS Pathfinder ProXT by Trimble (Westminster, CO 80021, USA, www.trimble.com) and were fixed for the entire study period. Locations of soil sampling points are presented in *Fig. 1*.

Soil samples were collected twice a year, in spring and autumn dates, from fields with a total area of not more than 4 ha. Soil sampling in spring were conducted in the period from February to April (before applying fertilizers), whereas in autumn in the period from September to October (after harvesting). Sampling done for 3 consecutive

years diverse in terms of meteorological conditions (*Tab. 2*), with 2010 being cold and wet, 2011 – very warm and dry and 2012 – warm and moderate (Statistical yearbook, 2011; 2012; 2013), two times per year, allow to average out the influence of year-by-year variations of these conditions and reveal more the influence of agronomic categories on N content. Each sample, weighing about 200 g, consisted of 15-20 primary soil samples collected from 60-90 cm layer using Egner stick from an area no larger than 100 m².

For each site selected, if the same crop was grown in successive years of the study, the average value for the respective period was calculated. In the case of sites located in grasslands, the same land use was continued over the entire study period and the average N_{min} content for the period 2010-2012 was considered.

Table 1. Number of analyzed soil samples taken from the 60-90 cm soil layer in grasslands on mineral soils, maize and mixed cereal (mostly oat and barley) crops

Crop type/land use		Number of samples
Grasslands (on mineral soils)	Total	859
	Meadows	521
	Pastures	160
	Hay and pasture	84
	Alternate	98
Maize		826
Mixed cereal (mostly oat and barley)		951

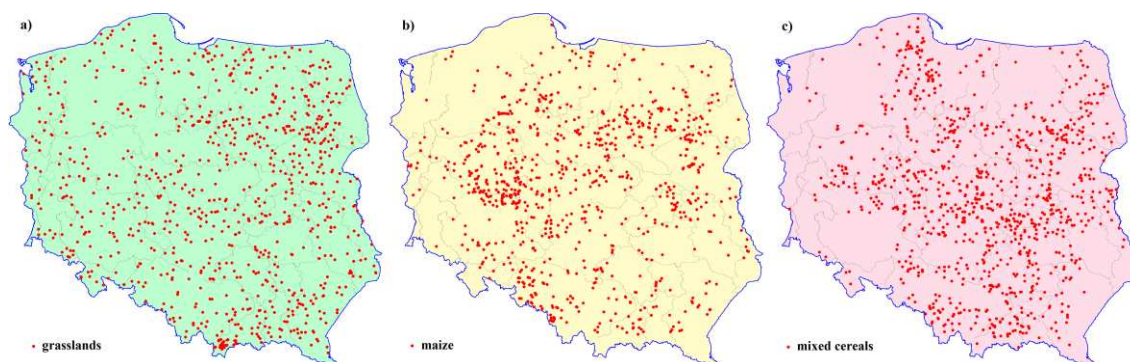


Figure 1. Location of soil sampling points from a) grasslands, b) maize and c) mixed cereals

Table 2. Basic meteorological conditions (on average) of the experimental years

Meteorological parameter	Year		
	2010	2011	2012
Temperature [°C]	7.1	8.5	8.1
Maximum temperature [°C]	36.6	34.3	36.5
Minimum temperature [°C]	-29.0	-25.1	-29.9
Precipitation [mm]	869.3	598.3	643.1
1 day maximum precipitation [mm]	186.2	140.5	66.2
Wind speed [m/s]	3.34	3.43	3.35
Sunshine hours [h]	1706.7	1973.7	1850.9

Soil samples analysis

Collected samples were delivered to the respective laboratory in tightly sealed containers and kept at a temperature of -18°C until an analysis of mineral nitrogen was performed. The soil samples with natural moisture content (after defrosting) were subjected to extraction with a 1% potassium sulfate solution at a ratio of 1:10. In the extracts obtained, nitrate and ammonium nitrogen content was determined spectrophotometrically using a Skalar San Plus System auto-analyzer (in accordance with the PN-R-04028:1997 norm, which is slightly modified, but equivalent to International Standard ISO 14256). Mineral nitrogen content (a sum of nitrate and ammonium nitrogen) was expressed in $\text{mg}\cdot\text{kg}^{-1}$ of dry matter of the soil sample (DM). Determination of dry matter was made using the gravimetric method after drying at 105°C (according to PN-ISO 11465:1999). In the air-dried samples, particle size distribution was determined using the laser diffraction method. As the extraction of nitrate and ammonium is carried out in a sample with natural moisture content, therefore obtained results were recalculated to the dry matter content using the empirical coefficient suitable for the soil of specific granulometric composition. Based on the content of particles with a diameter of <0.02 mm, one of four soil agronomic categories has been assigned to each soil sample (IUNG, 1990): very light soils ($< 10\%$ of fine particles), light soils (11-20%), medium soils (21-35%), and heavy soils ($> 35\%$ of fine particles).

Statistical analysis

To assess the relationship between soil agronomic category and content of mineral nitrogen in layer beyond the reach of roots of crop plants, N_{min} content in the 60-90 cm soil layer beneath ground surface in grasslands, as well as in soils under maize and mixed cereals was calculated as an annual average. Separately, averages were calculated for the spring and autumn sampling dates, depending on the assigned agronomic category and land use. Beside average values, standard deviations (SD) of mineral nitrogen content were calculated and presented on the figures. The relationships between N_{min} content and agronomic category were characterized by Pearson's correlation coefficients and assessed statistically using the one-way non-orthogonal analysis of variance classification with Tukey confidence intervals ($p = 0.05$). Additionally, simple regression analysis performed in SAS v. 9.1 software was carried out to obtain linear equations describing the relationship between the soil agronomic category and the N_{min} content in the 60-90 cm soil layer for varying land use. The goodness of fit of linear regression was evaluated using determination coefficients (R^2).

Results and discussion

The analyses show that indeed mineral nitrogen content in the 60-90 cm soil layer depends on agronomic category (*Fig. 2*). The highest mineral nitrogen content was observed in light soils, whereas a slightly lower one in very light soils. This trend persisted both in spring and in autumn, except for very light soils for which a higher content of this form of nitrogen was noted in spring than in autumn (*Fig. 3*). The effect of seasonality on nitrogen mineralization in soils of peatland ecosystems is discussed by Pawluczuk and Gotkiewicz (2003). They showed much higher amounts of soil N_{min} in spring than in summer and autumn. In their opinion, the reason for this is that in muck

and peat soils enhanced mineralization occurs also in winter and the quantities of nitrogen unused by plants (because of the non-growing period) are lost. Also, Arbačiauskas et al. (2014) obtained similar tendencies for the 60-90 cm soil layer of Lithuanian agricultural lands, irrespective of soil texture or nitrogen fertilisation rate.

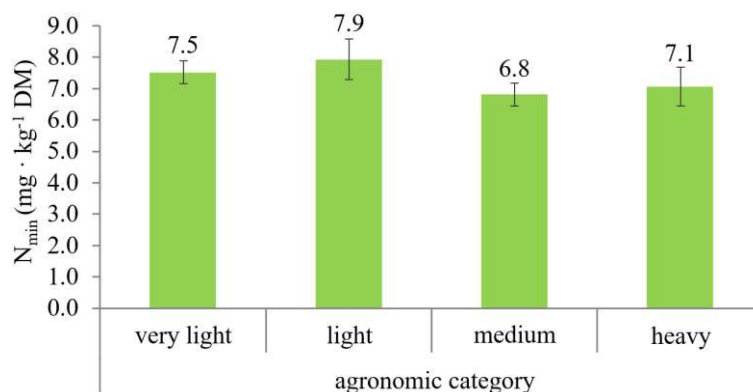


Figure 2. Average mineral nitrogen N_{min} content in the 60-90 cm soil layer with its standard deviation depending on soil agronomic category. DM stands for dry matter of the soil sample

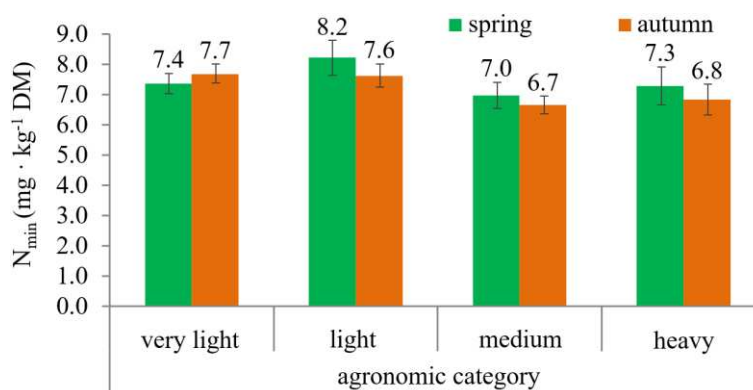


Figure 3. Average mineral nitrogen N_{min} content in the 60-90 cm layer of mineral soil with its standard deviation depending on agronomic category and soil sampling date. DM stands for dry matter of the soil sample

Higher mineral nitrogen contents in the 60-90 cm layer of very light and light soils relative to medium or heavy soils were also found in soil material taken from grassland soils and soils under mixed cereals. On the other hand, this relationship was opposite in the investigated layer in soils under maize because the highest N_{min} content was found in heavy soils (Fig. 4). A much higher N_{min} content in heavy soils relative to light soils was also found by Fotyma and Pietruch (2000). It was also shown that grassland soils accumulate less mineral nitrogen in the 60-90 cm layer than soils under mixed cereals or, which was even more evident, maize. Strong dependence of runoff and dissolved mineral nitrogen losses, and therefore differentiation of N_{min} content in the deeper soil layers, on vegetation cover was noticed by García-Díaz et al. (2017) for vineyards. Also De Notaris et al. (2017) showed that N leaching is influenced by vegetation cover, with spring wheat and potatoes being the two crops with highest N leaching.

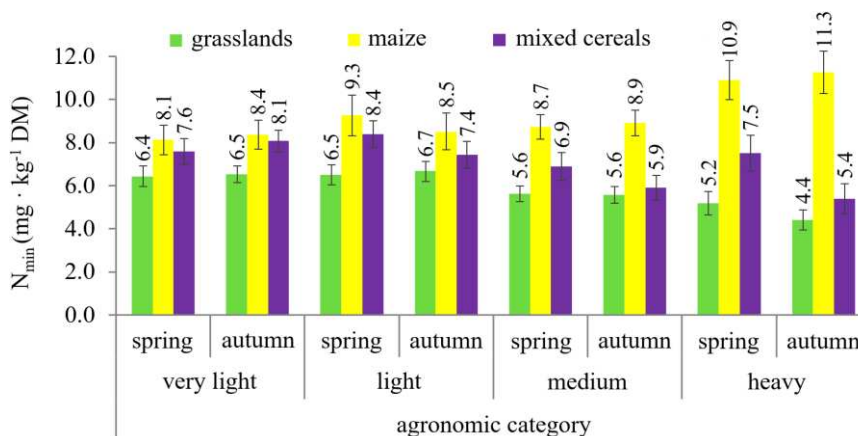


Figure 4. Average mineral nitrogen N_{min} content in the 60-90 cm layer of grassland soils and soils under maize and mixed cereals with its standard deviation depending on agronomic category and sampling date. DM stands for dry matter of the soil sample

Considering in turn mineral nitrogen content under different agronomic categories of grassland soils depending on land use, it was found that in most cases the highest content of this form of nitrogen at a depth of 60-90 cm was found in meadows (Fig. 5). The N_{min} contents in pasture grasslands as well as in hay and pastures grasslands were at a similar level, whereas the lowest amount of nitrogen was detected in alternate grasslands, which was particularly visible in heavy soils. Under the specific soil agronomic categories, greater differences in mineral nitrogen content between particular grassland uses were noted in autumn than in spring. Pawluczuk and Szymczyk (2008) obtained similar results. They found a lower mineral nitrogen content in muck and peat soils in extensively used meadows compared to this content in muck and peat soils in pastures. In the case of extensive grassland use, they found a higher nitrate content in groundwater under meadows than under pastures. These authors substantiate this fact by greater phytosorption of nitrogen by pasture vegetation and a low groundwater level. Above factors adversely affect the movement of the nitrate form of nitrogen deeper into the soil profile.

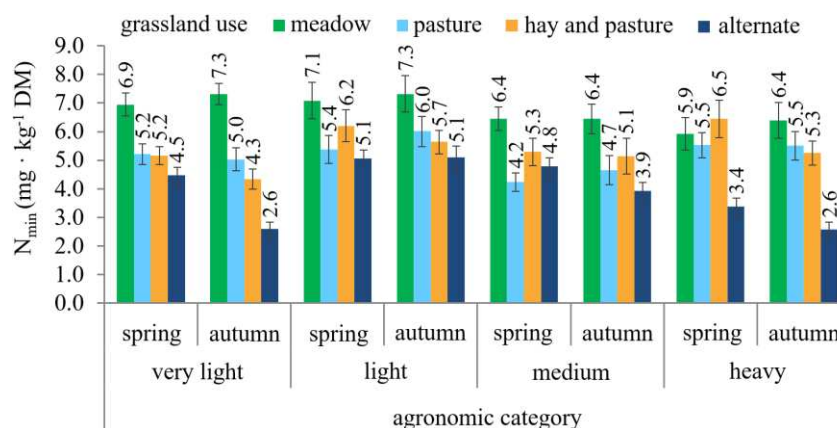


Figure 5. Average mineral nitrogen N_{min} content in the 60-90 cm layer of grassland soils with its standard deviation depending on grassland land use, sampling date and agronomic category. DM stands for dry matter of the soil sample

Observed relationships between soil agronomic category and mineral nitrogen content in the 60-90 cm soil layer (below the main root mass of the crops under investigation) were statistically confirmed (*Table 3*). Regardless of sampling date and land use, soil agronomic category had a significant effect on N_{\min} content ($R = -0.68$), but this relationship was weaker in spring ($R = -0.42$) and stronger in autumn ($R = -0.86$). It means that the N_{\min} losses decreased with the increase of percentage of fine particles with dimensions below 0.02 mm in soil, which is probably connected with lower permeability of heavier soils and therefore – reduced leaching. The dependence of N content on clay fraction (and, therefore, on agronomic category) was observed for USA, Australian rainforest, Denmark and the Netherlands, but those relations are not universal, however (Homann et al., 2007). According to Sapek and Kalińska (2004) the release of mineral forms during and after the growing season is increased due to the more intensive mineralization of nitrogen in the early summer months (May to July), which results in increased leaching in autumn and more pronounced relationships. The highest negative correlation was obtained for the relationship between the percentage of fine particles with dimensions below 0.02 mm and N_{\min} content for meadows ($R = -0.94$). In turn, a positive relationship was demonstrated for hay and pasture use. A negative correlation was also obtained for alternate grasslands, but for autumn sampling date this correlation was statistically insignificant. As far as the field crop plants in question are concerned, a positive relationship between N_{\min} content in the 60-90 cm layer and soil agronomic category was confirmed for maize crops. Opposite relationships were revealed for mixed cereal crops for both sampling dates and though for spring sampling these relationships are insignificant from the statistical point of view, a high and statistically significant correlation coefficient in the case of the autumn sampling date was obtained.

Table 3. Correlation coefficients between soil agronomic categories and mineral nitrogen N_{\min} content in the 60-90 cm soil layer with a breakdown into both land use and sampling date

Land use	Sampling date	
	spring	autumn
Grasslands (on mineral soils)	-0.96*	-0.95*
Meadows (on mineral soils)	-0.94*	-0.92*
Pastures (on mineral soils)	-0.02	-0.02
Hay and pasture grasslands (on mineral soils)	0.57*	0.45*
Alternate grasslands (on mineral soils)	-0.69*	-0.22
Maize	0.84*	0.89*
Mixed cereals	-0.40	-0.98*
Total soils	-0.42*	-0.86*
Total soils (on an annual basis)	-0.68*	

* correlation significant at significance level $p = 0.05$

After confirming that the relationship between soil agronomic category and content of mineral nitrogen in 60-90 cm soil layer exists, equations describing those relations were elaborated (*Figs 6-8*). The determined linear regression equations can be of great importance from the practical point of view, as they may be used to forecast changes in mineral nitrogen content depending on the percentage of fine particles in mineral soil. Therefore they may help the farmer to identify the optimal dose of mineral nitrogen in soils with different agronomic category and suppress nitrogen losses and thus adverse

impact on the environment. Significance of relationships described by obtained equations was confirmed by the high coefficients of determination.

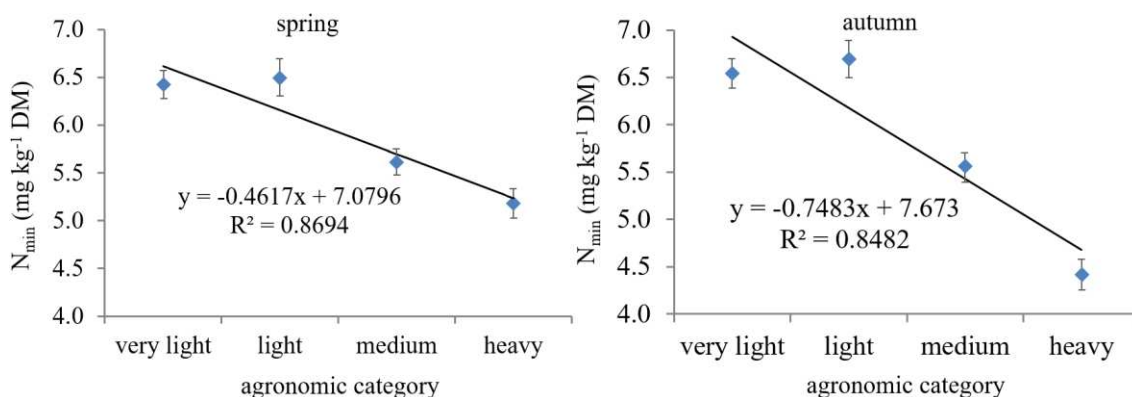


Figure 6. Relationship between agronomic category and average mineral nitrogen N_{min} content in the 60-90 cm layer of mineral soils under grasslands with its standard deviation for spring and autumn soil sampling dates. DM stands for dry matter of the soil sample

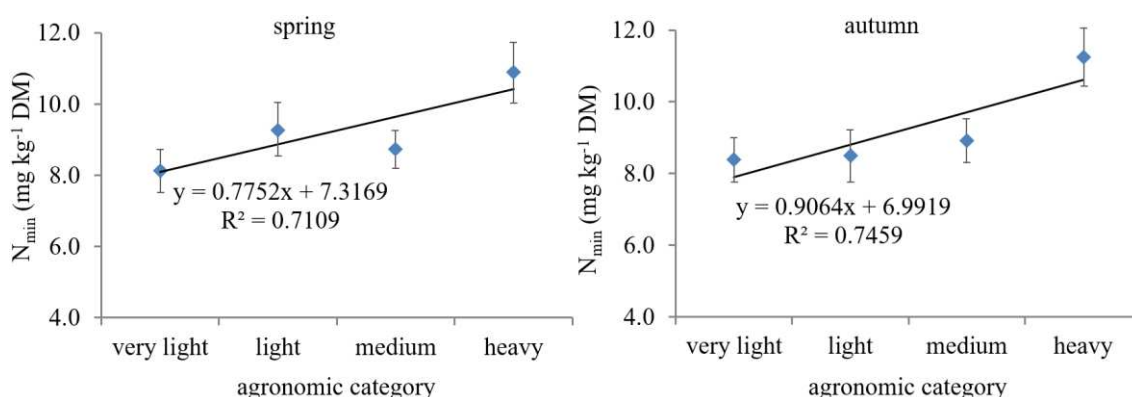


Figure 7. Relationship between agronomic category and average mineral nitrogen N_{min} content in the 60-90 cm layer of mineral soils under maize with its standard deviation for spring and autumn soil sampling dates. DM stands for dry matter of the soil sample

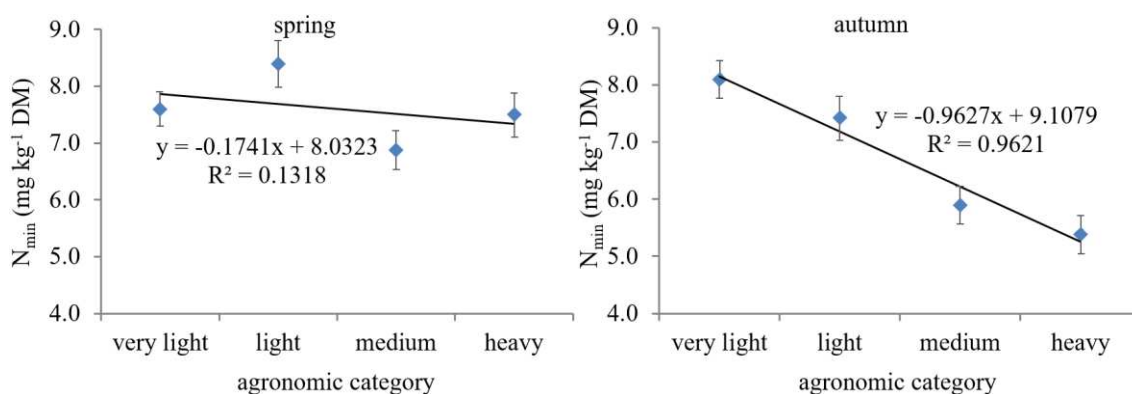


Figure 8. Relationship between agronomic category and average mineral nitrogen N_{min} content in the 60-90 cm layer of mineral soils under mixed cereals with its standard deviation for spring and autumn soil sampling dates. DM stands for dry matter of the soil sample

Conclusions

The results of this study confirm that significant differences in the content of mineral nitrogen can be observed in the soil layer beneath 60 cm, which is beyond the reach of the main root mass of crop plants in grassland soils and in arable soils, depending on agronomic categories and sampling date. It speaks for the fact that the leeching into deeper layers of soil occurs, which can have significant environmental consequences. Therefore, fertilization doses should take into account agronomic soil categories and type of land use. Regardless of observation period and the percentage of fine particles in mineral soils, the lowest content of N_{\min} was shown in grassland soils, whereas greater accumulation of this nutrient in the soil profile at a depth of 60-90 cm was observed in the soils under both maize and mixed cereals. This was especially evident for soils under maize. It was revealed that agronomic category and the content of N_{\min} in the 60-90 cm soil layer, regardless of the land use or sampling date, are strongly correlated. Elaborated equations describing those relationships for different land uses and sampling dates are characterized by very high coefficients of determination R^2 , which suggest that they may be successfully used in precision agriculture and contribute to sustainable management of fertilizers usage leading to reduction of nitrogen leaching from topsoil to groundwater, thus decreasing the negative impact of agricultural land use on environment.

Acknowledgements. This paper has been partly financed from the funds of the Polish National Centre for Research and Development in frame of the project BIO-FERTIL, contract number: BIOSTRATEG3/347464/5/NCBR/2017.

REFERENCES

- [1] Arbačiauskas, J., Staugaitis, G., Vaišvila, Z., Mažvila, J., Adomaitis, T., Šumskis, D., Enė, L. Ž., Lubytė, J., Mažeika, R. (2014): The interdependence of mineral nitrogen content in different soil layers of Lithuanian agricultural lands. – *Žemdirbystė (Agriculture)* 101(2): 133-138. <http://dx.doi.org/10.13080/z-a.2014.101.017>.
- [2] Baranowski, P., Krzyszczak, J., Sławiński, C., Hoffmann, H., Kozyra, J., Nieróbca, A., Siwek, K., Gluza, A. (2015): Multifractal analysis of meteorological time series to assess climate impacts. – *Climate Research* 65: 39-52. <https://doi.org/10.3354/cr01321>.
- [3] Bonin, C., Flores, J., Lal, R., Tracy, B. (2013): Root Characteristics of Perennial Warm-Season Grasslands Managed for Grazing and Biomass Production. – *Agronomy* 3: 508-523. <https://doi.org/10.3390/agronomy3030508>.
- [4] Coyne, M. S., Frye, W. W. (2005): Nitrogen in soil. Cycle. – In: Hillel, D. (ed.) *Encyclopedia of soil in the environment*. Elsevier Ltd., 13-21.
- [5] De Notaris, C., Rasmussen, J., Sørensen, P., Olesen, J.E. (2017): Nitrogen leaching: a crop rotation perspective on the effect of N surplus, field management and use of catch crops. – *Agriculture, Ecosystems and Environment* 255: 1-11. <https://doi.org/10.1016/j.agee.2017.12.009>
- [6] Fan, J., McConkey, B., Wang, H., Janzen, H. (2016): Root distribution by depth for temperate agricultural crops. – *Field Crops Research* 189: 68-74. <https://doi.org/10.1016/j.fcr.2016.02.013>.
- [7] Fotyma, E., Pietruch, Cz. (2000): Monitoring of the mineral nitrogen content in soils of arable land of Poland - the possibilities of practical use. – *Biuletyn Informacyjny IUNG* 12: 18-25. (in Polish)

- [8] Fotyma, M., Kęsik, K., Pietruch, C. (2010): Mineral nitrogen in soils of Poland as an indicator of plants nutrient requirements and soil water cleanness. – *Fertilizers and Fertilization* 38: 4-83. (in Polish).
- [9] Fronzek, S., Pirttioja, N., Carter, T. R., Bindi, M., Hoffmann, H., Palosuo, T., Ruiz-Ramos, M., Tao, F., Trnka, M., Acutis, M., Asseng, S., Baranowski, P., Basso, B., Bodin, P., Buis, S., Cammarano, D., Deligios, P., Destain, M. F., Dumont, B., Ewert, F., Ferrise, R., François, L., Gaiser, T., Hlavinka, P., Jacquemin, I., Kersebaum, K. C., Kollas, C., Krzyszczak, J., Lorite, I. J., Minet, J., Minguez, M. I., Montesino, M., Moriondo, M., Müller, C., Nendel, C., Öztürk, I., Perego, A., Rodríguez, A., Ruane, A. C., Ruget, F., Sanna, M., Semenov, M. A., Sławiński, C., Stratonovitch, P., Supit, I., Waha, K., Wang, E., Wu, L., Zhao, Z., Rötter, R. P. (2018): Classifying multi-model wheat yield impact response surfaces showing sensitivity to temperature and precipitation change. – *Agricultural Systems* 159: 209-224. <https://doi.org/10.1016/j.agsy.2017.08.004>.
- [10] García-Díaz, A., Bienes, R., Sastre, B., Novara, A., Gristina, L., Cerdà, A. (2017): Nitrogen losses in vineyards under different types of soil groundcover. A field runoff simulator approach in central Spain. – *Agriculture, Ecosystems & Environment* 236: 256-267. <https://doi.org/10.1016/j.agee.2016.12.013>.
- [11] Gleń-Karolczyk, K., Boligłowa, E., Antonkiewicz, J. (2018): Organic fertilization shapes the biodiversity of fungal communities associated with potato dry rot. – *Applied Soil Ecology* 129: 43-51. <https://doi.org/10.1016/j.apsoil.2018.04.012>.
- [12] Hoffmann, H., Baranowski, P., Krzyszczak, J., Zubik, M., Sławiński, C., Gaiser, T., Ewert, F. (2017): Temporal properties of spatially aggregated meteorological time series. – *Agricultural and Forest Meteorology* 234-235: 247-257. <https://doi.org/10.1016/j.agrformet.2016.12.012>.
- [13] Homann, P.S., Kapchinske, J.S. Boyce, A. (2007): Relations of mineral-soil C and N to climate and texture: regional differences within the conterminous USA. – *Biogeochemistry* 85: 303. <https://doi.org/10.1007/s10533-007-9139-6>
- [14] IUNG (1990): Fertilizer recommendations I: Limiting values to assess macro- and microelement contents in soils. – *Instytut Uprawy Nawożenia i Gleboznawstwa P(44): 26.* (in Polish)
- [15] Jadczyzyn, T., Pietruch, Cz., Lipiński, W. (2010): Soil monitoring in Poland for the content of mineral nitrogen in the years 2007-2009. – *Fertilizers and Fertilization* 38: 84-110. (in Polish)
- [16] Jarosiewicz, A., Tomaszewska, M. (2003): Controlled-release NPK fertilizer encapsulated by polymeric membranes. – *Journal of Agricultural and Food Chemistry* 51: 413-417.
- [17] Krzyszczak, J., Baranowski, P., Hoffmann, H., Zubik, M., Sławiński, C. (2017a): Analysis of Climate Dynamics Across a European Transect Using a Multifractal Method. – In: Rojas, I., Pomares, H., Valenzuela, O. (eds.) *Advances in Time Series Analysis and Forecasting: Selected Contributions from ITISE 2016. Contributions to Statistics.* Springer International Publishing, Cham, 103-116. https://doi.org/10.1007/978-3-319-55789-2_8.
- [18] Krzyszczak, J., Baranowski, P., Zubik, M., Hoffmann, H. (2017b): Temporal scale influence on multifractal properties of agro-meteorological time series. – *Agricultural and Forest Meteorology* 239: 223-235. <https://doi.org/10.1016/j.agrformet.2017.03.015>.
- [19] Krzyszczak, J., Baranowski, P., Zubik, M., Kazandjiev, V., Georgieva, V., Sławiński, C., Siwek, K., Kozyra, J., Nieróbca, A. (2018): Multifractal characterization and comparison of meteorological time series from two climatic zones. – *Theoretical and Applied Climatology* (in press). <http://dx.doi.org/10.1007/s00704-018-2705-0>.
- [20] Lamorski, K., Pastuszka, T., Krzyszczak, J., Sławiński, C., Witkowska-Walczak, B. (2013): Soil water dynamic modeling using the physical and support vector machine methods. – *Vadose Zone Journal* 12(4). <https://doi.org/10.2136/vzj2013.05.0085>.

- [21] Łoginow, W., Janowiak, J., Szychaj-Fabisiak, E. (1987): The variability of the total content of the individual forms of nitrogen in the soil. – *Zeszyty Naukowe ATR Bydgoszcz* 23: 13-24. (in Polish).
- [22] Mezhunts, B., Britt, C., McMillan, S., Givens D. (2005): The distribution of root biomass and energy yields in mountain grasslands in Armenia. – *Electronic Journal of Natural Sciences of the NAS of Armenia, Ecology* 1: 1-5.
- [23] Mosier, A.R., Doran, J.W., Freney, J.R. (2002): Managing soil denitrification. – *Journal of Soil and Water Conservation* 57(6): 505-513
- [24] Murat, M., Malinowska, I., Gos, M., Krzyszczak, J. (2018): Forecasting daily meteorological time series using ARIMA and regression models. – *International Agrophysics* 32(2): 253-264. <https://doi.org/10.1515/intag-2017-0007>.
- [25] Pawluczuk, J., Gotkiewicz, J. (2003): Evaluation of the mineralization process in soils of selected peat ecosystems of North-Eastern Poland in an aspect of soil resources protection. – *Acta Agrophysica* 1(4): 721-728. (in Polish)
- [26] Pawluczuk, J., Szymczyk, S. (2008): Dynamics of organic nitrogen mineralisation in muck soils of Dymerskie Meadows and the content of nitrate and ammonium nitrogen in groundwaters. – *Water-Environment-Rural Areas* 8, 2b(24): 105-115. (in Polish)
- [27] Paz, J. M., Ramos, C. (2004): Simulation of nitrate leaching for different nitrogen fertilization rates in a region of Valencia (Spain) using a GIS-GLEAMS system. – *Agriculture, Ecosystems & Environment* 103: 59-73.
- [28] Pietrzak, S. (2014): The amount of inorganic nitrogen in mineral meadow soils in Poland in the years 2008–2012. – *Water-Environment-Rural Areas* 14, 3(47): 113–124. (in Polish)
- [29] Pirttioja, N., Carter, T. R., Fronzek, S., Bindi, M., Hoffmann, H., Palosuo, T., Ruiz-Ramos, M., Tao, F., Trnka, M., Acutis, M., Asseng, S., Baranowski, P., Basso, B., Bodin, P., Buis, S., Cammarano, D., Deligios P., Destain, M. F., Dumont, B., Ewert, F., Ferrise, R., François, L., Gaiser, T., Hlavinka, P., Jacquemin, I., Kersebaum, K. C., Kollas, C., Krzyszczak, J., Lorite, I. J., Minet, J., Minguez, M. I., Montesino, M., Moriondo, M., Müller, C., Nendel, C., Öztürk, I., Perego, A., Rodríguez, A., Ruane, A. C., Ruget, F., Sanna, M., Semenov, M. A., Sławiński, C., Stratonovitch, P., Supit, I., Waha, K., Wang, E., Wu, L., Zhao, Z., Rötter, R. P. (2015): Temperature and precipitation effects on wheat yield across a European transect: a crop model ensemble analysis using impact response surfaces. – *Climate Research* 65: 87-105. <https://doi.org/10.3354/cr01322>.
- [30] Powlson, D. S. (1988): Measuring and minimising losses of fertilizer nitrogen in arable agriculture. – In: Jenkinson, D. S., Smith, K. A. (eds.) *Nitrogen Efficiency in Agricultural Soils*. Elsevier Applied Science, 231-245.
- [31] Regulation (2002): Regulation of the Minister of Environment concerning the criteria for designation of waters vulnerable to pollution by nitrogen compounds from agricultural sources. – *Dziennik Ustaw (Journal of Laws) of 2002, No. 241, item 2093*. (in Polish)
- [32] Rodríguez, A., Ruiz-Ramos, M., Palosuo, T., Carter, T. R., Fronzek, S., Lorite, I. J., Ferrise, R., Pirttioja, N., Bindi, M., Baranowski, P., Buis, S., Cammarano, D., Chen, Y., Dumont, B., Ewert, F., Gaiser, T., Hlavinka, P., Hoffmann, H., Höhn, J. G., Jurecka, F., Kersebaum, K. C., Krzyszczak, J., Lana, M., Mechiche-Alami, A., Minet, J., Montesino, M., Nendel, C., Porter, J. R., Ruget, F., Semenov, M. A., Steinmetz, Z., Stratonovitch, P., Supit, I., Tao, F., Trnka, M., de Wit, A., Rötter, R. P. (2019): Implications of crop model ensemble size and composition for estimates of adaptation effects and agreement of recommendations. – *Agricultural and Forest Meteorology* 264: 351-362. <https://doi.org/10.1016/j.agrformet.2018.09.018>.
- [33] Ruiz-Ramos, M., Ferrise, R., Rodríguez, A., Lorite, I. J., Bindi, M., Carter, T. R., Fronzek, S., Palosuo, T., Pirttioja, N., Baranowski, P., Buis, S., Cammarano, D., Chen, Y., Dumont, B., Ewert, F., Gaiser, T., Hlavinka, P., Hoffmann, H., Höhn, J. G., Jurecka, F., Kersebaum, K. C., Krzyszczak, J., Lana, M., Mechiche-Alami, A., Minet, J., Montesino, M., Nendel, C., Porter, J. R., Ruget, F., Semenov, M. A., Steinmetz, Z.,

- Stratonovitch, P., Supit, I., Tao, F., Trnka, M., de Wit, A., Rötter, R. P. (2018): Adaptation response surfaces for managing wheat under perturbed climate and CO₂ in a Mediterranean environment. – *Agricultural Systems* 159: 260-274. <https://doi.org/10.1016/j.agsy.2017.01.009>.
- [34] Sapek, B., Kalińska, D. (2004): Mineralization of soil organic nitrogen compounds in the light of long-term grassland experiments in IMUZ. – *Water-Environment-Rural Areas* 4, 1(10): 183-200. (in Polish).
- [35] Soon, Y. K., Clayton, G. W., Rice, W. A. (2001): Tillage and previous crop effects on dynamics of nitrogen in a wheat-soil system. – *Agronomy Journal* 93: 842-849.
- [36] Statistical Yearbook of the Republic of Poland (2011). Central Statistical Office. – Department of Statistical Publishing GUS, Warsaw.
- [37] Statistical Yearbook of the Republic of Poland (2012). Central Statistical Office. – Department of Statistical Publishing GUS, Warsaw.
- [38] Statistical Yearbook of the Republic of Poland (2013). Central Statistical Office. – Department of Statistical Publishing GUS, Warsaw.
- [39] Swanson, K. L., Tsonis A. A. (2009): Has the climate recently shifted? – *Geophysical Research Letters* 36: L06711. <https://doi.org/10.1029/2008GL037022>.
- [40] The World Bank (2015): World Development Indicators. Arable land (% of land area) [Data file]. – Food and Agriculture Organization, electronic files and web site. Retrieved from <https://data.worldbank.org/indicator/AG.LND.ARBL.ZS?locations=PL>.
- [41] Tkaczyk, P., Bednarek, W., Dresler, S., Krzyszczak, J., Baranowski, P., Sławiński, C. (2017): Relationship between assimilable-nutrient content and physicochemical properties of topsoil. – *International Agrophysics* 31(4): 551-562. <https://doi.org/10.1515/intag-2016-0074>.
- [42] Tkaczyk, P., Bednarek, W., Dresler, S., Krzyszczak, J. (2018a): The effect of some soil physicochemical properties and nitrogen fertilisation on winter wheat yield. – *Acta Agrophysica* 25(1): 107-116. <https://doi.org/10.31545/aagr0009>.
- [43] Tkaczyk, P., Bednarek, W., Dresler, S., Krzyszczak, J., Baranowski, P., Brodowska, M. S. (2018b): Content of certain macro and microelements in orchard soils in relation to agronomic categories and reaction of these soils. – *Journal of Elementology* 23(4): 1361-1372. <https://doi.org/10.5601/jelem.2018.23.1.1639>.
- [44] Tunbare, R., Benike, I., Tralmaka, L. (2005): The content of nitrate in soil and water in Latvia as a base for sustainable nitrogen management. – *Fertilizers and Fertilization* 1(22): 136-151.
- [45] Walkiewicz, A., Bulak, P., Brzezińska, M., Wnuk, E., Bieganowski, A. (2016): Methane oxidation in heavy metal contaminated Mollic Gleysol under oxic and hypoxic conditions. – *Environmental Pollution* 213: 403-411. <https://doi.org/10.1016/j.envpol.2016.02.048>.
- [46] Walkiewicz, A., Brzezińska, M., Bieganowski, A. (2018): Methanotrophs are favored under hypoxia in ammonium-fertilized soils. – *Biology and Fertility of Soils* 54(7): 861-870. <https://doi.org/10.1007/s00374-018-1302-9>.
- [47] Watros, A., Lipińska, H., Lipiński, W., Tkaczyk, P., Krzyszczak, J., Baranowski, P. (2018): The impact of fertilization on the mineral nitrogen content in grassland and fodder crop soils. – *Przemysł Chemiczny* 97(11): 1899-1905. <https://doi.org/10.15199/62.2018.11.17>. (in Polish).
- [48] Wnuk, E., Walkiewicz, A., Bieganowski, A. (2017): Methane oxidation in lead-contaminated mineral soils under different moisture levels. – *Environmental Science and Pollution Research* 24(8-9): 1-9. <https://doi.org/10.1007/s11356-017-0195-8>.
- [49] Yu, Z., Kraus, T. E. C., Dahlgren, R. A., Horwath, W. R., Zasoski, R. J. (2003): Mineral and dissolved organic nitrogen dynamics along a soil acidity-fertility gradient. – *Soil Science Society of America Journal* 67: 878-888.

STANDARD FOR ECOLOGICAL SUSTAINABILITY OF REGIONAL LAND UTILIZATION BASED ON ECOLOGICAL FOOTPRINT: ESTABLISHMENT AND EMPIRICAL STUDY

LIU, Y. Z.^{1,2*} – SUN, R. Z.¹ – CHEN, Z.¹ – CHEN, Y.^{1,2} – ZHANG, Z.³ – ZHU, X. N.¹ – SONG, G. F.¹
– LI, Z.¹ – WANG, Y. H.¹

¹*School of Resources and Environment Engineering, Wuhan University of Science and Technology, Wuhan 430081, China*

²*Hubei Key Laboratory for High-efficient Utilization and Agglomeration of Metallurgic Mineral Resources, Wuhan 430081, China*

³*College of Public Administration, Central China Normal University, Wuhan 430079, China*

**Corresponding author
e-mail: Liuyanzhong@wust.edu.cn*

(Received 11th Jan 2019; accepted 8th Mar 2019)

Abstract. The traditional ecological footprint model is found poorly applicable in the ecological sustainability assessment of regional land utilization. This paper designs a “consumption-output” ecological footprint model and establishes the standard for judging the ecological sustainability of regional land utilization with the sustainable ecological deficit of land as the assessment indicator. On this basis, this paper accounts and judges the ecological sustainability of land utilization in Linxiang City during the 2005-2013 period. The results showed: 1) The sustainable ecological deficit of the land in Linxiang City tended to grow amid fluctuation and remained at an ecological sustainability status; 2) The city has fully tapped the potential of available ecological capacity of cultivated land, pasture land and waters but has not made full use of that of construction lands and forest lands; 3) The ecological sustainability of regional land use is high in the north, low in the south and the weakest in the center. A comparison to the accounting results output from the traditional model shows that the improved model is more comprehensive and consistent with the reality in the assessment of ecological sustainability of regional land utilization. Finally, this paper provides corresponding suggestions for the city to realize ecological sustainability.

Keywords: *sustainable ecological deficit, ecological capacity, consumption-output, regional ecological sustainability, the assessment criterion*

Introduction

The indicator systems used for quantitative sustainability measurement have mushroomed, such as “drive-status-response” indicator system, sustainable economic welfare indicator, true development indicator and sustainability barometer, since the United Nations Conference on Environment and Development that took place in Rio de Janeiro, Brazil in 1992 (Xu and Zhang, 2000; Cha et al., 2013). Regional ecological sustainability means the long-term maintenance and development of the natural regional ecosystem as to the integrity of its structure and function (including supply of natural resources and ecosystem service) under the interference from nature and mankind (Peng et al., 2011, 2012). The natural ecosystem supports and regulates the life system of the earth and cannot be replaced by any artificial capital in this sense. Therefore, the concept of sustainability, which is derived from the concern over the depletion of natural resources and degradation of the ecological environment, can be realized only with regional ecological sustainability as an important condition precedent and basic way

(Franke, 1996; Parris, 2003), and the essence of regional ecological sustainability is to coordinate mankind's demand and the ecological capacity. William Rees, a Canadian ecological economist, invented the ecological footprint approach in 1992, and his doctoral student Mathis Wackernagel has gradually refined the approach (Rees, 1992; Wackernagel and Rees, 1996; Wackernagel et al., 1999). The new approach reflects the utilization status of the ecosystem and assesses the ecological sustainability of regional land utilization through quantitative measurement of the gap between the mankind demand for the natural ecological service and the supply of the ecological service provided by nature (Xu et al., 2006). The approach has quickly become a hot research topic in the area of sustainability assessment and promoted many scholars to perform extensive empirical studies, due to its advantages, including novelty of theory, visualization of concept, enrichment of connotation, operability, easy acceptance and global comparability (Lenzen and Murray, 2001; Monfreda, 2004; Chen et al., 2008a, b; Zhao et al., 2012, 2014a, b; Xiong et al., 2003; Tian et al., 2015; Wei and Wu, 2011; He et al., 2011; Lu, 2011; Zhang et al., 2009; Dai and He, 2013; Liu et al., 2015; Lai and Huang, 2005).

However, according to most of the studies, when the traditional model is used to assess regional ecological sustainability, it is often found that if a region has a lower consumption level and less developed economy, it will be more sustainable, which, however, is obviously contrary to the sustainability theory. Some scholars have studied on how to improve the model:

(1) In 2003, Xiong Deguo proposed to classify the ecological footprint into the ecological footprint of consumption and that of production and measure the stress of human activities on the local ecosystem with the ecological footprint of output for the purpose of judging the sustainability of the regional ecosystem and reflect the fairness of regional development with the ecological footprint of consumption (Xiong et al., 2003). Tian Long has calculated and assessed the ecological sustainability of land utilization in the Northwest Region of China in 2012 by replacing the ecological footprint with that of production and using the adjusted balancing factor and the output factor (Tian et al., 2015). Though the concept of ecological footprint of output has been put forward, no scholars have explored the internal relation between the ecological footprint of consumption and that of production. Moreover, most of the researchers have used the monotonous resource account to perform the ecological footprint accounting in related researches, but the decision on what resource account is used is rather discretionary and less justifiable.

(2) Wei Yuan, He Feng and other researchers have introduced the ecological footprint index, ecological footprint intensity, ecological moderate population, ecosystem utilization efficiency and other indicators on the basis of the ecological footprint model to make the model more suitable for the assessment of ecological sustainability of land utilization (Wei and Wu, 2011; He et al., 2011). Chen Chunfeng, Zhao Guishen and Lu Xiaoli suggested combining the theory of energy value and ecosystem service value with the ecological footprint model (Chen et al., 2008a; Zhao et al., 2014a; Lu, 2011). The improved model combined with other indicators and approaches can measure to what extent does mankind consume natural resources in a more comprehensive and accurate manner, but it cannot accurately reflect the ecological sustainability of land utilization in a specific region, as it does not take into account the true resource consumption of the region.

(3) Zhao Xingguo, Zhang Hengyi and Dai Yanan have adjusted and corrected the balancing factor and output factor based on the concept of “national hectare”, “provincial hectare” and “regional hectare” respectively (Zhao et al., 2014b; Zhang et al., 2009). Compared to the traditional model, the improved model based on the balancing factor and output factor can reflect the actual condition of the research region with the calculation of ecological footprint and ecological capacity. However, it always measures the sustainability status of a region with the ecological footprint of consumption as a scale and ignores the biological output the research region can obtain from the ecosystem.

The concept of ecological footprint in the traditional model is actually the ecological footprint of consumption, namely, the area of the land with an ecological production required to satisfy the resource demand of the population in the region. What corresponds to the ecological footprint of consumption is the ecological footprint of output, that is, the area of the land with an ecological production needed to produce resources of the regional ecosystem. The traditional ecological footprint theory is based on the global perspective. The global ecosystem can be seen as a closed system with self-sufficiency, and the resource consumption of mankind is equal to the resource output of the ecosystem. Therefore, the ecological footprint of consumption can be used to measure the pressure of mankind activities on the global ecosystem and further assess the sustainability of the ecosystem. However, a region always imports and exports resources, so the pressure generated from the ecological footprint of consumption does not all come from inside the region and the pressure derived from the ecological footprint of output will not be fully borne by the region. Therefore, during the assessment of ecological sustainability of regional land utilization, either the ecological footprint of consumption or that of production cannot alone reflect the pressure of human activities on the regional ecosystem, and thus cannot accurately reflect the sustainability of the regional ecosystem. In recent years, Liu Yanzhong has designed the sustainable ecological deficit of land on the basis of the classified accounting for ecological footprints of consumption and output to reflect the extent of sustainable utilization of the regional ecosystem (Liu et al., 2015). However, they have not thoroughly analyzed the relation between the ecological footprints of “consumption-production” and the ecological capacity, which makes it unable to accurately reflect the sustainability statuses under different situations.

To sum up, the researches on the improvement and application of the ecological footprint model only make some technical upgrades to the model in part and can realize more precise accounting of ecological footprints. However, there are no reasonable, scientific and uniform standards for judging the ecological sustainability of regional land utilization, which will usually deliver a serious impact on accurate judgment of regional ecological sustainability and cause the assessment result to deviate from the actual condition. Therefore, it is particularly important to establish the standard for judging the ecological sustainability of regional land utilization.

Based on the analysis above, this paper will further explore the connotations of the ecological footprint of consumption, ecological footprint of output and ecological capacity as well as internal relations among them. Moreover, this paper will, based on the improved “consumption-production” ecological footprint model, establish the standard for judging the ecological sustainability of regional land utilization with the sustainable ecological deficit of land as the assessment indicator. On this basis, the paper accounts and judges the ecological sustainability of land utilization in Linxiang City.

Materials and methods

Introduction of traditional ecological footprint model

The traditional ecological footprint model classifies various biological resources and energy consumption items required for human activities into the areas of six types of ecological production land (cultivated land, pasture land, forest land (including garden land), waters, fossil energy land and construction land), namely ecological footprint (*EF*). Then, the model calculates the area of the land with an ecological production that can be provided by one region, namely, ecological capacity (*EC*), and compares the difference between the *EC* and the *EF*, namely, ecological surplus (*ER*) or ecological deficit (*ED*) to judge whether the region is sustainable.

Improved “consumption-production” ecological footprint model

Analysis of connotations of related concepts

The improved ecological footprint model classifies ecological footprints into ecological footprint of consumption (*EF_c*) and ecological footprint of output (*EF_o*). The *EF_c* assesses the extent to which the population in the region demand the area of the land with an ecological production from the perspective of resource consumption. As one region may import resources when the supply of resources cannot satisfy the consumption demand in the region, the *EF_c* can reflect the extent to which the region demands the ecological production land inside and outside the region, and this can be expressed in terms of the difference between the *EC* and the *EF*, namely *ER_c* or *ED_c*. The *EF_o* accounts the ecological footprint from the perspective of corresponding output in the consumption resource account. One region may export resources to other regions after satisfying the internal consumption demand, so the *EF_o* reflects the extent to which the region and other regions demand the area of the land with an ecological production in the region, which represent the *EF_c* in broad sense. The difference between the *EF_o* and the usable *EC* is the *ER_o* or *ED_o*, and the *ED_o* represents the boundary of the ecological deficit borne by the regional ecosystem in the year. Specifically:

$$EF_c = Nr_j \sum (c_i / p_i) \quad (\text{Eq.1})$$

$$EF_o = Nr_j \sum (o_i / p_i) \quad (\text{Eq.2})$$

$$EC = N \sum (a_j r_j y_j) \quad (\text{Eq.3})$$

$$ER_c(ED_c) = EC - EF_c \quad (\text{Eq.4})$$

$$ER_o(ED_o) = EF_o - EC \quad (\text{Eq.5})$$

In the formulas: *N* is the population size, *j* is the ecological production land type (*j* = 1, 2, 3...6), *i* is the “consumption-output” item type (*i* = 1, 2, 3...*n*), *r_j* is the balancing factor, *c_i* is the per capita consumption of item *i*, *o_i* is the per capita output of item *i*, *p_i* is the global average capacity for item *i*, *a_j* is the per capita area of land type *j*, *y_j* is the output factor. When the ecological capacity is calculated, a 12% biodiversity production area shall be deducted to protect the biodiversity.

Classification of ecological production land types

In China, the land planning classifies lands into three tier-1 types, including (cultivated land, garden land, forest land and pasture land), construction land and other lands (including waters and nature reserves) in terms of purpose. Based on the characteristics of the land planning, this paper divides ecological production lands in the research region into seven types, namely, cultivated land, pasture land, forest land (including garden land), waters, fossil energy land, construction land and nature reserves (including unused grassland, alkaline land, marshland, sandy land, bare land and other unused lands). Nature reserves have important ecological values, and should be included in the ecological capacity calculation. However, these reserves do not directly provide human consumption products, so they can be excluded from the accounting of EF_c and EF_o .

Establishment of assessment indicators for ecological sustainability of land utilization

Based on the relation between the consumption surplus/deficit and output surplus/deficit, this paper has designed the sustainable ecological deficit (EL) of land as the indicator that is used to assess the regional ecological sustainability and perform quantitative measurement of ecological sustainability. The EL represents the deficit in the area of the land with an ecological production the region can still withstand from the time point of research (Liu et al., 2015). For concrete formula, please see Section 1.4 “Standard for judging ecological sustainability of land utilization” in this paper.

Establishment of standard for judging ecological sustainability of land utilization

This paper has established the standard for judging the ecological sustainability under eight scenarios in two statuses, based on the analysis of the internal relations among the EF_c , EF_o and EC (see Table 1).

Status 1: If EF_o is less than EC , the region will not make full use of the EC in the year, and the potential of the sustainable ecological deficit of the land will be the difference between the EC and the EF_o in the region. Below is the calculation formula of EL :

$$EL = EC - EF_o \quad (\text{Eq.6})$$

If: $EF_c < EF_o$, then: the region can export the ecological production land and display an ecological surplus. If: $EL > 0$, then: the region will remain at an ecological sustainability status;

If: $EF_c = EF_o$, then: the region will have no ecological production land available for export and display an ecological balance. If: $EL > 0$, then: the region will remain at an ecological sustainability status;

If: $EF_o < EF_c < EC$, then: the region will need to import the ecological production land and display an ecological deficit. If: $EL > 0$, then: the region will remain at an ecological sustainability status;

If: $EF_o < EF_c = EC$, then: the region will need to import the ecological production land and display an ecological deficit. If: $EL = 0$, then: the region will come at the critical point of ecological sustainability;

If: $EF_o < EC < EF_c$, then: the region will need to import the ecological production land and display an ecological deficit. If: $EL < 0$, then: the region will remain at an ecological non-sustainability status.

Table 1. Standard for judging ecological sustainability of regional land utilization based on “consumption-output” ecological footprint model

Status		Condition	Import & export capacity	Ecological balance status	EL formula	EL value	Annual judgment of sustainability
Status 1: $EF_o < EC$	The region will not make full use of the EC in the year, and the potential of the sustainable ecological deficit of the land will be the difference between the EC and the EF_o in the region	(1) $EF_c < EF_o$	It can export ecological production land	Ecological surplus	$EC - EF_c$	$EL > 0$	Sustainable
		(2) $EF_c = EF_o$	It cannot export ecological production land	Ecological balance		$EL > 0$	Sustainable
		(3) $EF_o < EF_c < EC$	It must import ecological production land	Ecological deficit		$EL > 0$	Sustainable
		(4) $EF_o < EF_c < EC$	It must import ecological production land	Ecological deficit		$EL = 0$	Critical point of sustainability
		(5) $EF_o < EC < EF_c$	It must import ecological production land	Ecological deficit		$EL < 0$	Unsustainable
Status 2: $EF_o > EC$	EF will be the maximum footprint the region can bear in the year, the potential of available ecological capacity will be fully utilized, and the corresponding ecological deficit of output will be the maximum deficit the region can tolerate in the year	(1) $EF_c < EF_o$	It can export ecological production land	Ecological surplus	$ER_o + (EC - EF_c)$	$EL > 0$	Sustainable

Status 2: If: $EF_o > EC$, then: the EF will be the maximum footprint the region can bear in the year, the potential of available ecological capacity will be fully utilized, and the corresponding ecological deficit of output will be the maximum deficit the region can tolerate in the year.

If: $EF_c < EF_o$, then: the region can export the ecological production land and display an ecological surplus. If: $EL > 0$, then: the region will remain at an ecological sustainability status. Below is the calculation formula of EL:

$$EL = ER_o + (EC - EF_c) \quad (\text{Eq.7})$$

If: $EF_c = EF_o$, then: the region will have no ecological production land available for export and display an ecological balance If: $EL = 0$, then: the region will come at the critical point of ecological sustainability. Below is the calculation formula of EL :

$$EL = ER_o + ED_c \quad (\text{Eq.8})$$

If: $EFC > EFO$, then: the region will need to import the ecological production land and display an ecological deficit. If: $EL < 0$, then: the region will remain at an ecological non-sustainability status. The EL calculation formula is the same as formula (Eq. 8).

Overview of research region

As a county-level city under Yueyang City, Hunan Province, Linxiang lies along the border between Hunan Province and Hubei Province, covers a total land area of 1,743.68 square kilometers and supervises 19 towns. The terrain is high in the south and low in the north with diversified land utilization types, including serial mountains in the northeast part, continuous hills in the central part and vast low-altitude lakes in the northwest part. The city has abundant resources, including nonferrous metals, and products, including bamboo products, and was identified as a resource city by the State Council in December 2013. Resource cities constitute important strategic bases assuring China's energy and resource security and represent an important support for sustainable development of the national economy. A research on the assessment of ecological sustainability of land utilization in these cities is necessary to promote sustainable development of these cities, accelerate the transformation of the economic development pattern and construct a comprehensive well-off society. This paper will perform the empirical study based on Linxiang City, so the results will be representative, suitable and promising for application to some extent.

Notes on calculation data

The EFC and EFO of Linxiang City during 2005-2013 are calculated in accordance with the statistical yearbooks (2005-2013), overall land planning data (2006-2020) and land change data (2005-2013) of Linxiang City. This paper converts various "consumption-output" items of Linxiang City into the areas of 7 types of ecological production lands, where the "consumption-output" items of cultivated land include grains, beans, yams, oil seeds, cotton, hemps, sugar canes, vegetables and fruits, those of forest land include tea, camellia seeds, palm sheets, dry bamboo shoots and woods, those of pasture land include meats and poultry eggs, those of waters include aquatic products, those of construction land are mainly electric power, and those of fossil energy lands include coal, liquefied petroleum gas and gasoline.

The balancing factor and output factor used in the ecological footprint accounting are mainly the values of the traditional accounting model designed by Wackernagel (Rees, 1992; Wackernagel and Rees, 1996; Wackernagel et al., 1999). In detail, the output factor of cultivated land is defined as the ratio of the average productivity of the cultivated land in Linxiang City to that in the world, or 1.73. As to nature reserves, the balancing factor is defined as 0.12 (Lai and Huang, 2005), which is calculated with the balancing factor formula proposed by Lai Li for the unused land, and the output factor is set to 1.

Results

Analysis of ecological sustainability of land utilization in Linxiang City

Analysis of time series trend for ecological sustainability of land utilization

The research has found (as shown in *Table 2*) that in Linxiang City, the aggregate ecological footprint of output always exceeded the aggregate available ecological capacity

and kept growing at a faster speed than that of the aggregate available ecological capacity. During the 8-year period, the aggregate ecological footprint of output grew at an average speed of 5.47%, which was higher than the annual average growth rate of 0.19% of the aggregate available ecological capacity and the aggregate ecological footprint of output at 2.42%. As a result, the aggregate ecological balance of consumption changed from an ecological surplus in the beginning to an ecological deficit in 2012. However, the aggregate ecological footprint of consumption was still less than the aggregate ecological footprint of output, and the sustainable ecological deficit of the land in Linxiang City tended to grow amid fluctuation and always remained at an ecological sustainability status.

Table 2. Sustainable ecological deficit of Linxiang City in 2005-2013. (Unit: Ghm²)

Year	2005	2006	2007	2008	2009	2010	2011	2012	2013	Annual average growth rate
Aggregate available ecological capacity	313516.82	314324.2	314677.59	314918.6	315419.88	316076.53	316742.82	317055.71	318218.38	0.19%
Aggregate ecological footprint of consumption	232016.89	245332.63	312281.29	252765.53	275107.04	310944.59	253813.23	317923.82	333521.87	5.47%
Aggregate ecological footprint of output	613110.44	691551.34	704095.32	682791.59	662248.58	677585.23	714238.99	736088.94	731911.39	2.42%
Aggregate ecological profit/loss of consumption	81499.93	68991.57	2396.3	62153.07	40312.83	5131.94	62929.59	-868.11	-15303.49	-14.85%
Aggregate ecological profit/loss of yield	299593.62	377227.13	389417.73	367872.99	346828.7	361508.7	397496.16	419033.23	413693.01	4.76%
Aggregate sustainable ecological deficit	381093.55	446218.71	391814.04	430026.06	387141.54	366640.64	460425.75	418165.12	398389.52	0.57%

Characteristics of spatial arrangement for ecological sustainability of land utilization

As illustrated in *Figure 1a*, the towns with strong sustainability included Huanggai Town, Chengfeng Town, Yuantan Town, Dinghu Town, Tandu Town, Wulipai Town, Yanglousi Town and Taolin Town, most of which lie in the central and northern parts of Linxiang City, in 2005. As illustrated in *Figure 1b*, the towns with strong sustainability included Huanggai Town, Jiangnan Town, Ruxi Town, Yuantan Town, Dinghu Town, Tandu Town, Nieshi Town and Taolin Town, most of which lie in the northern part of Linxiang City, in 2010. As illustrated in *Figure 1c*, the towns with strong sustainability included Huanggai Town, Jiangnan Town, Chengfeng Town, Ruxi Town, Yuantan Town, Dinghu Town, Tandu Town, Nieshi Town and Taolin Town, most of which lie in the northern part of Linxiang City, in 2013. Wulipai Town in the central part is a major town engaged in specialty agriculture and agricultural product processing as the pillar industry in the central economic zone of the city, Yanglousi Town is an important town

along the border engaged in bamboo product and tea processing as the pillar industry, and the river plain area in the northern part is home to major towns specializing in agricultural production and aquatic breeding. High output is the major reason why these towns maintained strong ecological sustainability. In 2005-2013, the ecological footprint of consumption of Chang'an Sub-district was always far higher than its ecological footprint of output and available ecological capacity, and the sustainable ecological capacity of the region was always negative. This made the region always at an ecological non-sustainability status and indicated the region mainly mitigated its pressure by importing the ecological production land from the outside. This is mainly because Chang'an Sub-district, the downtown of Linxiang City, specializes in tourism and comprehensive light industries as the pillar industry and has an industrial structure with inadequate resources. Tourism and industrial production drive rapid growth of the ecological footprint of consumption, while the low resource output renders the ecological footprint of output and available ecological capacity unable to support the rapid growth of the ecological footprint of consumption.

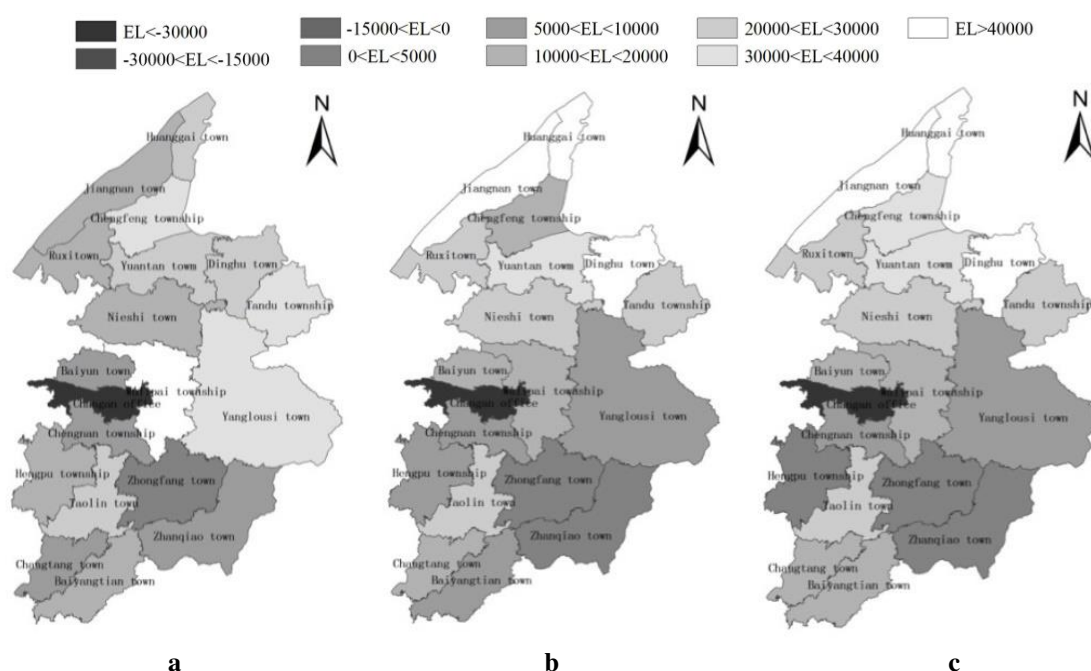


Figure 1. Spatial distribution of sustainable ecological deficit of Linxiang in **a** 2005, **b** 2010 and **c** 2013 (Ghm^2)

Analysis of ecological sustainability by land type

It can be inferred from *Table 3* that the ecological footprints of output of cultivated land, pasture land and waters all exceeded their available ecological capacities and ecological footprints of consumption over the years, indicating these three types of ecological production lands maintained an ecological surplus and could moderately export the output to mitigate the ecological sustainability pressure outside the region. These lands feature full use of their ecological capacity in the year, high utilization rate and high output ratio and kept ecologically sustainable with their sustainable ecological deficit above zero.

Table 3. Composition of “consumption-output” ecological footprint lands. (Unit: Ghm²)

Classification of ecological production lands		Cultivated land	Pasture land	Forest land	Waters	Construction land	Fossil energy land	Nature reserve
2005	Available ecological capacity	162536.11	5.1	85017.54	2190.78	63609.66	0	157.63
	Ecological footprint of consumption	101855.36	60328.35	270.26	32478.07	1471.18	35613.68	0
	Ecological footprint of output	210034.63	207716.31	25911.75	166689.66	2758.09	0	0
2010	Available ecological capacity	162361.08	5.03	84635.6	2185.17	66737.28	0	152.37
	Ecological footprint of consumption	108430.82	72967.13	1538.78	35430.32	3562.81	89014.73	0
	Ecological footprint of output	233407.77	231122.88	23199.91	187068.97	2785.71	0	0
2013	Available ecological capacity	162997.5	5.03	84414.94	2183.95	68467.77	0	149.18
	Ecological footprint of consumption	159653.76	79003.71	992.3	38214.13	4546.25	51111.73	0
	Ecological footprint of output	230487.79	240106.27	21418.29	237434.48	2464.56	0	0

During the period, the ecological footprint of consumption of the construction land kept growing and gradually overtook the ecological footprint of output to suffer an ecological deficit. However, the ecological footprint of consumption was always lower than the available ecological capacity, and the sustainable ecological deficit of the land was always above zero, indicating the ecological sustainability of the land. However, the available ecological potential of the construction land was not fully tapped, and Linxiang City can increase the utilization rate of the construction land to offset the ecological deficit and promote ecological sustainability. During the period, the ecological footprint of output of the forest land was smaller than the ecological capacity and bigger than the ecological footprint of consumption, and the sustainable ecological deficit of the land was above zero, indicating the land was ecologically sustainable. Therefore, Linxiang City can export the ecological surplus of the forest land to mitigate the ecological sustainability pressure of the external regions and promote its economic development.

Linxiang City has no fossil energy land but sees growing demand for consumption of fossil energy. Therefore, the growing demand for the ecological production land of fossil energy should be satisfied by exporting ecological resources of the ecological production land. This has delivered a huge pressure on the ecological sustainability of the region. Nature reserves do not supply direct products for mankind consumption, so this paper will only consider their ecological capacity. During regional development, Linxiang City can moderately adjust land utilization types to improve the contribution of nature reserves to the ecological capacity.

Comparison of assessment results output from the “consumption-output” ecological footprint model and traditional ecological footprint model

This paper has analyzed the assessment indicators with the “consumption-output” ecological footprint model as shown in *Table 2*, and discovered the time series trend in the ecological sustainability of land utilization. The result show that the sustainable ecological deficit of Linxiang City arrived at the peak value in 2011, then started falling

in the two years to follow but always remained above zero. This shows that Linxiang City has always maintained an ecological sustainable status, but the extent of ecological sustainability has tended to decline. Linxiang is a city with abundant mineral resources but only a few small mines are still under production after the Taolin Lead-Zinc Mine went bankrupt. The Ruxi Tiger Mountain Large Tungsten Mine has not started formal mining and the resource exploration cannot continue. This which will definitely affect the economic and social development of the city and further affect the ecological sustainability of land utilization in the region. According to the assessment standard of the traditional ecological footprint model, Linxiang City started incurring an ecological deficit in 2012 and the deficit kept rising. This shows that the region is ecologically unsustainable, which is still changing for the worse. In 2013, Linxiang City was defined as a mature resource city by the State Council. The Sustainable Development Planning for National Resource Cities (2013-2020) defines a mature resource city as follows: "A mature resource city stays at the stable stage of resource exploitation, has strong capacity to assure resource security and high level of economic and social development and represents the core area that assures China's energy and resource security at the current stage". Yet, the traditional ecological footprint model assesses Linxiang City as ecologically unsustainable, which is inconsistent with the positioning as a mature resource city.

When analyzing the spatial distribution of ecological sustainability of land utilization, this paper compares the results output from the two models for the year 2013. As illustrated in *Figure 1c*, the "consumption-out" ecological footprint model has output the following results: The ecological sustainability of regional land use is high in the north, low in the south and the weakest in the central, the towns in the northern part are strong in ecological sustainability, those in the southern part are general, the central part is weak and the downtown Chang'an Sub-district is even unsustainable. It can be inferred from *Figure 2* that the analysis results from the traditional model are bipolarized. The towns in the northern part are strong in ecological sustainability, those in the central and southern parts are not ecologically sustainable, and only a few towns maintain weak ecological sustainability. *Figure 2* shows that Chang'an Sub-district, Zhongfang Town, Taolin Town, Zhanqiao Town and Changtang Town are all ecologically unsustainable, indicating that these towns must import ecological production lands to satisfy their excessive ecological footprint of consumption. In contrast, Zhongfang Town, Taolin Town, Zhanqiao Town and Changtang Town are major forces in the economic development engaged in mineral resource exploitation and processing, mining, construction material and personalized agricultural products as pillar industries. They all export ecological production resources, meaning that their ecological production lands can both satisfy their own development needs and help mitigate the external ecological pressure. The results from the "consumption-output" ecological footprint model show that the ecological footprints of output of Zhongfang Town, Taolin Town, Zhanqiao Town and Changtang Town are bigger than their ecological footprints of consumption, so these towns maintain an ecological surplus and can export ecological production lands. At the same time, the sustainable ecological deficits of these four towns are all above zero, indicating they are all ecologically sustainable. These results are more consistent with the actual conditions.

As far as the ecological sustainability of different land types is concerned, it can be inferred from the "consumption-output" ecological footprint model has output the results below (see *Table 4*).

Table 4. Comparison of assessment results from the “consumption-output” ecological footprint model and traditional ecological footprint model. (Unit: Ghm²)

Classification of ecological production lands		Cultivated land	Pasture land	Forest land	Waters	Construction land	Fossil energy land	Nature reserve
2005	“Consumption-Output” model	108179.27	147387.96	84747.28	134211.59	62138.48	-35613.68	157.63
	Traditional model	60680.75	-60323.25	84747.28	-30287.29	62138.48	-35613.68	157.63
2010	“Consumption-Output” model	124976.95	158155.75	83096.82	151638.65	63174.47	-89014.73	152.37
	Traditional model	53930.26	-72962.1	83096.82	-33245.15	63174.47	-89014.73	152.37
2013	“Consumption-Output” model	70834.03	161102.56	83422.64	199220.35	63921.52	-51111.73	149.18
	Traditional model	3343.74	-78998.68	83422.64	-36030.18	63921.52	-51111.73	149.18

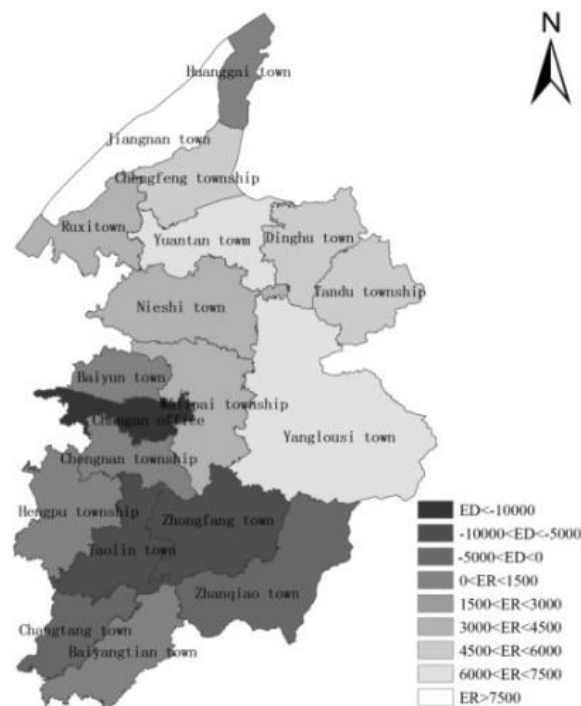


Figure 2. Spatial distribution of ecological surplus/deficit of Linxiang City in 2013 (Ghm²)

All the land types are ecologically sustainable, except that the sustainable ecological deficit of the fossil energy land is less than zero, indicating the land is ecologically unsustainable. According to the results from the traditional model, cultivated land, forest land, construction land and nature reserve all maintain an ecological surplus and are ecologically sustainable, while pasture land, waters and fossil energy land all record an ecological deficit and are ecologically unsustainable. Linxiang City has no fossil energy land but sees growing demand for consumption of fossil energy, so the fossil land is truly ecologically unsustainable. The ecological footprints of output of pasture land and waters are more than 3 times and about 6 times their ecological footprints of consumption in the years. This reveals that the biological resource outputs of pasture land and waters can fully satisfy the consumption demand in the region and reflects the status of ecological sustainability. This is because the traditional model measures the

ecological capacity of the ecological production land based on the true area of the land and compares the capacity to the ecological footprint of consumption to judge the ecological sustainability of the land. However, this approach ignores the fact that the output of biological resources changes with the advance of production technologies and the change in the input level. In contrast, the “consumption-output” model measures the relations among the ecological footprint of consumption, ecological footprint of output and ecological capacity and assesses the ecological sustainability of land utilization with the sustainable ecological deficit as the indicator to make the result more consistent with the reality.

Discussion

Based on the improved “consumption-production” ecological footprint model, this paper has established the standard for judging the ecological sustainability of regional land utilization with the sustainable ecological deficit of land as the assessment indicator. On this basis, this paper has performed an empirical study based on Linxiang City and drawn the following basic conclusions through the analysis above:

(1) In Linxiang City, the ecological footprints of consumption mainly come from people’s demand for cultivated land, pasture land, fossil energy land and waters, while cultivated land, pasture land and waters are principal contributors of ecological footprints of output. At present, cultivated land, pasture land and waters are all ecologically sustainable. However, as the ecological footprint of consumption keeps rising, the ecological surplus of the cultivated land will continuously decline and the ecological deficits of pasture land and waters will keep rising. The ecological footprints of output will grow annually, but the area of the lands with an ecological production will have a limited space for further expansion. Therefore, if mankind increases the output to satisfy the consumption without control, this will lead to the reduction of ecological capacity, ecological imbalance and other problems. To assure long-term sustainability of land utilization, Linxiang City should moderately implement intermittent suspension of farming, pasturing and fishing activities to recover the capacity of ecological production lands.

The construction land is ecologically sustainable in utilization, but its ecological footprint of output is far smaller than the ecological capacity. This reveals extensive utilization and low efficiency of the construction land. Therefore, Linxiang City should gradually lift the intensive utilization level of the construction land, and protect the areas of cultivated land and other lands with the function of ecological production to promote ecological sustainability of different types of lands.

The growing demand for fossil energy consumption has delivered a huge pressure on regional ecological sustainability. Linxiang City should consider reducing the use of fossil energies, develop green energies, encourage the production and use of energy-saving products. At the same time, it should improve the utilization rate and cleanness rate of fossil energies.

(2) Due to different spatial distribution and functional positioning, the towns in the northern river plain area are high in ecological sustainability. Yet, restricted by the industrial structure and consumption mode, the ecological footprints of consumption of the towns in the central urban area have quickly grown and overtaken their ecological capacity. Therefore, these towns are low in ecological sustainability and even unsustainable. Linxiang City should pay attention to adjusting the industrial structure,

optimizing the industrial arrangement and coordinating urban development and rural development, advocate sustainable consumption, and encourage the production and use of energy-saving products. It should save resources, develop the circular economy and protect the ecological environment. It should change the extensive economic development pattern, establish the production and consumption modes, intensive, economical and ecological, and promote the economic development to harmonize with resources and environment.

Conclusion

The “consumption-output” ecological footprint model is improved a lot as opposed to the traditional model as to suitability, integrity and reliability of the approach used to assess the ecological sustainability of regional land utilization. The analysis results based on the assessment indicators and judgment standards are more consistent with the reality and more reasonable than those from the traditional model.

This paper can to some extent solve the problem when the traditional ecological footprint model is employed to measure the ecological sustainability of regional land utilization. However, it is hard to collect related data used to calculate the balancing factor and output factor of ecological production lands. For this reason, these factors used in the research are both based on the “global hectare”, which restricts the precision of the research to some extent. Related indicators fluctuate over a broad band, which also restricts easy understanding of the rule to some extent. In future, we will still need to strengthen the research on the values of these factors. However, these points are not the major topics of this paper. When the indicator *EL* for ecological sustainability assessment of regional land utilization is applied to the horizontal comparison of ecological sustainability in different regions, the scientificity of comparative analysis will be affected by the difference of ecological footprint and ecological capacity. In other words, sustainable ecological deficit (*EL*) can only preliminarily judge the absolute ecological sustainability of land, but can not quantitatively evaluate the extent of sustainable utilization of the regional land, which is valuable for follow-up research. And we will discuss these more in-depth during future studies.

Acknowledgements. This research supported by National Natural Science Foundation of China (71774066).

REFERENCES

- [1] Cha, N., Wu, J. G., Yu, R. B. (2013): Analysis of subject trends in research on sustainable development. – *Acta Ecologica Sinica* 33(9): 2637-2644.
- [2] Chen, C. F., Wang, H. Y., Xiao, D. N. et al. (2008a): Comparison of sustainable development status in Heilongjiang Province based on traditional ecological footprint method and emergy ecological footprint method. – *Chinese Journal of Applied Ecology* 19(11): 2545-2549.
- [3] Chen, C. Z., Lin, Z. S., Liang, R. J. (2008b): Analysis of ecological sustainability in China based on the ecological footprint method. – *Journal of Natural Resources* 23(2): 230-236.
- [4] Dai, Y. N., He, X. G. (2013): Ecological sustainability in Chang-Zhu-Tan region: a prediction study. – *Acta Ecologica Sinica* 33(2): 595-602.

- [5] Franke, T. T (1996): Making future landscapes: defining a path to qualified sustainability. – *Landscape and Urban Planning* 35(4): 241-246.
- [6] He, F., Zhang, Q. F., Wang, L. et al. (2011): County-level ecological sustainability assessment based on improved ecological footprint model. – *Transactions of the CSAE* 27(5): 320-328.
- [7] Lai, L., Huang, X. J. (2005): Assessment of ecological footprint of national general land use planning in China. – *Transactions of the CSAE* 21(2): 66-71.
- [8] Lenzen, M., Murray, S. A. (2001): A modified ecological footprint method and its application to Australia. – *Ecological Economics* 37: 229-255.
- [9] Liu, Y. Z., Zhou, X., Chen, Y. et al. (2015): Ecological footprint-based environmental impact assessment of structural adjustment objectives for overall land utilization planning—take Linxiang City as an example. – *The Journal of Animal and Plant Sciences* 25(3 Suppl. 1): 99-106.
- [10] Lu, X. L. (2011): Ecological footprint model based on ecosystem services theory. – *Population Resources and Environment* 21(12): 115-120.
- [11] Monfreda, C. (2004): Establishing national natural capital accounts based on detailed ecological footprint and biocapacity assessments. – *Land Use Policy* 21: 231-246.
- [12] Parris, T. M., Kates, R. W. (2003): Characterizing a sustainability transition: Goals, targets, trends, and driving forces. US. – *Proceedings of the National Academy of Sciences of the United States of America* 100(14): 8068-8073.
- [13] Peng, J., Wang, Y. L., Wu, J. S. et al. (2011): Research progress on evaluation frameworks of regional ecological sustainability. – *Chinese Geographical Science* 21(4): 496-510.
- [14] Peng, J., Wu, J. S., Pan, Y. J. et al. (2012): Evaluation for regional ecological sustainability based on PSR model: conceptual framework. – *Progress in Geography* 31(7): 933-940.
- [15] Rees, W. E (1992): Ecological footprint and appropriated carrying capacity: What urban economics leaves out. – *UK Environment and Urbanization* 4(2): 121-130.
- [16] Tian, L., Zhang, Q. F., Zhang, X. et al. (2015): Assessment of ecological sustainability in northwest region based on improved ecological footprint model. – *Journal of Arid Land Resources and Environment* 29(8): 76-81.
- [17] Wackernagel, M., Rees, W. E. (1996): *Our Ecological Footprint: Reducing Human Impaction the Earth.* – New Society Publishers, Gabriola Island.
- [18] Wackernagel, M., Onisto, L, Bello, P. (1999): National natural capital accounting with the ecological footprint concept. – *Ecological Economics* 29: 375-390.
- [19] Wei, Y., Wu, C. Y. (2011): Dynamic analysis of ecological sustainability based on ecological footprint model in Guizhou province. – *Ecology and Environmental Sciences* 20(1): 102-108.
- [20] Xiong, D. G., Xian, X. F., Jiang, Y. D. (2003): Discussion on ecological footprint theory applied to regional sustainable development evaluation. – *Progress in Geography* 22(6): 618-626.
- [21] Xu, Z. M., Zhang, Z. Q. (2000): Review indicators of measuring sustainable development. – *Population Resources and Environment* 10(2): 60-64.
- [22] Xu, Z. M., Cheng, G. D., Zhang, Z. Q. (2006): A resolution to the conception of ecological footprint. – *Population Resources and Environment* 16(6): 69-78.
- [23] Zhang, H. Y., Liu, W. D., Wang, S. Z. et al. (2009): Calculation and analysis of equivalence factor and yield factor of ecological footprint based on sub-national hectare: a case study of Zhejiang. – *Journal of Natural Resources* 24(1): 82-92.
- [24] Zhao, G. S., Wang, Y. C., Tang, X. W. et al. (2014a): Evaluation of sustainability for intensive farmland ecosystem based on energy ecological footprint. – *Transactions of the CSAE* 30(18): 159-167.

- [25] Zhao, H. H., Wang, Y., Gu, X. M. et al. (2012): Establishment of environmental sustainability assessment indicators based on material flow and ecological footprint model in Tongling City of Anhui Province. – *Acta Ecologica Sinica* 32(7): 2025-2032.
- [26] Zhao, X. G., Pan, Y. J., Ding, S. et al. (2014b): Evaluation of regional land use sustainability and its spatial-temporal pattern among provinces in China. – *Transactions of the Chinese Society of Agricultural Engineering* 30(3): 196-204.

SOIL NUTRIENT CHARACTERISTICS OF GRAIN TO GREEN PROGRAM OF MAIN VEGETATION TYPES IN A SMALL WATERSHED, WULING MOUNTAIN AREA, CHINA

LUO, J.^{1,2} – NIU, Y.D.¹ – WANG, Y.¹ – ZHANG, Y.¹ – YAO, M.^{1,2} – TIAN, Y. X.^{1,2*} – ZHOU, X. L.^{1,2*}

¹Hunan Forestry Academy, Changsha, Hunan, China
(e-mail: luojia993@sina.com-- Jia Luo)

²Hunan Cili Forest Ecosystem State Research Station, Cili, Hunan, China
(e-mail: 6118408@126.com-- Min Yao)

*Corresponding authors
e-mail: tyx2019@sina.com-- Yuxin Tian; zxling36@263.net-- Xiaoling Zhou

(Received 11th Jan 2019; accepted 8th Mar 2019)

Abstract. In the present investigation, soil nutrient characteristics of three stands were studied. The soil organic matter content showed a hierarchy of *Pinus massoniana* forest > slope farmland > *Eucommia ulmoides* plantation > maple-*Cinnamomum camphora* mixed plantation in horizontal direction. However, with an increasing depth of soil layer, the soil organic matter content showed a decreasing pattern. The soil total nitrogen phosphorus and potassium contents of different vegetation types followed a pattern of *Eucommia ulmoides* plantation > maple-*Cinnamomum camphora* mixed plantation > *Pinus massoniana* forest > slope farmland. In this, the soil total nitrogen and phosphorus content decreased significantly with the increase in soil depths. The soil available nitrogen, potassium and phosphorus content of different vegetation types exhibited a pattern which follows slope farmland > *Eucommia ulmoides* plantation > maple-*Cinnamomum camphora* mixed plantation > *Pinus massoniana* forest. The soil available nitrogen, potassium and phosphorus content decreased with the soil depth increase. The pattern followed for soil trace elements of different vegetation types were *Eucommia ulmoides* plantation > slope farmland > *Pinus massoniana* forest > maple-*Cinnamomum camphora* mixed plantation. The average contents of trace elements in 0-10 and 10-20 cm of soil layer followed a gradation of Fe > Mn > Zn > Pb > Ni > Cu > Cd. 'Grain to Green Program' increased the soil nutrient content of different vegetation types, and soil nutrient content decreased with the soil depth increase. In this study, significant correlations were observed among soil nutrient elements in different vegetation types.

Keywords: organic matter and total nutrients contents, available nutrients contents, contents of soil microelements, correlation, three typical vegetation types

Introduction

The types of forest stands affect the accumulation, distribution and circulation of nutrients in soil. Thus, different vegetation types stimulate different soil nutrient contents (Xiang et al., 2014) and affect the formation and development of soil (Huang, 2000; David et al., 2018). Soil, as an essential component for supporting vegetation and is one of the important environmental factors affecting the survival, structure and function of plant communities (He et al., 2017). In forest ecosystem, soil nutrients serve as major factor affecting vegetation growth (Jiang et al., 2011). Since 1970s, with the rapid development of precision agriculture and introduction of geostatistics, the study on soil nutrients has drawn much attention. Chen et al. (2017) studied the soil nutrient content of different vegetation types which provides clues to understand the relationship between forest growth and soil nutrient formation. The study of soil nutrient change is significant to understand the soil fertility and nutrient cycling mechanisms of different vegetation types (Finzi et al., 1998; Augusto et al., 2002). Many authors have evaluated

the performances of different small-watershed forest stands in respect to water conservation and sediment yield reduction, the rules of sediment yield and runoff yield, and the regulation of vegetation restoration patterns for a long time (Lopes and Canfield, 2004; Yuan et al., 2006). The characteristics of soil nutrients and their influencing factors were also studied, but these works focused on the effects of variation of individual nutrient elements (Liu and Tong, 2005; Wei and Shao, 2007), spatial heterogeneity (Wang et al., 2002; Wang et al., 2007), soil types (Wen et al., 2005), land utilization patterns (Wang et al., 2001) and site conditions (McGrath et al., 2001; Latty et al., 2004) on the characteristics of soil nutrients. Some authors studied the soil nutrients, soil nutrient output mechanisms, microbial diversity and enzymatic activity of different forest stands (Peng et al., 2018; Hu et al., 2018; Zhang et al., 2018). However, the quantitative analysis of the availability of various soil nutrients to different forest stands was rarely studied (Yan et al., 2007). In China forest soil nutrients have been studied in a widespread manner extending from north to south (Gong et al., 2005; Huang et al., 2018). But the soil nutrient contents of different vegetation types after returning from farmland to forests and vertical heterogeneity of the soil nutrients were scarcely investigated (Cao et al., 2016). Especially, the hilly regions subjected to erosion in the south China with different water and soil erosion characteristics were rarely reported. Therefore, for the present study the Wuling Mountain small watershed was found as a typical example of hilly erosion regions of South China. A systematic study on the total and available nutrients and trace elements of soil covered by *Pinus massoniana* forest, *Eucommia ulmoides* plantation, maple-*Cinnamomum camphora* mixed plantation and slope farmland with different vegetation types was targeted. All these study sites were previously farmlands but returned to forests (the so called ‘Grain to Green’) later. Moreover, it was anticipated that the results of the present investigation could be beneficial for the soil conservation after returning farmland to forests as well as for vegetation optimization pattern selection and manual regulation in the hilly erosion regions of South China.

Field test region

The study area was located in the Nverzhai small watershed (111°12'42.836"E and 29°25'27.582"N) of Wuling mountain region in West Hunan Province of China. This watershed was well closed, containing a second-class small tributary of the Lishui River, and generally extended from north to south. It was a low mountain range with a total area of 3.15 km². The lowest elevation (outlet of the main ditch) was 210 m and the highest elevation was 917.4 m above MSL. The main ditch was about 1.2 km in length and the longitudinal slope of the main ditch was about 28.4‰. The forest coverage rate in this region was over 80%. The vegetation types were mainly characteristic to dense secondary forests after returning from farmland habitats. The soil-forming rock of the area was mainly sandy shale with yellow-red acidic soil. The light, heat and rainfall were abundant. The annual average sunshine time reached 1440 h, and the annual average temperature was 16°C. The annual average precipitation was about 1400 mm, and the annual frost-free period was 216–269 days. A prototype monsoon humid climate of the middle subtropical mountains prevailed in the area. The main vegetation types included *Eucommia ulmoides* plantation, *Pinus massoniana* forest, *Citrus reticulata* plantation and slope farmland.

Methods

Test fields and measurements

In August 2015, three typical vegetation types of *P. massoniana* forest, *E. ulmoides* plantation and maple-*cinnamomum camphora* mixed plantation under similar growing environmental conditions (such as slope, slope aspect and altitude) and after returning from farmland were selected. With reference to a slope farmland, three blocks of test fields (20 × 20 m) were selected for each vegetation type. The distance between two study sites was above 200 m. The height, diameter at breast height (DBH) and growing conditions of all trees with DBH values ≥ 5 cm were measured and recorded. Three shrub blocks (2 × 2 m) were randomly arranged in each test field, and the shrub species, number of plants and average height were recorded. Five herbaceous blocks (1 × 1 m) were also arranged in each test field, and the species, number, coverage and average height of the herbaceous plants were recorded. This work is guided on “Observation Methodology for Long-term Forest Ecosystem Research” of National Standards of the People's Republic of China (GB/T 33027-2016). The test field characteristics of each forest stand are shown in *Table 1*.

Table 1. Basic characteristics of vegetation in the experimental plots

Stand type	<i>Pinus massoniana</i> forest	<i>Eucommia ulmoides</i> plantation	Maple- <i>Cinnamomum camphora</i> mixed plantation	Slope farmland
Geographic coordinates	111°13'17"E, 29°25'21" N	111°12'46"E, 29°25'23"N	111°12'45"E, 29°25'22"N	111°12'45"E, 29°25'24"N
Elevation /m	400	313	333	305
Slope / (°)	35	15	18	25
Aspect	Southwest	Northeast	Northeast	Northeast
Soil parent materials	Malmstone	Malmstone	Plate shale	Shale
Soil type	Red Soil	Red Soil	Yellow Soil	Yellow Soil
Origin	Secondary forest	Plantation forest	Secondary forest	-
Density (individual·hm ⁻²)	2 366.7	5 005	3 507	-
Mean tree height /m	8	5.9	7	-
Mean DBH/cm	12.3	9	7.8	-
Canopy density	0.6	0.8	0.85	-
Main plants in shrub and herbaceous layer	<i>Quercus fabri</i> , <i>Rhododendron simsii</i> , <i>Stenoloma chusanum</i> , <i>Patrinia villosa</i>	<i>Rubus hirsutus</i> , <i>Rubus corchorifolius</i>	<i>Gynostemma pentaphyllum</i> , <i>Mallotus philippensis</i> , <i>Pteridium aquilinum</i>	<i>Camellia oleifera</i> , <i>Rhus chinensis</i> , <i>Agrimonia pilosa</i>

Soil sampling and processing

Three blocks (5 × 5 m) were selected in each forest stand. After removing dry branches and fallen leaves, the soil sampling was done following the "S"-shaped 5-point method. Soil layers at depths of 0-10 and 10-20 cm were separately sampled. The samplings were made in triplicates. After an air-drying process, the stones and roots in the soil samples were removed and the samples were crushed and screened with a screen (1 mm mesh size) for the measurements of relevant indicators.

Determination of soil chemical indicators

In October 2015, the soil nutrient indices were measured following Soil Agrochemical Analysis (Qi et al., 2008). The total nitrogen content was determined

with the semi-micro Kjeldahl method and NaOH-melting-molybdenum-antimony colorimetry was used to determine the total phosphorus content. For measuring total potassium content, NaOH-melting-flame-photometry was used. The alkali-hydrolyzed nitrogen content was determined with the alkali-hydrolyzed diffusion method. Available P was measured with the sodium-bicarbonate, extraction-molybdenum-antimony-colorimetry method while for the available potassium content, the NH₄OAc-leaching-flame-photometry was used. The organic matter content was determined with the potassium-dichromate-volumetry-heating-method. The iron, zinc and manganese contents were determined with the diethylene tri-amine penta acetic-acid-leaching-ICP (DTPA-ICP) method. For the determination of copper, cadmium, nickel and lead contents the ICP-MS method was used. The ICP-MS is displayed in *Figure 1*.

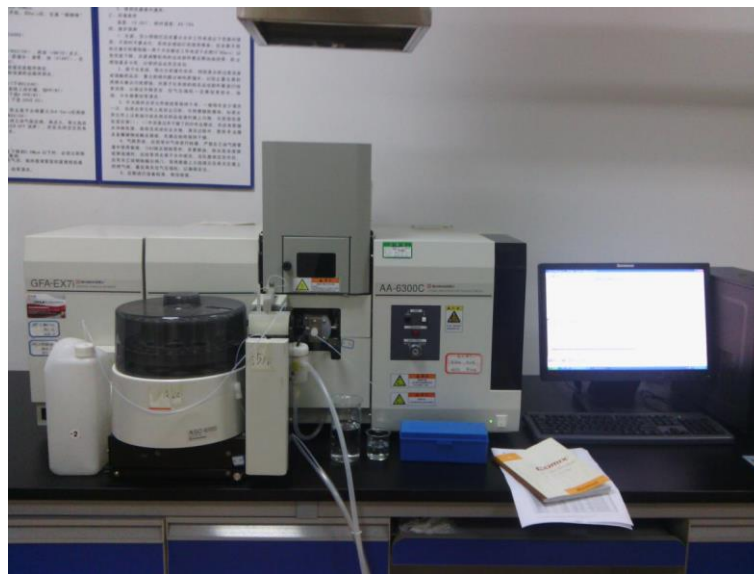


Figure 1. The equipment of ICP-MS used in this study

Data processing

The software SPSS 17.0 and R3.3.4 were used for data processing and analysis. One-way ANOVA and least significant difference (LSD) methods were applied for the comparison of the differences between the data groups. The software R3.3.4 was used to study the correlations between different soil nutrients.

Results and analysis

Organic matter and total nutrient contents in the soil of different forest stands

The differences in the contents of soil organic matter and total nutrients among different stands were significant (*Figure 2*). From 0–10 cm soil layers, the organic matter contents were ranked: *Pinus massoniana* forest > *Eucommia ulmoides* plantation > maple-Cinnamomum camphora mixed plantation > slope farmland. The organic matter content in the soil of *Eucommia ulmoides* plantation in the 10–20 cm soil layer reached a maximum, 1.80 times the lowest value (slope farmland). Its concentration in the soil of different stands through 0–20 cm soil layers were ranked as follows: The

Pinus massoniana forest ($27.44 \pm 9.37 \text{ g}\cdot\text{kg}^{-1}$) > *Eucommia ulmoides* plantation ($23.88 \pm 3.15 \text{ g}\cdot\text{kg}^{-1}$) > maple-*Cinnamomum camphora* mixed plantation ($16.98 \pm 1.98 \text{ g}\cdot\text{kg}^{-1}$) > slope farmland ($13.38 \pm 1.86 \text{ g}\cdot\text{kg}^{-1}$). With the increase of soil depth, the contents of soil organic matter in the soil of all stands decreased. For instance, the content of soil organic matter in the soil of the secondary *Pinus massoniana* forest decreased from 36.81 ± 0.002 to $18.07 \pm 0.22 \text{ g}\cdot\text{kg}^{-1}$.

The average contents of total nitrogen, total phosphorus and total potassium in the 0-20 cm soil layers of different forest stands followed the order of *Eucommia ulmoides* plantation > maple-*Cinnamomum camphora* mixed plantation > Masson Pine secondary forest > slope farmland. Besides, the contents of total nitrogen and total phosphorus in the soil of all stands decreased with the increase of soil depth, similar to the trend of the contents of organic matter against soil depth. For instance, the contents of total nitrogen and total phosphorus in the 0–10 cm soil layer of *Eucommia ulmoides* plantation were 1.64 ± 0.10 and $1.14 \pm 0.01 \text{ g}\cdot\text{kg}^{-1}$, respectively. While those in the 10–20 cm soil layer were lower (1.46 ± 0.15 and $1.07 \pm 0.03 \text{ g}\cdot\text{kg}^{-1}$, respectively). The contents of total nitrogen and phosphorus in the 10–20 cm soil layer of slope farmland was also lower than those in the 0–10-cm soil layer.

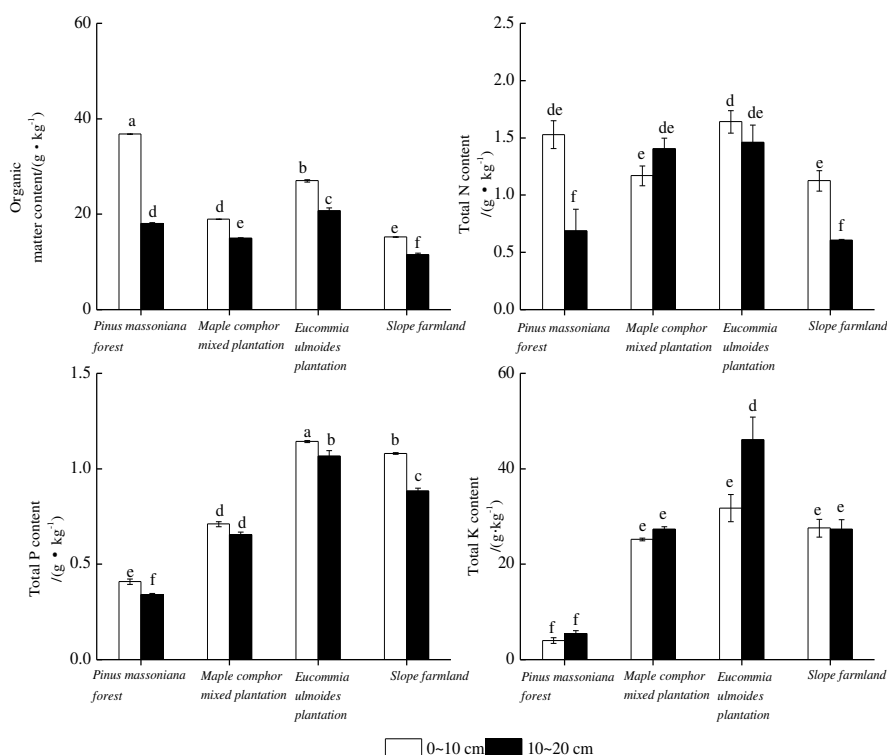


Figure 2. Soil organic matter and total nutrient content of different stand types (different lowercase letters represent the significance of difference between different vegetation types in the same soil layer, $P < 0.05$)

The contents of total potassium in the 0–10 cm soil layers of different vegetation types were ranked as follows: *Eucommia ulmoides* plantation ($31.79 \pm 2.85 \text{ g}\cdot\text{kg}^{-1}$) > slope farmland ($27.61 \pm 1.87 \text{ g}\cdot\text{kg}^{-1}$) > maple-*Cinnamomum camphora* mixed plantation ($25.22 \pm 0.30 \text{ g}\cdot\text{kg}^{-1}$) > *Pinus massoniana* forest ($4.02 \pm 0.60 \text{ g}\cdot\text{kg}^{-1}$). The contents in

the 10–20-cm soil layers were ranked as follows: *Eucommia ulmoides* plantation > maple-*Cinnamomum camphora* mixed plantation > slope farmland > *Pinus massoniana* forest. The contents of total potassium in soil of different stands increased with the increase of soil depth except for slope farmland. It can be conjectured that the accumulation of potassium in the *Pinus massoniana* forest was lower, while that in the *Eucommia ulmoides* plantation was higher; most of the potassium for uptake was concentrated on the upper soil.

Available nutrient contents in soil of different forest stands

Table 2 shows the total contents of available nitrogen, phosphorus and potassium in the 0-10 and 10-20 cm soil layers of different stands. These are ranked as follows: Slope farmland > *Eucommia ulmoides* plantation > maple-*Cinnamomum camphora* mixed plantation > *Pinus massoniana* forest. Soil available nitrogen from the study sites have been ranked as follows: *Pinus massoniana* forest > *Eucommia ulmoides* plantation > maple-*Cinnamomum camphora* mixed plantation > slope farmland. The state of available phosphorus was ranked as follows: Slope farmland > *Eucommia ulmoides* plantation > *Pinus massoniana* forest > maple-*Cinnamomum camphora* mixed plantation. The available potassium was ranked as follows: Slope farmland > *Eucommia ulmoides* plantation > maple-*Cinnamomum camphora* mixed plantation > *Pinus massoniana* forest. Both the contents of available phosphorus and available potassium in the soil of slope farmland were significantly higher than those in the soil of other vegetation types ($P < 0.05$), which may be related to the fertilization management. The available nitrogen content in the soil of maple-*Cinnamomum camphora* mixed plantation was higher, probably because its vegetation coverage was the highest. Liu et al. (2006) suggested that the vegetation coverage was positively affected by height, biomass, community species diversity and soil nutrient contents. In this study, the maple-*Cinnamomum camphora* mixed plantation had the highest vegetation coverage, so the available nutrient contents in the soil of this forest were higher.

Table 2. Soil available nutrient content of different stand types

Stand type	Soil layer/cm	Available Nitrogen/(mg·kg ⁻¹)	Available Phosphorus/(mg·kg ⁻¹)	Available Potassium/(mg·kg ⁻¹)
<i>Pinus massoniana</i> forest	0-10	108.36±2.11a	0.87±0.68bc	50.45±1.24c
	10-20	59.36±1.48b	0.58±0.04a	4.30±0.01a
Maple- <i>Cinnamomum camphora</i> mixed plantation	0-10	87.36±0.01cd	0.72±0.04ab	86.66±0.01d
	10-20	78.40±2.96de	0.50±0.14a	39.23±1.25b
<i>Eucommia ulmoides</i> plantation	0-10	96.60±0.84ab	1.42±0.01d	131.53±0.01g
	10-20	70.56±4.22c	1.08±0.02c	49.21±2.1c
Slope farmland	0-10	71.12±2.44ab	3.60±0.05f	116.56±0.01f
	10-20	62.70±2.01bc	1.97±0.02e	109.08±0.01f

The different lowercase letters indicate the significance of difference between different vegetation types in the same soil layer ($P < 0.05$)

As shown in Table 2, the average available nitrogen contents in the 0-20 cm soil layers were higher in *Eucommia ulmoides* plantation and *Pinus massoniana* forest i.e., 83.58 and 83.86 mg·kg⁻¹, respectively. The average nitrogen content in the slope farmland was the lowest (66.91 mg·kg⁻¹). In the 0–10-cm soil layer, the difference between the available nitrogen contents in the soil of the maple-*Cinnamomum*

camphora mixed plantation and *Eucommia ulmoides* plantation was significant ($P < 0.05$), but the difference between them in the 10–20-cm soil layer was not significant ($P < 0.05$). The content of available phosphorus in the soil of slope farmland was the highest ($2.79 \text{ mg}\cdot\text{kg}^{-1}$, $P < 0.05$), 4.5 times that in the soil of the maple-*Cinnamomum camphora* mixed plantation (the lowest, $0.61 \text{ mg}\cdot\text{kg}^{-1}$). On the other hand, the average available potassium content in the soil of slope farmland was also the highest ($112.82 \text{ mg}\cdot\text{kg}^{-1}$), followed by that of the *Eucommia ulmoides* plantation ($90.37 \text{ mg}\cdot\text{kg}^{-1}$).

The available nutrients of all stands decreased with the increase of soil depth. Especially, the soil available nitrogen content of *Pinus massoniana* forest and *Eucommia ulmoides* plantation decreased from 108.36 and $96.60 \text{ mg}\cdot\text{kg}^{-1}$ in the depth of 0–10 cm to 59.36 and $70.56 \text{ mg}\cdot\text{kg}^{-1}$ in the depth of 10–20 cm, respectively, indicating that the available phosphorus and potassium contents changed significantly with the soil depth among different forest stands.

Soil microelements among different forest stands

All the data on trace elements presented in Table 3 represents the average content from different forests stands within 0-10 and 10-20 cm soil depth profiles. The range of the trace elements followed a pattern like $\text{Fe} > \text{Mn} > \text{Zn} > \text{Pb} > \text{Ni} > \text{Cu} > \text{Cd}$. On the other hand, Fe, Mn, Zn, Pb, Ni, Cu and Cd content through 0-10 cm soil layers were ranked as *Eucommia ulmoides* plantation $>$ slope farmland $>$ *Pinus massoniana* forest $>$ maple-*Cinnamomum camphora* mixed plantation.

Table 3. Showing the content of soil trace elements in different forest stand types

Stand type	Soil layer(cm)	Cu ($\text{mg}\cdot\text{kg}^{-1}$)	Fe ($\text{mg}\cdot\text{kg}^{-1}$)	Zn ($\text{mg}\cdot\text{kg}^{-1}$)	Mn ($\text{mg}\cdot\text{kg}^{-1}$)	Cd ($\text{mg}\cdot\text{kg}^{-1}$)	Ni ($\text{mg}\cdot\text{kg}^{-1}$)	Pb ($\text{mg}\cdot\text{kg}^{-1}$)
<i>Pinus massoniana</i> forest	0-10	4.30	4582.05	32.13	83.24	0.53	9.24	32.58
	10-20	4.60	4483.64	28.31	60.97	0.14	8.01	29.97
Maple- <i>Cinnamomum camphora</i> mixed plantation	0-10	7.84	4941.38	48.49	478.68	0.53	16.63	37.81
	10-20	7.55	637.97	53.48	551.08	0.53	16.63	37.81
<i>Eucommia ulmoides</i> plantation	0-10	10.79	5001.27	54.40	718.17	0.27	25.87	29.97
	10-20	11.68	4997.00	53.71	729.31	0.40	24.64	29.97
Slope farmland	0-10	8.73	4958.49	51.04	695.89	0.40	21.56	29.97
	10-20	9.61	4937.11	50.93	662.47	0.40	24.03	24.74

In detail, Fe contents in 0–10 and 10-20cm soil layers showed a range of 637.98–5001.27 $\text{mg}\cdot\text{kg}^{-1}$. However, the average Fe content in the soil of *Eucommia ulmoides* plantation was the highest but the concentration of it in the soil of maple-*Cinnamomum camphora* mixed plantation was the lowest. On the other hand, Cu contents ranged from 4.30–11.68 $\text{mg}\cdot\text{kg}^{-1}$. It was highest in the soil of *Eucommia ulmoides* plantation but lowest in the *Pinus massoniana* forest. The Zn content varied from 28.31–54.40 $\text{mg}\cdot\text{kg}^{-1}$. In *Eucommia ulmoides* plantation, this parameter was the highest while in the *Pinus massoniana* forest it was lowest. Mn contents showed a range of 60.97–729.31 $\text{mg}\cdot\text{kg}^{-1}$ representing the highest value in the soil of *Eucommia ulmoides* plantation. Its concentration fell to a lower value in the soil of *Pinus massoniana* secondary forest. The recorded range of Cd content was 0.15–0.53 $\text{mg}\cdot\text{kg}^{-1}$. The soil of maple-*Cinnamomum camphora* mixed plantation showed the highest concentration of Cd. Another trace element Ni ranged from 8.01–25.87 $\text{mg}\cdot\text{kg}^{-1}$ showing its highest presence in the soil of

Eucommia ulmoides plantation. In the soil of *Pinus massoniana* forest low Ni concentration was seen. Pb varied from 24.74–37.81 mg·kg⁻¹ showing its highest concentration in the soil of maple-*Cinnamomum camphora* mixed plantation. The average Fe content in the soil of *Eucommia ulmoides* plantation decreased from 5001.27 mg·kg⁻¹ in the depth of 0–10 cm to 4995.55 mg·kg⁻¹ in the depth of 10–20 cm. While its concentration greatly decreased in the soil of maple-*Cinnamomum camphora* mixed plantation. The decreasing pattern was 4941.38 mg·kg⁻¹ in the depth of 0–10 cm to 637.97 mg·kg⁻¹ in the depth of 10–20 cm. In addition, the contents of trace elements in the soil of *Pinus massoniana* forest and slope farmland also showed the similar trend with the increase of soil depth. To sum up, it could be mentioned here that the contents of trace elements in the soil of different forest stands decreased with the increase of soil depth. It indicates that the contents of trace elements in the upper soil layer were much higher than those in the lower soil layer.

Correlation between soil nutrient contents

The results of correlation analysis between different soil nutrients for different stands are shown in Table 4.

Table 4. Showing the values of correlation coefficient (*r*) among different soil nutrient parameters

Index	Organic matter	Total N	Total P	Total K	Available nitrogen	Available phosphorus	Available potassium	Cu	Fe	Zn	Mn	Cd	Ni	Pb
Organic matter														
Total N	0.47													
Total P	-0.45	0.26												
Total K	-0.42	0.49	0.94*											
Available nitrogen	0.77	0.77	-0.41	-0.17										
Available phosphorus	-0.64	-0.60	0.59	0.32	-0.95*									
Available potassium	-0.72	-0.12	0.92*	0.79	-0.73	0.83								
Cu	-0.38	0.42	0.98*	0.98*	-0.25	0.44	0.85							
Fe	0.24	-0.14	0.40	0.11	-0.36	0.59	0.37	0.30						
Zn	-0.64	0.32	0.88	0.96*	-0.30	0.38	0.83	0.91*	-0.07					
Mn	-0.62	0.23	0.96*	0.96*	-0.43	0.55	0.92*	0.96*	0.16	0.97*				
Cd	-0.64	-0.07	-0.08	0.15	-0.05	-0.18	0.05	-0.02	-0.90	0.38	0.19			
Ni	-0.49	0.26	1.00**	0.95*	-0.41	0.58	0.92*	0.99*	0.35	0.91*	0.98*	-0.02		
Pb	0.01	0.37	-0.43	-0.10	0.60	-0.77	-0.50	-0.29	-0.96*	0.01	-0.23	0.76	-0.38	1

The symbol * is added if *P* was < 0.05; the symbol ** is added if *P* was < 0.01

Total phosphorus showed a positive correlation with total potassium ($r = 0.94$, $P < 0.05$). This parameter also showed significant positive correlation with the contents of Cu, Mn and Ni ($r = 0.98$, $P < 0.05$); $r = 0.96$, $P < 0.05$) and $r = 1$, $P < 0.01$, respectively). In the analysis, total potassium correlated significantly and positively ($P < 0.05$) with the contents of Cu, Zn, Mn and Ni, (the values of r were 0.98, 0.96, 0.96 and 0.95, respectively). Among these trace elements, Cu had significantly positive relationships with the contents of Mn and Ni ($P < 0.05$), and the correlation coefficients were 0.96 and 0.99, respectively. Zn correlated significantly and positively with Mn ($r =$

0.97, $P < 0.05$). Mn showed significant positive correlation with Ni ($r = 0.98$, $P < 0.05$). Significant negative correlation was observed between Fe and Pb ($r = -0.96$, $P < 0.05$).

Discussion

Effects of returning farmland to forest on the different soil nutrient contents

The interactions between soil and vegetation promote the change of spatial heterogeneity of soil and vegetation, and soil quality is the result of interactions between human and natural factors (Wang et al., 2010a). In the present work, the results showed that after returning farmland to forest, the organic matter contents in the soil of different forest stands were ranked as follows: *Pinus massoniana* forest > slope farmland > *Eucommia ulmoides* plantation > maple-*Cinnamomum camphora* mixed plantation. The reasons can be summarized as follows: The root system of *Pinus massoniana* secondary forest was more developed, and the canopy width was greater with more litter. Because of long-term fertilization, the organic matter content of slope farmland was high. Hence, the carbon source input of *Pinus massoniana* forest and slope farmland was high. The *Eucommia ulmoides* plantation accumulated abundant organic matter under the conditions of manual disturbance and cultivation management. The maple-*Cinnamomum camphora* mixed plantation was a secondary forest, of which the accumulation of organic matter was less affected by external factors. Therefore, its organic matter content was lower. The soil organic matter, as a cementing material between soil particles, can form water-resistant aggregates and large aggregates with moderate ratios and stable structures (Albiach et al., 2001). Hence, it has the ability to enhance soil and water conservation and to improve soil structure, thereby enhancing the ability of decomposing litter and leaves and improving the nutrients exchange rate between plants and soil. As a result, a benign circulation system will be formed.

The contents of total nitrogen, total phosphorus and total potassium in the soil of different forest stands after returning farmland to forest were relatively high, indicating that the soil in this area was not barren. Compared with the slope farmland, the total nitrogen content in the soil of *Eucommia ulmoides* plantation was the highest, principally because the soil nitrogen content mainly depended on the decomposition extent of organic matter and the accumulation of biomass. The *Eucommia ulmoides* plantation had high species diversity, and the biomass accumulation of shrubs and herbs was high also. Thereby, the return, decomposition and enrichment of nutrients were intense. Qi et al. (2007) also reported that the soil nitrogen content mainly depended on the decomposition extent of organic matter and accumulation of biomass. Except the slope farmland, the *Pinus massoniana* forest, *Eucommia ulmoides* plantation and the maple-*Cinnamomum camphora* mixed plantation were rich in understory vegetation, litter and biomass, which favored the accumulation of organic matter and nitrogen. The higher contents of organic matter also benefited the contents of nitrogen and phosphorus. The high contents of total potassium should be ascribed to the soil parent material in this area. The potassium in the soil mainly existed in the form of minerals. Thus, the supply level of potassium in the soil mainly depended on the amount of potassium minerals in the soil, so the potassium content in this area was enough. The results of our study showed that the soil organic matter in the woodlands, after returning farmland to forest, had been improved, indicating that the returning was beneficial to the accumulation of soil organic matter. This result is consistent with the results of Han et al. (2012) and Gong et al. (2005). Gong et al. (2005) also reported that the differences

between soil organic matter contents in different soil layers of various forest stands were significant.

It is assumed that the content of available nutrients serves as an indicator for the supply of soil nutrients (Wang et al., 2014). The results in this work showed that the average content of soil available nitrogen in 0-10 and 10-20 cm layers was higher than $78 \text{ g}\cdot\text{kg}^{-1}$. The average content of available phosphorus was lower than $1.35 \text{ g}\cdot\text{kg}^{-1}$ and the average content of available potassium was lower than $75 \text{ g}\cdot\text{kg}^{-1}$. The variation trend of the available nitrogen content in this region was in agreement with that of the total nitrogen content. According to the dynamic variation laws of nutrients in forest soil, the content of organic matter should be positively correlated with the content of soil available nitrogen to a certain extent (Yang and Zhang, 1986). Namely, the higher the organic matter content, the higher the available nitrogen content is. In the 0–10 cm soil layer, the contents of available nitrogen, available phosphorus and available potassium in the soil of *Eucommia ulmoides* plantation were relatively high. Because the litter fall from a relatively wide canopy of *Eucommia ulmoides* plantation was intense. This results a high content of organic carbon in the upper soil layer (Wang et al., 2010b), which was favorable to the accumulation of nitrogen and phosphorus.

After returning from farmland to forest, the contents of soil organic matter, total phosphorus and nitrogen and available potassium, phosphorus and nitrogen decreased with the increase of soil depth among various forest stands. This is because the soil nutrients generated mainly from soil minerals and soil organic matter and the latter compound is mainly generated from the litter of aboveground parts, underground roots, precipitation, slope infiltration, groundwater, fertilization and irrigation during cultivation. Therefore, most of the sources of soil nutrients were above ground, and these sources first contacted with the upper soil layer for enriched storage. Then, the nutrients were transported to the lower layer through leaching or uptake with roots. Consequently, the contents of organic matter, total phosphorus and nitrogen and available potassium phosphorus and nitrogen in the soil of different forest stands declined with the increase of soil depth.

Relationship between soil nutrients after returning farmland to forest

The contents of trace elements in the soil of different forest stands followed the order: $\text{Fe} > \text{Mn} > \text{Zn} > \text{Pb} > \text{Ni} > \text{Cu} > \text{Cd}$. The soluble Fe species could be involved in the growth of plants (Qi et al., 2008), so the content of Fe was high. All the organics and biological residues in the soil contained Zn and the acidic substances produced from organic matter during decomposition could increase the solubility of Zn compounds. The order of total contents of soil trace elements in the soil of different stands was ranked as follows: *Eucommia ulmoides* plantation > slope farmland > *Pinus massoniana* forest > maple-*Cinnamomum camphora* mixed plantation. In addition, generally the total contents of trace elements in the 0–10 cm soil layers were higher than those in the 10–20 cm soil layers. This is mainly due to the compensation effect of litter decomposition, nutrients release and return on the contents of trace elements in soil. This distribution phenomenon also reflects the weak leaching and deposition effects in the lower soil layers.

Based on the correlation analyses among soil nutrients of different forest stands after returning farmland to forest, the positive correlations between the content of soil organic matter and the contents of total and available nitrogen were found. This indicated that nitrogen and carbon elements were closely related in the accumulation

and storage process. This result is in accordance with the conclusion of Li et al. (2014) that the content of organic matter in soil had significantly positive correlations with the contents of total nitrogen, available nitrogen, total phosphorus and available phosphorus in the soil. On the other hand, Li et al. (2014) also found that the content of organic matter in soil correlated positively but weakly with the contents of soil total potassium and available potassium. This result was also consistent with the present study. Additionally, in the present work, we found that the content of phosphorus in soil was significantly positively correlated with the contents of trace elements Cu, Mn and Ni. This result agrees with the conclusions drawn by Huang et al. (2016), who reported that the contents of Cu, B, and N were significantly positively correlated with various minerals in the soil for the cultivation of wild tara vine. In this study, the content of total potassium was significantly positively correlated with contents of Cu, Zn, Mn and Ni, but Huang et al. (2016) suggested that the content of total potassium was significantly and negatively correlated with contents of Cu, Zn, Ni and other elements. This difference should be attributed to the reason that the soil used in Huang's study was acidic black loam located at the foot of the Changbai Mountain in Antu County, Yanbian Prefecture, Jilin Province, China, and the black loam, containing a small amount of soluble salts, had a great texture without salinization. As for the soil in our present work, the red and yellow soil had a parent material of shale and slate, and the soil texture was poor, compared to the black loam. These results show that the distribution of soil nutrients depends on the structural factors such as climate, topography, parent material and soil type which can lead to the spatial relationships between soil nutrients.

In this study, the content of Cu was correlated significantly and positively with Mn and Ni. On the other hand, Zn correlated significantly and positively with Mn. Mn however, correlated significantly and positively with Ni. In this study significant negative correlation was observed between Fe and Pb. These results indicate that the trace elements in various types of soil interacted with each other showing a pattern that, when the content of an element increased, the contents of relative trace elements changed.

Conclusion

After returning farmland to forest (i.e., Grain to Green), the accumulation of soil organic matter in the soil of the three vegetation types and slope farmland was increased, but the accumulation was different depending upon the vegetation types. The accumulation in the soil of *Pinus massoniana* forest was the highest, and that of the maple-*Cinnamomum camphora* mixed plantation was the lowest. In the vertical direction, the contents of organic matter in the soil of all forest stands were decreased. After returning farmland to forest, the contents of total nitrogen, phosphorus and potassium and organic matter in the soil of woodlands were the highest and those in the soil of the slope farmland were the lowest. This had indicated that the accumulation of nutrients in the soil of slope farmland was slower. Nevertheless, the accumulation of available nutrients in the soil of slope farmland was the fastest. The contents of available nitrogen and available phosphorus decreased with the increase of soil depth, but the content of available potassium increased with the increase of soil depth. After returning farmland to forest, the trace elements accumulated to a small extent but their differences based on different stands were negligible. The nutrient elements in the soil

of different vegetation types had significant correlations with each other and the soil trace elements interacted with each other following a pattern that when the content of an element increased, the contents of relative trace elements changed.

In addition, only the correlation between soil nutrients were studied in this research, and many other future studies such as dynamic changes of nutrient, change mechanism and so on would also play an important role in nutrient cycling research. And this needs to be studied further in the future. The result of this research can provide data support and theoretical basis for soil conservation, vegetation optimization model selection and artificial control in the erosion area of southern mountainous range of China.

Acknowledgements. The present research work was supported by the grant of Forestry Science and Technology Plan Project in Hunan (XLC201701-2), Major Research and Development Program in Hunan (2017NK2223), Forestry Science and Technology Plan Project in Hunan (XLKPT201703, XLKPT201706, XLKPT201707, XLKPT201710), National Science and Technology Plan for Twelfth Five-Year in the Countryside (2015BAD07B04), National Key R & D Program of China (2017YFC0505506), Forestry Science and Technology Project in Hunan (2012-HNLYKY-01) and CFERN & BEIJING TECHNO SOLUTIONS Award Funds on excellent academic achievements. All these supports are duely acknowledged with thanks.

REFERENCES

- [1] Albiach, R., Canet, R., Pomares, F. (2001): Organic matter components and aggregate stability after the application of different amendments to a horticulture soil. – *Bioresource Technology* 76(2): 125-129.
- [2] Augusto, L., Ranger, J., Binkley, D., Rothe, A. (2002): Impact of several common tree species of European temperate forests on soil fertility. – *Annals of Forest Science* 59(3): 233-253.
- [3] Cao, Y. S., Wu, F. Y., Xiao, Y. A. (2016): Effect of returning farmland to forests on soil nutrients contents and its vertical distribution. – *Ecology and Environmental Sciences* 25(2): 196-201.
- [4] Chen, S., Yuan, Z. L., Yao, S. (2017): Soil nutrients research on *Pinus tabulaeformis-Quercus aliena* var. *acuteserrata* mixed forest in Baotianman national nature reserve. – *Henan Science* 35(12): 1945-1951.
- [5] Finzi, A. C., Van Breemen, N., Canham, C. D. (1998): Canopy tree-soil interactions within temperate forests: species effects on soil carbon and nitrogen. – *Ecological Applications* 8(2): 440-446.
- [6] Gong, J., Chen, L. D., Fu, B. J., Hu, C. X., Wei, W. (2005): Effects of vegetation restoration on soil nutrient in a small catchment in Hilly Loess area. – *Journal of Soil and Water Conservation* 19(1): 93-96.
- [7] Han, X. H., Tong, X. G., Yang, G. H. (2012): Difference analysis of soil organic carbon pool in returning farmland to forest in loess hilly area. – *Transactions of the Chinese Society of Agricultural Engineering* 28(12): 223-229.
- [8] He, H. J., Wang, H. Q., Tao, Y. H. (2017): Study on soil nutrient of three types of plantations at Shatang forestry farm in Guangxi. – *Journal of Guangxi Science & Technology Normal University* 32(5): 127-130.
- [9] Hu, F., Du, H., Zeng, F. P. (2018): Dynamics of soil nutrient content and microbial diversity following vegetation in a typical karst peak-cluster depression landscape. – *Acta Ecologica Sinica* 38(6): 1-9.
- [10] Huang, C. Y. (2000): *Agrology*. – Beijing: China Agriculture Press.
- [11] Huang, Y. B., Cao, W. W., Xu, L. (2016): Wild actinidia arguta habitat soil nutrient content and correlation analysis. – *Journal of Anhui Agriculture Science* 44(18): 14-115.

- [12] Huang, K. C., Shen, Y. Y., Xu, G. P., Huang, Y. Q., Zhang, D. N., Sun, Y. J., Li, Y. Q., He, W., Zhou, L. W. (2018): Effects of reclamation on soil nutrients and microbial activities in huixian Karst Wetland in Guilin. – *Environmental Science* 22(4): 1813-1823.
- [13] Jiang, H. M., Li, M. Z., Wang, Q. (2011): Dynamics of soil nutrients under different vegetation types in the eastern Qilian Mountains. – *Research Soil and Water Conservation* 18(5): 166-170.
- [14] Latty, E. F., Canham, C. D., Marks, P. L. (2004): The effects of land-use history on soil properties and nutrient dynamics in northern hardwood forest of the Adirondack mountains. – *Ecosystems* 7(2): 193-207.
- [15] Li, Y., Man, X. L., Cai, T. J. (2014): Research on soil nutrient characteristic and correlation in different slope position of scotch pine forest in Da Hinggan Mountains. – *Journal of Anhui Agriculture Science* 42(5): 1413-1416,1420.
- [16] Liu, Q. Y., Tong, Y. P. (2005): Effects of land use type on soil nutrient distribution in northern agro-pasture ecotone. – *Chinese Journal of Applied Ecology* 16(10): 1849-1852.
- [17] Liu, Z. K., Wang, S. P., Chen, Z. Z., Wang, Y. F., Han, J. G. (2006): Properties of soil nutrients and plant community after rest grazing in Inner Mongolia steppe. – *Acta Ecologica Sinica* 26(6): 2048-2056.
- [18] Lopes, V. L., Canfield, H. E. (2004): Effects of watershed representation on runoff and sediment yield modeling. – *Journal of the American Water Resources Association* 40(2): 311-319.
- [19] McGrath, D. A., Smith, C. K., Gholz, H. L., Oliviera, F. (2001): Effects of land-use change on soil nutrient dynamics in Amazonian. – *Ecosystems* 4(7): 625-645.
- [20] Peng, X. D., Dai, Q. H., Li, C. L. (2018): Output mechanism of soil nutrients from karst slope farmland under simulated rainfall. – *Acta Ecologica Sinica* 38(2): 1-9.
- [21] Qi, L. H. (2007): Ecological characteristics of vegetation restoration for degraded lands in a watershed, Wulin mountain region. – Beijing: China Academy of Forestry Sciences.
- [22] Qi, L. H., Zhang, X. D., Peng, Z. H. (2008): Soil microelements under different vegetation restoration patterns in yellow soil slope region of mid-subtropics. – *Chinese Journal of Applied Ecology* 19(4): 735-740.
- [23] Wang, G. L., Liu, Z. B., Xu, M. X. (2001): Effect of vegetation restoration on soil nutrient changes in Zhifanggou watershed of loess hilly region. – *Bulletin of Soil and Water Conservation* 22(1): 1-5.
- [24] Wang, J., Fu, B. J., Qiu, Y., Chen, L., Yu, L. (2002): Spatial heterogeneity of soil nutrients in a small catchment of the Loess Plateau. – *Acta Ecologica Sinica* 22(8): 1173-1178.
- [25] Wang, Z. M., Zhang, B., Song, K. S., Liu, D. W., Li, J. P., Huang, J., Zhang, H. L. (2007): Analysis of related factors for soil nutrients in croplands of typical agricultural county, Northeast Plain, China. – *Journal of Soil and Water Conservation* 21(2): 73-77.
- [26] Wang, J., Lv, Z. Z., Qian, Y. (2010a): Soil nutrients under vegetation cover of different desert landscapes in junggar Basin, Xinjiang. – *Journal of Desert Research* 30(6): 1376-1373.
- [27] Wang, J. L., Wang, Z. H., Zhang, X. Z. (2010b): Effect on alpine vegetation of different grassland ecosystems composed of soil organic carbon and water stable aggregates content. – *Acta Agrestia Sinica* 18(6): 749-757.
- [28] Wang, Q. Y., Zhang, F. H. (2014): Soil nutrient properties under typical halophytic vegetation community in arid region. – *Journal of Soil and Water Conservation* 28(5): 235-241.
- [29] Ward, D., Trinogga, J., Wiegand, K., du Toit, J., Okubamichael, D., Reinsch, S., Schleicher, J. (2018): Large shrubs increase soil nutrients in a semi-arid savanna. – *Geoderma* 310: 153-162.
- [30] Wei, X. R., Shao, M. A. (2007): The distribution of soil nutrients on sloping land in the gully region watershed of the Loess Plateau. – *Acta Ecologica Sinica* 27(2): 603-612.

- [31] Wen, Z. M., Jiao, F., Liu, Z. Y. (2005): Natural vegetation restoration and soil nutrient dynamics of abandoned farmlands in forest-steppe zone on Loess Plateau. – *Chinese Journal of Applied Ecology* 16(11): 2025-2029.
- [32] Xiang, Z. Y., Zhang, L., Zhang, Q. F. (2014): Soil nutrients and microbial functional diversity of different stand types in Qinghai Province. – *Scientia Silvae Sinicae* 50(4): 22-31.
- [33] Yan, E. R., Wang, X. H., Chen, X. Y. (2007): Impacts of evergreen broad-leaved forest, degradation on soil nutrients and carbon pools in Tiantong, Zhejiang Province. – *Acta Ecologica Sinica* 27(4): 1646-1655.
- [34] Yang, C. D., Zhang, W. R. (1986): Research on forest soil organic matter in Wolong nature reserve. – *Acta Pedologica Sinica* 23(1): 30-38.
- [35] Yuan, Z. J., Cai, Q. G., Qing, J. (2006): Runoff and sediment characteristics of different land use in Heminguan watershed. – *Resources Science* 28(1): 70-74.
- [36] Zhang, H. X., Zeng, Q. C., An, S. S. (2018): Soil enzyme activities soil and leaf litter nutrients of typical vegetation in Ziwuling Mountain. – *Acta Ecologica Sinica* 38(7): 1-9.

ECOLOGICAL FLOW PROCESS EVALUATION OF A HYDROPOWER STATION'S DEHYDRATION RIVER

DAI, L. – FANG, G. – HUANG, X.* – ZHONG, J.

*College of Water conservancy and Hydropower Engineering, Hohai University
1 Xikang Rd. Nanjing, 210098 Jiangsu, P.R China*

**Corresponding author*

e-mail: hxhhuang2005@163.com; phone: +86-1-599-626-7968

(Received 11th Jan 2019; accepted 8th Mar 2019)

Abstract. We investigated the ecological restoration problems of dehydration river reaches, which are downstream of diversion-type hydropower station in medium and small watersheds. Based on this information, we calculated the ecological flow using the following five methods: the minimum monthly ecological flow method, the dynamic calculation method of ecological water demand, the Northern Great Plains Resource Program method (NGPRP), and the monthly frequency method. Then, we combined Matter Element Analysis (ME) and Tennant method to construct a ME-Tennant model. Furthermore, the ecological flow process of a river was evaluated with ME-Tennant model. The case study was performed at the Liujiaping Hydropower Station in Hunan Province, China. In this study, ME-Tennant evaluation model was applied to determine the ecological flow process, and the results were used to verify the validity and the applicability of the model. The study provides a basis for the ecological restoration of dehydration river reaches, which are downstream of the diversion-type hydropower stations. The proposed evaluation model does provide a new way to reasonably determine the ecological flow process of a river.

Keywords: *river reaches, minimum ecological flow, matter element analysis method, ME-Tennant method, Liujiaping hydropower station*

Introduction

Diversion-type hydropower stations are generally built in mountain reaches using a pipeline or artificial channels that lead water to the downstream. Diversion-type hydropower stations, which have small flow but large slope, utilizes the large water head to generate electricity. To construct the diversion-type hydroelectric power station, the runoff of the river is divided and dehydration river reaches are formed between the dumpsite and tail water stream. However, a diversion-type hydroelectric power station has adversely affected the quality of river water, causing harm to the ecological environment; moreover, it has negatively impacted the hydrology and the number of water resources in a given area. By maintaining the ecological runoff and its variation characteristics in a river, we can protect the ecosystem of a river and ensure its normal ecological functions. To offer protection to a river ecosystem and to restore its normal functioning, we need to essentially study the ecological runoff process of a river. Both Chinese and international scholars have proposed the idea of ecological runoff calculation. To fulfill this objective, they have used a variety of methods to calculate the ecological runoff of a river. After comparison and analysis of various methods, they have selected the calculation methods and results that reflect the actual situation of rivers. Zhang used five methods to study hydrology and ecological flow of the Pearl River basin. Thus, the ecological runoff of the Pearl River basin was calculated by five methods. By comparing the results with those of Tennant method, he preferred to use the minimum monthly ecological flow method and the monthly frequency method to calculate the minimum ecological runoff and the suitable ecological runoff, respectively

(Zhang, 2010); Shi used four hydrological methods to calculate the ecological flow, which was produced by the main rivers in Xiangyang City; the methods complied with the requirements of the river ecological water, and they were used to determine the basic ecological flow (Shi and Zuo, 2017). Yu used six methods to calculate the ecological base flow in Guanzhong section of Weihe River. Then, they analyzed the annual runoff distribution characteristics of Weihe River. The results indicated that the Tennant method produced the most accurate results, so it was the best method for calculating the ecological base flow of Weihe River (Palau and Alcázar, 2012). Palau used several methods to determine the minimum ecological flow, and they used BFM method to calculate it (Zhang, 2008).

Different methods may be used to calculate the ecological runoff of different rivers. A single method may produce unreasonable results for different rivers, so a variety of methods should be used to calculate and analyze the ecological runoff of different rivers. However, in this process, the evaluation is not accurate and intuitive enough as it subject to different factors, causing some difficulties in the final determination of ecological runoff. To tackle this situation, we combined Matter Element (ME) analysis and Tennant method to come up with an ME-Tennant model. This model was used to evaluate the ecological flow process of a river. Our main aim was to restore the ecology of dehydrated river reaches, which were located downstream of the diversion-type hydropower stations. Moreover, the ME-Tennant model was projected as a new way of reasonably determining the ecological flow process of a river.

Materials and Methods

Materials

The Liujiaping hydropower station is selected as the study area. Its coordinate is 11036'E-1100 42'E and 270 26'N-270 38'N. Liujiaping River is the primary tributary of Erdu River, which originates from Liangfengjie Mountain, Longhui County, Hunan Province, China. The river is zigzagged and it flows from the southeast to the northwest regions of China. In total, the area and length of the river basin area are 72 km² and 30 km, respectively. A large slope is a characteristic feature of the Erdu River basin. The conditions of the natural river are not conducive for fish farming, and there is no valuable and rare aquatic organism in the river. The basin belongs to the monsoon regions of Southeast Asia. Liujiaping reservoir is located in Longzhuangwan Village, Xupu County. In the reservoir, the rainwater harvesting area is 53.63 km², while the length of the mainstream above the dam site is 21.0 km. The average slope of the river is 91%, and the total reservoir capacity is 33.652×10^6 m³.

Liujiaping powerhouse is located approximately 3 km away in the downstream of the dam. It is a diversion-type hydroelectric power station, which should be regulated for multiple times in a year. There are dehydration river reaches between the dam site and the tail water stream, and a little pond is observed in the foundation pit; the riverbed sand is exposed and there is no habitat for the fish to survive and thrive. A definite ecological flow should be discharged to meet the requirements of ecological environment and water demands of the dehydration river reaches, which are downstream.

An ecological runoff refers to a flow of a certain quality, which is required to maintain the ecological function of a specific river ecosystem; it is affected by the river's ecohydrology and the changes inflicted with temporal and spatial variation. The ecological flow corresponds with the time axis. Therefore, we drew a response curve of

flow and time, which is known as ecological runoff process (Li, 2015). An ecological runoff process emphasizes the changing characteristics of an ecological flow, which is determined with respect to space and time scales and dynamic demands. It reflects the different requirements of ecological flow in different time-scales.

In order to protect the ecological conditions of dehydration river reaches, a certain ecological flow should be discharged (Wang, 2014); moreover, the ecological runoff process should be performed according to ecological flow requirements of each month. The ecological flow process of dehydration river reaches has many goals, and their implementation sequences are as follows: (1) ensure continuous flow; (2) provide a minimum living space for aquatic organisms; (3) provide suitable habitat conditions for aquatic organisms.

Calculation methods of ecological flow process

Presently, more than 200 kinds of calculation methods are used to determine the ecological flow of a river (Thame, 2003); these methods are mainly classified into four types: i) the hydrologic method is based on the historical hydrological flow data, such as the Tennant method; ii) the hydraulic method is based on hydraulic foundation and cross-section parameters used for calculation, such as the R2-Cross method and the wetted perimeter method; iii) the habitat simulation method is based on biological factors, which are combined with the results of hydraulic analysis and habitat evaluation. For example, the instream flow incremental method (IFIM method) and physical habitat model simulation method (PHABSIM method); and iv) the holistic analysis method is based on the theory of river system integrity, which is combined with the flow data and information. The overall evaluation method and the BBM method (Building Block Methodology) are the most commonly used methods of this type.

Due to a lack of ecological data, it is difficult to apply the following methods in China: the habitat simulation method, the hydraulic method, and the holistic analyze method. However, hydrology method only needs historical flow data to ascertain the ecological flow of a river, and most of China's regional historical flow data is sufficient; therefore, hydrology method is quite appropriate for use in China. Moreover, the method can be suitably used to analyze the research data of small and medium-sized rivers' ecological flow. In this study, we analyzed several common hydrological methods.

The minimum monthly ecological flow method

In the monthly minimum ecological flow method, the ecological flow of each month is calculated from the minimum monthly average flow observed in the historical runoff series of several years. With this method, we calculated the minimum ecological flow process (Yu, 2004). The formula is as follows:

$$q_i = \min(q_{ij}), j=1,2,\dots,n \quad (\text{Eq.1})$$

where, q_i is the minimum ecological flow of the month i , and it is expressed in m^3/s ; q_{ij} is the average monthly flow of the month i in the year j , and it is expressed in m^3/s ; n is the statistical year.

The dynamic calculation method of ecological water demand

The dynamic calculation method was based on the historical flow data, and it introduced the mean value ratio of the same period (Pan and Ruan, 2015; Pan, 2013); moreover, it was also used to determine the relationship between the monthly ecological flow and the annual average flow of each month. Thus, we determined the minimum ecological flow process. The concrete calculation process is as follows:

(1) Calculate the annual average and the minimum annual flow using a long series of natural flow data.

$$\bar{Q} = \frac{1}{12} \sum_{i=1}^{12} \bar{q}_i \quad (\text{Eq.2})$$

$$\bar{Q}_{\min} = \frac{1}{12} \sum_{i=1}^{12} q_{\min(i)} \quad (\text{Eq.3})$$

$$q_{\min(i)} = \min(q_{ij}), j=1,2,\dots,n \quad (\text{Eq.4})$$

where, \bar{Q} is the annual average flow, and it is expressed in m^3/s ; \bar{q}_i is the annual average monthly flow of each month i , and it is expressed in m^3/s ; \bar{Q}_{\min} is the minimum annual average flow, and it is expressed in m^3/s ; $q_{\min(i)}$ is the minimum monthly average flow of the month i in several years, and it is expressed in m^3/s ; q_{ij} is the monthly average flow of month i in year j , and it is expressed in m^3/s ; n is the statistical number.

(2) Calculate the mean value ratio of the same period according to the annual average flow and the minimum annual average flow:

$$\eta = \bar{Q}_{\min} / \bar{Q} \quad (\text{Eq.5})$$

(3) Calculate the monthly ecological flow according to the annual average monthly flow:

$$Q_i = \bar{q}_i \times \eta \quad (\text{Eq.6})$$

where, Q_i is the ecological flow of month i , and it is expressed in m^3/s .

NGPRP method

In the Northern Great Plains Resource Program method (NGPRP), the hydrological year group was classified into three types: low flow year group, normal flow year group, and flood year group. This method confirms that each month flow can be included in the normal flow year group, with a guaranteed rate of 90%. The minimum ecological flow is calculated by this approach (Wang, 2015). The anomaly percentage method was used to divide the group.

$$P_i = (Q_i - Q_a) / Q_a \quad (\text{Eq.7})$$

where, P_i is the anomaly percentage of annual average flow, and it is expressed in %. When $-10\% \leq P_i \leq 10\%$, it belongs to the normal flow year group; Q_i is the annual average flow of year i , and it is expressed in m^3/s ; Q_a is the annual average flow of several years, and it is expressed in m^3/s .

Monthly frequency method

In the monthly frequency method, the year is divided into different periods by referring to the historical monthly flow data. Then, different guarantee rates are selected to calculate the flow of each period, and this information is an estimate of the ecological flow process. To select different guarantee rates for each period, we referred to the main research studies of prominent scholars: Yu first proposed the monthly frequency method to calculate the ecological flow of Luohe River and Yihe River, and he assumed that the guaranteed rate of monthly flow was 80% in winter, 75% in spring and autumn, 50% in summer; these guaranteed rates of monthly flow were considered as the river's ecological flow in different seasons. Li proposed that the guaranteed rate of month flow was always greater than 50% in each month (Li, 2007). Guo assumed the guaranteed rate of monthly flow as 80% in the low water period and 50% in the normal flow period. For the flood period, he directly took the annual average flow as the ecological flow (Guo, 2008). In this study, the small river flow was divided into three phases: the low flow period, the normal flow period, and the flood period; the different selections of guaranteed rate are as follows: i) 90% in the low flow period, 80% in the normal flow period, and 50% in the flood period; ii) 50% guaranteed rate for each month; and iii) 80% in the low flow period, 50% in the normal flow period, and the annual average flow in the flood period.

Tennant method

The ecological flow was calculated using the Tennant method: a percentage of the annual average flow of the river channel was considered as the recommended flow (Xu, 2003), and different percentages were considered in different months. Moreover, the year was divided into the spawning period (April-September) and the general period (October-March) of water use. *Table 1* elucidates the relation between the channel flow and the river's ecological health in each period.

Table 1. The relation between the channel flow and the river ecological health

River ecological health	The percentage of channel flow accounts for annual average flow	
	General using water period (Oct-Mar.)	Spawning period (Apr-Sept.)
Maximum	200	200
Optimum range	60~100	60~100
very good	40	60
good	30	50
preferably	20	40
average or inferior	10	30
Poor or minimum	10	10
Severe degradation	<10	<10

In practical application, many Chinese scholars have modified the Tennant method to suit the specific conditions of the study area. Zhang Mei calculated ecological flow by dividing the year into non-flood period (November-May) and flood period (June-October) (Zhang, 2005). He considered the specific characteristics of the water diversion area in the west route of South-to-North Water Transfer Project. Zheng Zhihong emphasized the obvious seasons variations of North China River; the river's ecological water demand period was further classified into three different periods by considering a seasonal variation. For each period, the percentage of recommended base flow was reselected according to the expert suggestion (Zhen, 2010). Chen proved that the ecological flow of Yellow River was different in the following two periods: the non-flood period (November-July) and flood period (July-October). After analyzing the characteristics of Yellow River in each period, they further derived a new percentage coefficient by multiplying the bed gradient: this parameter was more suitable for the sandy river (Chen, 2011).

To perform the minimum monthly ecological flow method, we require hydrological data of more than 20 years; however, the calculation process is simple, and the minimum ecological flow can meet the minimum living conditions of aquatic organisms. Nevertheless, it is not conducive for the healthy development of the aquatic ecosystem in the long-term. To determine ecological water demand by the dynamic calculation method, we have to calculate the mean value ratio of the same period; this method rectifies the subjectivity and experience of the traditional hydrological method, and it reflects the change characteristics of river flow in times of abundance and drought; however, the method does not apply to strong seasonal rivers. Furthermore, NGPRP method takes into account climatic conditions, acceptable frequency factors, and the difference between the normal flows of different years, but the method lacks a biological basis. The monthly frequency method considers the different requirements of the ecological system in different periods; different assurance rates are chosen to ensure that the ecological flow process adapts with the natural flow process, but it is difficult to select the most reasonable assurance rate. The Tennant method is simple and convenient, but it does not analyze the flow characteristics from the river basin's characteristics; moreover, there are no formation rules. It is usually used to analyze a river of low priority or to inspect the results of other methods.

Both advantages and disadvantages are encountered when we use different methods to calculate ecological flow. The basin's geographical location, climate, underlying surface, and the influencing human activities are considered when we use a variety of calculation methods. Thus, an unreasonable result of ecological flow can be definitely avoided. However, the suitable methods used for calculating the ecological flow of different river types are different; therefore, the calculation results will be different when we use a variety of methods to calculate the ecological flow of a river. Furthermore, we also encountered some difficulties in the final determination of the ecological runoff process. Therefore, it is important to objectively evaluate the ecological flow process, which was calculated by different methods. The evaluation results can serve as the basis for the determination of ecological flow process. In this study, we proposed an evaluation model based on ME-Tennant method. This model was specifically developed to calculate the ecological flow process of a river.

Ecological flow process evaluation model based on ME-Tennant method

The matter element analysis method is based on the following principle: everything can be described by three elements-"things N, the characteristics of things C, the corresponding value of the characteristics X" which are basic elements of an ordered triple. These are known as matter elements. Using the ordered triple $R = (N, C, X)$, we describe things as basic elements (Feng and Hong, 2014).

(1) Construct the matter element matrix

The ecological flow conditions of 12 months were used as evaluation indexes of the ecological flow process, and we recorded them as 12 characteristics. The matter element matrix was established as follows:

$$R = \begin{pmatrix} P_0 & C_1 & X_1 \\ & C_2 & X_2 \\ & \vdots & \vdots \\ & C_n & X_n \end{pmatrix} \quad (\text{Eq.8})$$

where, R is the n-dimension matter element; P_0 is the unevaluated unit of the ecological flow process; C_i ($i = 1, 2 \dots n$) is the i-th evaluation index, which is the ecological flow condition of month i; X_i ($i = 1, 2 \dots n$) is the corresponding value of the evaluation index C_i , and the percentage of the ecological flow of month i accounts for the annual average flow.

(2) Construct the classical domain and the joint domain matter-element

The classical domain and the joint domain matter-element were constructed according to the evaluation criterion of the ecological flow process.

The classical domain matter-element R_j can be expressed as follows:

$$R_j(N_j, C, X_j) = \begin{pmatrix} N_j & C_1 & X_{j1} \\ & C_2 & X_{j2} \\ & \vdots & \vdots \\ & C_n & X_{jn} \end{pmatrix} = \begin{pmatrix} N_j & C_1 & [a_{j1}, b_{j1}] \\ & C_2 & [a_{j2}, b_{j2}] \\ & \vdots & \vdots \\ & C_n & [a_{jn}, b_{jn}] \end{pmatrix} \quad (\text{Eq.9})$$

where, N_j ($j = 1, 2 \dots m$) is the j-th grade of the ecological flow process; $X_{ji} = [a_{ji}, b_{ji}]$ is the classical domain, representing the percentage range of the ecological flow that accounts for the annual average flow corresponding with the j-th grade.

The joint domain matter-element can be expressed as follows:

$$R_p(N_p, C, X_p) = \begin{pmatrix} N_p & C_1 & X_{p1} \\ & C_2 & X_{p2} \\ & \vdots & \vdots \\ & C_n & X_{pn} \end{pmatrix} = \begin{pmatrix} N_p & C_1 & [a_{p1}, b_{p1}] \\ & C_2 & [a_{p2}, b_{p2}] \\ & \vdots & \vdots \\ & C_n & [a_{pn}, b_{pn}] \end{pmatrix} \quad (\text{Eq.10})$$

where, N_p is the set of evaluation grade; $X_{pi} = [a_{pi}, b_{pi}]$ is the joint domain, which represents the sum of the numerical range of the classical domain of each index.

(3) Determine the correlation function and the correlation degree.

The correlation function indicates that when the value of the matter element is taken as a point on the real axis, the conformity degree of the matter element lies within the required range of values. If $|X_o| = |b - a|$ is used to represent the length of the bounded interval $X_o = [a, b]$, the distance from x_i to $X_{ji} = [a_{ji}, b_{ji}]$ and x_i to $X_{pi} = [a_{pi}, b_{pi}]$, respectively:

$$\rho(x_i, X_{ji}) = \left| x_i - \frac{1}{2}(a_{ji} + b_{ji}) \right| - \frac{1}{2}(b_{ji} - a_{ji}) = \begin{cases} a_{ji} - x_i, & x_i \leq \frac{a_{ji} + b_{ji}}{2} \\ x_i - b_{ji}, & x_i > \frac{a_{ji} + b_{ji}}{2} \end{cases} \quad (\text{Eq.11})$$

$$\rho(x_i, X_{pi}) = \left| x_i - \frac{1}{2}(a_{pi} + b_{pi}) \right| - \frac{1}{2}(b_{pi} - a_{pi}) = \begin{cases} a_{pi} - x_i, & x_i \leq \frac{a_{pi} + b_{pi}}{2} \\ x_i - b_{pi}, & x_i > \frac{a_{pi} + b_{pi}}{2} \end{cases} \quad (\text{Eq.12})$$

The calculation formula of the correlation function $K_j(x_i)$ is as follows:

$$K_j(x_i) = \begin{cases} \frac{-\rho(x_i, X_{ji})}{|X_{ji}|} & x_i \in X_{ji} \\ \frac{\rho(x_i, X_{ji})}{\rho(x_i, X_{pi}) - \rho(x_i, X_{ji})} & x_i \notin X_{ji} \end{cases} \quad (\text{Eq.13})$$

where, $|X_{ji}| = |a_{ji} - b_{ji}|$.

(4) Determine the weight of each evaluation index

Weight refers to the importance of an index in the whole index system. Greater the value of the weight, more important it is in the system. To determine the weight of the index, we divided the method into two categories: the subjective weight method and the objective weight method. In this study, an analytic hierarchy process was used to determine the importance of each month's ecological flow (Fan and Jiang, 2001; Fan, 2001). The main steps are as follows:

- a) Determine the evaluation target and the evaluation index set
- b) Establish a fuzzy consistent judgment matrix

The fuzzy consistent judgment matrix reflects the relative importance degree of each two elements in $a_1, a_2, a_3, \dots, a_n$, and it is expressed as follows:

$$R = \begin{pmatrix} r_{11} & \cdots & r_{1n} \\ \vdots & \ddots & \vdots \\ r_{n1} & \cdots & r_{nn} \end{pmatrix} \quad (\text{Eq.14})$$

where, r_{ij} is the membership degree that indicates how much more important a_i is than a_j ; greater the value of r_{ij} , more important is a_i than a_j . We used the 0.1–0.9 scale method (Table 2) to determine it.

Table 2. Scale of 0.1~0.9 measure

Scale	0.5	0.6	0.7	0.8	0.9
Definition	equal important	slightly more important	obviously more important	much more important	extremely more important

The properties of fuzzy judgment consistency matrix R are as follows:

- 1) $r_{ii} = 0.5, i=1,2,3,\dots,n$;
- 2) $r_{ij} + r_{ji} = 1, i, j=1,2,3,\dots,n$;
- 3) $r_{ij} = r_{ik} - r_{jk} + 0.5, i, j, k = 1,2,3,\dots,n$.

For R to be a fuzzy consistent judgment matrix, the necessary and the sufficient condition is as follows: there exist an n-order non-negative normalized vector $W = (\omega_1, \omega_2, \dots, \omega_n)$ and a positive number a make $\forall i, j$ that satisfy the following condition:

$$r_{ij} = a(\omega_i - \omega_j) + 0.5 \quad (\text{Eq.15})$$

where, parameter $a \geq (n-1)/2$ (in this paper, set $a = (n-1)/2$); the value of a reflects the decision makers' personal preference. Smaller the value of a, more attention would experts pay to the difference between the weight of elements (Lv, 2002).

a) Calculate index weight

Fix the i in formula (15) and obtain the following equation:

$$\omega_i = \frac{1}{a} \left(r_{ik} - \frac{1}{2} \right) + \omega_k, \quad k = 1, 2, 3, \dots, n \quad (\text{Eq.16})$$

Calculate the sum of k and obtain the following equation:

$$n\omega_i = \frac{1}{a} \sum_{k=1}^n r_{ik} - \frac{n}{2a} + \sum_{k=1}^n \omega_k \quad (\text{Eq.17})$$

From the weight vector normalization condition, we obtained the following equation:

$$\omega_i = \frac{1}{n} - \frac{1}{2a} + \frac{1}{na} \sum_{k=1}^n r_{ik}, \quad i = 1, 2, 3, \dots, n \quad (\text{Eq.18})$$

In the formula, $0 \leq \omega_i \leq 1$.

(5) Calculate the comprehensive correlation degree

$$K_j(P_0) = \sum_{i=1}^n \omega_i K_j(x_i) \quad (\text{Eq.19})$$

where, $K_j(P_0)$ is the comprehensive correlation degree of the j-th evaluation grade.

(6) Grade evaluation

If $K_j = \max \{K_j(P_0)\} (j = 1, 2, \dots, m)$, the ecological flow process is in grade j. When $0 < K_j(P_0) < 1$, it indicates that the unevaluated unit meets the requirements of the standard object. When $-1 < K_j(P_0) < 0$, the evaluation unit can't meet the requirements of the evaluation grade; however, it has the capacity to transform into a form that conforms with the standard. When $K_j(P_0) < -1$, the evaluation unit neither meet the requirements nor can it transform. When $K_j(P_0) > 1$, the evaluation unit exceeds the upper limit of the standard grade.

(7) Determine the ecological flow process

The ecological flow process was determined reasonably using the evaluation grade of the ecological flow process, which was calculated by different calculation methods and combined with the ecological water requirement of the basin.

Results and discussion

Calculate the ecological flow process

In this paper, we selected measured monthly flow data of Liujiaping dam site from 1987 to 2015, which is period of 29 years in total. The annual average flow was $1.51 \text{ m}^3/\text{s}$. In theory, we must calculate the ecological flow process using natural flow data; however, since 1987, the river was more or less affected by human activities, so the ecological status might not have been restored to the original status. The altered ecosystem was further adapted to the present flow process. In fact, the so-called "natural state" was only considered as the state that was less affected by human activity. After analyzing the period 1987-2015, we found that the average flow of each year was slightly different from the average annual flow; moreover, there was no obvious mutation, indicating that the average annual flow was least affected by human activities. Therefore, the ecological flow process was calculated using the directly measured data instead of the natural flow data. After determining the multi-year average flow process at the dam site, we divided the whole year is divided into three periods: low water period (November-February), normal water period (March-April, September-October), and flood period (May-August). The hydrological frequency analysis was carried out using PIII curve. The minimum monthly ecological flow method, the dynamic calculation method of ecological water demand, the NGPRP method, and the monthly frequency method were used to calculate the ecological flow process of Liujiaping

hydropower station downstream of the dehydration river reaches. The calculation results are presented in *Table 3*.

Table 3. The calculation results of ecological flow process by different methods m^3/s

Month Method	1	2	3	4	5	6	7	8	9	10	11	12
Minimum monthly ecological flow method	0.301	0.368	0.332	0.613	1.166	1.292	1.180	0.566	0.191	0.234	0.230	0.200
Dynamic calculation method	0.311	0.362	0.423	0.520	0.751	0.910	1.031	0.726	0.543	0.412	0.357	0.324
NGPRP	0.400	0.560	0.550	0.830	1.080	1.630	1.350	0.830	0.450	0.450	0.380	0.430
monthly frequency method I	0.390	0.460	0.780	1.120	1.880	2.350	2.540	1.840	0.870	0.680	0.400	0.410
monthly frequency method II	0.750	0.830	1.040	1.340	1.880	2.350	2.540	1.840	1.240	0.940	0.790	0.750
monthly frequency method III	0.480	0.540	1.040	1.340	1.510	1.510	1.510	1.510	1.240	0.940	0.490	0.490

Monthly frequency method (i): 90% in the low flow period, 80% in the normal flow period, 50% in the flood period; monthly frequency method; (ii): 50% guaranteed rate for each month; monthly frequency method (iii): 80% in the low flow period, 50% in the normal flow period, and the annual average flow in the flood period

Evaluation of the ecological flow process based on ME-Tennant method

According to the present ecological situation of Liujiaping hydropower station downstream, the goals of discharging the ecological flow and their implementation sequences are as follows: (i) ensure a continuous flow; (ii) provide a minimum living space for aquatic organisms; and (iii) provide suitable habitat conditions for aquatic organisms. Because dry flow often occurs in the natural river reach of Liujiaping River during the dry season, we had to offer ecological protection and restoration; therefore, the order of ecological flow conditions and the importance degree of each period is as follows: low flow period > normal flow period > flood period. Drier the month, higher is its importance. Based on this finding, we constructed a fuzzy consistent judgment matrix to elucidate the relative importance of the ecological flow conditions observed in two consecutive months. Moreover, the weight of each month was determined by fuzzy analytic hierarchy process (AHP). The index value X_i is the percentage of ecological flow of month i , and it accounts for the annual average flow. The classical domain X_{ji} and the joint domain X_p were determined using the evaluation criteria laid down for the river's ecological flow process. As shown in *Table 4*, the values of indexes, the classical domain, and the joint domain were calculated by the six methods.

We calculated the correlation degree of each evaluation index with respect to each evaluation. By considering the weight of the index, we calculated the comprehensive correlation degree of each evaluation grade. As shown in *Table 5*, the comprehensive correlation degree and the evaluation results of an ecological flow process were calculated by six different methods.

Table 4. The values of indexes representing the ecological flow process; the classical domain and the joint domain calculated by different methods

Index	Index value Xi						Classical domain X _{ji}							Joint domain X _p
	Minimum monthly ecological flow method	Dynamic calculation method	NGPRP	monthly frequency method I	monthly frequency method II	monthly frequency method III	Poor X _{1i}	Average X _{2i}	Preferably X _{3i}	Good X _{4i}	Very good X _{5i}	Optimum X _{6i}	Maximum X _{7i}	
C1	19.90	20.61	26.49	25.83	49.67	31.79	[0,10]	[10,20]	[20,30]	[30,40]	[40,60]	[60,100]	[100,200]	[0, 200]
C2	24.37	23.98	37.09	30.46	54.97	35.76	[0,10]	[10,20]	[20,30]	[30,40]	[40,60]	[60,100]	[100,200]	[0, 200]
C3	21.96	28.02	36.42	51.66	68.87	33.11	[0,20]	[20,30]	[30,40]	[40,50]	[50,70]	[70,100]	[100,200]	[0, 200]
C4	40.57	34.42	54.97	74.17	88.74	53.64	[0,20]	[20,30]	[30,40]	[40,50]	[50,70]	[70,100]	[100,200]	[0, 200]
C5	77.19	49.71	71.52	124.50	124.50	94.70	[0,30]	[30,40]	[40,50]	[50,60]	[60,80]	[80,100]	[100,200]	[0, 200]
C6	85.54	60.29	107.95	155.63	155.63	98.10	[0,30]	[30,40]	[40,50]	[50,60]	[60,80]	[80,100]	[100,200]	[0, 200]
C7	78.15	68.29	89.40	168.21	168.21	100.66	[0,30]	[30,40]	[40,50]	[50,60]	[60,80]	[80,100]	[100,200]	[0, 200]
C8	37.46	48.09	54.97	121.85	121.85	86.75	[0,30]	[30,40]	[40,50]	[50,60]	[60,80]	[80,100]	[100,200]	[0, 200]
C9	12.76	35.99	29.80	57.62	82.12	38.41	[0,20]	[20,30]	[30,40]	[40,50]	[50,70]	[70,100]	[100,200]	[0, 200]
C10	15.53	27.27	29.80	45.03	62.25	31.79	[0,20]	[20,30]	[30,40]	[40,50]	[50,70]	[70,100]	[100,200]	[0, 200]
C11	15.20	23.62	25.17	26.49	52.32	25.17	[0,10]	[10,20]	[20,30]	[30,40]	[40,60]	[60,100]	[100,200]	[0, 200]
C12	13.25	21.46	28.48	27.15	49.67	25.17	[0,10]	[10,20]	[20,30]	[30,40]	[40,60]	[60,100]	[100,200]	[0, 200]

Table 5. The evaluation results of ecological flow process calculated by six different methods

Method	Comprehensive correlation degree							Evaluation results
	Poor	Average	Preferably	Good	Very good	Optimum	Maximum	
Minimum monthly ecological flow method	-0.1846	0.0423	-0.1483	-0.3904	-0.5098	-0.6452	-0.7658	Average
Dynamic calculation method	-0.3196	-0.0500	0.1935	-0.2254	-0.3874	-0.5787	-0.7220	Preferably
NGPRP	-0.3616	-0.1946	0.1193	-0.0622	-0.2277	-0.4612	-0.6423	Preferably
monthly frequency method I	-0.4078	-0.2743	0.0454	-0.0792	-0.205	-0.4107	-0.5503	Preferably
monthly frequency method II	-0.4534	-0.3956	-0.3233	-0.2302	0.2179	-0.0664	-0.3469	Very good
monthly frequency method III	-0.4141	-0.3182	-0.1756	0.0633	-0.1024	-0.2209	-0.4816	Good

Analysis of the evaluation result

Based on the evaluation results, we present the following observations: the minimum ecological flow process was calculated by different methods; the evaluation grade was "Average" when it was calculated by minimum monthly ecological flow method, but it was "Preferable" when calculated by dynamic calculation method and NGPRP method. In order to ensure a continuous flow and to provide the minimum living space for aquatic organisms, we selected and coupled only those ecological flow processes that had evaluation grades of "Preferable;" we considered the outer envelope curve as the minimum ecological flow process, which was no less than the 10% of the average annual flow. *Table 6* presents the ecological flow of each month in the minimum ecological flow process.

Table 6. *The ecological runoff process*

Month	1	2	3	4	5	6	7	8	9	10	11	12
Minimum flow	0.40	0.56	0.55	0.83	1.08	1.63	1.35	0.83	0.54	0.45	0.38	0.43
Suitable flow	0.48-0.75	0.54-0.83	1.04	1.34	1.51-1.88	1.51-2.35	1.51-2.54	1.51-1.84	1.24	0.94	0.49-0.79	0.49-0.75

The minimum ecological flow process is just used to meet the short-term hydrological condition, and it is used as the lower limit to satisfy the river ecosystem's stability and health conditions. Although it can ensure a continuous flow and provide the minimum living space for aquatic organisms, it seems to be harmful for the sustainable development of a river's ecosystem in the long-term. In order to maintain the stability of the basin ecosystem and its function, a suitable ecological flow process should be determined.

To evaluate a suitable ecological flow process, the conditions are as follows: i) the evaluation grade should be "Preferable" for the one calculated by monthly frequency method I; ii) the evaluation grade should be "Good" for the one calculated by the monthly frequency method III; and iii) the evaluation grade should be "Very good" for the one calculated by the monthly frequency method II. It is important to note that rare aquatic organisms and dense vegetation exist on both the sides of the Liujiaping River Basin, so it is relatively easy to conserve both soil and water in this region; moreover, natural precipitation occurs frequently and groundwater levels are sufficient to supply water. Therefore, when the monthly frequency method II and III have an evaluation grade of "Very good" and "Good," respectively, the ecological water requirements of the river are satisfied by both methods. Thus, we ensure a healthy development of the river's ecosystem. After coupling the two ecological flow processes, we considered the inner envelope curve and the outer envelope curve as the threshold of a suitable ecological flow process. *Table 6* presents the ecological flow of each month in the suitable ecological flow process.

At the Liujiaping hydropower station, scientists perform the most important task of power generation. By determining a suitable ecological flow process, we can ensure that the discharge of ecological flow is more flexible in nature. After combining the actual situation of the hydrological conditions and the demand of water and electricity, the generation benefit was considered as the basis of satisfying the ecological water

requirement. In this way, we improved the efficiency of water usage and the comprehensive benefits of electricity generation.

The minimum ecological flow process and the suitable ecological flow process were determined by taking into account following parameters: the evaluation results, the river's ecological status, and the demand for utilizing water resources in the dehydration river reaches. The minimum ecological flow process can maintain a certain amount of water in the river channel, and it can prevent the ecological condition of the river from deterioration or barrenness. A suitable ecological flow process can ensure that the ecosystem in its best condition, and it can sustain the development of a river's life and health. The two ecological flow processes can reflect the variation of an annual flow; they have a certain reference significance for the ecological protection and restoration of the lower reaches of hydropower stations.

Conclusion

In this study, we constructed the ME-Tennant model by combining Matter Element Analysis and Tennant method. This model was used to evaluate the ecological flow process of a river. The model was used to evaluate the ecological flow process of dehydration river reaches, which are downstream of Liujiaping Hydropower Station in Hunan Province, China. Furthermore, the minimum ecological flow process and the suitable ecological flow process were determined after analyzing the evaluation results of ecological flow process, which were obtained by six different calculation methods. To restore the ecology of the dehydration river reaches, we can use these evaluation results as a reference.

In the case study, we used the ME-Tennant model to evaluate the ecological flow of the dehydration river reaches. We found that the evaluation grade of a suitable ecological flow process method was greater than that of the minimum ecological flow process calculation method. Moreover, the evaluation results were in good agreement with the actual trends. This indicates that the evaluation results have certain credibility. A percentage of an ecological flow accounted for the annual average flow, which was calculated by the minimum monthly ecological flow method and the dynamic calculation method, were the same but the allocation of annual ecological flow was different. The evaluation model took into account the difference between the important ecological flow conditions of different months, so the evaluation grades were different. The evaluation results were more reasonable. To determine ecological flow process, we developed an evaluation model based on ME-Tennant method. This model was both reasonable and applicable; the evaluation process was simplified and the evaluation result was intuitive. Thus, the ecological flow process can be determined rationally with this innovative model.

Different rivers have different geographical locations, and hydrological conditions; moreover, the impact of human activity is different in different river basins. Furthermore, the ecological flow process method that is most suitable would be different for different rivers. In the evaluation model, the weight of each month, period division, and evaluation criteria should be adjusted according to the watershed situation. Moreover, the ecological data of most small and medium-sized watershed areas are scarce; therefore, the methods involved in this paper are largely based on the historical flow data and the hydrological data, so the hydrological sequence should be checked to ensure the reliability of the data.

The calculation method of ecological runoff process has high dependence on historical runoff data and requirements. The hydrological sequence should be tested to ensure the reliability of the data. In the process of evaluating and determining the ecological runoff process by applying the ME-Tennant method, due to the different geographical location, hydrological situation and the focus of the river ecological restoration target, the monthly weight, period division and evaluation criteria should be targeted to the basin. Information is adjusted.

Acknowledgements. This work was funded by the Key Project of Water Science and Technology Planning of Hunan Province ([2016]194-21), the fundamental Research Funds for the Central Universities (2019B11014), and the Project of Water Science and Technology Planning of Hunan Province ([2015]245-13).

REFERENCES

- [1] Chen, N., Zhang, D., Jiang, X. (2011): Calculation on eco-environmental water requirements in Huayuankou Station based on an improved Tennant Method. – *Journal of North China Institute of Water Conservancy and Hydroelectric Power* 32: 23-25.
- [2] Fan, Z., Jiang, Y. (2001): Review on the research of fuzzy judgment matrix ranking method. – *Systems Engineering* 19: 12-18.
- [3] Fan, Z., Jiang, Y., Xiao, S. (2001): Consistency of fuzzy judgement matrix and its properties. – *Control and Decision* 16: 69-71.
- [4] Feng, L., Hong, W. (2014): Application of matter element analysis in weather forecasting. – *Royal Meteorological Society* 21: 398-402.
- [5] Guo, L., Xia, Z., Li, J., Ma, G. (2008): Improvement of calculation methods for instream ecological runoff. – *Journal of Hohai University (Natural Sciences)* 4: 456-462.
- [6] Li, J., Xia, Z., Ma, G. (2007): A new monthly frequency computation method for instream ecological flow. – *Acta Ecologica Sinica* 27: 2916-2921.
- [7] Li, B., Yang, B. (2015): Study on ecological runoff process of Liaohe River. – *Northeast Water Conservancy and Hydroelectric Power* 33: 44-45.
- [8] Lv, Y. (2002): Weight calculation method of fuzzy analytical hierarchy process. – *Fuzzy Systems Mathematics* 16: 79-85.
- [9] Palau, A., Alcázar, J. (2012): The Basic Flow Method for Incorporating Flow Variability in Environmental Flows. – *River Research and Applications* 28: 93-102.
- [10] Pan, Z., Ruan, X., Xu, J. (2013): A new calculation method of instream basic ecological water demand. – *Journal of Hydraulic Engineering* 44: 119-126.
- [11] Pan, Z., Ruan, X. (2015): Spatio-temporal analysis of satisfactory degree of ecological water demand in Huaihe River Basin. – *Journal of Hydraulic Engineering* 46: 280-290.
- [12] Shi, Y., Zuo, Q. (2017): The estimation of ecological base flow of main rivers in Xiangyang Citu based on multiple hydrological methods. – *China Rural Water and Hydropower* 2: 50-54.
- [13] Thame, R. E. (2003): A global perspective on environmental flow assessment: emerging trends in the development and application of environmental flow methodologies for rivers. – *River Research and Applications* 19: 397-441.
- [14] Wang, H., Zhou, M., Liu, Y., Li, S. (2014): Hydraulic evaluation methods of ecological water demand by dehydration river reaches of small hydropower plants in Guangdong mountainous areas. – *Journal of Hydroelectric Engineering* 33: 154-161.
- [15] Wang, H., Zhou, M., Li, S., Zhu, J. (2015): Apply hydrological model to evaluation of ecological water demand of dehydration river reaches for small hydropower plants and water supplement. – *Journal of Hydroelectric Engineering* 34: 29-37.

- [16] Xu, Z., Dong, Z., Zhou, J., Su, F. (2003): Montana method of ecological water requirements and its application. – *Water Resources and Hydropower Engineering* 11: 15-18.
- [17] Yu, L., Xia, Z., Du, X. (2004): Connotation of minimum ecological runoff and its calculation method. – *Journal of Hohai University (Natural Sciences)* 32: 18-22.
- [18] Zhang, M., Jia, X., Wei, H. (2005): Ecological and environmental water demand in river channels of the first stage water diversion areas from the south to north via the western course. – *Resources Science* 4: 180-184.
- [19] Zhang, L., Li, Liang, L. (2008): Progress on the research of theory and calculation method of ecological water requirement. – *Transactions of the Chinese Society of Agricultural Engineering* 7: 307-312.
- [20] Zhang, Q., Cui, Y., Chen, Y. (2010): Evaluation of ecological instream flow of the Pearl River basin, south China. – *Ecology and Environmental Sciences* 19: 1828-1837.
- [21] Zhen, Z., Zhang, Z., Huang, Q., Qiu, L., Li, Q., Wei, M. (2010): Improvement and application on ecological water requirement Tennant Method. – *Journal of Sichuan University (Engineering Science Edition)* 42: 34-39.

DAMAGE ASSESSMENT OF NATURAL DISASTERS BASED ON CLOUD MODEL

LIU, Y.P.¹ – GAO, Y.Q.^{1*} – CHEN, H.Y.^{1,2} – LAI, L.J.¹

¹*College of Water Conservancy and Hydropower Engineering, Hohai University
1 Xikang Road, Nanjing 210098, P. R. China*

²*Nanjing Water Planning and Designing Institute Corp. Ltd
136 Honghuacun Road, Nanjing 210022, P. R. China*

**Corresponding author*

e-mail: yqgao@hhu.edu.cn; phone: +86-139-5188-9955

(Received 11th Jan 2019; accepted 8th Mar 2019)

Abstract. Natural disasters occur frequently in China and cause inordinate social and economic losses every year. Great attention has been paid to assessing the impact disasters has brought in order to take appropriate prevention as well as follow-up steps. The existing assessment indexes are not comprehensive and systematic enough to evaluate the disasters' social, economic and environmental impact. Besides, the assessment method and standard are not objective. A more comprehensive natural disaster evaluation index system is proposed and the weight determination and severity rating methods based on cloud model is presented in this paper to provide a reference to appropriately select the assessment method for different kinds of disasters. The index system and severity rating method are applied to 6 typical rainstorms and flood events. Five indicators on social and economic aspects are implemented to demonstrate the adaptability of the proposed method. The results of analysis and evaluation show that the weight set based on cloud model can gather all information from experts objectively, and the assessment method can achieve a reasonable standard of disaster grades reasonably and determine the grade level objectively.

Keywords: *evaluation of natural disaster situation, evaluation index system, weight determination method, disaster identification degree, rainstorm flooding*

Introduction

Natural disasters have an adverse impact on personal safety, agriculture, industry, society, economic and ecological environment. For example, in China, 190 million natural disaster victims were recorded in 2016, 1706 dead or missing, 9.1 million people needed emergency resettlement, 521,000 houses collapsed, 3.34 million houses were damaged, the affected area of crops reached 26220.7 thousand hectares, and the proportion of crop failure or death was 2902.2 thousand hectares. Direct economic losses amounted to 503.29 billion yuan (Liu et al., 2017). In recent years, vulnerability of China's natural environment has been increasing, ecological and environmental issues have become prominent, and natural disasters have been frequent and high-intensity. With the continuous growth of urbanization level and the development of social productive forces, population density continues to rise, economic aggregates and density increase rapidly, inter-regional economic linkages and cooperation increase, disaster prevention and rescue measures continue to improve, and economic losses and society caused by disasters The impact is constantly increasing. The characteristics of disaster losses are also changing: the number of deaths due to disasters has dropped, the number of people affected has risen, and direct and indirect economic losses have risen sharply. According to statistics, the average annual disaster loss in China since the

1990s is 40% higher than in the 1980s (Tang and Yu, 2016). In order to objectively and comprehensively reflect the damage severity and loss characteristics of natural disasters, and provide the basis for defensive measures optimization and disaster mitigation strategies, it is of absolute necessity to conduct disaster evaluation study.

At present, there have been numerous studies on disaster damage assessment such as floods, typhoons, storm surges and geological disasters. For example, Yang et al. (2010) selected indicators such as the number of death, the number of people affected, the number of collapsed houses, the area affected by crops, and the direct economic loss. The entropy method was used to calculate the weight, and the flood damage in 22 regions of China was evaluated in 1999. Gong et al. (2015) took 25 factors in disaster factors, disaster-bearing bodies and disaster prevention and mitigation capabilities with the number of deaths, the number of collapsed houses, the area affected by crops, the direct economic loss and the disaster index to conduct correlation analysis and studied the index selection of typhoon disaster damage assessment. Yin et al. (2012) established an index system from the aspects of casualties, fisheries and agriculture, and direct economic losses of living facilities, and applied the analytic hierarchy process and entropy method to determine the weights and assess the economic losses of 7 storm surge disasters in Guangdong Province. Cheng et al. (2011) selected the average earthquake intensity, the number of deaths missing, the death and disappearance rate of 10,000 people, the number of collapsed houses, the rate of collapsed houses, the risk of geological disasters, and the resettlement rate of 10,000 people to conduct county-wise grade evaluation of disasters in the earthquake-stricken areas; Shi et al. (2017) constructed the economic loss indicators and risk indicators for disaster relief based on the affected area of the disaster, the area planted with crops, the total production value and the frequency of disaster relief by the county of Xinjiang Statistics from 1984 to 2014, to assess the hail disaster in Xinjiang. In addition, the Ministry of Water Resources approved the Flood Disaster Assessment Standard (Standard) in 2012, mainly selecting the number of deaths, the number of people affected, the area affected by crops, the number of collapsed houses, the direct economic loss, and the economic loss of water conservancy facilities as a direct economic loss. Such indicators are employed to the assessment of the number of events and regional annual floods.

There are some shortcomings in the above research. The indicators selected for the disaster damage assessment are not comprehensive enough: only the agricultural impact is considered, the influence of industry and the tertiary industry is neglected; the socio-economic impact is considered, and the natural environmental impact is not considered; The indicators are scattered, without a comprehensive and systematic evaluation index system; At present, China's official disaster information reporting indicators also need to be fully expanded. On the other hand, the evaluation methods used mainly include fuzzy comprehensive evaluation method, entropy weight method, gray clustering method, gray correlation degree method, and matter element analysis method. However, weighting and rating criteria of most methods are often determined by experience and subjective. Although the entropy weight method can determine the objective weight, it depends on a large number of representative data information, and the effect is poor when the data representation is not strong. Secondly, the general method determines the case level by comparing the case evaluation value with the level threshold value, and the difference of the disastrous situation in different cases within the same disaster level is difficult to accurately express. Yu and Shen (1997) studied the ranking method of

different cases in the same level based on the grey clustering disaster classification model, but it is not intuitive enough..

The purpose of this paper is mainly as follows: it summarizes a comprehensive set of disaster damage assessment index system that considers the impact of various aspects, provides reference for the selection of indicators for damage assessment of different disasters, and reports indicators and contents for disaster information. The cloud model-based evaluation method is applied to the weight determination and model construction of the disaster damage assessment, thereby objectively transforming the expert weight evaluation information into quantitative data, and based on the basis of the level evaluation criteria and the intuitive and effective determination of the level.

Disaster damage assessment index system

The disaster damage assessment is to carry out hierarchical and comprehensive management according to the losses and impacts caused by various aspects. Based on the existing research, a systematic and comprehensive disaster damage assessment index system is constructed from the aspects of disaster attribute, social impact, economic impact and natural environment impact (*Table 1*).

Table1. Index system of disaster damages assessment

Target layer	Benchmark layer	Indicator layer	Key indicators
Assessment index system of natural disaster loss	Disaster properties	Time	Disaster duration Emergency resettlement time Disaster area repair time
		Space	Disaster coverage
	Social impact	Population	Death toll Missing Number of people affected Number of people to be resettled The age structure of the affected population The unemployment rate of the affected population The damage rate of the affected population
		Building facilities	Collapsed housing Damage housing Lifeline project Infrastructure
		Agricultural losses	Area affected Disaster area Failures area Agricultural production output
		Industrial and third industrial losses	Accumulated stagnation time Due to disaster number Due to disastrous bankruptcy
	Economic influence	Direct loss and its relative GDP ratio	
		Indirect loss and its relative GDP ratio	
	Natural environment influence	Rescue and reconstruction	Disaster relief put into disaster area restoration and reconstruction
		All kinds of resources loss or pollution Topographic geological landform influence or repair input Ecosystem influence or repair input	

Disaster attribute is a description of the scope, duration, emergency rescue and resettlement of disaster impacts. The societal impact mainly includes the damage to human health and life caused by disasters, the destruction of houses, lifeline projects and public infrastructure, and the direct and indirect effects of industrial activities such as agriculture, industry and service industries. Economic impacts are divided into direct losses, indirect losses, and emergency rescue and reconstruction efforts. The direct loss mainly refers to the direct loss or repair cost measured by the available monetary currency caused by the disaster. The indirect loss is mainly caused by the direct loss and destruction, which will not support and circulate the future sustainable development of the disaster area and the surrounding areas. The losses caused by emergency rescue and reconstruction in the disaster area refer to the investment in the rescue and resettlement of the affected people during the disaster, as well as the various inputs of the disaster-stricken areas to restore normal social order and restore production to the pre-disaster level. Ecological environmental impacts are mainly loss or pollution of water and soil resources, mineral resources, forest vegetation resources, landscape resources, biological resources, etc., changes in topographic geological features, and balanced destruction of local ecosystems. The natural ecological impact of a disaster can be understood as a loss of natural resources and a higher investment in environmental protection and ecological reconstruction.

Cloud model based disaster rating evaluation model

The weight determination method of expert evaluation information based on cloud model is proposed, and the cloud model correlation method is applicable to evaluation model construction and case level determination. This method can objectively synthesize the weight information given by all experts based on experience and reflect the fuzziness and randomness contained in subjective information.

Cloud model theory

The cloud model is an uncertainty transformation model between qualitative concept expressed by linguistic value and its quantitative numerical representation, which constitutes the uncertainty mapping between qualitative and quantitative, which is convenient for portraying the randomness and fuzziness in natural language description (Li et al., 2004; Gao et al., 2017; Li et al., 2010). Using the numerical characteristics of the cloud to reflect the overall characteristics of the concept plays an extremely important role in understanding the connotation and extension of the qualitative concept (Li et al., 2014). The cloud requires a three-dimensional feature of expected, entropy and super entropy to represent a concept in its entirety. The cloud model is the specific implementation of the cloud.

(1) According to the qualitative concept and the quantitative transformation direction, it is divided into a forward cloud model and a reverse cloud model.

(2) According to the symmetry, it is divided into a symmetric cloud model, a semi-cloud model, and a combined cloud model.

(3) Dimensions can be extended from one-dimensional cloud models to two-dimensional or even arbitrary dimensional cloud models.

The universal distribution of normal distribution and normal membership functions lays the theoretical foundation for the universality of the normal cloud model (Li and Liu, 2004). The normal cloud model is widely used in research.

Cloud model accuracy test and parameter correction

According to the reverse cloud model, it is possible that the cloud droplet dispersion is large, so it is necessary to make an accurate check and parameter correction.

The cloud drip that describe the qualitative concept are from the normal distribution $N(E_x, E_n^2 + H_e^2)$. It is well known from the central limit theorem that when any cloud drop $x \in [E_x - Z_{\alpha/2}\sqrt{E_n^2 + H_e^2}, E_x + Z_{\alpha/2}\sqrt{E_n^2 + H_e^2}]$ is used. The degree of certainty of the qualitative concept can be expressed by the confidence degree $1-\alpha$, where $Z_{\alpha/2}$ is the two-sided percentile of the standard normal distribution.

The accuracy test steps are as follows: (1) Use the forward cloud model to generate several cloud drops, such as the number of clouds with $n_1 = 1000$. (2) Select the qualitative concept to determine the degree and find the value $Z_{\alpha/2}$, if the degree of determination is 95%, $Z_{\alpha/2} = 1.96$. (3) Calculate $(x < E_x - Z_{\alpha/2}\sqrt{E_n^2 + H_e^2})$ is the mean of the cloud drop points X_L and $(x > E_x + Z_{\alpha/2}\sqrt{E_n^2 + H_e^2})$ the mean value of the cloud drop points X_H . When Equation 1 is met, the cloud model has higher precision, otherwise the cloud parameters need to be corrected (Xu et al., 2013; Ma et al., 2010).

$$\begin{aligned} |(d - d_0)/d| \times 100\% &\leq 20\% \\ d &= X_H - X_L, \quad d_0 = 2Z_{\alpha/2}\sqrt{E_n^2 + H_e^2} \end{aligned} \tag{Eq.1}$$

The cloud parameter correction steps are as follows: (1) Generates n_1 cloud droplet that belongs to the confidence interval $[E_x - Z_{\alpha/2}\sqrt{E_n^2 + H_e^2}, E_x + Z_{\alpha/2}\sqrt{E_n^2 + H_e^2}]$. (2) Calculates the sample mean \bar{X} and the variance of cloud droplets S^2 . (3) According to the Bayesian theory-based correction method to calculate (Liu et al., 2008):

$$\begin{cases} E_x^{(1)} = \left[\frac{\bar{X}}{(E_n^2 + H_e^2)/n_1} + \frac{E_x}{E_n^2} \right] / \left[\frac{1}{(E_n^2 + H_e^2)/n_1} + \frac{1}{E_n^2} \right] \\ E_n^{(1)} = \sqrt{\frac{\pi}{2}} \times \frac{\sum_{i=1}^{n_1} |x_i - E_x^{(1)}|}{n_1} \\ H_e^{(1)} = \sqrt{S^2 - (E_n^{(1)})^2} \end{cases} \tag{Eq.2}$$

In Equation 2: $E_x^{(1)}$, $E_n^{(1)}$ and $H_e^{(1)}$ are the revised expectation, entropy and hyper-entropy, respectively, x_i for the i cloud drops. After the correction, the new cloud model parameters are tested and modified to meet the accuracy requirement.

Cloud model based weight determination method

The weight determination steps of the expert evaluation information based on the cloud model are as follows:

(1) Invite n experts (to ensure the weight calculation results are convincing, need to invite more than 10 experts to evaluate) give the weight distribution results of m indicators, constitute the evaluation matrix $V = (V_{ij})(i = 1, 2, \dots, m; j = 1, 2, \dots, n)$.

(2) Using the inverse cloud algorithm without certainty, calculate the n weight evaluation values of the index i to obtain the weight cloud model parameters (E_x^i, E_n^i, H_e^i) .

(3) Perform accurate test and parameter correction on the weight cloud model of indicator.

(4) For the weighted cloud model of the modified indicator i , a forward cloud algorithm is used to randomly generate t (such as $t = 1000$) cloud drops, and the weights calculated x_i as the index i corresponding to the maximum degree of cloud drop point determination $\mu_i(x_i)$.

(5) Normalize the weight calculation values of the m indicators to obtain the weight vector $\Omega = (\omega_1, \omega_2, \dots, \omega_m)^T$.

Based on the weight calculation method of the cloud model, based on the existing expert evaluation values, the expert evaluation expectation (E_x) and the uncertainty eigenvalues (E_n and H_e) can be extracted to generate any number of evaluation values that meet the characteristics of the expert evaluation (Cloud drop). Finally calculate the weight vector, increase in the number of samples calculated by weight, and improve the credibility. As t increases, the weight calculated on the basis of the cloud model will tend to the expected value of the weight cloud model, which tends to the arithmetic mean of the expert weighting of the indicator. The weight vector calculated based on the cloud model considers the randomness and ambiguity of expert evaluation, and is of great importance for the study of the uncertainty method of qualitative evaluation weight calculation.

Cloud-based disaster damage assessment process

Different from the previous research, the disaster damage assessment level is directly determined in accordance with the expert experience. This model mainly determines the disaster level scale cloud with randomness and ambiguity based on the overall situation of the case evaluation, and determines the disaster level of each case. Proceed as follows:

(1) Indicator data are normalized. In order to measure the degree of disaster loss for a single indicator, the reference ceiling for each indicator has to be selected. The historical maximum value of each indicator in the existing historical data of the evaluation object can be invoked as the index reference for the upper limit. The ratio of the raw data to the reference upper limit of the corresponding indicator is the indicator value. Set the indicator data matrix $Y = Y_{ik}$ of p cases ($i = 1, 2, \dots, m; k = 1, 2, \dots, p$).

(2) Evaluation vector calculation. Calculate the disaster damage assessment value of each case to form a disaster damage assessment vector $Z = (z_1, z_2, \dots, z_p)^T$, where the element z_k of the vector can be expressed as Equation 3.

$$z_k = \sum_{i=1}^m (Y_{ik} \omega_i) \quad (\text{Eq.3})$$

(3) Cloud model generation. The overall disaster cloud model for Z using inverse cloud algorithm without a degree of certainty, and the accuracy test and correction are performed.

(4) High-level disaster clouds and low-level disaster cloud computing. Taking the E_x value of the overall disaster cloud as the dividing line, the case is split into high-level and low-level cases: the case where the disaster evaluation value is greater than E_x is a high-level case, and vice versa is a low-level case. Repeat step 3 for the disaster damage assessment values of all high-level cases to obtain a high-level disaster cloud model, and a low-level disaster cloud model.

(5) Disaster level scale clouds construction. First, based on the overall disaster situation cloud, high-level disaster situation cloud and low-level disaster situation cloud, combined with the case disaster situation, etc., the evaluation value interval of the evaluation level is established. Let the evaluation value interval of the s grade be $[a_s, b_s]$ ($s=1, 2, L, S'$), and the cloud parameter (E_{xs}, E_{ns}) is calculated according to the Equation 4 (Xu et al., 2011), H_{es} is specified according to the uncertainty of the evaluation language, and is generally regarded as 0.005.

$$\begin{cases} E_{xs} = (a_s + b_s) / 2 \\ E_{ns} = (b_s - a_s) / 6 \end{cases} \quad (\text{Eq.4})$$

Secondly, the accuracy test is made on each level of the cloud. Each level of cloud constitutes a disaster level scale and generates a scale cloud map.

(6) Each case level is determined. Calculate the case disaster evaluation value and the degree of the determination of the cloud, the k case Disaster damage assessment value and the second grade cloud model of the determination of $\eta_{k,s} = \exp\left(-\left(x_k - E_{xs}\right)^2 / 2E_{ns}'^2\right)$, where E_{ns}' is expected E_{ns} , H_{es} is the variance of the normal random number. The level of the most certain degree is the case level, and the second-largest level is the level deviation of the case, reflecting the difference in the disastrous situation of different cases in the same level. For example, the case of “middle disasters and partial disasters” is more serious than the case of “middle disasters and partial disasters”.

Example application

The cloud model-based disaster rating assessment model was applied to six typical storms and flood disaster damage assessments. Cases 1-3 are examples of three storms and floods that occurred in 2015 (China Meteorological Disaster Yearbook, 2016), and cases 4-6 were examples of evaluations in the standards.

According to the type of disaster and the actual situation of disaster loss, the indicators of population, building facilities, agricultural losses in social impact, and direct economic loss indicators in economic impact are selected for analysis. Due to

the lack of comprehensive statistical data, the disaster attribute and natural environmental impact indicators have not been selected yet. Based on available disaster loss data statistics, the population indicators have the number of people affected and the number of death, which are recorded as u_1 and u_2 respectively; the building facilities index selects the number of collapsed houses, which is recorded as u_3 ; the agricultural loss index selects the area affected by crops, recorded at u_4 ; and the direct economic loss is recorded as u_5 . Statistics of 6 typical storm flood disaster losses are shown in *Table 2*.

Weight determination

Ten experts were invited to evaluate the index weight, and the weights were calculated by the weighting method of the expert evaluation information based on the cloud model. The weight of the experts and the weight calculated based on the cloud model is shown in *Table 3*.

Table 2. *Statistic data of 6 rainstorm and flood disaster loss*

Case	Disaster details	Number of people affected (million)	Death toll (person)	House collapse (million rooms)	Area affected by crops (thousand hectares)	Direct economic losses (billion yuan)
1	May 18, 2015-22nd Fujian Rainstorm	29.9	11	0.28	34	30.6
2	July 20, 2015-25th Fujian Rainstorm	41.8	16	0.27	21	40
3	August 16, 2015-19th Sichuan rainstorm	148.1	30	0.36	91	8.8
4	2008.06 Zhujiang River basin flood	1842.96	50	5.24	957.85	131.07
5	2008.06 Zhujiang River basin flood	1106.3	36	1.60	368.9	84.6
6	2007 Henan Shaanxi Shanxi mountain torrent disaster	195.15	179	2.34	146.2	38.48

Table 3. *Index weight expert evaluation value and cloud model calculation value Indicator weight normalized weight*

Index	Weight										Normalized weights
	Prof.1	Prof.2	Prof.3	Prof.4	Prof.5	Prof.6	Prof.7	Prof.8	Prof.9	Prof.10	
u_1	0.12	0.11	0.13	0.09	0.11	0.1	0.15	0.1	0.11	0.1	0.1125
u_2	0.35	0.32	0.34	0.34	0.35	0.3	0.35	0.37	0.33	0.35	0.3394
u_3	0.08	0.1	0.09	0.12	0.09	0.12	0.08	0.08	0.1	0.1	0.0959
u_4	0.1	0.13	0.11	0.1	0.11	0.12	0.09	0.12	0.12	0.1	0.1100
u_5	0.35	0.34	0.33	0.35	0.34	0.36	0.33	0.33	0.34	0.35	0.3422

Case evaluation value and disaster situation cloud model calculation

The disaster damage assessment values of the six cases calculated in accordance with *Equation 3* were 0.1006, 0.1335, 0.1064, 0.6365, 0.3879, and 0.5304, respectively. For disaster damage assessment values of the six cases, inverse cloud algorithm (Ep.1~2) was used. After the accuracy test and parameter correction, the parameters of the overall disaster cloud model (E_x , E_n , H_e) were (0.3092, 0.2228, 0.0122). With the overall

disaster cloud $E_x=0.3092$ as the demarcation point, six cases were divided into low-level cases (Cases 1-3) and high-level cases (Cases 4-6). In the same way, the high-level disaster cloud parameters and the low-level disaster cloud parameters after the accuracy test and parameter correction are: (0.5236, 0.0899, 0.0258), (0.1135, 0.0167, 0.0054). Generate 1000 cloud drops for each of the three disaster clouds, and generate a cloud map in the [0,1] interval as showed in *Figure 1*.

Disaster level scale cloud computing

It can be seen from *Figure 1* that the disaster damage assessment values of the low-level cases are concentrated in [0.06, 0.16], and the closer the evaluation value is to the “low-level case disaster cloud” corresponding to 0.1135, the closer the determination is to 1. At the same time, the analysis of the disastrous situation in 1-3 cases found that the impact of the disaster situation was small, so the initial definition of the low-level case as a whole was a general disaster. The disaster damage assessment of high-level cases is concentrated in [0.25, 0.80], and the closer the evaluation value is to the “high-level case disaster cloud” corresponding to 0.5236, the closer the determination is to 1. The analysis of the disastrous situation in the 4-6 case found that the disaster situation had a great impact. The preliminary definition of the high-level case was a major disaster. The disaster damage assessment value of the overall disaster cloud is mainly concentrated in [0, 0.8], and the closer the evaluation value is to 0.3092, the closer determination of the “total disaster cloud” is to 1. The overall disaster situation cloud integrates the general disaster situation and major disaster situation, reflecting the average level of disaster losses. It is initially considered that the case where the evaluation value is around 0.3092 is a major disaster.

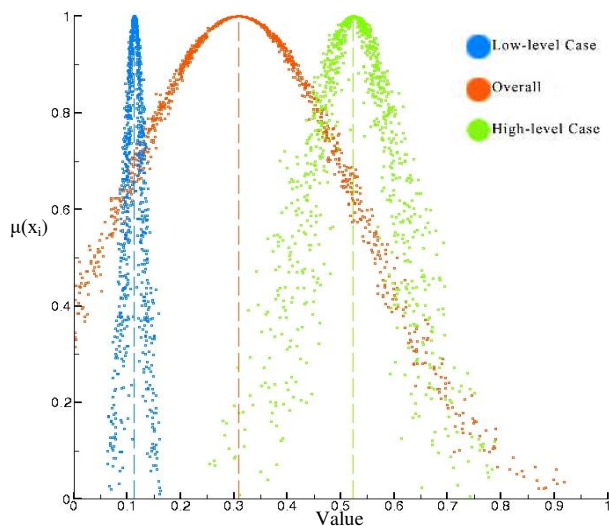


Figure 1. Each disaster cloud

According to the above analysis, considering the possibility of occurrence of disasters that are more serious than major disasters (i.e., “special major disasters”), and the construction of equidistant disaster scales, the assessment intervals for the classification of disasters are shown in *Table 4*. Among them, the straight line intervals [0, 0.115] and [0.805, 1] respectively indicate that the degree of certainty for “general

disaster” and “special major disaster” is 1 when the evaluation value belongs to the interval.

Table 4. Disaster damage assessment level

Interval type	Interval type	Evaluation interval
General disasters	Linear interval	[0, 0.115]
	Semi-descending cloud	[0.115, 0.345]
Large disasters	Symmetric cloud	[0.115, 0.575]
Major disasters	Symmetric cloud	[0.345, 0.805]
Special major disasters	Half-liter cloud	[0.575, 0.805]
	Straight zone	[0.805, 1]

According to the *Equation 4* cloud parameters are calculated for each cloud model interval, and the Cloud model parameters (E_x, E_n, H_e) of different disaster classes are obtained as follows: General disasters (0.115,0.077,0.005); Large disasters (0.345,0.077,0.005), Major Disasters (0.575,0.077,0.005), particularly major Disasters (0.805,0.077,0.005). Ching model accuracy test is in line with the requirements. Generate the ruler clouds as showed in *Figure 2*.

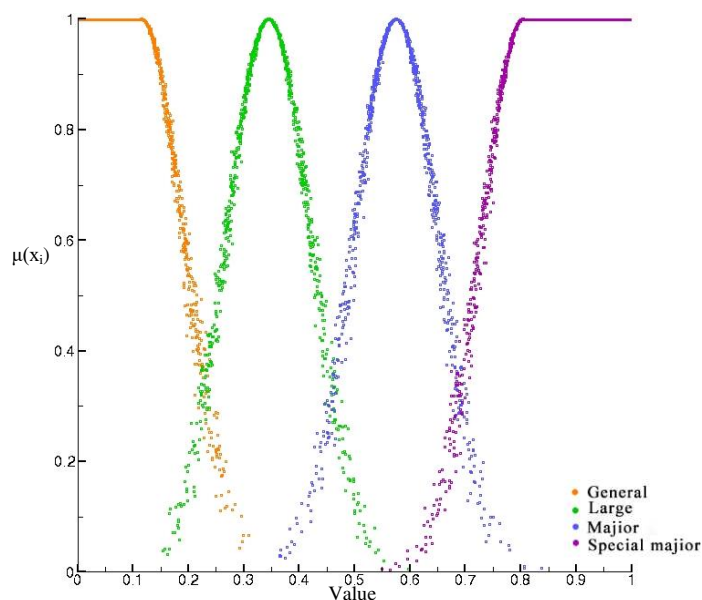


Figure 2. Disaster rating assessment ruler cloud

Case rating

Calculate the disaster damage assessment value of each case and the certain degree of cloud of each level in the scale cloud, and determine the case level according to the principle of maximum certainty. The results are presented in *Table 5* and *Figure 3*.

It can be seen from *Table 5* and *Figure 3* that the most certain grades in Case 4 and Case 6 are “major disasters”, and the second most important grades are “Special Major Disasters” and “Greater Disasters”. In addition to simply recognizing that both are

“significant disasters”, it can be said that the disaster level of Case 4 is “significant disasters and biased towards special major disasters”, and the disaster level of Case 6 is “significant disasters and biased towards larger disasters”. This is in line with the actual situation: in the Case 4 indicator data, except for the “number of death” is smaller than Case 6. The other indicators are 2.2-9.4 times of Case 6. Therefore, on the whole, the disastrous situation of Case 4 is more influential than Case 6. This shows that the cloud model method can express the disaster level deviation of different cases in the same level, and intuitively reflect the difference of the disastrous situation of the same level of disaster.

Table 5. The determination of each case level and grade evaluation results

Case	Determination				Cloud model evaluation results	Cloud model evaluation results
	General disasters	General disasters	Major disasters	Special major disaster		
1	1	0.0055	0	0	General disasters	General disasters
2	0.9743	0.0202	0	0	General disasters	General disasters
3	1	0.0173	0	0	General disasters	General disasters
4	0	0.0009	0.7173	0.1706	Major disasters	Major disasters
5	0.0005	0.8585	0.0553	0.0000	General disasters	General disasters
6	0	0.0906	0.8202	0.0019	Major disasters	Special major disaster

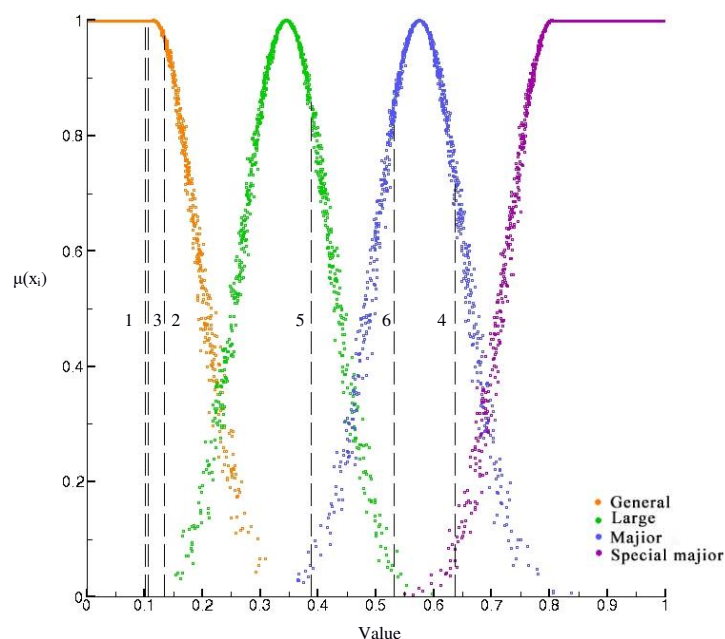


Figure 3. Case level determination chart. (The number in the figure indicates the case number, and the intersection of the dashed line with each level cloud model determines the degree of the value of the case evaluation for each level cloud)

It can be seen from *Table 5* that the evaluation results of the application cloud model method are compared with the results confirmed according to the “standard”: the results of Case 1-5 are the same, and the results of Case 6 are different. The consistency of the

results of Cases 1-5 indicates that the model is applied to the applicability and rationality of storm flood and flood disaster damage assessment. Case 6 is applicable to both the identification method of the indicator system and the direct identification method (“when the death population reaches 100 people or the direct economic loss reaches 20 billion yuan, it is recognized as a special major disaster; the death population reaches 50”. When there are less than 100 people or the direct economic loss reaches 10 billion yuan and less than 20 billion yuan, it is considered a “major disaster”. The former conclusion is the same as the result of this paper, which is “major disaster”; the latter conclusion is different from the result of this paper, and it is “special major disaster”. According to the principle of high, the conclusion that the evaluation of the Standard is adopted is “special major disaster”. The model of this paper is the same as the results obtained by the identification system of the Standards, which verifies the rationality and applicability of the model. When using the direct identification method to evaluate the disaster situation, the model may not be consistent with its evaluation results (for example, Case 6 in the example in this paper), and this situation will be further analyzed in subsequent studies.

Conclusion

This paper summarizes the disaster damage assessment index system of the aspects of disaster attribute, social impact, economic impact and natural environmental influence to form a comprehensive disaster damage assessment index system that considers the impact of various aspects. It can provide reference for the selection of disaster damage assessment indicators for different disasters. The shortcoming is that the topographic geological and geomorphological impacts and ecological environmental impacts in the natural environmental impact need to be further refined according to the characteristics of disaster losses, and more specific evaluation indicators are proposed.

Based on the weight determination method of cloud model, the correlation between randomness and fuzziness was revealed, and the expert evaluation was conducted with quantification, realizes the evaluation weight of multiple experts to the uncertainty conversion of comprehensive weight data, and can fully and comprehensively consider expert opinions and common weight determination methods. More objective than comparison.

A cloud model-based disaster rating model is proposed. The model evaluation results are basically consistent with the “standard” evaluation results, which verify the rationality and applicability of the model. The model can fully consider the overall situation of the disasters studied, and reduce the subjective dependence on expert experience. The case degree is determined by the principle of maximum certainty, and the degree of disaster level of different cases of the same level is reflected by the second largest degree of certainty level. Disaster identification degree of different cases of the same level is improved based on the effective classification of the disaster level, and the general evaluation method more objective and scientific. The case level determination process reflects the ambiguity and randomness of the cloud model when the quantitative evaluation data are converted into a graded comment. However, it is found that there may be a different evaluation result between the result obtained by the direct identification method and the cloud model is used for disaster assessment in the case study, and the specific reason for the difference is still unclear, which needs further analysis and discussion in the following research.

Acknowledgements. The study was supported by the National Natural Science Foundation of China Youth Science Foundation Project (No. 51309076), the Jiangsu General Fund(No. BK20181310), the Fundamental Research Funds for the Central Universities (No. 2014B05814), the Fundamental Research Funds for the Natural Science Foundation of Jiangsu Province(No. BK20130849). The project was also funded by the Priority Academic Program Development of Jiangsu Higher Education Institutions (No. 3014-SYS1401).

REFERENCES

- [1] Cheng, L.H., Tang, H., Zhou, T.G., Zhang, L., Zhang, M. (2011): Evaluation method of natural disaster intensity and its application: a research based on comprehensive disaster condition index. – *Journal of Natural Disasters* 2011(1): 46-50.
- [2] China Meteorological Administration Staff (2016): *China Meteorological Disaster Yearbook (2016)*. – Meteorological Press, Beijing.
- [3] Gao, Y.Q., Chen, H.Y., Xiao, X., Xu, J. (2017): Evaluation of management modernization of large and medium-sized sluices based on cloud theory. – *Journal of Economics of Water Resources* 35(2): 63-68.
- [4] Gong, Z.W., Hu, L. (2015): Influence factor analysis of typhoon disaster assessment. – *Journal of Natural Disasters* 2015(1): 203-213.
- [5] Li, D.Y., Liu, C.Y. (2004): Study on the Universality of the Normal Cloud Model. – *Engineering Science* 6(8): 28-34.
- [6] Li, D.Y., Liu, C.Y., Du, Y., Han, X. (2004): Artificial Intelligence with Uncertainty. – *Journal of Software* 15(11): 001583-1594.
- [7] Li, D.Y., Liu, C.Y., Gan, W. (2010): A new cognitive model: Cloud model. – *International Journal of Intelligent Systems* 24(3): 357-375.
- [8] Li, D.Y., Liu, C.W., Du, Y., Xu, J. (2014): *Uncertain Artificial Intelligence*. – National Defence Industry Press, Beijing.
- [9] Liu, J., Deng, G.S., Na, R.S. (2008): Analysis and design of Bayesian feedback cloud model. – *Systems Engineering - Theory & Practice* 28(7): 138-143.
- [10] Liu, N.J., Li, Q., Sun, Z. (2017): Analysis of natural disasters in China in 2016. – *Disaster Reduction in China* 2017(2): 50-53.
- [11] Ma, S.D., Han, L., Gong, G.H., Song, X. (2010): Target threat assessment technology based on cloud model. – *Journal of Beijing University of Aeronautics and Astronautics* 36(2): 150-153.
- [12] Ministry of Water Resources of the People's Republic of China Staff, 2012. *Flood Disaster Assessment (SL 579-2012)*. – China Water & Power Press, The Beijing.
- [13] Shi, L.M., Li, B., Li, Y.Y., Kong, L.W., Liu, W.P. (2017): Study on economic loss assessment and risk division of hail disaster in Xinjiang. – *Journal of Glaciology and Geocryology* 39(2): 299-307.
- [14] Tang, Y.D., Yu, W. (2016): *Disaster Economics 2*. – Tsinghua University Press, Beijing.
- [15] Xu, H.J., Wang, Z.Y., Su, H.Y. (2013): Dissolved gas analysis based feedback cloud entropy model for power transformer fault diagnosis. – *Power System Protection and Control* 2013(23): 115-119.
- [16] Xu, K.H., Meng, Q., Li, K. (2011). The comprehensive evaluation of attack formations of tank element base on cloud theory. – *Fire Control & Command Control* 36(10): 37-40.
- [17] Yang, X.L., Zhou, J.Z., Ding, J.H., Zhang, Y.Z. (2010): Attribute recognition model for comprehensive evaluation of flood grades based on entropy method. – *Yangtze River* 41(12): 16-19.
- [18] Yin, K.D., Wei, Q., Li, X.D. (2012). The evaluation techniques of the socio-economic loss caused by storm surge disaster. – *Marine Environmental Science* 31(6): 835-837.
- [19] Yu, Q.D., Shen, R.F. (1997). A grading model and its application of the comprehensive situation of natural disaster. – *Journal of Catastrophology* 1997(3): 12-17.

EFFECT OF PH AND SRT ON DENITRIFYING PHOSPHORUS REMOVAL IN A2N SEQUENCING BATCH REACTOR PROCESS

LI, W.^{1*} – GAO, M.¹ – ZENG, F.¹ – LIU, N.¹ – ZHU, X.¹ – ZHANG, C.^{2*}

¹*School of Municipal and Environmental Engineering, Shenyang Jianzhu University
No.9, Hunnan East Road, Hunnan New District, Shenyang, China*

²*School of Pharmaceutical Engineering, Shenyang Pharmaceutical University
Shenyang, China*

**Corresponding authors*

e-mail: liweilengjinyue@163.com (Wei Li), twyla666@sina.com (Conglu Zhang)

(Received 11th Jan 2019; accepted 8th Mar 2019)

Abstract. This research investigates the effect of pH and sludge retention time (SRT) on denitrifying phosphorus removal. A series of experiments were conducted using two 20L sequencing batch units with the following configuration: anaerobic/anoxic and aerobic sequencing batch reactors (SBRs). It was found that variation in pH from 6.5 to 8 resulted in obvious increase in phosphorus release and uptake, organic matter degradation [measured by the chemical oxygen demand (COD) and the percentage volatile suspended solid (VSS)] and polyhydroxybutyrate (PHB) accumulation also showed a rising trend in the anaerobic period, but sludge acclimatized under pH 8.5 condition exhibited a slightly lower denitrifying phosphorus removal capability. In addition, the rates of phosphorus release and uptake were 20.95 and 23.29 mg/g VSS / h in condition of pH 8 value. Activated sludge with the SRT of 16 days possessed better nitrite nitrogen utilization, organic matter degradation and phosphorus removal than sludge with the SRT of 6, 10 and 22 days, and polyphosphate concentration in anaerobic activated sludge per VSS decreased to 23.1 mg/g VSS, PHB concentration in anoxic activated sludge per VSS reduced to 16.3 mg/g VSS, thus, a dramatic denitrifying dephosphatation has occurred.

Keywords: *phosphorus removal, organic matter degradation, sludge, pH, SRT*

Introduction

In recent years, eutrophication caused by nitrogen and phosphorus pollution has attracted wide and intensive attention. Biological nutrient removal processes have been widely used in many municipal sewage treatment plants for several years (Wong et al., 2015). Conventional nitrogen and phosphorus removal were separately achieved by denitrifying bacteria and polyphosphate accumulating organisms (PAOs). Traditional biological nutrient removal processes have some problems between polyphosphate accumulating organism and denitrifying bacteria, such as external carbon source and sludge age. Kuba et al. (1993) reported that denitrifying polyphosphate accumulating organisms (DNPAOs) could achieve simultaneous nitrogen and phosphorus removal by using nitrate and/or nitrite as an electron donor. Denitrification and dephosphatation occur in sequencing batch reactor (SBR), which is different from continuous-flow-activated sludge system. DNPAOs have the similar metabolic characteristics to PAOs, degrade polyphosphate to orthophosphate and absorb organic compounds, are stored as polyhydroxyalkanoates (PHAs) in the cell under anaerobic condition. Under anoxic condition bacteria takes orthophosphate from liquid to synthesis polyphosphate with PHAs as electron donor and nitrate/nitrite as electron acceptor, meanwhile, achieves cell growth and maintenance. Compared with traditional anaerobic/aerobic phosphorus removal,

denitrifying phosphorus removal not only saves 50% organic carbon source and 30% energy consumption but also reduces 50% surplus sludge.

Nitrate as electron acceptor for denitrifying phosphorus removal has been recognized by scholars (Tayà et al., 2013; Wang et al., 2015a,b; Basset et al., 2016). However, in the early studies of biological nutrient removal processes, it was supposed that nitrite has been recognized as one of inhibitors in microbial metabolism (Zhou et al., 2011; Ge et al., 2016; Jabari et al., 2016). The nitrification reaction bath effluent may be not suitable for denitrifying phosphorus removal, it did not specially inoculate microorganisms with nitrite as electron acceptor under anoxic condition. Once up a time some people already realized that nitrite could also become electron acceptor of DNPAOs. Meinhold et al. (1999) showed that nitrite at low concentration levels (4-5 mg-NO₂⁻-N) was not detrimental to anoxic phosphorus uptake and could serve as electron acceptor for anoxic phosphorus uptake. Introduce an phosphorus uptake ability of denitrifying polyphosphate accumulating bacteria, phosphorus uptake amount was over 30 mg/L by dosing 20 mg/L NO₂⁻-N in the SBR (Liu et al., 2014). According to the above literatures, different scholars gave the controversial conclusions of the nitrite influence on the biological anoxic phosphorus removal. It is necessary to evaluate adequately whether denitrifying phosphorus removal is efficiency and stability with nitrite as electron acceptor.

Although the A²N process has the capacity of denitrifying dephosphatation, they differ in operational mode. The former operates in a single sludge system with nitrifiers and DPB mixed. In the A²N processes, only DPB will be present. In this process, the minimum SRT for nitrifiers no longer dominates the minimum SRT for DPB (Bortone et al., 1994; Kuba et al., 1996a).

Denitrifying phosphorus removal using nitrite as electron acceptor has been considered difficult due to the lack of available control parameters. It is reported that pH and sludge retention time (SRT) are critical factors, which affect the performance of denitrification and dephosphatation of DNPAOs-nitrite.

The pH value of biological nutrient removal systems respond to cell membrane permeability and electric charge of microorganisms. Microbe growth and multiplication are closely related to the pH in the environment. Obviously, the suitable pH is crucial to ensure the dominant position of functional bacteria in the wastewater treatment processes. Many scholars studied the relationship between pH and biological phosphorus removal characteristics, it was found that the efficiency of anoxic phosphate uptake enhanced with the increase of pH for DNPAOs sludge. (Smolders et al., 1994; Sun et al., 2015; Liu et al., 2015). However, there is no publication investigated the mechanism of denitrifying polyphosphate accumulating organisms with nitrite as electron acceptor under different pH values till now.

Phosphorus in wastewater is removed by surplus sludge discharge, the effect of anoxic phosphorus removal could decrease if SRT is too high or too low. SRT not only reflects the growth environment and the generation period of microorganisms, what's more, it also influences the efficiency of nutrient removal, effluent quality and sludge yield in the biological nutrient removal processes. Impact of SRT on the biological phosphorus removal process has always been studying with PAOs in recent years (Ge et al., 2013, 2015). Liu et al. (2008) discovered that the optimal SRT was 15 d for polyphosphate accumulating organism with nitrate as electron acceptor in modified A²N process. In accordance with a review of these literatures, it is found that few investigations have been conducted on the SRT influence on metabolic behavior of DNPAO with respect to anoxic phosphorus uptake using nitrites as electron acceptor.

The purpose of this study is to study the correlation between pH and nutrient removal efficiency, seek a reliable sludge retention time (SRT) for achieving a high-level denitrifying phosphorus removal by using nitrite as electron acceptor, investigate the effect of pH and SRT on metabolic mechanism of DNPAO-nitrite, and also establish the control strategies for denitrifying phosphorus removal processes.

Materials and methods

A²N-SBR system

The tow-sludge A²NSBR process consisted of A²SBR reactor and NSBR reactor which were made from transparent plexiglass, were fed with synthetic wastewater and operated under anaerobic/anoxic/shortcut nitrifying condition separately. Anoxic denitrifying phosphorus uptake occurred in A²SBR reactor by using nitrite as electron acceptor from NSBR reactor effluent. NSBR reactor with a working volume of 3 L, ran with two 4h-cycles per day to realize shortcut nitrification by micro oxygen aeration, each cycle consisted of instantaneous feeding, 180 min aerobic reaction, 45 min settling and 15 min decanting. The sludge retention time (SRT) was 14 days, COD/N and COD/P ratios were 0.2:1 and 23:1.

A²SBR reactor with a working volume of 10 L was inoculated with activated sludge from the secondary sedimentation tank of northern sewage treatment plant (Shenyang, China) and a laboratory-scale anaerobic-anoxic (A/A) reactor in which denitrifying polyphosphate accumulating organisms with nitrite electron acceptor were enriched. The denitrifying phosphorus removal reactor was conducted on 5.5h-cycle per day, operated with instantaneous feeding, 120 min anaerobic reaction, 150 min anoxic reaction, 45 min settling and 15 min drainage. All experiments were completed in the key laboratory of Liaoning university, China.

The operational critical factors of operation system were concluded as follow:

- 1) Effluent time of NSBR was consistent with anoxic phosphorus removal time of A²SBR, NO₂⁻-N provided by shortcut nitrification could be completely utilized by denitrifying phosphorus removal as electron acceptor, realized coupling link of shortcut nitrification reactor and denitrifying phosphorus removal reactor.
- 2) Effluent NO₂⁻-N concentration of NSBR met the need of anoxic phosphorus uptake and no interfering substance in the effluent flow was added to A²SBR.

Batch experiments

Activated sludge taken from the anaerobic-anoxic SBR was subjected to effect of pH on denitrifying dephosphatation, the batch experiments were conducted after the SBR with circulating steadily and good performance. The performance of SBRs operation was that nitrite and nitrate concentration and nitrite accumulation rate in NSBR effluent were 92.6 mg/L, 5 mg/L, and 94%, the denitrifying phosphorus removal rate in A²SBR was 95%. Amount of sewage was taken at the end of anoxic phase, and put in four 1-liter sealed glass bottles separately, domestic sewage was added to the glass as substrate. At different pH (6.5, 7.5, 8 and 8.5), some batch tests were operated to understand the effect of pH on metabolism of denitrifying polyphosphate accumulating organisms very well. The operation mode of batch experiments was agreement with A²SBR. The slurry mixture was stirred by magnetic stirring and mixed liquor suspended solid (MLSS) was 3300 mg/L. In initial anaerobic reaction, nitrogen was injected into

glass bottles to guarantee the anaerobic environment. In the anoxic phase nitrite and nitrate solution was continuously added into glass bottles as electron acceptor, and the concentrations of nitrite and nitrate could refer to A²SBR, which were 21.7 mg/L and 1.4 mg/L.

The pH was controlled by using pH detection probe, acid pump and alkali pump. The other reaction conditions, such as temperature, DO and stirring speed were the same as SBR reactor.

The nutrient removal efficiency was stable, and the average denitrifying dephosphatation was above 90%, effluent TN and P from the process can satisfy the GB effluent standards (P 0.5mg/L and TN 3mg/L), when the A²N-SBR ran to 80th day. A²SBR sludge was designed to study the denitrifying phosphorus removal performance without sludge discharge and effect of SBR (6d, 10d, 16d and 22d) on nutrients removal. Surplus Sludge discharged was 0.5L, 0.5L, 0.5L, and 0.5L, respectively. COD, TP, NO₂⁻-N, NO₃⁻-N, PHB, poly-P, MLSS, MLVSS were detected.

Synthetic wastewater

Synthetic wastewater was used in the experiment, the feed contained sodium acetate as carbon sources, KH₂PO₄ was used as phosphorus source, NH₄Cl was added to provide nitrogen source, additionally, the other components also included MgSO₄·7H₂O, CaCl₂, NaHCO₃, and trace elements. Characteristics of synthetic domestic sewage were NSBR influent: COD_{Cr} 20.2~27.5 mg/L, NH₄⁺-N 92.5~103 mg/L, TN 93~105.1 mg/L, TP 0.8~1.2 mg/L, pH 7~7.5; A²SBR influent: COD_{Cr} 141~158.7 mg/L, NH₄⁺-N 1.0~3.0 mg/L, TN 1.6~4.0 mg/L, TP 7.8~13 mg/L, pH 7.5~8.

Analytical methods

COD, TP, NO₂⁻-N, MLSS and MLVSS were analyzed in accordance with standard methods, and were measured according to the Chinese State Environmental Protection Agency Standard Methods (Chinese SEPA, 2002). The pH value and dissolved oxygen (DO) were measured online using pH and meters (DO530 and PH160, sinomeasure company, China), respectively. Glycogen was calculated according to Zhang et al. (2015). Biomass PHB content was detected by capillary-gas chromatography according to Cavaillé et al. (2013). GC working condition: A gas Perkin-Elmer gas chromatograph, equipped with a DB-5 column (30 m × 0.25 mm × 0.25 μm), and fitted with a flame ionization detector, 1:20 split, high purity nitrogen gas as carrier, 1:20 injection mode, sample volume 3 μl, furnace temperature 100°C. Biomass sample preparation: Added 2 to 3 drops of formaldehyde to sewage samples to inhibit the biochemical reaction, centrifuged and removed the supernatant, then washed with phosphate buffer solution, after centrifugation, the sewage samples were moved into ampere tube and then dried with a freeze dryer and stored in frozen tube seal at 4°C temperature. Esterification: The 50 mg dried sewage was placed in 10 mL glass tube, mixed with equal volumes of 1-propanol / HCl and dichloroethane, added 1mg benzoic acid as internal standard substance. Benzoic acid as internal standard substance was added to mixture, heated in 100°C for 2 hours. After esterification, the samples were left to be cooled at room temperature and distilled water was added to 5 ml, shocked and solution for 10 minutes for effective extraction of potential residual-free organic acid, mixed with Na₂SO₄ to remove water and stored with gas chromatography automatic sampling bottle at 4°C temperature.

Results and discussion

Effect of pH

Effect of pH on phosphorus concentration

pH is an important parameter for denitrifying phosphorus removal process, could affect the enzymes activity of denitrifying polyphosphate accumulating organisms, because it is related to the change of cell membrane charge (Nittami et al., 2011). The competition between glycogen accumulating organism and polyphosphate accumulating organism could lead to a decrease of phosphorus removal rate in inappropriate pH environment.

The effect of various pH values on anaerobic and anoxic transformations of TP concentration and efficiency was investigated (*Figure 1*). The phosphorus specific release rate and uptake rate, expressed as net amount of phosphorus release and uptake per unit amount of VSS per hour in reactor (mg phosphorus/g VSS/ hour). It can be seen from *Figure 1* that the anaerobic phosphate release increased from 27.52 mg/L to 42.69 mg/L when pH increased from 6.5 to 8.

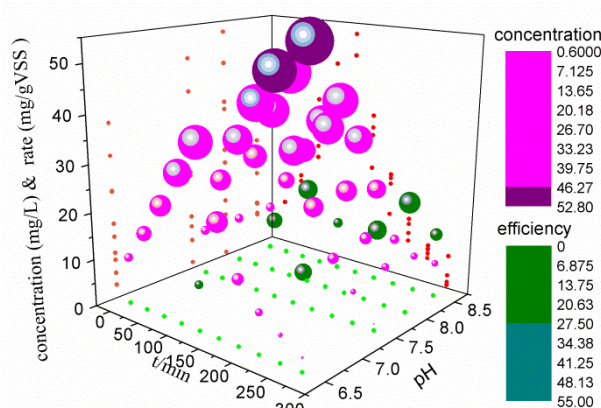


Figure 1. Effect of pH on phosphorus concentration and release and uptake rate

The scatter graph of phosphorus maximum specific anaerobic release rate showed upward trend with pH up to 8, but a plateau appeared to be reached 20.95 mg/g VSS/h at this value. The result was coincided well with previous investigation, in which it was assumed that acetic acid absorption need proton motive force, which need adenosine triphosphate (ATP) formed by polyphosphate degradation. Higher pH value could reduce proton motive force and more phosphate release (Zhao et al., 2016; Reza et al., 2016; Lu et al., 2016). However, when pH value increased to 8.5, anaerobic phosphorus release decreased to 28.69 mg/L. The phosphorus maximum specific anaerobic release rate began to decrease and reached 10.59 mg/g VSS/h in pH 8.5. The main possible reason was the formation of chemical precipitation phosphate compounds. Some phosphorus precipitations were absorbed on the surface of bacteria, it hindered the absorption and release of phosphate by denitrifying polyphosphate accumulating organisms (Sun et al., 2015). Experimental results showed that anaerobic phosphorus release was the maximum under pH 8. The pH also influences anoxic phosphorus uptake when using NO_2^- -N as electron acceptor, the concentration of effluent

phosphorus reduced, and the rate of anoxic phosphorus uptake increased with pH increase during anoxic denitrifying phosphorus uptake. The amount of phosphorus uptake was 34.63 mg/L, when pH was 6.5. There was a remarkable downtrend, phosphorus concentration reached nearly 0 mg/L sharply, and anoxic phosphorus uptake reached 52.02 mg/L when pH was kept at 8. When pHs were 6.5, 7.5 and 8, the corresponding phosphorus specific uptake rates were 18.92, 20.55, and 23.29 mg/g VSS/h. The influence of pH on the specific uptake velocity was rather moderate (as in the case of net phosphorus production), except at the highest pH 8.5, at which the specific uptake rate was reduced almost half of that calculated at pH 8. Similar phenomena took place in anaerobic phosphorus release reaction, but the effect of pH value on phosphorus specific uptake rate was not greater than specific release rate. The reason was that a large number of polyhydroxybutyrate (PHB) were synthesized under higher pH condition, which provided electron donor for anoxic phosphorus uptake. The batch tests indicated pH was an important influencing factor of denitrifying phosphorus removal, the amount of phosphorus uptake was directly proportional to pH (between 6.5 and 8).

Effect of pH on metabolic mechanism

The anaerobic acetic acid absorption, PHB production, and polyphosphate degradation of active sludge from batch tests in different pH condition were illustrated in *Figure 2*. Clearly, the columnar diagrams of anaerobic acetic acid absorption, PHB synthesis and polyphosphate decomposition per unit amount of VSS in reactor showed rising trend by pH condition in the range of 6.5~8. The rate of acetic acid absorption and PHB accumulation were 33.57 mg/g VSS/h and 20.73 mg/g VSS/h, poly-P degradation percentage was 62.32% at pH 6.5, and the rate of acetic acid absorption and PHB accumulation increased to 42.13mg/g VSS/h and 31.43 mg/g VSS/h, poly-P degradation percentage was 68.82% at pH 8.

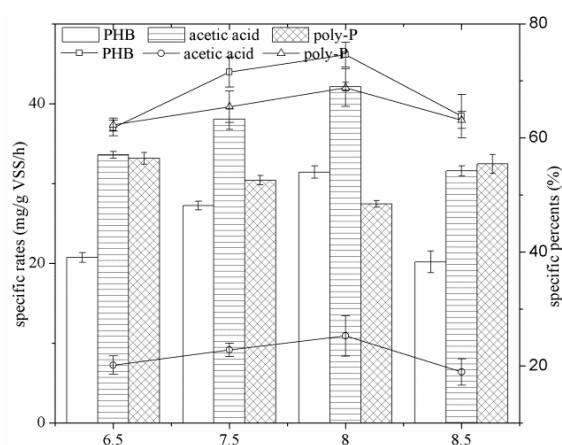


Figure 2. Specific rates and percents of PHB accumulation, acetic acid absorption and poly-P degradation

The trend curves of organic matter degradation, polyphosphate degradation rate and PHB conversion ratio along with pH value were the same as columnar diagrams. The main possible reason for different pH causing different PHB synthesis was related to

potential difference caused by pH gradient. The greater potential difference was, the more phosphate was released and the more PHB was transformed (Wang et al., 2015). The pH was adjusted to 8 by addition HCL or NaOH, it would be found that PHB conversion rate increased obviously, naturally acetic acid conversion rate and polyphosphate degradation ratio were also the largest. Thus increasing the anaerobic pH value would benefit to the microbial metabolism and phosphate removal. When pH was increased up to 8.5, because of chemical phosphorus precipitation, the rate of acetic acid absorption, PHB synthesis and poly-P degradation apparently decreased to 31.6 mg/g VSS/h, 20.17 mg/g VSS/h and 32.44 mg/g VSS/h. From the above considerations, it seems that pH should be strictly controlled below 8, it is the most favorable for biological denitrifying phosphorus removal.

The variation of COD, phosphorus, NO_2^- -N, PHB and polyphosphate concentration in stable anaerobic-anoxic SBR reactor at about pH 8 was highlighted in *Figure 3*. In 2 hours anaerobic P-release phase, sludge polyphosphate content showed downward trend in 2 hours anaerobic P-release sludge, the poly-phosphorus decomposition was 33.52 mg/g VSS, PHB production was 62.87 mg/g VSS. It has been demonstrated that propionic acid enhances the accumulation of polyhydroxyalkanoates (PHB) in sludge, which could apply electron donor for the simultaneous denitritation and phosphorus removal in the presence of nitrite (Oehmen et al., 2005a,b, 2006; Kishida et al., 2006; Katsou et al., 2015).

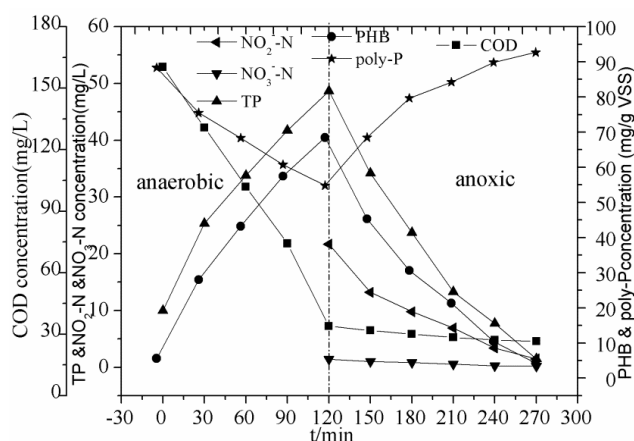


Figure 3. Variations of COD, TP, NO_2^- -N, PHB and poly-P in typical cycle

Meanwhile COD concentration gradually decreased, and phosphate concentration increased to 48.98 mg/L. The possible reason was that the higher energy demand for active uptake of acetic acid, which caused more polyphosphate degradation for producing more adenosine triphosphate (ATP) and resulted in more phosphorus release. In 2.5 hours anoxic P-uptake phase, sludge polyphosphate gradually accumulated to 92.67 mg/g VSS at the end of reaction, meanwhile, there were steadily decrease in the curves of PHB, NO_2^- -N, NO_3^- -N, and phosphorus, the concentrations of phosphate, NO_2^- -N and NO_3^- -N reached 1.47 mg/L, 1.5 mg/L and 0.21 mg/L in effluent. One explanation for this observation was that soluble orthophosphate (SOP) was absorbed and stored intracellular polyphosphate, which used PHB as electron acceptor and nitrite nitrogen as electron donor (Mielcarek et al., 2015). And additionally, the curve of COD concentration declined drastically in the anaerobic period, the curve of COD

concentration declined more sharply in P-release than P- uptake, COD concentration was 33.93 mg/L in anaerobic effluent, and anaerobic COD removal rate sped up to 78.84%. COD was removed mainly in anaerobic stage, which avoided the competition of traditional denitrification bacteria in anoxic stage. This experimental phenomenon was similar to the one of Liu et al. (2015). 22 mg/L NO_2^- -N and 1.5 mg/L NO_3^- -N as electron acceptors were removed by denitrifying phosphorus removal organisms, meanwhile 47.21 mg/L phosphorus was removed. The injections concentration of NO_2^- -N and NO_3^- -N were consistent with the A²SBR. It was shown that the majority of nitrite and nitrate were consumed by denitrifying phosphorus accumulating bacteria, but not by conventional denitrifying bacteria.

It is verified through batch experiment that 22 mg/L nitrite as the main electron acceptor has a good performance, these nitrite levels did not inhibit the DBPRN. It is completely suitable for applying to denitrifying phosphorus remove, and the results is quite similar to the A²N-SBR operation. Previous findings suggest that the nitrite levels at the end of the aerobic phase did not exceed 35 mg L and were usually in the range of 10~25 mg/L. Plotting $\text{sPUR}_{\text{anoxic}}$ versus the initial nitrite concentration at the end of the aerobic phase for a specific experimental period (i.e. period V) did not show any activity inhibition (Katsou et al., 2015).

Effect of SRT

Denitrifying phosphorus removal without sludge discharge

The effects of denitrifying phosphorus removal were investigated under condition of 18 days operation without sludge discharge that could make sure the optimum sludge age range. With reactor running continuously without sludge discharge, the effect of phosphorus removal was not stable. Results depicted in *Figure 4* indicated that phosphorus removal percentage fluctuated between 48% and 86.75%.

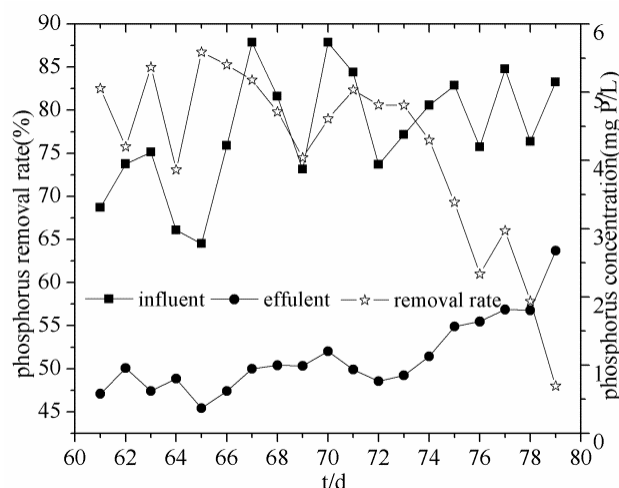


Figure 4. Performance of phosphorus removal of the system without sludge discharge

It was noted that the phosphorus concentration of the effluent was less than 3 mg/L, the average percentage of phosphorus removal reached 80.67% at the 16th day, over a period of 16 days, yield of phosphorus removal decreased gradually. It can be

concluded that there was a phenomenon of denitrifying phosphorus removal in condition of no sludge discharge. However, the phosphorus removal efficiency began to decline after the reactor was operated for more than 16 days without surplus sludge discharge. This result was not consistent with traditional theory of phosphorus removal, which argued that the shorter sludge age, the higher phosphorus removal efficiency. While Hatamoto et al. (2015) obtained the same conclusions, they believed that denitrifying poly-phosphorus accumulating microorganisms (DPAO) grew slowly and resulted in a longer sludge age.

The anaerobic/anoxic SBR ran continuously over 18 days and without sludge discharge, and the effect of SRT on NO_2^- -N and COD removal was shown in *Figure 5*. Unlike phosphorus, COD and NO_2^- -N removal ratios were 84.02%~92.71% and 75.83%~88.75% respectively, COD and NO_2^- -N average discharge concentration were 22.91 mg/L and 2.01 mg/L, implying that no excess sludge discharge would not instinct degradation of organic compounds, even if phosphorus bacteria decreased above 16 days' sludge age. The main reason is that organic compounds have been used as nutrients not only by denitrifying polyphosphate accumulating microorganisms but also other heterotrophic bacteria (Kuba et al., 1996b; Ge et al., 2015). Most of Nitrite nitrogen was absorbed as electron acceptor mainly by DPAO. Additionally, a small amount was removed by denitrification.

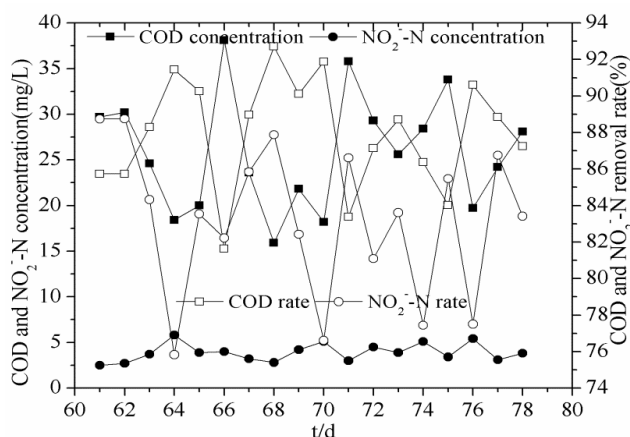


Figure 5. Performance of COD and NO_2^- -N removal in the system without sludge discharge

Effect of SRT on phosphorus removal

Figure 6 showed the removal rate and content variation of phosphorus achieved by sludge at different sludge age (6d, 10d, 16d and 22d). It was indicated that the average phosphorus removal ratio was 61.32% and average phosphorus concentration in effluent was 7.78 mg/L in average, when the sludge age was 6 days. Since SRT is shorter than generation period of bacteria, lots of DPB sludge was discharged and SRT was too short to metabolize actively for denitrifying polyphosphate accumulating organisms, this made DPB become non dominant strains. In addition, short SRT led to high sludge organic loading and residual carbon source, which inhibited microbial physiological activity of denitrifying polyphosphate accumulating organisms and traditional denitrifying bacteria grew rapidly. When the SRT was increased from 6d to 16d, the average denitrifying phosphorus removal ratio increased gradually and finally stabilized

at about 93.12%, with a decreased phosphorus effluent concentration of 0.69 mg/L. This is not consistent with the traditional view that at the smaller SRT, the better effect of phosphorus removal. However, when SRT reached 22d, sewage treatment performance of SBR got worse and phosphorus removal ratio decreased to 60.27%. The main reason is that the excessive sludge retention time resulted in reduction of organic load and ineffective phosphorus release (Luo et al., 2014). The literature suggests that denitrifying phosphorus removal sludge in strict anaerobic/anoxic systems showed the richest denitrifying phosphorus removal bacteria diversity when SRT were approximately 15-20d (Lv et al., 2013). A²N processes can accommodate denitrifying dephosphatation, in the range of SRT (15~20d), effluent N and P from the two processes can satisfy the EC effluent standards ($P < 1 \text{ g/m}^3$ and $N < 10 \text{ g/m}^3$) (Hao et al., 2001). Other works have also shown that a sludge retention time of 15~16 days was favorable for denitrifying phosphorus removal (Zeng et al., 2002; Peng et al., 2004).

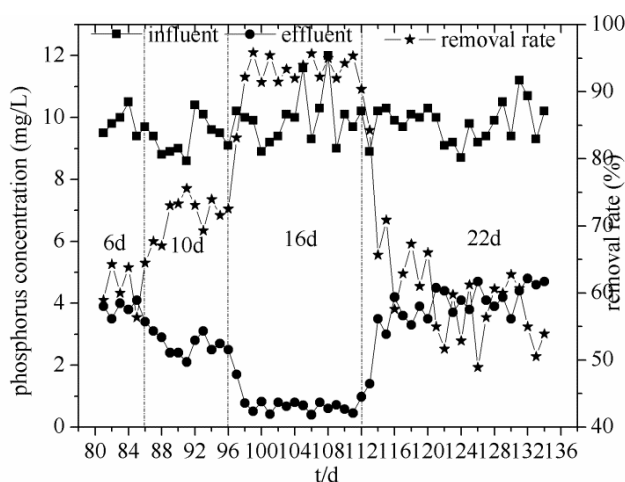


Figure 6. Effect of SRT on the performance of phosphorus removal

The anaerobic acetic acid degradation [measured by chemical oxygen demand (COD)] and PHB production were shown in *Figure 7*. It was found that activated sludge with an SRT of 16 days possessed better anaerobic acetic acid degradation and PHB production than other sludge time. The result was the same as the phosphorus variation. The average concentrations of COD and PHB in anaerobic effluent were 31.31 mg/L and 95.1 mg/L with an SRT of 16 days. The one possible reason is that SRT theoretically determines the microbial lifetime and microbial community. From our result, the shorter SRT may select microbial population with smaller COD consumption and PHB production ability compared with the longer SRT, this conclusion was in accord with literatures (Chen et al., 2016). Some a simulation SRT has been successful applied in A²N process, and total effluent COD is always below 45 g/m^3 , which satisfies the EC effluent standards (Hao et al., 2001). In addition, SRT could affect the PHB accumulation capability by sludge organic loading to biomass. In general, the SRT is proportional to biomass. But in this study, the concentration of COD and PHB in effluent with SRT of 22 days was similar to SRT of 16 days. This is probably because that the activated sludge with too long SRT contains aging microorganisms which might contribute to lower microbial activity. The growth of denitrifying polyphosphate accumulating organisms is inhibited with the too short or too long sludge retention time.

Microorganisms absorbed carbon source and stored by polyhydroxybutyrate are related to SRT and organic loading. In this study, 16 days is the most suitable sludge retention time for denitrifying polyphosphate accumulating organisms.

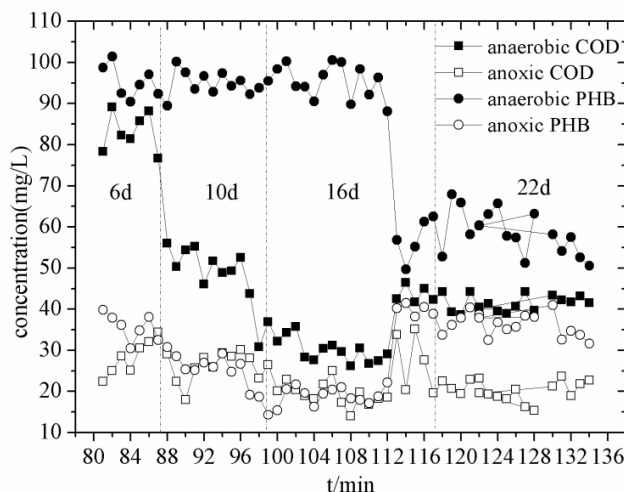


Figure 7. Effect of SRT on carbon removal

Effect of SRT on sludge concentration and metabolism mechanism

Activated sludge was the medium for microbial growth, results of SRT influence on mixed liquor suspended solid (MLSS), mixed liquor volatile suspended solid (MLVSS) and intracellular polymer content depicted in *Table 1* indicated that SRT was positively correlated to MLSS and MLVSS (6, 10, 16, 22 days). In this study, the MLSS in the anaerobic condition with an SRT of 6 days was around 1860 mg/L, and the value with a SRT of 22 days was around 4512 mg/L, the poly-P content amount per unit of MLVSS decreased from 40.7 to 24.2 mg/g VSS. The higher MLVSS promoted a complete phosphorus release and a lower content of phosphorus in the anaerobic sludge, but variation of phosphorus content per unit amount of MLVSS was less than the MLVSS. The main reason is that organic loading reduce with MLVSS increase, and phosphorus release per unit amount of MLVSS decrease. Accordingly, anaerobic phosphorus release per unit amount of MLVSS was proportional to SRT in condition of $SRT \leq 16d$ ($MLVSS \leq 2301$ mg/L), otherwise anaerobic phosphorus release per unit amount of MLVSS increased slightly with SRT enhancing in condition of $SRT > 16d$ ($MLVSS > 2301$ mg/L). Acetic acid are taken up into the cell and stored as PHB, energy (ATP) is required for this process, which is generated by degradation of the internal storage products polyphosphate and glycogen. In this case, anaerobic poly-P release would partly affect PHB synthesis, otherwise, intracellular glycogen of denitrifying phosphorus accumulating organisms could decompose PHB. The anaerobic PHB synthesis per unit amount of MLVSS was the most 63.8 mg/g VSS with an SRT of 16 days, the SRT had a little effect on anaerobic PHB synthesis. In theory, the content of PHB improves with SRT increasing, but there was no obvious influence on anaerobic PHB synthesis per unit amount of MLVSS because of organic load increase.

In the anoxic period, the MLVSS increased from 1342 mg/L to 3203 mg/L while SRT was from 6 to 22 days. The poly-P content increased gradually during anoxic denitrifying phosphorus uptake with the SRT increasing from 6 to 16 days, however,

these was a significant low at the point of SRT 22 days .Whereas SRT had less effect on anaerobic PHB production per unit amount of MLVSS in the reactor, it was because that MLVSS also increased with prolonged SRT, there was no significant difference in the amount of PHB synthesis of unit mass sludge. In the following electron acceptor phase, polyhydroxyalcanoates were degraded as electron for cell growth, polyphosphate synthesis. The system was slightly more effective in denitrifying phosphorus uptake at SRTs of 16 days than of 8, 10, 22 days, the PHB decomposition and polyphosphate accumulation were 16.3 mg/g VSS and 89.4 mg/g VSS at SRT of 16 days. PHB consumed more, phosphorus uptake more completely.

Table 1. Effect of SRT on MLSS, MLVSS, PHB and poly-P

t (d)	anaerobic concentration				anoxic concentration			
	MLSS (mg/L)	MLVSS (mg/L)	PHB (mg/g VSS)	poly-P (mg/g VSS)	MLSS (mg/L)	MLVSS (mg/L)	PHB (mg/g VSS)	poly-P (mg/g VSS)
6	1860	1380	55.7	40.7	1762	1342	35.9	58.3
10	2760	1915	61.6	35.9	2610	1835	26.7	76.7
16	3250	2301	63.8	23.1	3207	2237	16.3	89.4
22	4512	3158	31.2	24.2	4607	3203	18.4	61.8

Conclusions

In conclusion, our investigation showed that pH and SRT as the main operational conditions to improve anaerobic organic matter degradation, PHB accumulation and anoxic nitrite nitrogen utilization, polyphosphate synthesis in anaerobic/anoxic activated sludge process. The optimal pH for denitrifying poly-phosphorus accumulating bacteria was 8, the rate of anaerobic phosphorus release and anoxic phosphorus uptake was 20.95 and 23.29 mg/g VSS/h. Activated sludge with the SRT of 16 days possessed better nitrite nitrogen utilization, organic matter degradation and phosphorus removal than sludge with the SRT of 6, 10 and 22 days. Although the pH and SRT could affect denitrifying phosphorus removal, the exact mechanism of action is still unknown. Therefore, further research is needed to elucidate the exact mode of action of key factors on the activity of microorganisms in system.

Acknowledgements. This work was supported in part by the National Nature Science Foundation of China(No. 51776131 and 51678375).

REFERENCES

- [1] Basset, N., Katsou, E., Frison, N., Malamis, S., Dosta, J., Fatone, F. (2016): Integrating the selection of PHA storing biomass and nitrogen removal via nitrite in the main wastewater treatment line. – *Bioresour. Technol.* 200: 820-829.
- [2] Bortone, G., Malaspina, F., Stante, L., Tilche, A. (1994): Biological nitrogen and phosphorus removal in an anaerobic/anoxic sequencing batch reactor with separated biofilm nitrification. – *Water Sci. Technol.* 30, 303-313.
- [3] Cavallé, L., Grousseau, E., Pocquet, M., Lepeuple, A. S., Uribelarrea, J. L., Guillermina, H. R., Paul, E. (2013): Polyhydroxybutyrate production by direct use of waste activated sludge in phosphorus-limited fed-batch culture. – *Bioresour. Technol.* 149: 301-309.

- [4] Chen, Z. Q., Huang, L., Wen, Q. X., Zhang, H. C., Guo, Z. R. (2016): Effect of sludge retention time, carbon and initial biomass concentration on selection process: From activated sludge to polyhydroxyalkanoate accumulating cultures. – *J. Environ. Sci.* doi: org/10.1016/j.jes.2016.03.014.
- [5] GB 18918-2002. (2002): Discharge standard of pollutants for municipal wastewater treatment plant. – Chinese State Environmental Protection Administration, China.
- [6] Ge, H. Q., Batstone, D. J., Keller, J. (2013): Operating aerobic wastewater treatment at very short sludge ages enables treatment and energy recovery through anaerobic sludge digestion. – *Water Res.* 47: 6546-6557.
- [7] Ge, H. Q., Batstone, D. J., Keller, J. (2015): Biological phosphorus removal from abattoir wastewater at very short sludge ages mediated by novel PAO clade comamon adaceae. – *Water Res.* 69: 173-182.
- [8] Ge, Y., Wang, X. C., Dzakpasu, M. (2016): Characterizing phosphorus removal from polluted urban river water by steel slags in a vertical flow constructed wetland. – *Water Sci. & Technol.* 73: 2644-2653.
- [9] Hao, X. D., Van Loosdrecht, M. C. M., Meijer, S. C. F., Qian, Y. (2001): Model-based evaluation of two BNR processes - UCT and A2N. – *Wat. Res.* 35: 2851-2860.
- [10] Hatamoto, M., Saito, Y., Dehama, K. (2015): Microbial community structure of a simultaneous nitrogen and phosphorus removal reactor following treatment in a UASB-DHS system. – *Water Sci. Technol.* 71: 454-461.
- [11] Jabari, P., Munz, G., Yuan, Q., Oleszkiewicz, J. A. (2016): Free nitrous acid inhibition of biological phosphorus removal in integrated fixed-film activated sludge (IFAS) system. – *Chem. Eng. J.* 287: 38-46.
- [12] Katsou, E., Malamis, S., Frison, N., Fatone, F. (2015): Coupling the treatment of low strength anaerobic effluent with fermented biowaste for nutrient removal via nitrite. – *J. Environ. Manage.* 149: 108-117.
- [13] Kishida, N., Kim, J., Tsuneda, S., Sudo, R. (2006): Anaerobic/oxic/anoxic granular sludge process as an effective nutrient removal process utilizing denitrifying polyphosphate-accumulating organisms. – *Water Res.* 40: 2303-2310.
- [14] Kuba, T., Smolders, G. J. F., Loosdrecht, M. C. M. V., Heijnen, J. J. (1993): Biological phosphorus removal from wastewater by anaerobic–anoxic sequencing batchreactor. – *Water & Technol.* 27: 241-252.
- [15] Kuba, T., van Loosdrecht, M. C. M., Heijnen, J. J. (1996a): Phosphorus and nitrogen removal with minimal COD requirement by integration of nitrifying dephosphatation and nitrification in a two-sludge system. – *Water Res.* 30: 1702-1710.
- [16] Kuba, T., Murnleitner, E., Loosdrecht, M. C. M. V., Heijnen, J. J. (1996b): A metabolic model for biological phosphorus removal by denitrifying organisms. – *Biotechnol. Bioeng.* 52: 685-695.
- [17] Liu, H. B., Sun, L. P., Xia, S. Q. (2008): An efficient DPB utilization process: The modified A2N process. – *Biochem. Eng. J.* 38: 158-163.
- [18] Liu, Y. L., Li, X., Kang, X. R., Yuan, Y. X. (2014): Performance of denitrifying phosphorus removal of *Acinetobacter* strain at low temperature. – *Int. Biodeterior. Biodegrad.* 95: 135-138.
- [19] Liu, S. L., Li, J. Z. (2015): Accumulation and isolation of simultaneous denitrifying polyphosphate-accumulating organisms in an improved sequencing batch reactor system at low temperature. – *Int. Biodeterior. & Biodegrad.* 100: 140-148.
- [20] Lu, J. B., Yang, J. M., Xu, K., Hao, J., Li, Y. Y. (2016): Phosphorus release from coprecipitants formed during orthophosphate removal with Fe(III) salt coagulation: Effects of pH, Eh, temperature and aging time. – *J. Environ. Chem. Eng.* 4: 3322-3329.
- [21] Luo, J. Y., Feng, L. Y., Zhang, W., Li, X., Chen, H., Wang, D. B., Chen, Y. G. (2014): Improved production of short-chain fatty acids from waste activated sludge driven by carbohydrate addition in continuous-flow reactors: Influence of SRT and temperature. – *Appl. Energy* 113: 51-58.

- [22] Lv, X. M., Shao, M. F., Li, C. L., Li, J., Xia, X., Liu, D. Y. (2013): Bacterial diversity and community structure of denitrifying phosphorus removal sludge in strict anaerobic/anoxic systems operated with different carbon sources. – *Res. Article* 89: 1842-1849.
- [23] Meinhold, J., Arnold, E., Isaacs, S. (1999): Effect of nitrite on anoxic phosphate uptake in biological phosphorus removal activated sludge. – *Water Res.* 33: 1871-1883.
- [24] Mielcarek, A., Rodziewicz, J., Janczukowicz, W., Thornton, A. J., Jóźwiak, T., Szymczyk, P. (2015): Effect of the C:N:P ratio on the denitrifying dephosphatation in a sequencing batch biofilm reactor (SBBR). – *J. Environ. Sci.* 38: 119-125.
- [25] Nittami, T., Oi, H., Matsumoto, K., Seviour, R. J. (2011): Influence of temperature, pH and dissolved oxygen concentration on enhanced biological phosphorus removal under strictly aerobic conditions. – *New Biotechnol.* 29: 2-8.
- [26] Oehmen, A., Yuan, Z. G., Blackall, L. L., Keller, J. (2005): Comparison of acetate and propionate uptake by polyphosphate accumulating organisms and glycogen accumulating organisms. – *Biotechnol. Bioeng.* 91: 162-168.
- [27] Oehmen, A., Vives, M. T., Lu, H., Yuan, Z., Keller, J. (2005): The effect of pH on the competition between polyphosphate accumulating organisms and glycogen accumulating organisms. – *Water Res.* 39: 3727-3737.
- [28] Oehmen, A., Saunder, A. M., Vives, M. T., Yuan, Z., Keller, J. (2006): Competition between polyphosphate and glycogen accumulating organisms in enhanced biological phosphorus removal systems with acetate and propionate as carbon source. – *J. Biotechnol.* 123: 22-32.
- [29] Peng, Y. Z., Li, Y. Z., Wang, S. Y., Wang, Y. Y. (2004): Denitrification and dephosphatation by anaerobic/anoxic sequencing batch reactor. – *Chinese J. Chem. Eng.* 12: 877-880.
- [30] Reza, M., Cuenca, M. A. (2016): Simultaneous biological removal of nitrogen and phosphorus in a vertical bioreactor. – *J. Environ. Chem. Eng.* 4: 130-136.
- [31] Smolders, G. J. F., Meij, J. V. D., Loosdrecht, M. C. M. V., Heijnen, J. J. (1994): Model of the anaerobic metabolism of the biological phosphorus removal process: stoichiometry and pH influence. – *Biotechnol. Bioeng.* 43: 461-470.
- [32] Sun, L., Zhao, X. X., Zhang, H. F., Zhang, Y. Q. (2015): Biological characteristics of a denitrifying phosphorus-accumulating bacterium. – *Ecol. Eng.* 81: 82-88.
- [33] Tayà, C., Garlapati, V. K., Guisasola, A., Baeza, J. A. (2013): The selective role of nitrite in the PAO/GAO competition. – *Chemosphere* 93: 612-618.
- [34] Wang, Y. Y., Zhou, S., Wang, H., Ye, L., Qin, J., Lin, X. M. (2015a): Comparison of endogenous metabolism during long-term anaerobic starvation of nitrite/ nitrate cultivated denitrifying phosphorus removal sludge. – *Water Res.* 68: 374-386.
- [35] Wang, X. X., Wang, S. Y., Xue, T. L., Li, B. K., Dai, X., Peng, Y. Z. (2015b): Treating low carbon/nitrogen (C/N) wastewater in simultaneous nitrification-endogenous denitrification and phosphorus removal (SNDPR) systems by strengthening anaerobic intracellular carbon storage. – *Biochem. Eng. J.* 77: 147-153.
- [36] Wong, P. Y., Ginige, M. P., Kaksonen, A. H. (2015): Simultaneous phosphorus uptake and denitrification by EBPR-r biofilm under aerobic conditions: effect of dissolved oxygen. – *Water Sci. Technol.* 72: 1147-1154.
- [37] Zeng, R. J., Saunders, A. M., Yuan, Z. G., Blackall, L. L., Keller, J. (2003): Identification and Comparison of Aerobic and denitrifying polyphosphate-accumulating organisms. – *Biotechnol. Bioeng.* 83: 140-148.
- [38] Zhang, H. L., Sheng, G. P., Fang, W., Wang, Y. P., Fang, C. Y., Shao, L. M., Yu, H. Q. (2015): Calcium effect on the metabolic pathway of phosphorus accumulating organisms in enhanced biological phosphorus removal systems. – *Water Res.* 84: 171-180.
- [39] Zhao, W. H., Zhang, Y., Lv, D. M., Wang, M. X., Peng, Y. Z., Li, B. K. (2016): Advanced nitrogen and phosphorus removal in the pre-denitrification

- anaerobic/anoxic/aerobic nitrification sequence batch reactor (pre-A2NSBR) treating low carbon/nitrogen (C/N) wastewater. – Chem. Eng. J. 302: 296-304.
- [40] Zhou, Y., Oehmen, A., Lim, M., Vadivelu, V., Ng, W. J. (2011): The role of nitrite and free nitrous acid (FNA) in wastewater treatment plants. – Water Res. 45: 4672-4682.

EFFECTS OF THE PRECIPITATION PATTERN AND VEGETATION COVERAGE VARIATION ON THE SURFACE RUNOFF CHARACTERISTICS IN THE EASTERN TAIHANG MOUNTAIN

YUAN, Z.^{1*} – YAN, D. H.² – XU, J. J.¹ – WANG, Y. Q.¹ – YAO, L. Q.¹ – YU, Z. Q.¹

¹*Changjiang River Scientific Research Institute, Changjiang Water Resources Commission of the Ministry of Water Resources of China, #23 Huangpu Road, Wuhan, Hubei, China
(phone: +86-137-1656-5927; fax: +86-027-8282-9732)*

²*State Key Laboratory of Simulation and Regulation of Water Cycle in River Basin, China Institute of Water Resources and Hydropower Research, #1, Fuxing Road, Haidian District, Beijing, China*

**Corresponding author*

e-mail: yuanzhe@126.com; phone: +86-137-1656-5927; fax: +86-027-8282-9732

(Received 11th Jan 2019; accepted 8th Mar 2019)

Abstract. Water is a kind of important component in natural environment, while the ecological construction can influence the hydrological regime. A successful ecology construction is based on effective recognition of the relationship between the regional vegetation and surface water resources. This work used several datasets, including meteorological data, remote sensing data and hydrologic data. The objective of this work is to identify the effects of the precipitation and the ecological succession of vegetation on the surface runoff. The results indicated that: (1) the precipitation and surface runoff reduced by 4.8-7.3% and 20.6-43.2% during 1961-1985 and 1986-2011, respectively. The reduction of the surface runoff was higher than that of the precipitation; (2) the natural surface runoff of the Taihang Mountain is positively correlated with the precipitation and negatively correlated with NDVI. The natural surface runoff would increase by 16.6-66.7% with the hypothesis that vegetation during 1986-2011 was the same with that during 1961-1985; (3) considering the regional climate conditions, drought-tolerant native species should be chosen in landscape engineering of the Taihang Mountain. This effort can avoid exhaustion of water resource caused by the excessive construction of ecological project.

Keywords: *precipitation, NDVI, surface runoff, attribution assessment*

Introduction

Forest cover plays an important role in regulating land hydrological cycle, especially in precipitation redistribution, the impact of soil moisture movement and changing of runoff generation and confluence condition. Meanwhile, forest cover can reduce flood peak, increase runoff during dry season, control soil erosion and improve water quality. However, the relationship between forest and runoff has not reached a coincident conclusion. The main divergence is whether the forest cover will increase the soil moisture and decrease the runoff of the basin. There are two different views about this issue: the forest cover will increase the annual runoff for the retaining water capacity of forest, and the forest cover will increase precipitation and decrease ground surface evaporation. Hao, et al. (2004) did research in basin above Lushi hydrological station of the Luohe River, tributary of lower reaches of the Yellow River and the results indicated that the forest had increased the runoff. The annual runoff decreased obviously when most of the forest and grassland in the upper reaches of Mayinghe River Basin was turned into farmland (Wang et al., 2005). Because of the forest cover will increase evaporation and retain precipitation, enhance the use and exchange of deep

phreatic water, accelerate the partial hydrological cycle and reduce surface runoff, many researches also demonstrated that the forest cover can reduce annual runoff. Similarly, the river runoff and flood peak can also be reduced. Zhou, et al. (2001) found that evapotranspiration will be the main factor of losing water when the basin is small. Therefore, the runoff will decrease if the forest cover increases.

Based on the data from more than 600 observation stations in the southern hemisphere, the runoff within ten years will decrease to a large degree after planting trees for carbon sequestration (Jackson et al., 2005). This phenomenon would lead to bestrunking of the stream (Wang et al., 2006; Chen et al., 2009; Cao et al., 2009). After analyzing 94 basins around the world, Bosch, et al. (1982) found that the decrease of forest will result in the increase of runoff, while forestation in open field will cause the decrease of total runoff. Based on different methods, many other researches in different basins have reached the similar conclusion that the decrease of forest cover will lead to the increase of runoff (Siriwardena et al., 2006; Zhang and Schilling, 2006; Wang et al., 2008; Mao and Keith, 2009).

In addition, the annual runoff of the basin could be influenced by the forest vegetation change and the type of climatic region. For instance, the decrease of the forest cover rate would make the runoff coefficient markedly increase in the Loess Plateau. In arid and semi-arid areas, the evaporation capacity of forest is greater than the precipitation. The evaporation is the mainly moisture outlay of the ecosystem. Therefore, the forest coverage increase will result in the decrease of water yield of the drainage basin. Moreover, the variation of forest coverage exerts little effect on the annual runoff generation of the basin in the tropical and subtropical region. In the tropical and subtropical basin with abundant rainfall, the moisture evapotranspiration is depended on the climatic factor, and the vegetation coverage is not a key factor affecting the moisture evapotranspiration of the basin. The forest coverage variation had no significant influence on the runoff volume (Wang and Zhang, 2001). Currently, regional difference still exists in the relationship between vegetation coverage and runoff. Therefore, taking into account the response of streamflow after vegetation change and precipitation becomes necessary.

In this study, we (1) investigated the relationship between precipitation and runoff depth, and the variation characteristics of NDVI in typical basin for analyzing vegetation effects on surface runoff; (2) compared the runoff generation and runoff coefficient variation as estimated using different calibration periods; and (3) examined the restoring computation of natural runoff based on the approach to estimate the characteristic of the precipitation and runoff and explored a general framework to incorporate the effects of precipitation and vegetation variation on runoff in typical basin.

Materials and methods

Study area

The Taihang Mountain is situated in a topographical transforming region. The North China Plain is in its eastward, and the Loess Plateau is in the west. This mountain is roughly parallel with the coast line of eastern China. In the summer time, the warm, moist air from the Pacific Ocean will be raised up to cause rainfall in the area where the elevation is higher than 800 m. This is the reason why in the area where the elevation is higher than 800 m has a humid climate compared with places lower than 800 m in the

Taihang Mountain. When the elevation is lower than 800 m, the annual average temperature is around 12.3°C, precipitation is around 500 mm, and the annual potential evaporation is about 1700 mm. Based on the special environmental characteristics, the ecology system are more fragile in this region. The eastern Taihang Mountain, situated between 112°7'E and 115°30'E and between 37°17'N and 41°15'N, is the area investigated in this study, including the Yanghe River Basin, Yongdinghe Upriver Basin and Ziyahe Upriver Basin.

The daily precipitation data from 1961 to 2011 were gathered from the meteorological stations located in East Taihang Mountain Area (the stations close to the boundary were also included). Runoff data used in this research are collected from 3 typical hydrological stations of East Taihang Mountain. The representative hydrological stations are Xiangshuibao, Shixiali and Huangbizhuang reservoir, respectively (Table 1). Meanwhile, the actual measured streamflow data and natural streamflow data are available for the period of 1961-2011. The spatial distribution of 81 meteorological stations was screened in Figure 1.

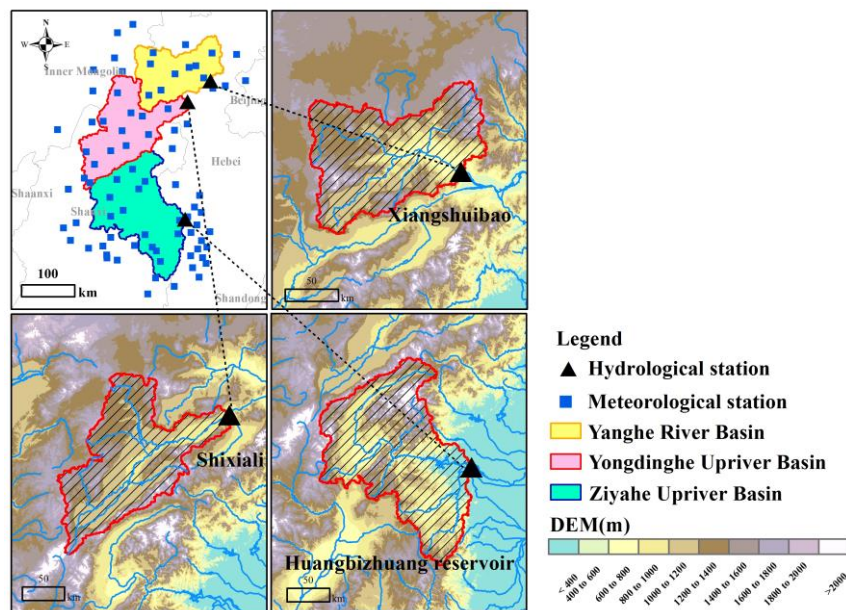


Figure 1. Locations of the paired catchments in Eastern Taihang Mountain

Table 1. Basic information of the 12 hydrological stations

Hydrological station	Longitude	Latitude	Control area (km ²)	River basin
Xiangshuibao	115°11'	40°31'	14507	Yanghe River Basin
Shixiali	114°33'	40°15'	23944	Yongdinghe Upriver Basin
Huangbizhuang reservoir	114°18'	38°15'	23272	Ziyahe Upriver Basin

In this study, GIMMS NDVI data and MODIS NDVI data are selected. These two data sets are provided by the Godard Space Flight Center in the National Aeronautics and Space Administration (NASA). The GIMMS data is 15 day compound product with 8 km resolution in global scale. MODIS NDVI data is calculated from MODIS

reflectance data based on the generalized algorithm. The preprocessing procedures include: quality assessment, region of interesting extraction, mosaicking and geometric rectification.

Time trend analysis of NDVI

According to the monthly NDVI data of the two datasets from 2000 to 2006, the monthly NDVI sequence (1982–2013) was derived through the per-pixel unary linear regression model. The per-pixel unary linear regression model can acquire the most appropriate regression equation for each pixel. The elementary structure form of the model for different data is calculated as *Equations 1* and *2* (Ma, 2009).

$$G_i = a + bV_i + \varepsilon_i \quad (\text{Eq.1})$$

where, parameter a and b are estimated by the least square method, and ε_i is random error.

$$b = \frac{\sum_{i=1}^n (G_i - \bar{V}) \times (G_i - \bar{G})}{\sum_{i=1}^n (V_i - \bar{V})} \quad a = \bar{G} - b \times \bar{V} \quad (\text{Eq.2})$$

where, G_i represents GIMMS NDVI in i th month, and V_i is MODIS NDVI ($8 \text{ km} \times 8 \text{ km}$) in i th month. \bar{G} is the mean of all monthly GIMMS data from 2000 to 2009 at corresponding pixel. \bar{V} is the mean of all monthly MODIS NDVI data ($8 \text{ km} \times 8 \text{ km}$) from 2000 to 2009 at corresponding pixel.

Zonal statistics for precipitation and NDVI

Since the meteorological stations are dense enough to capture the extent of East Taihang Mountain Area surface variation, the IDW (Inversed Distance Weighted) method is chosen to convert daily precipitation to grid surface data (Garcia et al., 2008). The spatial resolution of the interpolated areal daily precipitation is $5 \times 5 \text{ km}^2$. Data processing was carried out in the ArcInfo Workstation 10.0. The relative calculation is conducted by ARC Macro Language (AML). The key codes of IDW are listed as follows:

IDW = idw (point_cover, spot_item, #, 2, sample, 12, #, %cellsize%, %xmin%, %ymin%, %xmax%, %ymax%)

where, the point_cover indicates the source of the data containing points with z values to be converted to a grid surface; spot_item is the item in the point coverage to be used as the z value for the interpolation; cellsize is the width or height of a cell, in map units. cellsize is set as 5000 in this study, which means the spatial resolution of the grid file is $10 \times 10 \text{ km}^2$. {xmin, ymin, xmax, ymax} represents the interpolation within the data processing, and xmin, ymin, xmax, ymax are 560000, 4000000, 915000, 4510000, respectively.

According to the values of the enclosed grid cells, the mean value of annual precipitation and NDVI was calculated for each catchment. The code used in ZONALSTATS is shown as follows:

outtable = zonalstats(zonegrid, valuegrid, mean)

where, the zonegrid represents the integer grid that identifies the zone for each cell, valuegrid is the floating grid that defines the annual precipitation and NDVI values of the cells, and mean is a keyword for zonal mean calculations. The computation process was conducted in the ArcInfo Workstation 10.0 platform.

Determination of the streamflow decrease

The statistic model of precipitation (X_1), NDVI (X_2) and runoff (Y) was developed by the regression analysis method (Table 2). Then the responding relationship of precipitation, NDVI and runoff was analyzed through this statistic model.

Table 2. The responding relationship of precipitation, NDVI and annual runoff depth

Item	Factor	Variable
Dependent variable	Annual runoff depth	Y
Independent variable	Annual precipitation	X_1
	NDVI	X_2

According to the starting time of the landscape engineering in Taihang Mountain, the time sequence of this work is divided into two periods: natural period (1961-1985) and impacted period (1986-2011). The vegetation coverage remained natural during the natural period. However, the vegetation has gained relative recovery in the impacted period, and the relationship between the precipitation and streamflow was changed in a certain extent. After the break point, R_{nature} is indicated the average natural runoff (Fig. 2). Meanwhile, during the impacted period, the simulated natural runoff volume $R_{retrieve}$ could be obtained under the assumption that the relationship between precipitation and streamflow was the same as that in the natural period. Thus, decrement runoff volume caused by the vegetation recovery after 1985 can be derived from the function as Equation 3.

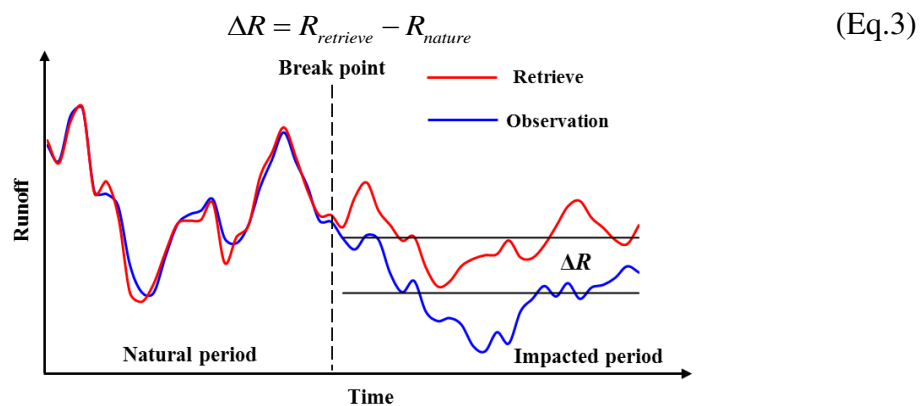


Figure 2. The framework for quantitative assessment of streamflow decrease

Results

The relationship between precipitation and runoff depth

During 1961-2011, the annual precipitation within the Yanghe River Basin, Yongdinghe Upriver Basin and Ziyahe Upriver Basin showed a decreasing tendency, and the changing rate of annual precipitation were -8.6 mm/10a, -8.0 mm/10a and -15.3 mm/10a, respectively. Compared with the period 1961-1985, the average annual precipitation of three catchments reduced by 5.1%, 4.8% and 7.3% during 1986-2011. The runoff and precipitation variation showed a similarity in the decreasing tendency. The variation rate of natural runoff of Yanghe River Basin, Yongdinghe Upriver Basin and Ziyahe Upriver Basin were -5.9 mm/10a, -3.9/10a and -9.9 mm/10a, respectively. The results demonstrated that the actual measured runoff depth decreased obviously within the study periods. The changing rates of actual measured runoff depth in the three typical basins were -7.2 mm/10a, -6.5 mm/10a and -16.1 mm/10a, respectively. After 1985, the natural runoff depth reduced by 43.2%, 30.7% and 20.6% compared with the average runoff depth during 1961-1985. Similarly, the actual measured runoff depths were 66.8%, 76.1% and 54.3% lesser than the average value before 1985. The difference between natural runoff and actual measured runoff is obvious under the pressure of anthropologic influence and it would be more obviously in the future (Fig. 3).

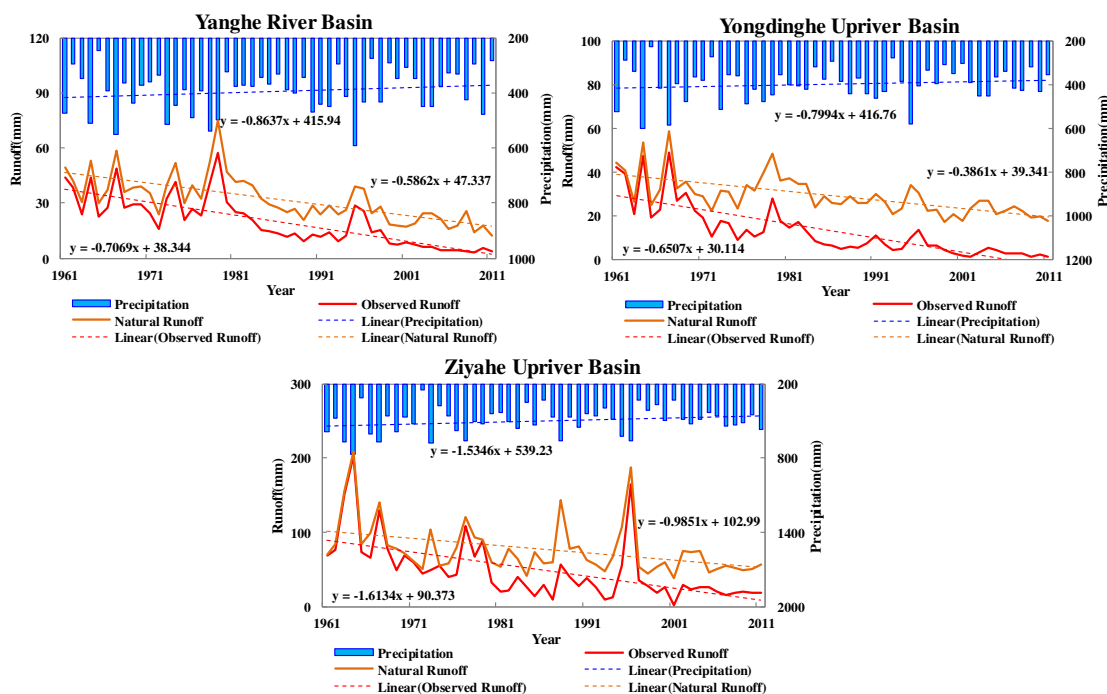


Figure 3. The annual precipitation and runoff depth variation in 1961-2011

The ratio of annual average intensive precipitation ($S > 25$ mm/d) was gradually increasing from north area to south area. The probability of intensive precipitation in Yanghe River Basin, Yongdinghe Upriver Basin and Ziyahe Upriver Basin were 13.4%, 15.0% and 23.0%, respectively. The intensive precipitation ratio in the Yanghe River Basin and Yongdinghe Upriver Basin presented decreasing tendency during the 1961-

2011 (Fig. 4). However, this ratio in Ziyahe Upriver Basin had an increasing tendency during the study period. Specially, the variation of intensive precipitation was obviously in the Yongdinghe Upriver Basin and Ziyahe Upriver Basin. With respect to the average intensive precipitation before 1985, the intensive precipitation ratio has reduced by 9.9% in the Yongdinghe Upriver Basin. Moreover, the intensive precipitation ratio has increased by 3.6% in the Ziyahe Upriver Basin.

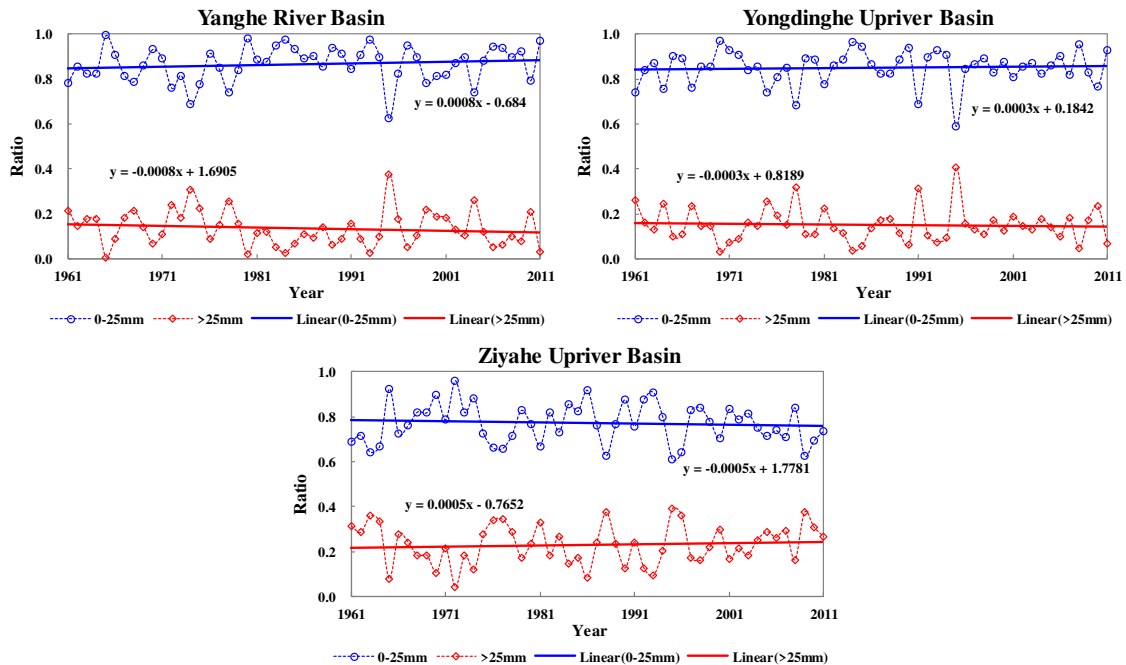


Figure 4. The probability of different intensive precipitation during 1961-2011

Characteristics of NDVI variation in typical basin

The NDVI of the Yanghe River Basin, Yongdinghe Upriver Basin and Ziyahe Upriver Basin presented an increasing tendency during 1983-2013 (Fig. 5), and their variation tendency rates were 0.017/10a, 0.015/10a and 0.009/10a, respectively. The results demonstrated that the increased range of NDVI value in the north region was obviously higher than that in the south region (Fig. 6). The variation tendency ratio of NDVI in the north area was generally above 0.010/10a. The large-scale vegetation recovery was mainly benefited by the landscape engineering in Taihang Mountain. The vegetation recovery project built 1.36 million hectares of forest from 1986 to 2000. As in the second stage (2001-2010), the recovery project built 1.78 million hectares of forest. During the third stage (2011-2050), the project aims to build 0.42 million hectares of forest. The forest cover rate will be enhanced from 15% to 35% after this project completed.

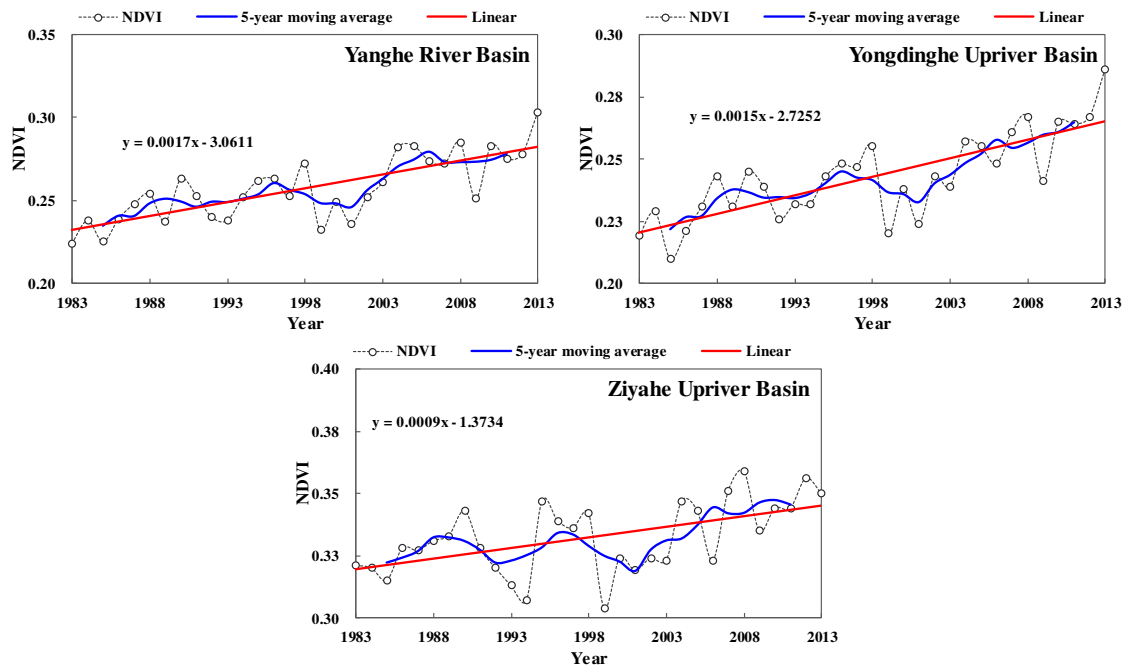


Figure 5. The variation of NDVI from 1983 to 2013

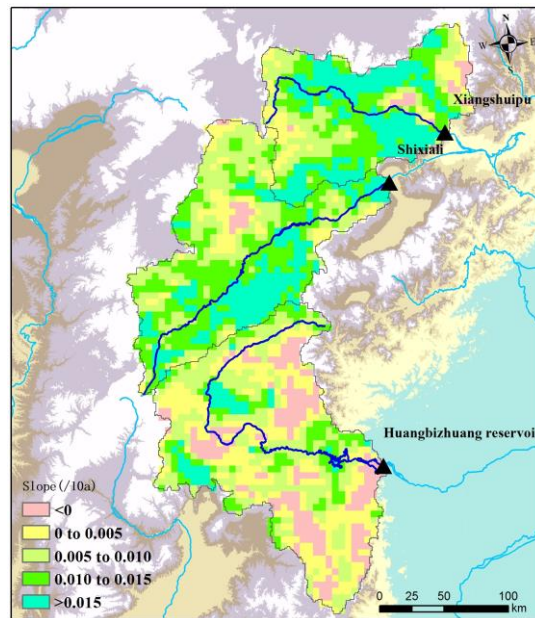


Figure 6. The variation tendency ratio of NDVI

Evidence for runoff generation and runoff coefficient variation

The runoff generation coefficient and runoff coefficient decreased obviously from 1961 to 2011. During the period, the runoff generation coefficients of Yanghe River Basin, Yongdinghe Upriver Basin and Ziyahe Upriver Basin reduced by $-0.014/10a$, $-0.009/10a$ and $-0.015/10a$, and the runoff coefficient in the typical basins were $-0.017/10a$, $-0.016/10a$ and $-0.029/10a$, respectively. The results indicated that the runoff

coefficient has more significant decreasing tendency since 1985 (Fig. 7). The average runoff generation coefficients in the Yanghe River Basin, Yongdinghe Upriver Basin and Ziyahe Upriver Basin were 0.10, 0.09 and 0.17 from 1961 to 1985. And the runoff coefficients in the typical basins were 0.07, 0.05 and 0.13, respectively. However, during 1986-2011, the average runoff generation coefficients/runoff coefficients were 0.06/0.03, 0.06/0.01 and 0.14/0.06, respectively. Meanwhile, the average runoff generation coefficients/runoff coefficients of the three typical basins have reduced by 40.1%/64.0%, 27.2%/74.9% and 14.3%/50.7% compared to the average value during 1961-1985 (Fig. 8). The runoff generation coefficient and runoff coefficient decreased obviously in the northern region.

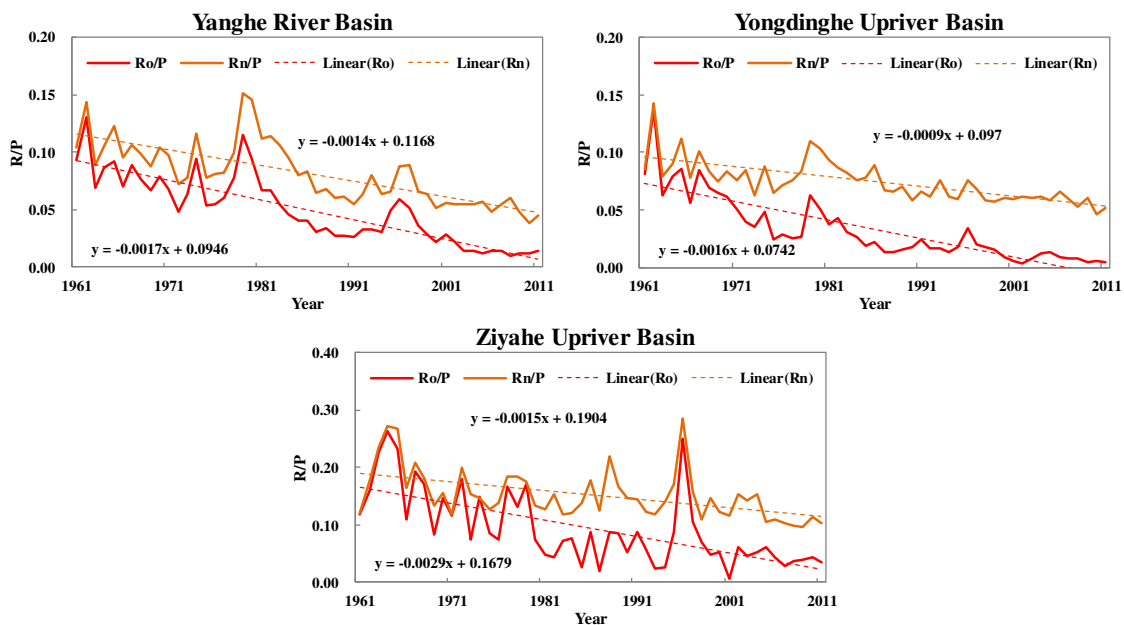


Figure 7. The interannual variation of runoff generation coefficient and runoff coefficient

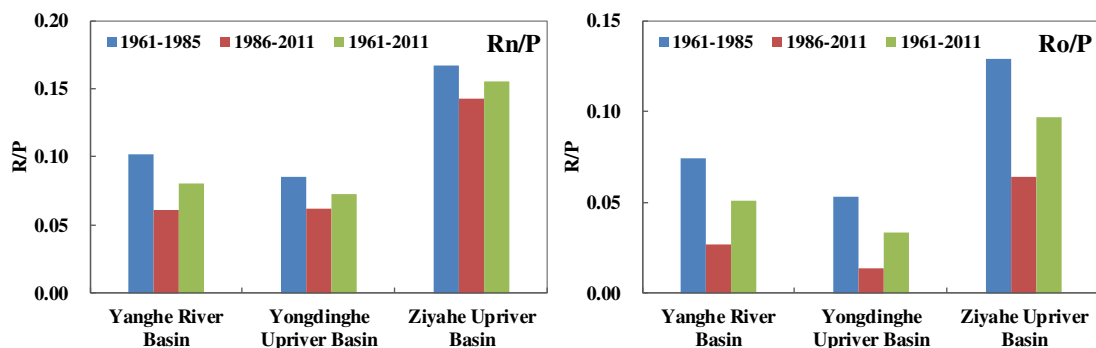


Figure 8. Different periods of runoff generation coefficient and runoff coefficient in typical basins

The least square method was carried out to conduct the regression analysis of precipitation (X_1), NDVI (X_2) and natural runoff depth (Y). The regression analysis results demonstrated that the volume of runoff has positive relationship with the

precipitation, and the NDVI has negative relationship with to the volume of runoff (Table 3). In conclusion, the vegetation in the eastern Taihang Mountain had greatly recovered due to the implement of landscape engineering. However, the forest covered area has unreasonable increased due to the excessive construction of vegetation. Thus, the volume of runoff in the typical basins was decreased to a certain degree for the influence of evapotranspiration increase.

Table 3. Regression analysis of precipitation, NDVI and natural runoff

River basin	Regression equation	R2
Yanghe River Basin	$Y = 0.07 X_1 - 198.59 X_2 + 47.93$	0.55
Yongdinghe Upriver Basin	$Y = 0.06 X_1 - 148.50 X_2 + 37.77$	0.68
Ziyahe Upriver Basin	$Y = 0.27 X_1 - 308.13 X_2 + 40.47$	0.55

Restoring computation of natural runoff

Compared with the period of 1961-1985, the precipitation in the typical basins had reduced by 4.8-7.3% during 1986-2011. Nevertheless, the volume of natural runoff has reduced by 27.2-40.1% (Table 4). The decreased runoff volume was greater than the amount of precipitation in the typical basins. Specifically, the reduction amplitude of runoff generation coefficient was 14.3-40.1%. Moreover, the reduction amplitude was increasing from south to north region, especially in the Yanghe River Basin. The relationship of precipitation and natural runoff in the typical basins are assumed to be similar with that during 1961-1985, and the precipitation still remained the level during 1986-2011. On this condition, the annual natural runoff depths of the Yanghe River Basin, Yongdinghe Upriver Basin and Ziyahe Upriver Basin were 39.0 mm, 33.1 mm and 80.1 mm. At the same time, the results demonstrated that the annual natural runoff depths within the typical basins has increased by 66.7%, 37.3% and 16.6% compared with that in the practical condition.

Table 4. Changes of annual mean precipitation and streamflow during the two periods in Yanghe River Basin, Yongdinghe Upriver Basin and Ziyahe Upriver Basin

River basin	Period	R/P	P _{mean} /mm	R _{mean} /mm	R _{retrieve} /mm
Yanghe River Basin	1961-1985	0.10	404.1	41.2	39.0
	1986-2011	0.06	383.3	23.4	
	Change	-40.1%	-5.1%	-43.2%	
Yongdinghe Upriver Basin	1961-1985	0.09	405.9	34.7	33.1
	1986-2011	0.06	386.4	24.1	
	Change	-27.2%	-4.8%	-30.7%	
Ziyahe Upriver Basin	1961-1985	0.17	518.7	86.4	80.1
	1986-2011	0.14	480.7	68.7	
	Change	-14.3%	-7.3%	-20.6%	

Conclusion

In the recent 50 years, the annual precipitation in the eastern Taihang Mountain presented the decreasing tendency. In the Yanghe River Basin, Yongdinghe Upriver

Basin and Ziyahe Upriver, the annual precipitation of the typical basins has reduced by 5.1%, 4.8% and 7.3%, respectively. The volume of the natural surface runoff has larger decrease compared with that of precipitation. On the basis of the Taihang Mountains afforestation project, the vegetation coverage was greatly recovered. The variation tendency rate of the regional averaged NDVI was 0.009~0.017/10a. The increase of the forest coverage can enhance the evapotranspiration of the surface, which is one of the major reasons for the runoff decrease. Similarly, the relationship of precipitation and natural runoff in the typical basins are assumed to be similar with those during 1961-1985, and the vegetation coverage remained the level before 1985. On this condition, the annual natural runoff depths of the Yanghe River Basin, Yongdinghe Upriver Basin and Ziyahe Upriver Basin were 39.0 mm, 33.1 mm and 80.1 mm. At the same time, the results demonstrated that the annual natural runoff depths within the typical basins increased by 66.7%, 37.3% and 16.6% compared with that during the practical condition. Thus, the vegetation's restoration causes the regional runoff's decrease by 16.6~66.7%.

The precipitation may continue decreasing in the future due to climate change and global warming. However, the surface evapotranspiration will be greatly enhanced for the continuous increasing temperature in this region. For this reason, the Taihang Mountain region may face the water shortage crisis in the future. Because of the water shortage tends to exist in long-term, how to balance water usage and vegetation restoration under the water shortage condition is becoming a challenge. In the future work, the selected vegetation species for afforestation project should consume less water and have a higher tolerance for water shortage condition. Furthermore, because of the water restrictions, the planted vegetation should keep lower densities to reduce water consume.

This research has adopted statistical methods to identify the impact of precipitation and vegetation variation on surface runoff. The formation of surface runoff is not only affected by precipitation and vegetation, but also by many other factors such as soil and temperature. Further research may use physically-based watershed eco-hydrological model to do more refined simulation of the eco-hydrological process, thus identifying the spatial difference of the impact of precipitation and vegetation variation on surface runoff. In the meantime, multi-set of vegetation restoration and repair scheme can be set. Optimal scheme which is the most suitable for the eastern Taihang Mountain can be selected.

Acknowledgements. This research was funded by [National Key Research and Development Project] grant number [2017YFC1502404]; [National Natural Science Foundation of China] grant number [51709008,51779013]; National Public Research Institutes for Basic R&D Operating Expenses Special Project (no. CKSF2017029 and no. CKSF2017061/SZ).

REFERENCES

- [1] Bosch, J. M., Hewlett, J. D. (1982): A review of catchment experiments to determine the effect of vegetation changes on water yield and evapotranspiration. – *Journal of Hydrology* 55(1): 3-23.
- [2] Cao, W. Z., Bowden, W. B., Davie, T. et al. (2009): Modelling impacts of land cover change on critical water resources in the Motueka river catchment, New Zealand. – *Water Resources Management* 23(1): 137-151.

- [3] Chen, Y., Xu, Y., Yin, Y. (2009): Simulation of the hydrologic response to land-use and land-cover changes scenarios: a case study of Xitiaoxi Basin. – *Journal of Natural Resources* 24(2): 351-357.
- [4] Hao, F., Chen, L., Liu, C., Dai, D. (2004): Impact of land use change on runoff and sediment yield. – *Journal of Soil and Water Conservation* 18(3): 5-8.
- [5] Jackson, R., B., Jobbagy, E. G., Avissar, R. et al. (2005): Trading water for carbon with biological carbon sequestration. – *Science* 310: 1944-1947.
- [6] Ma, M. G. (2009): Research of Monitoring and Simulation of Vegetation Dynamics in Northwest China, Based on Time Series Data. – *Academic Exchanges of Young Scholars in the Field of Geo-Information Science and Technology*, Beijing.
- [7] Mao, D., Keith, A. C. (2009): Impacts of land-use change on hydrologic responses in the Great Lakes region. – *Journal of Hydrology* 374(1-2): 71-82.
- [8] Siriwardena, L., Finlayson, B. L., McMahon, T. A. (2006): The impact of land use change on catchment hydrology in large catchments: the Comet River, Central Queensland, Australia. – *Journal of Hydrology* 326(1-4): 199-214.
- [9] Wang, L. X., Zhang, Z. Q. (2001): Impacts of forest vegetation on watershed runoff in dryland areas. – *Journal of Natural Resources* 16(5): 439-444.
- [10] Wang, S., Zhang, Z., Sun, G., Zhang, M., Yu, X. (2006): Effects of land use change on hydrological dynamics at watershed scale in the Loess Plateau. A case study in Lvergou watershed, Gansu Province. – *Journal of Beijing Forestry University* 28(1): 48-54.
- [11] Wang, S. F., Kang, S. Z., Zhang, L. et al. (2008): Modelling hydrological response to different land-use and climate change scenarios in the Zamu River basin of northwest China. – *Hydrological Processes* 22(14): 2502-2510.
- [12] Wang, G., Zhang, Y., Liu, G. et al. (2005): Effects of land use change on stream flow in Mayinghe River Basin during 1967-2000. – *Science in China D: Earth Science* 35(7): 671-681.
- [13] Zhou, X., Zhao, H., Sun, H. (2001): Proper assessment for forest hydrological effect. – *Journal of Natural Resources* 16(5): 420-426.
- [14] Zhang, Y. K., Schilling, K. E. (2006): Increasing stream flow and base flow in Mississippi River since the 1940s: effect of land use change. – *Journal of Hydrology* 324(1-4): 412-422.

SPATIAL VARIATION OF WITHIN-DAY AND BETWEEN-DAY CHLOROPHYLL A DYNAMICS DURING SUMMER IN GUANTING RESERVOIR, BEIJING, CHINA

JIANG, W. W.¹ – YU, J. S.^{1*} – LI, Z. J.¹ – NAKAMURA, T.² – YU, F. Q.¹ – ZHANG, J. Y.³

¹*College of Water Sciences, Beijing Normal University/Key Laboratory of Urban Hydrological Cycle and Sponge City Technology/Digital Watershed Laboratory, Beijing 100875, China*

²*Department of Global Engineering for Development, Environment and Society, Tokyo Institute of Technology, Yokohama 226-8502, Japan*

³*Shijiazhuang Hydrology and Water Resources Survey Bureau of Hebei Province, Shijiazhuang 050051, China*

**Corresponding author*

e-mail: yujingshanbnu@163.com; phone: +86-188-1091-5172; fax: +86-010-6225-1121

(Received 11th Jan 2019; accepted 8th Mar 2019)

Abstract. Recognizing intra- and inter-daily dynamics of chlorophyll a (Chl-a) and its related environmental variables on consecutive days is essential to assessing and managing water quality and eutrophication. In this study, the Chl-a concentration, nutrients, water temperature and meteorological factors in Guanting Reservoir in Beijing were collected at six sampling times during summer. The Chl-a concentration generally decreased from May to September. At both test times, thermal stratification and mixing in the water column controlled temporal and vertical variations in the maximum Chl-a concentration layer. The position of the maximum Chl-a concentration layer between days generally followed that of the thermocline. Daily stratifications were temporary and downwelling variations in the maximum Chl-a concentration layer were wind driven; therefore, the vertical distribution of Chl-a was homogenized at night. Surface Chl-a concentrations increased at night and decreased during the day, except on rainy days. Principal component analysis and Pearson's correlations indicated that daily average and raw surface Chl-a concentrations generally changed as a negative function of air temperature, solar radiation, wind speed and water temperature. However, when a 5-hour time lag was considered, the relationship between surface Chl-a concentration, all meteorological factors and water temperature became significantly positive.

Keywords: *eutrophication, reservoir stratification, phytoplankton occurrence, meteorological factors, short-term distribution*

Introduction

Chlorophyll a (Chl-a) is an important indicator of phytoplankton biomass that is of significance to analysis of the magnitude and extent of trophic state in lakes and reservoirs (Felip and Catalan, 2000; Bresciani et al., 2013; Wu et al., 2014). To adequately recognize the response of Chl-a to ecological changes in phytoplankton and its life cycle, spatial and temporal phytoplankton distributions have been analyzed and documented by many researchers (Pérez-Ruzafa et al., 2005; Wu and Kong, 2009; Zhou et al., 2016; Li et al., 2017). It is generally known that the dynamics of phytoplankton growth and algal blooms are controlled by combined environmental factors such as hydrodynamic conditions (wind speed and direction, bottom topography, stratification pattern, water velocity and discharge) (Cao et al., 2006; Cardoso and Motta-Marques, 2009; Li et al., 2017), nutrients (total nitrogen, total phosphorus, and TN:TP ratio) (Wang et al., 2008; Wu et al., 2014), physical variables (air temperature, light, water

temperature and turbidity) (Serra et al., 2007), characteristics of phytoplankton (species, size and buoyancy) (Lopes et al., 2005) and hydraulic management (León et al., 2016). Of these factors, nutrient supply and light are generally considered the primary variables limiting phytoplankton growth (Phlips et al., 1995; Becker et al., 2010; Zhou et al., 2016). However, the most influential or primary environmental factor controlling phytoplankton growth differs according to spatial and temporal scale and trophic state of the studied systems. León et al. (2016) demonstrated that stratification pattern and residence time are of great importance to reservoir trophic state and vertical distribution of Chl-a between seasons. Moreover, water temperature has been shown to be a more important factor in mesotrophic lakes than oligotrophic and eutrophic lakes (Rigosi et al., 2016). In shallow lakes, the negative effects of increasing wind on phytoplankton growth can be crucial because it leads to increased resuspension (Cardoso and Motta-Marques, 2009).

Investigating the phytoplankton dynamics in the short term is of great importance to recognizing the mechanism of phytoplankton growth for long term variations (Bresciani et al., 2013). It is well known that phytoplankton is characterized by obvious circadian variations (Neveux et al., 2003), which depend directly on their response to diurnal available solar radiation during the day (Wu and Kong, 2009). Serra et al. (2007) demonstrated that most processes involved in phytoplankton growth occur for less than 1 week. When investigating phytoplankton at short time intervals, previous studies have mainly focused on phytoplankton species and community structure (Lopes et al., 2005), the effects of stratification and wind on vertical mixing and advection movement of phytoplankton (Antenucci and Imerito, 2000; Marcé et al., 2006; León et al., 2016) and the relationship between Chl-a and environmental variables (Felip and Catalan, 2000; Cyr, 2017), as well as the time lag of Chl-a (Pérez-Ruzafa et al., 2005; Bresciani et al., 2013). For instance, León et al. (2016) reported that stratification changes the vertical profile of residence time, which is negatively correlated with phytoplankton biomass. Wind driven phytoplankton vertical downwelling (Cardoso and Motta-Marques, 2009) and night-time convective cooling would homogenize the vertical distribution of phytoplankton (Serra et al., 2007). Moreover, the interannual data ln (Chl-a) illustrated a positive correlation with average air temperature (Zhou et al., 2016); however, when the short-term data set was evaluated, Chl-a concentration was negatively correlated with average air temperature (Bresciani et al., 2013). These discrepancies in the association of Chl-a concentration and other environmental variables may be caused by differences in the time scales of the investigated datasets.

Before 1997, Guanting Reservoir was a source of drinking, industrial, and agricultural water in Beijing, China (Dai et al., 2008). However, the reservoir is now in a eutrophic state (He et al., 2008), and the concentration of phosphorus in the reservoir is much higher than the normal criterion for drinking water (Cui et al., 2005). Additionally, the trophic state index is higher than 50, which is based on total nitrogen (TN) and total phosphorus (TP) (He et al., 2011). Previous studies conducted in Guanting Reservoir have investigated the trophic state of its water body based on monitoring of sediment P-decomposing bacteria (Cui et al., 2005), water quality (He et al., 2008), cyanobacteria and their toxins (Dai et al., 2008), and microcystis water blooms (Chen et al., 2011), as well as water quality modeling (He et al., 2011). However, knowledge regarding short-term variations in phytoplankton distribution in the reservoir is relatively scarce and the relationship between Chl-a and other environmental variables is unclear. Therefore, continuous and multiple measurements

taken in the short term are needed to acquire a better understanding of the variability in Chl-a concentrations. Fluorescence method may not measure all phytoplankton activity (Bresciani et al., 2013). Distinct phytoplankton groups can be measured by fluorometric probes and the phytoplankton groups are summarized in Beutler et al. (2002). However, it has been used as a reliable alternative to the in situ and in vivo study of phytoplankton distribution and activity (Serra et al., 2007; Wu and Kong, 2009). According to a previous study, algal blooms in Guanting Reservoir began in late May and disappeared in early October (He et al., 2011). In the present study, samples were collected over six periods ranging from 2 to 3 days from late May to early September to detect vertical and surface variations in Chl-a concentration.

The specific objectives of this study were (1) to investigate vertical and surface distributions and diurnal variations in Chl-a, (2) to relate this variability of Chl-a to stratification patterns, nutrients and wind during the study period and (3) to correlate Chl-a data with water temperature and meteorological data during the study period.

Materials and methods

Reservoir and site description

This study was conducted in Guanting Reservoir, which is located in northwest Beijing (Fig. 1). The watershed area and storage capacity of the reservoir are approximately $4.34 \times 10^4 \text{ km}^2$ and $2.19 \times 10^{10} \text{ m}^3$, respectively. In the past 30 years, Guanting Reservoir has played an important role in local development through electricity generation, fishing, tourism, and other uses. More importantly, it has been a source of drinking, industrial, and agricultural water in Beijing. However, the rapid development of upriver and surrounding areas has led to serious pollution. As a result, Guanting Reservoir has not been used as a drinking water source since 1997 (Dai et al., 2008). The government made great efforts to restore the reservoir in 2006 and its water quality recovered to Level III according to the Environmental Quality Standards for Surface Water (He et al., 2008). Thus, Guanting Reservoir has the potential to once again be a drinking water source for Beijing.

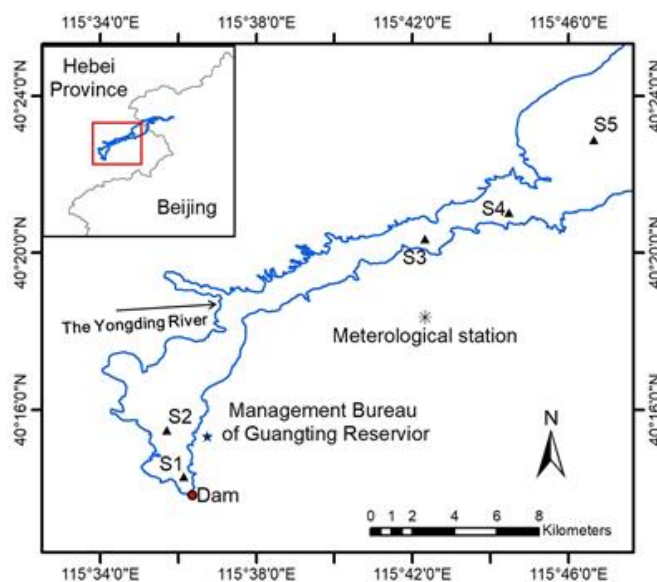


Figure 1. Map of sampling locations in Guanting Reservoir

Measurements of spatial and seasonal variations of Chl-a has been carried out in Guanting Reservoir in 2014 (Sun et al., 2015), which shows the algal blooms appeared in the area near the dam during summer in Guanting Reservoir (Figs. 1 and 2). Consequently, this present study extends the work of Sun et al. (2015) by investigating short-term variability of Chl-a concentrations in the area near the dam during summer. The average hydraulic residence time of Guanting reservoir is 467 days. A field sample site located in a relatively closed and calm area with maximum Chl-a concentration of 2014 that was suitable for in-situ testing was selected to investigate short-term vertical variations in Chl-a concentration (S1 in Fig. 2). The topography contour map of Guanting reservoir can be seen in He et al. (2011). The outlet discharge varies by time of week and draws off water at a depth of 8 m. The site was located near the dam in the deepest portion of the entire reservoir. The average water depth for each test time was about 11 m, which was ideal for investigation of the vertical dynamics of Chl-a concentration.

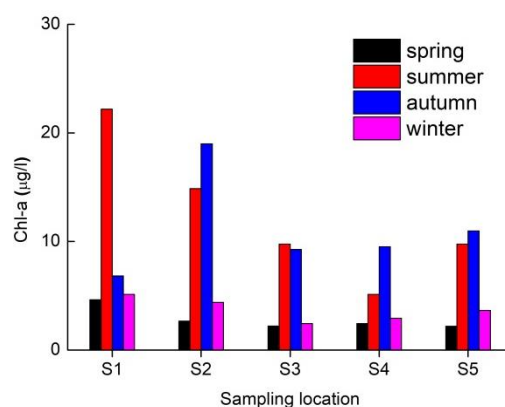


Figure 2. Spatial and seasonal variability of Chl-a in Guanting Reservoir. (Adapted from Sun et al., 2015)

Sampling and analysis

A total of six investigations including four rounds of vertical sampling and two rounds of surface sampling were conducted from 29 May to 9 Sep, 2015 (Figs. 3 and 4). On the vertical sampling days, the Chl-a concentration was obtained based on the fluorescent attributes of Chl-a concentration using an INFINITY water quality sensor (Onset, USA). The water temperature at each water depth was measured using a HOBO U20 recorder (Onset, USA), which had a measurement accuracy of ± 0.21 °C. A self-made lifting device was employed to move the aforementioned devices throughout each day (Fig. 5), six times during daytime (8:00 h, 10:00 h, 12:00 h, 14:00 h, 16:00 h and 18:00 h) and four times during night (21:00 h, 0:00 h, 3:00 h and 6:00 h). Chl-a concentration and water temperature data were vertically collected for each lifting time at 1-min intervals. Throughout all sampling times, a global positioning system (GPS, HOLUXGM-101, China) was used to precisely ensure the sampling location. It should be noted that few vertical samples were obtained from the water column during the last test period (Fig. 3d). This occurred because of a lack of power for the self-made lifting device from 6:00 h on 8/September, which caused it to stop lifting; therefore, only surface samples were collected from this point to the end of the study period. Water quality parameters including DO, pH and turbidity were determined in situ using a

Hydrolab Multi-parameter water quality sensor (Hach, USA). Based on He et al. (2011), the thermocline appeared at a depth of 4 m of Guanting reservoir during summer. Representative water samples (1500 ml) were collected from a depth of 2 m at noon during each test period and transported to the laboratory, where they were analyzed for total nitrogen (TN), ammonium (NH₄), total phosphorus (TP) and chemical oxygen demand (COD_{Mn}) according to the American Public Health Association (APHA, 1998). Furthermore, the daily discharge at the dam was obtained from Beijing Guanting Reservoir Management Bureau. A small meteorological sensor (JLC-QTF, China) was installed on shore (*Fig. 1*) and meteorological factors including air temperature, solar radiation, wind speed, wind direction and precipitation were recorded at 5-min intervals.

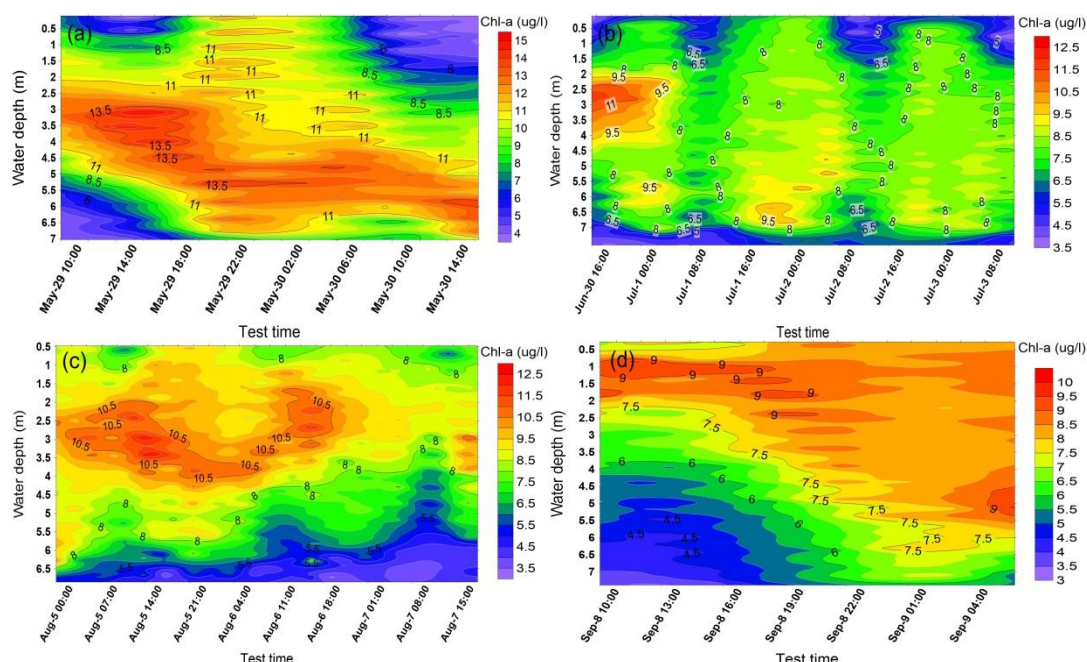


Figure 3. Interpolated contour maps of vertical Chl-a distributions for each test time

Data analysis

To detect short-term variations in Chl-a concentration and water temperature during each test time, isocline interpolation maps were prepared using the Surfer 8.0 package of Windows (Lopes et al., 2005). Additionally, SPSS 19.0 for Windows was used to conduct Pearson's correlations between Chl-a concentration and environmental variables (Wu et al., 2014), while principal component analysis (PCA) was performed using the CANOCO 4.5 software (Bresciani et al., 2013). It should be noted that PCA could not be applied to the water quality data because there were too few samples; therefore, the average daily Chl-a was set as an environment variable, and average daily values for each variable were used to test its relationship with water temperature, turbidity, discharge and meteorological data.

Results

Meteorological data during each test time is shown in *Figure 6*. The range of air temperature and wind speed (*Table 1*) of this study year is generally consistent with

meteorological factors reported in previous study (Xie and Xu, 2014). Generally, lower levels of solar radiation were recorded in May and July and the wind speed was mostly below 0.5 m/s at night (Fig. 6a and b). Because of the effects of cloudiness, solar radiation was largely half sinusoidal (Fig. 6c and f). However, the wind speed was clearly greater in May and July than August and September (Fig. 6d and e). Moreover, relatively high wind speeds (>5 m/s) were observed on 30/May and 1/July. Specifically, there was no obviously predominant wind direction in August and September, while the predominant wind direction and frequency were northwest and north (27% and 30%) on 30/May and 1/July, respectively (Table 1). The study period was rain free except for an event on 1/Jul from 18:00 h to 23:00 h and on 9/September from 8:00 to 22:00, during which time the daily precipitation was 16.5 mm and 5.4 mm, respectively.

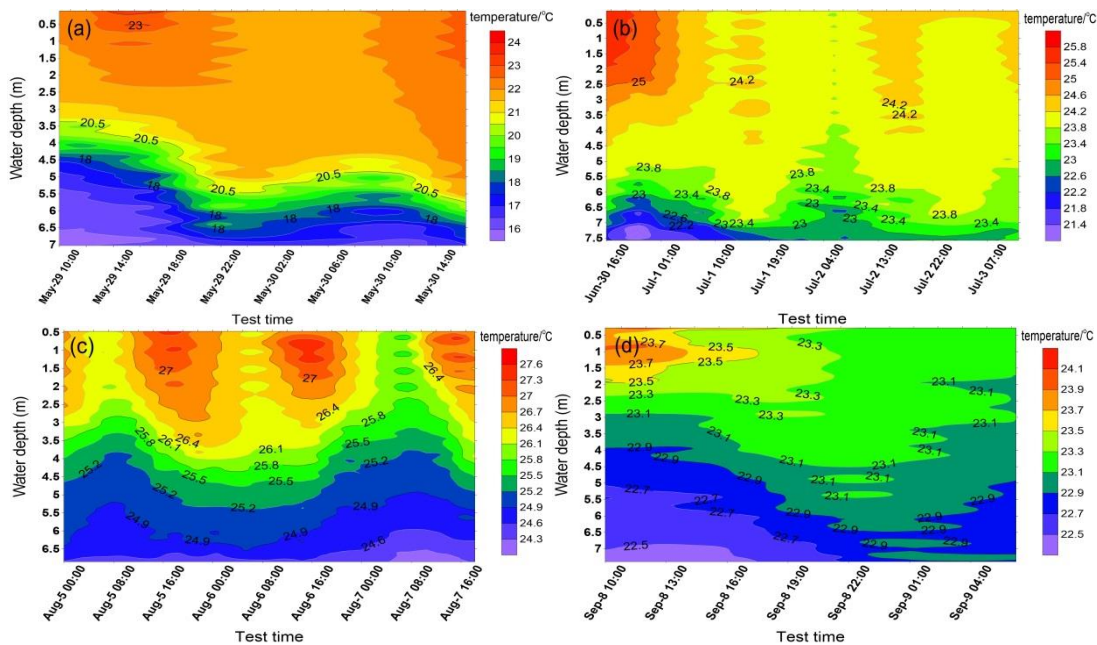


Figure 4. Interpolated contour maps of vertical water temperature for each test time

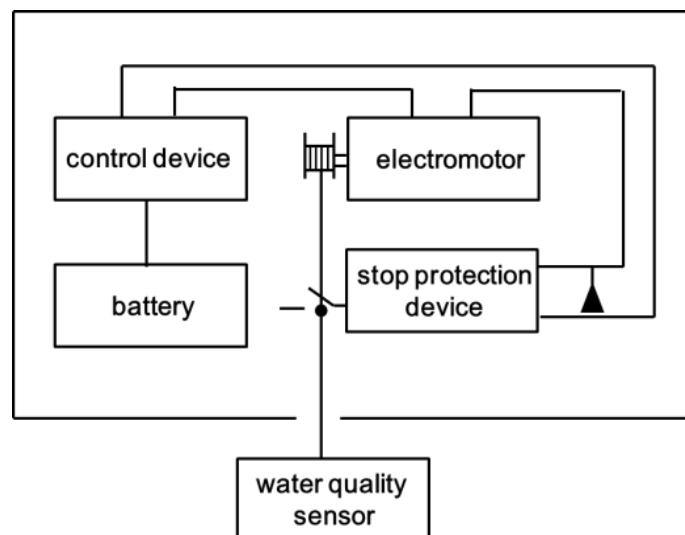


Figure 5. Schematic diagram of the self-designed lifting equipment

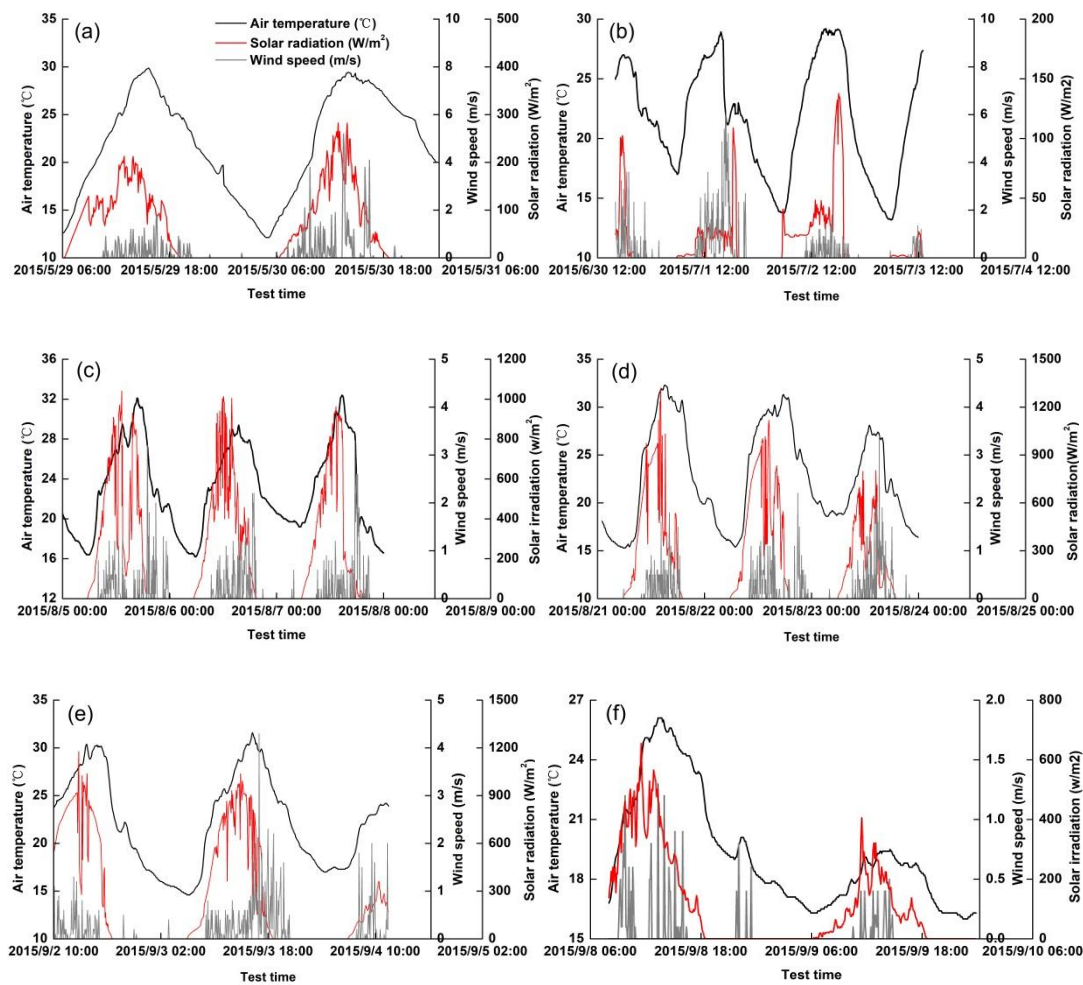


Figure 6. Meteorological data sequences for each test time including four times for vertical sampling (a, b, c and f) and two times (d and e) for surface water sampling

During investigation of vertical Chl-a, air temperature and average water temperature varied by only 0.6 °C in May, while they varied by up to 3.7 °C in August (Table 1). On the contrary, the difference in water temperature between the epilimnion and hypolimnion was much higher in May than August and September (Fig. 4a). These findings indicate that the reservoir was in the primary stages of thermal stratification in May and well stratified in August. However, because of the rain and higher discharge at the dam (Table 1), the stratifications broke down from 1/July (Fig. 4b). The reservoir outlet discharge at both test times (Table 1) is within the range of reservoir withdrawals (0.26-20.7 m³/s) during 2008. Besides, stratifications were temporary in the daytime, while the water column underwent mixing at night time (Fig. 4c and d). The depth of the mixing zone during night was smaller in August than in other surveys, indicating great water column stability in August. Taken together, these findings indicate that solar radiation increased water temperature, which drove thermal stratification and shoals the mixed layer.

Based on the criteria defined by Nürnberg (1996), Guanting Reservoir is a mesotrophic system. As shown in Figure 7, relatively low TP concentrations (<0.1

mg/l) were observed throughout the study period, and there were no significant differences in the TP and TN concentrations among water samples. All TN: TP ratios were greater than 16, which is regarded as the optimum ratio for phytoplankton growth (OECD, 2006).

Table 1. Mean and variation range of physical variables in Guanting Reservoir during each test time

Variables	29/May-30/May	30/Jun-3/Jul	5/Aug-8/Aug	21/Aug-23/Aug	2/Sep-4/Sep	8/Sep-9/Sep
Air temperature (°C)	21.1 (12.1-29.9)*	21.6 (13.2-29.1)	22.9 (16.2-32.4)	22.6 (15.3-32.3)	22.2 (14.6-31.6)	19.3 (16-26.1)
Solar radiation (W/m ²)	55.7 (0-282.7)	14.3 (0-137.8)	227 (0-1041.1)	225 (0-1320)	258 (0-1177)	112 (0-665)
Wind speed (m/s)	0.2 (0-5.2)	0.32 (0-6.1)	0.17 (0-3.5)	0.15 (0-3.4)	0.18 (0-4.3)	0.05 (0-1.3)
Chl-a concentration (µg/l)	9.8 (3.3-15.6)	6.7 (3.4-12.5)	7.6 (3.5-12.3)	6.8 (3.4-10.11)	5.1 (2.6-9.0)	7.0 (3.3-10.1)
Coefficient of variation of Chl-a	0.31	0.26	0.22	0.23	0.25	0.17
Water temperature (°C)	20.5 (15.9-23.9)	23.9 (18.0-25.9)	26.4 (23.8-28.0)	26.3 (25.6-27.1)	24.8 (23.9-27.1)	23.2 (22.1-24.3)
Turbidity (FTU)	3.7 (2.5-12.6)	3.6 (2.7-9.8)	4.6 (2.7-10.2)	4.3 (3.6-6.6)	3.9 (3.1-6.1)	4.7 (3.2-6.7)
Average discharge of the dam (m ³ /s)	0.971	6.721	0.885	1.285	2.13	1.51

*Brackets are corresponding to the range of measurements and displayed values are averages

In general, temporal variations in Chl-a concentrations varied slightly from May to September (*Table 1*); however, a general decrease in monthly Chl-a concentration was observed (*Fig. 8a*). Furthermore, the variations in Chl-a concentrations corresponded to differences in water temperature between the epilimnion and hypolimnion (*Fig. 8b*). Our results indicate that thermal stratification and mixing may limit phytoplankton growth vertically. Furthermore, a lower coefficient of variation (CV) of Chl-a vertical distribution was shown in August and September, when the reservoir was well stratified (*Table 1*).

In the four Chl-a vertical distribution investigations, the vertical profile of Chl-a concentration varied significantly between daytime and nighttime (*Fig. 3*). In May, the vertical profile of the Chl-a concentration primarily peaked around 3 m during daytime, with a maximum Chl-a concentration layer for thickness of 1.5 m (*Fig. 3a*). The maximum Chl-a concentration in the water column was about 1.5 times that in the surface water, whereas the depth of this layer changed with time and decreased to 7 m at night (*Fig. 3a*). At the same time, the surface Chl-a concentration increased at night. The surface Chl-a distribution recovered until sunset on the second day. However, this was not the case for the July survey. Specifically, the water column mixed from 1/Jul, at which time the Chl-a concentration was homogenous during the day and night (*Fig. 3b*). The reservoir was well stratified in August, when there was a shallow-surface mixing layer at the top of the water column (*Fig. 3c*) and there was a similar vertical profile of Chl-a concentration in the daytime as in May. However, the maximum Chl-a

concentration layer decreased slightly to 4 m at night (*Fig. 3c*). Therefore, the vertical profile of Chl-a was more stable through August. The Chl-a concentration showed a maximum concentration at around 1.5 m in the daytime on 8/September. Because of water mixing at night, the maximum Chl-a concentration layer decreased and its thickness increased to 5.5 m (*Fig. 3d*). The linear regression between the maximum Chl-a concentration and the thermocline for all test times is significant ($R^2 = 0.871$, $P < 0.001$). Specifically, although the position of the maximum Chl-a concentration layer varied temporally over the entire water column, it generally followed the same dynamics as the thermocline (*Figs. 3 and 4*).

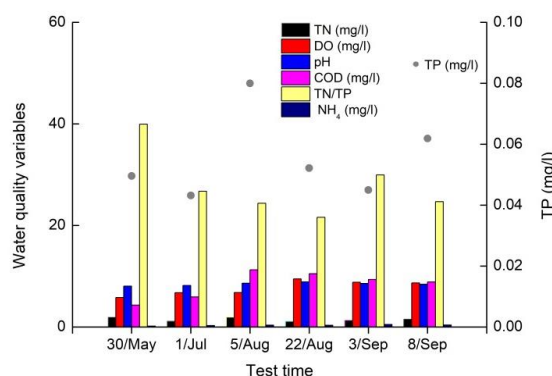


Figure 7. Water quality variables collected from a depth of 2 m at noon at S1 on each sampling day

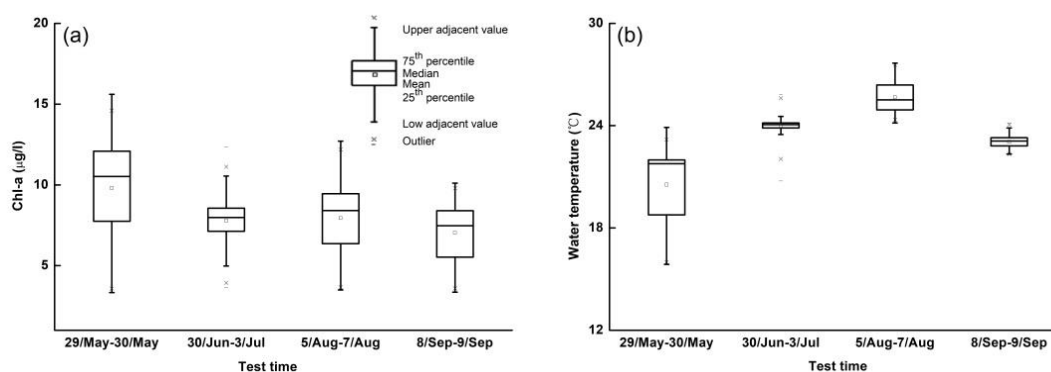


Figure 8. Box plots of vertical Chl-a concentration (a) and water temperature (b) at S1 for each test time

With the exception of July, the surface Chl-a concentration was inversely proportional to water temperature (*Fig. 9b*). Surface water temperature decreased during the rainfall events on 9/Sep and 1/July (*Fig. 9b and f*). With the exception of the rainy days, surface Chl-a showed a clearly diurnal variation in which concentration increased at night and decreased during the day (*Fig. 9a and c*). It is clear that the surface water temperature was correlated with Chl-a after an approximately 5-hour time lag, particularly in the August and September surveys (*Fig. 9d and e*). These findings suggest that phytoplankton took several hours to respond to the water temperature in the

surface water column. Pearson's correlation analysis was calculated directly from the raw surface Chl-a data and environmental variables (*Table 2*), which indicated that Chl-a was significantly negatively correlated with meteorological variables and water temperature for each test time and all data (all P values <0.01), except for wind speed and Chl-a on 8/Sep and 9/Sep (P > 0.05). However, when the 5-hour time lag was considered, the Chl-a values generally became significantly positively correlated with meteorological variables and water temperature (all P values <0.01), except for results of May and 8/Sep (*Table 2*).

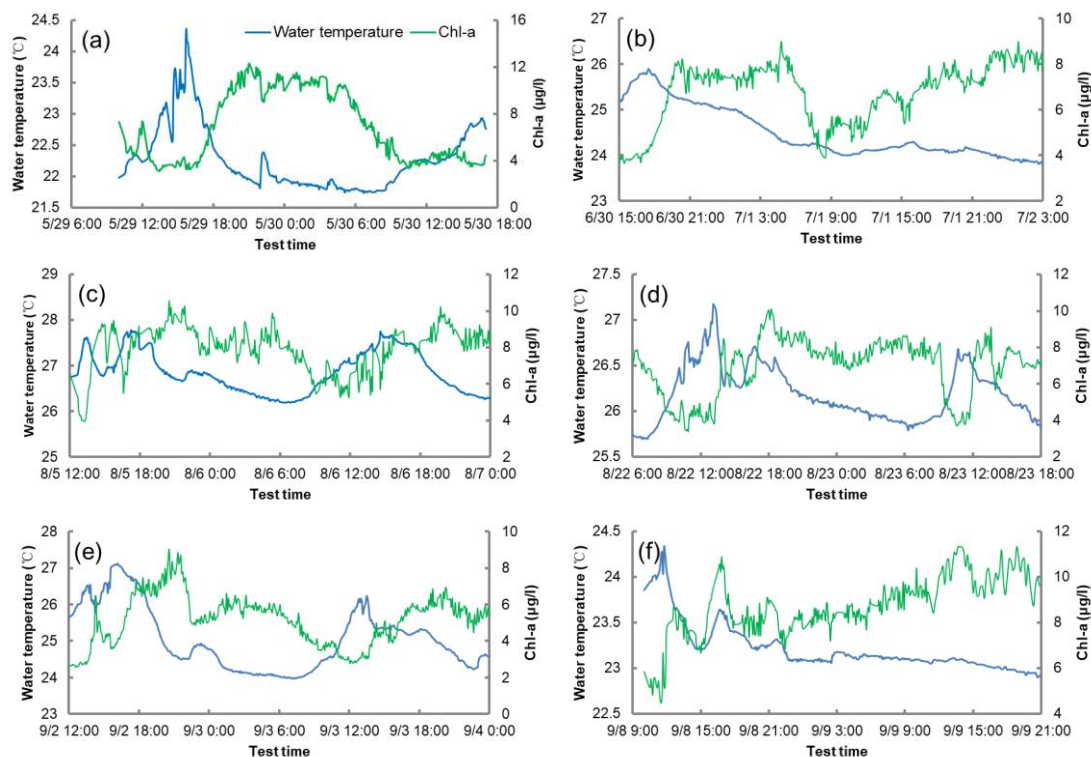


Figure 9. Variations in surface Chl-a concentration and surface water temperature during each test time

To identify the relationship between surface Chl-a and other environment variables, PCA was applied to daily Chl-a and water temperature, turbidity, discharge and meteorological data. *Figure 10* shows the biplot ordination of samples and environment variables. The biplot ordination explains 78.3% of this variation and exhibits well-defined spatial patterns. The first ordination (42.5%) was determined by most of the variables, particularly water temperature. Moreover, solar radiation and air temperature were on the positive side of the chart, while discharge and turbidity were on the negative side. The second ordination (35.8%) was positively related to wind speed, whereas it was inversely correlated with Chl-a. The relationship on the Y-axis likely illustrates the negative effects of wind speed, solar radiation and air temperature on daily average Chl-a concentration. Additionally, discharge and turbidity contributed slightly to Chl-a concentration. Hence, the results of PCA are generally in accordance with the correlation results of raw data describing surface Chl-a and meteorological variables.

Table 2. Pearson correlation coefficients between surface Chl-a concentration and environmental variables, both raw data and 5-hour lag time of Chl-a concentration were considered

Test time		Air temperature	Solar radiation	Wind speed	Water temperature
29/May-30/May (N = 303)	Raw data	-0.685**	-0.818**	-0.290**	-0.638**
	Time lag	0.400**	-0.226**	-0.037	0.406**
30/Jun-3/Jul (N = 828)	Raw data	-0.462**	-0.231**	-0.091**	-0.139**
	Time lag	0.453**	0.158**	0.177**	0.178**
5/Aug-8/Aug (N = 793)	Raw data	-0.308**	-0.188**	-0.596**	-0.101**
	Time lag	0.428**	0.202**	0.185**	0.369**
21/Aug-23/Aug (N = 590)	Raw data	-0.450**	-0.771**	-0.228**	-0.533**
	Time lag	0.490**	0.234**	0.127**	0.485**
2/Sep-4/Sep (N = 576)	Raw data	-0.375**	-0.755**	-0.135**	-0.265**
	Time lag	0.595**	0.376**	0.130**	0.699**
8/Sep-9/Sep (N = 315)	Raw data	-0.419**	-0.398**	-0.092	-0.640**
	Time lag	-0.398*	0.026	0.042	-0.373*
All data (N = 3405)	Raw data	-0.318**	-0.118**	-0.365**	-0.095**
	Time lag	0.298**	0.076**	0.055**	0.076**

**Significance at 99% confidence level

*Significance at 95% confidence level

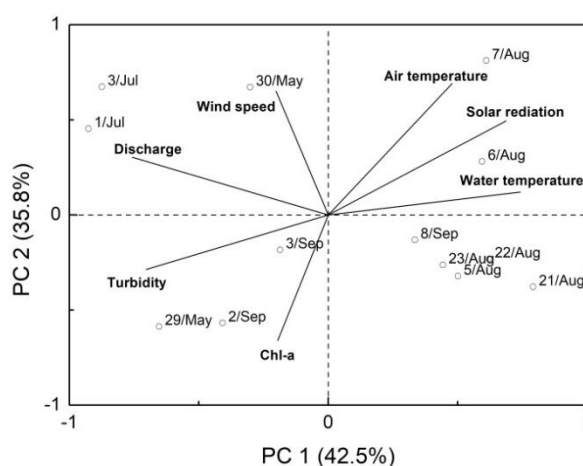


Figure 10. Principal component analysis ordination biplot. (Dots = samples, arrows = variables)

Discussion

The Chl-a concentrations observed from May to September showed a slight degree of variability from 2.6 to 15.6 $\mu\text{g/l}$ (Table 1), which was within the range of Chl-a values (about 2.5–20 $\mu\text{g/l}$) reported in an earlier study conducted in Guanting Reservoir from June to December (He et al., 2011). It is well known that the lower CV values of vertical distributions are calculated when relatively higher wind speeds occur (Wu and Kong, 2009). However, our results showed a lower CV of the Chl-a value appeared in August, when the reservoir was well stratified and there was great water column

stability. Several previous studies have reported that reservoir trophic state is controlled by metrological factors and stratification pattern (Wu et al., 2014; Bresciani et al., 2013; León et al., 2016). Generally, a decrease in monthly Chl-a concentration was shown for the four vertical Chl-a measurements in summer. Smaller variations in Chl-a concentration were in accordance with the smaller difference in water temperature between the epilimnion and hypolimnion. When lower water temperature difference existed in the water column, the phytoplankton tended to be homogenous, and therefore led to less variation of Chl-a concentration (Lopes et al., 2005; Serra et al., 2007).

It is well known that phytoplankton in lakes and reservoirs are recognized as limited by TP if the TN: TP ratio is relatively large, while they are limited by TN if the ratio is relatively small (Wang et al., 2008). These findings suggest that phytoplankton at both test times in Guanting Reservoir were probably limited by TP. Because of the limited water quality samples, the relationship between water quality parameters was not examined. The TP concentrations varied slightly at both test times (*Fig. 7*). It is likely the main reason to induce less difference of mean Chl-a concentration for each test time. In general, Chl-a concentration was significantly correlated with TP concentration (Zhou et al., 2016). Hence, the smaller Chl-a concentration observed in September was likely because of the lower TP (*Fig. 7*). According to Deng et al. (2012), a temperature range of 21–29 °C is suitable for phytoplankton growth. The TP concentration peak in August was likely the result of stronger activity of P-decomposing bacteria at higher temperature (Cui et al., 2005). However, the Chl-a in August was lower than that in May (*Fig. 8a*). Wu et al. (2014) reported that the effects of nutrients on Chl-a were not obvious. Therefore, seasonal variations in Chl-a during summer were not caused by the TP concentration and water temperature. In fact, highest light were observed in August (*Fig. 6c*), similar results were reported by Edwards et al. (2016), who confirmed that very strong light could restrain phytoplankton growth. Light might be a limiting factor when the euphotic zone is much smaller than the mixing zone (Kalff, 2002; Becker et al., 2010). The lowest solar radiation was recorded in July, indicating that it controlled phytoplankton growth (*Fig. 6b*). In addition, flow condition was inversely proportional to algal level in the short term (Kim et al., 2014), and the high discharge of the dam suggests that Chl-a may have been diluted during rainy days (*Table 1*).

Our investigations provide a broader understanding of short-term Chl-a vertical distribution within consecutive days. In both surveys, the lowest Chl-a appeared at the bottom of the water column, which is consistent with the findings of a previous study (Wu and Kong, 2009). Water temperature was the environmental variable that best explained vertical distributions of the phytoplankton community (Lopes et al., 2005). Variations in the position of the maximum Chl-a concentration layer between days generally followed the same dynamics as thermoclines, which is in accordance with the results reported by Serra et al. (2007). The Chl-a vertical distribution showed different behavior at each test time. Because of continuous mixing during the day and night in early July, Chl-a was likely directly influenced by rain and higher discharge. When the reservoir was primarily stratified in May (*Fig. 4a*), the developing thermocline was shallow and the epilimnion was easily mixed by winds and night-time convection, which tended to homogenize the vertical distribution of phytoplankton (Cyr, 2017). In contrast, stratification may decouple vertical circulation and mixing at night (Marcé et al., 2006). Guanting Reservoir was well stratified in August; therefore, the maximum Chl-a concentration layer was relatively stable at around 3 m during both the day and night. In September, the maximum concentration was located at the epilimnion during

the day, similar to the vertical distribution of phytoplankton suggested by Serra et al. (2007), who investigated phytoplankton that accumulated close to the surface during calm periods in September.

In the present study, stratifications were temporary and the maximum Chl-a concentration layer varied with downwelling at night. Wind speed (Cao et al., 2006), wind direction (Serra et al., 2007) and wind time (Cyr, 2017) play important roles in regulation of daily phytoplankton vertical downwelling (Cardoso and Motta-Marques, 2009) and horizontal movement (He et al., 2011). Minor stratifications can be easily broken down by wind (Li et al., 2007), and relatively strong winds of above 5 m/s directly induce vertical mixing and disturbance in the water column (Antenucci and Imerito, 2000). A few periods in which there were strong winds were recorded in our results. In particular, the test site is located near the south boundary of the entire reservoir, while on windy days (30/May and 1/July) the predominant wind direction was from the northwest and north, respectively. These results are similar to those reported by Cyr (2017), who suggested that when the wind was small but continuous, wind stress pushes the surface water downwind, creating downward flow at the downwind end of the basin.

Additionally, the surface Chl-a concentration exhibited diurnal periodic variation. It is well known that night-time vertical circulation and mixing as well as sinking of phytoplankton was induced by wind (Wu and Kong, 2009; Bresciani et al., 2013), consequently, this would homogenize the phytoplankton and enhance surface Chl-a concentrations at night. When considering seasonal and interannual data during long-term surveys, the relationship between Chl-a and light (Phlips et al., 1995), ln (Chl-a) and average air temperature (Zhou et al., 2016) was positively correlated. Moreover, interannual decreasing wind speed led to longer cyanobacterial bloom durations (Zhang et al., 2012). However, in the present short-term investigation, the results of PCA suggested that the daily average Chl-a was negatively correlated with daily average meteorological factors and water temperature. Our results agree with those of previous studies that showed Chl-a was negatively correlated with water temperature and light (Felip and Catalan, 2000) and wind speed (Serra et al., 2007). Our results demonstrate raw surface Chl-a values generally change as a negative function of meteorological factors and water temperature. However, when surface Chl-a was considered based on a 5-hour lag time, the relationship generally became significantly positive. Pérez-Ruzafa et al. (2005) found a 1-week time lag between Chl-a and nutrients and Bresciani et al. (2013) demonstrated that the time lags between Chl-a and solar radiation, water temperature and wind speed were 3 hours, 8–9 hours and 5 days, respectively. Therefore, time lag is a known phenomenon in short-term investigations, and the five-hour time lag in our study suggests a very rapid response of Chl-a to meteorological factors and water temperature in Guanting Reservoir.

Conclusions

This study describes the monthly and diurnal variation in vertical and surface distribution of Chl-a, as well as elucidates the quantitative relationships between Chl-a, water temperature, nutrients, meteorological factors and other physical variables in Guanting Reservoir during summer. In general, monthly Chl-a concentration exhibited a decreasing trend. Moreover, thermal stratification and mixing were found to be of great importance in controlling variation in the maximum Chl-a concentration layer in the

water column and variations in the position of the maximum Chl-a concentration layer between days generally followed the same dynamics as the thermocline. Furthermore, stratifications were temporary, with the maximum Chl-a concentration layer varying with downwelling and becoming homogenized at night because of wind driven mixing. The surface Chl-a concentration was also found to increase at night and decrease during the day, except on rainy days. The results of PCA and Pearson's correlation analysis indicated that the surface Chl-a concentration was significantly negatively correlated with air temperature, solar radiation, wind speed and water temperature. However, when a 5-hour time lag was considered, the relationships among surface Chl-a concentration, meteorological factors and water temperature became significantly positive.

Spatial and temporal variations in phytoplankton are always dynamic and highly variable, and more work is needed to assess the combined effects of environment variables on Chl-a concentration. Based on the species, size and buoyancy characteristics, further research will be devoted to hydrodynamics variables that drive phytoplankton communities spatially and temporally on a large scale.

Acknowledgements. This study was jointly supported by the National Key Research and Development Program of China (Grant Nos. 2016YFC0401308, 2018YFC0406502) and the National Natural Science Foundation of China (Grant Nos. 51779007, 41671018). We are grateful to the anonymous reviewers for their helpful suggestions, which have improved the quality of the manuscript.

REFERENCES

- [1] APHA (American Public Health Association) (1998): Standard Methods for the Examination of Water and Waste Water. 20th ed. – American Public Health Association, Washington, DC.
- [2] Antenucci, J., Imerito, A. (2000): The CWR Dynamic Reservoir Simulation Model DYRESM. Science Manual. – Centre for Water Research, The University of Western Australia, Perth.
- [3] Becker, V., Caputo, L., Ordóñez, J., Marcé, R., Armengol, J., Crossetti, L. O., Huszar, V. L. M. (2010): Driving factors of the phytoplankton functional groups in a deep Mediterranean reservoir. – *Water Research* 44: 3345-3354.
- [4] Beutler, M., Wiltshire, B., Meyer, C., Moldaenke, C., Luring, C., Meyerhofer, M., Hansen, U., Dau, H. (2002): A fluorometric method for the differentiation of algal populations in vivo and in situ. – *Photosynthesis Research* 72: 39-53.
- [5] Bresciani, M., Rossini, M., Morabito, G., Matta, E., Pinardi, M., Cogliati, S., Julitta, T., Colombo, R., Braga, F., Giardino, C. (2013): Analysis of within-and between-day chlorophyll-a dynamics in Mantua Superior Lake, with a continuous spectroradiometric measurement. – *Marine and Freshwater Research* 64: 303-316.
- [6] Cao, H. S., Kong, F. X., Luo, L. C., Shi, X. L., Zhou, Y., Zhang, X. F., Tao, Y. (2006): Effects of wind and wind-induced waves on vertical phytoplankton distribution and surface blooms of microcystis aeruginosa in Lake Taihu. – *Journal of Freshwater Ecology* 21: 231-238.
- [7] Cardoso, L. S., Motta-Marques, D. M. L. (2009): Hydrodynamics-driven plankton community in a shallow lake. – *Aquatic Ecology* 43: 73-84.
- [8] Chen, C., Zhang, Z., Ding, A., Wu, J., Xiao, J., Sun, Y. (2011): Bar-coded pyrosequencing reveals the bacterial community during microcystis, water bloom in Guanting Reservoir, Beijing. – *Procedia Engineering* 18: 341-346.

- [9] Cui, L. I., Yuan, H., Huang, H. (2005): Vertical distribution of phosphorus and P-dissolving/ decomposing bacteria in the sediment of Guanting reservoir. – *Science in China Series D (Earth Sciences)* 48: 285-294.
- [10] Cyr, H. (2017): Winds and the distribution of nearshore phytoplankton in a stratified lake. – *Water Research* 122: 114-127.
- [11] Dai, R., Liu, H., Qu, J., Ru, J., Hou, Y. (2008): Cyanobacteria and their toxins in Guanting Reservoir of Beijing, China. – *Journal of Hazardous Materials* 153: 470-477.
- [12] Deng, Y., Tang, X., Huang, B., Ding, L. (2012): Effect of temperature and irradiance on the growth and reproduction of the green macroalga, *Chaetomorpha valida* (Cladophoraceae, Chlorophyta). – *Journal of Applied Phycology* 24: 927-933.
- [13] Edwards, K. F., Thomas, M. K., Klausmeier, C. A., Litchman, E. (2016): Phytoplankton growth and the interaction of light and temperature: a synthesis at the species and community level. – *Limnology Oceanography* 61: 1232-1244.
- [14] Felip, M., Catalan, J. (2000): The relationship between phytoplankton biovolume and chlorophyll in a deep oligotrophic lake: decoupling in their spatial and temporal maxima. – *Journal of Plankton Research* 22: 1987-97.
- [15] He, G., Fang, H., Bai, S., Liu, X., Chen, M., Bai, J. (2011): Application of a three-dimensional eutrophication model for the Beijing Guanting Reservoir, China. – *Ecological Modelling* 222: 1491-1501.
- [16] He, W., Chen, S., Liu, X., Chen, J. (2008): Water quality monitoring in a slightly-polluted inland water body through remote sensing. Case study of Guanting Reservoir in Beijing, China. – *Frontiers of Environmental Science Engineering in China* 2: 163-171.
- [17] Kalff, J. (2002): *Limnology: Inland Water Ecosystems*. – Prentice Hall, New Jersey.
- [18] Kim, D. W., Min, J. H., Yoo, M., Kang, M., Kim, K. (2014): Long-term effects of hydrometeorological and water quality conditions on algal dynamics in the Paldang dam watershed, Korea. – *Water Science Technology Water Supply* 14: 601-608.
- [19] León, J. G., Beamud, S. G., Temporetti, P. F., Atencio, A. G., Diaz, M. M., Pedrozo, F. L. (2016): Stratification and residence time as factors controlling the seasonal variation and the vertical distribution of chlorophyll-a in a subtropical irrigation reservoir. – *International Review of Hydrobiology* 101: 36-47.
- [20] Li, T., Wang, D., Zhang, B., Liu, H., Tang, H. (2007): Morphological characterization of suspended particles under wind-induced disturbance in Taihu lake, China. – *Environmental Monitoring Assessment* 127: 79-86.
- [21] Li, Y., Zhang, Y., Shi, K., Zhou, Y., Zhang, Y., Liu, X. (2017): Spatiotemporal dynamics of chlorophyll-a, in a large reservoir as derived from Landsat 8 OLI data: understanding its driving and restrictive factors. – *Environmental Science Pollution Research* 25: 1359-1374.
- [22] Lopes, M., Bicudo, C. E., Ferragut, M. C. (2005): Short term spatial and temporal variation of phytoplankton in a shallow tropical oligotrophic reservoir, southeast Brazil. – *Hydrobiologia* 542: 235-247.
- [23] Marcé, R., Moreno-Ostos, E., Ordóñez, J., Feijóo, C., Navarro, E., Caputo, L., Armengol, J. (2006): Nutrient fluxes through boundaries in the hypolimnion of Sau reservoir: Expected patterns and unanticipated processes. – *Limnetica* 25: 527-540.
- [24] Neveux, J., Dupouy, C., Blanchot, J., Bouteiller, A. L., Landry, M. R., Brown, S. L. (2003): Diel dynamics of chlorophylls in high-nutrient, low-chlorophyll waters of the equatorial pacific (180°): interactions of growth, grazing, physiological responses, and mixing. – *Journal of Geophysical Research Oceans* 108: 1-17.
- [25] Nürnberg, G. K. (1996): Trophic state of clear and colored, soft and hardwater lakes with special consideration of nutrients, anoxia, phytoplankton and fish. – *Lake Reservoir Management* 12: 432-447.
- [26] OECD (2006): *Eutrophication of Waters. Monitoring, Assessment and Control*. Research of the Organization for Economic Cooperation and Development (OECD). – Prepared by

- Soil Water Conservation Society of Metro Halifax (SWCSMH).
<http://lakes.chebucto.org/TPMODELS/OECD/oecd.html>.
- [27] Pérez-Ruzafa, A., Fernández, A. I., Marcos, C., Gilabert, J., Quispe, J. I., García-Charton, J. A. (2005): Spatial and temporal variations of hydrological conditions, nutrients and chlorophyll a, in a Mediterranean coastal lagoon (Mar Menor, Spain). – *Hydrobiologia* 550: 11-27.
- [28] Philips, E. J., Aldridge, F. J., Schelske, C. L., Crisman, T. L. (1995): Relationships between light availability, Chlorophyll a, and tripton in a large, shallow subtropical lake. – *Limnology Oceanography* 40: 416-421.
- [29] Rigosi, A., Hanson, P., Hamilton, D. P., Hipsey, M., Rusak, J. A., Bois, J., Sparber, K., Chorus, I., Watkinson, A. J., Qin, B., Kim, B., Brookes, J. D. (2016): Determining the probability of cyanobacterial blooms: the application of Bayesian networks in multiple lake systems. – *Ecological Applications A Publication of the Ecological Society of America* 25: 186-199.
- [30] Serra, T., Vidal, J., Casamitjana, X., Soler, M., Colomer, J. (2007): The role of surface vertical mixing in phytoplankton distribution in a stratified reservoir. – *Limnology Oceanography* 52: 620-634.
- [31] Sun, Y. J., Chen, C., Ding, A. Z., Zhao, X. H., Zhang, H. C. (2015): The corresponding of microbial diversity on water quality and environmental variables of Guanting Reservoir. – *China Environmental Science* 35: 1547-1553 (in Chinese).
- [32] Wu, X., Kong, F. (2009): Effects of light and wind speed on the vertical distribution of *Microcystis aeruginosa* colonies of different sizes during a summer bloom. – *International Review of Hydrobiology* 94: 258-266.
- [33] Wu, Z., He, H., Cai, Y., Zhang, L., Chen, Y. (2014): Spatial distribution of chlorophyll-a and its relationship with the environment during summer in Lake Poyang: a Yangtze-connected lake. – *Hydrobiologia* 732: 61-70.
- [34] Wang, H. J., Liang, X. M., Jiang, P. H., Wang, J., Shi-Kai, W. U., Wang, H. Z. (2008): TN:TP ratio and planktivorous fish do not affect nutrient-chlorophyll relationships in shallow lakes. – *Freshwater Biology* 53: 935-944.
- [35] Xie, J., Xu, R. (2014): Variation characteristics analysis of the diurnal and monthly meteorological elements at different stations in Beijing. – *Meteorological and Environmental Sciences* 37: 20-28 (in Chinese).
- [36] Zhang, M., Duan, H., Shi, X., Yu, Y., Kong, F. (2012): Contributions of meteorology to the phenology of cyanobacterial blooms: implications for future climate change. – *Water Research* 46: 442-52.
- [37] Zhou, Q., Zhang, Y., Lin, D., Shan, K., Luo, Y., Zhao, L., Tan, Z. W., Song, L. R. (2016): The relationships of meteorological factors and nutrient levels with phytoplankton biomass in a shallow eutrophic lake dominated by cyanobacteria, Lake Dianchi from 1991 to 2013. – *Environmental Science Pollution Research International* 23: 15616-15626.

SPATIOTEMPORAL DYNAMICS OF AMMONIA NITROGEN AND ITS RESPONSE TO INFLOW RIVER BASED ON RANDOM FOREST MODEL IN NORTHWEST TAIHU LAKE, CHINA

XU, C.^{1,2} – YANG, G. S.^{1,2*} – WAN, R. R.^{1,2*} – LI, B.^{1,2} – MA, Q.³ – LU, X. M.³ – LV, W.⁴

¹*Key Laboratory of Watershed Geographic Sciences, Nanjing Institute of Geography and Limnology, Chinese Academy of Sciences, Nanjing 210008, P.R. China*

²*University of Chinese Academy of Sciences, Beijing 100049, P.R. China*

³*Jiangsu Province Hydrology and Water Resources Investigation Bureau Nanjing 210029, P.R. China*

⁴*Suzhou Substation of Jiangsu Province Hydrology and Water Resources Investigation Bureau Suzhou 215006, P.R. China*

**Corresponding authors*

e-mail: gsyang@niglas.ac.cn (Yang, G. S.), rrwan@126.com (Wan, R. R.)

(Received 11th Jan 2019; accepted 8th Mar 2019)

Abstract. Inflow rivers have crucial impact on lake eutrophication. Ammonia nitrogen (NH₄⁺-N) in inflow rivers have tightly coupled relationships with water quality in Lake Taihu, China. Based on the monthly concentrations from 2009 to 2015, this study focused on the spatiotemporal dynamics of NH₄⁺-N in northwest Taihu Lake and utilised random forest (RF) model to simulate its response to inflow rivers. Results indicated that (1) in northwest Lake Taihu, the spatiotemporal distribution patterns of NH₄⁺-N concentrations are distinct, and river inputs were the major source of NH₄⁺-N loadings. (2) Scenario simulation results in RF models indicated that the inflow loads should be controlled under 6427.38, 3248.01, 2206.92 and 1107.58 ta⁻¹ for the protective targets. (3) In 2015, NH₄⁺-N concentrations in four lake regions and NH₄⁺-N loads from inflow rivers were consistent with the simulation results in RF models. The NH₄⁺-N concentrations decreased approximately 6%, 34%, 44.44% and 6.67% in North Zone and Zhushan, Meiliang and Gonghu Bays, respectively, despite reduction in external NH₄⁺-N loads by 8.99%, 11.41%, 51.38% and 62.87%. This study provides further understand on quantifying the reduction of nutrient loading from inflow rivers and governing Lake Taihu or other typical eutrophic lakes.

Keywords: eutrophication, inflow river, load reduction, NH₄⁺-N, Taihu Lake, water quality

Introduction

With urbanisation development and population expansion, a large number of ecologically important freshwater bodies have experienced harmful water quality degradation and algal blooms, which have been a national concern in the recent decades (Schindler and Hecky, 2009; Qin et al., 2015; Wu et al., 2016). Previous research suggests that lake eutrophication is driven by physical, chemical and biological parameters and land use influences, including sediment dredging, aquatic organisms and hydrodynamic conditions (Wang et al., 2011; Bian et al., 2016). A great amount of nutrients and other contaminants enter lakes from river inputs, which are the main pollution route among all the influencing factors and considerably affecting the aquatic environment and ecosystem health of lakes (Rao and Schwab, 2007; Chen et al., 2011; Juma et al., 2014). Studies have found that the pollutant input from inflow rivers has a

meaningful effect on the nutrient concentration with certain relationships (Zhang et al., 2016).

As one of the five largest fresh lake and a long-term eutrophic water body in China, many efforts have been undertaken by researchers and government entities to restore the Lake Taihu since 1990, including sediment dredging, wetland construction, water transfer projects, the use of macrophytes and so on (Hu et al., 2010; Li et al., 2011a, 2013). Researchers have shown that increasing the amount of pollutant discharge into the lakes is crucial, and efforts to control the nutrient input from the catchment of Lake Taihu are essential (Chen et al., 2003; Qin et al., 2007; Wang et al., 2011). In addition to light, temperature and salinity, nitrogen (N) and phosphorus (P) are the most common factors of limiting algal growth and relevant control has been widely implemented to address eutrophication in many freshwater system (Nixon, 1995; Schindler and Vallentyne, 2008; Conley et al., 2009; Suttle and Harrison, 2010; Xu et al., 2010, 2015). With the tendency of being co-limited by N and P in Lake Taihu, evidence suggests that the lake has been in a nutrient-imbalance condition owing to focusing more on P reduction rather than together these two elements (Paerl, 2009; Lewis et al., 2011; Tang et al., 2016). In general, the pollution level of nitrogen and phosphorus is indicated by total nitrogen (TN) and total phosphorous (TP), and some studies have estimated the TN reduction in Lake Taihu and its inflow rivers (Du et al., 2017). Meanwhile, ammonia nitrogen ($\text{NH}_4^+\text{-N}$) is one of the three main forms of TN in natural water, and studies have indicated that $\text{NH}_4^+\text{-N}$ has tightly coupled relationships with TN and water quality in Lake Taihu Basin (Liang et al., 2008; Ferard and Blaise, 2013). Therefore, this study focuses on the spatiotemporal dynamics of $\text{NH}_4^+\text{-N}$ and its response to inflow river. In the interactional study of eutrophication, hydrodynamics and ecosystem in various freshwater bodies, lots of mathematical modelling approaches have been extensively applied to simulate the flow, water quality, spatiotemporal pattern of hydrodynamics and so on (Rasmussen et al., 2009; Min and Wise, 2010; Zhang et al., 2017). For instance, Mike21, a two-dimensional mathematic model, has been usually used to calculated aquatic environment capacity and total emission reduction according to aquatic environmental functions and targets (DHI, 2007; Zhu et al., 2013; Zhang, 2017). Several empirical models, such as the Wisconsin Department of Natural Resources' (WDNR) Wisconsin Lakes Modelling Suite, Seepage Lake Model and BATHTUB, have been previously developed and tested for predicting eutrophication-related water quality conditions in complex lakes and reservoirs (USEPA, 2000, 2010; WDNR, 2004; MPCA, 2006). However, these methods usually have certain data requirements or index restrictions (Wang et al., 2005). Random forest (RF) is a new machine learning algorithm and is combined with a predictor of multiple decision trees. It was proposed as a new soft computing method (Breiman et al., 1984). The RF has been developed to optimise predictive performance because of its several advantages, including a limited number of user defined parameters and the capability to model nonlinear relationships; reduce overfitting; remain robust despite of missing data and outliers; manage qualitative and quantitative variables; and evaluate, summarise and interpret final models (Breiman, 2001; Friedman, 2001; Friedman and Meulman, 2010). Over the past years, RF has been successfully applied to simulate soil organic carbon stocks, suspended sediment concentration, NO_2 concentration and nutrient concentrations (such as chemical oxygen demand); during these simulations, RFs have high tendency (Francke et al., 2008; Were et al., 2015; Rodriguez-Galiano et al., 2015; Ye et al., 2018; Muthukrishnan et al., 2018; Marttila et al., 2018; Kaminska, 2019).

The present work took the northwest Lake Taihu as an example for the analysis. Generally, this study aims to (1) analyse the temporal and spatial variations in $\text{NH}_4^+\text{-N}$ in the lake and its inflow rivers; (2) develop RF model to simulate the correspondence between the $\text{NH}_4^+\text{-N}$ concentrations in the lake and its inflow rivers; and (3) address the water quality in the northwest Lake Taihu response to the river inflow.

Materials and Methods

Study area

As the third largest freshwater lake in China, Lake Taihu is situated in Southeast Jiangsu Province and the lower reach of the Yangtze River Basin with a surface area of 2338 km² and drainage area of 36500 km² (Lake Taihu Basin Authority, 2012). Lake Taihu is the main drinking water source for its neighbouring residents despite being heavily polluted and inferior to Grade V in GB3838-2002 (Bai et al., 2009). With the deterioration of environment and water quality, it has caused serious pollution in the lake ecosystems and algal blooms have long been frequency and concerning phenomenon, especially northwest part of the lake, and rivers flowing into Lake Taihu are the crucial factor (Qin et al., 2008; Tao et al., 2018). Excessive nutrients from inflow rivers are the major source of pollutant loadings to the lake and subsequently lead to spatial heterogeneity (Li et al., 2013; Liu et al., 2017). Lake Taihu has a tanglesome river and channel network, and more than 200 rivers at different scales are connected to it (Zhang et al., 2014). As shown in *Fig. 1*, the inflow rivers are primarily located in the northwest regions, covering North Zone, Zhushan Bay, Meiliang Bay and Gonghu Bay, and the outflows in the eastern and southern part of the lake (Du et al., 2017; Li et al., 2019). Inflow rivers in northwest Lake Taihu contribute the most water discharge and nearly 80% of COD, N and P to the lake (Zhang and Chen, 2011). Eutrophication studies in Lake Taihu have often focused on P because it is the most universal limiting nutrient and is thus typically targeted for loading reduction (Morton et al., 2003; Niu et al., 2004; Schindler, 2006; Lewis and Wurtsbaugh, 2008). Nevertheless, it is fundamentally important and cannot be ignored to control N inputs. Therefore, the present work focuses on the $\text{NH}_4^+\text{-N}$ concentrations in northwest Lake Taihu and its inflow rivers based on the monthly monitoring data covering the period of 2009–2015.

Data analysis

Monthly $\text{NH}_4^+\text{-N}$ concentrations of inflow rivers and of northwest Lake Taihu during the period of 2009–2015 were provided by Jiangsu Province Hydrology and Water Resources Investigation Bureau. The locations of the monitoring sites distributed across northwest Lake Taihu and its inflow rivers are shown in *Fig. 1*. These monitoring stations were located by GPS, and water samples were collected monthly from 2009 to 2015, from approximately 1 m below the water. The samples were then delivered to a laboratory by cryopreservation, and their correlation processing, such as the sampling, preservation, transportation and analysis, were performed within 24 h. All the samples were measured three times, and results were expressed in average. All chemical analyses followed the standards established by the State Environmental Protection Bureau of China.

For the convenience of describing the influences of the inflow rivers, Lake Taihu was divided into seven sub-areas (*Fig. 1*), namely, North Zone, Zhushan Bay, Meiliang Bay,

Gonghu Bay, Southwest Zone, Central Zone, East Epigeal Zone and Dongtaihu Bay (Hu et al., 2008; Li et al., 2011b). This study focuses on the $\text{NH}_4^+\text{-N}$ concentration in northwest Lake Taihu and thus included only the sub-lakes of North Zone, Zhushan Bay, Meiliang Bay, Gonghu Bay and their inflow rivers. In view of data availability and the links between the sub-lakes and their inflow rivers, corresponding sites were selected, as shown in Fig. 2.

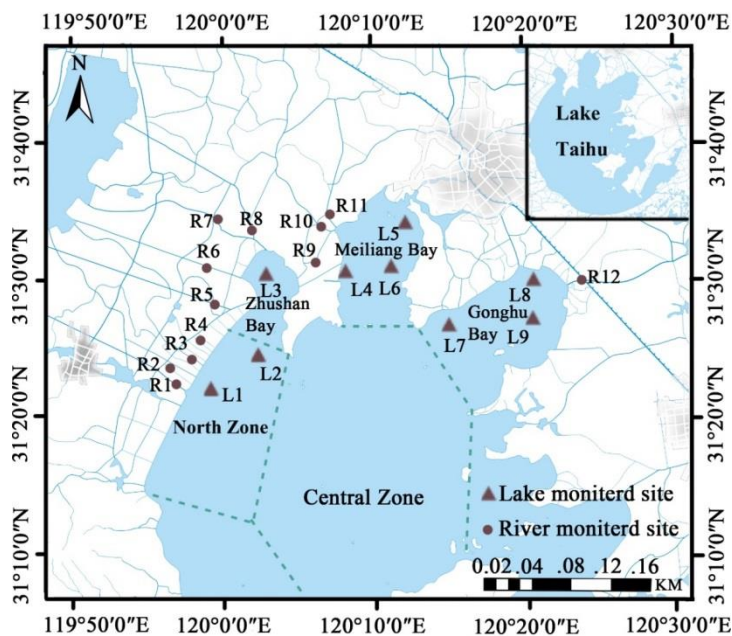


Figure 1. Study area and its monitoring sites

Model description

A RF model is made up of a number of simple (binary) decision trees, which were predetermined by a subset of predictors with the random selection strategy and grown on a bootstrap sample of the training set (Breiman, 2001). An RF makes no any additional assumptions about either the dependent or independent variables and could describe nonlinear and linear relationships (Cutler et al., 2007). The final model predictions are the average of the forest predictions and this method has been successfully used in analysis of many fields (Maraqqa et al., 2007; Paliwal and Patra, 2011). Despite the optimise predictive performance and wide potential, the complex relationship between pollutant concentrations and ambient conditions couldn't be provided and satisfactory described in this model (Khan et al., 2017; Kaminska, 2019).

Three important parameters, the number of trees to grow in the forests (ntree), the number of randomly selected predictor variables at each node (mtry) and the minimal number of observations at the terminal nodes of the trees (nodesize), must be specified in the RF model. Ntree is the most important one since its determination of the strength of each individual tree and correlation among trees (Peters et al., 2008). The random in an RF is performed by randomizing the observed subsets and mtry candidate variables both, which influence the tree and the split creation in the tree respectively. Multidimensional step function is produced by each individual tree, which results in that the average of the individual tree is a multidimensional step function, namely the whole

prediction of the forest. The multidimensional step function can predict smooth function as it has large number of sample values (Gromping and Ulrike, 2009).

In order to determine the fitting quality of each model, several possible error functions were computed and considered in the present work. As one of the basic measures to estimate a model's goodness of fit, the coefficient of determination R^2 is fundamental and the value ranges between $<0, 1>$. The closer it is to 1, the smaller are the differences between the empirical values and the estimated values.

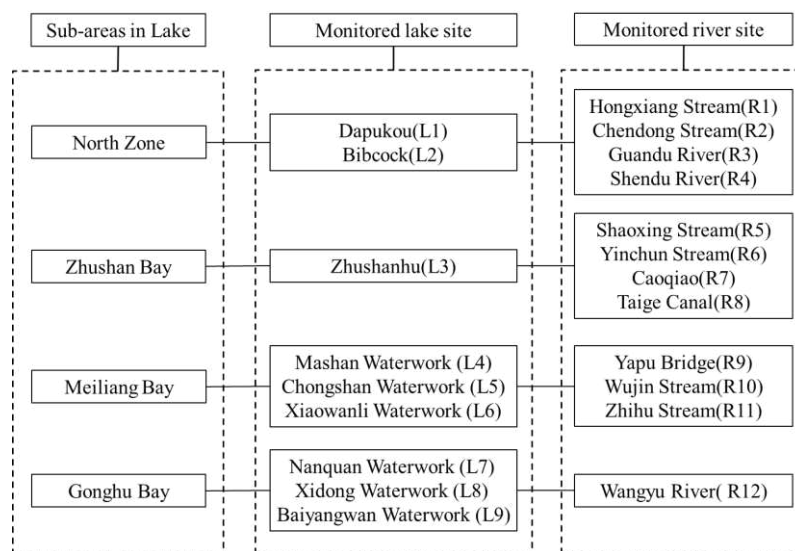


Figure 2. Sampling stations in Lake Taihu and its inflow rivers

Model scenarios

Developing effective and feasible nutrient reduction targets is necessary to improve trophic status and reduce bloom potentials. According to the Environmental Quality Standards for Surface Water in China (GB3838-2002) (Table 1), two nutrient reduction modeling scenarios were conducted to assess water quality response to nutrient load reductions in this study (Table 2).

Table 1. The standard of NH_4^+-N in the Environmental Quality Standards for Surface Water in China (GB3838-2002) (mg/L)

	Class I	Class II	Class III	Class IV	Class V
$NH_4^+-N (\leq)$	0.15	0.5	1.0	1.5	2.0

Table 2. Nutrient reduction scenarios and Water quality targets

	North Zone	Zhushan Bay	Meiliang Bay	Gonghu Bay
Scenario 1	Class III	Class III	Class II	Class II
Scenario 2	Class II	Class II	Class I	Class I

There is a possibility that water circumstances could be altered by climate change in the future which is not easy to control. Although the answers are clearer now that nutrients, light, temperature and hydrodynamic force have all have been shown to

influence formation of cyanobacterial blooms, the mechanism of a specific cyanobacterial bloom remains unknown (Qin et al., 2013). For example, temperature, precipitation and the distribution the runoff water have significant effect on the ammonium concentration and they are so complex and hard to predictable (Qin et al., 2010; Paerl et al., 2014). However, anthropogenic nutrient reduction to control water quality in lake is a direct and potentially achievable step that can be taken (Paerl et al., 2011; Xu et al., 2015). The two scenarios were made according to the water quality targets for the northwest Taihu Lake in the Master Plan of Integrated Regulation of Water Environment and the Water Function Zoning of the Lake Taihu Basin.

Results and Discussion

Spatiotemporal distribution of $\text{NH}_4^+\text{-N}$ in northwest Lake Taihu

The northwest Lake Taihu area is the most contaminated and has yet to be studied in detail. Thus, it was selected for the analysis of the spatial and temporal changes that occurred in 2009–2015. The spatiotemporal distribution of $\text{NH}_4^+\text{-N}$ in North Zone, Zhushan Bay, Meiliang Bay and Gonghu Bay are detailed as follows.

In the northwest Lake Taihu, the spatiotemporal distribution patterns of nutrient concentrations are distinct. In general, ammonia concentration tends to decrease gradually from 2009 to 2015 (*Fig. 3*).

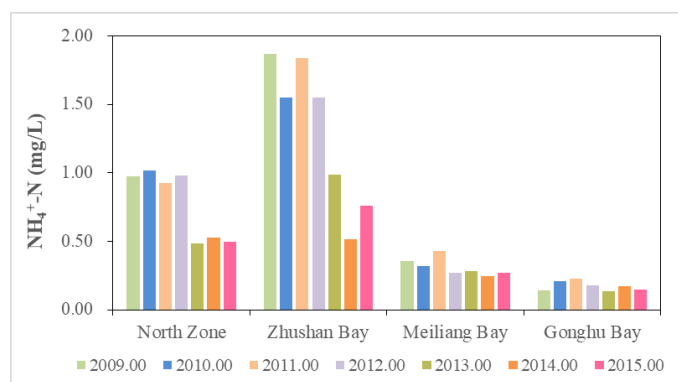


Figure 3. Yearly mean values of $\text{NH}_4^+\text{-N}$ concentration in northwest Lake Taihu

The North Zone and Zhushan Bay were the two heavily polluted areas, whereas Gonghu Bay was in the best and cleanest condition. The range of $\text{NH}_4^+\text{-N}$ concentration in the North Zone and Zhushan Bay was 0.5–2.5 mg/L, whereas those in Meiliang Bay and Gonghu Bay were approximately 0.5 mg/L (*Fig. 4*). The Environmental Quality Standards for Surface Water in China (GB3838-2002) has indicated that the $\text{NH}_4^+\text{-N}$ concentration in the North Zone and Zhushan Bay is classified as Class III–V, and that in the other two lake regions is classified as Class I or II; this classification indicates that the further consideration of the limiting nutrient in the North Zone and Zhushan Bay is important prior to other lake regions. The $\text{NH}_4^+\text{-N}$ content in the four seasons (that is, Winter: December, January and February; Spring: March, April and May; Summer: June, July and August; and Autumn: September, October and November) in northwest Lake Taihu were calculated (*Table 3*). The standard deviations of monthly mean values of $\text{NH}_4^+\text{-N}$ concentration in northwest Lake Taihu in *Fig. 4* are 0.52, 0.8,

0.1 and 0.09, separately. The results showed that season had a considerable effect on the $\text{NH}_4^+\text{-N}$ concentration of northwest Lake Taihu, which was remarkably higher in winter and spring than those in other seasons. In the studied area, the $\text{NH}_4^+\text{-N}$ concentration was the highest in winter. Therewith, the concentration started gradually decreasing in spring. Finally, it dropped to the minimum value in the summer or autumn. The seasonal tendency in the four regions was similar and especially evident in the North Zone and Zhushan Bay. The variations of concentrations in different seasons were in accordance with the change trend of air temperature. The solubility of ammonia nitrogen in water decreases with temperature increasing. What's more, these winter maxima possibly arise from (1) around lake, surface and subsurface catchment inputs are high in the non-growing season; (2) nutrients are concentrated in lower water levels; and (3) microbial activity is low due to low temperatures (Wang et al., 2017). It also may due to the relationships between ammonium loadings and rainfall, that's precipitation had a summer maximum and a fall minimum and followed an inverse seasonal cycle compared to $\text{NH}_4^+\text{-N}$ concentrations (Nöges et al., 2007).

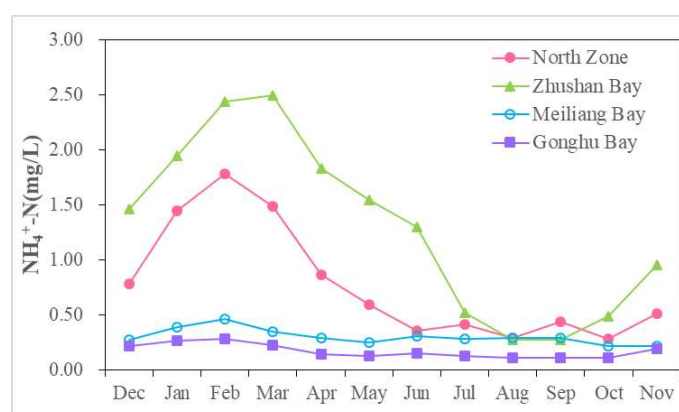


Figure 4. Monthly mean values of $\text{NH}_4^+\text{-N}$ concentration in northwest Lake Taihu

Table 3. Monthly mean values of $\text{NH}_4^+\text{-N}$ concentration in northwest Lake Taihu (mg/L)

	North Zone	Zhushan Bay	Meiliang Bay	Gonghu Bay
Winter	1.34	1.96	0.38	0.26
Spring	0.98	1.95	0.30	0.17
Summer	0.35	0.70	0.29	0.13
Autumn	0.41	0.57	0.24	0.14

$\text{NH}_4^+\text{-N}$ input from inflow rivers in northwest Lake Taihu

The annual $\text{NH}_4^+\text{-N}$ loads to the northwest Lake Taihu from its tributaries mean a large amount of nutrients and pollutant. Besides Gonghu Bay, $\text{NH}_4^+\text{-N}$ concentrations of inflow rivers in the regions were classified as Class IV–V or worse. By contrast, the water quality of inflow rivers in Gonghu Bay was relatively good. The $\text{NH}_4^+\text{-N}$ concentrations in the main inflow rivers in northwest Lake Taihu directly affected the northwest lake regions from 2009 to 2015, as shown in Fig. 5. The R^2 values of these scatter diagrams are all approximately 0.70 (that is, 0.763, 0.775, 0.641 and 0.758), and $p < 0.01$ (Fig. 5). In conclusion, river inputs are the major source of $\text{NH}_4^+\text{-N}$ loadings to the northwest Lake Taihu, and water quality in the lake is closely related to that in

inflow rivers. Declining water quality in inflow rivers have a considerable influence on lake restoration, and $\text{NH}_4^+\text{-N}$ concentrations evidently decrease with the reduction of inflow load.

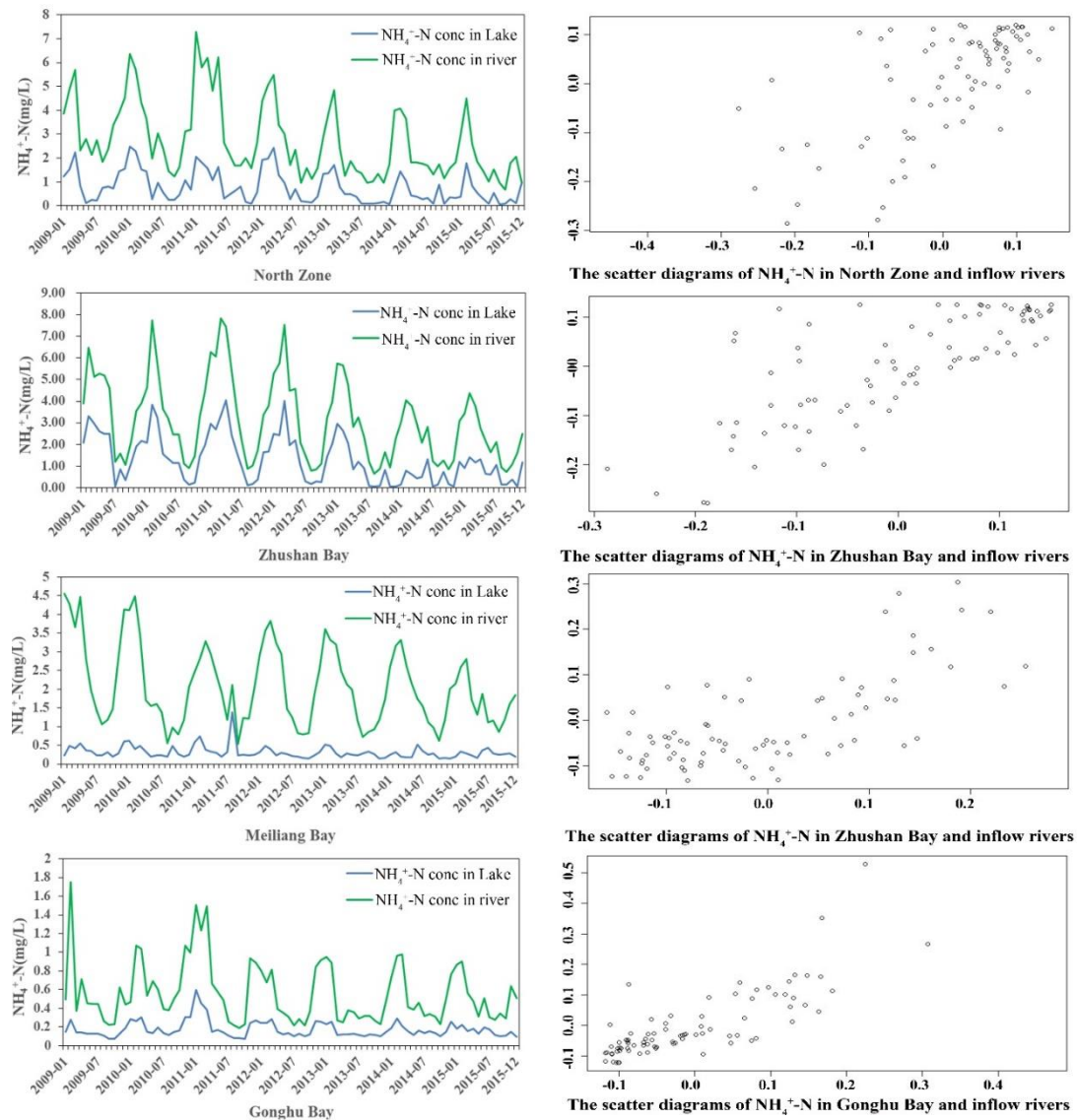


Figure 5. Monthly mean values of $\text{NH}_4^+\text{-N}$ concentration in northwest Lake Taihu and its inflow rivers from 2009 to 2015 and the scatter diagrams in corresponding regions

System response to nutrient reduction

Simulated results in RF model

By using the acquired monitoring data, the RF model set up the forecast model between the water quality of monitoring sites in the lake ($\text{NH}_4^+\text{-N}$ concentrations) and its inflow rivers ($\text{NH}_4^+\text{-N}$ loads). Given the relatively small dataset, every one of the seventh data were extracted as the testing stage, whereas the others are randomly assigned as the training stage after sorting the monthly monitoring data during 2009-2014, thereby ensuring that the RF model was fully calibrated. Then the data of

2015 in the inflow rivers were the independent validation set and used to test the model. The simulation results showed that the values of R^2 in the training stage of $\text{NH}_4^+\text{-N}$ were 0.87, 0.95, 0.73 and 0.97 in the RF model for the four pairs of lake and river stations. Meanwhile, the values of R^2 in the testing stage of $\text{NH}_4^+\text{-N}$ were 0.53, 0.52, 0.57 and 0.58 in the RF model. Moreover, the data of 2015 in the inflow rivers were used to the established model to stimulate the water quality in the lake. As shown in Fig. 6, the relationships between the measured $\text{NH}_4^+\text{-N}$ concentration and those predicted by the RF are proved to have good curve fitting characteristics. Consequently, the established RF model had a relatively high precision, and the forecast model could be used in the next step of stimulating the scene of water quality in the northwest Taihu Lake.

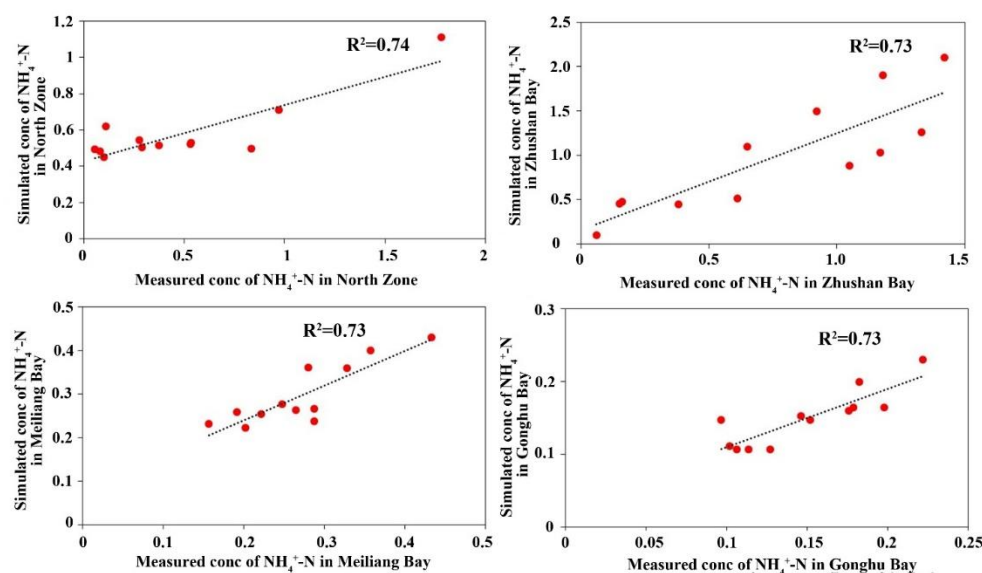


Figure 6. Measured and simulated $\text{NH}_4^+\text{-N}$ concentration in 2015 in the RF model (mg/L)

The Master Plan of Integrated Regulation of Water Environment of Taihu Basin, which was ratified by the State Council in 2008 and revised in 2013, had proposed the control targets of water quality indices in the lake (TN–Class V) for agricultural irrigation purpose. In addition, the Chinese State Council ratified the Master Plan of Integrated Regulation of Water Environment and the Water Function Zoning of the Lake Taihu Basin, thereby initiating the comprehensive treatment of the water environment in the basin. On the basis of the master plan, the $\text{NH}_4^+\text{-N}$ protective goals of the North Zone and Zhushan Bay belong to Class III, and those of Meiliang Bay and Gonghu Bay belong to Class II. As mentioned in Section 3.1, research has shown that $\text{NH}_4^+\text{-N}$ concentrations in the North Zone and Zhushan Bay were classified as Class III–V, whereas those in other two lake regions were classified as Class I or II. The setting of the $\text{NH}_4^+\text{-N}$ concentration in the lake as the target value should continuously debug the $\text{NH}_4^+\text{-N}$ concentration in the inflow rivers and allow the target value to be predicted in the debugged RF models (Table 4). Consequently, for the protective targets in the Master Plan of Integrated Regulation of Water Environment and the Water Function Zoning of the Lake Taihu Basin [Scenario 1: North Zone and Zhushan Bay (Class III), Meiliang Bay and Gonghu Bay (Class II)], the inflow loads should be

controlled under 6427.38, 3248.01, 2206.92 and 1107.58 $t a^{-1}$, respectively. The total NH_4^+-N loads in the northwest Lake Taihu should be maintained under **12989.89 $t a^{-1}$** . To achieve better water quality goal in Scenario 2 [North Zone and Zhushan Bay (Class II), and Meiliang and Gonghu Bays (Class I)], the inflow loads in the North Zone, Zhushan Bay, Meiliang Bay and Gonghu Bay should be maintained under 3304.64, 2466.53, 615.26 and 281.93 $t a^{-1}$, respectively. The total NH_4^+-N loads from the northwest Lake Taihu should be maintained under **6668.37 $t a^{-1}$** .

Table 4. Water quality goals in the lake and statistics of water quality values in different scenarios

Sub-lake	Water functional zone	Scenario 1		Scenario 2	
		Goal in lake (mg/L)	Inflow loads (ta^{-1})	Goal in lake (mg/L)	Inflow loads (ta^{-1})
North Zone	Conservation areas of Lake Taihu	1.0 (III)	6427.38	0.5 (II)	3304.64
Zhushan Bay	Conservation areas of Zhushan Lake	1.0 (III)	3248.01	0.5 (II)	2466.53
Meiliang Bay	Conservation areas of water scenery	0.5 (II)	2206.92	0.15 (I)	615.26
Gonghu Bay	Conservation areas of drinking water source	0.5 (II)	1107.58	0.15 (I)	281.93

Influences of loads on NH_4^+-N

The overall results indicated that the NH_4^+-N concentrations evidently decreased with the inflow loads in the lake regions. In 2015, the NH_4^+-N loads from inflow rivers were less than the standards in Scenario 1, and the NH_4^+-N concentrations in the four lake regions agreed with the simulation results in RF models in Table 5, that's the NH_4^+-N concentration in the North Zone and Zhushan Bay were classified as Class III and Meiliang Bay and Gonghu Bay were classified as Class II, which once again proved the practicability of the simulated results of the RF models. The NH_4^+-N concentrations in the four lake regions achieved the basic goals in the Master Plan of Integrated Regulation of Water Environment and the Water Function Zoning of the Lake Taihu Basin. Under 8.99% reduction of inflow loads in the North Zone, the water quality in this region could be suitable to Class II. Similarly, the NH_4^+-N loads from the inflow rivers of the North Zone, Zhushan Bay, Meiliang Bay and Gonghu Bay should be reduced by nearly 8.99%, 11.41%, 51.38% and 62.87%, respectively, for better water quality in the lake regions (the NH_4^+-N concentrations decreased by approximately 6%, 34%, 44.44% and 6.67%, respectively). The total NH_4^+-N loads from the inflow rivers of northwest Lake Taihu should be maintained under **6668.37 $t a^{-1}$** , which is 20.96% lower than that in 2015.

Table 5. Mass budgets for NH_4^+-N in inflow rivers in northwest Lake Taihu and load reductions in two scenarios in contrast to the situation in 2015

	NH_4^+-N loads from inflow rivers	NH_4^+-N concentrations in the lake regions	In comparison to Scenario 1	In comparison to Scenario 2
North Zone	3627.83	0.53 (III)	-77.17%	+8.91%
Zhushan Bay	2784.15	0.76 (III)	-16.66%	+11.41%
Meiliang Bay	1265.52	0.27(II)	-74.39%	+51.38%
Gonghu Bay	759.31	0.16(II)	-45.87%	+62.87%

Conclusions

In the present study, monthly $\text{NH}_4^+\text{-N}$ water quality data in inflow rivers and corresponding sub-lake were used to analyse the $\text{NH}_4^+\text{-N}$ distributions in northwest Lake Taihu. RF models were constructed to simulate the correspondence between the $\text{NH}_4^+\text{-N}$ concentrations in the lake and its inflow rivers in different scenarios.

In the northwest Lake Taihu, the spatiotemporal distribution patterns of nutrient concentrations are distinct, and river inputs were the major source of $\text{NH}_4^+\text{-N}$ loadings to the northwest Lake Taihu. The North Zone and Zhushan Bay were the most seriously polluted among the lake areas, whereas Gonghu Bay was the cleanest region. In winter and spring, $\text{NH}_4^+\text{-N}$ concentrations were significantly higher than in summer and autumn, and seasons had a significant effect on the $\text{NH}_4^+\text{-N}$ concentrations of northwest Lake Taihu. In the RF models, the R^2 and relationships between measured $\text{NH}_4^+\text{-N}$ concentrations and those predicted by the RF proved that the established RF models had a relatively high precision and that the forecast model could be used in the further stimulation of the scene of water quality in northwest Taihu Lake. In 2015, the $\text{NH}_4^+\text{-N}$ loads from inflow rivers were less than the standards in Scenario 1, and the $\text{NH}_4^+\text{-N}$ concentrations in the four lake regions agreed with the simulation results in RF models. For the protective targets [Scenario 1: North Zone and Zhushan Bay (Class III), Meiliang Bay and Gonghu Bay (Class II)], the inflow loads should be controlled under 6427.38, 3248.01, 2206.92 and 1107.58 t a^{-1} , respectively. To achieve better water quality goal for North Zone and Zhushan Bay (Class II), Meiliang Bay and Gonghu Bay (Class I), the inflow loads should be maintained under 3304.64, 2466.53, 615.26 and 281.93 t a^{-1} , respectively. The nutrient reduction scenarios showed that $\text{NH}_4^+\text{-N}$ concentrations decreased by approximately 6%, 34%, 44.44% and 6.67% in the North Zone, Zhushan Bay, Meiliang Bay and Gonghu Bay, despite the reduction of external $\text{NH}_4^+\text{-N}$ loads by 8.99%, 11.41%, 51.38% and 62.87%, respectively.

Eutrophication and algal blooms are worldwide environmental issues in lakes and the eutrophication process and forming mechanisms of algal blooms are particularly complicated in shallow lakes due to the strong lake–land, air–water and water–sediment interactions (Qin et al., 2007). This study provides further understand on the water quality distribution pattern in Lake Taihu, quantifying the reduction of nutrient loading from inflow rivers and governing Lake Taihu or other typical eutrophic lakes. However, only the northwest Lake Taihu Basin was studied instead of the entire lake, and only monthly $\text{NH}_4^+\text{-N}$ monitoring data during 2009–2015 were utilised as modelling variables instead of using other indices. Additional water quality indices and theoretical explorations are still needed in future works. Thus, stricter external nutrient managements and other ecological restoration tools must still be considered and investigated for the water environment recovery and protection in the Taihu basin. Under the control of exogenous nutrients, the variation characteristics and distribution of nutrient concentration in eutrophicated shallow lakes are closely related to the hydrodynamic process of shallow lakes and the action of underlying lake flow (Jing et al., 2000). At the same time, submerged plants can contain the dynamic suspension process of sediments, absorb nutrients in water and sediments, reduce the load of nutrients, and purify the water quality of lakes (Jöbgen et al., 2004; Wang et al., 2019). Therefore, it also shows that it is not enough to govern Taihu lake only by controlling external pollution, and the treatment of internal pollution of Taihu lake also needs to be strengthened.

Acknowledgements. This study was supported by the Strategic Priority Research Program of the Chinese Academy of Sciences (Grant No. XDA23020201), the Water Conservancy Science and Technology Project of Jiangsu Province (Grant No. 2018042 and No. 2014031). The authors would like to thank Jiangsu Province Hydrology and Water Resources Investigation Bureau for their assistance during the research.

REFERENCES

- [1] Bai, X., Ding, S., Fan, C., Liu, T., Shi, D., Zhang, L. (2009): Organic phosphorus species in surface sediments of a large, shallow, eutrophic lake, Lake Taihu, China. – *Environmental Pollution* 157: 2507-13.
- [2] Bian, B., Zhou, Y., Fang, B. B. (2016): Distribution of heavy metals and benthic macroinvertebrates: impacts from typical inflow river sediments in the Taihu basin, China. – *Ecological Indicators* 69: 348-359.
- [3] Breiman, L., Friedman, J., Stone, C. J., Olshen, R. A. (1984): *Classification and Regression Trees*, the Wadsworth and Brooks-cole Statistics-probability Series. – Taylor & Francis.
- [4] Breiman, L. (2001): Random forests. – *Machine Learning* 45: 5-32.
- [5] Chen, Y., Qin, B., Teubner, K., Dokulil, M. T. (2003): Long-term dynamics of phytoplankton assemblages: microcystis-domination in lake Taihu, a large shallow lake in China. – *Journal of Plankton Research* 25(4): 445-453.
- [6] Chen, S., Huang, W., Chen, W., Wang, H. (2011): Remote sensing analysis of rainstorm effects on sediment concentrations in Apalachicola Bay, USA. – *Ecological Informatics* 6(2): 147-155.
- [7] Conley, D. J., Paerl, H. W., Howarth, R. W., Boesch, D. F., Seitzinger, S. P., Havens, K. E., Lancelot, C., Likens, G. E. (2009): Controlling eutrophication: nitrogen and phosphorus. – *Science* 323(5917): 1014-1015.
- [8] Cutler, D. R., Edwards, T. C., Beard, K. H., Cutler, A., Hess, K. T., Gibson, J., Lawler, J. J. (2007): Random forests for classification in ecology. – *Ecology* 88: 2783-2792.
- [9] DHI (2007): *MIKE 21 Flow Model FM Hydrodynamic Module-User Guide*. – Danish Hydraulic Institute, Horsholm, Denmark.
- [10] Du, C., Li, Y., Wang, Q., Liu, G., Zheng, Z., Mu, M., Li, Y. (2017): Tempo-spatial dynamics of water quality and its response to river flow in estuary of Taihu Lake based on goci imagery. – *Environmental Science & Pollution Research* 24(36): 1-23.
- [11] Ferard, J. F., Blaise, C. (2013): *Encyclopedia of aquatic ecotoxicology*. – Springer Science, Dordrecht.
- [12] Francke, T., López-Tarazón, J., Schroder, B. (2008): Estimation of suspended sediment concentration and yield using linear models, random forests and quantile regression forests. – *Hydrological Processes* 22(25): 4892-4904.
- [13] Friedman, J. H. (2001): Greedy function approximation: A gradient boosting machine. – *Annals of Statistics* 29(5): 1189-1232.
- [14] Friedman, J. H., Meulman, J. J. (2010): Multiple additive regression trees with application in epidemiology. – *Statistics in Medicine* 22(9): 1365-1381.
- [15] Gromping, U. (2009): Variable Importance Assessment in Regression: Linear Regression versus Random Forest. – *The American Statistician* 63(4): 308-319.
- [16] Hu, W., Zhai, S., Zhu, Z., Han, H. (2008): Impacts of the Yangtze River water transfer on restoration of Lake Taihu. – *Ecological Engineering* 34: 30-49.
- [17] Hu, C., Lee, Z., Ma, R., Yu, K., Li, D., Shang, S. (2010): Moderate resolution imaging spectroradiometer (MODIS) observations of cyanobacteria blooms in Taihu Lake, China. – *Journal of Geophysical Research - Oceans* 2010: 261-263.
- [18] Jöbgen, A., Palm, A., Melkonian, M. (2004): Phosphorus removal from eutrophic lakes using periphyton on submerged artificial substrata. – *J Lake Sci* 528(1-3): 123-142.

- [19] Juma, D. W., Wang, H., Li, F. (2014): Impacts of population growth and economic development on water quality of a lake: case study of Lake Victoria Kenya water. – *Environ Sci Pollut R* 21: 5737-5746.
- [20] Kaminska, J. A. (2019): A random forest partition model for predicting NO₂ concentrations from traffic flow and meteorological conditions. – *Science of the Total Environment* 651: 475-483.
- [21] Khan, S., Ullah, R., Khan, A., Sohail, A., Wahab, N., Bilal, M., Ahmed, M. (2017): Random Forest-Based Evaluation of Raman Spectroscopy for Dengue Fever Analysis. – *Applied Spectroscopy* 71(9): 2111.
- [22] Lake Taihu Basin Authority (2012): Lake Taihu Basin and Southeast Rivers Water Resource Bulletin. – Lake Taihu Basin Authority, Shanghai.
- [23] Lewis, W. M., Wurtsbaugh, W. A. (2008): Control of lacustrine phytoplankton by nutrients: Erosion of the phosphorus paradigm. – *International Review of Hydrobiology* 93(4-5): 446-65.
- [24] Lewis, W. M., Wurtsbaugh, W. A., Paerl, H. W. (2011): Rationale for control of anthropogenic nitrogen and phosphorus to reduce eutrophication of inland waters. – *Environmental Science & Technology* 45(24): 10300-10305.
- [25] Li, Y., Acharya, K., Stone, M. C., Yu, Z., Young, M. H., Shafer, D. S., Zhu, J., Gray, K., Stone, A., Fan, L., Tang, C. (2011a): Spatiotemporal patterns in nutrient loads, nutrient concentrations, and algal biomass in lake Taihu, china. – *Lake & Reservoir Management* 27(4): 298-309.
- [26] Li, Y., Acharya, K., Yu, Z. (2011b): Modeling impacts of yangtze river water transfer on water ages in Lake Taihu, China. – *Ecological Engineering* 37(2): 325-334.
- [27] Li, Y., Tang, C., Wang, C., Anim, D. O., Yu, Z., Acharya, K. (2013): Improved yangtze river diversions: are they helping to solve algal bloom problems in Lake Taihu, China? – *Ecological Engineering* 51(1): 104-116.
- [28] Li, W., Yang, M., Liang, Z., Zhu, Y., Mao, W., Shi, J., Chen, Y. (2013): Assessment for surface water quality in Lake Taihu Tiaoxi River Basin China based on support vector machine. – *Stochastic Environmental Research & Risk Assessment* 27: 1861-70.
- [29] Li, A., aus der Beek, T., Schubert, M., Yu, Z., Schiedek, T., Schüth, C. (2019): Sedimentary archive of Polycyclic Aromatic Hydrocarbons and perylene sources in the northern part of Taihu Lake, China. – *Environmental Pollution* 246: 198-206.
- [30] Liang, T., Wang, S., Cao, H., Zhang, C., Li, H., Li, H., Song, W., Chong, Z. (2008): Estimation of ammonia nitrogen load from nonpoint sources in the xitiao river catchment, China. – *Journal of Environmental Sciences* 20(10): 1195-1201.
- [31] Liu, Y., Engel, B. A., Collingsworth, P. D., Pijanowski, B. C. (2017): Optimal implementation of green infrastructure practices to minimize influences of land use change and climate change on hydrology and water quality: Case study in Spy Run Creek watershed, Indiana. – *Science of the Total Environment* 601: 1400-11.
- [32] Lou, J., Schwab, D. J., Beletsky, D., Hawley, N. (2000): A model of sediment resuspension and transport dynamics in southern Lake Michigan. – *Journal of Geophysical Research* 105(C3): 6591-6610.
- [33] Maraqa, M. A., Ali, A., Khan, N. (2007): Modeling selected water quality parameters at Jebel Ali Harbour, Dubai- UAE. – *Journal of Coastal Research* 50: 794-799.
- [34] Marttila, H., Karjalainen, S. M., Kuoppala, M., Nieminen, M. L., Ronkanen, A. K. (2018): Elevated nutrient concentrations in headwaters affected by drained peatland. – *Science of the Total Environment* 643: 1304-1313.
- [35] Min, J. H., Wise, W. R. (2010): Depth-averaged, spatially distributed flow dynamic and solute transport modelling of a large-scaled, subtropical constructed wetland. – *Hydrological Processes* 24(19): 2724-2737.
- [36] Minnesota Pollution Control Agency (MPCA) (2006): Lake Pepin Watershed TMDL eutrophication and turbidity impairments project overview. – Minnesota.

- [37] Morton, S. C., Glindemann, D., Edwards, M. A. (2003): Phosphates, Phosphites, and Phosphides in Environmental Samples. – *Environmental Science & Technology* 37: 1169-74.
- [38] Muthukrishnan, R., Sleith, R. S., Karol, K. G., Larkin, D. J. (2018): Prediction of starry stonewort (*Nitellopsis obtusa*) invasion risk in upper Midwest (USA) lakes using ecological niche models. – *Acquatic Botany* 151: 43-50.
- [39] Niu, X., Geng, J., Wang, X., Wang, C., Gu, X., Edwards, M., Glindemann, D. (2004): Temporal and spatial distributions of phosphine in Taihu Lake, China. – *Acta Scientiae Circumstantiae* 323: 169-78.
- [40] Nixon, S. W. (1995): Coastal marine eutrophication: a definition, social causes, and future concerns. – *Ophelia* 41(1): 199-219.
- [41] Nõges, P., Kägu, M., Nõges, T. (2007): Role of climate and agricultural practice in determining matter discharge into large, shallow Lake Võrtsjärv, Estonia. – *Hydrobiologia* 581(1): 125-134.
- [42] Paerl, H. W. (2009): Controlling eutrophication along the freshwater-marine continuum: dual nutrient (N and P) reductions are essential. – *Estuaries & Coasts* 32(4): 593-601.
- [43] Paerl, H. W., Xu, H., McCarthy, M. J., Zhu, G., Qin, B., Li, Y., Gardner, W. S. (2011): Controlling harmful cyanobacterial blooms in a hyper-eutrophic lake (Lake Taihu, China): the need for a dual nutrient (N & P) management strategy. – *Water Res* 45(5): 1973-1983.
- [44] Paerl, H. W., Xu, H., Hall, N. S., Zhu, G., Qin, B., Wu, Y., Rossignol, K. L., Dong, L., McCarthy, M. J., Joyner, A. R. (2014): Controlling cyanobacterial blooms in hypertrophic Lake Taihu, China: will nitrogen reductions cause replacement of non-N₂ fixing by N₂ fixing taxa? – *PLoS One* 9(11):113-123.
- [45] Paliwal, R., Patra, R. R. (2011): Applicability of MIKE 21 to assess temporal and spatial variation in water quality of an estuary under the impact of effluent from an industrial estate. – *Water Science & Technology* 63(9): 1932-1943.
- [46] Peters, J., Verhoest, N. E. C., Samson, R., Boeckx, P., Baets, B. D. (2008): Wetland vegetation distribution modelling for the identification of constraining environmental variables. – *Landscape Ecology* 23(9): 1049-1065.
- [47] Qin, B., Xu, P., Wu, Q., Luo, L., Zhang, Y. (2007): Environmental issues of Lake Taihu, China. – *Hydrobiologia* 581(1): 3-14.
- [48] Qin, B. (2008): Lake Taihu, China: dynamics and environmental change. – *Spring Science & Business Media*.
- [49] Qin, B., Zhu, G., Gao, G., Zhang, Y., Li, W., Paerl, H. W., Carmichael, W. W. (2010): Drinking water crisis in Lake Taihu, China linkage to climatic variability and lake management. – *Environ Manage* 4: 105-112.
- [50] Qin, B., Gao, G., Zhu, G. W. (2013): Lake eutrophication and its ecosystem response. – *Chinese Science Bulletin* 58(9): 961-970.
- [51] Qin, B., Li, W., Zhu, G., Zhang, Y., Wu, T., Gao, G. (2015): Cyanobacterial bloom management through integrated monitoring and forecasting in large shallow eutrophic lake Taihu (China). – *Journal of Hazardous Materials* 287(2): 356-363.
- [52] Rao, Y. R., Schwab, D. J. (2007): Transport and mixing between the coastal and offshore waters in the great lakes: a review. – *J Great Lakes Res* 33: 202-218.
- [53] Rasmussen, E. K., Petersen, O. S., Thompson, J. R., Flower, R. J., Ahmed, M. H. (2009): Hydrodynamic-ecological model analyses of the water quality of Lake Manzala. – *Hydrobiologia* 622(1): 195-220.
- [54] Rodriguez-Galiano, V., Sanchez-Castillo, M., Chica-Olmo, M., Chica-Rivas, M. (2015): Machine learning predictive models for mineral prospectivity: An evaluation of neural networks, random forest, regression trees and support vector machines. – *Ore Geology Reviews* 71: 804-818.
- [55] Schindler, D. W. (2006): Recent advances in the understanding and management of eutrophication. – *Limnology & Oceanography* 51: 356-63.

- [56] Schindler, D. W., Vallentyne, J. R. (2008): The Algal Bowl: Overfertilization of the World's Freshwaters and Estuaries. – University of Alberta Press, Edmonton.
- [57] Schindler, D. W., Hecky, R. E. (2009): Eutrophication: more nitrogen data needed. – *Science* 324: 721-722.
- [58] Suttle, C. A., Harrison, P. J. (2010): Rapid ammonium uptake by freshwater phytoplankton. – *Journal of Phycology* 24(1): 13-16.
- [59] Tang, C., Li, Y., Acharya, K. (2016): Modeling the effects of external nutrient reductions on algal blooms in hyper-eutrophic Lake Taihu, China. – *Ecological Engineering* 94: 164-173.
- [60] Tao, Y., Yao, S., Xue, B., Deng, J., Wang, X., Feng, M., Hu, W. (2010): Polycyclic aromatic hydrocarbons in surface sediments from drinking water sources of Taihu Lake, China: sources, partitioning and toxicological risk. – *J Environ Monit* 12: 2282-2289.
- [61] United States Environmental Protection Agency (USEPA) (2000): Nutrient criteria technical guidance manual: lakes and reservoirs, Report no. EPA-822-B00-001. – Washington DC.
- [62] United States Environmental Protection Agency (USEPA) (2013): Surface water quality standards. – Washington DC.
- [63] Wang, S. H., Huggins, D. G., Frees, L., Volkman, C. G., Lim, N. C., Baker, D. S. (2005): An Integrated Modeling Approach to Total Watershed Management: Water Quality and Watershed Assessment of Cheney Reservoir, Kansas, USA. – *Water Air and Soil Pollution* 164(1-4): 1-19.
- [64] Wang, M., Shi, W., Tang, J. (2011): Water property monitoring and assessment for china's inland lake taihu from modis-aqua measurements. – *Remote Sensing of Environment* 115(3): 841-854.
- [65] Wang, J., Fu, Z., Qiao, H. (2019): Assessment of eutrophication and water quality in the estuarine area of Lake Wuli, Lake Taihu, China. – *Science of The Total Environment* 650: 1392-1402.
- [66] Were, K., Bui, D. T., Dick, O. B., Singh, B. R. (2015): A comparative assessment of support vector regression, artificial neural networks, and random forests for predicting and mapping soil organic carbon stocks across an Afri-montane landscape. – *Ecological Indicators* 52: 394-403.
- [67] Wisconsin Department of Nature Resources (WDNR) (2004): Phosphorus Total Maximum Daily Load (TMDL) for Half Moon Lake. – Eau Claire, Wisconsin.
- [68] Wu, P., Qin, B., Yu, G., Deng, J., Zhou, J. (2016): Effects of nutrient on algae biomass during summer and winter in inflow rivers of Taihu Basin, China. – *Water Environment Research* 88: 665-672.
- [69] Xu, H., Paerl, H. W., Qin, B., Zhu, G., Gao, G. (2010): Nitrogen and phosphorus inputs control phytoplankton growth in eutrophic Lake Taihu, China. – *Limnology & Oceanography* 55(1): 420-432.
- [70] Xu, H., Paerl, H. W., Qin, B., Zhu, G., Hall, N. S., Wu, Y. (2015): Determining critical nutrient thresholds needed to control harmful cyanobacterial blooms in eutrophic Lake Taihu, China. – *Environmental Science & Technology* 49(2): 1051-1059.
- [71] Ye, S., Chen, X., Dong, D., Wang, J., Wang, X., Wang, F. (2018): Rapid determination of water cod using laser-induced breakdown spectroscopy coupled with partial least-squares and random forest. – *Analytical Methods* 40(10): 4879-4885.
- [72] Zhang, X., Chen, Q. (2011): Spatial-temporal characteristic of water quality in Lake Taihu and its relationship with algal bloom. – *Journal of Lake Sciences* 23: 339-47.
- [73] Zhang, Y., Shi, K., Liu, X., Zhou, Y., Qin, B. (2014): Lake topography and wind waves determining seasonal-spatial dynamics of total suspended matter in turbid Lake Taihu, China: assessment using long-term high-resolution MERIS data. – *Plos One* 9(5): 98055.
- [74] Zhang, Y., Shi, K., Zhou, Y., Liu, X., Qin, B. (2016): Monitoring the river plume induced by heavy rainfall events in large, shallow, Lake Taihu using MODIS 250m imagery. – *Remote Sensing of Environment* 173: 109-121.

- [75] Zhang, T., Ban, X., Wang, X., Cai, X., Li, E., Wang, Z. (2017): Analysis of nutrient transport and ecological response in honghu lake, china by using a mathematical model. – Science of the Total Environment 575: 418-428.
- [76] Zhu, C., Liang, Q., Yan, F., Hao, W. (2013): Reduction of waste water in Erhai Lake based on MIKE21 hydrodynamic and water quality model. – The scientific world journal 5: 958506.

ASSESSING THE IMPACT OF CLIMATE CHANGE AND HUMAN ACTIVITIES ON RUNOFF IN THE DONGTING LAKE BASIN OF CHINA

ZHOU, J.^{1,2} – WAN, R. R.^{1,2*} – LI, B.¹ – DAI, X.^{1,2}

¹*Key Laboratory of Watershed Geographic Sciences, Nanjing Institute of Geography and Limnology, Chinese Academy of Sciences, Nanjing 210008, China*

²*University of Chinese Academy of Sciences, Beijing 100049, China
(phone: +86-151-9580-5305)*

**Corresponding author*

e-mail: rrwan@niglas.ac.cn; phone: +86-25-8688-2131

(Received 11th Jan 2019; accepted 8th Mar 2019)

Abstract. Global climate change and intensifying human activities have dramatically changed the runoff of Dongting Lake. This study investigated the runoff variations and associated impacts of climate change and human activity for the four inflow sub-basins of Dongting Lake. Multiple linear regression method and double-mass curve method were used to quantify the effects of climate change and human activities on water discharge. Results showed that the streamflow of the Xiangjiang, Zishui and Yuanjiang rivers exhibited an abrupt change in 2003, 2003 and 2005, respectively, whereas no significant turning year was detected for Lishui River. The impacts of climate factors and human activities were consistent using the two methods. The contribution rate of climate change to runoff reduction in Xiangjiang River was about 85–92% and the impact of human activities ranged from 8 to 15%. For the runoff changes in the Zishui and Yuanjiang River basins, results showed that the impact of climate factors ranged from 63 to 88% and from 62 to 82%, respectively. In comparison, the anthropogenic impact ranged from 12 to 37% and from 18 to 38%, respectively. This study will provide important insights into water resource management and planning for Dongting Lake basins.

Keywords: *streamflow, precipitation, evapotranspiration, human activities, Dongting Lake*

Introduction

River runoff changes are mainly affected by climate factors, such as precipitation and evapotranspiration. However, as an indirect influencing factor, increasing human activities (e.g. land utilisation change, water diversion for agricultural irrigation, hydropower engineering, water and soil conservation, etc.) have caused a change in water circulation (Allen and Ingram, 2002; Millán, 2014; Amin et al., 2016). Various studies have revealed a contradiction between water resources supply and demand due to the runoff changes in many river basins worldwide (Fu et al., 2004; Xu et al., 2010, 2013a, b). An analysis of the trends and characteristics of runoff changes and a quantitative evaluation on the effects of climate variability and human activities are important for the assessment and management of regional water resources.

Quantifying the impacts of climate change and anthropogenic activities on hydrological processes has become a hot topic in climatic and hydrologic studies (Zhang et al., 2015; Ahn and Merwade, 2014; Buendia et al., 2016; Griffioen, 2016). Extensive research has been conducted on several typical watersheds, such as the Nile River basin (Hasan et al., 2018), Columbia River basin, Colorado River basin, Mississippi River basin (Naik and Jay, 2011; Timilsena and Piechota, 2008), Mekong basin (Raghavan et al., 2012), Brahmani River basin (Islam et al., 2012), and in China,

the Yangtze River basin (Zhao et al., 2015), Yellow River basin (Wang et al., 2014; Kong, 2017), Wei River basin (Huang et al., 2016; Zhang et al., 2015) and Hei River basin (Luo et al., 2016). Two methods are commonly used for evaluating the contribution rates of the main influencing factors on runoff changes, including hydrological modelling (Huang et al., 2016; Liu et al., 2016) and quantitative evaluation method [e.g. climatic elastic coefficient method (Ahn and Merwade, 2014; Ye et al., 2013), multivariate regressive (Jiang et al., 2011), sensitivity analysis (Zuo et al., 2016) and double-mass curve (DMC) method (Li and Xu et al., 2016)]. Although these studies quantitatively evaluated the comprehensive effects of climate change and human activities on runoff change, some shortcomings and deficiencies were observed. For example, although the hydrological model has a good physical foundation, its structure and parameter sensitivity possess several uncertainties. Furthermore, while the quantitative evaluation method requires less data, a longer data series is needed to reach the effect of quantitative assessment, and noise in the long-time data series interferes with the evaluation results (Sankarasubramanian et al., 2001). Improvement of the accuracy to identify the change points of runoff variation and comprehensive application of various methods to quantify the contribution of climate change and human activities are necessary to obtain reasonable results.

Dongting Lake, the second largest freshwater lake in China, plays an important role in regulating the amount of water in Yangtze River, China's longest river. In recent decades, especially after the Three Gorges project operation, lake runoffs were changed greatly and the surrounding basins suffered from frequent droughts (Mao, 1998), which seriously disrupted water supply for agricultural production, human consumption and ecological water requirement. Several studies have discussed the variation trend of runoff and sediment discharge in Dongting Lake basin. Li and Gu et al. (2016) revealed that the annual discharge of the Dongting outlet lake has shown a decreasing trend since 1983, with the most obvious decrease from 2003 to 2014. The results also indicated that runoff and rainfall synchronised within a certain range of fluctuations. Qin et al. (2012) analysed the long-term changes of runoff and sediment discharge of the Four Rivers in Dongting Lake basin and pointed out that the annual runoff change is mainly affected by the abundance and deficiency of precipitation. Zhang and Liu (2018) investigated the runoff and sediment discharge change trend in Xiangjiang River basin and its relationship with rainfall, drought regime, dam engineering construction and vegetation change. These studies indicated that the variations of streamflow are considerably related to regional climate, especially precipitation. However, to our knowledge, the present studies have paid little attention to quantifying the contribution rate of the driving factors of runoff changes in Dongting Lake basin. Furthermore, quantifying the impacts of climate variability and human activities with a single method is challenging because of the complex processes involved. Thus, further studies are needed to provide a conclusive interpretation of the changes observed. The present study is essential not only for an improved understanding on the mechanism of hydrological response in the basin but also for local water resources management as well as flood and drought protection and disaster mitigation.

In this study, Sen's slope method, moving t-test, Pettitt test, multiple linear regression and DMC method were used to explore the streamflow variations of the Dongting Lake sub-basin and quantify the relative impacts of climate variability on human activity. The specific objectives of this study were as follows: (1) analyse the variability of long-term historical records of hydrological and climate data of the main

tributaries in Dongting Lake basin, (2) investigate the abrupt change points of runoff variations and (3) estimate quantitatively the contribution rate of climate factors and human activities to runoff changes.

Dataset and methodology

Study area

Dongting Lake, the second largest freshwater lake in China, is located at 28°30'N–30°20'N and 111°40'E–113°10'E (Fig. 1). With a drainage area of $2.63 \times 10^5 \text{ km}^2$, it occupies a large part of Hunan Province and a small part of Hubei, Chongqing, Guizhou, the Guangxi Zhuang Autonomous Region and Jiangxi provinces. Dongting Lake is connected to Yangtze River. The lake receives water flows mainly from Yangtze River and four tributaries from upstream (Xiangjiang, Zishui, Yuanjiang and Lishui) and discharges into Yangtze River through an outlet in the north. Runoffs from four rivers account for 54.6% of the total runoff (Qin et al., 2012), and changes in the runoffs directly impact the water quantity of Dongting Lake. The basin has well-developed river systems and includes four sub-basins: Xiangjiang, Zishui, Yuanjiang and Lishui River basins. Dongting Lake basin belongs to the subtropical monsoon climate zone. Its annual mean precipitation ranges from 1200 to 1400 mm depending on the position in the basin (Cui et al., 2012) and average annual runoff is $2608 \times 10^8 \text{ km}^3$.

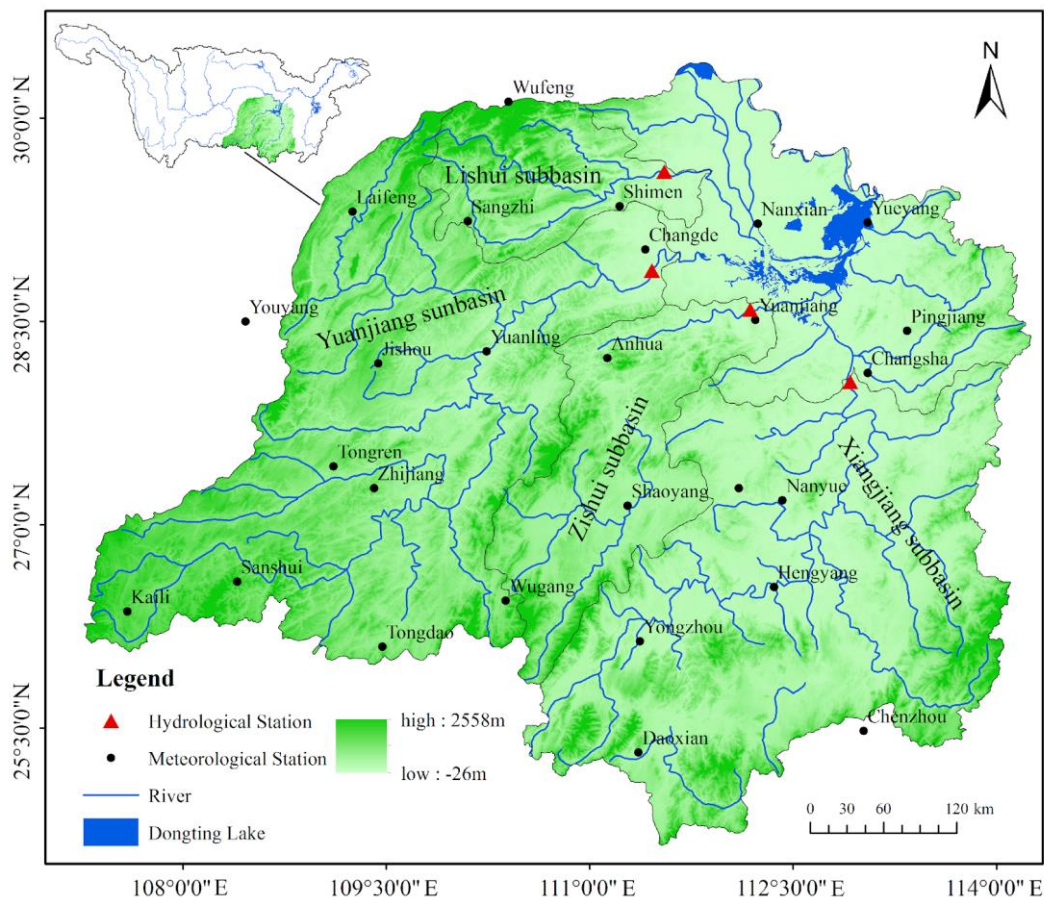


Figure 1. Location of the study area and the distribution of meteorological stations and hydrological stations

Dataset

Daily runoff observations (1980–2014) from four gauging stations, including Xiangtan, Taojiang, Taoyuan and Shimen stations, were derived from the *Yangtze River Hydrological Data*. The meteorological data from 25 weather stations inside the catchment (Fig. 1) were obtained from the National Meteorological Information Center (<http://data.cma.cn>). The stations provide daily observations on precipitation, temperature, maximum temperature, minimum temperature, actual vapour pressure, relative humidity, sunshine duration and wind speed. Potential evaporation is calculated using the Penman–Monteith formula (Penman, 1948). Considering the uneven distribution of meteorological stations, the precipitation and potential evaporation in each basin are calculated using the Thiessen polygon method on the ArcGIS platform.

Methodology

Trend test

Sen's slope, a non-parametric estimation method, can reflect the magnitude of the monotonic (Sen, 1968) trend and is given as Equation 1:

$$\beta = \text{Median}\left(\frac{X_i - X_j}{i - j} \mid 1 < j < i < n\right) \quad (\text{Eq.1})$$

where β is the median over all combinations of record pairs for the whole data set and is, therefore, not affected by extreme values in the observations (Hirsch et al., 1982). A positive value of β indicates the variables increase with time, whereas a negative value represents a decreasing trend.

Change-point analysis

Various methods can be used to detect abrupt climate change, such as Mann–Kendall method (Mann, 1945), moving t-test (Buishand, 1982), Pettitt test (Pettitt, 1979) and cumulative anomaly method (Weber and Stewart, 2010). According to the characteristics and virtues of these methods, moving t-test and Pettitt test methods are used to analyse the change points of runoff.

Moving t-test is used to test the significant difference of two random samples' mean. The method is simple, reliable and capable of avoiding artificial interference on the subsequence selection (Chen and Gupta, 2000). The method assumes the distribution functions before and after the change point as $F_1(x)$ and $F_2(x)$ and extracts two samples with the capacity of n_1 and n_2 from them, respectively. A T statistic is then constructed as follows:

$$T = \sqrt{\frac{\overline{x_1} - \overline{x_2}}{\frac{(n_1 - 1)S_1^2 + (n_2 - 1)S_2^2}{n_1 + n_2 - 2} \left(\frac{1}{n_1} + \frac{1}{n_2}\right)^{1/2}}} \quad (\text{Eq.2})$$

In the above equation, \bar{x}_i and S_i are the means and variances of the samples, respectively. At a given confidence level α , if $|T| > T_{\alpha/2}$, then the sequence has a significant difference. Among all the points satisfying $|T| > T_{\alpha/2}$, the point where T reaches the maximum is the most possible change point.

Pettitt test, put forward by A. N. Pettitt (1979), is used to determine the occurrence of a change point. This approach considers a time series as two samples represented by X_1, \dots, X_t and X_{t+1}, \dots, X_N . The Pettitt index $U_{t,N}$ is based on Mann–Whitney’s statistical function and can be calculated using Equation 3:

$$U_{t,N} = U_{t-1,N} + \sum_{j=1}^N \text{sgn}(x_t - x_j) \quad (t = 2, \dots, N) \quad (\text{Eq.3})$$

where if $x_t - x_j > 0$, then $\text{sgn}(x_t - x_j) = 1$; if $x_t - x_j = 0$, then $\text{sgn}(x_t - x_j) = 0$; and if $x_t - x_j < 0$, then $\text{sgn}(x_t - x_j) = -1$.

The test statistic counts the number of times a member of the first sample exceeds that of the second. Moreover, the null hypothesis does not change in the distribution of a sequence of random variables. The most significant change point is selected where the value of $U_{t,N}$ is the largest (Eq. 4), and a change point occurs at time t when the statistic $k(t)$ is significantly different from zero at a given level. For $P \leq 0.5$, the approximate significant level is given by Equation 5 (Pettitt, 1979).

$$k(t) = \text{Max}_{1 \leq t \leq N} |U_{t,N}| \quad (\text{Eq.4})$$

$$P \cong 2 \exp\left\{-6(K_N)^2 / (N^3 + N^2)\right\} \quad (\text{Eq.5})$$

Contribution rate analysis

Multi-regression method

Runoff changes involve the superposition of the effects of climate change and human activities, while climate factors influence the runoff mainly by precipitation and evaporation. Jiang et al. (2011) suggested a linear regression approach to estimate the monthly runoff using a function of precipitation and potential evapotranspiration (PET). On a monthly time scale, groundwater storage may play a role in runoff generation. Therefore, the original equation is modified by adding the precipitation from the previous month. Liu et al. (2016) showed that a three-variable linear regression model that considers precipitation, PET and precipitation from the previous month fitted well. The equation is given as

$$Q_i = aP_i + bP_{i-1} + cPET_i + d \quad (\text{Eq.6})$$

where Q, P and PET represent the runoff, precipitation and potential evapotranspiration during the natural period, respectively, for month i ; and a, b, c and d are constants estimated by least square estimation. Then, simulated runoff is estimated for the impact period using Equation 6. The difference between the observed runoff and the calculated

runoff will represent the contribution from human activities in the impact period. The runoff change caused by climate factors and human activities can be quantified respectively according to *Equations 7 and 8*.

$$\Delta Q_h = \left| \overline{O}_m - \overline{Q}_m \right| \quad (\text{Eq.7})$$

$$\Delta Q_c = \left| \overline{O}_n - \overline{Q}_m \right| \quad (\text{Eq.8})$$

$$\Delta Q_t = \Delta Q_c + \Delta Q_h \quad (\text{Eq.9})$$

where ΔQ_h and ΔQ_c represent the change in mean annual runoff due to human activities and climate factors, respectively; \overline{O}_m and \overline{O}_n are the average observed monthly runoff during the impact period and the natural period, respectively; and \overline{Q}_m represents the calculated average monthly runoff during the impact period.

Nash–Sutcliffe Coefficient (NSC) was used to evaluate the model performance as follows:

$$NSC = 1 - \frac{\sum_{t=1}^T (O_t - Q_t)^2}{\sum_{t=1}^T (O_t - \overline{O}_t)^2} \quad (\text{Eq.10})$$

where O and Q are the observed and simulated monthly runoffs, respectively. NSC changes between $-\infty$ and 1, and the closer this value is to 1, the higher the reliability of the model. Moriasi et al. (2007) suggested that the accuracy of simulations is satisfactory if the value of NCS is greater than 0.5.

Double mass curve analysis

DMC was first proposed by C. F. Merriam (1937) for the consistence analysis of a rainfall series in the Susquehanna Valley of the United States. Recently, DMC has been widely used in identifying the hydrological regime changes caused by anthropogenic disturbances (Huo et al., 2010; Gao et al., 2015). DMC is a plot of the accumulated values of one variable against the accumulated values of another related variable for the same period. Theoretically, it is a straight line when affected by climate change only. A break in the slope of the DMC indicates that human activities began to significantly influence runoff. In this study, precipitation and PET were the reference variable, and runoff was the tested variable. For a detailed description of this method, see Li et al. (2016).

Results

Variations of precipitation and potential evaporation

The results of Sen’s slope of annual precipitation and annual potential evaporation in Dongting Lake basin from 1980 to 2014 are shown in *Fig. 2a and b*, respectively. The

annual precipitation did not show the same upward or downward trending in the whole basin. Overall, the trend of precipitation change in the Xiangjiang River basin was more significant, and the precipitation of some weather stations in the Yuanjiang River basin had an upward tendency. The trend of precipitation change of weather stations failed to achieve a significant level, except for Wufeng Station (*Table 1*). As shown in *Fig. 2b*, potential evaporation in the whole basin showed an upward trend. From the spatial distribution, the trend of potential evaporation change decreased progressively from the eastern to the western region. Similarly, compared with the Lishui and Yuanjiang River basins, the increasing trend of PET in the Xiangjiang and Zishui River basins was more significant (*Table 1*).

Table 1. Sen's slope of precipitation and PET of meteorological stations in Dongting Lake

Basin	Station	Sen's slope	
		P (mm/a)	PET (mm/a)
Lishui	Sangzhi	1.31	0.20
	Shimen	-2.95	2.40
	Wufeng	-7.63	0.84
Yuanjiang	Jishou	-0.17	1.74
	Yuanling	0.01	1.49
	Changde	0.64	5.50
	Zhijiang	1.39	0.30
	Tongdao	-5.78	1.36
	Laifeng	-5.46	1.01
	Youyang	-2.22	1.71
	Tongren	-0.70	-0.08
	Kaili	-1.23	1.68
	Sansui	0.28	0.48
Zishui	Anhua	0.60	3.40
	Yuanjiang	-3.76	2.03
	Shaoyang	-4.34	2.77
	Wugang	-6.29	3.69
Xiangjiang	Changsha	-0.90	6.07
	Pingjiang	-4.69	3.17
	Shuangfeng	-1.26	0.76
	Nanyue	-4.75	2.88
	Yongzhou	-2.93	1.95
	Hengyang	-6.38	5.18
	Daoxian	1.58	0.12
Chenzhou	-2.45	1.51	

Positive values mean an increase, negative values mean a decrease. The bold font indicates the trend of change is significant at the 95% confidence interval

Figure 3a and *b* shows the respective long-term trends and mean annual value of annual precipitation and potential evaporation in Dongting Lake basin. The annual average precipitation in the basin was 1391.65 mm from 1980 to 2014 and great inter-annual variations could be observed, with the largest ratio at 1.89. Furthermore, the precipitation indicated a decreasing trend with a Sen of -1.57 mm/a ($P = 0.39$) (*Fig. 3a*).

Compared with other periods, rainfall was relatively abundant in the 1990s. However, the PET of Dongting Lake basin showed a significant increasing trend ($P < 0.05$) at a rate of 2.33 mm/a. The average PET was 1013.01 mm in 1980–2014, during which PET fluctuated greatly especially after 2000.

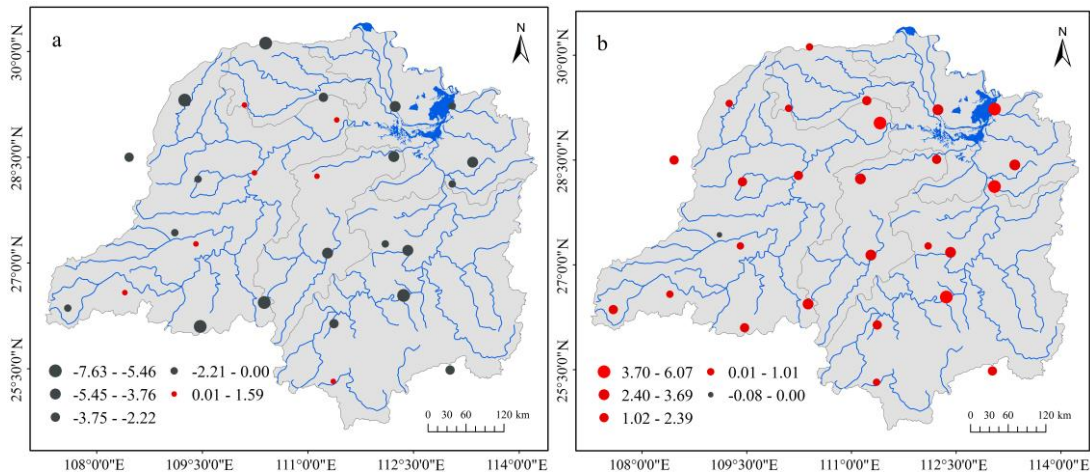


Figure 2. Spatial variations of precipitation and potential evaporation in Dongting Lake basin for 1980–2014 (a: Sen's slope of annual precipitation; b: Sen's slope of annual potential evaporation)

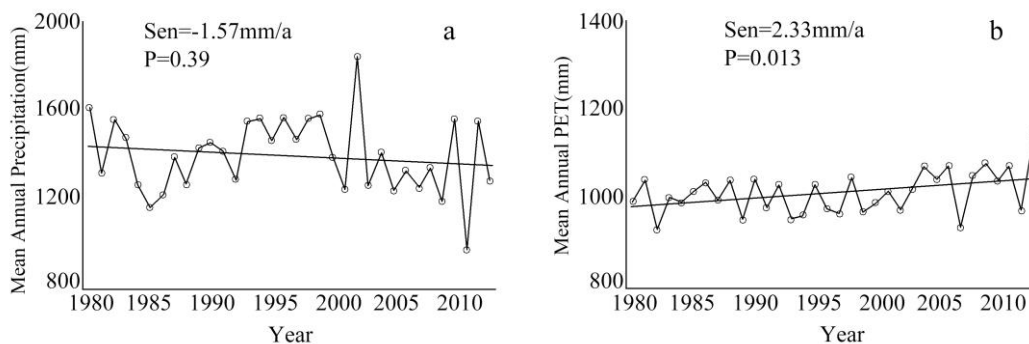


Figure 3. Variations of mean annual precipitation (a) and potential evaporation (b) from 1980 to 2014

Trend and change-point analysis of runoff

The variations of mean annual runoff for the four sub-basins in Dongting Lake basin are illustrated in *Figure 4a1, b1, c1 and d1*, respectively. Xiangjiang River basin had the highest annual runoff ($667 \times 10^8 \text{ m}^3$, about 40% of the total), followed by Yuanjiang ($629 \times 10^8 \text{ m}^3$) and Zishui ($227 \times 10^8 \text{ m}^3$) and the lowest was Lishui River basin at only $145 \times 10^8 \text{ m}^3$. Except for Lishui River basin, the runoff of the other three basins had similar inter-annual fluctuation patterns, firstly decreasing, then increasing and again decreasing. Similar to the precipitation changes, the annual runoff in the 1990s was significantly higher than that in the 1980s and the 2000s. The runoffs of four sub-basins were all lower than the previous record for the period after 2003. The annual runoff in Lishui had no clear increasing or decreasing trend.

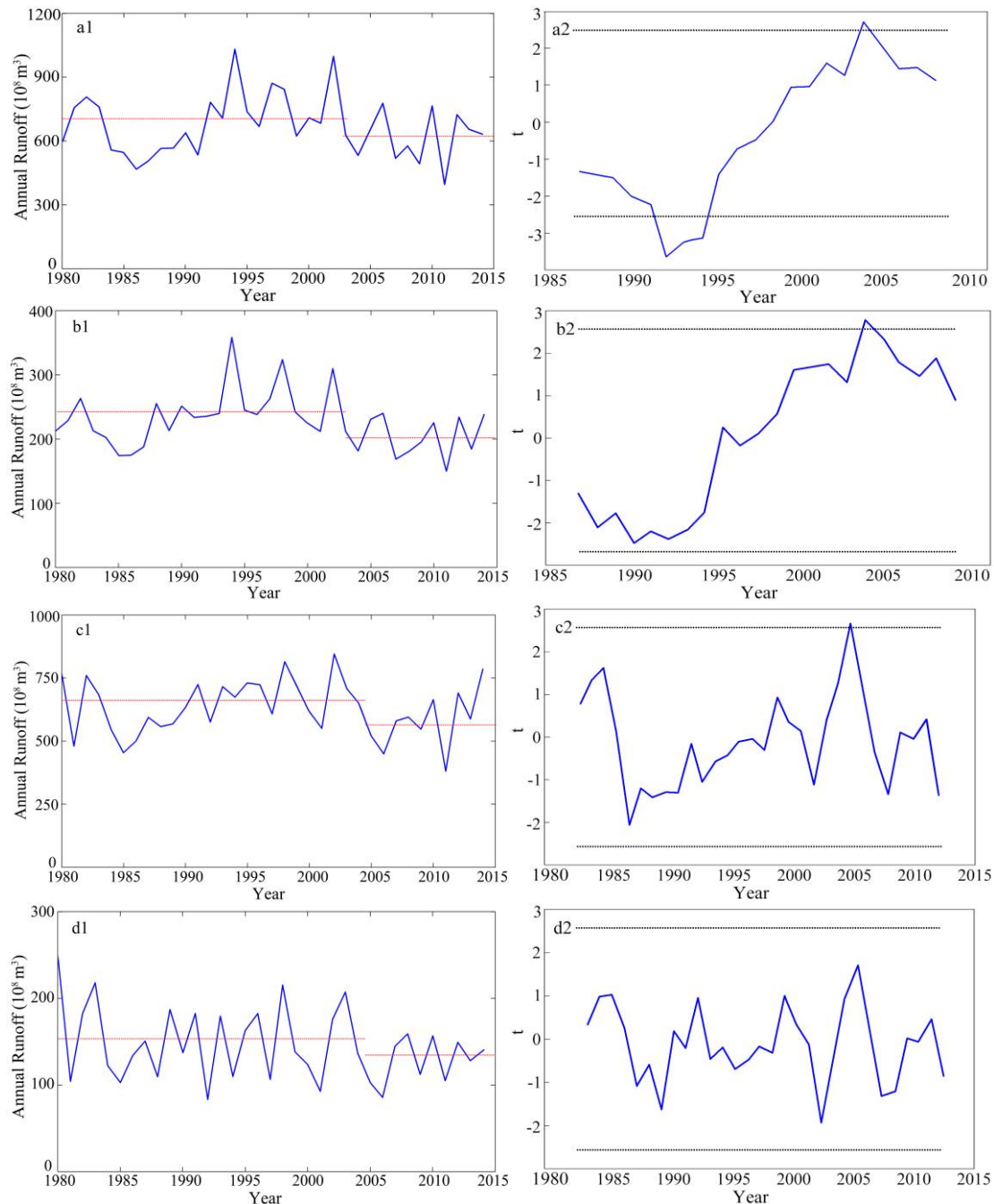


Figure 4. Variations and moving *t*-test on runoff in Dongting Lake basin (a: Xiangjiang River basin, b: Zishui River basin, c: Yuanjiang River basin and d: Lishui River basin). The red dotted line stands for mean annual runoff before and after the turning years on the left. The dotted line means the significance level of 0.05 on the right

The moving *t*-test and non-parametric Pettitt test were applied to detect the change point of the annual runoff series of the sub-basins. Similar results were obtained (Table 2). As shown in Figure 4a2, b2, c2, d2 and Table 2, the turning years in the runoff changes were 2003 for Xiangjiang River basin, 2003 for Zishui and 2005 for Yuanjiang River basin. No significant change point was found for Lishui River basin. On the basis of this finding, this study will analyse the runoff trend of the other three

sub-basins. Through trend and change-point analysis, the runoff series will be divided into a natural period series and an impact period series. The comparison and analysis of the mean runoff before and after the abrupt change indicated that the annual runoff of every sub-basin had a remarkable decline after the abrupt change. The drops were 11.46%, 14.87% and 8.77% in Xiangjiang, Zishui and Yuanjiang River basins, respectively.

Table 2. Summarised result of moving *t*-test and Pettitt test on the runoff change points for different sub-basins

Sub-basin	Moving <i>t</i> -test		Pettitt test	
	Change-point	<i>P</i>	Change-point	<i>P</i>
Xiangjiang	1992, 2003	0.05	2003	0.43
Zishui	2003	0.05	2003	0.12
Yuanjiang	2005	0.05	2005	0.45
Lishui	-	-	2003	1.06

‘-’ means the test results were not significant

Quantification of climatic and anthropogenic influences

Multi-regression method

The natural period was taken as a baseline, and the effects of climate change and human activities on runoff of each sub-basin were estimated for the impact period using two methods.

Multi-regression equations of the three sub-basins were developed based on the monthly average precipitation and potential evaporation of the natural period (Table 3). The coefficients of determination (R^2) were all greater than 0.75 (significance level of 0.001), and the NSCs were all greater than 0.65. These results indicate that the multi-regression models can accurately simulate runoff. The simulated runoff series was obtained with the use of precipitation and PET of the impact period as input. The contribution of climate factors and human activities to runoff were calculated according to Equations 7 and 8, respectively. The quantitative results are shown in Table 4.

Double mass curve analysis

The DMCs of precipitation–runoff and PET–runoff, along with the linear regression lines, are shown in Figures 5 and 6, respectively. Clearly, the DMCs showed the turning points for runoff, which indicated that the runoff changes were influenced by both climate factors and human activities in the three sub-basins of Dongting Lake. This result further verifies the correctness of the test for abrupt change.

The contribution rates of climate factors and human activities in runoff changes in these sub-basins were calculated and shown in Table 5. For Xiangjiang River basin, the annual average observed runoffs in the natural period and the impact period were $694.02 \times 10^8 \text{ m}^3$ and $611.40 \times 10^8 \text{ m}^3$, respectively. Based on the DMCs, the influence quantities of precipitation and evaporation on runoff reduction were $48.39 \times 10^8 \text{ m}^3$ and $27.56 \times 10^8 \text{ m}^3$, respectively. Accordingly, the contribution rates of precipitation and PET accounted for 58.58% and 33.35% of the runoff change, respectively. The reduction ratio due to human activities was only 8.07%. Similarly, the contribution rates

of climate factors and human activities to the runoff reduction in Zishui and Yuanjiang River basins were 62.56% and 37.44% and 61.68% and 38.32%, respectively.

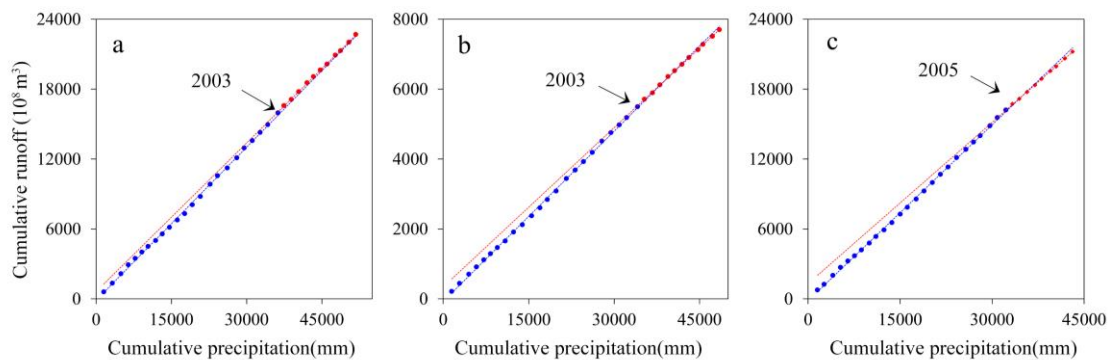


Figure 5. DMCs of annual runoff and precipitation at different sub-basins. The blue and red lines are the regression lines for the cumulative data before and after the change-point years, respectively (a: Xiangjiang River basin, b: Zishui River basin and c: Yuanjiang River basin)

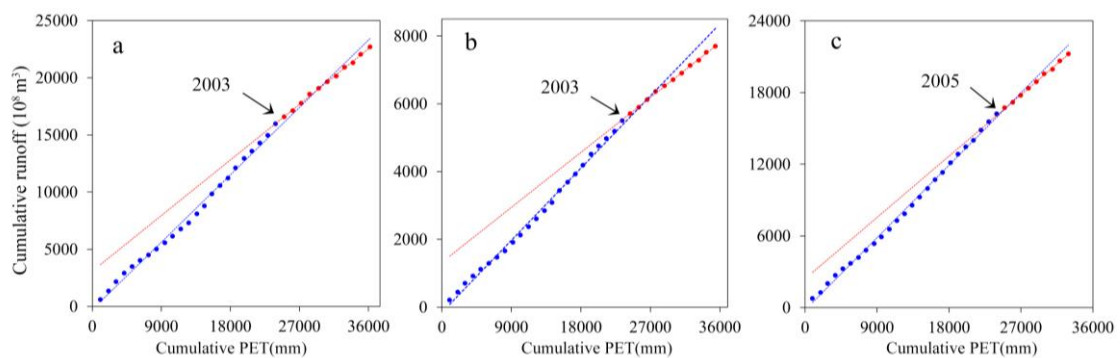


Figure 6. DMCs of annual runoff and PET at different sub-basins. The blue and red lines are the regression lines for the cumulative data before and after the change-point years, respectively (a: Xiangjiang River basin, b: Zishui River basin and c: Yuanjiang River basin)

Table 3. Multiple linear regressions for the series of monthly runoffs during the natural period in the three sub-basins of Dongting Lake basin

Sub-basin	Regression equation	R ²	Significance level	NSC
Xiangjiang	$Q=0.460P-0.117PET+0.255P'-12.855$	0.804	P < 0.001	0.805
Zishui	$Q=0.418P-0.123PET+0.206P'-3.157$	0.754	P < 0.001	0.716
Yuanjiang	$Q=0.524P-0.235PET+0.228P'-3.611$	0.839	P < 0.001	0.738

Table 4. Effects of climate variability and human activities on runoff change using multi-regression method

	Xiangjiang	Zishui	Yuanjiang
Climate change (%)	84.93	88.45	81.91
Human activities (%)	15.07	11.55	18.09

Table 5. Effects of climate variability and human activities on runoff change using DMC analysis

Sub-basin	Periods	\bar{O}	P			PET			C_H
			$\overline{Q_{m_P}}$	ΔQ_{c_P}	C_P	$\overline{Q_{m_PET}}$	ΔQ_{c_PET}	C_{PET}	
Xiangjiang	1980-2003	694.02							8.07
	2004-2014	611.40	645.62	48.39	58.58	666.47	27.56	33.35	
Zishui	1980-2003	239.06							37.44
	2004-2014	200.03	223.86	15.20	38.96	229.85	9.21	23.60	
Yuanjiang	1980-2005	648.39							38.32
	2006-2014	557.25	615.32	33.02	36.24	625.16	23.18	25.44	

The units \bar{O} , $\overline{Q_m}$, ΔQ_c : $\times 10^8 \text{ m}^3$; C_P , C_{PET} , C_H : %

Discussion

The results above showed that the annual runoff decreased significantly in Xiangjiang, Zishui and Yuanjiang River basins. Decreasing precipitation and increasing PET play critical roles in affecting the reduced runoff changes. Some studies showed that temperature and precipitation were the predominant factors that caused the shortage of water resources and drought and flood. Guo et al. (2001) indicated that the runoffs of semi-humid regions in the north of China are more sensitive to climate change than those of humid regions such as Yangtze River basin. In the present study, the climate variation features are consistent with those of the runoff series, providing further evidence that climate change are the dominant factor decreasing runoff. From the whole basin, the climate change trend in Xiangjiang and Zishui River basin are more significant, which corresponds to the conclusion that the contribution rate of climate change in decreasing runoff was larger in the two basins. No significant change point was detected in the runoff variation of Lishui River basin, consistent with the results of Liu et al. (2014) and Zheng and Sun (2014). Their studies showed that the annual runoff of Lishui River basin has not changed significantly since the 1980s. On the one hand, the annual rainfall of the study period has not changed significantly; on the other hand, although the underlying surface conditions of the middle and upper reaches of Lishui River have been changing, human activities have not affected the annual runoff. This outcome may be related to the well-developed river system and abundant runoff. While human activities are gradually intensifying, they have not caused significant changes to the hydrological characteristics of Lishui River. The relevant physical mechanisms need to be further verified and determined as well.

Through multi-regression method and DMC analysis, the contribution rates of climate change and human activities to runoff changes in the four sub-basins were obtained. The conclusions from the two methods are consistent: runoff reduction was mainly caused by climate change in the whole basin and human activities played an assisting role in such a change, a finding that is consistent with the conclusion of Xiao (2014). Zhang and Liu (2018) also indicated that regional climate change (precipitation and PET) are the main factors influencing the runoff of Xiangjiang River basin. The two kinds of methods confirm each other and improve the reliability of the evaluated results. With the results of the two methods combined, the impact of human activities on the runoff change was revealed to be negative. In addition, owing to the discrepancy in

regional climate and the intensive human activities in these sub-basins, the contribution of individual impacts varied under different regions. According to *Tables 4* and *5*, the contribution rate of human activities in decreasing runoff in Yuanjiang River basin was the largest at 18–38%. However, a percentage of the impact of climate change in Xiangjiang River basin was bigger than those in other sub-basins, and the impact of human activities accounted for 8–15% of decreasing runoff.

Human activities affect the basin hydrological process mainly through two aspects: changing the conditions of the underlying surface and developing hydropower engineering (Ye et al., 2009). The former involves the variation of land utilisation and land cover, urbanisation, water and soil conservation and vegetation restoration. Relevant documents show that the total population of Dongting Lake basin has increased by 12.07 million since 1980, and the areas for construction land have also increased (Xiao, 2014). In recent decades, according to statistics from the Hunan Water Conservancy Bureau (<http://www.hnwr.gov.cn>), the proportion of agricultural water use has dropped and industrial and domestic water use in urban and rural areas has increased. In addition, the forest coverage rate of the whole province increased from 36.7 to 57% during 1989–2010 (Xiao, 2014). Studies have shown that the implementation of soil and water conservation measures was conducive to increasing water storage capacity and reducing runoff (Ye et al., 2009). Water conservancy projects have a tremendous impact on runoff, in addition to changing channel characteristics. They likewise influence regional precipitation and evaporation by increasing the water area, especially through large reservoirs. According to the first water resources census of Hunan Province (<http://hnr.voc.com.cn>), by the end of 2011, there were 14,121 reservoirs of various types with a total reservoir capacity of 53.07 billion m³, of which the large reservoirs accounted for 68.2%. According to the statistical data of existing large reservoirs (Xiao, 2014), the ratio of control areas of reservoirs in Xiangjiang River basin was the smallest among all sub-basins. This fact is one of the possible causes for the results on the contribution rate of human activities in Xiangjiang River basin being the least. Overall, the effect of human activities on runoff is very complex, and the degree of influence of human activities on runoff change and the correlation between them need to be further verified.

Conclusions

On the basis of analysing the trend of runoff variation, this study used moving t-test and Pettitt method to detect turning points. Then, taking the natural period as the baseline, the impact of climatic factors and human activities on runoff variation was evaluated by multi-regression and DMC methods. The conclusions are as follows:

(1) During 1980–2014, the trend of runoff reduction in Dongting Lake basin was obvious. Besides Lishui River basin, the runoff of Xiangjiang, Zishui and Yuanjiang River basins showed abrupt changes in 2003, 2003 and 2005, respectively.

(2) Climate change was the dominant factor of runoff reduction in Dongting Lake basin, while human activities play a subsidiary role. The contribution rate of climate change to runoff reduction in Xiangjiang River Basin was approximately 85–92%, and the impact of human activities was 8–15%. In Zishui, the contribution of climate change accounted for 63–88% of the changes in runoff, while human activities were responsible for 12–37% of the change. Similarly, the impacts of climate change and human activities in Yuanjiang River basin were 62–82% and 18–38%, respectively.

The method adopted in this study can be easily used to quantify the impact of changing environments on runoff in areas that lack historical data. Some uncertainties exist because of the correlation of climate variability and anthropogenic activities. More attention should be directed to these uncertainties in future research on the quantitative estimation of influence of climate change and human activities on runoff in Dongting Lake basin. Furthermore, although the runoff reduction of Dongting Lake basin was caused by climate change, human disturbance will bring challenges to the utilisation of water resources. To maintain the ecosystem services of the river basin and ensure a certain degree of ecological water requirement, the dispatch and management of basin water resources should be strengthened.

Acknowledgements. This research received financial support from the National Key Research and Development Project of China (No. 2016YFC0402204) and the Key Research Program of the Chinese Academy of Sciences (No. KFZD-SW-318).

REFERENCES

- [1] Ahn, K.-H., Merwade, V. (2014): Quantifying the relative impact of climate and human activities on streamflow. – *Journal of Hydrology* 515(515): 257-266.
- [2] Allen, M. R., Ingram, W. J. (2002): Constraints on future changes in climate and the hydrologic cycle. – *Nature* 419(6903): 224-232.
- [3] Amin, M. Z. M., Shaaban, A. J., Ercan, A., Ishida, K., Kavvas, M. L., Chen, Z. Q., Jang, S. (2016). Future climate change impact assessment of watershed scale hydrologic processes in Peninsular Malaysia by a regional climate model coupled with a physically-based hydrology model. – *Science of the Total Environment* 575: 12-22.
- [4] Buendia, C., Batalla, R. J., Sabater, S., Palau, A., Marcé, R. (2016): Runoff trends driven by climate and afforestation in a Pyrenean Basin. – *Land Degradation & Development* 27(3): 823-838.
- [5] Buishand, T. A. (1982): Some methods for testing the homogeneity of rainfall records. – *Journal of Hydrology* 58(1): 11-27.
- [6] Chen, J., Gupta, A. K. (2000): *Parametric Statistical Change Point Analysis*. – Springer, Basel.
- [7] Cui, M., Zhou, J. X., Huang, B. (2012): Benefit evaluation of wetlands resource with different modes of protection and utilization in the Dongting Lake region. – *Procedia Environmental Sciences* 13(10): 2-17.
- [8] Fu, G. B., Chen, S. L., Liu, C. M., Shepard, D. (2004): Hydro-climatic trends of the Yellow River basin for the last 50 years. – *Climatic Change* 65(1-2): 149-178.
- [9] Gao, J. H., Jia, J., Kettner, A. J., Xing, F., Wang, Y. P., Li, J., Bai, F., Zou, X., Gao, S. (2015): Reservoir-induced changes to fluvial fluxes and their downstream impacts on sedimentary processes: the Changjiang (Yangtze) River, China. – *Quaternary International* 493: 187-197.
- [10] Griffioen, J. (2016): Enhanced weathering of olivine in seawater: the efficiency as revealed by thermodynamic scenario analysis. – *Science of the Total Environment* 575: 536.
- [11] Guo, S. L., Wang, J. X., Xiong, L. H., Ying, A. W., Li, D. F. (2002): A macro-scale and semi-distributed monthly water balance model to predict climate change impacts in china. – *Journal of Hydrology* 268: 1-15.
- [12] Hasan, E., Tarhule, A., Kirstetter, P.-E., Clark, R., Hong, Y. (2018): Runoff sensitivity to climate change in the Nile River Basin. – *Journal of Hydrology* 561: 312-321.

- [13] Hirsch, R. M., Slack, J. R., Smith, R. A. (1982): Techniques of trend analysis for monthly water quality data. – *Water Resources Research* 18(1): 107-121.
- [14] Huang, S. Z., Chang, J. X., Huang, Q., Chen, Y. T., Leng, G. Y. (2016): Quantifying the relative contribution of climate and human impacts on runoff change based on the Budyko hypothesis and SVM model. – *Water Resources Management* 30(7): 2377-2390.
- [15] Huo, Z. L., Feng, S. Y., Kang, S. Z, Li, W. C., Chen, S. J. (2010): Effect of climate changes and water-related human activities on annual stream flows of the Shiyang River basin in arid north-west China. – *Hydrological Processes* 22(16): 3155-3167.
- [16] Islam, A., Saha, B., Singh, A. (2012): Streamflow response to climate change in the Brahmani River basin, India. – *Water Resources Management* 26(6): 1409-1424.
- [17] Jiang, S. H., Ren, L. L, Yong, B., Singh, V. P., Yang, X. L., Yuan, F. (2011): Quantifying the effects of climate variability and human activities on runoff from the Laohahe basin in northern China using three different methods. – *Hydrological Processes* 25(16): 2492-2505.
- [18] Kong, D. X., Miao, C. Y., Wu, J. W., Duan, Q. Y. (2016): Impact assessment of climate change and human activities on net runoff in the Yellow River Basin from 1951 to 2012. – *Ecological Engineering* 91: 566-573.
- [19] Li, J. B., Gu, J. H., Dai, W., Lv, D. Q., Liu, W. (2016): Hydrologic regime variation and trend prediction in the typical sections of the middle reaches of the Yangtze River under the TGR operation. – *Journal of Glaciology and Geocryology* 38(5): 1373-1384.
- [20] Li, Z. W., Xu, X. L., Yu, B. F., Xu, C. H, Liu, M. X., Wang, K. L. (2016): Quantifying the impacts of climate and human activities on water and sediment discharge in a karst region of southwest China. – *Journal of Hydrology* 542: 836-849.
- [21] Liu, B. W., Nan, S., Geng, S. H., Chen, X. (2014): Evaluation characteristics and impacting factors of annual runoff and sediment in Lishui River during 1955-2009. – *Bulletin of Soil and Water Conservation* 34(6): 360-363.
- [22] Liu, J. Y., Zhang, Q., Deng, X. Y., Ci, H., Chen, X. H. (2016): Quantitative analysis the influences of climate change and human activities on hydrological processes in Poyang Basin. – *Journal of Lake Sciences* 28(2): 432-443.
- [23] Luo, K. S., Tao, F. L., Moiwo, J. P., Xiao, D. P. (2016): Attribution of hydrological change in Heihe River Basin to climate and land use change in the past three decades. – *Scientific reports* 6: 33704.
- [24] Mann, H. B. (1945): Nonparametric tests against trend. – *Econometrica* 13(3): 245-259.
- [25] Mao, D. H. (1998): Analysis of flood characteristics in Dongting Lake region. – *Journal of Lake Sciences* 10(2): 85-91.
- [26] Merriam, C. F. (1937): A comprehensive study of the rainfall on the Susquehanna Valley. – *Eos Transactions American Geophysical Union* 18(2): 471-476.
- [27] Millán, M. M. (2014): Extreme hydrometeorological events and climate change predictions in Europe. – *Journal of Hydrology* 518: 206-224.
- [28] Moriasi, D. N., Arnold, J. G., Liew, M. W. V., Bingner, R. L., Harmel, R. D., Veith, T. L. (2007): Model evaluation guidelines for systematic quantification of accuracy in watershed simulations. – *Transactions of the Asabe* 50(3): 885-900.
- [29] Naik, P. K., Jay, D. A. (2011): Distinguishing human and climate influences on the Columbia River: changes in mean flow and sediment transport. – *Journal of Hydrology* 404(3-4): 259-277.
- [30] Penman, H. L. (1948): Natural evaporation from open water, bare soil and grass. – *Proceedings of the Royal Society of London* 193(1032): 120-145.
- [31] Pettitt, A. N. (1979): A non-parametric approach to the change-point problem. – *Journal of the Royal Statistical Society* 28(2): 126-135.
- [32] Qin, H. Y., Xie, Y. H., Zou, D. S. (2012): Changes of runoff and sediment discharge into Dongting Lake from the four rivers in Hunan Province. – *Scientia Geographica Sinica* 32(5): 609-615.

- [33] Raghavan, S. V., Vu, M. T., Liong, S. Y. (2012): Assessment of future stream flow over the Sesan catchment of the Lower Mekong Basin in Vietnam. – *Hydrological Processes* 26: 3661-3668.
- [34] Sankarasubramanian, A., Vogel, R. M., Limbrunner, J. F. (2001): Climate elasticity of streamflow in the United States. – *Water Resources Research* 37(6): 1771-1781.
- [35] Sen, P. K. (1968): Estimates of the regression coefficient based on Kendall's tau. – *Publications of the American Statistical Association* 63(324): 1379-1389.
- [36] Timilsena, J., Piechota, T. (2008): Regionalization and reconstruction of snow water equivalent in the upper Colorado River basin. – *Journal of Hydrology* 352(1-2): 94-106.
- [37] Wang, S. J., Ling, L., Cheng, W. M. (2014): Variations of bank shift rates along the Yinchuan Plain reach of the Yellow River and their influencing factors. – *Journal of Geographical Sciences* 24(4): 703-716.
- [38] Weber, K., Stewart, M. (2010): A critical analysis of the cumulative rainfall departure concept. – *Ground Water* 42(6): 935-938.
- [39] Xiao, P. (2014): Attribution of Hydrological Trend in Dongting Lake Basin. – Tsinghua University, Beijing.
- [40] Xu, K. H., Milliman, J. D., Xu, H. (2010): Temporal trend of precipitation and runoff in major Chinese Rivers since 1951. – *Global & Planetary Change* 73(3-4): 0-232.
- [41] Xu, X. L., Liu, W., Rafique, R., Wang, K. L. (2013a): Revisiting continental U.S. hydrologic change in the latter half of the 20th century. – *Water Resources Management* 27(12): 4337-4348.
- [42] Xu, X. L., Scanlon, B. R., Schilling, K., Sun, A. (2013b): Relative importance of climate and land surface changes on hydrologic changes in the US Midwest since the 1930s: implications for biofuel production. – *Journal of Hydrology* 497(11): 110-120.
- [43] Ye, X. C., Zhang, Q., Liu, J., Li, L., Guo, H. (2009): Impacts of climate change and human activities on runoff of Poyang Lake catchment. – *Journal of Glaciology and Geocryology* 31(5): 835-842.
- [44] Ye, X. C., Zhang, Q., Liu, J., Li, X. H., Xu, C. Y. (2013): Distinguishing the relative impacts of climate change and human activities on variation of streamflow in the Poyang Lake catchment, China. – *Journal of Hydrology* 494: 83-95.
- [45] Zhang, H. B., Huang, Q., Zhang, Q., Gu, L., Chen, K. Y., Yu, Q. J. (2015): Changes in the long-term hydrological regimes and the impacts of human activities in the main Wei River, China. – *Hydrological Sciences Journal/Journal des Sciences Hydrologiques* 61(6): 1054-1068.
- [46] Zhang, X. Y., Liu, M. X. (2018): Effects of climate change and human activities on water and sediment discharge in Xiangjiang Basin. – *Research of Soil and Water Conservation* 25(1): 30-37.
- [47] Zhao, Y. F., Zou, X. Q., Gao, J. H., Xu, X., Wang, C. L., Tang, D. H., Wang, T., Wu, X. W. (2015): Quantifying the anthropogenic and climatic contributions to changes in water discharge and sediment load into the sea: a case study of the Yangtze River, China. – *Science of the Total Environment* 536: 803-812.
- [48] Zheng, M. G., Sun, L. Y. (2014): Recent change of runoff and its components of baseflow and surface runoff in response to climate change and human activities for the Lishui watershed of southern China. – *Geographical Research* 33(2): 237-250.
- [49] Zuo, D. P., Xu, Z. X., Yao, W. Y., Jin, S. Y., Xiao, P. Q., Ran, D. C. (2016): Assessing the effects of changes in land use and climate on runoff and sediment yields from a watershed in the Loess Plateau of China. – *Science of the Total Environment* 544: 238-250.

RESEARCH ON WATER DEMAND RULES AND YIELD OF MULTI-STOREY CROPPING HERBAGE GROUPS UNDER WATER STRESS CONDITIONS

LIU, H.^{1,2,4} – WEI, Z.^{1*} – YIN, C.^{3*} – WEI, Y.² – ZHAO, S.² – ZHANG, R.² – WANG J.² – ZHAO J.³

¹*Inner Mongolia Agricultural University
No. 306 Zhaowuda Road, Hohhot City, Inner Mongolia, China
(phone/fax: +86-471-431-9291)*

²*Institute of Water Resources for Pastoral Area Ministry of Water Resources
No. 128 University East Street, Saihan District, Hohhot City, Inner Mongolia, China
(phone: +86-471-469-0607; fax: +86-471-495-1331)*

³*Inner Mongolia Academy of Agricultural and Animal Husbandry Sciences
No. 22 Zhaojun Road, Yuquan District, Hohhot City, Inner Mongolia, China
(phone/fax: +86-471-590-0262)*

⁴*State Key Laboratory of Simulation and Regulation of Water Cycle in River Basin
Room 936, Block D, No. 1 Fuxing Road, Haidian District, Beijing, China
(phone/fax: +86-10-68781380)*

**Corresponding author
e-mail: 444841507@qq.com; phone/fax: +86-471-590-0262*

(Received 11th Jan 2019; accepted 8th Mar 2019)

Abstract. It is greatly significant to implement water-saving irrigation and establish a water-saving system for forage grass, on basis of non-full irrigation principles, in order to meet the demands for forage grass from the rapidly-developing Chinese dairy industry distributing in rural-urban fringes, and improve the utilization efficiency of limited water resources in the central dairy production area of Inner Mongolia. The paper targets four different planting patterns of maize/alfalfa, and discusses water demand rules of herbage groups, variation of evapotranspiration, influence of water shortage at different stages on evapotranspiration, and moisture sensitive period of the forage grass under multi-storey cropping conditions, based on the experimental data of forage multi-storey cropping field under different water stress conditions in the outskirts of Hohhot. According to the results, the change in water demand of maize/alfalfa belt type multi-storey cropping field presents a wavy rule during the whole growth period; compared to evapotranspiration of monocropping maize/alfalfa, the evapotranspiration of maize/alfalfa multi-storey cropping herbage group was not significantly variable. The moisture sensitive period of monoculture maize and alfalfa were respectively heading-milk ripe stage and branching-squaring stage, and the moisture sensitive period of 4//8-type multi-storey cropping pattern is branching-jointing stage.

Keywords: *water-saving irrigation, moisture sensitive period, designed moistening layer, water utilization efficiency, evapotranspiration, moisture sensitive period, water balance equation, modal coefficient*

Introduction

The development level of the dairy industry is deemed as a significant indicator of the quality of modern agriculture in a country, especially animal husbandry. Dairy industry is recognized as a food-saving, economic and efficient industry, among the animal by-products with the highest forage conversion intensity. The World Health Organization regards the average dairy consumption of the population as one of the key indicators to measure the standard of living of the people in a country, and many

countries worldwide, including China. In order to meet the demands for forage grass from the rapidly-developing Chinese dairy industry, it is very significant to research water-saving technologies on basis of non-full irrigation principles, implement water-saving irrigation on dairy forage grass, and improve utilization efficiency of limited water resources in production. Meanwhile, dairy industry mainly distributes in rural-urban fringes, the evapotranspiration for forage production and irrigation has been exhausting urban water resources, the proper distribution of limited water resources will become a critical issue in water management (Zhou et al., 2015; Wang et al., 2003; Chen et al., 1997; Li et al., 2003; Guo et al., 2005; Zhang et al., 2002; Zhao et al., 2008; Liu and Yin, 2013; Liu et al., 2016).

In Hohhot, well-known as “Chinese Dairy City”, the high-quality forage cultivated area reached 173,000 hm² in 2006, accounting for 33% of the city’s total arable land area. The paper analyzes the experimental data of forage multi-storey cropping field under different water stress conditions in the outskirts of Hohhot from 2011 to 2015, discusses water demand rules of herbage groups, variation of evapotranspiration, influence of water shortage at different stages of evapotranspiration, and determines the moisture sensitive period of the forage grass under multi-storey cropping conditions, based on analyzing the forage crops yield under different moisture treatment conditions. The research results provide the basis for the implementation of scientific water management on dairy forage production in Hohhot and even central Inner Mongolia.

Materials and methods

Experimental region

The experiment was conducted in Agricultural Technology Demonstration Park, Xigoumen Town, with coordinates of E111 59’38.97”, N40 37’56.48”. The experimental region is located in semi-arid temperate continental monsoon climate zone, the soil is sandy loam, the mass ratio of organic matter, total nitrogen and total phosphorus is respectively 1.0%, 0.7% and 0.1%, the dry bulk density is 1.4 g/cm³ and the field capacity is 22.2%.

Experimental design

The experimental materials adopt feed & storage dual-purpose type Jinshan No. 1 maize and mow-resistant high-protein content algonquin alfalfa, control index of soil moisture shown in *Table 1*. By adopting field comparison experimental method, total four kinds of crop combinations is planted, including monoculture maize, monoculture alfalfa, 2 rows of maize intercropped with 12 rows of alfalfa (2//12 type), 4 rows of maize intercropped with 8 rows of alfalfa (4//8 type). The total 17 treatment means are implemented, each treatment is made three times, each unit area is 32 m² as shown in *Table 2*. As for 2//12 type, the alfalfa/maize belt width is 2.4 m and 0.8 m, as for the 4//8 type, the alfalfa/maize belt width is 1.6 m, as for monoculture alfalfa/maize field, the belt width is 3.2 m. The climate condition is divided into non-drought and moderate drought, the soil moisture is regarded as the control index. Experimental photograph was shown in *Figure 1*.

Table 1. Control index of soil moisture. (Unit: field capacity %)

Experimental level	Maize monoculture	Alfalfa monoculture	Maize and alfalfa multi-storey cropping
Non-drought	70	65	65
Moderate drought	40~50	40~50	40~50

The moisture is a lower-limit value, the field capacity is an upper limit

Table 2. Experimental design for forage moisture stress

Trt.	Patterns	Moisture treatment			
		Sprouting-tillering period (sprouting (seedling establishment)- branching)	Tillering-jointing period (branching-squaring)	Heading-flowering period (squaring-flowering)	Grouting-mature period
1	Maize monoculture	Non-drought	Non-drought	Non-drought	Non-drought
2		Moderate drought	Non-drought	Non-drought	Non-drought
3		Non-drought	Moderate drought	Non-drought	Non-drought
4		Non-drought	Non-drought	Moderate drought	Non-drought
5		Non-drought	Non-drought	Non-drought	Moderate drought
6	Alfalfa monoculture	Non-drought	Non-drought	Non-drought	
7		Moderate drought	Non-drought	Non-drought	
8		Non-drought	Moderate drought	Non-drought	
9		Non-drought	Non-drought	Moderate drought	
10	2//12 type	Non-drought	Non-drought	Non-drought	
11		Moderate drought	Non-drought	Non-drought	
12		Non-drought	Moderate drought	Non-drought	
13		Non-drought	Non-drought	Moderate drought	
14	4//8 type	Non-drought	Non-drought	Non-drought	
15		Moderate drought	Non-drought	Non-drought	
16		Non-drought	Moderate drought	Non-drought	
17		Non-drought	Non-drought	Moderate drought	



Figure 1. Experimental photograph (heading-flowering period of maize and squaring- of alfalfa)

Experimental data acquisition

The meteorological data is obtained and purchased from local meteorological bureau. It is available to sample soil by manual earth boring auger, and determine soil water content by drying and weighing method. The quadrates is adopted to measure the yield before harvest. The tube irrigation method is adopted to record time, the meter is adopted to record irrigation water yield.

Results and analysis

Characteristic of water demand of forage groups under different planting patterns

In accordance with the principle of water balance, in any period of the whole growth term (t), the changes in moisture storage capacity in soil designed moistening layer (h) is expressed by the following water balance equation:

$$W_t - W_0 = W_r + P_0 + K + M + ET_a \quad (\text{Eq.1})$$

In Equation 1, W_0 , W_t represents moisture storage capacity in soil designed moistening layer at the beginning of time interval and at any time t ; W_r represents increased moisture storage capacity due to increase of soil designed moistening layer, if the soil designed moistening layer does not change, the option can be ignored; P_0 is rainfall; K is groundwater recharge within the period t , if in the experimental region, the groundwater level is below 10 m within a long period, K should be equal to 0; M is the irrigation water volume within the period t ; ET_a is the actual evapotranspiration.

Table 3 show the actual evapotranspiration and rules of water demand of maize/ alfalfa forage group of different cropping patterns under full irrigation conditions according to Equation 1.

Table 3. Forage group evapotranspiration of different planting pattern

Trt.	Items		Main technical parameters								Whole growth period
	Alfalfa	Growth period	Crop 1				Crop 2			Crop 3	
			Seeding-sprouting	Sprouting-branching	Branching-squaring	Squaring-flowering (clipping)	Seeding establishment-branching	Branching-squaring	Heading-flowering (clipping)	Seeding establishment-branching	
		Rainfall (mm)	25.6	34.4	29.2	62.6	134.2	48.4	6.6	16.5	357.5
	Maize	Growth period	Seeding-sprouting	Sprouting-jointing	Jointing-heading	Heading-milking maturity		Milking maturity-soft dough			
		Rainfall (mm)	21.5	44.6	48.6	224.6		11.9		351.2	
6	Soil Moisture		19.1-18.4	18.4-16.8	16.8-17.3	17.3~17.3	17.3-20.1	20.1-12.8	12.8-16.2	14.9-15.9	
	Irrigation amount (mm)				100	70			120	70	
	Consumption intensity (mm/d)		2.15	2.65	4.78	6.87	3.25	7.45	6.95	2.15	3.92
	Evapotranspiration (mm)		32.3	47.7	124.3	137.4	39	111.8	97.3	32.3	726.7
1	Soil moisture		19.2-20.0	20.0-19.9	19.9-14.0	14.0-14.1			14.1-13.5		
	Irrigation amount (mm)			70	120	180			80		
	Consumption intensity (mm/d)		1.82	3.05	6.65	8.25			6.45		5.95
	Evapotranspiration (mm)		17.6	92.4	124.5	289.6			76.5		600.6
10	Soil moisture		20.0-19.6	19.6-17.8	17.8-19.0	19.0-17.5	17.5-20.3	20.3-18.0	18.0-17.4	17.4-16.1	
	Irrigation amount (mm)				70	80		100	100	120	
	Consumption intensity (mm/d)		1.91	3.27	4.78	8.77	2.44	5.59	6.58	3.65	3.49
	Evapotranspiration (mm)		28.6	58.9	124.4	175.5	29.3	83.9	92.1	54.8	647.3
14	Soil moisture		18.9-18.4	18.4-16.7	16.7-17.7	17.7-16.5	16.5-20.3	20.3-16.15	16.2-15.4	54.8	
	Irrigation amount (mm)				70	80		100	100	120	
	Consumption intensity (mm/d)		2.0	2.9	5.7	7.6	4.9	7.5	6.9	4.4	3.6
	Evapotranspiration (mm)		29.8	49.6	98.5	151.0	57.3	112.4	96.3	65.7	660.5

The percentage of soil moisture in the total soil dry weight, %

Under full-irrigation conditions, the evapotranspiration of monoculture alfalfa is 726.7 mm as the maximum value, and the evapotranspiration of monoculture maize is 600.6 mm as the minimum value, the maize/alfalfa multi-storey cropping evapotranspiration is between the above data, the growing season of monoculture alfalfa within a year is longer than the monoculture maize, the evapotranspiration of monoculture alfalfa is also higher than the monoculture maize during the whole growth period; because mowing is implemented several times a year, evapotranspiration intensity is peaked with alfalfa mowing frequency, each peak occurs in alfalfa squaring-flowering stage, the maximum peak occurs between the first mowing and the Second mowing, during the branching-squaring stage, the evapotranspiration of alfalfa is maximum, accounting for 40.0% of the whole growth period; during the heading-milking stage, the evapotranspiration of monoculture maize is up to 289.6 mm, accounting for 48.2% of the whole growth period. The growing season of monoculture maize is relatively short, during the whole growth period, its total evapotranspiration is also lower than the monoculture alfalfa and multi-storey cropping alfalfa; the water demand rules show a single peak, the consumption intensity during heading-milking stage is maximum. The evapotranspiration of maize//alfalfa belt-type multi-storey cropping during the whole growth is greater than the monoculture maize; and is closer to monoculture alfalfa; the water demand rules of herbage group is impacted by alfalfa mowing, its evapotranspiration intensity is considerably unstable, the fluctuation trend is similar with monoculture alfalfa.

Variation analysis of evapotranspiration of forage grass under multi-storey cropping conditions

Because the dynamic evapotranspiration and evapotranspiration trend of forage grass has changed, the evapotranspiration of maize//alfalfa multi-storey cropping forage grass should not be equal to the sum of evapotranspiration of both two plants, the degree of variation (variability) is calculated by the following formula:

$$C_v = \frac{\sum_{i=1}^n \sqrt{(x - \bar{x})^2}}{x} \quad (\text{Eq.2})$$

In the formula: C_v -variability; x -sample evapotranspiration; \bar{x} -arithmetic mean of the two samples. The evapotranspiration indicators under monoculture conditions are taken as standard samples, the evapotranspiration indicators under multi-storey cropping are taken as comparison samples; C_v - the degree of variation of multi-storey cropping for monoculture.

The evapotranspiration variability calculated by *Equation 2* under the multi-storey cropping conditions are shown in *Table 4*. The results show that the evapotranspiration of forage grass group is not significantly variable from the evapotranspiration of monoculture maize and monoculture alfalfa, the variability is respectively 0.037 and 0.040, however, it is significantly variable, compared with monoculture alfalfa.

Evapotranspiration (ET) of monoculture maize under phased water shortage conditions

Under the maize monoculture conditions, the different water treatment has a significant impact on evapotranspiration. The treatment 4 is the water shortage at

heading-milking stage, the change in total evapotranspiration is the most obvious during the whole growth period, according for 75% of treatment 1. The treatment 2 is the water shortage at sprouting-jointing stage, the change in total evapotranspiration is minimum, according for 85% of treatment 1. In case of water shortage at a certain stage, the treatment may cause the increase of evapotranspiration at the next stage, there is a certain compensation effect, in this experiment, during the sprouting-jointing stage and heading-milking stage, the compensation effect for low moisture treatment is more obvious.

Table 4. Analysis on variation of ET of maize & alfalfa under multi-storey cropping conditions

Samples	Treatments	ET (mm)	C _v
Standard samples	1	600.6	0.0370
	6	726.7	0.0403
Comparison samples	14	660.5	

Water shortage at different growth stages on evapotranspiration of forage groups

It is found from Table 5 that the evapotranspiration at various growth stages under different water treatments is less at the preliminary stage, increase at the interim stage, the late small variation, and then decreases at the later stage, which mainly result from the growth and development of maize plants and influence from environment meteorological factors, the moisture shortage also affects daily evapotranspiration intensity, thereby affects the evapotranspiration at the reproductive stage. Treatment 2 and 3 is the drought conditions respectively at seedling/jointing stage, at this time, the maize seedling size is less, the evapotranspiration is less. At the heading-milking stage, the evapotranspiration of fully-irrigated treatment is maximum, other treatments are water deficit at other growth stages, although after rewatering in this stage, evapotranspiration increases obviously, but is always lower than treatment 1, because the jointing-heading stage is the peak of the growth of maize silage, if water deficit exists during this period, the growth of plants will be seriously affected, resulting in a less silage maize leaf area index, the plant evapotranspiration is less than other treatments; on the other hand, even if the stage is not affected by the drought, but before the stage have been affected, resulting in poor plant growth, and the evapotranspiration intensity and evapotranspiration will be ultimately affected in the later stage of treatment.

Table 5. Maize straw of different water treatment on evapotranspiration

Trt	Seeding-sprouting		Sprouting-jointing		Jointing-heading		Heading-milking maturity		Milking maturity-soft dough		Whole growth period (mm)
	ET (mm)	Modal coefficient (%)	ET (mm)	Modal coefficient (%)	ET (mm)	Modal coefficient (%)	ET (mm)	Modal coefficient (%)	ET (mm)	Modal coefficient (%)	
1	17.6	2.9	92.4	15.4	124.5	20.7	289.6	48.2	76.5	12.7	600.6
2	10.2	2	23.0	4.5	152.6	29.9	246.1	48.2	78.6	15.4	510.5
3	8.8	2	66.2	15.1	52.2	11.9	247.3	56.4	64.0	14.6	438.4
4	8.6	1.9	63.5	14.1	114.9	25.5	134.2	29.8	129.3	28.7	450.5
5	9.1	1.9	67.3	14	107.2	22.3	240.7	50.1	56.2	11.7	480.5

Evapotranspiration of monoculture alfalfa under phased water shortage conditions

Table 6 shows, the alfalfa high evapotranspiration period is between in the first crop and the second crop, in the stage, the evapotranspiration accounts for 47.82% and 40.49% of total amount of the whole growth period, under full-irrigation conditions. The low moisture treatments in seedling (seedling establishment)-branching, branching-squaring, squaring-flowering, and other growth stages has a great influence on the total evapotranspiration during the whole growth period, compared to treatment 1, the low moisture treatment at the branching-squaring stage decreases by 20%; at seedling (seedling establishment)-branching stage, the total evapotranspiration of whole growth period changes less, however, it can decrease by 18%, compared with treatment 6.

Table 6. *Evapotranspiration of monoculture alfalfa and maize/alfalfa intercropping at different water treatments*

Trt	Crop 1		Crop 2		Crop 3		Total ET (mm)
	ET (mm)	Modal coefficient (%)	ET (mm)	Modal Coefficient (%)	ET (mm)	Modal coefficient (%)	
6	347.5	45.9	294.3	38.8	84.9	11.2	726.7
7	250.1	40.5	266.2	43.1	76.6	12.4	592.9
8	270.2	44.7	206.0	34.1	103.5	17.1	579.7
9	262.1	43.1	229.5	37.8	91.5	15.1	583.1
14	326.5	43.0	276.9	36.5	57.1	7.5	660.5
15	279.7	42.6	257.8	39.2	33.8	5.1	571.3
16	303.8	45.5	235.9	35.3	40.6	6.1	580.3
17	275.5	42.9	247.3	38.5	35.0	5.5	557.8

Evapotranspiration of 4//8 type at intercropping stage under water shortage conditions

Table 6 shows, as same as monoculture alfalfa, the alfalfa high evapotranspiration period is between in the first crop and the second crop under full-irrigation conditions, however, the evapotranspiration ratio in the second crop is higher than monoculture alfalfa, in the stage, the evapotranspiration accounts for 49.43% and 41.92% of total amount of the whole growth period. The evapotranspiration of maize//alfalfa multi-storey cropping forage grass should not be equal to the sum of evapotranspiration of both two plants, this shows that the planting pattern changes growth environment, the field evapotranspiration changes. Under full irrigation conditions, the low water treatment has a greater impact on branching-squaring and squaring-flowering stages; and has poor impact on emergence-branching stage.

Influence of different water treatments on forage yield

Table 7 shows, at different growth stages, different forages show various response to water stress, but which is eventually reflected by forage yield differences. Ass for monoculture maize, the influence of water shortages on yield reduction is the greatest at heading-milking stage, and is the lowest at sprouting-jointing stage. The influence of phased water shortage on the yield (grain) is in compliance with the following rules: Treatment 4 > Treatment 3 > Treatment 5 > Treatment 2, the maize requires less moisture at seedling stage; at the jointing stage, the impact of water deficit on yield is

greater, in case of water shortage at jointing period, the yield reduction rate is 47.2%; at the heading and milking stages, the maize transfers from vegetative growth to reproductive growth, leaf area index and evapotranspiration reach its highest value during the whole period, reproductive growth and metabolism is being vigorous; at flowering, pollination and milking stages, the output efficiency is the highest, lack of water has a greatest impact, the yield reduction rate is up to 51.7%; after soft dough stage, the influence of water deficit on yield decreases gradually. At different stages, the water deficit treatment does not significantly affect moisture production efficiency of monoculture maize, which is basically the same between Treatment 1 and Treatment 2, Treatment 3 is slightly lower than Treatment 5, the influence of Treatment 4 is maximum.

Table 7. Analysis on forage yield under different water treatments

Treatments	ET (mm)	Total yield (dry weight kg/hm ²)	Moisture production efficiency (kg/m ³)	Yield reduction rate (%)
1	600.6	13250.0	2.2	—
2	510.5	11316.7	2.2	17.1
3	438.4	9000.0	2.1	47.2
4	450.5	8733.4	1.9	51.7
5	480.5	10316.7	2.1	28.4
6	726.7	21150.0	2.9	—
7	592.9	16031.7	2.7	24.2
8	579.7	13472.6	2.3	36.3
9	583.1	14212.8	2.4	32.8
14	660.5	2636.8	0.399	—
15	571.3	2136.8	0.289	19.0
16	580.3	1706.9	0.294	35.3
17	557.8	1693.9	0.304	35.8

As for monoculture alfalfa, when the water shortage is implemented at emergence-branching stage (the lower limit of soil moisture content is lower than 50%), the impact on the yield is minimum, the yield reduction rate is 24.2%, indicating under normal emergence seedling conditions, appropriate water shortage does not impact later yield; the branching- squaring stage is a critical period of alfalfa physiological change, water shortage has the greatest impact on later yield, the yield reduction rate is 36.35%; during the squaring-flowering period, the influence of water shortage on the total yield decreases, the yield reduction rate is 32.8%. under different moisture treatment conditions, if the water supply is sufficient, the water production efficiency of monoculture alfalfa is the highest, and 6.89% higher than that of water shortage at sprouting-branching stage, 20.69% higher than that of water shortage at branching-budding stage, and 17.24% higher than that of water shortage at budding-- flowering stage.

As for the intercropping maize/alfalfa, alfalfa has a longer growth period, under non-full irrigation experimental design is mainly base on phased water supply in alfalfa growth period. By conversion to the crude protein content in maize/alfalfa final product within one year, it is available to conclude that the water shortages at squaring-

flowering stage has the greatest impact on crude protein yield under intercropping conditions under different water treatments, which is different with the maximum influence period from water shortage of monoculture alfalfa of branching-squaring stage, indicating two kinds of forages jointly change the rules of nutrition production of the whole groups of plants in farmland.

Conclusions

As the main dairy forage, maize and alfalfa are completely different in water demands. During the whole growth period, the water demand rules of maize is a single peak parabola; during a growing season, the water demand rules of alfalfa shows multiple peaks as times of mowing increase; The evapotranspiration of maize//alfalfa multi-storey cropping forage grass should not be equal to the sum of evapotranspiration of both two plants, the rules of water demand change greatly, showing a wavy undulating state. compared to evapotranspiration of monoculture maize and monoculture alfalfa, the variation of evapotranspiration of maize//alfalfa multi-storey cropping forage groups is not very significant.

As for monoculture maize, the influence of phased water shortage on the yield is maximum at the jointing-heading and heading-milking stages (moisture sensitive period); the influence of phased water shortage is minimum at emergence-jointing stage; as for monoculture alfalfa, during the squaring-flowering and branching-squaring period (moisture sensitive period), the influence of phased water shortage on the yield is maximum; at emergence (seedlings establishment)-jointing stage, the influence of phased water shortage is minimum; as for 4//8-type multi-storey cropping, at the branching-jointing stage of alfalfa, the influence of phased water shortage on the yield is maximum, which is greatly different with monoculture alfalfa.

In future studies, in order to meet the requirements of large-scale popularization and application of multi-storey cropping, further test deepening, technology integration and demonstration of various technologies still need to be implemented., technological maturity and farmers' planting level need to be improved, and technological maturity and farmers' planting level need to be improved.

Acknowledgements. This research was supported by the Special funds projects of China Institute of water resources and Hydropower Research (MK2018J07, MK2017J05, MK2016J10), National Natural Science Foundation of China (51469024), National key research and development program (2018YFD0300400), Inner Mongolia Science and Technology Project (201701024).

REFERENCES

- [1] Chen, Y., Sun, J. (1997): Research on soil moisture control standards of water-saving irrigation. – *Irrigation and Drainage* 16(1): 24-28.
- [2] Guo, K., Li, H., Shi, H. et al. (2005): Research on optimization of water-saving irrigation system and evapotranspiration of forage crop in Mu Us sandland. – *Irrigation and Drainage* 2: 24-27.
- [3] Li, J., Wu, F., Fan, Y. (2003): Research on water-saving irrigation index and development mode. – *Water-Saving Irrigation* 5: 14-15.

- [4] Liu, H., Yin, C., Wei, Y., Zhang, R., Gao, T. (2016): Water production function of artificial grassland crop in arid desert area of Northern Xinjian. – *Agric. & Life Sci., Journal of Zhe Jiang University* 42(2): 169-178.
- [5] Wang, X., Ma, Y., Li, J. et al. (2003): Nutrients and biological characteristics of alfalfa. – *Pratacultural Science* 10: 39-40.
- [6] Zhang, X., Pei, D., Hu, C. (2002): Research on irrigation index of winter wheat and summer maize on Taihang Piedmont Plain. – *CSAE* 18(6): 36-41.
- [7] Zhao, S., Guo, K., Su, P. (2008): Comprehensive benefit evaluation on dairy forage under different cropping patterns. – *Water Economy* 26(6): 41-44.
- [8] Zhou, X., Luo, Q., Qu, B. (2005): Current situation and future development trends of China's dairy industry. – *Contemporary Animal Husbandry* 12: 1-3.
- [9] Liu, H., Wei, Y., Guo, K. (2013): Water requirement and its law of silage corn in northern Xinjiang arid desert grassland. – *Chinese Agricultural Science Bulletin* 29(33): 94-100.

CO₂ AND CH₄ PARTIAL PRESS AND FLUX ACROSS WATER-AIR INTERFACE IN THE DOWNSTREAM OF JINSHA RIVER, CHINA

QIN, Y.¹ – WANG, Z.¹ – LI, Z.² – YANG, B.¹

¹*Key Laboratory of Hydraulic and Waterway Engineering of the Ministry of Education, Chongqing Jiaotong University, Chongqing 400074, China*

²*Key Laboratory of Reservoir Environment, Chongqing Institute of Green and Intelligence Technology, Chinese Academy of Sciences, Chongqing 400714, China*

(Received 11th Jan 2019; accepted 8th Mar 2019)

Abstract. This paper takes some typical points at downstream of Jinsha River in China as examples for the overall evaluation of greenhouse gas emissions. In reference of previous literature, this study adopted the combination of headspace balance method and model estimation to obtain the partial pressures of carbon dioxide and methane in surface water and exchange fluxes of CO₂ and methane. Additionally, this paper also used field measuring instruments to measure the physical and chemical variables. The Spearman correlation index based on SPSS software are applied to analyse the relationship between the partial pressures and fluxes of CO₂ and methane and environment variables. Experiments' results showed that mean value for partial pressure of CO₂ ($p(\text{CO}_2)$) was (1785.87 ± 451.18) μatm , ranked medium in worldwide rivers. In contrast, the average value for $p(\text{CH}_4)$ was (22.63 ± 11.48) μatm ranked relatively low in worldwide rivers. Among all sampling sites, the $p(\text{CH}_4)$ for Linjiaba, Shaonvping, Lizhuang located in reservoir area were higher than that for other sites. And the diffusion of CO₂ flux was in medium level compared with other major rivers in the world, at (1.71 ± 0.55) $\text{mmol}/(\text{m}^2 \cdot \text{h})$, while that of CH₄ flux kept in low level at (0.0009 ± 0.0005) $\text{mmol}/(\text{m}^2 \cdot \text{h})$, and all benthic flux of CO₂ and CH₄ were positive indicated the Jinsha River was the source of producing greenhouse gas., the trend of the partial pressure and flux almost remained the same. Moreover, $p(\text{CO}_2)$ in surface waters showed positive correlations with alkalinity (TA) and dissolved organic carbon(DOC), and $p(\text{CH}_4)$ showed significant positive correlations with Chl-a and temperature. CO₂ flux showed positively correlation with the $p(\text{CO}_2)$, DOC, alkalinity (TA), and CH₄ flux is positively related to $p(\text{CH}_4)$, wind speed. Other environmental factors showed vague effects on the fluxes.

Keywords: carbon input, environmental indicators, greenhouse gas, greenhouse effect, river

Introduction

Although the water area takes up for approximately 2% of global inland area, it largely influences the global carbon cycle (Guo et al., 2011). As the crucial connection between terrestrial ecosystem and marine ecosystem which are two main carbon carriers, river has become vital part of global carbon cycle (Ludwig et al., 1996). The carbon output from rivers is closely responsible for the change of coastal environment, marine carbon cycle and the global climate system. However, in recent years, human activities accelerate land erosion-deposition, which to a large extent stimulates the disturbance and redeposition of carbon pool in land ecosystem, and strengthens carbon transport from rivers to ocean. About 1 Gt carbon containing 60% inorganic carbon and 40% organic carbon is estimated to be transported from river to sea (Ludwig et al., 1996; Zhang et al., 2013; Cole et al., 2007). Meanwhile, river releases and absorbs carbon dioxide and methane though air-water interface, of which the amount of released CO₂ can reach at least 10⁷ t/a (Li et al., 2013; Degens et al., 1991). These two typical gases emission significantly contributes 80–85% of greenhouse effect (Clarke et al., 2007). This percentage has not changed for the last 20–30 years, but the total radiative forcing which causes the increase in the planet's temperature has increased consistently

over this time window (Getoff, 2006). The primary effect for greenhouse effect gives Planet Earth its hospitable average temperature of c. 17 °C, and the smaller secondary effect which has been in existence for only 250–300 years and is caused by an increase in concentration of greenhouse gases (Yao and Gao, 2005). As a result, measuring CO₂ and CH₄ benthic flux among water-air interface in river in a right way contribute to a better understanding the role that river play in regional or global carbon cycle and a more systematical grasp of carbon budget in river basin. Considerable researches about gas fluxes in the last decades on water-air interface almost adopted eddy covariance method, model estimation method, remote sensing inversion, etc (Zhao et al., 2011b). Among these methods, field monitoring usually employs model estimation method for its simplicity, flexibility and practicality. Precisely, Model evaluation method applies the Fick law to evaluate the flux in accordance with Gas concentration gradient between air and water interface where difference of gas concentration between two medias Mass Transfer Coefficient are critical (Urabe et al., 2010; Jonsson et al., 2007; Huang and Wang, 2009).

Jinsha River is the upper reaches of the Yangtze River flowing through east northern of The Yunnan-Guizhou Plateau and west southern part of Sichuan Highland to the Minjiang River in Yibin City. Its length is 2326 km and its basin acreage which takes up 26% of the Yangtze River is 47.3×10^4 KM². In addition, it means annual discharge is 4750 m³/s. Due to the large area covered by Jinsha River, systematic and correct measure of greenhouse gas budget is critical for carbon cycle research. What should be noted is the processes of gas exchange between water-air interfaces are not only impacted by wind speed and temperature, but also related to depth and acreage of waters. Adopting the model estimation method to measure the CO₂ and CH₄ benthic flux, while there were few researches, should take the following factors into consideration, while there were few researches. In this paper, aiming at the downwards of Jinsha River from Panzhihua City to Yibin City, the research obtained the live data of CO₂ and CH₄ partial pressure in surface water and environmental parameters for field monitoring. Then the research used thin boundary layer method to estimate benthic flux of greenhouse gas and elementarily analyze the correlation between the environmental parameter and the partial pressure as well as the benthic flux. In downstream of Jinsha River, Wudongde hydropower station and Baihetan hydrogen station are being constructed, and Xiluodu hydrogen station and Xiangjiaba hydrogen station have been put into effect. The operation of newly-built hydropower stations will impact the carbon cycle in this area. A research on greenhouse flux on water-air interface is critical to illustrate variation change of carbon cycle after constructing plants and give information for reliability of hydropower energy system.

Materials and methods

Research objective

We researched at the downwards of Jinsha River (N24°29'—28°53' to E100°57'—104°38') from Panzhihua City (the junction of Yalong River and Jinsha River) to Yibin City (the junction of Min River and Jinsha River) in China, of which the length was 768 km and fall of water level was 719 m. From the upstream to downstream, a series of sampling positions were Geliping (GLP), Longjiedu (LJD), Jiaopingdu (JPD), Geledu (GLD), Yanziyan (YZY), Linjiaba (LJB), Shaonvping (SNP), Lizhuang (LZ), of which the locations were shown in *Table 1* and *Figure 1*. Among 8 sampling sites,

Shaonvping and Yanziyan are located in the reservoir area in front of Xiangjiaba hydropower station and Xiluodu hydropower station respectively, and Linjiaba site is located at the reservoir area between these two hydropower stations. We collected samples by taking local boat along the waterway in January 2016. Due to the rapid flow in Jinsha River, we gathered the water samples as well as relative environmental indicators in central of waterway. The scenes for sampling at Shaonvping, Gelefu, Yanziyan, Lizhuang are shown in *Figure 2*.

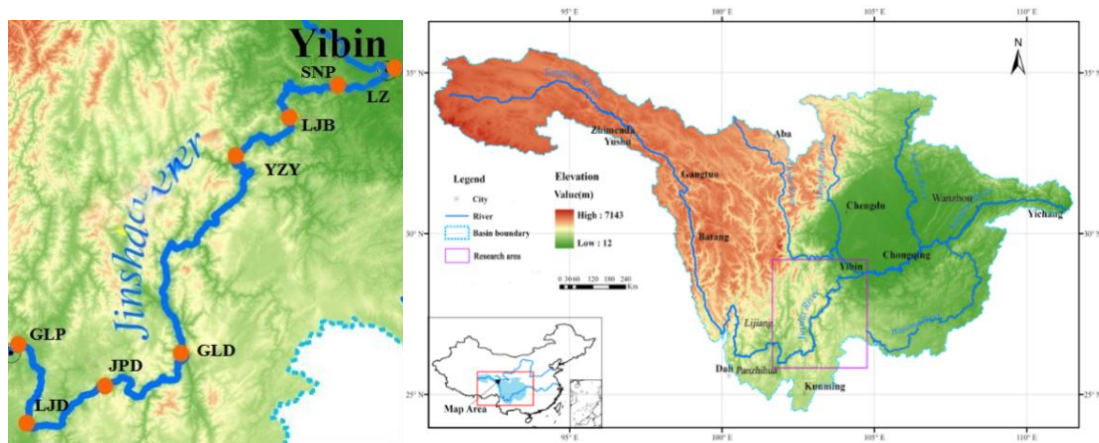


Figure 1. Sketch map of research area and sampling spots in the downstream of Jinsha River

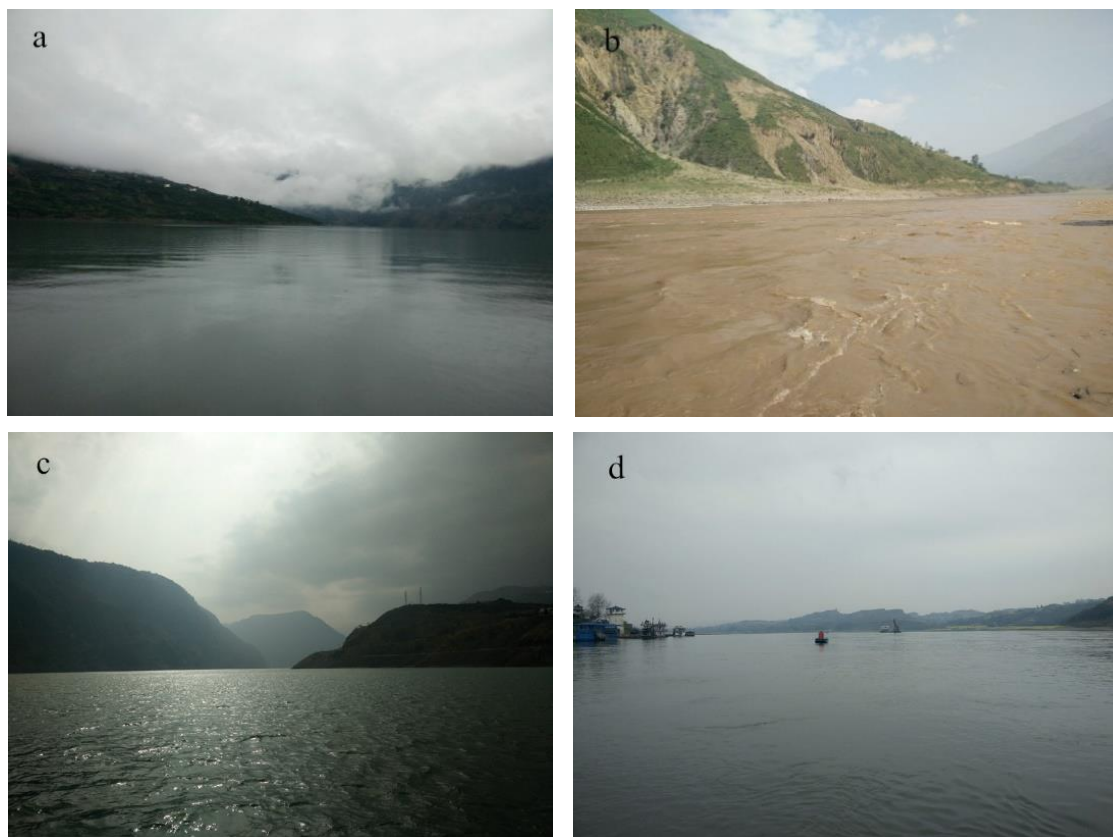


Figure 2. Photos of the sampling spots of Shaonvping (a), Geledu (b), Yanziyan (c) and Lizhuang (d) of the downstream of Jinsha River

Table 1. The locations of the sampling spots in downstream of Jinsha River

Sample site	$p(\text{CO}_2)/\mu\text{atm}$
Geliping (GLP)	N26°35.511', E101°31.857'
Longjiedu (LJD)	N25°57.729', E101°52.894'
Jiaopingdu (JPD)	N26°17.590', E102°22.912'
Geledu (GLD)	N26°31.251', E103°03.132'
Yanziyan (YZY)	N28°14.594', E103°36.370'
Linjiaba (LJB)	N28°39.347', E103°50.405'
Shaonvping (SNP)	N28°37.614', E104°19.174'
Lizhuang (LZ)	N28°48.933', E104°48.072'

Measure method for CH₄ and CO₂ in water-air interface

To measure water-air interface gas partial press, recent research mainly adopted following two methods: static closed chamber- Gas chromatography method and the headspace equilibrium method and thin boundary layer method. However, on the condition of wind blows and flowing water, the disturbance caused by friction between the chamber and surface water may cause extra emission of greenhouse gas which will influence the accuracy of experimental result from the former method (Pumpanen et al., 2004). And this method is labor-intensive and it is unfit for large-scale and long-term observation (Tremblay et al., 2005; Kolb and Etre, 2006). As a result, the static closed chamber technique only suits static water. Considering that the rapid flow of Jinsha River, long distance between sampling spots and poor weather condition during experiments, we use the latter method to observe the water-air interface greenhouse gas emission in the downstream of Jinsha River.

The principle of headspace equilibrium method

The principle of headspace equilibrium method is to obtain partial press of testing gas in water before equilibrium by measuring the concentration of the gas in upper space when gas concentration in water and air stay balance after rapid shake in the glass bottle filled with water sample and inert gas. The calculation is show as follows (Goldenfum, 2010):

$$p_{(Gas)} = \frac{(p_{final} \times K_{equilibrium}) + (\frac{HS}{S}) \times \frac{(p_{final} - p_{initial})}{V_m}}{K_{sample}} \quad (\text{Eq.1})$$

where the $p_{(Gas)}$ illustrates partial press of testing gas (μatm), and $p_{initial}$ and p_{final} denote testing gas partial press in upper part of bottle before and after equilibrium (μatm), and HS/S represents The volumetric properties for the gas mixture (mol/L), V_m demonstrate the molar volume of gas, K_{sample} and $K_{equilibrium}$ show solubility of testing gas at weather in bottle when sampling and experimenting respectively (mol/(L·atm)). And Henry coefficient of different gases can be calculated by following equations (Weiss, 1974; Weast and Astle, 1987):

$$\ln K_0(CO_2) = -58.0931 + 90.5069 \times \left(\frac{100}{T_K}\right) + 22.294 \times \ln\left(\frac{T_K}{100}\right) + \quad (\text{Eq.2})$$

$$s \times (0.027766 - 0.02588 \times \left(\frac{T_K}{100}\right) + 0.0050578 \times \left(\frac{T_K}{100}\right)^2)$$

$$\ln K_0(CH_4) = -115.6477 + \frac{155.5756}{(T_K/100)} + 65.2553 \times \ln\left(\frac{T_K}{100}\right) - 6.1698 \times \left(\frac{T_K}{100}\right) \quad (\text{Eq.3})$$

$$V_m = 1 \times 0.082057 \times (273.15 + T) \times \left(\frac{101.325}{p}\right) \quad (\text{Eq.4})$$

where T is temperature when sampling (°C) and p is atmospheric pressure when sampling (kpa). 2.2.2 Water-air interface gas benthic flux

The water-air interface gas benthic flux mainly impacted by partial press of gas in surface waters and gas transfer coefficient which is influenced by flowing speed, blowing speed and weather, etc. According to Fick Law, for freshwater bodies, the water-air interface gas benthic flux is obtained as follows (Weast and Astle, 1987):

$$Flux = k_x (C_{water} - C_{equilibrium}) \quad (\text{Eq.5})$$

with $Flux$ as greenhouse diffusion flux (mmol/(m²·h)), k_x as gas exchange coefficient (cm/h), C_{water} as the gas concentration in water (mmol/L), $C_{equilibrium}$ as greenhouse gas saturation concentration in site weather and atmospheric pressure (mmol/L).

And k_x is estimated worldwide mainly by following empirical equation adopted by Jähne et al. (1989):

$$k_x = k_{600} \left(\frac{600}{Sc}\right)^{0.67} \quad (\text{Eq.6})$$

with k_{600} as exchange coefficient of sulfur hexafluoride (SF₆) gas (cm/h). Considering sampling spots are being constructing or have been constructed hydraulic power plant, we choose the exchange coefficient for CO₂ and CH₄ for lakes and reservoir eco-system from empirical formula (shown as *Equations 7* and *8*, respectively (Cole and Caraco, 1998; Macintyre et al., 2006)

$$k_{600} = 2.07 + 0.215 \times U_{10}^{1.7} \quad (\text{Eq.7})$$

$$k_{600} = 2.07 + 0.215 \times U_{10}^{1.7} \quad (\text{Eq.8})$$

U_{10} illustrates wind speed on 10 m above the water (m/s). It is usually acquired by following formula using wind speed U_1 above water body measured at site (Crusius and Wanninkhof, 2003).

$$U_{10} = 1.22 \times U_1 \quad (\text{Eq.9})$$

where U_1 denotes instantaneous wind speed above water level from meteorological station (accuracy is 0.1 m/s).

And Sc denotes Schmidt constant at t °C. For freshwater, it can be calculated as follows (Roehm et al., 2009; Wanninkhof et al., 1992):

$$Sc(CO_2) = 1911.1 - 118.11t + 3.4527t^2 - 0.04132t^3 \quad (\text{Eq.10})$$

$$Sc(CH_4) = 1897.8 - 114.28t + 3.2902t^2 - 0.03906t^3 \quad (\text{Eq.11})$$

Then, greenhouse gas saturation concentration in water sample will be achieved by that partial press of greenhouse gas multiply by Henry coefficient shown as follows (Morel, 1982; Anderson, 2002; Zhang et al., 2009):

$$C_{equilibrium} = K_0 \times p(\text{Gas}) \quad (\text{Eq.12})$$

In Equation 12, K_0 denotes Henry coefficient which is defined as gas solubility (mol/(L·atm)) and $p(\text{Gas})$ show atmospheric pressure when experimenting (µatm).

The calculation procedure for greenhouse gas partial press and flux

The $p(\text{CO}_2)$ and $p(\text{CH}_4)$ in water were calculated within headspace equilibrium method though Agilent 7820A gas chromatograph according to Henry coefficient, water temperature, atmospheric pressure, volumetric property of gas and liquid in headspace bottle (5/7). And k_x is in connection with Schmidt constant from water weather and U_{10} obtained from Equation 11 (m/s). The downstream of Jinsha River was rarely impacted by farmland, wetlands and human, we determined the mean concentration of CO₂ and CH₄ in atmosphere as 390.5 ppm and 1.803 ppm respectively with reference to Gui's and Zhang's research on the Yellow River and the Yangtze river (Zhang et al., 2009; Gui, 2007). The whole process of calculation for greenhouse gas measurement by Headspace equilibrium method and Thin Boundary Layer Equation (TBL) method were shown in Figure 3. All field measuring apparatus had been calibrated standardly.

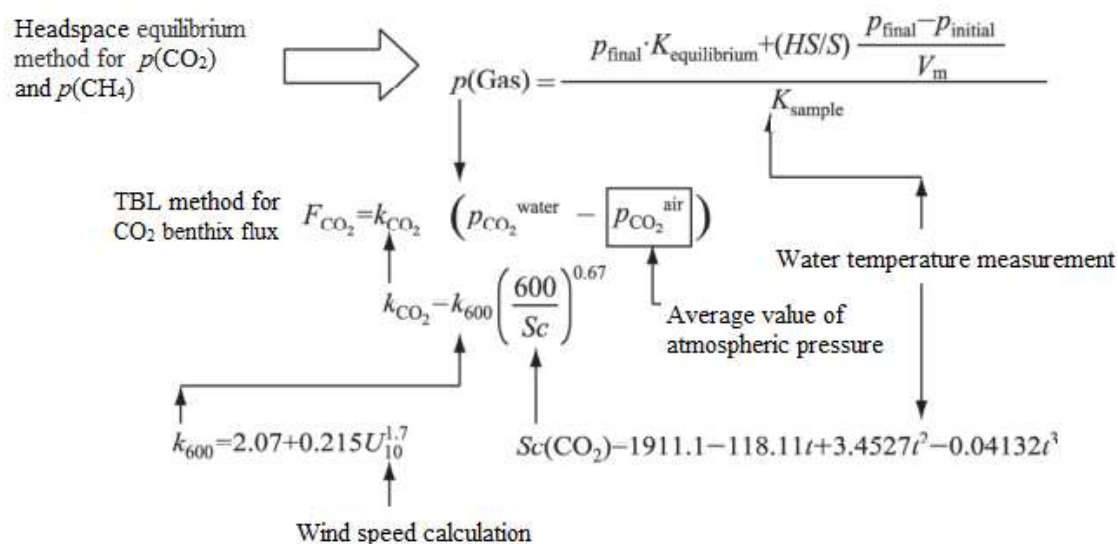


Figure 3. The process of calculation for greenhouse gas

Researching material and methods for sampling

Water sample was collected at 0.5 m depth by water sampler where headspace bottle was place inside to seal when submerging at each spot, and the water samples and headspace bottles were preserved at low temperature.

For environmental parameters measurements, pH, electrical conductivity and salinity were measured by YSI Multi-parameter instrument, temperature and atmospheric pressure were measured by handheld digital atmospheric pressure gauge, alkalinity (TA) was accessed from titration with standard sulfuric acid solution by microtiter from HACH Company (accuracy is 1.25 µl), the effective intensity of photosynthesis was measured by LI-COR190SA Light quantum instrument, the solar radiation intensity came from the illuminometer, water temperature and Dissolved Oxygen (DO) were obtained by site measurements with YSI ProODO Dissolved oxygen meter (accuracy is 0.1 °C, 0.01 mg/L respectively), Chlorophyll-a(Chl-a) adopted acetylacetone spectrophotometric method, concentration for Dissolved Total Nitrogen (DTN) and dissolved inorganic carbon (DIC) were measured by Shimadzu® TOC-V total carbon analyser from filtrates though What-man GF/F fibrous glass filter paper heated for 4 hours at 450 °C (Bates et al., 2011). Concentration for dissolved total phosphorus (DTP) measurements adopted Potassium persulphate- spectrophotometric method.

Researching method for analysis

The statistical analysis and calculation of this study data are proceeded by SPSS ® or Origin ®. And the spearman correlation analysis are adopted to understand the linear correlation between data changes and chlorophyll - a regression analysis relating to p (CO₂), p (CH₄), CO₂ and CH₄ fluxes and various physical and chemical indicators (pH, TA, DO, DOC, etc.), water temperature. The significant correlation are judged by the value for coefficient p shown as follow, when value for p which are below 0.05 means significant correlation and when value for p which are below 0.01 means extreme significant correlation.

$$\rho = \frac{\sum_i (x_i - \bar{x})(y_i - \bar{y})}{\sqrt{\sum_i (x_i - \bar{x})^2 \sum_i (y_i - \bar{y})^2}} \quad (\text{Eq.13})$$

Result and analysis

Partial press of CO₂ and CH₄ in surface water and water-air interface benthic flux

The partial press of carbon dioxide $p(\text{CO}_2)$ and methane $p(\text{CH}_4)$ in surface water in the downstream of Jinsha River in January 2016 are shown in *Figure 4*. Along the flowing orientation, $p(\text{CH}_4)$ approximately grew. The highest $p(\text{CH}_4)$ appeared at LZ sampling site (45.62 µatm), while the lowest point showed at GLD sampling site(12.01 µatm). The average value of $p(\text{CH}_4)$ was 22.63 ± 11.48 µatm. $p(\text{CO}_2)$ showed no definite change. The highest and lowest points are GLD (2491.23 µatm) and LJB (1030.11 µatm) respectively, and the mean value of $p(\text{CO}_2)$ was 1785.87 ± 451.18 µatm. The value of $p(\text{CH}_4)$ at YZY, LJB, SNP three sampling sites were relatively low.

The water-air interface benthic flux of carbon dioxide and methane in surface water at all sampling sites in the downstream of Jinsha River in January 2016 are shown in *Figure 5*. The flux of CO₂ and CH₄ were all positive which means the downstream of

Jinsha river was the source of greenhouse gas emission. The mean value of CH₄ and CO₂ were 0.0022 ± 0.0002 mmol/(m²·h) and 2.27 ± 0.48 mmol/(m²·h) respectively. The streamwise flux variation for each gas was similar to partial pressure variation of that gas. Because the TBL model method only concerned about the benthic partial press of gas and did not concern about the bubble diffusion which was the main diffuse means for CH₄, the measurement results of CH₄ flux might be smaller than actual level.

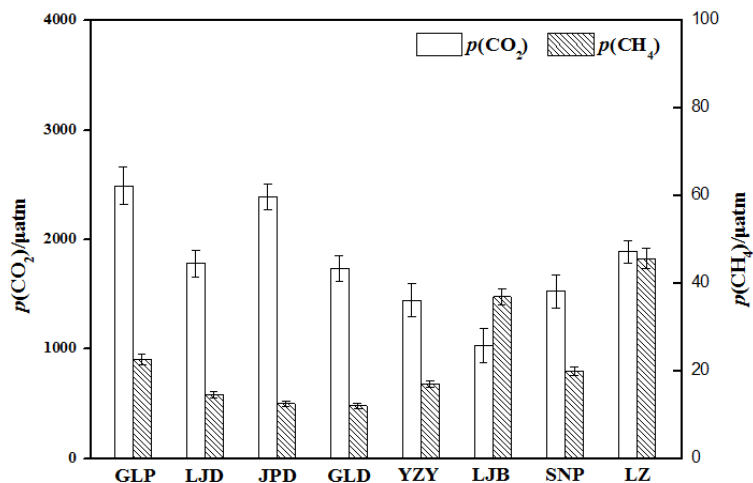


Figure 4. Variation of streamwise of surface water of $p(\text{CO}_2)$ with $p(\text{CH}_4)$

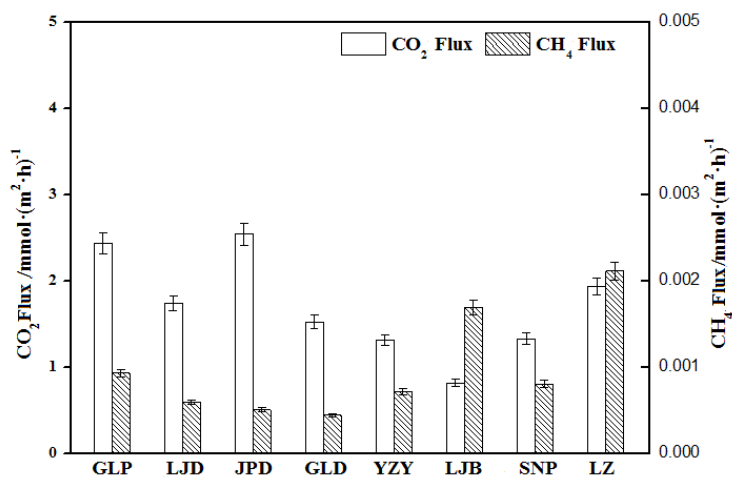


Figure 5. Variation of streamwise of exchange flux of CO₂ and CH₄ between water and air

Variation of environmental indicators

Water temperature and pH

The water temperature and pH variation along the river flowing route is shown in Figure 6. In January 2016, water weather changed a little in all sampling sites. The mean temperature was 14.7 ± 1.5 °C. The highest water weather was measured at GLP site, at 17.4 °C, in contrast, the water weather at GLD site was lowest, at 12.8 °C. The pH of surface water was almost same. The mean pH value was 7.14 ± 0.22 which

demonstrate the surface water of downstream of Jinsha River in winter was neutral. The pH value at LJD site was highest at 7.43 while the lowest pH value was at YZY site, at 6.78. And there was no obvious change tendency in all sampling sites on the flowing direction.

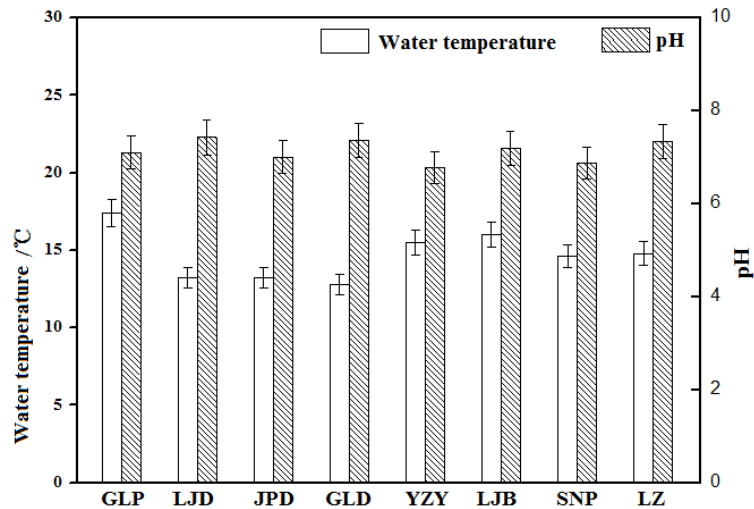


Figure 6. Variation of streamwise of water temperature and pH in the water

TA and Chl-a

The changes of TA and Chl-a along the river flowing route is shown in *Figure 7*. The highest Chl-a appeared at LJB site (30.456 mg·L⁻¹), and Chl-a values in YZY, LJB, SNP sampling sites were relatively high. Because SNP, YZY, LJB site are located at the reservoir area of Xiangjiaba and Xiluodu hydropower stations. In reservoir area, the flowing speed is lower than the other area, and water capacity is larger. As a result, the reservoir area is suitable for growth of phytoplankton, and Chl-a was relatively bigger than that in other area. On the other hand, TA showed no obvious change mode, and the value of TA changed a little in all sampling sites.

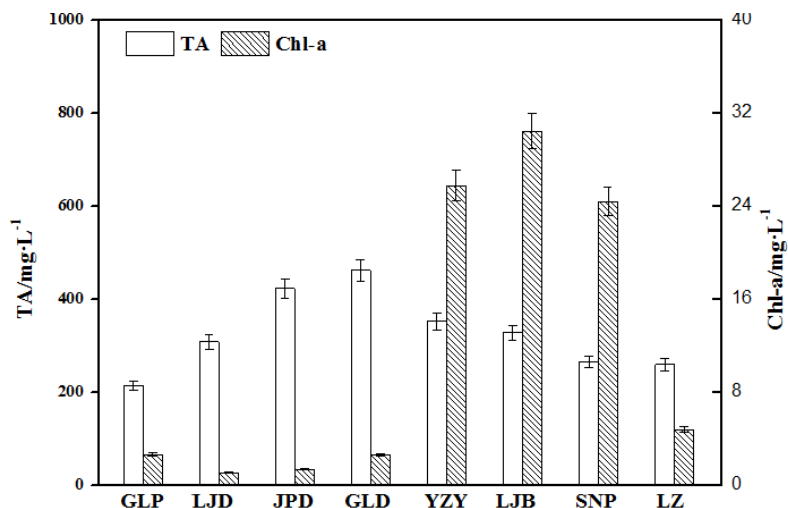


Figure 7. Variation of streamwise of TA and Chl-a in the water

DTN and DTP

The changes of DTN and DTP in 8 sampling sites along the river flowing route are shown in *Figure 8*. The fluctuation of DTP was similar to that of DTN among all sampling sites. The value of DTP and DTN in LJD were both highest, at 0.39 mg·L⁻¹ and 5.3709 mg·L⁻¹, respectively, in contrast, Chl-a in LJD site was lowest. And DTP and DTN in YZY, LJB and SNP were relatively low while Chl-a in these three sites were comparatively high. This proved phosphorus and nitrogen were absorbed adequately by phytoplankton.

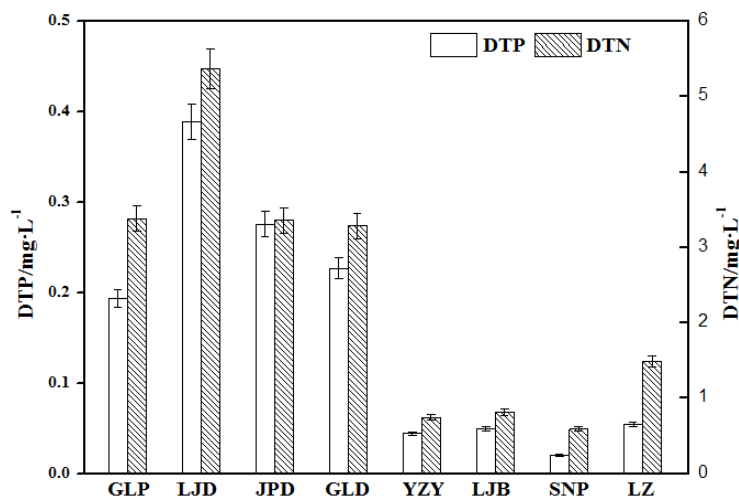


Figure 8. Variation of streamwise of DTN and DTP in the water

DO and DOC

The distribution of DO and DOC at all sampling sites in downstream of Jinsha River along the river flowing route are shown in *Figure 9*. DO in surface water generally climbed streamwise, accompanying with some decrease in last three sites. The average value for DO in water was (9.53 ± 1.00) mg·L⁻¹, the highest and lowest DO were measured at SNP site (11.22 mg·L⁻¹) and LJD site (7.94 mg·L⁻¹) respectively. DOC in water varied a little along the flowing route which showed no obvious law. The mean value for DOC in January 2016 was (3.37 ± 0.14) mg·L⁻¹, DOC in LJB and LZ sampling sites were highest 7 (3.60 mg·L⁻¹) and lowest (3.19 mg·L⁻¹) respectively among all sites in downstream of Jinsha River.

Discussion

The fluctuation of measured parameters on the streamwise

In the research, we focus on the partial pressure and flux of carbon dioxide and methane as well as the physical and physicochemical indicators at several sampling sites. From the experimental result, some changes appear along the river flowing direction, especially at last three sites near the reservoir. $p(\text{CH}_4)$ and flux of methane showed generally the same tendency of change, which have both increased at these three sites. This phenomenon indicates that these three sites have large water capacity contributing to low flowing speed, the stable water environment give rise to forming

strong microbial community construction. As a result, water provides suitable and better environment for microbial community construction. In addition, neighbour reservoir contains amount of organic matter after submerging the surrounding ecosystem, and these substances are the best nutrients for microorganism in surrounding area. After decaying and decomposing process, methane is generated and emitted (Wang, 2017; Jin and Wei, 2008). Similarly, Roehm and Tremblay (2006) found that there was a significant correlation between the concentration of methane between the environment in the deep water of the reservoir and environment in the downstream rivers ($R^2 = 0.80$ and 0.70). It is also estimated that about 70% of methane and 40% of carbon dioxide emissions have occurred in the river downstream of the Petit Saute reservoir in Guiala, France for more than a decade (Friedl and Wuest, 2002). In conclusion, existence of reservoir is proved to impact the greenhouse gas emission and ecosystem in surrounding water environment.

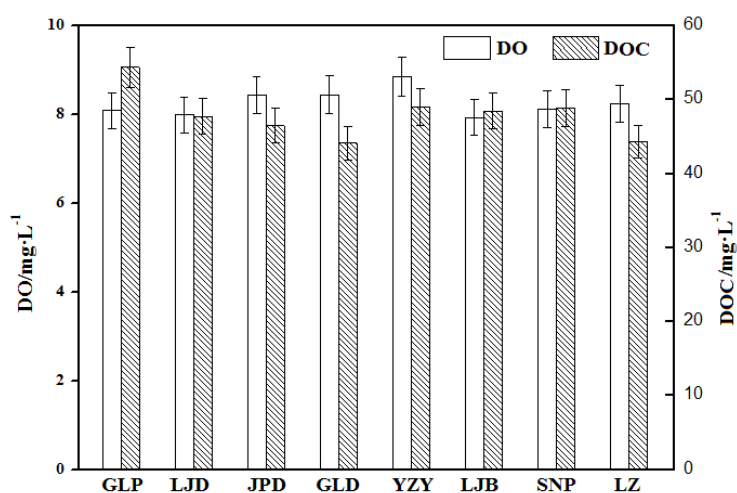


Figure 9. Variation of streamwise of DO and DOC in the water

Partial physical and chemical indexes also changed in these three sites. The concentration of Chl-a increased while DTN and DTP showed the reverse trend. The large capacity of water shapes better environment for photosynthesis contributing to the rise of concentration of Chl-a. Studies have shown that nitrogen content and nitrogen use efficiency of most plant leaves are positively correlated with photosynthetic capacity, which is one of the inherent physiological and ecological characteristics of plants (Evans, 2002; Cheng et al., 2012). Therefore, in the three sampling sites where photosynthesis effects increase, plants' utilization of ammonia nitrogen became stronger, so that DTN in water decreased (Wang and Xu, 2005). In terms of other estimators, the flux and partial pressure of carbon dioxide, water temperature, pH, TA and DOC showed no significant fluctuation law along streamwise orientation.

The correlation analysis between the partial press and flux of CO₂ and CH₄ and environmental indicators

We raised Spearman connection analysis method to illustrate the relationship between $p(\text{CO}_2)$, $p(\text{CH}_4)$, CO₂ flux, CH₄ flux and environmental indicators. The result given in Table 2 showed that $p(\text{CO}_2)$ in surface water has significant positive correlation

with DTN, DTP and negative correlation with DO, Chl-a, DOC. This proved the photosynthesis of phytoplankton in water was stronger than its respiration. The stronger photosynthesis worked, the more Chl-a was measured, the more CO₂ were fixed which decrease $p(\text{CO}_2)$ in water, the more nitrogen and phosphorus DTP and DTN in water was absorbed, the more DO and DOC were produced. The CO₂ flux demonstrated positive correlation with $p(\text{CO}_2)$, wind speed and negative correlation with DO, Chl-a, DOC which resemble $p(\text{CO}_2)$. And the wind blow would enhance the diffusion of CO₂. The $p(\text{CH}_4)$ showed negative correlation with Chl-a, TA and positive correlation with wind speed and water temperature. It is determined that the higher water temperature decreased the solubility of CH₄ in water, and naturally, $p(\text{CH}_4)$ increased when CH₄ diffused into surface water. In addition, relatively higher temperature and vigorous growth of phytoplankton provide a suitable metabolism environment for methanogen that contribute to producing CH₄ (Hong et al., 2004). Meanwhile, wind blowing will give rise to diffusion of CH₄ in surface water. The CH₄ flux showed positive correlation with $p(\text{CH}_4)$, wind speed, water temperature and negative correlation with Chl-a, TA which was similar to correlation of $p(\text{CH}_4)$. What can be proved is the larger value of $p(\text{CH}_4)$ indicated the larger CH₄ flux.

Table 2. Correlations between $p(\text{CO}_2)$, $p(\text{CH}_4)$, flux of CO₂, flux of CH₄ flux and environment factors

Indicators	$p(\text{CO}_2)$	$p(\text{CH}_4)$	CO ₂ flux	CH ₄ flux
Wind speed	-	0.819*	0.976**	0.819*
Water temperature	-	0.778*	-	0.778*
DO	-0.714*	-	-0.738*	-
Chl-a	-0.738*	-0.730*	-0.738*	-0.730*
TA	-	-0.762*	-	-0.762*
DTN	0.714*	-	-	-
DTP	0.712*	-	-	-
DOC	-0.833*	-	-0.857**	-
$p(\text{CO}_2)$	1	-	0.976**	-
$p(\text{CH}_4)$	-	1	-	1*

“-” indicates no obvious correlation, “*” showed obvious correlation (Sig. ≤ 0.05), “**” illustrated extreme correlation (Sig. ≤ 0.01)

Comparison of Jinsha River with other worldwide rivers for greenhouse gas concentration and flux

Comparison for CH₄ concentration and flux in Jinsha River and other rivers

Methane in general river mainly stem from direct produce, release from sediment and input of water enriching CH₄ in surrounding. Considering particulate organic carbons take minority of total suspended particulates, a small amount of CH₄ produced directly at site comparing to other two producing methods. Relative research indicated that concentration of CH₄ in surface water of downstream of Jinsha River was relatively low no matter in summer and in winter, because not only methane produced a little at site, but also a few human lived on the riverside of Jinsha River, and input of CH₄ from branch of Jinsha River is relatively low. In reference of previous researches, considering the wide river basin and large covering area of Jinsha River, we chose several typical

large rivers to make comparison. *Table 3* showed $p(\text{CH}_4)$ and CH₄ flux in the surface water of the world rivers. Average concentration of CH₄ in surface water was $(39.35 \pm 20.32) \text{ nmol}\cdot\text{L}^{-1}$, lower than other river worldwide. And average value for CH₄ diffusion flux in Jinsha River was $(23.36 \pm 0.67) \mu\text{mol}/(\text{m}^2\cdot\text{d})$, and it was lower than other river. It might be caused by measure method and calculation equation that need further research.

Table 3. The $p(\text{CH}_4)$ and exchange flux of CH₄ in the surface water of the world rivers

Country	River	$c(\text{CH}_4)/\text{nmol}\cdot\text{L}^{-1}$	CH ₄ exchange flux/ $(\mu\text{mol}/(\text{m}^2\cdot\text{d}))$	Reference
Germany	Weser River	830~8490	-	Grunwald et al. (2009)
USA	Yaquina River	276~1730	193.8~4437.5	Angelis and Lilley (2003)
USA	Mckenzie	5~79	75~225	Angelis and Lilley (2003)
USA	Willamette	155~298	343.8~2250	Angelis and Lilley (2003)
China	Yangze River	51~604	37.3~1125.3	Zhao et al. (2011a)
China	Downstream of Jinsha River	39.35 ± 20.32	23.36 ± 0.67	Author

Comparison for CO₂ concentration and flux in Jinsha River and other rivers

CO₂ in worldwide majority river were oversaturated where $p(\text{CO}_2)$ were measured at 2000 to 8000 μatm and $p(\text{CO}_2)$ in some tributary even surpassed 10000 μatm (Cole and Caraco, 2001; Richey et al., 2002). In recent years, there were some researches about $p(\text{CO}_2)$ in river. Gui's research demonstrates $p(\text{CO}_2)$ was 790-1600 μatm in mainstream of Yellow River in fall and Zhang's research showed $p(\text{CO}_2)$ was 860-1600 μatm in mainstream of Yangze River in a whole year (Gui, 2007; Zhang et al., 2009). Because these rivers are the typical worldwide rivers, through comparing the carbon dioxide emission in these rivers can understand the CO₂ emission level in Jinsha River. *Table 4* illustrated $p(\text{CO}_2)$ and CO₂ flux in the surface water of the these rivers. From *Table 4*, the average value of $p(\text{CO}_2)$ in surface water in downstream of Jinsha River was $1785.87 \pm 451.18 \mu\text{atm}$ that ranked medium comparing to worldwide other river such as Amazonian rivers, Hudson River. And average value of CO₂ diffusion flux on water-air interface was $(1.71 \pm 0.55 \text{ mmol}/(\text{m}^2\cdot\text{h}))$ ranked medium when comparing with other worldwide rivers.

Table 4. The $p(\text{CO}_2)$ and exchange flux of CO₂ in the surface water of the world rivers

Country	River	$p(\text{CO}_2)/\mu\text{atm}$	CO ₂ exchange flux/ $(\text{mmol}/(\text{m}^2\cdot\text{h}))$	Reference
Brazil	Amazonian rivers	4350 ± 1900	5.61~10.18	Grunwald et al. (2009)
USA	Hudson River	1014	0.67~1.5	Zhao et al. (2011b)
China	The Yellow River	790~1600	0.82	Bates et al., (2011)
China	Yangze River	860~1600	0.74	Zhang et al. (2009)
World	Worldwide river	679~9475	-	Cole and Caraco (2001)
China	Downstream of Jinsha River in winter	1785.87 ± 451.18	1.71 ± 0.55	Author

There are four hydropower stations being constructed and constructing in downstream of Jinsha River: XIangjiaba hydropower station and XIluodu hydropower station have been put into production since 2014, Baihexi hydropower station will begin working in 2020, and Wudongde hydropower station is going to be in operation by 2021. The operation of hydropower stations and reservoir storage might impact carbon

cycle in Jinsha River. It is vital to discover the impact of operation of hydropower station study upon greenhouse gas emission in downstream of Jinsha River, and it also plays crucial role of researching in carbon cycle development in this area. From our study, at Yanziyan site, Shaonvping site and Linjiaba site that located in reservoir district, $p(\text{CH}_4)$ and CH_4 exchange flux were relatively higher than other sites, while $p(\text{CO}_2)$ in these sites were lower than other sites and CO_2 flux showed no obvious change in these 3 sites. It can be proved from current data that the construction and operation of hydropower station did not cause severe greenhouse effect, and this need further research.

Conclusion

A systematic and correct acknowledge the greenhouse gas concentration and benthic flux in river can get a better understanding of the role river played in carbon cycle. And the construction of hydroelectric station may influence the carbon flow in eco system in surrounding area. There are 4 newly-built hydroelectric stations on the downstream of Jinsha River, the major river in China where measurement of CO_2 and CH_4 partial press and flux will illustrate the effect of hydroelectric plant upon carbon cycle and demonstrate whether hydroelectric plant will enhance the greenhouse effect. Considering the rapid current in Jinsha River, we adopted the headspace equilibrium method with combination of TBL model methods to obtain the partial press and concentration of carbon dioxide and methane.

At first, the brief introduction of research objective, Jinsha River and the specific sampling sites were illustrated. Then we reported the principle of headspace equilibrium method to obtain partial press and TBL model estimation method for benthic flux based on the Fick Law with gas transfer coefficient considering the impact of flow speed, wind speed and temperature. And we conclude the calculation procedure for partial press and flux from *Equations 1 to 12*. Moreover, environmental indicators measure method, apparatus and experimenting material were listed to show the measurement procedure.

In result and analysis part, firstly, we demonstrated the partial press and flux of CH_4 and CO_2 . The $p(\text{CH}_4)$ generally climbed with the mean value of $(22.63 \pm 11.48) \mu\text{atm}$ showed the methane increasing in reservoir sites. The $p(\text{CO}_2)$ showed no obvious changing trend along the flowing route with the mean value of $(1785.87 \pm 451.18) \mu\text{atm}$. And the flux of CH_4 and CO_2 variation trend was similar to $p(\text{CH}_4)$ and $p(\text{CO}_2)$ respectively, and them were both positive proved Jinsha River was the source of greenhouse gas emission. Then the variations of environmental indicators including water temperature, pH, Chl-a, TA, DTP, DTN, DO and DOC were displayed to show the differences between the natural sampling site (GLP, LJD, JPD, GLD, YZY) and sampling sites in reservoir area (LJB, SNP, LZ). From the fluctuation, Chl-a and flux and partial pressure of CO_2 increased in reservoir area while DTN and DTP dropped in reservoir area, and TA, DO and DOC showed no obvious variation which indicated phytoplankton grew prosperously would absorb N and P in suitable water temperature. And in winter, pH was neutral in downstream of Jinsha River. It is acknowledged the existence of reservoir will influence the surrounding water environment. Furthermore, the discussion part showed the correlation between partial press and flux of greenhouse gas and environmental indicators by Spearman correlation analysis method. The result came out that $p(\text{CO}_2)$ in surface waters showed positive correlations with alkalinity

(TA) and DOC, and $p(\text{CH}_4)$ showed significant positive correlations with Chl-a and temperature. CO₂ flux showed positively correlation with the $p(\text{CO}_2)$, DOC, alkalinity (TA), and CH₄ flux is positively related to $p(\text{CH}_4)$, wind speed. And $p(\text{CO}_2)$ and flux for CO₂ was ranked as medium while $p(\text{CH}_4)$ was ranked as low comparing to other worldwide rivers.

All in all, $p(\text{CH}_4)$ and CH₄ diffusion flux were relatively higher in reservoir area, $p(\text{CO}_2)$ was lower in reservoir area than that in natural area, and CO₂ diffusion was not obvious in reservoir area. So it can be demonstrated that the construction and operation of hydroelectric stations impact not much at greenhouse effect and this need more research to complement.

Acknowledgements. This work was supported by the National Natural Science Foundation Project of China (51609026), the Basic Science and Frontier Technology Research Project of Chongqing (cstc2017jcyjAX0280) and the Science and Technology Research Program of Chongqing Municipal Education Commission (KJ 1705146).

REFERENCES

- [1] Anderson, C. B. (2002): Understanding carbonate equilibria by measuring alkalinity in experimental and natural systems. – *Journal of Geoscience Education* 50(4): 389-403.
- [2] Angelis, M. A. D., Lilley, M. D. (2003): Methane in surface waters of Oregon estuaries and rivers. – *Limnology and Oceanography* 32(3): 716-722.
- [3] Bates, N. R., Mathis, J. T., Jeffries, M. A. (2011): Air-sea CO₂ fluxes on the Bering sea shelf. – *Biogeosciences Discussions* 8(5): 1237-1253.
- [4] Cheng, B., Hao, Q., Jiang, C. (2012): Research progress on greenhouse gas emissions from reservoirs and their influencing factors. – *Wetland Science* 10(1): 121-128.
- [5] Clarke, L., Edmonds, J., Jacoby, H., Pitcher, H., Reilly, J., Richels, R. (2007): Scenarios of Greenhouse Gas Emissions and Atmospheric Concentrations. – Sub-Report 2.1a of Synthesis and Assessment Product 2.1 by the U.S. Climate Change Science Program and the Subcommittee on Global Change Research, Department of Energy, Office of Biological & Environmental Research, Washington DC.
- [6] Cole, J. J., Caraco, N. F. (1998): Atmospheric exchange of carbon dioxide in a low-wind oligotrophic lake measured by the addition of SF₆. – *Limnology & Oceanography* 43(4): 647-656.
- [7] Cole, J. J., Caraco, N. F. (2001): Carbon in catchments: connecting terrestrial carbon losses with aquatic metabolism. – *Marine Freshwater Research* 52: 101-110.
- [8] Cole, J. J., Prairie, Y. T., Caraco, N. F., McDowell, W. H., Tranvik, L. J., Striegl, R. G. (2007): Plumbing the global carbon cycle: integrating inland waters into the terrestrial carbon budget. – *Ecosystems* 10(1): 172-185.
- [9] Crusius, J., Wanninkhof, R. (2003): Gas transfer velocities measured at low wind speed over a lake. – *Limnology & Oceanography* 48(3): 1010-1017.
- [10] Degens, E. T., Kempe, S., Richey, J. E. (1991): Biogeochemistry of Major World Rivers. SCOPE Report 42. – Wiley, Chichester.
- [11] Evans, J. R. (2002): Photosynthesis and nitrogen relationships in leaves of plants. – *Oecologia* 78: 9-19.
- [12] Friedl, G., Wuest, A. (2002): Disrupting biogeochemical cycles consequence of damming. – *Aquatic Sciences* 64(1): 55-65.
- [13] Getoff, N. (2006): Control of greenhouse gases emission by radiation-induced formation of useful products. Utilization of CO₂. – *Radiation Physics & Chemistry* 75(4): 514-523.

- [14] Goldenfum, J. (ed.) (2010): GHG Measurement Guidelines for Freshwater Reservoirs. – The International Hydropower Association, UK.
- [15] Grunwald, M., Dellwig, O., Beck, M., Dippner, J. W., Freund, J. A., Kohlmeier, C., et al. (2009): Methane in the southern North Sea: sources, spatial distribution and budgets. – *Estuarine Coastal and Shelf Science* 81(4): 445-456.
- [16] Gui, Z. S. (2007): Study on the Distribution and Influence Mechanism of p(CO₂) in the Yangtze River Mainstream and Estuary. – Ocean University of China, Shandong Sheng.
- [17] Guo, J. S., Jiang, T., Zhe, L. I., Chen, Y. B., Sun, Z. Y. (2011): Analysis on partial pressure of CO₂ and influencing factors during spring phytoplankton bloom in the backwater area of Xiaojiang River in Three Gorges Reservoir. – *Advances in Water Science* 22(6): 829-838.
- [18] Hong, Y., Ye, W, and Pei, X. (2004): Study on the effects of nitrogen and phosphorus in the water body of the Three Gorges Reservoir. – *China Water Resources* (20): 23-24.
- [19] Huang, J. W., Wang, X. X. (2009): Temporal variations in surface water CO₂ concentration in a boreal humic lake based on high-frequency measurements. – *Boreal Environment Research* 14(1): 48-60.
- [20] Jähne, B., Libner, P., Fischer, R., Billen, T., Plate, E. (1989): Investigating the transfer processes across the free aqueous viscous boundary layer by the controlled flux method. – *Tellus B* 41B(2): pp.177-195.
- [21] Jin, C., Wei, H. (2008): Preliminary study on greenhouse gas emissions from reservoirs. – *Journal of Yangtze River Scientific Research Institute* 25(6): 1-5.
- [22] Jonsson, A., Åberg, J., Jansson, M. (2007): Variations in p(CO₂) during summer in the surface water of an unproductive lake in northern Sweden. – *Tellus* 59(5): 797-803.
- [23] Kolb, B., Ettore, L. S. (2006): *Static Headspace-Gas Chromatography: Theory and Practice*. Second Ed. – Wiley, New York.
- [24] Li, Z., Bai, L., Guo, J. S., Fang, F., Jiang, T. (2013): Comparative study on water-air CO₂, CH₄ flux in two tributaries in the Three Gorges Reservoir, China. – *Environment Science* 34(3): 1008-1016.
- [25] Ludwig, W, Probst, J.-L., Kempe, S. (1996): Predicting the oceanic input of organic carbon by continental erosion. – *Global Biogeochemical Cycles* 10(1): 23-41.
- [26] Macintyre, S., Wanninkhof, R., Chanton, J. P. (2006): *Trace Gas Exchange Across the Air-Water Interface in Freshwater and Coastal Marine Environments*. – Matson and Harriss Blackwell Science, New York, pp. 52-97.
- [27] Morel, F. (1982): *Principles of Aquatic Chemistry*. – John Wiley and Sons, New York.
- [28] Pumpanen, J., Kolari, P., Minkkinen, K. (2004): Comparison of different chamber techniques for measuring soil CO₂ efflux. – *Agricultural and Forest Meteorology* 123: 159-176.
- [29] Richey, J. E., Melack, J. M., Aufdenkampe, A. K., Ballester, V. M., Hess, L. L. (2002): Outgassing from amazonian rivers and wetlands as a large tropical source of atmospheric CO₂. – *Nature* 416(6881): 617-620.
- [30] Roehm, C., Tremblay, A. (2006): Role of turbines in the carbon dioxide emissions from two boreal reservoirs, Québec, Canada. – *Journal of Geophysical Research* 111: 1-9.
- [31] Roehm, C. L., Prairie, Y. T., Del, G. P. A. (2009): The p(CO₂) dynamics in lakes in the boreal region of northern Québec, Canada. – *Global Biogeochemical Cycles* 23(3): 3013.
- [32] Tremblay, A., Varfalvy, L., Roehm, C. (2005): Greenhouse gas emissions—fluxes and processes. – *Apress* 7(2): 111-127.
- [33] Urabe, J., Iwata, T., Yagami, Y., Kato, E., Suzuki, T., Hino, S., Ban, S. (2010): Within-lake and watershed determinants of carbon dioxide in surface water: A comparative analysis of a variety of lakes in the Japanese Islands. – *Limnology and Oceanography* 56(1): 49-60.
- [34] Wang, G. (2017): Research progress on greenhouse gas in reservoirs. – *Science and Technology Innovation and Application* 5: 205-206.

- [35] Wang, Q., Xu, C. (2005): Effects of nitrogen and phosphorus on plant photosynthesis and carbon partitioning. – *Shandong Forestry Science and Technology* 2005(5): 59-62.
- [36] Wanninkhof, R. (1992): Relationship between wind speed and gas exchange over the ocean. – *Journal of Geophysical Research* 97(C5): 7373-7382.
- [37] Weast, R. C., Astle, M. J. (1987): 61st CRC handbook of chemistry and physics. – *American Journal of the Medical Sciences* 257(6): 423.
- [38] Weiss, R. F. (1974): Carbon dioxide in water and seawater: the solubility of a non-ideal gas. – *Marine Chemistry* 2(3): 203-215.
- [39] Yao, G., Gao, Q. (2005): Response and feedback of river carbon cycle to global change. – *Progress in Geography* 24(5): 50-60.
- [40] Zhang, C., Gao, Q., Tao, Z., Chen, X., Xie, C., Lin, P. (2013): Chemical weathering and CO₂ consumption in the Wuhua River basin, eastern Guangdong province. – *Journal of Lake Sciences* 25(2): 250-258.
- [41] Zhang, G., Zhang, J. L. S., Ren, J., Xu, J., Zhang, F. (2008): Methane in the Changjiang (Yangtze river) estuary and its adjacent marine area: riverine input, sediment release and atmospheric fluxes. – *Biogeochemistry* 91(1): 71-84.
- [42] Zhang, L. J., Xue, X. U., Wen, Z. C. (2009): Control factors of p(CO₂) and p(CH₄) degassing fluxes from the yellow river in autumn. – *Advances in Water Science* 20(2): 227-235.
- [43] Zhao, J., Zhang, G. L., Wu, Y., Yang, J. (2011a): Distribution and emission of methane from the Changjiang River. – *Environmental Science* 32(1): 18.
- [44] Zhao Y., Zeng Y., Wu B. F., Chen Y. B., Wang Q., Yuan C. (2011b): Review of methods for measuring greenhouse gas flux from the air-water interface of reservoirs. – *Shuikexue Jinzhan/Advances in Water Science* 22(1): 135-146.

USE OF THE BIOSTIMULATION OF INDIGENOUS MICROBIAL COMMUNITIES TO DEGRADE TOTAL PETROLEUM HYDROCARBONS IN CONTAMINATED SOIL

GUTIÉRREZ-ALCÁNTARA, E. J.¹ – TIRADO-TORRES, D.^{2*} – VÁZQUEZ-RODRÍGUEZ, G.² – DELGADILLO-RUÍZ, E.² – SALAZAR-HERNÁNDEZ, M.³ – RAMÍREZ-RAMÍREZ, N.⁴ – ZAMORATEGUI-MOLINA, A.²

¹*Faculty of Chemical-Biological Sciences, Autonomous University of Campeche, Av. Agustín Melgar S/N, Buena Vista, C.P.: 24039, Campeche, Cam., Mexico*

²*Department of Civil Engineering, Division of Engineering, Campus Guanajuato, University of Guanajuato, Av. Juárez N° 77, Col. Centro, Guanajuato, Gto., Mexico*

³*Department of Mines, Metallurgy and Geology, Division of Engineering, Campus Guanajuato, University of Guanajuato, Exhacienda de San Matías S/N Col. San Javier, Guanajuato, Gto., Mexico*

⁴*Department of Hydraulic and Geomatics Engineering, Division of Engineering, Campus Guanajuato, University of Guanajuato, Av. Juárez N° 77, Col. Centro, Guanajuato, Gto., Mexico*

**Corresponding author
e-mail: d.tirado@ugto.mx*

(Received 13th Jan 2019; accepted 8th Mar 2019)

Abstract. This study examined the best option for remediating soil contaminated with crude oil through the addition of the inorganic nutrients C:N:P (yeast extract-glucose, NH₄Cl-NaNO₃ and K₂HPO₄-K₃PO₄), in order to increase the degradation of TPHs in the soil. To the contaminated soil a physicochemical characterization was made to know the initial conditions of the inorganic nutrients. The controlled conditions in the biostimulation strategy were 20 days of incubation under uncontrollable ambient temperature conditions. Responses measured after the experiments were residual TPHs, surface tension, respiratory activity and microbial counting. After an incubation period of 20 days, the best treatments found were Y5, which contains the nutrient source glucose-NaNO₃-K₃PO₄, and Y4 (yeast extract-NH₄Cl-K₂HPO₄), with degradation efficiencies of 14.0 and 12.8%, respectively. Biostimulation with inorganic nitrogen and phosphorus increased the metabolic activity of indigenous microorganisms in the soil and thereby increased the degradation of petroleum hydrocarbons. The Y5 and Y4 treatments can be considered as suitable for use as a biostimulation strategy in soils contaminated with TPHs.

Keywords: *bioremediation, inorganic nutrients, crude oil, soil remediation, bacterial population*

Introduction

A vital raw material for the operation of industries and private businesses, oil has become the most important non-renewable resource for modern society (Costa et al., 2012). However, it is a potential source of pollution in the seas, soil and air (Liu et al., 2010), causing major environmental problems worldwide. The degradation of organic pollutants, such as petroleum hydrocarbons, is limited by the assimilation capacity of the native flora of the soil. In some cases, natural attenuation cannot sufficiently eliminate xenobiotics from the soil due to the potential effect of soil conditions, such as organic matter content, soil particle size and microbiota density (Abed et al., 2015). Bioremediation is a technique that uses the metabolism of microorganisms to transform

hydrocarbons into CO₂ and H₂O. It has been found that significant optimization of remediation parameters and increased microbial activity occur when strategies, such as biostimulation, are employed (Coulon et al., 2012).

This strategy entails the addition of nutrients to the indigenous community of microorganisms to incentivize metabolic action and improve the degradation of the pollutant being treated (Abed et al., 2014; Taccari et al., 2012). It should be noted that the application of this type of technique is recommended when the soil to be treated lacks the nutrients necessary for bioremediation. While bioaugmentation has resulted in higher rates of degradation in some cases (Ma et al., 2015; Taccari et al., 2012), the stimulation of indigenous microorganisms has resulted in the significant reduction of hydrocarbons in the soil (Suja et al., 2014; Silva et al., 2009). Thanks to biostimulation, groups of microorganisms native to the soil, such as archaeobacteria, contribute directly or indirectly to the elimination of petroleum hydrocarbons (Ghoreishi et al., 2017; Ghosal et al., 2016). Therefore, in some cases, bioremediation mechanisms are stimulated by increasing the growth of indigenous hydrocarbon-degrading microorganisms (Milic et al., 2009); however, in others, remediation is ineffective as the degradation effect requires too much time (Couto et al., 2010; Bento et al., 2005) due to the lack of limiting nutrients that accelerate the remediation carried out by indigenous microorganisms (Atlas and Hazen, 2011).

Research on biostimulation has been conducted on indigenous microorganisms from different types of soil, with different sources of nutrients applied to improve microbial activity and degrade petroleum hydrocarbons (Abed et al., 2015; Hassanshahian et al., 2014; Taccari et al., 2012). However, this research was conducted on a tropical soil lacking nutrients and with a low density of indigenous microorganisms. Therefore, this study aimed to evaluate both the efficiency of total petroleum hydrocarbons (TPHs) degradation by applying biostimulation with the addition of various sources of nutrients (carbon, nitrogen and phosphorus) and the effect of the production of biosurfactants in the soil.

Materials and methods

Selection of the study area and soil sampling

Soil with a history of spills with petroleum hydrocarbons was collected in the municipality of Poza Rica, Veracruz, located at 20° 32" north latitude and 97° 27" west longitude, at an altitude of 50 m.a.s.l., at a depth of 5 to 40 cm. Seven simple samples from different points in the contaminated site were collected, around 10 kg were taken per sample, the samples were collected before noon to avoid moisture loss and transported under shade. In the laboratory, all samples were mixed to form a composite sample. The soil is categorized as clay-sandy with conglomerate materials. The region has a warm climate, an average annual temperature of 24.2°C, average annual precipitation of 1,010 mm and relative moisture of 76 to 80% (INEGI, 2015).

Physicochemical characterization of the soil

Different physicochemical parameters of the soil were taken to verify that it was a soil type viable for the application of biostimulation. Each parameter was taken in triplicates (*Table 1*).

Table 1. Physical and chemical properties of the soil

Parameter	Value	Method
Moisture (%)	32.64 ± 0.46	Gravimetric
pH	7.85 ± 0.01	Potentiometric
Density (g/cm ³)	1.09 ± 0.03	Pycnometer
Total nitrogen (%)	0.25 ± 0.00	Micro-Kjeldahl
Assimilable phosphorous (mg/kg)	n/d	Bray I
Organic matter (%)	11.14 ± 0.26	Oxidation with chromic acid and sulphuric acid
Texture	Clay-sandy	Hydrometer
TPHs (mg/kg)	50,000 ± 852	Gravimetric
Total bacteria (CFU)	1.04 x 10 ⁴ ± 3.21 x 10 ²	CFUs
Total fungi (CFU)	1.06 x 10 ³ ± 3.06 x 10 ¹	CFUs

Note: n/d: not detected, ±: standard deviation.

The characterization of the contaminated soil revealed an unfavorable proportion between the main nutrients, namely nitrogen and phosphorus. According to Tindal (2005), the TPHs content shows that this a highly contaminated soil, with a slightly alkaline pH and a moisture content close to 30%. The presence of petroleum hydrocarbons causes higher proportions of C, resulting in a deficiency of both N and P (Atlas and Hazen, 2011). According to Abed et al. (2014), the concentration of indigenous microorganisms is low due to the N and P deficiency, as these nutrients are limiting factors in the growth of microorganisms. Given the low microbial mass, it was decided to apply nutrients to the soil in order to increase both microbial density and the degradation of TPHs.

Experimental development

From the composite sample we proceeded to make an experimental design of 2³ (Table 2), they were taken 2 kg of soil in wet base and placed in trays.

Table 2. Representation of factors and levels, the experimental matrix for the 2³ factorial design, the experimentation plan, and the responses measured

Factors (Independent Variables)				Levels			
Sources of:				-1 (g.kg ⁻¹)	+1 (g.kg ⁻¹)		
X ₁ : Source of carbon				Glucose (13.6)	Yeast extract (0.01)		
X ₂ : Source of nitrogen				NaNO ₃ (5.0)	NH ₄ Cl (1.0)		
X ₃ : Source of phosphorous				K ₂ HPO ₄ (2.0)	K ₃ PO ₄ (0.2)		
Experiment matrix				Experimentation plan		Response	
Treatment	X ₁	X ₂	X ₃	Source of carbon	Source of nitrogen	Source of phosphorous	
1	-	-	-	Glucose	NaNO ₃	K ₂ HPO ₄	Y ₁
2	+	-	-	Yeast extract	NaNO ₃	K ₂ HPO ₄	Y ₂
3	-	+	-	Glucose	NH ₄ Cl	K ₂ HPO ₄	Y ₃
4	+	+	-	Yeast extract	NH ₄ Cl	K ₂ HPO ₄	Y ₄
5	-	-	+	Glucose	NaNO ₃	K ₃ PO ₄	Y ₅
6	+	-	+	Yeast extract	NaNO ₃	K ₃ PO ₄	Y ₆
7	-	+	+	Glucose	NH ₄ Cl	K ₃ PO ₄	Y ₇
8	+	+	+	Yeast extract	NH ₄ Cl	K ₃ PO ₄	Y ₈
9	Not			Contaminated soil sterilized			C ₁
10	Not			Soil with natural attenuation			C ₂

The experimental design consists of 8 biostimulation treatments with different nutrients in order to obtain the best combination and apply to a bioremediation process of the sampling site. In addition, two controls (C1 and C2) were added, C1 contained contaminated soil sterilized and C2 was prepared with the same soil without addition of nutrient alone with the native microflora. For each treatment three replicates were made. The selection of inorganic nutrients was made according to Hassanshahian et al. (2014), with some modifications. The controllable parameters were: 20 days of incubation; humidity at 30%; and, soil contaminated with 50,000 mg/kg of TPHs, placing the samples under shade. The uncontrollable conditions in this work were the temperature that was presented throughout this design being of an average within 20 days of 30 ± 3 °C. The response variables that were measured after treatment were residual TPHs, surface tension, respiratory activity and the number of colony forming units (CFU) of microorganisms.

Measurement of response variables

Determination of TPHs

The extraction of TPHs from the soil was carried out according to Dias et al. (2012), with some modifications. In a conical centrifuge tube, to which 1 g of moisture base soil, 2 g of Na₂SO₄ and 10 ml of dichloromethane were added, mixed and vortexed for 45 seconds, and then centrifuged at 6,000 rpm for 15 minutes. This procedure was repeated 3 times for each sample and the supernatant was then collected and concentrated in a rotavapor at 740 mbar and 40°C until a volume of 2 ml was obtained. Once the extract had been concentrated, it was analyzed in both a Thermo Scientific Nicolet 380 FT-IR and a Smart Orbit spectrophotometer. Given the complex matrix of the soil, its extraction efficiency was evaluated, with a concentration of 2-fluorobiphenyl added to the soil prior to carrying out of the TPH extraction process.

Surface tension

The surface tension was measured using the hanging drop method in a model 200-00 Standard Goniometer with DROPimage Standard software (Ramé-Hart Instrument Co., EEUU) and Young-Laplace software, which is used to describe the shape of the drop under equilibrium conditions (Berry et al., 2015).

Respiratory activity (CO₂)

CO₂ evolution was measured using a Gow-Mac series 580 gas chromatograph, with an Alltech concentric column (CTR1) and a thermal conductivity detector coupled to a computer analyzing the samples via the Primary Computing Integration (CPI) Chromatography Data System program, version 6. The results were expressed as a percentage of CO₂. The working conditions of the system were as follows: 100°C detector; 30°C column; 40°C injector; 125 mV detector current; Helium as a mobile phase; 55 ml.min⁻¹ flow for the mobile phase; and, 40 lb/in² pressure for the mobile phase.

Microbial count

For the microbial count, nutrient agar was used for bacteria (Bioxón, México) and rose bengal agar (Disco, USA) for fungi. The microorganism count was assessed by

applying the plate count method on the CFUs, in which 1 g of soil was weighed and diluted in 9 ml of sterile saline water (0.9% NaCl w/v). A series of successive 1 ml dilutions were made in 9 ml of sterile distilled water (10^1 to 10^8) from the colloidal suspension obtained, with each dilution stirred before the subsequent dilution, and with each dilution inoculated in triplicates. The samples inoculated for bacteria growth were incubated at 37°C for 48 to 72 hours, while the Petri dishes inoculated for fungal growth were incubated at 28°C for 7 days in the dark (Gong, 2012).

Statistical analysis

The data were analyzed to detect significant differences ($P < 0.05$) among the treatments, using one-way analysis of variance (ANOVA). Minitab version 18 software was used to carry out the statistical analysis. The means were compared using LSD and Tukey tests.

Results and discussion

Removal of TPHs

The initial concentration of TPHs for all treatments was 50,000 mg/kg. *Figure 1* shows the results obtained for the removal of TPHs via the different treatments used in the experimental design, with their respective controls (C1: contaminated sterile soil; and, C2: natural attenuation). A decrease in non-significant TPHs was observed for C1, representing a loss of contaminant via chemical oxidation. C2 represents the soil with native flora, in which treatment a very minimal degradation rate was observed after 20 days of incubation, which is due to the low concentration of indigenous microorganisms present in the soil and the scarcity of nutrient sources. After an incubation period of 20 days, it was observed that the best treatments for the removal of TPHs were Y5 > Y4 = Y3, with residual concentrations of 43,000 > 43,666 and 44,000 mg/kg, respectively.

The LSD and Tukey statistical tests show significant differences among the treatments ($P \leq 0.05$), with the best TPH degradation percentage obtained being 12 to 14% in 20 days. These results coincide with Wu et al. (2016), who obtained 23.45 and 28.26% TPHs removal in bioaugmented and biostimulated systems, respectively, with an initial concentration of 46,000 mg/kg. This shows that the addition of inorganic nutrients such as N and P improve the action of indigenous microorganisms taken from contaminated soils and optimize the efficiency of soil remediation (Nikolopoulou and Kalogerakis, 2010). Stimulating the populations of indigenous microorganisms is vital for efficient TPHs degradation because the process requires many different bacterial species, as one single species is not capable of metabolizing more than two classes of compounds, in this instance hydrocarbons (Wu et al., 2013). Karamaladis et al. (2010), achieved 51.5% TPHs degradation, obtaining a concentration of 34,000 mg/kg after 20 days of incubation. This result is caused by the fact that lower concentrations of TPHs lead to the degradation of contaminants at a higher level (Sharma, 2012), which, in turn, generates a less toxic habitat for indigenous microorganisms and, thus, leads to higher microbial density and improved TPHs degradation (Wu et al., 2013). The results obtained here via biostimulation are significant compared to natural attenuation, which may be due to the C: N: P adjustment applied in this research, which stimulates both microbial growth and TPH degradation (Atlas and Hazen, 2011). This is consistent with previous studies, which found that the biostimulation of a soil contaminated with TPHs

obtained superior results than bioaugmentation (Abed et al., 2014; Taccari et al., 2012; Kauppi et al., 2011).

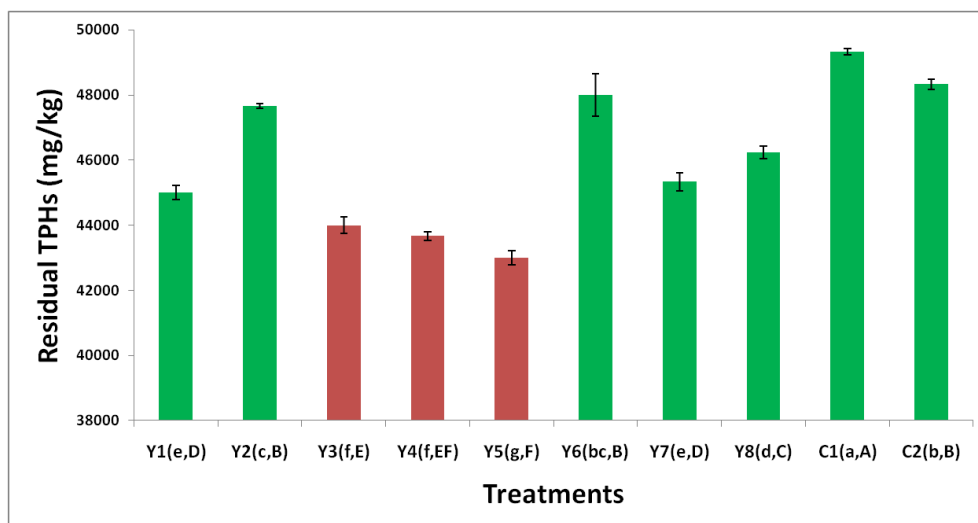


Figure 1. Removal of soil TPHs by applying the different biostimulation treatments. (a,A): Uppercase and lowercase letters within the parentheses correspond to the LSD and Tukey tests, respectively, ($P \leq 0.05$). The dark red bars show treatments with significant degradation of TPHs

Production of biosurfactants

The presence of biosurfactants was analyzed by means of the change in the surface tension of the extract in the soils using an extracting solution, the surface tension of which was measured and it was considered as the initial tension of the systems as well as the medium of culture of 72.30 mN/m at a temperature of 25°C according to Soares et al. (2017). Figure 2 shows the significant differences found for the treatments with respect to the surface tension values obtained ($P \leq 0.05$).

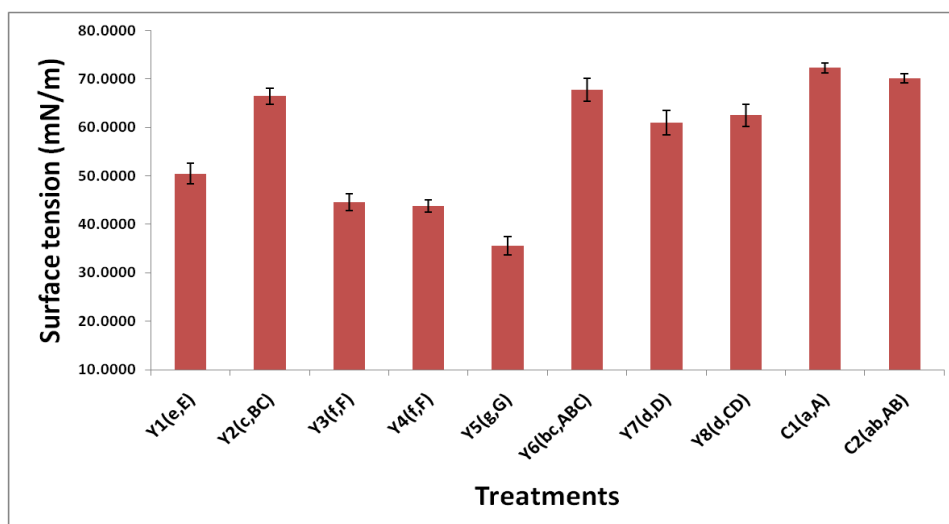


Figure 2. Surface tension in the different biostimulation treatments. (a,A): Uppercase and lowercase letters within the parentheses correspond to the LSD and Tukey tests, respectively ($P \leq 0.05$). Culture medium $\gamma = 72.30$ mN/m at 25°C

The LSD and Tukey tests show that there are significant differences between treatments ($P \leq 0.05$), with the treatments with the greatest surface tension change found to be $Y5 > Y4 = Y3$, with $35.63 > 43.82$ and 44.50 mN/m, respectively. These changes in surface tension confirm the production of biosurfactants by indigenous flora (Lin et al., 2009). The decrease in surface tension also has a direct relationship with the removal of TPHs, as it indicates a higher level of biosurfactant production, which enables the increased availability of petroleum hydrocarbons, thus generating a higher level of TPHs degradation.

Metabolic activity

This The metabolic activity of the microbial community was measured by the production of CO_2 , with each treatment measured on days 1, 3, 5, 10, 15 and 20. The results obtained are shown in *Figure 3* and reveal variable respiratory activity across all treatments. The results show an active microbial community (Diploick et al., 2009), while the treatments with the highest CO_2 production level were $Y5 = Y4 > Y3$, a finding which is directly related to the study of biosurfactant production and TPHs degradation.

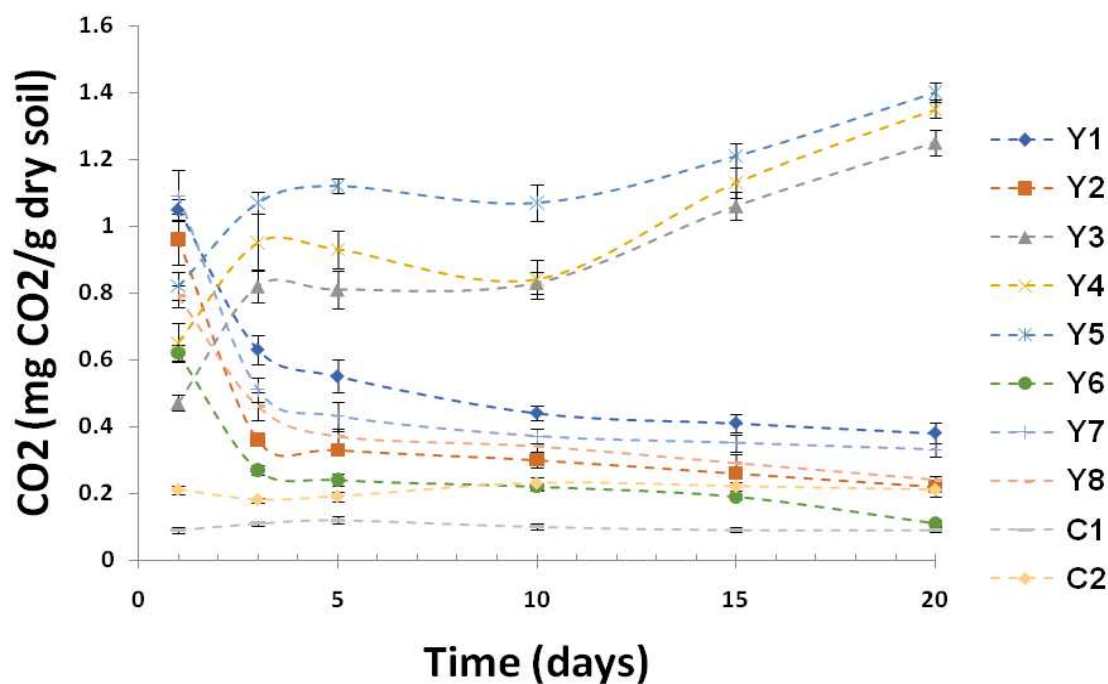


Figure 3. Release of CO_2 over 20 days of incubation

To verify that the production was caused by the action of the microbial community, a count of microorganisms was performed, which again found that the $Y5 = Y4 > Y3$ treatments had a higher microorganism population density, ranging from 6.36 to 9.83×10^7 CFU, compared to the initial concentration shown in *Table 1* (1.04×10^4 CFU) (*Figure 4*).

This proves not only that the bacterial populations were benefited by biostimulation with nutrients, but also that the populations of fungi presented greater population growth. Moreover, this study has observed a synergy effect between the bacterial and fungal populations, which improves the degradation of TPHs.

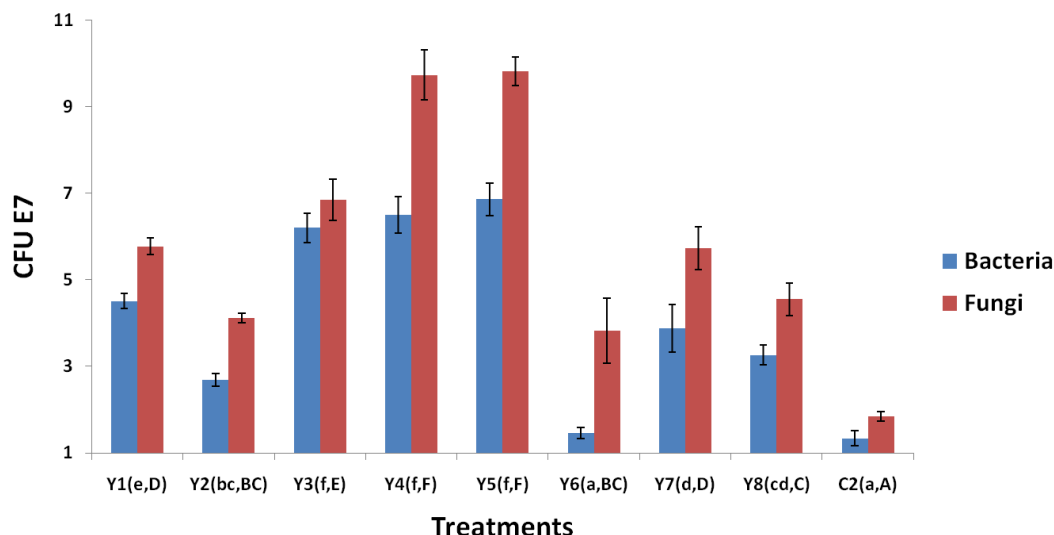


Figure 4. CFU of fungi and bacteria for each treatment in a biostimulated system

Conclusions

Based on previously obtained results with contaminated tropical soils, we can conclude that the success of bioremediation strategies depends on the properties of the contaminants, the nature of the nutrient products and the characteristics of the environment. Although several previous studies demonstrated the effectiveness of biostimulation, the present work could not demonstrate this fact since it took longer incubation time to be able to achieve a wider margin of degradation. Although in general, the treatments Y5 (Glucose-NaNO₃-K₃PO₄) and Y4 (yeast extract-NH₄Cl-K₂HPO₄) proved to be more effective than the other treatments to stimulate the degradation of the hydrocarbon. In this particular situation, the biostimulation strategy evidenced a better performance of the natural bacterial community, which constitutes a promising alternative for the restoration of tropical soil contaminated with hydrocarbons.

Acknowledgements. This project was financially supported by Programa para el Desarrollo Profesional Docente (PRODEP), NPTC- 2018, grant number 511-6/18-8876, Secretaría de Educación Pública (SEP). To University of Guanajuato for the availability of its infrastructure.

REFERENCES

- [1] Abed, R. M. M., Al-Kharusi, S., Al-Hinai, M. (2015): Effect of biostimulation, temperature and salinity on respiration activities and bacterial community composition in an oil polluted desert soil. – *Int. Biodeterior. Biodeg.* 98: 43-52. Available at: <https://doi.org/10.1016/j.ibiod.2014.11.018>.
- [2] Abed, R. M. M., Al-Sabahi, J., Al-Maqrashi, F., Al-Habsi, A., Al-Hinai, M. (2014): Characterization of hydrocarbon-degrading bacteria isolated from oil-contaminated sediments in the Sultanate of Oman and evaluation of bioaugmentation and biostimulation approaches in microcosm experiments. – *Int. Biodeterior. Biodeg.* 89: 58-66. Available at: <https://doi.org/10.1016/j.ibiod.2014.01.006>.

- [3] Atlas, R. M., Hazen, T. C. (2011): Oil biodegradation and bioremediation: a tale of the two worst spills in U.S. History. – *Environ. Sci. Technol.* 45(16): 6709-6715. Available at: <https://pubs.acs.org/doi/abs/10.1021/es2013227>.
- [4] Bento, F. M., Camargo, F. A., Okeke, B. C., Frankenberger, W. T. (2005): Comparative bioremediation of soils contaminated with diesel oil by natural attenuation, biostimulation and bioaugmentation. – *Bioresour. Technol.* 96: 1049-1055. Available at: <https://doi.org/10.1016/j.biortech.2004.09.008>.
- [5] Berry, J. D., Neeson, M. J., Dagastine, R. R., Chan, D. Y. C., Tabor, R. F. (2015): Measurement of surface and interfacial tension using pendant drop tensiometry. – *J. Colloid and Interface Sci.* 454: 226-237. Available at: <http://dx.doi.org/10.1016/j.jcis.2015.05.012>.
- [6] Costa, A., Romao, L., Araújo, B., Lucas, S., Maciel, S., Wisniewski, A., Alexandre, M. D. R. (2012): Environmental strategies to remove volatile aromatic fractions (BTEX) from petroleum industry wastewater using biomass. – *Bioresour. Technol.* 105: 31-39. Available at: <https://doi.org/10.1016/j.biortech.2011.11.096>.
- [7] Coulon, F., Brassington, K. J., Bazin, R., Linnet, P. E., Thomas, K. A., Mitchell, T. R., Lethbridge, G., Smith, J. W. N., Pollard, S. J. T. (2012): Effect of fertilizer formulation and bioaugmentation on biodegradation and leaching of crude oils and refined products in soils. – *Environ. Technol.* 33: 1879-1893. Available at: <https://doi.org/10.1080/09593330.2011.650221>.
- [8] Couto, M. N. P., Monteiro, E., Vasconcelos, M. T. S. (2010): Mesocosm trials of bioremediation of contaminated soil of a petroleum refinery: comparison of natural attenuation, biostimulation and bioaugmentation. – *Environ. Sci. Pollut. Res.* 17: 1339-1346. Available at: <https://doi.org/10.1007/s11356-010-0318-y>.
- [9] Dias, R. L., Ruberto, L., Hernández, E., Vázquez S. C., Lo Balbo, A., Del Panno, M. T., Mac Cormack, W. P. (2012): Bioremediation of an aged diesel oil-contaminated Antarctic soil: Evaluation of the “on site” biostimulation strategy using different nutrient sources. – *Int. Biodeterior. Biodegr.* 75: 96-103. Available at: <http://dx.doi.org/10.1016/j.ibiod.2012.07.020>.
- [10] Diploick, E. E., Mardlin, D. P., Killham, K. S., Paton, G. I. (2009): Predicting bioremediation of hydrocarbons: laboratory to field scale. – *Environ. Pollut.* 6: 1831-1840. Available at: [10.1016/j.envpol.2009.01.022](https://doi.org/10.1016/j.envpol.2009.01.022).
- [11] Ghoreishi, G., Alemzadeh, A., Mojarrad, M., Djavaheri, M. (2017): Bioremediation capability and characterization of bacteria isolated from petroleum contaminated soils in Iran. – *Sustainable Environ. Res.* 27: 195-202. Available at: <http://dx.doi.org/10.1016/j.serj.2017.05.002>.
- [12] Ghosal, D., Ghosh, S., Dutta, T. K., Ahn, Y. (2016): Current state of knowledge in microbial degradation of polycyclic aromatic hydrocarbons (PAHs): a review. – *Front. Microbiol.* 7: 1369-1389. Available at: <https://doi.org/10.3389/fmicb.2016.01369>.
- [13] Gong, X. B. (2012): Remediation of weathered petroleum oil-contaminated soil using a combination of biostimulation and modified fenton oxidation. – *Int. Biodeterior. Biodegr.* 70: 89-95. Available at: [10.1016/j.ibiod.2012.02.004](https://doi.org/10.1016/j.ibiod.2012.02.004).
- [14] Hassanshahian, M., Yakimov, M. M., Denaro, R., Genovese, M., Cappello, S. (2014): Using real-time PCR to assess changes in the crude oil degrading microbial community in contaminated seawater mesocosms. – *Int. Biodeterior. Biodegr.* 93: 241-248. Available at: <https://doi.org/10.1016/j.ibiod.2014.06.006>.
- [15] INEGI. (2015): Geographical and climatological aspects of Poza Rica, Veracruz. - Basic information notebook for the Mexican population, Mexico.
- [16] Karamalidis, A. K., Evangelou, A. C., Karabika, E., Koukkou, A. I., Drainas, C., Voudrias, E. A. (2010): Laboratory scale bioremediation of petroleum-contaminated soil by indigenous microorganisms and added *Pseudomonas aeruginosa* strain Spet. – *Bioresour. Technol.* 101: 6545-6552. Available at: [10.1016/j.biortech.2010.03.055](https://doi.org/10.1016/j.biortech.2010.03.055).

- [17] Kauppi, S., Sinkkonen, A., Romantschuk, M. (2011): Enhancing bioremediation of diesel-fuel-contaminated soil in a boreal climate: comparison of biostimulation and bioaugmentation. – *Int. Biodeterior. Biodegr.* 65: 359-368. Available at: <https://doi.org/10.1016/j.ibiod.2010.10.011>.
- [18] Lin, X., Li, X. J., Sun, T. H., Li, P. J., Zhou, Q. X., Sun, L. N., Hu, X. J. (2009): Changes in microbial populations and enzyme activities during the bioremediation of oil contaminated soil. – *Bull Environ. Contam. Toxicol* 83: 542-547. Available at: <https://doi.org/10.1007/s00128-009-9838-x>.
- [19] Liu, W., Luo, Y., Teng, Y., Li, Z., Ma, L. Q. (2010): Bioremediation of oily sludge contaminated soil by stimulating indigenous microbes. – *Environ. Geochem. health* 32: 23-29. Available at: <https://doi.org/10.1007/s00128-009-9838-x>.
- [20] Ma, X. K., Ding, N., Peterson, E. C. (2015): Bioaugmentation of soil contaminated with high-level crude oil through inoculation with mixed cultures including *Acremonium sp.* – *Biodegradation* 26: 259-269. Available at: <https://doi.org/10.1007/s10532-015-9732-7>.
- [21] Milic, J. S., Beskoski, V. P., Ilic, M., Ali, S. A., GojgicCvijovic, G. Đ., VRVIC, M. M. (2009): Bioremediation of soil heavily contaminated with crude oil and its products: composition of the microbial consortium. – *J. Serbian Chem. Soc.* 74: 455-460. Available at: <https://doi.org/10.2298/JSC0904455M>.
- [22] Nikolopoulou, M., Kalogerakis, N. (2010): Biostimulation strategies for enhanced bioremediation of marine oil spills including chronic pollution. In: Timmis, K. N. (ed.), *Handbook of Hydrocarbon and Lipid Microbiology* 9: 2521-2529, Springer-Verlag Berlin Heidelberg, Available at: https://doi.org/10.1007/978-3-540-77587-4_187.
- [23] Sharma, S. (2012): Bioremediation: features, strategies and applications. – *Asian J. Pharm. Life Sci.*: 2231-4423. Available at: <http://ajpls.com/admin/issues/issue131.pdf>.
- [24] Silva, I. S., Dos Santos, E. D. C., de Menezes, C. R., de Faria, A. F., Franciscan, E., Grossman, M., Durrant, L. R. (2009): Bioremediation of a polyaromatic hydrocarbon contaminated soil by native soil microbiota and bioaugmentation with isolated microbial consortia. – *Bioresour. Technol.* 100: 4669-4675. Available at: <https://doi.org/10.1016/j.biortech.2009.03.079>.
- [25] Soares, R. D. C. F., Almeida, D. G., Meira, H. M., Silva, E. J., Farias, C. B. B., Rufino, R. D., Luna, J. M., Sarubbo, L. A. (2017): Production and characterization of a new biosurfactant from *Pseudomonas cepacia* grown in low-cost fermentative medium and its application in the oil industry. – *Biocat. And Agricult. Biotech.* 12: 206-215.
- [26] Suja, F., Rahim, F., Raihan-Taha, M., Hambali, N., Razali, M. R., Khalid, A., Hamzah, A. (2014): Effects of local microbial bioaugmentation and biostimulation on the bioremediation of total petroleum hydrocarbons (TPH) in crude oil contaminated soil based on laboratory and field observations. – *Int. Biodeter. & Biodegrad.* 90: 115-122. Available at: <http://dx.doi.org/10.1016/j.ibiod.2014.03.006>.
- [27] Taccari, M., Milanovic, V., Comitini, F., Casucci, C., Ciani, M. (2012): Effects of biostimulation and bioaugmentation on diesel removal and bacterial community. – *Int. Biodeterior. Biodegr.* 66: 39-46. Available at: <https://doi.org/10.1016/j.ibiod.2011.09.012>.
- [28] Tindal, M. (2005): Environmentally Acceptable Endpoints for Weathered/Aged Petroleum Hydrocarbon CCME CWS Fraction 3. – Presentation prepared for: 2005 Soil and Groundwater Issues Forum, Petroleum Technology Alliance Canada, March 23, 2005. Calgary, Alberta.
- [29] Wu, M. L., Chen, L. M., Tian, Y. Q., Ding, Y., Dick, W. A. (2013): Degradation of polycyclic aromatic hydrocarbons by microbial consortia enriched from three soils using two different culture media. – *Environ. Pollut.* 178: 152-158. Available at: <https://doi.org/10.1016/j.envpol.2013.03.004>.
- [30] Wu, M., Dick, W. A., Li, W., Wang, X., Yang, Q., Wang, T., Xu, L., Zhang, M., Chen, L. (2016): Bioaugmentation and biostimulation of hydrocarbon degradation and the microbial community in a petroleum-contaminated soil. – *Int. Biodeter. & Biodegrad.* 107: 158-164. Available at: <http://dx.doi.org/10.1016/j.ibiod.2015.11.019>.

ISSR-BASED POPULATION GENETICS STUDY FOR TAGGING A DIVERSE POPULATION OF SHISHAM (*DALBERGIA SISSOO*) IN PAKISTAN

IJAZ, S.^{1*} – UL HAQ, I.² – RAZZAQ, H. A.¹ – NASIR, B.¹ – BABAR, M.¹

¹*Centre of Agricultural Biochemistry and Biotechnology (CABB), University of Agriculture, University Road, Faisalabad, Pakistan*

²*Department of Plant Pathology, University of Agriculture, University Road, Faisalabad, Pakistan*

**Corresponding author*

e-mail: siddraijazkhan@yahoo.com; phone: +92-333-166-1795

(Received 14th Jan 2019; accepted 26th Feb 2019)

Abstract. Population genetics is a subject of modelling the variations in gene and allele frequencies resulting genetic diversity between and within the population. The molecular marker assisted approaches in juxtaposition to computational biology have become powerful tools to explore the genetic pattern and diversity of a particular population. Therefore, population genetics of shisham population in terms of their diversity and genetic pattern was investigated. Twenty-one ISSR markers were used to investigate 30 shisham genotypes collected from Sindh, KPK and Balochistan. Genetic diversity analysis showed 337 loci were amplified with percent polymorphic loci, 99.41. Maximum diversity was found between genotypes SKP3 and KPK P3, however, genotypes TTP1 & TTP2 was found to be more similar. Principal Coordinate analysis depicted, first II coordinates accounted for 40.69% total genetic variation in 2-D plotting. AMOVA predicted high level of percent genetic variance within population (99%). Population genetic structure prediction using admixture model of Bayesian inference showed selected shisham population shared three gene pools ($K = 3$), with diverse genetic pattern that were grouped as distinct or even sharing maximum genetics. These findings could either be helpful for tagging and shaping scattered shisham population of Pakistan or a practical step toward identifying dieback disease resistant shisham germplasm.

Keywords: *molecular characterization, macropropagation, genetic structure, genetic diversity, dendrogram*

Introduction

Population genetics of trees is an imperative approach for characterizing, conserving and improving their dispersed population in a well-arranged manner. Evolutionary processes are the fundamental forces, which bring heterogeneity, existed in trees population. For exploring the forest biodiversity, their genetic study using molecular markers is of great impact (Tereba et al., 2017). Molecular markers have been employing to evaluate the genetic diversity based on allelic frequency present between and among the tree species (Zaya et al., 2017). These markers with the aid of computational biology well describe the genetic relationship of population at species as well as cultivar levels. These DNA markers, which determine the genetic relatedness in terms of diversity without environmental influence, are ISSR (Inter Simple Sequence Repeat), SSR (Simple Sequence Repeat), RAPD (Randomly Amplified Polymorphic DNA) etc. However, inter-SSR markers were identified as new and technically simple molecular marker technique that with small DNA template give results with robust and excellent repeatability (Nilkanta et al., 2017; Sheng et al., 2017).

Therefore, for determining the genetic diversity of *Dalbergia sissoo* (Shisham, tali) population of Sindh, KPK and Balochistan, ISSR marker analysis was made. Due to the fact that *Dalbergia sissoo* is economically the most important timber tree in Asia (Subedi et al., 2017). However, there is no well-defined categorization of its existed genotypes. Hence, ISSR based identification and tagging of diverse population of shisham from Punjab (Pakistan) has been attempted by Ijaz et al. (2018). In *Dalbergia* species SSR markers are not available, and characterization of shisham population in other countries has been documented using RAPD and ISSR markers (Bal and Panda, 2018). As literature supports that ISSR markers reveals high polymorphism rate with more reliability in comparison to RAPD markers (Wu et al., 2018), ISSR markers were used to study population genetics of shisham collected from Sindh, KPK and Balochistan (Pakistan).

Materials and methods

Germplasm collection and macropropagation

For the collection of healthy shisham germplasm, surveys were conducted across the three provinces of Pakistan viz., Sindh, KPK and Balochistan. Branch cuttings (3-5) were taken from healthy shisham trees and placed in differently labelled sampling bags. The selected shisham population size remained 15 from Sindh, 10 from KPK and 5 from Baluchistan (*Table 1*). Sandy loam soil was used to fill polythene bags (5-7" in length) after sterilization with 37% formalin solution. Cuttings from shisham trees (7-9 cm) with 3-5 nodes were planted in soil filled polythene bags and kept in green house for macropropagation (*Fig. 1*).

Table 1. List of shisham genotypes collected from three provinces (Sindh, KPK and Balochistan) Pakistan

Sr. #	Region	Plant code	Sr. #	Plant code
Sindh			Khyber Pakhtunkhwa (KPK)	
1.	Hyderabad	HP1	1.	KPK P1
2.		HP2	2.	KPK P2
3.		HP3	3.	KPK P3
4.	Jamshoro	JSP1	4.	KPK P4
5.		JSP2	5.	KPK P5
6.		JSP3	6.	KPK P6
7.	Khairpur	KPP1	7.	KPK P7
8.		KPP2	8.	KPK P8
9.	Naushahro Feroze	NFP1	9.	KPK P9
10.		NFP2	10.	KPK P10
			Balochistan	
11.	Sukkur	SKP1	1.	BLP1
12.		SKP2	2.	BP2
13.		SKP3	3.	BLP3
14.	Thatta	TPP1	4.	BLP4
15.		TPP2	5.	BLP5



Figure 1. Macropropagated shisham germplasm collected from Sindh, KPK and Balochistan at green house of Fungal Molecular Biology Laboratory (FMB Lab.), Department of Plant Pathology, University of Agriculture Faisalabad, Punjab, Pakistan

Molecular analysis

DNA of selected samples was isolated using modified CTAB method (Ijaz et al., 2018). Twenty one (21) ISSR markers were used for the amplification using PCR reaction conditions described by Ijaz et al., 2018. Polymerase Chain Reaction was performed on 96 well thermal cycler (peq STAR). The PCR products were resolved on agarose gel (2.5%) and visualized on gel documentation system (Bio Rad, USA). Band counting was scored as “1”, for presence and “0” for absence on excel sheet. Data was analyzed using different software packages (STRUCTURE v. 2.3.4, PopGen 32 v. 1.32, PAST v. 3.16, DARwin6 v. 6.0, GenAIExe v. 6.501 and Power Marker v. 3.25) available for genetic diversity and population genetics studies.

Results

ISSR marker based PCR products with reliability of DNA bands (depending on SSR motifs) were obtained (Fig. 2). In three province of Pakistan, these 21 ISSR markers amplify 337 loci in total among 30 selected shisham genotypes, of which recorded polymorphism percentage was 99.41 accounted for 335 polymorphic loci. Total amplified alleles were 5252 that ranging from 57 (ISSR-17) to 321 (ISSR-5), while an average alleles per primer were 250.09. However, average number of alleles per locus ranged as 10.28 (ISSR-14) to 21.89 (ISSR-9). The high level polymorphism was

exhibited from 8.60 (ISSR-15) to 18.61 (ISSR-14). To check marker diversity PIC (Polymorphic Information Content) was calculated, that ranged from 0.2493 (ISSR-14) to 0.4321 (ISSR-1) with average of 0.3435. However, the calculated value for gene diversity was ranged 0.3045 (ISSR-14) to 0.4986 (ISSR-1) with mid value of 0.4142 (Table 2).

Genetic diversity analysis

Genetic diversity was performed using two distance matrix based clustering analyses i.e. unweighted pair group method with arithmetic mean (UPGMA) based dendrogram using PAST v.3.16 (Euclidean matrices) and Unweighted Neighbor-Joining (NJ) based dendrogram using DARwin6 (bootstrap method). The UPGMA based hierarchical clustering of 30 shisham genotypes showed four major clusters (I, II, III & IV) (Fig. 3). The cluster I comprised of KPK genotypes, KPK P3, KPK P4, KPK P5, KPK P6, KPK P7, KPK P8, KPK P9 & KPK P10 (KPK genotypes). Cluster II, being the largest, included Sindh genotypes, TTP1 & TTP2 (Thatta genotypes), HP1, HP2 & HP3 (Hyderabad genotypes), NFP1 & NFP2 (Naushahro Feroze genotypes), KPP1 & KPP2 (Khairpur genotypes), JSP1, JSP2 & JSP3 (Jamshoro genotypes), SKP1 & SKP2 (Sukkur genotypes). Balochistan genotypes, BLP1, BLP2, BLP3, BLP4 & BLP5 were grouped in cluster III. While cluster IV was observed to be distinct one which comprised of KPK P1, KPK P2 (KPK genotypes) and SKP3 (Sukkur genotype, Sindh). The whole dendrogram was rooted by the three genotypes of cluster IV. Despite this dendrogram, Neighbor Joining (NJ) based clustering (using Darwin6 software) with 1000 bootstraps, also supported the UPGMA results (Fig. 4). Somehow, same clustering pattern was observed among selected genotypes of three provinces which validated the results as well.

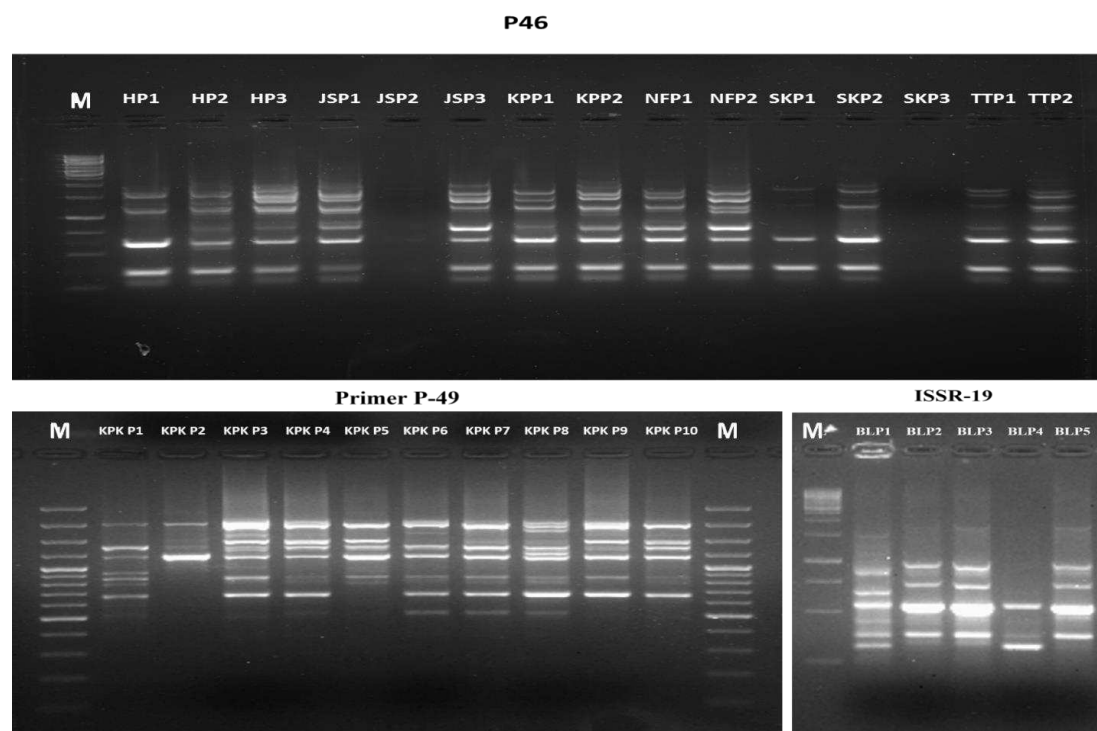


Figure 2. PCR amplification of shisham genotypes collected from Sindh, KPK and Balochistan using ISSR primers. (M = 1 kb DNA ladder)

Table 2. The number of scored bands and marker informativeness of 21 selected ISSR primers

Sr.#	Primers (Ijaz et al., 2018)	No. of loci	Total no. of allele	No. of alleles per locus	Total polymorphic allele	Polymorphism (%)	PIC*	EGD**
1	P-46	15	269	17.93	166	11.06	0.3539	0.4229
2	P-49	16	253	15.81	227	14.19	0.3209	0.4109
3	ISSR-1	17	221	13	238	14	0.4321	0.4986
4	ISSR-2	14	198	14.14	208	14.85	0.3333	0.3987
5	ISSR-3	15	170	11.33	250	16.67	0.3912	0.4571
6	ISSR-4	18	236	13.11	304	16.89	0.2985	0.3782
7	ISSR-5	17	321	18.88	189	11.12	0.3281	0.4215
8	ISSR-6	18	283	15.72	221	12.28	0.4126	0.4845
9	ISSR-7	20	250	12.5	310	15.5	0.3866	0.4511
10	ISSR-8	21	330	15.71	258	12.28	0.3646	0.4205
11	ISSR-9	18	394	21.89	110	6.47	0.2972	0.3316
12	ISSR-10	18	297	16.5	225	12.5	0.3505	0.4224
13	ISSR-11	18	379	21.05	161	8.94	0.2894	0.3598
14	ISSR-12	18	328	18.22	212	11.78	0.3110	0.3970
15	ISSR-13	15	193	12.87	242	16.13	0.3255	0.3850
16	ISSR-14	18	185	10.28	335	18.61	0.2493	0.3045
17	ISSR-15	15	309	20.6	129	8.6	0.3288	0.3930
18	ISSR-16	15	193	12.87	242	16.13	0.3725	0.4567
19	ISSR-17	4	57	14.25	59	14.75	0.3871	0.4733
20	ISSR-18	12	164	13.67	172	15.64	0.3442	0.4
21	ISSR-19	15	222	14.8	228	15.2	0.3370	0.4325
Total		337	5252	325.13	4486	---	7.2143	8.6998
Average		---	250.09	---	---	13.504	0.3435	0.4142

*Polymorphic information contents. **Expected gene diversity

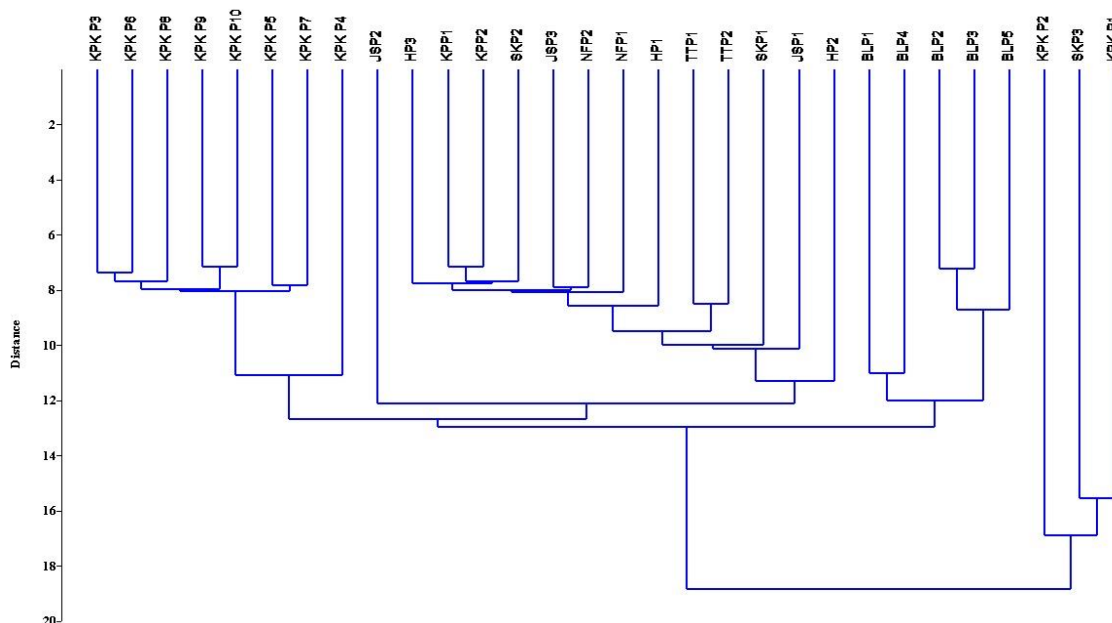


Figure 3. A UPGMA dendrogram based on Nei's genetic distance, showing clustering of 30 shisham samples collected across Sindh, KPK and Balochistan (Pakistan)

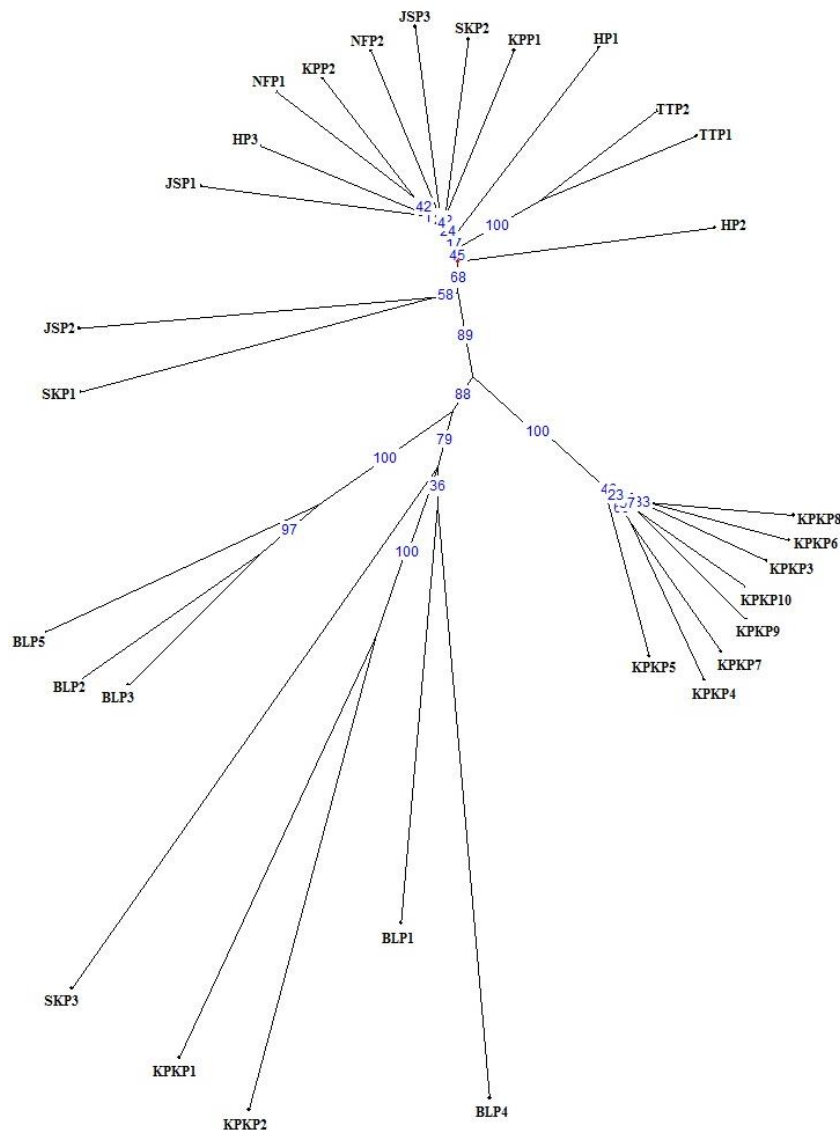


Figure 4. A dendrogram using DARwin6 software, based on unweighted neighbor joining (NJ), showing hierarchical clustering of 30 representative shisham genotypes from three provinces, Pakistan.

The similarity index retrieved from PopGen 32 also correlated with the results of dendrogram. The overall Nei's genetic distance ranged from 0.1594 to 1.1168. The maximum Nei's genetic diversity value of 1.1168 was scored by SKP3 and KPK P3 genotypes. Moreover, Sukkur genotype (SKP3) showed diversity value of 1.0197 and 1.0104 with KPK genotypes, KPK P6 and KPK P8, respectively. However, Thatta genotypes (TTP1 & TTP2) scored least Nei's genetic diversity value of 0.1594. These diversity values and the cladding of 30 genotypes were in accordance to each other. In addition, the values for total genetic diversity (H_t), number of alleles (n_a), effective number of alleles (n_e), Nei's gene diversity (h) and Shannon's information index (I) was also computed by PopGen32. The values for H_t , 0.3705, n_a 1.9941, n_e 1.6487, h 0.3705 and I 0.5469 were recorded on an average with standard deviation of 0.0169, 0.0769, 0.2968, 0.1301 and 0.1580, respectively.

Principle Coordinate Analysis (PCoA) was executed on Darwin6 program package to determine the spatial representation among and within selected shisham population based on genetic differences (Fig. 5). These results were in concurrence to the UPGMA based and NJ based clustering of selected genotypes. The two dimensional (2-D) plotting of 30 genotypes were observed from three provinces. These results revealed that first two coordinates (coords) accounted for genetic variation, 21.62% (Coord I) and 19.07% (Coord II). The genotypes found in intermixed as well as in scattered form. The SKP1, SKP3 (Sukkur genotypes, Sindh) and JSP2 (Jamshoro genotype, Sindh), BLP1, BLP2, BLP3, BLP4, BLP5 (Balochistan genotypes) KPK P1, KPK P2 (KPK genotypes) were showed to be scattered while all other genotypes were more or less closely related.

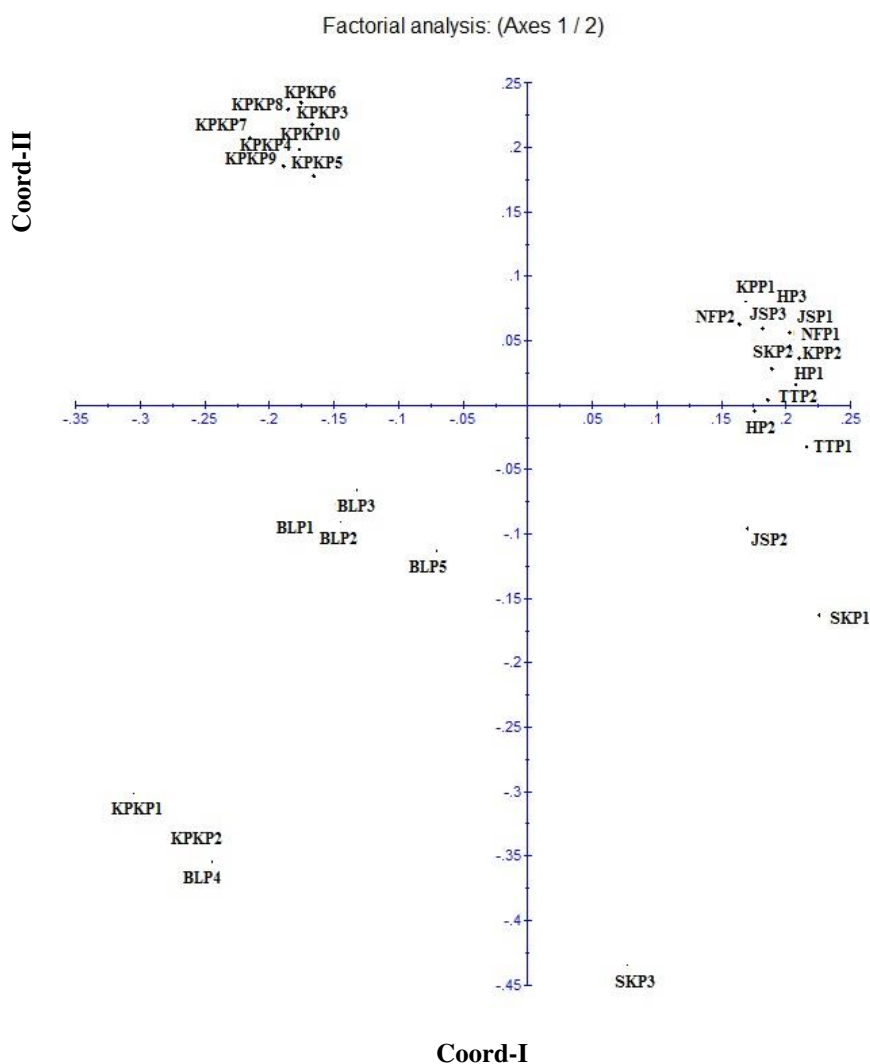


Figure 5. PCoA based 2-D plot of 30 shisham genotypes from Sindh, KPK and Balochistan, Pakistan

Analysis of molecular variance analysis (AMOVA) was performed using MS-Excel based program GenAlExe, on the whole ISSR data score of shisham genotypes without grouping by region or geographical location (Table 3). This analysis was performed to

understand the relationships within and among the populations (Fig. 6). AMOVA revealed high percentage credited to intra-population variation (99%) while the remaining in inter-population variation (1%). Therefore, in total, proportion of variation among shisham populations of three provinces was lower than within the populations, suggesting the collected shisham genotypes are highly diverse to each other but of same origin.

Table 3. Calculated variance for inter and intra populations with percent of the variance of each source to the total variance

Source	Degree of freedom (df)	Sum of square (SS)	Mean sum of square (MS)	Est. var.	Var. %
Among pops	2	185.800	92.900	1.032	1%
Within pops	27	2253.000	83.444	83.444	99%
Total	29	2438.800		84.476	100%

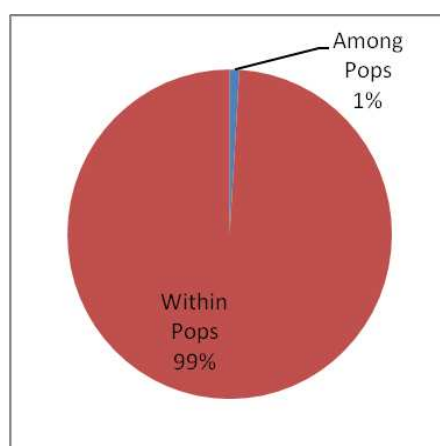


Figure 6. Percentile of molecular variance among and within studied shisham populations

Population genetic structure

The pattern of genetic structure among shisham population among three provinces has been observed using computer program STRUCTURE. The STRUCTURE HARVESTER suggested shisham population into appropriate subpopulation (K). The K was set from 2-5 with 10,000 burn-in and MCMC. Whereas the estimation of subpopulations was done by delta K (ΔK) value. For selected genotypes from three provinces (30 genotypes) the ΔK value was recorded as highest at $K = 3$, which conferred the shisham population into 3 subgroups (Fig. 7) (Table 4). This result depicted the sharing of three gene pools among investigated genotypes (Fig. 8).

Table 4. The Evanno table for 30 shisham genotypes (three provinces) showing maximum $\Delta K = 3$

K	Reps	Mean LnP (K)	St. dev LnP (K)	Ln' (K)	Ln'' (K)	ΔK
2	3	-4826.833333	150.394625	—	—	—
3	3	-3976.766667	1.504438	850.066667	892.966667	593.555027
4	3	-4019.666667	459.283021	-42.900000	118.133333	0.257212
5	3	-4180.700000	758.598715	-161.033333	—	—

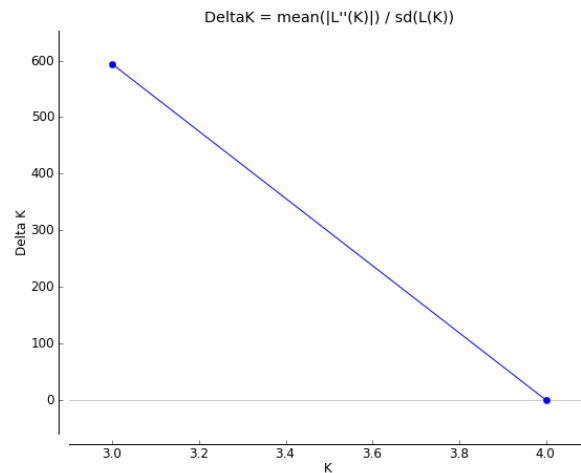


Figure 7. Result of *STRUCTUTE HARVESTER* in comparison to *Evanno* table suggest *K* cluster as *K* = 3

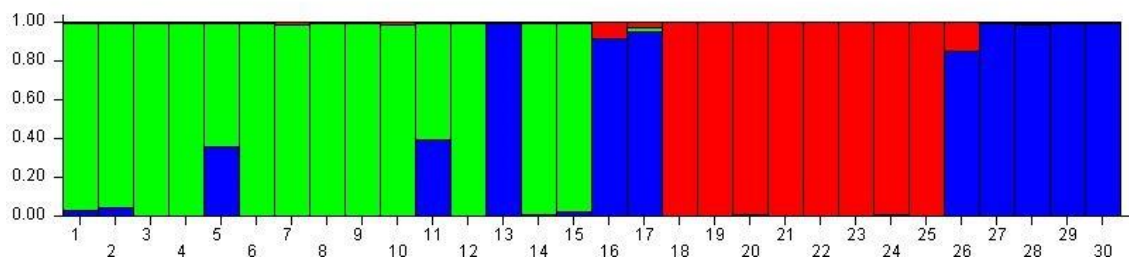


Figure 8. *STRUCTURE* analysis characterizes the shisham subpopulation into *K*3, represented in color codes in which each color illustrates the location of genotypes within its respective sub-group. Number on plane axis show the individuals belongs to shisham group and on perpendicular axis show the membership coefficient to sub population group

Discussion

Genetic diversity has of tremendous importance for any plant or tree species to survive in their natural habitat by providing the knowledge about novel strategies for their conservation. In recent years, DNA molecular markers proved to be a vital strategy for the assessment of inter and intra population interactions as well as variation which greatly contributed in conversation of endanger species (Gudeta, 2018). ISSR regions are present between the SSR motifs that are ubiquitous in genome of higher organism and have ability to discriminate the genotypes (Ijaz and Khan, 2009; Ijaz, 2011).

In the present study, 21 ISSR markers primers produced 337 loci among 30 selected shisham genotypes for which polymorphism percentage was recorded to be 99.41% accounted for 335 polymorphic loci. Similar study was conducted in Punjab population of Pakistan in which 21 ISSR markers showed 83.32% polymorphism among 60 selected shisham population (Ijaz et al., 2018). The UPGMA based clustering grouped this population of 30 genotypes in to four clusters and minimum Nei's genetic identity was observed as 0.3273 in SKP3 and KPK P3 while maximum showed to be 0.8487 in KPP2 and NFP2, KPP1 and KPP2, KPK P9 and KPK P10.

PCoA value was calculated through Drwin6 which showed to be 21.62% in first coordinate and 19.07% in second coordinate. However, for PCoA, in the study conducted by Ijaz et al. (2018) revealed the shisham populations of Punjab province, Pakistan showed 16.23% and 13.83% in coordinate I and coordinate II respectively. The delta K value was calculated by using STRUCTURE HARVESTER which was observed as K = 3 which revealed that 30 shisham genotypes were sharing three genetic pool, similar results were observed for Punjab shisham population (Ijaz et al., 2018) and for bamboo tree (Nilkanta et al., 2017). As for AMOVA, 99% and 1% variation was observed within and among population respectively. Similar results were observed in bamboo (Nilkanta et al., 2017) and pistachio (Meimand et al., 2017).

Conclusion

Maintenance of genetic diversity of forest trees is also of critical importance worldwide for its preservation, propagation and commercial cultivation. However, in the case of shisham (*Dalbergia sissoo*) cultivars and accessions there are no identified cultivars and accessions that have been identified as diverse and closely related as well as resistant and susceptible. Genetic diversity assessment of shisham would enable scientists to understand phylogenetic relationships among different genotypes, their geographical distribution and linkage of certain morphological traits with DNA markers linked to the genes controlling them. The information thus obtained may also be helpful in solving the problem of shisham. The research findings will be important in the development towards tagging and identifying *D. sissoo* germplasm on a molecular basis and a practical step for the sustainable management of diseases in shisham.

Acknowledgement. We highly acknowledge “Punjab Agriculture Research Board (PARB), Pakistan” for providing funds under the PARB project no. 952 “Resistance gene analogues based molecular identification for dieback disease resistance in shisham (*Dalbergia sissoo*)” to conduct this research work.

Conflict of interests. I declare that the submitted manuscript is our own work, which has not been published before and even is not currently being considered for publication elsewhere. And there is no conflict of interests.

REFERENCES

- [1] Bal, P., Panda, P. C. (2018): Molecular characterization and phylogenetic relationships of dalbergia species of eastern India based on RAPD and ISSR analysis. – International Journal of Innovative Science and Technology 3(7): 417-425.
- [2] Gudeta, T. B. (2018): Molecular marker based genetic diversity in forest tree populations. – Forestry Research and Engineering: International Journal 2(4): 176-182.
- [3] Ijaz, S. (2011): Microsatellite markers: an important fingerprinting tool for characterization of crop plants. – African Journal of Biotechnology 10(40): 7723-7726.
- [4] Ijaz, S., Khan, I. A. (2009): Molecular characterization of wheat germplasm using microsatellite markers. – Genetics and Molecular research 8(3): 809-815.
- [5] Ijaz, S., Razzaq, H. A., Babar, M., Haq, I. (2018): Assessment of population genetics of shisham (*Dalbergia sissoo*) based on genetic structure and diversity analysis. – International Journal of Biosciences 13(3): 209-222.
- [6] Mahmoodnia Meimand, M., Farzad Amirebrahimi, F., Karimi, H. R., Malekzadeh, K., Tajabadipour, A. (2017): Genetic diversity assessment of male and female pistachio genotypes based on ISSR markers. – Journal of Plant Molecular Breeding 5(1): 31-39.

- [7] Nilkanta, H., Amom, T., Tikendra, L., Rahaman, H., Nongdam, P. (2017): ISSR marker based population genetic study of *Melocanna baccifera* (Roxb.) Kurz: a commercially important bamboo of Manipur, North-East India. – Scientifica 2017. <https://doi.org/10.1155/2017/3757238>.
- [8] Sheng, F., Chen, S.-Y., Tian, J., Li, P., Qin, X., Wang, L., Luo, S.-P., Li, J. (2017): Morphological and ISSR molecular markers reveal genetic diversity of wild hawthorns (*Crataegus songorica* K. Koch.) in Xinjiang, China. – Journal of Integrative Agriculture 16(11): 2482-2495.
- [9] Subedi, G., Sah, C. K., Pokharel, D. K. J., Chaudhary, M. K., Aryal, P., Bhandari, I., Bhandari, R. (2017): Anti-bacterial guided fractionation of *Dalbergia sissoo*. – International Journal of Pharmaceutical Sciences and Research 8(10): 4325-4334.
- [10] Tereba, A., Konecka, A., Nowakowska, J.A. (2017): Application of selected molecular markers in studies on forest trees. – Folia Forestalia Polonica 59(2): 146-151.
- [11] Wu, W., Chen, F., Yeh, K., Chen, J. (2019): ISSR analysis of genetic diversity and structure of plum varieties cultivated in southern China. – Biology 8(1): 2.
- [12] Zaya, D. N., Molano-Flores, B., Feist, M. A., Koontz, J. A., Coons, J. (2017): Assessing genetic diversity for the USA endemic carnivorous plant *Pinguicula ionantha* RK Godfrey (Lentibulariaceae). – Conservation Genetics 18(1): 171-180.

UNDERSTANDING G × E INTERACTION OF ELITE BASMATI RICE (*ORYZA SATIVA* L.) GENOTYPES UNDER NORTH INDIAN CONDITIONS USING STABILITY MODELS

JAIN, B. T.¹ – SARIAL, A. K.² – KAUSHIK, P.^{3*}

¹Department of Genetics & Plant Breeding, CCS Haryana Agriculture University, Hisar, Haryana 125001, India

²CSK Himachal Pradesh Krishi Vishvavidyala, Palampur, Himachal Pradesh 176062, India

³Instituto de Conservación y Mejora de la Agrodiversidad Valenciana, Universitat Politècnica de València, Valencia 46022, Spain

*Corresponding author

e-mail: prakau@doctor.upv.es, prashantumri@gmail.com; phone: +34-96-387-7000

(Received 14th Jan 2019; accepted 6th Mar 2019)

Abstract. Information regarding the stability of genotypes is critical in expanding the adaptability of released genotypes. But, this information regarding the basmati (scented) rice genotypes cultivated under north Indian conditions are not well known. Therefore, here we have evaluated the twenty-two basmati rice genotypes for stability, based on important traits, and different production system. Genotypes were evaluated for two consecutive Kharif seasons under open field conditions in a randomized complete block design (RCBD). The genotypes were evaluated under four production systems namely, transplanted rice (TPR), system of rice intensification (SRI), direct seeded rice (DSR) in both settings, i.e. wet DSR (W) and dry DSR (D). The stability of genotypes was determined via Eberhart and Russell model, additive main effects and multiplicative interaction (AMMI), and genotype × environment interaction (GGE) biplot model. The stability and adaptability studied using Eberhart and Russell model, AMMI and GGE biplot identified Basmati-370 as the most stable genotype for biological weight; Pusa RH-10 for filled spikelet; CSR-30 for spikelet Number; and Traori Basmati for test grain weight. TPR was the most desirable test environment followed by SRI and DSR (W). Further, we have identified HKR 08-417 as the most suitable genotype for all of the production systems. Overall, this study provides information regarding stable basmati rice genotypes under the north Indian conditions.

Keywords: rice, G × E, GGE, AMMI, stability model, Eberhart and Russell, SRI, DSR

Introduction

Rice (*Oryza sativa* L.) production is vital for the growing population (Zhang, 2007; Wu and Cheng, 2014). Although, rice is grown worldwide over an area of around 163.24 mha with a production of around 740.95 mt. besides its productivity is around 4.54 t/ha (Anonymous, 2016). In India rice is cultivated over 43.99 mha which results in the production of 109.69 mt., with a productivity of 2.49 t/ha (Anonymous, 2017). The productivity of rice in India is around half of the world average. This low productivity of rice in the Indian subcontinent is a result of several factors like less water availability, the frequent occurrence of droughts, weed competition, insect pest, and diseases (Silalertruksa et al., 2017; Sreekanth et al., 2017). The rice production areas in India are highly diverse with different production systems due to the area specific soil and climatic features (Singh et al., 1997). Moreover, the improper commercialization of high yielding varieties for non-conventional systems of rice production like system of rice intensification (SRI), direct

seeded rice (DSR) etc. leads to below average yields under non-conventional systems (Wanjari et al., 2006).

Based on the aroma, rice is divided into two categories namely, basmati (scented) and non-basmati (non-scented) type. Basmati rice is comprised of long slender grain, pleasant aroma and fluffy rice texture (Ashfaq, 2015; Hinge et al., 2016). The scented aroma of basmati varieties is only perceived when basmati rice varieties are grown on the northwestern foothills of Himalayas (Bhattacharjee et al., 2002; Jena and Grote, 2012). Still, most of the basmati genotypes are limited to the environment of their developed institutes, due to less in-depth study regarding the performance of elite varieties under diverse environments from their developed institutes (Kamoshita et al., 2008). The researchers are primarily focused on configuring the input demand for the transplanted rice-based production system (Lin, 1994). The new production systems/non-conventional strategies like, SRI, DSR (are intended for the optimum yield per amount of input supplied (Jain et al., 2018).

Genotype × Environment interactions (GEI) plays a pivotal role in the positioning of genotypes from their native to non-native environment, which further hampers the plant breeding advancement (Pham and Kang, 1988). A genotype is termed as stable if it performs statically across different environments. Whereas, the theory of biological stability consider the concept of less variance for yield and yield related characters across unrelated environments (Becker and Leon's, 1988). Rice breeders and agronomists give little attention to biological stability concept (Xu, 2016).

A number of stability analyses models are used to determine the contribution of G × E interaction (GEI), also, to identify genotypes which perform superior under several environments (Génard et al., 2017; Malosetti et al., 2013). Stability model is defined in terms of mean value, regression coefficient, deviation from the regression, and principal component analysis (PCA) (Bernardo, 2002). Stability models like Finlay and Wilkinson (1963), and Eberhart and Russell (1966) are based on two parameter regression coefficient (bi), and deviation from regression (S^2_{di}). Whereas, the additive main effects and multiplicative interaction (AMMI) model is a combination of the main effect due to analysis of variance and their interactions (GEI) (Gauch, 1992).

Yan et al. (2000) created a biplot strategy known as GGE biplot which graphically indicates the genotype (G) primary effects and genotype × environment interaction (GGE). The G and GE are the two fundamental source of variation for genotype evolution under diverse environment. The GGE biplot analysis represents the G+GE of different environment records acquired by plotting the two (or more) PCA score of G × E interaction. The GGE biplot analysis allows the analysis of many characteristics of genotypes and environments (Samonte et al., 2005). Selection and identification of stable and high yielding genotypes over the different environments have been a continuous task to rice breeders (Balestre et al., 2010). Therefore, in our study, we have compared the Eberhart and Russell methodology, AMMI biplot, and GGE biplot analysis of the twenty-two popular basmati rice genotypes under north Indian conditions. Further, these approaches are applied under four different production systems transplanted rice (TPR), SRI, DSR (W) and DSR (D).

Materials and methods

Plant material and experiment layout

Experimental fields were settled at Regional Research Station, Kaul, India (29.98° N latitude and 79.66° E longitude) (Fig. 1). Field trials were conducted over two Kharif (July

to October) seasons in 2014-2015 and 2015-2016 respectively. During both of the years, the nursery was sown in June, for both TPR and SRI. After that, the seedlings were field transplanted in July for TPR and SRI. Whereas, the direct sowing of DSR (D) and DSR (W) was performed in June. Plants were harvested in the month of October for data analysis. The weather during the entire crop period is presented in *Figure 2*. The soil was analysed as a composite sample from the top 0-15 cm (Bandyopadhyay et al., 2012). The soil was sandy loam with the with different percentage of sand (81.4%), slit (7.3%), and clay (11.3%). All plant production related practices were followed based on the package of practices for rice cultivation.

The experimental materials comprised of popular basmati rice genotypes (*Table 1*). These genotypes were laid out in a randomized complete block design (RCBD) with three replications, using four production systems namely, TPR, SRI, DSR (W) and DSR (D) (*Table 2*). Each experimental plot consisted of five rows of 2 m long with 0.20 m row spacing (*Fig. 3*).

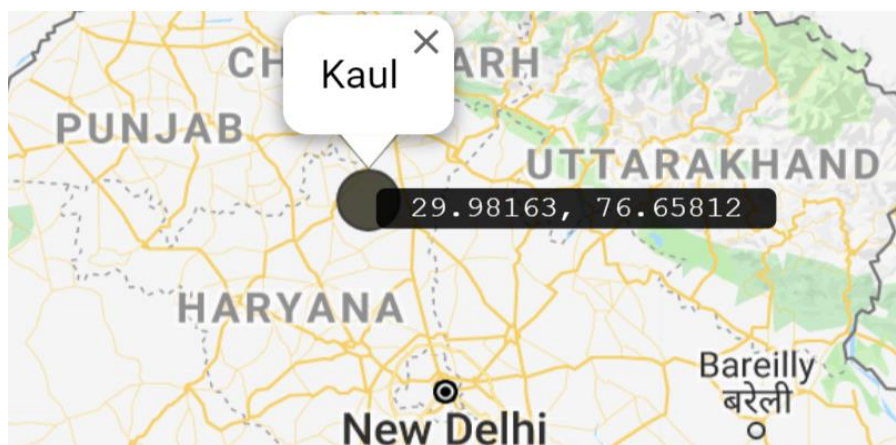
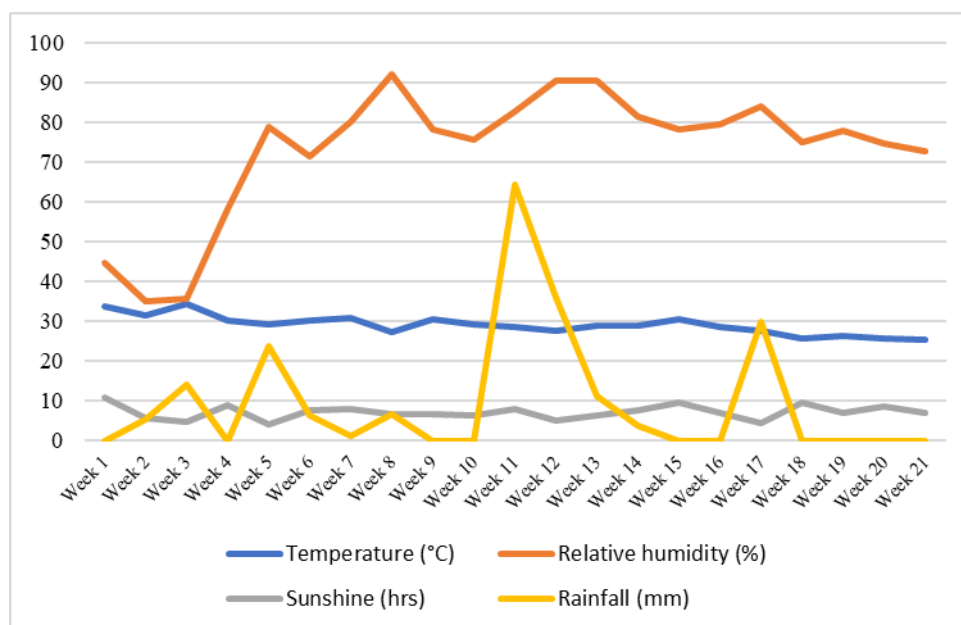
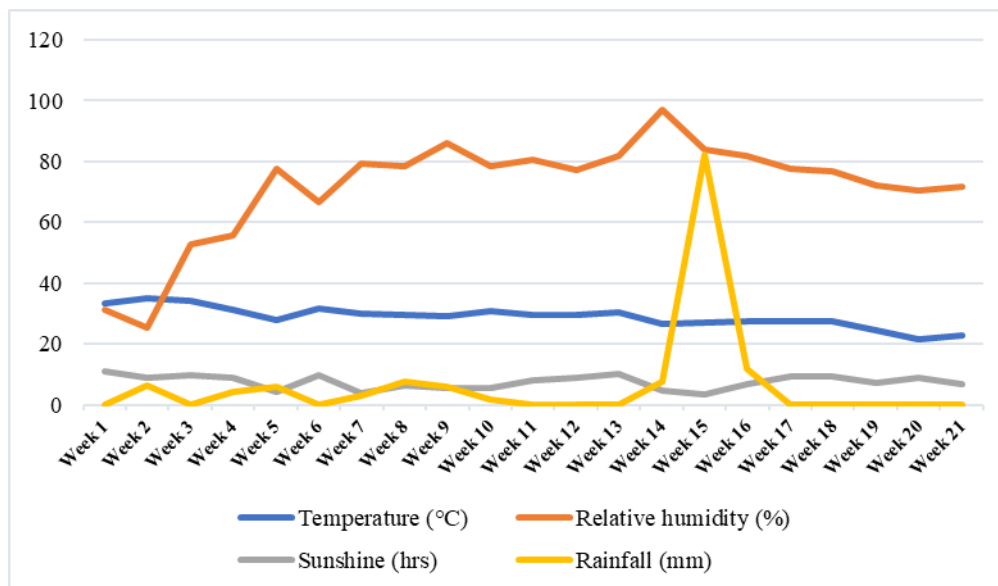


Figure 1. Location and coordinates of the experimental site in India



a



b

Figure 2. Temperature (°C), relative humidity (%), sunshine (h), and rainfall (mm) during first year and second year of the entire crop season

Table 1. List of basmati rice genotypes used in the study

Code	Genotypes
G1	Pusa Basmati 1121
G2	Pusa Basmati 1509
G3	Pusa Sugandh 2
G4	Pusa Sugandh 3
G5	Pusa Sugandh 5
G6	Pusa Basmati 6
G7	Pusa Basmati 1
G8	Improved Pusa Basmati 1
G9	HKR 98-476
G10	HKR 03-408
G11	HKR 06-434
G12	HKR 06-443
G13	HKR 06-487
G14	HKR 08-417
G15	HKR 08-425
G16	Haryana Mahek-1
G17	Haryana Basmati-1
G18	Traori Basmati
G19	Super Basmati
G20	CSR-30
G21	Basmati-370
G22	Pusa RH-10

Table 2. Description of environments

Environment	2014	2015
DSR (D)	E1	E2
DSR (W)	E3	E4
SRI	E5	*
TPR	E6	E7

Transplanted rice (TPR), system of rice intensification (SRI), direct seeded rice (DSR) in both conditions, i.e. wet (W) and dry (D)

*Filled damage during flood, so data was not included in the analysis

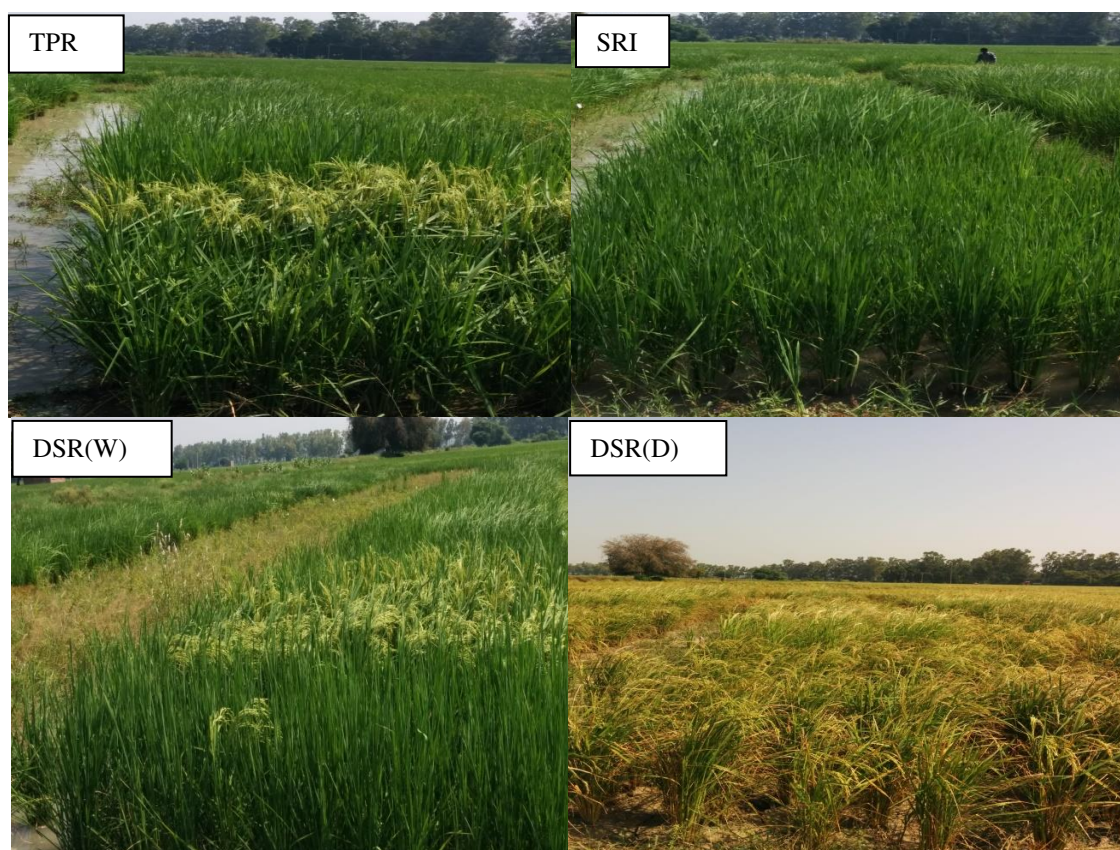


Figure 3. The four production systems used for the characterization of basmati rice genotypes. Transplanted rice (TPR), system of rice intensification (SRI), direct seeded rice wet (DSR (W)), and direct seeded rice dry (DSR (D))

Characterization and data analysis

In total seven characters were studied as the mean of five randomly chosen plants per plot. Biological weight is measured as the weight of plant biomass. The biological weight (g) per plant was recorded after harvesting and drying of mature plants. Whereas, the harvest index was determined as the ratio of grain yield/biological yield × 100. Test grain weight (g) was determined from the random sample of 1000 filled grains for each replication. Whereas, the number of spikelet per panicle were determined from a random sample of twenty panicles after harvesting. The percent of filled spikelet was

estimated as the percentage of grain filled spikelet to the total number of spikelet. While the days to 50% flowering were recorded based on the date of sowing to 50% flowering on a plot basis. Similarly, days to 75% maturity were recorded from the date of sowing until the day when a minimum 75% grains per panicle showed maturity.

The data analysis was performed using the software package PBTools version 1.4 (<http://bbi.irri.org/products>) and R Statistics (R Core Team, 2017). Unweighted Pair Group Method with Arithmetic Mean (UPGMA) method of hierarchical clustering was applied to the twenty-two genotypes in order to visualize how genotypes are related to each other based on all of the studied descriptors. The AMMI model (Gauch, 1988) is a combination of Additive (ANOVA) and multiplicative interaction (Principal component analysis). The Genotype × Environment interaction was evaluated by considering the first two PCA. The statistical model can be represented as:

$$Y_{ij} = \mu + g_i + e_j + \sum \lambda_n \alpha_{in} \gamma_{jn} + \theta_{ij} \quad (\text{Eq.1})$$

where:

Y_{ij} : mean yield of i^{th} genotype in the j^{th} environment;

μ : general mean;

g_i : i^{th} genotypic effect;

e_j : j^{th} location effect.

λ_n : eigenvalue of the Principal Component Axis n ;

α_{in} : and γ_{jn} are the i^{th} genotype, j^{th} environment Principle component analysis (PCA) scores for the PCA axis n ;

θ_{ij} : residual n is the number of PCA axes retained in the model.

Whereas GGE biplots are a combination of both G (Genotype) linear effect and G × E interaction and it is based on sites regression linear, bilinear model (Kang, 1993; Cornelius et al., 1996; Crossa and Cornelius, 1997; Crossa et al., 2002).

Results

Genotypic performance of different traits

A diverse range of variation in the means was detected for yield and yield-related traits for all of the 22 basmati rice genotype in a different production system. During the two seasons; wide-ranging genotypic fluctuation or variation was detected and ranged for biological weight (32.49 to 44.26); harvest Index (%) (27.54 to 41.17); test grain weight (19.62 to 29.95); number of Spikelet (57.49 to 109.71); filled spikelet (%) (73.06 to 87.62); 50% flowering (86.00 to 108.40); 75% maturity (107.60 to 137.60) among different genotype under study as shown in *Table 3*. Considering the two season average mean, genotypes G22 recorded the highest number of spikelet per plant, whereas, genotype G16 recorded the highest biological weight per plant. Genotype G2 was short duration with lowest unfilled grain and highest test grain weight in all the production system (*Table 3*). Further, using the Unweighted Pair Group Method with Arithmetic Mean (UPGMA) technique the clustering results of the twenty-two basmati rice genotypes are presented in *Figure 4*. More related genotypes were clustered together. Genotype G2 clustered apart from rest of the genotypes. Whereas, seven genotypes clustered together, while, the remaining fourteen genotypes were together (*Fig. 4*).

Table 3. Mean performance of genotypes for the studied characters over a period of two years

Genotype	Biological weight (g)	Harvest index (%)	50 flowering (%)	75 maturity (%)	Filled spikelet (%)	Test grain weight (g)	No. of spikelet
G1	43.76	32.32	101.60	128.30	75.41	27.46	62.05
G2	32.49	39.54	86.00	107.60	85.22	29.95	66.91
G3	36.63	36.66	89.50	113.60	81.39	27.45	91.05
G4	36.85	33.97	99.00	120.70	77.71	22.94	88.10
G5	35.86	35.43	99.80	119.60	79.21	25.44	92.38
G6	38.31	34.85	110.30	135.90	73.06	21.85	80.48
G7	35.52	34.84	107.50	136.80	77.42	21.85	89.10
G8	33.94	36.51	107.60	136.60	76.15	21.19	87.41
G9	39.55	30.16	107.40	135.40	77.21	21.50	57.50
G10	41.29	28.20	109.10	136.20	81.59	21.16	64.79
G11	44.11	27.55	111.40	137.00	82.17	22.63	66.00
G12	39.51	30.33	102.00	130.00	78.84	26.29	53.95
G13	39.14	30.02	108.40	134.10	84.26	19.62	84.95
G14	37.21	41.17	98.80	127.60	86.40	21.90	72.59
G15	40.14	37.31	99.40	129.10	84.67	21.52	81.10
G16	44.27	27.49	114.00	137.60	82.14	23.58	76.33
G17	36.63	34.13	101.50	127.90	79.42	22.61	83.77
G18	40.14	33.59	103.50	128.60	87.63	23.63	56.19
G19	38.88	32.71	96.70	127.80	82.54	21.44	77.58
G20	36.97	26.99	105.60	132.80	84.75	22.82	51.95
G21	43.83	29.20	101.00	130.10	83.23	22.10	81.24
G22	38.11	40.61	92.30	116.90	73.32	24.75	109.71
Mean	38.78	33.34	102.38	128.65	80.62	23.35	76.14
Standard error	3.19	2.18	1.70	2.30	2.20	0.95	4.99

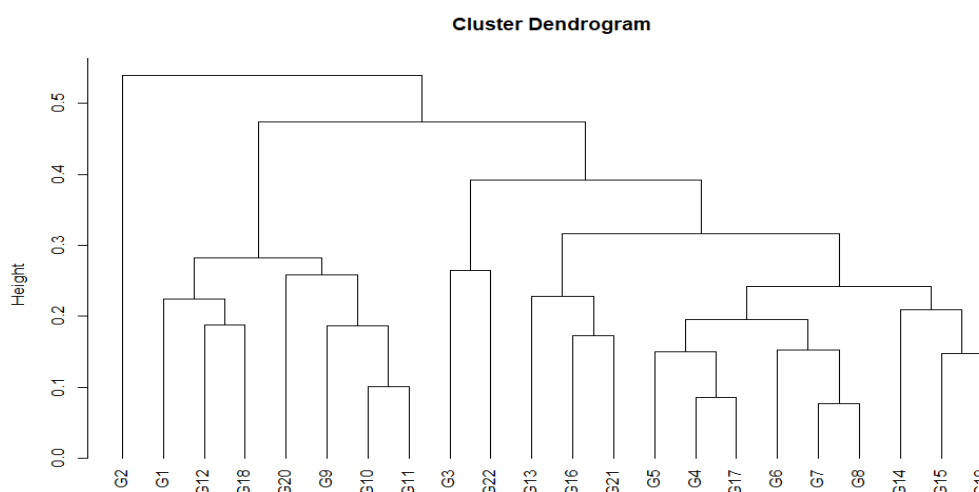


Figure 4. Clustering dendrogram of twenty-two basmati rice genotypes based on the Unweighted Pair Group Method with Arithmetic Mean (UPGMA) clustering method with on log-normalized descriptors values. The cophenetic correlation coefficient of clustering is 0.8

Pooled analysis and stability analysis

Interpretations on the yield-related traits for two-year data were then subjected to pooled analyses by using Eberhart and Russel (1966), Additive Main Effect and multiplicative interaction (Gauch and Zobel, 1989) and GGE Biplot (Yan and Kang, 2003). In the analysis, the environment defined by every arrangement of location or Kharif season with the production system. First Analysis of variance was conducted for each location (environment) then combined analysis of two-year data was subjected to stability analysis using PB tools and R software. The pooled analysis results showed that the genotypic and environmental variances were significant ($p < 0.05$) for all the traits. Similarly, the mean sum of squares due to $G \times E$ interaction was significant for all of the seven traits studied. Furthermore, the partitioning of the combined environment, and genotype × environment variance into linear and non-linear components showed that environment linear and combined deviation was significant given in Table 4.

Table 4. Pooled analysis of variance over different environments for different traits in rice (Eberhart and Russell, 1966 model)

Source of variations	DF	Biological weight (g)	Harvest index (%)	50 Flowering (%)	75 Maturity (%)	Filled spikelet (%)	Test grain weight (g)	No. of spikelets
Rep within Env.	14	3.5	1.81	0.81	0.5	8.23	0.53	13.32
Varieties	21	73.87*	127.58**	354.36**	480.49**	120.46**	45.29**	1536.44**
Env.+ (Var.* Env.)	132	249.73***	76.312**	32.56**	52.85**	63.66**	8.37*	435.22**
Environments	6	4600.33***	937.039**	325.86**	442.44**	679.10**	67.58**	5072.60**
Var.* Env.	126	42.56**	35.32*	18.59*	34.30*	34.35*	5.55*	214.39*
Environments (Lin.)	1	27601.99***	5622.23**	1955.21**	2654.67**	4074.60**	405.52**	30435.60**
Var.* Env.(Lin.)	21	63.49*	62.66**	20.33	44.27	54.03*	4.83015871	502.62**
Pooled Deviation	110	36.63***	28.50**	17.41**	30.84**	29.03**	5.44**	149.62**
Pooled Error	294	5.73	2.31	1.32	1.07	6.67	0.69	14.74
Total	153	225.59	83.34	76.72	111.55	71.45	13.44	586.37

*, **Significant at 5% and 1% respectively

The stability model proposed by Eberhart and Russell (1966) was adopted to analyse the data over different environments and in this model is the most popular technique of studying Genotype × Environment interaction and genotypic stability. It used two parameters (b_i and S^2d_i) to define stability. S^2d_i is primarily used to rank the relative stability of cultivars. The indication is that b_i may be utilized to depict the standard response to the goodness of environmental conditions though S^2d_i measures the predictability. According to this model, a stable variety is one that has a high mean (X_i), unit regression coefficient ($b_i=1$) and the deviation from regression as small as possible ($S^2d_i = 0$). The stability analysis revealed the genotypes in case of with significant regression coefficient (b_i) and non-significant deviation from the regression (S^2d_i) Genotype G21 (50% flowering) and G17 (filled spikelet (%)) exhibited non-significant S^2d_i , regression coefficient significantly greater than one and mean higher than the population mean was found suitable for a better environment (E6 and E5). Genotype G2 in biological weight, G18 and G21 in a filled spikelet (%), G2 and G12 in Number of spikelet with regression coefficient significantly less than one and non-significant deviation from regression and mean higher than the population mean was identified suitable for unfavourable environments E1, E2, E3, E4. Genotype G9 and G19 were

found stable for filled Spikelet (%) trait for all the environments that have high mean (Xi), unit regression coefficient (bi=1) and the deviation from regression as small as possible ($S^2di = 0$) given in Table 5.

Table 5. Stability parameters for yield contributing traits of rice genotypes tested over different environments

Genotypes	Parameter	Biological weight (g)	Harvest index (%)	50 flowering (%)	75 maturity (%)	Filled spikelet (%)	Test grain weight (g)	No. of spikelets
G1	Mean	43.762	32.323	101.571	128.286	75.414	27.462	62.048
	bi	1.22	1.273	0.830	1.022	1.123	0.666	0.229
	S ² di	29.395	25.010	5.55	6.638	9.777	0.579	21.705
G2	Mean	32.490	39.535	86.000	107.619	85.224	29.952	66.905
	bi	0.555	0.898	0.837	-0.019	-0.136	0.316	0.709
	S ² di	-0.537	49.719	2.062	39.809	9.969	4.788	13.008
G3	Mean	36.633	36.658	89.476	113.571	81.386	27.452	91.048
	bi	0.905	1.019	0.863	0.271	-0.256	0.657	1.399
	S ² di	12.465	29.494	6.785	51.342	22.906	-0.115	106.416
G4	Mean	36.848	33.966	99.000	120.714	77.714	22.943	88.095
	bi	0.800	0.814	1.827	0.010	1.351	0.001	1.462
	S ² di	26.09**	20.80**	34.35**	83.90**	163.25**	6.35**	202.05**
G5	Mean	35.857	35.430	99.762	119.571	79.205	25.438	92.381
	bi	0.563	0.077	1.448	0.542	0.496	0.927	1.176
	S ² di	33.21**	41.67**	67.98**	64.73**	4.772	4.63**	103.31**
G6	Mean	38.314	34.851	110.33	135.857	73.062	21.848	80.476
	bi	1.177	1.095	1.545	0.962	0.773	1.079	1.95*
	S ² di	1.449	65.10**	6.74**	7.94**	63.60**	7.64**	88.68**
G7	Mean	35.521	34.839	107.524	136.762	77.424	21.848	89.095
	bi	0.891	1.004	1.373	1.293	1.498	1.517	1.76*
	S ² di	13.74**	3.12*	11.95**	5.77**	22.20**	5.30**	96.96**
G8	Mean	33.943	36.507	107.571	136.619	76.148	21.186	87.410
	bi	0.95*	0.769	1.675	1.411	1.545	0.898	2.08*
	S ² di	5.064	25.12**	23.41**	5.19**	42.22**	12.85**	152.05**
G9	Mean	39.552	30.159	107.381	135.381	77.214	21.495	57.495
	bi	1.119	1.98*	1.368	1.85*	1.04*	0.940	0.649
	S ² di	33.88**	31.48**	4.035**	7.72**	5.894	6.11**	87.83**
G10	Mean	41.286	28.195	109.095	136.238	81.586	21.162	64.790
	bi	1.276	0.956	0.949	1.61*	0.765	1.22*	0.42*
	S ² di	53.30**	23.55**	3.42**	2.48**	6.991	0.352	23.62*
G11	Mean	44.114	27.547	111.380	137.048	82.167	22.633	66.000
	bi	1.393	0.844	0.710	1.456	0.887	1.565	0.639
	S ² di	84.97**	26.12**	0.019	8.31**	14.27**	10.01**	67.03**
G12	Mean	39.514	30.332	102.048	129.952	78.843	26.286	53.952
	bi	0.910	1.237	0.971	0.800	1.838	0.722	0.43**
	S ² di	35.55**	1.504	9.04**	26.35**	44.09**	0.86*	2.899
G13	Mean	39.143	30.022	108.381	134.143	84.257	19.624	84.952
	bi	0.863	1.126	0.424	1.618	1.312	1.26*	1.465
	S ² di	25.75**	6.71**	15.26**	31.78**	4.260	0.045	730.35**
G14	Mean	37.210	41.173	98.810	127.571	86.395	21.895	72.590
	bi	1.067	0.585	0.745	1.727	0.910	1.767	0.556
	S ² di	19.43**	11.83**	35.85**	29.08**	13.32*	1.34*	143.06**
G15	Mean	40.143	37.314	99.381	129.095	84.667	21.524	81.095
	bi	1.18*	1.283	0.547	1.054	0.40*	1.324	0.835
	S ² di	2.343	3.39*	29.93**	2.51*	6.654	0.824	194.79**
G16	Mean	44.267	27.488	114.048	137.571	82.138	23.576	76.333
	bi	1.356	1.482	0.818*	1.728	1.403	0.651	0.346
	S ² di	47.98**	29.54**	1.440	38.51**	12.31*	6.02**	90.42**
G17	Mean	36.631	34.130	101.476	127.905	79.419	22.614	83.767
	bi	0.929	1.252	1.639	-0.150	1.38*	2.220	1.839
	S ² di	21.85**	12.24**	12.94**	81.51**	4.067	8.47**	287.84**

G18	Mean	40.143	33.592	103.476	128.571	87.629	23.629	56.190
	bi	1.032	0.111	0.760	1.049	0.81*	0.846	0.503
	S ² di	25.98**	89.14**	5.79**	18.90**	-1.576	3.14**	76.25**
G19	Mean	38.876	32.708	96.667	127.762	82.537	21.438	77.581
	bi	0.959	1.58*	-0.178	1.450	1.01*	0.842	1.304
	S ² di	8.91*	8.95**	65.42**	26.44**	5.813	8.94**	162.68**
G20	Mean	36.971	26.992	105.571	132.810	84.752	22.819	51.952
	bi	1.163	1.74*	0.555	1.079	1.186	1.340	0.035*
	S ² di	68.91**	16.08**	5.47**	27.05**	12.07*	6.64**	170.01**
G21	Mean	43.829	29.196	101.048	130.143	83.233	22.095	81.238
	bi	0.839	0.708	1.18*	0.787	0.83*	0.965	0.874
	S ² di	96.98**	14.17**	0.789	4.49**	-1.604	7.06**	32.28*
G22	Mean	38.114	40.610	92.333	116.905	73.324	24.752	109.714
	bi	0.828	0.149	1.104	0.439	1.796	0.270	1.304
	S ² di	35.11**	41.67**	6.27**	84.99**	25.17**	2.65**	115.49**

*, **Significant at 5% and 1% respectively

Genotypes or general genotypic adaptation

GGE and AMMI biplots described stability across genotypes or general genotypic adaptation. Comparative position of diverse genotypes on the biplots is based on its projection onto the O-axis in AMMI Biplot and GGE biplot. Biplots can identify GEI effects on each trait which contribute towards yield. AMMI1 biplot interpreted results by main effect and IPCA1 of both genotype and environment revealed that genotypic differences were important in term of direction and magnitude along both axis (X axis and Y axis). AMMI biplot represent that shift along the X-axis reflected changes in main effects, however, shift along the Y-axis reflected differences in interaction effects and adaptation of a genotype to specific environment showed by high PCA score, IPCA scores nearly to zero gave information about stable genotype in different environments. The AMMI biplot analysis is provided in *Table 6*.

Table 6. AMMI analysis for different traits in rice across different production system

Source of variations	Biological weight (g)	*SS (%)	Harvest index (%)	SS (%)	50 Flowering (%)	SS (%)	75 maturity (%)	SS (%)	Filled spikelet (%)	SS (%)	Test grain weight (g)	SS (%)	No. of spikelets	SS (%)
Trials	225.60		83.35		76.73		111.55		71.46		13.44		586.37	
Genotypes	73.87*	4.49	127.58*	21.01	354.36*	63.39	480.50*	59.12	120.46*	23.14	45.30*	46.24	1536.45*	35.96
Environments	4600.33*	79.97	937.02*	44.09	325.87*	16.65	442.45*	15.55	679.10*	37.27	67.59*	19.71	5072.60*	33.92
G × E interaction	42.56*	15.54	35.33*	34.90	18.59*	19.96	34.30*	25.32	34.36*	39.59	5.56*	34.04	214.40*	30.11
PCA I	81.72*	39.62	69.32*	40.49	69.68*	77.33	92.63*	55.72	60.61*	36.40	8.61*	31.96	423.70*	40.78
PCA II	45.87*	20.53	40.67*	21.93	14.60*	14.96	66.63*	37.00	41.36*	22.93	7.00*	24.00	352.16*	31.29
PCA III	40.34*	16.55	36.31*	17.95	3.66*	3.44	7.61*	3.88	39.00*	19.82	5.64*	17.72	148.17*	12.07
PCA IV	27.33*	10.19	19.02*	8.55	2.59*	2.21	4.01*	1.86	24.37*	11.26	4.85*	13.84	88.33*	6.54
PCA V	25.72*	8.63	16.19*	6.55	1.57*	1.21	2.44*	1.02	13.37*	5.56	3.45*	8.87	90.64*	6.04
Residual	15.00	4.48	12.60	4.53	1.24	0.85	1.44	0.53	10.90	4.03	1.58	3.60	55.52	3.29
Pooled residual	23.14*		22.01*		18.59*		34.30*		34.36*		5.56*		214.40*	
Error	5.64		2.30		1.30		1.05		6.74		0.69		14.68	
Total	78.64		29.20		26.33		37.72		28.22		4.92		204.42	

*, **Significant at 5% and 1%, respectively. *Mean sum of squares (SS)

AMMI analysis (*Figs. 5, 6, 7, 8 and 9*) showed that genotype G22 for filled spikelet (%); G20 for number of spikelets; G18 for test grain weight; G8 for Harvest index.

Environment E5, E6 were more responsive for the traits Biological weight, number of Spikelets, Test Grain Weight, filled Spikelet (%) and environment E7 was responsive for traits filled Spikelet (%), Test grain weight, Harvest index. From the AMMI biplot was concluded that environment interaction was extremely diverse and entirely the four Production systems were extremely interactive for most of the yield-related traits. Environment E5, E6 seemed to be a favourable environment for all the yield-related traits; E7, E2 for filled spikelet (%), Test Grain Weight, Harvest Index. Environment E1 and E3 unfavourable for Harvest Index, Test grain weight, number of spikelet and filled spikelet (%).

Specific genotypic adaptation

Specific genotypic evaluation centred on two GGE biplots “which-won-where pattern” biplot and adaptation biplot displayed specific genotypic adaptation to limited environment condition or the adaptability of genotypes for each environment. The biplot *Figure 10* represents a polygon where some of the genotypes were placed on the crests, while the rest were surrounded by the polygon. As the genotypes placed on the peak had the longest detachment from the biplot origin and they were expected to be the most responsive. The genotypes on the crests could be called the ideal/vertex genotype. In the present study, the genotypes G15 in E1 and E5 are the vertex genotype, which had the highest test grain weight. The genotype G20 is only apex genotype for environment E4 and Genotype G14 for E2 and E6 environment. None of the environments fell in the sectors with genotypes G1, G7 and G3 that these genotypes were not appropriate for growing in these environments.

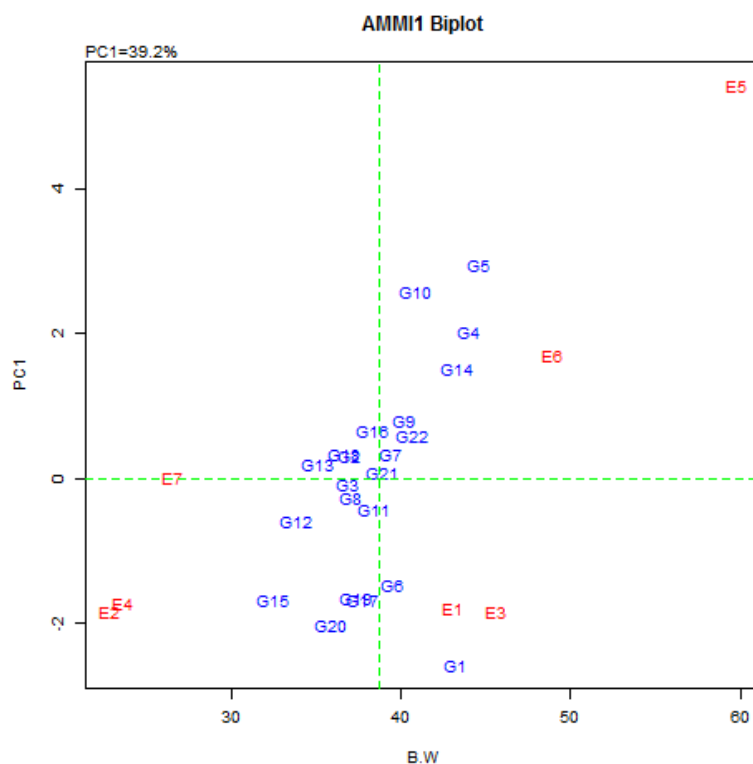


Figure 5. AMMI1 biplot for biological weight (g)

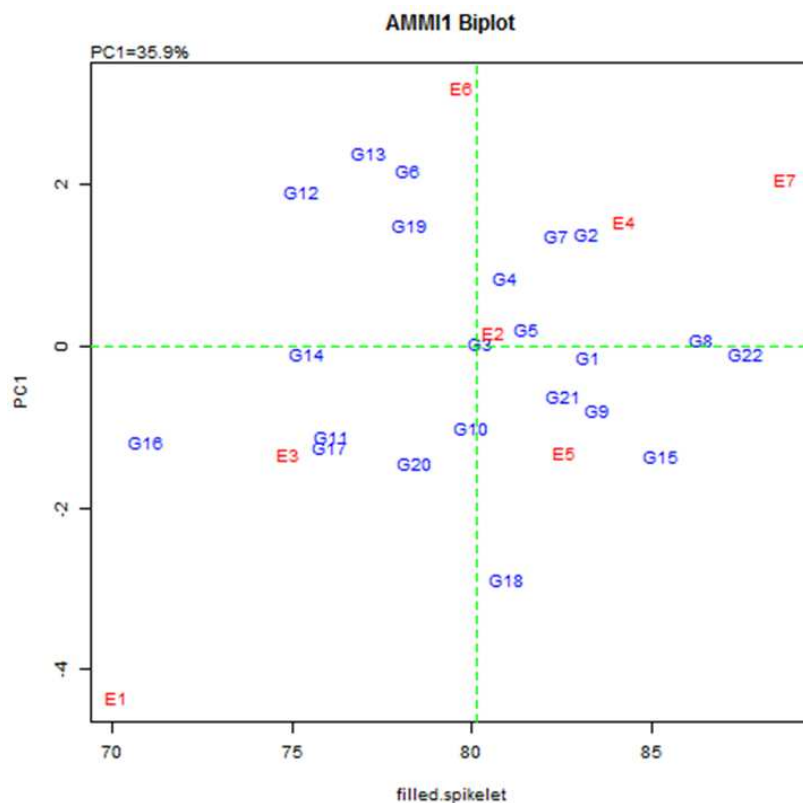


Figure 6. AMMI1 biplot for filled spikelet (%)

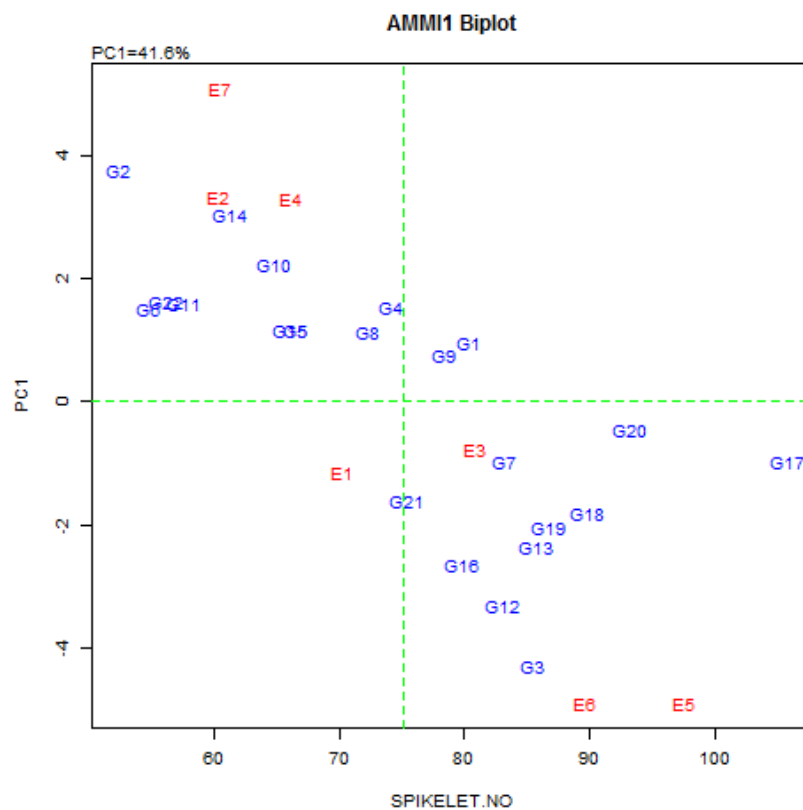


Figure 7. AMMI1 biplot for number of spikelets

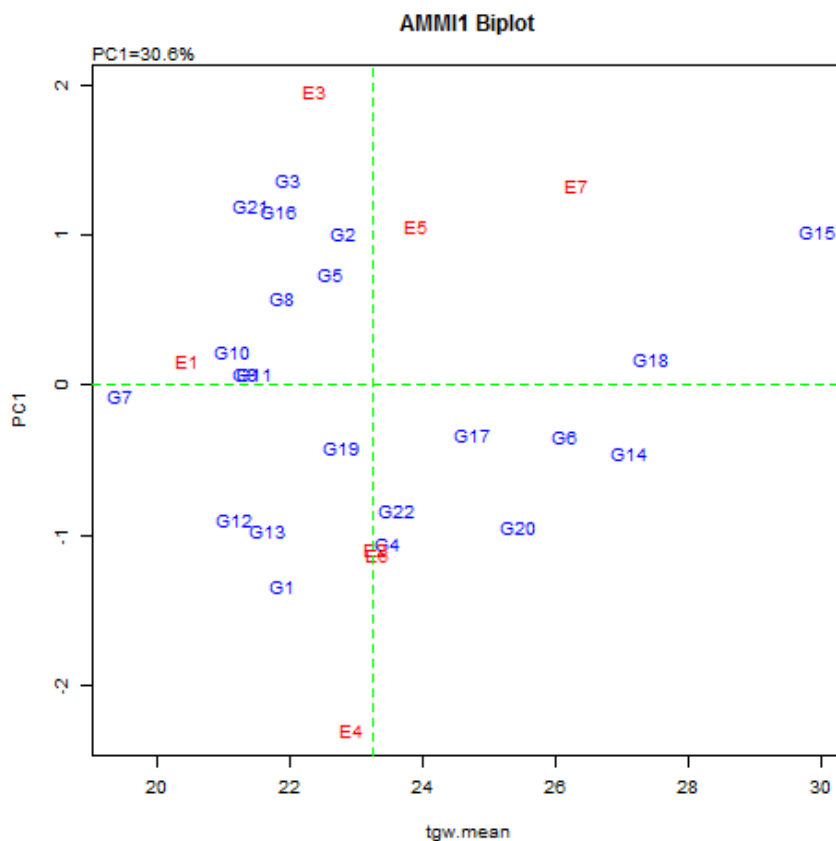


Figure 8. AMMI1 biplot for test grain weight (g)

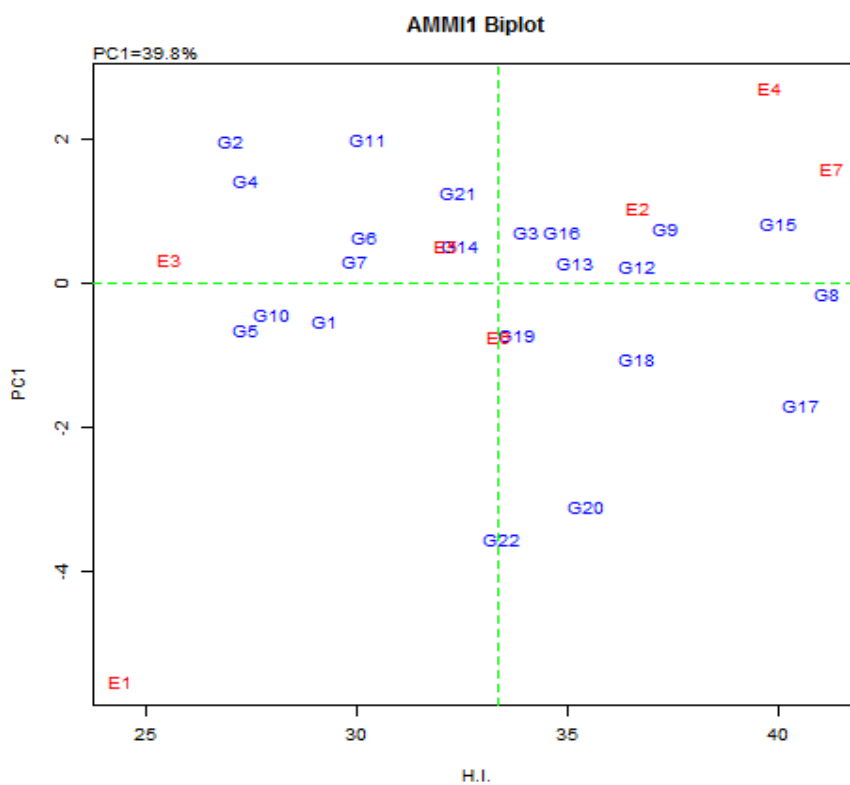


Figure 9. AMMI1 biplot for harvest index (%)

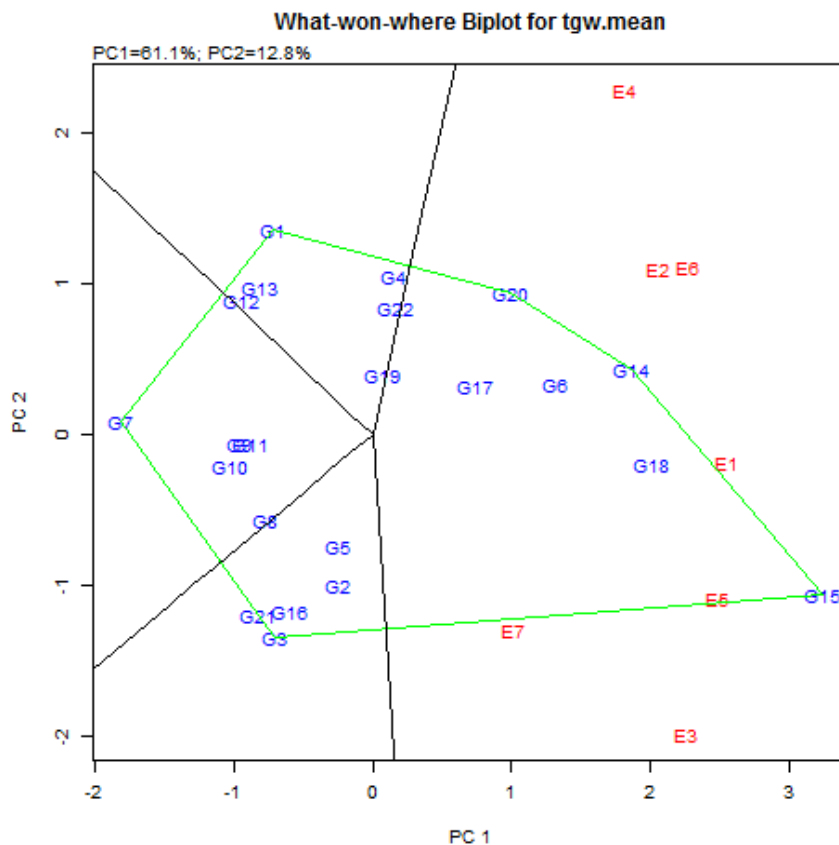


Figure 10. Polygon views of the GGE biplot based on symmetrical scaling for “which-won-where” pattern of rice genotypes in three environments “which-won-where pattern biplot test grain weight (g)”

In case of biological weight (*Fig. 11*) Vertex genotypes are G4, G5, G10 and G1 at E6, E5, E7 and E1 respectively. In case filled spikelet (*Fig. 12*) Vertex genotypes are G22, G2, G12, G18 and G15 at E2, E4, E7, E1 and E3, E5 respectively.

In *Figure 13* average tester coordinate (ATC X-axis) or the performance line passes through the biplot origin with an arrow indicating the positive end of the axis. The average biological Weight of the genotypes is estimated by the projections of their markers to the ATC X-axis. Genotypes G2 and G5 had the highest biological Weight and genotype G15 had the poorest biological Weight. Mean biological weight of the genotypes were in the following order: G2 > G5 > G14 > G1 > G10 > G9 > G11 > G22 > G2 > G16 (*Fig. 13*). The performance of genotypes G10 and G1 were the most variables (least stable), whereas genotypes G4, G9 and G22 were highly stable with high biological weight.

The discriminating power vs representativeness view of the GGE biplot as shown in *Figure 14* indicated that environments E1 and E5 with the most extended projection from the biplot origin were found large discriminating power of the genotypes (i.e., provided information regarding differences among genotypes). On the other hand, E2 and E3 with its shortest vector from the biplot origin was found less discriminating of the different genotypes. Environments E2, E3, E4 and E6 were found to be more representative of other test environments because they have smaller angles with the AEAs (*Fig. 14*). E6 was therefore identified as an ideal environment that has both discriminating abilities of

the genotypes and representative of the other test environments. Therefore, environment E6 can be used to effectively select superior rice genotypes that can perform consistently across environments.

Ranking genotypes relative to the ideal genotypes

An ideal genotype is one that has both high mean yield and high stability. The centre of the concentric circles (*Fig. 15*) represents the position of an ideal genotype, which is defined by a projection onto the mean-environment axis that equals the longest vector of the genotypes that had above-average mean biological weight and by a zero projection onto the perpendicular line (zero variability across environments). Therefore, genotypes G21 and G16 which fell into the centre of concentric circles, were ideal genotypes in terms of higher yield ability and stability, compared with the rest of the genotypes. In addition G6, G7, G22, G9, G2 located on the next concentric circle, may be regarded as desirable genotypes.

Ranking environment relative to the ideal environment

The GGE biplot way of measuring representativeness is to define an average environment and use it as a reference or benchmark. The average environment is indicated by small circle (*Fig. 16*). The ideal environment, represented by the small circle with an arrow pointing to it, is the most discriminating of genotypes and yet representativeness of the other tests environments. Therefore, E1, E2 and E3 were the most desirable test environment followed by E7.

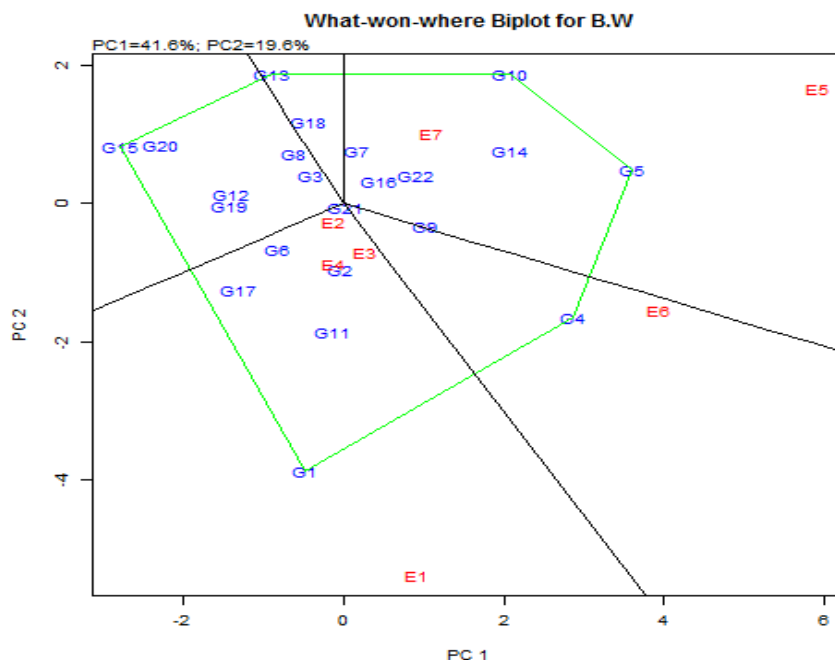


Figure 11. Polygon views of the GGE biplot based on symmetrical scaling for “which-won-where” pattern of rice genotypes in three environments “which-won-where biplot biological weight (g)”

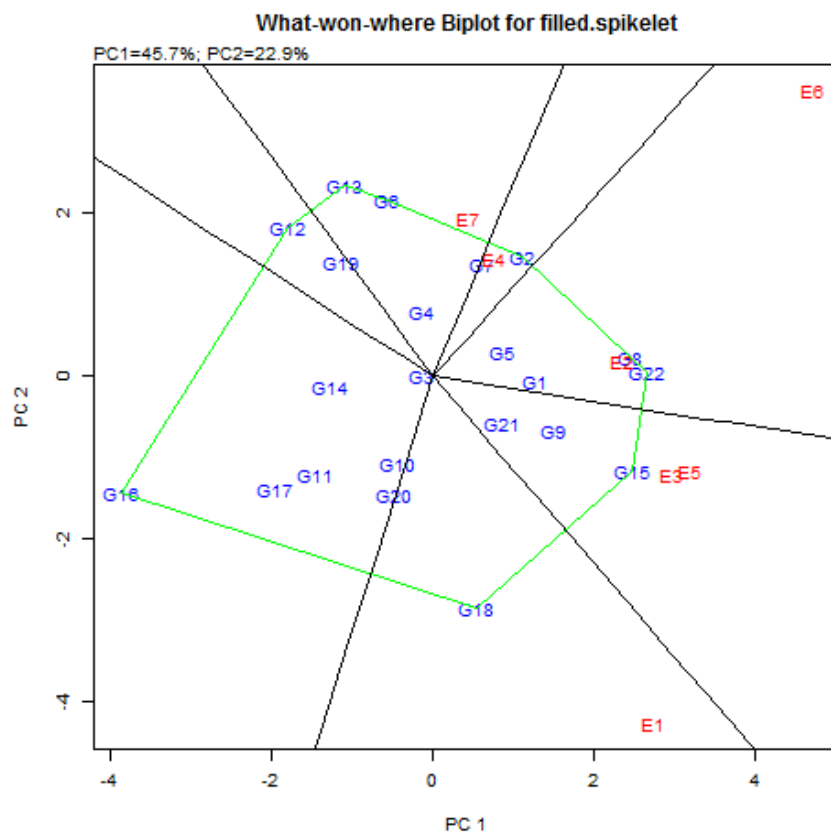


Figure 12. Polygon views of the GGE biplot based on symmetrical scaling for “which-won-where” pattern of rice genotypes in three environments “which-won-where biplot filled spikelet (%)”

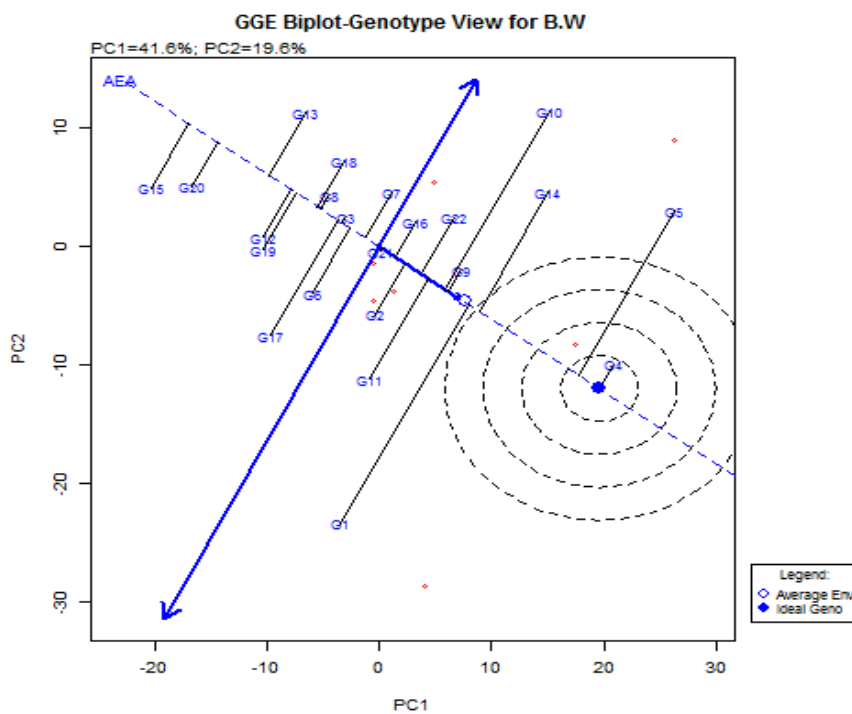


Figure 13. Polygon view biological weight (g)

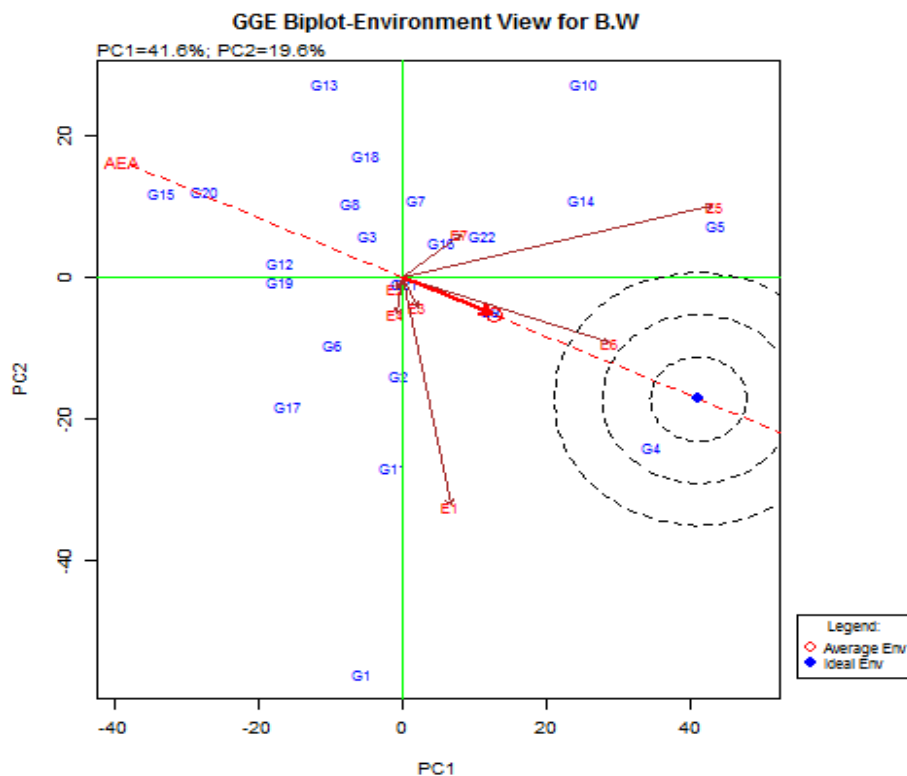


Figure 14. GGE biplot for biological weight (g)

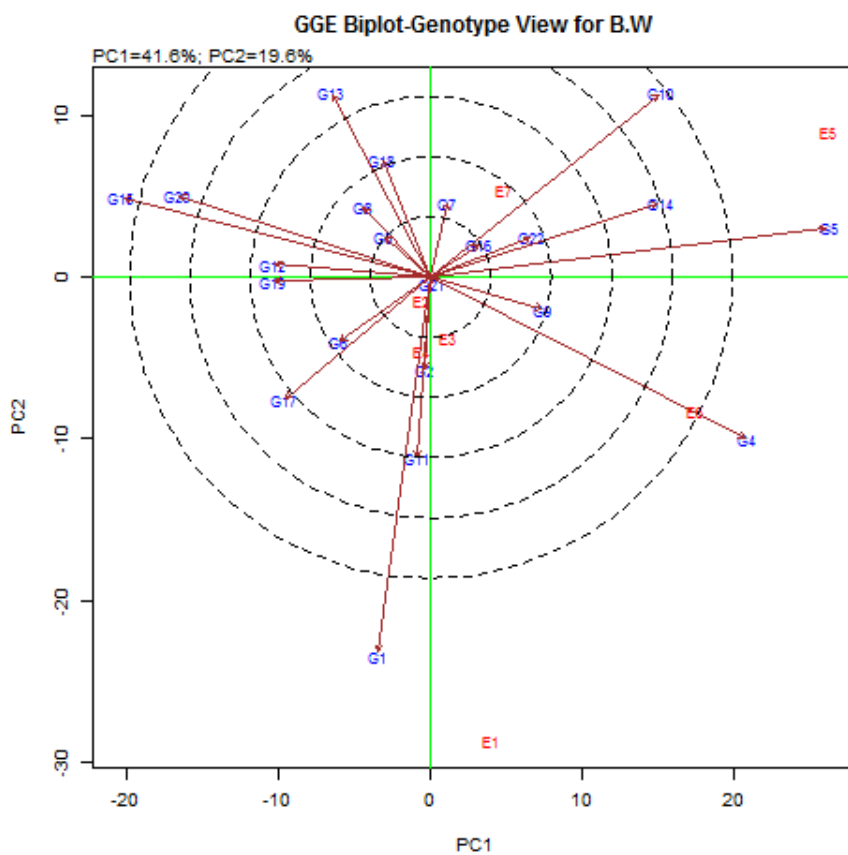


Figure 15. Ranking genotypes relative to the ideal genotypes

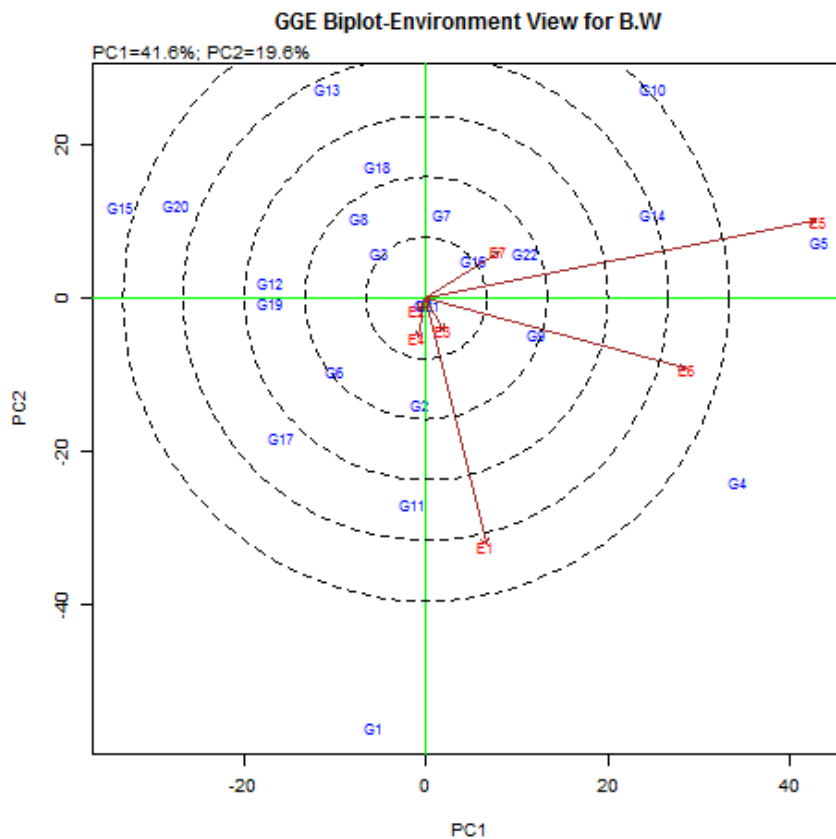


Figure 16. Ranking environment relative to the ideal environment

Discussion

Due to the Cultivation of rice under several agroecological zones and in different production systems the evaluation of rice genotypes for stability and adaptability is of prime importance (Bose et al., 2012). The changes in environmental conditions significantly affect rice production (Bose et al., 2014). Therefore, here we have identified stable rice genotype to sustain with innovative production systems like the system of rice intensification, and direct seeded rice using stability models. Previously, researchers have used GGE biplot analysis mainly for assessment of varietal stability cultivar evaluation and mega-environment evaluation (Kang, 1993; Yan and Hunt, 2001; Yan and Kang, 2003; Dehghani et al., 2006; Navabi et al., 2006; Blanche et al., 2007; Ding et al., 2007; Jalata, 2011; Mohammadi et al., 2012; Rakshit et al., 2012; Amiri et al., 2015). The simultaneous selection for stability and high mean results in the selection of better genotypes with non-significant stability variance, and it enhances the quality of selection (Nassir, 2013). Pooled analysis study stipulates that a significant basis of variation in the basmati rice genotypes was due to genotype by environment interaction. In the present study, two-year data under four production system of rice was primarily subjected to stability analysis of the traits.

The GGE and AMMI1 biplots recognised Genotype G21 most stable genotype for biological weight; G22 for Filled spikelet (%); G20 for Number of spikelets; G18 for Test Grain weight; G8 for Harvest index was identified as most stable genotypes. Similarly, it has been proved that for multi-environment trails both GGE and AMMI biplots were important for judging stable and adaptable genotypes (Hagos and Abay,

2013; Stojaković et al., 2010; Mitrovic et al., 2012; Rad et al., 2013). Genotypes G21 and G16 were ideal genotypes for biological weight. Further, E1, E2 and E3 were the top three most desirable test environments. Whereas, the GGE biplot analysis has identified E3 as the ideal environment having a long vector length (discriminating ability) and a small angle (representativeness) and G18 as a superior genotype across environments. Similar research finding by Khalil et al. (2011).

This study uncovered that the GGE biplot hence clarified better Genotype + Genotype-Environment interaction than the AMMI1 biplot so that better precise explanation of the GGE of the basmati rice genotype in a diverse production system. This might likely be due to the truth that in spite of the fact that, the AMMI1 biplot (Zobel et al., 1988) has been demonstrated to be exceptionally effective in identifying significant sources of variation of Genotype × Environment interaction effects and has moreover been pronounced as either superior or equal GGE biplot analysis (Gauch, 2006), but it isn't capable to successfully show the virtual execution of each genotype in each environment i.e., does not have the foremost critical property of a true biplot. As a result, the performance of a given genotype in a given environment cannot be precisely visualized even in case it completely shows the data.

Also, Yan et al. (2007) concluded that the GGE biplot is predominant in the AMMI1 biplot in mega-environment analysis and genotype assessment, as it clarifies more G+GE and pinpointed that, the AMMI1 biplot is way better seen as a tool for displaying conclusions instead of as a tool for finding which-won-where designs. Contrastingly, the GGE biplot was criticised by Ebdon and Gauch (2002) and Gauch (2006) for not being able to uncover which-won-where designs in case more than two PCs are required to surmise the information.

Conclusion

We showed the significance of Genotype × Environment interaction by evaluating the genotypic potential of twenty-two basmati rice genotypes using stability models. Basmati rice genotypes were compared for their stability under different production systems (both conventional and non-conventional) for yield-related traits. Results from the analysis with Eberhart and Russell model, AMMI and GGE biplots showed Genotype G21 as the most stable genotype for biological weight; G22 for filled spikelet (%); G20 for number of spikelets; G18 for test grain weight; and G8 for harvest index. Whereas, among the different environments E7 was the most desirable test environment followed by E5 and E4. Overall, a summary list of best genotypes under all of the four production system is provided in *Table 7*. Further, the HKR 08-417 (G14) was determined to be stable under all of the production systems.

Table 7. List of best three genotypes for all of the four production system

Production system	Genotype
TPR	HKR 98-476 (G9)
	Haryana Mehak-1 (G16)
	HKR 08-417 (G14)
SRI	HKR 98-476 (G9)
	Imp Pusa Basmati 1,(G8)
	HKR 08-417 (G14)

DSR (W)	Imp Pusa Basmati1, (G8) Haryana Mehak-1 (G16) HKR 08-417 (G14)
DSR (D)	Super Basmati (G19) HKR 06-487 (G13) HKR 08-417 (G14)

REFERENCES

- [1] Amiri, R., Bahraminejad, S., Sasani, S., Jalali-Honarmand, S., Fakhri, R. (2015): Bread wheat genetic variation for grain's protein, iron and zinc concentrations as uptake by their genetic ability. – *European Journal of Agronomy* 67: 20–26.
- [2] Anonymous (2016): Food and Agriculture Organisation of the United Nations. – <http://www.FAOstat.fao.org.com>.
- [3] Anonymous (2017): Agricultural Statistics. – Directorate of Economics and Statistics, Department of Agriculture and Cooperation, Ministry of Agriculture, GOI, New Delhi, pp. 99-100.
- [4] Ashfaq, M. (2015): Basmati–rice a class apart (a review). – *Rice Research: Open Access* 03(04). doi:10.4172/2375-4338.1000156.
- [5] Balestre, M., Santos, V. B., Soares, A. A., Reis, M. S. (2010): Stability and adaptability of upland rice genotypes. – *Crop Breeding and Applied Biotechnology* 10(4): 357–363.
- [6] Bandyopadhyay, K., Aggarwal, P., Chakraborty, D., Pradhan, S., Narayan Garg, R., Singh, R. (2012): Practical Manual on Measurement of Soil Physical Properties Practical. – Indian Agricultural Research Institute, New Delhi, India, pp. 8–25.
- [7] Becker, H. C., Leon, J. (1988): Stability analysis in plant breeding. – *Plant Breeding* 101: 1–23.
- [8] Bernardo, R. (2002): Quantitative Traits in Plants. – Stemma Press, Bowsens Lanne, Woodbury, MN.
- [9] Bhattacharjee, P., Singhal, R. S., Kulkarni, P. R. (2002): Basmati rice: a review. – *International Journal of Food Science & Technology* 37(1): 1–12.
- [10] Blanche, S. B., Myers, G. O., Kang, M. S. (2007): GGE biplots and traditional stability measures for interpreting genotype by environment interactions. – *Journal of Crop Improvement* 20: 123–135.
- [11] Bose, L. K., Nagaraju, M., Singh, O. N. (2012): Genotype × Environment interaction and stability analysis of low land rice genotypes. – *Journal of Agriculture Science* 57: 1–8.
- [12] Bose, L. K., Jambhulkar, N. N., Singh, O. N. (2014): Additive main effects and multiplicative interaction (AMMI) analysis of grain yield stability in early duration rice. – *Journal of Animal and Plant Science* 24: 1885–1897.
- [13] Cornelius, P. L., Crossa, L., Seyedsadr, M. S. (1996): Statistical Test and Estimators of Multiplicative Models for Genotype-by-Environment Interaction. – In: Kang, M. S., Gauch, H. G. (eds.) *Genotype-by-Environment Interaction*. CRC Press, Boca Raton, FL, pp. 199–234.
- [14] Crossa, J., Cornelius, P. L. (1997): Sites regression and shifted multiplicative model clustering of cultivar trials sites under heterogeneity of variances. – *Crop Science* 37: 406–415.
- [15] Crossa, J., Cornelius, P. L., Yan, W. (2002): Biplots of linear-bilinear models for studying crossover genotype × environment interaction. – *Crop Science* 42: 619–633.
- [16] Dehghani, H., Ebadi, A., Yousefi, A. (2006): Biplot analysis of genotype by environment interaction for barley yield in Iran. – *Agronomy Journal* 98: 388–393.
- [17] Ding, M., Tier, B., Yan, W. (2007): Application of GGE biplot analysis to evaluate genotype (G), environment (E) and G×E interaction on *P. radiata*: case study. –

- Australasian Forest Genetics Conference, 11–14 April 2007, The Old Woolstore, Hobart, Tasmania, Australia.
- [18] Ebdon, J. S., Gauch, H. G. Jr. (2002): Additive main effect and multiplicative interaction analysis of national turfgrass performance Trials: II. Cultivar recommendations. – *Crop Science* 42: 497–506.
- [19] Eberhart, S. A., Russell, W. A. (1966): Stability parameters for comparing varieties. – *Crop Science* 6: 36–40.
- [20] Finlay, K. W., Wilkinson, G. N. (1963): The analysis of adaptation in a plant breeding programme. – *Australian Journal of Agriculture Research* 14: 742–754.
- [21] Gauch, H. G. (1988): Model selection and validation for yield trials with interaction. – *Biometrics* 44: 705–715.
- [22] Gauch, H. G. (1992): Statistical analysis of regional yield trials: AMMI analysis of factorial designs. – Elsevier Amsterdam The Netherlands: 53–110.
- [23] Gauch, H. G. (2006): Statistical analysis of yield trials by AMMI and GGE. – *Crop Science* 46: 1488–1500.
- [24] Gauch, H. G., Zobel, R. W. (1989): Accuracy and selection success in yield trials analysis. – *Theoretical and Applied Analysis* 77: 443–481.
- [25] Génard, M., Lescourret, F., Bevacqua, D., Boivin, T. (2017): Genotype-by-environment interactions emerge from simple assemblages of mathematical functions in ecological models. – *Frontiers in Ecology and Evolution* 5. <https://doi.org/10.3389/fevo.2017.00013>.
- [26] Hagos, G. H., Abay, F. (2013): AMMI and GGE biplot analysis of bread wheat genotypes in the northern part of Ethiopia. – *Journal of Plant Breeding and Genetics* 1(1): 12–18.
- [27] Hinge, V. R., Patil, H. B., Nadaf, A. B. (2016): Aroma volatile analyses and 2AP characterization at various developmental stages in Basmati and Non-Basmati scented rice (*Oryza sativa* L.) cultivars. – *Rice* 9. <https://doi.org/10.1186/s12284-016-0113-6>.
- [28] Jain, B. T., Sarial, A. K., Kaushik, P. (2018): Stability analysis utilising AMMI model and regression analysis for grain yield of basmati rice (*Oryza sativa* L.) genotypes. – *Journal of Experimental Biology and Agricultural Sciences* 6: 522–530.
- [29] Jalata, Z. (2011): GGE-biplot analysis of multi-environment yield trials of barley (*Hordeum vulgare* L.) genotypes in south eastern Ethiopia high lands. – *International Journal of Plant Breeding and Genetics* 5: 59–75.
- [30] Jena, P. R., Grote, U. (2012): Impact evaluation of traditional Basmati rice cultivation in Uttarakhand State of northern India: what implications does it hold for geographical indications? – *World Development* 40(9): 1895–1907.
- [31] Kamoshita, A., Babu, R. C., Boopathi, N. M., Fukai, S. (2008): Phenotypic and genotypic analysis of drought-resistance traits for development of rice cultivars adapted to rainfed environments. – *Field Crops Research* 109(1–3): 1–23.
- [32] Kang, M. S. (1993): Simultaneous selection for yield and stability in crop performance trials: consequences for growers. – *Agronomy Journal* 85: 754–757.
- [33] Khalili, I. A., Rahman, H., Rehman, N. U., Arif, M., Khalili, I. H., Iqbal, M., Ullah, H., Afridi, K., Sajjad, M., Ishaq, M. (2011): Evaluation of maize hybrids for grain yield stability in north-west Pakistan. – *Sarhad Journal of Agriculture* 27(2): 213–218.
- [34] Lin, J. Y. (1994): Impact of hybrid rice on input demand and productivity. – *Agricultural Economics* 10(2): 153–164.
- [35] Malosetti, M., Ribaut, J.-M., van Eeuwijk, F. A. (2013): The statistical analysis of multi-environment data: modeling genotype-by-environment interaction and its genetic basis. – *Frontiers in Physiology* 4. <https://doi.org/10.3389/fphys.2013.00044>.
- [36] Mitrovic, B., Stanisavljevi, D., Treski, S., Stojakovic, M., Ivanovic, M., Bekavac, G., Rajkovic, M. (2012): Evaluation of experimental maize hybrids tested in multi-location trials using AMMI and GGE biplot analyses. – *Turkish Journal of Field Crops* 17: 35–40.
- [37] Mohammadi, M., Karimizadeh, R., Hosseinpour, T., Falahi, H. A., Khanzadeh, H., Sabaghnia, N. et al. (2012): Genotype × Environment interaction and stability analysis of

- seed yield of durum wheat genotypes in dry land conditions. – *Notulae Scientia Biologicae* 4: 57–64.
- [38] Nassir, A. L. (2013): Genotype × Environment analysis of some yield components of upland rice (*Oryza sativa* L.) under two ecologies in Nigeria. – *International Journal of Plant Breeding and Genetics* 7: 105–114.
- [39] Navabi, A., Yang, R. C., Helm, J., Spaner, D. M. (2006): Canspring wheat-growing mega or niche-adapted genotypes?. – *Crop Science* 46: 1107–1116.
- [40] Pham, H. N., Kang, M. S. (1988): Intercorrelations among and repeatability of several stability statistics estimated from international maize trails. – *Crop Science* 28: 925–928.
- [41] R Core Team (2017): R A Language and Environment for Statistical Computing. – <https://www.R-project.org/>.
- [42] Rad, N. M., Kadir, M. A., Rafii, M. Y., Jaafar, H. Z., Naghavi, M. R., Ahmadi, F. (2013): Genotype x environment interaction by AMMI and GGE biplot analysis in three consecutive generations of wheat (*Triticum aestivum*) under normal and drought stress conditions. – *Australian Journal of Crop Science* 7: 956–961.
- [43] Rakshit, S., Ganapathy, K. N., Gomashe, S. S., Rathore, A., Ghorade, R. B., Nagesh Kumar, M. V. et al. (2012): GGE biplot analysis to evaluate genotype, environment and the interactions in sorghum multi-location data. – *Euphytica* 185: 465–479.
- [44] Samonte, S. O. P. B., Wilson, L. T., McClung, A. M., Medley, J. C. (2005): Targeting cultivar onto rice growing environment using AMMI and SREG GGE biplot analysis. – *Crop Science* 45: 2414–2424.
- [45] Silalertruksa, T., Gheewala, S. H., Mungkung, R., Nilsalab, P., Lecksiwilai, N., Sawaengsak, W., Sawaengsak, W. (2017): Implications of water use and water scarcity footprint for sustainable rice cultivation. – *Sustainability* 9(12): 2283. <https://doi.org/10.3390/su9122283>.
- [46] Singh, B. N., S. Fagade, M. N. Ukwungwu, C. Williams, S. S. Jagtap, O. Oladimeji, et al. (1997): Rice growing environment and biophysical constraint in rice agroecological Zones of Nigeria. – *Meteorology Journal* 2: 35–44.
- [47] Sreekanth, M., Hakeem, A. H., Peer, Q. J. A., Rashid, I. (2017): Low productivity of Indian agriculture with special reference on cereals. – *Journal of Pharmacognosy and Phytochemistry* 6(5): 239–243.
- [48] Stojaković, M., Ivanović, M., Jocković, Đ., Bekavac, G., Purar, B., Nastasić, A., Stanislavljević, D., Mitrović, B., Treskić, S., Laišić, R. (2010): NS maize hybrids in production regions of Serbia. – *Field and Vegetable Crops Research* 47: 93–02.
- [49] Wanjari, R. H., Mandal, K. G., Ghosh, P. K., Adhikari, T., Rao, N. H. (2006): Rice in India: present status and strategies to boost its production through hybrids. – *Journal of Sustainable Agriculture* 28(1): 19–39.
- [50] Wu, W., Cheng, S. (2014): Root genetic research, an opportunity and challenge to rice improvement. – *Field Crops Research* 165: 111–124.
- [51] Xu, Y. (2016): Envirotyping for deciphering environmental impacts on crop plants. – *TAG Theoretical and Applied Genetics (Theoretische und Angewandte Genetik)* 129: 653–673. <https://doi.org/10.1007/s00122-016-2691-5>.
- [52] Yan, W., Hunt, L. A. (2001): Interpretation of genotype × environment Interaction for winter wheat yield in Ontario. – *Crop Science* 41: 19–25.
- [53] Yan, W., Kang, M. S. (2003): GGE biplot analysis: a graphical tool for breeders, geneticists and agronomists. – CRC Press, Boca Raton, FL.
- [54] Yan, W., Hunt, L. A., Sheng, Q., Szlavnic, Z. (2000): Cultivar evaluation and mega-environment investigation based on GGE biplot. – *Crop Science* 40: 596–605.
- [55] Yan, W., Kang, M. S., Ma, B., Woods, S., Cornelius, P. L. (2007): GGE biplot vs. AMMI analysis of genotype-by-environment data. – *Crop Science* 47: 641–653.
- [56] Zhang, Q. (2007): Strategies for developing green super rice. – *Proceeding of the National Academy of Sciences USA* 104: 16402–16.

- [57] Zobel, R. W., Wright, M. J., Gauch, H. G. (1988): Statistical analysis of a yield trial. – *Agronomy Journal* 80: 388–393.

LONG-TERM ABANDONMENT OF MOUNTAIN MEADOWS AFFECTS BUMBLEBEES, TRUE BUGS AND GRASSHOPPERS: A CASE STUDY IN THE AUSTRIAN ALPS

WALCHER, R.^{1*} – HUSSAIN, R. I.¹ – SACHSLEHNER, L.² – BOHNER, A.³ – JERNEJ, I.¹ – ZALLER, J. G.¹ – ARNBERGER, A.⁴ – FRANK, T.¹

¹*Institute of Zoology, University of Natural Resources and Life Sciences Vienna
Gregor-Mendel-Straße 33, A-1180 Vienna, Austria*

²*Büro für Naturschutzpraxis und Forschung, An der Scheibenwiese 1/1/2
A-1160 Vienna, Austria*

³*Agricultural Research and Education Centre Raumberg-Gumpenstein
Raumberg 38, A-8952 Irdning Donnersbachtal, Austria*

⁴*Institute for Landscape Development, Recreation and Conservation Planning, University of
Natural Resources and Life Sciences Vienna, Peter-Jordan-Straße 65, A-1180 Vienna, Austria*

*Corresponding author

e-mail: ronnie.walcher@boku.ac.at, ronnie.walcher@gmx.at; phone: +43/1/47654-83315

(Received 16th Jan 2019; accepted 28th Feb 2019)

Abstract. We investigated how abandonment of mountain meadows influences bumblebees, true bugs and grasshoppers in two years in the Eisenwurzen region (Austria). We surveyed abandoned (20-40 years old) and annually mown unfertilized meadows. Bumblebees were observed in 20 m² plots, bugs were collected by sweep netting and grasshoppers identified with a soundscape approach. The insect groups were analysed in relation to plant species richness, flower cover, vegetation cover and the surrounding landscape. Bumblebee species richness and richness of long-tongued species were significantly higher in managed meadows. Similarly, we found significantly more phytophagous bug species in managed meadows, whereas grasshoppers showed no difference between meadow types. Bumblebee species richness and abundance, the abundance of phytophagous bugs and total grasshopper species richness were associated with total flower cover. Surrounding forest area negatively affected bugs, while open landscape positively affected bugs, both regarding species richness and abundance, number of phytophagous species and individuals and individuals overwintering as egg. Species assemblages of the three insect groups did not significantly differ between meadow types. Extensive management is important to preserve bumblebee and bug richness. However, abandoned meadows, which are not yet re-grown into forest can still act as suitable habitats for the three insect groups.

Keywords: *extensive management, management cessation, grasslands, Bombus sp., Heteroptera, Orthoptera*

Introduction

More than 40 % of the earth's terrestrial surface is covered by grasslands (Suttie et al., 2005). In Central European landscapes, they represent valuable ecosystems harbouring a high plant diversity (Dengler et al., 2013; Chytrý et al., 2015). Semi-natural grasslands were maintained for hundreds of years by local farmers and traditional land-use systems (Maurer et al., 2006; Fischer et al., 2008; Poschlod et al., 2009; Hejcman et al., 2013; Price et al., 2015). In Austria, 60% of the agriculturally used area is made up of grasslands, 90% of which are not ploughed for at least 20 years (Pötsch et al., 2005). Changes in farming practice and intensity have led to a reduction

of semi-natural grasslands throughout European landscapes (Wesche et al., 2012). Main causes of this reduction are agricultural intensification and abandonment (e.g. Strijker, 2005; Baur et al., 2006a; Gellrich et al., 2007; Tasser et al., 2007; Prévosto et al., 2011; Graf et al., 2014). The reasons for the abandonment of extensively managed mountain meadows are manifold. Rey Benayas et al. (2007) identified some of the main drivers of land-use abandonment and mentioned socio-economic factors like rural depopulation and ecological factors like slope, altitude and accessibility as factors for management cessation. Especially, slopes with a high inclination are more often abandoned (Tasser et al., 2007; Niedrist et al., 2009). Land-use abandonment, and the consequent process of secondary succession (Komac et al., 2013), leads to forest-regrowth (Gellrich et al., 2007; Prévosto et al., 2011). Abandoned meadows undergo several successional stages (Tasser et al., 2007). Some of these stages remain stable for decades and abandoned grassland remains open for a long time (Walcher et al., 2017). Usually, regular mowing or grazing is necessary to maintain semi-natural grasslands without encroachment of woody vegetation (Hansson and Fogelfors, 2000; Maurer et al., 2006).

While there is a great body of evidence regarding the effects of abandonment on plants, knowledge regarding insect species is scarce. The effects of human-induced land-use changes strongly depend on the insect taxa being considered (Bonari et al., 2017; Lessard-Therrien et al., 2018). Therefore, studies taking different insect groups into account, are important in order to understand the consequences of management measures and to develop conservation strategies (Van Noordwijk et al., 2017).

The three insect groups investigated in the present study are scarcely studied in mountainous grasslands, and especially data on true bugs in mountainous grassland ecosystems are largely missing. This is surprising because bumblebees, bugs and grasshoppers are suitable organisms to study the effects of land-use abandonment in grassland ecosystems. The reduction of foraging resources and loss of suitable nesting sites are the main causes for bumblebee decline (Carvell, 2002; Goulson et al., 2005; Carvell et al., 2006; Nieto et al., 2014; Goulson et al., 2015). Long-tongued bumblebee species, in particular, often have specialized diets and are known to be in decline in many European countries (Goulson et al., 2005; Kosior et al., 2007). The true bugs are a diverse group, including generalist and specialist species, which are assumed to react differently to land-use changes such as abandonment. Along with grasshoppers, they respond sensitively to altered environmental conditions (Schwab et al., 2002; Frank and Kuenzle, 2006; Fartmann et al., 2012) and are suitable indicators for land-use changes (Duelli and Obrist, 2003; Fartmann et al., 2012). Especially, grasshoppers require specific habitat conditions (Baur et al., 2006b). They are particularly affected by the cessation of management (e.g. Marini et al., 2009; Uchida et al., 2016).

In the present study, we aimed at investigating how abandonment impacts richness and abundance of bumblebees, true bugs and grasshoppers. Therefore, we compared extensively managed annually mown meadows (no fertilizer application) with abandoned meadows in an Austrian region. The Eisenwurzen region is one of the largest nature reserve areas in Austria. This area contains a range of semi-natural habitats and is facing severe challenges due to abandonment (Haberl, 2009). We investigated the three insect taxa for the same reasons as in Walcher et al. (2017), but collected an additional year of data and one additional meadow per treatment. Data sampling over multiple years in mountainous grassland ecosystems is highly important in order to possibly give recommendations for management schemes and conservation strategies in the future. Thus, in the present study, we picked up the highly topical issue

of land-use abandonment by conducting a 2-years research in such an important nature reserve area.

We hypothesized that (i) species richness and assemblages of the three insect groups differ significantly between meadow types and, (ii) surrounding landscape structure and vegetation parameters significantly influence the three insect groups.

Methods

Study region

The study was carried out in 2015 and 2016 in the Styrian part of the Eisenwurzen region (Austria). Sampling was carried out once in June (between 16th and 18th of June) and once in August (between 16th and 18th of August) in both years. The mean annual temperature in this region is 6.9°C and the mean annual precipitation is 1 087 mm. Eight southerly exposed meadows – four extensively managed and four abandoned – were selected in the three municipalities St. Gallen, Stainach, and Pürgg (Fig. 1, Table 1).

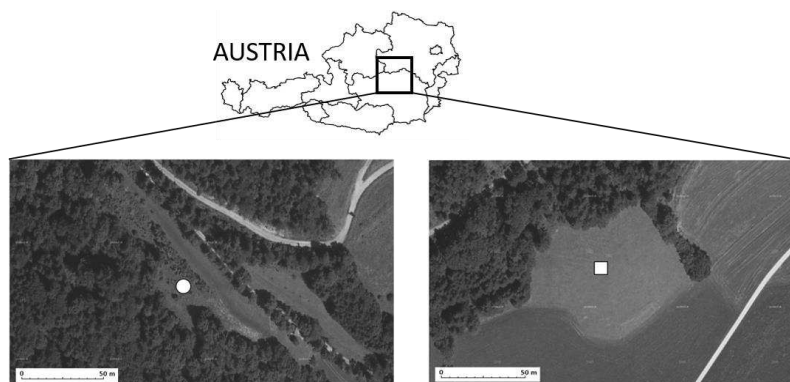


Figure 1. Location of the study region Eisenwurzen. Orthophotos are shown for one abandoned (○) and one managed meadow (□) (data source: www.basemap.at)

Table 1. Coordinates of the investigated meadows in the Eisenwurzen region. Meadow A1-A4 are abandoned and meadows M1-M4 are managed meadows

Meadow	Latitude	Longitude
A1	47°40'03.8" N	14°35'43.9" E
A2	47°39'51.5" N	14°35'39.6" E
A3	47°31'46.2" N	14°04'23.8" E
A4	47°31'01.1" N	14°07'26.9" E
M1	47°40'06.2" N	14°35'48.8" E
M2	47°39'53.3" N	14°35'42.7" E
M3	47°31'45.6" N	14°04'27.0" E
M4	47°31'01.8" N	14°07'31.4" E

Photos of the studied meadows give an impression of managed (Fig 2 a and b) and abandoned (Fig 2 c and d) meadows.

Due to technical problems with the soundscape method, we could only survey grasshoppers in three managed and three abandoned meadows, making a total of six meadows (n=6). The annually mown, non-fertilized managed meadows are usually

mown at the beginning of August. In both years, 2015 and 2016, the meadows were mown mid-July. Thus, sampling in August took place four weeks after the last cut, thus ensuring new plants in flower for the second sampling round in August. Meadows are usually mown manually with bar mowers or, on very steep parts of the meadows, using a scythe. Abandoned meadows are between 20 and 40 years old and were used extensively before cessation of management. Information about former and current management of the investigated meadows and age of abandoned meadows was gathered by interviewing the land owners. The meadows were located at an average elevation of 670 m above sea level. The size of managed meadows ranged from 1095 to 4500 m², while the size of abandoned meadows ranged from 573 to 3370 m². The sizes of managed and abandoned meadows were not significantly different ($F=0.959$, $p=0.365$; ANOVA). We measured the percentage of surrounding open landscape (pastures, extensively and intensively used meadows) and the percentage of forest cover (closed forest) within a 500 m radius around the centre of each meadow, using ArcGIS (orthophotos, updated in 2017, ArcGIS basemap).



Figure 2. Photos of study sites in the Eisenwurzen region (a and b are managed and c and d are abandoned meadows), Photos © R. Walcher

Insect sampling

We sampled bumblebees and bugs in June and August 2015 and 2016 and grasshoppers in August 2015 and 2016. We assessed richness and abundance of bumblebees in four rectangular 20 m² (4 * 5) plots at each meadow. Sampling plots were selected randomly in the centre of the meadows. In order to guarantee standardisation of the sampling method, we selected distances of 3, 9 and 27 meters between the plots. Sampling was performed for 15 minutes per plot, summing up to 1 hour of observation time, and individual bumblebees were counted and identified on-site at the species level using an identification key by Gokcezade et al. (2015). However, single individuals had to be collected for complete confident identification in

the lab. Furthermore, we grouped bumblebees into long- and short-tongued species and individuals. This classification is important because tongue length plays a major role in food plant selection.

For true bug sampling we carried out sweep-netting along defined transects. The distance between two transects was 15 metre. Specifically, we conducted 90 sweeps per meadow subdivided into 3 * 30 sweeps covering an area of total 90 m² (3 transects of 15 metre length * 2 m width of the transect). Collected bugs were identified using identification literature of Wagner (1952, 1966, 1967) and Strauss (2010). We gathered information on food preference (zoo- and phytophagous) and overwintering strategy (overwintering as egg or imagoes) from Wagner (1952, 1966, 1967).

To assess number of grasshopper species, we used digital recorders (Olympus LS-12, Olympus Europa SE & CO. KG, Hamburg, Germany) and connected them to bat detectors (Batbox III D, Batbox Ltd. Steyning, UK). We adjusted a frequency of 27 kHz on the detectors with a bandwidth of 16 kHz. We installed both devices on 80 cm high platforms. The records, which were conducted between 10 a.m. and 5 p.m., were afterwards analysed at the office by comparing them with acoustic material (e.g. Roesti and Keist, 2009). The recording range was approximately 30 meters. No analysis of grasshopper abundance can be made with the soundscape approach. All identified grasshoppers were assigned to Ensifera and Caelifera according to Baur et al. (2006b). All samples were taken during suitable weather conditions (low wind, sunny conditions, temperatures above 20°C, dry vegetation).

For bumblebee and true bug sampling, we carried out sampling in the meadows successively and not parallel. However, to avoid that the meadows were always sampled at the same time of the day, we investigated meadows, which were sampled in June in the morning, in August in the afternoon 2015. In the following year (2016) we sampled the meadows vice versa to 2015. A sketch showing the experimental setup of insect sampling is shown in *Figure 3*.

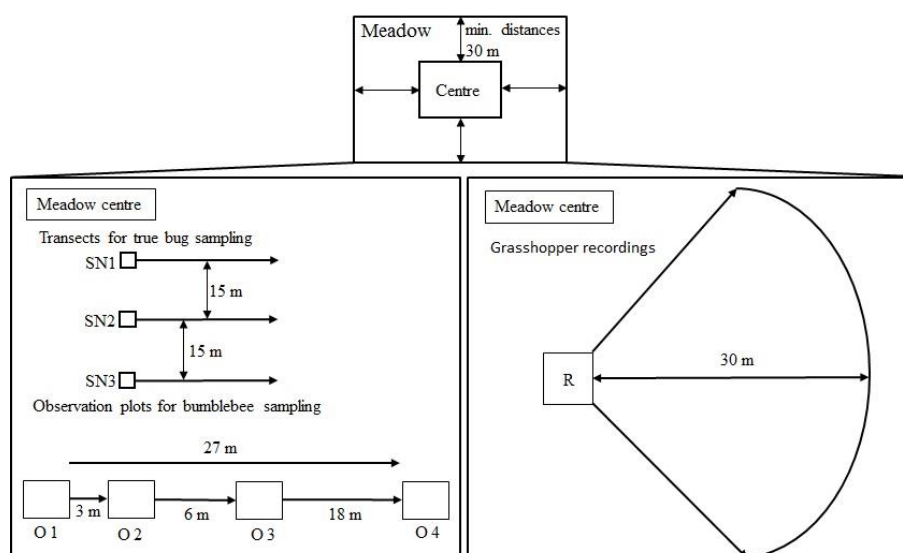


Figure 3. Sketch showing sampling locations within one meadow. SN1-SN3 denotes transects for sweep sampling of true bugs. O1-O4 denotes observation plots for bumblebees. R denotes location of the recording devices. Measurements were carried out in the centre of each meadow keeping distances of minimum 30 meter to adjacent habitats

Plant sampling

To estimate the influence of vegetation parameters on the three insect groups, we examined vegetation cover as well as total flower cover and diversity of vascular plants in each meadow. Sampling was carried out in June and August 2015 and 2016. We selected four 1 m² plots in the centre of the meadows. For the purpose of vegetation assessments, we placed a 1 * 1 m frame on the ground and identified each plant to the species level. We recorded percentage of vegetation cover (including living biomass, necromass and open soil) and percentage of flower cover within the total plot area (1 m²). We subdivided individual plant species into plant species providing open or hidden nectar flowers, which is an especially important vegetation parameter for bumblebees and their different tongue-length.

Statistical analysis

We used Shapiro-tests to check for normal distribution, and Bartlett- and Fligner-tests to check for homogeneity of variances of the data. We used generalized linear mixed models (GLMMs) to investigate the management effect on species richness and abundance of the three insect groups. Management was chosen as a fixed factor, and month (June and August) and year (2015 and 2016) as random factors. We investigated overdispersion in GLMMs by including an observation-level random effect (Harrison, 2014; Meyer et al., 2017). GLMMs were performed using the R-package *lme4* (Bates et al., 2015). We conducted generalized linear models (GLMs) to investigate differences between management types regarding tongue-length of bumblebees, feeding and hibernating strategy types of true bugs, suborders of grasshoppers, effects of vegetation parameters (vegetation and flower cover, plant species richness, plants providing hidden and open nectar flowers) and the structure of the surrounding landscape (open landscape and forest) on the three investigated insect groups. To test for over- or underdispersion, we used the *P__disp()* function (R-package “msme” version 0.5.1, Hilbe and Robinson, 2014) and the *dispersion.test()* function in R (R-package “AER”, version 1.2-4, Kleiber et al., 2015). We specified quasi-poisson errors to correct for over- or underdispersion in GLMs (Crawley, 2013). Before calculating GLM models, we investigated possible correlations between plant parameters and surrounding landscape structures. Since plant parameters and surrounding landscape structures were correlated, we decided to test them in single GLM-models. Furthermore, the point-biserial correlation coefficient r_{pb} was computed to detect possible significant associations of any individual species of the three insect groups with the two meadow types. This procedure calculates the strength (R-function *strassoc()*) and significance (R-function *signassoc()*) of possible associations. Both functions are included in the package “indicspecies” version 1.7.5 in R (De Cáceres and Jansen, 2015). Two-sided permutation tests were conducted to assess significant associations. We calculated confidence intervals and bootstrapped data 999 times with replacement (Walcher et al., 2017).

We analysed possible differences in species composition of the three insect groups conducting a principal coordinate analysis (PCO). We included month and year as random factors, similar to the univariate analysis. A permutational ANOVA (PERMANOVA) was conducted to evaluate significant differences in species assemblages of the three insect groups. We permuted residuals 9999 times under a reduced model. Furthermore, by conducting the SIMPER-routine (similarity

percentages), we investigated how individual species contribute to the differences between meadow types.

We used the version 6.1.13 of the software Primer including PERMANOVA+ (PRIMER-E Ltd. Plymouth, UK) to conduct PCO, PERMANOVA, and SIMPER routines. We performed all other statistical analysis in R, version 3.1.3 (R Core Team, 2015).

Results

Bumblebees

In total, we collected 98 bumblebee individuals of 13 species (*Bombus* sp., Appendix A). Twelve species with 64 individuals were found in managed, and 8 species with 34 individuals in abandoned meadows. We identified three cuckoo bumblebees (*Bombus* [*Psithyrus*] sp.). Further, we distinguished between 5 long- and 8 short-tongued species.

Managed meadows harboured a significantly higher total bumblebee richness and higher numbers of long-tongued species (GLMM, $z=2.479$, $p=0.0132$ and $z=2.147$, $p=0.0318$ respectively; Fig. 4 a and b).

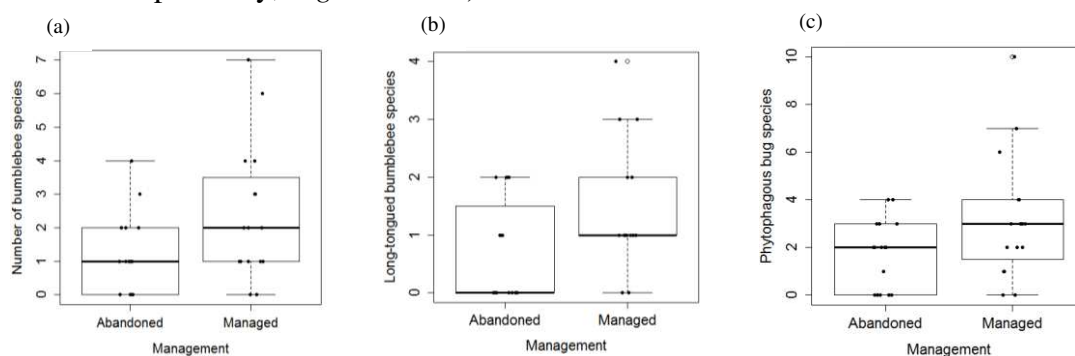


Figure 4. Response of (a) total bumblebee species richness, (b) long-tongued bumblebee species richness and (c) phytophagous bug species richness on management. Boxplots show the median and the 25 % and 75 % percentiles. The dashed lines indicate the 10 % and 90 % percentiles. Outliers are indicated by (○). Data points are included as jitter-overlay

Higher total flower cover increased total bumblebee species richness and abundance, and both number of short- and long-tongued species and individuals (Table 2, Fig. 5a-f).

Higher plant species with hidden nectar flowers significantly increased total bumblebee species richness as well as number of long-tongued species (Table 2, Fig. 6 a and b).

No relationship was found between number of bumblebee species and individuals, abundance of short- and long-tongued species and individuals and total plant species richness, surrounding landscape (open landscape and forest cover), vegetation cover and number of plant species with open nectar flowers. The point-biserial correlation did not show a significant association between individual bumblebee species and meadow types.

There was no significant difference between meadow types regarding bumblebee species assemblages (PERMANOVA, main-test: $p = 0.145$). We found an average

similarity of 15.30 in annually mown meadows (SIMPER-analysis). 92.17% of the similarity was described by *B. lapidarius*, *B. hortorum*, *B. humilis* and *B. terrestris*. *Bombus humilis*, *B. pascuorum*, *B. hypnorum* and *B. terrestris* explained 91.42% of the similarity of 7.22 in abandoned meadows. Both meadow types revealed a dissimilarity of 91.49. *Bombus humilis*, *B. hortorum*, *B. lapidarius*, *B. pascuorum* and *B. terrestris* described 70.34% of the dissimilarity.

Table 2. Generalized Linear Models (GLM, significance level: $p < 0.05$) showing the effects of vegetation parameters on the three insect groups. The table shows the relationships between flower classes and bumblebees and the relationship between surrounding landscape structure, true bugs and grasshoppers. P-values which are significant are highlighted in bold (n.s.: not significant, (-) indicates a negative effect, (+) indicates a positive effect, Res.dev. = Residual deviance, df = degrees of freedom)

Bumblebees									
	Flower cover			Flower classes			Hidden nectar		
	Res.dev.	df	p	Res.dev.	df	p	Res.dev.	df	p
Total species	39.32	30	<0.001 (+)	51.05	30	n.s.	47.37	30	0.022 (+)
Total individuals	103.48	30	0.004 (+)	123.43	30	n.s.	124.14	30	n.s.
Long-tongued species	32.17	30	0.008 (+)	37.40	30	n.s.	32.85	30	0.033 (+)
Short-tongued species	37.02	30	<0.001 (+)	40.88	30	n.s.	44.64	30	n.s.
Long-tongued individuals	77.70	30	0.044 (+)	82.49	30	n.s.	86.32	30	n.s.
Short-tongued individuals	73.33	30	0.008 (+)	90.66	30	n.s.	84.19	30	n.s.

Bugs									
	Flower cover			Surrounding landscape structure					
	Res.dev.	df	p	Open landscape			Forest cover		
	Res.dev.	df	p	Res.dev.	df	p	Res.dev.	df	p
Total species	57.73	30	n.s.	57.26	30	n.s.	54.69	30	0.034 (-)
Total individuals	280.76	30	n.s.	273.40	30	0.049 (+)	247.04	30	0.011 (-)
Phytophagous species	62.66	30	n.s.	60.41	30	0.035 (+)	56.72	30	0.004 (-)
Overwinter egg species	44.03	30	n.s.	43.47	30	n.s.	42.93	30	n.s.
Overwinter imago species	64.30	30	n.s.	65.08	30	n.s.	62.92	30	n.s.
Phytophagous individuals	303.24	30	0.048 (+)	289.55	30	0.032 (+)	258.92	30	0.007 (-)
Overwinter egg individuals	309.44	30	n.s.	290.30	30	0.026 (+)	262.88	30	0.008 (-)
Overwinter imago indiv.	122.18	30	n.s.	123.65	30	n.s.	122.32	30	n.s.

Grasshoppers									
	Flower cover			Surrounding landscape structure					
	Res.dev.	df	p	Open landscape			Forest cover		
	Res.dev.	df	p	Res.dev.	df	p	Res.dev.	df	p
Total species	1.95	10	0.009 (+)	3.72	10	n.s.	3.76	10	n.s.
Caelifera	2.52	10	n.s.	1.99	10	n.s.	1.74	10	0.046 (-)
Ensifera	7.15	10	n.s.	7.82	10	n.s.	7.67	10	n.s.

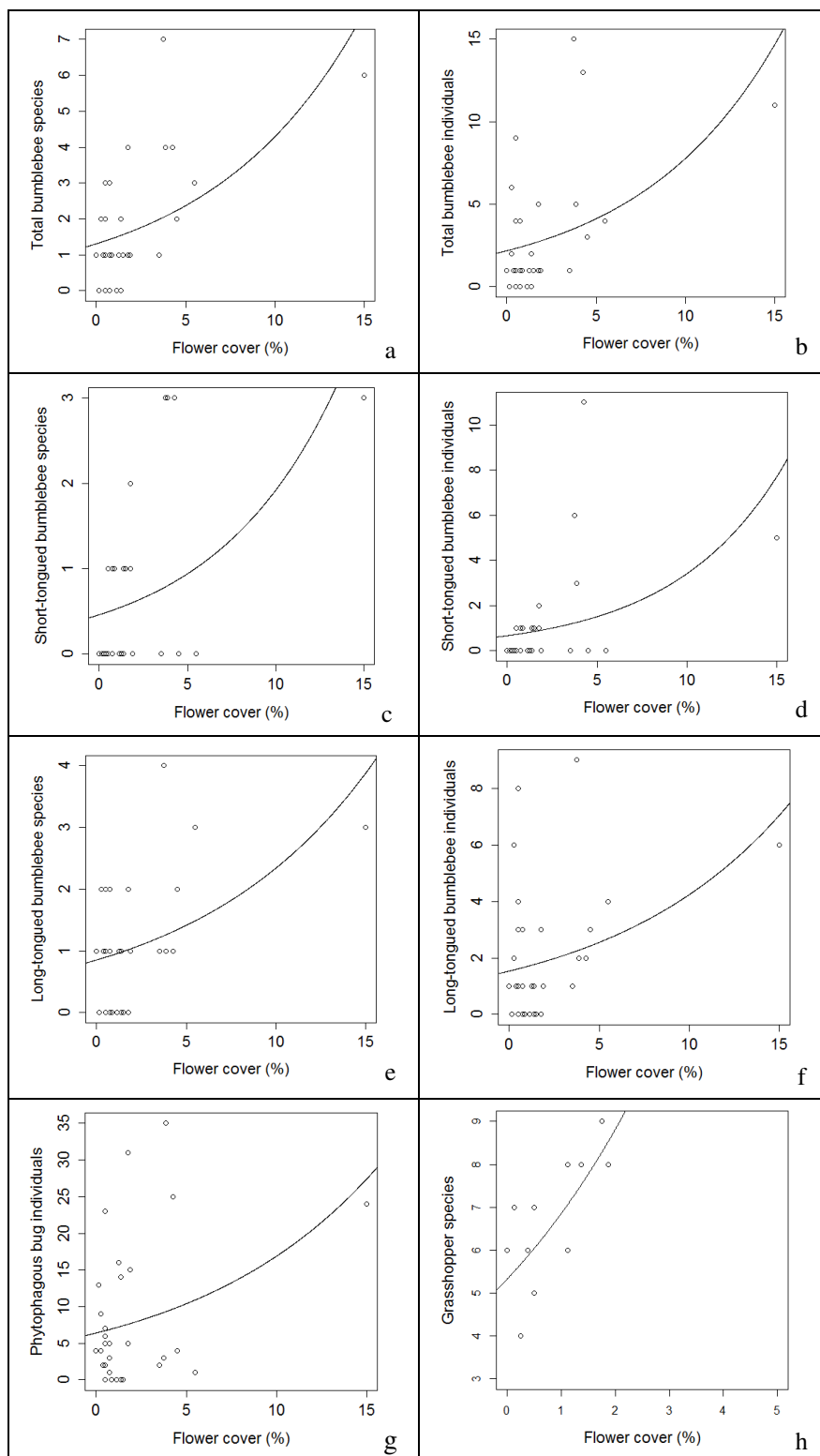


Figure 5. Relationship between flower cover (in %) and (a) total bumblebee species, (b) total bumblebee abundance, (c) short-tongued bumblebee species, (d) short-tongued bumblebee abundance, (e) long-tongued bumblebee species, (f) long-tongued bumblebee abundance, (g) abundance of phytophagous bugs and (h) total grasshopper species. Fitted lines were drawn through the scatterplot using the predict-function in R

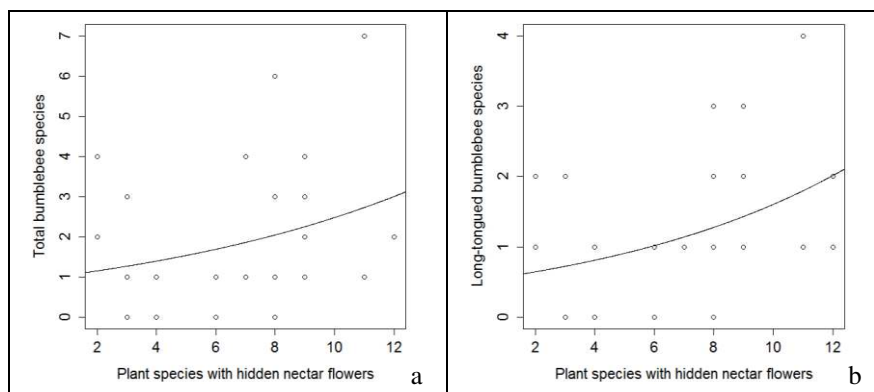


Figure 6. Relationship between plant species with hidden nectar flowers and (a) total bumblebee species and (b) long-tongued bumblebee species. Fitted lines were drawn through the scatterplot using the predict-function in R

True bugs

In total, we found 281 bug individuals of 32 species (*Appendix B*). We found 165 individuals of 27 species in managed, and 116 individuals of 13 species in abandoned meadows. Twenty-nine species were classified as phytophagous and three species as zoophagous. We classified 12 species as overwintering as eggs and 20 species as overwintering as imagos. We did not further include zoophagous bug species in the analysis due to the underrepresentation of this trophic group.

Managed meadows harboured significantly higher phytophagous bug species than abandoned meadows (GLMM, $z=1.970$, $p=0.0488$; *Fig. 4c*). Richness and abundance of true bugs, number of phytophagous bug species and individuals and individuals hibernating as eggs decreased with an increasing amount of forest cover in the surrounding landscape (*Table 2*). A larger proportion of open landscape in the surrounding landscape positively affected total number of individuals, individuals overwintering as eggs and species and individuals belonging to the phytophagous trophic group (*Table 2*). Increasing flower cover increased the number of phytophagous individuals (*Table 2*, *Fig. 5g*). No individual bug species was associated with either annually mown or abandoned meadows.

True bug species assemblages did not significantly differ between meadow types (PERMANOVA, main-test: $p=0.565$). The average Bray-Curtis similarity in the SIMPER-analysis in managed meadows was 7.19, with *Leptopterna dolobrata*, *Carpocoris purpureipennis*, *Orthops kalmii*, *Dolychoris baccarum*, *Graphosoma lineatum* and *Halticus apterus* explaining 91.58% of the similarity. Abandoned meadows revealed a similarity of 9.13. 91.11% of the similarity was due to the species *Nabis rugosus*, *Leptopterna dolobrata*, *Polymerus microphtalmus* and *Graphosoma lineatum*. We found an average dissimilarity of 92.30 between meadow types, where 62.70% of the dissimilarity was explained by the species *Leptopterna dolobrata*, *Nabis rugosus*, *Halticus apterus*, *Polymerus microphtalmus* and *Carpocoris purpureipennis*.

Grasshoppers

We detected a total of 15 grasshopper species in both meadow types (*Appendix C*). We found 12 species in managed and 13 species in abandoned meadows. We found eight Caelifera species and seven Ensifera species.

There was no management effect on total species richness or on richness of Caelifera and Ensifera. Increasing total flower cover increased total grasshopper species richness (Table 2, Fig. 5h). Caelifera were significantly negatively affected by higher amounts of forest cover in the surrounding landscape (Table 2). We found *Stenobothrus lineatus* to be significantly associated with managed meadows.

Grasshopper species assemblages did not differ between meadow types (PERMANOVA, main-test: $p=0.257$). 94.01% of the similarity of 61.63 in managed meadows was due to the species *Chorthippus biguttulus*, *Stenobothrus lineatus*, *Pseudochorthippus parallelus*, *Metrioptera brachyptera*, *Roeseliana roeselii* and *Euthystira brachyptera*. 84% of the similarity of 53.42 in abandoned meadows was explained by the species *Euthystira brachyptera*, *Pholidoptera griseoptera*, *Gomphocerippus rufus*, *Pseudochorthippus parallelus*, *Roeseliana roeselii*, and *Chorthippus biguttulus*. The average dissimilarity between meadow types was 52.36, with *Stenobothrus lineatus*, *Metrioptera brachyptera*, *Pholidoptera griseoptera*, *Gomphocerippus rufus*, *Chorthippus biguttulus*, *Roeseliana roeselii*, *Barbitistes serricauda* and *Pholidoptera aptera* explaining 67.13% of the dissimilarity.

Landscape structure and vegetation parameters

Managed meadows comprised a significantly higher total plant species richness as well as a higher total flower cover compared to abandoned meadows ($F=38.17$, $p<0.001$ and $F=6.06$, $p=0.019$, respectively, ANOVA). Similarly, managed meadows harboured a significantly higher number of plant species with hidden nectar flowers ($F=88.05$, $p<0.001$). Vegetation cover as well as number of plant species with open nectar flowers did not differ between habitat types. Surrounding open landscape and surrounding forest cover were significantly negatively correlated ($R^2=-0.96$; $p<0.001$). Flower cover significantly increased with increasing numbers of plant species ($R^2=0.44$; $p=0.012$). Number of plant species were significantly positively correlated with number of plants with hidden nectar flowers ($R^2=0.74$; $p<0.001$) and number of plants with open nectar flowers ($R^2=0.37$; $p=0.037$). Numbers of hidden nectar plants marginally significantly increased with increasing flower cover ($R^2=0.34$; $p=0.057$). A list of the recorded plant species, the mean values for vegetation and flower cover and mean numbers of plant species providing open and hidden nectar flowers are given in Appendix D.

Discussion

Our results showed a positive effect of extensive management on total bumblebee species richness, particularly on long-tongued bumblebee species. This positive effect is mainly attributable to the higher total flower cover and the higher number of plant species which provided hidden nectar flowers in the investigated annually mown meadows. As a consequence of abandonment, it is likely that plant species richness decreased (e.g. Stampfli and Zeiter, 1999; Pykälä et al., 2005), which subsequently led to a reduction of floral resources (Maurer et al., 2005). In our study, there was also a positive association between total flower cover and plant species richness. This illustrates the importance of maintaining extensively managed, species-rich meadows to preserve local bumblebee richness. In addition, these meadows provide an adequate supply of suitable foraging resources throughout almost the entire activity period of bumblebees, except for the time between mowing and the emergence of new flowers. The importance of providing flower-rich habitats for bumblebees has already been

stressed by numerous authors (e.g. Dramstad and Fry, 1995; Carvell et al., 2006; Ahrné et al., 2009). Similar species assemblages between meadow types suggests the provision of a sufficient amount of suitable foraging plants in abandoned meadows (Walcher et al., 2017). Further, bumblebees are highly mobile organisms which use a wide range of habitat types (e.g. Darvill et al., 2004; Westphal et al., 2006; Carvell et al., 2017), and both meadow types lay within their flight range.

Managed meadows contained significantly higher numbers of phytophagous bug species compared to abandoned meadows. Effects of management on several bug species were also shown in other studies (e.g. Di Giulio et al., 2001). Due to a reduced plant species richness in abandoned meadows we assume that suitable host plants for phytophagous bug species might be lost during the process of secondary succession (Tasser and Tappeiner, 2002). The managed meadows provided a range of suitable host plants for many bug species, as many of them were polyphagous species using a range of different plant species and families (e.g. Di Giulio and Edwards, 2003; Wachmann et al., 2004, 2007, 2008). True bugs were positively related with surrounding open landscape, revealing the importance of this landscape factor for the observed bugs (Torma et al., 2017). Most of the examined bug species in the present study are associated with open grassland habitats (e.g. Wachmann et al., 2004, 2007, 2008). This might explain the positive relationship with surrounding open landscape, because these species can utilize the supplementary resources in the surrounding meadows depending on their food specialization (Torma et al., 2017). In addition, these habitats can also be regarded as suitable refuges during mowing of the extensively managed meadows or as supplementary overwintering habitats. Most of the detected species were found in both habitat types. True bugs are usually very mobile organisms with a high dispersal potential (Bröring and Wiegand, 2005; Yanhui et al., 2007; Reynolds et al., 2013). In addition, many of the bug species found in both managed and abandoned meadows were generalist species which do not depend on a specific habitat (e.g. Di Giulio et al., 2001; Wachmann et al., 2004, 2007, 2008). This and the ability to migrate over long distances might explain the lack of differences in species assemblages between both habitat types. The positive relationship between bug species and total flower cover confirms the results of some other studies (Frank and Kuenzle, 2006; Zurbrügg and Frank, 2006). Around 70% of the collected bugs are reported to feed or stay mainly on inflorescences (Wachmann et al., 2004, 2007, 2008). This explains the positive relationship between bugs and flower cover in the present study. In general, both managed and abandoned meadows are beneficial for various bug species, while abandoned meadows, which are not yet regrown with woody plants, are still a valuable habitat for many bug species inhabiting open landscapes.

Several studies on grassland habitats revealed a negative influence of land-use abandonment on grasshoppers, in which abandonment led to a decline in grasshopper species richness (Marini et al., 2009; Uchida and Ushimaru, 2014; Uchida et al., 2016). Our results, on the other hand, supports the findings of other studies (Bonari et al., 2017; Walcher et al., 2017), in that grasshoppers did not show any response to land-use abandonment. Most of our observed grasshopper species are considered to be habitat generalists. Therefore, we assume that they are well adapted to the habitat conditions of both managed and abandoned meadows. Interestingly, there was a positive relationship between total grasshopper species richness and flower cover. We interpret this as an indirect effect of management, as there is no evidence in literature of grasshoppers using inflorescences as a direct food source. Zahn et al. (2010) showed a positive correlation

between grasshopper abundance and total flower cover. More likely, the factor flower cover is an indicator of habitat conditions and vegetation development in the two management types. Managed meadows are particularly important habitats for some of the observed grasshopper species. For example, *Stenobothrus lineatus* was found to be a characteristic species of the managed meadows. This species requires regularly mown meadows with a low sward height and some places of bare ground (Behrens and Fartmann, 2004). However, abandoned meadows were characterized by taller vegetation and the presence of certain bushes and small trees. In general, Ensifera prefer more structured habitat types containing trees and shrubs (Baur et al., 2006b; Marini et al., 2009) and some of the Ensifera species were exclusively or almost exclusively detected in abandoned meadows. A species which showed a particular preference for abandoned meadows was *Tettigonia cantans*. This species requires well-structured habitat types with dense vegetation (Baur et al., 2006b). The negative relationship between Caelifera and surrounding forest cover is due to the fact that none of the observed Caelifera species would choose closed forest as habitat type, since they are known to have an affinity for open habitats. There was no difference between species assemblages in managed and abandoned meadows. This result is in contrast to other studies (e.g. Fartmann et al., 2012; Walcher et al., 2017) who found that species assemblages differed between successional stages of grasslands. Most of the grasshopper species we observed have no special preference for a specific habitat type (Baur et al., 2006b) but are more sensitive to vegetation characteristics (Gardiner et al., 2002). It can be assumed that most of the observed grasshopper species found suitable microhabitats in both meadow types, and thus contain similar species assemblages.

Conclusion

Extensive management of meadows turned out to be an important management scheme to sustain bumblebee and true bug richness in the nature reserve Eisenwurzen region. High plant richness in the extensively mown meadows was associated with high flower cover, which contributed to high richness and abundance of the three insect groups studied. Both types of meadows harboured a similar composition of the three insect taxa. This shows that abandoned meadows, as long as they are not yet re-grown into forest, can act as suitable habitat for many of the observed species. However, a conversion into closed forest would deteriorate habitat conditions which are suitable for most species inhabiting open habitats. Thus, a regular removal of shrubs and trees is required for the maintenance of this meadow type.

Acknowledgements. We want to thank the land owners and farmers for their permission to investigate insects and plants on their meadows. Thanks to the Austrian Academy of Sciences (project: Healthy Alps) for supporting this study.

REFERENCES

- [1] Ahn , K., Bengtsson, J., Elmqvist, T. (2009): Bumble bees (*Bombus* spp) along a gradient of increasing urbanization. – PLoS ONE 4: e5574.
- [2] Bates, D., Maechler, M., Bolker, B., Walker, S. (2015): Fitting linear mixed-effects models using lme4. – Journal of Statistical Software 67: 1-48.

- [3] Baur, B., Cremene, C., Groza, G., Rakosy, L., Schileyko, A. A., Baur, A., Stoll, P., Erhardt, A. (2006a): Effects of abandonment of subalpine hay meadows on plant and invertebrate diversity in Transylvania, Romania. – *Biological Conservation* 132: 261-273.
- [4] Baur, B., Baur, H., Roesti, C., Roesti, D. (eds.) (2006b): *Die Heuschrecken der Schweiz*. – Haupt, Bern, Switzerland.
- [5] Behrens, M., Fartmann, T. (2004): Habitatpräferenzen und Phänologie der Heidegrashüpfer *Stenobothrus lineatus*, *Stenobothrus nigromaculatus* und *Stenobothrus stigmaticus* in der Medebacher Bucht (Südwestfalen/Nordhessen). – *Articulata* 19: 141-165.
- [6] Bonari, G., Fajmon, K., Malenovský, I., Zelený, D., Holuša, J., Jongepierová, I., Kočárek, P., Ondřej, K., Uříčář, J., Chytrý, M. (2017): Management of semi-natural grasslands benefiting both plant and insect diversity: The importance of heterogeneity and tradition. – *Agriculture Ecosystems and Environment* 246: 243-252.
- [7] Bröring, U., Wiegleb, G. (2005): Soil zoology: Colonization, distribution, and abundance of terrestrial Heteroptera in open landscapes of former brown coal mining areas. – *Ecological Engineering* 24: 135-147.
- [8] Carvell, C. (2002): Habitat use and conservation of bumblebees (*Bombus* spp.) under different grassland management regimes. – *Biological Conservation* 103: 33-49.
- [9] Carvell, C., Roy, D. B., Smart, S. M., Pywell, R. F., Preston, C. D., Goulson, D. (2006): Declines in forage availability for bumblebees at a national scale. – *Biological Conservation* 132: 481-489.
- [10] Carvell, C., Bourke, A. F. G., Dreier, S., Freeman, S. N., Hulmes, S., Jordan, W. C., Redhead, J. W., Sumner, S., Wang, J., Heard, M. S. (2017): Bumblebee family lineage survival is enhanced in high-quality landscapes. – *Nature* 543: 547-549.
- [11] Chytrý, M., Dražil, T., Hájek, M., Kalníková, V., Preislerová, Z., Šibík, J., Ujházy, K., Axmanová, I., Bernátová, D., Blanár, D., Dančák, M., Dřevojan, P., Fajmon, K., Galvánek, D., Hájková, P., Herben, T., Hrivnák, R., Janeček, Š., Janišová, M., Jiráská, Š., Kliment, J., Kochjarová, J., Lepš, J., Leskovjanská, A., Merunková, K., Mládek, J., Slezák, M., Šeffler, J., Šefflerová, V., Škodová, I., Uhlířová, J., Ujházyová, M., Vymazalová, M. (2015): The most species-rich plant communities in the Czech Republic and Slovakia (with new world records). – *Preslia* 87: 217-278.
- [12] Crawley, M. J. (ed.) (2013): *The R Book*. – Wiley, New York.
- [13] Darvill, B., Knight, M. E., Goulson, D. (2004): Use of genetic markers to quantify bumblebee foraging range and nest density. – *Oikos* 107: 471-478.
- [14] De Cáceres, M., Jansen, F. (2015): *Indicspecies: Relationship between species and group of sites*. – R Package version 1.7.5.
- [15] Dengler, J., Bergmeier, E., Willner, W., Chytrý, M. (2013): Towards a consistent classification of European grasslands. – *Applied Vegetation Science* 16: 518-520.
- [16] Di Giulio, M., Edwards, P. J., Meister, E. (2001): Enhancing insect diversity in agricultural grasslands: the roles of management and landscape structure. – *Journal of Applied Ecology* 38: 310-319.
- [17] Di Giulio, M., Edwards, P. J. (2003): The influence of host plant diversity and food quality on larval survival of plant feeding heteropteran bugs. – *Ecological Entomology* 28: 51-57.
- [18] Dramstad, W., Fry, G. (1995): Foraging activity of bumblebees (*Bombus*) in relation to flower resources on arable land. – *Agriculture Ecosystem Environment* 53: 123-135.
- [19] Duelli, P., Obrist, M. K. (2003): Biodiversity indicators: the choice of values and measures. – *Agriculture Ecosystem Environment* 98: 87-98.
- [20] Fartmann, T., Krämer, B., Stelzner, F., Poniowski, D. (2012): Orthoptera as ecological indicators for succession in steppe grassland. – *Ecological Indicators* 20: 337-344.
- [21] Fischer, M., Rudmann-Maurer, K., Weyand, A., Stöcklin, J. (2008): Agricultural land use and biodiversity in the Alps: how cultural tradition and socioeconomically motivated

- changes are shaping grassland biodiversity in the Swiss Alps. – *Mountain Research and Development* 28: 148-155.
- [22] Frank, T., Künzle, I. (2006): Effect of early succession in wildflower areas on bug assemblages (Insecta: Heteroptera). – *European Journal of Entomology* 103: 61-70.
- [23] Gardiner, T., Pye, M., Field, R., Hill, J. (2002): The influence of sward height and vegetation composition in determining the habitat preferences of three *Chorthippus* species (Orthoptera: Acrididae) in Chelmsford, Essex, UK. – *Journal of Orthoptera Research* 11: 207-213.
- [24] Gellrich, M., Baur, P., Koch, B., Zimmermann, N. E. (2007): Agricultural land abandonment and natural forest re-growth in the Swiss mountains: a spatially explicit economic analysis. – *Agriculture Ecosystems and Environment* 118: 93-108.
- [25] Gokcezade, J. F., Gereben-Krenn, B-A., Neumayer, J., Krenn, H. W. (2015): Feldbestimmungsschlüssel für die Hummeln Österreichs, Deutschlands und der Schweiz (Hymenoptera, Apidae). – *Linzer Biologische Beiträge* 47: 5-42.
- [26] Goulson, D., Hanley, M. E., Darvill, B., Ellis, J. S., Knight, M. E. (2005): Causes of rarity in bumblebees. – *Biological Conservation* 122: 1-8.
- [27] Goulson, D., Nicholls, E., Botias, C., Rotheray, E. L. (2015): Bee declines driven by combined stress from parasites, pesticides, and lack of flowers. – *Science* 347: 1435-1444.
- [28] Graf, R., Müller, M., Korner, P., Jenny, M., Jenni, L. (2014): 20% loss of unimproved farmland in 22 years in the Engadin, Swiss Alps. – *Agriculture Ecosystems and Environment* 185: 48-58.
- [29] Haberl, H. (2009): Towards an integrated model of socioeconomic biodiversity drivers, pressures and impacts. A feasibility study based on three European long-term socio-ecological research platforms. – *Ecological Economics* 68: 1797-1812.
- [30] Hansson, M., Fogelfors, H. (2000): Management of a semi-natural grassland; results from a 15-year-old experiment in southern Sweden. – *Journal of Vegetation Science* 11: 31-38.
- [31] Harrison, X. A. (2014): Using observation-level random effects to model overdispersion in count data in ecology and evolution. – *PeerJ* 2: e616.
- [32] Hejman, M., Hejmanová, V., Pavlů, V., Beneš, J. (2013): Origin and history of grasslands in Central Europe - a review. – *Grass and Forage Science* 68: 345-363.
- [33] Hilbe, J., Robinson, A. (2014): msme: Functions and Datasets for “Methods of Statistical Model Estimation”. – R Package version 0.5.1.
- [34] Kleiber, C., Zeileis, A., Zeileis, M. A. (2015): AER: Applied econometrics with R. – R Package version 1.2-4.
- [35] Komac, B., Kéfi, S., Nuche, P., Escós, J., Alados, C. L. (2013): Modeling shrub encroachment in subalpine grasslands under different environmental and management scenarios. – *Journal of Environmental Management* 121: 160-169.
- [36] Kosior, A., Celary, W., Olejniczak, P., Fijał, J. (2007): The decline of the bumblebees and cuckoo bees (Hymenoptera: Apidae: Bombini) of Western and Central Europe. – *Oryx* 41: 79-88.
- [37] Lessard-Therrien, M., Humbert, J-Y., Hajdamowicz, I., Stańska, M., van Klink, R., Lischer, L., Arlettaz, R. (2018): Impacts of management intensification on ground-dwelling beetles and spiders in semi-natural mountain grasslands. – *Agriculture Ecosystems and Environment* 251: 59-66.
- [38] Marini, L., Fontana, P., Battisti, A., Gaston, K. J. (2009): Response of orthopteran diversity to abandonment of semi-natural meadows. – *Agriculture Ecosystems and Environment* 132: 232-236.
- [39] Maurer, K., Weyand, A., Fischer, M., Stöcklin, J. (2006): Old cultural traditions, in addition to land use and topography, are shaping plant diversity of grasslands in the Alps. – *Biological Conservation* 130: 438-446.
- [40] Meyer, S., Unternährer, D., Arlettaz, R., Humbert, J-Y., Menz, M. H. M. (2017): Promoting diverse communities of wild bees and hoverflies requires a landscape

- approach to managing meadows. – *Agriculture Ecosystems and Environment* 239: 376-384.
- [41] Niedrist, G., Tasser, E., Lüth, C., Dalla Via, J., Tappeiner, U. (2009): Plant diversity declines with recent land use changes in European Alps. – *Plant Ecology* 202: 195-210.
- [42] Nieto, A., Ralph, G. M., Comeros-Raynal, M. T., Kemp, J., García Criado, M., Allen, D. J., Dulvy, N. K., Walls, R. H. L., Russell, B., Pollard, D., García, S., Craig, M., Collette, B. B., Pollom, R., Biscoito, M., Labbish Chao, N., Abella, A., Afonso, P., Álvarez, H., Carpenter, K. E., Clò, S., Cook, R., Costa, M. J., Delgado, J., Dureuil, M., Ellis, J. R., Farrell, E. D., Fernandes, P., Florin, A-B., Fordham, S., Fowler, S., Gil de Sola, L., Gil Herrera, J., Goodpaster, A., Harvey, M., Heessen, H., Herler, J., Jung, A., Karmovskaya, E., Keskin, C., Knudsen, S. W., Kobylansky, S., Kovačić, M., Lawson, J. M., Lorange, P., McCully Phillips, S., Munroe, T., Nedreaas, K., Nielsen, J., Papaconstantinou, C., Polidoro, B., Pollock, C. M., Rijnsdorp, A. D., Sayer, C., Scott, J., Serena, F., Smith-Vaniz, W. F., Soldo, A., Stump, E., Williams, J. T. (2014): European Red List of bees. – Publication Office of the European Union, Luxembourg.
- [43] Poschlod, P., Baumann, A., Karlik, P. (2009): Origin and development of grasslands in Central Europe. – In: Veen, P., Jefferson, R., de Schmidt, J., Van der Straaten, J. (eds.) *Grasslands in Europe of high nature value*. KNNV Publishing, Zeist.
- [44] Pötsch, E. M., Blaschka, A., Resch, R. (2015): Impact of different management systems and location parameters on floristic diversity of mountainous grassland. – *Grassland Science in Europe* 10: 315-318.
- [45] Prévosto, B., Kuiters, L., Bernhardt-Römermann, M., Dölle, M., Schmidt, W., Hoffmann, M., Van Uytvanck, J., Bohner, A., Kreiner, D., Stadler, J., Klotz, S., Brandl, R. (2011): Impacts of land abandonment on vegetation: successional pathways in European habitats. – *Folia Geobotanica* 46: 303-325.
- [46] Price, B., Kienast, F., Seidl, F., Ginzler, C., Verburg, P. H., Bolliger, J. (2015): Future landscapes of Switzerland: Risk areas for urbanisation and land abandonment. – *Applied Geography* 57: 32-41.
- [47] Pykälä, J., Luoto, M., Heikkinen, R. K., Kontula, T. (2005): Plant species richness and persistence of rare plants in abandoned semi-natural grasslands in northern Europe. – *Basic and Applied Ecology* 6(1): 25-33.
- [48] R Core Team (2015): R: A language and environment for statistical computing. – R Foundation for Statistical Computing, Vienna, Austria. <https://www.R-project.org/>.
- [49] Rey Benayas, J. M., Martins, A., Nicolau, J. M., Schulz, J. (2007): Abandonment of agricultural land: an overview of drivers and consequences. – *CAB Reviews* 2: 1-14.
- [50] Reynolds, D. R., Nau, B. S., Chapman, J. W. (2013): High altitude migration of Heteroptera in Britain. – *European Journal of Entomology* 110: 483-492.
- [51] Roesti, C., Keist, B. (2009): *Die Stimmen der Heuschrecken*. – Haupt, Bern, Switzerland.
- [52] Schwab, A., Dubois, D., Fried, P. M., Edwards, P. J. (2002): Estimating the biodiversity of hay meadows in north-eastern Switzerland on the basis of vegetation structure. – *Agriculture Ecosystems and Environment* 93: 197-209.
- [53] Stampfli, A., Zeiter, M. (1999): Plant species decline due to abandonment of meadows cannot easily be reversed by mowing. A case study from the southern Alps. – *Journal of Vegetation Science* 10: 151-164.
- [54] Strauss, G. (2010): *CORISA Wanzenabbildungen*. Biberach. – www.corisa.de.
- [55] Strijker, D. (2005): Marginal lands in Europe-causes of decline. – *Basic and Applied Ecology* 6: 99-106.
- [56] Suttie, J. M., Reynolds, S. G., Batello, C. (2005): *Grasslands of the world*. – Plant Production and Protection Series 34, Food and Agriculture Organization of the United Nations, Rome.
- [57] Tasser, E., Tappeiner, U. (2002): Impact of land use changes on mountain vegetation. – *Applied Vegetation Science* 5: 173-184.

- [58] Tasser, E., Walde, J., Tappeiner, U., Teutsch, A., Noggler, W. (2007): Land-use changes and natural reforestation in the Eastern Central Alps. – *Agric. Ecosyst. Environ.* 118: 115-129.
- [59] Torma, A., Bozsó, M., Tölgyesi, C., Gallé, R. (2017): Relationship of different feeding groups of true bugs (Hemiptera: Heteroptera) with habitat and landscape features in Pannonic salt grassland. – *Journal of Insect Conservation* 21: 645-656.
- [60] Uchida, K., Ushimaru, A. (2014): Biodiversity declines due to abandonment and intensification of agricultural lands: patterns and mechanisms. – *Ecological Monographs* 84: 637-658.
- [61] Uchida, K., Takahashi, S., Shinohara, T., Ushimaru, A. (2016): Threatened herbivorous insects maintained by long-term traditional management practices in semi-natural grasslands. – *Agriculture Ecosystems and Environment* 221: 156-162.
- [62] Van Noordwijk, C. G. E., Baeten, L., Turin, H., Heijerman, T., Alders, K., Boer, P., Mabelis, A. A., Aukema, B., Noordam, A., Remke, E., Siepeö, H., Berg, M. P., Bonte, D. (2017): 17 years of grassland management leads to parallel local and regional biodiversity shifts among a wide range of taxonomic groups. – *Biodiversity and Conservation* 26: 717-734.
- [63] Wachmann, E., Melber, A., Deckert, J. (2004): Die Tierwelt Deutschlands. Wanzen Band 2 Cimicomorpha. – Goecke & Evers, Keltern.
- [64] Wachmann, E., Melber, A., Deckert, J. (2007): Die Tierwelt Deutschlands. Wanzen Band 3 Pentatomorpha I. – Goecke & Evers, Keltern.
- [65] Wachmann, E., Melber, A., Deckert, J. (2008): Die Tierwelt Deutschlands. Wanzen Band 4 Pentatomorpha II. – Goecke & Evers, Keltern.
- [66] Wagner, E. (1952): Blindwanzen und Miriden. Die Tierwelt Deutschlands und der angrenzenden Meeresteile. – Fischer, Jena.
- [67] Wagner, E. (1966): Die Tierwelt Deutschlands und der angrenzenden Meeresteile nach ihren Merkmalen und nach ihrer Lebensweise, Wanzen oder Heteroptera I, Pentatomorpha. – Fischer, Jena.
- [68] Wagner, E. (1967): Die Tierwelt Deutschlands und der angrenzenden Meeresteile nach ihren Merkmalen und nach ihrer Lebensweise, Wanzen oder Heteroptera II, Cimicomorpha. – Fischer, Jena.
- [69] Walcher, R., Karrer, J., Sachslehner, L., Bohner, A., Pachinger, B., Brandl, D., Zaller, J. G., Arnberger, A., Frank, T. (2017): Diversity of bumblebees, heteropteran bugs and grasshoppers maintained by both: abandonment and extensive management of mountain meadows in three regions across the Austrian and Swiss Alps. – *Landscape Ecology* 32: 1937-1951.
- [70] Wesche, K., Krause, B., Culmsee, H., Leuschner, C. (2012): Fifty years of change in Central European grassland vegetation: Large losses in species richness and animal-pollinated plants. – *Biological Conservation* 150: 76-85.
- [71] Westphal, C., Steffan-Dewenter, I., Tschardtke, T. (2006): Bumblebees experience landscapes at different spatial scales: possible implications for coexistence. – *Oecologia* 149: 289-300.
- [72] Yanhui, L., Wu, K., Guo, Y. (2007): Flight potential of *Lygus lucorum* (Meyer-Dür) (Heteroptera: Miridae). – *Environmental Entomology* 36: 1007-1013.
- [73] Zahn, A., Englmaier, I., Drobny, M. (2010): Food availability for insectivores in grasslands – arthropod abundance in pastures, meadows and fallow land. – *Applied Ecology and Environmental Research* 8: 87-100.
- [74] Zurbrugg, C., Frank, T. (2006): Factors influencing bug diversity (Insecta: Heteroptera) in semi-natural habitats. – *Biodiversity and Conservation* 15: 275-294.

APPENDICES

Species lists of bumblebees, heteropteran bugs, grasshoppers and plants (with related vegetation parameters) in the study region Eisenwurzen.

Appendix A. Number of individuals of bumblebees in managed and abandoned meadows in the Eisenwurzen region in 2015 and 2016 (M1-M4...managed meadows, A1-A4...abandoned meadows)

Bumblebee species	Eisenwurzen							
	Managed				Abandoned			
	M1	M2	M3	M4	A1	A2	A3	A4
<i>Bombus hortorum</i>	5	6	0	3	0	1	0	1
<i>Bombus humilis</i>	2	1	2	1	0	0	15	2
<i>Bombus hypnorum</i>	0	0	0	1	0	0	0	2
<i>Bombus lapidarius</i>	4	2	2	0	0	0	3	0
<i>Bombus lucorum</i>	3	1	0	8	0	0	0	0
<i>Bombus mucidus</i>	0	0	3	0	0	0	0	0
<i>Bombus pascuorum</i>	3	3	0	0	0	1	3	0
<i>Bombus pratorum</i>	0	0	2	0	1	0	0	0
<i>Bombus terrestris</i>	3	3	0	0	1	0	2	0
<i>Bombus wurflenii</i>	1	0	1	0	0	0	0	0
<i>Psithyrus barbutellus</i>	0	0	0	0	0	0	1	1
<i>Psithyrus bohemicus</i>	0	1	0	2	0	0	0	0
<i>Psithyrus campestris</i>	0	0	1	0	0	0	0	0

Appendix B. Number of individuals of heteropteran bugs in managed and abandoned meadows in the Eisenwurzen region in 2015 and 2016 (M1-M4...managed meadows, A1-A4...abandoned meadows)

Bug species	Eisenwurzen							
	Managed				Abandoned			
	M1	M2	M3	M4	A1	A2	A3	A4
<i>Adelphocoris lineolatus</i>	0	0	0	0	0	0	0	1
<i>Adelphocoris seticornis</i>	0	4	3	0	0	0	0	0
<i>Aelia accuminata</i>	0	0	3	0	0	0	0	0
<i>Capsus ater</i>	0	0	1	0	0	0	0	0
<i>Carpocoris purpureipennis</i>	2	0	4	2	3	0	2	0
<i>Catoplatus fabricii</i>	0	0	0	1	0	0	0	0
<i>Charagochilus gyllenhalii</i>	0	0	0	0	0	1	0	1
<i>Corizus hyoszyami</i>	0	0	2	0	0	0	0	0
<i>Dolychoris baccarum</i>	0	2	7	1	0	0	0	0
<i>Eurydema oleracea</i>	0	7	0	0	0	0	0	0
<i>Eurygaster maura</i>	0	2	0	0	0	0	0	0
<i>Exolygus rutilans</i>	0	4	0	0	0	0	0	0
<i>Graphosoma lineatum</i>	0	1	2	0	0	1	3	0
<i>Halticus apterus</i>	0	0	11	2	0	1	23	0
<i>Holcostethus vernalis</i>	0	0	1	0	0	0	0	0
<i>Leptopterna dolobrata</i>	2	21	30	23	0	1	27	5
<i>Lygus rugulipennis</i>	0	2	0	0	0	0	0	0
<i>Megalonotus chiragra</i>	0	0	1	0	0	0	0	0
<i>Myrmus miriformis</i>	0	1	0	0	4	0	6	1
<i>Nabis ferus</i>	0	0	0	0	0	1	0	2
<i>Nabis limbatus</i>	0	0	0	0	1	0	0	0
<i>Nabis rugosus</i>	0	3	1	0	4	3	2	3
<i>Orthops kalmii</i>	2	0	2	0	0	0	1	0
<i>Palomena prasina</i>	0	1	2	0	0	0	0	0
<i>Plagiognathus crysanthemi</i>	1	0	0	1	0	0	0	0

Bug species	Eisenwurzen							
	Managed				Abandoned			
	M1	M2	M3	M4	A1	A2	A3	A4
<i>Polymerus microphtalmus</i>	0	0	0	1	0	1	2	7
<i>Polymerus unifasciatus</i>	0	3	0	0	0	0	0	0
<i>Rhopalus subrufus</i>	1	0	0	0	0	0	0	0
<i>Rubiconia intermedia</i>	1	0	0	0	0	0	0	0
<i>Stenodema calcarata</i>	0	0	0	0	8	1	0	0
<i>Stictopleurus crassicornis</i>	0	0	3	0	0	0	0	0
<i>Stictopleurus punctatonervosus</i>	0	0	1	0	0	0	0	0

Appendix C. Presence/absence of grasshopper species in managed and abandoned meadows in the Eisenwurzen region in 2015 and 2016 (M1-M4...managed meadows, A1-A4...abandoned meadows)

Grasshopper species	Eisenwurzen						
	Managed			Abandoned			
	M1	M2	M3	A1	A2	A3	
<i>Barbitistes serricauda</i>	0	1	0	1	1	1	
<i>Chorthippus biguttulus</i>	1	1	1	1	0	1	
<i>Chorthippus dorsatus</i>	0	0	1	0	0	0	
<i>Chrysochraon dispar</i>	0	1	0	0	0	1	
<i>Decticus verrucivorus</i>	1	0	1	0	1	0	
<i>Euthystira brachyptera</i>	1	1	0	1	1	1	
<i>Gomphocerippus rufus</i>	0	0	0	1	1	0	
<i>Metrioptera brachyptera</i>	1	0	1	1	0	0	
<i>Omocestus sp.</i>	0	0	0	1	0	0	
<i>Pholidoptera aptera</i>	1	0	0	1	1	1	
<i>Pholidoptera griseoaptera</i>	1	1	1	1	1	1	
<i>Pseudochorthippus parallelus</i>	1	1	1	0	1	1	
<i>Roeseliana roeselii</i>	1	1	1	0	1	1	
<i>Stenobothrus lineatus</i>	1	1	1	0	0	0	
<i>Tettigonia cantans</i>	0	0	0	1	1	1	

Appendix D. Presence/absence of plant species and the means of vegetation cover (in %) and flower cover (in %) and mean numbers of plants with open nectar flowers and plants with hidden nectar flowers in managed and abandoned meadows in the Eisenwurzen region in 2015 and 2016 (M1-M4...managed meadows, A1-A4...abandoned meadows)

Vegetation parameters	Eisenwurzen							
	Managed				Abandoned			
	M1	M2	M3	M4	A1	A2	A3	A4
Vegetation cover (in %)	84.925	78.93	71.75	77.77	75.915	85	80.475	74.175
Flower cover (in %)	2.53	5.53	1.8725	2.2175	0.74875	0.74875	0.75	0.875
Plants with open nectar flowers	5	6.5	3	6	5	5.5	3	4
Plants with hidden nectar flowers	11.5	8.5	7.5	7.5	3	5	2	3.5

Plant species	Eisenwurzen							
	Managed				Abandoned			
	M1	M2	M3	M4	A1	A2	A3	A4
<i>Acer pseudoplatanus</i>	1	0	0	0	0	0	0	0
<i>Achillea millefolium</i> agg.	1	1	1	1	0	1	1	1
<i>Acinus alpinus</i>	1	0	0	0	0	0	0	0
<i>Aegopodium podagraria</i>	0	1	0	1	0	1	1	1
<i>Agrostis capillaris</i>	1	1	0	1	0	1	1	1
<i>Ajuga genevensis</i>	0	0	1	0	0	0	0	0

	Managed				Abandoned			
	M1	M2	M3	M4	A1	A2	A3	A4
Plant species								
<i>Ajuga reptans</i>	0	1	1	1	0	1	0	0
<i>Alchemilla monticola</i>	0	1	0	1	0	0	0	0
<i>Allium carinatum carinatum</i>	1	0	1	0	1	1	1	1
<i>Allium lusitanicum montanum</i>	0	0	1	0	0	0	1	0
<i>Anacamptis pyramidalis</i>	1	0	0	0	0	0	0	0
<i>Anthericum ramosum</i>	0	0	0	0	1	0	0	0
<i>Anthoxanthum odoratum</i>	0	1	0	1	0	1	0	1
<i>Anthriscus sylvestris</i>	0	1	0	0	0	0	0	0
<i>Anthyllis vulneraria carpatica</i>	1	1	0	1	0	0	0	0
<i>Aquilegia atrata</i>	1	0	0	0	0	0	0	0
<i>Arabidopsis halleri</i>	0	1	0	0	0	1	0	0
<i>Arabis hirsuta</i>	0	1	0	1	0	0	0	0
<i>Arenaria serpyllifolia</i>	0	0	1	0	0	0	0	1
<i>Arrhenatherum elatius</i>	0	1	1	1	0	0	1	1
<i>Astrantia major major</i>	1	1	0	1	1	1	0	1
<i>Avenula pubescens pubescens</i>	1	1	1	1	0	1	1	0
<i>Betonica alopecurus</i>	1	0	0	0	1	1	0	0
<i>Betonica officinalis</i>	0	1	0	1	0	1	0	1
<i>Betula pendula</i>	1	0	0	0	0	0	0	0
<i>Brachypodium pinnatum</i>	1	1	1	1	1	1	1	1
<i>Briza media</i>	1	1	1	1	0	1	0	0
<i>Bromus erectus</i>	1	1	1	1	0	0	1	1
<i>Bupthalmum salicifolium</i>	1	1	1	1	1	1	1	0
<i>Calamagrostis varia</i>	0	0	0	0	1	0	0	0
<i>Campanula patula</i>	0	1	0	1	0	0	0	0
<i>Campanula persicifolia</i>	0	1	0	0	0	0	0	0
<i>Campanula rapunculoides</i>	0	0	1	0	0	0	1	0
<i>Campanula rotundifolia</i>	1	1	0	1	0	1	1	1
<i>Cardamine pratensis</i>	0	0	0	1	0	1	0	0
<i>Carduus defloratus viridis</i>	1	0	1	0	0	0	0	1
<i>Carex alba</i>	1	0	0	0	1	1	0	0
<i>Carex caryophyllea</i>	1	0	1	1	0	0	0	0
<i>Carex flacca</i>	1	0	0	1	1	1	1	0
<i>Carex montana</i>	0	1	1	0	0	0	0	0
<i>Carex ornithopoda ornithopoda</i>	1	0	0	0	1	0	0	0
<i>Carex pallescens</i>	0	0	0	0	0	1	0	0
<i>Carex panicea</i>	1	0	0	0	1	1	0	0
<i>Carex spicata</i>	0	0	1	0	0	0	1	0
<i>Carex sylvatica</i>	0	0	0	0	0	1	0	0
<i>Carlina acaulis acaulis</i>	1	0	0	0	1	1	0	0
<i>Centaurea jacea</i>	1	1	0	1	1	1	0	0
<i>Centaurea scabiosa scabiosa</i>	1	1	1	1	1	1	0	0
<i>Cephalanthera damasonium</i>	0	0	0	0	1	0	0	0
<i>Cerastium holosteoides</i>	0	1	1	1	0	0	0	0
<i>Cerinthe minor</i>	0	0	0	0	0	0	1	0
<i>Chaerophyllum aureum</i>	0	0	0	0	0	0	1	0
<i>Chaerophyllum hirsutum</i>	0	0	0	1	0	0	0	0
<i>Cirsium erisithales</i>	0	0	0	1	0	0	0	0
<i>Clinopodium vulgare</i>	0	1	0	1	1	1	1	1
<i>Colchicum autumnale</i>	0	0	0	0	0	1	0	0
<i>Convolvulus arvensis</i>	0	0	0	0	0	0	1	0
<i>Corylus avellana</i>	0	0	0	0	1	0	0	0
<i>Crataegus monogyna</i>	0	0	1	0	0	0	0	0
<i>Crepis biennis</i>	0	1	0	1	0	0	0	0
<i>Cruciata laevipes</i>	0	1	0	1	0	0	1	0
<i>Cyclamen purpurascens</i>	0	0	0	0	1	0	0	0
<i>Cynosurus cristatus</i>	0	1	0	1	0	0	0	0
<i>Dactylis glomerata</i>	1	1	0	1	0	1	1	1
<i>Danthonia decumbens decumbens</i>	1	1	0	0	0	0	0	0
<i>Daucus carota</i>	0	1	0	0	0	0	0	0
<i>Dianthus carthusianorum carthusianorum</i>	0	1	1	1	0	0	1	0

	Managed				Abandoned			
	M1	M2	M3	M4	A1	A2	A3	A4
Plant species								
<i>Erica carnea</i>	0	0	0	0	1	0	0	0
<i>Euphorbia amygdaloides</i>	0	0	0	0	1	0	0	0
<i>Euphorbia cyparissias</i>	1	0	0	0	1	1	0	0
<i>Euphrasia officinalis rostkoviana</i>	1	0	1	1	0	0	0	0
<i>Festuca pratensis</i>	1	1	1	1	0	1	0	1
<i>Festuca rubra rubra</i>	1	1	1	1	1	0	1	1
<i>Festuca rupicola</i>	1	1	1	0	1	1	1	1
<i>Fraxinus excelsior</i>	0	0	1	1	0	1	1	1
<i>Galeopsis tetrahit</i>	0	0	0	0	0	0	0	1
<i>Galeopsis speciosa</i>	0	0	0	0	0	1	0	1
<i>Galium album</i>	1	1	1	1	1	1	1	1
<i>Galium pumilum</i>	1	1	0	1	1	1	1	1
<i>Galium verum</i>	0	1	0	0	0	0	0	1
<i>Gentiana verna</i>	0	0	0	1	0	0	0	0
<i>Gentianella aspera</i>	1	0	0	0	0	0	0	0
<i>Geranium phaeum phaeum</i>	0	1	0	0	0	0	0	0
<i>Glechoma hederacea</i>	0	1	1	0	0	0	0	0
<i>Gymnadenia conopsea conopsea</i>	1	1	0	1	1	0	0	0
<i>Helianthemum nummularium obscurum</i>	1	1	0	1	1	0	1	0
<i>Helleborus niger</i>	0	0	0	0	1	0	0	0
<i>Hieracium pilosella</i>	0	0	1	0	0	0	0	0
<i>Hieracium spec.</i>	0	0	1	0	0	0	0	0
<i>Hippocrepis comosa</i>	1	0	0	0	1	0	0	0
<i>Holcus lanatus</i>	0	1	0	1	0	0	0	0
<i>Hypericum maculatum</i>	0	0	0	0	0	1	0	0
<i>Hypericum perforatum</i>	0	0	0	0	0	0	1	0
<i>Knautia arvensis arvensis</i>	1	1	1	1	0	1	1	0
<i>Knautia drymeia intermedia</i>	1	1	1	1	1	0	0	1
<i>Knautia maxima</i>	1	1	1	1	0	0	0	1
<i>Koeleria pyramidata pyramidata</i>	1	1	1	1	1	1	1	1
<i>Laserpitium latifolium</i>	1	0	0	0	1	0	0	0
<i>Lathyrus pratensis</i>	0	1	1	1	0	1	1	1
<i>Leontodon hispidus hispidus</i>	1	1	1	1	1	0	0	1
<i>Leucanthemum ircutianum</i>	1	1	1	1	0	0	0	0
<i>Lilium bulbiferum bulbiferum</i>	0	0	0	0	0	0	0	1
<i>Linum catharticum</i>	1	1	0	1	0	0	0	0
<i>Lotus corniculatus</i>	1	1	1	1	1	1	1	0
<i>Luzula multiflora</i>	0	1	0	0	0	0	0	0
<i>Medicago falcata</i>	1	1	1	1	0	1	1	1
<i>Medicago lupulina</i>	1	1	1	1	0	0	0	0
<i>Melampyrum sylvaticum</i>	0	0	0	0	1	0	0	0
<i>Mercurialis perennis</i>	0	0	0	0	0	0	1	0
<i>Molinia caerulea</i>	1	0	0	0	1	0	0	0
<i>Myosotis arvensis</i>	0	1	0	1	0	0	0	0
<i>Orchis coriophora</i>	0	1	0	0	0	0	0	0
<i>Origanum vulgare vulgare</i>	0	0	0	0	1	0	0	0
<i>Orobanche gracilis</i>	0	1	0	1	0	0	0	0
<i>Phyteuma orbiculare</i>	1	0	0	0	1	1	0	0
<i>Pimpinella major major</i>	1	1	0	1	0	1	0	0
<i>Pimpinella saxifraga saxifraga</i>	1	1	1	1	1	0	1	1
<i>Plantago lanceolata</i>	1	1	1	1	0	1	0	0
<i>Plantago media</i>	0	0	1	0	0	0	0	0
<i>Poa angustifolia</i>	0	1	1	1	0	1	1	1
<i>Poa trivialis</i>	0	1	0	1	0	0	0	0
<i>Polygala amarella</i>	1	0	0	0	0	0	0	0
<i>Polygala chamaebuxus</i>	1	0	0	0	1	0	0	0
<i>Polygala comosa</i>	1	1	0	0	0	0	0	0
<i>Polygonatum odoratum</i>	0	0	0	0	1	0	0	1
<i>Potentilla erecta</i>	1	1	0	1	1	1	0	1
<i>Potentilla reptans</i>	0	0	1	0	0	0	0	0
<i>Primula elatior</i>	0	1	0	1	0	1	0	0

	Managed				Abandoned			
	M1	M2	M3	M4	A1	A2	A3	A4
Plant species								
<i>Prunella grandiflora</i>	1	1	0	1	1	0	0	0
<i>Prunella vulgaris</i>	0	0	0	1	0	0	0	0
<i>Quercus robur</i>	0	1	0	0	0	0	0	0
<i>Ranunculus acris acris</i>	0	1	0	1	0	0	0	0
<i>Ranunculus bulbosus</i>	0	0	1	0	0	0	1	0
<i>Ranunculus nemorosus</i>	1	0	0	0	1	1	0	0
<i>Ranunculus repens</i>	0	1	0	0	0	0	0	0
<i>Rhinanthus alectorolophus alectorolophus</i>	0	1	0	0	0	1	0	0
<i>Rhinanthus glacialis</i>	1	0	0	1	1	0	0	0
<i>Rhinanthus minor</i>	0	1	0	1	0	0	0	1
<i>Rubus caesius</i>	0	0	0	0	0	0	0	1
<i>Rubus idaeus</i>	0	0	0	0	0	0	0	1
<i>Rumex acetosa</i>	0	1	1	1	0	0	1	0
<i>Salvia glutinosa</i>	0	0	0	0	1	0	0	0
<i>Salvia verticillata</i>	0	1	1	0	0	0	1	0
<i>Sanguisorba minor</i>	1	0	0	0	0	0	0	0
<i>Scabiosa columbaria</i>	1	1	1	1	0	0	0	0
<i>Seseli libanotis</i>	1	0	0	0	0	0	0	0
<i>Sesleria caerulea</i>	1	0	0	0	1	0	0	0
<i>Silene nutans nutans</i>	0	1	1	1	0	0	0	1
<i>Silene vulgaris vulgaris</i>	0	0	1	0	0	0	0	1
<i>Stellaria graminea</i>	0	0	0	0	0	0	0	1
<i>Taraxacum officinale agg.</i>	0	1	0	1	0	1	0	1
<i>Teucrium chamaedrys</i>	0	0	0	0	1	0	1	0
<i>Thymus pulegioides pulegioides</i>	1	1	1	1	1	0	1	0
<i>Tragopogon orientalis</i>	0	0	0	1	0	0	0	1
<i>Trifolium medium medium</i>	0	0	0	0	1	1	1	0
<i>Trifolium montanum</i>	1	1	0	1	1	0	0	1
<i>Trifolium pratense pratense</i>	1	1	1	1	0	0	0	0
<i>Trifolium repens</i>	0	1	1	1	0	0	0	0
<i>Trisetum flavescens</i>	0	1	1	1	0	1	1	0
<i>Trollius europaeus</i>	0	0	0	0	0	1	0	0
<i>Valeriana officinalis</i>	0	0	0	0	0	1	0	0
<i>Verbascum nigrum</i>	0	0	0	0	0	0	1	0
<i>Veronica chamaedrys chamaedrys</i>	0	1	1	1	0	1	1	1
<i>Vicia cracca</i>	0	1	1	1	1	0	1	1
<i>Vicia sepium</i>	0	0	0	0	0	1	0	0
<i>Vincetoxicum hirundinaria</i>	1	0	0	0	1	0	0	0
<i>Viola arvensis arvensis</i>	0	0	0	0	0	0	0	1
<i>Viola hirta</i>	1	1	1	1	1	0	1	1
<i>Viola rupestris</i>	1	1	0	1	1	1	1	1

CHANGES IN MICROMORPHOLOGICAL CHARACTERS OF *PLATANUS ORIENTALIS* L. LEAVES IN TURKEY

SEVIK, H.¹ – CETIN, M.^{2*} – OZTURK, A.³ – YIGIT, N.³ – KARAKUS, O.⁴

¹*Department of Environmental Engineering, Faculty of Engineering and Architecture,
Kastamonu University, Kastamonu, Turkey*

²*Department of Landscape Architecture, Faculty of Engineering and Architecture, Kastamonu
University, Kastamonu, Turkey*

³*Department of Forest Engineering, Faculty of Forestry, Kastamonu University
Kastamonu, Turkey*

⁴*Programs of Sustainable Agriculture and Natural Plant Resources, Institute of Science,
Kastamonu University, Kastamonu, Turkey*

**Corresponding author
e-mail: mcerin@kastamonu.edu.tr*

(Received 19th Jan 2019; accepted 29th Mar 2019)

Abstract. In this study, it is aimed to determine the variation of some leaf characters of *Platanus orientalis* L. depending on the climate type. For this purpose, in a country dominated by three climate types (Terrestrial, Black Sea and Mediterranean), leaves samples of *Platanus orientalis* trees were collected. Scaled images were obtained with the help of electron microscope (SEM = Scanning Electron Microscope) of collected leaf samples. Thus, with measurements made on these images, stoma length (μm), stoma width (μm), por length (μm), por width and stoma density (1 mm^2 area). The obtained data were evaluated as statistic and the change of these characters according to climate type and city was evaluated. In addition, by applying correlation analysis to the data, it was attempted to determine the relations between the subject characters and climate data. As a result of the study, no significant effect of the climate could be detected on the characteristics examined. This situation can be interpreted that morphological characteristics are shaped by many environmental factors and genetic structure besides climate. The authors suggest an increase and diversification in studies on the subject in order to determine how and under which conditions micromorphological characteristics are shaped. For this reason, it can be shown that the subjects of the study are collected from the individuals which were primarily raised for landscaping, and the practices in landscape studies change the micro ecological conditions in a clear way.

Keywords: *climate, correlation, flora, plant, landscape plant*

Introduction

In parallel with the rapid increase in urbanization across the globe, green areas are destroyed. However, the increase in the average global incomes and awareness levels of people has led to more efforts and legislations to preserve and increase green areas wherever possible. This is evident in major cities around the world where local authorities are planning to turn their cities greener by announcing schemes and plans to plant six and seven-figure trees in the short and long terms. The importance of plants and trees cannot be overstressed. Their environmental and social benefits such as reducing air and noise pollution, balancing the climate, and contributing to the ecosystem are just a few of many (Cetin and Sevik 2016a,b; Cetin et al., 2017). Furthermore, they perform many functions such as being an economic resource, reducing the speed of the wind and supporting wildlife (Kantarcı et al., 2011; Özel,

2008; Ertuğrul et al., 2014). In fact, one of the factors that affect the value of properties in cities nowadays is the amount of green areas and their proximity to them (Tilki et al., 2008; Erna, 2009; Ökmen and Yurtsever, 2010; Yiğit et al., 2014; Öztürk et al., 2017).

When designing open green places in urban areas, plant species, composition, cultivar, and even form are of great importance besides their sizes. In addition to their functional purposes, plants are desired to be aesthetically valuable, and more often than not, people tend to prefer non-native plants. As a result of this, plant species are used outside of their natural distribution areas, which is a situation frequently encountered in landscape architecture. They are confronted with stress factors arising from different habitats (Sevik and Cetin, 2016; Sevik et al., 2017, 2018; Cetin and Sevik 2016a,b; Cetin et al., 2017; Turkyilmaz et al., 2018a, b, c).

It is possible that the stress that may occur in plants as a result of their cultivation in the climatic conditions they are not accustomed to, may affect their micromorphological features that are not visible as well as their morphological features that are visible (Sevik and Cetin, 2015; Sevik et al., 2017, 2018; Cetin et al., 2018a, b; Kaya et al., 2018) because Turkey is under the influence of three main climates, which are quite different from each other. These climate types include the Black Sea climate type, continental climate type, and Mediterranean climate type. The effects of these climate types are combined with topographical conditions, resulting in many different types of local climates (Cetin et al., 2018a; Akkemik, 2014). According to the results of the study, the micromorphological characteristics of the areas working on the climate of the cities of the climate conditions or even the microclimate conditions of the areas of the plant is more effective than the main climate type. In this study, it has been shown that the environmental conditions affect the micromorphological characteristics of the leaves. The results of the study show that the local and micro-conditions are more effective on the micromorphological characteristics of the leaves than the main climate type. In landscape studies, there are many plants grown in the area where all three climate types are dominant. These plants are not morphologically different from each other. However, there is not enough information about how they differ in morphometric and micromorphological terms. However, these changes can provide insight into many issues, from the stress level of the plant to the habitat and the adaptation level (Sevik et al., 2017). However, in order to determine how these micromorphological changes should be interpreted, it is necessary to determine under what conditions these changes are shaped.

In this study, it was aimed to determine the change in some micromorphological characteristics in *Platanus orientalis* individuals grown in different climate types dominant in Turkey.

Materials and methods

Materials

The study was performed on the leaves of *Platanus orientalis* L. Plane tree (*Platanus orientalis* L.) belonging to Platanaceae family and is known for its grandeur and longevity. *Platanus orientalis* is one of the most common plane varieties in the world and it is the most widespread plane tree growing in Turkey. The common name of this variety is oriental plane. Among plane trees, it was the first variety to be discovered. The oriental plane is widely used as an ornamental tree, especially in urban areas and is also cultivated sometimes for timber (Guler et al., 2017).

Each of the city areas from each of the leaves collected from each leaf and each leaf was made from one to three pieces. Leaf specimens are collected from mature trees but it can be stated that the trees are at least 50-60 years of age.

Platanus orientalis (Oriental plane) leaves were collected from the areas dominated by the three climate types prevailing in Turkey. The Black Sea climate, which is one of the climate types prevailing in Turkey, is defined as wet and humid every season, while the Mediterranean climate has dry and hot summers as well as warm and rainy winters. In continental climate, summers are hot and dry, while winters are cold and snowy (Karakus, 2018). However, there are huge differences between the climate data of the cities in the regions where these climate types are dominant. The general climate characteristics of the cities included in the study were examined separately, and average temperature (T_a), average maximum temperature (T_{max}), average minimum temperature (T_{min}), average sunshine duration (ASD), average number of rainy days (ANRD), monthly average total precipitation (MATP), maximum temperature (MaxT) and minimum temperature (MinT) values obtained from the records of the General Directorate of Meteorology are presented in tables (URL, 1). The average meteorological data of the cities included in the study are given in *Table 1*.

Table 1. Annual average meteorological data of the cities included in the study

Cities	Black Sea climate type			Mediterranean climate type			Continental climate type		
	Bartın	Samsun	Rize	Çanakkale	Antalya	İzmir	Ankara	Kayseri	Van
T_a (°C)	12.8	14.5	14.3	15.0	18.6	17.8	11.9	10.7	9.2
T_{max} (°C)	19.0	18.2	18	19.6	24.1	22.6	17.8	18.0	14.9
T_{min} (°C)	7.6	11	11.1	10.7	13.7	13.4	6.2	2.9	3.6
ASD (hrs)	67.2	61	49.4	87.0	100.3	94.5	80.3	83.5	92.8
ANRD	140.0	135.6	172.5	83.6	75.1	77.7	102.3	107.2	93.0
MATP (mm)	1040.5	717.5	2304.1	616.2	1066.9	695.9	387.2	384.9	388.5
MaxT (°C)	42.8	39	38.2	39.0	45	43	41	40.7	37.5
MinT (°C)	-18.6	-9.8	-7	-11.5	-4.6	-8.2	-24.9	-32.5	-28.7

T_a (°C) = average temperature (°C); T_{max} (°C) = average maximum temperature (°C); T_{min} (°C) = average lowest temperature (°C); ASD = average sunshine duration (h); ANRD = average number of rainy days; MATP = monthly average total precipitation (mm); MaxT= maximum temperature (°C); MinT = minimum temperature (°C)

Upon examining the results of the table, it is observed that there are big differences between the meteorological data of the cities. The most significant difference is the amount of precipitation which is very important for plant development. While the annual average precipitation in Rize province is 2304.1 mm, this figure decreases to 384.9 mm in Kayseri, where the continental climate is dominant. There is approximately a 6-time difference between the two figures. A similar situation is observed between the temperature values. It is noteworthy that there are huge differences between the cities, especially in minimum temperatures. For example, the minimum temperature is -4.6 °C in Antalya, where the Mediterranean climate type is observed, while this figure is -32.5 °C in Kayseri where the continental climate is observed (*Fig. 1*).

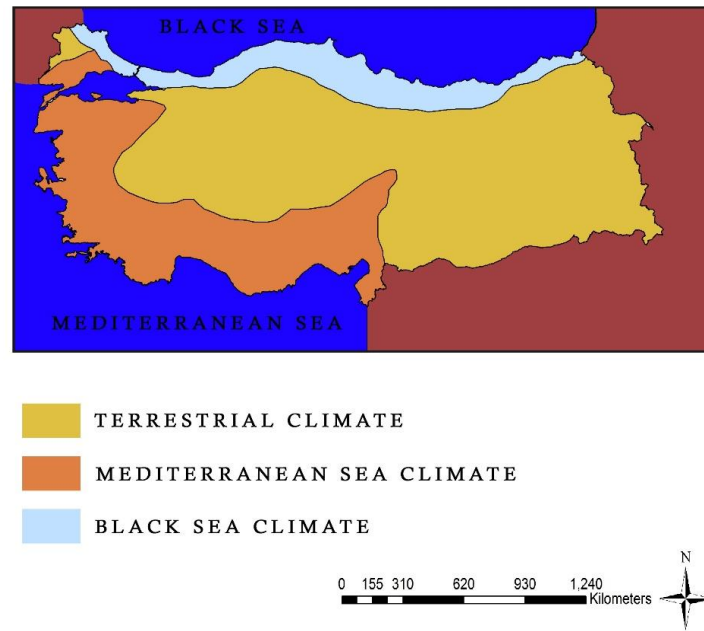


Figure 1. Showing climate type in Turkey

Method

Within the scope of the study, plane leaves were collected from the parks in the centers of the provinces at the end of September. A total of ten pieces of leaves were collected from each city and each leaf was made up of three pieces. Leaf specimens were collected from mature trees. The areas where the samples were collected are also shown in the map (Fig. 2). The GPS coordinates of the sampling of cities are following: Bartın 41° 38' 15.3744" N 32° 20' 1.7268" E; Samsun 40° 50' 12.5"N 34° 52' 28.9" E; Rize 41° 1' 31.8468" N 40° 31' 3.5976" E; Canakkale 39° 27' 12.0"N 26° 03' 48.9"E; Ankara 38° 40' 11.9"N 30° 50' 03.2"E; İzmir 37° 49' 06.9"N 26° 13' 48.7"E; Antalya 36° 05' 32.8"N 29° 15' 36.4"E; Kayseri 37° 39' 00.5"N 34° 53 '41.3"E; Van 37° 43' 48.4"N 42° 39' 42.8"E



Figure 2. The locations of cities where the leaves samples were taken

The samples of the mature leaves collected were pressed and brought to the laboratory. Samples were taken from the leaves brought to the laboratory and examined under an electron microscope. With the help of a Scanning Electron Microscope (SEM), scaled images were obtained from the lower side of the leaf blades and areas close to the middle sections. Files with the “.jpeg” extension were created from the obtained images. The points, where the measurements that were made using the “ImageJ” computer measurement program in order to perform micromorphological measurements of the leaves after these processes were completed, are shown in *Figure 3*.

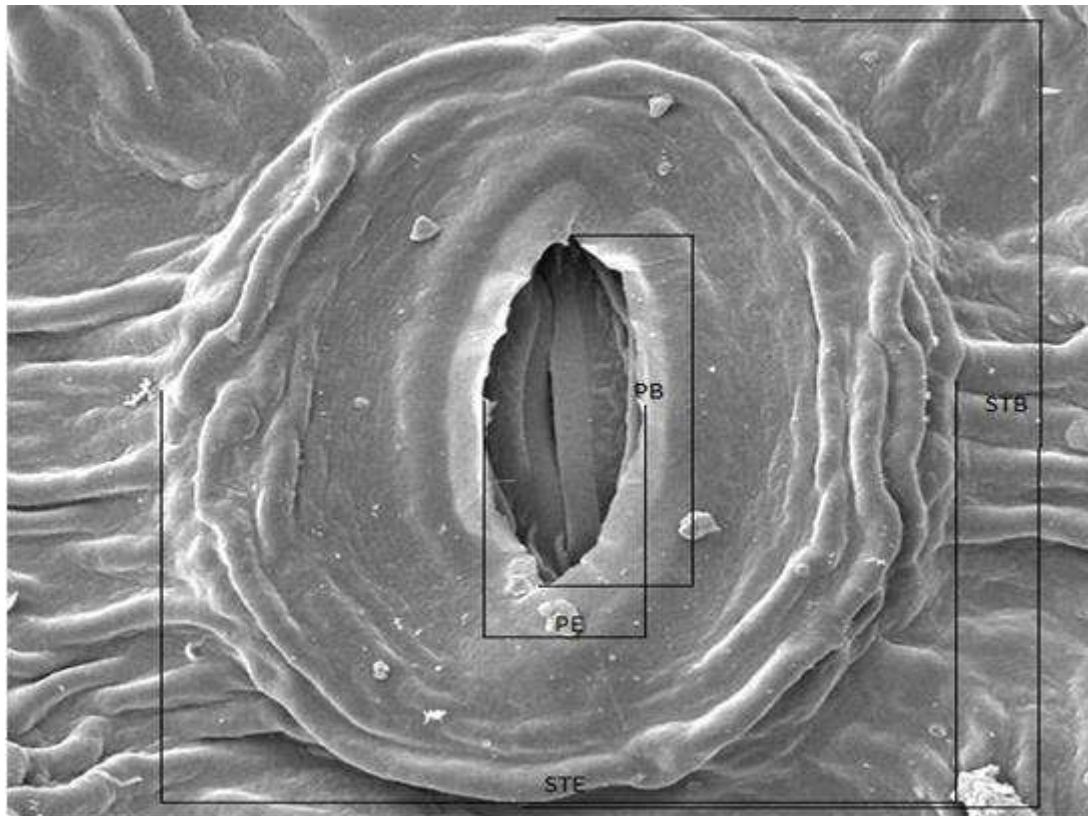


Figure 3. Measurement of micromorphological characteristics. *STL*: stoma length, *STW*: stoma width, *PL*: pore length, *PW*: pore width, *STD*: stoma density (1 mm² in area)

The data were analyzed with the help of SPSS packaged software, and the variance analysis and Duncan’s test were applied to the data. As a result, correlation analysis was applied to the data in order to reveal the correlation of the characteristics with each other and with the climate parameters. The correlation coefficient varies between 0 and -1 or +1 and determines the direction of the correlation. If the sample correlation coefficient is equal to 0, it means that there is no linear connection between the two variables. As this value increases, the correlation between the two variables begins to increase and reaches the highest level when it is 1 (Cohen, 1988). According to Cohen, the correlation between the two variables is weak if the correlation coefficient is between 0.10-0.29 and moderate between 0.30-0.49 and strong between 0.50-1.0. The correlation analysis results obtained in the study were interpreted, and whether the correlation between the characteristics and climate parameters was statistically significant, the correlation direction and strength were interpreted.

Results

Change in micromorphological characteristics depending on climate types

Together with the results of the variance analysis and Duncan's test performed in order to determine the change in micromorphological characteristics of the species grown in different climate types depending on the climate type, the average values of the micromorphological characteristics based on the climate type are presented in *Table 2*.

Table 2. *Change in micromorphological characteristics depending on climate type*

Climate Type	Characters				
	STL (µm)	STW (µm)	PL (µm)	PW (µm)	STD (µm)
Continental	30.776	25.364 b	14.764	7.037	391.56
Mediterranean	28.687	21.956 a	13.382	6.441	313.78
Black Sea	29.105	24.448 ab	13.279	6.842	340.00
F Value	1.303 ns	3.736*	2.064 ns	0.414 ns	1.480 ns

*Significant level is at 0.05. The letters a, b, c, etc. means according to Duncan test results; show that the group is located. The means of following abbreviations are STL: stoma length; STW: stoma width; PL: pore length; PW: pore width; STD: stoma density

Upon examining the table values, it is observed that there is no statistically significant difference between climate types with at least 95% confidence level in terms of characteristics other than STW. On the other hand, there are significant differences at a 99% confidence level between the climate types in terms of STW. As a result of Duncan's test, two homogeneous groups were formed. The lowest value (21.956 µm) was obtained in the Mediterranean climate type, while the value obtained in the Black Sea climate type (24.448 µm) took place in both homogeneous groups. The value obtained in the continental climate type (25.364 µm) took place in the last homogeneous group.

Change in micromorphological characteristics depending on cities

Variance analysis was performed to determine the micromorphological characteristics of the species collected from the aforementioned cities. The F value and significance level obtained as a result of the variance analysis and the groupings consisting of the average values and Duncan's test are presented in *Table 3*.

Upon examining the table values, it is observed that there are statistically significant differences between the cities with at least 95% confidence level in terms of all characteristics except for STD. In terms of STD, there are no statistically significant differences between the cities at least 95% confidence level.

According to Duncan's test results, STL values were collected in three homogeneous groups. As a result of Duncan's test, Antalya with the lowest value (23.481 µm) took place in the first homogeneous group, while Bartın, Kayseri, and Samsun took place in the second homogeneous group, and Ankara and Çanakkale with the highest value (33.163 µm) took place in the third homogeneous group. Izmir, Rize, and Van took place in both the second and third homogeneous groups. In terms of STW, Antalya with the lowest value (17.669 µm) formed the first homogeneous group, while Ankara with

the highest value (27.274 μm) formed the last homogeneous group together with Van, Samsun, Çanakkale, and Rize. Bartın, Kayseri, and Rize formed the second homogeneous group.

Table 3. Change in micromorphological characteristics depending on cities

Climate	Provinces	STL (μm)	STW (μm)	PL (μm)	PW (μm)	STD (μm)
Mediterranean	Antalya	23.481 a	17.669 a	10.522 a	4.506 a	301.33
	İzmir	29.536 bc	21.765 b	14.473 bc	6.675 bcd	349.33
	Çanakkale	33.045 c	26.435 c	15.152 c	8.142 de	290.67
Black Sea	Samsun	28.756 b	27.049 c	14.309 bc	8.764 e	378.67
	Bartın	28.402 b	20.773 b	13.359 bc	5.597 ab	321.33
	Rize	30.158 bc	25.521 c	12.168 ab	6.167 abc	320.00
Continental	Van	31.433 bc	27.164 c	14.872 c	7.120 bcde	457.33
	Kayseri	27.732 b	21.655 b	13.551 bc	5.952 ab	290.67
	Ankara	33.163 c	27.274 c	15.867 c	8.039 cde	338.67
	F Value	5.924***	18.324***	3.979**	5.051***	0.727ns

*Significant level is at 0.05; **significant level is at 0.01; ***significant level is at 0.001 level. The letters a, b, c, etc. means according to Duncan test results; show that the group is located. The means of following abbreviations are STL: stoma length; STW: stoma width; PL: pore length; PW: pore width; STD: stoma density

PL values were collected in three homogenous groups based on cities. Antalya which had the lowest value (10.522 μm) took place only in the first homogeneous group, while Ankara (15.867 μm), Çanakkale (15.152 μm) and Van (14.872 μm) which had the highest values were only in the last homogeneous group. Rize which had the second lowest value (12.168 μm) took place in the second homogeneous group, while other cities, Bartın, Kayseri, Samsun, and Izmir took place in both the second and third homogeneous groups. The cities were gathered in five homogeneous groups in terms of the PW value. Antalya which had the lowest value (4.506 μm) took place only in the first homogeneous group, while Samsun which had the highest value (8.764 μm) took place only in the last homogeneous group. Regarding the other cities, Bartın and Kayseri were included in the first and second homogeneous groups, Rize was included in the first, second and third homogeneous groups, Izmir was included in the second, third and fourth homogeneous groups, Van was included in the second, third, fourth and fifth homogeneous groups, Ankara was included in the third, fourth and fifth homogeneous groups, and Çanakkale was included in the fourth and fifth homogeneous groups.

As a result of the variance analysis of the STD characteristic based on cities, it was determined that the change in the STD values based on cities was not statistically significant at least 95% confidence level. Therefore, Duncan's test was not applied to

the change in STD characteristic based on cities. When the change in STD based on cities is examined, it is observed that the values vary between 290.67 units/mm² and 457.33 units/mm². The lowest STD value was obtained in Çanakkale, while the highest STD value was obtained in Van.

Results of the correlation analysis

Correlation analysis was performed to determine the correlation between micromorphological characteristics and climate values, and the results are presented in Table 4.

Table 4. Results of the correlation analysis related to micromorphological characteristics

	STL (µm)	STW (µm)	PL (µm)	PW (µm)	STD (µm)
STL	0.740**				
PL	0.730**	0.594**			
PW	0.397**	0.618**	0.562**		
STD	0.110	0.128	0.115	0.150	
T _a (°C)	-0.347*	-0.450**	-0.329*	-0.188	-0.326
T _{max} (°C)	-0.450**	-0.665**	-0.359*	-0.342*	-0.323
T _{min} (°C)	-0.240	-0.267	-0.285	-0.079	-0.308
ASD (hrs)	-0.128	-0.326*	0.037	-0.156	0.056
ANRD	0.046	0.223	-0.124	0.021	-0.020
MATP (mm)	-0.159	-0.120	-0.429**	-0.276	-0.214
MaxT (°C)	-0.497**	-0.777**	-0.318*	-0.457**	-0.236
MinT (°C)	-0.233	-0.211	-0.325*	-0.081	-0.303

*Significant level is at 0.05; **significant level is at 0.01; ***significant level is at 0.001 level. The means of following abbreviations are STL: stoma length; STW: stoma width; PL: pore length; PW: pore width; STD: stoma density

Upon examining the table values, it is observed that the correlations between all characteristics other than STD are statistically significant. Only the correlation of STD with STL was statistically significant. It was determined that all of the correlations between micromorphological characteristics were positive, only the correlation between STL and PW was moderate and the correlations between the other characteristics were strong.

When the correlation between climate data and micromorphological characteristics is examined, it is observed that no correlation of STD with the climate parameters is statistically significant. In addition to this, it is observed that the correlation of MaxT (°C) and T_{max} (°C) with all micromorphological characteristics and the correlation of T_a (°C) with micromorphological characteristics other than PW are statistically significant. In addition to these, it was determined that the correlation of MinT (°C) with PL, the correlation of ASD (hrs) with STW, and the correlation of MATP (mm) with PL were statistically significant.

It is noteworthy that the statistically significant correlations found between climate data and micromorphological characteristics are all negative. The strongest correlations among these are between STW and ANRD, and T_{max} (°C). While these correlations are negative and strong, other correlations are moderate and strong.

Discussion

The plants used in the study were collected from plants that were planted for landscaping in city centers. In landscape studies, practitioners may change micro-environmental conditions to a certain extent. This situation causes species to be cultivated outside of their natural distribution areas (Cetin et al., 2018a). In this case, the effects of the dominant climate type in the area where the plant is grown are limited. For example, in this study, there was no correlation found between the amount of precipitation and the characteristics examined at the expected level. However, there is a very strong correlation between precipitation, namely water status, and plant development (Sevik and Cetin, 2015; Biber and Kara, 2012; Li et al., 2015; Marathe and Babu, 2017; Dixon et al., 2015).

Studies on the micromorphological characteristics of plants indicate that the water status and stomatal characteristics are closely related (Yang and Wang, 2001; Zhang et al., 2006; Liu et al., 2006). The fact that there was no significant difference between the characteristics examined and the climatic parameters in this study is probably due to the alteration of micro conditions by maintenance work on plants in landscape applications because irrigation applications, climatic, fertilizing applications, edaphic, spraying and pruning applications may also change biological conditions significantly.

In the studies, it is stated that the morphological and micromorphological characteristics of plant leaves are related to stress conditions. Factors such as high and low temperatures, salinity, oxygen shortage, and light stress as well as water status can significantly affect plant growth performance and characteristics (Kulaç, 2010; Xu and Zhou, 2008; Sevik et al., 2016; Topacoglu et al., 2016; Sevik and Karaca, 2016; Zhao et al., 2001; Romero-Aranda et al., 2001). Therefore, stomatal characteristics may change depending on many environmental conditions such as light, humidity, drought, and CO₂ (Banon et al., 2004; Beerling et al., 1997). In fact, it is stated that stomatal characteristics may change depending on factors such as traffic density because many unpredictable environmental factors may affect the growth, development and morphological characteristics of plants by creating stress effects (Sevik et al., 2017, 2018; Cetin et al., 2018a, b; Turkyilmaz, 2018a, b, c).

Plants do not easily encounter stress factors due to the climate in their natural habitats. However, since the plants used in landscape studies are cultivated outside of their natural habitat, they are more likely to encounter climate-induced stress conditions. The damages and effects on plant morphology caused by stress factors vary depending on the type, tolerance, and adaptability of the plant (Madhova Rao, 2005; Kadioğlu, 2004).

Besides the mentioned conditions, the effect of external factors on plants can also affect plant development and its morphological characteristics. Factors such as pruning, hormone applications, spraying, shading and fertilization were demonstrated to be effective on the morphological and micromorphological characteristics of the plant (Knecht and Orton, 1970; Ferris et al., 1996; Pearson et al., 1995; Guney et al., 2016; Sevik and Cetin, 2016; Aydemir Özcan, 2017).

In addition, one of the factors that determine the reaction of the plant to the environmental conditions is the genetic structure. Morphological and physiological characteristics in plants are shaped by the interaction of genetic structure and environmental factors. Therefore, there are many factors affecting morphological characteristics. Many factors such as precipitation, temperature, stress factors, light, air pollution and soil structure affect the morphological characteristics of plants (Gratani,

2014; Peguero-Pina et al., 2014; Jochner et al., 2015; Majeed et al., 2015; Jud et al., 2016; Ren et al., 2018). The response of the plant to these factors is closely related to the genetic structure of the plant (Sevik et al., 2016, 2017). Plants of the same species can react differently to different stress conditions (Topacoglu et al., 2016). This is related to the genetic structure of the plant. As a matter of fact, it is stated that there may be significant differences between morphological and micromorphological characteristics of the plants grown in the same environment besides their growth performance (Sevik et al., 2016, 2017; Hrivnák et al., 2017).

Conclusion

As a result of the study, it was determined that there were huge differences between the data obtained from the cities located in the regions where the same climate type is dominant. For example, while the lowest value for STL was obtained in Antalya province, the second highest value was obtained in Çanakkale. On the other hand, the lowest value for PL was obtained in Antalya, while the second highest value was obtained in Izmir. However, three of the cities of Antalya, Çanakkale, and Izmir are located in areas where the Mediterranean climate type is dominant.

The results of the correlation analysis also support these results. According to the results of the correlation analysis, there was no correlation between the climate parameters and micromorphological characteristics at the expected level. Similar results were obtained for morphometric characteristics. It may be interpreted that factors other than climate are more effective on micromorphological and morphometric characteristics.

As a result of the study, no significant effect of the climate could be detected on the characteristics examined in the study. The possible causes are explained above. This situation can be interpreted as morphological characteristics are shaped by many environmental factors and genetic structure besides climate. In this case, it can be suggested to increase and diversify studies on the subject in order to determine how and under which conditions micromorphological characteristics are shaped in particular. In these studies, the diversification of the effects of environmental and genetic factors and examination of the changes caused by only one factor may provide more accurate data.

If a plant with high water demand is grown in a dry area, its water needs can be met by regular irrigation. Therefore, the micro conditions in which the plant is grown may be quite different from the main climate type. A similar situation applies to edaphic factors. Thus, micro-environmental conditions in plants used for landscaping can be quite different from the edaphic and climatic conditions of the region, and the micro-environmental conditions can strongly affect the growth performance of the plant. Therefore, it is difficult to determine the effect of climate on micromorphological characteristics of the plant in the studies conducted on the plants collected from these areas. Therefore, future studies to be carried out on natural plant species if they cannot be conducted in control environments may lead to more accurate data for determining the effect of climate on the micromorphological characteristics of the plant.

REFERENCES

- [1] Akkemik, Ü. (ed.) (2014): Natural-Exotic Trees and Shrubs of Turkey. – Publications of the General Directorate of Forestry, Ankara.

- [2] Aydemir Özcan, A. G. (2017): Effect of Shading and Fertilization Applications on Flower Yield and Growth in Lavender (*Lavandula angustifolia* Miller.). – Kastamonu University, Graduate School of Natural and Applied Sciences, Department of Forest Engineering, Master Thesis, Kastamonu.
- [3] Banon, S., Fernandez, J. A., Franco, J. A., Torrecillas, A., Alarcón, J. J., Sánchez-Blanco, M. J. (2004): Effects of water stress and night temperature preconditioning on water relations and morphological and anatomical changes of *Lotus creticus* plants. – *Scientia Horticulturae* 101(3): 333-342.
- [4] Beerling, D. J., Kelly, C. K., Salisbury, E. J. (1997): Stomatal density of temperature woodland plants over the past seven decades of CO₂ increase: a comparison of Salisbury (1927) with contemporary data. – *American Journal of Botany* 84: 1572-1583.
- [5] Biber, Ç., Kara, T. (2012): Plant water consumption of maize plant and limited irrigation practices. – *Journal of Anatolian Agricultural Sciences* 21(1): 140-146.
- [6] Cetin M, Sevik H, Saat A (2017): Indoor air quality: the samples of Safranbolu Bulak Mencilis Cave. – *Fresenius Environmental Bulletin* 26(10): 5965-5970.
- [7] Cetin, M., Sevik, H. (2016a): Assessing Ecotourism Potential Areas through a Case Study in Ilgaz Mountain National Park. – In: Butowski, L. (ed.) *Tourism - From Empirical Research towards Practical Application*. Chapter 5. InTech, London. DOI: 10.5772/62573.
- [8] Cetin, M., Sevik, H. (2016b): The change of air quality in Kastamonu city in terms of particulate matter and CO₂ amount. – *Oxidation Communications* 39(4-II): 3394-3401.
- [9] Cetin, M., Sevik, H., Yigit, N., Ozel, H. B., Aricak, B., Varol, T. (2018a): The variable of leaf micromorphological characters on grown in distinct climate conditions in some landscape plants. – *Fresenius Environmental Bulletin* 27(5): 3206-3211.
- [10] Cetin, M., Onac, A. K., Sevik, H., Sen, B. (2018b): Temporal and regional change of some air pollution parameters in Bursa. – *Air Quality, Atmosphere & Health*. <https://doi.org/10.1007/s11869-018-00657-6>.
- [11] Cohen, J. (1988): *Statistical Power Analysis for the Behavioral Sciences* (2nd Ed.). – Lawrence Erlbaum Associates, Hillsdale, NJ.
- [12] Dixon, E. K., Strik, B. C., Valenzuela-Estrada, L. R., Bryla, D. R. (2015): Weed management, training, and irrigation practices for organic production of trailing blackberry: I. Mature plant growth and fruit production. – *HortScience* 50(8): 1165-1177.
- [13] Erna, L. (2009): Factors affecting upper-middle and upper-income housing prices in urban development areas of Istanbul. – Master Thesis, Istanbul Technical University, Institute of Science and Technology, Istanbul.
- [14] Ertuğrul, M., Varol, T., Özel, H. B. (2014): Climate changes in prospect for the West Black Sea Forests. – *International Journal of Bartın Faculty of Forestry* 16(23-24): 35-43.
- [15] Ferris, R., Nijs, I., Beaghe, T., Impens, I. (1996): Elevated CO₂ and temperature have different effects on leaf anatomy of perennial ryegrass in spring and summer. – *Annals of Botany* 78: 489-497.
- [16] Gratani, L. (2014): Plant phenotypic plasticity in response to environmental factors. – *Advances in Botany 2014*: 1-17.
- [17] Güler, Z., Dursun, A., Ozkan, D. (2017): Volatile compounds in the leaf of plane tree (*Platanus orientalis*) with solid phase microextraction (SPME) technique. – *Int. J. Sec. Metabolite*, Vol. 4(3): 167-176.
- [18] Guney, K., Cetin, M., Sevik, H., Guney, K. B. (2016): Influence of germination percentage and morphological properties of some hormones practice on *Lilium martagon* L. seeds. – *Oxidation Communications* 39(1-II): 466-474.
- [19] Hrivnák, M., Paule, L., Krajmerová, D., Kulac, S., Sevik, H., Turna, I., Tvauri, I., Gömöry, D. (2017): Genetic variation in Tertiary relics: The case of eastern-Mediterranean *Abies* (Pinaceae). – *Ecology and Evolution* 7(23): 10018-10030.

- [20] Jochner, S., Markevych, I., Beck, I., Traidl-Hoffmann, C., Heinrich, J., Menzel, A. (2015): The effects of short-and long-term air pollutants on plant phenology and leaf characteristics. – *Environmental Pollution* 206: 382-389.
- [21] Jud, W., Vanzo, E., Li, Z., Ghirardo, A., Zimmer, I., Sharkey, T. D., Hansel, A., Schnitzler, J. P. (2016): Effects of Heat and drought stress on post-illumination bursts of volatile organic compounds in isoprene-emitting and non-emitting poplar. – *Plant, Cell & Environment* 39(6): 1204-1215.
- [22] Kadioğlu, A. (2004): *Bitki Fizyolojisi*. – Lokman Yayın, Trabzon.
- [23] Kantarcı, M. D., Özel, H. B., Ertekin, M., Kırdar, E. (2011): An evaluation on the adaptation of six tree species used in the afforestation of Konya-Karapınar to the steppe habitat. – *The Journal of Bartın Forestry Faculty* 13(19): 107-127.
- [24] Karakuş, O. (2018): Variation of some leaf micromorphological characteristics in *Platanus orientalis* L. individuals grown in different growing conditions. – Master Thesis, Kastamonu University, Kastamonu.
- [25] Kaya, L. G., Kaynakci-Elinc, Z., Yuçedag, C., Cetin, M. (2018): Environmental outdoor plant preferences: a practical approach for choosing outdoor plants in urban or suburban residential areas in Antalya, Turkey. – *Fresenius Environmental Bulletin* 27(12): 7945-7952.
- [26] Knecht, G. N., Orton, E. R. (1970): Stomata density in relation to winter hardiness of *Ilex opaca* Ait. – *Journal of the American Society for Horticultural Science* 95: 341-345.
- [27] Kulaç, Ş. (2010): Investigation of some morphological physiological and biochemical changes in yellow pine (*Pinus sylvestris* L.) seedlings exposed to drought stress. – Ph.D. Thesis, Karadeniz Technical University, Institute of Science and Technology, Trabzon.
- [28] Li, C., Lei, J., Zhao, Y., Xu, X., Li, S. (2015): Effect of saline water irrigation on soil development and plant growth in the Taklimakan Desert highway shelterbelt. – *Soil and Tillage Research* 146: 99-107.
- [29] Liu, S., Liu, J., Cao, J., Bai, C., Shi, R. (2006): Stomatal distribution and character analysis of leaf epidermis of jujube under drought stress. – *Journal of Anhui Agricultural Science* 34: 1315-1318.
- [30] Madhova-Rao, K. V., Raghavendra, A. S., Janardhan-Reddy, K. (2005): *Physiology and Molecular Biology of Stress Tolerance in Plants*. – Springer, Netherlands.
- [31] Majeed, A., Abbasi, M. K., Hameed, S., Imran, A., Rahim, N. (2015): Isolation and characterization of plant growth-promoting rhizobacteria from wheat rhizosphere and their effect on plant growth promotion. – *Frontiers in Microbiology* 6: 198.
- [32] Marathe, R. A., Babu, K. D. (2017): Plant growth, nutrient uptake, water use efficiency and yield of pomegranate as affected by irrigation scheduling in loamy soils of semi-arid regions. – *The Horticultural Society of India (Regd.)* 74(2): 204-209.
- [33] Ökmen, M., Yurtsever, H. (2010): Taxation of public rent in the process of urban planning. – *Journal of Finance* 158: 58-74.
- [34] Özel, H. B. (2008): The effect of forest restoration applications on some soil properties of Bartın-Ardıç region. – *Journal of Ecology* 17(69): 14-19.
- [35] Öztürk, A., Seki, N., Yiğit, N. (2017): Woody plant variety in parks and gardens of Taşköprü (Kastamonu) district and evaluation of local compliance. – *International Journal of Current Research* 9(11): 60857-60861.
- [36] Pearson, M., Davies, W. J., Mansfield, T. A. (1995): Asymmetric responses of adaxial and abaxial stomata to elevated CO₂ impacts on the control of gas exchange by leaves. – *Plant, Cell & Environment* 18: 837-843.
- [37] Peguero-Pina, J. J., Sancho-Knapik, D., Barrón, E., Camarero, J. J., Vilagrosa, A., Gil-Pelegrín, E. (2014): Morphological and physiological divergences within *Quercus ilex* support the existence of different ecotypes depending on climatic dryness. – *Annals of Botany* 114(2): 301-313.

- [38] Ren, X., Zhu, J., Liu, H., Xu, X., Liang, C. (2018): Response of antioxidative system in rice (*Oryza sativa*) leaves to simulated acid rain stress. – *Ecotoxicology and Environmental Safety* 148: 851-856.
- [39] Romero-Aranda, R., Soria, T., Cuartero, J. (2001): Tomato plant-water uptake and plant-water relationships under saline growth conditions. – *Plant Science* 160(2): 265-272.
- [40] Sevik, H., Cetin, M. (2015): Effects of water stress on seed germination for select landscape plants. – *Polish Journal of Environmental Studies* 24(2): 689-693.
- [41] Sevik, H., Cetin, M. (2016): Effects of some hormone applications on germination and morphological characters of endangered plant species *Lilium artvinense* L. onion scales. – *Bulgarian Chemical Communications* 48(2): 256-260.
- [42] Sevik, H., Karaca, U. (2016): Determining the resistances of some plant species to frost stress through ion leakage method. – *Fresenius Environmental Bulletin* 25(8): 2745-2750.
- [43] Sevik, H., Cetin, M., Kapucu, O. (2016): Effect of light on young structures of Turkish Fir (*Abies nordmanniana* subsp. *bornmulleriana*). – *Oxidation Communications* 39(1-II): 485-492.
- [44] Sevik, H., Cetin, M., Kapucu, O., Aricak, B., Canturk, U. (2017): Effects of light on morphologic and stomatal characteristics of Turkish fir needles (*Abies nordmanniana* subsp. *bornmulleriana* Mattf.). – *Fresenius Environmental Bulletin* 26(11): 6579-6587.
- [45] Sevik, H., Ozel, H. B., Cetin, M., Ozel, H. U., Erdem, T. (2018): Determination of changes in heavy metal accumulation depending on plant species, plant organism, and traffic density in some landscape plants. – *Air Quality, Atmosphere & Health*. <https://doi.org/10.1007/s11869-018-0641-x>.
- [46] Tilki, F., Güner, S., Tüfekçioğlu, A. (2008): Urban forestry and Artvin city urban forestry applications. – *Artvin Coruh University, Journal of Forestry Faculty* 9(1-2): 92-100.
- [47] Topacoglu, O., Sevik, H., Akkuzu, E. (2016): Effects of water stress on germination of *Pinus nigra* Arnold. Seeds. – *Pakistan Journal of Botany* 48(2): 447-453.
- [48] Turkyilmaz, A., Cetin, M., Sevik, H., Isinkaralar, K., Ahmida Saleh, E. A. (2018a): Variation of heavy metal accumulation in certain landscaping plants due to traffic density. – *Environment, Development and Sustainability*. DOI: <https://doi.org/10.1007/s10668-018-0296-7>.
- [49] Turkyilmaz, A., Sevik, H., Cetin, M. (2018b): The use of perennial needles as biomonitors for recently accumulated heavy metals. – *Landscape and Ecological Engineering* 14(1): 115-120.
- [50] Turkyilmaz, A., Sevik, H., Cetin, M., Ahmida Saleh, E. A. (2018c): Changes in heavy metal accumulation depending on traffic density in some landscape plants. – *Pol. J. Environ. Stud.* 27(5): 2277-2284. DOI: 10.15244/pjoes/78620.
- [51] Xu, Z., Zhou, G. (2008): Responses of leaf stomatal density to water status and its relationship with photosynthesis in a grass. – *Journal of Experimental Botany* 59(12): 3317-3325.
- [52] Yang, H. M., Wang, G. X. (2001): Leaf stomatal densities and distribution in *Triticum aestivum* under drought and CO₂ enrichment. – *Acta Phytoecologica Sinica* 25: 312-316.
- [53] Yiğit, N., Öztürk, A., Sevik, H. (2014): Ecological impact of urban forests (example of Kastamonu urban forest). – *International Journal of Engineering Sciences & Research Technology* 3(12): 558-562.
- [54] Zhang, Y. P., Wang, Z. M., Wu, Y. C., Zhang, X. (2006): Stomatal characteristics of different green organs in wheat under different irrigation regimes. – *Acta Agronomica Sinica* 32: 70-75.
- [55] Zhao, R. X., Zhang, Q. B., Wu, X. Y., Wang, Y. (2001): The effects of drought on epidermal cells and stomatal density of wheat leaves. – *Inner Mongolia Agricultural Science and Technology* 6: 6-7.

EFFECT OF LAND CREATION ON REGIONAL ECOLOGICAL ENVIRONMENT: A CASE STUDY FOR LANZHOU CITY, CHINA

SHI, Y. F.^{1*} – MA, C.¹ – KONG, D. J.² – ZHAO, J.¹

¹*College of Geography and Environment Science, Northwest Normal University
Lanzhou, Gansu Province 730070, China*

²*School of Foreign Languages, Lanzhou Jiaotong University
Lanzhou, Gansu Province 730070, China*

**Corresponding author
e-mail: shiyfgis@126.com*

(Received 21st Jan 2019; accepted 27th Feb 2019)

Abstract. With the accelerating process of urbanization, the contradiction between the shortage of land resources and the expansion of cities has become increasingly prominent. Many cities have expanded the area of development by “cutting mountains and building land”. Taking Lanzhou city of China, a typical valley-type city as the study area, land use change data obtained from remote sensing imagery in 1995, 2000, 2005, 2010, and 2015 were quantified by land use transfer matrix, land use change intensity index, ecosystem service value, and regional eco-environmental quality index method. The study on the characteristics of land use change and its impact on the ecological environment in Lanzhou City shows that the land use change in Lanzhou City during the period of 1990 to 2015 years is mainly reflected by the decrease of cultivated land and grassland, the increase in construction land and unused land area; The quality of eco-environment in Lanzhou City was negative developed from 1990 to 2015. The spatial expansion caused by urbanization had the most profound impact on land use types; the minimum value of eco-environmental index of all counties in Lanzhou City appeared in 2015, and Grassland and Farmland occupied by a large amount of construction land is the main reason for the deterioration of ecological environment quality. Based on the study, we expected to provide reference for the development and construction, and ecological environment protection of similar areas, especially the cities with extremely shortage of land resources such as the typical river-valley cities in the future development.

Keywords: *land creation, ecological environmental effect, land use, TM image, Lanzhou City of China*

Introduction

The fundamental national condition that China has Limited Farmland per Capita has led to a strong contradiction between supply and demand for land resources. Nowadays, the process of urbanization in our country is accelerating, and cities are rapidly expanding. However, limited land resources and urban expansion space have limited the expansion of cities. Especially in the valley-cities, the expandable area is relatively limited due to the restrictions of the terrain. Under the background of increasingly conspicuous contradiction between limited land resources, increasing population and land use demand, some cities in our country carry out the project of “Bulldoze Mountains to Build New City” to expand the urban area, thus obtaining better development space. For example, Yan’an expands the scale of the city through the method of “Foundation in the mountains” and builds a Yan’an New Area (Cui, 2015); the “industry terrace” project was implemented in Fujian, Guizhou, etc. (Huang, 2014; Jiang et al., 2007). The main method is to combine “truncating the mountain” and filling land with flat land in order to expand the area; the new district of Lanzhou and Gaolan county in Gansu Province have expanded the area of development by “truncating the

mountain”. However, various scholars have different opinions on whether the “Bulldoze Mountains to Build New City” is feasible or not. Cui (2015) believes that the construction of Yan’an New District will continue to expand land for urban construction, at the same time, it causes changes in land use types, destruction of vegetation resources and ecological environment. Li et al. (2014) considered that the “cutting the mountain and building the city” project was not mature in terms of economy, technology, and ecological protection. Liu and Li (2014) considered that the implementation of the government’s plan, “Cutting off hilltops and moving mountains to build city in Yan’an”, is feasible and provides references for other cities. That because detailed planning, hydrology and water resources, have demonstrated from all sides of ecology by experts.

“Bulldoze Mountains to Build New City” will cause changes in the land use types. Changes in land use types (Li et al., 2017; Tan et al., 2010) will have an impact on the regional ecological environment. The quality of the ecological environment will directly affect human well-being and the sustainable development of the region (Chang et al., 2017; Ma et al., 2015; Liu et al., 2005, 2009; Terefe et al., 2017). Domestic and foreign scholars have studied the impact of changes in land use types on the value of ecological services. For example, such as Terefe et al. (2017) believed that the reduction of forest land in Ethiopia has resulted in huge losses in ecosystem service value; Lawler et al. (2014) studied land use change in the United States. The impact of changes on ecosystem services suggests that changes in land use have promoted the fixation of carbon but led to the destruction of ecological environment. Xie et al. (2008) studied the land use changes in the suburbs of Tongchuan City on the eco-environment with the value of ecosystem services as indicators. Zhou et al. (2017) studied the effect of ecosystem service value of valley-city in Lanzhou, and concluded that the invading of farmland ecosystems by land for urban construction led to a drastic decline in ecosystem service value in Qinwangchuan basin. However, ecosystem service value is used to measure the quality of the ecological environment as an important indicator (Rong et al., 2017; Zhang et al., 2017; Hu et al., 2008).

As a typical valley-city, Lanzhou City has limited land resources, urban development is restricted, and the contradiction between growing population and demand for land is becoming increasingly prominent. In the past two decades, many cities such as Qinwangchuan and the new district of Lanzhou have carried out a number of “Bulldoze Mountains to Build New City projects”, thereby expanding the urban land area. Therefore, the thesis uses Lanzhou City as an object of study to use the Landsat image data from 1990 to 2015 to analyze the characteristics of spatio-temporal changes in land use, and estimate the value of ecosystem services, continue to evaluate the impact of land use changes on ecology caused by “Bulldoze Mountains to Build New City”.

Material and methods

Background of the study area

Lanzhou City, the capital of Gansu Province, is the political, economic and cultural center of Gansu Province and it is also an important central city in the northwestern China. It is located in the upper reaches of the Yellow River and is located at longitude 102°36'-104°34' E and latitude 35°34'-37°07' (Fig. 1), with an average elevation of 1500 m. It belongs to the loess hilly and gully region, temperate semi-arid continental monsoon climate, and large temperature difference between day and night, less

precipitation (Guo et al., 2016). Lanzhou is an important support for the Western Long Hai-Lan Xin Economic Zone. The core of the upper Yellow River economy is mainly composed 34 towns and 27 villages. It currently governs five districts such as Chengguan District, Qilihe District, Anning District, Xigu District, and Honggu District and three counties including Yuzhong County, Gaolan County and Yongdeng County. The total land area of Lanzhou City is 1311.9 thousand hm^2 . Due to the constraints of the canyon topography and the two mountains in the north and the south, Lanzhou's urban space development is greatly constrained. The geographical space is relatively narrow and its integrity is poor. It is a typical valley-city in China (Zhang et al., 2013). The human settlement environment formed by this influence is special.

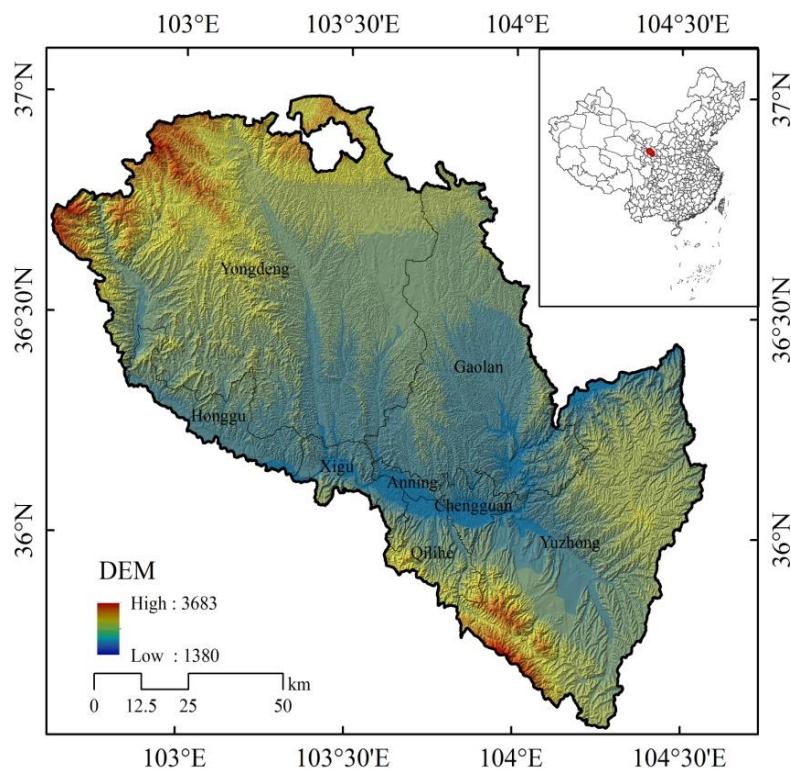


Figure 1. The location of study area

Data sources and processing

The research data used in this paper includes:

Remote Sensing Data: Landsat remote sensing images of Lanzhou City were selected in 1990, 1995, 2000, 2005, 2010 and 2015. The coordinates are 130/35, 131/34, and 131/35, and the spatial resolution is 30 m. All these data are from Geospatial Data Cloud (<http://westdc.westgis.ac.cn>).

Through radiation correction and FLAASH atmospheric correction, the processed remote sensing images were stitched and cropped to obtain remote sensing images in the study area from 1990 to 2015. By classification, the land use type map was obtained. In this study, the overall accuracy (OA), and another discrete multivariate index KAPPA (K) coefficient are used in accuracy assessments. The OA and K statistics can be calculated as *Equations 1* and 2, respectively (Wei et al., 2010):

$$OA = \frac{\sum_{i=1}^k n_{ii}}{n} \quad (\text{Eq.1})$$

$$K = \frac{n \sum_{i=1}^k n_{ii} - \sum_{i=1}^k n_{i+} n_{+i}}{n^2 - \sum_{i=1}^k n_{i+} n_{+i}} \quad (\text{Eq.2})$$

where, n is the total number of observations; k is the number of rows in the matrix, and n_{ii} is the number of observations in row i and column i ; n_{i+} and n_{+i} are the total numbers of pixels in i -th row and i -th column, respectively. The results of statistics and accuracy analysis are shown in *Table 1*.

Table 1. The classification supervision accuracy evaluation

Year	2015	2010	2005	2000	1995	1990
Kappa coefficient	0.8699	0.8384	0.8248	0.8735	0.9024	0.9231
Overall accuracy	89.38%	90.16%	85.96%	91.25%	92.25%	85.59%

From *Table 1*, we can see that the classification accuracy of land use types in Lanzhou City during the period from 1990 to 2015 is all above 85.5%, which satisfies the accuracy requirements for follow-up studies.

Boundary data: National Geographic Center released.

Research methods

Land use change intensity index

The land use intensity index refers to the change in certain land-use types per unit area in the study area during a certain period of time. The land use change index (Xie et al., 2008) is calculated as *Equation 3*:

$$K_i = \frac{U_{ai}}{U_{bi}} \times \frac{1}{T} \times 100\% \quad (\text{Eq.3})$$

where K_i denotes the i -th land use type change intensity index in the study area, U_{ai} denotes the i -th land use type area in the initial stage of the study period, U_{bi} denotes the i -th land use type area in the end of the research period, and T denotes the initial period of the study and the end of the study period. The time is apart and the unit is year.

Calculation of ecological service value

Xie et al. (2005) divided China's ecosystem services into nine categories such as climate regulation, water conservation, and food production, and formulated a table of ecological service values per unit area of different terrestrial ecosystems in China to calculate the ecological service value of the research area in different periods. The formula is as *Equation 4*:

$$ESV = \sum_{i=1}^n A_i \times VC_i \quad (\text{Eq.4})$$

ESV is the total value of ecological services of different land-use types (yuan), i refers to land-use types, A_i refers to the area of the i -th land-use type in the study area (hm^2), and VC_i is the unit ecological service value of the i -th land-use type ($\text{Yuan}/\text{hm}^2 \cdot \text{a}$).

Eco-environmental quality index

Taking into consideration the ecological environment quality and area ratio of land use types in various regions, the eco-environmental index are used to quantitatively characterize the overall situation of the ecological environment quality in a certain region. The expression (Zhang et al., 2018) is as *Equation 5*:

$$EV_t = \frac{\sum_{i=1}^n A_i C_i}{\sum_{i=1}^n A_i} \quad (\text{Eq.5})$$

where A_i , C_i is the area and eco-environmental index of the i -th land-use type in the period t , and n is the number of land-use types in the area.

Results and discussion

Analysis of land use change

(1) Overall land use change from 1990 to 2015

Based on the remote sensing imagery data from 1990 to 2015, using a combination of supervised classification and artificial visual interpretation, the land use type map of Lanzhou was interpreted, as shown in *Figure 2*.

The overall classification accuracy of different periods is between 85.59 and 92.25%, which meets the research needs. Overall, in the past 20 years, the land use structure in Lanzhou City underwent significant changes, mainly reflected in the increase in construction land and unused land, and the corresponding reduction in the area of cultivated land and grassland. From the point of view of spatial distribution, the increased construction land mainly shows two situations of agglomeration and scattered distribution. The increased construction land is mainly distributed in Gaolan County and Yongdeng County, that is, the construction of Lanzhou New District in December 2010 is consistent; The border between Anning District and Gaolan County is mainly the construction of Poly Xiuling Mountain, which is in line with the situation of the field investigation. Judging from the time series, the land for construction increased from 1990 to 2015. With 2010 as the demarcation point, the area of construction land in 2015 increased significantly.

In order to further study the characteristics of land use structure in Lanzhou City from 1990 to 2015, the area and proportion of each type of land use were calculated separately. The results are shown in *Table 2*.

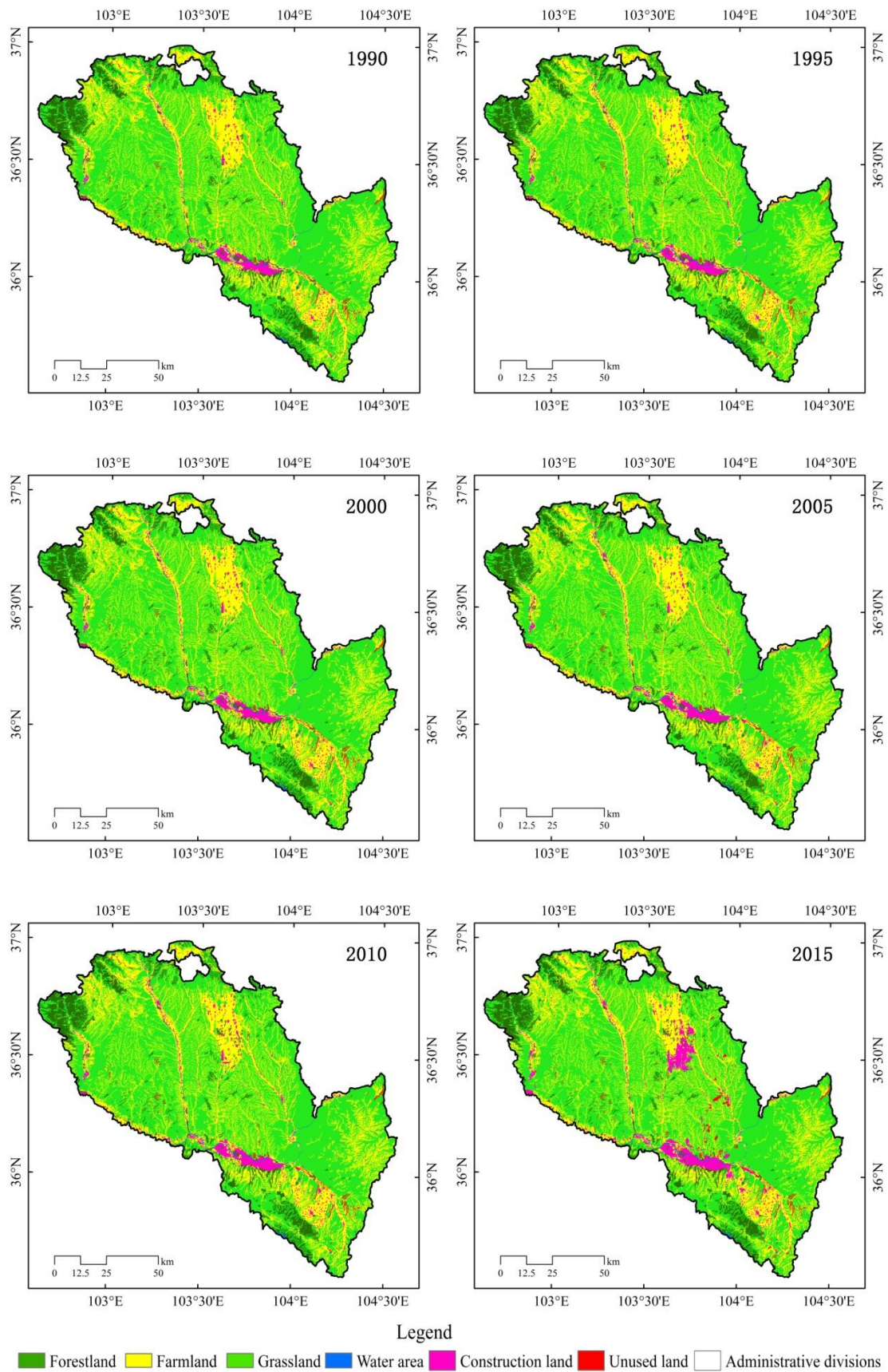


Figure 2. Spatial distribution of land use types in Lanzhou city during 1990-2015

Table 2. Land use structural feature of Lanzhou city during 1990-2015 (unit: km²)

Year		Farmland	Forestland	Grassland	Water area	Construction land	Unused land
1990	Area (km ²)	3853.51	900.91	8012.09	68.71	315.07	52.62
	Proportion (%)	29.19	6.82	60.68	0.52	2.39	0.40
1995	Area (km ²)	3841.26	901.55	8007.88	69.38	328.75	54.08
	Proportion (%)	29.09	6.83	60.65	0.53	2.49	0.41
2000	Area (km ²)	3850.19	904.19	7987.62	68.10	340.19	52.62
	Proportion (%)	29.16	6.85	60.50	0.52	2.58	0.40
2005	Area (km ²)	3816.61	899.11	7993.48	68.17	369.81	55.73
	Proportion (%)	28.91	6.81	60.54	0.52	2.80	0.42
2010	Area (km ²)	3788.53	918.96	7993.81	68.39	377.95	55.26
	Proportion (%)	28.69	6.96	60.55	0.52	2.86	0.42
2015	Area (km ²)	3642.95	909.63	7917.97	70.04	558.40	103.91
	Proportion (%)	27.59	6.89	59.97	0.53	4.23	0.79
1990-2015	Net variable (km ²)	-210.56	8.72	-94.12	1.33	243.33	51.29
	Change rate (%)	-1.6	0.07	-0.71	0.01	1.84	0.39

From *Table 2*, we can see that during the period from 1990 to 2015, grassland was the main type of land use in Lanzhou, accounting for about 60% of the total area; in 2005, as the boundary, it decreased first and then increased. In 2015, it decreased drastically, and its value was 94.12 km². This is mainly caused by cutting mountains and land; arable land accounts for about 30% of the total area of land use. Since 2005, the area of cultivated land has been decreasing, which has decreased by nearly 210.56 km² compared with that of 1990. Construction land has been on an increasing trend. Compared with 1990, it has increased by 243.33 km² with a rate of change of 1.84%. Unused land and forest lands have been fluctuating. The change of Forest land was relatively small, while unutilized land increased nearly more than doubled in 2015. That is mainly because the land, which used for construction has not been used yet, increased obviously after the bulldoze mountains.

(2) Land use transfer characteristics and change intensity analysis

From the spatial distribution and structural characteristics of land use, we can see that the land use structure of Lanzhou City has undergone significant changes from 1990 to 2015. Therefore, the land use transfer situation in Lanzhou City from 1990 to 2015 was analyzed. The results are shown in *Table 3*.

From *Table 3*, it can be seen that various types of land use types have changed from 1990 to 2015. The types of land converted into construction land are the unused land <water area <woodland <grassland <cultivated land, and the area of water and unused land converted into construction land is 0.93 km² and 0.3 km² respectively; the area of cultivated land converted into construction land is 179.02 km², accounting for 73.34% of the conversion area. The conflict of the shortage of land resources and the large area of land for urban construction leads to create land from mountains, which caused the majority of grassland and a little few of the farmland reduced. This is similar to Lanzhou New District and Poly Lingxiushan. The Country Garden, which is still under

construction, has close ties with other construction projects. On the other hand, due to the need for the construction of educational resources, large-scale arable land has been lost, such as Pengjiaping, Qiujiawan and so on.

Table 3. Land use transfer matrix of Lanzhou city during 1990-2015 (unit: km²)

		2015					
		Farmland	Forestland	Grassland	Water area	Construction land	Unused land
1990	Farmland	3614.73	19.96	18.24	1.77	179.02	19.78
	Forestland	1.05	883.70	0.26	0.15	15.19	0.55
	Grassland	26.70	5.39	7898.95	0.52	48.63	31.89
	Water area	0.21	0.01	0.00	67.56	0.93	0.00
	Construction land	0.00	0.57	0.03	0.03	314.33	0.10
	Unused land	0.25	0.00	0.48	0.00	0.30	51.59

In order to further reveal the changes of land use types in Lanzhou City during the past 25 years, the change intensity of land use types in Lanzhou City during different research periods was calculated and the results are shown in *Table 4*.

Table 4. The intensity of Land use change of Lanzhou city during 1990-2015 (unit: %)

Year	Farmland	Forestland	Grassland	Water area	Construction land	Unused land
1990-1995	-0.06	0.01	-0.01	0.20	0.87	0.55
1995-2000	0.05	0.06	-0.05	-0.37	0.70	-0.54
2000-2005	-0.17	-0.11	0.01	0.02	1.74	1.18
2005-2010	-0.15	0.44	0.00	0.07	0.44	-0.17
2010-2015	-0.77	-0.20	-0.19	0.48	9.55	17.61
1990-2015	-0.22	0.039	-0.047	0.08	3.09	3.90

According to *Table 4*, from 1990 to 2015, the intensity index of land use change in forest land, water area, construction land, and unused land is positive, indicating that the overall area is increasing. In terms of different time periods, except for the intensity index of land use change during the period from 1995 to 2000, the rest is negative, indicating that the area of cultivated land has decreased during the past 15 years, and has decreased significantly from 2010 to 2015; The intensity index of construction land use change is positive, that is to say, the area of construction land in Lanzhou has increased at different degrees in the past 25 years. From 1990 to 2015, the positive value of the unexploited land use change index (19.34%) was much greater than the negative value (0.71%), and the unutilized land increased significantly. Most of the land obtained through the cut-to-earth land reclamation project has not yet been put into use in 2010-2015. Construction has led to a significant increase in unused land.

Eco- services value measurement and analysis

(1) Land use transfer characteristics and change intensity analysis

According to the research of Xie et al. (2005) in China's terrestrial ecosystem service value-equivalent factor table and correction factors of different provinces, the ecological

service value of different land-use types in Lanzhou City is estimated, as shown in *Table 5*.

Table 5. *The intensity of Land use change of Lanzhou city during 1990-2015 (unit: million yuan)*

Year	Forestland	Grassland	Farmland	Water area	Construction land	Unused land	Total value
1990	73156.2	215583.8	98958.4	11737.8	491.5	82.1	400009.7
1995	73208.4	215470.4	98643.8	11852.5	512.8	84.4	399772.4
2000	73422.5	214925.2	98873.2	11633.5	530.7	82.1	399467.1
2005	73010.2	215083.0	98010.7	11645.5	576.9	86.9	398413.2
2010	74622.5	215091.8	97289.8	11684.4	589.6	86.2	399364.2
2015	73864.4	213051.2	93551.3	11965.7	871.0	162.1	393465.7

From *Table 5*, we can see from the total value of ecosystem services, the total value of ecosystem services in Lanzhou City decreased and then increased from 1990 to 2015. The total value of ecosystem services continued to decline during 1990-2005, which was reduced by 1596.5 million yuan. From 2005-2010, the total value of ecosystem services showed an increasing trend. From 2010-2015, the total value of ecosystem services declined drastically 5898.5 million yuan.

From the single type of land use, the ESV for forest land is similar to the change in the total value of ecosystem services in Lanzhou City. From 1990 to 2005, there was a trend of “increase-decrease-increase”, of which in 2010 and 1990, the forest ecosystem service value peaked in 1990 and 2010 at the highest and lowest values, which were 74622.5 million yuan and 73156.2 million yuan respectively. In the past 25 years, the ecosystem service value of grassland and farmland showed a decreasing trend. The maximum values all appeared in 1990, and the minimum values all appeared in 2015. This is mainly due to the large number of Bulldoze Mountains to Build New City projects destroyed in Lanzhou City. Grassland and farmland have resulted in a significant reduction in the area of these two types of land use, which has led to a reduction in the value of ecosystem services. Due to the needs of urban construction, the area of construction land continues to increase. As a result, the ecosystem service value of construction land continues to rise. The speed of land creation is faster than the speed of construction. As a result, the area of unused land continues to expand, leading to a significant increase in the value of ecosystem services of unused land from 2010 to 2015.

(2) *Regional comprehensive ecological environmental quality change*

According to *Equation 3*, the eco-environmental indices of land use types in Lanzhou and its counties are calculated to analyze the impact of land use changes on the eco-environmental quality. The results are shown in *Table 6*.

From *Table 6*, we can see that the overall eco-environmental quality of Lanzhou City is basically stable, but it shows a downward trend. In addition to the increase trend from 2005 to 2010, the eco-environmental quality index of Lanzhou during the four periods of 1990-1995, 1995-2000, 2000-2005, and 2010-2015 both showed a downward trend. The ecological quality indices have been significantly reduced. The statistical analysis

of the changes in eco-environmental index in all counties and counties of Lanzhou City in the past 25 years was the largest in Anning District, followed by Chengguan District, and Gaolan County ranked the third; the minimum eco-environmental index values of all counties appeared in 2015, including grassland and the large amount of cultivated land occupied by construction land is the main reason for the decline in the quality of the ecological environment.

Table 6. *The ecological environment quality index of Lanzhou city during 1990-2015*

	1990	1995	2000	2005	2010	2015
Chengguan District	0.3283	0.3273	0.3273	0.3204	0.3218	0.3091
Qilihe District	0.3502	0.3508	0.3507	0.3493	0.3498	0.3465
Anning District	0.3145	0.3128	0.3128	0.3022	0.3021	0.2932
Xigu District	0.3499	0.3479	0.3482	0.3469	0.3463	0.3454
Red Ancient District	0.3341	0.3341	0.3339	0.3336	0.3333	0.3306
Yongdeng County	0.3491	0.3490	0.3490	0.3489	0.3495	0.3481
Gaolan County	0.3330	0.3331	0.3327	0.3330	0.3339	0.3280
Yuzhong County	0.3394	0.3392	0.3390	0.3387	0.3387	0.3378
Lan'Zhou City	0.3426	0.3425	0.3424	0.3421	0.3425	0.3401

Conclusions

(1) From the land use type spatial distribution map, we can see that the area of construction land has increased significantly. It is mainly located in Yongdeng County and Gaolan County, and is used for the construction of Lanzhou New District and Poly Xiuling Mountain.

(2) In 2015, construction land and unused land increased rapidly. The project of "land creation" led to the conversion of large areas of farmland and grassland into construction land, which was mainly used for urban construction and educational resource construction.

(3) From the total value of ecosystem services, the total value of ecosystem services in Lanzhou City decreased and then increased from 1990 to 2015. From 2010 to 2015, the total value of ecosystem services declined drastically and its value was 5898.5 million yuan.

(4) During the period from 1990 to 2015, the overall eco-environmental quality in Lanzhou City was relatively stable, but overall it showed a deteriorating trend. Within the local area of each county, the quality of ecological environment changed significantly. Among them, the influence of cultivated land and grassland on the ecological environment quality played a leading role.

(5) This paper lacks the improvement research on the existing evaluation methods. How to consider other factors to the quantitative calculation of the ecological environment index, and accurately assess the effect of the land use changes on ecological environment. The influence of different scales and different land use classification systems on the evaluation results remains to be further studied in the future.

Acknowledgements. This work was funded by the National Natural Science Foundation of China (41661084, 41761083, 41661035) and the project of Northwest Normal University (5007-355).

REFERENCES

- [1] Chang, Z. B., Qin, F., Han, Z. G., Lu, Y., Yu, Y. Y. (2017): Dynamic evaluation of eco-environmental quality in He'nan province based on RS and GIS. – *Bulletin of Soil and Water Conservation* 37: 132-137+345.
- [2] Cui, Y. J. (2015): Study on the Benefit of Resources and Environment in Yan'an New Area. – Chang'an University, Xi'an.
- [3] Guo, X. Y., Liu, X. L., Wang, L. G. (2016): Land use optimization in order to improve ecosystem service: a case of Lanzhou city. – *Acta Ecologica Sinica* 36: 7992-8001.
- [4] Huang, R. (2014): The effect of land creation on atmospheric environment using numerical simulation in valley city: a case study for Lanzhou. – Lanzhou University, Lanzhou.
- [5] Hu, H. B., Liu, W. J., Cao, M. (2008): Impact of land use and land cover changes on ecosystem services in Menglung, Xishuangbanna, Southwest China. – *Environmental Monitoring and Assessment* 146(1): 147-156.
- [6] Jiang, H., Yin, Q., Luo, Y. X. (2007): Industry terrace-a new pattern of land use in China. – *Agricultural Mechanization Research* 05: 28-30+45.
- [7] Lawler, J. J., Lewis, D. J., Nelson, E., Plantinga, A. J., Polasky, S., Withey, J. C., Helmers, D. P., Martinuzzi, S., Pennington, D., Radeloff, V. C. (2014): Projected land-use change impacts on ecosystem services in the United States. – *Proc. Natl. Acad. Sci. USA* 111: 7492-7497.
- [8] Li, P. Y., Qian, H., Wu, J. H. (2014): Environment: accelerate research on land creation. – *Nature* 510: 29-31.
- [9] Li, X., Chen, G. Z., Liu, X. P., Liang, X., Wang, S. J., Chen, Y. M., Pei, F. S., Xu, X. C. (2017): A new global land-use and land-cover change product at a 1-km resolution for 2010 to 2100 based on human-environment interactions. – *Annals of the American Association of Geographers*. DOI: 10.1080/24694452.2017.1303357.
- [10] Liu, J. Y., Zhang, Z. X., Xu, X. L., Kuang, W. H., Zhou, W. C., Zhang, S. W., Li, R. D., Yan, C. Z., Yu, D. S., Wu, S. X., Jiang, N. (2009): Spatial patterns and driving forces of land use change in China in the early 21st Century. – *Acta Geographica Sinica* 64: 1411-1420.
- [11] Liu, Y. B., Li, R. D., Song, X. F. (2005): Analysis of coupling degrees of urbanization and ecological environment in China. – *Journal Natural Resources* 01: 105-112.
- [12] Liu, Y. S., Li, Y. H. (2014): Environment: China's land creation project stands firm. – *Nature* 511: 410.
- [13] Ma, W. J., Pu, C. L., Su, L. L., Jiang, L. (2015): Analysis of impact of land use change on ecological environment in Changji city. – *Tianjin Agricultural Sciences* 21: 29-32+36.
- [14] Rong, Y., Li, C., Xu, C., Yan, Y. (2017): Ecosystem service values and spatial differentiation changes during urbanization: a case study of Huanghua city. – *Chinese Journal of Ecology* 05: 1374-1381.
- [15] Tan, K. C., Lim, H. S., MatJafri, M. Z., Abdullah, K. (2010): Landsat data to evaluate urban expansion and determine land use/land cover changes in Penang Island, Malaysia. – *Environmental Earth Sciences* 60(7): 1509-1521.
- [16] Terefe, T., Feyera, S., Moges, K. (2017): The impact of land use/land cover change on ecosystem services in the central highlands of Ethiopia. – *Ecosystem Services* 47-54.
- [17] Wei, Y. C., Tang, G. A., Yang, X. (2010): The Tutorial of Remote Sensing Digital Image Processing. – Science Press, Beijing, pp. 208-251.
- [18] Xie, G. D., Xiao, Y., Zhen, L., Lu, C. X. (2005): Study on ecosystem services value of food production in China. – *Chinese Journal of Eco-Agriculture* 03: 10-13.
- [19] Xie, H. X., Li, R., Ren, Z. Y., Yang, Q. K. (2008): Quantitative assessment of the effect on the eco-environment from LUCC in a region scale-a case in the city proper and the suburbs of Tongchuan. – *Journal Natural Resources* 03: 458-466.

- [20] Zhang, Q., Gao, S. F., Gao, C. Q., Wang, J. Z., Niu, L., Zhang, N. (2018): Ecological land of Pingdingshan city and its ecosystem services evolution over the past 20 years. – *Ecological Science* 37: 159-168.
- [21] Zhang, Y. J., Han, H. Q., Gao, H. J., Cai, G. P., Zhang, C. X. (2017): Coordination degree between ecosystem services value and land ecological security level in Zunyi. – *Journal of Southwest Forestry University (Natural Science)* 05: 141-146.
- [22] Zhang, Z. B., Pan, J., Li, X. H. (2013): The spatial evolution and formation mechanism of population density in Lanzhou city over the past 30 years. – *Scientia Geographica Sinica* 33: 36-42.
- [23] Zhou, W. X., Shi, P. J., Wang, Y. N., Liang, B. B., Tang, X. (2017): Effect of Ecosystem service values of river valley city: a case study of Lanzhou. – *Arid Zone Research* 01: 232-241.

OCCURRENCE, ECOLOGY AND PHYLOGENY OF BANANA STREAK BADNAVIRUS (BSV) AND CUCUMBER MOSAIC CUCUMOVIRUS (CMV) IN *MUSA SP.* PRODUCTION AREAS OF THE MEDITERRANEAN COASTLINE OF TURKEY

FIDAN, H.^{1*} – KOÇ, G.²

¹*Plant Protection Department, Faculty of Agriculture, Akdeniz University, 07070, Antalya, Turkey*

²*Subtropical Fruits Research and Experimental Center, Çukurova University, Adana, Turkey*

**Corresponding author
e-mail: hakanfidantr@hotmail.com.tr*

(Received 31st Jan 2019; accepted 6th Mar 2019)

Abstract. The Banana infecting viruses have an importance in the movement and propagation of plant germplasm, especially in areas where banana is propagated vegetatively. During field surveys 118 banana leaf samples have been tested by DAS-ELISA, PCR and RT-PCR have shown malformation, necrosis, chlorotic streak and mosaic symptoms collected from Mediterranean Coast Line (Adana, Antalya and Mersin provinces) of Turkey in 2015 and 2016. For diagnosis of CMV, BBTV, BSV, TMV, PVY, WMMV, PRSV, BCMV and TSWV pathogens that cause severe crop loss in banana plantations firstly, serological tests have been conducted using DAS-ELISA immune kit. Further identification and confirmation studies by PCR and RT-PCR from leaf samples exhibiting mild chlorotic streaks and mosaics on leaves, typical infection of *Banana streak mosaic virus* (BSV) and *Cucumber mosaic cucumovirus* (CMV) were used. Their symptoms were truly matched in PCR (BSV & CMV) and DAS-ELISA (CMV) analyses. Disease incidence was consequently estimated between 17.79% (CMV) and 4.23% (BSV). This is the first molecular evidence for BSV or BSV mixed with CMV in banana in Turkey. Sequence information of PCR products were obtained from Hplotypes and searched on BLAST system of NCBI. Phylogenetic analyses have informed the origin and ecology of CMV in bananas which were infected by vegetables grown inside the banana greenhouses The banana BSV isolate was in the same group isolates that were obtained in Kenya, Congo, Australia, China and India.

Keywords: *molecular ecology of banana viruses, BSV, CMV, PCR, DAS-ELISA*

Introduction

Banana (*Musa spp.*) is an economically important fruit, which is grown in tropical and subtropical climates and are widely consumed in both fresh and preserved form. Production is not only concentrated in the Mediterranean area of Turkey, but it is also produced worldwide (FAO, 2015). Around the world, roughly 145 million tons of bananas are grown each year (Baggaley, 2017). In Turkey according to the Ministry of Food, Agriculture and Livestock, 369009 tons of banana fruit was produced at the Mediterranean Coast Line (Adana, Mersin and Antalya provinces) in 2017. Additionally, an increase (14.4%) in banana production has been forecasted for this year (TUIK, 2017). There are many factors decreasing the quantity and quality of banana production more likely than in other fruit crops. One of the most important restrictive factors including plant diseases and pests, are viral agents. Among the important agronomic traits, virus resistance is one of the major breeding objectives, as several diseases caused by viruses have great economic impact on production.

Banana bunchy top virus (BBTV), *Banana streak virus* (BSV), *Cucumber mosaic virus* (CMV), *Banana bract mosaic virus* (BBrMV), *Banana mild mosaic virus* (BanMMV), *Banana virus X* (BVX) are major banana infecting viral agents (Tripathi et al., 2016). Morphology, taxonomy, symptomatology, cytopathology, epidemiology, diagnosis and sanitation of these *Musa spp* infecting species were reviewed by Teycheney and Lescot (2004). Furthermore, *Water melon mosaic virus*, *Papaya ringspot virus*, *Tobacco mosaic virus*, *Bean common mosaic virus*, *Tomato spotted wilt virus*, Potygroup and *Potato virus Y* could cause diseases in bananas. Nevertheless, based on the symptoms observed, Gambley and Thomas, (2001) has been underlined some viral infections.

Banana bunchy top virus was first recorded in Fiji in 1889, and has spread broadly in banana production areas. It has been transmitted by sucker, and black aphid (*Pentalonia nigronervosa*). Also tissue culture propagation has an importance on transmission, due to noneradicated infections. The *Banana bunchy top virus* can cause major economic yield loss. Another major threat is *Banana streak virus* that can cause leaf streak disease, it is a member of genus *Badnavirus*, and was first recorded in 1986. There are two main distinct strains of BSV (Lockhart and Olszewski, 1993). The Onne strain of BSV, now renamed BSV-OL (R Hull, personal communication), in Africa, Central and South America. The other strain is called as the Cavendish strain of BSV (BSV-Cav), which has been found in commercial banana plantations in Australia. BSV is transmitted by *Planococcus citri* (Risso) and possibly other species of mealybug (Lockhart and Jones, 1999). The characteristic symptoms of BSV infection are mainly chlorotic and necrotic streaks on the leaves. Other symptoms may include narrowing and thickening of the leaf, internal pseudostem necrosis, splitting of the base of the leaf sheaths and detachment of leaves, overall stunting of the plant, smaller bunches and abnormally shaped fruit with a thinner peel that is prone to splitting. The symptoms are probably diverged by factors such as environmental conditions, and host and virus genotypes (Lockhart and Jones, 1999).

BSV is transmitted by infected mother plants and through tissue-culture propagation of infected explants and by several mealybug (Hemiptera: Coccoidea: Pseudococcidae) species, but not mechanically (Lockhart and Jones, 1999). Mealybug species which have been confirmed as vectors include the citrus mealybug, *Planococcus citri* Russo (Lockhart and Olszewski, 1993), *Pseudococcus comstiki* Kuwana (Su, 1998), both the pineapple mealybug *Dysmicoccus brevipes* Cockerell and the sugarcane mealybug *Sacchirococcus sacchari* Cockerell (Kubiriba et al., 2001b), and the vine mealybug *Planococcus ficus* Signoret (Meyer et al., 2008).

Sison et al. (2017) underlined that BSV can be transmitted to uninfected banana by mealybugs of *Musa sp.* (*Pseudo-coccus elisae* and *Dysmicoccus brevipes*), *Manilkara zapota* (unreported), *Anonna muricata*, *Ananas comosus* (*Dysmicoccus brevipes*) and *Nephelium napaceum*. Infection transmission proficiency and mean effect seriousness was eminently most astounding utilizing the vectors from the last two yields. Mealybugs assume a noteworthy job in the characteristic spread of the infection. Since bananas in the Philippines are likewise planted close by the previously mentioned harvests, the board systems ought to tend to decrease the number of inhabitants in these mealybug species from fields.

The prevalent infection by CMV (Cucumovirus), has been classified by serology and symptomology (mosaic, line patterns and ringspot at leaf), and has three subgroups (IA, Ib and II) regarding coat protein gene. Interveinal chlorosis is also caused by CMV

strains. If strain severity is higher, plant mortality may become by CMV infections. CMV has been transmitted by sucker, and aphids. Eradication, certified material and vector management are important strategies to overcome the menace. CMV has many host species even ornamentals in Turkey (Koç. et al., 2016; Karanfil et al., 2016)

The aims of the paper are to determine the presence and distribution of common banana viruses, including BSV, BBTV and CMV in the Mediterranean Area of Turkey. Existence of banana viruses has not yet been explored by reliable* laboratory assays (i.e. more sensitive current techniques for detection and characterization such as serological (DAS-ELISA) and molecular (PCR) methods) other than those used in this study in our country.

Materials and methods

The research was conducted in the Mediterranean Coast Line of Turkey in 2015-2016 years. A total of 118 samples were collected from suspected plants in banana plantains at different locations in the line. During the surveys, small and shapeless malformed leaves, light colored areas resembling mosaic with streaks of necrotic areas of the leaves and small bunchy formations were observed on plants. Surveys were conducted during the growing season and only symptomatic samples were collected randomly throughout the area in Turkey (Fig. 1).

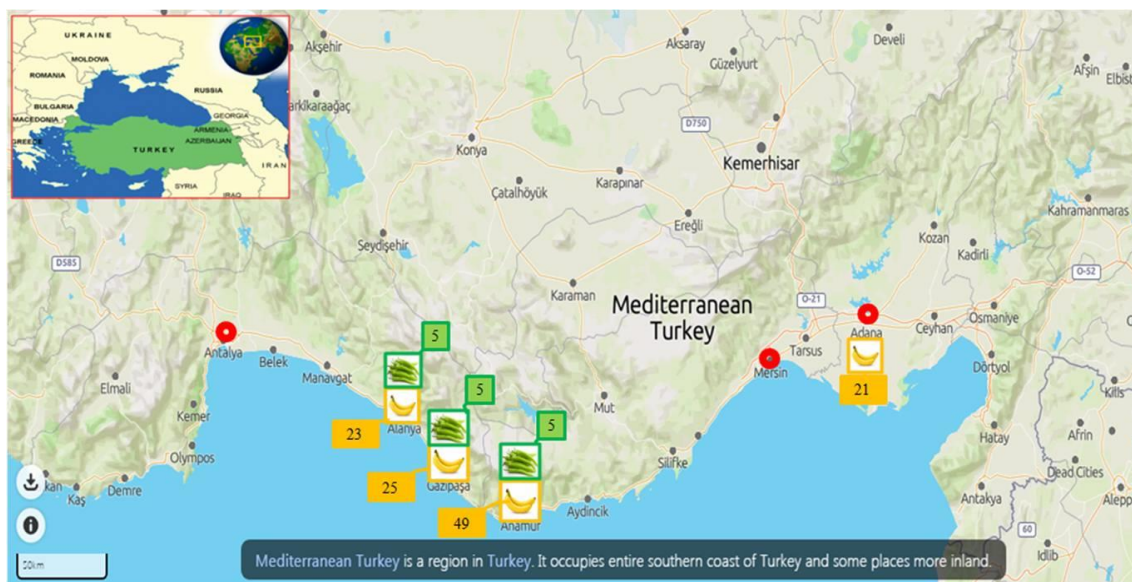


Figure 1. Origin and number of samples per site from sampling area.
(<https://www.countryreports.org/travel/Turkey.html>;
https://mapcarta.com/Mediterranean_Turkey/Map)

Green pepper plants, has been sampled which are grown for non commercial purposes at suitable places of the banana plantations. The typical symptom showing banana and pepper plants PCR product used for analyses.

Serological tests

The samples, were labelled and placed in separate plastic bags, they were brought to the Virology Laboratory placed in ice bucket and kept at 4 °C. All samples were processed within 24 h.

Double antibody sandwich enzyme linked immunosorbent assay (DAS-ELISA)

For the identification of viruses infecting *Musa spp.*, leaf samples were tested by DAS-ELISA using polyclonal antiserum specific to the following viruses: BBTV (*Banana bunchy top virus*), CMV (*Cucumber mosaic cucumovirus*), TMV (*Tobacco mosaic tobamovirus*), TSWV (*Tomato spotted wilt orthotospovirus*), PVY (*Potato Y potyvirus*), BCMV (*Bean common mosaic potyvirus*), WMV-2 (*Watermelon mosaic 2 potyvirus*), PRSV (*Papaya ringspot virus*) *Potygroup* and Orthotospovirus Etc. specific antisera purchased from Agdia USA, Bioreba AG, Switzerland and Loewe® Biochemica GmbH, Germany, respectively.

Tests involved detection of viruses in infected young leaves and were carried out according to Clark and Adams (1977). Polystyrene microtiter plates were coated with 1:200 dilution of gamma globulin. The leaves of infected young plants were grounded in the extraction buffer (phosphate buffered saline, PBS, pH 7.0). Plant samples were applied at a dilution of 1/5 (Wff) in PBS (pH 7.0), containing 0.05 volumes Tween-20, 0.2% polyvinyl pyrrolidone (PVP-40) and 2% bovine serum albumin (BSA). IgG-conjugate was applied at the concentration of 1 ul/200 ul (Agdia and Loewe) and 1 ul/1000 ul (Bioreba). Alkaline phosphatase conjugate was used at a 1/1000 dilution.

Results were acquired spectrophotometrically at 405 nm wave length with a Medispec ESR 200 ELISA microplate reader. Also, negative controls (healthy samples), twice the mean value of healthy specimen were considered as positive. Positive controls of all viruses were supplied in lyophilized form with the kits and were resuspended in the sample buffer as recommended by the manufacturer (Agdia, Inc.).

Total RNA isolation, reverse-transcription polymerase chain reaction (RT-PCR) and phylogenetic analysis

Total RNA extracts (Dellaporta et al., 1983) of BSV, CMV and BBTV suspected banana samples were used in a PCR and RT-PCR (Reverse-Transcription Polymerase Chain Reaction) with BSV5466 5'-AGAGTGGGTTTCATCAAGTAGC and primer BSV 6196 5'-GAATTTCCCGCTCGCATAAG). The primer number indicates 731 bp positions (one cycle of 94 °C denaturation for 4 min, 30 cycles each at 94 °C for 30 s, gradient temp 58 °C for 30 s and 72 °C for 30 s followed by one cycle of final extension for 10 min.) in the BSV genome (Cherian et al., 2004); partially 513 bp CMV CP genes were cloned by sense CMVf TAACCTCCCAGTTCTCACCGT and antisense CMVr CCATCACCTTAGCTTCCATGT primers (95 °C, 45 s.; 52 °C, 30 s; and 72 °C, 45 s and final extension 72 °C for 10 min totally 35 cycles) according to Buzkan and Yüzer (2009); CP.F1 5'ATGGCTAGGTATCCGAAG 3' and CP.R1 5'CCAGAACTACAATAGAATGCC 3'primers, designed for BBTV virus indexing, were cloned partially 530 bp (denaturation for 5 min at 94 °C, then 35 cycles of: 1 min at 94 °C, 1 min at 57 °C, 90 s at 72 °C, and then a final extension for 10 min at 72 °C.) by Mahadev et al. (2013). CP genes of each viruses have been subjected to processing at PCR thermocycler by using Thermo Scientific Verso 1-Step RT-PCR Hot-Start Kit according to manufacturer's protocol.

Standard PCR for DNA viruses and RT-PCR for RNA viruses were used and total RNA was isolated from leaf tissue by the RNeasy Plant Mini Kit (Qiagen).

Analysis of PCR products

PCR reaction mixture (Ten microlitres) was combined with gel loading buffer and analyzed on a 1.5% agarose gel containing 0.5 mg/ml of ethidium bromide and photographed (Sambrook et al., 1989). 100 bp DNA ladder (thermo) or Bio Marker™ Low (Bio Ventures, Inc.) were used on each gel to determine the length of the amplified product. PCR-amplicons run at 100 V for 70 to 80 min, and the gel was stained with ethidium bromide.

Phylogenetic analysis

The PCR products were obtained and directly sequenced by Commercially Sequencing Service. Sequences were compared via databank BLAST on NCBI server (www.ncbi.nlm.nih.gov). Dnasp5 program was conducted for diversification, genetic distance and neighbourhood analyses. According to these analyses, a phylogenetic tree has established by MEGA 7 Program and Neighbours joining method.

Results

Type of symptoms

Mosaic and chlorotic streaking along the veins of the leaves, leading to necrosis, are common.

Virus infected leaves in the fields reduced in size and light colored yellowish necrotic leaf margin areas resembling to mosaic with streaks occurred (*Fig. 2*); There were also, leaf mosaics, necrotic streaks, small narrowed and shapeless malformed leaves (*Fig. 3*), bunchy head formation and general discoloration were observed on the plants (*Fig. 4*). Leaf mosaics, marginal necrosis on banana plants are shown in *Fig. 5*. During harvesting, the plant was cut from the beginning to the end of line. The agricultural worker has not changed or sterilized all cutting equipments. Therefore, all harvested plants could have shown severe disease symptoms. This is clearly indicated that mechanically harvesting will spread the viruses.



Figure 2. Light colored yellowish necrotic leaf margin areas resembling to streaks



Figure 3. Leaf mosaics, necrotic streaks, mosaic, small narrowed and shapeless malformed leaves

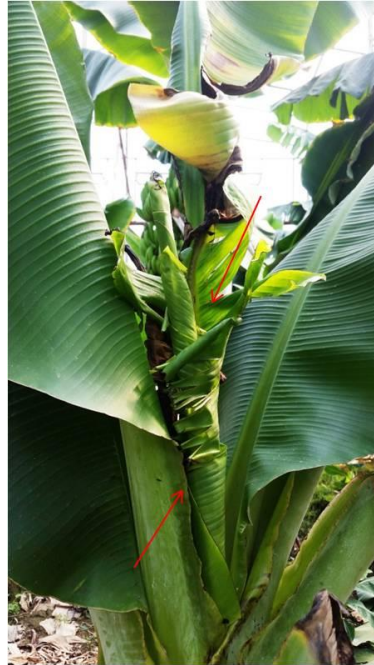


Figure 4. Small-bunchy formation and general discoloration on banana plants



Figure 5. Leaf mosaics, streaks, marginal necrosis on banana plants

Occurrence and detection of viruses by ELISA

As a result of DAS-ELISA, positive results were obtained from CMV (*Cucumber mosaic virus*). While one samples gave suspected BBTV value by DAS-ELISA. In performed serological analyses, 21 out of 118 (with 17.79% incidence) tested samples produced positive reaction with the specific antiserum to CMV. However, none of the

BBTV (*Banana bunchy top virus*), TMV (*Tobacco mosaic tobamovirus*), TSWV (*Tomato spotted wilt tospovirus*), PVY (*Potato Y potyvirus*), BCMV (*Bean common mosaic potyvirus*), WMV-2 (*Watermelon mosaic 2 potyvirus*), PRSV (*Papaya ringspot virus*) *Potygroup* and *Orthotospo* viruses have had strict positive reaction.

CMV is a member of the genus *Cucumovirus* and the family of *Bromoviridae* and have been reported on banana worldwide previously.

There is no commercial antiserum available to study BSV with immune test analyses. BSV can be tested with PCR analyses using DNAs obtained from banana plants.

The RT-PCR amplification

In order to verify the infection, RT-PCR analyses have been done. The target RNA regions (CMV; 513bp and BSV; 731bp) on coat protein partial genes of both viruses, identical for detection, were amplified in the RT-PCR assay. The Amplified RNAs, symptomologically selected from two samples, were yielded an expected product of 513 bp (*Fig. 6*) on agarose gel (2%) electrophoresis. Consequently, RT-PCR results confirmed infections of CMV in DAS-ELISA for positive plants. Additionally, 731 bp cDNA bands of BSV, 5 samples with 4.23% incidence via PCR, were observed. A mix infection by CMV+BSV was verified among them. However, none of the samples that were tested on suspicion of BBTV symptom (*Banana bunchy ball virus*) did not give positive PCR reaction. Symptoms may be related to zinc deficiency.

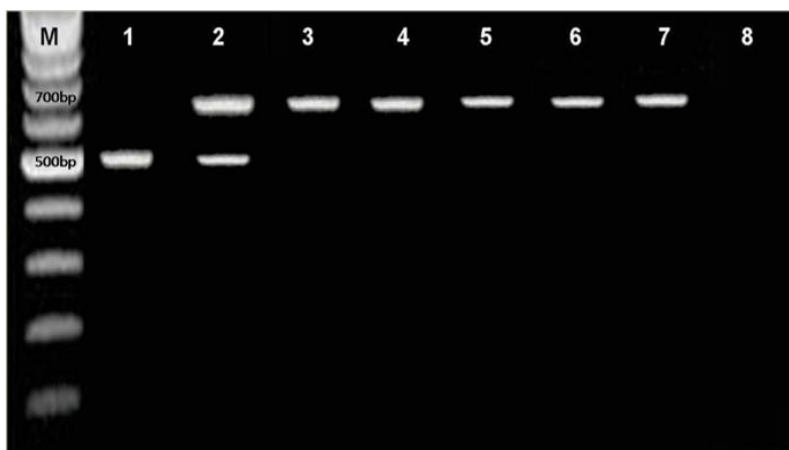


Figure 6. First lane M DNA ladder; RT-PCR product of 513 bp of CMV CP (Lane 1, Lane 2); RT-PCR product of 731 bp of BSV CP (Lane 3 to Lane 7); Also Lane 2 stand as mix infection by CMV+BSV positive samples of *Musa spp.* in Turkey. Lane 8 negative control on agarose gel (2%)

In the light of the observed symptoms, DAS-ELISA and PCR were conducted against nine viruses. Positive results were obtained only against CMV and BSV among all viruses (*Tables 1 and 2*). In addition to species specific ELISA, *Potygroup* and *Orthotospo* group specific polyclonal antisera were not given positive results for all collected samples.

Table 1. The sample distribution by province, presence of viruses assayed by ELISA-PCR

Provinces	Collected samples	CMV	BBTV	BSV	TMV	PVY	WMMV2	PRSV	BCMV	TSWV
Antalya	48	48/6⁺	48/0	48/2⁺	48/0	48/0	48/0	48/0	48/0	48/0
Adana	21	21/0	21/0	21/0	21/0	21/0	21/0	21/0	21/0	21/0
Mersin	49	49/15⁺	49/0	49/3⁺	49/0	49/0	49/0	49/0	49/0	49/0
Toplam	118	118/21		118/5						

⁺Infected samples assayed by DAS-ELISA and RT-PCR

According to DAS-ELISA and RT-PCR assays, only four major symptom types are associated with CMV and BSV (Table 2) which were recorded in Gazipaşa, Alanya and Anamur districts. All three of these districts have banana production plantains along the Mediterranean coastline of Turkey.

Table 2. Observed symptom types and test results by province in terms of CMV and BSV

Provinces/districts	Symptom types			
	Mosaic	Chlorosis	Streaking	Necrosis
Antalya/Gazipaşa	11/2 ^{a,b}	4/1 ^{a,b}	6/1 ^b	4/1 ^{a,b}
Antalya/Alanya	10/2 ^{a,b}	3	7/1 ^b	3/1 ^{a,b}
Mersin/Anamur	19/7 ^{a,b}	10/5 ^{a,b}	14/3 ^b	6/3 ^{a,b}
Adana	13	4	-	4

^aELISA, ^bPCR

Phylogenetic analysis

Sequence and phylogenetic analyses have been shown that banana CMV and pepper CMV isolates are viruses with exactly the same haplotype. Banana and pepper plants include same CMV isolate sequences (Fig. 7) and the virus isolate has spread from pepper to banana. Virus infestation may also occur mechanically or via aphid vectors.

Phylogenetic tree was performed by MEGA 7 Program and Neighbour joining method from 2 symptomologically selected banana and pepper plants. The banana sample (TRAnCMVB, accessed as new record to NCBI system with accession number: MH931390) is a Banana CMV isolate (Fig. 7; Tables 3 and 4). A different haplotype was determined by RT-PCR and sequences. The results of comparison with isolates from other countries were submitted to NCBI system as new records. The results were clarified that these isolates have similar homology with pepper CMV isolate as TRAnCMVP (accessed as new record to NCBI system with accession number: MH931391) (100%-Turkey) and HE971674.1 pepper isolate (88%-Tunisia); KC559757.1 melon isolate (87% Bosnia and Herzegovina); KT270571.1 melon isolate (88% Serbia) and KJ789892.1 squash isolates (87% South Africa) were grouped into Ia (Fig.7; Tables 3 and 4). This result shows that the pepper and banana isolates are the same.

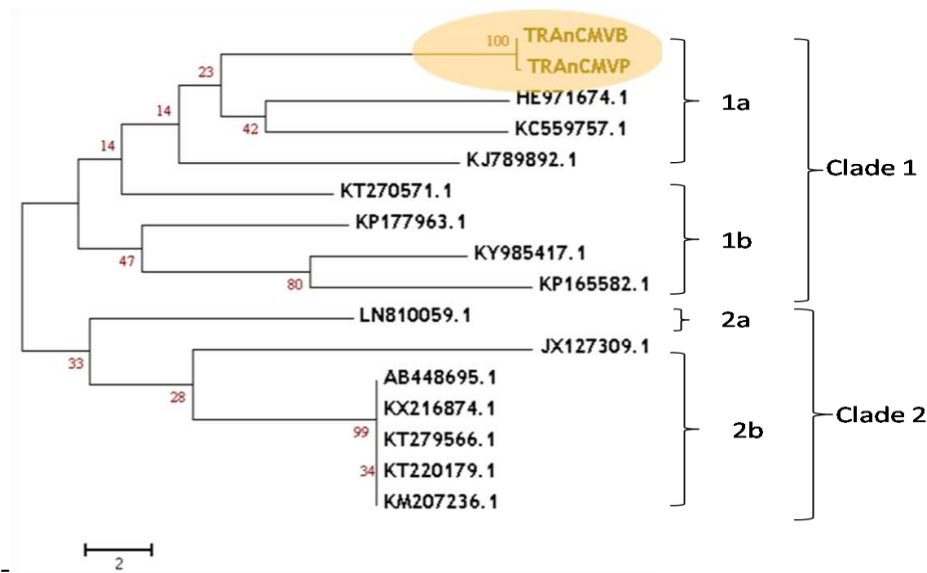


Figure 7. Phylogenetic tree of Turkish Antalya Banana CMV haplotype had branched with Group 1a

Another phylogenetic tree was performed by MEGA 7 Program and Neighbour joining method for one BSV banana isolates as TRAnBSV (accessed as new record to NCBI system with accession number: MH931389) (Fig. 8; Tables 5 and 6). Two different haplo group (CladeI and CladeII) were determined by sequences. This different isolate was compared with the isolates of other countries. Their results were submitted to the NCBI system as new records. The results were clarified that this isolate have similar CladeIb homology with AM905905.1 (97% - Kenya) and KU759865.1 (98% - Democratic Republic of Congo).

Table 3. Phylogenetic tree pair wise distance matrix of CMV haplotypes of different countries and Turkish CMV banana and pepper isolates from Antalya

TRAnCMVB	0.02	17.80	21.69	16.41	27.88	17.58	30.79	27.83	27.91	19.46	30.15	27.83	18.86	17.98	27.92
TRAnCMVP		17.36	27.12	15.97	27.35	17.40	31.03	27.31	27.32	19.13	30.47	27.31	19.32	17.80	27.40
HE971674.1			28.78	21.62	26.67	17.83	26.74	26.62	26.71	27.18	17.74	26.62	15.71	14.73	26.67
KY985417.1				17.39	27.12	21.13	18.17	27.17	27.08	16.85	11.51	27.17	20.22	18.83	27.12
JX127309.1					15.89	29.98	26.36	15.89	15.89	17.98	21.40	15.89	26.41	20.46	15.86
KX216874.1						18.86	15.67	0.01	0.00	21.50	28.49	0.01	26.29	27.96	0.00
KT270571.1							20.12	18.86	18.83	18.65	18.95	18.86	16.34	21.54	18.83
LN810059.1								15.67	15.67	20.18	32.96	15.67	17.70	18.68	15.67
KT220179.1									0.01	21.50	28.44	0.00	26.24	27.91	0.01
KT279566.1										21.48	28.52	0.01	26.29	27.92	0.01
KP177963.1											17.42	21.50	20.11	21.53	21.47
KP165582.1												28.44	19.62	26.11	28.44
KM207236.1													26.24	27.91	0.01
KJ789892.1														20.65	26.29
KC559757.1															27.96

Table 4. The isolates which are listed in phylogenetic tree with Turkey Banana CMV isolate

Bootstrap code	Origin	Host	Identity %
TRAnCMVP	Anamur/Turkey	<i>Capsicum annuum</i>	100
TRAnCMVB	Anamur/Turkey	Banana	100
HE971674.1	Tunisia	<i>Capsicum annuum</i>	88
KY985417.1	Macedonia	<i>Capsicum annuum</i>	88
JX127309.1	Serbia	<i>Solanum lycopersicum</i> (Tomato)	88
KX216874.1	Democratic Republic of the Congo	<i>Musa acuminata</i>	87
KT270571.1	Serbia	<i>Cucumis melo</i>	87
KT279566.1	Iran	Cucumber	87
LN810059.1	Greece-Lesvos	<i>Citrullus lanatus</i>	87
KT220179.1	Egypt	Banana	87
KP177963.1	India	<i>Canna generalis</i> Cv. Allengheny	87
KP165582.1	Germany		87
KM207236.1	Egypt-Giza, Governorate	Tomato	87
KJ789892.1	South Africa	<i>Cucurbita pepo</i> L	87
KC559757.1	Bosnia and Herzegovina	<i>Cucumis melo</i> (Melon)	87
AB448695.1	Syria-Hama	<i>Solanum tuberosum</i>	87

Table 5. Phylogenetic tree pair wise distance matrix of BSV haplotypes of different countries and Turkish BSV banana and pepper isolates from Antalya

TRAnBSV	4.02	6.26	4.06	5.76	5.91	4.39	4.71	4.44	5.84	7.07	4.10	3.76	6.33
KJ013506.1		1.74	0.02	5.93	5.95	4.70	3.89	4.07	5.74	4.42	4.45	3.70	6.06
DQ859899.1			1.84	4.24	4.29	4.41	4.02	3.57	4.18	3.91	4.39	3.61	3.68
AJ002234.1				6.03	6.05	4.70	4.04	4.03	5.86	4.55	4.47	3.57	5.91
KF545102.1					0.05	6.30	6.08	4.28	0.08	4.28	6.14	3.63	4.69
KF545124.1						6.18	6.14	4.27	0.11	4.32	6.18	3.74	4.62
JQ346523.1							3.99	3.83	6.14	5.88	5.72	3.52	3.83
FJ594909.1								3.35	5.86	4.08	4.35	3.91	4.63
EU076424.1									4.23	4.24	3.82	2.65	3.92
KF545103.1										4.40	5.88	3.64	4.68
KT339346.1											4.20	4.17	5.72
AM905905.1												3.93	5.82
KU759865.1													4.15
AF215816.1													

Table 6. The isolates which are listed in Phylogenetic tree with Turkish Banana BSV isolate

Bootstrap code	Origin	Host	Identity %
TSAnBSV	Turkey-Anamur	Banana	
KJ013506.1	France: Montpellier	"	97
DQ859899.1	India	"	97
AJ002234.1	Nigerian	"	97
KF545124.1	Uganda	"	97
KF545103.1	Tanzania	"	93
KT339346.1	China: Guangzhou	"	97
KF545102.1	Kenya	"	97
JQ346523.1	India	"	98
FJ594909.1	South China	"	98
EU076424.1	Colombia	"	99
AF215816.1	Australia: N. Queensland	"	97
KF548092.1	Brazil	"	98
AM905905.1	Kenya	"	97
KU759865.1	Dem. Rep. of the Congo	"	98

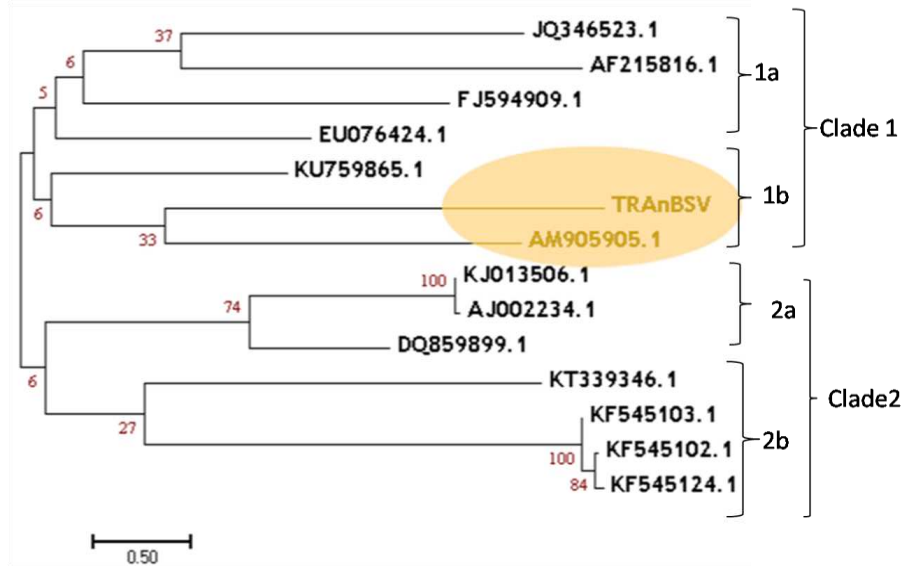


Figure 8. Phylogenetic tree of Turkish Antalya Banana BSV haplotype had branched with Group 1b

Discussion

The Mediterranean coast line is an important agricultural production area and all kind of commercial ships are visiting for trade. This study revealed the natural distribution and occurrence of banana viruses in this area. Our results pointed out that the sanitary conditions in banana growing fields are very important in Turkey to prevent the spreading of common plant viruses. CMV is the most widely spread virus, infecting banana crops in Turkey, it belongs to the genus Cucumovirus and it is transmitted by aphids. Management of these vectors are difficult. The symptoms on collected plants have been assigned to CMV and BSV by mixed infection. CMV infection causes typical leaf mosaic symptoms, mosaic may become necrotic when mixed infection occurs with BanMMV or BSV (Teycheney et al., 2005). These results fit with our results where our collected samples from Antalya samples generally showed a severe mosaic and became necrotic, when had CMV mixed infection with Banana streak mosaic virus (BSV). Similarly, Daniells et al. (2001) pointed out BSV infection have caused yield losses and severe mosaic symptoms. Discrete dark spots may appear on the petiole of the infected plants, pseudostem splitting, fruit bunch emerges from pseudostem, cracks on the skin of fruits occur, which become impossible to commercialize (Teycheney et al., 2005). The most characteristic symptoms of BSV infection are chlorotic and necrotic streaks on the leaves which have been recorded from Turkey BSV banana isolates by Lockhart and Jones (1999). Severe symptoms are correlated with high virus titres (Dahal et al., 1998a, b; 1999). With increasing concern about BSV, there is relatively little information on the effect of virus infection on yield of bananas. In one study in the Ivory Coast, the reduction in yield of cv. Poyo bananas (*Musa spp.* AAA group, Cavendish subgroup) was estimated to be from 7% to 90%, depending on the severity of symptoms (Lassoudière, 1974). Banana streak infections (BSVs) involve a complex of badnaviruses from the family Caulimoviridae known to contaminate *Musa sp.* around the world (Bhat et al., 2016).

The study was focused on BSV due to first occurrence on banana, cultivated in Turkey; Although BSV has a narrower host range than CMV, the BSV may survive in various banana plantains that are imported materials and cuttings as a reservoir. In addition, the presence of vector mealybug in the greenhouse and outside, and the lack of biological and chemical control agents, increase the risk of infection. These results allow CMV to be spread more by aphids from cultivated vegetable crops such as; pepper, melon, squash, tomatoes, are cultivated by farmers in the local area or near the banana greenhouse to meet household consumption need. It also originates progressively from different weed species and occurs after infection with infected seedlings or inoculum sources. Previous studies have found CMV in Turkey (Yılmaz, 1976). The destructive effect of CMV on Turkish banana production has been detailed by same researcher. If It's not well controlled. The current results have verified the previous results that banana plants infected with CMV could be limiting banana production. But overall, CMV has a low impact on production as it can be well controlled (Teycheney et al., 2005)

This is the first report of BSV and BSV+CMV mix infection infected banana in the Eastern Mediterranean Coastline of Turkey. Also it confirms reliable laboratory molecular methods that previous reports include of CMV on banana using serological, symptomologically and biological indexing in Turkey by Yılmaz (1976), Sertkaya (2016) and Tohumcu and Kamberoğlu (2018). BSV have been transmitted not only by mealy bug but also by sucker. Also tissue culture propagation has an importance. It can cause major economic yield loss. Eradication, Certified Material and Vector Management are important strategies to overcome the BSV.

In Cuba, Higginson et al. (2016) focused on some BSV strains on tetraploid banana cvs. FHIA 23. Banana leaf tests were gathered at arbitrary from symptomatic or potentially non-symptomatic plants in four FHIA 23 plots situated in El Mambí in Ciego de Avila area, Bayamo in Granma, Quivicán in Mayabeque and Santo Domingo in Villa Clara areas. Gathered samples were prepared and recorded for the nearness of BSV species BSOLV, BSGFV, and BSIMV by multiplex immunocapture PCR (M-ICPCR), An aggregate of 84 tests were gathered. Just a single plant at El Mambí was symptomatic with indications comprising of slight chlorotic leaf streaks. While BSOLV and BSGFV species were recognized in 12% of the 84 filed FHIA 23 tests, the species BSIMV did not show up in any example of this cultivar. Contaminated FHIA 23 tests were just recognized in the eight-month manor of El Mambí in Ciego de Avila. 17% (9/52) of the examples were distinguished contaminated by BSOLV in this area, including the plant showing chlorotic leaf streaking. An extra FHIA 23 non-symptomatic example of the same area was contaminated by BSGFV.

We have hypothesized that the BSV might come with ornamental plants which are relatives of banana plants. It is not able to coincidence that the BSV appeared in the banana grown area which is also a very popular place for the ornamental plants at the Eastern Mediterranean Coastline of Turkey. The CMV is commonly seen all over vegetable and fruit grown regions. Our results have clearly indicated that the virus could come from vegetable grown areas to banana grown places.

Bunchy top symptoms can be recorded on young suckers Infected plants are dwarfed and their emerging leaves are small and narrow with brittle, yellow edges. The leaves grow upright and have a stunted, bunched appearance similarly to the results of Teycheney et al. (2005). But there is no obvious result from ELISA and symptomologically suspected samples against Banana bunchy top virus in Turkey.

This paper also indicates that uncontrolled distribution of Banana plants in countries will create the viral problems.

The PCR technique was standardized and successfully applied for CMV and BSV detection. PCR-based detection methods will have the advantage of amplifying the target nucleic acid present even at very low level and it is an attractive technique for the early diagnosis of plant viral agents (Mahadev et al., 2013). Sison et al. (2017) reported four episomal BSV species either in single or mixed infections in the Philippines by Molecular assays.

Molecular analyses have distinguished that there is one CMV haplotype present in Turkey according to their sequences alignments at NCBI system. Sequence alignments have shown Turkey's banana CMV haplotypes (TRAnCMVB) have similar homology with pepper CMV isolate from Turkey as TRAnCMVP and HE971674.1 pepper isolate from Tunisia; KC559757.1 melon isolate from Bosnia and Herzegovina; KT270571.1 melon isolate from Serbia (that could have same origin with Bosnia And Herzegovina) and KJ789892.1 squash isolates from South Africa clustered into Ia although isolates belong to different geographic origins.

To verify BSV banana isolate as TRAnBSV two different haplo group (CladeI and CladeII) were determined by sequences. Results were submitted to the NCBI system as new records, were clarified that this isolate have similar CladeIb homology with AM905905.1 from Kenya and KU759865.1 from Democratic Republic of the Congo. It is concluded that as evidence by phylogenetic analysis, both all CMV and BSV isolates are not identified as belong to new population or groups.

Both CMV and BSV Turkish isolates which are focused on in this study, have been placed to the NCBI system with new accession numbers (NCBI, 2018).

The results have indicated that all exported plant materials can be distributed through any quarantine regulation.

Conclusion

Further studies should be planned for identifying respective vectors and unknown epidemiological features and characteristics of the viruses (Islam et al, 2016). There are new viruses perpetuating in weeds and adjacent crop species in plantains. Novel management strategies for diseases will be devised upon these studies to protect sanitized and resistant plants, often depends on the virulence of pathogen (Razukas et al., 2007). Therefore, the infection pathway and transmissibility of major viruses could be prevented. This can be done by determining the virus ecology and molecular origin, which were another outcome of this study.

Thomas et al. (2015) description of virus diseases emerging from mass spread of contaminated plant materials or from mealybug transmission from neighbouring contaminated plants is obscure. Regardless, it is important to perform more precise and valid analytical strategies to screen the condition of planting material. On the off chance that in vitro culture is utilized, the meristem micropropagation joined with cryotherapy methods will guarantee the evacuation of tainting infections. Sison et al. (2017) determined some preventions, such as host resistance and removal of infected plants, against BSV infections are suitable control practices.

Banana bunchy top virus (BBTV), banana streak virus (BSVs) and cucumber mosaic (CMV) infections are announced to be contaminating bananas habitually all around the world. Successful control of their spread relies upon strong discovery of these infections

in engendering stock, planting material, contaminated nursery plants, and through strict quarantine Zhang et al. (2018).

Tripathi et al. (2019), reported a strategy to inactivate the eBSV by editing the virus sequences, named as CRISPR/Cas9 is a novel approach, as well as editing of endogenous banana streak virus in the B genome of *Musa spp.* Seventy-five percent of the altered plants stayed asymptomatic in contrast with the non-altered control plants. This examination prepares for the improvement of B genome germplasm and its utilization in rearing projects to deliver cross breeds that can be comprehensively spread.

All positive samples detected in this study, have been eradicated. Thus, it was tried to maintain or protect the country's disease free status with the definite destruction of the sources of infection, which were detected on a limited or limited level to comply with agricultural quarantine legal measures.

This report is the primary step to initiate research on the impact of the virus in banana production and germplasm exchange.

Acknowledgements. Thanks to Assoc.Prof. Ozer Çalış and Prof.Dr.Nedim Mutlu for critical review of the publication.

Conflict of interests. The authors declare that they have no conflict of interests.

Ethical approval. This article does not contain any studies with human participants or animals performed by any of the authors.

REFERENCES

- [1] Baggaley, K. (2017): The world's bananas are under attack. But no, they're not about to go extinct. – Environment 13 September. <https://www.popsoci.com/worlds-bananas-under-attack-disease>.
- [2] Bhat, A. I., Hohn, T., Selvarajan, R. (2016): Badnaviruses: the current global scenario. – Viruses 8: 177.
- [3] Buzkan, N., Yüzer, D. (2009): Molecular detection of seed-borne viruses in Kahramanmaraş red peppers. – Alatarım 8(1): 1-7.
- [4] Cherian, A. K., Baranwal, V. K., Malathi, V. G., Pant, R. P., Ahlawat., Y. S. (2004): *Banana streak virus* from India and its detection by polymerase chain reaction. – Indian Journal of Biotechnology 3: 409-413.
- [5] Clark, M. F., Adams, A. N. (1977): Characteristic of microplate method of enzyme-linked immunosorbent assay for detection of plant viruses. – J. Gen. Virol. 34: 475-483.
- [6] Dahal, G., Hughes, J. d. A., Thottappilly, G., Lockhart, B. E. L. (1998a): Effect of temperature on symptom expression and reliability of banana streak badnavirus detection in naturally infected plantain and banana (*Musa spp.*). – Plant Disease 82: 16-21.
- [7] Dahal, G., Pasberg-Gauhl, C., Gauhl, F., Thottappilly, G., Hughes, J. d. A. (1998b): Studies on a Nigerian isolate of banana streak badnavirus: II. Effect of intraplant variation on virus accumulation and reliability of diagnosis by ELISA. – Annals of Applied Biology 132: 263-275.
- [8] Dahal, G., Gauhl, F., Pasberg-Gauhl, C., Hughes, J., d. A., Thottappilly, G., Lockhart, B. E. L. (1999): Evaluation of micropropagated plantain and banana (*Musa spp.*) for banana streak badnavirus incidence under field and greenhouse conditions in Nigeria. – Ann. Appl. Biol. 134: 181-191.

- [9] Daniells, J. W., Geering, A. W. D., Bryde, N. J., Thomas, J. E., Ferguson, M. E. (2001): The effect of *Banana streak virus* on the growth and yield of dessert bananas in tropical Australia. – *Ann Appl Biol* 139: 51-60.
- [10] Dellaporta, S. L., Wood, J., Hicks, J. B. (1983): A plant DNA mini-preparation: version 2. – *Plant Mol Biol Rep* 1(4): 19-21. DOI: 10.1007/BF02712670.
- [11] FAO Data (2015): Food and Agriculture Organization of the United Nations. The Statistics Division of FAO. – <http://faostat.fao.org/>.
- [12] Gambley, C. F., Thomas, J. E. (2001): Molecular characterization of banana mild mosaic virus, a new filamentous virus in *Musa spp.* – *Arch. Virol.* 146: 1369-1379.
- [13] Higginson, E. J., Font, C., Quiala, I., Gonzalez, G., Fonseca, M. A., Echemendía, A. L., Teycheney, P. Y. (2016): Presence of banana streak viruses on the cultivar FHIA 23 in Cuba. – *Fitosanidad* 20(2): 93-94.
- [14] Islam, W., Zhang, J., Adnan, M., Noman, A., Zaynab, M., Wu, Z. (2016): Plant virus ecology: a glimpse of recent accomplishments. – *Applied Ecology And Environmental Research* 15(1): 691-705.
- [15] Karanfil, A., Soylu, B., Korkmaz, S. G. (2016): Çanakkale İli ve İlçelerindeki Soğanlı Süs Bitkilerinde Hıyar Mozaik Virüsü (Cucumber mosaic virüs; CMV) Enfeksiyonunun Araştırılması, Turkey. – 6th Plant Protection Congress with International Participation September 5-8, 2016 Konya, Turkey.
- [16] Koç, G., Fidan, H., Baloğlu, S. (2016): *Zinnia elegans*, Türkiye de *Cucumber mosaic virus* (CMV) için Bir Ara Konukçu Turkey. – 6th Plant Protection Congress with International Participation September 5-8, 2016 Konya, Turkey.
- [17] Lassoudière, A. (1974): La mosaïque dite “à tirets” du bananier Poyo en Côte d’Ivoire. – *Fruits* 29: 349-357.
- [18] Lockhart, B. E. L., Jones, D. R. (1999): Banana Streak. – In: Jones, D. R. (ed.) *Diseases of Banana, Abaca and Enset*. CABI, Wallingford, UK, pp. 263-274.
- [19] Lockhart, B. E. L., Olszewski, N. E. (1993): Serological and Genomic Heterogeneity of Banana Streak Badnavirus: Implications for Virus Detection in *Musa* Germplasm. – In: Ganry, J. (ed.) *Breeding Banana and Plantain for Resistance to Diseases and Pests*. International Network for the Improvement of Banana and Plantain, Montpellier, France, pp. 105-113.
- [20] Mahadev, S. R., Thamilarasan, S. K., Kathithachalam, A. (2013): PCR detection of banana bunchy top virus (BBTV) at tissue culture level for the production of virus-free planting materials. – *International Research Journal of Biological Sciences* 2(6): 22-26.
- [21] Meyer, J. B., Kasdorf, G. G. F., Nel, L. H., Pietersen, G. (2008): Transmission of activated episomal Banana streak OL (badna) virus (BSOLV) to cv. Williams banana (*Musa sp.*) by three mealybug species. – *Plant Dis.* 92: 1158-1163.
- [22] NCBI (2018): Submissions to GenBank/Bankit. – The National Center for Biotechnology Information. <https://www.ncbi.nlm.nih.gov/WebSub/?tool=genbank>.
- [23] Razukas, A., Jundulas, J., Asakaviciute, R. (2007): Potato cultivars susceptibility to potato late blight (*Phytophthora infestans*). – *Applied Ecology And Environmental Research* 6(1): 95-106.
- [24] Saitou, N., Nei, M. (1987): The neighbor-joining method—a new method for reconstructing phylogenetic trees. – *Mol Biol Evol* 4: 406-425.
- [25] Sambrook, J., Fritsch, E. F., Maniatis, T. (1989): *Molecular Cloning: A Laboratory Manual*. – Cold Spring Harbor Laboratory Press, New York.
- [26] Sertkaya, G. (2016): Hatay ilinde Muz Yetiştiriciliğinin Durumu ve Muz Bitkilerinde CMV (Cucumber mosaic virüs) nin Araştırılması, Turkey. – 6th Plant Protection Congress with International Participation September 5-8, 2016 Konya, Turkey.
- [27] Sison, M. L. J., Cueva, F. M. D., Pozon, A. P. M. (2017): Transmission of episomal *banana streak virus* by mealybugs of different host plants. – *J. ISSAAS* 23(2): 203-214.
- [28] Su, H. J. (1998): First Occurrence of Banana Streak Badnavirus and Studies on Its Vectorship in Taiwan. – In: Frison, E. A., Sharrock, S. L. (eds.) *Banana Streak Virus: A*

- Unique Virus–Musa Interaction? Proc. Workshop Promusa Virology Working Group. INIBAP, Montpellier, pp. 20-25.
- [29] Tamura, K., Peterson, D., Peterson, N., Stecher, G., Nei, M., Kumar, S. (2011): MEGA5: Molecular evolutionary genetics analysis using maximum likelihood, evolutionary distance and maximum parsimony methods. – *Mol. Biol. Evol.* 28: 2731-2739.
- [30] Teycheney, P. Y., Lescot, T. (2004): *Viral Diseases of Banana and Plantain*. – CIRAD, Montpellier.
- [31] Teycheney, P. Y., Marais, A., Savanella-Dumas, L., Dulucq, M. J., Candresse, T. (2005): Molecular characterization of banana virus X (BVX) a novel member of Flexiviridae family. – *Arch Virol* 150: 1715-1727. DOI: 10.1007/s00705-005-0567-0.
- [32] Thomas, J. E. (2015): *MusaNet Technical Guidelines for the Safe Movement of Musa Germplasm*, 3rd Ed. – Bioversity International, Italy, Rome.
- [33] Tohumcu, E., Kamberoğlu, A. M. (2018): Türkiye’de muz üretim alanlarında Cucumber mozaik virüs (CMV)’ün RT-PCR tekniği ile teşhisi. – Türkiye VII. Bitki Koruma Kongresi.
- [34] Tripathi, J. N., Ntui, V. O., Ron, M., Muiruri, S. K., Britt, A., Tripathi, L. (2019): CRISPR/Cas9 editing of endogenous banana streak virus in the B genome of *Musa spp.* overcomes a major challenge in banana breeding. – *Communications Biology* 2: 46. <https://doi.org/10.1038/s42003-019-0288-7>.
- [35] Tripathi, S., Patil, B. L., Verma, R. (2016): *Viral Diseases of Banana and Their Management*. – In: Gaur, R. et al. (eds.) *Plant Viruses: Evolution and Management*. Springer, Singapore, pp. 289-308.
- [36] TUIK (2017): Türkiye İstatistik Kurumu Haber Bülteni, Bitkisel Üretim 2. Tahmini. – 2017 Sayı: 24583 27 Ekim 2017.
- [37] Yılmaz, M. A. (1976): Akdeniz Bölgesinde Muzlarda Muz Mozaik Virüsü ve Özçürüklüğü Yapan Fungal Etmenler Üzerine Araştırmalar. – Ç. Ü. Ziraat Fakültesi Bitki Koruma Bölümü Doçentlik Tezi.
- [38] Zhang, J., Borth, W., Lin, B., Melzer, M., Shen, H., Pu, X., Sun, D., Nelson, S., Hu, J. (2018): Multiplex detection of three banana viruses by reverse transcription loop-mediated isothermal amplification (RT-LAMP). – *Tropical Plant Pathology* 43(6): 543-551. <https://doi.org/10.1007/s40858-018-0257-6>.

POTENTIAL OF FLOW CYTOMETRY IN SEX DETERMINATION AND *IN VITRO* MICROPROPAGATION OF *LAURUS NOBILIS* L.

ROYANDAZAGH, D. S.

Department of Agricultural Biotechnology, Faculty of Agriculture, Tekirdağ Namik Kemal University, Degirmenaltı Campus 59030 / Suleymanpasa-Tekirdag, Turkey
e-mail: sdaneshvar@nku.edu.tr; phone: 00905314318608

(Received 31st Jan 2019; accepted 21st Mar 2019)

Abstract. Perennial bay laurel (*Laurus nobilis* L.) is a dioecious economic plant. Its leaves and fruits are considered as important non-wood forest products that are used in food, pharmaceutical, and cosmetic industries. However, it is not possible to distinguish males and females at an early age and this can hinder its multiplication in a planned way. The aim of the present study is to determine the sex of bay laurel at an early stage by analyzing the nuclear DNA (Deoxyribonucleic acid) contents using flow cytometry. The findings of the study showed that the male DNA content is $\geq 7.95 \pm 0.13$ pg and the female nuclear DNA content is $\leq 7.84 \pm 0.10$ pg. After sex determination, female green axillary buds were cultured on MS (Murashige and Skoog) medium containing different combinations including BAP (6-Benzylaminopurine), NAA (1-Naphthaleneacetic acid) and GA3 (Gibberellic acid) for 42 days to induce micropropagation of the buds. The results indicated 100% shoot regeneration with 2.5 ± 0.85 shoots per explant on MS medium containing 6.6 μ M BAP, 5.4 μ M NAA, and 0.6 μ M GA3. Each randomly selected 45 female shoots were rooted on MS medium containing 4.90 μ M IBA (Indole-3-butyric acid) for 12 weeks. Only 16 among them induced roots. However, 13 female plantlets, upon their transfer to pots, showed continuing viability and successful acclimatization to external conditions. Distinguishing sex of bay laurel plants at an early age and establishment of a rapid propagation protocol could offer a significant benefit in breeding and plant production.

Keywords: bay laurel, *Laurus nobilis* L., DNA content, dioecious plant, micropropagation, acclimatization, sex determination, adult plants

Introduction

The family of Lauraceae has 45 genera and 2850 known species worldwide (Maarten and Christenhusz, 2016). Different ploidy levels have been described, in *Laurus* with tetraploidy ($2n = 4x = 48$), as the most frequent karyotype (Ehrendorfer et al., 1968). Bay laurel has spread over Tropical Asia, America, Africa, and Mediterranean countries (Darlington and Wylie, 1955). It can resist temperatures as low as -15°C in natural distribution areas (Lanzara, 1978). The hairless dark green leaves and black fruits are highly aromatic due to the presence of oil-filled cavities (Villar, 1986). Both fruits and leaves contain different types of essential oils with different quantities in them. These contain 25-30% green, aromatic oil consisting of a variety of fatty acids, including glycerides of acetic, oleic, linoleic, stearic, palmitic, myristic, and lauric acids, and free acetic acid oil (Panza et al., 2011). Both, its fruits and leaves are significantly important in pharmaceutical, food and cosmetics industries (Ercan, 1983). The dried leaves exclusively used to flavor foods as they produce about 1.3% essential oils containing 45% eucalyptol, 12% terpenes, 8-12% terpinyl acetate, 3-4% sesquiterpenes, 3% methyleugenol, and other α - and β -pinenes, phellandrene, linalool, geraniol, and terpineol. Their concentrations are inconsistent and differ with the antagonistic stage of plant growth. Generally, the highest oil percentage is obtained from dried leaves during mid-summer harvest (Tanrıverdi et al., 1993; Konukçu, 2001; Kilic et al., 2004). Therefore, early identification of the plants is of significant importance. The strategies

to multiply male and female plants have significant importance and could be planned at an advanced stage of growth and with a purposeful and positive contribution to the economy of Turkey (Ercan, 1983). Anatolia and Balkans are considered as the origin of bay laurel. Nowadays, it grows in all of the Mediterranean countries (Algeria, Turkey, Italy, Greece, Morocco, Portugal, Spain, Albania, Romania and in the Greek islands in the Aegean Sea, on the eastern coasts of Libya, the western part of Syria, Israel, Palestine), Northern Europe (Belgium, France), The Black Sea coast of Russia, Georgia, Crimea, and Mexico at altitude of 600-800 m above sea level in temperate regions (Göker and Acar, 1983; Demir et al., 2004). The bay laurel Essential Oils (eugenol, cineol and geraniol), account for the distinctive spicy aroma and are extracted from its fruits and leaves (Konukçu, 2001). It is also considered in manufacturing perfumes and soap in many parts of the world (Tanrıverdi et al., 1993; Dhifi et al., 2018). Phenotypic sex determination is practically not possible during the early stages of the development of dioecious plants. It is possible to determine the ploidy level of plants by using flow cytometry for measuring the amount of nuclear DNA in plants. The data Information about genome size is a very important factor in determining the biodiversity of a large number of biological fields (Zonneveld, 2005). The flow cytometry could be used for plants' early sex determination studies. The identification and sex determination of dioecious plants could provide a significant advantage in production, multiplication, and breeding of plants (Bennett and Smith, 1976; Tuna, 2016). Therefore, the purpose of this study is to develop a protocol for sex determination of bay laurel seedling after their germination and establish micropropagation protocol in female sapling through axillary stem buds.

Materials and Methods

Plant material

The fresh bay laurel seeds were purchased from Yalova seed vendor in the open market. The number of chromosomes was determined as 48 in different studies. These seeds were stored at room temperature for 2 weeks and were, then, germinated at + 4°C for 6 weeks. All treatments of sex determination, regeneration and rooting experiments were carried out in Department of Agricultural Biotechnology and Department of filed crop Tekirdağ Namik Kemal University, Tekirdağ, Turkey.

Sterilization and germination

The seeds were first rinsed with 2% solution of Tween 20, followed by sterilizing with 20, 40, 60, 80, and 100 percent commercial bleach (containing active 5% NaOCl – Ace, Turkey), and ensued by 4× 4 times rinsing with bidistillated and sterilized water. Seeds with 100 less pericarp were, then, germinated on MS medium (Murashige and Skoog, 1962) and supplemented with 30 g/l sucrose in glass tubes (1 seed/test tube) of adjusted pH to 5.7±0.1 For germination, these seeds were cultured in Sony versatile environmental chambers under 24 ± 1°C using 16 hours' light/ 8 hours' dark photoperiod.

After seed germination, the leaf samples of *in vitro* germinated plants were taken for sex determination analysis by flow cytometry. Adult male and female plants were also analyzed for the purpose of comparison along the freshly germinated seedlings for

comparison purpose and validate the results. The regeneration studies were initiated by taking green shoot buds from respective female seedlings.

Flow Cytometry and Sex Determination

Fully developed bay laurel leaf samples were taken from 2-month-old seedlings and were cultivated under *in vitro* conditions; barley (*Hordeum vulgare*) 2C DNA=10.65 pg was used for estimation of genome size in *Laurus nobilis* in flow cytometry with the fluorescing DNA stain 4',6-diamidino-2-phenylindole (DAPI) as per manufacturer's instructions (Thermofisher Scientific Waltham, Massachusetts USA). The nuclear DNA quantification studies were set up using 3 replications.

Estimation of nuclear DNA content

The 10-15 mg samples were taken from the leaf tissues of barley grown by the standard *in vivo* and leaf tissues of bay laurel germinated by *in vitro* conditions; they were cultured in Petri dishes on MS medium afterwards. By adding 1 ml of A stock solution (20 ml MgSO₄ buffer, 20 mg Dithiothreitol, 500 µl DAPI stock, 550 µl TritonX-100) to the petri dish (Arumuganathan and Earle, 1991; Noirot et al., 2002), the plant tissues were decomposed with razor blades until they were crumbled away in the solution. The solution was filtered (30-33 µm) and followed by micro-centrifuging. The Supernatant, formed in the bottom of the micro-centrifuge tube, was dissolved in 400 µl B solution (5 ml solution A, 10 µl RNase and DNase free). Thereafter, the prepared samples were incubated in 5 ml glass tubes for 15 minutes at 37°C temperature. The samples were analyzed by flow cytometry (Partec) device (Tuna et al., 2001; Savas Tuna et al., 2017). The absolute DNA content of 58 germinated bay laurel seedlings was calculated by using the values of the fluorescence intensities of the M1 peaks at the selected standard and the following formula, as a picogram (Zonneveld et al., 2005; Aydın Akbudak et al., 2018), was used for this purpose:

$$\text{Sample DNA content 2C} = \frac{\text{mean of sample peak (M1)}}{\text{mean of sample peak (M1}_i\text{)}} * \text{Standard DNA content 2C (Eq.1)}$$

The data used in the formula was obtained from flow cytometry analyses. The separation of the male and female plant, by measuring their DNA content quantities, were conducted and the results were later compared with the results of Parlar (2017).

In vitro Micropropagation

The plant is difficult to multiply due to high oxidation of phenolic compounds (25-30% essential oil in female plants compared to males with 1.3% essential oils only). The idea was to use female plants that are more prone to necrosis and compared to male plants with lesser concentrations of essential oils and phenolic compounds. Therefore, axillary bud explants from the female seedlings, grown under *in vitro* conditions, were cultured on MS medium containing different combinations and concentrations of BAP, NAA and GA3.

Rooting and acclimatization

The growing shoots were re-cultured on MS medium containing 4.4 µM BAP. The 45 regenerating shoots were rooted in MS medium containing 2.24, 4.90 and 7.35 µM

IBA in sterile glass jars. At this stage, the bay laurel seedlings (5-10 cm in length) were washed with tap water without harming the leaves and roots. These were transferred to sterilized peat moist in 500 ml paper cups. The pots were covered with transparent polythene bags and were left to grow in an environmental chamber. The bags were gradually perforated at the end of the second week to increase air circulation and to reduce the humidity 40-50% at +25±2°C (Dewir et al., 2015). This was done to adapt the plants to external conditions. The polythene bags were completely removed later and the plants were left to grow and harden in the environmental chamber. These plants were watered with liquid MS medium once in a month.

Statistical analysis of regeneration studies

All treatments of regeneration and rooting experiments used 15 explants (unless otherwise mentioned) which were divided equally into three replicates containing 5 explants each (3 replications x 5 explants = 15 explants); treatments were repeated twice afterwards. Statistical analysis of the data was carried out by using IBM SPSS18 (Statistical Package for the Social Sciences) computer software. The means were separated by using the Duncans Multiple Range Test and the percentage values were subjected to “arcsine transformation”, before carrying out the statistical analysis (Snedecor and Cochran, 1982).

Results

Surface Sterilization and Germination of bay laurel

Out of different commercial bleach concentrations used for sterilization of bay laurel seeds, 60-100% commercial bleach concentration showed the most optimum results with 80% seed germination and development of no fungus or bacterial contamination of the seeds. However, the 80-100% commercial bleach concentration had negative impacts on the growth and development of seeds. The results are given in *Table 1*.

Table 1. Effects of different concentrations of Sodium of Sodium hypochlorite (NaOCl) on contamination and germination of with pericarp and without pericarp seed of *Laurus nobilis* L.

Concentration of in percentage Sodium hypochlorite (NaOCl) (%) for sterilization of Seeds with pericarp	Contamination percentage (%)Seeds with pericarp	Germination percentage (%)Seeds with pericarp
100	26.5±0.0b	0.0±0.0c
80	39.2±0.0c	0.0±0.0c
60	50.7±0.0d	0.0±0.0c
40	63.4±0.0e	0.0±0.0c
20	90.0±0.0f	0.0±0.0c
0 (control)	90.0±0.0f	0.0±0.0c
Without pericarp	Without pericarp	Without pericarp
100	0.0±0.0a	22.7±10c
80	0.0±0.0a	71.5±20a ←
60	0.0±0.0a	63.4±28a
40	30.0±10b	45.0 ±11b
20	77.0±10f	12.9±5.7c
0 (control)	90.0±0.0f	0.0±0.0c

Means shown by different small letters in a single column are statistically different at 0.01 level of significance using Duncans multiple

The contamination percentage had a range of 26.57–90%, however, the concentration was decreased by each increase in the commercial concentration of commercial bleach on seeds with pericarps. No seed germination was noted irrespective of the commercial bleach concentration treatment and control treatment. The contamination percentage had a range of 0.00–77.08% and decreased with each increase in the concentration of commercial bleach on seeds without pericarps. No contamination was noted on seeds treated with 60-100% commercial bleach. The study indicates seed sterilization and their germination behavior with and without pericarps. The contamination rate was lower and the germination percentage was higher on the seeds. On pericarps removal, germination percentage had to be ranged between 0-80%.

Flow cytometry and sex determination

In seeds without a pericarp, 60% NaOCl concentration was applied and 58 stable bay laurel seeds were germinated. The DNA content and average of bay laurel was calculated by in flow cytometry with the fluorescing DNA stain 4',6-diamidino-2-phenylindole (DAPI) analysis with Partec device on the Fully developed bay laurel leaf samples of these seedlings. The obtained DNA content of 58 bay laurel seedlings and 50 samples each from known male and female plants were taken as control treatment and were, then, compared with the studies. The number of chromosome $2n = 2x = 48$ in the female and male plants, in the average DNA content of the plant, showed a 0.05 difference between male and female plants. It was observed that the male DNA contents of the male and female plant were slightly, a small margin of 0.11 pg, higher than the female plants. According to Parlar (2017), determined DNA contents of 84 male and female plants, were separated into independent groups by being subjected to t-test analysis, whereby the DNA content of the female plants was reported as 7.84 ± 0.10 pg and the DNA content of the male plants was 7.95 ± 0.13 pg. The results of this study showed that the DNA content of bay laurel, ranged between 7.04–8.14 pg, was divided into two groups; the male plants had nuclear DNA content of $\geq 7.95 \pm 0.13$ pg and the female ones had nuclear DNA content of $\leq 7.84 \pm 0.10$ pg. The result of this study showed that 43 out of the 58 seedlings were females and 16 of them were males (Fig. 1). The DNA content of the previously known males of $\geq 7.95 \pm 0.13$ pg and females of $\leq 7.84 \pm 0.10$ pg also showed the same threshold level in their DNA contents.

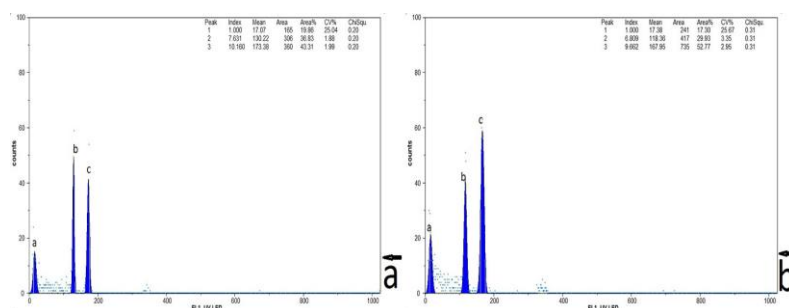


Figure 1. Comparative schematic representation of *Laurus nobilis* histograms showing flow cytometry analysis of isolated nuclei of male and female plants (a) peak a- fragmented nuclei, chromosomes, plastids and other organeller; peak b- M1, *L. nobilis*, male seedlings DNA content of 7.99 pg, peak c- M2 nuclear DNA content of Barley (*H. vulgare*) (b) peak a- fragmented nuclei, chromosomes, plastids and other organeller; peak b- M1, female seedling nuclear DNA content of 7.51 pg, peak of *L. nobilis*, peak c- M2 nuclear DNA content of Barley (*Hordeum vulgare*)

In vitro Micropropagation

The axillary bud explants, obtained from 2-month-old female bay laurel seedlings, germinated under *in vitro* conditions using by flow cytometry, were transferred to MS medium containing different doses and combinations of BAP, NAA, and GA₃. The shoot regeneration was noted on all shoot buds irrespective of their concentrations and combinations of BAP+NAA+GA₃. The best shoot regeneration was noted on MS medium as containing 6.6 μM BAP+ 5.4 μM NAA+ 0.6 μM GA₃ (Fig. 2a, b).

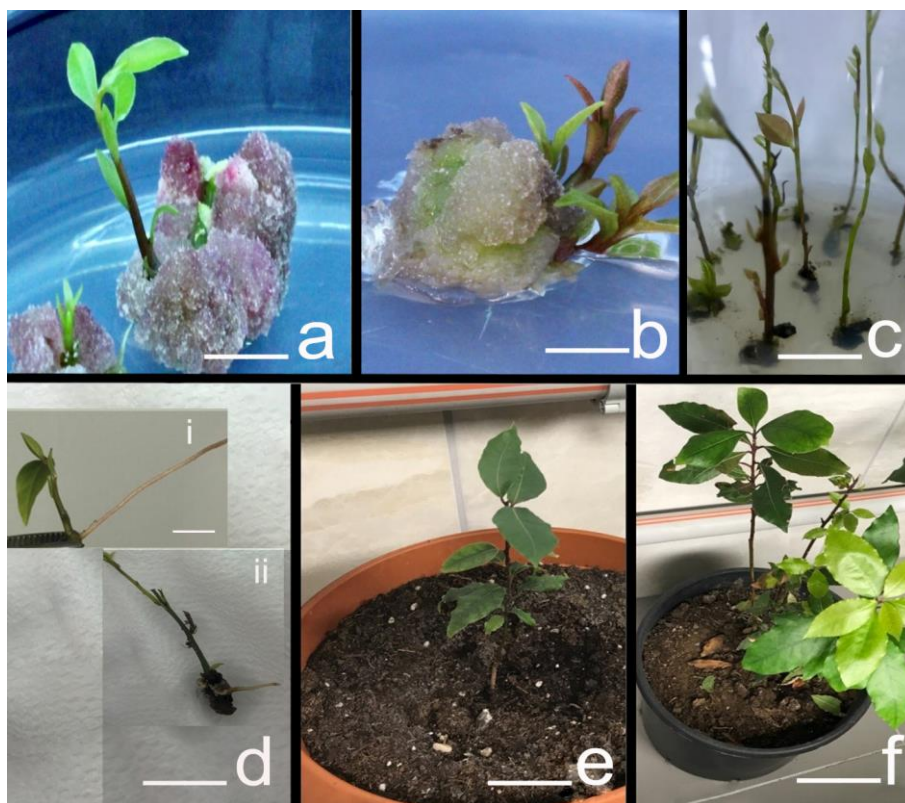


Figure 2. *In vitro* regeneration from female shoot buds on axillary bud explants of *L. nobilis* (a) induction of shoots on axillary buds induced calli of female using 6.6 μM BAP+ 5.4 μM NAA+ 0.6 μM GA₃ (c) rooting of *in vitro* regenerated shoots using 4.90 μM IBA (d) rooted shoots of female shoots (e) the saplings transferred to pots after 3 months in environmental chamber (d) the saplings ready for transfer to fields with profuse growth of leaves. bar in frame (a,b) 1.1 cm (c)1.25 cm (d-i) 1cm (d-ii) 1.2cm (e) 1.5 cm (f) 2cm

After 42 days (2 × subcultures), the data were collected by testing the growth of the regenerating female shoots. The shoots regenerating on the explants, after their excision as single female shoots, were transferred to MS medium for 28 days. The Analysis of variance results showed that shoot regeneration percentage (%), the average number of shoots per explant, and their shoot length showed significant differences among treatment means. The maximum number of shoot induction per explant was obtained as 2.5±0.85 on MS nutrient medium containing 6.6 μM BAP+5.4 μM NAA +0.6 μM GA₃. In terms of shoot percentage, the best results were obtained on the MS medium containing 8.8 μM BAP+2.7μM NAA +0.6 μM GA₃. The longest shoots were obtained on MS medium containing 6.6 μM BAP+ 5.4 μM NAA + 0.6 μM GA₃ (Table 2).

Table 2. Effects of different concentrations of NAA, BAP and GA3 on regeneration of shoots after 42 days of culture from axillary buds of *Laurus nobilis*

Medium (μ M)			Shoot regeneration percentage (%)**	Number of shoots per explant*	Shoot length (cm)*
BAP	NAA	GA3			
4.4	2.7	0.6	60.0 \pm 26.61abc	1.0 \pm 0.0b	0.2 \pm 0,0bc
4.4	5.4	0.6	26.5 \pm 0.0 c	1.0 \pm 0.0b	0.2 \pm 0,1bc
4.4	8.1	0.6	21.9 \pm 20.0c	0.6 \pm 0.5b	0.1 \pm 0,0c
6.6	0.5	0.6	35.0 \pm 7.3bc	1.2 \pm 0.2b	0.3 \pm 0.2abc
6.6	5.4	0.6	54.9 \pm 7.3abc	2.5\pm0.8a ←	0.4\pm0,2a ←
6.6	8.1	0.6	30.0 \pm 26.6bc	0.6 \pm 0.5b	0.1 \pm 0,0c
8.8	2.7	0.6	76.9\pm22.6a ←	1.3 \pm 0.4b	0.3 \pm 0,1abc
8.8	5.4	0.6	68.8 \pm 36.6ab	1.2 \pm 0.2b	0.2 \pm 0,1bc
8.8	8.1	0.6	71.1 \pm 15.3ab	1.1 \pm 0.1b	0.2 \pm 0,0bc
Control (MS medium)			0.0 \pm 0.0	0.0 \pm 0.0	0.0 \pm 0.0

*Means shown by different small letters in a single column are statistically different at 0.05 level of significance using Duncans multiple range test

**Means shown by different small letters in a single column are statistically different at 0.01 level of significance using Duncans multiple range test

Rooting and acclimatization of bay laurel shoots

In vitro regenerated female shoots of 3-5 cm long that was rooted on 4.90 μ M IBA (Fig. 2c). The first indications of rooting appeared after 4 weeks on MS medium containing 4.90 μ M IBA. The increase in the number of roots was very evident after 12 weeks, with the highest rooting on MS medium containing 4.90 μ M IBA (Fig. 2d-i and 2d-ii) on female shoots. Out of 45 female shoots used for rooting only 16/90 (17.77%) of them induced roots. The other concentrations of IBA were not suitable for rooting compared with this concentration. 2.24 μ M IBA was non-inducing and 7.35 μ M IBA showed necrosis and burning on the treated shoots. The number of roots increased when the rooted plantlets were cultured on MS medium. Prolonged culture of shoots on 4.90 μ M IBA containing medium tended to induce callus formation that had negative effects on root growth and development.

Out of 16 rooted female plantlets, as mentioned above, only 13 could be acclimatized to external conditions after their transfer to pots (Fig. 2e). After the hardening period of 3 months in the environmental chamber, these female plants were ready for transfer to the fields (Fig. 2f).

Discussion

Sex determination cannot be ensured phenotypically at the first stage of the development of dioecious plants like bay laurel, in general. The literature reports no studies relating to sex determination in bay laurel at the seedling stage with highly limited *in vitro* micropropagation studies. It is highly significant to determine the sex and production protocols in bay laurel for the establishment of planned breeding and production programs.

The elimination of micro-organisms from the tissues has great importance in *in vitro* cultures of plants. During seed or tissue sterilization, surface contact of NaOCl must be adjusted to the level that it doesn't have any hazardous effect. This depends on the

Careful adjustment of the concentration of disinfectant, duration of application, and the surrounding temperature. The researchers report high sterilization and germination of seeds without pericarps. The contamination rate was lower and the germination percentage was higher on the seeds if the pericarps were not removed. It was also found that diluted 30% commercial bleach (5% NaOCl) is suitable as a sterilizing agent of bay laurel seeds without pericarps. Additionally, that high-frequency of seed germination was highly affected by seed health during sterilization. The optimization of appropriate seed sterilization procedure is a prerequisite for carrying out any tissue culture experiment. The high (40-100% concentration) dose of commercial bleach was hazardous to the health of the seeds and resulted in a reduction of seed germination. The results of the study are in agreement with previous studies (Sari et al., 2006; Şenyay, 2008; Erkmén, 2009; Chaari Rkhis et al., 2011; Cavusoglu et al., 2014). These studies suggest that sodium hypochlorite exhibits a broad spectrum of anti-microbial activity and effectively disinfect or inactivate bacterial, fungal, and viral organisms adhering to the surface of explants. Contrary to Chourfi et al. (2014), who has reported germination of laurel seeds using kinetin and IAA (indole acetic acid), NAA on WMP (woody plant medium), this study did not need any phytohormonal treatment to germinate seeds.

Sex determination

DNA content was determined by using flow cytometry method on the leaf samples taken from bay laurel seedlings germinated under *in vitro* conditions and as a result of this study, it was determined that DNA content of bay laurel changes between 7.04 to 8.14 and it was showed that 43 out of the 58 seedlings were female and 16 of them were male. DNA content of male and female plant are not significantly different in statistical terms but is different numerically. The results were confirmed by finding the amount of DNA on adult male and female plants. Therefore, it is assumed that the method of determining sex would work. Sex determination was performed by comparing the DNA content of the plant following (Parlar, 2017). Doležel and Göhde (1995) have confirmed the sex determination of chalk plants by using flow cytometry. They used young leaves of two different chalk plants (*Melandrium. album* and *Melandrium. rumrum*), and noted that the nuclear DNA content of cells of female plants was lower compared to the DNA content in the cells of male plants. The nuclear DNA content of male and female plants differed at a rate of 3.7% (Costich et al., 1991). It was shown that the DNA content of male *Silene latifolia* plants was larger compared to the DNA content of female plants. Furthermore, the researchers reported a difference in AT/GC contents of the males and females. Whereas Vagera et al. (1994) have shown androgenesis under *in vitro* conditions, by using ripe microspores of *M. album*. Supermales were crossed with normal female plants under *in vitro* conditions, to obtain female plants. Flow cytometry analysis was positively used for the determination of sex and the ploidy level. However, the researcher (Cepeda-Cornejo et al., 2012) did not find any significant differences between male and female individuals in terms of DNA during content sex analysis study of four *Chamaedorea* palm species.

Micropropagation

Micropropagation studies on axillary buds showed the induction of an average number of shoots per explant. The best regeneration was noted on MS medium containing 8.8 µM BAP, 2.7 µM NAA, and 0.6 µM GA3. The results are supported by the findings of Stanica et al. (1992), who used axillary buds of one-year bay laurel,

lateral shoots of 2-3 cm in length, apical meristems, and 1 node fragments of developing shoots as explants. They took explants' starting material at 6 different times between February and May and regenerated them on MS medium containing 0.01 mg/l NAA + 0.3 mg/L BA + 250 mg/L Ascorbic acid + 1 mg/L MS medium containing adenine sulphate, and DKW nutrient media containing 0.2 mg/L IBA + 1 mg/L BA. They found that MS medium showed induction of callus at the rate of 62%. This was ensued by shoot formation on DKW medium. On the contrary, Souayah et al. (2002) reported that the best shoot development in axillary buds occurred on $1/3 \times$ MS medium containing 1 mg/L BAP + 1 mg/L GA3. Callus development was observed in medium containing BAP and NAA; it was reported that the addition of activated coal to nutrient medium enhanced the development of root and callus. Cobo et al. (2019) reported that the significantly higher numbers of shoots per bud in mortio (*Vaccinium floribundum Kunth*) were observed on mWPM (modified Woody Plant medium) with 3.0 mg/L 2iP (N6-isopentenyladenine) or with 5.0 mg/L 2iP + 0.1 mg/L NAA (1-naphthaleneacetic acid).

In decade-long studies of *in vitro* regeneration, conducted by Boza and Altun (2013), the rate of shoot, root, and callus induction was examined on shoot tips, buds, and nodal cuttings; *in vivo* were taken from laurels located in the Turkish provinces of İzmir and Aydın. They used MS medium, DKW medium (Driver and Kuniyuki, 1984), and Heller and WPM (Woody Plant Medium) containing NAA, BAP, IBA; Kinetin plant, in different concentrations and combinations, could be used for micropropagation of the plant. They recommended that MS medium, having 0.3-4 mg/l BA and 0.5-5 mg/l NAA for the rooting of the micropropagated shoots. The rooting from woody plants is difficult due to the carry over effect of cytokinins (Huetteman and Preece., 1993). Although no study reported the rooting of bay laurel under *in vitro* conditions, the results are supported by the findings of Chourfi et al. (2014), Grigoriadou et al. (2002) on olive, Spahiu et al. (2013) on peach using IBA, and Sriskandarajah et al. (1982) on apples using 10 μ M NAA or 750 μ M IBA; all of them used IAA, IBA or NAA for rooting of woody shoots of different plants.

Rooting and acclimatization

The rooting and acclimation stages on plants affect the plants' development quality after acclimatization (McClelland, 1990). Adaptation studies of rooted bay laurel plants to external conditions are rare. The study confirms successful acclimatization of female bay laurel, when the humidity around the plants was gradually reduced to 50% and the first indications of rooting appeared after 4 weeks on MS medium containing 4.90 μ M IBA. The increase in the number of roots was very evident after 12 weeks, the results are supported by Grigoriadou et al. (2002), who acclimatized *in vitro* regenerated *Chondrolia chalkidikis* plants to a soil substrate containing peat moss and perlite (1:4) with 90% success. Binet et al. (2007) found that shoots of olive were successfully adjusted to external conditions after rooting (Nas, 2004) and reported that IBA applications in different concentrations to different hazelnut species have positive impacts on *in vitro* rooting. Khater and Benbouza (2019) have reported that the highest root numbers and lengths in *Juniperus thurifera* L. were produced on $1/2$ MS medium supplemented with IBA and NAA (5.0mg L⁻¹ each) and During transfer to acclimatization, rates of plant losses of 50% occurred.

Conclusion

It is important to develop mass production technologies, suitable for different purposes, for non-wood forest products, especially bay laurel. For instance; in order to obtain bay laurel leaves and Essential Oils, generally female plants are preferred or male plants have the inside track to be grown due to being easier in terms of shaping and due to female plants being crumbled and causing pollution in landscape studies. With the results achieved from the study are, especially; it is considered that it would be possible to conduct early sex determination studies on perennial and diecious plants like bay laurel. It is assumed that optimization of *in vitro* micropropagation methods will help conscious commercial cultivation and easy breeding of bay laurel.

Acknowledgements. This study was supported by Agriculture, Forestry and Veterinary Research Grant Committee (TOVAG) of Scientific and Technical Research Council of Turkey (TUBITAK, Project No. 2150251) and Department of Agricultural Biotechnology Namik Kemal University, Tekirdag, Turkey. The author is pleased to thank Prof. Dr. Metin TUNA for flow cytometry analysis in his laboratory.

REFERENCES

- [1] Arumuganathan, K., Earle, E. D. (1991): Estimation of nuclear DNA content of plants by flow cytometry. – *Plant Molecular Biology Reporter* 9: 229-241.
- [2] Aydın Akbudak, M., Şakiroğlu, M., Tuna, M. (2018): Estimation of nuclear dna content and determination of relationship between altitude and genome size of usda turkish oat (*avena spp.*) collection. – *Gesunde Pflanzen* 70: 171-178.
- [3] Bennett, M. D., Smith, J. B. (1976): Nuclear DNA amounts in angiosperms. – *Phil. Trans. R. Soc. Lond* 274: 227-276.
- [4] Binet, M. N., Lemoine, M. C., Martin, C., Chambon, C., Gianinazzi, S. (2007): Micropropagation of olive (*Olea europaea* L.) and application of mycorrhiza to improve plantlet establishment. – *In Vitro Cell.Dev.Biol.Plant* 43: 473-478.
- [5] Boza, A., Altun, Z. G. (2013): Propagation possibilities of bay laurel (*Laurus nobilis* L.) by Tissue Culture Method. – Ege Forestry Research Institute, İzmir.
- [6] Cavusoglu, A., Sulusoglu, M. (2014): Effects of indole-3-butyric acid (IBA) and 1-naphthaleneacetic acid (NAA) on rooting of female and male *Laurus nobilis* L. cuttings. – *International Journal of Biosciences* 4: 206-216.
- [7] Cepeda-Cornejo, V., Palomino, G., Méndez, I. (2012): Intersexual comparison of DNA content by flow cytometry and chromosome number in four dioecious chamaedorea palms from Mexico. – *Caryologia* 65: 263-270.
- [8] Chaari Rkhis, A., Maalej, M., Drira, N., Alvaro, S. (2011): Micropropagation of olive tree (*Olea europaea* L.) oveslati. – *Turk J Agric For* 35: 403-412.
- [9] Chourfi, A., Alaoui, T., Echchgadda, G. (2014): *In vitro* propagation of the Bay Laurel (*Laurus nobilis*. L) in Morocco. – *South Asian Journal of Experimental Biology* 4: 96-103.
- [10] Cobo, M. M., Gutierrez, B., Torres, M. D. (2019): Regeneration of mortio (*Vaccinium floribundum* Kunth) plants through axillary bud culture. – *In vitro cellular & developmental biology-plant* Volume 54: 112-116.
- [11] Costich, D. E., Thomas, R., Meagher, E. J., Yurkow, A. (1991): Rapid means of sex identification in *Silene latifolia* by use of flow cytometry. – *Plant Molecular Biology Reporter* 9: 359-370.
- [12] Darlington, C. D., Wylie, A. P. (1956): Chromosome atlas of flowering plants. – George Alien & Unwin Ltd, London.

- [13] Demir, V., Gunhan, T., Yagcioglu, A. K., Degirmencioglu, A. (2004): Mathematical modelling and the determination of some quality parameters of air-dried bay leaves. – Biosyst. Eng 88: 325-335.
- [14] Dewir, Y. H., El-Mahrouk, M. E., Murthy, H. N., Paek, K. Y. (2015): Micropropagation of cattleya: improved *in vitro* rooting and acclimatization. – Horticult Environ Biotechnol 56: 89-93.
- [15] Dhifi, W., Bellili, S., Jazi, S., Ben Nasr, S., El Beyrouthy, M., Mnif, W. (2018): Phytochemical composition and antioxidant activity of tunisian *Laurus nobilis*. – Pakistan journal of pharmaceutical sciences 31: 2397-2402.
- [16] Doležel, J., Göhde, W. (1995): Sex determination in dioecious plants *Melandrium Album* and *Melandrium Rubrum* using high-resolution flow cytometry. – Cytometry 19: 103-106.
- [17] Driver, J. A., Kuniyuki, A. H. (1984): *In vitro* propagation of paradox walnut rootstock. – HortSci 4:507-509.
- [18] Ehrendorfer, F., Krendl, F., Habeler, E., Sauer, W. (1968): Chromosome numbers and evolution in primitive angiosperms. – Taxon 17(4): 337-353.
- [19] Ercan, A. (1983): Defne yaprağı ve yağı ihracatının geliştirilmesi, ihracatı. – Geliştirme Etüd Merkezi, Ankara.
- [20] Erkmen, S. (2009): The effects of cold stratification pretreatment on germination of tatar maple (*Acer tataricum* L.) seeds. – M.Sc. Dissertation–Ankara university, institute of sciences.
- [21] Göker, Y., Acar, İ. (1983): Orman yan ürünlerinden (*Laurus nobilis* L.) Akdeniz Defnesi. – İ.Ü. Orman Fakültesi Dergisi 33: 124-140.
- [22] Grigoriadou, K., Vasilakakis, M., Eleftheriou, E. P. (2002): *In vitro* propagation of the greek olive cultivar “*Chondrolia Chalkidikis*. – Plant Cell, Tissue and Organ Culture 71(1): 47-54.
- [23] Huetteman, C. A., Preece, J. E. (1993): Thidiazuron: a potent cytokinin for woody plant tissue culture. – Plant Cell, Tissue and Organ Culture 33: 105-119.
- [24] Khater, N., Benbouza, H. (2019): Preservation of *Juniperus thurifera* L.: a rare endangered species in Algeria through *in vitro* regeneration. – Journal of forestry research 30: 177-86.
- [25] Kilic, A., Hafizoglu, H., Kollmannsberger, H., Nitz, S. (2004): Volatile constituents and key odorants in leaves, buds, flowers, and fruits of (*Laurusnobilis*L). – Journal of Agricultural and Food Chemistry 52: 1601-1606.
- [26] Konukçu, M. (2001): Ormanlar ve ormancılığımız. – Ankara Devlet Planlama Teşkilatı Yayınları, Ankara.
- [27] Lanzara, P., Pizetti, M. (1989): Les arbres. – Nathan, Milan.
- [28] Maarten, J. M., Christenhusz, J. W. B. (2016): The number of known plants species in the world and its annual increase. – Phytotaxa 261(3): 201-217.
- [29] McClelland, M. T., Smith, M. A. L., Carothers, Z. B. (1990): The effects of *in vitro* and ex vitro root initiation on subsequent microcutting root quality in three woody plants. – Plant Cell Tissue and Organ Culture 23: 115-123.
- [30] Murashige, T., Skoog, F. (1962): A revised medium for rapid growth and bioassays with tobacco tissue cultures. – Physiol Plant 15: 473-497.
- [31] Nas, M. N. (2004): Inclusion of polyamines in the medium improves shoot elongation in hazelnut (*Corylus avellana* L.) micropropagation. – Turkish Journal of Agriculture and Forestry 428: 189-194.
- [32] Noiro, M., Barre, P., Louarn, J., Duperray, C., Hamon, S. (2002): Consequences of stoichiometric error on nuclear DNA content evaluation in *Coffea liberica* var. dewevrei using DAPI and propidium iodide. – Ann. Bot 89: 385-389.
- [33] Panza, E., Tersigni, M., Iorizzi, M., Zollo, F., De Marino, S., Festa, C., Napolitano, M., Castello, G. (2011): Laurosides B, a megastigmane glycoside from *Laurus nobilis* L. (bay laurel) leaves, induces apoptosis in human melanoma cell lines by inhibiting NF-κB activation. – Journal of Natural Products 74: 228-33.

- [34] Parlar, E. (2017): Sex determination in *Laurus nobilis* L. using flow cytometry method. – M.Sc. Dissertation, Tekirdağ Namık Kemal university.
- [35] Sari, A., Oğuz, B., Bilgiç, A. (2006): Breaking seed dormancy of laurel (*Laurus nobilis* L.). – *New Forests* 31: 403-408.
- [36] Savas Tuna, G., Duyu, G., Uzun, K., Yucel, G., Tuna, M. (2017): Determination of nuclear DNA content and ploidy of *Hypericum perforatum* L. accessions collected from western Turkey. – *Journal of agricultural sciences* 23: 395-403.
- [37] Snedecor, G. W., Cochran, W. G. (1982): *Statistical methods*. – The Iowa State University Press, Iowa.
- [38] Souayah, N., Khouja, L. M., Khaldi, A., Rejeb, N. M., Bouzid, S. (2002): Breeding Improvement of *Laurus nobilis* L. by Conventional and *In vitro* Propagation Techniques. – *Journal of Herbs Spices & Medicinal Plants* 9: 101-105.
- [39] Spahiu, E., Hodaj, B., Rama, P. (2013): The influence of season collection of explants on micropropagation of peach rootstock GF-677. – *Journal Agriculture Sci* 12: 15-18.
- [40] Sriskandarajah, S., Mullins, M. G., Nair, Y. (1982): Induction of adventitious rooting *in vitro* in difficult to propagate cultivars of apple. – *Plant Science Letters* 24: 1-9.
- [41] Stanica, F., Standardi, A., Hoza, D., Tudor, T. A. (1992): Studies on micropropagation of laurel (*Laurus nobilis* L.). – *Seria B, Horticultura* 35: 83-90.
- [42] Şenyay, D. (2008): Researches on *in vitro* regeneration of mastic tree (*pistacia lentiscus* L.). – M.Sc. Dissertation, Ege university.
- [43] Tanrıverdi, H. (1993): Defne meyvası sabit yağının ekstraksiyon verimi ve kalitesinin belirlenmesi üzerine bir araştırma. – *FABAD-J, Pharm.Sci* 18: 107-113.
- [44] Tuna, M., Vogel, K. P., Arumuganathan, K., Gill, K. S. (2001): DNA content and ploidy determination of bromegrass germplasm accessions by flow cytometry. – *Crop Sci* 41: 1629-1634.
- [45] Tuna, M. (2016): Flow cytometry and use in agricultural research. II. Flow Cytometry and Use in Agricultural Research. – *Handbook, Tekirdag*.
- [46] Vagera, J., Paulíková, D., Doležel, J. (1994): The development of male and female regenerants by *in vitro* androgenesis in dioecious plant (*Melandrium albüm*). – *Annals of Botany* 73: 455-459.
- [47] Villar, L. (1986): Lauraceae. – In: *Castroviejo. Flora Iberica*. Madrid: Real Jardin Botanico, C.S.I.C. 199- 200.
- [48] Zonneveld, B. J., Leitch, M. I. J., Bennett, M. D. (2005): First nuclear DNA amounts in more than 300 angiosperms. – *Annals of Botany* 96: 229-244.

ASSESSMENT OF FRUIT DEFECTS AND ECONOMIC LOSS OF SOME SOFT DATE PALM CULTIVARS (*PHOENIX DACTYLIFERA* L.) IN NORTH DELTA, EGYPT

EL-ANSARY, M. A. – OMAR, A. K. – SALAMA, A. * – HELAL, S. M.

*Horticulture Department, Faculty of Agriculture, Kafrelsheikh University
Kafr Elsheikh 33516, Egypt*

*(e-mail/phone: mohamed.elansary@agr.kfs.edu.eg, +20-100-659-1818;
alaa.omr@agr.kfs.edu.eg, +20-109-740-8240)*

**Corresponding author*

e-mail: abdelmoety.salama@gmail.com; phone: +20-109-513-1735

(Received 2nd Feb 2019; accepted 21st Mar 2019)

Abstract. This research was carried out to quantify the amount of defected fruits, outlining the causes of defect, and their negative economic impact, in terms of total fruit loss (US\$), production cost (US\$), total area of cropping land (hectare), and irrigation water (m³) of ‘*Samani*’, ‘*Hayani*’, ‘*Bent Aisha*’, ‘*Oreebi*’, and ‘*Zaghloul*’ soft date palm (*Phoenix dactylifera* L.) cultivars grown in North Delta, Egypt. Random fruit samples were taken at harvest date of each cultivar from Rasheed and Baltim districts and divided into two sets; sound fruit (free of visible defects) and defected/discarded fruit. The defected fruits set was classified based on the type of defect into; misshape, unpollinated fruit (shees), decay and mold, dirt, discolored, dry fruit, insect damage, over-ripped fruit, shrivelling, under size, unripe fruit, no calyx, and mechanical injuries. Each type of defect was calculated as a percentage of the total weight of the defected fruit. Fruit loss was determined as follow; ‘*Hayani*’ (19.66–26.77%), ‘*Samani*’ (23.03–25.33%), ‘*Oreebi*’ (16.79–25.00%), ‘*Bent Aisha*’ (9.66–15.68%) for 2015/2016–2016/2017 seasons respectively, ‘*Zaghloul*’ (5.55%) for 2016-2017. Total monetary loss based on the farm price was about 8,641,908–9,232,793 for the studied cultivars. Total loss in terms of cropping land was about 1,771–1,939 ha with a total loss of 1,511,616–1,654,890 in production cost and 11,2–12,3 million (m³) of the irrigation water. Fruit without calyx was the main defect of all the studied cultivars, except ‘*Oreebi*’ during both seasons.

Keywords: *postharvest loss, date defects, losses cost evaluation, irrigation water loss, fruit loss*

Abbreviations: EGP: Egyptian pounds, MALR: Ministry of Agriculture and Land Reclamation

Introduction

Date palm (*Phoenix dactylifera* L.) is one of the key fruits in dry and semidry regions (Chao and Krueger, 2007). Egypt considers the highest country for date production over the world with 1590414 ton (FAO, 2019), around 18% of the global date production. There are three types of date fruits, soft, semi-dry and dry, about 45% of date fruits in Egypt are soft (MALR, 2018). The most common soft types in Egypt are ‘*Hayani*’, ‘*Zaghloul*’, ‘*Samani*’, ‘*Bent Aisha*’, and ‘*Oreebi*’, (they present around 43% of the soft types in Egypt) (MALR, 2018). In cooperation with FAO and other international agencies, Egypt has developed, in September 2016, strategy for the development of date palm and dates sector. One of its main pillars is to enhance dates export through high quality fruits (FAO, 2016). An important step to produce and maintain high quality date fruits and reduce loss and waste is to know the volume and types of defects (El-Habbab et al., 2017). Yahia et al. (2014) concluded that some of the vital means to produce good quality dates and to maintain its postharvest quality include: selecting the right type of male clones for pollination, developing appropriate date palm mechanization, especially for pollination and harvesting, adequate use of the cold chain, packaging and packages,

food safety measures, insect control and prevention of re-infestation during postharvest processes. The results of FAO (2011) study pointed out that roughly one-third of food produced for human consumption is lost or wasted globally. The types of food loss and waste in low-income countries are primarily linked to the limited financial resources, low managerial and technical capacities in harvesting performances, storage and cooling facilities in hard climatic conditions, inferior infrastructure, packaging and marketing systems. Yahia et al. (2014) reported that only about 10% of the world production of dates is handled in global trade due to various factors including inadequate handling practices and insufficient information for small farmers, who are the main producers. They also pointed out to the need to investigate and refine several subjects such as: improvements of harvesting systems; safe means for insect and pathogen control; adequate packaging and storage conditions; and more biochemical studies on sugar interactions, tissue softening, and browning. In Arabian Peninsula countries, fermentation, insect infection, birds and mechanical damage are the common types of postharvest loss of dates; the produced dates do not fulfil International Regulations and Standards required for export. Elsayed and Abdel Gleel (2013), in Egypt, had reported that, the average dates loss of ten-year (2000–2010) at harvesting were 10-15% and 8.1% during postharvest processes, this is due to mechanical (harvesting, sorting, grading, and transportation) or biological (pests and insects) reasons. El-Habbab et al. (2017) investigated dates loss at harvest time of three cultivars in four locations in Saudi Arabia, that include shees & besr, bird's damage, falling, insects and dust mite. They found that the loss varied from location to location as well as within cultivars in the same location. The average level of loss during the marketing stage was about 5-10% in most varieties and locations except Ajweh in Riyadh (2.7% only). Lemlem et al. (2018) found that conventional procedures of date palm production were applied in Afar Regional State, Ethiopia and constrained with high incidence of insect pests. They recommended training sessions on good agricultural practices and to improve management, and postharvest handling practices. As a result of thirty years working on postharvest loss prevention, Boye and Muck (2015) concluded that a series of prerequisites including reliable funding over extended period, continuity in science-based programs and project approaches, considerations of technical and socio-economic factors are needed for implementing sustainable postharvest loss prevention. Identification of main causes of date defects and determination its percentage might contribute in filling the information gap of support to overcoming the weaknesses of date palm sector identified in Egypt date palm strategy (FAO, 2016), specifically weak tendency towards good agricultural practices to produce high quality dates.

The objectives of this work were to evaluate the cost, magnitude and type of main defects for some soft date palm cultivars at harvesting date, in North Delta, Egypt.

Materials and methods

The work was carried out in two main areas for soft date production in Egypt, Rasheed and Baltim districts which are located in North of Behira and Kafr El-Sheikh governorate respectively, at the North of Nile Delta, Egypt, on date palm fruits (*Phoenix dactylifera*, L.) of 'Samani', 'Hayani', 'Bent Aisha', and 'Oreebi', soft cultivars during 2015/16 and 2016/17 seasons and on 'Zaghloul', only 2016/17 season. Three random crates samples, 16 kg each, which represent about 5% of total harvested amount daily that, weighs around 1000 kg of above-mentioned cultivars at commercial harvesting

date of each cultivar usually practiced in the farm for many years. Each sample was examined and separated into two sets, sound fruits (free of visible defects) and defected/discarded set, the percentages of sound and discarded fruits were calculated.

The defected fruit set was examined and separated according to the type of defect; each defect in the discarded set was calculated as a percentage of the total weight of the defected fruit set. The following are the types of defects were used for the examination and separation: 1) Misshape, the fruit was considered misshaped when it shows abnormal/irregular characteristic of the cultivar. 2) Unpollinated dates (shees), dates not pollinated as evidenced by thin flesh, immature characteristics and no pit in unpitted dates (Codex Stan 143-1985). 3) Decay, dates that are in a state of decomposition and very objectionable in appearance, (Codex Stan 143-1985). 4) Dirt, dates contaminated with sand, soil, dust or other field debris and particles are not easy to be removed. 5) Discolored, when the color of dates does not present the possess characteristic color for the cultivar 6) dry dates, 7) Insect damage, dates damaged by insects or mites or contaminated by damage and contamination the presence of dead insects or mites, fragments of insects or mites or their excreta (Codex Stan 143-1985). 8) Over ripped, fruits transformed from Bisir into Rutab stage 9) Shrivelling, date loses the moisture content causing wrinkling in fruit surface. 10) Under size, when number of fruits in half kg are more than 23 fruits for 'Samani' and 'Zaghloul' cultivars and more than 100 fruits for 'Oreebi', 'Hayani' and 'Bent Aisha' cultivars (Codex Stan 143-1985). 11) Unripe dates, dates which may be light in weight, light in color, have shrivelled or little flesh or a decidedly rubbery texture (Codex Stan 143-1985). 12) Without calyx, 13) Mechanical injuries, any type of mechanical cracked or mashed or bruises on fruit surface. The data were managed as a randomized complete block design with three replicates ($n = 3$). Data were analyzed by Assistat software version 7.7, program **last** update was on 08/10/2014 according to Little and Hills (1972). Means were compared using Duncan's new multiple-range test at P value ≤ 0.05 (Duncan, 1965).

Financial value of defected date fruits (loss) at harvesting in Egyptian pounds (EGP): was calculated for each cultivar as follows:

$$\text{Production (ton)} \times \% \text{ of loss at harvesting} \times \text{Farm get price/ton (US\$)} \quad (\text{Eq.1})$$

Loss in cropping-land (area used to produce lost amount of dates) Fed, was calculated as follows:

$$\text{Total production area (hectare)} \times \% \text{ of loss at harvesting} \quad (\text{Eq.2})$$

Loss of production cost was calculated as follows:

$$\text{Loss in cropping-land (hectare)} \times \text{production cost (US\$/Fed)} \quad (\text{Eq.3})$$

Loss of irrigation water (m^3) used to produce the lost amount of date fruits of each cultivar as follows:

$$\text{Loss in cropping-land (hectare)} \times \text{Water requirements per Fed (m}^3\text{)} \quad (\text{Eq.4})$$

Results and discussion

Amount of sound and defected (loss) date palm fruits at harvesting time

The results in *Tables 1* and *2* showed that, the percentages of the sound, non-defected fruits at harvesting time and total discarded percentage/defected fruits of 'Samani', 'Oreebi', 'Hayani', 'Bent Aisha' and 'Zaghloul' cultivars during 2016 and 2017 seasons. The sound date palm fruits percentage was 84.32, 83.21, 76.97, and 73.23% for 'Bent Aisha', 'Oreebi', 'Samani', and 'Hayani' in 2016 season, respectively. While during second season (2017), it recorded 94.50, 90.34, 80.34, 75.00% and 74.67% for 'Zaghloul', 'Bent Aisha', 'Hayani', 'Oreebi' and 'Samani' respectively. Regarding the defected fruits, 'Hayani' cultivar showed that, the highest fruit loss at harvesting time was 26.77 percentage during 2016 season more than one quarter of its production, followed by 'Samani' cultivar (23.03%), the differences were not significant. On the other hand, losing fruits of 'Oreebi' and 'Bent Aisha' cultivars were 16.79 and 15.68% during harvesting time in the same season, respectively, with no significant differences between them. The losses of both cultivars at harvested time were significantly lower than 'Hayani' and 'Samani' cultivars.

In 2017 season, loss fruit of 'Samani' and 'Oreebi' cultivars were almost equal quantities; 25% of the produced fruits at harvested time and the differences between them was not significant followed by 'Hayani' 19.66 and 'Bent Aisha' 9.00%, respectively. While the lowest fruit loss was recorded by 'Zaghloul' cultivar (5.50%).

The obtained results showed that loss at harvested of soft dates is substantial. These results are in consistent with those of Kader and Rolle (2004) who found that the magnitude of fruit losses depends, among other factors, on the nature of the commodities and the conditions of the produce at the time of collections. This also accords with FAO study in 2011 and Yahia et al. (2014), they reported that, low technical capacities in harvesting performances is one of the reasons of fruit loss, also El-Habbab et al. (2017) concluded that, the level of loss at harvesting time differs from area to area and from cultivar to another. Similar findings were observed on orange (Salama et al., 2015). So, the management practices of harvesting process play significant role in reducing loss during this stage and next stages in dates supply chain. The relatively low loss of 'Zaghloul' could be attributed to the differences between growers in practicing harvesting techniques and processes.

Type of soft date fruit defects (loss) at harvesting time

Results in *Tables 1* and *2* present the percentages of different types of defects in the discarded fruit set. Fruits without calyx (*Fig. 1*) are the main defect of all studied cultivars in both seasons except 'Oreebi' cultivar, it was discoloration in both seasons. In the first seasons 2016 (*Table 1*), 'Hayani' cultivar, showed the highest without calyx defect (41.70%) followed by 'Bent Aisha' (39.93%), the difference between them were not significant, while 'Samani' cultivar (20.48%) was significantly lower than both. 'Oreebi' cultivar showed the lowest significant without calyx defect. In the second 2017 season (*Table 2*), 'Hayani' cultivar, also showed the highest without calyx defect (56.29%) followed by 'Bent Aisha' (55.38%) and 'Samani' (53.78%) cultivars respectively, the differences between them were not significant. 'Zaghloul' cultivar (31.08%) was significantly lower than 'Hayani', 'Bent Aisha' and 'Samani' while 'Oreebi' showed the lowest significant difference. This is could be attributed to the harsh way of fruit separation from the strands, which led mostly to the separation of part

of the fruit flesh with the cap (calyx), as shown in Photo 1. Fruits without calyx (cap) are more subjected to microorganisms and insect's infestation.

Table 1. Sound, defected date fruits and types of defects as percentage of total sample weight of some soft date palm cultivars at harvesting time in North Delta, Egypt during 2016 season

Defect %	Cultivars			
	'Samani'	'Bent Aisha'	'Hayani'	'Oreebi'
Sound fruits (%)	76.97 ab	84.32 a	73.23 b	83.21 a
Defected fruits (%)	23.03 a	15.68 b	26.77 a	16.79 b
Causes of defects				
Misshaped	0.57 b	0.00b	0.61b	3.72 a
Unpollinated dates (Shees)	0.00 a	0.00 a	0.00 a	0.67 a
Decay and mold	2.56 a	0.00 b	0.32 b	0.00 b
Dirt	0.00	0.00	0.00	0.00
Discolored	9.36 b	3.74b c	1.72c	69.83 a
Dry dates	0.46 b	5.64 a	0.24 b	0.62 b
Insect damage	4.59 a	2.89 ab	0.00 b	0.85 ab
Over ripped	0.58 b	0.52 b	0.00 b	11.80 a
Shriveling	0.50c	7.31 a	0.77c	2.58b
Unripe Dates	0.00	0.00	0.00	0.00
Without calyx	20.48 b	39.93 a	41.70 a	5.76c
Wounds	3.63 a	0.00b	0.35 b	0.00b

Values with the same letter in the same raw are not significant at ($P \geq 0.05$)

Table 2. Sound, defected date fruits and types of defects as percentage of total sample weight of some soft date palm cultivars at harvesting time in North Delta, Egypt during 2017 season

Defect %	Cultivars				
	'Samani'	'Bent Aisha'	'Hayani'	'Oreebi'	'Zaghloul'
Sound fruits (%)	75.33 d	90.33b	80.33 c	75.00 d	94.50 a
Defected fruits (%)	25.33 a	9.66 c	19.66 b	25.00 a	5.50 d
Causes of defects					
Misshaped	8.70 b	0.00 c	2.83 c	0.00c	21.17 a
Unpollinated dates (Shees)	1.19b	0.00 d	0.42c	5.02a	1.45b
Decay and mold	3.87 a	0.00c	0.39 bc	0.60b	0.00c
Dirt	3.52 a	0.43b	0.00b	0.00 b	0.00 b
Discolored	6.97 bc	2.02 c	5.32bc	55.52 a	9.93 b
Dry dates	0.11 a	0.17 a	0.42 a	0.25 a	0.00 a
Insect damage	4.23 ab	1.80 bc	1.44 bc	0.40 c	0.00 c
Over ripped	0.00 b	0.55 b	4.70 a	0.60 b	0.00 b
Shriveling	1.68 b	1.82 b	9.13 a	0.30 b	0.00 b
Unripe dates	0.17 a	0.00 a	0.00 a	0.00 a	0.00 a
Without calyx	53.78 a	55.38 a	56.29 a	13.34c	31.08 b
Wounds	0.37 b	0.00 b	0.14 b	0.00 b	2.27 a

Values with the same letter in the same raw are not significant at ($P \geq 0.05$)



Figure 1. Severe losses occurred due to careless rough handling of dates by farmers. A) rough way of separating the fruits from the branches (strands) using stick, B) separation of part of the fruit flesh with the cap (calyx), C) strands full of caps

Discoloration defect was significantly the highest in ‘*Oreebi*’ cultivar during both seasons, 69.83% and 55.52% respectively. In the first season, the difference between ‘*Bent Aisha*’, ‘*Hayani*’ was not significant while ‘*Samani*’ was significantly higher than both. In the second season, there was no significant difference neither between ‘*Hayani*’, ‘*Zaghloul*’ and ‘*Samani*’ cultivars nor ‘*Hayani*’ ‘*Bent Aisha*’ and ‘*Samani*’ while the difference between ‘*Zaghloul*’ and ‘*Bent Aisha*’ was significant.

During the both seasons, unpollinated dates (shees), decay, dirt, insect damage, unripe fruit and mechanical injuries defects for all cultivars were low and ranged from around 0.00 to almost 5.00%. The same was also observed for dry dates defect except for ‘*Bent Aisha*’ cultivar in the first season, 5.64% significantly higher than the rest of the studied cultivars. Over ripening defect showed the same lower trend except for ‘*Oreebi*’ cultivar in the first season (11.80%), it was significantly higher than the other studied cultivars. Shriveling defect showed also the same lower trend except for ‘*Bent Aisha*’ cultivar during the first season (7.31%) and ‘*Hayani*’ (9.13%) in the second season, significantly higher than the rest of the studied cultivars.

Results showed that the main causes of fruit loss at harvest under North Delta conditions were fruit without calyx (cap) for ‘*Samani*’, ‘*Bent Aisha*’, ‘*Hayani*’, and ‘*Zaghloul*’ cultivars and discoloration defect for ‘*Oreebi*’ cultivar. Fruit of the studied cultivars were less susceptible to insect damage, decay, dry dates, misshape, and unpollinated fruit (shees). These results are in consistent with those of Kereth et al. (2013) who stated that mechanical damages were the main type of fruit defect at harvest (79%) in Tanzania. El-saedy (2011) found that the fallen cap (calyx) of ‘*Hallawy*’ and ‘*Zaghloul*’ fruit triggered a high increase in polyphenol oxidase and peroxidase activity that resulted in negative effect on fruit weight loss, peel anthocyanin content, soluble solids, malic acid and total phenol content, which in turn led to quick fruit deterioration during cold storage at 1 °C. This is pointed out to the need of improving harvest methods, Yahia et al. (2014) and Kader and Awad (2009) reported that in Arabian Peninsula countries, mechanical damage are the common types of postharvest loss of dates. El-Habbab et al. (2017) stated that dates loss at harvest time of three cultivars in four locations in Saudi Arabia, include shees & besr, birds damage, falling, insects and dust mite which is not the case for the studied soft dates cultivars under North Delta conditions. Elsayed and Abdel Gleel (2013), in Egypt, have reported that, the average

dates loss of ten-year (2000–2010) at harvesting were 10-15% and 8.1% during postharvest processes, this is due to mechanical (harvesting, sorting, grading, and transportation) or biological (pests and insects) reasons.

Financial value of the defected (loss) date fruits at harvesting

The Total value of dates loss of the studied cultivars during 2016 and 2017 were 9,232,793 and 8,641,908.89 (US\$) based on farm gate price of 2014, (Table 3). The results showed that, the highest value loss in both seasons were corresponding to ‘Hayani’ cultivar, 6,546,601.99 and 4,634,720.74 (US\$) respectively, followed by ‘Samani’ cultivar 1,986,639.19 and 2,185,044.32 (US\$) for both seasons respectively. ‘Zaghloul’ ranked the third with 1,215,153.39 US\$ in 2017 followed by ‘Bent Aisha’ 497,908.44 and 306,747.16 US\$ for 2016 and 2017 respectively.

Table 3. Financial value (EGP) of date fruits loss at harvesting of some soft date palm cultivars in North Delta, Egypt during 2016 and 2017 seasons

Cultivar	Total ¹ Production (ton)	% loss ²		Farm gate price/ton in 2016 (US\$) ³	Loss (US\$), based on farm gate price/ton ⁴	
	2016	2016	2017		2016	2017
‘Zaghloul’	170,025	-	5.50	129.94	-	1,215,153.39
‘Hayani’	335,699	27.77	19.66	70.22	6,546,601.99	4,634,720.74
‘Bent Aisha’	45,327	15.68	9.66	70.06	497,908.44	306,747.16
‘Samani’	101,486	23.03	25.33	85.00	1,986,639.19	2,185,044.32
‘Oreebi’	17,143	16.79	25.00	70.06	201,643.38	300,243.27
Total					9,232,793.00	8,641,908.89

¹Source: Ministry of Agriculture and Land Reclamation, Economic Affairs Sector (2018). The last available statistical issue for production is 2016, so we used it for both 2016 & 2017 seasons

²Results of this work in Table 1

³Source: Ministry of Agriculture and Land Reclamation, Economic Affairs Sector (2016). The last available statistical issue for Farm gate price is 2016, so we used it for both 2016 & 2017 seasons

⁴Calculated by Equation 1 from columns 1, 2 and 3 (1 US\$ = 17.8 Egyptian pound (EGP))

Loss of irrigation water and cropping-land and production cost (EGP) as a result of fruit defects (Loss) of some soft date palm cultivars at Harvesting

The irrigation water that has been used to produce the lost percentage of date fruits at harvesting, is considered an important lost as well taking into consideration that Egypt suffers from water shortage (Omar and Moussa, 2014). It was 5,242,919, 3,987,674, 1,325,155 and 666,340 m³ for ‘Hayani’, ‘Samani’, ‘Oreebi’ and ‘Bent Aisha’ in 2016 respectively. In 2017, it was 4,385,922, 3,711,768, 1,973,132, 1,804,411 and 410,513 m³ for ‘Samani’, ‘Oreebi’, ‘Hayani’, ‘Zaghloul’ and ‘Bent Aisha’ respectively (Table 4). These differences due to the differences in the cultivated areas. The average water loss was 11,222,087 and 12,285,744 m³ for 2016 and 2017 respectively. This amount of water was used to irrigate around 14% and 15% of date palm cropland during 2016 and 2017 seasons.

Water requirements for date palm vary from region to another according to climate conditions as well as the irrigation method, where it is 15,000–35,000 m³/ha in Algeria,

23,600 in Tunisia, 13,000–20,000 in Morocco, 15,000–20,000 in Iraq, where it is 22,300 m³/ha in Egypt (Albaker, 1972; Liebenbag and Zaid, 2002; Kassem, 2007).

Table 4. Estimated loss of irrigation water (million m³), cropping land (ha) and production cost (US\$) because of defected fruits (loss) at harvesting of some soft date palm cultivars in North Delta, Egypt during 2016 and 2017 seasons

Cultivar	Total ¹ cultivated area (ha)	Loss (%) ²		Loss in cropping-land (ha) ³		Production cost Loss (US\$) ⁴		Loss of irrigation water (million m ³) (water requirement equal to 6333.18 m ³ /ha) ⁵	
		2016	2017	2016	2017	2016	2017	2016	2017
‘Zaghloul’	5,180.25	0	5.5	0.00	284.91	-	243,054	-	1,804,410
‘Hayani’	2,981.09	27.77	19.66	127.85	586.08	706,221	499,957	5,242,915	3,711,765
‘Bent Aisha’	671.01	15.68	9.66	105.85	64.82	89,756	55,296	666,342	410,514
‘Samani’	2,734.03	23.03	25.33	629.65	692.53	537,139	590,783	3,987,668	4,385,916
‘Oreebi’	1,246.22	16.79	25	209.24	311.56	178,499	265,782	1,325,157	1,973,134
Total	12,812.60			1,771.9	1,939.9	1,511,616	1,654,890	11,222,082	12,285,738

¹Source: Ministry of Agriculture and Land Reclamation, Economic Affairs Sector (EAS), Bulletin of the Agricultural Statistics, Part (2) 2018

²Results of this work in Table 1

³Calculated by Equation 2, from columns 1 & 2

⁴Calculated by Equation 3, based on production cost/Fed equal to 15,185 EGP, source: Ministry of Agriculture and Land Reclamation, Economic Affairs Sector (EAS), 2017

⁵Calculated by Equation 4. Water requirements for Date palm in North Delta Region = 2661 m³/Feddan and 6333.18 m³/ha as One Feddan (Fed), equal to 0.39 ha. Source: Hassanien et al. (2012)

Conclusion

1. The percentages of fruit loss was 19.66- 26.77, 23.03–25.33, 16.79–25.00, 9.66–15.68, and 5.55% for ‘Hayani’, ‘Samani’, ‘Oreebi’, ‘Bent Aisha’ and ‘Zaghloul’ cultivars respectively.
2. The total financial value of date fruit loss was based on farm price (US\$), which was 9,232,793 and 8,641,908 US\$.
3. The total loss in terms of cropping land was 1764.44–1931.38 ha with a total loss in production cost = 3.59 - 3.93 million US\$ and a loss in irrigation water = 11,2–12,3 million m³.
4. The main fruit defect of ‘Hayani’, ‘Samani’, ‘Bent Aisha’ and ‘Zaghloul’ at harvesting in north delta area is Fruits without calyx (cap), while for ‘Oreebi’ cultivars is discoloration.
5. At harvesting, defects because of insect damage, decay, dry dates, misshape, and unpollinated fruit (shees) were low and ranged from around 0 to 5%.
6. There is a need for training programs on good agricultural practices of dates.

Acknowledgements. The authors would like to thank Dr. Samahy, Vegetable Crop Research Station, Horticulture Research Institute, for his help in statistical analysis.

REFERENCES

- [1] Albaker, A. (1972): Date Palm Trees. – Ministry of Higher Education, Baghdad, Iraq (in Arabic).
- [2] Boye, J., Muck, O. (2015): Conclusions from 30 Years of Practical Postharvest Loss Prevention Work. – Abstract #ADMI024 P. 55-57 The First International Congress on Postharvest Loss Prevention. Development Measurement Approaches and Intervention Strategies for Smallholders. Rome, Italy, October 4-7, 2015.
- [3] Chao, C. T., Krueger, R. R. (2007): The date palm (*Phoenix dactylifera* L.): overview of biology, uses, and cultivation of biology, uses, and cultivation. – Hortscience 42(5): 1077-1082.
- [4] Codex Standard for Dates (Codex Stan 143-1985): <https://www.google.com/search?q=Codex+for+dates&oq=Codex+for+dates&aqs=chrome.69i57j0l2.20051j0j4&sourceid=chrome&ie=UTF-8>. – Accessed at 03. 01. 2019.
- [5] Duncan, D. B. (1965): Multiple ranges and multiple F test. – Biomet. 11: 1-42.
- [6] El-Habbab, M. S., Al-Mulhim, F., Al-Eid, S., Abo El-Saad, M., Aljassas, F., Sallam, A., Ghazzawy, H. (2017): Assessment of post-harvest loss and waste for date palms in the Kingdom of Saudi Arabia. – International Journal of Environmental & Agriculture Research (IJOEAR) 3(6): 1-11.
- [7] El-saedy, R. M. A. (2011): Pomological characteristics and postharvest behavior of Hallway and ‘Zaghloul’ date fruits during cold storage. – Zagazig, J. Agric. Res. 38(3): 587-606.
- [8] El-Sayed, E. A., Abdel Gleel, S. S. (2013): An economic analysis for production and exports of date in Egypt. – J. Agric. Econom. Social Sci., Mansoura Univ. 4(9): 1771-1783.
- [9] FAO (2011): Global Food Losses and Food Waste. Extent, Causes and Prevention. – FAO, Rome.
- [10] FAO (2016): Strategy for the Development of Date Palm and Dates Sector in Egypt. – <http://www.fao.org/egypt/resources/ar/> (accessed on 29.01.2019).
- [11] FAO (2019): Data for Crop Production in 2017. – <http://www.fao.org/faostat/en/#data> (accessed on 25/1/2019).
- [12] Hassanien, M. K., Ahmed, M. A., Hashem, F. A., Khalil, A. A., Refaie, K. M. (2012): Management of Deficit Water for Crops in Egypt. – Central Laboratory for Agricultural Climate, Agriculture Research Center, Giza, Egypt.
- [13] Kader, A. A., Awad, H. (2009): Harvesting and Postharvest Handling of Dates. – ICARDA, Aleppo, Syria.
- [14] Kader, A., Rolle, R. S. (2004): The Role of Post-Harvest Management in Assuring the Quality and Safety of Horticultural Produce. – FAO, Rome, Italy.
- [15] Kassem, M. A. (2007): Water requirements and crop coefficient of date palm trees “Sukariah CV.”. – Misr Journal Agricultural Engineering 24(2): 339-359.
- [16] Kereth, G. A., Monica Lyimo, M., Hadijah, A. Mbwana, H. A., Mongi, R. J., Carolyne, C. Ruhembe, C. C. (2013): Assessment of post-harvest handling practices: knowledge and losses of fruits in Bagamoyo District of Tanzania. – Food Science and Quality Management 11: 8-15.
- [17] Lemlem, A., Alemayehu, M., Endris, M. (2018): Date palm production practices and constraints in the value chain in Afar Regional State, Ethiopia. – Hindawi Advances in Agriculture 6469104. <https://doi.org/10.1155/2018/6469104>.
- [18] Liebenbag, P. J., Zaid, A. (2002): Date Palm Irrigation. – FAO Plant Production and Protection Papers, 156 Rev. 1.
- [19] Little, T. M., F. J. Hills. (1972): Statistical Methods in Agricultural Research. – Univ. California, Davis, CA, USA.

- [20] Ministry of Agriculture and Land Reclamation, Economic Affairs Sector (EAS) (2016): Bulletin of the Agricultural Statistics, Part (2), Summer & Nili Crops, 2015. – Ministry of Agriculture and Land Reclamation, Dokka.
- [21] Ministry of Agriculture and Land Reclamation, Economic Affairs Sector (EAS) (2017): Bulletin of The Agricultural Statistics, Part (2), Summer & Nili Crops, vegetables & Fruits, 2016. – Ministry of Agriculture and Land Reclamation, Dokka.
- [22] Ministry of Agriculture and Land Reclamation, Economic Affairs Sector (EAS) (2018): Bulletin of The Agricultural Statistics, Part (2), Summer & Nili Crops, vegetables & Fruits, 2016. – Ministry of Agriculture and Land Reclamation, Dokka
- [23] Omar, M. E. M., Moussa, A. M. A. (2014): Water management in Egypt for facing the future challenges. – Journal of Advanced Research 7(3): 403-412.
- [24] Salama, A., Ansary, M., Elmorsy, A., El-Hamady, M. (2015): Survey of defects of orange in Egypt that affect its acceptability for exportation. – 1st International Congress in Postharvest Loss Prevention held in Rome, Italy (4-7 October).
- [25] Yahia, E. M., Lobo, M. G., Kader, A. A. (2014): Harvesting and Postharvest Technology of Dates. – In: Siddiq, M., Aleid, S. M. (eds.) – Dates: Postharvest Science, Processing Technology and Health Benefits. Wiley Blackwell, Hoboken, NJ, pp.108-113.

GRAFTING PERFORMANCE OF SOME WINE GRAPE (*VITIS VINIFERA* L.) CULTIVARS GRAFTED ON DIFFERENT AMERICAN GRAPEVINE ROOTSTOCKS

BEKAR, T.

*Siirt University, Faculty of Agriculture, Horticulture Department, 56000 Siirt, Turkey
(e-mail: tubabekar@gmail.com, tubabekar@siirt.edu.tr; phone: 05422272137)*

(Received 7th Feb 2019; accepted 29th Mar 2019)

Abstract. This study was conducted in the vine sapling production unit of "Kazova Vasfi Diren Agricultural Enterprise" located in central town of Tokat province in Turkey. The article attempted to graft five wine grape cultivars (Narince, Chardonnay, Merlot, Syrah, Öküzgözü) with five different American grapevine rootstocks (1103 Paulsen, 5BB, 41B, 110 R, 140 Ru) in order to combat mainly Phylloxera, but also provide protection against nematodes, lime and salinity-like soil-borne problems. Sapling yields of different cultivar/rootstock combinations were investigated. While the greatest sapling yield was observed in Narince/1103 Paulsen combination (98.03%), the lowest sapling yield was observed in Chardonnay/110R combination (43.64%).

Keywords: *vine rootstock, grapevine sapling, omega grafting, stratification room, sapling yield*

Introduction

Phylloxera (*Viteus vitifolii* Fitch.) was first encountered in France in 1863, then spread to European and Turkish lands. This pest feeds on the roots of culture vines and causes the termination of several grape cultivars (Yayla, 2008). Therefore, viticulture through direct rooting of scions of the local grape cultivars will not be economical. Laliman observed that some American grapevine rootstocks were resistant to Phylloxera, thus resistance to Phylloxera was achieved through grafting culture cultivars on these rootstocks (Winkler et al., 1974). For an economic viticulture, it is more appropriate to establish vineyards with vine saplings grafted on American grapevine rootstocks. American vine rootstocks are not only resistant to Phylloxera, but also serve alternative solutions for the problems related to nematodes, lime, salinity and the other soil-borne problems (Çelik et al., 1998).

Success of grafting is generally understood as callus layer formation between the rootstock and scion tissues and full-bonding and cohesion of them into a single plant (Janick, 1986; Çelik, 2007). In vine sapling production, sapling quality and final take ratios are largely dependent on whether or not the vines from which grafting materials were taken are free of pests and diseases, nutritional status of grafting materials, pre-grafting storage conditions of the rootstocks and scions, grafting method, attention paid to grafting, time of grafting, ambient conditions at stratification and following stages of grafted scions, mulching treatments, care and maintenance conditions after planting and the most important of all, cultivar/rootstock combinations (Kısmalı, 1978; Çelik and Ağaoğlu, 1982; Eriş et al., 1989; Kelen, 1994; Baydar and Ece, 2005).

Bhujbal (1993) used 1103P, 41B, SO4, Dogridge and Salt Creek rootstocks and Thompson Seedless cultivar and reported the best rooting and the greatest final take ratio for 1103P rootstock.

Dardeniz and Şahin (2005) grafted Uslu and Yalova İncisi grape cultivars on 1103P, 5BB, 41B and 140 Ru rootstocks and reported the greatest final take ratios as 44.61% and 37.47% for Uslu cultivar respectively grafted on 41B and 5BB rootstocks.

Ağaoğlu and Çelik (1982) grafted Hamburg Misketi, Hafızali and Hasandede grape cultivars on Kober 5BB and 99R rootstocks and reported total final take ratios varied as between 20-60%.

Kavak (2006) investigated the effects of Mycorrhiza and humic acid treatments on sapling final take ratios and reported the greatest grafting success (70.00%) for Yalova İncisi/1103P combinations and the lowest success ratio (52.67%) for Kalecik Karası/1103 P and Kalecik Karası/Fercal combinations.

Günen (2008) compared combinations of Cabernet Sauvignon and Syrah cultivars with five different rootstocks under open-field and greenhouse conditions and reported that ambient growth was significant. The greatest success was reported for Cabernet Sauvignon cultivar/1103 Paulsen combination as 90.08% in the first year and as 63.33% in the second year and for Syrah cultivar/1103 Paulsen combination as 91.67% in the first year and as 60.42% in the second year.

In this study, open-root sapling production was performed to assess the compatibility problems of commercially valuable wine grape cultivars of Narince, Chardonnay, Merlot, Syrah and Öküzgözü grafted on 1103 P, 5 BB, 41 B, 110 R and 140 Ru rootstocks commonly used in Turkey to propose solutions for Phylloxera, nematode, lime and salinity-like soil-born problems.

Material and method

This study was conducted in 2017 at the vine sapling production facility of Kazova Vasfı Diren Agricultural Enterprise in central town of Tokat province in Turkey (*Figure 1*). The 1103 P, 5 BB, 41 B, 110 R and 140 Ru American vine rootstocks and Narince, Chardonnay, Merlot, Syrah and Öküzgözü wine grape cultivars were used as the plant material of the study.

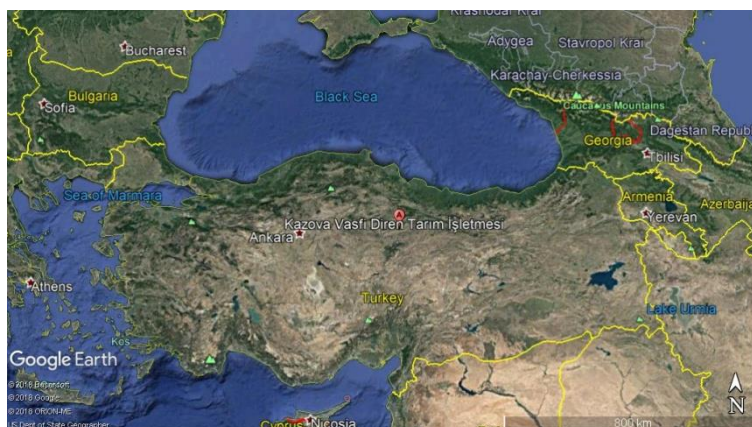


Figure 1. Study site

Shoots were taken from well-lignified mid-sections of annual branches, they were cut into single-bud scions and classified based on their thickness (7-8 mm, 9-10 mm and 11-12 mm thick) (Roux, 1988). Scions were treated with perlite moistened with water with

500 g/l Fenhexamid active ingredient against grey mold disease (*Botrytis cinerea*). Treated scions were then placed into plastic bags and stored in a cold storage at +4°C temperature for 2 months until the time of grafting (*Figure 2*).

Scions were cut into 30 cm long pieces as to have a single bud at the bottom and classified based on their thickness (7-8 mm, 9-10 mm and 11-12 mm thick). As can be seen in *Figure 3*, all buds were blunted except for the bottom one. Scions were then tied in bunches of 100 scions, placed into aseptic sacks and stored in a cold storage.



Figure 2. Processes applied to grafting scions



Figure 3. Processes applied to rootstocks

The scions (washed from the perlite over them) and rootstocks taken out of cold storage were kept outside (in a closed place) for three days. Rootstocks were kept in water-filled barrels and pools for two days (48 hours) and scions of the cultivars were kept in these places for one day (24 hours) (*Figure 4*). Just 6 hours before the end of this processes, 50% Benomyl was added only to holding water of scions to prevent the development of fungal diseases.

In this study, 37 500 grafted scions were produced [5 wine cultivars (Narince, Chardonnay, Merlot, Syrah and Öküzgözü) X 5 American Vine Rootstocks (1103 Paulsen, 5 BB, 41 B, 110 R and 140 Ru) X 3 replications X 500 grafted scions in each replicate] with omega bench grafting technique. Right after grafting, about 6 cm top section of grafted scions were coated with commercial paraffin prepared by using 1-5% wax, Vaseline, resin, bitumen, tar, mineral oil as well as efficient rate of fungicide and auxin and melted at 82°C. Following paraffin coating, grafted scions were taken into germination media and they were stacked into poplar shavings in Richter crates as recommended by Cangi et al. (2000) (*Figure 5*).

Richter crates were then taken into stratification room for callusing. Stratification room conditions were arranged as 28-29°C temperature, 85-90% relative humidity and ventilation at every 6 hours (Çelik, 1982). The grafted scions left in Richter crates in stratification room for 21 days were taken out and placed in a closed facility for 2 days. Richter crates were opened, cleaned and second paraffin coating was applied to scions with full overall callusing. Grafted scions were placed into water pools for 12 days (a night) and they were removed from the water and rested for 2 days (Figure 6).



Figure 4. Pre-grafting processes applied to rootstocks and scions



Figure 5. Omega grafting, paraffin coating and placement into Richter crates



Figure 6. Processes applied after stratification room

Before to take the grafted scions to the field on 25th of April, they were subjected to 2000 ppm IBA (indole-3 butyric acid) and planted onto previously mulch-covered seed beds at 20 x 10 cm (row spacing x on-row plant spacing) spacing (Figure 7).



Figure 7. Plantation of grafted scions to the field

Following the defoliation, saplings were removed from the field on 23rd of November. Saplings offered for sale were counted and sapling yield (final take) (%) for five wine grape cultivars and five American vine rootstock combinations was calculated as the ratio of number of saplings offered for sale to number of grafted scions.

$$SY = \left[\frac{NSOS}{NGS} \right] \times 100 \quad (\text{Eq.1})$$

where; SY= Sapling Yield (%), NSOS= Number of Saplings Offered for Sale, NGS= Number of Grafted Scions.

Statistical analysis

Experiments were conducted in randomized plots design with 3 replications. Following the analysis of variance, means were compared with Tukey's multiple range test at 1% significance level. JMP software was used in statistical analyses. Significant differences were indicated with the small letters by the data.

Standard deviation (SD)

Standard deviation calculations were performed to compare all experimental data in themselves.

Results and discussion

The results obtained for different cultivars are provided in *Tables 1, 2, 3, 4 and 5*. There were significant differences in number of saplings offered for sale and sapling yields of the cultivars ($p < 0.01$).

In Narince cultivar, the greatest number of saplings offered for sale and sapling yield (491.33 and 98.27%, respectively) were obtained from 1103 P combination and the lowest values (265.33 and 53.07%) were obtained from 110 R combination (*Table 1*).

Table 1. Sapling yields for Narince cultivar with different rootstocks (Mean \pm SD)

CULTIVAR	ROOTSTOCKS	NGS	NSOS	SY (%)
NARINCE	1103 P	500	491.33 \pm 2.60 a	98.27 \pm 0.52 a
	5 BB	500	424.00 \pm 2.08 c	84.80 \pm 0.42 c
	41 B	500	457.00 \pm 3.21 b	91.40 \pm 0.64 b
	110 R	500	265.33 \pm 1.45 e	53.07 \pm 0.29 e
	140 Ru	500	294.67 \pm 2.91 d	58.93 \pm 0.58 d

The means indicated with different letters in the same column are significantly different according to Tukey's test at $p < 0.01$. NGS: Number of Grafted Scions, NSOS: Number of Saplings Offered for Sale, SY: Sapling Yield

In Chardonnay cultivar, the greatest number of saplings offered for sale and sapling yield (399.00 and 79.80%, respectively) were obtained from 1103 P combination and the lowest values (218.67 and 43.73%) were obtained from 110 R combination (*Table 2*). The differences between 5 BB and 41 B rootstocks were not found to be significant.

Table 2. Sapling yields for Chardonnay cultivar with different rootstocks (Mean ± SD)

CULTIVAR	ROOTSTOCKS	NGS	NSOS	SY (%)
CHARDONNAY	1103 P	500	399.00±5.20 a	79.80±1.04 a
	5 BB	500	375.33±1.45 b	75.07±0.29 b
	41 B	500	373.67±2.60 b	74.73±0.52 b
	110 R	500	218.67±1.20 d	43.73±0.24 d
	140 Ru	500	277.33±1.20 c	55.47±0.24 c

The means indicated with different letters in the same column are significantly different according to Tukey's test at $p < 0.01$. NGS: Number of Grafted Scions, NSOS: Number of Saplings Offered for Sale, SY: Sapling Yield

In Merlot cultivar, the greatest number of saplings offered for sale and sapling yield (413.00 and 82.60%, respectively) were obtained from 1103 P combination and the lowest values (269.00 and 53.80%) were obtained from 110 R combination. The differences between 1103 P and 5 BB rootstocks were not found to be significant (Table 3).

Table 3. Sapling yields for Merlot cultivar with different rootstocks (Mean ± SD)

CULTIVAR	ROOTSTOCKS	NGS	NSOS	SY (%)
MERLOT	1103 P	500	413.00±2.08 a	82.60±0.42 a
	5 BB	500	407.67±2.03 a	81.53±0.41 a
	41 B	500	373.67±5.21 b	74.73±1.04 b
	110 R	500	269.00±2.08 d	53.80±0.42 d
	140 Ru	500	297.33±4.33 c	59.47±0.87 c

The means indicated with different letters in the same column are significantly different according to Tukey's test at $p < 0.01$. NGS: Number of Grafted Scions, NSOS: Number of Saplings Offered for Sale, SY: Sapling Yield

In Syrah cultivar, the greatest number of saplings offered for sale and sapling yield (391.33 and 78.27%, respectively) were obtained from 1103 P combination and the lowest values (254.33 and 50.87%) were obtained from 110 R combination (Table 4).

Table 4. Sapling yields for Syrah cultivar with different rootstocks (Mean ± SD)

CULTIVAR	ROOTSTOCKS	NGS	NSOS	SY (%)
SYRAH	1103 P	500	391.33±2.33 a	78.27±0.47 a
	5 BB	500	364.00±2.52 b	72.80±0.50 b
	41 B	500	379.00±1.53 ab	75.80±0.31 ab
	110 R	500	254.33±3.76 d	50.87±0.75 d
	140 Ru	500	310.33±1.20 c	62.07±0.24 c

The means indicated with different letters in the same column are significantly different according to Tukey's test at $p < 0.01$. NGS: Number of Grafted Scions, NSOS: Number of Saplings Offered for Sale, SY: Sapling Yield

In Öküzgözü cultivar, the greatest number of saplings offered for sale and sapling yield (376.67 and 75.33%, respectively) were obtained from 1103 P combination and the lowest values (248.67 and 49.73%) were obtained from 110 R combination (Table 5).

In a previous study comparing different cultivar/rootstock combinations under Isparta conditions, grafted vine saplings were produced through omega bench grafting and the greatest final take values were respectively reported for Razakı/SO4 combination (97.22%), Alphonse Lavallée/SO4 combination (98.33%) and Italia/1103 Paulsen combination (98.04%) (Baydar and Ece, 2005). In present study, the greatest final take values (yield) of all cultivars were reported for 1103 Paulsen combination.

Table 5. Sapling yields for Öküzgözü cultivar with different rootstocks (Mean ± SD)

CULTIVAR	ROOTSTOCKS	NGS	NSOS	SY (%)
ÖKÜZGÖZÜ	1103 P	500	376.67±0.33 a	75.33±0.07 a
	5 BB	500	355.67±2.60 b	71.13±0.52 b
	41 B	500	367.33±2.33 ab	73.47±0.47 ab
	110 R	500	248.67±1.45 d	49.73±0.29 d
	140 Ru	500	322.00±2.31 c	64.40±0.46 c

The means indicated with different letters in the same column are significantly different according to Tukey's test at $p < 0.01$. NGS: Number of Grafted Scions, NSOS: Number of Saplings Offered for Sale, SY: Sapling Yield

The greatest number of saplings offered for sale (491.33%) was obtained from Narince/1103 P interaction and the lowest value (218.67%) was obtained from Chardonnay/110 R interaction. The greatest sapling yield (98.27%) was obtained from Narince/1103 P interaction and the lowest value (43.73%) was obtained from Chardonnay/110 R interaction. While the greatest number of saplings offered for sale and sapling yields were observed in scions grafted on 1103 P rootstock and the lowest values were observed in scions grafted on 110 R rootstock. The differences in relevant values of Chardonnay/5 BB, Chardonnay/41 B, Merlot/41 B, Öküzgözü/1103 P, Chardonnay/140 Ru and Merlot/110 R interactions were not found to be significant (Table 6).

İşçi and Altındişli (2006) cleft-grafted different grape cultivars on rooted American vine rootstocks in place and reported final take ratios in 41 B and 110 R rootstocks respectively as 83 and 100% for Yuvarlak Çekirdeksiz cultivar, as 77 and 83% for Red Globe cultivar, as 84 and 80% for Buca Razakısı cultivar, as 100 and 81% for Trakya İlkereni cultivar and as 96 and 87% for Alphonse Lavallée cultivar. Similar different values were also observed in this study for different cultivars.

Alço et al. (2015) investigated the grafting room performance of different cultivar/rootstock combinations and reported grafting room performance of Cardinal, Merlot and Cabernet Sauvignon grape cultivars grafted on 110 R rootstock respectively as 96.50, 98.75 and 98.75% in 2012 and as 97.75, 96.25 and 86.25% in 2013. Researchers reported the grafting room performance of the same grape cultivars grafted on 5 BB rootstock respectively as 99.50, 99.75 and 99.50% in 2012 and as 74.25, 70.50 and 86.75% in 2013. Present values obtained for Merlot/110 R and 5 BB combinations were lower than those values.

Günen and Altındişli (2017) compared combinations of Cabernet Sauvignon cultivar with three different rootstocks in open field and undercover conditions. Researchers indicated that growth ambient did not have significant effects on grafting success ratios

and reported the greatest grafting success for 1103 Paulsen rootstock as 90.08% in the first year and as 63.33% in the second year, the lowest grafting success for 110 R rootstock in the first year (53.18%) and for 99 R rootstock in the second year (23.34%). Present findings were parallel to those results obtained for 1103 R rootstock.

Table 6. Sapling yields of cultivar/rootstock interactions (Mean \pm SD)

CULTIVARS	ROOTSTOCKS	NGS	NSOS	SY (%)
Narince	1103 P	500	491.33 \pm 2.60 a	98.27 \pm 0.52 a
	5 BB	500	424.00 \pm 2.08 c	84.80 \pm 0.42 c
	41 B	500	457.00 \pm 3.21 b	91.40 \pm 0.64 b
	110 R	500	265.33 \pm 1.45 mn	53.07 \pm 0.29 mn
	140 Ru	500	294.67 \pm 2.91 l	58.93 \pm 0.58 l
Chardonnay	1103 P	500	399.00 \pm 5.20 de	79.80 \pm 1.04 de
	5 BB	500	375.33 \pm 1.45 gh	75.07 \pm 0.29 gh
	41 B	500	373.67 \pm 2.60 gh	74.73 \pm 0.52 gh
	110 R	500	218.67 \pm 1.20 p	43.73 \pm 0.24 p
	140 Ru	500	277.33 \pm 1.20 m	55.47 \pm 0.24 m
Merlot	1103 P	500	413.00 \pm 2.08 cd	82.60 \pm 0.42 cd
	5 BB	500	407.67 \pm 2.03 d	81.53 \pm 0.41 d
	41 B	500	373.67 \pm 5.21 gh	74.73 \pm 1.04 gh
	110 R	500	269.00 \pm 2.08 m	53.80 \pm 0.42 m
	140 Ru	500	297.33 \pm 4.33 kl	59.47 \pm 0.87 kl
Syrah	1103 P	500	391.33 \pm 2.33 ef	78.27 \pm 0.47 ef
	5 BB	500	364.00 \pm 2.52 hi	72.80 \pm 0.50 hi
	41 B	500	379.00 \pm 1.53 fg	75.80 \pm 0.31 fg
	110 R	500	254.33 \pm 3.76 no	50.87 \pm 0.75 no
	140 Ru	500	310.33 \pm 1.20 jk	62.07 \pm 0.24 jk
Öküzgözü	1103 P	500	376.67 \pm 0.33 gh	75.33 \pm 0.07 gh
	5 BB	500	355.67 \pm 2.60 i	71.13 \pm 0.52 i
	41 B	500	367.33 \pm 2.33 gh ₁	73.47 \pm 0.47 gh ₁
	110 R	500	248.67 \pm 1.45 o	49.73 \pm 0.29 o
	140 Ru	500	322.00 \pm 2.31 j	64.40 \pm 0.46 j

The means indicated with different letters in the same column are significantly different according to Tukey's test at $p < 0.01$. NGS: Number of Grafted Scions, NSOS: Number of Saplings Offered for Sale, SY: Sapling Yield

Çelik and Gider (1991) grafted Alphonse Lavallée and Cardinal grape cultivars on 1103 Paulsen, 5 BB and S04 rooted rootstocks and indicated that grafting success varied with the cultivar/rootstock combinations and reported the greatest grafting success (98.08%) for Cardinal/1103P combination. Present findings were similar with those findings.

Eroğlu (2014) grafted Alphonse Lavallée and Red Globe grape cultivars on 110 R and 1103 P rootstocks and investigated the effects of different biological preparates on sapling performance. Researcher reported grafting success in 110 R and 1103 P rootstocks respectively as 97.00 and 99.00% for Alphonse Lavallée cultivar and as 97.60 and 97.90%

for Red Globe cultivar. While present findings were lower than those findings on 110 R and were parallel to findings on 1103 P rootstock.

Çoban and Kara (2003) investigated sapling quality of combinations of four different grape cultivars and three different American vine root stocks and reported sapling performance of Lival, Ribol, Danam and Datal cultivars respectively as 51.0, 60.0, 61.0 and 70.0% in 5 BB rootstock, as 45.0, 65.0, 60.0 and 65.0% in 99 R rootstock and as 48.6, 50.0, 60.0 and 60.0% in 110 R rootstock.

Çakır and Yücel (2016) investigated grafting performance of Narince and Kalecik Karası grape cultures on 1103 Paulsen rootstock and reported callus formation ratios as 77% in Narince and as 60% in Kalecik Karası grape cultivar.

Yağcı and Gökkaynak (2016) investigated sapling performance of Sultani Seedless grape cultivar on different rootstocks (110 R, 140 Ruggeri, 1613 C, 5 BB and Ramsey) and reported total sapling performance respectively as 51.5, 40.4, 50.3, 57.3 and 50.2%. While present findings were lower than those findings on 5 BB rootstock, they were parallel to findings on 110 R rootstock.

Conclusion

With the intrusion of Phylloxera pest into vineyards, local viticulture practices have become impossible in Turkey. Therefore, growers had to establish their vineyards with American vine rootstocks resistant to Phylloxera, well-adapted to ecological conditions and with a good affinity to grape cultivars to be grown. This study was conducted through omega bench grafting of five different wine grape cultivars (Narince, Chardonnay, Merlot, Syrah and Öküzgözü) on five different American vine rootstocks (1103 P, 5 BB, 41 B, 110 R and 140 Ru) compatible with different soil characteristics of Turkish vineyards. While the greatest sapling yield (98.03%) was observed in Narince/1103 Paulsen combination, the lowest yield (43.64%) was observed in Chardonnay/110R combination. Present findings provide significant background information against potential incompatibilities in grafted vine saplings. Before to decide on any combinations, compatibility and affinity of the available rootstocks to the cultivar, adaptation of the rootstocks to local ecological conditions, effects of the rootstocks on yield, quality, growth, development and nourishment of the cultivar all should be well put forth. Such attributes of the rootstocks should be taken into consideration while recommending rootstocks to growers for the cultivars they wish to grow. Such appropriate recommendations will have great contributions to success and yield in viticulture activities of the growers.

REFERENCES

- [1] Ağaoglu, Y. S., Çelik, H. (1982): Effect of grafting machines on success of grafted vine production. – U.Ü. Zir. Fak. Dergisi. 1: 25-32.
- [2] Alço, T., Dardeniz, A., Sağlam, M., Özer, C., Açıkbaz, B. (2015): The effects of different cultivar/rootstock combinations on grafting room efficiency and callus formation in grafted vines (Aşılı asma fidanı üretiminde farklı çeşit/anaç kombinasyonlarının aşısı odası randımanı ile kallus gelişim düzeyi üzerine etkileri). – Selçuk Üniversitesi, Selçuk Tarım ve Gıda Bilimleri Dergisi-A 27 (Türkiye 8. Bağcılık ve Teknolojileri Sempozyumu Özel Sayısı): s. 8-16.

- [3] Baydar, N. G., Ece, M. (2005): Comparison of different scion/rootstock combinations in the production of grafted grapevines in Isparta condition (Isparta koşullarında aşılı asma fidanı üretiminde farklı çeşit/anaç kombinasyonlarının karşılaştırılması). – Süleyman Demirel Üniversitesi, Fen Bilimleri Enstitüsü Dergisi, 9-3.
- [4] Bhujbal, B. G. (1993): Performance of five grape rootstocks for rooting and grafting. – Maharashtra Journal of Horticulture 7(1): 7-9.
- [5] Cangı, R., Balta, F., Doğan, A. (2000): Anatomical and histological investigations on the effects of stratification substrates on final take and quality of grafted vines (Aşılı asma fidanı üretiminde kullanılan katlama ortamlarının fidan randıman ve kalitesi üzerine etkilerinin anatomik ve histolojik olarak incelenmesi). – Türk JagricFor. 24: 393-398.
- [6] Çakır, A., Yücel, B. (2016): Determination of Narince and Kalecik Karası grape varieties with paulsen 1103 grapevine rootstocks grafting performance (Narince ve Kalecik Karası üzüm çeşitlerinin 1103 Paulsen amerikan asma anacı ile aşı performanslarının belirlenmesi). – Türk Tarım ve Doğa Bilimleri Dergisi 3(4): 311-317.
- [7] Çelik, H. (1982): The effects of different stratification room and NAA applications in the production of grafted-rooted grapevine sapling in greenhouse conditions for Kalecik Karası/41 B grafting combination (Kalecik karası/41 B aşı kombinasyonu için ser koşullarında yapılan aşılı-köklü fidan üretiminde değişik köklenme ortamları ve NAA uygulamalarının etkileri). – Doçentlik tezi (basılmamış), Ankara, s. 73.
- [8] Çelik, S., Gider, S. (1991): Grafting the rooted-rootstocks, planted to establish a vineyard, within same year (Bağ kurmak amacıyla dikilen köklü anaçların aynı yıl içinde aşılınması). – T.C. Tarım ve Köyüşleri Bakanlığı Türkiye 1. Fidancılık Sempozyumu, Ankara, 113-121.
- [9] Çelik, H., Ağaoglu, Y. S., Fidan, Y., Marasalı, B., Söylemezoğlu, G. (1998): General Viticulture (Genel Bağcılık). – Sun Fidan A. Ş. Mesleki Kitaplar Serisi: 1, Ankara, s. 253.
- [10] Çelik, S. (2007): Viticulture Ampelology [Bağcılık (Ampeloloji)]. – Namık Kemal Üniversitesi, Ziraat Fakültesi, Bahçe Bitkileri Bölümü. Cilt I. Genişletilmiş 2. Baskı. 428 s. Tekirdağ.
- [11] Çoban, H., Kara, S. (2003): Investigations on the effect of some grape (*Vitis vinifera* L.) varieties grafted on different rootstocks on the quality of grapevine saplings (Bazı üzüm (*Vitis vinifera* L.) çeşitlerinin asma anaçları ile aşı tutma durumu ve fidan kalitesine etkileri üzerine araştırmalar). – Journal of Aegean Agricultural Research Institute 13(1): 176-187.
- [12] Dardeniz, A., Şahin, A. O. (2005): The effects of the combinations of different varieties and rootstocks on the vegetative growth and nursery plant ratio for the production of grafted vine rootstocks (Aşılı asma fidanı üretiminde farklı çeşit ve anaç kombinasyonlarının vejetatif gelişme ve fidan randımanı üzerine etkileri). – Bahçe Dergisi. 34(2): 1-9.
- [13] Eriş, A., Soylu, A., Türkben, C. (1989): The effects of some applications on callus formation and rooting at the grafted site in the production of grafted-rooted grapevine sapling (Aşılı köklü asma fidanı üretiminde bazı uygulamaların aşı yerinde kallus oluşumu ve köklenme üzerine etkileri). – Bahçe 18(1-2): 29-34.
- [14] Eroğlu, D. (2014): The effects of different biological preparation applications on grafted sapling propagation in pots of some grape cultivars (Bazı üzüm çeşitlerinin aşılı tüplü fidan üretimlerinde farklı biyolojik preparat uygulamalarının etkileri). – Adnan Menderes Üniversitesi, Fen Bilimleri Enstitüsü (Yüksek Lisans Tezi), 81 s., Aydın.
- [15] Günen, E. (2008): Investigations on the effects of different rootstock-scion relations and propagation types on yield and quality of tubed vine grafts (Bazı şaraplık üzüm çeşitlerinin aşılı köklü asma fidanlarının üretiminde anaç kalem ilişkileri ve üretim şekillerinin fidan randımanı ile kalitesine etkileri üzerinde araştırmalar). – Ege Üniversitesi, Fen Bilimleri Enstitüsü (Doktora Tezi), s. 217. Bornova, İzmir.
- [16] Günen, E., Altındışli, A. (2017): An assesment of tube sapling performance of graft combinations of Cabernet Sauvignon grape variety with some american rootstocks under greenhouse and open field conditions (Cabernet Sauvignon üzüm çeşidinin bazı amerikan asma anaçları ile aşı kombinasyonlarının örtü altı ve açıkta yetiştiricilik koşullarında tüplü fidan performanslarının değerlendirilmesi). – Ege Üniv. Ziraat Fak. Derg. 54(1): 91-99.

- [17] İşçi, B., Altındişli, A. (2006): A research on take ratio of some grapes varieties of 41B and 110 R american rootstock (Bazı üzüm çeşitlerinin 41 B ve 110 R amerikan asma anaçları ile aşılı tutma yüzdesi üzerine araştırmalar). – Ege Üniv. Ziraat Fak. Derg., 43(2): 13-25.
- [18] Janick, J. (1986): Horticultural Science. – 4th. ed., W. H. Freeman and Company, New York, 39: 346. 746.
- [19] Kavak, O. (2006): The effects of mychorriza and humic acid applications on quality of grafted and potted plant propagation in grapes (Aşılı köklü ve tüplü asma fidanı üretiminde fidan kalite özelliklerine mikoriza ve humik asit uygulamalarının etkileri). – Selçuk Üniversitesi, Fen Bilimleri Enstitüsü (Yüksek Lisans Tezi), KONYA. s. 52.
- [20] Kelen, M. (1994): Investigations on the effects of some applications on the yield and quality of sapling in the production of grafted-rooted grapevine sapling, on the anatomical and histological investigation of grafted fusion (Bazı uygulamaların aşılı-köklü asma fidanı üretiminde fidan randımanı ve kalitesi üzerine etkileri ile aşılı kaynaşmasının anatomik ve histolojik olarak incelenmesi üzerine araştırmalar). – Y.Y.Ü. Fen Bil. Ens. (Doktora Tezi), VAN, 131 s.
- [21] Kısmalı, İ. (1978): Investigations on the production of grafted-rooted grapevine sapling made with Yuvarlak Çakirdeksiz grape varieties and different American grapevine rootstocks (Yuvarlak Çakirdeksiz üzüm çeşidi ve farklı Amerikan asma anaçları ile yapılan aşılı köklü asma fidanı üretimi üzerinde araştırmalar). – Basılmamış Doçentlik Tezi. 102 s.
- [22] Roux Le, D. J. (1988): The collection and storage of vineyard grafting material. – VORI leaflet, 209. Stellenbosch, South Africa, 2 p.
- [23] Winkler, A. J., Cook, J. A., Kliewer, W. M., Lider, L. A. (1974): General Viticulture. – University of California Press., Berkeley and Los Angeles, 633 p.
- [24] Yağcı, A., Gökkaynak, A. G. (2016): The effect of rootstock and shading ratio on seedling performance and quality of Sultani Çakirdeksiz grape cultivar (Sultani Çakirdeksiz üzüm çeşidinin fidan randımanı ve kalitesi üzerine anaç ve gölgeleme oranının etkisi). – Ege Üniv. Ziraat Fak. Derg. 53(1): 109-116.
- [25] Yayla, F. (2008): Investigation of wine characteristics of grape varieties in local collection vineyards (project intermediate report) [Milli koleksiyon bağındaki üzüm çeşitlerinin şaraplık özelliklerinin araştırılması (proje ara sonuç raporu)]. – s. 4, Bağcılık Araştırma Enstitüsü Müdürlüğü, Tekirdağ.

COMPARISON OF BIOACTIVITIES OF NATIVE DIATOMACEOUS EARTH AGAINST TURKESTAN COCKROACH [*BLATTA LATERALIS* WALKER (BLATTODEA: BLATTIDAE)] NYMPHS

ALKAN, M.^{1*} – ATAY, T.² – ERTÜRK, S.¹ – KEPENEKÇI, I.²

¹*Plant Protection Central Research Institute, 06172 Yenimahalle, Ankara, Turkey*

²*Tokat Gaziosmanpaşa University, Faculty of Agriculture, Department of Plant Protection, Tokat, Turkey*

*Corresponding author
e-mail: alkan0101@gmail.com

(Received 7th Feb 2019; accepted 29th Mar 2019)

Abstract. Cockroaches, *Blatta lateralis* Walker (Orthoptera: Blattidae) have been one of the important groups of insect pests in urban environments. In this study, it was investigated that the effects of different native diatomaceous earths samples against Turkestan cockroach, *Blatta lateralis* Walker (Blattodea: Blattidae) nymph in the laboratory conditions. For this purpose, three different diatomaceous earths (Turco000, Turca004 and Turco020), obtained from domestic sources, were tested in seven different doses (0.50 g/m², 0.75 g/m², 1 g/m², 1.25 g/m², 1.50 g/m², 1.75 g/m² and 2.00 g/m²). It was concluded that the increase in the application dose increased the mortality. Turco020 caused 100% mortality rate at the end of the 28th hour at the application dose of 1.25 g/m². Similarly, the dose of 1.25 g/m² of Turco004 and the dose of 0.75 g/m² of Turco000 at the same treatment period produced 100% mortality. Based on the statistical analysis, a positive interaction between particle size and biological activity was detected. These results showed that the diatomite obtained from local sources have an important role in the control of this household pest.

Keywords: *Turkestan cockroach, bioactivity, native, control, particle size, efficiency, household pest*

Introduction

The Turkestan cockroach, *Blatta lateralis* Walker (Blattodea: Blattidae), also known as the rusty red cockroach, red runner cockroach or simply rusty red, red runner is native to a large area of the Middle East extending from Libya eastward to Central Asia including Afghanistan, Pakistan, Uzbekistan, and southern Russia (Alesho, 1997). In addition, Kim and Rust (2013) reported that this species has become an important invasive species throughout the southwestern United States. The adults of Turkestan cockroach are three cm tall and adult females are shorter than male. The Turkestan cockroach females produce between two and 25 ootheca or egg capsules over their life span. Each ootheca contains about 18 eggs. The species becomes adult after five molts, the nymphal developmental period at 26.7°C is about 224 d. Five generations of Turkestan cockroaches require about 3 years (Kim and Rust, 2013).

Because of the species cause water and food contamination, transfer pathogens that cause diseases in human to induce allergic reactions and diseases (Shahraki et al., 2013). There is also a risk of damage to common household plants and crops that Turkestan cockroach feeds on once the cockroach reaches pest extents (Kim and Rust, 2013). In addition, Cranshaw (2011) reported that this species was known as a nuisance invader of homes in the United States. The use of insecticides is primarily preferred for

the control of cockroaches. However, alternative control methods have gained importance due to reasons such as the use of insecticides in indoor areas, threatening human and environmental health and developing resistance of cockroaches to insecticides. Some of the strains have shown resistance to up to 8-12 insecticide (Cochran, 2000; Kambayi et al., 2006).

In this context, there is growing interest in diatomaceous earth, which is known to be particularly effective against indoor pests (Faulde et al., 2006a; Alves et al., 2008; Hosseini et al., 2014; Islam and Rahman, 2016; Akhtar and Isman, 2016; Ertürk et al., 2017; Agnew and Romero, 2017; Atay et al., 2018). The mode of action of DE is generally accepted as desiccation affect on the insects (Faulde et al., 2006b). The effect primarily depends on its physical properties. There are different mechanisms of action such as abrasion of the cuticle, absorption of cuticular waxes, damage to the digestive tract, blockage of the spiracles and tracheae, and surface enlargement combined with dehydration (Ebeling, 1971; Faulde et al., 2006b).

The effectiveness of DEs for killing and controlling insect populations can vary depending on geographical origin, formulation process, oil absorption capacity, and chemical/mechanical modification of DEs, test conditions used and the species being tested (Quarles, 1992; Faulde et al., 2006b). This study was carried out to determine the efficacy of insecticidal activity of DE, which is obtained from domestic sources, against *B. lateralis* nymphs under laboratory conditions.

Material and methods

Rearing of Blatta lateralis

Turkestan cockroach nymphs were produced in 30 L plastic containers with 5 cm high peat at the base. A mixture of wheat flour and milk powder was used as a nutrient and water-absorbed paper for water needs (Figure 1). The colony was maintained in the climate room at $25 \pm 2^\circ\text{C}$, $65 \pm 5\%$ relative humidity and 12:12 (L:D) photoperiod.

Diatomaceous earth

Diatomaceous earth (DE)'s used in this study were acquired from a local commercial company operating in Ankara-Kazan and Beypazarı counties (Beg-tuğ Mineral). The particle sizes of the diatomaceous earth were ranged 1-10 μm , 10-30 μm , 43-65 μm , for Turco000, Turco004 and Turco020, respectively. Local diatomaceous earth mainly composes of SiO_2 (83-95%) and other minerals were found oxidized form of calcium, aluminum, iron in small amounts.

Bioassay tests

Turco000, Turco004 and Turco020 local diatomaceous earth were weighed in seven different doses (0.50 g/m^2 , 0.75 g/m^2 , 1 g/m^2 , 1.25 g/m^2 , 1.50 g/m^2 , 1.75 g/m^2 and 2.00 g/m^2) and added to 20 cm^2 glass bottles (Hosseini et al., 2014). Five of Turkestan cockroach nymphs in the same period (60-day-old) were placed into glass bottles. Honey was applied to the inner edges of the bottles to feed of the insects, the mouth of the bottle was covered with insect proof mesh and incubated at $25 \pm 2^\circ\text{C}$ and $65 \pm 5\%$ r.h. conditions. At the end of the fourth, eighth, 12, 16, 20, 24, 28, 32 and 36 hours live and dead insects were counted and recorded. In the experiment, the control group

were not treated with the DE. Trials were set up with randomized block design with 18 replications.



Figure 1. Rearing of *Blatta lateralis* in laboratory conditions

Statistical analysis

Contact toxicity test results were first converted into percent mortality and then were subjected to arcsine ($nR = \arcsin\sqrt{n}$) transformation and ANOVA. Variance analysis was carried out with transformed data and additionally, the differences among treatments were analysed by means of Tukey multiple comparison tests ($p < 0.05$). All statistical analyses were conducted with MINITAB® Release 16 package program.

Results

It was determined that different doses of Turco020 showed activity in varying proportions against Turkestan cockroach nymphs (*Table 1*).

In all of the studied periods 2.00 g/m² showed significant activity on the mortality of the nymphs. After four hours of treatment, the dose of 2.00 g/m² had a mortality rate of 72.33%, at the end of the eight hours treatment mortality rate reached 100%. The dose of 1 g/m² caused 97.39% mortality rate at the end of the 24th hours and took place in a different statistical group from the control. All doses showing with significant activity were in a different statistical group than the control group. The doses of 0.50 g/m², 0.75 g/m² and 1 g/m² did not provide 100% mortality rate in any time period.

Turco004 showed similar bio-activity together with Turco020 on Turkestan cockroach nymphs (*Table 2*). The lowest dose and the shortest duration time in terms of 100% mortality were 1.25g/m² dose and 28 hours of treatment, respectively. However, based on the treatment time, 2.00g/m² dose gave 100% mortality rate at the end of the 12th hour. This dose was statistically different from the control group. The doses of 1.25g/m², 1.50g/m², 1.75g/m² and 2.00g/m² gave 100% mortality rate different application time period.

Table 1. Mortality rates of Turco020 against Turkestan cockroaches

HAT	Mortality (%) ± SE*								
	Control	0.50g/m ²	0.75g/m ²	1g/m ²	1.25g/m ²	1.50g/m ²	1.75g/m ²	2.00g/m ²	
4	0.00±0.00c ¹	0.07±0.28c	1.06±0.91c	0.80±1.03c	4.05±2.19c	4.50±2.49c	23.85±3.95b	72.33±2.75a	F=27.98, df=7.143, P<0.05
8	0.00±0.00e	4.14±1.70de	11.50±1.61d	38.26±2.28c	78.58±2.02b	90.09±1.73b	99.74±0.53a	100.00±0.00a	F=124.71, df=7.143, P<0.05
12	0.00±0.00e	7.04±1.88d	33.44±1.27c	65.40±2.04b	98.94±0.91a	99.93±0.28a	100.00±0.00a	-	F=211.62, df=7.143, P<0.05
16	0.00±0.00e	18.56±1.73d	41.54±1.90c	79.57±2.21b	99.93±0.28a	100.00±0.00a	-	-	F=204.44, df=7.143, P<0.05
20	0.07±0.28e	20.61±1.45d	50.00±2.61c	89.62±3.10b	99.93±0.28a	-	-	-	F=153.42, df=7.143, P<0.05
24	0.07±0.28d	22.64±1.55c	58.56±1.77b	97.39±2.38a	100.00±0.00a	-	-	-	F=200.31, df=7.143, P<0.05
28	0.07±0.28d	22.64±1.55c	64.55±2.10b	98.09±1.81a	-	-	-	-	F=207.85, df=7.143, P<0.05
32	0.07±0.28d	24.53±1.85c	71.23±2.28b	98.38±1.46a	-	-	-	-	F=199.34, df=7.143, P<0.05
36	0.07±0.28d	27.88±1.50c	74.61±2.64b	98.38±1.46a	-	-	-	-	F=194.04, df=7.143, P<0.05

*Standard Error; HAT: Hour after treatment; ¹Different letters in the same line indicate statistically different from each other (Anova P < 0.05. Tukey test)

Table 2. Mortality rates of Turco004 against Turkestan cockroaches

HAT	Mortality (%)±SE*								
	Control	0.50g/m ²	0.75g/m ²	1g/m ²	1.25g/m ²	1.50g/m ²	1.75g/m ²	2.00g/m ²	
4	0.00±0.00d ¹	0.00±0.00d	0.07±0.28cd	1.65±1.06cd	3.66±1.48cd	5.74±2.01c	23.30±2.33b	53.91±1.91a	F=30.55, df=7.143, P<0.05
8	0.00±0.00e	5.79±1.91de	15.53±2.38d	46.32±2.70c	81.61±2.24b	94.21±1.91ab	94.16±1.51ab	98.67±1.19a	F=74.51, df=7.143, P<0.05
12	0.00±0.00d	13.95±1.97c	45.10±3.03b	66.99±2.57b	95.31±1.51a	98.02±1.32a	98.94±0.91a	100.00±0.00a	F=95.54, df=7.143, P<0.05
16	0.00±0.00e	21.42±2.02d	61.09±3.33c	86.89±1.86b	99.40±0.74a	99.93±0.28a	100.00±0.00a	-	F=138.81, df=7.143, P<0.05
20	0.00±0.00e	32.28±1.84d	72.33±2.27c	92.31±2.06b	99.74±0.53a	100.00±0.00a	-	-	F=163.61, df=7.143, P<0.05
24	0.00±0.00e	37.82±2.26d	76.42±1.95c	95.31±1.51b	99.93±0.28a	-	-	-	F=180.24, df=7.143, P<0.05
28	0.00±0.00d	40.34±1.72c	77.46±1.91b	98.02±1.32a	100.00±0.00a	-	-	-	F=221.59, df=7.143, P<0.05
32	0.00±0.00d	41.54±1.65c	84.38±1.98b	98.94±0.92a	-	-	-	-	F=240.78, df=7.143, P<0.05
36	0.00±0.00d	42.76±1.82c	86.96±1.96b	99.73±0.53a	-	-	-	-	F=255.58, df=7.143, P<0.05

*Standard Error; HAT: Hour after treatment; ¹Different letters in the same line indicate statistically different from each other (ANOVA P<0.05 Tukey test)

Turco 000 having the smallest particle size, showed that dose-dependent activity in varying proportions. In terms of the highest activity and the shortest application time, the dose of 0.75 g/m² provided 100% mortality at the end of the 28th hours. Besides, at the end of 12th hours, complete mortality was obtained at doses of 1.25 g/m² and above (Table 3). All doses and times showing significant bioactivity were in a different statistical group with the control group.

Table 3. Toxicity of Turco 000 against Turkestan cockroaches

HAT	Mortality (%)±SE*								
	Control	0.50g/m ²	0.75g/m ²	1g/m ²	1.25g/m ²	1.50g/m ²	1.75g/m ²	2.00g/m ²	
4	0.00±0.00c ¹	0.14±0.61c	1.65±1.06c	0.80±1.03c	3.22±1.25bc	3.66±1.48bc	16.53±2.08ab	19.18±2.52ab	F=9.19, df=7.143, P<0.05
8	0.00±0.00e	27.97±1.63d	64.12±1.83c	77.55±2.08c	83.39±1.67bc	94.88±2.21ab	96.34±1.48ab	99.40±0.74a	F=70.41, df=7.143, P<0.05
12	0.00±0.00d	48.77±1.14c	96.83±1.65b	99.73±0.53ab	100.00±0.00a	100.00±0.00a	100.00±0.00a	100.00±0.00a	F=329.37, df=7.143, P<0.05
16	0.00±0.00c	60.76±1.67b	99.40±0.74a	100.00±0.00a	-	-	-	-	F=446.07, df=7.143, P<0.05
20	0.00±0.00c	76.53±2.12b	99.93±0.28a	-	-	-	-	-	F=426.91, df=7.143, P<0.05
24	0.00±0.00c	77.47±1.97b	99.93±0.28a	-	-	-	-	-	F=455.25, df=7.143, P<0.05
28	0.00±0.00c	88.58±2.01b	100.00±0.00a	-	-	-	-	-	F=497.8, df=7.143, P<0.05
32	0.00±0.00c	91.64±2.22b	-	-	-	-	-	-	F=447.41, df=7.143, P<0.05
36	0.00±0.00c	95.91±2.10b	-	-	-	-	-	-	F=474.63, df=7.143, P<0.05

*Standart Error; HAT: Hour after treatment; ¹Different letters in the same line indicate statistically different from each other (Anova P<0.05. Tukey test)

Statistical analysis showed that there was a significant interaction between diatomaceous earth*dose and diatomaceous earth*time. Interactions of dose, time, and diatoms, both individually and with each other, were found to be statistically significant (Table 4).

Table 4. ANOVA parameters for main effects and interactions for mortality of Turkestan cockroach

Source	DF	Seq SS	Adj SS	Adj MS	F	P
Diatomaceous earth	2	4830	2959	1480	10.45	0.00
Doses	6	178891	49931	8322	58.78	0.00
Time	8	1318661	1034576	129322	913.5	0.00
Diatomaceous earth * Dose	12	39469	6830	569	4.02	0.00
Diatomaceous earth * Time	16	110531	55313	3457	24.42	0.00
Dose * Time	48	496830	443475	9239	65.26	0.00
Diatomaceous earth * Dose * Time	96	536729	536729	5591	39.49	0.00
Error	3213	454856	454856	142		
Total	3401	3140798				

Discussion

In this study was tested the effectiveness of the native diatomaceous earth, which is a biorational control method, for the Turkestan cockroach nymphs that are important indoor and outdoor pest, in terms of an alternative control method to the chemical compounds. In the trials, the insecticidal properties of local diatomaceous earth were initially tested in different doses and times against Turkestan cockroach nymphs and in this aspect, this study is a first in literature. Results from contact bioassays revealed that nymphs of the Turkestan cockroaches are sensitive to the diatomaceous earth at different rates. The most toxic formulation was Turco000 with the highest mortality rate and minimum exposure time (*Table 3*). It is known that the effect of the particle size on the effectiveness against insects is significant; smaller particles are significantly more effective than larger ones (Korunic et al., 2011). Similarly, Turco004 and Turco020 were less effective because of the having larger particle size than Turco000. The results we found supporting Bhan et al. (2014) findings showed that developed temephos and imidacloprid containing polyethylene glycol encapsulated nanopesticide with the melt-dispersion method and find more active against larvae of *Culex quinquefasciatus* (Diptera: Culicidae).

It is generally known for the diatomaceous earth that high relative humidity content effects the rate of mortality due to the desiccation (Fields, 1998; Subramanyam and Roesli, 2000; Fields and Korunic, 2000; Mewis and Ulrichs, 2001; Athanassiou et al., 2011; Frederick and Subramanyam, 2016). In our study, we used $65 \pm 5\%$ r.h. conditions in terms of determining the effect of the r.h. for the toxicity test. However, this relative humidity value needs to be diversified in future studies. Faulde et al. (2006a) revealed that seven kinds of DE formulation have been showing different toxicity at 25 g DE powder per m^2 to the adults of German cockroach, *Blattella germanica* (L.) (Orthoptera: Blattellidae) in a humid climate (85% r.h.), complete populations were eliminated within 10 days with FS 90.0S White, FS 90.0S, and FS 95.0 DE formulations tested. Our findings showed that the doses of $1g/m^2$ of Turco000 killed the Turkestan cockroach nymphs at the end of the 16th hour's treatment. It is estimated that morphological differences of different types of cockroaches and the origin of the diatomaceous affects the mortality rates of insects at several rates.

The reactions of biological stages of insects to diatomaceous earth are also different. It is known that larval or nymphal stages of insect more susceptible to the DE formulations. Older larvae or nymph stages are significantly more resistant than young larval periods (Vayias and Athanassiou, 2004). Although the adult cockroach was not used in this study, it can be said that the nymphal periods of Turkestan cockroach are more sensitive to diatomaceous earth. Similarly, Hosseini et al. (2014) reported that the dose of $25 g/m^2$ of DE completely kills the nymphal stages of German cockroaches at 72 hours, while LC_{50} and LC_{90} values for adults determined as a $12.9034 g/m^2$ and $626.0942 g/m^2$, respectively. Vayias and Athanassiou (2004) stated that all larvae of *Tribolium castaneum* Herbst, 1797 (Coleoptera: Tenebrionidae) were killed at the dose of 1.5 g/kg of SilicoSec whereas this rate was 50% in adults after 48 hours exposure period.

As a result, cockroaches emerge as a problem in terms of hygiene in areas where human activity and habitats are intense. Cockroaches are the potential carrier of human diseases, a pathogenic organism such as bacteria, protozoa, fungi, and helminths (Tatfeng et al., 2005; Baumholtz et al., 2008). In addition, increased awareness of side effect of the synthetic pesticides to the society, the resistance statues of insects against

pesticides, has also led to the need to investigate safe control methods for the cockroaches that can be used in the integrated pest management system.

Conclusions

Diatomaceous earth can be regarded, as have strongly insecticidal properties against Turkestan cockroach. The results show that there is a negative correlation between particle size and activity. In view of these findings, native diatomaceous earth should be investigated in different humidity and temperature conditions against an invasive species Turkestan cockroach adults and nymphs.

REFERENCES

- [1] Agnew, J., Romero, A. (2017): Behavioral responses of the common bed bug, *Cimex lectularius*, to insecticide dusts. – *Insects* 8(3): 83.
- [2] Akhtar, Y., Isman, M. B. (2016): Efficacy of diatomaceous earth and a DE-aerosol formulation against the common bed bug, *Cimex lectularius* Linnaeus in the laboratory. – *Journal of pest science* 89(4): 1013-1021.
- [3] Alesho, N. A. (1997): Synanthropic cockroaches of Russia. – *Proc. Inter. Coll. Social Insects* 34: 45-50.
- [4] Alves, L. F., Oliveira, D. G., Neves, P. M. (2008): Factors affecting diatomaceous earth effectiveness in the control of *Alphitobius diaperinus* (Panzer) (Coleoptera: Tenebrionidae) adults. – *Neotrop Entomol* 37(6): 716-722.
- [5] Atay, T., Akın, A., Alkan, M., Ertürk, S. (2018): Pre-Studies on Contact Toxicity of Some Local Diatomaceous Earths on Mealworm, *Tenebrio molitor* L. (Coleoptera:Tenebrionidae), Larvae. – I. International Agricultural Science Congress, 09-12 May 2018, Van/Turkey, p494.
- [6] Athanassiou, C. G., Kavallieratos, N. G., Vayias, B. J., Tomanovic, Z., Petrovic, A., Rozman, V., Adler, C., Korunic, Z., Milovanovic, D. (2011): Laboratory evaluation of diatomaceous earth deposits mined from several locations in central and southeastern Europe as potential protectants against coleopteran grain pests. – *Crop Prot.* 30: 329-339.
- [7] Baumholtz, M. A., Parish, L. C., Witkowski, J. A., Nutting, W. B. (2008): The medical importance of cockroaches. – *Int J Dermatol.* 36: 90-6.
- [8] Bhan, S., Mohan, L., Srivastava, C. N. (2014): Relative larvicidal potentiality of nano-encapsulated Temephos and Imidacloprid against *Culex quinquefasciatus*. – *Journal of Asia-Pacific Entomology* 17(4): 787-791.
- [9] Cochran, D. G. (2000): Cockroach: their biology, distribution, and control. – WHO/CDS/CPC/ WHO st ed, 2000. <http://www.who.int/iris/handle/10665/65846>.
- [10] Cranshaw, W. (2011): A review of nuisance invader household pests of the United States. – *American Entomologist* 57(3): 165-169.
- [11] Ebeling, W. (1971): Sorptive dusts for pest control. – *Annu Rev Entomol.* 16: 123-158.
- [12] Ertürk, S., Ferizli, A. G., Emekci, M. (2017): Depolanmış çeltikte piriç biti, *Sitophilus oryzae* L., 1763 (Coleoptera: Curculionidae)'nin mücadelesinde diyatom toprağı formülasyonlarının değerlendirilmesi. – *Türkiye Entomoloji Dergisi* 41(3): 347-354.
- [13] Faulde, M. K., Tisch, M., Scharninghausen, J. J. (2006a): Efficacy of modified diatomaceous earth on different cockroach species (Orthoptera, Blattellidae) and silverfish (Thysanura, Lepismatidae). – *J Pest Sci.* 79: 155-161.
- [14] Faulde, M. K., Scharninghausen, J. J., Cavaljug, S. (2006b): Toxic and behavioural effects of different modified diatomaceous earths on the German cockroach, *Blattella germanica* (L.) (Orthoptera: Blattellidae) under simulated field conditions. – *Journal of Stored Products Research* 42: 253-263.

- [15] Fields, P. (1998): Diatomaceous earth: advantages and limitations. – In: Zuxun, J., Quan, L., Yongsheng, L., Xianchang, T., Lianghua, G. (eds.) Proceedings of the seventh international working conference of stored products protection. Sichuan Publishing House of Science & Technology, Peoples Republic of China. I, pp 781-789.
- [16] Fields, P., Korunic, Z. (2000): The effect of grain moisture content and temperature on the efficacy of diatomaceous earths from different geographical locations against stored-product beetles. – J Stored Prod Res. 36: 113.
- [17] Frederick, J. L., Subramanyam, B. (2016): Influence of temperature and application rate on efficacy of a diatomaceous earth formulation against *Tribolium castaneum* adults. – Journal of Stored Products Research 69: 86-90.
- [18] Hosseini, S. A., Bazrafkan, S., Vatandoost, H., Abaei, M. R., Ahmadi, M. S., Tavassoli, M., Shayeghi, M. (2014): The insecticidal effect of diatomaceous earth against adults and nymphs of *Blattella germanica*. – Asian Pacific journal of tropical biomedicine 4: 228-232.
- [19] Islam, M. S., Rahman, M. M. (2016): Diatomaceous earth induced alterations in the reproductive attributes in the housefly *Musca domestica* L. (Diptera: Culicidae). – Elixir Appl. Zool 2(5).
- [20] Kamyabi, F., Vatan Doost, H., Abolhassani, M., Aghasi, M., Telmadarehei, Z., Abaei, M. R. (2006): Susceptibility of different strains of German cockroach, (*B. Germanica*) to three insecticides in hospitals affiliated to Kerman University of Medical Sciences. – Journal of Mazandaran University of Medical Sciences 16: 108-98.
- [21] Kim, T., Rust, M. K. (2013): Life history and biology of the invasive Turkestan cockroach (Dictyoptera: Blattidae). – Journal of economic entomology 106(6): 2428-2432.
- [22] Korunic, Z., Rozman, V., Halamic, J., Kalinovic, I., Hamel, D. (2011): Insecticide potential of diatomaceous earth from Croatia. – IOBC-WPRS Bulletin 69: 389-397.
- [23] Mewis, I., Ulrichs, C. H. (2001): Action of amorphous diatomaceous earth against different stages of the stored product pests *Tribolium confusum*, *Tenebrio molitor*, *Sitophilus granarius* and *Plodia interpunctella*. – J Stored Prod Res. 37: 153-164.
- [24] Quarles, W. (1992): Diatomaceous earth for pest control. – The IPM Practitioner 14(5/6): 1-11.
- [25] Shahraki, G. H., Parhizkar, S., Nejad, A. R. S. (2013): Cockroach Infestation and Factors Affecting the Estimation of Cockroach Population in Urban Communities. – International Journal of Zoology 2013: 1-6.
- [26] Subramanyam, B. H., Roesli, R. (2000): Inert dusts. – In: Subramanyam, B. H., Hagstrum, D. W. (eds.) Alternatives to pesticides in stored-product IPM. Dordrecht: Kluwer Academic Publishers. p. 321-373.
- [27] Tatfeng, Y. M., Usuanlel, M. U., Orukpe, A., Digban, A. K., Okodua, M., Oviasogie, F. (2005): Mechanical transmission of pathogenic organisms: the role of cockroaches. – J Vect Born Dis. 42: 129-34.
- [28] Vayias, B. J., Athanassiou, C. G. (2004): Factors affecting the insecticidal efficacy of the diatomaceous earth formulation Silico-Sec against adults and larvae of the confused flour beetle, *Tribolium confusum* Du Val (Coleoptera: Tenebrionidae). – Crop Protection 23: 565-573.

PROFICIENCY OF BILOT METHODS (AMMI AND GGE) IN THE APPRAISAL OF TRITICALE GENOTYPES IN MULTIPLE ENVIRONMENTS

KENDAL, E.^{1*} – TEKDAL, S.² – KARAMAN, M.³

¹*Mardin Artuklu University, Department of Plant and Animal Production, Kiziltepe Vocational and Training High School, Mardin, Turkey*

²*GAP International Agricultural Research and Training Center, 21100 Diyarbakir, Turkey*

³*Muş Alparslan University, Faculty of Applied Sciences, Department of Plant and Production Technologies, Muş, Turkey*

**Corresponding author
e-mail: enver21_1@hotmail.com*

(Received 8th Feb 2019; accepted 21st Mar 2019)

Abstract. The AMMI (additive main effect and multiplicative interaction) and GGE (genotype, genotype x environment) biplot analyses were used to evaluate and identify stability and yield of Triticale genotypes at three different locations throughout two years (2014-15-2015-16). The AMMI analysis of variance showed significant genotype, environment and GE interaction and indicated 1.31, 98.40 and 0.28% of total variation, respectively. The GGE bi-plot analysis indicated 78.19% of the total variation (PC1 (principle component) 50.01%, and PC2 26.08%). This study has been useful to discriminate genotypes with superior and stable yield evaluated by the AMMI analysis and yield stability index incorporating the AMMI stability value and yield capacity in a single non-parametric index. The AMMI analysis indicated that G4, G8 (candidate) and G6 were found to be quite promising genotypes. In the GGE biplot analysis genotypes were investigated in two mega-environments, and the first mega-environment covered E3, E5 and E6, and the second mega-environment covered E1, E2 and E4. The genotypes G6, G8, G9 and G11 were the winning genotypes in ME (mega-environment) I, G3, G4 and G12 and in ME II. The GGE and AMMI biplot approaches let us to describe the best genotypes, and G8 to be stable and high yielding for both ME, G6 only for ME I, G4 only for ME II and can be recommended to release as a cultivar.

Keywords: *stability, interaction, yield, multi, approach*

Introduction

In order to ensure an adequate and balanced diet of the growing world population, food production should be increased in parallel. This is possible through the development and application of new cultivation techniques and also by the development of more efficient and high quality plant species. For this purpose, Triticale (x *Triticosecale Wittmack*), was developed as a new species, a hybrid of wheat and rye, used as an alternative cereal crop for growing in marginal areas (Kendal and Sayar, 2016). This new species is known that it is tolerant to diseases, pests, dry conditions, acid and problematic soils and it was determined that it could replace cereal forage crops. Triticale is mostly used in animal feeding and it is also evaluated as grain, roughage, silage and straw. The feed value of triticale is equivalent to corn, wheat, barley, rye and sorghum or better than them, while in feed rations, it can be preferred instead of corn, wheat, barley, rye and oats. Triticale is used primarily as animal feed,

and in recent years it has also been used in human food and ethanol production (Oral, 2018).

Triticale cultivation in the world has shown an increase of over 40% in the last a decade years. The area of cultivation of triticale is 3.8 million ha, and the production is around 14.7 million tons in the world, and this rate is increasing day by day (Anonymus 2; Ayalew et al., 2018). In Turkey, statistical data related to triticale production have started to be given after 2004, and in 2016, about 38.000 ha area was planted and about 125.000 tons of product was obtained from this area. However, in our country, Triticale is the highest yield in cereals and grain yields approximately 3360 kg per hectare (Anonymous 1; Kizilgeci, 2019). Therefore, triticale is gaining more and more attention both in the world and in our country.

The exploiting of heredity instability is one of the very significant issues in terms of breeding strategies and this situation can only be explained by phenotypically phrase (Rad et al., 2013). In order to explain the phenotypic variations, it is highly dependent on the effect of the environments. Explaining this diversity is upwards sophisticated by the fact that all genotypes don't react in the same way as change in circles and the two environments do not have exactly the same conditions (Neisse et al., 2018). If the performance of genotypes changes in different location, then the interaction of the genotype location is an important factor in plant breeding strategies. Therefore, analysis of any variance combined can measure GEI and identify main effectiveness, however it is not enough to declare the GEI effectiveness. A convenient analytic pattern like the additive main effects and multiplicative interaction (AMMI) can cure both the additive main effect and multiplicative interaction constituent utilize the ANOVA (analysis of variance) and IPCA (Interaction Principal Components), respectively (Kilic, 2014; Mohammadi et al., 2018). The GGE biplot exploits the PCA approach to investigate the multi environment data and allow the visual presentation of the relationship among genotypes, environments and interaction as well as.

The aim of this study were to (i) analyses the effect of GEI on grain yield of 12 triticale genotypes by two new biplot models (AMMI and GGE) (ii) identifying high yielding and stable triticale genotype(s) across locations and (iii) to detect appropriate genotype(s) for every location or environment.

Material and Methods

The ten spring triticale advanced lines and two local check were evaluated in three locations across two years (2014-2015 and 2015-2016 growing seasons). The information of genotypes showed in *Table 1*. The trials were planted following a randomized complete block design with four replications at each location. The information about test location is given in *Table 2*. Each parcel was set in a six row plot of 6 meter length and 1.2 m diameter with plant spacing of 20 cm. Sowing of trials were done in autumn and sowing density was used 500 seeds in per m⁻². The fertilization of planting time, 60 kg N ha⁻¹ and 60 kg P ha⁻¹ were used, and 60 kg N ha⁻¹ was used to each plots at tillering time for all plots. The grain yield was recorded from each plot after harvesting of the materials and measured extrapolated to ton/ha.

The described growing seasons 2014-2015

The rainfall was the same with long term in all location and it was enough for germination of plant after sowing time in October, the triticale had good weather in

winter days. Seasonal conditions were favorable for triticale cultivation in the development period in March and April in all location. Therefore, the expected high yield was obtained in all location of 2014-15 growing season. All location had good growing season, but in Ceylanpınar location the rainfall is very low than other location and it was partially heat stress during after heading time, in Adiyaman location during the spring period there was partially heat stress, In Diyarbakir location, conditions were more favorable than other locations.

Table 1. The code, name/pedigree of triticale genotypes

Code	Name of cultivar and pedigree of lines	Orijin
G1	LIRON_2/5/DIS B5/3/SPHD/PVN/YOGUI_6/4/ CTSS04Y00163S-102Y-06M-06Y-2M-3Y-0M-0SD-0SD-0SD	CIMMYT
G2	PRESTO//2*TESMO_1/MUSX 603/4/ARDI_1/... CTSS03Y00091T-050TOPY-5M-2Y-06Y-5M-1Y-0M-0SD-0SD-0SD	CIMMYT
G3	LIRON_2/5/DIS B5/3/SPHD/PVN/YOGUI_6/4/ CTSS03Y00033T-A-62M-1Y-06Y-2M-4Y-0M-0SD-0SD-0SD	CIMMYT
G4	TURACO/CENT.SARDEV/7/LIRON_2/5/DIS B5/3/... CTSS02B00186T-8Y-3M-3Y-4M-1Y-0M-0SD-0SD-0SD	CIMMYT
G5	Tacettinbey(check) -----Cukurova University	TURKEY
G6	DRIRA/2*CMH77A.1165/8/NIMIR_3/ERIZO_12/5/... CTSS02B0028T-6Y-3M-3Y-4M-2Y-0M-0SD-0SD-0SD	CIMMYT
G7	LIRON_2/5/DIS B5/3/SPHD/PVN/YOGUI_6/4/ CTSS02B00413S-22Y-2M-3Y-1M-2Y-0M-0SD-0SD-0SD	CIMMYT
G8	HX87-244/HX87-255/5/PRESTO//2*TESMO_1/... CTSS03SH00028S-25Y-2M-4Y-3M-1Y-0M-0SD-0SD-0SD	CIMMYT
G9	HX87-244/HX87-255/7/LIRON_2/5/DIS B5/3/SPHD/... CTSS03SH00030S-17Y-3M-4Y-3M-1Y-0M-0SD-0SD-SD	CIMMYT
G10	Presto(check) Transitional Zone Agricultural Research Institute	TURKEY
G11	LIRON_2/5/DIS B5/3/SPHD/PVN/YOGUI_6/4/... CTSS03Y00036T-A-1M-2Y-06Y-2M-4Y-0M-0SD-0SD-0SD	CIMMYT
G12	LIRON_2/5/DIS B5/3/SPHD/PVN/YOGUI_6/4/... CTSS03Y00036T-A-1M-4Y-06Y-4M-1Y-0M-0SD-0SD-0SD	CIMMYT

Table 2. Years, sites, codes and coordinate status of environments

Years	Code of Sites	Sites	Altitude (m)	Latitude	Longitude	Averag. of pers. (mm)
2014-2015	E1	Diyarbakır	612	37° 55' N	40° 14' E	584.2
	E2	Adiyaman	669	37° 76' N	38° 27' E	540.3
	E3	Ceylanpınar	366	36° 84' N	40° 05' E	306.0
2015-2016	E4	Diyarbakır	612	37° 55' N	40° 14' E	417.2
	E5	Adiyaman	669	37° 76' N	38° 27' E	402.4
	E6	Ceylanpınar	366	36° 84' N	40° 05' E	217.0

The described growing seasons 2015-2016

The rainfall of second season was late in planting time and it was low, in development of plant time, when we compare it with long term rainfall of locations. On the other hand; the temperature was high. Genotypes were exposed to drought in Ceylanpınar location. In the Adiyaman location, it was partially exposed to temperature stress. In Diyarbakır, heat stress was effective after heading period in April. Therefore, the grain yield of 2014-2015 season was suitable than 2015-16 growing season in all locations. The conditions of Ceylanpınar location is usually hard than other location, because the total of rainfall of seasons usually is low (Table 2).

Statistical analysis (AMMI and GGE)

The AMMI analysis was carried out using the adjusted mean values of grain yield to detect the relation among genotypes, locations and GEI over model designated by Zobel et al. (1988). The adopted method uses PCA to decompose the multiplicative effects of GEI into a number of IPCA. The two models (AMMI and GGE) analysis were carried out by Genstat software (version 12). The Additive mean effect and multiplicative interaction model analysis is based on the following formula; $Y_{ger} = \mu + \alpha_g + \beta_e + \sum_n \lambda_n \gamma_{gn} \delta_{en} + \epsilon_{ger} + \rho_{ge}$; where, Y_{ger} is the monitored grain yield of genotype (g) in environment (e) for replication (r); Additive parameters: μ is the grand mean; α_g is the deviation of genotype g from the grand mean, β_e is the deviation of the environment e; Multiplicative parameters: λ_n is the singular value for IPCA, γ_{gn} is the genotype eigenvector for axis n, and δ_{en} is the environment eigenvector; ϵ_{ger} is error term and ρ_{ge} is PCA residual.

AMMI Stability Value (ASV) is the space from the origin to the coordinate point in a two dimensional plot of to IPCA scores (Purchase, 1997). Because the IPCA1 score contributes to the sum of squares of GEI, a weighted value is needed. This weighted value was calculated for each genotype and each environment according to the relative contribution of IPCA1 to IPCA2 to the interaction sum of squares as follows:

$$ASV = \sqrt{\left[\frac{SS_{IPCA1}}{SS_{IPCA1} + SS_{IPCA2}} (IPCA1Score)^2 \right] + (IPCA2Score)^2} \quad (Eq.1)$$

Where, SS_{IPCA1} / SS_{IPCA2} is the weight given to the IPCA1-value by dividing the IPCA1 sum of squares by the IPCA2 sum of squares (Purchase, 1997).

Genotypic stability index (GSI) incorporate mean and stability index in a single criteria and calculated as: $GSI = RASV + RY$ where, RASV is the rank of ASV and RY is the rank of mean yield of genotypes across environments. This index considered the rank of AMMI stability value to rank genotypes based on grain yield across environments.

On the other hand; data were graphically analyzed to interpret GEI to identify stable and adaptive genotypes using the GGE biplot described by Yan and Tinker (2006). The GGE biplot methodology (Yan et al., 2000) was applied for analysis of GE interaction of grain yield. The GGE biplot model is based on the following formula:

$$E(Y_{ij}) = \mu + \beta_j + K \sum_k \delta_k \gamma_{ik} \eta_{jk} \quad (Eq.2)$$

where $E(Y_{ij})$ is the expectation value of genotype i in environment j ; μ is the grand mean; β_j is the environment effect; K stand for the number of principal the environment effect; K stand for the number of principal components (PC) needed to provide an adequate explanation of G + GE; δ_k is singular value for the kth PC; and stands for the $\delta_k \gamma_{ik} \eta_{jk}$ ith genotype score and stands for the jth environmental score for the kth PC. Singular value η_{jk} partitioning is achieved by providing a scaling factor f to obtain alternative genotype ($c_{ik} = \delta_k^f$ and environment scores. The symmetric scaling ($f = 0.5$) was used in γ_{ik} ($d_{jk} = \delta_k^{1-f} \eta_{jk}$) visualizing which-wins-where pattern of MET data, due to its compliance with most of the features related to other benchmarking methods (Yan, 2002).

Result

The AMMI analysis

The variance of AMMI analysis showed that genotype, environment, GEI and IPCA (Interaction principle component analysis) had significant ($p < 0.01$) effect on triticale grain yield of 12 genotypes tested in six environments (*Table 3*). The environment main effect accounted for 98.40% of total variation, compared with 1.31% for genotype and 0.28% for GE interaction effects in the analysis of combined variance (*Table 3*). The quantity of genotypic effect was about two times greater than the GEI effect, which indicates different possible presence of MEs in the METs data. The major differences between the circles influenced the average of squares and caused the grain yield of each environment to change. The multiplicative variance of the treatment sum of squares due to interaction was partitioned into the fourth interaction principal components and the only one of them significant effect. The first PCs accounted for 56.75%, the second for 17.56%, the third for 17.11%, and the fourth only 8.55% of G+GE total variation for triticale data. Except the first IPCA-I, the remaining three IPC axes were non-significant and contributed 43.22% of the GEI (*Table 3*).

Table 3. *The analysis of variance for grain yield using AMMI model*

Source	df	SS	MS	F	G+E+GE SS explained (%)
Total	287.00	1091.60	3.80	-	-
Treatments	71.00	1024.40	14.43	55.80	-
Genotypes	11.00	28.40	2.58	9.98**	1.31
Environments	5.00	965.60	193.11	216.61**	98.40
Block	18.00	16.00	0.89	3.45	-
Interactions	55.00	30.40	0.55	2.14**	0.28
IPCA 1	15.00	19.00	1.26	4.89**	56.75
IPCA 2	13.00	5.00	0.39	1.50ns	17.56
IPCA 3	11.00	4.20	0.38	1.46ns	17.11
IPCA 4	9.00	1.80	0.19	0.75ns	8.55
Residuals	7.00	0.50	0.07	0.27	-
Error	198.00	51.20	0.26	-	-

df - degrees of freedom; SS - sum of squares; MS - mean square. **, $p < 0.01$; G - genotypes; E - environments

In the AMMI model, the figure interpret by two direction and x-axis represents the genotypes and environment main effect and y-axis represents the effects of interaction (*Fig. 1*). The genotypes and environment indicated much more variability in both main effect and interaction. The environment located above the y-axis mean that they are desirable and high-efficient, whereas the environments, which are located under of y-axis mean that they are unfavorable and low-yielding (Kendal and Tekdal, 2016). According to these definitions, in the AMMI (*Fig. 1*) indicated that grain yield of the first year (7.244 t/ha) is higher than in the second year (3.979 t/ha) in all locations (*Fig. 1 and Table 4*). When we evaluate the locations based on grain yield average, all locations were located above average (y axis) in the first crop season (2014-15), while all location were located under average (y axis) in the second crop season (2015-16). This implies that grain yield of first year in all locations were higher than the second year. On the other hand, when we evaluate the environments independently, the highest yield average is obtained from E1 and the lowest yield average is obtained from E6.

According to the location averages, Diyarbakir location (6.529 t/ha) is found to be more efficient than the other two locations in both years (Fig. 1 and Table 5). The AMMI (Fig. 1) also shows the stability of genotype based on mean grain yield of multiple environments. The genotypes located near the x-axis and on the right of the y-axis mean that they are stable and high-efficient, whereas the genotypes, which are located far from x-axis and left side of y-axis mean that they are unstable and low-yielding (Crossa et al., 1990). Accordingly, G7, G4 and G8 placement of near x axis and on the right of the y-axis, therefore it mean that these genotypes are quite stable and yielding. Moreover; G1, G3, G10 (check) and placement of far from x axis, so these genotypes are unstable across environments. The AMMI (Fig. 1) biplot showed that G4, G6 and G8 are quite yielding, while both of check used in the study (G5 and G10) are poorest genotypes across test environments (Table 4).

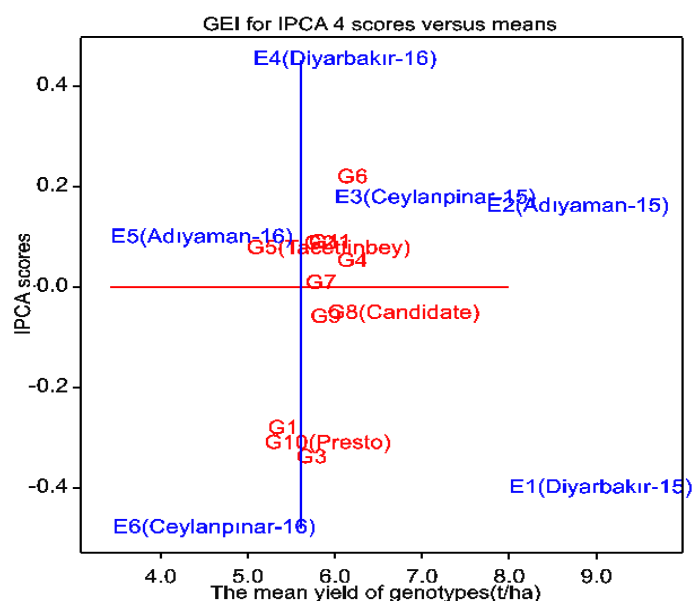


Figure1. The AMMI shows the stability of genotype based on mean grain yield of multiple environments. The genotypes located near the x-axis and on the right of the y-axis mean that they are stable and high-efficient, whereas the genotypes, which are located far from x-axis and left side of y-axis mean that they are unstable and low-yielding. G1-G12 is the codes for the triticales disomic addition lines and G5 and G10 used as the control, respectively. E1- E3 are environment codes for 2014-15, E4-E6 for 2015-16 growing season

Table 4. The genotype means and IPCA scores based on six environments

Genotypes	Gen mean	IPCAg[1]	IPCAg[2]	IPCAg[3]	IPCAg[4]
G1	5.228	0.31884	0.21680	-0.37392	-0.28371
G2	5.644	0.35121	-0.47205	0.00288	0.08386
G3	5.553	-0.62687	-0.41001	0.10880	-0.34148
G4	6.022	-1.08531	0.33717	0.08051	0.04918
G5	4.984	0.34995	0.37082	0.64101	0.07483
G6	6.022	0.29643	0.34783	-0.12295	0.21614
G7	5.660	0.16724	-0.40324	0.39346	0.00543
G8	5.911	0.05858	-0.04726	-0.23521	-0.05409
G9	5.714	-0.03673	0.29583	-0.09229	-0.06228
G10	5.188	0.32915	0.08225	0.11694	-0.31300
G11	5.699	0.04626	-0.12553	-0.44469	0.08626
G12	5.713	-0.16875	-0.19261	-0.07455	0.53887

Table 5. AMMI-estimates per environment(yield(t/ha) across years and locations)

Geno- types	Diyarbakır				Adıyaman				Ceylanpınar			
	(E1) 2014-15		(E4) 2015-16		(E2) 2014-15		(E5) 2015-16		(E3) 2014-15		(E6) 2015-16	
	Yield	Rank	Yield	Rank	Yield	Rank	Yield	Rank	Yield	Rank	Yield	Rank
G1	7.324	G4	4.364	G12	7.348	G4	3.418	G6	5.485	G6	3.429	G6
G2	7.927	G3	5.337	G4	7.196	G6	3.797	G8	6.044	G7	3.563	G8
G3	8.766	G8	5.165	G8	7.776	G9	2.911	G11	5.572	G4	3.127	G9
G4	9.105	G7	5.471	G2	9.178	G8	2.978	G2	6.127	G8	3.272	G2
G5	6.991	G12	4.261	G6	6.910	G12	2.601	G12	6.105	G5	3.034	G7
G6	7.914	G9	5.333	G7	8.246	G11	4.072	G9	6.581	G9	3.986	G11
G7	8.147	G11	5.332	G11	7.256	G3	3.434	G7	6.277	G2	3.515	G1
G8	8.258	G2	5.339	G3	8.033	G1	3.910	G1	6.122	G12	3.806	G10
G9	8.008	G6	4.976	G9	8.097	G7	3.498	G10	6.093	G10	3.613	G4
G10	7.419	G10	4.414	G10	7.041	G2	3.117	G4	5.762	G11	3.376	G12
G11	8.003	G1	5.220	G1	7.867	G10	3.841	G3	5.752	G3	3.511	G3
G12	8.089	G5	5.529	G5	7.945	G5	3.543	G5	6.007	G1	3.165	G5
Mean	7.996		5.062		7.741		3.427		5.994		3.450	
Mean	6.529				5.584				4.722			
Mean	7.244						3.979					

The GGE Biplot analysis

The mean grain yield across two years (2014-15-2015-2016) in three location (Diyarbakır, Adıyaman, Ceylanpınar) of 12 triticale genotypes were showed in *Table 5*. These table data was used to generated a GGE biplot (*Fig. 2-Fig. 6*), although the genotype is compatible with biplot, it represents only 78.19% of the variation. In the present study, the first two IPCAS were used to portray genotype by environment interaction and placement on the (*Fig. 2-Fig. 6*). The GGE biplot provides good explanation of the pattern, regarding first two IPCs.

The relationships among and between genotypes and environments visualize in *Fig. 2*. A biplot such a graph to be interpreted bi-directionally has the following comments (Yan et al., 2000; Yan and Tinker, 2006). 1) The cosine of the angle between the vectors of the two environments approaches the Pearson correlation between them. Therefore, an angle of less than 90° shows a positive correlation, an angle greater than 90° shows a negative correlation and an angle of 90° shows zero correlation. 2) If the vector of a environment is longer than other vectors, the variation of this environment on genotypes is higher than the other environments, if the vector length of any environment is very short than other traits vector then the variation of this environment is very low. 3) The angle between the vector of any genotype and any environment gives information about the state of the genotypes to environments.

If the angle is quite sharp and narrow indicates that the genotype is desirable for that environment if the angle is too large then the genotype is undesirable for that environment. 4) The length of the vector of a genotype indicates the strength or weakness of the genotype for all environments. According to these explanations there are high correlation among E3, E5, E6 and G6 is desirable for these environment, while there are high correlation E1, E2 and E4 and G6 is desirable genotype for these

environments, and G8 (candidate) is desirable for all environments (*Fig. 2 and Table 6*). In *Fig. 3*, five sectors are created, with two sectors each of them consisting of three environments. These sectors stand for different MEs, because the winning genotypes for each sector are those positioned at the vertex we can say that G4 is winning genotype for sector II (E3, E5 and E6), G6 for sector I (E1, E2 and E4).

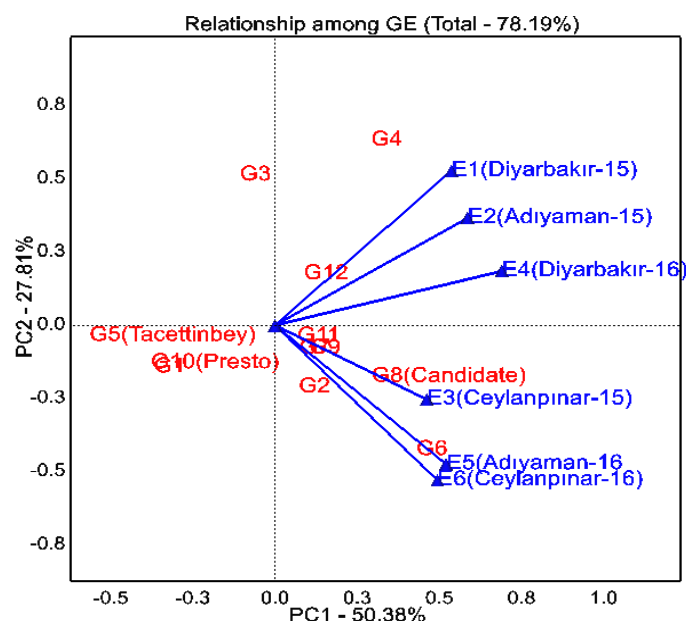


Figure 2. The GGE biplot which shows the relationships among test environments. The correlation coefficient between any two environments is approximated by the cosine of the angle between their vectors. Acute angles indicates a positive correlation, obtuse angles a negative correlation and right angles no correlation. G1-G12 is the codes for the triticales disomic addition lines and G5 and G10 used as the control, respectively. E1- E3 are environment codes for 2014-15, E4-E6 for 2015-16 growing season

Table 6. The first four AMMI selections for per environments, variance and IPCA scores

Env	Mean	Score	1	2	3	4	IPCAe[1]	IPCAe[2]	IPCAe[3]	IPCAe[4]	Variance
E1	7.996	-0.79	G4	G3	G8	G7	-0.78881	-0.44311	0.14583	-0.40141	0.6423
E2	7.741	-0.75	G4	G6	G9	G8	-0.74728	0.69354	-0.32960	0.15858	0.5670
E3	5.994	0.41	G6	G7	G4	G8	0.41209	0.30484	0.73113	0.17556	0.4741
E4	5.062	-0.14	G12	G4	G8	G2	-0.14082	-0.53822	0.06581	0.45130	0.4142
E5	3.427	0.70	G6	G8	G11	G2	0.69460	-0.18457	-0.59209	0.09693	0.3242
E6	3.450	0.57	G6	G8	G9	G2	0.57021	0.16753	-0.02109	-0.48096	0.2598

Similar situation (two mega- environment) occurred among environments presented in *Fig. 4*. The stability of genotypes also showed in *Fig. 5*, and generated by GGE biplot. The AEC is showing the stability genotypes based on across environment. The similar results indicated on *Fig. 6*, and G8 and G6 are favorable genotypes because they located near of center ideal center of biplot. The result showed that G8 (candidate) is quite stable and yielding, G6 and G4 are yielding as well as. The biplot showed that the selection of genotypes can be done both on specific and general goals.

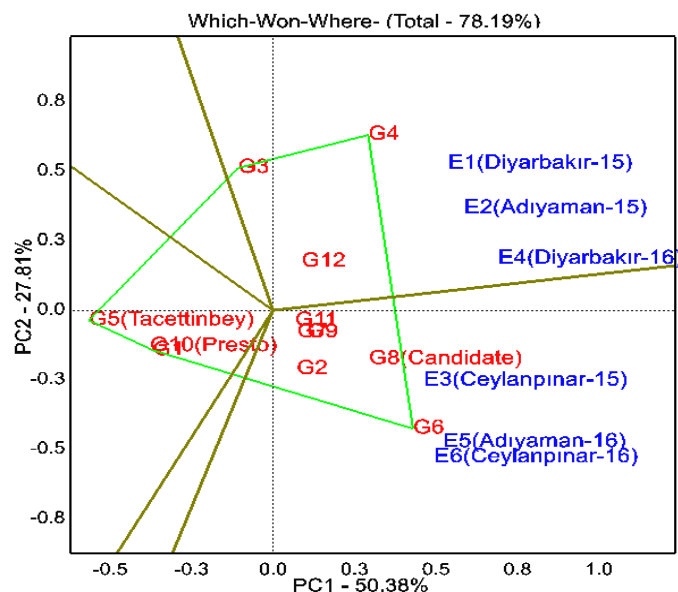


Figure 3. Which-won-where for genotypes and environments. The Polygon view of genotype-environment interaction for wheat-barley disomic addition lines over six test environments. The vertex genotype in each sector is the best genotype at environments whose markers fall into the respective sector. Environments within the same sector share the same winning genotype, and environments in different sectors have different winning genotypes. G1-G12 is the codes for the triticales disomic addition lines and G5 and G10 used as the control, respectively. E1- E3 are environment codes for 2014-15, E4-E6 for 2015-16 growing season

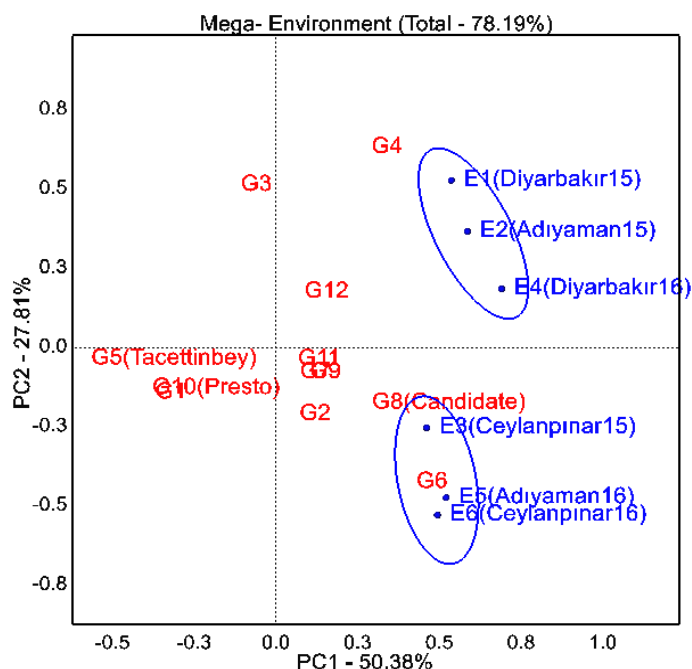


Figure 4. The potential mega-environments and ideal for mega environments. The environments which have same conditions located in the same mega-environment, and the genotypes which located in the center mega-center mean is desirable for this mega-environments. G1-G12 is the codes for the triticales disomic addition lines and G5 and G10 used as the control, respectively. E1- E3 are environment codes for 2014-15, E4-E6 for 2015-16 growing season

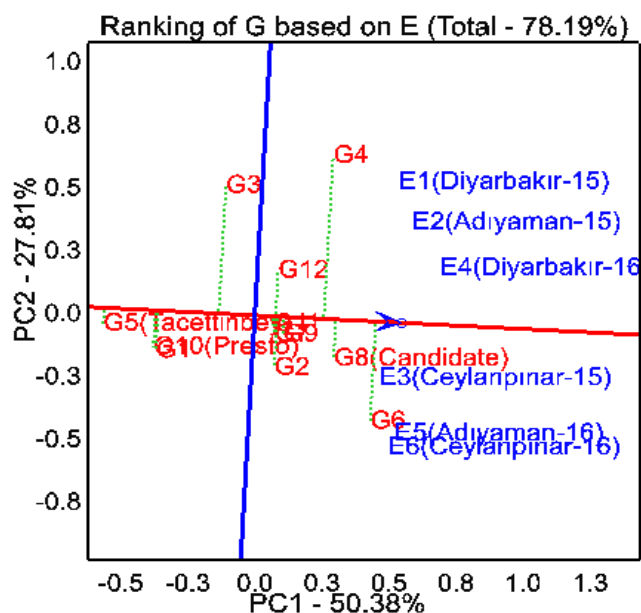


Figure 5. The GGE biplot showing the ranking of genotypes for both yield and stability performance over environments. The line passing through the biplot origin is called the average environment coordinate (AEC). More close to concentric circle indicates higher mean yield. The line which passes through the origin and is perpendicular to the AEC with arrows represents the stability of genotypes. Either direction away from the biplot origin, on this axis, indicates greater GE interaction and reduced stability. G1-G12 is the codes for the triticale disomic addition lines and G5 and G10 used as the control, respectively. E1- E3 are environment codes for 2014-15, E4-E6 for 2015-16 growing season

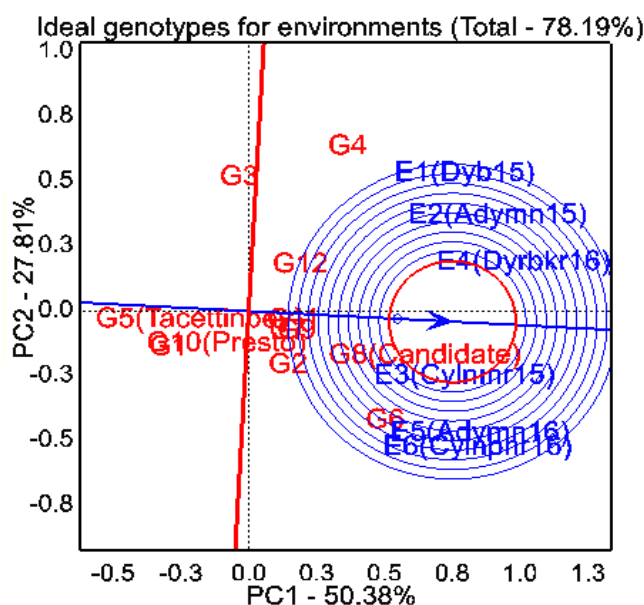


Figure 6. The comparison method rank the genotypes to an ideal genotype. The ideal genotype can be used as a reference for genotype evaluation. Thus, using the ideal genotype as the center, concentric circles were drawn to help visualize the distance between each genotype and the ideal genotype. G1-G12 is the codes for the triticale disomic addition lines and G5 and G10 used as the control, respectively. E1- E3 are environment codes for 2014-15, E4-E6 for 2015-16 growing season

Discussion

The multiple environments experiments aims to identify superior genotypes for different conditions. Due to the unpredictable environmental factors, different models (GE, GEI, GGE, AMMI) were developed to elucidate the effect of genotype, environment or interaction, and are still used in breeding studies (Kendal and Sayar, 2016; Kendal et al., 2016). In addition, The AMMI and GGE biplot techniques have been used for a long time by many researchers to understand the effect of genotype, environment and GEI based on grain yield (Yan and Tinker, 2006; Kendal and Dogan, 2015; Akcura et al., 2016; Oral et al., 2018). The AMMI analysis was used to identify the stability and superiority of genotypes, favorable and yielding environments based on multiple environments (Tekdal and Kendal, 2018). In the study AMMI analysis indicated that G4 and G6 were yielding genotypes, while G7 and G8 (candidate) were stable in tested environments. On the other hand, the study showed that the grain yield is fluctuation depend on factors of environmental and years. In addition, some locations (Diyarbakır) have proven to be highly yielding, some other locations (Ceylanpınar) have proven to be low-yielding even if the year conditions change. Some studies on AMMI commented that this model can be used to describe a two-way table of GE means. When the GE means are independent and homoscedastic, ordinary least squares (OLS) gives optimal estimates of the model (Gauch et al., 2008), this model could be used to evaluate genotypes at different locations over the years in breeding program (Sadeghzadeh et al., 2017). The magnitude of environment effect was higher than genotype effect (Rad et al., 2013). In triticale the locations that are both descriptive and representative are good test locations for the selection of adapted genotypes (Bilgin et al., 2018). According to GGE biplot biplot showed that the selection of genotypes can be done both on spesific and general goals. In the study, two mega-environment were occurred in the test environments and G4 was the best yielding in the poorest environments or years, and G6 for yielding crop seasons or environments, while G8 (candidate) is stable for general testing environments. According to results of a study indicated that an ideal genotype should have both high mean yield and high stability within a mega-environment (Yan and Tinker, 2006). In studies conducted in different years or environments, if there is no difference between two or more environments and within the same circle, this is called mega environment and it is recommended to work in one of these environmental groups in later studies. Fortunately, more than two mega-environments are often sufficient to allow GE to capture a sizeable portion of the interaction signal (Gauch, 2013; Hongyu et al., 2015). According to the results of the AMMI and GGE biplot models had similar results in view of specific adaptability to environmental conditions. Nevertheless, contrary results were obtained for environmental contribution to the stability of genotypes (Lule et al., 2014; Shahriari et al., 2018). Both AMMI and GGE were able to efficiently explore the variability present in MET data due to genotype-environment interaction and both models proved to be approximately equivalent, leading to substantially the same conclusions about the genotypes with the highest yield and stability (Neisse et al., 2018).

Conclusion

The results of study revealed that grain yield of triticale was highly influenced by environment effect followed by genotypic effects and GEI contributed the least. This study demonstrated that AMMI model was found effective for determining the yielding

and stabilize triticale genotypes and discriminating ability and representativeness of the test environments. According of the study, G4 and G6 showed specific ability, while G8 general adaptability in test environments. Moreover; G4 can be recommend for yielding (mega-env II), while G6 for low-yielding (Mega-env. I) seasons or environments. On the other hand, G8 can be registered as variety for study area, because this genotype is quite stable and yielding among genotypes in test environments. Both AMMI and GGE biplot model were proved to be approximately equivalent, leading to substantially the same conclusions about the genotypes with the highest yield and stability.

REFERENCES

- [1] Akcura, M., Kokten, K., Akcacik, A. G., Aydogan, S. (2016): Pattern analysis of Turkish bread wheat landraces and cultivars for grain and flour quality. – Turkish J. of Field Crops 21(1): 120-130.
- [2] Anonymus 1. (2018): <http://www.fao.org/home/en/>.
- [3] Anonymus 2. <http://www.factfish.com/statistic/triticale%2C%20production%20quantity>.
- [4] Ayalew, H., Kumssa, T. T., Butler, T. J., Ma, X. F. (2018): Tritical improvement for forage and cover crop uses in the Southern Great Plains of the United States. – Frontiers in plant science 9.
- [5] Bilgin, O., Balkan, A., Korkut, Z. K., Başer, I. (2018): Multi-environmental evaluation of Triticale, Wheat and Barley genotypes by GGE biplot analysis. – Journal of Life Sciences 12: 13-23.
- [6] Crossa, J., Gauch, H. G., Zobel, R. W. (1990): Additive main effects and multiplicative interaction analysis of two international maize cultivar trials. – Crop Sci. 30: 493-500.
- [7] Gauch, H. G., Piepho, H. P., Annicchiarico, P. (2008): Statistical analysis of yield trials by AMMI and GGE: further considerations. – Crop Science 48: 866-889.
- [8] Gauch, H. G. (2013): A simple protocol for AMMI analysis of yield trials. – Crop Science 53(5): 1860-1869.
- [9] Hongyu, K., Silva, F. L., Oliveira, A. C. S., Sarti, D. A., Araújo, L. C., Dias, C. T. S. (2015): Comparação entre os modelos AMMI e GGE Biplot para os dados de ensaios multi-ambientais. – Rev. Bras. Biom., São Paulo 33(2): 139-155.
- [10] Kendal, E., Dogan, Y. (2015): Stability of a candidate and cultivars (*Hordeum vulgare* L) by GGE Biplot analysis of Multi-environment yield trials in spring barley. – Agriculture & Forestry 61(4): 307-318.
- [11] Kendal, E., Sayar, M. S. (2016): The stability of some spring triticale genotypes using biplot analysis. – The J. of Animal & Plant Sci. 26(3): 754-765.
- [12] Kendal, E., Sayar, M. S., Tekdal, S., Aktas, H., Karaman, M. (2016): Assessment of the impact of ecological factors on yield and quality parameters in triticale using GGE biplot and AMMI analysis. – Pak. J. Bot. 48(5): 1903-13.
- [13] Kendal, E., Tekdal, S. (2018): AMMI model to assess durum wheat genotypes in multi-environment trials. – J. Agr. Sci. Tech. 20: 153-166.
- [14] Kilic, H. (2014): Additive main effect and multiplicative interactions (AMMI) Analysis of grain yield in barley genotypes across environments. – J. Agr. Sc. 20: 337-344.
- [15] Kizilgeçi, F. (2019): Assessment of yield and quality of some Triticale genotypes in South-Eastern Anatolia. Journal of the Institute of Sci. and Technology, 9(1): 545-551.
- [16] Lule, D., Tesfaye, K., Mengistu, G. (2014): Genotype by environment interaction and grain yield stability analysis for advance triticale (*X. Triticosecale Wittmack*) genotypes in western Oromia, Ethiopia. – SINET: Ethiopian Journal of Science 37(1): 63-68.
- [17] Mohammadi, R., Armion, M., Zadhasan, E., Ahmadi, M. M., Amri, A. (2018): The use of AMMI model for interpreting genotype \times environment interaction in durum wheat. – Experimental Agriculture 54(5): 670-683.

- [18] Neisse, A. C., Kirch, J. L., Hongyu, K. (2018): AMMI and GGE Biplot for genotype \times environment interaction: a medoid-based hierarchical cluster analysis approach for high-dimensional data. – *Biometrical Letters* 55(2): 97-121.
- [19] Oral, E. (2018): Effect of nitrogen fertilization levels on grain yield and yield components in triticale based on AMMI and GGE biplot analysis. – *Applied Ecology and Environmental research* 16(4): 4865-4878.
- [20] Oral, E., Kendal, E., Dogan, Y. (2018): Selection the best barley genotypes to multi and special environments by AMMI and GGE biplot models. – *Fresenius Environmental Bulletin* 27(7): 5179-5187.
- [21] Purchase, J. L. (1997): Parametric analysis to describe $G \times E$ interaction and yield stability in winter wheat. – PhD. Thesis, Department of Agronomy, Faculty of Agriculture, University of the Orange Free State, Bloemfontein, South Africa.
- [22] Rad, M. N., Kadir, M. A., Rafii, M. Y., Jaafar, H. Z., Naghavi, M. R., Ahmadi, F. (2013): Genotype environment interaction by AMMI and GGE biplot analysis in three consecutive generations of wheat (*Triticum aestivum*) under normal and drought stress conditions. – *Australian J. of Crop Science* 7(7): 956.
- [23] Sadeghzadeh, B., Mohammadi, R., Ahmadi, H., Abedi, A. G., Khalilzadeh, G., Mohammadfam, M., Hasanpour, H. M. (2017): Efficiency of GGE biplot and AMMI analyses for adaptability and grain yield stability of durum wheat lines under different environments. – *Journal of Crop Ecophysiology (agriculture science)* 11, 2(42): 413-436.
- [24] Shahriari, Z., Heidari, B., Dadkhodaie, A. (2018): Dissection of genotype \times environment interactions for mucilage and seed yield in *Plantago* species: Application of AMMI and GGE biplot analyses. – *PloS one* 13(5): e0196095.
- [25] Tekdal, S., Kendal, E. (2018): AMMI model to assess durum wheat genotypes in multi-environment trials. – *J. Agr. Sci. Tech.* 20: 153-166.
- [26] Yan, W., Hunt, L. A., Sheng, Q., Szlavnic, Z. (2000): Cultivar evaluation and mega-environment investigation based on the GGE biplot. – *Crop Science* 40(3): 597-605.
- [27] Yan, W., Rajcanw, I. (2002): Biplot analysis of test sites and trait relations of Soybean in Ontario. – *Crop Sci.* 42: 11-20.
- [28] Yan, W., Tinker, N. A. (2006): Biplot analysis of multi-environment trial data: Principles and applications. – *Canadian journal of plant science* 86(3): 623-645.
- [29] Zobel, R. W., Wright, M. S., Gauch, H. G. (1988): Statistical analysis of a yield trial. – *Agronomy Journal* 80: 388-393.

APPENDIX



Picture 1. The locations of research was presented in Southeast Anatolia of Turkey

FACTORS AFFECTING BACTERIA CONTAMINATION AMONG FOOD HANDLERS AT A PUBLIC HOSPITAL IN SOUTH SUMATRA, INDONESIA

UTARI, S.^{1,2*} – HERMANSYAH³ – SALEH, I.⁴ – PAMBAYUN, R.⁵

¹*Environmental Science Department, Sriwijaya University, Palembang, Indonesia*

²*The South Sumatera Provincial Health Office, Health Training Center, Palembang, Indonesia*

³*Department of Chemistry, Faculty of Mathematics and Natural Science, Sriwijaya University, Palembang, Indonesia*

⁴*Department of Medical, Faculty of Medical Science, Sriwijaya University, Palembang, Indonesia*

⁵*Department of Agricultural Technology, Faculty of Agriculture, Sriwijaya University, Palembang, Indonesia*

**Corresponding author*

e-mail: utariutari76@yahoo.com; phone: +62-813-677-70208

(Received 11th Feb 2019; accepted 28th Mar 2019)

Abstract. Food-borne diseases caused by pathogenic bacteria (especially *Escherichia coli*) are one of the main causes of mortality in some developing countries. Hospitals are one of the potential places from where food-borne diseases might spread. The food handlers working in the hospital have a major role in the distribution of pathogenic bacteria because they are directly involved in the hospital's food chain. This study aimed to determine bacteria contamination among 30 food handlers based on some influencing factors, such as education level, work experience, worker's behavior, and hygiene training at a public hospital in South Sumatra, Indonesia. To study the correlation between some factors with the level of *E. coli* contamination, the bivariate analysis was performed. The results of the bivariate analysis revealed that there was a significant relationship between the education level and work experience of the food handlers with the level of *E. coli* contamination (p -value ≤ 0.05). In the other hand, there was no significant relationship between behavior and hygiene training with the level of *E. coli* contamination (p -value ≥ 0.05). This study indicates the importance of socialization about food hygiene and regular rectal swab test for food handlers to ensure their health level.

Keywords: *Escherichia coli, rectal swab, hygiene, infection, bivariate analysis*

Introduction

Food handlers working in hospitals are people who directly involved in the food chain processing until the food distribution to the patients. The role of food handlers in spreading diseases is the contact between food handlers suffering infectious diseases with the food source itself. Subsequently, the food is consumed by the patient and causes nosocomial infections.

Food handlers who work in the food service sector with poor personal hygiene are the potential source of pathogenic organism infection (Acikel et al., 2008; Mukhopadhyay et al., 2016; Anjum et al., 2017; Gameda et al., 2018). The food contamination occurs during food chain process including preparation, production, processing, and the food distribution (Permenkes RI, 2011; Anuradha and Dandekar, 2014; Mukhopadhyay et al., 2016). The risk of bacteria contamination to the food

handlers depends on their health status, personal hygiene, knowledge, and the hygiene practice (Esparar et al., 2010; Dahiru et al., 2016).

Foodborne disease is defined as illness resulting from the consumption of contaminated food; food can be contaminated with microbial pathogens or a toxic substance (Unicomb, 2009). Most of the foodborne diseases happen because the food handlers have transmitted the bacteria or viruses through improper food handling and poor sanitation. The hands of food-handlers can serve as vectors in the spread of foodborne diseases due to poor personal hygiene or cross-contamination. Recent days, the food-borne diseases become a major health problem in developing countries, such as Ethiopia (Girma et al., 2017; Gameda et al., 2018), Nigeria (Dahiru et al., 2016), Iran (Heydari-Hengami et al., 2018), and Indonesia (Chantika, et al., 2016; Kurniasih et al., 2015). The global incidence of food-borne diseases is difficult to estimate, but it was reported that in 2005 there were 1.8 million people killed from diarrheal diseases. This case can be linked to food and drinking water pollution (WHO, 2007, 2008).

As located in a developing country, the health problem is one of the concerning issues in Palembang, South Sumatra-Indonesia. The public hospital in South Sumatra serves many patients every day. Based on the preliminary research, the supervision of food hygiene and sanitation by the Environmental Health Department and the Nutritional Departments should be improved to ensure the public hospital sanitation. In the other hand, the Department of Infectious Disease only evaluates adherence of the hygiene activities in the food sanitation. Therefore, further study is required to perform the synergistic responsible of the three departments for food sanitation and hygiene. The food processing at a public hospital in South Sumatra should be improved to ensure the quality of food services, especially for patients.

Commonly, the parameter of hygiene is the presence of *Staphylococcus aureus* bacteria, while the parameter of sanitation is *Escherichia coli* contamination. This research is focused on *E. coli* contamination which is found in food handlers due to the poor sanitation of the hospital's workers (Hanekom et al., 2010; Kurniasih et al., 2015; Switaj et al., 2015; Dahiru et al., 2016; Nasrolahei et al., 2016). *Escherichia coli* or commonly abbreviated as *E. coli* is one of the common gram-negative bacteria. In general, these bacteria can be found in the human colon and feces (Switaj et al., 2015; Nasrolahei et al., 2017). Most of *E. coli* is harmless, however, *E. coli* type O157: H7 can cause bloody diarrhea because produces verotoxins (Lourenco et al., 2011; Switaj et al., 2015).

This study was to overview the *E. coli* contamination among food handlers at a public hospital in South Sumatra and also analyzes the factors affecting *E. coli* contamination among food handlers at the Nutrition Department at a public hospital in South Sumatra. In addition, this research also offers an effort to reduce the risk of *E. coli* contamination in the food handlers.

Materials and methods

This study was a cross-sectional design including data collection simultaneously with a descriptive quantitative approach, bacteria investigation, and factors that influence the health rate of food handlers at a public hospital in South Sumatra. The study was conducted to determine bacteria contamination among 30 food handlers at a public hospital in South Sumatra, as the population in this study. The dependent variable was *E. coli* contamination on food handler's sample. The independent variables were

education level, work experience, behavior, and hygiene training. The education level was divided into two sub-variables, which consisted of a middle (senior high school) and low (elementary and junior high school). The work experience was divided into two sub-variables which consisted of more and less than 3 years. The worker's behavior was divided into two sub-variables which consist of following and not following Standard Operation Procedure. The hygiene training was also divided into two sub-variables, which consist of attending and not attending the training related to the hygiene process.

Interviews were conducted with all food handlers working at the hospital. Total of 30 respondents was interviewed and 30 samples of rectal swabs were obtained from the corresponding workers for further testing. Preparation of the bacteria samples follows the WHO standard (WHO, 2003) using a rectal swab for *E. coli* bacteria (Esparar et al., 2004). Swab sampling and laboratory identification were analyzed in the Laboratory of Environmental Health Center Palembang.

Bivariate analysis was carried out to investigate the quantitative distribution of independent and dependent variables. Bivariate analysis was also performed to examine the correlation between each of the independent variables and the dependent variable. This was achieved by comparing the p-value to study the level of significance (Emzir, 2009). The factors investigated were education level, work experience, behavior, and hygiene training for staff at a public hospital in South Sumatra.

Results

The *E. coli* contamination shows the sanitation rate of the hospital's employees. *Table 1* shows that 36.7% of the food handlers staff at a public hospital in South Sumatra are positively contaminated with *E. coli*, while 63.3% of them are not indicated to be contaminated with *E. coli*.

Table 1. Analysis of *E. coli* contamination among the food handlers a public hospital in South Sumatra

No	Results	Food handlers	
		Quantity	Percent (%)
1.	Not contaminated	19	63.3
2.	Contaminated	11	36.7
	Total	30	100

Bivariate analysis was carried out on the characteristics of respondents and risk factors for *E. coli* exposure, especially those with a probability value less than 0.05 ($p < 0.05$). The analysis results will describe the risk factors for *E. coli* contamination without considering the existence of other independent variables. The bivariate analysis was carried out by making a double crosstab (2×2), the respondent's characteristics, and the risk factors which estimated to affect the *E. coli* contamination.

Table 2 shows the correlation between education levels and *E. coli* contamination. The p-value is 0.015 or $p \leq 0.05$ indicating that there is a significant correlation between the education level and *E. coli* contamination incident.

Table 3 reveals a correlation between work experience and *E. coli* contamination incident. The obtained p-value is 0.02 or $p \leq 0.05$ indicating the significant correlation between work experience and the *E. coli* contamination.

Table 4 shows correlation between food handler's behavior and *E. coli* contamination. The p-value is 0.37 or $p \geq 0.05$ indicating no significant correlation between worker's behavior and the *E. coli* contamination.

Table 5 shows the correlation between training related to the food handler's job and *E. coli* contamination. The p-value is 0.15 or $p \geq 0.05$ indicating that there is no significant correlation between the training profile and *E. coli* contamination incident.

Table 2. Correlation between education level and *E. coli* contamination

<i>E coli</i>	Education level				p-value
	Low	%	Middle	%	
Negative	1	5	19	95	0.015
Positive	4	40	6	60	
Total	5	16.7	25	83.3	

Table 3. Correlation between work experience and *E. coli* contamination

<i>E coli</i>	Work experience				p-value
	< 3 years	%	> 3 years	%	
Negative	6	30	14	70	0.02
Positive	9	90	1	10	
Total	15	50	15	50	

Table 4. Correlation between behavior of food handlers and *E. coli* contamination

<i>E coli</i>	Behavior				p-value
	Following SOP	%	Not following SOP	%	
Negative	6	30	14	70	0.37
Positive	7	70	3	30	
Total	13	43.3	17	56.7	

Table 5. Correlation between food handler's training and *E. coli* contamination

<i>E coli</i>	Training				p-value
	No	%	Yes	%	
Negative	2	10	18	90	0.15
Positive	5	50	5	50	
Total	7	23.3	23	76.7	

Discussion

E. coli contamination is exclusively coming from fecal. It is transmitted through the fecal contamination of food and water, as well as cross-contamination, and by human contact during the food preparation. Meanwhile, the primary contamination source is the consumption of contaminated food, such as undercooked food or raw milk. For this reason, Lambrechts et al. (2014) proposed that *E. coli* contamination of the hands of

food handlers as an indicator of a hand-washing efficiency. The hands of ready-to-eat food service food handlers have been the main vector for spreading food-borne diseases. Furthermore, Howes et al. (1996) stated that improper food handlers practice contributed up to 97% of foodborne illnesses in food service establishments and homes. Even, the study of Wilson et al. (2017) revealed that food poisoning originated from the catering industry contributed 70% higher than that caused by other sectors.

Factors affecting *E. coli* contamination of food handlers include the knowledge and the food handling process. The food handler's responsibilities include providing the foodstuffs, storing the foodstuffs, processing the food, and distributing the food to patients or other hospital staffs. Our investigation reveals that there are still less than 50% of food handlers at a public hospital in South Sumatra who work not in accordance with the SOP. The reason given by workers regarding this problem is they are not familiar and they feel uncomfortable when using the work equipment (apron, gloves, head cover, etc.).

A total of 63.3% of food handlers are not indicated in *E. coli* contamination, while 36.7% of food handlers are indicated *E. coli* contamination. In general, 75% of the food handlers worker a public hospital in South Sumatra have a high school education background, 33.3% of them still have work experience less than 3 years, 26.7% of them do not follow the SOP in their work, and 33.3% of them have never attended the formal training related to their work.

These results are in accordance with the previous study conducted by Lazarevic et al. (2013). They revealed that the most general isolated bacteria in food handler's cases are *E. coli*. Another study by Nasrolahei et al. (2016) showed that there were 29.2% of 220 respondents contaminated with *E. coli* bacteria. Oundo et al. (2008) studied *E. coli* contamination of food handlers in three different locations in Kenya. They got 1.2% samples in Diani, 4% samples in Malindi, and 1.8% samples in Nairobi are contaminated by *E. coli*.

By finding a significant relationship between work experience, the food handler's behavior, and the *E. coli* contamination; special attention is required to improve the employee's behavior. The effort to reduce contamination of *E. coli* bacteria at a public hospital in South Sumatra is by providing socialization or related training about hygiene implementation as well as regular health checks for the food handlers. Because 36.7% of food handlers at a public hospital in South Sumatra are infected with *E. coli*, it is necessary to have rectal swab test intensively to check the health level of the food handlers. This suggestion is in accordance with several studies conducted by El Derea et al. (2008), Lazarevic et al. (2013), Ngivu (2016), Sande et al. (2014), Sharif et al. (2013, 2015), and Zaglool, et al. (2011).

Conclusion

A total of 36.7% of food handlers at a public hospital in South Sumatra are indicated to have *E. coli* contamination. The results of the bivariate analysis show that some factors including the education level and work experience significantly affected the risk of *E. coli* contamination. In the other hand, there is no significant correlation between the behavior of the food handlers and hygiene training with the *E. coli* contamination level. This study revealed the importance of socialization about food hygiene and regular rectal swab test for food handlers to reduce the risk of *E. coli* contamination among the food handlers. Future studies may include investigation of other bacteria and

viruses that might contaminate the food handlers as well as the effectiveness of lathering on bacteria removal from hands.

REFERENCES

- [1] Acikel, C. H., Ogur, R., Yaren, H., Gocgeldi, E., Ucar, M., Kir, T. (2008): The hygiene training of food handlers at a teaching hospital. – *Food Control* 19: 186-190.
- [2] Anjum, W., Kalasker, P. S., Bhaskar, K. (2017): Prevalence of intestinal parasites and its associated socio-demographic factors among the food handlers of Bagalkot city, Karnataka, India. – *Int J Community Med Public Health* 4(1): 1-4.
- [3] Anuradha, M., Dandekar, R. H. (2014): Knowledge, attitude and practice among food handlers on food borne diseases: a hospital based study in tertiary care hospital. – *IJBAR* 5(4): 196-198.
- [4] Chantika, I., Sumardianto, D., Sumaningrum, N. D. (2016): Higiene penjamah dan sanitasi pengeloan makanan di Instalasi Gizi Rumah Sakit Umum Daerah Gambiran Kota Kediri. – *Jurnal Preventia* 1(1): 7-13.
- [5] Dahiru, J. Y., Abubakar, F. A., Idris, H., Abdullahi, S. A. (2016). Bacterial contamination of food handlers at various restaurants in Kano State Metropolis, Kano Nigeria. – *Int. J. Curr. Microbiol. App. Sci.* 5(5): 165-170.
- [6] El Derea, H., Salem, E., Fawzi, M., Azeem, M. A. (2008): Safety of patient meals in 2 hospitals in Alexandria, Egypt before and after training of food handlers. – *Eastern Mediterranean Health Journal* 14(4): 941 – 952.
- [7] Emzir (2009): *Metodologi Penelitian Pendidikan*. – PT Raja Grafindo Persada, Jakarta.
- [8] Esparar, D. G., Belizario, V. Y., Relos, J. R. D. (2004): Prevalence of intestinal parasitic infections among food handlers of a tertiary hospital in manila using direct faecal smear and formalin ether concentration technique. – *Phil J Microbiol Infect Dis* 33(3): 99-103.
- [9] Gemeda, T. I., Asayehu, T. T., Abdisa, M., Fekadu, H. (2018): Assessment of knowledge, attitude and practices of food handlers in Nekemte Referral Hospital, Wollega, Ethiopia. – *J Nutr Health Food Eng.* 8(1): 87-92.
- [10] Girma, H., Beyene, G., Mekonnen, Z. (2017): Prevalence of intestinal parasites among food handlers at cafeteria of Jimma University Specialized Hospital, Southwest Ethiopia. – *Asian Pac J Trop Dis* 7(8): 467-471.
- [11] Hanekom, S. M., Vermeulen, E. E., Oldewage-Theron, W. (2010): Food safety risk factors in a hospital food service unit serving low microbial diets to immune-compromised patients. – *African Journal of Food Agriculture, Nutrition and Development* 10(9): 4000-4015.
- [12] Heydari-Hengami, M., Hamed, Y., Najafi-Asl, M., Sharifi-Sarasiabi, K. (2018): Prevalence of intestinal parasites in food handlers of Bandar Abbas, Southern Iran. – *Iran J Public Health* 47(1): 111-118.
- [13] Howes, M., McEwen, S., Griffiths, M., Harris, L. (1996): Food handler certification by home study: Measuring changes in knowledge and behaviour. – *Dairy Food Environ San.* 16: 737-744.
- [14] Kurniasih, R. P., Nurjajuli, Hanani, Y. D. (2015): Hubungan Higiene dan Sanitasi Makanan Dengan Kontaminasi Bakteri *Escherichia coli* dalam makanan di warung makan sekitar terminal Borobudur, Magelang. – *Jurnal Kesehatan Masyarakat* 3(1): 549-558.
- [15] Lambrechts, A. A., Human, I. S., Doughari, J. A., Lues, J. F. R. (2014): Bacterial contamination of the hands of food handlers as indicator of hand washing efficacy in some convenient food industries in South Africa. – *Pak. J. Med. Sci.* 30(4): 755-758.
- [16] Lazarevic, K., Stojanovic, D., Bogdanovic, D. C., Dolicanin, Z. C. (2013): Hygiene training of food handlers in hospital settings: Important factor in the prevention of nosocomial infections. – *Cent Eur J Public Health* 21(3): 146-149.

- [17] Lourenco, A., Carneiro, S., Pinto, J., Rocha, M., Ferreira, E. C., Rocha, I. (2011): A study of the short and long-term regulation of *E. coli* metabolic pathways. – Journal of Integrative Bioinformatics 8(3): 183-198.
- [18] Mukhopadhyay, S., Malpekar, K., Shastri, J. (2016): Intestinal parasitic and bacterial infection among food handlers in a metropolitan tertiary care hospital. – J. Evolution Med. Dent. Sci. 5(62): 4327-4331.
- [19] Nasrolahei, M., Mirshafiee, S., Kholdi, K., Salehian, S., Nasrolahe, M. (2017): Bacterial assessment of food handlers in Sari City, Mazandaran Province, North of Iran. – Journal of Infection and Public Health 10: 171-176.
- [20] Ngivu, J. (2016): Impact of food handlers' food safety training in a paediatric hospital in East Africa. – American Journal of Infection Control 44: S28-S82.
- [21] Oundo, J. O., Kariuki, S. M., Boga, H. I., Muli, F. W., Iijima, Y. (2008): High incidence of enteroaggregative *Escherichia coli* among food handlers in three areas of Kenya: A possible transmission route of travelers diarrhea. – Journal of Travel Medicine 15(1): 31-38.
- [22] Permenkes RI No 1096 (2011): Higiene Sanitasi Jasaboga – Kementerian Kesehatan Republik Indonesia, Jakarta.
- [23] Sande, S., Basak, S., Sande, V., Tawade, V. (2014): Screening of food handlers for intestinal parasites and enteropathogenic bacteria in a tertiary care hospital. – International Journal of Health Sciences & Research 4(5): 88-94.
- [24] Sharif, L., Obaidat, M. M., Al-Dalalah, M. R. (2013): Food hygiene knowledge, attitudes and practices of the food handlers in the military hospitals. – Food and Nutrition Sciences 4: 245-251.
- [25] Sharif, M., Daryani, A., Kia, E., Rezaei, F., Nasiri, M., Nasrolahei, M. (2015): Prevalence of intestinal parasites among food handlers of Sari, Northern Iran. – Rev. Inst. Med. Trop. Sao Paulo 57(2): 139-144.
- [26] Switaj, T. L., Winter, K. J., Christensen, S. R. (2015): Diagnosis and management of foodborne illness. – Am. Fam. Physician 92(5): 358-365.
- [27] Unicomb, L. E. (2009): Food Safety: Pathogen transmission routes, hygiene practices and prevention. – J. Health Popul. Nutr. 27(5): 599-601.
- [28] WHO (2003): Basic Laboratory Procedures in Clinical Bacteriology. – World Health Organization, Geneva.
- [29] WHO (2007): Food Safety and Foodborne Illness. Fact Sheet No. 237. – World Health Organization, Geneva.
- [30] WHO (2008): WHO Initiative to Estimate the Global Burden of Foodborne Diseases. – World Health Organization, Geneva.
- [31] Wilson, M., Murray, A. E., Black, M. A., McDowell, D. A. (1997): The implementation of hazard Analysis and critical control points in hospital catering. – Manag Serv Qual 7(3): 150-156.
- [32] Zagloul, D. A., Khodari, Y. A., Othman, R. A. M., Farooq, M. U. (2011): Prevalence of intestinal parasites and bacteria among food handlers in a tertiary care hospital. – Nigerian Medical Journal 52(4): 266-270.

BEEKEEPING AS A RURAL DEVELOPMENT ALTERNATIVE IN TURKISH NORTHWEST

ALTUNEL, T.^{1*} – OLMEZ, B.²

¹*Faculty of Forestry, Kastamonu University, Kuzeykent Campus, 37200 Kastamonu, Turkey
(phone: +90-532-570-9455; fax: +90-366-215-2316)*

²*Kastamonu Regional Directorate of Forestry, Halime Cavus st. No 7, 37100, Kastamonu, Turkey
(phone: +90-542-337-1364; fax: +90-366-214-1508)*

**Corresponding author*

e-mail: taltunel@kastamonu.edu.tr; +90-532-570-9455; fax: +90-366-215-2316

(Received 12th Feb 2019; accepted 28th Mar 2019)

Abstract. Turkey is one of the best areas for beekeeping because of its geography, climate, and the diversity of flora and fauna. Beekeeping is a traditional and socio-economic activity which is performed throughout Anatolia and has a place in our culture. Besides this, bee-keeping is very important to protect biodiversity and pass it onto the next generations, and also to provide and enhance food security. There are more than 100,000 families with 6.6 million colonies in Turkey. With all those, bee-keeping contributes to Turkish economy around US\$ 5-6 billion, not only through bee products but also pollination. As a part of the national policy, ORKÖY (the office of forest-village relations) provides micro-credits to villagers, who live in and around forested areas. In this study, ORKOY branch office distributed 30 beehives to 80 villagers with beekeeping certificates (in 2016 and 2017) and let them put their hives in the “honey forest” which was established in the region by the Forest Directorate. Face-to-face surveys, interviews and observations were conducted with 80 participants who benefited from beehive support and “honey forest.” At the end of the study, socio-economic effects and welfare improvement of local people through beekeeping and producing of bee products are analyzed in the northwest of Turkey.

Keywords: *honey production, villagers, socio-economic, social forestry, Turkey*

Introduction

Nowadays, the world population and the amount and quality of the produced goods and services do not increase at the same rate. The increase in the population increases demands and expectations, and thus it increases the expectations of people from agriculture and forest areas. Forests have versatile benefiting opportunities in terms of variety and quantity. The concept of “agricultural forestry” (agroforestry) was defined for the first time in the 1980s by some international organizations such as FAO. Agricultural forestry is the research and development of the possibilities of multi-faceted utilization from the same plot of land and the planning of agricultural and forest-related products, mostly animal husbandry, in the same field together. In this context, beekeeping and production of bee products are among the best examples of agricultural forestry practices. When the effect of bees on pollination is considered, it is observed that the beekeeping sector is also supported by forestry institutions to conserve biological diversity in forests, prevent erosion by the development of forest areas, and increase the quality of honey and honey products (OGM-1, 2018; FAO-1, 2018).

The first findings on obtaining bee products by human beings were found in nest paintings in the Mesolithic rocks which are thought to be about 8000 years old. In 1919, in the Arana Cave in the city of Valencia in Spain, the Mesolithic rock paintings dated

to 6000 BC and demonstrating a human figure harvesting honey from the bee colony in the tree cavity were determined. Similar depictions, older than the Mesolithic period, were also found in the rock paintings in India. Based on these depictions dating back to many years ago, it could be stated that the history of beekeeping traces back to 16,000 years ago (Genç, 2003). Furthermore, according to the information on the tablets, the ancient Egyptians used honey in food, medicine, and religious ceremonies 4000 years ago. The Sumerians, who lived in Mesopotamia, are known to accept honey as medicine in 3000 years BC (Bakan, 2009; Nakamura, 2009).

Literature review

In a study conducted in Japan, a significant decrease in the number of bees detected due to environmental factors, infectious diseases, and pesticides (Kohsaka et al., 2017). Beekeeping, which is an important way to protect biodiversity and to transfer it safely to future generations, is also very important in terms of providing food security in the world and increasing its diversity. However, with the extinction of bee colonies in the world in recent years, food security and continuity of the ecosystem have become endangered (Phillips, 2014). Therefore, beekeeping is a strategic sector that needs to be supported as a state policy.

With its different climate and soil types, flowering opportunities for different trees throughout the year, large flora areas, topographic structure, highlands, meadows and pastures, various fruit species, industrial plants (such as sunflower and cotton), forage crops and legume fields, trees of many species such as chestnut, pine, acacia, linden, spindle, eucalyptus, rhododendron, etc., shrubs, maquis shrublands and mixed forests, Turkey represents a magnificent country in terms of natural resources required for beekeeping, honey variety, and quantity. Because of these features, beekeeping has been one of the ancient and common production varieties in Anatolia (Sıralı, 2015).

Since beekeeping is an activity that requires knowledge but does not need muscle power and intensive workforce, children, the elderly or women who cannot be sufficiently effective in other production works can be directed to beekeeping activities. Furthermore, since it is an activity generating revenue in a short time, it is also an activity with high socio-economic importance which enables the income of people living in forests or adjacent villages to increase. Therefore, beekeeping is regarded as an alternative source of livelihood for people from all sociologically different segments, such as nuclear families, retirees, farmers with little or no land, teachers or village imams (OGM-2, 2018).

Beekeeping can be performed in two ways. Beekeeping, which is performed without changing the location of hives throughout the year, is called stationary beekeeping. Migratory beekeeping is a way of beekeeping in which bee colonies are carried to areas with more favorable nectar and pollen resources throughout the year and in which productivity is higher (Özkırım, 2018). Migratory beekeepers carry about half of their bee colonies in winter to the coastal areas of the Mediterranean, Aegean, and Black Sea regions. These beekeepers, who travel around Turkey throughout the season and change places of their hives three times a year, move primarily to the Central Anatolian plateau with the beginning of April, then to high plateaus in the summer months, and finally to the areas in Muğla and İzmir for pine honey production since September (TAB-1, 2018).

Since the beekeeping activity produces directly or indirectly the foods needed by people by playing a significant role in the pollination of plants, whether it is stationary or migratory beekeeping, it is also indispensable for herbal product agriculture. Approximately 85% of pollination in flowering plants in nature occurs through honey bees (Ghamdi et al., 2017).

Honey is composed of many components, such as approximately 82% carbohydrate, 17% water, 0.7% minerals, and 0.3% proteins, vitamins, phenolic compounds, free amino acids, and organic acids (Karabagias et al., 2014; Ozmen and Alkin, 2006; Islam et al., 2012). As a result of beekeeping activities, products such as honey, pollen, propolis, royal jelly and bee venom, which are very important for people and used in the treatment of various diseases, are produced. A method of treatment with bee products, which is called “Apitherapy,” has become a rapid trend in the world, especially in China. Among these products, propolis is known as a potent antibiotic, and royal jelly is known as an energy supply and hormonal source. Honey and pollen also have high nutritional value and are known to be effective in the treatment of diseases and infections (OGM-3, 2018; TAB-2, 2018).

The quality and quantity of nectar sources depend on the season, environmental, meteorological conditions, blooming stage of the plant, and even time of the day (Farkas and Zajacz, 2007). There are about 200 kinds of components in honey. Honey is a versatile consumption product which has high nutritional value and which displays easy digesting, disease-protective and therapeutic properties due to vitamins, minerals, flavonoids, phenolic and organic acids, amino acids and enzymes in its content. Moreover, in a study conducted, heavy metals were determined in honey samples, and it was stated that bee products could be an effective and cheap method in the prevention of environmental pollution as an indicator substance (Ozmen and Alkin, 2006; Spilioti et al., 2014).

Regarding its source, honey is divided into two as nectar honey (flower honey) and secretion honey (pine honey). Flower honey is obtained from many forest trees, shrub florals, and shrub species such as chestnut, linden, acacia, rhododendron, and from herbaceous plants inside the gaps in forests or on the edges of forests, and depending on the season, flower honey can be obtained in all parts of Turkey (DPT, 2018). Pine honey is obtained in Muğla and its vicinity, in the Mediterranean region where Calabrian pines are intense, and its source is pine, oak and abies species. Approximately one-fourth of the honey produced in Turkey is pine honey (DPT, 2018; Subaşı, 2004).

Beekeeping in the world and Turkey

According to the figures of FAO, the total number of beehives in the world is around 79.9 million, and approximately 1 million 592 thousand tons of honey is produced annually from these beehives. One-fourth of the total honey produced in the world is the subject of trade. When countries in the world are ranked according to the number of their hives, India ranks first with 11.5 million hives. However, China, which has 9 million hives, is the most honey-producing country in the world, with approximately 466 thousand tons of honey produced per year. After China, Turkey ranks second with 114 thousand tons, Argentina produces 80 thousand tons, Ukraine 74 thousand tons, and the Russian Federation produces 68 thousand tons of honey. China and Argentina are prominent in the export of honey, while the American and European Union countries are prominent in the import of honey (FAO-2, 2018; Karasin and Kaptan, 2015).

The countries, where honey production per hive is more than the world average of 22 kg, are Canada with 56 kg/hive, China with 52 kg/hive, Mexico with 39 kg/hive, Argentina with 27 kg/hive, and the USA with 26 kg/hive. In Turkey which ranks 12th in the world with its 15 kg of honey production per hive, despite the great hive presence, production per hive is low since the efficiency of honey production is low. With the highest number of hives in the world, India is the last among the world countries with an average of 4 kg of honey production per hive (Sıralı, 2015).

There are different principles and rules on this subject in each of the 12 countries that perform 80% of the export of honey and bee products in the world; therefore, production at international standards is not possible. For example, while the most important factor in the European countries is honey's being GMO-free, in North America, filtered, pasteurized, and liquid honey is preferred. In the Middle East, people consider crystallized honey as fake honey and do not prefer it (Kuvancı et al., 2017).

In Turkey, beekeeping is a socio-economic activity that has been traditionally performed in every region of Anatolia and has become a part of the culture. Turkey is the homeland of approximately 70% of honey-giving plant species and 22% of bee breeds. In Turkey, more than 100 000 families have a total of 6.6 million bee colonies. 10% of these families earn a livelihood solely from beekeeping, and 30% of them continue beekeeping as a side income activity. The remaining 60% are engaged in beekeeping activities as a hobby (TUIK, 2018).

According to the data of TÜİK (Turkish Statistical Institute) (2017), 114 thousand tons of honey is produced annually in Turkey. Twenty thousand tons of this amount are pine honey, and 100% of it is produced in forest areas. When it is considered that such varieties of honey as chestnut honey, linden honey, acacia honey, rhododendron honey, thyme honey are also produced in our forests besides pine honey, honey can be stated to be a significant “non-wood forest product.” The first ten provinces in Turkey in terms of honey production are Muğla, Ordu, Adana, Aydın, Sivas, Antalya, İzmir, İçel, Erzurum and Samsun provinces, respectively, and about half of the honey production is provided from these provinces (Sıralı, 2018).

In Turkey, to increase the sources of income of forest villagers by encouraging them to perform beekeeping, the General Directorate of Forestry has put 270 “honey production forest” lands into the service of beekeepers across the country. Moreover, with the protocol signed between the Ministry and the Beekeepers Association, it was decided to make water ponds in forest areas and to plant fire-resistant plants that give honey in fire lanes and forest roads. While 85% of honey production takes place in forest areas, only 15% takes place in agricultural areas (OGM-1, 2015).

Beekeeping contributes to the economies of countries directly as an agricultural activity and indirectly by contributing to plant production. Beekeeping is also important as a not land-dependent activity because in rural areas it can alone be a livelihood source for families without land (Kuvancı et al., 2016).

According to the 2017 data of TÜİK, 114, 471 tons of honey was produced in Turkey, and the revenue of US\$ 24,720,000 was obtained with the exportation of 1,236 tons of this production. If the honey remaining in the country is considered to be sold at a minimum sales price of US\$ 20 per kilogram, the total value will be about US\$ 2,264,700.000, and the total contribution of the produced honey to the country's economy will be about US\$ 2 billion 289 million. When this figure, which is obtained only with the honey data from beekeeping products, includes products such as pollen, beeswax, and royal jelly, the contribution of beekeeping products to the country's

economy is determined to be approximately US\$ 3 billion in a year. Considering that the contribution of beekeeping to the economy by pollination is at least 10-12 times of the income obtained from beekeeping products, it can be stated that beekeeping makes an essential contribution to Turkey's economy annually at about US\$ 30-35 billion (TUIK, 2018).

The objective of this study is to determine whether the support of government policies, such as ORKOY credits, establishing honey forests and providing education on beekeeping, helps villagers to improve their social, cultural, and economic welfare.

Materials and methods

Within the scope of the activities carried out by Kastamonu Regional Directorate of Forestry ORKÖY Branch to support forest villagers, the social and economic individual project types that can be applied in forest villages were determined pursuant to the regulations with regard to “providing support for the social and economic development of forest villagers for the protection, development, and expansion of forests”, and the study program was created. Within this context, in the years 2015 and 2016, in the areas with the stand area of pure and mixed chestnut (*Castanea sativa* Mill.) within the borders of Kastamonu Regional Directorate of Forestry, face-to-face surveys, interviews, and observational studies were conducted with 80 individuals benefiting from the support of “scientific beekeeping.” While determining the beekeepers to be included in the study, attention was paid to the fact that they were forest villagers who had not received ORKÖY support before, had a certificate of beekeeping, and resided in the region. To analyze the socio-economic structure of chestnut honey producers and to determine honey and other beekeeping products' contributions to the social and cultural life of local people and their effects on the welfare level, the survey questions were asked to the people of the region.

Chestnut, which is called *Castanea* (*Castanea sativa* Mill.) in Latin, is from the family of Fagaceae. It grows in all temperate regions of the North Hemisphere. Although 10-12 species of chestnut are known to be in the world, the species that grows naturally in Turkey is Anatolian chestnut (*Castanea sativa* Mill) (Conedera et al., 2016). Chestnut tree, as a valuable species with its fruit and wood, is of great importance for its region from ecological, economic, social and cultural aspects (Doğanay, 2007).

In this study, to analyze the socio-economic structures of chestnut honey producers in Kastamonu, the contribution of chestnut honey production and beekeeping activities to the local people was determined by face-to-face surveys and interviews. First of all, the participants' demographic characteristics, product mix, production quantities, sales price, and obtained revenues and perceptions and opinions about beekeeping were attempted to be determined with the questions prepared for this purpose. While preparing the questions, a literature survey was conducted on the subject, and the opinions of the participants were obtained with 30 closed and open-ended questions. In the survey, apart from the questions regarding the study, questions related to the demographic characteristics of participants such as age, gender, education, etc. were also included. After the questionnaires were transferred to the computer in Excel format, in the analyses of the collected data, straight and cross-analyses were performed using SPSS (Statistical Package for Social Sciences) statistical program, and the results were presented and interpreted with the help of graphs (Orhunbilge, 2014).

Results

About 85% of the local people who deal with beekeeping in the study area are aged between 31 and 60 years. Beekeeping activities are mostly conducted by men in the region, and although women are involved in these activities together with men, they prefer to remain in the background. Furthermore, most of the people engaged in beekeeping (75%) are primary school graduates.

40% of the beekeepers, who participated in the study, stated that their total annual income is between US\$ 4,000-5,000, and 45% stated that it is over US\$ 5,000. According to the land amount owned by the beekeepers to whom the survey was applied, while 80% have 0-15 acres of land, only 8.5% have 26 acres of land and more.

Of the participants benefiting from beekeeping-related support, 32.5% have been engaged in beekeeping for 6-10 years, 21.3% for 11-15 years, and 25% for over 16 years. It was found out that almost all of the beekeepers were performing the beekeeping activity with one or two people, and these people were mostly their spouses or children, in other words, their family members.

Upon examining the ownership status of lands where beekeeping activities were carried out, 90% of the participants stated that they carried out beekeeping activities on their land, 10% in forest area or honey forests. 65% of the beekeepers participating in the study stated that beekeeping education was insufficient and that the relevant ministries and NGOs should attach importance to the subject of training.

Upon examining the number of hives owned by beekeepers including 30 hives provided by ORKÖY, it was found out that 50% of the beekeepers have 1-50 hives, 33.7% have 51-80 hives, 5% have 81-100 hives, 6.3% have 101-130 hives, and 5% have 130 hives and more. In 80% of the hives, there are 9 and more frames. In the region where half of the beekeepers have a maximum of 50 hives, before increasing the number of hives, the number of colonies under controlling and registration can be increased by determining the flora of the region. Thus, studies not only on yield but also on quality will be useful for beekeeping and will increase the amount of production.

Within the scope of the study, the beekeepers were asked about their seasonal expenses per hive, and 75% of the participants stated that their expenses were US\$ 20-35, and 15% stated that the expenses were US\$ 40 and above.

It was stated that the maximum amount of harvest received (*Fig. 1*) by the beekeepers participating in the survey from one hive was between 7-10 kg with a rate of 80%, in case the meteorological conditions in the region were good and the chestnut tree nectar at the end of May and the beginning of June was optimal. In the case of adverse climate conditions, the minimum amount of harvest from one hive was recorded to be between 1 and 3 kg at a rate of 95%.

80% of the 80 beekeepers who received hives stated the sale price of the produced honey as US\$ 20-25 and 17.5% stated it as US\$ 25-40. Regarding the marketing method of the produced beekeeping products, 98.8% of the participants stated that they sell the produced honey directly to consumers, and very few of them stated that they sell it to intermediaries. Beekeepers (96%), who did not experience any problem with the marketing of produced beekeeping products, stated that the customer was ready in the market.

While 37.5% of the participants who carry out beekeeping activities and benefit from ORKÖY support are members of beekeeping cooperatives, 62.5% do not have cooperative membership. 53.8% of the beekeepers benefited from the support granted

for two years in 2015, and 46.2% benefited from it in 2016, and the number of applications for support in the second year was higher than in the previous year.

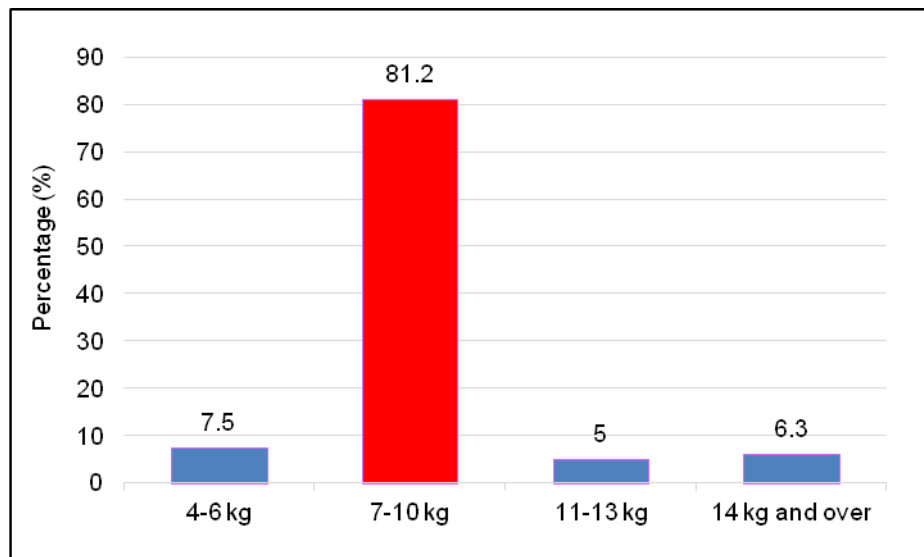


Figure 1. Maximum honey harvest under good meteorological conditions (kg)

76.2% of the beekeepers benefiting from the ORKÖY support stated that they generated profit and 20% stated that they did not make any profit or loss. The beekeepers were asked whether they wanted to use the ORKÖY support again, and 81.2% of them stated that they wanted to take advantage of it again and 18.8% stated that they did not want to take advantage of it again. When the participants were asked whether they had heard the term “honey forest,” 51.2% stated that they had not heard it and 48.8% stated that they knew it. When the beekeepers were asked about the “future of beekeeping,” 81.2% stated that they were hopeful about the future, 10% stated they were hopeless, and 8.8% stated that they did not have a positive or negative opinion.

In the comparison of the land amount owned by the beekeepers with their annual income, an increase was observed in the income levels as the amount of the land they owned increased (*Fig. 2*). As the land amount owned by the beekeepers increased, the number of their hives also increased.

When the relationship between the educational level of the beekeepers participating in the study and their cooperative memberships was examined, it was observed that while 22 primary school graduates and 7 secondary school graduates were not members of cooperatives, 38 primary school graduates and 7 secondary school graduates had cooperative membership. Accordingly, no relationship was determined between educational level and cooperative membership.

Upon examining the desire of the participants who carry out beekeeping activities and have benefited from the ORKÖY support to reuse the support according to their profit/loss status, it was determined that 53 individuals generated profit and could reuse the support, 8 individuals did not want to reuse the support although they generated profit, and 11 individuals did not make any profit or loss but could reuse the support. Therefore, any relationship between making profit or loss and ORKÖY support was not determined.

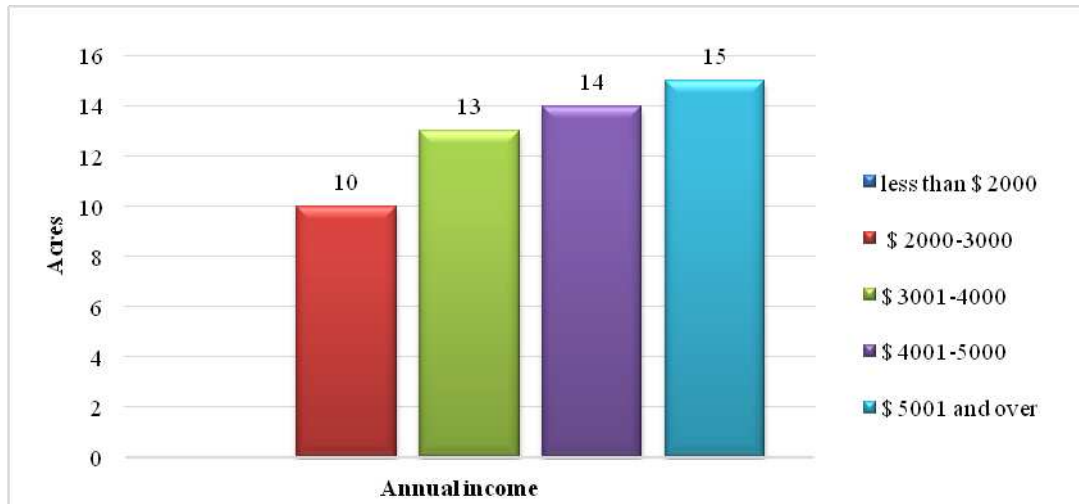


Figure 2. The relationship between the amount of the land owned and total income

Beekeepers who carry out beekeeping activities with the ORKÖY support sell honey directly to consumers at an average price of US\$ 21-25 (Fig. 3). There is no sale of honey to intermediaries, factories or on export markets in the region.

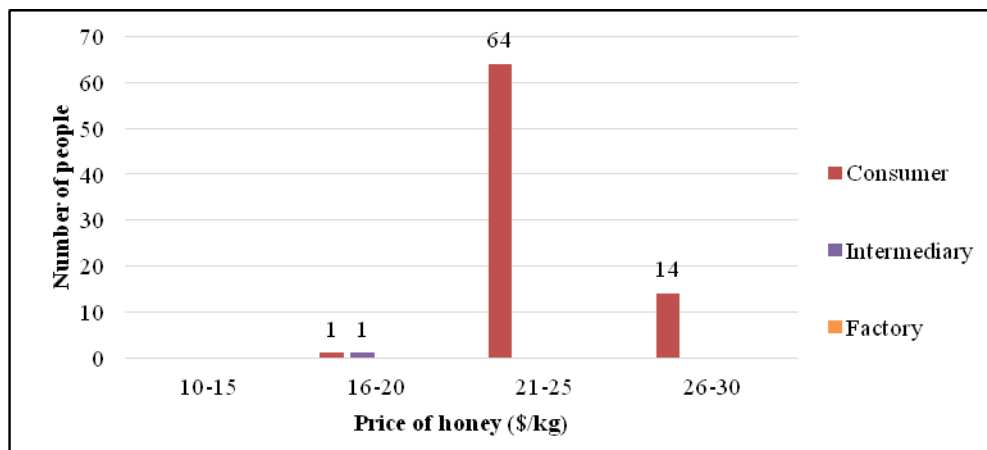


Figure 3. The relationship between the sale price of honey and the marketing method

Of the beekeepers who said that beekeeping-related training was sufficient, 17 beekeepers said that they learned beekeeping from the family, four beekeepers said that they learned it from other beekeepers, and four beekeepers said that they learned it in the course. Of the beekeepers who stated that the training was insufficient, 22 beekeepers stated that they learned beekeeping from the family, 16 beekeepers stated that they learned it in the course, and 14 beekeepers stated that they learned it from other beekeepers (Fig. 4). In general, the participants stated that they learned beekeeping from their families that beekeeping training was insufficient, and that beekeeping could not be learned from sources such as TV, books, and brochures, and that productivity could be increased through more visual and practical training.

Upon examining the relationship between the beekeeping activity and the total annual income, it was observed that the individuals who participated in the study did not

produce beekeeping products such as propolis, pollen, beeswax, royal jelly, and bee venom, but produced only honey. Providing the necessary support, carrying out studies, and attaching importance to educational activities related to the subject to produce other beekeeping products in addition to honey in the study area will be effective in increasing the income and welfare of the people in the region.

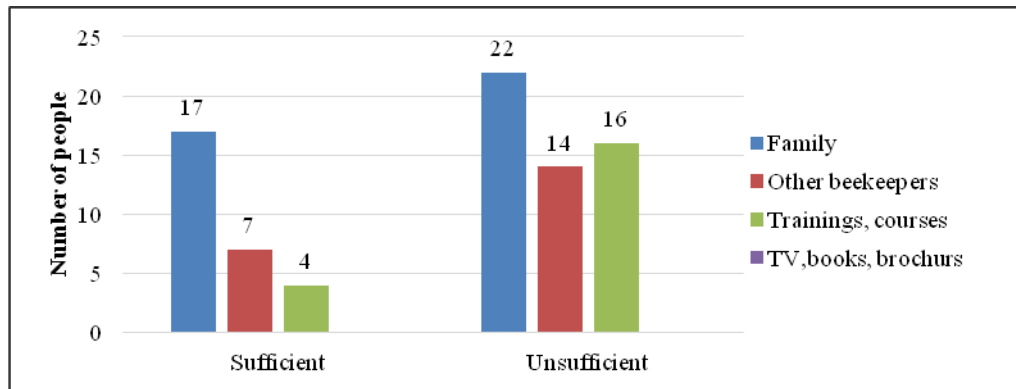


Figure 4. Sufficiency of beekeeping training according to the beekeeping learning style

Discussion

The production power of the honey bee, which offers valuable products for human life and health, has become much more critical with the increase in the world population. Besides its importance in the universal dimension, beekeeping also offers essential opportunities concerning the local development of forest villagers, since it is a field that provides middle or high-income opportunities with low investment and labor force. As Ayan et al. concluded in a study (2014), beekeepers/forest villagers have to have organic, brand name and certified bee products to increase their income.

In a study conducted by Önal and Bekiroğlu in 2011, the participants stated that they found the support provided by ORKÖY positive and that the economic and social village development projects implemented in the region increased the welfare level of the villages (82). Similarly, in this study, the villagers dealing with beekeeping stated that they were satisfied with ORKÖY support (96%), that their welfare level increased with the received support, and that they wanted the support to be repeated. In the same study by Önal and Bekiroğlu (2011) who emphasized the importance of being organized as a cooperative in rural areas, it was stated that the fact that villagers have a say in their works and the sales of products in the market and an increase in their efficiency should be provided through cooperatives. In this study, the ratio of becoming a member of a cooperative was determined as low as 37.5%, and it was stated that by increasing this ratio beekeepers would receive a say on the regional and national scale. Although in Turkey there are Provincial Unions established in the provinces and TAB (Turkey Beekeepers Association) that was established at the national level; locally, the memberships of beekeepers to these associations are inadequate.

Training of beekeepers/villagers on sustainable beekeeping is very important to improve their income level and sustainable usage of forest resources, in addition to providing food security (FAO-1, 2018). In our study, 52 (65%) out of 80 beekeepers stated that practical training and experience are important for sustainable beekeeping and sustainable usage of natural resources.

In the study conducted by Kuvancı et al. in the Eastern Black Sea Region (2017), it was stated that the average age of beekeepers was high, and to give momentum to this sector, the entrepreneurship and dynamism of the young people were needed. Similar results were also obtained in the study conducted in Kastamonu, and it was determined that 61% of the participants performing beekeeping activities were in the 40-60 age range. This result also indicates that the young population in villages migrates to cities due to unemployment. Again, the opinions in the same study which argued that the mix of goods related to beekeeping products should be diversified and that the level of income in the region should be increased by producing high value-added products show parallelism with the results of our study.

In another study conducted in the Netherlands, it was determined that producers, who perform plant production, pay beekeepers bee rent to provide pollination in plants and that they generate 3.5 times more of yield from bees' contribution to plant production in return (Hilmi et al., 2011). In Turkey, there is no study carried on this subject. The subject of making payment to beekeepers by determining the contribution of beekeeping to plant production should be put on the agenda by both the Ministry of Agriculture and Forestry and the Beekeepers Association.

Because of the low yield in the production of honey per hive, Turkey could not reach its beekeeping potential and the desired position in the world honey trade yet. Although the colony presence has increased by 41% over the last decade, the prices of bee products remain high due to reasons such as insufficient bee product variety, the lack of added value, unorganized marketing, and consumer demand. Although Turkey is in the second rank in the world in the amount of honey production, it could not reach the deserved position in the export of honey products due to imbalances in prices and supply amount (TUIK, 2018).

As it is stated by Seijo and Jato (2001), chestnut trees are a very important nectar and pollen resource to produce bee products both by quality and quantity. That is why *Castanea Sativa* Miller trees are important for beekeepers in northern Turkey economically, ecologically, and socially.

Conclusions

The fact that beekeeping activities have reached the targeted level will provide benefits such as the continuation of biodiversity, the development of citizens living in rural areas and the increase in their welfare level, the increase in the economic input to the region, the decrease in migration from the village to the city, the development of the relationship between forests and public, the decrease in illegal activities in forests, and many other ecological, social and economic aspects.

Since beekeeping is not a land-dependent branch of agriculture, it can solely be a source of income for farmers with little or no land. It is possible to state the main reasons which make beekeeping activities attractive as the opportunity to carry out beekeeping activities with limited resources in budget and capital, low maintenance and management costs, opportunity to generate income in a short time, opportunity of the easy sale of bee products due to the high demand in the market, and chance to procure materials that are necessary for beekeeping such as hives, bees, breeding bees, etc. within the country.

The forest ecosystem is not just areas which provide the industrial wood product. The products and services provided by forest ecosystems are more needed nowadays

than in the past due to reasons such as population growth, quality of life, changes in consumer preferences, and the decrease in natural resources. To meet the people's increasing expectations from forests in a sustainable manner, each element of forests should be operated within the framework of efficiency principles.

Due to its rich plant diversity, Turkey has a great potential for the production and export of quality honey and other bee products obtained as a result of beekeeping activities. Although Turkey takes the second place in honey production in the world, we do not produce and export value-added honey products such as wax, pollen, propolis, and bee milk. It is necessary to conduct studies on how to produce those products and how we can market them worldwide instead of consuming them locally or nationally. To contribute more to the economy and environment, studies should be carried out on beekeeping activities to develop joint action plans with the Ministry of Food, Agriculture and Livestock, the Ministry of Forestry, universities, producer unions, cooperatives and exporting companies according to the results of these studies.

For the purpose of the national and international recognition of “chestnut honey,” which is produced with great devotion by the local people in Kastamonu, has its unique aroma and taste, and determination of its standards, the process of branding was initiated by the local government, and an application for “geographical sign” registration was made.

REFERENCES

- [1] Al-Ghamdi, A. A., Adgaba, N., Herab, A. H., Ansari, M. J. (2017): Comparative Analysis of profitability of honey production using traditional and box hives. – *Saudi Journal of Biological Sciences* 24: 1075-1080.
- [2] Ayan, S., Ayan, Ö., Altunel, T., Yer, E. N. (2009): Honey forests as an example of agroforestry practices in Turkey. – *Forestry Ideas* 20(48): 141-150.
- [3] Bakan, A. (2009): The mystery of honey. – *Journal of Science and Technology, TUBITAK* 10: 8-11.
- [4] Conedera, M., Tinner, W., Krebs, P., de Rigo, D., Caudullo, G. (2016): *Castanea sativa* in Europe: distribution, habitat, usage and threats. – *European Atlas of Forest Tree Species*. Publication office of EU: 78-79.
- [5] DPT (State Planning Organization). Onuncu beş yıllık Kalkınma Planı, Bitkisel Üretim Özel İhtisas Komisyonu Raporu. – http://www.sbb.gov.tr/wp-content/uploads/2018/10/10_BitkiselUretim-2.pdf. Accessed on: 22.07.2018.
- [6] Doğanay, H. (2007): *Ekonomik Coğrafya 3 – Ziraat Coğrafyası*. Aktif Yayınları.
- [7] FAO and FDA (Forest Development Authority of Liberia). (2013): *Farmer Level Tech-Note for: Beginner Beekeeping*. – FAO, Liberia.
- [8] FAO-1: Agroforestry. <http://www.fao.org/forestry/agroforestry/80338/en/>. – Accessed on: 23.08.2018.
- [9] FAO-2: Food and agricultural data. <http://www.fao.org/faostat/en/#home>. – Accessed on: 25.10.2018.
- [10] Farkas, A., Zajacz, E. (2007): Nectar production for the Hungarian honey Industry. – *The European Journal of Plant Science and Biotechnology* 1(2): 125-151.
- [11] Genç, F. (2003): *Basic Principles of Beekeeping*. – Atatürk University Faculty of Agriculture Press, Erzurum.
- [12] Hilmi, M., Bradbear, N., Mejia, D. (2011): *Beekeeping and Sustainable Livelihoods*. – FAO, Rural Infrastructures and Agro-Industries Division, Diversification Booklet Number 1: 62.

- [13] Islam, A., Khalil, I., Islam, N., Moniruzzaman, M., Mottalib, A., Sulaiman, S. A., Gan, S. H. (2012): Physicochemical and antioxidant properties of Bangladeshi honeys stored for more than one year. – *BMC Complementary and Alternative Medicine* 12(1): 177.
- [14] Karabagias, I. K., Badeka, A., V., Kontakos, S., Karabournioti, S., Kontominas, M. G. (2014): Botanical discrimination of Greek unifloral honeys with physico-chemical and chemometric analyses. – *Food Chemistry* 165: 181-190.
- [15] Karasin, K., Kaptan, A. (2015): Dünyada bal üretimi ve kovan sayıları. – *Journal of KA* 1(3): 34-37.
- [16] Kohsaka, R., Park, M., S., Uchiyama, Y. (2017): Beekeeping and honey production in Japan and South Korea: past and present. – *Journal of Ethnic Foods* 4(2): 72-79.
- [17] Kuvanci, A., Güler, A., Aksoy, F., Karaoglan, Y. (2016): Bal arasının kivi bitkisinin polenlerinden yararlanma düzeyleri. – *Journal of Beekeeping Research, Arıcılık Araştırma Enstitüsü Müdürlüğü* 8(1): 15-21.
- [18] Kuvanci, A., Yılmaz, F., Öztürk, S., Konak, F., Buldağ, M. (2017): Doğu Karadeniz Bölgesi Arıcılığına Genel Bakış. – *Journal of Beekeeping Research, Arıcılık Araştırma Enstitüsü Müdürlüğü* 9(2): 47-55.
- [19] Michener, C., D. (2007): *The Bees of the World*. – The Johns Hopkins University Press, Baltimore, Maryland.
- [20] Miguel, M. G., Antunes, M. D., Faleiro, M. L. (2017): Honey as a complementary medicine. – *Integrative Medicine Insights* 12: 1-15.
- [21] Nakamura, J. (2009): *Apiculture. Development of Beekeeping in Developing Countries and Practical Procedures*. – JAICAF (Japan Association for International Collaboration of Agriculture and Forestry), Tokyo.
- [22] OGM-1 (General Directorate of Forestry) Workshop (2015): Ormanlarımız ve arıcılık çalıştayı. – Department of Non-Wood Forest Products Publications, Ankara.
- [23] OGM-2: Ministry of Agriculture and Forestry. Action Plan of Honey Forest. – <https://www.ogm.gov.tr/ekutuphane/Yayinlar/Orman>. Accessed on: 12.06.2018.
- [24] OGM-3 (General Directorate of Forestry): ORKÖY (Forest–Village Relations) Introductory Booklet. – <https://www.ogm.gov.tr/Baskanliklar/OrmanveKoyIliskileri/>. Accessed on: 22.08.2018.
- [25] Önal, P., Bekiroğlu, S. (2011): Orman Köylerinde ORKÖY tarafından gerçekleştirilen Köy Kalkındırma Projelerinin Uygulama Sonuçlarının Araştırılması (Şile-İstanbul). – *Journal of the Faculty of Forestry, İstanbul University* 61(2): 53-66.
- [26] Orhunbilge, N. (2014): *Tanımsal İstatistik, olasılık ve olasılık dağılımları*. – Nobel Academic Publishing, Ankara.
- [27] Ozkirim, A. (2018): Beekeeping in Turkey: Bridging Asia and Europe. – In: Chantawannakul, P. et al. (eds.) *Asian Beekeeping in the 21st Century*. Springer, Singapore, pp. 41-70.
- [28] Ozkok, A., Sorkun, K. (2001): Important bee products used in apitherapy: honey, pollen and propolis. – *Journal of Technical Beekeeping* 2001: 4-10.
- [29] Ozmen, N., Alkin, E. (2006): Balın antimikrobiyal özellikleri ve insan sağlığına etkileri. – *Uludağ Beekeeping Journal* 4: 155-160.
- [30] Phillips, C. (2014): Following beekeeping: more-than-human practice in agrifood. – *Journal of Rural Studies* 36: 149-159.
- [31] Seijo, M. C., Jato, M. V. (2001): Distribution of castanea pollen in Galician honeys (NW Spain). – *Aerobiologia* 17(3): 255-259.
- [32] Sirali, R. (2015): Arıcılığın Ordu yöresi için ekonomik önemi. – *Journal of Beekeeping Research, Arıcılık Araştırma Enstitüsü Müdürlüğü* 7(2): 18-20.
- [33] Sirali, R., Cinbirtoglu, S. (2018): Bal arılarının tozlaşmada ve bitkisel üretimdeki önemi. *Journal of Beekeeping Research*. – *Arıcılık Araştırma Enstitüsü Müdürlüğü* 10(1): 28-33.
- [34] Spilioti, E., Jaakkola, M., Tolonen, T., Lipponen, M., Virtanen, V., Chinou, I., Kassi, E., Karabournioti, S., Moutsatsou, P. (2014): Phenolic acid composition, anthiatherogenic

- and anticancer potential of honeys derived from various regions in Greece. – PloS One 9(4): e94860.
- [35] Subasi, B. (2004): Kestane sektör profili. – ITO (İstanbul Ticaret Odası), Etüt ve Araştırma Şubesi, İstanbul.
- [36] TAB-1 (Turkish Association of Beekeepers): Göçer arıcılık ve konaklamalar. – <http://www.tab.org.tr/apimondia>. Accessed on: 25.06.2018.
- [37] TAB-2 (Turkish Association of Beekeepers): Apiterapi çalışmayı sonuç raporu. – <http://www.tab.org.tr/apiterapi-calistayi-sonuc-raporu.html>. Accessed on: 15.11.2018.
- [38] TUIK (Turkish Standards Institute): Beekeeping statistics. – http://www.tuik.gov.tr/PreTablo.do?alt_id=1001. Accessed on: 17.04.2018.

INVESTIGATING THE QUALITY OF DURUM WHEAT LANDRACES AND DETERMINATION OF PARENTS TO USE IN BREEDING PROGRAMS

KENDAL, E.^{1*} – EREN, A.¹ – DOĞAN, Y.¹ – ORAL, E.² – KOYUNCU, M.³

¹*Department of Seed Production, Kızıltepe Vocational Training High School, Mardin Artuklu University, 21500 Kızıltepe, Mardin, Turkey*

²*Department of Field Crops, Faculty of Agriculture, Van Yüzüncü Yıl University, Van, Turkey*

³*Department Engineering of Food, Karamanoğlu Mehmetbey University, Karaman, Turkey*

**Corresponding author
e-mail: enver21_1@hotmail.com*

(Received 15th Feb 2019; accepted 21st Mar 2019)

Abstract. The study was conducted to evaluate the quality of durum wheat grain. For this reason, genetic resources are crucial for the identification of parents and the enrichment of the gene pool that can be used in the development of new varieties for better nutrition of people. For this purpose, 131 populations of landraces, 9 promising line and 5 new varieties were used. The experiment was set up in randomized blocks with 7 replications, according to the augmented (increased) experimental design in 2015-2016 growing season. In the study, we examined total nitrogen content, protein ratio, CIE (Commission Internationale Eclairage) wheat color analysis (L* brightness, b* jaundice, a* redness) of 145 genotypes of durum wheat seeds. According to analysis of variance, highly significant differences ($P < 0.05$ or $P < 0.01$) were determined for total nitrogen, protein content and CIE L* value, while differences were not significant for b* value and a* value. The superiority of the genotypes was determined by the first two principal components (IPC1 (principle component) and IPC2) in order to create a two-dimensional GT biplot. The sum squares of the first two components were accounted by 45.34% (PC1) and 40.03% (PC2) for genotypes. The GT (genotype x trait) biplot indicated that 9 (nine) sectors occurred among genotypes and quality parameters. On the other hand, three groups occurred among the quality parameters based on the genotypes. The scatter plot demonstrated that there is a high correlation between b* jaundice, and a* redness. The results showed that cultivars and more landraces have general adaptability for all quality parameters, while some genotypes (G79, G78), (G22, G102), (G3) and (G121, G5) showed specific adaptation for N (nitrogen), PC (protein content) and L*, a* and b* values, respectively. According to the biplot techniques, G36 came forward with the N, P and a* value and desirable landraces, G5 for b* value, G30 stable line for all quality parameters, while (G128, G61) and the majority of promising lines (L4, L6) did not come forward with any quality parameters. The results of the study indicated that the majority of landraces can be used as parents to improve the quality of durum wheat varieties. The study indicated that GT biplot can be used to evaluate the genotypes graphically to select the best genotypes for parents to use in breeding programs.

Keywords: *GT biplot, quality parameters, Southeastern Anatolia, Turkey*

Introduction

Global biodiversity and plant genetic diversity compose of the genetic resources which are crucial for the identification of parents and the enrichment of the gene pool that can be used in the development of new varieties for better nutrition of people. For this reason, landraces are very important as genetic resources for identity of parents to improve gene pool and develop new quality varieties for better people's health. Nowadays, quality of durum wheat is most substantial for healthy fed in Middle East countries, because majority of people are fed from durum wheat product (bulghur,

macaroni, bread). Therefore, landraces are considerable for breeding program of durum wheat, because most people care to use the healthy-products (bulghur, macaroni, and bread) of wheat. Upon domestication, it was estimated that initial diversity was reduced by 84% in durum wheat (Jaradat, 2013).

Turkey is located at a unique position from the view point of plant genetic diversity. Due to both in terms of environmental conditions and in terms of culture is very suitable for wheat cultivation. Turkey is one of the Centers of Origin of wheat and wheat has been grown around 8.5 million ha with production of around 20 million tons annually (<http://www.tuik.gov.tr/PreHaberBultenleri.do?id>; Karaman, 2019). The total 50% of durum wheat is produced in Southeastern Anatolia region where is center (Karacadag) origin of durum wheat. Southeastern Anatolia region follows the Southeastern Taurus Mountains and the valley of the Tigris River. Frequency of durum wheat exceeds 60%, with a high diversity of morph types dominated by murkiness (Morgounov et al., 2016).

The nutrient content of wheat grain can vary from genetic resources (landraces population, wild wheat, the origin of cultivars) to regions and continents. Domestication and deep selecting in breeding progression significantly influenced to the depletion of nutritional content and in minimizing the genetic diversity of crops. An analysis of the nutritional value, especially micronutrients in the CIMMYT (International Maize and Wheat Improvement Center)-developed germplasm displayed that a declining trend in the micronutrient levels of the varieties (Velu et al., 2014; Pandey et al., 2016).

Nowadays, over three billion people suffer from “malnutrition”, a locution used to define shortage of micronutrients (FAO, 2013). At the present time, nutrient shortcoming is a problem both common in developing countries, but extensive in developed countries where diet is mainly dependent on cereals. Therefore, the durum wheat program need to progressive revelation studies of nutritional in breeding. Throughout the last century, the input of high-yielding cultivars, led to the loss of genetic diversity. Wheat landraces are comprised of complex, variable, genetically dynamic and diverse populations, for both biotic, abiotic stresses in their environment and micro-macronutrient.

On the other hand, durum wheat breeding programs should have focuses on the develop of new varieties for high quality which are important for modern pasta and bulgur industry, because of changing consumption habits and undernourishment places where this is based on durum wheat. To achieve this goal, durum wheat landraces keeps its importance inside genetic diversity in Middle east and Southeastern Anatolia region. Because local durum wheat populations have adequate quality characteristics (nitrogen content, protein ratio, wheat color analysis (L* brightness, b* jaundice, a* redness) for the development of new varieties that can be used in the pasta and bulgur industries. For this reason, durum wheat breeders have recently given more importance to the durum wheat landraces in order to raise the quality criteria in durum wheat.

Among quality criteria seed quality is one of the important factor effecting plant growth, yield and nutrient uptake by the plants. For a good and healthy growing start seed quality is important. Seed quality is one of the best criteria for cereal productions and qualified seeds led to about 25 to 40 percent yield increase. During the early stage, plants meet their nutrient and energy demand from the reserves in their seeds mostly. So, huge nutrient stocks in the seeds are vitally important for plants to be able to survive their growth healthy (Erdal et al., 2017).

The aims of the present study were to assess the importance of the local durum of wheat landraces that are about to disappear in nature and constitute the source of the

gene for durum wheat in terms of quality criteria to determine the parents which can be used in durum wheat breeding programs.

Materials and methods

Plant material and experimental arrangement

The study was conducted using a total of 131 populations of landraces; 9 promising landraces and 5 new varieties were used. The populations of landraces were collected from Southeastern Anatolia region of Turkey where is centers for origin of durum wheat. The cultivars are used registered by International Agricultural Research and Training Center during last decades. The varieties used in the study both have good quality criteria and very common cultivating in this region. The coordinate data of the used genotypes indicated in *Table 1*. The meteorological data showed in *Figure 1*. The map to overview of the areas of collected landraces of durum wheat presented in *Figure 2*.

Table 1. The coordinate of landraces which collected places Shout Eastern of Anatolia

No	Altitude (m)	Coordinates		No	Altitude (m)	Coordinates	
		X	Y			X	Y
1	803	596291	4222874	71	1016	634008	4301447
2	710	596898	4221585	72	1090	584410	4293758
3	700	599901	42209007	73	1283	485371	4269859
4	709	599954	42 1682	74	1348	485612	4270632
5	735	600531	4222173	75	811	522958.63	4194028.75
6	725	600386	4222039	76	715	519141.53	4193911.25
7	687	598988	4218628	77	715	519141.53	4193911.25
8	685	63610	4220816	78	762	519532.25	4191512.25
9	703	605131	4222688	79	762	524911.00	4180531.50
10	777	606500	4228778	80	668	513518.31	4150858.75
11	838	606226	4231796	81	728	526140.69	4150528.00
12	863	625538	4251067	82	925	664595.38	4146901.00
13	872	626115	4251110	83	925	664595.38	4146901.00
14	862	627655	4251196	84	925	664595.38	4146901.00
15	884	619904	4251715	85	848	662635.94	4154887.00
16	907	618144	4252344	86	828	662583.94	4156068.50
17	910	614216	4251336	87	836	662792.13	4156608.25
18	888	610797	4260263	88	1002	670122.88	4157678.03
19	853	610396	4249353	89	1094	682464.10	4158560.50
20	796	610891	4248325	90	1089	682464.10	4158560.50
21	787	611954	4248357	91	978	692842.94	4148766.75
22	785	611951	4248355	92	997	687266.91	4149245.25
23	1064	650497	4237654	93	988	686129.00	4149423.25
24	1050	650164	4237395	94	1094	679879.00	4146845.75
25	679	681780	4237283	95	1069	675314.00	4143407.00
26	681	681781	4237284	96	917	634.514.94	4152010.25

27	895	68456	4266685	97	1041	617647.80	4142738.75
28	895	684652	4246867	98	950	708362.06	4135393.00
29	897	683593	4249088	99	911	708190.01	4136542.20
30	853	668840	4260416	100	882	708019.88	4137244.75
31	786	594207	422878	101	921	707595.06	4141429.25
32	837	594634	42275550	102	934	707360.75	4143376.50
33	931	592344	4231601	103	965	70935.75	4150709.25
34	873	588191	4241045.50	104	986	708496.50	4153507.00
35	812	588895	4241660	105	990	708098.13	4154453.25
36	865	635665	4253198.50	106	986	708146.00	4154610.50
37	1025	636301	4259395	107	986	708146.00	4154610.50
38	890	636017	4254531.50	108	723	715642.15	4227401.15
39	876	650340.75	4258239.50	109	723	715642.15	4227401.15
40	978	556997.56	4236808.00	110	573	Unknown	Unknown
41	1032	555252.81	4236790.50	111	628	749524.25	4208746.00
42	814	547904.19	4234858.50	112	970	760148.05	4204095.09
43	862	541615.56	4232495.50	113	970	760148.05	4204095.09
44	884	540057.13	4231857.50	114	496	753207.81	4191005.25
45	677	541118.75	4224902.50	115	496	753207.81	4191005.25
46	723	536671.00	4219466.00	116	462	749122.01	4187300.25
47	729	496012	4195229	117	462	749122.01	4187300.25
48	828	502219.75	4201199.50	118	461	748892.38	4186918.01
49	805	502337.59	4201143.50	119	542	747895.05	4878340.50
50	805	502337	4201143.50	120	723	754523.31	4177849.50
51	755	502776.56	4202023.50	121	723	754523.31	4177849.50
52	722	502318.59	4202746.00	122	787	759218.71	4175591.72
53	1045	500979.00	4210611.50	123	841	759326.81	4176481.75
54	925	498985.97	4210780.00	124	1003	239151.64	4170548.75
55	1025	496297.66	4210493.50	125	1202	244929.83	4173425.00
56	1032	496144.84	4210521.50	126	875	760055.31	415805.50
57	1032	496144.84	421052.50	127	1005	756303.63	4155465.75
58	1077	492395.16	4209038	128	792	756828.00	4153671.25
59	890	488445.31	4207384.00	129	730	753644.69	415549.00
60	819	449332.03	4204385.00	130	883	741775.94	4158370.25
61	835	450771.00	4203501.50	131	896	738389.38	4158352.50
62	858	452118.34	4203644.00	132	896	738389.38	4158352.50
63	858	452118.34	4203644.00	133	978	727246.69	4155708.75
64	893	458033	4203095	134	978	727246.69	4155708.75
65	867	528384	4272667	135	978	727246.69	4155708.75
66	862	546436	4274936	136	978	727246.69	4155708.75
67	857	565288	4278407	137	978	727246.69	4155708.75
68	1031	577881	4280381	138	951	724918.13	4154284.00
69	1095	625437	4289576	139	951	724918.13	4154284.00
70	1164	625998	4288948	140	951	724918.13	4154284.00

Checks: 1-Artuklu, 2-Hasanbey, 3-Hasanbey, 4-Şahinbey, 5-Zühre. All control varieties released from GAP International Research and Training Center

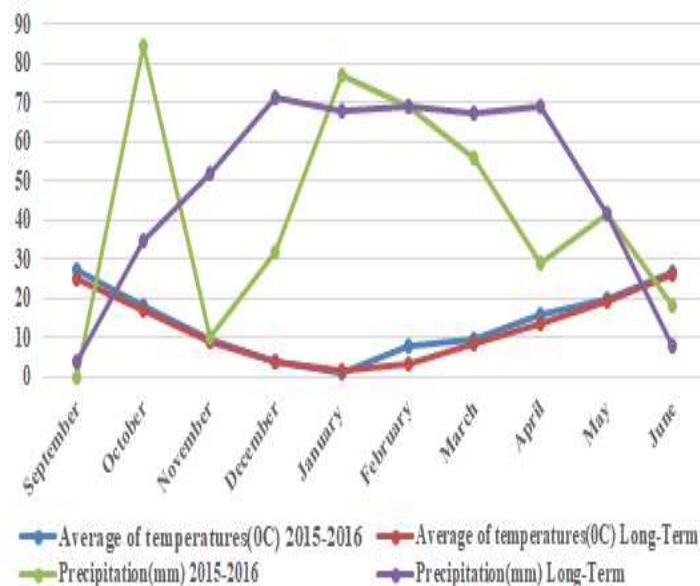


Figure 1. The values of meteorological data of 2015-16 season and average of long term in research area

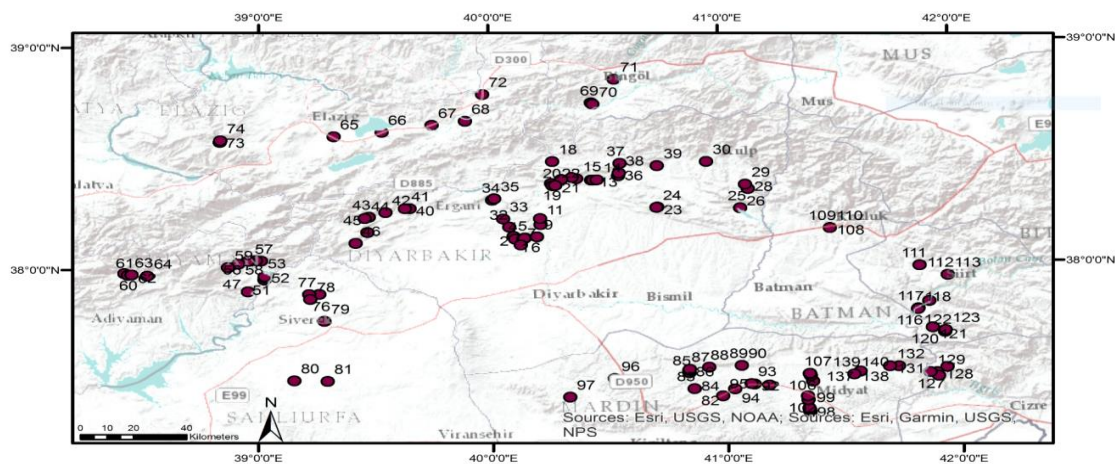


Figure 2. The map to overview of the areas of collected landraces of durum wheat used in the research

The experiment was set up in randomized blocks with 7 replications, according to the augmented (increased) experimental design in Diyarbakir conditions in 2015-2016 growing season. The seeding rates were 450 seeds m⁻². Plot size was 0.4 m² (20 cm × 1 m) consisting of 2 rows spaced 20 cm apart. Sowings were made by hands. The fertilization rates for all plots were 60 kg N ha⁻¹ and 60 kg P ha⁻¹ with sowing time and 60 kg N ha⁻¹ was applied to plots at the early stem elongation. Harvests were made using Hege 140 harvester.

In the study, we examined total nitrogen content, protein ratio, wheat color analysis (L* brightness, b* jaundice, a* redness) of 145 genotypes of durum wheat seeds. All analysis was done in the lab of Department Engineering Food of Karamanoğlu Mehmetbey University.

Total nitrogen content (N%)

Data were recorded for grain protein content. It was estimated from a random sample of 100 gm of hand-threshed seeds of each genotype per samples. The seeds were milled and total Nitrogen percent (N%) was determined by Kjeldahl method as described in the manual by Sertsu and Bakele (2000).

Total protein content (%)

Data were recorded for grain protein content. It was estimated from a random sample of 100 gm of hand-threshed seeds of each genotype per samples. The seeds were milled and total Nitrogen percent (N%) was determined by Total nitrogen (N) contents of the samples were measured using a nitrogen analyzer (Velp Scientifica, Dumas Nitrogen Analyzer - NDA 701, Italy) running on a Dumas incineration method (AACC Method 46-30) and protein contents calculated using a 5.7 nitrogen-protein conversion factor AACC, 2000). There is a linear relationship between protein ratio and total nitrogen (Nuttall et al., 2017).

L*, a* and b* color

Wheat samples of 300-g grain portions were cleaned and tempered overnight to 16.5% moisture and milled on a QC-109 laboratory mill into semolina as described by Petrova (1993). L* and color (a*, b*) values were measured (AACC Method 14-22) using Hunter colorimetric (Color Flex A60-1010-615, Hunter Lab, VA, USA) of samples ground using a 1 mm size sieve (AACC, 2000). Yellow pigment content of wheat, semolina and pasta disc was determined according to ICC method 152 as β -carotene from a standard curve. Semolina color was measured by the CIE 1976 (Commission Internationale de l' Eclairage) L*a*b* color system. L* indicates lightness, a* represents redness, and b* represents yellowness of color. The colors of semolina and flours are expressed using the L* a* b* color system. L* is a measure of brightness, it can ranges from 0, completely non-reflective or black and 100, perfect white or total reflection. Bread wheat flours have reading values around 90, while semolina has lower values. The b* value is the blue-yellow chromaticity coordinate, it can go from -60, pure blue, to +60, pure yellow. Usual b* values for bread wheat flours are around 9.5. For semolina the higher the b* value the more yellowness. Good quality durum has a b* of approx. 27.3 or more. The b* value is the red-green coordinate.

Statistical analyses

The data obtained from the study related the investigated quality parameters were analyzed by using the JMP 5.0.1 statistical software package (SAS Institute, 2002), and the differences between means were compared using a least significant difference (LSD) test at the 0.05 probability level (Steel and Torrie, 1980). GT biplot analyses were carried out using GT biplot software to assess quality parameters (Yan and Thinker, 2006). In multi-traits (MT) for genotypes, biplots were constructed by plotting the first two principal components (PC1 and PC2) derived from centered quality criteria data to singular value separation. Also, with the GT biplot analysis graphs in the study: It was aimed at revealing relation among examined traits and genotypes means by scatter plot (*Fig. 3*), and grouped quality parameters and performance of each genotype at each trait (*Fig. 4*), which-won-where of sector analysis (*Fig. 5*), the stable and high

performance of genotypes quality parameters by ranking model (Fig. 6), compare the desirable genotypes to ideal center on parameters by comparison model (Fig. 7).

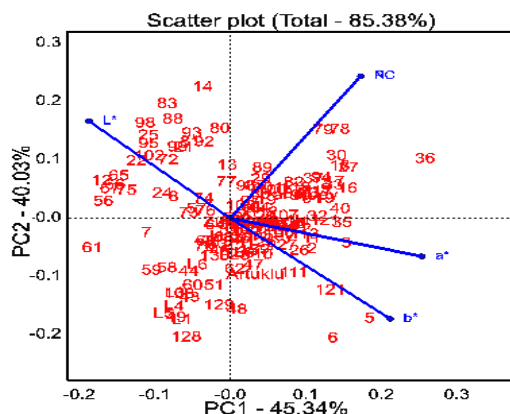


Figure 3. Relation among quality traits and genotypes. (PC: protein content, N: total nitrogen, L*: brightness, a*: redness, b*: yellowness)

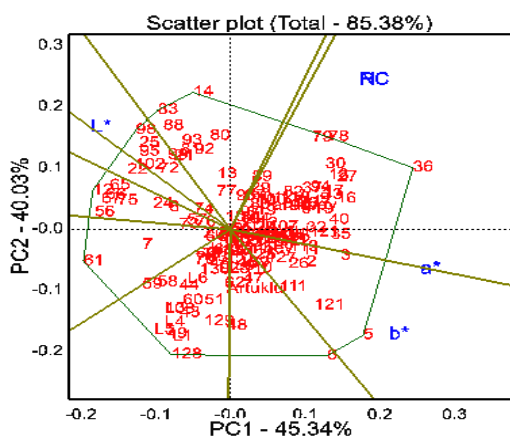


Figure 4. Sectors on genotypes and quality traits. (PC: protein content, N: total nitrogen, L*: brightness, a*: redness, b*: yellowness)

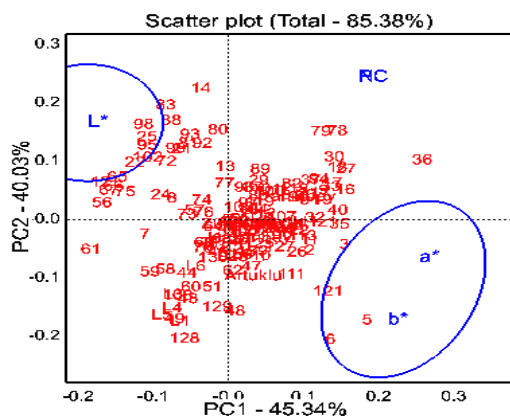


Figure 5. Groups on genotypes and quality traits. (PC: protein content, N: total nitrogen, L*: brightness, a*: redness, b*: yellowness)

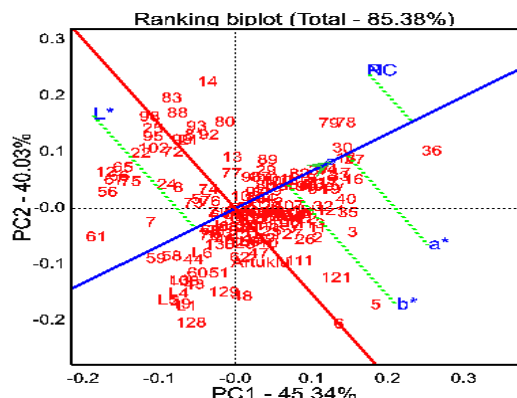


Figure 6. Ranking of genotypes on means of quality traits. (PC: protein content, N: total nitrogen, L*: brightness, a*: redness, b*: yellowness)

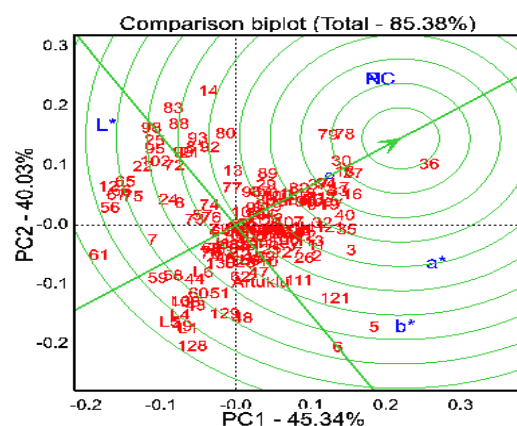


Figure 7. Comparison of genotypes on means of quality traits. (PC: protein content, N: total nitrogen, L*: brightness, a*: redness, b*: yellowness)

Results

The analysis of augmented (increased) experimental design revealed highly significant differences among the 145 genotypes of durum wheat for total nitrogen percent (N %), protein content L*(lightness color of semolina) ($p < 0.05$), while it was not significant for a* (represents redness color of semolina) and b* (represents yellowness color of semolina), as shown in *Table 2*. Moreover, significant interactions among the tested genotypes indicated that the genotypes had difference genotypic structures in terms of examined quality parameters. Usually, the wheat breeders interested in the landraces with high genotypic main effect (high values than average) and with low fluctuation in examined parameters (stable). The results variance analysis of sum of squares of quality parameters showed in *Table 2*.

The results of the data reviewed

The total nitrogen (N) percent of genotypes ranged from 2.07% (G1) to 3.18% (G79) and the mean of total nitrogen percent of genotypes was found 2.65% (*Table 4*). The results of the total nitrogen percent indicated that 79 genotypes have higher values than the five standards used as the control in the study. On the other hand; Güneyyıldızı and

Zühre varieties were the best on total nitrogen percent of among standards which used in the study. The landraces which collected in same province of Southeastern Anatolia Region showed different performance on total nitrogen percent, but the landraces which collected in Diyarbakır city (Dicle, Hani and Lice province) and Siirt city (Eruh province) had good results of total nitrogen percent respectively. Moreover; the landraces (G59-G64) collected in Gerger province of Adıyaman city had low value of total nitrogen percent. The results of total nitrogen percent showed that Southeastern Anatolia Region of Turkey is one of the Centers of origin of durum wheat showed a unique position from the view point of genetic diversity of durum wheat by landraces. Therefore, it is possible to can select the best landraces which have the best results in the study to improve the total of nitrogen and enrich the gene pool and develop quality varieties.

Table 2. The variance analysis of sum of squares of quality parameters

Source	df	N (%)	PC (%)	CIE (Semolina color results)		
				L* brightness	a* redness	b* yellowness
Genotype	144	6.310*	191.467*	842.325*	38.752ns	1125.964ns
Blok	6	0.452	14.698	24.438	13.038	109.694
Model	150	9.230	286.832	1019.069	82.101	1339.982
Error	24	0.558	18.136	67.202	5.448376	126.678
C Total	174	9.789	304.967	1086.271	87.550	1466.66
LSD (0.05)		0.360	2.071	3.959	0.621	5.436
CV (%)		5.790	5.78	2.05	20.81	13.81

LSD: least significant effect, CV: Coefficient of variation, d.f.: degree of freedom *: Value significant at 0.05 probability level, ns: not significant, N (%): total nitrogen, PC (%): Protein content

The protein content of 145 genotypes varied from 12.22% (G77) to 18.11% (G79) and the average of the genotypes was found 15.14% and nearly 80 genotypes (all of them are landraces) had high value of protein content% (Table 3). The consequence of protein content showed that more than half of landraces have high protein content results than 5 varieties which used in the study as check. However, Güneyyıldızı and Zühre varieties were the best on protein content of among standards. These two varieties registries (2010) the last time in the region and they are used in farming area, because of high quality parameters. There was diversity on protein content among landraces which collected in same province, but the landraces showed good performance which collected in Şanlıurfa (Siverek) Diyarbakır city (Dicle, Hani and Lice province) and Siirt city (Eruh province) on protein content respectively. Moreover; the landraces (G61-G64) collected in Sincik province of Adıyaman city had low value of crude protein content. The outcome of protein content indicated that Centers of Origin of durum wheat (Southeastern Anatolia Region of Turkey) is one of the unique positions from the view point of genetic diversity of durum wheat by landraces. On the other hand the study showed that there is high and positive correlation (Fig. 3) between protein content and total nitrogen percent of genotypes. Range of protein contents defined in this study was in accordance to that reported by Simmonds (1989), reported that average protein content of durum wheat may vary from 9-18%. Matsuo and Irvine (1970) reported that wheat with 13% or higher protein content made a satisfactory

pasta, whereas a protein content lower than 11% gave a pasta with poor cooking quality. The results of our study showed that majority of landraces had high value of protein content that made a satisfactory pasta (= and >13%).

Table 3. The result of correlation analysis among quality parameters

		N (T. Nitr.)	P. content	L* brightness	a* redness
CIE	L* brightness	0.13ns	-0.25ns		
	a* redness	0.19*	0.17**	-0.47**	
	b* yellowness	-0.08ns	-0.25ns	-0.58**	0.69**

** : Value significant at 0.01, * : Value significant at 0.05 probability level, ns: not significant, N %: total nitrogen

L value, brightness of semolina color* of 145 genotypes ranged from 71.11 (G122) to 89.12 (G13) and the average of the genotypes was found 81.29 value and nearly 30 landraces had high value on CIE L* brightness of semolina color than the best variety which used in the study as control% (Table 4). On the other hand, the results demonstrated that Güneyyıldızı and Zühre varieties were the best on L* brightness of semolina color of among standards. These two varieties released last time, because of high value L* brightness of semolina color. The results indicated that there is high diversity among local populations collected in the region. Especially, the landraces which collected in the Hani, Lice provinces which located the north of Diyarbakır city where consist of Karacadağ mountain which Centers of Origin of durum wheat were the best among genotypes with regard to L* semolina color. Furthermore, the first genotypes (landraces) which collected in around Diyarbakır city plain places and the genotypes which collected in Kulp province were very poor on L* semolina color. The result of study showed that there was high genetic heterogeneity among durum wheat landraces and it can be support to improve genetic pool for breeder of durum wheat.

a value, redness of semolina color* of 145 genotypes varied from 0.35 (G13) to 3.85 (G41) and the average of the genotypes was found 2.32 value. The results indicated that there is high negative correlation (-0.47**) between a* redness of semolina color and L* brightness of semolina color (Table 3 and Fig. 3).

b value, yellowness of semolina color* of 145 genotypes ranged from 6.76 (G13) to 22.13 (G6) and the average of the genotypes was found 16.44 value (Table 4). The results indicated that there is high negative correlation between b* and L* and high positive correlation between b* and a* semolina colors (Table 3 and Fig. 3).

Graphically the association between genotypes and quality parameters

Principal component analysis was used to show the distribution of genotypes based on quality traits. The two dimensional PCA score plot, derived from multi-traits and accounted for 85.38% (45.34% and 40.03% for PC1 and PC2, respectively) of the total variation (Figs. 3-7). The scatter plot showed that three groups were occurred among quality traits and genotypes showed a wide distribution on traits, and also it was showed high correlation between b* jaundice, a* redness (Fig. 3). The results showed that cultivars and more landraces have general adaptability for all quality parameters (Fig. 4), while some genotypes (79, 78, etc.), (22, 102, etc.), (3..) and 121, 5, etc.) showed specific adaptation for N, PC, L*, a* and b* respectively (Figs. 5 and 6).

According to the biplot techniques, G36 came forward with the N, P and a* and desirable landraces, G5 for b*, 30 stable line for all quality parameters, while (128, 61, etc.) and majority of promising lines (L4, L6) came not forward with any quality parameters (Fig. 7). The study indicated that GT biplot can be used to evaluate the genotypes as graphically to select the best genotypes for parents to use in breeding program (Oral, 2018).

Table 4. The rank and means of the quality parameters of durum wheat genotypes

Genotype	Rank	N (%)	Rank	PC (%)	CIE (semolina color results)					
					Rank	L*	Rank	a*	Rank	b*
1	145	2.07	65	15.38	144	74.53	127	1.66	126	12.08
2	70	2.68	71	15.25	142	75.25	143	0.92	130	11.40
3	52	2.74	52	15.63	114	79.97	96	2.14	105	15.63
4	24	2.83	24	16.15	118	79.85	57	2.50	99	16.91
5	81	2.64	82	15.04	28	82.91	125	1.78	131	11.28
6	83	2.64	84	15.02	139	76.36	86	2.23	1	22.13
7	115	2.45	116	13.98	140	76.31	71	2.41	10	19.48
8	123	2.42	124	13.82	18	83.86	142	1.02	144	7.33
9	87	2.62	88	14.92	10	85.71	141	1.20	142	8.37
10	9	3.01	9	17.15	55	81.55	111	2.02	112	14.45
11	58	2.72	58	15.50	20	83.70	122	1.83	114	14.03
12	50	2.75	50	15.66	57	81.50	64	2.44	110	14.79
13	106	2.52	107	14.36	1	89.12	145	0.35	145	6.76
14	20	2.86	20	16.32	11	85.49	140	1.22	137	10.16
15	3	3.13	3	17.86	2	88.22	144	0.49	143	7.62
16	98	2.56	99	14.62	24	83.28	121	1.84	115	13.96
17	7	3.04	7	17.32	90	80.80	82	2.28	113	14.20
18	6	3.04	6	17.33	35	82.36	105	2.08	109	14.89
19	4	3.11	4	17.74	29	82.80	106	2.07	111	14.67
20	12	2.95	12	16.80	34	82.37	101	2.11	108	15.07
21	107	2.51	108	14.32	82	81.02	38	2.69	102	16.41
22	94	2.59	95	14.79	17	83.93	118	1.89	140	9.65
23	121	2.44	122	13.89	12	85.39	129	1.57	141	9.01
24	64	2.70	64	15.39	86	80.97	14	2.94	72	17.67
25	134	2.36	135	13.45	23	83.46	110	2.03	138	10.15
26	95	2.58	96	14.71	6	85.85	138	1.30	139	9.70
27	113	2.46	114	14.03	141	76.04	11	3.00	104	15.78
28	16	2.90	16	16.55	131	78.97	18	2.92	83	17.43
29	100	2.56	101	14.61	128	79.08	30	2.78	84	17.39
30	79	2.66	80	15.15	48	81.87	78	2.34	107	15.34
31	13	2.93	13	16.68	113	79.97	33	2.75	93	17.11
32	73	2.67	74	15.25	102	80.47	48	2.62	96	16.97
33	85	2.63	86	14.98	121	79.66	8	3.05	40	18.40
34	33	2.79	33	15.93	110	80.03	15	2.94	45	18.32
35	105	2.52	106	14.37	96	80.62	44	2.65	57	17.95
36	75	2.67	76	15.20	138	76.69	6	3.18	73	17.63

37	5	3.09	5	17.60	136	78.26	2	3.80	5	19.78
38	38	2.78	38	15.84	104	80.44	37	2.69	86	17.34
39	114	2.46	115	14.03	50	81.74	98	2.13	92	17.16
40	129	2.39	130	13.62	132	78.69	65	2.44	100	16.87
41	11	2.95	11	16.82	45	82.00	1	3.85	2	20.74
42	26	2.82	26	16.10	120	79.68	12	2.97	14	19.24
43	89	2.61	90	14.88	87	80.91	56	2.50	61	17.87
44	137	2.32	138	13.20	69	81.25	80	2.30	34	18.54
45	125	2.42	126	13.80	38	82.31	102	2.11	43	18.36
46	97	2.57	98	14.64	60	81.42	79	2.33	54	17.96
47	47	2.75	47	15.68	76	81.07	59	2.47	64	17.85
48	96	2.57	97	14.67	108	80.17	25	2.87	22	18.76
49	133	2.36	134	13.45	122	79.64	17	2.92	4	19.83
50	142	2.21	143	12.57	49	81.83	81	2.28	9	19.49
51	62	2.70	62	15.41	67	81.28	103	2.09	81	17.46
52	126	2.42	127	13.80	79	81.06	72	2.38	11	19.41
53	60	2.71	60	15.47	70	81.17	84	2.26	29	18.60
54	54	2.74	54	15.60	62	81.39	92	2.18	89	17.23
55	45	2.76	45	15.71	63	81.36	89	2.19	62	17.86
56	44	2.76	44	15.74	61	81.41	90	2.19	58	17.92
57	110	2.49	111	14.22	4	86.00	136	1.39	128	11.68
58	66	2.69	67	15.36	21	83.62	126	1.77	95	16.97
59	130	2.39	131	13.60	40	82.10	116	1.95	101	16.43
60	135	2.33	136	13.29	81	81.03	108	2.05	116	13.72
61	141	2.22	142	12.68	77	81.07	62	2.44	18	19.10
62	144	2.14	145	12.22	16	84.34	128	1.62	117	13.50
63	131	2.38	132	13.55	98	80.57	29	2.79	3	19.95
64	116	2.45	117	13.97	105	80.28	76	2.35	63	17.86
65	103	2.53	104	14.44	53	81.66	104	2.08	27	18.64
66	109	2.50	110	14.23	7	85.84	135	1.40	121	12.90
67	117	2.45	118	13.97	5	85.96	133	1.41	118	13.26
68	122	2.43	123	13.84	9	85.72	137	1.35	119	13.14
69	111	2.49	112	14.21	80	81.06	73	2.36	24	18.70
70	118	2.44	119	13.93	56	81.51	94	2.16	36	18.53
71	127	2.42	128	13.79	66	81.33	93	2.16	28	18.64
72	119	2.44	120	13.93	83	81.01	67	2.43	76	17.56
73	77	2.66	78	15.15	27	82.95	117	1.95	133	11.21
74	104	2.52	105	14.39	30	82.75	123	1.79	78	17.52
75	88	2.61	89	14.89	31	82.63	119	1.88	85	17.35
76	120	2.44	121	13.92	19	83.70	124	1.79	135	11.04
77	99	2.56	100	14.61	42	82.03	112	2.02	87	17.31
78	57	2.73	57	15.56	39	82.29	115	1.98	80	17.48
79	1	3.18	1	18.11	111	80.02	26	2.87	44	18.33
80	2	3.14	2	17.91	99	80.53	39	2.68	50	18.06
81	25	2.83	25	16.13	54	81.64	88	2.20	132	11.24
82	61	2.71	61	15.45	22	83.51	113	2.00	123	12.19

83	36	2.78	36	15.87	117	79.89	22	2.90	69	17.72
84	27	2.82	27	16.10	8	85.80	134	1.41	127	11.82
85	91	2.60	92	14.81	94	80.68	52	2.56	71	17.68
86	112	2.49	113	14.18	91	80.78	46	2.64	55	17.95
87	71	2.68	72	15.25	95	80.67	58	2.48	60	17.89
88	65	2.70	66	15.37	75	81.13	69	2.42	79	17.49
89	40	2.78	40	15.83	14	85.29	132	1.51	122	12.59
90	37	2.78	37	15.85	64	81.36	66	2.44	97	16.97
91	48	2.75	48	15.68	126	79.38	16	2.93	25	18.69
92	42	2.77	42	15.81	133	78.66	19	2.91	13	19.31
93	53	2.74	53	15.62	43	82.02	97	2.14	129	11.43
94	51	2.75	51	15.65	26	82.99	109	2.03	136	11.03
95	21	2.86	21	16.32	127	79.25	7	3.11	38	18.44
96	86	2.62	87	14.93	13	85.30	131	1.52	124	12.16
97	72	2.68	73	15.25	59	81.43	75	2.36	90	17.22
98	90	2.61	91	14.87	68	81.27	42	2.66	82	17.44
99	63	2.70	63	15.40	3	86.15	139	1.27	125	12.12
100	78	2.66	79	15.15	25	83.23	114	1.99	134	11.16
101	15	2.91	15	16.61	84	81.00	41	2.67	41	18.39
102	14	2.92	14	16.63	103	80.45	49	2.61	75	17.60
103	39	2.78	39	15.83	15	85.24	130	1.56	120	13.10
104	35	2.78	35	15.87	65	81.34	63	2.44	59	17.92
105	30	2.81	30	15.99	71	81.16	50	2.61	31	18.59
106	67	2.69	68	15.35	101	80.51	36	2.70	47	18.22
107	46	2.75	46	15.70	119	79.69	10	3.01	6	19.65
108	23	2.84	23	16.17	112	80.02	21	2.91	8	19.53
109	138	2.28	139	13.02	89	80.88	51	2.56	56	17.95
110	55	2.73	55	15.57	116	79.92	40	2.68	65	17.84
111	84	2.63	85	14.98	130	78.99	23	2.89	16	19.16
112	82	2.64	83	15.02	143	75.08	4	3.33	48	18.19
113	28	2.81	28	16.03	109	80.11	43	2.66	35	18.53
114	29	2.81	29	16.00	137	78.01	5	3.24	7	19.62
115	31	2.80	31	15.95	129	79.03	13	2.96	12	19.31
116	68	2.69	69	15.35	85	80.98	60	2.47	26	18.67
117	41	2.77	41	15.81	125	79.56	28	2.80	39	18.41
118	8	3.01	8	17.18	134	78.50	9	3.03	20	18.92
119	10	2.99	10	17.03	135	78.47	32	2.77	77	17.56
120	18	2.87	18	16.38	124	79.56	77	2.35	51	18.04
121	32	2.80	32	15.93	74	81.13	61	2.46	74	17.60
122	56	2.73	56	15.56	145	71.11	3	3.44	106	15.42
123	17	2.89	17	16.47	123	79.57	27	2.86	32	18.58
124	22	2.84	22	16.20	97	80.58	47	2.62	53	18.02
125	19	2.86	19	16.32	106	80.26	24	2.88	70	17.68
126	49	2.75	49	15.67	88	80.90	31	2.78	52	18.03
127	59	2.72	59	15.49	73	81.15	68	2.43	98	16.96
128	34	2.79	34	15.88	107	80.18	20	2.91	19	18.97

129	143	2.20	144	12.53	92	80.71	35	2.71	46	18.29
130	128	2.41	129	13.71	115	79.97	34	2.72	49	18.16
131	92	2.60	93	14.79	52	81.71	70	2.41	94	17.03
132	139	2.28	140	12.97	46	81.96	55	2.52	17	19.12
133	76	2.67	77	15.19	93	80.68	85	2.23	42	18.39
134	132	2.37	133	13.52	47	81.90	83	2.27	88	17.30
135	136	2.33	137	13.27	37	82.34	95	2.14	15	19.21
136	140	2.27	141	12.93	36	82.34	87	2.21	37	18.48
137	102	2.54	103	14.50	41	82.08	91	2.18	66	17.81
138	43	2.77	43	15.76	58	81.46	74	2.36	21	18.90
139	74	2.67	75	15.22	78	81.07	53	2.55	33	18.58
140	69	2.69	70	15.32	72	81.16	45	2.64	30	18.60
Artuklu	124	2.42	125	13.81	100	80.52	54	2.53	23	18.71
Güneyyıldızı	80	2.64	81	15.04	33	82.38	100	2.12	67	17.80
Hasanbey	101	2.56	102	14.57	51	81.73	99	2.12	68	17.74
Şahinbey	108	2.50	109	14.26	44	82.00	107	2.05	103	16.34
Zühre	93	2.59	94	14.79	32	82.47	120	1.86	91	17.20
Mean		2.65		15.14		81.29		2.32		16.44
Min.		2.07		12.22		71.11		0.35		6.76
Max.		3.18		18.11		89.12		3.85		22.13

L*: brightness, a*: Redness, b*: yellowness, N %: total nitrogen, PC: protein content

Discussion

Nowadays, a number of study have focused on nutrient shortcoming in people who are fed from durum wheat product and to improve the quality of new varieties which came from hybrids made genetic resources in successful breeding programs (Akcura, 2011; Aktas, 2016; Mohammed et al., 2011; Pandey et al., 2016; Kendal and Sener, 2016). For this purposes the durum wheat landraces is very important and these days, they have been largely replaced, in their centers of diversity by monocultures of pure genotypes. This genetic erosion resulted in significant loss of valuable genetic diversity for quality traits (Jaradat, 2013). To improve the quality of new durum varieties, landraces keeps its importance inside genetic diversity in Middle east and Southeastern Anatolia region. Because landraces have adequate quality characteristics for the development of new varieties that can be used in the pasta and bulgur industries. For this reason, durum wheat breeders have recently given more importance to the durum wheat landraces in order to raise the quality criteria in durum wheat (Tekdal et al., 2014; Kiliç et al., 2012).

The genotypes used in the research showed high variability in the maintenance of all the quality parameters examined. The still prefer of some wheat landraces shows that they have more competitive advantage on quality parameters relative to modern varieties and it is very imported that modern durum wheat cultivars are superior among cereals to providing high quality protein for billions of people around the world (Jaradat, 2013). Therefore, the need is urgent to improve nutritive quality (Koshgoftarmanesh et al., 2010). The wide variation of genotypes of durum wheat quality parameters were described by more researchers (Tekdal et al., 2014; Kiliç et al., 2012; Kendal and Sener, 2016). The researchers working on durum wheat in different

years and places have provided some results in support of our study on the quality of durum wheat. To summarize of these studies; as in most grain quality traits in wheat, protein content is known to be affected by genetic and environment mainly location (Bement et al., 2003). However, durum wheat is richer in protein, as this is crucial for pasta making (Nuttal et al., 2017), in Mediterranean areas, durum wheat has a significantly higher average grain N concentration under the same climatic conditions (Cossani et al., 2011). As a result of the study, grain color and protein content that are durum wheat quality traits were related with bulgur quality properties. Therefore both quality properties can be used indirect selection criterion to develop high quality bulgur genotypes (Tekdal et al., 2014). Durum wheat is a good source of protein and grain protein content of 13% for durum is a standard in quality throughout the grain industry (Riley et al., 1998). On the other hand; in the pasta industry, high protein content are required to process semolina into a suitable final product because the protein content is responsible for the cooking quality of pasta products (Reddecliffe, 2001). Durum wheat is used in bulgur sector, because it has bright yellow color and contains more protein than other wheat varieties (Bayram, 2000).

Color content has to be increased to avoid artificial coloration, which is reported to be a major problem for pasta and bulgur consumers and industrialists with pasta wheat breeding programs (Schulthess, 2013). In recent years, efforts to obtain yellow bulgur and pasta in the direction of consumers' demands mechanical annealing operations were introduced (Oner, 2002). The color of pasta and bulgur is a result of the relative proportions of pigments in the wheat grain. The color of durum wheat and flour came from the carotenoid pigments (Reddecliffe, 2001). The color of pasta and bulgur is the most important factor that consumers associate with quality and consumers believe that pasta and bulgur with a golden appearance has higher quality than sallow pasta. High yellow pigment content is desirable to ensure that the pasta has an intense amber color (Clarke et al., 1998; Tekdal et al., 2014). The L* value gives an idea of the yellow color and value the brightness of the product in durum wheat, and is considered as an important quality criterion (Sahin et al., 2006). Genotypes with high b* and L* values indicate that the quality of durum wheat increases and studies have shown that the yellow b* value is 86.6% and the L* value is under the genotype effect of 12.6% (Coşkun et al., 2010; Hailu and Mereker, 2008). Yellow pigment concentration in durum wheat is determining particularly in the commercial and nutritional quality of end-products and very important criterion in the assessment of semolina quality (Digesu et al., 2009). The semolina yellow pigment concentration is defining factor for amber color of the commercial value of durum wheat pasta (Blanco et al., 2011). Pasta quality was assessed by determining color (L*, a* and b* values) furosine, and quaking quality (stickiness, bulkiness, firmness (Marconi et al., 2002). The colour relationship between wheat fractions were that in all groups, the flour colour values (CIE L*, a*, b*) were well defined by those of the whole-meal fraction, and this was attributed to the predominance of the flour fraction in the wheat grain. It is, therefore, possible to extrapolate colour values from the easily accessible, whole-meal samples, to those of the flour fraction, which is the main portion consumed (Humphires et al., 2004).

Principal component analysis (GT Biplot) graphically showed that there is high correlation between genotypes and quality parameters and also relation among quality parameters (Figs. 3-7). The GT biplot mainly allows the visualization of any crossover GT interaction, which is very important for the breeding program (Goyal et al., 2011; Kendal and Sener, 2015; Sayar and Han, 2015). The GT (genotype-trait) biplot provides

an excellent tool for visualizing genotype \times trait data (Adjabi et al., 2014). In the biplot, a vector was drawn from the biplot centered to each marker of the traits to facilitate visualization of the relationships between genotypes and traits, and the angle of vectors among traits. If the angle of the vector was less than 90° , there was a positive correlation between genotypes and traits. If the angle was equal to 90° , they were not correlated. There was a negative correlation if the angle was less than 90° (Yan and Kang, 2003). In this study, there was a positive correlation between CIE a* and CIE b*, and total N and PC, while negative correlations among CIE a*, b* and L* (Fig. 3 and Table 3). Nuttall et al. (2017) reported that there is linear correlation between total nitrogen and protein content, Tekdal et al. (2014) reported that there is negative correlation between CIE L* and CIE a* values and positive correlation between CIE a* and CIE b* values. On the other hand, there was high and special correlation among some genotype and quality traits. We can select the G6, G5 and G121 for CIE b* and G3 for b* and G25, G98 for L* and G78, G79 for total N and PC (Fig. 4). Kendal et al. (2016), The GGE biplot also ranks the traits for their ability to discriminate among genotypes. Sectors of the biplot formed COI groups based on the winning genotypes in each group of traits. So in the study, the features which examined were in four sectors and located in three different mega-traits. CIE a*, CIE b* located in sector 1 and total N and PC located in sector 2, while CIE L* only located in sector 3 (Fig. 5). On the other hand, CIE a*, CIE b* located in group 1 and CIE L* only located in group 2, total N and PC located in group 3 (Fig. 5). The GT biplot method provides considerable flexibility, allowing plant breeders to simultaneously select genotypes for quality and stability (Sabaghnia et al., 2013). Haile et al. (2007), the main goals of breeding programs is one of that producing durum wheat genotypes with high and stable grain protein content in Principal component analysis. In the study showed that G30 is stable genotype for all quality parameters, while G5, G14, G61 and majority of other genotypes were not stable for quality parameters (Fig. 6). Yan and Tinker (2006), the GGE biplot was accurate in interpreting the comparing genotypes and traits. The genotype with both high mean performance and high stability for all of the traits was called an ideal genotype (Kendal and Sayar, 2016; Karaman, 2019). Therefore the center of the concentric circles (i.e., ideal genotype) was the AEA in the positive direction. Genotypes located closer to the ideal genotype were more desirable than others. In the study, G36 located the center of ideal circle, it means that this genotype is ideal and desirable for all quality parameters (Fig. 7). On the other hand, G61 and G128 located under means line and far from center of circle, it means that these genotype are undesirable for all parameters. The results of the study indicated that majority of landraces can be used as parents to improve the quality of durum wheat varieties.

Conclusion

The study showed that durum wheat landraces still is very importance to raise the quality criteria in durum wheat for breeding programs. The results showed that cultivars and more landraces have general adaptability for all quality parameters, while some genotypes showed special adaptation and G79, G78, for N and PC, G22, G102 for L*, G3 for a* and G121, G5 for b*. Moreover, G30 was stable and G36 was ideal for all quality parameters. According to the biplot techniques indicated that there is high correlation between CIE a* value and CIE b* value and between N and PC, while negative correlation with these traits to CIE L* Therefore the study showed that

majority of landraces can be used as parents to improve the quality of durum wheat varieties on special or general quality parameters.

Acknowledgements. This research was supported by Mardin Artuklu University (MAU-BAP-17-KMYO-15). We want thanks to GAP International Agricultural Research Center, Department of wheat breeding program and Karamanoğlu Mehmetbey University, Department Engineering of Food for project contributions and support.

REFERENCES

- [1] Adjabi, A., Bouzerzour, A., Benmahammed, A. (2014): Stability analysis of durum wheat (*Triticum durum* desf.). – *Grain Yield J. of Agr.* 13(3): 131-139.
- [2] Akçura, M. (2011): The relationships of some traits in Turkish winter bread wheat landraces. – *Turkish Journal Agriculture* 35(2): 115-125.
- [3] Aktaş, H. (2016). Drought tolerance indices of selected landraces and bread wheat (*Triticum aestivum* L.) genotypes derived from synthetic wheats. – *Applied Ecology and Environmental Research* 14(4): 177-189.
- [4] Bayram, M. (2000): Bulgur around the world. – *Cereal Foods World* 45(2): 80-82.
- [5] Bement, G., Ameha, Y., Alemayehu, Z., Jemanesh, K., Tekalign, T., Bekele, M. (2003): Fertilizer N effects on yield and grain quality of durum wheat. – *Trop. Agric. (Trinidad)* 80: 146–151.
- [6] Blanco, A., Colasuonno, P., Gadaleta, A., Mangini, G., Schiavulli, A., Simeone, R., Digesù, A. M., Vita, P. D., Mastrangelo, A. M., Cattivelli, L. (2011): Quantitative trait loci for yellow pigment concentration and individual carotenoid compounds in durum wheat. – *Journal of Cereal Science* 54: 255-264.
- [7] Clarke, J. M., Marchylo, B. A., Kovacs, M. I. P., Noll, J. S., McCaig, T. N., Howes, N. K. (1998): Breeding Durum Wheat for Pasta Quality in Canada. – In: Braun, H. J., Altay, F., Kronstad, W. E., Beniwal, S. P. S., McNab, A. (eds.) *Wheat: Prospects for Global Improvements*. –Kluwer Academic Publishers, Boston, pp. 229-236.
- [8] Cossani, C. M., Slafer, G. A., Savin, R. (2011): Do barley and wheat (bread and durum) differ in grain weight stability through seasons and water-nitrogen treatments in a Mediterranean location? – *Field Crops Research* 121: 240–247.
- [9] Digesu, A. M., Platani, C., Cattivelli, L., Mangini, G., Blanco, A. (2009): Genetic variability in yellow pigment components in cultivated and wild tetraploid wheats. – *Journal of Cereal Science* 50: 210–218.
- [10] Erdal, I., Küçükyumuk, Z., Kurt, S. S, Değirmenci, M. (2017): Effects of seed weights on plant growth and mineral nutrition of wheat and bean plants. – *Suleyman Demirel University, Journal of Natural and Applied Sciences* 21(3): 749-755.
- [11] FAOSTAT (2013): <http://faostat.fao.org/>. – FAO, Rome.
- [12] Goyal, A., Beres, B. L., Randhawa, H. S., Navabi, A., Salmon, D. F., Eudes, F. (2011): Yield stability analysis of broadly adaptive triticale germplasm in southern and central Alberta. – *Canadian J. Plant Sci.* 91: 125-135.
- [13] Haile, J. K., Sarial, A. K., Assefa, S. (2007): AMMI analysis for stability and locations effect on grain protein content of durum wheat genotypes. – *Cereal Research Communications* 35(4): 1661–1673.
- [14] Hailu, F., Mereker, A. (2008): Variation in gluten strength yellow pigment in Ethiopian tetraploid wheat germplasm. – *Genetic Resources and Crop Evolution* 55: 277-285.
- [15] Humphries, J. M., Graham, R. D., Mares, D. J. (2004): Application of reflectance colour measurement to the estimation of carotene and lutein content in wheat and triticale. – *Journal of Cereal Science* 40(2): 151-159.

- [16] Jaradat, A. A. (2013): Wheat landraces: wheat landraces: a mini review. – Emir. J. Food Agric. 25(1): 20-29.
- [17] Karaman, M. (2019). Evaluation of bread wheat genotypes in irrigated and rainfed conditions using biplot analysis. – Applied Ecology and Environmental Research 17(1): 1431-1450.
- [18] Kendal, E., Sayar, M. S. (2016): The stability of some spring triticale genotypes using biplot analysis. – The Journal of Animal & Plant Sciences 26(3): 754-765.
- [19] Kendal, E., Sener, O. (2015): Examination of genotype × environment interactions by GGE biplot analysis in spring durum wheat. – Indian J. Gen. & Plant Breed. 75(3): 341-348.
- [20] Kendal, E., Sayar, M. S., Tekdal, S., Aktas, H., Karaman, M. (2016): Assessment of the impact of ecological factors on yield and quality parameters in triticale using GGE biplot and AMMI analysis. – Pak. J. Bot 48(5): 1903-1913.
- [21] Kilic, H., Tekdal, S., Kendal, E., Aktas, H. (2012): Evaluation of advanced triticum wheat (*Triticum turgidum* ssp durum) Lines based on augmented trial design with biplot analysis method. – Kahramanmaraş Sutcu Imam University, Natural Science Journal 15(4): 18-25.
- [22] Marconi, E., Carcea, M., Schivone, M., Cubadda, R. (2002): Spelt (*Triticum spelta* L.) pasta quality: Combined effect of flour properties and drying conditions. – Cereal Chemistry 79(5): 634.
- [23] Matsuo, R. R., Irvine, G. N. (1970): Effect of gluten on the cooking quality of spaghetti. – Cereal Chemistry 47: 173-176.
- [24] Mohammed, A., Geremew, B., Amsalu, A. (2011): Variation and associations of quality in ethiopian durum wheat (*Triticum turgidum* L. var. durum) genotypes. – International Journal Breeding and Genetics. DOI: 1039223/ijpbg.2011.
- [25] Morgounov, A., Keser, M., Kan, M., Küçükçongar, M., Özdemir, F., N Gummadov., Muminjanov, H., Zuev, E., Qualset, C. O. (2016): Wheat landraces currently grown in Turkey: distribution, diversity and use. – Crop Sci. 56: 3112–3124.
- [26] Nuttall, J. G., O’Leary, G. J., Panozzo, J. F., Walker, C. K., Barlow, K. M., Fitzgerald, G. J. (2017). Models of grain quality in wheat—a review. – Field Crops Research 202: 136-145.
- [27] Oner, M. D. (2002): Bulgur industry, problems and solution proposal. – Grain Products Technology Congress and Exhibition, Gaziantep, Turkey, pp.39-48.
- [28] Oral, E. (2018): Effect of nitrogen fertilization levels on grain yield and yield components in triticale based on AMMI and GGE biplot analysis. – Applied Ecology and Environmental Research 16(4): 4865-4878.
- [29] Pandey, A., Khan, M. K., Hakki, E. E., Thomas, G., Hamurcu, M., Gezgin, S., Gizlenci, O., Akkaya, A. S. (2016): Assessment of genetic variability for grain nutrients from diverse regions: potential for wheat improvement. – SpringerPlus 5: 1912.
- [30] Redcliffe, T. M. (2001): Optimizing durum wheat yield and quality. – Master of Science Digital Thesis, Lincoln University, Lincoln New Zealand.
- [31] Riley, E. A., Thompson, T. L., White, S. A., Ottman, M. J. (1998): Late Season Tissue Tests for Critical grain Protein Content in Durum, Maricopa. – In: Ottman, M. (ed.) Forage and Grain. A college of Agriculture Report Series. University of Arizona, Tucson, Arizona, pp. 43-50.
- [32] Sabaghnia, N., Karimizadeh, R., Mohammadi, M. (2013): GGL biplot analysis of durum wheat yield in multi-environment trials. – Bulgarian J. Agri. Sci. 19(4): 756-765.
- [33] Sahin, M., Akcura, M., Gocmen, Aydogan, S. (2006): Assessment of parameters measured by color spectrophotometer in durum wheat breeding. – Botanical Research Journal 2: 17-21.
- [34] Sayar, M. S., Han, Y. (2015): Determination of seed yield and yield components of grass pea (*Lathyrus sativus* L.) lines and evaluations using GGE biplot analysis method. – Tarım Bilimleri Dergisi- J. Agri. Sci. 21(1): 78-92.

- [35] Simmonds, D. H. (1989): Inherent Quality Factors in Wheat. *Wheat and Wheat Quality in Australia*. – CSIRO, Australia, pp. 31–61.
- [36] Stehno, Z. (2000): Evaluation of Durum Wheat in the Czech Gene Bank: Quality Parameters. – In: Royo, C., Nachit, M., Di Fonzo, N., Araus, J. L. (eds.) *Durum Wheat Improvement in the Mediterranean Region: New Challenges*. CIHEAM, Zaragoza, pp. 173-176.
- [37] Tekdal, S., Kendal, E., Aktas, H., Ayana, B., Bayram, M., Kilic, H., Yildirim, M. (2014): Status Screening of Wheat Varieties With Some of the Lines in the Local Population and Advanced Level Results in Terms of Quality in Turkey. – TUBITAK-1001, Project No: 111O246.
- [38] Velu, G., Ortiz-Monasterio, I., Cakmak, I., Hao, Y., Singh, R. P. (2014): Biofortification strategies to increase grain zinc and iron concentrations in wheat. – *J Cereal Sci* 59(3): 365–372.
- [39] Yan, W., Kang, M. S. (2003): *GGE Biplot Analysis: A graphical Tool for Breeders, Geneticists and Agronomists*. – CRC Press, Boca Raton.

DETERMINATION OF RELATIONSHIP BETWEEN LAND SURFACE TEMPERATURE AND DIFFERENT LAND USE BY CHAID ANALYSIS

KOÇ, A.^{1*} – KARAHAN, A. E.² – BİNGÜL, M. B.¹

¹*Iğdir University, Faculty of Agriculture, Department of Landscape Architecture
76000 Iğdir, Turkey*

²*Iğdir University, Faculty of Agriculture, Department of Zootechnic, 76000 Iğdir, Turkey*

**Corresponding author
e-mail: ahmetkoc0625@hotmail.com*

(Received 22nd Feb 2019; accepted 29th Mar 2019)

Abstract. The increasing average air temperatures and the change of climate elements pose negative threats to human and its life. Human beings develop different methods and plans to eliminate and minimize the threats that occur. Satellite imagery is the tool of these methods and plans. Through existing satellite imagery, land surface temperatures and land uses are determined by remote sensing methods to provide sustainable planning. Surface temperatures of the land are such a parameter that concerns the climate, fauna, flora and interaction of human beings with the environment. This study aimed to establish the bond between the surface temperature of the land and the different land uses. The data was collected from Erzurum province, which is located in Turkey, with a surface area of 25066 km². Thermal Band data obtained from four different dates which represents the four seasons and Coordination of Information on the Environment (CORINE) Land Cover (CLC) maps were digitized and interpreted statistically in Geographic Information Systems (GIS) package program. The results showed that forest areas 12.2°C, water surfaces 13.8°C, agricultural areas 17.9°C, open areas 15.7°C and residential areas 18.7°C has average surface temperature values. Statistically, the bonds between land uses and other variables were evaluated using Chi-square Automatic Interaction Detector (CHAID) analysis. As a result, this study will contribute planners and decision makers develop climate-sensitive strategies and policies regarding basin planning and urban planning.

Keywords: *thermal band, CORINE, CHAID analysis, surface temperature, land use, Turkey*

Introduction

Scientifically proven that temperatures have increased over the current century and this increase will continue in the future (Becker et al., 2012; Fearnside, 2015). In climate change scenarios for the years between 1990-2050 some hypotheses were developed and according to these hypotheses, it is asserted that the temperature will increase by 2-2.9°C on a global basis (van der Knaap et al., 2018). Climate change causes increased temperature, irregular precipitation and therefore a significant change in the climate cycle (Alexander et al., 2006; van Haren et al., 2013; Rajczak and Schar, 2017). Climate change with increased temperature forces people to live in places close to different land use areas in order to sustain their comfortable lives. The differences in land uses arise as a result of a mechanism created by the human and natural processes. Land changes over existing ecosystems has led to the emergence of surface temperature differences (Arnfield, 2003; Wu et al., 2012; Gonzalez et al., 2013). It has also caused a decrease in water quality and quantity due to varying climate in different land uses (Felzer, 2012; Tong et al., 2012; Seung-Hwan et al., 2013; El-Khoury et al., 2015). Recently, scientists are working on large areas with thermal band analyses

based on remote sensing methods, while generating future scenarios and hypotheses (Zhan et al., 2011; Chen et al., 2014; Cho et al., 2018). Monitoring global climate change and its impacts with remote sensing methods has made it possible to make urban climate assessments (Zhang et al., 2004; Weng, 2009; Masiello et al., 2015). At the same time, the surface temperature, which is the basic climate parameter, has a great importance. Surface temperature is one of the physical parameters of land surface processes from local scale to global scale (Li et al., 2013). The surface temperature, surface radiation, and therefore the energy, has a great proposition in terms of its optimal use (Voogt and Oke, 2003; Yang et al., 2012; Feng and Myint, 2016). It is also stated in previous studies that the effect of surface temperature that directly influences the air temperature as a result of the division of anthropogenic effects is of great importance at spatial scale (Chrysoulakis et al., 2013; Song et al., 2017). Given the importance of surface temperature in terms of location and environmental sciences, temporal change provides a remarkable source of information (Li et al., 2013). The surface temperature of the land represents a unit of climate change from the "Land Surface Temperature" (LST) remote sensing platforms (Gallego-Elvira et al., 2016; Rosas et al., 2017). To monitor the effects of global warming and climate change, it is necessary to make assessments in different land uses (Zhang et al., 2004; Masiello et al., 2015; Blasi et al., 2016).

In thermal satellites, land surface temperature measurements are somewhat difficult because satellites are influenced by both surface temperatures and atmospheric conditions (Prata et al., 1995). In order to avoid measurement constraints, it is possible to achieve atmospheric correction of the thermal data with well developed split window approaches using two TIR bands (Becker and Li, 1990). With a swath width of 2,330 km, The Moderate Resolution Imaging Spectroradiometer (MODIS) satellite module is capable of displaying every single point in the world every day or two with the help of 36 different spectral bands (Xia et al., 2018). Indeed, the MODIS satellite provides a choice for scientific studies in order to be able to work on a regional scale between land uses and surface temperature (Justice et al., 2002; Jacob et al., 2004). Using MODIS satellite data, the linkages between the seasonal temperature distributions of the areas and land uses within the study area boundaries were investigated. The main purpose of this study is to investigate the compatibility of the thermal comfort with the environment in different land uses. As study site, Erzurum Province, which accommodates 3 different basin areas and topographic structure ranging from 850-3500 m, were selected. The results of the study will contribute planners and decision makers develop climate-sensitive strategies and policies regarding basin planning and urban planning.

Material and Method

Erzurum Province (approximately 25066 km², 40°15"-42°35"E, 40°57"-39°10"N), which is located in Turkey, has a terrestrial climate. The average air temperature is -7°C in January and 16.2°C in July. The average annual air temperature is 6.1°C and is below -4.4°C from December to March. The average annual precipitation is 39.6 mm, and the wet season is from April to January. Short summer and a long winter lead to a high thermal exposure for the city. Land topography in the study area is constantly changing. Topography, which varies from 3200 m to 780 m, supports the formation of different climatic areas (*Figure 1*).

Land Use Classification of the Study Site

The land use classification map of the study area was created as a result of the digitization of Corine level 3 1/25000 scaled raster maps which obtained from Provincial Directorate of Agriculture (*Figure 2*). There are 44 different category of Corine level 3 in Turkey (İT, 2004). Within the Erzurum province, there are 27 sub-categories regarding to Corine level 3. These categories are reduced by simplifying to level 1 (Yildiz et al., 2018). As a result of this classification, the study site is divided into 5 different categories, including open areas, agricultural areas, forests, water surfaces and residential areas (*Figure 2*).



Figure 1. The study site

Thermal Satellite Images of the Study Site

In the lower scale land surface temperature (LST) studies, researchers mostly use Landsat-7 and Landsat-8 thermal sensors (Mallick et al., 2008; Mallick et al., 2012; Yıldız et al., 2018). Although the Landsat data sets that provide highly reliable and precise results in lower scale studies have also used in the upper scale, some problems can occur due to the area occupied by each raster data set and the bandwidth. For instance, in the upper scale LST studies if you use Landsat data set, four or five raster images are needed to define your study site, but MODIS data set, one raster image is enough to define it. This is one of the reasons why we used the MODIS data set in this study. Another reason why we preferred the MODIS satellite, because the satellite completes its tour around the globe in one day, offering unique opportunities for users.

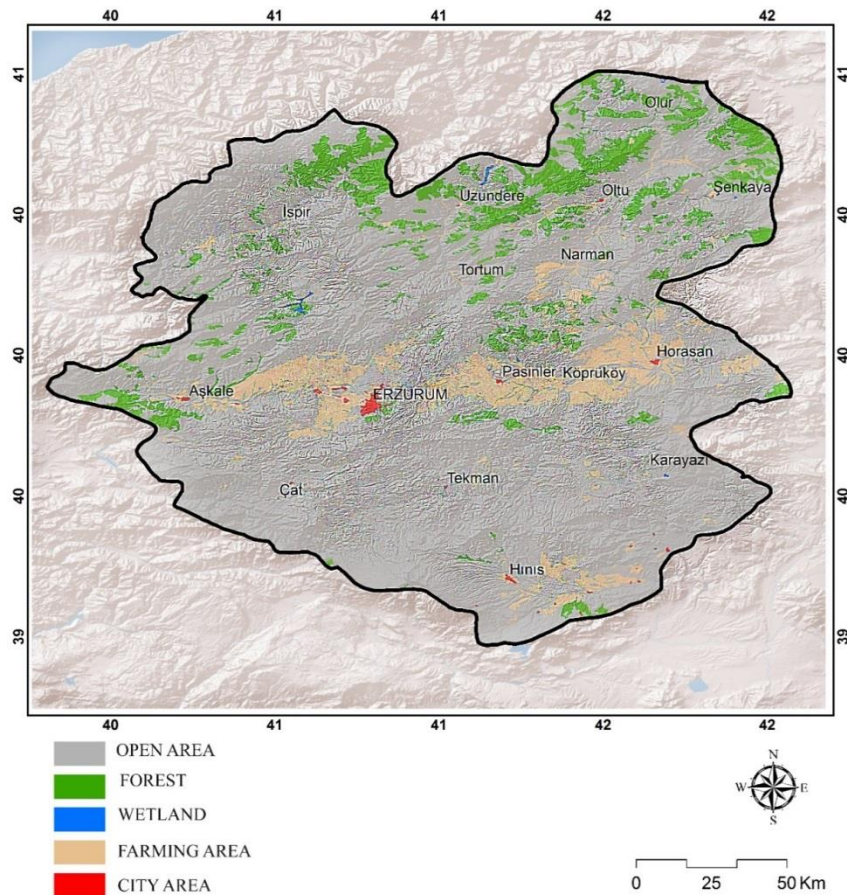


Figure 2. Land use classification map of the study site

Thermal images for the study site have 1000 m spatial resolution and 21st Band of MODIS satellite thermal infra-red data, 3,929 μm -3,989 μm , is used. In order to verify the surface temperature of the radiation intensity of the obtained data the Stefan-Boltzmann law was used (Montvay and Pietarinen, 1982; Narimanov and Smolyaninov, 2012; Rosas et al., 2017).

$$T_s = \sqrt[4]{\frac{T_m^4 - (1-\epsilon)T_{sky}^4}{\epsilon}} \quad (\text{Eq.1})$$

where

- T_m = Surface temperature measured by radiometer.
- T_s = Surface temperature.
- T_{sky} = Sky temperature.
- ϵ = Surface emissivity.

Thermal infra-red images of the validated data were obtained by processing the ARC-GIS 10.2 Package program with a controlled classification method (Eastman, 2001) (Figure 3). Pixel spacing has been utilized when controlled classification is performed. The 255-bit RGB-size thermal image indicates the highest bit range of

350 Kelvin degrees and 200 Kelvin degrees at the lowest 1-bit size. The following equation has been used to convert the RGB image to degrees Celsius. Data from the 2nd band of the MODIS satellite were digitized with the following formula (<https://worldview.earthdata.nasa.gov>).

$$^{\circ}\text{C} = \left[T_{\min} + \left(\frac{T_{\max} - T_{\min}}{255} \right) \times \text{RGB} \right] - 273.15 \quad (\text{Eq.2})$$

where

- °C: Celsius.
- RGB: Value at point of measurement.
- T_{\max} : Maximum Kelvin degree indicated by thermal band.
- T_{\min} : The minimum Kelvin degree indicated by thermal band.

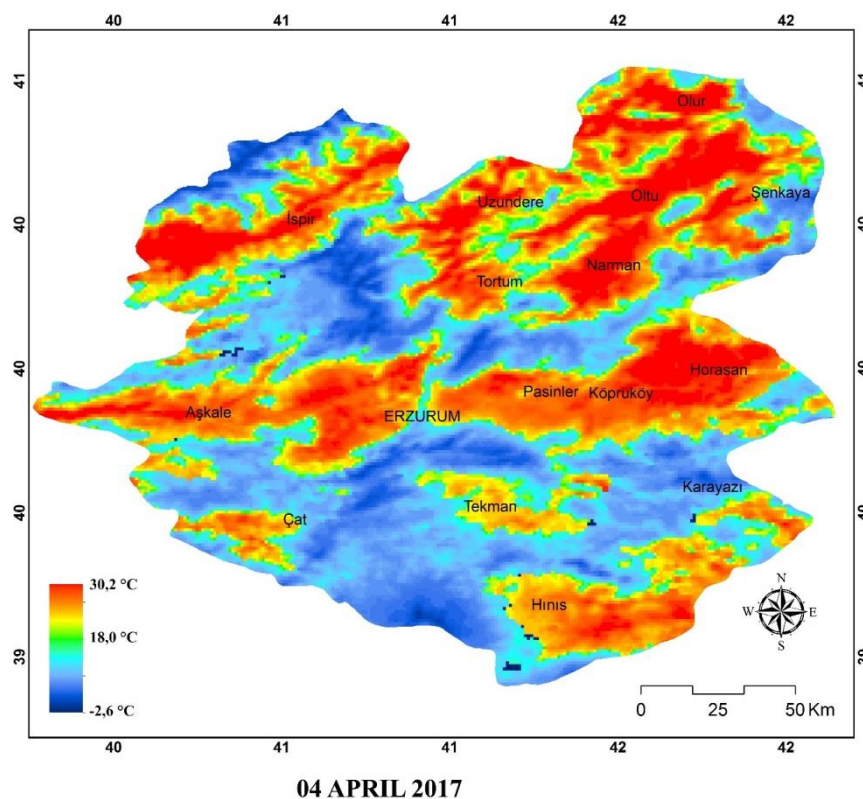


Figure 3. Thermal Band Analysis of the study area on 4 April 2017

In this study, four different dates were selected for thermal data. The selected dates are equal to the average temperatures of the seasons in which they belong. The average temperatures of the winter, spring, summer and autumn seasons were obtained from the General Directorate of Meteorology Affairs. The thermal data set of each day was obtained from the MODIS satellite.

Landsat satellites pass through a point every 16-days (Feng et al., 2013). The thermal band analyses of the MODIS satellite are obtained on a daily basis, especially on land surface temperatures (LST) (Rawat et al., 2018). The data obtained from the MODIS satellite is not suitable for use at lower scales due to the resolution, but in the upper

scales or in the wide range of fields, the MODIS satellite offers different opportunities in terms of LST (Rawat et al., 2018). Our study was conducted in a large area of approximately 25,066 km² which is categorized as upper scale class

Three different watershed structures were taken into account when receiving thermal temperature data for different land classification in the study site. Thermal temperature values were obtained from 10 different locations of each different land use. Besides, 4 different time intervals were determined to be compatible with the study on a seasonal basis. These time intervals were matched with data from the General Directorate of State Meteorology. As a result of this pairing, each date carries similar qualities with the average temperature of the season.

Statistical Analysis of the Data of the Study Site

Decision trees are a widely used method for data mining and machine learning. The Chaid analysis technique is a decision tree algorithm that summarizes the relationships of arguments with each other and the dependent variable in a tree-shaped diagram. In the tree model, decision-making points are called nodes. In this model, the diagram begins to branch with the root node, which encompasses all relationships and is the most complex node. After that, the arguments are separated into the child nodes, which are heterogeneous among each other, homogeneous each time. When adequate homogeneity is ensured, the division stops, and these nodes are called terminal nodes. In the Chaid analysis, which is a Non-parametric test, dependent and independent variables can be continuous, discrete, or categorical and does not require preconditions and assumptions, such as normalcy and linearity required by parametric tests. When the tree diagram is divided into nodes, if the dependent variable is categorical, the chi-square statistic or if it is continuous the F-test are used (Akin et al., 2017). The reason for the selection of Chaid analysis in this study is that two of the independent variables are categorical (land use and month) and one is a constant variable (altitude). The determination coefficient (R^2) between the observed temperature values and the expected temperature values was calculated as 0.82. Minimum parental node count 20, child node count 10, maximum tree depth set as 3 and statistical analysis was done in SPSS 17.0 package program.

$$R^2(\%) = \left[1 - \frac{\sum_{i=1}^n (Y_i - \hat{Y}_i)^2}{\sum_{i=1}^n (Y_i - \bar{Y})^2} \right] * 100 \quad (\text{Eq.3})$$

Results

The thermal band Analysis taken on April 4, 2017 showed that open areas have minimum -1.15°C maximum is 32.4°C surface temperature and the surface temperature difference 33.6°C is measured. Forests surface temperature is minimum 1.2°C, maximum of 18.0°C and the temperature difference is 16.8°C. For water surfaces the temperature minimum 1.2°C, maximum 29.4°C and the difference is 28.2°C. Surface temperature parameters for agricultural land use minimum 4.2°C, maximum of 27.6°C and the temperature difference is 23.4°C. Residential areas; the surface temperature is similar to other land uses; minimum 2.4°C, maximum 29.4°C and the difference is 27°C (Table 1 and Figure 3). If we handle the study site on the basin scale, it is determined that the surface temperature is colder than the Çoruh Basin on the east of the Araz Basin and the Euphrates-Tigris Basin on April 4.

Table 1. The values of thermal band analysis results of the study area on 4 April 2017

Points	Open Areas (°C)	Forests (°C)	Water Surfaces (°C)	Agricultural Areas (°C)	Residential Areas (°C)
1	21.0	7.2	1.2	22.8	20.4
2	4.2	15.6	18.6	25.8	20.8
3	16.8	1.25	3.0	4.2	25.8
4	8.4	14.4	1.8	25.2	2.4
5	7.2	4.2	29.4	20.4	29.4
6	32.4	6.0	19.2	22.8	26.4
7	-1.1	10.2	1.2	4.2	22.8
8	5.4	18.0	6.0	15.0	25.8
9	6.6	7.8	21.0	27.6	18.6
10	14.4	6.1	14.4	21.6	10.8

For the thermal band analysis taken on June 17 2017, when we examined in terms of the land uses, open area sampling points are maximum 30.6°C, minimum 20.4°C and the difference is 10.2°C. Forests minimum surface temperature is 18.0°C, maximum of 27.6°C and the temperature difference is 9.6°C. The temperature of the water surfaces is minimum -3.5°C, maximum 31.8°C and the total difference is 35.4°C. In terms of agricultural areas are observed at a minimum temperature of 24.6°C, while the temperature difference is observed at a maximum of 33.0°C. The total temperature difference in agricultural land use is 8.4°C. Similarly, the surface temperature observed at minimum 24.6°C in the residential area is 31.2°C and the difference is 6.6°C (Table 2 and Figure 4). On the basin scale, the surface temperature of the Aras Basin is seen to be significantly higher than the other 2 basins. In some points, air corridors in the form of deep canyons in basin bases cause wind mobility to cool down the surface cover and this is an evident in the north-west strip of Aras Basin and in the northern of the Çoruh Basin.

Table 2. The values of thermal band analysis results of the study area on June 17 2017

Points	Open Spaces (°C)	Forests (°C)	Water Surfaces (°C)	Agricultural Areas (°C)	Residential Areas (°C)
1	24.6	18.6	20.4	27.0	27.6
2	20.4	18.0	21.6	28.2	31.2
3	20.4	20.4	21.0	25.2	30.0
4	27.6	21.6	-3.5	25.8	27.6
5	30.6	21.6	31.8	25.8	28.2
6	26.4	21.6	25.2	30.0	24.6
7	23.4	18.0	20.4	24.6	29.4
8	30.0	27.6	21.0	25.8	25.8
9	25.2	23.4	29.4	24.6	30.0
10	24.6	18.0	26.4	33.0	30.6

The study site was examined in the thermal band Analysis taken on October 6. 2017. The minimum 20.6°C, maximum 28.8°C is measured for open areas is and a total surface temperature difference is 8.2°C. For forests surface temperature is minimum 12.6°C maximum 30.0°C and the temperature difference is 17.4°C. On water surfaces minimum temperature is 17.4°C maximum 28.8°C and the total difference is 8.4°C.

Surface temperature parameters in agricultural areas; minimum 19.8°C, maximum of 33.0°C and the temperature difference is 13.2°C. In residential areas, the surface temperature is similar to other land uses; minimum 22.8°C, maximum 27.0°C and the total difference was 4.2°C (Table 3 and Figure 5).

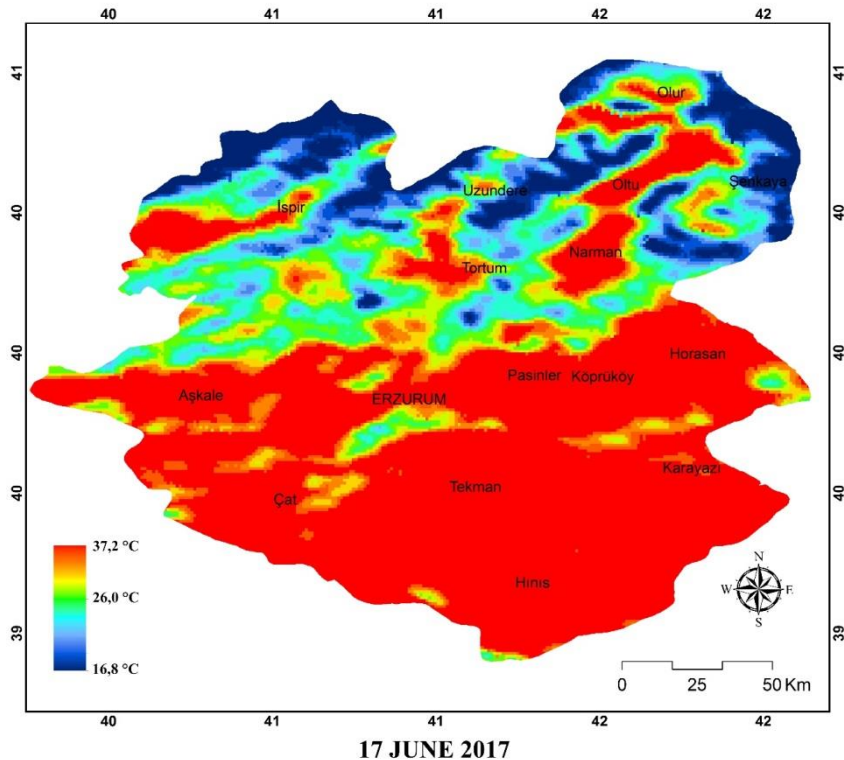


Figure 4. Thermal Band Analysis of the study area on 17 June 2017

Table 3. The values of thermal band analysis results of the study area on 6 October 2017

Points	Open Spaces (°C)	Forests (°C)	Water Surfaces (°C)	Agricultural Areas (°C)	Residential Areas (°C)
1	21.6	16.2	21.6	27.0	22.2
2	23.4	18.0	20.4	26.4	24.6
3	22.8	13.2	17.4	23.4	25.2
4	24.6	15.6	23.4	25.8	25.8
5	28.2	19.8	25.8	25.8	24.0
6	27.6	23.4	25.8	25.2	22.8
7	20.4	12.6	21.6	19.8	25.2
8	24.6	30.0	24.6	25.8	24.0
9	28.8	22.2	23.4	24.6	27.0
10	22.2	13.2	22.2	33.0	25.8

When we examine the thermal band analysis on 2 December 2017; a maximum of 9.8°C is observed at open areas sampling points. While a minimum of -3.5°C with a difference of 13.4°C, a minimum temperature of -4.1°C is determined when a maximum surface temperature of 6.0°C in the forest areas. The temperature difference is 10.2°C. On the water surface, the minimum temperature is -9.5°C, maximum -4.1°C and the

total difference is 5.4°C. For the agricultural areas a minimum temperature is -4.7°C and a maximum temperature 9.0°C. The total temperature difference in agricultural areas is 13.8°C. In the same way, the minimum surface temperature of the residential area is -7.75°C, maximum surface temperature is 6.0°C and the difference is 13.8°C (Table 4 and Figure 6).

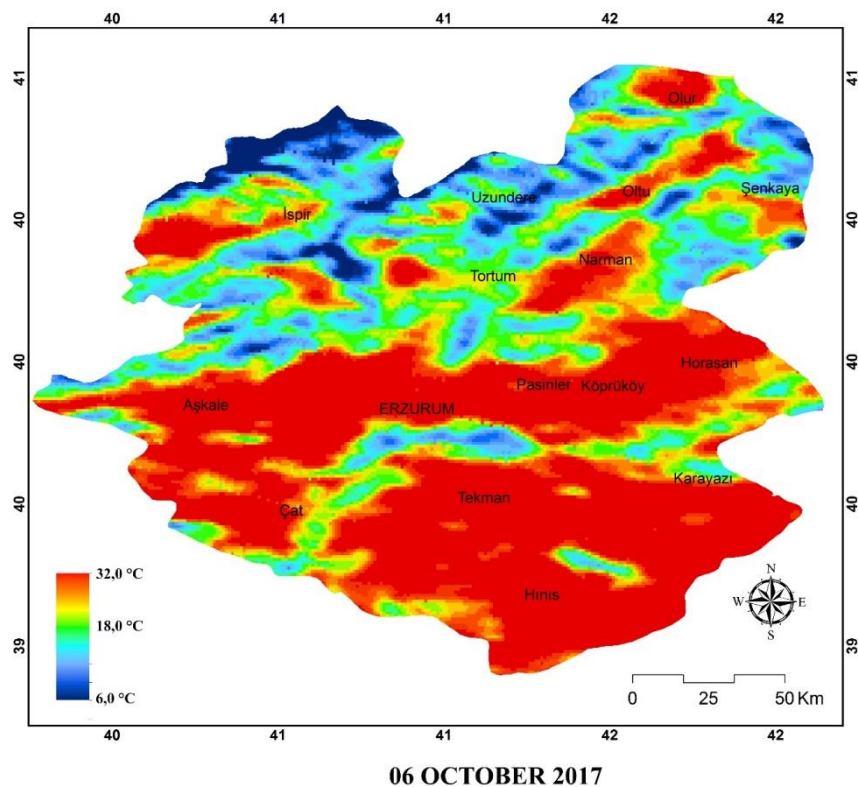


Figure 5. Thermal band analysis of the study area on 6 October 2017

Table 4. The values of thermal band analysis results of the study area on 2 December 2017

Points	Open Spaces (°C)	Forests (°C)	Water Surfaces (°C)	Agricultural Areas (°C)	Residential Areas (°C)
1	4.2	3.0	-4.1	-2.9	-0.5
2	-2.9	2.4	6.6	-2.9	6.0
3	9.8	-1.7	-1.7	-3.5	4.2
4	-0.5	2.4	-9.5	-1.1	-2.3
5	-0.5	-4.1	7.2	1.2	5.4
6	6.6	-0.5	2.4	5.4	6.6
7	-3.5	0.6	-5.3	-4.7	0.0
8	-2.3	6.0	-2.3	-2.3	6.0
9	5.4	-2.3	4.2	2.4	-2.3
10	-1.1	0.0	-2.3	9.0	-7.7

When we examined the thermal band images on the basin scale on December 2 2017; Erzurum Province is covered with snow cover in general. However, the thermal band analyses show in areas where there is little or no snow cover. The surface temperature is

higher than other areas (Figure 6). Coruh Basin has a lot of elevation differences in terms of topographic properties. Therefore, there are some formations of micro-climatic areas due to these characteristics. Micro-climatic areas are seen to be warmer in terms of surface temperature. On the other hand, Aras Basin and Fırat-Dicle basin consist of very flat areas in terms of topography. Flat areas are very cold because they are covered with snow cover in terms of surface temperature. However, in some rugged areas of the Aras Basin. The surface temperature is partly warmer than other areas (Figure 6).

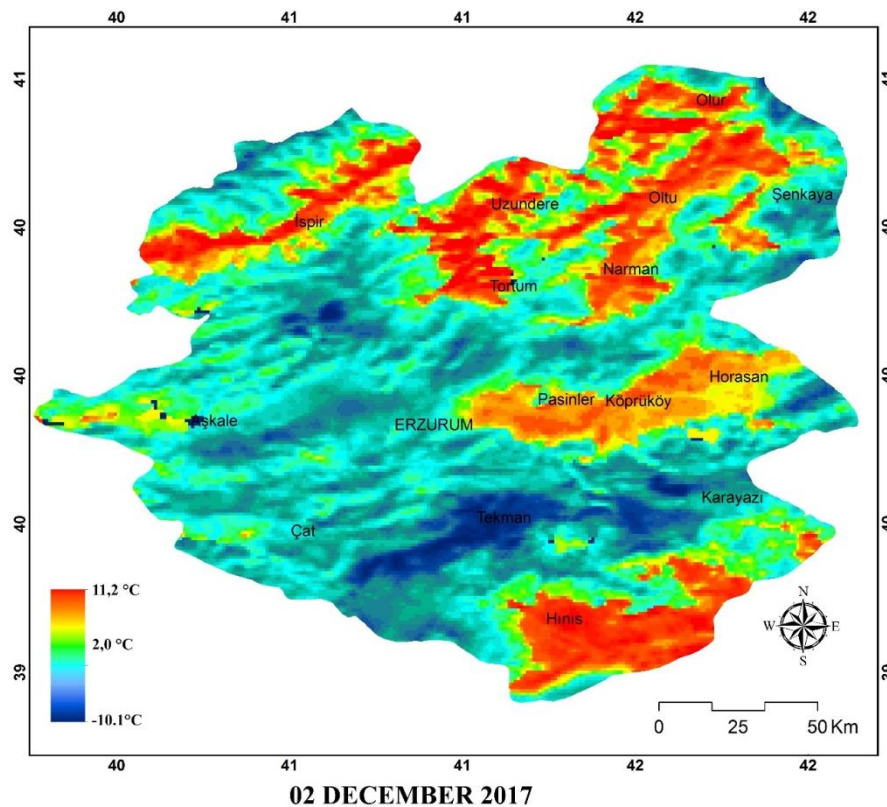


Figure 6. Thermal band analysis of the study area on 2 December 2017

In the study area, sampling points were obtained from 10 different locations, homogeneously distributed for each different land use. MODIS satellite sensors with a spatial resolution of 1000 m cause a large standard deviation in small areas. Therefore, while obtaining the data, sampling area was considered. The sampling areas sizes ranges from 2.3 km² to 14 km². The areas are not smaller than 1 km²; hence it resulted in low standard deviation of LST data from the MODIS satellite sensors. In addition, the thermal data was obtained from the 4 different stations of the General Directorate of Meteorology Affairs for the accuracy of the sensor data used in the study (Table 5). On the basis of the resulting data, the difference of average surface temperature between stations was 1.9°C.

In the statistical analysis of this study, the effects of land use, month, and altitude were examined from the factors affecting the surface temperature. Because month and land use factors used as categorical, altitude factor used as continuous variables, CHAID analysis was preferred, which is a method use both categorical and continuous

variables. Beside this, the values of the altitude continuous variable divided into homogenous subgroups are automatically performed.

Table 5. Temperature values obtained from thermal band analysis and meteorology stations

Date/Place		4 Apr 2017 (°C)	17 Jun 2017 (°C)	6 Oct 2017 (°C)	2 Dec 2017 (°C)
İspir	Radio-meter	19.6	27.2	23.8	7.9
	Station	18.4	24.9	22.9	6.7
Erzurum	Radio-meter	12.8	22.3	16.1	-3.2
	Station	11.7	21.0	14.8	-1.0
Tekman	Radio-meter	12.3	26.4	15.1	-8.2
	Station	8.5	21.4	14.3	-6.4
Hınıs	Radio-meter	12.1	24.3	18.1	5.2
	Station	10.5	21.9	16	4.9

According to the results of the statistical analysis, the most effective factors on the temperature of the months of June and October formed a homogeneous group in itself, and the temperature average is 23.9°C. It is determined that the month of December (0.6°C) with the lowest temperature average has an altitude effect (Figure 7).

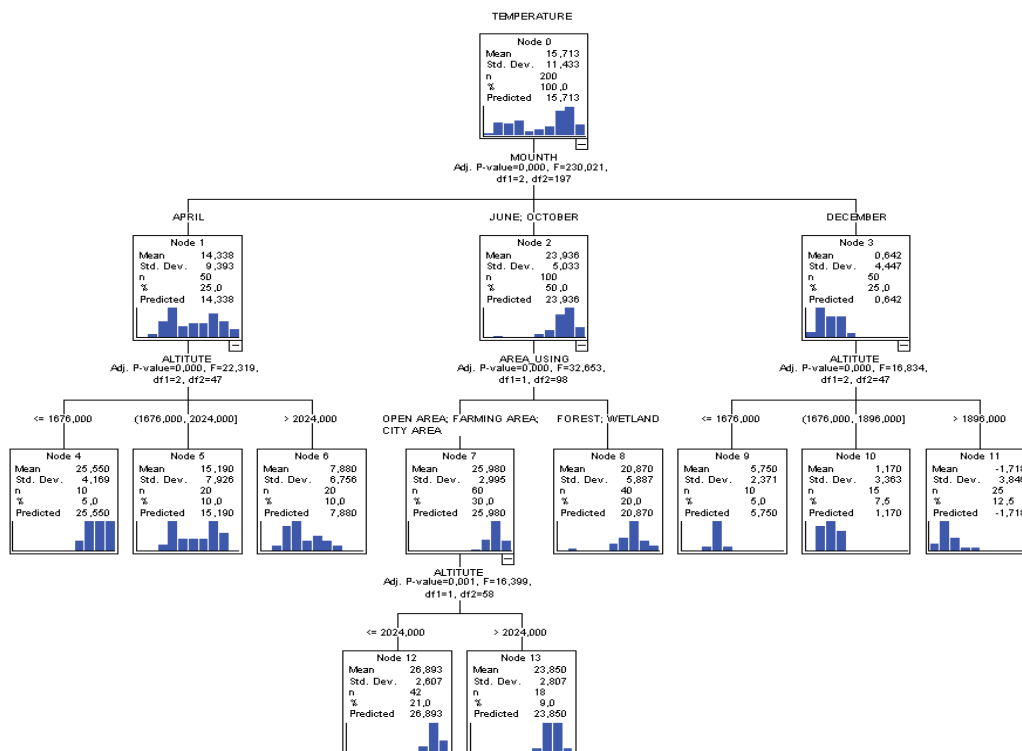


Figure 7. Statistical analysis of thermal band data

The altitude is divided into 3 heterogeneous groups while forming a homogeneous group in itself. While the average temperature of December is 5.7°C at a height lower than 1676 m, the temperature is between 1676-1896 m is 1.1°C and the temperature in the altitude above 1896 m is determined as -1.1°C (Figure 7).

$P < 0.00$ has been effective in the land uses on the months of June and October. Among all land uses categories, open spaces and residential areas created one group. Forests and water surfaces created another group. Average surface temperature in open areas and residential areas is 25.9°C . In the other group, the surface temperature of the forest and water surfaces is 20.8°C (Figure 7).

The group formed by the open areas, agricultural areas and residential areas has been affected by height and the surface temperature of the area, which is less than 2024 m in altitude, is 26.89°C over 2024 m is 23.8°C . In the month of April only altitude was effective. The surface temperature at a height lower than 1676 m is 25.55°C , while the temperature is between 1676-2024 m is 15.1°C and over 2024 m is 7.8°C (Figure 7).

Overall, the most effective factor on the surface temperature was the month which comprise June, October, April and December. June and October were creating a homogeneous sub-group with the average surface temperature 23.9°C . On the other hand, April with a range of 14.3°C and December with a range of 0.6°C were creating separate group. The highest average surface temperature was seen at node 12. On this node, the average surface temperature obtained from 42 different observation points when open areas, farming areas and city areas and the altitude were lower than 2024 m for June and October as 26.9°C .

Discussion

One of the biggest problems facing seasonal determination of surface temperature is to distinguish between seasonal and sudden changes (Verbesselt et al., 2010; Ghazaryan et al., 2016; Muro et al., 2018). As a matter of fact seasonal timelines are divided into consideration of the 1-year urban meteorology data of 2017. It is also stated in previous studies that the measured value between 2 different single points to determine the surface temperature change is not an ecological indication (McVicar and Jupp, 1998). This study was evaluated by taking 10 different points in 5 different categories in 4 different time intervals on the province-scale. Surface temperature is used as an ideal tool for temporal analysis in the basin and other scales. although the resolution of the MODIS satellite in thermal band analyses is low quality (Neteler, 2010).

The reason for the selection of Chaid analysis in this study is that two of the arguments (land use and month) are categorical and one (altitude) is a constant variable. The determination coefficient between the temperature values observed and the expected temperature values (R^2) was calculated as 0.82. In another similar study the value of correlation between the two variables (R^2) was calculated as 0.65 (Muro et al., 2018).

Areas with the highest average surface temperature in the study site were determined as residential areas and they had a surface temperature of 18.7°C . At the same time the forest surfaces 12.2°C water surfaces 13.8°C agricultural areas 17.9°C and open areas 15.7°C were determined to have an average surface temperature. When the bonding between land uses and average surface temperatures is examined an average surface temperature difference was observed as 3.4°C between open areas and forests. Similarly, in previous studies, this difference was between 12 and 1.8°C (Falahatkar et al., 2011; Li et al., 2012; Mallick et al., 2012). In some studies, the difference between water surfaces and forests temperatures was found to be less important (Van and Bao, 2016). Indeed, in this study surface temperature values were close to each other in the water surfaces and forests. However, in another group study the difference between the

forests and water surface temperatures was observed over 10°C (Falihatkar et al., 2011). In different studies the causes of different surface temperatures in similar land uses are topographic status of land structure, change in land use and humidity (Yuksel and Yilmaz, 2008). In this study, we have done on the provincial scale accommodates within the boundaries of 3 different basins. Even on the inside of these basins the land heights and climatic conditions are constantly differentiating from each other. Therefore, it causes different surface temperature values in the same land use.

Conclusion

In our study, we investigated the link between different land surface covers and surface temperature (LST) statistically. As a matter of fact, in the scientific studies that were made before, the method of statistical multi-linear regression analysis and correlation calculations were used for determining links between land surface temperature and land use (Choudhury et al., 2018; Wang et al., 2018). The point that makes our study different from other studies; we have been annotated with CHAID analysis by adding height and 4 different time zones in order to determine links between land surface temperature and land use. The reason for choosing CHAID analysis is that the month and land use factors used as the categorical variables, and the altitude factor used as continuous variables. In addition, using thermal band images in different time periods has supported the consistency of the links between LST and the land use.

In this study, Erzurum Province located in the eastern part of Turkey were investigated and also the 3 basin examples within the provincial boundaries were discussed. According to the results of the statistical analysis of the study, the most effective factor on surface temperature is the month of June and October in which a homogeneous group and the temperature average of this group is 23.9°C. It is determined that the month of December (0.64°C) with the lowest temperature average has an altitude effect.

If we look at the land use categories, the average surface temperature in the open areas and residential areas is 25.9°C. in the other group, the surface temperature of the forests and water surfaces is 20.8°C. When we discussed the study results in the basin scale, the surface temperature was higher at Coruh basin than Aras and Dicle basin due to altitude.

In addition, the results of this study can be used as a preliminary study in the planning activities for the future basin planning, urban planning, water resources conservation and uses and the planning of nature conservation.

REFERENCES

- [1] Akin, M., Eydurhan, E., Reed, B. M. (2017): Use of RSM and CHAID data mining algorithm for predicting mineral nutrition of hazelnut. – *Plant Cell Tissue and Organ Culture* 128(2): 317-317.
- [2] Alexander, L. V., Zhang, X., Peterson, T. C., Caesar, J., Gleason, B., Tank, A. M. G. K., Haylock, M., Collins, D., Trewin, B., Rahimzadeh, F., Tagipour, A., Kumar, K. R., Revadekar, J., Griffiths, G., Vincent, L., Stephenson, D. B., Burn, J., Aguilar, E., Brunet, M., Taylor, M., New, M., Zhai, P., Rusticucci, M., Vazquez-Aguirre, J. L. (2006): Global observed changes in daily climate extremes of temperature and precipitation. – *Journal of Geophysical Research-Atmospheres* 111(D5).

- [3] Arnfield, A. J. (2003): Two decades of urban climate research: A review of turbulence, exchanges of energy and water, and the urban heat island. – *International Journal of Climatology* 23(1): 1-26.
- [4] Becker, F., Li, Z. L. (1990): Towards a Local Split Window Method over Land Surfaces. – *International Journal of Remote Sensing* 11(3): 369-393.
- [5] Becker, A., Inoue, S., Fischer, M., Schwegler, B. (2012): Climate change impacts on international seaports: knowledge, perceptions, and planning efforts among port administrators. – *Climatic Change* 110(1-2): 5-29.
- [6] Blasi, M. G., Liuzzi, G., Masiello, G., Serio, C., Telesca, V., Venafrà, S. (2016): Surface parameters from SEVIRI observations through a Kalman filter approach: application and evaluation of the scheme in Southern Italy. – *Tethys-Journal of Mediterranean Meteorology & Climatology* (13): 3-10.
- [7] Chen, Y. H., Zhan, W. F., Quan, J. L., Zhou, J., Zhu, X. L., Sun, H. (2014): Disaggregation of Remotely Sensed Land Surface Temperature: A Generalized Paradigm. – *Ieee Transactions on Geoscience and Remote Sensing* 52(9): 5952-5965.
- [8] Cho, K., Kim, Y., Kim, Y. (2018): Disaggregation of Landsat-8 Thermal Data Using Guided SWIR Imagery on the Scene of a Wildfire. – *Remote Sensing* 10(1).
- [9] Choudhury, D., Das, K., Das, A. (2018): Assessment of land use land cover changes and its impact on variations of land surface temperature in Asansol-Durgapur Development Region. – *The Egyptian Journal of Remote Sensing and Space Science*.
- [10] Chrysoulakis, N., Lopes, M., San Jose, R., Grimmond, C. S. B., Jones, M. B., Magliulo, V., Klostermann, J. E. M., Synnefa, A., Mitraka, Z., Castro, E. A., Gonzalez, A., Vogt, R., Vesala, T., Spano, D., Pigeon, G., Freer-Smith, P., Staszewski, T., Hodges, N., Mills, G., Cartalis, C. (2013): Sustainable urban metabolism as a link between bio-physical sciences and urban planning: The BRIDGE project. – *Landscape and Urban Planning* 112: 100-117.
- [11] Eastman, J. (2001): IDRISI 32 release 2. guide to GIS and image processing volumes 1 and 2. – Clark Labs, Clark University, Worcester.
- [12] El-Khoury, A., Seidou, O., Lapen, D. R., Que, Z., Mohammadian, M., Sunohara, M., Bahram, D. (2015): Combined impacts of future climate and land use changes on discharge, nitrogen and phosphorus loads for a Canadian river basin. – *Journal of Environmental Management* 151: 76-86.
- [13] Falahatkar, S., Hosseini, S. M., Soffianian, A. R. (2011): The relationship between land cover changes and spatial-temporal dynamics of land surface temperature. – *Indian Journal of Science and Technology* 4(2): 76-81.
- [14] Fearnside, P. M. (2015): Emissions from tropical hydropower and the IPCC. – *Environmental Science & Policy* 50: 225-239.
- [15] Felzer, B. S. (2012): Carbon, nitrogen, and water response to climate and land use changes in Pennsylvania during the 20th and 21st centuries. – *Ecological Modelling* 240: 49-63.
- [16] Feng, M., Sexton, J. O., Huang, C. Q., Masek, J. G., Vermote, E. F., Gao, F., Narasimhan, R., Channan, S., Wolfe, R. E., Townshend, J. R. (2013): Global surface reflectance products from Landsat: Assessment using coincident MODIS observations. – *Remote Sensing of Environment* 134: 276-293.
- [17] Feng, X., Myint, S. W. (2016): Exploring the effect of neighboring land cover pattern on land surface temperature of central building objects. – *Building and Environment* 95: 346-354.
- [18] Gallego-Elvira, B., Taylor, C. M., Harris, P. P., Ghent, D., Veal, K. L., Folwell, S. S. (2016): Global observational diagnosis of soil moisture control on the land surface energy balance. – *Geophysical Research Letters* 43(6): 2623-2631.
- [19] Ghazaryan, G., Dubovyk, O., Kussul, N., Menz, G. (2016): Towards an Improved Environmental Understanding of Land Surface Dynamics in Ukraine Based on Multi-Source Remote Sensing Time-Series Datasets from 1982 to 2013. – *Remote Sensing* 8(8).

- [20] Gonzalez, A., Donnelly, A., Jones, M., Chrysoulakis, N., Lopes, M. (2013): A decision-support system for sustainable urban metabolism in Europe. – *Environmental Impact Assessment Review* 38: 109-119.
- [21] Imhoff, M. L., Zhang, P., Wolfe, R. E., Bounoua, L. (2010): Remote sensing of the urban heat island effect across biomes in the continental USA. – *Remote Sensing of Environment* 114(3): 504-513.
- [22] İT, L. B. (2004): CORINE Arazi Kullanımı Sınıflandırma Sistemine Göre Arazi Kullanım Haritasının Hazırlanması: Isparta Örneği. – *TARIM BİLİMLERİ DERGİSİ* 10(4): 366-374.
- [23] Jacob, F., Petitcolin, F., Schmugge, T., Vermote, E., French, A., Ogawa, K. (2004): Comparison of land surface emissivity and radiometric temperature derived from MODIS and ASTER sensors. – *Remote Sensing of Environment* 90(2): 137-152.
- [24] Justice, C. O., Townshend, J. R. G., Vermote, E. F., Masuoka, E., Wolfe, R. E., Saleous, N., Roy, D. P., Morisette, J. T. (2002): An overview of MODIS Land data processing and product status. – *Remote Sensing of Environment* 83(1-2): 3-15.
- [25] Li, Y. Y., Zhang, H., Kainz, W. (2012): Monitoring patterns of urban heat islands of the fast-growing Shanghai metropolis. China: Using time-series of Landsat TM/ETM+ data. – *International Journal of Applied Earth Observation and Geoinformation* 19: 127-138.
- [26] Li, Z. L., Tang, B. H., Wu, H., Ren, H. Z., Yan, G. J., Wan, Z. M., Trigo, I. F., Sobrino, J. A. (2013): Satellite-derived land surface temperature: Current status and perspectives. – *Remote Sensing of Environment* 131: 14-37.
- [27] Mallick, J., Kant, Y., Bharath, B. (2008): Estimation of land surface temperature over Delhi using Landsat-7 ETM+. – *J. Ind. Geophys. Union* 12(3): 131-140.
- [28] Mallick, J., Singh, C. K., Shashtri, S., Rahman, A., Mukherjee, S. (2012): Land surface emissivity retrieval based on moisture index from LANDSAT TM satellite data over heterogeneous surfaces of Delhi city. – *International Journal of Applied Earth Observation and Geoinformation* 19: 348-358.
- [29] Masiello, G., Serio, C., Venafrà, S., Liuzzi, G., Gottsche, F., Trigo, I. F., Watts, P. (2015): Kalman filter physical retrieval of surface emissivity and temperature from SEVIRI infrared channels: a validation and intercomparison study. – *Atmospheric Measurement Techniques* 8(7): 2981-2997.
- [30] McVicar, T. R., Jupp, D. L. B. (1998): The current and potential operational uses of remote sensing to aid decisions on drought exceptional circumstances in Australia: a review. – *Agricultural Systems* 57(3): 399-468.
- [31] Montvay, I., Pietarinen, E. (1982): The Stefan Boltzmann Law at High-Temperature for the Gluon Gas. – *Physics Letters B* 110(2): 148-154.
- [32] Muro, J., Strauch, A., Heinemann, S., Steinbach, S., Thonfeld, F., Waske, B., Diekkruger, B. (2018): Land surface temperature trends as indicator of land use changes in wetlands. – *International Journal of Applied Earth Observation and Geoinformation* 70: 62-71.
- [33] Narimanov, E. E., Smolyaninov, I. I. (2012): Beyond Stefan-Boltzmann Law: Thermal Hyper-Conductivity. – 2012 Conference on Lasers and Electro-Optics (CLEO).
- [34] Neteler, M. (2010): Estimating Daily Land Surface Temperatures in Mountainous Environments by Reconstructed MODIS LST Data. – *Remote Sensing* 2(1): 333-351.
- [35] Prata, A., Caselles, V., Coll, C., Sobrino, J., Otlle, C. (1995): Thermal remote sensing of land surface temperature from satellites: Current status and future prospects. – *Remote Sensing Reviews* 12(3-4): 175-224.
- [36] Rajczak, J., Schar, C. (2017): Projections of Future Precipitation Extremes Over Europe: A Multimodel Assessment of Climate Simulations. – *Journal of Geophysical Research-Atmospheres* 122(20): 10773-10800.
- [37] Rawat, K. S., Sehgal, V., Ray, S. (2018): Downscaling of MODIS thermal imagery. – *The Egyptian Journal of Remote Sensing and Space Science*.

- [38] Rosas, J., Houborg, R., McCabe, M. F. (2017): Sensitivity of Landsat 8 Surface Temperature Estimates to Atmospheric Profile Data: A Study Using MODTRAN in Dryland Irrigated Systems. – *Remote Sensing* 9(10).
- [39] Schott, J. R., Hook, S. J., Barsi, J. A., Markham, B. L., Miller, J., Padula, F. P., Raqueno, N. G. (2012): Thermal infrared radiometric calibration of the entire Landsat 4, 5, and 7 archive (1982–2010). – *Remote Sensing of Environment* 122: 41-49.
- [40] Seung-Hwan, Y., Jin-Yong, C., Sang-Hyun, L., Yun-Gyeong, O., Koun, Y. D. (2013): Climate change impacts on water storage requirements of an agricultural reservoir considering changes in land use and rice growing season in Korea. – *Agricultural Water Management* 117: 43-54.
- [41] Song, J., Wang, Z. H., Myint, S. W., Wang, C. Y. (2017): The hysteresis effect on surface-air temperature relationship and its implications to urban planning: An examination in Phoenix, Arizona, USA. – *Landscape and Urban Planning* 167: 198-211.
- [42] Streutker, D. R. (2003): Satellite-measured growth of the urban heat island of Houston, Texas. – *Remote Sensing of Environment* 85(3): 282-289.
- [43] Tomlinson, C. J., Chapman, L., Thornes, J. E., Baker, C. J. (2012): Derivation of Birmingham's summer surface urban heat island from MODIS satellite images. – *International Journal of Climatology* 32(2): 214-224.
- [44] Tong, S. T. Y., Sun, Y., Ranatunga, T., He, J., Yang, Y. J. (2012): Predicting plausible impacts of sets of climate and land use change scenarios on water resources. – *Applied Geography* 32(2): 477-489.
- [45] Tran, T. V., Ha, D. X. B. (2008): A study on urban development through land surface temperature by using remote sensing: in case of Ho Chi Minh City. – *VNU Journal of Science* 24: 160-167.
- [46] van der Knaap, Y. A., Bakker, M. M., Alam, S. J., Witte, J.-P. M., Aerts, R., van Ek, R., van Bodegom, P. M. (2018): Projected vegetation changes are amplified by the combination of climate change, socio-economic changes and hydrological climate adaptation measures. – *Land Use Policy* 72: 547-562.
- [47] van Haren, R., van Oldenborgh, G. J., Lenderink, G., Collins, M., Hazeleger, W. (2013): SST and circulation trend biases cause an underestimation of European precipitation trends. – *Climate Dynamics* 40(1-2): 1-20.
- [48] Van, T. T., Bao, H. D. X. (2016): A study on urban development through land surface temperature by using remote sensing: in case of Ho Chi Minh City. – *VNU Journal of Science: Earth and Environmental Sciences* 24(3).
- [49] Verbesselt, J., Hyndman, R., Newnham, G., Culvenor, D. (2010): Detecting trend and seasonal changes in satellite image time series. *Remote Sensing of Environment* 114(1): 106-115.
- [50] Voogt, J. A., Oke, T. R. (2003): Thermal remote sensing of urban climates. – *Remote Sensing of Environment* 86(3): 370-384.
- [51] Wang, Y. C., Hu, B. K. H., Myint, S. W., Feng, C. C., Chow, W. T. L., Passy, P. F. (2018): Patterns of land change and their potential impacts on land surface temperature change in Yangon, Myanmar. – *Science of the Total Environment* 643: 738-750.
- [52] Weng, Q. H. (2009): Thermal infrared remote sensing for urban climate and environmental studies: Methods, applications, and trends. – *Isprs Journal of Photogrammetry and Remote Sensing* 64(4): 335-344.
- [53] Wu, L., Long, T. Y., Liu, X., Guo, J. S. (2012): Impacts of climate and land-use changes on the migration of non-point source nitrogen and phosphorus during rainfall-runoff in the Jialing River Watershed, China. – *Journal of Hydrology* 475: 26-41.
- [54] Xia, L., Zhao, F., Chen, L., Zhang, R., Mao, K., Kylling, A., Ma, Y. (2018): Performance comparison of the MODIS and the VIIRS 1.38 μm cirrus cloud channels using libRadtran and CALIOP data. – *Remote Sensing of Environment* 206: 363-374.

- [55] Yang, X. Y., Li, Y. G., Yang, L. N., (2012): Predicting and understanding temporal 3D exterior surface temperature distribution in an ideal courtyard. – *Building and Environment* 57: 38-48.
- [56] Yildiz, N. D., Avdan, U., Yilmaz, S., Matzarakis, A. (2018): Thermal map assessment under climate and land use changes; a case study for Uzundere Basin. – *Environmental Science and Pollution Research* 25(1): 940-951.
- [57] Yuksel, U. D., Yilmaz, O. (2008): A study on determining and evaluating summertime urban heat islands in Ankara at regional and local scale utilizing remote sensing and meteorological data. – *Journal of the Faculty of Engineering and Architecture of Gazi University* 23(4): 937-952.
- [58] Zhan, W. F., Chen, Y. H., Zhou, J., Li, J., Liu, W. Y. (2011): Sharpening Thermal Imageries: A Generalized Theoretical Framework From an Assimilation Perspective. – *Ieee Transactions on Geoscience and Remote Sensing* 49(2): 773-789.
- [59] Zhang, X. Y., Friedl, M. A., Schaaf, C. B., Strahler, A. H. (2004): Climate controls on vegetation phenological patterns in northern mid- and high latitudes inferred from MODIS data. – *Global Change Biology* 10(7): 1133-1145.

HIGH TRANSPLANT DENSITY CAUSE LOSS YIELD AND QUALITY DECREMENT BY AFFECTING PHOTOSYNTHESIS, DRY MATTER ACCUMULATION AND TRANSPORTATION IN SUPER RICE

DUAN, M. Y.^{1,2#} – LUO, H. W.^{1,2#} – PAN, S. G.^{1,2} – MO, Z. M.^{1,2} – YANG, X. J.^{1,2} – TIAN, J. Y.^{1,2} – NIE, J.^{1,2} – WANG, H. X.^{1,2} – LI, L.^{1,2} – TANG, X. R.^{1,2*}

¹*Department of Crop Science and Technology, College of Agriculture, South China Agricultural University, 2018, 510642, PR China*

²*Scientific Observing and Experimental Station of Crop Cultivation in South China, Ministry of Agriculture, 2018, 510642, PR China*

#These author have contributed equally to this work.

**Corresponding author
e-mail: tangxr@scau.edu.cn*

(Received 23rd Feb 2019; accepted 21st Mar 2019)

Abstract. Transplant density is an important factor which has impacts on rice growth and development in transplanted rice production system. Present study used three transplant densities in paddy field experiment and set as D1 (transplant spacing of 20 cm × 24 cm, about 2.085 hundred thousand hills for each hectare), D2 (transplant spacing of 20 cm × 20 cm, about 2.603 hundred thousand hills for each hectare) and D3 (transplant spacing of 20 cm × 16 cm, about 3.120 hundred thousand hills for each hectare). The results showed that high density (D3) not only reduced the net photosynthetic rate and *LAI* values at heading stage, but also decreased dry matter accumulation and transportation compared to D1 density. The highest yield was recorded in D1 density and the lowest yield was recorded in D3 density. Study also revealed that high density caused yield loss by decreasing the grain number and seed-setting rate. Furthermore, high density also increased chalk rice rate and chalkiness while reducing the amylose content. The activity of sucrose synthase (SS) in D3 was significantly lower than D1 and it might relate to the reduction of grain quality.

Keyword: *rice, density, yield, quality, net photosynthetic rate, dry matter accumulation and transportation*

Introduction

Rice (*Oryza sativa* L.) is a main crop which has been cultivated in China, its production plays an important role in Chinese food security. In recent years, because the area of arable lands is in rapid decline, how to maintain the rice productivity and promote the yield potential had been the main research direction for many experts in last decade (Tao et al., 2019; Tang et al., 2019). There are a lot of factors that could affect grain yield and quality of rice. For example, the transplant density is a key part which affects grain yield and quality significantly in rice production.

Rational close planting is one of the important strategies for high yield and good quality cultivation of rice. A suitable transplanted density not only could give full play to the strong tillering and self-regulation ability of rice population, reduce the competition of inter-row and inter-plant growth in rice population, and avoid the overgrowth of early growth, but also ensure that the rice field can make full use of light energy, carry out photosynthesis, accumulate more organic matter, thereby increasing

rice yield (Zhou et al., 2018; Huang et al., 2018; Tareq et al., 2018). In 2001, Yuan demonstrated that low plant density enlarged the growth space of above-ground and below-ground parts of rice, enlarges individual strength and panicle size, thus gaining high yield. The study of Hayashi et al. (2006) revealed that over-dense planting strengthens the competition of photosynthetic nutrients among rice individuals and promotes early flowering of rice. Furthermore, Mobasser et al. (2009) indicated that low density treatment could increase the conversion rate and output rate of stem and sheath substances and finally increased rice yield.

High yield and good quality of rice are the major goals in rice production and in transplanted rice production system, suitable transplant density is an important part to gain those two goals. Thus, we explored the process of photosynthesis, dry matter accumulation and transportation in order to study the response of super rice yield and quality under high transplant density in present study.

Materials and Methods

Plant materials and growing condition

A super hybrid rice variety, *Huahang31*, a well-known and widely grown in South China, were in planted during the late season (July-November) in 2010 and the early season (March-July) in 2011 at the College of Agriculture's Experimental Farm, South China Agricultural University (SCAU), Guangzhou, Guangdong Province, China (23°16' N, 113°23' E, elevation 11 m). The air temperature was shown in *Figure 1*.

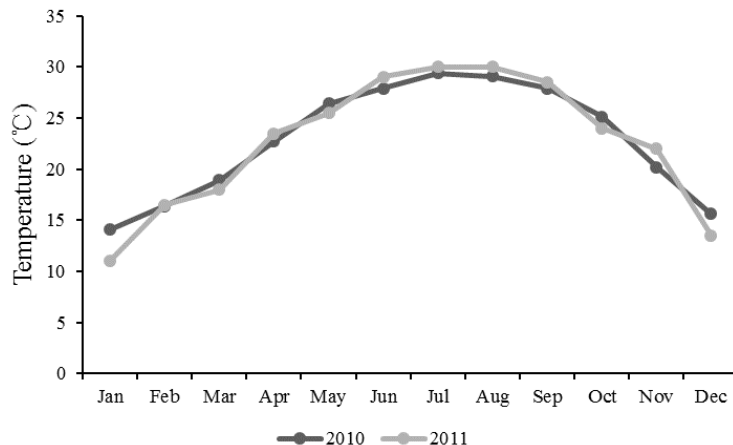


Figure 1. Mean monthly air temperature in Guangzhou during 2010 and 2011 (Annual average temperature in 2010 was 22.81°C and in 2011 was 22.63°C)

Before sowing, the seeds were soaked in water for 24 h, germinated in manual climatic box for the next 24 h, shade dried and the germinated seeds were sown in PVC trays for nursery raising. 15-day-old seedlings and 25-day-old seedlings were transplanted to the field in 2010 and 2011, respectively. The experimental soil has been planted rice for many years and it was sandy loam with of 16.80 g kg⁻¹ organic matter content, 1.032 g kg⁻¹ total N, 0.998 g kg⁻¹ total P, 13.598 g kg⁻¹ total K, 84.60 mg kg⁻¹ available N, 43.58 mg kg⁻¹ available P, and 106.10 mg kg⁻¹ available K.

Treatments descriptions

Three transplanted densities were applied at the experiment and set as blow.

- D1: Seedlings were transplanted at the rate of 2 seedlings per hill at a spacing of 20cm × 24cm, about 0.2085 million hills per hectare.
- D2: Seedlings were transplanted at the rate of 2 seedlings per hill at a spacing of 20cm × 20cm, about 0.2505 million hills per hectare.
- D3: Seedlings were transplanted at the rate of 2 seedlings per hill at a spacing of 20cm × 16cm, about 0.3120 million hills per hectare.

Commercial compound fertilizer (Total nitrogen contents TN = 15%, K₂O contents = 12%, P₂O₅ contents = 7.2%) was applied at the same amount of 1500 kg ha⁻¹. 80% of fertilizer was applied as basal and 20% was top-dressed at tillering stage.

Plant sampling and determination of biomass accumulation

At tillering stage, heading stage and maturity, the rice plants were harvested from fifteens hills in each plot. The leave, stems and grain were separated from the plants and dried Under the condition of 80°C respectively in order to get the estimation of dry matter. The output rate of stem matter (OPRS) was calculated as:

$$\text{OPRS} = \frac{(\text{stem weight at heading stage} - \text{stem weight at maturity})}{\text{stem weight at heading stage}} \quad (\text{Eq.1})$$

The conversion rate of stem matter (CRS) was calculated as:

$$\text{CRS} = \frac{(\text{stem weight at heading stage} - \text{stem weight at maturity})}{\text{grain weight at maturity}} \quad (\text{Eq.2})$$

The fresh grains were separated and collected from the rice plants 7th day after heading stage, washed with double distilled water and stored Under the condition of -80°C for the estimation of sucrose synthase (SS), soluble starch synthase (SSS) and Bound starch synthase (GBSS).

Determination of photosynthesis, SPAD and Leaf area index (LAI)

Portable photosynthesis system (LI-6400, LI-COR, USA) was used to determine net photosynthetic rate at 09:00–10:30 a.m. according to the standard method (Pan et al., 2016). SPAD meter ‘SPAD-502’ (Konica Minolta, Japan) was used for precise, rapid and non-destructive estimation of leaf chlorophyll contents. At tillering stage, heading stage and maturity, the rice plants were harvested from ten hills in each plot. The leaves were separated from main plants and the green leaves area was measured by a leaf area meter (CID-202, Lincoln, NE, USA) to determine the leaf area index (LAI).

Determination of activities of sucrose synthase (SS)

The activity of SS was measured according to the method described by Li et al. (2008). The activity of SS was determinate in both saturating and selective (limiting) conditions. The limiting assay consisted of the same reaction mixture except that 10 mmol L⁻¹ Pi was added and the concentrations of uridine diphosphate glucose

(UDPG), fructose, and glucose-6-P were reduced to 2, 2 and 10 mmol L⁻¹. The reaction was terminated by using 1 mol L⁻¹ NaOH and the mixture was boiled to degrade any unreacted fructose-6-P. After cooling, 0.20 mL of 0.1% (w/v) resorcinol in 95% ethanol and 0.80 mL of 9 mmol L⁻¹ HCl were added and the tubes were incubated at 80°C for 10 min. Three separate extractions of grain powder were assayed for the activities of enzymes. The activities of SS were shown as specific activities (g⁻¹ FW h⁻¹).

Determination of activities of soluble starch synthase (SSS) and granule-bound starch synthase (GBSS)

The activity of SSS and GBSS was determined by Nakamura and Yuki (1992). Twenty shelled grains of the same part were accurately weighed and placed in a pre-cooled mortar. The supernatant was extracted with 4 ml extract (containing 100 mmol L⁻¹ Ph7.5 Hepes-NaOH buffer, 8 mmol L⁻¹ MgCl₂ 6H₂O, 2 mmol L⁻¹ EDTA-Na₂, 12.5% (v/v) glycerol, 1% (w/v) PVP-40, 50 mmol L⁻¹ mercaptoethanol) by grinding in an ice bath. The supernatant was extracted by centrifugation at 12000 G for 30 min.

SSS activity determination: 1.5 ml centrifuge tube was taken and 20 ml crude enzyme solution was added in turn into 20 ml crude enzyme liquid, 36 µl reaction liquid A (containing 50 mmol L⁻¹ pH7.4 Hepes-NaOH, Hepes-NaOH, 1.6 mmol L⁻¹ ADPG, 0.7 mg amylose and 15 mmol L⁻¹ DTT) was reacted at 30°C for 20 minutes and then boiling water for 30 s to stopped reaction and ice bath cooled; 20 µl reaction liquid B (containing 50 mmol L⁻¹ pH7.4 Hepes-NaOH, 4 mmol L⁻¹ mmol L⁻¹ MgCl₂6H₂O and 1.2 unit pyruvate kinase reacted at 30°C for 20 minutes, then boiling water terminated the reaction for 30 seconds and centrifuged for 10000 g for 10 minutes. The supernatant was extracted at 60 µl and added to 43 µl reaction liquid C (containing 50 mmol L⁻¹ pH7.4 Hepes-NaOH, 10 mmol L⁻¹ glucose, 20 mmol L⁻¹ MgCl₂6H₂O, 2 mmol L⁻¹ NADP, 1.4 unit hexokinase and 0.35 unit glucose-6-phosphate dehydrogenase) for 10 minutes. The absorbance at 340 nm was determined after reaction at 30°C.

GBSS activity determination: The subsoil of SSS crude extract was washed twice with 1 ml extract and centrifuged for 20 minutes at 4°C for 3000 g. Then the crude enzyme solution of GBSS was obtained by centrifuging the 3 ml extract at 4°C for 24 hours and 12000 g at 2°C for 30 minutes. A 1.5 ml centrifugal tube was used, 20 µl GBSS crude enzyme was added in turn, 36 µl reaction liquid A (containing 50 mmol L⁻¹ pH7.4 Hepes-NaOH, 1.6 mmol L⁻¹ ADPG, 15 mmol L⁻¹ DTT), the other two reaction liquids and reaction process were the same as SSS determination.

Estimation of rice yield and related attributes

At maturity stage, the rice grains were harvested from ten unit sampling area (10.00 m²) in each plot and then threshed by machine. The harvested grains were sundried and weighed in order to determinate the grain yield. Twenty hills of rice from different locations in each plot were sampled for estimating the average effective panicles number per hill. Then, three hills representative plants were taken for estimation of the yield related traits.

Estimation of grain quality

Dry grains were stored at room temperature for two months to determine grain quality attributes. About 1.00 kg rice grains from each treatment was taken from storage and brown rice rate was determined by rice huller (Jiangsu, China) while brown rice and

head rice rates were calculated by using a Jingmi testing rice grader (Zhejiang, China). Grains with chalkiness and chalkiness degree were determined using an SDE-A light box (Guangzhou, China) while an Infratec-1241 grain analyzer (FOSS-TECATOR) was used to measure the grain amylose and protein contents.

Statistical analysis

Data were analyzed by using statistical software ‘Statistix 8.1’ (Analytical Software, Tallahassee, FL, USA) while differences amongst means were separated by using least significant difference (LSD) test at 5% probability level. Graphical representation was conducted via Sigma Plot 14.0 (Systat Software Inc., California, USA).

Result

Yield and yield components

As shown in *Table 1*, transplant densities affected rice yield and its components differently. High density could significantly increase panicle number and the highest panicle number was recorded in D3 in both years. However, we observed that the lowest yield was recorded in D3 for 2010 and 2011 and the yield in D3 was significantly lower than D1. The decrement of yield was due to the reduction in both grains number and seed setting rate. Compared to D1, D3 treatment remarkably reduced seed setting rate and grain number. Moreover, there was no significant difference among D1, D2 and D3 in 1000-grain weight.

Table 1. Effect of transplant densities on rice yield and its components

Year	Transplant density	Panicle number 10 ⁴ hm ⁻²	Grain number per panicle	Seed setting rate (%)	1000-grain weight (g)	Yield (t ha ⁻²)
2010	D1	270.83b	132.33a	88.56a	22.99a	7.30a
	D2	271.67b	133.67a	88.18a	23.37a	6.92b
	D3	295.14a	120.00b	87.90b	23.26a	7.02b
2011	D1	230.67c	153.33a	91.25a	23.43a	7.70a
	D2	273.33b	138.00b	88.18b	23.49a	7.55a
	D3	298.00a	117.67c	88.57b	23.29a	7.12b
Analysis of variance						
	Density (D)	**	**	ns	ns	ns
	Year (Y)	ns	ns	*	**	*
	D × Y	ns	ns	ns	*	ns

Data are expressed as the mean of three replications. Values followed by different letters within the same column are significant different at $P < 0.05$ probability level. NS means non-significant differences; * and ** indicated significant differences at 0.05 and 0.01 probability levels, respectively. The same as belowed

Grain quality and its attributes

As shown in *Table 2*, there was no significant difference among D1, D2 and D3 in both brown rice rate and head rice rate. However, compared to D1 treatment, D2 and D3 treatments significant increased chalky rice rate in 2010 and 2011. D3 treatment also

increased chalkiness remarkably for both years. Furthermore, the lower amylose content was recorded in D3 than D1 for 2010 and 2011.

Table 2. Effect of transplant densities on grain quality and its attributes

Year	Transplant density	Brown rice rate (%)	Head rice rate (%)	Chalky rice rate (%)	Chalkiness (%)	Amylose content (%)
2010	D1	81.72a	44.64a	4.00b	2.13b	18.07a
	D2	81.55a	43.64a	5.33a	3.35a	18.10a
	D3	81.82a	45.80a	5.67a	3.6a	17.77b
2011	D1	80.67a	41.99a	8.00b	5.10b	18.00a
	D2	80.57a	40.65a	10.67a	5.33ab	18.00a
	D3	80.80a	42.67a	11.33a	5.70a	17.80b
Analysis of variance						
	Density (D)	**	ns	*	*	*
	Year (Y)	**	**	**	*	ns
	D × Y	ns	ns	*	**	ns

Net photosynthetic rate, LAI and SPAD values

The difference in transplant density could significantly affect rice photosynthesis (Figure 2). At tillering stage, heading stage and maturity in 2010, the net photosynthetic rate in D3 was significantly lower than D1 whilst in 2011, only at heading stage the net photosynthetic rate in D3 was remarkably lower than D1. Compared to D1, D3 treatment significantly decreased LAI values at heading stage for both years. Furthermore, we observed that the SPAD values in D2 and D3 were remarkably lower than D1 at heading stage and maturity in 2010. However, in 2011, there was no significant difference among D1, D2 and D3 in all growth stages.

Dry matter accumulation and transportation

As shown in Table 3, different densities affected dry matter weight differently. At tillering stage, D3 density significantly decreased leaf weight and stem weight compared to D1 in 2010. The leaf weight, stem weight and grain weight at both heading stage and maturity in D3 were remarkably lower than D1 for 2010 and 2011. Furthermore, we observed that high density (D3) had negative impact on transportation of stem matter while the lowest OPRS and CRS were also recorded in D3 treatments for both years while there was no significant difference between D1 and D2.

Enzymes involved sucrose biosynthesis

As shown in Figure 3, different densities affected sucrose biosynthesis in grain in terms of SS, SSS and GBSS activities. For SS activity, D3 and D2 had lower acidity than D1 in 2010 while the trend in 2011 was recorded as: D1 > D2 > D3. Compared to D1, D3 treatment also significant decreased the GBSS and SSS activity in 2010 whilst in 2011, there was no significant difference among D1, D2 and D3 in both GBSS and SSS activity.

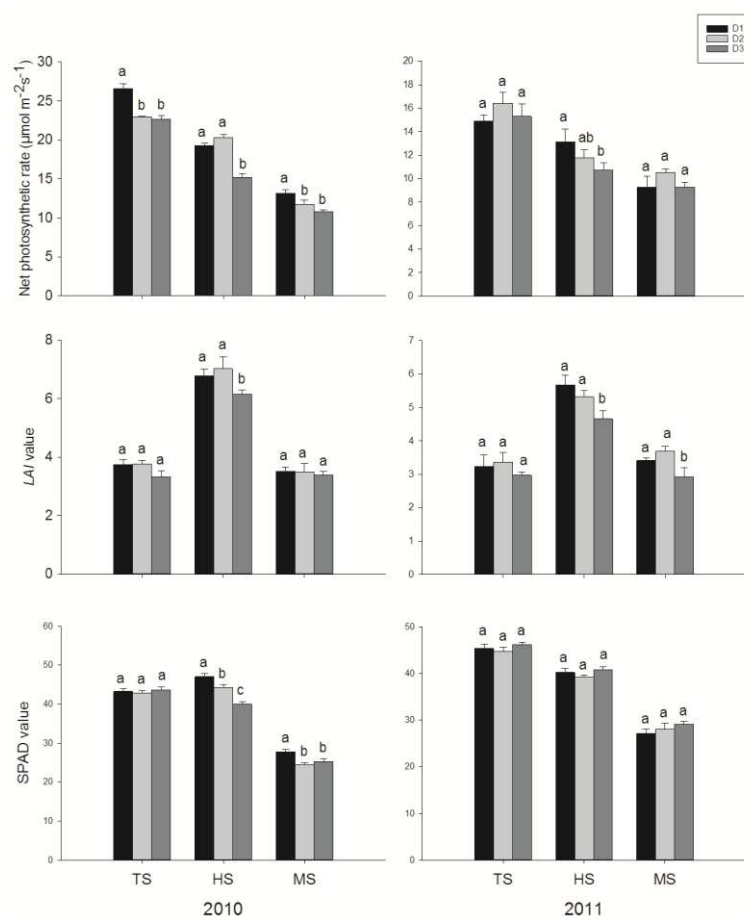


Figure 2. Effect of transplant densities on net photosynthetic rate, LAI and SPAD values. Capped bars represent S.E. of three replicates. Means sharing a common letter don't differ significantly at ($P \leq 0.05$) according to least significant difference (LSD) test for both the years. The same as below

Table 3. Effect of transplant densities on dry matter accumulation and transportation

Year	Transplant density	TS		HS			MS			OPRS (%)	CRS (%)
		Leaf weight (g hill ⁻¹)	Stem weight (g hill ⁻¹)	Leaf weight (g hill ⁻¹)	Stem weight (g hill ⁻¹)	Grain weight (g hill ⁻¹)	Leaf weight (g hill ⁻¹)	Stem weight (g hill ⁻¹)	Grain weight (g hill ⁻¹)		
2010	D1	7.74a	6.16a	14.07a	29.69a	9.02a	10.69a	24.36a	36.10a	17.95a	19.68a
	D2	6.38b	5.73a	13.11a	25.25b	6.62b	9.07b	19.27b	33.08a	23.68a	22.60a
	D3	4.97c	4.77b	8.50b	15.95c	4.71c	7.43c	15.62b	29.31b	2.07b	1.34b
2011	D1	7.22a	6.16a	11.85a	22.02ab	18.49a	11.85a	18.74a	47.66a	14.90a	11.24a
	D2	6.90a	5.42a	12.21a	23.15a	17.88ab	12.21a	19.94a	53.52a	13.87a	10.01a
	D3	6.59a	6.34a	9.46b	18.64b	12.45b	9.46b	16.51b	38.25b	11.43b	8.26b
Analysis of variance											
	Density (D)	**	ns	**	**	**	**	**	*	**	**
	Year (Y)	ns	ns	ns	ns	**	ns	ns	**	**	**
	D × Y	ns	ns	ns	*	ns	ns	ns	**	**	**

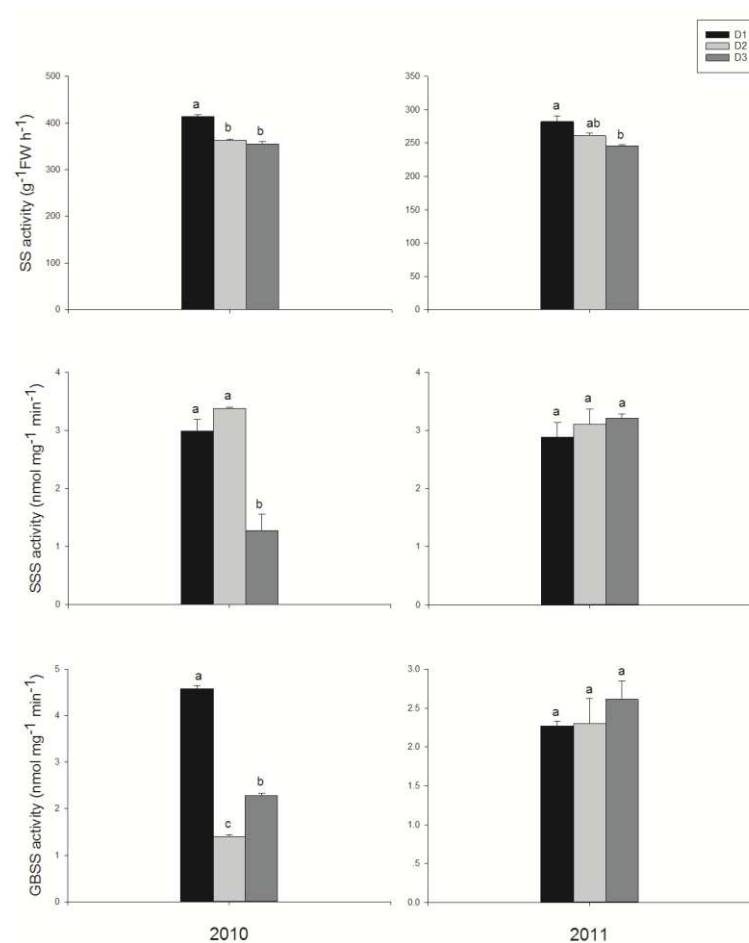


Figure 3. Effect of transplant densities on SS, SSS and GBSS activity

Discussion

A suitable plant density is one of the decisive factors for harvesting higher grain yield in rice production (Peng et al., 2018; Lee et al., 2018). Normally, the transplant density determines the competition of nutrients such as photosynthesis and fertilizer uptake among rice individuals in the middle and late growth stages among different rice individuals. In our study, we observed that compared to D1, D2 density significantly decreased rice yield in 2010 but there was no difference between D1 and D2. The D3 density remarkably reduced yield by decreasing the grain number and seed setting rate in both years. Present study showed that high density was able to significantly increase panicle number in paddy field, but it would also have negative impacts on other yield components and then still cause the yield loss without yield increment. Similar result was also reported by Zhao (2011) who demonstrated that the yield of super rice, *Y-liangyou 302*, was mainly affected by panicles and spikelets per panicle, while the spike length and 1000-grain weight did not showed any significant influence on yield and high nitrogen and low planting density is conducive to increase the yield of rice variety *Y-liangyou 302* in north region of Guangxi. The further reason in reduction of yield might be the increment in competition for photosynthesis among rice individuals under high density. Present study showed that D3 treatment not only decreased the net

photosynthetic rate, but also reduced the *LAI* values. Leaf area index (*LAI*) is an important parameter in crop growth status monitoring and yield forecasting (Xue and Wang, 2004). Normally, the values of *LAI* and net photosynthetic rate represent the intensity of population photosynthesis. In our study, the result indicated that the lower population photosynthesis under high density induced the decrement in dry matter accumulation and inadequate supply of dry matter eventually led to a decline in production. Our finding was also consistent with the research of Sultana et al. (2001) who indicated that dry matter accumulation was an important factor in determining rice yield.

Furthermore, worse grain quality was recorded in D3 treatment than D1. Present study revealed that not only D2 and D3 densities would increase both chalky rice rate and chalkiness, but also D3 density would significantly decreased amylose content. The increment in chalkiness and chalky rice rate might be due to the decrement of net photosynthetic rate at heading stage and the matter transportation from stem to grain. The study of Mo et al. (2015) showed that photosynthesis during the filling stage might had a great impact on grain chalkiness of rice. In 2015, the study of Zhou et al. (2015) found that there was a positive correlation among low amylose content, high degree of endosperm chalkiness and percentage of grains with chalkiness in grain and similar conditions were also observed in our study. The lower amylose content in D3 than D1 could be explained by the reduction in SS activity. Moreover, lower OPRS, CRS and net photosynthetic rate in heading stage also could be responsible for amylose content decrement.

Conclusion

Present study showed that high transplanted reduced the rice photosynthesis decreased the dry matter accumulation and transportation and finally caused the loss of grain yield. For revealing the mechanism of rice yield and quality formation by transplant density treatments, much work should be done at molecular and physiological level at the field trials.

Acknowledgements. This study was supported by Guangdong science and technology planning project (2011AO2020001), National Natural Science Foundation of China (31271646), the World Bank Loan Agricultural Pollution Control Project in Guangdong (0724-1510A08N3684) and the Technology System of Modern Agricultural Industry in Guangdong (2017LM1098).

REFERENCES

- [1] Hayashi, S., Kamoshita, A., Yamagishi, J. (2006): Effect of planting density on grain yield and water productivity of rice (*Oryza sativa* L.) grown in flooded and non-flooded fields in Japan. – *Plant Production Science* 9: 298-311.
- [2] Huang, M., Chen, J., Cao, F., Zou, Y. (2018): Increased hill density can compensate for yield loss from reduced nitrogen input in machine-transplanted double-cropped rice. – *Field Crops Research* 221: 333-338.
- [3] Lee, J., Wissuwa, M., Zamora, O. B., Ismail, A. M. (2018): Novel Sources of aus Rice for Zinc Deficiency Tolerance Identified Through Association Analysis Using High-Density SNP Array. – *Rice Science* 25: 293-296.

- [4] Li, J. Y., Liu, X. H., Cai, Q. S., Gu, H., Zhang, S. S., Wu, Y. Y., Wang, C. J. (2008): Effects of Elevated CO₂ on Growth, Carbon Assimilation, Photosynthate Accumulation and Related Enzymes in Rice Leaves during Sink-Source Transition. – *Journal of Integrative Plant Biology* 50: 723-732.
- [5] Mo, Z., Li, W., Pan, S., Fitzgerald, T. L., Xiao, F., Tang, Y., Wang, Y., Duan, M., Tian, H., Tang, X. (2015): Shading during the grain filling period increases 2-acetyl-1-pyrroline content in fragrant rice. – *Rice* 8: 1-10.
- [6] Mobasser, H. R., Yadi, R., Azizi, M., Ghanbari, A. M., Samdaliri, M. (2009): Effect of density on morphological characteristics related-lodging on yield and yield components in varieties rice (*Oryza sativa* L.) in Iran. – *American-Eurasian Journal of Agricultural and Environmental Science*.
- [7] Nakamura, Y., Yuki, K. (1992): Changes in enzyme activities associated with carbohydrate metabolism during the development of rice endosperm. – *Plant Science* 82: 15-20.
- [8] Pan, S., Liu, H., Mo, Z., Patterson, B., Duan, M., Tian, H., Hu, S., Tang, X. (2016): Effects of Nitrogen and Shading on Root Morphologies, Nutrient Accumulation, and Photosynthetic Parameters in Different Rice Genotypes. – *Scientific Reports* 6.
- [9] Peng, B., Feng, G. N., Zhen, Q., Qiu, M. (2018): EFFECTS OF OZONE AND DENSITY INTERACTION ON THE GROWTH, DEVELOPMENT AND YIELD FORMATION OF RICE. – *Applied Ecology and Environmental Research* 16: 4199-4215.
- [10] Sultana, N., Ikeda, T., Kashem, M. A. (2001): Effect of foliar spray of nutrient solutions on photosynthesis, dry matter accumulation and yield in seawater-stressed rice. – *Environmental & Experimental Botany* 46: 129-140.
- [11] Tang, S., Zhang, H., Liu, W., Dou, Z., Zhou, Q., Chen, W., Wang, S., Ding, Y. (2019): Nitrogen fertilizer at heading stage effectively compensates for the deterioration of rice quality by affecting the starch-related properties under elevated temperatures. – *Food Chemistry* 277: 455-462.
- [12] Tao, F., Palosuo, T., Valkama, E., Makipaa, R. (2019): Cropland soils in China have a large potential for carbon sequestration based It on literature survey. – *Soil & Tillage Research* 186: 70-78.
- [13] Tareq, T. M., Rahman, M. S., Jewel, N. A., Islam, T., Shimono, H., Seraj, Z. I. (2018): Relative Response of Indigenous Rice Genotypes to Low Versus Normal Planting Density for Determination of Differential Phenotypic Plasticity in Traits Related to Grain Yield. – *Plant Tissue Culture & Biotechnology* 28: 109-124.
- [14] Xue, L. H., Wang, S. H. (2004): Relationship between spectral vegetation indices and LAI in rice. – *Acta Phytocologica Sinica* 28: 47-52.
- [15] Yuan, L. (2001): The Strategy for Hybrid Rice Development. – *Hybrid Rice* 4-6.
- [16] Zhao, R. D. (2011): Effects of transplanting density and nitrogen fertilizer rate on yield and its components in super-high-yielding early rice variety Y-liangyou 302. – *Journal of Southern Agriculture*.
- [17] Zhou, L., Liang, S., Ponce, K., Marundon, S., Ye, G., Zhao, X. (2015): Factors affecting head rice yield and chalkiness in indica rice. – *Field Crops Research* 172: 1-10.
- [18] Zhou, C., Huang, Y., Jia, B., Wang, Y., Wang, Y., Xu, Q., Li, R., Wang, S., Dou, F. (2018): Effects of Cultivar, Nitrogen Rate, and Planting Density on Rice-Grain Quality. – *Agronomy-Basel* 8.

APPENDIX



Figure A1. Photo of the experiment

PROTEASE PRODUCING *PSEUDOMONAS AERUGINOSA* STRAIN (IBC-2) FROM COAL MINES OF ORAKZAI AGENCY, PAKISTAN

AFRIDI, M. I.¹ – ALI, N.^{1*} – MEMON, A. R.² – QASIM, M.³ – JAMAL, Q.³ – KHATTAK, B.³ –
ADNAN, M.⁴ – KHAN, S. N.⁵ – ULLAH, A.⁶ – YOUNAS, F.⁷ – ULLAH, F.⁸

¹*Department of Biotechnology and Genetic Engineering, Kohat University of Science & Technology (KUST), 26000 Kohat, Pakistan*

²*Department of Biochemistry, Liaquat Medical University of Health Sciences Jamshoro 76090 Sindh, Pakistan*

³*Department of Microbiology, Kohat University of Science & Technology (KUST) 26000 Kohat, Pakistan*

⁴*Department of Botany, Kohat University of Science & Technology (KUST) 26000 Kohat, Pakistan*

⁵*Department of Zoology, Kohat University of Science & Technology (KUST) 26000 Kohat, Pakistan*

⁶*Department of Pharmacy, Forman Christian College, Lahore, Pakistan*

⁷*Sulaiman Bin Abdullah Aba Al-Khail Center for Interdisciplinary Research in Basic Sciences (SA-CIRBS), International Islamic University, Islamabad, Pakistan*

⁸*Department of Biosciences, COMSATS University (CIIT), 45550 Islamabad, Pakistan*

**Corresponding author*

e-mail: nawabali_1857@yahoo.com; phone: +92-344-303-5006; fax: +92-922-554-556

(Received 31st Oct 2018; accepted 8th Feb 2019)

Abstract. Microbial proteolytic enzymes are used to hydrolyze proteins in various bio-industrial applications but most of the enzymes are not active in extreme temperature conditions, pH and salt concentrations. This increases the demand to explore enzymes to show activity at such extreme environments. Exciting findings have been described about the extremophilic bacteria isolated first time from coal mines of Orakzai Agency, Pakistan, having protease producing properties. Among various extracted isolates, ~6 isolates were purified based on showing proteolytic activity using 2% skim milk agar media at 37 °C for 24 hrs, to identify various morphological and biochemical characteristics. The isolate, IBC-2 showed maximum zonal activity (21 mm) and was identified as *Pseudomonas aeruginosa* (JCM 5962) using 16S rRNA gene sequencing. The strain IBC-2 exhibited significantly ($P \leq 0.05$) maximum growth and protease production (335 U/ml) at 37 °C and at pH 7 after 24 hrs of incubation. The strain was also significantly ($P \leq 0.05$) more active for protease production at neutral pH (435 U/ml) than at high or low pH, reflected neutral nature of the bacteria. In conclusion, the strain IBC-2 has highest protease producing ability with distinctiveness, which can be used for wide range bio-industrial applications.

Keywords: *extremophiles, gram negative bacteria, 16s rRNA, proteolytic enzyme, natural resource*

Introduction

Microbial proteases are widely used for various physiological and biochemical purposes in a variety of industrial applications worldwide. Proteases having proteolytic

nature, catalyze the breakdown of peptide bonds between amino acids forming proteins (Rawlings and Barrett, 2013). The overwhelming importance of proteases is due to substrate specificity, active site, catalytic mechanism and stability (Maurer, 2004). Owing to various industrial applications, proteases have marked contribution among global enzyme market (Maurer, 2004).

Commercially, protease has many applications in leather, food and pharmaceutical industries as well as also used for bioremediation purposes (Jellouli et al., 2009; Kirk et al., 2002). Two third of the commercial proteases have been collected from microbial sources (Gupta et al., 2002). Commercial proteases are mostly obtained from bacterial origin and there are copious bacterial strains having protease producing potential, such as *Flavobacterium clostridium*, *Achromobacter*, *Actinomyces species*, *Staphylococcus aureas* and *Thermoactinomyces including Pseudomonas aurigenosa* (Prakasham et al., 2006). Bacterial proteases are usually preferred source over other sources like plant and animal on the basis of fast-growing nature as well as require minimum space for culturing. Moreover, they can be easily modified genetically for large scale purification compared to plants and animals, in order to get new enzymes with assorted characteristics (Gupta et al., 2002).

Currently, very limited (1-2%) microbes have been explored having commercial importance including extremophiles as well. Extremophiles can significantly tolerate a wide range of environmental conditions like high or low temperature (-2-121 °C), acidic and basic pH, high saline stress, a wide range of radiation as well as unusual conditions such as drought and nutrients limitations (Gomes and Steiner, 2004; Jadhav et al., 2013). In present time, researcher have focused their keen interest to investigate microbes of novel extremophile characteristics having distinctive adaptation and products that further used in stern industrial conditions. Therefore, microbes of such extreme environments need to be targeted and to be screened for novel extremozymes activities.

Coal mines are among those sources that can provides such acid-tolerant and obligate acidophilic extremophiles bacteria (Johnson and McGinness, 1991) and have greater odds to explore novel species in such hostile environments (Roohi et al., 2014). Interestingly, our lab also reported some novel halotolerant bacterial strains from salt mines of Karak (Pakistan) that have significant potential to produce both protease and amylase enzymes (Ali et al., 2016; Shah et al., 2017). Therefore, this further increased our incessant curiosity for exploring cheap microbial source of extremozymes in coal mines.

Materials and methods

Sampling and isolation of bacterial strains

The coal samples (500 g) were collected from the coal mines of Feroz Khel (33.885652°N 71.187346°E); located in Orakzai Agency, Kyber Pakhtunkhwa, Pakistan in sterilized plastic boxes and transported to laboratory (Department of Microbiology, KUST Kohat) for further processing. Before isolation, entire samples of coal were crushed using a clean & sterilized grinder and powdered samples were serially diluted to 10⁻³, 10⁻⁶ and 10⁻⁹ working solutions in sterilized autoclaved distilled water. The dilutions were cultured on nutrient agar plates using pour-plate technique. The colonies having contrasting culture features (n = 62) were sub cultured by frequent streaking at

same conditions to acquire pure colonies or isolates (Jamal et al., 2016; Roohi et al., 2012).

Screening and identification of proteolytic isolates

Pure isolates (n = 6) were observed for proteolytic activities using 2% skim milk (SM) agar media incubated at 37 °C for 24 hrs (Xiong et al., 2007) following Bergey's manual of systematic bacteriology for morphological and biochemical properties (Buchanan and Gibbons, 1974). Despite of producing larger proteolytic inhibitory zone and other differences like shape and color of colony, the zone of the IBC-2 was very clear comparative to IBC-5 (little turbid) which makes IBC-2 a best choice for our onward analysis (*Table 1; Figs. 1 and S1*). Moreover, 16S rRNA sequence analysis was performed for further recognition of the chosen IBC-2 strain(s). Genomic DNA was extracted from IBC-2 strain(s) using phenol/chloroform method (Ali et al., 2016) and was amplified against 16S rRNA universal primer; 9F (5'-GA GT TT GA TC CT GG CT CA G-3') and 1510R (5'-GG CT AC CT TG TT AC GA-3') using DreamTaq™ Green PCR Master Mix (2X) (Thermo Scientific™) as described by Ali et al. (2016). The thermocycler (Veriti™ Applied Biosystems, Foster City, CA, USA) conditions were; a single cycle of initial denaturation (96 °C for 5 min), followed by 25 cycles (95 °C for 45 s, 52 °C for 45 s and 72 °C for 90 s), while the final elongation phase was performed at 72 °C for 10 min. The PCR amplified product of IBC-2 strain(s) was confirmed on 2% agarose gel followed by sequencing from Macrogen Lab, South Korea (<http://dna.macrogen.com/eng/index.jsp>). The bacterial strain (IBC-2) was BLAST on the server EZ-Biocloud (EZ-Taxon) in order to find out nomenclature (Yoon et al., 2017), whereas the phylogenetic tree was constructed using bioinformatics software MEGA 6.0 (Molecular Evolutionary Genetics Analysis version 6.0) (Tamura et al., 2013).

Partial purification and quantification of protease enzyme

For partial purification of protease enzyme, 1 ml of fresh inoculum was added to 2% SM broth media and was subjected to incubation at 37 °C for 36 hrs using shaking incubator. The cellular enzymes were partially purified by centrifugation of culture for 20 min at 4 °C for 4000g using filter injection (22 µ). Furthermore, ammonium sulphate (70% w/v) precipitation of enzymes was performed from supernatant overnight at 4 °C in a shaking incubator followed by centrifugation (4000g) at 4 °C. The pellets were dissolved in sterile water that were tested for their proteolytic activity (Nadeem et al., 2007).

Moreover, for protease quantification, a modified assay described by Nadeem et al. (2007) was used. Briefly, 1 ml (2% w/v) of the substrate casein (0.05 M glycine-NaOH pH 10) and 1 ml of crude enzyme were incubated at 40 °C for 20 min. The reaction was stopped by adding 3 ml of 10% (w/v) trichloro acetic acid (TCA) at room temperature for 30 min followed by centrifugation (100g) for 10 min at 4 °C. Afterwards, 0.5 ml supernatant was taken and dissolved in 4.5 ml of 0.05 M glycine-NaOH buffer (pH 10) and the absorbance were checked spectrophotometrically (UV-VIS 1800, Shimadzu, Kyoto, Japan) at 280 nm. The calibration curve was plotted using tyrosine (CAS number 60-18-4, Sigma Aldrich, USA) as standard on increasing concentrations of tyrosine such as 1, 2, 3, 4, 5 and 6 µg dissolved in 0.05 M glycine-NaOH buffer. One

proteolytic unit (1U) was defined as the quantity of the enzyme that released 1 µg of tyrosine each minute under the defined assay conditions.

Table 1. Isolate (IBC-2) showing casein hydrolysis zone formation on skim milk agar (2%) plate

Bacterial isolates	Colony color	Colony shape	Proteolytic zone (mm)
IBC-1	Off white	Circular	17.5
IBC-2	White	Irregular	21
IBC-5	Off white	Circular	20.5
IBC-6	Off white	Circular	18
IBC-7	Off white	Circular	18.5
IBC-10	Yellow	Circular	19

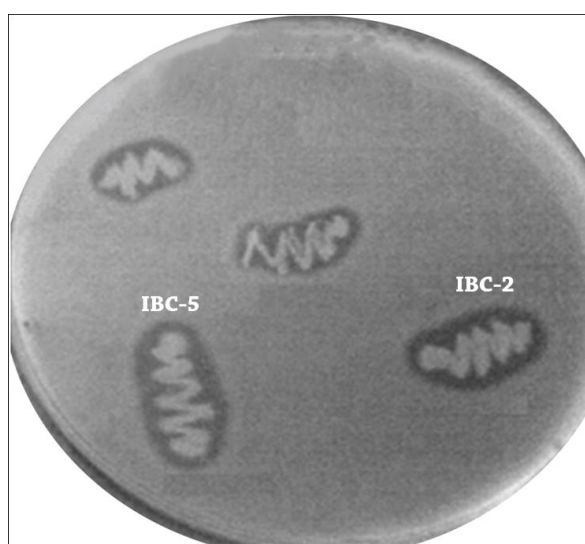


Figure 1. Isolate (IBC-2) showing casein hydrolysis zone formation on skim milk agar (2%) plate



Figure S1. Different proteolytic isolates have different shape and color of colony

Electrophoretic protease separation

Molecular weight of the protease was determined using SDS-PAGE (12%) as depicted by Laemmli (1970). The protease enzyme (partially purified) was assayed

with loading dye (0.5 M Tris–HCl pH 8.0, SDS 10% (w/v), glycerol 6% (v/v), 2- β -mercaptoethanol and bromophenol blue 0.3% (v/v) after heating at 95 °C for 5 min. The crude protease was resolved with Pre-stained PageRuler™ Protein Ladder 10–180 KDa (Thermo Fisher Scientific™, Rockford, IL, USA) at 120 V for 2-2.5 hrs using Bio-Rad Mini Gel apparatus (Bio-Rad, Hercules, CA, USA). After resolving, SDS-PAGE, gel was stained by Coomassie Brilliant Blue (R-250) and proteins (protease enzyme) bands patterns were observed using white light apparatus.

Growth optimization

The isolate IBC-2 had been further optimized for its growth and protease production at varying physical factors. Pure inoculum (1 ml) of IBC-2 strain(s) was grown in Lauria-Bertani (LB) culture media (50 ml) under different incubation temperatures such as 20, 37, 50 and 60 °C using discrete media pH like 4, 5, 7, 9 and 11. After 24 hrs incubation, optimum growth of bacteria and protease production was calculated at 600 nm and the protease production was measured as per assay procedure (Ali et al., 2016).

Statistical analysis

All tests were carried out in replicates (n = 3) and statistically analyzed using SPSS v.21 (IBM SPSS Inc., Chicago, IL, USA). The results were taken in means and standard error (SE), while Tukey's honest significant difference (HSD) post hoc test were applied using ANOVAs.

Results

Identification and proteolytic potential of IBC-2 bacterial strain

In current study, a total of sixty-two (n = 62) bacterial strains were isolated, first time from coal mines of Orakzai Agency. Among them, thirty-three (n = 33) exhibit proteolytic zones (11-15 mm) but six (n = 6) out of thirty-three (n = 33) had a great potential of producing inhibitory zone with more than 15 mm (*Table 1*) (Sharmin et al., 2005). All the selected six isolates were further analyzed through biochemical and morphological identity (*Tables 1 and 2; Fig. 1*) for tentative identification. Because of largest and clear inhibitory zone, the isolate IBC-2 was with rod shaped, gram negative and showed positive tests for oxidase, catalase and gelatinase that was tentatively acknowledged as *Pseudomonas* (*Tables 1 and 2; Fig. 1*) and was selected to analysed further for their proteolytic optimization and molecular identification of the strain.

Molecular and phylogenetic analysis of isolate IBC-2

The isolate regarding IBC-2, were further evaluated at molecular level (*Fig. 2*). DNA extracted from IBC-2 isolate was amplified with 16S rRNA specific marker from EZ-Taxon server, bearing 99% sequence similarity with *Pseudomonas aeruginosa* JCM 5962(T) with accession number BAMA01000316. Moreover, phylogenetic tree demonstrated that IBC-2 strain is closely allied with *Pseudomonas aeruginosa* JCM 5962(T) as illustrated in *Figure 3*. The phylogenetic analysis involved 63 nucleotide sequences that targets 990 positions and data with gaps were removed after alignment by CLUSTAL X.

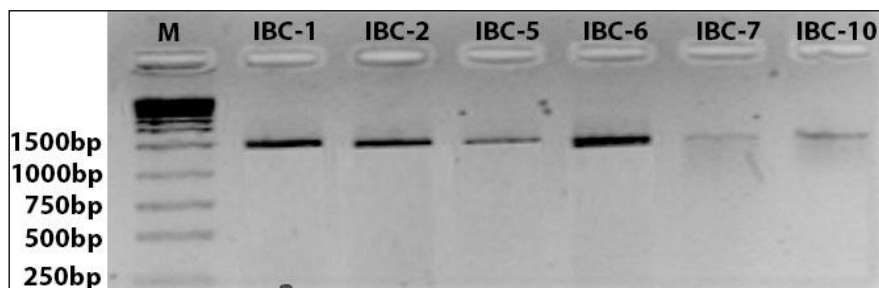


Figure 2. PCR amplification of 16S rRNA (1.5 K bp) from IBC-2 isolate

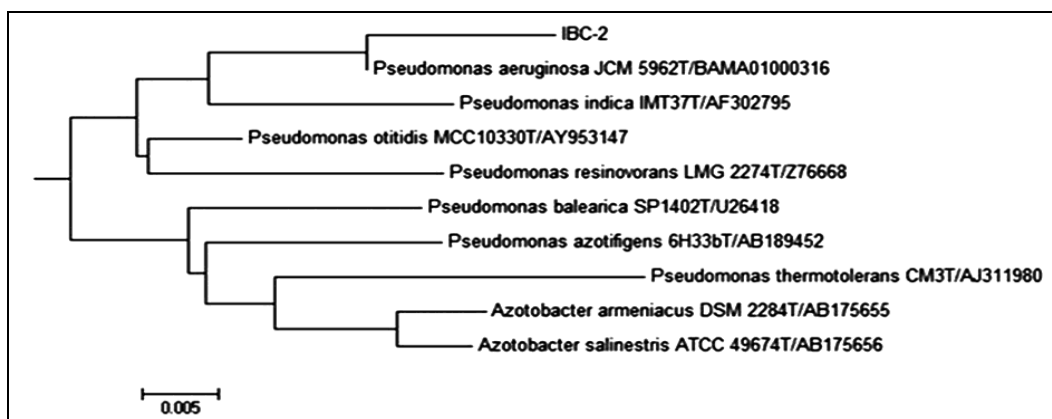


Figure 3. Phylogenetic tree showing the interrelationships of isolate IBC-2 and its close relatives inferred from 16SrRNA gene sequence. (Evolutionary analysis was conducted in MEGA 6. Scale bar = 0.005 changes per nucleotide position)

Table 2. Tentative identification of the selected isolates (n = 6) on the basis of gram staining and different biochemical tests

Bacterial isolates	Gram staining/shape	Oxidase	Catalase	Citralase	Sugar fermenter	Gas formation	H ₂ S formation	Motility test	Indole test	Urease test	Tentative identification (genus)
IBC-1	Gram -ve rod shape	+	+	+	+	+	-	+	-	-	<i>Pseudomonas spp.</i>
IBC-2	Gram -ve rod shape	+	+	+	+	+	-	+	-	-	<i>Pseudomonas spp.</i>
IBC-5	Gram -ve rod shape	+	+	+	+	+	-	+	-	-	<i>Pseudomonas spp.</i>
IBC-6	Gram +ve rod shape	-	+	+	-	+	-	+	-	+	<i>Bacillus spp.</i>
IBC-7	Gram -ve rod shape	+	+	+	+	+	-	+	+	+	<i>Proteobacteria spp.</i>
IBC-10	Gram +ve cocci	-	+	-	+	+	-	-	-	+	<i>Staphylococcus spp.</i>

Enzymatic activity and SDS-PAGE analysis of protease enzyme

The enzymatic activities of partially purified enzymes from all six (n = 6) bacterial isolate were spectrophotometrically performed. Among these, the isolate IBC-2 showed significantly higher proteolytic activity (300 U/ml) compared to other isolates (Fig. 4).

Moreover, all isolates were further resolved using polyacrylamide/bis-acrylamide (SDS-PAGE) and confirmed that the isolate IBC-2 belongs from *Pseudomonas aeruginosa* (30-50 KDa; Fig. 5) as per reported literature (Aqel et al., 2009; Dutta and Banerjee, 2006; Raj et al., 2012; Sevinc and Demirkan, 2011; Zambare et al., 2010).

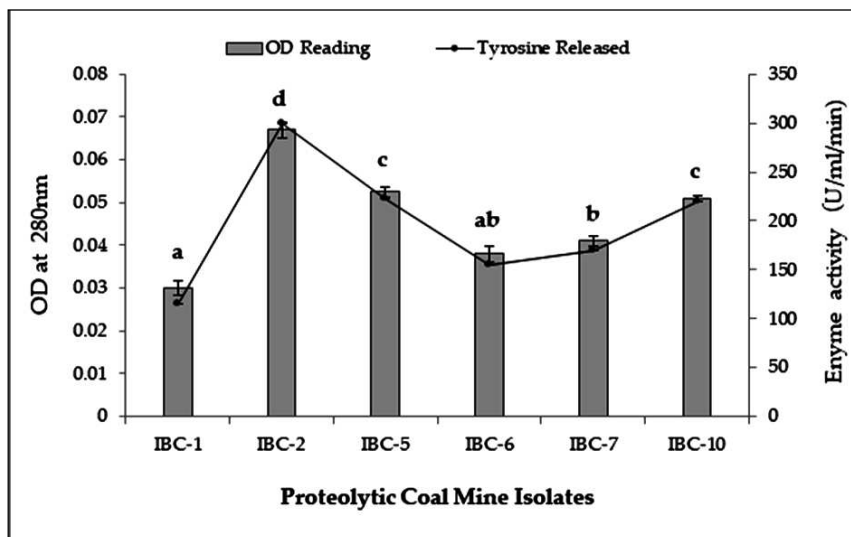


Figure 4. Enzyme quantification of the six (IBC 1, 2, 5, 6, 7 and 10) proteolytic coal mine isolates. Data shown in bars represents mean OD of replicates ($n = 3$). Different alphabetical letters represent statistically significant differences (based on ANOVA) among the different isolates according to Tukey's honest significant difference (HSD) post-hoc test ($P \leq 0.05$)

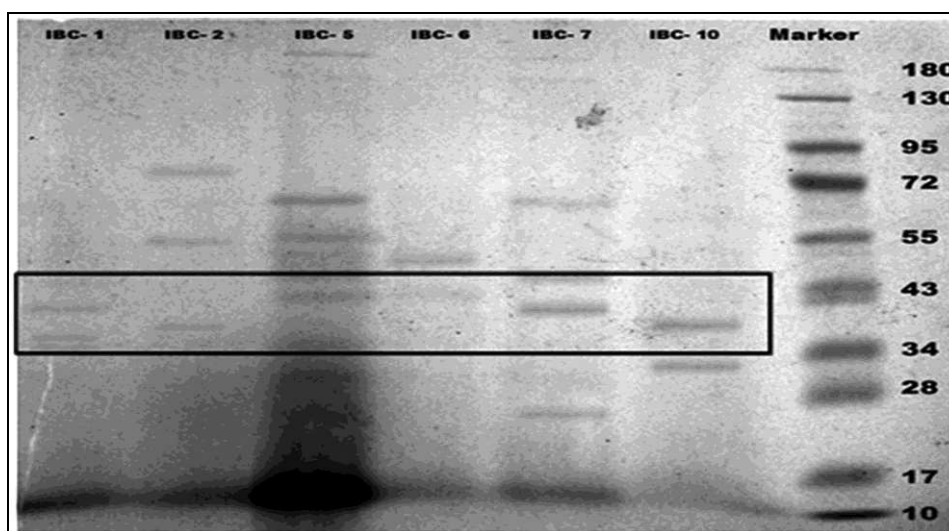


Figure 5. SDS-PAGE gel analysis of partially purified protease enzymes extracted from different isolates of coal bacteria

Growth optimization and protease production of selected IBC-2 isolates

The optimum growth factors (temperature and pH) were calculated for the selected IBC-2 isolates using varying degree of temperature (20, 37, 50 and 60 °C) and pH (4-

11) in order to find out optimum bacterial growth and protease production using similar conditions in each case. Among the isolated bacterial stains, IBC-2 showed highest growth concentration at 37 °C at 600 nm after 24 hrs of incubation. Incubation at dissimilar temperatures notably affects the growth as well as protease production of the bacteria and in our study and maximum protease production (335 U/ml) was recorded at 37 °C while at temperatures lower or higher than 37 °C, low growth and lesser protease production was observed (Fig. 6).

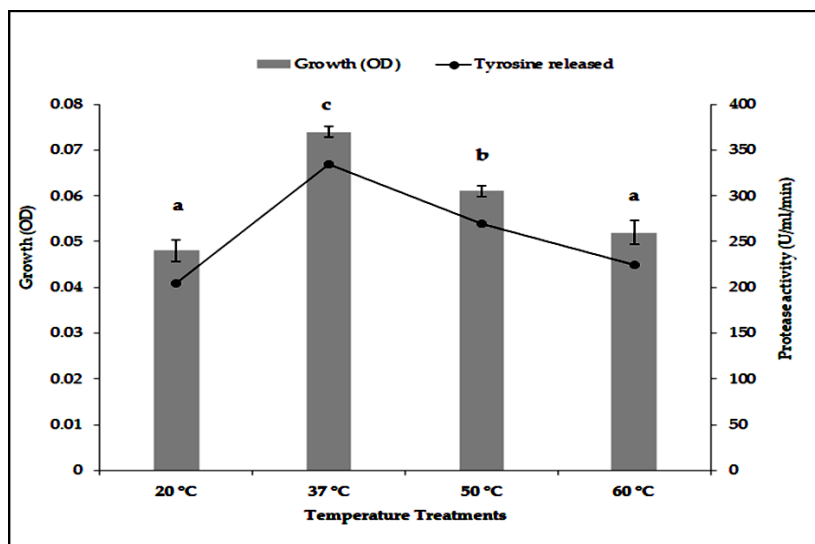


Figure 6. *Pseudomonas aeruginosa* strain IBC-2 growth and protease production optimization at different incubation temperatures. Bars and line dots illustrate mean values of replicates \pm standard error ($n = 3$). Different alphabetical letters represent statistically significant differences (based on ANOVA) at different temperature treatments according to Tukey's HSD post-hoc test ($P \leq 0.05$)

Similarly, to find out the pH effects, incubation was performed at 37 °C using different pH conditions (pH4-11). It was observed that the isolate IBC-2 favoured a pH of 7, giving optimum bacterial growth as well as significant protease production (435 U/ml). The protease production was found substantially higher than protease produced at either acidic pH (4 and 5) or alkaline pH (9 and 11) as shown in Figure 7. Therefore, it was concluded that IBC-2 gives best growth and maximum protease production at 37 °C while keeping the media pH neutral i.e. pH 7.

Discussion

Proteases have a wide range of commercial applications, including leather industries, food confectionaries and pharmaceuticals as well as also used in bioremediation processes (Jellouli et al., 2009; Kirk et al., 2002). Moreover, microbes, especially bacteria are among the easiest and cheapest source of proteases. On this regard, the coal mines of Orakzai Agency were screened for the isolation of commercially valuable bacteria. In our study, 33 bacterial isolates were found to have protease producing ability among total ($n = 62$) isolated bacterial strains. Moreover, among these 33 isolates, only 6 isolates had greater potential of casein hydrolyzing using skim milk agar

by producing larger zones (above 15 mm) as shown in *Tables 1* and *2*. Usually, various components such as caseins, gelatine and proteins are not utilized by bacteria, because these cannot penetrate into bacterial cell wall. This reveals the importance of extracellular proteases to solubilize the proteins and other components. The formation of zones on media containing proteins has been revealed in several scientific reports, showed that protease is usually excreted from microbial sources (Ali et al., 2016; Rajeeva et al., 2015).

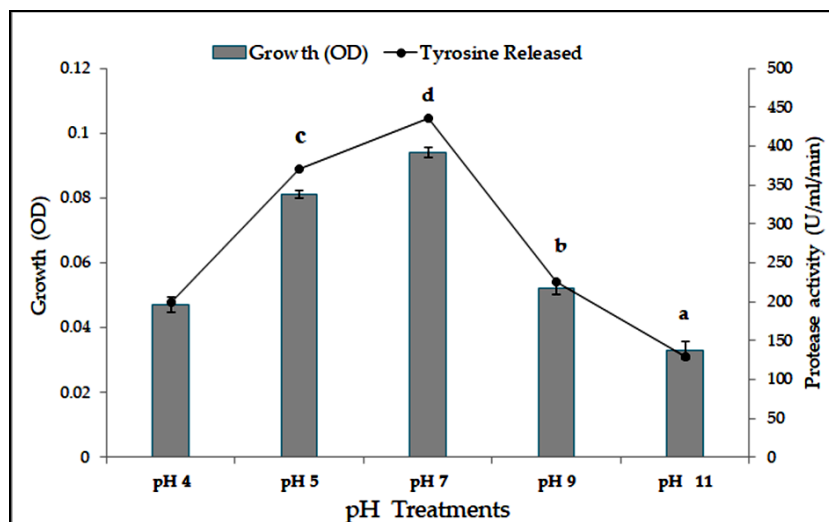


Figure 7. *Pseudomonas aeruginosa* strain IBC-2 growth and protease production optimization at different pH culture conditions. Bars and line dots illustrate mean values of replicates \pm standard error ($n = 3$). Different alphabetical letters represent statistically significant differences (based on ANOVA) at different pH treatments according to Tukey's HSD post-hoc test ($P \leq 0.05$)

The studies for morphological characteristics of selected bacterial isolates ($n = 6$) showed differences in colony size, shape and color (*Table 2*) reflecting the bacterial diversity in coal mines. Furthermore, these characteristics revealed that the isolated bacteria might belong to *Bacillus*, *Pseudomonas*, *Arthrobacter*, *Brachy bacterium* and *Staphylococcus* genus. Previously, these methods found standard for identification of various microbial species such as *Bacillus*, *Staphylococcus* and *Pseudomonas* spp. on the basis of morphology and different biochemical tests (Jamal et al., 2016; Jasuja et al., 2013; Roohi et al., 2014; Sethy and Behera, 2012). Although morphological and biochemical screening reveals initial microbial identification, but molecular methods such as 16S rRNA, provides precise identification of microbes (Wei Wang, 2009). In our study, the presence of *Pseudomonas aeruginosa* strain IBC-2 was first time reported as coal mine dwelling species and since very little studies have been conducted on coal mines micro flora regarding isolation of *Pseudomonas* species to be used for protease production.

Partial purification of protease from crude extract is possible by ammonium sulphate precipitation and this method is widely used for enzymes purifications (Yossan et al., 2006). As shown in *Figure 1*, all the selected six isolated strains showed clear zones on SM agar media and revealed protease activity. The protease purified from the selected isolated stain(s) were functional and effective after purification and parallel findings

were also revealed by Josephine et al. from different *Bacillus* sp., where the samples were collected from soil (Rajeeva et al., 2015). Among the six isolates, IBC-2 apparently revealed high protease productions and protease activity (300 U/ml/24 hrs). Analogous to our findings, maximum protease production (432 U/ml/24 hrs) was reported from *Pseudomonas aeruginosa* (Arioleand and Ilega, 2013), including *Pseudomonas aeruginosa* strain RGSS-09 as well (Rajeeva et al., 2015).

In our analysis, additional confirmation of crude purified enzymes (34-45 KDa) was performed using SDS PAGE for all selected isolates. SDS-PAGE was performed for separation of proteins and protease were found in range of 17 to 60 KDa, which is reported range for proteases (Yossan et al., 2006). Moreover, many *Pseudomonas* species showed specific molecular weights of proteases ranging from 35-50 KDa (Raj et al., 2012). In correlation to our results, a couple of study reported the molecular weight regarding protease enzymes were in the range of 30-52 KDa from various *Bacillus* sp (HS08A, HUTBS71) (Aqel et al., 2009; Dutta and Banerjee, 2006; Sevinc and Demirkan, 2011; Zambare et al., 2010).

Enzymatic activities and growth of microorganisms are significantly ($P \leq 0.05$) correlated with various incubation temperatures and has shown prominent effects on secretion of extracellular proteolytic enzymes using various microbes (Balaji et al., 2012). Similarly, IBC-2 strain significantly ($P \leq 0.05$) revealed that dense bacterial growth occurs at 37 °C when incubated for 24 hrs (Fig. 6). This inferred the direct relationship of bacterial growth with protease production. Different researchers worked on proteases and reported the relationship between protease production and bacterial growth under different laboratory conditions such as temperature, media and pH (Ali et al., 2016; Shah et al., 2017; Zambare et al., 2010). The optimum temperature for protease production was reported as 30 °C produced by an extremophilic *Bacillus* sp (MIG) isolated from marine water (Mohapatra et al., 2003). The specific protease producing bacteria (e.g. *Bacillus* spp.) was reported to have different range of optimum temperatures such as 35 °C (Gerze et al., 2005), 40 °C (Josephine et al., 2012), 50 °C (Anwar and Saleemuddin, 2000) and 70 °C (Sookkheo et al., 2000; Morya and Yadav, 2010). An increase in the production of protease was reported when temperature was increased up to 37 °C for *Pseudomonas* sp. from abattoir soil has been reported by Kalaiarsi and Sunitha (2009) and Akujobi et al. (2012), respectively. The decrease in protease production beyond 37 °C reported by these researchers has supported our results and it has been reported that optimum temperature has key role in the production of protease. In similar fashion, time of incubation is also important to have high protease production and it varies for different microorganisms (Mukesh Kumar et al., 2012).

Like temperature, optimum pH also contributes to protease expression and activity. In this study, protease production was observed at pH range 4-11 and bacterial growth is reported in high amount at neutral pH 7 for IBC-2 (Fig. 7). In similar approach, Ravishankar et al. (2012) reported high production and enzyme activity of *Bacillus subtilis* AKR3 up to pH 7 and has been found declined beyond the pH from 9-11. Supporting our work, the optimum pH 7 and temperature 37 °C was also previously reported for protease production of *Pseudomonas aeruginosa* (Raj et al., 2012). In case of *Bacillus subtilis* strain reported by Ali et al. (2016), pH 10 was the optimum pH for high protease production. These findings revealed that different bacteria need different conditions as most favourable. The bacteria under study have shown high protease

activity at temperature 37 °C and pH 7, which are the most suitable conditions for broad range of bio-industrial applications (Grbavcic et al., 2011; Najafi et al., 2005).

Conclusion

Finally, our finding is the first inveterate report from coal mines of Orakzai Agency that investigated protease producing bacteria. Based on morphological, biochemical and 16S rRNA sequencing, and the bacteria with high protease activity; IBC-2 strain was identified as *Pseudomonas aeruginosa*. The highest protease activity was observed at temperature 37 °C and pH 7 which makes the bacteria as the better producer at conditions favoured/used in most of the bio-industrial applications. Moreover, natural resources need to be further explored in an attempt to find out novel bacterial strain(s), with an exceptional capability of surviving and maintain their hydrolytic activity within harsh condition in order to overcome the bio-industrial problems.

Acknowledgements. The authors are grateful to the Directorate of Science and Technology (DoST) Peshawar, Khyber Pakhtunkhwa-Pakistan for financial aid to implement this research work.

Conflict of interests. All authors declared no conflict of interests, and also the funding body had no role in the experiment design, methodology or data interpretation.

REFERENCES

- [1] Akujobi, C. O., Odu, N. N., Okorundu, S. I., Ike, G. N. (2012): Production of protease by *Pseudomonas aeruginosa* and *Staphylococcus aureus* isolated from abattoir environment. – *J. Res. Biol.* 2(2): 077-082.
- [2] Ali, N., Ullah, N., Qasim, M., Rahman, H., Khan, S. N., Sadiq, A., Adnan, M. (2016): Molecular characterization and growth optimization of halo-tolerant protease producing *Bacillus Subtilis* Strain BLK-1.5 isolated from salt mines of Karak, Pakistan. – *Extremophiles* 20(4): 395-402.
- [3] Anwar, A., Saleemuddin, M. (2000): Alkaline protease from *Spilosoma obliqua*: potential applications in bio-formulations. – *Biotechnol Appl Biochem* 31(Pt 2): 85-9.
- [4] Aqel, H., Farouk, Q., Yousef, T. K. (2009): Characterization of a purified thermostable protease from hyperthermophilic *Bacillus* strain HUTBS71. – *European Journal of Scientific Research* 31(2): 280-288.
- [5] Arioleand, C. N., Ilega, E. (2013): Alkaline protease production by *Pseudomonas aeruginosa* isolated from the gut of pilaovate. – *J. Glob. Biosci.* 2(5): 126-131.
- [6] Balaji, N., Rajasekaran, K. M., Kanipandian, N., Vignesh, V., Thirumurugan, R. (2012): Isolation and screening of proteolytic bacteria from freshwater fish *Cyprinus carpio*. – *International Multidisciplinary Research Journal.* 2(6): 56-59.
- [7] Buchanan, R. E., Gibbons, N. E. (1974): *Bergey's Manual of Determinative Bacteriology.* 8th Ed. – Williams & Wilkins Co, Baltimore, USA.
- [8] Dutta, J. R., Banerjee, R. (2006): Isolation and characterization of a newly isolated *Pseudomonas* mutant for protease production. – *Braz Arch Biol Techn* 49(1): 37-47.
- [9] Gerze, A., Omay, D. Guvenilir, Y. (2005): Partial Purification and Characterization of Protease Enzyme from *Bacillus subtilis megatherium*. – *Appl Biochem Biotechnol Spring*(121-124): 335-345.
- [10] Gomes, J., Steiner, W. (2004): The biocatalytic potential of extremophiles and extremozymes. – *Food Technol. Biotechnol.* 42(4): 223-235.

- [11] Grbavcic, S., Bezbradica, D., Izrael-Zivkovic, L., Avramovic, N., Milosavic, N., Karadzic, I., Knezevic-Jugovic, Z. (2011): Production of lipase and protease from an indigenous *Pseudomonas aeruginosa* strain and their evaluation as detergent additives: compatibility study with detergent ingredients and washing performance. – *Bioresour. Technol.* 102(24): 11226-33.
- [12] Gupta, R., Beg, Q. K., Lorenz, P. (2002): Bacterial alkaline proteases: molecular approaches and industrial applications. – *Appl Microbiol Biotechnol* 59(1): 15-32.
- [13] Jadhav, A. G., Jaybhaye, A. A., Musaddiq, A. A. (2013): Salt tolerant protease produced by an aerobic species belonging to the *Bacillus* genus isolated from saline soil. – *IJSRP* 3(2): 1-8.
- [14] Jamal, Q., Ahmed, I., Rehman, S., Abbas, S., Yong Kim, K., Anees, M. (2016): Isolation and characterization of bacteria from coal mines of Dara Adam Khel, Pakistan. – *Geomicrobiology* 33(1): 1-9.
- [15] Jasuja, N. D., Saxena, R., Chandra, S., Joshi, S. C. (2013): Isolation and identification of microorganism from polyhouse agriculture soil of Rajasthan. – *African Journal of Microbiology Research* 7(41): 4886-4891.
- [16] Jellouli, K., Bougatef, A., Manni, L., Agrebi, R., Siala, R., Younes, I., Nasri, M. (2009): Molecular and biochemical characterization of an extracellular serine-protease from *Vibrio metschnikovii* J1. – *J Ind Microbiol Biotechnol* 36(7): 939-48.
- [17] Johnson, D. B., Mcginness, S. (1991): A highly efficient and universal solid medium for growing mesophilic and moderately thermophilic, iron-oxidizing, acidophilic bacteria. – *Journal of Microbiological Method.* 13(2): 113-122.
- [18] Josephine, F. S., Ramya, V. S., Devi, N., Ganapa, S. B., Siddalingeshwara, K. G., Venugopal, N., Vishwanatha, T. (2012): Isolation, production and characterization of protease from *Bacillus* Sp isolated from soil sample. – *J. Microbiol. Biotech. Res.* 2(1): 163-168.
- [19] Kalaiarsi, K., Sunitha, P. U. (2009): Optimization of alkaline protease production from *Pseudomonas fluorescens* isolated from meat waste contaminated soil. – *Afri. J. Biotechnol.* 8(24): 7035-7041.
- [20] Kirk, O., Borchert, T. V., Fuglsang, C. C. (2002): Industrial enzyme applications. – *Curr Opin Biotechnol* 13(4): 345-51.
- [21] Laemmli, U. K. (1970): Cleavage of structural proteins during the assembly of the head of bacteriophage T4. – *Nature* 227(5259): 680-5.
- [22] Maurer, K. H. (2004): Detergent proteases. – *Curr Opin Biotechnol* 15(4): 330-4.
- [23] Mohapatra, B. R., Bapuji, M., Sree, A. (2003): Production of industrial enzymes (Amylase, Carboxymethylcellulase and Protease) by bacteria isolated from marine sedentary organisms. – *Acta Biotechnol* 23(1): 75-84.
- [24] Morya, V. K., Yadav, D. (2010): Production and partial characterization of neutral protease by an indigenously isolated strain of *Aspergillus tubingensis* NIICC-08155. – *Internet Journal of Microbiology.* 8(1): 53-55.
- [25] Mukesh Kumar, D. J., Venkatachalam, P., Govindarajan, N., Balakumaran, M. D., Kalaichelvan, P. T. (2012): Production and purification of alkaline protease from *Bacillus* sp. MPTK 712 Isolated from dairy sludge. – *Global Veterinaria* 8(5): 433-439.
- [26] Nadeem, M., Qazi, J. I., Baig, S., Syed, Q. (2007): Studies on commercially important alkaline protease from *Bacillus lichniformis* N-2 isolated from decaying organic soil. – *Turk J Biochem* 32(4): 171-177.
- [27] Najafi, M. F., Deobagkar, D., Deobagkar, D. (2005): Potential application of protease isolated from *Pseudomonas aeruginosa* PD100. – *Electronic Journal of Biotechnology* 8(2): 79-85.
- [28] Prakasham, R. S., Rao Ch, S., Sarma, P. N. (2006): Green gram husk--an inexpensive substrate for alkaline protease production by *Bacillus* sp. in solid-state fermentation. – *Bioresour Technol* 97(13): 1449-54.

- [29] Raj, A., Khess, N., Pujari, N., Bhattacharya, S., Das, A., Sundara Rajan, S. (2012): Enhancement of protease production by *Pseudomonas aeruginosa* isolated from dairy effluent sludge and determination of its fibrinolytic potential. – *Asian Pacific Journal of Tropical Biomedicine* 2(3): S1845-S1851.
- [30] Rajeeva, G., Soni, T., Sheffalika, S. (2015): Production and characterization of thermotolerant-organic solvent resistant acidic protease by *Pseudomonas aeruginosa* RGSS-09 isolated from dairy sludge. – *Asian J. Biochem.* 10(2): 52-66.
- [31] Ravishankar, K., Kumar, M. A., Saravanan, K. (2012): Isolation of alkaline protease from *Bacillus subtilis* AKRS3. – *Afri J. Biotechnol.* 11(69): 13415-13427.
- [32] Rawlings, N. D., Barrett, A. J. (2013): *Handbook of Proteolytic Enzymes*. 3rd Ed. – Academic Press, New York.
- [33] Roohi, A., Ahmed, I., Iqbal, M., Jamil, M. (2012): Preliminary isolation and characterization of halotolerant and halophilic bacteria from salt mines of Karak, Pakistan. – *Pak. J. Bot.* 44(Special Issue March): 365-370.
- [34] Roohi, A., Ahmed, I., Paek, J., Sin, Y., Abbas, S., Jamil, M., Chang, Y. H. (2014): *Bacillus pakistanensis* sp. nov., a halotolerant bacterium isolated from salt mines of the Karak Area in Pakistan. – *Antonie Van Leeuwenhoek* 105(6): 1163-72.
- [35] Sethy, K., Behera, N. (2012): Antimicrobial activity of thermotolerant bacterial isolate from coal mine spoil. – *AJMR* 6(26): 5459-5463.
- [36] Sevinc, N., Demirkan, E. (2011): Production of protease by *Bacillus* sp. N-40 isolated from soil and its enzymatic properties. – *J. Biol. Environ. Sci.* 5(14): 95-103.
- [37] Shah, I., Azam, N., Din, G., Ali, N., Ullah, W., Qasim, M., Shehzad, A., Muhammad, N. (2017): Isolation and characterization of protease producing bacteria from soil samples of District Kohat, Pakistan. – *JBMS* 2(1): 1-5.
- [38] Sharmin, S., Hossain, M. T., Anwar, M. N. (2005): Isolation and characterization of a protease producing bacteria *Bacillus amovivorus* and optimization of some factors of culture condition for protease production. – *J. Biol. Sci.* 5(3): 358-362.
- [39] Sookkheo, B., Sinchaikul, S., Phutrakul, S., Chen, S. T. (2000): Purification and characterization of the highly thermostable proteases from *Bacillus stearothermophilus* TLS33. – *Protein Expr Purif.* 20(2): 142-51.
- [40] Tamura, K., Stecher, G., Peterson, D., Filipski, A., Kumar, S. (2013): MEGA6: Molecular Evolutionary Genetics Analysis version 6.0. – *Mol Biol Evol* 30(12): 2725-9.
- [41] Wei Wang, M. S. (2009): Phylogenetic relationships between *Bacillus* species and related genera inferred from 16s rDNA sequences. – *Braz J Microbiol* 40(3): 505-21.
- [42] Xiong, H., Song, L., Xu, Y., Tsoi, M. Y., Dobretsov, S., Qian, P. Y. (2007): Characterization of proteolytic bacteria from the Aleutian deep-sea and their proteases. – *J Ind Microbiol Biotechnol* 34(1): 63-71.
- [43] Yoon, S. H., Ha, S., M., Kwon, S., Lim, J., Kim, Y., Seo, H., Chun, J. (2017): Introducing EzBioCloud: a taxonomically united database of 16S rRNA gene sequences and whole-genome assemblies. – *Int J Syst Evol Microbiol* 67(5): 1613-1617.
- [44] Yossan, S., Reungsang, A., Yasuda, M. (2006): Purification and characterization of alkaline protease from *Bacillus megaterium* isolated from Thai fish sauce fermentation process. – *Science Asia* 32(2006): 377-383.
- [45] Zambare, V., Nilegaonkar, S., Kanekar, P. (2010): A novel extracellular protease from *Pseudomonas aeruginosa* MCM B-327: enzyme production and its partial characterization. – *N Biotechnol.* 28(2): 173-81.

ADVANCES IN RESEARCH OF LODGING AND EVALUATION IN SUGARCANE

LI, X.^{1,2#} – LIN, S. H.^{2#} – HUANG, Q. Y.² – LIANG, Q.² – LI, Y. J.² – YANG, L. T.^{1,2*} – LI, Y. R.^{1,2*}

¹*Agricultural College, Guangxi University, Nanning 530005, China*

²*Key Laboratory of Sugarcane Biotechnology and Genetic Improvement (Guangxi), Ministry of Agriculture, Guangxi Key Laboratory of Sugarcane Genetic Improvement, Sugarcane Research Center, Chinese Academy of Agricultural Sciences, Sugarcane Research Institute, Guangxi Academy of Agricultural Sciences, Nanning 530007, China*

[#]*Li, X. and Lin, S. H. have contributed equally to this manuscript.*

**Corresponding authors*

e-mail: litao61@hotmail.com(Litao Yang); liyr@gxaas.net(Yangrui Li)

(Received 3rd Apr 2019; accepted 23rd Apr 2019)

Abstract. Sugarcane is the largest sugar crop in China and the world, and one of the important commercial crops in southern China. However, the influence of sugarcane lodging is more and more serious with increasing cane yield. After lodging, the plant growth and sugar accumulation in stalk was seriously affected, resulting in considerable losses in cane and sugar yield, and difficulty in machine operation in the field. At present, there is no perfect evaluation method for sugarcane lodging, and little has been done on research of related physiological and biochemical indexes, microscopic structures and so on although there have been some reports on the effects of sugarcane lodging. But there has been a lot of research on lodging in rice, corn and wheat, which could be referred for studying the resistance mechanism and evaluation method in sugarcane.

Keywords: *lodging resistance, agronomic character, yield, sugar content, lignin, cellulose*

Introduction

Guangxi Province had been ranking the first in sugarcane planting area, cane and sugar production, and economic benefit in China (Ye et al., 2016; Li, 2010). With tall plant and large biomass above ground, at the late elongation and maturation stages after October, the plant height of sugarcane exceeds 300 cm, the higher the plant is, the greater the risk of lodging meets (Li et al., 2018a). After lodging, the cane yield and sugar content was declined, the photosynthesis, water metabolism, mineral absorption and conversion in plants, and mechanical and hand harvesting were also affected. The relationships between lodging and lignin, cellulose and microscopic structure were closely correlated.

Cause of lodging

Lodging is the phenomenon that crop stem changes from natural upright state to permanent dislocation. Wind and rain were the direct induction factor for lodging. In addition, environmental factors and cultivation measures also played a role in lodging (Merugumala et al., 2019; Ishimaru et al., 2008). According to the occurrence location, lodging was generally divided into two types: root lodging and stem lodging (Tian et al., 2016). Root lodging referred to whole-plant falling down when the load above ground exceeds the misspecified strength of the root system, and stem lodging referred

to base stem breaks when the load on the upper part of the stem exceeds the mechanical support power of the base stem (Mizuno et al., 2018; Mulsanti, et al., 2018). For rice, stem lodging occurs frequently because the mechanical strength of the stem was weakened due to the weak base of the stem and the underdeveloped mechanical tissue (Sowadan et al., 2018; Li, 2012).

Effect of lodging on agronomic characters

The lodging of sugarcane was affected by the number of leaves, planting furrow depth, planting density, row spacing and other factors (Singkham et al., 2016). Park et al. (2005) and Cock et al. (1997) found that the relationship between the number of sugarcane leaves and sugarcane yield and lodging was closely related. The results showed that the lodging of sugarcane decreased after removing leaves due to the reduction of wind area, and the lodging of sugarcane decreased with the decline of sugarcane leaves. Meanwhile, each sugarcane plant remaining 4 to 6 leaves could ensure yield and effectively reduce lodging. Berding et al. (2005) conducted a comparative experiment on sugarcane planting with different planting depths and varieties. The results showed that the lodging of sugarcane was less when the row spacing was at 260 mm, the sugarcane was prone to lodging when the row spacing was at 120 mm, and there was less lodging in Q152 than Q187 and Q174. Babu et al. (2010) conducted an experiment to study on the relationship between hardness of sugarcane peel and lodging, and the results showed that sugarcane with high hardness of sugarcane peel was not easy to get lodging. By adding silicon fertilizer, the hardness of sugarcane epidermis could be effectively strengthened, so that the stalk could obtain good supporting force and the lodging rate could be reduced (Brienzo et al., 2014). Loganandhan et al. (2013) conducted a comparative experiment on planting depth and earth-up condition of sugarcane, and the results showed that deep planting could reduce lodging of sugarcane. Sugarcane was not prone to lodging when the number of seedcane buds and millable stems were controlled (Neto et al., 2018). Chiluwal et al. (2018) found that it was useful for improving the lodging resistance when the planting row spacing was more than 1 m.

Effect of lodging on cane yield

Different degrees of lodging had different effects on sugarcane growth. For slightly inclined and semi-inclined sugarcane, their growth have been affected because the plant head was loosened and some sugarcane roots are broken, the sugarcane plants have to grow in bending (Heerden et al., 2014; Singh et al., 2002). For inclined and lodging sugarcane, their stem tips grow upward because sugarcane plants strive for gaining more sunlight, so that the meristematic tissue outside the region of growth on the sugarcane node proliferates rapidly, resulting in tender, fragile, bending and easy-broken outer parts (Paraskevopoulos et al., 2016). The serious lodging causes the sugarcane plant to turn over, break or stop growing. If things go on liked this, the sugarcane stem would become dry. Moreover, rats liked to nest in the sugarcane bushes and steal sugarcane in large quantities. In addition, it was hard to conduct field management after sugarcane lodging, so the early lodging not only caused losses at that time, but also affected the later growth and reduces the cane yield due to the failure to fertilize and control pests such as aphids (Yang et al., 2016). Even worse, the perennial

root of sugarcane could not be reserved for the next year after lodging due to root breakage, stool turnover, heavy damage in sugarcane stool, excessive nutrient consumption and rotten sugarcane stool with many germs, most sugarcane stools remaining perennial roots for the next year would have no buds to sprout, which resulted in plant deficiency and yield reduction in the ratoon crops (Shanmuganathan, et al., 2017).

Effect of lodging on sucrose content

The growth of sugarcane would be inhibited in root and tip after lodging, and sugarcane plants would be stacked together to give out heat. Together with sufficient water after rain, the root region of sugarcane stem germinated into air roots and lateral buds germinate (Jacobsen et al., 2015). Furthermore, the part above ground was exposed after lodging. When the sun shined directly, soil temperature would increase, resulting in the increase of ineffective tillers in later stage, nutrient consumption, hollow stem, decline of sucrose content, dry sugarcane plant and stem gradually that turned over or broke, rapid conversion of sugar and decline of sugar yield rate (Mcintyre et al., 2015). Therefore, the dry sugarcane stems not only are absorbed sugar content, but also increase the acidity of sugarcane juice while making sugar, which makes it difficult to make sugar and causes certain losses to factories (Singh, 2002).

Sucrose is the main form of carbohydrate transport in sugarcane plants. However, sugarcane plants after lodging have weak photosynthetic capacity, less carbohydrate synthesis and insufficient sunlight, which affect transportation, slow down the sugar accumulation in segmental storage tissues, so that the brix of sugarcane juice was low at harvest time. For instance, sugarcane plants lodged in late September had a full-stem brix 6.13% lower than that of normal plants when harvesting in January next year, and the lower segment was the area where sugar accumulation was seriously affected (Huang, et al., 2014).

Effect of lodging on physiological and biochemical indexes

Sugarcane was a C₄ plant with high photosynthetic intensity and light saturation point (Marchiori et al., 2014). After lodging of sugarcane plants, the leaves could not obtain sufficient light energy due to the deterioration of light conditions in the field, which could not meet the direct needs of photosynthesis for light energy, but also hinder the stomatal opening, increased the diffusion resistance of CO₂ into the leaves and reduce the photosynthetic intensity significantly (Liu et al., 2016a). Moreover, lodging was also not conducive to leaf extension. Zhao et al. (2014) reported that the average leaf area and single stem green leaf area of sugarcane plants after lodging declined by 25.3% and 22.7% respectively compared with normal plants. The reduction of photosynthetic area would inevitably lead to the decrease of synthetic amount of photosynthetic product in the whole sugarcane plant (Mo, 1979).

The water metabolism of sugarcane plants is composed of three closely-related links: water absorption, water transport and water loss, and there are two mechanisms of water absorption in sugarcane plants: active absorption and passive absorption (Jangpromma et al., 2010). After lodging of sugarcane plants, some of the roots are broken by mechanical force and the root system could not get enough carbohydrates from the ground, so the activity of life is weak and the amount of active water absorption

decreases (Zhang et al., 2015). Meanwhile, sugarcane plants after lodging are squeezed together with weak light and high relative humidity, as well as weak transpiration, which greatly affect the passive water absorption ability. Since the water absorption and loss (mainly transpiration) of sugarcane plants after lodging are adversely affected, water transport has to proceed gradually, which destroys the normal water metabolism of sugarcane plants and is extremely harmful to their growth and tissue enrichment (Heerden et al., 2015).

After lodging of sugarcane plants, the life activities of root system are adversely affected, and the absorption and transport of mineral nutrients are weakened. According to Chand et al. (2010), the amount of potassium chloride absorbed by the root system of sugarcane plants after lodging and transported by xylem to parts above ground was about half of that of normal plants, and the amount of phosphorus was only 1/4 of that of normal plants. After lodging, the normal physiological condition of phosphorus and potassium absorption and transport from outside during the whole growth process of sugarcane plants was changed obviously, which was an important reason for poor growth, low yield and poor quality (Yanai et al., 2010).

The relationship between lodging and lignin and cellulose

During the period of internode enrichment, a large number of photosynthetic products would flow to the stem, and the cell wall is significantly thicker accompanied by fibrosis and lignification. In the mean time, a large amount of starch accumulated in parenchyma cells significantly increases the dry weight per unit length of stem, which is the key period to determine lodging resistance (Ferreira et al., 2016).

Lignin

As a phenolic polymer synthesized from cinnamom alcohol and other monomers, lignin is the organic component next only to cellulose on the earth, which has a relatively high content in wood plants, generally accounting for 15% to 35% of dry weight (Stewart et al., 2015). With the biological functions of strengthening the mechanical strength of cell wall, improving transport capacity of cells and resisting microbial invasion, lignin exists in the cell walls of tracheids and xylem vessels of various supporting and leading tissues in plants, which is mainly accumulated in the thickened secondary cell wall, cross-linked and arranged with cellulose and hemicellulose (Zhao et al., 2015; Cao et al., 2015). The initial properties of lignin could enhance the hardness of stem and leading tissue so as to maintain the upward growth of plants and the upward transport of water and nutrients through the xylem (Kanran et al., 2018; Tian et al., 2017). Although lignin could improve the mechanical strength and stress tolerance of the stem, its content was closely related to the rigidity of the stem (Hu et al., 2017a), so the varieties with strong lodging resistance had high lignin content. Hasan et al. (1993) reported that there was no significant correlation between lodging resistance and lignin content in different types of rice varieties, but it was generally believed that lignin content significantly affected the mechanical strength of plant stems based on a large number of studies on rice, wheat and maize (Zhang et al., 2017; Kamran et al., 2018a, b).

Cellulose

As the main component of plant skeleton (cell wall), the basic structural unit of cellulose is microfibril, and the content of cellulose affects the degree of thickening of cell wall and further determines the mechanical strength of stem (Hoang et al., 2017; William et al., 2017). For example, Wang et al. (2006) showed that the stem strength of wheat variety was significantly higher than that of its parents, which mainly attributed to higher cellulose content. Subsequently, Wang et al. (2012) and Liu et al. (2016b) drew the similar conclusion in wheat, soybean and rice respectively. Recently, Okuno et al. (2014) considered that, the adverse effect of insufficient lignin content on stem hardness could be compensated by increasing cellulose content so as to improve the lodging resistance of forage rice, which might result from the molecular compensation mechanism in the bio-synthesis pathway of cellulose and lignin. According to Robertson et al. (2017), the contribution of cellulose content under panicle internodes to maize stem reached by 85%, which was in accordance with the study of Ma et al. (2012), indicating that it was an important method to improve the physical strength of maize stem and enhance the lodging resistance of maize by increasing cellulose content. Hernández et al. (2018) showed that the lodging rate of maize was negatively correlated with the crude fiber content of stem.

The relationship between lodging and microscopic structure

At present, there is no report about analysis of microscopic structure with sugarcane lodging, but a lot of research has been done on crops such as maize and rice (Tian et al., 2015; Du et al., 2016). From the perspective of cytology, the mechanical strength of stem mainly came from thick-walled cells, and plant cell walls were divided into primary and secondary walls. Wang et al. (2015) studied the morphological structure in stem, anatomical characteristics and chemical composition of cell wall of 10 maize varieties, and analyzed the correlation between these variables. The results shown that the cortex/radius, thick-walled tissue ratio, mechanical tissue ratio, cellulose content and lignin content of stem were positively correlated with stress tolerance, while the thick-walled tissue ratio, stem length/stem diameter and number of vascular bundles were negatively correlated with stress tolerance. According to Liu et al. (2011), the arrangement of rapeseed longitudinal xylem cells in the main stem of lodging resistant variety was relatively neat, which was distributed in a linear manner parallel to the main stem, the length-width ratio of most horizontal cortical cells was greater than two with compact and ordered arrangement, and the ray of vascular column penetrated the cambium. However, a material with common lodging resistance had irregular longitudinal arrangement of xylem cells, the length-width ratio of most horizontal cortical cells was less than the two with disordered arrangement, and the ray of vascular column had poor coherence with extra-cambium cells.

Evaluation methods of lodging resistance in crops

Crop lodging is the result of plant itself and environmental factors, and there are significant differences in lodging resistance in different crop genotypes, but the phenotypic identification of crop lodging resistance could only be carried out under certain environmental conditions. However, since the environmental conditions could

not be accurately predicted, it is necessary to establish a mechanical evaluation system based on the physical and morphological characteristics of the plant itself, which is not depended on climate conditions, so could better evaluate the lodging resistance of crops (Corbin et al., 2014; Tian, 2013).

Tilting angle method

Tilting angle method (Zhang et al., 1999) is to show the lodging resistance of plants by the angle between the stem at the mature stage and the vertical line of the ground. According to tilting angle, degree of lodging could be divided into 3 types: lodging type (60-90 degrees), inclined type (30-60 degrees) and vertical type (0-30 degrees).

Bending moment method

When discussing the lodging resistance of rice with different panicle types, the bending moment method could be adopted (Xu et al., 2004).

Resistance force method

In this method, the dynamometer is placed vertically with the stem and 20 cm away from the ground. Then, the dynamometer is pushed slowly to an angle of 45° between the plant and the ground, so the value showed by the instrument is the bending resistance of the stem. The larger the value is, the stronger the lodging resistance is. Otherwise, the worse the lodging resistance is. The advantage of this method is to evaluate the lodging resistance of rice by measuring the bending resistance of each stem, which was close to the real situation in the field (Li et al., 2018b; Xiao et al., 2015).

Lodging resistance index method

Sun (1987) proposed an acknowledged formula: rice stem lodging resistance index (CLRI), it was calculated with basal stem resistance, stem length and grain weight per panicle. According to this formula, the lodging resistance of rice stem could be divided into four types, that is, none lodging resistant, more lodging resistant, lodging resistant and high lodging resistant. The higher the CLRI was, the greater the lodging resistance was, and vice versa (Li, 2015).

Application of the lodging resistance index

Among the above anti-lodging evaluation methods, the lodging resistance index method is used most frequently, which can effectively reflect severity of corn lodging and yield after harvesting (Chu et al., 2017). Zhao et al. (2017) selected the best combination of silicon application amount by using the anti-lodging index. Zhang et al. (2019) and Hu et al. (2017b) found that lodging resistance coefficient of maize and wheat was closely related to stem folding resistance. Hu et al. (2018) found in the wheat comparative experiment that the four lodging indexes were all significantly positively

correlated with the length of the second and third stem segments, and the lodging indexes bending moment and resistance force showed better effects.

Conclusion

After sugarcane lodging, its cane yield and sugar content would reduce seriously. Meanwhile, it reduces the quality of mechanical harvesting, go against to photosynthesis, make destruction of water metabolism, affects mineral absorption and conversion. Lignin and cellulose affect the degree of thickening of cell wall and further determine the mechanical strength of stem. The mechanical strength of stem mainly come from thick-walled cells. There are a lot of evaluation methods of lodging resistance in crops, and lodging resistance index method is used most frequently. It could be used for reference in sugarcane.

Acknowledgements. This research was supported by the Fund for the Guangxi Innovation Teams of Modern Agriculture Technology (gjnytxgxcxt-d-03), Fund of Guangxi (2016GXNSFBA380138), Fund of Guangxi Science and Technology Base and Special Foundation (AD17195100), Funds of Guangxi Academy of Agricultural Sciences (2015JZ93, 2015YT02; G2014YZ01).

REFERENCES

- [1] Babu, C., Koodalingam, K., Natarajan, U. S. (2010): Genetic enhancement of sugarcane (*saccharum* sp. hybrids) for resistance to red rot disease and economic traits. – Research Gate 4(3): 97-107.
- [2] Berding, N., Hurney, A. P. (2005): Environmental stimuli promoting sucker initiation in sugarcane. – Hurneyd Field Crops Research 92(2): 219-230.
- [3] Brienzo, M., Ferreira, S., Vicentim, M. P., Souza, W. D., Sant’Anna, C. (2014): Comparison study on the biomass recalcitrance of different tissue fractions of sugarcane culm. – Bioenergy Research 7(4): 1454-1465.
- [4] Cao, C., Yang, Z., Han, L., Jiang, X., Ji, G. (2015): Study on in situ analysis of cellulose, hemicelluloses and lignin distribution linked to tissue structure of crop stalk internodal transverse section based on FTIR microspectroscopic imaging. – Cellulose 22(1): 139-149.
- [5] Chand, M., Lal, R., Khippal, A., Singh, R., Narang, A. K. (2010): Drought management in sugarcane during pre-monsoon period. – Sugar Tech 12(1): 64-66.
- [6] Chilawal, A., Singh, H. P., Sainju, U., Khanal, B., Whitehead, W. F., Singh, B. P. (2018): Spacing effect on energy cane growth, physiology, and biomass yield. – Crop Science 58(3): 1-14.
- [7] Chu, T. X., Michael, J. S., Michael, J. B., Seth, C. M., Luke, S. P. (2017): Assessing lodging severity over an experimental maize (*Zea mays* L.) field using UAS images. – Remote Sensing 9(9): 923-946.
- [8] Cock, J. H., Amaya, A., Bohorquez, C., Munchmeyer, B. (1997): Simulation of production potential of self-defoliating sugarcane cultivars. – Field Crops Research 54: 1-8.
- [9] Corbin, J. L. (2014): Evaluation of management practices to mitigate lodging for ‘c1151’ rice (*Oryza sativa*, L.). – Mississippi State University Dissertations & Theses. Gradworks 1: 22-23.
- [10] Du, J., Zhang, Y., Guo, X., Ma, L., Shao, M., Pan, X., Zhao, C. (2016): Micron-scale phenotyping quantification and three-dimensional microstructure reconstruction of

- vascular bundles within maize stalks based on micro-CT scanning. – *Functional Plant Biology* 44: 10-22.
- [11] Ferreira, S. S., Hotta, C. T., Poelking, V. G. D. C., Leite, D. C. C., Buckeridge, M. S., Loureiro, M. E. (2016): Co-expression network analysis reveals transcription factors associated to cell wall biosynthesis in sugarcane. – *Plant Molecular Biology* 91(1-2): 15-35.
- [12] Hasan, S., Shimojo, M., Goto, I. (1993): Chemical components influencing lodging resistance of rice plant and its straw digestibility in vitro. – *Asian-Australasian Journal of Animal Sciences* 6: 41-44.
- [13] Heerden, P. D. R. V. (2014): Effects of lodging and anti-lodging chemicals on the productivity of variety N25: preliminary findings. – *Proceedings of South African Sugar Technologists' Association* 84: 169-172.
- [14] Heerden, P. D. R. V., Singels, A., Paraskevopoulos, A., Rosslera, R. (2015): Negative effects of lodging on irrigated sugarcane productivity. An experimental and crop modelling assessment. – *Field Crops Research* 180: 135-142.
- [15] Hernández, A. J. M., Largo, G. A., Martínez, R. R., Pereda, D., Álvarez, J. M., Acebes, J. L. (2018): Effect of ancymidol on cell wall metabolism in growing maize cells. – *Planta* 247(4): 987-999.
- [16] Hoang, N. V., Furtado, A., O'Keefe, A. J., Botha, F. C., Henry, R. J. (2017): Association of gene expression with biomass content and composition in sugarcane. – *PloS ONE* 12(8): 8-14.
- [17] Hu, D., Liu, X. B., She, H. Z., Gao, Z., Ruan, R. W., Wu, D. Q., Yi, Z. L. (2017a): The lignin synthesis related genes and lodging resistance of *Fagopyrum esculentum*. – *Biologia Plantarum* 61(1): 138-146.
- [18] Hu, H., Li, S. S., Hua, H., Sun, M. M., Kang, J., Xiang, G. J., Wang, C. Y. (2017b): Research on stalk morphological structure characteristics and its relationship between with the lodging of different wheat varieties. – *Journal of Triticeae Crops* 10: 83-88.
- [19] Hu, W. G., Cao, T. J., Wang, X. C., Zhang, Y. E., Chang, P., Zhan, H. (2018): Qualitative and quantitative study on lodging resistance of wheat varieties in Henan Province. – *Acta Agriculturae Boreali-Sinica* 33(05): 164-171.
- [20] Huang, W. W., Li, W. J., He, G. B., Pan, T. Y., Han, L. X., Luo, F. F. (2014): Regional trial reports on sugarcane varieties in Baise, Guangxi (2011-2012). – *Journal of Southern Agriculture* 45(2): 194-199.
- [21] Ishimaru, K., Togawa, E., Ookawa, T., Kashiwagi, T., Yuka, M., Naoki, H. (2008): New target for rice lodging resistance and its effect in a typhoon. – *Planta* 227(3): 601-609.
- [22] Jacobsen, K. R., Fisher, D. G., Maretzki, A., Moore, P. H. (2015): Developmental changes in the anatomy of the sugarcane stem in relation to phloem unloading and sucrose storage. – *Plant Biology* 105(1): 70-80.
- [23] Jangpromma, N., Kitthaisong, S., Lomthaisong, K., Daduang, S., Jaisil, P., Thammasirirak, S. (2010): A proteomics analysis of drought stress-responsive proteins as biomarker for drought-tolerant sugarcane cultivars. – *American Journal of Biochemistry & Biotechnology* 6(2): 89-102.
- [24] Kamran, M., Ahmad, I., Wang, H., Wu, X., Jing, X., Liu, T., Ding, R., Han, Q. (2018a): Mepiquat chloride application increases lodging resistance of maize by enhancing stem physical strength and lignin biosynthesis. – *Field Crops Research* 224: 148-159.
- [25] Kamran, M., Ahmad, I., Wu, X., Liu, T., Ding, R., Han, Q. (2018b): Application of paclobutrazol: a strategy for inducing lodging resistance of wheat through mediation of plant height, stem physical strength, and lignin biosynthesis. – *Environmental Science and Pollution Research* 25(29): 366-378.
- [26] Li, F., Liu, S., Xu, H., Xu, Q. (2018b): A novel *fc17/cesa4* mutation causes increased biomass saccharification and lodging resistance by remodeling cell wall in rice. – *Biotechnology for Biofuels* 11(1): 298-306.

- [27] Li, H. (2012): Mechanical model with varying stiffness and critical grain load of wheat stalk. – Transactions of the Chinese Society for Agricultural Machinery 43(2): 70-74.
- [28] Li, X., Li, Y. J., Liang, Q., Lin, S. H., Huang, H. R., Huang, Q. Y. (2018a): Adaptability of sugarcane clone in Nanning ecological region. – Guangxi Sugar Industry 22: 129-130.
- [29] Li, Y., Liu, G., Li, J., You, Y. L., Zhao, H. M., Liang, H., Mao, P. (2015): Acid detergent lignin, lodging resistance index, and expression of the caffeic acid O-methyltransferase gene in brown midrib-12 sudangrass. – Breeding Science 65(4): 291-297.
- [30] Li, Y. R. (2010): Modern Sugarcane Science. – China Agriculture Press, Beijing, pp. 121-122.
- [31] Liu, T., Liu, W. G., Ren, M. L., Du, Y. L., Deng, Y. C., Zou, J. L. (2016a): Effects of shade degrees on photosynthesis and lodging resistance degree of different shade tolerance soybean. – Scientia Agricultura Sinica 49(8): 1466-1475.
- [32] Liu, T. X., Guan, C. Y., Li, Y. X. (2011): Preliminary study on the relationship between stem microstructure and lodging resistance in rapeseed (*Brassica napus* L.). – Chinese Agricultural Science Bulletin 27(5): 139-143.
- [33] Liu, W., Deng, Y., Hussain, S., Zou, J., Yuan, J., Luo, L., Yang, C., Yuan, X., Yang, W. (2016b): Relationship between cellulose accumulation and lodging resistance in the stem of relay intercropped soybean [*Glycine max* (L.) Merr.]. – Field Crops Research 196: 261-267.
- [34] Loganandhan, N., Gujja, B., Goud, V. V. (2013): Sustainable sugarcane initiative (SSI): a methodology of ‘more with less’. – Sugar Tech 15(1): 98-102.
- [35] Ma, Y. H., Sun, D. Q., Li, T. Y., Lin, H., Pan, L. Y., Zhang, C. Y. (2012): Correlation analysis between rind penetration resistance and morphological characters and chemical contents in maize stalk. – Heilongjiang Agricultural Sciences 4: 1-4.
- [36] Marchiori, P. E. R., Machado, E. C., Ribeiro, R. V. (2014): Photosynthetic limitations imposed by self-shading in field-grown sugarcane varieties. – Field Crops Research 155: 30-37.
- [37] McIntyre, C. L., Goode, M. L., Cordeiro, G., Bundock, P., Elliott, F., Henry, R. J. (2015): Characterisation of alleles of the sucrose phosphate synthase gene family in sugarcane and their association with sugar-related traits. – Molecular Breeding 35(3): 1-14.
- [38] Merugumala, G. R., Satyanarayana, P. V., Narne, C., Ravikumar, B. N. V. S. R., Ramana, R. P. V., Pavani, L., Deepika, V. (2019): Molecular breeding of “swarna,” a mega rice variety for lodging resistance. – Molecular Breeding 39(4): 39-55.
- [39] Mizuno, H., Kasuga, S., Kawahigashi, H. (2018): Root lodging is a physical stress that changes gene expression from sucrose accumulation to degradation in sorghum. – BMC Plant Biology 18(1): 1-12.
- [40] Mo, J. Y. (1979): Preliminary analysis of adverse physiological effects of sugarcane lodging. – Sugar Industry 12: 22-24.
- [41] Mulsanti, I. W., Yamamoto, T., Ueda, T., Samadi, A. F., Kamahora, E., Rumanti, I. A., Thanh, V. C., Adachi, S. (2018): Finding the superior allele of japonica-type for increasing stem lodging resistance in indica rice varieties using chromosome segment substitution lines. – Rice 11(1): 1-14.
- [42] Neto, J. R., Souza, Z. M. D., Kölln, O. T., Carvalho, J. L. N., Ferreira, D. A., Barbosa, L. C. (2018): The arrangement and spacing of sugarcane planting influence root distribution and crop yield. – Bioenergy Research 4: 1-14.
- [43] Okuno, A., Hirano, K., Asano, K., Takase, W., Masuda, R., Morinaka, Y., Ueguchi, T. M. (2014): New approach to increasing rice lodging resistance and biomass yield through the use of high gibberellin producing varieties. – PLoS ONE 9: 1-5.
- [44] Paraskevopoulos, A. L., Singls, A. L., Tweddle, P. B. (2016): Quantifying the negative impact of lodging on irrigated sugarcane productivity: a crop modelling assessment. – Africa Sugarcane Technology 89: 154-158.

- [45] Park, S. E., Robertson, M., Inmanbamber, N. G., Inmanbamber, N. G., Bonnett, G. D., Thorburn, P. J. (2005): Decline in the growth of a sugarcane crop with age under high input conditions. – *Field Crops Research* 92(2): 305-320.
- [46] Robertson, D. J., Julias, M., Lee, S. Y., Cook, D. D. (2017): Maize stalk lodging: morphological determinants of stalk strength. – *Crop Science* 57(2): 926.
- [47] Shanmuganathan, M., Baskaran, V., Chandrasekaran, R. (2017): Evaluation of mid-late sugarcane clones for their yield and quality characters in advanced selection stage in plant and ratoon crops. – *Electronic Journal of Plant Breeding* 8(3): 992-997.
- [48] Singh, G. (2002): Constraints to high yield and CCS in large and lodged cane crops. – Ph.D. Thesis of James Cook University, Queensland, pp. 28-30.
- [49] Singh, G., Chapman, S. C., Jackson, P. A., Lawn, R. J. (2002): Lodging reduces sucrose accumulation of sugarcane in the wet and dry tropics. – *Australian Journal of Agricultural Research* 53(11): 1183.
- [50] Singkham, N., Songsri, P., Jaisil, P. (2016): Diversity of characteristics associated with lodging resistance in sugarcane germplasm. – *Sabrao Journal of Breeding Genetics* 48: 97-104.
- [51] Sowadan, O., Li, D., Zhang, Y., Zhu, S., Hu, X., Bhanbhro, L. B., et al. (2018): Mining of favorable alleles for lodging resistance traits in rice (*Oryza sativa*) through association mapping. – *Planta* 248(1): 155-169.
- [52] Stewart, C. E., Moturi, P., Follett, R. F., Halvorson, A. D. (2015): Lignin biochemistry and soil n determine crop residue decomposition and soil priming. – *Biogeochemistry* 124(1-3): 335-351.
- [53] Sun, X. C. (1987): Study on the resistance of the culm of rice to lodging. – *China Agriculture Science* 20(4): 32-37.
- [54] Tian, B., Liu, Y., Zhang, L., Li, H. (2017): Stem lodging parameters of the basal three internodes associated with plant population densities and developmental stages in foxtail millet (*Setaria italica*) cultivars differing in resistance to lodging. – *Crop Pasture Science* 68(4): 349-357.
- [55] Tian, B. H. (2013): The methods of lodging resistance assessment in cereal crops and their application in foxtail millet. – *Journal of Plant Genetic Resources* 14(2): 265-269.
- [56] Tian, B. H., Liu, L. Y., Zhang, L. X., Song, S. X., Wang, J. G., Wu, L. F. (2015): Characterization of culm morphology, anatomy and chemical composition of foxtail millet cultivars differing in lodging resistance. – *Journal of Agricultural Science* 153(8): 1437-1448.
- [57] Tian, Z. M., Huang, Z. H., Chen, J. X., Shi, B. L., Wei, D., Zhai, W. H., Li, H. (2016): Effects of planting density on lodging resistance and yield of three erectophile maize varieties. – *Journal of Maize Sciences* (5): 83-88.
- [58] Wang, J., Zhu, J. C., Lin, Q. Q., Li, X. J., Teng, N. J., Li, Z. S., Li, B., Zhang, A. M., Lin, J. X. (2006): The effect of stem structure and cell wall chemical composition on the stress resistance of wheat stem. – *Chinese Science Bulletin* 51(6): 679-685.
- [59] Wang, J., Zhu, J., Huang, R., Yang, Y. S. (2012): Investigation of cell wall composition related to stem lodging resistance in wheat (*Triticum aestivum* L.) by FTIR spectroscopy. – *Plant Signaling Behavior* 7(7): 856-863.
- [60] Wang, T. J., Zhang, L., Han, Q. (2015): Effects of stalk cell wall and tissue on the compressive strength of maize. – *Plant Science Journal* 33(1): 109-115.
- [61] William, P. B., Heather, D. C. (2017): Cell wall composition and lignin biosynthetic gene expression along a developmental gradient in an Australian sugarcane cultivar. – *Peer J* 5: 4141.
- [62] Xiao, Y., Liu, J., Li, H., Cao, X., Xia, X., He, Z. (2015): Lodging resistance and yield potential of winter wheat: effect of planting density and genotype. – *Frontiers Agricultural Science and Engineering* 2(2): 168-177.

- [63] Xu, Z. J., Chen, W. F., Ma, D. R., Lu, Y. N., Zhou, S. Q., Liu, L. X. (2004): Correlations between rice grain shapes and main qualitative characteristics. – *Acta Agronomica Sinica* 30(9): 894-900.
- [64] Yanai, J., Nakata, S., Funakawa, S., Nawata, E., Katawatin, R., Kosaki, T. (2010): Effect of NPK application on growth, yield and nutrient uptake by sugarcane on a sandy soil in northeast Thailand. – *Tropical Agriculture Development* 54: 113-118.
- [65] Yang, W., Mo, X. W., Yang, J., Yuan, F. W., Huang, S. C. (2016): Experimental study on the basic parameters of sugarcane on easy lodging period – *Journal of Agricultural Mechanization Research* 12: 143-148.
- [66] Ye, J., Yang, Y. Y., Xu, L. P., Li, Y. R., Que, Y. X. (2016): Economic impact of stem borer-resistant genetically modified sugarcane in Guangxi and Yunnan provinces of China. – *Sugar Tech* 18(5): 1-9.
- [67] Zhang, F. J., Zhang, K. K., Du, C. Z., Li, J., Xing, Y. X., Yang, L. T., Li, Y. R. (2015): Effect of drought stress on anatomical structure and chloroplast ultrastructure in leaves of sugarcane. – *Sugar Tech* 17(1): 41-48.
- [68] Zhang, H. N., Yu, Q., Du, X. Y., Liu, M. Q., Xu, E. J., Liu, Z. Q. (2019): The effect of straw mulching and pre-sowing irrigation on resistance of summer maize against lodging. – *Journal of Irrigation and Drainage* 38(2): 9-14.
- [69] Zhang, W., Wu, L., Ding, Y., Yao, X., Wu, X., Weng, F., Li, G., Liu, Z., Tang, S., Ding, C., Wang, S. (2017): Nitrogen fertilizer application affects lodging resistance by altering secondary cell wall synthesis in japonica rice (*Oryza sativa*). – *Journal of Plant Research* 130(5): 1-13.
- [70] Zhang, Z. X., Chen, W. F., Yang, Z. Y., Hua, Z. T., Gao, R. L., Gao, Y., Zhao, Y. C. (1999): Effect of lodging resistance on yield and its relationship with stalk physical characteristics. – *Journal of Shenyang Agricultural University* 30(2): 81-85.
- [71] Zhao, D., Glaz, B., Irej, M. S., Hu, C. J. (2014): Sugarcane genotype variation in leaf photosynthesis properties and yield as affected by mill mud application. – *Agronomy Journal* 107(2): 506-517.
- [72] Zhao, Q., Zeng, Y., Yin, Y., Pu, Y., Jackson, L. A., Engle, N. L., Martin, M. Z., Tschaplinski, T. J., Ding, S. Y., Ragauskas, A. J., Richard, A. Dixon, R. A. (2015): Pinorensinol reductase 1 impacts lignin distribution during secondary cell wall biosynthesis in arabidopsis. – *Phytochemistry* 112(1): 170-178.

EVALUATION OF LODGING RESISTANCE IN SUGARCANE (*SACCHARUM SPP. HYBRID*) GERMPLASM RESOURCES

LI, X.^{1,2#} – LI, Y. J.^{2#} – LIANG, Q.² – LIN, S. H.² – HUANG, Q. Y.² – YANG, R. Z.² – YANG, L. T.^{1,2*}
– LI, Y. R.^{1,2*}

¹*Agricultural College, Guangxi University, Nanning 530005, China*

²*Key Laboratory of Sugarcane Biotechnology and Genetic Improvement (Guangxi), Ministry of Agriculture, Guangxi Key Laboratory of Sugarcane Genetic Improvement, Sugarcane Research Center, Chinese Academy of Agricultural Sciences, Sugarcane Research Institute, Guangxi Academy of Agricultural Sciences, Nanning 530007, China*

[#]*Li, X. and Li, Y. J. have contributed equally to this manuscript.*

**Corresponding authors*

e-mail: litao61@hotmail.com(Litao Yang); liyr@gxaas.net(Yangrui Li)

(Received 3rd Apr 2019; accepted 23rd Apr 2019)

Abstract. In order to observe the performance of lodging-related traits, evaluate the lodging-resistant ability of different combinations of sugarcane, a field experiment was conducted in 2018. Thirty sugarcane combinations were used as the materials, and the lodging grade, fracture resistance force, basal stem diameter, middle stem diameter and brix were investigated. With the data of lodging classification, the lodging resistance index was established. It was found that the lodging resistance index was significantly and positively correlated with the ratio of basal and middle stem diameters and brix. A cluster analysis was conducted, for the thirty sugarcane combinations by the lodging resistance index, which showed sixteen were lodging resistant, thirteen half-lodging, and two complete-lodging.

Keywords: *lodging resistance, combination, stem diameter, fracture resistance force, index*

Introduction

Sugarcane (*Saccharum spp. hybrid*) is the largest sugar crop in China and the world, during the 2017/2018 milling season, the planting area was 1.38 million ha and the sugar yield was 10.48 million tones in China. Guangxi is the first in sugarcane planting area, sugar yield, and economic benefit in Chinese sugar industry (Li et al., 2010). Due to the tall plant and large biomass above ground, lodging occurs very common, which seriously affects the yield and sucrose content in cane, in some areas, the cane yield was reduced by 10% to 20% in light, and more than 50% in severe. The sucrose content was reduced by 15% to 35%, and the number of millable canes was reduced by 0.8 stalks/m² (Li et al., 2018; Singh et al., 2002). Meanwhile, lodging reduces the quality of mechanical harvesting, results in more harvesting loss, and increases broken rate of stools by 24.8% on average, which seriously hinders the popularization and application of machine harvest in sugarcane (Li, 2010; Mo, 1979) as well as the development of sugarcane industry (Liu and Fan, 2011; Zhang et al., 2010). There have been a lot of research about lodging resistance evaluation of germplasm resources for other crops, such as rice, maize, wheat, etc. (Wang et al., 2014; Kamran et al., 2018; Piñera-Chavez et al., 2016). Up to day, however, there has been no perfect evaluation method for sugarcane lodging at home and abroad, and very few reports about sugarcane lodging research could be referred. Considering the changes of climatic and ecological regions and the status of main cultivars, it is necessary to carry out comprehensive and specific

evaluation and research on lodging resistance of different sugarcane genotypes and the mechanisms in sugarcane lodging resistance (Kimbeng et al., 2000; Singh et al., 1999). This study was done by using thirty sugarcane combinations as materials to study the features of sugarcane lodging, establish classification standards for sugarcane lodging, and evaluate the lodging-resistant ability of the combinations, in order to provide a reference for selection of lodging-resistant parent and varieties in sugarcane.

Materials and methods

Plant materials

The tested materials were the seedlings from Sugarcane Research Institute, Guangxi Academy of Agricultural Sciences, Nanning in 2017. Thirty combinations were randomly selected, and the sugarcane variety ROC22 was used as control (*Table 1*). GT and SWS parents were from Sugarcane Research Institute, Guangxi Academy of Agricultural Sciences. YT and ZZ parents were from Guangzhou Sugarcane Industry Research Institute. YZ and DZ parents were from Sugarcane Research Institute of Yunnan Academy of Agricultural Sciences. CP parents were from USDA Canal Point Sugarcane Field Station. FN, LC and ROC parents were from Fujian Agriculture and forestry university, Sugarcane Research Center of Liucheng and Taiwan Sugarcane Research Institute. C1, Co, FR, PR and NongL were imported from Brazil, Franch, Puerto Rico and Japan, respectively.

Table 1. Sugarcane combinations tested

No.	Combination	No.	Combination
142	CP07-1618×YG22	975	GT05-ym3×LC03-1137
229	GT04-112×YC90-33	977	YT94-128×GT09-1163
283	GT06-3283×LT07-95	981	SWS09-001×CP92-1641
289	NongL8×GT09-1009	989	C1-2003×YZ95-128
327	GT04-1023×FN39	1124	GT02-761×YF90-95
370	CP07-1618×FN39	1245	GT01-25×CP09-4707
371	CP07-1618×LC03-1137	1252	GT05-3661×CP09-4256
381	GT05-wm48×GT07-229	Y12	ROC28×YT00-236
399	Co1001×GT10-2018	Y44	YT00-318×YT93-159
430	YZ99-596×GT10-2018	Y50	YT01-71×DZ93-88
506	GT06-1264×YT96-833	Y57	YT91-976×ROC23
564	GT02-761×YC07-71	Y65	YT93-159×YC07-71
593	GT06-3283×YZ06-80	Y70	YT94-128×ROC22
643	GT02-901×GT06-178	Y86	ZZ33×GT92-66
670	CP00-1630×GT06-1184	ROC22	ROC5×69-463
875	FR93-865×PR83-1248		

Experimental site

The experiment was carried out in Dingdang base of Sugarcane Research Institute Guangxi Academy of Agricultural Sciences in Long'an County. The soil was neutral sandy loam.

Experiment design

The seeds of the tested combinations were sowed in late March, 2017, and the seedlings were transplanted to nursery cups in the middle of April when they had two to four leaves. On June 15th, they were planted in the field. Sixty nine individual plants were randomly selected in each combination. Repeated planting was carried out for 3 times in randomized block design. Each plot contained one row of 7 m long, and the space between rows was 1.2 m. Twenty three plants were planted in each plot. Compound fertilizer (N:P:K = 8:6:6) 750 kg/ha was applied as the base fertilizer at the time of planting and urea 75 kg/ha was dressed at tillering stage.

Investigation index and method

From November to December, the resistance grade, lodging resistance index, fracture resistance, basal stem diameter, middle stem diameter, and brix were estimated by measuring 21 seedlings in each plot excluding the first and last seedlings to avoid the marginal effect in each row.

Resistance grade: It was estimated by referring to the partition method of Hao et al. (2008) with modification. The classification was done based on the lodging angle formed by the link between the top and the base of the stem, and the perpendicular line of the ground (Table 2).

Lodging resistance index (LRI): It was estimated according to the method of Li et al. (2012) and Xie et al. (2009). The equation is as follows:

$$LRI = \sum(g_i \times n_i) / N \times 100\% \quad (\text{Eq.1})$$

where n is the number of lodging stalks in a lodging grade, g is the lodging grade, and N is the total number of stalks investigated.

Stem diameter: The middle parts of basal and middle stem internode were measured with vernier caliper at mature stage.

Brix: Cane juice was extracted and measure with ATAGO handheld saccharimeter at mature stage.

Fracture resistance force: Ten upright and uniform plants were selected in each row, not including the plants on the sides. A PROSTRATETESTER DIK-7401 was kept vertically to the middle of the stem and push it hard to the plant to form a 45° included angle. The data showing on the prostrate tester were recorded.

Table 2. The grading standard of sugarcane lodging resistance in field

Lodging grade	Lodging angle
Grade 1	> 60°
Grade 2	30-60°
Grade 3	0-30°

Data analysis

The data were processed by Excel 2010 and subjected to ANOVA, and mean values were separated using Duncan's multiple range test. All statistical analyses were performed using the DPS 14.15 statistical package. The correlation between

combinations and lodging indexes were evaluated using Person correlation analysis. The lodging resistance index was used for cluster analysis which was carried out with the method of the distance of χ^2 and sum of squares of deviation. The grading standard of sugarcane lodging resistance was made by the observation of the sugarcane lodging and relevant research results (*Table 3*).

Table 3. The grading standard of sugarcane lodging resistance

Resistance grade	Lodging resistance index	Lodging level
Grade 1	1.00-1.60	High lodging
Grade 2	1.61-2.30	Middle lodging
Grade 3	2.31-3.00	Erect

Results

Relationship between different agronomic traits and resistance grade

It data in *Table 4* showed that the differences were significant in different lodging types for all the agronomic traits. The differences in brix in the erect, half lodging and complete lodging types suggested that the impact of lodging on brix was salient, and lodging would certainly reduce the brix in cane juice. The basal and middle stem diameters also significantly and negatively affected sugarcane lodging. The larger the stem, the higher the lodging resistance was, regardless of middle or basal part. The ratio between basal and middle stem diameter was an important index. Obviously, the stem with consistency from top to base possesses excellent lodging resistance. The stem with thin base and thick middle parts was easy to get lodging.

Table 4. The relationship of different agronomic traits and lodging

Type	Brix (°BX)	Basal stem diameter (cm)	Middle stem diameter (cm)	Ratio of middle and basal stem diameter
Erect	19.8±0.9 a	237±21 a	236±20 a	1.00±0.05 a
Half lodging	19.6±1.0 b	225±17 b	231±17 b	0.98±0.05 b
Complete lodging	19.3±1.2 c	206±18 c	219±19 c	0.94±0.05 c

Data in the table are the means of three replicates. Different low case letters in the same column represent the significant difference at 5% in Duncan's multiple range test

The resistance force test was not effective in this experiment. As shown in *Table 5*, the differences in repetitions were very significant, but those in combinations were not significant.

Table 5. The relationship of resistance force and different combinations in sugarcane

Item	Df	Sum Sq	Mean Sq	F value	Pr (>F)
Repetition	2	307.5	153.8	14.85	0.000007**
Combination	30	471.9	15.7	1.52	0.0876
Residuals	56	579.7	10.4		

** represent the significance at 1% levels

Analysis on relevance between agricultural traits and lodging resistance index

The lodging index resistance and the diameters of basal and middle stem were highly significantly and positively correlated ($r = 0.419^{**}$ and 0.356^{**}), indicating the thicker the stem was, the more lodging resistant the plant was. The lodging resistance index was significantly and positively correlated with the brix, suggesting that erect stalks had higher sugar content in cane. The lodging resistance index showed significantly positive correlation ($r = 0.201^*$ and $r = 0.232^*$) with the ratio of middle and basal stem diameter, indicating that the sugarcane genotypes with uniform stem were more lodging resistant. Though the correlation coefficients were moderate, they were significant in this study. The larger the ratio of middle and basal stem diameter was, the higher lodging resistance the sugarcane genotypes possessed (*Table 6*).

Table 6. Correlation coefficients between different traits

Correlation coefficient	Lodging resistance index	Resistance force	The ratio of middle in basal stem diameter	Brix	Basal stem diameter	Middle stem diameter
Lodging resistance index	1					
Resistance force	-0.02	1				
The ratio of middle in basal stem diameter	0.201*	-0.037	1			
Brix	0.232*	0.052	-0.168	1		
Basal stem diameter	0.419**	0.294**	0.432	0.093	1	
Middle stem diameter	0.356**	0.223*	-0.049	0.19	0.87	1

* and ** represent the significance at 5%, and 1% levels, respectively

Cluster analysis

Systematic cluster analysis was done based on the lodging resistance index, and the results were shown in *Figure 1*. The 30 tested combinations were divided into three categories, among them, 16 were in level 3, 13 in level 2, and 2 in level 1 (*Table 7*). GT and YT parents were accounted for 56% and 44% in level 3 respectively, and CP parents were accounted for 30% in level 2. The control variety ROC 22 belonged to the middle lodging type was classified in level 2 in this study, which was in line with its performance in commercial production.

Discussion

Three or more classifications were established according to the angle in other crops (Wang et al., 2015; Stamp and Kiel, 2010; Nakajima et al., 2008). By far, there has been no confirmed classification for lodging in sugarcane. In this study, the lodging of 30 sugarcane was classified into three levels, that is, level 1 (lodging), level 2 (half-lodging) and level 3 (erect) referring to other crops and sugarcane production reality. Meanwhile, the lodging index was brought up, and supported by the test data. The index could be used to judge the capability of lodging resistance of sugarcane rapidly. In the past, many sugarcane breeders had been deducing the lodging resistance trait by visual observation, and deducing whether the sugarcane was lodging resistant or not according to the approximate growth of sugarcane stalks in the field. But it was difficult for breeders to distinguish the status of some sugarcane genotypes which looked either like

lodged or erect, unless they were all erect or lodged. If the plants of a clone tended to lodging, which would be classified as complete lodging. With the lodging resistance index established in this study, we can quickly determine the lodging resistance of a clone and greatly improve the efficiency of sugarcane breeding.

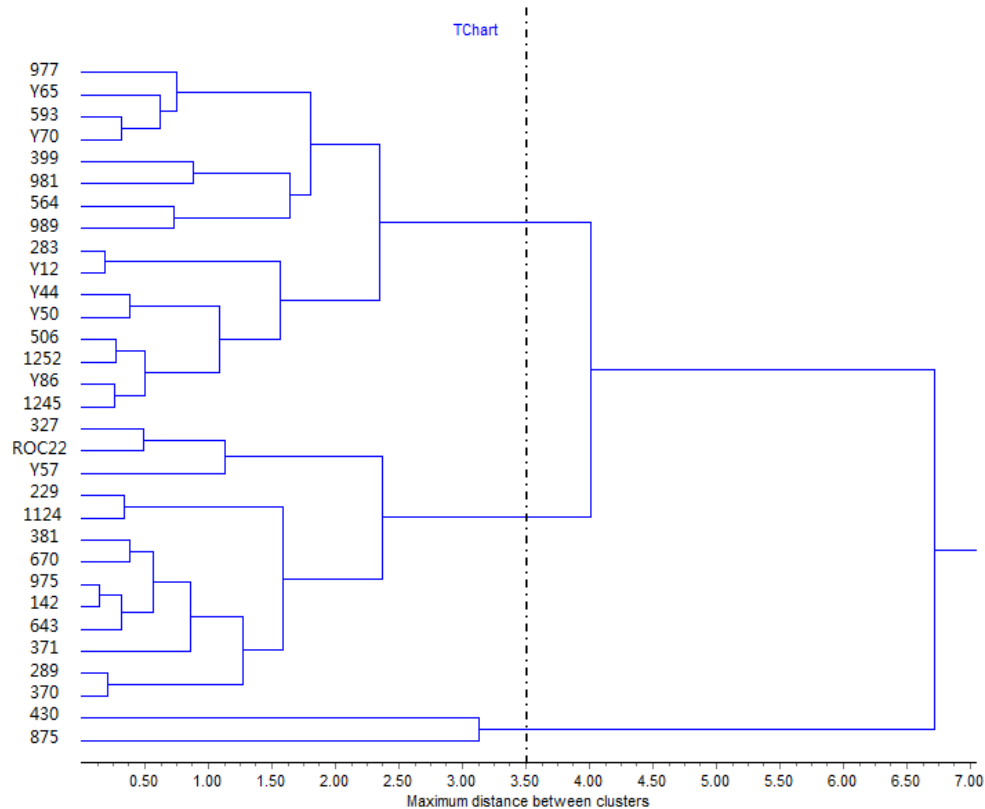


Figure 1. Clustering of lodging for different sugarcane combinations

Table 7. The lodging level of different combinations

No.	Combination	Level	No.	Combination	Level
977	YT94-128×GT09-1163	3	ROC22	ROC5×69-463	2
Y65	YT93-159×YC07-71	3	Y57	YT91-976×ROC23	2
593	GT06-3283×YT06-80	3	229	GT04-112×YC90-33	2
Y70	YT94-128×ROC22	3	1124	GT02-761×YF90-95	2
399	Co1001×GT10-2018	3	381	GT05-wm48×GT07-229	2
981	SWS09-001×CP92-1641	3	670	CP00-1630×GT06-1184	2
564	GT02-761×YC07-71	3	975	GT05-ym3×LC03-1137	2
989	C1-2003×YZ95-128	3	142	CP07-1618×YG22	2
283	GT06-3283×LT07-95	3	643	GT02-901×GT06-178	2
Y12	ROC28×YT00-236	3	371	CP07-1618×LC03-1137	2
Y44	YT00-318×YT93-159	3	289	NongL8×GT09-1009	2
Y50	YT01-71×DZ93-88	3	370	CP07-1618×FN39	2
506	GT06-1264×YT96-833	3	430	YZ99-596×GT10-2018	1
1252	GT05-3661×CP09-4256	3	875	FR93-865×PR83-1248	1
Y86	ZZ33×GT92-66	3			
1245	GT01-25×CP09-4707	3			
327	GT04-1023×FN39	3			

In this study, we identified the relationship between the lodging level and brix and stem diameter in sugarcane. When lodging occurred, the brix was down. Mo (1979) reported that the brix declined after lodging in sugarcane, which is in accordance to the results of this study. In addition, for the first time, this research used the data of the ratio of basal and middle stem diameter. The higher the ratio was, the higher lodging resistance index of sugarcane was. Apparently, they were positively correlated. When the ratio was lower than one, the lodging resistance index decreased and the degree of lodging was significantly higher, caused by the heavy top and light base (Peng, 1988; Feng et al., 2006). In the breeding process of sugarcane or other stalk crops, the breeders preferred to choose the ideal plant type – “tower type” (Liu, 2017). This structure was stable and could minimize losses even in bad weather such as strong wind (Johnson et al., 1998). Especially for the large leafed sugarcane, it is necessary to maintain the stability by selecting the “tower” structure. Therefore, the introduction of the ratio of basal and mid stem diameters would help the breeders to judge sugarcane lodging resistance more comprehensively.

There had been many studies on breeding and selecting resistance traits such as drought resistance, cold resistance and smut resistance by sugarcane germplasm resources (Agboire et al., 2000; Cai et al., 2008; Pan et al., 2006; Zhou et al., 2012). An excellent sugarcane variety was always selected from hundreds of sugarcane combinations (Yang et al., 2011). High yield, high sucrose content, strong ratoon ability and multi-resistance were the breeding targets (Mbuma et al., 2018; Huang et al., 2016; Zhou et al., 2017). However, the most prominent problem encountered in conventional breeding was the narrow genetic basis and insufficient parental innovation, which greatly affects the selection of new breakthrough sugarcane varieties. It is even more difficult to obtain new sugarcane varieties with specific characteristics (Duan et al., 2017; Ramburan et al., 2010). For lodging resistant breeding, it was necessary to have lodging resistant sugarcane germplasm resources (Sengwayo et al., 2018). In this research, based on the lodging resistance index, 30 combinations were classified into three levels, sixteen in level 3, thirteen in level 2, and two in level 1. In the combinations of lodging resistant, GT and YT parents were accounted for 56% and 44% respectively; In the combination of middle lodging, CP parents were accounted for 30%, indicating that the sugarcane varieties (clones) selected and planted in the local climate zone could better adapt to the cultivation environment. In China, the breeders consider more about the effect of lodging on commercial sugarcane production, so they prefer to select the clones with lodging resistance (Yang et al., 2019; Wu et al., 2019). Because of the complete sugarcane mechanization in the USA, the sugarcane breeders mainly considered yield and sugar, and the lodging resistance of sugarcane might be not the main target (Zhou and Li, 2012). Continuous evaluation of the lodging resistance of germplasm resources, statistical analysis of excellent combinations and excellent parents would be helpful to breed lodging resistant sugarcane varieties.

The instrument for measuring the resistance force, DIK7401, did not produce good results in sugarcane. Considering the limit of measurement range of the instrument, and that sugarcane is relatively high and the stem has strong tenacity, the thrust required should be much higher than that for rice (Xiong et al., 2018) and wheat (He, 2018). In the next step, we will consider to use a broader ranged resistance force tester for the study, and NKK-4005 computer-controlled universal testing machine may be used to measure the mechanical indexes of different lodging forms of sugarcane, such as leaf, skin endurance and stem bending resistance (Yang et al., 2016).

Conclusion

In this study, lodging grades and lodging resistance index were established for sugarcane. According to the lodging degree, sugarcane lodging could be divided into three grades, that is, grade 1 (complete lodging), grade 2 (half lodging) and grade 3 (erect). The established lodging resistance index could be used to evaluate the lodging resistance of sugarcane quickly. The relationship between lodging and brix and stem diameter was confirmed. The brix in cane juice decreased when lodging occurred. The ratio of basal and mid stem diameters was found highly significantly correlated with the lodging resistance in sugarcane. When the ratio was less than one, the lodging resistance index of sugarcane was low and the lodging degree was obviously heavy. With the lodging resistance index, the thirty combinations used in this study were divided into three categories, sixteen in grade 3, thirteen in grade 2, and two in grade 1.

Acknowledgements. This research was supported by the Fund for the Guangxi Innovation Teams of Modern Agriculture Technology (gjnytxgxcxt-d-03), Fund of Guangxi (2016GXNSFBA380138), Fund of Guangxi Science and Technology Base and Special Foundation (AD17195100), Funds of Guangxi Academy of Agricultural Sciences (2015JZ93, 2015YT02; G2014YZ01).

REFERENCES

- [1] Agboire, S., Wada, A. C., Ishaq, M. N. (2000): Evaluation and characterisation of sugar cane germplasm accessions for their breeding values in Nigeria. – *Journal of Food Technology in Africa* 7(1): 33-35.
- [2] Cai, Q., Aitken, K. S., Deng, H. H., Chen, X. W., McIntyre, C. L. (2008): Verification of the introgression of *erianthus arundinaceus* germplasm into sugarcane using molecular markers. – *Plant Breeding* 124(4): 322-328.
- [3] Duan, W. X., Huang, Y. X., Zhou, S., Zhang, B. Q., Luo, T., Yang, C. F., Gao, Y. J., Zhang, G. M. (2017): Transmission of parental chromosomes in F₁, BC₁ and BC₂ progeny between *Saccharum spp. hybrid* and *Narenga porphyrocoma* (Hance) Bor. - *Chinese Journal of Tropical Crops* 38(12): 2201-2005.
- [4] Feng, Y. X. (2006): Planting good autumn sugarcane to develop sugar industry. – *Guangxi Sugar Industry* 4: 43-45.
- [5] Hao, W. L., Liu, H. X., Zhu, L., Meng, Q. H. (2008): General provisions for methods for determining conditions of agricultural machinery test. – *PRC National Standard* 65: 2.
- [6] He, H. H. (2018): Physical and chemical characteristics related to lodging resistance in wheat. – Wuhan: M. S. Thesis of Huazhong Agricultural University 35: 1023.
- [7] Huang, J. Y., Li, X., Tan, F., Tang, S. Y., Wang, L. W., Huang, H. R. (2016): Breeding and characterization of a new sugarcane variety Guitang 49. – *Subtropical Agriculture Research* 12(2): 73-78.
- [8] Johnson, D. E., Dingkuhn, M., Jones, M. P., Mahamane, M. C. (1998): The influence of rice plant type on the effect of weed competition on *Oryza sativa* and *Oryza glaberrima*. – *Weed Research* 38(3): 207-216.
- [9] Kamran, M., Ahmad, I., Wang, H., Wu, X., Jing, X., Liu, T. (2018): Mepiquat chloride application increases lodging resistance of maize by enhancing stem physical strength and lignin biosynthesis. – *Field Crops Research* 224: 148-159.
- [10] Kimbeng, C. A., Mcrae, T. A., Stringer, J. K., Hogarth, D. M. (2000): Gains from family and visual selection in sugarcane, particularly for heavily lodged crops in the Burdekin region. – *Conference of the Australian Society of Sugar Cane Technologists* 37: 68-72.

- [11] Li, C. S., Huo, X. J., Wei, S. L., Wei, D., Wei, H. F., Huang, S. M. (2012): Evaluation of 5 banana varieties for resistance to Fusarium wilt. – Journal Of Southern Agriculture 43(4): 449-453.
- [12] Li, X., Li, Y. J., Liang, Q., Lin, S. H., Huang, H. R., Huang, Q. Y. (2018): Adaptability of sugarcane clone in Nanning ecological region. – Guangxi Sugar Industry 22: 129-130.
- [13] Li, Y. R. (2010): Modern Sugarcane Science. – China Agriculture Press, Beijing, pp. 121-122.
- [14] Li, Y. R., Mao, C. C., Tang, Q. Z. (2010): Reasons and countermeasures for sugar yield decrease in Asian countries in 2008-2009. – Guangxi Agricultural Science 41(1): 80-84.
- [15] Liu, F. X. (2017): Discussion on the reasonable combination of maize plant type and dense planting. – Agricultural Service 22: 103.
- [16] Liu, G. L., Fan, H. W. (2011): A better active design for optimizing grinding parameters of aviation spiral bevel gears. – Journal of Northwestern Polytechnical University 32(3): 92-97.
- [17] Mbuma, N. W., Zhou, M., Merwe, R. V. D. (2018): Evaluating parents for cane yield in sugarcane breeding using best linear unbiased prediction analysis of progeny data derived from family plots. – South African Journal of Plant and Soil 13: 1-8.
- [18] Mo, J. Y. (1979): Preliminary analysis of adverse physiological effects of sugarcane lodging – Sugar Industry (12): 22-24.
- [19] Nakajima, T., Yoshida, M., Tomimura, K. (2008): Effect of lodging on the level of mycotoxins in wheat, barley, and rice infected with the fusarium graminearum species complex. – Journal of General Plant Pathology 74(4): 289-295.
- [20] Pan, S. M., Chen, Y. Q., Wu, J. S., Zhang, M. Q. (2006): Screening and evaluation of the drought resistant genotypes in sugarcane. – Journal of Jiangxi Agricultural University 28(6): 838-843.
- [21] Peng, S. G. (1988): Review of 30 years of sexual crossbreeding of sugarcane in Guangxi. – Southwest Agricultural Journal (3): 15-22.
- [22] Piñera-Chavez, F. J., Berry, P. M., Foulkes, M. J., Molero, G., Reynolds, M. P. (2016): Avoiding lodging in irrigated spring wheat. ii. genetic variation of stem and root structural properties. – Field Crops Research 196: 64-74.
- [23] Ramburan, S., Paraskevopoulos, A., Saville, G., Jones, M. (2010): A decision support system for sugarcane variety selection in south africa based on genotype-by-environment analyses. – Experimental Agriculture 46(2): 243.
- [24] Sengwayo, S., Zhou, M., Labuschagne, M. (2018): Trends in broad-sense heritability and predicted selection gains for the coastal short cycle breeding sugarcane programmes in South Africa. – South African Journal of Plant & Soil 35(2): 89-99.
- [25] Singh, G., Chapman, S. C., Jackson, P. A., Lawn, R. J., Hogarth, D. M. (1999): Yield accumulation in sugarcane under wet tropical conditions - effect of lodging and crop age. – Proceedings of the Australian Society of Sugar Cane Technologists 21: 241-245.
- [26] Singh, G., Chapman, S. C., Jackson, P. A., Lawn, R. J. (2002): Lodging reduces sucrose accumulation of sugarcane in the wet and dry tropics. – Australian Journal of Agricultural Research 53(11): 1183-1195.
- [27] Stamp, P., Kiel, C. (2010): Root morphology of maize and its relationship to root lodging. – Journal of Agronomy & Crop Science 168(2): 113-118.
- [28] Wang, X. D., Wang, M. Q., Wang, H. X. (2014): Analysis on the relationship between yield components and yield of rice germplasm in cold region. – Heilongjiang Agricultural Sciences 6(3): 153-172.
- [29] Wang, Y., Wei, Z. W., Shao, P., Tian, X. H., Wang, X. L., Ma, G. H. (2015): Research status on relationship between culm characteristics and lodging resistance of rice. – Hubei Agricultural Sciences 34: 2054-2057.
- [30] Wu, J. Y., Huang, J. J., Ling, Q. P., Chen, Y. S., Zeng, Q. Y., Yang, Z. D., Qi, Y. W., Li, Q. W. (2019): Preliminary identification and evaluation of 12 strains of HoCP series in sugarcane germplasm resources. – Journal of Tropical and Subtropical Botany 1: 53-59.

- [31] Xie, Z. S., Zhang, X., Chen, Y. Y., Luo, S. R., Wei, S. Y. (2009): Assessment of banana germplasm for resistance to fusarium wilt. – Chinese Journal of Tropical Crops 30(3): 362-364.
- [32] Xiong, W., Fengying, X. U., Wang, X. (2018): Effect of different nitrogen application rate on rice stem characteristics. – Agricultural Biotechnology 40(2): 56-62.
- [33] Yang, R. Z., Li, Y. R., Wang, W. Z., Zhu, Q. Z., Zhou, H., Tang, S. Y. (2011): Evaluation of cold tolerance of sugarcane under drought frost condition. – Agricultural Science & Technology 24: 1303-1307.
- [34] Yang, R. Z., Zhou, H., Lei, J. C., Duan, W. X., Li, Y. R., Tang, S. Y., Li, W. J., Yang, C. F., Gao, Y. J., Zhou, S. (2019): The harvest index of different sugarcane varieties. – Sugar Crops of China 41(1): 8-12.
- [35] Yang, W., Mo, X. M., Yang, J., Yuan, F. W., Huang, S. C. (2016): Experimental study on the basic parameters of sugarcane on easy lodging period. – Journal of Agricultural Mechanization Research 12: 143-148.
- [36] Zhang, X. C., Hu, Y., Yang, Z. J. (2010): Cutting movement analysis of spiral bevel gear based on the tooth generating line. – Journal of Beijing University of Technology 28(11): 63-67.
- [37] Zhou, H., Li, Y. R. (2012): Analysis on sugarcane varieties bred in the United States of America. – Journal of Southern Agriculture 43(5): 570-577.
- [38] Zhou, H., Lei, J. C., Gui, Y. Y., Xian, W., Liang, Q., Yang, R. Z., Li, Y. R. (2012): Evaluation on cold tolerance of sugarcane varieties under field conditions. – Journal of Plant Genetic Resources 13(6): 968-973.
- [39] Zhou, Z. F., Deng, Y. C., Wang, L. W., Xian, W., Tan, F., Huang, H. R. (2017): Selection and species evaluation of sugarcane variety Guitang 47. – China Seed 2: 62-64.

MORPHOLOGICAL RESPONSES OF ORNAMENTAL SUNFLOWER TO PUTRESCINE TREATMENT UNDER DROUGHT CONDITIONS

KAHROBAIYAN, M.¹ – NEMATI, S. H.^{1*} – RAHEMI, M.² – KHOLDEBARIN, B.³ – TEHRANIFAR, A.¹

¹*Department of Horticultural Sciences and Landscape, Faculty of Agriculture, Ferdowsi University of Mashhad, Mashhad, Iran*

²*Department of Horticultural Sciences, Faculty of Agriculture, Shiraz University, Shiraz, Iran*

³*Department of Biology, Faculty of Sciences, Shiraz University, Shiraz, Iran*

**Corresponding author
e-mail: nematish@yahoo.com*

(Received 1st Aug 2018 ; accepted 16th Jan 2019)

Abstract. Drought is one of the most important abiotic stresses that affects plant growth and development. Polyamines (PAs) can have an active key role in improving plants tolerance to various stresses. Based on global ecological conditions, plants growing in about one third of the potentially viable lands such as Iran are exposed to drought stress during growing season. The objective of the present study was to investigate the enhancing effects of foliar application of Putrescine (PUT) on short-term tolerance against water stress in ornamental sunflowers. This study was conducted in the experimental greenhouse of the Department of Horticultural Sciences and Landscape, Ferdowsi University of Mashhad, Iran. Plant materials used in this study were the F₁ seeds of ornamental sunflower (*Helianthus annuus* L. cv. Sunbright kids). The experiment was conducted as a factorial (2 × 3) in complete randomized block design with four replications and 8 plants in each replicate. Plants were irrigated at 40 and 80% field capacity (FC). Foliar spray of PUT (0, 75 and 150 mg l⁻¹) was applied twice during plants growing period. Water stress at 40% FC as compared with 80% FC, significantly affected reproductive and vegetative characteristics of plants. The effects of exogenous application of PUT (75 and 150 mg l⁻¹) in comparison with control, significantly increased leaves number per plant, leaves fresh and dry weight, leaves area, stems fresh and dry weight, stems diameters at soil surface, plants height, roots fresh and dry weight, roots area, number of flowers, flowers longevity, seeds number per head and seeds weight. In this study, there was no significant difference between the effects of PUT levels on most of the reproductive and vegetative characteristics of sunflower plants under water stress conditions. The results confirmed that foliar application of PUT protected plants against drought stress and increased specially flowers retention. Therefore, to improve parameters of the studied plants under drought stress, the commercial application of PUT (75 mg l⁻¹) is recommended for this cultivar.

Keywords: *flower longevity, Helianthus annuus, polyamine, reproductive and vegetative parameters, water stress*

Introduction

About one-third of the global potentially viable lands are subject to an inadequate water supply (Zhang and Huang, 2013). Plants are usually exposed to different environmental stress conditions in their life cycles. Drought is one of the most important abiotic stresses that affect plant growth and development. Decrease in water availability to plants due to low soil water potential followed by leaves transpiration will result in an increase in stomatal resistance, low CO₂ influx and a decrease in photosynthesis (Kotakis et al., 2014 and Zgallai et al., 2005).

Polyamines (PAs) have great influence on plant development and stress tolerance (Hussain et al., 2011; Urano et al., 2003). The most important polyamines are diamine

putrescine (PUT), triamine spermidine (Spd) and tetramine spermine (Spm) (Marco et al., 2011). There is a direct correlation between drought tolerance and the total plants PUT content which is in agreement with the inherent function of PUT in improving drought resistance regardless of plants Spd and Spm contents (Alcázar et al., 2010).

It is believed that the biosynthesis of PAs especially that of PUT will improve plants abiotic stress-tolerance as compared to non-tolerant ones (Hussain et al., 2011). Since cationic PAs' are inherently capable of binding to cellular polyanions including DNA, RNA and proteins, they can influence the synthesis, structure and function of these macromolecules and also by interacting with other cell components, PAs widely affect plant growth and development and also plants responses to environmental stresses (Kanayama and Kochetov, 2015). PAs are involved in signal transduction leading to a change in other hormones (Bitrian et al., 2012), such as Abscisic acid (ABA) (Hussain et al., 2011) and ethylene (Kaur–Sawhney et al., 2003). PAs maintain cell stability (Legocka and Kluk, 2005), and regulate root growth (Wang et al., 2011). It has been found that PA concentrations are higher in the roots and leaves of stressed plants. This implies that PA metabolism in drought-tolerant plants is an adaptive mechanism to drought stress (Zhang and Huang, 2013). Previous studies have shown that there is a close relation between the PUT levels and the biochemical and morphological responses to dehydration. In addition, it has been observed that by manipulating at the transcriptional level, PUT increases ABA biosynthesis in plants in response to drought stress. It has also been reported that PUT accumulation enhances drought tolerance since the levels of Spm and Spd have not increased during the dehydration period (Espasandin et al., 2014).

Considering the adverse climatic conditions in Iran, and plants in landscapes being exposed to drought stress during growing season, the objective of this study was to investigate whether the direct PUT application on ornamental sunflowers plants can enhance short-term tolerance against water stress in such plants.

Materials and methods

This study was conducted in the experimental greenhouse of the Department of Horticultural Sciences and Landscape, Faculty of Agriculture, Ferdowsi University of Mashhad, Iran, under controlled conditions with relative humidity of 60%, and 25 °C/18 °C (day/night) temperature. The light intensity inside the greenhouse was 500-700 $\mu\text{mol m}^{-2} \text{s}^{-1}$. The environmental conditions of the greenhouse were relatively constant during the whole period of the experiments from germination to vegetative and reproductive growth phases.

Plant materials used in this study were the F₁ seeds of ornamental sunflower (*Helianthus annuus* L. cv. Sunbright kids) purchased from Sokata Company, Japan. Seeds were planted in trays containing coco peat, peat moss and perlite (1:1:1, v/v/v). After seedlings were at 6 leaf stage (after one month), they were transplanted into plastic pots containing 4.6 kg of soil, leaf mould, vermicompost and sand (7:1:1:1, v/v/v/v). Before starting the experiments, the physical properties of the soil mixture used were determined (*Table 1*). Forty days after seeds germination, plants were sprayed with Putrescine (PUT) (0, 75 and 150 mg l⁻¹). The amount sprayed was enough to soak the leaves and the solution started to drip and applied 10 times for each plant. Control plants were sprayed with the same amount of distilled water. As the seedlings entered the reproductive phase (60 days after seed germination), soil moisture contents

were kept at 40 and 80% field capacity (FC). One month after the first foliar PUT spray (10 days after plants entered the reproductive phase), the second spray was applied, same way as the first one (Figs. 1 and 2). At the end of the experiments, the following morphological characters were determined: Flowers number and diameters (Digital calliper), petals length, flowers longevity on the plants, seeds number and seeds weight in each head, leaves number and area (Leaf Area Meter, Model: L1-3100C. LI-COR Biosciences, USA), plants height and stems diameter at soil surface. Roots area and length and mean roots diameter were measured by Root Analyser (Model: DELTA-T DEVICES LTD. CAMBRIDGE. ENGLAND). Plants aerial parts were cut from soil surface and their roots were washed with tap water to remove the soil. After wiping the moisture, roots were separated from each other and put on the surface of Root Analyser for parameters determination. Also, the fresh weight (FW) and dry weight (DW) of flowers, leaves, stems and roots were determined. Dry weights were determined after keeping the samples in an oven at 75 °C for 72 h.



Figure 1. Ornamental sunflower plants used in the experiments



Figure 2. Method used to apply PUT on ornamental sunflower plants

Table 1. Physico-chemical characteristics of the potting soil

EC (dS/m)	pH	N (%)	K (mg/Kg)	P (mg/Kg)	Sand (%)	Clay (%)	Silt (%)
3.53	7.15	0.1428	482.3	36.8	42	18	40

The experiments were conducted as a factorial (2×3) in complete randomized block design with four replications and 8 plants in each replicate. Statistical differences between measurements were analyzed following the analysis of variance (ANOVA) using Minitab 16.0 software. Analysis of variance was performed based on Fischer S test. Fischer-LSD test was used to compare means and differences ($P \leq 0.05$).

Results

Effects of water stress on plants reproductive characteristics are shown in *Table 2* and *Figures 3* and *4*. Water stress at 40% FC in comparison with 80% FC significantly reduced flowers number (3.26%), flowers diameter (8.58%), petals length (6.17%), flowers FW (7.5%), flowers longevity (11.11%), seeds number per head (14.38%) and seeds weight (50%).

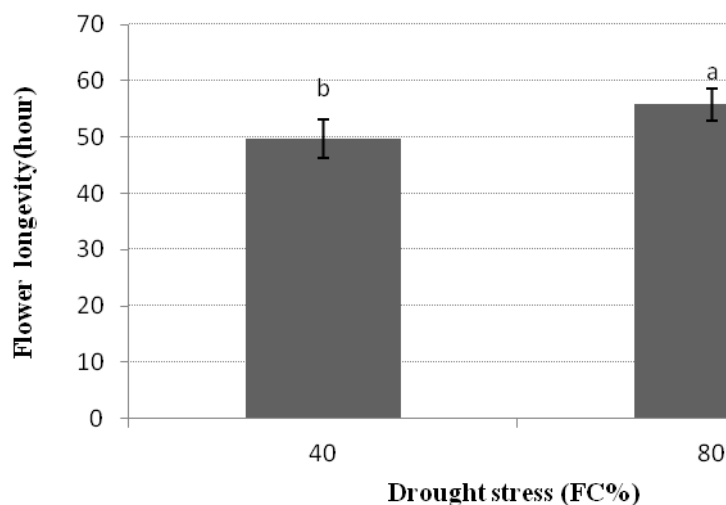


Figure 3. Effects of drought stress on flower longevity. Histograms with different letters are statistically significant based on LSD test at $P \leq 5\%$ level

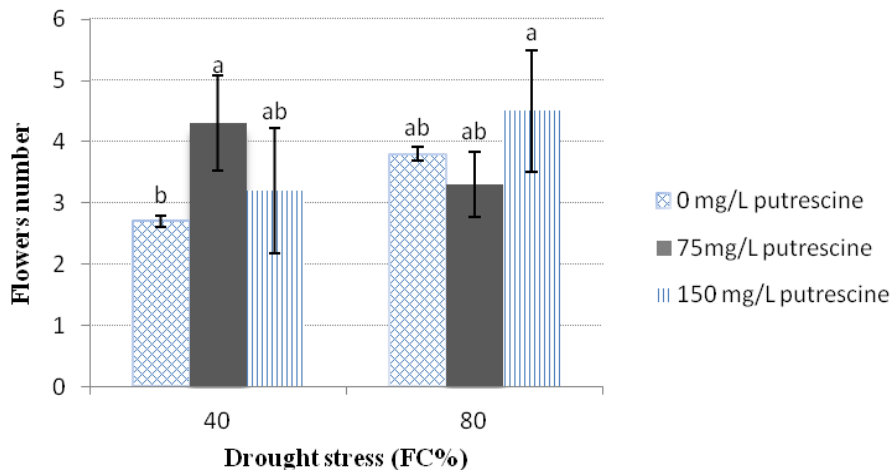


Figure 4. Interaction effects of drought stress levels and Putrescine on flowers number. Histograms with different letters are statistically significant based on LSD test at $P \leq 5\%$ level

Table 2. Effects of drought stress on flowers parameters

Drought stress (FC %)	Parameters					
	Flower diameter (mm)	Petal length (mm)	Flower fresh weight (g)	Flower dry weight (g)	Seed numbers per head	Seeds weight (g)
40	53.3 b*	22.8 b	4.0 a	0.5 a	39.9 b	0.1 b
80	58.3 a	24.3 a	3.7 b	0.5 a	46.6 a	0.2 a

*Means with different letters in a column are statistically significant based on LSD test at $P \leq 5\%$ level

The results of water stress effects on plants vegetative parameters are shown in *Tables 3 and 4* and *Figure 5*. Water stress at 40% FC in comparison with 80% FC significantly reduced leaves number per plant (23.90%), leaves FW (37.5%), leaves DW (32%), leaves area (37.08%), stems FW (35.11%), stems DW (28.20%), stems diameter at soil surface (15.22%), plants height (9.24%), total roots length (32.51%), roots FW (25.30%), roots DW (15.38%) and roots area (27.45%).

The effects of PUT spray on flower parameters are shown in *Table 5* and *Figures 4* and *6*. PUT at 75 and 150 mg l⁻¹ in comparison with control, significantly increased flowers number (18.75% and 37.5% respectively), flowers longevity (25.9% and 9.77% respectively), seeds number per head (26.2% and 0.76% respectively) and seeds weight (100% by both PUT concentrations used).

Table 3. Effects of drought stress on plants vegetative parameters

Drought stress (FC %)	Parameters						
	Stem diameter at soil surface (mm)	Stem fresh weight (g)	Stem dry weight (g)	Leaves number per plant	Leaves fresh weight (g)	Leaves dry weight (g)	Plants height (cm)
0	7.8 b*	17.0 b	2.8 b	12.1 b	8.5 b	1.7 b	16.7 b
80	9.2 a	26.2 a	3.9 a	15.9 a	13.6 a	2.5 a	18.4 a

*Means with different letters in a column are statistically significant based on LSD test at $P \leq 5\%$ level

Table 4. Effects of drought stress on roots parameters

Drought stress (FC %)	Parameters				
	Average roots diameter (mm)	Total roots length (mm)	Roots fresh weight (g)	Roots dry weight (g)	Roots area (mm ²)
40	0.6 a*	127273.2 b	18.9 b	2.2 b	76796.0 b
80	0.6 a	188578.2 a	25.3 a	2.6 a	105857.6 a

*Means with different letters in a column are statistically significant based on LSD test at $P \leq 5\%$ level

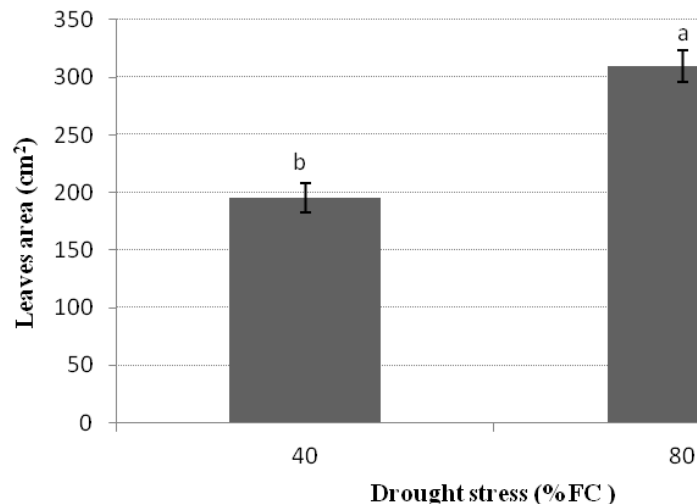


Figure 5. Effects of drought stress on leaves area. Histograms with different letters are statistically significant based on LSD test at $P \leq 5\%$ level

The effects of exogenous application of PUT on plants under water stress are shown in Tables 6 and 7 and Figure 7. PUT (75 and 150 mg l⁻¹) spray in comparison with control (distilled water), significantly increased leaves number per plant (6.15% and 16.22% respectively), leaves FW (23.40% and 29.79% respectively), leaves DW (15.79% and 15.79% respectively) and leaves area (17.58% and 28.49% respectively). Also seedlings stems parameters under water stress conditions were affected by Put spray. PUT (75 and 150 mg l⁻¹) in comparison with control significantly increased stems FW (18.03% and 36.61% respectively), stems DW (14.29% and 39.29% respectively), stems diameter at soil surface (10% and 3.66% respectively), plants height (5.88% and 3.53% respectively), roots FW (23.40% and 28.72% respectively), roots DW (47.37% and 31.58% respectively) and roots area (39.06% and 39.75% respectively).

Table 5. Effects of Putrescine on flowers parameters

PUT (mg l ⁻¹)	Parameters					
	Flower diameter (mm)	Petal length (mm)	Flower fresh weight (g)	Flower dry weight (g)	Seeds number per head	Seeds weight (g)
0	54.4 a*	23.4 a	3.7 a	0.5 a	39.7 b	0.1 b
75	58.0 a	23.8 a	3.8 a	0.5 a	50.1 a	0.2 a
150	54.9 a	23.6 a	4.0 a	0.5 a	40.0 b	0.2 a

*Means with different letters in a column are statistically significant based on LSD test at $P \leq 5\%$ level

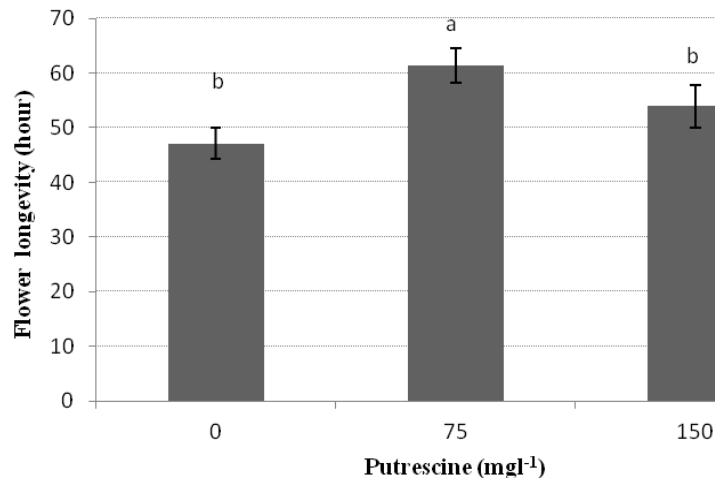


Figure 6. Effects of Putrescine on flower longevity. Histograms with different letters are statistically significant based on LSD test at $P \leq 5\%$ level

Table 6. Effects of Putrescine on plants vegetative parameters

PUT (mg l ⁻¹)	Parameters						
	Stem diameter at soil surface (mm)	Stem fresh weight (g)	Stem dry weight (g)	Leaves number per plant	Leaves fresh weight (g)	Leaves dry weight (g)	Plant height (cm)
0	8.2 a*	18.3 b	2.8 b	13.0 b	9.4 b	1.9 b	17.0 b
75	8.7 a	21.6 ab	3.2 ab	13.8 ab	11.6 ab	2.2 ab	18.0 a
150	8.5 a	25.0 a	3.9 a	15.2 a	12.2 a	2.2 a	17.6 ab

*Means with different letters in a column are statistically significant based on LSD test at $P \leq 5\%$ level

Table 7. Effects of Putrescine on roots parameters

PUT (mg l ⁻¹)	Parameters				
	Average roots diameter (mm)	Total roots length (mm)	Roots fresh weight (g)	Roots dry weight (g)	Roots area (mm ²)
0	0.6 a*	118798.9 a	18.8 b	1.9 b	72326.0 b
75	0.6 a	171249.0 a	23.2 ab	2.8 a	100578.8 a
150	0.6 a	183729.2 a	24.2 a	2.5 ab	101075.6 a

*Means with different letters in a column are statistically significant based on LSD test at $P \leq 5\%$ level

In this study, there were no significant differences between the effects of the two PUT levels used on most of the vegetative and reproductive parameters under water stress conditions. It was only the seeds number per head which was affected by the two PUT levels.

The interaction effects of water stress levels (40% and 80% FC) and PUT levels (75 and 150 mg l⁻¹) significantly increased plants height, flowers number and seeds number per head (Table 8 and Fig. 4).

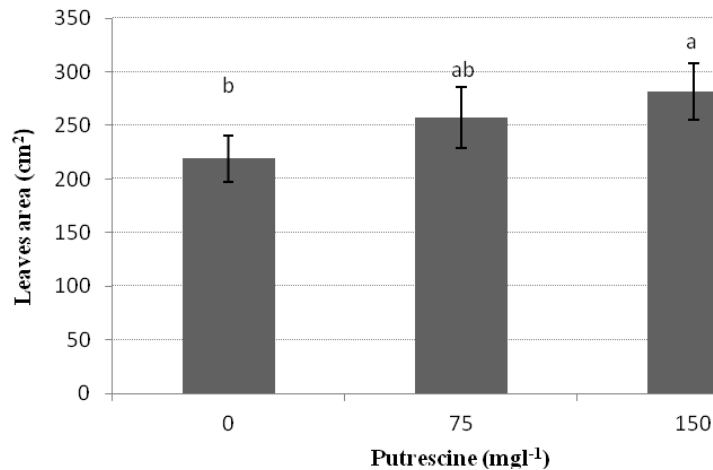


Figure 7. Effects of Putrescine on leaves area. Histograms with different letters are statistically significant based on LSD test at $P \leq 5\%$ level

Table 8. Interaction effects of Putrescine and drought stress on some plants morphological parameters

Treatments		Parameters	
Drought stress	PUT*	Seeds number per head	Plants height (cm)
DS1	0	36.00±8.34 ^{bc**}	16.60±0.31 ^{bc}
	75	53.50±11.64 ^a	16.60±0.26 ^c
	150	30.40±10.31 ^c	17.00±0.94 ^{bc}
DS2	0	43.40±3.55 ^{abc}	17.50±1.21 ^{bc}
	75	46.80±6.45 ^{abc}	19.40±0.13 ^a
	150	49.60±4.57 ^{ab}	18.30±1.12 ^{ab}

DS (Drought stress): DS1: 40%FC; DS2: 80%FC

*PUT (0, 75, 150 mg l⁻¹)

**Data are means ± SD (standard deviation). Means with different letters in a column are statistically significant based on LSD test at $P \leq 5\%$ level

Discussion

In the present study, water stress caused a number of changes in ornamental sunflower plants such as leaves number per plant, leaves area, leaves, stems and roots fresh and dry weight, plants height, roots length and roots area. Leaves drop was significantly higher at 40% FC as compared with 80% FC (Table 3 and Fig. 5). Drought induced plant growth inhibition such as plants height and leaves senescence which has also been reported for white clover (Li et al., 2016). The decrease in plants growth and increase in leaves senescence under drought conditions could be due to a decline in plants cytokinin content (Clark et al., 2004; Peleg and Blumwald, 2011). In our study, water stress decreased both plants FW and DW (Tables 2, 3 and 4). The reduction in plants FW under drought stress has also been reported for other plants such as wheat (Rane et al., 2001). The reduction in plants FW under drought stress is mainly due to loss of cell turgor required for cell growth and cell expansion. It has also been reported

that PAs play important roles in cell division and elongation (Hummel et al., 2004; Mattoo et al., 2010; Paschalidis and Roubelakis-Angelakis, 2005).

The decrease in plants DW in response to drought stress (*Tables 2, 3 and 4*), is probably due to decline in plant growth, reduction in photosynthetic activity due to increase in stomatal resistance and leaves senescence (Manivannan et al., 2007; Zgallai et al., 2005).

We found that water stress significantly reduced flowers number, flowers diameter and flowers longevity, but foliar application of PUT significantly increased flowers number and flowers longevity (*Table 2 and 5 and Figs. 3, 4 and 6*). Changes in flower parameters under drought stress, might be due to the cytokinin and gibberellin decline and leaves senescence. Application of PUT somehow counteracted the inhibitory effects of drought stress on flowers parameters (*Table 5 and Figs. 4 and 6*). It has been reported that increase in endogenous PAs leads to the up-regulation of plants cytokinin and gibberellin biosynthesis mechanisms (Li et al., 2016).

In our study, seeds number and seeds weight per head were significantly reduced by water stress (*Table 2*). Our results are in agreement with previous reports which have indicated that drought stress increases the ethylene (ETH) evolution rate of wheat grain leading to the inhibition of wheat grain filling (Liu et al., 2016).

It has been reported that external application of PAs is responsible for the increase in endogenous ABA levels (Steiner et al., 2007). Increase in ABA promotes the transport of carbohydrate from stem to the grain (Liu et al., 2016). It has also been reported that increase in PUT accumulation in plants promotes drought tolerance. However, no increase in plants Spm and Spd contents were observed during dehydration period (Espasandins et al., 2014).

Exogenous application of PUT at both concentrations (75 and 150 mg l⁻¹) significantly increased most sunflowers plants vegetative and reproductive parameters (*Tables 5, 6 and 7 and Figs. 4, 6 and 7*). The protective effects of PUT on cell membrane stability index (MSI) and leaves chlorophylls content as well as on photosynthetic activity (PN) have also been reported by Rahemi et al. (2017).

Application of PUT significantly increased flowers retention in sunflower plants (*Fig. 6*). Similar results have been reported by Baninasab and Rahemi (2008) for flower bud retention in pistachio plants. It has been reported that PAs inhibit the biosynthesis of ETH in plants since S-adenosylmethionine, the precursor of both PA and ETH synthesis will be used mainly for the synthesis of PAs rather than ETH (Liang and Lur, 2002). Exogenous application of PAs has blocked ETH synthesis in rice panicles (Yang et al., 2008).

Conclusion

Our study has indicated that ornamental sunflower Sunbright kids cultivar, is highly sensitive to water stress. PUT treatments before the onset of drought stress, protects plant against drought and inhibits plants water loss, confirming the key role of PUT in its ability to protect plants against water stress. The effect of exogenous application of PUT (75 and 150 mg l⁻¹) in comparison with control, significantly increased leaves number per plant, leaves fresh and dry weight, leaves area, stems fresh and dry weight, stems diameter at soil surface, plants height, roots fresh and dry weight, roots area, number of flowers, flower longevity, seeds number per head and seeds weight. In this study, there was no significant difference between the effects of PUT levels on most of

the reproductive and vegetative parameters of sunflower plants under water stress conditions. Therefore, to improve the vegetative and reproductive parameters of the studied plants under drought stress, the commercial application of PUT (75 mg l⁻¹) is recommended for this ornamental sunflower cultivar.

The results of our study originally indicate that PUT treatment under drought conditions improves flowers longevity and other plants parameters such as flowers number and leaves number per plant and leaves area which are important in urban landscape.

The determination of the intercellular titer of PUT and other polyamines and analyses of endogenous plant growth substances such as cytokinins, gibberellins and abscisic acid during experiments are suggested. Furthermore, studying some plants physiological parameters under these conditions such as photosynthetic rate (Pn), transpiration rate (Tr), stomatal conductance of CO₂ (gs), stomatal size, plants carbohydrates, proline, chlorophylls and carotenoids contents are recommended.

Acknowledgements. This research was supported by Ferdowsi University of Mashhad. The authors are very grateful to Professor Mehdi Nassiri-Mahallati for his guidance in statistical data analysis.

REFERENCES

- [1] Alcázar, R., Planas, J., Saxena, T., Zarza, X., Bortolotti, C., Cuevas, J., Bitrián, M., Tiburcio, A. F., Altabella, T. (2010): Putrescine accumulation confers drought tolerance in transgenic Arabidopsis plants overexpressing the homologous arginine decarboxylase 2 gene. – *Plant Physiol. Biochem.* 48: 547-552.
- [2] Baninasab, B., Rahemi, M. (2008): Effect of exogenous polyamines on flower bud retention in pistachio. – *Korean Soc. Hort. Sci.* 49: 149-154.
- [3] Bitrián, M., Zarza, X., Alterabella, T., Tiburcio, A. F., Alcázar, R. (2012): Polyamines under abiotic stress: metabolic crossroads and hormonal crosstalks in Plant. – *Metabolites* 2: 516-528.
- [4] Clark, D. G., Dervinis, C., Barrett, J. E., Klee, H., Jones, M. (2004): Drought-induced leaf senescence and horticultural performance of transgenic PSAG12-IPT petunias. – *J. Amer. Soc. Hort. Sci.* 129: 93-99.
- [5] Espasandins, F. D., Maia, S. J., Calzadilla, P., Ruiz, O. A. (2014): Transcriptional regulation of 9-cis-epoxycarotenoid dioxygenase (NCED) gene by putrescine accumulation positively modulates ABA synthesis and drought tolerance in *Lotus tenuis* plants. – *Physiol. Biochem.* 76: 29-35.
- [6] Hummel, I., Gouesbet, G., El Amrani, A., Aïnouche, A., Couée, I. (2004): Characterization of the two arginine decarboxylase (polyamine biosynthesis) paralogues of the endemic subantarctic cruciferous species *Pringlea antiscorbutica* and analysis of their differential expression during development and response to environmental s. – *Gene.* 342: 199-209.
- [7] Hussain, S. S., Ali, M., Ahmad, M., Siddique, K. H. (2011): Polyamines: natural and engineered abiotic and biotic stress tolerance in plants. – *Biotechnol. Adv.* 29: 300-311.
- [8] Kanayama, Y., Kochetov, A. (2015): *Abiotic Stress Biology in Horticultural Plants.* – Springer, Japan.
- [9] Kaur-Sawhney, R., Tiburcio, A. F., Alterabella, T., Galston, A. W. (2003): Polyamines in Plants an overview. – *J. Cell. Mol. Biol.* 2: 1-12.
- [10] Kotakis, C., Theodoropoulou, E., Tassis, K., Oustamanolakis, C., Ioannidis, N. E., Kotzabasis, K. (2014): Putrescine, a fast-acting switch for tolerance against osmotic stress. – *J. Plant Physiol.* 171: 48-51.

- [11] Legocka, J., Kluk, A. (2005): Effect of salt and osmotic stress on changes in polyamine content and arginine decarboxylase activity in *Lupinus luteus* seedling. – J. Plant Physiol. 169: 662-668.
- [12] Li, Z., Zhang, Y., Zhang, X., Peng, Y., Merewitz, E., Ma, X., Huang, L., Yan, Y. (2016): The alterations of endogenous polyamines and phytohormones induced by exogenous application of spermidine regulate antioxidant metabolism, metallothionein and relevant genes conferring drought tolerance in white clover. – Environmental and Experimental Botany 124: 22-38.
- [13] Liang, Y. L., Lur, H. S. (2002): Conjugated and free polyamine levels in normal and aborting maize kernels. – Crop Sci. 42: 1217-1224.
- [14] Liu, Y., Liang, H., Lv, X., Liu, D., Wen, X., Liao, Y. (2016): Effect of polyamines on the grain filling of wheat under drought stress. – Plant Physiology and Biochemistry 100: 113-129.
- [15] Manivannan, P., Jaleel, C. A., Sankar, B., Kishorekumar, A., Somasundaram, R., Lakshmanan, G. M. A., Panneerselvam, R. (2007): Growth, biochemical modifications and proline metabolism in *Helianthus annuus* L. as induced by drought stress. – Colloids and Surfaces B: Biointerfaces 59: 141-149.
- [16] Marco, F., Alcázar, R., Tiburcio, A. F. P. (2011): Carrasco, Interactions between polyamines and abiotic stress pathway responses unraveled by transcriptome analysis of polyamine overproducers. – OMICS 15: 775-781.
- [17] Mattoo, A. K., Minocha, S. C., Minocha, R., Handa, A. K. (2010): Polyamines and cellular metabolism in plants: transgenic approaches reveal different responses to diamine putrescine versus higher polyamines spermidine and spermine. – Amino Acids. 38: 405-413.
- [18] Paschalidis, K. A., Roubelakis-Angelakis, K. A. (2005): Spatial and temporal distribution of polyamine levels and polyamine anabolism in different organs/tissues of the tobacco plant. Correlations with age, cell division/expansion, and differentiation. – Plant Physiol. 138: 142-152.
- [19] Peleg, Z., Blumwald, E. (2011): Hormone balance and abiotic stress tolerance in crop plants. – Curr. Opin. Plant Biol. 14: 290-295.
- [20] Rahemi, M., Rostami, A. A., Kholdebarin, B., Sedaghat, S. (2017): Role of polyamines in caprifig drought tolerance. – Inter: J. Sci. Technol. 6: 822-829.
- [21] Rane, J., Maheshwari, M., Nagarajan, S. (2001): Effect of pre-anthesis water stress on growth, photosynthesis and yield of six wheat cultivar different in draught tolerance. – Indian J. Plant Physiol. 6: 53-60.
- [22] Steiner, N., Santa-Catarina, C., Silveira, V., Floh, E. I. S., Guerra, M. P. (2007): Polyamine effects on growth and endogenous hormones levels in *Araucaria angustifolia* embryogenic cultures. – Plant Cell Tiss. Org. 89: 55-62.
- [23] Urano, K., Yoshiba, Y., Nanjo, T., Igarashi, Y., Seki, M., Sekiguchi, F., Yamaguchi-Shinozaki, K., Shinozaki, K. (2003): Characterization of Arabidopsis genes involved in biosynthesis of polyamines in abiotic stress responses and developmental stages. – Plant Cell Environ. 26: 1917-1926.
- [24] Wang, J., Sum, P., Chen, C., Wang, Y., Fu, X., Liu, J. H. (2011): An arginine decarboxylase gene PtADC from *Poncirus trifoliata* confers abiotic stress tolerance and promotes primary root growth in Arabidopsis. – J. Exp. Bot. 62: 2899-2914.
- [25] Yang, J. C., Cao, Y. Y., Zhang, H., Liu, L. J., Zhang, J. H. (2008): Involvement of polyamines in the post-anthesis development of inferior and superior spikelets in rice. – Planta 228: 137-149.
- [26] Zgallai, H., Steppe, K., Lemeur, R. (2005): Photosynthetic, physiological and biochemical responses of tomato plants to polyethylene glycol-induced water deficit. – Journal of Integrative Plant Biology 47: 1470-1478.
- [27] Zhang, C., Huang, Z. (2013): Effects of endogenous abscisic acid, jasmonic acid, polyamines, and polyamine oxidase activity in tomato seedlings under drought stress. – Scientia Horticulturae 159: 172-177.

PHYTOEXTRACTION AND PHYTOSTABILISATION APPROACHES OF HEAVY METAL REMEDIATION IN ACID MINE DRAINAGE WITH CASE STUDIES: A REVIEW

MANG, K. C. – NTUSHELO, K.*

*Department of Agriculture and Animal Health, University of South Africa, South Africa
(e-mail: kaluchimdimang@yahoo.com; phone: +27-(0)-748-366-063)*

**Corresponding author
e-mail: ntushk@unisa.ac.za; phone: +27-(0)-789-027-944*

(Received 5th Aug 2018; accepted 5th Oct 2018)

Abstract. This review discusses phytoextraction and phytostabilisation of acid mine drainage (AMD) alongside with their benefits and limitations with case studies. Furthermore, plants associated with these two approaches of phytoremediation and impact of AMD on aquatic macrophytes used for phytoremediation were also reviewed. Both phytoextraction and phytostabilisation approaches are promising technologies in remediating AMD. However, their limitation of low metal removal and the lack of knowledge of minimum amendments required for their effective remediation call for the proposal, herein made, to combine aquatic macrophytes, as well as include plants from a wide range of families capable of phytoextraction and phytostabilisation in the remediation of AMD.

Keywords: *aquatic macrophytes, conventional treatment, hyperaccumulators, phytoremediation*

Introduction

The activities of the mine cause the production of acidic water that flows down to nearby water bodies causing long term impairment to biodiversity and waterways. The acidic water produced by the mines is termed acid mine drainage (AMD). Acid mine drainage also known as acid rock drainage is a process that occurs as a result of the contact between oxygenated water and mineral pyrite which leads to the oxidation of the pyrite and the production of acids (Evangelou, 1995; Blowes et al., 2003). Because of its environmental impact, acid mine drainage has attracted great attention all over the world, especially in countries where mining activity is very high. Acid mine water is characterized by low pH and a very high concentration of sulphates, iron and heavy metals. Many researchers have pointed out that the metal load of the acid mine drainage is of greater concern than the acidity with respect to the environmental damage (Kleinman, 1990; Fyson et al., 1994; Clarke, 1996; Kuyucak, 2002; Filipek et al., 2003). Furthermore, the source of the AMD may remain active for decades or even centuries after the closure of the mine (Modis et al., 1998). Individually mine have unique conditions and ability to produce AMD and therefore interventions should vary from mine to mine. The impact of AMD is dependent on local conditions and varies widely, depending on the geomorphology, the climate and the extent and distribution of the AMD generating deposits. There are no known standard methods for ranking, measuring and reducing the risk of AMD.

Water, air and soil constitute our environment and the process of removing any contaminants or pollutants from the environment is termed environmental remediation. Various technologies which cut across physical, chemical and biological processes have been employed for adequate remediation of polluted water, air and soil. The application of the various technologies depends on the nature of the pollutants. This is also

applicable to environment polluted with acid mine waters. The conventional technologies which involves the neutralization of the acid in AMD using calcium carbonate, lime, hydrated lime, caustic soda and soda ash often cause the production of voluminous sludge. This sludge represents further environmental problems and an increase in the cost of remediation (Fiset et al., 2003). The high cost of this conventional method of AMD remediation has produced economic pressure and caused more research work to be done by many researchers in order to discover cost-effective and environmentally sound ways to treat AMD.

Phytoremediation is a form of bioremediation studied by many researchers for the treatment of AMD that proved to be cost-effective when compared to the conventional method of treatment (Pilon-Smits, 2005). It applies to all chemical and physical processes that involve plants in degrading or immobilizing contaminants in the environment especially in soil and groundwater. Phytoextraction, phytovolatilization, phytostabilization, rhizodegradation, phytohydraulics, and phytodegradation are the six major types of phytoremediation. However, the focus of this review article is phytoextraction and phytostabilization.

Phytoextraction is also known as phytoaccumulation. Hyperaccumulation of contaminants through the roots of plants and the storage of those contaminants in their stem or leaves tissues is the mechanism of contaminants removal in this phytoremediation method. The contaminants are removed from the environment alongside with the plants when harvested. This phytoremediation method is useful particularly for removing metals from soil. It also provides an avenue of recovering the metals through the incineration of the plants, a process called phytomining. Phytovolatilization involves the taking up of volatile compounds by the plants through their roots. The volatile compounds are transpired directly or converted to metabolites that is capable of being transpired by the plants through their leaves. The contaminants are released to atmosphere.

Phytostabilization is also known as phytosequestration. This method involves the absorption of the contaminants by the roots, and adsorption to the surface of roots. It also involves the production of biochemicals by the plant which are then released into the soil or groundwater around the roots. The biochemicals have the ability to sequester, precipitate, or otherwise, immobilize nearby contaminants. Rhizodegradation occurs in the soil or groundwater that surrounds the plant roots. The exudates from the plants stimulate rhizosphere bacteria surrounding the root of plants to initiate biodegradation of contaminants in the soil. Phytohydraulics also involves the sequestration and degradation of contaminants that come in contact with the deep root of trees. In the work done by Hong et al. (2001), poplar trees were used to contain groundwater plume of methyl-tert-butyl-ether. Phytodegradation applies the mechanism of metabolism or biotransformation of the contaminants as they are taken up into the plant tissues. The transformation of the contaminants can occur in root, stem or leaves of plant depending on the type of plants involved in the phytodegradation.

The Indian Mustard, *Brassica juncea* (Brassicaceae), a plant familiar to the ones found in Sri Lanka, is found to be the most promising and well-tested plant for phytoextraction. This weedy mustard is successfully cultivated or naturalised in India, Western Egypt, Central Asia and Europe (Prasad and Freitas, 2003). It produces 18 tons of biomass/hectare/crop and it is able to accumulate and translocate high concentrations of Cr, Cu, Cd, Ni, Zn, and Pb at the same time to the shoot system (Kumar et al., 1995; Blaylock et al., 1997; Begonia et al., 1998; Zhu et al., 1999). Work done by many

researchers have shown that this plant has the ability to accumulate heavy metals and the field trial done in the United State of America has shown that this plant can be successfully used in the field remediation of heavy metals and radionuclides (Huang et al., 1998; Lasat et al., 1998; Tucker and Shaw, 2000; Dushenkov, 2003; Qadir et al., 2004). The biomass of Indian Mustard growing in mine soil can be increased by the application of a combination of technosol and biochar and this can improve its effectivity as a bioremediator (Forján et al., 2017). Vetiver grass (*Chrysopogon zizanioides*) has been successfully grown and used in phytoremediation of gold mine tailings in South Africa (Melato et al., 2016). The good qualities of vetiver grass as a bioremediator are well accepted and a compendious account of this is found in Banerjee et al. (2018). This review examines the use of phytoextraction and phytostabilisation approaches for the treatment of mine tailings alongside with their associated benefits and limitations. Phytoextraction and phytostabilisation of mine tailings in temperate and arid environment were considered alongside with the impact of acid mine drainage on aquatic macrophytes used for phytoremediation.

Impact of Acid Mine Drainage (AMD) on Aquatic Macrophytes: A Case Study of *Eichhornia crassipes*, *Pistia stratiotes* and *Spirodela polyrhiza*

Activities of the mining industries in the world cause pollution of the surrounding areas. Mining tailings and piles of refuse may contain sulphide minerals such as arsenopyrite. This arsenopyrite is one of the main contamination sources in mining industries. Their exposure to the atmospheric water and oxygen causes their oxidation with the release of potential toxic elements to the environment through AMD system. Sulphur, iron, manganese and arsenic are common elements associated with acid mine drainage and are believe to be highly toxic even at low concentrations (Duker et al., 2005).

Acid mine drainage is believed to influence aquatic systems and alter the biological community structure through the elimination of species in the food chain. In this stance, phytoremediation, an *in situ* remediation technology, is a low cost option for the reclamation of contaminated environments through the use of plants (Pilon-Smits, 2005). Among all the forms of phytoremediation, phytoextraction and phytostabilisation are the commonly used forms of phytoremediation technology. Macrophytes that freely float in water are mostly used plant species for phytoremediation because of their ability to grow fast, accumulate heavy metals and metalloids in large quantities, survive under harsh conditions and tolerate high concentrations of toxic elements (Mishra et al., 2008a; 2008b).

The major setback of phytoremediation studies is that they are limited to some selected plant species and few metals (Hassan et al., 2007; Rahman et al., 2007). As a result, there is an information paucity on the simultaneous absorption of several contaminants especially, in acid mine drainage. *Eichhornia crassipes*, *Pistia stratiotes* and *Spirodela polyrhiza* species possess the ability to absorb several different elements to some extent and simultaneously accumulate heavy metals and toxic metalloids from acid mine drainage. Preliminary work done by Michelle et al. (2010) showed that *Pistia stratiotes* and *Spirodela polyrhiza* were susceptible to low pH in the aquatic medium which is the main characteristic of acid mine drainage. Furthermore, they observed that *E. crassipes* was more tolerant to acidic environment (*Figure 1*). The decrease in the chlorophyll a content was also observed to be another effect of acid mine

drainage on plants as seen in *P. stratiotes* and *S. polyrhiza*, due to the necrosis on the leaves.

Eichhornia crassipes plants were also observed to accumulate part of the soluble arsenic from acid mine drainage in their different tissues with the root accumulating more of the heavy metals. Furthermore, the work done by Mokhtar et al. (2011) indicated that *E. crassipes* showed 97.3% efficiency for copper removal in an aqueous solution containing various concentrations of copper. *Pistia stratiotes* and *S. polyrhiza* die when exposed to acid mine drainage. The work done by Michelle et al. (2010) gave an insight on the ability of some aquatic macrophytes to accumulate heavy metals. However, there exists the need to further evaluate the simultaneous absorption of other heavy metals by aquatic macrophytes and their interactions to enhance the development of a better phytoremediation technology for acid mine drainage while preserving the aquatic macrophytes capable of accumulating the heavy metals.

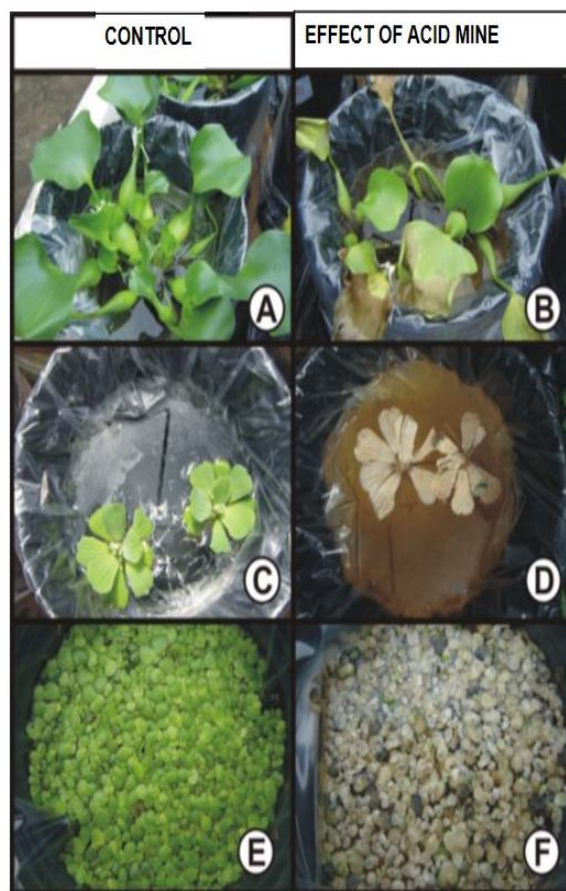


Figure 1. Phytotoxic effects of acid mine drainage in aquatic floating macrophytes. (A-B, *E. crassipes*; C-D, *P. stratiotes*; E-F, *S. polyrhiza*) Source: Michelle et al., 2010

Limitations of Phytoremediation Using Aquatic Plants

Various research endeavours have shown phytoremediation to be a better environmentally friendly and cost-effective method for the treatment of wastewater and polluted environments with respect to conventional methods (Sood et al., 2012; Sharma et al., 2014; Newete and Byrne, 2016). The production of biomass through its fast

growth ability gave more advantages to this method of remediation however, its inability to tolerate high concentrations of metal and the influence of seasons on its effectiveness is disadvantageous (Rai, 2008; Mannino et al., 2008).

Sharma et al. (2014) stated that phytoremediation is used either as a secondary or a tertiary treatment method for industrial or mine wastewater treatment because of high concentration of heavy metals and the toxicity of the metals. As a result of this, Rai (2008) encouraged regular harvest and safe disposal of the biomass for effective phytoremediation treatment in order to avoid the release of the absorbed or adsorbed metals back into their source when the plant dies and decompose.

Plants Associated with Phytoextraction and Phytostabilisation of Heavy Metals: A case study of Sri Lanka and South Africa

The success of phytoextraction and phytostabilisation is dependent on the plant species available. Baker and Whiting (2002) also indicated that those plants that can carry out these two phytoremediation approaches in remedying acid mine drainage are those native to the region of interest and are able to tolerate and accumulate high concentrations of heavy metals. Baker et al. (2000) further pointed out that many hyperaccumulators of heavy metals such as Cu, Co, As, Zn, Pb, Mn, Se, Cd, and Ni are characterised by their ability to survive high concentrations of these heavy metals and always endemic to metal-rich substrates. Over 420 species of heavy metals hyperaccumulators that belong to about 45 plant families have been identified (Cobbett, 2003). In addition, Krämer (2003) reported that new hyperaccumulators are being discovered from field collections with only few number of them tested in the laboratory for their behaviour and mechanisms of hyperaccumulation. Several fascinating patterns have been observed since the events of hyperaccumulators discovery (Ernst, 2000; Baker and Whiting, 2002). First, many families of plants such as Asteraceae, Brassicaceae, Euphorbiaceae, Fabaceae, Flacourtiaceae, and Violaceae were found to contain large numbers of hyperaccumulators. This implied that several genera within the families may be predisposed or preadapted to tolerate high level of heavy metals. The second pattern observed was the high percentage of these hyperaccumulators in tropical regions of the world. About 320 species of Ni hyperaccumulators discovered, two-thirds were found in the tropical regions of the world (Reeves, 2003; Proctor, 2003). The third pattern indicated that more than 80% of the identified hyperaccumulators take up more Ni than the other metals. The reasons behind this observed pattern of hyperaccumulators occurrence could be attributed to the combination of the following factors:

- Availability of time for the evolution of these species of hyperaccumulators in the tropical regions.
- High weathering of naturally occurring ore-bodies in tropical regions which imposes a greater selective pressures on indigenous floras.
- Provision of a selective advantage in dealing with other stresses of tropical regions due to the heavy metal accumulation traits in the hyperaccumulators.
- The availability of Ni over the other metals due to the presence of many tracts of Ni-enriched serpentine outcrops along continental margins.
- The interest of researchers in discovering hyperaccumulators in tropical regions.

Reeves (2003) reported that over 50 species of Ni hyperaccumulators have been found endemic to the metal-rich serpentine outcrops of New Caledonia (an island). These include species from genera such as *Cledion* (Euphorbiaceae), *Argophyllum*

(Grossulariaceae), *Casearia* (Flacourtiaceae), *Geissois* (Cunoniaceae), *Homalium* (Flacourtiaceae), *Hybanthus* (Violaceae), *Oncotheca* (Oncothecaceae), *Pancheria* (Cunoniaceae), *Phyllanthus* (Euphorbiaceae), and *Xylosma* (Flacourtiaceae) (Jaffré et al., 1979; Reeves, 2003). Jaffré et al. (1976) found that the latex of a small tree called *Seberita acuminata* (Sapotaceae) that is endemic in the island contains more than 20% Ni by dry weight. Proctor (2003) reported that the Asian region have few identified hyperaccumulator and most of them are closely related to the ones found in Sri Lanka. *Myristica* (Myristicaceae), *Planchonella* (Sapotaceae), and *Trichospermum* (Tiliaceae) are the genera of Ni hyperaccumulator found in Indonesia. Another Asian genus called *Rinorea* (Violaceae) has two Ni hyperaccumulating species (Brooks and Wither, 1977a,b; Wither and Brooks, 1977). Wither and Brooks (1977) identified that *Rinorea benghalensis* collected from Sri Lanka's herbarium has 1% Ni hyperaccumulation by dry weight. Rajakaruna and Baker (2004) was in the opinion that this species may have been collected from the serpentinized areas of Katupotha in the south-central part of island. The same species was also found in Sabah (Jopony and Tongkul, 1999) and found to hyperaccumulate Ni. The genera such as *Brackenridgea* (Ochnaceae), *Dichapetalum* (Dichapetalaceae), *Walsura* (Meliaceae) as well as *Phyllanthus* (Euphorbiaceae) and *Shorea* (Dipterocarpaceae) widely represented in the Sri Lankan flora were found to hyperaccumulate Ni in Sabah and Phillipines (Proctor et al., 1989; Baker et al., 1992). Jayasekera and Rossbach (1994, 1996) suggested that there may be several taxa in Sri Lanka with the capacity to accumulate high concentrations of heavy metals.

Sri Lankan endemic plants such as *Crotalaria biflora* (Fabaceae), *Evolvulus alsinoides* (Convolvulaceae), *Hybanthus enneaspermus* (Violaceae) showed high level of whole-plant Ni hyperaccumulation; and *Clerodendrum infortunatum* (Verbenaceae), *Croton bonplandianus* (Euphorbiaceae), *Geniosporum tenuiflorum* (Lamiaceae), *Tephrosia villosa* (Fabaceae), and *Waltheria indica* (Sterculiaceae) showed high level of whole-plant Cu hyperaccumulation (Rajakaruna and Bohm, 2002). It is worth noting that Cu hyperaccumulation is a rare and the taxa shown to accumulate Cu need further review to confirm these preliminary findings. *Cassia kleinii* (Fabaceae), a woody shrub well-suited, found in Ni- and Cr-enriched serpentine outcrop of Ussangoda, has shown Ni hyperaccumulation (Rajakaruna and Bohm, 2002; Iqbal et al., 2006).

Combretum erythrophyllum (River Bush-willow), an indigenous South African tree species that may reach a height of approximately 5 m within 5 years and can further grow to a height of about 15 m after 50 years (Stoffberg et al., 2008), has been used as a phytoextraction and phytostabilisation option on several tailings dams in Johannesburg. This tree can survive in high salinity areas and bears seed. McGaw et al. (2001) reported that the leaves and bark of this tree is used in traditional medicine around southern Africa. Based on this, care needs to be taken in the harvest of this tree for traditional medicine when used for phytoremediation.

Eucalyptus camaldulensis (Red River gum) is an invasive plant with Australia as its native country. It is also found in South Africa. This tree is able to thrive well in a high salt and acidic conditions and other harsh conditions including drought. It is a hyperaccumulator of Mn and Pb. Singh et al. (2010) found out that *E. camaldulensis* showed high productivity and great reduction in most soil mineral concentrations in an experiment done to assess mineral uptake of *Acacia nilotica* L. (babool), *Dalbergia sissoo* L. (sissoo) and *Eucalyptus camaldulensis* seedlings. From the findings

of this work, it was indicated that *E. camaldulensis* was the best option for the rehabilitation of soil because it can tolerate high salt concentration in the soil and water. It is important that sterile plants are planted for phytoextraction to minimise the risk of invasion of the surrounding environment.

Tamarix usneoides (Wild Tamarix) is native to South Africa and can thrive well in highly saline environments. The plant possesses a good root system that can penetrate deep water tables in arid environments and an adaptive salt glands that can secrete excess salts. In South Africa, this plant is used for phytoremediation with success around tailings dams. *Sporobolus spicatus* (Salt Grass) is adapted to growing salt pan edges, marsh and river edges as perennial grass. The salt accumulation by the shoots of this grass increases with increasing soil salinity (Ramadan, 2001). This plant is recommended to be used for phytoremediation because of its ability to survive in adverse and wet conditions.

Phytoextraction of Metals in Mine Tailings: A Case Study of Temperate and Arid Environments

Phytoextraction of metals especially from mine tailings entails the application of metal-hyperaccumulating plants that accumulate the metals either in their root, leaves or stem. This accumulation of heavy metals is followed by the harvesting of the plants. The harvested plants could either be destroyed or the accumulated heavy metals are recycled and reused. Plants that concentrate metals into above-ground biomass at a very high concentrations are known as hyperaccumulators. These hyperaccumulators have the tendency to accumulate metals at levels of 0.01–1% of the plant biomass produced. This is dependent on the specific metal being absorbed by these plants (Brooks, 1998; Baker et al., 2000). High biomass production and fast growth rates are the key characteristics of these hyperaccumulators that enhances maximum accumulation of metals. Accumulation factor which is the ratio of metals in the shoot tissue to the metal in the contaminated environment, and translocation factor which is defined as the ratio of the metals in the shoot to the metals in the root of the plants are other measures used to identify and define hyperaccumulators. Based on accumulation factors, translocation factors, high biomass and fast growing rate, over four hundred species of hyperaccumulators that belong to 45 families have been identified as effective hyperaccumulators of metals from contaminated soils with species specifically capable of phytoextraction in mine tailings being identified (Baker et al., 2000; Deng et al., 2007; Turnau et al., 2007). The general method of identifying and defining hyperaccumulators is the metal concentration in the shoot tissues of plants. Furthermore, accumulation factor is also necessary for identifying the feasibility of phytoextraction. This feasibility of phytoextraction means the number of cropping cycles required for the metal removals to the level that is accepted (Zhao et al., 2003).

For the identification of potential plants candidates for phytoextraction in acid mine drainage, several surveys of plants colonizing mine tailings together with hyperaccumulators grown in mine tailings have been done. However, phytoextraction of metals from mine tailings are faced with major challenges. Phytoextraction of metals in mine tailings is known to be generally poor because of low metal bioavailability in tailings amended with compost to enhance the growth of plants (Knight et al., 1997; Meerts and Van Isacker, 1997; Salt et al., 1997; Bennett et al., 2003). Furthermore, Krzaklewski and Pietrzykowski (2002) observed that some plant species have the ability

to survive and colonize mine tailings but their metal accumulation was not sufficient for them to be used as hyperaccumulators. In order to enhance hyperaccumulation of metals by hyperaccumulators, metal chelators have been tested and used to enhance hyperaccumulation. However, their use posed a problem of phytotoxicity for the plants. Based on this, chelators are applied generally after good plant biomass production is achieved (Berti and Cunningham, 2000). Another challenge faced when chelators are applied is the leaching of metals into the groundwater especially in temperate environments due to increase solubility of metals in the mine tailings (Wu et al., 1999; Schmidt, 2003). This leaching of metals into groundwater leads to their pollution.

Transgenic hyperaccumulator plants have been researched and explored for remediation of mine tailings in many countries of the world. However, the major drawback of these transgenic hyperaccumulators is their adverse impacts on species diversity, soil ecosystems, and the food chain (Wolfenbarger and Phifer, 2000; Wolfe and Bjornstad, 2002). Furthermore, their invasive potentials and ability to colonize disturbed areas in desert environments and establishment of late successional species is also a major concern in the use of transgenic hyperaccumulators (Castellanos et al., 2005). In order to enhance the proper management of this transgenic hyperaccumulators, the use of sterile clones, harvesting of plants before flowering, selection of species that will not outcompete indigenous plants have been encouraged (Pilon-Smits and Pilon, 2002; Snow et al., 2005). Wolfe and Bjornstad (2002) finally observed that poor public acceptance may pose a problem in the implementation of transgenic hyperaccumulators.

Plants growing in temperate environments where there are mine tailings experience low pH, metal toxicity, lack of soil structure, and low nutrient content as challenges that oppose their developments. Those plants that are able to tolerate and overcome the challenges in temperate environments often face the problems of low biomass production. This low biomass production impedes the success of phytoextraction in the temperate environments as the success of metal accumulation by the plants depend on the biomass production. A typical example is found in Europe where the populations of *Thlaspi caerulescens* were found to be thriving in metal contaminated sites and mine tailing sites with the ability to accumulate the metals. In the United Kingdom, *T. caerulescens* were found to thrive in mine tailings and mine spoils. The plant was found to accumulate 50 - 160 mg kg⁻¹ Cd and 13,000 - 19,000 mg kg⁻¹ Zn with accumulation factors of Zn >1 (Baker et al., 1994). The accumulation factors of the plant was observed to increase up to 73 and 40 for Cd and Zn respectively when the plant was exposed to a lower level of Cd to Zn ratio (Zhao et al., 2003).

Study done in greenhouse using *T. caerulescens* exposed to a mine spoil containing up to 3300 mg kg⁻¹ Zn and 58 mg kg⁻¹ Cd to evaluate its phytoextraction potential showed that the plant accumulated 250 mg Cd kg plant biomass⁻¹ and 8,000 mg Zn kg plant biomass⁻¹ (Knight et al., 1997). As a result of low biomass production of the plant in mine tailings, an approximate 100 - 1200 cropping cycles would be needed to remove Cd and 200 - 600 cropping cycles to remove Zn from the studied mine tailings. These cropping cycles translated into decades for complete remediation of the mine tailings. The obtained results showed that *T. caerulescens* may be useful for the remediation of environment contaminated with low Cd and Zn and may not be suitable for more highly contaminated mine spoil that was studied.

In the quest to improve phytoextraction efficiency in mine tailings, two transgenic strains of *Brassica juncea* (L.) Czern were discovered and observed to accumulate up to

1.5 to 3-fold more metal (Cd, Cr, Cu, Pb, Zn) than the wild type strain in a greenhouse study (Bennett et al., 2003). The enzymes *c*glutamylcysteine synthetase (ECS) and glutathione synthetase (GS) that affect production of the metal-binding thiol peptides, phytochelatin and glutathione, respectively were overproduced by the transgenic strains. Twenty five per cent and five per cent of Cd and Zn respectively were reduced by the strains of this transgenic *B. juncea* from compost-amended tailings however, leaching was later discovered as the primary reason for metal reduction in this study (Ernst, 2005). Bennett et al. (2003) indicated that the addition of compost and lime required for growth of *B. juncea* in the mine tailings decreased plant metal bioavailability and hence the overall phytoextraction efficiency of the transgenic plants.

The growth of plants in arid environment is also faced with the challenges of lack of water and often saline conditions in addition to low pH, metal toxicity, low nutrients and lack of soil structure. Despite the challenges faced by the plants in this environment, a promising list of natural hyperaccumulators that have the ability to colonize mine tailings have been identified however, few of them have been studied in the greenhouse to evaluate their hyperaccumulation potentials (Leita et al., 1989; Bech et al., 2002; Gonzalez and Gonzalez-Chavez, 2006). In Spain, *Cichorium intybus* L. and *Cynodon dactylon* (L.) Pers. which naturally colonize the mine tailings were evaluated for lead (Pb) accumulation. This study was carried out on artificially Pb contaminated potting soils. The shoot Pb accumulation was observed to be 800 - 1500 and 400 - 1200 mg kg⁻¹ Pb for *C. intybus* and *C. dactylon*, respectively. Furthermore, it was observed that shoot accumulation of the metal had no inhibition effect on the plant growth and biomass production. However, the limitation of this study was that the authors were not able to show how this phytoextraction ability of these plants would translate to a mine tailings environment (Del Rio-Celestino et al., 2006).

Conesa et al. (2007b) carried out a field and greenhouse study on *Lygeum spartum* L. a grass known to colonize mine tailings site in Mediterranean regions, to evaluate the phytoextraction ability of the grass. It was observed in the field and greenhouse that the metal accumulation was low with the exception of zinc which was extremely high and between 3000 to 6000 mg kg⁻¹ when plants were irrigated and fertilized in the greenhouse. Frérot et al. (2006) observed in their work that contrary to the believe that *Armeria arenaria* (Pers.) Schult., *Festuca arvernensis* Auquier, and *Koeleria vallesiana* (Honck.) Gaudin are non-hyperaccumulators, they were found to hyperaccumulate Pb at 1,000 - 2,000 mg kg⁻¹ in the field.

Elevated salinity is the most common characteristics of mine tailings in arid environments. The electrical conductivity of the environment is believed to influence by the salinity and this electrical conductivity was observed in arid environments with high salinity (22 dS m⁻¹) to be greater than the tolerant level for plants (Munshower, 1994; Marschner, 1995). *Atriplex* spp accumulate sodium and potassium at a high concentrations in mine tailings and uncontaminated soils and as a result, they are referred to as halophytes (Osmond et al., 1980; Mendez et al., 2007). The work done by Lutts et al. (2004) in a hydroponic greenhouse study using *Atriplex halimus* L. showed that the plant can take up 830 and 440 mg kg plant tissue⁻¹ of Cd and Zn respectively in shoot biomass and did not display symptoms of toxicity during growth. This high concentration of the accumulated metals may have been influenced by the low concentrations of cations (Na⁺/K⁺) in the hydroponic growth medium. However, the occurrence of the same result in the field study is not known.

Limitations of Phytoextraction

The widespread use of phytoextraction as a remediation strategy for mine tailings is faced with major drawbacks. The time taken for a complete phytoextraction might be so long especially with a highly metal polluted mine tailings. Plant metal bioavailability and metal extraction efficiency may decrease as a result of the distribution of different metals in mine tailings alongside with compost amendments required for the plant growth. Ernst (2005) indicated the polymetallic nature of mine tailings as another drawback to the success of the spread of phytoextraction as hyperaccumulators can only accumulate one or two metals and as a result, multiple plant species and ecotypes are required. This drawback is further strengthened in arid regions with high saline content of mine tailings and the preference of Na^+/K^+ by many halophytes (Osmond et al., 1980; Munshower, 1994; Marschner, 1995). Characteristics of plants can also decrease the efficiency of plants to metals from mine tailings. Keller et al. (2003) pointed out that hyperaccumulators generally possess shallow root zone which limit metal removal by plant rooting depth. Metal extraction efficiency may be reduced in tailings with high metal concentrations. Generally, the harsh conditions of mine tailings influences biomass production of plants and consequently, the efficiency of phytoextraction (Ernst, 2005; Audet and Charest, 2007).

Wildlife is in danger of metal exposure as a result of the accumulation of the metals in the shoot system of the hyperaccumulators eatable by wildlife animals. Wood et al. (1995) pointed out that the worst scenario can be seen in arid regions where food sources are limited. All these drawbacks are believed to influence the cost of implementing phytoextraction by making it high and optimisation of this process may also require expensive inputs. Furthermore, the cost of harvesting, disposing and re-seeding of hyperaccumulators which may be required for many cropping cycles add to the total cost of the technology (Cunningham and Berti, 2000). In conclusion, there is the need to consider the safety of wildlife. This do not remove the remediation application of phytoextraction in mine tailings. However, there is the need to balance the costs associated with this strategy and the potential value of the land once it is reclaimed.

Phytostabilization of Mine Tailings: A Case Study of Temperate and Arid Environments

Phytostabilization of mine tailings involves the establishment of plants that have extensive root system which will enable them to create steady vegetative cap that does not accumulate metals into above-ground tissues. The mechanism of action of established plants in the mine tailings include sorption of metals onto the root surfaces, accumulation of metals in the root tissue and stabilization of metals through precipitation (Cunningham et al., 1995; Wong, 2003). Furthermore, established plants in the mine tailings for phytostabilization should have the ability to enhance diverse heterotrophic microbial community interaction that will encourage the growth of plants and promote the transformation of the materials in the mine tailings necessary for the improvement of the soil structure (Mummey et al., 2002a; Glick, 2003; Wong, 2003; Mendez et al., 2007). The established plants also provide the initial plant cover that enhances the growth and establishment of other plants in the environment leaving the environment with diversified and self-sustaining vegetative cap that reduces water erosion, leaching processes and eolian.

The plants used for phytostabilization varies from region to region and depends on the nature of metal contaminants in the mine tailings. Furthermore, physicochemical factors influences the stability and diversity of naturally established plant communities in the same regions (Conesa et al., 2007a). As a result, physicochemical characteristics of individual mine tailings sites need to be considered before the establishment of plants required for phytostabilization. There is also the need to amend the mine tailings with compost manure or lime required for the growth of the plants so as to remove any toxic effect and decrease metal bioavailability. The plants selected for phytostabilization need not to translocate metals to shoot tissues. This is to safe guard the life of wildlife animals that may depend on them for survival and also to prevent surface contamination. In view of this, the ratio of shoot metal concentrations to root metal concentration or soil metal concentration should be less than one. The plants should also meet the US Domestic Animal Metal Toxicity Limits to prevent exposure to foraging animals (Wood et al., 1995; NRC, 2005).

Grasses are mostly used for phytostabilization in temperate environments because of their rapid growth and extensive rooting systems. In Europe, *Festuca* spp. and *Agrostis* spp. are native grass species that are mostly used for phytostabilization. They are also used in the US and China for phytostabilization (Smith and Bradshaw, 1979; Ye et al., 1999; Pierzynski et al., 2002; Von Willert and Stehouwer, 2003). A greenhouse experiment done in Scotland by Pichtel and Salt (1998) showed that application of NPK fertilizer only enhances the growth of *Festuca ovina* L. and *F. rubra* in a moderately acidic Pb/Zn mine waste sample.

Several field trials done in the UK indicated successful establishment of *F. rubra* and *Agrostis tenuis* Sibthorp in Pb/Zn and Cu mine tailings with a combination of fertilizers and lime (Smith and Bradshaw, 1979). Furthermore, native plants have been explored by many studies in combination of soil cover to achieve phytostabilization. This was seen in the work done in Washington, US by Kramer et al. (2000) using *Alnus viridis* subsp. *sinuate* (Regel) and *Anaphalis margaritacea* (L.) where they observed the two plants demonstrating adequate plant biomass and shoot tissue exclusion of high concentrations of Al and Zn when grown in copper mine tailings amended with biosolids-woodchip mixture before the planting of the plants. Similarly, in China, Shu et al. (2001) carried out a study using 41 native seed species from a soil seed bank obtained from nearby uncontaminated areas. They established the plants in a Pb/Zn mine tailings following application of an 8-cm top-soil layer over the tailings material and observed that 9 of the plants survived with three of them showing both good plant coverage and low metal accumulation.

Drought-, salt- and metal-tolerant plants are required for effective phytostabilization of mine tailings in arid and semiarid climates. Addition of an organic amendment and irrigation enhance the success of re-vegetation in arid environment. In semiarid Western Australia *Atriplex* spp. are known pioneer plants on mine tailings (Osmond et al., 1980; Jefferson, 2004). An irrigated greenhouse study conducted by Mendez et al. (2007), showed that a minimum of 10% compost addition was required for adequate growth of *Atriplex lentiformis* (Torr.) in both moderately acidic and extremely acidic Pb/Zn mine tailings. They also observed that shoot uptake of metals did not exceed US Domestic Animal Metal Toxicity Limits.

Sabey et al. (1990) also conducted a greenhouse study using biosolids which indicated that a sludge application of 60 Mg ha⁻¹ was required for growth of *Atriplex canescens* (Pursh) in copper mine tailings. One disadvantage of the high sludge

application observed by them was elevated Cu concentrations tissues of the leaves that exceeded recommended US Domestic Animal Metal Toxicity Limits by 5-fold. Rosario et al. (2007) conducted a field experiment to examine the impact of compost on establishment of *A. canescens* in an alkaline mine tailing site in southern Arizona, US. Forty four litres of water over the first eight months of growth was administered to the individual plants. Similar plant growth results were obtained in both composted and uncomposted tailings and 80% of transplants survived. Further observation in this study was that Pb exceeded the US Domestic Animal Metal Toxicity Limits in some plants by up to 3-fold. The information obtained from these studies implied that plant growth requirements and physicochemical factors of the mine tailings determines the amount and type of amendment required by the plants. Therefore, amendment requirements are both site- and plant species-specific.

Re-vegetation through the use of direct-seeding in field studies that have been performed in an arid environment was promising. Study performed in Zimbabwe by Piha et al. (1995) using direct seeding method with no irrigation in a tin mine tailings site where the seeds were subjected initially to seven weeks of drought produced 40% plant cover with a mixture of grasses and legumes after the first growing season using only an initial addition of NPK fertilizer. The study done in South Africa by Van Rensburg and Morgenthal (2004) in a platinum tailings with seeds from a mixture of grasses and amended with fertilizer produced average plant cover of 2%. However, the authors suggested that lack of irrigation and poor timing that did not take advantage of the seasonal rainfall are the cause of these poor results. The seeding study done by Windsor and Clements (2001) in a gold mine tailing site in where the seeds were irrigated showed that seedling density was 3-fold greater in irrigated plots compared to plots without irrigation. This implied that in arid and semi-arid environments, irrigation significantly increases the plant establishment. If irrigation is not feasible, direct seeding studies require precise timing to take advantage of the normal rainfall season.

Limitations of Phytostabilization of Mine Tailings

Phytostabilization being a long-term field studies makes it difficult to evaluate the overall success of this strategy. A 20-year study carried out by Mummey et al. (2002b) showed that both plant and microbial diversity in a re-vegetated mining site was low compared to an adjacent undisturbed site in a semiarid grassland. However, plant cover gave a promising result of the use of this technology because it was higher than the ones found in the undisturbed site. Complete plant coverage is dependent on the environment. Semi-arid and arid shrublands are not likely to produce a complete plant coverage when compared to the temperate environments. This becomes a limitation to the success of the use of phytostabilization to remedy acid mine tailings. The difference in plant coverage in arid and temperate environment is dependent on nitrogen availability, water use efficiency and light. Availability of nitrogen and efficiency of water use influences plant dynamics in semi-arid and arid environment whereas light and nitrogen availability influences plant dynamics in temperate environment (Tilman, 1988; Gebauer and Ehleringer, 2000). Therefore, infrequent rainfall could result to increase mortality of the secondary successional plant communities in semi-arid and arid environment (Watson et al., 1997; Castellanos et al., 2005). To overcome some of the limitations it is recommended that a comprehensive approach which employs various strategies can be embarked upon. Emenike et al. (2018) explores the combined

use of plants and microbes to biotransform contaminated soils and similar mechanisms including the addition of nutrients and nanoremediation as suggested by Das (2018) may prove sustainable. The table below gives a summary of plants and their bioremediation potentials (*Table 1*).

Table 1. Summary of plant species used in phytoextraction and phytostabilization of metals in acid mine drainage

Plant species	Family	Remediation Mechanism	Achieved Results	References
<i>Chrysopogon zizanioides</i>	Poaceae	Phytoextraction	Zn, Cu, and Ni removal	Melato et al. (2016)
<i>Brassica juncea</i>	Brassicaceae	Phytoextraction	Cr, Cu, Cd, Ni, Zn, and Pb accumulation and removal	Kumar et al. (1995); Blaylock et al. (1997); Begonia et al. (1998); Zhu et al. (1999)
<i>Eichhornia crassipes</i>	Pontederiaceae	Phytoextraction	97.3% Cu removal efficiency in aqueous solution, arsenic hyperaccumulation	Mokhtar et al. (2011); Michelle et al. (2010)
<i>Waltheria indica</i>	Malvaceae	Phytoextraction	High level of whole-plant Cu removal	Rajakaruna and Bohm (2002)
<i>Cassia kleinii</i>	Fabaceae	Phytoextraction	Ni removal	Iqbal et al. (2006); Rajakaruna and Bohm (2002)
<i>Thlaspi caerulescens</i>	Brassicaceae	Phytoextraction	Accumulation of 50 - 160 mg kg ⁻¹ Cd and 13,000 - 19,000 mg kg ⁻¹ Zn	Baker et al. (1994); Zhao et al. (2003)
<i>Seberita acuminata</i>	Sapotaceae	Phytoextraction	Removal of over 20% of Ni	Jaffré et al. (1976)
<i>Rinorea benghalensis</i>	Violaceae	Phytoextraction	1% removal of Ni	Wither and Brooks (1977)
<i>Cichorium intybus</i> L.	Asteraceae	Phytoextraction	Removal of 800 -1500 mg kg ⁻¹ Pb through shoot accumulation	Del Rio-Celestino et al. (2006)
<i>Cynodon dactylon</i> (L.) Pers.	Poaceae	Phytoextraction	Removal of 400 -1200 mg kg ⁻¹ Pb through shoot accumulation	Del Rio-Celestino et al. (2006)
<i>Armeria arenaria</i> (Pers.) Schult., <i>Festuca arvernensis</i> Auquier, and <i>Koeleria vallesiana</i> (Honck.)	Plumbaginaceae, Poaceae, and Poaceae respectively	Phytoextraction	Removal of 1,000 - 2,000 mg kg ⁻¹ Pb	Frérot et al. (2006)
<i>Crotalaria biflora</i> , <i>Evolvulus alsinoides</i> , and <i>Hybanthus enneaspermus</i>	Fabaceae, Convolvulaceae, and Violaceae respectively	Phytoextraction	Whole-plant hyperaccumulation of Ni	Rajakaruna and Bohm, (2002)
<i>Clerodendrum infortunatum</i> , <i>Croton bonplandianus</i> , <i>Geniosporum tenuiflorum</i> , <i>Tephrosia villosa</i> , and <i>Waltheria indica</i>	Verbenaceae, Euphorbiaceae, Lamiaceae, Fabaceae, and Sterculiaceae respectively	Phytoextraction	Whole-plant hyperaccumulation of Cu	Rajakaruna and Bohm, (2002)
<i>Atriplex halimus</i> L.	Amaranthaceae	Phytoextraction	Accumulation of 830 and 440 mg kg plant tissue ⁻¹ of Cd and Zn respectively in shoot biomass	Lutts et al. (2004)
<i>Lygeum spartum</i> L.	Poaceae	Phytoextraction	Removal of 3000 - 6000 mg kg ⁻¹ Zn	Conesa et al. (2007b)

Plant species	Family	Remediation Mechanism	Achieved Results	References
<i>Festuca rubra</i> and <i>Agrostis tenuis</i> Sibthorp	Both belongs to Poaceae	Phytostabilization	Successful establishment in Pb/Zn and Cu mine tailings with a combination of fertilizers and lime	Smith and Bradshaw (1979)
<i>Alnus viridis</i> subsp. <i>sinuate</i> (Regel) and <i>Anaphalis margaritacea</i> (L.)	Betulaceae, and Asteraceae respectively	Phytostabilization	Demonstration of adequate plant biomass and shoot tissue exclusion of high concentration of Al and Zn in Cu mine tailings amended with biosolids-woodchip mixture	Kramer et al. (2000)
<i>Atriplex lentiformis</i>	Amaranthaceae	Phytostabilization	Demonstrated adequate growth in moderately acidic and extremely acidic Pb/Zn mine tailings with 10% compost addition	Mendez et al. (2007)
<i>Atriplex canescens</i>	Chenopodiaceae	Phytostabilization	Successfully grown in Cu mine tailings with sludge application of 60 Mg ha ⁻¹ and displayed high Cu concentrations in the leaves tissues	Sabey et al. (1990)

Conclusion

Remediation of mine tailings through phytoremediation approaches is a promising strategy. Work done on phytoextraction indicated that the approach will be limited to sites where the land values are high, and the time of restoring the site will be long due to high cost and lengthy treatment times. Phytostabilization provides a more suitable generation phytoremediation approach because of its easy nature of implementation and lower cost. However, both approaches need further review and optimization to enhance complete restoration of AMD.

The Indian mustard, *Brassica juncea* (Brassicaceae), *Chrysopogon zizanioides* and an aquatic macrophyte *Eichhornia crassipes* have been identified to be successful in the remediation of AMD. This review suggests further research on their mechanisms of heavy metal remediations, the climatic influence, and the nutrient requirements for the development of enough biomass for phytoremediation. Furthermore, the combination of these three plant species in the remediation of most areas or mine tailings contaminated with heavy metals needs further research.

Acknowledgements. The authors wish to thank the National Research Foundation and the Agricultural Research Council - University of South Africa Climate Change Collaboration Centre for their financial support.

REFERENCES

- [1] Audet, P., Charest, C. (2007): Heavy metal phytoremediation from a meta-analytical perspective. – Environmental Pollution 147: 231-237.
- [2] Baker, A. J. M., Proctor, J., Reeves, R. D. (1992): The Vegetation of Ultramafic (Serpentine) Soils. – Proceedings of the First International Conference on Serpentine Ecology, University of California, Intercept, Hampshire, UK.

- [3] Baker, A. J. M., Reeves, R. D., Hajara, A. S. M. (1994): Heavy metal accumulation and tolerance in British populations of the metallophyte *Thlaspi caerulescens* J. & C. Presl (Brassicaceae). – *New Phytology* 127: 61-68.
- [4] Baker, A. J. M., McGrath, S. P., Reeves, R. D., Smith, J. A. C. (2000): Metal hyperaccumulator plants: a review of the ecology and physiology of a biological resource for phytoremediation of metal-polluted soils. – In: Terry, N., Banuelos, G. (eds.) *Phytoremediation of contaminated soil and water*. Lewis Publishers, Boca Raton.
- [5] Baker, A. J. M., Whiting, S. M. (2002): In Search for the Holy Grail—another step in understanding metal hyperaccumulation? – *New Phytologist* 155: 1-7.
- [6] Banerjee, R., Goswami, P., Mukherjee, A. (2018): Chapter 22 - Stabilization of Iron Ore Mine Spoil Dump Sites With Vetiver System. – In: *Bio-Geotechnologies for Mine Site Rehabilitation*: 393-413. Elsevier, Kolkata.
- [7] Bech, J., Poschenrieder, C., Barcelo, J., Lansac, A. (2002): Plants from mine spoils in the South American area as potential sources of germplasm for phytoremediation technologies. – *Acta Biotechnology* 1-2: 5-11.
- [8] Begonia, G. B., Davis, C. D., Begonia, M. E. T., Gray, C. N. (1998): Growth responses of Indian Mustard (*Brassica juncea* (L.) Czern.) and its phytoextraction of lead from a contaminated soil. – *Bulletin of Environmental Contamination and Toxicology* 61: 38-43.
- [9] Bennett, L. E., Burkhead, J. L., Hale, K. L., Terry, N., Pilon, M., Pilon-Smits, E. A. H. (2003): Analysis of transgenic Indian mustard plants for phytoremediation of metal-contaminated mine tailings. – *Journal of Environmental Quality* 32: 432-440.
- [10] Berti, W. W. R., Cunningham, S. D. (2000): Phytostabilization of metals. – In: Raskin, I., Ensley, B. D. (eds.) *Phytoremediation of toxic metals - using plants to clean up the environment*. John Wiley & Sons, Inc., New York 71-88.
- [11] Blaylock, M. J., Salt, D. E., Dushenkov, S., Zakharova, O., Gussman, C., Kapulnik, Y., Ensley, B. D., Raskin, I. (1997): Enhanced accumulation of Pb in Indian mustard by soil-applied chelating agents. – *Environmental Science and Technology* 31: 860-856.
- [12] Blowes, D. W., Ptacek, C. J., Jambor, J. L., Weisener, C. G. (2003): The geochemistry of acid mine drainage. – In: Holland, H. D., Turekian, K. K. (eds.) *Treatise on geochemistry*. Oxford: Elsevier: 150-204.
- [13] Brooks, R. R., Wither, E. D. (1977a): Nickel hyperaccumulation by *Rinorea bengalensis* (Wall.) O.K. – *Journal of Geochemical Exploration* 7: 295-300.
- [14] Brooks, R. R., Wither, E. D. (1977b): Balt and nickel in *Rinorea* species. – *Plant and Soil* 47: 707-712.
- [15] Brooks, R. R. (1998): Plants that hyperaccumulate heavy metals: their role in phytoremediation, microbiology, archaeology, mineral exploration and phytomining. – CAB International, Wallingford.
- [16] Castellanos, A. E., Martinez, M. J., Llano, J. M., Halvorson, W. L., Espiricueta, M., Espejel, I. (2005): Successional trends in Sonoran Desert abandoned agricultural fields in northern Mexico. – *Journal of Arid Environment* 60: 437-455.
- [17] Clarke, L. (1996): Coal mining and water quality. – *Journal of Mines Metals and Fuels* 44: 181-183.
- [18] Cobbett, C. (2003): Heavy metals and plants—model systems and hyperaccumulators. – *New Phytologist* 159: 289-293.
- [19] Conesa, H. M., Garcia, G., Faz, A., Arnaldos, R. (2007a): Dynamics of metal tolerant plant communities' development in mine tailings from the Cartagena-La Union Mining District (SE Spain) and their interest for further revegetation purposes. – *Chemosphere* 68: 1180-1185.
- [20] Conesa, H. M., Robinson, B. H., Schullin, R., Nowack, B. (2007b): Growth of *Lygeum spartum* in acid mine tailings: response of plants developed from seedlings, rhizomes, and at field conditions. – *Environmental Pollution* 145: 700-707.
- [21] Cunningham, S. D., Berti, W. R., Huang, J. W. W. (1995): Phytoremediation of contaminated soils. – *Trends in Biotechnology* 13: 393-397.

- [22] Cunningham, S. D., Berti, W. W. R. (2000): Phytoextraction and phytostabilization: technical, economic, and regulatory considerations of the soil-lead issue. – In: Terry, N., Banuelos, G. (eds.) *Phytoremediation of contaminated soil and water*. CRC Press LLC, Boca Raton.
- [23] Das, P. K. (2018): Phytoremediation and Nanoremediation: Emerging Techniques for treatment of acid mine drainage water. – *Defence Life Science Journal* 3(2): 190-196.
- [24] Del Rio-Celestino, M., Font, R., Moreno-Rojas, R., De Haro-Bailon, A. (2006): Uptake of lead and zinc by wild plants growing on contaminated soils. – *Industrial Crop and Products* 24: 230-237.
- [25] Deng, J. C., Liao, B., Ye, M., Deng, D. M., Lan, C. Y., Shu, W. S. (2007): The effects of heavy metal pollution on genetic diversity in zinc/cadmium hyperaccumulator *Sedum alfredii* populations. – *Plant Soil* 297: 83-92.
- [26] Duker, A. A., Carranza, E. J. M., Hale, M. (2005): Arsenic geochemistry and health. – *Environmental International* 31: 631-641.
- [27] Dushenkov, S. (2003): Trends in phytoremediation of radionuclides. – *Plant and Soil* 249: 167-175.
- [28] Emenike, C. U., Jayanthi, B., Agamuthu, P., Fauziah, S. H. (2018): Biotransformation and removal of heavy metals: a review of phytoremediation and microbial remediation assessment on contaminated soil. – *Environmental Reviews* 26(2): 156-168.
- [29] Ernst, W. H. O. (2000): Evolution of metal hyperaccumulation and the phytoremediation hype. – *New Phytologist* 146: 357-358.
- [30] Ernst, W. H. O. (2005): Phytoextraction of mine wastes - options and impossibilities. – *Chemie der Erde-Geochemistry* 65(1): 29-42.
- [31] Evangelou, V. P. (1995): *Pyrite Oxidation and its Control*. – CRC Press, New York: 275.
- [32] Filipek, L. H., Hatton, C., Gusek, J., Tsukamoto, T. (2003): Passive treatment of acid rock drainage (ARD): state of the practice. – In: *Proceedings of the Tenth International Conference on Tailings and Mine Waste*, Colorado, USA, 293-303.
- [33] Fiset, J. F., Zinck, J. M., Nkinamubanzi, P. C. (2003): Chemical stabilization of metal hydroxide sludge. – In: *Proceedings of the X International Conference on Tailings and Mine Waste*, Vail, CO, USA, AA Balkema: 329-332.
- [34] Forján, R., Rodríguez-Vila, A., Covelo, E. F. (2017): Increasing the nutrient content in a mine soil through the application of technosol and biochar and grown with *Brassica juncea* L. – *Waste and Biomass Valorization*: 1-17.
- [35] Frérot, H., Lefévre, C., Gruber, W., Collin, C., Santos, A., Escarré, J. (2006): Specific interactions between local metalicolous plants improve the phytostabilization of mine soils. – *Plant Soil* 282: 53-65.
- [36] Fyson, A., Kalin, M., Adrian, L. W. (1994): Arsenic and nickel removal by wetland sediments. – In: *Proceedings of the International Land Reclamation and Mine Drainage Conference and Third International Conference on the Abatement of Acidic Drainage*, vol. 1. Pittsburgh, PA: 109-118.
- [37] Gebauer, R. L. E., Ehleringer, J. R. (2000): Water and nitrogen uptake patterns following moisture pulses in a cold desert community. – *Ecology* 81: 695-712.
- [38] Glick, B. R. (2003): Phytoremediation: synergistic use of plants and bacteria to clean up the environment. – *Biotechnology Advances* 21: 383-393.
- [39] Gonzalez, R. C., Gonzalez-Chavez, M. C. A. (2006): Metal accumulation in wild plants surrounding mining wastes: soil and sediment remediation (SSR). – *Environmental Pollution* 144: 84-92.
- [40] Hasan, S. H., Talat, M., Rai, S. (2007): Sorption of cadmium and zinc from aqueous solutions by water hyacinth (*Eichhornia crassipes*). – *Bioresource Technology* 98(4): 918-928.
- [41] Hong, M. S., Farmayan, W. F., Dortch, I. J., Chiang, C. Y., McMillan, S. K., Schnoor, J. L. (2001): Phytoremediation of MTBE from groundwater plume. – *Environmental Science and Technology* 35: 1231-1239.

- [42] Huang, J. W., Blaylock, M. J., Kapulnik, Y., Ensley, B. D. (1998): Phytoremediation of uranium-contaminated soils: role of organic acids in triggering uranium hyperaccumulation in plants. – *Environmental Science and Technology* 32: 2004-2008.
- [43] Iqbal, M. C. M., Kulasekara, L., Rajakaruna, N., Iqbal, S. S. (2006): Plant-soil relations of a serpentine site in the southern coast of Sri Lanka. – Fifth International Conference on Serpentine Ecology. Siena, Italy, 09-13 May. (Abstract).
- [44] Jaffré, T., Brooks, R. R., Lee, J., Reeves, R. D. (1976): *Seberita acuminata*: a hyperaccumulator of nickel from New Caledonia. – *Science* 193: 579-580.
- [45] Jaffré, T., Kersten, W., Brooks, R. R., Reeves, R. D. (1979): Nickel uptake by Flacourtiaceae of New Caledonia. – *Proceedings of the Royal Society of London B205*: 385-394.
- [46] Jayasekera, R., Rossbach, M. (1994): Trace elements in plants growing in contrasting ecosystems in Sri Lanka: analytical aspects. – *Environmental Geochemistry and Health* 16: 171-179.
- [47] Jayasekera, R., Rossbach, M. (1996): Background levels of heavy metals in plants of different taxonomic groups from a montane rain forest in Sri Lanka. – *Environmental Geochemistry and Health* 18: 55-62.
- [48] Jefferson, L. V. (2004): Implications of plant density on the resulting community structure of mine site land. – *Restoration Ecology* 12: 429-438.
- [49] Jopony, M., Tongkul, F. (1999): Hyperaccumulation of nickel by *Rinorea benghalensis* in ultrabasic soils of Sabah, Malaysia. – Third International Conference on Environmental Chemistry and Geochemistry in the Tropics. Hong Kong, 24-26 November. (Abstract).
- [50] Keller, C., Hammer, D., Kayser, A., Richner, W., Brodbeck, M., Sennhauser, M. (2003): Root development and heavy metal phytoextraction efficiency: comparison of different plant species in the field. – *Plant Soil* 249: 67-81.
- [51] Kleinman, R. L. P. (1990): Acid mine drainage, US bureau of mines researches and develops: control methods for both coal and metal mines. – *Environmental Science and Technology* 24(9): 1278-1285.
- [52] Knight, B., Zhao, F. J., McGrath, S. P., Shen, Z. G. (1997): Zinc and cadmium uptake by the hyperaccumulator *Thlaspi caerulescens* in contaminated soils and its effects on the concentration and chemical speciation of metals in soil solution. – *Plant Soil* 197: 71-78.
- [53] Kramer, P. A., Zabowski, D., Scherer, G., Everett, R. L. (2000): Native plant restoration of copper mine tailings: I. Substrate effect on growth and nutritional status in a greenhouse study. – *Journal of Environmental Quality* 29: 1762-1769.
- [54] Krämer, U. (2003): Phytoremediation to phytochelatin—plant trace metal homeostasis. – *New Phytologist* 158: 4-6.
- [55] Krzaklewski, W., Pietrzykowski, M. (2002): Selected physicochemical properties of zinc and lead ore tailings and their biological stabilisation. – *Water Air Soil Pollution* 141: 125-142.
- [56] Kumar, P. B. A. N., Dushenkov, V., Motto, H., Raskin, I. (1995): Phytoextraction: the use of plants to remove heavy metals from soils. – *Environmental Science and Technology* 29: 1232-1238.
- [57] Kuyucak, N. (2002): Acid mine drainage prevention and control options. – *CIM Bulletin* 95(1060): 96-102.
- [58] Lasat, M. M., Fuhrmann, M., Ebbs, S. D., Cornish, J. E., Kochian, L. V. (1998): Phytoremediation of a radiocesium-contaminated soil: evaluation of cesium-137 bioaccumulation in the shoots of three plant species. – *Journal of Environmental Quality* 27: 165-169.
- [59] Leita, L., De Nobili, M., Pardini, G., Ferrari, F., Sequi, S. (1989): Anomalous contents of heavy metals in soils and vegetation of a mine area in S.W. Sardinia, Italy. – *Water Air Soil Pollution* 48: 423-433.

- [60] Lutts, S., Lefevre, I., Delperee, C., Kivits, S., Dechamps, C., Robledo, A., Correal, E. (2004): Heavy metal accumulation by the halophyte species Mediterranean saltbush. – *Journal of Environmental Quality* 33: 1271-1279.
- [61] Mannino, I., Franco, D., Piccioni, E., Favero, L., Mattiuzzo, E., Zanetto, G. (2008): A cost-effectiveness analysis of seminatural wetlands and activated sludge wastewater-treatment systems. – *Environmental Management* 41: 118-129.
- [62] Marschner, H. (1995): Mineral nutrition of higher plants. – Academic Press Inc., San Diego.
- [63] McGaw, L. J., Rabe, T., Sparg, S. G., Jäger, A. K., Eloff, J. N., van Staden, J. (2001): An investigation on the biological activity of *Combretum* species. – *Journal of Ethnopharmacology* 75(1): 45-50.
- [64] Meerts, P., Van Isacker, N. (1997): Heavy metal tolerance and accumulation in metalicolous and non-metallicolous populations of *Thlaspi caerulescens* from continental Europe. – *Plant Ecology* 133: 221-231.
- [65] Melato, F. A., Mokgalaka, N. S., McCrindle, R. I. (2016): Adaptation and detoxification mechanisms of Vetiver grass (*Chrysopogon zizanioides*) growing on gold mine tailings. – *International Journal of Phytoremediation* 18(5): 509-520.
- [66] Mendez, M. O., Glenn, E. P., Maier, R. M. (2007): Phytostabilization potential of quailbush for mine tailings: growth, metal accumulation, and microbial community changes. – *Journal of Environmental Quality* 36: 245-253.
- [67] Michelle, B.da-C., Rosane, A., Jaime, W. V.de-M. (2010): Phytoremediation of acid mine drainage by aquatic floating macrophytes. – Institute of Science and Technology for Mineral Resource, Water and Biodiversity, INCT-ACQUA - Annual Report 1-4.
- [68] Mishra, V. K., Upadhyaya, A. R., Pandey, S. K., Tripathi, B. D. (2008a): Heavy metal pollution induced due to coal mining effluent on surrounding aquatic ecosystem and its management through naturally occurring aquatic macrophytes. – *Bioresource Technology* 99: 930-936.
- [69] Mishra, V. K., Upadhyaya, A. R., Pandey, S. K., Tripathi, B. D. (2008b): Phytoremediation of mercury and Arsenic from Tropical open cast coalmine effluent through naturally occurring aquatic *macnophytes*. – *Water, Air and Soil Pollution* 192: 303-314.
- [70] Modis, K., Adam, K., Panagopoulos, K., Komtopoulos, A. (1998): Development and Validation of a geostatistical model for prediction of acid mine drainage in underground sulphide mines. – *Journal of Transaction of the Institute of Mining and Metallurgy (Sect A: Min. Industry)* A102-A107.
- [71] Mokhtar, H., Morad, N., Ahmad Fizri, F. F. (2011): Hyperaccumulation of copper by two species of aquatic plants. – *International Conference on Environmental Science and Engineering IPCBEE 8*. IACSIT Press, Singapore.
- [72] Mummey, D. L., Stahl, P. D., Buyer, J. S. (2002a): Microbial biomarkers as an indicator of ecosystem recovery following surface mine reclamation. – *Applied Soil Ecology* 21: 251-259.
- [73] Mummey, D. L., Stahl, P. D., Buyer, J. S. (2002b): Soil microbiological properties 20 years after surface mine reclamation: spatial analysis of reclaimed and undisturbed sites. – *Soil Biology and Biochemistry* 34: 1717-1725.
- [74] Munshower, F. F. (1994): Practical handbook of disturbed land revegetation. – Lewis Publishing, Boca Raton.
- [75] National Research Council. (2005): Mineral tolerance of animals. – National Academies Press, Washington.
- [76] Newete, S. W., Byrne, M. J. (2016): The capacity of aquatic macrophytes for phytoremediation and their disposal with specific reference to water hyacinth. – *Environmental Science and Pollution Research* 23(11): 10630-10643.
- [77] Osmond, C. B., Bjorkman, O., Anderson, D. J. (1980): Physiological processes in plant ecology: toward a synthesis with *Atriplex*. – Springer-Verlag, New York.

- [78] Pichtel, J., Salt, C. A. (1998): Vegetative growth and trace metal accumulation on metalliferous wastes. – *Journal of Environmental Quality* 27: 618-624.
- [79] Pierzynski, G. M., Lambert, M., Hetrick, B. A. D., Weeney, D. W., Erickson, L. E. (2002): Phytostabilization of metal mine tailings using tall fescue. – *Practical Periodical Hazard and Toxic Radioactive Waste Manage* 6: 212-217.
- [80] Piha, M. I., Vallack, H. W., Michael, N., Reeler, B. M. (1995): A lowinput approach to vegetation establishment on mine and coal ash wastes in semiarid regions. 2. Lagooned pulverized fuel ash in Zimbabwe. – *Journal of Applied Ecology* 32: 382-390.
- [81] Pilon-Smits, E., Pilon, M. (2002): Phytoremediation of metals using transgenic plants. – *Critical Review in Plant Science* 21: 439.
- [82] Pilon-Smits, E. A. H. (2005): Phytoremediation. – *Annual Review of Plant Biology* 56: 15-39.
- [83] Prasad, M. N. V., Freitas, H. M. O. (2003): Metal hyperaccumulation in plants— Biodiversity prospecting for phytoremediation technology. – *Electronic Journal of Biotechnology* 6: 285-321.
- [84] Proctor, J. (2003): Vegetation and soil and plant chemistry on ultramafic rocks in the tropical Far East. – *Perspectives in Plant Ecology, Evolution, and Systematics* 6: 105-124.
- [85] Proctor, J., Phillipps, C., Duff, G. K., Heaney, A., Robertson, F. M. (1989): Ecological studies in Gunung Silam, a small ultrabasic mountain in Sabah, Malaysia. II. Some forest processes. – *Journal of Ecology* 77: 317-331.
- [86] Qadir, S., Qureshi, M. I., Javed, S., Abdin, M. Z. (2004): Genotypic variation in phytoremediation potential of *Brassica juncea* cultivars exposed to Cd stress. – *Plant Science* 167: 1171-1181.
- [87] Rahman, M. A., Hasegawa, H., Ueda, K., Maki, T., Okumura, C., Rahman, M. M. (2007): Arsenic accumulation in duckweed (*Spirodela polyrhiza* L.): a good option for phytoremediation. – *Chemosphere* 69(3): 493-499.
- [88] Rai, P. K. (2008): Heavy metal pollution in aquatic ecosystems and its phytoremediation using wetland plants: an Eco-sustainable approach. – *International Journal of Phytoremediation* 10(2): 131-158.
- [89] Rajakaruna, N., Bohm, B. A. (2002): Serpentine and its vegetation: a preliminary study from Sri Lanka. – *Journal of Applied Botany* 76: 20-28.
- [90] Rajakaruna, N., Baker, A. J. M. (2004): Serpentine: A model habitat for botanical research in Sri Lanka. – *Ceylon Journal of Science (Biological Sciences)* 32: 1-19.
- [91] Ramadan, T. (2001): Dynamics of Salt Secretion by *Sporobolus spicatus* (Vahl) Kunth from Sites of Differing Salinity. – *Annals of Botany* 87: 259-266.
- [92] Reeves, R. D. (2003): Tropical hyperaccumulators of metals and their potential for phytoextraction. – *Plant and Soil* 249: 57-65.
- [93] Rosario, K., Iverson, S. L., Henderson, D. A., Chartrand, S., McKeon, C., Glenn, E. P., Maier, R. M. (2007): Bacterial community changes during plant establishment at the San Pedro River mine tailings site. – *Journal of Environmental Quality* 36: 1249-1259.
- [94] Sabey, B. R., Pendleton, R. L., Webb, B. L. (1990): Effect of municipal sewage-sludge application on growth of two reclamation shrub species in copper mine spoils. – *Journal of Environmental Quality* 19: 580-586.
- [95] Salt, D. E., Pickering, I. J., Prince, R. C., Gleba, D., Dushenkov, S., Smith, R. D., Raskin, I. (1997): Metal accumulation by aquacultured seedlings of Indian mustard. – *Environmental Science and Technology* 31: 1636-1644.
- [96] Schmidt, U. (2003): Enhancing phytoextraction: the effect of chemical soil manipulation on mobility, plant accumulation, and leaching of heavy metals. – *Journal of Environmental Quality* 32: 1939-1954.
- [97] Sharma, S., Singh, B., Manchanda, V. K. (2014): Phytoremediation: role of terrestrial plants and aquatic macrophytes in the remediation of radionuclides and heavy metal contaminated soil and water. – *Environmental Science and Pollution Research* 22(2): 946-962.

- [98] Shu, W. S., Ye, Z. H., Lan, C. Y., Zhang, Z. Q., Wong, M. H. (2001): Acidification of lead/zinc mine tailings and its effect on heavy metal mobility. – *Environmental International* 26: 389-394.
- [99] Singh, G., Bhati, M., Rathod, T. (2010): Use of tree seedlings for the phytoremediation of a municipal effluent used in dry areas of north-western India: Plant growth and nutrient uptake. – *Ecological Engineering* 36(10): 1299-1306.
- [100] Smith, R. A. H., Bradshaw, A. D. (1979): The use of metal tolerant plant populations for the reclamation of metalliferous wastes. – *Journal of Applied Ecology* 16: 595-612.
- [101] Snow, A. A., Andow, D. A., Gepts, P., Hallerman, E. M., Power, A., Tiedje, J. M., Wolfenbarger, L. L. (2005): Genetically engineered organisms and the environment: current status and recommendations. – *Ecological Application* 10: 377-404.
- [102] Sood, A., Uniyal, P. L., Prasanna, R., Ahluwalia, A. S. (2012): Phytoremediation potential of aquatic macrophyte, *Azolla*. – *Ambio* 41: 122-137.
- [103] Stoffberg, G. H., van Rooyen, M. W., van der Linde, M. J., Groeneveld, H. T. (2008): Predicting the growth in tree height and crown size of three street tree species in the City of Tshwane, South Africa. – *Urban Forestry and Urban Greening* 7: 259-264.
- [104] Tilman, D. (1988): *Plant strategies and the dynamics and structure of plant communities*. – Princeton University Press, New Jersey.
- [105] Tucker, R. K., Shaw, J. A. (2000): Phytoremediation and public acceptance. – In: Raskin, I., Ensley, B. D. (eds.) *Phytoremediation of toxic metals. Using plants to clean up the environment*. J. Wiley & Sons, New York, USA: 33-42.
- [106] Turnau, K., Henriques, F. S., Anielska, T., Renker, C., Buscot, F. (2007): Metal uptake and detoxification mechanisms in *Erica andevalensis* growing in a pyrite mine tailing. – *Environmental and Experimental Botany* 61: 117-123.
- [107] Van Rensburg, L., Morgenthal, T. (2004): The effect of woodchip waste on vegetation establishment during platinum tailings rehabilitation. – *South African Journal of Science* 100: 294-300.
- [108] Von Willert, F. J., Stehouwer, R. C. (2003): Compost and calcium surface treatment effects on subsoil chemistry in acidic minespoil columns. – *Journal of Environmental Quality* 32: 781-788.
- [109] Watson, I. W., Westoby, M., Holm, A. M. (1997): Continuous and episodic components of demographic change in arid zone shrubs: models of two *Eremophila* species from Western Australia compared with published data on other species. – *Journal of Ecology* 85: 833-846.
- [110] Windsor, D. M., Clements, A. (2001): A germination and establishment field trial of *Themeda australis* (kangaroo grass) for mine site restoration in the Central Tablelands of New South Wales. – *Restoration Ecology* 9: 104-110.
- [111] Wither, E. D., Brooks, R. R. (1977): Hyperaccumulation of nickel by some plants of Southeast Asia. – *Journal of Geochemical Exploration* 8: 579-583.
- [112] Wolfe, A. K., Bjornstad, D. J. (2002): Why would anyone object? An exploration of social aspects of phytoremediation acceptability. – *Critical Review in Plant Science* 21: 429-438.
- [113] Wolfenbarger, L. L., Phifer, P. R. (2000): Biotechnology and ecology-the ecological risks and benefits of genetically engineered plants. – *Science* 290: 2088-2093.
- [114] Wong, M. H. (2003): Ecological restoration of mine degraded soils, with emphasis on metal contaminated soils. – *Chemosphere* 50: 775-780.
- [115] Wood, M. K., Buchanan, B. A., Skeet, W. (1995): Shrub preference and utilization by big game on New Mexico reclaimed mine land. – *Journal of Range Management* 48: 431-437.
- [116] Wu, J., Hsu, F. C., Cunningham, S. D. (1999): Chelate-assisted Pb phytoextraction: Pb availability, uptake, and translocation constraints. – *Environmental Science and Technology* 33: 1898-1904.

- [117] Ye, Z. H., Wong, J. W. C., Wong, M. H., Lan, C. Y., Baker, A. J. M. (1999): Lime and pig manure as ameliorants for revegetating lead/ zinc mine tailings: a greenhouse study. – *Bioresource Technology* 69: 35-43.
- [118] Zhao, F. J., Lombi, E., McGrath, S. P. (2003): Assessing the potential for zinc and cadmium phytoremediation with the hyperaccumulator *Thlaspi caerulescens*. – *Plant Soil* 249: 37-43.
- [119] Zhu, Y. L., Pilon-Smits, E. A. H., Jouanin, L., Terry, N. (1999): Overexpression of glutathione synthetase in *Brassica juncea* enhances cadmium tolerance and accumulation. – *Plant Physiology* 119: 73-79.

SILICON-MEDIATED IMPROVEMENT IN TOLERANCE OF ECONOMICALLY IMPORTANT CROPS UNDER DROUGHT STRESS

PANG, Z.^{1,2} – TAYYAB, M.^{1,2} – ISLAM, W.^{3,4,5} – TARIN, M. W. K.⁶ – SARFARAZ, R.⁷ – NAVEED, H.⁸
– ZAMAN, S.⁹ – ZHANG, B.¹⁰ – YUAN, Z.^{1,2*} – ZHANG, H.^{1,2*}

¹*Key Laboratory of Sugarcane Biology and Genetic Breeding, Ministry of Agriculture, Fujian Agriculture and Forestry University, Fuzhou 350002, China*

²*College of Crop Science, Fujian Agriculture and Forestry University, Fuzhou 350002, China*

³*Key Laboratory for Humid Subtropical Eco-Geographical Processes of the Ministry of Education, Fujian Normal University, Fuzhou 350007, China*

⁴*Institute of Geography, Fujian Normal University, Fuzhou 350007, China*

⁵*Agriculture Department, Govt. of Punjab, Lahore, Pakistan*

⁶*College of Forestry, Fujian Agriculture and Forestry University Fuzhou 350002, China*

⁷*College of Resources and Environment, Fujian Agriculture and Forestry University, Fuzhou 350002, China*

⁸*Institute of Entomology, College of Life Sciences, Nankai University, Tianjin 300071, China*

⁹*Institute of Entomology, University of Agriculture, Faisalabad 38000, Pakistan*

¹⁰*College of Biological Science and Biotechnology, Shenyang Agricultural University, Shenyang, China*

**Corresponding authors*

e-mail: yzn05@sina.com (Z. Yuan); zhanghua4553@sina.com (H. Zhang)

(Received 30th Aug 2018 ; accepted 8th Apr 2019)

Abstract. Drought is considered as one of the significant threats to food security worldwide as it inhibits the growth, yield and quality of economically important crops. An increase in crop yield is considered a tremendous achievement as it will be helpful to meet the current growing demand for food in drought-stressed areas. Silicon (Si) is the second most abundant component in the soil. Recent research has revealed that Si can enhance plant tolerance against drought stress. In addition, application of Si can increase seed germination, underground and aboveground biomass, photosynthetic pigments, quality and yield of grains. Therefore, we have summarized the importance of Si in improving the drought tolerance in plants. Furthermore, we have explained the Si-mediated mechanisms which led to modifications in gas exchange properties, homeostasis of the nutrient element, synthesis of compatible solute, osmotic adjustments, antioxidant stimulation and enzymatic action in plants under drought stress. We believe that the current study will help in understanding the importance of Si application in plants under drought stress conditions.

Keywords: *seed germination, antioxidants enzymes, drought tolerance, gene expression, soil*

Introduction

The increasing demand for food day by day is one of the significant challenges for agricultural scientists worldwide (Warner and Jones, 2017). On the other hand, the world's crop productivity is continually decreasing due to extreme climate changes and shrinking resources. In view of that, finding the new options to improve the crop productivity is a challenging task for all nations across the world (George et al., 2018; Lesk et al., 2016; Rizwan et al., 2018). Abiotic stresses (salt, drought, and extreme temperature stress) are the challenging problems for plant development and its productivity in many parts of the world (Khalil et al., 2016, 2018; Suzuki et al., 2014). Among these abiotic stresses, drought is one of the most harmful environmental factors which inhibit growth, yield and quality of economically important crops (Ali et al., 2016; Calvo-Polanco et al., 2016). Therefore, it is estimated to be one of the severe threats for future agricultural crop production (Khalil et al., 2018; Tayyab et al., 2018a). The negative impacts of drought stress on many plants have become the central debate in recent years (Tayyab et al., 2018a). Drought along with other abiotic stresses including heavy metal contamination not only restricts plant production but also poses severe threats to human health (Arshad et al., 2016; Noman and Aqeel, 2017). For example, Liu et al. (2017) revealed that under different growth stages, the translocation and redistribution of cadmium have a different influence for drought in peanut plants. It can affect the processes such as cell dehydration, the inhibition of cell expansion and division, stem elongation, leaf size, root proliferation, disturbed stomatal oscillations, water and nutrient absorption in plants (Kaushal and Wani, 2016; Khalil et al., 2018; Tayyab et al., 2018a). Furthermore, it also reduces photosynthesis (Khan et al., 2017; Zang et al., 2014), soil water potential, water use efficiency (WUE) (Kaushal and Wani, 2016), and induce oxygen deficiency by the production of reactive oxygen species (ROS) (Fukao et al., 2011). Consequently, combating the stress caused by drought is a serious matter to achieve food security in changing climate conditions around the world.

Si is found to be the second most abundant element in soil (Sommer et al., 2006). However, it comprises up to 10% dry weight of many plants. In the past, researchers could not find Si as an essential element for normal development and growth of the plant (Epstein, 1994; Hodson et al., 2005). However, concerning the Si efficiency on the plant's life cycle, Epstein and Bloom (2005) recommended that the proper need of Si element is significant for normal plant growth. Recently, numerous researches have demonstrated that Si mitigates the destructive effects of biotic stresses (pests and diseases) (Dann and Le, 2017; Yang et al., 2017) and abiotic stresses (drought, heavy metal toxicity and salinity) in plants (Biju et al., 2017; Hasanuzzaman et al., 2018; Tayyab et al., 2018b). These benefits are attributed to Si application; thus, Si can play a serious role in order to mitigate drought stress in plants. Moreover, sustainable agriculture has got great importance so it can be used as a high-quality fertilizer because of its non-corrosive and non-polluted nature. Si effect for plant growth and development in unfavorable climatic conditions has been reviewed by many researchers recently around the globe (Guntzer et al., 2012; Tayyab et al., 2018b; Van Bockhaven et al., 2012). Van Bockhaven et al. (2012) reviewed the role of Si for plant disease resistance. However, the mechanisms of Si-mediated mitigation of drought stress in plants are still debatable and need to be reviewed. Si application as a fertilizer for plants also has gained momentum recently. In order to enhance drought tolerance, Si application in term of soil amendment is expected to become a new approach in agricultural farming in the future. Therefore, we have reviewed the current status and progress in understanding the mechanisms of Si-mediated

drought tolerance in plants. The review unveils the various mechanisms involved in the plant's protection during drought stress as well as suggests guidelines for further research.

History of silicon application

Si is widely distributed as silica or alumino-silicates – better known as rocks and sand. Si is not readily available for plants to use; instead plants can only absorb Si as a monosilicic acid (Marafon and Endres, 2013). Si is beneficial for plants, such as protecting against diseases, insects attacks, reinforcing nutrients and safeguarding under unfavorable conditions like drought, salt or heavy metals toxicity (Debona et al., 2017; Tayyab et al., 2018b). Kutschera and Niklas (2018) highlighted the function of Si in plant biology as “whether silicic acid is an indispensable substance for those plants that contain silica, whether it takes part in the nutritional processes, and what is the relationship that exists between the uptake of silicic acid and the life of the plant?” (Lewin and Reimann, 1969). In the 20th century, several trials were directed on Si to demonstrate its beneficial role in agriculture owing to its safe behavior and presence in nature. For the first time in the world, rice (*Oryza sativa*) soils in Japan were treated with Si in 1955 (Takahashi et al., 1990). Si fertilizers commonly contain neutral or slightly alkaline pH which has the neutralizing effect for acidic soils (Savant et al., 1999). Several kinds of Si fertilizers are applied in the field usually in the form of solids as well as liquids such as calcium silicates, calcium and magnesium silicates wollastonite, potassium silicate and sodium silicate.

Silicon in soils

Si contributes to the second major element existing in soil (Sommer et al., 2006). Si reacts with oxygen and turns into silicates, i.e., feldspars and quartz (*Fig. 1*). Silicate formed by oxygen and pure Si is known as silica (i.e., quartz) whereas other silicates (i.e., feldspars) have some elements (sodium, potassium, aluminum, and calcium) including oxygen and Si. Soils are formed as the results of weathering of rocks made from alumino-silicates and silicates minerals. By biological and physical weathering silicate minerals release Si into soil solution that formulates silicic acid (H_4SiO_4). Then, plant roots absorb silicic acid from soil solution (Epstein, 2009). The plant contains a significant amount of Si owing to its ubiquitous nature and abundance (Epstein, 1999). Si abundance and concentration fluctuates with the soil type. Typically, upper horizons frequently have low Si concentrations in the sandy soils (Marschner, 2011), whereas clay soils have higher phyllo-silicates quantities that release Si. The quartz (SiO_2) mineral is abundantly present in sandy soils which are less prone to decomposition. The complexity of quartz mineral makes sandy soil more responsive to Si application than clayey soil (Dematté et al., 2011). In tropical and subtropical soils, Si commonly is found very low due to desilication because of leaching and some weathering processes (Epstein, 1999). Additionally, it is predicted that 210 to 224 million tons of Si have been removed by intensive arable cultivation throughout the world (Meena et al., 2014).

Silicon uptake and accumulation in plants

Plants differ in their ability to uptaking the Si. Some plants can accumulate more Si in their leaves and those with more than 1.5% of their total dry biomass are known as

accumulators. Plants containing Si levels less than 0.5% in their leaves are considered as non-accumulators (Marafon and Endres, 2013). Variation of Si concentration in plants is attributed to their Si uptake capability and roots xylem loading (Ma et al., 2001a). The plasma membrane present in plant root cells might provide a path for uncharged monomeric H_4SiO_4 uptake by diffusion. Thus, H_4SiO_4 permeability coefficient of $10^{-10}ms^{-1}$ throughout a plasma membrane (Raven, 2001), does not clarify experimentally measured Si contents in plants (Tamai and Ma, 2003). Passive and active transporters are involved in the Si uptake and transport from growth medium to xylem tissues (Mitani et al., 2005). This hypothesis was confirmed due to Si uptake inhibition as plants were exposed to metabolic inhibitors (i.e., 2,4- dinitrophenol, potassium cyanide) or low temperature (Mitani et al., 2005; Tamai and Ma, 2003). A low-affinity silicic acid transporter involves Si transportation from root medium to cortical cells. Kinetic studies for Si uptake in rice (*O. sativa*), tomato (*Solanum lycopersicum*) and cucumber (*Cucumis sativus*) confirmed that the density of transporters present in the plasma membrane is responsible for Si uptake changes (Mitani et al., 2005). Recently, *Lsi1*, *Lsi2*, and *Lsi6* genes are associated with Si uptake and distribution in rice (*O. sativa*), barley (*Hordeum vulgare*), maize (*Z. mays*), and cucumber (*C. sativus*) (Ma and Yamaji, 2015). Si-influx transporters (*Lsi1* and *Lsi6*) are associated with Si distribution in the tissues of root and shoot (Mitani et al., 2011). Whereas, putative anion transporter (*Lsi2*) is commonly expressed in roots endodermis (Ma et al., 2007). Ma et al. (2007) reported that *Lsi2* transporter activity is proton-driven and acts as a Si/H^+ antiport.

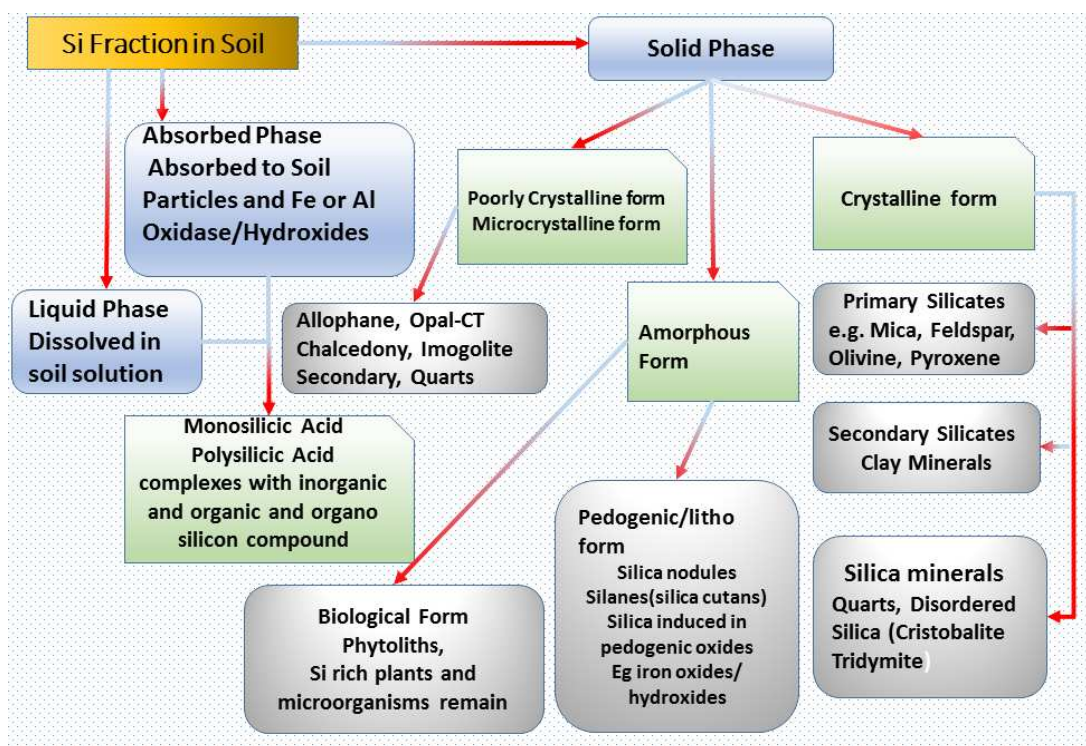


Figure 1. Various sources of silicon in the soil. (Modified from Zia, 2018)

Silicon and drought stress

Drought commonly reduces plant growth and its yield in semiarid and arid regions throughout the world (Zandalinas et al., 2018). It adversely affects plant biomass and

growth of all crops cultivated in main fields as well (Kaushal and Wani, 2016). In contrast, various researchers have demonstrated that Si should consider being a practical approach to overcome these opposing effects stimulated by drought (Guo et al., 2017; Shi et al., 2014). The mechanisms in order to enhance drought tolerance in the plant by Si application at the morphological, physiological and biochemical levels are summarized below (see also Fig. 2).

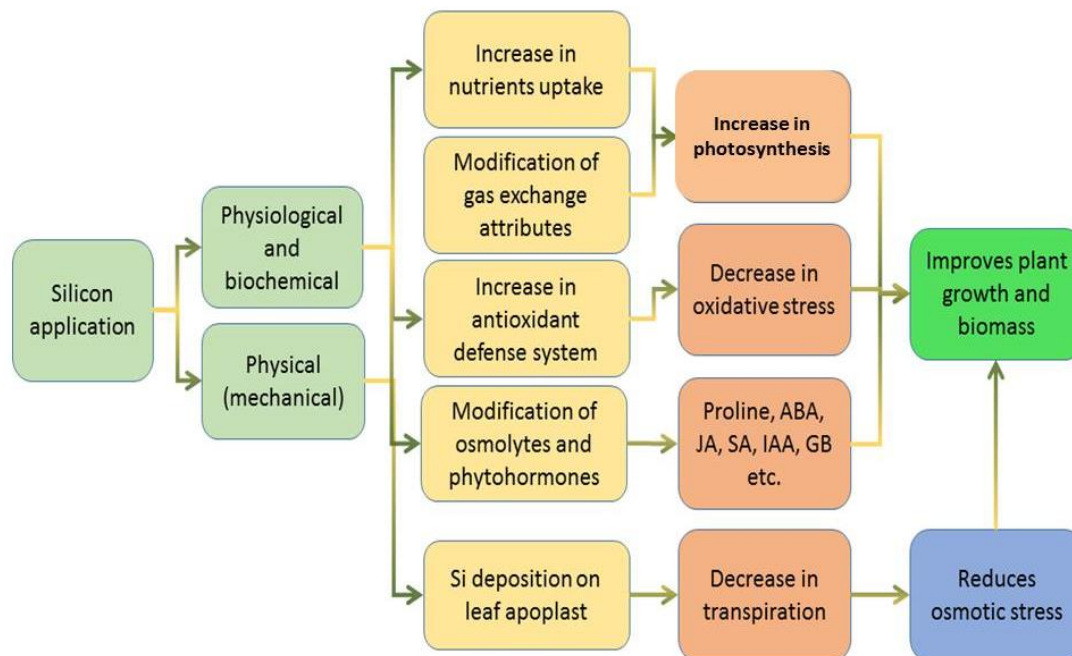


Figure 2. The mechanism for the Si-mediated alleviation of drought stress tolerance in plants. (Modified from Rizwan et al., 2015; Tayyab et al., 2018b)

Si-mediated improvement in seed germination under drought condition

Drought stress negatively affects the seed germination leading to considerable reduction in crop yield (Guo et al., 2017; Shi et al., 2014). Until now, a little research was conducted to study the Si effects for seed germination under drought conditions (Ahmed et al., 2016; Hasanuzzaman et al., 2018). On the contrary, Si not only mitigates the adverse effect induced by drought stress on seed germination but also promotes seed development. For instance, seed priming with sodium silicate contributed to recovering wheat (*Triticum aestivum*) seed germination compared to untreated seeds (Hameed et al., 2013). The authors described that soaking of seeds for 8 h in aerated solutions of 20 mM, 40 mM and 60 mM sodium silicate resulted in 97% improvement in seed germination under water-deficit stress induced by 15% polyethylene glycol (PEG)-6000 (Hameed et al., 2013). Similarly, Ahmed et al. (2016) reported seeds priming with Si (silicic acid, sodium silicate, and silica gel) at different concentration (0.5%, 1.0%, and 1.5%) to explore its potential benefits for couple of wheat (*T. aestivum*) varieties. The authors have shown that silica gel can be used as an active priming practice at 1.5% concentration for better development of a plant under drought conditions. Likewise, calcium silicate employed in the soil in the same conditions enhanced seed germination of maize (*Z. mays*; 15 different cultivars) up to 80.96% under water stress (under rain-fed conditions) (Zargar and Agnihotri, 2013). Shi et al. (2014) reported that the Si

application improved the seed germination in four tomatoes (*S. lycopersicum*) cultivars under drought as compared to control (without Si). The authors investigated the effects of exogenous Si (0.5 mM) to tomato (*S. lycopersicum*) bud seedlings under water deficit stress simulated by 10% (w/v) PEG-6000 in four different cultivars ('Jinpengchaoguan', 'Zhongza No.9', 'Houpi L402' and 'Oubao318'), which significantly improved the seed germination by 21.9% - 38.2% (Shi et al., 2014). Similarly, in a recent study, Hasanuzzaman et al. (2018) revealed that application of Si is also an active practice for the alleviation of the destructive effects of drought on seed germination in *Brassica napus*. Furthermore, Si application improved the vigor of seedlings. These reports demonstrate that Si can be effective to mitigate the destructive effects of drought on seed germination of crop plants. However, the general mechanisms must be explored for well understanding of Si functions in seedlings under drought conditions.

Silicon-mediated improvement in plant growth, biomass, and photosynthesis under drought stress

Plant biomass and growth is severely reduced by drought (Amin et al., 2016; Noman et al., 2015), hence the application of Si under drought stress can be considered a practical approach to improve plant biomass and growth. Si should be used in conditions effective for its activity and approach to improve plant growth and biomass under drought stress (Hajiboland et al., 2017; Merwad et al., 2018). Si employed in wheat (*T. aestivum*) grown soil resulted in increased root biomass, shoots, spike weight and dry weight (Ahmad et al., 2007; Gong et al., 2003; Xu et al., 2017). Ratnakumar et al. (2016) reported that foliar application of Si (0, 8, 16, 32 ppm at different plant growth stages such as vegetative, booting and seed development stage) on wheat (*T. aestivum*) in the form of ortho-silicic acid improved the root length, density and growth. In another study shoot and root lengths were improved via seed priming by sodium silicate under PEG-6000-induced drought (Hameed et al., 2013). Similarly, Si supply improved roots and shoot fresh weight of Kentucky bluegrass (*Poa pratensis*) under water stress. The daily amount of water or Si solution was 250 mL per pot. For 14 d, plants were treated with 0, 0.1, and 1.0 mM Si solution for Si treatments and with distilled water for the control (Bae et al., 2017). Application of Si (seed priming) provided the better results of grain yield of wheat (*T. aestivum*) grown under drought in hydroponics in pots and field experiments (Ahmed et al., 2016; Gharineh and Karmollachaab, 2013; Pei et al., 2010). Seed priming combined with other sources of Si improved the grain yield and spike length of the wheat (*T. aestivum*) crop as compared to control without seed priming under drought (Ahmed et al., 2016). The authors used seeds of two wheat varieties, i.e., NARC-2009 and Chakwal-50 which were sown in pots after priming with distilled water and different concentration (0.5%, 1.0%, 1.5%) of Si sources (silicic acid, sodium silicate and silica gel). Maximum Si uptake at three leaves (0.028 $\mu\text{g g}^{-1}$ dry weight (DW), anthesis (0.072 $\mu\text{g g}^{-1}$ DW) and maturity (0.103 $\mu\text{g g}^{-1}$ DW) were recorded for silica gel (15%) (Ahmed et al., 2016). Similarly, the use of Si (potassium silicate) employed on sorghum (*Sorghum bicolor*) resulted in improved roots dry weight by 30% under drought (Ahmed et al., 2011). In a recent study, Si used as fertilizer in sugarcane field enhanced sugarcane (*Saccharum officinarum*) stalk yield, dry biomass and provided the best product under drought (de Camargo et al., 2017). Si applied in soil or through foliar application in the field (five sprays of 1.425 mM Si water solution), resulted in improved potato (*Solanum tuberosum*) yield and dry tuber weight just similar to well-irrigated potato (S.

tuberosum) plants (Pilon et al., 2014). Similarly, the application of Si improved the total root length, root surface area, volume and dry weight of rice (*O. sativa*) plants under drought (Ming et al., 2012). However, Nolla et al. (2012) and Moro et al. (2015) demonstrated rice (*O. sativa*) grain yield and plant height improvement by adopting the silicate in soil under drought conditions. Soybean (*Glycine max*) plant shoot length and dry and fresh weight were improved by use of Si under drought (Hamayun et al., 2010). The authors further explained that the adverse effects of PEG-induced drought were alleviated by adding and 200 mg L⁻¹ Si to the drought-stressed treatments (Hamayun et al., 2010). Diatomite application in soil provided effective results by improving growth parameter (shoots and roots length) and yield parameters (number of pods, fresh and dry weight of pod) in white lupine (*Lupinus albus L.*) under drought (Abdalla, 2011). Si increased leaf area index in numerous plant species, e.g., wheat (*T. aestivum*) and Fennel (*Foeniculum vulgare Mill*) under drought (Asgharipour and Mosapour, 2016; Gong et al., 2003). The application Si (300 kg of ha⁻¹) increased the quantity of spikelet panicle and grain yield of rice; furthermore, dry matter recovery and yield had a positive linear relationship with shoot Si under drought (Ullah et al., 2017). The application of Si on two maize (*Z. mays*) varieties (hybrid P-33H25 and FH-810) increased the height of plant, stem diameter, number of leaves, cob length, the number of grain/cob, grain yield, and biological yield, which ultimately contributed to better growth and yield (Amin et al., 2016). The application of Si for tobacco (*Nicotiana Rustica L.*) has increased the biomass particularly aboveground parts in drought and control conditions (Hajiboland et al., 2017). Correspondingly, Si application on cowpea increased the yield per plant (Merwad et al., 2018).

Additionally, Si has also progressive influences on straw and grain quality of plants in drought conditions, but unfortunately, the studies are minimal. For example, Si (0.03 mM sodium selenite/1.5 mM potassium silicate) application has a direct relation to levels of phenolic compounds, amylose and flavonoid contents of rice grains. It also increased the lignin, cellulose, pectin, carbohydrates, proteins and fat contents of rice straw under drought conditions in a field experiment (Emam et al., 2014). So, it is necessary to clarify further mechanisms to improve the quality of cereals mediated by Si application under drought, especially at the molecular level. Drought stress is the primary driver which significantly reduces the photosynthesis in plants. On the other hand, various studies have exposed that by absorbing Si, photosynthetic pigments can be increased in various plant species (Hasanuzzaman et al., 2018; Merwad et al., 2018). The application of Si on wheat (*T. aestivum*) plants showed better result by improving the leaves chlorophyll content (Ma et al., 2016), and photosynthesis rate (Sattar et al., 2017). Likewise, Maghsoudi et al. (2016) demonstrated that Si leaf application increased photosynthesis pigments (chlorophyll a, b and total land carotenoids) and chlorophyll stability index (CSI) in different wheat (*T. aestivum*) cultivars under drought conditions. Similarly, Si foliar application on wheat increased leaf chlorophyll content (Ratnakumar et al., 2016). Si usage protected rapeseed (*B. napus*) leaves photosynthetic pigments (Hasanuzzaman et al., 2018), and increased total chlorophyll content of soybean (*G. max*) leaves under drought (Shen et al., 2010). Si was also observed to improve the allocation of light absorbed between PSII and PSI in the chloroplasts of tomato (*S. lycopersicum*) leaves and maintain the chloroplast membrane structure under drought (Cao et al., 2015). Moreover, Si (K₂SiO₃ at the rate of 2.25 mM) increased photosynthesis and chlorophyll content of two cucumber cultivars (*C. sativus*) under drought (Ouzounidou et al., 2016).

In a recent study, Merwad et al. (2018) revealed that Si foliar application on cowpea (*Vigna unguiculata*) leaves improved chlorophyll (a, b, and total carotenoids) contents. Moreover, chlorophyll content and chlorophyll ratio (a:b) in chestnut leaves was improved under drought condition, when Si (Sili-K® solution containing 0.12% Si and 0.15% K) was repeatedly ($\times 3$) sprayed onto leaves of potted chestnut plantlets and irrigation was suspended for 7 weeks (Zhang et al., 2013). Application of Si on two different rice cultivars (Curinga and IAC-202) enhanced the photosynthetic rate which was reduced by the lack of water (Moro et al., 2015). Soil or foliar applied Si enhanced chlorophyll (a and carotenoids) concentration and chlorophyll (a/b ratio) similar to well-irrigated potato (*S. tuberosum*) plants (Pilon et al., 2014). Si foliar application significantly increased the net photosynthesis rate, green leaf color of Blue Kentucky grass (*P. pratensis*) leaves (Saud et al., 2014), whereas enhanced photochemical efficiency and photosynthetic rate of Cacao (*Theobroma cacao*) leave under drought conditions (Zanetti et al., 2016).

Impacts of Si application under drought stress

Si use exhibited positive influences on seed germination, photosynthesis, plant growth and biomass under drought circumstances in the previous segment. These affirmative effects can be owing to various mechanisms such as enhancement of nutrient uptake by plants, by adjusting osmotic potential, by modifying the gaseous exchange attributes, decrease the oxidative stress and by an alteration in expressing of the gene in plants. Details of these mechanisms are given in (Fig. 2).

Oxidative stress

Dry conditions damage the photosynthetic pigments and disturb the balance between ROS production and antioxidants thus affect overall crop production (Kim et al., 2017). Through up-regulation of antioxidant activities of catalase (CAT), superoxide dismutase (SOD), and growth regulators (GR), Si treatment of wheat plants resulted in higher drought tolerance (Gong et al., 2005). Si supplements in wheat plants of wheat (*T. aestivum*) shown lesser contents of glutathione, lipid peroxidation and total flavonoid while raised content of ascorbate with Si application (Ma and Takahashi, 2002). Similarly, in tomato plants, Si supplementation upon polyethylene glycol (PEG) induced drought stress resulted in tolerance through increased activities of CAT and SOD along with the enhanced roots ability of water uptake (Shi et al., 2014). Moreover, Si reduced the activities of ascorbate peroxidase (APX), under drought conditions in sunflower (*Helianthus annuus*) (Gunes et al., 2008b).

Drought stress produces ROS in plants triggering oxidative stress damage (Fukao et al., 2011; Noman et al., 2015). Various research communities revealed that Si supply increases the antioxidant enzymes activities while decreased oxidative damage stress in plants which can be adequate to the progression of plant drought tolerance (Bae et al., 2017; Hajiboland et al., 2017; Ma et al., 2016). Si application reduced the lipid peroxidation and hydrogen peroxide (H_2O_2) of sunflower (*H. annuus*), chickpea (*Cicer arietinum*) (Gunes et al., 2007, 2008b), and lentil (*Lens culinaris*) plants leave under drought conditions (Biju et al., 2017). Similarly, H_2O_2 and lipid peroxidation were reduced in rapeseed (*B. napus*) leaves (Hasanuzzaman et al., 2018), decreased H_2O_2 contents in tobacco (*Nicotiana tabacum*) (Hajiboland et al., 2017), and wheat (*T. aestivum*) leaves (Gong et al., 2008; Ma et al., 2016). Xu et al. (2017) described that

usage of Si (potassium silicate 1.0 mM) significantly decreased H₂O₂, malondialdehyde (MDA) contents, and increased superoxide dismutase (SOD) activities in leaves of wheat during drought by Si supplementation (Gharineh and Karmollachaab, 2013). In addition, Pei et al. (2010) stated that the Si (1 mM)-supplying reduced H₂O₂, MDA in wheat (*T. aestivum*) leaves and Chinese liquorice (*Glycyrrhiza uralensis*), under drought conditions induced by 100 mM NaCl with 0, 10 and 20% of PEG-6000 (Zhang et al., 2017). Si supplementation in soil decreased the Lipid peroxidation (LP) in white lupin (*L. albus*) (Abdalla, 2011). Shi et al. (2014) demonstrated that Si addition improved superoxide dismutase (SOD), catalase activities (CAT), and H₂O₂ in bud radicles than non-Si treated tomato (*S. lycopersicum*) seedlings. Similarly, Si supply enhanced antioxidant activity, including SOD, CAT and decreased H₂O₂ & MDA contents in tomato (*S. lycopersicum*) (Cao et al., 2017). Additionally, Si application considerably enhanced peroxidase (POD) and SOD in the Canola (*B. napus*) plants activities (Habibi, 2014). Furthermore, the application of Si improved ascorbate peroxidase activity (APX) and glutathione (GSH) contents in Chinese liquorice (*Glycyrrhiza uralensis*) under drought than non-Si treatments (Zhang et al., 2017). The antioxidant enzyme's activity (e.g., SOD and CAT) was increased by Si application in wheat (*T. aestivum*) (Sattar et al., 2017), Cowpea (*V. unguiculata*) (Merwad et al., 2018) and in potato's plants (*S. tuberosum*) by foliar application of Si under drought (Pilon et al., 2014).

Moro et al. (2015) revealed that the use of Si was effective to increase rice SOD, CAT and APX activities and similarly, CAT, POD, SOD and H₂O₂ were enhanced in soybean (*G. max*) (Shen et al., 2010) and Kentucky bluegrass (*P. pratensis*) during drought stress (Bae et al., 2017). Hasanuzzaman et al. (2018) noted that CAT, APX enhanced in rapeseed (*B. napus*) and similarly SOD activity of mango (*Mangifera indica*) leaves (Helaly et al., 2017). Moreover, SOD, CAT, APX, and POD were enhanced in the wheat (*T. aestivum*) (Tale and Haddad, 2011), chickpea (*C. arietinum*) shoot (Gunes et al., 2007) and tomato (*S. lycopersicum*) as compared to non-Si supplemented plants (Shi et al., 2014). Actions of SOD and POD decreased by the Si use and increased CAT activity of cucumber (*C. sativus*) plants than to Si-deficient plants (Ma et al., 2004). Impact of Si on the antioxidant enzyme of plants not only fluctuates with the changes of plant species but also depends on the plant stages of growth during drought (Gong et al., 2008). However, reports are limited on Si's functions on the antioxidant enzyme actions at various growth periods of the plant. For instance, the activities of APX, SOD and the CAT were not improved at the booting stage however improved the SOD while decreased APX activity at the filling stage of wheat (*T. aestivum*) during drought (Gong et al., 2008). Improvement of non-enzymatic antioxidants contents can provide best results to decrease the plant oxidative stress. Various reports revealed that levels of the nonenzymatic antioxidants of different species of plant could be affected by the Si application (Gong et al., 2005; Pei et al., 2010). For example, the Glutathione reductase (GSH) activity (Gong et al., 2005) and ascorbic acid (AA) concentration were improved through the use of the Si during drought conditions in wheat (*T. aestivum*) (Pei et al., 2010). In deduction, Si application reduced the oxidative stress and increased antioxidant enzymes activities.

Plant nutrients uptake

The plants need sufficient quantity of the essential nutrients for proper development and growth, but nutrients uptake in plants is disturbed under drought conditions (Emam et al., 2014; Merwad et al., 2018; Ratnakumar et al., 2016). However, Si has positive

effects on nutrients uptake in plants under drought. For instance, by the application of Si, Potassium (K) and the total Phosphorus (P) level were enhanced straw of wheat (*T. aestivum*) seed (Ratnakumar et al., 2016), and rice (*O. sativa*) straw (Emam et al., 2014) and leaf P in wheat (*T. aestivum*) (Gong and Chen, 2012). Additionally, it was also effective to improve N, P and K of seed and shoot of cowpea (*V. unguiculata*) plants (Merwad et al., 2018). In addition, Calcium (Ca) and K content increase in wheat (*T. aestivum*) leaf and roots was observed (Kaya et al., 2006). Correspondingly, Kentucky Bluegrass (*P. pratensis*) (root, shoot and leaf) C: N ratio improved by the supply of Si under drought (Saud et al., 2014). Gunes et al. (2008a) noted that Si supply in soil enhanced the macronutrients (Ca, K, P, Mg) and the micronutrients (Cu, Fe, and Mn) uptake of sunflower (*H. annuus*) cultivar under drought. Exogenous Si supply was effective for wheat (*T. aestivum*) plant growth by modifying the nutrient uptake (Si, Na and Mg) (Xu et al., 2017), and improve (N, P, and K) uptake in different species of grass (Eneji et al., 2008). Contrarily, reports show that the nutrients uptake reduced in a plant with the supply of Si (Chen et al., 2011). For instance, in rice (*O. sativa*) plants Ca, K, Mg, and Fe contents were increased by drought, on the other hand, Si supply reduces these nutrients in plants (Chen et al., 2011).

Regulating osmotic potential

Optimal water level plays a significant role in plants existence under drought. Generally, plants maintain a high water level through osmotic adjustment under dry stress circumstances (Blum, 2017). Although, high drought circumstances trigger a considerable reduction in water content of leaf including water potential in various plants (Abid et al., 2018; Paz-Kagan et al., 2017; Sattar et al., 2017). Various literature highlighted that Si supply extensively enhanced the water potential of plant's leaf and water content under a dry spell (Hasanuzzaman et al., 2018; Ming et al., 2012; Ratnakumar et al., 2016). For instance, supply of Si enhanced water contents in wheat (*T. aestivum*) (Ratnakumar et al., 2016; Sattar et al., 2017; Tale and Haddad, 2011), rapeseed (*B. napus*) (Hasanuzzaman et al., 2018), rice (*O. sativa*) (Ming et al., 2012), chickpea (*C. arietinum*) (Fawaz and Mohammad, 2013), sunflower (*H. annuus*) (Gunes et al., 2008b), cucumber (*C. sativus*) (Ma et al., 2004), and sorghum (*S. bicolor*) (Sonobe et al., 2010) under drought.

Application of Si enhanced the osmotic, relative water contents, turgor and water potential of wheat (*T. aestivum*) flag leaf (Sattar et al., 2017). Such as the water content of wheat (*T. aestivum*) was increased during drought (Ratnakumar et al., 2016). Si use improved the leaf relative water content in cowpea (*V. unguiculata*) (Merwad et al., 2018), rapeseed (*Brassica napus L.*) (Hasanuzzaman et al., 2018), Kentucky bluegrass (*P. pratensis*) (Saud et al., 2014) and maize (*Z. mays*) plants (Amin et al., 2014). On the other hand, under drought Si reduced the osmotic potential of roots in sorghum (*S. bicolor*) without interrupting water contents (Sonobe et al., 2010). Osmotic adjustment is consequence owing to soluble amino acids (alanine and glutamic acid) and sugars. Yin et al. (2014) revealed that Si reduced the proline content and osmotic potential of sorghum (*S. bicolor*) leaf whereas enhanced soluble sugar. Authors proposed that the osmotic adjustment does not contribute to Si mediated rise in drought tolerance in the sorghum (*S. bicolor*). The water content of leaf and the water potential improved by the supply of Si are accredited to a thickness of wheat (*T. aestivum*) leaves (Gong et al., 2003). Furthermore, leaf water potential enhancement might be triggered by Si

deposition in the leaves. Additionally, deposition of Si on leaf surface might reduce transpiration through controlling molecules of water (Keller et al., 2015).

Regulation of osmolytes and phytohormones

Osmolytes and phytohormones roles have been already well described for tolerance of plants at different stresses (Kurepin et al., 2017; Zhang et al., 2017). Various studies demonstrated about Si application improving plant tolerance against drought through modifications of osmolytes in different species of plants (Hamayun et al., 2010; Hasanuzzaman et al., 2018; Xu et al., 2017). Si was effective to enhance proline, a non-protein amino acid, but total sugar and soluble protein were decreased in potato (*S. tuberosum*) leaves (Crusciol et al., 2009). On a similar note, use of Si improved proline contents in the wheat (*T. aestivum*) (Gong et al., 2005), pepper (*Capsicum annuum*) (Pereira et al., 2013) and rapeseed (*B. napus*) plant (Hasanuzzaman et al., 2018). Proline is frequently measured as an osmotic protector which may be effective to support plants against drought. However, studies associated with Si supply effects on plants growth hormones are limited under drought condition. Si supply declined Jasmonic acid (JA) level but enhanced salicylic acid (SA) levels in shoots of soybean plant (Hamayun et al., 2010) and pepper (*C. annuum*) plants, nitrate reductase activity (Pereira et al., 2013). The study demonstrated that the Si could be effective to enhance tolerance against drought in the plant through improvement in nitrogen metabolism and signaling of phytohormones. Yin et al. (2014) revealed that the use of Si increased sorghum (*S. bicolor*) drought resistance through regulation of 1-aminocyclopropane-1-carboxylic acid and polyamine synthesis.

Regulation of gene expression

In the first report, Si supply was effective to enhance aquaporin genes expression under drought which prompted water uptake in sorghum (*S. bicolor*) roots (Liu et al., 2014). Also, the Si supply enhanced up-regulation of conjugated polyamines synthesis genes in sorghum (*S. bicolor*) during drought condition (Yin et al., 2014). Khattab et al. (2014) demonstrated that Si supply improved expression of the ring domain carrying protein (OsRDCP1), drought-related protein (OsCMO) and coding choline mono-oxygenase and dehydrin (OsRAB16b) in rice (*O. sativa*) plants of rice. So far, a mechanism of Si-mediated gene expression under alleviation of drought stress is poorly understood; therefore more efforts are required to uncover this aspect.

Regulating gaseous exchange

Leaf gas exchange attributes to deliver beneficial evidence on plant mechanisms in stressed conditions (Chen et al., 2011; Liu et al., 2014). Especially under drought conditions, the stomata regulate the water level of the plant by adjusting the rate of transpiration. Countless studies revealed that supply of the Si regulates plant's gaseous exchange attributes as plant are exposed to the drought (Hajiboland et al., 2017; Ming et al., 2012; Pereira et al., 2013; Saud et al., 2014). For example, the supply of diatomite in the soil provided a reduction in white lupine plants transpiration rate by improving stomatal conductance and the rate of photosynthesis (Abdalla, 2011). Similarly, Hattori et al. (2005) noted a higher transpiration rate and stomatal conductance in plants of sorghum (*S. bicolor*) during drought than without Si supply control plants. The authors concluded that maintenance of higher water level in sorghum (*S. bicolor*) plants was

because of higher water absorption in the existence of Si. Correspondingly, under drought Si use improved the transpiration and net photosynthesis rate in the rice (*O. sativa*) (Ming et al., 2012), pepper (*C. annuum*) plants (Pereira et al., 2013) and soybean (*G. max*) (Shen et al., 2010).

Furthermore, the use of Si enhanced rate of transpiration and the stomatal conductance in sorghum (*S. bicolor*) seedling (Liu et al., 2014). Gao et al. (2005) noted that Si supply improved WUE in the drought stress maize (*Z. mays*) through a reduction in transpiration rate of the leaf by stomata showed that the Si effects stomatal drive in the plant. Authors suggested that the rate of stomatal transpiration was decreased whereas stomatal density and morphology cannot clarify Si to decrease the rate of stomatal transpiration in maize (*Z. mays*) (Gao et al., 2006). Si use improved the rate of photosynthesis whereas the reduced rate of transpiration under drought condition in Tobacco (*N. Rustica*) (Hajiboland et al., 2017) and in plants of maize (Amin et al., 2014). Furthermore, the increase in WUE by Si supply was noted in chickpea (*C. arietinum*), (Fawaz and Mohammad, 2013), cacao (*Theobroma cacao*) grown in pots (Zanetti et al., 2016), wheat (*T. aestivum*) grown-up in the hydroponics (Ding et al., 2007) and wheat (*T. aestivum*) grown in field condition in drought (Gong and Chen, 2012). Gong et al. (2005) proposed that the use of Si on wheat (*T. aestivum*) was grown in the pots, shown an increased level in net CO₂ incorporation rate of the leaves during drought. The study is limited associated with the diurnal changes of plant gas exchanges characteristics with a supply of Si in drought. Gong and Chen (2012) revealed that Si use was effective for diurnal change in the net photosynthetic rate of leaf, the rate of transpiration and the stomatal conductance of plants of wheat (*T. aestivum*) in the field condition under drought. Likewise, Ma et al. (2004) noted Si mediated diurnal change in the gas exchange characteristic in plants of cucumber (*C. sativus*) in drought.

Conclusion and perspective

Since 1999, many studies have been carried out to enlist benefits of Si for plant growth, but still, there is a lack of application of Si as a fertilizer for agronomic and horticulture benefits. Here is a dire need to create awareness about Si benefits among the masses and estimate its economic prospects. Therefore, the main aim of this review is to explain the mechanisms of the Si mediated mitigation of droughts in the plant. Available literature demonstrated that Si supplementation was sufficient to improve biomass, plant growth, seed germination, and photosynthesis drought stress condition. Si supply increased biomass and plant growth during a drought might be due to various mechanisms. This review can assist in well understanding mechanism of Si-arbitrated development in plants drought tolerance. Moreover, it could be effective to understand how crop production can be increased in drought stresses. We think that in the era of the 21st century where molecular tools are being incorporated at every step in all the field of studies, which genes are expressed under drought stresses in various plant species and which genes are playing their active part in plant growth improvement while Si usage and uptake by plant should be focused. This can take us to modify genetically economically significant crops to generate the drought stress tolerant cultivar which can be very beneficial in the future. Moreover, in all the studies, Si supplementation was in the form of potassium/calcium/sodium silicate. The need is to separate the Si from other anions and it can be applied at indigenous levels so that we may better understand the particular role of Si during plant development.

Funding. This research was funded by the Modern Agricultural Industry Technology System of China via grant number CARS-170208.

Acknowledgements. We acknowledge the Modern Agricultural Industry Technology System of China for funding (CARS-170208). We want to praise the donor agencies of China for supporting this project.

REFERENCES

- [1] Abdalla, M. M. (2011): Beneficial effects of diatomite on growth, the biochemical contents and polymorphic DNA in *Lupinus albus* plants grown under water stress. – *Agriculture and Biology Journal of North America* 2: 207–220.
- [2] Abid, M., Hakeem, A., Shao, Y., Liu, Y., Zahoor, R., Fan, Y. et al. (2018): Seed osmopriming invokes stress memory against post-germinative drought stress in wheat (*Triticum aestivum* L.). – *Environmental and Experimental Botany* 145: 12–20.
- [3] Ahmad, F., Aziz, T., Maqsood, M. A., Tahir, M. A., Kanwal, S. (2007): Effect of silicon application on wheat (*Triticum aestivum* L.) growth under water deficiency stress. – *Emirates Journal of Food and Agriculture* 19(2): 1–7.
- [4] Ahmed, M., Qadeer, U., Aslam, M. A. (2011): Silicon application and drought tolerance mechanism of sorghum. – *African Journal of Agricultural Research* 6: 594–607.
- [5] Ahmed, M., Qadeer, U., Ahmed, Z. I., Hassan, F. (2016): Improvement of wheat (*Triticum aestivum*) drought tolerance by seed priming with silicon. – *Archives of Agronomy and Soil Science* 62: 299–315.
- [6] Ali, Q., Haider, M. Z., Iftikhar, W., Jamil, S., Javed, M. T., Noman, A. et al. (2016): Drought tolerance potential of *Vigna mungo* L. lines as deciphered by modulated growth, antioxidant defense, and nutrient acquisition patterns. – *Brazilian Journal of Botany* 39: 801–812.
- [7] Amin, M., Ahmad, R., Basra, S., Murtaza, G. (2014): Silicon induced improvement in morpho-physiological traits of maize (*Zea mays* L.) under water deficit. – *Pakistan Journal of Agricultural Sciences* 51(7): 187–196.
- [8] Amin, M., Ahmad, R., Ali, A., Hussain, I., Mahmood, R., Aslam, M. et al. (2016): Influence of silicon fertilization on maize performance under limited water supply. – *Silicon* 10(2): 1–7.
- [9] Arshad, M., Ali, S., Noman, A., Ali, Q., Rizwan, M., Farid, M. et al. (2016): Phosphorus amendment decreased cadmium (Cd) uptake and ameliorates chlorophyll contents, gas exchange attributes, antioxidants, and mineral nutrients in wheat (*Triticum aestivum* L.) under Cd stress. – *Archives of Agronomy and Soil Science* 62: 533–546.
- [10] Asgharipour, M. R., Mosapour, H. (2016): A foliar application silicon enhances drought tolerance in fennel. – *JAPS, Journal of Animal and Plant Sciences* 26: 1056–1062.
- [11] Bae, E.-J., Hong, A., Choi, S.-M., Lee, K.-S., Park, Y.-B. (2017): Silicon pretreatment alleviates drought stress and increases antioxidative activity in Kentucky bluegrass. – *International Turfgrass Society Research Journal* 13: 591–600.
- [12] Biju, S., Fuentes, S., Gupta, D. (2017): Silicon improves seed germination and alleviates drought stress in lentil crops by regulating osmolytes, hydrolytic enzymes and antioxidant defense system. – *Plant Physiology and Biochemistry* 119: 250–264.
- [13] Blum, A. (2017): Osmotic adjustment is a prime drought stress adaptive engine in support of plant production. – *Plant, Cell & Environment* 40: 4–10.
- [14] Calvo-Polanco, M., Sánchez-Romera, B., Aroca, R., Asins, M. J., Declerck, S., Dodd, I. C. et al. (2016): Exploring the use of recombinant inbred lines in combination with

- beneficial microbial inoculants (AM fungus and PGPR) to improve drought stress tolerance in tomato. – *Environmental and Experimental Botany* 131: 47–57.
- [15] Cao, B., Ma, Q., Zhao, Q., Wang, L., Xu, K. (2015): Effects of silicon on absorbed light allocation, antioxidant enzymes and ultrastructure of chloroplasts in tomato leaves under simulated drought stress. – *Scientia Horticulturae* 194: 53–62.
- [16] Cao, B., Wang, L., Gao, S., Xia, J., Xu, K. (2017): Silicon-mediated changes in radial hydraulic conductivity and cell wall stability are involved in silicon-induced drought resistance in tomato. – *Protoplasma* 254: 2295–2304.
- [17] Chen, W., Yao, X., Cai, K., Chen, J. (2011): Silicon alleviates drought stress of rice plants by improving plant water status, photosynthesis and mineral nutrient absorption. – *Biological trace element research* 142: 67–76.
- [18] Crusciol, C. A. C., Pulz, A. L., Lemos, L. B., Soratto, R. P., Lima, G. P. P. (2009): Effects of silicon and drought stress on tuber yield and leaf biochemical characteristics in potato. – *Crop Science* 49: 949–954.
- [19] Dann, E. K., Le, D. P. (2017): Effects of silicon amendment on soilborne and fruit diseases of avocado. – *Plants* 6: 51.
- [20] de Camargo, M. S., Bezerra, B. K. L., Vitti, A. C., Silva, M. A., Oliveira, A. L. (2017): Silicon fertilization reduces the deleterious effects of water deficit in sugarcane. – *Journal of Soil Science and Plant Nutrition*. <http://dx.doi.org/10.4067/S0718-95162017005000008>.
- [21] Debona, D., Rodrigues, F. A., Datnoff, L. E. (2017): Silicon's role in abiotic and biotic plant stresses. – *Annual Review of Phytopathology*. DOI: 10.1146/annurev-phyto-080516-035312.
- [22] Demattê, J. L. I., Paggiaro, C. M., Beltrame, J. A., Ribeiro, S. S. (2011): Uso de silicatos em cana-de-açúcar. – *Informações Agronômicas* 133: 7–12.
- [23] Emam, M. M., Khattab, H. E., Helal, N. M., Deraz, A. E. (2014): Effect of selenium and silicon on yield quality of rice plant grown under drought stress. – *Australian Journal of Crop Science* 8: 596.
- [24] Eneji, A. E., Inanaga, S., Muranaka, S., Li, J., Hattori, T., An, P. et al. (2008): Growth and nutrient use in four grasses under drought stress as mediated by silicon fertilizers. – *Journal of Plant Nutrition* 31: 355–365.
- [25] Epstein, E. (1994): The anomaly of silicon in plant biology. – *Proceedings of the National Academy of Sciences* 91: 11–17.
- [26] Epstein, E. (1999): Silicon. – *Annual Review of Plant Biology* 50: 641–664.
- [27] Epstein, E. (2009): Silicon: its manifold roles in plants. – *Annals of Applied Biology* 155: 155–160.
- [28] Epstein, E., Bloom, A. J. (2005): *Mineral Nutrition of Plants: Principles and Perspectives*. 2nd Ed. – Sinauer Assoc. Inc., Sunderland, UK.
- [29] Fawaz, K., Mohammad, A.-C. (2013): Growth and nitrogen fixation in silicon and/or potassium fed chickpeas grown under drought and well watered conditions. – *Journal of Stress Physiology & Biochemistry* 9(1): 14-27.
- [30] Fukao, T., Yeung, E., Bailey-Serres, J. (2011): The submergence tolerance regulator SUB1A mediates crosstalk between submergence and drought tolerance in rice. – *The Plant Cell* 23: 412–427.
- [31] Gao, X., Zou, C., Wang, L., Zhang, F. (2005): Silicon improves water use efficiency in maize plants. – *Journal of plant nutrition* 27: 1457–1470.
- [32] Gao, X., Zou, C., Wang, L., Zhang, F. (2006): Silicon decreases transpiration rate and conductance from stomata of maize plants. – *Journal of Plant Nutrition* 29: 1637–1647.
- [33] George, S., Manoharan, D., Li, J., Britton, M., Parida, A. (2018): Drought and salt stress in *Macrotyloma uniflorum* leads to common and specific transcriptomic responses and reveals importance of raffinose family oligosaccharides in stress tolerance. – *Gene Reports* 10: 7–16.

- [34] Gharineh, M. H., Karmollachaab, A. (2013): Effect of silicon on physiological characteristics wheat growth under Water-Deficit Stress Induced by PEG. – *International Journal of Agronomy and Plant Production* 4: 1543–1548.
- [35] Gong, H., Chen, K. (2012): The regulatory role of silicon on water relations, photosynthetic gas exchange, and carboxylation activities of wheat leaves in field drought conditions. – *Acta Physiologiae Plantarum* 34: 1589–1594.
- [36] Gong, H., Chen, K., Chen, G., Wang, S., Zhang, C. (2003): Effects of silicon on growth of wheat under drought. – *Journal of Plant Nutrition* 26: 1055–1063.
- [37] Gong, H., Zhu, X., Chen, K., Wang, S., Zhang, C. (2005): Silicon alleviates oxidative damage of wheat plants in pots under drought. – *Plant Science* 169: 313–321.
- [38] Gong, H. J., Chen, K. M., Zhao, Z. G., Chen, G. C., Zhou, W. J. (2008): Effects of silicon on defense of wheat against oxidative stress under drought at different developmental stages. – *Biologia Plantarum* 52: 592–596.
- [39] Gunes, A., Pilbeam, D. J., Inal, A., Bagci, E. G., Coban, S. (2007): Influence of silicon on antioxidant mechanisms and lipid peroxidation in chickpea (*Cicer arietinum* L.) cultivars under drought stress. – *Journal of Plant Interactions* 2: 105–113.
- [40] Gunes, A., Kadioglu, Y. K., Pilbeam, D. J., Inal, A., Coban, S., Aksu, A. (2008a). Influence of silicon on sunflower cultivars under drought stress, II: essential and nonessential element uptake determined by polarized energy dispersive X-ray fluorescence. – *Communications in Soil Science and Plant Analysis* 39: 1904–1927.
- [41] Gunes, A., Pilbeam, D. J., Inal, A., Coban, S. (2008b). Influence of silicon on sunflower cultivars under drought stress, I: growth, antioxidant mechanisms, and lipid peroxidation. – *Communications in Soil Science and Plant Analysis* 39: 1885–1903.
- [42] Guntzer, F., Keller, C., Meunier, J.-D. (2012): Benefits of plant silicon for crops: a review. – *Agronomy for Sustainable Development* 32: 201–213.
- [43] Guo, Q., Wang, Y., Zhang, H., Qu, G., Wang, T., Sun, Q. et al. (2017): Alleviation of adverse effects of drought stress on wheat seed germination using atmospheric dielectric barrier discharge plasma treatment. – *Scientific Reports* 7: 16680.
- [44] Habibi, G. (2014): Silicon supplementation improves drought tolerance in canola plants. – *Russian Journal of Plant Physiology* 61: 784–791.
- [45] Hajiboland, R., Cheraghvareh, L., Poschenrieder, C. (2017): Improvement of drought tolerance in tobacco (*Nicotiana rustica* L.) plants by silicon. – *Journal of Plant Nutrition* 40: 1661–1676.
- [46] Hamayun, M., Sohn, E.-Y., Khan, S. A., Shinwari, Z. K., Khan, A. L., Lee, I.-J. (2010): Silicon alleviates the adverse effects of salinity and drought stress on growth and endogenous plant growth hormones of soybean (*Glycine max* L.). – *Pak. J. Bot.* 42: 1713–1722.
- [47] Hameed, A., Sheikh, M. A., Jamil, A., Basra, S. M. A. (2013): Seed priming with sodium silicate enhances seed germination and seedling growth in wheat (*Triticum aestivum* L.) under water deficit stress induced by polyethylene glycol. – *Pak. J. Life Soc. Sci.* 11: 19–24.
- [48] Hasanuzzaman, M., Nahar, K., Anee, T. I., Khan, M. I. R., Fujita, M. (2018): Silicon-mediated regulation of antioxidant defense and glyoxalase systems confers drought stress tolerance in *Brassica napus* L. – *South African Journal of Botany* 115: 50–57.
- [49] Hattori, T., Inanaga, S., Araki, H., An, P., Morita, S., Luxová, M. et al. (2005): Application of silicon enhanced drought tolerance in *Sorghum bicolor*. – *Physiologia Plantarum* 123: 459–466.
- [50] Helaly, M. N., El-Hoseiny, H., El-Sheery, N. I., Rastogi, A., Kalaji, H. M. (2017): Regulation and physiological role of silicon in alleviating drought stress of mango. – *Plant Physiology and Biochemistry* 118: 31–44.
- [51] Hodson, M. J., White, P. J., Mead, A., Broadley, M. R. (2005): Phylogenetic variation in the silicon composition of plants. – *Annals of Botany* 96: 1027–1046.

- [52] Kaushal, M., Wani, S. P. (2016): Rhizobacterial-plant interactions: strategies ensuring plant growth promotion under drought and salinity stress. – *Agriculture, Ecosystems & Environment* 231: 68–78.
- [53] Kaya, C., Tuna, L., Higgs, D. (2006): Effect of silicon on plant growth and mineral nutrition of maize grown under water-stress conditions. – *Journal of Plant Nutrition* 29: 1469–1480.
- [54] Keller, C., Rizwan, M., Davidian, J.-C., Pokrovsky, O. S., Bovet, N., Chaurand, P. et al. (2015): Effect of silicon on wheat seedlings (*Triticum turgidum* L.) grown in hydroponics and exposed to 0 to 30 μ M Cu. – *Planta* 241: 847–860.
- [55] Khalil, F., Rauf, S., Monneveux, P., Anwar, S., Iqbal, Z. (2016): Genetic analysis of proline concentration under osmotic stress in sunflower (*Helianthus annuus* L.). – *Breeding Science* 66: 463–470. DOI: 10.1270/jsbbs.15068.
- [56] Khalil, F., Naiyan, X., Tayyab, M., Pinghua, C. (2018): Screening of EMS-induced drought-tolerant sugarcane mutants employing physiological, molecular and enzymatic approaches. – *Agronomy* 8: 1–13. DOI: 10.3390/agronomy8100226.
- [57] Khan, A., Anwar, Y., Hasan, M. M., Iqbal, A., Ali, M., Alharby, H. F. et al. (2017): Attenuation of drought stress in brassica seedlings with exogenous application of Ca^{2+} and H_2O_2 . – *Plants* 6: 20.
- [58] Khattab, H. I., Emam, M. A., Emam, M. M., Helal, N. M., Mohamed, M. R. (2014): Effect of selenium and silicon on transcription factors NAC5 and DREB2A involved in drought-responsive gene expression in rice. – *Biologia Plantarum* 58: 265–273.
- [59] Kim, Y.-H., Khan, A. L., Waqas, M., Lee, I.-J. (2017): Silicon regulates antioxidant activities of crop plants under abiotic-induced oxidative stress: a review. – *Frontiers in Plant Science* 8: 510.
- [60] Kurepin, L. V, Ivanov, A. G., Zaman, M., Pharis, R. P., Hurry, V., Hüner, N. P. A. (2017): Interaction of Glycine Betaine and Plant Hormones: Protection of the Photosynthetic Apparatus during Abiotic Stress. – In: Hou, H. J. M. et al. (eds.) *Photosynthesis: Structures, Mechanisms, and Applications*. Springer, Berlin, pp. 185–202.
- [61] Kutschera, U., Niklas, K. J. (2018): Julius Sachs (1868): The father of plant physiology. – *American Journal of Botany* 105: 656–666.
- [62] Lesk, C., Rowhani, P., Ramankutty, N. (2016): Influence of extreme weather disasters on global crop production. – *Nature* 529: 84–87.
- [63] Lewin, J., Reimann, B. E. F. (1969): Silicon and plant growth. – *Annual Review of Plant Physiology* 20: 289–304.
- [64] Liu, C., Yu, R., Shi, G. (2017): Effects of drought on the accumulation and redistribution of cadmium in peanuts at different developmental stages. – *Archives of Agronomy and Soil Science* 63: 1049–1057.
- [65] Liu, P., Yin, L., Deng, X., Wang, S., Tanaka, K., Zhang, S. (2014): Aquaporin-mediated increase in root hydraulic conductance is involved in silicon-induced improved root water uptake under osmotic stress in *Sorghum bicolor* L. – *Journal of Experimental Botany* 65: 4747–4756.
- [66] Ma, C. C., Li, Q. F., Gao, Y. B., Xin, T. R. (2004): Effects of silicon application on drought resistance of cucumber plants. – *Soil Science and Plant Nutrition* 50: 623–632.
- [67] Ma, D., Sun, D., Wang, C., Qin, H., Ding, H., Li, Y. et al. (2016): Silicon application alleviates drought stress in wheat through transcriptional regulation of multiple antioxidant defense pathways. – *Journal of Plant Growth Regulation* 35: 1–10.
- [68] Ma, J. F., Takahashi, E. (2002): – *Soil, Fertilizer, and Plant Silicon Research in Japan*. – Elsevier, Amsterdam.
- [69] Ma, J. F., Yamaji, N. (2015): A cooperative system of silicon transport in plants. – *Trends in Plant Science* 20: 435–442. DOI: 10.1016/j.tplants.2015.04.007.

- [70] Ma, J. F., Goto, S., Tamai, K., Ichii, M. (2001a). Role of root hairs and lateral roots in silicon uptake by rice. – *Plant Physiology* 127: 1773–1780.
- [71] Ma, J. F., Miyake, Y., Takahashi, E. (2001b). Silicon as a Beneficial Element for Crop Plants. – In: Datnoff, L. E. et al. (eds.) *Studies in plant Science*. Elsevier, Amsterdam, pp. 17–39.
- [72] Ma, J. F., Yamaji, N., Mitani, N., Tamai, K., Konishi, S., Fujiwara, T. et al. (2007): An efflux transporter of silicon in rice. – *Nature* 448: 209.
- [73] Maghsoudi, K., Emam, Y., Pessarakli, M. (2016): Effect of silicon on photosynthetic gas exchange, photosynthetic pigments, cell membrane stability and relative water content of different wheat cultivars under drought stress conditions. – *Journal of Plant Nutrition* 39: 1001–1015.
- [74] Marafon, A. C., Endres, L. (2013): Silicon: fertilization and nutrition in higher plants. – *Embrapa Tabuleiros Costeiros-Artigo em periódico indexado (ALICE)*. <http://www.alice.cnptia.embrapa.br/alice/handle/doc/980846>.
- [75] Marschner, H. (2011): *Marschner's Mineral Nutrition of Higher Plants*. – Academic Press, Cambridge, MA.
- [76] Meena, V. D., Dotaniya, M. L., Coumar, V., Rajendiran, S., Kundu, S., Rao, A. S. (2014): A case for silicon fertilization to improve crop yields in tropical soils. – *Proceedings of the National Academy of Sciences, India Section B: Biological Sciences* 84: 505–518.
- [77] Merwad, A.-R. M. A., Desoky, E.-S. M., Rady, M. M. (2018): Response of water deficit-stressed *Vigna unguiculata* performances to silicon, proline or methionine foliar application. – *Scientia Horticulturae* 228: 132–144.
- [78] Ming, D. F., Pei, Z. F., Naeem, M. S., Gong, H. J., Zhou, W. J. (2012): Silicon alleviates PEG-induced water-deficit stress in upland rice seedlings by enhancing osmotic adjustment. – *Journal of Agronomy and Crop Science* 198: 14–26.
- [79] Mitani, N., Ma, J. F., Iwashita, T. (2005): Identification of the silicon form in xylem sap of rice (*Oryza sativa* L.). – *Plant and Cell Physiology* 46: 279–283.
- [80] Mitani, N., Yamaji, N., Ago, Y., Iwasaki, K., Ma, J. F. (2011): Isolation and functional characterization of an influx silicon transporter in two pumpkin cultivars contrasting in silicon accumulation. – *The Plant Journal* 66: 231–240.
- [81] Moro, A. L., Broetto, F., Moro, E. (2015): Antioxidative responses, physiological and productive of rice grown under water deficit and silicon fertilization. – *Semina: Ciências Agrárias* 36: 3013–3028.
- [82] Nolla, A., Faria, R. J., Korndorfer, G. H., Silva, T. R. B. (2012): Effect of silicon on drought tolerance of upland rice. – *Journal of Food, Agriculture & Environment* 10: 269–272.
- [83] Noman, A., Aqeel, M. (2017): miRNA-based heavy metal homeostasis and plant growth. – *Environmental Science and Pollution Research*. DOI: 10.1007/s11356-017-8593-5.
- [84] Noman, A., Ali, S., Naheed, F., Ali, Q., Farid, M., Rizwan, M. et al. (2015): Foliar application of ascorbate enhances the physiological and biochemical attributes of maize (*Zea mays* L.) cultivars under drought stress. – *Archives of Agronomy and Soil Science* 61: 1659–1672.
- [85] Ouzounidou, G., Giannakoula, A., Ilias, I., Zamanidis, P. (2016): Alleviation of drought and salinity stresses on growth, physiology, biochemistry and quality of two *Cucumis sativus* L. cultivars by Si application. – *Brazilian Journal of Botany* 39: 531–539.
- [86] Paz-Kagan, T., Vaughn, N. R., Martin, R. E., Brodrick, P. G., Stephenson, N. L., Das, A. J. et al. (2017): Landscape-scale variation in canopy water content of giant sequoias during drought. – *Forest Ecology and Management*. <https://doi.org/10.1016/j.foreco.2017.11.018>.

- [87] Pei, Z. F., Ming, D. F., Liu, D., Wan, G. L., Geng, X. X., Gong, H. J. et al. (2010): Silicon improves the tolerance to water-deficit stress induced by polyethylene glycol in wheat (*Triticum aestivum* L.) seedlings. – *Journal of Plant Growth Regulation* 29: 106–115.
- [88] Pereira, T. S., da Silva Lobato, A. K., Tan, D. K. Y., da Costa, D. V., Uchoa, E. B., do Nascimento Ferreira, R. et al. (2013): Positive interference of silicon on water relations, nitrogen metabolism, and osmotic adjustment in two pepper (*capsicum annum*) cultivars under water deficit. – *Australian Journal of Crop Science* 7: 1064.
- [89] Pilon, C., Soratto, R. P., Broetto, F., Fernandes, A. M. (2014): Foliar or soil applications of silicon alleviate water-deficit stress of potato plants. – *Agronomy Journal* 106: 2325–2334.
- [90] Ratnakumar, P., Deokate, P. P., Rane, J., Jain, N., Kumar, V., Berghe, D. V. et al. (2016): Effect of ortho-silicic acid exogenous application on wheat (*Triticum aestivum* L.) under drought. – *Journal of Functional and Environmental Botany* 6: 34–42.
- [91] Raven, J. A. (2001): Silicon Transport at the Cell and Tissue Level. – In: Datnoff, L. E. et al. (eds.) *Studies in Plant Science*. Elsevier, Amsterdam, pp. 41–55.
- [92] Rizwan, M., Ali, S., Ibrahim, M., Farid, M., Adrees, M., Bharwana, S. A. et al. (2015): Mechanisms of silicon-mediated alleviation of drought and salt stress in plants: a review. – *Environmental Science and Pollution Research* 22: 15416–15431. DOI: 10.1007/s11356-015-5305-x.
- [93] Rizwan, M., Ali, S., Abbas, T., Adrees, M., Zia-ur-Rehman, M., Ibrahim, M. et al. (2018): Residual effects of biochar on growth, photosynthesis and cadmium uptake in rice (*Oryza sativa* L.) under Cd stress with different water conditions. – *Journal of Environmental Management* 206: 676–683.
- [94] Sattar, A., Cheema, M. A., Abbas, T., Sher, A., Ijaz, M., Wahid, M. A. et al. (2017): Physiological response of late sown wheat to exogenous application of silicon. – *Cereal Research Communications* 45: 202–213.
- [95] Saud, S., Li, X., Chen, Y., Zhang, L., Fahad, S., Hussain, S. et al. (2014): Silicon application increases drought tolerance of Kentucky bluegrass by improving plant water relations and morphophysiological functions. – *The Scientific World Journal* 2014.
- [96] Savant, N. K., Korndörfer, G. H., Datnoff, L. E., Snyder, G. H. (1999): Silicon nutrition and sugarcane production: a review. – *Journal of Plant Nutrition* 22: 1853–1903.
- [97] Shen, X., Zhou, Y., Duan, L., Li, Z., Eneji, A. E., Li, J. (2010): Silicon effects on photosynthesis and antioxidant parameters of soybean seedlings under drought and ultraviolet-B radiation. – *Journal of Plant Physiology* 167: 1248–1252.
- [98] Shi, Y., Zhang, Y., Yao, H., Wu, J., Sun, H., Gong, H. (2014): Silicon improves seed germination and alleviates oxidative stress of bud seedlings in tomato under water deficit stress. – *Plant Physiology and Biochemistry* 78: 27–36.
- [99] Sommer, M., Kaczorek, D., Kuzyakov, Y., Breuer, J. (2006): Silicon pools and fluxes in soils and landscapes—a review. – *Journal of Plant Nutrition and Soil Science* 169: 310–329.
- [100] Sonobe, K., Hattori, T., An, P., Tsuji, W., Eneji, A. E., Kobayashi, S. et al. (2010): Effect of silicon application on sorghum root responses to water stress. – *Journal of Plant Nutrition* 34: 71–82.
- [101] Suzuki, N., Rivero, R. M., Shulaev, V., Blumwald, E., Mittler, R. (2014): Abiotic and biotic stress combinations. – *New Phytologist*. DOI: 10.1111/nph.12797.
- [102] Takahashi, E., Ma, J. F., Miyake, Y. (1990): The possibility of silicon as an essential element for higher plants. – *Comments on Agricultural and Food Chemistry* 2: 99–102.

- [103] Tale, A., Haddad, R. (2011): Study of silicon effects on antioxidant enzyme activities and osmotic adjustment of wheat under drought stress. – *Czech Journal of Genetics and Plant Breeding* 47: 17–27.
- [104] Tamai, K., Ma, J. F. (2003): Characterization of silicon uptake by rice roots. – *New Phytologist* 158: 431–436.
- [105] Tayyab, M., Caifang, Z., Islam, W., Khalil, F., Ziqin, P., Caifang, Z. et al. (2018a). Biochar: an efficient way to manage low water availability in plants. – *Applied Ecology and Environmental Research* 16: 2565–2583.
- [106] Tayyab, M., Islam, W., Zhang, H. (2018b). Communications in Soil Science and Plant Analysis Promising role of silicon to enhance drought resistance in wheat. DOI: 10.1080/00103624.2018.1547394.
- [107] Ullah, H., Luc, P. D., Gautam, A., Datta, A. (2017): Growth, yield and silicon uptake of rice (*Oryza sativa*) as influenced by dose and timing of silicon application under water-deficit stress. – *Archives of Agronomy and Soil Science*, 1–13.
- [108] Van Bockhaven, J., De Vleeschauwer, D., Höfte, M. (2012): Towards establishing broad-spectrum disease resistance in plants: silicon leads the way. – *Journal of Experimental Botany* 64: 1281–1293.
- [109] Wang, H.-S., Yu, C., Fan, P.-P., Bao, B.-F., Li, T., Zhu, Z.-J. (2015): Identification of two cucumber putative silicon transporter genes in *Cucumis sativus*. – *Journal of Plant Growth Regulation* 34: 332–338.
- [110] Warner, K. J., Jones, G. A. (2017): A population-induced renewable energy timeline in nine world regions. – *Energy Policy* 101: 65–76. DOI: 10.1016/j.enpol.2016.11.031.
- [111] Xu, L., Islam, F., Ali, B., Pei, Z., Li, J., Ghani, M. A. et al. (2017): Silicon and water-deficit stress differentially modulate physiology and ultrastructure in wheat (*Triticum aestivum* L.). 3 – *Biotech* 7: 273.
- [112] Yang, L., Han, Y., Li, P., Li, F., Ali, S., Hou, M. (2017): Silicon amendment is involved in the induction of plant defense responses to a phloem feeder. – *Scientific Reports* 7: 4232.
- [113] Yin, L., Wang, S., Liu, P., Wang, W., Cao, D., Deng, X. et al. (2014): Silicon-mediated changes in polyamine and 1-aminocyclopropane-1-carboxylic acid are involved in silicon-induced drought resistance in *Sorghum bicolor* L. – *Plant Physiology and Biochemistry* 80: 268–277.
- [114] Zandalinas, S. I., Mittler, R., Balfagón, D., Arbona, V., Gómez-Cadenas, A. (2018): Plant adaptations to the combination of drought and high temperatures. – *Physiologia Plantarum* 162: 2–12.
- [115] Zanetti, L. V., Milanez, C. R. D., Gama, V. N., Aguilar, M. A. G., Souza, C. A. S., Campostrini, E. et al. (2016): Leaf application of silicon in young cacao plants subjected to water deficit. – *Pesquisa Agropecuária Brasileira* 51: 215–223.
- [116] Zang, U., Goisser, M., Häberle, K., Matyssek, R., Matzner, E., Borken, W. (2014): Effects of drought stress on photosynthesis, rhizosphere respiration, and fine-root characteristics of beech saplings: a rhizotron field study. – *Journal of Plant Nutrition and Soil Science* 177: 168–177.
- [117] Zargar, S. M., Agnihotri, A. (2013): Impact of silicon on various agro-morphological and physiological parameters in maize and revealing its role in enhancing water stress tolerance. – *Emirates Journal of Food and Agriculture* 25(2): 138–141. DOI: 10.9755/ejfa.v25i2.10581.
- [118] Zhang, C., Moutinho-Pereira, J. M., Correia, C., Coutinho, J., Gonçalves, A., Guedes, A. et al. (2013): Foliar application of Sili-K® increases chestnut (*Castanea* spp.) growth and photosynthesis, simultaneously increasing susceptibility to water deficit. – *Plant and Soil* 365: 211–225.

- [119] Zhang, W., Xie, Z., Wang, L., Li, M., Lang, D., Zhang, X. (2017): Silicon alleviates salt and drought stress of *Glycyrrhiza uralensis* seedling by altering antioxidant metabolism and osmotic adjustment. – *Journal of Plant Research* 130: 611–624.
- [120] Zia, Z. (2018): Crop protection silicon mitigates biotic stresses in crop plants: A review. – *Crop Protection* 104: 21–34. DOI: 10.1016/j.cropro.2017.10.008.

THE ROLE OF ODONATE NYMPHS IN ECOFRIENDLY CONTROL OF MOSQUITOES AND SENSITIVITY OF ODONATE NYMPHS TO INORGANIC NUTRIENT POLLUTANTS

ILAH I, I.^{1*} – YOUSAFZAI, A. M.² – ATTAULLAH, M.¹ – HAQ, T. U.³ – ALI, H.¹ – RAHIM, A.¹ – SAJAD, MA.² – NAJEEB, S.¹ – ZAMAN, S.⁴ – ULLAH, S.⁴ – AHMAD, A.¹ – BEGUM, R.¹ – WAQAS¹ – BIBI, H.¹ – HUSSAIN, S.¹ – AHMAD, B.¹

¹Department of Zoology, University of Malakand, Chakdara, Dir Lower, Khyber Pakhtunkhwa, Pakistan

²Department of Zoology, Islamia College Peshawar, Peshawar, Khyber Pakhtunkhwa, Pakistan

³Department of Biotechnology, University of Malakand, Chakdara, Dir Lower, Khyber Pakhtunkhwa, Pakistan

⁴Department of Botany, University of Malakand, Chakdara, Dir Lower, Khyber Pakhtunkhwa, Pakistan

*Corresponding author
e-mail: ikramilahi@uom.edu.pk

(Received 27th Oct 2018; accepted 25th Jan 2019)

Abstract. During the present research, the predatory efficiency of nymphs of six coexisting odonate species i.e., *I. elegans*, *T. aurora*, *P. flavescens*, *L. fulva*, *S. decoloratum* and *C. servilia* was studied by using the 3rd instar larvae of *Cx. quinquefasciatus* as prey. Among the odonate species, there was observed variation in the daily feeding rate. The highest number of mosquito larvae was ingested by the *P. flavescens* nymph (47.0 ± 5.1 mosquito larvae/day). The predation performance of the odonate nymph was also compared between the day and night times. The feeding rate of nymphs of most odonate species was significantly higher during the daytime as compared to night-time ($P \leq 0.05$). During the present research, feeding rates of odonate nymphs on *Cx. quinquefasciatus* 3rd instar larvae were also studied under varied condition of prey and predator density and water volume. Feeding rate of nymphs of each odonate species was positively correlated with increase in predator and prey density but was negatively correlated with increase in water volume. During the present research, odonate nymphs i.e., *I. elegans*, *T. aurora* and *P. flavescens* were exposed to various concentration of NH_4^+ and NO_3^- in the laboratory for seven days. Nymph of *P. flavescens* species was found least sensitive to both, NH_4^+ and NO_3^- . From the findings of the present research it was concluded that *P. flavescens* species is more efficient predator of *Cx. quinquefasciatus* 3rd instar larvae and is highly resistant to increasing water level of NH_4^+ and NO_3^- .

Keywords: damselfly, dragonfly, predation, feeding rate, ammonium, nitrate

Introduction

Control of mosquitoes is mostly practiced by using conventional synthetic chemical insecticides such as organochlorine and organophosphate compounds (Ghosh et al., 2012). The frequent application of synthetic chemical insecticides has caused the development of insecticide resistance in insect pests, contamination of the environment, and adverse effects on non-target organisms (Lee et al., 2001). There is the requirement of adopting environment friendly approaches for the control of mosquito population (Ghosh et al., 2012). Biological control is the application of living organisms that can be used as control agents against insect pests. Several living organisms can act as biological control agents against mosquitoes such as bacteria (Phillips, 2001), plants

(Ajaegbu et al., 2016), protozoans (Das et al., 2016), larvivorous fish (Walton, 2007) and predatory insects (Mandal et al., 2008).

Predators of mosquito larvae can play important role in regulation of mosquito population (Knight et al., 2004). They not only attack on mosquito larvae but also kill and eat several other co-existing organisms however the presence of alternate preys has no negative influence on the role of predators in regulation of mosquito larval population (Stav et al., 2005). The natural predators that can play role in regulation of mosquito larval population include some larvivorous fish (Chandra et al., 2008), some aquatic bugs (Saha et al., 2007), tadpole shrimps (Su and Mulla, 2002), diving beetles (Lundkvist et al., 2003), Toxorhynchites mosquito larvae (Kumar and Hwang, 2006) and odonate nymphs (Damsselfly and dragonfly) (Chatterjee et al., 2007).

Odonate nymphs are important voracious predators and they capture their prey such as mosquito larvae and other smaller aquatic invertebrates and even larvae of fish and amphibians with the help of specialized protractible labium (Boyd, 2005). These nymphs can play important role in the regulation of mosquito population (Din et al., 2013). Due to predatory role against mosquito larvae, they have gained attention for their use in ecofriendly control of mosquitoes (Mitra, 2006). To the best of author knowledge, very few studies have been conducted on the predatory ability of odonate nymphs against mosquito larvae (Mandal et al., 2008; Akram and Ali-Khan, 2016). During the present study, the predatory ability of one species of damselfly (order Odonata, sub order Zygoptera) i.e., *Ischnura elegans* (Vander Linden, 1820) and five species of dragonfly (order Odonata, sub order Anisoptera) i.e., *Trithemis aurora* (Burmeister, 1839), *Pantala flavescens* (Fabricius, 1798), *Libellula fulva* (Muller, 1764), *Sympetrum decoloratum* (Selys, 1884) and *Crocothemis servilia* (Drury, 1770) were studied against *Culex quinquefasciatus* larvae under laboratory conditions during the day and night times. The predatory ability of odonate nymphs under varied conditions of prey and predator density and water volume were also studied.

Odonate nymphs that share the aquatic habitat with mosquito larvae, face increasing environmental pressure due to increasing urbanization and human activities. Ammonium and nitrate are the important nutrient pollutants and their levels in surface water are increasing (Rabalais, 2002; Du et al., 2017). Ammonium, nitrate and other ionic forms of inorganic nitrogen enter the surface water both from natural sources and anthropogenic sources (Wetzel, 2001; Rabalais, 2002; Du et al., 2017). Increased level of different forms of inorganic nitrogen in water is toxic to fresh water invertebrates, fishes and amphibian (Hickey and Vickers, 1994; Camargo et al., 2005). Odonate nymphs are sensitive to environmental pollutants (Clark and Samways, 1996). To the best of author knowledge, a single study has been reported on the effect of ammonium on odonate nymphs such as *Erythromma najas*, *Lestes sponsa* and *Sympetrum flaveolum* (Beketov, 2002). Dida et al. (2015) recently studied the diversity of predators and mosquito larval habitats and the range of their adaptive capacity to water physico-chemical parameters along the Mara River. It was concluded that the invasion of aquatic habitats by the predators of mosquito larvae is driven by the presence of mosquito larvae and the water physico-chemical characteristics. It was suggested that understanding the biotic and abiotic characteristics of aquatic habitats that favor the co-occurrence of mosquito larvae and predators may contribute to the effective control of mosquito borne diseases. During the present study, the sensitivity of nymphs of three odonate species i.e., *Ischnura elegans*, *Trithemis aurora* and *Pantala flavescens* to ammonium and nitrate was studied.

The present research aimed to explore the comparative predatory efficacy of different odonate nymphs against mosquito larvae and the predatory ability of odonate nymphs under varied conditions of prey and predator density and water volume. The present research also aimed to determine the sensitivity of odonate nymphs to inorganic nutrient pollutants i.e., ammonium and nitrate.

Materials and methods

Laboratory rearing of Cx. quinquefasciatus

Laboratory colonies of *Cx. quinquefasciatus* were maintained during April 2017 (max temperature 29 °C) and September 2017 (max temperature 31 °C). Larvae of *Cx. quinquefasciatus* were collected by using a rectangular plastic dipper (38 cm length, 28 cm width and 6.5 cm height) from a ditch containing stagnant water at the campus of university of Malakand, Chakdara, Dir Lower, Khyber Pakhtunkhwa, Pakistan. The larvae were brought in 700 ml plastic containers with water from the collection site to the laboratory at the University of Malakand and reared for establishing a colony. The larvae were provided with larval food comprising of dog biscuit and dry yeast powder in the ratio of 3:2. The pupae emerged were transferred to a 500 ml plastic jar containing 300 ml non-chlorinated tap water and placed in mosquito cage (45 cm × 45 cm × 45 cm). The adults emerged were fed with carbohydrate food by providing cotton pad soaked in 10% sucrose solution. The female adult mosquitoes laid eggs in the jar containing water inside the cage. The eggs hatched into larvae, thus larvae of each instars were available for experiments. For confirmation of species proper literature was used for identification of both larvae and adults (Harbach, 1988).

Collection and identification of odonate nymphs

Several puddles on the bank of River swat near the campus of University of Malakand, were visited during April and May 2017 and September 2017 for collection of damselfly and dragonfly nymphs. Damselfly and dragonfly nymphs of 8 to 10 instars were collected by using a rectangular plastic dipper (38 cm length, 28 cm width and 6.5 cm height) on the bank of River swat near the campus of University of Malakand, during April 2017, and September 2017. The nymphs were transported in plastic jars containing water of the collection site to the laboratory at University of Malakand within 1 h of capture. In the laboratory damselfly and dragonfly nymphs were separately maintained in small fish aquaria (45 cm length, 40 cm width and 40 cm height) containing water brought from the collection site in large plastic bottles. Aquaria were receiving solar illumination through windows and oxygenated by using air pumps. Few strings of aquatic plants brought from the collection site were also added to the aquaria which provided clinging sites for the nymphs. Before conducting experiments, the nymphs were fed with dried yeast powder and mosquito larvae. The specimens were identified to the species level with the help of literature (Gardner, 1960; Yousuf et al., 1996; Anjum, 1997; Mitra, 2002; Din et al., 2013). During the identification of odonate nymph, help was also taken from the literature and unpublished documents provided by Dr. Ahmad Zia (personal communication), Senior Scientific Officer and Taxonomist in the Insect National Museum at National Agricultural Research Council (NARC), Islamabad, Pakistan. During April 2017 collection of odonate nymphs, one species of damselflies namely *Ischnura elegans* and two species of dragonflies namely *Trithemis*

aurora and *Pantala flavescens* were identified. During September 2017 collection, dragonfly nymphs of *Libellula fulva*, *Sympetrum decoloratum* and *Crocothemis servilia* were identified and found in sufficient number; therefore, experiments were conducted on nymphs of these genera. All the odonate species identified and studied are shown in *Figure 1*.

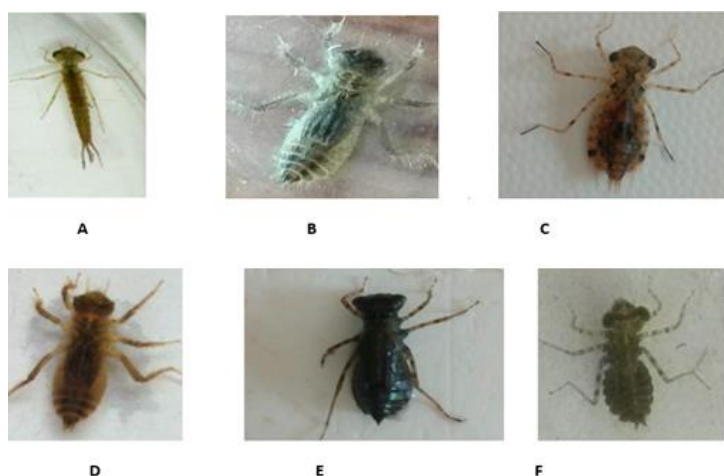


Figure 1. Pictures of nymphs of different odonate species collected and used during the present research. A - *Ischnura elegans*, B - *Trithemis aurora*, C - *Pantala flavescens*, D - *Libellula fulva*, E - *Sympetrum decoloratum*, F - *Crocothemis servilia*

24-h feeding rate of donate nymphs during April, 2017

During April 2017, three nymphs of three odonate species (one nymph of each Species) i.e., *Ischnura elegans*, *Trithemis aurora* and *Pantala flavescens*, were placed separately into three labelled 1000 ml plastic jars each jar was containing 700 ml sieved water of collection site. To each container 80 3rd instar larvae were added. Twelve replicates were run for each predator species. The experiments were started at 05:00 h of Pakistan standard time and the results were checked next day at 05:00 h (after 24 h). The number of larvae consumed by each predator species was counted after 24 h.

24-h feeding rate of donate nymphs during September, 2017

During September 2017, the feeding efficiencies of dragonfly nymphs of *L. fulva*, *S. decoloratum* and *C. servilia* on 3rd instar larvae of *Culex quinquefasciatus* were compared. These three dragonfly nymphs were placed separately into three labelled 1000 ml plastic jars each containing 700 ml sieved water of collection site. To each container 50 3rd instar larvae were added. Six replicates were run for each predator species. The experiments were started at 07:00 h of Pakistan standard time and the results were checked next day at 07:00 h (after 24 h). The number of larvae consumed by each predator species was counted after 24 h.

Feeding rate of odonate nymphs during light and dark phases in April, 2017

During April 2017, the feeding rates of *Ischnura elegans*, *Trithemis aurora* and *Pantala flavescens* on 3rd instar larvae of *Cx. quinquefasciatus* were studied during the light (day time) and dark (night time) phases. The durations of light phase (5:00 to

19:00 h) was 14 h and dark phase (19:00 to 5:00 h) was 10 h. Per hour feeding rate was calculated. One nymph each of *Ischnura elegans*, *Trithemis aurora* and *Pantala flavescens*, were placed separately into three labelled 1000-ml plastic jars each containing 700 ml sieved water of collection site. Eighty 3rd instar larvae of *Cx. quinquefasciatus* were added to each jar at 05:00 h (sunrise time) and the number of larvae consumed by each nymph was noted at 19:00 h (sunset time). The laboratory was receiving sufficient light during the day through windows. To determine the feeding rate of nymphs during the dark phase, 80 3rd instar larvae of *Cx. quinquefasciatus* were added to each jar at 19:00 h (sunset time) and the number of larvae consumed by each nymph was noted at next 05:00 h (sunrise time). The experiment was run in 12 replicates.

Feeding rate of odonate nymphs during light and dark phases in September, 2017

During September 2017 study, three nymphs of three dragonfly species i.e., *Libellula*, *Sympetrum* and *C. servilia* were placed separately into three labelled 700 ml plastic jars (one nymph of one odonate species/jar) each containing 400 ml sieved water of collection site. Fifty 3rd instar larvae of *Cx. quinquefasciatus* were added to each jar at the morning (06:00 h, Pakistan standard time). The duration of light phase (6:00 h to 18:09 h) and dark phase (18:09 to 6:00 h) was 12 h each. Therefore the 12-h feeding rate of dragonfly nymphs was compared between light and dark phases.

Feeding pattern of odonate nymphs after every 3 h interval in day and night

The feeding activities of dragonfly nymphs were also noted after every 3 h for 24 h (6:00–9:00 h, 9:00–12:00 h, 12:00–15:00 h, 15:00–18:00 h, 18:00–21:00 h, 21:00–24:00 h, 24:00–3:00 h, 3:00–6:00 h Pakistan standard time). Sieved water of collection site was utilized for experiment.

Feeding rate under varied condition of predator density, water volume and prey density

The predation of damselfly and dragonfly nymphs on 3rd instar *Cx. quinquefasciatus* larvae with variation in predator density, water volume and prey density were evaluated during April 2017. For each odonate nymph, six 4 L plastic jars were arranged with varied predator density, water volume and prey density. The experiment for each predator species was conducted on three different dates and in triplicate. The six combinations for each odonate species are shown in *Table 1*.

Table 1. Various combinations of predator density, water volume and prey density

S. No. of combinations	Combinations
1	1 predator, 1 L and 50 Prey
2	1 predator, 2L and 50 Prey
3	1 predator, 1 Land 100 Prey
4	2 predators, 1 L and 50 Prey
5	2 predators, 2 L and 50 Prey
6	2 predators, 1 Land 100 Prey

The number of larvae consumed was noted after 24 h. The predation performance data obtained during September 2017 experiments have been presented separately from the data obtained during April 2017 experiments due to differences in timing and number of replicas.

Sensitivity of odonate nymphs to inorganic nutrient pollutants

During the present research, the sensitivity of nymphs of *I. elegans*, *T. aurora* and *P. flavescens* to various concentrations of inorganic nutrient pollutants i.e., ammonium (NH_4^+) and nitrate (NO_3^-) was investigated. These nymphs were exposed to various concentrations of NH_4^+ and NO_3^- in water.

Sensitivity of odonate nymphs to Ammonium

Stock solution of NH_4^+ was prepared by dissolving ammonium chloride (NH_4Cl) in non-chlorinated tap water. The molecular weight of NH_4Cl is 53.5 g which contains 18 g of NH_4^+ . 2.9 g of NH_4Cl was required for preparation of 1000 ml NH_4^+ solution of 1000 ppm. From this stock solution, testing solutions of different concentrations of NH_4^+ were prepared by applying the dilution equation $C_1V_1 = C_2V_2$.

According to the WHO (2006) standards for wastewater reuse in the Eastern Mediterranean Region, the maximum permissible concentration of NH_4 in effluents for reuse in agricultural irrigation is 5 ppm. Therefore, during the present research, the minimum concentration of NH_4^+ to which odonate nymphs were exposed was 5 ppm. Thus, *I. elegans*, *T. aurora* and *P. flavescens* were initially exposed to testing solutions of 5, 10, 25, 50 and 100 ppm concentrations of NH_4^+ in 400 ml polyethylene containers for finding concentration range to be used for determining the LC50 values. The ecological effects test guidelines of Environmental Protection Agency, USA (US EPA, 1996) were followed with some modifications for determining the concentration range. Volume of testing solution in each polyethylene container was 250 ml. A 400 ml polyethylene control container containing 250 ml non-chlorinated tap water was also kept. Nymphs of each species were exposed individually in containers to avoid cannibalism. Due to individual placement, limited laboratory space and limited availability of nymphs, the method of Hardersen and Wratten (1996) was followed. The detail is as under: six intact 8th to 10th instar nymphs of each species were placed in six plastic containers (five NH_4^+ concentrations and one control). In short, 18 containers were arranged for the nymphs of three odonate species, six for each species. Experiment was run in five replicates. The period of exposure was 7 days. Following standard toxicity protocols, the nymphs were not fed during the 7 days exposure (ASTM, 2008). At day 7th of exposure period, the numbers of dead and live nymphs were noted. The criterion for death was lack of response to prodding. During preliminary experiment, no mortality of nymphs occurred up to 50 ppm. Therefore, further experiments were performed using high concentrations. Therefore, nymphs of each species were exposed to higher concentrations (100, 200, 400 and 600 ppm) of NH_4^+ solution for determining LC50 values. Five intact last instar nymphs of each species were placed individually in their respective five containers (four concentrations and one control). This experiment was run in triplicate. After 7 days of exposure, the number of dead and live nymphs was noted. Several trips were conducted for collection of nymphs and experiments were repeated continuously till the number of nymphs in each replica for each concentration reached 20. In total 20 independent experiments were conducted.

Sensitivity of odonate nymphs to nitrate

Stock solution of NO_3^- was prepared by dissolving sodium nitrate (NaNO_3) in non-chlorinated tap water. The molecular weight of NaNO_3 is 85.5 g which contains 62 g of NO_3^- . 1.4 g of NaNO_3 was required for preparation of 1000 ml NO_3^- solution of 1000 ppm. From this stock solution, testing solutions of different concentrations of NO_3^- were prepared by applying the dilution equation $C_1V_1 = C_2V_2$.

According to the standards for wastewater reuse in the Eastern Mediterranean Region, the maximum permissible concentration of NO_3^- in effluents for reuse in agricultural irrigation is 45 ppm (WHO, 2006). Therefore, during the present research, the minimum concentration of NO_3^- to which odonate nymphs were exposed was 45ppm. The concentrations of NO_3^- to which nymphs were exposed during range finding bioassay were 45, 100, 150, 200, 400 ppm. The rest of detail of range finding bioassay was the same as described for NH_4^+ . During preliminary experiment no mortality of nymphs occurred up to 150 ppm NO_3^- solution. However, at 200 ppm NO_3^- concentration, mortality in nymphs of each Odonate species was observed. Therefore, nymphs of each species were exposed to higher concentrations (200, 400, 550 and 700 ppm) of NO_3^- solution for determining LC_{50} values. The rest of detail of experiment for determining LC_{50} values are the same as described for NH_4^+ .

Statistical analysis

The 24 h feeding rate of odonate nymphs were compared by applying Tukey test in One Way ANOVA. The difference in feeding rate of each odonate nymph species between light and dark phases was analyzed by Independent Samples t-Test. The effects of variation in predator density, water volume and prey density on daily feeding rate of each odonate nymph was analyzed by multiple linear regression test. During the study on sensitivity of odonate nymphs to inorganic nutrient pollutants, the average of percent mortality data was subjected to log probit analysis (Finney, 1971) for calculating LC_{50} . SPSS 16 software was used for the analysis of the data. The LC_{50} values were compared by 95% confidence limits overlap method.

Results

24-h feeding rate of donate nymphs during April, 2017

During April 2017 experiments, the 24-h feeding rates of *I. elegans*, *T. aurora* and *P. flavescens* on *Cx. quinquefasciatus* 3rd instar larvae were studied in the laboratory (Table 2). Significantly higher ($P>0.05$) number of *Cx. quinquefasciatus* 3rd instar larvae were consumed by *P. flavescens* (47.0 ± 5.1 larvae/24-h) followed by *T. Aurora* (17.8 ± 4.2 larvae/24-h) and *I. elegans* (10.5 ± 3.1 larvae/24-h).

Feeding rate of odonate nymphs during light and dark phases in April, 2017

During April 2017 study, the per hour feeding rates of *I. elegans*, *T. aurora* and *P. flavescens* on 3rd instar larvae of *Cx. quinquefasciatus* were compared between the daytime and night-time (Table 3). The nymphs of *I. elegans* species consumed 0.52 ± 0.19 larvae /hour at the day time and 0.35 ± 0.16 larvae/hour at the night time. The difference in feeding rate between the day and night time was significant. Similar trend was also observed in *P. flavescens*. However, *T. aurora* showed insignificantly

($P > 0.05$) higher feeding rate during the night time (1.03 ± 0.24 larvae /hour) as compared to its feeding rate during the day time (0.91 ± 0.11 larvae/hour).

24-h feeding rate of donate nymphs during September, 2017

The 24-h feeding rates of *L. fulva*, *S. decoloratum* and *C. servilia* on *Cx. quinquefasciatus* 3rd instar larvae were studied during September 2017 (Table 4). Maximum number of mosquito larvae was consumed by *S. decoloratum* (17.2 ± 4.2 larvae/24 h) followed by *L. fulva* (14.2 ± 2.3 larvae/24 h) and *C. servilia* (11.8 ± 2.1 larvae/24 h). The difference in consumption rate between *S. decoloratum* and *C. servilia* was significant ($P < 0.05$) but the difference between the *S. decoloratum* and *L. fulva* or *L. fulva* and *C. servilia* was not significant ($P > 0.05$).

Feeding rate of odonate nymphs during light and dark phases in September, 2017

During September 2017 study, the 12-h feeding rates of *L. fulva*, *S. decoloratum* and *C. servilia* were compared between the day and night times (Table 5). The feeding rate of each of these odonate specie was significantly higher ($P < 0.05$) during the daytime as compared to the night-time.

Feeding pattern of odonate nymphs after every 3 h interval

The feeding pattern of nymphs of *L. fulva*, *S. decoloratum* and *C. servilia* were also noted after every 3 h interval at day and night times for 24 h (Fig. 2). Each nymph consumed maximum larvae during the first 3-h interval (6:00 to 9:00 h Pakistan standard time).

Table 2. 24-h feeding rate of odonate nymphs against *Cx. quinquefasciatus* 3rd instar larvae during April 2017 experiments

Odonate Sp.	No. of larvae consumed per 24 h (mean + Sd)	95% confidence interval		F value
		Lower bound	Upper bound	
<i>I. elegans</i>	10.5 ± 3.1^c	8.6	12.4	251.6
<i>T. aurora</i>	17.8 ± 4.2^b	15.2	20.5	
<i>P. flavescens</i>	47.0 ± 5.1^a	43.7	50.3	

Different letters in superscript represent that the 24-h feeding rate of different odonate nymphs is significantly different at $P < 0.05$ (Tukey Test)

Table 3. Feeding rate of odonate nymphs during light and dark phases in April 2017

Species	No. of larvae consumed per hour at day time (mean + Sd)	No. of larvae consumed per hour at night time (Mean + Sd)	T value	Significance 2-tailed
<i>I. elegans</i>	$0.52 + 0.19^*$	$0.35 + 0.16$	1.895	$P < 0.05$
<i>T. aurora</i>	$0.91 + 0.11$	$1.03 + 0.24$	-1.317	$P > 0.05$
<i>P. flavescens</i>	$2.2 + 0.5^*$	$1.8 + 0.28$	-2.7	$P < 0.05$

* represents that the hourly feeding rate of a nymph during the day time is significantly higher from the night time (independent sample T-test)

Table 4. 24-h feeding rate of odonate nymphs against *Cx. quinquefasciatus* 3rd instar larvae during September 2017 experiments

Odonate Sp.	No. of larvae consumed per 24-h (mean + Sd)	95% Confidence Interval		F value
		Lower bound	Upper bound	
<i>L. fulva</i>	14.2 ± 2.3 ^{ab}	11.7	16.6	21.9
<i>S. decoloratum</i>	17.2 ± 4.2 ^b	12.8	21.5	
<i>C. servilia</i>	11.8 ± 2.1 ^a	9.8	13.9	

Different letters in superscript represent that the 24-h feeding rate of different odonate nymphs is significantly different at P < 0.05 (Tukey Test)

Table 5. Feeding rate of odonate nymphs during light and dark phases in September 2017

Species	No. of larvae consumed per 12-h at day time (mean + Sd)	No. of larvae consumed per 12-h at night time (mean + Sd)	T value	Significance 2-tailed
<i>L. fulva</i>	8.8 ± 1.5*	5.3 ± 1.03	4.8	P < 0.05
<i>S. decoloratum</i>	11.6 ± 4.1*	5.5 ± 1.04	3.6	P < 0.05
<i>C. servilia</i>	7.83 ± 1.5*	4.0 ± 0.89	-5.4	P < 0.05

* represents that the 12-h feeding rate of a nymph during the day time is significantly higher from the night time (independent sample T-test)

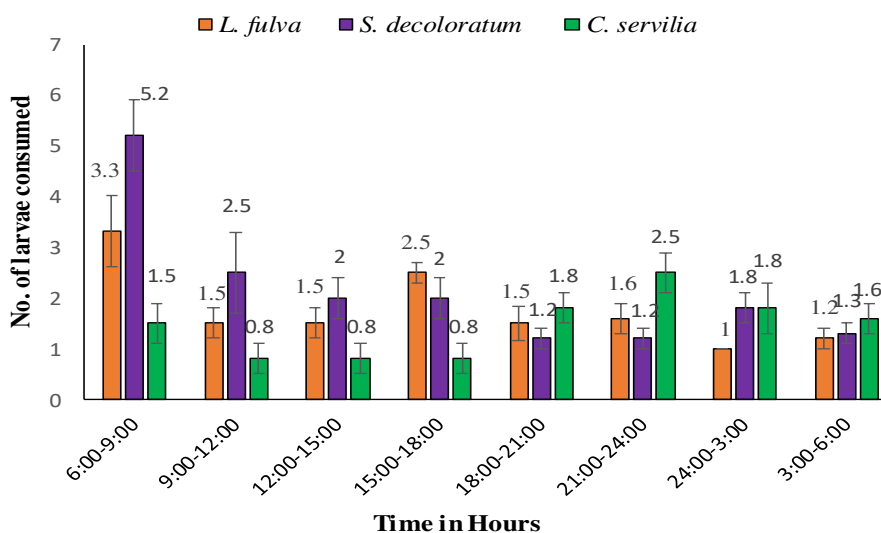


Figure 2. Feeding pattern of nymphs of three odonate species after every 3 h interval during light and dark phases for 24 h

Feeding rate under varied condition of predator density, water volume and prey density

The 24-h feeding rate of *I. elegans*, *T. aurora* and *P. flavescens* on 3rd instar larvae of *Cx. quinquefasciatus* was also studied under varied conditions (combinations) of

predator density, water volume and prey (mosquito larvae) density (Table 6). Nymph of each odonate species consumed significantly higher number ($P < 0.05$) of mosquito larvae in combination no. 6 (condition of increased predator and prey density and decreased water volume) as compared to other combinations. In this combination, *I. elegans*, *T. aurora* and *P. flavescens* consumed 22.0 ± 2.6 , 45.3 ± 4.1 and 63.0 ± 7.5 larvae/day (larvae consumed/24-h), respectively. Strong correlation ($R^2 > 0.70$) was observed during determination of correlation of feeding rate of each odonate species with variation in predator density, water volume and prey density. The regression equation for nymphs of each odonate species clearly indicated that the feeding rate is positively correlated with increase in prey and predator density but negatively correlated with increase in water volume.

Sensitivity of predators of mosquito larvae to ammonium (NH_4^+)

During the present research, the sensitivity of *I. elegans*, *T. aurora* and *P. flavescens* was studied during exposure to various concentrations of NH_4^+ for seven days (Table 7). During range finding study, the highest concentration of NH_4^+ that caused no mortality of odonate nymphs was 50 ppm. The lowest concentration of NH_4^+ that caused some mortality among the odonate nymphs was 100 ppm. At this concentration of NH_4^+ , lowest mortality ($3.3 \pm 1.6\%$) was observed in *P. flaviscans* followed by *T. aurora* ($5.0 \pm 0\%$) and *I. elegans* ($6.6 \pm 1.6\%$). Similar trend was noted during exposure to highest concentration i.e., 600 ppm. At this concentration, the mean percent mortality of *P. flaviscans*, *T. aurora* and *I. elegans* were $43.3 \pm 1.6\%$, $58.3 \pm 7.2\%$ and $71.6 \pm 1.6\%$, respectively. Maximum LC_{50} value was shown by *P. flaviscans* (740.3 ppm) followed by *T. aurora* (516.7 ppm) and *I. elegans* (425.7 ppm).

Table 6. Feeding rate of odonate nymphs on mosquito larvae under varied conditions of predator density, water volume and prey density

Species	S. No of combinations	Combination	Larvae consumed/24 h	F value	R ² value	Y-equation
<i>I. elegans</i>	1	1 predator, 1 L and 50 Prey	10.3 ± 2.1b	59.7	0.78	7.6 + 6.3 (predator) – 7.16 (volume) + 0.07 (prey)
	2	1 predator, 2L and 50 Prey	5.0 ± 1.7a			
	3	1 predator, 1 Land 100 Prey	11.3± 4.1b			
	4	2 predators, 1 L and 50 Prey	16.3 ± 1.5c			
	5	2 predators, 2 L and 50 Prey	7.3 ± 4.1b			
	6	2 predators, 1 Land 100 Prey	22.0 ± 2.6d			
<i>T. aurora</i>	1	1 predator, 1 L and 50 Prey	20.6 ± 4.1a	80.9	0.77	0.6 + 20.2 (predator) – 4.3 (volume) + 0.05 (prey)
	2	1 predator, 2L and 50 Prey	16.6 ± 5.8a			
	3	1 predator, 1 Land 100 Prey	18.6 ± 3.2a			
	4	2 predators, 1 L and 50 Prey	38.0 ± 5.3d			
	5	2 predators, 2 L and 50 Prey	33.3± 11.5c			
	6	2 predators, 1 Land 100 Prey	45.3 ± 4.1e			
<i>P. flavescens</i>	1	1 predator, 1 L and 50 Prey	38.6± 10.1a	55.8	0.73	18.3 + 21.1 (predator) – 5.16 (Vol) + 0.06 (prey)
	2	1 predator, 2L and 50 Prey	32.3 ± 6.8a			
	3	1 predator, 1 Land 100 Prey	38.6 ± 3.2a			
	4	2 predators, 1 L and 50 Prey	57.0 ± 7.0c			
	5	2 predators, 2 L and 50 Prey	53.0 ± 11.2c			
	6	2 predators, 1 Land 100 Prey	63.0 ± 7.5d			

Means having different letters are significantly different at $P < 0.05$ (Tukey Test)

Table 7. Sensitivity of nymphs of three different odonate species to ammonium (NH_4^+)

Species	Concentration (ppm)/% mortality (mean+ SE)					LC ₅₀ (ppm)	95% confidence limits
	50 ppm	100 ppm	200 ppm	400 ppm	600 ppm		
<i>I. elegans</i>	0	6.6 ± 1.6	20.0 ± 2.8	38.3 ± 4.4	71.6 ± 1.6	425.7a	369.1–507.2
<i>T. aurora</i>	0	5.0 ± 0	16.7 ± 1.6	36.7 ± 4.4	58.3 ± 7.2	516.7b	446.5–625.8
<i>P. flaviscans</i>	0	3.3 ± 1.6	10.0 ± 2.9	26.7 ± 1.6	43.3 ± 1.6	740.3c	648.1–879.3

The alphabetical order of letters in column of LC₅₀ is according to increasing LC₅₀ values. LC₅₀ values sharing no letter are significantly different

Sensitivity of predators of mosquito larvae to nitrate (NO_3^-)

During the present research, the sensitivity of *I. elegans*, *T. aurora* and *P. flavescens* was studied during exposure to various concentrations of NO_3^- for seven days (Table 8). During range finding study, the highest concentration of NO_3^- that caused no mortality of odonate nymphs was 150 ppm. The lowest concentration of NO_3^- that caused some mortality among the odonate nymphs was 200 ppm. During exposure to this concentration of NO_3^- , minimum mortality ($5.0 \pm 0.0\%$) was observed in *P. flaviscans* followed by *T. aurora* ($10.0 \pm 0.0\%$) and *I. elegans* ($11.6 \pm 1.7\%$). Similar trend was noted during exposure to highest concentration i.e., 700 ppm. At highest concentration of NO_3^- , the mean percent mortality of *P. flaviscans*, *T. aurora* and *I. elegans* were $28.3 \pm 1.6\%$, $50.0 \pm 5.8\%$ and $65.0 \pm 2.7\%$, respectively. Maximum LC₅₀ value was shown by *P. flaviscans* (LC₅₀ = 1353.1 ppm) followed by *T. aurora* (LC₅₀ = 678.4 ppm) and *I. elegans* (LC₅₀ = 597.8 ppm).

Table 8. Sensitivity of nymphs of three different odonate species to nitrate (NO_3^-)

Species	Concentration (ppm)/% mortality (mean± SE)					LC ₅₀ (ppm)	95% confidence limits
	150	200	400	550	700		
<i>I. elegans</i>	0	11.6 ± 1.7	26.6 ± 3.3	40.0 ± 2.8	65.0 ± 2.7	597.8 ^a	391.4–2595.6
<i>T. aurora</i>	0	10.0 ± 0.0	20.0 ± 2.9	28.3 ± 4.4	50.0 ± 5.8	678.4 ^{ab}	463.4–3167.3
<i>P. flaviscans</i>	0	5.0 ± 0.0	10.0 ± 0.0	21.6 ± 4.4	28.3 ± 1.6	1353.1 ^{abc}	969.1–4338.3

The alphabetical order of letters in column of LC₅₀ is according to increasing LC₅₀ values. LC₅₀ values sharing no letter are significantly different

Discussion

For the control of mosquitoes and other insect pests, alternative approaches that are ecofriendly should be adopted (Ghosh et al., 2012). Biological control strategies are environment friendly, sustainable and targeting a range of different mosquito species which help in reduction of reliance on application of synthetic chemical insecticides (Benelli et al., 2016). Historically, Biological control involves the application of natural predators which is particularly important for the control of mosquito-borne arboviruses, which normally do not have specific antiviral therapies available (Huang et al., 2017). Damselfly and dragonfly nymphs have the predatory ability and share aquatic habitat with the immature stages of mosquitoes therefore they can be considered good biological control agents against mosquitoes (Mitra, 2006; Chatterjee et al., 2007). During the present research, the predatory efficiencies of nymphs of six coexisting

odonate species i.e., *I. elegans*, *T. aurora*, *P. flavescens*, *L. fulva*, *S. decoloratum* and *C. servilia* were studied by using *Cx. quinquefasciatus* 3rd instar larvae as prey. There was observed variation in the daily (24-h) feeding rate of nymphs of various odonate species (Tables 2 and 4). Highest number of mosquito larvae was ingested by the *P. flavescens* nymph (47.0 ± 5.1 mosquito larvae/day). To the best of author knowledge, the predatory ability of *T. aurora*, *P. Flavescens*, *L. fulva*, *S. decoloratum* and *C. servilia* nymphs have been studied for the first time during the present study. The predation performance of few other odonate nymph species have been reported. For example, Miura and Takahashi (1988) studied the predatory ability of damselfly nymph, *Enallagma civile*, against the *Culex tarsalis* larvae. The average 24 h feeding rate of last instar nymph of *E. civile* on 3rd instar larvae of *Cx. tarsalis* was 6.06 larvae. Mandal et al. (2008) studied the predatory efficiency of nymphs of two dragonfly species i.e., *Aeshna flavifrons* and *Sympetrum durum*, and three damselfly species i.e., *Coenagrion kashmirum*, *Ischnura forcipata* and *Rhinocypha ignipennis*, against 4th instar larvae of *Cx. quinquefasciatus*. *I. forcipata* nymph consumed highest number of mosquito larvae (64.3 ± 1.8). Akram and Ali-Khan (2016) studied the predation performance of five odonate nymphs, *Anax parthenope*, *Bradinopyga geminate*, *Ischnura forcipata*, *Rhinocypha quadrimaculata* and *Trithemis aurora* against the 4th instar larvae of *Aedes aegypti* in the laboratory. *Ischnura forcipata* consumed highest number of mosquito larvae (56 larvae/ day). Chandra et al. (2006) studied the predatory efficiency of a dragonfly nymph, *Brachytron pratense*, against the larvae of *Anopheles subpictus* in the laboratory conditions. *Brachytron pretense* consumed up to 66 mosquito larvae through 24 h. The predatory ability of odonate nymphs against non insect pests have also been studied. For example, Younes et al. (2016) studied the predation performance of odonate nymphs of the species *Hemianax ephippiger* against two species of fresh water snail, *Bulinus truncatus* and *Biomphalaria alexandrina* which act as intermediate hosts of *Schistosoma* species. Odonata nymph consumed both species of the fresh water snail, however the odonate nymphs consumed more *Bulinus truncatus* than *Biomphalaria alexandrina*. Consumption rate also differed according to the snail type, density and size. Odonate nymphs preferred small sized prey.

The predation performance of nymphs of different odonate species was also compared between the day and night times. During the April 2017 study, the per hour feeding rates of *I. elegans*, *T. aurora* and *P. flavescens* on 3rd instar larvae of *Cx. quinquefasciatus* were compared between the day and night times. The nymphs of *I. elegans* and *P. flavescens* species consumed significantly higher ($P \leq 0.05$) number of mosquito larvae during the day time as compared to the night time. The feeding rate of *T. aurora* was also higher during the day time but the difference from the night time was insignificant ($P > 0.05$) (Table 3). During the September 2017 study, the 12-h feeding rates of *L. fulva*, *S. decoloratum* and *C. servilia* on 3rd instar larvae of *Cx. quinquefasciatus* were compared between the day and night times. Each nymph consumed maximum larvae during the first 3-h interval (6:00 to 9:00 h Pakistan standard time). Similar trend has also been reported by Venkatesh and Tyagi (2013) during their study on the predatory performance of *Bradinopyga geminata* and *Ceragrion coromandelianum* larvae on *Aedes aegypti* larvae in the laboratory conditions. During the present study, the duration of the day and night time was 12 h each. Therefore, the feeding rate of nymphs of *L. fulva*, *S. decoloratum* and *C. servilia* was compared between the day and night times (Table 5). Nymphs of all these odonate species consumed significantly higher number of mosquito larvae during the day time

as compared to the night time ($P < 0.05$). Mandal et al. (2008) reported higher feeding rate of different odonate nymph species at the light phase as compared to the dark phase. A dragonfly nymph, *Brachytron pretense* consumed more *Anopheles subpictus* larvae during the day time compared to the night time (Chandra et al., 2006). Chandra et al. (2008) reported that feeding rate of *A. sulcatus* did not differ between the light and dark phases. Eyes in odonate nymphs are known to be very helpful in capturing prey but mechanoreceptors also play equal role in predation (Mandal et al., 2008). Backswimmers use both mechanoreceptor and vision for detecting their prey (Dieguez and Gilbert, 2003). Mechanoreceptors play role in detecting waves and providing accurate information for discriminating between prey and non-prey vibrations and adjusting their orientation or displaying prey catching behavior (Lang, 1980). In several odonate species, the nymphs come out from perches at night and wander for predation (Corbet, 1980). Dieguez and Gilbert (2003) studied the effect of light and dark on the predation efficiency of Backswimmer, *Buenoa macrotibialis*. It was noted that *Buenoa macrotibialis* can feed on small prey such as *Brachionus calyciflorus* and *Tropocyclops extensus* in presence of light but cannot feed well on these small preys in dark. It was further noted that *Buenoa macrotibialis* can feed equally in light and dark conditions on the largest prey such as *Daphnia pulex*. Their findings show the importance of both visual and mechanical cues in detecting prey of different sizes.

The 24-h feeding rate of *I. elegans*, *T. aurora* and *P. flavescens* on 3rd instar larvae of *Cx. quinquefasciatus* was also studied under varied conditions of predator density, water volume and prey (mosquito larvae) density (Table 6). The feeding rate of nymphs of each odonate species was positively correlated with increase in density of predator and prey but negatively correlated with increase in volume of water. This showed that the independent variables i.e., predator density, water volume and prey density are strong predictors of feeding rate of odonate nymphs on mosquito larvae. The negative impact of increased water volume (search area) on the feeding rate of odonate nymphs on mosquito larvae may be probably due to the evasion tactics of the mosquito larvae (Bhattacharjee et al., 2009). The positive correlation of increase in predator density with increase in predation rate on mosquito larvae may be probably due to intra-specific completion (Chandra et al., 2006). The positive correlation of increase in prey density with increase in predation rate of odonate nymphs on mosquito may be probably due to increase in chances of availability of prey to the odonate nymphs. Similar results have also been reported by other researchers in other odonate nymph species or other predatory insects against mosquito larvae. For example, Chandra et al. (2006) observed a decrease in the feeding rate of a dragonfly nymph (*Brachytron pratense*) on *Anopheles subpictus* larvae with increase in water volume. On the other hand, there occurred an increase in feeding rate of *Brachytron pretense* nymph on *Anopheles subpictus* larvae with increase in predator and prey (mosquito larvae) density. Mandal et al. (2008) studied variation in feeding rate of nymphs of five odonate species on 4th instar larvae of *Culex quinquefasciatus* (as prey) with variation in predator density, water volume (search area) and prey density. The predation rate was negatively correlated with increases in water volume (increase in search area) but linearly related to the increase in the density of predator and density. In the study of Chandra et al. (2008), the feeding rate of *Acilius sulcatus* larvae (predator) on the 4th instar larvae of *Culex quinquefasciatus* (prey) decreased with increase in water volume but increased with increase in the density of prey and predators.

During the present research, *I. elegans*, *T. aurora* and *P. flavescens* nymphs were exposed to various concentrations of NH_4^+ and NO_3^- for seven days for testing their sensitivity to these pollutants. Nymphs of all the species survived up to 50 ppm concentration of NH_4^+ . Nymphs of *P. flavescens* were found less sensitive to NH_4^+ . The LC_{50} value of NH_4^+ for *P. flavescens* was significantly higher when compared to the LC_{50} values of NH_4^+ for *T. aurora* and *I. elegans* (Table 7). To the author knowledge there are no reports about the toxicity of NH_4^+ or ammonia (NH_3) with *I. elegans*, *T. aurora* and *P. flavescens* nymphs. However, NH_3 toxicity with other odonate nymphs such as *Erythromma najas*, *Lestes sponsa* and *Sympetrum flaveolum* has been reported by Beketov (2002). These nymphs showed high tolerance to NH_3 . Toxicity of NH_4^+ is dependent on pH (Körner et al., 2001). Both, un-ionized (NH_3) and ionized (NH_4^+) forms of ammonia may exist in aqueous solution. The ratio of NH_3 to NH_4^+ increases with rise in pH and temperature (Körner et al., 2001). Uncharged ammonia (NH_3) can cross biological membrane more easily than charged NH_4^+ , therefore NH_3 is more toxic (Levit, 2010). The toxic effects of NH_3 to aquatic invertebrate is mediated by damaging the respiratory surfaces and changing the pH of hemolymph (Colt and Armstrong, 1981). NH_4^+ become toxic at higher concentration (Monselise and Kost, 1993). During the present study, solutions of NH_4Cl were prepared in non-chlorinated tap water with neutral pH (pH 7.3) and experiment was conducted at room temperature (17 to 23 °C), thus the existence of NH_3 would be less likely. Martinelle and Häggström (1993) presented a model that explains the mechanism of NH_4^+ toxicity. According to the model, NH_4^+ competes with potassium ions for inward transport over the cell membrane through potassium transport proteins such as Na^+/K^+ -ATPase and the Na^+/K^+ -2(Cl^-)-co-transporter. It was concluded that one important toxic effect of NH_4^+ is the need for maintaining ion gradients across the membrane that require energy.

During the study of susceptibility of *I. elegans*, *O. sabina* and *P. flavescens* nymphs to different concentrations of NO_3^- , all the nymphs survived up to 150 ppm concentration of NO_3^- (Table 8). However, exposure to higher NO_3^- concentrations resulted in mortality. Nymphs of *P. flavescens* were found least susceptible to NO_3^- . For example, maximum LC_{50} value was shown by *P. flaviscans* (1353.1 ppm) followed by *O. sabina* (678.4 ppm) and *I. elegans* (597.8 ppm). During the present research, the LC_{50} values of NO_3^- against odonate nymphs were higher than the LC_{50} values of ammonium against these nymphs. This might be explained by the fact that biological membranes are less permeable to NO_3^- than to NH_4^+ , therefore there occurs limited uptake of NO_3^- in aquatic animals, which contribute to relatively low toxicity of NO_3^- (Cheng and Chen, 2002; Alonso and Camargo, 2003). The main toxic action of NO_3^- on aquatic animals is due to the conversion of oxygen-carrying pigments (e.g., hemoglobin, hemocyanin) to forms that are incapable of carrying oxygen (e.g., methemoglobin) (Scott and Crunkilton, 2000; Cheng and Chen, 2002).

To the author knowledge there are no reports about the toxicity of NO_3^- with the odonate nymphs. However, NO_3^- toxicity with other aquatic invertebrates has been reported. For example, Alonso and Camargo (2003) studied short-term toxicity of ammonia, nitrite, and NO_3^- to the aquatic snail, *Potamopyrgus antipodarum* (Hydrobiidae, Mollusca). The 4 days LC_{50} values of NO_3^- for *P. antipodarum* was 1042 ppm. Camargo et al. (2005) studied NO_3^- toxicity to two freshwater Amphipod species, *Eulimnogammarus toletanus* and *Echinogammarus echinosetosus* and a caddisfly (*Hydropsyche exocellata*). The 5 days LC_{50} of NO_3^- for *E. toletanus*, *E. echinosetosus* and *H. exocellata* were 73.1 ppm, 56.2 ppm and 230.2 ppm, respectively.

The LC₅₀ values of NO₃⁻ reported by Camargo et al. (2005) for *E. toletanus*, *E. echinosetosus* and *H. exocellata* are much lower than the LC₅₀ values of NO₃⁻ for Odonate nymphs observed during the present research. The LC₅₀ values of NO₃⁻ reported by Alonso and Camargo (2003) for *P. antipodarum* are comparable to the LC₅₀ values of NO₃⁻ observed during the present research for odonate nymphs. The toxicity of NO₃⁻ may decrease with increase in body size, water salinity, and environmental adaptation (Camargo et al., 2005). The effects of other environmental pollutants on aquatic insects have also been reported. For example, Lacerda et al. (2014) exposed *Chironomus kiiensis* lar larvae of *Chironomus kiiensis* larvae to crude oil. During their study, the 48-h LC₅₀ was 26.5 ppm. Maximum mortality for most of the tested concentrations was observed during the first 24 h of the experiment. Similarly, Miles et al. (2017), exposed predatory insects to different concentrations of clothianidin, a neonicotinoid, in a semi-natural mesocosm. They observed high mortality of predatory invertebrates and increasing prey density with increase in clothianidin concentration.

Conclusion

1) From the findings of the study of predatory ability of damselfly and dragonfly nymphs, it was concluded that *I. elegans*, *T. aurora*, *P. flavescens*, *L. fulva*, *S. decoloratum* and *C. servilia* nymphs can play an important role in the eco-friendly control of the *Cx. quinquefasciatus* mosquito, and *P. flavescens* nymph is more efficient predator of *Cx. quinquefasciatus* 3rd instar larvae.

2) From the findings of the study of sensitivity of odonate nymphs to inorganic nutrient pollutants, it was concluded that *I. elegans*, *T. aurora* and *P. flavescens* nymphs can tolerate high concentration of NH₄⁺, and NO₃⁻ under condition of neutral pH and room temperature. *P. flavescens* species is highly resistant to increasing water level of NH₄⁺ and NO₃.

Authors contribution and Acknowledgements. This article has been prepared from the first author's (Ikram Ilahi) PhD thesis entitled "Ecofriendly control of *Culex quinquefasciatus* (Say, 1823) and susceptibility of its larvae and predators to different environmental pollutants" at the Department of Zoology, Islamia College, Peshawar, Khyber Pakhtunkhwa, Pakistan. Ali Muhammad Yousafzay acted as the supervisor. The remaining authors participated during collection in fields and/or in statistical analysis of data and preparation of manuscript. The help of Dr. Ahmad Zia, Senior Scientific Officer and Taxonomist in the Insect National Museum at National Agricultural Research Council (NARC), Islamabad, Pakistan, in providing literature and unpublished documents for identification of odonate nymphs is highly acknowledged.

REFERENCES

- [1] Ajaegbu, E. A., Danga, S. P. Y., Chijoke, I. K., Okoye, F. B. C. (2016): Mosquito adulticidal activity of the leaf extracts of *Spondias mombin* L. against *Aedes aegypti* L. and isolation of active principles. – J. Vector Borne Dis. 53: 17-22.
- [2] Akram, W., Ali-Khan, H. A. (2016): Odonate nymphs: generalist predators and their potential in the management of dengue mosquito, *Aedes aegypti* (Diptera: Culicidae). – J. Arthropod-Borne Dis. 10(2): 252-257.
- [3] Alonso, A., Camargo, J. A. (2003): Short-term toxicity of ammonia, nitrite, and nitrate to the aquatic snail *Potamopyrgus antipodarum* (Hydrobiidae, Mollusca). – Bull. Environ. Contam. Toxicol. 70: 1006-1012.

- [4] Anjum, S. A. (1997): Biosystematics of odonate naiads of the Punjab by rearing techniques. – MSc Thesis, Department of Agriculture Entomology University of Agriculture Faisalabad, Pakistan.
- [5] ASTM - American Society for Testing and Materials (2008): Guide for Conducting Acute Toxicity Tests on Aqueous Ambient Samples and Effluents with Fishes, Macroinvertebrates, and Amphibians. – ASTM International, West Conshohocken, Pennsylvania.
- [6] Beketov, M. A. (2002): Ammonia toxicity to larvae of *Erythromma najas* (Hansemann), *Lestes sponsa* (Hansemann) and *Sympetrum flaveolum* (Linnaeus) (Zygoptera: Coenagrionidae, Lestidae; Anisoptera: Libellulidae). – *Odonatologica* 31(3): 297-304.
- [7] Benelli, G., Jeffries, C. L., Walker, T. (2016): Biological control of mosquito vectors: past, present, and future. – *Insects* 7: 52.
- [8] Bhattacharjee, I., Aditya, G., Chandra, G. (2009): Laboratory and field assessment of the potential of larvivorous, air-breathing fishes as predators of culicine mosquitoes. – *Biol. Control*. 49: 126-133.
- [9] Boyd, S. (2005): Damselflies and Dragonflies. Scientific Illustration Major. – University of Georgia, Athens. <http://www.discoverlife.org/nh/tx/Insecta/Odonata/>.
- [10] Camargo, J. A., Alonso, A., Salamanca, A. (2005): Nitrate toxicity to aquatic animals: a review with new data for freshwater invertebrates. – *Chemosphere* 58: 1255-1267.
- [11] Chandra, G., Chatterjee, S. N., Ghosh, A. (2006): Role of dragonfly (*Brachytron pratense*) nymph as a biocontrol agent of larval mosquitoes. – *Bul. Penel Kesehatan* 34(4): 147-151.
- [12] Chandra, G., Bhattacharjee, I., Chatterjee, S. N., Ghosh, A. (2008): Mosquito control by larvivorous fish. – *Indian J Med Res.* 127: 13-27.
- [13] Chatterjee, S. N., Ghosh, A., Chandra, G. (2007): Eco-friendly control of mosquito larvae by *Brachytron pratense* nymph. – *J Environ Health* 69(8): 44-49.
- [14] Cheng, S. Y., Chen, J. C. (2002): Study on the oxyhemocyanin, deoxyhemocyanin, oxygen affinity and acid–base balance of *Marsupenaeus japonicus* following exposure to combined elevated nitrite and nitrate. – *Aquatic Toxicol.* 61: 181-193.
- [15] Clark, T. E., Samways, M. J. (1996): Dragonflies (Odonata) as indicators of biotope quality in the Kruger National Park, South Africa. – *J. Appl. Ecol.* 33: 1001-1012.
- [16] Colt, J. E., Armstrong, D. A. (1981): Nitrogen toxicity to crustaceans, fish and molluscs. – *Bio-Engineering Symposium for Fish Culture (FCS Publ.1)*, pp 34-47.
- [17] Corbet, P. S. (1980): Biology of Odonata. – *Ann Rev Entomol.* 25: 189-218.
- [18] Das, B. P., Deobhankar, K., Pohekar, K. N., Marathe, R., Husain, S. A., Jambulingam, P. (2016): Laboratory bioassay of *Chilodonella uncinata*, an entomopathogenic protozoan, against mosquito larvae. – *Journal of Mosquito Research* 6(10): 1-10.
- [19] Dieguez, M. C., Gilbert, J. J. (2003): Predation by *Buenoa macrotibialis* (Insecta, Hemiptera) on zooplankton: effect of light on selection and consumption of prey. – *J. Plankton Res.* 25(7): 759-769.
- [20] Dida, G. O., Gelder, F. B., Anyona, D. N., Abuom, P. O., Onyuka, J. O., Matano, A., Adoka, S. O., Kanangire, C. K., Owuor, P. O., Ouma, C., Ofulla, A. V. (2015): Presence and distribution of mosquito larvae predators and factors influencing their abundance along the Mara River, Kenya and Tanzania. – *Springer plus* 4: 136.
- [21] Din, A. U., Zia, A., Bhatti, A. R., Khan, M. N. (2013): Odonata naiads of Potohar Plateau, Punjab, Pakistan. – *Pakistan J. Zool.* 45: 695-700.
- [22] Du, Y., Ma, T., Deng, Y., Shen, S., Lu, Z. (2017): Sources and fate of high levels of ammonium in surface water and shallow groundwater of the Jiangnan Plain, Central China. – *Environ. Sci. Process Impacts* 19: 161.
- [23] Finney, D. J. (1971): Probit Analysis. – Cambridge University Press, London, pp 68-78.
- [24] Gardner, A. E. (1960): A Key to the Larvae of the British Odonata. The New Naturalist Dragonflies. – Collins St. James, London, pp. 190-225.

- [25] Ghosh, A., Chowdhury, N., Chandra, G. (2012): Plant extracts as potential mosquito larvicides. – Indian J. Med. Res. 135(5): 581-598.
- [26] Harbach, R. E. (1988): The mosquitoes of the subgenus *Culex* in South West Asia and Egypt (Diptera: Culicidae). – Contribution of American Entomological Institute 24(1).
- [27] Hardersen, S., Wratten, S. D. (1996): The sensitivity of the nymphs of two New Zealand Damselfly Species (Odonata: Zygoptera) to Azinphos-Methyl and Carbaryl. – Australian Journal of Ecotoxicology 2: 55-60.
- [28] Hickey, C. W., Vickers, M. L. (1994): Toxicity of Ammonia to Nine Native New Zealand freshwater Invertebrate Species. – Arch. Environ. Contain. Toxicol. 26: 292-298.
- [29] Huang, Y. S., Higgs, S., Vanlandingham, D. L. (2017): Biological Control Strategies for Mosquito Vectors of Arboviruses. – Insects 8: 21.
- [30] Knight, T. M., Chase, J. M., Goss, C. M., Knight, J. J. (2004): Effects of interspecific competition, predation, and their interaction on survival and development time of immature *Anopheles quadrimaculatus*. – J. Vector Ecol. 29: 277-284.
- [31] Körner, S., Das, S. K., Veenstra, S., Vermaat, J. E. (2001): The effect of pH variation at the ammonium/ammonia equilibrium in wastewater and its toxicity to *Lemna gibba*. – Aquat. Bot. 71: 71-78.
- [32] Kumar, R., Hwang, J. S. (2006): Larvicidal efficiency of aquatic predators: a perspective for mosquito biocontrol. – Zool. Stud. 45(4): 447-466.
- [33] Lacerda, A. C. F., Gusmão, G. A., Hamada, N. (2014): Tests of chronic and acute toxicity of crude oil on larvae of *Chironomus kiiensis* Tokunaga (Diptera: Chironomidae). – Braz. J. Biol. 74(3): S70-S77.
- [34] Lang, H. H. (1980): Surface wave discrimination between prey and non-prey by the backswimmer *Notonecta glauca* L. (Hemiptera: Heteroptera). – Behav. Ecol. Sociobiol. 6: 233-246.
- [35] Lee, S. E., Kim, J. E., Lee, H. S. (2001): Insecticide resistance in increasing interest. – Agric. Chem. Biotechnol. 44: 105-112.
- [36] Levit, S. M. (2010): A Literature Review of Effects of Ammonia on Fish. – The Nature Conservancy, Montana. pp 1-10.
- [37] Lundkvist, E., Landin, J., Jackson, M., Svensson, C. (2003): Diving beetles (*Dytiscidae*) as predators of mosquito larvae (Culicidae) in field experiments and in laboratory tests of prey preference. – Bull. Entomol. Res. 93: 219-226.
- [38] Mandal, S. K., Ghosh, A., Bhattacharjee, I., Chandra, G. (2008): Biocontrol efficiency of odonate nymphs against larvae of the mosquito, *Culex quinquefasciatus* Say, 1823. – Acta. Trop. 106: 109-114.
- [39] Martinelle, K., Häggström, L. (1993): Mechanisms of ammonia and ammonium ion toxicity in animal cells: transport across cell membranes. – J. Biotechnol. 30(3): 339-50.
- [40] Miles, J. C., Hua, J., Sepulveda, M. S., Krupke, C. H., Hoverman, J. T. (2017): Effects of clothianidin on aquatic communities: Evaluating the impacts of lethal and sublethal exposure to neonicotinoids. – PLoS One 12(3): e0174171.
- [41] Mitra, A. (2006): Current status of the Odonata of Bhutan: a checklist with four new records. – Bhu. J. RNR. 2(1): 136-143.
- [42] Mitra, T. R. (2002): Geographical distribution of Odonate (Insecta) of Eastern India. – Memoirs Zool. Survey India 19(1): 1-171.
- [43] Monselise, B. E., Kost, D. (1993): Different ammonium uptake, metabolism and detoxification efficiencies in two Lemnaceae. – Planta 189: 167-173.
- [44] Phillips, R. S. (2001): Current status of malaria and potential for control. – Cim. Microbial Rev. 14(1): 208-226.
- [45] Rabalais, N. N. (2002): Nitrogen in aquatic ecosystems. – Ambio. 31: 102-112.
- [46] Saha, N., Aditya, G., Saha, G. K. (2007a): A comparative study of predation of three aquatic heteropteran bugs on *Culex quinquefasciatus* larvae. – Limnology 8: 73-80.

- [47] Scott, G., Crunkilton, R. L. (2000): Acute and chronic toxicity of nitrate to fathead minnows (*Pimephales promelas*), *Ceriodaphnia dubia* and *Daphnia magna*. – Environ. Toxicol. Chem. 19: 2918-2922.
- [48] Stav, G., Blaustein, L., Margalit, Y. (2005): Individual and interactive effects of a predator and controphic species on mosquito populations. – Ecol. Appl. 15(2): 587-598.
- [49] US EPA-United States Environmental Protection Agency (1996): Ecological Effects Test Guidelines: Aquatic Invertebrate Acute Toxicity Test, Freshwater Daphnids. – US EPA, Washington, DC, pp. 712C–96-114.
- [50] Venkatesh, A., Tyagi, B. K. (2013): Predatory potential of *Bradinopyga geminate* and *Ceriagrion coromandelianum* Larvae on dengue vector, *Aedes aegypti* under controlled conditions (Anisoptera: Libellulidae; Zygoptera: Coenagrionidae; Diptera: Culicidae). – Odonatologica 42(2): 139-149.
- [51] Walton, W. E. (2007): Larvivorous fish including *Gambusia*. – J. Amer. Mosq. Cont. Assoc. 23(sp2): 184-220.
- [52] Wetzel, R. G. (2001): Limnology. 3rd Ed. – Academic Press, New York.
- [53] WHO (2006): A Compendium of Standards for Wastewater Reuse in the Eastern Mediterranean Region. – WHO, Geneva.
- [54] Yousuf, M., Khan, M. J., Khaliq, A. (1996): Description of some final instar naiads (Libellulidae: Odonata) from Punjab and Sindh. – Pak. Entomol. 18(1-2): 17-23.
- [55] Zia, A. (2010): Biosystematics of damselflies (Zygoptera: Odonata) of Pakistan. – Ph.D. Thesis, Department of Agriculture Entomology, Pir Mehr Ali Shah Arid Agriculture University, Rawalpindi, Pakistan.

OPTIMUM CROP CULTIVATION AT DIFFERENT LEVELS OF IRRIGATION WATER ALLOCATION (CASE STUDY: QAZVIN PLAIN)

SHIRSHAHI, F.¹ – BABAZADEH, H.^{1*} – EBRAHIMIPAK, N. A.² – KHALEDIAN, M. R.³

¹*Department of Water Science and Engineering, Science and Research Branch, Islamic Azad University, Tehran, Iran
(phone: +98-919-313-3541 – F. Shirshahi)*

²*Department of Irrigation, Soil and Water Research Institute, Agricultural Research, Education and Promotion Organization, Tehran, Iran
(phone: +98-912-181-7169)*

³*Department Water Engineering, Faculty of Agricultural Sciences, University of Guilan, and Caspian Sea Basin Research Center, Rasht, Iran
(phone: +98-911-248-1285)*

**Corresponding author*

e-mail: h_babazadeh@hotmail.com; phone: +98-912-699-0105

(Received 4th Nov 2018 ; accepted 28th Jan 2019)

Abstract. Designing and implementing a crop pattern is necessary not only to cope with water deficit, but also to control the limiting factors and optimal utilization of available facilities, which have been addressed in many countries of the world. The current study was conducted at five levels of irrigation including I₁, I₂, I₃, I₄ and I₅ (100, 90, 80, 70 and 65% of crop evapotranspiration) and at three different levels of cultivation including S₁, S₂ and S₃ (current cultivated area, 10% increase in cultivated area and 10% decrease in cultivated area compared to current conditions). Optimum crop levels were estimated for each crops of crop pattern. The results show that the model in S₂ allocates a higher level to strategic crops, and in S₃ it allocates a higher level to higher-yielding crops. The S₃I₁ has the highest income among all scenarios. I₂ increased economic productivity at an average level of 7.5% while maintaining income. Therefore, it is possible to allocate a lower amount of area and a lower amount of water, and to earn more income. Also, I₄ and I₅ levels are not recommended due to reduced income and yield. If there is a decrease in available water and I₅ is reached, cropping tomato, beet and alfalfa are not recommended considering economic level.

Keywords: *cropping pattern, drought, linear programming, productivity, water deficit*

Introduction

Regarding world statistic, the greatest water consumption in countries can be found in the agriculture section (Kang et al., 2016; Programme, 2012; Mancosu et al., 2015). Consumed water in agriculture sector guarantees food security of the countries (Dai and Li, 2013). Therefore, optimal usage of water and maintaining the existing water resources are necessary (Garg and Dadhich, 2014). Cultivation pattern has a key role in water management and it can be determined that what level of cultivation and how much water could be allocated to what crops in order to receive more profit, water storage and providing food security (Niu et al., 2016; Zeng et al., 2010).

Amount of cultivation of agricultural products must be determine regarding the existing resources, price of products, cost of production, yield of production, demand of the country and correct policies. Also, in order to supply countries fundamental

demands, choosing agronomical and horticultural productions must be based on the existing infrastructures, social-economic issues and level of technologies maintaining basic resources of production.

Jiang et al. (2016) have developed PBREOP model in west north of China. Results of optimization through this model led to 15% increase in profit. In addition, analyzing scenarios including five level of water allocation has shown that allocation of water could be decreased to 23% without declining profit. Mushtaq and Moghaddasi (2011) have investigated the effect of deficit irrigation to respond climate changes and environmental water demands in Murray-Darling basin of Australia. Three scenarios have been compared in this research: Optimization with full irrigation, optimization with deficit irrigation and deficit irrigation without optimization. Results have shown that deficit irrigation is effective to maximize gross yield and increase water consumption efficiency.

About four decades ago, Qazvin plain was one of the five fertile plains of Iran. Agriculture in this plain has supposed to become one of the industrial poles of the country, but it has become the main occupation of people living in the region. Exactly for this reason and while some of the surface waters of the area are transported through the construction of the Taleghan Dam to supply Tehran's drinking water. The utilization of Qazvin plain surface water and groundwater resources has been expanded to the extent. According to the existing reports, it is far beyond the capacity of the water system. The aquifers are progressing towards irreversible degradation. At present, usage of groundwater in the whole consuming sectors is estimated to be 1.8 billion cubic meters, while the authentic limit to use the water resources of Qazvin province is 880 million cubic meters (Shokoohi et al., 2014). In order to resolve the water crisis in Qazvin plain, revise of crop pattern and water management is required especially in the agricultural sector (Shokoohi, 2012; RamezaniEtedali et al., 2015).

Using a single-objective mathematical model, Shirdeli and Dastavar (2014) have dealt with optimization of crop patterns of the lands in the down part of BoinZahra (Qazvin, Iran) dam. The aim of this study had been to maximize the income of farmers in this area and they developed four 5-year programs for future analysis. The results of their study showed that there is a possibility for a significant increase in farmers' income in this area. Also, farmers' income increases during the second to fourth 5-year program will be 20, 44.7 and 50.3% respectively in compare with the first 5-year period. Upon completion of the last five-year program, water productivity will increase from 50 to 77%.

Yousefdost et al. (2016) turned to optimization for managing the water resources of the Taleghan dam and determining the maximum yield of crop production in Qazvin Plain under different climate conditions. One of the most important results of the research is to determine the new cultivar pattern, so that both objectives which are providing the farmer's profit and allocation of water resources to the other needs by its saving, become available. According to the presented results, 2.81, 2.62, 1.34 and 1.355% profit have obtained for farmers with the new culture pattern in hot and dry, dry, normal, and wet weather situation, respectively.

Parhizkari et al. (2016) have considered three methods of irrigation including full irrigation, 5% deficit irrigation and 10% deficit irrigation for studying the effect of deficit irrigation on crop pattern and farmers profit in Qazvin. The results of using deficit irrigation method have showed that by applying this strategy under different scenarios, it is possible to reduce the area under cultivation of products that are less

economic (wheat and water barley) and increase the area under cultivation of those products with more gross profit through the saved volume of water.

The plan of water allocation in irrigation and drainage networks is one of the main issues of optimal management of economic efficiency of water. Therefore, a model that could assess the plan of water allocation in the constraints and ruled conditions in the network, would enjoy of a great importance. Mathematical models and planning methods can help planners and managers in decision making. In previous studies, deficit irrigation has been dealt with, but deficit irrigation and decreasing or increasing the area under cultivation has not been studied at the same time. The purpose of current study is to manage the pattern of cultivation to achieve higher income with less water consumption in Qazvin plain.

Materials and methods

The case study

The area of Qazvin province is 15820 km² and is in central sphere of Iran between 48°44' to 50°51' E length and 35°24' to 36° to 36°48' N latitude (QPG, 2016). Qazvin plain is belonging the Central Salt Lake basin. This area has the highest level of cropping of various types of products in the plains of this basin (Shokoohi et al., 2014). Qazvin Plain with an area of 440 thousand ha is in the central plateau of Iran and has semi-arid climates and hot summer and relatively cold winters. The main aim of constructing Taleghan dam is to provide agricultural water in Qazvin Plain, to provide drinking water to Tehran and Karaj, to artificially recharge Qazvin aquifer and to control the seasonal floods of the Taleghan River. *Figure 1* shows the location of the studied area (Yousefdost et al., 2016).

The required statistics were obtained from statistics of the Ministry of Agricultural Jihad or from the Organization of Agricultural Jihad of Qazvin province. *Table 1* shows the current level of cultivation area, income, maximum yield, sensitivity coefficients (K_y), Crop Evapotranspiration (ET_c), water requirement and proportion of areas under cultivation of important products in the studied area in the crop year 2015. The K_y and ET_c in the study area suggested by Taftah et al. (2014) were used. Monthly weather data for three years (2012–2015), including maximal and minimal temperature and monthly average rainfall were collected from Feizabad (36°8' N, 50°15' E, 1240 m) station in this study area and they are shown in *Figure 2*.

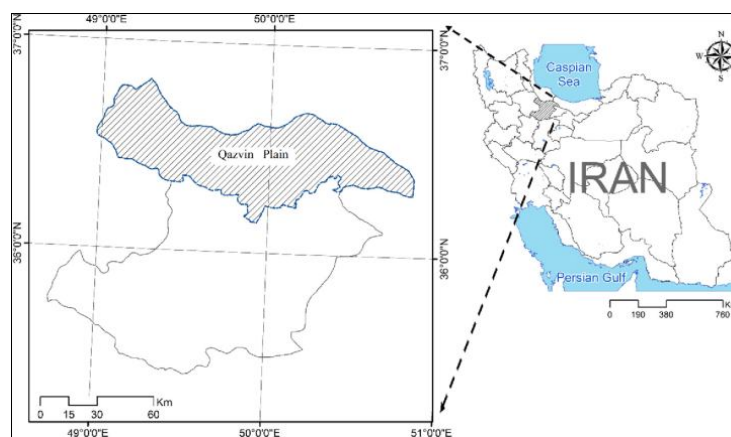


Figure 1. Location of the study area in Iran map

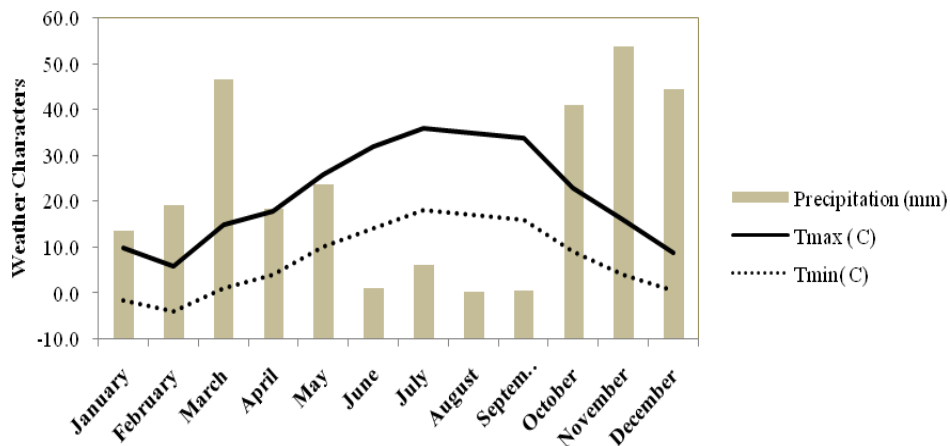


Figure 2. Distribution of monthly temperatures and monthly average rainfall in the Qazvin District over 3 years (2012–2015)

Table 1. Basic data used in optimization model based on the year 2015

Crop	Area ha	Yield kg/ha	Marketing price USD/Kg	Income USD	K _y	ET _c mm	Water requirement MCM	Area under cultivation ratio
Wheat	18118	5069	0.32	828	0.79	542.0	9.82	0.42
Barely	9170	4417	0.30	573	0.79	400.7	3.67	0.21
Seed corn	892.9	9604	0.36	1560	0.92	760.0	0.68	0.02
Sugar beet	1650	54109	0.61	1307	0.94	1038.4	1.71	0.04
Tomato	630	48317	0.91	1330	0.88	1092.1	0.69	0.01
Alfalfa	5094	17672	0.19	1826	1.00	1336	6.81	0.12
Maize	7850	51443	0.05	1077	0.96	696	5.46	0.18
Total	43404.9			8502			28.84	

Defining the model and its dependent variables

The method of linear programming modeling which involves the parameters of crop pattern designing including crop water requirement, cultivation frequency and etc., requires designing a model that initially consists of three principles, i.e. objective or objectives, variables, constraints, and limitations, also the relationship between these principles must be defined in a matrix called the planning matrix. In the framework of the program’s objective function and by using a linear planning approach, a designer can follow many lateral objectives within the framework of variables and constraints, in addition to what is considered as the ultimate objective.

In current study, the maximum income in thousand USD was considered as the objective function (Eq. 1). The objective function was the most economic benefit with considering the decline in yield caused by water shortage, which is presented in the following relation (Eqs. 1-2):

$$Max Z : \sum_{i=1}^n \alpha_i \cdot A_i (P_i \cdot Y_i - C_i - Q \cdot C_w) \quad (Eq.1)$$

$$Y_i = Y_i^{\max} \left[1 - k_y \left(1 - \frac{W_i}{ET_i} \right) \right] \quad (\text{Eq.2})$$

where Z : the objective function, α_i : the percentage of the surface area under cultivation for each product, i : the product, A_i : the total area of the lands (Ha), P_i : marketing price of each kg of product (USD), Y_i : the product yield function (Eq. 2), $Y_{i\max}$: Maximum product yield (kg), K_y : Coefficient of the crop yield response to water deficit, W_i : the amount of water entered into the earth (mm), ET_i : the water demand of the product (mm), Q : water used (liter), C_w : Cost of each litre of water (USD), C_i : Cost of production per product (USD). Applying the constraints was done with the following assumptions:

1. Wheat is a strategic product and the least supposed culture is 30%.
2. Products which are below 5% in the current state are determined at least 1% and utmost 15%. The basis for selection 15% is based on the capability to crop yields in the region.
3. Products whose cultivation in the region is less than 20% and are cultivated after strategic crops, their minimum cultivation is as the same as the current cultivation and their maximum area under cultivation is selected 2 times more than the current cultivation.
4. Percent of the present area under cultivation of barely is 21%. Considering the importance of this crop, it is chosen at least 15% and utmost 30%.
5. Total cultivation area was considered as a limitation in different scenarios.
6. The allocated water was considered as water constraint in the five water scenarios.

The crop production function is a function of the relative yield of the product according to the evapotranspiration of the crop. The researchers have presented the K_y of the products in general after analyzing experimental data. In current research, *Equation 3*, which is based on the relative reduction of the product and the relative lack of evapotranspiration, was used to investigate the effect of the reduced water allocated to the crop yield (Doorenbos and Kassam, 1979).

$$1 - \frac{y_i}{y_{i\max}} = k_y \left(1 - \frac{ET_a}{ET_m} \right) \quad (\text{Eq.3})$$

where Y_i : the product yield function, $Y_{i\max}$: Maximum product yield (kg), $\frac{y_i}{y_{i\max}}$:

Actual yield ratio to maximum yield (relative yield), $\frac{ET_a}{ET_m}$: Actual evapotranspiration

to the maximum evapotranspiration of the crop (mm), k_y : Coefficient of the crop yield response to water deficit.

The current study was optimized considering five irrigation scenarios including I_1 , I_2 , I_3 , I_4 and I_5 (regarding water allocation of 100, 90, 80, 70 and 65% of crop water requirement, respectively) and three different levels of cultivation including S_1 , S_2 and S_3 (respectively equivalent to the existing cultivated area, 10% increase in cultivated

area and 10% decrease in cultivated area compared to the current situation) and the optimal amount of cropping levels were estimated for each crop pattern of the products. The total cultivation area and water used of fifteen defined scenarios are presented in *Figure 3*.

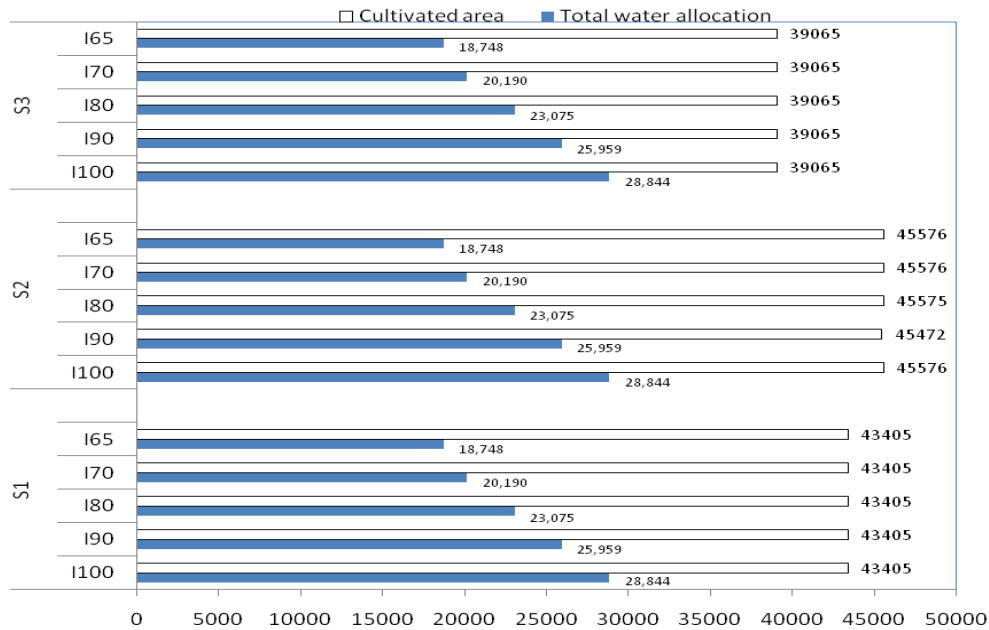


Figure 3. Cultivated area and total water allocated to each scenario in Qazvin District (the amount of allocated water was calculated based on crop evapotranspiration)

Since farmers generally pay attention to the economic yield of crop cultivation, the economic productivity index (WP_s) has also been studied and calculated in this research from different scenarios. The WP_s index was defined and calculated based on thousand USD per cubic meter of crop water requirement as follows (Eq. 4):

$$WP_s = \frac{(\$ \text{ kg}^{-1}) (\text{kg ha}^{-1})}{ET(\text{m}^3 \text{ha}^{-1})} \quad (\text{Eq.4})$$

where \$ has been considered equal to thousand USD.

Results

Relative yield of the products in different water allocations is the most important of water allocation modeling. In the case that the water allocated to the crop is equal to the maximum water requirement of the crop, the relative yield is equal to one. Also, if the water allocated is less than the crop water requirement, its relative yield will be less than one. In *Figure 4*, the relative yield of the products is shown in various water scenarios. The economic level of products yield is 0.7 (Papamichi et al., 2008); therefore, in I_5 , the estimated yield for most products is at the level of 0.7, and for the tomato, alfalfa and sugar beet is 0.69, 0.68 and 0.69 respectively, these values are less than those of their economical level. This means that the cultivation of these products in

these water conditions is not economic due to high water requirements and decrease in yield. The relative yield of different crops at all cultivation scenarios has been reduced by decreasing the amount of water allocated (*Fig. 5*). The main output of the model, which is related to the objective function of the model, is the income and the area under cultivation ratio for each product. Total income for different irrigation and cultivations scenarios as well as the optimal cultivation ratio is presented in *Table 2*. The income of I_1 at S_1 cultivation level was less than S_3 with income of 91 and 96 thousand USD respectively, while by increasing the level under cultivation (S_2) the amount of income (78 thousand USD) fell down.

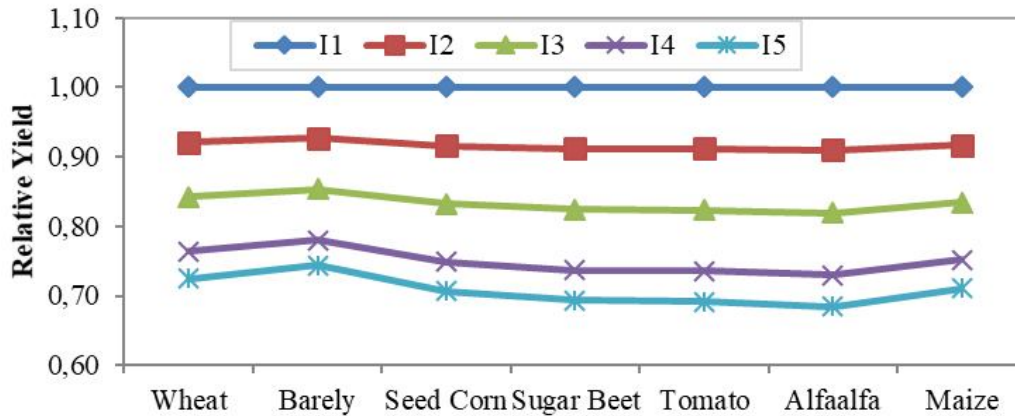


Figure 4. Relative yield of crops in different water scenarios

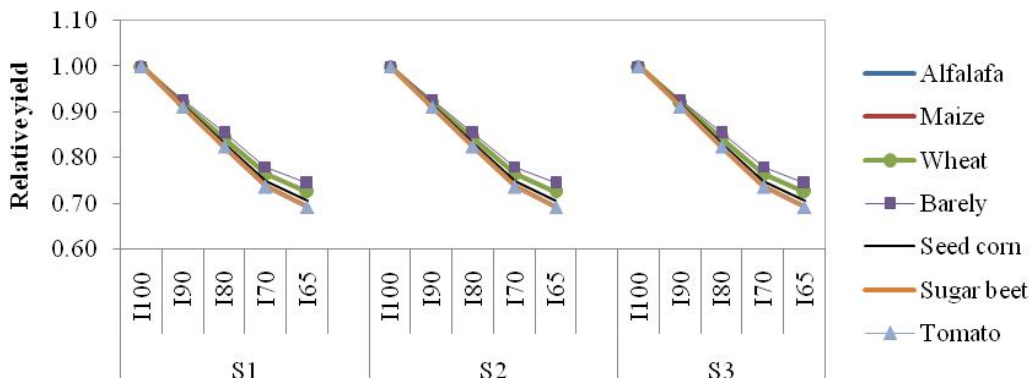


Figure 5. Relative yield of crops in different water scenarios and cultivations

The percentage of optimal cultivation area for products with higher incomes in the S_3 is in highest so far as the water allocated is not limited. The highest cultivation areas were for alfalfa, tomato and sugar beet cultivars that are 16.20, 4.70 and 2.40%, respectively in S_3 and the lowest in were 1₂, 1 in S_2 . The highest ratio of optimum cultivation area for seed corn was found to be 7% in S_1 and the lowest was observed at S_2 , i.e. 1%. However, in S_2 , products with high water consumption are at the minimum of the specified constraint domain and strategic products such as wheat and barley are at the maximum specified range in the model. In wheat and barley, the highest culture percentage was observed in S_2 , i.e. 47.00% and 30.00%, respectively.

Table 2. Comparison of the average total income for different irrigation and the cultivars scenarios and the optimal percentage of crop cultivation

		Income USD*10 ³	Optimized area under cultivation %						
			Wheat	Barely	Seed corn	Sugar beet	Tomato	Alfalfa	Maize
S ₁	I ₁	91bc	30.60	25.70	7.00	1.80	1.00	12.00	22.00
	I ₂	90c	30.30	26.00	3.00	2.60	1.10	12.00	25.40
	I ₃	75e	31.75	27.00	3.50	2.20	2.40	12.15	21.15
	I ₄	66hi	35.70	24.10	2.70	3.00	1.30	12.10	21.10
	I ₅	61j	30.70	29.00	2.75	3.20	1.90	12.75	19.80
S ₂	I ₁	78e	43.00	30.00	1.10	1.00	1.00	12.10	18.00
	I ₂	75e	40.75	30.00	1.00	1.00	1.00	12.00	20.25
	I ₃	63ij	44.00	30.00	1.00	1.00	1.00	12.20	21.00
	I ₄	56k	43.50	28.50	1.00	1.00	1.00	12.00	18.00
	I ₅	52l	42.70	29.00	1.10	1.00	1.00	12.50	18.30
S ₃	I ₁	96a	31.80	15.00	1.70	2.40	4.70	16.20	18.30
	I ₂	93ab	30.40	15.00	1.00	5.30	3.60	15.00	19.70
	I ₃	84d	27.65	16.20	2.20	3.70	4.60	15.10	20.60
	I ₄	71f	29.60	15.75	2.00	3.20	4.35	15.80	19.35
	I ₅	67g	30.70	15.00	1.00	2.90	4.50	15.80	20.10

The letters are used to determine the results of scenario adaptation

Figure 6a shows the final income per different levels of area under cultivation for each irrigation scenario and Figure 6b shows the final income per different levels of irrigation for each area under cultivation. In Section A, we can see that the difference between income in I₁ and I₂ is insignificant subtle and income has fallen from I₁ to I₅ totally.

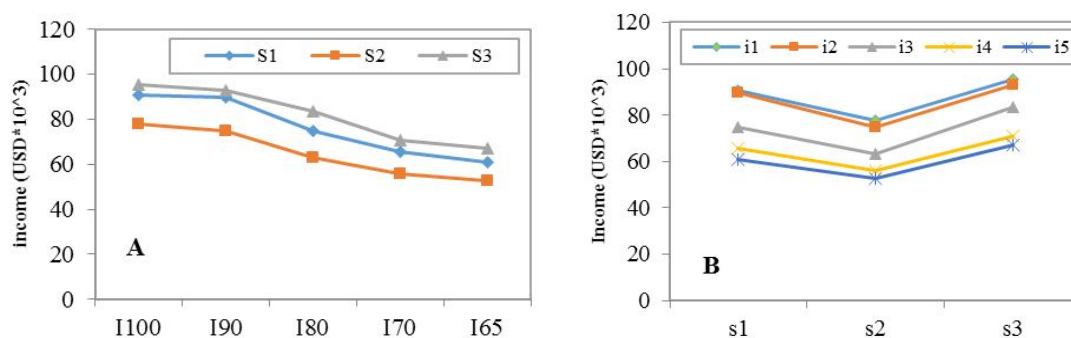


Figure 6. The final income in (a) cultivar scenarios, (b) irrigation scenarios

Table 3 shows binary comparison matrix in different products related to the total income. Studies showed that the total income (based on million Rials) has positive correlation with all products except barley (with coefficient equal to -0.072) and they were 0.011, 0.387, 0.449, 0.425, 0.885 and 0.829 for wheat, seed corn, beet, tomato, alfalfa, respectively. Total income has significant correlation with all products except wheat and barley. The highest correlation of total income was with alfalfa, i.e. 0.855.

Table 3. Binary comparison matrix in different scenarios of area under cultivation and water allocation

	TR	MZ	AF	TO	SB	CR	BL	WT
WT: Wheat	0.011	0.214	0.129	-0.289	-0.400	-0.383	0.550	1
BL: Barely	-0.072	0.314	-0.246	-0.465	-0.473	0.267	1	
CR: Seed corn	0.387	0.583	0.060	-0.080	0.021	1		
SB: Sugar beet	0.449	0.136	0.433	0.065	1			
TO: Tomato	0.425	-0.130	0.423	1				
AF: Alfalfa	0.855	0.573	1					
MZ: Maize	0.829	1						
TR: Total income	1							

Figure 7 shows the required water for each crop and total income in a diagram. In I_1S_2 the required water for wheat, barley and alfalfa were increased in compare with I_1S_1 which shows allocating more area under cultivation for these three productions in this scenario. It can be observed that, in this section, income has decreased. This issue reminds two results: first that despite high importance of strategic products, they are not economic necessarily and second that more water consumption and high cultivation area necessarily do not lead to more income. In I_1S_3 water requirement has increased in tomato, beet and Alfalfa which shows allocating more area under cultivation to these three productions in compare with the conditions I_1S_1 and I_2S_2 . Income increase has observed in this section.

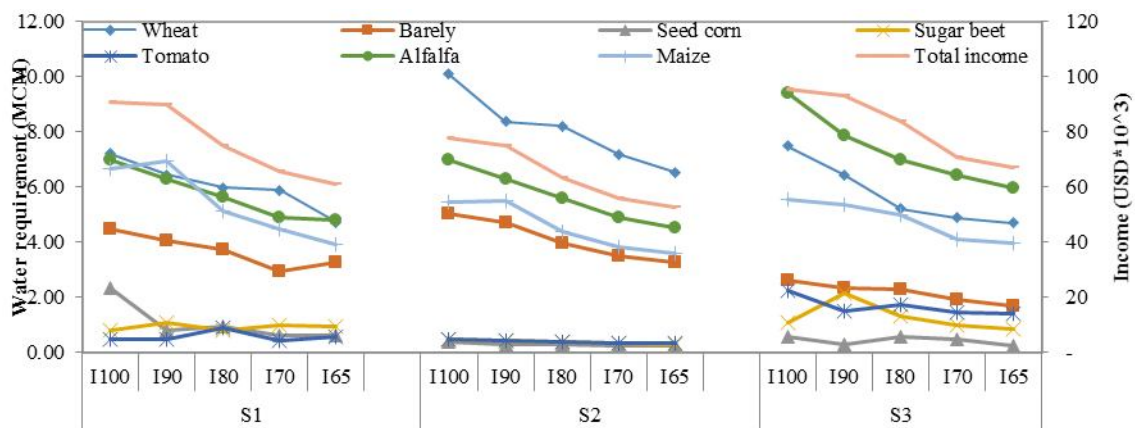


Figure 7. Water requirement by crops and total income

In Figure 8, economic productivity and total income has been presented in all scenarios. Economic productivity was calculated in different scenarios from 2.7 to 3.6 thousand USD in cubic meter. In addition of maintaining the income, I_2 has averagely increased economic productivity in different levels, i.e. 0.43 thousand USD per cubic meter water. Economic productivity is in the minimum level in S_2 . S_3 obtained more income while its water consumption was equal to S_1 and S_2 . Economic productivity was more observed in S_3 . Generally, water allocation to products with high income in S_3 has increased income.

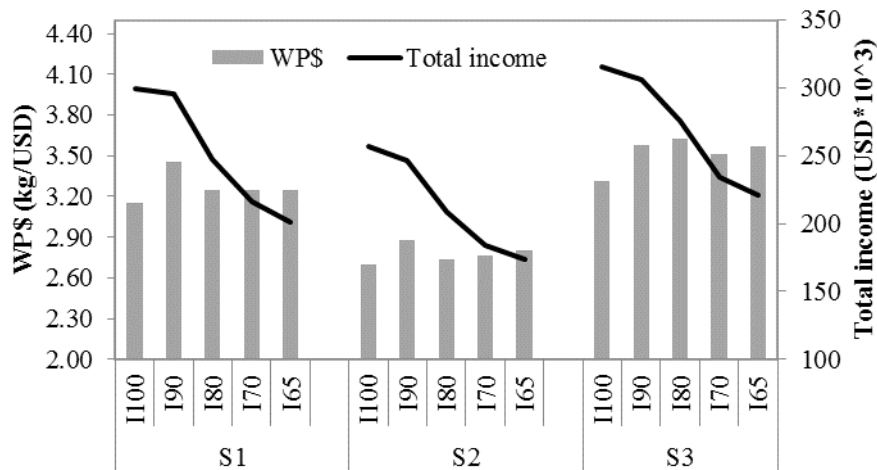


Figure 8. Total income and economic productivity by scenarios

Discussion

Using study results, we can now answer the question which of the strategies ‘increasing cultivated area’ or ‘reducing cultivated area’ will result in the highest WP or economic benefit. Reducing the cultivated area will result in higher water productivity. However, it is seen that even a decrease in the area under cultivation and the optimal use of water at a lower level have resulted in an increase of 5.3% of income. Lalezari et al. (2016) reported that the result of applying deficit irrigation plan and increasing economic profit plan at the same time for allocating water and land shows providing more water requirement and decreasing area under cultivation is a more proper strategy for managing water in agriculture in drought condition.

With increasing the cultivation area, since the allocation of water is constant or less than the existing conditions, the model has optimized the high water-consuming products such as tomato and beet at the minimum ratio of the defined area for scenario and developed cultivation area of strategic products such as wheat and barley toward higher bound of cultivation range. The results of this study are not in line with the results of the studies conducted by Jafarzadeh et al. (2016) and Alizadeh et al. (2012) as all concluded that optimization leads to high levels of cultivation for strategic products in the region. It is recommended that greenhouse products and products that can be cultivated in the greenhouse become transferred to the greenhouse and the stored water from removing these products become allocated to strategic products.

I₂, we can save 10% of water consumption with only 1.2% reduction in income. A study in the West of the Palestine Region revealed that optimal cultivation pattern reduces water consumption by as much as 10%, which contributes to the sustainability of water resources (Nazer et al., 2010). In addition, as compared to the previously published results (García-Vila and Fereres, 2012; Zhanget al., 2014), objective function could not only have a feasible computation, but also well consider the benefit coordination between different water conditions and the various cultivated area in the district.

Results showed that it is possible to have more income with lower area and even lower water allocation by managing the cultivation area.

Conclusion

Crop pattern is supposed to be one the most important effective components in management of water resources. This study has determined an optimal Crop pattern in Qazvin plain in order to decrease water allocation and increase or decrease the area under cultivation. I_4 and I_5 are not recommended due to decrease in income and yield. In order of decrease in existing water and reaching to I_5 amount, with regard to economic limit, cultivating of high water consuming products such as tomato, beet and alfalfa is not recommended. According to the results if there were enough cultivation area, Model recommend higher area for strategic products. Also with regard to the higher cultivation area and decrease in water allocation related to the current situation and due to high water demand of crops such as beet, alfalfa and corn, the cultivation area of these products were decreased. Unlike, when the cultivation area is limited constrain, the model would increase area under cultivation of economic products with higher income and allocate water to them. So it has been observed that income in S_2 and S_3 has been decreased and increased in compare with S_1 , respectively. In addition of retaining income, I_2 increased economic productivity in different levels, i.e. 0.82 million Rials per cubic meter water averagely. These results could decrease lots of tests and it could be used as a certain criterion for the future research works and management of crop pattern.

REFERENCES

- [1] Alizadeh, A., Majidi, N., Ghorbani, M., Mohammadian, F. (2012): Cropping pattern optimization with target balancing of ground water resources: case study of Mashhad-Chenaran plain, Iran. – Iranian Journal of Irrigation and Drainage 6: 55-68 (in Persian).
- [2] Dai, Z. Y., Li, Y. P. (2013): A multistage irrigation water allocation model for agricultural land-use planning under uncertainty. – Agricultural Water Management 129: 69-79.
- [3] Doorenbos, J., Kassam, A. H. (1979): Yield response to water. – Irrigation and Drainage Paper 33: pp. 257.
- [4] García-Vila, M., Fereres, E. (2012): Combining the simulation crop model AquaCrop with an economic model for the optimization of irrigation management at farm level. – European Journal of Agronomy 36: 21-31.
- [5] Garg, N. K., Dadhich, S. M. (2014): Integrated non-linear model for optimal cropping pattern and irrigation scheduling under deficit irrigation. – Agricultural Water Management 140: 1-13.
- [6] Jafarzadeh, A., Khaseii, A., Shahidi, A. (2016): Designing a multi-objective decision-making model to determine optimal crop pattern influenced by climate change phenomenon (case study: Birjand plain). – Iranian Journal of Soil and Water Research 47: 849-859. (In Persian). doi: 10.22059/ijswr.2016.59991.
- [7] Jiang, Y., XU, X., Huang, Q., Huo, Z., Huang, G. (2016): Optimizing regional irrigation water use by integrating a two-level optimization model and an agro-hydrological model. – Agricultural Water Management 178: 76-88.
- [8] Kang, S. Z., Hao, X. M., Du, T. S., Tong, L., Su, X. L., Lu, H. N., Li, X. L., Huo, Z. L., Li, S. E., Ding, R. S.(2016): Improving agricultural water productivity to ensure food security in China under changing environment: from research to practice. – Agricultural Water Management. <http://dx.doi.org/10.1016/j.agwat.2016.05.007>.
- [9] Lalehzari, R., Nasab, S. B., Moazed, H., Haghghi, A. (2016): Multiobjective management of water allocation to sustainable irrigation planning and optimal cropping

- pattern. – *Journal of Irrigation and Drainage Engineering*. DOI: 10.1061/(ASCE)IR.1943-4774.0000933.
- [10] Mancosu, N., Snyder, R. L., Kyriakakis, G., Spano, D. (2015): Water scarcity and future challenges for food production. – *Water* 7: 975-992.
- [11] Mushtaq, S., Moghaddasi, M. (2011): Evaluating the potentials of deficit irrigation as an adaptive response to climate change and environmental demand. – *Environmental Science and Policy, Australia College of Agriculture* 14: 1139-1150.
- [12] Nazer, W., Tilmant, D., Mimi, Z. (2010): Optimizing irrigation water use in the West Bank Palestine. – *Agricultural Water Management* 97: 339-345.
- [13] Niu, G., Li, Y. P., Huang, G. H., Liu, J., Fan, Y. R. (2016): Crop planning and water resource allocation for sustainable development of an irrigation region in China under multiple uncertainties. – *Agricultural Water Management* 166: 53-69.
- [14] Parhizkari, A., Saboohi, M., Ahmadpoor, M., Badi, H. (2016): Assessment of the effects of deficit irrigation and decrease in water allocation on agricultural sector production in Qazvin Province. – *Journal of Water Research in Agriculture* 30(2): 173-185 (in Persian). DOI: 10.22092/jwra.2016.106642.
- [15] Papamichail, D. M., Georgiou, P. E., Vougioukas, S. G. (2008): Optimal model irrigation reservoir operation and simultaneous multi-crop cultivation area selection using single reservoir operation and simulated annealing. – *Journal of Irrigation and Drainage* 55: 129-144.
- [16] Programme, W. W. A. (2012): *The United Nations World Water Development Report 4: Managing Water under Uncertainty and Risk*. – UNESCO, Paris.
- [17] Qazvin Province Governor (QPG) (2016). <http://ostan-qz.ir>.
- [18] RamezaniEtedali, H., Ahmadaali, K., Liaghat, A., Parsinejad, M., Tavakkoli, A. R., Ababaei, B. (2015): Optimum water allocation between irrigated and rain fed lands in different climatic conditions. – *Biological Forum - An International Journal* 7: 1556-1567.
- [19] Shirdeli, A., Dastvar, S. (2014): An optimization technique for cropping patterns and land consolidation: A case study for irrigation network. – *Management Science Letters* 4: 2087-2092.
- [20] Shokoohi, A. (2012): Comparison of SPI and RDI in drought analysis in local scale with emphasizing on agricultural drought (Case study: Qazvin and Takestan). – *Iranian of Irrigation & Water Engineering* 9: 111-122. (In Persian).
- [21] Shokoohi, A. R., Razinei, T., Daneshkar Arasteh, P. (2014): On the effects of climate change and global warming on water resources in Iran. – *International Bulletin of Water Resources & Development* 2: 1-9.
- [22] Yosefdost, I., Mohammadrezapour, O., Ebrahimi, M. (2016): Applying genetic algorithms in determining optimal cropping pattern in different weather conditions in Qazvin Plain. – *Journal of Water Research in Agriculture* 30: 317-331 (in Persian). DOI: 10.22092/jwra.2016.107153.
- [23] Zhang, L., Li, C. Y. (2014): An inexact two-stage water resources allocation model for sustainable development and management under uncertainty. – *Water Resour. Manage.* 28: 3161-3178.
- [24] Zeng, X. T., Kang, S. Z., Li, F. S., Zhang, L., Guo, P. (2010): Fuzzy multi-objective linear programming applying to crop area planning. – *Agricultural Water Management* 98: 134-142.

EFFECT OF TEMPERATURE ON CLOSTRIDIUM SP. STRAIN PXL2 AND REMOVAL OF ARSENIC AND NITRATE FROM GROUNDWATER

LI, B. H.^{1,2} – PAN, X. L.^{2,3*}

¹*Xinjiang Institute of Engineering, Urumqi 830091, China*

²*Laboratory of Environmental Pollution and Bioremediation, Xinjiang Institute of Ecology and Geography, Chinese Academy of Science, Urumqi 830011, China*

³*College of Environment, Zhejiang University of Technology, Hangzhou 310014, China*

*Corresponding author

e-mail: panxl@zjut.edu.cn; phone: +86-0571-88871577

(Received 5th Nov 2018 ; accepted 4th Feb 2019)

Abstract. Anaerobic Fe(II) Oxidation DeNitrifiers (AFODN) have recently been proposed as an option to treat groundwater contaminated by arsenic and nitrates through oxidation of microbiological nitrate-dependent ferrous oxidation. In previous studies, a pure strain of AFODN bacteria, Clostridium sp. Strain PXL2, was isolated from anoxic activated sludge. In this paper, the growth curve of strain PXL2 is studied under different temperature conditions, along with its Fe(II) oxidation, nitrate reduction, and arsenic removal efficiency. The results showed that at 5°C, the growth of the strain was significantly inhibited. At 15°C, the metabolic rate of growth, denitrification and Fe (II) oxidation rate were optimum and the total arsenic removal rate was high at 51.1%. The strain PXL2 can remove nitrate and arsenic contamination at the same time under normal groundwater temperature conditions. These analyses provide the necessary data to support the application of AFODN in engineering projects.

Keywords: *denitrification, iron oxide minerals, heavy metal, bioremediation, synchronize*

Introduction

Section title Arsenic contamination in water bodies due to the release of untreated industrial wastewaters has been on the rise due to excessive mining and smelting. The prevalence of arsenic and its compound in water bodies grows more serious every day and currently threatens the lives of more than 140 million people around the world (Karim, 2000; Smedley and Kinniburgh, 2002; Singh et al., 2007; Song et al., 2017). In China alone, it is estimated that more than 3 million people are exposed to elevated levels of As (Sun, 2004). New endemic areas have been progressively identified, such as the Huhot Basins in Inner Mongolia (Guo et al., 2001) and the Datong Basin in Shanxi Province (Wang et al., 2007) since the first case of chronic As poisoning was observed in the Xinjiang autonomous region in 1980 (Wang and Huang, 1994). Populations in affected areas suffer from melanosis, keratosis in their palms and soles, gangrene, and even skin cancer.

Among the numerous reduction processes of the soluble matrix, NO₃⁻ reduction plays a key role in the nitrogen cycle and has important implications for agriculture, environmental health, and public health (Shen et al., 2010; Xing et al., 2010). Natural nitrate attenuation is driven by microbial enzyme reduction, although, the abiotic reduction of nitrate also occurs under some extreme conditions (Hansen et al., 1996; Ottley et al., 1997; Zhang et al., 2014). Oxidation of microbiological nitrate-dependent Fe(II) to Fe(III) has been recently described with ferrous iron as the only electron donor

and with nitrate as the electron acceptor (Straub et al., 1996; Hafenbradl et al., 1996; Straub et al., 2004; Weber et al., 2006; Chakraborty et al., 2011; Li et al., 2015). These microorganisms are called the Anaerobic Fe(II) Oxidation DeNitrifiers (AFODN) (Wu et al., 2010). Enrichments of AFODN were successfully established with a variety of marine, brackish, or freshwater sediment samples (Kappler, 2005). The metabolism of AFODN is affected by many external factors (Chen et al., 2018). The major environmental factors include temperature, salinity, carbon source, pH, dissolved oxygen, and iron source. The oxidation of ferrous oxide directly affects the removal efficiency of heavy metals. To achieve the highest removal efficiency of nitrate and heavy metals and the best governance effect, it is necessary to provide optimum conditions for the ferrous oxidation and nitrate reduction by AFODN, which will help activate the microorganisms and lay the foundation for its application.

The response of different microorganisms to heavy metals is dependent on their physiologies (Li, 2017). Various treatment technologies to mitigate the severe problem of arsenic tainted groundwater have been extensively studied during last few decades (Hu et al., 2015; Niazi et al., 2018; Cui et al., 2018). Previous studies showed that low concentrations of arsenic promoted the growth of heterotrophic microorganisms. However, the growth of heterotrophic microorganisms was inhibited with the increase of As(III) concentration. While under the same exogenous arsenic concentration, it has a stronger inhibitory effect on autotrophic microorganisms than on heterotrophic microorganisms.

In this study, a novel AFODN species, the Clostridium sp. strain PXL2, was isolated from anaerobic activated sludge (Li et al., 2016), and its growth curve was studied under different temperature conditions. Fe(II) oxidation, nitrate reduction, and arsenic removal efficiency by strain PXL2 were observed under different temperature conditions. The resistance of strain PXL2 to arsenic, as well as its ability to oxidize microbiological nitrate-dependent Fe(II) to Fe(III) in an arsenic contaminated environment made it ideal for application in practical engineering. These analyses can provide the data necessary to support the application of AFODN in engineering projects.

Experimental materials and methods

An anaerobic nitrate-reducing Fe(II) oxidizing bacteria *C. freundii* PXL2 could synchronously remove As(III) and nitrate from water, associated with Fe(II) oxidation. Batch experiments were conducted to study the effect of temperature on ferrous oxidation and denitrification of PXL2 strains. SEM-EDS analyzed the morphologies under different temperature conditions. The removal of arsenic under different temperature conditions was studied at the same time. The selection medium (Li et al., 2014) was used as the culture medium with three repetitions for each sample.

Three tubes of mediums inoculated with AFODN culture were set to determine the efficiency of Fe(II) oxidation and nitrate reduction. The whole experiment was carried out in the G250 anaerobic, insuring microbial metabolism in the absence of oxygen. The amount of inoculation was 4% (vol/vol). All the tubes were sampled every 24 hours to determine the nitrate, nitrite, and Fe(II) concentrations. The effect of temperature on the denitrification of AFODN was performed. The initial concentrations of $\text{FeCl}_2 \cdot 4\text{H}_2\text{O}$ and KNO_3 were 1 mM and 20 mM, respectively.

Arsenic pollution was simulated by NaAsO₂ to study the removal of arsenic by strain PXL2 at different temperatures. The initial concentration of As (III) was 60-70 μM (about 5 mg L⁻¹). To improve arsenic removal rate, the experimental analysis was extended to seven days. In addition to the analysis of total arsenic concentrations, the concentrations of As (III) and As (V) were also analyzed separately.

Concentrations of nitrate, nitrite, and Fe(II) were measured by a spectrophotometer (DU 800 UV/Vis Spectrophotometer, Beckman Coulter, United States). N-(α-naphthyl)-ethylenediamine spectrophotometry was used to determine the concentrations of nitrite at 540 nm (Geng et al., 1996). Nitrate concentration was measured by UV spectrophotometry at 220 nm and 275 nm (Veena and Narayana, 2009). Phenanthroline spectrophotometry was used to determine Fe(II) concentration at 510 nm (Gendel and Lahav, 2008). For the modified phenanthroline assay, the samples were mixed with 40 mM sulfamic acid (pH approximately 1.8) instead of 25 vol% HCl because the sulfamic acid reacted rapidly with nitrite and prevented Fe(II) oxidation by the nitrite at an acidic pH (Klueglein and Kappler, 2013). All the samples were measured within 2 h after sampling. Total As concentration was measured by an AFS-8X atomic fluorescent spectrophotometer (Jitian Instruments Co., Ltd., Beijing, China). Ten ml of 5% thiourea and 5% vitamin C mixture and 2.5 ml of concentrated HCl were added to 50 ml of sample as As(V) reducing agent and stabilizer, respectively, and 2.0% (W/V) KBH₄ and 0.5% (W/V) KOH were used to transform the ion state As(III) to AsH₃. The flow carrier of samples was 5% (V/V) HCl. The original As(III) concentration in the water samples was measured by the same method without the addition of the 5% thiourea and 5% vitamin C mixture. Microbial morphology was observed by a Scanning Electron Microscope (SEM) (Zeiss Super 55VP, Germany) equipped with an energy dispersive X-ray (EDX) (Bruker XFlash 5010, Germany) spectroscope. Accelerating voltages ranged from 15 to 35 kV.

All the experiments were performed in triplicates. Error bars on graphs show the standard deviation. The data were analyzed by analysis of variance and the means were compared by Tukey's test ($p < 0.05$).

Results and discussion

Growth curve of PXL2 strains at different temperatures

Temperature is a major environmental factor that affects the growth of microorganisms. The temperature at which fastest microbial growth and reproduction occur is called the optimum growth temperature. The reaction rate increases with rising temperature, however, increasing temperature leads to the destruction of intracellular enzymes and nucleic acids and eventually, microbial death. Lower temperatures decrease cellular metabolic activity and lead to slow growth. A temperature that is too low triggers the formation of intracellular ice crystals that would lead to dehydration of the microorganisms and ultimately microbial death.

Based on the variation of groundwater temperature in seasonal alternations, three temperature gradients of 5°C, 15°C and 30°C were selected to study the growth and reproduction ability of PXL2 strains at different temperatures. In the selected medium access, 2% bacterial suspension were placed in 5°C, 15°C, 30°C anaerobic environment static cultures for 72 h and the absorbance of the bacterial liquid was measured at 600 nm. The results are shown in *Figure 1*. As can be seen from the figure, 5°C obviously inhibited the growth of the strain, and the OD value of the 96 h bacterial

liquid continued to decline, indicating that the strain cannot complete its metabolism at 5°C. At 15°C, some microbes could not adapt to the low-temperature environment and died after about 8 h of inoculation, after which the OD of the bacteria began to increase, indicating that the surviving microbes gradually adapted to the ambient temperature and the growth and metabolism rates were consistent with those at 30°C. The growth, propagation and metabolism rate are the highest, the bacterial stagnation period is short, and the logarithmic phase can be quickly achieved at this temperature.

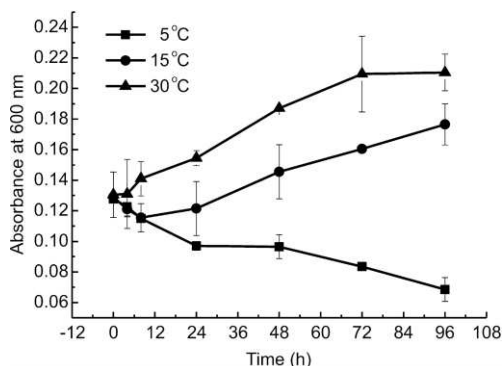


Figure 1. Growth curves of PXL2 strains at different temperatures

The optimal temperature for bacterial oxidization under ferrous anaerobic conditions is mainly related to the source of separation. Ehrenreich et al. (1994) isolated two strains of Chromatium strain L7 and Rhodobacter strain SW2 from the sediments of freshwater ditches whose optimal temperature range for growth was 18-20°C, and found that they did not thrive at temperatures above 24°C. Hafenbradl et al. (1996) isolated an extremely thermophilic archaeon named Ferroglobus Placidus gen. Sp. Nov. from a hydrothermal system. The optimal temperature range of this strain was 65°C to 95°C and its doubling time was about 2.8 h. The bacteria could not grow when the environment temperature was under 63°C or exceeded 96°C. AFODN strain HidR2, which was isolated from seabed sediments grew at temperatures of 5 to 40°C while the optimum temperature was 33°C (Benz et al., 1998). For two strains of photosynthetic non-ferrous anaerobic oxidative bacteria, strain N1 and strain N2, which were also separated from seafloor sediments, the optimal temperature ranges were similar to strain HidR2. The optimal growth temperature of strain N1 was 20-25°C, while the optimal growth temperature of strain N2 was 25-28°C (Straub et al., 1999). For AFODN strains BrG1 and BrG2, which were isolated from brackish water lakes and urban ditches, their growth rate at 15°C was greater than that at 28°C (Straub et al., 1996).

The strain PXL2 was isolated from the ditch sediments. It is a normal temperature living environment. So the strain PXL2 can grow at temperatures of 5 to 30°C. And the growth rate increases with temperature within the scope of the study.

Ferrous Oxidation and Nitrate Reduction of PXL2 Strains at Different Temperatures

The effect of temperature on the ferrous oxidation and nitrate reduction of AFODN is primarily due to the metabolic activity of the microorganism (Leahy and Colwell, 1990). The ferrous oxidation of AFODN and nitrate reduction is based on specific metabolic methods of microorganisms, and the catalytic effect of the enzyme is most efficient only within the optimum temperature range.

Figures 2A, B and C show the changes of Fe (II), NO₃⁻ and NO₂⁻ concentrations in the medium inoculated with PXL2 strains with time at different temperatures, respectively.

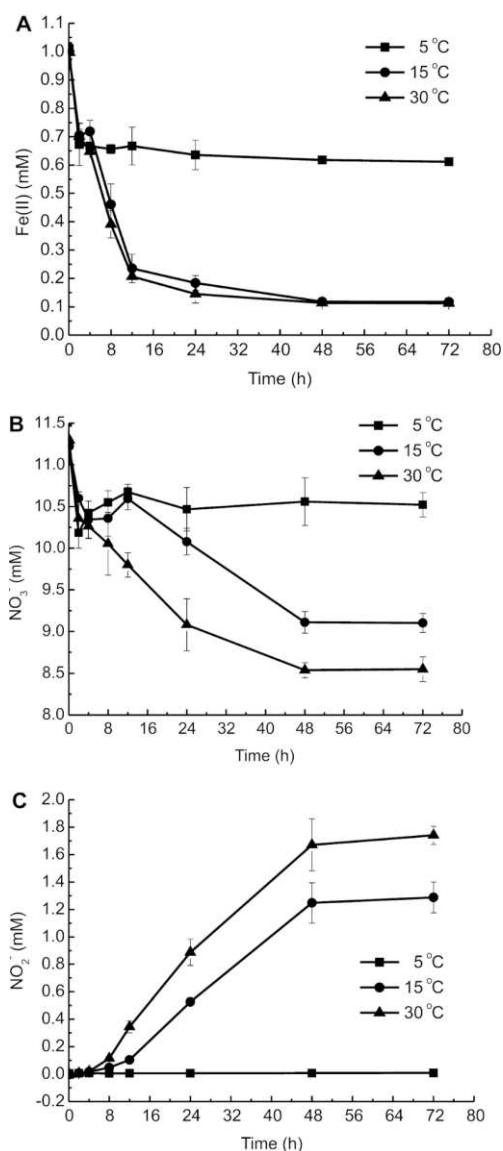


Figure 2. Time profile of Fe(II), NO₃⁻ and NO₂⁻ concentrations in the strain PXL2 culture at different temperatures

It can be seen from the figure that at the same oxidation rate, the temperature has little or no effect on the oxidation of ferrous ions within 4 h after inoculation. However, with time, the low temperature (5°C) sample significantly inhibits the oxidation of Fe (II). At 5°C, the ferrous oxidation rates were significantly lower than those at 15°C and 30°C. The oxidation rates of ferrous iron at 15°C and 30°C were almost the same as the initial Fe (II) concentration of 1 mM. About 90% of Fe (II) was oxidized after 24 h. Fe(II) oxidation was completed and nitrate degradation was also completed. As shown in Figure 2B, the nitrate degradation ability of PXL2 strains did not change significantly within 4 h after the completion of Fe (II) oxidation. However, with the duration of

inoculation, nitrate degradation ability was quite different. At 5°C, the biomass stagnated after 12 h of inoculation and no longer had the ability to degrade nitrate. The same degradation rate was maintained at 15°C and 30°C, but strain PXL2 completed 19.5% nitrate degradation at 15°C after 72 h of inoculation, While at 30°C, 24.8% nitrate degradation was completed, which is slightly higher than that at 15°C. The trend of accumulation of nitrite coincides with the trend of degradation of nitrate. Higher accumulation of nitrite, 1.7 mM, was observed in 30°C environments. The second highest concentration is the concentration of nitrite at 15°C reached 1.3 mM. No nitrite was accumulated in the environment at 5°C.

The PXL2 strains showed different rates of ferrous oxidation and nitrate degradation at different temperatures, which may affect the reproduction of microorganisms. At the same time, the oxidative degradation ability of AFODN at low temperature was greatly reduced. The low temperature inhibited the growth of microorganism's intracellular enzyme activity, so that it reduced the ability of oxidation and degradation.

SEM-EDS Analysis of Sediments at Low Temperatures

SEM analysis of microbial antioxidant sediments at 5°C, 15°C and 30°C (*Fig. 3*) shows that the morphology of the cells changed significantly at 5°C, the bacillus coarsened and shortened, and obvious dents generally appear, possibly as a response to the low temperature.

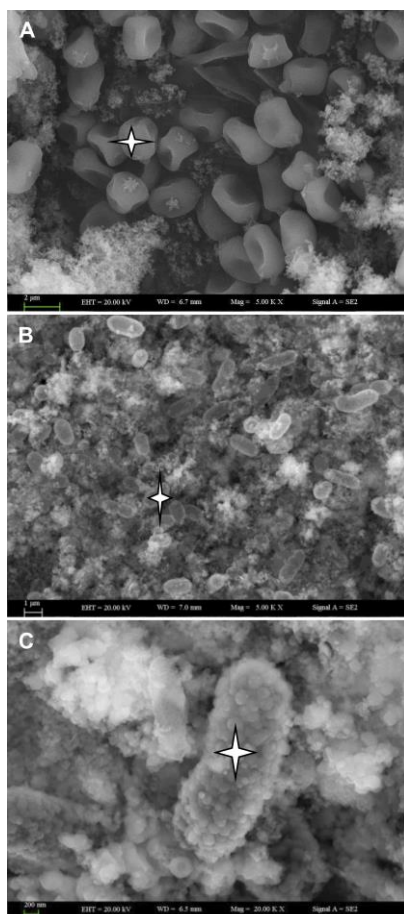


Figure 3. SEM analysis of microbial ioxidant sediments--strain PXL2 at different temperatures (The star indicated the point of EDS analysis in Figure 4. A: 5°C; B: 15°C; C: 30°C)

At 30°C, the cells were incrustated in nanosize Fe(III) oxides with only few cells being completely free of surface precipitates (*Fig. 3c*). The average diameter of the Fe(III) oxides was between 100~200 nm.

EDS analysis of ferrous oxide products at 5°C, 15°C and 30°C. *Figure 4* shows that the sediments formed at 5°C mainly consist of C and O, with only a small amount of Fe. The highest C content was 62.41%, the content of O was 33.15% and the content of iron was only 0.35%. The contents of Fe in the sediments formed at 15°C were higher at about 9.64%, which far exceeded the content of Fe in the sediments formed at 5°C. At 30°C, EDS analysis showed that the precipitates were mainly composed of C (22.85%), O (40.68%) and Fe (22.41%). Iron content exceeds at the first two temperatures.

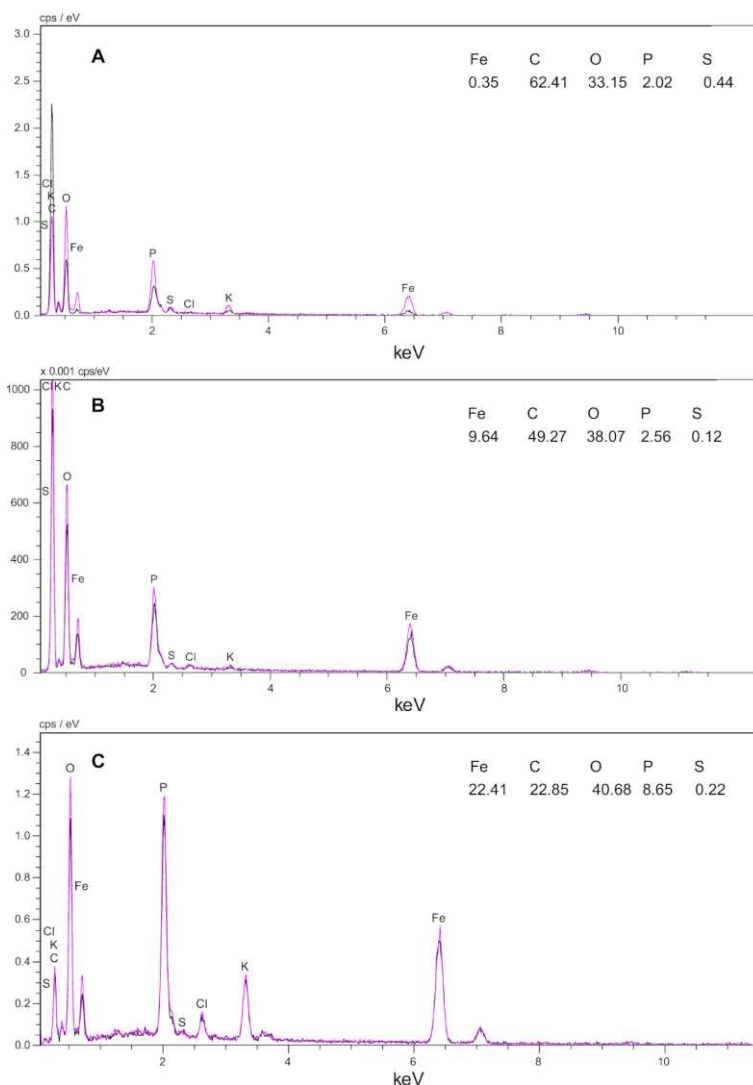


Figure 4. EDS analysis of strain PXL2 sediments at different temperatures (A corresponding *Fig. 3A*; B corresponding *Fig. 3B*; C corresponding *Fig. 3C*)

Based on the above analysis, we can see that low temperature environments had inhibitory effects on strain PXL2. At 5°C, the cell morphology changed and the Fe content in sediment was extremely low and mainly existed in pericellular region instead of the cell surface while Temperature of 15°C seemed to have less of an effect on the

metabolism of microorganisms, and the morphology of the cells remains the same, but the content of Fe was at least 50% lower than the sediment at 30°C. Thus, 30°C is most suitable for the growth and metabolism of strain PXL2. Under this temperature, microbial metabolism is the fastest, and the rate of Fe oxidation and the content of Fe in sediment are the highest.

Removal of arsenic by strain PXL2 at different temperatures

The removal of arsenic at different temperatures is shown in *Figure 5*. The different amounts of arsenic are removed at different temperatures over time. After 7 days of treatment, total arsenic concentrations decreased from 70 µM to 54.9 µM, 34.2 µM and 49.0 µM at 5°C, 15°C and 30°C, the removal rates were 21.6%, 51.1% and 30.0%, respectively. The highest rate was at 15°C.

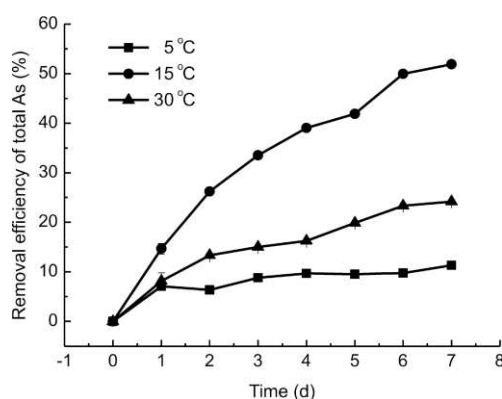


Figure 5. Total arsenic removal efficiency at different temperatures

Strain PXL2 has the ability to remove arsenic by arsenic oxidation. As seen in *Figure 6*, as total arsenic is removed, some As (III) is oxidized to As (V). At 5°C and 30°C, with the removal of total arsenic, the concentration of As (III) decreased and the concentration of As (V) increased continuously. The percentage of As (III) in total arsenic dropped from the original 90% to 62.1% and 54.0%, respectively. The corresponding As (V) concentrations increased from 10% to 37.9% and 46.0%, respectively. The conversion of As (III) to As (V) at 15°C is less pronounced with respect to the other conversions at two temperature, but some of the As (V) production can be seen.

From the above analysis we can see that temperatures that are too high or too low are not suitable for strain PXL2 arsenic removal, with 15°C being the most suitable temperature. One of the reasons may be that enzyme catalysis in microbial metabolism is inhibited severely at extreme low and high temperatures. Compared with the medium temperature, microbial metabolism is active in high temperature environments, and therefore results in the fastest ferrous oxide oxidation rate. The rate of ferrous oxidation directly affects the type of oxidation product. Different types of iron oxides have different arsenic adsorption capacities. The environment of oxidative denitrification of AFODN anaerobic ferrous compounds is mainly for the pollution of nitrate and arsenic in groundwater. The perennial groundwater temperature is maintained at 15°C~17°C, which is very conducive to AFODN reproductive metabolism and enzyme catalysis. Therefore, strain PXL2 is suitable for applications to groundwater pollution control.

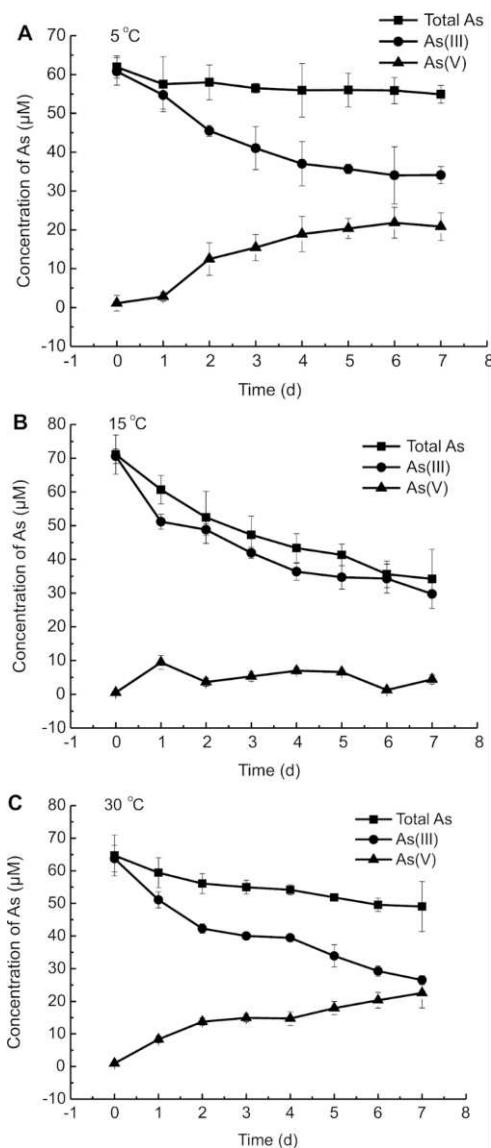


Figure 6. Time profile of As concentrations in the strain PXL2 culture at different temperatures

Conclusion

Growth of strain PXL2 was significantly inhibited at 5°C. At this temperature, morphological changes were also seen, where a rod-like shape changed to a spherical one, and dents appeared on the bacterial surface. Under this condition, the denitrification ability and Fe (II) capacity of the strain decreased significantly. The As removal ability was also affected. The total arsenic removal rate was at 21.6%. At 15°C, the metabolic rate of growth, denitrification and Fe (II) oxidation rate were slightly lower than 30°C, but the total arsenic removal rate was the highest at this temperature, at 51.1%. The total arsenic removal rate at 30°C was 30.0%. On the whole, the strain PXL2 metabolized well at 15°C, and was found to be suitable for treating nitrate and arsenic contamination in groundwater. This biological treatment has promising applications in future projects. This research promotes the research of ferrous anaerobic micro-organisms in this new field of research.

Acknowledgements. This work was supported by National Science Foundation of Xinjiang Uygur Autonomous Region, China (2016D01A028).

REFERENCES

- [1] Benz, M., Brune, A., Schink, B. (1998): Anaerobic and aerobic oxidation of ferrous iron at neutral pH by chemoheterotrophic nitrate-reducing bacteria. – Archives of Microbiology 69: 159-165.
- [2] Chakraborty, A., Roden, E. E., Schieber, J. (2011): Enhanced Growth of Acidovorax sp. Strain 2AN during Nitrate-Dependent Fe(II) Oxidation in Batch and Continuous-Flow Systems. – Applied and Environmental Microbiology 77: 8548-8556.
- [3] Chen, D. D., Liu, T. X., Li, X. M. (2018): Biological and chemical processes of microbially mediated nitrate-reducing Fe(II) oxidation by Pseudogulbenkiania sp. strain 2002. – Chemical Geology 476: 59-69.
- [4] Cui, J. L., Du, J. J., Tian, H. X. (2018): Rethinking anaerobic As(III) oxidation in filters: Effect of indigenous nitrate respirers. – Chemosphere 196: 223-230.
- [5] Ehrenreich, A., Widdel, F. (1994): Anaerobic oxidation of ferrous iron by purple bacteria, a new type of phototrophic metabolism. – Applied and Environmental Microbiology 60: 4517-4526.
- [6] Gendel, Y., Lahav, O. (2008): Accurate determination of Fe(II) concentrations in the presence of a very high soluble Fe (III) background. – Applied Geochemistry 23: 2123-2129.
- [7] Geng, Y. J., Wu, Q., Muszynski, M. (1996): Apoptosis of Vascular Smooth Muscle Cells Induced by In Vitro Stimulation with Interferon- γ , Tumor Necrosis Factor- α , and Interleukin-1 β . -Arteriosclerosis, Thrombosis, and Vascular Biology 16: 19-27.
- [8] Guo, X. J., Fujino, Y., Kaneko, S. (2001): Arsenic contamination of groundwater and prevalence of arsenical dermatosis in the Hetao plain area, Inner Mongolia, China. – Molecular and Cellular Biochemistry 222: 137-140.
- [9] Hafenbradl, D., Keller, M., Dirmeier, R. (1996): Ferroglobus placidus gen. nov., sp. nov., a novel hyperthermophilic archaeum that oxidizes Fe²⁺ at neutral pH under anoxic conditions. – Archives of Microbiology 166: 308-314.
- [10] Hansen, H. C. B., Koch, C. B., Nancke-Krogh, H. (1996): Abiotic nitrate reduction to ammonium: key role of green rust. – Environmental Science & Technology 30: 2053-2056.
- [11] Hu, S., Shi, Q. T., Jing, C. Y. (2015): Groundwater arsenic adsorption on granular TiO₂: integrating atomic structure, filtration, and health impact. – Environmental Science & Technology 49: 9707-9713.
- [12] Kappler, A., Schink, B., Newman, D. K. (2005): Fe (III) mineral formation and cell encrustation by the nitrate-dependent Fe (II)-oxidizer strain BoFeN1. – Geobiology 3: 235-245.
- [13] Karim, M. M. (2000): Arsenic in groundwater and health problems in Bangladesh. – Water Research 34: 304-310.
- [14] Klueglein, N., Kappler, A. (2013): Abiotic oxidation of Fe(II) by reactive nitrogen species in cultures of the nitrate-reducing Fe(II) oxidizer Acidovorax sp. BoFeN1 – questioning the existence of enzymatic Fe(II) oxidation. – Geobiology 11: 180-190.
- [15] Leahy, J. G., Colwell, R. R. (1990): Microbial Degradation of Hydrocarbons in Environment. – Microbiological Reviews 54: 305-315.
- [16] Li, B. H., Tian, C. Y., Zhang, D. Y. (2014): Anaerobic Nitrate-Dependent Iron (II) Oxidation by a Novel Autotrophic Bacterium, *Citrobacter freundii* Strain PXL1. – Geomicrobiology Journal 31(2): 138-144.

- [17] Li, B. H., Pan, X. L., Zhang, D. Y. (2015): Anaerobic nitrate reduction with oxidation of Fe(II) by *Citrobacter Freundii* strain PXL1—a potential candidate for simultaneous removal of As and nitrate from groundwater. – *Ecological Engineering* 77: 196-201.
- [18] Li, B. H., Deng, C. N., Zhang, D. Y. (2016): Bioremediation of Nitrate- and Arsenic-Contaminated Groundwater Using Nitrate-Dependent Fe(II) Oxidizing *Clostridium* sp. Strain pxl2. – *Geomicrobiology Journal* 33: 185-193.
- [19] Li, Y. F., Long, X. X., Chong, Y. X. (2017): Characterization of the cell Fe mineral aggregate from nitrogen removal employing ferrous and its adsorption features to heavy metal. – *Journal of Cleaner Production* 156: 538-548.
- [20] Niazi, N. K., Bibi, I., Shahid, M. (2018): Arsenic removal by perilla leaf biochar in aqueous solutions and groundwater: an integrated spectroscopic and microscopic examination. – *Environmental Pollution* 232: 31-41.
- [21] Ottley, C. J., Davison, W., Edmunds, W. M. (1997): Chemical catalysis of nitrate reduction by iron(II). – *Geochimica et Cosmochimica Acta* 61: 1819-1828.
- [22] Shen, X. Y., Zhang, L. M., Shen, J. P. (2010): Soil type determines the abundance and community structure of ammonia-oxidizing bacteria and archaea in flooded paddy soils. – *Journal of Soils and Sediments* 10: 1510-1516.
- [23] Singh, N., Kumar, D., Sahu, A. (2007): Arsenic in the environment: effects on human health and possible prevention. – *Journal of Environmental Biology* 28: 359-365.
- [24] Smedley, P. L., Kinniburgh, D. G. (2002): A review of the source, behaviour and distribution of arsenic in natural waters. – *Applied Geochemistry* 17: 517-568.
- [25] Song, P. P., Yang, Z. H., Zeng, G. M. (2017): Electrocoagulation treatment of arsenic in wastewaters: A comprehensive review. – *Chemical Engineering Journal* 317: 707-725.
- [26] Straub, K. L., Benz, M., Schink, B. (1996): Anaerobic, nitrate dependent microbial oxidation of ferrous iron. – *Applied and Environmental Microbiology* 62: 1458-1460.
- [27] Straub, K. L., Rainey, F. A., Widdel, F. (1999): *Rhodovulum iodolum* sp. Nov. and *Rhodovulum robiginosum* sp. Nov., two new marine phototrophic ferrous-iron-oxidizing purple bacteria. – *International Journal of Systematic Bacteriology* 49: 729-735.
- [28] Straub, K. L., Schonhuber, W. A., Buchholz-Cleven, B. E. E. (2004): Diversity of ferrous iron-oxidizing, nitrate reducing bacteria and their involvement in oxygen independent iron cycling. – *Geomicrobiology Journal* 21: 371-378.
- [29] Sun, G. F. (2004): Arsenic contamination and Arsenicosis in China. – *Toxicology and Applied Pharmacology* 198: 268-271.
- [30] Veena, K., Narayana, B. (2009): Spectrophotometric determination of nitrite using new coupling agents. – *Indian Journal of Chemical Technology* 16: 89-92.
- [31] Wang, L. F., Huang, J. Z. (1994): Chronic arsenism from drinking water in some areas of Xinjiang, China. – In: Nriagu, J. O. (ed.) *Arsenic in the Environment, Part II: Human Health and Ecosystem Effects*. John Wiley and Sons Inc.: New York 159-172.
- [32] Wang, S. X., Wang, Z. H., Cheng, X. T. (2007): Arsenic and fluoride exposure in drinking water: children's IQ and growth in Shanyin County, Shanxi Province, China. – *Environmental Health Perspectives* 115: 643-647.
- [33] Weber, K. A., Pollock, J., Cole, K. A. (2006): Anaerobic nitrate-dependent iron (II) bio-oxidation by a novel lithoautotrophic betaproteobacterium, strain 2002. – *Applied and Environmental Microbiology* 72: 686-694.
- [34] Wu, G. Y., Zhang, D. Y., Pan, X. L. (2010): Anaerobic oxidation of ferrous iron by microbial mixture and its potential to remove mercury and nitrate from the groundwater. – *Research Journal of Chemistry and Environment* 14: 36-39.
- [35] Xing, S. H., Chen, C. R., Zhou, B. Q. (2010): Soil soluble organic nitrogen and microbial processes under adjacent coniferous and broadleaf plantation forests. – *Journal of Soils and Sediments* 10: 748-757.
- [36] Zhang, W., Li, X. M., Liu, T. X. (2014): Competitive reduction of nitrate and iron oxides by *Shewanella putrefaciens* 200 under anoxic conditions. – *Colloids and Surfaces A: Physicochemical Engineering Aspects* 445: 97-104.

SPATIAL ASSOCIATIONS AND SPECIES COLLOCATION OF DOMINANT TREE SPECIES IN A NATURAL SPRUCE-FIR MIXED FOREST OF CHANGBAI MOUNTAINS IN NORTHEASTERN CHINA

ZHANG, M.¹ – LIU, Y.² – GUO, W.³ – KANG, X.^{3*} – ZHAO, H.⁴

¹College of Forestry, Shanxi Agriculture University, Shanxi 030801, P. R. China

²College of Forestry, Inner Mongolia Agriculture University
Inner Mongolia 010019, P. R. China

³Key Laboratory for Silviculture and Conservation Ministry of Education, Beijing Forestry University, Beijing 100083, P.R. of China

⁴Forest police college, Nanjing 210023, P.R. of China

*Corresponding author

e-mail: zmt0411@163.com; phone: +86-018503444094; fax: +86-03546288329

(Received 5th Nov 2018; accepted 4th Feb 2019)

Abstract. In order to achieve of the spatial association and optimum collocation, a 1-ha natural spruce-fir mixed forest plot which was established on Changbai Mountains, PR China. Diameter at breast height, height, and the crown width of the standing free trees with >1 cm DBH trees were measured, and species were identified. *O*-ring statistics and the nearest neighbor analysis were applied to test the spatial correlations and distribution of number of dominant species at different vertical layers. We found that: (1) according to the importance values, the top four species were *Abies nephrolepis* (Trautv.) Maxim., *Picea koraiensis* Nakai, *Pinus koraiensis* Sieb. et Zucc. and *Tilia amurensis* Rupr.; (2) most of species pairs have positive associations at small scales, while few are no relevance or have negative associations; (3) the number of juveniles and lower layer trees showed positive skewness under the upper layer trees and the maximum number for coniferous species was at a distance 4.5-6.5 m, while it was 6.5-8.5 m for broadleaved species. Our results provide a new insight into the development of reforestation technique in spruce-fir forests in the Changbai Mountains.

Keywords: *inter-specific association, scale, O-ring statistics, nearest neighbor analysis*

Introduction

Studying forest regeneration processes is essential in understanding forest diversity and dynamics, which follows a forest life cycle from germination to death (Darrigo et al., 2016). The information of forest regeneration, moreover, is fundamentally important because it reflects the stability of the structure and composition of overstory, and provides the prerequisites for the developing of ecological, social and economic benefits of forest continuously (Mostacedo et al., 2009; Lydersen et al., 2015). Forest management must change radically to maintain biodiversity and enough juveniles (Liu et al., 2015).

However, natural regeneration of seedlings and species cannot fulfill the requirements for the healthy growth of the forest due to landscape fragmentation, and the limitation of seed dispersal (Levesque et al., 2011; Holeksa et al., 2017). Artificial regeneration, therefore, can supplement the lack of woodland seedling individuals and the number of species (Wagner et al., 2010; Hejel et al., 2016). However, adaptive

species must be chosen according to characteristics of alternative tree species (Gonzalez-Rodriguez et al., 2011).

A mount of studies, therefore, have been focused on the species niche and interspecific association of classical ecology with the objective to understand their optimal collocation of species effects on the forest ecosystem (Zhao et al., 2012; Su et al., 2015; Wright et al., 2016). In addition, more studies also have been focused on spatial structure, but only limited to a quantitative description of the forest spatial pattern (Li et al., 2014; Lydersen et al., 2015; Nguyen et al., 2016). Vertical spatial structure, however, is closely related to and affects the different ecological processes which include intra-specific and inter-specific competition, disturbance reaction, and environmental heterogeneity, regeneration mechanisms and understory development (Hao et al., 2007; Zhang et al., 2015). Ecology rules of spatial structure were rarely applied to forest management.

In this study, species spatial associations and distribution were analyzed with the distance at different vertical layers in a 1-ha spruce-fir mixed forest plot, to provide a scientific basis for the best collocation of different forest vertical layers of the mixed forest. We hoped to fulfill three objectives: (1) evaluate mechanisms of species coexistence though calculate species spatial associations between juveniles, lower and upper height class trees; (2) clarify the dependency relationship according to distributions of number of the species with the distance among different height layers; (3) indicate the distance or scale is an important factor among different tree height classes in the forest.

Materials and methods

Study area

Jin Gouling forest farm is our study area, which is located in Changbai Mountain in northeastern PR China ($43^{\circ}22' N$, $130^{\circ}10' E$) (Fig. 1). The annual precipitation is 500–600 mm, with most of the rain falling in July. The altitude ranges from 300 to 1200 m and the slopes mostly vary between 5° and 25° . A gray–brown podzolic soil is present on the low and intermediate mountains in the area and is derived from the parent basalt rock.

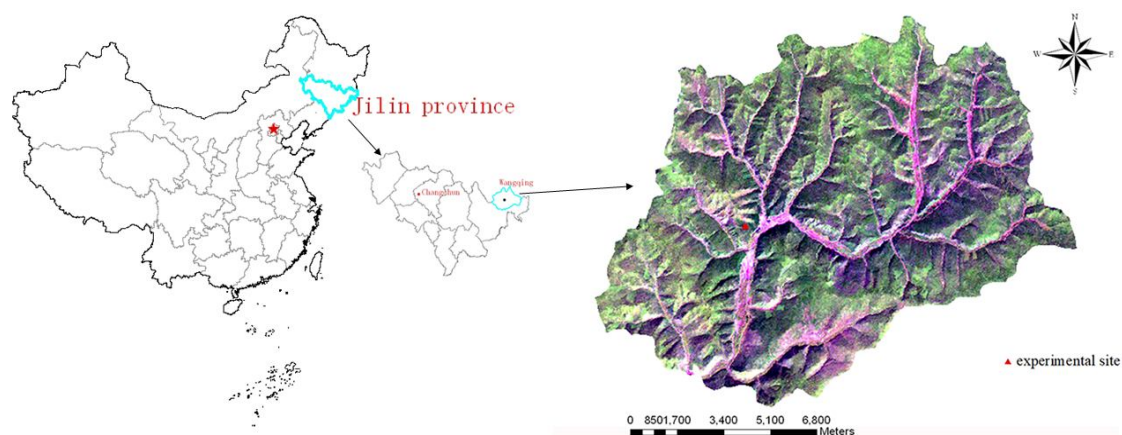


Figure 1. Location of study site within the Changbai Mountain in northeastern China

Plot establishment and data collection

A 100m×100m plot was established in natural spruce-fir forest which suffered little distance because of its difficult accessibility. Twenty-five 20 m×20 m subplots were set in above-mentioned plot. All detailed information of stand description factors can be found in (Zhang, 2017).

Data analysis

Forest spatial associations analysis

O-ring statistic model was broadly employed to investigate structural forest processes (Wiegand and Moloney, 2004; Xu et al., 2009). Therefore, O-ring statistic model was used to explore the spatial associations of the dominant tree species. The O-ring statistics includes both univariate and bivariate statistics (Getzin et al., 2006). The O-ring statistic model $O_{12}(r)$ is calculated as:

$$\hat{O}_{12}^w(r) = \frac{\frac{1}{n_1} \sum_{i=1}^{n_1} \text{Po int } s_2 [R_{1,i}^w(r)]}{\frac{1}{n_1} \sum_{i=1}^{n_1} \text{Area} [R_{1,i}^w(r)]} \quad (\text{Eq.1})$$

where n_1 is the number of points of pattern 1 (the object 1 of univariate statistic), $R_{1,i}^w(r)$ means the ring with radius r and ring width w centered on the i th point of pattern 1; $\text{Points}_2[X]$ (Equation 2) calculate the number of points in regional X of pattern 2 (the object 2 of univariate statistic), $\text{Area}[X]$ (Equation 4) means the area of the study regional X.

$$\text{Po int } s_2 [R_{1,i}^w(r)] = \sum_{allx} \sum_{ally} S(x, y) P_2(x, y) I_r(x_i, y_i, x, y) \quad (\text{Eq.2})$$

$$I_r^w(x_i, y_i, x, y) = \begin{cases} 1 & \text{if } r - \frac{w}{2} \leq \sqrt{(x - x_i)^2 + (y - y_i)^2} \leq r + \frac{w}{2} \\ 0 & \text{otherwise} \end{cases} \quad (\text{Eq.3})$$

$$\text{Area} [R_{1,i}^w(r)] = z^2 \sum_{allx} \sum_{ally} S(x, y) I_r(x_i, y_i, x, y) \quad (\text{Eq.4})$$

In these equations, (x_i, y_i) is the coordinate of point i in pattern 1. When the coordinate of point i is inside the study regional X, $S(x, y) = 1$, otherwise, $S(x, y) = 0$. $P_2(x, y)$ means the number of points in pattern 2, I_r (Equation 3) is a counter variable to define the circle with radius r that is centered at the i th point of pattern 1, z^2 means the area of one cell. The univariate statistic $O_{ii}(r)$ is calculated by setting the pattern 1 equal to the pattern 2.

Nearest neighbor analysis

Supposing that in a large enough forest stand, which existed plenty of juveniles of species A and adult tree of species B, the number of juveniles of A is N. Di is the

distance from random juveniles of species A to the nearest adult tree of species B, and the average distance between juveniles of species A and nearest adult trees of species B with the following formula:

$$\bar{D} = \frac{1}{N} \sum_{i=1}^N Di \quad (\text{Eq.5})$$

where \bar{D} is the mean distance from juvenile tree to mature individual, which is used to analyze the attachment relationship between juvenile and mature tree, σ^2 is the standard variance of Di .

Because of the limited area of the plot and number of individuals (juveniles and mature trees), it is difficult to calculate Di . The central limit theorem, therefore, was used here, which assumed that a juvenile and a nearest adult tree constitute a sample unit, when the sample number ≥ 50 , the average distance showed an approximately normal distribution (Rice, 2007).

$$\frac{(\bar{d} - \bar{D})}{\sigma / \sqrt{n}} \cdot \frac{\text{approximately}}{n \geq 50} \sim N(0,1) \quad (\text{Eq.6})$$

and the formula can be obtained:

$$p \left\{ \left| \bar{d} - \bar{D} \right| \leq U_{\alpha} \cdot \frac{S}{\sqrt{n-1}} \right\} = 1 - \alpha \quad (\text{Eq.7})$$

where U_{α} is the expected value of the sample distance, S is the variance of the standard sample distance, and the confidence interval is $[\bar{d} - U_{\alpha} \cdot \frac{S}{\sqrt{n-1}}, \bar{d} + U_{\alpha} \cdot \frac{S}{\sqrt{n-1}}]$. In

addition, the distribution area was divided into juveniles of species A around the nearest adult tree of species B into several annular zones, and the center point was under the stem of adult tree. The ratio of number of juveniles of species A in each annular zone was counted. The distance, which distributed the maximal number of juveniles, was the optimal distance for replanting juveniles of species A under adult trees of species B (Zhao et al., 2012).

The spatial scale was set 0-20 m, and in this case, 199 randomizations in Monte Carlo simulations were used to provide 95% confidence envelopes. In addition, the nearest neighbor was used to analyzed to test the distribution of number of dominant species with distance and identified the strength of the association among juvenile, lower height class and upper height class.

Results

Stand structure

Table 1 presents the descriptive statistics of species for the entire plot. According to important value, *A. nephrolepis* (Fir) ranked first and had the largest number (1638) and basal area (12.90 m² hm⁻¹). *P. jezoensis* (Spruce) followed second with number (415),

basal area ($6.18 \text{ m}^2 \text{ hm}^{-1}$). Although *P. koraiensis* (Korean pine) had only 278 individuals, it ranked third in terms of important value. *T. amurensis* (Linden) had the largest DBH (64 cm) and its important value ranked fourth. It is basically the same data base that has been used in the study of (Zhang, 2017).

Table 1. Basic structural characteristics of tree species in a 1-ha uneven-aged natural spruce-fir forest plot in Changbai Mountain

Species	No. of trees	DBH(cm)		Standard deviation	Basal area ($\text{m}^2 \text{ hm}^{-1}$)	Important value
		Max	Mean			
<i>A. nephrolepis</i> (Trautv.) Maxim. (Fir)	1638	45.2	9.9	9.79	12.90	69.67
<i>P. jezoensis</i> Carr. (Spruce)	415	48.3	16.4	11.90	6.18	45.55
<i>P. koraiensis</i> Sieb. et Zucc. (Korean pine)	278	55.5	13.9	13.22	4.37	40.46
<i>T. amurensis</i> Rupr. (Linden)	342	64.0	6.7	7.88	2.15	39.15
<i>B. platyphylla</i> Suk. (White birch)	33	30.4	17.7	5.73	1.35	10.85
<i>P. amurense</i> Rupr. (Yellow pineapple)	4	11.8	15.2	3.47	0.07	4.20
<i>P. davidiana</i> Dode (Elm)	3	30.4	19	9.95	0.09	4.19

Intra- and interspecies spatial associations of dominant tree species were analyzed among different height classes (Table 2). All standing free trees were firstly divided the height into juvenile ($h < 5 \text{ m}$), lower ($5 \text{ m} \leq h < 10 \text{ m}$), intermediate ($10 \text{ m} \leq h < 15 \text{ m}$) and upper ($h \geq 15 \text{ m}$) layer but most species were distributed at the juvenile trees and few individuals were found in the lower, intermediate and upper layer (Zhang, 2017).

Table 2. Basic quantity characteristics of four dominant tree species at four height classes

Species	Height (m)			Numbers of different height classes				Total
	Maximum	Minimum	Mean	J	L	M	U	
<i>A. nephrolepis</i>	21.9	0.3	4.58	1185	142	141	170	1638
<i>P. jezoensis</i>	24.4	0.6	5.7	265	101	20	69	415
<i>P. koraiensis</i>	21.0	0.3	5.17	175	50	31	22	278
<i>T. amurensis</i>	19.2	0.4	4.92	224	62	46	10	342

J- juvenile height class ($h < 5 \text{ m}$), L-lower height class ($5 \text{ m} \leq h < 10 \text{ m}$), M-intermediate height class ($10 \text{ m} \leq h < 15 \text{ m}$), U-upper height class ($h \geq 15 \text{ m}$)

Intra- and interspecies spatial association of dominant tree species between juvenile and upper layer trees (juvenile layer vs. upper layer trees)

The spatial associations of the juvenile (J) and upper (U) layer trees varied with the scale that be examined (Fig. 2). The most dominant species of juvenile height class were positive correlations at small scales, and with scaling up, no relevance or even negative associations emerged. For instance, *Tilia* (J) was positive associations to *Tilia* (U) and *Pinus* (U) both at scales 0-2 m and 8-9 m scales, *Abies* (U) and *Picea* (U) at 0-7 m and 0-6 m scales, respectively (Fig. 2a-2d). Similarly, *Pinus* (J) was positive associations to *Tilia* (U) and *Picea* (U) at 0-10 m and 0-7 m scales (Fig. 2e, 2h). *Abies* (J)

and *Picea* (J), furthermore, were positive correlations to *Tilia* (U) at scales ≤ 7 m and ≤ 3 m. *Abies* (J) was also positive associations to *Abies* (U) and *Picea* (U) at scales ≤ 8 m and ≤ 10 m (Fig. 2i, 2k-2m).

Three different associations were observed as follows: (1) *Pinus* (J) and *Picea* (J) were significant positive associations to *Abies* (U) at the majority of scales, so did *Abies* (J) to *Pinus* (U) and *Picea* (J) to *Pinus* (U) (Fig. 2g, 2j, 2n and 2o); (2) *Pinus* (J) exhibited no relevance and negative association to *Pinus* (U) at scales, and with the scales increased, positive association emerged (Fig. 2f); (3) *Picea* (J) was negative correlation to *Picea* (U) at 0-3 m and 9-10 m scales (Fig. 2p).

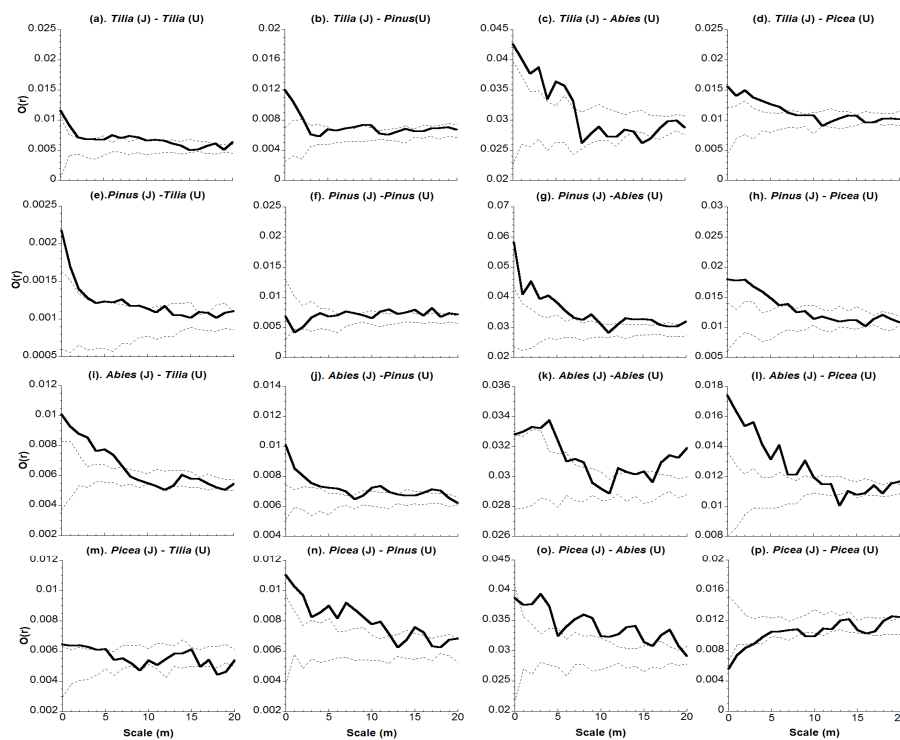


Figure 2. Spatial associations of juvenile height class to the upper height class. Black lines indicate ring statistics $O(r)$; dashed lines indicate upper and lower of the limit 95% confidence envelopes. Above the dashed lines indicate positive association between species pairs, below the dashed lines indicate positive association, and in the interval of dashed lines indicate independence between species pairs (similarly hereinafter). J: the juvenile height class, U: the upper height class

Intra- and interspecies spatial association of dominant tree species between lower and upper layer trees (lower vs. upper layer trees)

The spatial associations of the lower (L) height class and upper (U) height class at different vertical layers (Fig. 3). *Tilia* (L) tended to show negative association to *Tilia* (U) at 4-6 m and 10-11 m, and was positive correlation to *Abies* (U) at scales ≤ 1 m, while no relevancies was observed to *Pinus* (U) and *Abies* (U) at the most scales. *Pinus* (L) was positively associated to *Pinus* (U) only at scales ≤ 3 m and with scaling up, more scales exhibited independence or even inhibition, (Fig. 3a-3d, 3f). It was found that *Pinus* (L) was significant positive association was showed at the most scales

(≤ 15 m, ≤ 15 m and ≤ 11 m) to *Tilia* (U), *Abies* (U) and *Picea* (U) (Fig. 3e, 3g, 3h). Similarly, *Abies* (L) was positive correlation to all four species at scales ≤ 14 m, ≤ 3 m and 7-10 m, ≤ 16 m and ≤ 8 m (Fig. 3i-3l). *Picea* (L) was positive correlation to *Tilia* (U), *Pinus* (U) and *Abies* (U) at scales ≤ 5 m, ≤ 4 m, and ≤ 6 m, while negative association to *Picea* (U) at scales ≤ 3 m, respectively (Fig. 3m-3p).

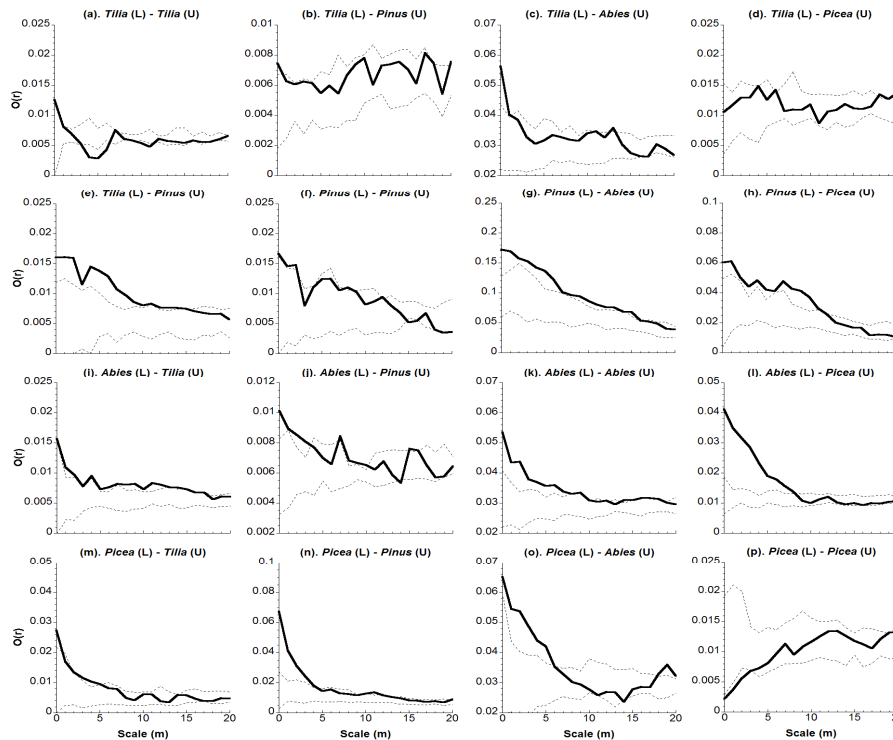


Figure 3. Spatial associations of lower height class to the upper height class. Black lines indicate ring statistics $O(r)$; dashed lines indicate upper and lower of the limit 95% confidence envelopes. L: the lower height class, U: upper height class

Distribution of the number of the dominant species with the distance at different height classes

Four dominant species (J) were nearest to *A. nephrolepis* (U), while furthest to *T. amurensis* (U). In addition, the average distances among species (J) and species (U) were observed: (1) *Tilia* (U): *Pinus* (J) < *Tilia* (J) < *Picea* (J) < *Abies* (J); (2) *Pinus* (U): *Picea* (J) < *Abies* (J) < *Pinus* (J) < *Tilia* (J); (3) *Abies* (U): *Picea* (J) < *Pinus* (J) < *Abies* (J) < *Tilia* (J); (4) *Picea* (U): *Tilia* (J) < *Pinus* (J) < *Abies* (J) < *Picea* (J). The average distance between species (L) and species (U) was from 4.729 m to 8.877 m. The average distance to species (U) specific to species (L) were showed: (1) *Tilia* (U): *Tilia* (L) < *Pinus* (L) < *Abies* (L) < *Picea* (L); (2) *Pinus* (U): *Pinus* (L) < *Abies* (L) < *Tilia* (L) < *Picea* (L); (3) *Abies* (U): *Picea* (L) < *Abies* (L) < *Pinus* (L) < *Tilia* (L); (4) *Picea* (U): *Abies* (L) < *Pinus* (L) < *Tilia* (L) < *Picea* (L).

The results of distribution of the number between juvenile were shown that lower and upper height class trees (Fig. 4 and Fig. 5). All skewness values were greater than zero. Positive skewness, therefore, was observed (Tab.3). The number of species (J) and species (L) under the upper layer trees was first gradually increased with the distance,

and then decreased beyond a certain critical point. It was found that the distributions of the greatest number of species (J) and species (L) from 4.5 m to 10.5 m scales. For instance, four species (J) were mainly distributed in the range of 4.5 to 6.5 m scales under *Picea* (U), 4.5 to 8.5 m under *Pinus* (U) and *Abies* (U), while 6.5 to 10.5 m under *Tilia* (U) (Fig. 4). Furthermore, all the species (L) were distributed in the range of 4.5 to 8.5 m under *Tilia* (U), *Abies* (U) and *Picea* (U), while 4.5 to 10.5 m scales under *Pinus* (U) (Fig. 5).

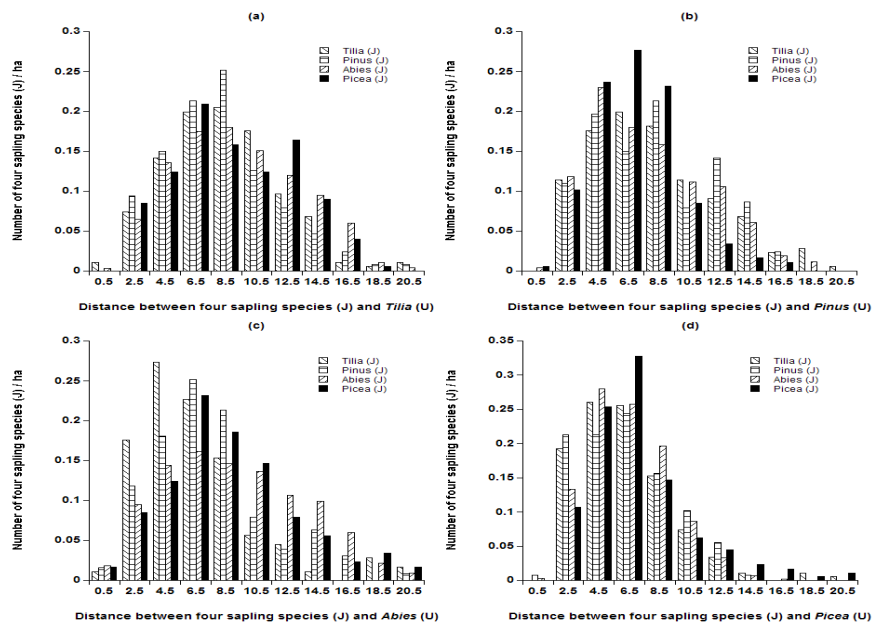


Figure 4. Distribution between juvenile (J) and upper (U) height classes of four dominant species with the distance

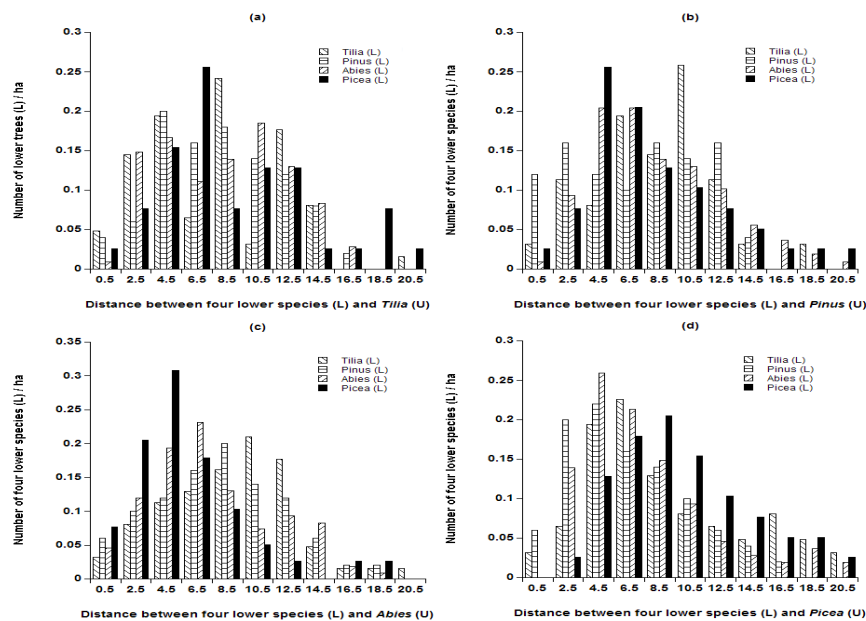


Figure 5. Distribution between lower (L) and upper (U) height classes of four dominant species with the distance

Discussion

The study site is an uneven-aged spruce-fir mixed forest where has abundant tree species and complicated stand structure. According to importance value index, the dominant species are ranked to *A. nephrolepis*, *P. jezoensis*, *P. koraiensis* and *T. amurensis*. The same result has been reported in previous study (Gong, 2009), which according to analysis of forest dynamic (succession and restoration), the dominant trees were above mentioned species, and they will not change much with the development process.

Forest spatial association is closely related to scales (Navarro-Cerrillo et al., 2013; Zhang et al., 2015). Generally, juvenile and lower height classes tended to be positive association at smaller scales, with scales increased, it was changed by no relevance or even negative association (*Fig. 2 and Fig. 3*). The same results have been reported in some researches (Hao et al., 2007; Zhang et al., 2009). Some researchers thought that habitat heterogeneity and seeds dispersal ability with mother tree which resulted in positive association (Hubbell et al., 1999; Lin et al., 2011; Basnou et al., 2016). In addition, effect of intra specific competition was also important factor (Petritan et al., 2014).

Tilia (J) and *Abies* (J) are positive associations around their mother upper trees at small scales, while with scales increase, no relevance or negative association emerge (*Fig. 2a and 2k*). Limited seed dispersal ability and their shade tolerant characteristics ensure them grow well under the canopy of parent trees in weak light. Although the coexistence may lead to competition and increase mortality, more juveniles can grow well under the canopy of the upper layer trees. Since then, with juveniles grow continually, few nutrients can be supplied for juveniles, more deaths appear. Distance among juveniles increase, therefore, the degree of aggregation decline (Kobe and Vriesendorp, 2011). In addition, positive associations between other three juvenile species and *Tilia* (U) explain coniferous species which can keep exuberant vitality under *Tilia* canopies (*Fig. 2e, 2i and 2m*), which supported the previous researches (Zhang et al., 2007; Chen et al., 2009). Except above-mentioned reasons, positive association of three juvenile and lower layer species to other upper species may suggest two reasons: (1) they have broad niches; (2) complex structure of branches of upper layer trees blocks the seeds dispersal, which leads to wind propagation insignificant. The same results are argued in previous researches (Li et al., 2007; Sebkova et al., 2012).

Strongly positive associations at the most scales were observed between species (J), (L) and species (U) suggest that the canopy of upper layer trees may provide suitable recruitment conditions for the understory. For instance, *Pinus* (J), *Picea* (J) and *Abies* (U), *Abies* (J), *Picea* (J) and *Pinus* (U) (*Fig. 2g, 2j, 2o and 2n*), *Pinus* (L) and Species (U) except *Pinus* (U) (*Fig. 3e, 3g, and 3h*), *Abies* (L) and *Tilia* (U), *Abies* (L) and *Abies* (U) (*Fig. 3i and 3k*), etc. Zhao et al. (2012) argued that these four species were the dominant species in this community, and trees of species pairs needed similar growth environment. Although their niches overlapped with each other, they can coexistence though competition of mutually promotive.

Negative associations for a few species (J) and (L) to their upper layer trees at small scales were observed. Take *Pinus*, *Picea* and *Tilia* for example, the negative association among *Pinus* might be attributable to human interference. Most pinecones were harvested, because of great economic value and this led to the lack of understory trees (Tao et al., 1995; Liu et al., 2004). The reason of exclusion among *Picea* different height class may be unsuited micro environmental conditions for their survival,

establishment, and growth of juveniles and lower trees. The same result reported in previous research (Gilbert, 2002). Juvenile of *Tilia* has shade tolerant characteristic, with tree height increases, however, the growth of *Tilia* needs more light, which cannot develop under the overstory (Zhang et al., 2007).

The average distance of different tree height layers (Tab.3) are showed that *Pinus* (J) and *Tilia* (J) are most likely to growth under the canopy of *Picea* (U) and *Tilia* (U); similarly, *Picea* (J) establish under the canopy of *Pinus* (U) and *Abies* (U) easily, but difficultly under *Picea* (U). These results are consistent with the spatial association analysis. Nevertheless, the analyses of mean distance are observed that *Tilia* (L), *Pinus*(L) are most favored growth under their parent trees, which is inconsistent with the result of the spatial association. The difference between two analytical of two methods may be led to different results.

The distributions of the number among different tree height class were observed that the number of species (J) and (L) increased with distance until a maximum value reached, and then decreased with distance gradually (Fig. 3 and Fig. 4). The distribution of maximum number mainly kept in a range, rather than in their immediate vicinity, the same result was reported in previous research (Schupp and Jordano, 2011). In addition, maximum number of juveniles of four dominant species was distributed from 4.5 m to 10.5 m, and this finding can be illustrated in Janzen-Connell theory in a certain extent, which high mortality is likely to occur near the mature trees (Matthesius et al., 2011; Steinitz et al., 2011). Meanwhile, the distribution of number of juveniles were influenced significantly by the crown widths, because of the canopy inhibited the growth of shrubs and herbs, more understory trees, therefore, can grow well in upper height trees (Pretzsch and Dieler, 2012). The distribution of maximum number for coniferous trees (*Pinus*, *Abies* and *Picea*) was at distance 4.5-6.5 m, while 6.5-8.5 m for broadleaved tree (*Tilia*) (Fig. 3 and Fig. 4). (Zhao et al., 2012) considered the length of coniferous tree is longer than broadleaved tree and the larger the crown width, therefore, the longer optimum distance occurred.

Conclusions

Our major aim was to understand the spatial reciprocity among different tree-height classes of dominant species in a mixed forest. The conclusions were shown that: (1) vertical structure plays an important role in population regeneration and community dynamics; (2) relative to the natural regeneration, artificial regeneration by enrichment planting is an expensive method, but has an obvious advantage in terms of the flexibility of either species combinations or spatial arrangements; (3) distance or scale is an important factor for distribution of trees. In different distance or scale, result of distribution of trees may be different. To obtain the optimum result, suitable distance or scale should be chosen according to situation of research in the plot. In addition, environmental factors, natural or human interference factors and the long-term monitoring data should also be considered and examined.

Acknowledgements. This study was supported by the project of applied basic research of Shanxi Province (Grant No. 201801D221302) and the planning subject of science and technology innovation of Shanxi agricultural university in China (Grant No. 2015YJ17). The author also thanked the editor and all anonymous reviewers for their constructive suggestions.

REFERENCES

- [1] Basnou, C., Vicente, P., Espelta, J. M., Pino, J. (2016): Of niche differentiation, dispersal ability and historical legacies: what drives woody community assembly in recent Mediterranean forests? – *Oikos* 125: 107-116.
- [2] Chen, L., Zhao, X. H., Zhang, Y. (2009): Spatial distribution patterns and associations of *Pinus koraiensis* and *Tilia amurensis* in Tilia-Korean pine forest on the north slope of Changbai Mountain, northeastern China. – *Journal of Beijing Forestry University* 31: 6-10. (in Chinese).
- [3] Darrigo, M. R., Venticinque, E. M., dos Santos, F. A. M. (2016): Effects of reduced impact logging on the forest regeneration in the central Amazonia. – *Forest Ecology and Management* 360: 52-59.
- [4] Getzin, S., Dean, C., He, F. L., Trofymow, J. A., Wiegand, K., Wiegand, T. (2006): Spatial patterns and competition of tree species in a Douglas-fir chronosequence on Vancouver Island. – *Ecography* 29: 671-682.
- [5] Gilbert, G. S. (2002): Evolutionary ecology of plant diseases in natural ecosystems. – *Annual Review of Phytopathology* 40: 13-43.
- [6] Gong, Z. W. (2009): Dynamics of Forest Succession and Restoration Strategies for Degraded Spruce-fir Forest in Changbai Mountain. – [PhD dissertation] Beijing, China: Beijing Forestry University (in Chinese).
- [7] Gonzalez-Rodriguez, V., Navarro-Cerrillo, R. M., Villar, R. (2011): Artificial regeneration with *Quercus ilex* L. and *Quercus suber* L. by direct seeding and planting in southern Spain. – *Annals of Forest Science* 68: 637-646.
- [8] Hao, Z. Q., Zhang, J., Song, B., Ye, J., Li, B. (2007): Vertical structure and spatial associations of dominant tree species in an old-growth temperate forest. – *Forest Ecology and Management* 252: 1-11.
- [9] Hejäl, P., Katona, K., Békési, S., Szemethy, L. (2016): Effects of natural and artificial beech regeneration methods on food diversity and browsing intensity in the Inner Western Carpathians. – *Austrian Journal of Forest Science* 133: 139-156.
- [10] Holeska, J., Jaloviar, P., Kucbel, S., Saniga, M., Svoboda, M., Szewczyk, J., Szwagrzyk, J., Zielonka, T., Zywiec, M. (2017): Models of disturbance driven dynamics in the West Carpathian spruce forests. – *Forest Ecology and Management* 388: 79-89.
- [11] Hubbell, S. P., Foster, R. B., O'Brien, S. T., Harms, K. E., Condit, R., Wechsler, B., Wright, S. J., Loo de Lao, S. (1999): Light-Gap disturbances, recruitment limitation, and tree diversity in a neotropical forest. – *Science* 283: 554-557.
- [12] Kobe, R. K., Vriesendorp, C. F. (2011): Conspecific density dependence in seedlings varies with species shade tolerance in a wet tropical forest. – *Ecology Letters* 14: 503-510.
- [13] Levesque, M., McLaren, K. P., McDonald, M. A. (2011): Recovery and dynamics of a primary tropical dry forest in Jamaica, 10 years after human disturbance. – *Forest Ecology and Management* 262: 817-826.
- [14] Li, Z., Xie, Z. Q., Li, Q. M., Zhao, C. M., Li, C. L. (2007): Spatial and temporal pattern of seed rain of *Abies fargesii* in Shennongjia Nature Reserve, Hubei. – *Biodiversity Science* 15(5): 500-509. (in Chinese).
- [15] Li, Y. F., Hui, G. Y., Zhao, Z. H., Hu, Y., Ye, S. (2014): Spatial structural characteristics of three hardwood species in Korean pine broad-leaved forest-Validating the bivariate distribution of structural parameters from the point of tree population. – *Forest Ecology and Management* 314: 17-25.
- [16] Lin, Y. C., Chang, L. W., Yang, K. C., Wang, H. H., Sun, I. F. (2011): Point patterns of tree distribution determined by habitat heterogeneity and dispersal limitation. – *Oecologia* 165: 175-184.
- [17] Liu, Z. G., Ji, L. Z., Hao, Z. Q., Zhu, J., Kang, H. (2004): Effect of cone-picking on natural regeneration of Korean pine in Changbai Mountain Nature Reserve. – *Chinese Journal of Applied Ecology* 15: 958-962. (in Chinese).

- [18] Liu, X. Z., Lu, Y. C., Xie, Y. S., Xue, Y. (2015): The positive interaction between two nonindigenous species, *Casuarina* (*Casuarina equisetifolia*) and *Acacia* (*Acacia mangium*), in the tropical coastal zone of south China: stand dynamics and soil nutrients. – *Tropical Conservation Science* 8: 598-609.
- [19] Lydersen, J. M., Collins, B. M., Knapp, E. E., Roller, G. B., Stephens, S. (2015): Relating fuel loads to overstorey structure and composition in a fire-excluded Sierra Nevada mixed conifer forest. – *International Journal of Wildland Fire* 24: 484-494.
- [20] Matthesius, A., Chapman, H., Kelly, D. (2011): Testing for Janzen-Connell Effects in a West African Montane Forest. – *Biotropica* 43: 77-83.
- [21] Mostacedo, B., Putz, F. E., Fredericksen, T. S., Villca, A., Palacios, T. (2009): Contributions of root and stump sprouts to natural regeneration of a logged tropical dry forest in Bolivia. – *Forest Ecology and Management* 258: 978-985.
- [22] Navarro-Cerrillo, R. M., Manzanedo, R. D., Bohorque, J., Sánchez, R., Sánchez, J., de Miguel, S., Solano, D., Qarro, M., Griffith, D., Palacios, G. (2013): Structure and spatio-temporal dynamics of cedar forests along a management gradient in the Middle Atlas, Morocco. – *Forest Ecology and Management* 289: 341-353.
- [23] Nguyen, H. H., Uria-Diez, J., Wiegand, K. (2016): Spatial distribution and association patterns in a tropical evergreen broad-leaved forest of north-central Vietnam. – *Journal of Vegetation Science* 27: 318-327.
- [24] Petritan, I. C., Marzano, R., Petritan, A. M., Lingua, E. (2014): Overstorey succession in a mixed *Quercus petraea*-*Fagus sylvatica* old growth forest revealed through the spatial pattern of competition and mortality. – *Forest Ecology and Management* 326: 9-17.
- [25] Pretzsch, H., Dieler, J. (2012): Evidence of variant intra- and interspecific scaling of tree crown structure and relevance for allometric theory. – *Oecologia* 169: 637-649.
- [26] Rice, J. A. (2007): *Mathematical statistics and data analysis*. – China machine press, Beijing.
- [27] Schupp, E. W., Jordano, P. (2011): The full path of Janzen-Connell effects: genetic tracking of seeds to adult plant recruitment. – *Molecular Ecology* 20: 3953-3955.
- [28] Sebkova, B., Samonil, P., Valtera, M., Adam, D., Janik, D. (2012): Interaction between tree species populations and windthrow dynamics in natural beech-dominated forest, Czech Republic. – *Forest Ecology and Management* 280: 9-19.
- [29] Steinitz, O., Troupin, D., Vendramin, G. G., Nathan, R. (2011): Genetic evidence for a Janzen-Connell recruitment pattern in reproductive offspring of *Pinus halepensis* trees. – *Molecular Ecology* 20: 4152-4164.
- [30] Su, S. J., Liu, J. F., He, Z. S., Zheng, S. Q., Hong, W., Xu, D. W. (2015): Ecological species groups and interspecific association of dominant tree species in Daiyun Mountain National Nature Reserve. – *Journal of Mountain Science* 12(3): 637-646.
- [31] Tao, D. L., Zhao, D. C., Zhao, S. D., Hao, Z. Q. (1995): Dependence of natural regeneration of Korean Pine on animals-An out closure experiment. – *Chinese Biodiversity* 3: 131-133. (in Chinese).
- [32] Wagner, S., Collet, C., Madsen, P., Nakashizura, T., Nyland, R. D., Sagheb-Talebi, K. (2010): Beech regeneration research: From ecological to silvicultural aspects. – *Forest Ecology and Management* 259: 2172-2182.
- [33] Wiegand, T., Moloney, K. A. (2004): Rings, circles, and null-models for point pattern analysis in ecology. – *Oikos* 104: 209-229.
- [34] Wright, S. J., Calderon, O., Hernandez, A., Detto, M., Jansen, P. A. (2016): Interspecific associations in seed arrival and seedling recruitment in a Neotropical forest. – *Ecology* 97: 2780-2790.
- [35] Xu, X. M., Harwood, T. D., Pautasso, M., Jeger, M. J. (2009): Spatio-temporal analysis of an invasive plant pathogen (*Phytophthora ramorum*) in England and Wales. – *Ecography* 32: 504-516.
- [36] Zhang, J., Hao, Z. Q., Song, B., Ye, J., Li, B. H., Yao, X. L. (2007): Spatial distribution patterns and associations of *Pinus koraiensis* and *Tilia amurensis* in broad-leaved Korean

- pine mixed forest in Changbai Mountains. – Chinese Journal of Applied Ecology 18: 1681-1687. (in Chinese).
- [37] Zhang, J., Hao, Z. Q., Sun, I. F., Song, B., Ye, J., Li, B., Wang, X. (2009): Density dependence on tree survival in an old-growth temperate forest in northeastern China. – Annals of Forest Science 66(204): 1-9.
- [38] Zhang, M. T., Kang, X. G., Meng, J. H., Zhang, L. X. (2015): Distribution patterns and associations of dominant tree species in a mixed coniferous-broadleaf forest in the Changbai Mountains. – Journal of Mountain Science 12: 659-670.
- [39] Zhang, M. T. (2017): Spatial Association and Optimum Adjacent Distribution of Trees In a Mixed Coniferous-Broadleaf Forest In Northeastern China. – Applied Ecology and Environmental Research 15: 1551-1564.
- [40] Zhao, H. Y., Kang, X. G., Guo, Z. Q., Yang, H., Xu, M. (2012): Species Interactions in Spruce-Fir Mixed Stands and Implications for Enrichment Planting in the Changbai Mountains, China. – Mountain Research and Development 32: 187-196.

ECOLOGICAL FITNESS OF TRIBENURON METHYL (ALS-INHIBITOR HERBICIDE) SUSCEPTIBLE AND RESISTANT BIOTYPES OF WILD MUSTARD IN COMPETITION WITH WHEAT

HAGHIGHI, A.¹ – MOHAMADDOUST CHAMANABAD, H. R.^{1*} – ZAND, E.² – BIABANI, A.³ – ASGHARI, A.¹

¹*Department of Agronomy and Plant Breeding, Faculty of Agriculture and Natural Resource, University of Mohaghegh Ardabili, Ardabil, Iran
(phone: +98-911-179-3043 – A. H.; +98-914-304-2117 – A. A.)*

²*Iranian Research Institute of Plant Protection, Agricultural Research, Education and Extension Organization, AREEO, Tehran, Iran
(phone: +98-912-300-3132)*

³*Department of Agronomy and Plant Breeding, Faculty of Agriculture, Gonbad-Kavous University, Gonbad-Kavous, Iran
(phone: +98-911-374-0583)*

**Corresponding author*

e-mail: hr_chamanabad@yahoo.com; phone: +98-915-108-2239

(Received 14th Nov 2018 ; accepted 25th Jan 2019)

Abstract. The occurrence of ALS-herbicide-resistant *Sinapis arvensis* in wheat crops causes crop yield losses, which makes it necessary to understand the factors that influence the interference of this weed to develop safer management strategies. This study was aimed to evaluate the ecological fitness of wild mustard that is susceptible (S biotypes) and resistant (R biotypes) to Tribenuron Methyl herbicide in competition with wheat in 2014-2017. The experiments were conducted in a greenhouse using a completely randomized design with four replications. The treatments were placed in pots and arranged in replacement series for three experiments: 1) wheat with the R biotype; 2) wheat with the S biotype; and 3) the R biotype with the S biotype) at the following ratios: 100:0, 75:25, 50:50, 25:75, and 0:100. The results showed that S biotype of wild mustard was more competitive than R biotype. There was no significant difference between S biotype and R biotype with accordance of the aggressivity index. The difference between the relative yield of wheat and biotypes of *S. arvensis* was significant, and regarding relative yield total, the S biotype was superior. Relative seed production index as the resultant index of competition at similar densities was not significant.

Keywords: *aggressivity index, herbicide resistance, relative yield total, Sinapis arvensis, Triticum aestivum*

Introduction

Since the advent of agriculture, crops have been at risk of weed invasion and damaged quantitatively and qualitatively. Thus, there have been ongoing efforts to reduce the negative impact of weeds on plant production (Vila-Aiub et al., 2015). Wild mustard is one of the most significant weed reducing the quantity and quality of wheat in Iran (Minbashi Moeini et al., 2006). For more than 40 years, relying too much on the technology of herbicides to reduce the amount of damage caused by weed, resulting in obtaining adaptive traits by weeds that help them survive and reproduce under herbicides application condition (Powles and Yu, 2010). As a consequence, more than 200 species of resistant weeds have been reported in the world (Heap, 2018) and this

trend of increasing weed resistance is spreading at a high pace (Norsworthy et al., 2012).

The organisms that genetically earn resistance to some environmental stresses may be ecologically inferior under non-stress conditions compared to susceptible plants (Bazzaz et al., 1987). Theoretically, weed resistance to herbicides is along with fitness cost that has been evaluated in several studies (Van Etten et al., 2016). Fitness cost (which is also called resistance cost) can be defined as reduced fitness of the plant in environments without herbicides (Deyle et al., 2013a). When the fitness costs are created by ecological interferences such as competition, it is termed ecological costs (Vila-Aiub et al., 2009). As an example, Gassmann and Futuyama (2005) stated that resistant plants had less fitness than susceptible plants due to less attraction of pollinators or the increase of pest damage. Also, Vila-Aiub et al. (2009) concluded that resistant plants pay more ecological cost due to the reduced competitiveness to capture resources. Based on the theory of resource allocation, plants show a reaction for the increase in ecological success with the approach of adaptability under environmental selection by directing resources to different organs, i.e. stem and root, and cell metabolism (Van Etten et al., 2016). Resistance due to mutation has been reported to reduce the allocation of resources to growth organs (Vencill et al., 2012). This theory helps to understand the phenomenon “resource trade-off” between plant growth, defensive duties, and reproduction (Coley et al., 1985). When a biotype of weed becomes resistant to herbicide, in most cases, its ability to compete for growth resources decreases (Vila-Aiub et al., 2015). The potential mechanism causing resistance cost is determined with the traits such as the plant size and tolerance to the availability of resources that one of these sources is nitrogen (Frenkel et al., 2017).

Competitive interferences in plants consist of two components: the impact of the plant on the availability of resources and plant response to changes in the availability of resources. Effect of a plant on environmental resources to overcome neighboring plants (competitive effects) or to survive regardless of the competitor’s presence (competitive response) depends on the ability of a plant (Goldberg, 1995). Fitness is one of the most effective factors in the creation and persistence of resistant and susceptible biotypes of weeds (Gressel and Segel, 1990; Maxwell et al., 1990). Fitness is defined as the ability of an organism to establish, survive and reproduce successfully (Radosevich et al., 1997). Therefore, the difference between the fitness of R biotypes and S biotypes might be due to the difference in survival, fertility (Putwain and Mortimer, 1989), or the ability to compete (Massinga et al., 2005; Marshall et al., 2005).

The reason for estimating the fitness costs about herbicides resistance is that this may reduce the frequency of resistant genotypes in weed communities without herbicide application and it may result in the identification of approaches to managing resistant weeds (Vila-Aiub et al., 2009). The evolution of herbicide resistance in weeds provides an appropriate model to examine the phenomenon “resource trade-off” (development, defense, reproduction) predicted by the theory of resource allocation (Bergelson and Purrington, 1990). Knowing the biological properties of resistant masses and also the mechanisms resulting in resistance may be useful in the management of them (Jordan et al., 1999). Measuring the difference between the fitness of resistant weeds and susceptible weeds, the evolution of resistance to herbicides can be predicted and also, the management strategies can be developed in order to use the traits reducing the ecological traits of resistant masses (Vila-Aiub, et al., 2015). Also, it can be effective in reducing the frequency of resistant plants in the affected population (Gill et al., 1996).

The difference between the fitness of resistant and susceptible species is an essential factor in predicting the evolution of resistance to the herbicide. In the case of removal of selective pressure of herbicide, if the fitness of resistant plant is less than susceptible plant, the resistant plant is replaced by the susceptible plant (Weiderholt and Stoltenberg, 1996). In this case, after the occurrence of the resistance in weed population, it is hoped that the resistance will be reduced (Zand et al., 2008). However, if this difference is not effective, the frequency of resistant plants will not probably decrease in population, in this case, long-term management of resistant plant needs to adopt the strategies reducing the severity of selection which is desirable for resistant plants and also, needs to combine other management strategies. These strategies are the rational application of herbicides, using the unique biological aspects of resistant weeds and manipulating the farming systems in order to maximize the effectiveness of chemical and non-chemical weed management (Weiderholt and Stoltenberg, 1996). Survival, competitiveness and reproductive success are the criteria of fitness (Massinga et al., 2005). Therefore, this can be performed by performing tests and evaluating the competitive ability and seed production.

As a result, it has been hypothesized that wild mustard has a superior competitive ability than wheat and that there may be differences in the competitiveness among biotypes of wild mustard that are resistant and susceptible to ALS-inhibitor herbicides. Thus, this study aimed to investigate the competitive ability of wheat in coexistence with biotypes of wild mustard that are susceptible and resistant to ALS-inhibitor herbicides and to determine whether there are differences in the competitiveness between the different biotypes.

Materials and methods

This study consisted of two phases: a) collecting the wild mustard seeds of populations which were suspicious to be resistant to Tribenuron Methyl herbicide from the wheat fields of Golestan Province of Iran and gathering the histories of the fields (Fig. 1) and then, screening the masses and determining their possible resistance in the greenhouse of Agriculture School of Gonbad-Kavous University, Iran (according to Moss et al., 1999).

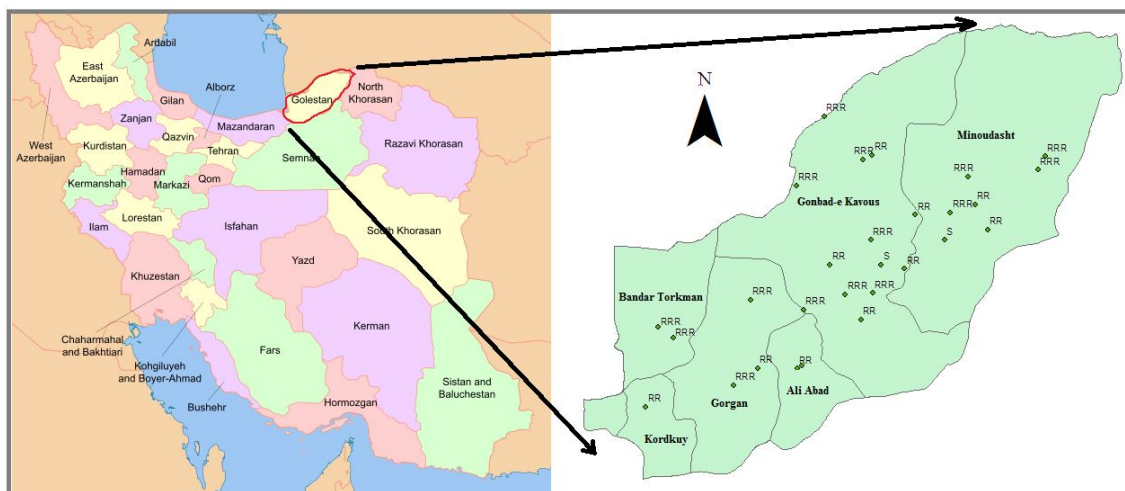


Figure 1. Geographic location and resistance rates of wild mustard seeds

b) Selecting a resistant biotype (R biotype) along with susceptible biotype (S biotype) and examining the possible relative fitness of them in competition with wheat after identifying the results of screening at Gonbad-Kavous Agricultural Research Station, Iran (Table 1).

Table 1. Specifications of surveyed farms, geographic location and resistance rates based on the Moss method

Wild mustard biotype	Longitude	Altitude	Weight relative to the control	Resistance type (Moss et al., 1999)
Sr-btm	54-15-59.68	37-0-12.08	0.86	RRR*
Sr-ems	54-51-12.97	37-6-13.63	0.83	RRR
Sr-aam	54-36-56-42	37-8-24.62	0.80	RRR
Sr-nsh	55-9-57.54	37-9-41.02	0.89	RRR
Sr-azs	54-11-58.76	37-2-33.01	0.88	RRR
Sr-ndm	54-38-41.30	36-53-36.97	0.27	R?*
Sr-gjn	54-32-15.33	36-50-0.07	0.78	RRR
Sr-aak	54-50-44.59	36-54-10.92	0.36	RR**
Sr-fza	54-49-25.87	36-53-27.28	0.63	RR
Sr-rmn	55-6-45.57	37-3-58.45	0.26	R?
Sr-kok	54-8-30.37	36-45-19083	0.36	RR
Sr-dak	55-31-22.01	37-26-51.14	0.76	RRR
Sr-Bsh	55-41-26.47	37-23-5.16	0.50	RR
Sr-Igr	55-18-46.16	37-14-49.35	0.41	RR
Sr-Gzl	54-57-21.47	37-48-3.77	0.73	RRR
Sr-Gbj	54-57-40.26	37-15-56.10	0.95	RRR
Sr-Gmt	55-9-44.70	37-21-9.62	0.87	RRR
Sr-Cpg	55-7-52.45	37-38-38.55	0.92	RRR
Sr-Ylb	55-36-15.67	37-34-39.74	0.93	RRR
Sr-Dsb	54-49-32.29	37-33-2.76	0.90	RRR
Sr-Mrt	55-55-21.57	37-35-46.68	0.90	RRR
Sr-Gld	55-57-19.73	37-38-41.57	0.90	RRR
Sr-Blm	55-2-35.74	37-9-24.27	0.94	RRR
Sr-Kgn	55-29-42.67	37-20-58.75	0.12	S****
Ss-Ykg	55-38-8.45	37-28-31.77	0.64	RR
Sr-Agj	55-21-51.90	37-26-28.49	0.45	RR
Sr-Abd	55-10-20.25	37-39-33.10	0.25	R?
Ss-Gad	55-12-24.49	37-15-45.06	0.11	S

*RRR: complete resistant, *R?: suspecting resistant, **RR: resistant, ****S: susceptible

First phase: in June 2014, the seeds of Wild mustard were collected from the fields in which Tribenuron Methyl herbicide was used for at least 7-years by knowing the history of wheat fields. Totally, from each of 28 fields, 500-gram seeds were collected from the parts which were not controlled by Tribenuron Methyl herbicide. The masses of seeds were planted in the pots with the diameter of 30 cm and depth of 35 cm in fall in the same year to determine the possible resistance to Tribenuron Methyl herbicide. Firstly, in order to break dormancy, the seeds were treated with 2 mg of Gibberellic acid

(Abdollahpour et al., 2013). For each biotype, 20 seeds were planted in prepared pots, and they were placed in the open air. After the appearance of true leaves, the density of each pot was reduced to 10 seeds. At 5-7 leaf stage of wild mustard, the common dose of Tribenuron Methyl herbicide (Nezamabadi et al., 2007), 25 g per hectare (commercial form) was used to determine the possible resistance of masses. According to the method provided by Moss et al. (1999) which is used to determine the resistance in a single dose, the possible resistance of masses was determined. In this method, four weeks after spraying, the live plants of each pot were pruned, and after recording the number of plants, their fresh weight was recorded. With comparing the fresh weight of plant of each mass (W_t) treated by herbicide to the control sample not treated (W_o) with herbicide, the possible resistance was estimated by *Equation 1*. In the method provided by Moss et al. (1999), less than 36% reduction, 36-72% reduction, 72-81% reduction and 81-100% reduction in fresh weight are considered as completely resistant (RRR), resistant (R), susceptible to be resistant (R?) and susceptible (S), respectively.

$$W_i = \frac{W_t}{W_o} \times 100 \quad (\text{Eq.1})$$

In screening the collected masses by the mentioned method, 57.14%, 25%, 10.71% and 7.14% of samples were resistant (RRR), resistant (R), susceptible to be resistant (R?) and susceptible (S), respectively. Because of collecting the S biotype to Tribenuron Methyl herbicide from the region of Gonbad-Kavous, the most resistant mass of this region was selected as the R biotype so that they have least genetic differences, and these biotypes were used to examine the ecological fitness and possible costs of herbicide resistance. 2nd phase: After selecting the seeds, the steps of dormancy breaking and planting in pots were done under the previous method. The experiment was performed in a randomized complete block design with four replications and nine treatments and the form of replacement series in larger pots with a diameter of 40 cm and a depth of 35 cm. The soil of pots was prepared with a combination of frost soil, manure and washed sand in equal ratios to ensure that there were no seeds of wild mustard. The treatments consisted of R and S biotypes of wild mustard and wheat (*Triticum aestivum*) in replacement ratios of 0:100, 75:25, 50:50, 25:75 and 100:0 (S and R biotypes of wild mustard and wheat). The total number of pots was 36 (each replication contained nine pots, one pot of wheat, four pots with different densities of S biotype of wild mustard and four pots with different densities of R biotype of wild mustard). Planting dates were 5th January 2014 and 11th November 2015. After examining the wheat and biotypes of wild mustard physiologically, all of them were pruned, and their dry weight and yield components were measured separately. They were weighted by weighing scales with the accuracy of 0.001, and the amount of reproduced seeds of wild mustard was estimated by *Equation 1*. After variance analysis and comparing the means, the indices of competitiveness were used for weeds and crops. With mathematical indices, the features of plant competition, including the intensity of competition and its importance, the effects of competition, reactions, and results of the competition can be examined quantitatively. The indices facilitate the expression and explanation of results, and the results of different studies can be compared by purifying and concentrating the test data (Weigelt and Jolliffe, 2003). Competition indices were divided into three parts of the intensity of competition, the

impact of competition and the results of the competition. SAS software was used to analyze the data.

$$S_n = TSw \times 50 / S_w \quad (\text{Eq.2})$$

Equation 2 was used to determine the amount of reproduced seeds per wild mustard plant (Vila-Aiub et al., 2009). In this equation, S_n is the number of reproduced seeds per wild mustard plant, TS_w is the total weight of reproduced seeds per wild mustard plant, and S_w is the mean weight of 50 reproduced seeds of wild mustard biotypes.

A) In examining the intensity of competition, the indices of aggressivity and competition ratio were used. In examining the intensity of competition, the changes in the competition of the densities of the population are necessary (Sackville and Hamilton, 2001), so, in all equations related to the intensity of competition, the density was not calculated. However, this does not mean that the intensity of competition is independent of density because, in these indices, the variables depend on the density and frequency naturally (Weigelt and Jolliffe, 2003).

Aggressivity was examined by *Equation 3*.

$$A = 1/2[(S_{mix}/W_{mono}) - (W_{mix}/S_{mono})] \quad (\text{Eq.3})$$

S_{mix} : wild mustard at different ratios with wheat

W_{mix} : wheat at different ratios with S and R biotypes

S_{mono} : wild mustard in mono culture

W_{mono} : wheat in mono culture

Competition ratio was examined by *Equation 4*.

$$CR = \left[\frac{S_{mix}/S_{mono}}{W_{mix}/W_{mono}} \right] \quad (\text{Eq.4})$$

S_{mix} : wild mustard at different ratios with wheat

W_{mix} : wheat at different ratios with S and R biotypes

S_{mono} : wild mustard in mono culture

W_{mono} : wheat in mono culture

B) The competition effects of S and R biotypes were examine with Relative Yield and Relative Yield Total (*Eq. 5*).

$$RY = \frac{A_{mix}}{A_{mono}} \quad (\text{Eq.5})$$

A_{mix} : Different combinations of wheat and wild mustard biotypes

A_{mono} : wheat and S and R biotypes in pure culture

C) The outcome of competition was examined by Relative seed production index (*Eq. 6*).

$$RRR = S_r / S_s \quad (\text{Eq.6})$$

S_r : the amount of seeds per resistant wild mustard biotype

Ss: the amount of seeds per S biotype

Fitness Cost of R biotype to S biotype was examined by (Eq. 7).

$$FC = 1 - (WR / WS) \times 100 \quad (\text{Eq.7})$$

The analysis of variance, comparison of mean squares and Orthogonal contrasts were performed by SAS software Ver. 9.1 and the figures were designed via Microsoft Excel 2013.

Results

Results showed that with reduction wild mustard ratio, wild mustard dry weight increased significantly for two biotypes, resulting reduction in wheat dry matter. The reduction of wheat dry matter in competition with biotypes of has been almost uniform and in comparing the S and R biotypes was not significant (Fig. 2(A) and Fig. 2(B)). Comparing these two figures showed that this increase of wild mustard dry matter in S biotype was greater than R biotype. At same wild mustard ratio, the S biotype had greater dry matter than R biotype, and this shows that the increased intraspecific competition in the S biotype compared to R biotype.

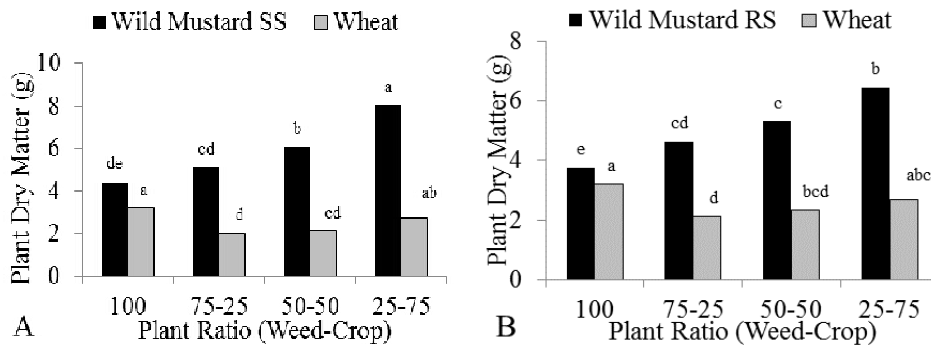


Figure 2. The impression of wheat and wild mustard (A: S biotype, B: R biotype)

As shown in Figure 3, it was observed that the decrease in the number of the wheat spikelet in competition with S biotype was more than the R biotype, but the difference was significant only at the 50:50 ratios.

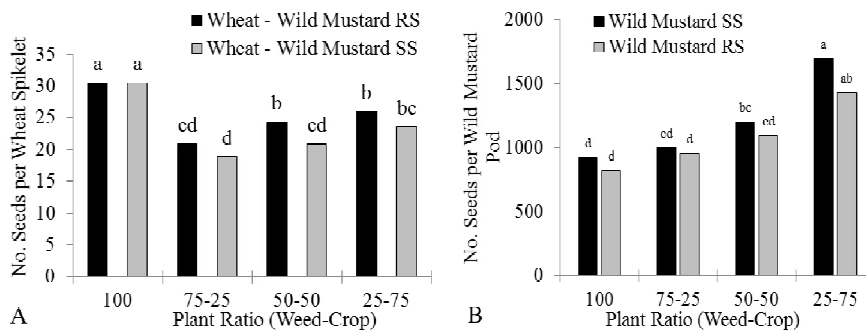


Figure 3. Number of seeds; A: per wheat spikelet in competition with wild mustard, B: number of seeds per wild mustard pod in competition with wheat

Figure 4 is related to the number of seeds in the biotypes of wild mustard, the difference between these two types of biotypes was not significant at the density ratio of 50:50, but the amount of reproduced seeds in S biotype was greater than R biotype.

In accordance the variance analysis of the competition indices (Table 2), it was observed that the differences between the competition ratios of S and R biotypes of wild mustard were significant at the confidence level of 5% in terms of dry weight, but they were not significant in terms of the number of reproduced seeds. The difference between the indices of aggressivity of S and R biotypes of wild mustard was not statistically significant concerning dry weight (Table 2). About wheat, the difference between the relative yields was significant at the confidence level of 5% and about S and R biotypes of wild mustard, it was significant at the confidence level of 1% (Table 2). The differences between the indices of RYT of S and R biotypes of wild mustard were not statistically significant (Table 2).

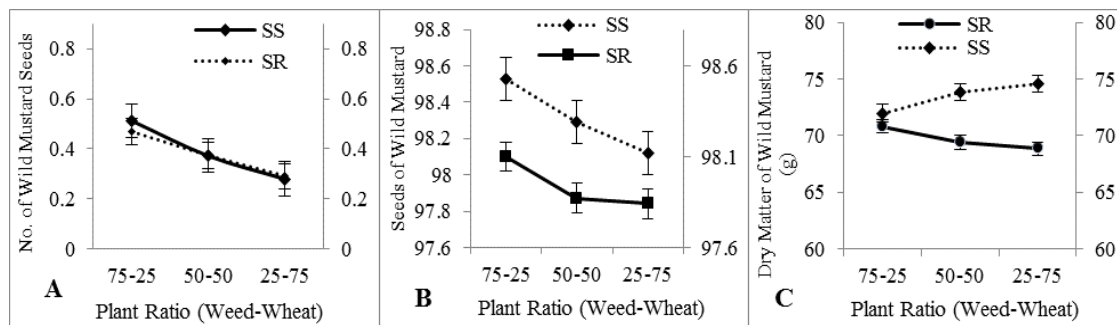


Figure 4. Relative seed reproduction of wild mustard biotypes based on reproduced seeds (A) and competition ratio of wheat and wild mustard biotypes in seed reproduction (B) and dry matter (C)

Table 2. Analysis of variance of competition indices in wild mustard biotypes and wheat at various planting ratios and group comparisons of ratios of S and R wild mustard biotypes with wheat

Source of variation	Degree of freedom	CR ¹ /dry matter of wild mustard	CR/seed of wild mustard	A ² /wild mustard	RY ³ /wheat	RY/wild mustard	RYT ⁴ /wild mustard
YEAR	1	2.702**	3.56**	0.057*	0.283 ^{ns}	1.641*	1.641**
R(Y)	6	0.071*	0.57 ^{ns}	0.002 ^{ns}	0.093**	1.187 ^{ns}	4.95 ^{ns}
TREAT	5	0.574 ^{ns}	3.93*	0.016*	0.069 ^{ns}	3.071 ^{ns}	43.21*
T*Y	5	0.056 ^{ns}	0.35 ^{ns}	0.001 ^{ns}	0.089 ^{ns}	1.050 ^{ns}	4.39 ^{ns}
Error	30	0.269	0.34	0.006	0.069	0.93	16.07
C.V. (%)		17.21	22.60	19.54	23.19	0.31	5.60
Orthogonal contrasts							
(0.75)Ss+(0.25)W vs. (0.75)Rs+(0.25)W	1	1.248*	1.735*	0.04*	0.026 ^{ns}	99.5*	0.801**
(0.50)Ss+(0.50)W vs. (0.50)Rs+(0.50)W	1	0.074 ^{ns}	0.1008 ^{ns}	0.001*	0.146**	5.3 ^{ns}	0.001 ^{ns}

(0.25)Ss+(0.75)W vs. (0.25)Rs+(0.75)W	1	1.476*	2.002*	0.041*	0.077*	107.22**	2.197**
Ss vs.Sr	1	1.414*	0.944*	0.043*	0.025**	108.33*	1.834**

¹Competition ratio, ²Aggressivity, ³Relative yield, ⁴Relative yield total. * and **: significant difference at 1% and 5% probability; ns: not significant

Table 3 shows the results of the examination of competition ration based on dry weight. It was observed that the S biotype was superior to the R biotype. In the combination of relative densities of S biotype with wheat, with the decrease in the ratio of combination, the competition index increased and with the increase in it, the index reduced. This shows the increase in the intraspecific competition of S biotype. Nevertheless, in R biotype, in addition to the reduced index, the changes in the ratio in total combination had no significant impact on the competition ratio.

Table 3. Mean comparison of competition parameters on R and S biotypes in different plant ratios

Comparison of mean	CR ¹ /dry matter of wild mustard	CR/seed of wild mustard	A ² /wild mustard	RY ³ /wheat	RY/wild mustard	RYT ⁴ /wild mustard	RRR/wild mustard
(0.25)Ss+(0.75)W	74.58 a ⁵	98.53 a	0.512 a	0.343 c	3.023 a	3.36 a	1.86 a
(0.5)Ss+(0.5)W	73.85 a	98.29 ab	0.372 ab	0.357 c	2.94 ab	3.29 ab	1.42 bc
(0.5)Ss+(0.25)W	71.98 ab	98.12 ab	0.280 b	0.393 bc	2.63 bc	3.03 bc	1.105 c
(0.25)Rs+(0.75)W	70.83 bc	98.10 ab	0.47 a	0.415 ab	2.48 cd	2.89 c	1.77 ab
(0.5)Rs+(0.5)W	69.41 bc	97.87 b	0.374 ab	0.444 a	2.31 cd	2.76 c	1.36 bc
(0.5)Rs+(0.25)W	68.86 c	97.84 b	0.290 b	0.458 a	2.28 d	2.74 c	1.20 c
LSD	2.69	0.589	0.177	0.055	0.34	0.30	0.33

¹Competition ratio, ²Aggressivity, ³Relative yield, ⁴Relative yield total. ⁵Means within each column followed by the same letter are not significantly different at 0.05 probability level according to LSD

The difference between the aggressivity index of susceptible wild mustard biotype and R biotype was not significant, but this index in S biotype was greater than R biotype. In this index, the degrees of aggressivity of both S and R biotypes increased by the reduction in the ratio in total density. The relative yield of wheat was statistically significant at the confidence level of 5% (Table 3). The relative yield of wheat in combination with R biotype was greater. At the highest density of R biotype of wild mustard with wheat (25%:75%), the greatest relative yield was obtained. The relative yield of wheat in combination with S biotype was significantly less than R biotype. It was observed in S biotype that with the increase in the ratio of total density for wild mustard, the relative yield of wheat increased. About this index, it can be said that the S biotype in compared with the R biotype significantly reduced the relative yield of wheat, but with the increase in the density of wild mustard biotypes and also the increase in the intraspecific competition, the relative yield of wheat increased. The difference between the relative yields of wild mustard biotypes was significant at the confidence level of 1%. The differences between the relative yields of S biotype of wild mustard in different combination with wheat were not significant. In orthogonal

comparisons of *Table 3*, it was observed that the indices of competition significantly changed with the changes in the ratio of wild mustard biotypes and or wheat at different density ratios. This shows the indirect impact of relative density and total density on the estimation of indices.

However, concerning the S biotype, it was observed that the increase in the ratio of this biotype at the different ratios with wheat reduced the relative yield. The highest relative yield of S biotype was obtained at the ratio of 25% of total density.

Figure 5A shows the fitness cost of R biotype in seed reproduction and *Figure 5B* shows it in the biological yield. The fitness cost of R biotype was greater than S biotype in both cases. Cost of resistance for R biotype at different intercropping ratios (resistant wild mustard: Wheat) of 100%: 0%, 25%: 75%, 50%: 50% and 75%: 25% resulted in 14.73, 9.39, 12.21, 19.67 percent decrease in biological yield and 4.60, 10.76, 8.71 and 15.75 percent decrease in seed reproduction, respectively.

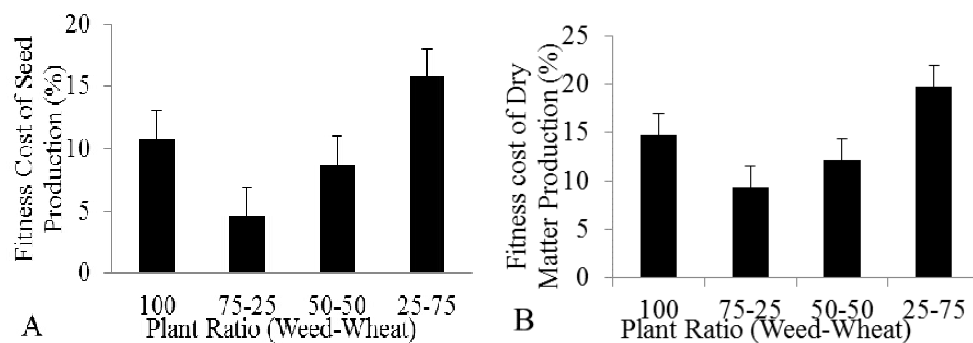


Figure 5. Percentage of the fitness cost of wild mustard R biotype in seed reproduction (A), and dry mass production (B)

Discussion

The results of this study showed that the ecological costs are related to the resistance of wild mustard to Tribenuron Methyl herbicide. The R biotype of wild mustard in competition with wheat had fewer damages compared to S biotype (competitive effects). Besides, the capacity of vegetative and reproductive resource allocation in competition with wheat (competitive reaction) in R biotype was significantly less than S biotype. The ecological costs related to the herbicide resistance were in line with the theory of resource allocation that predicts a negative correlation between plant growth and resistance to environmental stresses (Bazzaz et al., 1987; Lerdaud and Gershenson, 1997). Also, the results of this study showed that in conditions of intense competition, the cost of herbicide resistance is higher (*Figs. 1* and *2*). In the higher ratios of wild mustard, the amount of dry matter of R biotypes was less than S biotype. In competition with wheat, S and R biotypes of wild mustard showed different effects. Conard and Radosevich (1979) found dry matter production of S biotypes (*Senecio vulgaris* and *Amaranthus retroflexus*) was higher than that of R biotypes, under both competitive and non-competitive conditions. Costa and Rizzardi (2014) also reported that R and S biotypes of *Raphanus raphanistrum* significantly decreased the wheat shoot dry matter.

Results showed that in the intense competition, R biotype has less fitness than S biotype in attracting resources. This result is consistent with the result of the study by Herms and Mattson (1994) that believed the cost of resistance increases regarding

resource constraints. The ability of a plant to reduce the growth of neighboring plants (competitive effect) and to continue to grow despite the presence of neighboring plants (competitive reaction) depends on the capacity of attracting resources (Goldberg, 1995). Such processes, which are related to the difference in the amount of dry matter of the plant height, the potential ability of a plant to attract the light and the continuation of this positive feedback, result in disproportionate resources allocation. Ranking competitive effects based on the ability to reduce the growth of targeted species is associated with ranking the maximum potential of measures between R and S biotypes. So, the larger plants, i.e., S biotypes, overcome the wheat with greater power. In nature, due to this problem, the S biotypes overcome the R biotypes over a long time. This result is consistent with the results of other studies on different competitive effects of plant species in terms of plant size (Goldberg, 1995).

The results showed that intraspecific competition between the S biotypes was more than R biotypes. By accepting that the capacity of attracting the resources is greatly related to the size of a plant, it can be predicted that competitive effects and reaction will have a positive correlation with larger plants and they will have more competitive reactions than smaller plants (Goldberg, 1995). In conditions of competition with wheat, S biotypes clearly showed more competitive reaction than the R biotypes, and this resulted in more reduction in wheat dry matter and yield. Different tolerance to low levels of resources can result in different competitive reactions between S and R biotypes. This potential ability of S biotype to continue the growth regarding resources constraints may appear in the conditions in which there is intense competition for resources. For example, the competitive effects of wheat on R biotype were more compared to S biotype. Its signs can be observed in the effects of vegetative and reproductive organs of R biotype compared to S biotype. The differences in the dry matter of targeted plant showed that the competitive reaction of R biotypes might appear concerning intense competition or significant environmental resource constraints. In the diminished competitive reaction for resources is related to the effect of herbicide resistance, it can reduce the fitness of plant that finally will result in a reduction in R biotype compared to S biotype with natural selection. Therefore, this fitness cost in keeping genetic polymorphism is related to the herbicide resistance (Antonovics and Thrall, 1994). Despite the diminished ability of R biotypes in competition with wheat, herbicide resistant plants showed poor intraspecific competition with the capacity of growth continuation in response to different cultures. This may be related to poor intraspecific competition due to the smaller size. Stoll and Prati (2001) reported that less intraspecific spatial density might be an approach to advance the survival of weaker competitors (R biotype) compared to stronger competitors (S biotype) and also, to prevent the replacement. Vila-Aiub et al. (2009) believed that apart from the concept of evolution of herbicide resistance, the intensity of selective pressure that is caused by humans can change the approaches in the history of plant life during only a few generations. These approaches are different methods of resources allocation in growth, defense, and reproduction models. Now, it is proved that revolutionary changes can earn a place on ecological time scales (Carrol et al., 2007) and this process can be accelerated by human activities (Palumbi, 2001).

Conclusion

The results showed that the R biotype of wild mustard caused significant damage to dry weight and economic yield of wheat, although the damage was less than the S biotype. The trend of variations in the dry weight of resistant and susceptible wild mustard biotypes at different ratios of density showed that the intra-specific competition in the resistant biotype was higher than that of the susceptible biotype. The competitive indices and relative yield of susceptible biotypes of wild mustard were higher than those of resistant biotypes, but the invasive index was not significant. Seed production of the resistant biotype was lower than that of the susceptible biotype of wild mustard, but since the seed production of this weed is very high, this biological characteristic of the R biotype could hardly be used for short-term management of this weed. Due to the fact that the frequency of resistant wild mustard plants in the short term will not be reduced because of reduced fitness cost, the use of integrated methods such as chemical, agronomic and mechanical ones, along with the use of biological and ecological aspects, could be used as a strategy to reduce the population of wild mustard R biotype. It is suggested that the ecological dynamics and fitness cost of wild mustard R and S biotypes should be investigated in infected fields, both practical and long-term.

REFERENCES

- [1] Bazzaz, F. A., Chiariello, N. A., Coley, P. D., Pitelka, L. F. (1987): Allocating resources to reproduction and defense. – *Bioscience* 37: 58-67.
- [2] Bergelson, J., Purrington, C. B. (1995): Surveying patterns in the cost of resistance in plants. – *American Naturalist* 148: 536-558.
- [3] Carrol, S. P., Hendry, A. P., Reznick, D. N., Fox, C. W. (2007): Evolution on ecological time scales. – *Functional Ecology* 21: 387-393.
- [4] Chapin, F. S., Autumn, K., Pugnaire, F. (1990): Evolution of suites of traits in response to environmental-stress. – *American Naturalist* 142: 278-292.
- [5] Coley, P. D., Bryant, J. P., Chapin, F. S. (1985): Resource availability and plant anti-herbivore defense. – *Science* 230: 895-899.
- [6] Conard, S. G., Radosevich, S. R. (1979): Ecological fitness of *Senecio vulgaris* and *Amaranthus retroflexus* biotypes susceptible or resistant to atrazine. – *Journal of Applied Ecology* 16: 171-177. DOI: 10.2307/2402736.
- [7] Costa, L. O., Rizzardi, M. A. (2014): Resistance of *Raphanus raphanistrum* to the herbicide metsulfuron-methyl. – *Planta Daninha* 32(1): 181-187. <http://dx.doi.org/10.1590/S0100-83582014000100020>.
- [8] Delye, C., Jasieniuk, M., Le Corre, V. (2013): Deciphering the evolution of herbicide resistance in weeds. – *Trends Genetics* 29: 649-658.
- [9] Frenkel, E., Matzrafi, M., Rubin, B., Peleg, Z. (2017): Effects of environmental conditions on the fitness penalty in herbicide resistant *Brachypodium hybridum*. – *Frontiers in Plant Science* 8: 94-105. DOI: 10.3389/fpls.2017.00094.
- [10] Gassmann, A. J., Futuyma, D. J. (2005): Consequence of herbivore for the fitness cost of herbicide resistance: photosynthetic variation in the context of plant-herbivore interaction. – *Journal of Evolutionary Biology* 18: 447-454.
- [11] Gill, G. S., Cousense, R. D., Allan, M. R. (1996): Germination, growth and development of herbicide resistant and susceptible population of rigid ryegrass (*Lolium rigidum*). – *Weed Science* 44: 252-256.
- [12] Goldberg, D. E. (1995): Components of Resource Competition in Plant Communities. – In: Grace, J. B., Tilman, D. (eds.) *Perspectives in Plant Competition*. Academic Press, San Diego, pp. 27-49.

- [13] Gressel, J., Segel, I. A. (1990): Modeling the effectiveness of herbicide rotation and mixtures as strategic to delay or to percole resistance. – *Weed Technology* 4: 186-195.
- [14] Heap, I. M., 2018. The International Survey of Herbicide Resistant Weeds. – www.weedscience.org (accessed Nov 24, 2018).
- [15] Herms, D. A. Mattson, W. J. (1994): Plant-growth and defense. – *Trends in Ecology Evolution* 9: 488-498.
- [16] Jordan, N., Kelrick, M., Brooks, J., Kinerk, W. (1999): Biorational management tactics to select a gimst triazine-resistant *Amaranthus hybridus*: a field trial. – *Journal of Applied Ecology* 36: 123-13.
- [17] Lerdaun, N., Gershenson, J. (1997): Allocation Theory and Chemical Defense. – In: Bazzaz, F., Grace, T. (eds.) *Plant Resource Allocation*. Academic Press, London.
- [18] Marshall, M., Khatib, K., Loughin, T. (2005): Gene flow, growth, and competitiveness of imazethapyr resistant common sunflower. – *Weed Science* 49: 14-21.
- [19] Massinga, R. A. M., Al-Khatib, K. P., Amand, S. T., Miller, J. F. (2005): Relative fitness of imazamox-resistant common sunflower and prairie sunflower. – *Weed Science* 53: 166-175.
- [20] Maxwell, B. D., Roush, M. L., Radosevich, S. R. (1990): Predicting the evolution and dynamics of herbicide resistance in weed populations. – *Weed Technology* 4: 2-13.
- [21] Minbashi Moeini, M., Nezamabadi, N., Zand, E. (2007): Analysis approach for weed management of irrigated wheat fields. – Key articles of 2nd Conference on Weeds in Iran, 30th and 31th October, Mashhad.
- [22] Moss, S. R., Clarke, J. H., Blair, A. M. Culley, T. N. Read, M. A. Ryan, P. J., Turner, M. (1999): The occurrence of herbicide-resistant grass-weeds in the United Kingdom and a new system for designating resistance in screening assay. – *Proceeding of the Brighton Crop Protection Conference on Weeds*. BCPC, Hampshire, UK, 179-184.
- [23] Nezamabadi, N., Zand, E., Pourazar, R., Baghestani Torshiz, N., Baghestani Meybodi, M. A. (2007): Dose-response of the number of broadleaf weeds in wheat fields to different formulations of Tribenuron Methyl herbicide. – *Journal of Pajouhesh va Sazandegi* 74: 99-107.
- [24] Norsworthy, J. K., Ward, S. M., Shaw, D. R., Llewellyn, R. S., Nichols, R. L., Webster, T. M., Bradley, K. W., Frisvold, G., Powles, S. B., Burgos, N. R., Witt, W. W., Barrett, M. (2012): Reducing the risks of herbicide resistance: best management practices and recommendations. – *Weed Science* 60: 31-62. <http://dx.doi.org/10.1614/WS-D-11-00155.1>.
- [25] Palumbi, S. R. (2001): Evolution humans as the world's greatest evolutionary force. – *Science* 293: 1786-1790.
- [26] Powles, S. B., Yu, Q. (2010): Evolution in action: plants resistant to herbicides. – *Annual Review of Plant Biology* 61: 317-347.
- [27] Putwain, P. D., Mortimer, A. M. (1989): The resistance of weeds to herbicides: Rational approaches for containment of a growing problem. – *Proceedings of the Brighton Crop Protection Conference - Weeds*, pp. 432-438.
- [28] Radosevich, S., Holt, J. Ghersa, C. (1997): *Weed Ecology, Implications for Management*. 2nd Ed. – John Wiley and Sons, Inc., New York.
- [29] Stoll, P., Prati, D. (2001): Interference aggregation alters competitive interactions in experimental plant communities. – *Ecology* 82: 319-327.
- [30] Van Etten, M. L., Kuester, A., Chang, S. M., Baucom, R. S. (2016): Fitness costs of herbicide resistance across natural populations of the common morning glory, *Ipomoea purpurea*. – *Evolution* 70: 2199-2210.
- [31] Vencill, W. K., Nichols, R. L., Webster, T. M., Soteris, J. K., Mallory-Smith, C., Burgos, N. R., Johnson, W. G., McClelland, M. R. (2012): Herbicide resistance: toward an understanding of resistance development and the impact of herbicide-resistant crops. – *Weed Science* 60: 2-30.

- [32] Vila-Aiub, M. M., Powles, N. P. (2009): Evidence for one ecological cost of enhanced herbicide metabolism in *Lolium rigidum*. – *Journal of Ecology* 97: 772-780.
- [33] Vila-Aiub, M. M., Gundel, P. E., Preston, C. (2015): Experimental methods for estimation of plant fitness costs associated with herbicide resistance genes. – *Weed Science* 63: 203-216.
- [34] Weiderholt, R. J., Stoltenberg, D. E. (1996): Absence of differential fitness between Giant foxtail (*Setaria faberi*) Accessions resistant and susceptible to Acetyl-coenzyme A carboxylase inhibitors. – *Weed Science* 44(1): 18-24.
- [35] Weigelt, A., Jolliffe, P. (2003): Indices of plant competition. – *Journal of Ecology* 91: 707-720.
- [36] Zand, E., Baghestani, M. A., Mousavi, S. K., Oveisi, M., Ebrahimi, M., Rastgoo, M. M., Labbafi Hoseinabadi, R. (2008): *Weed Management Guide*. – Jahad Daneshgahi Press, Mashhad (in Persian with English summary).

IMPACT OF ARBUSCULAR MYCORRHIZAL FUNGI ON SOME DEFENSE ENZYME ACTIVITIES AT AN EARLY STAGE OF MAIZE (*ZEAMAYS*. L) UNDER DIFFERENT ABIOTIC STRESSES

MAYER, Z.¹ – JUHÁSZ, Á.¹ – VO TRUNG, A.¹ – POSTA, K.^{1,2*}

¹*Institute of Genetics, Microbiology and Biotechnology, Szent István University
Páter Károly u. 1, Gödöllő 2100, Hungary
(phone: +36-28-522-000)*

²*Industrial University of Ho Chi Minh City, 12 Nguyen Van Bao Street
Ho Chi Minh City, Vietnam*

*Corresponding author

e-mail: posta.katalin@mkk.szie.hu; phone: +36-28-522-000/ext. 2105

(Received 1st Dec 2018; accepted 14th Feb 2019)

Abstract. Environmental impacts on plants are becoming more extreme and their response to these effects is a key factor in plant production. Promoting the adaptability of plants is a priority area, one of the opportunities is the symbiotic system of mycorrhizal fungi with plants. Arbuscular mycorrhizal (AM) fungi have beneficial effects on plants' water and nutrient uptake and increasing plant defense mechanisms to alleviate different oxidative stresses. The aim of this study was to investigate how arbuscular mycorrhizal fungi influence the changes in some plant defense enzymes (catalase (CAT), peroxidase (PER), glutathione S-transferase (GST), polyphenol oxidase (PPO)) together with gene expressions under salt, high temperature and drought stresses at an early stage of maize (*Zea mays* L.). The results suggest that AM fungi inoculation may take part in the alleviation processes caused by high temperature, salt and drought stresses. However, these mechanisms are influenced by the age of the plants which is most likely justified by energy considerations.

Keywords: *drought stress, salinity stress, AM fungi inoculation, peroxidase, catalase*

Introduction

Maize (*Zea mays* L.) is one of the most important widely grown crops. According to the latest statistical data on maize growing in Hungary, the total harvested area and output was 0.99 Mha and 6.8 Tg in 2017. Several studies show the dramatically negative impact of climate change on crop production, and similar trend can be found in Hungarian maize production caused by the frequency of extreme agrometeorological phenomenon (Nagy, 2010; Lobell et al., 2012; Pepó and Vári, 2016). However only few works have been done at an early stage, where plants not yet adapted to these conditions. Various biotic and abiotic stresses such as salt, extreme temperature and drought are the most limiting factors on plant growth and decrease crop yield (Molazem and Azimi, 2015). Under stress conditions highly reactive oxygen species (ROS) are generated in plant and ROS-scavenging enzymes (catalase, peroxidase, glutathione S-transferase etc.) together with non-enzymatic way (ascorbic acid, glutathione etc.) are able to detoxify these toxic molecules (Choudhury et al., 2017). Several studies have reported changes in defense enzyme activities and transcriptional alterations of maize under different stress conditions such as drought (Chugh et al., 2011; Song et al., 2017; Zenda et al., 2018), temperature (Zhu et al., 2010; Cetinkaya et al., 2014; Shi et al., 2017), salinity (Estrada et al., 2013; Carrasco-Ríos and Pinto, 2014; AbdElgawad et al., 2016; Forieri et al., 2016). There are some opportunities including the inoculation with

arbuscular mycorrhizal (AM) fungi for helping the plants to tolerate extreme environmental conditions and alleviate reactive oxygen species. This symbiotic relationship has established more than 400 million years ago and offer some benefits to target plant, including enhanced uptake of water and nutrients - mostly phosphorus - as well as reduction of weeds and protection against pathogens (Feddermann et al., 2010; Ruiz-Sánchez et al., 2010; Smith et al., 2011; Smith and Smith, 2011; Bowles et al., 2016). Several studies suggest that AM fungi induce a plant-wide systemic defense mechanism called mycorrhiza-induced resistance (MIR) (Cameron et al., 2013; Dehghan et al., 2013). The MIR is associated with a more effective activation of JA-dependent system helping plants to alleviate various biotic and abiotic stresses (Chen et al., 2013; Anjum et al., 2016). However, the increased resistance caused by AM fungi is dependent on plant species, arbuscular mycorrhizal fungi and environmental conditions (Pozo and Azcón-Aguilar, 2007; Azcón and Barea, 2010; Vos et al., 2013). Some studies clearly suggest that amelioration of stress resistance by AM fungi symbiosis related to the raising of antioxidant activities in colonized plants (Hajiboland et al., 2010; Baslam and Goicoechea, 2012; Abdel Latef, 2013; Liu et al., 2015; Păun et al., 2015). The mechanisms by which AM fungi alter the production of defense enzymes are still not clarified and only few studies have been carried out at an early stage of plants concerning low level of mycorrhizal colonization.

Therefore, our aim was to investigate how arbuscular mycorrhizal fungi influence the changes in some plant defense enzymes together with gene expressions (catalase (*CAT*), peroxidase (*PER*), glutathione S-transferase (*GST*), polyphenol oxidase (*PPO*)) under salt, high temperature and drought stresses at an early stage of maize (*Zea mays* L.).

Materials and methods

Plant material and growth conditions

The experiment was carried out in Institute of Genetics, Microbiology and Biotechnology, Szent István University (SZIU), Gödöllő, Pest County, Hungary. Seeds of maize ('Golda F1') were sterilized in 1% NaOCl then washed with sterilized water five times and germinated on wet filter paper. Three days after germination the seedlings were transferred to plastic pots containing 0.75 kg sterilized peat and sand 1:2 (v/v) as substrate. Half of the transplanted plants were inoculated with 15 g of a commercial mycorrhizal product, Symbivit® (mixture of *Rhizophagus irregularis*, *Funneliformis mosseae*, *Claroideoglossum etunicatum*, *Claroideoglossum claroideum*, *G. microaggregatum*, *Funneliformis geosporum*) produced by Symbiom Ltd. (Lanskroun, Czech Republic; www.symbiom.cz). For non-mycorrhizal treatments sterilized mycorrhizal inoculant were prepared at the same rate (15 g plot⁻¹) and were then used in mycorrhizal treatment. Both treatments were transferred to a climatic chamber EKOCHL 1500 (24/26°C, 60% RH, 16 h light / 8 h dark) for 21 or 42 days. Plants (mycorrhizal and non-mycorrhizal) were exposed to different stress conditions. Plants were irrigated daily with 25 ml of 100 mM NaCl, representing salinity stress. Additional plants were exposed to drought stress (FC 20 ± 5%) compared to control (FC 85 ± 3%). Healthy 20 and 41 days-old seedlings were selected and exposed to 42°C for 24 h as high temperature stress (HT). Altogether eight treatments with two harvest time were designed replicated five times: 21 or 42 days old mycorrhizal inoculated plants (+AM) and non-mycorrhizal plants (-AM) under salt (Salt), high temperature

(HT), drought (D) and control (C) conditions, respectively. Plants were harvested after 21 or 42 days of growth, fresh and dry weight of shoots and roots were estimated.

RNA isolation and cDNA synthesis

Total RNA was extracted from maize leaves using Vantage Total RNA Purification Kit (Origene, USA) following the manufacturer's instructions, followed by DNase I (Fermentas) digestion the genomic DNA in the total RNA was eliminated. For qRT-PCR analysis from all treatments first-strand cDNA was synthesized using First-Strand cDNA Synthesis for Quantitative RT-PCR kit (Origene, USA). QRT-PCR was performed on Stratagene Mx3000P QPCR System (Agilent Technologies). Each reaction was performed in a final volume of 25 μ l containing 12.5 μ l SYBR Green Master Mix reagent (Applied Biosystems), 1 μ l of diluted cDNA sample (equal concentration in final volume, 4 ng/ μ l), 70 nM gene-specific primers and 8 μ l nuclease-free water. Gene-specific primers sequences listed in *Table 1*.

Table 1. Primers for qRT-PCR analysis

Gene	Primer set (5' to 3')	Product size (bp)
catalase (<i>CAT</i>)	forward: ATCAAGTTCCCCGACGTGATCC reverse: AGAAGAAGGTGTGCAGGCTCTC	118
peroxidase (<i>PER</i>)	forward: CGCCTCCAAGAACCTCAGTATC reverse: AGTTGTAGAGCCGGTCAACG	128
polyphenol oxidase (<i>PPO</i>)	forward: ATCTTCTTCCCGCACCACAC reverse: TCCTCGTCGTAGAACAGGAACG	125
glutathione S-transferase (<i>GST</i>)	forward: ACCGACTCGTTGCCTACTTCAC reverse: GATAAACAAGCGTTTGCACCC	105
<i>actin</i>	forward: CAGTGGTCTGAACAACGGGTA reverse: GGTAAGGTCACGACCAGCAA	127

PCR cycle procedure was: 95°C for 15 min, followed by 40 cycles at 95°C for 15 sec, 58°C for 30 sec and 72°C for 16 sec, finally 1 cycle at 95°C 60 sec, 58°C 30 sec and 95°C 30 sec. The real-time PCR experiment was conducted under identical conditions with three replications. As internal reference amplification of *actin* gene was used (*Table 1*). The gene expression of *CAT*, *PER*, *GST*, *PPO* was calculated using the $2^{-\Delta\Delta CT}$ method.

Enzyme assays

In order to determine the enzyme activity of *PER* and *PPO* plant extract was prepared using 0.2 g fresh plant leaves in Tris-HCl (3 ml; 50 mM; pH 7.8); polyvinylpyrrolidone-K 25 (7.5% (w/v) and EDTA-Na₂ (1 mM)) buffer. Peroxidase enzyme activities are performed by Rathmell and Sequeira (1974), the change in absorbance is observed at 436 nm wavelength. For the measurement, 1.1 ml of 0.1 M sodium phosphate buffer solution (pH 6.0), 50 μ l of 50 mM guaiacol, 50 μ l of 12 mM hydrogen peroxide, and 5 μ l of plant extract were added to the reaction mixture. The concentration of polyphenol oxidase enzyme - more specifically the degree of the formation of quinone compounds - was carried out by Fehrmann and Dimond (1967).

The change in absorbance was monitored at 400 nm for 10 minutes. The reaction mixture contained 1.1 ml of buffer solution and 100 µl of plant extract. The buffer solution was prepared by adding 0.1 M sodium phosphate buffer (pH 6.0), 1 mM EDTA and 20 mM catechol. Plant extract for CAT and GST protocol was prepared using 0.2 g fresh leaves in 1.2 ml 0.2 M sodium phosphate buffer (pH 7.8, 0.1 mM EDTA). The catalase enzyme activity was measured by the method of Aebi (1984), based on the dissociation ability of hydrogen peroxide. For measuring 995 µl of 50 mM sodium phosphate buffer (pH 7.0), 500 µl of 10 mM hydrogen peroxide and 5 µl of extract were mixed. The change of absorbance was followed at 240 nm wavelength for 5 minutes. Glutathione S-transferase enzyme activities were measured using Glutathione S-transferase (GST) Assay Kit (Sigma-Aldrich-Merck, Darmstadt, Germany) established on the method of Habig et al. (1974). The concentration of total soluble protein in plant extract solution was determined using Bradford reagent, bovine serum albumin as a standard (Bradford, 1976).

Assessment of mycorrhizal colonization of AM fungi

Root colonization was estimated in five plants both from mycorrhizal and non-mycorrhizal per treatments. Fine roots from each plant were stained with Trypan Blue (Vierheilig et al., 1998). Stereomicroscope at × 100 magnification was used to examine the internal fungal structures (hyphae, arbuscules) and the percentage of root colonization was calculated using grid line intersect method (Giovannetti and Mosse, 1980).

Statistical analysis

Statistical analysis was performed with R Statistical Software 3.3.1 (R Development Core Team, 2011). Values were expressed as means ± SD. Differences between treatments were determined by one-way analysis of variance (ANOVA). A *p*-value < 0.05 was considered to indicate statistical significance.

Results and discussion

No colonization was recognized when sterilized inoculant were used for inoculation. 21 days after AM fungi inoculation, external hyphae together with germinated spores were only detected, however internal hyphae together with arbuscules were recorded at older age of plants. The highest level of mycorrhizal colonization (52% ± 4) was measured after 6 weeks of growth under drought stress following under high temperature (42% ± 2) and salt stresses (35% ± 3), respectively.

Significant differences in fresh shoots and roots weights were observed in arbuscular mycorrhizal inoculated plants under control conditions and high temperature stresses. Drought and salt stress reduced the biomass of AM fungi inoculated and non-mycorrhizal plants, as well. Generally, lower biomass production of plants caused by drought and salt stress is associated with inhibition of leaf development and consequently reduced light interception (Anjum et al., 2011; Kaya et al., 2013a). The mycorrhizal inoculated salt treated plants did not show statistical difference in the shoot and root biomass compared to the non-mycorrhizal ones. Under drought conditions only the root biomass was affected by mycorrhizal colonisation after 21 days of growth (Table 2).

Table 2. Biomass of mycorrhizal (+AM) and non-mycorrhizal (-AM) plants after 21 days of growth

Age of plant 21 days		Shoots		Roots	
Treatments		Fresh weight (g plant ⁻¹)	Dry weight (g plant ⁻¹)	Fresh weight (g plant ⁻¹)	Dry weight (g plant ⁻¹)
Control (C)	-AM	1.58 ± 0.05b	0.58 ± 0.12b	0.68 ± 0.18c	0.34 ± 0.08b
	+AM	1.76 ± 0.07c	0.82 ± 0.07c	0.97 ± 0.06d	0.72 ± 0.10c
Salt (S)	-AM	0.42 ± 0.06a	0.19 ± 0.08a	0.12 ± 0.03a	0.07 ± 0.01a
	+AM	0.50 ± 0.07a	0.25 ± 0.09a	0.25 ± 0.05ab	0.10 ± 0.02a
High temperature (HT)	-AM	1.57 ± 0.05b	0.57 ± 0.10b	0.66 ± 0.04c	0.30 ± 0.03b
	+AM	1.75 ± 0.04c	0.80 ± 0.11bc	0.98 ± 0.07d	0.78 ± 0.03c
Drought (D)	-AM	0.42 ± 0.09a	0.17 ± 0.01a	0.22 ± 0.05ab	0.13 ± 0.01a
	+AM	0.48 ± 0.01a	0.18 ± 0.04a	0.38 ± 0.07b	0.29 ± 0.04b

Different lower-case letters within the same column indicate significant differences

Significantly higher fresh and dry shoots and fresh roots biomass were obtained in the inoculated plants (+AM) under control, salt and high temperature stress conditions compared to the non-mycorrhizal ones (-AM) (Table 3). Beneficial effects of AM fungi to target plant including enhanced nutrient uptake mostly phosphorus and water uptake, thereby stimulating the growth of the plant are well known (Bowles et al., 2016). Salt stress causes interfere in the homeostasis of the ions wherewith reactive oxygen species release in the plant cell. By the fact that AM fungi reduces the negative effects of salt stress by hyphae network, it promotes the growth of the plant (Wu et al., 2010). However, in this study the mycorrhizal plants under drought condition did not keep higher shoot biomass compared to non-mycorrhizal ones, which can be related to carbon drain effect or dysfunction of maize metabolism (Liu et al., 2004) and correlated with results were reported by Kohler et al. (2008) and Zhu et al. (2012).

Table 3. Biomass of mycorrhizal (+AM) and non-mycorrhizal (-AM) plants after 42 days of growth

Age of plant 42 days		Shoots		Roots	
Treatments		Fresh weight (g plant ⁻¹)	Dry weight (g plant ⁻¹)	Fresh weight (g plant ⁻¹)	Dry weight (g plant ⁻¹)
Control (C)	-AM	4.27 ± 0.11c	2.66 ± 0.27b	1.50 ± 0.17d	0.69 ± 0.03d
	+AM	6.06 ± 0.21d	3.70 ± 0.11c	3.29 ± 0.19e	1.61 ± 0.06e
Salt (S)	-AM	0.84 ± 0.08a	0.43 ± 0.01a	0.20 ± 0.06a	0.13 ± 0.03a
	+AM	1.23 ± 0.16b	0.69 ± 0.01a	0.62 ± 0.09bc	0.35 ± 0.05b
High temperature (HT)	-AM	4.37 ± 0.15c	2.70 ± 0.23b	1.52 ± 0.17d	0.67 ± 0.04d
	+AM	6.04 ± 0.17d	3.76 ± 0.08c	3.27 ± 0.22e	1.60 ± 0.07e
Drought (D)	-AM	0.75 ± 0.05a	0.52 ± 0.04a	0.27 ± 0.06ab	0.10 ± 0.02a
	+AM	1.01 ± 0.08ab	0.78 ± 0.12a	0.75 ± 0.02c	0.49 ± 0.02c

Different lower-case letters within the same column indicate significant differences

One of the earliest responses in plants by the colonization of AM fungi is the rapid accumulation of reactive oxygen species (ROS) (Choudhury et al., 2017). ROS is not

only harmful to plant cells, but also to mycorrhizal fungi. Under different stress conditions at different rates of enhanced enzyme activities together with gene expressions were found among various treatments. Changing in the activities of antioxidant enzymes as peroxidase, catalase etc. are not exclusive specificity of arbuscular mycorrhizal fungi during colonization process, presumably playing the key role the specific feature of each strain, instead of the colonization.

Catalase is playing a role in the production of monomers, dimers and phenoxy-free radicals and regulates the harmful accumulation of hydrogen peroxide (H_2O_2). In general, higher CAT enzyme activity of non-mycorrhizal plants were measured under different stresses compared to mycorrhizal plants after 21 days of growth. Reverse tendency was observed in CAT enzyme activity under salt and high temperature stresses at older plants (*Fig. 1c,d*).

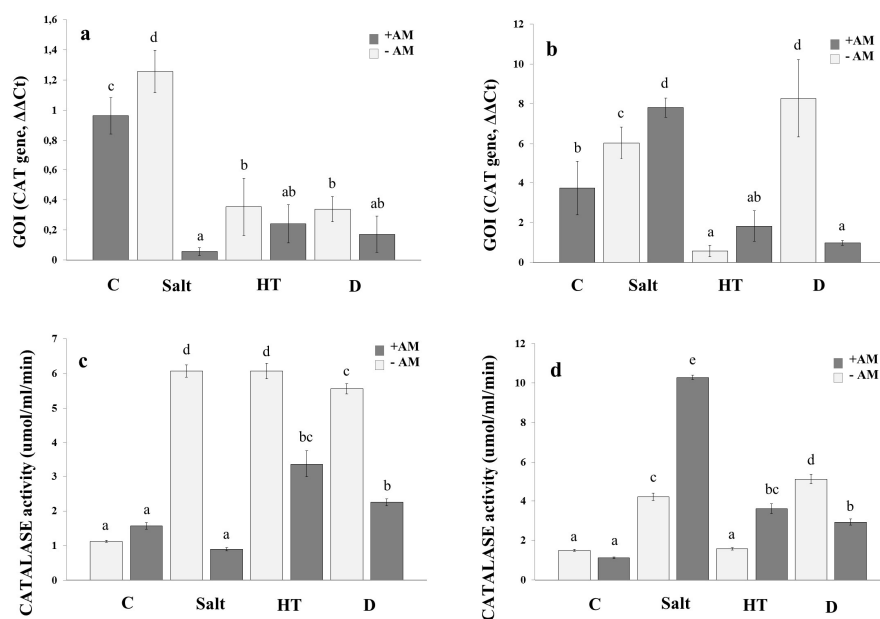


Figure 1. Catalase gene expression and enzyme activity of mycorrhizal and non-mycorrhizal plants under different stress conditions. a) CAT gene expression in 21-day-old plant b) CAT gene expression in 42-day-old plant c) CAT enzyme activity in 21-day-old plant d) CAT enzyme activity in 42-day-old plant; different letters represent significantly different ($p < 0.05$) values

At an early stage of plant, mycorrhizal fungi often seems to parasites, which due to the not sufficient production of energy from plant photosynthesis to cover the growth of mycorrhizal fungi together with plant requirement. Without stress the mycorrhizal and non-mycorrhizal control plants showed same enzyme activity. Under stress conditions at early-growth stages of mycorrhizal plants could produce less energy to respond. This could be one of the reasons for the lower enzyme activity of mycorrhizal plants compared to non-mycorrhizal ones after 21 days of growth. In line with the progressing of the incubation time leaf surface increases, plants produce more energy which can be used by both the production of enzymes and by the fungi for growth. As detected during salt and high temperature stress conditions in mycorrhizal plants after 42 days of growth compared to non-mycorrhizal ones. Similar tendency was found measuring 1.3 times higher *CAT* gene expression under salt stress after 42 days of growth. Our results,

regarding increased catalase enzyme activity under salt stress condition are agreed with the results of AbdElgawad et al (2016) and Chaparzadeh et al. (2004) who treated *Calendula officinalis* with 100 mM NaCl solution. Higher enzyme activity under salt and high temperature stresses in inoculated older plants are often found (Zhu et al., 2010). Under drought stress condition, non-mycorrhizal plants showed higher enzymatic activity at both age of plants. Due to the increased uptake of water resulting from higher AM fungi colonization rate could moderate the drought effect during 42-days term stress. The tendency of gene expression under drought stress was the same as the results of enzyme activity and besides in 21 days old plants no significant difference was observed (Fig. 1a). However, significantly higher (7.8 times) gene expression was measured in 42 days old non-mycorrhizal plants under drought condition compared to inoculated ones (Fig. 1b).

The increased PER activity of plants can occur not only in mycorrhizal plants but also during various abiotic stresses (Borde et al., 2011; Rahmaty and Khara, 2011; Pfeiffer et al., 2013). Interestingly, non-mycorrhizal plants after 42 days of growth had higher peroxidase enzyme activity compared to the inoculated ones under high temperature (Fig. 2d).

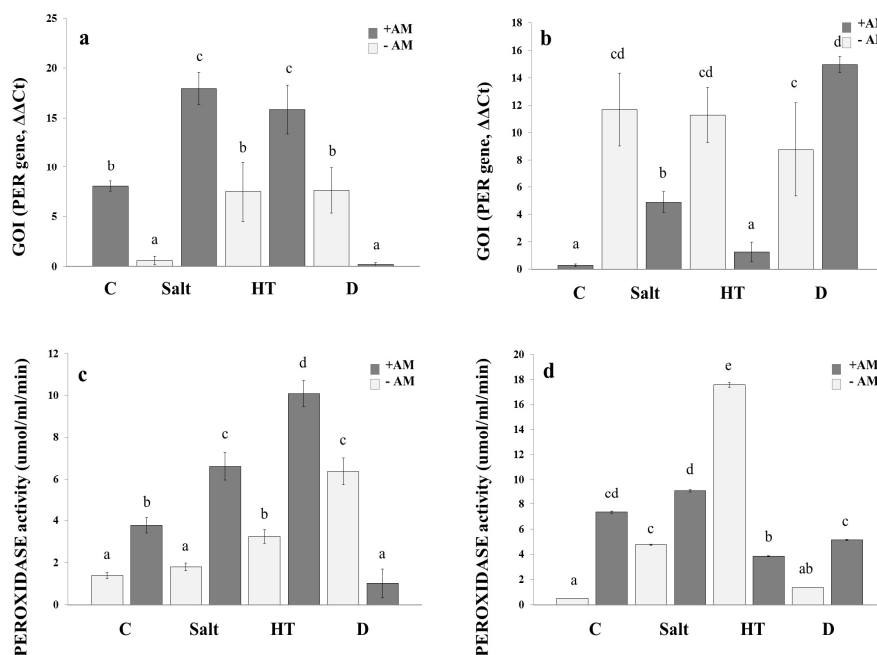


Figure 2. Peroxidase gene expression and enzyme activity of mycorrhizal and non-mycorrhizal plants under different stress conditions. a) PER gene expression in 21-day-old plant b) PER gene expression in 42-day-old plant c) PER enzyme activity in 21-day-old plant d) PER enzyme activity in 42-day-old plant; different letters represent significantly different ($p < 0.05$) values

Different results of enzymes activities reported during the colonization of AM fungi indicating that the enzyme activity are somehow connect to the symbiotic processes (Younesi et al., 2013). After 21 days of growth inoculated plants demonstrated higher enzyme activity and gene expression under salt (3 times) and high temperature stresses (2.8 times) compared to non-mycorrhizal ones (Fig. 2a,c). At the age of 42-day old mycorrhizal plants showed higher enzyme activity under salt and drought stress

compared to non-mycorrhizal treated plants. Under high temperature stress, non-mycorrhizal plants showed higher activity and gene expression than the inoculated ones (Fig. 2b,d). Stomatal conductance and transpiration rates of colonized plants are higher than non-colonized ones under high temperature stress, indicating that AM fungi colonization play a role in the gas exchange metabolism improvement with open stoma and increase the rate of transpiration (Zhu et al., 2010). During temperature stress symbiosis improves water retention, preventing the plant of the negative effects of dehydration (Zhu et al., 2012).

Under control condition after 21 and 42 days of incubation, there was no difference in CAT activity regardless of mycorrhization compared to the higher PER activity in mycorrhizal plants. However, under salt stress CAT activity of 21 days old mycorrhizal plants is lower (Fig. 1a,c) than PER activity (Fig. 2a,c). This strategy of an early stage of plant most likely due to the activity and role function of PER and CAT in the plant defense system. Both are involved in the degradation of H₂O₂, besides Estrada et al. (2013) and Abeer et al. (2015) observed in mycorrhizal plants exhibited much higher activity of PER than CAT enzyme in the elimination of H₂O₂.

Glutathione S-transferases are among the most well-known and most frequently used detoxification enzymes (Nianiou-Obeidat et al., 2017). They play a role in the inactivation of oxidative stress metabolites, which process protects the cell from oxidative damages (Mohsenzadeh et al., 2011). GST in plants neutralize not only toxic substances but also promote a number of defensive mechanisms in the plant. It may facilitate the intracellular storage and transport of hydrophobic non-substrate compounds such as metabolites. Under the various stresses there were no significant differences in GST enzyme activity between mycorrhizal and non-mycorrhizal plants after 21 days of growth (Fig. 3c).

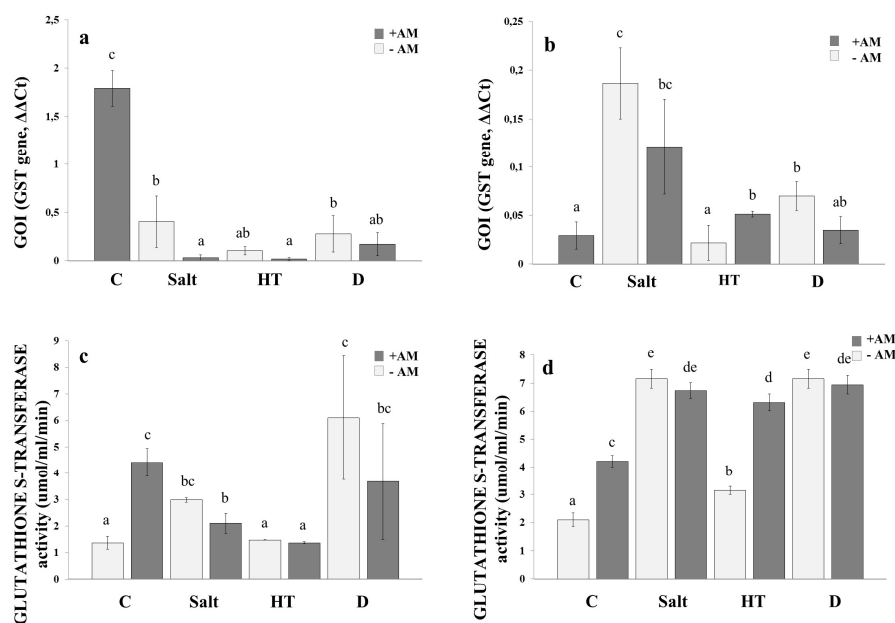


Figure 3. Glutathione S-transferase gene expression and enzyme activity of mycorrhizal and non-mycorrhizal plants under different stress conditions. a) GST gene expression in 21-day-old plant b) GST gene expression in 42-day-old plant c) GST enzyme activity in 21-day-old plant d) GST enzyme activity in 42-day-old plant; different letters represent significantly different ($p < 0.05$) values

By the increase of incubation time all the stress effects induced higher enzyme activity in the plant compared to the control, which trend was previously reported by Haluskova et al. (2009). Depending on the age of the plants Wagner et al. (2002) found also different *GST* gene expression under different stress conditions similar to our results (Fig. 3a,b). In the present study, the *GST* gene expression and the GST enzyme activity showed the same tendency under high temperature after 42 days of growth in agreement with the studies of Cetinkaya et al. (2014) and Mayer et al. (2017) (Fig. 3b,d).

After three weeks of incubation drought stress induced significantly increased enzyme activity in mycorrhizal plants (Fig. 4c). The enzyme activity of PPO is increased in general with the age of the plants. In this study the changes in *PPO* gene expression correlated with the enzyme activity under different stress conditions (Fig. 4a,c). Different stresses caused various changes in enzyme activities but only salt stress increased at high rate (8 times) of this enzyme accumulation in mycorrhizal plant after 42 days of growth (Fig. 4b,d). The higher polyphenol oxidase activity under salt stress was also observed by Kaya et al. (2013b) and Demir and Kocacaliskan (2001).

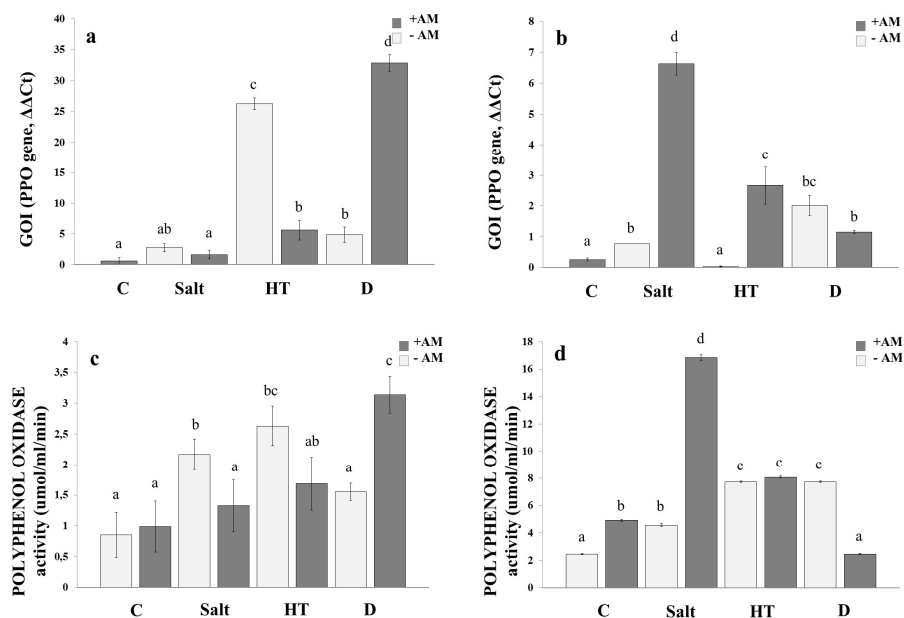


Figure 4. Polyphenol oxidase gene expression and enzyme activity of mycorrhizal and non-mycorrhizal plants under different stress conditions. a) PPO gene expression in 21-day-old plant b) PPO gene expression in 42-day-old plant c) PPO enzyme activity in 21-day-old plant d) PPO enzyme activity in 42-day-old plant; different letters represent significantly different ($p < 0.05$) values

Our result suggests that measured defense enzymes are working together in a complex network, influencing to each others. At an early stage of inoculation, when low colonization level but active arbuscule formation could be observed in mycorrhizal plants the highest accumulation of tested enzymes altogether were measured in non-mycorrhizal plants under drought stress. It is almost two times more, than measured in mycorrhizal plants. It shows opposite tendency than expected from mycorrhizae offered balance activity under stresses. Explanation of less damage caused in mycorrhizal plant

than in non-mycorrhizal one under drought condition most likely due to the increased surface offered by external hyphae of mycorrhizal fungi increase the water uptake and water efficiency (Smith and Read, 2010; Zhao et al., 2015). It could be one reason for lower defense enzyme activities measured in mycorrhizal treatment under dry condition. Similar tendency was found applying salt stress, when the mycelium network of AM fungi could also attenuate the strength of this stress using different mechanisms (Mardukhi et al., 2015). Out of the tested stresses, the high temperature caused the biggest change in measured defense enzymes between mycorrhizal and non-mycorrhizal treatments.

Conclusions

Our results suggest that AM inoculation could take part in the alleviation processes caused by high temperature, salt and drought stresses. However, these mechanisms are influenced by the age of the plants which is most likely justified by energy considerations. Besides increased defense enzymes activities of mycorrhizal plants compared to non-mycorrhizal one, the AM fungi could offer some other strategies to increased tolerance of plants against salt and drought stresses. Nevertheless, the activity of CAT, PER, GST and PPO concerning degradation of toxic ROS molecules in plant defense system under various stresses, should be investigated in more detail. Especially the CAT and PER related expression system and not well documented PPO activity supports further studies in plant – AM fungi symbiotic relationship.

Acknowledgements. This work was supported by „ÚNKP-17-3 New National Excellence Program of the Ministry of Human Capacities”, “GLIA: 2017-1.3.1-VKE-2017 has been implemented with the support provided from the National Research, Development and Innovation Fund of Hungary, financed under the 00030 funding scheme” and „Higher Education Institutional Excellence Program (1783-3/2018/FEKUTSTRAT) awarded by the Ministry of Human Capacities within the framework of water related researches of Szent István University”.

REFERENCES

- [1] AbdElgawad, H., Zinta, G., Hegab, M., Pandey, R., Asard, H., Abuelsoud, W. (2016): High salinity induces different oxidative stress and antioxidant responses in maize seedling organs. – *Front. Plant. Sci.* 24: 134-141.
- [2] Abdel Latef, A. A. H. (2013): Growth and some physiological activities of pepper (*Capsicum annum* L.) in response to cadmium stress and mycorrhizal symbiosis. – *J. Agr. Sci. Tech.* 15: 1437-1448.
- [3] Abeer, H., Abd Allah, E. F., Alqarawi, A. A., El-Didamony, G., Alwhibi, M., Egamberdieva, D., Ahmad, P. (2014): Alleviation of adverse impact of salinity on faba bean (*Vicia faba* L.) by arbuscular mycorrhizal fungi. – *Pak. J. Bot.* 46(6): 2003-2013.
- [4] Aebi, H. (1984): Catalase in vitro. – *Method. Enzymol.* 105: 121-126.
- [5] Anjum, S. A., Xie, X. Y., Wang, L. C., Saleem, M. F., Man, C., Lei, W. (2011): Morphological, physiological and biochemical responses of plants to drought stress. – *Afr. J. Agric. Res.* 6(9): 2026-2032.
- [6] Anjum, S. A., Tanveer, M., Ashraf, U., Hussain, S., Shahzad, B., Khan, I., Wang, L. (2016): Effect of progressive drought stress on growth, leaf gas exchange, and antioxidant production in two maize cultivars. – *Environ. Sci. Pollut. R.* 23: 17132-17141.

- [7] Azcón, R., Barea, J. M. (2010): Mycorrhizosphere interactions for legume improvement. – In: *Microbes for legume improvement*. Springer, Vienna, pp. 237-271.
- [8] Baslam, M., Goicoechea, N. (2012): Water deficit improved the capacity of arbuscular mycorrhizal fungi (AMF) for inducing the accumulation of antioxidant compounds in lettuce leaves. – *Mycorrhiza* 22: 347-359.
- [9] Borde, M., Dudhane, M., Jite, P. (2011): Growth photosynthetic activity and antioxidant responses of mycorrhizal and non-mycorrhizal bajra (*Pennisetum glaucum*) crop under salinity stress condition. – *Crop Prot.* 30: 265-271.
- [10] Bowles, T. M., Barrios-Masias, F. H., Carlisle, E. A., Cavagnaro, T. R., Jackson, L. E. (2016): Effects of arbuscular mycorrhizae on tomato yield, nutrient uptake, water relations, and soil carbon dynamics under deficit irrigation in field conditions. – *Sci. Total Environ.* 566: 1223-1234.
- [11] Bradford, M. (1976): A rapid and sensitive method for the quantitation of microgram quantities of protein utilizing the principle of protein-dye binding. – *Anal. Biochem.* 72: 248-254.
- [12] Cameron, D. D., Neal, A. L., van Wees, S. C., Ton, J. (2013): Mycorrhiza-induced resistance: more than the sum of its parts? – *Trends Plant Sci.* 18: 539-545.
- [13] Carrasco-Ríos, L., Pinto, M. (2014): Effect of salt stress on antioxidant enzymes and lipid peroxidation in leaves in two contrasting corn, ‘Lluteño’ and ‘Jubilee’. – *Chilean J. Agr. Res.* 74: 89-95.
- [14] Cetinkaya, H., Tasci, E., Dinler, B. S. (2014): Regulation of glutathione S-transferase enzyme activity with salt pre-treatment under heat stress in maize leaves. – *Res. Plant Biol.* 4: 5.
- [15] Chaparzadeh, N., D’Amico, M. L., Khavari-Nejad, R. A., Izzo, R., Navari-Izzo, F. (2004): Antioxidative responses of *Calendula officinalis* under salinity conditions. – *Plant Physiol. Bioch.* 42: 695-701.
- [16] Chen, S., Jin, W., Liu, A., Zhang, S., Liu, D., Wang, F., Lin, X., He, C. (2013): Arbuscular mycorrhizal fungi (AMF) increase growth and secondary metabolism in cucumber subjected to low temperature stress. – *Sci. Hortic-Amsterdam* 160: 222-229.
- [17] Choudhury, F. K., Rivero, R. M., Blumwald, E., Mittler, R. (2017): Reactive oxygen species, abiotic stress and stress combination. – *Plant J.* 90: 856-867.
- [18] Chugh, V., Kaur, N., Gupta, A. K. (2011): Evaluation of oxidative stress tolerance in maize (*Zea mays* L.) seedlings in response to drought. – *Indian J. Biochem Bio.* 48: 47-53.
- [19] Dehghan, G., Amjad, L., Nosrati, H. (2013): Enzymatic and non-enzymatic antioxidant responses of alfalfa leaves and roots under different salinity levels. – *Acta Biol. Hung.* 64: 207-217.
- [20] Demiř, Y., Kocaçalışkan, İ. (2001): Effects of NaCl and proline on polyphenol oxidase activity in bean seedlings. – *Biol. Plantarum* 44: 607-609.
- [21] Estrada, B., Aroca, R., Barea, J. M., Ruiz-Lozano, J. M. (2013): Native arbuscular mycorrhizal fungi isolated from a saline habitat improved maize antioxidant systems and plant tolerance to salinity. – *Plant Sci.* 201: 42-51.
- [22] Feddermann, N., Finlay, R., Boller, T., Elfstrand, M. (2010): Functional diversity in arbuscular mycorrhiza – the role of gene expression, phosphorous nutrition and symbiotic efficiency. – *Fungal Ecol.* 3: 1-8.
- [23] Fehrmann, H., Dimond, A. E. (1967): Peroxidase activity and phytophthora resistance in different organs of the potato plant. – *Phytopathology* 57: 69-72.
- [24] Forieri, I., Hildebrandt, U., Rostás, M. (2016): Salinity stress effects on direct and indirect defence metabolites in maize. – *Environ. Exp. Bot.* 122: 68-77.
- [25] Giovannetti, M., Mosse, B. (1980): An evaluation of techniques for measuring vesicular arbuscular mycorrhizal infection in roots. – *New Phytol.* 84: 489-500.
- [26] Habig, W. H., Pabst, M. J., Jakoby, W. B. (1974): Glutathione S-transferases the first enzymatic step in mercapturic acid formation. – *J. Biol. Chem.* 249: 7130-7139.

- [27] Hajiboland, R., Aliasgharzadeh, N., Laiegh, S., Poschenrieder, C. (2010): Colonization with arbuscular mycorrhizal fungi improves salinity tolerance of tomato (*Solanum lycopersicum* L.) plants. – *Plant Soil* 331: 313-327.
- [28] Halušková, L. U., Valentovičová, K., Huttová, J., Mistrík, I., Tamás, L. (2009): Effect of abiotic stresses on glutathione peroxidase and glutathione S-transferase activity in barley root tips. – *Plant Physiol. Biochem.* 47(11-12): 1069-1074.
- [29] Kaya, C., Ashraf, M., Dikilitas, M., Tuna, A. L. (2013a): Alleviation of salt stress-induced adverse effects on maize plants by exogenous application of indoleacetic acid (IAA) and inorganic nutrients-A field trial. – *Aust. J. Crop Sci.* 7(2): 249.
- [30] Kaya, C., Sonmez, O., Aydemir, S., Ashraf, M., Dikilitas, M. (2013b): Exogenous application of mannitol and thiourea regulates plant growth and oxidative stress responses in salt-stressed maize (*Zea mays* L.). – *J. Plant Interact.* 8: 234-241.
- [31] Kohler, J., Hernández, J. A., Caravaca, F., Roldán, A. (2008): Plantgrowth-promoting rhizobacteria and arbuscular mycorrhizal fungi modify alleviation biochemical mechanisms in water- stressed plants. – *Funct. Plant Biol.* 35: 141-151.
- [32] Liu, A., Wang, B., Hamel, C. (2004): Arbuscular mycorrhiza colonization and development at suboptimal root zone temperature. – *Mycorrhiza* 14: 93-101.
- [33] Liu, T., Sheng, M., Wang, C. Y., Chen, H., Li, Z., Tang, M. (2015): Impact of arbuscular mycorrhizal fungi on the growth, water status, and photosynthesis of hybrid poplar under drought stress and recovery. – *Photosynthetica* 53: 250-258.
- [34] Lobell, D. B., Sibley, A., Ortiz-Monasterio, J. I. (2012): Extreme heat effects on wheat senescence in India. – *Nature Climate Change* 2: 186-189.
- [35] Mardukhi, B., Rejali, F., Daei, G., Ardakani, M. R., Malakouti, M. J., Miransari, M. (2015): Mineral uptake of mycorrhizal wheat (*Triticum aestivum* L.) under salinity stress. *Commun. – Soil Sci. Plan.* 46: 343-357.
- [36] Mayer, Z., Duc, N. H., Sasvári, Z., Posta, K. (2017): How arbuscular mycorrhizal fungi influence the defense system of sunflower during different abiotic stresses. – *Acta Biol. Hung.* 68: 376-387.
- [37] Mohsenzadeh, S., Esmaeili, M., Moosavi, F., Shahrtash, M., Saffari, B., Mohabatkar, H. (2011): Plant glutathione S-transferase classification, structure and evolution. – *Afr. J. Biotechnol.* 10: 8160-8165.
- [38] Molazem, D., Azimi, J. (2015): Morpho-physiological characterization in eight varieties of maize (*Zea mays* L.) under soil salinity. – *Pol. J. Environ. Stud.* 24: 6.
- [39] Nagy, J. (2010): Impact of fertilization and irrigation on the correlation between the soil plant analysis development value and yield of maize. – *Commun. Soil Sci. Plant Anal.* 41(11): 1293-1305.
- [40] Nianiou-Obeidat, I., Madesis, P., Kissoudis, C., Voulgari, G., Chronopoulou, E., Tsaftaris, A., Labrou, N. E. (2017): Plant glutathione transferase-mediated stress tolerance: functions and biotechnological applications. – *Plant Cell Rep.* 36: 791-805.
- [41] Păun, A., Neagoe, A., Păun, M., Baciu, I., Iordache, V. (2015): Heavy metal-induced differential responses to oxidative stress and protection by mycorrhization in sunflowers grown in lab and field scales. – *Pol. J. Environ. Stud.* 24(3).
- [42] Pepó, P., Vári, E. (2016): Evaluation of the yield production of C3 (*Triticum aestivum* L.) and C4 (*Zea mays* L.) cereals with a new plant physiological parameter. – *J. Anim. Plant. Sci.* 26(3): 716-724.
- [43] Pfeiffer, T., Štolfa, I., Žanić, M., Pavičić, N., Cesar, V., Lepeduš, H. (2013): Oxidative stress in leaves of two olive cultivars under freezing conditions. – *Acta Biol. Hung.* 64: 341-351.
- [44] Pozo, M. J., Azcón-Aguilar, C. (2007): Unravelling mycorrhiza-induced resistance. – *Curr. Opin. Plant Biol.* 10: 393-398.
- [45] Rahmaty, R., Khara, J. (2011): Effects of vesicular arbuscular mycorrhiza *Glomus intraradices* on photosynthetic pigments, antioxidant enzymes, lipid peroxidation, and

- chromium accumulation in maize plants treated with chromium. – Turkish J. Biol. 35: 51-58.
- [46] Rathmell, W. G., Sequeira, L. (1974): Soluble peroxidase in fluid from the intercellular spaces of tobacco leaves. – Plant Physiol. 53: 317-318.
- [47] R Core Team (2011): R: A language and environment for statistical computing. – R Foundation for Statistical Computing, Vienna, Austria. <https://www.r-project.org/>.
- [48] Ruiz-Sánchez, M., Aroca, R., Munoz, Y., Armada, E., Polón, R., Ruiz-Lozano, J. M. (2010): The arbuscular mycorrhizal symbiosis enhances the photosynthetic efficiency and the antioxidative response of rice plants subjected to drought stress. – J. Plant Physiol. 167(11): 862-869.
- [49] Shi, J., Yan, B., Lou, X., Ma, H., Ruan, S. (2017): Comparative transcriptome analysis reveals the transcriptional alterations in heat-resistant and heat-sensitive sweet maize (*Zea mays* L.) varieties under heat stress. – BMC Plant Biol. 17(1): 26.
- [50] Smith, S. E., Read, D. J. (2010): Mycorrhizal symbiosis. – Academic press.
- [51] Smith, S. E., Smith, F. A. (2011): Roles of arbuscular mycorrhizas in plant nutrition and growth: new paradigms from cellular to ecosystems scales. – Annu. Rev. Plant Biol. 62: 227-250.
- [52] Smith, S. E., Jakobsen, I., Grønlund, M., Smith, F. A. (2011): Roles of arbuscular mycorrhizas in plant phosphorus nutrition: interactions between pathways of phosphorus uptake in arbuscular mycorrhizal roots have important implications for understanding and manipulating plant phosphorus acquisition. – Plant Physiol. 156: 1050-1057.
- [53] Song, K., Kim, H. C., Shin, S., Kim, K. H., Moon, J. C., Kim, J. Y., Lee, B. M. (2017): Transcriptome analysis of flowering time genes under drought stress in maize leaves. – Front. Plant. Sci. 8: 267.
- [54] Vierheilig, H., Coughlan, A. P., Wyss, U., Piché, Y. (1998): Ink and vinegar, a simple staining technique for arbuscular-mycorrhizal fungi. – Appl. Environ. Microb. 64: 5004-5007.
- [55] Vos, C., Schouteden, N., van Tuinen, D., Chatagnier, O., Elsen, A., de Waele, D., Panis, B., Gianinazzi-Pearson, V. (2013): Mycorrhiza-induced resistance against the root knot nematode *Meloidogyne incognita* involves priming of defense gene responses in tomato. – Soil Biol. Biochem. 60: 45-54.
- [56] Wagner, U., Edwards, R., Dixon, D. P., Mauch, F. (2002): Probing the diversity of the *Arabidopsis* glutathione S-transferase gene family. – Plant Mol. Biol. 49: 515-532.
- [57] Wu, Q. S., Zou, Y. N. (2010): Beneficial roles of arbuscular mycorrhizas in citrus seedlings at temperature stress. – Sci. Hortic. 125: 289-293.
- [58] Younesi, O., Moradi, A., Namdari, A. (2013): Influence of arbuscular mycorrhiza on osmotic adjustment compounds and antioxidant enzyme activity in nodules of salt-stressed soybean (*Glycine max*). – Acta Agri. Sloven. 101(2): 219.
- [59] Zenda, T., Liu, S., Wang, X., Jin, H., Liu, G., Duan, H. (2018): Comparative proteomic and physiological analyses of two divergent maize inbred lines provide more insights into drought-stress tolerance mechanisms. – Int. J. Mol. Sci. 19(10): 3225.
- [60] Zhao, R., Guo, W., Bi, N., Guo, J., Wang, L., Zhao, J., Zhang, J. (2015): Arbuscular mycorrhizal fungi affect the growth, nutrient uptake and water status of maize (*Zea mays* L.) grown in two types of coal mine spoils under drought stress. – Appl. Soil Ecol. 88: 41-49.
- [61] Zhu, X. C., Song, F. B., Xu, H. W. (2010): Influence of arbuscular mycorrhizae on lipid peroxidation and antioxidant enzyme activity of maize plants under temperature stress. – Mycorrhiza 20: 325-332.
- [62] Zhu, X. C., Song, F. B., Liu, S. Q., Liu, T. D., Zhou, X. (2012): Arbuscular mycorrhizae improves photosynthesis and water status of *Zea mays* L. under drought stress. – Plant Soil Environ 58: 186-191.

A FRAMEWORK FOR HAZARD ASSESSMENT OF DEBRIS-FLOW ACCUMULATION AREAS

LE, M. H.^{1,2*} – HAN, Q. W.^{1,2} – FANG, C. M.^{1,2} – GUAN, J. Z.^{1,2}

¹*State Key Laboratory of Simulation and Regulation of Water Cycle in River Basin
China Institute of Water Resources and Hydropower Research
A-1 Fuxing Rd., Haidian dist, Beijing 100038, China*

²*Department of Sediment Research
China Institute of Water Resources and Hydropower Research
No.20 Chegongzhuang West Rd., Haidian dist., Beijing 100048, China*

**Corresponding author*

e-mail: lemaohua@gmail.com; phone: +86-10-68786624; fax: +86-10-68786624

(Received 5th Dec 2018; accepted 21st Mar 2019)

Abstract. An increasing demand for assessing the hazard of debris-flow accumulation areas is critical to risk management and policy implication for debris-flow hazard mitigation. In this paper, a framework for hazard assessment in debris flow-prone areas is proposed. Based on the hazard definition, debris-flow hazard is computed by its occurrence probability and disruptive intensity. Debris-flow occurrence probability is defined as a joint probability considering both hydrological and debris supply condition. Debris-flow disruptive intensity is introduced to express the inundated and impact damage of debris flow by the distribution of flow depth and velocity. The distribution is based on an extended geometric model of debris-flow fans, including the maximum length, width, and thickness (or flow depth) of debris-flow fans, and the channel outlet width. A hazard matrix, correlated to debris-flow occurrence probability and disruptive intensity, is used to map the hazard on debris-flow accumulation areas. The proposed procedure is applied to assess the debris-flow hazard on the accumulation area of Shuida gully, located in the Longchi town, Sichuan province of China. Finally, the article considers the effects of hazard maps.

Keywords: hazard recognition, debris-flow fan configuration, occurrence probability, debris-flow disruptive intensity, Shuida gully

Introduction

Debris flows are common phenomena in mountainous regions throughout the world (Coussot and Meunier, 1996). Their accumulation flooding processes always make the foothills of the landform change, and form the alluvial fans which are a preferred location for urban development owing to their good drainage conditions and gently slope. In many densely developed mountainous regions, fans provide the only readily developable land (Jakob and Hungr, 2005). Unfortunately, many fans in active mountains are prone to debris flows, which can constitute a widespread hazard to people and property (Davies and McSaveney, 2008). Therefore, there is an increasing demand for assessing the hazard of debris-flow accumulation areas, which is critical to risk management and policy implication for debris-flow hazard mitigation.

According to the International Union of Geological Sciences definition (IUGS, 1997), a hazard in a given point on an alluvial fan is defined as the probability that a debris flow of a defined intensity will occur. Based on this definition, the hazard assessment mainly includes two parts: one is the debris-flow occurrence probability related to its basin characteristics and hydrological conditions, the other is the debris-flow intensity described by means of variables characterizing its destructive power.

Over the past few decades, the debris-flow hazard assessment has been generally carried out either by using empirical approaches or applying physical and numerical methods. The empirical models (Okunishi and Suwa, 2001; Iverson, 2014; Rickenmann, 2016) are based on few parameters and consequently allow generalized conclusions only. However, they generally offer a readily applicable and verifiable approach. The most common empirical relationships estimate the maximum run-out distance of debris flow. In recent years, data mining has been utilized for assessing debris flow hazards (Lin et al., 2012; Liang et al., 2012). With the development of rheological and physical-mathematical based modeling of debris flows, numerical techniques and geographical information science, quantitative approaches are widely used to assess the hazard of debris-flow. For example, Wei et al. (2003) simulated the movement process of debris flow out of the outlet, and established the momentum model for debris flow risk zoning. Liu and Huang (2006) introduced the concept of separating the boundary layer and the main flow in fluid mechanics to debris flows, and developed a numerical program for field application on hazard area mapping. Tsai et al. (2011) considered large-scale debris flow simulations in various volumes at the same area by using the DEBRIS-2D numerical program for hazard assessment.

Taking into account the triggering, propagation and stoppage of debris flows, Calvo and Savi (2009) applied a Monte Carlo procedure to quantify debris flow hazard. De Scally et al. (2010) conducted discriminant analysis for identifying controls on fan depositional processes, and implications for the assessment of debris-flow hazard on fans. Hürlimann et al. (2008) reviewed various different run-out and intensity calculation methods and discussed their implication for generating debris-flow hazard maps. In quantitative approaches, Guzzetti et al. (2005) proposed a probabilistic model to determine landslide hazard at the basin scale. Based on debris supply conditions, the basins where debris flows occur can be classified as either supply-limited (or weathering-limited) or supply-unlimited (or transport-limited) (Glade, 2005; Jakob et al., 2005). However, the existing debris-flow occurrence probability calculation methods were generally on the assumption of unlimited sediment availability, neglecting the requirement of a significant recharge period prior to each debris flow event. In addition, the determination of debris-flow magnitude and intensity is also necessary during the hazard assessment (Jakob and Hungr, 2005). Typically, the characteristic parameters such as area inundated, maximum flow velocity, and maximum flow depth are related.

In this study, a framework for hazard assessment of debris-flow accumulation areas was developed. Four key components of this framework were discussed: (i) the debris-flow occurrence probability was estimated by combining the critical hydro-climatic thresholds and debris supply conditions; (ii) the fan configurations were classified as complete, partial and unformed types, and an extended geometric model of debris-flow fans was provided for hazard assessment; (iii) the disruptive intensity was introduced to express the inundated and impact damage of debris flows; (iv) the debris-flow occurrence probability and destructive power were correlated in a hazard matrix which can represent hazard qualitatively by hazard degree classes or quantitatively by a value ranging from zero to unity. Finally, the developed framework was applied to evaluate the debris-flow hazard on the accumulation area of Shuida gully, located in the Longchi town, Sichuan province of China.

Methods and Materials

Methods

The framework for hazard assessment of debris-flow accumulation areas includes the following steps (*Fig. 1*):

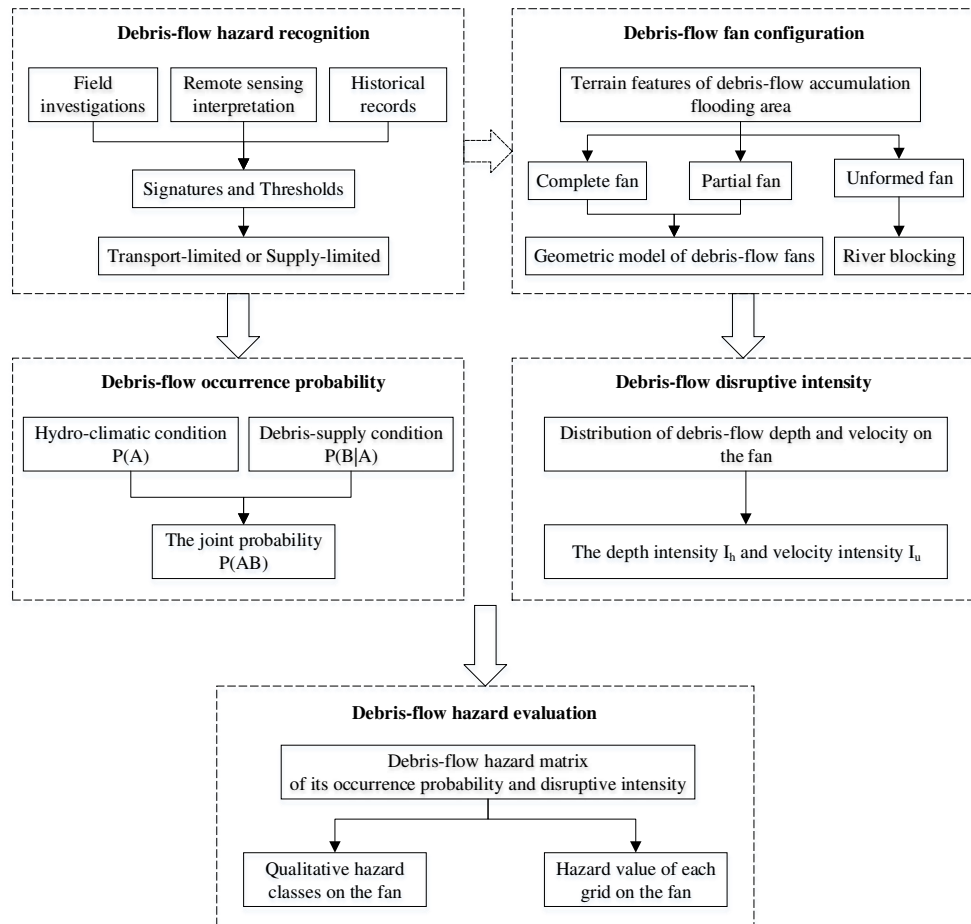


Figure 1. The framework for hazard assessment of debris-flow accumulation areas

- Debris-flow hazard recognition is the first, and possibly most important segment. The causes of debris flows, and their behavior once initiated, are known in outline but poorly understood to date (Iverson, 1997; Takahashi, 2009). However, it is clear that a debris flow occurrence requires large volumes of sediment to be available, either on slopes or in a stream channel, and steep slopes to allow rainfall and/or stream-flow of sufficient magnitude to mobilize the sediment (Welsh and Davies, 2011). Thus, we propose a reference method for debris-flow hazard identification based on its occurrence signatures or thresholds (*Table 1*). Additionally, it is necessary for the following probability estimation to divide gullies into transport-limited and supply-limited by field investigation of catchment characteristics.
- Debris-flow occurrence probability is a function of the critical hydro-climatic thresholds and debris supply conditions. Therefore, the authors defined a joint

probability to estimate the hazard occurrence probability considering both hydrological and geomorphic characteristics.

- Debris-flow fan configuration is the basis of hazard evaluation. According to the different terrain features of debris-flow accumulation flooding area, the fan configurations may unfold in various spatial patterns. In order to establish a geometric model of debris-flow fans for the following calculations, the fan configurations are classified as complete, partial and unformed types, and an extended geometric model of debris-flow fans is provided.

Table 1. The reference method for debris-flow hazard recognition

Criterion	Description	References
Signatures	Steep channel Narrow channel, small width-to-depth ratio Semi-circular to U-shaped channel Accumulation of unconsolidated sediment in the channel Channel scoured to bedrock, or filled with coarse rock-fall debris with high hydraulic conductivity (supply-limited) Scour marks, mud-lines and debris impact scars on the trees well above the flood limit Inverse grading of fan or levee deposits Coarse deposits beyond the channel on the fan Poorly sorted or imbricated deposits on the fan	Meyer et al. (2014); Jakob and Hungr (2005)
Thresholds	Melton ratio $R > 0.5$ Watershed length $WL \leq 2.7\text{km}$ Empirical formula $P = RT^{0.2}/G^{0.5} \geq 0.47$, R, T, G is the dimensionless factor related to hydrology, topography, and geology respectively	Wilford et al. (2004); Welsh and Davies (2011); Yu et al. (2014)

- Dividing debris-flow fans into many grids with equal area, we can evaluate hazard of each grid by the disruptive intensity, which is introduced to express the inundated and impact damage of debris flow by the distribution of flow depth and velocity.
- Debris-flow occurrence probability and destructive power are correlated in a hazard matrix which can represent hazard qualitatively by hazard degree classes or quantitatively by a value ranging from zero to unity. For practical use, administrations always use qualitative hazard classes to better correlate with building codes and urbanization plans (Raetzo et al., 2002). However, quantitative methods have their advantages of objectivity.

Debris-flow occurrence probability

Debris flow initiation requires steep slopes, availability of erodible sediments, and a storm of sufficient magnitude. Thus, we apply a joint probability $P(A \cap B)$ to calculate the probability of debris-flow occurrence using Equation 1:

$$P_H = P(A \cap B) = P(B|A) \cdot P(A) \quad (\text{Eq.1})$$

where P_H is the debris-flow occurrence probability; A represents the local hydro-climatic condition or rainfall exceeding the critical value; B represents the availability of erodible sediments under the given slope channel; $(B|A)$ indicates the occurrence of B under the triggering condition A; $A \cap B$ indicates the simultaneous occurrence of A and B; and P is the event occurrence probability.

As an approximation, rainfalls can be considered as independent random-point events in time (Cowpertwait et al., 1996), the occurrence probability of a rainfall during a period of n years can be estimated using the binomial equation:

$$P(A) = 1 - (1 - 1/T)^n \quad (\text{Eq.2})$$

where T is the return period of rainfalls. It can be obtained from a historical catalogue of local rainfalls or from the local hydrological handbook.

To determine the occurrence probability of sediment entrainment under condition A , it is necessary to discuss the debris supply condition and the magnitude (or transport capacity) of A in a given basin. In transport-limited gullies, abundant readily entrainable sediment is present, and whenever a rainfall of sufficient magnitude occurs, a debris flow will result. On the contrary, in supply-limited gullies, the volume of entrainable sediment is limited, and a rainfall of sufficient magnitude may not initiate a debris flow unless enough sediment is available (Brayshaw and Hassan, 2009). In the conceptual model for supply-limited gullies (Glade, 2005), an extrinsic hydro-meteorological threshold is not a sufficient condition, but an intrinsic sediment recharge threshold must be reached for debris flows to occur. Otherwise, there is an inherent danger of overestimating debris-flow occurrence when considering rainfall events only. Generally, rainfall will not necessarily trigger debris flows but floods or hyper-concentrated flows. The sediment recharge threshold is related to channel recharge rate, which can be determined by knowledge of debris storage and the elapsed time since the last debris flow in the basin (Jakob et al., 2005).

Consequently, we set the conditional probability for quantitative hazard assessment as: $P(B|A) = 1$ in transport-limited basins; and $P(B|A)$ values in the interval (0,1) in supply-limited basins. Owing to the difficulty in evaluating sediment recharge rate in gullies, we refer the existing quantitative study on the effect of geological conditions on debris-flow occurrence (Yu et al., 2014), and roughly estimate $P(B|A) = 0.6$ in supply-limited basins where weathering are strong and precipitation are abundant, while $P(B|A) = 0.2$ elsewhere.

Debris-flow fan configuration

Delimiting the spatial extent of potential damage from debris flows relies on understanding of the fan evolution, which is mainly governed by the terrain features of debris-flow accumulation flooding areas, and the physical properties of debris flows, such as rheology, sediment concentration. Since the different depositing conditions for debris flows, fan configurations may unfold in various surficial patterns. We categorize the fan configurations as complete, partial and unformed types. The latter two types always result in river blocking, and the last one may fail to form a fixed shape. Therefore, the authors only proposed a geometric model for the first two types.

Generally, natural debris-flow fans cannot be easily sorted in a precise and uniform shape. In the past, the fan shape has been represented by a semi-circle or semi-ellipse (Tsai, 2006; Takahashi, 2014), which assumes the maximum width of debris-flow fan locates at the outlet of the main channel. In other words, the circumferential angle corresponding to the plane of debris-flow fan is always equal to 90° . To further promote the utilization of the geometric model of debris-flow fans, the authors assumed debris-flow fans as a sector planar, where the effect of hydraulic structures, roads, and buildings on the flowing direction is not considered, and the path of the flow

downstream from the mouth is straight. In this study, the maximum length l_m , width b_m , and thickness (or flow depth) h_m of debris-flow fan, and the channel outlet width b_0 are used to derive the geometric model for debris-flow fans, as shown in a rectangular Cartesian coordinate system (Fig. 2). For practical use, the channel outlet width can be measured by field investigation, and other parameters can be estimated by empirical formulas (Table 2). Additionally, if debris flows occur under the same formation conditions, the four parameters can be valued by the existing field survey record.

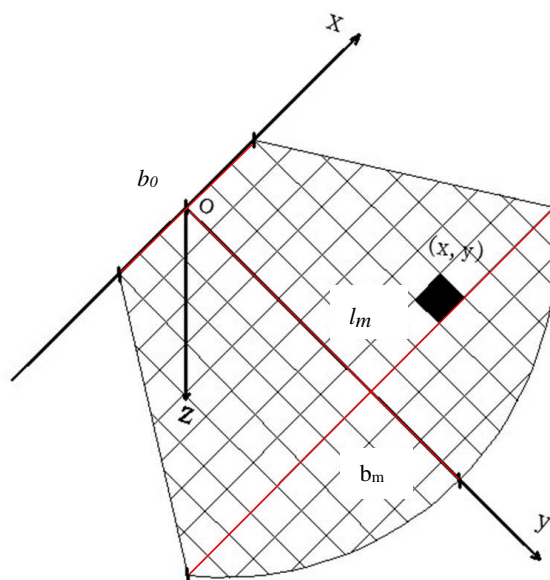


Figure 2. The coordinate system of the debris-flow fan (The origin is at the outlet center, x is parallel to the transverse section, y points down the fan slope, and z points into the slope, normal to the x - y plane)

Table 2. Empirical formulas for estimation of the maximum length, width, and thickness of the debris-flow fan

Formulations	Scope	References
$l_m = 15V_c^{1/3}$	Worldwide	Rickenmann (1999)
$l_m = -143.3387 + 29.8536 \ln V_c$ $b_m = -149.0417 + 25.6293 \ln V_c$ $h_m = 0.7067 + 0.0001 \ln V_c$	The slope of accumulation area is about 5° ; debris flow density is 1.82g/cm^3	Liu et al. (1993)
$l_m = 0.36A^{0.06} + 0.03(V_L \cdot H)^{0.54} - 0.18$ $b_m = 0.40A^{0.08} + 0.04(V_L \cdot H)^{0.35} - 0.23$	Wenchuan earthquake area	Tang et al. (2012)

Based on the above coordinate system, the corresponding circumferential angle of the fan plane is firstly derived:

$$\theta = \arcsin \frac{b_m}{\sqrt{4l_m^2 + b_0^2}} - \arctan \frac{b_0}{2l_m} \quad (\text{Eq.3a})$$

where $0^\circ < \theta < 90^\circ$.

Then, the fan shape can be described mathematically by the width of each transverse section, the calculation can be expressed as follows:

$$b = \begin{cases} b_0 + 2y \tan \theta & 0 \leq y \leq \frac{b_m - b_0}{2} \cot \theta \\ \frac{\sqrt{b_m^2 - (2y \sin \theta + b_0 \cos \theta)^2}}{\sin \theta} & \frac{b_m - b_0}{2} \cot \theta < y \leq l_m \end{cases} \quad (\text{Eq.3b})$$

where y is the longitudinal axis value of each grid center.

When $\theta = 90^\circ$, the fan shape is a semi-circle or semi-ellipse, whose width will be calculated as:

$$b = b_m \sqrt{1 - \left(\frac{y}{l_m}\right)^2} \quad (\text{Eq.3c})$$

According to the experimental results (Tsai, 2006; Takahashi, 2014), the non-dimensional longitudinal profile of fans can be approximated using a half-Gaussian curve, the calculation can be expressed as:

$$\frac{z_c}{h_m} = \exp \left[-\frac{1}{2C_L^2} \left(\frac{y}{l_m}\right)^2 \right] \quad (\text{Eq.3d})$$

The non-dimensional transverse profile can be approximated by a Gaussian curve:

$$\frac{z}{z_c} = \exp \left[-\frac{1}{2C_T^2} \left(\frac{x}{b}\right)^2 \right] \quad (\text{Eq.3e})$$

where Z_c denotes the thickness at the center point $(0, y)$ along the longitudinal axis; Z represents the thickness at any grid (x, y) ; and C_L, C_T are empirical coefficients, given approximately as 0.389 and 0.211.

Thus, if l_m, b_m, h_m, b_0 are given, we can obtain the three-dimensional topography of debris-flow fans using *Equations 3a-3e*.

Debris-flow disruptive intensity

In order to describe the damage degree of debris flow, a relatively disruptive intensity is introduced:

$$I_\xi = \frac{\xi(x,y)}{\xi_m} \quad (\text{Eq.4})$$

where I_ξ is the debris-flow disruptive intensity represented by variable ξ characterizing the debris-flow destructive power; $\xi(x,y)$ is the variable value of each grid on the fan; and ξ_m is the maximum. For expressing the inundated and impact damage of debris flow, ξ can be considered as flow depth and velocity.

United *Equations 3a-3e*, the inundated damage intensity can be deduced:

$$I_h = \begin{cases} \exp \left[-\frac{y^2}{2C_L^2 l_m^2} - \frac{x^2}{2C_T^2 (b_0 + 2y \tan \theta)^2} \right] & 0 \leq y \leq \frac{b_m - b_0}{2} \cot \theta \\ \exp \left[-\frac{y^2}{2C_L^2 l_m^2} - \frac{x^2 \sin^2 \theta}{2C_T^2 (b_m^2 - (2y \sin \theta + b_0 \cos \theta)^2)} \right] & \frac{b_m - b_0}{2} \cot \theta < y \leq l_m \end{cases} \quad (\text{Eq.5a})$$

When $\theta = 90^\circ$, the intensity can be calculated as:

$$I_h = \exp \left[-\frac{y^2}{2C_L^2 l_m^2} - \frac{x^2 l_m^2}{2C_T^2 b_m^2 (l_m^2 - y^2)} \right] \quad (\text{Eq.5b})$$

Considering the impact damage intensity, the distribution of velocity on the fan should be known. The authors assumed the debris-flow depositing processes in the mainstream line (along the maximum length) are uniform deceleration motion, and the attenuation processes of flow velocity in the transverse section are linear with the distance from the mainstream line, which will be decelerated to zero at the edge of the fans. Thus, the flow velocity at any grid (x,y) on the fan can be expressed as:

$$u(x, y) = \frac{b - 2|x|}{b} \cdot u_m \cdot \sqrt{1 - \frac{y}{l_m}} \quad (\text{Eq.6a})$$

where u_m is the maximum of flow velocity.

According to Equation 4, the impact damage intensity can be expressed as:

$$I_u = \frac{b - 2|x|}{b} \cdot \sqrt{1 - \frac{y}{l_m}} \quad (\text{Eq.6b})$$

As a result, debris-flow disruptive intensity can be obtained by l_m, b_m, b_0 , including two empirical coefficients C_L, C_T .

Debris-flow hazard evaluation

Based on the above derivation, debris-flow hazard of each unit on the fan can be computed as:

$$P(\xi) = P_H \cdot I_\xi \quad (\text{Eq.7})$$

where $P(\xi)$ is a probability function of variable ξ characterizing the debris-flow destructive power.

According to the definition of hazard, the necessary parameters at each grid in a hazard map are occurrence probability and disruptive intensity of debris flows (Hürlimann et al., 2008). Thus, these two parameters are correlated in a hazard matrix which can represent hazard qualitatively by hazard degree classes or quantitatively by a value ranging from zero to unity. An example of a debris-flow hazard matrix is given in Table 3.

In this hazard matrix, the debris-flow occurrence probability is classified into two groups. When the occurrence probability is smaller, the alluvial fan scale may be larger, and its disruptive intensity is greater. Therefore, we rank hazard degree classes with different intensity intervals in the groups.

Table 3. Example of debris-flow hazard matrix

Class	Occurrence probability, P_H	Disruptive intensity, I_E	Occurrence probability, P_H	Disruptive intensity, I_E
Very high	[0.01,1)	[0.7,1]	(0,0.01)	[0.5,1]
High		[0.5,0.7)		[0.2,0.5)
Medium		[0.2,0.5)		[0.05,0.2)
Low		[0,0.2)		[0,0.05)

Materials

The proposed framework is applied to evaluate the debris-flow hazard on the accumulation area of Shuida gully, located in the Longchi town, Sichuan province of China (N31°04'30", E103°33'44"). In the Shuida catchment (Fig. 3), which is situated in the Wenchuan earthquake area, a debris flow was triggered by a rainstorm on 13 August 2011.



Figure 3. (a) Photography showing the whole Shuida catchment and co-seismic landslides developed upslope; (b) The debris-flow scoured channel; (c) The deposited fan

Field investigations indicated that the gully was transport-limited, where abundant loose materials deposited after the earthquake. According to the local hydrological handbook, the return period of the rainstorm was 50 years. The 0.5 km² catchment has 650 m of relief with a mean catchment slope of 0.20. The necessary parameters for hazard assessment of debris flow are reported in Table 4.

Table 4. Parametric values used in the hazard assessment

b_0 (m)	b_m (m)	l_m (m)	h_m (m)	u_m (m/s)
35	154	180	7	5

Results

According to the above methods, the annual exceedance probability of Shuida gully debris flow is 0.02. The fan plane can be described by the width of each transverse section, which is deduced from *Equations 3a-3b*, as follows:

$$b = \begin{cases} 35 + 0.71y & 0 \leq y \leq 166.67 \\ \frac{\sqrt{23716 - (0.67y + 32.96)^2}}{0.34} & 166.67 < y \leq 180 \end{cases} \quad (\text{Eq.8})$$

According to *Fig. 4*, the actual deposited area can be measured at 22832 m², and the calculated area is 17118 m², while the overlapping area is 17068 m². Thus, the accuracy of the proposed geometric model is 75%, and it can be calculated as:

$$A_m = \frac{S_b}{S_n} \cdot \frac{S_b}{S_m} \quad (\text{Eq.9})$$

where A_m is the accuracy of model; S_a is the actual deposited area; S_b is the overlapping area; and S_m is the area calculated by the above geometric model of debris-flow fan.

Due to the fan partially unfolding, the accuracy of the model may be affected. However, the calculated area basically overlaps the actual accumulation area. In the calculated area, the fan domain is divided into many grids with equal area of 5 m×5 m, and the debris-flow disruptive intensity of each grid was calculated by *Equations 5a* and *6b*. The calculation process was carried out on ArcGIS 10.2. The final hazard maps are shown in *Fig. 4*.

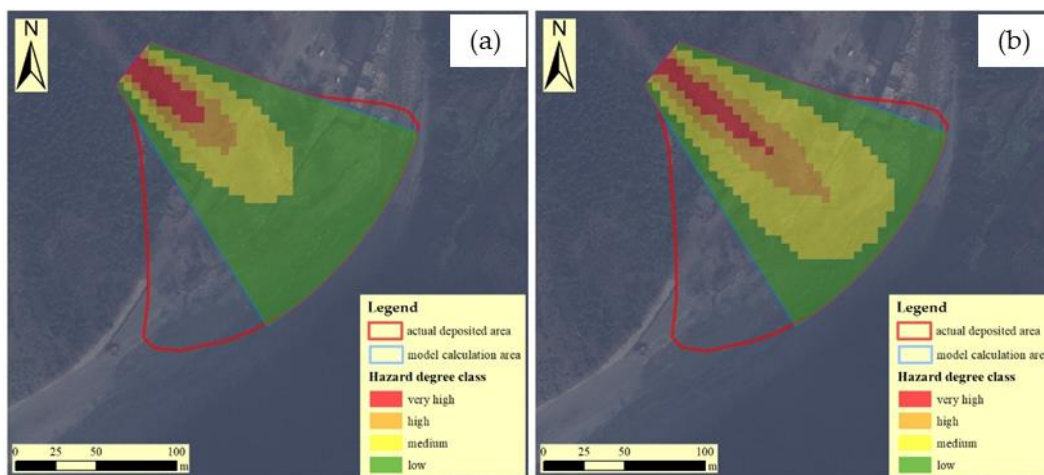


Figure 4. Hazard map of Shuida gully debris flow according to the proposed methods depending on (a) Flow depth; (b) Flow velocity

According to *Fig. 4(a)*, the area proportion of hazard grades from very high to low is 4.9%, 5.8%, 18.2%, and 71.1%, respectively. The proportion of flow depth greater than 1.4 m is 28.9%, which represents the inundated damage of Shuida gully debris flow. *Fig. 4(b)* shows the debris-flow impact damage, and the proportion of flow velocity greater than 1m/s is 54.9%.

Discussion

The developed methods appear useful and efficient for mapping the hazard on debris-flow accumulation area. These methods allow to emphasize and estimate the hazard component of debris flow, including the calculations of debris-flow occurrence probability and disruptive intensity. The hazard matrix, correlated to debris-flow occurrence probability and destructive power, can satisfy different evaluation requirements by hazard degree classes or by a value ranging from zero to unity. Meanwhile, the proposed framework, including five steps in a quantitative way to evaluate hazard of each grid on debris-flow fans, also points out some directions to be further studied:

- During the recognition of debris-flow hazard, it is useful to distinguish the debris supply condition of gullies. In supply-limited gullies, the importance of the recharge rate of sediments that may influence the frequency of occurrence and the magnitude of debris flows should be investigated. Moreover, the appropriate and reliable quantitative methods are expected to put forward for debris-flow hazard recognition.
- The conditional probability $P(B|A)$ is related to the triggering mechanism of debris flow. So it is important to introduce the initiation law of sediment under different hydro-climatic conditions, and establish the relationship between the conditional probability and the triggering condition of debris flow.
- The fan-forming process is difficult to be described mathematically in a precise shape, owing to the diversity of the terrain features of debris-flow accumulation areas and the complexity of the physical properties of debris flows. Although the developed geometric model of debris-flow fans further promotes the existing model, a more reliable numerical simulation is still regarded as a better method. Thus, the depositing processes of debris flows should be studied by governing equations for more accurate simulation of debris-flow fans.
- The above disruptive intensity is a relative value, which should be measured combined with its maximum. Other variables such as flow discharge, impact force, or momentum may also be available as indicators characterizing debris-flow destructive power.

Conclusion

According to the hazard definition, a framework for hazard assessment of debris-flow accumulation areas was proposed, including the calculations of debris-flow occurrence probability and disruptive intensity. A joint probability was defined to estimate debris-flow occurrence probability considering both hydrological and geomorphic characteristics, which was carried out on dividing basins into transport-limited or supply-limited by debris-flow occurrence signatures or thresholds. A relatively disruptive intensity was introduced to describe the damage degree of debris

flows by the distributions of flow depth and velocity. The distributions were obtained by an extended geometric model of debris-flow fans, and a hypothesis of uniform deceleration motions on fans.

The application for mapping the hazard on Shuida alluvial fan indicates that the developed geometric model can reflect the debris-flow accumulation flooding area, and the hazard evaluation by the given hazard map can show the inundated and impact damage of the debris flow in reality. Meanwhile, a numerical simulation, considering accumulation processes of debris flows, will be inspired in the future.

Acknowledgements. This work was funded by (1) National Key R&D Plan (Grant No. 2017YFC0405301); (2) International S&T Cooperation Program of China (Grant No. 2015DFR70980); (3) Scientific Program of China Institute of Water Resources and Hydropower Research (Grant No. SE0145B792017), and (4) Open Research Fund of State Key Laboratory of Simulation and Regulation of Water Cycle in River Basin, China Institute of Water Resources and Hydropower Research (Grant No. SKL2018ZY07). The materials were obtained with the help of Prof. Tang Chuan from State Key Laboratory of Geohazard Prevention and Geoenvironment Protection (Chengdu University of Technology).

REFERENCES

- [1] Brayshaw, D., Hassan, M. A. (2009): Debris flow initiation and sediment recharge in gullies. – *Geomorphology* 109: 122-131.
- [2] Calvo, B., Savi, F. (2009): A real-world application of Monte Carlo procedure for debris flow risk assessment. – *Computers & Geosciences* 35(5): 967-977.
- [3] Coussot, P., Meunier, M. (1996): Recognition, classification and mechanical description of debris flows. – *Earth-Science Reviews* 40: 209-227.
- [4] Cowpertwait, P. S. P., O'Connell, P. E., Metcalfe, A. V., Mawdsley, J. A. (1996): Stochastic point process modelling of rainfall. I. Single-site fitting and validation. – *Journal of Hydrology* 175: 17-46.
- [5] Davies, T. R., McSaveney, M. J. (2008): Principles of sustainable development on fans. – *Journal of Hydrology (New Zealand)* 47: 43-65.
- [6] De Scally, F. A., Owens, I. F., Louis, J. (2010): Controls on fan depositional processes in the schist ranges of the Southern Alps, New Zealand, and implications for debris-flow hazard assessment. – *Geomorphology* 122: 99-116.
- [7] Glade, T. (2005): Linking debris-flow hazard assessments with geomorphology. – *Geomorphology* 66: 189-213.
- [8] Guzzetti, F., Reichenbach, P., Cardinali, M., Galli, M., Ardizzone, F. (2005): Probabilistic landslide hazard assessment at the basin scale. – *Geomorphology* 72: 272-299.
- [9] Hürlimann, M., Rickenmann, D., Medina, V., Bateman, A. (2008): Evaluation of approaches to calculate debris-flow parameters for hazard assessment. – *Engineering Geology* 102: 152-163.
- [10] IUGS (International Union of Geological Sciences). (1997): Working group on landslides, committee on risk assessment, quantitative risk assessment for slopes and landslides: state of the art. – *Proceedings of the International Workshop on Landslides Risk Assessment, Rotterdam, Netherlands*: 3-12.
- [11] Iverson, R. M. (1997): The physics of debris flows. – *Reviews of geophysics* 35(3): 245-296.
- [12] Iverson, R. M. (2014): Debris flows: behaviour and hazard assessment. – *Geology today* 30(1): 15-20.

- [13] Jakob, M., Bovis, M., Oden, M. (2005): The significance of channel recharge rates for estimating debris-flow magnitude and frequency. – *Earth Surface Processes and Landforms* 30: 755-766.
- [14] Jakob, M., Hungr, O. (2005): *Debris-flow hazards and related phenomena*. – Springer, Berlin.
- [15] Liang, W. J., Zhuang, D. F., Jiang, D., Pan, J. J., Ren, H. Y. (2012): Assessment of debris flow hazards using a Bayesian Network. – *Geomorphology* 171: 94-100.
- [16] Lin, J. W., Chen, C. W., Peng, C. Y. (2012): Kalman filter decision systems for debris flow hazard assessment. – *Natural Hazards* 60: 1255-1266.
- [17] Liu, X. L., Zhang, S. L., Tang, C., Chen, M. (1993): A preliminary research on the model experiments of the risk range of debris fan. – *Geographical research* 12(2): 77-85. (In Chinese).
- [18] Liu, K. F., Huang, M. C. (2006): Numerical simulation of debris flow with application on hazard area mapping. – *Computational Geosciences* 10: 221-240.
- [19] Meyer, N. K., Schwanghart, W., Korup, O., Romstad, B., Etzelmüller, B. (2014): Estimating the topographic predictability of debris flows. – *Geomorphology* 207: 114-125.
- [20] Okunishi, K., Suwa, H. (2001): Assessment of debris-flow hazards of alluvial fans. – *Natural Hazards* 23: 259-269.
- [21] Raetzo, H., Lateltin, O., Bollinger, D., Tripet, J. P. (2002): Hazard assessment in Switzerland-Codes of Practice for mass movements. – *Bulletin of Engineering Geology and the Environment* 61: 263-268.
- [22] Rickenmann, D. (1999): Empirical relationships for debris flow. – *Natural Hazards* 19: 47-77.
- [23] Rickenmann, D. (2016): Debris-flow hazard assessment and methods applied in engineering practice. – *International Journal of Erosion Control Engineering* 9(3): 80-90.
- [24] Takahashi, T. (2009): A review of Japanese debris flow research. – *International Journal of Erosion Control Engineering* 2(1): 1-14.
- [25] Takahashi, T. (2014): *Debris flow: mechanics, prediction and countermeasures*. – CRC Press, London.
- [26] Tang, C., Zhu, J., Chang, M., Ding, J., Qi, X. (2012): An empirical-statistical model for predicting debris-flow runout zones in the Wenchuan earthquake area. – *Quaternary International* 250: 63-73.
- [27] Tsai, Y. F. (2006): Three-dimensional topography of debris-flow fan. – *Journal of Hydraulic Engineering* 132(3): 307-318.
- [28] Tsai, M. P., Hsu, Y. C., Li, H. C., Shu, H. M., Liu, K. F. (2011): Application of simulation technique on debris flow hazard zone delineation: a case study in the Daniao tribe, Eastern Taiwan. – *Natural Hazards and Earth System Sciences* 11: 3053-3062.
- [29] Wei, F. Q., Hu, K. H., Lopez, J. L., Cui, P. (2003): Method and its application of the momentum model for debris flow risk zoning. – *Chinese Science Bulletin* 48(6): 594-598.
- [30] Welsh, A., Davies, T. (2011): Identification of alluvial fans susceptible to debris-flow hazards. – *Landslides* 8: 183-194.
- [31] Wilford, D. J., Sakals, M. E., Innes, J. L., Bergerud, W. A. (2004): Recognition of debris flow, debris flood and flood hazard through watershed morphometrics. – *Landslides* 1: 61-66.
- [32] Yu, B., Zhu, Y., Wang, T., Chen, Y. J., Zhu, Y. B., Tie, Y. B., Lu, K. (2014): A prediction model for debris flows triggered by a runoff-induced mechanism. – *Natural hazards* 74: 1141-1161.

ASSESSING NDVI SPATIAL PATTERN RELATED TO MANAGEMENT ZONES

LIU, H. – WANG, X.*

*Heilongjiang Bayi Agricultural University, No. 5 Xinfeng Road, Daqing High-Tech Zone,
Heilongjiang Province, China
(phone: +86-139-3694-2710; fax: +86-459-681-9210)*

**Corresponding author*

e-mail: ndwangxi@163.com; phone: 86-138-3696-1962; fax: +86-459-681-9210

(Received 19th Dec 2018 ; accepted 6th Mar 2019)

Abstract. The NDVI of GreenSeeker has proven to be an effective tool for Management Zoning. An optimal method on the basis of NDVI was proposed to establish Management Zoning accurately in this study. First, the coefficient of variation of time series distance difference of Greenseeker and UAV NDVI was tested, it was significant to evaluate the accuracy of Greenseeker NDVI for large-areas. On this basis, optimal partition numbers and partitioning algorithm were identified according to the Silhouette Coefficient of data structure, the accuracy of estimation of agronomic parameters and the difference of agronomic parameters in each plot under different partition numbers. Results demonstrate that the difference among the points of the distance sequence is not significant ($F = 0.641 > 0.05$). The NDVI of Greenseeker has high reliability. When the partitioning algorithm and the number of partitions are K-means and four, respectively, the Silhouette Coefficient and the accuracy of estimation of agronomic parameters (plant height, nitrogen content) are higher than in other treatments. At the same time, the agronomic parameters in each plot showed the significant differences. The proposed method provides a good prospect to optimize the establishment of management zones.

Keywords: *nitrogen top dressing, clustering algorithm, the number of cluster, Greenseeker, UAV*

Abbreviations: NDVI: normalized difference vegetation index; GS-NDVI: NDVI was detected by Greenseeker; UAV-NDVI: NDVI was detected by UAV; *Si*: Silhouette Coefficient; NCE: normalized classification entropy; FPI: fuzzy performance index; FCM: fuzzy c-means algorithm; HC: hierarchical clustering; RMSSDT: root mean square standard deviation; RS: R square

Introduction

Nitrogen top dressing is a promising approach to improve yield and quality of maize in the early stages of growth (Sun et al., 2018). Site-specific application of nitrogen top dressing should lead to more efficient use and reduced the load on the environment (Zhou et al., 2018; Jin and Zhou, 2018). Management zones is a common intermediate step of moving from a uniform ‘field average’ management system to a site-specific crop management system (Ingerstad, 1982; Raun et al., 2002; Aavidai, 2016). The NDVI has a strong correlation with maize nitrogen content. The quest for precision in N management has prompted numerous recent investigations exploring the potential of NDVI by improved prediction of crop N needs (i.e., fertilizer Rate) (Rajkovich et al., 2012; Abbasi et al., 2012; Herbst et al., 2009; Cilia et al., 2014; Allen et al., 1973). Therefore, the NDVI can be regarded as a basis for management zones.

The acquisition methods of NDVI mainly include satellite remote sensing, aerial remote sensing and ground remote sensing. The spectral image sensor of satellite remote sensing and aerial remote sensing uses daylight as a light source to accurately describe the state of plant growth by NDVI and image information. However, due to the influence of cloud, atmosphere and meteorological conditions, it is difficult for them to

meet the strict requirements of nitrogen top dressing time (Cao et al., 2012). The UAV platform can solve previous problems, and its NDVI has been proved to have high accuracy, but its recharge mileage is limited (McKinion et al., 2009; Cruppe et al., 2017; Ren et al., 2008). The active spectrum sensor of ground remote sensing contains light emitting diodes (LEDs) that emit modulated light onto the canopy (thus, the term active) and detect reflectance of the modulated light from the canopy with photodiodes. Both visible and near-infrared wavelengths are typically included. With their own light sources, these sensors are less sensitive to diurnal variations than sensors that rely on ambient sunlight (Mulla et al., 1992; Fleming et al., 2000). Operationally, these sensors can be mounted on N fertilizer applicators equipped with computer processing and variable rate controllers, so that sensing and fertilization are accomplished in one pass over the crop. Commercial passive spectroscopy sensors mainly include Yara N-Sensor (Yara, Dulmen, Germany), GreenSeeker (Trimble, Sunnyvale, CA., USA), CropCircle (Holland Scientific Inc., Lincoln, NE, USA), and all of the above-mentioned sensors can output NDVI.

At present, there are several approximations for the development of site-specific management zones. For example, the chemical and physical properties (nitrogen content, conductivity) of soil were used to characterize spatial variability (Gerard et al., 1997; John et al., 2007; Wang et al., 2001), including topographic maps (Fu et al., 2010), direct soil sampling (Coque et al., 2006), non invasive soil sampling by electrical conductivity equipment (Colaco et al., 2017). The second approach is based on yield maps, which was established through the difference between the average of yield for many years and the current year's output. The third method is the integration of the two previous approaches and considers soil and/or relief information plus the use of yield maps (Beckie et al., 1997; Jia et al., 2004). More practical approaches have also considered farmers' knowledge in order to delineate management zones (Yang et al., 2009). All of the above information can be performed using different algorithms, such as K-mean, fuzzy clustering analysis, hierarchical clustering, etc (Orteg and Santibáñez, 2007; Yang et al., 2016; Cai et al., 2006; Chuang et al., 2006). However, the problems, such as high labor intensity and cumbersome operation, make it difficult to obtain the approximations. At the same time, the performance evaluation method of partition method is relatively single.

It is evident that NDVI is strongly associated with plant growth and soil nutrients. In this paper, the clustering method was studied based on the large-area corn canopy NDVI by the ground remote sensing sensor Greenseeker. At the same time, the NDVI of the unified location was obtained by the remote sensing image of the UAV. This study mainly completes the following two research contents.

(1) The accuracy of NDVI of Greenseeker was verified by comparing the different of data between NDVI and UAV.

(2) The optimal of partitioning algorithm and the number of partitions was proposed to establish a reasonable management zones and describe the group differences in corn growth

Materials and methods

Experiment location

The test site was located at Zhao Guang Farm, Hei He City, Heilongjiang Province (E 126°38'-127°38'5", N 47°1'-48°1') in northeastern China. The frost-free period is

about 120 days. The annual rainfall is 570 mm, the annual average sunshine is more than 2,700 h, and the soil type is mainly black soil. The Institute is located at No. 12-2, Zhao Guang Farm. The corn planting adopts a double ridge with a ridge width of 1.1 m. The area was surrounded by a space to ensure the accuracy of GPS data acceptance. The data collection time was June 12, 2016. The yellow border shows the ground-sensing Greenseeker working area (*Fig. 1*). The corn variety was Demei Ya No. 3, and it is 55 days after emergence. It needs to be ≥ 10 °C and the accumulated temperature of activity is about 2200 °C. It is a common early maize variety.

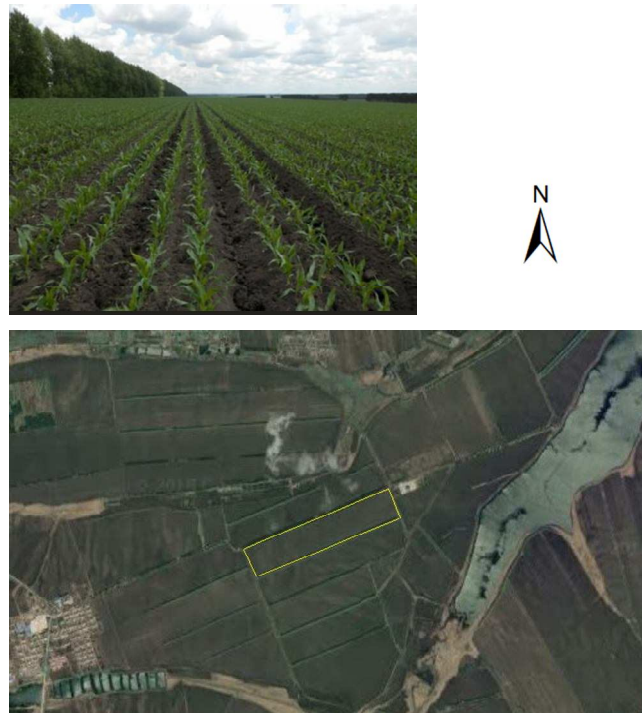


Figure 1. Sampling area

Data measurement and acquisition

The data of corn canopy was obtained by the ground remote sensing Greenseeker and the UAV remote sensing platform, respectively (*Fig. 2*). The ground remote sensing platform consists of six Greenseeker (Trimble, USA), Tractor (191, Valmet, Finland), Global positioning system (AG332, Trimble, USA) and VMC 1000 on-board computer (Xin Han, China). The Greenseeker was equipped with a narrow-band LED source with red light 660 nm and near-infrared light of 770 nm, which can obtain NDVI of plant canopy under two bands. It has a measurement area of 61 cm \pm 10 cm (width) \times 1.5 cm \pm 0.5 cm (length). The Greenseeker vertical distance was 70 cm from the canopy and the detection direction was consistent with the ridge (*Fig. 2a*). The measurement accuracy of GPS receiver was centimeter level. The update rate of GS and GPS was 1 Hz. The Valmet 191 tractors with manual throttle mode and speed digital display mode has the ability to work at a constant speed. According to the actual production situation, the test set the working speed to be 9 km/h and the working area is 416000 m².

The UAV has a battery life of 30 minutes, and its gyroscope ensures the stability of the spectral image sensor (Fig. 2b). At the same time, the route can be planned to achieve automatic flight. The spectrum image sensor of the UAV was an agricultural-specific multi-spectral camera (SEQUIOA, Mica Sense, USA). It has four wavelengths, Green (540-570) nm, Red (630-670) nm, Red-edge (730-750) nm and NIR (780-820) nm, respectively. The flight height of UAV was 500 m and the measurement area was 39600 m².



Figure 2. Ground remote sensing platform (a); UAV remote sensing platform (b)

Spectral image processing method for UAV

The spectral images have different degrees of distortion due to the imaging principle, external state and surface condition of the SEQUIOA spectral image sensor. The Agisoft Photoscan software was used to process and splicing spectral images of different channels. The spectral images were processed and spliced by Agisoft Photoscan software to obtain the orthophoto map of the four bands in the detection area, and RED and NIR images synthesized the NDVI images. In order to compare the different of NDVI between UAV and Greenseeker, the spectral image was split into a single zone using meshing methods (Fig. 3). The area of the zone was the same as that of the GS detection area. The NDVI of each zone of the spectral image was extracted and use the whiteboard to correct the coordinates of the initial zone and Greenseeker data points. Therefore, the GS-NDVI corresponds to UAV-NDVI one by one, and the difference analysis was carried out. Figure 3 is the spectral images processing flow chart.

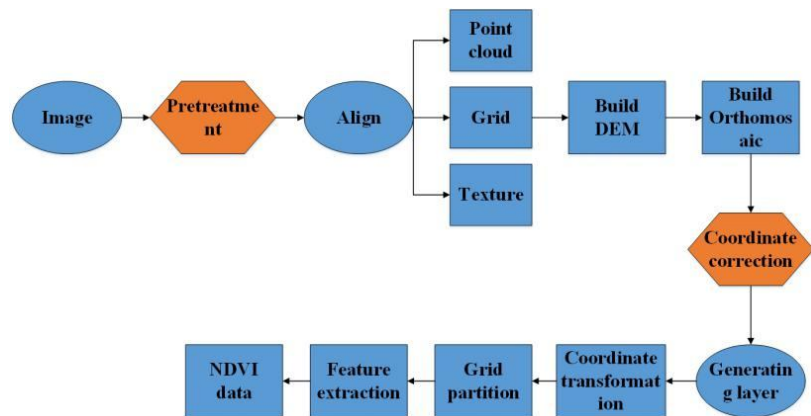


Figure 3. Spectral images processing flow chart

Partition method

The unsupervised clustering algorithm was used to divide the MANAGEMENT ZONING of variable fertilization. The purpose of clustering was to have high similarity between objects of the same category, and highly dissimilar with objects in other clusters. This study uses the following three partition clustering algorithms.

Algorithm 1: The K-mean clustering algorithm minimizes the sum of the squares of the Euler distances from the objective function x_j to the cluster center point u_i based on the randomly selected cluster number and the cluster center, and the partition was generated (Zhang et al., 2010). The function was as follows:

$$\operatorname{argmin} \sum_{i=1}^k \sum_{x_j \in C_i} \|x_j - u_i\|^2 \quad (\text{Eq.1})$$

The number of clusters was determined by ai and bi (ai : Average distance from i to other samples in the same cluster; bi : Average distance from i to samples of different clusters). The smaller the ai , the more accurate classification. The smaller the bi , the less accurate classification (Sangalli et al., 2010). The cluster center value will collapse to its cluster data center value after the algorithm runs converged.

Algorithm 2: The fuzzy c-means algorithm obtains the membership degree of each class point to all class centers by finding the iterative minimization of the objective function, and achieves the purpose of clustering (Huang, 1998). The most commonly used objective function is:

$$J(MC) = \sum_{k=1}^n \sum_{j=C_i}^c \mu_{ik} d_{ik}^2 \quad (\text{Eq.2})$$

C was the clustering category execution matrix $c \times p$. M was the sample fuzzy membership matrix $n \times c$. μ_{ij} is the membership value of the sample attribute of the i -th sample to the j -th cluster category. φ (fuzziness exponent) is a constant that controls the degree of overlap between clustering results and categories. d_{ij}^2 is the square of the distance between the i -th sample attribute and the j -th category center. The selection of the fuzzy category number C and the fuzzy weighted index φ directly affects the output of the continuous classification. The principle of φ selection is greater than 1, and 1.3 is taken here (Schepers et al., 2004; Ramchandran et al., 2015; Hassan et al., 2018). The clustering number is determined by fuzzy clustering index and normalized classification entropy. The division of the cluster was evident when the value of FPI is close to 0. NCE has similar results. The equation is as follows:

$$FPI = 1 - \frac{c}{(c-1)} \left[1 - \sum_{k=1}^n \sum_{i=1}^c (u_{ik})^2 / n \right] \quad (\text{Eq.3})$$

$$NCE = \frac{1}{(c-1)} \left[\sum_{k=1}^n \sum_{i=1}^c u_{ik} \log_a(u_{ik}) \right] \quad (\text{Eq.4})$$

Algorithm 3: Hierarchical Clustering divides the nearest two samples into a family, repeating the division until there is only one family left, so there was no need to specify

the number of classes (Di Gennaro et al., 2017). The distance between the samples can be calculated by the class average method. The order of hierarchical decomposition is in the bottom-up mode.

In order to define the optimal number of clusters, the following two indices have been used to calculate the cluster validity indicators, which are the root mean square standard deviation and the R square validity index (Condorelli et al., 2018). Since the purpose of clustering is to define homogeneous groups, the lower RMSSTD value in clustering analysis is better. The value ranges from 0-1. The high value of RS indicates that there is a significant difference between the clusters, and the classification effect was better.

$$RMSSTD = \sqrt{\frac{\sum_{i=1}^{n_c} \sum_{j \in C_i} (x_j - \bar{x}_i)^2}{\sum_{i=1}^n (r_i - 1)}} \quad (\text{Eq.5})$$

$$RS = \frac{\left[\sum_{j=1}^n (x_j - \bar{x}) \right] - \left[\sum_{i=1}^{n_c} \sum_{j \in C_i} (x_j - \bar{x})^2 \right]}{\sum_{i=1}^n (x_j - \bar{x})^2} \quad (\text{Eq.6})$$

n_c was the number of clusters; \bar{x}_i was the cluster center.

Evaluation method

Difference between GS-NDVI and UAV-NDVI

The NDVI between Greenseeker and UAV cannot be directly quantified, because the two sensors work differently, the trends were changed. Since the NDVI data is an isochronous sequence, the data only changes on the Y-axis. Therefore, the difference value of the two pairs of data was taken as a single set of random variable sample sequences. If there is no difference in the effect of the two data, the difference between each pair should be an unbiased estimator of the population mean difference. The method was T test.

Performance evaluation method for different clustering algorithms

(1) Clustering performance comprehensive evaluation parameter

The Silhouette Coefficient combines a_i and b_i and can be used to evaluate the impact of different algorithms or operating modes on clustering results based on the same raw data (Omran et al., 2005). It only considers dataset geometry as shown in Equation 7.

$$s(i) = \begin{cases} 1 - \frac{a(i)}{b(i)}, & a(i) < b(i) \\ 0, & a(i) = b(i) \\ \frac{b(i)}{a(i)} - 1, & a(i) > b(i) \end{cases} \quad (\text{Eq.7})$$

(2) Rationality verification of clustering method based on agronomic parameters

According to the Site-specific fertilizer management method, a reasonable Management Zoning should have the following characteristics. The crops in the same plot have consistent growth status, and the growth status of crops between different plots have significantly different. There was a significant correlation between plant height and biomass of maize and NDVI. There the rationality of Management Zoning of NDVI was verified base on plant height and biomass of maize. The method was as follows, a multi-management partition map with location information was generated by clustering algorithms when the number of partitions is 2-6. In each plot on the map, 100 sets of sample information were collected randomly. (The height of the corn was measured by the distance of the ground to the highest stretch of all the leaves when the blade was naturally stretched. The fresh matter of the aboveground tissue was used as the corn biomass). Regression models of plant height and biomass of Maize in the same plot were established based on the total sample. The consistency of the corn growth status was evaluated by the estimated error RMSE of regression models. Based on the sample mean of plant height and biomass in each plot, comparing the differences in plant height and biomass between the various plots, and evaluating whether the corn growth status between the plots was significantly different. Through the analysis of corn agronomic parameters, the optimal clustering method was proposed to establish a reasonable management partition.

Results

Comparative analysis of differences between UAV-NDVI and GS-NDVI

A significant difference can be clearly seen between soil reflectance (1 in *Fig. 4*) and maize reflectance (2 in *Fig. 4*), and the resolution is relatively high, which shows that the NDVI based on UAV has high accuracy. Red part in *Figure 4a* stands for UAU's working area and the blue part shows the meshing. Based on the whiteboard (3 in *Fig. 4*). UAV mesh and GS mesh are in one-to-one correspondence (4 in *Fig. 4*).

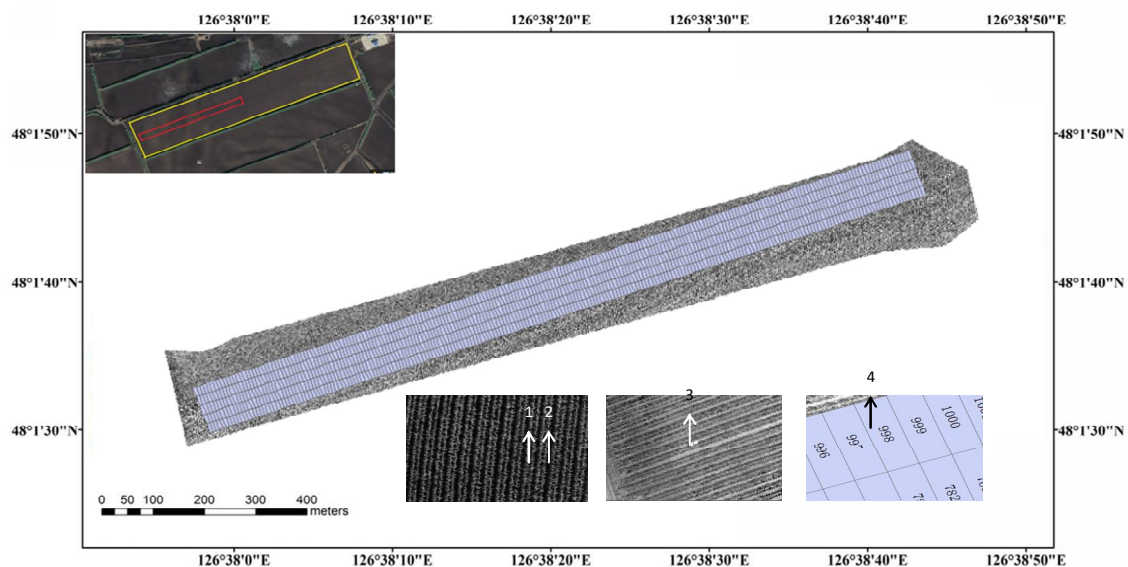


Figure 4. The image of NIR

Figure 5a shows the NDVI time series. GS-NDVI was significantly higher than UAV-NDVI, because the detection of GS is closer to the object than the UAV, and the scattering and refraction of light have less effect on GS-NDVI. The Sig > 0.05 of the two sets of data was tested by K-S, indicating that the array belongs to a normal distribution and satisfies the preconditions of the T test (Fig. 5b and c). Univariate T-tests were performed on the arrays. The results showed that the single factor variation was not significant (Sig > 0.05) (Table 1), indicating that GS-NDVI and UAV-NDVI had similar trends throughout the time series.

Performance comparison of clustering algorithms

The GS-NDVI of detection area was described (Table 2). The variation was 17.8%, which satisfies the preconditions for the precise agricultural division and implementation of MANAGEMENT ZONING.

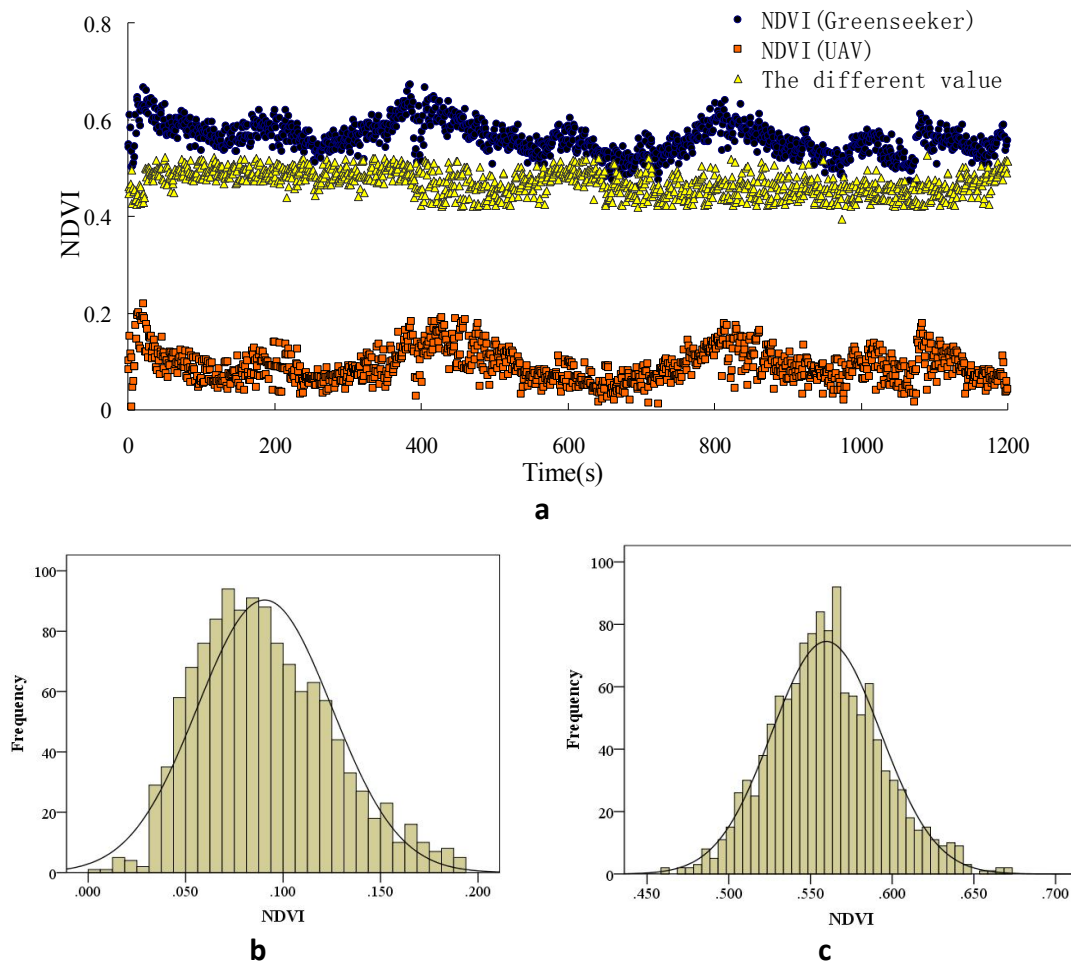


Figure 5. The NDVI trend with time (a); frequency distribution map of GS-NDVI (b); frequency distribution map of UAV-NDVI (c)

Table 1. Statistical analysis table

Sequence	Number of data	Mean	Standard deviation	Sig
Difference value	1249	.46834	.025884	0.848

Table 2. Descriptive statistics of the sample area

Data	Number of data	Maximum value	Minimum value	Standard deviation	Variability (%)	Time consumed (h)
GS-NDVI	27153	0.84	0.108	0.089	17.8	7.62

The effect of clustering number and clustering method on partitioning results

The initial cluster number was set to 2-6 and the cluster center was randomly selected. When K-mean algorithm was applied, the b_i begins to increase, but then again decreased with the increase in a number of clusters, the maximum value was reached when the number of clusters was 4. The change of a_i under different cluster numbers was gentle. Therefore, when the number of clusters was 4, the K-mean clustering has a better effect (Fig. 6a). PFI and NCE reached a minimum when the number of clusters was 3, so the FCM optimal cluster number was 3 (Fig. 6b). In RMSSTD and RS, we searched the map for the critical “knee” to find out that the optimal cluster number was 3 of Hierarchical Clustering (Fig. 6c). According to the optimal number of clusters, the a_i and b_i of each clustering algorithm was calculated. Then the S_i was explained by Formula 8. The results were shown in (Table 3), the a_i and b_i of FCM was the minimum values, it indicates the data in the cell was compact and the cell division was reasonable. However, the difference between each cell in the whole region was small, resulting in lower S_i . The FCM clustering algorithm could not clearly describe the overall trend of NDVI, and management zone could not be accurately established. Due to the difference in the number of partitions between K-mean and HC, there was a difference between a_i and b_i , but S_i were basically the same and significantly higher than FCM. Both K-mean and HC have excellent ability to create management zone. Although K-mean and HC have similar performance, but the calculation time of HC was significantly longer than that of K-mean.

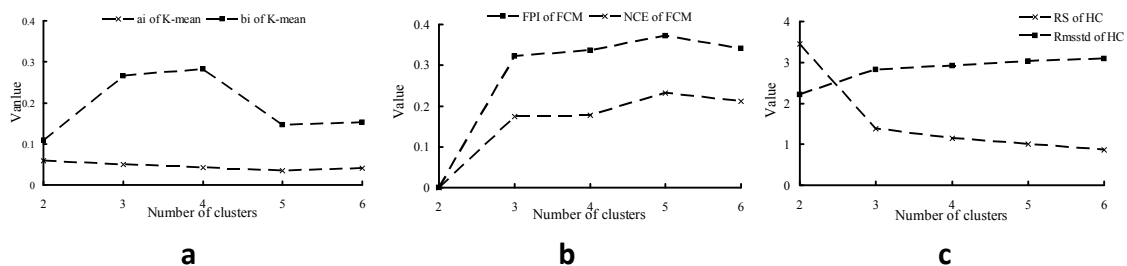


Figure 6. The a_i and b_i under different clustering numbers of K-mean (a); the FPI and NCE under different clustering numbers of FCM (b); the RMSSTD and RS under different clustering numbers of HC (c)

Table 3. Comparison of different clustering algorithm results

Cluster	Number of partitions	a_i	b_i	S_i
FCM	3	0.0356	0.169	0.427
K-mean	4	0.0399	0.299	0.817
HC	3	0.0439	0.323	0.811

The variation trend of RMSE of plant height under different treatments was shown in *Figure 7a*. With the increase of the number of clusters, the RMSE trend of each clustering algorithm were gentle. The RMSE of K-mean was significantly smaller than that of HC and FCM. Therefore, clustering method was more important than clustering number in estimating maize plant height. K-means performance was stronger. When using biomass data, the RMSE of each algorithm show a trend of decreasing first and then increasing with the increase of clustering number (*Fig. 7b*). The RMSE have the minimum value when the cluster number was 4, which indicates that the number of clusters was more important than the clustering algorithm in the estimation of biomass.

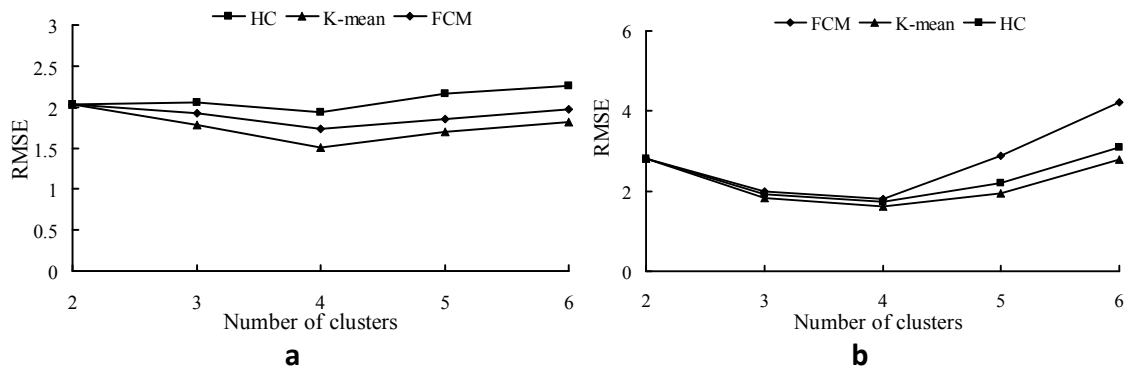


Figure 7. Plant height and biomass estimation error of different algorithms under different cluster numbers

The differences of plant height and fresh matter weight in different plots were shown under different clustering methods and cluster numbers (*Fig. 8*). The performance of each algorithm is basically the same when the partition number are 2 and 3, respectively. When using K-mean for partitioning, the results showed that there was a significant difference in plant height and biomass between each plot when the number of clusters was 4. As the number of partitions increases further, several plots with similar growth status of corn appeared (Same Letter), there were no significant differences in the plant height and the weight of fresh matter between them. The optimal result was still 4 partitions (*Fig. 8a*). HC was similar to K-mean results (*Fig. 8b*), but its computational complexity is significantly higher than K-mean. When using Fcm for partitioning, the partition result was similar to K-mean when the number of clusters was 6. But the SD of each plot was higher than K-mean, this indicates that the difference in corn growth in each cell of FCM has a large impact on the accuracy of the partition (*Fig. 8c*). In summary, four partitions can accurately express the population differences of corn growth status when use the K-mean.

Regression analysis of plant height and biomass was conducted by GS-NDVI. The R^2 of fitting curves of plant height and biomass were 0.8655 and 0.9002, respectively (*Fig. 9*). It shows that NDVI prediction is effective. It can be seen from the trend of the curve that the slope of the curve does not change significantly when NDVI is in the range of 0.118-0.246 and 0.658-0.792, respectively. The NDVI value with high or low cannot accurately predict corn plant height and fresh matter weight at this time.

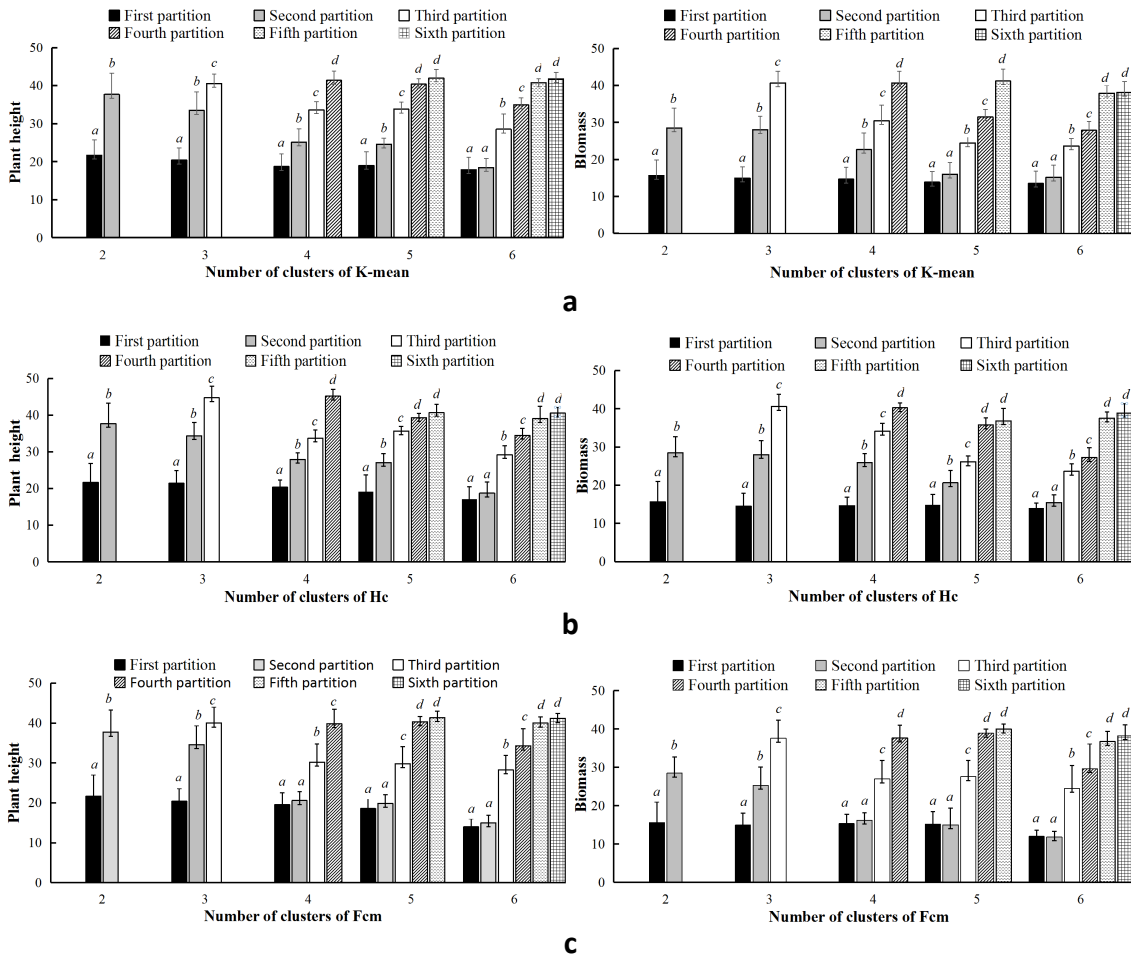


Figure 8. The difference in plant height and biomass of each plot under different cluster numbers; K-mean (a); Hc (b); Fcm (c). Marking the same letter (such as a and ab) means that the difference is not significant, and different letters (such as a and b) are significant differences. The lower-case letters (a, b, c) indicate a significant level of $f = 0.05$

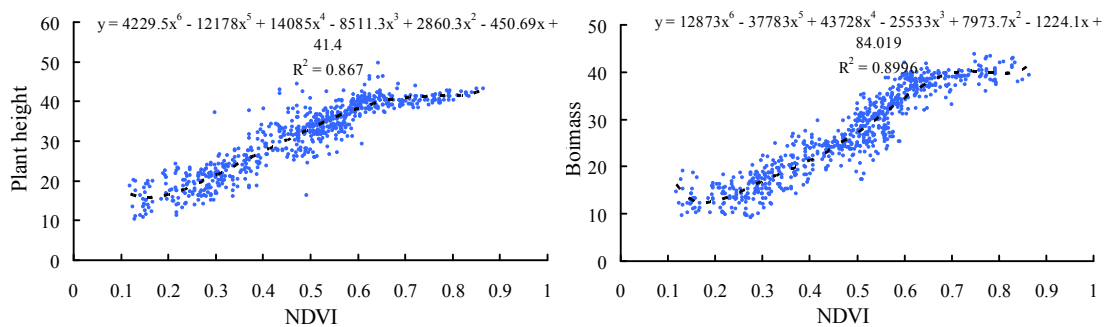


Figure 9. Prediction models of plant height and biomass by GS-NDVI

Four partitions can accurately express the group difference of corn growth status when using the K-mean. Although the HC algorithm can achieve better classification results, it has a large amount of computation. Distribution map of maize growth status difference was built by K-mean and 4 cluster numbers based on GS-NDVI (Fig. 10).

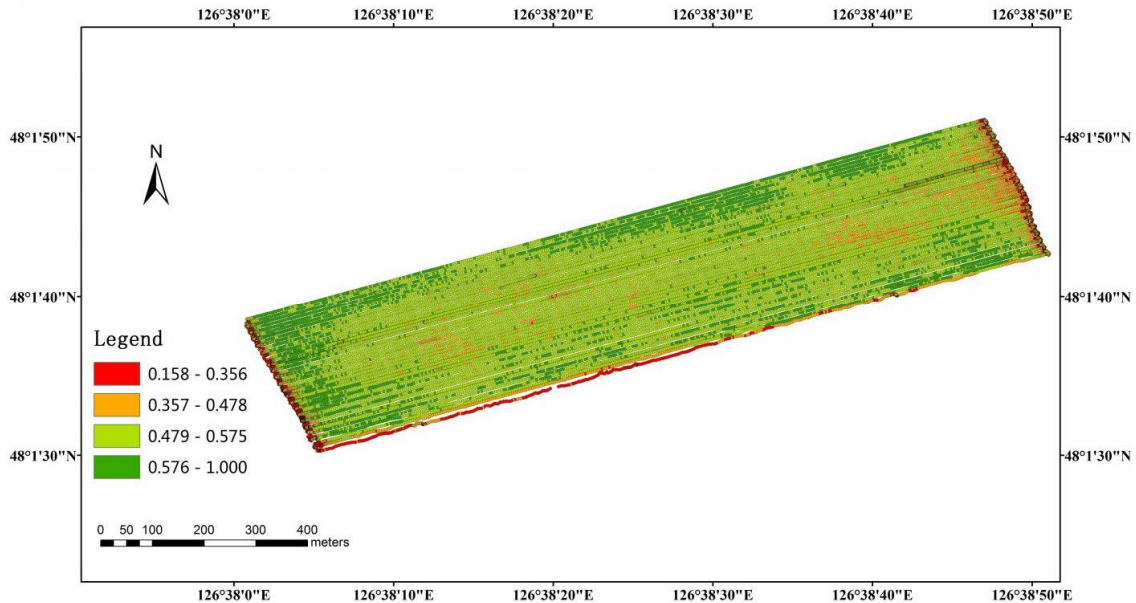


Figure 10. Maize growth map based on NDVI

Discussion

The definition of a specific location MANAGEMENT ZONING depends on spatial information that is stable or predictable over time. In this paper, the time series NDVI data were used to reflect the differences of maize growth. The overall variation of NDVI was 12%, and the result is similar to that of previous research (Park and Moon, 2007; Zhang and Qiu, 2012).

Due to the differences in the working methods of the platform and the sensor, there are also differences in the NDVI data obtained in the crop canopy. Previous articles have discussed the differences in large-area plant canopy NDVI data acquired by different sensors. In this investigation, the trend of GS-NDVI and UAV-NDVI time series was compared. We found that there was no significant difference in the change trend of them on the whole plot, the accuracy of large-area GS-NDVI data was proved. Existing methods for comparing NDVI differences between different types of sensors were cumbersome. For example, compare the estimation errors of nitrogen content (Caturegli et al., 2016), the correlation between NDVI and crop yield (Duan et al., 2017). The method of this study directly compares NDVI data without the need to collect large-scale crop samples and test their chemical composition and the results were satisfactory.

K-mean is more effective at expressing corn population differences than Fcm. The results is different from other studies such as NDVI data clustering based on remote sensing images (Yang et al., 2012; Bandyopadhyay et al., 2007; Cammaran et al., 2011; Glass, 2007). The reason for this difference was that the NDVI data of the spectral image is more accurate (such as using image processing, texture features, etc. to remove outliers in the NDVI). In this investigation, we select the m value of Fcm concerning spectral image clustering, but the GS-NDVI collected in real time was greatly disturbed in the field, such as the reflectance of bare soil (Ghobadi et al., 2015). There are many abnormal data, which causes the selected m value of Fcm to be unsuitable for GS-NDVI.

The effectiveness of the number of partitions can be assessed by several criteria. The measure of variance reduction of the MANAGEMENT ZONING when compared to the within-field variance can be calculated (Sarangi, et al., 2015). Alternatively, the Variable Rate (VR) fertilization nutrients was applied based on a recommendation map derived from data associated with the MANAGEMENT ZONING. Then, a cost-benefit was analyzed based on the nutrients used (input) and yield obtained (output) to evaluate the effectiveness of the number of partitions (Halcro et al., 2013). The evaluation method SC used in this study is based on the same principle as the variance evaluation method. According to the existing research, the agronomic parameters of corn under different growth conditions have significant differences. Therefore, this paper uses agronomic parameters to evaluate the accuracy of the number of partitions and determine the optimal number of partitions. In conclusion, the research methods and evaluation methods used in this paper are feasible, and the result is effective for MANAGEMENT ZONING.

Plant height and biomass are important parameters for expressing corn growth status, and NDVI has a significant relationship with them. However, the GS-NDVI values were not accurate for plant height and biomass evaluation in the lower range (0.118-0.293) and higher range (0.718-0.841). Other scholars have also obtained similar results when studying the correlation between NDVI and corn traits (Hansen et al., 2003; Yang et al., 2010, 2012). The reason for this result was due to excessive soil reflection from the corn canopy NDVI of small leaf area. Conversely, the NDVI high value appears saturated. At this time, NDVI cannot accurately estimate the corn trait.

According to K Lawton research (Lawton, 1946), the air permeability in the edge of the field was conducive to corn growth. The growth status of corn in the edge of lower left corner of experimental field was consistent with his conclusion. However, the growth status of corn in the edge of upper right corner of experimental field has poor growth. This problem may be due to the semi-sloping land, and upper right corner of the area with a low topographical position, the water stress affecting the growth of the corn. The corn in the lower edge of the field near the windbreak was poorly grown. According to the research of Reynolds et al. (2007), tree competition significantly reduced corn photosynthetic radiation (PAR), net assimilation (NA), and individual growth and yield. Relevant scholars have also researched the reasons for the difference in growth in other locations, but there is no unified answer at present.

Conclusions

The comparative method of NDVI time series trend was proposed to Indicate the effectiveness of the large-area NDVI of Greenseeker was worthy of recognition. At the same time, the optimal partition method of NDVI for management zone based on plant height and biomass of maize was discussed. The plant height evaluation accuracy results show that the contribution of cluster algorithm is greater than the number of partitions. The opposite result of biomass performance. When the number of partitions is 4, a reasonable management partition map of NDVI was established based on K-mean.

In this paper, based on the NDVI data of Greenseeker, a reasonable management partition was established by clustering method, but data is processed offline. Therefore, the future research focuses on the development of online clustering methods. Develop a more intelligent and simple management partition real-time creation method.

Acknowledgements. The authors would like to thank Edanz Editing and anonymous reviewers for their constructive comments and suggestions to improve the quality of the study. This work was partially supported by National Key R & D project (2016YFD020060802).

REFERENCES

- [1] Aavudai, A. (2016): Growing degree days-Ecosystem indicator for changing diurnal temperatures and their impact on corn growth stages in Kansas. – *Ecological Indicators* 61: 149-158.
- [2] Abbasi, M. K., Tahir, M. M., Sadiq, A., Iqbal, M., Zafar, M. (2012): Yield and nitrogen use efficiency of rainfed maize response to splitting and nitrogen rates in Kashmir, Pakistan. – *Agronomy Journal* 104(2): 448-457.
- [3] Allen, W. A., Gausman, H. W., Richardson, A. J. (1973): Theory of Leaf Reflectance Evaluated by Ray Tracing. – *Appl. Opt* 12(10): 2448-2453.
- [4] Bandyopadhyay, S., Maulik, U., Mukhopadhyay, A. (2007): Multiobjective genetic clustering for pixel classification in remote sensing imagery. – *IEEE Transactions on Geoscience and Remote Sensing* 45(5): 1506-1511.
- [5] Beckie, H. J., Moulin, A. P., Pennock, D. J. (1997): Strategies for variable rate nitrogen fertilization in hummocky terrain. – *Canadian Journal of Soil Science* 77(4): 589-595.
- [6] Cai, W., Chen, S., Zhang, D. (2006): Fast and robust fuzzy c-means clustering algorithms incorporating local information for image segmentation. – *Pattern Recognition* 40(3): 825-838.
- [7] Cammarano, D., Fitzgerald, G., Basso, B., O’Leary, G., Chen, D., Gracee, P., Fiorentinoc, C. (2011): Use of the canopy chlorophyll content index (CCCI) for remote estimation of wheat nitrogen content in rainfed environments. – *Agronomy Journal* 103(6): 1597-1603.
- [8] Cao, Q., Cui, Z., Chen, X., Khosla, R., Dao, T. H., Miao, Y. (2012): Quantifying spatial variability of indigenous nitrogen supply for precision nitrogen management in small scale farming. – *Precision Agriculture* 13(1): 45-61.
- [9] Caturegli, L., Corniglia, M., Gaetani, M., Grossi, N., Magni, S., Migliazzi, M., Angelini, L., Mazzoncini, M., Silvestri, N., Fontanelli, M., Raffaelli, M., Peruzzi, A., Volterrani, M. (2016): Unmanned aerial vehicle to estimate nitrogen status of turfgrasses. – *Plos One* 11(6).
- [10] Chuang, K., Tzeng, H., Chen, S., Wu, J., Chen, T. (2006): Fuzzy c-means clustering with spatial information for image segmentation. – *Computerized Medical Imaging and Graphics* 30(1): 9-15.
- [11] Cilia, C., Panigada, C., Rossini, M., Meroni, M., Busetto, L., Amaducci, S., Boschetti, M., Picchi, V., Colombo, R. (2014): Nitrogen status assessment for variable rate fertilization in maize through hyperspectral imagery. – *Remote Sensing* 6(7): 6549-6565.
- [12] Colaço, A. F., Molin, J. P. (2017): Variable rate fertilization in citrus: a long term study. – *Precision Agriculture* 18(2): 169-191.
- [13] Condorelli, G. E., Maccaferri M., Newcomb, M., Andrade, P. -Sanchez, White, J. W., French, A. N., Sciara, G., Ward, R., Tuberosa, R. (2018): Comparative aerial and ground based high throughput phenotyping for the genetic dissection of NDVI as a proxy for drought adaptive traits in durum wheat. – *Frontiers in Plant Science*. <https://doi.org/10.3389/fpls.2018.00893>.
- [14] Coque, M., Gallais, A. (2006): Genomic regions involved in response to grain yield selection at high and low nitrogen fertilization in maize. – *Theoretical and Applied Genetic* 112(7): 1205-1220.
- [15] Cruppe, G., Edwards, J. T., Lollato, R. P. (2017): In-season canopy reflectance can aid fungicide and late-season nitrogen decisions on winter wheat. – *Agronomy Journal* 109(5): 2072-2086.

- [16] Di Gennaro, S. F., Rizza, F., Badeck, F. W., Berton, A., Delbono, S., Gioli, B., Toscano, P., Zaldei, A., Mates, A. (2017): UAV-based high-throughput phenotyping to discriminate barley vigour with visible and near-infrared vegetation indice. – *International Journal of Remote Sensing* 39(15-16): 5330-5344.
- [17] Duan, T., Chapman, S. C., Guo, Y., Zheng, B. (2017): Dynamic monitoring of NDVI in wheat agronomy and breeding trials using an unmanned aerial vehicle. – *Field Crops Research* 15(8): 71-80.
- [18] Fleming, K. L., Westfall, D. G., Wiens, D. W., Brodahl, M. C. (2000): Evaluating farmer defined management zone maps for variable rate fertilizer application. – *Precision Agriculture* 2(2): 201-215.
- [19] Fu, W., Tunney, H., Zhang, C. (2010): Spatial variation of soil nutrients in a dairy farm and its implications for site-specific fertilizer application. – *Soil and Tillage Research* 106(2): 185-193.
- [20] Gérard, B., Buerkert, A., Hiernaux, P., Marschner, H. (1997): Non-destructive measurement of plant growth and nitrogen status of pearl millet with low-altitude aerial photography. – *Plant Nutrition for Sustainable Food Production and Environment* 373-378.
- [21] Ghobadi, Y., Pradhan, B., Shafri, H. Z. M., Kabiri, K. (2015): Assessment of spatial relationship between land surface temperature and landuse/cover retrieval from multi-temporal remote sensing data in South Karkheh Sub-basin, Iran. *Arabian Journal of Geosciences* 8(1): 525-537.
- [22] Glass, A. D. M. (2003): Nitrogen use efficiency of crop plants: physiological constraints upon nitrogen absorption. – *Critical Reviews in Plant Science* 24: 453-470.
- [23] Halcro, G., Corstanje, R., Mouazen, A. M. (2013): Site-specific land management of cereal crops based on management zone delineation by proximal soil sensing. – *Precision Agriculture* 13: 475-481.
- [24] Hansen, P. M., Schjoerring, J. K. (2003): Reflectance measurement of canopy biomass and nitrogen status in wheat crops using normalized difference vegetation indices and partial least squares regression. – *Remote Sensing of Environment* 86(4): 542-553.
- [25] Hassan, M. A., Yang, M., Rasheed, A., Yang, G., Reynolds, M., Xia, X., Xiao, Y., He, Z. (2018): A rapid monitoring of NDVI across the wheat growth cycle for grain yield prediction using a multi-spectral UAV platform. – *Plant Science* (2): 152-158.
- [26] Herbst, M., Protingheuer, N., Graf, A., Huisman, J. A., Weihermüller, L., Vanderborght, J. (2009): Characterization and understanding of bare soil respiration spatial variability at plot scale. – *Vadose Zone J* 8(3): 762-771.
- [27] Huang, Z. (1998): Extensions to the k-means algorithm for clustering large data sets with categorical values. – *Data Mining and Knowledge Discovery* 2(3): 283-304.
- [28] Ingerstad, T. (1982): Relative addition rate and external concentration; Driving variables used in plant nutrition research. – *Cell & Environment* 5(6): 443-453.
- [29] Jia, L., Buerkert, A., Chen, X., Roemheld, V., Zhang, F. (2004): Low-altitude aerial photography for optimum N fertilization of winter wheat on the North China Plain. – *Field Crops Research* 89(2-3): 389-395.
- [30] Jin, S., Zhou, F. (2018): Zero growth of chemical fertilizer and pesticide use: china's objectives, progress and challenges. – *Journal of Resources and Ecology* 9(sp1): 50-58.
- [31] John, R., Dalling, J. W., Harms, K. E., Yavitt, J. B., Stallard, R. F., Mirabello, M., Hubbell, S. P., Valencia, R., Navarrete, H., Vallejo, M., Foster, R. B. (2007): Soil nutrients influence spatial distributions of tropical tree species. – *PNAS* 104(3): 864-869.
- [32] Lawton, K. (1946): The Influence of soil aeration on the growth and absorption of nutrients by corn plants. – *Soil Science Society of America Journal*, 263-268.
- [33] McKinion, J. M., Jenkins, J. N., Willers, J. L., Zumanis, A. (2009): Spatially variable insecticide applications for early season control of cotton insect pests. – *Computers and Electronics in Agriculture* 67(1-2): 71-79.

- [34] Mulla, D. J., Bhatti, A. U., Hammond, M. W., Benson, J. A. (1992): A comparison of winter wheat yield and quality under uniform versus spatially variable fertilizer. – *Agriculture, Ecosystems & Environment* 38(4): 301-311.
- [35] Omran, M., Engelbrecht, A. P., Salman, A. (2005): Particle swarm optimization method for image clustering. – *International Journal of Pattern Recognition and Artificial Intelligence* 19(3): 297-321.
- [36] Orteg, R. A., Santibáñez, O. A. (2007): Determination of management zones in corn (*Zea mays*, L.) based on soil fertility. – *Computers and Electronics in Agriculture* 88(1): 49-59.
- [37] Park, S., Moon, W. M. (2007): Unsupervised classification of scattering mechanisms in polarimetric SAR data using fuzzy fuzzy logic in entropy and alpha plane. – *IEEE Transactions on Geoscience and Remote* 45(8): 2652-2664.
- [38] Rajkovich, S., Enders, A., Hanley, K., Hyland, C., Zimmerman, A. R., Lehmann, J. (2012): Corn growth and nitrogen nutrition after additions of biochars with varying properties to a temperate soil. – *Biology and Fertility of Soils* 48(3): 271-284.
- [39] Ramchandran, D., Johnston, D. B., Tumbleson, M. E., Rausch, K. D., Singh, V. (2015): Seasonal variability in ethanol concentrations from a dry grind fermentation operation associated with incoming corn variability. – *Industrial Crops and Products* 64: 155-160.
- [40] Ramirez, M. B., Allen, P. B., Freeland, R. S., Wilkerson, J. B. (2017): Cotton canopy NDVI: reducing the ground exposure effect. – *Transactions of the ASABE* 60(2): 293-301.
- [41] Raun, W. R., Solie, J. B., Johnson, G. V., Stone, M. L., Mullen, R. W., Freeman, K. W., Thomason, W. E., Lukina, E. V. (2002): Improving nitrogen use efficiency in cereal grain production with optical sensing and variable rate application. – *Agronomy Journal* 94(4): 815-827.
- [42] Ren, J., Chen, Z., Zhou, Q., Tang, H. (2008): Regional yield estimation for winter wheat with MODIS-NDVI data in Shandong, China. – *International Journal of Applied Earth Observation and Geoinformation* 10(4): 403-413.
- [43] Reynolds, P. E., Simpson, J. A., Thevathasan, N. V., Gordon, A. M. (2007): Effects of tree competition on corn and soybean photosynthesis, growth, and yield in a temperate tree-based agroforestry intercropping system in southern Ontario, Canada. – *Ecological Engineering*, 29(4): 362-371.
- [44] Sangalli, L. M., Secchi, P., Vantini, S., Vitelli, V. (2010): K-mean alignment for curve clustering. – *Computational Statistics & Data Analysis* 54(5): 1219-1233.
- [45] Sarangi, S. K., Maji, B., Singh, S., Sharma, D. K., Burman, D., Mandal, S., Singh, U. S., Ismail, A. M., Haefele, S. M (2015): Using improved variety and management enhances rice productivity in stagnant flood-affected tropical coastal zones. – *F. Crop. Res* 190: 70-81.
- [46] Schepers, A. R., Shanahan, J. F., Liebig, M. A., Schepers, J. S., Johnson, S. H., Luchiaric, A. (2004): Appropriateness of management zones for characterizing spatial variability of soil properties and irrigated corn yields across years. – *Agronomy Journal* 9(1): 195-203.
- [47] Sun, S. K., Lu, Y. J., Gao, H., Jiang, T. T., Du, X. Y., Shen, T. X., Wu, P. T., Wang, Y. B. (2018): Impacts of food wastage on water resources and environment in China. – *Journal of Cleaner Production* 185: 732-739.
- [48] Wang, J., Fu, B., Qiu, Y., Chen, L. (2001): Soil nutrients in relation to land use and landscape position in the semi-arid small catchment on the loess plateau in China. – *Journal of Arid Environments* 48(4): 537-550.
- [49] Yang, F., Sun, J., Fang, H., Yao, Z., Zhang, J., Zhu, Y., Kaishan, S. et al. (2012): Comparison of different methods for corn LAI estimation over northeastern China. – *International Journal of Applied Earth Observation and Geoinformation* 18: 462-471.
- [50] Yang, J., Parikh, D., Batra, D. (2016): Joint unsupervised learning of deep representations and image clusters. – *The IEEE Conference on Computer Vision and Pattern Recognition* 5147-5156. DOI: 10.1109/CVPR.2016.556.

- [51] Yang, W., Li, M., Sigrimis (2010): Nick estimating nitrogen content of cucumber leaves based on nIR spectroscopy. – *Sensor Letters* 8(1): 145-150.
- [52] Yang, Y., Fulin, W., Jie, Z. (2009): Intelligent fertilization decision support system based on knowledge model and WebGIS: Decision for fertilization. – *Computer Science and Information Technology* 8(11): 232-235.
- [53] Zhang, C., Qiu, F. (2012): Hyperspectral image classification using an unsupervised neuro-fuzzy system. – *Journal of Applied Remote Sensing* 6(1): 112-121.
- [54] Zhang, X., Shi, L., Jia, X., Seielstad, G., Helgason, C. (2010): Zone mapping application for precision-farming: a decision support tool for variable rate application. – *Precision Agriculture* 11(2): 103-114.
- [55] Zhou, K., Sui, Y., Xu, X., Zhang, J., Chen, Y., Hou, M., Jiao, X. (2018): The effects of biochar addition on phosphorus transfer and water utilization efficiency in a vegetable field in Northeast China. – *Agricultural Water Management* 210: 324-329.

DIFFERENTIAL RESPONSE OF FABA BEAN (*VICIA FABA* L.) PLANTS TO WATER DEFICIT AND WATERLOGGING STRESSES

AL-AMRI, S. M.

*Biology Department, Shaqra Faculty of Science and Arts, Shaqra University
Shaqra, Saudi Arabia
(e-mail: asenany203@yahoo.com)*

(Received 23rd Dec 2018 ; accepted 11th Apr 2019)

Abstract. Most of literature on water deficit and water logging tolerance and resistance in faba bean, have not be widely studied. Therefore, it is important to study the different plant responses to these abiotic stresses to understand the mechanisms of tolerance. Towards this goal faba bean plants were cultivated in soil culture at different levels of field capacity, FC (Control), 2FC (flooding), 75% of FC, low water deficit (LWD) and 50% of FC, high water deficit (HWD), for 2 weeks. Fresh and dry weights of plant roots and shoots were significantly decreased under both water stresses (flooding and water deficit). Number of plant nodules was affected as exposed to high and low water deficit levels (75% & 50% FC) by about 47% and 5%, respectively. Alcohol dehydrogenase specific activity of bean roots grown under flooding stress was significantly increased as compared to absolute control while the specific activity of alcohol dehydrogenase activity (ADH) under the two levels of drought (75% & 50% FC) was less affected as compared to reference control. Also, Michael's constant (K_m) and maximum velocity (V_{max}) of ADH in bean roots was decreased under the two levels of drought (75% & 50% FC) and flooding stress (2FC) compared to absolute control. Transfers cross sections stained with safranin examined and photographed at 25 X of 3-weeks old roots of flooded faba bean plants showing loosely parenchymal cell of cortex containing many and large intercellular spaces as compared to control and droughted plants. We concluded that flooding cause damage to *Vicia faba* plant more than water deficit through its effects on nodule formation and activity.

Keywords: *water stress, legumes, alcohol dehydrogenase activity (ADH)*

Introduction

Abiotic stress is a major constraint for agricultural production allover the world and drought is the most important limiting factor (Asgher et al., 2017; Hussain et al., 2018). Water deficit and flooding stresses have a negative impact on the living organisms in a specific environment (Armstrong, 1971a, b; El-Enany et al., 2014). The combination of environmental stresses always leads to cellular damage and causes a series of morphological, physiological, biochemical and molecular changes in plant growth, development and productivity (Gao et al., 2007; Mittler et al., 2006). Boyer (1982) and Araus et al. (2002) stated that exposure to water deficit or waterlogging stresses cause metabolism disturbance and damage to biomolecules. Frequent occurrence of climatic extremes water deficit and/or flooding every year in several parts of the world has adversely affected production of may crops (Candian and Tarhan, 2012). As a result, water deficit and waterlogging of the soil have become apparent in crop yields (Parent et al., 2008; Ashraf and Irm, 2005). Plants respond to environmental stresses at morphological, anatomical, cellular and molecular levels, leaf development (Cutler et al., 1980), maintain root development and soil moisture extraction and delayed leaf senescence (Hsiao et al., 1985).

Waterlogging process often prevents plant productivity by inhibiting oxygen diffusion to the roots (Sorrell et al., 2002). The anatomical structure of the roots is important to adapt to anoxic environments for wetland types (Sorrell et al., 2002; Colmer, 2003). Also, some advanced research has shown that the response of plants to waterlogging may be

due to roots morphology modifications like thickness of root, absence of lateral roots and reduction in root system (Wheeler, 1999; Visser et al., 2000; Romeu et al., 2019). Root propagation is important for plant growth, and the ability of nutrient acquisition depend on root length and structure in heterogeneous environments (Wahl et al., 2001). Vartapetian and Jackson (1997) stated that growth of roots under hypoxia or oxygen deficiency leads to confusion in oxygen-dependent pathways, especially the power generation system, functional relationships between roots and stem and both carbon absorption and photosynthesis. Wetland plants adapt to anaerobic conditions by formation of air roots containing intensive aerenchyma cavities to promote internal oxygen transport (Jackson and Armstrong, 1999; Visser et al., 2000; Colmer, 2003). Lysigenous and schizogenous aerenchyma disturbed in many important crop plant species and tissues (Justin and Armstrong, 1987; Jackson and Armstrong, 1999; Gunawardena et al., 2001). Also, schizogeneous aerenchyma was recorded in some wetland species like *Rumex palustris* and *Ranunculus sceleratus* (Visser et al., 2000). Some species such as *Sagittaria lancifolia* tend to form both schizogenous and lysigenous aerenchyma (Schussler et al., 1997). Our objective was to study the response of growth, nodulation, nodule activity and anatomy of faba bean plant roots under the effect of both water stresses (water deficit or waterlogging). Also, this study aimed to compare the differential response of *Vicia faba* plants to water deficit and waterlogging.

Materials and methods

Surface sterilized seeds of faba bean (*Vicia faba*) plants were conducted at the greenhouse chamber. Ten seeds were sown in culture pots containing 3 kg clay (Three pots for each treatment) and treated as follow. The pots were irrigated with tap water until reach field capacity is referred as control. Two weeks old seedlings were subjected to the following treatment: First group of pots irrigated until reach flooding, 2 FC (WL), second group of pots were irrigated till reach 75% of FC (LWD) and the third group of pots irrigated tell reach 50% of FC (HWD) for two weeks. At the early vegetative stage and after 2-weeks of treatments, plants were separated into roots and shoots. Results of fresh and dry weights of the roots and shoots will be recorded. Another part of fresh roots and shoots were stored in liquid nitrogen and stored at -80°C for experimental analysis. Nodule number, nodule fresh and dry weights were recorded. The activity nitrogenase enzyme was measured as described previously by Abd-Alla (1992) using the method recorded by Larue and Kurz (1973). Save each bottle at room temperature with 5% (T/T) acetylene for 1 hour and the emitted ethylene in the reaction bottle was measured by a gas chromatograph (Thermo Scientific TRACE GC Ultra equipped with FID detector). The enzyme activity was calculated as the μmol acetylene/h/g nodule fresh weight. Determination of nodules leghemoglobin was recorded after 45 days of plant growth by the method of Becana et al. (1986). One gram of detached nodules were ground in a mortar and pestle under cooling and macerated with 2 ml KCN, then centrifuged at 10,000 rpm for 30 min in a refrigerated centrifuge. The supernatants were reduced with sodium dithionate and the absorbance was recorded at 540 nm. Oxhemoglobin was used as a standard for calculations.

Alcohol dehydrogenase activity and its kinetics

0.5 g of leaf tissues were mined in 5 ml of 100 mM K-phosphate buffer (pH 7.8) containing 0.1 EDTA and 0.1 g polyvinylpyrrolidone. The mixture was centrifuged at

15,000 rpm for 15 min and the supernatants were used for measuring the activity of alcohol dehydrogenase enzyme (ADH). The enzyme activity was measured by monitoring NADH oxidation at 340 nm according to Yamanoshita et al. (2005) and modified by Govinda and Shanta (2011). The reaction medium was activated by addition of different volumes (50, 100, 150 and 200 μ l of 2.4 mM NADH and extract) and the reaction was initiated with 0.3 M acetaldehyde.

Root anatomy

Five root sections were collected from different plant treatment and immediately fixed in 2% paraformaldehyde, 2% glutaraldehyde, and 100 mM sodium cacodylate buffer, pH 7.35 for sectioning. Fixed prepared tissues were then rinsed with 100 mM sodium cacodylate buffer (pH 7.35) containing 10 mM 2-mercaptoethanol and 130 mM sucrose. These sections were stained using Sato's triple lead solution stain and 5% aqueous uranyl acetate (Sato, 1968). After infiltration with Spurr's resin (Spurr, 1969) and polymerization, ultrathin sections (60–90 nm) were cut with an ultramicrotome, contrasted with uranyl acetate and lead citrate, and examined with a transmission electron microscope (JEOL TEM 100 CXII, Electron Microscope Unit, Assiut University).

Statistical analysis

One-way ANOVA using the SPSS 10.0 software program. Means and standard errors were calculated for three replicate values. Means were compared by the Duncan's multiple range test and statistical significance was determined at 5% level.

Experimental results

Growth criteria

Faba plants grow under controlled conditions did not show any symptoms of leaf damage over the longest experimental period. Waterlogging stress induce visible leaf damage was apparent after 20 days of planting, like midrib yellowing, leaf yellow spots and finally wilting, their progression was very rapid. The results of roots and shoots of bean plants grown under water logging and water deficit stresses are presented in *Figure 1*. These results indicate that the stress of water deficit significantly reduced the fresh and dry weights of the roots and shoots of faba bean plants, especially developing at high droughted level (50% FC).

Both stresses flooding and high water deficit reduced significantly the total biomass of faba bean (*Vicia faba*) plants. Water deficit level (50% FC) significantly reduced roots fresh and dry weights more than low water deficit level (75% FC) as compared to control plants. Whereas, roots dry weight of flooded treatment was seems higher and this sometimes occurs at least in part as the result of initiation of several new lateral roots under flooding condition on the sub-merged part of shoot.

Number of nodules

The results of nodule number are presented in *Table 1*, these results showed that the levels of drought (75% & 50% FC) was significantly lowered the number of nodules per plant by about 5% and 47%, respectively. Also, the waterlogging stress significantly decreased the number of nodules by about 52.2%.

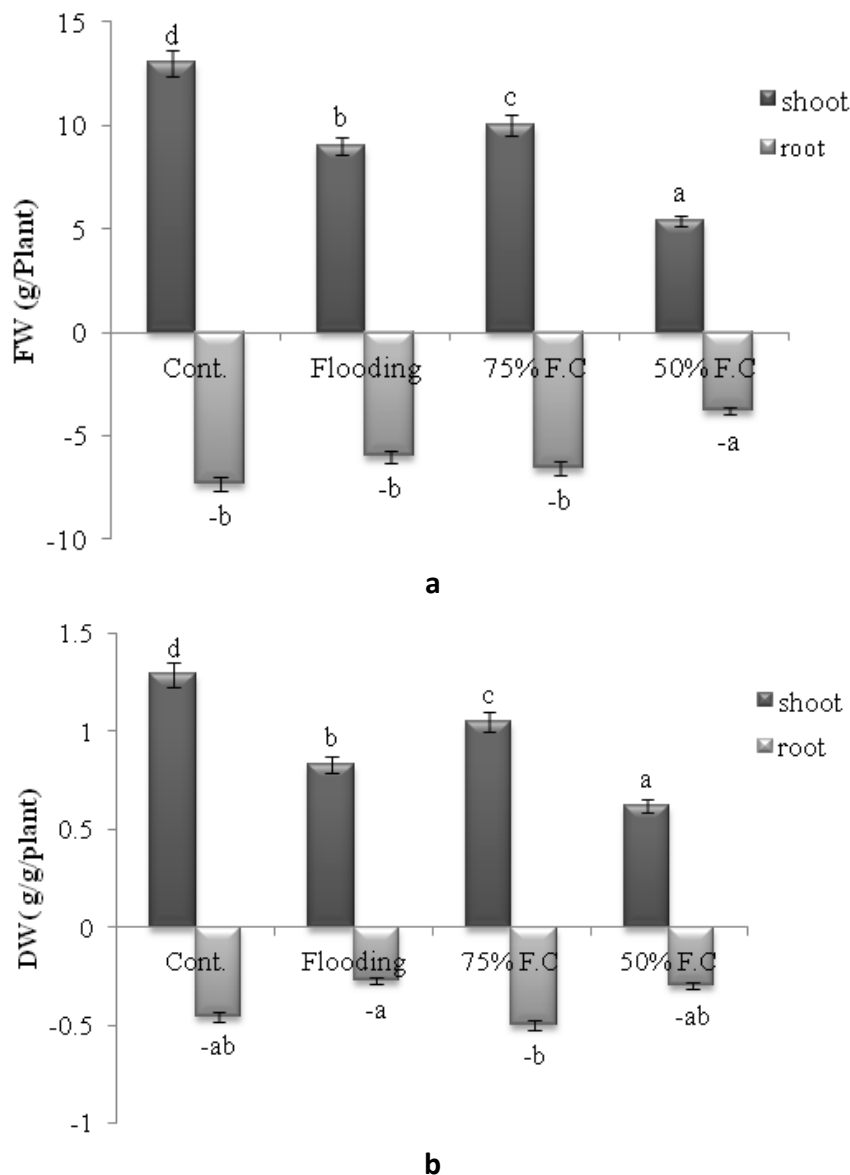


Figure 1. Fresh weights of roots and shoots (a) and roots and shoots dry weights (b) of faba bean plants grown under different levels of field capacity for two weeks. The same letters indicate non-significant differences between treatments at $P < 0.01$

Table 1. Effect of water deficit and waterlogging on nodules number, nodule leghemoglobin and nitrogenase activity of faba bean plants grown under different levels of field capacities for two weeks

Treatments	<i>Vicia faba</i> plants		
	Number of nodules/plant	Nodule leghemoglobin	Nitrogenase activity
Control	115±8.3 ^d	0.33±0.02 ^c	6.32±7.36 ^c
Flooding (2 FC)	60±4 ^c	0.19±0.01 ^a	0.69±0.17 ^a
LWD (57% FC)	35±6.2 ^b	0.27±0.1 ^b	5.38±3.11 ^c
HWD (50% FC)	13±2 ^a	0.23±0.01 ^b	1.16±0.3 ^b

The same letters indicate non-significant differences between treatments at $P < 0.05$

Nodule leghemoglobin content

Table 1 showed that the number of nodules significantly reduced at highest level of drought (50% FC) and flooding (2 FC). Also, nodule leghemoglobin content was decreased significantly as a result water stress imposed to the both levels of drought (75% & 50% FC) and flooding. The percentage of reduction in nodule leghemoglobin content of root nodules was 81% and 63% respectively. The results also showed that, nodule leghemoglobin content was decreased significantly under waerlogging.

The results in Table 1 revealed that the activity of nitrogenase enzyme was significantly decreased especially at the level of 50% FC. The percentage of decrease was reached 85%. Also, the data showed that, a significant decrease in the activity of nitrogenase enzyme in faba bean under flooding treatment.

ADH activity and kinetics

Alcohol dehydrogenase (ADH) activity and specific activity are presented in Figure 2. The data expressed as Δ abs. at 340 nm $\text{min}^{-1} \text{mg}^{-1}$ FW and Δ abs. at 340 nm $\text{min}^{-1} \text{mg}^{-1}$ protein, respectively. The specific activity of ADH (Δ abs. at 340 nm $\text{min}^{-1} \text{mg}^{-1}$ FW) of plant roots grown under flooding treatment was increased as compared to control. Whereas, the activity and specific activity of ADH enzyme was significantly decreased under the two level of water deficit (75% and 50%FC) as compared to absolute control.

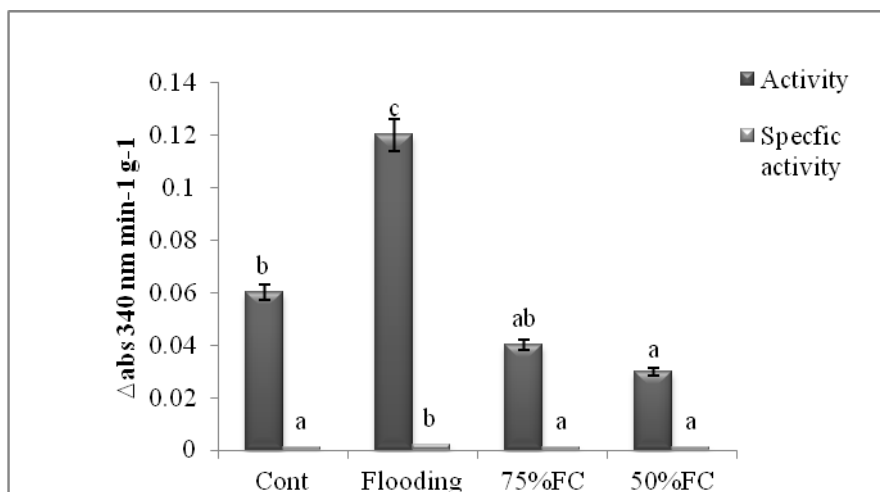


Figure 2. Alcohol dehydrogenase activity (Δ abs. at 340 nm $\text{min}^{-1} \text{mg}^{-1}$ FW) and specific activity (Δ abs. at 340 nm $\text{min}^{-1} \text{mg}^{-1}$ protein) of faba bean plant roots grown under the different level of field capacity. The same letters indicate non-significant differences between treatments at $P < 0.01$

Lineweaver-Burk plots for Alcohol dehydrogenase (ADH; EC 1.11.1.11) enzyme that was extracted from roots of bean plants grown under flooding and drought are result in the production of lines with different slops and intercepts for ADH activity which presented in Figure 3. The intercepts on X-axis (K_m), intercepts of y-axis (V_{\max}) and Kcat of the different lines. Michael's constant (K_m) and maximum velocity (V_{\max}) of ADH in roots of bean plants grown under both level of drought (75% & 50%FC) of treatments were decreased as compared to absolute control.

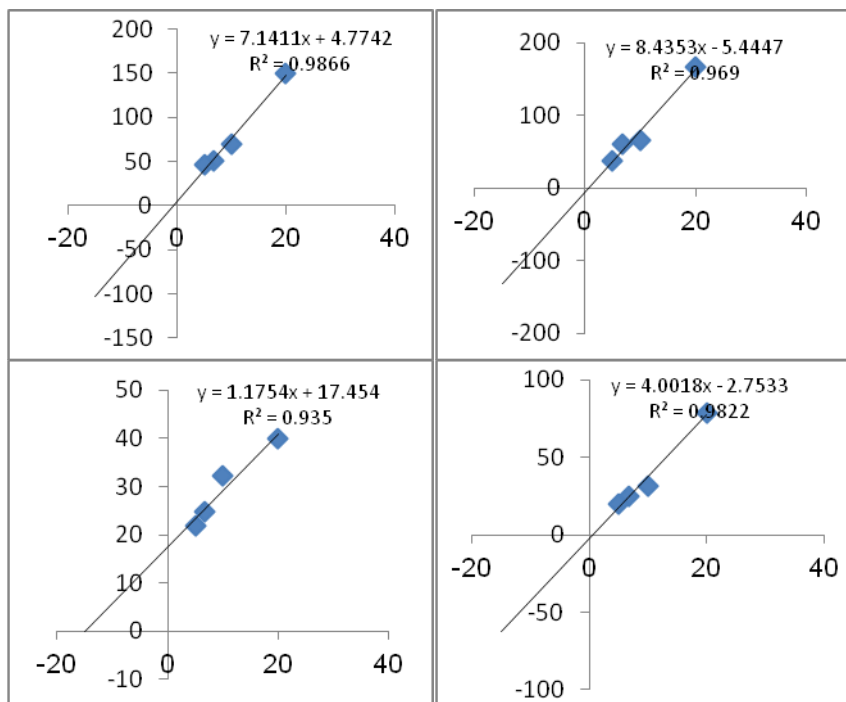


Figure 3. Lineweaver-Burk plots for alcohol dehydrogenase (ADH; EC 1.11.1.11) enzyme of *Vicia faba* plants grown for 2- weeks under water deficit (LWD & HWD) and flooding

Anatomy of root

Transverse sections of plant roots grown under high water deficit and flooding compared to control plant were investigated (Fig. 4). The photos showed that aerenchyma was found in the T.S root tested plants under flooding stress as shown in Figure 4 as compared to plant control. However, under drought we found accumulation of solutes in the parenchyma cells compared to plant control, but didn't recorded in bean plants as shown in the same Figure 4. A cross section of control plants section of central tissue cells contains normal parenchymal cells. B-Cortical tissue showing compact parenchymal cells with few intercellular spaces. C- Cortical cells showing loosely parenchymal cell containing many and large intercellular spaces (aerenchyma).

Discussion

The effectiveness of WL and WD on roots and shoots growth of tested faba bean plants are shown in Figure 1. The results showed that water stress (WD or WL) significantly reduced the fresh and dry weights of the roots and shoots of faba bean plants, especially when the water shortage reached (50% FC).

Waterlogging and high water deficit stresses significantly decreased the total biomass of faba bean (*Vicia faba*) plants grown under the both stresses. These data are in agreement with many investigators (Sorrell et al., 2000; Chen et al., 2002). Water stress affects the growth of plant organs by alteration of morphological features of the plants (French and Turner, 1991; Cox and Conran, 1996). The mechanisms involved in the adaptation of plants to water deficit is the change in root to shoot dry mass ratio (Turner, 1997; El-Enany et al., 2013). The reduction in water availability results in

growth inhibition, reduced shoot and root growth of bean plant. Reduction in tissue dry weights during drought stress may be due to decrease in plant growth, photosynthesis, cell expansion and cell division (Sundaravalli, et al., 2005; Rodriguez et al., 2008).

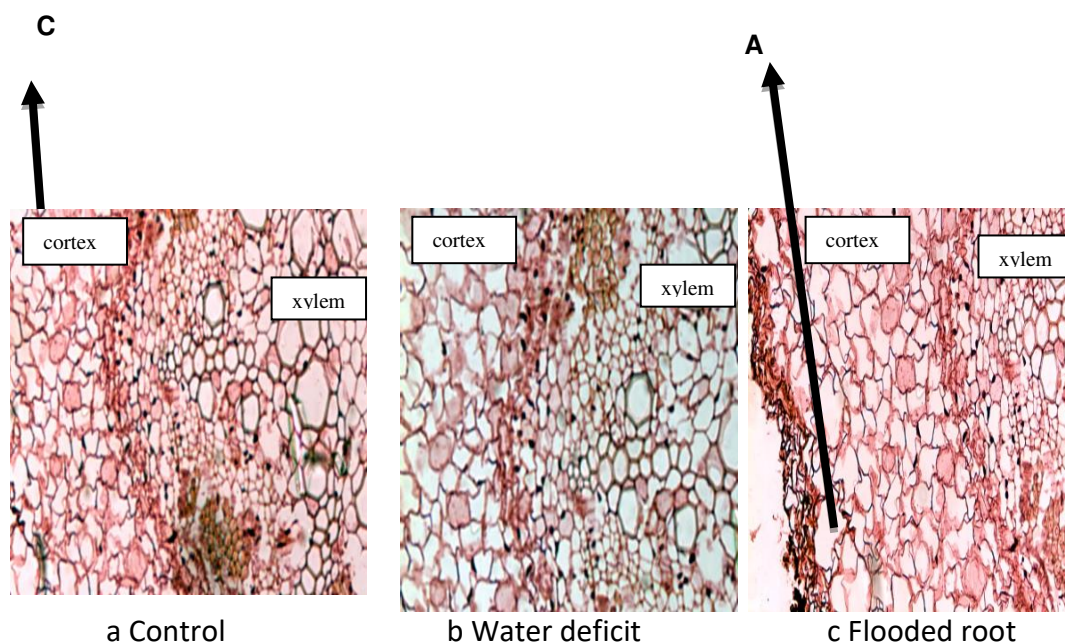


Figure 4. Transverse cross sections of 3-weeks old of faba bean roots stained with safranin examined and photographed at 25 X. A: aerenchyma resulted from lyses of some cortex parenchyma as compared to C: normal cortex in control roots

Our results indicated that the no. of nodules per plant was significantly decreased under both drought and flooding (Table 1). Streeter (2003) and González et al. (2010) concluded that the severely effects on nodulation occur during the establishment of the symbiosis and formation of nodules. Many studies have shown that water deficit negatively affects the stabilization of biological nitrogen fixation by reducing the number of nodules and the activity of nitrogen fixing enzymes (Abd-Alla et al., 2001; Ashraf and Iram, 2005; Christophe et al., 2011; Silvente et al., 2012). In addition, stress may reduce the invasion of leguminous plant roots by living rhizobia in the soil (Latrach et al., 2014; Mouradi et al., 2016). Charlson et al. (2009) reported that the nitrogen fixation in legume plants reduced under drought stress and may due to (i) the accumulation of ureides in both nodules and shoots, (ii) minimize in shoot nitrogen demand, (iii) reduce transpiration rate and thus lower xylem translocation rate and (iv) the decline of metabolic enzyme activity.

Table 2 showed that nitrogenase activity was significantly affected by drought and flooding, This may be due to lowered oxygen diffusion to the bacteroids, thus depressing nodule respiration and consequently nitrogenase activity (Guerin et al., 1990). This process usually involves increased production of oxygen free radicals species such as H_2O_2 , O_2 , and OH (Becana et al., 1986). Legume nodules possess a number of enzymatic mechanisms to minimize the toxicity of active oxygen species, including superoxide-dismutase, catalase and peroxidase (Becana et al., 1986). Inhibition of the nitrogen-fixing activities of nodules by waterlogging may by the

decreased by the bacteroids synthesis of nitrogenase (Bisseling et al., 1980), or by minimizing carbohydrate metabolism of host tissue in the nodule and/or decline in leghemoglobin content (Huang and LaRue, 1985). Higher leghemoglobin content was observed in the nodules of waterlogged plant (Table 2) and this may be facilitates the diffusion of oxygen from the nodule surface to the bacteriod and increase biological nitrogen fixation. This was also observed by Huang and LaRue (1985).

Table 2. *V_{max} and K_m and K_{cat} and K_m/K_{cat} of alcohol dehydrogenase activity (ADH) of faba bean plant roots grown under water deficit and waterlogging*

Parameters	Faba bean plants			
	Cont.	Flooding	75% F.C.	50% F.C.
V _{max}	3.13	0.06	0.18	0.21
K _m	12.42	0.07	1.55	1.50
K _{cat}	62.50	1.15	3.67	4.19
K _m /K _{cat}	0.20	0.06	0.42	0.36

The results in Figure 3 show that waterlogging activate alcohol dehydrogenase activity in roots more than shoots, whereas its activity not affected under different levels of water deficit. These results are consistent with Kato-Noguchi and Morokuma (2007) and Yamanoshita et al. (2005) who observed that waterlogging stimulates sugar fermentation by stimulating the activity of dehydrogenase of roots. Also, (Kang et al., 2009) found that activation of ethanolic fermentation was found in bean and cowpea plant to survive anaerobiosis and considered one of the strategies for growing cucumber seedling under waterlogging. The survival of seedling for many days of waterlogging may due to the oxygen available to roots through aerenchyma (Nada, et al., 2004; Yin et al., 2010). Aerenchyma formation is an important way to increase oxygen penetration from the shoots to the roots, and is essential for maintaining air diffusion, to provide a source of energy for alcoholic fermentation.

The results in Figure 4 show that formation of aerenchyma in plant roots grown under waterlogging treatment as compared with control plants. Whereas, plant roots sections appear a narrow cortex cells for faba bean plants grown under high water deficit as compared by control plant root. These results are in accordance with many investigators (Ashraf, 2003; Voesenek et al., 2006; Justin and Armstrong, 1987). Jackson and Armstrong (1999) showed that the improvement of the aeration of the rhizosphere in plants grown under flooding induced by formation of aerenchyma. Drew et al. (2000) stated that there are two different processes in plants to form aerenchyma schizogeny or lysigeny, or by their combination. Schizogenous aerenchyma involves cell wall reorganization and cell separation, whereas lysigenous aerenchyma formed by cell death) and cell wall autolysis (Gunawardena et al., 2001; Evans, 2003). Suralta and Yamauchi (2008) and Joshi and Kumer (2012) explained that the formation of aerenchyma tissue may facilitate oxygen aggregation in submerged tissues and reduce hypoxia of waterlogged seedlings. Larger intercellular spaces formed in faba bean plants may improved the plant's capacity for oxygen aggregation and exchange gases within the submerged parts of plants.

Conclusion

Faba bean plant is significantly affected by water deficit and waterlogging during the vegetative stage. Our data stated that the flooding cause damage to *Vicia faba* plant more than water deficit through its effects on nodule formation and activity. The findings of current study support previous conclusion that ADH enzyme activity and root anatomy can be used as a bioindicator for waterlogging or water deficit stress in legume plants and thereby playing an important role in flooding stress tolerance and signaling in crop plant.

REFERENCES

- [1] Abd-Alla, M. H. (1992): Nodulation and nitrogen fixation in faba bean (*Vicia faba* L.) plants under salt stress. – *Symbiosis* 12: 311-319.
- [2] Armstrong, W. (1971a): Radial oxygen losses from intact rice roots as affected by distance from the apex, respiration and waterlogging. – *Physiologia Plantarum* 25: 192-197.
- [3] Armstrong, W. (1971b): Oxygen diffusion from the roots of rice grown under non waterlogged conditions. – *Physiologia Plantarum* 24: 242-247.
- [4] Araus, J. L., Slafer, G. A., Reynolds, M. P., Royo, C. (2002): Plant breeding and drought in C₃ cereals: What should we breed for? – *Annals of Botany* 89: 925-940.
- [5] Asgher, M., Per, T. S., Masood, A., Fatma, M., Freschi, L., Corpas, F. J., Khan, N. A. (2017): Nitric oxide signaling and its crosstalk with other plant growth regulators in plant responses to abiotic stress. – *Environmental Science Pollution Research* 24: 2273-2285.
- [6] Ashraf, M. (2003): Relationships between leaf gas exchange characteristics and growth of differently adapted populations of Blue panicgrass (*Panicum antidotale* Retz) under salinity or waterlogging. – *Plant Science* 165: 69-75.
- [7] Ashraf, M., Iram, A. (2005): Drought stress induced changes in some organic substances in nodules and other plant parts of two potential legumes differing in salt tolerance. – *Flora* 200: 535-546.
- [8] Becana, M. S., Aparicio-Tejo, P., Pena, J., Aguirreolea, J., Sánchez, D. M. (1986): N₂-fixation and leghemoglobin content during nitrate and water stress induced senescence of *Medicago sativa* root nodules. – *J of Experimental Botany* 37: 597-605.
- [9] Bisseling, S. T., van Staveren, W., van Kammen, A. (1980): The effect of waterlogging on the synthesis of the nitrogenase components in bacteroids of *Rhizobium leguminosarium* in root nodules of *Pisum*. – *Biochemical and Biophysical Research Communication* 93: 687-693.
- [10] Boyer, J. S. (1982): Plant productivity and environment. – *Science*, 218: 443-448.
- [11] Candan, N., Tarhan, L. (2012): Tolerance or sensitivity responses of *Mentha pulegium* to osmotic and waterlogging stress in terms of antioxidant defense systems and membrane lipid peroxidation. – *Environmental and Experimental Botany* 75: 83-88.
- [12] Charlson, D. V., Bhatnagar, S., King, C. A., Ray, J., Sneller, C., Carter, T. (2009): Polygenic inheritance of canopy wilting in soybean (*Glycine max* (L.) Merr). – *Theoretical and Applied Genetics* 119: 587-594.
- [13] Chen, H., Qualls, R. G., Miller, G. C. (2002): Adaptive responses of *Lepidium latifolium* to soil flooding: biomass allocation, adventitious rooting, aerenchyma formation and ethylene production. – *Environmental and Experimental Botany* 48: 119-128.
- [14] Christophe, S., Jean-Christophe, A., Annabelle, L., Alain, O., Marion, P., Anne-Sophie, V. (2011): Plant N Fluxes and Modulation by Nitrogen, Heat and Water Stresses: A Review Based on Plants. – In: Shanker, A., Venkateswarlu, B. (eds.) *Abiotic Stress in Plants. Mechanisms and Adaptations*. InTech, Rijeka, Croatia.

- [15] Colmer, T. D. (2003): Aerenchyma and an inducible barrier to radial oxygen loss facilitate root aeration in upland, paddy and deepwater rice (*Oryza sativa* L.). – *Annals of Botany* 91: 301-309.
- [16] Cox, J. A., Conran, J. G. (1996): The effect of water stress on the life cycles of *Erodium crinitum* Carolin and *Erodium cicutarium* (L.) L'Herit. ex Aiton (Geraniaceae). – *Australia Journal of Ecology* 21: 235-240.
- [17] Cutler, J. M., Shahan, K. W., Steponkus, P. L. (1980): Influence of water deficits and osmotic adjustment on leaf elongation in rice. – *Crop Science* 20: 314-318.
- [18] Drew, M. C. (1997): Oxygen deficiency and root metabolism: injury and acclimation under hypoxia and anoxia. – *Annual Review Plant Biology* 48: 223-250.
- [19] El-Enany, A. E., AL-Anazi, A. D., Dief, N., Al-Taisan, W. A. (2013): Role of antioxidant enzymes in amelioration of water deficit and waterlogging stresses on *Vigna sinensis* plants. – *Journal of Biology and Earth Sciences* 3: B144-B153.
- [20] El-Enany, A. E., Morsy, F., Dief, N. (2014): Impact of water stress on growth criteria and alcohol dehydrogenase activity of three legume plants. – *Minia Science Bulletin* 25: 29-51.
- [21] Evans, D. E. (2003): Aerenchyma formation. – *New Phytol.* 161: 35-49.
- [22] French, R. J., Turner, N. C. (1991): Water deficits change dry matter partitioning and seed yield in narrow-leaved lupins (*Lupinus angustifolius* L.). – *Australian Journal of Agricultural Research* 42: 471-484.
- [23] Gao, J.-P., Chao, D.-Y., Lin, H.-X. (2007): Understanding abiotic stress tolerance mechanisms: recent studies on stress response in rice. – *Journal of Integrative Plant Biology* 49: 742–750.
- [24] Gonzalez, E. M., Gordon, A. J., James, C. L., Arrese-Igor, C. (1995): The role of sucrose synthase in the response of soybean nodules to drought. – *Journal of Experimental Botany* 46: 1515-1523.
- [25] Govinda, R., Shanta, K. (2011): Alcohol dehydrogenase (ADH) activity in soybean (*Glycine max* L.] Merr.) under flooding stress Electronic. – *Journal of Plant Breeding* 2: 50-57.
- [26] Gunawardena, A., Pearce, D. M., Jackson, M. B., Hawes, C. R., Evans, D. E. (2001): Characterization of programmed cell death during aerenchyma formation induced by ethylene or hypoxia in roots of maize (*Zea mays* L.). – *Planta* 212: 205-214.
- [27] Hsiao, T. C., Silk, W. K., Jing, J. (1985): Leaf Growth and Water Deficits: Biophysical Effects. – In: Baker, N. R., Davies, W. J., Ong, C. K. (eds.) *Control of Leaf Growth*. Society for Exp. Biol. Seminar Series 27. Cambridge University Press, Cambridge, pp 239-266.
- [28] Huang, C. Y., LaRue, T. A. (1985): Effects of waterlogging on the nitrogen fixation and carbohydrate metabolism in nodules of soybean plant. – *Proceeding of The National Science Council B. ROC* 9: 82-88.
- [29] Hussain, M., Farooq, S., Hasan, W., Ul-Allah, S., Tanveer, M., Farooq, M., Nawaz, A. (2018): Drought stress in sunflower: physiological effects and its management through breeding and agronomic alternatives. – *Agricultural Water Management* 201: 152-166.
- [30] Jackson, M. B., Armstrong, W. (1999): Formation of aerenchyma and the processes of plant ventilation in relation to soil flooding and submergence. – *Plant Biology* 1: 274-287.
- [31] Joshi, R., Kumar, P. (2012): Lysigenous aerenchyma formation involves non-apoptotic programmed cell death in rice (*Oryza sativa* L.) roots. – *Physiology and Molecular Biology of Plants* 18: 1-9.
- [32] Justin, S. H., Armstrong, W. (1987): The anatomical characteristics of roots and plant response to soil flooding. – *New Phytologist* 106: 465-495.
- [33] Kang, T. W., Adesogan, A. T., Kim, S. C., Lee, S. S. (2009): Effects of esterase-producing inoculants on fermentation, aerobic stability, and neutral detergent fiber digestibility of corn silage. – *Journal of Dairy Science* 92: 732-738.

- [34] Kato-Noguchi, H., Morokuma, M. (2007): Ethanol fermentation and anoxia tolerance in four rice cultivars. – *Journal of Plant Physiology* 164: 168-173.
- [35] LaRue, T. A., Kurz, W. G. W. (1973): Estimation of nitrogenase using a colorimetric determination for ethylene. – *Plant Physiology* 51: 1074-1075.
- [36] Latrach, L., Farissi, M., Mouradi, M., Makoudi, B., Bouizgaren, A., Ghoulam, C. (2014): Growth and nodulation of alfalfa-rhizobia symbiosis under salinity: electrolyte leakage, stomatal conductance, and chlorophyll fluorescence. – *Turkish Journal of Agriculture and Forestry* 38: 320-326.
- [37] Mittler, R. (2006): Abiotic stress, the field environment and stress combination. – *Trends in Plant Science* 11: 15-19.
- [38] Mouradi, M., Farissi, M., Bouizgaren, A., Makoudi, B., Kabbadj, A. Very, A. A Sentenac, H., Qaddourya, A., Ghoulam, C. (2016): Effects of water deficit on growth, nodulation and physiological and biochemical processes in *Medicago sativa*-rhizobia symbiotic association. – *Arid Land Research and Management* 30: 193-208.
- [39] Nada, K., Iwatani, E., Doi, T., Tachibana, S. (2004): Effect of putrescine pretreatment to roots on growth and lactate metabolism in the root of tomato (*Lycopersicon esculentum* Mill.) under root-zone hypoxia. – *Journal Japanese of Society for Horticultural Science* 73: 337-339.
- [40] Parent, C., Berger, A., Folzer, H., Dat, J., Crevecoeur, M., Badot, P-M., Capelli, N. (2008): A novel nonsymbiotic hemoglobin from oak: Cellular and tissue specificity of gene expression. – *New Phytologist* 177: 142-154.
- [41] Rodriguez, H. J., Volkenburgh, E. V., Hoy, M., Wright, L., Beckwith, F., Kim, Y-K., Regina, S. R. (2008): Stress tolerance in plants via habitat-adapted symbiosis. – *The ISME Journal* 2: 404-416.
- [42] Romeu, d. S. L., Marilza, N. d. N., Tamara, T. T., Lourival, P. G. N., Cristiane, A. d. S. R., Alismrio, L. d. S. (2019): Alleviation of water deficit in *Physalis angulata* plants by nitric oxide exogenous donor. – *Agricultural Water Management* 216: 98-104.
- [43] Sato, T. (1968): A modified method for lead staining of thin sections. – *Journal Electron Microscope* 17: 158.
- [44] Schussler, E. E., Borkhsenius, O. N., Longstreth, D. J. (1997): Formation of root aerenchyma involves programmed cell death in *Sagittaria lancifolia*. – *Plant Physiology* 114: 456-456.
- [45] Silvente, S., Sobolev, A. P., Lara, M. (2012): Metabolite adjustments in drought tolerant and sensitive soybean genotypes in response to water stress. – *PLoS One* 7: 38554.
- [46] Sorrell, B. K., Downes, M. T., Stanger, C. L. (2002): Methanotrophic bacteria and their activity on submerged aquatic macrophytes. – *Aquatic Botany* 72: 107-119.
- [47] Spurr, A. R. (1969): A Low-Viscosity epoxy resin embedding medium for electron microscopy. – *Journal of Ultrastructure Research* 26: 31-43.
- [48] Streeter, J. G. (2003): Effects of drought on nitrogen fixation in soybean root nodules. – *Plant Cell Environment* 26: 1199-1204.
- [49] Sundarvalli, M. V., Paliwal, K., Ruckmani, A. (2005): Effect of water stress on photosynthesis, protein content and nitrate reductase activity of *Albizia* seedlings. – *Journal of Plant Biology* 32: 13-17.
- [50] Suralta, R., Yamauchi, A. (2008): Root growth, aerenchyma development and oxygen transport in rice genotypes subjected to drought and waterlogging. – *Environmental and Experimental Botany* 64: 75-82.
- [51] Turner, N. C. (1997): Further progress in crop water relations. – *Advances in Agronomy* 58: 293-338.
- [52] Vartapetian, B. B., Jackson, M. B. (1997): Plant adaptation to anaerobic stress. – *Annals of Botany* 79: 3-20.
- [53] Visser, E. J. W., Colmer, T. D., Blom, C. W. P. M., Voeselek, L. A. C. J. (2000): Changes in growth, porosity, and radial oxygen loss from adventitious roots of selected

- mono and dicotyledonous wetland species with contrasting types of aerenchyma. – *Plant, Cell and Environment* 23: 1237-1245.
- [54] Voeselek, L. A. C. J., Colmer, T. D., Pierik, R., Millenaar, F. F., Peeters, A. J. M. (2006): How plants cope with complete submergence. – *New Phytologist* 170: 213-226.
- [55] Wahl, S., Ryser, P., Edwards, P. J. (2001): Phenotypic plasticity of grass root anatomy in response to light intensity and nutrient supply. – *Annals of Botany* 88: 1071-1078.
- [56] Wheeler, B. D. (1999): *Water and Plants in Freshwater Wetlands*. – In: Baird, A. J., Wilby, R. L. (eds.) *Eco-Hydrology*. Routledge, London, pp. 127-180.
- [57] Yamanoshita, T., Masumori, M., Yagi, H., Kojima, K. (2005): Effects of flooding on downstream processes of glycolysis and fermentation in roots of *Melaleuca cajuputi* seedlings. – *Journal of Forest Research* 10: 199-204.
- [58] Yin, D., Fadi, C. S., Zhi, C., Fang, W. (2010): Morpho-anatomical and physiological responses of two *Dendranthema* species to waterlogging. – *Environmental and Experimental Botany* 68(2): 122-130.

IDENTIFICATION OF CYCLO(L-PRO-D-TYR) FROM *BACILLUS AMYLOLIQUEFACIENS* Y1 EXHIBITING ANTIFUNGAL ACTIVITY AGAINST *FUSARIUM GRAMINEARUM* TO CONTROL CROWN ROT IN WHEAT

JAMAL, Q.^{1,2*} – MONKHUNG, S.³ – MUNIR, S.⁴ – CHO, J. Y.⁵ – MOON, J. H.⁶ – KHATTAK, B. U.² – MALIK, M. S.² – YOUNIS, F.⁷ – KIM, K. Y.^{1*}

¹*Division of Food Technology, Biotechnology and Agrochemistry, Institute of Environmentally-Friendly Agriculture, Chonnam National University, Gwangju 61186, South Korea*

²*Department of Microbiology, Kohat University of Science and Technology, Kohat, KP 26000, Pakistan*

³*Crop Production Technology Program, Faculty of Animal Science and Agricultural Technology, Silpakorn University, Phetchaburi Information Technology Campus, Phetchaburi 76120, Thailand*

⁴*Faculty of Plant Protection, Yunnan Agricultural University, Kunming 650201, Yunnan, PR China*

⁵*Department of Food Engineering, Mokpo National University, Mokpo, South Korea*

⁶*Department of Food Science and Technology, BK21 Plus Program, Chonnam National University, Gwangju 61186, Republic of Korea*

⁷*Sulaiman Bin Abdullah Aba Al-Khail Centre for Interdisciplinary Research in Basic Sciences, International Islamic University, Islamabad, Pakistan*

**Corresponding authors*

e-mail: qaiserjamal71@yahoo.com; kimkil@jnu.ac.kr

(Received 24th Dec 2018 ; accepted 28th Feb 2019)

Abstract. In this study, evidence for antagonism of antifungal metabolites produced by *Bacillus amyloliquefaciens* Y1 was described, as they actively inhibit growth of *Fusarium graminearum* under *in vitro* and *in vivo* condition. The culture supernatant and crude butanol extract inhibit the mycelial growth of *F. graminearum*. In addition, an antifungal compound was purified from the metabolites of Y1 and identified as cyclo(L-Pro-D-Tyr) using ¹H and ¹³C NMR spectroscopic analysis. For the first time, cyclo(L-Pro-D-Tyr) displayed potent antifungal activity against *F. graminearum* under *in vitro* condition. The hyphae of this fungal pathogen became deformed with cyclo(L-Pro-D-Tyr). Exposure of *F. graminearum* to various concentrations of cyclo(L-Pro-D-Tyr) on wheat seeds significantly inhibit fungal colonization. Furthermore, during *in vivo* wheat pot experiment, Y1 results in 27% higher total yield and showed a protective effect against *F. graminearum* by reducing low discoloration symptoms on stems. The grain yield per pot was five times higher compared to control pots (water only) infected with *F. graminearum*. To our knowledge, the antifungal activity of the cyclo(L-Pro-D-Tyr) is reported for the first time against the plant pathogenic fungus *F. graminearum*. The present study demonstrated the potential of *B. amyloliquefaciens* Y1 as a biocontrol agent against the wheat crown rot fungal pathogen as well as a plant growth promoter for wheat.

Keywords: *biological control, wheat disease, chemistry, antifungal, pathogen*

Introduction

Two major destructive fungal diseases that posing a serious threat to wheat cultivation and production are head blight and crown rot caused by the mycotoxin-producing fungal pathogen *Fusarium graminearum*. *Fusarium* crown rot (FCR) is characterized by dry rot of crown, necrosis of root tissue and basal stem, and limited grain yield. *Fusarium* crown rot has never gotten much attention as it is mainly considered to be limited in its geographical distribution, but according to latest reports, it occurs in many cereal producing regions (Smiley et al., 2005 a,b). A severe intensive infection can result in more than 50% yield loss, and reduced grain quality. It is known that this fungus is harmful to animals and humans because it produces several mycotoxins in wheat such as zearalenone (ZEA) (Cowger and Arellano, 2013) and deoxynivalenol (DON), that can cause embryotoxic, neurotoxic, immunosuppressive and teratogenic effects (Cowger and Arellano, 2013; Pestka, 2007; Pestka and Smolinski, 2005).

Conventional methods such as crop rotation and inter-row sowing can be used to control diseases caused by *F. graminearum*. Crop rotation is effective, but there are also economic limitations, as *F. graminearum* can reside inside the stubble for several years (Burgess, 2005). The recent reports revealed that there is a remarkable reduction in the *Fusarium* crown rot (FCR) damage due to inter-row sowing (Simpfendorfer et al., 2012). Due to limitations, FCR has recently been reported in cereal-growing regions. Moreover, chemical management is effective but the application of chemicals such as acephate, carbendazim, chlorothalonil, chlopyrifos, Dichlorodiphenyltrichloroethane (DDT), and diazinon causes environmental pollution, affects human health, and enables pathogens to build resistance to these chemicals (Baldwin and Rathmell, 1988). Few studies have been done about the losses caused by *F. graminearum* and more information is needed to manage this phytopathogenic fungus through the application of antagonistic microorganisms (Palazzini et al., 2016).

Several bacteria are available commercially including strains of the genera *Pseudomonas* and *Bacillus*, and have been used successfully as alternative to chemical pesticides in crop production (Choudhary and Johri, 2009). *Bacillus* species are among the most important bacteria that can be most promising for plant protection (Pérez-García et al., 2011). Their most notable characteristics include their ability to survive for extended periods of time, their spore formation, the wide range of biochemically active molecules that can significantly inhibit phytopathogen growth and ease of formulating their commercial products (Broggini et al., 2005). *Bacillus subtilis*, *Bacillus amyloliquefaciens* and *Paenibacillus polymyxa* mostly found in soil are considered to be safe for use in environment and with mammals (Stabb et al., 1994; Zhao et al., 2015). Two new cyclic lipopeptides (3 and 4) were isolated from the culture filtrate of *Bacillus amyloliquefaciens* strain SD-32, together with two known metabolites, iso-C15 and iso-C16 bacillomycin D (Tanaka et al., 2014). They can provide higher protection to plants (Falcão et al., 2014; Krebs et al., 1993), because of their antifungal and antibacterial activities against several phytopathogens (Ben Abdallah et al., 2015; Krebs et al., 1998). They produce various types of secondary metabolites (antibiotics) (Asaka and Shoda, 1996; Stabb et al., 1994) and most of them have been identified as low molecular weight dipeptide or cyclic peptides (Dolej and Bochow, 1996; Nakano and Zuber, 1990; Vanittanakom et al., 1986). Among cyclic peptides, diketopiperazines (DKPs) are relatively simple cyclic dipeptides consisting of two α -amino acids produced by bacteria, fungi, mammals, and plants (Ström et al., 2002).

More attention has paid to study about diversity and biological roles of more than 100 DKPs found in nature (McClelland et al., 2004). Four DKPs from *B. thuringiensis* strain and two from *B. endophyticus* demonstrated their antifungal activities (Sansinenea et al., 2016). Beside their antimicrobial properties, cyclic peptides are involved in root colonization and the systemic stimulation of immune system of the host plant (Ongena and Jacques, 2008). In general, the activities of cyclic peptides from *Bacillus spp.* against fungal phytopathogens have been frequently described. Synthetic DKPs has also been reported to have antibacterial and antifungal activities (Graz, 2002; Pitchen, 2002).

The present study was aimed to evaluate antifungal potential of *B. amyloliquefaciens* Y1 against *F. graminearum* under *in vitro* and *in vivo* condition. In addition, identification of an antifungal compound may have a role in its probable mechanism to control *Fusarium* crown rot in wheat.

Materials and methods

Microorganisms and culture conditions

B. amyloliquefaciens Y1 was isolated previously with accession number KP967704. *Fusarium graminearum* KACC 41040, was obtained from Korea Agriculture Culture Collection (KACC). For *in vitro* and *in vivo* study, a spore suspension was prepared by growing *F. graminearum* in carboxymethyl cellulose (CMC) broth at 25 °C in shaking incubator for 10 days.

Antifungal characterization

Antifungal activity of culture supernatant

Antifungal activities were detected by growing strain Y1 in Luria-Bertani 33 (Palazzini et al., 2016) broth at 40 °C for 7 days at 170 rpm. The culture broth was centrifuged at 7,000 × g for 20 min. The supernatant collected was filtered through Whatman filter paper No. 2 (0.45 µm) and finally with 0.20 µm syringe filter. The resulting supernatant was mixed with sterile PDA to make final concentration of 0, 10, 30, and 50%. A 5 mm diameter mycelial plug of *F. graminearum* from a 7-days-old culture was placed in the centre of the PDA plate and incubated at 28 °C in the dark. Mycelial growth was measured as colony diameter of *F. graminearum* hyphae after 6 days inoculation and growth inhibition percentage were evaluated by using the following formula:

$$\text{Growth inhibition percentage (GI \%)} = [(R - r) / R] \times 100$$

where R is the radius/ diameter of the colony on the control plates and r is the radius of the colony on the treatment plate. Experiment was carried out in triplicate and repeated three times.

Antagonistic activity of bacterial crude extract against the plant pathogens

Strain Y1 was inoculated into the LB broth at 40 °C for 10 days. The pH of Y1 culture broth was adjusted to 3 using concentrated HCl and used to obtain the crude extract by active fractionation (1:1, vol/vol) with an elutropic series of solvents: ethyl

acetate and n-butanol. The partially isolated butanol solvent was concentrated through a rotary evaporator to get crude extract (48 g) (Büchi, Rheinstetten, Germany). A 20% stock solution of crude extract was prepared. From the stock solution, 3, 4 and 5 mg was added on paper disc to check antifungal activity against *F. graminearum*. A 5 mm diameter mycelial plug from 7 days old culture was placed in the centre of the PDA plate. The control consists of an equal volume of methanol added to another paper disc on the same PDA plate. Mycelial growth was measured as colony diameter of *F. graminearum* and growth inhibition was evaluated by using the following formula:

$$(\text{GI } \%) = [(R - r)/R] \times 100$$

where R is the radius/diameter of the fungal growth towards the paper disc on the control side and r is the radius of the fungal colony growth towards the paper disc on the treatment side. Experiment was carried out in triplicate.

Extraction and purification of the antifungal compound

The butanol crude extract (48 g) was prepared from cell free culture supernatant (36 L) of strain Y1 and was dissolved in methanol and subjected to silica gel column chromatography (Kieselgel 60, 70-230 mesh, Merk, Darmstadt, Germany) with stepwise elution of CHCl_3 : MeOH (100:0, 90:10, 70:30, 40:60, 50:50, and 0:100; v/v). Total of 3L solvent was used in each step of elution. The vacuum (EYELA rotary vacuum evaporator) was used to concentrate all fractions to a semisolid mass, and each fraction was assayed for antifungal activity. The bioactive fraction CHCl_3 : MeOH (100:0) was further purified by HPLC (high-performance liquid chromatography) using a system with a PrepHT C18 column (7 × 300 mm, 10 μm). The SPD-10 UV-VIS detector (Shimadzu, Japan) was used to monitor elution with manual injection at 210 and 254 nm using acetonitrile and water as a mobile phase (35:65) at a flow rate of 2 mL/min. All peaks were collected and concentrated using a centrifugal evaporator (Hanil Scientific Inc, South Korea) at 40 °C. The purities of the collected fractions were further analysed using an HPLC analytical C18 column (5 μL, 4.6 × 250 mm). The pure compound with a single peak was used for antifungal activity. The active compound was used for further structural analysis.

Identification of the purified antifungal compound

The ^1H and ^{13}C nuclear magnetic resonance (NMR) was used to determine the structure of the purified compound. Briefly, the purified antifungal compound (approx. 12 mg) was dissolved in 0.6 mL methanol-*d*₄ (CD_3OD) and used for spectral analysis. NMR spectra were recorded on a DRX 500 NMR instrument (Bruker, Rheinstetten, Germany) operating at 500 MHz for ^1H and 125 MHz for ^{13}C at room temperature. Chemical shifts are reported in ppm (δ) using CD_3OD as the solvent (unless otherwise indicated) and tetramethylsilane (CH_3)₄Si as an internal standard.

Determination of antifungal activity of the purified compound and its effect on hyphal deformation

The purified compound was assayed against *F. graminearum* growth. A 4% stock solution of the purified compound was prepared in methanol. A total of 1000 μL (a mixture of 300 μL conidial suspension + 700 μL CMC broth) was added to each well of

a 24-well microplate except for the first well, which contained 600 μL of the conidial suspension of *F. graminearum* (4×10^6 spores/mL) and 1300 μL CMC. After addition of the conidial suspension, 100 μL of the compound was added to the first well. Further, serial dilution was performed to obtain the desired concentration of 2000, 1000, 500, 250, 125, 62.5, 31.25, 15.625, 7.81, 3.90, and 1.95 ppm in each well. The conidial suspension of *F. graminearum* and methanol were used as a control. The well plate was kept for one h in clean bench to evaporate methanol. The direct effect of the antifungal compound on hyphae was examined using light microscope (Olympus BX41TF, Japan).

Assessment of the purified compound to control F. graminearum on wheat seeds

Wheat seeds ($n = 30$) per treatment were immersed in 100 mL of DW (distilled water) for 1 h, followed by immersing 1 min in a dilute solution of NaOCl (sodium hypochlorite) for surface sterilization. They were then washed with distilled water and placed in petri dish to dry. Solutions of the purified compound at various concentration were prepared in methanol using serial dilution to obtain serial doses (2000, 1000, 500, 250, 125, 62.5, 31.25 ppm). Then, wheat seeds were soaked for 1 h in various concentration of compound and left in open petri dish to evaporate excess methanol. Seeds soaked in methanol were used as a control. A spore suspension of *F. graminearum* was prepared (4×10^6 spores/ml) and approximately 10 μl of the spore suspension was spread on each wheat seed. The inoculated wheat seeds were incubated at 28 °C on moisten cotton in petri dish, and the inhibition of fungal growth was recorded as white mycelia appeared on all seeds ($30 = 100\%$) in the control treatment. All tests were performed in triplicate.

Glasshouse experiment

The growth promotion and biocontrol effect of strain Y1 in wheat plants were also focused. Two types of pot experiment were performed in a greenhouse at Chonnam national university, South Korea. A glasshouse potting mix was prepared by mixing soil, sand, vermiculite, and compost at a ratio of 2:1:1:0.04 (v/v), respectively. The soil was air-dried and ground to pass through a 2-mm sieve and mixed thoroughly. The potting mixture was transferred to 20 L pots containing 20-25 kg soil. A total 60 seeds per pot were sown in four rows. In one type of pot experiment, at two weeks interval, after 14, 28, and 42 days of seeds sowing, each pot was amended by pouring 300 ml of water, or fertilizer media (M) (KH_2PO_4 0.08 g, KCl (0-0-60) 0.02 g, K_2SO_4 0.1 g, CaCl_2 0.1 g, water soluble fertilizer 2.66 ml, blue fertilizer (20-20-20-2, 4g) per litre of water) or Y1 culture grown for 7 days at 40 °C in media known as BB media (chitin 0.5 g, gelatin 0.5 g, Yeast 0.1 g, KH_2PO_4 0.08 g, KCl (0-0-60) 0.02 g, K_2SO_4 0.1 g, CaCl_2 0.1 g, water soluble fertilizer 2.66 ml, blue fertilizer (20-20-20-2, 4 g) and sugar 4 g/L of water) for a total of three times. The treatments were arranged in a randomized complete block design and replicated four times. To assess growth promotion in wheat, plant height, plant weight, root weight and grains per pot was calculated after four months.

To assess the biocontrol of crown rot in wheat by Y1, pots were amended with *F. graminearum* in the soil. One month after seed sowing, one mL of *F. graminearum* suspension containing 4×10^6 spores per mL was drench in each seedling. At 14, 28 and 42 days after seeds sowing, each pot was amended by pouring 300 mL of water (C + Fg), or fertilizer media (M + Fg), or strain Y1 culture grown in BB media

(Y1 + Fg) or commercial fungicide (F + Fg). A total of 60 wheat tillers were randomly collected from each replicate after harvesting and assessed for the incidence of crown rot by recording the percentage of tillers with brown discoloration on the lower stems (Liu and Ogbonnaya, 2015). After harvesting the plants, reduction in yield due to crown rot was also measured by measuring plant height, plant weight/pot, root weight, and grains weight/pot.

Statistical analysis

The data were statistically analysed through SAS 9.1 software (SAS Institute, 2003). The least significant difference (LSD) was used to calculate mean values among treatments at a 5% level ($p = 0.05$) of significance.

Results

Antifungal characterization

The cell-free culture supernatant displayed antifungal activity at various concentrations mixed in PDA as it inhibited the growth of *F. graminearum*. The inhibitory effects increased with concentration increased (Fig. 1a). At 10% concentration, the cell-free culture supernatant showed more than 30% growth inhibition of *F. graminearum*. Higher concentration increased the growth inhibition, as 40 and 45% growth inhibition were recorded for the 30 and 50% concentration, respectively.

The paper disc method assessed the antifungal effect of the bacterial *n*-butanol crude extract. The Y1 crude extract at various concentrations had good inhibition effect on the pathogenic fungi (Fig. 1b). The crude extract (3 mg) affected the growth of the tested fungi by 13%. An increase in the inhibitory effect was found as the amount of treatment increased. The highest growth inhibition rates of 20% and 17% were obtained when 5 mg and 4 mg of crude extract were added to the paper disc respectively. The antifungal compound-enriched extract revealed interesting antifungal activities.

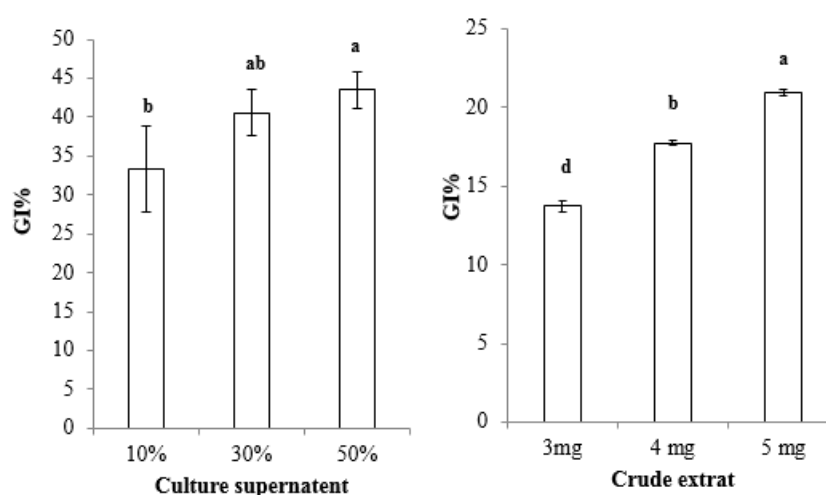


Figure 1. Effect of Y1 culture filtrate (a) at various concentrations on growth of *F. graminearum*. Effect of different crude extracts (b) concentration of Y1 on growth of *F. graminearum*. Calculated mean in chart values are from three replicates. Error bars represent standard deviation of mean

Extraction and purification of antifungal compound

The Y1 crude extract displayed antifungal activity against *F. graminearum* according to paper disc assay. A bioactive fraction was found because of silica gel column chromatography. The bioactive fraction (2 g) was further subjected to prep HPLC. The purity of the compound was confirmed with a single peak on an analytical HPLC column (Fig. 2). The antifungal activity of pure compound was checked and confirmed by testing against *F. graminearum* using paper disc method. The 12 mg of pure active compound obtained from *n*-butanol crude extract of Y1 strain. The bioactive antifungal compound showed a single peak with a 4.93 min retention time.

<Chromatogram>

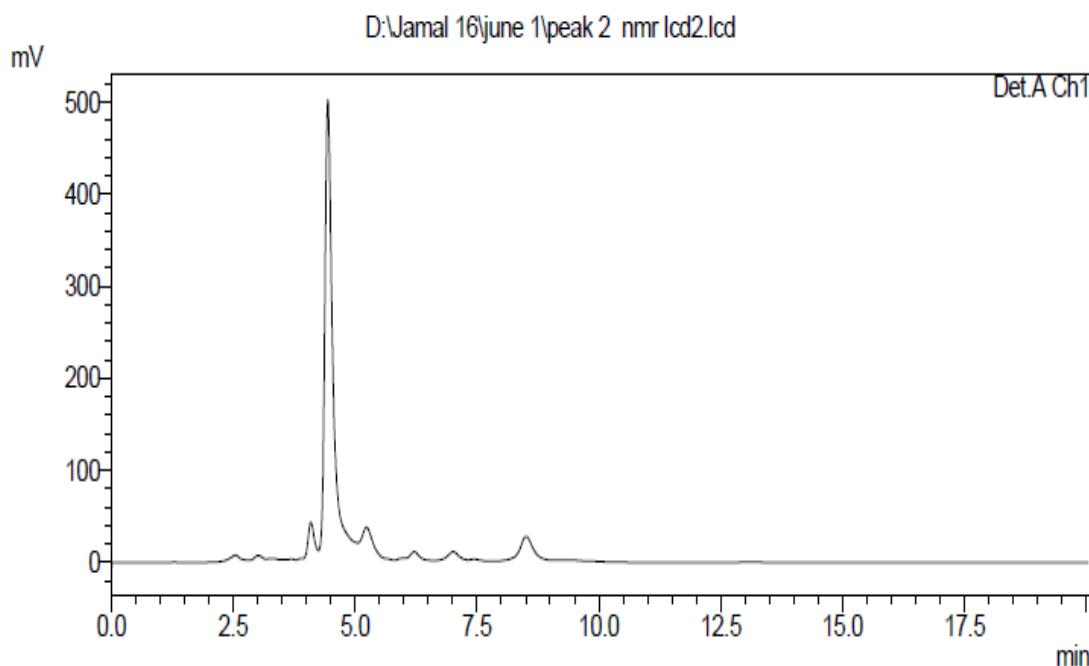


Figure 2. The high-performance liquid chromatography (HPLC) spectrum of the purified antifungal compound from strain Y1

Identification of the purified antifungal compound

The structure of the purified antifungal compound was identified according to its ^1H - and ^{13}C -NMR spectra (Fig. 3a and b). Peak data were as follows. ^1H NMR (500MHz, CD_3OD , δ , J/Hz): 4.37 (1H, dt, 5.0, 2.0, H-2), 2.11 (1H, m, H-4a), 1.80 (1H, m, H-4b), 2.09 (1H, m, H-5a), 1.82 (1H, m, H-5b), 3.49-3.61 (1H, m, H-6), 7.04 (2H, d, 8.5, H-2',6'), 6.71 (2H, d, 8.5, H-3',5'), 3.06 (1H, ddd, 11.0, 6.5, 1.0, H-7'a), 4.05 (1H, ddd, 11.0, 6.5, 2.0, H-8'), ^{13}C -NMR (125 MHz, CD_3OD): δC (ppm) 170.8 (C-1), 60 (C-2), 46.062 (C-3), 29.4 (C-4), 37.831 (C-5), 45.9 (C-6), 127.6 (C-1'), 132.1 (C-2',6'), 116.2 (C-3',5'), 157.7 (C-4'), 37.7 (C-7), 57.9 (C-8') and 167 (C-9'). From the NMR spectra, the compound was identified as cyclo(L-Pro-D-Tyr) (Fig. 4). The NMR spectrum was found to be similar to that reported by Kumar et al. (2013a).

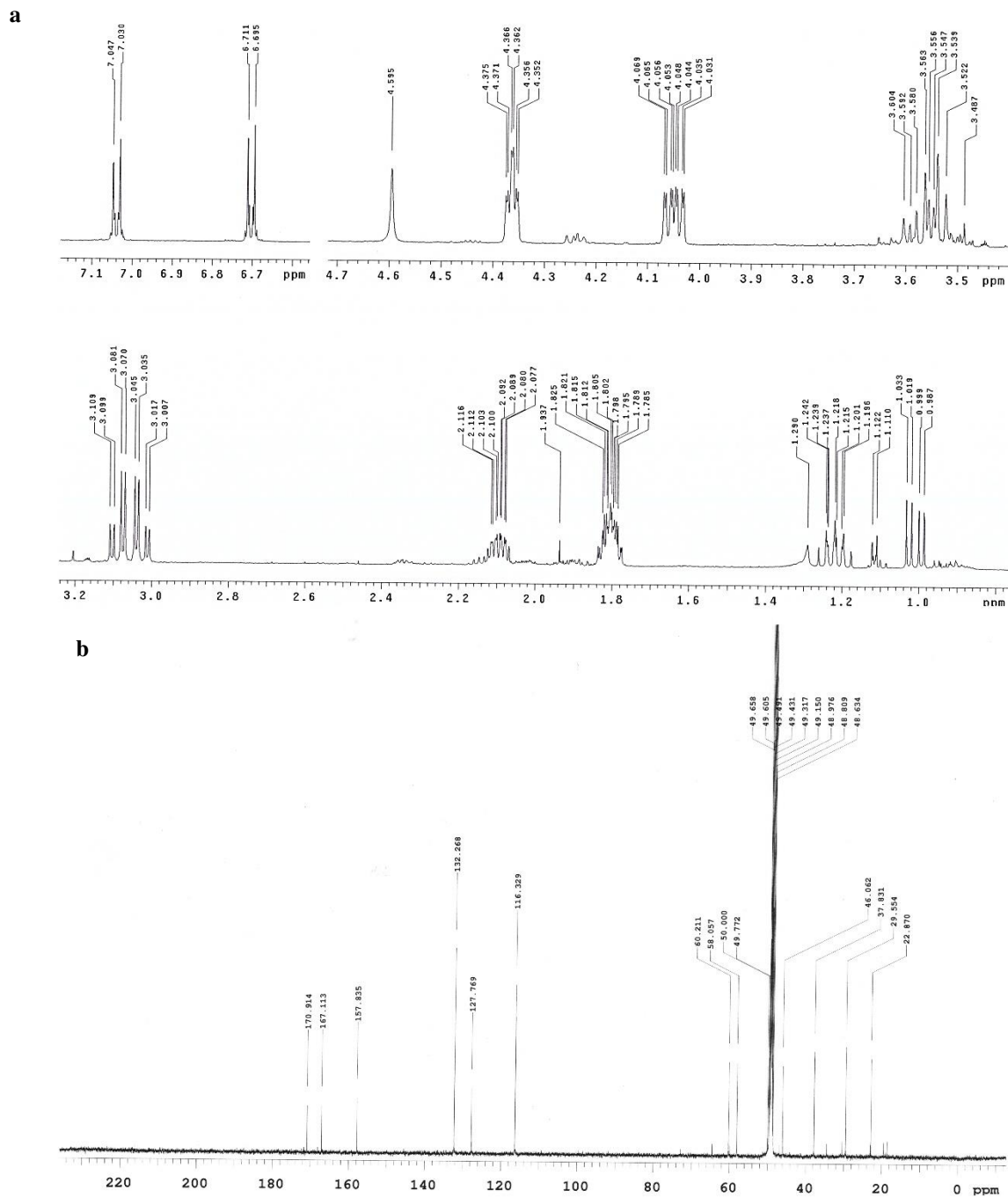


Figure 3. ^1H (a) and ^{13}C (b) nuclear magnetic resonance (NMR) spectra of the purified antifungal compound cyclo(L-Pro-D-Tyr) from strain Y1

Determination of antifungal activity of the purified compound and its effect on fungal hyphae

Antifungal activity assay showed that various concentration of cyclo(L-Pro-D-Tyr) inhibited growth of *F. graminearum*, as evidenced by decreasing turbidity in wells with increasing treatments concentration. Microscopic examination revealed that the hyphae of *F. graminearum* were altered because of the cyclo(L-Pro-D-Tyr) treatment. The results clearly highlight that 125 ppm affected the mycelia growth of *F. graminearum*,

and the effects increased with increasing concentration of compound: at 250 ppm and 500 ppm, there was more visible hyphae deformation. Alterations in the shape, including deformation and degradation of hyphae, were observed under light microscopy (Fig. 5).

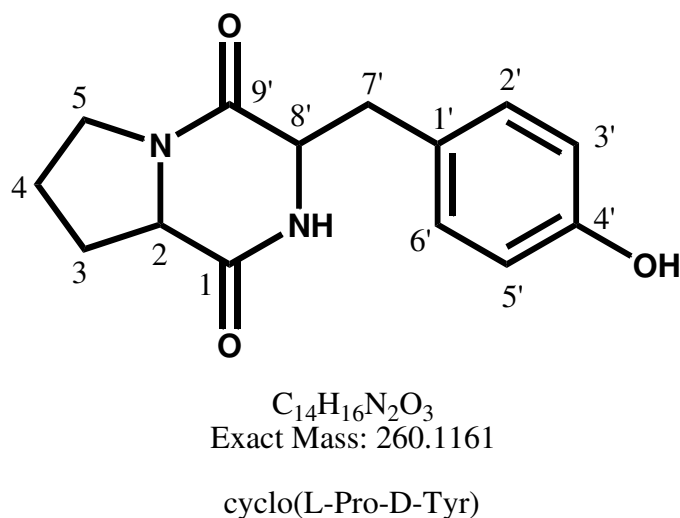


Figure 4. The structure of purified compound cyclo(L-Pro-D-Tyr) from strain Y1

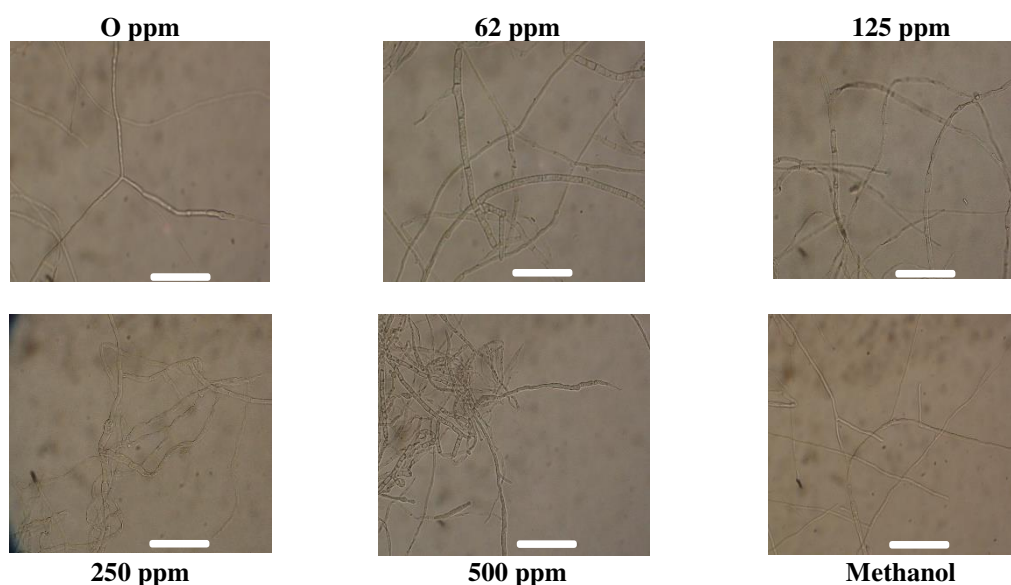


Figure 5. Microscopically evident of changes in hyphae morphology of *F. graminearum* when treated with cyclo(L-Pro-D-Tyr). The carboxy methyl cellulase (CMC) containing *F. graminearum* conidial suspension only as control 0, 62, 125, 250, 500 ppm of Cyclo (L-Pro-D-Tyr) and methanol incubated for 5 days at 30 °C. All bars = 100 μ m

Assessment of the purified compound to control *F. graminearum* on wheat seeds

The ability of secondary metabolites of strain Y1 to inhibit the growth of *F. graminearum* on wheat seeds would be of major concern to the agricultural economy. Thus, the ability of cyclo(L-Pro-D-Tyr) produced by strain Y1 to protect wheat seeds

from diseases caused by *F. graminearum* was investigated. Wheat seeds soaked in various concentration of cyclo(L-Pro-D-Tyr) demonstrated marked delay and inhibited seeds colonization compared to the control (Fig. 6). White mycelia were observed in the control wheat seeds 2 days after fungal inoculation, whereas seeds treated with 125 ppm or more of cyclo(L-Pro-D-Tyr) were found with low or no fungal growth.

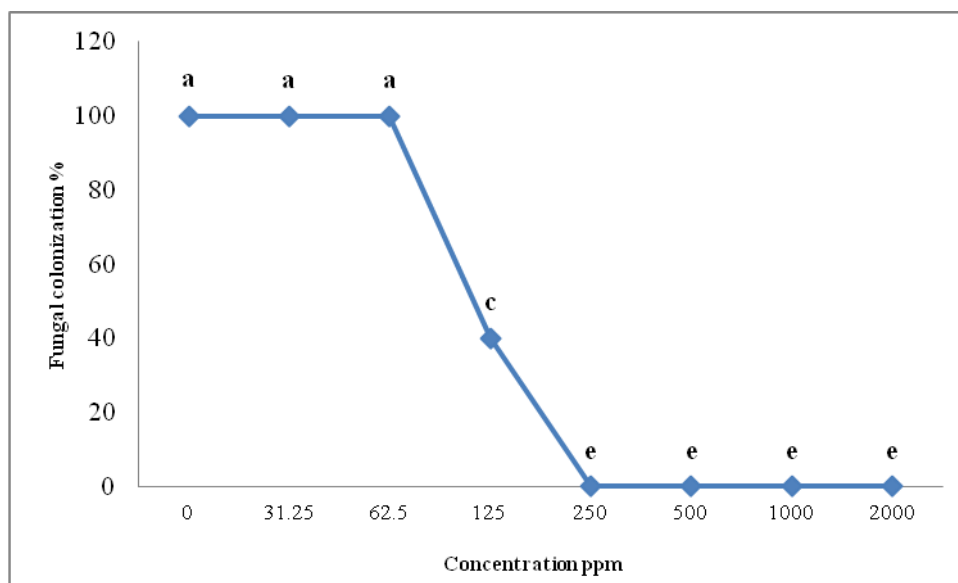


Figure 6. *F. graminearum* colonization on wheat seeds with various concentration of cyclo(L-Pro-D-Tyr). Means with the same letter are not significantly different at $P = 0.05$ when compared by LSD

Glasshouse experiment

The plant growth-promoting ability of strain Y1 was assessed *in vivo* using pot experiment with fertilizer media and bacterial inoculum. The results obtained from the pot experiment are shown in Table 1. The results indicated that at four months after sowing seeds, there were significant differences between the control and strain Y1 treatments. For vegetative growth, total yield significantly improved with the application of strain Y1, as the plant height, weight and root weight were higher with the Y1 treatment. Strain Y1 also caused an increase in the reproductive growth of wheat. The numbers of grains per spike were significantly higher in strain Y1-treated pots compared to all other treatments.

In the biocontrol of FCR, strain Y1 was found to reduce the percentage of disease in plant. The results showed that harvesting plants after four months, the strain Y1 group had the higher plant stand average against crown rot (Table 1). Pots treated with strain Y1 displayed high values for plant height, plant weight, root weight, and total grains per pot due to the better response of the plants to the effects of *F. graminearum* in the soil. *F. graminearum* exhibited crown rot symptoms in the control and reduced wheat yield, as the C (without *F. graminearum*) had higher values for plant height, plant weight, root weight, and total grains per pot compared to C + Fg (with *F. graminearum* spores) (Table 1). The level of control of crown rot in the pots treated with fertilizer medium was significantly lower (55%) compared to the pots treated with strain Y1 (28%). Total

grain weight per pot increased with the application of medium (40 g) compared to the control only C + Fg (9 g) but was lower compared to the application of strain Y1 (48 g).

Table 1. Effect of Y1 culture on crown rot severity of wheat in glass house experiment

Treatment	Disease incidence %	Plant height (cm)	Plant weight/pot (g)	Root weight (g)	Grains weight/pot (g)
C	NR	61.6 ab	71 bc	1.13 b	21 c
Y1	NR	67.4a	174 a	1.64 a	68 a
M	NR	61.5 ab	148 ab	1.21 b	42 b
C + Fg	65 a	49.1 b	37d	0.98 bc	9 d
Y1 + Fg	28 c	64.24 a	148 ab	1.52 a	48 ab
M + Fg	55 b	56.1 a	126 b	0.93 c	40 b
F + Fg	8 d	66.6 a	137 ab	1.03 bc	42 ab

Means with the same letter are not significantly different at $P \leq 0.05$ when compared by LSD
NR = Not Recorded, C = Water control, Y1 = *Bacillus amyloliquefaciens* Y1 culture, M = Fertilizer medium, C + Fg = Water + *F. graminearum*, Y1 + Fg = *B. amyloliquefaciens* Y1 + *F. graminearum*, M + Fg = Fertilizer medium + *F. graminearum*, F + Fg = Fungicide + *F. graminearum*

Discussion

In *in vitro* study, the culture supernatant and crude extract of *B. amyloliquefaciens* Y1 indicated fungicidal activity against *F. graminearum*. The increase in concentration of culture supernatant and crude extract displayed more growth inhibition. Several studies have reported that antagonistic bacteria showed antifungal properties by producing secondary metabolites in their culture broth against pathogens (Blin et al., 2013; Ehteshamul-Haque and Ghaffar, 1993; Liu et al., 2017). Increase in concentration of secondary metabolites produced by *B. amyloliquefaciens* Y1 were likely involve in increases activity (Jamal et al., 2015).

Recently, natural products have been investigated to report biocontrol mechanism of antagonistic microorganisms. In this study, we purified and identified cyclo(L-Pro-D-Tyr) as natural antifungal product from the culture supernatant of Y1 based on ^1H and ^{13}C -NMR spectra. To our knowledge, this is the first report of cyclo(L-Pro-D-Tyr) from *B. amyloliquefaciens* strain as an antifungal compound. Cyclo(L-Pro-D-Tyr) is a diketopiperazine (DKP) compound (De Rosa et al., 2003) previously purified from body fluids, sponges, microorganisms, and a variety of tissues (Rudi et al., 1994; Ström et al., 2002). Cyclo(L-Pro-D-Tyr) has been isolated from *Callyspongia* sp., a specie of marine sponge in the South China Sea (Huang et al., 2010). Kumar et al. identified cyclo(L-Pro-D-Tyr) in the secondary metabolites of *Bacillus* spp. and reported its antifungal and antibacterial properties (Kumar et al., 2013a).

Both synthetic and natural DKPs displayed biological activities, including antiviral (Sinha et al., 2004), antifungal (Houston et al., 2004), antitumor (Nicholson et al., 2006) and antibacterial (Kwon et al., 2000). The antimicrobial activities of cyclo(L-Pro-D-Tyr) has been less explored; however, here we reported its antifungal activity against *F. graminearum*. The bio-preservative properties of the cyclo(L-Pro-D-Tyr) was also evaluated on growth suppression of *F. graminearum* on wheat seeds. To the best of our knowledge, there is no previous report of DKP cyclo(L-Pro-D-Tyr) to be used as bio-preservative to report antagonistic mechanism to control *F. graminearum* causing foliar disease on wheat seeds. The bio-preservative property of DKP, cyclo(L-Pro-D-Leu) to

inhibit growth of *A. flavus* and *A. niger* on soybeans was also reported (Kumar et al., 2013b). Previously, we identified cyclo(D-Pro-L-Val) in Y1 as antifungal metabolites against *F. graminearum* (Jamal et al., 2017). *Bacillus subtilis* L1-21 was also reported to control this pathogen *in vitro* (Munir et al., 2018). These findings showed that Y1 could control wheat foliar disease by producing DKPs and other antifungal metabolites.

The effectiveness of strain Y1 under *in vivo* condition was also evaluated for growth promotion of wheat plants and reduction in wheat crown rot. It has also been reported that many strains of *B. subtilis*, *B. amyloliquefaciens*, and *B. cereus* interact with plants and suppress plant pathogens (Choudhary and Johri, 2009; Jamal et al., 2017). *Pseudomonas fluorescens* LY1–8 was also reported to control the FHB and FCR in greenhouse and field (Wang et al., 2015). Application of *Chlonostachys rosea* ACM941 (10^8 cfu/ml) reduced the disease index in wheat by 30–46% (Xue et al., 2014b). The wheat stalks with several *Fusarium* species was successfully control with *Clonostachys rosea* (Palazzini et al., 2013). Moreover, biocontrol species of *Chlonostachys* suppress the disease on maize debris (Luongo et al., 2005), soybean debris and wheat, (Xue et al., 2014a) and floral crops (Morandi et al., 2008).

Bacteria suppress disease by producing a number of antibiotics (Nelson et al., 2014; Roitman et al., 1990; Xu et al., 2018). Cyclic dipeptides were reported to influence the quorum sensing signalling and has strong inhibitory effect against *Vibrio anguillarum* (Campbell et al., 2009; Fdhila et al., 2003; Yan et al., 2004). Similarly, our *in vitro* study demonstrated that cyclo(L-Pro-D-Tyr) act as an antibiotic to suppress growth of *F. graminearum*. The production of cyclo(L-Pro-D-Tyr) as an antifungal compound by Y1 in its culture broth may partially explain its biocontrol mechanism in wheat pot experiment. The production of cyclic peptides responsible for antimicrobial activity of the *B. licheniformis* N1 strain in the control of tomato gray mold, tomato late blight, and pepper anthracnose were also investigated (Kong et al., 2010). The biocontrol of *Fusarium* dry rot in wounded potato tubers is due to an antibiotic, pyrrolnitrin, produced by *B. cepacia* in its culture broth (Burkhead et al., 1994).

The strain Y1 not only control wheat crown rot but also improve plant growth, as evidenced by increase in plant weight, plant height, and grain yield per pot. The present study agree with the findings of Huang and Wong that *Burkholderia cepacia* (A3R) reduced wheat crown rot significantly in under glasshouse and field condition and increase grain yield (Huang and Wong, 1998). Many plant-growth promoting bacteria improve plant growth by producing antimicrobial compounds (Sopheareth et al., 2013; Xu et al., 2018). Briefly, the current and our previous study (Jamal et al., 2017) provides enough evidence to consider Y1 strain as a promising biocontrol agent to control FHB and FCR in wheat by producing antifungal DKPs cyclo(L-Pro-D-Tyr) and cyclo(D-Pro-L-Val) in its culture broth.

Conclusions

In conclusion, isolation of DKP cyclo(L-Pro-D-Tyr) from *B. amyloliquefaciens* Y1, is a new finding in biocontrol literature with its antifungal characterization against *F. graminearum*. Both *in vitro* and *in vivo* study resulted that application of Y1 suppressed growth of *F. graminearum*. Cyclo(L-Pro-D-Tyr) isolated from Y1 can serve as a role model to uncoil the antagonistic mechanism of biocontrol agent. In pot experiment, addition of Y1 significantly inhibited pathogen growth and enhanced wheat plant growth. Thus, our result indicated that Y1 can serve as successful substitute over

synthetic chemicals which are detrimental to control pathogenic fungi causing serious health and environmental concerns. In addition, these biocontrol agents may serve as a potential antagonist to manage other important wheat diseases in the greenhouse and fields.

Acknowledgements. This research was supported by IPET (Institute of Planning and Evaluation for Technology in Food, Agriculture, Forestry and Fisheries for which this work was funded under grant no: 316032-5), Ministry for Food, Agriculture, Forestry and Fisheries, Republic of Korea.

REFERENCES

- [1] Asaka, O., Shoda, M. (1996): Biocontrol of *Rhizoctonia solani* damping-off of tomato with *Bacillus subtilis* RB14. – *Applied and Environmental Microbiology* 62: 4081-4085.
- [2] Baldwin, B., Rathmell, W. (1988): Evolution of concepts for chemical control of plant disease. – *Annual Review of Phytopathology* 26: 265-283.
- [3] Ben Abdallah, D., Frikha-Gargouri, O., Tounsi, S. (2015): *Bacillus amyloliquefaciens* strain 32a as a source of lipopeptides for biocontrol of *Agrobacterium tumefaciens* strains. – *Journal of Applied Microbiology* 119: 196-207.
- [4] Blin, K., Medema, M. H., Kazempour, D., Fischbach, M. A., Breitling, R., Takano, E., Weber, T. (2013): antiSMASH 2.0—a versatile platform for genome mining of secondary metabolite producers. – *Nucleic Acids Research* 41: W204-W212.
- [5] Brogгинi, G., Duffy, B., Holliger, E., Schärer, H.-J., Gessler, C., Patocchi, A. (2005): Detection of the fire blight biocontrol agent *Bacillus subtilis* BD170 (Biopro®) in a Swiss apple orchard. – *European Journal of Plant Pathology* 111: 93-100.
- [6] Burgess, L. (2005): Intermediate hosts and the management of crown rot and head blight. Annual Report of GRDC Strategic Initiative on Crown Rot, Common Root Rot and *Fusarium* Head Blight. – Grains Research and Development Corporation, Kingston, Australia, pp. 34-36.
- [7] Burkhead, K. D., Schisler, D. A., Slininger, P. J. (1994): Pyrrolnitrin production by biological control agent *Pseudomonas cepacia* B37w in culture and in colonized wounds of potatoes. – *Applied and Environmental Microbiology* 60: 2031-2039.
- [8] Campbell, J., Lin, Q., Geske, G. D., Blackwell, H. E. (2009): New and unexpected insights into the modulation of LuxR-type quorum sensing by cyclic dipeptides. – *ACS Chemical Biology* 4: 1051-1059.
- [9] Choudhary, D. K., Johri, B. N. (2009): Interactions of *Bacillus* spp. – and plants – with special reference to induced systemic resistance (ISR). – *Microbiological Research* 164: 493-513.
- [10] Cowger, C., Arellano, C. (2013): *Fusarium graminearum* infection and deoxynivalenol concentrations during development of wheat spikes. – *Phytopathology* 103: 460-471.
- [11] De Rosa, S., Mitova, M., Tommonaro, G. (2003): Marine bacteria associated with sponge as source of cyclic peptides. – *Biomolecular Engineering* 20: 311-316.
- [12] Dolej, S., Bochow, H. (1996): Studies of the Mode of Action of *Bacillus Subtilis* Culture Filtrates in the Model Pathosystem Tomato Seedling-*Fusarium Oxysporum* f. sp. *Radicis-Lycopersici*. – Mededelingen-Faculteit Landbouwkundige en Toegepaste Biologische Wetenschappen Universiteit, Gent (Belgium).
- [13] Ehteshamul-Haque, S., Ghaffar, A. (1993): Use of rhizobia in the control of root rot diseases of sunflower, okra, soybean and mungbean. – *Journal of Phytopathology* 138: 157-163.
- [14] Falcão, L., Silva-Werneck, J., Vilarinho, B., da Silva, J., Pomella, A., Marcellino, L. (2014): Antimicrobial and plant growth-promoting properties of the cacao endophyte *Bacillus subtilis* ALB629. – *Journal of Applied Microbiology* 116: 1584-1592.

- [15] Fdhila, F., Vázquez, V., Sánchez, J. L., Riguera, R. (2003): dd-Diketopiperazines: Antibiotics active against *Vibrio anguillarum* isolated from marine bacteria associated with cultures of *Pecten maximus*. – *Journal of Natural Products* 66: 1299-1301.
- [16] Graz, C. J. M. (2002): Cyclic dipeptides as novel antimicrobial agents. – <http://hdl.handle.net/20.500.11892/156232>
- [17] Houston, D. R., Synstad, B., Eijsink, V. G., Stark, M. J., Eggleston, I. M., Van Aalten, D. M. (2004): Structure-based exploration of cyclic dipeptide chitinase inhibitors. – *Journal of Medicinal Chemistry* 47: 5713-5720.
- [18] Huang, R.-M., Ma, W., Dong, J.-D., Zhou, X.-F., Xu, T., Lee, K. J., Yang, X., Xu, S.-H., Liu, Y. (2010): A new 1: 4-diazepine from South China Sea marine sponge *Callyspongia* species. – *Molecules* 15: 871-877.
- [19] Huang, Y., Wong, P. (1998): Effect of *Burkholderia* (*Pseudomonas*) *cepacia* and soil type on the control of crown rot in wheat. – *Plant and Soil* 203: 103-108.
- [20] Jamal, Q., Lee, Y. S., Jeon, H. D., Park, Y. S., Kim, K. Y. (2015): Isolation and biocontrol potential of *Bacillus amyloliquefaciens* Y1 against fungal plant pathogens. – *Korean Journal of Soil Science and Fertilizer* 48: 485-491.
- [21] Jamal, Q., Cho, J.-Y., Moon, J.-H., Munir, S., Anees, M., Kim, K. Y. (2017): Identification for the First Time of Cyclo (d-Pro-l-Leu) Produced by *Bacillus amyloliquefaciens* Y1 as a nematocide for control of *Meloidogyne incognita*. – *Molecules* 22: 1839.
- [22] Kong, Q., Shan, S., Liu, Q., Wang, X., Yu, F. (2010): Biocontrol of *Aspergillus flavus* on peanut kernels by use of a strain of marine *Bacillus megaterium*. – *International Journal of Food Microbiology* 139: 31-35.
- [23] Krebs, B., Junge, H., Ockhardt, A., Hoding, B., Heubner, D., Erben, U. (1993): *Bacillus subtilis*-an effective biocontrol agent. – *Pesticide Science* 37: 427-433.
- [24] Krebs, B., Höding, B., Kübart, S., Workie, M. A., Junge, H., Schmiedeknecht, G., Grosch, R., Bochow, H., Hevesi, M. (1998): Use of *Bacillus subtilis* as biocontrol agent. I. Activities and characterization of *Bacillus subtilis* strains/Anwendung von *Bacillus subtilis* als Mittel für den biologischen Pflanzenschutz. I. Aktivitäten und Charakterisierung von *Bacillus subtilis*-Stämmen. – *Zeitschrift für Pflanzenkrankheiten und Pflanzenschutz/Journal of Plant Diseases and Protection* 105(2): 181-197.
- [25] Kumar, N., Mohandas, C., Nambisan, B., Kumar, D. S., Lankalapalli, R. S. (2013a): Isolation of proline-based cyclic dipeptides from *Bacillus* sp. N strain associated with rhabditid entomopathogenic nematode and its antimicrobial properties. – *World Journal of Microbiology and Biotechnology* 29: 355-364.
- [26] Kumar, S. N., Mohandas, C., Nambisan, B. (2013b): Purification of an antifungal compound, cyclo (L-Pro-D-Leu) for cereals produced by *Bacillus cereus* subsp. *thuringiensis* associated with entomopathogenic nematode. – *Microbiological Research* 168: 278-288.
- [27] Kwon, O. S., Park, S. H., Yun, B.-S., Pyun, Y. R., Kim, C.-J. (2000): Cyclo (Dehydroalanyl-L-Leu), an ALPHA.-Glucosidase Inhibitor from *Penicillium* sp. F70614. – *The Journal of Antibiotics* 53: 954-958.
- [28] Liu, C., Ogbonnaya, F. C. (2015): Resistance to *F. usarium* crown rot in wheat and barley: a review. – *Plant Breeding* 134: 365-372.
- [29] Liu, K., Newman, M., McInroy, J. A., Hu, C.-H., Kloepper, J. W. (2017): Selection and assessment of plant growth-promoting rhizobacteria for biological control of multiple plant diseases. – *Phytopathology* 107: 928-936.
- [30] Luongo, L., Galli, M., Corazza, L., Meekes, E., Haas, L. D., Van Der Plas, C. L., Köhl, J. (2005): Potential of fungal antagonists for biocontrol of *Fusarium* spp. in wheat and maize through competition in crop debris. – *Biocontrol Science and Technology* 15: 229-242.
- [31] McClelland, K., Milne, P., Lucieto, F., Frost, C., Brauns, S., Venter, M., Plessis, J., Dyason, K. (2004): An investigation into the biological activity of the selected

- histidine-containing diketopiperazines cyclo (His-Phe) and cyclo (His-Tyr). – *Journal of Pharmacy and Pharmacology* 56: 1143-1153.
- [32] Morandi, M. A., Mattos, L. P., Santos, E. R., Bonugli, R. C. (2008): Influence of application time on the establishment, survival, and ability of *Clonostachys rosea* to suppress *Botrytis cinerea* sporulation on rose debris. – *Crop Protection* 27: 77-83.
- [33] Munir, S., Li, Y., He, P., He, P., He, P., Cui, W., Wu, Y., Li, X., He, Y. (2018): *Bacillus subtilis* L1-21 possible assessment of inhibitory mechanism against phytopathogens and colonization in different plant hosts. – *Pakistan Journal of Agricultural Sciences* 55(4): 996-1002.
- [34] Nakano, M. M., Zuber, P. (1990): Molecular biology of antibiotic production in *Bacillus*. – *Critical Reviews in Biotechnology* 10: 223-240.
- [35] Nelson, B. A., Ramaiya, P., de Leon, A. L., Kumar, R., Crinklaw, A., Jolkovsky, E., Crane, J. M., Bergstrom, G. C., Rey, M. W. (2014): Complete genome sequence for the *Fusarium* head blight antagonist *Bacillus amyloliquefaciens* strain TrigoCor 1448. – *Genome Announcements* 2: e00219-00214.
- [36] Nicholson, B., Lloyd, G. K., Miller, B. R., Palladino, M. A., Kiso, Y., Hayashi, Y., Neuteboom, S. T. (2006): NPI-2358 is a tubulin-depolymerizing agent: in-vitro evidence for activity as a tumor vascular-disrupting agent. – *Anti-Cancer Drugs* 17: 25-31.
- [37] Ongena, M., Jacques, P. (2008): *Bacillus* lipopeptides: versatile weapons for plant disease biocontrol. – *Trends in Microbiology* 16: 115-125.
- [38] Palazzini, J., Groenenboom-de Haas, B., Torres, A., Köhl, J., Chulze, S. (2013): Biocontrol and population dynamics of *Fusarium* spp. on wheat stubble in Argentina. – *Plant Pathology* 62: 859-866.
- [39] Palazzini, J. M., Alberione, E., Torres, A., Donat, C., Köhl, J., Chulze, S. (2016): Biological control of *Fusarium graminearum* sensu stricto, causal agent of *Fusarium* head blight of wheat, using formulated antagonists under field conditions in Argentina. – *Biological Control* 94: 56-61.
- [40] Pérez-García, A., Romero, D., De Vicente, A. (2011): Plant protection and growth stimulation by microorganisms: biotechnological applications of *Bacilli* in agriculture. – *Current Opinion in Biotechnology* 22: 187-193.
- [41] Pestka, J. J. (2007): Deoxynivalenol: toxicity, mechanisms and animal health risks. – *Animal Feed Science and Technology* 137: 283-298.
- [42] Pestka, J. J., Smolinski, A. T. (2005): Deoxynivalenol: toxicology and potential effects on humans. – *Journal of Toxicology and Environmental Health, Part B* 8: 39-69.
- [43] Pitchen, R. (2002): The medicinal chemistry of the cyclic dipeptides cyclo (Met-Met) and cyclo (Met-Gly). – MSc Thesis, Faculty of Health Sciences, University of Port Elisabeth.
- [44] Roitman, J. N., Mahoney, N. E., Janisiewicz, W. J. (1990): Production and composition of phenylpyrrole metabolites produced by *Pseudomonas cepacia*. – *Applied Microbiology and Biotechnology* 34: 381-386.
- [45] Rudi, A., Kashman, Y., Benayahu, Y., Schleyer, M. (1994): Amino acid derivatives from the marine sponge *Jaspis digonoxea*. – *Journal of Natural Products* 57: 829-832.
- [46] Sansinenea, E., Salazar, F., Jiménez, J., Mendoza, Á., Ortiz, A. (2016): Diketopiperazines derivatives isolated from *Bacillus thuringiensis* and *Bacillus endophyticus*, establishment of their configuration by X-ray and their synthesis. – *Tetrahedron Letters* 57: 2604-2607.
- [47] Simpfendorfer, S., Brettell, R., Nicol, J. (2012): Inter-row sowing reduces crown rot in winter cereals. – First International Crown Rot Workshop for Wheat Improvement¹. Narrabri. Organising Committee of the 1st International Crown Rot Workshop.
- [48] Sinha, S., Srivastava, R., De Clercq, E., Singh, R. K. (2004): Synthesis and antiviral properties of arabino and ribonucleosides of 1: 3-Dideazaadenine, 4-Nitro-1: 3-dideazaadenine and Diketopiperazine. – *Nucleosides, Nucleotides and Nucleic Acids* 23: 1815-1824.

- [49] Smiley, R. W., Gourlie, J. A., Easley, S. A., Patterson, L.-M. (2005a): Pathogenicity of fungi associated with the wheat crown rot complex in Oregon and Washington. – *Plant Disease* 89: 949-957.
- [50] Smiley, R. W., Gourlie, J. A., Easley, S. A., Patterson, L.-M., Whittaker, R. G. (2005b): Crop damage estimates for crown rot of wheat and barley in the Pacific Northwest. – *Plant Disease* 89: 595-604.
- [51] Sopheareth, M., Chan, S., Naing, K. W., Lee, Y. S., Hyun, H. N., Kim, Y. C., Kim, K. Y. (2013): Biocontrol of Late Blight (*Phytophthora capsici*) disease and growth promotion of pepper by *Burkholderia cepacia* MPC-7. – *The Plant Pathology Journal* 29: 67-76.
- [52] Stabb, E. V., Jacobson, L. M., Handelsman, J. (1994): Zwittermicin A-producing strains of *Bacillus cereus* from diverse soils. – *Applied and Environmental Microbiology* 60: 4404-4412.
- [53] Ström, K., Sjögren, J., Broberg, A., Schnürer, J. (2002): *Lactobacillus plantarum* MiLAB 393 produces the antifungal cyclic dipeptides cyclo (L-Phe-L-Pro) and cyclo (L-Phe-trans-4-OH-L-Pro) and 3-phenyllactic acid. – *Applied and Environmental Microbiology* 68: 4322-4327.
- [54] Tanaka, K., Ishihara, A., Nakajima, H. (2014): Isolation of anteiso-C17, iso-C17, iso-C16, and iso-C15 Bacillomycin D from *Bacillus amyloliquefaciens* SD-32 and their antifungal activities against plant pathogens. – *Journal of Agricultural and Food Chemistry* 62(7): 1469-1476.
- [55] Vanittanakom, N., Loeffler, W., Koch, U., Jung, G. (1986): Fengycin-a novel antifungal lipopeptide antibiotic produced by *Bacillus subtilis* F-29-3. – *The Journal of Antibiotics* 39: 888-901.
- [56] Wang, L.-Y., Xie, Y.-S., Cui, Y.-Y., Xu, J., He, W., Chen, H.-G., Guo, J.-H. (2015): Conjunctively screening of biocontrol agents (BCAs) against fusarium root rot and fusarium head blight caused by *Fusarium graminearum*. – *Microbiological Research* 177: 34-42.
- [57] Xu, D., Deng, Y., Han, T., Jiang, L., Xi, P., Wang, Q., Jiang, Z., Gao, L. (2018): In vitro and in vivo effectiveness of phenolic compounds for the control of postharvest gray mold of table grapes. – *Postharvest Biology and Technology* 139: 106-114.
- [58] Xue, A., Chen, Y., Sant'anna, S., Voldeng, H., Fedak, G., Savard, M., Längle, T., Zhang, J., Harman, G. (2014a): Efficacy of CLO-1 biofungicide in suppressing perithecial production by *Gibberella zeae* on crop residues. – *Canadian Journal of Plant Pathology* 36: 161-169.
- [59] Xue, A. G., Chen, Y., Voldeng, H. D., Fedak, G., Savard, M. E., Längle, T., Zhang, J., Harman, G. E. (2014b): Concentration and cultivar effects on efficacy of CLO-1 biofungicide in controlling *Fusarium* head blight of wheat. – *Biological Control* 73: 2-7.
- [60] Yan, P.-S., Song, Y., Sakuno, E., Nakajima, H., Nakagawa, H., Yabe, K. (2004): Cyclo (L-leucyl-L-prolyl) produced by *Achromobacter xylosoxidans* inhibits aflatoxin production by *Aspergillus parasiticus*. – *Applied and Environmental Microbiology* 70: 7466-7473.
- [61] Zhao, L., Xu, Y., Lai, X.-H., Shan, C., Deng, Z., Ji, Y. (2015): Screening and characterization of endophytic *Bacillus* and *Paenibacillus* strains from medicinal plant *Lonicera japonica* for use as potential plant growth promoters. – *Brazilian Journal of Microbiology* 46: 977-989.

EFFECTS OF ANTIMICROBIAL INTERVENTIONS AND BRINING ON MICROBIOLOGICAL QUALITY OF 6 MONTHS' QUICK FROZEN CHICKEN MIXED PORTIONS

MASHISHI, M. D.¹ – OKORO, V. M. O.^{1*} – MBAJIORGU, C. A.¹

¹*Department of Agriculture and Animal Health, College of Agriculture and Environmental Sciences, University of South Africa, Florida, 1710, South Africa*

**Corresponding author*

e-mail: melavicong@gmail.com, phone: +27-78-938-9749

(Received 27th Dec 2018; accepted 14th Feb 2019)

Abstract. This study was to know the effects of abattoir, chlorinated antimicrobial intervention and brining on microbiology of post 6 months' frozen (-10 ± 2 °C) and thawed mixed chicken portions, as well as determine the optimal brining levels. Broilers (5-6 weeks old, $n = 180$, 1.12-1.25kg carcass weight) processed at 3 different processing plants ($n = 60$ per abattoir) into chicken portions of breasts, thighs and wings were packaged in 1 kg bags after applying antimicrobial intervention and brining before quick freezing them. After 6 months quick freezing at -10 °C and thawing, standard plate counts (SPC), spore counts and psychrophilic counts (log cfu/g) were evaluated and subjected to ANOVA in a randomized complete block design (RCBD). No coliforms, molds, staphylococci, and yeasts were not detected due to abattoir, antimicrobial and brining interventions. Also no significant SPC, spore count and psychrophilic bacterial count ($P > 0.05$) effects was recorded due to abattoirs. ASC significantly ($P < 0.05$) lowered all the counts compared to Aq. Cl and ClO₂. The 0% brine had highest ($P < 0.05$) counts (3.33, 3.25 and 3.63 logCFU/g) for SPC, spores and psychrophilic bacteria respectively, while 30 and 35% levels had the least ($P < 0.05$) counts (ranges from 1.06 – 1.87 logCFU/g) per sample tested with no significant interaction effects recorded. There is a significant optimal brining levels of 13.27, 35.87 and 34.10 (%) for SPC, spores and psychrophilic counts based on the quadratic regression model.

Keywords: *psychrophilic bacteria, quadratic function, aqueous chlorine, standard plate count, freezing*

Introduction

Food preservation using low temperatures is the most commonly used method for storing fresh foods as well as its distribution. Fresh meat is among the most perishable foods and chill temperatures are mostly used to delay the spoilage process by spoilage bacteria after slaughter, processing cuts and portions, transportation to distributors and the final storage at various retail sites (Xia et al., 2009). The basic aim of cooling techniques for fresh meat preservation is to slow or limit the spoilage rate as temperature below the optimal range can inhibit the microbial growth (Cassens, 1994). The methods of temperature regulation for storage are chilling, freezing and super-chilling which help to inhibit or completely stop bacterial growth (Zhou et al., 2010). However, the growth of psychrophilic group of bacteria, yeasts and molds is not prevented by all levels of refrigeration (Neumeyer et al., 1997) and both enzymatic and non-enzymatic changes will continue at a much slower rate (Van Berkel et al., 2004). During freezing, about 60% of the viable microbial population dies but the remaining population gradually increases during longer frozen storage periods (Rahman, 1999b). Modi et al. (2006) and Sudheer et al. (2011) reported an increase in psychrophilic bacterial count in prolonged freezing storage of spiced chicken.

Most psychrophilic bacteria belong to the microbial genera of both gram positive, such as lactic acid bacteria, and gram-negative bacteria such as *Pseudomonas* spp. and

Enterobacteriaceae (Holzapfel, 1998). Particular species involved in the spoilage of meat preserved at chill temperature are of *Pseudomonas* spp. (Ercolini et al., 2007), while the microflora of vacuum packaged frozen-preserved meat is characterized mostly by psychotropic lactic acid bacteria (Nychas et al., 1998). It is assumed that antimicrobial intervention and brining before freezing could significantly reduce such spoilage microbes during long frozen preservation periods, however there is paucity of information on spoilage microbial load of chicken portions thawed after quick frozen at -10 °C for 6 months.

The poultry processing plants make use of antimicrobial interventions (chlorine antimicrobials) such as aqueous chlorine, chlorine dioxide and Acidified Sodium Chlorite to abate the effects of spoilage bacteria as the storage period increases (Alonso-Hernando et al., 2013). Also, the poultry processing industry had introduced the method of brining for processed chicken with an objective of improving the flavour, taste and tenderness of chicken through different liquid additive solutions (Venter, 2015). Although, there is paucity of scientific report on the effect of high levels of brining on the portion's microbial load and its effects on the chicken, it had been speculated that increased brining levels above 60% could result in high levels of salts in the products which could affect the consumer's health (Alvarado and McKee, 2007; Ellinger, 1972). However, there is paucity of information on the effects of antimicrobial intervention and brining on the level of standard plate counts (SPC), spore counts and psychrophilic counts (log cfu/g) in 6 months frozen chicken portions, as well as the optimum levels of inclusion to attain the lowest microbial count in frozen chicken portions.

Therefore, this study is aimed at determining the relative effects of antimicrobial intervention and brining on spoilage microbial load in long term (6 months) frozen chicken portions; determine the best chlorinated antimicrobial to be used among the commonly used ones in the market; as well as determine the optimal brining levels that will lead to the lowest spoilage bacterial levels in frozen chicken portions.

Materials and methods

Sources of experimental materials and laboratory analysis

This research was carried out following the ethical approval given by the College of Agriculture and Environmental Sciences (CAES) research ethics review committee of University of South Africa (Ethics ref no: 2016/CAES/066). 180 freshly slaughtered broiler chickens from 3 different abattoirs (60 per abattoir) was used for this experiment. They were processed into chicken portions comprising of breasts, thighs and wings per chicken. These abattoirs were high through-put commercial poultry abattoirs, referred to as sources A, B and C. The standard plate, spore and psychrophilic bacterial count were carried out in a Biotechnology laboratory.

Chicken sample preparation, chlorinated antimicrobial and brining applications at the abattoir

The freshly slaughtered and processed mixed chicken portions from each abattoir was divided equally into 2 portions for antimicrobial intervention and brining. Three types of chlorinated antimicrobial were purchased from suppliers - Chlorine dioxide, Aqueous Chlorine, and Acidified Sodium Chlorite and applied at the rate of 50 mg/g to the chicken portions with brush (aseptically) after sub-dividing the portions into 3 equal

parts aseptically. Thereafter, they were bagged into 1 kg cellophane bags and labelled for identification, and a total of 12 bags per abattoir were randomly selected for refrigeration, comprising of 4 bags per treatment. A total of 24 bags per plant was randomly selected, with 12 bags each for antimicrobial intervention and brining respectively, replicated 3 and 2 times per treatment accordingly. Chlorine antimicrobials - Aqueous Chlorine (Aq. Cl), Acidified Sodium Chlorite (ASC) and Chlorine Dioxide (ClO₂) all sprayed before packaging while the other 12 bags were assigned to 6 brining levels (0%, 15%, 20%, 25%, 30%, and 35% of 1 kg chicken portion) per treatment before quick freezing them for 6 months at -10 °C and thawing thereafter for standard plate counts (SPC), spore counts and psychrophilic counts (log cfu/g).

The brine solutions were prepared in the abattoirs at the following brining concentration levels of 0%, 15%, 20%, 25%, 30% and 35% of 1 kg chicken portion as treatments (*Table 1*). The brine solutions were prepared separately for each brining level in stainless steel tanks that were automated and transported through a flexible hose to the brine injection unit. The processed portion per abattoir for brining were subsequently divided into 6 parts after weighing out 1 kg each, before brining and packaging in a cellophane bag and identified with an indelible marker. A total of 12 bags comprising of 2 bags per treatment were randomly selected for refrigeration at -10 °C for 6 months.

Table 1. Graded levels of brine mixes applied to each replicate of 1 kg chicken portion

Ingredients	Brining (%)*					
	0	15	20	25	30	35
Salt (g)	0	5.5	7.3	9.1	10.9	12.7
Sugar (g)	0	2.6	3.5	4.4	5.3	6.2
Water (L)	0	24.2	34.9	43.7	52.4	61.1

*Chicken to brine ratio = 80:20 in percentage of 1 kg

After 6 months of refrigeration, cold water thawing procedure at 26 °C was applied to thaw the samples. All of the frozen samples were firmly tied and placed in a leak-proof plastic bag, before submerging in a sterile large bowl filled with water and allowed to thaw for 24 h. The samples were then removed aseptically and sampled for standard plate counts (SPC), spore counts and psychrophilic counts (log CFU/g) in the laboratory which were recorded and analyzed for mean effects.

Standard plate counts (SPC), spore counts and psychrophilic counts (log cfu/g)

The procedure of Woteki (1998) was used to determine the microbiological quality by aseptically collected (60 ± 0.1 g) of the sample (either the breast, wing or thigh randomly) from each replicate. The total plate count was conducted using the procedure of (AOAC, 1995). Psychrophilic bacterial count was carried out according to the procedure of (APHA, 2001). The counting was achieved using the same procedure as in Total Plate count; 1 ml of the series dilutions, then the plates were incubated at 5-7 °C for 10 days. The blended samples were then tested for standard plate counts (SPC), bacterial spores, coliform, staphylococci and yeast and molds by pour-plate method as per APHA (2001) procedures (*Fig. 1*).

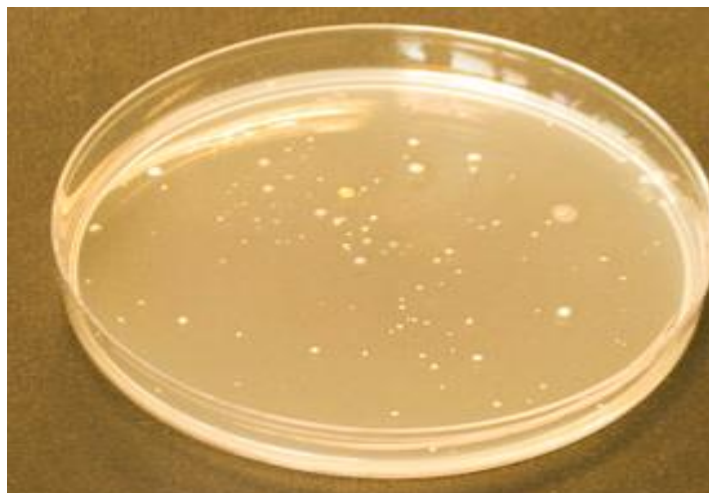


Figure 1. A petri dish showing a sample colony of psychrophilic bacteria from chicken portions rinsates using the procedure of APHA (2001)

Statistical analysis

The effects of source, antimicrobial intervention and brining levels on microbiological quality of chicken were analyzed with the general linear model (GLM) procedures of the (SPSS, 2017). The statistical model was:

$$Y_{ijk} = \mu + T_i + B_j + C_k + (TB)_{ij} + (TC)_{ik} + \Sigma_{ijk} \quad (\text{Eq.1})$$

where Y_{ijk} = the overall observation (Bacterial load); μ = population means; T_i = effect of abattoir source; B_j = effect of antimicrobials; C_k = effect of brining levels; $(TB)_{ij}$ = interaction effect of abattoir source and antimicrobials; $(TC)_{ik}$ = interaction effects of abattoir source and brining and Σ_{ijk} = residual effect.

A breakdown of the experimental design is as shown below:

Treatment 1 = Abattoirs effects only

Treatment 2 = Antimicrobial effects only

Treatment 3 = Brining effects only

Treatment 4 = Abattoirs and antimicrobial agents.

Treatment 5 = Abattoirs and brining levels

Where there was a significant F-test ($P < 0.05$), the Duncan New Multiple Range test method was used to separate the means according to SPSS (2017).

The related responses in Psychrophilic bacterial count to antimicrobial and brining levels were modeled using the quadratic regression model below:

$$Y = a + b_1x + b_2x^2 \quad (\text{Eq.2})$$

where Y = microbiological load; a = intercepts on Y axis; b = co-efficient of the quadratic equation; x = brining levels in percentages and $b_1/2b_2 = x$ value for optimal or minimal responses. The quadratic model was fitted to the experimental data by means of the regression using curve estimation procedure of SPSS (2017). The quadratic model was used because it gave the best fit (Okoro and Mbajiorgu, 2017).

Results

The application of chlorine antimicrobials had a significant effect ($P < 0.05$) on the chicken portions from within abattoirs used in the study (Table 2), they however did not differ between different abattoirs within treatments. Although the values of samples treated with acidified sodium chlorite were consistently lower in all the samples from different abattoirs than those treated with aqueous chlorine and chlorine dioxide, no statistical significant differences were recorded between them. However, between the three chlorine antimicrobials, the ASC consistently recorded a significantly lowest SPC, spores and psychrophilic bacterial count while Aq.Cl recorded the highest ($P < 0.05$) But there were no significant difference between values of spore counts generated from abattoir C. This could be due to all three antimicrobials being made from chlorine, resulting in their effectiveness appearing to be the same in terms of reducing standard plate counts (SPC), spore counts and psychrophilic counts.

Table 2. Effects of chlorine antimicrobials on standard plate count, spores and psychrophilic bacteria count (logCFU/g) of frozen chicken from 3 commercial chicken abattoirs sampled

Microbial* counts (logCFU/g)	Abattoirs	Chlorine antimicrobials (50 mg/g)				
		ASC	Aq. Cl.	ClO ₂	SEM	P-Value
SPC	A	1.33 ^c	2.50 ^b	2.98 ^a	0.189	0.030
	B	1.33 ^c	2.67 ^b	2.92 ^a	0.221	0.029
	C	1.17 ^c	2.92 ^b	3.11 ^a	0.367	0.045
Spores	A	1.36 ^c	2.72 ^b	3.18 ^a	0.379	0.050
	B	1.37 ^c	3.07 ^b	3.22 ^a	0.221	0.052
	C	2.76	3.02	3.21	0.367	0.560
Psychrophiles	A	1.37 ^c	2.60 ^b	2.98 ^a	0.389	0.030
	B	1.51 ^c	2.57 ^b	2.92 ^a	0.321	0.034
	C	1.42 ^c	2.52 ^b	3.09 ^a	0.467	0.025

^{a,b,c}Means in the same row and column not sharing a common superscript are significantly different ($P < 0.05$) SEM = standard error of mean, P- value = probability value, Aq. Cl = aqueous chlorine, ASC = acidified sodium chlorite, ClO₂ = chlorine dioxide

The effect of the brining levels on standard plate count, spores and psychrophilic bacterial count was the same across all three major abattoirs (Table 3). However, at 0% brine, the microbiological quality was significantly higher ($P < 0.05$) than any other levels in all three abattoirs. Furthermore, the results have indicated no significant difference of SPC, spores and psychrophilic bacterial count between 15, 20 and 25% across all samples from the three abattoirs. The brining levels between 30 and 35% also has no significant differences ($P < 0.05$) among them for the microbial loads.

The levels of brining and chlorine antimicrobials affected the levels of standard plate count, spores and psychrophilic bacterial load in the frozen chicken portions (Table 4). The control samples (0% brine) had significantly higher ($P < 0.05$) bacterial load than all samples injected with various brining levels. At 20% and 25% brining levels however, there was no difference ($P > 0.05$) in bacterial count except for SPC where 20% is significantly higher than 25%.

Application of quadratic regression model to identify optimal brining levels to achieve the least SPC, spore and psychrophilic bacterial count resulted in a significant

($P < 0.05$) optimum levels (Table 5). The effect of percentage brining on average SPC, spore and psychrophilic bacteria count had optimum quadratic values of $20.67 + 20.578 \text{ brining} - 7.986 \text{ brining}^2$, $80.142 - 31.793 \text{ brining} + 2.178 \text{ brining}^2$ and $31.77 + 5.909 \text{ brining} - 3.748 \text{ brining}^2$ respectively. The optimal brining levels were 13.27, 35.87 and 34.10 for SPC, spore and psychrophilic counts respectively. These are the optimal brining level to give the lowest microbial count in 6 months frozen ($-10 \pm 2 \text{ }^\circ\text{C}$) chicken portions. The co-efficient of determination (R^2) which is very high, implies that the optimum brining levels have significant influence in reducing microbial load.

The result of the optimization function indicates that brining has a direct effect on the amount of microbial counts that develop during long term refrigeration; hence, the best brining level of inclusion to achieve the fewest number of bacterial loads is determined (Figs. 2 and 3).

Table 3. Effects of brining levels on standard plate count, spores and Psychrophilic bacteria count (logCFU/g) of frozen chicken from 3 commercial chicken abattoirs sampled

Microbial* counts (logCFU/g)	Abattoirs	Brining levels (%)						SEM	P-value
		0	15	20	25	30	35		
SPC	A	3.23 ^a	2.67 ^b	2.27 ^{bc}	2.11 ^c	1.92 ^d	1.33 ^d	0.352	0.001
	B	3.00 ^a	2.33 ^b	2.19 ^c	2.09 ^c	1.89 ^d	1.67 ^d	0.584	0.001
	C	3.13 ^a	1.97 ^b	2.33 ^{bc}	2.12 ^c	1.87 ^d	1.17 ^d	0.419	0.001
Spores	A	3.18 ^a	2.47 ^b	2.28 ^{bc}	2.10 ^c	1.89 ^d	1.23 ^d	0.552	0.021
	B	3.25 ^a	2.43 ^b	2.27 ^c	2.11 ^c	1.88 ^d	1.56 ^d	0.444	0.035
	C	3.30 ^a	2.52 ^b	2.25 ^{bc}	2.08 ^c	1.90 ^d	1.47 ^d	0.319	0.033
Psychrophiles	A	3.93 ^a	3.17 ^b	2.87 ^{bc}	2.21 ^c	1.52 ^d	1.13 ^d	0.252	0.041
	B	3.60 ^a	3.33 ^b	2.79 ^c	2.14 ^c	1.69 ^d	1.07 ^d	0.384	0.044
	C	4.13 ^a	2.97 ^b	2.43 ^{bc}	2.02 ^c	1.47 ^d	1.11 ^d	0.219	0.026

^{a,b,c}Means in the same row and column not sharing a common superscript are significantly different ($P < 0.05$). SEM = standard error of mean, P-value = probability value, ClO_2 = chlorine dioxide, Aq. Cl = aqueous chlorine, ASC = acidified sodium chlorite

Table 4. Effects of antimicrobial intervention and brining on microbial counts of mixed chicken portions frozen ($-10 \text{ }^\circ\text{C} \pm 2$) for 6 months

Microbial* counts (logCFU/g)	Antimicrobial intervention* (50mg/g)			Brining (%)						SEM	P-value
	ASC	Aq. Cl.	ClO_2	0	15	20	25	30	35		
SPC	1.17 ^c	2.52 ^b	3.21 ^a	3.33 ^a	2.87 ^b	2.63 ^b	2.32 ^c	1.76 ^d	1.57 ^d	0.267	0.023
Spores	1.47 ^c	3.01 ^b	3.42 ^a	3.25 ^a	2.43 ^b	2.12 ^c	2.11 ^c	1.87 ^d	1.56 ^d	0.412	0.044
Psychrophilic	1.39 ^c	2.30 ^b	3.08 ^a	3.63 ^a	3.32 ^b	2.40 ^c	2.13 ^c	1.70 ^d	1.06 ^d	0.321	0.001

^{a,b,c}Means in the same row not sharing a common superscript are significantly different ($P < 0.05$). SEM = standard error of mean, P-value = probability value, Aq. Cl = aqueous chlorine, ASC = acidified sodium chlorite, ClO_2 = chlorine dioxide, *SPC = standard plate count, ASC = acidified sodium chlorite, Aq. Cl = aqueous chlorine, ClO_2 = chlorine dioxide

Table 5. The optimal brining levels on standard plate count, spores and psychrophilic bacteria count (logCFU/g) using quadratic regression model

Microbial* counts (logCFU/g)	R ² values	Optimal Y levels of bacteria	Optimal brining levels (%)	P - Value
SPC	0.988	1.289	13.27	0.001
Spore	0.980	7.299	35.87	0.003
Psychrophile	0.938	0.788	34.10	0.016

SPC = standard plate count, R² = co-efficient of determination, P-value = probability value

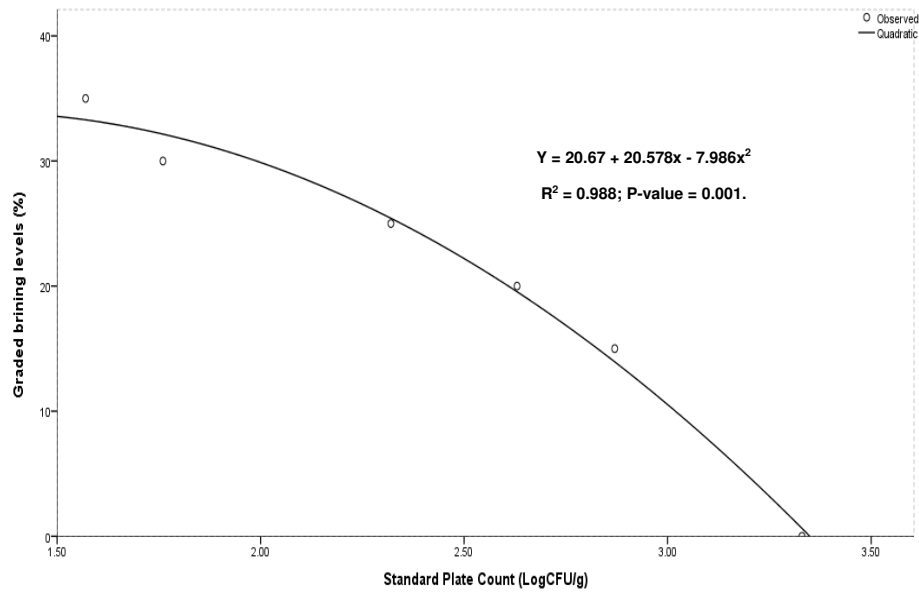


Figure 2. Quadratic function showing the optimum brining levels of quick frozen chicken for standard plate count

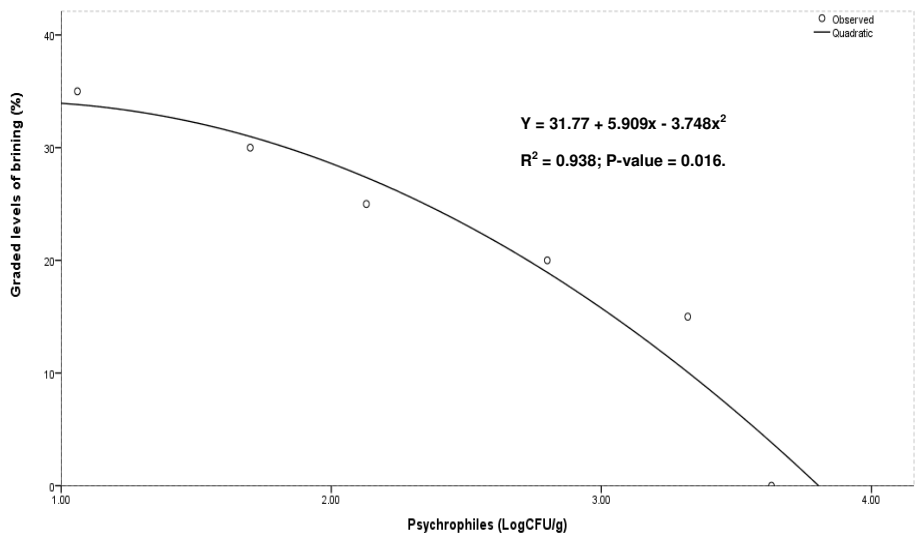


Figure 3. Quadratic function showing the optimum brining levels of quick frozen chicken for psychrophilic bacterial count

Discussion

Antimicrobial intervention and brining of chicken portions are important in preservation and storage of meat as Perez-Chabela and Mateo-Oyague (2004) reported that pathogenic microorganisms are commonly isolated from thawed frozen raw meat with larvae of *Taenia* spp. and *Trichinella spiralis* killed after 1-3 weeks of refrigeration at -18 °C or after ultra-rapid freezing at -29 °C of raw meat. Also Lowry and Gill (1984) reported that moulds grew at temperatures lower than -10 °C with Knöchel et al. (2007) also reporting the development of spoilage microbes in non-marinated chicken which increases rapidly when refrigerated. Chlorine is a major antimicrobial intervention agent and its widely used in poultry processing industry being effective against a whole range of microorganism in poultry processing (Purnell et al., 2014) and is regarded as the most effective antimicrobial to control bacterial, viral and protozoan pathogens (Duan et al., 2017; Purnell et al., 2014). However, it is reported that the efficacy of the antimicrobials is determined by the level of attachment of bacterial infection on the chicken skin. This factor might have a slight contribution to the results as the samples were sprayed directly on each sample before the portions were packed. It is reported that chlorine dioxide, when used under commercial operations, has the potential to reduce up to 2- 3 logCFU/g in microbial levels in frozen poultry (Tamblyn and Conner, 1997). The present study indicates that all the abattoirs were not affected by the effects of the antimicrobials when they were compared. However, among the antimicrobials, there was a significant difference in terms of the microbial load of the samples tested with acidified sodium chlorite having the least load while chlorine dioxide having the most load. Although all three chosen antimicrobials originated from chlorine as a base, acidified sodium that reduced more bacteria than all other antimicrobials is in acidic format, a form which is very convenient to lactic acid bacteria that is capable of causing great reduction of microbial load in white meat (Oyarzabal, 2008; Vlahova-Vangelova and Dragoev, 2014). This is also in agreement with the findings of Purnell et al. (2014) showing that acidified sodium chloride could be the most effective antimicrobial to be used in the poultry processing industry.

Brining of chicken slows formation of colony for spoilage bacteria and the bacterial development remains below 1.03 logCFU/g (Knöchel et al., 2007; Vlahova-Vangelova and Dragoev, 2014) for a period of 3 months. Different amounts of brine required for use in chicken preservation has been reported by different authors. Alvarado and McKee (2007) reported that salt within brine was meant to reduce rate of deterioration by reducing the growth of microorganisms in the chicken with higher concentration of salt proven to inhibit the microbial spoilage in white meat. This study has shown that higher level of brining consistently reduces the levels of microbial organisms causing spoilage. Although 5% brine is reported for best quality of meat products when assessing the chicken from sensory properties (Venter, 2015); it did not consider levels of spoilage microbes effect on the meat due to longer periods of storage. This study has shown that at lower levels of inclusion of brine (0-10%), the level of spoilage microbes is still within safe limits after 6 months of refrigeration, implying that higher levels might not be necessary. But as the period of refrigeration increases beyond 6 months, the spoilage bacteria level could increase, hence The United States Food and Drug Administration (USFDA) recommended a storage period of 9 months for chicken and turkey parts (FDA, 2017). Meanwhile, Venter (2015) reported the prohibition of abattoirs from exceeding 15% level of brining by the country's regulatory body resulting in a suggested 20% brining levels by the abattoirs as the most accommodative

amount for inclusion when considering longer preservation periods. This study however suggests an inclusion of up to 34.10% brining level to optimally remove psychophilic microbes, and 13.27 for optimal eradication of standard plate count of microbes. Brining at levels up to 60% may reduce the quality of the chicken through dilution of nutrients such as proteins, fat and energy (Tamblyn and Conner, 1997; Whitman and Marshall, 1971). Farber and Idziak (1984) had reported high moisture content in the 60% brining level treated samples resulting in lower salt which has been diluted by the moisture. However, Farber and Idziak (1984) reported that the highest injection level of 60% was tenderer than lower inclusion levels.

The primary preservation agents of brine are salt and sugar, which do not only prevent spoilage of the chicken but serve to inhibit growth of pathogens and spoilage bacteria when applied correctly (Pichpol, 2009; Purnell et al., 2014). These preservative agents have antimicrobial mechanisms which capacitate them to disrupt microbial enzyme activity and weaken their DNA structure. Sugar's preservative mechanism is to accelerate accumulation of antimicrobial compounds from the growth of spoilage microorganisms. This includes conversion of sugar molecules to organic acids by lactic acid bacteria (Vlahova-Vangelova and Dragoev, 2014). Moreover, Vlahova-Vangelova and Dragoev (2014) had reported that development of spoilage bacteria depend on the presence of lactic acid bacteria solutions not sugars. This may explain why the greatest reduction of spoilage microbes is found between 30-35% of brining level in this study.

Conclusion

Generally, this study has shown that usage of antimicrobial intervention and brining could achieve the same level of microbial reduction, hence either of the two could be used when preserving chicken portions. An antimicrobial intervention of acidified sodium chlorite could be used in the preservation of chicken portions, while brining up to the level of 13.27% for reduced standard plate count and 34.10% for optimum psychophilic bacterial count reduction could be important. Therefore, ASC could be used interchangeably while brining, as it is easily accessible in the market and relatively cheap, making it a better preservative commercially for chicken preservation than other antimicrobials.

Acknowledgements. The authors wish to acknowledge the active participation of the meat processing plants that allowed the use of their facilities in conducting this experiment.

REFERENCES

- [1] Alonso-Hernando, A., Alonso-Calleja, C., Capita, R. (2013): Effectiveness of several chemical decontamination treatments against Gram-negative bacteria on poultry during storage under different simulated cold chain. – *Food Control* 34: 574–580.
- [2] Alvarado, C., McKee, S. (2007): Marination to improve functional properties and safety of poultry meat. – *Journal of Applied Poultry Research* 16: 113–120.
- [3] AOAC (1995): *Official Methods of Analysis*. – Association of Official Analytical Chemists, Washington DC.
- [4] APHA (2001): *Compendium of Methods for the Microbiological Examination of Food*. – American Public Health Association, Washington DC.

- [5] Cassens, R. G. (1994): Meat Preservation Preventing Losses and Assuring Safety. Departement of Meat and Animal Sciences. – University of Wisconsin, Food and Nutrition Press, Inc, Madison, WI.
- [6] Duan, D., Wang, H., Xue, S., Li, M., Xu, X. (2017): Application of disinfectant sprays after chilling to reduce the initial microbial load and extend the shelf-life of chilled chicken carcasses. – *Food Control* 75: 70–77.
- [7] Ellinger, R. (1972): Phosphates in Food Processing. – In: Furia, T. E. (ed.) *Handbook of Food Additives*. CRC, Boca Raton, FL, pp. 617–780.
- [8] Ercolini, D., Russo, F., Blaiotta, G., Pepe, O., Mauriello, G., Villani, F. (2007): Simultaneous detection of *Pseudomonas fragi*, *P. lundensis*, and *P. putida* from meat by use of a multiplex PCR assay targeting the *carA* gene. – *Applied and Environmental Microbiology* 73: 2354–2359.
- [9] Farber, J. M., Idziak, E. S. (1984): Attachment of psychrotrophic meat spoilage bacteria to muscle surfaces. – *Journal of Food Protection* 47: 92–95.
- [10] FDA (2017): Food Code. – U. S. Public Health Services of US Food and Drug Administration, College Park, MD.
- [11] Holzapfel, W. (1998): The Gram-positive bacteria associated with meat and meat products. – *The Microbiology of Meat and Poultry* 31: 35–74.
- [12] Knöchel, S., Mach, N., Karlsson, A. (2007): Microbial and physical changes in marinated beef of high and normal pH during storage in different atmospheres. – *International 53rd Congress of Meat Science and Technology*, Beijing, 5-10 August, pp. 37–38.
- [13] Lowry, P. D., Gill, C. O. (1984): Mould growth on meat at freezing temperatures. – *Int. J. Refrigeration* 7: 133–136. [https://doi.org/DOI: 10.1016/0140-7007\(84\)90026-4](https://doi.org/DOI: 10.1016/0140-7007(84)90026-4).
- [14] Modi, V. K., Sachindra, N. M., Sathisha, A. D., Mahendrakar, N. S., Narasimha Rao, D. (2006): Changes in quality of chicken curry during frozen storage. – *Journal of Muscle Foods* 17: 141–154. <https://doi.org/10.1111/j.1745-4573.2006.00034.x>.
- [15] Neumeyer, K., Ross, T., Thomson, G., McMeekin, T. A. (1997): Validation of a model describing the effects of temperature and water activity on the growth of psychrotrophic pseudomonads. – *International Journal of Food Microbiology* 38: 55–63.
- [16] Nychas, G., Drosinos, E., Board, R. (1998): Chemical Changes in Stored Meat. – In: Board, R. J., Cavies, A. R. (eds.) *Microbiology of Meat and Poultry*. Springer, New York.
- [17] Okoro, V. M. O., Mbajiorgu, C. A. (2017): Crossbreeding parameter estimates for growth and conformation traits in a three pig diallel cross. – *Applied Ecology and Environmental Research* 15: 117–128. http://dx.doi.org/10.15666/aeer/1504_117128.
- [18] Oyarzabal, O. (2008): Antimicrobials to control *Campylobacter* in broilers. – Department of Poultry Science. MSc Dissertation, Auburn University, USA.
- [19] Perez-Chabela, M. L., Mateo-Oyague, J. (2004): Frozen Meat: Quality and Shelf Life. – In: Hui, Y. H., Cornillon, P., Legaretta, I. G., Lim, M. H., Murrell, K. D., Kit Nip, W. (eds.) *Handbook of Frozen Foods*. Marcel Dekker Inc, New York.
- [20] Pichpol, D. (2009): Experimental reduction of salmonella in raw chicken breasts. – MSc Dissertation, Faculty of Veterinary and Animal Sciences, Freien University, Berlin.
- [21] Purnell, G., James, C., James, S., Howell, M., Corry, J. (2014): Comparison of acidified sodium chlorite, chlorine dioxide, peroxyacetic acid and tri-sodium phosphate spray washes for decontamination of chicken carcasses. – *Food and Bioprocess Technology* 7: 2093–2101.
- [22] Rahman, S. F. (1999): Food Preservation by Freezing. – In: Rahman, S. F. (ed.) *Handbook of Food Preservation*. Marcel Dekker, New York, pp: 259, 262, 268.
- [23] SPSS (2017): IBM SPSS Statistics Software 24. – IBM, Armonk, NY.
- [24] Sudheer, K., Das, C., Mandal, P. K., Pal, U., Rao, V. (2011): Effect of frozen storage on the physico-chemical, microbiological and sensory quality of low fat restructured chicken block incorporated with gizzard. – *International Journal of Meat Science* 1: 62–69.

- [25] Tamblyn, K., Conner, D. (1997): Bactericidal activity of organic acids in combination with transdermal compounds against *Salmonella typhimurium* attached to broiler skin. – *Food Microbiology* 14: 477–484.
- [26] Van Berkel, B. M., Boogaard, B., Heijnen, C. (2004): Preservation of Fish and Meat. – Technical Centre for Agricultural and Rural Co-operation, Agromisa Foundation, Wageningen.
- [27] Venter, Z. (2015): Bid to halt chicken brine regulations fails. – IOL News. <https://www.iol.co.za/news/bid-to-halt-chicken-brine-regulations-fails-2071194>.
- [28] Vlahova-Vangelova, D., Dragoev, S. (2014): Marination: effect on meat safety and human health. A review. – *Bulgarian Journal of Agricultural Science* 20: 503–509.
- [29] Whitman, P. A., Marshall, R. T. (1971): Isolation of psychrophilic bacteriophage-host systems from refrigerated food products. – *Applied Microbiology* 22: 220–223.
- [30] Woteki, C. (1998): USDA FSIS: Food Safety Research Priorities and Challenges. – Food Safety and Inspection Service, United States Department of Agriculture Washington, DC.
- [31] Xia, X., Kong, B., Liu, Q., Liu, J. (2009): Physicochemical change and protein oxidation in porcine *Longissimus dorsi* as influenced by different freeze–thaw cycles. – *Meat Science* 83: 239–245.
- [32] Zhou, G. H., Xu, X. L., Liu, Y. (2010): Preservation technologies for fresh meat. A review. – *Meat Science* 86: 119–128.

APPENDIX

OUTPUTS FROM SPSS2017

ANOVA for independent variable: chlorine antimicrobials and abattoirs for SPC, spore count and psychrophilic bacterial count

SPC

Descriptive									
ABT	ATM2	N	Mean	Std. dev.	Std. error	95% confidence interval for mean		Min.	Max
						Lower bound	Upper bound		
A	1.00	12	1.33072	3.12856	.189034	1.1789	1.1545	1.1789	1.4545
A	2.00	12	2.5012	4.31611	.224595	1.1743	1.6590	2.1743	2.6590
A	3.00	12	2.98324	4.26046	.367299	1.4597	1.8736	2.4597	3.2396
	Pr.	.87	.0301	3.76552	.073	1.933	.004	.9822	.3236
	Total	36	2.45500	.00268	.66711	1.3957	1.1043	2.00	3.00
B	1.00	12	1.33072	2.12856	.19034	1.3789	1.1545	1.1789	1.545
B	2.00	12	2.6712	3.10611	.324595	1.7743	1.6590	2.1743	2.5590
B	3.00	12	2.92445	3.30046	.465299	1.3797	1.8736	2.4597	3.0391
	Pr.	.87	.02901	.34552	.303	1.633	.005	.9812	.13226
	Total	36	2.3510	4.1268	.86711	1.2157	1.2043	1.40	2.780
C	1.00	12	1.17204	2.89856	.179034	1.3289	1.2345	1.2739	1.2545
C	2.00	12	2.9212	3.71611	.52595	1.3443	1.4290	2.2243	2.1190
C	3.00	12	3.11324	3.62046	.26299	1.1957	1.3436	2.8507	3.2766
	Pr.	.87	.045201	.76552	.003	.933	.054	.9822	.2136
	Total	36	2.65500	4.00268	.66711	1.3057	1.2043	2.100	3.00

ANOVA						
	ATM2	Sum of squares	df	Mean square	F	Sig.
	Between groups	48.500	17	24.250	1.562	.025
	Within groups	512.250	35	15.523		
	Total	560.750	52			

1 = ASC, 2 = AQ.CL, 3 = CLO2, ATM = Antimicrobial intervention, ABT = Abattoir

SPORES

Descriptive									
ABT	ATM2	N	Mean	Std. dev.	Std. error	95% confidence interval for mean		Min.	Max
						Lower bound	Upper bound		
A	1.00	12	1.37233	3.12856	.191034	1.2789	1.6545	1.2789	1.2545
A	2.00	12	2.7212	4.21611	.324595	1.5543	1.8910	2.5743	2.4590
A	3.00	12	3.18324	4.23046	.417299	1.4976	1.9936	2.8597	3.1396
	Pr.	.87	.0501	3.36552	.093	1.7303	.024	.5822	.4246
	Total	36	2.67500	.03268	.46711	1.4157	1.2043	1.90	2.170
B	1.00	12	1.37202	2.33856	.29034	1.1789	1.2545	1.1289	1.745
B	2.00	12	3.0712	3.00611	.34595	1.2743	1.4390	2.1243	2.990
B	3.00	12	3.22445	3.29046	.40299	1.4797	1.9736	2.9197	3.4391
	Pr.	.87	.0521	.324552	.3503	1.833	.2005	.9212	.12226
	Total	36	2.3510	4.1268	.86711	1.2157	1.2043	1.40	3.780
C	1.00	12	2.7604	2.89856	.179034	1.3289	1.2345	1.2739	1.2545
C	2.00	12	3.0212	3.71611	.52595	1.3443	1.4290	2.2243	2.1190
C	3.00	12	3.21324	3.62046	.26299	1.1957	1.3436	2.8507	3.2766
	Pr.	.87	.045201	.76552	.003	.933	.054	.9822	.2136
	Total	36	2.15500	4.00268	.66711	1.3057	1.2043	2.100	3.00

ANOVA						
	ATM2	Sum of squares	df	Mean square	F	Sig.
	Between groups	55.300	17	124.250	1.62	.015
	Within groups	432.870	35	418.523		
	Total	487.170	52			

PSYCHROPHILES

Descriptive									
ABT	ATM2	N	Mean	Std. dev.	Std. error	95% confidence interval for mean		Min.	Max
						Lower bound	Upper bound		
A	1.00	12	1.37211	3.02856	.129034	1.8189	1.1445	1.1389	1.2345
A	2.00	12	2.6012	4.11611	.204595	1.6243	1.3590	2.1543	2.4490
A	3.00	12	2.98024	4.46046	.37299	1.3497	1.4736	2.3397	3.4396

	Pr.	.87	.0301	3.36552	.083	1.833	.124	.9722	.3636
	Total	36	2.45500	.01268	.44711	1.3457	1.223	2.30	3.20
B	1.00	12	1.51072	2.02856	1.19034	1.2989	1.2545	1.1389	1.445
B	2.00	12	2.5712.	3.30611	.624595	1.3343	1.4890	2.2743	2.4190
B	3.00	12	2.9215	3.10046	.565299	1.6597	1.5636	2.6597	3.0791
	Pr.	.87	.03009	.31552	.5303	1.233	.105	.9512	.13226
	Total	36	2.3510	4.1268	.86711	1.2157	1.2043	1.40	2.380
C	1.00	12	1.42204	2.59856	.179034	1.3289	1.2345	1.2739	1.2545
C	2.00	12	2.5212.	3.91611	.52595	1.3443	1.4290	2.2243	2.1190
C	3.00	12	3.09124	2.62046	.26299	1.1957	1.3436	2.8507	3.2766
	Pr.	.87	.045201	.76552	.003	.933	.054	.9822	.2136
	Total	36	2.65500	4.20268	.66711	1.3057	1.2043	2.150	3.33

ANOVA						
	ATM2	Sum of squares	df	Mean square	F	Sig.
	Between groups	79.100	17	44.250	1.62	.005
	Within groups	603.015	35	85.513		
	Total	682.110	52			

Post hoc tests

Homogeneous Subsets

SPC

ATM2 Duncan ^a					
ABT	ATM2	N	Subset for alpha = 0.05		
			1	2	3
A	3.00	12	2.98167		
A	2.00	12		2.50327	
A	1.00	12			1.33067
	Sig.	.025			
B	3.00	12	2.92017		
B	2.00	12		2.67027	
B	1.00	12			1.33017
	Sig.	.025			
C	3.00	12	3.11167		
C	2.00	12		2.92027	
C	1.00	12			1.36721
	Sig.	.025			

Means for groups in homogeneous subsets are displayed

^aUses harmonic mean sample size = 12.000

ANOVA for dependent variable: SPC, spore count and psychophilic bacterial count on brining levels in different abattoirs

SPC

		Descriptives							
ATM	PSC1	N	Mean	Std. dev.	Std. error	95% confidence interval for mean		Min.	Max.
						Lower bound	Upper bound		
A	.00	6	3.2333	.75277	.30732	.5432	1.7661	2.0433	3.6233
A	15.00	6	2.6667	.75277	.30732	.5565	1.4331	1.3767	2.9567
A	20.00	6	2.2733	.81650	.33333	.0986	1.8932	2.1765	2.1902
A	25.00	6	2.1133	1.4719	.60093	.7821	.98821	1.8886	2.3781
A	30.00	6	1.9166	.51640	.21082	.6786	1.7699	1.9127	2.8086
A	35.00	6	1.3336	.75227	.30732	.5698	1.9883	1.0767	1.9567
	Pr	.87	.00121	1.1912	.61911	1.987	1.8990	.04521	.1765
	Total	36	2.0166	3.7148	.35321	1.007	1.7236	1.2310	3.231
B	.00	6	3.0013	.63277	.32782	.4332	1.6961	2.3343	3.7633
B	15.00	6	2.3334	.72277	.31332	.6715	1.7731	1.4467	2.5467
B	20.00	6	2.1902	.91250	.41333	.4216	1.5932	2.2765	2.7702
B	25.00	6	2.0913	1.5719	.71093	.3891	1.7821	1.6667	2.4481
B	30.00	6	1.8916	.51640	.43182	.5092	1.6699	1.5127	2.7686
B	35.00	6	1.6713	.55177	.35732	.5923	1.7983	1.3767	1.5867
	Pr	.87	.00111	1.1912	.51914	.7637	1.8954	.07521	.1965
	Total	36	2.0166	3.3348	.58371	.4007	1.5636	1.4210	3.7631
C	.00	6	3.1333	.43237	.29732	.4332	1.6543	2.0433	3.9933
C	15.00	6	1.9667	.76271	.31402	.6665	1.5441	1.5767	2.7867
C	20.00	6	2.3333	.71650	.41933	.8986	1.9344	2.0765	2.5502
C	25.00	6	2.1123	.94719	.61593	.8621	1.4821	1.6986	2.6581
C	30.00	6	1.8726	.41620	.33482	.7686	1.5455	1.4427	2.3486
C	35.00	6	1.1726	.65237	.45732	.7598	1.7881	1.6767	1.9067
	Pr	.87	.00111	1.2912	.44321	.6987	1.7691	.06521	.1865
	Total	36	2.0166	3.1148	.4192	.6707	1.8236	1.410	3.731

ANOVA

PSC1	Sum of squares	df	Mean square	F	Sig.
Between groups	459.000	11	91.800	10.5420	.000
Within groups	524.000	30	.800		
Total	983.000	41			

Spores count

Descriptives								
ATM	PSC1	N	Mean	Std. dev.	Std. error	95% confidence interval for mean	Min.	Max.

						Lower bound	Upper bound		
A	.00	6	3.1833	.75277	.30732	.5432	1.7661	2.0433	3.6233
A	15.00	6	2.4737	.75277	.30732	.5565	1.4331	1.3767	2.9567
A	20.00	6	2.2833	.81650	.33333	.0986	1.8932	2.1765	2.1902
A	25.00	6	2.1033	1.4719	.60093	.7821	.98821	1.8886	2.3781
A	30.00	6	1.8916	.51640	.21082	.6786	1.7699	1.9127	2.8086
A	35.00	6	1.2336	.75227	.30732	.5698	1.9883	1.0767	1.9567
	Pr	.87	.02121	1.1912	.61911	1.987	1.8990	.04521	.1765
	Total	36	2.6236	3.7148	.55211	1.007	1.7236	1.2310	3.231
B	.00	6	3.2513	.63277	.32782	.4332	1.6961	2.3343	3.7633
B	15.00	6	2.4334	.72277	.31332	.6715	1.7731	1.4467	2.5467
B	20.00	6	2.2702	.91250	.41333	.4216	1.5932	2.2765	2.7702
B	25.00	6	2.1113	1.5719	.71093	.3891	1.7821	1.6667	2.4481
B	30.00	6	1.8816	.51640	.43182	.5092	1.6699	1.5127	2.7686
B	35.00	6	1.5613	.55177	.35732	.5923	1.7983	1.3767	1.5867
	Pr	.87	.03521	1.1912	.51914	.7637	1.8954	.07521	.1965
	Total	36	2.3166	3.3348	.44441	.4007	1.5636	1.4210	3.7631
C	.00	6	3.3033	.43237	.29732	.4332	1.6543	2.0433	3.9933
C	15.00	6	2.5227	.76271	.31402	.6665	1.5441	1.5767	2.7867
C	20.00	6	2.2533	.71650	.41933	.8986	1.9344	2.0765	2.5502
C	25.00	6	2.0823	.94719	.61593	.8621	1.4821	1.6986	2.6581
C	30.00	6	1.9026	.41620	.33482	.7686	1.5455	1.4427	2.3486
C	35.00	6	1.4726	.65237	.45732	.7598	1.7881	1.6767	1.9067
	Pr	.87	.03312	1.2912	.44321	.6987	1.7691	.06521	.1865
	Total	36	2.0106	3.1148	.4192	.6707	1.8236	1.410	3.731

ANOVA

PSC1	Sum of squares	df	Mean square	F	Sig.
Between groups	513.139	11	102.628	136.837	.000
Within groups	22.500	30	.750		
Total	535.639	41			

Psychrophilic

Descriptives

ATM	PSC1	N	Mean	Std. dev.	Std. error	95% confidence interval for mean		Min.	Max.
						Lower bound	Upper bound		
A	.00	6	3.9333	.75277	.30732	.5432	1.7661	2.0433	3.6233
A	15.00	6	3.1667	.75277	.30732	.5565	1.4331	1.3767	2.9567
A	20.00	6	2.8733	.81650	.33333	.0986	1.8932	2.1765	2.1902
A	25.00	6	2.2133	1.4719	.60093	.7821	.98821	1.8886	2.3781
A	30.00	6	1.5216	.51640	.21082	.6786	1.7699	1.9127	2.8086
A	35.00	6	1.1336	.75227	.30732	.5698	1.9883	1.0767	1.9567

	Pr	.87	.04121	1.1912	.61911	1.987	1.8990	.04521	.1765
	Total	36	2.3157	3.7148	.25213	1.007	1.7236	1.2310	3.231
B	.00	6	3.6013	.63277	.32782	.4332	1.6961	2.3343	3.7633
B	15.00	6	3.3334	.72277	.31332	.6715	1.7731	1.4467	2.5467
B	20.00	6	2.7902	.91250	.41333	.4216	1.5932	2.2765	2.7702
B	25.00	6	2.1413	1.5719	.71093	.3891	1.7821	1.6667	2.4481
B	30.00	6	1.6916	.51640	.43182	.5092	1.6699	1.5127	2.7686
B	35.00	6	1.0713	.55177	.35732	.5923	1.7983	1.3767	1.5867
	Pr	.87	.04411	1.1912	.51914	.7637	1.8954	.07521	.1965
	Total	36	2.0166	3.3348	.38371	.4007	1.5636	1.4210	3.7631
C	.00	6	4.1333	.43237	.29732	.4332	1.6543	2.0433	3.9933
C	15.00	6	2.9667	.76271	.31402	.6665	1.5441	1.5767	2.7867
C	20.00	6	2.4333	.71650	.41933	.8986	1.9344	2.0765	2.5502
C	25.00	6	2.0213	.94719	.61593	.8621	1.4821	1.6986	2.6581
C	30.00	6	1.4726	.41620	.33482	.7686	1.5455	1.4427	2.3486
C	35.00	6	1.1126	.65237	.45732	.7598	1.7881	1.6767	1.9067
	Pr	.87	.02611	1.2912	.44321	.6987	1.7691	.06521	.1865
	Total	36	2.0166	3.1148	.2192	.6707	1.8236	1.410	3.731

ANOVA

PSC1	Sum of squares	df	Mean	F	Sig.
Between groups	28.389	11	14.194	1.146	.003
Within groups	408.583	33	12.381		
Total	436.972	41			

Post hoc tests

Homogeneous subsets

SPC

BRINE1 Duncan^a

ATM	BRINE1	N	Subset for alpha = 0.05			
			1	2	3	4
A	35.00	6	1.33333			
A	30.00	6	1.92167			
A	25.00	6		2.11333		
A	20.00	6			2.27333	
A	15.00	6			2.67333	
A	.00	6				3.23167
	Sig.		.341	.341	.117	.112
B	35.00	6	1.67333			
B	30.00	6	1.89167			
B	25.00	6		2.09333		
B	20.00	6		2.19333		

B	15.00	6			2.3316	
B	.00	6				3.0017
	Sig.		.341	.341	.117	.112
C	35.00	6	1.17333			
C	30.00	6	1.87167			
C	25.00	6		2.12333		
C	20.00	6		2.33333		
C	15.00	6			1.97333	
C	.00	6				3.13167
	Sig.		.341	.341	.117	.112

Means for groups in homogeneous subsets are displayed

^aUses harmonic mean sample size = 6.000

ANOVA for dependent variable: SPC, spore count and psychrotrophic bacterial load for antimicrobial intervention and brining

Antimicrobials intervention

Descriptives									
ABT	ATM2	N	Mean	Std. dev.	Std. error	95% confidence interval for mean		Min.	Max.
						Lower bound	Upper bound		
SPC	1.00	12	1.1733	.93361	.84686	1.4694	2.1973	.063	1.00
SPC	2.00	12	2.4720	.77793	1.09059	2.0996	2.9004	1.50	2.50
SPC	3.00	12	2.3048	.77692	1.09030	1.1836	2.9831	2.50	2.50
	Pr.	.87	.023	.33729	.26711	.4457	.6674	.987	.0887
	Total	36	1.772	1.53340	.58890	4.2767	14.6678	7.00	21.00
Spores	1.00	12	1.4733	.45361	.23446	1.3294	2.9273	1.00	3.00
Spores	2.00	12	3.0107	.87293	1.5932	2.1236	3.1004	.605	2.70
Spores	3.00	12	3.4203	.76692	1.0370	1.2656	2.8651	1.09	3.50
	Pr.	.87	.044	1.8762	.4121	.6652	.8875	.876	.987
	Total	36	2.2072	1.61120	.36790	3.4267	7.6678	2.340	8.201
PSY	1.00	12	1.3933	.77461	.67186	1.3344	3.1373	.090	3.00
PSY	2.00	12	2.3040	.59193	.99059	1.4316	2.8704	1.00	1.52
PSY	3.00	12	3.0831	.68222	.43030	1.2836	1.6831	2.50	1.30
	Pr.	.87	.001	1.2331	.3211	.9982	.5542	.4333	.3244
	Total	36	2.0612	1.3140	1.0090	3.5437	6.3378	4.030	5.00

ANOVA						
	ATM2	Sum of s	df	Mean	F	Sig.
	Between groups	28.389	8	14.194	1.146	.003
	Within groups	408.583	26	12.381		
	Total	436.972	34			

Post hoc tests

Homogeneous subsets

ATM2 Duncan^a					
Microbe	ATM2	N	Subset for alpha = 0.05		
			1	2	3
	3.00	12	3.21		
SPC	2.00	12		2.25	
	1.00	12			1.17333
	Sig.		.003		
	3.00	12	3.42		
	2.00	12		3.01	
Spores	1.00	12			1.47
	Sig.		.003		
	3.00	12	3.08		
	2.00	12		2.30	
PSY	1.00	12			1.39
	Sig.		.003		

Means for groups in homogeneous subsets are displayed

^aUses harmonic mean sample size = 12.000

BRINING

Descriptives									
ABT Microbes	Brine	N	Mean	Std. dev.	Std. error	95% confidence interval for mean		Min.	Max.
						Lower bound	Upper bound		
SPC	.00	6	3.33333	.93361	.84686	1.4694	2.1973	.063	1.00
SPC	15.00	6	2.87267	.77793	1.09059	2.0996	2.9004	1.50	2.50
SPC	20.00	6	2.63167	.77692	1.09030	1.1836	2.9831	2.50	2.50
SPC	25.00	6	2.32223	.66792	.44592	2.0882	2.6551	0.87	3.12
SPC	30.00	6	1.76333	1.2331	.67552	1.7763	2.0898	1.45	3.08
SPC	35.00	6	1.57333	.98872	.43552	0.8778	1.6652	2.45	2.99
	Pr.	.87	.02311	.33729	.26711	.4457	.6674	.987	.0887
	Total	36	11.1944	1.53340	.58890	4.2767	14.6678	7.00	21.00
Spore	.00	6	3.25012	.45361	.23446	1.3294	2.9273	1.00	3.00
Spore	15.00	6	2.43771	.87293	1.5932	2.1236	3.1004	.605	2.70
Spore	20.00	6	2.12111	.76692	1.0370	1.2656	2.8651	1.09	3.50
Spore	25.00	6	2.11066	.93361	.84686	1.4694	2.1973	.063	1.00
Spore	30.00	6	1.87122	.77793	1.09059	2.0996	2.9004	1.50	2.50
Spore	35.00	6	1.56233	.77692	1.09030	1.1836	2.9831	2.50	2.50
	Pr.	.87	0.044	1.2331	.3211	.9982	.5542	.4333	.3244
	Total	36	11.6772	1.3140	1.0090	3.5437	6.3378	4.030	5.00
PSC	.00	6	3.63122	.77461	.67186	1.3344	3.1373	.090	3.00
PSC	15.00	6	3.32122	.59193	.99059	1.4316	2.8704	1.00	1.52

PSC	20.00	6	2.79341	.68222	.43030	1.2836	1.6831	2.50	1.30
PSC	25.00	6	2.13021	.45361	.23446	1.3294	2.9273	1.00	3.00
PSC	30.00	6	1.69872	.87293	1.5932	2.1236	3.1004	.605	2.70
PSC	35.00	6	1.05782	.76692	1.0370	1.2656	2.8651	1.09	3.50
	Pr.	.87	0.001	1.8762	.4121	.6652	.8875	.876	.987
	Total	36	12.7662	1.61120	.36790	3.4267	7.6678	2.340	8.201

ANOVA

BRINE

	Sum of s	df	Mean	F	Sig.
Between groups	28.389	8	14.194	1.146	.003
Within groups	408.583	26	12.381		
Total	436.972	34			

Post hoc tests

Homogeneous subsets

BRINE1

Duncan^a

Microbes	BRINE	N	Subset for alpha = 0.05			
			1	2	3	4
SPC	35.00	6	1.57333			
SPC	30.00	6	1.76333			
SPC	25.00	6		2.32333		
SPC	20.00	6			2.6311	
SPC	15.00	6			2.8711	
SPC	.00	6				3.3333
	Sig.		.325	.106	.325	1.000
Spores	35.00	6	1.56112			
Spores	30.00	6	1.87122			
Spores	25.00	6		2.11322		
Spores	20.00	6		2.11876		
Spores	15.00	6			2.42981	
Spores	.00	6				3.6321
	Sig.		.145	.056	.325	1.000
PSC	35.00	6	1.06211			
PSC	30.00	6	1.70212			
PSC	25.00	6		2.13321		
PSC	20.00	6		2.40121		
PSC	15.00	6			3.32112	
PSC	.00	6				3.63112
	Sig.		.325	.106	.325	1.000

Means for groups in homogeneous subsets are displayed

^aUses harmonic mean sample size = 6.000

Optimization outputs

Curve fit

Quadratic for SPC

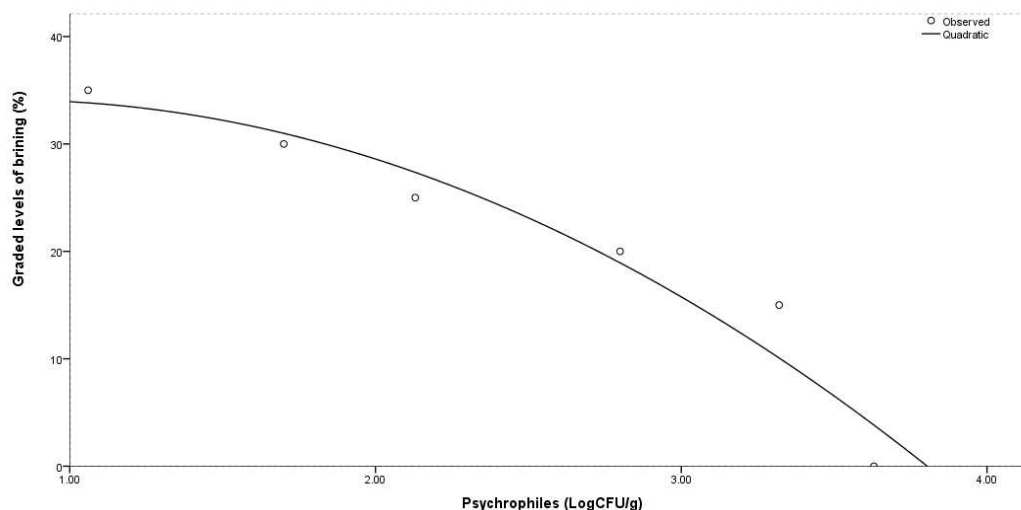
Model summary			
R	R	Adjusted R	Std. error of the estimate
.968	.938	.896	3.999

The independent variable is psychrophiles

ANOVA					
	Sum of s	df	Mean	F	Sig.
Regression	722.869	2	361.434	22.606	.016
Residual	47.964	3	15.988		
Total	770.833	5			

The independent variable is psychrophiles

Coefficients					
	Unstandardized coefficients		Standardized coefficients	t	Sig.
	B	Std. Error	Beta		
Psychrophiles	5.909	12.090	.470	.489	.659
Psychrophiles ** 2	-3.748	2.518	-1.430	-1.488	.233
(Constant)	31.774	13.013		2.442	.092



```
* Curve Estimation.
TSET NEWVAR=NONE.
CURVEFIT
/VARIABLES=Levels WITH spores
/CONSTANT
/MODEL=QUADRATIC
/PRINT ANOVA
/PLOT FIT.
```

Curve fit

Quadratic for spores

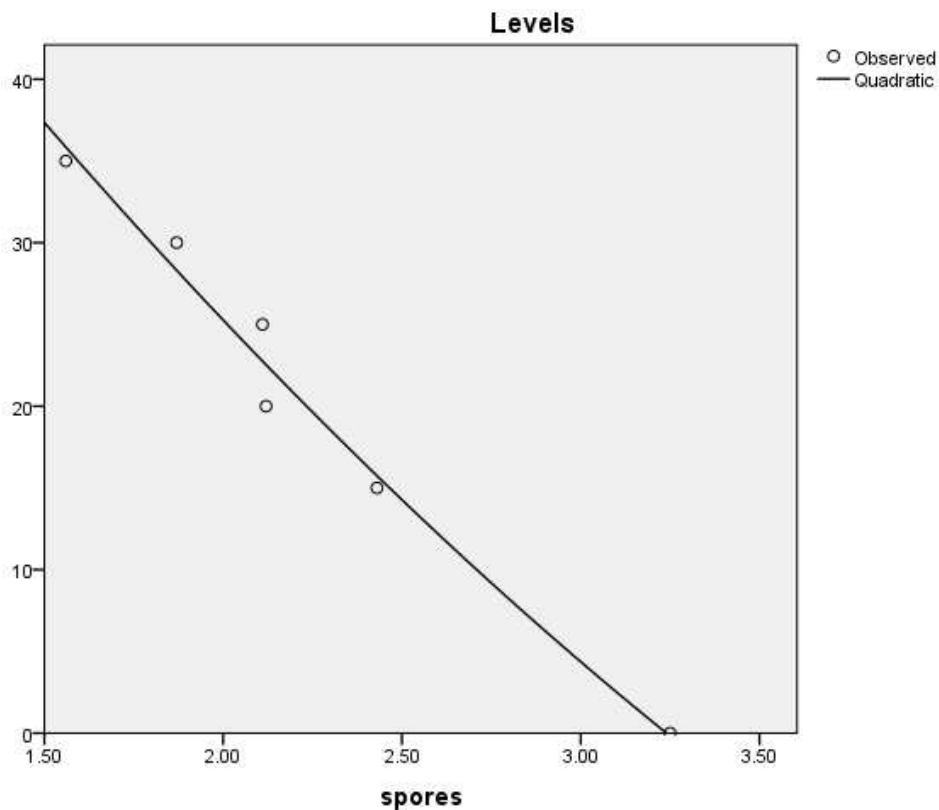
Model Summary			
R	R	Adjusted R	Std. Error of the Estimate
.990	.980	.966	2.281

The independent variable is spores

ANOVA					
	Sum of s	df	Mean	F	Sig.
Regression	755.221	2	377.611	72.560	.003
Residual	15.612	3	5.204		
Total	770.833	5			

The independent variable is spores

Coefficients					
	Unstandardized coefficients		Standardized coefficients	t	Sig.
	B	Std. error	Beta		
spores	-31.793	15.683	-1.487	-2.027	.136
spores ** 2	2.178	3.185	.501	.684	.543
(Constant)	80.142	18.453		4.343	.023



```
* Curve Estimation.
TSET NEWVAR=NONE.
CURVEFIT
/VARIABLES=Levels WITH SPC
/CONSTANT
/MODEL=QUADRATIC
/PRINT ANOVA
/PLOT FIT.
```

Curve fit

Quadratic for psychrophilic

Model summary

R	R	Adjusted R	Std. error of the estimate
.994	.988	.980	1.773

The independent variable is SPC

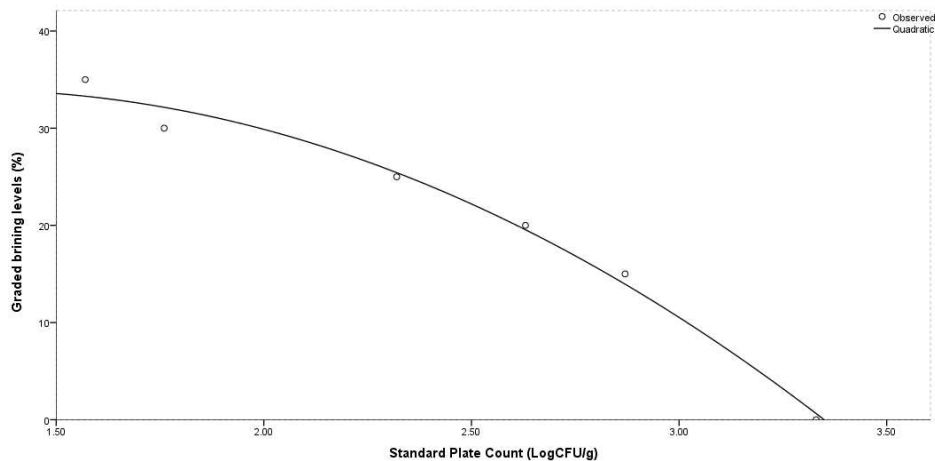
ANOVA

	Sum of s	df	Mean	F	Sig.
Regression	761.401	2	380.700	121.082	.001
Residual	9.432	3	3.144		
Total	770.833	5			

The independent variable is SPC

Coefficients

	Unstandardized coefficients		Standardized coefficients	t	Sig.
	B	Std. Error	Beta		
SPC	20.578	11.093	1.110	1.855	.161
SPC ** 2	-7.986	2.286	-2.090	-3.494	.040
(Constant)	20.670	12.794		1.616	.205



BIOLOGICAL, SEROLOGICAL AND MOLECULAR DETECTION OF *TOMATO MOSAIC VIRUS* INFECTING PEPPER PLANTS FROM TURKEY

ÇULAL-KILIÇ, H.

*Department of Plant Protection, Faculty of Agricultural Sciences and Technologies, Isparta
Applied Sciences University, Isparta, Turkey
(e-mail: handankilic@isparta.edu.tr)*

(Received 3rd Jan 2019; accepted 27th Feb 2019)

Abstract. This study was carried out to detect the presence *Tomato mosaic virus* (ToMV) by biological, serologic and molecular methods in the pepper production areas in Burdur and Denizli provinces. Symptoms related with virus infections on the pepper plants were observed during the surveys. Mechanical inoculation studies, DAS-ELISA (Double-antibody sandwich enzyme linked immunosorbent assay) tests, IC-RT-PCR (Immunocapture Reverse transcription polimerase chain reaction) studies were carried out during the work carried out to define the virus. The plants collected from the field that were suspicious with regards to being infected with the virus were first tested by the ELISA method. It was determined that 10 of the 209 tested samples were infected with ToMV. The samples that gave positive results during ELISA tests were used in the mechanical inoculation studies. Symptoms were observed in the indicator plants within a period of 7-10 days. 20 plant samples that gave negative ToMV values in the ELISA tests but had absorbance values close to positive along with the 10 samples that were tested as positive in the DAS-ELISA were used in the IC-RT-PCR method. All of the 30 samples produced expected amplification size of band with 318 bp as observed on agarose gel electrophoresis.

Keywords: *vegetables viruses, identification, DAS-ELISA, IC-RT-PCR*

Introduction

Pepper (*Capsicum annum* L.) is a member of the Solanaceae family and is a hot and mild climate plant. The homeland of pepper is stated to be tropical South America and especially Brazil. Pepper was brought England from Spain in the 1500s from where it spread to the rest of Europe. China is the leader in worldwide pepper production as of 2016 with 13.189.303 tons. It is followed by Mexico with 2.335.560 tons whereas Turkey is ranked three with 1.986.700 tons. Turkey is followed by Indonesia and USA (TUIK, 2016; FAO, 2016).

Pepper is rich in vitamins A and C. Peppers can be used as fresh or as canned, in pastes, as pickled, in concentrated tomato soups, ready soups, in making powdered or chili peppers, in paint industry, pharmaceutical industry etc. (Anonymous, 2017).

Burdur and Denizli are important in vegetable production due to their soil and climate properties as well as irrigation options. Especially Kale district of Denizli cultivates good quality peppers.

Significant efficiency losses occur in pepper cultivation due to wrong or insufficient agricultural applications as well as biotic and abiotic disease factors. There are many fungi, bacteria and virus based diseases in the vegetable cultivation areas which limit cultivation. Virus diseases are significant among these factors due to their chemical and physical structures, sizes, types of infection, symptom formation, transport and the lack of an effective struggle against them (Agrios, 1997).

Kenyon et al. (2014) have stated that there are about 68 viruses that cause diseases in peppers. The viruses that are observed in pepper which cause significant losses in

efficiency are as follows: *Tobacco mosaic virus* (TMV), *Tomato mosaic virus* (ToMV), *Cucumber mosaic virus* (CMV), *Potato Y virus* (PVY), *Tomato spotted wilt virus* (TSWV), *Alfalfa mosaic virus* (AMV), *Pepper mild mottle* (PMMoV), *Pepper vein mottle virus* (PVMV), *Pepper ringspot virus* (PRSV) (Ryu et al., 2009; Arogundade et al., 2012).

ToMV belongs to the Tobamovirus type. Virus includes linear single helical RNA genome. It has a rod shaped particle structure. The virus has a length of about 300 nm and a width of about 18 nm. Virus particles consist of 5% nucleic acid; 95% protein. The genome is single pieced. ToMV can be spread between plants on workers' hands, tools and clothes with normal activities such as plant tying, harvest. Seed can be infected and pass the virus to the plant. *Tomato mosaic virus* can survive in infected root debris in the soil for up to two years (Silva et al., 2011).

TMV, ToMV, CMV, PMMoV, TSWV, PVY, AMV have been determined during the studies carried out related with the diseases of peppers in our country (Şevik, 2011; Sertkaya, 2012; Özdağ and Sertkaya, 2017; Geyik, 2017).

The existence of virus diseases, their harms and their symptoms vary in accordance with the type of the pepper plant as well as the environmental conditions. That is why, first the detection of the viruses in the culture plant that is cultivated should be made in order to minimize the damages caused by virus disease and to develop control methods. It is not correct to carry out diagnosis based only on observation for virus detection. In recent years, PCR methods have been developed in parallel with molecular techniques which enable sensitive and accurate diagnosis of pepper viruses from plant tissues (Jacobi et al., 1998; Vinayarani et al., 2011; Kumar et al., 2011; Gümüş and Paylan, 2013).

The aim of this study is to determine ToMV in the pepper production areas of Burdur and Denizli provinces by DAS-ELISA, mechanical inoculation and IC-RT-PCR method.

Materials and methods

Plant material

The main material of this study consists of 209 leaf samples (115 samples from Denizli + 84 samples from Burdur) which show virus disease symptoms and which are thought to be infected with virus. The samples were collected from the pepper production areas (8 locations) during June-September in 2012-2013. The samplings were made from plants with leaf deformation, leaf curling, necrosis formation on the leaves, mosaic symptoms and stunting symptoms. There is no difference between sampling sites during surveys. The samples were labeled inside polyethylene bags and brought to the laboratory in ice boxes to be preserved in deep freezer (-20 °C) until the required tests were carried out.

Serological test method (DAS-ELISA)

ToMV-DAS-ELISA (BIOREBA AG, Switzerland) commercial kit was used in the study. The application were performed were performed as described by Clark and Adams (1977).

Accordingly, 200 µl of IgG was added to each of the hole of ELISA plate, which was diluted in the coating buffer at a ratio of 1:1000 which was then kept at +4 °C for

overnight. Afterwards the ELISA plates were washed with the washing buffer. The washing was repeated 3 times. The plant extracts prepared by diluting at a ratio of 1/10 using extraction buffer was added to each hole as 200 µl and was kept overnight at +4 °C. Washing was repeated the next day. After washing process, conjugated antibody was diluted at a ratio of 1:1000 in the conjugate buffer, 200 µl was added to each hole and was kept at 37 °C for 4 h. After the washing process, each substrate prepared as 1 mg/ml in the substrate solution was added to each hole as 200 µl and was left to wait at room temperature. Finally, p-nitrophenyl phosphate in diethanolamine substrate buffer; (pH: 9.8) was added and 405 nm values were measured at a microplate reader VersaMax microplate reader (Molecular Devices, Sunnyvale, CA) after 60-120 min. Samples with absorbance values greater than twice the mean absorbance reading of healthy controls obtained from (Bioreba, Switzerland) were considered positive for ToMV (Şevik, 2016).

Mechanical inoculation studies

Mechanical inoculation was carried out on test plants during the 3-4 leaf stage using the samples that yielded positive reaction as a result of the ELISA tests of ToMV infection suspicious leaf samples collected during the survey. To this end, plant tissues acquired from ToMV infested plants were prepared at a ratio of 1:1 (W/V) in 0.01 M phosphate buffer solution (pH; 7.2) including 0.01% 'lik 2-Mercaptoethanol and was inoculated to the leaves of the test plants. *Capsicum annuum*, *Chenopodium amaranticolor*, *Nicotiana glutinosa*, *Nicotiana tabacum* L. "Xanthii", *Nicotiana tabacum* "White Burley" were used as test plants (Aghamohammadi et al., 2013). Plant growth cabins at 18- 20 °C temperature were used to observe symptoms in test plants. Mechanical inoculation studies were repeated until symptoms were seen.

Molecular test method (IC-RT-PCR)

Immunocapture-RT-PCR method was used as molecular test method since it is more advantageous due to the direct usage of plant extracts after mixing with water without any need for nucleic acid isolation. Antibodies specific to the virus were used, viral forms in the crushed plant material were captured immunologically and were used in viral RNA amplification. The DAS-ELISA positive samples (10 samples) and the samples with absorbance values close to positive (20 samples) were used in molecular studies for a total of 30 samples. In the Immunocapture-RT-PCR method:

- PCR tubes were coated with the antibody specific to the virus during ELISA studies and were left for incubation at 4° C for the overnight.
- Tubes were washed with PBS-Tween Buffer for 3 times after incubation and they were left to wait in the deep freezer until molecular studies.
- During molecular studies.
- plant tissue extract, as prepared above for ELISA, was loaded into the antibody-coated tubes and incubated. The samples were left for incubation at +4 °C overnight.
- Tubes were washed with PBS-Tween Buffer for 3 times after incubation and were also washed once with sterile pure water.
- RT-PCR mixture was added to these PCR tubes afterwards.

RT-PCR was performed using a One Step RT-PCR Kit (Bio Basic, Canada Inc). Reverse transcription was performed in a 50 µl reaction mixture containing, 21 µl H₂O, 25 µl 2x1 PrimeScript One Step RT-PCR buffer (containing dNTP mixture, One step Enhancer solution), 2 µl Prime Script 1 step enzyme mix, 1 µl 20 Mm primers. RT-PCR of ToMV replicase gene portion of approximately 318 bp were amplified.

An approximately 318 bp DNA fragment was amplified from ToMV-infected plants by IC-RT-PCR with a ToMV specific primer pairs. Oligonucleotide primer sequences were used to detect ToMV reported by Kumar et al. (2011):

F-5-CGAGAGGGGCAACAAACAT-3

R-5-ACCTGTCTCCATCTCTTTGG-3

Thermocycling (Techne-TC-5000) was programmed as 1 cycle at 50 °C for 30 min, at 94 °C for 2 min and 40 cycles at 94 °C for 30 s, at 54 °C for 30 s, at 72 °C for 30 s and finally at 72 °C for 1 min.

Pepper plant leaves infected with ToMV in DAS-ELISA studies and ToMV-infected *C. amaranticolor* and *Capsicum annuum* plant leaves were used as positive control in molecular studies; whereas healthy pepper plant leaves were used as negative control.

IC-RT-PCR products were separated on a 1% agarose gel by electrophoresis (Bio-Rad) and stained in a 0.5 µg/ml ethidium bromide solution. An image was captured after the exposure of ethidium-bromide-stained gel on a transilluminator with a digital camera (UVP-Doc-It). 100 bp DNA ladder (Thermoscientific, GeneRuler) was used as marker.

Results

Symptoms such as leaf deformation, leaf curling, decoloring of the leaves, necrosis formation on the leaves, mosaic symptoms and stunting symptoms have been observed and these plants have been photographed during the survey (*Fig. 1*).

Firstly, ELISA tests were carried out on the leaf samples collected from 209 plants with virus infection symptoms in order to determine the existence of ToMV. The results showed that 10 out 209 samples were infected with ToMV. Whereas ToMV infection rate for 209 of the collected samples was determined as 4.78%.

Mechanical inoculation studies were carried out using ToMV infected leaves that were detected after ELISA tests. Chlorotic local lesion symptoms were observed in *Chenopodium amaranticolor* of the plants one week after inoculation; whereas local lesion symptoms were observed at *Nicotiana glutinosa* 10 days after inoculation and the symptoms have been photographed (*Figs. 2 and 3*). On the other hand, *Capsicum annuum* directly developed systemic symptoms as mosaic, stunting (Cherian and Muniyappa, 1998; Aghamohammadi et al., 2013; Ullah et al., 2017) (*Fig. 4*). The presence of ToMV was further confirmed through mechanical inoculation and IC-RT-PCR.

IC-RT-PCR method is one of the molecular methods that is widely used in many studies to detect virus diseases in plants and this was used on pepper samples to detected the ToMV. 10 samples yielded positive results as a result of the testing of the 209 leaf samples collected from the pepper cultivation area by DAS-ELISA. At this stage of the study, 20 isolates which yielded negative results in the DAS-ELISA tests but which had absorbance values close to positive along with 10 samples that yielded positive results in DAS-ELISA were used in the IC-RT-PCR studies which is more sensitive in comparison to ELISA. It was determined a result of the RT-PCR works on

plant samples that all of the samples yielded the expected band specific to ToMV (318 bp) and that all of the 30 samples (100%) were infected with ToMV. No fragment was amplified from negative control (Figs. 5, 6 and 7).



Figure 1. Mosaic and deformation symptoms observed in pepper leaves



*Figure 2. Necrotic local lesion on *Nicotiana glutinosa**

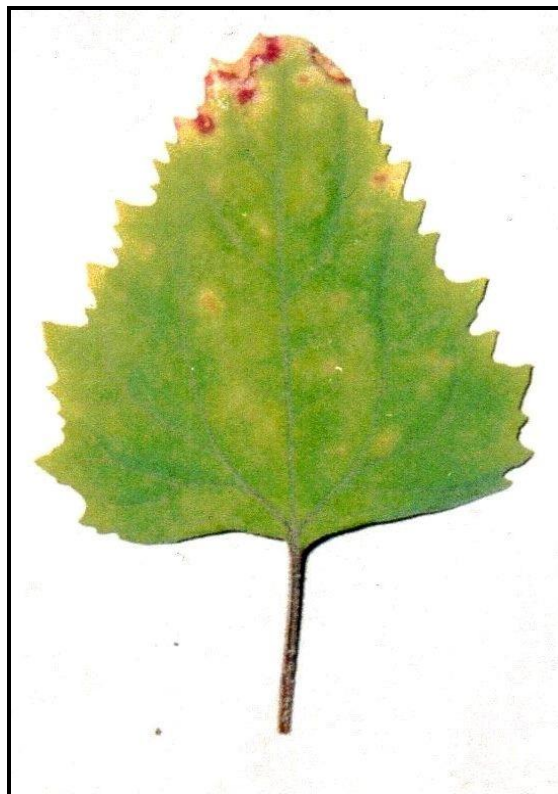


Figure 3. Chlorotic local lesion on *Chenopodium amaranticolor*



Figure 4. Mosaic and deformation on *Capsicum annuum*

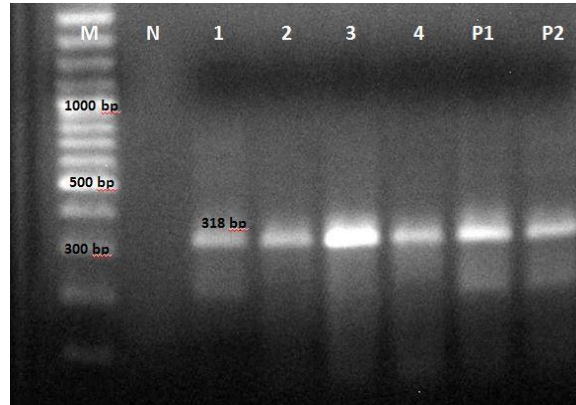


Figure 5. Detection of *Tomato mosaic virus* by IC-RT-PCR. M: 100 bp DNA ladder; N: healthy pepper. Lane 1-4: Sample of pepper plants; P1: ToMV- infected *C. amaranticolor*; P2: ToMV- infected pepper

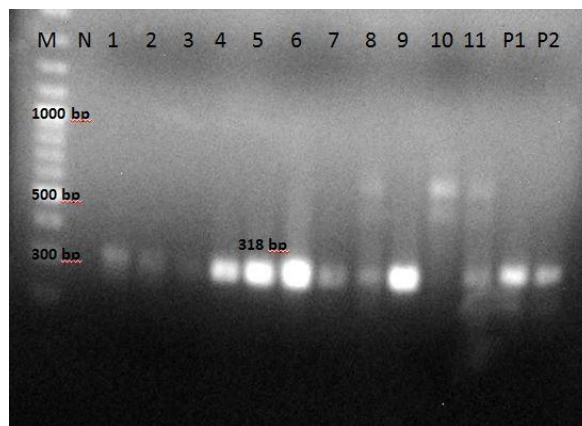


Figure 6. Detection of *Tomato mosaic virus* by IC-RT-PCR. M: 100 bp DNA ladder; N: healthy pepper. Lane 1-11: Sample of pepper plants; P1: ToMV- infected *C. amaranticolor*; P2: ToMV- infected pepper

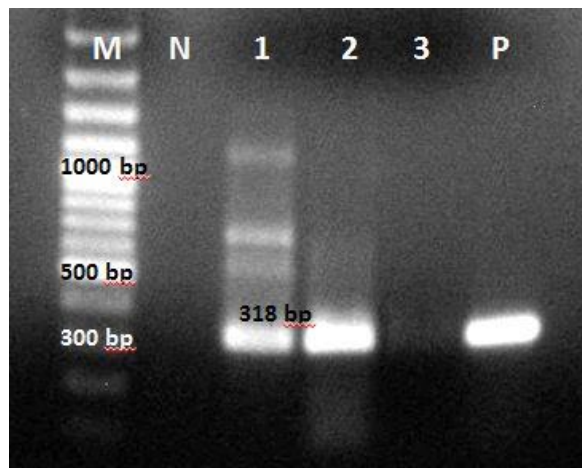


Figure 7. Detection of *Tomato mosaic virus* by IC-RT-PCR. M: 100 bp DNA ladder; N: healthy pepper. Lane 1-2: Sample of pepper plants; P: ToMV- infected *C. amaranticolor*; Lane 3: healthy *C. amaranticolor*

Discussion

Virus based diseases are quite significant due to the facts that their control is mostly hard and indeed impossible, that there is no effective chemicals and that the viruses spread far and wide via vector insects.

It is essential to first detected the viruses found in the cultivated culture plant in order to minimize the damages due to viruses and to develop control strategies. The symptomatologic studies that will be carried out based on observation for defining the viruses should be supported with serologic and molecular tests that will be carried out. It is possible to take precautions for the control of this virus disease only after carrying out the diagnosis of this factor. Biological, serological, and molecular assays have generally been used for identification of plant viruses. Although ELISA is preferred assay for routine virus detection, RT-PCR has increasingly been used for detection and identification of viruses due to higher level of sensitivity (Almeida et al., 2018). Among the molecular methods, the most widely used is the RT-PCR (Liu et al., 2014). The IC-RT-PCR technique has as an advantage the fact that crushing of the plants for the viral RNA extraction is unnecessary, since only the viral particles that lie on the outside are captured by the specific antiserum (Mulholland, 2009). Another advantage of IC-RT-PCR, compared to RT-PCR, would be the speed of testing. The RNA obtained by IC-RT-PCR is performed in fewer steps when compared with RT-PCR (Chikh-Ali and Karasev, 2015; Çulal-Kılıç et al., 2017).

The mosaic, contraction in the nervures, spotting, leaf and fruit deformations as well as necrosis formation on the leaves observed during the surveys carried out at Burdur and Denizli pepper cultivation areas were in accordance with the symptoms reported in previous studies mosaic symptoms and stunting symptoms (Kumar et al., 2011; Svoboda and Svobodova-Leisova, 2012).

The symptoms that occur in *Capsicum annuum*, *Chenopodium amaranticolor* and *Nicotiana glutinosa* as a result of mechanical inoculation put forth the existence of ToMV in leaf samples collected. The acquired symptoms were in accordance with previous study results and supports the view that the virus can be ToMV (Aghamohammadi et al., 2013; Ullah et al., 2017).

However, it is a fact that sometimes symptoms cannot be observed in mechanical inoculation method due to various reasons. That is why, detection studies should be supported with more sensitive methods since the use of this method by itself might lead to errors.

The positive reactions acquired during the serologic test carried out to diagnose the virus signify the existence of ToMV in the plant. The ELISA tests used in the diagnosis work for many plant viruses have widely been used by researchers (Geyik, 2017; Kapoor et al., 2018). The fact that it is fast, sensitive, economical and reliable makes this method a preference (Vinayarani et al., 2011; Almeida et al., 2018).

It has been found in this study as a result of carrying out DAS-ELISA tests on the leaf samples that 10 of the 209 samples were infected with ToMV. ToMV infection has been detected in studies carried out at various parts of our country (Gümüş and Paylan, 2013; Özdağ and Sertkaya, 2017).

Özdağ and Sertkaya and (2017) has carried out survey studies to determine the virus diseases in pepper areas in Hatay province and it has been found as a result that of the 303 plant samples, CMV, PLRV, PVX, PVY, PMMoV, PepMoV, ToMV and TSWV. DAS-ELISA method has been used to detect the viruses.

20 samples that yield absorbance values close to positive and 10 samples that yield positive results DAS-ELISA have been handled in IC-RT-PCR work. In these studies, base pairs that amplify the 318 bp of ToMV and the replicase gene have been used. As a result, expected band was observed in all of the 30 isolates (%100) which put forth that the samples are infected with ToMV. The results of this study were in accordance with the study by Kumar et al. (2011) carried out using primer pairs designed for ToMV. The same researchers have acquired a 318 bp band in molecular studies. Similarly, Gümüş and Paylan (2013); Almeida et al. (2018) have used IC-RT-PCR method to determine the presence of ToMV in their studies.

10 of the 209 samples used in DAS-ELISA tests were determined to be infected with ToMV, whereas it was determined in IC-RT-PCR studies that all 30 samples (%100) were infected with ToMV putting forth that PCR method is much more sensitive with respect to ELISA especially when virus density is low. IC-RT-PCR showed greater sensitivity in detecting to ToMV.

According to results of symptom inspections on plants, IC-RT-PCR, DAS-ELISA and mechanical inoculation studies, ToMV in Burdur and Denizli provinces was caused by more than one agent. ToMV was not detected in all the symptomatic samples, it is thought those symptoms were also caused by other viruses. Studies on those potential viruses must be carried out to find out the causal virus of pepper in this region. 179 pepper samples that showed virus-like symptoms did not react with the antiserum of ToMV used in serological test and IC-RT-PCR method indicating that they were possibly infected with other pepper viruses.

Conclusions

In this study, the existence of ToMV in the pepper production areas at Burdur and Denizli provinces have been found out using biological, serological and molecular methods. Previous studies also identified TSWV as common virus infecting pepper (Çulal-Kılıç et al., 2017) in same zone. ToMV in peppers in this region were firstly identified in this study.

REFERENCES

- [1] Aghamohammadi, V., Rakhshandehroo, F., Shams-Bakhsh, M., Palukaitis, P. (2013): Distribution and genetic diversity of tomato mosaic virus isolates In Iran. – *Plant Pathol J* 95(2): 339-347.
- [2] Agrios, G. N. (1997): *Plant Pathology*. – Academic Press Inc., New York.
- [3] Almeida, J. E. M., Figueira, A. R., Duarte, P. G., Lucas, M. A., Alencar, N. E. (2018): Procedure for detecting tobamovirus in tomato and pepper seeds decreases the cost analysis. – *Bragantia* 77(4): 590-598.
- [4] Anonymous (2017): <http://megep.meb.gov.tr>. – Accessed on 25 Oct 2017.
- [5] Arogundade, O., Balogun, O. S., Kareem, K. T. (2012): Occurrence and distribution of pepper veinal mottle virus and cucumber mosaic virus in pepper in Ibadan, Nigeria. – *Virology* 19: 79.
- [6] Cherian, S., Muniyappa, N. (1998): ELISA based survey and host range of Tomato mosaic tobamovirus. – *Indian J Virol* 14: 65-69.
- [7] Chikh-Ali, M., Karasev, A. V. (2015): Immunocapture-Multiplex RT-PCR for the Simultaneous Detection and Identification of Plant Viruses and Their Strains: Study Case,

- Potato Virus Y (PVY). – In: Lacomme, C. (ed.) Plant Pathology. Methods in Molecular Biology. Humana Press, New York, pp. 177-186.
- [8] Clark, M. F., Adams, A. N. (1977): Characteristics of the microplate method of enzyme linked immunosorbent assay for the detection of plant viruses. – *J Gen Virol* 34: 475-483.
- [9] Çulal Kiliç, H., Yardımcı, N., Bal, A., Güneş, A., Deniz, F. (2017): Sensitive detection of *tomato spotted wilt virus* from pepper plants by DAS-ELISA, RT-PCR and IC-RT-PCR. – *Rom Biotech Lett* 22(5): 12934-12939.
- [10] FAO (2016): <http://faostat.fao.org/site/567/Desktop>. – Accessed on 11 Apr 2016.
- [11] Geyik, S. (2017): Investigation on tomato virus diseases of virus in tomato growing areas in the Marmara Region of Turkey. – MSc Thesis, Namık Kemal University, Graduate School of Natural and Applied Sciences, Department of Plant Protection.
- [12] Gümüş, M., Paylan, I. C. (2013): Detection of viruses in seeds of some vegetables by reverse transcriptase polymerase chain reaction (RT-PCR). – *Afr J Biotechnol* 12(25): 3891-3897.
- [13] Jacobi, V., Bachand, G. D., Hamelin, R. C., Castello, J. D. (1998): Development of multiplex Immunocapture RT-PCR assay for detection and differentiation of tomato and tobacco mosaic viruses. – *J Virol Methods* 74: 167-178.
- [14] Kapoor, S., Sharma, A., Handa, A. 2018. Correlation between symptoms and ELISA for the detection of cucumber mosaic virus in bell pepper. – *Int J Curr Microbiol App Sci* 7(6): 400-406.
- [15] Kenyon, L., Kumar, S., Tsai, W. S., Hughes, J. (2014): Virus diseases of peppers (*Capsicum* spp.) and their control. – *Adv Virus Res* 90: 297-354.
- [16] Kumar, S., Udaya Shankar, A. C., Nayaka, S. C., Lund, O. S., Prakash, H. S. (2011): Detection of Tobacco mosaic virus and Tomato mosaic virus in pepper and tomato by multiplex RT-PCR. – *Lett Appl Microbiol* 53: 359-363.
- [17] Liu, H. W., Luo, L. X., Li, J. Q., Liu, P. F., Chen, X. Y., Hao, J. J. (2014): Pollen and seed transmission of *Cucumber green mottle mosaic virus* in cucumber. – *Plant Pathol* 63: 72-77.
- [18] Mulholland, V. (2009): Immunocapture-PCR for Plant Virus Detection. – In: Burns, R. (ed.) Plant Pathology. – Methods in Molecular Biology, Totowa, Humana Press, pp. 183-192.
- [19] Özdağ, Y., Sertkaya, G. (2017): Investigation on viruses causing yellowing disease in pepper in Hatay-Turkey. – *Journal of Agricultural Faculty of Mustafa Kemal University* 22(1): 16-22.
- [20] Ryu, J. G., Ko, S. J., Lee, Y. H., Kim, M. K., Kim, K. H., Kim, H. T., Choi, H. S. (2009): Incidence and distribution of virus diseases on paprika (*Capsicum annuum* var. *grossum*) in Jeonnam province of Korea. – *Plant Pathol J* 25(1): 95-98.
- [21] Sertkaya, G. (2012): Studies on the *Tomato mosaic virus* (ToMV) on red pepper production areas in Hatay, Turkey. – 9th National Symposium on Vegetable, 12-14 September, Konya.
- [22] Silva, P. P., Freitas, R. A., Nascimento, W. M. (2011): Detection of *Tomato mosaic virus* in tomato seed and treatment by thermotherapy. – *Acta Hort* 917: 303-308.
- [23] Svoboda, J., Svobodová-Leišová, L. (2012): Occurrence of viruses on pepper plantations in the Czech Republic. – *Hortic Sci* 39(3): 139-143.
- [24] Şevik, M. A. (2011): Occurrence of pepper mild mottle virus in greenhouse grown pepper (*Capsicum annuum* L.) in the West Mediterranean region of Turkey. – *Afr J Biotechnol* 10(25): 4976-4979.
- [25] Şevik, M. A. (2016): *Turnip mosaic virus* infecting kale plants in Ordu, Turkey. – *Phyton Int J Exp Bot* 85: 231-235.
- [26] Tuik (2016). Crop Production Statistics. Turkish Statistical Institute. Turkey. – <http://tuikrapor.tuik.gov.tr/reports>. Accessed on 04 May 2016.

- [27] Ullah, N., Ali, A., Ahmad, M., Fahim, M., Din, N., Ahmed, F. (2017): Evaluation of tomato genotypes against tomato mosaic virus (ToMV) and its effect on yield contributing parameters. – Pak J Bot 49(4): 1585-1592.
- [28] Vinayarani, G., Madhusudhan, K. N., Deepak, S. A., Niranjand, S. R., Prakash, H. S. (2011): Detection of mixed infection of tobamoviruses in tomato and bell pepper by using RT-PCR and duplex RTR-PCR. – Int J Plant Pathol 2(2): 89-95.

THE IMPACT OF FLOODPLAIN VEGETATION ON THE EROSION-SEDIMENTATION PROCESSES IN FLUVISOLS DURING FLOOD EVENTS

BELČÁKOVÁ, I.¹ – VOJTKOVÁ, J.^{2*} – PAUKOVÁ, Ž.³ – OFFERTÁLEROVÁ, M.¹

¹*Faculty of Ecology and Environmental Sciences, Technical University in Zvolen
T. G. Masaryka 24, 960 53 Zvolen, Slovakia
(phone: +421-455-206-492; fax: +421-455-206-279)*

²*Faculty of Civil Engineering, Slovak University of Technology in Bratislava
Radlinského 11, 810 05 Bratislava, Slovakia
(phone: 421-2-5927-4471; fax: +421-2-5296-7027)*

³*Faculty of European Studies and Regional Development, Slovak Agricultural University
tr. A. Hlinku 2, 949 76 Nitra, Slovakia
(phone: +421-376-415-7292; fax: +421-376-531-522)*

**Corresponding author
e-mail: belcakova@tuzvo.sk; phone: 421-908-899-229*

(Received 4th Nov 2018; accepted 21st Mar 2019)

Abstract. Limiting factors for riparian ecosystem were previously considered to be riparian habitat structure, water flow variability, sedimentation and erosion. Recent scientific research have started to focus their attention to the feedback between form and function in fluvial ecosystems considering that not only geomorphology controls riparian vegetation dynamics, but also riparian vegetation controls geomorphology. Erosion-sedimentation processes significantly change the channel of the river and its surroundings and the sediment movement indicator is the critical value of the shear stress. This contribution deals with the impact of vegetation on the erosion-sedimentation processes in fluvisols during flood events. Selected vegetation characteristics and their effects on the humus horizons in fluvisols were assessed at the selected area of the River Schwechat followed by modelling of the shear stress during flood events.

Keywords: *riparian ecosystem, floodplain water, biogeomorphic processes, landform dynamics, hydraulic modelling, Schwechat River*

Introduction

Riparian ecosystems are transitional semiterrestrial areas regularly influenced by fresh water, usually extending from the edges of water bodies to the edges of upland communities. Because of their spatial position, they integrate interactions between the aquatic and terrestrial components of the landscape. They are dynamic environments characterized by strong energy regimes, substantial habitat heterogeneity, a diversity of ecological processes, and multidimensional gradients (Daigneault et al., 2017). Habitat for riverine and riparian organisms is a constantly changing mosaic biophysically dynamic in space and time. In his context, the biota is uniquely adapted to the dynamics of the system (Dufour et al., 2015). Riparian ecosystems are often locations of concentrated biodiversity at regional to continental scales.

Interactions between riparian vegetation and fluvial hydraulic processes are regulated by the flow regime which is one of the primary drivers shaping morphological patterns and ecological integrity (Wohl et al., 2015; Claude et al., 2018). One of the outcomes of

these complex interactions are discrete vegetation units that represent snapshots in time characterized by stands of different age and structural features (Egger et al., 2013a, b). Riparian species have developed adaptations and synchronized life history traits with the variable conditions of the river dynamics (Kui et al., 2014; Kui and Stella, 2016). When fluvial characteristics are modified, riparian plant communities and vegetation structure change favouring less bio-diverse environments, worse water quality and more exposed river beds (Stallings et al., 2015), definitely leading to a poor or bad ecological status. In many cases, to achieve a good ecological status of water body can be crucial for the riparian vegetation protection in order to support its hydrological and ecological functions (Garcia-Arias and Francés, 2015; Macura et al., 2012).

As pointed out by Sponseller et al. (2013), running water ecosystems illustrate several principles governing the interaction of landscape form and ecological function. Whereas the control of sediment dynamics by hygromorphic plants has been identified as an important component of intertidal ecosystem function (Passarelli et al., 2014; O'Brian et al., 2018; Kazakova, 2018; Varigin, 2018), the effect of riparian vegetation on sediment erosion and deposition within fluvial systems has been studied mainly from the geomorphic perspective of landform dynamics (Bywater-Reyes et al., 2015).

Fluvial biogeomorphic studies suggested that the geomorphic effects (flow resistance, sediment stabilization and accretion) and biomechanical and life history responses (mechanical resistance, reproduction, dispersion, and growth) of riparian vegetation within and between floods may represent key controls on both the riparian ecosystem and landscape dynamics. Thus, the effects of riparian vegetation on sediment erosion/deposition dynamics may form a biogeomorphic function regulating conjointly succession, biodiversity and landform dynamics within fluvial corridors (van Dijk et al., 2014; Corenblit et al., 2014a). Biogeomorphic approaches are recently investigating back mechanisms between biota, topography and landscape dynamics (Correnblit et al., 2014b; van Oorschot et al., 2017; Dyderski et al., 2015; Gonzales et al., 2014, 2015; Arnold and Toran, 2018).

Riparian ecosystems often represent locations of concentrated biodiversity, and flooding is one of the most important factors accounting for the remarkably high biodiversity associated with the riparian zones (Tagwirey and Sullivan, 2015). Floods recharge the floodplain water table and provide seedlings with access to moist soils, create new sites for plant recruitment, flush organic material such as woody debris, deposit nutrients onto the floodplain and disperse seeds of riparian plants (Warner et al., 2014). The physiological effect of a flood event depends on an individual plant tolerance (Egger et al., 2013a). The most important flood factors affecting plants are flood level and relative water depth, flood duration, flood timing and time since the last flood event.

Because of the sensitivity to the hydrological regime, riparian vegetation composition, structure and vigour respond rapidly to flow regime changes (Boudell et al., 2015; Wohl et al., 2015). Hydrological changes sometimes result in the encroachment of river margins by native riparian species (e.g. Merrit, 2013; Sankey et al., 2015). In other cases, native species may lose their vigour (e.g. Havel et al., 2015; Li, 2013; Gonzalez et al., 2014) and may be replaced by other native or alien species that have different hydrological requirements and tolerances (e.g. Garssen et al., 2014; Capon et al., 2013; Catford et al., 2014).

Morphodynamic processes associated with floods such as sediment deposition/aggradation and fluvial erosion result in the physical disturbances. These

disturbances determine species diversity, population recruitment and survival, and the age structure of stands (Solari et al., 2015; Kath et al., 2014; Kondolf and Piégay, 2016). The extent and intensity of flood disturbance can be measured by its destructive impact on the vegetation (Mobaied et al., 2016).

Erosion of sediments during flood events can be estimated by a critical shear stress. When the flow conditions exceed a critical value, sediment particles on the stream bed start to move. The ability of a particle to move is related to hydraulic shear stress, frictional forces, water depth and the specific weight of the particle (Lamb et al., 2017). Riparian vegetation dynamics depends on hydrogeomorphologic parameters (Operman et al., 2017), and, in return, on living and dead riparian plants modulate sediment, diaspore, nutrient and water flows within fluvial corridors (Funk et al., 2018; Habersack et al., 2016). Fluvial corridors are constituted of river channels, their margins and the zone of expansion of frequent floods, occupied by riparian vegetation (Kim and Kupfer, 2016). The ability of some riparian plants to grow on deposited sediment implies that sediment deposition favours plant biomass production. In return, biomass production then increases surface roughness and sediment deposition (Thomas et al., 2015; Corenblit et al., 2014a). Many studies (Camporeale et al., 2013; Clarke et al., 2014; Eichel et al., 2013) suggest that vegetation plays key roles in determining fluvial ecosystem structure, function and channel geometry. During floods many riparian species reproduce both vegetatively and sexually and a lot of sediments are transported with the flow. Vegetation reduces velocity and shear stress on the interface between vegetation patch and flow (Rössler et al., 2018; Hession et al., 2013; Gilyear et al., 2017) that causes increasing sediment deposition within and behind vegetation patches (Surian et al., 2015). The decrease of the shear stress depends on the vegetation density (Rivaes et al., 2014).

The main goal of our research was to find out how important role can riparian vegetation have when it comes to protection of the floodplain soils in the selected area. The research investigates the impact of riparian vegetation on the sediment erosion in floodplain area of River Schwechat in Austria. Another part of our research aimed at the determination of shear stress values exerted in the soil surface during flood events using hydraulic modelling and, also, to assess its impact on erosion-accumulation processes. This impact was surveyed during one big flood, which occurred in spring of 2014 being the biggest flood event in the area of River Schwechat since year 2007.

Materials and methods

The focus of the work consisted of the application of theoretical and methodological approaches in the field of landscape ecology, biogeomorphology, hydrology, geobotany, geographic information systems (GIS) and remote sensing. Furthermore, applied methodology of our research was adopted and modified from the paper of Corenblit et al. (2009, 20014a, b, 2015).

Based on field measurements, a first task was to distinguish different vegetation types and groups followed by series of phytocoenological relevés that were conducted not only in the measured area but in the whole surrounding. That gave us quite clear idea about vegetation types and their characteristics present in the area of interest. Subsequently, humus horizon thickness was calculated and particle size survey was performed.

Selected vegetation characteristics and their effects on the humus horizons in fluvisols were then statistically assessed followed by modelling of the shear stress during flood events.

The study area

The study site at River Schwechat is located in the Baden district at the south-eastern part of lower Austria about 20 km south of Vienna. Our reference site is located near the Traiskirchen village (starts at N 48°0.065' E 16°17.456' and ends at N 47°59.891', E 16°16.921', see *Fig. 1*). The area is part of the floodplain forest around the river Schwechat and is protected as a natural monument. Schwechat flows through most of the south-eastern part of lower Austria. The highest point is at Schwechat Schöpfl at 893 m above sea level. With a slight bow, it flows from its origin in the north-east ending at Mannswörth (Schwechat) at 162 m above sea level with its water mouth into the Danube.

A large part of the catchment area is the southern part of the Wienerwald. Within the streams of Agsbach, Lammeraubach and Sattelbach the runoff flows into Schwechat near Baden. The Sattelbach, which joins in the same named village, is the largest tributary stream.

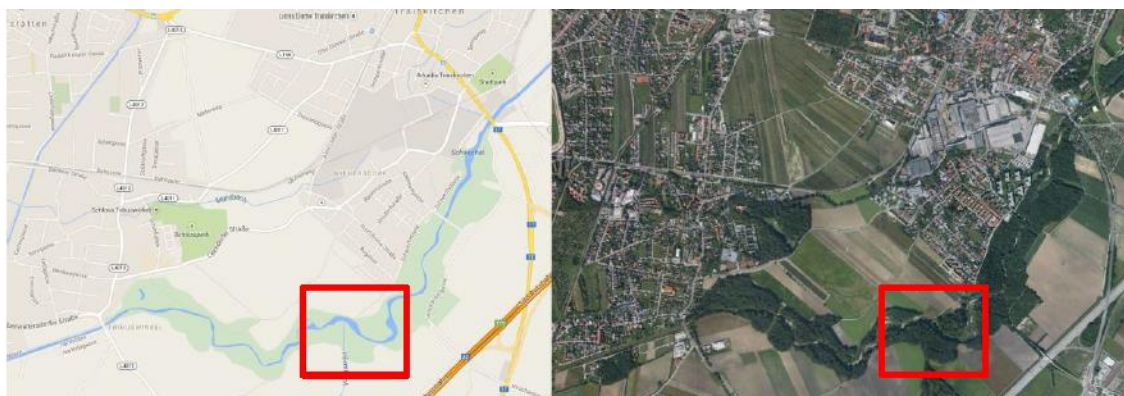


Figure 1. Study site at the Schwechat River. (Source: Google Maps)

The Wienerwald region is in the transition zone between the Pannonian climate in the east and the mainly oceanic swayed middle European climate in the west. The study area is located at about 200 m above sea level.

The summers are warm; the winters are very cold, dry, and windy; and it is partly cloudy year round. Over the course of the year the temperature reaches the annual average of about 12 °C. The monthly mean minimum and maximum daily temperature of Baden district is presented in *Figure 2*.

The annual precipitation in this area is around 600 mm (2011) with minimum numbers in winter (February) and the maximum ones in summer (June and July). *Figure 3* shows the average monthly rainy days over the year.

The perceived humidity level in Baden district, as measured by the percentage of time in which the humidity comfort level is *muggy*, *oppressive*, or *miserable*, does not vary significantly over the course of the year, staying within 2% of 2% throughout. The mean monthly relative humidity is displayed in *Figure 4*. All presented averages are based on weather reports collected during 2005–2015.

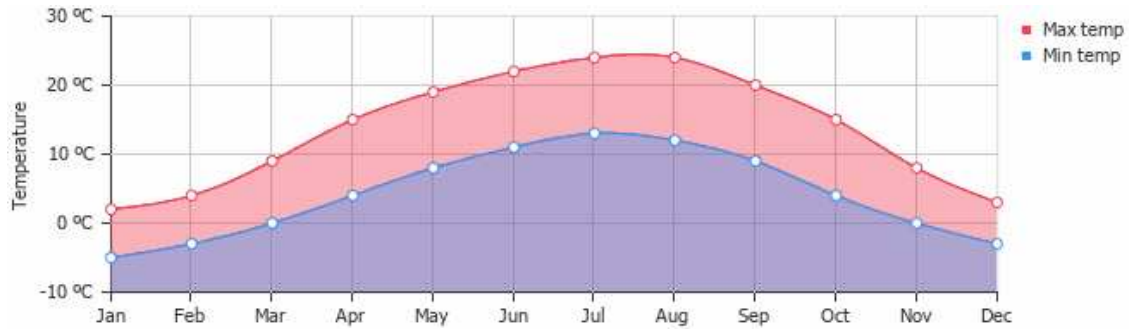


Figure 2. Monthly mean minimum and maximum daily temperature in Wiener Neustadt, Baden district. (Source: www.weather-and-climate.com)

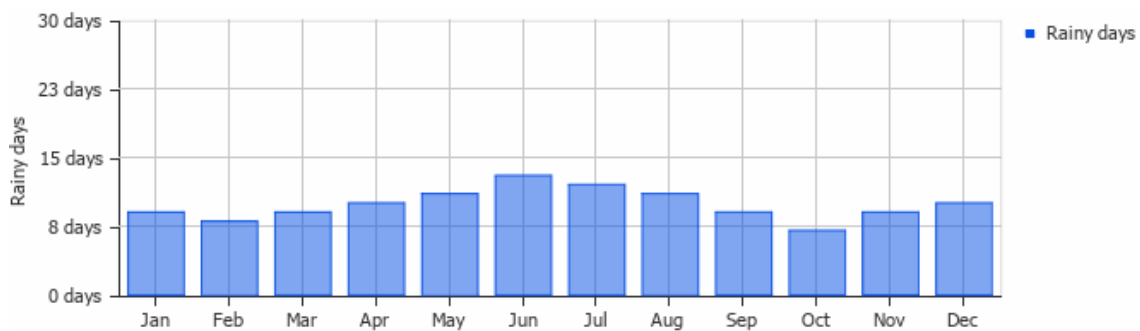


Figure 3. Average days with precipitation per month in Wiener Neustadt, Baden district. (Source: www.weather-and-climate.com)



Figure 4. Average relative humidity in Wiener Neustadt, Baden district. (Source: www.weather-and-climate.com)

As the considered section for our research is close to the Traiskirchen the deciding discharge site is “Cholerakapelle” which is upstream of Baden. *Table 1* shows recurrence intervals and correspondent discharges at this hydrological station. Run off data before and during the flood are displayed in *Figure 5*.

The flood occurred in May 2014 (peak May 16th, 2014). Maximum discharge that occurred during the flood was $91.7 \text{ m}^3 \text{ s}^{-1}$ (<http://ehyd.gv.at>) which corresponds to the 4.5 year discharge. Historical maximum discharges are represented in *Table 2*.

Table 1. Recurrence intervals and correspondent discharges. (Source: <http://ehyd.gv.at>)

HQ	Discharge Q (m ³ /s)
100	260
30	200
10	140
5	100
2	53
1	40
MQ	1.5

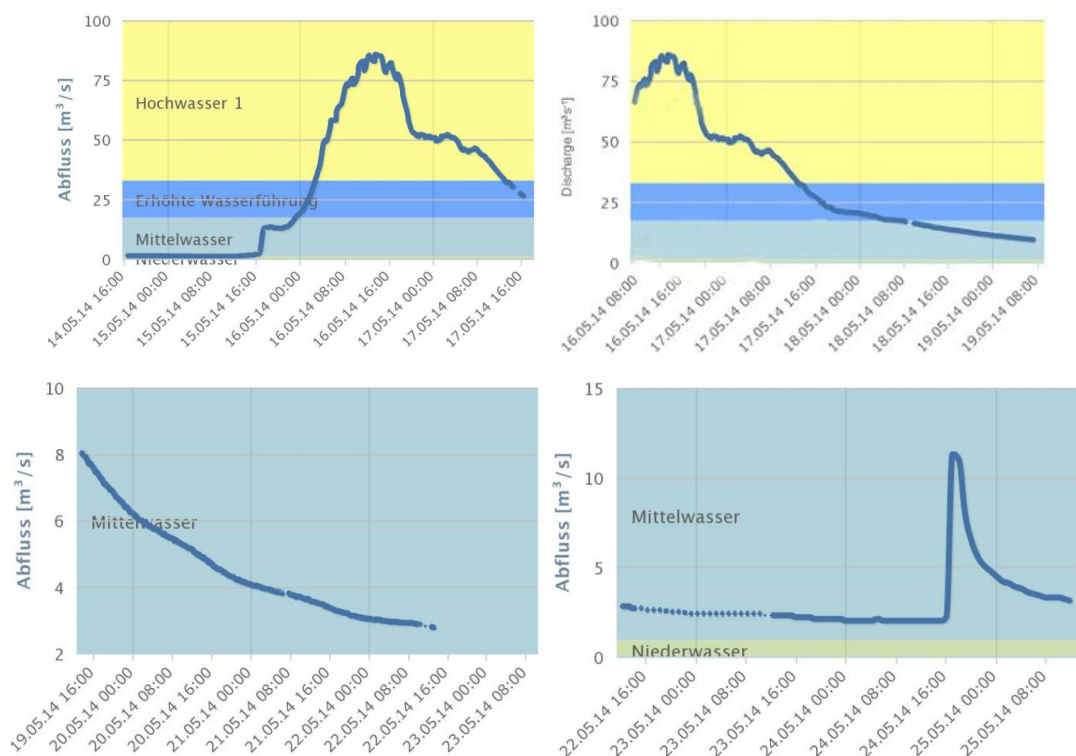


Figure 5. Run off data before and during the flood

Table 2. Historical maximum discharges. (Source: <http://ehyd.gv.at>)

Date	Q (m ³ /s)	W (cm)	x-year discharge
8.7.1997	257	533	100
1.7.1975	150	412	12
7.9.2007	147	446	12
8.8.2006	143	443	10
7.6.2002	129	430	8.5
13.8.2002	106	408	5.5
18.5.1991	104	350	5.5
16.5.2014	91.7	394	4.5
18.4.1994	83.2	385	4
9.2.1987	65.1	302	3

Field measurements

Observations were made along one transect (T1) located at River Schwechat; the transect was chosen appropriately to represent characteristics needed in this survey. Eight measuring plots within T1 transect were distinguished.

The research started in June and July 2013 when we determined the position of the transect and the measured plots. The comprehensive survey and field measurements of the floodplain vegetation continued in May and June 2014. Data measured in May 2014 were used to capture the transect state before the flood while data measured in June 2014 were used for defining the changes after the flood.

Plots were determined as areas of 2 m × 2 m, limited by using wooden removable frame (Fig. 6) fixed in one corner by an iron stake and three adjustable corners which were levelled using a spirit level. These frames were subdivided into a regular 0.2 m mesh defining 100 sampling subplots. Iron stakes driven into the substrate guided precise relocation of the plots, with starting position of 40 cm above the ground level. Each plot and its surroundings were documented by high-resolution photographs.



Figure 6. Frame design

The first step was to estimate total vegetation coverage in each plot followed by precise estimation in each subplot based on photographs. The key for the mapping units is based on the characterization of polygons in the aerial photo. The delimitation of the polygons with similar land cover was done before starting the mapping in the field. The data collection was focused on structural features. The dominant species and their coverage percentages were recorded. Furthermore, maximum plant height, median plant height, vegetation coverage and humus horizon thickness were measured in each subplot. Humus horizon thickness serves as a parameter to estimate amount of eroded/accumulated material, thus to estimate the changes of the humus horizon thickness.

The chosen study site is characterised by both a strong natural meandering and a high occurrence of wood and sediment transport during floods. Trees and debris that were transported during floods were deposited after stage decline and large areas with bare sand. Gravel banks were also observed.

Phytocoenological survey

One of the most important part of the research was vegetation mapping provided by series of phytocoenological relevés which were conducted not only in the measured transect, but in the whole surrounding. That gave us quite clear idea about vegetation types present in the area of interest. As the riparian areas are considered to be valuable ecosystems because of their biodiversity and functions, part of our research was dedicated to the invasive species which can significantly lower the biodiversity and other important functions of these ecosystems.

Our phytocoenological research followed results of vegetation mapping obtained in Ecoriver project (Egger et al., 2013a). According to this project, 10 vegetation types were distinguished in the whole research area (Fig. 7).

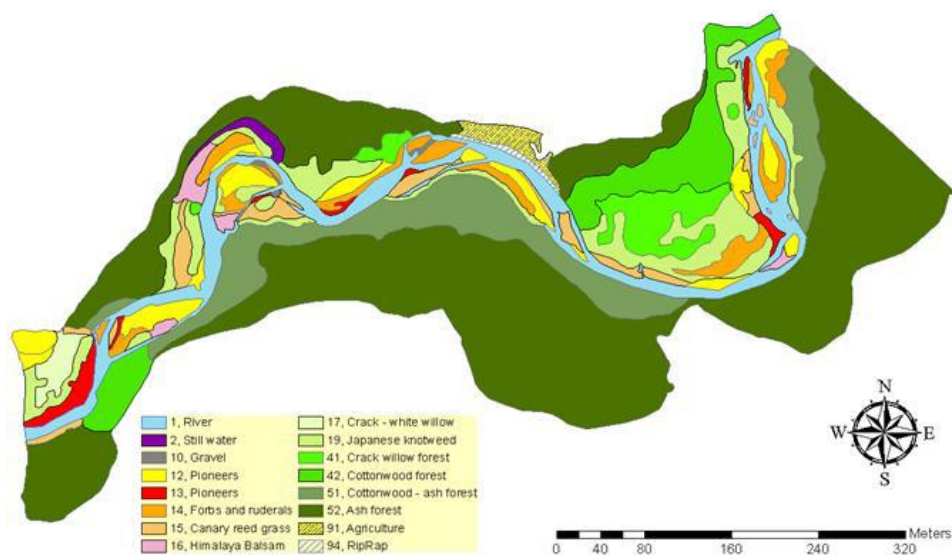


Figure 7. Mapped vegetation types. (Egger et al., 2013a)

Vegetation types were investigated by performing a phytocoenological relevés to define a floristic composition of these sites. Abundance of each plant species were classified according to the 7-points Braun-Blanquet classification (Braun-Blanquet, 1964). Nomenclature of plant taxa is presented according to the program TURBOVEG for Windows (Henekens, 1998-2012). This computer software package was developed in The Netherlands for processing of phytocoenological data. The package comprises of an easy-to-use database management system. The data bank to be managed can be divided into several databases which may consist of up to 100.000 relevés each. The program provides methods for input, import, selection and export of relevés. In 1994, TURBOVEG was accepted as the standard computer package for the European Vegetation Survey. Currently it has been installed in more than 25 countries throughout Europe and overseas (Henekens, 1998-2012). Relevés were used for defining the floristic composition of the site.

Particle size survey

Samples were taken from individual plots before the flood event (May, 2014). As the first step samples were dried and fine grained components were divided. Subsequently,

saturated hydraulic conductivity was measured. Then the percentage of the different sized particles in each sample were determined using the Cassagrande densimetric method.

The areometric Cassagrande method is based on the use of special densimeters (areometers) that monitor changes in the density of a soil suspension in water and in various soil particle diameters in terms of the sedimentation time changes. Density changes are caused by the sedimentation process; the density of the hydro-suspension falls with the increasing length of measurement. This method is one of the non-repeated sedimentation methods, which means, that all of the measurements must be performed within one sedimentation process. An appliance for this method consisted of an analytical balance, porcelain dish, laboratory spoon, timer, calibrated cylinder (1000 ml; *Fig. 8*), funnel, manual mixer, densimeter, thermometer, dispersing agent (sodium hexamethaphosphate) and distilled water.



Figure 8. Calibrated cylinders (1000 ml)

The charge of fine grained soil differs according to the amount of clay particles in the soil. In the case of clayey soils, the charge ranges from 20 to 30 g (in clays it is 10 g), as far as sandy-clay, loamy and clay-loamy soils are concerned, the charge is approximately 30-50 g and in case of sandy soils it is 100 g. The soil was weighed, placed in a porcelain dish and mixed with distilled water (200 ml). Dispersing agent was then added (10 ml of agent for every 10 g of fine grained soil) and was boiled for 1 h. The suspension was mullied at the bottom of the dish after cooling while the muddy part was poured directly into a graduated cylinder (1000 ml). The suspension in the graduated cylinder was mixed by a glass rod for one minute before the measurement started. When the glass rod was taken out, an areometer was put in its place and the first density measurement started after 30 s.

The results were analysed with a nomogram in which the size of settling particles is determined depending on the individual sedimentation time. The process is followed by a percentual determination of individual fractions.

The soil type was identified according to the given values based on the classification system used in Slovak Republic. It is being applied to particles with diameters below 0.01 mm (*Table 3*).

Table 3. Soil texture classification

Particle content < 0.01 mm (%)	Soil type nomenclature	Basic soil type
0	Sand	Light soil
0-10	Sandy	
10-20	Loamy sand	
20-30	Sandy loam	Medium heavy soil
30-45	Loamy	
45-60	Clayey loam	
60-75	Clayey	Heavy soil
> 75	Clay	

There were 8 measuring plots placed (T1-1, T1-2, T1-3 up to T1-8) in the evaluated transect. However, due to the huge development of invasive species stands (mostly by *Fallopia japonica*) it was not possible to measure all the parameters in three plots (T1-1, T1-2, T1-3) and they were not assessed.

Statistical evaluation

Similarly, due to the huge development of invasive species of *Fallopia japonica* it was not possible to measure all the parameters in three plots (T1-1, T1-2, T1-3) and they were not statistically evaluated. Therefore, data from 5 plots (T1-4 to T1-8) were evaluated, each plot was divided to 100 subplots (0.2 m × 0.2 m), and in each subplot 4 parameters were measured. That makes 400 datasheets for each plot, altogether 2000 data for 5 evaluated plots. The relationships between parameters (dominant species and their coverage, maximum plant height, median plant height, vegetation coverage and humus horizon thickness) in the transect and also in the individual plots were analysed.

Fallopia japonica was quickly spreading after 2013, especially close to flood areas. That is why differences in the area of distribution were measured before and after flood. Measurements were performed in our area of interest.

Hydraulic modelling

The next step of our research was the modelling of the flood discharge from May 2014 using a MIKE 21 model together with Mud Transport Module (MT). Such module can simulate the processes of erosion, transport, setting and deposition in marine, brackish and fresh water areas. The module takes into account fine non-cohesive materials.

The aim of the hydraulic modelling was to find out the value of the shear stress, which was affecting the plots during the flood event. The model inputs were represented by the digital elevation model, which was created from the topographic data measured at the site, the flood characteristic discharges and the information about sediment character. The output of the model is the point mesh with shear stress values. The output was exported to the GIS and used for creating graphic outputs of the modelling.

The critical shear stress τ_{crit} can be determined from the shields curve (Fig. 9). The shields curve presents the relation between non-dimensional critical shear stress and boundary Reynolds number Re which is the Reynolds number on the interface between flowing water and surface. For higher Reynolds numbers the critical shear stress decreases and for Reynolds numbers $Re \gg 500$ the shields parameter is constant at 0.057.

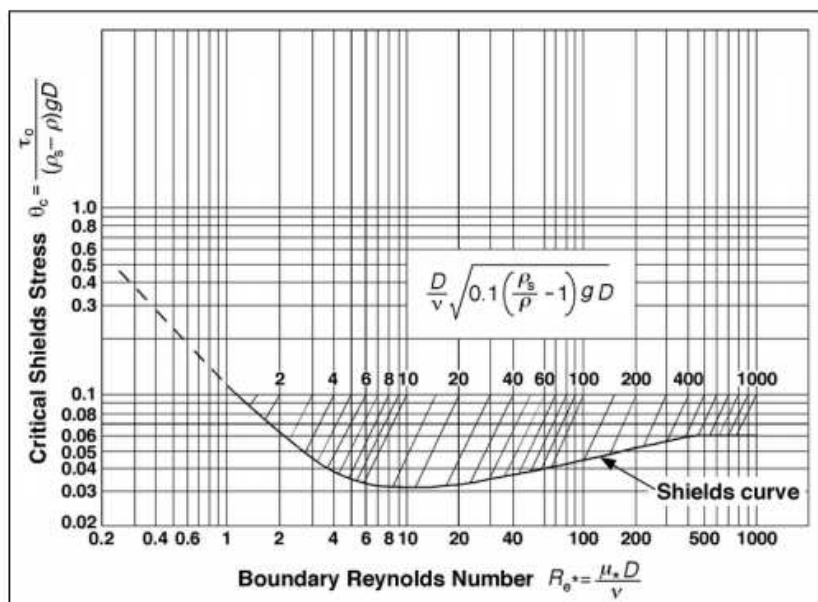


Figure 9. The shields curve

Results

Phytocoenological survey of distinct vegetation types

Phytocoenological characterization was performed in order to distinguish all the vegetation types present in the surroundings of T1 transect. Only herb vegetation occurred in the area of transect therefore the effect of herb vegetation on the erosion – sedimentation processes are presented. Hopefully research will continue in the future, when there will be more localities and effect of woody vegetation evaluated, so the research can follow by characterization of the vegetation presented in this study.

Pioneer site at the transect is typically dominated by species of *Saponaria officinalis* usually followed by species of *Chenopodium album*, *Echium vulgare*, *Impatiens glandulifera*, *Melilotus officinalis*, *Papaver rhoeas*, *Persicaria dubia*, *Phalaris arundinacea*, *Poa pratensis*, *Arctium* sp., *Polygonum aviculare* and young tree seedlings of *Populus x canadensis* and *Salix fragilis*. The second type of pioneer site is dominated by species of *Impatiens glandulifera*, subdominated by *Saponaria officinalis* or *Urtica dioica* following with species like *Echium vulgare*, *Galium aparine*, *Phalaris arundinacea*, *Artemisia vulgaris*, *Hedera helix*, *Melilotus album*, *Plantago lanceolata*, *P. major* and *Poa pratensis*.

Closer to the poplar forest edge a pioneer site dominated by seedlings of young *Populus nigra* trees with few individuals with shrub height were found, sometimes subdominated in herb and also in shrub layer by tree species of *Robinia pseudoacacia*

followed by species *Phalaris arundinacea*, *Saponaria officinalis*, *Urtica dioica* and *Plantago major*, *Hedera helix*, *Chelidonium majus*, *Ulmus laevis*.

There were three types of forbs and ruderals stands in our study site – the first one dominated by *Echium vulgare* and/or *Arrhenatherum elatius* (on the drier stands), the second one dominated by *Impatiens glandulifera* and the third type of forbs and ruderals is dominated by *Phalaris arundinacea*.

Wetter type of forbs and ruderals are stands dominated by *Phalaris arundinacea* often followed by *Urtica dioica*, typical are also young poplar and willow trees in herb or shrub layer, also *Saponaria officinalis* with higher abundance. Among other species found here were for example *Impatiens glandulifera*, *Rumex obtusifolius*, *Juglans nigra*, *Lapsana communis*, *Lolium perenne*, *Scrophularia umbrosa*, *Lythrum salicaria*, *Stellaria sp.*, *Mentha longifolia*, *Taraxacum* sect. *Ruderalia*, *Petasites hybridus*, *Trifolium hybridum*.

There were just few localities with crack-white willow stands in our study area and they had small coverage. Tree layer is formed by *Salix fragilis*, *S. alba*, *Robinia pseudoacacia*. Shrub layer is typically covered by *Fallopia japonica* that is present also in herb layer together with *Impatiens glandulifera*. Few patches with the crack willow forest were found at the site with *Salix fragilis* species. *Vitis vinifera* was typical in tree, shrub and also in herb layer. This site has typical shrub layer in crack willow stands, because in most cases it invaded by *Fallopia japonica* that is typical also in herb layer.

Large stands of poplar forest vegetation type were not found so it was possible to put together only one phytocoenological relevé. There was significant dominance of poplar trees in the low tree layer followed with *Fraxinus excelsior*, *Acer platanoides*, *Ulmus minor*, *Acer campestre*, *Acer negundo*, *Prunus avium* and *Prunus padus*. Shrub layer was dominated by *Sambucus nigra* and also species of *Cornus sanguinea*, *Juglans regia*, *Ulmus minor*, *Fallopia japonica*, *Prunus padus* and *Corylus avellana* were found here. Herb layer was dominated by species of *Aegopodium podagraia* with *Urtica dioica*, *Alium ursinum* and *Galeobdolon luteum*.

Poplar – ash forest occurred in both higher and lower tree layers with dominant species of *Fraxinus excelsior*, *Populus nigra*, *Acer campestre*, *Acer platanoides*, *Ulmus minor*, *Ulmus laevis*, *Robinia pseudoacacia* and *Juglans nigra*. Shrub layer was represented by *Cornus sanguinea*, *Acer platanoides*, *Acer campestre*, *Crataegus monogyna*, *Sambucus nigra*, *Ulmus minor*, *Ulmus glabra*, *Cornus mas*, *Juglans regia*, *Ligustrum vulgare* and *Acer negundo*. Herb layer was dominated by *Lonicera xylosteum* and subdominated by *Aegopodium podagraria*. All the above mentioned species from tree and shrub layers can also be found in herb layer together with species of *Salvia glutinosa*, *Knautia arvensis*, *Arum maculatum*, *Rubus caesius*.

Typical maple species in higher tree layer were represented by *Acer campestre*, *A. platanoides* and *A. negundo*, ash *Fraxinus excelsior* was dominant in lower tree layer where also *Populus alba*, *Ulmus laevis*, *Tilia platyphyllos* and less *Ulmus minor*, *Prunus padus* were found. Shrub layer is also formed by these tree species and seedlings were also found in the herb layer. Typical shrub species in these forests are *Sambucus nigra*, *Ligustrum vulgare*, *Acer campestre*, *Ulmus minor*, *Crataegus monogyna*, *Rosa canina*, *Cornus sanguinea*, *Juglans regia*, *Fraxinus excelsior*. In herb layer a presence of *Lonicera xylosteum*, *Aegopodium podagraria*, *Hedera helix*, *Allium ursinum* were noticed as well as species like *Arrhenatherum elatius*, *Arum maculatum*, *Calystegia sepium*, *Chenopodium bonus-henricus*, *Elymus caninus*, *Euonymus europaeus*, *Rubus caesius*, *Ranunculus repens*, *Polygonatum latifolium* and seedlings of tree species.

Phytocoenological relevés were performed in the surroundings of the measured plots (not directly at plots measured) in order to have a better picture of phytocoenological composition of the transect surroundings. Relevés were used for defining the floristic composition of the site. The example of phytocoenological table with relevé is presented in the phytocoenological *Tables 4* and *5*.

Table 4. Phytocoenological table. R1., R2., R3. - *Impatiens glandulifera*; R4., R5. - *Phalaris arundinacea*

Species	Relevé No.				
	1.	2.	3.	4.	5.
Shrub layer					
<i>Salix fragilis</i>	-	-	-	1	-
Herb layer					
<i>Ranunculus repens</i>	-	-	-	+	-
<i>Impatiens glandulifera</i>	4	3	4	+	r
<i>Phalaris arundinacea</i>	3	2	2	3	4
<i>Plantago major</i>	+	-	-	-	-
<i>Saponaria officinalis</i>	1	+	3	1	+
<i>Urtica dioica</i>	2	1	3	3	1
<i>Clematis vitalba</i>	-	-	+	+	-
<i>Fallopia japonica</i>	-	-	+	-	-
<i>Hedera helix</i>	-	-	+	-	-
<i>Poa nemoralis</i>	-	-	r	-	-
<i>Populus nigra</i>	-	-	r	2	-
<i>Robinia pseudacacia</i>	-	-	1	-	-
<i>Lolium perenne</i>	-	-	-	+	-
<i>Melilotus albus</i>	-	1	-	-	-
<i>Arctium species</i>	-	-	-	-	1
<i>Artemisia vulgaris</i>	-	-	-	2	-
<i>Plantago lanceolata</i>	-	-	-	+	-
<i>Sisymbrium strictissimum</i>	-	r	-	-	-
<i>Anthemis arvensis</i>	-	-	-	1	-
<i>Arctoa species</i>	-	-	-	+	-
<i>Barbarea vulgaris</i>	-	-	-	+	-
<i>Juglans nigra</i>	-	-	-	r	-
<i>Lapsana communis ssp. communis</i>	-	-	-	r	-
<i>Lythrum salicaria</i>	-	r	-	+	+
<i>Mentha longifolia</i>	-	-	-	+	-
<i>Petasites hybridus</i>	-	-	-	+	-
<i>Poa trivialis</i>	-	-	-	1	-
<i>Populus alba</i>	-	-	-	r	+
<i>Rumex crispus</i>	-	-	-	r	+
<i>Rumex obtusifolius</i>	-	-	-	+	-
<i>Scrophularia umbrosa</i>	-	-	-	r	-
<i>Stellaria species</i>	-	-	-	r	-
<i>Taraxacum sect. Ruderalia</i>	-	-	-	r	-
<i>Trifolium hybridum</i>	-	-	-	r	-
<i>Elymus caninus</i>	-	-	-	r	-
<i>Fallopia convolvulus</i>	-	-	-	-	+
<i>Persicaria species</i>	-	-	-	-	+
<i>Poa palustris</i>	-	-	-	-	1
<i>Salix purpurea</i>	-	-	-	-	r
<i>Setaria pumila</i>	-	-	-	-	+

Table 5. Phytocoenological table header (R1 – R5)

Relevé number	1.	2.	3.	4.	5.
Date (year/month/day)	2013/07/26	2013/06/15	2013/07/26	2013/06/16	2013/07/18
Relevé area (m ²)	10.00	4.00	12.00	16.00	16.00
Cover total (%)	95	40	80	95	85
Cover shrub layer (%)	0	0	0	4	0
Cover herb layer (%)	95	40	80	95	85
Height shrub layer (m)	0.0	0.0	0.0	1.7	0.0
Height herb layer (cm)	110	40	130	100	70
Max. height herb layer (cm)	140	160	150	170	100
Richness	5	7	10	28	14
Shannon	1.08	1.17	1.53	2.41	1.31
Evenness	0.67	0.60	0.66	0.72	0.50
Simpson	0.59	0.56	0.73	0.84	0.48

Particle size survey

Particle size survey was performed in the laboratory, The Casagrande's method was used for evaluation (Table 6) of 5 samples, each representing one plot (T1-4 to T1-8). Based on our field measurements performed in 2014, 3 plots (T 1-1, T 1-2 and T 1-3) were not assessed due to the presence of *Fallopia japonica*.

From the particle size analysis shown in Table 6 the soil types in each of our measured plots can be characterized The amount of the sand in the samples is greatest in the last two plots T1 -7 and T1-8.

Table 6. Particle size analysis

Particles	T1-4	T1-5	T1-6	T1-7	T1-8
Silt (%)	< 1	< 1	6	< 1	< 1
Clay (%)	16	21	23	6	7
Clayic sand (%)	8	9	2	2	1
Sand (%)	76	70	69	92	92

Statistical evaluation

Analysis of the relationships between individual parameters consisted of the evaluation in the whole transect and within the plots using the linear regression analysis. Data were obtained in May 2014 in two different time periods. The status before and after flood had to be compared as it was necessary to find out the effect of the vegetation on soil during flooding. Flood was culminating on May 16th, 2014 and it was not possible to get to the transect because of the flooded access, Figures 10 and 11 represent localities upstream and downstream from the research site. Data from 5 plots in T1 transect (T1-4 to T1-8) have been evaluated and, also, analyses of individual

parameters dependence on the channel distance and dependence of humus horizon difference on the vegetation parameters (height, coverage) were performed.



Figure 10. Flood - downstream



Figure 11. Flood - upstream

The graph and the regression line of the dependence between vegetation coverage and the distance from the water body is presented in *Figure 12*. Correlation coefficient is negative and equals to -0.542 , reflecting strong negative relationship between these

two parameters. This value means that with the increasing distance from the water, vegetation coverage is getting lower in the area within 12-30 m distance from the water body.

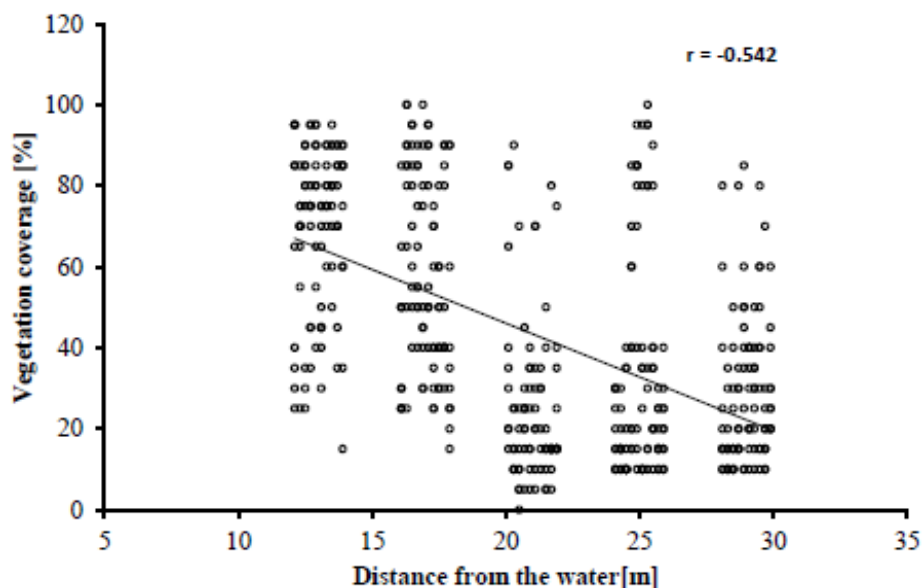


Figure 12. Dependence of the vegetation coverage on the distance from the water body

In *Figure 13* the graph of the dependence of the maximum plant height and the distance from the water body is presented. Similar results to the one in the previous case were observed; correlation coefficient is negative and equals -0.454. This value can be interpreted as a strong negative relationship between variables. We can conclude, that in the plots T1-4 to T1-8, the greater is the distance from the river the lower is the maximum plant height.

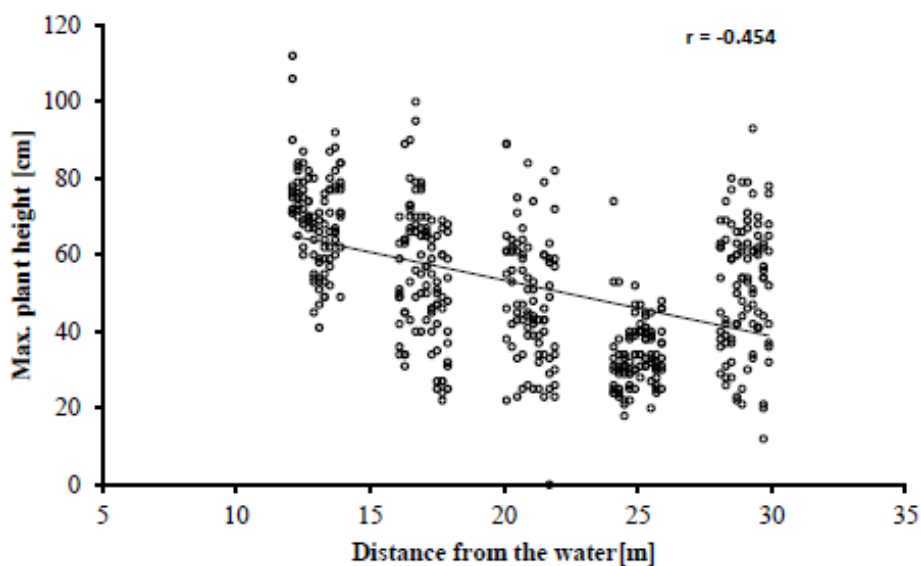


Figure 13. Dependence of the maximum plant height on the distance from the water body

Figure 14 shows dependence of the humus horizon thickness difference (difference before and after flood) and distance from the water body. In this case, the correlation coefficient result was a positive value equal to 0.779. This value reflects positive relationship; with greater distance from the river the humus horizon thickness difference is increasing. Erosion is decreasing and deposition of material is starting to occur with increased distance from the water body. In this case, the effect of the distance from the river on the changes in the humus horizon thickness is more important than other measured vegetation parameters (height, coverage).

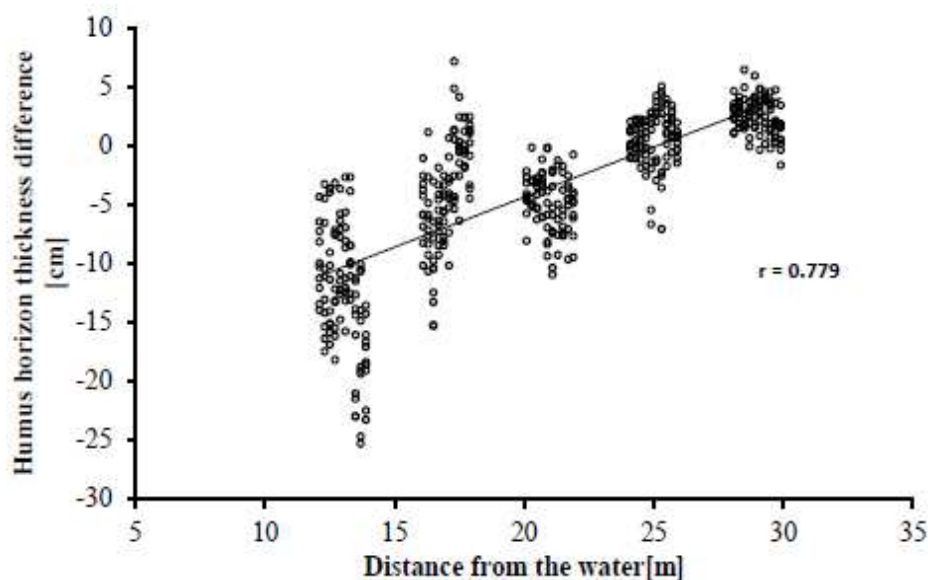


Figure 14. Dependence of the humus horizon thickness difference on the distance from the water body

Figure 15 shows dependence between maximum plant height and vegetation coverage. Correlation coefficient value is $r = 0.5$ and it can be concluded that there is a positive correlation between these two parameters; value of the maximum plant height is increasing with increased vegetation coverage.

In Figures 16 and 17 relationships between humus horizon thickness differences and vegetation parameters; vegetation coverage and maximum plant height are presented. In both cases the correlation coefficient had negative values (-0.498 and 0.471) reflecting negative relationship between variables. It can be concluded that with higher percentage of vegetation coverage in measured plots the erosion in humus horizons of fluvisols increased and the deposition decreased. Similar conclusion can be confirmed for plant height; erosion is higher with higher maximum plant height.

The above presented results show that distance from the water body was the most important effect on the thickness of the humus horizon in fluvisols at the chosen site. Taking into account the conditions during flood event in spring 2014, the vegetation did not have such important role. It must be noticed that we are dealing with a complex system and complicated process, thus other involved factors (e.g. species composition, size of the root system, roughness of the vegetation cover) were not considered in this study.

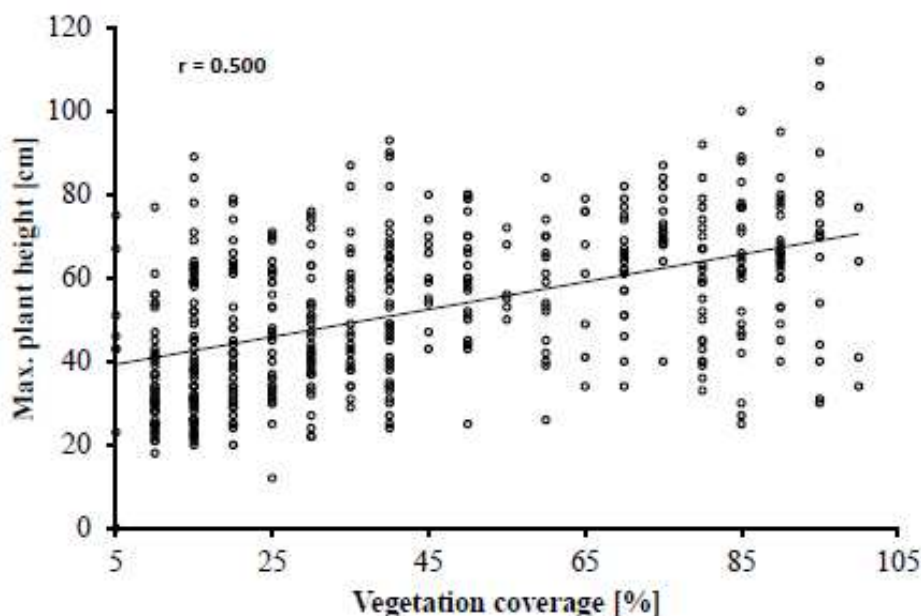


Figure 15. Dependence of the maximum plant height and the vegetation coverage

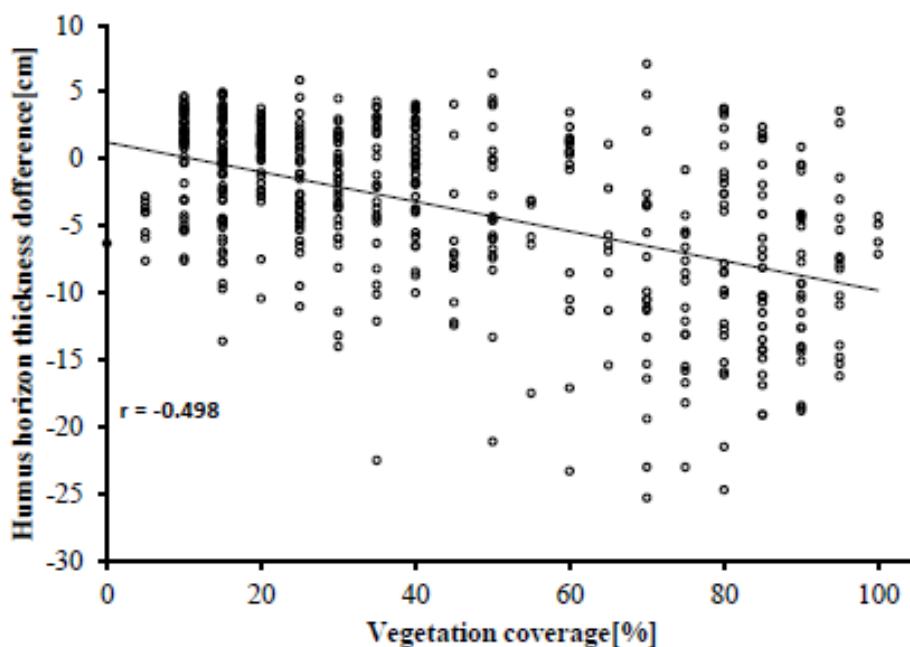


Figure 16. Dependence of the humus horizon thickness difference and the vegetation coverage

Our results of the relationship analysis between vegetation characteristics and changes in the humus horizon thickness are in contradictions with the published information. Surprisingly, there are mainly negative correlations between the change in the thickness of humus horizon and vegetation coverage, respectively maximum plant height. The results indicate, that vegetation promote erosion and negatively affect sediment accumulation. Such correlation relationships apparently cannot be a causal relationship but it is only a seeming correlation. Effect of vegetation in the studied

riparian zone is masked by the influence of spatial change of vegetation characteristics. In the matter of fact, very strong negative correlation was recorded for the relationship between the distance from the water body and vegetation coverage, respectively maximum plant height.

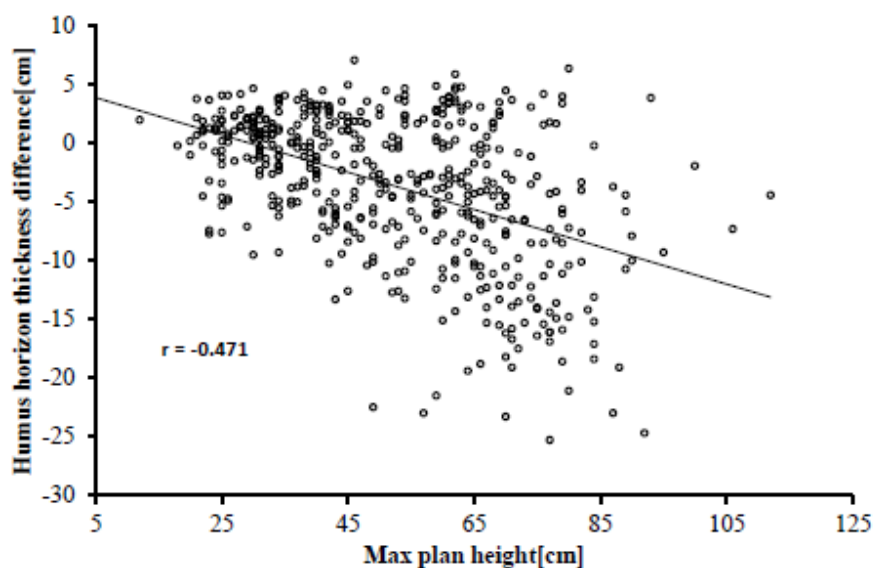


Figure 17. Dependence of the humus horizon thickness and maximum plant height

Hydraulic modelling

Shear stress was modelled using MIKE21 processed in the GIS environment; *Figure 18* represents the output from model with shear stress values for whole area while *Figure 19* shows the shear stress values simulated for individual plots. The highest values of shear stress were simulated in the T1-4 and T1-5 plots, in the plot T1-4 shear stress values were equal to 19 N.m^{-2} and in the plot T1-5 there were equal to 17 N.m^{-2} . During flooding of such intensity (app. Q4.5), the humus horizon is eroded in the area of these plots. The plot T1-6 appeared to be a “transition zone” between erosion and sedimentation, shear stress values were equal to $16 - 9 \text{ N.m}^{-2}$ and humus horizon sunk to minimal values.

Discussion

River channel significantly changes during the flood. The influence of vegetation on the channel transport and dynamics was analysed in few studies (Gurnell, 2014, 2016a, b; Rinaldi et al., 2013, 2015). It can be concluded that vegetation plays significant role in shaping the river channel and morphodynamic river development (Liu and Neph, 2016). Presence of vegetation causes that with lowering the velocity flow the shear stress is lowering and the river bank is stabilizing.

There are few types of erosion occurring around the river during the floods, while thanks to the surface erosion; also plants can be eroded together with soil particles (Rivaes et al., 2014).

Surface erosion can be found on bigger areas closer to the channel, with evenly distributed, high shear stress on the surface.

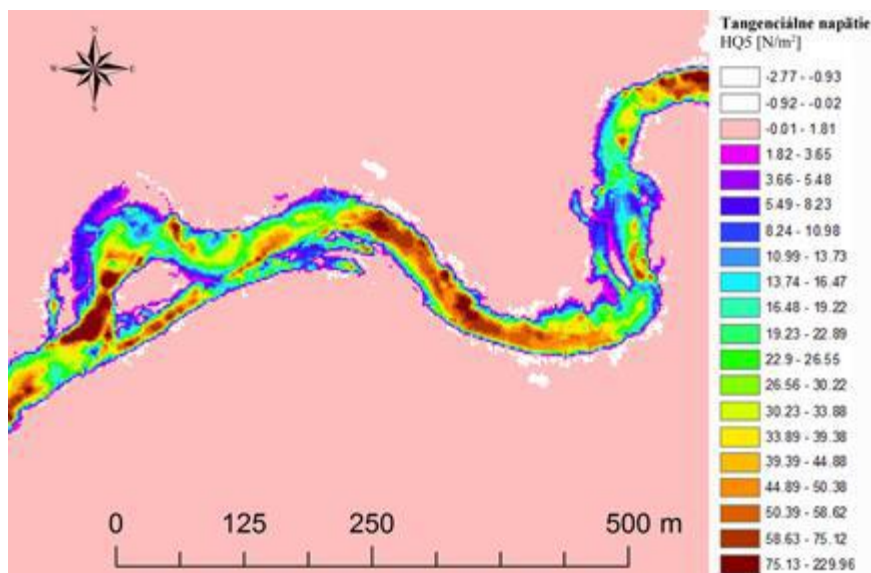


Figure 18. Modeled shear stress in the evaluated plots of the Schwechat River Q 4,5 (Arc Map)

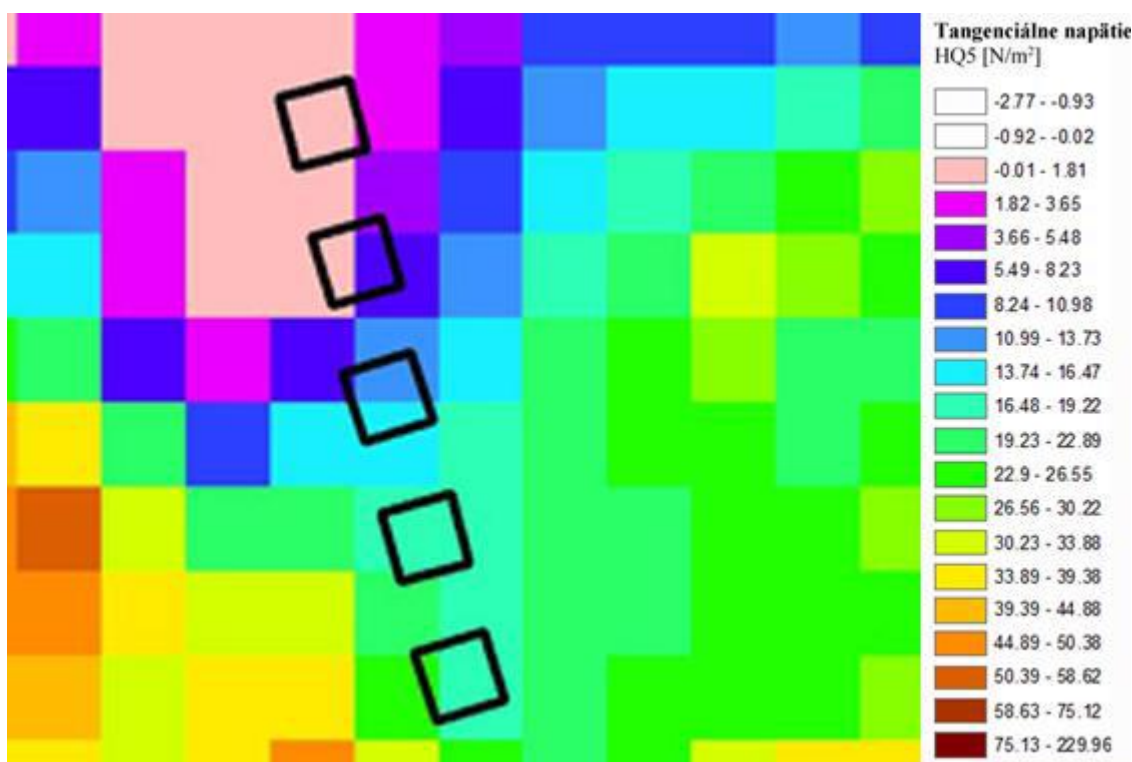


Figure 19. Modelled shear stress in the evaluated plots of the Schwechat River Q4,5

Aforementioned studies proved that vegetation, according to its lowering of the flow velocity and the shear stress values, has a significant anti-erosive function. Presence of the vegetation can also support deposition of sediments and cohesive particles brought by water during the floods.

As already mentioned, our results of the relationship analysis between vegetation characteristics and changes in the humus horizon thickness are in contradictions with

the published information. Surprisingly, there are mainly negative correlations between the change in the thickness of humus horizon and vegetation coverage, respectively maximum plant height. Effect of vegetation in the studied riparian zone is masked by the influence of spatial change of vegetation characteristics. In the matter of fact, very strong negative correlation was recorded for the relationship between the distance from the water body and vegetation coverage, respectively maximum plant height.

As shown by shear stress modelling, changes in the thickness of humus horizons are influenced mainly by a significant decline in the values of shear stress exerted by water during flood events on the soil surface. The sharp decline in shear stress with increasing distances of the water flow has resulted in a gradual shift from erosion processes with a negative change in the thickness of humus horizons, to the accumulation process with a positive change in the thickness of the research areas furthest from the water flow. The impact of changes shear stress on erosion-accumulative processes in the studied area is in addition highlighted by the spatial variation of grain composition of soils. Since with increasing distance from the water flow is the proportion of the lighter particles in the soil lowering, and on the other hand the proportion of heavier sand particles is increasing. The impact of this physical process is so powerful that it completely obscures the effect of vegetation present in the research plots, resulting in the aforementioned correlation relations.

Conclusion

The main aim of this research was to find out how important is the influence of vegetation in floodplain areas on deposition and erosion of the sediment, thus on the thickness of the humus horizon during floods. In the selected site of the river Schwechat in Lower Austria we observed different parameters required for this analysis. Among many data, those that meet the objectives of our study were selected and these were also statistically evaluated.

Statistical evaluation had two stages; the first step was to evaluate the variability across the transverse profile, the second step was to evaluate variability in individual squares - plots. In this case, we can conclude, that the variability within the plots was not as significant; thus, the distance between the pads within a square were not big enough to be able to see any significant difference in the effects of various parameters on the thickness of the humus layer.

From the evaluated data it was obvious that on the T1-4 plot erosion of sediment during the flood originally appeared, but that decreases with a distance from the shore and is changing to sedimentation on the plots T1-7 and T1-8. The role of the statistical evaluation was to determine which factors have the greatest impact on erosion accumulative processes affecting the variations in thickness of humus horizons of fluvisols. The investigated factors on the results of field research were especially distance from the water flow and the plants height and vegetation coverage. There were also modelled values of shear stress exerted by water on the soil surface during flood events.

Trying to characterize a specific process of such a complex system is certainly a difficult task and we have to keep in mind that the thickness of humus horizon of fluvisols in the offshore area is affected by many more factors, which was not taken into account in this work; such as the nature of vegetation, its detailed species composition

and distribution, foliar coverage, the coverage and the nature of the root system of vegetation.

Unfortunately, it was not possible to evaluate all the selected transect areas as it was not possible to collect data for the amount of sediment during the second measurement thanks to massive distribution of species *Fallopia japonica*. The selected plots with complete data provide characteristics for remote area 16 to 40 meters from a watercourse, with predominantly sandy-loamy to sandy soil and the herb community, with a dominant species *Echium vulgare*, or *Arrhenatherum elatius*. Therefore plots closest to the river, where the positive effect of vegetation is expected is settled by *Fallopia japonica* which can contrariwise support the erosion of sediments. As we calculated, the rate of spread might be very dangerous and lowering the ecological quality in this protected area.

The flood of May 2014 had an intensity of about 4.5 years water ($91.7 \text{ m}^3 \text{ s}^{-1}$), and during this kind of flood with those growing and soil conditions, the thickness of the humus horizon on the evaluated plots is mostly affected by the distance from the water flow. When evaluating vegetation parameters, it was found that, surprisingly, a higher cover reduces the amount of settled material and increases erosion in the humus horizon.

Similarly surprising, dependence concerns also affect the maximum height of plants. Erosion increases and sedimentation reduces with increasing maximum plant height. These surprising dependences are not the result of vegetation effect but are related to the dominant influence of distance from a watercourse on erosion-accumulative processes. Distance from water has a strong impact on the decrease of the shear stress which during the flood effects on the soil surface. At the same time the negative correlation between the distance from a watercourse and vegetation coverage/maximum plant height was observed. The impact of this factor therefore masks the effect of vegetation characteristics.

From the recorded changes in the humus layer thicknesses during flood events it can be concluded, that the erosion-accumulative processes were dominantly controlled by changes in shear stresses, that were affecting the soil surface during the flood. Influence of shear stress has also enhanced by the spatial variation of grain composition of soils.

As already mentioned, the results indicate that vegetation promote erosion and negatively affect sediment accumulation. Such correlation relationships apparently cannot be a causal relationship but it is only a seeming correlation. Effect of vegetation in the studied riparian zone is masked by the influence of spatial change of vegetation characteristics. In the matter of fact, very strong negative correlation was recorded for the relationship between the distance from the water body and vegetation coverage, respectively maximum plant height.

Phytocoenological characterization can help when performing future research in this area and monitoring of the invasive species spreading is suggested for evaluation during future flood events.

Acknowledgements. This research was supported by the Scientific grant Agency of the Ministry of Education, Science and Sport of the Slovak Republic (VEGA 1/0096/16).

REFERENCES

- [1] Arnold, E., Toran, A. (2018): Effects of bank vegetation and incision on erosion rates in an urban stream. – *Water* 10(4): 482. DOI: 10.3390/w10040482.
- [2] Boudell, J. A., Dixon, M. D., Rood, S. B., Stromberg, J. C. (2015): Restoring functional riparian ecosystems: concepts and applications. – *Ecohydrology* 8: 747-752. DOI: 10.1002/eco.1664.
- [3] Braun-Blanquet, J. (1964): *Pflanzensoziologie. Grundzüge der Vegetationskunde*. Ed. 3. – Springer, Wien-New York.
- [4] Bywater-Reyes, S., Wilcox, A. C., Stella, J. C., Lightbody, A. F. (2015): Flow and scour constraints on uprooting of pioneer woody seedlings. – *Water Resources Research* 51(11): 9190-9206. DOI: 10.1002/2014WR016641.
- [5] Camporeale, C., Perucca, E., Ridolfi, L., Gurnell, A. M. (2013): Modelling the interactions between river morphodynamics and riparian vegetation. – *Reviews of Geophysics* 51(3): 379-414. DOI: 10.1002/rog.20014.
- [6] Capon, S. J., Chambers, L. E., Mac Nally, R., Naiman, R. J., Davies, P; Marshall, N. et al. (2013): Riparian ecosystems in the 21st Century: hotspots for climate change adaptation? – *Ecosystems* 16(3): 1-23. DOI: 10.1007/s10021-013-9656-1.
- [7] Catford, J. A., Morris, W. K., Vesk, P. A., Gippel, C. J., Downes, B. J. (2014): Species and environmental characteristics point to flow regulation and drought as drivers of riparian plant invasion. – *Diversity and Distributions* 20: 1084-96. DOI: 10.1111/ddi.12225.
- [8] Clarke, L. E. (2014): The use of live vegetation in geomorphological experiments: how to create optimal growing conditions. – *Earth Surface Processes and Landforms* 39(5): 705-710. DOI: 10.1002/esp.3534.
- [9] Claude, N., Leroux, C., Duciercq, M., Tassi, P., Abderrezzak, K. K. (2018): Limiting the development of riparian vegetation in the Isère River: A physical modelling study. – *E3S Web of Conferences* 40: 02015. DOI: 10.1051/e3sconf/20184002015.
- [10] Corenblit, D., Steiger, J., Gurnell, A. M., Tabacchi, E., Roques, L. (2009): Control of sediment dynamics by a vegetation as a key function driving biogeomorphic succession within fluvial corridors. *Earth Surf. Process.* – *Landforms* 34: 1790-1810. DOI: 10.1002/esp.1876.
- [11] Corenblit, D., Steiger, J., Tabacchi, E., Gonzáles, E., Planty-Tabacchi, A. M. (2014a): Ecosystem engineers modulate exotic invasions in riparian plant communities. – *River Research and Applications* 30(1): 45-59. DOI: 10.1002/rra.2618.
- [12] Corenblit, D., Steiger, J., González, E., Gurnell, A. M., Charrier, G., Darrozes, J., Dousseau, J., Julien, F., Lambs, L., Larrue, S., Roussel, E., Vautier, F., Voldoire, O. (2014b): The biogeomorphological life cycle of poplars during the fluvial biogeomorphological succession: a special focus on *Populus nigra*. – *Earth Surface Processes and Landforms* 39(4): 546-563. DOI: 10.1002/esp.3515.
- [13] Daigneault, A. J., Eppink, F. V., Lee, W. G. (2017): A national riparian restoration programme in New Zealand: Is it value for money? – *Journal of Environmental Management* 187(1): 166-177. DOI: 10.1016/j.jenvman.2016.11.013.
- [14] van Dijk, W. M., Teske, R., van de Lageweg, W. I., Kleinhans, M. G. (2013): Effects of vegetation distribution on experimental river channel dynamics. – *Water Resources Research* 49: 7558-7574. DOI: 10.1002/2013WR013574.
- [15] Dufour, S., Massimo, R., Piégay, H., Amael, M. (2015): How do river dynamics and human influences affect the landscape pattern of fluvial corridors? Lessons from the Magra River, Central -Northern Italy. – *Landscape and Urban Planning* 134: 107-118. DOI: 10.1016/j.landurban.2014.10.007.
- [16] Dyderski, M. K., Gdula, A. K., Jagodziński, A. M. (2015): “The rich get richer” concept in riparian woody species. A case study of the Warta River Valley (Poznań, Poland). – *Urban Forestry & Urban Greening* 14(1): 107-114. DOI: 10.1016/j.ufug.2014.12.003.

- [17] Eichel, J., Krautblatter, M., Schmittlein, S., Dikau, R. (2013): Biogeomorphic interactions in the Turtmann Glacier forfield, Switzerland. – *Geomorphology* 201: 98-110. DOI: 10.1016/j.geomorph.2013.06.012.
- [18] Egger, G., Politi, E., Angermann, K., Schneider, M., Kopecki, I., Habersack, H., Blamauer, B., Sattler, S., Mayr, P. (2013a): EcoRiver Linking riparian vegetation and hydrodynamic processes: an integrated dynamic simulation model. – Technical Report 2112650: 2013.
- [19] Egger, G., Politi, E., Garófano-Gómez, V., Blamauer, B., Ferreira, M. T., Rivalles, R., Benjankar, R. et al. (2013b): Embodying Interactions of Riparian Vegetation and Fluvial Processes into a Dynamic Floodplain Model: Concepts and Applications. – In: Maddock, I., Harby, A., Kemp, P., Wood, P. (eds.) *Ecohydraulics: An Integrated Approach*. John Wiley & Sons Ltd, New York.
- [20] Funk, A., Martínéz-Lopéz, J., Borgwardt, F., Trauner, D., Bagstad, K. J., Balbi, S., Magrach, A., Villa, F., Hein, T. (2019): Identification of conservation and restoration priority areas in the Danube River based on the multi-functionality of river-floodplain systems. – *Science of the Total Environment* 654: 763-777. DOI: 10.1016/j.scitotenv.2018.10.322.
- [21] Garcia-Arias, A., Francés, F. (2015): The RVDM model: modelling impacts, evolution and competition processes to determine riparian vegetation dynamics. – *Ecohydrology* 9(3): 438-459. DOI: 10.1002/eco.1648.
- [22] Garssen, A. G., Verhoeven, J. T. A., Soons, M. B. (2014): Effects of climate-induced increases in summer drought on riparian plant species: a meta-analysis. – *Freshwater Biology* 59(5): 1052-1063. DOI: 10.1111/fwb.12328.
- [23] Gilyear, D. J., Greenwood, M. T., Thoms, M. C. (2017): Large wood produced by riparian forests can also protect reinforce and stabilise landforms. – *Front Plant Science* 8: 1612. DOI: 10.3389/fpls.2017.01612.
- [24] Gonzáles, E., Cabezas, A., Corenblit, D., Steiger, J. (2014): Autochthonous versus allochthonous organic matter in recent soil C accumulation along a floodplain biogeomorphic gradient: an exploratory study. – *Journal of Environmental Geography* 7(1-2): 29-38. DOI: 10.2478/jengeo-2014-0004.
- [25] González, E., Sher, A. A., Tabacchi, E., Masip, A., Poulin, M. (2015): Restoration of riparian vegetation: A global review of implementation and evaluation approaches in the international, peer-reviewed literature. – *Journal of Environmental Management* 158: 85-94. DOI: 10.1016/j.jenvman.2015.04.033.
- [26] Gurnell, A. M. (2014): Plants as river system engineers. – *Earth Surface Processes and Landforms* 39(1): 4-25. DOI: 10.1002/esp.3397.
- [27] Gurnell, A. M., Corenblit, D., García de Jalón, D., González del Tánago, M., Grabowski, R. C., O'Hare, M. T., Szewczyk, M. (2016a): A conceptual model of vegetation-hydrogeomorphology interactions within river corridors. – *River Research and Applications* 32(2): 142-163. DOI: 10.1002/rra.2928.
- [28] Gurnell, A. M., Rinaldi, M., Buijse, A. D., Brierley, G., Piégay, H. (2016b): Hydromorphological frameworks: emerging trajectories. – *Aquatic Sciences: Research Across Boundaries* 78(1): 135-138. DOI: <http://dx.doi.org/10.1007/s00027-015-0436-1>.
- [29] Habersack, H., Hein, T., Stanica, A., Liska, I., Mair, R., Jager, E., Hauer, C., Bradley, C. (2016): Challenges of river basin management: Current status of, and prospects for, the River Danube from a river engineering perspective. – *Science of the Total Environment* 543(A): 828-845. doi: 10.1016/j.scitotenv.2015.10.123
- [30] Havel, J. E., Kovalenko, K. E., Thomaz, S. M., Amalfitano, S., Kats, L. B. (2015): Aquatic invasive species: challenges for the future. – *Hydrobiologia* 750(1): 147-170. DOI: 10.1007/s10750-014-2166-0.
- [31] Hennekens, S. (1998-2012): *Turboveg for Windows*. – Version 2.
- [32] Hession, W. C., Curran, J. C. (2013): The Impacts of Vegetation on Roughness in Fluvial Systems. – In: Shroder, J. F., Butler, D. R., Hupp, C. R. (eds.) *Treatise on*

- Geomorphology. Vol 12. Ecogeomorphology. Academic Press, San Diego. DOI: 10.1016/B978-0-12-374739-6.00323-7.
- [33] Kazakova, A. I., Semikolennykh, A. A., Gornov, A. V., Gornova, M. V., Lukina, N. V. (2018): Influence of vegetation on the lability characteristics of sandur areas of the Bryansky Les Nature Reserve. – Moscow University Soil Science Bulletin 73(3): 100-106. <https://doi.org/10.3103/S0147687418030055>.
- [34] Kath, J., Reardon-Smith, K., Le Brocq, A. F., Dyer, F. J., Dafny, E., Fritz, L., Batterham, M. (2014): Groundwater decline and tree change in floodplain landscapes: Identifying non-linear threshold responses in canopy condition. – *Global Ecology and Conservation* 2: 148-160. <https://doi.org/10.1016/j.gecco.2014.09.002>.
- [35] Kim, D., Kupfer, J. A. (2016): Tri-variate relationships among vegetation, soil and topography along gradients of fluvial biogeomorphic succession. – *PLoS One* 11(9): e0163223. DOI: 10.1371/journal.pone.0163223.
- [36] Kondolf, M. G., Piégay, H. (eds.) 2016: *Tools in Fluvial Geomorphology*. – Wiley-Blackwell, New York.
- [37] Kui, L., Stella, J. C. (2016): Fluvial sediment burial increases mortality of young riparian trees but induces compensatory growth response in survivors. – *Forest Ecology and Management* 366: 32-40. DOI: 10.1016/j.foreco.2016.02.001
- [38] Kui, L., Stella, J. C., Lightbody, A., Wilcox, A. C. (2014): Ecogeomorphic feedbacks and food loss of riparian tree seedlings in meandering channel experiments. – *Water Resources Research* 50: 9366-9384. DOI: 10.1002/2014WR015719.
- [39] Lamb, M. P., Brun, F., Fuller, B. M. (2017): Hydrodynamics of steep streams with planar coarse-grained beds: Turbulence, flow resistance, and implications for sediment transport. – *Water Resources Research* 53(3): 2240-2263. DOI: 10.1002/2016WR019579.
- [40] Li, S., Xia, X., Tan, X., Zhang, Q. (2013): Effects of catchment and riparian landscape setting on water chemistry and seasonal evolution of water quality in the Upper Han River Basin, China. – *PLoS ONE* 8(1): e53163. <https://doi.org/10.1371/journal.pone.0053163>
- [41] Liu, C., Neph, H. (2016): Sediment deposition within and around a finite patch of model vegetation over a range of channel velocity. – *Water Resources Research* 52(1): 600-612. DOI: 10.1002/2015WR018249.
- [42] Macura, V., Škrinár, A., Kalúz, K., Jalčovníková, M., Škrovinová, M. (2012): Influence of the morphological and hydraulic characteristics of mountain streams on fish habitat suitability curves. – *River Research and Applications* 28(8): 1161-1178.
- [43] Merritt, D. M. (2013): Reciprocal Relations between Riparian Vegetation, Fluvial Landforms, and Channel Processes. – In: Shroder, J. F., Wohl, E. (eds.) *Fluvial Geomorphology. Vol. 9. Treatise on Geomorphology*. Academic Press, San Diego. DOI: 10.1016/B978-0-12-374739-6.00323-7.
- [44] Mobaied, S., Geoffroy, J. J., Machon, N. (2016): The importance of spatiotemporal heterogeneity for biodiversity in forest heathland mosaics and implications for heathland conservation. – *Journal of Environmental Protection* 7: 1317-1332. DOI: 10.4236/jep.2016.710115.
- [45] O'Brian, R., Shephard, S., Coghlan, B. (2018): A river vegetation quality metric in ecohydromorphology philosophy. – *River Research and Applications* 34(3): 207-217. DOI: 10.1002/rra.3244.
- [46] van Oorschot, M., Kleinhans, M. G., Geerling, G. W., Egger, G., Leuven, R. S. E. W., Middelkoop, H. (2017): Modeling invasive alien plant species in river systems: Interaction with native ecosystem engineers and effects on hydro-morphodynamic processes. – *Water Resources Research* 53(8): 6945-6969.
- [47] Opperman, J. J., Moyle, P., Larsen, E. W., Florsheim, J. L., Manfree, A. D. (2017): *Floodplains: Processes and Management for Ecosystem Services*. – University of California Press, California.

- [48] Passarelli, C., Olivier, F., Paterson, D. M., Meziane, T., Hubas, C. (2014): Organisms as cooperative ecosystem engineers in intertidal flats. – *Journal of Sea Research* 92: 92-101. DOI: 10.1016/j.seares.2013.07.010.
- [49] Rinaldi, M., Surian, N., Comiti, F., Bussetini, M. (2013): A method for the assessment and analysis of the hydromorphological condition of Italian streams: the morphological quality index (MQI). – *Geomorphology* 180-181(0): 96-108. DOI: 10.1016/j.geomorph.2012.09.009.
- [50] Rinaldi, M., Surian, N., Comiti, F., Bussetini, M. (2015): A methodological framework for hydromorphological assessment, analysis and monitoring (IDRAIM) aimed at promoting integrated river management. – *Geomorphology* 251(15): 122-136. DOI: 10.1016/j.geomorph.2015.05.010.
- [51] Rivaes, R., Pinheiro, A. N., Egger, G., Ferreira, T. (2014): The role of river morphodynamic disturbance and groundwater hydrology as driving factors of riparian landscape patterns in Mediterranean Rivers. – *Freshwater Biology* 59(5): 1052-1063. DOI: 10.1111/fwb.12328.
- [52] Rössler, N., Egger, G., Drescher, A. (2018): Fluvial processes and changes in the floodplain vegetation of the Vjosa River (Albania). – *Acta ZooBot Austria* 155: 73-84.
- [53] Sankey, J. B., Ralston, B. E., Grams, P. E., Schmidt, J. C., Cagney, L. E. (2015): Riparian vegetation, Colorado River, and climate: five decades of spatiotemporal dynamics in the Grand Canyon with river regulation. – *Journal of Geophysical Research G: Biogeosciences* 120(8): 1532-1547. DOI: 10.1002/2015JG002991.
- [54] Solari, L., Van Oorschot, M., Hendriks, D., Rinaldi, M., Vargas-Luna, A. (2015): Advances on modelling riparian vegetation-hydromorphology interactions. – *River Research and Applications* 32(2): 164-178. DOI: 10.1002/rra.2910.
- [55] Sponseller, R. A., Heffernan, J. B., Fisher, S. G. (2013): On the multiple ecological roles of water in river networks. – *Ecosphere* 4(2): 17. <http://dx.doi.org/10.1890/ES12-00225.1>
- [56] Stallings, K. D., Seth-Carley, D., Richardson, R. J. (2015): Management of aquatic vegetation in the southeastern United States. – *Journal of Integrated Pest Management* 6(1): 3. <http://dx.doi.org/10.1093/jipm/pmv002>.
- [57] Surian, N., Barban, M., Ziliani, L., Monegato, G., Bertoldi, W., Comiti, F. (2015): Vegetation turnover in a braided river: frequency and effectiveness of floods of different magnitude. – *Earth Surface Processes and Landforms* 40(4): 542-558. <https://doi.org/10.1002/esp.3660>.
- [58] Tagwireyi, P., Sullivan, M. P. (2015): Riverine landscape patch heterogeneity drives riparian ant assemblages in the Scioto River Basin, USA. – *PLoS ONE* 10(4): e0124807. DOI: 10.1371/journal.pone.012480.
- [59] Thomas, L. K., Mosner, E., Leyer, I. (2015): River dynamics and invasion: distribution patterns of native and invasive woody vegetation at the Río Negro, Argentina. – *Riparian Ecol. Conserv.* 2: 45-57. DOI: 10.1515/remc-2015-0001.
- [60] Varigin, A. Y. (2018): Biotic links in the fouling community of Odessa Bay (Black Sea). – *Biosystems Diversity* 26(1): 24-29. DOI: 10.15421/011804.
- [61] Warner, A. T., Bach, L. B., Hickey, J. T. (2014): Restoring environmental flows through adaptive reservoir management: planning, science and implementation through the Sustainable Rivers Project. – *Hydrological Sciences Journal* 59(3-4): 770-785.
- [62] Wohl, E. E., Bledsoe, B. P., Jacobson, B. R., Poff, N. L., Ratburn, S. L., Walters, D. M., Wilcox, A. C. (2015): The natural sediment regime in rivers: broadening the foundation for ecosystem management. – *BioScience* 65(4): 358-371. DOI: 10.1093/biosci/biv002.

ASSESSMENT OF PLANT COMMUNITIES AND IDENTIFICATION OF INDICATOR SPECIES OF AN ECOTONAL FOREST ZONE AT DURAND LINE, DISTRICT KURRAM, PAKISTAN

HUSSAIN, M.^{1,2} – KHAN, S. M.^{1*} – ABD_ALLAH, E. F.^{3*} – UL HAQ, Z.¹ – ALSHAHRANI, T. S.³ – ALQARAWI, A. A.³ – UR RAHMAN, I.⁴ – IQBAL, M.¹ – ABDULLAH¹ – AHMAD, H.⁵

¹Department of Plant Sciences, Quaid-i-Azam University, Islamabad, Pakistan

²College of Forestry, Guangxi University, Daxuedonglu 100, Nanning, Guangxi 530004, China

³Department of Plant Production, College of Food & Agricultural Sciences, P. O. Box. 2460, Riyadh 11451, Saudi Arabia

⁴Department of Botany, Hazara University, Mansehra, Pakistan

⁵Islamia College, Peshawar, Pakistan

*Corresponding authors

e-mail: shuja60@gmail.com, eabdallah@ksu.edu.sa

(Received 3rd Jan 2019 ; accepted 21st Mar 2019)

Abstract. There must be unique indicator vegetation at Ecotonal Zone in the border region of Pakistan and Afghanistan. Keeping this hypothesis in mind the forest zone of District Kurram at Durand Line was ecologically surveyed. Stations were established, GPS readings, environmental gradients were recorded and soil samples were collected. Data was statistically analysed using PC-ORD version-5 and CANOCO version-4.5. Indicator Species Analysis (ISA), constancy and fidelity level were used to find indicator species of communities. Preliminary results showed that study area hosts 195 vascular plant species belonging to 145 genera and 60 families. Cluster Analysis classified vegetation into four plant communities; (a) *Elaeagnus angustifolia-Rosa chinensis-Seriphidium kurramense* (b) *Platanus orientalis-Rosa moschata – Epilobium hirsutum* (c) *Quercus baloot – Jasminum auriculatum-Foeniculum vulgare* (d) *Quercus dilatata-Hedera nepalensis-Calamintha umbrosa*. Nitrogen, Sodium and Potassium were the strongest Physico-chemical factors ($P \leq 0.05$) determining plant communities composition. Interestingly, *Vincetoxicum cardiostephanum* was reported as narrow endemic species. Distinguished indicator species had significant environmental preferences. Variables like grazing and fodder chopping were the major vegetation drivers. Altitude was one of the most important determinants, influencing directly species distribution; Current study could be potentially used elsewhere for vegetation management and conservation strategies.

Keywords: Indicators of Transitional Zone; Kurram Agency at Pak Afghan Border; Edaphic Factors

Introduction

The “ecotone” term was coined by Clements (1905) for transition zone and considered it as a basic unit of landscape ecology (Hansen et al., 1992; Casalini et al., 2019), having extremely unique vegetation, sensitive ecosystems and sharp communities boundaries (Walker et al., 2003; Gonçalves and Souza, 2014), due to abrupt environmental changes (Arellano et al., 2017). These characteristics enhanced significance to check competing ecological theories (Neilson, 1991) and especially climate change management (Kupfer and Cairns, 1996; Judi et al., 2018). The sensitivity and mechanisms of response are differentially varied among ecosystems and

communities (Huang et al., 2016). The ecosystem continuations particularly for food security are indispensable, not merely to mountainous highland but for lowlands ecosystem; particularly who are dependent on these mountains resources (Rasul, 2010; Dolezal et al., 2016). Therefore, understanding plant and environmental variables correlations, highlighting leading threats and conservation managements are the fascinating research field for ecologists and environmentalists (Tavili and Jafari, 2009; Khan et al., 2016).

Vegetation structure and composition are persuaded by numerous natural and anthropogenic activities (Shaheen et al., 2012; Lyu et al., 2017). Thus, ecosystem services quantification and evaluating vegetation distribution and mapping are important for conservation (Biondi, 2011). Vegetation classification into possible plant communities is also a mandatory part of ecosystem ecology, natural resource management and habitats degradation and fragmentation studies (Khan et al., 2015). It would visualise heterogeneity insights of particular vegetation's type (Haq et al., 2015b). Plant ecologists often hypothesized vegetation driving mechanism and environmental gradients (Willig et al., 2003; Haq et al., 2015a). In mountainous region topography and elevation had strong effects on species diversity, richness and community structures (Khan et al., 2015; Ullah et al., 2015). Anthropogenic disturbances may trigger species shifting (Johnstone and Chapin, 2003) and/or probably eliminate forest products (Brown and Johnstone, 2012) and alter ecosystem function (D'Amato et al., 2011). Long-term overgrazing could have legacial effects on plant diversity, biomass production and edaphic factors (Sher et al., 2010; Sternberg et al., 2017). The soil micro and macro nutrients level can significantly affect species richness and communities Byrne et al. (2017) examined plant's responses against precipitational change and concluded comparatively high level sensitivity. Chang et al. (2018) and Skagen et al. (2018) emphasized forest sensitivity and responses against precipitation variation in ecotones over a time scale.

The indicator species identification ultimately helps in management and restoration of natural resources (Ahmad and Khan, 2004; Mashwani et al., 2011). Keeping the hypothesis in mind; there must be unique indicator vegetation at Ecotonal Zone. The current study was designed to evaluate the vegetation and communities, indicator species and to determine whether soil characteristics and/or anthropogenic activities influences on community distribution in the ecotonal zone. The aim was designed with three main objectives; to quantify vegetation of the ecotonal region, to classify vegetation in major communities along the geo-climatic and altitudinal environmental gradients and to assess the indicator species under the influence of disturbances for future generation management. Additionally, current study documented suggestions for the mountainous plant biodiversity conservation under the scenario of continuous anthropogenic activities.

Material and methods

Study area description

The Kurram Valley is situated in the far West of the Khyber Pukhtunkhwa (KP), Pakistan, projecting like a neck in Afghanistan and touching Pukthia, Nangarhar and Khost provinces on its West. Previously, study area was called as FATA but on 24 May 2018 in 25th Constitutional amendment, has been merged to KP and give it agency status, It lies between 33° 20' to 34° 10' N-latitudes and 69° 50' to 70° 50' E-longitude,

with a total length of 115 km and covering 3380 km² area (Fig. 1). District Orakzai and Khyber are lies on its East, District Hangu is situated at southeast, while District North Waziristan is bordered at south. “Koh-e-Sufaid” the part of Western Himalayas, situated on its North. The highest known peak is Sikaram with an altitude of 4728 m a.s.l. This mountainous range results high annual average precipitation and hence summers remain pleasant. The valley is relatively dry and mostly represents the dry temperate-type of habitat. Heavy snowfall has been experienced in winter with a freezing temperature (Fig. 6). The study area, floristically the part of Western Irano-Turanian region of the Western Himalayan province. Moreover, it gains distinctive position to act as botanical buffer zone between the dry temperate and moist temperate vegetation zones of the Himalayan and Hindu Kush mountainous ranges, respectively. Thus, due to this unique transitional locality, the valley hosts typical vegetation and position in the region. Vegetation is predominated by oak, blue pine, cheer pine forests and chilgoza pine in the extreme border with Afghanistan. Despite of high phytogeographic status factor like; geopolitical conflicts, harsh terrain, long history of Afghan war, low literacy rate and feudal tribal laws divert the concentration of the scientific societies to evaluate the region ecologically. Therefore, project was lunched to evaluate quantitatively.

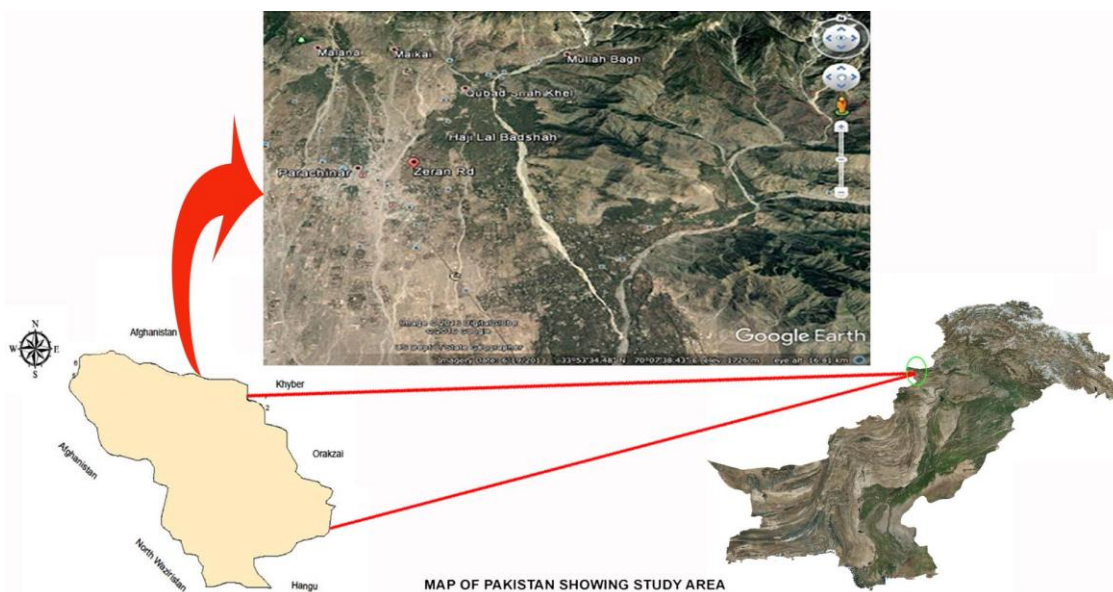


Figure 1. . Map of the Zeran valley (Border region of Pakistan and Afghanistan).

Field sampling techniques for vegetation quantification

During the summer season of 2016 to 2017, phytosociological techniques were used for vegetation assessment along edaphic and other related environmental transects (Laurance et al., 2004; Khan et al., 2012). The area was divided into seven different stations on the basis of floristic composition, physiognomy, topography and altitudinal variation (McMahon et al., 2011). Mature and least disturbed vegetation of the study area was focused (Laurance et al., 2004). A mixture of transect and quadrats method was frequently used. Square shape quadrats 1 × 1 m², 5 × 5 m² and 10 × 10 m² for herbs, shrubs and trees respectively were laid in each station. The plant species were collected from respective habit type, vernacular names, family names and other relevant

information were recorded in the field note books. The collected plant specimens were properly pressed, dried using blotting papers, poisoned and finally mounted on the standard herbarium sheets. All specimens were preserved in the Herbarium of Quaid-I-Azam University, Islamabad, Pakistan for future reference. The specimens were identified with help of the Flora of Pakistan (Ali et al., 1972–2009; Ali and Qaiser, 1986, 1995–2010) and available literatures at Islamabad Herbarium, Quaid-I-Azam University and National Herbarium at National Agriculture Research Centre (NARC), Pakistan. The scientific names of all plant species were confirmed from the plant list website (<http://www.theplantlist.org>).

The quantitative vegetation attributes i.e., density, cover, frequency and their relative values were recorded. Importance Value Indices of species were also calculated (Curtis and McIntosh, 1950). Various environmental variables like grazing pressure, soil depth and condition, number of stumps, elevation and aspects were recorded with special concentration. Geographical co-ordinates of each site were noted using GPS. The community's names were based on ISA, species constancy and faithfulness.

Soil sampling and analyses

Since the top-soil soil contains greater nutrient concentration and highest organic matter contents. Mostly roots biomass is accumulated throughout this soil profile (Vallés et al., 2015; Jobbágy and Jackson, 2001). Within each quadrat, soil samples were randomly collected from each microsite, and then mixed accordingly to make a unique pooled. Pebbles and wood pieces were removed. The samples were shade dried, sieved, air dried, ground and analysed for the selective physico-chemical edaphic factors in a Fauji Fertilizer Company (FFC) limited farm advisory centre, Hasan Abdal, Pakistan. The soil texture was determined by the hydrometer method of particle-size analysis (Day, 1965). The Organic carbon (O.M) contents were analysed via (Nelson and Sommers, 1996) methodology and Nitrogen was measured following the semi-micro Kjeldahl procedure of (Bremner and Mulvaney, 1982). Electric conductivity (E.C) was analysed in saturation extract using (Rhoades, 1982) protocol. Potassium and Phosphorus were analysed according to (Soltanpour, 1985), whilst Sodium was measured via (Rhoades and Miyamoto, 1990) methodology.

Data statistical analyses

The data obtained from field work needs to be examined in a statistical framework (Kent and Coker, 2002). It helps ecologists to analyse the effect of environmental factors, vegetation classification and mapping for conservation and management purposes (Anderson et al., 2006). Data of 252 quadrats (84 for each trees, shrubs and herbs species respectively) were alphabetically arranged in MS Excel spread sheet 2010. The utilities of PC-ORD version_5 i.e., Cluster Analysis (CA) and Indicator Species Analysis (ISA) were applied to classify plant communities (Dufrene and Legendre, 1997), analyse distribution pattern and identify indicator species respectively. CA brings stations with similar floristic composition close to each other (Sorensen, 1948; Dalirsefat et al., 2009). The ISA identified indicator plant species with statistical significance ($\leq .05$) of each habitat type, defined by the environmental variable. It also constructed indicator values for each species using Monte Carlo techniques. Each species was evaluated for its ability to categorize among all the treatments of environmental variables and attributed to its suitable habitat type. ISA

provided suggestions of how well the presence of a species would indicate a specific station or plant community (Dufrene and Legendre, 1997).

Mantel test as a utility of PCORD was used to estimate the strength of the relationship between species and environmental data matrices. These tests help to test hypothesis, whether variation in factors like aspect and elevation etc would have any impact on the diversity of plant species as well as communities qualitatively as well as quantitatively. The naming of plant communities was based on the indicator plant species, having significant P value ≤ 0.05 , identified by ISA, as recommended by Dufrene and Legendre (1997). Beside this, constancy and fidelity level of the characteristics species of the communities were also checked for further authentication of indicator, to use in naming the communities (Malik and Husain, 2006).

Ordination analyses for identification of ecological responsible gradients

Ordination is a multivariate statistical method that summarizes communities data by constructing a low dimensional space in which similar samples and species come closer together along the specific environmental gradients complex and dissimilar ones goes further apart from each other (Gauch, 2010). Keeping the objectives in mind, we analysed plant species data with measured environmental variables in CANOCO (Ter Braak and Barendregt, 1986). Canonical Correspondence Analyses (CCA) is the most meaningful direct ordination gradient technique (Braak, 1988). It is widely used to examine environmental factors influence (Dufrene and Legendre, 1997). The CANOCRAW, utility of CANOCO was used to construct CCA plots of species-environmental and community-environmental variables.

Results

Species diversity and dominant species

Preliminary findings confirmed total of 195 vascular plant species belongs to 144 genera of 60 Families in the study area (*Table A1* in the *Appendix*). The recorded 195 plant species belong to 144 genera and 60 families (*Table A1*). In which 3 and 5 species belongs pteridophytes and gymnosperms, whilst angiosperms dominating the area with 186 species. Within angiosperms, dicotyledons dominated the region having 160 members whilst 27 species were the representative of monocotyledons (see *Appendix*). The dominant species were evaluated on the basis of the IVI. The lower altitude (1500-2000 m) subtropical evergreen elements like *Olea ferruginea* (7.60%) and deciduous Treelets species like *Cotoneaster bacillaris* (3.79) dominated the area. In the middle attitude (2000-2500 m) broad leaved evergreen, *Quercus baloot* (8.63%) found to be dominant whilst at the higher elevational zone (2500-3000 m) moist temperate element and western Himalayan native species *Quercus dilatata* (17.11%) and *Cedrus deodara* (6.37%) forming close gregarious association. The forest thickness was positively correlated whilst species diversity and richness were negatively correlated along the elevational gradient in the study area. The lower xeric elevation was mostly occupied by habitat *Daphne mucronata* (8.58%), *Sophora mollis* (12.17%) and *Berberis lyceum* (7.99%). On the other hand higher elevational zones were dominated by, *Indigofera heterantha*, *plectranthus rugosus* and *Berberis parkeriana* by 19.04%, 14.81% and 7.39% of IVI total weightage of 21 recorded shrub species. The forest ground flora was dominated by representatives of Poaceae includes; cynodon dactylon (7.73%), *Stipa sibirica* (3.72%), *Setaria pumila* (3.26), *Piptatherum laterale*

(2.69%), *Apluda mutica* (2.56%), *Agrostis vinealis* (2.11%) with associated species; *Medicago sativa* (6.16%), *Cirsium arvense* (3.91%) *Oxalis corniculata* (2.71%) and *Viola odorata* (2.44%) in 142 recorded herbs species (Appendix). The *V. cardiostephanum* was reported after 122 years and confirms their occurrence with a rarity in Pakistan. Harsukh, collected for the first time but in non-flowering stage (Fig. 6C). Our study re-confirms the occurrence of *V. cardiostephanum* in Pakistan. Its holotype Rechinger 35614 (W) belongs to Afghanistan. Hence, it is a narrow endemic to this ecotonal region of Pak-Afghan border, with a limited distribution; probably less than 100 km². According to the IUCN red list categories and criteria it has been declared as Critically Endangered species.

Community's classification

The application of PC-ORD version-5 packages with 1,0 data gave rise to Cluster Analyses (CA); precisely divide the plant species into four major communities (Fig. 2). The communities' nomenclatures were based on the species constancy, fidelity level and Indicator Species Analyses (ISA). Each indicator species was studied under the influence of environmental variables. The Monte Carlo test result showed that; Nitrogen (N), Sodium (Na), Soil texture (S.T) and altitude played significant role in communities' composition. The Monte Carlo test result shows the strength of the environment-species relationship. The first community; *Elaeagnus angustifolia-Rosa chinensis-Seriphidium kurramense* was found at the lower altitude. The habitat of this community was mostly xeric. The second community; *Platanus orientalis-Rosa moschata-Epilobium hirsutum* found, where mostly agricultural practices were noticed. The third community; *Quercus baloot-Jasminum auriculatum-Foeniculum vulgare* and fourth communities *Quercus dilatata-Hedera nepalensis-Calamintha umbrosa* were found at the high elevation (Table 1).

Table 1. Detail information of the indicator species of the all communities along with fidelity level, constancy classes and Indicator species analyses

S No.	Indicator species	Com	Constancy		F. C.	Var	I.V	P*
			C.C	C%				
1	<i>Elaeagnus angustifolia</i>	1 st	C4	68.75	72.3	N	47	0.05
						S.T	46	0.01
2	<i>Rosa chinensis</i>	1 st	C1	12.5	100	K	47	0.02
3	<i>Seriphidium kurramense</i>	1 st	C3	43.75	100	N	49	0.04
						O.M	13	0.04
4	<i>Platanus orientalis</i>	2 nd	C2	26.09	61.02	Na	25.8	0.0302
5	<i>Rosa moschata</i>	2 nd	C1	8.7	67.61	Na	66.3	0.001
						EC	19.7	0.0562
6	<i>Epilobium hirsutum</i>	2 nd	C1	4.35	100	Na	33.3	0.0358
7	<i>Quercus baloot</i>	3 rd	C2	29.17	50.52	pH	56.1	0.0528
8	<i>Jasminum auriculatum</i>	3 rd	C1	12.5	100	pH	33.3	0.0386
9	<i>Foeniculum vulgare</i>	3 rd	C1	4.17	100	Na	33.3	0.032
						EC	20	0.0526
10	<i>Quercus dilatata</i>	4 th	C3	52.38	100	K	33.7	0.0196
11	<i>Hedera nepalensis</i>	4 th	C1	4.76	100	ST	33.3	0.0308
12	<i>Calamintha umbrosa</i>	4 th	C1	14.29	76.67	K	43.9	0.011
						Na	32.8	0.0196

Com = community, C.C = Constancy class, C% = Constancy%, F.C = Fidelity class, Var = Variables, I.V = Indicator Value, P* = significant value

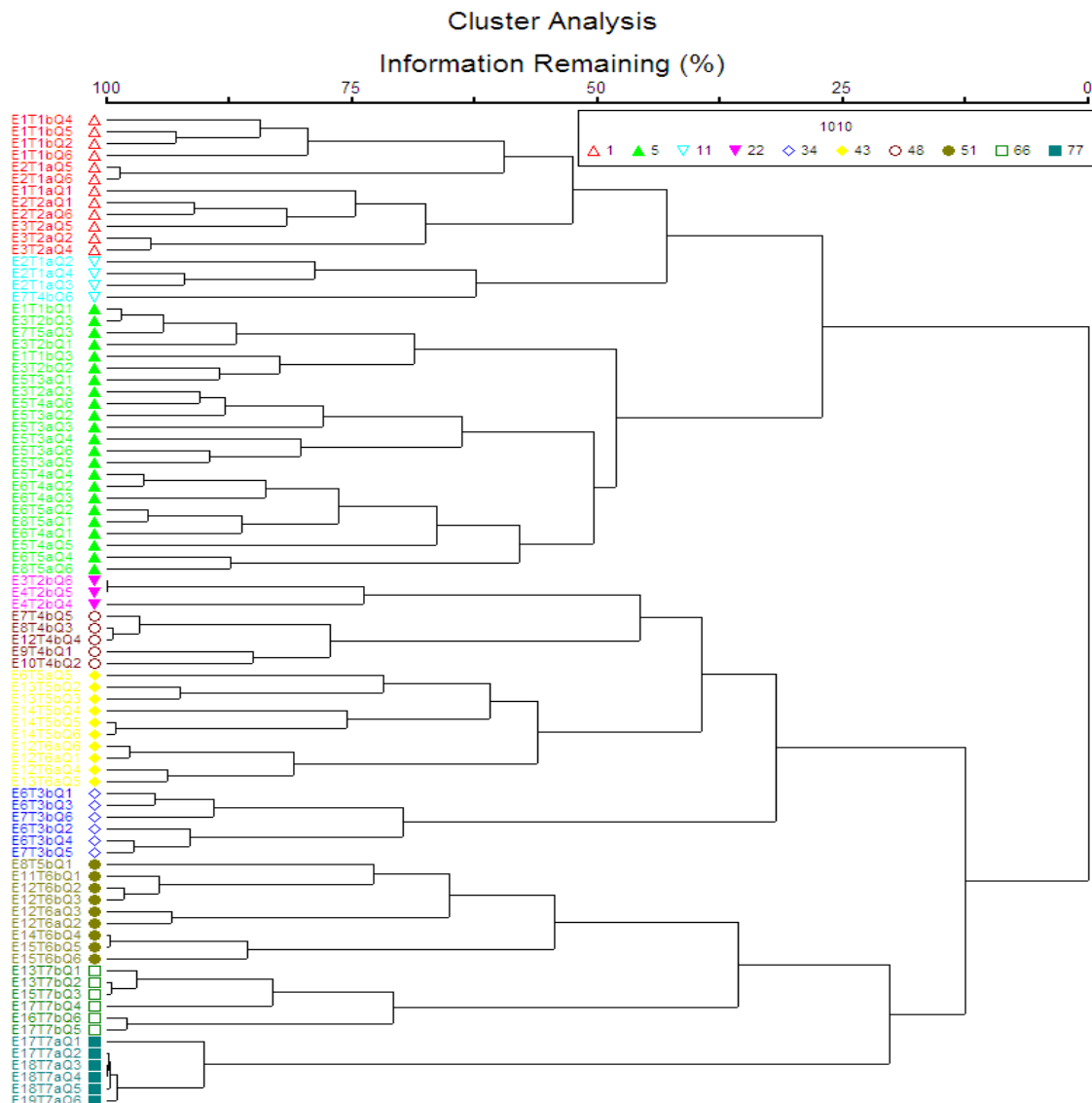


Figure 2. Cluster Analysis classifying the study sites into four communities.

1. *Elaeagnus angustifolia* – *Rosa chinensis* – *Seriphidium kurramense* community

The application of CA and TWCA based on Sorenson Similarity Index, a total of 48 releves clustered in this community. It was found at the elevation range of 1550-1900 m above sea level (a.s.l). The name was given based on significant indicator species (P^* value ≤ 0.05) i.e., *Elaeagnus angustifolia*, *Rosa chinensis* and *Seriphidium kurramense* respectively (Table 1). Impacts of edaphic factors were also analysed and found that higher Nitrogen and Potassium concentration and medium Organic matter were the most prominent driving environmental variables in determination of these indicator species (Fig. 5). Moreover, these species have higher constancy fidelity within this community (Table 1). The concentration of N and pH in this community is higher as it comprises of the cultivated land, where use of fertilizers like Di-Ammonium Phosphate (Muthuramkumar et al.), Nitro-Phos (NP) and Potassium sulphate are repeatedly used for higher yields. Based on IVI values the dominant tree species includes *Robinia*

pseudoacacia, *Punica granatum* and *Populus nigra*. Amongst the shrubby layer *Daphne mucronata* and *Berberis lycium* were the dominant whereas in the herbaceous layer *Cynodon dactylon*, *Sanguisorba minor* and *Dichanthium annulatum* were reported as dominated species of this community.

Being located at lower elevation numbers of anthropogenic activities i.e., deforestation for fuel and fodder purposes, over grazing and agricultural land expansion are the main threats to the vegetation of this community. It was easily accessible to vicinity of human settlement to utilize the local plant resources. The physio-chemical analyses of this community revealed that pH ranges from 6.8 to 7.8, Nitrogen (0.032-0.87%), Sodium (0.5-1.4 mmolc/100 g), Electrical Conductivity (0.17-0.33 dS/m), Phosphorous (1-4 ppm), Potassium (106-420 ppm) and Organic matter (0.51-1.39%).

2. *Platanus orientalis* – *Rosa moschata* – *Epilobium hirsutum* community

This community was found at the middle elevation (1950-2300 m) of the valley. It hosts 84 different quadrats. The characteristic species of tree, shrub and herb layers were *Platanus orientalis*, *Rosa moschata* and *Epilobium hirsutum* respectively. Sodium and EC were the main environmental variables determining the indicator species of this community (Fig. 5). We observed that *Rosa moschata* was found in higher while other indicator species observed at a moderate concentration of Sodium and Electrical Conductivity respectively. The indicator species was found with relatively lower constancy level and higher fidelity level within this community (Table 1). The other important tree species present were *Populus nigra*, and *Diospyros lotus*. These species were cultivated, therefore gains dominancy in this community as well. Abundant shrub species reported were *Sambucus nigra*, *Rubus fruticosus* and *Indigofera heterantha*. Dominant herbs species were *Medicago sativa* and *Impatiens edgeworthii* in this community.

Agricultural practices were found as the top disturbing elements in this community. Analysing of soil showed that pH ranges from 7.1 to 7.9, Nitrogen (0.043-0.078%), Sodium (0.6-1.5 mmolc/100 g), Electrical Conductivity (0.15-1.18 dS/m), Phosphorous (2-6 ppm), Potassium (84-900 ppm) and Organic matter (0.69-1.25%).

3. *Quercus baloot* – *Jasminum auriculatum* – *Foeniculum vulgare* community

Based upon Sorenson index of similarity measurement this community was established relatively at the higher elevation, i.e., 2350-2780 m. Vegetation of this community was dominated by woody plants. Diagrammatic presentation of cluster dendrogram show total 72 releves clustered together in this community. The principle indicator species of this community were *Quercus baloot*, *Jasminum auriculatum* and *Foeniculum vulgare*. The important environmental variables responsible for the community establishment were slightly higher pH, moderate Sodium and higher concentration of EC (Fig. 5). All the characteristic species of this community show higher level of faithfulness (Table 1). This community comprises of a thick forest dominated by ever green tree species i.e., *Quercus semicarpifolia*, *Olea ferruginea* and deciduous tree species like *Celtis caucasica*. *Indigofera heterantha*, *Plectranthus rugosus* and *Sophora mollis* were the dominant shrubs. *Piptatherum laterale* and *Thymus linearis* were the dominant herb species.

Fodder, fuel wood, chopping and grazing were observed as main anthropogenic activities disturbing the natural vegetation equilibrium. Soil analyses of this community

indicates that pH ranges from 6.8 to 7.8, Nitrogen (0.048-0.079%), Sodium (0.3-2.4 mmolc/100 g), Electrical Conductivity (0.07-1.33 dS/m), Phosphorous (2-10 ppm), Potassium (42-560 ppm) and Organic matter (0.76-1.26%).

4. *Quercus dilatata* – *Hedera nepalensis* – *Calamintha umbrosa* community

This was the community of highest elevation range, that is 2800-3000 m a.s.l. It was represented by 63 quadrats. The analysis inveterate that; *Quercus dilatata*, *Hedera nepalensis* and *Calamintha umbrosa* were the strongest indicator species with a p values < 0.05, under the influence of high Potassium and moderate Sodium concentration (Fig. 5). The characteristic species showed high fidelity and moderate constancy level (Table 1). This was tree dominating community comprised of the principle indicator of moist temperate vegetation i.e., *Cedrus deodara*, *Quercus baloot* and *Pinus brutia* as dominant tree species. Dominant shrub species were *Indigofera heterantha*, *Plectranthus rugosus* and *Berberis parkeriana*. This community has slightly lower species richness in comparison to the other communities. *Thymus linearis* and *Apluda mutica* were dominating the herbaceous layer of this community.

Soil depth was shallow, due to rugged topography and steep slopes. Higher grazing pressure make this community very prone for soil erosion. Lower temperature prevails throughout the year. These condition results low plant species diversity. Medicinal plant collectors for commercial purposes were the major anthropogenic activities. Large No of stumps were reported as people collect wood for timber and fuel purposes mainly from this elevation range. Physio-chemical analyses revealed pH ranges from 7.2-8, Nitrogen (0.052-0.072%), Sodium (0.-1.4 mmolc/100 g), Electrical Conductivity (0.08-0.28 dS/m), Phosphorous (2-6 ppm), Potassium (60-8690 ppm) and Organic Matter (0.15-1.12%). Due to thick forest layer soil texture of this community was sandy clay loam.

Direct environmental gradient analyses

The plant and environmental data treatment via CCA identified the core factors; showing high significant p-value < 0.002. The CCA bi-plot showed that both vegetation variations and communities' variations were mainly driven by; stumps, grazing pressure, Phosphorous, Sodium and Nitrogen (Table 2). The CCA ordination procedures for species and communities (Figs. 3, 4 and 5) indicated that 1st axis strongly correlated with altitude and partially with pH; the 2nd axis was mainly correlated with stumps (due to immense deforestation), high concentration of sodium and strong EC; 3rd quadrat correlated with high Phosphorous and medium organic matter (O.M) whilst the 4th axis was under the immense grazing pressure (Figs. 3 and 4). Similarly stations CCA bi-plot (Fig. 5) demonstrated clear reflection of altitudinal and latitudinal gradient complexes of the region. The 1st and 2nd community were clustered at the lower altitude. Moreover, it also describes stations of woody and evergreen vegetation was mostly found at the higher elevation. The physiographic and geomorphologic gradient complexes describes that depth soils and sunlight exposures loving vegetation were frequently distributed at lower parts whilst relatively thin soils an shad loving species favoured the high elevated habitats. The sum of all Eigen value Monte Carlo test were 14.312. The 1st axis eigen value was quite high (0.469), which showed the slope in spreading species along with the axis. The 1st axis cumulative percentage of Species-environment relation was 21.6%

of total unexplained variance. This value of 4th axis was the highest with 65.1% (Table 2).

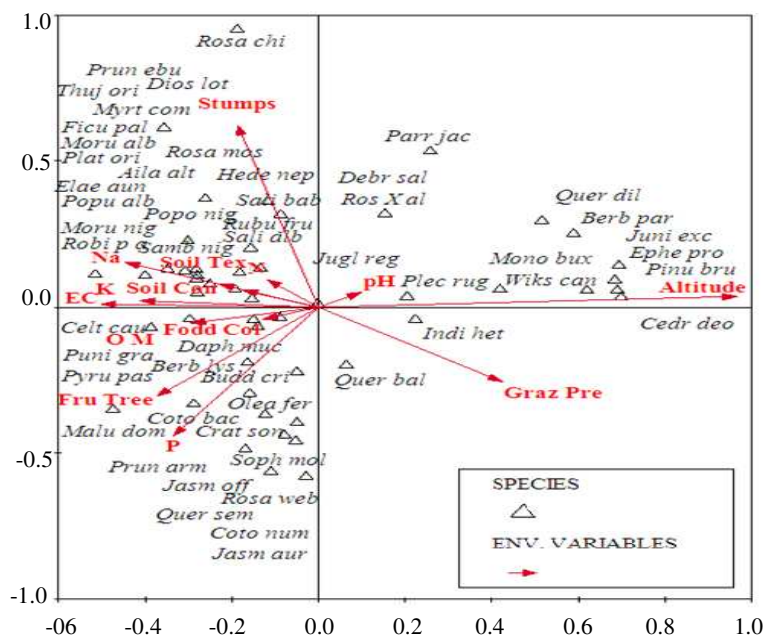


Figure 3. CCA diagram showing distribution trees and shrubs species along the environmental gradients. P = Phosphorous, Na = Sodium, K = Potassium, OM = Organic Matter, Soil Tex = Soil Texture, N= Nitrogen and EC = Electric Conductivity, Fru tree= Fruit trees, Soi Tex= Soil texture, Graz Pre= Grazing pressure, Soil con= Soil Condition

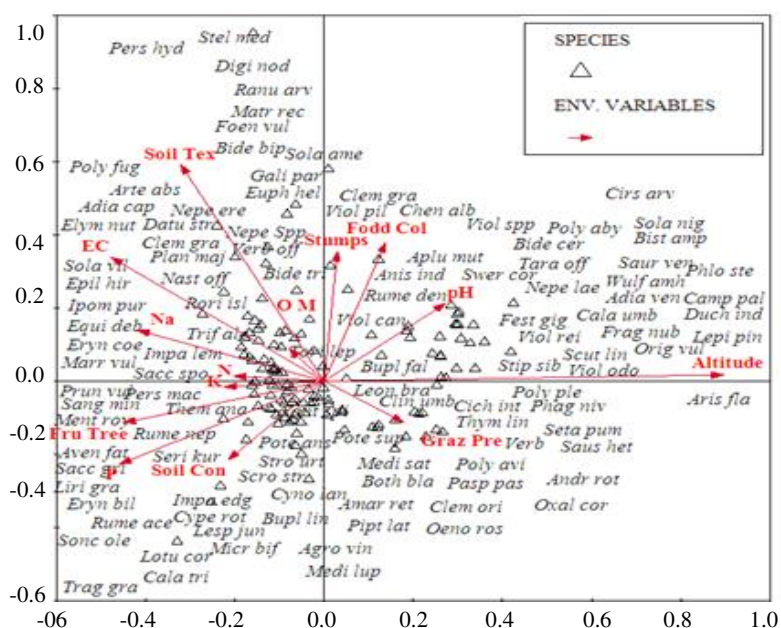


Figure 4. CCA diagram showing distribution herbs species along the environmental gradients. P = Phosphorous, Na = Sodium, K = Potassium, OM = Organic Matter, Soil Tex = Soil Texture, N = Nitrogen and EC = Electric Conductivity, Fru tree = Fruit trees, Soi Tex = Soil texture, Graz Pre = Grazing pressure, Soil con = Soil Condition

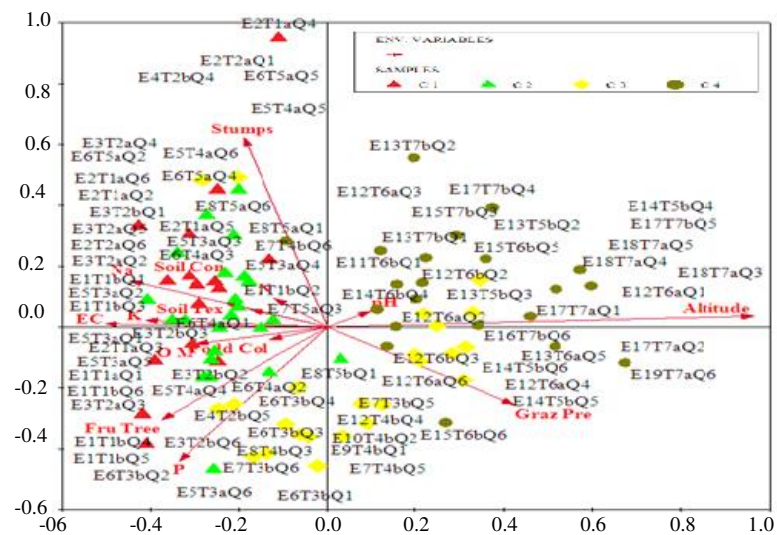


Figure 5. CCA diagram showing distribution selected stations along the environmental gradients. P = Phosphorous, Na = Sodium, K = Potassium, OM = Organic Matter, Soil Tex = Soil Texture, N = Nitrogen and EC = Electric Conductivity, Fru tree = Fruit trees, Soi Tex = Soil texture, Graz Pre = Grazing pressure, Soil con= Soil Condition, C1 = Community 1st, C2 = Community 2nd, C3 = Community 3rd and C4 = Community 4th

Table 2. Summary of the CCA bi-plot four axes of Monte Carlo test for the ecotonal vegetation using IVI data

Axes	1	2	3	4	Total inertia
Eigen values	0.469	0.394	0.288	0.262	14.312
Species-environment correlations	0.903	0.880	0.909	0.836	
Cumulative percentage					
Variance of species data	3.3	6.0	8.0	9.9	
Species-environment relation	21.6	39.7	53.0	65.1	
Sum of all eigen values					14.312
Sum of all canonical eigen values					2.170
Summary of Monte Carlo test (499 permutations under reduced model)			Test of significance of all canonical axes		
Eigen value	0.469		Trace		2.473
F-ratio	2.539		F-ratio		1.675
P-value	0.002		P-value		0.002

Discussion

Biological assemblages could evaluate significantly the deteriorative impacts of anthropogenic activities on natural ecosystems (Kusnierz et al., 2015). Ecotones can be differentiated on the bases of the sharpness of their communities (Lloyd et al., 2000). The most appropriate causes are; sharp climatic gradient, elevation, invasion of dominant, steep topography and environmental factor especially human influences (Walker et al., 2003; Casalini, 2017). Results strongly support our hypothesis to have unique indicator vegetation at Ecotonal Zone and edaphological factors affecting

community composition. A total of 195 belongs to 60 families of vascular plant species, were reported in varied ecological zones of the valley (*Appendix*). Altitude was one of the most important determinants, influencing directly species distribution; because it governs the micro climate of the habitats (Casalini, 2017; Singh et al., 2009). In the lower altitude (1500-2000 m) subtropical evergreen elements like *Olea ferruginea* (7.60%) in an association with deciduous Treelets species *Cotoneaster bacillaris* (3.79) were recorded as dominated. In the middle attitude (2000-2500 m) broad leaved evergreen species, *Quercus baloot* (8.63%) whilst moist temperate element and western Himalayan native species *Quercus dilatata* (17.11%) and *Cedrus deodara* (6.37%) at the elevation of 2500-3000 m were reported as dominant. *Daphne mucronata* (8.58%), *Sophora mollis* (12.17%) and *Berberis lyceum* (7.99%, sub-tropical indicator) dominated the lower xeric elevation, whilst *Indigofera heterantha* (19.04%), *Plectranthus rugosus* (14.81%) and *Berberis parkeriana* (7.39%) find as dominant shrub species. The herbaceous flora was dominated mostly Poaceae members; cynodon dactylon (7.73%), *Stipa sibirica* (3.72%), *Setaria pumila* (3.26), *Piptatherum laterale* (2.69%), *Apluda mutica* (2.56%), *Agrostis vinealis* (2.11%) along with *Medicago sativa* (6.16%), *Cirsium arvense* (3.91%) *Oxalis corniculata* (2.71%) and *Viola odorata* (2.44%) in 142 recorded herbs species (*Appendix*). The *V. cardiostephanum* occurrence was reconfirmed after Harsukh (122 years later) and who collected it in non-flowering stage (*Fig. 6C*). We collect it in flowering stage and occupying less than 100 km², so applying IUCN category and criteria; declared it as its holotype Rechinger 35614 (W) belongs to Afghanistan. Hence, it is a narrow endemic to this ecotonal region of Pak-Afghan border, with a limited distribution; probably less.

The species richness and Diversity Index were optimum at middle elevations (2000-2400 m a.s.l) as compare to the lower (1500-150 m a.s.l), and higher altitudes due to various pressures and xeric conditions at these areas. Reporting moist indicator climatic species like; *Cedrus deodara*, *Indigofera heterantha*, *Bistorta amplexicaulis* and *Trifolium repen* (*Appendix*) in the high elevation is supported by Saima et al. (2009) and Ahmed et al. (2006) studies. The gradual decreasing in species richness along the increasing altitude is considered as a general pattern Shaheen et al. (2011, 2012). Such phenomena of species distribution have also been reported from other mountainous locations using more or less same techniques, i.e., Anderson et al. (2006), Ahmad et al. (2015) and Haq et al. (2017). The micro climatic conditions of the valley vary from sub-tropical to cool temperate zone is in accordance to and Shen et al. (2015) and Zhou et al. (2018). The vegetation of Irano-Toranian and Western Himalayan types for example *Parrotiopsis jacquemontiana* is one of such indicator from the Current location as well. Comparison with previous researches in the adjacent areas indicates similar vegetation zones Khan and Ahmad (2015), Khan et al. (2016) and Haq et al. (2015a).

The multivariate statistical analysis via PCORD V-5 software sorted out the vegetation into 4 plant communities (*Fig. 2*) on the bases of indicator plant species. Approach to the communities naming based on statistical approaches, specifically Indicator Species Analysis in conjunction with fidelity (faithfulness) and constancy measurements of Bergmeier (2002) is one of the technical feature of our finding. The use of indicator species to determine environmental conditions and community types is an emerging technique in vegetation ecology for both theoretical and applied purposes. This use of multispecies environmental or ecological indications instead of single or repetitive indicator has enormously contributed in the bio-indication system and its reliability (Carignan and Villard, 2002; Niemi and McDonald, 2004; Butler et al., 2012;

Rahman et al., 2019). The characteristic species of each community was confirmed through Indicator Species Analyses, Species fidelity Level and constancy classes. Similar procedure for communities composition were also adopted by Shaheen et al. (2011) Khan et al. (2012), Khan (2012), Ahmad et al. (2016), Bano et al. (2017), Pharswan and Mehta (2010) and Ilyas et al. (2012) in their respective research. Indicator species analyses revealed that Nitrogen, Phosphorous, Sodium, EC and pH were the strongest and significant edaphic factors ($p \leq 0.05$) for the constitutions plant communities and determination of indicator species (Table 1). Khan et al. (2016) used the same method with unique results from Thandiani Sub-Forest Division of the Western Himalayas. Soil factors influences over plant distribution in the ecotonal region agreed with the previous studies of El-Keblawy et al. (2015) and Grellier et al. (2014).

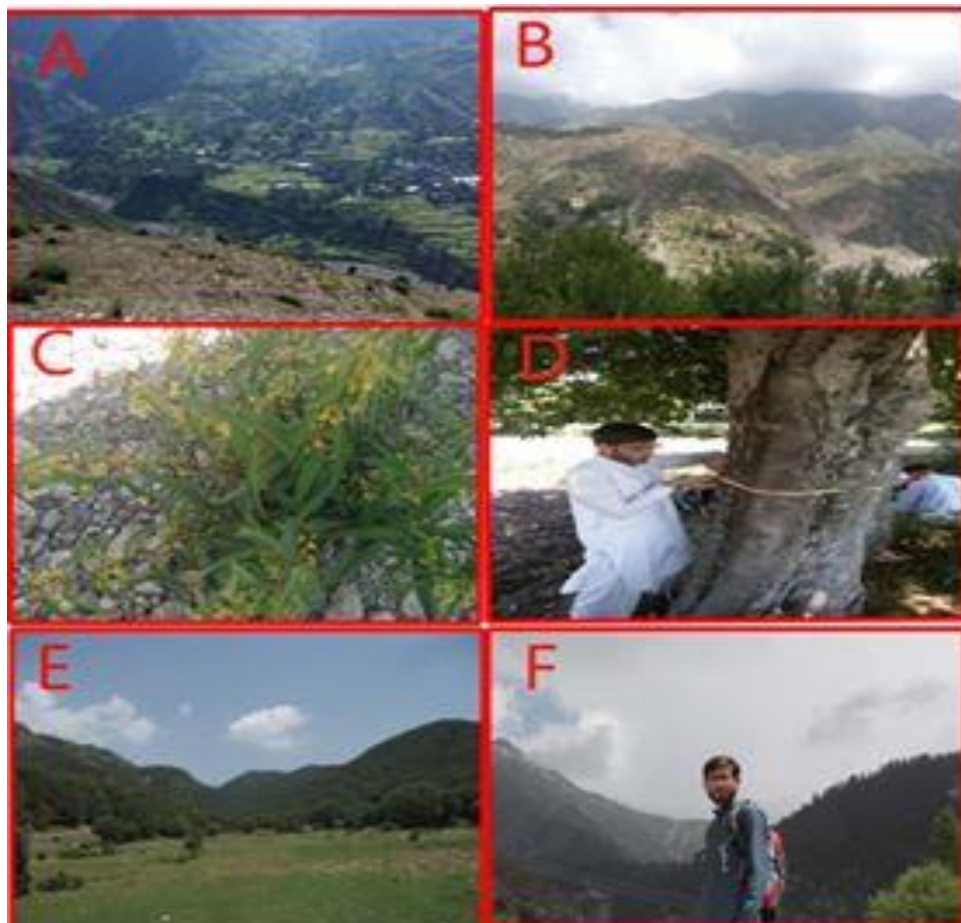


Figure 6. Pictorial view of the ecotonal region, (A) settlements with agricultural practices, (B) South facing Barren mountains range (C) *Vincetoxicum cardiostephanum* in flowering stage (D) measuring DBH of *Crataegus songarica*, (E) *Quercus dilatata* thick forest and pastures zone, (F) Snow covered high elevated mountains peak

CANOCO version 4.5 was used to analyse the effect of biotic and abiotic factors on species composition, diversity and community structure (Figs. 3, 4 and 5). Use of these Software packages can be seen in the studies of Brown and Bezuidenhout (2005) and Khan et al. (2012b). The elevation, longitude and latitude were responsible for microclimatic variations. Dense vegetation was observed on the north facing slopes as

compared to south facing slopes in the high elevation of the valley. The environmental gradients like elevation, soil conditions, grazing pressure and soil texture clearly indicates strong impacts on species diversity and composition of the region (Figs. 4 and 5; Table 2). Soil depth decreases with the high elevation due to steep slopes in areas where soil erodes during rainy seasons. The Organic matter concentration in the lower region (Figs. 3, 4 and 5) is quite high, it was the prime factor retaining higher species diversity and thick vegetation cover, is in accordance to the Casalini (2017) and Bao-Liang et al. (2009) because it is reliable to retain greater humidity and moisture concentration in landform (Pei et al., 2010). Ecologists recommended such ecosystems to support higher biodiversity and combat with climatic challenges. CCA bi-plot also revealed that species were highly sensitive to EC, Phosphorous and sodium (Fig. 3 and 4). These findings are in agreements with Khan et al. (2013) and Shaukat et al. (2014). Furthermore, increasing herbaceous vegetation along the elevation gradients indicates the positively correlation with eco-physiological stresses along the increasing altitude. The physiographic elements altitudinal range variations and edaphic factors have great effect on vegetation structure and its distribution pattern (Fig. 5). Plant species restricted to a particular habitat due to the availability of their requirements and optimum environmental factors. These factors clearly change the community structure and their distribution from point to point. Now a-days such studies have been adopted by numerous of ecologists and environmentalists to correlate the communities with the environmental factors (Chawla et al., 2008 and Khan et al., 2015).

Amongst the anthropogenic stimuli (counting stumps) repeated fuel-wood chopping is considered the major factor having huge impacts on the structure of the vegetation and results declining and almost disappearance of large old trees (Fig. 3 and 4). The most preferred species for fuel wood consumptions includes; *Quercus dilatata*, *Q. baloot*, *Olea ferruginea*, *Morus nigra* and *M. alba*. The greater wood extraction level than the carrying capacity causes a proportional changes in structure and community composition. Moreover, harvesting scenarios also increase ecological impacts. Once they become lost, large gap will be created; so forest fragmentation will be enhanced and probably susceptibility to invasion will be promoted (Rüger et al., 2008); and will inhibit the native seedlings regeneration (Cochrane, 2003). The grazing pressure has negatively affected the species diversity and vegetation structure (Fig. 3 and 4), this happen because over grazing can alter soil chemistry and also make it prone for the erosion (Rooney and Waller, 1998). The heavy and uncontrolled grazing and trampling by large amount of cattle on daily by local nomads is alarming situation. For best management legislation, the regeneration patterns and the main governing factors should be addressed (Wangda, 2003). Moreover, subsequent soil erosion and harsh climate during winter season also had catastrophic affect. The dense lush green vegetation of the region are now slowly and steadily replaced by stripped steep ridges, with increasing number of houses, roads and terracing fields. Our finding suggests priorities for the biodiversity conservation via indicator species approaches. Border Area of Afghanistan is geopolitically zone of tension that makes it an Ecotonal territory with rich diversity and must be evaluated taxonomically for probable new species. Recently, ecotones have gained greater attention because also species has narrow ecological amplitude (Silva and Souza, 2018; Corenblit et al., 2011) and expected future climatic changes could affect ecotonal vegetation very strongly (Camarero et al., 2017; Gebrekirstos et al., 2014).

Conclusion

The species distribution, communities composition using edaphic and environmental variables contributed valuable information for understanding ecotonal vegetation. We concluded that fragile vegetation of this sensitive region is under tremendous pressure due to diverse anthropogenic activities. It enhanced understanding of phyto-diversity that could potentially lead for conservation, especially in the perspective of anthropogenic impacts. The robustic multivariate statistical tools recognized indicator for micro-climatic and micro-ecological zonation. Results could be improved further if; soil moisture contents studied along the topographical gradient. It will ultimately enhance edaphological and geomorphological role for vegetation management and conservation strategies in landscape ecology. Moreover, presence of endemic species required detail taxonomic and micro-ecological investigation.

Acknowledgments. The authors would like to extend their sincere appreciation to the Deanship of Scientific Research at King Saud University for its funding to this Research group NO (RG-1435-014).

REFERENCES

- [1] Ahmad, H., Khan, A. A. (2004): Conservation and sustainable use of medicinal and aromatic plants of Pakistan. – Proceedings of the International Workshop held in Islamabad, December 2, 2003.
- [2] Ahmad, H., Öztürk, M., Ahmad, W., Khan, S. M. (2015): Status of Natural Resources in the Uplands of the Swat Valley Pakistan. – In: Öztürk, M. et al. (eds.) Climate Change Impacts on High-Altitude Ecosystems. Springer, Cham, pp. 49-98.
- [3] Ahmed, M., Husain, T., Sheikh, A. H., Hussain, S. S., Siddiqui, M. F. (2006): Phytosociology and structure of Himalayan forests from different climatic zones of Pakistan. – Pakistan Journal of Botany 38(2): 361.
- [4] Ali, S., Khatoon, S. (1982): Genus *Vincetoxicum* von Wolf (Asclepiadaceae) in Pakistan. – Pakistan Journal of Botany 14: 61-68.
- [5] Ali, S., Nasir E., Qaiser M. (1972–2009): Flora of Pakistan. – Pakistan Agricultural Research Council and The University of California, USA.
- [6] Ali, S. I., Qaiser, M. (1986): A phytogeographical analysis of the phanerogams of Pakistan and Kashmir. – Proceedings of the Royal Society of Edinburgh, Section B: Biological Sciences 89: 89-101.
- [7] Ali, S. M., Qaiser M. (1995-2010): Flora of Pakistan. – Fakhri Printing Press, Karachi.
- [8] Anderson, M. J., Ellingsen, K. E., McArdle, B. H. (2006): Multivariate dispersion as a measure of beta diversity. – Ecology Letters 9(6):.683-693.
- [9] Arellano, G., Umaña, M. N., Macía, M. J., Loza, M. I., Fuentes, A., Cala, V., Jørgensen, P. M. (2017): The role of niche overlap, environmental heterogeneity, landscape roughness and productivity in shaping species abundance distributions along the Amazon–Andes gradient. – Global Ecology and Biogeography 26: 191-202.
- [10] Bano, S., Khan, S. M., Alam, J., Alqarawi, A. A., Abd_Allah, E. F., Ahmad, Z., Rahman, I. U., Ahmad, H., Aldubise, A., Hashem, A. (2017): Eco-floristic studies of the Beer Hills along the Indus River in the districts Haripur and Abbottabad, Pakistan. – Saudi Journal of Biological Sciences. <https://doi.org/10.1016/j.sjbs.2017.05.001>
- [11] Bao-Liang, C. H. I., Cheng-Si, B. I. N. G., Walley, F., Yates, T. (2009): Topographic indices and yield variability in a rolling landscape of western Canada. – Pedosphere 19(3): 362-370.
- [12] Bergmeier, E. (2002): The vegetation of the high mountains of Crete a revision and multivariate analysis. – Phytocoenologia 32(2): 205-249.

- [13] Biondi, E. (2011): Phytosociology today: methodological and conceptual evolution. – *Plant-Biosystems - An International Journal Dealing with all Aspects of Plant Biology* 145(suppl. 1): 19-29.
- [14] Braak, C. J. (1988): CANOCO—an extension of DECORANA to analyze species-environment relationships. – *Plant Ecology* 75(3): 159-160.
- [15] Bremner, J. M., Mulvaney, C. (1982): Nitrogen—Total 1. – In: Page, A. L. et al. (eds.) *Methods of Soil Analysis. Part 2: Chemical and Microbiological Properties*. SSSA, Madison, WI, pp. 595-624.
- [16] Brown, C. D., Johnstone, J. F. (2012): Once burned, twice shy: Repeat fires reduce seed availability and alter substrate constraints on *Picea mariana* regeneration. – *Forest Ecology and Management* 266: 34-41.
- [17] Brown, L. R., Bezuidenhout, H. (2005): The vegetation of the farms Ingleside and Welgedacht of the Mountain Zebra National Park, Eastern Cape. – *Koedoe* 48(2): 23-42.
- [18] Butler, S. J., Freckleton, R. P., Renwick, A. R., Norris, K. (2012): An objective, niche-based approach to indicator species selection. – *Methods in Ecology and Evolution* 3(2): 317-326.
- [19] Byrne, K. M., Adler, P. B., Lauenroth, W. K. (2017): Contrasting effects of precipitation manipulations in two Great Plains plant communities. – *Journal of Vegetation Science* 28(2): 238-249.
- [20] Camarero, J. J., Linares, J. C., García-Cervigón, A. I., Batllori, E., Martínez, I., Gutiérrez, E. (2017): Back to the future: the responses of alpine treelines to climate warming are constrained by the current ecotone structure. – *Ecosystems* 20(4): 683-700.
- [21] Carignan, V., Villard, M. A. (2002): Selecting indicator species to monitor ecological integrity: a review. – *Environmental Monitoring and Assessment* 78(1): 45-61.
- [22] Casalini, A. I. (2017): Heterogeneity of the vegetation in the ecotone between the phytogeographic provinces of the mountains and Patagonia. Description and associated factors. – *Revista Mexicana de Biodiversidad* 86: 72-79.
- [23] Casalini, A. I., Bouza, P. J., Bisigato, A. J. (2019): Geomorphology, soil and vegetation patterns in an arid ecotone. – *Catena* 174: 353-361.
- [24] Chang, C.-T., Wang, H.-C., Huang, C.-Y. (2018): Assessment of modis-derived indices (2001–2013) to drought across Taiwan's forests. – *International Journal of Biometeorology* 62: 809-822.
- [25] Chawla, A., Rajkumar, S., Singh, K. N., Lal, B., Singh, R. D., Thukral, A. K. (2008): Plant species diversity along an altitudinal gradient of Bhabha Valley in western Himalaya. – *Journal of Mountain Science* 5(2): 157-177.
- [26] Clements, F. E. (1905): *Research Methods in Ecology*. – University Publishing Company, Lincoln, NE.
- [27] Cochrane, M. A. (2003): Fire science for rainforests. – *Nature* 421: 913.
- [28] Curtis, J. T., McIntosh, R. P. (1950): The interrelations of certain analytic and synthetic phytosociological characters. – *Ecology* 31(3): 434-455.
- [29] D'Amato, A. W., Fraver, S., Palik, B. J., Bradford, J. B., Patty, L. (2011): Singular and interactive effects of blowdown, salvage logging, and wildfire in sub-boreal pine systems. – *Forest Ecology and Management* 262(11): 2070-2078.
- [30] Dalirsefat, S. B., da Silva Meyer, A., Mirhoseini, S. Z. (2009): Comparison of similarity coefficients used for cluster analysis with amplified fragment length polymorphism markers in the silkworm, *Bombyx mori*. – *Journal of Insect Science* 9(1).
- [31] Day, P. R. (1965): *Particle Fractionation and Particle-Size Analysis*. – American Society of Agronomy, Soil Science Society of America, Madison, WI.
- [32] Dolezal, J., Dvorsky, M., Kopecky, M., Liancourt, P., Hiiesalu, I., Macek, M., Altman, J., Chlumská, Z., Rehakova, K., Capkova, K. (2016): Vegetation dynamics at the upper elevational limit of vascular plants in Himalaya. – *Scientific Reports* 6: 24881.
- [33] Dufrene, M., Legendre, P. (1997): Species assemblages and indicator species: the need for a flexible asymmetrical approach. – *Ecological Monographs* 67(3): 345-366.

- [34] El-Keblawy, A., Abdelfattah, M. A., Khedr, A. H. A. (2015): Relationships between landforms, soil characteristics and dominant xerophytes in the hyper-arid northern United Arab Emirates. – *Journal of Arid Environments* 117: 28-36.
- [35] Ewald, J. (2003): A critique for phytosociology. – *Journal of Vegetation Science* 14(2): 291-296.
- [36] Francis, A. P., Currie, D. J. (1998): Global patterns of tree species richness in moist forests: another look. – *Oikos* 18(3): 598-602.
- [37] Gauch, H. G. (2010): Multivariate analysis in community ecology. – *Journal of the American Statistical Association* 78(383): 735.
- [38] Gauch, H. G., Gauch Jr, H. G. (1982): *Multivariate Analysis in Community Ecology* (No. 1). – Cambridge University Press, Cambridge, UK.
- [39] Gebrekirstos, A., Teketay, D., Mitlöhner, R. (2014): Responses of *Dobera glabra* and eight co-occurring species to drought and salinity stress at a savanna-scrub ecotone: implications in the face of climate change. – *Open Journal of Forestry* 4: 327-337.
- [40] Gonçalves, E. T., Souza, A. F. (2014): Floristic variation in ecotonal areas: patterns, determinants and biogeographic origins of subtropical forests in South America. – *Austral Ecology* 39: 122-134.
- [41] Grellier, S., Florsch, N., Janeau, J. L., Podwojewski, P., Camerlynck, C., Barot, S., Ward, D., Lorentz, S. (2014): Soil clay influences *Acacia* encroachment in a South African grassland. – *Ecohydrology* 7(6): 1474-1484.
- [42] Hansen, A. J., Risser, P. G., di Castri, F. (1992): Epilogue: Biodiversity and Ecological Flows across Ecotones. – In: Hansen, A. J., DiCastri, F. (eds.) *Landscape Boundaries*. Springer, New York, pp. 423-438.
- [43] Haq, F., Ahmad, H., Iqbal, Z. (2015a): Vegetation composition and ecological gradients of subtropical-moist temperate ecotonal forests of Nandiar Khuwar catchment, Pakistan. – *Bangladesh Journal of Botany* 44(2): 267-276.
- [44] Haq, F., Ahmad, H., Iqbal, Z. (2015b): Vegetation description and phytoclimatic gradients of subtropical forests of Nandiar Khuwar catchment District Battagram. – *Pakistan Journal of Botany* 47(4): 1399-1405.
- [45] Haq, F., Ahmad, H., Iqbal, Z., Alam, M., Aksoy, A. (2017): Multivariate approach to the classification and ordination of the forest ecosystem of Nandiar valley western Himalayas. – *Ecological Indicators* 80: 32-241.
- [46] Huang, L., He, B., Chen, A., Wang, H., Liu, J., Lü, A., Chen, Z. (2016): Drought dominates the interannual variability in global terrestrial net primary production by controlling semi-arid ecosystems. – *Scientific Reports* 6: 24639.
- [47] Ilyas, M., Shinwari, Z. K., Qureshi, R. (2012): Vegetation composition and threats to the montane temperate forest ecosystem of Qalagai hills, Swat, Khyber Pakhtunkhwa, Pakistan. – *Pakistan Journal of Botany* 44: 113-122
- [48] Jobbágy, E. G., Jackson, R. B. (2001): The distribution of soil nutrients with depth: global patterns and the imprint of plants. – *Biogeochemistry* 53: 51-77.
- [49] Johnstone, J. F., Chapin, F. S. (2003): Non-equilibrium succession dynamics indicate continued northern migration of lodgepole pine. – *Global Change Biology* 9(10): 1401-1409.
- [50] Judi, D., Rakowski, C., Waichler, S., Feng, Y., Wigmosta, M. (2018): Integrated modeling approach for the development of climate-informed, actionable information. – *Water* 10(6): 775.
- [51] Kent, M. (2011): *Vegetation Description and Data Analysis: A Practical Approach*. – John Wiley & Sons, Chichester.
- [52] Khan, S. M. (2012): *Plant communities and vegetation ecosystem services in the Naran Valley, Western Himalaya*. – Doctoral Dissertation, University of Leicester.
- [53] Khan, S. M., Ahmad, H. (2015): Species Diversity and Use Patterns of the Alpine Flora with Special Reference to Climate Change in the Naran, Pakistan. – In: Öztürk, M. et al.

- (eds.) *Climate Change Impacts on High-Altitude Ecosystems*. Springer, Cham, pp. 155-175.
- [54] Khan, S. M., Page, S., Ahmad, H., Shaheen, H., Harper, D. M. (2012): Vegetation dynamics in the Western Himalayas, diversity indices and climate change. – *Science Technology and Development* 31(3): 232-243.
- [55] Khan, S. M., Page, S., Ahmad, H., Ullah, Z., Shaheen, H., Ahmad, M., Harper, D. M. (2013): Phyto-climatic gradient of vegetation and habitat specificity in the high elevation Western Himalayas. – *Pakistan Journal of Botany* 45: 223-230.
- [56] Khan, W., Khan, S. M., Ahmad, H. (2015): Altitudinal variation in plant species richness and diversity at Thandiani sub forests division, Abbottabad, Pakistan. – *Journal of Biodiversity and Environmental Sciences* 7: 46-53.
- [57] Khan, W., Khan, S. M., Ahmad, H., Ahmad, Z., Page, S. (2016): Vegetation mapping and multivariate approach to indicator species of a forest ecosystem: A case study from the Thandiani sub Forests Division (TsFD) in the Western Himalayas. – *Ecological Indicators* 71: 336-351.
- [58] Kupfer, J. A., Cairns, D. M. (1996): The suitability of montane ecotones as indicators of global climatic change. – *Progress in Physical Geography* 20(3): 253-272.
- [59] Kusnierz, P. C., Holbrook, C. M., Feldman, D. L. (2015): An evaluation of a bed instability index as an indicator of habitat quality in mountain streams of the northwestern united states. – *Environmental Monitoring and Assessment* 187: 511-530.
- [60] Laurance, W. F., Oliveira, A. A., Laurance, S. G., Condit, R., Nascimento, H. E., Sanchez-Thorin, A. C., Lovejoy, T. E., Andrade, A., D'angelo, S., Ribeiro, J. E., Dick, C. W. (2004): Pervasive alteration of tree communities in undisturbed Amazonian forests. – *Nature* 428(6979): 171-174.
- [61] Lloyd, K. M., Mcqueen, A. A., lee, B. J., Wilson, R. C., Walker, S., Wilson, J. B. (2000): Evidence on ecotone concepts from switch, environmental and anthropogenic ecotones. – *Journal of Vegetation Science* 11(6): 903-910.
- [62] Lyu, L., Suvanto, S., Nöjd, P., Henttonen, H. M., Mäkinen, H., Zhang, Q.-B. (2017): Tree growth and its climate signal along latitudinal and altitudinal gradients: comparison of tree rings between Finland and the Tibetan Plateau. – *Biogeosciences* 14: 3083-3095.
- [63] Malik, R. N., Husain, S. Z. (2006): Classification and ordination of vegetation communities of the Lohibehr reserve forest and its surrounding areas, Rawalpindi, Pakistan. – *Pakistan Journal of Botany* 38(3): 543.
- [64] Mashwani, Z. R., Arshad, M., Ahmad, M., Khan, M. A. (2011): Diversity and Distribution Pattern of Alpine Vegetation along Lake Saif-ul-Mulook, Western Himalaya, Pakistan. – In: *International Conference on Environmental, Biomedical and Biotechnology IPCBEE (Vol. 16)*. IACSIT Press Singapore, pp. 155-163.
- [65] McMahon, S. M., Harrison, S. P., Armbruster, W. S., Bartlein, P. J., Beale, C. M., Edwards, M. E., Kattge, J., Midgley, G., Morin, X., Prentice, I. C. (2011): Improving assessment and modelling of climate change impacts on global terrestrial biodiversity. – *Trends in Ecology & Evolution* 26(5): 249-259.
- [66] Muthuramkumar, S., Ayyappan, N., Parthasarathy, N., Mudappa, D., Raman, T., Selwyn, M. A., Pragasan, I. A. (2006): Plant community structure in tropical rain forest fragments of the western Ghats, India. – *Biotropica* 38: 143-160.
- [67] Neilson, R. P. (1991): Climatic Constraints and Issues of Scale Controlling Regional Biomes. – In: Holland, M. M. et al. (eds.) *Ecotones*. Springer, Boston, MA, pp. 31-51.
- [68] Nelson, D. W., Sommers, I. E. (1996): Total Carbon, Organic Carbon, and Organic Matter. – In: Page, A. L. et al. (ed.) *Methods of Soil Analysis. Part 3: Chemical Methods*. SSSA, Madison, WI, pp. 961-1010.
- [69] Niemi, G. J., McDonald, M. E. (2004): Application of ecological indicators. – *Annual Review of Ecology, Evolution, and Systematics* 35: 89-111.
- [70] Pei, T., Qin, C. Z., Zhu, A. X., Yang, L., Luo, M., Li, B., Zhou, C. (2010): Mapping soil organic matter using the topographic wetness index: a comparative study based on

- different flow-direction algorithms and kriging methods. – *Ecological Indicators* 10(3): 610-619.
- [71] Pharswan, K., Mehta, J. P., Subodh (2010): Floristic composition and biological spectrum of vegetation in alpine meadows of Kedarnath: Garhwal Himalaya. – *Nature and Science* 8(7): 109-115.
- [72] Rahman, I. U., Hart, R., Afzal, A., Iqbal, Z., Ijaz, F., Ali, N., Abdallah, E. F., Khan, S. M., Alqarawi, A. A., Alsubeie M. S., Bussmann, R. W., 2019. A new ethnobiological similarity index (ESI) for the analysis of quantitative data. – *Applied Ecology and Environmental Research*, 17(2):2765-2777
- [73] Rasul, G. (2010): The role of the Himalayan mountain systems in food security and agricultural sustainability in South Asia. – *International Journal of Rural Management* 6(1): 95-116.
- [74] Rhoades, J. (1982): Soluble Salts. – In: Page, A. L. et al. (eds.) *Methods of Soil Analysis. Part 2: Chemical and Microbiological Properties*. SSSA, Madison, WI, pp. 167-178.
- [75] Rhoades, J., Miyamoto, S. (1990): Testing Soils for Salinity and Sodicity. – In: Weterman, R. L. (ed.) *Soil Testing and Plant Analysis*. SSSA, Madison, WI, pp. 299-336.
- [76] Rooney, T. P., Waller, D. M. (1998): Local and regional variation in hemlock seedling establishment in forests of the upper Great Lakes region, USA. – *Forest Ecology and Management* 111(2-3): 211-224.
- [77] Rüger, N., Williams-Linera, G., Kissling, W. D., Huth, A. (2008): Long-term impacts of fuelwood extraction on a tropical montane cloud forest. – *Ecosystems* 11(6): 868-881.
- [78] Saima, S., Dasti, A. A., Hussain, F., Wazir, S. M., Malik, S. A. (2009): Floristic compositions along an 18-km long transect in Ayubia National Park district Abbottabad, Pakistan. – *Pakistan Journal of Botany* 41(5):2115-2127.
- [79] Shaheen, H., Khan, S. M., Harper, D. M., Ullah, Z., Allem Qureshi, R. (2011): Species diversity, community structure, and distribution patterns in western Himalayan alpine pastures of Kashmir, Pakistan. – *Mountain Research and Development* 31: 153-159.
- [80] Shaheen, H., Ullah, Z., Khan, S. M., Harper, D. M. (2012): Species composition and community structure of western Himalayan moist temperate forests in Kashmir. – *Forest Ecology and Management* 278: 138-145.
- [81] Shaukat, S. S., Khan, M. A., Mett, M., Siddiqui, M. F. (2014): Structure, composition and diversity of the vegetation of Hub dam catchment area, Pakistan. – *Pakistan Journal of Botany* 46(1): 65-80.
- [82] Shen, M., Piao, S., Jeong, S. J. et al. (2015): Evaporative cooling over the Tibetan Plateau induced by vegetation growth. – *Proceedings of the National Academy of Sciences of the United States of America* 112(30): 9299.
- [83] Sher, H., Ahmad, A., Eleyemini, M., Fazl-i-Hadi, S., Sher, H. (2010): Impact of nomadic grazing on medicinal plants diversity in Miandam, Swat-Pakistan (Preliminary results). – *International Journal of Biodiversity and Conservation* 2(6): 146-154.
- [84] Singh, H., Kumar, M., Sheikh, M. A. (2009): Distribution pattern of oak and pine along altitudinal gradients in Garhwal Himalaya. – *Nature and Science* 7: 81-85.
- [85] Skagen, S. K., Augustine, D. J., Derner, J. D. (2018): Semi-arid grassland bird responses to patch-burn grazing and drought. – *The Journal of Wildlife Management* 82: 445-456.
- [86] Soltanpour, P. N. (1985): Use of ammonium bicarbonate DTPA soil test to evaluate elemental availability and toxicity. – *Communications in Soil Science and Plant Analysis* 16(3): 323-338.
- [87] Sorensen, T. (1948): A Method of Establishing Groups of Equal Amplitude in Plant Sociology Based on Similarity of Species Content and Its Application to Analyses of the Vegetation on Danish Commons. – I kommission hos E. Munksgaard, København, pp. 1-34.
- [88] Sternberg, M., Golodets, C., Gutman, M., Perevolotsky, A., Kigel, J., Henkin, Z. (2017): No precipitation legacy effects on above-ground net primary production and species

- diversity in grazed Mediterranean grassland: a 21-year experiment. – *Journal of Vegetation Science* 28(2): 260-269.
- [89] Tavili, A., Jafari, M. (2009): Interrelations between plants and environmental variables. – *International Journal of Environmental Research* 3(2): 239-246.
- [90] Ter Braak, C. J., Barendregt, L. G. (1986): Weighted averaging of species indicator values: its efficiency in environmental calibration. – *Mathematical Biosciences* 78(1):57-72.
- [91] Ullah, Z., Ahmad, M., Sher, H., Shaheen, H., Khan, S. M. (2015): Phytogeographic analysis and diversity of the grasses and sedges (Poales) of northern Pakistan. – *Pakistan Journal of Botany* 47: 93-104.
- [92] Vallés, S. M., Cambrollé, J., Gallego-Fernández, J. B. (2015): Effect of soil characteristics on plant distribution in coastal ecosystems of SW Iberian Peninsula sand spits. – *Plant Ecology* 216: 1551-1570.
- [93] Walker, S., Wilson, J. B., Steel, J. B., Rapson, R., Smith, B., King, W. M., Cottam, Y. H. (2003): Properties of ecotones: evidence from five ecotones objectively determined from a coastal vegetation gradient. – *Journal of Vegetation Science* 14: 579-590.
- [94] Wangda, P. (2003): Forest zonation along the complex altitudinal gradients in a dry valley of Punatsang-Chu, Bhutan. – Master's Thesis, The University of Tokyo, Japan.
- [95] Willig, M. R., Kaufman, D. M., Stevens, R. D. (2003): Latitudinal gradients of biodiversity: pattern, process, scale, and synthesis. – *Annual Review of Ecology, Evolution, and Systematics* 34(1): 273-309.
- [96] Zhou, C. W., Yang, R., Yu, L. F., Zhang, Y., Yan, L. B. (2018): Hydrological and ecological effects of climate change in Caohai watershed based on SWAT model. – *Applied Ecology and Environmental Research* 17(1): 161-172.

APPENDIX

Table A1. Plant check of the ecotonal region, along with a detail of their families, habit and IVI%

S/No.	Botanical name	Family	Habit	IVI%	S/No.	Botanical name	Family	Habit	IVI%
1	<i>Adiantum capillus veneris</i>	Pteridaceae	Herb	0.34	99	<i>Morus nigra</i>	Moraceae	Tree	0.52
2	<i>Adiantum venustum</i>	Pteridaceae	Herb	0.77	100	<i>Myrtus communis</i>	Myrtaceae	Shrub	2.38
3	<i>Agrostis vinealis Schreb</i>	Poaceae	Herb	2.11	101	<i>Nasturtium officinale</i>	Brassicaceae	Herb	0.16
4	<i>Ailanthus altissima</i>	Simaroubaceae	Tree	3.53	102	<i>Nepeta Spp</i>	Lamiaceae	Herb	0.05
5	<i>Amaranthus retroflexus</i>	Amaranthaceae	Herb	0.08	103	<i>Nepeta erecta</i>	Lamiaceae	Herb	0.32
6	<i>Amaranthus viridis</i>	Amaranthaceae	Herb	0.08	104	<i>Nepeta laevigata</i>	Lamiaceae	Herb	0.46
7	<i>Androsace rotundifolia</i>	Primulaceae	Herb	0.27	105	<i>Oenothera rosea</i>	Onagraceae	Herb	1.16
8	<i>Anisomeles indica</i>	Lamiaceae	Herb	0.21	106	<i>Olea ferruginea</i>	Oleaceae	Tree	7.60
9	<i>Apluda mutica</i>	Poaceae	Herb	2.56	107	<i>Origanum vulgare</i>	Lamiaceae	Herb	0.46
10	<i>Arisaema flavum</i>	Araceae	Herb	0.29	108	<i>Oxalis corniculata</i>	Oxalidaceae	Herb	2.71
11	<i>Artemisia absinthium</i>	Asteraceae	Herb	0.11	109	<i>Parrotiopsis jacquemontiana</i>	Hamamelidaceae	Tree	1.13
12	<i>Arthraxon prionodes</i>	Poaceae	Herb	0.10	110	<i>Paspalum paspalodes</i>	Poaceae	Herb	0.13
13	<i>Avena fatua</i>	Poaceae	Herb	0.40	111	<i>Persicaria hydropiper</i>	Polygonaceae	Herb	0.04
14	<i>Berberis lysium</i>	Berberidaceae	Shrub	7.99	112	<i>Persicaria maculosa</i>	Polygonaceae	Herb	0.82
15	<i>Berberis parkeriana</i>	Berberidaceae	Shrub	7.39	113	<i>Phagnalon niveum</i>	Asteraceae	Herb	0.22
16	<i>Bidens bipinnata</i>	Asteraceae	Herb	0.09	114	<i>Phlomis stewartii</i>	Lamiaceae	Herb	1.66
17	<i>Bidens cernua</i>	Asteraceae	Herb	0.23	115	<i>Pinus brutia</i>	Pinaceae	Tree	1.37
18	<i>Bidens tripartite</i>	Asteraceae	Herb	0.20	116	<i>Piptatherum laterale</i>	Poaceae	Herb	2.69
19	<i>Bistorta amplexicaulis</i>	Polygonaceae	Herb	0.43	117	<i>Plantago lanceolata</i>	Plantaginaceae	Herb	2.12
20	<i>Bothriochloa bladhii</i>	Poaceae	Herb	1.66	118	<i>Plantago major</i>	Plantaginaceae	Herb	0.15
21	<i>Bromus japonicas</i>	Poaceae	Herb	0.38	119	<i>Platanus orientalis</i>	Platanaceae	Tree	1.30

22	<i>Buddleja crispa</i>	Buddlejaceae	Shrub	0.16	120	<i>Plectranthus rugosus</i>	Lamiaceae	Shrub	14.81
23	<i>Bupleurum falcatum</i>	Apiaceae	Herb	1.93	121	<i>Polygala abyssinica</i>	Polygalaceae	Herb	0.27
24	<i>Bupleurum linearifolium</i>	Apiaceae	Herb	0.10	122	<i>Polygonum aviculare</i>	Polygonaceae	Herb	0.44
25	<i>Calamintha umbrosa</i>	Lamiaceae	Herb	0.45	123	<i>Polygonum plebejum</i>	Polygonaceae	Herb	0.24
26	<i>Calanthe tricarinata</i>	Orchidaceae	Herb	0.05	124	<i>Polypogon fugax</i>	Poaceae	Herb	0.08
27	<i>Campanula pallida</i>	Campanulaceae	Herb	0.36	125	<i>Populus nigra</i>	Salicaceae	Tree	6.08
28	<i>Cannabis sativa</i>	Cannabaceae	Herb	1.38	126	<i>Populus alba</i>	Salicaceae	Tree	0.19
29	<i>Cedrus deodara</i>	Pinaceae	Tree	6.37	127	<i>Potentilla anserina</i>	Rosaceae	Herb	0.55
30	<i>Celtis caucasica</i>	Ulmaceae	Tree	3.63	128	<i>Potentilla supina</i>	Rosaceae	Herb	0.79
31	<i>Centaurea calcitrapa</i>	Asteraceae	Herb	0.08	129	<i>Prunella vulgaris</i>	Lamiaceae	Herb	0.29
32	<i>Centaurea iberica</i>	Asteraceae	Herb	0.20	130	<i>Prunus armeniaca</i>	Rosaceae	Tree	0.67
33	<i>Chenopodium album</i>	Chenopodiaceae	Herb	0.11	131	<i>Prunus eburnea</i>	Rosaceae	Tree	2.51
34	<i>Cichorium intybus</i>	Asteraceae	Herb	0.29	132	<i>Punica grantum</i>	Lythraceae	Tree	5.04
35	<i>Cirsium arvense</i>	Asteraceae	Herb	3.91	133	<i>Pyrus pashia</i>	Rosaceae	Tree	0.10
36	<i>Cirsium vulgare</i>	Asteraceae	Herb	0.24	134	<i>Quercus baloot</i>	Fagaceae	Tree	8.63
37	<i>Clematis grata</i>	Ranunculaceae	Herb	0.41	135	<i>Quercus dilatata</i>	Fagaceae	Tree	17.11
38	<i>Clematis graveolens</i>	Ranunculaceae	Herb	0.44	136	<i>Quercus semecarpifolia</i>	Fagaceae	Tree	0.80
39	<i>Clematis orientalis</i>	Ranunculaceae	Herb	0.32	137	<i>Ranunculus arvensis</i>	Ranunculaceae	Herb	0.55
40	<i>Clinopodium umbrosum</i>	Lamiaceae	Herb	0.58	138	<i>Ranunculus laetus</i>	Ranunculaceae	Herb	0.16
41	<i>Convolvulus arvensis</i>	Convolvulaceae	Herb	0.67	139	<i>Ranunculus repens</i>	Ranunculaceae	Herb	0.60
42	<i>Cotoneaster bacillaris</i>	Rosaceae	Tree	0.33	140	<i>Raphanus raphanistrum</i>	Brassicaceae	Herb	0.13
43	<i>Cotoneaster nummularia</i>	Rosaceae	Tree	3.79	141	<i>Robinia pseudoacacia</i>	Fagaceae	Tree	11.01
44	<i>Crataegus songarica</i>	Rosaceae	Tree	0.67	142	<i>Rorippa islandica</i>	Brassicaceae	Herb	0.03
45	<i>Cymbopogon jwarancusa</i>	Poaceae	Herb	0.42	143	<i>Rosa chinensis</i>	Rosaceae	Shrub	3.70
46	<i>Cynodon dactylon</i>	Poaceae	Herb	7.73	144	<i>Rosa moschata</i>	Rosaceae	Shrub	1.17
47	<i>Cynoglossum lanceolatum</i>	Boraginaceae	Herb	0.09	145	<i>Rosa webbiana</i>	Rosaceae	Shrub	0.30
48	<i>Cyperus rotundus</i>	Cyperaceae	Herb	0.22	146	<i>Rosa X alba</i>	Rosaceae	Shrub	0.18
49	<i>Daphne mucronata</i>	Thymelaeaceae	Shrub	8.58	147	<i>Rubia cordifolia</i>	Rubiaceae	Herb	0.98
50	<i>Datura stramonium</i>	Solanaceae	Herb	0.05	148	<i>Rubus fruticosus</i>	Rosaceae	Shrub	4.31
51	<i>Debregeasia salicifolia</i>	Urticaceae	Shrub	0.16	149	<i>Rumex acetosa</i>	Polygonaceae	Herb	0.05
52	<i>Dichanthium annulatum</i>	Poaceae	Herb	0.45	150	<i>Rumex dentatus</i>	Polygonaceae	Herb	0.67
53	<i>Digitaria nodosa</i>	Poaceae	Herb	0.07	151	<i>Rumex nepalensis</i>	Polygonaceae	Herb	0.06
54	<i>Diospyros lotus</i>	Ebenaceae	Tree	2.14	152	<i>Saccharum griffithii</i>	Poaceae	Herb	0.07
55	<i>Duchesnea indica</i>	Rosaceae	Herb	0.78	153	<i>Saccharum spontaneum</i>	Poaceae	Herb	1.17
56	<i>Elaeagnus aungustifolia</i>	Elaeagnaceae	Tree	3.18	154	<i>Salix alba</i>	Salicaceae	Tree	3.48
57	<i>Elymus nutans</i>	Poaceae	Herb	0.09	155	<i>Salix babylonica</i>	Salicaceae	Tree	0.87
58	<i>Ephedra procera</i>	Ephedraceae	Shrub	3.40	156	<i>Sambucus nigra</i>	Sambucaceae	Shrub	7.90
59	<i>Epilobium hirsutum</i>	Onagraceae	Herb	0.04	157	<i>Sanguisorba minor</i>	Rosaceae	Herb	0.79
60	<i>Equisetum debile</i>	Equisetaceae	Herb	0.18	158	<i>Sauromatum venosum</i>	Araceae	Herb	0.16
61	<i>Eragrostis pilosa</i>	Poaceae	Herb	0.08	159	<i>Saussuria heteromalla</i>	Asteraceae	Herb	2.41
62	<i>Eragrostis tenella</i>	Poaceae	Herb	0.05	160	<i>Scrophularia striata</i>	Scrophulariaceae	Herb	0.44
63	<i>Erigeron bonariensis</i>	Asteraceae	Herb	0.21	161	<i>Scutellaria linearis</i>	Lamiaceae	Herb	0.77
64	<i>Erigeron canadensis</i>	Asteraceae	Herb	0.98	162	<i>Seriphidium kurramense</i>	Asteraceae	Herb	0.49
65	<i>Eryngium billardieri</i>	Apiaceae	Herb	0.14	163	<i>Setaria pumila</i>	Poaceae	Herb	3.26
66	<i>Eryngium coeruleum</i>	Apiaceae	Herb	0.11	164	<i>Solanum americanum</i>	Solanaceae	Herb	0.12
67	<i>Euphorbia helioscopia</i>	Euphorbiaceae	Herb	0.17	165	<i>Solanum nigrum</i>	Solanaceae	Herb	0.06
68	<i>Festuca gigantea</i>	Poaceae	Herb	0.38	166	<i>Solanum nigrum var. villosum</i>	Solanaceae	Herb	0.05
69	<i>Ficus palmata</i>	Moraceae	Tree	0.47	167	<i>Sonchus asper</i>	Asteraceae	Herb	0.14
70	<i>Foeniculum vulgare</i>	Apiaceae	Herb	0.09	168	<i>Sonchus oleraceus</i>	Asteraceae	Herb	0.29
71	<i>Fragaria nubicola</i>	Rosaceae	Herb	0.07	169	<i>Sophora mollis</i>	Papilionaceae	Shrub	12.17
72	<i>Galinsoga parviflora</i>	Asteraceae	Herb	0.29	170	<i>Stellaria media</i>	Caryophyllaceae	Herb	0.22
73	<i>Hedera nepalensis</i>	Araliaceae	Shrub	0.39	171	<i>Stipa sibirica</i>	Poaceae	Herb	3.72
74	<i>Impatiens edgeworthii</i>	Balsaminaceae	Herb	1.50	172	<i>Strobilanthes urticifolia</i>	Acanthaceae	Herb	0.29
75	<i>Impatiens lemarii</i>	Balsaminaceae	Herb	0.20	173	<i>Swertia cordata</i>	Gentianaceae	Herb	0.92

76	<i>Indigofera heterantha</i>	Papilionaceae	Shrub	19.04	174	<i>Tagetes minuta</i>	Asteraceae	Herb	0.77
77	<i>Ipomoea purpurea</i>	Convolvulaceae	Herb	1.03	175	<i>Taraxacum officinale</i>	Asteraceae	Herb	0.70
78	<i>Jasminum auriculatum</i>	Oleaceae	Shrub	0.24	176	<i>Themeda anathera</i>	Poaceae	Herb	0.15
79	<i>Jasminum officinale</i>	Oleaceae	Shrub	0.62	177	<i>Thuja orientalis</i>	Cupressaceae	Shrub	0.59
80	<i>Juglans regia</i>	Juglandaceae	Tree	2.73	178	<i>Thymus linearis</i>	Lamiaceae	Herb	5.03
81	<i>Juniperus excelsa</i>	Cupressaceae	Tree	0.97	179	<i>Torilis leptophylla</i>	Apiaceae	Herb	1.07
82	<i>Leontopodium brachyactis</i>	Asteraceae	Herb	0.08	180	<i>Tragopogon gracilis</i>	Asteraceae	Herb	0.03
83	<i>Lepidium pinnatifidum</i>	Brassicaceae	Herb	0.38	181	<i>Trifolium alexandrianum</i>	Papilionaceae	Herb	0.19
84	<i>Lepedeza juncea</i>	Papilionaceae	Herb	1.44	182	<i>Trifolium repens</i>	Papilionaceae	Herb	0.76
85	<i>Liriope graminifolia</i>	Haemodoraceae	Herb	0.10	183	<i>Urtica dioica</i>	Urticaceae	Herb	0.07
86	<i>Lotus corniculatus</i>	Papilionaceae	Herb	0.96	184	<i>Verbena officinalis</i>	Verbenaceae	Herb	0.15
87	<i>Malus domestica</i>	Rosaceae	Tree	0.21	185	<i>Verbena Linn.</i>	Verbenaceae	Herb	0.05
88	<i>Malva neglecta</i>	Malvaceae	Herb	0.36	186	<i>Vincetoxicum cardiostephanum</i>	Apocynaceae	Herb	0.78
89	<i>Marrubium vulgare</i>	Lamiaceae	Herb	0.05	187	<i>Viola canescens</i>	Violaceae	Herb	0.70
90	<i>Matricaria recutita</i>	Asteraceae	Herb	0.54	188	<i>Viola odorata</i>	Violaceae	Herb	2.44
91	<i>Medicago lupulina</i>	Papilionaceae	Herb	0.50	189	<i>Viola pilosa</i>	Violaceae	Herb	0.71
92	<i>Medicago sativa</i>	Papilionaceae	Herb	6.16	190	<i>Viola reichenbachiana</i>	Violaceae	Herb	0.14
93	<i>Mentha arvensis</i>	Lamiaceae	Herb	0.13	191	<i>Viola spp.</i>	Violaceae	Herb	0.09
94	<i>Mentha longifolia</i>	Lamiaceae	Herb	1.52	192	<i>Wikstroemia canescens</i>	Thymelaeaceae	Shrub	4.51
95	<i>Mentha royleana</i>	Lamiaceae	Herb	0.54	193	<i>Wulfeniopsis amherstiana</i>	Plantaginaceae	Herb	0.13
96	<i>Micromeria biflora</i>	Lamiaceae	Herb	0.09	194	<i>Xanthium spinosum</i>	Asteraceae	Herb	1.91
97	<i>Monothea buxifolia</i>	Sapotaceae	Tree	2.56	195	<i>Xanthium strumarium</i>	Asteraceae	Herb	0.40
98	<i>Morus alba</i>	Moraceae	Tree	1.03					

CARBON EMISSION PREDICTION MODEL OF AGROFORESTRY ECOSYSTEM BASED ON SUPPORT VECTOR REGRESSION MACHINE

CAI, J. – MA, X. *

College of Economics and Management, Anhui Agricultural University, Hefei 230036, China

**Corresponding author
e-mail: maxiaoqian4568@163.com*

(Received 29th Dec 2018 ; accepted 8th Mar 2019)

Abstract. The carbon emission prediction model of agroforestry ecosystem based on least squares regression method has no learning process for data samples, it is difficult to accurately describe the non-linear relationship among them, and the prediction accuracy is poor. A carbon emission prediction model of agroforestry ecosystem based on support vector regression was designed. Seven carbon sources, including root decomposition, chemical fertilizer, pesticide, agricultural film, agricultural irrigation, agricultural machinery and farmland tillage, were selected as influencing factors of carbon emissions in agroforestry ecosystem. The SVR model for carbon emissions prediction in agroforestry ecosystem was constructed, and the regression function of sample data was solved by optimizing the training sample data based on the basic principle of support vector regression machine. On this basis, the data of influencing factors of agroforestry ecosystem were normalized and substituted into the model to predict the carbon emission results of agroforestry ecosystem system. Experiments show that the errors of the designed model in predicting the average carbon emissions of agroforestry ecosystems in the two experimental provinces from 2010 to 2017 are $5.9/10^4$ t and $6.4/10^4$ t, respectively, which are lower than those of other models. The average time of predicting the carbon emissions of agroforestry ecosystems in the two experimental provinces from 2006 to 2015 is about 4.15 s, which shows that the model can predict agriculture. The results of forest ecosystem carbon emissions have the advantages of high efficiency, high precision and comprehensiveness.

Keywords: *support vector regression machine, agroforestry ecosystem, carbon emission, prediction, model, regression function*

Introduction

Since the late nineteenth century, the global surface temperature has risen by 0.4-0.8 °C. Global warming, an environmental change problem, has attracted widespread attention in the international community. Greenhouse gas emissions are the main causes of climate warming (Grinblat et al., 2015). The main greenhouse gases produced by human activities are carbon dioxide, methane, nitrous oxide and fluoride, among which carbon dioxide is the most important anthropogenic greenhouse gas (Babaranti, 2019). Fluoride itself does not contain Greenhouse Effect, but a greenhouse gas. The IPCC Fourth Assessment Report pointed out that the increase of global carbon dioxide concentration was mainly attributed to the use of fossil fuels (Onwuka et al., 2019). The increase of nitrogen monoxide concentration was mainly attributed to the use of agriculture and fossil fuels. The increase of nitrogen monoxide concentration was mainly attributed to the agroforestry ecosystem (Zhang et al., 2016). With the progress and extension of agroforestry ecological science and technology, the industrialization trend of agroforestry ecosystem has been strengthened. For example, the United States is a typical modern country of agroforestry ecosystem. Its development of agroforestry ecosystem is essentially based on technology and energy. The degree of mechanization

and chemistry of agroforestry ecological production is quite high, and its income and input of agroforestry ecological energy is as high as 1:15, which is the most in the world. Facing the increasingly serious contradiction between land and population, China with a large population is also vigorously promoting the development of modern agroforestry ecology. It can be seen that the agroforestry and ecological production sector has become an important area of fossil energy consumption. In 2014, the share of agricultural greenhouse gas emissions calculated by carbon dioxide equivalent accounted for 13.5% of total greenhouse gas emissions. It can be seen that agroforestry ecosystem has become one of the main sources of greenhouse gas emissions (Ouyang et al., 2019).

Scholars in China and abroad have shown that the broad definition of agroforestry ecosystem refers to the five industrial forms of planting, forestry, animal husbandry, fisheries and sideline (Franzluebbers et al., 2016). Carbon emissions from agroforestry ecosystems mainly come from the following aspects: (1) The use of chemical fertilizers will produce greenhouse gas emissions such as nitrous oxide, methane and so on. At the same time, the production and transportation of chemical fertilizers will produce carbon emissions. (2) The use of pesticides, including their carbon emissions during production and transportation. (3) The use of agricultural film products, including carbon emissions in the production process. (4) Carbon emissions from fossil fuels directly consumed, including the use of agricultural machinery and irrigation equipment. (5) Loss of soil organic carbon during farming. (6) Combustion of crop straw (Khanchoul et al., 2019).

Agroforestry ecosystem is a special ecosystem: it is not only a carbon source manufacturing system, but also a carbon sink absorption system (Vignola et al., 2015). Carbon sources in agroforestry ecosystems mainly come from planting and aquaculture, which are closely related to human beings. Carbon sinks mainly come from forestland and agricultural land (Anderegg et al., 2015). In recent years, the world's agroforestry ecosystem has entered the era of low-carbon economy, while the development of low-carbon agroforestry ecosystem in China is still in its infancy, and low-carbon agroforestry ecosystem is an important issue facing our country at present. In this context, the study of carbon emissions from agroforestry ecosystems in China has a certain practical significance (Oyedotun et al., 2019).

At present, there are many ways to predict carbon emissions in agroforestry ecosystems. Because there are some technical and practical difficulties in observing and counting carbon emissions flux, the existing methods are based on some easy statistical data. Wall et al. (2015) predicted carbon emissions from agroforestry ecosystems through tillage data and meteorological information. Brogniez et al. (2015) predicted carbon emissions from agroforestry ecosystems according to the fertilization on farmland. Maas et al. (2015) predicted carbon emissions from agroforestry ecosystems by testing soil organic carbon content (Roslee, 2019). The least squares regression method and ridge regression method are mostly used in the above-mentioned carbon emission models of agroforestry ecosystems. They have the problems of weak stability and explainability, and are difficult to determine parameters. At the same time, the forecasting model has no learning process for data samples, and it is difficult to accurately describe the non-linear relationship among them, so the forecasting accuracy is poor. Now the mainstream carbon emission prediction method is based on the carbon emissions of fossil energy. The main carbon emissions of agroforestry ecosystem are mainly caused by the use of agricultural, chemical fertilizer, agricultural film and diesel

oil, so the carbon emissions are predicted from the perspective of input (Sharma et al., 2019).

Support Vector Machine (SVM) is a new machine learning algorithm based on statistical learning theory. Because of its excellent learning performance, it has been successfully applied in many fields such as face recognition, handwritten numeral recognition and image retrieval, which can be used for classification and regression problems. In order to solve the defects existing in the prior method, an effective carbon emission prediction method is found, and the basis for the implementation of the high-efficiency energy-saving emission reduction decision is provided. In this paper, a prediction model of carbon emissions in agroforestry ecosystem based on SVM is designed, which provides an important basis for making efficient energy-saving and emission reduction decisions (Khanchoul et al., 2019).

Materials and methods

Selection of influencing factors of carbon emission in agroforestry ecosystem

When the carbon source of the ecosystem was predicted, the carbon emissions of the selected two experimental provinces increased at a constant rate. GDP is the final result of the production activities of all permanent units in a country (or region) calculated by market price. and obtaining the GDP data according to the GDP accounting system. There are seven kinds of carbon sources for predicting carbon emissions in agroforestry ecosystems (Sinare and Gordon, 2015): first, the carbon emissions caused by the use of chemical fertilizers; second, the carbon emissions caused by the use of pesticides; third, the carbon emissions caused by the decomposition of residual roots after harvesting crops; fourth, the carbon emissions from indirect consumption of fossil fuels during irrigation; fifth, carbon emissions caused by the use of agricultural film; Sixth, the destruction of soil organic carbon pools by farmland tillage, resulting in the loss of a large amount of organic carbon into the air and carbon emissions; seventh, the direct or indirect consumption of fossil fuels (diesel, electricity, etc.) by agricultural machinery (Michael et al., 2015). These seven carbon sources were selected as independent variables of carbon emission prediction in the studied agroforestry ecosystem.

Figure 1 depicts the proportion of different carbon sources in total carbon emissions in the agroforestry ecosystem of China. It can be concluded that the carbon emissions of agroforestry ecosystem in this province are mainly caused by root decomposition after harvesting (accounting for 59.8712% of the carbon emissions of agroforestry ecosystem). In agroforestry ecosystem, the proportion of carbon emissions of various types in total emissions is in the order of root decomposition (59.8712%), chemical fertilizer (28.0495%), pesticide (4.9972%), agricultural film (3.0612%), agricultural irrigation (2.2927%), agricultural machinery (1.7519%) and farmland tillage (0.0123%). The proportion of root decomposition in agricultural carbon emissions is prominent due to the large agricultural planting area and unscientific farmland management in the province (Carsan et al., 2015).

SVR model for prediction of carbon emissions in agroforestry ecosystem

The SVR model for carbon emission prediction of agroforestry ecosystem was established. The results of carbon emission of agroforestry ecosystem were predicted

based on the above seven factors: root decomposition, chemical fertilizer, pesticide, agricultural film, agricultural irrigation, agricultural machinery and farmland tillage.

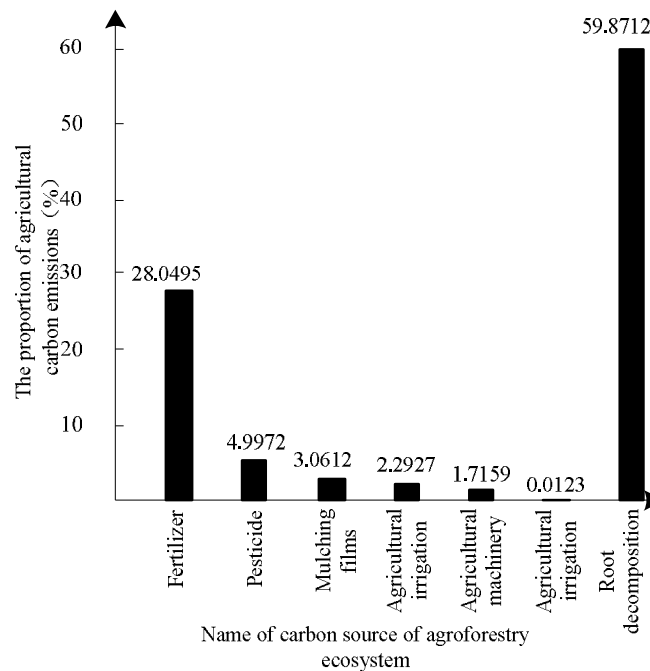


Figure 1. Emission ratio of agroforestry ecosystem in a province

Basic principle of support vector regression machine

SVR is a machine learning method based on statistical learning theory (Sloat et al., 2015). Because it is especially suitable for limited samples, it can obtain global optimum theoretically and has a good generalization ability. Moreover, its computational complexity is independent of the dimension of samples. It has been well applied in function approximation and regression estimation (Helen, 2016). Given the training set $T = \{(x_1, y_1), \dots, (x_n, y_n)\}$, $x_i \in R^m$, $y_i \in R$, $i = 1, \dots, n$, where x_i and y_i represent the input factor and the expected value, respectively, and n is the total number of data points. If we can deduce the y value of any model x by a linear function $y = f(x) = (w \bullet x) + b$ on R^m , it is called linear regression problem. The linear regression problem can be converted to the following optimization problem (Rueda et al., 2015):

$$\left\{ \begin{array}{l} \min \frac{1}{2} \|w\|^2 + C \frac{1}{n} \sum_{i=1}^n (\xi_i + \xi_i^*), \\ s.t. \\ ((w \bullet x_i) + b) - y_i \leq \varepsilon + \xi_i, \\ i = 1, 2, \dots, n \\ y_i - ((w \bullet x_i) + b) \leq \varepsilon + \xi_i^*, \\ i = 1, 2, \dots, n \\ \xi_i, \xi_i^* \geq 0, i = 1, 2, \dots, n \end{array} \right. \quad (\text{Eq.1})$$

In the formula, C is the penalty parameter, ξ_i and ξ_i^* are the relaxation variables, ε is the threshold of insensitive loss function, which is used for fitting accuracy (He and Rong, 2015). $\|w\|^2$ is the confidence risk; b is the parameter to be identified.

Generally, the dual problem of model (Eq.1) is introduced instead of solving model directly.

$$\begin{cases} \min \frac{1}{2} \sum_{i,j=1}^n (\alpha_i^* - \alpha_i)(\alpha_j^* - \alpha_j)(x_i - x_j) + \\ \varepsilon \sum_{i=1}^n (\alpha_i^* + \alpha_i) - \sum_{i=1}^n y_i (\alpha_i^* - \alpha_i), \\ \text{s.t.} \quad \sum_{i=1}^n (\alpha_i - \alpha_i^*) = 0, \\ 0 \leq \alpha_i, \alpha_i^* \leq \frac{C}{n}, i = 1, 2, \dots, n \end{cases} \quad (\text{Eq.2})$$

In the formula, α_i and α_i^* are the support vector parameters.

If $\bar{\alpha}_i \neq 0$ or $\bar{\alpha}_i^* \neq 0$ is the optimal solution, the input x_i in the training set is called support vector. The correlation coefficients of regression function are: $S_1 = \{i | \bar{\alpha}_i \in (0, C/n)\}$, $S_2 = \{i | \bar{\alpha}_i^* \in (0, C/n)\}$, find $j \in S_1$ or $k \in S_2$, and it can be calculated:

$$\bar{b} = y_i - \sum_{i=1}^n (\bar{\alpha}_i^* - \bar{\alpha}_i)(x_i \bullet x_j) + \varepsilon \quad (\text{Eq.3})$$

or

$$\bar{b} = y_k - \sum_{i=1}^n (\bar{\alpha}_i^* - \bar{\alpha}_i)(x_i \bullet x_k) - \varepsilon \quad (\text{Eq.4})$$

Finally, the linear regression function of the training sample is obtained as follows:

$$f(x) = \sum_{i=1}^n (\bar{\alpha}_i^* - \bar{\alpha}_i)(x_i \bullet x) + \bar{b} \quad (\text{Eq.5})$$

It is not difficult to see that the dual problem (Eq.2) and regression function (Eq.5) only involve the inner product operation ($x_i \bullet x_j$) between sample inputs. Therefore, the inner product kernel function $K(x_i, x_j)$ can be introduced to transform the linear regression problem into the non-linear regression problem in the high dimensional space (Hilbert space) (Dressler et al., 2015). The support vector regression model (ε -SVR) can be constructed (Marilice et al., 2015).

$$\begin{cases} \min \frac{1}{2} \sum_{i,j=1}^n (\alpha_i^* - \alpha_i)(\alpha_j^* - \alpha_j)K(x_i, x_j) + \\ \varepsilon \sum_{i=1}^n (\alpha_i^* + \alpha_i) - \sum_{i=1}^n y_i (\alpha_i^* - \alpha_i), \\ \text{s.t.} \quad \sum_{i=1}^n (\bar{\alpha}_i - \bar{\alpha}_i^*) = 0, \\ 0 \leq \alpha_i, \alpha_i^* \leq \frac{C}{n}, i = 1, 2, \dots, n \end{cases} \quad (\text{Eq.6})$$

When the optimal solution $\bar{\alpha} = (\bar{\alpha}_1, \bar{\alpha}_1^*, \dots, \bar{\alpha}_n, \bar{\alpha}_n^*)^T$ is obtained, the corresponding training sample regression function becomes as follows:

$$f(x) = \sum_{i=1}^n (\bar{\alpha}_i^* - \bar{\alpha}_i) K(x_i, x) + \bar{b} \quad (\text{Eq.7})$$

Choose $\bar{\alpha}_j$ or $\bar{\alpha}_k^*$ in $(0, \frac{C}{n})$, and the corresponding \bar{b} is:

$$\bar{b} = y_j - \sum_{i=1}^n (\bar{\alpha}_i^* - \bar{\alpha}_i) K(x_i, x_j) + \varepsilon \quad (\text{Eq.8})$$

or

$$\bar{b} = y_k - \sum_{i=1}^n (\bar{\alpha}_i^* - \bar{\alpha}_i) K(x_i, x_k) - \varepsilon \quad (\text{Eq.9})$$

Establishment of SVR carbon emission prediction model

A multi-input and single-output support vector regression model is constructed by constructing the relationship between the input and the output through the SVR model, as shown in *Figure 2* (Benjamin et al., 2018). The specific steps are as follows:

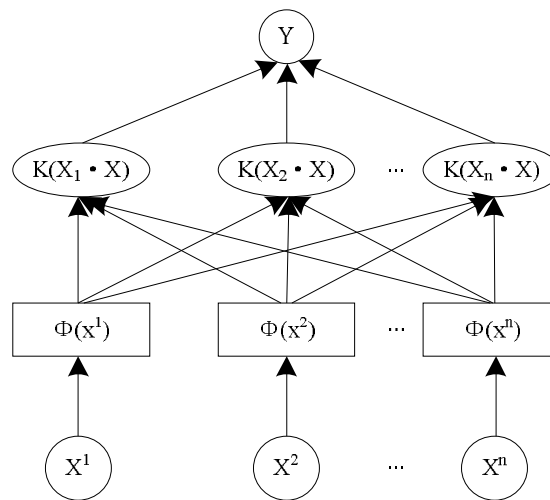


Figure 2. Support vector regression machine model

In *Figure 2*, carbon emissions and their influencing factors are input, and carbon emission values are outputted. The first step is to classify the samples (Ping et al., 2015). Taking an agroforestry ecosystem in a province of China as an example, the data of carbon emissions and their influencing factors from 1990 to 2010 and 2011 to 2017 were taken as training samples and testing samples respectively. The influencing factors were root decomposition, chemical fertilizer, pesticide, agricultural film, agricultural irrigation, agricultural machinery and farmland tillage (carbon emissions and their shadows due to space limitation). Sound factor data sheet is not described in detail.

The second step is to normalize all sample data, that is, to normalize the independent variables and dependent variables in all samples with the following formula, so that all data are in [0, 1] (Terrado et al., 2015).

$$x_{il} = \frac{x_{il}^0 - \min x_{il}^0}{\max x_{il}^0 - \min x_{il}^0}, i = 1, 2, L, n, l = 1, 2, L, 7 \quad (\text{Eq.10})$$

$$y_i = \frac{y_i^0 - \min y_i^0}{\max y_i^0 - \min y_i^0}, i = 1, 2, L, n \quad (\text{Eq.11})$$

The third step is to select the best penalty coefficients C and γ of training samples and test samples. Firstly, the parameters C and γ are selected roughly, and the range of their values are $lbC \in [-10, 10]$, $lb\gamma \in [-10, 10]$, which are substituted into the model to get the rough map. According to the printed rough map, the range of parameters are $lbC \in [-8, 8]$, $lb\gamma \in [-10, 10]$, and then substituted into the SVR carbon emission prediction model to get the fine map. The grid width m , cross validation fold k and regression bandwidth ε remain unchanged, which are 1, 5 and 0.05, respectively. The optimum values C^* and γ^* of C and γ are 9.18959 and 0.0358968, respectively.

The fourth step is to construct and test the SVR carbon emission prediction model. The SVR carbon emission prediction model was constructed by using the above optimal parameters C^* , γ^* and all training samples. The regression function was obtained as follows:

$$\begin{aligned} f(x) = & 2.5460K(x_2, x) + 1.3375K(x_3, x) - 9.1896K(x_4, x) \\ & + 4.9274K(x_5, x) + 9.1896K(x_6, x) - 9.1896K(x_7, x) \\ & - 7.3493K(x_{10}, x) + 5.0624K(x_{12}, x) - 9.1896K(x_{13}, x) \\ & - 9.1896K(x_{14}, x) - 9.1896K(x_{15}, x) + 9.1896K(x_{16}, x) \\ & + 9.1896K(x_{17}, x) - 0.4126K(x_{19}, x) + 1.7260K(x_{21}, x) \\ & + 9.1896K(x_{22}, x) - 1.7442K(x_{24}, x) + 0.9176 \end{aligned} \quad (\text{Eq.12})$$

x is the input sample whose model parameters are not zero, that is, support vector; $f(x)$ is the set of output vectors. After the regression function $f(x)$ is obtained, the correlation coefficients of training samples and test samples are substituted into $f(x)$ to get $S_1 = 0.997601$ and $S_2 = 0.976871$, respectively. At the same time, the training sample and the test sample are substituted into the model to obtain the comparison chart between the original data and the fitting data, as shown in *Figure 3*. Therefore, the regression function $f(x)$ can be used as a carbon emission prediction model of agroforestry ecological coefficient in a province of China.

Results

Accuracy analysis of model prediction results

In order to verify the accuracy of the carbon emission prediction model of agroforestry ecosystem based on vector regression machine, two provinces in China are

represented by experimental object 1 and experimental object 2. The carbon emissions of agricultural and forestry ecosystems in 2010-2017 in two experimental provinces were predicted by using this model, the carbon emission prediction model of agricultural and fore ecosystems based on tillage data and meteorological information, the carbon emission prediction model of agricultural and forestry ecosystems based on least square regression method and the carbon emission prediction model of agricultural and forestry ecosystems based on ridge regression method, respectively. The results are shown in *Tables 1* and *2*.

In order to reflect the predicted results of different models more clearly, the data in *Tables 1* and *2* are described in the form of polyline graphs, and the results are shown in *Figures 4* and *5*.

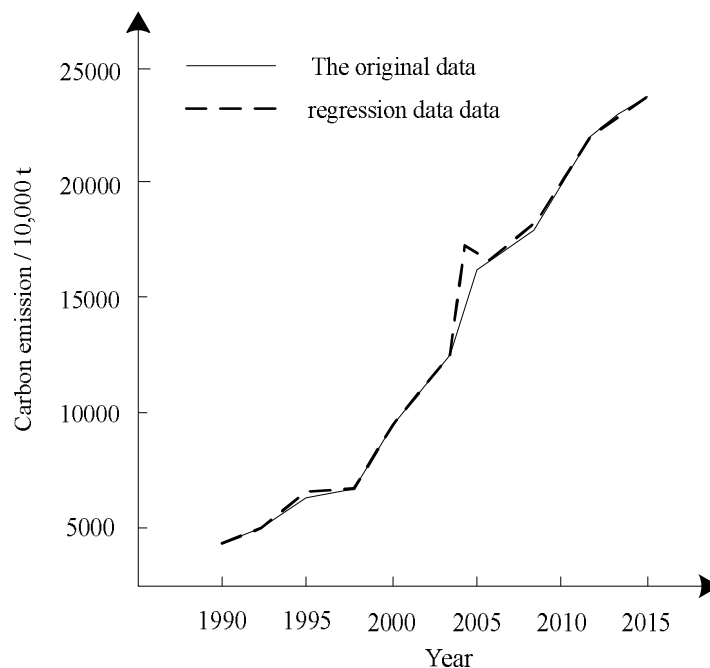


Figure 3. Comparison of original data and regression data

Table 1. Prediction of carbon emissions from agroforestry ecosystem in Provinces 1, 2010-2017

Particular year	Actual emissions /10 ⁴ t	Paper model /10 ⁴ t	Prediction model based on tillage data and meteorological information /10 ⁴ t	Prediction model based on least square regression /10 ⁴ t	Forecasting model based on ridge regression method /10 ⁴ t
2010	7033.5	7046.0	7139.4	7126.0	7239.1
2011	7637.3	7729.9	7806.7	7772.0	7523.2
2012	8209.8	8255.1	8276.4	8185.3	7612.2
2013	8979.1	8823.2	8806.5	8756.2	8706.5
2014	9282.6	9315.8	9326.6	9207.8	8806.2
2015	9457.3	9471.1	9401.3	9360.4	9493.6
2016	9736.5	9699.7	9815.5	9682.7	9677.0
2017	9642.7	9685.4	9722.9	9697.4	9581.4

Table 2. Prediction of carbon emissions from agroforestry ecosystem in Provinces 2, 2010-2017

Particular year	Actual emissions /10 ⁴ t	Paper model /10 ⁴ t	Prediction model based on tillage data and meteorological information /10 ⁴ t	Prediction model based on least square regression /10 ⁴ t	Forecasting model based on ridge regression method /10 ⁴ t
2010	6342.8	6315.4	6426.2	6259.9	6418.6
2011	6675.4	6708.7	6759.8	6601.7	6724.3
2012	6848.2	6872.2	6930.5	6779.2	6781.0
2013	7350.5	7329.4	7287.6	7311.4	7393.8
2014	7961.8	7969.3	7885.3	8006.2	7992.4
2015	8400.6	8426.5	8492.3	8457.1	8351.5
2016	8792.4	8817.8	8726.4	8869.5	8730.5
2017	9033.0	9016.4	9106.6	9002.5	9084.3

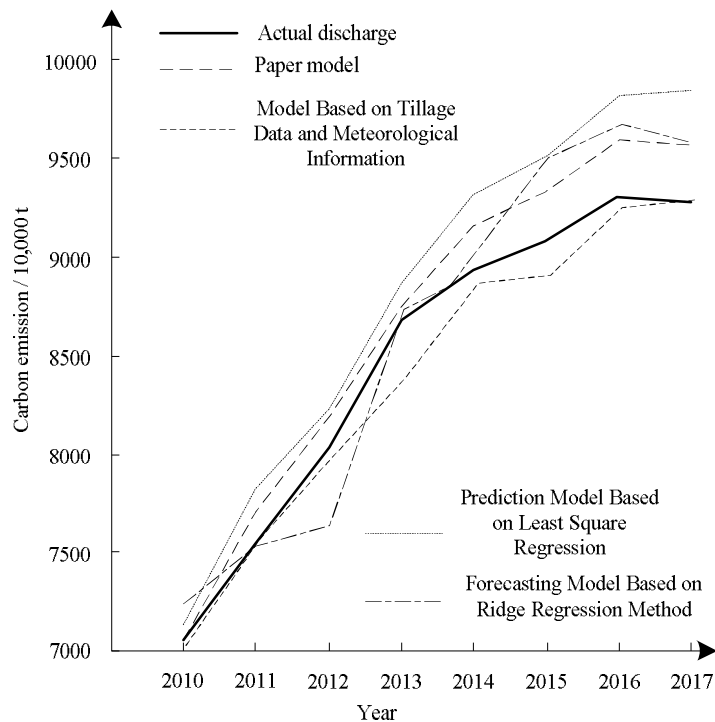


Figure 4. Prediction of carbon emissions from agroforestry ecosystem in Provinces 1, 2010-2017

Analysis *Table 1* and *Figure 4* show that the average carbon emissions of agroforestry ecosystem in the first province from 2010 to 2017 are about $8747.4/10^4$ t. The difference between the average carbon emissions predicted by this model and the average actual carbon emissions is the smallest, about $5.9/10^4$ t, while the differences between the other models and the actual emissions are $39.5/10^4$ t, $23.9/10^4$ t and $167.5/10^4$ t, respectively. *Table 2* and *Figure 5* show that the average carbon emissions

of agroforestry ecosystems in the two provinces from 2010 to 2017 are about $7675.6/10^4$ t. The prediction results of this model are about $7682.0/10^4$ t and the error is about $6.4/10^4$ t. The prediction results of the other three models are $7701.8/10^4$ t, $7660.9/10^4$ t and $7684.6/10^4$ t, respectively. The prediction results of this model are the closest to the actual results. The experimental results show that the prediction accuracy of carbon emissions from agroforestry ecosystems is high.

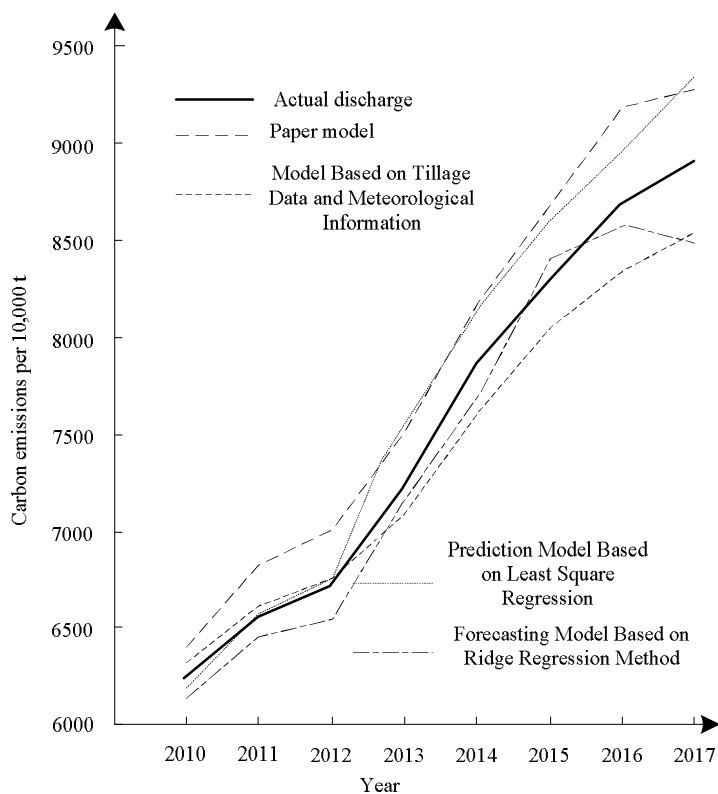


Figure 5. Prediction of carbon emissions from agroforestry ecosystem in Provinces 2, 2010-2017

Analysis of correlation between of GDP and carbon emissions

In order to analyze the correlation between GDP and carbon emissions of agroforestry ecosystem, the factors influencing carbon emissions in China in 2010, the factors predicted at different GDP growth rates and different agroforestry ecological consumption rates in 2011-2015 were normalized into the model, and the output results were inversely normalized. The predicted value of carbon emissions in China in 2010 was 1.026×10^7 t. The predicted carbon emissions during the 12th Five-Year Plan period at different GDP growth rates and different carbon emission ratios are shown in *Table 3*.

From the above analysis, the projected carbon emissions by 2030 can reach 10.49 billion tons. The model predicts that under the same GDP growth rate, the larger the proportion of agricultural and forestry ecological consumption decreases, the less carbon emissions, and the slower the growth of carbon emissions will be over time. This indicates that the optimization of agricultural and forestry ecological energy structure,

especially the development and utilization of low-carbon energy, will be conducive to reducing the proportion of carbon dioxide in energy consumption, thereby slowing down the growth trend of carbon emissions. Under the same decline rate of ecological consumption of agriculture and forestry, the greater the growth rate of GDP, the more carbon emissions, and the faster the growth rate of carbon emissions over time, which shows that if we pursue the rapid growth of GDP too much, the carbon emissions in China will increase rapidly. Therefore, in the future, China can appropriately reduce the GDP growth target and continuously promote the optimization of energy structure to ensure the effective realization of carbon emission reduction targets.

Table 3. Carbon emission forecast value for 2011-2015 under different situations (10^4 t)

GDP growth rate /%	The ratio of agricultural and forestry ecological consumption decreases /%	In 2011	In 2012	In 2013	In 2014	In 2015
7.0	0.80	8398	8765	9156	9573	10023
	1.12	8355	8680	9014	9389	9796
	1.40	8313	8595	8901	9233	9597
7.5	0.80	8423	8831	9255	9748	10025
	1.12	8386	8742	9107	9544	10002
	1.40	8338	8668	8992	9371	9820
8.0	0.80	8461	8893	9359	9890	10454
	1.12	8424	8822	9215	9682	10227
	1.40	8375	8730	9113	9547	10022
8.5	0.80	8488	8963	9173	10063	10628
	1.12	8450	8891	9344	9878	10399
	1.40	8404	8800	9230	9696	10195
9.0	0.80	8521	9034	9591	10187	10848
	1.12	8489	8950	9450	10036	10618
	1.40	8439	8861	9327	9868	10414

Analysis of model practicability

In order to verify the practicability of the model, the model was used to predict soil carbon emissions under different vegetation cover in the agroforestry ecosystem of the experimental object 1. Vegetation coverage refers to the ratio of the vertical projected area of plants to the area of a region, expressed as a percentage. The results are shown in *Table 4*.

Table 4 shows that the prediction errors are less than $9.80/10^4$ t when the model is used to predict the soil carbon emissions under different vegetation cover in the agroforestry ecosystem. The experimental results show that the model can predict the soil carbon emissions in the agroforestry ecosystem comprehensively and has strong practicability.

Analysis of model prediction efficiency

In order to test the prediction efficiency of this model, the carbon emissions of agroforestry ecosystems in two provinces from 2006 to 2015 were predicted by using this model and the other three models respectively. The time required for different

models to predict carbon emissions was compared. The results are shown in *Tables 5 and 6*.

Analysis *Tables 5 and 6* show that the time used to predict carbon emissions from agroforestry ecosystems in different years of the experimental object 1 is 3.64-4.53 s, and the average time spent is 4.07 s, while the average time spent by the other three systems is 7.39 s, 9.41 s and 8.20 s respectively. The model predicted the carbon emissions of agroforestry ecosystems in different years of the experimental subjects 2 in 3.85-4.69 s, and the average time spent was 4.23 s. The average time needed for the other three systems to predict carbon emissions was 7.65 s, 9.60 s and 8.55 s, respectively. The experimental results show that it takes less time to predict the carbon emissions of agroforestry ecosystem by using the proposed model. The average time to predict the carbon emissions of different experimental objects is about 4.15 s, which is the highest efficiency.

Table 4. Comparison of soil carbon emission rates under different vegetation covers in agroforestry ecosystem ($10^4 t$)

Vegetation	Actual value of carbon emissions	Minimum predictive value	Predicted maximum
Degraded meadow	256.2	253.66	261.69
Degraded shrub	350.81	346.52	354.95
Kobresia meadow	352.17	349.97	358.52
Shrub meadow	400.09	398.64	406.62
Abandoned land	612.25	607.08	616.19
Young trees	691.95	686.69	695.26
Spring highland barley	922.39	916.61	926.41
Fir forest	965.77	961.48	969.5
Winter wheat	1064.9	1060.25	1069.17
Cutting slash	1302.96	1298.72	1305.19

Table 5. Time comparison of different models for predicting carbon emissions of experimental object 1

Particular year	Paper model /s	Prediction model based on tillage data and meteorological information /s	Prediction model based on least square regression /s	Forecasting model based on ridge regression method /s
2006	4.53	6.86	9.52	8.66
2007	3.98	6.97	8.86	7.37
2008	3.64	6.92	8.93	9.25
2009	4.22	7.63	9.25	7.48
2010	4.15	7.37	10.06	8.52
2011	3.96	8.03	10.24	8.34
2012	4.03	7.55	9.37	7.98
2013	4.17	7.21	9.66	7.26
2014	4.11	7.36	9.28	8.02
2015	3.98	8.00	8.94	9.11

Table 6. Time comparison of different models for predicting carbon emissions of experimental object 2

Particular year	Paper model /s	Prediction model based on tillage data and meteorological information /s	Prediction model based on least square regression /s	Forecasting model based on ridge regression method /s
2006	4.48	7.53	9.65	7.96
2007	4.51	7.96	10.2	8.05
2008	4.69	8.11	9.37	8.44
2009	3.98	8.27	9.51	8.93
2010	3.96	7.54	8.83	7.99
2011	4.22	6.68	9.42	8.42
2012	4.16	7.92	10.06	9.38
2013	4.37	8.05	8.9	8.76
2014	3.85	7.44	9.92	8.35
2015	4.03	6.99	10.11	9.24

Discussion

This paper puts forward policy suggestions on carbon emission reduction in agroforestry ecosystem from four aspects: developing agroforestry ecosystem economy, improving agroforestry ecosystem efficiency, adjusting agroforestry ecosystem structure and scientific management. China ranks first among the world's largest carbon emitters, the United States second, and India third, according to data. According to a 2016 report by the American Lung Association, more than half of people in the United States face the risk of breathing air pollution, with carbon dioxide emissions of 54.14 million tons. Although India has signed agreements to reduce emissions and use clean energy, 1.2 million people die every year from respiratory diseases (Deo et al., 2016; Tian and Wang, 2016; Xiao et al., 2018).

Improving the development level of agroforestry ecosystem and vigorously developing low-carbon agroforestry ecosystem

Carbon emissions of agroforestry ecosystems in China are increasing year by year, and the level of economic development of agroforestry ecosystems plays the most important role in promoting the scale of carbon emissions of agroforestry ecosystems expands with the rapid development of agroforestry ecosystems. But the hard measures to restrain economic growth are not advisable. The key is to improve the quality of economic development of agroforestry ecosystem. As long as agroforestry ecosystem takes the road of sustainable development, we can get economic growth and environmental quality improvement at the same time (Brahma et al., 2018; Norhayati Rashid, 2017).

First of all, it needs to be supported by a good policy and legal environment, a perfect training system for new farmers and practical talents, a modern agroforestry ecosystem production and management system, and diversified farmers' cooperative organizations. It exploratively brings the emission reduction of agroforestry ecosystem into the track of legalization, so that the emission reduction of agroforestry ecosystem can be legalized. Secondly, we should increase investment in the development of low-carbon agroforestry

ecosystems. It will increase investment in agroforestry ecosystem infrastructure and vigorously develop core technologies in the field of low-carbon agroforestry ecosystem.

Improving the productivity of agroforestry ecosystem and reducing the carbon emission intensity of agroforestry ecosystem

The improvement of production efficiency of agroforestry ecosystem plays a positive role in reducing carbon emission of agroforestry ecosystem. Although the intensity of carbon emission of agroforestry ecosystem in China is decreasing year by year, the production efficiency of agroforestry ecosystem in China is still low. Improving the productivity of agroforestry ecosystem does not only mean scale and mechanization. For example, the scale and mechanization model of the United States brings about high land productivity and commodity efficiency, but also high pollution and high consumption. Therefore, our efficient agroforestry ecosystem should be a technological route with biochemical technology as the main and mechanical technology, promoting the research and development and application of scientific research and innovation, and improving the utilization efficiency of various agricultural funds.

In order to achieve a reasonable combination of nitrogen, phosphorus and potassium fertilizers, it is necessary to apply fertilizers strategically according to different soil nutrient conditions, so as to reduce carbon emissions in the production and transportation of chemical fertilizers, as well as direct carbon emissions in the application process. Promoting the comprehensive utilization of straw resources, strengthening recycling and returning straw to the field will help to improve the soil nutrient status, increase organic matter and improve the soil fertility level (Saleh et al., 2016). Straw can be silage, ammoniation, compaction, microbial fermentation and other ways to produce breeding feed, effectively improve the utilization efficiency of straw resources; biological insecticide-repellent method is used to replace pesticides, using the medicinal properties of various plants in nature and the intergrowth of organisms to achieve the method of resisting pests.

Adjusting the industrial structure of agroforestry ecosystem and reducing the carbon emission of agroforestry ecosystem

The adjustment of industrial structure of agroforestry ecosystem is helpful to reduce carbon emission of agroforestry ecosystem. On the basis of ensuring basic food security, regions should base themselves on resource advantages, face market demand, and develop their own advantages and characteristic departments according to their own resource enjoyment.

First, we should increase the gross domestic product of forestry, fishery and animal husbandry, change the traditional agroforestry ecosystem model and develop diversified agroforestry ecosystems. For example, the emerging agroforestry ecosystem, which combines the traditional agroforestry ecosystem with tourism, meets the requirements of the development of ecological economy, and improves the comprehensive capacity of agroforestry ecosystem production by promoting the comprehensive development of various sectors of agriculture, forestry, animal husbandry and fishery. In the process of structural adjustment of agroforestry ecosystem, each subject should be clearly positioned to give full play to their respective effects. Secondly, we should combine the actual situation, find out the advantages and breakthroughs, scientifically and rationally adjust the structure of planting industry, and combine with aquaculture. Under the condition of

guaranteeing the supply of basic grain, efforts should be made to develop the planting industries of peanut, cotton, rape and other cash crops, such as building dry and fresh fruit bases, expanding industrial and vegetable bases, and vigorously planting characteristic horticultural crops.

Implementing scientific farmland management technology

The dynamic change of organic carbon in agroforestry ecosystem is not only affected by natural factors such as temperature, precipitation and vegetation types, but also by agricultural management measures such as fertilization, straw returning, no-tillage and irrigation. Under the current planting mode, the space for increasing the carbon sequestration effect of agroforestry ecosystem through the improvement of existing management measures has been very small, and the potential for further carbon sequestration is limited. In order to further improve the carbon sequestration capacity of agroforestry ecosystem, we must implement scientific agroforestry ecosystem management technology, reduce the carbon dioxide emissions from the residual root decomposition after harvesting, and further improve the carbon sequestration capacity to the residual root decomposition after harvesting, such as scientific irrigation, rational fertilization and so on.

Conclusions

In this paper, a prediction model of carbon emissions in agroforestry ecosystem based on support vector regression machine is designed. Seven different kinds of carbon sources in root system are selected as influencing factors of carbon emissions in agroforestry ecosystem. According to the basic principle of support vector regression machine, a prediction model of carbon emissions in agroforestry ecosystem is established. The prediction model predicts carbon emissions in agroforestry ecosystem based on seven influencing factors data. Experiments show that the difference between the average carbon emission and the actual average carbon emission of agricultural and forestry ecosystems in the two provinces are $5.9/10^4$ t and $6.4/10^4$ t respectively, which is lower than that of other prediction models. The prediction model predicts that under the same GDP growth rate, the optimization of the energy structure of agricultural and forestry ecosystems is conducive to reducing the proportion of carbon dioxide in energy consumption, thus reducing the proportion of carbon dioxide in energy consumption. The average time used to predict the carbon emissions of agricultural and forestry ecosystems in different years was 4.07 s and 4.23 s, respectively, which was lower than the average time of other prediction models. The experimental results showed that the model in this paper can predict carbon emissions of agroforestry ecosystem quickly and completely.

Acknowledgements. The article takes study cases in Anhui province of China.

REFERENCES

- [1] Anderegg, W., Schwalm, C., Biondi, F. (2015): Forest ecology. Pervasive drought legacies in forest ecosystems and their implications for carbon cycle models. – *Science* 349(6247): 528-32.

- [2] Babaranti, O., Horn, S., Jowett, T., Frew, R. (2019): Isotopic signatures in *Mytilus galloprovincialis* and *Ulva latuca* as bioindicators for assessing discharged sewage effluent in coastal waters along Otago Peninsula, New Zealand. – *Geology, Ecology, and Landscapes* 3(1): 53-64. DOI: 10.1080/24749508.2018.1485079.
- [3] Benjamin, E., Ola, O., Buchenrieder, G. (2018): Does an agroforestry scheme with payment for ecosystem services (PES) economically empower women in sub-Saharan Africa? – *Ecosystem Services* 31(A): 1-11.
- [4] Brahma, B., Pathak, K., Lal, R. et al. (2018): Ecosystem carbon sequestration through restoration of degraded lands in Northeast India. – *Land Degradation & Development* 29(1): 41-64.
- [5] Brogniez, D., Ballabio, C., Stevens, A. (2015): A map of the topsoil organic carbon content of Europe generated by a generalized additive model. – *European Journal of Soil Science* 66(1): 121-134.
- [6] Carsan, S., Stroebel, A., Dawson, I. (2015): Can agroforestry option values improve the functioning of drivers of agricultural intensification in Africa? – *Annals of Physics* 99(2): 434-458.
- [7] Deo, R. C., Samui, P., Kim, D. (2016): Estimation of monthly evaporative loss using relevance vector machine, extreme learning machine and multivariate adaptive regression spline models. – *Stochastic Environmental Research & Risk Assessment* 30(6): 1769-1784.
- [8] Dressler, W., Wilson, D., Clendenning, J. (2015): Examining how long fallow swidden systems impact upon livelihood and ecosystem services outcomes compared with alternative land-uses in the uplands of Southeast Asia. – *Journal of Development Effectiveness* 7(2): 210-229.
- [9] Franzluebbers, A., Chappell, J., Wei, S. (2016): Greenhouse gas emissions in an agroforestry system of the southeastern USA. – *Nutrient Cycling in Agroecosystems* 10(1): 1-16.
- [10] Grinblat, G., Uzal, L., Verdes, P. (2015): Nonstationary regression with support vector machines. – *Neural Computing & Applications* 26(3): 641-649.
- [11] He, J., Rong, L. (2015): Limits of state-led programs of payment for ecosystem services: field evidence from the sloping land conversion program in Southwest China. – *Human Ecology* 43(5): 1-10.
- [12] Helen, K. (2016): Commodification of natural resources and forest ecosystem services: examining implications for forest protection. – *Environmental Conservation* 44(1): 24-33.
- [13] Khanchoul, K., Boubehziz, S. (2019): Spatial variability of soil erodibility at El Hammam catchment, Northeast of Algeria. – *Environment & Ecosystem Science* 3(1): 17-25.
- [14] Khanchoul, K., Boukhrissa, Z. A. (2019): Assessing suspended sediment yield in the Saf Saf Gauged catchment, Northeastern Algeria. – *Malaysian Journal of Geosciences* 3(2): 07-11.
- [15] Maas, B., Tschardtke, T., Saleh, S. (2015): Avian species identity drives predation success in tropical cacao agroforestry. – *Journal of Applied Ecology* 52(3): 735-743.
- [16] Marilice, C., Mendonça, S., Horokoski, T. (2015): Carbon sequestration and riparian zones: assessing the impacts of changing regulatory practices in Southern Brazil. – *Land Use Policy* 42(42): 329-339.
- [17] Michael, A., Terry, R., Eric, D., Zakiya, L., Eric, B. (2015): Loblolly pine age and density affects switchgrass growth and soil carbon in an agroforestry system. – *Forest Science* 58(5): 485-496.
- [18] Norhayati, I., Rashid, M. (2017): Adaptive neuro-fuzzy prediction of carbon monoxide emission from a clinical waste incineration plant. – *Neural Computing & Applications* 2017: 1-13.
- [19] Ogunkunle, T. J., Adewumi, A. A., Adeyinka, O. (2019): Biodiversity: overexploited but underutilized natural resource for human existence and economic development. – *Environment & Ecosystem Science* 3(1): 26-34.

- [20] Onwuka, O. S., Ezugwu, C. K., Ifediegwu, S. I. (2019): Assessment of the impact of onsite sanitary sewage system and agricultural wastes on groundwater quality in Ikem and its environs, south-eastern Nigeria. – *Geology, Ecology, and Landscapes* 3(1): 65-81. DOI: 10.1080/24749508.2018.1493635.
- [21] Ouyang, H., Liu, Z., Wang, L., Peng, W., Deng, H., Ashraf, M. A. (2018): Fungicidal activity and bamboo preservation of *Pinus elliottii* needles extracts. – *Wood Research* 63(4): 533-546.
- [22] Oyedotun, T. D. T., Johnson-Bhola, L. (2019): Beach litter and grading of the coastal landscape for tourism development in sections of Guyana's coast. – *Journal Clean WAS* 3(1): 01-09.
- [23] Ping, Z., Liang, H., Xin, F. (2015): Ecosystem service value assessment and contribution factor analysis of land use change in Miyun County, China. – *Sustainability* 7(6): 7333-7356.
- [24] Roslee, R. (2019): Engineering Geological investigation on Karambunai-Lok Bunuq landslides, Kota Kinabalu, Sabah. – *Malaysian Journal of Geosciences* 3(2): 01-06.
- [25] Rueda, X., Thomas, N., Lambin, E. (2015): Eco-certification and coffee cultivation enhance tree cover and forest connectivity in the Colombian coffee landscapes. – *Regional Environmental Change* 15(1): 25-33.
- [26] Saleh, C., Dzakiyullah, N. R., Nugroho, J. B. (2016): Carbon dioxide emission prediction using support vector machine. – *IOP Conference Series: Materials Science and Engineering* 114(1): 012148.
- [27] Sharma, S., Upadhyay, S., Singh, B. (2019): Employment opportunities with promoting waste management in India. – *Journal Clean Was* 3(1): 10-15.
- [28] Sinare, H., Gordon, L. (2015): Ecosystem services from woody vegetation on agricultural lands in Sudano-Sahelian West Africa. – *Agriculture Ecosystems & Environment* 200(200): 186-199.
- [29] Sloat, L. L., Henderson, A., Lamanna, C. (2015): The effect of the foreshummer drought on carbon exchange in Subalpine meadows. – *Ecosystems* 18(3): 533-545.
- [30] Terrado, M., Tauler, R., Bennett, E. (2015): Landscape and local factors influence water purification in the Monteregian agroecosystem in Québec, Canada. – *Regional Environmental Change* 15(8): 1743-1755.
- [31] Tian, Y., Xu, Y. P., Wang, G. (2018): Agricultural drought prediction using climate indices based on support vector regression in Xiangjiang River basin. – *Science of the Total Environment* 622-623: 710-720.
- [32] Vignola, R., Harvey, C., Bautista-Solis, P. (2015): Ecosystem-based adaptation for smallholder farmers: Definitions, opportunities and constraints. – *Agriculture Ecosystems & Environment* 211(211): 126-132.
- [33] Wall, G., Garcia, R., Kimball, B. (2015): Interactive effects of elevated carbon dioxide and drought on wheat. – *Agronomy Journal* 98(2): 354-381.
- [34] Xiao, X., Zhang, T., Zhong, X. et al. (2018): Support vector regression snow-depth retrieval algorithm using passive microwave remote sensing data. – *Remote Sensing of Environment* 210: 48-64.
- [35] Zhang, Y., Xiao, Q., Huang, M. (2016): Temporal stability analysis identifies soil water relations under different land use types in an oasis agroforestry ecosystem. – *Geoderma* 271: 150-160.

EFFECTS OF HEAVY METAL PB AND CD STRESS ON PHYSIOLOGICAL CHARACTERISTICS OF JAPANESE HONEYSUCKLE

MAO, X. F. – XU, X. B. – CHEN, L. L.*

School of Life Science and Technology, Xinxiang University, Xinxiang 453000, China

**Corresponding author
e-mail: 3193175505@qq.com*

(Received 29th Dec 2018 ; accepted 8th Mar 2019)

Abstract. To evaluate physiological changes of Japanese honeysuckle under lead and cadmium stress, pot-plant experiment was adopted to discover heavy metal Pb or Cd single stress and Pb+Cd combined stress on part of physiological parameters of Japanese honeysuckle. The results showed that under the same treatment, as time prolonged, the content of soluble sugar and soluble protein was decreased, the activity of SOD declined, the amount of free proline and MDA increased and the activity of CAT elevated. Under Pb stress only, total Chlorophyll content rose first and dropped afterwards and POD activity increased, however, under Cd stress only and Pb+Cd stress, both THCL content and POD activity first rose and then declined. In addition, under Pb or Cd single stress and combined stress, as treatment concentration increased, the contents of soluble sugar, soluble protein, free proline and MDA increased accompanied by POD, CAT and SOD activity increased while TCHL content decreased. All these indicate that under certain range of heavy metal stress, Japanese honeysuckle can reduce metabolic disorder plant damage caused by heavy metal stress through increasing osmotic regulating substances of leaves and inducing scavenging system of active oxygen.

Keywords: *Japanese honeysuckle, heavy metal stress, antioxidative enzyme, chlorophyll, osmosis substances*

Abbreviations: SOD: superoxide dismutase, MDA: malondialdehyde, CAT: catalase, POD: peroxidase, CHL a: chlorophyll a, CHL b: chlorophyll b, TCHL: total chlorophyll, Pb: lead, Cd: cadmium

Introduction

With the acceleration of industrialization and urbanization in China, the issue of environmental pollution has become increasingly prominent, especially air, soil and water pollution caused by man-made factors, which have not only influenced urban ecosystem, but also greatly changed the quality of farmland. Among all the factors, heavy metals in the soil are main sources of pollution and the situation is getting worse (Liu et al., 2016).

Pb and Cd are two main heavy metal pollutants in soil from industrial and agricultural activities such as mining and smelting of metalliferous ores, wastewater irrigation and abuse of chemical fertilizers and pesticides (Wang et al., 2015; Abad-Valle et al., 2016). Both of them, which can stay in the soil for a long time, are easy to accumulate and be absorbed by plants. In plants, they accumulate a lot in various organs not only to cause changes in morphology, physiology and biochemistry, structure, but also to endanger human health through the food chain (Khan et al., 2018). In soil, Cd is easily absorbed by plant roots and transported to other parts of plants, which is harmful to organisms even at very low concentration (Hu et al., 2014; Ran et al., 2016). In many cases, photosynthetic organs are damaged, inducing net photosynthesis rate decreased and leaf senescence accelerated, thus plant growth is inhibited, causing decrease of

chlorophyll content (Liu et al., 2015; Silva et al., 2017), stomatal closure and affecting water metabolism and nutrient imbalance caused (Schmidt et al., 2015; Anjum et al., 2016) by Cd can also change the activities of several enzymes relating to nitrogen metabolism, carbohydrate metabolism and sulfur metabolism (Mostofa et al., 2015). Pb is another kind of common harmful heavy metal (Okpoli, 2019). Pb entering into plants can alter cell membrane osmosis and cause a certain degree of damage to sub-micro structures like chloroplast, mitochondria and nucleus (Muhammad et al., 2018). Pb can competitively replace metal elements in the active sites of some enzymes and affect the normal activities of enzymes, thereby causing a series of disorders of physiological processes such as photosynthesis, respiration, nitrogen metabolism, nucleic acid metabolism (Hossain, 2019). It indirectly affects plant growth through antagonism leading to element imbalance and nutritious stress.

Japanese honeysuckle (*Lonicera japonica* T.) belongs to Caprifoliaceae Lonicera. Its flower buds, which can be used as medicine with heat-clearing, detoxifying and anti-inflammatory effects (Li et al., 2017; Wang et al., 2017) is a famous Chinese herbal medicine and widely planted in China. Japanese honeysuckle of Fengqiu county, Henan province, which is famous for its long planting history and high quality, has become the largest planting and export base in China. Their products are exported to Japan, Singapore and southeast Asia, etc. In recent years, the phenomenon of heavy metal exceeded in Chinese herbal medicine has caused great concern. It is closely related to Chinese herbal medicine quality and safety (Chen et al., 2017). As the main origin of Japanese honeysuckle, the farmland of Fengqiu is also polluted with the acceleration of industrialization and urbanization in Henan, affecting the production and quality of Japanese honeysuckle (Sarker et al., 2019). For previous studies of Japanese honeysuckle, the focuses were mostly on the efficacy of its medicinal ingredients, extraction and processing and seldom on heavy metal's physiological influence. The purpose of our research is to probe the physiological and biochemical reactions and tolerance of Japanese honeysuckle, which may provide research basis for the further study of the accumulation characteristics of heavy metals in it and to provide evidence for its scientific planting to ensure its quality, production and clinical medication safety (Ogunkunle et al., 2019).

Materials and methods

Materials

The tested yearling seedling of tree-shaped Japanese honeysuckle was provided by the Four Seasons Honeysuckle Seedlings Company in Jia Zhuang, Fengqiu County, Henan province and the tested soil was also collected from the farmland in the Japanese honeysuckle plant base in Jia Zhuang. After naturally dried, the soil was sieved, crushed and put over 5 mm sieve with the physiological and chemical values and the background values of Pb, Cd were determined (see *Table 1*).

Table 1. The physiological and chemical values of tested soil

pH	Organics (mg/kg)	Main nutrients (mg/kg)			Heavy metals (mg/kg)	
		Available N	Available P	Available K	Cd	Pb
7.8	11.40	91.40	20.40	376	0.035	92.40

Research design

The experiment was conducted in Xinxiang University, Hongqi District, Xinxiang City, Henan Province, China (35.26°N, 113.97°E). It is a warm temperate continental monsoon climate with an average annual temperature of 14.2 °C, an average annual precipitation of 573.4 mm, an average annual sunshine time of 2400 h, an average annual humidity of 68.0%, and a frost-free period of 220 days (Sufiyan et al., 2018).

Test soil was polluted by Pb(NO₃)₂ and CdCl₂ as sources of Pb and Cd. The four treatments of this research were designed according to the amount of pure heavy metals in each pot of soil, which was measured by its weight in each kilo of dry soil. Treatment one was taken as control with no Pb and Cd added (CK). Treatment two only had Pb stress of different concentrations: L₁ (Pb 400 mg/kg), L₂ (Pb 600 mg/kg), L₃ (Pb 800 mg/kg), L₄ (Pb 1000 mg/kg). Treatment three was under Cd stress of different concentrations: C₁ (Cd 0.5 mg/kg), C₂ (Cd 1.0 mg/kg), C₃ (Cd 5.0 mg/kg), C₄ (Cd 10.0 mg/kg). Treatment four had Pb and Cd combined stress of different concentrations: L₁+C₁(400 mg/kg Pb+0.5 mg/kg Cd), L₂+C₂(600 mg/kg Pb+1.0 mg/kg Cd), L₃+C₃(800 mg/kg Pb+5.0 mg/kg Cd), L₄+C₄ (1000 mg/kg Pb+10.0 mg/kg Cd). There were 12 treatments in total and each one repeated five times. All the reagents were added to the prepared 7 kg soil in pots (25 cm × 14 cm × 18 cm) according to the concentration of each treatment. In order to ensure sufficient nutrients for plant growth, 0.2 g of urea and 0.1 g of potassium dihydrogen phosphate were applied to every kg of soil (Samsudin et al., 2018). The soil was permitted to equilibrate for 30 d after lead and cadmium contamination. 30 d later, one healthy seedling of similar growth status was planted in each pot, which were placed in greenhouse in February, 2017 and given 300-500 ml Deionized water each pot every day during the research. In order to simulate the natural growth conditions of Japanese honeysuckle, the greenhouse uses natural light source and keep ventilation. At the same time, the temperature is consistent with the external temperature (Monteiro Junior et al., 2019).

Determining items and methods

At 45 and 90 days after stress respectively, leaf determination was conducted for each plant. 4-5 pairs of mature leaves under the top buds of new shoots Japanese honeysuckle were quickly packed into plastic bags, sealing tightly for determination. In the whole research, 8 items were determined with different procedures, including acetone extraction method for Chlorophyll content (Arnon, 1949). anthrone method for soluble sugar content (Fairbairn, 1953). Determination of proline by Acidic Ninhydrin (Walter and John, 1955). coomassie blue staining for soluble protein content (Sedmak and Grossberg, 1977). Thiobarbituric acid method for MDA, malanodialdehyde (MDA) content was determined from the difference (A532-A600) in absorbance by using Beerand Lambert's equation and expressed in terms of $\mu\text{mol g}^{-1}$ (Jambunathan, 2010). Guaiacol colorimetric method (Bestwick et al., 1998) for POD activity with each OD value changes 0.01 per minute as a enzyme activity unit (U), NBT illumination method for SOD activity with the amount of enzymes for inhibiting 50% of NBT illumination as an enzyme activity unit (U) (Elavarthi and Martin, 2010). Catalase activity was measured according to (Aebi, 1984) where H₂O₂ decomposition is followed spectrophotometrically at 240 nm (Oyedotun, 2019). One enzyme activity unit is equal to 1 mmol H₂O₂ decomposed per minute (Elavarthi and Martin, 2010). Each procedure

was repeated three times to get the mean value. Data processing and analysis were conducted by Excel 2007 and SPSS 19.0.

Results and analysis

Chlorophyll content

As the pigment for photosynthesis, the content of chlorophyll is a predominant reflective parameter for photosynthetic capacity of plant leaves (Riccardi et al., 2014). See Table 2, at 45 d and 90 d, under single and combined stress, Chl a appears an apparent tendency of declining. When cadmium concentration was 1.0 mg/kg and stress was 90 days, Chl a decreased by 59.11% compared to CK, and Chl b decreased by 77.89% when lead concentration was 1000 mg/kg and stress was 90 days. The content of Chl b decreased more than Chl a. Therefore, Chl b is more sensitive than Chl a under heavy metal stress. Nevertheless, under the same treatment, CHL a, CHL b and TCHL showed downtrend with time increased, manifesting the inhibition effect of heavy metal stress for chlorophyll synthesis.

Table 2. Effect of Pb, Cd stress on chlorophyll content mg/g

Element	Treatment	Chl a		Chl b		Total Chl	
		45d	90d	45d	90d	45d	90d
Cd	CK	1.385±0.030a	1.230±0.059a	0.986±0.007a	0.882±0.019a	2.371±0.064a	2.112±0.083a
	1	1.021±0.052b	0.528±0.044b	0.793±0.060a	0.323±0.005b	1.814±0.210b	0.851±0.017b
	2	0.956±0.027bd	0.503±0.029b	0.710±0.045a	0.308±0.004c	1.666±0.085bd	0.811±0.014b
	3	0.869±0.004bd	0.521±0.021b	0.629±0.065ac	0.266±0.010d	1.498±0.035bd	0.787±0.017b
	4	0.807±0.060cd	0.549±0.013b	0.475±0.045bc	0.236±0.001e	1.282±0.025cd	0.785±0.014b
Pb	CK	1.385±0.030a	1.230±0.059a	0.986±0.007a	0.882±0.019a	2.371±0.064a	2.112±0.083a
	1	0.976±0.022b	1.023±0.019b	0.296±0.009b	0.328±0.042b	1.272±0.017b	1.351±0.114b
	2	0.833±0.025c	0.794±0.004c	0.275±0.005bd	0.246±0.068b	1.108±0.007c	1.040±0.063c
	3	0.821±0.007c	0.770±0.051c	0.258±0.001cd	0.214±0.049b	1.079±0.022c	0.984±0.060c
	4	0.823±0.013c	0.745±0.042c	0.226±0.009e	0.195±0.050b	1.049±0.010c	0.94±0.038c
Cd+Pb	CK	1.385±0.030a	1.230±0.059a	0.986±0.007a	0.882±0.019a	2.371±0.064a	2.112±0.083a
	1	0.872±0.031b	0.765±0.049b	0.236±0.008b	0.274±0.036b	1.108±0.026b	1.039±0.011b
	2	0.850±0.016be	0.754±0.006bd	0.258±0.001bd	0.230±0.033b	1.108±0.023b	0.984±0.078b
	3	1.051±0.015c	0.835±0.011b	0.303±0.008c	0.182±0.058b	1.354±0.012c	1.017±0.033b
	4	0.791±0.008de	0.618±0.036c	0.234±0.006bd	0.205±0.062b	1.025±0.006b	0.886±0.028b

Data are mean ± SD (n = 5). Different lowercase letters in the same column indicate significant difference at p < 0.05 levels between different treatments according to the LSD

Free proline content

As one of the most important osmotic substances in plants, the accumulation of free proline plays an important role for osmotic regulation of cells, stabilization of cell structure and reduction of oxidation (Dawood et al., 2014). Under normal circumstances, the content of free proline keeps at comparatively low level. However, under the adverse conditions such as salinization, drought, heavy metal pollution, etc., free proline will accumulate in cytoplasm to resist stress and carry out osmotic adjustment (Ali et al., 2015). Under Pb, Cd single and combined stress, the contents of free proline were all higher than CK and increased with concentration during 45 d and 90 d treatment processes. Under the same treatment, when the concentration of

Pb > 800 mg/kg and Cd > 5 mg/kg, the amount of free proline decreased with time, yet under Pb+Cd stress, free proline content increased with time (see *Table 3*).

Table 3. Effect of Pb, Cd stress on the content of free proline mg/g

Treatment	Element					
	Cd		Pb		Cd + Pb	
	45d	90d	45d	90d	45d	90d
CK	0.112±0.004a	0.131±0.010a	0.112±0.004a	0.131±0.010a	0.112±0.004a	0.131±0.010a
1	0.141±0.014a	0.164±0.042b	0.145±0.021ac	0.168±0.003ac	0.168±0.005a	0.174±0.035a
2	0.162±0.036a	0.343±0.003c	0.260±0.034bc	0.366±0.021bc	0.170±0.056a	0.184±0.008a
3	0.390±0.054b	0.351±0.023c	0.468±0.017d	0.281±0.065bc	0.894±0.097b	1.183±0.108b
4	0.711±0.026c	0.543±0.045c	0.750±0.077e	0.473±0.005d	1.208±0.078d	1.263±0.016b

Data are mean ± SD (n = 5). Different lowercase letters in the same column indicate significant difference at p < 0.05 levels between different treatments according to the LSD

Soluble sugar content

Soluble sugar, the main osmotica for plants, has a stabilization effect for cell membrane and protoplasmic colloid and a protective effect when the concentration of inorganic ions is high in cells. Under osmotic stress, plants can reduce osmosis by accumulating soluble sugar to adapt to changes of environment (Nawaz et al., 2015) According to data in *Table 4*, soluble sugar content showed a downtrend as treatment time prolonged under the same treatment of Pb, Cd single and combined stress at 45 d and 90 d. For concentration, when it increased, soluble sugar content of each group all showed a gradually rising tendency compared to CK and reached the highest at treatment 4. For Pb stress only, soluble content increased 43.94% and 46.09% respectively in contrast to CK at 45 d and 90 d. For Cd stress, the percentages were 61.36% and 54.69%, whereas 70.45% and 57.81% for Pb+Cd combined stress.

Table 4. Effect of Pb, Cd stress on soluble sugar mg/g

Treatment	Element					
	Cd		Pb		Cd + Pb	
	45d	90d	45d	90d	45d	90d
CK	0.132±0.014a	0.128±0.012a	0.132±0.014a	0.128±0.012a	0.132±0.014a	0.128±0.012a
1	0.145±0.015a	0.138±0.023a	0.143±0.002a	0.132±0.044a	0.149±0.008a	0.144±0.022a
2	0.160±0.007a	0.153±0.034a	0.159±0.042a	0.155±0.130a	0.170±0.015ac	0.163±0.004a
3	0.174±0.021ac	0.163±0.050a	0.170±0.003a	0.164±0.026a	0.194±0.015ad	0.183±0.050a
4	0.213±0.005bc	0.198±0.033a	0.190±0.034a	0.187±0.033a	0.225±0.027bcd	0.202±0.020a

Data are mean ± SD (n = 5). Different lowercase letters in the same column indicate significant difference at p < 0.05 levels between different treatments according to the LSD

Soluble protein content

Soluble proteins are typical enzymes that specifically bind to the membrane system. Under certain stresses, the higher the content of soluble protein in plants, the stronger the physiological and biochemical reactions and metabolic activities of the plant, which can be used as an indicator of plant's relative resistance. In *Table 5*, Soluble protein

content decreased with the increase of time when under the same treatment at 45 d and 90 d separately, The soluble protein content of each treatment was higher than control no matter single or combined stress and increased with concentration.

Table 5. Effect of Pb, Cd stress on soluble protein mg/g

Treatment	Element					
	Cd		Pb		Cd + Pb	
	45d	90d	45d	90d	45d	90d
CK	0.302±0.027a	0.181±0.003a	0.302±0.027a	0.181±0.003a	0.302±0.027a	0.181±0.003a
1	0.493±0.033ac	0.282±0.210ac	0.545±0.035b	0.438±0.019b	1.148±0.187b	1.124±0.196b
2	0.660±0.046bc	0.453±0.025ad	0.759±0.036b	0.555±0.066b	1.270±0.109b	1.163±0.098b
3	0.820±0.044b	0.633±0.075bcd	0.870±0.058b	0.764±0.036c	2.194±0.202c	2.183±0.311c
4	1.102±0.142d	0.188±0.001a	1.200±0.113c	0.188±0.101a	3.218±0.237d	3.195±0.214d

Data are mean ± SD (n = 5). Different lowercase letters in the same column indicate significant difference at p < 0.05 levels between different treatments according to the LSD

MDA content

MDA is the main decomposition product of membrane lipid peroxidase and one of the main parameters reflecting the degree of damage to membrane system (Magwanga et al., 2018). In *Table 6*, the result showed that MDA contents of both single and combined stress were higher than CK at high concentrations. which pointed that high concentrations treatments had damage to plant. Under Pb, Cd single stress, MDA contents of Japanese honeysuckle leaves were higher than CK by 2.62% to 124.8%. While under combined stress, it was higher than CK by 14.24% to 104.31%. At different treatment time, MDA content increased as treatment time increased, which meant that as time prolonged, the damage of membrane lipid peroxidation increased and the ability to clear active oxygen decreased. For single treatment, MDA content increased as treatment concentration increased, indicating that Japanese honeysuckle growth was inhibited to a certain extent. Whereas MDA content had no apparent increase with concentration increase under combined stress, indicating that Japanese honeysuckle was not sensitive to the aggravation of adverse stress under the combined stress.

POD content

POD, a common redox enzyme in plants, is a kind of enzyme with high activity. As a type of enzyme that is very sensitive to environmental factors (Ashraf et al., 2017). It can catalyze the oxidative decomposition of toxic substances. At the 45 d and 90 d, POD activity of Japanese honeysuckle leaves increased as treatment concentration increased under single and combined stress (see *Table 7*). Particularly at 90 d of Pb₄ of single stress, POD activity increased by up to 107.45%, which manifested that under high concentration of Pb treatment, POD acted as protection for heavy metal damage. When under Cd stress, POD activity first increased with treatment concentration. As treatment time prolonged, its activity dropped when Cd concentration ≥ 5.0 mg/kg, but was still higher than CK, indicating that when Cd concentration was beyond the tolerance of plant, POD activity was inhibited. POD activity under combined stress was similar to that under Cd stress. When the concentration of

Pb+Cd > 1.0 mg/kg + 600 mg/kg, POD activity began to drop, however, it was still higher than CK and Pb, Cd stress, indicating synergistic effect of Pb and Cd. At low concentration, POD activity's increase shows raise in its capacity of scavenging oxygen free radicals and its decrease at high concentration indicates its limitation of defense mechanism.

Table 6. Effect of Pb, Cd stress on MDA content $\mu\text{mol/g}$

Treatment	Element					
	Cd		Pb		Cd+Pb	
	45d	90d	45d	90d	45d	90d
CK	0.344±0.020a	0.371±0.071a	0.344±0.020a	0.371±0.071a	0.344±0.020a	0.371±0.071a
1	0.353±0.021a	0.447±0.031ac	0.353±0.052a	0.437±0.044ac	0.393±0.063a	0.667±0.031bd
2	0.378±0.023ac	0.576±0.035bc	0.458±0.026ac	0.478±0.047ac	0.478±0.047ac	0.676±0.038bc
3	0.399±0.024ac	0.664±0.037bc	0.566±0.031bc	0.568±0.035bc	0.499±0.045ac	0.567±0.027b
4	0.449±0.026bc	0.753±0.039de	0.770±0.042d	0.834±0.053d	0.639±0.049bc	0.758±0.057cde

Data are mean \pm SD (n = 5). Different lowercase letters in the same column indicate significant difference at p < 0.05 levels between different treatments according to the LSD

Table 7. Effect of Pb, Cd stress on POD activity U/g

Treatment	Element					
	Cd		Pb		Cd+Pb	
	45d	90d	45d	90d	45d	90d
CK	311.43±35.54a	350.56±20.58a	311.43±35.54a	350.56±20.58a	311.43±35.54a	350.56±20.58a
1	419.88±37.70ac	454.83±70.56ac	324.56±29.56ac	368.84±21.20ac	431.56±17.72ac	458.84±25.47ac
2	420.52±23.64bc	438.88±12.68ad	335.67±20.84ad	378.42±28.27ad	511.47±35.73bc	522.42±33.44ad
3	483.49±13.82bc	472.56±41.23ac	426.97±32.85bcd	482.63±60.65bcd	567.66±22.87b	544.34±80.57bcd
4	600.76±32.13d	582.34±19.64bcde	648.53±33.67e	727.22±29.56e	569.56±53.16b	545.72±26.51bcd

Data are mean \pm SD (n = 5). Different lowercase letters in the same column indicate significant difference at p < 0.05 levels between different treatments according to the LSD

SOD content

SOD is one of the most important protective enzymes for scavenging active free radicals in plants. It can effectively clear excessive oxygen free radicals in plants and reduce its peroxide degree on membrane lipids (Malar et al., 2014). According to the data in Table 8, compared between 45 d and 90 d, the activity of enzyme decreased with the prolong of treatment time. The activity of SOD increased as the treatment concentration increased under single and combined stress, however, it was not so apparent compared to the control, indicating that the influence of Pb, Cd stress was not so obvious on the activity of SOD.

CAT content

As an important redox enzyme in plants as well as a key enzyme for biological defense system, CAT can scavenge superfluous active oxygen, maintain the balance of active oxygen metabolism and protect the integrity of cell membrane (Khan et al., 2018; Anjum et al., 2015). Under single and combined treatment, with the increase of treatment time and concentration, the activity of CAT showed an increasing trend,

indicating that Japanese honeysuckle leaves can adapt to long time adverse environment by increasing the activity of CAT. The activity of CAT increased more when the concentration of Cd > 1.0 mg/kg, Pb > 600 mg/kg, Pb+Cd > 600 mg/kg + 1.0 mg/kg at 90 d. The increase amplitudes were 50.31%, 45.6% and 70.14% respectively, among which the combined stress had the highest increase (see *Table 9*). The results showed that high concentrations of Pb and Cd stress could promote the increase of CAT activity in leaves of Japanese honeysuckle and the Pb and Cd combined stress had corresponding synergistic effect.

Table 8. Effect of Pb, Cd stress on SOD activity U/g

Treatment	Element					
	Cd		Pb		Cd+Pb	
	45d	90d	45d	90d	45d	90d
CK	580.98±35.54a	540.77±28.93a	580.98±35.54a	540.77±28.93a	580.98±35.54a	540.77±28.93a
1	544.46±32.63a	589.32±28.56a	594.56±29.56a	558.64±28.76a	621.56±40.72a	588.84±29.33a
2	591.52±15.23a	548.77±22.58a	605.47±37.66a	568.42±28.27a	641.47±39.90a	612.42±33.44a
3	625.46±32.65a	582.73±0.023a	613.48±32.65a	605.46±32.65ac	666.73±32.87a	633.43±50.52a
4	621.88±35.31a	571.34±29.56a	739.56±33.67b	697.77±29.56bc	689.56±43.16a	655.23±43.11a

Data are mean ± SD (n = 5). Different lowercase letters in the same column indicate significant difference at p < 0.05 levels between different treatments according to the LSD

Table 9. Effect of Pb, Cd stress on CAT activity U/g

Treatment	Element					
	Cd		Pb		Cd+Pb	
	45d	90d	45d	90d	45d	90d
CK	14.34±0.86a	14.67±1.87a	14.34±0.86ac	14.67±1.87a	14.34±0.86a	14.67±1.87a
1	14.94±2.18ac	15.72±1.05ac	12.32±0.43ac	14.63±1.21a	16.45±0.27a	17.76±0.29ac
2	17.60±1.12ad	17.78±1.18ad	15.33±0.23ac	16.78±0.14ac	18.51±0.31ac	19.87±0.16bc
3	20.21±0.39bc	21.13±1.42bc	18.81±1.29b	19.88±0.51bc	20.81±1.51bc	22.92±0.63bc
4	20.92±1.79bd	22.05±0.64bd	19.31±0.25b	21.36±0.12b	21.36±1.72b	24.96±0.15de

Data are mean ± SD (n = 5). Different lowercase letters in the same column indicate significant difference at p < 0.05 levels between different treatments according to the LSD

Discussion

Under heavy metal stress, three kinds of osmosis substances, free proline, soluble sugar, soluble protein, accumulated quickly in leaves to reduce osmotic potential in cells, increase osmotic adjustment ability, promote moisture absorption and ensure the norm growth of plants. However, after 45 d of single treatment, the contents of soluble sugar, soluble protein and free proline increased. Both soluble sugar and soluble protein contents decreased after 90 d of single and combined stress. These results are correlated with work of Janmohammadi et al. (2013). This might be caused by physiological mechanism damage of plants after long time single or combined stress, which might inhibit the accumulation of soluble sugar and soluble protein, accelerate their decomposition and reduce their contents. One reason, which might explain the increase of soluble sugar, is that plants can regulate osmotic potential to reduce damage caused

by outside environment through increasing soluble sugar content. Since a large number of increased organic small solutes like soluble protein can reduce water potential in cells so as to achieve the purpose of water absorption from the surrounding cells. The other reason might be that under heavy metal stress, the absorption of some essential ions weakened, leading to accelerated decomposition of substances such as starch, protein and nucleic acids, thus plant growth was inhibited. The content of soluble sugar in leaves of Japanese honeysuckle treated with heavy metal stress decreased 90 days compared with 45 days, which may be due to the consumption of plant respiration as time went by. Soluble sugar content in Japanese honeysuckle leaves under Pb, Cd single stress or Pb+Cd combined stress was comparatively high, which might improve the capacity of stress tolerance of plants. Free proline can still maintain a higher concentration. These findings are correlated with work of Jayasri et al. (2017). Their study of Pb stress on *Lemna minor* demonstrated that the decomposition of soluble protein accelerated under adverse circumstances and separated into various amino acid including free proline, etc., resulting in the rise of proline content. Due to the low osmotic potential of the external environment under heavy metal stress, plants will lose water. In order to avoid infiltration injury, plant cells will take the initiative to absorb and accumulate inorganic salts and soluble substances such as free proline to reduce intracellular osmotic potential and avoid water loss damage. In our study, the higher content of free proline under high concentration of heavy metal stress may be related to this, however, the specific reasons still need further analysis. Stress changes substances metabolism of plants and generates osmotic adjustment substances to accumulate in plants, such as macro molecular substances like starch, protein, which further break down into small molecules such as soluble sugar, soluble protein and free proline. These substances have strong hydrophilic property, stabilizing colloidal property, protecting plant cells from damage or reducing damage in tissue metabolism. The capacity of osmotic adjustment of these substances can directly reflect the strength of stress resistance of plants.

When the reactive oxygen species produced in plant cells under heavy metal stress are beyond scavenging activity of protective enzyme system, free radicals will accumulate in leaf cells, thereby inducing peroxidase damage of plant cells. As one of the antioxidant enzymes, POD plays an important role for plants to resist adversity stress. In our study, Pb, Cd stress have effects for SOD, POD and CAT activities. However, the activity of POD increased more than that of SOD and CAT. 45 d after treatment, under low concentration and high concentration of Pb, Cd single and combined stress, the activities of SOD, POD and CAT all increased to protect Japanese honeysuckle from injury. When the concentration of stress was higher as time prolonged, POD activity further increased whereas SOD and CAT activities began to drop, indicating that POD played a major protective role in stress as the treatment time prolonged. When Cd concentration is in the range of 0.05-0.5 mol/L, the activity of POD and SOD increased with the increase of Cd concentration, but the content of MDA and the permeability of cell membrane also showed an upward trend (Santos et al., 2015). Although Cd increased the activity of POD and SOD to a certain extent, it did not prevent the occurrence of membrane hyperperoxide. Our study indicated that although Pb, Cd stress have influence on SOD, POD and CAT activities, POD activity increased more than that of SOD and CAT. At 45 d of treatment, under low and high concentrations of Pb, Cd stresses or Pb+Cd combined stress, the activities of SOD, POD, CAT all increased to protect Japanese honeysuckle from injury. At 90 d of

treatment, when Pb, Cd stress or combined stress were of high concentrations, POD activity further increased while SOD and CAT activities began to drop, manifesting that POD act as the main protector under stress with the increase of time. The study showed that Japanese honeysuckle reduce metabolism imbalance damage through increasing osmotic adjustment substances of leaves and inducing the scavenging system of reactive oxygen in a certain range of heavy metal stress.

Conclusions

1. In our study, heavy metal stress hindered CHL synthesis to different extents at 45 d and 90 d. At 90 d, the content of CHL was lower than 45 d, which illustrated that heavy metal stress inhibited CHL synthesis as treatment time prolonged.

2. In our study, all the evidence pointed to the fact that under heavy metal stress, three kinds of osmosis substances, free proline, soluble sugar, soluble protein, accumulated quickly in leaves of Japanese honeysuckle to reduce osmotic potential in cells, increase osmotic adjustment ability, promote moisture absorption and ensure the norm growth of plants. The contents of soluble sugar, soluble protein and free proline increased after 45 d of single treatment. Both soluble sugar and soluble protein contents decreased after 90 d of single and combined stress. This might be caused by physiological mechanism damage of plants after long time single or combined stress, which might inhibit the accumulation of soluble sugar and soluble protein, accelerate their decomposition and reduce their contents. Free proline can still maintain a higher concentration.

3. In our study, Pb, Cd stresses have effects for SOD, POD and CAT activities. However, the activity of POD increased more than that of SOD and CAT. 45 d after treatment, under low concentration and high concentration of Pb, Cd single and combined stress, the activities of SOD, POD and CAT all increased to protect Japanese honeysuckle from injury. When the concentration of stress was higher as time prolonged, POD activity further increased whereas SOD and CAT activities began to drop, indicating that POD played a major protective role in stress as the treatment time prolonged. With the increase of Cd concentration, the content of MDA and the permeability of cell membrane also showed an upward trend. Although Cd increased the activity of POD and SOD to a certain extent, it did not prevent the occurrence of membrane hyperperoxide.

4. The study showed that Japanese honeysuckle can reduce metabolism imbalance damage through increasing osmotic adjustment substances of leaves and inducing the scavenging system of reactive oxygen in a certain range of heavy metal stress.

Acknowledgements. This work was supported by the Science and Technology Key Projects of Henan Province (152102310018); Key Scientific Research Project of colleges and university in Henan Province (16A180049).

REFERENCES

- [1] Aebi, H. (1984): Catalase in vitro methods. – *Enzymol* 105: 121-126.
- [2] Ali, N., Hadi, F. (2015): Phytoremediation of cadmium improved with the high production of endogenous phenolics and free proline contents in *Parthenium*

- hysterophorus plant treated exogenously with plant growth regulator and chelating agent. – Environmental Science Pollution Research 22(17): 13305-13318.
- [3] Anjum, S. A., Tanveer, M., Hussain, S. et al. (2015): Cadmium toxicity in maize (*Zea mays* L.): consequences on antioxidative systems, reactive oxygen species and cadmium accumulation. – Environmental Science and Pollution Research 22(21): 17022-17030.
- [4] Anjum, S. A., Tanveer, M., Hussain, S. et al. (2016): Morpho-physiological growth and yield responses of two contrasting maize cultivars to cadmium exposure. – Clean-Soil Air Water 44(1): 29-36.
- [5] Arnon, D. I. (1949): Copper enzymes in isolated chloroplasts. Polyphenoxidase in *Beta vulgaris*. – Plant Physiol 24(1): 1.
- [6] Ashraf, U., Hussain, S., Anjum, S. A. et al. (2017): Alterations in growth, oxidative damage, and metal uptake of five aromatic rice cultivars under lead toxicity. – Plant Physiol Biochem 115: 461-471.
- [7] Bestwick, G. S., Brown, I. R., Mansfield, J. W. (1998): Localized changes in peroxidase activity accompany hydrogen peroxide generation during the development of an anohost hypersensitive reaction in lettuce. – Plant Physiology 118: 1067-1078.
- [8] Chen, D. D., Xie, X. F., Ao, H., Liu, J. L., Peng, C. (2017): Raman spectroscopy in quality control of Chinese herbal medicine. – Journal of the Chinese Medical Association 80: 288-296.
- [9] Dawood, M. G., Taie, H. A. A., Nassar, R. M. A. et al. (2014): The changes induced in the physiological, biochemical and anatomical characteristics of *Vicia faba* by the exogenous application of proline under seawater stress. – South African Journal of Botany 93: 54-63.
- [10] Elavarthi, S., Martin, B. (2010): Spectrophotometric assays for antioxidant enzymes in plants, in plant stress tolerance. – Methods and Molecular Biology 639: 273-280.
- [11] Fairbairn, N. J. (1953): A modified anthrone reagent. – Chem and Ind. 4: 86.
- [12] Hossain, S. (2019): Seismic geomorphology as a tool for reservoir characterization: a case study from Moragot Field of Pattani Basin, Gulf of Thailand. – Malaysian Journal of Geosciences 3(1): 45-50.
- [13] Hu, Y., Nan, Z., Jin, C., Wang, N., Luo, H. (2014): Phytoextraction potential of poplar (*Populus alba* L. var. *pyramidalis* Bunge) from calcareous agricultural soils contaminated by cadmium. – Int J Phytorem 16(5): 482-495.
- [14] Jambunathan, N. (2010): Determination and detection of reactive oxygen species (ROS), lipid peroxidation, and electrolyte leakage in plants. – Methods in Molecular Biology 639: 292-298.
- [15] Janmohammadi, M., Bihanta, M. R., Ghasemzadeh, F. (2013): Influence of rhizobacteria inoculation and lead stress on the physiological and biochemical attributes of wheat genotypes. – Cercet. Agron. in Mold. XLVI(1). DOI: <https://doi.org/10.2478/v10298-012-0074-x>.
- [16] Jayasri, M. A., Suthindhiran, K. (2017): Effect of zinc and lead on the physiological and biochemical properties of aquatic plant *Lemna minor*: its potential role in phytoremediation. – Appl. Water Sci. 7(3):1247-1253.
- [17] Khan, M. M., Islam, E., Irem, S. et al. (2018a): Pb-induced phytotoxicity in para grass (*Brachiaria mutica*) and Castorbean (*Ricinus communis* L.): Antioxidant and ultrastructural studies. – Chemosphere 200: 257-265.
- [18] Khan, J., Siddiq, M., Akram, B., Ashraf, M. A. (2018a): In-situ synthesis of CuO nanoparticles in P(NIPAM-co-AAA) microgel, structural characterization, catalytic and biological applications. – Arabian Journal of Chemistry 11(6) 897-909.
- [19] Li, C. L., Yang, M. Y., Zhu, L. J., Zhu, Y. Q. (2017): Honeysuckle flowers extract loaded bombyx morisilk fibroin films for inducing apoptosis of Hela cells. – Microscopy Research and Technique 80: 1297-1303.
- [20] Liu, Z., Yang, Y., Bai, Y., Huang, Y., Nan, Z., Zhao, C., Ma, J., Wang, H. (2016): The effect of municipal sludge compost on the mobility and bioavailability of Cd in a

- sierozem-wheat system in an arid region northwest of China. – *Environmental Science and Pollution Research* 23(20): 20232-20242.
- [21] Liu, Z. L., Chen, W., He XY. (2015): Influence of Cd²⁺ on growth and chlorophyll fluorescence in a hyperaccumulator: *Lonicera japonica* Thunb. – *Plant Growth Regul* 34(3): 672-676.
- [22] Magwanga, R., Lu, P., Kirungu, J. et al. (2018): Whole genome analysis of cyclin dependent kinase (CDK) gene family in cotton and functional evaluation of the role of CDKF4 gene in drought and salt stress tolerance in plants. – *International Journal of Molecular Sciences* 19(9): 2625.
- [23] Malar, S., Shivendra Vikram, S., Jc Favas, P., Perumal, V. (2014): Lead heavy metal toxicity induced changes on growth and antioxidative enzymes level in water hyacinths [*Eichhornia crassipes* (Mart.)]. – *Botanical Studies* 55(1): 54.
- [24] Monteiro Junior, J. J., Silva, E. A., De Amorim Reis, A. L., Souza Santos, J. P. M. (2019): Dynamical spatial modeling to simulate the forest scenario in Brazilian dry forest landscapes. – *Geology, Ecology, and Landscapes* 3(1): 46-52: DOI: 10.1080/24749508.2018.1481658.
- [25] Mostofa, M. G., Rahman, A., Ansary, M. D., Mesbah, U. et al. (2015): Hydrogen sulfide modulates cadmium-induced physiological and biochemical responses to alleviate cadmium toxicity in rice. – *Scientific Reports* 5: 14078.
- [26] Muhammad, S., Hafiz, N. A., Zahir, A. Z., Muhammad, S. (2018): Impact of lead tolerant plant growth promoting rhizobacteria on growth, physiology, antioxidant activities, yield and lead content in sunflower in lead contaminated soil. – *Chemosphere* 195: 606-614.
- [27] Nawaz, F., Ahmad, R., Ashraf, M. Y. et al. (2015): Effect of selenium foliar spray on physiological and biochemical processes and chemical constituents of wheat under drought stress. – *Ecotoxicology and Environmental Safety* 113: 191-200.
- [28] Ogunkunle, T. J., Oyelami, O. A., Adepoju, A. O. (2019): Study of the phytodiversity along Antorun Reservoir, near Ogbomoso, Nigeria. – *Environment & Ecosystem Science* 3(1): 1-12.
- [29] Okpoli, C. C. (2019): Delineation of high-resolution aeromagnetic survey of Lower Benue Trough for lineaments and mineralization: case study of Abakikili Sheet 303. – *Malaysian Journal of Geosciences* 3(1): 51-60.
- [30] Oyedotun, T. D. T. (2019): Land use change and classification in Chaohu Lake catchment from multi-temporal remotely sensed images. – *Geology, Ecology, and Landscapes* 3(1): 37-45. DOI: 10.1080/24749508.2018.1481657.
- [31] Ran, J., Wang, D., Wang, C., Zhang, G., Zhang, H. (2016): Heavy metal contents, distribution, and prediction in a regional soil-wheat system. – *Sci Total Environ* 544: 422-431.
- [32] Riccardi, M., Mele, G., Pulvento, C. et al., (2014): Non-destructive evaluation of chlorophyll content in quinoa and amaranth leaves by simple and multiple regression analysis of RGB image components. – *Photosynth Res* 120(3): 263-272.
- [33] Samsudin, M. S., Azid, A. (2018): Assessment of marine water quality index in mangrove estuarine: case study in Setiu River estuary. – *Journal Clean WAS* 2(2): 16-18.
- [34] Santos, D., Duarte, B., Cacador, I. (2015): Biochemical and photochemical feedbacks of acute Cd toxicity in *Juncus acutus* seedlings: the role of non-functional Cd-chlorophylls. – *Estuarine Coastal and Shelf Science*.167: 228-239.
- [35] Sarker, M. K. U., Majumder, A. K., Haque, M. Z., Hossain, M. S., Al Nayeem, A. (2019): Assessment of inland water quality parameters of Dhaka City, Bangladesh. – *Environment & Ecosystem Science* 3(1): 13-16.
- [36] Schmidt, E. C., Felix, M. R. D. L., Polo, L. K. et al. (2015): Influence of cadmium and salinity in the red alga *Pterocladia capillacea*: cell morphology, photosynthetic performance and antioxidant systems. – *Brazilian Journal of Botany* 38(4): 737-749.
- [37] Sedmak, J. J., Grossberg, S. E. (1977): A rapid, sensitive, and versatile assay for protein using Coomassie brilliant blue G-250. – *Anal. Biochem* 79: 544-552.

- [38] Silva, A. J., Nascimento, C. W. A., Gouveia-Neto, A. S. (2017): Assessment of cadmium phytotoxicity alleviation by silicon using chlorophyll a fluorescence. – *Photosynthetica* 55(4): 648-654.
- [39] Sufiyan, I., Magaji, J. I. (2018): Modeling flood hazard using swat and 3d analysis in Terengganu watershed. – *Journal Clean Was* 2(2): 19-24.
- [40] Walter, T., John, L. (1955): A photometric methods for the determination of proline. – *J. Biol. Chem.* 215: 655-660.
- [41] Wang, D. Y., Zhao, X. M., Liu, Y. L. (2017): Hypoglycemic and hypolipidemic effects of a polysaccharide from flower buds of *Lonicera japonica* Thunb in streptozotocin-induced diabetic rats. – *International Journal of Biological Macromolecules* 102: 396-404.
- [42] Wang, Y., Wang, S., Nan, Z., Ma, J., Zang, F., Chen, Y., Li, Y., Zhang, Q. (2015): Effects of Ni stress on the uptake and translocation of Ni and other mineral nutrition elements in mature wheat grown in sierozems from northwest of China. – *Environ Sci Pollut Res* 22(24): 19756-19763.

EVALUATING ECONOMIC GROWTH EFFICIENCY AND ITS DETERMINANTS UNDER LOW CARBON ECONOMY IN THE CHINESE CONTEXT

LIU, X.¹ – WEN, T. Q.² – LIU, S. S.^{3*} – ZHONG, X.^{1*}

¹*Institute of Finance, Guangzhou University, Guangzhou 510006, China*

²*Library, Zhongnan University of Economics and Law, Wuhan 430073, China*

³*School of Management, Hubei University of Education, Wuhan 430205, China*

**Corresponding authors*

e-mail: liusishi@whut.edu.cn (S. S. Liu); zhongxiong1218@hotmail.com (X. Zhong)

(Received 29th Dec 2018; accepted 8th Mar 2019)

Abstract. This research aims to find out effective approaches to improve the low carbon economy efficiency of China and to promote its low carbon economy development. This paper utilizes two kinds of data envelopment analysis models to estimate the economic efficiency and low carbon economy efficiency of China. It takes carbon dioxide emissions as an undesirable output and compares them to find out the different performances of economic growth in various regions in China in the context of low carbon economy development, and then explores the potential determinants of low carbon economy efficiency for different regions in different periods. The results show that low carbon economy efficiency is much lower than economy efficiency in most areas in China. Additionally, both low carbon economy efficiency and economy efficiency show a slow downward trend in most provinces in China from 2000 to 2011, which was followed by a slight increase in 2012. Moreover, low carbon economy efficiency and economy efficiency show obvious geographic characters. We propose some policy implications. Several policy implications are also provided for various areas to improve low carbon economy efficiency.

Keywords: *economic efficiency, carbon emissions, data envelopment analysis model, low-carbon economy, China*

Introduction

Since the reform and opening-up policies in 1978, China has become the second-largest economy in the world and seen an average annual economic growth rate of 9.9% from 1979 to 2010, which arouses the interest of many researchers (Xing et al., 2018; Mutlu et al., 2018). Some of these studies have reported a prolonged slowdown in China's total factor productivity. Many studies calculate the economic efficiency with different data envelopment analysis (DEA) models (Deilmann et al., 2016; Xing et al., 2018), super-efficiency DEA window analysis (Huang et al., 2018a), integrated DEA/AHP model etc. In most of these studies, labor, capital, and energy consumption are used as the inputs, while GDP is used as the output to calculate economic efficiency (Ashraf et al., 2018).

However, the rapid economic growth of China brings about increasingly more energy consumption, which results in rapid increase in CO₂ emissions (Dong et al., 2018). China is the largest CO₂ emitter in the world which accounts for 26.7% of global emission in 2012, and consequently, faces significant pressure to reduce carbon emission (Zhang et al., 2014). The carbon intensity goal announced by Chinese government in 2009 shows that the Chinese government pursues the win-win target of GDP growth and carbon emission reduction in the process of economic development.

However, most previous studies ignored the impact of CO₂ emission constraints on the efficiency of China's economic growth (Haque et al., 2019).

Both GDP and CO₂ emissions are simultaneously produced in the process of production. However, different from GDP which is a desirable output, carbon emission is an undesirable output. As such, traditional DEA models may not be appropriate. The undesired input can be evaluated by both indirect and direct methods (Scheel, 2001). The former one means using the inverse value of undesirable output as desirable output (Golany and Roll, 1989) or seeing the undesirable output as input (Tyteca, 1997) in standard DEA models. However, the direct approach treats the undesirable outputs more appropriately (Wu et al., 2018). Moreover, the slack-based measure (SBM) model with more desirable outputs and less undesirable outputs relative to fewer inputs should be recognized as efficient (Xie et al., 2018).

Therefore, this paper first estimates the Low Carbon Economy Efficiency of China by taking CO₂ emissions as the undesirable output and GDP as the desirable output in the undesirable output DEA model (Kumar et al., 2019). And then, Low Carbon Economy Efficiency with Economy Efficiency is compared to find out the different performances of economic growth in various regions in China in the context of low carbon economy. Moreover, the potential determinants of Low Carbon Economy Efficiency for different regions in different periods are explored to find out the effective ways to improve Low Carbon Economy Efficiency and to promote low carbon economy development (Jeegatheesan et al., 2018).

Plenty of studies contribute to indicate determinants influencing CO₂ emissions and economic growth in China. The following factors are of great importance (Suhaili et al., 2018).

(1) Industry structure. In general, industrial is more energy intensive than tertiary industry. It is estimated that the rapid growth of energy consumption and CO₂ emissions are consistent with the continuing heavy industrialization in China. In this paper, the proportion of industrial added value in GDP is taken as an indicator for measuring industry structure.

(2) Urbanization. The urbanization rate of China expanded from 36.2% in 2000 to 52.6% in 2012 and is estimated to reach 70% in 2030 (World Bank, 2014). The rapid growth of urbanization rate makes carbon emission reductions very difficult (Song et al., 2018a). In this paper, the proportion of urban population residents in the total population is represented as the urbanization rate (Ali et al., 2018).

(3) Research and Development (R&D) support. Extensive studies emphasize the importance of R&D to improve productivity and environmental performance (Song et al., 2018b). Moreover, the literature on climate policy modeling has also indicated the core role that R&D is playing in industrializing countries such as China because R&D exerts opposing influences on energy and emission intensities (Huang et al., 2018b). Therefore, the proportion of R&D expenditure in GDP is taken as a proxy for scientific and technical support (Nordin et al., 2018).

(4) Government support. China is an investment-driven country, as such, the government's attitude towards the environmental problems can be seen from the amount of money invested. In this paper, the proportion of financial expenditure in GDP is considered as a proxy indicator (Majumder et al., 2019).

(5) International trade. The ongoing raising of international trade is a significant driver for GDP growth and carbon dioxide emissions in China (Xu et al., 2017). It is estimated that CO₂ emissions in trade accounted for 19% of its total production-based

emissions in 2008 (Zhang, 2014) due to more exports of energy-intensive products. The ratio of the amount of imports and exports to GDP is taken as a proxy indicator in this paper. *Table 1* shows the details of these indicators.

Table 1. Summary of determinants of low carbon economy efficiency

Factors	Max	Min	Mean	S.D
The proportion of industrial added value in GDP (IS)	0.530	0.134	0.395	0.080
Urbanization rate (UR)	0.893	0.232	0.468	0.149
Gross domestic expenditure on R&D in GDP (RD)	0.429	0.001	0.024	0.068
The proportion of financial expenditure in GDP (GS)	0.612	0.069	0.177	0.079
The ratio of imports and exports to GDP (IE)	1.632	0.026	0.316	0.367

The objective of this research is to find out effective approaches to improve the low carbon economy efficiency of China and to promote its low carbon economy development. The remainder of this paper is organized as follows. 2 different DEA models are employed to estimate Economy Efficiency and Low Carbon Economy Efficiency, as well as their inputs and outputs, are briefly introduced (Nouaim et al., 2019). Afterwards, the paper presents and discusses in details the results of Economy Efficiency and Low Carbon Economy Efficiency from the viewpoint of different regions in various periods in China. Conclusions and several policy implications can be found in the last section.

Materials and methods

DEA models

As one of the most widely used efficiency evaluation methods, DEA models provide a mechanism for measuring relative efficiency of similar economic production systems. Different DEA models and their applying requirements and advantages have been discussed in details by Wu et al. (2018), Liu and Liu (2016) and Jiang et al. (2016). In this paper, BCC DEA model is employed to estimate Economy Efficiency which aims at constant inputs producing more outputs (GDP). In contrast, undesirable output DEA model is utilized to estimate Low Carbon Economy Efficiency, which implies that constant inputs producing more desirable output (GDP) and fewer undesirable output (CO₂ emissions).

BCC DEA model

BCC DEA model was first proposed by Banker et al. (1984) and largely applied in the situation of “variable returns to scale” (VRS). BCC DEA model can classify the DMUs into efficient and inefficient ones according to the rule that whether the efficiency score equals one.

According to Banker et al. (1984), the envelopment form of BCC DEA model can be expressed as *Equation 1*:

$$\theta^* = \text{Min}(\theta - \varepsilon(e^- S^- + e^+ S^+))$$

$$s.t. \begin{cases} \sum_{j=1}^n X_j \lambda_j + S^- = \theta X_0 \\ \sum_{j=1}^n Y_j \lambda_j - S^+ = Y_0 \\ \sum_{j=1}^n \lambda_j = 1 \\ \lambda, S^+, S^- \geq 0 \end{cases} \quad (\text{Eq.1})$$

where X_j and Y_j in the model respectively represent inputs and outputs of the j^{th} DMU, λ_j denotes the weights, θ is technological efficiency, $\theta < 1$ means the DMU is inefficient, while $\theta = 1$ shows the DMU is efficient in BCC DEA.

Undesirable output SBM DEA model

Based on Tone (2001) and Zhou et al. (2006), the undesirable output SBM DEA model can be defined as follows.

Given that there are n DMUs in production system P , and each DMU has m inputs, s_1 desirable outputs, and s_2 undesirable outputs.

$$X = [x_1, x_2, \dots, x_n] \in R^{m \times n}, Y^g = [y_1^g, y_2^g, \dots, y_n^g] \in R^{s_1 \times n} \text{ and } Y^b = [y_1^b, y_2^b, \dots, y_n^b] \in R^{s_2 \times n}$$

Matrices represent inputs, desirable outputs and undesirable outputs respectively. Moreover, $X > 0$, $Y^g > 0$, and $Y^b > 0$. The production possibility set (P) is defined as:

$$P = \left\{ (x, y^g, y^b) \mid x \geq X\lambda, y^g \leq Y^g\lambda, y^b \geq Y^b\lambda, \sum \lambda = 1 \right\}$$

where $\lambda \in R^n$ is the intensity vector, and $\sum \lambda = 1$ represents the assumption of variable returns to scale (VRS).

We suppose that the DMU₀ (x_0, y_0^g, y_0^b) is efficient if there is no vector $(x, y^g, y^b) \in P$ that simultaneously satisfies $x_0 \geq x$, $y_0^g \leq y^g$ and $y_0^b \geq y^b$. And the SBM DEA models with undesirable outputs can be written as

$$\rho = \text{Min} \frac{1 - \frac{1}{m} \sum_{i=1}^m \frac{s_i^-}{x_{i0}}}{1 + \frac{1}{s_1 + s_2} \left(\sum_{r=1}^{s_1} \frac{s_r^g}{y_{r0}^g} + \sum_{r=1}^{s_2} \frac{s_r^b}{y_{r0}^b} \right)}$$

$$s.t. \begin{cases} x_0 - X\lambda - s^- = 0 \\ y_0^g - Y^g\lambda + s^g = 0 \\ y_0^b - Y^b\lambda - s^b = 0 \\ s^- \geq 0, s^g \geq 0, s^b \geq 0, \lambda \geq 0 \end{cases} \quad (\text{Eq.2})$$

where, s^- , s^g and s^b correspond to slack variables of inputs, desirable outputs, and undesirable outputs respectively. The objective function is strictly decreasing with respect to $s_i^-(\forall i)$, $s_r^g(\forall r)$, $s_r^b(\forall r)$ and the objective value satisfies $0 < \rho \leq 1$. Let the optimal solution of the above program be $(\lambda^*, s^{-*}, s^{g*}, s^{b*})$, and if and only if $\rho = 1$, $s^{-*} = 0$, $s^{g*} = 0$ and $s^{b*} = 0$, the DMU is efficient.

Using the transformation by Charnes and Cooper (1962), the equivalent linear program of Equation 1 can be obtained to calculate efficiency scores.

Data for inputs and outputs

The empirical study covers 30 provinces in the Chinese mainland, excluding Tibet because of energy consumption data loss. The 30 provinces in China can be aggregated to four areas, the Eastern (E), Northeast (NE), Central (C) and Western (W) areas. The Eastern area is the richest and most developed region in China. The Northeast area is one of the earliest and most important industrial base in the country. The Central area is considered to be a connecting link between the booming Eastern region and the relatively poor Western region by the Chinese government. The Western area is relatively backward but the resource-rich region.

The amount of energy consumption (E), labor force (L), and capital stock (K) are taken as inputs in both DEA models. Moreover, GDP is considered as the only output in BCC DEA model and the desirable output in undesirable DEA model, which presents the performance of economic development. In addition, the amount of CO₂ emissions is taken as the undesirable output in the undesirable DEA model, which reflects the objective to reduce carbon emissions.

CO₂ emissions

The amount of CO₂ emissions of different types of fossil fuel can be calculated. According to the national standard from the National Development and Reform Commission (NDRC) (Guidance for Compiling Provincial Greenhouse Gas Emission Lists (Trial), 2011), eight types of fossil fuel are considered, including coal, coke, crude, gasoline, kerosene, diesel oil, fuel oil, and natural gas. Thus, according to the approach recommended by IPCC (2006), CO₂ emissions from fossil fuel burning can be calculated based on

$$Q_{CO_2} = \sum_{i=1}^8 Q_i \times NCV_i \times CEF_i \times COF_i \times (44/12) \quad (\text{Eq.3})$$

where Q_{CO_2} is the quantity of CO₂ emissions from all eight types of fossil fuel consumption; i represents different types of fossil fuel, Q_i is the total consumption of fuel i ; NCV_i , CEF_i and COF_i represent the default net calorific value, carbon content factor, and carbon oxidization factor of fuel i ; $NCV_i \times CEF_i \times COF_i \times (44/12)$ is CO₂ emission factor of fuel i . All these data can be got from NDRC as shown in Table 2.

All the data on fossil fuel are compiled from China Statistical Yearbook. However, the latest China Statistical Yearbook 2013 only provides energy consumption data by fuel by provinces in the year of 2011. As a consequence, we estimated these data in 2012 using the average annual growth rate of 2000-2011. Thus, the amount of CO₂

emissions for each province can be calculated by Equation 3 and the descriptive statistics are shown in Figure 1.

Table 2. CO₂ emission factors by fuel

Fuel	Coal	Coke	Crude	Fuel oil	Gasoline	Kerosene	Diesel	Natural gas
NCV (kJ/kg)	20908	28435	41816	41816	43070	43070	42652	38931
CEF (tonne C/TJ)	26.37	29.5	20.1	21.1	18.9	19.5	20.2	15.3
COF	0.94	0.93	0.98	0.98	0.98	0.98	0.98	0.99
Emission factor k_i	1.9003	2.8604	3.0202	3.1705	2.9251	3.0179	3.0959	2.1622

The unit of k_i is kg-CO₂/kg except natural gas, which is kg-CO₂/m³

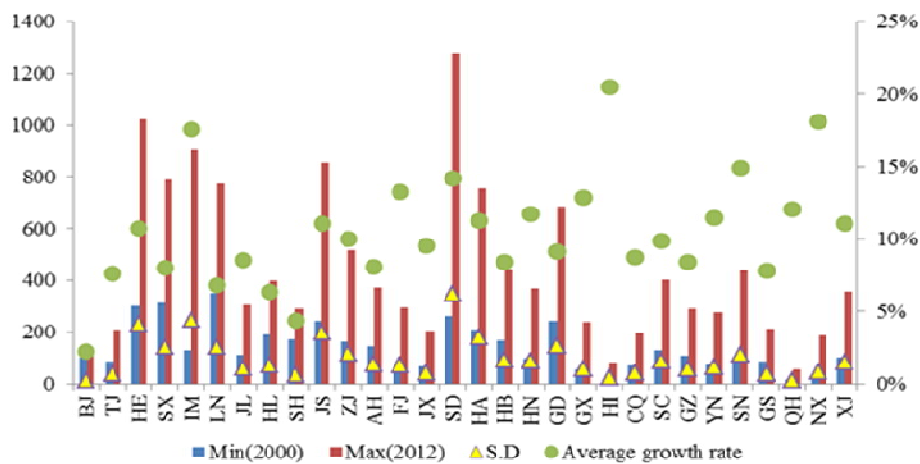


Figure 1. Total amount of CO₂ emissions for 30 provinces in China (million tons)

Summary of inputs and outputs

The data on E, L, and GDP are obtained from China Statistical Yearbook. Data for K from 2000 to 2006 are directly acquired from Shan (2008), and the rest of the data from 2007 to 2012 are estimated by perpetual inventory method according to Shan (2008). Considering the fact that Chongqing used to be a part of Sichuan Province before 1997, Shan (2008) estimated their K value on the basis that considering Chongqing still as part of Sichuan. In order to separate the two different regions, K is divided according to gross fixed capital formation in these two provinces. All price values are converted to 2000 prices according to GDP deflator. Table 3 shows descriptive statistics of the input and output variables by region.

Analysis of impact factors

To further discover the determinants influencing China’s economic growth efficiency under carbon emissions constraint, regression analysis method for panel data is applied to measure the relationship between the efficiency and the impact factors mentioned in 2.2.2. Specifically, the econometric model can be defined as:

$$LCEE_{i,t} = C + C_i + \beta_1 * IS_{i,t} + \beta_2 * UR_{i,t} + \beta_3 * RD_{i,t} + \beta_4 * GS_{i,t} + \beta_5 * IE_{i,t} + \varepsilon_{i,t} \quad (\text{Eq.4})$$

where, $LCEE_{i,t}$ is carbon efficiency of province i in year t . IS , UR , RD , GS , IE represent the five determinants mentioned before, C is a common intercept, C_i represents the individual effect, $C + C_i$ indicates the varying efficiency among different provinces, $\varepsilon_{i,t}$ is the error term.

Table 3. Summary statistics of input and output variables by region (2000–2012)

Region	Inputs						Output		Undesirable output	
	E (100 Mtce)		K (100 million USD)		L (1 million)		GDP (100 million USD)		CO ₂ (100 million tonnes)	
	Mean	SD	Mean	SD	Mean	SD	Mean	SD	Mean	SD
E_BJ	57.32	10.61	2756.249	1262.043	10.07	2.54	100.3045	35.91916	120.65	13.76
E_TJ	48.25	17.11	1891.827	1362.055	4.56	0.54	60.34284	28.67891	136.27	39.37
E_HE	207.91	65.58	4063.016	2601.682	35.74	1.87	144.9277	53.2488	607.43	225.32
C_SX	133.49	37.97	2071.075	1556.405	15.27	0.96	62.70013	26.46932	569.19	138.01
W_IM	110.56	54.25	2673.29	2467.961	10.86	0.89	70.20476	40.61602	417.28	237.79
NE_LN	158.13	45.09	3454.778	2433.889	20.24	1.69	126.6616	50.07473	526.93	138.47
NE_JL	63.46	18.20	2184.257	1793.164	11.48	0.85	58.7078	25.20205	191.20	60.86
NE_HL	88.42	22.35	1858.744	1067.398	16.83	0.69	77.80098	24.09578	269.91	69.53
E_SH	87.15	21.13	3450.929	1494.084	8.43	1.02	126.7916	37.54386	229.29	35.72
E_JS	182.27	69.92	7431.195	4755.302	41.00	4.92	278.0748	117.1187	494.09	192.97
E_ZJ	127.22	39.67	4941.707	2779.458	33.42	4.86	193.6125	71.19288	327.55	113.74
C_AH	74.30	20.37	2261.005	1489.445	36.19	2.50	84.56416	35.16442	235.35	72.67
E_FJ	69.52	25.75	2710.772	1808.361	19.33	2.10	102.3354	38.79931	154.96	71.54
C_JX	46.68	15.67	1807.2	1267.894	21.43	1.66	63.65722	27.85474	127.13	43.49
E_SD	250.61	94.26	7677.597	4827.992	51.69	3.97	268.8539	107.6881	744.34	334.36
C_HA	157.52	54.20	5033.007	3872.653	57.54	2.45	156.9017	63.60701	450.71	175.46
C_HB	111.26	37.15	3167.432	2131.834	28.20	3.38	106.5139	47.12221	273.47	88.24
C_HN	102.63	42.22	2572.21	1809.053	37.23	2.25	106.7428	47.37182	219.89	85.48
E_GD	194.25	68.14	6641.326	3890.437	48.52	7.62	324.8159	117.0079	429.23	141.29
W_GX	54.96	21.23	2149.302	1822.175	27.34	1.59	64.10032	27.88576	119.16	56.64
E_HI	9.86	3.79	546.5904	309.1981	3.92	0.45	14.41257	5.550566	35.29	22.25
W_CQ	54.17	22.55	1502.283	792.4238	17.67	1.23	54.5722	23.56849	116.55	42.80
W_SC	130.22	45.85	2943.216	1607.141	46.85	2.37	117.2177	49.52972	254.64	86.15
W_GZ	65.13	16.37	1186.849	835.3971	22.34	1.36	31.99477	14.18511	185.77	56.29
W_YN	64.77	21.37	1729.01	1175.067	25.43	2.07	52.83377	19.43141	176.38	64.35
W_SN	62.59	23.86	2415.456	1896.651	19.06	0.62	65.09878	32.83076	224.19	110.49
W_GS	46.72	12.60	872.2084	572.9711	13.35	0.85	29.27414	11.08636	139.13	39.20
W_QH	19.00	7.92	422.3674	317.9981	2.71	0.23	8.944712	4.144462	31.97	12.85
W_NX	27.47	10.51	596.5249	503.7929	3.04	0.21	10.68166	5.416159	91.10	46.81
W_XJ	62.23	22.50	1506.54	962.5757	7.81	0.77	38.53641	14.59276	192.47	82.70
Northeast	310.00	85.40	7497.779	5291.441	48.56	3.11	263.1704	99.2544	988.04	268.55
Eastern	1234.36	414.70	42111.21	25034.48	256.67	29.40	1614.472	611.2801	3279.10	1183.08
Central	625.88	206.74	16911.93	12122.06	195.86	12.39	581.0799	246.8879	1875.75	595.65
Western	697.84	258.26	17997.05	12910.5	196.47	11.99	543.4562	242.996	1948.64	826.84

E, NE, C, and W represent Eastern, Northeast, Central and Western area of China respectively. BJ: Beijing, TJ: Tianjin, HE: Hebei, SX: Shanxi, IM: Inner Mongolia, LN: Liaoning, JL: Jilin, HL: Heilongjiang, SH: Shanghai, JS: Jiangsu, ZJ: Zhejiang, AH: Anhui, FJ: Fujian, JX: Jiangxi, SD: Shandong, HA: Henan, HB: Hubei, HN: Hunan, GD: Guangdong, GX: Guangxi, HI: Hainan, CQ: Chongqing, SC: Sichuan, GZ: Guizhou, YN: Yunnan, SN: Shannxi, GS: Gansu, QH: Qinghai, NX: Ningxia, XJ: Xinjiang

The results of Hausman test indicates Fixed Effects estimator should be taken in this study. As such, the estimated coefficients between Low Carbon Economy Efficiency and determinants can be calculated according to *Equation 4* by Eviews software. As a calculation result, the estimated coefficients by region are shown in *Table 4*.

Table 4. The estimated coefficients in Table 1 by region

	Whole country	Eastern	Northeast	Central	Western
IS	-0.625***	-1.470***	0.025	-1.247**	0.516
UR	0.677***	0.763***	-0.128	-0.137	2.074***
RD	-0.195*	-5.559***	9.000*	-0.240***	-13.653***
GS	0.593***	-1.135**	-0.916*	1.483***	0.981***
IE	0.282***	0.241***	-0.278**	-0.292	-0.011
C	0.379***	1.060***	0.725***	0.877***	-0.531***
Observations	390	130	39	104	117
Adj R2	0.619	0.75	0.677	0.692	0.624
D.W.	1.945	2.264	2.232	2.862	2.573

***, **, * indicates 1%, 5%, and 10% significant, respectively

(1) The dependence on the proportion of industrial added value in GDP (IS) has a negative influence on Low Carbon Economy Efficiency in the whole country, which agrees with most research (Hao and Peng, 2017). The high proportion of energy intensive industry in the secondary industry accounts for a large amount of carbon emissions in China (Fan et al., 2018). However, IS has a negative effect on the Eastern and Central areas but a positive effect on the Northeast and Western area. For the Eastern and Central area, the desirable output GDP is huge and presents an upward trend, so the core task of promoting Low Carbon Economy Efficiency improving should be concentrated on carbon abatement. However, in the Northeast and Western area, where the economics are relative backwardness, industrial structure which shifts from industrial to other industries will damage economic growth rather than decrease carbon emissions.

(2) Urbanization rate (UR) is one of the most vital positive factors impact Low Carbon Economy Efficiency of the whole country, as well as the Eastern and Western areas. Low Carbon Economy Efficiency in these areas will respectively go up by 0.677%, 0.763%, 2.074% with the value of UR increase 1%. The fast growing UR in Eastern area can promote the concentration of population lives and improve the efficiency of public infrastructure. Therefore, economies of scale of energy consumption can improve the energy efficiency. For the Western area, where the intensity of population is much smaller than the Eastern, the economies of scale of energy consumption are much more obvious. Therefore, a positive correlation can be seen in UR and Low Carbon Economy Efficiency there. However, UR had a negative and non-significant effect on the Northeast and Central areas. The reason is that with the process of urbanization, residents in urban have a growing demand for higher levels of energy services as living standards rise, which should greatly promote the total energy consumption and ultimately promote CO₂ emissions.

(3) The ratio of R&D expenditure to GDP (RD) contributes to Low Carbon Economy Efficiency in China was negative for every area but the Northeast. Firstly, energy

rebound effect can be seen in these areas. Energy rebound effect means that although technological innovations improved the energy efficiency and energy savings, it also promoted rapid economic development and resulted in energy consumption increasing, and the volumes of increased over that of decreased. Secondly, R&D expenditure in China, which covers all aspects of science and technology, should be improved both in volume and structure.

(4) The relationship between the proportion of financial expenditure in GDP (GS) and Low Carbon Economy Efficiency is positive except for the Eastern and Northeast areas. The amount of investment in financial expenditure such as environmental pollution treatment seeing a continuing increase in recent years, which showed the efforts and determination of the government to reduce energy overuse and waste. However, it can be seen from *Table 5* that the government's efforts are negative in the Eastern and Northeast areas. For one thing, the amount of the investment may not be enough, especially for the Eastern area with the largest GDP in China; for another, investing in subsidy of equipment and technologies using have not been effectively used.

Table 5. The estimated coefficients in Table 1 by period

	Whole Country		Eastern		Northeast		Central		Western	
	00-07	08-12	00-07	08-12	00-07	08-12	00-07	08-12	00-07	08-12
<i>IS</i>	-0.885***	-0.035	-1.850***	-0.414	0.478**	0.481	-1.421***	-1.372***	-2.451***	2.035***
<i>UR</i>	0.586***	1.321***	0.963***	0.607	-2.106***	1.766	0.857**	-0.247	2.190***	0.706***
<i>RD</i>	-0.204	-0.276	-6.600***	-0.871	3.250	-7.324	-36.953***	-10.908**	0.134	-0.195
<i>GS</i>	0.671***	0.724***	-2.881***	0.942	0.415***	1.121	-1.147	-0.484**	1.832*	1.521
<i>IE</i>	0.299***	0.229***	0.242***	0.235***	0.244	-0.416	0.144	0.886	-0.577***	0.241
<i>C</i>	0.532***	-0.261*	1.305***	0.338	1.347	-0.756	1.151***	1.335***	0.340	-1.074***
<i>Obs</i>	240	150	80	50	24	15	48	30	88	55
<i>Adj R²</i>	0.673	0.718	0.867	0.708	0.634	0.613	0.656	0.791	0.666	0.736
<i>D.W.</i>	2.074	2.200	2.290	2.358	2.386	2.042	1.591	2.349	2.115	2.629

***, **, * indicates 1%, 5%, and 10% significant respectively

(5) The ratio of imports and exports to GDP (IE) has a positive impact on Low Carbon Economy Efficiency of China. International trade can impact Low Carbon Economy Efficiency through introducing advanced technology, equipment, and management experience, as well as embodied carbon (Kang et al., 2018). The former factors' effects can be seen from a long horizon while the latter can be seen in the initial stage of IE development. It can be seen that IE showed a positive and significant relationship with Low Carbon Economy Efficiency in the Eastern area where the vast majority of imports and exports in China are produced. The other three areas only account for 13.03% of the total amount of imports and exports in China from 2000 to 2012, and the majority of export-oriented factories in these areas are transferred from the Eastern area because of high energy consumption and environmental pollution. These factories contribute much more carbon emissions rather than GDP. International trade in these three areas was still in the initial stage and saw a negative impact on Low Carbon Economy Efficiency.

Moreover, this paper divides the period of 2000-2012 into two periods (2000-2007 and 2008-2012) to discover different determinants affecting Low Carbon Economy Efficiency of different areas in different periods. The results are shown in *Table 5*.

(1) IS sees decreased negative affect on Low Carbon Economy Efficiency in all areas except the Northeast, which means that energy and resource saving during the process of industrialization should be taken into account. However, increased positive correlation between IS and Low Carbon Economy Efficiency still can be seen in the Northeast area, for the reason that as an old industry base in China, industrialization is the basis of economic development in the Northeast area. Consequently, they should promote Low Carbon Economy Efficiency improvement during the process of industrialization through means of upgrading the industrial production from high investment, high energy consumption and high emissions to low investment, low energy consumption, and low emissions.

(2) Urbanization shows a further strengthened positive impact on Low Carbon Economy Efficiency improvement in the whole country and the Northeast area, while decreased affection in other three areas. Especially for the Central area, urbanization shows a negative impact on Low Carbon Economy Efficiency in the period of 2008-2012. The average annual growth rate of urbanization in the Central area rose from 1.46% in the period of 2000-2007 to 1.6% in the period of 2008-2012, with an increase of 0.14%, while the Eastern, Northeast and Western areas seeing an increase of 0.5%, 0.16%, 0.3% respectively. The change of average annual growth rate of urbanization in the Central area is the smallest and the rate in the Northeast area is the slowest, where UR has a positive impact on improving economic efficiency under carbon emissions constraints. The results indicate that pursuing the urbanization speed while ignoring its quality should be avoided in the process of urbanization.

(3) RD showed a slightly increased negative impact on Low Carbon Economy Efficiency in the whole country while greatly decreased negative effect on the Eastern and Central areas, and became a negative factor in the period of 2008-2012 in the Northeast and Western areas. Besides the reason of volumes and structure of R&D expenditure mentioned above, the different performances of RD in various areas in China also contribute to these differences. The growth rate of RD in the whole country, Eastern and Central areas increased by 38.11%, 44.39% and 57.52% from the period of 2000-2007 to 2008-2012. However, the Northeast and Western areas only saw 14.83% and 17.87% increase, less than a half comparing with other areas.

(4) Government support plays an increasingly more important role in improving Low Carbon Economy Efficiency in all areas but the Western. These results indicate that local governments paying more attention to the development of Low Carbon Economy Efficiency, and implying the importance of government support in the initial stage of low carbon economy development. However, for a small amount of financial expenditure in the Western area (198.82 billion per year per provinces in 2008-2012, only accounts for 78.27% of that in the whole country), the importance of government support is not obvious.

(5) International trade can be seen a decreased correlation with Low Carbon Economy Efficiency in the whole country, Eastern and Northeast areas in these two periods, especially for the Northeast area where the coefficient turned from positive in 2000-2007 to negative in 2008-2012. However, the correlation between Low Carbon Economy Efficiency and IE went up from 0.144, -0.577 to 0.886 and 0.241 in the Central and Western areas at the same time. The reason is that imports and exports can be seen a

decreased importance in these two areas. Although the amount of imports and exports increased by 2.3 and 2.6 times per province in the Central and Western areas from the period of 2000-2007 to 2008-2012, the proportion in GDP dropped from 10% to 9.74% in the Central area and slightly increased from 11.12% to 11.49% in the Western area. For the Eastern, Northeast, and the whole country, the amount of imports and exports increased by 1.67, 1.57 and 1.72 times, while the proportion in GDP decreased from 84.3%, 27.89%, 56% to 72.64%, 22.73%, 49.43%.

Results

With the two different DEA models, both Economy Efficiency and Low Carbon Economy Efficiency of different regions from 2000 to 2012 can be calculated. The calculation results show that the majority of provinces in China saw a smaller Low Carbon Economy Efficiency than Economy Efficiency except for Guangdong, Shanghai, Beijing, Tianjin, Hainan, Qinghai, and Ningxia. Jiangsu, Zhejiang, Shandong, Chongqing and Sichuan witnessed an upward trend in both Low Carbon Economy Efficiency and Economy Efficiency. In contrast, both the Low Carbon Economy Efficiency and Economy Efficiency declined in Inner Mongolia, Jilin and Guangxi. Although Low Carbon Economy Efficiency in Hainan and Qinghai pointed at efficiency frontier (the score of Low Carbon Economy Efficiency is one), their Economy Efficiency showed a downward trend, which implied poor economic conditions there. However, most provinces demonstrate gradually increased Low Carbon Economy Efficiency with declined Economy Efficiency after 2007, when the Chinese government proposed the first national plan and policy-based document National Climate Change Program on climate changes.

As shown in *Table 6*, the majority of provinces in the Eastern area are high-efficiency regions, and most provinces in the Central and Western area of China are low efficiency. These results imply that the Low Carbon Economy Efficiency shows obvious geographic characters. Furthermore, the whole period can be divided into four periods, as shown in *Table 7*.

Table 6. Average efficiency scores and rank by region (2000-2012)

Regions	EE		LCEE		Regions	EE		LCEE	
	Score	Ranking	Score	Ranking		Score	Ranking	Score	Ranking
Northeast (NE)	0.808		0.550		Central (C)	0.771		0.780	0.505
Eastern (E)	0.892		0.843		Western (W)	0.644		0.660	0.550
China	0.777		0.638						

LCEE – low carbon economy efficiency; EE – economy efficiency

Table 7. Regional economic efficiency by period

	9 th Plan (2000)		10 th Plan (2001-05)		11 th Plan (2006-10)		12 th Plan (2011-12)	
	EE	LCEE	EE	LCEE	EE	LCEE	EE	LCEE
China	0.812	0.674	0.791	0.651	0.763	0.623	0.760	0.627
Northeast (NE)	0.859	0.559	0.829	0.571	0.789	0.540	0.779	0.517
Eastern (E)	0.897	0.860	0.900	0.851	0.886	0.831	0.884	0.842
Central (C)	0.828	0.537	0.797	0.524	0.762	0.492	0.761	0.479
Western (W)	0.716	0.613	0.669	0.562	0.642	0.528	0.653	0.542

China's Economy Efficiency had decreased from 0.812 in 2000 to 0.76 in the 12th five-year with a percentage decline of 6.38%. The Western area saw its efficiency rising from 0.642 in the 11th five-year to 0.653 in the 12th five-year, while the other three areas saw downward trends. China's Low Carbon Economy Efficiency had gradually decreased from 0.674 in the period of 9th five-year to 0.623 in the period of 11th five-year, and then slightly increased to 0.627 in the period of 12th five-year. Seeing the same trends as the whole country, Low Carbon Economy Efficiency of the Eastern and Western areas experienced a slight rise in the period of 12th five-year, while the Northeast and Central area had declined from 0.559, 0.537 in 2000 to 0.517, 0.479 in the 12th five-year. Comparing Economy Efficiency with Low Carbon Economy Efficiency, it can be found that Low Carbon Economy Efficiency is smaller than Economy Efficiency in any areas at any time.

Discussion

The analytical methodology of this paper is innovative and can be utilized in similar research. It utilizes two kinds of data envelopment analysis models to estimate the economic efficiency and low carbon economy efficiency of China. It takes carbon dioxide emissions as an undesirable output and compares them to find out the different performances of economic growth in various regions in China in the context of low carbon economy development, and then explores the potential determinants of low carbon economy efficiency for different regions in different periods.

As can be seen in the previous section, it is still a long and tough journey for China to achieve the win-win goal of high GDP growth and low CO₂ emissions, for Low Carbon Economy Efficiency is lower than Economy Efficiency in most provinces in China, which means unbalanced development of high GDP growth and low CO₂ emissions, and implied that most policy makers and implementers prefer increasing desirable output of GDP than decreasing undesirable output of CO₂ emissions. This is because provincial leaders in China pay more emphasis on the quantity of GDP growth over the quality of economic performance because the likelihood of promotion of them increases with GDP growth in their provinces (Chen et al., 2017). Therefore, the quality of economics development, such as carbon emissions, should be considered as the next goal to achieve after getting a high value of GDP. This conclusion has also been supported by the evidence that the richest Eastern area also has the highest Low Carbon Economy Efficiency in China. Consequently, it is necessary to reform the performance evaluation system of policy maker and implementers from the quantity of economic growth to the quality of economic performance. Therefore, the environment protection, energy efficiency, as well as resources and other indicators, should be considered as important as GDP in the performance evaluation system, so as to stimulate policy makers and implementers to take decreasing undesirable outputs equally important as increasing desirable outputs.

Moreover, Low Carbon Economy Efficiency and its determinants vary with regions in China. As a consequence, different provinces should implement different policies and actions based on their actual situation to improve the Low Carbon Economy Efficiency. Provinces in the most developed and richest Eastern area see the highest Low Carbon Economy Efficiency for higher levels of environmental concern than other areas (Lin and Xu, 2018). Also, they have sufficient economic strength to realize the balanced development of GDP growth and CO₂ emissions. Provinces in the Western area have

the advantage of the natural ecological environment and benefit from more stringent constraints of promoting GDP growth due to the requirements to protect the natural ecological environment. Therefore, the core task for eastern and western areas to improve Low Carbon Economy Efficiency is expected to maintain a balance between GDP growth and CO₂ emissions. In addition, the reason that the Northeast and Central area saw a continuing decrease Low Carbon Economy Efficiency in recent years is that these two areas emphasis on increasing the desirable output GDP while ignoring the reduction of undesirable output CO₂ emissions. Consequently, the Northeast and Central regions need to treat carbon emissions abatement as important as GDP growth, which can be promoted through the reform of performance evaluation system for policy makers and implementers. In addition, different policies and actions have different effects on Low Carbon Economy Efficiency of various areas. For the Northeast area, the likelihood of promoting efficiency increases with RD, while RD has a negative impact on the Eastern and Western areas. For the Eastern and Western areas, the process of urbanization is more critical to improving Low Carbon Economy Efficiency, they should emphasize the quality of urbanization. Government support, especially financial support, sees more positive and obvious impact for the Central area.

Finally, it is necessary to introduce market-based policy instruments to simultaneously control CO₂ emissions and promote GDP growth. Both the central and local governments play key roles in promoting economic development in China, through the ways of making policy, planning, resources input and allocation and so on (McMillan and Naughton, 1992). However, according to the law of diminishing marginal returns, expanding the volume of production factors input would yield lower per-unit returns at some time, which means relying on factors-driven to promote economic development is unsustainable and possibly increasing CO₂, so as to exacerbate the difficulty of economic efficiency improvement. As a result, market-based policy tools, such as environmental tax and emissions trading, should be introduced to provide incentives for carbon emitters to reduce carbon emissions without damaging economic development. For one thing, the revenue from environmental taxes can be reallocated to investment in energy saving technologies, or expanding the amount of funds invested in environmental pollution control, so as to promote Low Carbon Economy Efficiency improvement. For another, emissions permit trading is also a financial instrument. Several carbon emission trading systems such as EUETS and CCX introduced a series of financial derivative products (Helm, 2014). The purpose of developing emission trading market not only can control carbon emissions but also can be used as a financial instrument to promote the development of the financial market.

Conclusions

Improving the efficiency of economic development is of vital importance of China to achieve sustainable development, and CO₂ emissions impact the development of economics as well. This research compared two kinds of economics development efficiency based on whether considering CO₂ emissions or not (Economy Efficiency or Low Carbon Economy Efficiency). Furthermore, we analyzed in details that the determinants of Low Carbon Economy Efficiency of different areas in China. The following basic conclusions can be obtained:

(1) There is still a long and tough journey for China to achieve the win-win goal of high GDP growth and low CO₂ emissions.

(2) Low Carbon Economy Efficiency and its determinants vary with regions in China.

(3) It is necessary to introduce market-based policy instruments to simultaneously control CO₂ emissions and promote GDP growth.

Most importantly, the analytical methodology of this paper is innovative and can be utilized in similar research.

Acknowledgements. This work is funded by the National Natural Science Foundation of China (No. 71601148 and 71271159), the China Postdoctoral Science Foundation (No. 2016M592393), and the Projects of the Social Science Foundation of Guangdong Province (No. GD16YYJ02).

REFERENCES

- [1] Ali, A. J., Akbar, N. J., Arun Kumar, M. S., Vijayakumar, S., Akbar John, B. (2018): Effect of cadmium chloride on the haematological profiles of the freshwater ornamental fish, *Cyprinus carpio* Koi (Linnaeus, 1758). – *Journal Clean Was* 2(2): 10-15.
- [2] Ashraf, M. A., Hanafiah, M. M. (2018): Sustaining life on earth system through clean air, pure water, and fertile soil. – *Environmental Science & Pollution Research*
- [3] Banker, R. D., Charnes, A., Cooper, W. W. (1984): Some models for estimating technical and scale inefficiencies in data envelopment analysis. – *Management Science* 30(9): 1078-1092.
- [4] Charnes, A., Cooper, W. W. (1962): Programming with linear fractional functionals. – *Naval Research Logistics* 9(3-4): 181-186.
- [5] Chen, W., Chen, J., Xu, D., Liu, J., Niu, N. (2017): Assessment of the practices and contributions of China's green industry to the socio-economic development. – *Journal of Cleaner Production* 153(1): 648-656.
- [6] Deilmann, C., Lehmann, I., Reißmann, D., Hennesdorf, J. (2016): Data envelopment analysis of cities—investigation of the ecological and economic efficiency of cities using a benchmarking concept from production management. – *Ecological Indicators* 67: 798-806.
- [7] Dong, K., Sun, R., Dong, X. (2018): CO₂ emissions, natural gas and renewables, economic growth: assessing the evidence from China. – *Science of the Total Environment* 640: 293-302.
- [8] Fan, J. L., Wang, J. D., Kong, L. S., Zhang, X. (2018): The carbon footprints of secondary industry in China: an input-output subsystem analysis. – *Natural Hazards* 91(2): 635-657.
- [9] Golany, B., Roll, Y. (1989): An application procedure for DEA. – *Omega* 17: 237-250.
- [10] Hao, Y., Peng, H. (2017): On the convergence in China's provincial per capita energy consumption: new evidence from a spatial econometric analysis. – *Energy Economics* 68: 31-43.
- [11] Haque, D. M. E., Hayat, T., Tasnim, S. (2019): Time series analysis of subsidence in Dhaka City, Bangladesh using Insar. – *Malaysian Journal of Geosciences* 3(1): 32-44.
- [12] Helm, D. (2014): The European framework for energy and climate policies. – *Energy Policy* 64(1): 29-35.
- [13] Huang, J., Liu, Q., Cai, X., Hao, Y., Lei, H. (2018a): The effect of technological factors on China's carbon intensity: new evidence from a panel threshold model. – *Energy Policy* 115: 32-42.
- [14] Huang, J., Xia, J., Yu, Y., Zhang, N. (2018b): Composite eco-efficiency indicators for china based on data envelopment analysis. – *Ecological Indicators* 85: 674-697.
- [15] Jegatheesan, J., Zakaria, Z. (2018): Stress analysis on pressure vessel. – *Environment & Ecosystem Science* 2(2): 53-57.

- [16] Jiang, W., Liu, J., Liu, X. (2016): Impact of carbon quota allocation mechanism on emissions trading: an agent-based simulation. – *Sustainability* 8(8).
- [17] Kang, Z. Y., Li, K., Qu, J. Y. (2018): The path of technological progress for China's low-carbon development: evidence from three urban agglomerations. – *Journal of Cleaner Production* 178: 644-654.
- [18] Kumar, P., Joshi, V. (2019): A geospatial- statistical approach to alienate priority area of upper watershed of River Subarnarekha using morphometric assessment framework. – *Malaysian Journal of Geosciences* 3(1): 21-31.
- [19] Lin, B., Xu, M. (2018): Regional differences on CO₂ emission efficiency in metallurgical industry of China. – *Energy Policy* 120: 302-311.
- [20] Liu, X., Liu, J. (2016): Measurement of low carbon economy efficiency with a three-stage data envelopment analysis: a comparison of the largest twenty CO₂ emitting countries. – *International Journal of Environmental Research and Public Health* 13(11): 1116.
- [21] Majumder, S. C., Islam, K., Hossain, M. M. (2019): State of research on carbon sequestration in Bangladesh: a comprehensive review. – *Geology, Ecology, and Landscapes* 3(1): 29-36. DOI: 10.1080/24749508.2018.1481656
- [22] McMillan, J., Naughton, B. (1992): How to reform a planned economy: lessons from China. – *Oxford Review of Economic Policy* 8(1): 130-143.
- [23] Mutlu, C. C., Essen, M. V., Peng, M. W., Saleh, S. F., Duran, P. (2018): Corporate governance in China: a meta-analysis. – *Journal of Management Studies* 55(6): 943-979.
- [24] Nordin, N. F. H., Tg Mahassan, T. S. H., Chowdhury, A. J. K. (2018): Bacterial population study in oil-contaminated and uncontaminated soils. – *Journal Clean Was* 2(2): 06-09.
- [25] Nouaim, W., Chakiri, S., Rambourg, D., Karaoui, I., Ettaqy, A., Chao, J., Allouza, M., Razoki, B., Yazidi, M., El Hmidi, F. (2019): Mapping the water erosion risk in the Lakhdar river basin (central High Atlas, Morocco). – *Geology, Ecology, and Landscapes* 3(1): 22-28. DOI: 10.1080/24749508.2018.1481655
- [26] Scheel, H. (2001): Undesirable outputs in efficiency valuations. – *European Journal of Operational Research* 132: 400-410.
- [27] Shan, H. J. (2008): Re-estimating the capital stock of China: 1952-2006. – *The Journal of Quantitative & Technical Economics* 25(10): 17-31.
- [28] Solomon, S. (Ed.) (2007): *Climate Change 2007-the Physical Science Basis: Working Group I Contribution to the Fourth Assessment Report of the IPCC. Volume 4.* – Cambridge University Press, Cambridge, UK.
- [29] Song, C. J., Liu, Q. L., Gu, S., Wang, Q. (2018a): The impact of China's urbanization on economic growth and pollutant emissions: an empirical study based on input-output analysis. – *Journal of Cleaner Production* 198: 1289-1301.
- [30] Song, M., Wang, S., Sun, J. (2018b): Environmental regulations, staff quality, green technology, R&D efficiency, and profit in manufacturing. – *Technological Forecasting & Social Change* 133: 1-14.
- [31] Suhaili, M. Z., Samsudin, M. D. M. (2018): Utilization of wastewater for corrosion prevention of carbon steel pipe using single chamber microbial fuel cells. – *Environment & Ecosystem Science* 2(2): 47-52.
- [32] Tone, K. (2001): A slacks-based measure of efficiency in data envelopment analysis. – *European Journal of Operational Research* 130: 498-509.
- [33] Tyteca, D. (1997): Linear programming models for the measurement of environmental performance of firms-concepts and empirical results. – *Prod Analysis* 8: 183-197.
- [34] World Bank, DRC. China: A new approach for efficient, inclusive, sustainable urbanization. – <http://www.worldbank.org/en/news/press-release/2014/03/25/china-a-new-approach-for-efficient-inclusive-sustainable-urbanization>.

- [35] Wu, X., Chen, Y., Guo, J., Gao, G. (2018): Inputs optimization to reduce the undesirable outputs by environmental hazards: a DEA model with data of PM2.5 in China. – *Natural Hazards* 90(1): 1-25.
- [36] Xie, B. C., Wang, J. Y., Ma, J. J., Duan, N. (2018): Efficiency evaluation of china's provincial power systems based on the dynamic network slacks-based measure model. – *Journal of Cleaner Production* 174: 650-660.
- [37] Xing, Z. C., Wang, J. G., Zhang, J. (2018): Expansion of environmental impact assessment for eco-efficiency evaluation of China's economic sectors: an economic input-output based frontier approach. – *Science of the Total Environment* 635: 284-293.
- [38] Xu, J., Zhang, M., Zhou, M., Li, H. (2017): An empirical study on the dynamic effect of regional industrial carbon transfer in China. – *Ecological Indicators* 73: 1-10.
- [39] Zhang, B., Chen, G. Q., Li, J. S., Tao, L. (2014): Methane emissions of energy activities in China 1980–2007. – *Renewable and Sustainable Energy Reviews* 29(0): 11-21.
- [40] Zhou, P., Ang, B. W., Poh, K. L. (2006): Slacks-based efficiency measures for modeling environmental performance. – *Ecological Economics* 60: 111-118.

CHARACTERIZATION OF *ZEA MAYS* L. THROUGH MORPHOLOGICAL, BIOCHEMICAL AND MOLECULAR MARKERS

RAHIM, F.^{1*} – KHAN, M. Q.² – ASHRAF, N.² – SHAFI, N.² – KHAWAJA, S.² – KHALID, S.² – ZAHID, G.² – AHMED, M.¹ – AHMED, M. S.³

¹*Department of Agriculture, Azad Jammu and Kashmir, Pakistan
(e-mail/phone: mumtaz.uel@googlemail.com/+92-333-513-7525 – M. Ahmed)*

²*University of Azad Jammu and Kashmir, Muzaffarabad, Pakistan
(e-mail/phone: mqkhan2004@yahoo.com/+92-344-581-7395 – Q. Khan;
nasra.ashraf@yahoo.com/+92-347-328-2515 – N. Ashraf;
nuzhatshafi@gmail.com/+92-333-524-0171 – N. Shafi;
sundus_kh@yahoo.com/+92-334-572-8558 – S. Khawaja;
saba_ak01@yahoo.com/+92-335-538-6999 – S. Khalid;
ghassanzahid@gmail.com/+92-334-509-3453 – G. Zahid;)*

³*Crop Science Institute, NARC, Islamabad, Pakistan
(e-mail/phone: ms.ahmedgenes@gmail.com/+92 321 5295691)*

**Corresponding author
e-mail: sardarfaisalrahim@gmail.com; phone: +92-348-536-4771*

(Received 5th Jan 2019 ; accepted 27th Feb 2019)

Abstract. 18 open-pollinated maize accessions were assessed for variability under randomized complete block design with 3 replications. Each plot comprised of two rows each 5 m in length with a plant to plant distance of 30 cm and a row to row distance of 75 cm. Data on morpho-biochemical traits were collected and subjected to statistical analysis to find out the variability among the maize accessions and association of increasing protein and oil content with the agronomic traits. From the source population 5 varieties with a high percentage of oil and protein, were selected and analyzed for total seed protein profile using Sodium Dodecyl Sulphate Polyacrylamide Gel Electrophoresis. Significant results of variance and covariance were observed for all morpho-biochemical traits, which revealed significant variation among the maize accessions. SDS-PAGE showed considerable variation in protein banding among the maize accessions. Correlation results showed an independent association of morphological traits with oil and protein contents in almost all the source population. This indicated that oil and protein content of maize grain can be increased without negatively affecting the important agronomic traits. Based on the results, the variability could be utilized to develop commercial maize varieties with improved quality of grain utilizing the conventional techniques of selection and hybridization.

Keywords: *biodiversity, correlation, oil content, protein content, SDS-PAGE*

Introduction

Maize is the 3rd most important crop in Pakistan after wheat and rice with an average yield of 4.3 ton ha⁻¹ (Farooq, 2013) below the worldwide maize yield of 5.2 ton ha⁻¹ (FAOSTAT, 2012). Therefore, it is very important to screen the new indigenous and exotic lines with an improved yield to be used in maize breeding programs (Iqbal et al., 2015). Genetic diversity is a basic tool for crop improvement (Iqbal et al., 2014) which could be managed, maintained and explained by morphological, biochemical and molecular markers (Vojka et al., 2016; Iqbal et al., 2015).

Pakistan imports 75% of edible oil (Zaidi, 2014) and could save billions by promoting local edible oil. Besides carbohydrates corn grain also has a considerable percentage of oil (3.77 to 11.56%) and protein (5.7 to 11.60%) (Deif et al., 2012; Singh et al., 2005; Mittelman et al., 2003; Okporie et al., 2002) and annually gives almost 15% of the proteins obtained from food-crops throughout the world (Li and Vassal, 2004). Oil content and protein content of maize grain are positively associated with yield and its components (Sreckov, 2011; Obi and Onysishi, 1994), therefore, could be increased without adversely affecting yield (Okporie et al., 2007). Oil and protein of corn grain can be increased by different breeding techniques, e.g. recurrent selection method, which has been one of the most effective and successful methods used in breeding programs for maize improvement (Berner, et al., 2006; Uguru, 2005; Obi, 1991).

Many studies investigated variability among maize germplasm through morphological (Kariuki et al., 2016; Iqbal et al., 2015; Shrestha, 2014) and biochemical markers (Deif et al., 2012; Mittelman et al., 2003). These experiments determined variability through morphological and biochemical characterization of maize varieties under RCBD with 3 replications and reported a wide range of variation for different morpho-biochemical characters investigated. Vojka et al. (2016) used morphological and molecular markers to study the variation among 29 inbred lines and reported that morphological and molecular markers are equally effective and accurate practices to determine the pedigree information of tested maize lines.

Other studies (Mittelman et al., 2003) evaluated oil content, protein content and grain yield in a group of maize test-crosses under RCBD with three replications. Results showed weak association and significant variation for oil content, protein content and grain yield. Deif et al. (2012) set an experiment to study the variability of 14 maize inbred lines and 15 crosses for oil and protein content. Results showed significant differences for protein content and oil content ranging from 8.34% to 11.60% and 7.67 to 11.56%, respectively. On the other hand, in crosses protein and oil content ranges from 8.22% to 13.94% and 9.27% to 11.29%, respectively. The highest values for protein content (13.94%), oil content (10.65%) and grain yield per plant (128.73 g) were reported by a cross.

Previous studies suggested that plant height is strongly associated with maize yield (Hegy et al., 2002; Sangoi et al., 1998; Aldrich et al., 1986), while 100-kernel weight and ear length predict yield components, whereas days to 50% silking predicts the maturity time of maize plants (Okporie et al., 2007). Furthermore, maize forage yield is preferred by farmers because it contains sufficient quantities of protein and minerals and possesses high digestibility as compared to other non-legume fodders (Chaudhary et al., 2014). Therefore, Plant height, grain yield, ear length, days to 50% silking and dry forage yield are among the most important agronomic traits to be assessed and should not be adversely affected in the maize breeding programs. Okporie et al. (2007) investigated 8 maize varieties to find out the correlation of increasing oil and protein content with five important agronomic parameters viz., plant height, ear height, 100-kernel weight, kernel density and days to 50% silking, under RCBD with 3 replications. They reported an independent association among the traits investigated and concluded that oil and protein content of maize can be increased without adversely affecting these agronomic traits.

Pakistan is not only facing the problem of having low maize yield ha^{-1} but also the poor quality of corn grain. Therefore, to achieve the goal efforts need to develop high

yielding maize varieties with an improved percentage of oil and protein which can be obtained by the determination of variability among the local and exotic germplasm to be used in future breeding programs.

The objectives of this study are: (1) to determine variation among selected maize varieties through morphological, biochemical and molecular markers; (2) to determine the association of oil and protein content with selected agronomic markers.

Materials and methods

The experimental material comprised of 10 open pollinated maize varieties viz., Sadaf, Islamabad Yellow, Agati-2002, SG-2002, Soan-3, Sahiwal-2002, Margala, Rakaposhi, Islamabad white and Kashmir Gold and 8 advance maize lines viz., BS-1, EV-7004 Q, EV-5098, EV-1097, BS-2, EV-6089, EV-6098, and EV-1098. The Seed of 8 open pollinated varieties and 9 advance maize lines were collected from National Agriculture Research Council (NARC) Islamabad and one local variety 'Kashmir Gold' was used as a check. The experiment was carried out using randomized complete block design with three replications at the research area of Faculty of Agriculture, Rawalakot, Department of Plant Breeding and Molecular Genetics. Each plot comprised of two rows each 5 m in length with a plant to plant distance of 20 cm and a row to row distance of 75 cm. All recommended agronomic practices were followed to raise an ideal crop. Data on 5 competitive plants of the selected one-meter square area from each plot was recorded on maturity. Nitrogen and phosphorus fertilizers were applied @ 60 and 90 kg ha⁻¹, respectively. Data was recorded before and after harvesting of the crop for five morphological traits viz., days to 50% silking, plant height, 1000-grain weight, ear length and dry forage yield and two biochemical traits viz., oil content and protein content. Morphological parameters were recorded by using the standard descriptors formulated by IBPGR (1980). The protein content was determined by the Micro-Kjeldahl method as described by Pearson (1976). While the oil content was obtained with the help of Soxhlet's extractor as described by Anon (1978).

From the source population two advance maize lines viz., EV-5098, EV-1097, EV-6089, two commercial varieties viz., Agaiti-2002, Rakaposhi and a Local Check (Kashmir Gold) with a high percentage of oil and protein were selected and analyzed for total seed protein profile using Sodium Dodecyl Sulphate Polyacrylamide Gel Electrophoresis (SDS-PAGE) as described by Laemmli (1970). The gel picture was taken, uploaded to ImageJ software and the distance covered by protein bands was calculated and scored by assigning + or – sign for the presence or absence of bands, respectively.

Data for agronomic and biochemical traits were submitted to analysis of variance using the GLM procedure of the SAS system v9.2 (SAS Institute, 2007) and the treatment means were compared by the Tukey's test at 5% level of significance. Correlation associations of oil content and protein content of maize kernel with plant height, days to silking, ear length, 1000-grain weight, and dry forage yield and correlation coefficients were calculated as given by Okpori (2006).

Results

The mean values for days to silking, plant height, ear length, 1000-grain weight, and dry forage yield are given in *Table 2*. Data for these morphological characters were

analyzed statistically and genotypic and phenotypic variance and covariance were estimated (*Table 1*). Significant differences were observed among maize accessions for days to silking, plant height, ear length, 1000-grain weight and dry forage weight (*Table 1*). The genotypic and phenotypic variances were significantly different for all the traits (*Table 1*). Genotypic and phenotypic variability values for days to silking (0.22% and 0.23%, respectively), plant height (1.4% and 1.4%, respectively), ear length (0.09% and 0.10%, respectively), 1000-grain weight (7.4% and 7.9%, respectively) and dry forage yield (281.25% and 326%, respectively) showed less environmental influence on these tested characters.

Table 1. Estimates of parameters of variability for yield and its components

Characters	Mean	Range	Genotypic variance	Phenotypic variance	GCV	PCV
Days to 50% silking	81.9	71.5-87.8	17.9	18.9	0.2	0.2
Plant height (cm)	199.9	170-241	274	278	1.4	1.4
Ear length (cm)	15.35	12.8-18	1.3	1.6	0.1	0.1
1000 grain weight (g)	232.8	180.83-345	1717	1839	7.4	7.9
Dry matter yield (kg ha ⁻¹)	12640.3	8564-16295	3555051	4120678	281.3	326.0
Oil content (%)	5.2	2.10 – 8.40	3.72	3.73	36.85	36.88
Protein content (%)	4.80	2.07 – 7.80	3.19	3.20	37.13	37.15

The minimum days to silking were taken by Rakaposhi with an average value of 73, whereas variety EV-1097 took maximum 86.9 days, similarly, Aguiti-2002 attained maximum plant height of 238.0 cm, whereas variety EV-1097 was short stature variety with 172.6 cm plant height. Agaiti-2002 and local check attained the maximum ear length with an average of 17.8 cm and 17.65 cm, respectively, and EV-7004Q attained minimum ear length of 13.10 cm. Maximum grain weight with an average value of 308.8 g was obtained from Agaiti-2002, whereas the minimum weight of 100-grains was presented by Sahiwal-2002 (181.1 g). EV-1098 produced maximum dry matter yield (16190 kg ha⁻¹), whereas the variety EV-7004Q yielded less dry matter ha⁻¹ with an average value of 9342.0 kg.

The mean values for oil content and protein content are given in *Table 2*. Data for these biochemical characters were analyzed statistically and significant differences were observed among maize varieties for oil content and protein content and genotypic and phenotypic variance and covariance were estimated (*Table 1*) for oil content (36.85% and 36.88%, respectively) and protein content (37.13% and 37.15%, respectively). Results showed less environmental influence on the traits of oil content and protein content. Maximum values for oil content and protein content were obtained by EV-6089 (8.40%) and Agaiti-2002 (11.80%), respectively. Meanwhile, minimum values were obtained by EV-1098 (2.10%, 6.06%, respectively). The coefficient of variation (CV %) for days to silking (1.15), plant height (1.5), ear length (3.15), 1000-grain weight (4.53), dry forage yield (5.95) oil content (2.83) and protein content (1.78) indicates the excellent experimental precision.

From the photograph of the protein gel (photograph not presented) banding pattern drawn and the distance covered by protein bands measured (*Table 3*). The protein gel expressed nine bands at the marginally variable distance. At the distance of 1 cm (10 kDa) and 1.6 cm (15 kDa), all the varieties showed a common band. EV-6089, Rakaposhi and Local check (Kashmir Gold) recorded one band each at the distance of 2.7 cm (25 kDa). EV-6089 and Local check shared one common band at the distance of 3.1 cm (30 kDa) in

the protein profile. Agaiti-2002, EV-5098 and EV-1097 gave one band each travelled the distance of 3.4 cm (40 kDa). Rakaposhi had two isolated bands at the distance of 4 cm (70 kDa) and 6.4 cm (130 kDa). Similarly, EV-5098 expressed a solitary band at the distance of 4.8 cm (100 kDa) in the protein profile. EV-5098 and EV-1097 both had one band each at a distance of 7.3 cm (170 kDa).

Table 2. Mean values of different morphological traits of maize (*Zea mays* L.) varieties

SN	Variety	Days to silking	Plant height (cm)	Ear length (cm)	1000-grain weight (g)	Dry forage yield (g)	Protein content (%)	Oil content (%)
1	Rakaposhi	86.90 A	201.5 EF	14.85 BCDEF	206.5 CD	14010.0 ABCDE	10.11 C	3.10 EF
2	Islamabad white	86.70 AB	178.0 H	15.20 BCDEF	204.7 CD	14880.0 AB	7.97 G	1.8 G
3	Sadaf	85.70 ABC	197.1 F	15.40 BCDE	234.0 C	10750.0 FGH	8.66 F	3.30 EF
4	Islamabad yellow	85.05 ABC	196.5 F	16.50 AB	214.3 CD	9884.0 GH	9.26 DE	4.50 C
5	EV-7004 Q	85.00 ABC	203.3 DE	13.10 G	274.5 AB	9342.0 H	8.10 G	4.00 D
6	BS-2	84.85 ABC	177.3 H	13.80 EFG	202.7 CD	12260.0 CDEFG	9.47 D	3.97 D
7	BS-1	84.45 ABCD	189.0 G	15.20 BCDEF	208.8 CD	12140.0 DEFG	6.47 I	1.40 GH
8	Local check (XY)	83.90 ABCD	219.9 B	17.65 A	298.8 AB	14200.0 ABCDE	11.27 B	6.20 AB
9	EV-6089	83.50 BCD	212.7 C	16.30 ABC	300.9 AB	11190.0 FGH	11.17 B	6.37 A
10	SG-2002	83.40 BCD	220.1 B	13.70 FG	278.8 AB	9984.0 GH	6.70 I	3.50 E
11	Sahiwal-2002	82.80 CDE	204.4 DE	16.45 AB	181.1 D	11040.0 FGH	10.20 C	0.47 I
12	Margala	82.65 CDE	188.3 G	14.85 BCDEF	198.5 CD	12700.0 BCDEF	6.17 J	1.17 H
13	EV-6098	81.30 DE	208.3 CD	14.50 DEFG	269.5 B	14440.0 ABCD	7.30 H	2.87 F
14	EV-5098	79.80 E	187.4 G	15.40 BCDE	208.4 CD	14700.0 ABC	10.10 C	3.97 D
15	EV-1097	75.00 F	172.6 H	15.85 BCD	186.0 D	11750.0 EFGH	9.17 E	4.80 C
16	EV-1098	75.00 F	199.6 EF	15.00 BCDEF	214.4 CD	16190.0 A	6.07 J	0.10 I
17	Agaiti-2002	74.80 F	238.0 A	17.75 A	308.3 A	14980.0 AB	11.76 A	5.80 B
18	Soan-3	73.95 F	204.9 DE	14.75 CDEF	200.4 CD	13090.0 BCDEF	8.70 F	3.00 H
	LSD_{0.05}	2.89	9.21	1.48	5.11	2311	0.26	0.45
	CV (%)	1.15	1.50	3.15	4.53	5.95	1.78	2.83

*Means with similar letters are statistically non-significant

Table 3. Tabulated representations of SDS-PAGE results of six maize varieties

Distance (cm)	kDa	Agaiti-02	EV-5098	EV-1097	EV-6089	Rakaposhi	Local check
1	10	+	+	+	+	+	+
1.6	15	+	+	+	+	+	+
2.7	25	-	-	-	+	+	+
3.1	30	-	-	-	+	-	+
3.4	40	+	+	+	-	-	-
4	70	-	-	-	-	+	-
4.8	100	-	+	-	-	-	-
6.4	130	-	-	-	-	+	-
7.3	170	-	+	+	-	-	-

+ Presence of protein band. - Absence of protein band

Almost all the maize varieties from the source population expressed negative or positive but non-significant correlation of oil and protein with agronomic traits viz., days to silking, plant height, ear length, 1000-grain weight and dry forage yield (Table 4a and 4b). For some traits maize varieties viz., BS-2, Agaiti-2002 and EV-6089, Sahiwal-2002 for days to silking, EV-6089, Islamabad white, EV-1098, Rakaposhi,

Agaiti-2002, BS-2 and EV-6089 for plant height, Margala, Soan-3, EV-704 Q, SG-2002, Soan-3 and Kashmir Gold for ear length, Sadaf, EV-5098, Islamabad yellow, Agaiti-2002 and Sahiwal-2002 for 1000-grain weight, EV-7004 Q and Soan-3 for forage yield, showed positive or negative and significant results.

Table 4a. Correlation (*r*) between oil content and five morphological traits

Varieties	Dry matter	Ear length (cm)	Plant height (cm)	Days to silking	1000-grain weight
Sadaf	-0.705	-0.592	0.461	-0.165	-0.982*
BS-1	0.279	0.277	-0.277	0.867	0.287
Islamabad yellow	-0.260	-0.397	0.705	0.962	0.986*
Agaiti-2002	0.608	0.719	0.798	-0.984*	0.602
EV-7004 Q	1.000**	-0.348	0.721	0.327	0.146
EV-5098	-0.321	0.619	0.823	-0.741	-1.000*
EV-1097	-0.849	0.645	-0.549	0.902	-0.189
BS-2	-0.371	0.037	0.915	1.000**	0.655
Margala	0.191	0.973*	0.856	0.886	-0.756
EV-6089	-0.602	-0.786	0.975*	-0.990*	-0.735
Islamabad white	-0.710	-0.803	0.999**	0.560	-0.350
EV-6098	0.951	0.189	1.000**	0.911	-0.800
Rakaposhi	-0.716	-0.209	0.999**	-0.795	-0.867
SG-2002	0.405	0.803	-0.674	0.444	-0.884
EV-1098	-0.965	-0.866	-0.995**	0.972	0.822
Soan-3	-0.416	-0.998**	-0.873	0.406	-0.956
Sahiwal-2002	0.294	-0.397	-0.669	0.842	0.979*
Local check (Kashmir Gold)	-0.472	0.914	-0.511	0.812	-0.588

Table 4b. Correlation (*r*) between protein content and morphological traits

Varieties	Dry matter	Ear length	Plant height	Days to silking	1000-grain weight
Sadaf	-0.256	-0.916	0.843	0.350	-0.945
BS-1	-0.627	-0.629	0.629	0.905	0.949
Islamabad yellow	0.612	0.721	-0.376	-0.782	-0.846
Agaiti-2002	0.988*	0.041	0.993*	-0.836	-0.116
EV-7004 Q	-0.409	0.999**	0.350	0.737	-0.966
EV-5098	-0.659	0.371	-0.904	0.952	0.500
EV-1097	0.807	-0.700	0.485	-0.932	0.115
BS-2	-0.664	0.374	0.998**	0.931	0.359
Margala	0.477	0.998**	0.661	0.706	-0.918
EV-6089	0.481	0.866	-0.933	1.000**	0.824
Islamabad white	-0.954	-0.439	0.865	0.878	-0.742
EV-6098	-0.919	-0.277	-0.995**	-0.945	0.742
Rakaposhi	-0.519	-0.447	0.956	-0.922	-0.964
SG-2002	-0.343	0.992*	0.027	0.941	-0.961
EV-1098	-0.641	0.091	-0.329	0.620	-0.172
Soan-3	-0.309	-0.985*	-0.923	0.298	-0.983*
Sahiwal-2002	-0.110	0.000	-0.319	0.987*	0.818
Local check (Kashmir Gold)	0.158	-0.997**	0.764	-0.576	0.820

Discussion

Morphological comparisons were made to know the extent of variation among maize varieties under investigation to estimate the genetic diversity. Statistical analysis of the data reflected a high level of variation for all the morphological traits. This is in agreement with the results reported by Hussain et al. (2011) who have screened the same maize varieties and reported the wide range of variation for all the morphological markers used and reported values ranged from 69 to 84 and 145 to 205 for days to silking and plant height, respectively. Present results for days to silking, plant height and ear length also showed resemblance with the findings of Koirala and Gurung (2002), who reported a significant amount of variability for days to silking, plant height and ear length. Koirala and Gurung (2002) recorded days to silking varied from 72 to 77 days, 198 to 230.0 cm plant height and a similar range of values for ear length. Similar findings were also reported by Borrás et al. (2007), Baqa et al. (2014) and Ghimire and Timsina (2015) for days to silking. Present investigation showed that 1000-grain weight results were closer to the findings of Koirala and Gurung (2002) and Sabeena and Dar (2005), who reported a wide range of variability for 1000 grain weight, values ranged from 340 to 325 g. Similarly, significant variations for grain yield were reported by other investigations (Mubeen et al., 2015; Charles et al., 2013; Adebayo and Menkir, 2015). High variability for important agronomic traits, i.e. days to silk, plant height, ear length, 1000-kernel weight and grain yield in our investigation was also supported by the results of previous studies (Sonmez, 2018; Iqbal et al., 2015; Shrestha, 2013; Ranatunga et al., 2009; Miguel et al., 2008; Ihsan et al., 2005; Beyene et al., 2005; Dijak et al., 1999). Results for dry matter yield in this study do not resemble with the findings of Sabeena and Dar (2005), who reported the values ranged from 8150 to 12000 kg ha⁻¹ for this trait. These findings also show deviation with the findings of Koirala and Gurung (2002), who observed the maximum dry forage yield of 14000 kg ha⁻¹. Genotypic and phenotypic variances are presented in *Table 1*. For all the traits studied, genotypic and phenotypic variances were significant, which is a piece of evidence that variability within the maize varieties is sufficiently divergent and constitutes potential candidate varieties on which improvement program can be initiated.

The values for oil content and protein content were significantly different and varied between 0.10% - 6.40% and 6.06% - 11.80%, respectively. The results were in clear agreement with the previous findings reported significantly different percentage of oil and protein values ranged from 3.77% to 11.56% and 5.7% to 12.08%, respectively (Sonmez, 2018; Deif et al., 2012; Seiam and Khalifa, 2007; Mittelmann et al., 2003; Singh et al., 2005). Varieties in the present study showed less percentage of oil content as compared to the previous studies. This difference may be due to the environmental factors and plant growth conditions which could modify the percentage of oil percentage (Villalobos et al., 1996).

Use of SDS-PAGE markers for the determination of variability and identification of varieties by extensive study of seed storage protein in many crop species became an efficient tool (Shah et al., 2003; Tawab, 2004; Anjali and Sanjay, 2012; Iqbal et al., 2014). In this study, the variability within selected varieties was confirmed by molecular investigations on the basis of gene product extracted from the seed of six maize accessions using SDS-PAGE markers. At the distance of 1 cm (10 kDa) and 1.6 cm (15 kDa) similar varieties could be an indication of their evolutionary interrelationship. EV-6089, Rakaposhi and Local check (Kashmir Gold) recorded one

band each at the distance of 2.7 cm (25 kDa) in the protein gel which indicated their similar genetic makeup. EV-6089 and Local check were different from the others as they shared one common band at the distance of 3.1 cm (30 kDa) in the protein profile. Agaiti-2002, EV-5098 and EV-1097 gave one band each travelled the distance of 3.4 cm (40 kDa) in the protein gel which showed their genetic resemblance as well as evidence that these varieties could have some common heritage. Rakaposhi had two isolated bands at the distance of 4 cm (70 kDa) and 6.4 cm (30 kDa) that showed Rakaposhi is genetically different from all other varieties studied so far. Similarly, EV-5098 expressed a solitary band at a distance of 4.8 cm (100 kDa) in the protein profile and showed that EV-5098 has a different genetic background as compared to other varieties studied so far. EV-5098 and EV-1097 both had one band each at a distance of 7.3 cm (170 kDa) which indicated that these maize accessions have some common genes and genetically they are different from other varieties. Similar results were reported in other investigations which exploited high level of genetic variability among studied germplasm and revealed that some bands are scored by all varieties and some bands shared by one or more than one variety (Khan et al., 2014; Osman et al., 2013; Verma, 2006; Laura, 2006; Haider, 2002; Tubajika, 2001; Gorinstein, 1999). In the present study, 22% of total visible protein bands were monomorphic and 78% were polymorphic. Results are in clear agreement with other findings (Vivodik et al., 2016; Iqbal et al., 2014; Rashed et al., 2010) which reported a wide range of variability among maize germplasm and recorded 31% to 39% monomorphic and 61% to 65% polymorphic protein bands.

The positive or negative and significant results of correlation suggest that an increase in oil content of maize can adversely affect the important agronomic traits. But these results are negligible as not even a single genotype has significant results for all the traits studied and only a few lines showed significant results for few traits. Since no significant relationship existed in the majority of remaining varieties of the source population, it indicates that high oil maize can be bred without adversely affecting the studied agronomic traits. Similar results were reported by Okporie and Oselebe (2007), Okporie and Obi (2002), Obi and Onish (1994) and Rajni et al. (1983). For 1000-grain weight, the present finding was contrary to the work reported by Okporie and Obi (2002) and Obi and Onish (1994), who found oil content to be positively and significantly correlated with 1000-grain weight.

Results of some morphological and biochemical traits deviate from the previous findings. This departure may be due to the environmental factors, variable sample size, and source population. For reliable detection of contrasted varieties usually experiments were performed in two or more consecutive years but the present experiment has not been repeated in consecutive years because Hussain et al. (2011) have previously evaluated the performance of the same varieties which have been screened in the present study and they also recorded significant differences for all the morphological traits studied and reported that these varieties had a wide genetic background, therefore, the results of the present investigation have sufficient and the real scientific interest.

Conclusion

In this study, morphological and biochemical markers confirmed a high level of variability among all the maize varieties investigated. Similarly, molecular markers (SDS-PAGE) also confirmed the wide range of variation among selected maize

varieties. The variability can be used in future breeding programs to improve maize varieties. Further, results showed non-significant association between oil and protein content with days to 50% silking, plant height, ear length, 1000-grain weight and dry forage yield, which indicated that oil and protein content that are among the most important and desirable traits of maize grain could be increased by using effective breeding methods without negatively affecting the important agronomic traits studied. Finally, recurrent selection and hybrid breeding might be recommended for developing high yielding maize varieties with the improved percentage of oil content and protein content.

Acknowledgements. We are thankful to NARC Islamabad, HEC Pakistan and Department of Food Science and Technology, University of Poonch for their financial and technical support.

Author contribution. All authors contributed equally.

Conflict of interests. The authors declare that they have no conflict of interests.

REFERENCES

- [1] Adebayo, M. A., Menkir, A. (2015): Assessment of hybrids of drought tolerant maize (*Zea mays* L.) inbred lines for grain yield and other traits under stress managed conditions. – Nigerian Journal of Genetics 20: 1-5.
- [2] Aldrich, S. R., Scott, W. O., Hoelt, R. G. (1986): Modern Maize Production. 3th Ed. – A and L Publications, Inc., Champaign, Illinois.
- [3] Anjali, C., Sanjay, C. (2012): Genetic diversity estimation of maize cultivars based on protein profiles in different conditions. – Indian Journal of Agriculture and Biochemistry 25: 52-56.
- [4] FAOSTAT (2012): Food and Agricultural commodities production. – Food and Agriculture Organization of the United Nations. <http://faostat.fao.org/site/339/default.aspx>.
- [5] Anon (1978): Determination of Oil in Feeding Stuffs. Laboratory Manual. – Department of Animal Science, University of Nigeria, Nsukka.
- [6] Baqa, S., Haseeb, A., Ahmed, M., Ahmed, A. (2014): Evaluation of growth of different maize varieties in field under the climatic conditions of Peshawar. – Journal of Natural Sciences Research 4: 22-27.
- [7] Berner, D. K., King, J. G., Singh, B. B. (2006): Striga research and control. A prospective from Africa. – Plant Disease 79: 652-660.
- [8] Beyene, Y., Botha, A. M., Myburg, A. A. (2005): A comparative study of molecular and morphological method of describing genetic relationships in traditional Ethiopian highland maize. – African Journal of Biotechnology 4: 586-595.
- [9] Borrás, L., Westgate, M. E., Astini, J. P., Echarte, L. (2007): Coupling time to silking with plant growth rate in maize. – Field Crops Research 102: 73-85.
- [10] Charles, M. K., Fredrick, N. M., George, O. A., Odongo, O. M. (2013): Genetic variability analysis for growth and yield parameters in double cross maize (*Zea mays* L.) genotypes in Kitale County of Kenya. – Journal of Plant Breeding and Genetics 01: 7-11.
- [11] Chaudhary, D. P., Jat, S. L., Kumar, R., Kumar, A., Kumar, B., (2014): Fodder Quality of Maize: Its Preservation. – In: Chaudhary, D. P. et al. (eds.) Maize: Nutrition Dynamics and Novel Uses. Springer, New Delhi.
- [12] Deif, A. M. H., Mekki, B. B., Mostafa, E. A. H., Esmail, R. M., Khattab, S. A. M. (2012): The genetic relationship between proteins, oil and grain yield in some maize hybrids. – World Journal of Agricultural Sciences 8: 43-50.

- [13] Dijak, M., Modarres, A. M., Hamilton, R. I., Dwyer, L. M., Stewart, D. W., Mather, D. E., Smith, D. L. (1999): Leafy reduced-stature maize hybrids for short- season environments. – *Crop Science* 39: 1106-1110.
- [14] Farooq, O. (2013): Agriculture. – Pakistan Economic Survey. Government of Pakistan. http://finance.gov.pk/survey_1213.html.
- [15] Ghimire, B., Timsina, D. (2015): Analysis of yield and yield attributing traits of maize genotypes in Chitwan, Nepal. – *Scrutiny International Research Journal of Agriculture, Plant Biotechnology and Bio Products* 2: 153-162.
- [16] Gorinstein, S., Jaramillo, N., Medina, O., Rogrigues, W., Tosello, G., Paredes, O. (1999): Evaluation of some cereals, plants and tubers through protein composition. – *Journal of Protein Chemistry* 18: 687-693.
- [17] Haider, A., Shanshoury, A. (2002): Variation of storage proteins and isozymes within maize inbred lines. – *Biologia Plantarum* 43: 199-203.
- [18] Hegyi, G. Z., Pok, I., Kizmus, L., Zsubori, Z., Nagy, E., Marton, L. C. (2002): Plant height and height of the main ear in maize (*Zea Mays* L.) at different locations and different plant densities. – *Acta Agronomica Hungarica* 50: 75-84.
- [19] Hussain, N., Khan, Y., Baloch, M. S. (2011): Screening of maize varieties for grain yield at Dera Ismail Khan. – *Journal of Animal and Plant Science* 21: 626-628.
- [20] IBPGR (1980): Maize Descriptors. – Food and Agriculture Organization, The International Board for Plant Genetic Resources, Rome, pp. 6-8.
- [21] Iqbal, J., Shinwari, Z. K., Rabbani, M. A. (2014): Investigation of total seed storage proteins of Pakistani and Japanese maize (*Zea Mays* L.) through SDS-PAGE markers. – *Pakistan Journal of Botany* 46: 817-822.
- [22] Iqbal, J., Shinwari, Z. K., Rabbani, M. A. (2015): Maize (*Zea Mays* L.) Germplasm agro-morphological characterization based on descriptive, cluster and principal component analysis. – *Pakistan Journal of Botany* 47: 255-264.
- [23] Ihsan, H., Khalil, I. H., Rahman, H., Iqbal, M. (2005): Genotypic variability for morphological and reproductive traits among exotic maize hybrids. – *Sarhad Journal of Agriculture* 21: 599-602.
- [24] Kariuki, J. K., Githiri, S. M., Wesonga, J. M., Tesfamichael, T. S. (2016): Assessment of variation in agro-morphological traits in M3 and M4 maize lines. – *International Journal of Agronomy Agriculture Research* 9: 147-161.
- [25] Khan, S. A., Iqbal, J., Khurshid, H., Saleem, N., Rabbani, M. A., Zia, M., Shinwari, Z. K. (2014): The extent of intra-specific genetic divergence in *Brassica napus* L. population estimated through various agro-morphological traits. – *European Academic Research* 2: 2255-2275.
- [26] Koirala, R., Gurung, D. (2002): Heterosis and combining ability of seven yellow maize populations in Nepal. – Asian Regional Maize Workshop, Bangkok, Thailand, August, 5-8.
- [27] Laemmli, U. K. (1970): Cleavage of structural proteins during assembly of head of bacteriophage 14. – *Nature* 227: 680-685.
- [28] Laura, M. M., Paulo, A. (2006): Characterization of different maize varieties using SDS-PAGE. – *Science of Agricultural Genetics* 3: 25-27.
- [29] Li, J. S., Vassal, S. K. (2004): Quality Protein Maize. – In: Wrigley, C., Walker, C. E. (eds.) *Encyclopedia of Grain Science*. Elsevier, Amsterdam, pp. 212-216.
- [30] Miguel, C., Simoes, M., Oliveira, M. M., Rocheta, M. (2008): Envelope-like retrotransposons in the plant kingdom: evidence of their presence in gymnosperms (*Pinus pinaster*). – *Journal of Molecular Evolution* 67: 517-525.
- [31] Mittelman, A., José, B. M. F., Gustavo, J. M. M. L., Claudete, H. K., Ricardo, T. T. (2003): Potential of the ESA23B maize population for protein and oil content improvement. – *Scientia Agricola* 60: 319-327.

- [32] Mubeen, S., Rafique, M., Munis, M. F. H., Chaudhary, H. J. (2015): Study of southern corn leaf blight (SCLB) on maize genotypes and its effect on yield. – Journal of the Saudi Society of Agricultural Sciences 16: 210-217.
- [33] Vojka, B., Nikolic, A., Andjelkovic, V., Kovacevic, D., Filipovic, M., Vasic, V., Drinic, S. M. (2016): UPOV morphological versus molecular markers for maize inbred lines variability determination. – Chilean Journal of Agricultural Research 76: 417-426.
- [34] Obi, I. U. (1991): Maize its Agronomy, Diseases, Pest and Food Values. – Optimal Computers Solutions Ltd., Enugu, Nigeria.
- [35] Obi, I. U., Onyishii, G. C. (1994): Development of high protein population maize from two cycles of reciprocal recurrent selection. – Journal of Agricultural Research 11: 63-68.
- [36] Okporie, E. O. (2006): Statistics for Agricultural and Biological Sciences. – Chestnut Agency Limited, Enugu, Nigeria.
- [37] Okporie, E. O., Obi, I. U. (2002): Estimation of genetic gains in protein and oil of eight populations of maize after three cycles of reciprocal recurrent selection. – Journal of Science and Agricultural Food Technology 2: 40-45.
- [38] Okporie, E. O., Oselebe, H. O. (2007): Correlation of protein and oil contents with five agronomic traits of maize after three cycles of reciprocal recurrent selection. – World Journal of Agricultural Sciences 3: 639-641.
- [39] Osman, G., Munshi, A., Altf, F., Mutawie, H. (2013): Genetic variation and relationships of *Zea mays* and *Sorghum* species using RAPD-PCR and SDS-PAGE of seed proteins. – African Journal of Biotechnology 12: 4269-4276.
- [40] Pearson, D. (1976): The Chemical Analysis of Foods. 7th Ed. – Churchill Livingstone Pub. Co., London and New York.
- [41] Rajni, R., Sarkar, D. K., Singh, R. (1983): Correlations and regressions among oil content, grain yield and yield components in maize. – Indian Journal of Agriculture Research 11: 63-68.
- [42] Ranatunga, M. A. B., Meenakshisundaram, P., Arumungachamy, S., Maheswaran, M. (2009): Genetic diversity of maize (*Zea mays* L.) inbreds determined with morphomeric traits and simple sequence repeat markers. – Maydica 54: 113-123.
- [43] Rashed, M. A., Deif, A. M. H., Atta, A. H., Mohamed, F. I., Mahmoud, F. E. (2010): Protein fingerprinting and heat shock proteins detection in some maize inbred lines (*Zea mays* L.). – Journal of Genetic Engineering and Biotechnology 8: 1-7.
- [44] Sabeena, N., Dar, Z. (2005): Genetic divergence among local maize cultivars of Kashmir Valley. – S. K. University of Agriculture Sciences & Technology of Kashmir. K. D. Research Station.
- [45] Sangoi, L., Salvador, R. J. (1998): Influence of plant height and of leaf number on maize production at high plant densities. – Pesquisa Agropecuária Brasileira 33: 297-306.
- [46] SAS, I. (2007): The SAS System for Windows, Version 9.2. – SAS Institute Inc., Cary.
- [47] Seiam, M. A., Khalifa, K. I. (2007): Heterosis and phenotypic correlation for oil, protein and starch content in 81 maize inbreds, hybrids and populations. – Egyptian Journal of Plant Breeding 11: 209-221.
- [48] Shah, A. H., Khan, M. F., Khaliq, A. (2003): Genetic characterization of some maize (*Zea mays* L.) varieties using SDS-PAGE. – Asian Journal of Plant Sciences 2: 1188-1191.
- [49] Shrestha, J. (2013): Agro-morphological characterization of maize inbred lines. – Sky Journal of Agriculture Research 2: 85-87.
- [50] Singh, P., Sain, D., Dwivedi, V. K., Kumar, Y., Sangwan, O. (2005): Genetic divergence studies in maize (*Zea mays* L.). – Annals of Agriculture Biological Research 10: 43-46.
- [51] Sonmez, C. (2018): Effect of phosphorus fertilizer on some yield components and quality of different anise (*pimpinella anisum* L.) populations. – Turkish Journal of Field Crops 23: 100-106.

- [52] Sreckov, Z., Nastastic, A., Bocanski, J., Djalovic, I., Vukosavljev, M., Jockovic, B. (2011): Correlation and path analysis of grain yield and morphological traits in test-cross populations of maize. – *Pakistan Journal of Botany* 43: 1729-1731.
- [53] Tawab, A. Y. M. (2004): Molecular markers of some maize genotypes. – Ph.D. Thesis. Faculty of Agriculture, Ain Shams University, Egypt.
- [54] Tubajika, K., Damann, K. (2001): Sources of resistance to aflatoxin production in maize. – *Journal of Agricultural and Food Chemistry* 49: 2652-2656.
- [55] Uguru, M. I. (2005): *Crop genetics and Breeding*. Revised Ed. – Epharata Press, Nsukka, Enugu State, Nigeria.
- [56] Verma, V. L. K., Reddy, N. M., Keshavulu, K., Ankaiah, R. (2006): Characterization of maize genotypes through SDS-PAGE. – *Crop Research Hisar* 30: 124-27.
- [57] Vivodik, M., Galova, Z., Balazova, Z., Petrovicova, L., Hlozakova, T. K. (2016): Genetic variation and relationships of old maize genotypes (*Zea mays* L.) detected using SDS-PAGE. – *Potravinarstvo* 10: 532-536.
- [58] Villalobos, D. F., Hall, A. J., Ritchie, J. T., Orgaz, F. (1996): A development, growth and yield model of the sunflower crop. – *Agronomy Journal* 88: 403-415.
- [59] Zaidi, S. M. H. (2014): Edible oil imports in Pakistan. – *South Asian Journal of Management Sciences* 8: 1-8.

DIALLEL ANALYSIS OF ELITE TOMATO LINES COMPRISING LEAF CURL VIRUS RESISTANCE GENES

VIJETH, S.¹ – DHALIWAL, M. S.¹ – JINDAL, S. K.¹ – GARG, N.² – KAUSHIK, P.^{3*} – SHARMA, A.¹

¹*Department of Vegetable Science, Punjab Agricultural University, Ludhiana 141 004, India*

²*Regional Research Station, Punjab Agricultural University, Bathinda 151 001, India*

³*Instituto de Conservación y Mejora de la Agrodiversidad Valenciana, Universitat Politècnica de València, Valencia 46022, Spain*

**Corresponding author*

e-mail: prakau@doctor.upv.es, prashantumri@gmail.com; phone: +34-96-387-7000

(Received 12th Jan 2019 ; accepted 21 Mar 2019)

Abstract. Tomato leaf curl virus is a serious threat to an autumn-winter crop of tomato in North India, causing yield losses up to 90-100%. Therefore, nine resistant and one susceptible line (Punjab Chhuhara) of tomato were crossed in half-diallel fashion to develop 45 F₁ hybrids. Parents and their hybrids were evaluated for yield and quality traits under natural epiphytotic field conditions. There were extensive differences in the performance of parental lines carrying similar and different resistance genes (*Ty-X*). Of three parental lines carrying *Ty-2* gene, CLN 17 performed better than 2123D and 2123C in respect of mean and general combining ability (GCA) for total yield and fruit weight. Likewise, out of three parental lines incorporating two resistance genes (*Ty-1* and *Ty-2*), the line CLN 138B had better mean values and GCA for total yield and fruit weight than CLN 138A and CLN 104. However, the parental line CLN 154 with three different resistance genes (*Ty-1*, *Ty-2*, *Ty-3*) showed the best GCA for total yield, and it was followed by genotype CLN 138B comprising of two resistance genes (*Ty-1* and *Ty-2*). However, the parental lines carrying *Ty-2* gene alone produced three useful hybrids expressing 19 to 28% heterosis over top parent for total yield. Four highly significant cross-combinations can be recommended for pedigree selection to develop superior inbred lines. The top parent CLN 154 yielding significantly higher than released varieties along with seven F₁ hybrids manifesting 16 to 31% top parent heterosis for total yield can be recommended after multi-location evaluations. Overall, this study provides useful information on the successful leaf curl virus resistant gene combinations under the north-Indian conditions.

Keywords: *begomovirus, combining ability, diallel cross, heterosis, leaf curl virus resistance, Solanum lycopersicum*

Introduction

Tomato (*Solanum lycopersicum* L.) is one of the most important vegetable crops of India and the world. India contributes 11.1% to world tomato production and is the second largest tomato producer in the world after China (FAOSTAT, 2018). In North Indian plains, the autumn-winter crop of tomato is transplanted during second fortnight of August. The main constraint in this crop is the incidence of tomato leaf curl virus (ToLCV) which may cause yield losses up to 90-100% (Gaikwad et al., 2011a; Kaushik and Dhaliwal, 2018; Moriones et al., 2017). The disease is transmitted by whitefly (*Bemisia tabaci* Gennadius), the population of which is usually high during July to October under Punjab conditions (Kaushik and Dhaliwal, 2018). Management of the whitefly using systemic insecticides has proved futile because of rapid turnover rate of the vector population in the tomato crop (Shankarappa et al., 2008; Singh et al., 2015) and frequent development of resistance against insecticides (Horowitz et al., 2005). Therefore, breeding for disease resistance is the best approach to control this disease

(Picó et al., 1996). In this direction, the Punjab Agricultural University has so far developed and released three open-pollinated resistant varieties of tomato viz., Punjab Varkha Bahar 1 (PVB-1), Punjab Varkha Bahar 2 (PVB-2) (Cheema and Dhaliwal, 2010) and Punjab Varkha Bahar 4 (PVB-4). However, it is important to develop F₁ hybrids resistant to ToLCV because tomato hybrids generally outperform open-pollinated varieties and are therefore widely cultivated by farmers in India (Prasanna et al., 2015). Although a few hybrid combinations have been identified by Shankarappa et al. (2008) for cultivation in South India, there is a need to develop and identify resistant hybrids for each geographical region because of the occurrence of a different isolate of the virus in each area. The earlier work on the geographical distribution of tomato leaf curl begomovirus species within India suggested that viruses with bipartite genomes (DNA-A and DNA-B components) were prevalent in North India while those with monopartite genomes (DNA-A) were found in South India (Hong and Harrison, 1995; Kirthi et al., 2002; Muniyappa et al., 2000).

Tomato leaf curl virus is a geminivirus belonging to the *Begomovirus* genus of the family Geminiviridae (Varma and Malathi, 2003). Five different leaf curl viruses predominantly infecting tomato crop have been reported in India. These include tomato leaf curl New Delhi virus (ToLCNDV), tomato leaf curl Palampur virus (ToLCPMV), tomato leaf curl Bangalore virus (ToLCBV), tomato leaf curl Karnataka virus (ToLCKV) and tomato leaf curl Gujarat virus (ToLCGV). A recent survey and molecular characterization of ToLCV revealed that three begomovirus species, viz., ToLCNDV, ToLCPMV and ToLCKV are predominant under Punjab conditions (Gaikwad et al., 2011b; Kaushik et al., 2015).

Six *Ty*-genes (*Ty-1* to *Ty-6*) conferring the variable degree of resistance to ToLCV are available in cultivated tomato (Hanson et al., 2016). Two partially dominant genes *Ty-1* and *Ty-3* are mapped on chromosome 6 (Ji et al., 2007a; Zamir et al., 1994) and are reported to be at the same locus (Verlaan et al., 2013). A dominant gene *Ty-2* was mapped on chromosome 11 (Hanson et al., 2006). The *Ty-4* is a minor QTL on chromosome 3 that accounted for only 16% variation in symptom severity (Ji et al., 2009). Besides, a recessive gene *ty-5* was mapped on chromosome 4 (Hutton et al., 2012). Of late, Hutton and Scott (2014) have identified a *Ty-6* gene on chromosome 10 that confers resistance against the bipartite TYLCV. Of these genes, the dominant *Ty-2* and partially dominant *Ty-3* carrying lines could be potential resources for developing resistant or tolerant hybrids due to the nature of their gene action (Prasanna et al., 2015). The present study was, therefore, undertaken to evaluate ten parental lines along with their 45 F₁ hybrids incorporating *Ty-1*, *Ty-2* and *Ty-3* genes in respect of yield and quality traits under natural field conditions (against local isolate of ToLCV) and to identify superior inbred lines and F₁ hybrids based on their combining ability, heterosis and *per se* performance for yield and other horticultural traits.

Materials and methods

The present investigations were conducted at Vegetable Research Farm, Punjab Agricultural University, Ludhiana, coordinates at 30°55' North latitude, 75°54' East longitude and 247 m altitude. The plant material comprised ten advance generation lines of tomato (Table 1). Of these, nine lines, viz., PVB-2, CLN 138A, CLN 138B, CLN 104, CLN 17, 2123D, 2123C, PVB-1 and CLN 154, had a varying degree of resistance to ToLCV. The tenth parental line, viz., Punjab Chuhara, was susceptible to ToLCV

(Gaikwad et al., 2011a; Kaushik and Dhaliwal, 2018). All the ten parental lines were crossed manually during February-March, 2014 in a diallel mating design (Griffing, 1956) without reciprocals to generate 45 F₁ hybrids. The seed of all the 55 entries were sown on 29th July, 2014 after treatment with Thiram @ 2-3 g·kg⁻¹ of seed. The seedlings were transplanted on 2nd September, 2014 in a randomized complete block design (RCBD) with three replications. Ten plants of each entry were planted in a single row. Planting was done on one side of the raised beds, and row × plant spacing was maintained at 1.35 m × 0.30 m. The beds were covered with steel gray plastic mulch of 25 µm thickness. The insecticides were not sprayed in the trial so as to enhance the population of whitefly. To increase inoculum pressure, one row of ToLCV susceptible cv. Punjab Chhuhara was planted after every 10 rows in the experimental plots.

Table 1. Particulars of ten parental lines of tomato evaluated in half-diallel for yield and quality traits

Parental line	Pedigree/alternate name	Resistance gene(s)	Source	References
PVB-2	Punjab Varkha Bahar-2	Unknown	PAU	-
CLN 138A	CLN 3022 F ₂ -138-6-2-0	Ty-1, Ty-2	AVRDC	Zamir et al. (1994)
CLN 138B	CLN 3022 F ₂ -138-6-7-0	Ty-1, Ty-2	AVRDC	Hanson et al. (2006); Zamir et al. (1994)
CLN 104	CLN 3024 F ₂ -104-48-1-0	Ty-1, Ty-2	AVRDC	Hanson et al. (2006); Zamir et al. (1994)
CLN 17	CLN 3008 F ₂ -17-10-0	Ty-2	AVRDC	Hanson et al. (2006)
2123D	CLN 2123D	Ty-2	AVRDC	Hanson et al. (2006)
2123C	CLN 2123C	Ty-2	AVRDC	Hanson et al. (2006)
PVB-1	Punjab Varkha Bahar-1	Unknown	PAU	-
CLN 154	CLN 3022 F ₂ -154-11-11-0	Ty-1, Ty-2, Ty-3	AVRDC	Hanson et al. (2006); Ji et al. (2007b); Zamir et al. (1994)
PC	Punjab Chhuhara	Nil	PAU	-

PAU: Punjab Agricultural University, Ludhiana, India; AVRDC: The World Vegetable Center, Shanhua, Tainan, Taiwan

The plants were characterized based on the scale shown in *Figure 1*. After that, potential disease incidence (PDI) was determined with the formula as (number of infected plants/total number of plants) × 100 (Kaushik and Dhaliwal, 2018). The observations were recorded for ten traits. Total yield (kg plant⁻¹) was calculated by adding the weight of fruits obtained from all pickings and dividing by number of plants per entry per replication. A random sample of five fruits from second picking was taken and fruit weight (g) was estimated by dividing the weight of the sample with the number of fruits in the sample. Five randomly selected fruits from second harvest were used to determine polar diameter of fruit (distance between stem end and blossom end of the fruit), equatorial diameter of fruit (transversal distance of the fruit) and pericarp thickness (after dissecting the equatorial plane of the fruit) with the help of an Absolute Digimatic Vernier Caliper (Mitutoyo Corporation) and average was worked out. The same fruits were used to count the number of locules per fruit and average was worked out. For quality evaluation, five red ripe fruits were taken from second picking and cut longitudinally. Juice was squeezed from the blossom end and filtered through a double

layer of muslin cloth. Total soluble solids ($^{\circ}$ Brix), titratable acidity (mg/100 ml juice), lycopene (mg/100 g fresh weight) and dry matter (%) were estimated according to the procedure described elsewhere (Garg and Cheema, 2011).

Analysis of variance was performed for each trait, and the differences among mean values of all 55 entries for each trait were tested for significance using standard error of difference. Diallel analysis was carried out according to Griffing (1956) method II, model 1 (fixed effect model) to estimate general combining ability (GCA) and specific combining ability (SCA) effects. Heterosis over mid-parent (MPH), better parent (BPH) and top parent (TPH) was estimated and tested for significance using standard formulas (Garg and Cheema, 2011).



Figure 1. ToLCV symptoms severity rating in tomato on 0-4 scale, where 0 = Symptomless, 1 = Resistant, 2 = Tolerant, 3 = Susceptible and 4 = Highly susceptible

Results

Under open field conditions, seven out of ten parents showed a nil PDI (%) (Fig. 2). Remaining, one parent PC was susceptible to ToLCV infestation and remaining two parents showed the PDI (%) of 35-45% (Fig. 2). Whereas, twenty hybrids out of total forty-five demonstrated nil infection (Fig. 2). While for the remaining hybrids the PDI (%) ranged from 25-80% (Fig. 2). The analysis of variance for the experimental design revealed that the mean squares for genotypes were significant for all the traits indicating potential genetic differences among genotypes i. e. parents and their F_1 hybrids. The analysis of variance for combining ability revealed that variances for GCA and SCA were significant for all the traits indicating the importance of additive as well as non-additive types of gene effects in the inheritance of the traits studied. The GCA effects represent the additive nature of gene action. A high general combiner parent is characterized by its better breeding value when crossed with several other parents. Besides, mean performance of the parent is also considered in unison with GCA since the former offers reliability to GCA as a guide to the selection of parent (Sharma, 2006; Singh et al., 2014). Four parental lines viz., CLN 154, CLN 138B, PVB-2 and PVB-1 had shown significant positive values of GCA for total yield along with correspondingly

high mean yield (*Table 2*) reflecting their true breeding value. These lines also showed significant and positive GCA for fruit weight and quality traits. The GCA of parental lines was in consonance with their mean performance. For example, parental lines having high GCA for total yield had high mean yield too. However, there were differences in the combining ability of parental lines carrying the same resistance gene. For example, CLN 17, 2123D and 2123C had the same resistance gene *Ty-2*, but CLN 17 was a better combiner for total yield than the other two parental lines. Likewise, the line CLN 138B was a better combiner than CLN 138A and CLN 104 although all these three lines incorporated same resistant genes, viz., *Ty-1* and *Ty-2*.

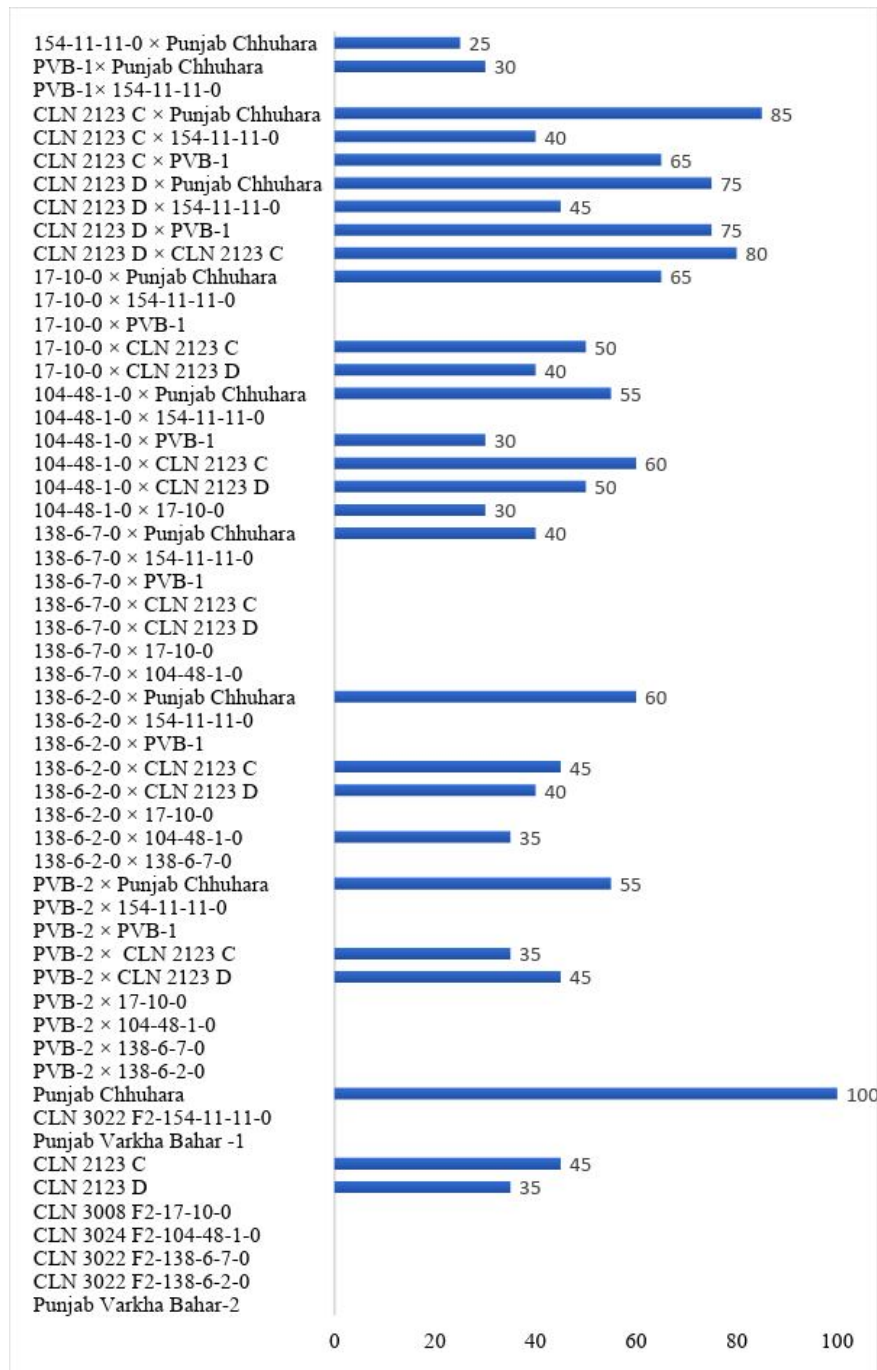


Figure 2. Per cent disease incidence (PDI) reaction of parents and their hybrids

Table 2. General combining ability (GCA) effects and mean values of ten parental lines of tomato evaluated in half-diallel for yield and quality traits

Parental line	Total yield (kg plant ⁻¹)		Fruit weight (g)		Number of locules		Pericarp thickness (mm)		Polar diameter (cm)	
	GCA	Mean	GCA	Mean	GCA	Mean	GCA	Mean	GCA	Mean
PVB-2	0.22*	2.13	6.15*	96.67	0.52*	4.22	-0.10	5.58	-0.09*	5.61
CLN 138A	-0.03	1.17	-3.41*	67.67	-0.28*	3.03	-0.65*	4.33	-0.05	4.88
CLN 138B	0.42*	1.97	12.27*	102.00	0.26*	3.50	1.18*	6.33	0.49*	6.30
CLN 104	-0.07	1.30	-0.07	61.33	-0.03	2.92	-0.42*	3.57	-0.29*	3.94
CLN 17	0.07	1.60	1.36*	86.33	0.25*	4.00	0.43*	6.57	-0.03	5.93
2123D	-0.20*	1.20	-4.32*	64.67	-0.52*	2.93	-0.71*	3.77	-0.18*	4.67
2123C	-0.34*	0.97	-8.74*	60.33	-0.53*	2.80	-0.43*	4.10	-0.12*	4.44
PVB-1	0.14*	1.97	7.71*	94.00	0.45*	3.98	0.42*	5.60	0.14*	6.00
CLN 154	0.43*	2.50	3.54*	89.33	0.53*	4.00	0.23*	6.20	0.09*	5.50
PC	-0.63*	0.26	-14.50*	34.33	-0.65*	2.30	0.05	4.60	0.02	4.92
**CD (g _i) (P≤0.05)	0.07		1.11		0.08		0.13		0.09	
CD (g _i -g _j) (P≤0.05)	0.10		1.65		0.12		0.19		0.14	
CD (P≤0.05)		0.36		5.69		0.43		0.65		0.50

*Significant at P ≤ 0.05, **Critical difference (CD)

Table 2. contd.

Parental line	Equatorial diameter (cm)		Total soluble solids (°Brix)		Titratable acidity (mg/100 ml)		Lycopene (mg/100 g)		Dry matter (%)	
	GCA	Mean	GCA	Mean	GCA	Mean	GCA	Mean	GCA	Mean
PVB-2	0.46*	5.97	0.01	4.17	-0.04*	0.53	0.53*	3.20	0.14*	5.01
CLN 138A	-0.10*	4.35	-0.02	3.85	-0.03*	0.66	0.27*	3.57	0.03	4.69
CLN 138B	0.65*	6.09	0.11*	4.30	-0.08*	0.43	0.09*	3.00	0.15*	4.17
CLN 104	-0.34*	3.62	0.42*	4.80	0.10*	0.75	0.56*	3.97	0.22*	3.04
CLN 17	-0.06	5.59	-0.01	3.71	0.07*	0.66	-0.06	3.30	0.07	4.44
2123D	-0.50*	4.19	-0.13*	2.97	-0.06*	0.69	-1.14*	2.13	-0.48*	3.93
2123C	-0.28*	4.18	-0.38*	3.30	0.04*	0.65	-0.90*	1.96	-0.59*	3.28
PVB-1	0.31*	6.24	-0.17*	4.50	-0.01*	0.48	0.40*	3.50	0.16*	4.90
CLN 154	0.81*	5.45	0.40*	4.47	-0.06*	0.47	0.24*	3.87	-0.16*	4.32
PC	-0.32*	4.22	-0.23*	4.11	0.08*	0.51	0.00	3.10	0.48*	4.40
**CD (g _i) (P≤0.05)	0.08		0.10		0.01		0.08		0.11	
CD (g _i -g _j) (P≤0.05)	0.12		0.14		0.02		0.12		0.16	
CD (P≤0.05)		0.43		0.50		0.07		0.43		0.56

*Significant at P ≤ 0.05, **Critical difference (CD)

The F₁ hybrids had a higher mean and wider range than their parental lines for all the traits. However, the maximum increase was recorded in total yield (47.68%) followed by fruit weight (20.27%), number of locules (15.13%) and titratable acidity (13.73%). For other traits, the average heterosis was less than 10% (Table 3). Heterosis of both positive and negative magnitudes was observed for all the traits. For total yield, 38, 19 and 7 hybrids exhibited significant positive values of MPH, BPH and TPH, respectively. Not even a single hybrid manifested significant negative MPH whereas only 3 hybrids recorded significant negative BPH (Table 4). The promising hybrids along with their TPH were CLN 138A × CLN 138B (31.20%), CLN 138B × 2123C (28.00%), CLN 138A × CLN 154 (24.00%), CLN 138B × PVB-1 (22.80%), CLN 17 × PVB-1 (20.80%), CLN 138B × 2123D (18.80%) and CLN 104 × CLN 154 (16.00%). All of these seven hybrids had significant positive SCA effects (Table 4) reflecting the importance of non-additive gene action in heterosis manifestation for total yield. For fruit weight, 34, 16 and 5 hybrids exhibited significant positive values of MPH, BPH and TPH, respectively. Whereas, there were 3, 15 and 27 hybrids manifesting significant negative values of MPH, BPH and TPH, respectively (Table 4). Out of five hybrids exceeding the top parent for fruit weight, three (CLN 138B × PVB-1, CLN 138A × CLN 154 and CLN 138B × 2123C) were the same that recorded significant positive TPH for total yield revealing that increase in total yield was accompanied by an increase in fruit weight. All of these five hybrids manifested significant positive SCA values (Table 4) signifying the role of non-additive gene action in the expression of heterosis for fruit weight.

Table 3. Mean, and range of parental lines and their F₁ hybrids along with average heterosis for yield and quality traits in ten parental lines of tomato evaluated in half-diallel

Parameter	Total yield (kg plant ⁻¹)	Fruit weight (g)	Number of locules	Pericarp thickness (mm)	Polar diameter (cm)	Equatorial diameter (cm)	TSS (°Brix)	Titratable acidity (mg/100 ml)	Lycopene (mg/100 g)	Dry matter (%)
Parental mean	1.51	75.67	3.37	5.07	5.22	4.99	4.02	0.51	3.16	4.22
Parental range	0.26-2.50	34.33-102.00	2.30-4.22	3.57-6.57	3.94-6.30	3.62-6.24	2.97-4.80	0.43-0.75	1.96-3.97	3.04-5.01
Hybrid mean	2.23	91.01	3.88	5.32	5.27	5.16	4.30	0.58	3.40	4.32
Hybrid range	0.61-3.28	59.67-129.00	2.23-5.70	3.13-8.17	4.30-6.50	3.40-7.20	2.90-5.67	0.27-0.82	1.03-5.50	2.77-5.80
Average heterosis (%)	47.68	20.27	15.13	4.93	0.96	3.41	6.97	13.73	7.59	2.37

Of 45 hybrids, 15 involved low × low combiner parents for total yield. Although none of these exhibited significant positive TPH, there were 13 and 8 hybrids manifesting 27.94-130.77% and 34.38-102.86% MPH and BPH, respectively. This result raises the importance of low combiner parents in heterosis breeding. On the contrary, there were a few cross-combinations viz., PVB-2 × CLN 138B, PVB-2 × CLN 154, CLN 138B × CLN 154, and PVB-1 × CLN 154, which could not express significant heterosis for commercialization but involved parents having medium × high and high × high combiner parents for total yield. In the present study, three parental lines were incorporating *Ty-2* gene viz., CLN 17, 2123D and 2123C. The yield potential of these three lines was significantly different. The line CLN 17 yielded 1.60 kg plant⁻¹ which was substantially higher than 2123D (1.20 kg plant⁻¹)

and 2123C (0.97 kg plant⁻¹). Likewise, the fruit weight of CLN 17 was 86.33g which was significantly higher than that of 2123D (64.67g) and 2123C (60.33g). The line CLN 17 performed better in hybrid combinations than 2123D and 2123C did, making it a better general combiner for fruit yield and fruit weight. Hence, the line CLN 17 performed better than 2123D and 2123C in respect of yield, fruit weight and GCA for yield & fruit weight. However, there were three promising F₁ hybrids involving these lines viz., CLN 138B × 2123C, CLN 138B × 2123D and CLN 17 × PVB-1 which recorded 28.00, 18.80 and 20.80% increase in total yield over top parent, respectively. Therefore, the parental lines carrying *Ty-2* gene alone should not be considered useless and may yield useful hybrid combinations and hence may be included in tomato breeding programs aimed at developing resistance to ToLCV.

There were three parental lines viz., CLN 138A, CLN 138B and CLN 104 carrying two resistant genes *Ty-1* and *Ty-2*. Of these three lines, the yield and fruit weight of CLN 138B (1.97 kg plant⁻¹ and 102.00g) was significantly higher than that of CLN 104 (1.30 kg plant⁻¹ and 61.33g) and CLN 138A (1.17 kg plant⁻¹ and 67.67g). The line CLN 138B had significant positive GCA for yield and fruit weight whereas the other two lines exhibited negative values of GCA for these two traits. So, the line CLN 138B was better than CLN 138A and CLN 104 concerning yield, fruit weight and GCA for yield & fruit weight. The parental line CLN 154 incorporated three resistant genes *Ty-1*, *Ty-2* and *Ty-3* whereas the lines PVB-1 and PVB-2 had unknown resistance genes. The fruit weight of these three lines was at par with each other. However, CLN 154 yielded 2.50 kg plant⁻¹ which was significantly higher than that of PVB-2 (2.13 kg plant⁻¹) and PVB-1 (1.97 kg plant⁻¹). Although all of these three lines had significant positive values of GCA for yield and fruit weight, CLN 154 was better combiner for yield and PVB-1 for fruit weight. The superior performance of CLN 154 as compared to released cultivars (PVB-1 and PVB-2) offers the scope of its commercial release and is, therefore, recommended for multi-location testing across the state.

High yield is one of the most important breeding objectives under disease epiphytotic conditions. Among parents, the line CLN 154 incorporating three resistance genes was the highest yielder (58.65 t ha⁻¹). To cover up the cost of hybrid seeds, it was desirable to identify hybrids yielding significantly higher than the top parent. In this context, seven hybrids exhibiting 16.00-31.20% heterosis over top parent for total yield were identified. These seven hybrids also manifested 16.00-66.95% heterosis over better parent and 52.63-108.92% over mid-parent for total yield. The fruit weight of promising hybrids varied from 82.33 g to 117.33 g which is well within acceptable limits and comparable with that of top parent CLN 154 (89.33 g). The number of locules and pericarp thickness of promising hybrids ranged from 3.33-5.40 and 4.23-7.37 mm, respectively, which were comparable to top parent CLN 154 (4.0, 6.20 mm). The fruit shape of all the promising hybrids was round just like the top parent and round-fruited hybrids are highly acceptable for table purpose. Similarly, the total soluble solids, titratable acidity, lycopene and dry matter of promising hybrids varied from 3.47-5.00°Brix, 0.32-0.59 mg/100 ml, 3.03-5.50 mg/100 g and 3.87-5.30%, respectively, which were comparable with CLN 154 (4.47°Brix, 0.47 mg/100 ml, 3.87 mg/100 g, 4.32%). The desirable horticultural traits of the promising hybrids enhance the feasibility of their commercial acceptability.

Table 4. Specific combining ability (SCA) and heterosis over mid-parent (MPH), better parent (BPH) and top parent (TPH) exhibited by forty five F_1 hybrids of ten parental lines of tomato crossed in half-diallel for total yield and fruit weight

F ₁ hybrid	Total yield					Fruit weight				
	SCA	GCA of parents	MPH	BPH	TPH	SCA	GCA of parents	MPH	BPH	TPH
PVB-2 × CLN 138A	0.11	M × L	45.45*	12.5	-4	-10.29*	H × L	-1.83	-16.55*	-20.91*
PVB-2 × CLN 138B	-0.81*	M × H	-5.85	-9.38	-22.80*	-18.97*	H × H	-11.74*	-14.05*	-14.05*
PVB-2 × CLN 104	-0.09	M × L	26.53*	1.56	-13.2	0.03	H × L	19.41*	-2.41	-7.52*
PVB-2 × CLN 17	0.11	M × L	34.05*	17.19*	0	6.26*	H × M	11.48*	5.52	0
PVB-2 × 2123D	0.08	M × L	32.13*	3.12	-12	4.94*	H × L	17.76*	-1.72	-6.86*
PVB-2 × 2123C	0.62*	M × L	67.74*	21.88*	4	-0.3	H × L	8.70*	-11.72*	-16.34*
PVB-2 × PVB-1	0.05	M × M	22.44*	17.66*	0.4	17.25*	H × H	25.17*	23.45*	16.99*
PVB-2 × CLN 154	-0.11	M × H	13.61*	5.33	5.2	-15.85*	H × M	-11.75*	-15.10*	-19.54*
PVB-2 × PC	0.85*	M × L	111.72*	18.75	1.2	24.66*	H × L	59.59*	8.14*	2.48
CLN138A × CLN138B	0.80*	L × H	108.92*	66.95*	31.20*	0.26	L × H	14.73*	-4.58	-4.58
CLN 138A × CLN 104	-0.42*	L × L	27.94*	21.79	-36.80*	8.26*	L × L	44.19*	37.44*	-8.82
CLN 138A × CLN 17	0.13	L × L	63.90*	41.67*	-9.2	5.33*	L × M	18.83*	5.98	-10.29*
CLN 138A × 2123D	0.40*	L × L	91.56*	88.89*	-9.2	19.17*	L × L	50.63*	47.29*	-2.28
CLN 138A × 2123C	0.64*	L × L	121.50*	102.86*	-5.2	2.93	L × L	23.44*	16.75*	-22.55*
CLN 138A × PVB-1	-0.07	L × M	35.67*	8.29	-14.80*	-12.52*	L × H	-1.03	-14.89*	-21.57*
CLN 138A × CLN 154	0.61*	L × H	68.94*	24.00*	24.00*	22.65*	L × M	41.40*	24.25*	8.82*
CLN 138A × PC	-0.47*	L × L	35.66	-17.14	-61.20*	-8.31*	L × L	21.57*	-8.37	-39.22*
CLN 138B × CLN 104	-0.15	H × L	40.67*	16.95	-8	28.58*	H × L	57.96*	26.47*	26.47*
CLN 138B × CLN 17	-0.01	H × L	44.54*	31.19*	3.2	-3.52*	H × M	4.42	-3.59	-3.6
CLN 138B × 2123D	0.65*	H × L	87.38*	50.85*	18.80*	1.83	H × L	17.60*	-3.92	-3.92
CLN 138B × 2123C	1.02*	H × L	117.69*	62.71*	28.00*	16.91*	H × L	33.89*	6.54*	6.54*
CLN 138B × PVB-1	0.41*	H × M	55.84*	55.67*	22.80*	9.13*	H × H	19.72*	15.03*	15.03*
CLN 138B × CLN 154	-0.14	H × H	25.28*	12	12	-22.03*	H × M	-14.28*	-19.61*	-19.61*
CLN138B × PC	0.18	H × L	85.65*	5.08	-17.20*	9.34*	H × L	39.85*	-6.54*	-6.54*
CLN 104 × CLN 17	0.36*	L × L	70.34*	54.17*	-1.2	-14.85*	L × M	1.14	-13.51*	-26.79*
CLN 104 × 2123D	0.45*	L × L	82.40*	75.64*	-8.8	19.83*	L × L	64.56*	60.31*	1.64
CLN 104 × 2123C	0.54*	L × L	96.48*	71.79*	-10.8	16.91*	L × L	58.36*	57.07*	-5.56
CLN 104 × PVB-1	-0.21	L × M	19.88*	-0.68	-21.60*	-3.54*	L × H	18.88*	-1.77	-9.48*
CLN 104 × CLN 154	0.44*	L × H	52.63*	16.00*	16.00*	-9.37*	L × M	9.29*	-7.84*	-19.28*
CLN 104 × PC	0.40*	L × L	130.77*	38.46*	-28.00*	7.67*	L × L	70.04*	32.61*	-20.26*
CLN 17 × 2123D	0.18	L × L	53.57*	34.38*	-14	-6.27*	M × L	4.64	-8.49*	-22.55*
CLN 17 × 2123C	0.1	L × L	50.19*	20.83	-22.80*	-4.85*	M × L	3.64	-11.97*	-25.49*
CLN 17 × PVB-1	0.71*	L × M	69.19*	53.13*	20.80*	8.03*	M × H	16.82*	12.06*	3.26
CLN 17 × CLN 154	-0.13	L × H	20.49*	-1.33	-1.2	13.87*	M × M	21.83*	19.78*	4.9
CLN 17 × PC	-0.17	L × L	47.31*	-14.58	-45.20*	5.24*	M × L	33.15*	-6.95*	-21.25*
2123D × 2123C	-0.61*	L × L	-12.44	-20.83	-62.00*	-15.50*	L × L	-4.53	-7.73	-41.50*
2123D × PVB-1	-0.27*	L × M	11.67	-10.32	-29.20*	-9.29*	L × H	3.78	-12.41*	-19.28*
2123D × CLN 154	0.24*	L × H	38.92*	2.67	2.8	14.55*	L × M	32.47*	14.18*	0
2123D × PC	-0.14	L × L	53.42*	-6.39	-55.20*	0.59	L × L	41.41*	8.25	-31.37*
2123C × PVB-1	-0.54*	L × M	-7.48	-30.80*	-45.60*	-3.03	L × H	9.08*	-10.46*	-17.48*
2123C × CLN 154	-0.32*	L × H	7.78	-25.33*	-25.20*	6.44*	L × M	19.56*	0.15	-12.28*
2123C × PC	-0.52*	L × L	-0.81	-36.90*	-75.60*	1.34	L × L	40.14*	9.94	-34.97*
PVB-1 × CLN 154	0.01	M × H	19.46*	6.67	6.8	2.85	H × M	11.63*	8.87*	0.32
PVB-1 × PC	0.70*	M × L	106.28*	16.75	-8	10.40*	H × L	43.12*	-2.3	-9.97*
CLN 154 × PC	0.31*	H × L	59.42*	-12	-12	-1.15	M × L	23.11*	-14.79*	-25.37*
**CD ($P \leq 0.05$)	0.21	-	0.31	0.36	0.36	3.34	-	4.96	5.73	5.73
SE (S_{ij})	0.12					1.9				
SE ($S_{ij} - S_{ik}$)	0.17					2.8				
SE ($S_{ij} - S_{kl}$)	0.16					2.67				

*Significant at $P \leq 0.05$, **Critical difference (CD)

Discussion

The cultivated tomato has provided little resistance to the ToLCV (Pico et al., 1998; Ji et al., 2007a). Tolerance was found in Nova (Mayee et al., 1974) and EC 104395 (Varma et al., 1980). Breeding begomovirus-resistant cultivars have involved the introgression of resistance genes from wild tomato species. Among the wild species *L. hirsutum f glabratum* and *L. peruvianum* were highly resistant (Banerjee and Kalloo, 1987). Resistance in *L. pimpinellifolium* LA1921 was found to be monogenic and incompletely dominant, and two epistatic genes governed resistance in *L. hirsutum f glabratum* (B 6013). Two independent genes for resistance seem to be involved in these two-wild species with that of *L. hirsutum f glabaratum* dominant over the other (Banerjee and Kalloo, 1990). Pilowsky and Cohen (1974) studied crosses between a tomato yellow leaf curl virus (ToYLCV) homozygous resistant line of *L. pimpinellifolium* and the susceptible tomato cv Pearson. Inheritance of ToYLCV was studied by Hassan et al. (1984) in the interspecific crosses between *L. esculentum* Mill. cv UC 82 × *L. cheesmanii* ssp. *minor* (Hook) C H Mill. cv LA 1401, and *L. esculentum* cv. VF 145-B-7879 × *L. hirsutum* Humb. & Bonpl. cv LA 386. They artificially inoculated the genetic population with ToYLCV before transplanting and later evaluated under field conditions. They found that resistance derived from *L. cheesmanii* seems to be recessive, and resistance derived from *L. hirsutum* is dominant and controlled by more than one gene. Dhaliwal and Cheema (2011) have also reported 20.93-58.75% heterosis over better parent for total yield in promising F1 hybrids tested under ToLCV infested conditions. The high yield and disease resistance of F1 hybrids must be accompanied by good horticultural traits like shape, size, flavour etc. for them to become commercially acceptable. Furthermore, these results are in accordance with the result for the other member of Solanaceae, i.e. eggplant (Kaushik et al., 2018; Kaushik 2019)

Banerjee and Kalloo (1987) studied the inheritance of ToLCV resistance in interspecific crosses between ToLCV resistant *L. hirsutum f glabratum* line B6013 and five susceptible cultivars (HS101, HS102, HS110, Pusa Ruby and Punjab Chhuhara) of *L. esculentum*. They reported that resistance derived from *L. hirsutum f glabratum* B6013 based on two epistatic genes one from the wild parent and another from the cultivated one. The inheritance of tolerance of ToYLCV, deriving from the wild tomato *L. peruvianum*, was studied by Pilowsky and Cohen (1990) crossing the cultivated tomato (*L. esculentum* Mill.) line M-60 (ToYLCV-tolerant) with line M-10 (ToYLCV-susceptible line). Genetic data indicated that 5 recessive genes controlled tolerance. Nagaraja et al. (1996) estimated the gene effects for fruit yield, its components and inheritance of leaf curl virus resistance in two interspecific crosses between *L. esculentum* cultivars Arka Saurabh and Arka Vikas and tomato leaf curl virus resistant *L. hirsutum*. They concluded that an additive-dominance model accounted for most of the variation among generations for days to tomato leaf curl virus symptoms expression in both the crosses.

The inheritance of resistance to ToLCV disease was assessed by Nainar and Pappiah (2002) under field conditions in eight crosses involving susceptible tomato cultivars PKM1, CO.2, CO.3 and Pusa Ruby and resistant wild parent's *L. hirsutum* and *L. pimpinellifolium*. They reported that the resistance in *L. hirsutum* was controlled by three recessive genes and a single incomplete dominant gene in *L. pimpinellifolium*.

Shekara et al. (2003) studied the inheritance of resistance to tomato leaf curl virus in tomato using triple test cross analysis. The genotypes consisted of crosses between 148

resistant testers and the susceptible cultivar Arka Abha and crosses between the resistant cultivar ATY-1 and the susceptible cultivars Arka Sourabh. The importance of the additive genetic variance for resistance was observed. The magnitude of the additive genetic component was higher than the dominance component and suggested pedigree selection method for the development of cultivars resistant to tomato leaf curl virus.

Resistance to ToYLCV was studied by Castro et al. (2007) in a cross between *S. lycopersicum* × *S. pimpinellifolium* UPV16991. Crosses between four breeding lines susceptible to ToYLCV and L102 were also performed to study the dominance of the resistance in *S. lycopersicum* genetic backgrounds. Response to ToYLCV infection of P₁, P₂, F₁, F₂, BC₁, and BC₂ generations fitted, for this line, a monogenic control with partial recessiveness and incomplete penetrance. Hazra and Nath (2008) conducted an experiment to evaluate 25 tomato genotypes for resistance to tomato leaf curl virus and concluded that percent disease incidence and co-efficient of infection in the genotypes was highest in early autumn (planting in last week of August), followed by spring-summer (planting in first week of February) and autumn-winter (planting in second week of October) seasons. The extent of heterosis for tospovirus resistance, yield and associated characters was studied by Kumar et al. (2009) by using line × tester mating. The lines carrying Ty-2 gene have been reported to be susceptible to bipartite tomato-infecting begomoviruses (Giordano et al., 1998; Prasanna et al., 2015).

Ji and Scott (2006) mapped Ty-3 gene on the long arm of chromosome 6, between cLED-31-P16 and T1079 markers. Recently, Kadirvel et al. (2013) identified new locus (qTy10.1) on chromosome 10 in the line FLA456, named it as Ty-6. Similar to our results a series of lines pyramided by Prasanna et al. (2014) using *S. habrochaites* derived resistance (Ty-2), and *S. chilense* derived resistance (Ty-3). The pyramided lines and Ty-3 carrying lines exhibited a high level of resistance that could be used as critical genetic stocks for resistance breeding. Also, Shankarappa et al. (2008) developed two hybrids viz., BLRH-3 and BLRH-16 resistant to ToLCV both in the glasshouse and the field conditions. Based on phenotypic survey and virus quantification two highly resistant hybrids SJ12 and RFT112 were identified (Tabein et al., 2017). Recently, Elbaz et al. (2016) found that the entries with Ty-1/Ty-3 + Ty-2 offered the highest levels of resistance to TYLCV. Whereas, Rubio et al. (2016) determined and quantified the effect of Ty-1 gene introgression on yield and quality of tomatoes. Ty-1 introgression negatively affected the yield attributes.

Tomás et al. (2011) screened for ToYLCVD resistance under high disease pressure generated by natural infection in the field. They have concluded two independent loci, one dominant and one recessive, were associated with EELM- 889 resistance. The study showed these loci to be distinct from that of the resistance gene (Ty-1) deployed in resistant tomato cultivars. Therefore, both kinds of resistance could be combined to provide improved resistance to ToYLCVD. Dhaliwal and Cheema (2011) have also reported that hybrids were manifesting significant standard heterosis for yield in tomato also expressed significant standard heterosis for fruit weight. Therefore, it is advisable to handle these cross-combinations by pedigree selection to exploit additive gene action to find significant desirable improvement in yield along with resistance to ToLCV (Dhaliwal and Cheema, 2011). In our study, the hybrids identified should not be resorted to selection in segregating generations as their superior performance is attributed to the involvement of non-fixable gene effects.

Conclusions

Extensive and significant difference in the performance of lines carrying different combinations of resistance genes (Ty-X) against ToLCV. The top parent CLN 154 yielding significantly higher than released varieties along with seven F₁ hybrids manifesting 16 to 31% top parent heterosis for total yield can be recommended after multi-location evaluations. Overall, this study provides useful information on the successful leaf curl virus resistant gene combinations under the north-Indian conditions.

Acknowledgements. Authors are thankful to AVRDC – The World Vegetable Centre, Taiwan, for kindly providing the seeds of CLN lines having variable degree of resistance to ToLCV.

REFERENCES

- [1] Banerjee, M. K., Kalloo, G. (1987a): Inheritance of resistance to tomato leaf curl virus in *Lycopersicon hirsutum* f. *glabratum*. – Euphytica 36: 581-84.
- [2] Banerjee, M. K., Kalloo, G. (1987b): Sources and inheritance of resistance to leaf curl virus in *Lycopersicon*. – Theoretical and Applied Genetics 73: 707-10.
- [3] Banerjee, M. K., Kalloo, G. (1990): Nature of resistance to tomato leaf curl virus (TLCV) in two species of *Lycopersicon*. – Haryana Agricultural University Journal of Research 20: 225-28.
- [4] Castro, P. A., Diez, M. J., Nuez, F. (2007): Inheritance of tomato yellow leaf curl virus resistance derived from *Solanum pimpinellifolium* UPV16991. – Plant Disease 91: 879-85.
- [5] Cheema, D. S., Dhaliwal, M. S. (2010): Punjab Varkha Bahar 1 and Punjab Varkha Bahar 2: New varieties of tomato resistant to ToYLCV. – Journal of Research, Punjab Agricultural University 47: 116-117.
- [6] Elbaz, M., Hanson, P., Fgaier, S., Laarif, A. (2016): Evaluation of tomato entries with different combinations of resistance genes to tomato yellow leaf curl disease in Tunisia. – Plant Breed. 55(6): 1-7.
- [7] FAOSTAT (2018): <http://www.fao.org/faostat/en/#data/QC>. – Accessed 12.11.18.
- [8] Gaikwad, K. A., Cheema, D. S., Sharma, A., Dhaliwal, M. S. (2011a): Reaction of elite tomato (*Solanum lycopersicum* L.) germplasm against tomato leaf curl virus disease. – Acta Horticulturae 157-161. <https://doi.org/10.17660/ActaHortic.2011.914.28>.
- [9] Gaikwad, K. A., Sharma, A., Cheema, D. S. (2011b): Molecular detection and characterization of leaf curl virus infecting tomato in Punjab India. – Acta Horticulturae 153-156. <https://doi.org/10.17660/ActaHortic.2011.914.27>.
- [10] Garg, N., Cheema, D. S. (2011): Assessment of fruit quality attributes of tomato hybrids involving ripening mutants under high temperature conditions. – Scientia Horticulturae 131: 29-38.
- [11] Giordano, L. de B., Bezerra, I. C., Ferreira, P. T. O., Borges Neto, C. R. (1998): Breeding tomatoes for resistance to whitefly-transmitted geminivirus with bipartite genome in Brazil. – VI International Symposium on Processing Tomato & Workshop on Irrigation & Fertigation of Processing Tomato, pp. 357-360.
- [12] Griffing, B. (1956): Concept of general and specific combining ability in relation to diallel crossing systems. Australian Journal of Biological Sciences – 9: 463-493. <https://doi.org/10.1071/bi9560463>.
- [13] Hanson, P., Green, S. K., Kuo, G. (2006): Ty-2, a gene on chromosome 11 conditioning geminivirus resistance in tomato. – Tomato Genetics Cooperative Report 56: 17-18.
- [14] Hanson, P., Lu, S.-F., Wang, J.-F., Chen, W., Kenyon, L., Tan, C.-W., Tee, K. L., Wang, Y. Y., Hsu, Y. C., Schafleitner, R. (2016): Conventional and molecular marker-assisted

- selection and pyramiding of genes for multiple disease resistance in tomato. – *Scientia Horticulturae* 201: 346-354.
- [15] Hassan, A. A., Laterrot, H., Mazyed, H. M., Nassor, S. H., Sims, W. L., Nakhla, M. K. (1984): Genetics and heritability of tomato yellow leaf curl virus tolerance derived from *Lycopersicon pimpinellifolium*. – European Assn. for Res. on Plant Breeding. Tomato Working Group, Wageningen, Netherlands.
- [16] Hazra, P., Nath, S. (2008): Source of resistance in tomato (*Lycopersicon esculentum* Mill.) and inheritance of host resistance for tomato leaf curl disease. – *Indian Journal of Agricultural Sciences* 78: 690-94.
- [17] Hong, Y. G., Harrison, B. D. (1995): Nucleotide sequences from tomato leaf curl viruses from different countries: evidence for three geographically separate branches in evolution of the coat protein of whitefly-transmitted geminiviruses. – *Journal of General Virology* 76(Pt 8): 2043-2049. <https://doi.org/10.1099/0022-1317-76-8-2043>.
- [18] Horowitz, A. R., Kontsedalov, S., Khasdan, V., Ishaaya, I. (2005): Biotypes B and Q of *Bemisia tabaci* and their relevance to neonicotinoid and pyriproxyfen resistance. – *Archives of Insect Biochemistry and Physiology* 58: 216-225. <https://doi.org/10.1002/arch.20044>.
- [19] Hutton, S. F., Scott, J. W. (2014): Ty-6, a major begomovirus resistance gene located on chromosome 10. – *Tomato Genetics Cooperative Report* 64: 14-18.
- [20] Hutton, S. F., Scott, J. W., Schuster, D. J. (2012): Recessive resistance to tomato yellow leaf curl virus from the tomato cultivar Tyking is located in the same region as Ty-5 on Chromosome 4. – *HortScience* 47: 324-327.
- [21] Ji, Y. F., Scott, J. W., Hanson, P., Graham, E., Maxwell, D. P. (2007a): Sources of Resistance, Inheritance and Location of Genetic Loci Conferring Resistance to Members of the Tomato-Infecting Begomoviruses. – In: Czosnek, H. (ed.) *Tomato Yellow Leaf Curl Disease*, Springer, Dordrecht, pp: 343-62.
- [22] Ji, Y., Schuster, D. J., Scott, J. W. (2007b): Ty-3, a begomovirus resistance locus near the Tomato yellow leaf curl virus resistance locus Ty-1 on chromosome 6 of tomato. – *Molecular Breeding* 20: 271-284.
- [23] Ji, Y., Scott, J. W., Schuster, D. J., Maxwell, D. P. (2009): Molecular mapping of Ty-4, a new tomato yellow leaf curl virus resistance locus on chromosome 3 of tomato. – *Journal of the American Society for Horticultural Science* 134: 281-288.
- [24] Kadirvel, P., de la Pana, R., Schaffeitner, R., Huang, S., Geethanjali, S., Kenyon, L., Tsai, W., and Hanson, P. (2013): Mapping of QTLs in tomato line FLA456 associated with resistance to a virus causing yellow leaf curl disease. – *Euphytica* 190: 297-308.
- [25] Kaushik, P., Dhaliwal, M. S. (2018): Diallel analysis for morphological and biochemical traits in tomato cultivated under the influence of tomato leaf curl virus. – *Agronomy* 8: 153. <https://doi.org/10.3390/agronomy8080153>.
- [26] Kaushik, P., Dhaliwal, S. M., Jindal, K. S., Srivastava, A., Tyagi, V., Brar, S. N., Rana, K. M. (2015): Heterosis and leaf curl virus resistance in rainy season tomato under North Indian conditions. – *African Journal of Agricultural Research* 10: 2763-2772. <https://doi.org/10.5897/AJAR2014.9133>.
- [27] Kaushik, P., Plazas, M., Prohens, J., Vilanova, S., Gramazio, P. (2018): Diallel genetic analysis for multiple traits in eggplant and assessment of genetic distances for predicting hybrids performance. – *Plos One* 13: e0199943. <https://doi.org/10.1371/journal.pone.0199943>.
- [28] Kaushik, P. (2019): Line × Tester Analysis for Morphological and Fruit Biochemical Traits in Eggplant (*Solanum melongena* L.) Using Wild Relatives as Testers. – *Agronomy* 9: 185. doi:10.3390/agronomy9040185.
- [29] Kirthi, N., Maiya, S. P., Murthy, M. R. N., Savithri, H. S. (2002): Evidence for recombination among the tomato leaf curl virus strains/species from Bangalore, India. – *Archives of Virology* 147: 255-272.

- [30] Kumar, K. H. Y., Patil, S. S., Dharmatti, P. R., Byadagi, A. S., Kajjidoni, S. T., Patil, R. H. (2009): Estimation of heterosis for tospovirus resistance in tomato. – Karnataka Journal of Agricultural Sciences 22: 1073-75.
- [31] Mayee, C. D., Kanwar, J. S., Nandpuri, K. S. (1974): The comparative performance of different genotypes of tomato vis-a-vis leaf curl and mosaic. – Journal of Research (PAU) 11: 362-64.
- [32] Moriones, E., Praveen, S., Chakraborty, S. (2017): Tomato Leaf Curl New Delhi Virus: An emerging virus complex threatening vegetable and fiber crops. – Viruses 9. <https://doi.org/10.3390/v9100264>.
- [33] Muniyappa, V., Venkatesh, H. M., Ramappa, H. K., Kulkarni, R. S., Zeidan, M., Tarba, C. Y., Ghanim, M., Czosnek, H. (2000): Tomato leaf curl virus from Bangalore (ToLCV-Ban4): sequence comparison with Indian ToLCV isolates, detection in plants and insects, and vector relationships. – Archives of Virology 145: 1583-1598.
- [34] Nagaraja, T. E., Kulkarni, R. S., Prasad, S. G., Basavaraja, G. T. (1996): Estimates of gene effects for fruit yield its components and inheritance in two interspecific crosses of tomato. – Crop Improvement 23: 71-74.
- [35] Nainar, P., Pappiah, C. M. (2002): Inheritance of resistance to tomato leaf curl virus disease (ToLCV) in the segregating generations of eight crosses of tomato (*Lycopersicon esculentum* Mill.). – South Indian Horticulture 50: 72-77.
- [36] Pico, B. M., Diez, J., Nuez, F. (1998): Evaluation of whitefly-mediated inoculation techniques to screen *Lycopersicon esculentum* and wild relatives for resistance to tomato yellow leaf curl virus. – Euphytica 101: 259-71.
- [37] Picó, B., Díez, M. J., Nuez, F. (1996): Viral diseases causing the greatest economic losses to the tomato crop. II. The tomato yellow leaf curl virus - a review. – Scientia Horticulturae 67: 151-196. [https://doi.org/10.1016/S0304-4238\(96\)00945-4](https://doi.org/10.1016/S0304-4238(96)00945-4).
- [38] Pilowsky, M., Cohen, S. (1974): Inheritance of resistance to tomato yellow leaf curl virus in tomatoes. – Phytopathology 64: 632-672.
- [39] Pilowsky, M., Cohen, S. (1990): Tolerance to tomato yellow leaf curl virus derived from *Lycopersicon peruvianum*. – Plant Disease 4: 248-50.
- [40] Prasanna, H. C., Sinha, D. P., Rai, G. K., Krishna, R., Kashyap, S. P., Singh, N. K., Singh, M., Malathi, V. G. (2014): Pyramiding Ty-2 and Ty-3 genes for resistance to monopartite and bipartite tomato leaf curl viruses of India. – Plant Pathol. 10: 1-10.
- [41] Prasanna, H. C., Kashyap, S. P., Krishna, R., Sinha, D. P., Reddy, S., Malathi, V. G. (2015): Marker assisted selection of Ty-2 and Ty-3 carrying tomato lines and their implications in breeding tomato leaf curl disease resistant hybrids. – Euphytica 204: 407-418. <https://doi.org/10.1007/s10681-015-1357-8>.
- [42] Rubio, F., Alonso, A., Martínez, S. G., Ruiz, J. R. (2016): Introgression of virus-resistance genes into traditional Spanish tomato cultivars (*Solanum lycopersicum* L.): Effects on yield and quality. – Scientia Horticulturae 198: 183-190.
- [43] Shankarappa, K. S., Sriharsha, Rangaswamy, K. T., Aswathanarayana, D. S., Prameela, H. A., Kulkarni, R. S., Muniyappa, V., Rao, A. M., Maruthi, M. N. (2008): Development of tomato hybrids resistant to tomato leaf curl virus disease in South India. – Euphytica 164: 531-539. <https://doi.org/10.1007/s10681-008-9750-1>.
- [44] Sharma, J. R. (2006): Statistical and Biometrical Techniques in Plant Breeding. – New Age International Publisher, New Delhi.
- [45] Shekara, A. C. C., Kulkarni, R. S., Muniyappa, V. (2003): Triple test cross analysis of tomato leaf curl virus resistance in tomato (*Lycopersicon esculentum* Mill.). – Indian Journal of Genetics 63: 185-86.
- [46] Singh, R. K., Rai, N., Singh, M. J. I., Singh, S. N., Srivastava, K. (2014): Genetic analysis to identify good combiners for ToLCV resistance and yield components in tomato using interspecific hybridization. – J Genet 93(3): 623-629.

- [47] Singh, R. K., Rai, N., Singh, M., Saha, S., Singh, S. N. (2015): Detection of tomato leaf curl virus resistance and inheritance in tomato (*Solanum lycopersicum* L.). – *The Journal of Agricultural Science* 153: 78-89. <https://doi.org/10.1017/S0021859613000932>.
- [48] Tabein, S., Behjatnia, S. A., Laviano, L., Pechioni, N., Accotto, G. P., Noris, E., Miozzi, L. (2017): Pyramiding Ty-1/Ty-3 and Ty-2 in tomato hybrids dramatically inhibits symptom expression and accumulation of tomato yellow leaf curl disease inducing viruses. – *Arch. Phytopathol. Plant Prot.* 315: 1-15.
- [49] Tomás, D. M., Cañizares, M. C., Abad, J., Muñoz, R. F., Moriones, E. (2011): Resistance to Tomato yellow leaf curl virus accumulation in the tomato wild relative *Solanum habrochaites* associated with the C4 viral protein. – *Molecular Plant-Microbe Interactions Journal* 24: 849-61.
- [50] Varma, A., Malathi, V. G. (2003): Emerging geminivirus problems: a serious threat to crop production. – *Annals of Applied Biology* 142: 145-164.
- [51] Verlaan, M. G., Hutton, S. F., Ibrahim, R. M., Kormelink, R., Visser, R. G. F., Scott, J. W., Edwards, J. D., Bai, Y. (2013): The Tomato Yellow Leaf Curl Virus resistance genes Ty-1 and Ty-3 are allelic and code for DFDGD-Class RNA-dependent RNA Polymerases. – *PLOS Genetics* 9: e1003399. <https://doi.org/10.1371/journal.pgen.1003399>.
- [52] Zamir, D., Ekstein-Michelson, I., Zakay, Y., Navot, N., Zeidan, M., Sarfatti, M., Eshed, Y., Harel, E., Pleban, T., van-Oss, H., Kedar, N., Rabinowitch, H. D., Czosnek, H. (1994): Mapping and introgression of a tomato yellow leaf curl virus tolerance gene, TY-1. – *Theoretical and Applied Genetics* 88: 141-146. <https://doi.org/10.1007/BF00225889>.

ELEVATED TEMPERATURE INDUCED CHANGE OF NON-POINT SOURCE POLLUTANTS IN PADDY WATER

HONG, S.-C.* – JANG, E. S. – CHOI, S.-K. – CHOI, D.-H. – HUR, S. O.

*Climate Change & Agroecology Division, National Institute of Agricultural Sciences
Wanju 55365, Republic of Korea*

**Corresponding author*

e-mail: schongcb@korea.kr; phone: +82-63-238-2501; fax: +82-63-238-3823

(Received 14th Jan 2019; accepted 28th Feb 2019)

Abstract. Higher temperature could induce biological effects in many areas of agriculture. The objective of this study is to investigate the effects of elevated temperature on nutrients and non-point source pollutants in paddy water and soil. Nitrogen and phosphorus were applied based on the recommended application amounts for rice cultivation and there was an unfertilized plot as a control. Paddy soils were flooded with distilled water in an incubator for eight weeks. Temperature treatments included ambient as a control, ambient plus 2°C, and ambient plus 4°C. Soil NH₄-N content after elevated temperature treatment was high in sandy loam soil and soil NO₃-N content after elevated temperature treatment was high in clay loam soil. Elevated temperatures induced increments of water total nitrogen (T-N) concentration for no chemical fertilization, standard fertilization, and standard fertilization + 100% in sandy loam soil. T-N concentration dissolved in distilled water in rice straw of ambient + 2°C temperature increased by 24% more than that of the control temperature treatment, and total phosphorus (T-P) concentration of ambient + 4°C temperature increased by 16%. Thus, it was considered that water soluble T-N and T-P of rice residue could be released easily by rain from agricultural fields.

Keywords: *higher temperature, nutrient, rice paddy, straw, water soluble nutrient*

Introduction

The Special Report on Global Warming of 1.5°C (SR15) was approved on October 5, 2018 at the 48th session of the Intergovernmental Panel on Climate Change (IPCC) held in Incheon, Republic of Korea. This IPCC report was prepared by 99 authors and editors from 40 countries from around the world, and it is based on over 6,000 scientific references. The key point of this special report is that human activity has induced about 1°C (0.8~1.2°C) global warming at present compared with pre-industrialization times; and, if the current speed of warming continues, the rise will be over 1.5°C in 2030~2052. Also, global warming is different depending on region and time, and extreme weather changes were detected during global warming of 0.5°C to the present. In order to reduce global warming within 1.5°C, carbon dioxide (CO₂) emissions should achieve net zero. Temperature is the most important factor affecting plant growth and yield and every biological process changes depending on temperature (Cross and Zuber, 1972; Yan and Hunt, 1999). Generally, the relationship between air temperature and soil temperature is positive (Groffman et al., 2009), increasing temperature lowers soil moisture (Brzostek et al., 2012), and net nitrogen mineralization was shown to increase depending on higher temperature in an incubation experiment (Pendall et al., 2004), or not (Niklinska et al., 1999). Elevated temperature increases nitrogen mineralization by 45%~52% (Rustad et al., 1998) and net nitrification by 32% (Bai et al., 2013). Higher temperature affects nitrogen leaching by increasing NO₃⁻ solubility and affects the frequency of soil freezing and thawing (Bai and Houlton, 2009).

Nutrient input materials for crop cultivation are chemical fertilizers, cow manure compost, pig manure compost, and various types of organic compost. Leaching of total nitrogen (T-N) and total phosphorus (T-P) by runoff from cultivated land acts as a non-point pollution source when they move out of the agricultural water system. The amount of non-point pollution sources from rice paddy is estimated at 3 kg·ha⁻¹ of nitrogen and 2 kg·ha⁻¹ of phosphorus (Shin, 2001; Kim, 2008; Jung, 2013). Soil loss and muddy water from rain are the factors that most affect management of the aqua-ecosystem and water quality control for drinking water sources in an increasingly significant way.

In a higher temperature environment, there could be changes in the decomposition, uptake by crop, volatilization, and runoff of nutrient input materials for crop cultivation. Therefore, this study was conducted to investigate changes in rice cultivation water as a non-point pollutant source under an elevated temperature environment.

Materials and Methods

Fertilization

This study was conducted from June to November 2017 at the National Institute of Agricultural Sciences (NIAS) in Wanju (Lat 35.834, Lon 127.038), Republic of Korea. The soils used were sandy loam and clay loam. Treatment consisted of a control with no added chemical fertilizer, chemical fertilizer, and chemical fertilizer plus 100% increase of the chemical fertilizer. A 50 ml plastic tube was filled with 40 g of soil, which was treated with chemical fertilizer and then distilled water was poured into the tube. The chemical properties of the soils used in this study are shown in *Table 1*.

Table 1. Chemical properties of soils used in this study

Soil property	pH (1:5)	EC (dS/m)	OM (g/kg)	Av. P ₂ O ₅ (mg/kg)	Ca	Mg	K	Na
					Ex. cations (Cmol ⁺ /kg)			
Sandy loam	6.8	0.74	4	54	1.3	3.7	0.54	1.49
Clay loam	6.5	0.53	22	82	4.3	1.8	0.35	0.13

Temperature treatment

The weather data used for the elevated temperature manipulation was provided by the Buraeing weather station located in Buraeing-myeon, Kimje-si, Jeonbuk province.

In order to calculate the day temperature treatment, the average maximum temperatures from July to September over a ten-year period (2007~2016) were calculated; and to calculate the night temperature treatment, the average minimum temperatures from July to September over a ten-year period (2007~2016) were calculated.

Temperature treatment was conducted from May 23, 2017 for eight months using an incubator. Temperature treatment with the incubator was over ten steps a day for 144 minutes each. Day and night temperatures of the ambient were 25°C /18°C, ambient + 2°C were 27°C /20°C, and ambient + 4°C were 29°C /22°C, respectively (*Table 2*).

Table 2. Elevated temperature treatment in this study at each time by using an incubator

Time (hour : minute)	Ambient	Ambient + 2°C	Ambient + 4°C
01 : 44	18	20	22
04 : 08	17	19	21
06 : 32	19	21	23
08 : 56	19	21	23
11 : 20	24	26	29
13 : 44	26	28	30
16 : 08	26	28	30
18 : 32	25	27	29
20 : 56	24	26	28
23 : 20	19	21	23

Sampling and analysis

Soil pH and EC were measured by using a pH meter (Model 720A, Orion) and an EC meter (Model 145A, Orion). NH₄-N concentration of soil was measured by the indophenol-blue method, NO₃-N concentration of soil was measured by the chromotropic acid method, and available phosphorus concentration of soil was measured by the Lancaster method (RDA, 2010). For analysis of nutrient content, 80 ml of distilled water was added to 40 g of soil, and the treated water was analysed every two weeks for a total of 4 times on June 6, June 20, July 4, and July 18.

In order to analyse the amount of T-N and T-P concentration of straw leachate in response to elevated temperature, 2 g of straw was soaked with 70 ml of distilled water, and then after 1, 3, 5, and 7 days the water was sampled. T-N concentrations were measured by using a chromotropic acid method kit (C-mac, Korea) at 410 nm, and T-P concentrations were measured by using a molybdovanadate method kit (C-mac, Korea) at 420 nm.

Results and Discussion

Soil Nitrogen

Accumulated NH₄-N concentration was determined every two weeks in soil applied with chemical fertilizer under elevated temperature. The results (*Figure 1*) show that the NH₄-N concentration of no fertilization and standard fertilization treatment with ambient + 2°C and ambient + 4°C treatment was higher than that with the control temperature treatment in sandy loam soil. The NH₄-N concentration of no fertilization with ambient + 2°C and ambient + 4°C treatment was higher than that with the control temperature treatment in clay loam soil.

The NH₄-N concentration of standard fertilization and standard fertilization + 100 % with ambient + 2°C and ambient + 4°C treatment was lower than the control temperature treatment in clay loam soil.

Also, the NH₄-N concentration of no fertilization and standard fertilization was higher in sandy loam than in clay loam soil with an elevated temperature (ambient + 2°C and ambient + 4°C treatment).

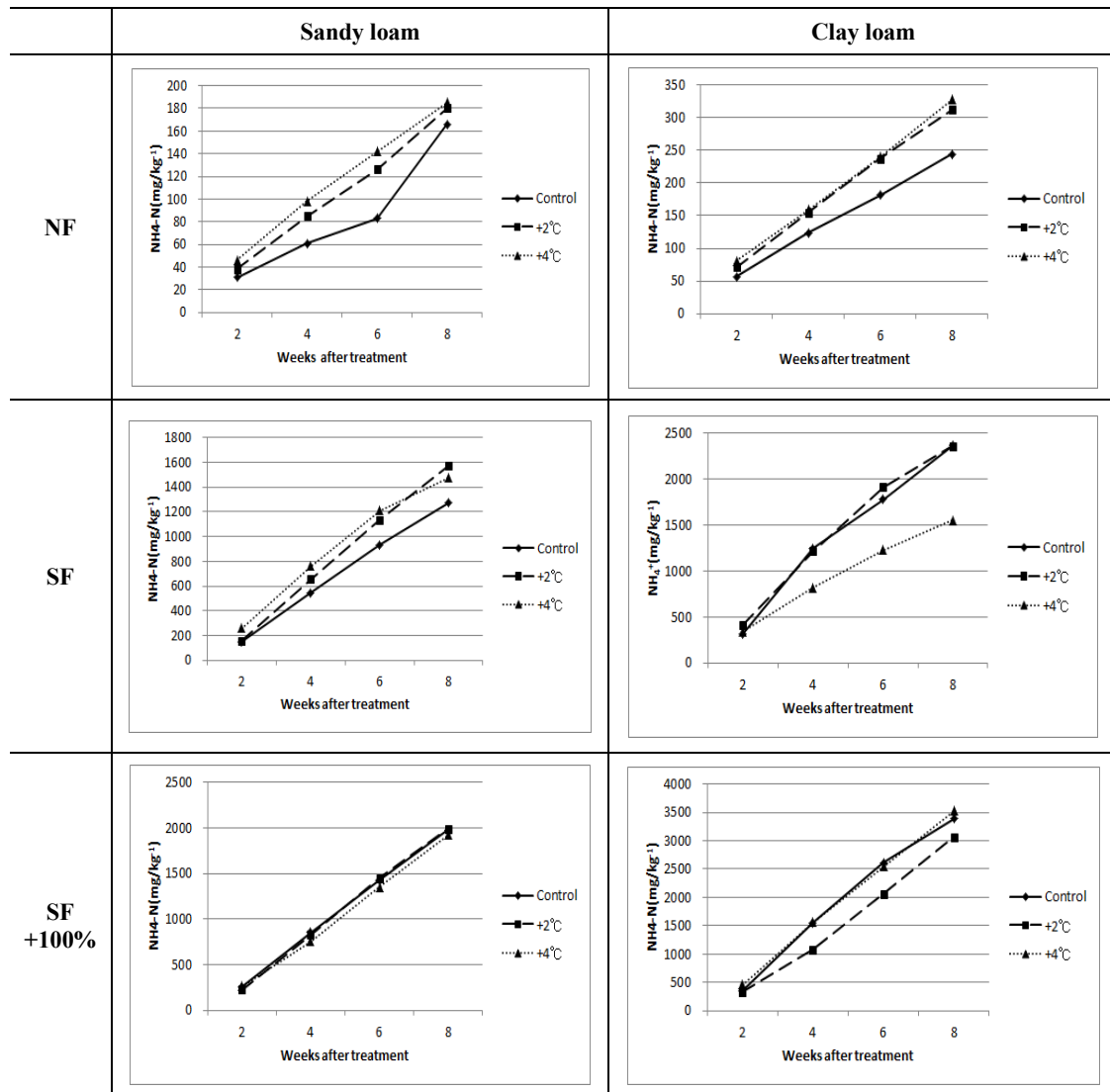


Figure 1. Concentration of $\text{NH}_4\text{-N}$ of soil treated with elevated temperature for 8 weeks, NF: No fertilization, SF: Standard fertilization, SF + 100%: Standard fertilization plus 100 percent increase

Accumulated $\text{NO}_3\text{-N}$ concentration was determined every two weeks in soil with applied chemical fertilizer under elevated temperature. The results (Figure 2) show that the $\text{NO}_3\text{-N}$ concentration of no fertilization treatment in ambient + 2°C and ambient + 4°C was higher than that with the control temperature treatment in sandy loam soil. The $\text{NO}_3\text{-N}$ concentration of standard fertilization treatment in ambient + 4°C was higher than that of the control temperature treatment in sandy loam soil.

The $\text{NO}_3\text{-N}$ concentration of no fertilization, standard fertilization, standard fertilization + 100% under ambient + 2°C and ambient + 4°C was higher than that of the control temperature treatment in clay loam soil.

Rustad et al. (2001) reported that elevated temperature increases soil net mineralization by 45%~52%, and Bai et al. (2013) reported that elevated temperature increases net nitrification by 32%. Rising temperature increase the availability of $\text{NO}_3\text{-N}$ and affects nitrogen leaching by changing the frequency of soil freezing and thawing (Bai and

Houlton, 2009). Through various incubation experiments, net nitrogen mineralization increased in relation to increasing temperature (Pendall et al., 2004), or not (Niklinska et al., 1999).

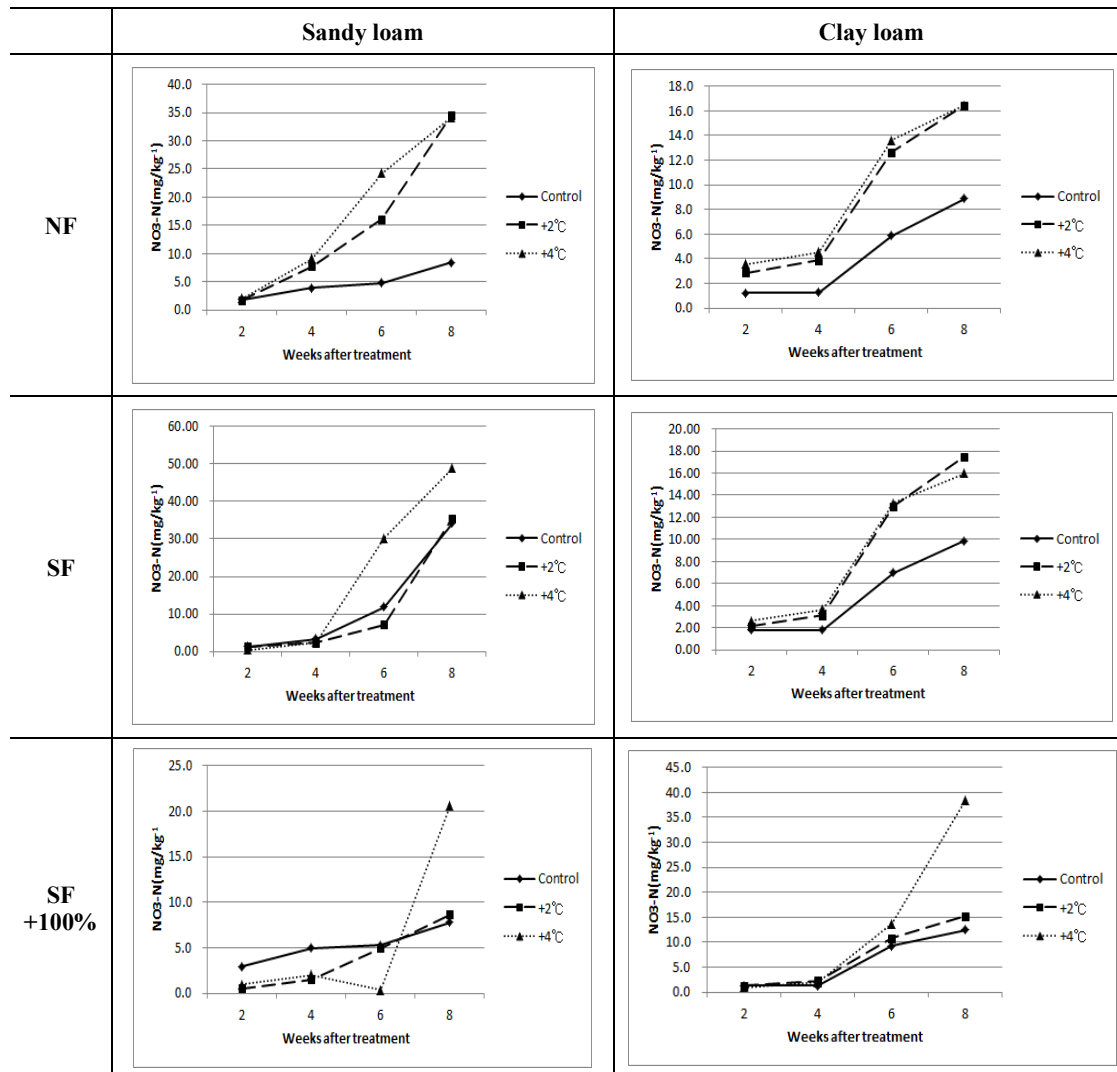


Figure 2. Concentration of NO₃-N of soil treated with elevated temperature for 8 weeks, NF: No fertilization, SF: Standard fertilization, SF + 100 %: Standard fertilization plus 100 percent increase

Nitrogen, Phosphorus of Water

In an elevated temperature environment, accumulated T-N concentration was determined every two weeks in soil water treated with chemical fertilizer. The results (Figure 3) show that elevated temperature induced T-N concentration increases with no chemical fertilizer treatment, standard fertilization, and standard fertilization + 100 % in sandy loam soil. Elevated temperature showed a T-N concentration increase only with standard fertilization in clay loam soil.

These results are similar to results from research showing that nitrification is activated by up-regulated soil temperature treatment (Verburg et al., 1999), nitrogen mineralization

and amount of nitrification increase in relation to time at a depth of 15~30 cm, and nitrogen mineralization and amount of nitrification are greater at the surface soil layer than the deep soil layer (Shin and Reddy, 1997). Also, Saad and Conrad (1993) reported that 25~30°C was the optimal temperature range for nitrification and denitrification in a microbial experiment.

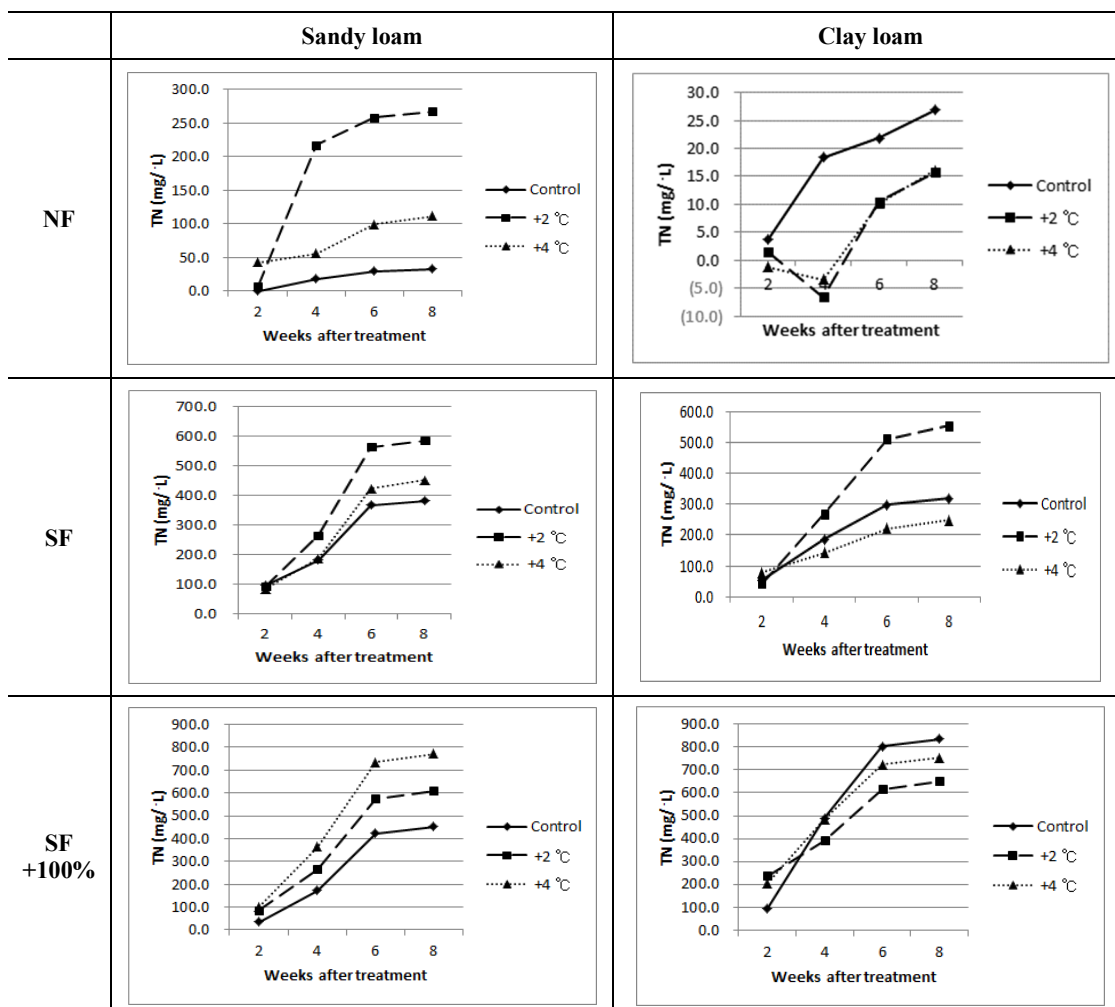


Figure 3. Concentration of total nitrogen (T-N) of water treated with elevated temperature for 8 weeks. NF: No fertilization, SF: Standard fertilization, SF + 100 %: Standard fertilization plus 100 percent increase

In an elevated temperature environment, accumulated T-P concentration was determined every two weeks in soil water treated with chemical fertilizer. The results (Figure 4) show that elevated temperature treatment of ambient + 2°C and ambient + 4°C with no fertilization treatment increased T-P in sandy soil, but no such tendency was shown for T-P content of water in clay loam soil.

Nutrient leaching of straw

The accumulated nutrient concentration of leachate from straw was determined after treatment in an elevated temperature environment for seven days. The results (Figure 5)

show that T-N concentration with the control temperature treatment was 3.2 mg/L⁻¹, while that with the ambient + 2°C treatment was 4.0 mg/L⁻¹, an increase of 24%.

T-P concentration with the control temperature treatment was 3.4 mg/L⁻¹, while that with the ambient + 4°C treatment was 4.1 mg/L⁻¹, an increase of 16%.

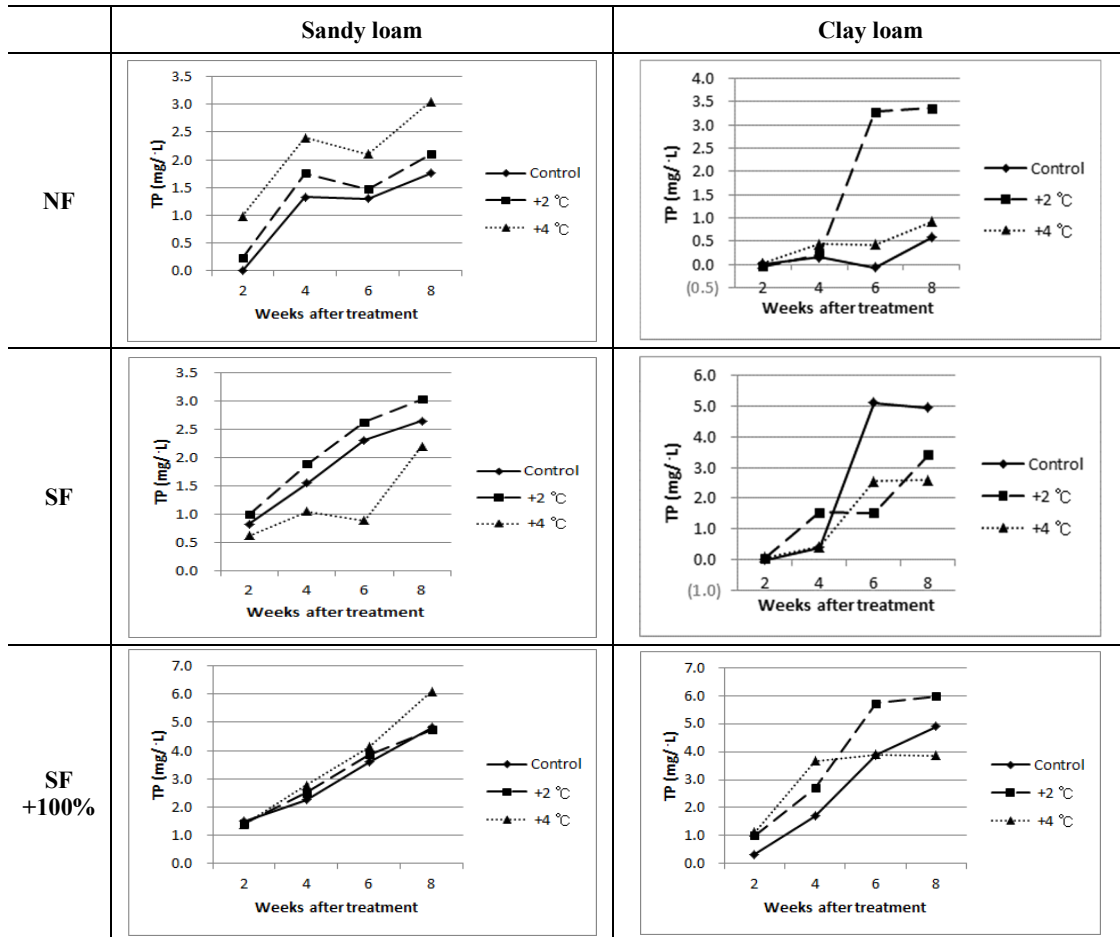


Figure 4. Concentration of total phosphorus (T-P) of water treated with elevated temperature for 8 weeks. NF: No fertilization, SF: Standard fertilization, SF + 100 %: Standard fertilization plus 100 percent increase

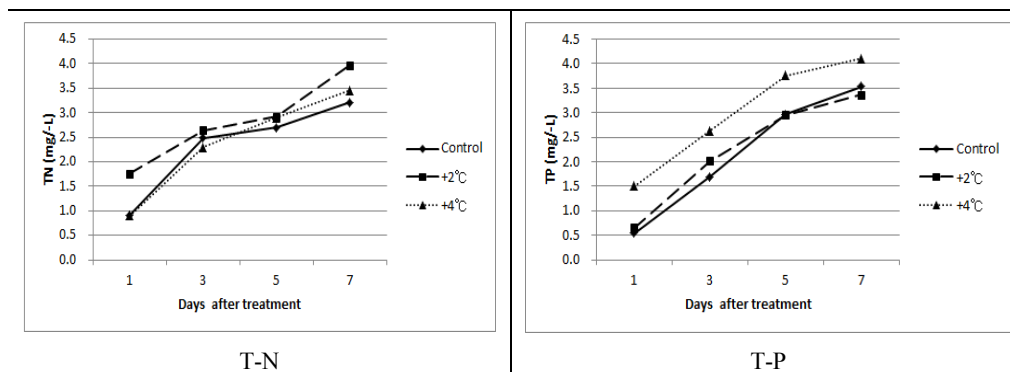


Figure 5. Concentration of T-N and T-P eluted from straw soaked in distilled water for seven days at three different temperatures

Cowen and Lee reported (1973) that 5.4% of total phosphorus of oak tree leaves was soluble and elutable. Schreeg (2013) reported that there is a relationship between solubility and tropical tree leaf amount with $r^2 = 0.79$ for K, $r^2 = 0.51$ for Na, and $r^2 = 0.66$ for P with the weakest relationship of $r^2 = 0.36$ for N. Additionally, when total K content was 100, that of P was 35%, Na 28%, and N 5%. The mineral content of straw was reported to be 0.71% for T-N and 0.16% for P₂O₅ with the T-N and T-P of straw leached well in water; the longer the soaking of the straw, the higher the T-P concentration in the water (Hong, 2016). Hong et al. (2015) also reported that when red pepper furrows were covered with straw, the solubility of phosphorus in rain water led to excess runoff of phosphorus from uplands.

Therefore, under the elevated temperature environment in future in comparison with the current climate, more leaching of soluble nitrogen and phosphorus from crop residues and runoff from crop land can be expected.

Conclusion

Elevated temperatures induced increments of water total nitrogen (T-N) concentration for no chemical fertilization, standard fertilization, and standard fertilization + 100 % in sandy loam soil. Under the elevated temperature environment in future in comparison with the current climate, more leaching of soluble nitrogen and phosphorus from crop residues and runoff from crop land can be expected. These results can be used as the basis for the development of technology in response to climate change that can reduce nutrient runoff and improve water quality at the watershed. There is a need for paddy field scale experiments under a near natural environment for factors such as temperature, precipitation, sunlight, humidity, and wind by using a practically scaled open-top chamber.

Acknowledgements. This study was carried out with the support of the "Research Program for Agricultural Science & Technology Development (Project No. PJ012546)" of the National Institute of Agricultural Sciences, Rural Development Administration, Republic of Korea.

REFERENCES

- [1] Bai, E., Houlton, B. Z. (2009): Coupled isotopic and process-based modeling of gaseous nitrogen losses from tropical rain forests. – *Global Biogeochemical Cycles* 23: doi: 10.1029/2008GB003361.
- [2] Bai, E., Li, S., Xu, W., Li, W., Dai, W., Jiang, P. (2013): A meta-analysis of experimental warming effects on terrestrial nitrogen pools and dynamics. – *New Phytol.* 199 : 441-451.
- [3] Brzostek, E. R., Blair, J. M., Dukes, J. S., Frey, S. D., Hobbie, S. E., Melillo, J. M., Mitchell, R. J., Pendall, E., Reich, P. B., Shaver, G. R. (2012): The effect of experimental warming and precipitation change on proteolytic enzyme activity: positive feedbacks to nitrogen availability are not universal. – *Global Change Biology* 18: 2617-2625.
- [4] Cowen, W. F., Lee, G. F. (1973): Leaves as source of phosphorus. – *Environmental Science & Technology* 7(9): 8539-8540.
- [5] Cross, H. Z., Zuber, M. S. (1972): Prediction of flowering dates in maize based on different methods of estimating thermal units. – *Agronomy journal* 64: 351-355.
- [6] Groffman, P., Butterbach-Bahl, K., Fulweiler, R., Gold, A., Morse, J., Stander, E., Tague, C., Tonitto, C., Vidon, P. (2009): Challenges to incorporating spatially and temporally

- explicit phenomena (hotspots and hot moments) in denitrification models. – *Biogeochemistry* 93: 49-77.
- [7] Hong, S. C., Kim, M. K., Jung, G. B., So, K. H. (2016): Furrow covering effects with rice straw on nutrient discharge from upland soil used for red pepper cultivation. – *Journal of the Korea Organic Resource Recycling Association* 24(1): 11-19.
- [8] Joung, D. S., Reddy, G. B. (1997): Nitrogen mineralization and nitrification of selected piedmont soils in north carolina. – *Korean Journal of Soil Sciences and fertilizer* 30(1): 23-28.
- [9] Jung, C. G., Ahn, S. R., Kim, S. J., Yang, H. J., Lee, H. J., Park, G. A. (2013): HSPF and SWAT modelling for identifying runoff reduction effect of non-point source pollution by rice straw mulching on upland crops. – *Journal of Korean Society of Agricultural Engineering* 55(2): 47-57.
- [10] Kim, J. H., Han, K. H., Lee, J. S. (2008): Characteristics of agricultural non-point source pollutants by rainfall events in rural watersheds. – *Journal of Korean Society of Agricultural Engineering* 24(1): 69-77.
- [11] *Methods of Soil Chemical Analysis*. 2010. p.68-85. NIAST. RDA.
- [12] Niklinska, M., Maryanski, M., Laskowski, R. (1999): Effect of temperature on humus respiration rate and nitrogen mineralization: implications for global climate change. – *Biogeochemistry* 44: 239-257.
- [13] Pendall, E., Bridgham, S., Hanson, P. J., Hungate, B., Kicklighter, D. W., Johnson, D. W., Law, B. E., Luo, Y., Megonigal, J. P., Olsrud, M. (2004): Below-ground process responses to elevated CO₂ and temperature: a discussion of observations, measurement methods, and models. – *New Phytologist* 162: 311-322.
- [14] Rustad, L. E., Fernandez, I. J. (1998): Experimental soil warming effects on CO₂ and CH₄ flux from a low elevation spruce–fir forest soil in Maine, USA. – *Global Change Biology* 4: 597-605.
- [15] Saad, O. A. L. O., Conrad, R. (1993): Temperature dependence of nitrification, denitrification, and turnover of nitric oxide in different soils. – *Biology and Fertility of Soils* 15: 21-27.
- [16] Saxe, H., Cannell, M. G. R., Johnsen, Ø., Ryan, M. G., Vourlitis, G. (2001): Tree and forest functioning in response to global warming. – *New Phytologist* 149: 369-399.
- [17] Schreeg, L. A., Mack, M. C., Turner, B. L. (2013): Nutrient-specific solubility patterns of leaf litter across lowland tropical woody species. – *The Ecological Society of America* 94(1): 94-105.
- [18] Shin, E. S., Choi, J. Y., Lee, D. H. (2001): Characteristics of non-point source pollutants in surface runoff from rural area. – *Journal of Korean Society of Water Quality* 17(3): 299-311.
- [19] Verburg, P. S. J., Van Loon, W. K. P., Lukewille, A. (1999): The CLIMEX soil-heating experiment: soil response after 2 years of treatment. – *Biology and Fertility of Soils* 28: 271-276.
- [20] Yan, W., Hunt, L. A. (1999): An Equation for modeling the temperature response of plants using only the cardinal temperature. *Ann Bot.* 84: 607-614.

PREDICTION OF DIEBACK DISEASE OF *DALBERGIA SISSOO* (SHISHAM) BASED UPON ENVIRONMENTAL FACTORS AND TREE AGE

AHMAD, I.^{1*} – ATIQ, M.² – NAWAZ, M. F.¹ – AHMED, S.³ – ASIF, M.¹ – GULL, S.⁴ – TANVIR, M. A.¹ – ABDULLAH, M.⁵ – AZHAR, M. F.⁶ – RAJPUT, N. A.²

¹*Department of Forestry and Range Management, University of Agriculture, Faisalabad 38000, Punjab Province, Pakistan*

²*Department of Plant Pathology, University of Agriculture, Faisalabad, Punjab, Pakistan*

³*Department of Plant Pathology, University College of Agriculture, University of Sargodha, Sargodha, Pakistan*

⁴*Department of Botany, University of Karachi, Karachi, Pakistan*

⁵*Cholistan Institute of Desert Studies, The Islamia University of Bahawalpur, Bahawalpur, Pakistan*

⁶*Department of Forestry, Range and Wildlife Management, Bahauddin Zakariya University, Multan, Pakistan*

**Corresponding author*

e-mail: irfan_uaf@yahoo.com, irfanahmad@uaf.edu.pk; phone: +92-333-650-2933

(Received 20th Jan 2019 ; accepted 4th Mar 2019)

Abstract. Dieback of forest trees is considered as serious problem in most parts of the world. Shisham an important multipurpose tree of the Indian subcontinent is suffering from dieback. Changing climate in most parts of the world is considered an important factor of ecosystem disturbance. Impact of environmental variables, tree age and water table on the dieback of shisham was examined in different regions of Punjab, Pakistan. Significant correlation was observed between environmental variables and dieback in minimum, moderate and maximum infected trees among three age classes. Water table and rainfall expressed non- significant correlation. A multiple regression model was developed to determine the relationship between environmental variables and dieback. Coefficient of determination value ($R^2 = 0.89$) depicts that model is statistically good. Model indicated that most of the predictor variables has minor role in disease development except age and time span. With one unit increase in age and time span disease will increase 4.15 and 5.25 units respectively. Values of partial R-square indicated that age class (0.5253), time span (0.2943) and relative humidity (0.0552) are major contributors in disease development. It was concluded from the study that age and time span are significant predictor of dieback.

Keywords: *characterization, disease incidence, correlation, climatic factors, predictive model*

Introduction

Dieback of forest trees is a periodic event caused by premature loss of tree health and forest stand vitality (Clatterbuck, 2006). Forest decline and dieback have been reported from different forest ecosystems and climatic zones of the world (Lowman, 1991; Jump et al., 2006) and in the recent past mortality rate has increased in many forest ecotypes of the world (Hosking, 1989; Jursik, 2004). Natural disturbances, including biotic and abiotic stresses are inherent components of forest ecosystems affecting their functioning and biodiversity (Boydet et al., 2013; Thom and Seidl, 2016). About two to three

decades ago dieback of *Dalbergia sissoo* was reported in different regions of Pakistan (Ciesla, 1994). *D. sissoo* being a nitrogen fixing tree and multiple uses is an important tree of social forestry with good economic returns (Lal and Singh, 2012; Ahmad et al., 2013; Farooq et al., 2018; Rashid et al., 2019). Dieback is a major threat to this multipurpose tree (Ahmad et al., 2016, 2017) and has affected millions of trees in Southern Asia (Vogel et al., 2011). Symptoms of shisham dieback are approximately similar to dieback of mango in southern Punjab of Pakistan (Khan et al., 2014) Climate change, fungal pathogens and nutrient deficiencies have been considered as the major causes of tree decline and dieback (Simpson, 1993; Rajput et al., 2008). In different regions of the world fungal pathogens have been recognized as the responsible causal organisms of tree decline and climate change has also been found associated with forest dieback (Ahmad et al., 2016). Environmental stresses contribute to tree mortality and occurrence of forest diseases due to different pathogens will probably become more common and severe in the near future, as different biotic and abiotic factors are strongly influenced by climatic change (Sturrock et al., 2011; Raza et al., 2015). Dieback in northern hardwood forests was strongly linked with the global climatic change; the coefficient of determination value ($R^2 = 0.49$) in the regression analysis showed that climatic changes were responsible for 49% of the dieback occurring in northern hardwood forests (Auclair et al., 2005). An increasing trend in the forest mortality and dieback due to drought was observed. The linear regression model suggested a very strong association between tree mortality and drought conditions due to low rainfall and high temperature (Phillips et al., 2009; Allen et al., 2010). The extent of forest dieback linked with global climate change would be greater than that observed in the past (National Research Council, 2001). High rate of shisham mortality in India was linked with changing climatic conditions, such as increased drought, extremes of winter and summer, with severe foggy conditions which adversely affected the photosynthesis and other physiological processes of the trees (Singh, 1980; Kaushal et al., 2002).

Age is also considered an important factor in development of forest dieback. Nepstad et al. (2008) reported that as trees are perennial woody plants which grow slowly but the mortality rate of trees was very much higher, even within a period of few months as compared to its growth rate which is very interesting. Older trees were more susceptible to dieback compared with younger trees (Auclair et al., 2010). Little scientific information is known about the spread and development of the disease in individual forest trees in different age groups (Timmermann et al., 2017). Sperry et al., 1991 suggested that in older trees, the membranes associated with vessels and tracheids rupture easily under ecological stresses. Acharya and Subedi (2000) recorded mortality of over-mature dieback-affected *D. sissoo* trees in a short period of even few weeks. Along with tree age, certain species of fungi, such as *F. solani* and *G. lucidum*, killed over 20% of older trees of *D. sissoo* under abiotic stresses in Bihar (Chaturvedi et al., 2002).

The effective use of chemical agents against plant diseases requires knowledge of the epidemiology of disease. Understanding disease dynamics, including the pathogen life cycle, provides the basis for forecasting disease outbreaks. Because shisham decline massively reduces both the economic gains and the social uses of this tree, the aim of integrated disease management must be to reduce these losses. Approaches are required which aim to avoid frequent recurrence of shisham decline epidemics. Much research, therefore, remains to be done. Disease severity in relation to different age classes of shisham has not been assessed, and no correlation has been determined between disease

occurrence and the water table. The impact of varying environmental conditions in relation to spread of disease has not been studied quantitatively. Therefore the objective of study was to assess the relationship between shisham dieback, environmental variables and tree age.

Materials and methods

D. sissoo dieback disease data collection

A comprehensive survey of different *D. sissoo* (shisham) growing regions of Punjab province of Pakistan was carried out to collect the data regarding incidence of dieback disease (Fig. 1). Data were collected for the three consecutive years. Furthermore on the basis of disease severity we categorized the trees into three categories i.e. minimum infected, moderately infected and dead or fully affected trees.

Characterization of environmental factors conducive for shisham dieback in field conditions

Data collected for the incidence of shisham dieback from the different ecological zones of Punjab were subjected to correlation analysis with different climatic variables. The influence of each environmental variable (maximum and minimum air temperature, rainfall, relative humidity wind velocity, age and water table) on the severity of shisham dieback occurrence was determined by correlation.

Regression analysis

Regression analysis was used to determine any link between environmental/climatic factors and disease incidence/development (Chatterjee and Hadi, 2006). There are two types of models i.e. simple and multiple regression models (Eqs. 1 and 2). For developing simple linear regression models, the response variable (Y), in this case disease, was a function of the single predictor or explanatory variable (X), here an environmental/climatic variable. The equation for simple linear regression is:

$$Y = \beta_0 + \beta_1 X \quad (\text{Eq.1})$$

where β_0 is the intercept and β_1 is the slope. In multiple linear regression, however, there are more explanatory or predictor variables when compared with simple linear regression. The relationship is described by:

$$Y = \beta_0 + \beta_1 x_1 + \beta_2 x_2 + \dots + \beta_i x_i + \epsilon \quad (\text{Eq.2})$$

where x represents the collection of i predictors x_1, x_2, \dots, x_i in the model, and $\beta_1, \beta_2, \dots, \beta_i$ are the corresponding regression coefficients and ϵ is the random error or disturbance.

Development of disease predictive model for the field study

A predictive model for the field data on disease incidence and severity was also developed. Weekly environmental data comprising of maximum and minimum air

temperatures, relative humidity, average rainfall and wind speed were collected from the Regional Meteorological Station, Lahore. All the collected environmental data, tree age, underground water table data and dieback disease incidence data in the different districts of Punjab (Faisalabad, Lahore, Sargodha, Sahiwal, Okara, Rawalpindi, Multan, Bahawalpur, Rahim yar khan and Dera Ghazi Khan) from November 2009 to April 2010 and the same months during 2010-11, were subjected to analysis of variance to evaluate the effect of abiotic factors on disease incidence by using the Least Significant Difference Test (LSD at $P < 0.05$).

The influence of these environmental conditions on disease severity was determined by correlation analyses (Steel et al., 1997). R^2 , Mallows C_p and mean square error (MSE) were the criteria used to select the best models (Khan and Illayas, 1999).

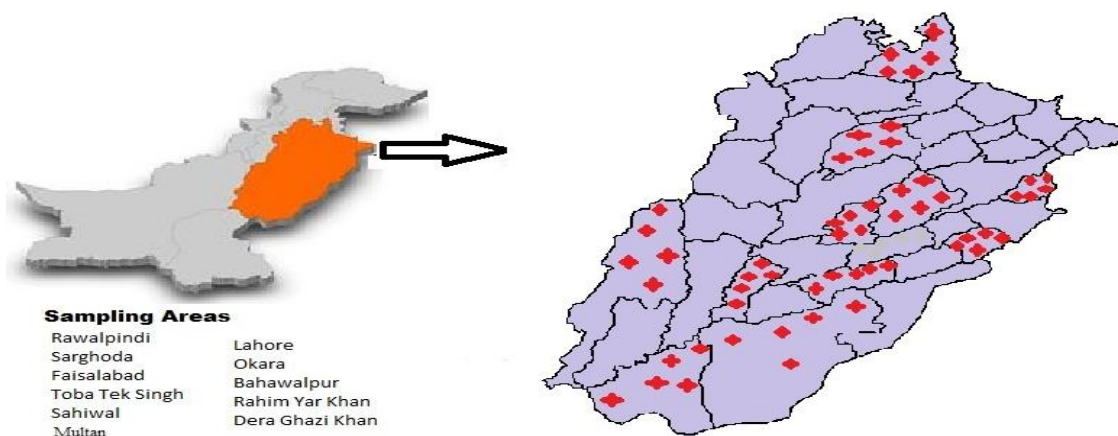


Figure 1. Study area map showing eleven districts of Punjab province

Results

Correlation between environmental variables and host (minimum, moderate and maximum infected trees of shisham) in different ecological zones of Punjab

There was a significant correlation between environmental variables (rainfall, relative humidity, minimum temperature, maximum temperature, wind velocity and water table) and host (minimum, moderate and maximum infected with dieback disease) of three age classes in different areas of Punjab ($P < 0.05$). Water table and rainfall expressed non-significant correlation with dieback disease in all categories of host (minimum, moderate and maximum infected with dieback). A weak and negative association was found between maximum temperature and minimum infected ($r = -0.190$), positive in moderately infected ($r = 0.176$) and fully infected trees ($r = 0.175$) followed by wind velocity in minimum infected ($r = -0.166$), moderately affected ($r = 0.184$) and fully infected trees ($r = 0.129$). Similar results were expressed by maximum temperature (minimum infected, $r = -0.105$; moderately infected, $r = 0.150$; maximum infected, $r = 0.138$) and relative humidity in minimum infected ($r = 0.106$), moderately infected ($r = -0.125$) and maximum infected ($r = -0.076$) trees (Figs. 2, 3 and 4).

Regression analyses of environmental variables against dieback disease were carried out independently to observe the effects of each environmental variable separately on the disease development in the major shisham grown areas of the Punjab province. Table 1 showed the regression equations and R^2 of the correlations of environmental

variables with the minimum trees. R^2 value shows that 39.2% of variation in dieback disease was explained by the host categories', followed by time span (20.5%), maximum temperature (3.6%), wind speed (2.7%), minimum temperature (2.4%), relative humidity (1.1%), rainfall (0.3%) and water table (0.2%). For minimum infected trees, category of host was responsible for 29.1% of variation, followed by time (15.7%), wind speed (3.4%), maximum temperature (3.0%), minimum temperature (2.2%), relative humidity (1.5%), water table (0.2%); rainfall did not explain any variation. Similar trend was detected in maximum infected trees, where as 37.6% variation was explained by age class, followed by time span (18.6%), maximum temperature (3.1%), minimum temperature (1.9%), wind speed (1.7%), relative humidity (0.6%), rainfall (0.5%) and 0.2% by water table.

Table 1. Regression equations of minimum, moderate and maximum infected trees with different variables

Categories of host								
Trees with minimum infection			Moderately affected trees			Trees with maximum infection		
Regression equation	R ²	S.E	Regression equation	R ²	S.E	Regression equation	R ²	S.E
Min.I= 86.6 - 8.47	39.2	8.61	Mod.I=6.59 + 3.50	29.1	4.46	Max.I = 6.80+4.95	37.6	5.21
Time = 84.7 - 10.0	20.5	9.85	Time = 7.30 +4.20	15.7	4.87	Time = 8.15 + 5.70	18.6	5.94
W T= 68.7+0.0416	0.2	11.03	W T =14.1-0.0221	0.2	5.29	W T = 17.2-0.022	0.2	6.59
RF= 69.5+0.491	0.3	11.03	RF=13.6-0.086	0.0	5.30	RF = 16.9-0.410	0.5	6.58
R.H = 63.7+0.078	1.1	10.98	RH=16.9-0.0432	1.5	5.26	RH= 19.3 - 0.0331	0.6	6.57
Min.T = 72.8-0.262	2.4	10.91	Mini.T=12.2+0.120	2.2	5.24	Mini.T = 15.1+0.139	1.9	6.53
Max.T = 77.1+0.273	3.6	10.84	Max.T=10.4+0.120	3.0	5.23	Max.T = 12.6+0.150	3.1	6.49
WS= 71.1-1.50	2.7	10.89	WS=12.9+0.797	3.4	5.21	WS = 16.0+0.706	1.7	6.53

WT: Water table; Mini. T: Minimum temperature (°C); Max. T: Maximum temperature (°C); WS: Wind speed (Km/h); RF: Rainfall (mm); Min.I: Trees with minimum infection; Max. I: Maximum infected trees; Mod.I: Moderately infected trees

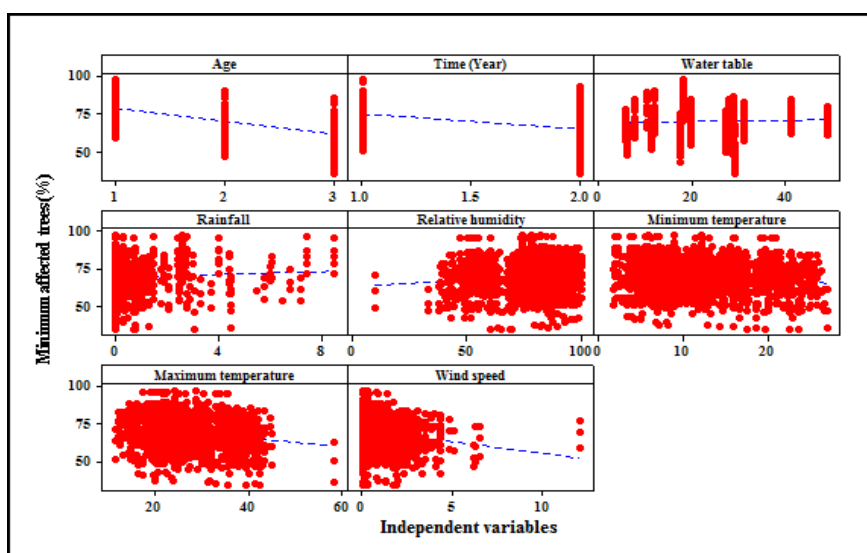


Figure 2. Effect of different environmental variables on proportions of minimum affected *D. sissoo* trees in Punjab

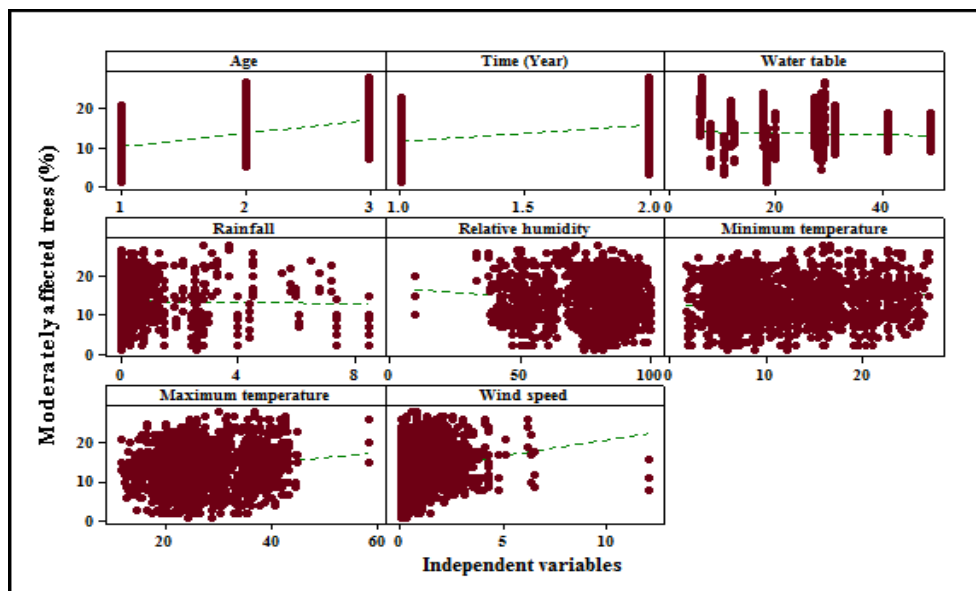


Figure 3. Effect of different environmental variables on proportions of moderately affected *D. sissoo* trees in Punjab

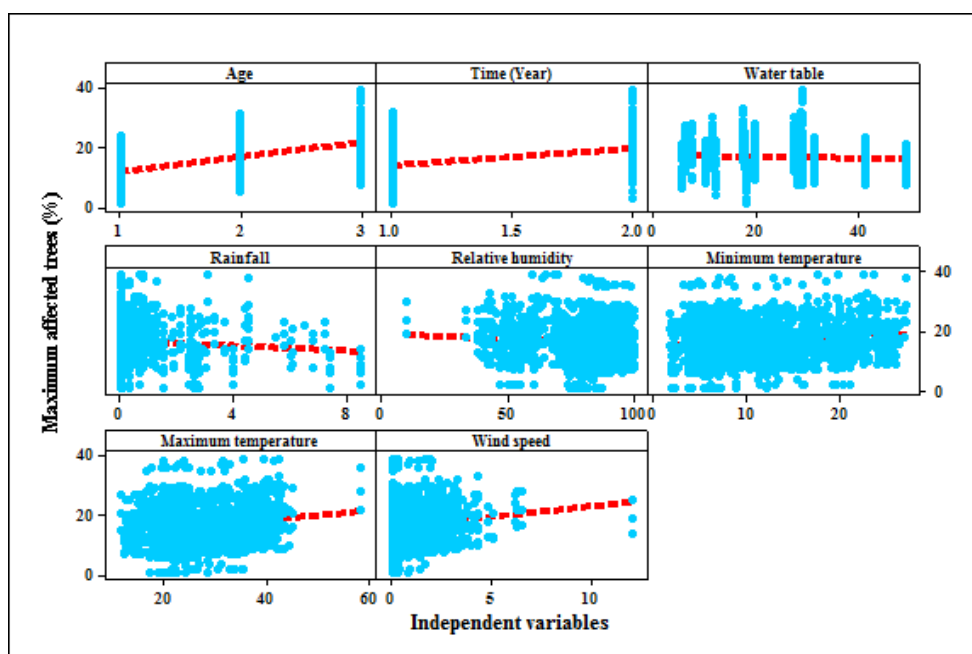


Figure 4. Effect of different environmental variables on proportions of maximum affected *D. sissoo* trees in Punjab

***Dalbergia sissoo* dieback disease predictive model based on field survey data**

Data of dead shisham trees due to dieback disease about different categories of host were collected from different shisham grown areas of Punjab (Pakistan) through a comprehensive survey. The effect of host category, environmental variables (Minimum and maximum temperature, rainfall, relative humidity, wind velocity and water table)

and years (time) on dieback disease development was determined by correlation and regression analysis. A multiple regression model was developed to determine the inter-relationships between environmental and the development of dieback disease (Eq. 3). With R^2 value of 0.89, the model was statistically justified at $P < 0.05$ and, therefore, can be used to predict the likelihood of dieback occurring under a given set of environmental and other variables.

$$Y = 2.51 + 4.15 x_1 + 5.25 x_2 + 0.00866 x_3 - 0.113 x_4 - 0.0611 x_5 - 0.0115 x_6 - 0.0092 x_7 + 0.514 x_8 \quad (\text{Eq.3})$$

$R^2 = 0.89$, $x_1 =$ host category, $x_2 =$ year (time), $x_3 =$ water table, $x_4 =$ rainfall, $x_5 =$ relative humidity, $x_6 =$ minimum temperature, $x_7 =$ maximum temperature, $x_8 =$ wind velocity.

The model indicated that most predictor variables had a small role in disease development. Age class and time span, however, had an important role. The model equation suggests that with one unit increase in age, dieback incidence will increase by 4.15 units in shisham plantations; with a single unit increase in time span (years), the change in dieback would be 5.25. For rainfall, relative humidity, minimum and maximum temperature, the negative values indicate that an increase in these variables will reduce disease incidence. In the principle component analysis, using the forward selection method, an optimum model was developed. The summary of the forward selection process (Table 2) shows that the partial R^2 value after entering the age variable was 0.5253 and for year, relative humidity and wind velocity it was 0.2943, 0.0552 and 0.0154, respectively. Beyond these variables, there was negligible increase in the R^2 value. The R^2 value for both the full model and optimum models was the same (0.89).

Then model was evaluated according to the procedures described by the Chaterjee and Hadi (2006) by a) through comparison of the dependent variable (Dieback disease) and regression coefficients with physical theory b) comparison of observed and predicted data.

Table 2. Summary of forward selection

Sr#	Variable entered	Partial R-square	Model R-square	Pr > F
1	Host category (minimum, moderate and maximum infected)	0.5253	0.5253	<0.000
2	Time (year)	0.2943	0.8196	<0.000
3	Relative humidity (%)	0.0552	0.8748	<0.000
4	Wind speed (Km/h)	0.0154	0.8902	<0.000
5	Rainfall (mm)	0.0009	0.8911	<0.000
6	Water table	0.0004	0.8915	<0.023
7	Min Temperature (°C)	0.0003	0.8919	<0.040

Comparison of the dependent variable (dieback disease) and regression coefficients with physical theory

Coefficient of determination (R^2) was an important parameter derived from the present work. Standard error was good with 1.5532 value (Table 3) The regression model was significant at $P < 0.05$ (Tables 4 and 5). Minimum and maximum

temperatures were non- significant in the full predictive model. Role of water table and rainfall were also not much significant and summary of forward selection represents the same (Table 2) while all other parameters were significant. In the optimum model age, year, relative humidity and wind velocity were the major contributors in the disease development (Eq. 4). The coefficients, standard error, t stat and P values of full and optimum models are given in Tables 3, 4 and 5, respectively. It has been concluded from the above results that the model is very good for prediction.

Optimum predictive model for field data:

$$Y = 1.65 + 4.15 \text{ Age} + 5.20 \text{ Year} - 0.0523 \text{ RH} + 0.544 \text{ WS} \quad (\text{Eq.4})$$

$$R^2 = 0.89.$$

The model was also assessed by comparing the observed and predicted data. Figure 5 shows that majority of the predictions fell between the 95% confidence intervals and 95% predictive intervals, demonstrating a very good relationship between predicted and observed data. Based on the R^2 (89%), the CI and PI model can be used for forecasting the dieback disease of shisham in various climatic conditions in the future.

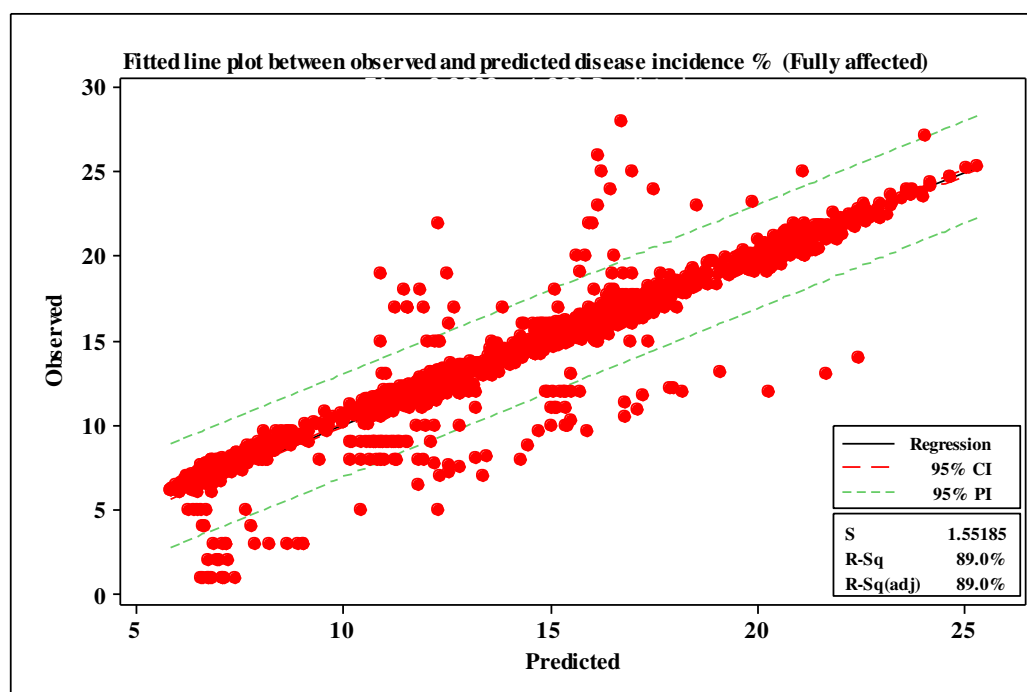


Figure 5. Fitted line plot for dieback disease in maximum affected trees of Shisham with predicted and observed data points at 95% confidence and predictive interval

Table 3. Regression statistics of optimum predictive model for the maximum infected trees

Regression statistics	
R-square	0.89
Adjusted R-square	0.89
Standard error	1.5532
Observations	1583

Table 4. ANOVA for optimum predictive model of maximum infected trees

SOV	Df	SS	MS	F	P value
Regression	4	30889.5	7722.4	3200.57	<0.000
Error	1579	3809.8	2.4		
Total	1583	34699.3			

Table 5. Coefficient of variables, standard error, t stat and P-value

Predictors	Coefficients	Standard error	T stat	P-value
Constant	1.65	0.29	5.57	0.000
Age	4.15	0.047	86.91	0.000
Year	5.20	0.078	66.44	0.000
Relative humidity	-0.052	0.0029	-17.62	0.000
Wind velocity	0.54	0.036	14.87	0.000

Discussion

Dieback is a major threat to *D. sissoo* and has caused huge damage in all areas where this tree is cultivated. In Pakistan dieback of shisham has been recorded in different regions but severity differs with region (Gill and Aziz, 2004; Ahmad et al., 2016). In present study, a detailed survey of *D. sissoo* in four different agro-ecological zones of Punjab, Pakistan was conducted and considerable variation was observed in the incidence of dieback disease in the different zones of Punjab. Similar results were reported by Bajwa et al. (2003) from shisham plantations in all regions of Punjab. In present study incidence of disease was observed in different age classes of host (minimum, moderately and maximum infected trees).

The current work showed that tree age, and climatic factors including relative humidity, minimum and maximum temperature and wind velocity, were significantly correlated ($P < 0.05$) with incidence of dieback disease in the different agro-ecological zones. Tree age showed a prominent and strong association with dieback disease in all the examined districts and zones. Amongst the climatic factors, maximum temperature and wind velocity were more important compared to other variables. Baksha and Basak (2000) and Sharma et al. (2000) correlated mortality of *D. sissoo* with different ages of trees, and found low disease incidence in the early stages of growth, but greater susceptibility in older and larger trees leading to a high mortality rate compared to young plants. These results also support the conclusions of Boland et al. (2004) and Sturrock (2007), Dukes et al. (2009), Tubby and Webber (2010), Timmermann et al. (2017). The disease predictive model developed through regression analysis of the field survey data in this work utilized age class, environmental variables (minimum and maximum temperature, rainfall, relative humidity and wind velocity), time span (years) and underground water table to generate the model. Age class and time span played very important roles in the development of dieback under the field conditions. Hosking and Hutcheson (1992) showed that dieback of *Cordyline australis* was associated with old trees and attack of pathogens. Acharya and Subedi (2000) reported mortality of over mature dieback affected *D. sissoo* trees in a short period of even few weeks. Phillips et al. (2009) and Allen et al. (2010) observed an increasing trend in forest dieback and mortality due to drought on the basis of literature available from 1984 to 2010. In 1984,

only 1% tree mortality was linked with drought, whereas in 2010 the figure was 4%; the value of $R^2 = 0.61$ in the linear regression model showed a very strong association between tree mortality and drought conditions due to low rainfall and high temperature. These results support the findings reported here, that with the passage of time environmental stresses increased forest mortality. Different researchers (Negi, 2002; Sidhu et al., 2002; Chaudhry, 2006; Thom and Seidl, 2016) observed that the reoccurrence of climatic changes in *D. sissoo* plantations for more than two years may seriously disturb plant growth and reduce resistance of plants to different pathogens which ultimately causes the death of the trees. These findings are confirmed in this present study.

Conclusions

Mortality of *Dalbergia sissoo* due to dieback disease is linked with tree age as disease incidence in different age classes were observed and correlated with various environmental factors. Association was observed between disease and different climatic factors. Varying level of water table in different agro ecological zones of Punjab Province of Pakistan was not considered as a major threat to shisham dieback. Time span in regression equations indicates that with the passage of time disease severity will increase. Farmers and foresters should be careful about the symptoms of disease and harvesting will be a better option for the most affected trees. In future changing climatic conditions of Pakistan can spread disease to least affected areas.

Acknowledgements. We thank Abdul Hannan for guidance with predictive modeling and analysis; Muhammad Kashif, Lecturer Statistics for statistical support; and Amjad Saeed from Punjab Forestry Research Institute, Faisalabad for field assistance. Authors are grateful to the Meteorological Department, Lahore, Punjab for providing climatic data of selected districts.

REFERENCES

- [1] Acharya, K. P., Subedi, N. (2000): A survey on the dieback *Dalbergia sissoo* in Nepal. Field Document No. 18. – Proc. Sub Regional seminar on Dieback of *sissoo* (*Dalbergia sissoo*), Kathmandu, Nepal, pp. 22-25.
- [2] Ahmad, I., Khan, R. A., Siddiqui, M. T. (2013): Incidence of dieback disease following fungal inoculations of sexually and asexually propagated shisham (*Dalbergia sissoo*). – Forest Pathology 43(1): 77-82.
- [3] Ahmad, I., Gul, S., Hannan, A., Siddiqui, M. T., Nawaz, M. F., Asif, M., Salman, A. (2016): Dieback disease predictive model for sexually and asexually propagated *Dalbergia sissoo* (Shisham). – Pakistan Journal of Botany 48(4): 1645-1650.
- [4] Ahmad, I., Hannan, A., Ahmad, S., Asif, M., Nawaz, M. F., Tanvir, M. A., Azhar, M. F. (2017): Fungi associated with decline of kikar (*Acacia nilotica*) and red river gum (*eucalyptus Camaldulensis*) in Faisalabad. – International Journal of Biological, Biomolecular, Agricultural, Food and Biotechnological Engineering 11(2): 171-174.
- [5] Allen, C. D., Macalady, A. K., Chenchouni, H., Bachelet, D., McDowell, N., Vennetier, M., Kitzberger, T., Rigling, A., Breshears, D. D., Hogg, P., Gonzalez, R., Fensham, Z., Zhangm, J., Castro, N., Demidova, J., Hwan Lim, G., Allard, S. W., Running, A., Cobb, N. (2010): A global overview of drought and heat induced tree mortality reveals emerging climate change risks for forests. – Forest Ecology and Management 259: 660-84.

- [6] Auclair, A. N. D., Jhon, T., Revenga, C. (2005): The role of climatic variability and global warming in the decline of northern hardwoods. – *Water Air Soil Pollution* 91: 163-186.
- [7] Auclair, A. N. D., Heilman, W. E., Blondel, B. (2010): Predicting forest dieback in Maine, USA: a simple model based on soil frost and drought. – *Canadian Journal of Forest Research* 40: 687-702.
- [8] Bajwa, R., Javaid, A., Shah, M. B. M. (2003): Extent of shisham (*Dalbergis sissoo*) decline in Sialkot, Gujranwala, Lahore and Sargodha districts. – *Mycopathology* 1: 1-5.
- [9] Baksha, M. W., Basak, A. C. (2000): Mortality of sissoo (*Dalbergia sissoo*) in Bangladesh. Field Document No. 18. – Proc. Sub Regional seminar on Dieback of sissoo (*Dalbergia sissoo*), Kathmandu, Nepal, pp. 1-4.
- [10] Boland, G. J., Melzer, M. S., Hopkin, A., Higgins, V., Nassuth, A. (2004): Climate change and plant diseases in Ontario. – *Canadian Journal of Plant Pathology* 26: 335-350.
- [11] Boyd, I. L., Freer-Smith, P. H., Gilligan, C. A., Godfray, H. C. J. (2013): The consequences of tree pests and diseases for ecosystem services. – *Science* 342: 1235773.
- [12] Chatterjee, S., Hadi, A. S. (2006): *Regression Analysis by Example*. Fourth Ed. – John Wiley and Sons, Chichester.
- [13] Chaturvedi, O. P., Ali, M. S., Das, D. K. (2002): Studies on Shisham Mortality and Its Management in Bihar. – Department of Forestry and Natural Resources Punjab Agricultural University, Ludhiana, pp. 22-25.
- [14] Chaudhary, A. K. (2006): Abiotic and biotic stresses on shisham trees. – Proc. of the Second National Seminar on Shisham Dieback, June 29, 2004. Punjab Forestry Research Institute, Faisalabad, pp. 111-118.
- [15] Ciesla, W. M., Donaubauer, M. E. (1994): Decline and dieback of trees and forests: a global overview. – *FAO Forestry Paper* 120: 90.
- [16] Clatterbuck, W. K. (2006): *Dieback and Decline of Trees*. – University of Tennessee, Agricultural Extension Service, Knoxville.
- [17] Dukes, J. S., Pontius, J., Orwig, D. (2009): Responses of insect pests, pathogens, and invasive plant species to climate change in the forests of northeastern North America: what can we predict. – *Canadian Journal of Forest Research* 39: 231-248.
- [18] Farooq, T. H., Gautam, N. P., Rashid, M. H. U., Gillani, M. M., Nemin, W., Nawaz, M. F., Islam, W., Zainab, M., Wu, P. (2018): Contributions of agroforestry on socioeconomic conditions of farmers in central Punjab, Pakistan - a case study. – *Cercetări Agronomice în Moldova* 2: 91-101.
- [19] Gill, M. A., Aziz, T. (2004): Evaluation of soil properties for their role in shisham dieback. In proceedings of second National seminar on Shisham dieback. – Punjab Forestry Research Institute Faisalabad 36-39.
- [20] Hosking, G. P. (1989): Beech forest health- implications for management. – *New Zealand Journal of Forestry Science* 19: 290-293.
- [21] Hosking, G. P., Hutcheson, J. A. (1992): Sudden Decline of Cabbage Tree (ti kouka) - How Bad, How Extensive? What's New in Forest Research no 227. – Zealand Forest Research Institute, Rotorua.
- [22] Jump, A., Hunt, J. M., Peñuelas, J. (2006): Rapid climate change-related growth decline at the southern range edge of *Fagus sylvatica*. – *Global Change Biology* 12: 2163-2174.
- [23] Jurskis, V. (2004): Overview of forest decline in coastal New South Wales. – Proc. Colloquium at Batemans, Bay Sydney, Australia, pp. 4-7.
- [24] Kaushal, P., Banyal, R., Kant, C. (2002): – Role of climatic conditions on mortality of Kikar and shisham in Punjab. In Proc: Regional Symposium on Mortality of Shisham and Kikar in Northern States of India. Gill, S. S., Chauhan, S. K., Khajuria, H. N., Dhanda, R.S., Chauhan, R. (eds.). March 3-4, 2002. Punjab Agriculture University, Ludhiana, pp. 51-64.
- [25] Khan, M. A., Ilyas, M. B. (1999): A two environmental variable model to forecast leaf rust on wheat. – *Proceeding of 2nd National Conference Plant Pathology*, pp. 72-89.

- [26] Khan, A. I., Khan, A., Asif, H., Jiskani, M. M., Muhlbach, H. P., Azim, M. K. (2014): Isolation and 16s rDNA sequence analysis of bacteria from dieback affected mango orchards in southern Pakistan. – Pakistan Journal of Botany 46: 1431-1435.
- [27] Lal, H. S., Singh, S. (2012): Ethnomedicinal uses of *Dalbergia sissoo* Roxb in Jharkhand. – International Journal of Ayurvedic & Herbal Medicine 2(1): 198-201.
- [28] Lowman, M. D. (1991): The dieback crisis - tree declines throughout the world. – Centre for Environmental Studies Journal, Williams College, pp. 28-31.
- [29] National Research Council (2001): Economic and Ecological Impacts of Abrupt Climate Change. – In: Committee on Abrupt Climate Change, Ocean Studies Board, Polar Research Board, Board on Atmospheric Sciences and Climate (eds.) Abrupt Climate Change: Inevitable Surprises. National Research Council, Washington, DC, Chapter 5, pp. 90-117.
- [30] Negi, J. D. S. (2002): Shisham Mortality in India - Case Study. – Department of Forestry and Natural Resources Punjab Agricultural University, Ludhiana 19-21.
- [31] Nepstad, D. C., Stickler, C. M., Soares-Filho, B., Merry, F. (2008): Interactions among Amazon land use, forests and climate: prospects for a near-term forest tipping point. – Philosophical Transactions of the Royal Society of London, Series B 363: 1737-1746.
- [32] Phillips, O. L., Aragão, L. E. O. C., Lewis, S. L., Fisher, J. B., Lloyd, J., pez-González, G., Ló Malhi, Y., Monteagudo, A., Peacock, J., Quesada, C. A., van der Heijden, G., Almeida, S., Amaral, I., Arroyo, L., Aymard, G., Baker, T. R., Bánki, O., Blanc, L., Bonal, D., Brando, P., Chave, J., Alves de Oliveira, A. C., Dávila Cardozo, N., Czimczik, C. I., Feldpausch, T. R., Freitas, M. A., Gloor, E., Higuchi, N., Jiménez, E., Lloyd, G., Meir, P., Mendoza, C., Morel, A., Neill, D. A., Nepstad, D., Patinão, S., Peñuela, M. C., Prieto, A., Ramírez, F., Schwarz, M., Silva, J., Silveira, M., SotaThomas, A., Ter Steege, H., Stropp, J., Vásquez, R., Zelazowski, P., Alvarez Dávila, E., Andelman, S., Andrade, A., Chao, K., Erwin, T., Di Fiore, A., Honorio, C., Keeling, E., Killeen, H., Laurance, T. J., Peña Cruz, W. F., Pitman, A., Núñez Vargas, N. C. A., Ramírez-Angulo, P., Rudas., Salamão, H., Silva, R., Terborgh, N., Torres- Lezama, J. A. (2009): Drought sensitivity of the Amazon rainforest. – Science 323: 1344-1347.
- [33] Rajput, N. A., Pathan, M. A., Jiskani, M. M., Rajput, A. Q., Arain, R. R. (2008): Pathogenecity and host range of *Fusarium solani* (MART) SACC. Causing dieback of shisham (*Dalbergia sissoo* ROXB.). – Pakistan Journal of Botany 40(6): 2631-2639.
- [34] Rashid, M. H. U., Asif, M., Farooq, T. H., Gautam, N. P., Nawaz, M. F., Ahmad, I., Gilani, M. M., Wu, P. (2019): Cuttings growth response of *Dalbergia Sissoo* (Shisham) to soil compaction stress. – Applied Ecology and Environmental Research. DOI: http://dx.doi.org/10.15666/aer/1701_10491059.
- [35] Raza, M. M., Khan, M. A., Ahmad, I., Bajwa, A. A., Aslam, H., Ullah, B. A., Riaz, K. (2015): Forest pathogens and diseases under changing climate-a review. – Pakistan Journal of Agricultural Research 28: 318-337.
- [36] Sharma, M. K., Singhal, R. M., Pokhariyal, T. C. (2000): *Dalbergia sissoo* in India. Field Document No. 18. – Proc. Sub Regional Seminar on Dieback of Sissoo (*Dalbergia sissoo*), Kathmandu, Nepal.
- [37] Simpson, P. (1993): The Cabbage Trees (*Cordyline australis*) are Dying: Investigations of Sudden Decline in New Zealand. – In: Huetti, R. F., Muller-Dombois, D. (eds.) Forest Decline in the Atlantic and Pacific Region. Springer-Verlag, Berlin and Heidelberg, pp. 280-292.
- [38] Sidhu, D. S., Dhillon, G. P. S., Singh, B. (2002): Shisham Mortality and Its Remedial Measures through Genetic Manipulations. Mortality of Shisham and Kikar in India. – Department of Forestry and Natural Resources, Punjab Agricultural University, Ludhiana, pp. 31-36.
- [39] Singh, S. (1980): Shisham (*Dalbergia sissoo*) mortality and its remedial measure through genetic manipulations. – Proc. Regional Symposium on Mortality of Shisham and Kikar in Northern States of India. March 3-4, 2002. Punjab Agriculture University, Ludhiana.

- [40] Sperry, J. S., Perry, A. H., Sullivan, J. E. M. (1991): Pit membrane degradation and air-embolism formation in ageing xylem vessels of *Populus tremuloides* Michx. – *Journal of Experimental Botany* 42(11): 1399-1406.
- [41] Steel, R. G. D., Torrie, J. H., Dicky, D. A. (1997): *Principles and Procedures of Statistics. A Biometrical Approach*. 3rd Ed. – McGraw Hill Book Co., New York.
- [42] Sturrock, R. N. (2007): Climate change effects on forest diseases: an overview. – Proc. 54th Annual Western International Forest Disease Work Conf, Smithers, British Columbia, 2-6 October, 2006.
- [43] Sturrock, R. N., Frankel, S. J., Frankel, J., Brown, A. V., Hennon, P. E., Lliejunas, J. T., Lewis, K. J., Worrall, J. J., Woods, J. (2011): Climate change and forest diseases. – *Plant Pathology* 60: 133-149.
- [44] Thom, D., Seidl, R. (2016): Natural disturbance impacts on ecosystem services and biodiversity in temperate and boreal forests. – *Biological Reviews* 91: 760-781.
- [45] Timmermann, V., Nagy, N. E., Hietala, A. M., Børja, I., Solheim, H. (2017): Progression of ash dieback in Norway related to tree age, disease history and regional aspects. – *Baltic Forestry* 23: 150-158.
- [46] Tubby, K. V., Webber, J. F. (2010): Pests and diseases threatening urban trees under a changing climate. – *Forestry* 83: 451-459.
- [47] Vogel, S., Tantau, H., Mielke-Ehret, N., Hoque, M. I., Sarker, R. H., Saha, M. L., Alam, S. K. S., Khan, S., Muhlbach, H. P. (2010): Detection of virus particles and double stranded RNA in dieback affected *Dalbergia sissoo* from Bangladesh. – *Bangladesh Journal of Botany* 40: 57-65.

TESTING THE IMPACT OF BANKING SECTOR DEVELOPMENT ON TURKEY'S CO₂ EMISSIONS

SAMOUR, A. * – ISIKSAL, A. Z. * – RESATOGLU, N. G.

*Banking and Finance Department, Near East University, Nicosia, Northern Cyprus, via Mersin 10
Turkey*

**Corresponding authors*

e-mail: aliya.isiksal@neu.edu.tr, ahmad.samour@neu.edu.tr

(Received 21st Jan 2019; accepted 10th Apr 2019)

Abstract. This article aims to introduce a new research topic by investigating the role of banking sector development on Turkey's CO₂ emissions for the time period 1980-2014. Autoregressive Distributed Lag (ARDL), Fully Modified-OLS (FMOLS), and Canonical Co-integrating Regression (CCR) models are applied to test the coefficients between the variables. The newly-developed Bayer-Hanck combined co-integration test is used to support the robustness of the ARDL bounds test. The results show that banking sector development led to an increase in CO₂ emissions. The improvements in the Turkish banking sector development could lead to increased investment and energy consumption, which would subsequently cause raise in CO₂ emissions. Furthermore, the results show that an increase in the RIN would lead to decrease in CO₂ emissions. RIN has fundamental repercussions for the economy by either impacting the cost of capital or influencing the availability of credit, which in turn determines the level of savings as well as that of investment in an economy, which may subsequently affect CO₂ emissions. It is suggested that policy-makers should use the banking sector development and RIN channels to reduce environmental degradation by introducing monetary policy reforms, while also encouraging energy investment and the production of electricity using renewable sources.

Keywords: *Bayer-Hanck combined co-integration test, structural breaks, ARDL, environmental degradation, carbon dioxide*

Abbreviations: B.R.S.A: Banking Regulation and Supervision Agency, GDP: Gross domestic product, ARDL: Autoregressive Distributed Lag, CO₂: Carbon emissions, OECD: Organisation for economic co-operation and development, RIN: Real interest-rate, GHG: Greenhouse gas emissions, FDI: Foreign direct investment, E.K.C: Environmental Kuznets curve, VECM: Vector Error Correction Model, SB: Structural break, CMR: Clemente-Montanes-Reyes, A.I.C: Akaike information criterion, S.B.C: Schwarz-Bayesian criteria, CV: critical values, BH: Bayer-Hanck, FMOLS: Fully modified ordinary least square, CCR: Canonical co-integrating regression

Introduction

Since its economy has been liberalized in 1980, Turkey has undergone several key changes in its banking sector. The first major change was introduced in 1985 through the issuance of major banking reform legislation, which was related to the structural problems of the Turkish banking system (Ganioglu, 2008). The second major change in the banking sector was initiated after the economic crisis of 1994. This crisis had a severe impact on the sector due to accumulated risks, including RIN risks, currency risks, liquidity risks and credit risks (Akinci et al., 2013). The third main change in the banking sector occurred in 1999 when the banking sector act was fundamentally reformed in order to support its supervisory authority of the sector and to provide a suitable framework to deal with banks' problems, such as the establishment of the Banking Regulation and Supervision Agency (B.R.S.A.) as an independent agency that aimed to regulate and supervise the sector. The fourth main change happened after the 2001 crisis, whereby the government initiated a comprehensive banking sector restructuring program (Repkova

and Stavarek, 2014). According to the Banks Association of Turkey, the banking sector experienced positive developments from 2001 to 2014, the share of non-performing loans to total loans substantially decreased.

Sustainable development, particularly in the banking sector is a critical issue for Turkey, which aims to be among the world's top ten-largest economies (Pata, 2018). It has made efforts to promote economic growth by increasing GDP and investment, and this has caused a rise in greenhouse gas emissions (GHG) and CO₂ emissions. Environmental degradation is an important barrier preventing sustainable development in Turkey (Pata, 2018). The main strategic objective for Turkey is to alleviate the harmful influence of CO₂ emissions. The policy makers play an important role in promoting investments in low emission projects. Moreover, they can enforce different techniques to minimize CO₂ emissions, such as by promoting the use of clean energy technologies like solar and wind (Viebahn et al., 2007). In this respect, this study aims to instigate a new discussion by testing the association among banking sector development, RIN and CO₂ emissions in Turkey through examining the environmental Kuznets curve hypothesis (E.K.C.)

Turkey is an emerging economy; it represents an ideal case to examine the influence of banking sector development, RIN, energy consumption and real income on Turkey's CO₂ emissions for several reasons. Firstly, the International Energy Agency (IEA) has shown that Turkey has one of the most energy intensive industries among the organisation for economic co-operation and development (OECD) countries. Uzlu et al. (2014) stated that a fundamental part of primary energy consumption in Turkey is supported by imported oil and gas, thus leading to an increase in the budget deficit. Ates (2015) stated that Turkey had the greatest rate of increase in greenhouse gas emissions (GHG) in the period from 1990 to 2010, primarily consisting of CO₂ emissions. Secondly, Turkey's economy has faced prime economic structural changes over the last decades, mainly in the 1980s. Turkey had liberalized its economy, as a result of which, the economic growth was driven by several factors, particularly the free market economy and the increase in international trade. In this respect, the structure of international trade has changed radically, where trade as a percentage of GDP has risen from 17.08% in 1980 to 51.14% in 2014. Furthermore, the total exports in 1980 were 2.9 billion USD, whereas it reached 157.6 billion USD in 2014 (Guloglu, 2016). In addition, foreign direct investment (FDI) has also increased in Turkey over the last three decades (Isiksal et al., 2017). Net cumulative FDI inflows in Turkey reached 127 billion dollars in the period from 2001 to 2012 (Seker et al., 2015). Thirdly, even though Turkey has faced periods of crisis after the introduction of its liberalization program, the banking sector has experienced positive developments, particularly in the period between 2001 and 2014. Finally, after the 2001 Turkish economic crisis, Turkey changed its exchange rate system from a fixed system to a floating exchange rate regime, which is determined by supply and demand processes in the market (Central bank of Turkey).

This study seeks to examine the dynamic relationship between banking sector development, RIN, income, energy use and Turkey's CO₂ emissions from 1980 to 2014. Banking sector development is measured by credits provided by banks as a percentage to GDP. There are few studies that have used this variable to measure the impact of banking sector development on CO₂ emissions. This study argues that the impact of banking sector development and the RIN on CO₂ emissions can be positive or negative depending on how these variables affect economic growth and energy consumption.

Positive developments in the banking sector, such as an increase in the credits provided by banks to the private sector, may lead to an increase in total assets, an increase in the shareholders' equity of the sector, improvements in the risk management systems, and a decrease in the share of non-performing loans to total loans, which may affect economic growth and energy consumption and cause a subsequent rise in CO₂ emissions.

On other hand, RIN may affect CO₂ emissions in three channels. Firstly, low interest-rate helps corporations to minimize financing costs and also optimizes asset/liability structure management (Isiksal et al., 2018), which causes an expansion of the operation and production through the purchase of new equipment and increased investments in new projects, which leads to an increase in energy consumption and causes an increase in CO₂ emissions. Secondly, RIN can affect trade and FDI, as the boost in economic growth thus may lead to an increase in energy consumption and an increase in CO₂ emissions (Riti et al., 2017). Finally, when RIN has a significant impact on the real income, it may lead to an increase in consumer loans as well as the consumption of electrical machines, automobiles, etc. which would also increase CO₂ emissions (Beck and Demirguc-Kunt, 2006).

The remainder of this study is organized as follows: Section 2 is a literature review focusing on the relationship between real income, energy consumption, the banking sector, RIN and CO₂ emissions; Section 3 presents the materials and methods; Section 4 is the results and discussion; and Section 5 provides conclusion.

Literature review

Real income, energy consumption and CO₂ emissions

The existing empirical studies show that there is a linkage between energy consumption, real income and CO₂ emissions. Recent empirical studies seem to present varied empirical evidence on linkage between energy consumption, real income and CO₂ emissions. Say and Yucel (2006) found that energy consumption led to an increase in CO₂ emissions and proposed that the E.K.C. hypothesis exists in Turkey. Yavuz (2014) examined the linkage between energy, income and CO₂ emissions in Turkey over the period from 1960 to 2007. Seker et al. (2015) used the ARDL model and found that energy consumption led to an increase in CO₂ emissions. Recent studies by Katircioglu and Katircioglu (2018) and Pata (2018) used the ARDL testing model and they found that energy consumption led to an increase in CO₂ emissions in Turkey. They suggested that real income is the primary driver for consumption of energy and it was suggested that the policy makers in Turkey should boost and support energy efficiency in order to promote sustainable growth.

Unlike these studies, some authors argue that the inverted U-shaped linkage between CO₂ emissions and income is not valid. Akbostanci et al. (2009) applied the time series model and Ozturk and Acaravci (2010) used a linear logarithmic model. They also did not find that the E.K.C. hypothesis holds for Turkey and they suggested that energy conservation policies such as rationing energy consumption and controlling CO₂ emissions were not likely to have any evident effect on the economic growth in Turkey.

RIN and CO₂ emissions

RIN is an important factor affecting the economy and the spillover effect of RIN on CO₂ emissions depends on how this variable will affect real income, investment, and how

it may lead to an increase (decrease) in energy consumption and then subsequently affect CO₂ emissions. According to many empirical studies, RIN can affect economic performance by macroeconomic channels (Sokolov et al., 2011; Missio et al., 2015; Almahadin and Tuna, 2017; Sehrawat, 2017). The authors showed that the interest rate can have a different impact on economic performance in developing and developed economies; the mixed results can be attributed to different economic structures (Backhaus et al., 2016), different interest rate policies (tight vs expansive) and different inflation levels (Chari et al., 2002). The authors mainly suggested that the stability of the interest rate might lead to better economic performance (Danish et al., 2017; Backhaus and Isiksal, 2016).

Hence, if there is a real impact of RIN on economic activities, it will affect energy consumption and energy prices. Tolis et al. (2010) analyzed the impact of RIN and inflation rates on energy investments and argued that volatility in RIN affected energy investment. That could have a controversial effect on sustainability and could lead to an increase in CO₂ emissions. By using the US interest rate, Ziaei (2018) indicated that a decrease in RIN was accepted as a positive signal in the energy market and the energy consumed by the residential sector.

Banking sector development and CO₂ emissions

Many empirical studies (Beck and Levine, 2004; Wachtel, 2001; Petkovski and Kjosevski, 2014) have stated that development of the financial sector including developed banking performance accelerates the economic growth rate. Beck et al. (2000) stated that more funds are available for distribution as loans, which should stimulate and support consumption, investment, economic growth, and energy demand, and may cause an increase in energy consumption. Aslan et al. (2014) showed a positive relationship between banking development and energy consumption, and stated that deposit money bank assets and domestic credit to the private sector increases energy consumption, which may cause an increase in CO₂ emissions.

Development of the banking sector is a part of financial development; generally, the role of financial development in ecological degradation has received increased attention in the recent literature. Zhang (2011) tested the role of financial development on CO₂ emissions in China for the period 1980 to 2009 and found that China's financial development acts as an important driver for the increase in CO₂ emissions. Similar results were found in India by Shahbaz et al. (2015), who used the Vector Error Correction Model (VECM) approach and supported the assertion that financial development has a positive impact on CO₂ emissions in India over the time period of 1970–2012. Haseeb et al. (2018) used fully modified ordinary least square (FMOLS) panel data and examined the relationship between financial development measured by domestic credit to the private sector (% of GDP) and CO₂ emissions in the BRICS countries from 1995 to 2014 and found that domestic credit to the private sector (% of GDP) led to an increase in CO₂ emissions. Pata (2018) applied the FMOLS and ARDL models and found that financial development had a positive impact on CO₂ emissions in Turkey over the period from 1974 to 2014. These studies confirmed that financial development plays an important role in increasing and improving the economic efficiency of the financial systems and this can affect economic activities and the demand for energy, thus causing an increase in CO₂ emissions.

In contrast, Saidi and Mbarek (2017) used the GMM panel method to analyze 19 emerging countries and found a negative impact of financial development on CO₂

emissions for the period from 1990 to 2013. Park et al. (2018) used PMG estimates and data from the period 2001 to 2014 for selected European Union (EU) countries, and their findings showed that financial development led to a decrease in CO₂ emissions. In these studies, the authors suggested that financial development may increase energy efficiency and then decrease energy consumption and CO₂ emissions. Ozturk and Acaravci (2013) used the ARDL bounds test and stated that financial development did not affect CO₂ emissions in Turkey over the period from 1960 to 2007.

However, most of the studies focused on financial development measured by domestic credit provided by the financial sector to the private sector and only a minimal number of studies have focused on the banking sector development variable. Tamazian et al. (2009) analysed the role of financial development on CO₂ emissions in the BRIC countries over the period from 1992 to 2004. The authors found that capital market and banking sector development led to a reduction in CO₂ emissions. Sadorsky (2011) used the dynamic panel demand model and examined the nexus between financial development and CO₂ emissions and stated that deposit money bank assets led to an increase in CO₂ emission in nine Central and Eastern European counties. A summary of the EKC hypothesis and other studies is presented in *Table 1*.

Table 1. Summary of the studies

Authors	Period	Country	Methodology	Findings
Zhang (2011)	1980-2009	China	Granger causality	FD is significant.
Shahbaz et al. (2015)	1970–2012	India	VECM	FD is significant.
Saidi and Mbarek1 (2017)	1990-2013	19 counties	GMM panel	FD is significant.
Haseeb et al. (2018)	1995-2014	BRICS	FMOLS Panel	FD is significant.
Tamazian et al. (2009)	1992-2004	BRIC	SSRF Model	BD is significant.
Sadorsky (2011)	1990-2013	EU counties	GMM Model	BD is significant.
Ozturk and Acaravci (2013)	1960-2007	Turkey	ARDL Model	FD is not significant
Jalil and Mahmud (2009)	1971-2005	China	ARDL Model	FD is significant
Yavuz (2014)	1960-2007	Turkey	Time series	Y is significant
Seker et al. (2015)	1974-2010	Turkey	ARDL Model	Y is significant
Pata (2018)	1974-2014	Turkey	ARDL Model	Y is valid
Akbostanci et al. (2009)	1992-2001	Turkey	Time series	Y is not valid
Ozturk and Acaravci (2010)	1968-2005	Turkey.	linear log model	Y is not valid
Say and Yucel (2006)	1970-2005	Turkey	IPCC - TCO2	EN is significant.
Katircioglu and Katircioglu (2018)	1974-2014	Turkey	ARDL Model	EN is significant.

Y is real income, FD is financial development, BD is bank development, EN is energy consumption

Materials and methods

After Grossman and Krueger (1995) proposed the first theoretical linkage between CO₂ emissions and income, many empirical studies (Say and Yucel, 2006; Jalil and Mahmud, 2009; Yavuz, 2014; Katircioglu and Katircioglu, 2018; Pata, 2018) have used the following model:

$$\ln CO_{2it} = \beta_0 + \gamma_1 \ln Y_{it} + \gamma_2 \ln Y_{it}^2 + \varepsilon_{it} \quad (\text{Eq.1})$$

where CO_2 is carbon dioxide emissions (measured in metric tons per capita), Y is GDP per capita (constant 2010 US-dollar), Y^2 is the square of GDP, ε_t is the error-term, while i and t represent the country and years, respectively.

This study is different from the existing literature as it uses other economic factors, namely bank development and RIN. Thus, bank development and RIN are external proxies added to the conventional EKC model. The empirical model of this paper is presented as follows:

$$\ln CO_{2t} = \beta_0 + \gamma_1 \ln Y_t + \gamma_2 \ln Y_t^2 + \gamma_3 \ln EG_t + \gamma_4 \ln BD_t + \gamma_5 \ln RIN_t + \varepsilon_{it} \quad (\text{Eq.2})$$

where $\ln CO_{2t}$ represents the logarithm of CO_2 , $\ln Y$ and $\ln Y^2$ are the logarithms of Y (GDP) and Y^2 (square of GDP), $\ln EG_t$ is the logarithm of energy consumption, $\ln BD$ represents the logarithm of banking sector development, and RIN is the real interest rate. The data is annual data covering the years between 1980 and 2014. Descriptive statistics of the variables are represented in Table 2. A summary of the descriptions of the variables and sources of the data is represented in Table 3.

Table 2. Descriptive statistics of the variables

	Mean	Median	Maximum	Minimum	Standard deviation
CO_{2t}	1.093758	1.149764	1.502182	0.54398	0.273282
Y_t	8.963046	8.952993	9.496421	8.51459	0.275895
Y^2_t	80.41015	80.15609	90.18201	72.49824	4.960866
EG_t	6.986357	7.026588	7.368592	6.557903	0.242447
BD_t	3.12257	2.916845	4.093362	2.648661	0.437009
RIN	-0.00272	0.0458	0.2414	-0.85	0.220229

Table 3. Summary of the variables' descriptions and sources of the data

Variables	Description	Source of the data
CO_{2t}	CO ₂ emissions (metric-tons-per capita)	World-Bank (website)
Y_t	GDP-per-capita (constant-2010-USD)	World-Bank (website)
Y^2_t	the square of GDP	World-Bank (website)
EG_t	Energy consumption (kt of oil-equivalent)	World-Bank (website)
BD_t	Credits provided by banks to the private-sector as a % of GDP	World-Bank (website)
RIN	RIN (interest rate of the time-deposit minus inflation-rate)	World-Bank (website)

Unit root tests and co-integration tests

This paper uses the Perron-Vogelsang (1999) with one structural break (SB) and Clemente-Montanes-Reyes (CMR) (Clemente et al., 1998) with two SBs to estimate the order of integration of the variables.

To examine the long-term relationship between CO_2 and the Y , Y^2 , En , BD , RIN variables, this paper uses the ARDL bounds test within the ARDL methodology introduced by Pesaran et al. (2001). The model is distinguished from other models as it uses different lags to estimate the parameters by employing a single reduced form

equation. Considering the sensitivity of this methodology to the number of lags, the Akaike-information-criterion (A.I.C) and Schwarz-Bayesian-criteria (S.B.C) were applied to select the optimal lag length (p). Additionally, in this test, all variables are treated as endogenous, thus excluding the endogeneity problem. Therefore, by employing this test, the paper aims to determine if there is cointegration or not in three options: I(0), I(1) or mixed. In this vein, the *F*-statistics value was compared to the theoretical values introduced by Pesaran et al. (2001). If the *F*-statistics value exceeds the upper bound I(1), the null-hypothesis will be rejected, indicating that there is cointegration among the variables. If the *F*-statistics value is less than the lower bound I(0), the null-hypothesis will be accepted, indicating that there is no cointegration among the variables. Furthermore, if the *F*-statistics value lies between I(0) and I(1), this means that the result is inconclusive. The ARDL approach equation is as follows:

$$\Delta \ln CO_{2t} = \beta_0 + \sum_{i=1}^n \gamma_1 \Delta \ln CO_{2t-j} + \sum_{i=1}^n \gamma_2 \Delta \ln Y_{t-j} + \sum_{i=1}^n \gamma_3 \Delta \ln Y_{t-j}^2 + \sum_{i=1}^n \gamma_4 \Delta \ln EG_{t-j} + \sum_{i=1}^n \gamma_5 \Delta \ln BD_{t-j} + \sum_{i=1}^n \gamma_6 \Delta \ln RIN_{t-j} + \sigma_1 \ln CO_{2t-1} + \sigma_2 \ln Y_{t-1} + \sigma_3 \ln Y_{t-1}^2 + \sigma_4 \ln En_{t-1} + \sigma_5 \ln BD_{t-1} + \sigma_6 \ln RIN_{t-1} + \varepsilon_{1t} \quad (\text{Eq.3})$$

In Equation 4, Δ represents the operator of the first difference. $\ln CO_{2t}$, $\ln Y_t$, $\ln Y_t^2$, $\ln EG_t$, $\ln BD_t$, $\ln RIN_t$ are the dependent and independent variables, *n* is the maximum number of lags, and ε_t represents the error-term. Once the existence of co-integration is validated, in order to capture the speed of adjustment of the dependent variable, the error correction model is estimated using the following equation:

$$\Delta \ln CO_{2t} = \beta_0 + \sum_{i=1}^n \gamma_1 \Delta \ln CO_{2t-j} + \sum_{i=1}^n \gamma_2 \Delta \ln Y_{t-j} + \sum_{i=1}^n \gamma_3 \Delta \ln Y_{t-j}^2 + \sum_{i=1}^n \gamma_4 \Delta \ln EG_{t-j} + \sum_{i=1}^n \gamma_5 \Delta \ln BD_{t-j} + \sum_{i=1}^n \gamma_6 \Delta \ln RIN_{t-j} + \omega ECT_{t-1} + \varepsilon_{1t} \quad (\text{Eq.4})$$

ECT_{t-1} is the one period lagged error correction-term. It is expected that the *ECT* will be significant with a negative sign (Gujarati, 2003). *ECT* shows the speed of adjustment among the short-term and long-term levels of the dependent variable.

The Bayer-Hanck (BH) (2013) combined cointegration test is utilized to investigate the robustness of the ARDL model. It is applied to the data with a unique order of integration. It combines four different cointegration tests, namely Engle and Granger (1987) (EG_t), Johansen (1988) (JO_t), Boswijk (1994) (BO_t), and Banerjee et al. (1998) (BA_t). This test combines the outcomes of previous co-integration tests and provides the *Fisher-F* statistics for more reliable and conclusive outcomes. BH provides functional estimates by disregarding the nature of multiple testing proceedings. This test is a combination of the computed *p*-values with the significance level of cointegration tests based on Fisher's formula as follows:

$$EG_t - JOH_t = -2[IN(P_{EG_t}) + (P_{JOH_t})] \quad (\text{Eq.5})$$

$$EG_t - JOH_t - BO_t - BDM_t = -2[IN(P_{EG_t}) + (P_{JO_t}) + (P_{BO_t}) + (P_{BA_t})] \quad (\text{Eq.6})$$

where *p* are the values of individual cointegrations tests (EG_t, JO_t, BO_t, BA_t). The estimated long-run combined cointegration *Fisher F*-statistics will be compared with the critical values (CV), which were presented by Bayer and Hanck (2013). The null hypothesis of the BH test is no long-run combined co-integration. It will be rejected if the computed *Fisher F*-statistics value is higher than the critical values.

The paper uses other techniques to estimate long-run coefficient, namely fully modified ordinary least square (FMOLS) and canonical co-integrating regression (CCR), which were introduced by Phillips and Hansen (1990) and Park (1992). These tests consider endogeneity and the serial correlation problems, which may appear in the existence of cointegration. These tests can only be utilized when the variables are I(1).

The direction of the causal relationship between CO₂ emissions, Y , Y^2 , EG , BD , and RIN is tested by using Granger causality within *VECM*. This test identifies if there is co-integration among the time series variables and if so, it is possible to analyze the direction of the causal effect linkage by using the error correction model (ECM) since it includes information about the causality in both the short and long run. This test allows for the addition of an (*ECT*) to capture the short-term deviations of the time series from their long-term equilibrium path. The (ECM) equation is as follows:

$$\Delta \ln CO_{2t} = \beta_0 + \sum_{i=1}^n \gamma_1 \Delta \ln CO_{2t-j} + \sum_{i=1}^n \gamma_2 \Delta \ln Y_{t-j} + \sum_{i=1}^n \gamma_3 \Delta \ln Y^2_{t-j} + \sum_{i=1}^n \gamma_4 \Delta \ln EG_{t-j} + \sum_{i=1}^n \gamma_5 \Delta \ln BD_{t-j} + \sum_{i=1}^n \gamma_6 \Delta \ln RIN_{t-j} + ECT_{t-1} + \varepsilon_{1t} \quad (\text{Eq.7})$$

$$\ln Y_t = \beta_0 + \sum_{i=1}^n \gamma_1 \Delta \ln Y_{t-j} + \sum_{i=1}^n \gamma_2 \Delta \ln CO_{2t-j} + \sum_{i=1}^n \gamma_3 \Delta \ln Y^2_{t-j} + \sum_{i=1}^n \gamma_4 \Delta \ln EG_{t-j} + \sum_{i=1}^n \gamma_5 \Delta \ln BD_{t-j} + \sum_{i=1}^n \gamma_6 \Delta \ln RIN_{t-j} + ECT_{t-1} + \varepsilon_{1t} \quad (\text{Eq.8})$$

$$\Delta \ln Y^2_t = \beta_0 + \sum_{i=1}^n \gamma_1 \Delta \ln Y^2_{t-j} + \sum_{i=1}^n \gamma_2 \Delta \ln CO_{2t-j} + \sum_{i=1}^n \gamma_3 \Delta \ln Y_{t-j} + \sum_{i=1}^n \gamma_4 \Delta \ln EG_{t-j} + \sum_{i=1}^n \gamma_5 \Delta \ln BD_{t-j} + \sum_{i=1}^n \gamma_6 \Delta \ln RIN_{t-j} + ECT_{t-1} + \varepsilon_{1t} \quad (\text{Eq.9})$$

$$\Delta \ln EG_t = \beta_0 + \sum_{i=1}^n \gamma_1 \Delta \ln EG_{t-j} + \sum_{i=1}^n \gamma_2 \Delta \ln CO_{2t-j} + \sum_{i=1}^n \gamma_3 \Delta \ln Y_{t-j} + \sum_{i=1}^n \gamma_4 \Delta \ln Y^2_{t-j} + \sum_{i=1}^n \gamma_5 \Delta \ln BD_{t-j} + \sum_{i=1}^n \gamma_6 \Delta \ln RIN_{t-j} + ECT_{t-1} + \varepsilon_{1t} \quad (\text{Eq.10})$$

$$\Delta \ln BD_t = \beta_0 + \sum_{i=1}^n \gamma_1 \Delta \ln BD_{t-j} + \sum_{i=1}^n \gamma_2 \Delta \ln CO_{2t-j} + \sum_{i=1}^n \gamma_3 \Delta \ln Y_{t-j} + \sum_{i=1}^n \gamma_4 \Delta \ln Y^2_{t-j} + \sum_{i=1}^n \gamma_5 \Delta \ln EG_{t-j} + \sum_{i=1}^n \gamma_6 \Delta \ln RIN_{t-j} + ECT_{t-1} + \varepsilon_{1t} \quad (\text{Eq.11})$$

$$\Delta \ln RIN_t = \beta_0 + \sum_{i=1}^n \gamma_1 \Delta \ln RIN_{t-j} + \sum_{i=1}^n \gamma_2 \Delta \ln CO_{2t-j} + \sum_{i=1}^n \gamma_3 \Delta \ln Y_{t-j} + \sum_{i=1}^n \gamma_4 \Delta \ln Y^2_{t-j} + \sum_{i=1}^n \gamma_5 \Delta \ln EG_{t-j} + \sum_{i=1}^n \gamma_6 \Delta \ln BD_{t-j} + ECT_{t-1} + \varepsilon_{1t} \quad (\text{Eq.12})$$

In *Equations 7-12*, Δ represents the operator of the first difference, $\ln CO_2$, $\ln Y$, $\ln Y^2$, $\ln EG$, $\ln BD$, and RIN are the dependent and independent variables, ε_t represents the error-term, and ECT_{t-1} is the lagged error correction-term added to the equations. The short-term causality is examined by Wald test's F -statistics to define the significance of the related coefficient by applying the first difference of the stationary variables (Masih, 1996). To examine the long-run causality, the test of the related coefficient of the lagged *ECT* is used.

Results and discussion

Unit root test results

The results of Perron and Vogelsang and CMR with one and two SBs are reported in *Tables 4* and *5*. The results of the Perron and Vogelsang and CMR unit root test with one and two SBs show that all the variables are stationary at first-difference, I(1). *Figure 1* shows the time series plot of the series at the natural logarithm indicating various economic fluctuations and policy changes in Turkey.

The results of the F bounds tests are represented in *Table 6*. The results show that the F -statistics is higher than 5% (Pesaran et al., 2001). This confirms that there is co-integration among all the variables.

Table 6 provides powerful evidence on the level relationship for Equation 2 of this study. The null hypothesis ($\sigma_1 = \sigma_2 = \sigma_3 = \sigma_4 = \sigma_5 = \sigma_6 = 0$) in Equation 3 can be rejected and this shows that CO₂ emissions in Turkey are in a long-run relationship with the regressed variables (Y, Y², En, BD and RIN).

Table 4. Perron and Vogelsang unit root test results with one SB

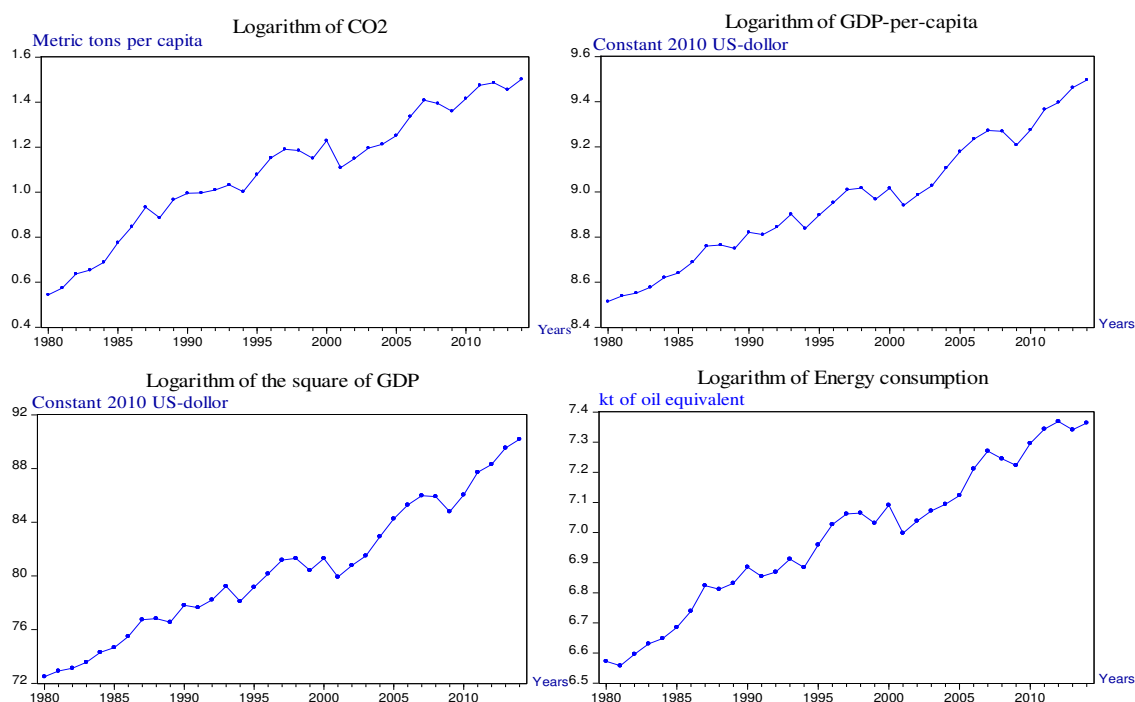
	At level	SB		At 1st difference	SB
<i>lnCo2</i>	-3.488	2002	$\Delta \ln CO_2$	-6.611**	1999
<i>lnY</i>	-3.791	2005	$\Delta \ln Y$	-6.709**	2009
<i>Ln Y²</i>	-3.655	2005	$\Delta \ln Y^2$	-5.655**	2009
<i>lnEG</i>	-2.772	2010	$\Delta \ln EG$	-6.751**	1999
<i>lnBD</i>	-2.579	2008	$\Delta \ln BD$	-5.965**	2003
<i>RIN</i>	-3.120	1990	ΔRIN	-7.276**	1999

* and ** denote significantly level at the 5% and 10% levels, respectively

Table 5. CMR with two structural breaks unit root tests

	At level	SB 1	SB 2		At 1st difference	SB	SB 2
<i>lnCO2</i>	-4.189	1998	1999	$\Delta \ln CO_2$	-7.222**	1986	2000
<i>lnY</i>	-4.219	1994	2002	$\Delta \ln Y$	-7.780**	2000	2008
<i>Ln Y²</i>	-4.210	1994	2002	$\Delta \ln Y^2$	-7.941**	2000	2008
<i>lnEG</i>	-5.261	1996	2010	$\Delta \ln EG$	-6.353**	1996	2003
<i>lnBD</i>	-5.360	2000	2006	$\Delta \ln BD$	-8.359**	1996	2000
<i>RIN</i>	-5.390	1988	1997	ΔRIN	-9.979**	1997	2001

* and ** denote significantly level at the 5% and 10% levels, respectively



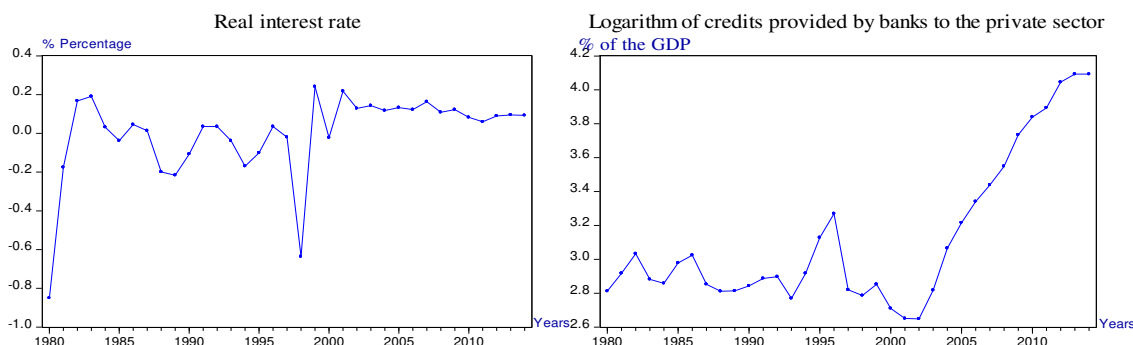


Figure 1. Time series plot of series

Table 6. ARDL bounds test results (*F*-bound-test)

	Level		t statistics
	I (0)	I (1)	
Critical value at 1% sign level	2.86	4.57	6.502970***
Critical value at 5% sign level	2.39	3.38	

* and ** denote significantly level the 5% and 10%, respectively

The results of the BH combined co-integration test are reported in Table 7. The results show that the computed *F*-statistics value is higher than the tabulated *F*-statistics in both $EG_t - JO_t$ and $EG_t - JO_t - BO_t - BA_t$ at 5% and 10% levels of significance. Therefore, the results of the BH (2013) co-integration tests confirm the robustness of the ARDL model. These results imply that there is a long-run association and all the variables are corresponding together in the long term.

Table 7. BH combined co-integration test results

	Fisher- <i>F</i> statistics		Co-integration results
	<i>EGT-JOT</i>	<i>EGT-JOT-BOT-BAT</i>	
	14.863**	19.252*	Co-integration exists
Sig level at (5)%	10.711	20.788	
sig level at (10)%	8.352	16.239	

*, **shows significantly level at 10%, and 5%, respectively

The normality test results confirm that the model is normally distributed. Furthermore, ARCH, LM and the Breusch-Pagan Godfrey, tests results confirm that the model is homoscedastic and there is no autocorrelation. Furthermore, the Ramsey-Reset test results confirm the stability of the results. The results show that the model is correctly formulated. Moreover, Figures 2 and 3 show the stability tests using CUSUM and CUSUM squares. The figures show that the blue lines are between the two red lines at the 5% significant level, which means that there is stability in the long-run coefficients.

Table 8 shows that the speed of adjustment is negative and statistically reliable; the rate of convergence from the short-run to long-run equilibrium is 85.5%. The results

from ARDL, FMOLS and CCR are presented in *Tables 8* and *9*. The results show that the coefficient of GDP(*Y*) is highly elastic, positive and statistically significant, while the squared GDP(*Y*²) is negative and statistically significant in the long-run. This finding strongly confirms that the E.K.C. hypothesis is valid for Turkey.

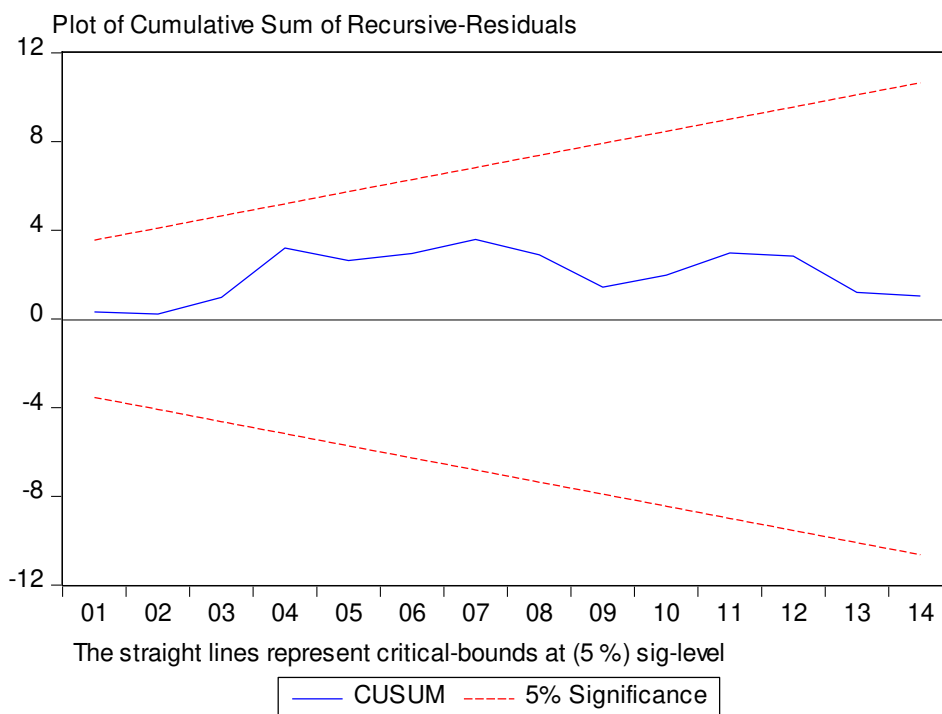


Figure 2. Plot of CUSUM test

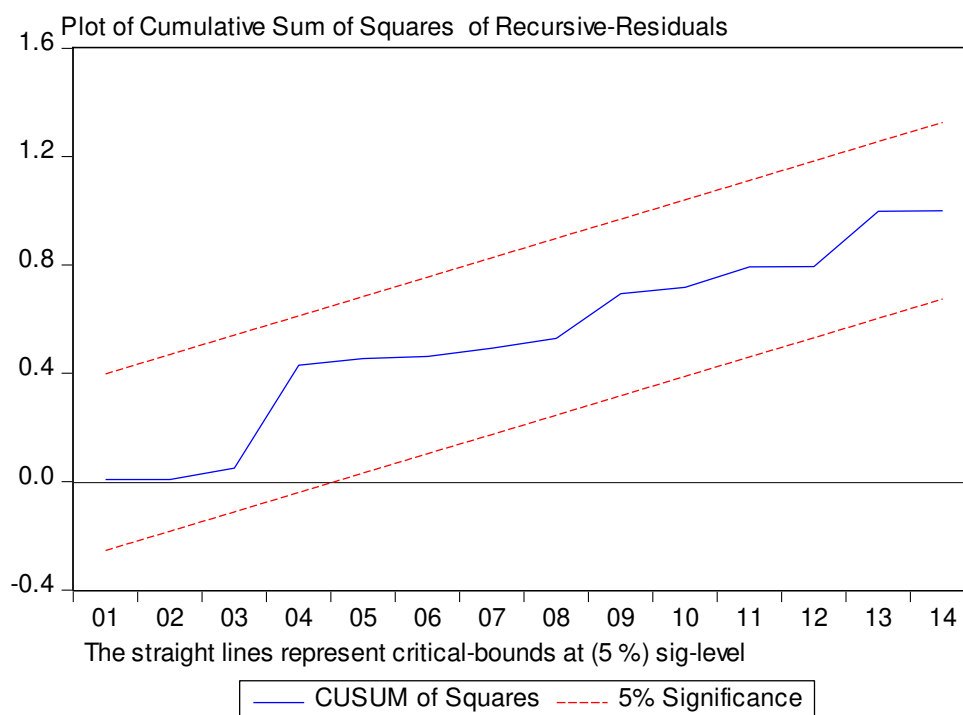


Figure 3. Plot of CUSUM of squares test

Table 8. Estimated short and long-term coefficients using ARDL (1,3, 3,2, 3,3)

Variables	Coefficient	t-statistics	p-value
$\Delta \ln Y$	1.5566***	6.2321	0.0001
$\Delta \ln Y^2$	-0.4688*	-1.8351	0.0963
$\Delta \ln EG$	1.1468***	2.9691	0.0000
$\Delta \ln BD$	0.1042***	5.4067	0.0003
ΔRIN	-0.0007***	-5.4502	0.0003
$\ln Y$	2.2224*	1.8532	0.0935
$\ln Y^2$	-0.4079*	-2.2750	0.0571
$\ln EG$	1.2652***	7.2595	0.0000
$\ln BD$	0.0648***	3.3028	0.0080
RIN	-0.0008*	-1.8841	0.0889
$ECT(-1)$	-0.8551***	-8.5342	0.0000
χH^{BPC}	1.215(0.3881)	R.sq	0.98
χH^{Ar}	1.139(0.350)	Adjusted	0.96
χN^{JB}	1.952(0.376)	D.W.	2.301
χR^{RT}	0.3075(0.760)		
χB^{CS}	2.075(0.1879)		

χH^{BPC} is heteroscedasticity F-test, χH^{Ar} is ARCH test, χN^{JB} is normality test, χR^{RT} is Ramsey RESET, χB^{CS} is B-Godfrey serial correlation. DW is Durbin-Watson
*, **, *** shows significantly level at 10%, 5% and 1%, respectively

Table 9. FMOLS and CCR model results

Regressor	FMOLS				CCR		
	Coeff.	t-ratio	p-value		Coeff.	t-ratio	p-value
$\ln Y$	1.992***	3.577	0.001	$\ln Y$	3.014***	4.170	0.000
$\ln Y^2$	-0.204***	-2.959	0.006	$\ln Y^2$	-0.332***	-3.708	0.001
$\ln EG$	1.093***	16.908	0.000	$\ln EG$	1.089***	14.653	0.000
$\ln BD$	0.013**	2.261	0.033	$\ln BD$	0.014**	2.617	0.015
RIN	-0.001***	-4.626	0.000	RIN	-0.002***	-6.595	0.000
Adjusted R2	0.985	-	-	-	0.985	-	-

*, **, *** shows significantly level at 10%, 5% and 1%, respectively

The coefficient of energy consumption in both the short and long run has a positive significant effect on the level of CO₂ emissions. Furthermore, the proxy for banking sector development is positive and significant in both the short and long run. Thus, an increase in credits provided by banks as a percentage of GDP led to an increase in CO₂ emissions. On the other hand, the proxy of RIN is negative and statistically significant in the short and long run. Therefore, an increase in the RIN leads to a decrease in CO₂ emissions.

The coefficient of GDP makes the highest impact on CO₂ emissions, which shows that a 1% increase in GDP will lead to a 2.22%-3.01% increase in emissions. The second highest impact is made by energy consumption, which indicates that a 1% increase in energy consumption will lead to 1.09%-1.26% increase in emissions. The

results also show that a 1% increase in bank credits will increase the emissions by 0.01%-0.06%; however, with a 1% increase in RIN, the emissions will decline by 0.0008%-0.02%.

Granger causality test results

Table 10 reports the Granger causality results. The null hypothesis of the causality test is that x and y are independent, or there is no linkage between x and y . As shown in Table 10 there is a long-run unidirectional causality from Y , EG , BD and RIN to CO_2 (Y , EN , BD , $RIN \rightarrow CO_2$). The results strongly confirm that the E.K.C. hypothesis is valid for Turkey. Furthermore, the results show that there is a unidirectional short-run causality running from RIN to the bank credits to the private sector and energy consumption ($RIN \rightarrow BD$, $RIN \rightarrow EG$), which confirms that the RIN may cause banking sector development and energy consumption, which may lead to an increase in CO_2 emissions in Turkey. There is a unidirectional causality from the bank credits to the private sector and energy consumption ($BD \rightarrow EG$). These results confirm our findings for a strong relationship between banking sector development and CO_2 emissions in Turkey.

Table 10. Granger causality results

	Short Run causality F-statistics					Long Run causality t statistics	
	$\Delta \ln CO_2$	$\Delta \ln Y$	$\Delta \ln Y^2$	$\Delta \ln EG$	$\Delta \ln BD$	ΔRIN	$ECT_t - 1$
$\Delta \ln CO_2$	-	6.342**	3.451	7.078**	7.221**	6.006**	-2.1940**
$\Delta \ln Y$	0.472	-	0.033	4.634*	0.655	0.767	-1.1409
$\Delta \ln Y^2$	0.605	0.034	-	3.983	0.655	0.424	-0.7070
$\Delta \ln EG$	0.789	7.154**	1.333	-	5.358*	16.781***	-1.1091
$\Delta \ln BD$	0.891	0.244	0.21	0.156	-	5.247*	-0.8843
ΔRIN	1.499	0.112	0.108	0.476	0.326	-	-0.9528

*, **, ***shows significantly level at 10%, 5% and 1%, respectively

Conclusion

This article aims to introduce a new research topic by investigating the role of banking sector development, RIN , real income, and energy consumption on Turkey's CO_2 emissions for the time period 1980-2014. This article is different from the existing literature as it introduces a new discussion concerning the role of banking sector development on CO_2 emissions in Turkey. The sophisticated econometric models, Autoregressive Distributed Lag (ARDL), Fully Modified-OLS (FMOLS), and the Canonical Cointegrating Regression (CCR) tests are applied to test the short and long-run coefficients between the variables. The ARDL model was preferred due to its advantages compared to the other models. Firstly, the ARDL model has superior features in small data in particular, and it is not important to test the integration order of the series. This test enables simultaneous analysis of both the short-run and long-run effects of independent variables on the dependent variable. In order to confirm and support the results in the long run, the paper uses the FMOLS, and CCR tests. These tests consider endogeneity and the serial correlation problems, which may appear in the existence of cointegration. The new approach involving the Bayer-Hanck (BH)

combined co-integration test is used to enhance and support the robustness of the ARDL bounds test. Moreover, the Granger causality test within the VECM model is applied to examine the causality direction among the variables of this study. The empirical results and policy recommendations are as follows:

Real income and energy consumption

The empirical results from the ARDL, FMOLS and CCR models show strong evidence to confirm that the E.K.C. hypothesis holds for Turkey. The results from the ARDL and causality tests show that the increase in real income and energy consumption led to an increase CO₂ emissions. These results are consistent with Say and Yucel (2006), Yavuz (2014), Katircioglu and Katircioglu (2018), and Pata (2018) who found positive relation between energy consumption and real income CO₂ emissions in Turkey, the policy market should design long-term energy strategies to reduce emissions through efficient energy consumption channels and should also implement some strategies that promote the use of the renewable energy sources.

Banking sector development and RIN

The study can make a significant impact in terms of the policies intended to diminish the carbon dioxide emissions in Turkey. The planning of emission levels by using energy consumption and income association might underestimate the real amount of the pollution produced if the financial development variables like bank development and RIN are not considered. Therefore, while banking sector development has lower long-run elasticity than the long-run coefficients of income and energy consumption, it has a positive and statistically significant impact on carbon dioxide emissions. The empirical findings show that increases in banking sector development increase pollution. These results are consistent with Sadorsky (2011) and Pata (2018). These studies confirmed that financial development plays an important role in increasing the economic efficiency of the financial systems and this can affect economic activities and the demand for energy, thus causing an increase in CO₂ emissions. The long-run elasticity of RIN is smaller than the long-run coefficient of credits provided by banks, although it is negative and significant. The larger amount of credits provided by banks as a percentage of GDP shows that there are more funds available as loans for the private sector and this increases consumption, economic growth, energy use, and emissions. However, even a small increase in RIN discourages the consumption of durables like automobiles, mobile phones, etc. and therefore worsens the emissions.

The findings of this article are important for several reasons. Emerging economies like Turkey might experience increases in carbon emissions because of the increase in energy consumption and income levels. Making projections of GHG that do not consider bank credits to the private sector and RIN may underestimate or overestimate the real emissions. It will be difficult to meet greenhouse gas emission targets if the impacts of banking sector development and RIN are not considered.

This study has introduced a new research topic by investigating the role of banking sector development and RIN on Turkey's CO₂ emissions; further research for the developing and developed countries or regions is suggested for comparison purposes. Furthermore, different proxies and other methodologies not only via time series models but also panel data can also be adapted as further researches in order to examine the role of banking sector development and RIN in the environmental concerns of countries.

Acknowledgements. We would like to thank the editor and the anonymous reviewers for their valuable comments, which helped us to improve the paper. We would like to thank Simon Thompson from Near East University, North Cyprus for his assistance with the proofreading of our paper.

REFERENCES

- [1] Akbostanci, E., Turut-Asik, S., Tunc, G. I. (2009): The relationship between income and environment in Turkey: is there an environmental Kuznets curve? – *Energy Policy* 37(3): 861-867.
- [2] Akinci, D. A., Matousek, R., Radic, N., Stewart, C. (2013): Monetary policy and the banking sector in Turkey. – *Journal of International Financial Markets, Institutions and Money* 27: 269-285.
- [3] Almahadin, H. A., Tuna, G. (2017): Dynamic impact of interest rate volatility and spillover effect of the US interest rate on banking sector development of Turkey: empirical evidence from cointegration and causality analysis. – *Asia-Pacific Journal of Accounting & Economics*. <https://doi.org/10.1080/16081625.2017.1354709>.
- [4] Aslan, A., Apergis, N., Topcu, M. (2014): Banking development and energy consumption: Evidence from a panel of Middle Eastern countries. – *Energy* 72: 427-433.
- [5] Ates, S. A. (2015): Energy efficiency and CO₂ mitigation potential of the Turkish iron and steel industry using the LEAP (long-range energy alternatives planning) system. – *Energy* 90: 417-428.
- [6] Backhaus, A., Isiksal, A. (2016): The impact of momentum factors on multi asset portfolio. – *Romanian Journal of Economic Forecasting* 19(4): 146-169.
- [7] Backhaus, A., Zhakanova, A., Fiedler, M. (2016): The robustness of momentum as an asset allocation instrument. – *Asia Life Sciences: The Asian International Journal of Life Sciences* 25(1): 349-366.
- [8] Banerjee, A., Dolado, J., Mestre, R. (1998): Error-correction mechanism tests for cointegration in a single-equation framework. – *Journal of Time Series Analysis* 19(3): 267-283.
- [9] Bayer, C., Hanck, C. (2013): Combining non-cointegration tests. – *Journal of Time Series Analysis* 34(1): 83-95.
- [10] Beck, T., Demircuc-Kunt, A. (2006): Small and medium-size enterprises: access to finance as a growth constraint. – *Journal of Banking & Finance* 30(11): 2931-2943.
- [11] Beck, T., Levine, R. (2004): Stock markets, banks, and growth: panel evidence. – *Journal of Banking & Finance* 28(3): 423-442.
- [12] Beck, T., Levine, R., Loayza, N. (2000): Finance and the sources of growth. – *Journal of Financial Economics* 58(1-2): 261-300.
- [13] Boswijk, H. P. (1994): Testing for an unstable root in conditional and structural error correction models. – *Journal of Econometrics* 63(1): 37-60.
- [14] Chari, V. V., Kehoe, P. J., McGrattan, E. R. (2002): Can sticky price models generate volatile and persistent real exchange rates? – *The Review of Economic Studies* 69(3): 533-563.
- [15] Clemente, J., Montanes, A., Reyes, M. (1998): Testing for a unit root in variables with a double change in the mean. – *Economic Letters* 59: 175-82.
- [16] Danish, Zhang, B., Wang, B., Wang, Z. (2017): Role of renewable energy and non-renewable energy consumption on EKC: evidence from Pakistan. – *Journal of Cleaner Production* 855-864.
- [17] Engle, R. F., Granger, C. W. (1987): Co-integration and error correction: representation, estimation, and testing. – *Econometrica: Journal of the Econometric Society* 251-276.
- [18] Ganioglu, A. (2008): Understanding banking sector reforms in Turkey: assessing the roles of domestic versus external actors. – *Journal of Southern Europe and the Balkans* 10(3): 363-376.

- [19] Grossman, G. M., Krueger, A. B. (1995): Economic growth and the environment. – *The Quarterly Journal of Economics* 110(2): 353-377.
- [20] Gujarati, D. N., Porter, D. C. (2003): *Basic Econometrics*. – McGraw Hill, New York.
- [21] Guloglu, B., Bayar, G. (2016): Sectoral exports dynamics of Turkey: evidence from panel data estimators. – *The Journal of International Trade & Economic Development* 25(7): 959-977.
- [22] Haseeb, A., Xia, E., Baloch, M. A., Abbas, K. (2018): Financial development, globalization, and CO₂ emission in the presence of EKC: evidence from BRICS countries. – *Environmental Science and Pollution Research* 25(31): 31283-31296.
- [23] Isiksal, A. Z., Isiksal, H., Jalali, H. (2017): The impact of foreign direct investment on Turkish economy 2010–2016. – *Economics* 5(2): 69-81.
- [24] Isiksal, A. Z., Samour, A., Resatoglu, N. G. (2018): Monetary policy and exchange rates pre-and post-global financial crisis: the case of Turkey. – *Journal of History Culture and Art Research* 7(5): 83-91.
- [25] Jalil, A., Mahmud, S. F. (2009): Environment Kuznets curve for CO₂ emissions: a cointegration analysis for China. – *Energy Policy* 37(12): 5167-5172.
- [26] Johansen, S. (1988): Statistical analysis of cointegration vectors. – *Journal of Economic Dynamics and Control* 12(2-3): 231-254.
- [27] Katircioglu, S., Katircioglu, S. (2018): Testing the role of fiscal policy in the environmental degradation: the case of Turkey. – *Environmental Science and Pollution Research* 25(6): 5616-5630.
- [28] Kuznets, S. (1955): Economic growth and income inequality. – *The American Economic Review* 45(1): 1-28.
- [29] Masih, A. M. and Masih, R. (1996): Energy consumption, real income and temporal causality: results from a multi-country study based on cointegration and error-correction modelling techniques. – *Energy Economics* 18(3): 165-183.
- [30] Missio, F. J., Jayme, F. G., Britto, G., Luis Oreiro, J. (2015): Real exchange rate and economic growth: new empirical evidence. – *Metroeconomica* 66(4): 686-714.
- [31] Ozturk, I., Acaravci, A. (2010): CO₂ emissions, energy consumption and economic growth in Turkey. – *Renewable and Sustainable Energy Reviews* 14(9): 3220-3225.
- [32] Ozturk, I., Acaravci, A. (2013): The long-run and causal analysis of energy, growth, openness and financial development on carbon emissions in Turkey. – *Energy Economics* 36: 262-267.
- [33] Park, J. Y. (1992): Canonical cointegrating regressions. – *Econometrica: Journal of the Econometric Society* 119-143.
- [34] Park, Y., Meng, F., Baloch, M. A. (2018): The effect of ICT, financial development, growth, and trade openness on CO₂ emissions: an empirical analysis. – *Environmental Science and Pollution Research* 25(30): 30708-30719.
- [35] Pata, U. K. (2018): Renewable energy consumption, urbanization, financial development, income and CO₂ emissions in Turkey: Testing EKC hypothesis with structural breaks. – *Journal of Cleaner Production* 187: 770-779.
- [36] Perron, P., Vogelsang, T. J. (1992): Nonstationarity and level shifts with an application to purchasing power parity. – *Journal of Business & Economic Statistics* 10(3): 301-320.
- [37] Pesaran, M. H., Shin, Y., Smith, R. J. (2001): Bounds testing approaches to the analysis of level relationships. – *Journal of Applied Econometrics* 16(3): 289-326.
- [38] Petkovski, M., Kjosevski, J. (2014): Does banking sector development promote economic growth? An empirical analysis for selected countries in Central and South Eastern Europe. – *Economic Research-Ekonomska istraživanja* 27(1): 55-66.
- [39] Phillips, P. C., Hansen, B. E. (1990): Statistical inference in instrumental variables regression with I(1) processes. – *The Review of Economic Studies* 57(1): 99-125.
- [40] Repkova, I., Stavarek, D. (2014): Concentration and competition in the banking sector of Turkey. – *Amfiteatru Economic* 16(36): 625.

- [41] Riti, J. S., Song, D., Shu, Y., Kamah, M. (2017): Decoupling CO₂ emission and economic growth in China: Is there consistency in estimation results in analyzing environmental Kuznets curve? – *Journal of Cleaner Production* 166: 1448-1461.
- [42] Sadorsky, P. (2011): Financial development and energy consumption in Central and Eastern European frontier economies. – *Energy Policy* 39(2): 999-1006.
- [43] Saidi, K., Mbarek, M. B. (2017): The impact of income, trade, urbanization, and financial development on CO₂ emissions in 19 emerging economies. – *Environmental Science and Pollution Research* 24(14): 12748-12757.
- [44] Say, N. P., Yucel, M. (2006): Energy consumption and CO₂ emissions in Turkey: empirical analysis and future projection based on an economic growth. – *Energy Policy* 34(18): 3870-3876.
- [45] Sehrawat, M., Giri, A. K. (2017): Financial structure, interest rate, trade openness and growth: time series analysis of Indian economy. – *Global Business Review* 5: 1278-90.
- [46] Seker, F., Ertugrul, H. M., Cetin, M. (2015): The impact of foreign direct investment on environmental quality: a bounds testing and causality analysis for Turkey. – *Renewable and Sustainable Energy Reviews* 52: 347-356.
- [47] Shahbaz, M., Mallick, H., Mahalik, M. K., Loganathan, N. (2015): Does globalization impede environmental quality in India? – *Ecological Indicators* 52: 379-393.
- [48] Sokolov, V., Lee, B. J., Mark, N. C. (2011): Linkages between exchange rate policy and macroeconomic performance. – *Pacific Economic Review* 16(4): 395-420.
- [49] Tamazian, A., Chousa, J. P., Vadlamannati, K. C. (2009): Does higher economic and financial development lead to environmental degradation: evidence from BRIC countries. – *Energy Policy* 37(1): 246-253.
- [50] Tolis, A., Doukelis, A., Tasiopoulos, I. (2010): Stochastic interest rates in the analysis of energy investments: Implications on economic performance and sustainability. – *Applied Energy* 87(8): 2479-2490.
- [51] Uzlu, E., Kankal, M., Akpınar, A., Dede, T. (2014): Estimates of energy consumption in Turkey using neural networks with the teaching-learning-based optimization algorithm. – *Energy* 75: 295-303.
- [52] Viebahn, P., Nitsch, J., Fishedick, M., Esken, A., Schuwer, D., Supersberger, N., Edenhofer, O. (2007): Comparison of carbon capture and storage with renewable energy technologies regarding structural, economic, and ecological aspects in Germany. – *International Journal of Greenhouse Gas Control* 1(1): 121-133.
- [53] Wachtel, P. (2001): Growth and Finance: what do we know and how do we know it? – *International Finance* 4(3): 335-362.
- [54] Yavuz, N. C. (2014): CO₂ emission, energy consumption, and economic growth for Turkey: Evidence from a cointegration test with a structural break. – *Energy Sources, Part B: Economics, Planning, and Policy* 9(3): 229-235.
- [55] Zhang, Y. J. (2011): The impact of financial development on carbon emissions: an empirical analysis in China. – *Energy Policy* 39(4): 2197-2203.
- [56] Ziaei, S. M. (2018): US interest rate spread and energy consumption by sector (evidence of pre and post implementation of the Fed's LSAPs policy). – *Energy Reports* 4: 288-3.

CDNA-AFLP ANALYSIS REVEALS INDUCIBLE GENE EXPRESSION IN TOMATO LEAVES IN RESPONSE TO SIMULATED ACID RAIN

LIU, T. T. – MA, J. – LI, M. – PAN, T. F. – MA, C. L. – QIU, D. L.*

College of Horticulture, Fujian Agriculture and Forestry University, Fuzhou 350002, China

**Corresponding author*

e-mail: qiudl1970@fafu.edu.cn; phone: +86-591-8378-9379

(Received 21st Jan 2019 ; accepted 27th Feb 2019)

Abstract. Acid rain as an important environmental problem in China and a stressor may cause gene expression, and tomato is one of model plants and the most important vegetable crops in middle and south China. Tomato seedlings were exposed for 7 days to simulated acid rain (SiAR) of pH 3.0 and control (pH 5.6). The cDNA-amplified fragment length polymorphism (cDNA-AFLP) was carried out to separate differentially expressed gene fragments by using selective base pairs including 8 Mse I primers and 8 EcoR I primers, which allowed the identification and cloning of 45 differential expression transcript-derived fragments (TDFs) corresponding to SiAR, among of which 45 TDFs were successfully cloned and sequenced. 31 of them were found homologies in the NCBI, and 19 displayed homology to genes with known functions, 12 to genes with uncharacterized function. 8 TDFs played significant role in tomato resistance to acid rain-stress. Among of them, TDF5 and TDF8 were stress- inducible transcription factor. TDF4 and TDF20 played important role in resistance to SiAR stress. TDF2 was related to isoprenoid biosynthesis, TDF7 to transcription regulation, TDF11 to metabolism, TDF24 to plant development and defense. Possible roles of the 8 TDFs in the response of tomato to SiAR are also discussed. Moreover, Homologous of amino acid encoded in TDF5 and TDF8 were analyzed.

Keywords: *SiAR stress, Lycopersicon esculentum, cDNA-amplified fragment length polymorphism, transcript-derived fragments*

Abbreviations: SiAR: simulated acid rain, cDNA-AFLP: cDNA-amplified fragment length polymorphism, TDFs: transcript-derived fragments

Introduction

Acid rain emerged as an important environmental problem in China in the late 1970s. The frequency of acid rain has kept increasing since then. It was reported that the loss of forest ecological benefits caused by acid rain exceeded 16 billion Yuan (2.4 billion dollars) per year only in 11 provinces of south China (Feng, 2000). Previous studies have documented acid rain stress causing the leaching of leaf nutrients; changes of physiological and biochemical process; and inhibition of growth and yield of plants (Bellani et al., 1997; Chen et al., 2013; Odiyi et al., 2014; Percy et al., 1990; Qiu et al., 2002, 2005; Ramlall et al., 2015; Wang et al., 2014a, b) Acid rain as an environmental stressor may cause gene differential expression. Gene expression profiles were reported in *Dimocarpus longan* Lour (Zheng et al., 2017), *Synechocystis sp* PCC 6803 (Ohta et al., 2005) and *Arabidopsis thaliana* (L.) Heynh (Liu et al., 2013) in response to acid rain stress. Changes in the total protein profile of *Dimocarpus longan* leaves in response to simulated acid rain (SiAR) stress were documented by Pan et al. (2015).

Tomato (*Lycopersicon esculentum*) is one of model plants and the most important vegetable crops in middle and south China. Previous study has shown that the pigment synthesis, growth and biomass of tomato was inhibited under SiAR stress (Shaukat et al., 2008). One way to study the cellular response to acid rain on a large scale is to

examine gene expression at the mRNA level using the PCR-based technique of cDNA-amplified fragment length polymorphism (cDNA-AFLP) which has often been described as an extremely efficient method for isolation of differentially expressed genes (Baisakh et al., 2006) and is a less labor-intensive mRNA fingerprinting method for isolation of differentially expressed genes (Bachem et al., 1996). Due to its high sensitivity, it is possible to identify rare transcripts (Fukumura et al., 2003). This technique has been further improved to avoid the possibility of several transcript-derived fragment (TDFs) arising from a single gene/cDNA. Keeping the above in view, the objective of this study was to identify some of the key genes that were differentially expressed in response to SiAR.

Materials and methods

Plant materials and treatments

Tomato seeds (*Lycopersicon esculentum* cv. 'Fudan') were sown in plug trays with peat-based substrate with peat, vermiculite, and perlite medium (3:1:1). 7 days after emergence (DAE), each seedling was transferred to a pot containing a 3:1:1 mixture of peat, vermiculite, and perlite. The plants were kept in a net house with a natural photoperiod at Fujian Agriculture and Forestry University. Simulated acid rain was applied to plants at 42 DAE.

Sulfuric acid and nitric acid were selected for the preparation of SiAR, based on the mole ratio 1:5 of sulfuric acid to nitric acid in the precipitation of southern Fujian, China (Tang et al., 1996). Normal rain has a pH of about 5.6; it is slightly acidic because carbon dioxide (CO₂) dissolves into it forming weak carbonic acid, and the solution with pH value of 5.6 was regarded as the control (Qiu et al., 2005). Solution of SiAR with pH 3.0 was also prepared. Dilution of reagent grade acid was done with distilled water and determined by Orion 828 acidity analyzer (made in America). A sprayer was used to apply the acid solutions. The spray was repeated 7 times during 7 days, at each application, leaves were thoroughly wetted. There were 9 pots in each treatment, and each treatment was repeated triple. Each replicate consisted of 9 plants. After 7 days of application, one leaf from each tested plant (symptoms appeared) and control plant (*Fig. 1*) was sampled and immediately frozen in liquid nitrogen and then stored at -80 °C until use.



Figure 1. Tomato leaves after treated by pH 3.0 and control (pH 5.6) for 1 week

RNA preparation and cDNA synthesis

Total RNA was isolated from each sample of frozen tissue (0.1 g). The frozen tissue was homogenized with 0.5 ml of isopropyl alcohol (1:10, v/v) per 1 ml with Trizol extraction method (Invitrogen, Shanghai). The RNA concentration was determined by measuring absorbance at 260 nm. RNA integrity was determined by running 5 μ L of total RNA in a 1.0% agarose gel electrophoresis. 4 μ g of total RNA was used initially for first strand synthesis, followed by second strand synthesis using SuperScriptTM III double stranded cDNA synthesis kit (Invitrogen), according to the manufacturer's protocol.

cDNA-AFLP reaction

The cDNA-AFLP procedure was conducted as described by Bachem et al. (1998) with some modifications. Approximately 100 ng cDNA from from each treatment was digested with EcoRI and MseI restriction enzymes in a three-step reaction at 37 °C for 55 min, 65 °C for 55 min and 80 °C 10 min, respectively. The digested products were ligated to adapters with sequences as follows: EcoRI adapter, 5' CTC GTA GAC TGC GTA CC 3', 3'CAT CTG ACG CAT GGT TAAP5'; MseI adapter, 5'GAC GAT GAG TCC TGA G 3', 3'TAC TCA GGA CTC ATP5'. The ligated products were pre-amplified with the corresponding pre-amplification primers (EcoRI: 5' GAC TGC GTA CCA ATT CA 3', MseI: 5'GAT GAG TCC TGA GTAA C 3'5). Equal amounts of pre-amplified products were amplified with primers having selective nucleotides at the 3' end (EcoRI: 5' GAC TGC GTA CCA ATT CA AC 3'; MseI: 5'GAT GAG TCC TGA GTAA C AA 3' (Table 1). Altogether 128 different primer combinations were tested. 4 μ L of the AFLP products were heat-denatured and resolved in a 6% denaturing polyacrylamide sequencing gel run with 1 \times TBE electrophoresis buffer. The gels were silver-stained according to the Silver SequenceTM DNA Sequencing System Technical Manual.

Transcript-derived fragment (TDF) isolation and re-amplification

The bands of interest were marked, removed from the gel and soaked in ddH₂O (50 μ L) initially at 100 °C for 15 min and then hydrated overnight at 4 °C. 10 μ L of the aliquot was used for re-amplification in a total volume of 50 μ L, with the same set of corresponding selective primers and the same PCR conditions as for the selective amplification except that an annealing temperature of 56 °C, 35 cycles and a final 4 min extension were used. The PCR products were resolved in a 1.5% 1 \times TBE-agarose gel, and each single band corresponding to the selected TDFs was isolated, soaked to elute the DNA according to agarose gel DNA Purification Kit (TAKARA).

Cloning and sequencing of TDFs

The eluted TDFs were cloned into the plasmid pMD₁₈-T vector (TaKaRa Biotechnology (Dalian) Co., Ltd., China) following the manufacturer's protocol. Positive clones were inoculated, and PCR positive cultures from every TDF were sequenced with an ABI automated sequencer.

Analysis of sequences

The sequences of the TDF were analyzed for their homology against the publicly available non-redundant genes/ESTs/Transcripts in GeneBank using the BLASTN and BLASTX algorithms. Multiple sequence alignment was performed with ClustalX2.0

algorithm with default parameters (<http://www.clustal.org/clustal2/>). The phylogenetic tree was constructed using the neighbor-joining method in MEGA5.0 package (Tamura et al., 2011).

Table 1. Primers used for cDNA-AFLP amplification

Adaptor\primers	Primer NO.	Primer sequence
Mse I Adapter		5'GAC GAT GAG TCC TGA G 3' 3'TAC TCA GGA CTC ATP5'
Mse I Pre-amp	M00	5'GAT GAG TCC TGA GTAA C 3'
Mse I Sel-smp	M0	5'GAT GAG TCC TGA GTAA C AA 3'
	M1	5'GAT GAG TCC TGA GTAA C AC 3'
	M2	5'GAT GAG TCC TGA GTAA C AG 3'
	M3	5'GAT GAG TCC TGA GTAA C AT 3'
	M4	5'GAT GAG TCC TGA GTAA C TA 3'
	M5	5'GAT GAG TCC TGA GTAA C TC 3'
	M6	5'GAT GAG TCC TGA GTAA C TG 3'
	M7	5'GAT GAG TCC TGA GTAA C TT 3'
EcoR I Adapter		5' CTC GTA GAC TGC GTA CC 3' 3'CAT CTG ACG CAT GGT TAAP5'
EcoR I Pre-amp	E00	5' GAC TGC GTA CCA ATT CA 3'
EcoR I Sel-smp	E0	5' GAC TGC GTA CCA ATT CA AC 3'
	E1	5' GAC TGC GTA CCA ATT CA AG 3'
	E2	5' GAC TGC GTA CCA ATT CA CA 3'
	E3	5' GAC TGC GTA CCA ATT CA CT 3'
	E4	5' GAC TGC GTA CCA ATT CA CC 3'
	E5	5' GAC TGC GTA CCA ATT CA CG 3'
	E6	5' GAC TGC GTA CCA ATT CA GC 3'
	E7	5' GAC TGC GTA CCA ATT CA GG 3'

Results

Isolation of the TDFs responsive to SiAR stress

A total of 128 primer combinations were used for the AFLP analysis of cDNAs from simulated acid rain-stressed leaves. cDNAs were obtained from the treatments of pH 5.6 (Control) and pH 3.0 (Fig. 2). A total of 45 transcript-derived fragments (TDFs) were isolated from the silver-stained cDNA-AFLP gels based on their presence, and identified as inducibly expressed. Sequence alignment of these 45 cloned TDFs against NCBI databases showed that 31 had a homologous gene in the database. Due to incompleteness of tomato gene annotation and the conservation of gene families between tomato and *Arabidopsis*, *Vitis vinifera*, *Populus*, *Ricinus communis*, *Phaeosphaeria nodorum*, *Glycine max*, *Ipomoea batatas*, *Sorghum*, *Zea mays*, *Artemisia annua*.

We used these matches of the identified inducibly expressed genes as surrogates for function annotation (Fig. 3). 14 of 45 TDFs had no annotation in the database. Fourteen of the TDFs had no similar sequences in the NCBI databases. The genes with unknown functions consist of those that have not yet been associated with a response to abiotics stress, and some of these novel genes did not match any sequence from the GenBank

databases. In general, our results indicated that multiple defense strategies lead to an enhanced defense capacity of tomato plants to SiAR.

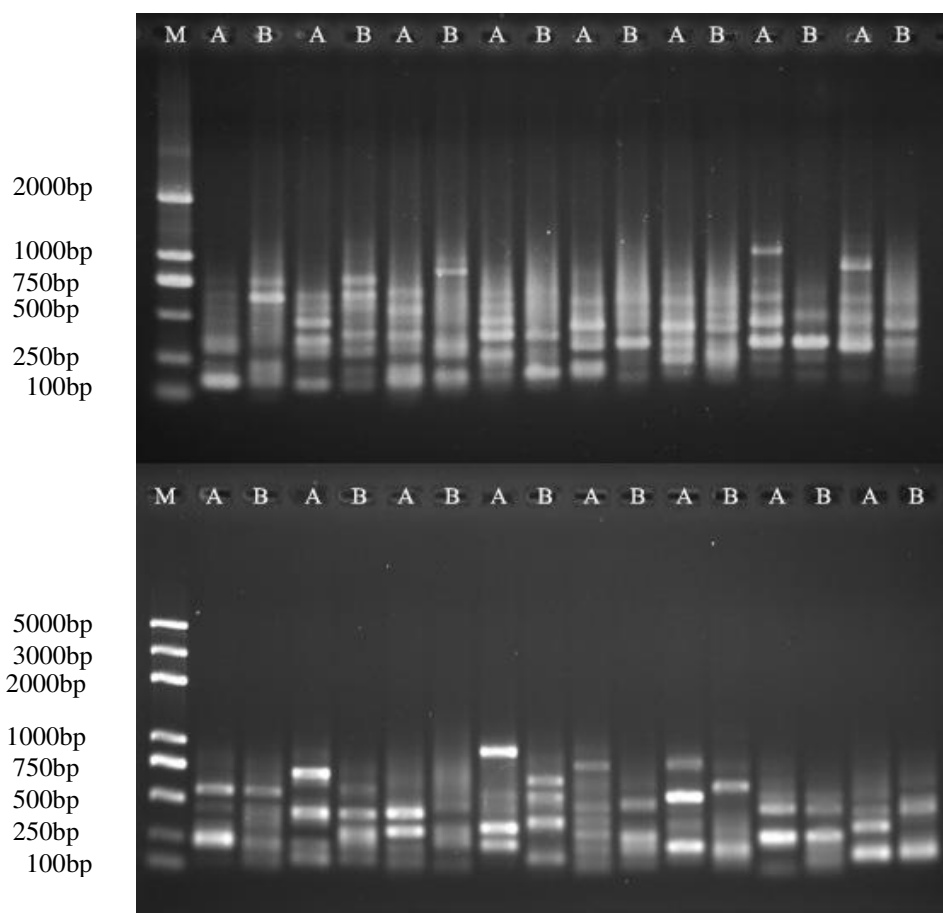


Figure 2. The result of electrophoresis of selectivity amplification products amplified with pair primers of *EcoR I* and *Mse I* (A: pH 3.0, B: pH 5.6) M: DL2000

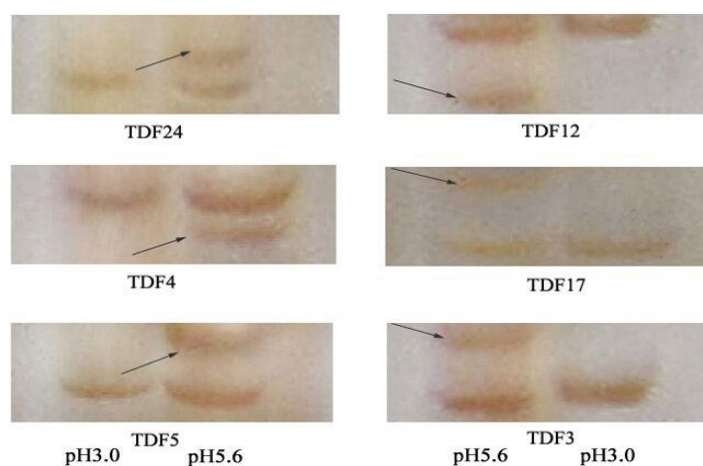


Figure 3. Inducible expression of genes of tomato treated under SiAR and control (pH 5.6). Arrow in TDF3, TDF12, and TDF17 showed their down-regulated expression of tomato leaves in response to SiAR, while TDF4, TDF5 and TDF24 showed their up-regulated expression, respectively

Sequencing and classification of cDNA

The expression profile was compared between pH 3.0 and control on the basis of their either complete presence or absence (*Fig. 2*). 31 TDFs above 100 bp were eluted from the gel, re-amplified, and sequenced (*Fig. 4* and *Fig. A1* in the *Appendix*).

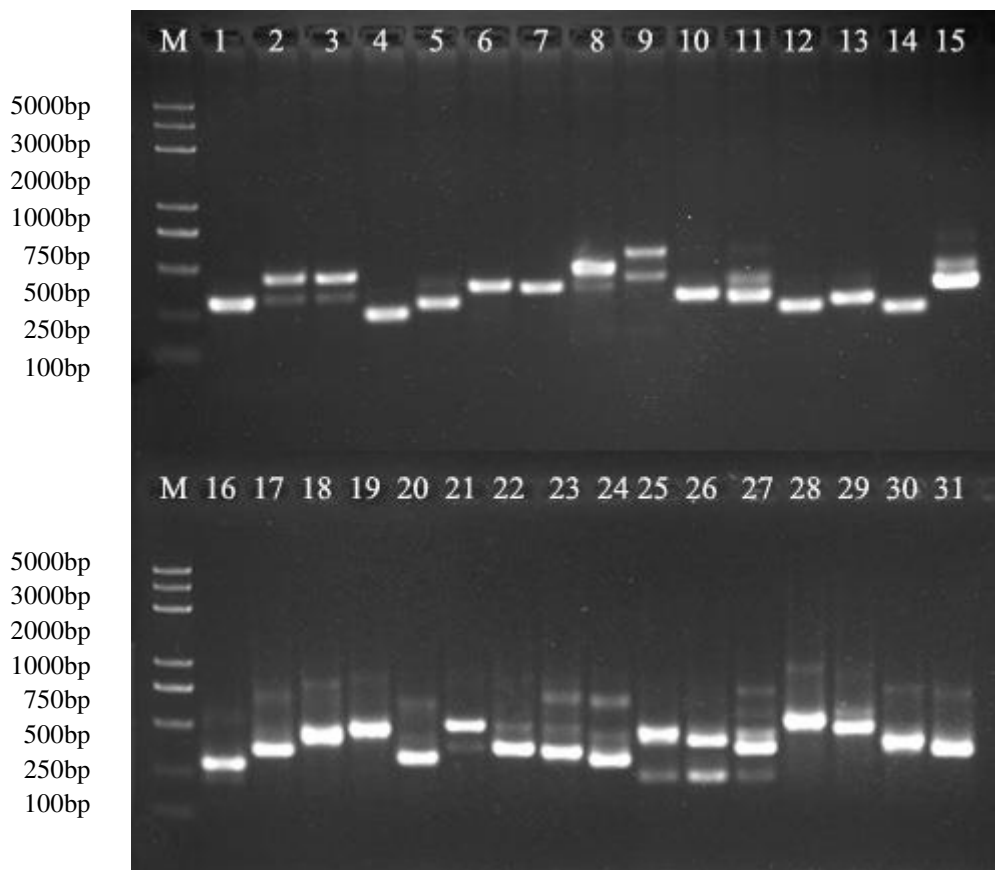


Figure 4. Agarose gel of re-amplified TDFs from tomato in response to SiAR. M: 2000 bp marker; 1-31 showing TDF1-TDF31, respectively

The TDFs with known or putative function were submitted to the NCBI database and are presented in *Table 2* with GenBank Accession numbers. The up- and down-regulated genes are also categorized into these functional groups (*Table 2*). *Figure 5* shows the percentages of acid rain induced genes assigned to different functional categories. Comparison of the homologies of these sequences and those in the database suggested that most of them (about 68.9%) had homology with genes involved in functions like UBA and UBX domain-containing protein (12.9%, TDF1, TDF6, TDF9, TDF19), Inositol-1, 4, 5 -triphosphate-5-phosphatase (3.2%, TDF15), Inositol polyphosphate 5-phosphatase (3.2%, TDF26), Tobamovirus multiplication protein (3.2%, TDF13), Hypothetical protein (9.7%, TDF11, TDF16, TDF28), RING/U-box superfamily protein (3.2%, TDF7), Stress transcription factor A-6b (6.5%, TDF5, TDF8), Receptor protein (3.2%, TDF27), Plastidic aldolase (3.2%, TDF30), Phenylalanine ammonia-lyase (3.2%, TDF24), Solanesyl diphosphate synthase (3.2%, TDF2), Peroxidase (6.5%, TDF4, TDF20).

Table 2. Transcript-derived fragments (TDFs) from tomato in response to simulated acid rain

TDF No.	TDF size (bp)	Sequence name	GeneBank accession no.	Annotation	Similarity	E-value	Organism	Expression ^a
UBA and UBX domain-containing protein								
1	175	M0E0-1	AK327205.1	cDNA, clone: LEFL2024113, HTC in fruit	74%	4e-15	<i>Solanum lycopersicum</i>	-
6	220	M5E2	AK321642.1	cDNA, clone: LEFL1027AF01, HTC in leaf	87%	1e-68	<i>Solanum lycopersicum</i>	-
9	264	M6E2-3	AK247661.1	cDNA, clone: LEFL1085DG07, HTC in leaf	100%	1e-05	<i>Solanum lycopersicum</i>	-
19	387	M5E3	AK247676.1	cDNA, clone: LEFL1089BC10, HTC in leaf	79%	4e-90	<i>Solanum lycopersicum</i>	-
Inositol-1,4,5-triphosphate-5-phosphatase								
15	170	M5E0	EU159402.1	Inositol-1,4,5-triphosphate-5-phosphatase (5PT1) mRNA, complete cds	100%	4e-22	<i>Solanum lycopersicum</i>	-
Inositol polyphosphate 5-phosphatase								
26	225	M7E2-3	XM_010326266.2	Putative inositol polyphosphate 5-phosphatase At5P2	81%	4e-18	<i>Solanum lycopersicum</i>	-
Tobamovirus multiplication protein								
13	360	M2E3	XP_010318614.2	Tobamovirus multiplication protein 1	100%	0	<i>Populus trichocarpa</i>	-
Hypothetical protein								
11	267	M0E3	XM_001793885.1	SN15 hypothetical protein partial mRNA	72%	1e-26	<i>Phaeosphaeria nodorum</i>	+
16	301	M2E2	XM_002264451.1	Predicted: hypothetical protein LOC100244254, mRNA	77%	3e-59	<i>Vitis vinifera</i>	-
28	350	M5E3	XM_002513344.1	Cyclin-L2, putative, mRNA	85%	2e-30	<i>Ricinus communis</i>	-
RING/U-box superfamily protein								
7	338	M6E2-1	NM_123389.3	Zinc finger (C3HC4-type RING finger) family protein (AT5G40250) mRNA, complete cds	73%	4e-19	<i>Arabidopsis thaliana</i>	+
Stress transcription factor A-6b								
8 ^b	290	M6E2-2	XM_002517024.1	Heat shock factor protein HSF30, putative, mRNA	76%	1e-37	<i>Ricinus communis</i>	+
5 ^b	202	M5E0-2	CU227021.1	EST from severe drought-stressed leaves	76%	2e-48	<i>Populus</i>	+
Receptor protein								
27	344	M3E3	AF401036.1	Receptor-like protein 9DC gene, complete cds	78%	3e-66	<i>Lycopersicon pimpinellifolium</i>	+
Plastidic aldolase								
30	365	M7E3-1	AB027001.1	mRNA for plastidic aldolase NPALDPI, complete cds	80%	5e-50	<i>Nicotiana glauca</i>	+
Phenylalanine ammonia-lyase								
24	298	M7E2-1	M90692.1	Phenylalanine ammonia-lyase (PAL5) gene, complete cds	95%	8e-129	<i>Lycopersicon esculentum</i>	+
Solanesyl diphosphate synthase								
2	338	M0E0-2	DQ889204.1	Solanesyl diphosphate synthase (SppS) gene, complete cds	100%	1e-171	<i>Lycopersicon esculentum</i>	+
Peroxidase								
4	341	M5E0-1	BAG09369.1	Peroxisomal acyl-CoA oxidase	87%	3e-14	<i>Glycine max</i>	+
20	206	M1E0-2	AY206413.1	Anionic peroxidase swpb2 mRNA, complete cds	78%	3e-30	<i>Ipomoea batatas</i>	+

Uncharacterized								
14	154	M1E0-1	HG975443.1	Chromosome ch04, complete genome	100%	2e-71	<i>Solanum lycopersicum</i>	-
12	247	M1E1	AC239572.2	Strain Heinz 1706 clone hba-139d12, complete sequence	82%	5e-61	<i>Solanum lycopersicum</i>	-
17	258	M3E2	AC212438.2	Chromosome 11 clone C11HBa0168B23, complete sequence	100%	2e-128	<i>Solanum lycopersicum</i>	-
18	211	M4E3	CU468016.3	DNA sequence from clone LE_HBa-187P23, complete sequence	86%	6e-65	<i>Solanum lycopersicum</i>	-
21	274	M7E0	CU457804.4	DNA sequence from clone SL_Mbof-121C14 on chromosome 4, complete sequence	85%	7e-79	<i>Solanum lycopersicum</i>	-
22	292	M1E2	EU180574.1	Clone BAC C09HBa0179M08, complete sequence	72%	3e-13	<i>Solanum lycopersicum</i>	-
23	281	M2E2	CU326380.7	DNA sequence from clone LE_HBa-75M11, complete sequence	86%	7e-85	<i>Solanum lycopersicum</i>	-
25	310	M7E2-2	AP011551.1	DNA, chromosome 8, clone: C08SLe0087H10, complete sequence	80%	9e-40	<i>Solanum lycopersicum</i>	-
31	193	M7E3-2	AP011553.1	DNA, chromosome 8, clone: C08SLm0050D24, complete sequence	75%	1e-04	<i>Solanum lycopersicum</i>	-
29	169	M6E3	AC239435.2	Strain Heinz 1706 chromosome 1 clone hba-305j13 map 1, complete sequence	89%	3e-49	<i>Solanum lycopersicum</i>	-
10	212	M6E2-4	CU302232.4	DNA sequence from clone LE_HBa-29F16 on chromosome 4, complete sequence	74%	4e-23	<i>Solanum lycopersicum</i>	-
3	164	M0E0-3	AP010799.1	DNA, chromosome 8, clone: C08HBa0112M02, complete sequence	88%	2e-47	<i>Solanum lycopersicum</i>	-

a: The TDF up-regulated under SiAR stress were indicated with plus (+), while the TDFs down-regulated were indicated with minus (-); b: TDFs selected for homologous analysis of amino acid

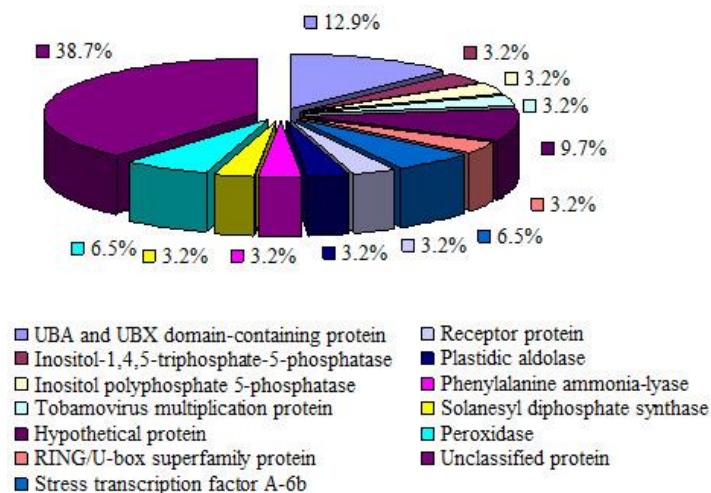


Figure 5. Distribution of inducibly expressed genes of tomato under SiAR stress. A total of 31 TDFs were grouped into 13 functional categories. The percentages of gene transcripts in each group are listed

The homologous analysis of TDF5 and TDF8

Multiple sequence alignment revealed that the predicted nucleotide sequence of TDF5 displayed homology with other species (Fig. 6), including *Populus* (0.09935), *Vitis vinifera* (0.21868), *Ricinus communis* (0.08232), *Daucus carota* (0.24211), *Arabidopsis* (0.23250), *Lycopersicum esculentum* (0.00804), *Soybean* (0.29692) (Fig. 7), while TDF8 had homology with *Lycopersicum esculentum* (0.12116), *Vitis vinifera* (0.13402), *Artemisia annua* (0.71636), *Sorghum* (0.05429), *Zea mays* (0.08618), *Ricinus communis* (0.101665), *Populus* (0.04893), *Arabidopsis* (0.22726) (Figs. 8 and 9).

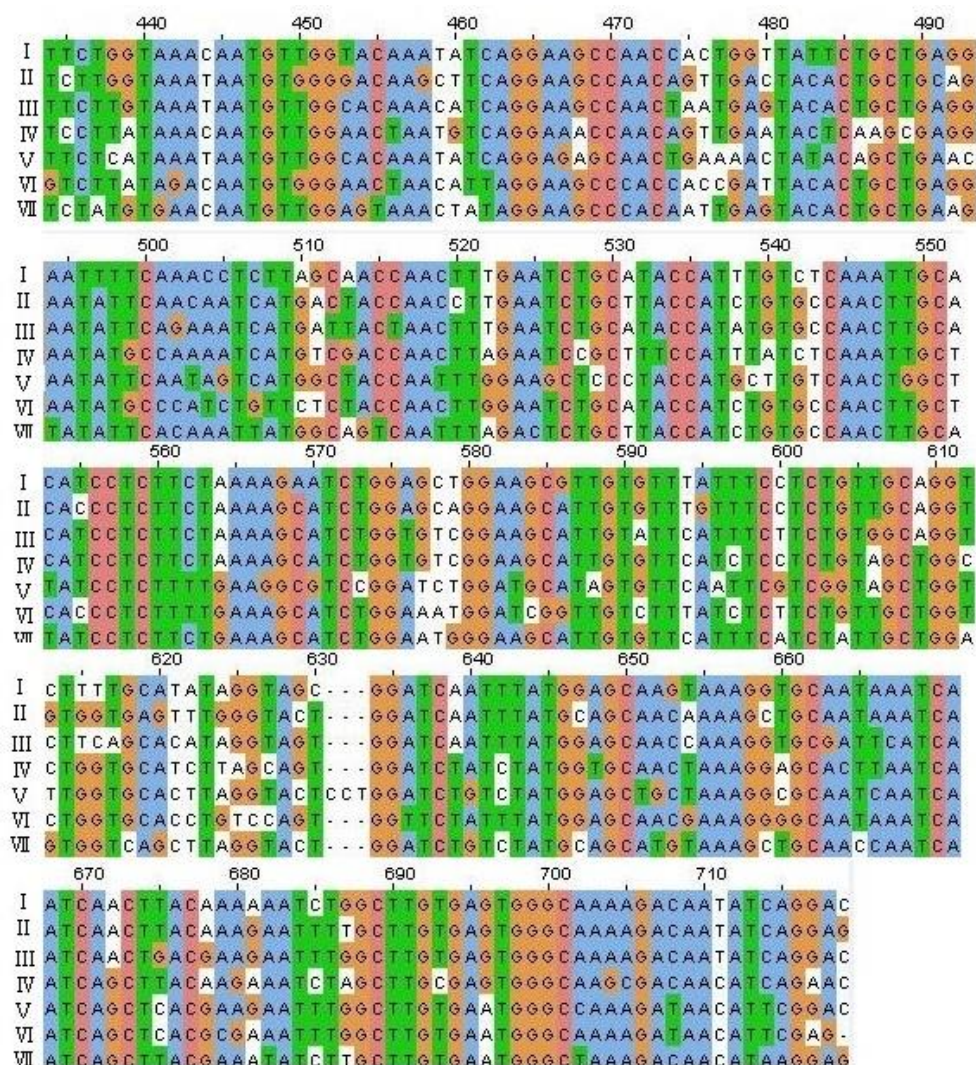


Figure 6. Homologous analysis of TDF5

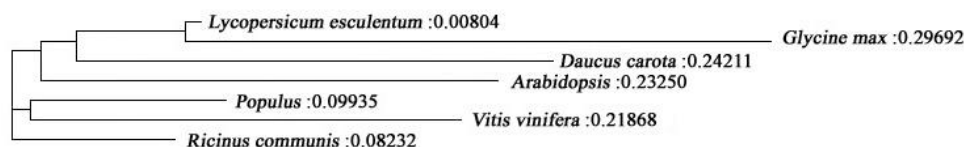


Figure 7. Homologous tree of TDF5

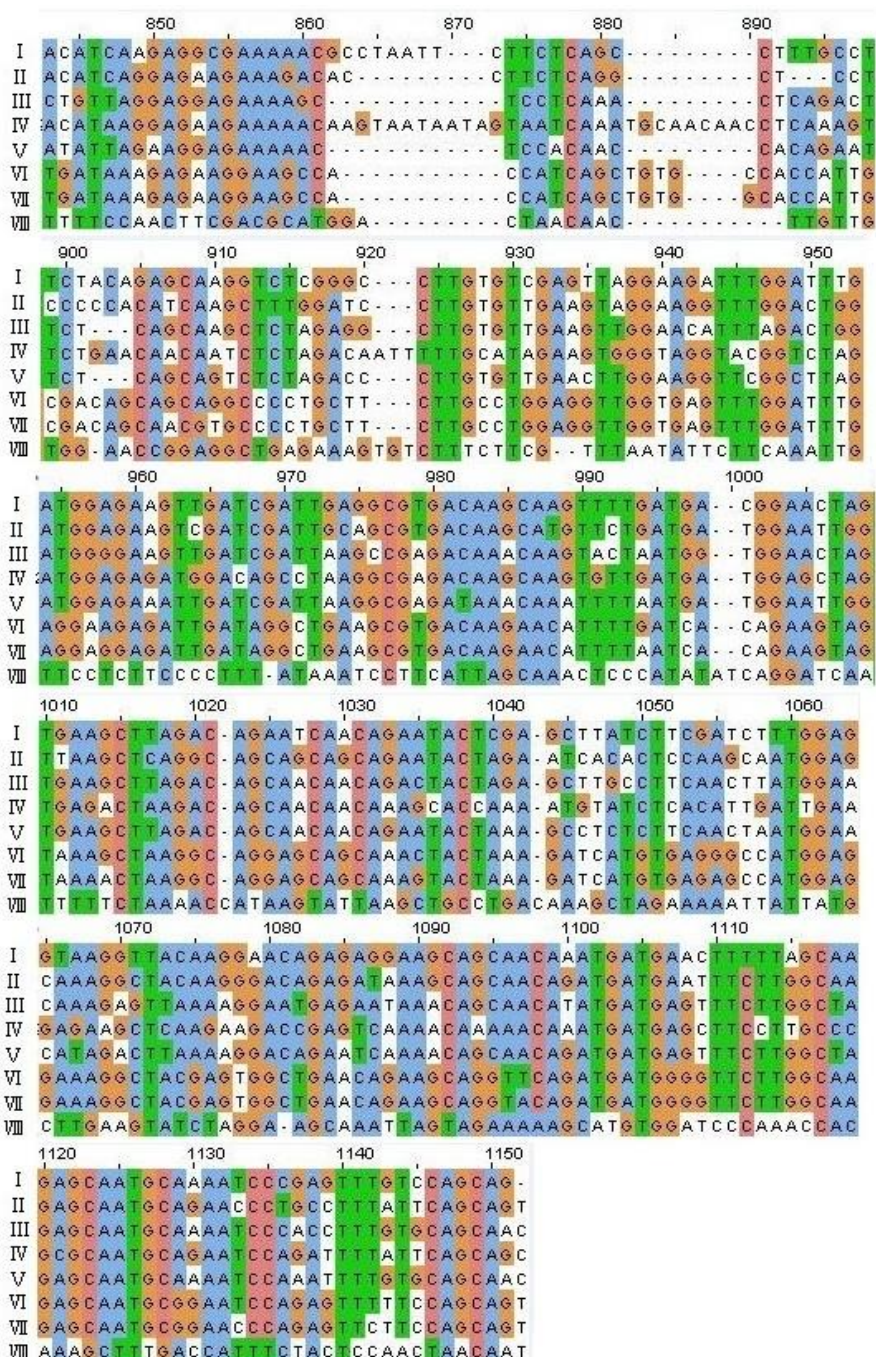


Figure 8. Homologous analysis of TDF8. I: *Lycopersicum esculentum*; II: *Vitis vinifera*; III: *Populus*; IV: *Arabidopsis*; V: *Ricinus communis*; VI: *Sorghum*; VII: *Zea mays*; VIII: *Artemisia annua*

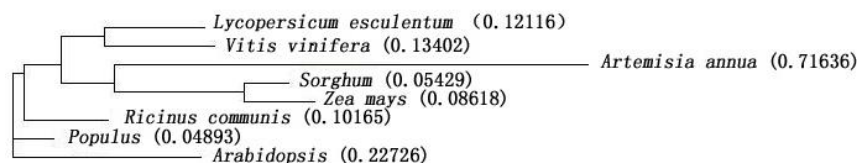


Figure 9. Homologous tree of TDF8

Discussion

The biological functions of identified SiAR-responsive genes were categorized according to transcriptional levels. The putative functions of the TDFs that were differentially expressed in SiAR treatments were analyzed. The largest categories with ascribed function are stress-related genes (68.9%) involved in functions like UBA and UBX domain-containing protein (12.99%), peroxidase (6.5%), inositol-1, 4, 5 - triphosphate-5-phosphatase (3.2%), inositol polyphosphate 5-phosphatase (3.2%), tobamovirus multiplication protein (3.2%), hypothetical protein (9.7%), RING/U-box superfamily protein (3.2%), stress transcription factor A-6b (6.5%), receptor protein (3.2%), plastidic aldolase (3.2%), phenylalanine ammonia-lyase (3.2%), solanesyl diphosphate synthase (3.2%). Among of them, the expression of TDFs in tomato leaves under SiAR stress were up-regulated, including TDF2, TDF4, TDF5, TDF7, TDF8, TDF11, TDF20, TDF24, TDF27, TDF30. The results of the differentially regulated TDFs reported to have direct or indirect relation with simulated acid rain stress response are discussed below.

Responses of isoprenoid biosynthetic genes to simulated acid rain

As a part of the plant defense machinery, isoprenoids are employed, among others, to protect plant cells from abiotic stress (Munne-Bosch et al., 2003). TDF2 showed high similarity with the enzymatic proteins in the pathway of isoprenoid biosynthesis, which were down-regulated in the seedlings subjected to simulated acid rain stress. Plastoquinone is regulated by solanesyl diphosphatesynthase (SPPS) (Phatthiya et al., 2007). Simulated acid rain stress affecting phosphorylation of the chloroplast of longan leaves was documented by Qiu et al. (2002). These indicated that simulated acid rain stress influenced photophorylation by the way of inhibiting isoprenoid production. The same result was documented that isoprenoids in Sitka spruce are induced after mechanical wounding due to increased transcription or enzymatic activities of genes and enzymes participating in the biosynthetic pathways of these metabolites (McKay et al., 2006).

Phenylalanin ammonia-lyase

TDF24 showed similarity with phenylalanin ammonia-lyase (PAL-5) gene. Phenylalanine ammonia-lyase catalyzes the conversion of L-phenylalanine into trans-cinnamate, the initial committed step of the multi-branched phenylpropanoid pathway in higher plants. This is a key biochemical reaction in both plant development and defense. In tomato, at least five different classes of PAL genes were isolated. PAL 5 was distinctly (5-6-fold) more common. TDF24 was up-regulated after simulated acid rain stress. This type of PAL gene sequence also was found to be strongly expressed and differentially regulated in response to changes in light or wounding or to infection by a plant pathogen (Chang et al., 2008).

Glycosyltransferase

Glycosyltransferases, which catalyze the transfer of a sugar residue from an activated donor to an acceptor molecule, are found in all living organisms. Since plants, in contrast to animals, are sessile organisms and cannot move away from adverse environmental conditions they need to adapt themselves to environmental stresses

(Wang et al., 2015). TDF11 expressed in tomato which evolved distinct mechanisms by which tolerance against acid rain can be achieved.

Zinc finger protein kinase

About two to three-fold increase in the expression of the cDNA (TDF7) encoding a cys2/his2 zinc finger protein kinase conferred tolerance to simulated acid rain stress in tomato. Over-expression of the members of zinc finger protein kinase family was also documented during salt tolerance in transgenic *Arabidopsis* and tobacco (Mukhopadhyay et al., 2004; Ragueh et al., 1989; Sakamoto et al., 2004). Stress-responsive zinc finger gene playing a role was reported in drought tolerance in *petunia* (Sugano et al., 2003).

Peroxisomal acyl-CoA oxidase

The peroxisomal acyl-CoA oxidase family plays an essential role in lipid metabolism by catalyzing the conversion of acyl-CoA into trans-2-enoyl-CoA during fatty acid beta-oxidation (Fabi et al., 2010). The TDFs including TDF4, TDF5, TDF8, TDF20, TDF27 and TDF30 were differentially regulated under simulated acid rain, indicating that these proteins may take part in the mechanism of anti-SiAR and play important role in the resistance to the stress.

Unknown genes

The large group of signal transduction, transcription regulation-related protein, stress- inducible proteins (68.9% of the 31 known or predicted genes) suggested that tomato can rapidly initiate the regulatory system and control the expression of simulated acid rain resistance-related genes. Also, many unknown genes, 31.1% of the total, had not been reported and consist of those that have not yet been associated with a response to abiotics stress, and some of these novel genes did not match any sequence from the GenBank databases, and might play important roles in the response of tomato to SiAR, indicating that multiple defense strategies lead to an enhanced SiAR defense capacity in tomato.

This work helped us to identify the responsive transcripts expressed under SiAR. Most of them are related with their previously studied genes involved in stress responses such as abiotic and biotic factors. The induction of these genes under SiAR suggests their function in possible regulation of acid rain adaptation in tomato. This is suggested by the association of most of the cDNAs with genes involved in biosynthesis of isoprenoid and phenylpropanoid, zinc finger protein kinase family, and lipid metabolism. Knowledge of acid rain tolerance can be enriched by studying the genes involved in the interconnected aspects like preventing or controlling the damage caused by acid rain, establishing the homeostatic environment in the stressful environment and resuming the normal growth at the reduced rate.

TDFs identified in our work revealed the genes related to lipid metabolism and biosynthesis of anti-oxidants of isoprenoid and phenylpropanoid, zinc finger protein kinase conferred tolerance to simulated acid rain stress in tomato which help in establishing homeostatic environment. However, some of the TDFs in the study did not show homology with any other known genes, indicating that further work is necessary to elucidate the mechanism of acid rain and biological roles of these genes in seedlings

of tomato. This progress will bring to the research community a huge wealth of information on novel acid rain-related genes.

Conclusions

Among of which 31 TDFs in leaves of tomato under simulated acid rain stress were cloned and sequenced. TDF5 and TDF8 were stress- inducible proteins. TDF4 and TDF20 played important role in resistance to SiAR stress. TDF2 was related to isoprenoid biosynthesis, TDF7 to transcription regulation, TDF11 to metabolism, TDF24 to plant development and defense. These 8 TDFs may play significant role in tomato resistance to acid rain-stress. Further study is necessary to elucidate the roles of these genes in tomato under SiAR stress.

Acknowledgments. This work was supported by the National Natural Science Grant of China (Award no. 30400061), Natural Science Foundation of Fujian Province, China (2011J01082) and Special fund for science and technology innovation of FAFU (CXZX2016107).

Conflict of interests: The authors declare that they have no conflict of interests.

REFERENCES

- [1] Bachem, C. W. B., VanderHoeven, R. S., DeBrujin, S. M., Vreugdenhil, D., Zabeau, M., Visser, R. G. F. (1996): Visualization of differential gene expression using a novel method of RNA fingerprinting based on AFLP: analysis of gene expression during potato tuber development. – *Plant Journal* 9: 745-753.
- [2] Bachem, C. W. B., Oomen, R. J. F. J., Visser, R. G. E. (1998): Transcript imaging with cDNA-AFLP: a step-by-step protocol. – *Plant Molecular Biology Reporter* 16: 157-173.
- [3] Baisakh, N., Subudhi, P. K., Parami, N. P. (2006): cDNA-AFLP analysis reveals differential gene expression in response to salt stress in a halophyte *Spartina alterniflora* Loise. – *Plant Science* 170: 1141-1149.
- [4] Bellani, L. M., Rinallo, C., Muccifora, S., Gori, P. (1997): Effects of simulated acid rain on pollen physiology and ultrastructure in the apple. – *Environmental Pollution* 95: 357-362.
- [5] Chang, A., Lim, M. H., Lee, S. W., Robb, E. J., Nazar, R. N. (2008): Tomato Phenylalanine Ammonia-lyase gene family, highly redundant but strongly underutilized. – *Journal of Biological Chemistry* 283: 33591-33601.
- [6] Chen, J., Wang, W. H., Liu, T., Wu, F. H., Zheng, H. L. (2013): Photosynthetic and antioxidant responses of *Liquidambar formosana* and *Schima superba* seedlings to sulfuric-rich and nitric-rich simulated acid rain. – *Plant Physiology and Biochemistry* 64: 41-51.
- [7] Fabi, J. P., Mendes, L. R. B. C., Lajolo, M., Nascimento, J. R. O. (2010): Transcript profiling of papaya fruit reveals differentially expressed genes associated with fruit ripening. – *Plant Science* 179: 225-233.
- [8] Feng, Z. W. (2008): Ecological effects and control strategies of acid deposition on ecosystems in China. – *Yunnan Environmental Science* 19: 1-6.
- [9] Fukumura, R., Takahashi, H., Saito, T., Tsutsumi, Y., Fujimori, A., Sato, S., Tatsumi, K., Araki, R., Abe, M. (2003): A sensitive transcriptome analysis method that can detect unknown transcripts. – *Nucleic Acids Research* 31: e94.
- [10] Liu, T. W., Niu, L., Fu, B., Chen, J., Wu, F. H., Chen, J., Wang, W. H., Hu, W. J., He, J. X., Zheng, H. L. (2013): A transcriptomic study reveals differentially expressed genes

- and pathways respond to simulated acid rain in *Arabidopsis thaliana*. – *Genome* 56: 49-60.
- [11] McKay, S., K. A., Toudefallah, M., Martin, D. M., Alfaro, R., King, J., Bohlmann, J., Plant, A. L. (2006): Wound-induced terpene synthase gene expression in Sitka spruce that exhibit resistance or susceptibility to attack by the white pine weevil. – *Plant Physiology* 140: 1009-1021.
- [12] Mukhopadhyay, A., Vij, S., Tyagi, A. K. (2004): Overexpression of a zinc-finger protein gene from rice confers tolerance to cold, dehydration, and salt stress in transgenic tobacco. – *Proceedings of the National Academy of Science of United States of America* 101: 6309-6314.
- [13] Munne-Bosch, S., Alegre, L. (2003): Drought-induced changes in the redox state of atocopherol, ascorbate, and the diterpene carnolic acid in chloroplasts of *Labiatae* species differing in carnolic acid content. – *Plant Physiology* 131: 1816-1825.
- [14] Odiy, B. O., Bamidele, J. F. (2014): Effects of simulated acid rain on growth and yield of cassava *Manihot esculenta* (Crantz). – *Journal of Agricultural Science* 6: 96-101.
- [15] Ohta, H., Shibata, Y., Haseyama, Y., Yoshino, Y., Suzuki, T., Kagasawa, T., Kamei, A., Ikeuchi, M., Enami, I. (2005): Identification of genes expressed in response to acid stress in *Synechocystis sp.* PCC 6803 using DNA microarrays. – *Photosynthesis Research* 84: 225-230.
- [16] Pan, T. F., Li, Y. Y., Ma, C. L., Qiu, D. L. (2015): Calcium affecting protein expression in long an undersimulated acid rain stress. – *Environmental Science and Pollution Research* 22: 12215-12223.
- [17] Percy, K. E., Baker, E. A. (1990): Effects of simulated acid rain on epicuticular wax production, morphology, chemical composition and on cuticular membrane thickness in two clones of Sitkaspruce [*Picea sitchensis* (Bong.) Carr.]. – *New Phytologist* 116: 9-87.
- [18] Phatthiya, A., Takahashi, S., Chareonthiphakorn, N., Koyama, T., Wititsuwannakul, D., Wititsuwannakul, R. (2007): Cloning and expression of the gene encoding solanesyl diphosphate synthase from *Hevea brasiliensis*. – *Plant Science* 172: 824-831.
- [19] Qiu, D. L., Liu, X. H. (2002): Effects of simulated acid rain on photosynthetic function and calcium regulation. – *Chinese Journal of Applied Ecology* 3: 1072-1076.
- [20] Qiu, D. L., Liu, X. H., Guo, S. Z. (2005): Effects of simulated acid rain on fertility of litchi. – *Journal of Environmental Sciences* 17: 1034-1037.
- [21] Ragueh, F., Fescur, N., Roby, D., Marco, Y. (1989): Gene expression in *Nicotiana tabacum* in response to compatible and incompatible isolates of *Pseudomonas solanacearum*. – *Physiological and Molecular Plant Pathology* 35: 23-33.
- [22] Ramlall, C., Varghese, B., Ramdhani, S., Pammenter, N. W., Bhatt, A., Berjak, P. (2015): Effects of simulated acid rain on germination, seedling growth and oxidative metabolism of recalcitrant-seeded *Trichilia dregeana* grown in its natural seed bank. – *Physiologia Plantarum* 153: 149-160.
- [23] Sakamoto, H., Maruyama, K., Sakuma, Y., Meshi, T., Iwabuchi, M., Shinozaki, K., Yamaguchi-Shinozaki, K. (2004): *Arabidopsis* cys2/his2-type zincfinger proteins function as transcription repressors under drought, cold, and high salinity conditions. – *Plant Physiology* 136: 2734-2746.
- [24] Shaukat, S. S., Khan, M. A. (2008): Growth and physiological responses of tomato (*Lycopersicon esculentum* Mill.) to simulated acid rain. – *Pakistan Journal of Botany* 40: 2427-2435.
- [25] Sugano, S., Kaminaka, H., Rybka, Z., Catala, R., Salina, J. (2003): Stress-responsive zinc finger gene *ZPT2-3* plays a role in drought tolerance in petunia. – *Plant Journal* 36: 830-41.
- [26] Tamura, K., Peterson, D., Peterson, N., Stecher, G., Nei, M., Kumar, S. (2011): Mega5: Molecular evolutionary genetics analysis using maximum likelihood, evolutionary distance, and maximum parsimony methods. – *Molecular Biology and Evolution* 28: 2731-2739.

- [27] Tang, D. G., Wang, W., Pang, Y. B., Liu, H. J., Wang, S. S., Wang, R. M. (1996): Contribution of NO_x to acid rain in the area of south Fujian province. – Research of Environmental Science 9: 38-40.
- [28] Wang, L. H., Wang, W., Zhou, Q., Huang, X. H. (2014a): Combined effects of lanthanum (III) chloride and acid rain on photosynthetic parameters in rice. – Chemosphere 112: 355-361.
- [29] Wang, L. Q., Yang, L. T., Guo, P., Zhou, X. X., Ye, X., Chen, E. J., Chen, L. S. (2015): Leaf cDNA-AFLP analysis reveals novel mechanisms for boron-induced alleviation of aluminum-toxicity in *Citrus grandis* seedlings. – Ecotoxicology and Environmental Safety 120: 349-359.
- [30] Wang, Y. P., Wang, Y., Kai, W. B., Zhao, B., Chen, P., Sun, L., Ji, K., Li, Q., Dai, S. J., Sun, Y. F., Wang, Y. D., Pei, Y. L., Leng, P. (2014b): Transcriptional regulation of abscisic acid signal core components during cucumber seed germination and under Cu²⁺, Zn²⁺, NaCl and simulated acid rain stresses. – Plant Physiology and Biochemistry 76: 67-76.
- [31] Zheng, S., Pan, T. F., Ma, C. L., Qiu, D. L. (2017): Differential gene expression of longan under simulated acid rain stress. – Bulletin of Environmental Contamination and Toxicology 98: 726-731.

APPENDIX

Figure A1. The sequence of transcript-derived fragments (TDFs) from tomato in response to simulated acid rain

1 M0E0-1 (175bp) GGTCGCTGCTTGCTGATCATGTGAACACTACATTCCCTGTTACCC
TCATTGACCCTACAGATATTTTGTCTTCATTTGAGGTTCTCTTGC
TCTCGTATGTCTCATATCATATTCCCAAAGCATCAGACCGCCTT
GTTTCATGGAGTTGTAAAATATTTTCATCAAGCTATTGCAGATC

2 M0E0-2 (338bp) GCAGAACCTAAAATGCCTTCCATCTAGTCCTTTTCAAGCAGCA
CTTGAGGAAATCGTGAAGTATAATCTGGAGAGAATTGAATAGA
CGAAAACAAAGGACGAAACTATACAACTTTGGTTTATTATTCT
CTGAAAGCTCTTCATATCTAACAATATCTGGAGCACAGAGTAG
AAGCTATTACTATAGTTTGAATGGCAACAACGATCAGAACGAA
AGTGCTTCACTATGTTTCATATATTATACCCATACAGGTTGTAAT
TTTCAGTTCCTAATACAGCAATATGGTGTTCAGCATTCTTTAT
AATTTGGCTAATAAATTGTCAAATTTCAACTGTTG

3 M0E0-3 (164bp) ACTCATATACGCCGAGCAGATGGTGTGCGAACGCATCAAT
TGGACGTTTCGTTGACTGGTTAGAACCCTGATTCAAGATACAGG
TATACCAAATATTTATGGGCTGAACTGCCTGCTACTGCTGTCT
ACATGCTGAAAATTTCAACCACCAATGCTGTTGT
TTGGTAGATTGGTTCTCTATTGTGAGGGTGCAAATAATGTTATT
TATGAGAGGTTGCGTGAAGGAGACACTGATTTGTTGAAACGAC

4 M5E0-1 (341bp) TAGGACCCTCTTGGGTATTCTTGGTGGCGCTGTCCTCCAATGCC
TTTGCCACGGCGAGAGTGGTCTTAACCCTGTCACCACATAAAA
ATCCCGTCCAAAAAAATTCCTCACTTCCCTCCATCCATTCC
ATGACTTCCCCAAGGTAGCCTGGCCGGAAGTCATTTTACCACT
CTCATACAACCTTGCGAAGACGCCATCCAACAAGAAGCATAGCC
TGAATGTTGCTCAACATCTGAACAAGCTTCTGTTGAG

- 5 M5E0-2 (202bp) GTCTTATAGACAATGTGGGAACTAACATTAGGAAGCCCACCAC
CGATTACACTGCTGAGGAATATGCCCATCTGTTCTCTACCAACT
TGGAATCTGCATACCATCTGTGCCAACTTGCTCACCCCTCTTTTG
AAAGCATCTGGAAATGGATCGGTTGTCTTTATCTCTTCTGTTGC
TGGTCTGGTGCACCTGTCCAGTGGTTCTATTTATGGAGCAACGA
AAGGGGCAATAAATCAGCTCACGCGAAATTTGGCTTGTGAATG
GGCAAAAGATAACATTCGAG
- 6 M5E2 (220bp) AAACAGGTGAGACACGGCAACCAAAGGACTTCAACTGGTGCC
AACCGAGAACATGGCATCCCCACTTCACAGCACATGTGAATC
TACAAGCTGAGATAAATAAATTTGATTCTACTATTTTGATTTGG
GTTTTCAAATTGGGCACAAATTGAAGGACAAAATCACCTCCAC
CAGGAAAACCAACATATGATTGGGTATTTTTTTCCTCATCAAATT
ATTT
- 7 M6E2-1 (338bp) AAAAATACAAGTAATGCATCAATAAACGCTTGATCAAAACTAG
AATTATGTAGGTGGAATAACTATTGAAAGCTTCTTTGCAAAGT
ATTCACACTAGAACTTCAGGGTATCCATTAGATTGACATGAT
GCTGAAGAAAAAAGGTGTTTCATAAGAATCCTAACTAGCAAAT
GAAGCAGGCCACACATGAAAAATAAGACAAATAATACAAGTA
TAATAAAAAGAACAACCTGTCCGAATATTGTTTCCATATGGAGA
GCACAACCATGTAAGTGTCTAACTCTATGAAGGTTTGTGATA
ATGCTGAAATTTTGTAGTAGTGAAGCGCATTTCAG
- 8 M6E2-2 (290bp) ACATCAAGAGGGCGAAAACGCCTAATCCTTCTCAGCCTTTGCC
TTCTACAGAGCAAGGTCTCGGGCCTTGTGTGCGAGTTAGGAAGA
TTTGGATTTGATGGAGAAGTTGATCGATTGAGGCGTGACAAGC
AAGTTTTGATGACGGAAGTGAAGCTTAGACAGAATCAACA
GAATACTCGAGCTTATCTTCGATCTTTGGAGGTAAGGTTACAA
GGAACAGAGAGGAAGCAGCAACAATGATGAACTTTTTAGCA
AGAGCAATGCAAAATCCCGAGTTTGTCCAGCAG
- 9 M6E2-3 (264bp) CTTGGAGACTTGCTTTTTCCCTGAAATTCTACCCCATTTTAAA
GAGGAAATGTTGCATCGATGGCTTGGATTATCTCCATCGTCCTT
GGTGTGACGTGGAACAATCTCACACCACCAAGGACGATTATG
GTGCTCTGGGAGCTGCTGAAAGTCGTAATAATGGAAAGGGAC
GGAGAAAAAATGATAAAGGGACAAGTTGTCTTCTACTCTTCA
TATATTCTGTGTTACGTCGTGATGAGAACGTTGGAGGTTGAC
GCAT
- 10 M6E2-4 (212bp) TCTTGGAGCTCAATACTGCAAGGTAGTGGCAATCGTCTACCCC
AAACGATGGCCAGTCCACCAGACGATGGCCTGTCGATGGGTGG
CATCGATGTGTTTTGAAGGTTGAGGAGTTTCAAGAGAAACCAA
CAAACCTCATCGATGGGATGTGGTCTTACCCACGGACCGTCTGA
TGATGATGTCGATTGGGTTGTGATTTCTTGCAGTTTTTCAG
- 11 M0E3 (267bp) GCTCCTGGCGATGTGCAACTCGTGGCTGGTGAGTTCATGCCTTC
GGCCGGACGTGATGGCTTAGCATCATCAATTGAAAGATGGGCG
ATATACTGGTTTAACGCTCTGTCTTGCCGGAGGAAAACCTAGCG
GGTTGCGCGTGAACGTGGAGTGTACGGCATCGCTACGTGTGAC
AATCTCAGACACGGTTCGACCCGAGCTCATAATCTTCTGTGTC
AATGTGGCGACTTGGATCACCACGACCTTGTCTTCCACTGCG
GGTTCTTG

- 12 M1E1 (247bp) AATATGAGAGACGATTGATACGCCTTGTTGGTAACCTCACCTC
ATGACGATTATATGTGCTGGAAGATCTCATTGCTAATCAATGG
GTGCGTTGCTCAACTTCGTTTTCTTTACGTACTTCAGAGTTGAC
TCAAACATTATGGAATCTTGCTTCTATTTATGAGGTTTACTCAA
ATCTTTACATAACCGGTCACCTCTTTCTTTACTTGATGAAATGT
AAATTTGACCTTACATTATTATCTTGGTG
- 13 M2E3 (360bp) TTTCACTTGATGATTGGATCTTCAAATTTGGGTTATTTCTTTAT
TTTATTTTGACAATTGTTGCCGCATGTAATGGTTGGATTTTCTG
GTCGCACTCCTGTGGCTTTGTCGTTATGGCTTTCCCCAAAATTC
TTTTCTTGCGGCATTCTTCTTCTCTTTCTTTCTGGGTTGATC
TTTGTATCAGTCAAATGATGAAGAAGATGAAGATGATGTATA
TAGCCCTCGAGAAGCTTTGTTGGAGAAGAACAAGCCAAATTCA
AATGCTGATAGTCGCCGAAGATGCTGCTCTTTTCGTGCTGTCAA
AGTGGGAAGCCGCCAAAAGTTGTGGTTCTGGTTACCCTGTTA
GTTTTTCTG
- 14 M1E0-1 (154bp) GTGAGGACCATAATCATGAGCTTACTTGGATCCACTAGATACT
GTCTATTTGAGACAAATCCTATGGGGGCATGTAGTTATGCGAC
AAGGTGATTGCTTCTAAAATATTCTATTTCTACTAATGGGTAAT
CTCCATTCTAAATTTACCCAGTG
- 15 M5E0 (170bp) AGAAGAGATCACCAGCATGGTAAGCAACAAGTACTTTGGTAGT
CTACAAGAATCGCGAGAAGCATTGCATAAATTTTAGTAACTGA
GTGTCCTCTTCGTGTTTATGCAGGTGTGATCGTATACTATGGTT
AGGGAAAGGTATAAAAACAGATGTTTTACAAGCGCGCAGAG
- 16 M2E2 (301bp) AACTGAGGTTTCCGTGGTGTCTTTCTATATCCAGTAGCAAATC
AATTACATTAGGGGACTCAAGACCCTGGCCAATCAGAAATAAT
ACGGCAACCATGCACCGGACTTGATGCCAAAGGAAAGCACTG
CCTTTGATTTTCATTATCATGAGTTGATCATCATTGTCTCTTTCA
TTGAAGGGGACAATTTCAAACGATATTATGTGCCGCCGGTAGT
TGTGCACATTGTCTGCATCCATTTTGCAAAAATTTCTGAAATCA
TGTTCCCCTAAGAATTTCTTCGCAGCAGTTTGCATGGCTG
- 17 M3E2 (258bp) CAGCTTGCCCCACCTCGACTATTTCACTAGGTACCTTGCTATCT
CCCACCAGCATAGACCATCGGGCAACTTTGCCACTAAGGCTTA
GGCAGATAAAAAAGCACCTAATGGTTTTGTCTCTGCTGGAATT
TAGACCCTGATCTCTATGATTTGAACTCACTTCATTATCTAAAC
CACACCCTTAGGTGCAAATACACTCCCACATATATTATCAATC
AGTTATATTATCAACCAAGATTTTATCTCACCAAAAACATG
- 18 M4E3 (211bp) TTCATCAACAATGAAGAGTTCAACAAGAAGAAAGTGATCATCA
TAATGGGGGCCACACGAACGGGAAAATCCCGTCTCTCTGTTGA
CTTTGCCACCCATTTTCGAGGAGAAATAATAAACTTGAACAAA
ATGCAAGTTTACAAGGGACTTGAAATTGTTACAAACAAGATAA
CACACACTGAGAAACAAGGTGAACGACACTATTTGTTAG
- 19 M5E3 (387bp) GGAGTGACTCCGATGAGCCTCAAGAGTATTATACTGGCGGAGA
GAAAAGCGGAATGCTTGTTC AAGATCCATCTAAGGCAAATGAT
GTGAACTCAATATTCGATCAAGCTAGACAACATGCAACTGTTG
AAGGACCTCCAGCATCATCTGGCTCTAGAAGCTTTATTGGAAC
TGCTAGAAGACTTACGGGTGAGACTGTGTCTGCTGCTCCTCAG
CCACCTGAGAGTGTTACTCATAACCATCACTTTCTGGACCAATGG
GTTCACTATTGATGATGGACCCTTGCGGAGGTTTGATGATCCA

- 20 M1E0-2
(206bp)
GAAAATGCCCTTTCTTAGAGAGTATCCGGAAGTCTGAGTGCC
CAAAGAAGTCTGAGCCAGAAGACAGGAGGACGTCTGTCCGAG
CAATTTTGTGGGGAAACAAAGTCCAAGAACAATAACTTTTGG
TCACCACCAGATTTTGGGCATCTATTGCGCAATTGGACAACAT
ATGATTCATCCAGAGTTAATTCTGGTTTATTATTTCCCTGACTGG
TTGTAGAGCCTTTGTCTGAACCTGGTACATCTTGAATTTCCAAT
TGTGTGGCTTCCCTGCATTACAACCTTATCGGTG
- 21 M7E0
(274bp)
TGAAATGGGATTCATATCGTGTAACAAGTCGATACCAATATCA
ATTTTCCGTTTCGCGAGGAATACCAGGGATATAATTAGGTAAGA
CCTATAGAAATTTCCCTCAATACGGGGACCGACTCAATTAGAGG
AATTTCAATTTCTAAATCTTGGACTCTTACAATATGGTATAAAC
ACCCTTCAGAGATCATTTTACAAGCTTTGAAATAAGAAATGAT
ACGACCTCTAGGAATAGAGTTTCCCCTCTTCCACACTAAAACG
GGCTCATCTGGAAAG
- 22 M1E2
(292bp)
TCCTTGCTTGAGGAATATATACTTGGGTTGATGATATACTGCTC
AATGGTGCTCATTGTTGCACCTCTCCTTATTGGCTTCCCGATC
AATAGTCAATTGTGCCCTGATGGAAGACTGGTGTGCGACTATGC
AATGCATCGAATTTGAATGAGTGTGAGCTTGATGGGCCACTTA
TGGGTGTCTATTTTTGAATATAAATTACTGCTCTTTGGTCATGAC
TGATACTAATACTCCCTTTTTTTCTCTTCGGATGCCTACAATAT
AAATTATGTTTCCAACCTGTGTTACTTTGGT
- 23 M2E2
(281bp)
CTGCTGGACTGGATTGGAAGGAAAAAAGTGAGGATACATGAC
TTTCATGGTTGCTTCTACTTCCCTAAGTATCTCCCTTTATGGACTG
ACTCCTTCACAGAACCTTGACTGAATCGACTTCTTTGTTTATCA
ACCTTCTAAACTGATGGTCAAGAATCTCAACTGGTACATCCTTA
TAAAAAAGCCTATCTTTCACAGCCACACTCTCTAATGGCATCAT
ATAATCTGGATCACCAACACACTACTTCAAAAAGTGAGATATGG
AAGACCGGATGCAATGCAG
- 24 M7E2-1
(298bp)
CTTAGTCACTGGGTTTGCAAGGGATTGAAGTTCTGAGCAGTAA
GAAGCCATTGCAATTTTCAGCTCCCTTGAGTCCATAATCCAAGCT
TGGATTCCTTCCCTGCTGTGAGATTATATGGCAACACATTGTTGT
AATAGTCGTTGACAAGTTCCAAAAAATTGGGCAAACATCAATTT
CCCAATATATGCAAGGGCCAATCTTGTATTATCCATGGACACA
CCAATAGGGGTACCTTGGAATTTCCACCGTGTAAGGCCTTGT
TTCTTGAAACATCGATCAATGGGTTGTCGTTCACTAAA
- 25 M7E2-2
(310bp)
AATTGATTGATCCTTGCTGTAAATTCGTGGTTTTATATACAAA
TTGAGTTTGAGATGGATGTTGCATGTTCAAAAAAATTTCAATG
ATCCGATGGCTTGAAGAATTGTTTTCTCGTCACTTGAGGACAA
GAAATGGTTCTATGTTGAGGGTTTTGATGTGCCGTCAAATCTTG
CTACATTTGATGCTTGAAAATAAATACTGATTTCCCTCATCAAG
TGTTTTATGTGTATATAGTTTGGTTTGGTACTTTTTTTACATGTGG
ACATAAAAGAGGAATGAAAAGAAGATTGTTGATAACCAAATG
CTAAA
- 26 M7E2-3
(225bp)
TCTGCAACGTCCGAGGCTATCCGATATTGCTTTTCTGGAATGG
TCGGAATATATGTATCTATTTGGGGGCTTATTAAGTACACAAG
GCACGTATCTGCTTTGCAAGTGTCCCCGTTGCAATCGGACTTA
TGGCACACAGGGGAAACACTGTACTGCTTCCCTTTCCAGAAC

TTCATTGAATCAAACATCGCCATTCAATAAAGAATTTTGGTGA
AATCCTTC
27 M3E3 CTAATCATCTTTGGACGGTTTCTTCATCAATCTGTTGCTGAAAA
(344bp) CTTTGATGGTGTATTTTTGGGTCGTAACAATTTGTTCCGGTCCC
ATCCCCCAAGGAGTGGGTGAGAGGAATGATACCTTTTGGATTT
GGATTTTAGCCTTTTGAACCTTAATGGGAAAATCAATACAACCTTT
TATTATTGGAACTCTTTCAAGGTCTTTAGCTTGATTGGCAATA
AACTAACGGGGAAAGTCCCACGATCTGTGATCTTTTGTGAGTA
TTTGAACACTACTTGATCTATGCAACTTTCAGTTGAATGACACGT
TTCCAAACTGAATGGTATACCTATCTCAGTTGCACAGG
28 M5E3 GCCCGGGATGCATGTTCTAGCAGGAAAGGTTGAAGAACTCC
(35bp) TCGTCCCCTGAAACATGTTATACTTGTTTCTTATGAAATCATT
ATAAAAAGGATTCTGAAGCTATTCAGAGGATCAAGCAAAGG
TATTGCTCATTGCCCTGGTGGTTGTGCTCTGTACATACCTATTT
GTTCCATGTTCTAATTTTAGGTCCTCTTGAAAGTTGCCATTTTC
AAAAATAAAATAAAATTTAAGTCCTCTTGAATTTTTTTTGGCCT
ATAAATTTGCTTCATCATGCTTATACCTGAAAGATTTTGCTTGT
ATGGTCATTTGACGGTTGTTTCAGTTTGGAG
29 M6E3 AGGAGAAGGGTGAGCCCTGGAGGATGATCTGGACAACAAAAA
(169bp) TCCCCTCCACCGTGAATTACTTCGATGGCTTTTGGAAAGGAGG
CAGTCTTGCCACATGAAAACCTTGAACAAGAAGAAATCTTATCT
ACATTCTAGATGCTTTTTATGTAAAAAACGGGTGATAACCG
30 M7E3-1 CATCATTGCTCTTGGTTTTGTAATCTGCCATACACAATATTCTT
(365bp) GACGATTTACTGCTAAATTTTTATGCACCGCGACTCCATCATGA
ATTCTGTATGAGAACTTCCTGGCGTACTTTCTAATATCTTAGT
ACACATATCCTTTCCCAAACATTCCCTCCTTGGCCTCCTCAAAC
TCACCTTCACCGGTGTATTTGCCTAGTGGCCCAATATAGTTGGC
ACCTGCTCAAGTAAAACAAGCTTTCTGAGCTGCCTCAAAATTTT
CTGGTCTTCCACCCCATGTCTTGAGACATGTGTTCTGAAAGCCT
CTTGGATATGAAAACGATACATGTCAGGGGGTGAGAGATTGGT
TCTTCGAGTTCAGT
31 M7E3-2 AAGCAACGATAAAGTGTTCTCGTTTATAAACCCCTTTGTTGGTTC
(193bp) ATGACGCTATCCTGCCCCTGAGGACAGATTGGAACCCTTCCTC
TCCTACATGGAAAAGTATCACTCCCTAACCATGCGACGTCAAT
GAAACCTTTCTTCCTTATCTGCAAATTCCTCCCCCTTGTTCCAAC
AACATCACTAGGTGCCAAG

ACTUAL EVAPOTRANSPIRATION OF GRASSLANDS AND PLANTATIONS IN ARID ZONES

NIZIŃSKI, J. J.* – ZIERNICKA-WOJTASZEK, A. – KSIĄŻEK, L. – GAWROŃSKI, K. – SKOWERA, B. –
ZUŚKA, Z. – WOJKOWSKI, J.

*Faculty of Environmental Engineering and Land Surveying, University of Agriculture in
Krakow, Al. Mickiewicza 24-28, 30-059 Krakow, Poland*

**Corresponding author
e-mail: georges.nizinski@ird.fr*

(Received 23rd Jan 2019; accepted 29th Mar 2019)

Abstract. In models of global change, the course of the general circulation of the atmosphere is dependent on the planetary distribution of sources and sinks of energy; during periods of balance, energy is transported by atmospheric air and the water of the oceans. The atmosphere must thus transport the energy of the continents towards the oceans during the summer and that of the oceans towards the continents during the winter. The study of these phenomena on the continents uses data related to studies of actual evapotranspiration on a local level, which is the level presented here. Recent models of actual evapotranspiration dissociate evaporation of the soil from canopy transpiration and interception, and simulate the evolution of the structure of cover, stomatal resistances, and factors which govern vapour water flux resistance and the balance between evaporation and transpiration. In today's models which take a mechanistic approach, the difficulty of choosing income parameters has become significant, especially the problem of their initial state under a given set of environmental conditions. The objective of this paper is to point out the potential use of the Penman-Monteith formula, which has worked well for the actual evapotranspiration phenomenon of close covers and can be adapted to sparse vegetation (herbaceous savannah with areas of bare soil), while treating leaf transpiration and bare-soil evaporation separately. The actual evapotranspiration of the herbaceous savannah is limited by a boundary layer resistance of the same order of magnitude as surface resistance plotted to the stomata and leaf area index, whereas that of woody covers is limited only by surface resistance: the stomata of trees are more sensitive to the drying of the air and soil than those of herbaceous plants.

Keywords: *drylands, Sudano-Sahel, sparse vegetation, Penman-Monteith equation, evapotranspiration, surface resistance*

Introduction

In actual evapotranspiration models of plant cover with mechanistic vocation, the problems are (a) the choice of the most significant input parameters; and (b) their initial calibration in a given set of environmental conditions. The purpose of this paper is to present the advantages of using the Penman-Monteith formula (Monteith and Unsworth, 1990).

The actual evapotranspiration of herbaceous savannahs is limited by boundary layer resistance which is of the same order of magnitude as cover resistance, which in turn is related to stomata resistance and leaf area index, whereas the actual evapotranspiration of plantations is limited only by cover resistance: the stomata of trees are more sensitive to drying of air and soil than those of herbaceous plants.

In this article, for the estimation and modelling of actual evapotranspiration, the time-step resolution is one day; conditions are equivalent to so-called 'conservative flux' in which absorption is equal to transpiration, which is rarely the case in reality for a time-step resolution of less than one day, during which the plant is subject to dehydration and rehydration, but which is realistic for a 24-h time-step resolution.

Historically Penman (1948) and Monteith (1965) laid the physical foundations for calculating the evaporation of a wet surface and subsequently the actual evapotranspiration of closed plant cover.

The aim of the work described in this paper is to highlight the quality and relevance of the Penman-Monteith model. Nevertheless, on the one hand, even for continuous covers, it is necessary to refine the parameters of the canopy resistance. On the other hand, it was relevant to check the Penman Monteith model for sparse covers crops using the field experience (here the savannahs of the Sahel and the Atlantic coast of Congo); this model makes it possible to account for the actual evapotranspiration of closed plant cover (woody plants) and ought be adapted to sparse cover (woody herbaceous savannah with bare soil surfaces) by treating leaf transpiration and evaporation of bare soil separately.

Materials and methods

Theory of evapotranspiration measurements

For uniform and sufficiently large surfaces with very small slope values, sensible heat and latent heat fluxes are considered vertical and are subject to the principle of ‘similarity’ between the coefficients of sensible heat transfer (k_H) and latent heat (k_E); thus $k_H \approx k_E$. Empirical relationships between flows and vertical gradients of sensible and latent heat can be expressed in the form known as the Penman-Monteith equation (1965):

$$Ea = \frac{ET_0}{\left(1 + \left(\frac{\gamma}{\Delta + \gamma}\right) \cdot \left(\frac{r_{st}}{LAI \cdot r_a}\right)\right)} \quad (\text{Eq.1})$$

where: Ea is actual evapotranspiration (mm day^{-1}); ET_0 is potential evapotranspiration (mm day^{-1}) (in this paper, we applied an equation associated with the FAO formula used by Allen et al., 1998); γ is the psychrometric constant (mb K^{-1}); Δ is the slope of the saturation vapour pressure vs temperature curve (bar K^{-1}); r_{st} is stomatal resistance (s cm^{-1}); LAI is leaf area index; ($\text{m}^2 \text{m}^{-2}$); r_a is aerodynamic resistance (s cm^{-1}).

Crop boundary layer diffusion resistance

The Penman-Monteith equation involves the quantification of *aerodynamic resistance* of plant cover (r_a), *crop cover resistance* (cover resistance) (r_c), and climatic variables. Aerodynamic resistance is a physical quantity that accounts for the diffusion of heat or water vapour from leaf surfaces into the atmosphere (*Fig. 1*).

Cover resistance (r_c) is chiefly a biological term that accounts for the diffusion of water vapour from leaves in terms of a leaf’s stomatal resistance to such diffusion, r_{st} . The following simplified equations are used for closed plant cover (Saugier, 1996):

$$r_a = \frac{r_b}{LAI} + r_{a(1)} \quad (\text{Eq.2})$$

$$r_c = \frac{r_b + r_{st}}{LAI} + r_{a(1)} \quad (\text{Eq.3})$$

where: r_b is leaf boundary layer resistance (s cm^{-1}); LAI is leaf area index ($\text{m}^2 \text{m}^{-2}$); $r_{a(1)}$ is aerodynamic resistance (s cm^{-1}); r_{st} is stomatal resistance (s cm^{-1}).

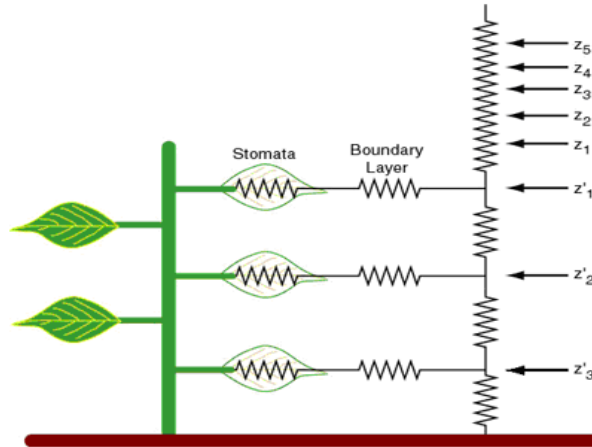


Figure 1. Model schematically showing the resistance of given vegetation cover (r_c). Resistance levels are represented by serrated segments. In the ‘big leaf’ model (Monteith, 1965) the resistance of the vegetation cover (r_c) refers to one vegetation layer

These equations assume that the leaf resistances of the entire canopy are identical at all times, but this is not actually the case: from the top to the bottom of the canopy, r_b increases due to a decrease in wind speed, and r_{st} increases due to a decrease in global radiation (R_g) (see the detailed analysis by Saugier, 1996); in addition, leaf growth conditions depend on the position of leaves in the canopy architecture; the top and bottom leaves do not share the same physiological characteristics (leaves are designated ‘shadow’ and ‘light’).

Aerodynamic resistance

Aerodynamic resistance is composed of leaf boundary layer resistance to the diffusion of heat or water vapour and resistance of the air between the middle of the canopy (average height of the canopy) and the height above the canopy where it is technically possible to measure meteorological variables. We calculate r_a or its inverse, $1/r_a = g_a$, and aerodynamic conductance, assuming equality between the transfer coefficients for heat (k_H) and for momentum (k_V):

$$r_a = \left(\frac{1}{(k^2 \cdot u_{2M})} \right) \cdot \left[\ln \left(\frac{z-d}{z_0} \right) \right]^2 \quad (\text{Eq.4})$$

where r_a is aerodynamic resistance (s cm^{-1}); k is the von Kármán constant (0.39); u_{2M} is wind speed (m s^{-1}); z is height above ground (m); z_0 is roughness height (m); d is zero plane displacement height (m).

For tree-covered areas we calculated g_a from stand height as well:

$$d = 0.75 h \quad (\text{Eq.5})$$

$$z_0 = 0.1 h \quad (\text{Eq.6})$$

where h is mean tree height (m).

Cover resistance

Canopy resistance depends on the stomatal resistance of the leaves and the leaf area index of the canopy in question. Canopy transpiration is the sum of transpirations of all leaves; each leaf is characterised by instantaneous stomatal resistance which is dependent on its own physiological characteristics and the microclimate to which it is subjected.

In terms of stomatal resistance: stomatal movements (depending on the turgor of the guard cells) are governed by global radiation, air vapour pressure, soil water content, and leaf water status.

The mechanisms through which stomata respond to the last three factors are still being discussed:

- Humidity of the atmosphere: more and more often, it is said that stomata are dependent on relative air humidity, and may also be dependent on the deficit of saturation of the air associated with the flow of water inside the leaf; however, it is unclear what kind of mechanism is involved;
- Soil water content status: the influence of soil water content on stomatal movements has long been explained by its action on leaf water status, i.e. a decrease in soil water potential leads to a decrease in leaf water potential resulting from a threshold potential stomatal closure. However, today we know that a plant that is adequately supplied with water but subject to high soil water potentials will close its stomata: roots, in contact with dry soil, synthesise abscisic acid which acts directly on the stomata, irrespective of the water status of the plant. Among the species we studied, *Balanites aegyptiaca* may correspond to this scenario: in the course of soil drying, when higher soil layers contain no more water available for the plant, but deeper layers still contain available water, *Balanites aegyptiaca* will close its stomata during the days, even from late at night until sunrise, there may be no stomatal opening);
- Plant water status: there is no simple causal relationship between stomatal movements and leaf water potential. Thus, with equal leaf water potential, the stomata are closed at night and open during the day. Depending on the species, soil drying causes stomatal closure, with or without an impact on leaf water potential. The species we worked on correspond to the first case, with the exception of *Balanites aegyptiaca*. During a period of soil drying, *Balanites aegyptiaca* employs a leaf area index modification strategy (falling leaves) associated with maintaining a high level of leaf water potential for the remaining leaves (during a period corresponding to a drought). Among the strategies of a plant subject to drought are those relating to the flow of water in the plant and those relating to the distribution of assimilated materials; however, in general, a larger share of carbon goes to the roots, and/or reduction of leaf growth and acceleration of senescence occurs.

Stomatal resistance is usually systematically measured in the field, as we have done here, but currently only empirical models are available to account for variations in this resistance along with environmental factors. The stomatal resistance of a leaf can be calculated, using

the empirical models of Jarvis (1976), from the relationships between the minimal stomatal resistance of a leaf, leaf water potential, global radiation, air saturation deficit, and soil water content.

Stomatal resistance depends on *minimal stomatal resistance*, a specific point value corresponding to a situation characterised by the absence of water stress (soil and plant). Minimal stomatal resistance changes over time, from a leaf's appearance to its senescence; it decreases to a minimum value, then rises again (morphological and physiological evolution of the leaf), as we have observed in the species we studied (*Fig. 6a-d*). In deciduous species (oaks, *Acacia*, Rubber tree), where all of the leaves of the canopy evolve grosso modo synchronously, canopy resistance is a function of minimum stomatal resistance and leaf area index.

In evergreen species (*Eucalyptus* spp.), the degree of dependence of canopy resistance on minimum stomatal resistance depends on the renewal rate of the leaves, since leaves of varying ages coexist in the cover (sampling problem).

To estimate historical *crop cover resistance*, we began by assuming that all leaves were similar (i.e. shared the same physiological characteristics, even microclimate).

- Katerji and Perrier (1985) estimated the variability of stomatal resistance throughout the canopy and divided the cover into several layers to which they applied the equation given above (*Eqs. 2 and 3*).
- Saugier and Katerji (1991) proposed a calculation based on the exponential decay of global radiation and the cumulative leaf area index from the top of the canopy, as well as on integration of the variation of stomatal resistance with received global radiation.
- Other authors calculate cover resistance (r_c) from latent heat flux measurements above the canopy using micrometeorologic methods, reversing the Penman-Monteith equation; closed crop cover is considered a 'big leaf' whose aerodynamic resistance must be a known value.

We started by using the Jarvis (1976) model. Then, for the savannah of the Congolese littoral, we used an inverse Penman-Monteith equation, with parallel measures of stomatal resistance and environmental factors; this latter approach enables deterministic analysis of cover resistance. Measurement of leaf area index is decisive in estimating this resistance.

Climate variables

Another variable which is difficult to estimate using the Penman-Monteith equation is the air saturation deficit, which should theoretically and ideally be measured above the vegetation in the layer of the atmosphere constantly modified by evapotranspiration (surface boundary layer) and various meteorological station values (short and well-watered lawns).

Some models exist for the estimation of air saturation deficit from the characteristics of the planetary boundary layer, a global layer subject to the exchange of energy and mass with the surface but not yet subject to the Earth's rotation (20-40 m at night and up to 3,000 m during the day).

Study sites and measurements

Study sites field work was carried out:

1) On a 1-ha plot (*Fig. 2*) situated on a dune's rise (including the dune's crest and hollow with 1.6% slope). The plot was located near Souilène, about 400 km from Dakar and 20 km from Dagana (16°20'30"N, 15°25'40"W). The study area is a Sahelian zone

in the northern Ferlo region (North Senegal, West Africa). The climate of the region is dry tropical with mean annual precipitation (1918-1990, Dagana) of 282 mm year⁻¹. This Mimosaceae thorn scrub has three main vegetation layers: a herbaceous layer (mainly composed of annual grasses) dominated by shrub and small trees layers. The landscape is typically a gently undulating surface composed of low magnitude non-oriented dunes that end in small hollows. The overstore canopy is mainly 20 year old *Acacia tortilis* (Forsk.) Hayne ssp *raddiana* (Savi) Brenan and 25 year old *Balanites aegyptiaca* (L.) Del; stand density is 151 trees ha⁻¹ and the total basal area is 3.87 m² ha⁻¹. On the 1 ha plot we selected agroforestry with *Acacia tortilis*, a grove with *Balanites aegyptiaca* and a herbaceous zone outside the tree crown shade (without trees). Mean height of *Acacia tortilis* and *Balanites aegyptiaca* trees was 6.60 m and 6.40 m, respectively, and mean stem diameter at soil level was 0.56 m and 0.61 m. The age of selected trees, (20 and 25 years, respectively) correspond to the most important populations in the pyramid-shaped diagrams representing the populations of *Acacia tortilis* and *Balanites aegyptiaca* by age-groups. Every grove possessed its characteristic herbaceous layer (annuals). The plot's soils belong to the brown sub-arid sandy soils which are slightly acid (pH 6-6.5) and poor in clay, organic matter, nitrogen and phosphorus. The study zone is a rangeland with average annual primary production of the herbaceous layer (2895 kg DM ha⁻¹ year⁻¹) being 10% lower than the actual demand of the grazing livestock. The continuous livestock presence destroys the crust at the soil surface and promotes infiltration of rainfall.



Figure 2. Experimental site located in the Ferlo region (northern Senegal). Landscape formed by a very open thorny steppe, including a herbaceous layer composed of annual species, dominated by grasses (average dry-matter yield, 2,895 kg ha⁻¹ year⁻¹) and dotted with trees and shrubs (*Acacia tortilis* and *Balanites aegyptiaca*) with an average height of 6.5 m, a density of 151 trees ha⁻¹, and a total basal area of 3.87 m² ha⁻¹ (Nizinski et al., 1994)

(2) On two plots located (Fig. 3a) near Kondi (latitude 4°34'S, longitude 11°54'E, altitude 80–120 m above sea level), about 40 km north from Pointe Noire (Congo). The Kouilou region (covered 13315 km²) is situated on the Atlantic Ocean front of the Congo between Cabinda in the South and Gabon in the North; the climate of the region

is subequatorial tropical with mean annual rainfall $Pi_{49-98} = 1188$ mm, potential evapotranspiration $Ep_{92-98} = 1390$ mm year⁻¹ ($Ep_{92-98} = 3.8$ mm day⁻¹; $Ep_{\text{RAINY SEASON}} = 4.2$ mm day⁻¹, $Ep_{\text{DRY SEASON}} = 3.2$ mm day⁻¹), mean air temperature 24.9 °C ($t_{\text{max}} = 28.2$ °C, $t_{\text{min}} = 21.9$ °C), relative air humidity 81.1% ($H_{\text{max}} = 95.5\%$, $H_{\text{min}} = 66.4\%$) (long-term values estimated over the period of 1949–98, meteorological station, Pointe Noire). The rainy season, which lasts about 180 days, starts in November and ends in April, the dry season from June to September; May and October are the months of transition. The study area is situated on thick detritic formations of continental origin, dating from the plioleistocene. The soils are ferrallitic and highly desaturated, on sandy to sandy clay material (grayish-ochre colour, more than 90% of sand content and particular structure).

Sampling and measurement techniques: water balance, plant water status and environmental measurements

- Weekly measurements: gross precipitation, throughfall (22 rain gauges “Association”; collecting area 8800 cm²), stemflow (10 stemflow collars), soil water content (neutron probe “Solo25”, Centre d’Etudes Nucléaires, Cadarache, France; 8 permanent access tubes).
- Hourly measurements: leaf water potential (pressure chamber PMS, Inst. Co., Corvallis, Oregon, USA), leaf transpiration, stomatal resistance (porometer AP4, Delta-T-Devices, UK), soil water potential (tensiometers, Soil Moisture Equipment Corporation, Oh, USA).
- Leaf area index (*Fig. 3b*): maximal leaf area index and leaf area distribution will be reported, the total leaf area divided by the area covered by the leaf area, obtained by direct measurements of the number of leaves of the year harvested (litter fresh).
- Stomatal resistance (r_s): measurements were made using an AP4 porometer, Delta-T-Devices® (*Fig. 4*). Porometers measure gaseous exchanges between the leaf and the atmosphere. These fluxes are proportional to the surface of the leaf, to the concentration gradients of the gas between the inside and the outside of the leaf, and to the conductivity (= 1 / resistance) of the leaf. In open systems, a constant flow of air and a known water vapor concentration enters the chamber where the leaf is located, and the concentration of outgoing water vapor is then measured. It is then possible to calculate perspiration and stomatal resistance.

Results and discussion

Impact of leaf area index on actual evapotranspiration: The actual/potential evapotranspiration ratio increases with increasing leaf area index according to the function:

$$E_a/ET_0 = 1 - e^{(-k \text{ LAI})} \quad (\text{Eq. 7})$$

where k is the extinction coefficient of light in the cover (Saugier, 1996) and LAI is leaf area index (m² m⁻²).

Depending on the type of vegetation, the differences in this curve (*Eq. 7*) are larger or smaller. The measurement and modelling of leaf area index are therefore essential.

We will illustrate the influence of leaf area index on actual evapotranspiration with two situations: a temperate oak forest, representing a deciduous forest that we followed several years from bud break until the leaves fell, and the Sahelian steppe, representing heterogeneous vegetation.



Figure 3 a. Experimental site located in the watershed of Kouilou on the Atlantic coast of Congo (view from the study site). **b.** LAI measurement of savannah 90% dominated by *Loutetia arundinacea* (average height, 1.5 m; maximum biomass, 3.5 tonnes ha^{-1} ; maximum dead biomass, 4.6 tonnes ha^{-1} ; leaf area index, 4.3; root zone, 3 m in depth; field capacity (R_{FC}), 363 mm; permanent wilting point (R_{WP}), 182 mm; available water content (R_{AW}), 181 mm)



Figure 4. Stomatal resistance measurements were made using an AP4 porometer, Delta-T-Devices®

For the savannahs (Sahelian steppe, Fig. 2; savannah of the Congolese littoral, Fig. 3a), we estimated g_a from the profiles of the wind speeds above these herbaceous covers (from 2.5 to 5.0 $cm\ s^{-1}$).

The overall values of aerodynamic resistance reflect the fact that resistance decreases with roughness of the canopy and wind speed. For sparse vegetation, no formula has been developed as yet for the calculation of aerodynamic resistance. For the Sahelian steppe, composed of 80% herbaceous areas (groves of low trees), we assumed the equality of aerodynamic resistance in herbaceous zones and groves, which, given the

low density of trees within groves, is reasonable: resistance is even higher than density is low; otherwise, regarding estimates of interception (in which only aerodynamic resistance occurs), it can be assumed that there is no overestimation here either, because rains are of great intensity and the water retention capacity of crowns and trunks is low (2.9-3.8 mm for *Balanites aegyptiaca* and *Acacia raddiana*, respectively) (Fig. 2).

The maximum values of interception of *Balanites aegyptiaca* and *Acacia raddiana* groves equal 8.4 and 12.4% of incident rainfall (Pi), respectively. These values can reach 40% of Pi for oaks in the temperate zone (forest of Fontainebleau). The maximum values of interception of groves (8.4 and 12.4% of Pi, respectively) are of the same order of magnitude as that of the herbaceous zones of the Sahel savannah (7.5% of Pi) (Fig. 2) and the savannah of the Congolese littoral (7% of Pi) (Fig. 3a).

In the case of *deciduous species*, it is a question of modelling various phenological stages: the day of bud burst; the period of leaf growth up to maximum leaf area index; the adult phase during which the leaf area index is equivalent to the maximum value ($LAI = LAI_{max}$); the beginning of senescence from the first fall of leaves until the leaf area index equals zero. For *Quercus petraea*, using two simple input variables [mean air temperature and photoperiod] we modelled the day of budburst, the day marking the end of surface growth of the leaves, and the evolution of leaf area index.

In terms of the relationship of minimal stomatal resistance to leaf area index in deciduous species, with the exception of Eucalyptus, the species we studied are deciduous. The leafless period is the cold season in the temperate zone and the dry season in the tropical zone. Thus we were able to analyse the following phenomenon: when setting up the canopy, the minimal stomatal resistance of a leaf decreases with increasing leaf area index and generally continues to decrease to its minimum value as long as the leaf area index is maximal (Fig. 5). The leafless period may be longer or shorter depending on the species ($LAI_{max} - \text{minimum values } r_{st-min}$; in *Quercus petraea*, $LAI = 100\%$, $r_{st-min} = 3.6 \pm 0.9 \text{ s cm}^{-1}$ and $LAI = 8\%$, $r_{st-min} = 8.7 \pm 3.6 \text{ s cm}^{-1}$, respectively) (Fig. 6a-d); for example, in oaks, it is very short (two to three weeks). Subsequently, r_{st-min} increases throughout the period of LAI_{max} (two and a half months for the oak) and continues to increase during senescence.

In deciduous forests, actual evapotranspiration follows changes in leaf area index; as there is a gap between the points when $LAI = LAI_{max}$ and when r_{st-min} reaches its minimum value, actual evapotranspiration reaches its maximum (when not subjected to water stress) when r_{st-min} is at its minimum value for oaks, i.e. about a month after $LAI = LAI_{max}$ (Fig. 7).

Balanites aegyptiaca offers an example of adaptation to drought. To summarise the characteristics that may explain its distribution (this species 'goes up' to the northernmost part of Senegal) and the current increase in its frequency compared to other shrub and tree species of the Sahelian steppe: in the dry season, when water availability becomes limited, we observed that *Balanites aegyptiaca* employed a strategy of maintaining high leaf water potential through increased stomatal resistance ('ABA message' from the roots) and a leaf area index modification strategy (falling leaves). Thus, at the end of the dry season when *Balanites aegyptiaca* no longer has leaves, soil water that was available but not used (increased stomatal resistance, decreased transpiration) remains in the deep layers of the soil (deeper than 2.0 m).

Subsequently, bud break and leaf growth occur prior to the rainy season, during a period when the relative air humidity increases; this leaf growth is possible because there is water available deep in the soil.

This leads us to make two assumptions:

(1) We posit the existence of a chemical ‘message’ related to detection of the increase in relative air humidity. This message participates in the chemical equilibrium of induction at bud break. This detection must be performed by an above-ground organ, possibly the photosynthetic stalk (thorns), which remains in place.

(2) We suppose that this message has priority over the ‘ABA message’ from the roots, since the leaves are being put in place while the soil water content of the upper layers are at the permanent wilting point, in ‘soil conditions’ identical to those of the end of the dry season. Here, we can question the adaptive advantage of setting up the leaves prior to the arrival of the rainy season.

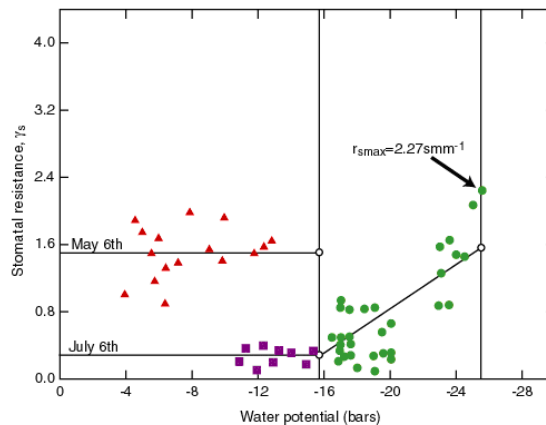


Figure 5. Evolution of minimal stomatal resistance (r_{st-min} , $s\ cm^{-1}$) with leaf water potential (Ψ_m , bars) for oak leaves in the forest of Fontainebleau and in the park of the Orsay University of during the growing seasons of 1983 and 1987, respectively ($r_{st-min} = 78.501\ SF^{0.7505}$; $r^2 = 0.905$; $N = 12$)

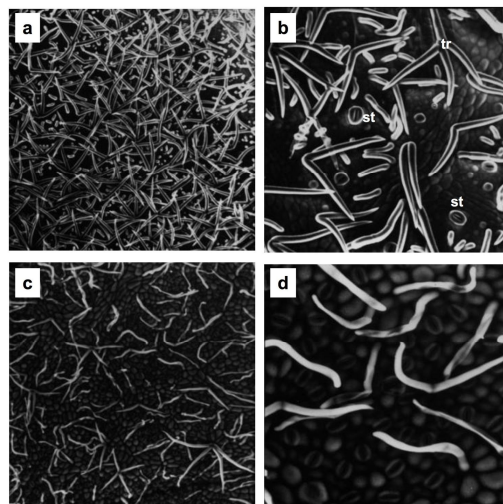


Figure 6 a-d. Images acquired via scanning electron microscopy showing two morphological stages of stomata and trichomes of *Quercus petrea* leaves growing in the park of the Orsay University: **a** low- and **b** high-resolution images for the morphological stage of 24 April 1987 ($SF = 8\%$ of SF_{max} , $r_{st-min} = 8.7 \pm 3.6\ s\ cm^{-1}$, $N = 50$); **c** low- and **d** high-resolution images for the morphological stage of 14 May 1987 ($SF = 100\%$ of SF_{max} , $r_{st-min} = 3.6 \pm 0.9\ s\ cm^{-1}$, $N = 50$). The location of some stomatas (st) and trichomes (tr) is indicated in **b**

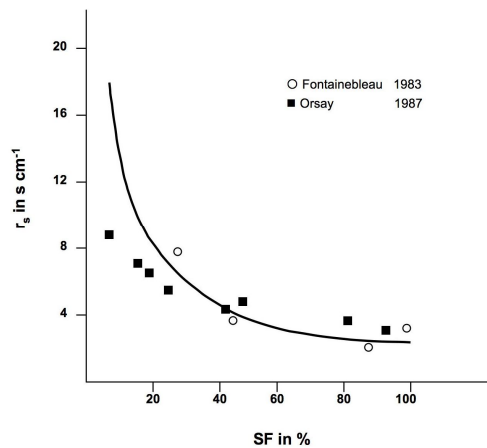


Figure 7. Evolution of minimal stomatal resistance (r_{st-min} , $s\ cm^{-1}$) along with leaf area (SF, %) for oak leaves during the growing season of 1983 in the forest of Fontainebleau

Conclusion

Humankind has changed and continues to change plant cover; globally, there has been an increase in herbaceous and bare-soil areas to the detriment of areas that had been populated with trees and shrubs since the Neolithic. Changes in vegetation cover have involved changes in local and regional climates as well as in the global climate.

Climate models of the general circulation of the atmosphere require actual evapotranspiration models which incorporate ‘vegetation-atmosphere’ exchanges as realistically as possible. Our studies of *Acacia raddiana* and *Balanites aegyptiaca* in the steppes of Senegal (Nizinski et al., 1994) and of *Loudetia arundinacea* in the savannah and eucalyptus plantations on the coast of the Congo (Nizinski et al., 2011) offer two examples of the impact of a change in cover on actual evapotranspiration: in Senegal, the groves of the steppe (20% of the surface) may be assimilated into the ‘clear forest’ of *Acacia senegal* in Northern Senegal before this forest disappears and an 80% herbaceous area represents the new ecosystem.

In Congo, on the coast, there are remnants of pure savannah adjoining the planted eucalyptus forests in the original savannah. The replacement of the forest with a herbaceous ecosystem is increasing drainage and reducing actual evapotranspiration over a complete cycle of vegetation (with seasonal variations which may be marked, since the two ecosystems differ less in periods of water deficit than in wet seasons, when evaporation of intercepted water is greater in the forest due to its high degree of roughness).

For example, the ‘boundary layer resistance’ of the Congolese savannah is $Z_H \approx 3.0 \times$ stand height of plant cover in the case of sensible heat flux, and $Z_{\lambda,E} \approx 3.5 \times$ stand height of plant cover in the case of latent heat flux. Methodologically, any fetch effects should be omitted, so that classical aerodynamic formulas can be applied.

The surface conductance of the two covers differs little; what differs is aerodynamic conductance, in which the two covers differ by a factor of two (from 2.5 to 5.0 $cm\ s^{-1}$ for ‘herbaceous’ and from 5.0 to 10.0 $cm\ s^{-1}$ for ‘forest’). The two covers also differ in their albedo (superior in the case of the herbaceous ecosystem) and energy balance (inferior in the case of the herbaceous ecosystem). Actual evapotranspiration of the

herbaceous ecosystem depends mostly on net radiation, actual evapotranspiration of the forest on deficit of air saturation.

Soil plays a major role: the surface state of the soil governs the existence (or absence) of runoff due to the presence (or absence) of a crust on the soil surface in sparse herbaceous ecosystems. The steppe occupied by *Acacia raddiana* in the first year after the experimental plot was set aside was characterised by a crust on the soil surface and non-renewal of the herbaceous layer, because this surface was no longer being trampled by herds of animals; in the second year, weeds replaced trampling. The hydraulic conductivity of the saturated soil also governs the existence (or absence) of runoff; this variable is generally lower in herbaceous ecosystems, which are often subjected to trampling by animals, than in forests.

The depth of soil colonised by tree roots is generally greater than that of soil colonised by grass roots: available water remaining in the soil of the steppe occupied by *Acacia raddiana* could be used if the steppe was forested. Lean and Rowntree (1997) give an example of the replacement of a forest (Amazon rainforest) with a meadow, pointing out that reducing the depth of the exploited soil does not affect the water balance. The Amazon rainforest contains areas where the potentially exploitable soil around the roots is shallow (existence of an impermeable horizon for the roots). In this case the forest has little available soil water content comparable to that of the grassland which succeeds it and whose soil is often characterised by significant underground water circulation. Here we see the importance of soil in regional water balance.

In models of global change, the course of the general circulation of the atmosphere is dependent on the planetary distribution of sources and sinks of energy; during periods of balance, energy is transported by atmospheric air and the water of the oceans. The atmosphere must thus transport the energy of the continents towards the oceans during the summer and that of the oceans towards the continents during the winter.

The study of these phenomena on the continents employs data relating to studies of actual evapotranspiration on a local level, which is the level presented here. Recent models of actual evapotranspiration dissociate evaporation of the soil, canopy transpiration, and interception, and simulate the evolution of the structure of cover, stomatal resistance, and factors which govern the vapour water flux resistances and the balance between evaporation and transpiration. In today's models which take a mechanistic approach, the difficulty of choosing income parameters has become significant, especially the problem of their initial state under a given set of environmental conditions. Currently, from a methodological point of view, for shrubs and tree species, estimation of the transpiration of individual trees using the sap-flow method opens up new perspectives.

The aim of the work described in this paper is to highlight the quality and relevance of the Penman-Monteith model. Nevertheless, on the one hand, even for continuous covers, it is necessary to refine the parameters of the canopy resistance. On the other hand, it was relevant to check the Penman Monteith model for sparse covers crops using the field experience (here the savannahs of the Sahel and the Atlantic coast of Congo); this model makes it possible to account for the actual evapotranspiration of closed plant cover (woody plants) and can be adapted to sparse cover (woody herbaceous savannah with bare soil surfaces) by treating leaf transpiration and evaporation of bare soil separately.

We conclude by stating that the fieldwork parallel to the modelling work is far from complete. We have shown that, for *Quercus petraea*, there is a factor of three between

the minimum and maximum values of minimal stomatal resistance or from the range that one may assume very extensive drought adaptation characteristics such as those described for *Balanites aegyptiaca*.

REFERENCES

- [1] Allen, R. G., Pereira, L. S., Raes, D., Smith, M. (1998): Crop Evapotranspiration: Guidelines for Computing Crop Water Requirements. – Paper no. 56. Food and Agriculture Organization, Rome, Italy.
- [2] Jarvis, P. G. (1976): The interpretation of the variations in leaf water potential and stomatal conductance found in canopies in the field. – Philosophical Transactions of the Royal Society of London, Series B, 273: 593-610.
- [3] Katerji, N. Perrier, A. (1985): Détermination de la résistance globale d'un couvert végétal à la diffusion de la vapeur d'eau et de ses différentes composantes. Approche théorique et vérification expérimentale sur une culture de luzerne. – Agricultural Meteorology 34: 105-120.
- [4] Lean, J., Rowntree, P. R. (1997): Understanding the sensitivity of a GCM simulation of Amazonian deforestation to the specification of vegetation and soil characteristics. – Journal of Climate 10: 1216-1235.
- [5] Monteith, J. L. (1965): Evaporation and Environment in the State and Movement of Water in Living Organisms. – Proceedings of the Soc. Exp. Biol., Symposium No. 19. Cambridge Univ. Press, Cambridge, pp. 205-234.
- [6] Monteith, J. L., Unsworth, M. H. (1990): Principles of Environmental Physics (2nd Ed.). – Edward Arnold, London.
- [7] Niziński, J. J., Morand, D., Saugier, B. (1989): Variation of stomatal resistance with leaf age in *Quercus petraea*: effect on the soil-water balance of an oak forest. – Annales des Sciences Forestières 46(suppl.): 429-432.
- [8] Niziński, J. J., Morand, D., Fournier, C. (1994): Actual evapotranspiration of a thorn scrub with *Acacia tortilis* and *Balanites aegyptiaca* (North Senegal). – Agricultural and Forest Meteorology 69: 93-111.
- [9] Niziński, J. J., Galat, G., Galat-Luong, A. (2011): Water balance and sustainability of Eucalyptus plantations in the Kouilou basin (Congo-Brazzaville). – Russian Journal of Ecology - Ekologiya 42: 40-50.
- [10] Penman, H. L. (1948): Natural evaporation from open water, bare soil, and grass. – Proceedings of the Royal Society of London, Series A 193: 120-145.
- [11] Saugier, B. (1996): Evapotranspiration des prairies et des cultures. – Comptes Rendus de l'Académie d'agriculture de France 82: 133-153.
- [12] Saugier, B., Katerji, N. (1991): Some plant factors controlling evapotranspiration. – Agricultural and Forest Meteorology 54: 263-277.

ALGORITHM TO CALCULATE SUSPENDED SEDIMENT CONCENTRATION USING LANDSAT 8 IMAGERY

HERNÁNDEZ-CRUZ, B.^{1*} – VÁSQUEZ-ORTIZ, M.² – CANET, C.³ – PRADO-MOLINA, J.⁴

¹*Facultad de Ingeniería, Universidad Nacional Autónoma de México, Ciudad Universitaria, Coyoacán, C. P. 04510, Ciudad de México, Mexico.*

²*Instituto Nacional de Pesca y Acuicultura, SAGARPA, Av. México 190, Del Carmen, Coyoacán, C. P. 04100, Ciudad de México, Mexico.
(e-mail: Mariogeo190192@gmail.com)*

³*Centro de Ciencias de la Atmósfera, Universidad Nacional Autónoma de México, Ciudad Universitaria, Coyoacán, C. P. 04510, Ciudad de México, Mexico.
(e-mail: ccanet@atmosfera.unam.mx; phone: +52-55-5622-4059; fax: +52-55-5622-5009)*

⁴*Laboratorio Nacional de Observación de la Tierra, Universidad Nacional Autónoma de México, Ciudad Universitaria, Coyoacán, C. P. 04510, Ciudad de México, Mexico.
(e-mail: jprado@igg.unam.mx; phone: +52-55-5623-0222 ext. 45475)*

**Corresponding author*

e-mail: gberehc@ingenieria.unam.mx; phone: +52-55-5622-8001 ext. 1028

(Received 24th Jan 2019; accepted 10th Apr 2019)

Abstract. Satellite imagery was used to assess the suspended sediment concentration (SSC) of the plume at the Grijalva river mouth, Gulf of Mexico. The SSC was calculated with the algorithm of Topliss. The algorithm was created for Landsat 5 MSS. For this study it was validated the results for Landsat 7 ETM+ and Landsat 8 OLI. The depth of the ocean floor was measured using the speedtech sounder. The spectral response was registered with a GER-1500 spectroradiometer (with a measurement range of 296.71–1092.08 nm). The spectral responses were used to determine the size of the suspended particles and to perform the atmospheric correction. Spectral responses indicate that silt size particles predominate near the river mouth, whereas clay overtakes further towards the open sea. The trend in the river when water meets seawater, means an increase of suspended sediment towards the surface due to the lower density of fresh water, and the amount of sediment rises in the open sea. The correlation between the measurements in situ and SSC values produced by the algorithm demonstrates that the operation is suitable to estimate suspended sediments.

Keywords: *Grijalva River, spectral response, sediments decrease, particles size, speedtech sounder*

Introduction

Suspended sediments in the plume of a river mouth control the delta morphology and ecology. In water bodies suspended sediments are quantified as a concentration, as the total amount of solids suspended in the mixture water-sediment, generally expressed in mg/l (Carbonneau and Piégay, 2012; Qu, 2016).

The importance of the study of suspended sediment concentration (SSC) in the delta and sediment plume of the Grijalva River, southwestern Gulf of Mexico, lies in the volume of water transported (140 km³ per year; the river length: 1521 km), and the vulnerability that it represents in physical-geographic terms (Kemp and Piégay, 2016). A serious vulnerability issue in the delta is the coastline retraction; this phenomenon occurs at the State of Tabasco, southern Mexico, from Sanchez Magallanes (3 to 5 m

per year) to the mouth of the San Pedro River, with 8–9 m per year (Hernández et al., 2008; Nooren et al., 2017).

The assessment of SSC could be done with sensors capable of detecting the electromagnetic radiations that arrive at Earth's surface from the atmosphere, where its reflectance can be recorded and processed (Sobrino, 2000; Zhou et al., 2017). Remote detection of water body's properties, as suspended and diluted matter, is based in the interaction between the electromagnetic waves and the molecules of water and its components (Bukata et al., 2018; Domínguez et al., 2011). Sediments suspended in water produce an increase in reflection of visible radiation, varying for different particle diameters, mainly in the blue and green bands (Chuvienco, 2008). Hence, remote sensing techniques have been used to measure the SSC, through models and algorithms showing potential at regional, multi-temporal and synoptic levels; costs involved in this procedure are considerably lower than those of in situ sampling and laboratory analysis (Nooren et al., 2017; Ritchie et al., 1987; Topliss et al., 1990; Wang, 2007; Long and Pavelsky, 2013).

Algorithms for SSC quantifying can be used in some cases to predict sediment concentrations under other rivers with similar conditions (Long and Pavelsky, 2013). Some studies had developed universal algorithms to estimate suspended sediments using sensors such as MODIS and MERIS; however, such algorithms require a minimum calibration (Ritchie and Cooper, 1991; Nechad et al., 2015).

Topliss et al. (1990) developed an algorithm to quantify the SSC for concentration ranges of 5–100 and 100–1000 mg/l with the Landsat MSS sensor (bands: green, red and infrared). The data derived from Landsat 7 ETM+ and Landsat 8 OLI TIRS—the sensors employed in this study—are compatible with the data at level 1 (orthorectified) created using Landsat 1 to 5 (Ariza, 2015).

This research has three main objectives. First, to determine the validity of new generation of Landast sensors (ETM+ OLI/TIRS) using the Topliss algorithm, which was designed and calibrated for Landsat 5 MSS sensor (Topliss et al., 1990). Second, to establish the statistical relationship of the algorithm for sensor OLI with the in situ SSC measurements in the Grijalva delta and plume. The third objective was to determine the size of the sedimentary particles suspended in river and sea water in the study area, through reflectance measurements obtained in the field by spectroradiometer, and to compare them with library theoretical signatures. Depending on the reflectance percentage the spectral signature, it is possible to determine of particle size and concentration of sediment.

Review of literature

So far there are only a few works available in the literature regarding suspended sediment concentration calculus. Most of the studies and algorithms developed, using satellite imagery, were carried-out in the 2000-2010 decade. Nevertheless, between current works, we can mention:

He et al. (2013): the authors implemented a monitoring of diurnal dynamics of sediments in the ocean employing meteorological images of GOCI. The variables adjusted in the model were those related with the atmosphere. They found results with differences of less than 5000 mg/l, except during typhoon season.

For the study areas of deltas connecting fresh water to the sea, Long and Pavelsky (2013) used MODIS imagery to determine SSC in the Peace-Athabasca, delta in

Canada. They applied 31 empiric equations using band 1 (620-670 nm) and band 2 (841-876 nm), obtaining a Spearman's correlation of $\rho = 0.95$ in 29 years of sampling.

Loisel et al. (2014) studied, over a period of 11 years, the SSC in the west of the Vietnam Sea. They used MERIS (Medium Resolution Imaging Spectrometer) data, with a spatial resolution of 300 m. They applied three algorithms, which allowed to eliminate atmosphere interferences and to differentiate fluvial sediments from those of the sea.

Time series allowed them to recognize the season of the year with the highest SSC (Monsoon season, in September-October). In November SSC starts to decrease, and in March and May is when drier periods appear. Results obtained with MERIS imagery were satisfactory, even with the spatial resolution of 300 meters per pixel. Algorithms employed has been successfully applied in other regions of the world, and with the modifications they made on some variables, they found a correlation coefficient of 0.7 between remote sensing techniques and in situ measurements, which is a good result for a remote sensing methodology (Loisel et al., 2014).

Material and methods

Study area

The delta and plume of the Grijalva river lie to the north of the Centla Municipality, State of Tabasco, southeastern Mexico (*Fig. 1*), between 525221.38 and 535316.162 m N and between 2066918 and 2054176 m W; (UTM North zone 15). The size of the study area is $\sim 60 \text{ km}^2$, and the furthest sampling point was 10 km away from the coastline.

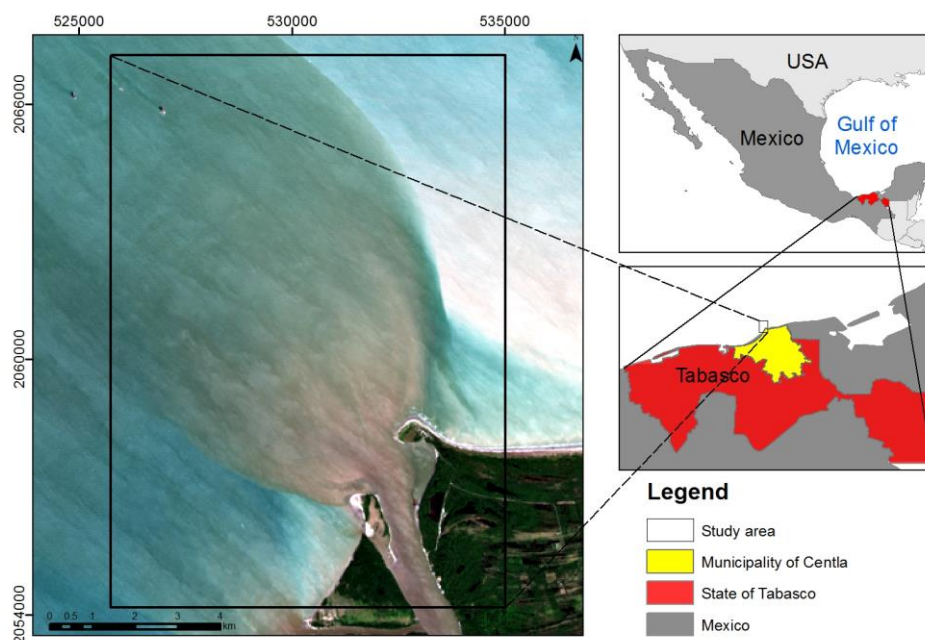


Figure 1. Plume and delta of Grijalva River, Southeast Mexico. This river flows into the Gulf of Mexico

The climate is $Am(w)$, that is, warm-humid with abundant rain in the summer, leading to marked periods of precipitation and drought (GET, 2006). Near the river

mouth there are coastal cords, roughly parallel to the coastline, formed by sediments supplied by the Grijalva River during the last 5000 years, since the stabilization of the current sea level. Vegetation grows between the cordons formed in the water. The type of vegetation is a riparian forest of white poplar (*Populus alba*) and tulle (*Schoenoplectus acutus*) (Buena and Santiago, 2005; Nooren et al., 2017; Psuty, 1965); there are, in addition, mangrove swamps in zones nearby the river mouth.

Field data gathering and laboratory analysis

Sampling points were selected considering the dynamic distribution of sediments in the plume when entering in contact with seawater (cf. Arche, 2010), to avoid the effect of the soil and vegetation of the riverbank, with at least 1000 m distance between points (Fig. 2). Timing of sample collection considered the passing of the Landsat 8 satellite together with the presence of optimal meteorological conditions. Both conditions were encountered on January 25, 2016, when sampling activity was performed.

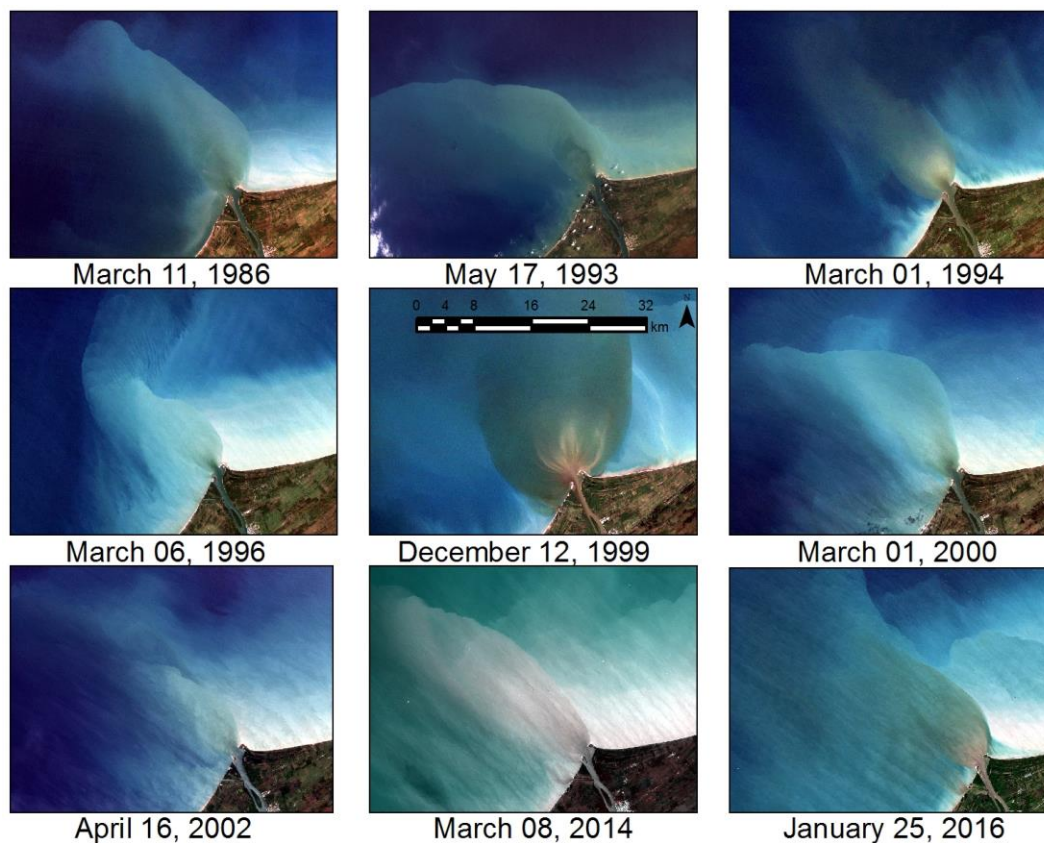


Figure 2. Historical distribution of the Grijalva river plume. The last map (January 25, 2016) corresponds to the date of sampling

Samples between 0.6 and 1.0 l of water were collected at a depth of 15 to 30 cm. Depth was measured with a Speedtech instrument and spectral response of the suspended sediments with a GER-1500 spectroradiometer whose measurement range is between 296.71 and 1092.08 nm in intervals of ~1.5 nm (Fig. 3).

In the laboratory, sediments were separated by a gravimetric method according to the Mexican norm NMX-AA-034-SCFI-2015. The method allows the quantitative

measurement of the solids, dissolved solids, as well as the amount of organic matter contained in natural waters, residual, and treated wastewater.

In concordance with international standards, above mentioned norm coincides with ISO 11923:1997, Water quality – Determination of suspended solid by filtration through glass-fiber filters. However, some differences between them are found in the concepts; international method principle broaden solids determinations, drying device is different, reference suspension used has major concentration, and storage time of the sample is larger in the ISO standard. Mexican Norm maintains calculations for total suspended solids and incorporate them to another species not covered by ISO (Norma Oficial Mexicana, 2016).

Regarding the samples, every crucible with a Whatman 2 μm filter had a constant weight. A vacuum pump in a flask was used to filter 100 ml of each sample. A constant weight of sediment on a Whatman filter (2 μm) in a filtering crucible was dried in a stove at 105 °C for more than 12 h. From the weight of the residue, the concentration of suspended solids (mg/l) was calculated. Correlation and regression analyses compared these data with those obtained by remote sensing.

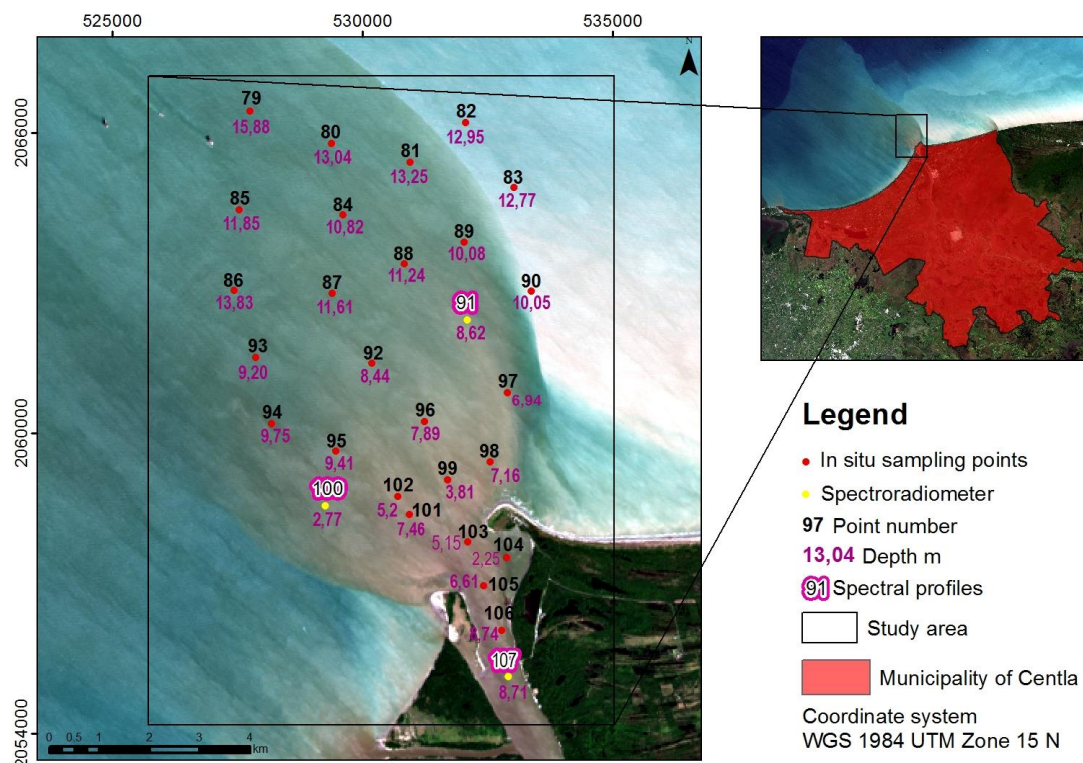


Figure 3. Distribution of sampling sites in the Grijalva river sediment plume

Remote sensing data

Satellite imagery of the study area (U.S. Geological Survey, 2016) corresponds to Path 22 and Row 47 for OLI sensor, and Path 21 Row 47 for ETM+. The ETM+ sensor revisits the same place with a difference of eight days. Imagery with adequate meteorological conditions was searched from various dates with no clouds present (0% of clouds). The image that corresponds to the date of sampling was obtained on January 26, 2016 for Landsat 8, with the time in the central scene at 16:35:21 hours and

February 03, 2016 with a time in the central scene at 16:13, for ETM+. Downloaded images were geometrically corrected with the cartographic projection WGS 1984 UTM zone 15 N.

Atmospheric corrections

The atmospheric conditions affect the radiometric response of the recorded images (Richards, 2013). Radiometric and atmospheric corrections eliminate these effects and convert digital levels in physical and biophysical variables (Padró et al., 2017). In the present study, images were corrected using physical models of radiative transference, usually based on a series of standard atmospheres (Chuvieco, 2008; Sobrino, 2000).

The FLAASH method (*Fast Line-of-sight Atmospheric Analysis of Spectral Hypercubes*) eliminates the effects of the atmosphere, the illumination, and other factors in the reflectance of the surface, and thereby generates more precise values; it combines directly the code of atmospheric radiative transference MODTRAN4, which allows direct selection of atmospheric models such as MODTRAN standard, and the diverse types of aerosols. Furthermore, the method can be applied to correct the adjacency effect and to calculate the visibility in the whole image (Liang and Wang, 2012).

Image processing

After the atmospheric and radiometric corrections, the image was cut according to the study area. The so-called salt and pepper error was corrected applying a media filter with a 3×3 kernel.

Land covers not belonging to water were masked with the application of NDVI and NDWI indexes. In the first case the water presents values less than zero and helps in the separability; in the second one higher values correspond to the water. NDWI method is based in the quotient of the reflectance of the near-infrared and the radiation emitted in the green portion of the visible part of the electromagnetic spectrum. This enhancement minimizes the reflectance of the soil and vegetation, highlighting water bodies (Feeters, 2013). NDVI index was developed to separate the reflectance of the green portion of vegetation from any other surface. However, it was proven useful to detect water surfaces (Rokni et al., 2014).

Hence, the two indexes together allow a better separation and identification of water bodies. Finally, the algorithm proposed by Topliss et al. (1990) was applied, this being a transformation of images to generate new variables not available on the original imagery.

Results

Dispersion graphics

The correlation coefficient between the SSC obtained in the laboratory and the SSC captured from satellite imagery using the algorithm (*Fig. 4a*) was 0.47; thus, the relationship between the two measurements is low. The determination coefficient R^2 was 0.228, which suggests that the model explains 23% of the variance. Results from Landsat 7 were very similar, correlation coefficient was 0.52, with a lineal coefficient R^2 of 0.279.

However, if 9 points (80, 81, 83, 84, 87, 90, 91, 92 and 95) were ruled out, because they had depths less < 15 cm. It is possible to have an interference with the basement in

shallow depth. The correlation coefficient without the discarded samples is 0.65, with $R^2 = 0.42$; this increases the possibility of the estimation of the sediments using the algorithm, since the model here explains 42% of the variance. Results from Landsat 7 without the discarded samples were $R^2 = 0.34$ and the correlation coefficient 0.58 (Fig. 4b).

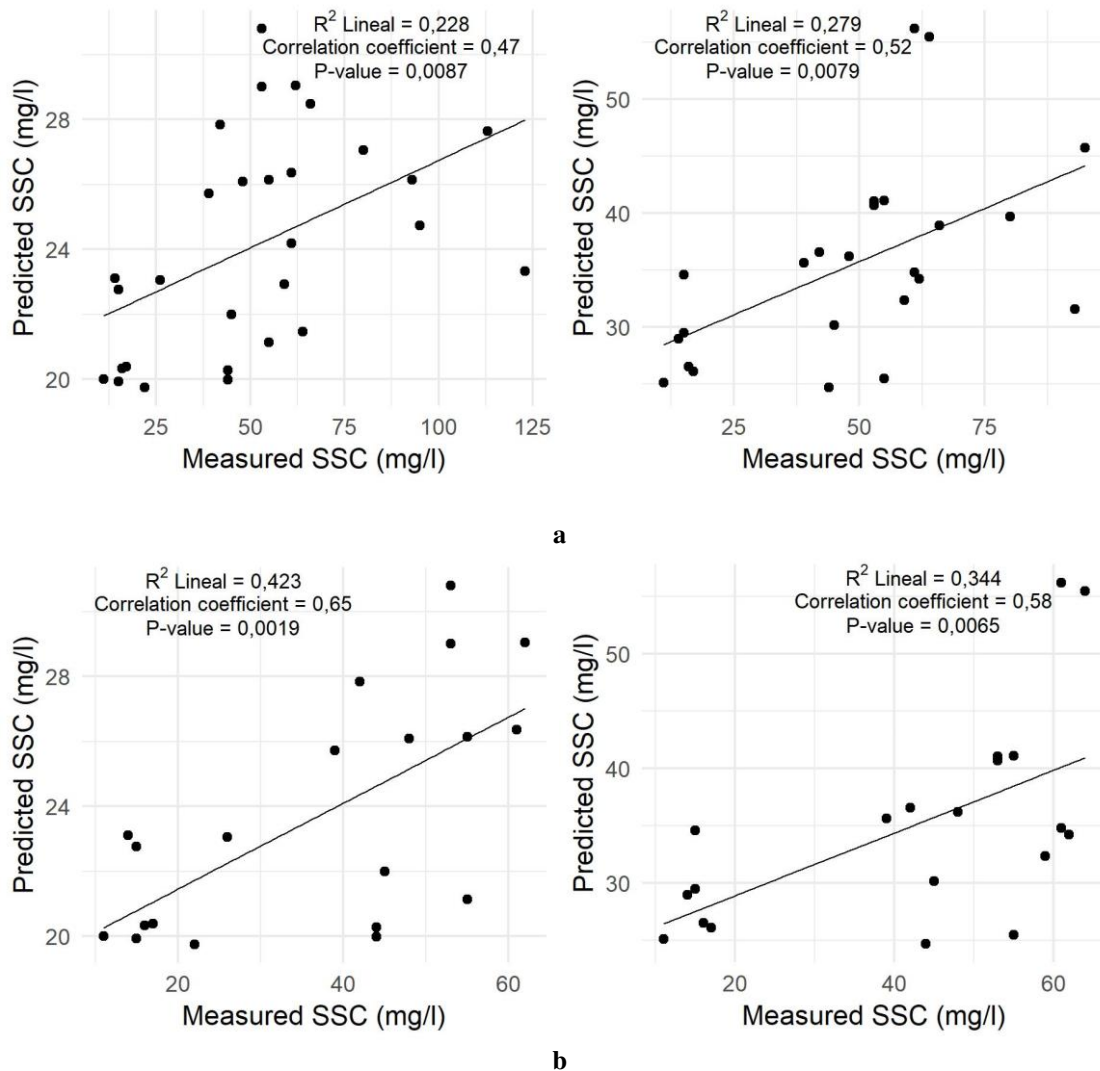


Figure 4. Dispersion diagrams of SSC measured in situ vs. results obtained by algorithm. **a** Results with 29 samples. In these plots data obtained from OLI sensor (left) and from ETM+ sensor (right) are shown. **b** Results with 20 samples are depicted on the left with data obtained from OLI sensor and on the right with data gathered from ETM+ sensor

The mean squared root (MSR) error between the two methods was 38.71 mg/l, in agreement with the poor correspondence between the algorithm results and the observations, as indicated by the correlation coefficient. When the anomalous points are omitted, the MSR error falls to 17.01 mg/l. The correlation levels indicated by P values suggest that the test statistics are significant and that it is possible to apply the algorithms for Landsat 7 ETM+ and for Landsat 8 OLI.

Mapping SSC

The measurements recorded in situ were geographically represented by kriging interpolation. Maps of the SSC distribution in the delta and the plume of the Grijalva River on 25 January 2016 (Fig. 5A) show concentrations to be low at the river mouth and gradually increase as the stream flows out to the open sea. The results of measurements show that SSC at points on the continental shelf are greater than those at the river mouth or in the river channel. This suggests that sediments moving along the river are transported by the water column likely near the bottom, and that when fresh water encounters seawater the difference in their densities causes former to rise, carrying the sediments up towards the surface. These sediments are subsequently distributed to form the plume of the river.

The concentration of suspended sediments measured in the laboratory (Fig. 5B) and mapped using kriging interpolation gradually increased in the direction of the open sea. Nevertheless, the result of the interpolation does not show the whole structure of the plume, particularly between 2062000 N and 2066464 N, because this method estimates the data of non-sampled spaces and therefore does not adhere to the shape of the plume.

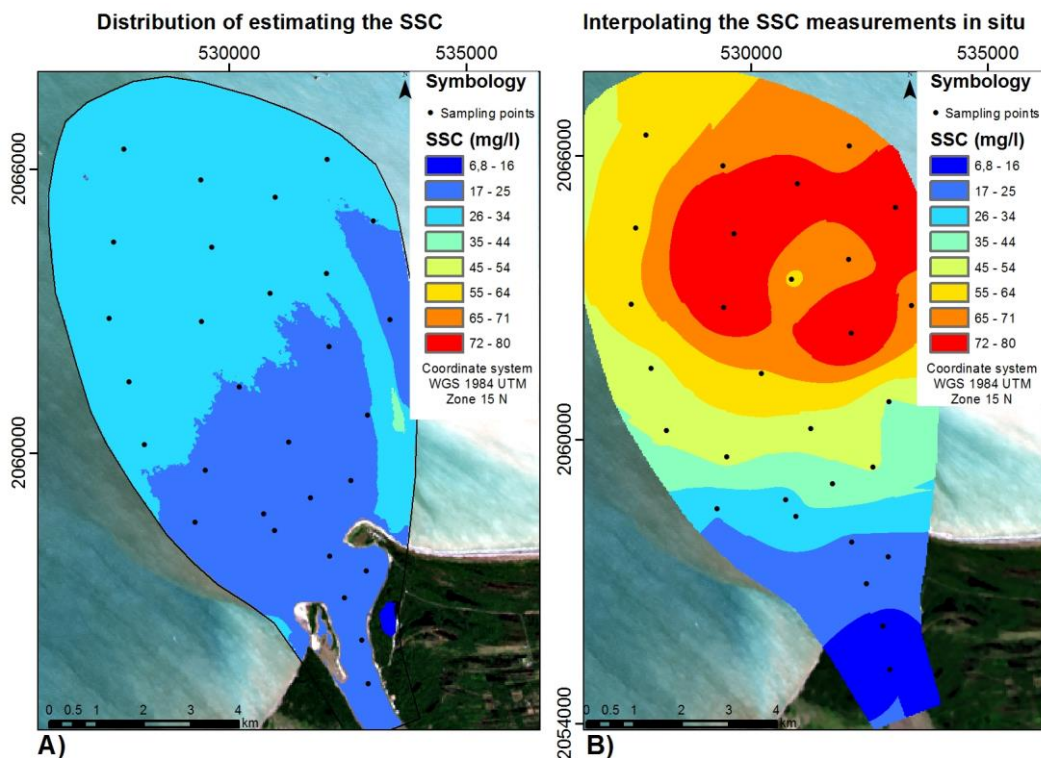


Figure 5. Cartographic representation of (A) results in laboratory and (B) Kriging interpolation

Spectral response analysis

In the spectral response analysis of suspended sediments, a comparison of in situ spectral signature against that one extracted from Landsat 8 was carried-out. A covariance between these two variables was found (Fig. 6). It is important to mention that the spectral response of Landsat 8 image was obtained using only seven

atmospherically corrected bands, meanwhile with the spectroradiometer, 316 bands with intervals of approximately 1.5 nm were used.

Figure 6 shows the spectral responses of the five sampling sites where the spectroradiometer was used; one point with the spectral response obtained from the satellite image is located 35.5 km before of the end of the plume of sediments and another is in the river mouth, where the water is practically free of suspended materials (*Fig. 6*).

At Point 91, the spectroradiometer showed the highest reflectance (16.5%; *Fig. 6a*). This sampling point also coincides with the site of the highest SSC obtained in the laboratory (123 mg/l). However, according to the theoretical signature of SSC, at this point concentration should be 600–1000 mg/l. Measured concentration from the field sample compared against theoretical signature value registered a difference of ± 870 mg/l. At point 100 (*Fig. 6b*), reflectance was 8.1% and the concentration was 15 mg/l, whereas the theoretical value is 100–150 mg/l (Jensen, 2007; Rose et al., 2015). In this point, measured difference in the field sample and theoretical oscillated between 85 and 135 mg/l. At point 107 (*Fig. 6c*), reflectance was 12.5% and the concentration was 16 mg/l, whereas the theoretical value is ± 500 mg/l. Thus, difference of concentrations between field sample and theoretical value was 484 mg/l. Difference between theoretical and in situ reflectance of the SSC gave a high correlation, $R^2 = 0.71$.

From a comparison of in situ observations of spectral responses (*Fig. 6*) and theoretical signatures, the size of suspended particles can be estimated (Jensen, 2007). The measured reflectance ($> 5\%$) suggests that particle sizes correspond to silt or mud. However, in the response extracted from the image at a point almost at the end of the plume (*Fig. 6d*) reflectance is $< 5\%$, indicating that the dominant particles are clays.

Discussion

Values obtained in the measurement of the suspended sediments in the laboratory are greater than those calculated using the algorithm proposed by Topliss et al. (1990); Chen et al. (1992) found a high correlation ($R^2 = 0.98$ with $n = 29$; $R^2 = 0.83$ with $n = 20$) between the SSC and the reflectance measured in the laboratory, where the environmental effects are scarce. However, correlation between the SSC and the reflectance at the ocean surface was weak ($R^2 = 0.46$), because of the environmental effects (atmosphere, aerosols, tides etc.) (Qu et al., 2016). Data obtained in the delta of the Grijalva river using Landsat 7 and the most recent Landsat 8 satellites, has a correlation of $R^2 = 0.279$ with 29 samples and $R^2 = 0.334$ with 20 samples of Landsat 7 and $R^2 = 0.228$ with 29 samples and $R^2 = 0.423$ with 20 samples of Landsat 8.

Results obtained for Landsat 5 with the algorithm proposed by Topliss et al. (1990), has an average correlation coefficient of $R^2 = 0.70$ (Harrington et al., 1992; Ritchie and Cooper, 1991; Lodhi et al., 1998). The algorithm showed a very good correlation in lakes and the sea, but in 2013 this satellite was no longer acquiring images. Actually, Landsat 7 and Landsat 8 have similar spectral bands, which allowed us to apply the algorithm developed by Topliss et al. (1990) although the results have very low correlations for both satellites.

First calculations of sediments concentrations were based mainly on atmospheric variables due to the fact that they represented major variations in these estimations, however, between 1950 and 1970, rivers in the world with big flows started to show a

decrement in the sediments they were transporting, this provoked that spectral responses had variations (Qu et al., 2016; Tessler et al., 2015).

In 1983 building of hydroelectric dam Chixoy, caused a decrement in the concentration of the sediments transported by the Grijalva River. Between 1983 and 2009 accumulation of sediments drop from $158 \times 10^6 \text{ m}^3$ to $6.1 \times 10^6 \text{ m}^3 \text{ yr}^{-1}$ (Nooren et al., 2017). Nowadays, the algorithms and models developed to calculate SSC take into account changes in the spectral response of the sediments, as well as atmospheric variables (Lu et al., 2013; Qu et al., 2016; Zhang et al., 2015).

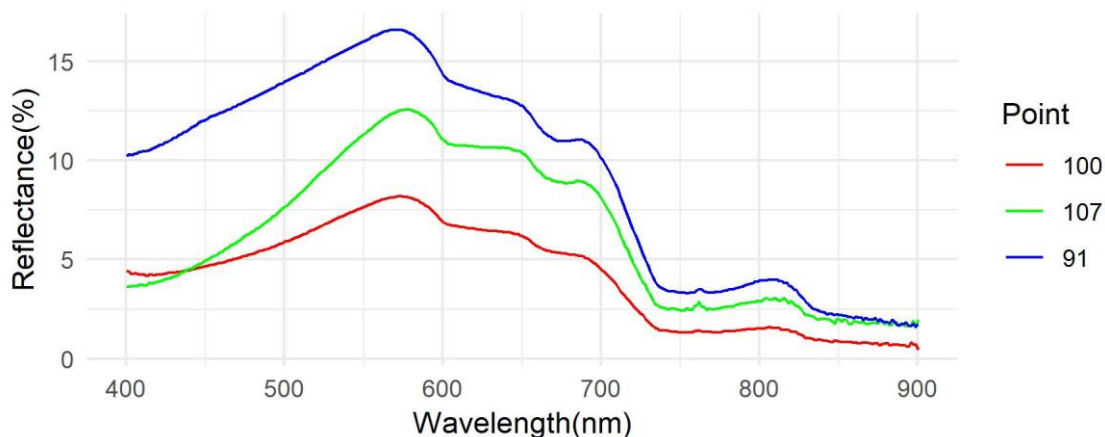


Figure 6. Three spectral responses in situ and the last spectral response using landsat 8. The blue line is the Fig. 6a; the red line is the sample 100 is the Fig. 6 b and the green line is the Fig. 6c

In the dispersion diagram the relationship between both variables is low due the high atmospheric interference between the satellite and water surface; additionally, water vapor and aerosols are present, which causes the sensor not to detect the total reflectance of the sediments.

It is possible that the algorithm cannot be applied at latitudes far from the one for which it was proposed (45° North). Furthermore, the climate where the algorithm was originally applied (Dfc, subpolar without dry season; and ET, tundra) differs from the tropical conditions of the present study, where suspended solids dominate. Under tundra climate bottom loading dominates (Arche, 2010). Hence, in the present study area, prediction of suspended sediments by the algorithm is less precise than that obtained in the laboratory.

Distribution analysis of the suspended sediments by kriging showed anisotropy in the river mouth because water transport usually is in one direction (Fig. 5). However, the zone with the highest SSC was distinct because the prediction suffered a circular tendency differing from the other points. Nevertheless, water discharged by a river generally has a preferred direction of flow (Arche, 2010).

The SSC can increase along the route to the open sea because a sediment wedge forms in the river mouth (Arche, 2010), where the superficial layer is fresh water brought by the river and this water column also carries suspended sediments that are subsequently exposed. The smaller particles (clays) travel a long distance before sinking to the bottom of the sea.

The analysis of spectral responses obtained in situ with the spectroradiometer and those obtained with the bands of the image allow calculating the increase in reflectance due to suspended sediments. Likewise, determination of the size of particles in suspension allows the comparison with the signatures allocated in spectral libraries or in the literature that match a reflectance value (%) to the SSC in mg/l (Novo, 1989; Jensen, 2007).

Based on the reflectance, the particle size that dominates in the river mouth corresponds to silt. On the other hand, the signature extracted from the image (*Fig. 6*), with a reflectance value less than 5% at the end of the plume, shows that particle size that dominate are clays (Jensen, 2007). The low percentage of reflectance encountered in clayey sediments is due to the organic matter content.

According to the spectral responses measured in situ at the sampling points, concentrations are lower than those supposed to be present regarding the volume of sediments, which increase the value of the reflectance (Novo, 1989). Because of the above and the low linear relationship between both variables, there are two important points to consider:

- a) Since solar radiation interacts with organic and inorganic compounds in the water, the suspended sediments in the water column should be sampled according to the penetrating capacity of the bands in the visible spectrum or at established depths down the column.
- b) The relative positions of the Sun and the sensor should be considered because reflection by water surface can be specular. The sensor receives the maximum reflected energy from the surface only if it is situated in the direction of the reflection angle. In the present study the relative positions of the Sun (43° from the horizon) and the satellite precluded measuring all the radiation reflected from the water surface. Consequently, in situ reflectance is 2–4% greater than the reflectivity of the spectral bands of the image. Therefore, the amount estimated by the algorithm is lower than that quantified in the laboratory. Additionally, local variations such as tides can suddenly change the transportation of suspended sediments.

In this study it was shown that the SSC estimation of sediments travelling in the surface can be done using bands 3 and 4. If sampling is performed by water column, the SSC are overestimated and could be calculated using the red and infrared bands for a range of concentrations of 100 to 1000 mg/l.

Conclusions

Although suspended sediments are usually quantified by in situ sampling, this task is time consuming and not economically viable for studies in remote areas. Thus, a good alternative is to use remote sensing techniques for quantification of SSC through spectral images.

This study used a spectroradiometer to obtain spectral responses in situ; real reflectance values at the water surface could be compared with values derived from the atmosphere-corrected image. Additionally, silt and clay particle size were determined in situ. Likewise, in situ reflectance indicated that most of the suspended particles were travelling in the water column rather than on the surface.

Cartographic representation of the SSC, calculated with satellite imagery and through interpolation with in situ data, indicated a gradual increase in SSC along the route to the open sea, despite the low linear relationship between those two measurements.

For analysis of superficial sediments, according to the statistical significance obtained, the algorithm proposed by Topliss et al. (1990) can be used, with green and red bands. For sediments sampled within the water column, at concentrations exceeding 100 mg/l, red and infrared bands would be used.

Taking into account the recent changes of the sedimentary regime and fluvial dynamics of the Grijalva River, the spectral responses of the sediments are mixed with the water, the shallow oceanic floor, and the predominant minerals. Therefore, it is necessary to carry-out a more extensive sampling in the study area to modify the algorithm of Topliss et al. (1990) based in spectral mixtures of the SSC.

Acknowledgements. The authors would like to thank Ing. Hernández Ordóñez Rodrigo by the support for this publication paper.

REFERENCES

- [1] Arche, A. (2010): Sedimentología del proceso físico a la cuenca sedimentaria. – Consejo Superior de Investigaciones Científicas, Madrid.
- [2] Ariza, A. (2015): Instituto Geográfico Agustín Codazzi. – <http://www.unspider.org/sites/default/files/LDCM-L8.R1.pdf>.
- [3] Bueno, J., Álvarez, F., Santiago, S. (2005): Biodiversidad del Estado de Tabasco. – CONABIO, Mexico.
- [4] Bukata, R. P., Jerome, J. H., Kondratyev, A. S., Pozdnyakov, D. V. (2018): Optical Properties and Remote Sensing of Inland and Coastal Waters. – CRC Press, Boca Raton.
- [5] Carbonneau, P. E., Piégay, H. (2012): Fluvial Remote Sensing for Science and Management (1st Ed.). – Wiley-Blackwell, Chichester.
- [6] Chen, Z., Curran, P. J., Hansom, J. D. (1992): Derivative reflectance spectroscopy to estimate suspended sediment concentration. – Remote Sensing of Environment 40(1): 67-77.
- [7] Chuvieco, E. (2008): Teledetección Ambiental (3rd Ed.). – Ariel, Barcelona.
- [8] Domínguez-Gómez, J., Marcos-Martín, C., Chao-Rodríguez, Y., Delgado-Rojas, G., Rodríguez Pérez, D. (2011): Estudio de aguas continentales mediante teledetección. – UNED, Madrid.
- [9] Feeters, S. (2013): Using the normalized difference water index (NDWI) within a geographic information system to detect swimming pools for mosquito abatement: a practical approach. – Remote Sensing 5(7): 3544-3561.
- [10] GET (2006): Programa de Ordenamiento Ecológico del Estado de Tabasco. – Villahermosa, Gobierno del Estado de Tabasco, Tabasco.
- [11] Harrington, J. A., Schiebe, F. R., Nix, J. F. (1992): Remote sensing of Lake Chicot, Arkansas: Monitoring suspended sediments, turbidity, and Secchi depth with Landsat MSS data. – Remote Sensing of Environment 29(1): 15-27.
- [12] He, X., Bai, Y., Pan, D., Huang, N., Dong, X., Chen, J., Chen-Tung, A., Cui, Q. (2013): Using geostationary satellite ocean color data to map the diurnal dynamics of suspended particulate matter in coastal waters. – Remote Sensing of Environment 133: 225-239.
- [13] Hernández-Santana, J. R., Ortiz-Pérez, M. A., Méndez Linares, A. P., Gama-Campillo, L. (2008): Morfodinámica de la línea de costa del estado de Tabasco, México: tendencias desde la segunda mitad del siglo XX hasta el presente. – Investigaciones Geográficas 65: 7-21.

- [14] Jensen, J. R. (2007): *Remote Sensing of the Environment* (2nd Ed.). – Pearson Prentice Hall, South Carolina.
- [15] Kemp, G., Day, J., Yáñez-Arancibia, A., Peyronnin, N. (2016): Can continental shelf river plumes in the northern and southern Gulf of Mexico promote ecological resilience in a time of climate change. – *Water* 8(3) 83.
- [16] Liang, S., Li, X., Wang, J. (2012): *Advanced Remote Sensing: Terrestrial Information Extraction and Applications*. – Academic Press, Netherland.
- [17] Lodhi, M. A., Rundquist, D. C., Han, L., Kuzila, M. S. (1998): Estimation of suspended sediment concentration in water using integrated surface reflectance. – *Geocarto International* 13(2): 11-15.
- [18] Loisel, H., Mangin, A., Vantrepotte, V., Dessailly, D., Dinh, D. N., Garnesson, P., Ouillon, S., Lefebvre, J. P., Mériaux, X., Phan, T. M. (2014): Variability of suspended particulate matter concentration in coastal waters under the Mekong's influence from ocean color (MERIS) remote sensing over the last decade. – *Remote Sensing of Environment* 150: 218-230.
- [19] Long, C. M., Pavelsky, T. M. (2013): Remote sensing of suspended sediment concentration and hydrologic connectivity in a complex wetland environment. – *Journal Remote Sensing of Environment* 129: 197-209.
- [20] Lu, Y., Zheng, G., Tian, Q., Lyu, C., Sun, S. (2013): Analyzing the effects of particle size on remotely sensed spectra: a study on optical properties and spectral similarity scale of suspended particulate matters in water. – *Applications Optical* 52(4): 879-888.
- [21] Nechad, B., Ruddick, K. G., Schroeder, T., Oubelkheir, K., Blondeau-Patissier, D., Cherukuru, R. C. N., Brando, V. E., Dekker, A. G., Clementson, L. A., Banks, A. C., Maritorea, S., Werdell, J., Sa, C., Brotas, V., Caballero de Frutos, I., Ahn, Y.-H., Salama, S., Tilstone, G. H., Martinez-Vicente, V., Foley, D., McKibben, M., Nahorniak, J., Peterson, T., Silio-Calzada, A., Röttgers, R., Lee, Z. P., Peters, M., Brockmann, C. (2015): Coast Colour Round Robin datasets: a database to evaluate the performance of algorithms for the retrieval of water quality parameters in coastal waters. – *Earth System Science Data* 7: 319-348.
- [22] Nooren, K., Hoek, W. Z., Winkels, T. G., Huizinga, A., van der Plicht, J., Van-Dam, R., Van-Heteren, S., Van-Bergen, M., Prins, M. A., Reimann, T., Wallinga, J., Cohen, K., Minderhoud, P., Middelkoop, H. (2017): The Usumacinta-Grijalva beach-ridge plain in southern Mexico: A high-resolution archive of river discharge and precipitation. – *Earth Surface Dynamics* 5(3): 529-556.
- [23] Norma Oficial Mexicana, NMX-AA-034 (2016): Análisis de agua -Medición de sólidos y sales disueltas en aguas naturales, residuales y residuales tratadas - Métodos de prueba. – *Diario Oficial de la Federación*, 11 de febrero de 2016, CDMX.
- [24] Novo, E. M. M., Hansom, J. D., Curran, P. J. (1989): The effect of sediment type on the relationship between reflectance and suspended sediment concentration. – *Remote Sensing* 10(7): 1283-1289.
- [25] Padró, J. C., Pons, X., Aragonés, D., Díaz-Delgado, R., García, D., Bustamante, J., Pesquer, L., Domingo-Marimon, C., González-Guerrero, Ó., Cristóbal, J., Doktor, D., Lange, M. (2017): Radiometric correction of simultaneously acquired Landsat-7/Landsat-8 and Sentinel-2A imagery using pseudoinvariant areas (PIA): Contributing to the Landsat time series legacy. – *Remote Sensing* 9(12): 1319.
- [26] Psuty, N. P. (1965): Beach-ridge development in Tabasco, Mexico 1. – *Annals of the Association of American Geographers* 55(1): 112-124.
- [27] Qu, L., Lei, T., Ning, D., Civco, D., Yang, X. (2016): A spectral mixing algorithm for quantifying suspended sediment concentration in the Yellow River: a simulation based on a controlled laboratory experiment. – *International Journal of Remote Sensing* 37(11): 2560-2584.
- [28] Richards, A. J. (2013): *Remote Sensing Digital Image Analysis* (5th Ed.). – Springer, Berlin.

- [29] Ritchie, J. C., Cooper, C. M. (1991): Algorithm for estimating surface suspended sediment concentrations with Landsat MSS digital data. – *Journal of the American Water Resources Association* 27: 373-379.
- [30] Ritchie, J. C., Cooper, C. M., Yongqing, J. (1987): Using Landsat multispectral scanner data to estimate suspended sediments in Moon Lake, Mississippi. – *Remote Sensing of Environment* (23): 65-81.
- [31] Rokni, K., Ahmad, A., Selamat, A., Hazini, S. (2014): Water feature extraction and change detection using multitemporal imagery. – *Remote Sensing* 6(5): 4173-4189.
- [32] Rose, C. W., Shellberg, J. G., Brooks, A. P. (2015): Modelling suspended sediment concentration and load in a transport limited alluvial gully in northern Queensland, Australia. – *Earth Surface Processes and Landforms* 40(10): 1291-1303.
- [33] Sobrino, A. J. (2000): Teledetección. – Universidad de Valencia, Valencia.
- [34] Tessler, Z. D., Vörösmarty, C. J., Grossberg, M., Gladkova, I., Aizenman, H., Syvitski, P. M., Foufoula-Georgiou, E. (2015): Profiling risk and sustainability in coastal deltas of the world. – *Science* 349(6248): 638-643.
- [35] Topliss, B. J., Almos, C. L., Hill, P. R. (1990): Algorithms for remote sensing of high concentration, inorganic suspended sediment. – *International Journal of Remote Sensing* 11(6): 947-966.
- [36] Wang, J., Lu, X., Zhou, Y. (2007): Retrieval of suspended sediment concentrations in the turbid water of the Upper Yangtze River Using Landsat ETM+. – *Chinese Science Bulletin* 52: 273-280.
- [37] Zhang, Y., Huang, Z., Chen, C., He, Y., Jiang, T. (2015): Particle size distribution of river suspended sediments determined by in situ measured remote sensing reflectance. – *Applied Optics* 54(20): 6367-6376.
- [38] Zhou, Z., Bian, C., Wang, C., Jiang, W., Bi, R. (2017): Quantitative assessment on multiple timescale features and dynamics of sea surface suspended sediment concentration using remote sensing data. – *Journal of Geophysical Research: Oceans* 122: 8739-8752.

SEASONAL VARIATIONS IN SOIL CO₂ EMISSIONS UNDER CONTINUOUS FIELD CROP PRODUCTION IN SEMI ARID SOUTHEASTERN TURKEY

YILMAZ, G.

*Department of Environmental Engineering, Faculty of Engineering, Harran University, Osmanbey Campus, Şanlıurfa, Turkey
(e-mail: gyilmaz@harran.edu.tr; phone: +90-414-318-3789; fax: +90-414-318-3190)*

(Received 24th Jan 2019; accepted 29th Mar 2019)

Abstract. Quantification of soil CO₂ emission under different cropping designs and relating it to the climate parameters can help better understanding the main mechanisms controlling its magnitude and mitigating its release to the atmosphere. Wheat and corn are the most produced crops worldwide contributing highly to total CO₂ emissions from agricultural lands to atmosphere. Long term fluctuations in the soil CO₂ emissions under continuous wheat and corn cropping and bare land were monitored for 509 weeks from 2009 to 2018 in semi arid conditions in the Harran Plain located in southeastern Turkey. The soil CO₂ emissions were modeled for each cropping seasons separately using available meteorological parameters (air temperature (AT), soil temperatures (ST), relative humidity (RH) and rainfall) and field soil moisture (SM) data. The quantity of long term soil CO₂ emission were following order; corn, wheat and bare land and it was around 38% higher (574 vs 792 kg ha⁻¹ week⁻¹) in soils under field crops than bare soils. Overall there were n increasing trends in seasonal, yearly cumulative and average weekly soil CO₂ emissions over the years. The weekly soil CO₂ emission values were positively correlated with AT and ST but negatively with RH and SM. The linear models were able to explain variations in the long term weekly soil CO₂ emissions obtained during wheat, corn cultivations and bare land up to 77%, 55% and 50%, respectively.

Keywords: *global warming, soil CO₂ emission, wheat, corn, meteorological data, stepwise regression*

Introduction

Global warming increases the soil respiration causing the release of more CO₂ emissions (Lu and Cheng et al., 2009). Among other three greenhouse gases CO₂ has the highest concentration in the atmosphere. Measurements and modeling of the soil CO₂ emissions under different soil types and crop managements are cost effective and crucial for global warming, carbon cycling as well as international agreements that aim to mitigate the amount of carbon released to atmosphere (Allaire et al., 2012). Quantification of the CO₂ emission from soils under different land uses is also important for developing strategies for reducing the CO₂ emissions to atmosphere. A number of researchers have shown atmospheric CO₂ increase very recently. The soil CO₂ respiration consists of basically two parts; roots respiration and microbial respiration as a result of organic matter decomposition (Morell et al., 2012; Zhang et al., 2015). Roots and microbial activities are responsible of 40% and 60% of total the soil respiration, respectively (Kuzyokav and Larionova, 2006).

Methods such as edycovariance or with closed chamber combined with gas chromatography are generally used for measurement of the soil CO₂ emissions. Another most commonly used technique in measuring the soil CO₂ emissions is soda lime (Edwards, 1982). This is advantageous, because it is cheap and easy to perform, enabling the soil CO₂ measurements at higher number of locations simultaneously compare to aforementioned methods which can only be obtained only at limited number of locations.

In addition, the earlier researchers comparing soda lime method reported that there is no statistically significant different between soda lime method and them (Raich et al.1990).

There are nearly two times more carbon in the soils than atmosphere (Lehmann and Joseph, 2009) and according to Lal (2004) that may be more than that. Depending upon agricultural management, soils can either be source or sink for CO₂ in the atmosphere and the amount of CO₂ released from soils to atmosphere can change based on the soil type, land use type or vegetation type, agricultural management as well as the time of measurement (i.e. seasonal variability) (Iqbal et al., 2009; Panosso et al., 2009, 2011; Mancinelli et al., 2010). Soil CO₂ emissions in the agricultural soils are generally between 0.1 and 6 g CO₂ m⁻² h⁻¹ (Sauerbeck, 2001).

Average soil CO₂ emissions reported by earlier studies were 59 to 527 mg m² h⁻¹, 37-498 mg m² h⁻¹, 32-397 mg m² h⁻¹ for forest, grassland and cropland (Wang et al., 2008). The amount of soil CO₂ emissions in peat, sandy and clay soils respectively were obtained as 650 mg m² d⁻¹, 300 mg m² h⁻¹ and 500 mg m² h⁻¹ (Koizumi et al., 1999). Bauer et al. (2006) for the soils under conservation tillage measured soil CO₂ emissions as 840 mg m² h⁻¹. Akbolat et al. (2009) reported as 300-700 mg m² h⁻¹. The cropped soils release CO₂ 2 to 3 fold higher than bare soils (Rastogi, 2002).

The soil CO₂ emissions are mostly impacted from the factors such as soil temperature and moisture (Bauer et al., 2006; Ngao et al., 2012; Xu et al., 2016; Iqbal et al., 2009; Reth et al., 2005), weather parameters, soil organic matter, C/N ratio, bulk density (Lin et al., 2008; Morell et al., 2012).

Wheat and corn are the most produced grain crops in the world and Turkey is one of the largest producers of both. Yearly around 653 355 000 and 19 674 000 tonnes wheat is produced in 217 312 000 ha and 8 103 000 ha areas in the world and in Turkey, respectively (FAOSTAT, 2010). Worldwide wheat grows on 215 million hectares of land each year (CGIAR, 2017).

Emissions of CO₂ from most of the forest crops, orchards, grasses are well documented (Frank et al., 2006; Almaraz et al., 2009). On the other hand, soil CO₂ emissions from soils under field crops with long terms field studies are limited. The studies available are mostly performed in a short term period which may not be sufficient to construct reliable models. Therefore, information about soil CO₂ emissions of soils under wheat plantation makes it significant.

The goals of this study were to: 1) quantify weekly and seasonal distributions of the long terms (from 2009 to 2018) CO₂ emissions from the soil under wheat and corn plantation 2) compare CO₂ emissions estimations obtained from the soils under field conditions compared with bare soils located nearby field crops, and 3) model the relationships between the soil CO₂ emissions from the soils under different managements (wheat, corn cultivation and uncultivated bare soils) and meteorological parameters and field moisture data at the same locations with soil CO₂ measurements.

Materials and methods

Study site and field management

The study was performed in a field under continuous wheat (2009-2017) and corn (2016-2018) cultivations, in addition to bare land located in the experimental farm of the Harran University, southeastern Turkey (37° 10' N Lat; 38° 59' E Long; *Fig. 1*). The study area has a semi arid climate with an average annual temperature, precipitation, evaporation and altitude values of 17.2 °C, 365.2 mm, 1848 mm and 520 m, respectively.

The soils of the study area are high in percent clay content, pH, percent CaCO₃ content and cation exchange capacity (CEC) but low in soil organic matter (<1.5 g kg⁻¹) (Dinç et al., 1998). Detailed information about the soil properties of the area is given in *Table 1*. Soils were clay loam and classified as Vertisol, according to Soil Taxonomy (Dinç et al., 1998).

Table 1. Soil properties of bare field and the experimental areas under field crops

Location	Sampling depth (cm)	EC (dS/m)	CaCO ₃ (%)	pH	P	K	Organic matter	Total N (%)	Sand	Clay	Silt	Texture
Bare area	(0-30)	0.73	17.40	7.70	2.71	112.5	1.36	0.09	22	60	18	Clay
Bare area	(30-60)	0.82	17.40	7.76	0.82	82.0	0.85	0.08	22	60	18	Clay
Field crops	(0-30)	0.83	23.50	7.76	3.04	82.0	1.45	0.09	32	50	18	Clay
Field crops	(30-60)	0.82	25.40	7.84	0.41	36.70	1.01	0.09	26	56	18	Clay

Wheat crops were planted in 2009-2017. Also during the experiment, in 2016-2018, corn crop following wheat was planted. Wheat and corn received regular care which included application of water as flood irrigation, fertilizer and pest control with sowing, 40 kg da⁻¹ compose fertilizer as 20+20+Zn has been applied as base fertilizer and as top fertilizer 50 kg da⁻¹ urea was applied. The same fertilizer practice was repeated in each year.

Soil laboratory analysis

A composite soil sample was taken as representative of orchard field at the surface (0-30 cm) and subsurface soil (30-60, 60-90 cm). Soil samples were air dried and passed through a 2 mm sieve and analyzed according to the routine soil analyses methods. Particle size distributions were determined by the hydrometer method (Bouyoucos, 1926); organic matter content by the Walkley-Black method (Nelson and Sommers, 1982); CaCO₃ content using a calcimeter (Kacar, 1994); soil pH with a 1:2.5 from soil/water suspension using pH meter (McLean, 1982); electrical conductivity (EC) in soil extraction using a conductivity meter (Janzen, 1993), soil N according to Kjeldahl method (Kacar, 1994). Soil available P and K were determined using an ICP-AEAS (Varian-Vista, Palo Alto, CA, USA), after NaHCO₃ extraction (pH 8.5) (Olsen and Sommers, 1982) and NH₄OAc extraction (Knudsen et al., 1982), respectively.

Soil CO₂ emissions and meteorological variables

In addition to soil CO₂ emission measurements under wheat and corn plantation, the measurements were also performed in bare soils with no cultivation fields. The soil CO₂ emissions measurements were performed as weekly basis during total of 509 weeks between January, 2009 and October, 2018, using soda lime method (Edwards, 1982).

Soda lime method is advantageous because it is easy to perform and also does not require expensive equipments. Around 40 g soda lime was oven dried at 105 °C during 24 h, weighted and added in the numbered plastic PVC containers (3 cm tall, and 100 cm² area top). The containers that have a known amount of soda lime was placed under a chamber (23 cm width and 33 cm length) inserted 2 cm in soils in order to prevent interaction between soda lime and atmosphere in order to avoid any gas leakage underneath of the chamber as much as possible. A PVC lid (50 cm by 50 cm) was used to provide shadow for the chambers to reduce the temperature difference between inside

and outside of the chambers. After one week in the field, the chambers were left and PVC containers with soda lime were weighted in the laboratory to measure changes in weight during one week incubation period. The soil CO₂ emissions were performed with five replications and then averaged to obtain a final emission values.

The amount CO₂ emission was obtained as below:

$$F_{CO_2} = \frac{(C_{adsorbed} - C_{initial}) * W}{t_{incubation} * A} \quad (\text{Eq.1})$$

Here:

F_{CO_2} = emitted CO₂ g⁻¹ cm² h⁻¹

$C_{adsorbed}$: Weight of soda lime after incubation (g)

$C_{initial}$: Weight of soda lime before incubation (g)

W: coefficient of water, taken as 1.69

$t_{incubation}$: Incubation period (week)

A: Area of the chamber, cm²

Emission of CO₂ calculated as g cm² hour was converted into total weekly and monthly amounts.

Meteorological variables used in the study were obtained from Sanliurfa city meteorological station located around 5 km away from the study site. Daily measurements were converted to weekly basis. The meteorological variables included air temperature (AT), soil temperature (ST) at different depths (5, 10, 20, 50 and 100 cm), relative humidity (RH) and rainfall (mm). Field soil moisture data were obtained gravimetrically from the soils samples taken at the same location where soil CO₂ emissions were measured.



Figure 1. Photo showing the experimental design set up for soil CO₂ emissions

Statistical analyses and modeling

The relationships between CO₂ emissions at different sites (wheat and corn fields, and bare soils) and meteorological parameters and field soil moisture data were examined using correlation analyses and multiple linear regression (MLR) models.

MLR models the relationships between response (soil CO₂ emissions) and predictor variables (meteorological parameters and field soil moisture data) using a linear function between two (Eq. 2):

$$y_i = \beta_0 + \beta_1 X_{1i} + \dots + \beta_p X_{pi} + \varepsilon_i \quad (\text{Eq.2})$$

where y_i refers to response variable which is modeled by a linear function of predictor variables; X_i , β are coefficients; ε is error term.

The models were also validated using independent data set splitting the whole data into two groups; as 70 and 30%; while the former was used for calibration, the latter was used for validation of the model which was constructed using General Linear Model (GLM).

The models were constructed for the data in each sampling sites and each year separately and also for complete years (2009-2018). Correlation analyses and MLR modeling were performed using SPSS program. GLM model used in model validation (testing) was performed using R program.

Results

Soil properties

Averaged soil properties measured at different depths and sites are given in *Table 1*. Soils are high in CaCO₃ (>15%) and low in soil organic matter (<2%) contents. These were due to no organic residues given in to soils, conventional tillage and warm climate environment of the study area. Soils have a basic soil pH, a heavy clay texture and do not have any salinity problem which is indicated by low soil EC values (<4 dS m⁻¹). While total nitrogen and plant available P contents in the soils were low, K levels were high. Soil P and organic matter were higher in the soils under field crop rotation but it was opposite for K which was found higher in bare soils compare to the soils under wheat and corn crop rotation. It may be because of plant uptake.

Soil CO₂ emissions

Average, minimum and maximum of the soil CO₂ emissions (kg ha⁻¹ week⁻¹) measured in the soil during the study periods (2009–2018) are given in *Table 2*. Long term weekly, seasonal and cumulative yearly fluctuations of the soil CO₂ emissions are given in *Figures 2-5*. The results showed that CO₂ emissions were highly variable and the higher emission peaks were obtained in the summer seasons.

The soil CO₂ emissions were highly variable, both seasonally and locally ranging from 54 to 2504 kg ha⁻¹ week⁻¹. The CO₂ emissions in bare soils ranged from 57 to 1690 kg ha⁻¹ week⁻¹ with average values of 791 and 523 kg ha⁻¹ week⁻¹, respectively (*Table 2*). When the fields are under either wheat or corn plantation (excluding the weeks when there is no crop in the field), average soil CO₂ emissions were 534 and 850 kg ha⁻¹ week⁻¹ for bare soils (CO₂-Bare) and field soils (CO₂-Field), respectively.

Average weekly CO₂ emissions of the soils under wheat plantations in 2009-2017 were 310, 480, 516, 481, 400, 535, 680 and 696 kg ha⁻¹ week⁻¹, respectively, which showed a consistent increase over time. Similar to the soils under wheat plantations, average weekly CO₂ emissions of soils under corn plantation were higher compared to the previous years. It was 914 and 1056 kg ha⁻¹ week⁻¹ in 2016 and 2017, respectively. The average weekly soil CO₂ emissions from bare soils (CO₂-Bare) were always lower than those obtained in the soils under both wheat and corn cultivation (*Table 2*). Average weekly soil CO₂ emissions from the bare soils corresponding to the same weeks when fields under wheat plantation were 310, 480, 516, 481, 400, 535, 680 and 696 kg ha⁻¹ week⁻¹, respectively in 2009-2017. Average weekly soil CO₂ emissions from bare soils corresponding to the same weeks when the fields under corn plantation in 2016 and 2017 were 687 and 621 kg ha⁻¹ week⁻¹, respectively.

Table 2. Descriptive statistics of long term soil CO₂ emissions under different field management and meteorological parameters

		CO ₂ -B	CO ₂ -F	SM-B	SM-F	AT	RH	ST5	ST10	ST20	ST50	ST100	Rainfall
		kg ha ⁻¹ week ⁻¹		%		°C	%	°C					mm
2009 WHEAT (n [†] =25)	Avg.	310	506	24	29	15	53	16	16	15	15	15	8.1
	Min.	93	195	9	10	2	21	3	4	5	8	11	0.0
	Max.	505	1041	33	49	30	80	33	31	29	28	25	38.6
2010 WHEAT (n=34)	Avg.	480	575	28	24	15	56	16	16	16	16	17	10.7
	Min.	257	274	10	5	5	25	6	6	7	10	12	0.0
	Max.	860	1000	36	35	30	85	35	33	30	28	26	57.0
2011 WHEAT (n=28)	Avg.	516	1128	27	24	14	55	15	15	15	15	15	12.8
	Min.	366	275	9	6	5	31	6	7	8	9	11	0.0
	Max.	1015	2316	34	36	29	79	29	29	27	27	23	57.2
2012 WHEAT (n=29)	Avg.	481	786	27	31	14	50	14	14	14	14	14	14.3
	Min.	68	54	14	21	3	15	5	5	6	7	9	0.0
	Max.	831	1476	42	42	33	87	34	32	30	29	24	84.7
2013 WHEAT (n=30)	Avg.	400	853	28	30	14	58	14	14	14	15	15	14.6
	Min.	225	278	13	20	3	24	6	6	7	8	11	0.0
	Max.	746	1396	37	37	28	85	28	27	26	26	22	52.0
2014 WHEAT (n=23)	Avg.	535	769	24	22	16	47	16	16	15	15	15	8.2
	Min.	223	421	8	6	7	28	7	7	8	8	11	0.0
	Max.	783	1144	39	36	26	82	29	29	27	27	23	74.2
2016 WHEAT (n=23)	Avg.	680	886	23	24	15	51	16	16	16	15	15	7.3
	Min.	364	335	6	7	1	26	5	6	7	7	10	0.0
	Max.	992	1941	40	40	28	79	29	29	28	27	24	36.6
2016 CORN (n=22)	Avg.	687	914	12	14	27	33	29	29	28	28	27	1.8
	Min.	334	243	3	4	12	19	12	12	14	15	19	0.0
	Max.	1690	2504	33	38	34	66	36	35	34	34	30	39.6
2017 WHEAT (n=24)	Avg.	696	952	22	26	15	48	16	16	16	16	15	6.2
	Min.	512	550	10	7	4	25	6	6	6	7	9	0.0
	Max.	945	1327	31	37	30	73	32	31	30	29	25	60.8
2017 CORN (n=25)	Avg.	621	1056	12	31	21	43	23	23	23	23	24	2.9
	Min.	396	548	5	4	6	22	7	8	10	10	14	0.0
	Max.	911	1854	24	51	34	72	36	36	34	33	30	27.9
PLANTED & UNPLANTED (n=509)	Avg.	524	792	19	21	20	45	21	21	20	20	20	7.1
	Min.	57	54	1	1	1	15	3	4	5	7	9	0.0
	Max.	1690	2504	44	51	36	88	41	39	36	34	32	89.4
PLANTED (n=289)	Avg.	534	850	23	26	17	49	19	18	18	18	18	8.5
	Min.	68	54	3	4	1	15	3	4	5	7	9	0.0
	Max.	1690	2504	42	51	34	87	38	36	34	34	31	84.7

†The number of total weeks between planting and harvesting of with corresponding field crop

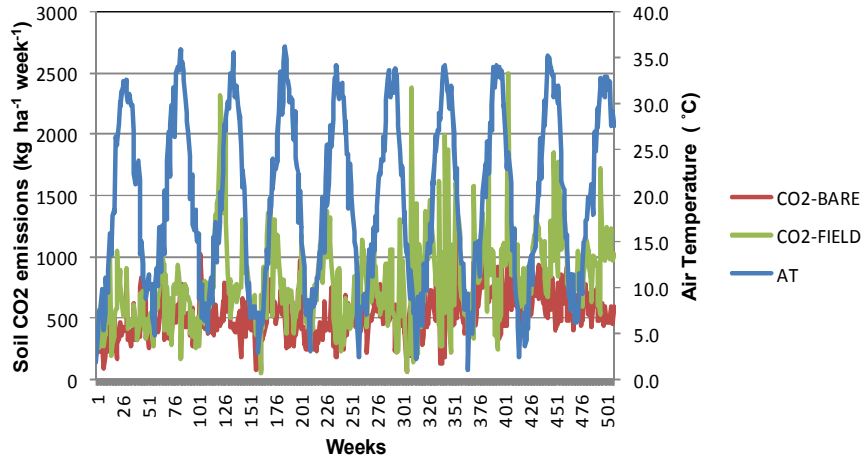


Figure 2. The weekly fluctuations of field soil CO₂, bare soil CO₂ emissions and air temperature from 2009 to 2018 (509 weeks)

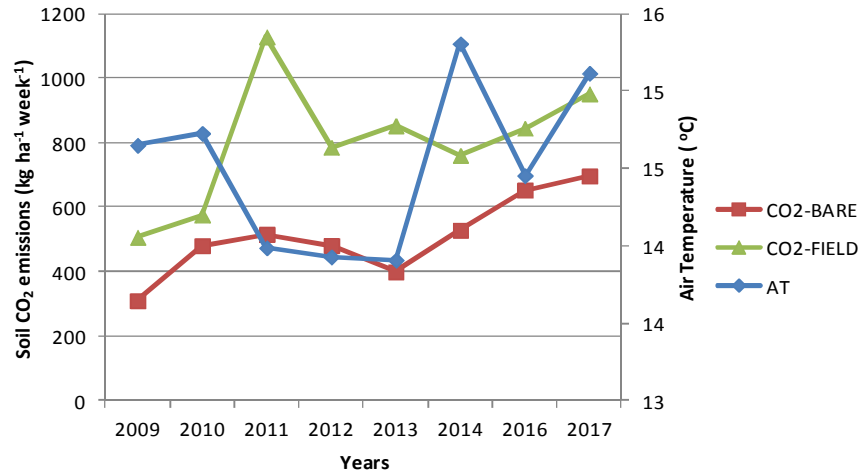


Figure 3. Changes in yearly mean soil CO₂ emissions from two different sites and air temperature

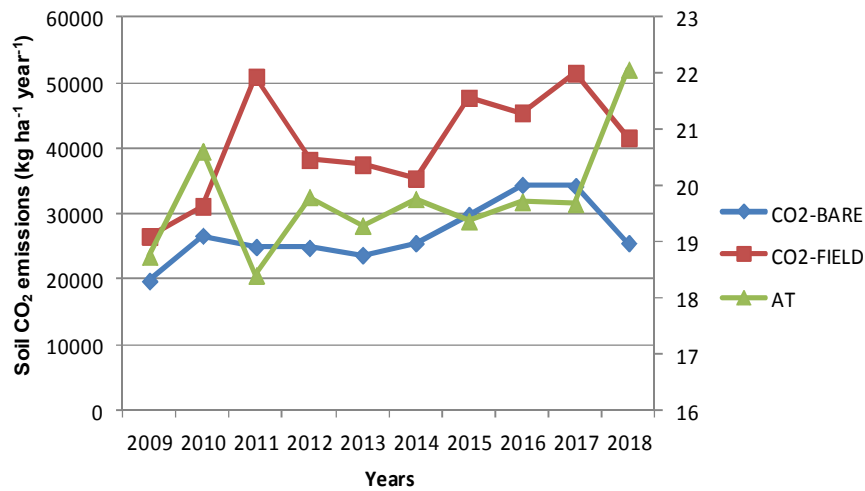


Figure 4. Variations in cumulative yearly soil CO₂ emissions

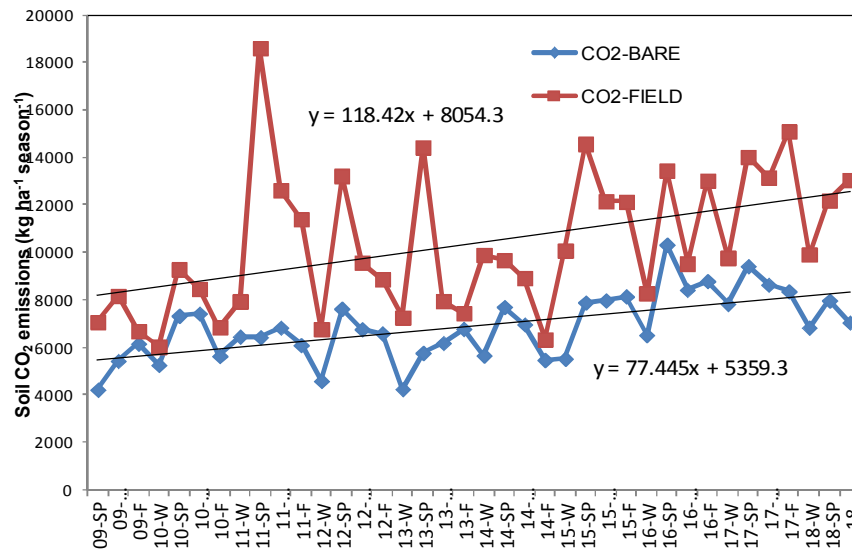


Figure 5. Seasonal (each points corresponding to seasons starting from spring and followed by summer-fall-winter seasons) variations in soil CO₂ emissions from 2009 to 2018

Correlations between the soil CO₂ emissions from the bare soils and wheat and corn plantations for each year separately and combined are given in *Table 3*. When all years were considered together, weekly CO₂-field values were significantly correlated ($p < 0.05$) with all meteorological parameters except rainfall, soil temperature at 100 cm and soil moisture data. While weekly CO₂-bare soil values were significantly correlated ($p < 0.05$) with all meteorological and soil moisture parameters (*Table 3*).

In the 2012, 2013, 2016 and 2017 years, weekly soil CO₂ emission values obtained had a statistically significant positive correlations ($p < 0.05$) with air and soil temperatures at different depths while significant negative correlations ($p < 0.05$) with relative humidity. They had statistically significant negative correlation with soil moisture values in 2012 and 2013 and insignificant negative correlations in 2016 and 2017.

In the 2009 and 2011 years, only weekly soil CO₂ emission values obtained from the soils under wheat cultivation had statistically significant negative and positive correlations ($p < 0.05$) with the same variables. The same situation was valid for only weekly soil CO₂ emission values obtained from the bare soils in 2014 (*Table 3*). Rainfall values had statistically ($p < 0.05$) significant negative correlations with weekly soil CO₂ emission values obtained from the soils under wheat cultivation in 2010, 2012 and 2016 years (*Table 3*).

Correlations between the soil CO₂ emissions under corn plantation both in 2016 and 2018 and environmental parameters were mostly insignificant ($p > 0.05$) (*Table 3*). As opposed to bare land and soils under wheat cultivation, the soil CO₂ emissions measured during corn plantation in 2016 had negative correlations with air and soil temperatures but positive correlations with rainfall, relative humidity and soil moisture.

Modeling of soil CO₂ emissions

Multiple Linear Regression models were constructed between the soil CO₂ emissions at different locations (bare land and field crops) and available climate parameters; air

temperature, soil temperature, relative humidity, precipitation and field soil moisture data. For different land managements the models were constructed for all weeks in whole years (from 2009 to 2018), for only weeks when the field is planted with wheat or corn (from 2009 and 2018) and for weeks during crop season in each year, separately. Coefficient of Determination (R²) values showing the per cent variations in soil CO₂ emissions at different time and locations explained by each models and significance of independent variables in terms of contribution to the model are given in Table 4. Model R² values for complete years considering both planted and also unplanted weeks and considering only planted weeks were 0.16 and 0.22, respectively. They were 0.1 and 0.23 respectively for bare land. For the models constructed separately for each crop season in different years, R² values ranged from 0.47 to 0.77 for wheat plantation, between 0.19 and 0.55 for corn plantation and 0.12 to 0.66 for bare land (Table 4).

Table 3. Correlations between soil CO₂ emissions and climatic variables and soil moisture field data

		CO ₂ -F	SM-B	SM-F	AT	RH	ST5	ST10	ST20	ST50	ST100	Rainfall
		kg ha ⁻¹ week ⁻¹	%		°C	%	°C					mm
2009 WHEAT	CO2-B	0.48*	-0.36	-0.20	0.40*	-0.32	0.36	0.36	0.35	0.35	0.36	0.21
	CO2-F	-	-0.37	-0.29	0.59**	-0.55**	0.59**	0.58**	0.58**	0.58**	0.56**	-0.09
2010 WHEAT	CO2-B	0.82**	-0.18	-0.24	0.14	-0.33	0.18	0.19	0.18	0.16	0.13	-0.28
	CO2-F	-	-0.17	-0.28	0.22	-0.34*	0.26	0.27	0.26	0.22	0.16	-0.37*
2011 WHEAT	CO2-B	0.13	-0.10	-0.07	0.28	-0.17	0.26	0.27	0.28	0.30	0.42*	0.06
	CO2-F	-	-0.01	0.20	0.81**	-0.52**	0.83**	0.82**	0.81**	0.80**	0.67**	-0.13
2012 WHEAT	CO2-B	0.75**	-0.43*	-0.38*	0.59**	-0.66**	0.55**	0.54**	0.53**	0.52**	0.46*	-0.37*
	CO2-F	-	-0.46*	-0.47**	0.61**	-0.56**	0.59**	0.59**	0.58**	0.56**	0.47**	-0.40*
2013 WHEAT	CO2-B	0.49**	-0.75**	-0.69**	0.46*	-0.39**	0.52**	0.53**	0.52**	0.52**	0.44*	-0.26
	CO2-F	-	-0.61**	-0.63**	0.76**	-0.59**	0.75**	0.76**	0.75**	0.74**	0.63**	-0.33
2014 WHEAT	CO2-B	0.34	-0.22	-0.38	0.55**	-0.37	0.51*	0.52*	0.52*	0.52*	0.50*	-0.13
	CO2-F	-	0.40	0.52*	-0.36	0.36	-0.40	-0.40	-0.39	-0.39	-0.36	-0.15
2016 WHEAT	CO2-B	0.18	-0.31	-0.42*	0.51*	-0.58**	0.53**	0.53**	0.52*	0.52*	0.48*	-0.24
	CO2-F	-	-0.34	-0.27	0.55**	-0.47*	0.55**	0.54**	0.54**	0.53**	0.48**	-0.45*
2017 WHEAT	CO2-B	0.69**	-0.38	-0.35	0.44*	-0.57**	0.41*	0.41*	0.41*	0.40	0.38	-0.22
	CO2-F	-	-0.35	-0.32	0.57**	-0.29	0.56**	0.56**	0.56**	0.55**	0.53**	0.16
2016 CORN	CO2-B	0.70**	-0.03	0.02	-0.23	-0.04	-0.26	-0.26	-0.27	-0.28	-0.25	-0.07
	CO2-F	-	-0.11	0.05	-0.34	0.10	-0.32	-0.31	-0.31	-0.31	-0.25	0.01
2017 CORN	CO2-B	0.36	-0.22	-0.51**	0.18	-0.21	0.19	0.20	0.20	0.21	0.24	-0.09
	CO2-F	-	-0.63**	-0.25	0.58**	-0.48*	0.61**	0.62**	0.63**	0.64**	0.68**	-0.15
2018 CORN	CO2-B	0.36	0.02	0.07	-0.20	-0.01	-0.27	-0.28	-0.29	-0.30	-0.32	0.12
	CO2-F	-	-0.58**	0.40*	0.29	-0.23	0.29	0.29	0.30	0.31	0.34	-0.12
PLANTED & UNPLANTED	CO2-B	0.51**	-0.15**	-0.10*	0.17**	-0.21**	0.15**	0.15**	0.16**	0.15**	0.13**	-0.14**
	CO2-F	-	0.01	0.14**	0.14**	-0.10*	0.12**	0.12**	0.12**	0.11*	0.06	-0.07
PLANTED	CO2-B	0.49**	-0.37**	-0.31**	0.31**	-0.40**	0.30**	0.30**	0.31**	0.31**	0.30**	-0.24**
	CO2-F	-	-0.30**	-0.07	0.40**	-0.36**	0.38**	0.38**	0.38**	0.38**	0.35**	-0.19**

AT: Air temperature (°C); ST5, ST10 and ST100 are soil temperature at 5, 10 and 100 cm, respectively; SM: Soil Moisture; RH: Relative; * significant at p < 0.05 level; ** significant at p < 0.01 level

Both SM and ST at different depths were found significant (p < 0.05) in the models constructed for the soils under field crops (Table 4). For models constructed for soil CO₂ emissions in bare land, the ST20 and ST100 were significant when considering

whole weeks (planted and unplanted), the SM, RH and ST5 were statistically significant when considering only weeks in crop seasons (planted) (Table 4).

Table 4. MLR modeling results for soil CO₂ emissions under different land managements

	2009 Wheat	2010 Wheat	2011 Wheat	2012 Wheat	2013 Wheat	2014 Wheat	2016 Wheat	2017 Wheat	2016 Corn	2017 Corn	2018 Corn	Planted & Unplanted	Planted
CO ₂ -FIELD													
R2	0.54	0.47	0.77	0.53	0.60	0.66	0.60	0.48	0.19	0.55	0.27	0.16	0.22
SM-F	ns	ns	ns	ns	ns	**	ns	ns	ns	ns	ns	**	*
AT	ns	**	ns	ns	ns	**	*	ns	ns	ns	ns	ns	ns
RH	ns	ns	ns	ns	ns	*	*	ns	ns	ns	ns	ns	ns
ST5	ns	ns	ns	ns	ns	ns	ns	ns	ns	ns	ns	ns	*
ST10	ns	ns	ns	ns	ns	s	ns	ns	ns	ns	ns	ns	ns
ST20	ns	ns	ns	ns	ns	ns	ns	ns	ns	ns	ns	**	*
ST50	ns	ns	ns	ns	ns	ns	ns	ns	ns	ns	ns	ns	ns
ST100	ns	ns	ns	ns	ns	ns	ns	ns	ns	ns	ns	ns	*
Rainfall	ns	ns	ns	ns	ns	*	ns	ns	ns	ns	ns	ns	ns
CO ₂ -BARE													
R2	0.55	0.48	0.43	0.54	0.62	0.50	0.66	0.47	0.28	0.12	0.34	0.07	0.23
SM-B	ns	ns	ns	ns	**	ns	ns	ns	ns	ns	*	ns	**
AT	ns	**	ns	ns	ns	*	ns	ns	ns	ns	ns	ns	ns
RH	ns	*	ns	ns	ns	ns	ns	ns	ns	ns	ns	ns	**
ST5	ns	ns	ns	ns	ns	ns	ns	ns	ns	ns	ns	ns	**
ST10	ns	*	ns	ns	ns	ns	ns	ns	ns	ns	ns	ns	ns
ST20	ns	ns	ns	ns	ns	ns	ns	ns	ns	ns	ns	**	ns
ST50	ns	ns	ns	ns	ns	ns	*	ns	ns	ns	ns	ns	ns
ST100	ns	ns	*	ns	ns	ns	*	ns	ns	ns	ns	**	ns
Rainfall	ns	ns	ns	ns	ns	ns	*	ns	ns	ns	ns	ns	ns

R²: coefficient of determination; AT: air temperature (°C); ST5, ST10 and ST100 are soil temperature at 5, 10 and 100 cm, respectively; SM: soil moisture; RH: relative humidity

For the models constructed for each crop seasons in different years separately, the significance of independent variables in the models changed based on different crop types and also years. Air temperature were found significant only in the models constructed for soils under wheat plantation in 2010, 2014 and 2016 years and for bare soils in 2010 and 2014 years. Relative humidity values were significant only for models constructed for soils under wheat plantation in 2014 and 2016 and bare soils in 2019. ST at different depths were not found significant in the models constructed for each cropping season year separately for field crops but found significant for bare soils in 2010 (ST10), 2011 (ST100) and 2016 (ST50 and ST100) years. Rainfall was found statistically significant for the models constructed for soils under wheat plantation in 2014 and for bare land in 2016 cropping season (Table 4).

Stepwise regression was used to select the most important variables in modeling the soil CO₂ emissions in different cropping seasons and managements. The most significant variables selected by stepwise regressions are shown in Table 5. Accordingly, when all weeks (planted and unplanted weeks) considered, the method selected SM and AT as the most important variables explaining the variations in the soil CO₂ emissions under field crops and RH in soil CO₂ emissions from bare land. When considering only planted weeks, the result did not change for soils under field crops but

SM, ST5 and ST10 variables in addition to RH were also found as the most significant in modeling the soil CO₂ emissions from bare land.

Table 5. Significant meteorological parameters in modeling soil CO₂ emissions determined by stepwise regression

		VARIABLES	R ²	P
2009 WHEAT	CO ₂ -FIELD	AT	0.35	**
	CO ₂ -BARE	AT	0.16	*
2010 WHEAT	CO ₂ -FIELD	Rainfall	0.14	*
	CO ₂ -BARE	-	-	-
2011 WHEAT	CO ₂ -FIELD	ST5, SM-Field	0.75	**
	CO ₂ -BARE	ST100	0.18	*
2012 WHEAT	CO ₂ -FIELD	AT	0.38	**
	CO ₂ -BARE	RH	0.44	**
2013 WHEAT	CO ₂ -FIELD	AT	0.57	**
	CO ₂ -BARE	SM-Bare	0.57	**
2014 WHEAT	CO ₂ -FIELD	SM-Field	0.27	*
	CO ₂ -BARE	AT	0.31	**
2016 WHEAT	CO ₂ -FIELD	AT	0.31	**
	CO ₂ -BARE	RH	0.33	**
2017 WHEAT	CO ₂ -FIELD	AT	0.32	**
	CO ₂ -BARE	RH	0.32	**
2016 CORN	CO ₂ -FIELD	-	-	-
	CO ₂ -BARE	-	-	-
2017 CORN	CO ₂ -FIELD	ST100	0.46	**
	CO ₂ -BARE	-	-	-
2018 CORN	CO ₂ -FIELD	SM-Field	0.16	*
	CO ₂ -BARE	-	-	-
PLANTED	CO ₂ -FIELD	AT,SM-Field,	0.18	**
	CO ₂ -BARE	RH,SM-Bare,ST5,ST10	0.21	**
PLANTED & UNPLANTED	CO ₂ -FIELD	SM-Field, AT,	0.10	**
	CO ₂ -BARE	RH	0.04	**

R²: coefficient of determination; *p significant at p < 0.05 level; **significant p < 0.01 level
Variables selected according to stepwise regression; AT: air temperature (°C); ST5, ST10 and ST100 are soil temperatures at 5, 10 and 100 cm, respectively; SM: soil moisture; RH: relative humidity

In other stepwise regression models performed for each crop season separately, the model selected AT as the most significant variable in 2009, 2012, 2013, 2016 and 2017 in explaining the variations in CO₂ emissions from the soils under wheat cultivation, in 2009 and 2014 years from bare land. Rainfall was only found as the most significant parameter in explaining the variations in CO₂ emissions from the soils under wheat cultivation in 2010, when stepwise regression is used. The RH was found the most significant parameter for the variations in soil CO₂ emissions from bare land. Soil temperatures at 5 cm and 100 cm were found the most significant variables for the variations in CO₂ emissions in 2011 from the soils under wheat cultivation and bare land. The ST100 was also found the most significant variable for the variations in soil

CO₂ emissions from the corn field in 2017. Soil moisture was selected as the most significant variable by stepwise regression in explaining variations in the soil CO₂ emissions from wheat plantation in 2011 and 2014 years and from bare land in 2013 (Table 5).

Seasonal variations in the soil CO₂ emissions from both field and also bare land were also estimated using GLM model and available meteorological parameters and soil moisture data. For this purpose, the data was first split into two groups. 70% of the data was used for model construction and the rest 30% was estimated using constructed model. R² and RMSE values showing the accuracy of the estimations of soil CO₂ emissions of the samples in validation set (test set) were 0.15 and 0.05 and 253 and 178 kg ha⁻¹ week⁻¹ for field and bare area, respectively. Figure 6 shows the consistency between actual and model predictions for the CO₂ values in both locations.

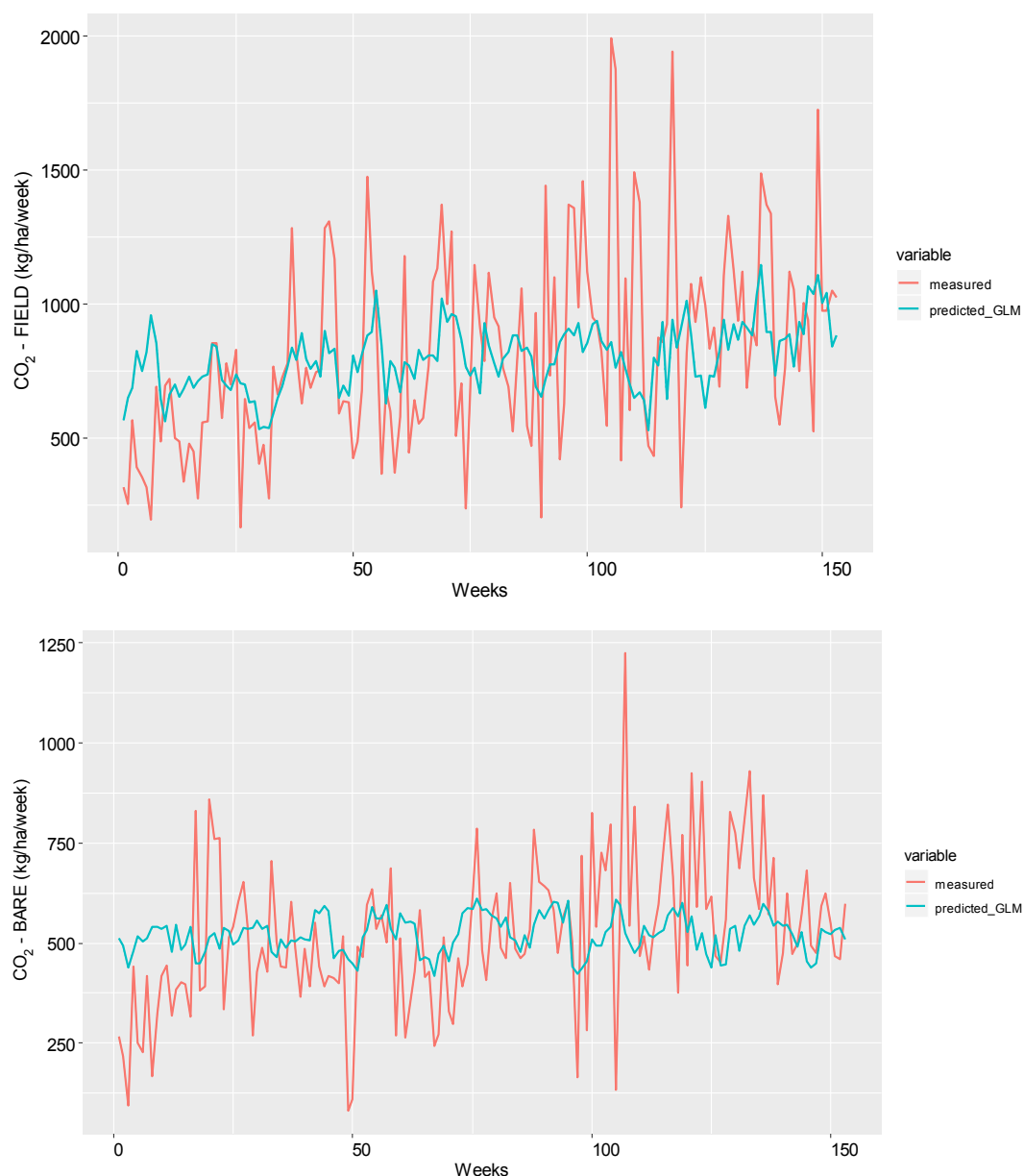


Figure 6. Actual and GLM model predictions of soil CO₂ emissions in field (CO₂-FIELD; R²: 0.148; RMSE: 253) and bare areas (CO₂-BARE; R²: 0.05; RMSE: 178)

Discussion

Around 20% of atmospherically CO₂ is due to agricultural activities (Lal and Bruce, 1999) and grain crops such as wheat and corn are the most produced grain crops worldwide therefore the quantification of soil CO₂ emissions under these types of vegetation are important in terms of accuracy of carbon budgets and modeling.

Long term weekly soil CO₂ emission amounts from field crops and bare land had a distinct trend in seasonal fluctuation. Higher in summer and lower in winter seasons similar to air temperature (*Fig. 2*). Seasonal trends have been often reported for CO₂ emissions from soil under various other crops (Raich et al., 2002).

Soil CO₂ emissions under field crops showed a clearly higher release compare to bare soils. The relation between soil CO₂ emissions over the years and mean air temperature can be observed in *Figure 3*.

The soil CO₂ emissions showed an increase over time, as can be observed in *Figures 4* and *5*. The yearly cumulative soil CO₂ emissions could be explained with increased temperature over years. In addition, the plant residuals increased causes increase in soil organic matter. In some years the rates showed a decrease compared to previous year, however there was a general trend toward the higher cumulative emission.

Soil CO₂ emissions measured varied highly based on time of measurement (seasonal-climate), management (field crop vs. bare land) and cropping season (type of crop). Guo et al. (2013) also showed that the quantity of the soil CO₂ emissions under field cropping (wheat) can change depending on different growing stage of the crop in addition to environmental parameters such as soil temperature and rainfall.

The soil CO₂ emissions obtained from field crop plantation of our study were in a similar range with other ecosystems. Meng-yang et al. (2014) reported soil CO₂ emissions as 829, 629 and 474 g CO₂ m⁻² from July 1 to September 30 (921, 698 and 526 kg ha⁻¹ week⁻¹, respectively) for fields under 20- year continuous maize, wheat and soybean cultivation in a similar semi arid area located in northeast China. Gu et al. (2016) reported the soil CO₂ emissions under wheat plantation ranging from 372 to 418 mg m⁻² h⁻¹ (equals to 625-702 kg ha⁻¹ week⁻¹). Chen et al. (2004) indicated soil CO₂ emissions in wheat field ranging from 10 to 606 mg m⁻² h⁻¹ (equals to 17-1019 kg ha⁻¹ week⁻¹). The average soil CO₂ emissions from under semi-arid continuous wheat was 2.34 μ mol m⁻² s⁻¹ (equals to 622 kg ha⁻¹ week⁻¹) by Zhang et al. (2011).

The CO₂ emissions obtained in our study were relatively lower than other ecosystems such as orchards, forests or pastures. In arid region in China for grassland in the Black Chinese soils, Li et al. (2009) measured average weekly soil CO₂ emissions during growing season as 1680 kg ha⁻¹ week⁻¹. Lessard et al. (1994) measured the soil CO₂ emissions under forest vegetation and found a range between 158 and 1037 kg ha⁻¹ week⁻¹ and also compared with nearby cultivated fields, which provided soil CO₂ emissions between 18 and 495 kg ha⁻¹ week⁻¹. This is three times lower than emissions in the soils under forest. As opposed to these researchers, Iqbal et al. (2009) comparing the soil CO₂ fluxes under different land management, such as vegetables, forest, uplands and orchard stated that the soils under forest and orchard management provided relatively lower CO₂ emissions compare to other agricultural land uses.

According to average weekly emissions, the soils in continuous wheat and corn emitted 38% more CO₂ than the bare soils. The CO₂ emission from soil is the combination of root and soil microbial activities (Kuzyakov and Larionova, 2006). The root contributions to soil emissions are known as 48% (Raich and Tufekcioglu, 2000).

Soils under plantation can provide 2 to 3 fold higher CO₂ emissions compared to bare soil.

When considering the years for both corn and wheat; the mean soil CO₂ emissions measured during corn production was higher than wheat production in both 2016 and 2017. This may be due to differences in time of growing wheat and corn. Wheat grows in winter and spring seasons, corn is grown in summer season, mostly when the air and soil temperatures are higher. The researcher who compared the soil CO₂ emissions from wheat and corn cultivation in a field experiment specifically designed for comparison purpose reported that emissions were higher in corn than both wheat and also soybean cultivations. The researcher attributed the increase to that of higher residues incorporated into the soil in corn cultivation. Our study was completely under farmer conditions with regular field cares. Relatively higher emissions from the soil under corn crops have been attributed to higher residue incorporation under corn vegetation compare to other crops compared such as wheat and soybean.

We found statistically significant correlations between the soil CO₂ emissions and meteorological variables available and field soil moisture data. Except a few cases, the soil CO₂ emissions had mostly significant positive correlations with AT and ST while significant negative correlations found with RH, rainfall and soil moisture. Significance of variables such as the soil temperature and moisture in modeling the soil CO₂ emissions have been mostly emphasized by earlier researchers. The negative correlations between soil the CO₂ emissions and soil moisture content and rainfall could be due to optimum moisture conditions during the study period which was provided by irrigation. Earlier researchers reported that as long as soil moisture are at optimum level, its impact may be insignificant in the soil CO₂ emissions (Morell et al., 2010; Mancinelli et al., 2010).

Modeling of soil CO₂ emissions

Although the models used to estimate the soil CO₂ emissions at different locations, crop managements and seasons were found statistically significant ($p < 0.05$). The R² values showing capability of MLR models for explaining variations in the long terms soil CO₂ emissions were relatively lower, indicating that there are other factors that may involve in overall variations in the emissions. Zhang et al. (2011) emphasized that soil management practices such as tillage had high control over the quantity of soil CO₂ emissions under field conditions in addition to environmental factors such as soil temperature and moisture.

Lower R² values have been also found by earlier researchers. Mapanda et al. (2010) obtained R² values between the soil CO₂ emissions and various environmental parameters were between 0.12 and 0.48 from the models. Mancinelli et al. (2010) received R² values between 0.25 and 0.28 using the soil temperature and moisture as controlling parameter.

According to the MLR and stepwise regression models, the significant and most significant parameters selected in modeling relationships between long terms fluctuations in soil CO₂ emissions from different crop management and climatic parameters along with field soil moisture data were not same for the models constructed for different seasons and cropping managements. All variables included into the models were once selected as the most significant variables in modeling, however in most cases, AT was selected as the most significant variable in modeling the soil CO₂

emissions, which was followed by soil moisture, soil temperatures at different depth, RH and rainfall data.

Overall the accuracies of the soil CO₂ estimations using GLM models and available meteorological data were low. However the model estimations closely followed the actual observations (*Fig. 6*). Low estimation accuracies were mostly due to the higher emission values within the data sets which were not being able to be captured by the model and were underestimated. In addition to climate variables, agricultural practices such as plowing which are not included in the model may impact magnitude of the distribution of soil CO₂ emissions and cause occurrence of extreme values.

Conclusions

This study evaluated the long term (from 2009 to 2018) seasonal fluctuations in the soil CO₂ emissions under wheat and corn plantation and compared their results with ones obtained from bare soils located nearby. The CO₂ emissions from the soils under field crops were always about 38% higher than bare soils. The soil CO₂ emissions showed an increasing trend over the years which can be explained by increases in air temperature and accumulations of plant residues in the soil. Up to 77% of variations in the soil CO₂ emissions were explained with combined use of MLR model and available meteorological parameters and soil moisture data. Air temperature, soil temperatures at different depth and soil moisture were found the most significant parameters impacting the overall variations in long terms fluctuations in the soil CO₂ emissions under different cropping and bare soils. Overall the results indicated that per cent of variations explained by modeling could be improved by incorporating the soil management factors into models.

Acknowledgements. Financial support of this study has been provided by Harran University Scientific Research Commissions (HUBAK). The author would like to thank Prof. Dr. Ahmet Ruhi Mermut for his suggestion to improve the text and Dr. A. V. Bilgili, in Harran University, Turkey, for his contributions to the manuscript preparation and support.

REFERENCES

- [1] Akbolat, D. Evrendilek, F., Coskan, A., Ekinçi, K. (2009): Quantifying soil respiration in response to shortterm tillage practices: a case study in southern Turkey. – *Acta Agriculturae Scandinavica Section B-Soil and Plant Science* 59: 50-56.
- [2] Almaraz, J. J., Mabood, F., Zhou, X., Madramootoo, C., Rochette, P., Ma, B., Smith, D. L. (2009): Carbon dioxide and nitrous oxide fluxes in corn grown under two tillage systems in southwestern Quebec. – *Soil Science Society of America Journal* 73: 113-119.
- [3] Allaire, S. E., Lange, S. F., Lafond, J. A., Pelletier, B., Cambouris, A. N., Dutilleul, P. (2012): Multiscale spatial variability of CO₂ emissions and correlations with physico-chemical soil properties. – *Geoderma* 170: 251-260.
- [4] Bauer, P. J., Frederick, J. R., Novak, J. M., & Hunt, P. G. (2006): Soil CO₂ flux from a Norfolk loamy sand after 25 years of conventional and conservation tillage. – *Soil & Tillage Research* 90: 205-211.
- [5] Bouyoucos, G. J. (1926): Estimation of the colloidal material in soils. – *Science* 64: 362.
- [6] CGIAR (2017): 2016 Annual Report to CGIAR Consortium. Copenhagen, Denmark: CGIAR Research Program on Climate Change. – *Agriculture and Food Security (CCAFS)*, Wageningen.

- [7] Dinç, U., Şenol, S., Sayın, M., Kapur, S., Güzel, N., Dericci, R., Yeşilsoy, M. Ş. et al. (1988): Güneydoğu Anadolu Bölgesi Toprakları (GAP), I. Harran Ovası (in Turkish). – TÜBİTAK, Şanlıurfa (Project No: TOAG-534).
- [8] Edwards, N. T. (1982): The use of soda-lime for measuring respiration rates in terrestrial systems. – *Pedobiologia* 23: 321 – 330.
- [9] FAOSTAT (2010): Food and Agricultural Organization of the United Nations, Rome. – FAOSTAT@fao.org.
- [10] Frank, A. B., Liebig, M. A., Tanaka, D. L. (2006): Management effects on soil CO₂ efflux in northern semiarid grassland and cropland. – *Soil & Tillage Research* 89: 78-85.
- [11] Guo, Q., Li, W. W., Liu, D. D., Wu, W., Liu, Y., Wen, X. X., Liao, Y. C. (2013): Seasonal characteristics of CO₂ fluxes in a rain-fed wheat field ecosystem at the Loess Plateau. – *Spanish Journal of Agricultural Research* 11: 980-988.
- [12] Iqbal, J., Lin, S., Hu, R., Feng, M. (2009): Temporal variability of soil-atmospheric CO₂ and CH₄ fluxes from different land uses in mid-subtropical China. – *Atmospheric Environment* 43: 5865-5875.
- [13] Janzen, H. H. (1993): Soluble Salts. – In: Carter, M. R. (ed.) *Soil Sampling and Methods of Analysis*. – Canadian Society of Soil Science, Crc Pres Inc. Boca Raton, FL.
- [14] Kacar, B. (1994): *Soil and Plant Analysis III. Soil Analysis*. – Ankara Uni. Agricultural Fac., Ankara.
- [15] Knudsen, D., Peterson, G. A., Pratt, P. F. (1982): Lithium, Sodium, and Potassium. – In: Page, A. L., Miller, R. H., Keeney, D. R. (eds.) *Methods of Soil Analysis, Part 2*. ASA, Madison, WI.
- [16] Koizumi, H., Kontturi, M., Mariko, S., Nakadai, T., Bekku, Y., Mela, T. (1999): Soil respiration in three soil types in agricultural ecosystems in Finland. – *Acta Agriculturae Scandinavica, Section B—Soil & Plant Science* 49: 65-74.
- [17] Kuzyakov, Y. V., Larionova, A. A. (2006): Contribution of rhizomicrobial and root respiration to the CO₂ emission from soil (A review). – *Eurasian Soil Sci.* 39: 753.
- [18] Lal, R., Bruce, J. P. (1999): The potential of world cropland soils to sequester C and mitigate the greenhouse effect. – *Environmental Science & Policy* 2: 177-185.
- [19] Lehmann, J., Joseph, S. (2009): *Biochar for Environmental Management: Science and Technology*. – Earthscan, London.
- [20] Lessard, R., Rochette, P., Topp, E., Pattey, E., Desjardins, R. L., Beumont, G. (1994): Methane and carbon dioxide fluxes from poorly drained adjacent cultivated forest sites. – *Can J Soil Sci* 74: 139-146.
- [21] Li, H., Han, X., Qiao, Y., Ho, X., Xing, B. (2009): Carbon dioxide emission from black soil as influenced by land-use change and long-term fertilization. – *Commun in Soil Sci Plan Analysis* 40: 1350-1368.
- [22] Lin, T. B., Wang, Z. Q., Song, X. L., Qu, Y. W., Meng, Z. Y. (2008): CO₂ flux and impact factors in winter wheat field ecosystem. – *Chin Eco Agr* 16: 458-1463.
- [23] Lu, X., Cheng, G. (2009): Climate change effects on soil carbon dynamics and greenhouse gas emissions in *Abies fabri* forest of subalpine, southwest China. – *Soil Biology and Biochemistry* 4: 1015-1021.
- [24] Lu, X., Lu, X., Tanveer, S. K., Wen, X., Liao, Y. (2016): Effects of tillage management on soil CO₂ emission and wheat yield under rain-fed conditions. – *Soil Research* 54: 38-48.
- [25] Mancinelli, R., Campiglia, E., Di Tizio, A., Marinari, S. (2010): Soil carbon dioxide emission and carbon content as affected by conventional and organic cropping systems in Mediterranean environment. – *Appl Soil Ecol* 46: 64-72.
- [26] McLean, E. O. (1982): Soil pH and Lime Requirement. – In: Page, A. L., Miller, R. H., Keeney, D. R. (eds.) *Methods of Soil Analysis, Part 2*. ASA, Madison, WI.
- [27] Morell, F. J., Alvaro-Fuentes, J., Lampurlanes, J., Cantero-Martinez, C. (2010): Soil CO₂ fluxes following tillage and rainfall events in a semiarid Mediterranean agroecosystem: effects of tillage systems and nitrogen fertilization. – *Agr Ecosyst Environ* 139: 167-173.

- [28] Morell, F. J., Whitmore, A. P., Álvaro-Fuentes, J., Lampurlanés, J., Cantero-Martínez, C. (2012): Root respiration of barley in a semiarid Mediterranean agroecosystem: field and modelling approaches. – *Plant Soil* 351: 135-147.
- [29] Meng-yang, Y., Ya-ru, Y., Lu-jun, L., Yan-Li, X., Xiao-zeng, H. (2014): Soil CO₂ emissions as affected by 20-year continuous cropping in Mollisols. – *Journal of Integrative Agriculture* 13: 615-623.
- [30] Nelson, D. W., Sommers, L. E. (1982): Chemical and Microbiological Properties. – In: Page, A. L., Miller, R. H. Keeney, D. R. (eds.) *Methods of Soil Analysis, Part 2*. ASA, Madison, WI.
- [31] Ngao, J., Epron D., Delpierre N., Bréda N., Granier A., Longdoz B. (2012): Spatial variability of soil CO₂ efflux linked to soil parameters and ecosystem characteristics in a temperate beech forest. – *Agricultural and Forest Meteorology* 154: 136-46.
- [32] Olsen, S. R., Sommers, L. E. (1982): Phosphorus. – In: Page, A. L., Miller, R. H., Keeney, D. R. (eds.) *Methods of Soil Analysis, Part 2*. ASA, Madison, WI.
- [33] Panosso, A. R., Marques, J. Jr., Pereira, G. T., La Scala, N. Jr. (2009): Spatial and temporal variability of soil CO₂ emission in a sugarcane area under green and slash-and-burn managements. – *Soil Till Res.* 105: 275-282.
- [34] Panosso, A. R., Marques Jr, J., Milori, D. M. B. P., Ferraudo, A. S., Barbieri, D. M., Pereira, G. T., La Scala Jr., N. (2011): Soil CO₂ emission and its relation to soil properties in sugarcane areas under slash-and-burn and green harvest. – *Soil and Tillage Research* 111: 190-196.
- [35] Raich, J. W., Potter, C. S., Bhagawati, D. (2002): Interannual variability in global soil respiration, 1980-94. – *Global Change Biol* 8: 800-812.
- [36] Rastogi, M., Singh, S., Pathak, H. (2002): Emission of carbon dioxide from soil. – *Current Science* 82: 510-517.
- [37] Reth, S, Reichstein, M., Falge, E. (2005): The effect of soil water content, soil temperature, soil pH-value and the root mass on soil CO₂ efflux—a modified model. – *Plant Soil* 268: 21-33.
- [38] Sauerbeck, D. R., (2001): CO₂ emissions and C sequestration by agriculture. Perspectives and limitations. – *Nutrient Cycling in Agroecosystems* 60: 253-266.
- [39] Xu, Q., Yang, R., Dong, Y.-X., Liu, Y.-X., Qiu, L.-R. (2016): The influence of rapid urbanization and land use changes on terrestrial carbon sources/sinks in Guangzhou, China. – *Ecological Indicators* 70: 304-316.
- [40] Wang, L. G., Qiu, J. J., Tang, H. J., Hu, L., Li, C. S., Eric, V. R. (2008): Modeling soil organic carbon dynamics in the major agricultural regions of China. – *Geoderma* 147: 47-55.
- [41] Zhang, H., Zhou, X., Lu, F., Pang, J., Feng, Z., Liu, W., O, Z., Wang, X. (2011): Seasonal dynamics of soil CO₂ efflux in a conventional tilled wheat field of the Loess Plateau, China. – *Ecol Res* 26: 735-743.
- [42] Zhang, T., Wang, G., Yang, Y., Mao, T., Chen, X. (2015): Non-growing season soil CO₂ flux and its contribution to annual soil CO₂ emissions in two typical grasslands in the permafrost region of the Qinghai-Tibet Plateau. – *European Journal of Soil Biology* 71: 45-52.

STUDY OF ENZYME ACTIVITY CHANGING PATTERN IN LIVESTOCK MANURES COMPOSTING

FENG, L.¹ – LI, X.¹ – ZHEN, X.^{2*} – DONG, H.² – ZHENG, J.³ – WANG, Y.³

¹Liaoning Province Clean Energy Key Laboratory, Shenyang Aerospace University,
Shenyang Daoyi Street 37, Shenyang 110136, China
(phone: +86-180-4003-8889)

²School of New Energy and Power Engineering, Lanzhou Jiaotong University,
No. 88, Anning West Road, Anning District, Lanzhou 730070, China
(phone: +86-139-1930-2012)

³School of Energy and Power Engineering, Lanzhou University of Technology,
No. 287, Langongping Road, Qilihe District Lanzhou, 730050, China
(phone: +86-139-1925-7393)

*Corresponding author

e-mail: zxf283386515@163.com ; phone: +86-139-1930-2012

(Received 28th Jan 2019 ; accepted 29th Mar 2019)

Abstract. Aerobic static composting was conducted for 21 days with cattle, pig and chicken manure along with the leavening agent of 10% corn stalk. In the composting process, the changing trend of parameters: temperature, pH and water content and quantities of microorganism including bacteria, fungi and actinomycetes were studied. It showed that the composting treatment of the three types of livestock manure entered the high temperature period of 45 °C on the 6th day and reached the maximum temperature on the 15th day. The number of days with temperature above 55 °C was 6, 6 and 9 d, which all satisfied the maturity standards. At the end of the composting process, the total nutrient content of pig manure was the highest (6.33%), the total nutrient content of cattle manure was the lowest (5.04%). Throughout the composting process, the changes of activities of urease and invertase were the same with a decreasing trend as a whole. However, the activity of catalase increased with the process of composting. At the end of the composting reactions, concentrations of catalase, urease and invertase were the highest with corresponding values of $62.18 \pm 0.45/0.002 \text{ mol}\cdot\text{L}^{-1}\cdot\text{g}^{-1}$, $54.28 \pm 8.35 \text{ mg}\cdot\text{g}^{-1}\cdot\text{d}^{-1}$ and $11.28 \pm 0.14 \text{ mg}\cdot\text{g}^{-1}\cdot\text{d}^{-1}$, respectively.

Keywords: livestock manures, aerobic compost, process parameters, enzyme reaction, biochemical reactions

Introduction

Since 1978 onward, the industries related to livestock and poultry breeding have increased exponentially (Awasthi et al., 2018). Their rapid development produced benefit economic benefits, improved human food structure and nutrition comprehensively with enhanced life quality (Wang et al., 2013). However, the unprocessed livestock manure originated from the breeding industries creates huge environmental challenge. In comparison with the traditional dispersed feeding system, extensive feeding decreases the growth cycle of livestock and poultry. Extensive feeding increases the yield and reduces the breeding cost significantly (Yasuda et al., 2017). However, it has been proved that intensive breeding results in the separation of planting and breeding. Thus, the environmental pollution created by animal husbandry is severe. Nowadays, livestock manure has been considered as one of the three non-point sources of environmental pollution.

There are stocks of livestock manure in China with a wide range of environmental effects. However, the utilization level of livestock manure is low (Xi et al., 2011). With the low utilization efficiency, the promotion of resource utilization out of livestock manure has been neglected. To overcome this problem, researches are urgently needed targeting the livestock manure stocks arising. Livestock manure is the main agricultural waste with large quantity and wide distribution. It is urgent to solve the current utilization status of livestock manure as well as to find the optimum utilization pathway in different districts of China (Zhang et al., 2011; Feng et al., 2015). Recent studies on the microbial aerobic conversion processes of compost have been focused on the single livestock manure as raw material. There has been no report on the enzyme activities involved in the composting using raw materials of different livestock manure. The present study aimed to compare the changing pattern of enzyme activities in composting with different livestock manures. The research could provide theoretical evidence and technical support for organic fertilizer production to the local entrepreneurs.

Experiments and methods

Materials

Cattle manure, pig manure and chicken manure used in the composting process with livestock manures were procured at a breeding farm near Shenyang Aerospace University in Shenbei New District, Shenyang, Liaoning. Corn stalks were also provided by the same breeding farm. Corn stalks were cut into pieces of 2-4 cm (length) by the knife mill before use.

The physicochemical properties of composting materials are shown in *Table 1*.

Table 1. Agrochemical characters of different compost materials

Raw materials	Water content (%)	pH	Total carbon (%)	Total nitrogen (%)	Total potassium (K ₂ O%)	Total phosphorus (P ₂ O ₅ %)	C/N
Cattle manure	68.9	7.64	38.32	1.78	1.48	1.45	21.53
Pig manure	73.4	7.35	39.41	1.80	1.58	1.78	21.89
Chicken manure	70.8	7.28	41.15	2.99	1.52	2.98	13.76
Corn stalk	21.5	7.19	54.82	1.04	0.98	0.46	52.71

Experimental schemes

An aerobic static composting was conducted using the composting materials of three livestock manures, including cattle manure (R1), pig manure (R2) and chicken manure (R3). The 21 d composting reaction was conducted with six self-designed aerobic composting boxes among which two composing boxes were considered as a group to contain a single type of livestock manure.

The results of every parameter data in the experiments were taken as an average. Additives of 10% corn stalk adjusted the porosity and organic matter content of the livestock manure. In the whole composting process, different parameters like temperature, oxygen concentration, carbon dioxide concentration, density, were monitored. Besides, the gas produced during the composting process was treated using a

bio-filter. The authors compared and analyzed the change in every parameter and the law of enzyme activities in the composting process with different livestock manures.

Experiment apparatus

The self-designed composting box was used in the composting experiment. The experiment apparatus of the composting is shown in *Figure 1*.

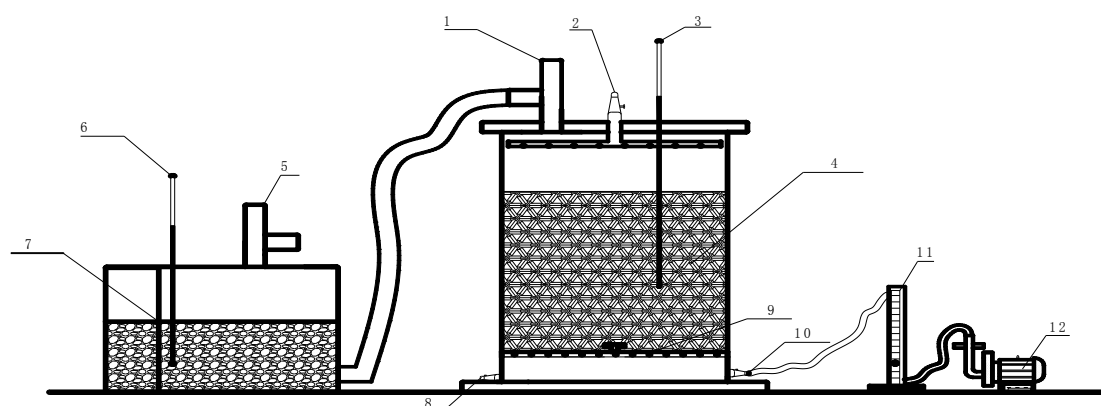


Figure 1. Experimental apparatus used in the aerobic composting with livestock manures. 1. The vent of the composting box. 2. Back-ejecta nozzle of leachate. 3. Thermometer. 4. Composting box. 5. The gas outlet of bio-filter. 6. Thermometer. 7. Bio-filter. 8. Discharge pipe of leachate. 9. Grid plate. 10. Inlet pipe. 11. The flow meter. 12. Fan

The livestock manure was mixed evenly and sampled to determine the density, pH value, conductivity, moisture content, organic content and ash content of raw materials. Then in proportion to add additives (straw), full mixing, sampling, determination of mixed materials of the above indicators.

Fill the compost box with the mixed materials, press gently to ensure the material is even, then weigh and measure the height of the material in the box and the diameter of the box. Seal the box with bolts, insert thermometer, add insulation layer, put the box on the reaction rack, connect the air pump and flow meter, and breathe air into the reactor. The first data was recorded from the time the air was pumped in; temperature was recorded every 2 h, O₂ and CO₂ concentrations in the compost bin and biofilter were recorded every 4 h.

Analysis method

Determination of total solid content (TS)

The determination of TS aims to enable the evaporation of material under the condition of 110 °C until the material is completely in the dry state. With the measurement of precise balance, the weight of dry crucible was recorded as m_1 . Then the experimental materials were weighed together with precise balance, and the weight was denoted as m_2 . Crucible was dried until its mass is no longer changed, and the mass was recorded as m_3 .

The equation for the total solid content is as follows (Zhang et al., 2011):

$$TS = \frac{m_3 - m_1}{m_2 - m_1} \times 100\% \quad (\text{Eq.1})$$

Determination of volatile solids (VS) content

According to the definition of volatile solid, under the condition of 650 °C, high temperature heat comes out of that part of the solid. When the sample is heated and cooled, the portion of the lost weight is the volatile solid, and the non-volatile residue is called ash (expressed as a percentage or g/L). The drying samples were put in the muffle furnace under the high temperature of 550 °C for 3 h (Feng et al., 2015). Subsequently, the samples were removed for half an hour cooling after being weighted, and the average quality was recorded as m_4 . The calculation of volatile solid can be expressed as:

$$VS = \frac{m_3 - m_4}{m_2 - m_1} \times 100\% \quad (\text{Eq.2})$$

where: VS represents the volatile solid content of the sample, %;

M_1 is the mass of the crucible, g;

M_2 represents the total mass of the sample and crucible before drying, g;

M_3 represents the total mass of the sample and crucible after drying (before putting it into the muffle furnace), g;

M_4 represents the total mass of sample and crucible after putting into a muffle furnace, g.

Determination of pH value

The samples were tested in a special centrifugal tube, and after centrifugation for 30 minutes, the supernatant was removed for pH determination. PH meter was used to measure the supernatant and record the data.

Determination of enzyme activity

The KMnO_4 titration method was used to determine the enzyme and catalase activities in soil. The results were demonstrated by the quantity of KMnO_4 consumed in ml by unit composting weight with the unit of $0.002 \text{ mol} \cdot \text{L}^{-1} \cdot \text{g}^{-1} \cdot 20 \text{ min}^{-1}$ (Seal et al., 2012).

The determination of urease activity was done via colorimetric method utilizing phenol sodium and sodium hypochlorite. The results were demonstrated by the milligram quantity of NH_4^+ -N per 100 g composting with the unit of $\text{mg} \cdot \text{g}^{-1} \cdot \text{d}^{-1}$ (Gray F, 2015).

The determination of invertase was carried out with the 3,5-dinitrosalicylic acid method and the results were demonstrated by the milligram quantity of glucose produced by 1 g composting in 1 d with the unit of $\text{mg} \cdot \text{g}^{-1} \cdot \text{d}^{-1}$ (Margaritis et al., 2017).

Results and discussion

The change of temperature, pH and water content in the composting process with different livestock manure

Temperature changes

Composting is a biochemical process dominated by microorganisms. In this process, the temperature is an important index that affects both the microbial activity and the microbial

community structure. The duration of the high-temperature stage in the composting process largely determines the composting effect and the quality of the composting product (Chen, 2012; Jieying et al., 2017).

Figure 2 shows the temperature changes during the composting processes of three types of manures. For all three types of manure, the composting process exhibited the high-temperature period (45 °C) at the same time (6 days), and they were subjected at these conditions for 15 days. R1, R2 and R3 reached the highest temperature on the 15th day, with values of 56.1 °C, 58.3 °C and 59.3 °C, respectively. Among them, R3 (chicken manure) treatment stayed at the high-temperature stage for the longest time, while the high-temperature periods for R1 (cattle manure) and R2 (pig manure) treatments were relatively short. After 18 days, all piles entered the cooling stage after lowering for three days, during which the temperature dropped to 45–47 °C at the end of the composting.

During the composting process, the temperature increase of the pile is an accumulative result of the heat generated by the microbial metabolism; therefore it reflects the metabolic intensity of microorganisms and the conversion rate of the composting substances (Jieying et al., 2017). If the temperature is too low or the high-temperature stage is too short, the pest eggs and weed seeds cannot be effectively erased. On the other hand, if the temperature is too high, the production efficiency of the enterprise is compromised, and some medium-temperature microorganisms that mainly decompose cellulose and lignin may not be able to survive, thus affecting the composting process. Research (Wei et al., 2018) suggested that the preferred high-temperature for the solid organic waste composting is 60–65 °C, and that it needs to be maintained for more than 7 days. In this experiment, the composting treatments of the three types of manures showed a rapid heating feature, and the high-temperature (55 °C) duration was 16–18 days.

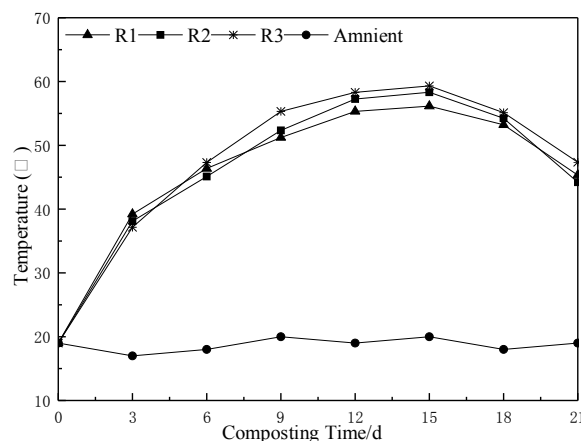


Figure 2. Temperature changes of the three manures of composting

Changes in pH during composting of the livestock and poultry manure

Figure 3 shows the changes in pH during the composting of the livestock and poultry manures. For all three types of manures, the pH increased initially and decreased later. At the end of the composting process, the pH showed an increase again. Until day 3, the pH change of R1 was 7.27-7.55. In addition, the corresponding pH change of R2 was 7.29-7.65. Moreover, the pH change of R3 was 7.33-7.87. These changes were mainly

due to the decomposition of amino acids in the manure, as deamination of the amino acids could cause a slight increase of pH in the whole piles. From day 4, the pH of all the composting reactions started to drop. The lowest pH of R3 (chicken manure) compost was 6.07 during the whole composting process. In addition, the lowest pH of R1 was 6.07 which appeared on day 15. Besides, the lowest pH of R2 was 6.31 which appeared on the day 12. Such low pH was mainly due to the decomposition of the organic matter in the compost material of livestock and poultry that produced organic acids, organic acids led to a decrease of pH. It is worth noting that the organic matter from the chicken manure is more susceptible to hydrolysis and acidification, thus the pH value of R3 decreased to a highest degree.

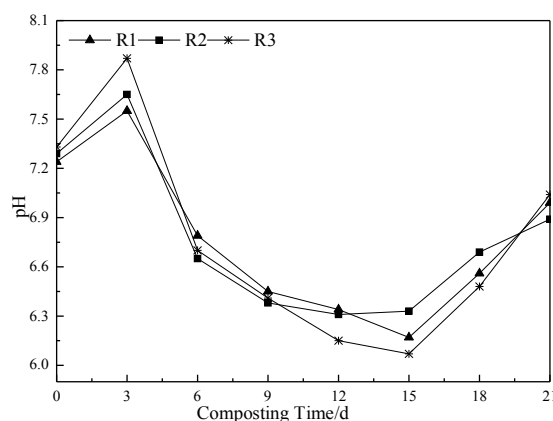


Figure 3. Changes in pH of three kinds

On day 15, starting from 6.17 (R1), 6.31 (R2) and 6.07 (R3), the pH values of all the composting reactions began to rise again, during the high-temperature stage, the organic acids in the piles were efficiently decomposed by the thermophilic bacteria to produce CO₂, and the decrease of organic acid content, therefore, led to a rise in pH. At the end of composting, the pH values of the three piles were 6.99 (R1), 6.89 (R2), and 7.04 (R3). These change patterns was due to the oxidative decomposition of the decomposable organic matter in the piles. The produced nitrogen (ammonium) accumulated continuously, causing an increase in the pH of the piles. At the same time, the increase of pH gave rise to the volatilization of ammonium nitrogen; therefore, at the end of composting, the pH values of all the manures were in the range of 6.9–7.1.

Changes in moisture content during composting of manures

Figure 4 shows the changes in moisture content during the composting of the livestock and poultry manure. For all three manure types, the initial moisture percentages were 64–67%. The moisture content reduced, as the composting process started, and the percentage of the moisture content in all piles in the end was 30–32%. R1 (cattle manure) showed a significant moisture loss (about 35%). The period with the largest decrease in the moisture content was the high-temperature stage, probably due to the high metabolic activity of the microorganisms during the heating-stage and high-temperature stage. In particular, during the high-temperature stage, the thermophilic bacteria dominated the microbial community, and at this stage, they rapidly utilized and degraded the organic matter. Consequently, the demand for oxygen significantly

increased. Because of the cold incoming air and the hot outgoing air, the water saturation of the outgoing air increased significantly, resulting in a faster use of water and more marked evaporation. At the end of the composting experiment, the moisture percentages were 30.11 (R1), 32.22 (R2) and 30.01 (R3). If too much water evaporates during the high-temperature period, the moisture in the late composting period and the rate of decomposing can significantly reduce, thus prolonging the composting cycle. Therefore, appropriate water replenishment needs to be applied when the moisture percentage in the maturity period is less than 20%.

Moisture content and pH are the two important indices of the composting process. Moisture can dissolve the organic matter during composting, participate in microbial metabolism, and regulate the compost temperature. Neither a high moisture content, nor low moisture content is beneficial to the survival of the microorganisms. If the moisture content is too high, it indicates that the ventilation and permeability are poor, and this can lead to partial hypoxia of the pile and produce acid odor. Furthermore, it is not conducive to the export of nutrients, thus resulting in an economic loss. On the other hand, a dry environment restricts the metabolism of the microorganisms. Studies have shown that the optimum moisture percentage in the early stage of composting is 50–65%, and in the later stage of composting, in order to maintain the speed of composting and shorten the composting cycle, the moisture percentage should not be less than 20%. The optimal pH for composting is 5.5–8.5. It is interesting that the initial moisture content and the pH measured in this experiment are in the optimal range.

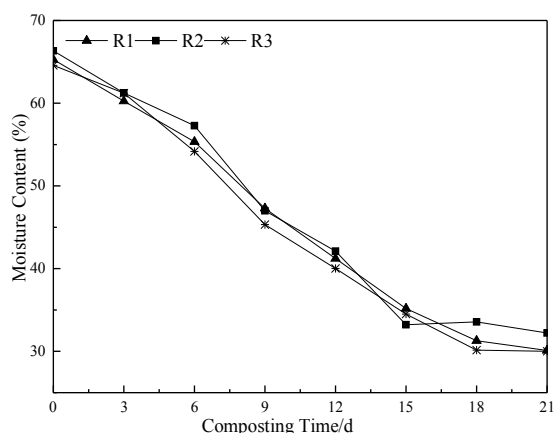


Figure 4. Change in moisture content of the three manures of three kinds of composting

The change of C-N-P-K content in the composting process with different livestock manure

The total nutrient of $N+P_2O_5+K_2O$ is an essential index for the quantity of organic fertilizer (Awasthi et al., 2015). There are three pathways of nitrogen transformation in the composting process. The first one is the emission of ammonia gas to the atmosphere, resulting in a loss of nutrients from the composting system. The second one is the transformation of nitrogenous compounds to nitrate or nitrite by nitrifying bacteria or nitrite bacteria, respectively. The third one is the assimilation of nitrogen by microorganisms. The content of total nutrients ($N + P_2O_5 + K_2O$) shows an increasing trend in the composting process due to two reasons. The first reason is the emission of the organic state released and transformed to the inorganic state due to the

decomposition of organic matters in the composting process. The second reason is the quantity of organic carbon decreased due to the functions of microorganisms which caused an increase in the concentration effect. Thus, the total nutrient content increased (Zhuotong et al., 2018; Wang et al., 2017, 2014). According to *Table 2*, the total nutrient content of pig manure was the highest with the value of 6.33% and that of the cattle manure was lowest (5.04%).

According to the *Organic Fertilizer Industry Standards* (NY525-2012) issued in 2012, the mass fraction of organic matters in the qualified products should be larger than 45%. In addition, the mass fraction of the total nutrients (N + P₂O₅ + K₂O) should be larger than 5%. Besides, the mass fraction of water content should be smaller than 30%. Besides, values of pH in the qualified products should be in the range of 5.5-8.5. According to *Table 2*, all the four composting products from the present study satisfied the requirements of *Organic Fertilizer Industry Standards* (NY525-2012) (Jain et al., 2018).

Table 2. The total nutrients in the composting products with different livestock manure

The composting products	TN/%	TP/%	TK/%	(N+P ₂ O ₅ +K ₂ O)/%
R1 (cattle manure)	1.93±0.18	1.57±0.19	1.54±0.19	5.04
R2 (pig manure)	2.25±0.18	2.41±0.15	1.67±0.12	6.33
R3 (chicken manure)	2.14±0.15	1.83±0.16	1.78±0.19	5.75

The enzyme activity changes in the composting process with different livestock manure

Composting is a biochemical process where decomposition and transformation of organic matters to stable humus take place. The process follows the utilization of the secreted enzymes in the growth and reproduction processes as well as metabolic activities of microorganisms. So, different enzymes are involved in the whole composting process (Hannum et al., 2017). Enzymes are composed of apoenzyme and the cofactor has characteristics of specificity, high efficiency and diversity. In the present study, the relationships between the enzyme activity change of catalase, urease and invertase and the quantity of microorganisms were systematically compared. For the purpose, composting process with four livestock manure was investigated targeting to provide theoretical evidence for the composting mechanism.

The enzyme activity change of catalase in the composting process with different livestock manure

Catalase demonstrates the intensity of the degree of composting oxidation, because catalase can decompose hydrogen peroxide produced in the composting process and thus decrease its poisoning effect to microorganism (Ukalska-Jaruga et al., 2018).

Figure 5 showed the changing trend of the enzyme activity of catalase in the composting process with different livestock manure. It showed that the initial concentration of catalase in the initial composting reaction of R1 (cattle manure) was $48.21 \pm 1.11 \text{ mol}\cdot\text{L}^{-1}\cdot\text{g}^{-1}$. Besides, the initial concentration of catalase of R2 (pig manure) was $45.04 \pm 0.85 \text{ mol}\cdot\text{L}^{-1}\cdot\text{g}^{-1}$. Moreover, the initial concentration of catalase of R3 (chicken manure) was $44.29 \pm 0.65/0.002 \text{ mol}\cdot\text{L}^{-1}\cdot\text{g}^{-1}$. With the process of the

composting, the concentration of catalase gradually increased. At the end of the reaction, the concentration of catalase were in descending order of R1 (cattle manure) > R2 (pig manure) > R3 (chicken manure) with corresponding values of 62.18 ± 0.45 , 55.21 ± 0.58 and $54.28 \pm 0.14/0.002 \text{ mol}\cdot\text{L}^{-1}\cdot\text{g}^{-1}$, respectively. The main reason for the gradual increase of catalase concentration in the composting process with livestock manure was the increase of biochemical metabolism activity. This activity was carried out by the thermophilic bacterium as a replacement for the mesophilic bacterium. The latter bacterium happened to be the active microbial flora with the increase of the pile temperature. Besides, the temperature was also an important factor which influenced enzymatic reactions. Thus, the concentration of catalase increased gradually with the process of reactions.

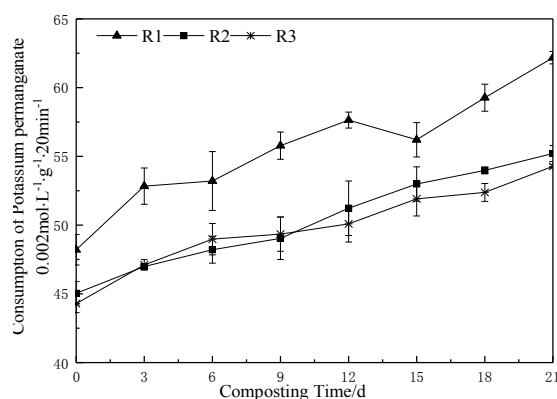


Figure 5. Activity change in catalase

The enzyme activity change of urease in the composting process with different livestock manure

Figure 6 shows the changing trend of the enzyme activity of urease in the composting process with different livestock manure. Urease could catalyze the transformation and decomposition of urea to ammonia and CO_2 as well as promote the transformation and decomposition of nitrogenous organic matter. Thus, it was the key index to evaluate the transformation velocity of nitrogen in the composting process. It showed that the initial urease concentrations in the primary reaction period of the composting were 258.47 ± 8.35 , 249.78 ± 3.98 and $4261.87 \pm 4.28 \text{ mg}\cdot\text{g}^{-1}\cdot\text{d}^{-1}$ for R1 (cattle manure), R2 (pig manure) and R3 (chicken manure), respectively. This illustrates the high activities of microorganisms in the initial composting period which secreted urease rapidly to decompose and transform susceptible nitrogenous organic matters. With the process of the reaction, urease activity became passive with the increase in temperature and demonstrated negative correlation with the change of temperature (Jain et al., 2018; Hannum et al., 2017). The urease content decreased gradually due to the decrease of the mesophilic microorganism quantities. The decrease of urease activities and the slowdown of decomposition and mineralization of nitrogenous organic matters occurred when the process entered into the high temperature period of the composting. At the end of the reaction, the urease concentrations in the pile were in a descending order of R1 (cattle manure) > R3 (chicken manure) > R2 (pig manure) with values of 54.28 ± 8.35 , 51.24 ± 1.25 and $50.24 \pm 5.36 \text{ mg}\cdot\text{g}^{-1}\cdot\text{d}^{-1}$, respectively.

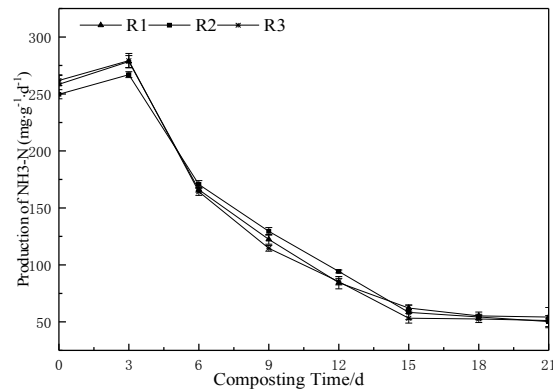


Figure 6. Activity change of urease in three kinds of livestock dung composting kinds of livestock dung composting

The change of invertase activity in the composting with different livestock manure

Figure 7 shows the changing trend of invertase activity in the composting with different livestock manures. Results show that the changing trends of invertase and catalase were the same. The initial catalase concentrations of the composting with R1 (cattle manure), R2 (pig manure) and R3 (chicken manure) were 50.28 ± 1.21 , 42.27 ± 1.25 and $44.54 \pm 1.01 \text{mg} \cdot \text{g}^{-1} \cdot \text{d}^{-1}$, respectively. Results indicate that the high activity of microorganism in the initial period of composting, which secreted invertase rapidly to decompose and transform susceptible nitrogenous organic matters (Li et al., 2016; Kazemi et al., 2016). With the process of the reaction, the invertase content in the pile decreased gradually, mainly due to the decrease in quantities of mesophilic microorganisms. Therefore, a decrease of invertase activities and the slowdown of the decomposition and mineralization rate of nitrogenous organic matters also occurred when the reaction phases entered into the high-temperature period of the composting. At the end of the reaction, the urease concentrations were in descending order of R2 (pig manure) > R3 (chicken manure) > R1 (cattle manure) with values of 11.28 ± 0.14 , 10.94 ± 1.11 and $10.45 \pm 0.97 \text{mg} \cdot \text{g}^{-1} \cdot \text{d}^{-1}$, respectively (Teutscherova et al., 2017; Sharma et al., 2017).

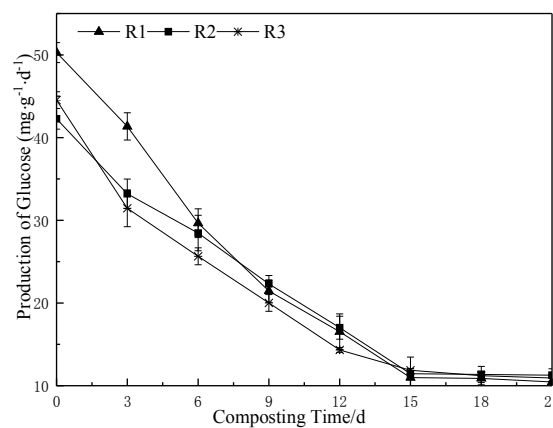


Figure 7. Activity change of sucrase in three

Conclusions

The composting treatment of three livestock manure entered the high-temperature period (45 °C) on the 6th day. Besides, their temperatures reached the maximum of 56.1, 58.3 and 59.3 °C, respectively. The number of days with temperature above 55 °C were 6, 6 and 9 d, respectively. Among them, the treatment of R3 (chicken manure) had the most days which belonged to the high temperature period, whereas the treatment of R1 (cattle manure) and R2 (pig manure) had relatively fewer days for belonging high-temperature period. All of them could satisfy the requirement of maturity standards.

pH values of the composting process with three livestock manure demonstrated the trend of initial increase, then decrease and final increase rally. pH of the R3 composting (chicken manure) was the lowest in the whole composting process. The value was 6.07 on the 15th day. Besides, pH values recorded were in the range of 6.9-7.1 at the end of the composting. Furthermore, the change of water content of three composting manures demonstrated the decreasing trend with the decreasing amplitude of 34-36%.

At the end of the composting with livestock manure, the total nutrients of pig manure composting were the highest with the value of 6.33%. The total nutrients of cattle manure composting were the lowest with the value of 5.04%.

Different types of enzymes were involved in different stages in the composting process. In the whole composting system, the activity change of urease and invertase was same with a decreasing trend as a whole. However, the catalase activity increased gradually with the process of composting. At the end of the composting reaction, the concentrations of catalase, urease and invertase were the highest in the piles of R1 (cattle manure), R1 (cattle manure) and R2 (pig manure), respectively, with corresponding values of $62.18 \pm 0.45/0.002 \text{ mol} \cdot \text{L}^{-1} \cdot \text{g}^{-1}$, $54.28 \pm 8.35 \text{ mg} \cdot \text{g}^{-1} \cdot \text{d}^{-1}$ and $11.28 \pm 0.14 \text{ mg} \cdot \text{g}^{-1} \cdot \text{d}^{-1}$.

Recommendation

The paper compared the changing pattern of enzyme activities in composting with different livestock manures added 10% straw as bulking agent and provided theoretical evidence for temperature, pH, moisture content and nutrition parameters. Future studies should focus on the change of microbial population and the correlation between microbial quantity and enzyme activity, so as to further analyze the mechanism of microbial enzymatic reaction and study the biochemical reaction activity of livestock and poultry manure compost.

Acknowledgements. This work was funded by the National Natural Science Foundation project (51509122), and Gansu Provincial Higher Education Science and Technology Achievements Transformation Project (2018D-04), Gansu Natural Science Foundation (18JR3RA154), 2018 Yangling Demonstration Zone Collaborative Innovation Major Project (2018CXY-14).

REFERENCES

- [1] Awasthi, M. K., Pandey, A. K., Bundela, P. S. et al. (2015): Co-composting of organic fraction of municipal solid waste mixed with different bulking waste: characterization of physicochemical parameters and microbial enzymatic dynamic. – *Bioresource Technology* 182: 200-207.

- [2] Awasthi, M. K., Awasthi, S. K., Wang, Q. et al. (2018): Influence of biochar on volatile fatty acids accumulation and microbial community succession during biosolids composting. – *Bioresource Technology* 251: 158.
- [3] Chen Yajuan, C. A. U. (2012): Effects of different C/N of composting materials on main indexes of high-temperature aerobic composting of chicken manure and sawdust. – *Journal of China Agricultural University* 17(5): 118-123.
- [4] Feng, R., Yin, Y., Zi-Fu, L. I. et al. (2015): Experimental study on composting of dewatered sewage sludge by addition of low ratio lime mixture. – *China Environmental Science* 35(5): 1442-1448.
- [5] Gray, N. F. (2015): *Biotechnology and Wastewater Treatment*. – In: Gray, N. F. (ed.) *Biology of Wastewater Treatment*. OUP, Oxford.
- [6] Hannum, H., Hasanah, Y. (2017): Effect of straw compost and phosphorus and zinc fertilizer on the content of phosphorus and zinc in paddy. – <http://repository.usu.ac.id/handle/123456789/69356>.
- [7] Jain, M. S., Jambhulkar, R., Kalamdhad, A. S. (2018): Biochar amendment for batch composting of nitrogen rich organic waste: effect on degradation kinetics, composting physics and nutritional properties. – *Bioresource Technology* 253: 204.
- [8] Jieying, H., Zixuan, Y., Hongjian, G. et al. (2017): Chemical structures and characteristics of animal manures and composts during composting and assessment of maturity indices. – *Plos One* 12(6): e0178110.
- [9] Kazemi, K., Zhang, B., Lye, L. M. et al. (2016): Design of experiment (DOE) based screening of factors affecting municipal solid waste (MSW) composting. – *Waste Management* 58: 107-117.
- [10] Li, S., Li, J., Zhang, B. et al. (2016): Influence of inoculants on content and quality of humus during chicken manure composting. – *Transactions of the Chinese Society of Agricultural Engineering*. DOI: 10.11975/j.issn.1002-6819.2016.z2.037.
- [11] Margaritis, M., Psarras, K., Panaretou, V. et al. (2017): Improvement of home composting process of food waste using different minerals. – *Waste Management* 73: 87-100.
- [12] Seal, A., Bera, R., Chatterjee, A. K. et al. (2015): Evaluation of a new composting method in terms of its biodegradation pathway and assessment of compost quality, maturity and stability. – *Archives of Agronomy & Soil Science* 58(9): 995-1012.
- [13] Sharma D., Varma, V. S., Yadav, K. D. et al. (2017): Evolution of chemical and biological characterization during agitated pile composting of flower waste. – *International Journal of Recycling of Organic Waste in Agriculture* 6(1): 89-98.
- [14] Teutscherova, N., Vazquez, E., Santana, D. et al. (2017): Influence of pruning waste compost maturity and biochar on carbon dynamics in acid soil: Incubation study. – *European Journal of Soil Biology* 78: 66-74..
- [15] Ukalska-Jaruga, A., Debaene, G., Smreczak, B. (2018): Particle and structure characterization of fulvic acids from agricultural soils. – *Journal of Soils and Sediments*. DOI: 10.1007/s11368-018-2008-1.
- [16] Wang, C., Guo, X., Deng, H. et al. (2014): New insights into the structure and dynamics of actinomycetal community during manure composting. – *Applied Microbiology and Biotechnology* 98(7): 3327-3337.
- [17] Wang, X., Selvam, A., Chan, M. et al. (2013): Nitrogen conservation and acidity control during food wastes composting through struvite formation: biomass, bioenergy, biowastes, conversion technologies, biotransformations, production technologies. – *Bioresource Technology* 147(8): 17-22.
- [18] Wang, X., Cao, A., Zhao, G. et al. (2017): Microbial community structure and diversity in a municipal solid waste landfill. – *Waste Management* 66: 79.
- [19] Wei, H., Wang, L., Hassan, M. et al. (2018): Succession of the functional microbial communities and the metabolic functions in maize straw composting process. – *Bioresource Technology* 256: 333-341.

- [20] Xi, B., Dang, Q., Wei, Z. et al. (2011): Effects of microbial inoculants on actinomycetes communities diversity during municipal solid waste composting. – Transactions of the Chinese Society of Agricultural Engineering 27(13): 227-232.
- [21] Yasuda, T., Waki, M., Fukumoto, Y. et al. (2017): Characterization of the denitrifying bacterial community in a full-scale rockwool biofilter for compost waste-gas treatment. – Applied Microbiology & Biotechnology 101(17): 1-14.
- [22] Zhang H., Lv D., Wei, L. (2011): Characteristics of dewatered sewage sludge and green waste co-composting. – Second International Conference on Digital Manufacturing & Automation, 5-7 August, Zhangjiajie, Hunan, China.
- [23] Zhuotong, Z., Xueying, G., Piao, X. et al. (2018): Responses of microbial carbon metabolism and function diversity induced by complex fungal enzymes in lignocellulosic waste composting. – Science of the Total Environment 643: 539-547.

A STUDY ON THE UTILIZATION OF THE EXOTIC INVASIVE SPECIES *HYPOCHAERIS RADICATA* L. AS MANAGEMENT PERSPECTIVE

HWANG, H. J.^{1#} – LEE, M.^{1#} – KIM, J. H.¹ – LEE, S.¹ – SON, D.² – OH, J. M.¹ – SONG, U.^{1,2*}

¹*Department of Biology, Jeju National University, Jeju 63243, Republic of Korea*

²*Research Institute for Basic Sciences, Jeju National University, Jeju 63243, Republic of Korea*

**Corresponding author*

e-mail: uhrami@gmail.com; phone: +82-64-754-3525; fax: +82-64-756-3541

#These authors contributed equally to this work (co-first authors)

(Received 1st Feb 2019 ; accepted 21st Mar 2019)

Abstract. Although *Hypochaeris radicata* L. is a noxious alien species in Korea, there is no effective way to prevent it from spreading. Therefore, this study aims to study the possibility of using *H. radicata* as an effective natural compound source which will contribute to the utilization of the invasive alien species and some extent to prevent invasion. Hot water and ethanol extracts of *H. radicata* showed high efficiency as a natural antioxidant indicating the species may be used as a natural antioxidant material. Extracts of *H. radicata* has shown no toxic effects on cells. Rather, *H. radicata* extract has an function of inhibiting the generation of NO in high concentrations of extracts which means that *H. radicata* extract has a function of anti-inflammatory effect. When the research on the effect of *H. radicata* finds out more, the utilization of this species will be increased and the environmentally friendly public participation management will be possible due to an increase in its collection. Also, it is meaningful that we have attempted to find an ecological engineering approach through utilization methods of alien species that has been spread widely in Korea.

Keywords: *cat's-ear, natural compounds, antioxidant, anti-inflammatory, alien species*

Introduction

Invasive alien plants are species that are dispersed outside their original habitats through intentional or unintentional means, which can harm the environment. This destruction will result in loss of ecosystem function and extinction of native species, eventually reducing biodiversity, ultimately resulting in socioeconomic decline (Samways et al., 1996). However, these exotic species can be used as sources of natural compound (medicine, cosmetic etc.), that such development of these uses may help to manage such exotic species through increase the harvest of this species in the wild (Maema et al., 2016), as a kind of ecological engineering. The free radical and properties containing natural antioxidants that metabolize the endogenous products of several oxidizing species are facilitated by ecological stress (Grassmann et al., 2002) for most plants, and studies of these natural products are useful for confirming the availability of plants. Recently, there has been an increasing interest in natural antioxidants, which can protect humans from damage caused by oxidative stress (Scalbert et al., 2005). This study attempts to approach *Hypochaeris radicata* L., which causes many problems in Jeju Island and some inland regions (Kim et al., 2006), as a new perspective. *H. radicata* is managed because it is designated as a harmful species in the Ministry of Environment. However, in Jeju Island, *H. radicata* is already the most dominant species. Thus, realistic removal and management of this species are difficult

and showed no results so far (Ryu et al., 2017). From the discovery of *H. radicata* in Chungcheong and Jeolla, it shows that diffusion and settlement have already occurred inland (Hyun et al., 2018). Therefore, the case of *H. radicata* shows that there is a limitation in the existing management methods for general harmful species. Therefore, we investigated the medicinal efficacy of *H. radicata* through the view as a resource. Through this, the research applying the idea that increasing the use of these alien species is a positive management of alien species (Li et al., 2015). For this purpose, we conducted a study on the efficacy of *H. radicata*.

Materials and methods

Plant sampling

In October 2018, 10 habitats from the northern part of Jeju island, Korea were randomly selected and the *H. radicata* used for the experiment were collected. Every sampling sites were unmanaged areas inside of agricultural fields, mostly close to roads. Sampling sites were relatively flat areas and dominated by *H. radicata*. The geographic coordinates of the center of the sampling sites are 33°27'49"N, 126°29'07"E. Ten plant samples were collected from each site and used as one large sample. Harvested plants were washed and then dried for 24 h. The stems and leaves except roots were cut into the crusher and used as experimental material.

Total antioxidant capacity (TAC) the superoxide dismutase activity (SOD) using raw plant

From plant leaves, crude extracts were prepared by re-suspending the frozen cells in 50 mM phosphate buffer (pH 7.2). The plant samples (0.1 g) were washed and then the cells were quick-frozen in liquid N₂ and milled subsequently. Phosphate buffer (1 ml; Sigma-Aldrich Corp.) was added and the suspension was stirred using Vortex mixer. Waited more than 30 min for protein extraction. After centrifuging at 14,000 rpm at 4 °C for 20 min, 400 µl of the supernatant was collected for the experiments. Absorption was measured using SpectraMax (Molecular Devices, USA). Protein quantities were determined by using Bradford assay (Bradford, 1976) to obtain a standard curve. Total Antioxidant capacity was measured by the antioxidant activity of an organic liquid using bathocuproine (Jaramillo-Flores et al., 2003) with a slight modification of the protocol. Our method comprises the following steps. First, mix a sample of the liquid (15 µl) with bathocuproine (200 µM; 585 µl) and stir using Vortex mixer and Pour a predetermined quantity (200 µl) of each of the samples into the wells of a multi-well plate. Then, Perform spectrophotometric measurements of the samples at 490 nm (S1). Add a predetermined quantity (50 µl) of copper sulfate solution to each well and incubate it at room temperature for 5 min; terminate the reaction using ethylenediaminetetraacetic acid (EDTA). Then again, Perform the second round of spectrophotometric measurements at 490 nm (S2). Total Antioxidant Capacity is calculated as $TAC = S2 - S1$ (µM/ml). Finally, convert units using the Bradford assay results (µM/mg). The superoxide dismutase activity was measured using the methods established by Peskin and Winterbourn (2000) and protocols of the WST assay by Donindo, Japan.. Using a WST-1 (2-(4-Iodophenyl)- 3-(4-nitrophenyl)-5-(2,4-disulfophenyl)- 2H-tetrazolium, monosodium salt) solution (Dojindo, Japan) and an

Enzyme Working Solution (Dojindo, Japan), SOD activities were calculated under the Dojindo's protocols.

Extract preparation

The dried aboveground plant parts (i.e., leaves and branches) were coarsely powdered by using an electric blender. 32.6 g of dried plant powder was then, a) extracted with 500 ml of 70% (v/v) ethanol for 24 h (EtOH) or b) extracted with 500 ml of 90 °C distilled water (HW: Hot Water) for 2 h. Then extracted solutions were filtered (Whatman No.1), and then concentrated with a rotary evaporator. Then the solution was freeze-dried to make the final product as powder.

Radical scavenging assay for testing antioxidant effects of extracts

DPPH (1,1-diphenyl-2-picrylhydrazyl) radical scavenging activity of the *H. radicata* were measured by a method suggested by Blois (1958). 180 µL of DPPH solution in 0.4 mM in ethanol was mixed with 20 µL of the extract (DW and ethanol) and incubated in the dark at 25 °C for 10 min. Then, the absorbance of the sample (A sample) and negative control (A control) consisting of only ethanol alone was measured at 517 nm. The DPPH radical scavenging activity of the sample was calculated by using *Equation 1*.

$$\text{Scavenging activity (\%)} = 100 \times \frac{(\text{A control} - \text{A sample})}{\text{A control}} \quad (\text{Eq.1})$$

ABTS (2,2'-azino-bis-(3-ethylbenzothiazoline-6-sulphonicacid)) radical scavenging activity of the subtropical plant extracts was measured as a method by Zhu et al. (2011). ABTS and potassium persulfate solutions (7 and 2.45 mM, respectively) were mixed and then incubated in the dark at 25 °C for 16 h. The ABTS solution was diluted with ethanol to obtain the working solution with an absorbance at 745 nm. Then, 20-µL aliquots of the plant extract samples were dissolved in ethanol at different concentrations (10–500 µg/mL), mixed with 180 µL of the working solution, incubated in the dark at 25 °C for 10 min, and then the Abs sample and Abs control (ethanol only) were measured. The ABTS radical scavenging activity was calculated by using *Equation 1*.

High performance liquid chromatography (HPLC)

High Performance Liquid Chromatography (HPLC) was analyzed at NICEM (Seoul National University, South Korea) using Ultimate 3000 model, (Thermo Fisher Scientific, Waltham, MA USA). The flow rate was 0.8 mL/min and the gradient was given using Buffer A [0.3% trifluoroacetic acid (TFA)] and Buffer B (Acetonitrile). C-18 column (4.6*250,5 µm) was used and wavelength of 280 nm [190-800 nm diode array detection (DAD) scanning] was used for analysis. 12 standards that often used for phenolic compounds were used to detect natural compounds of *H. radicata* (syringic acid, salicylic acid, *p*-coumaric acid 4, ferulic acid, naringin, myricetin, hesperidin, *trans*-cinnamic acid, quercetin, naringenin, confertin, scopoletin).

Cell culture

Murine RAW 264.7 macrophages were obtained from the Korean Cell Line Bank (Seoul, South Korea). Cells were cultured in Dulbecco's modified Eagle's medium, supplemented with 10% fetal bovine serum, penicillin, and streptomycin sulfate (all from

GIBCO, Grand Island, NY, USA), in an incubator at 37 °C in a humidified atmosphere of 95% air and 5% CO₂. For this study the cells were mechanically passaged by dissociation every other day; they underwent fewer than 25 passages.

Toxicity of plant extract (MTT assay)

A 3-(4,5-dimethylthiazol-2-yl)-2,5-diphenyltetrazolium bromide (MTT) assay was undertaken as described previously by Yang et al. (2013). Cells were counted with a haemocytometer, and the number of viable cells was assessed by trypan blue dye exclusion method. The RAW 264.7 macrophages were seeded in 24-well plates for 18 h and then stimulated with various treatments (250, 500, 1000, 1500 µg/mL of HW and 50, 100, 200, 500 µg/mL of 70% EtOH) or LPS (lipopolysaccharide) (1 µg/mL) for 1 h. On the day of collection, cells were incubated with MTT solution for 24 h at 37 °C in a humidified atmosphere of 95% air and 5% CO₂. The MTT-containing supernatant was removed and the formazan crystals were solubilized in dimethylsulfoxide. The absorbance of each well at 540 nm was measured using an automatic microplate reader (PowerWave X340, Bio-tech Instruments, Inc., Winooski, VT, USA).

NO (nitric oxide) concentration as indicator of anti-inflammatory effects

The NO concentration in treatments was determined based on the method of Yang et al. (2013). RAW 264.7 cells (5×10^5 cells/well) were cultured on 24-well dishes with 1 µg/mL of LPS and various treatments (250, 500, 1000, 1500 µg/mL of HW and 50, 100, 200, 500 µg/mL of 70% EtOH). After 18 h, culture supernatants were collected and nitrite, a stable oxidized product of NO, was measured by a modified Griess (1879) method. Equal volumes (100 µL) of the Griess (1879). Reagent [1% sulfanilamide and 0.1% *N*-(1-naphthyl)-ethylenediamine dihydrochloride in 5% phosphoric acid] and *D. divaricate*, *D. prolifera*, *P. cornea*, *G. lanceolata*, or *G. filicina* were incubated together at room temperature for 10 min. The absorbance of each well at 540 nm was measured using an automatic microplate reader (PowerWave X340, Bio-tech Instruments).

Statistical analysis

Differences between multiple groups were evaluated using oneway PROC analysis of variance (ANOVA). When a significant treatment effect was detected, post hoc comparisons of the means were performed using Tukey's honest significant difference test (SAS v. 9.1, SAS Institute Inc., USA). Differences were considered significant if $p < 0.05$.

Results and discussion

Total antioxidant capacity (TAC) and superoxide dismutase activity (SOD)

TAC and SOD were measured using fresh plant leaves instead of extracts (*Table 1*). To see the functions of the plant itself as a medicinal herb not the effects of extracts, TAC and SOD were selected. However, most other TAC studies of leaves of plants, results are re-directed to extracts by calculation, so it is difficult to make a direct comparison because the unit is L (liter). Rarely, among the existing studies using the same method as we did, there are results of *Brassica campestris* ssp. *napus* var. *nippo-oleifera* Makina (oilseed rape) and *Lactuca sativa* L. (lettuce), a leaf-eating crop (Song

et al., 2013). *H. radicata* is expected to have higher efficacy than conventional plants because it shows a high value of three times higher than that of this crop. In addition, the result can have the meaning of the archive showing the antioxidant value of the fresh leaf of *H. radicata*. In the case of SOD, it was possible to make a direct comparison with other papers since it came out as a unit. In the case of overseas studies using the same Dojindo SOD kit for medicinal herbs (Rafat et al., 2010), five herbicides showed an average value of about 60 unit (SOD unit). On the other hand, *H. radicata* has a value of 90 or more. Therefore, the antioxidant effect of *H. radicata* is expected to be high and gave us expectation for noticeable efficacy.

Table 1. Total antioxidant capacity and superoxide dismutase activity of *H. radicata*

Sample	Value
TAC ($\mu\text{M}/\text{mg}$ protein)	389.35 ± 41.34
SOD (U/mg protein)	94.03 ± 2.21

Each value represents mean \pm S. D. (n = 4)

Radical scavenging assay for testing antioxidant effects of extracts

Free radicals are known to cause various diseases by causing oxidative stress in the body. Therefore, DPPH and ABTS radical scavenging activities were measured to confirm the free radical inhibitory activity of HW extract and 70% EtOH extract on the aboveground part of *H. radicata*. As a result, the DPPH radical scavenging activity of EtOH extract ($\text{IC}_{50} = 139.63 \pm 5.30 \mu\text{g}/\text{mL}$) was higher than that of HW extract ($\text{IC}_{50} = 167.91 \pm 3.94 \mu\text{g}/\text{mL}$) (Table 2). In the ABTS radical scavenging activity, HW extract ($\text{IC}_{50} = 58393 \pm 13.31 \mu\text{g}/\text{mL}$) was higher than EtOH extract ($\text{IC}_{50} = 155.94 \pm 35.27 \mu\text{g}/\text{mL}$) (Table 2). When DDPH radical scavenging activity of *H. radicata* was compared with other popular medicinal plants such as *Trigonella foenum-graecum* and *Elettaria cardamomum* (Khalaf et al., 2008). The IC_{50} value of *H. radicata* was lower. Therefore, it can be said that *H. radicata* showed higher efficiency as a natural antioxidant than popular medicinal plants (*T. foenum-graecum* and *E. cardamomum*). This suggests that *H. radicata* may be used as a natural antioxidant material. After conducting this experiment, we've found a new reference that has investigated DPPH and ABTS of *H. radicata* extract (Ko et al., 2017). This paper also showed that *H. radicata* extract has strong antioxidant effects, which is consistent with our results. However, our DPPH value of HW extract is low compared to other paper from a research group who have studied this plant steadily (Senguttuvan et al., 2014) while the local paper (Ko et al., 2017) showed similar value (EtOH) to our results. As Korea and India are very distant counties, ecotypes of *H. radicata* in India could be different. Also as climate condition of Korea is different from India (cold winter in Korea), it would affect the chemical composition of plants.

Anti-inflammatory activity and toxicity of HW and EtOH extracts in RAW 264.7 cells

To determine the toxicity and anti-inflammatory effects of extracts, the most common method is to examine the cell viability by RAW 264.7 cells using NO production and MTT assay. In the HW extract, NO production was significantly increased in LPS only treatment (LPS +, Sample 0 $\mu\text{g}/\text{mL}$) compared to control (LPS -, Sample 0 $\mu\text{g}/\text{mL}$), but HW extracts treated with 500, 1000, and 1500 $\mu\text{g}/\text{mL}$ showed

that NO production decreased by concentration compared to LPS only treatment (Fig. 1). This shows that the higher the concentration, the stronger resistant the inflammation by NO product inhibition. Cell viability was also reduced in all treatments compared to control (LPS -, Sample 0 µg/mL) and all values are lower than the value of LPS only treatment (LPS +, Sample 0 µg/mL), but with the exception of 1500 µg/mL treatment. As the LPS itself is toxic, it is a normal response. However, when the extract is added, the toxicity is alleviated considering low values in most concentration range. In general, when the cell viability is 80% or more, it is considered that there is no problem, so that the overall extract, even including 1500 µg/mL treatment are safe to be considered as none toxic.

Table 2. Antioxidant activities of *H. radicata* extracts

Sample	DPPH radical scavenging activity	ABTS radical scavenging activity
HW	167.91 ± 3.94	187.04 ± 11.54
EtOH	139.63 ± 5.30	203.6 ± 4.68
Ascorbic acid	6.48 ± 0.25	22.34 ± 0.87

Each value represents mean ± S. D. (n = 4). IC50 (IC50 = µg/mL) values were calculated from regression lines using eight different concentrations in triplicate experiments. HW; hot water extracts. EtOH; 70% ethanol extract

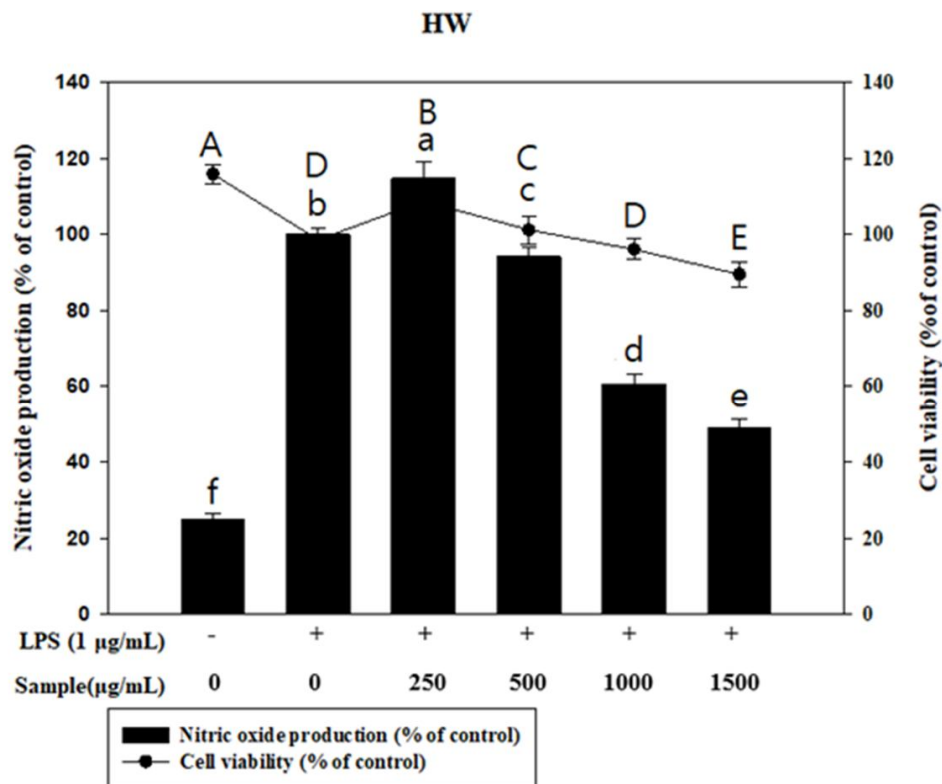


Figure 1. Effect of HW extract on cell viability and nitric oxide production in LPS-stimulated RAW 264.7 cells. Raw 264.7 cell were incubated with 250, 500, 1000 and 1500 µg/mL of HW extract for 1 h, and then incubated with LPS (1 µg/mL) for 24 h. The data expressed as a mean ± SD (n = 4). Symbols or bars having the same letter are not significantly different at the 0.05 level. Uppercase letters show difference between symbols, while lowercase letters show difference between bars

In the 70% EtOH extract, NO production was significantly increased in the LPS only treatment (LPS +, Sample 0 $\mu\text{g/mL}$) compared to the control (LPS -, Sample 0 $\mu\text{g/mL}$). However, EtOH extracts treated with 500, 1000, and 1500 $\mu\text{g/mL}$ showed that NO production decreased (Fig. 2). Therefore, EtOH extract appears to have anti-inflammatory effect like HW treatment and its effects are considered to be stronger than HW extract. The cell viability was significantly higher in the 50 $\mu\text{g/mL}$ to 200 $\mu\text{g/mL}$ treatment groups, and these results are showing alleviated toxicity at this concentration. And the highest concentration (500 $\mu\text{g/mL}$) did not show any significant difference with control. Therefore, this suggests that *H. radicata* extract induces cell proliferation by minimizing the effect of cytotoxicity. As a result, the *H. radicata* extract has not been shown to be toxic to the cell. Rather, in some treatments, it can protect cells by reducing the harmful effects on cells. And the *H. radicata* extract can be regarded as a function of inhibiting the generation of NO in high concentrations of extracts. In other words, *H. radicata* extract has a function of anti-inflammatory effect.

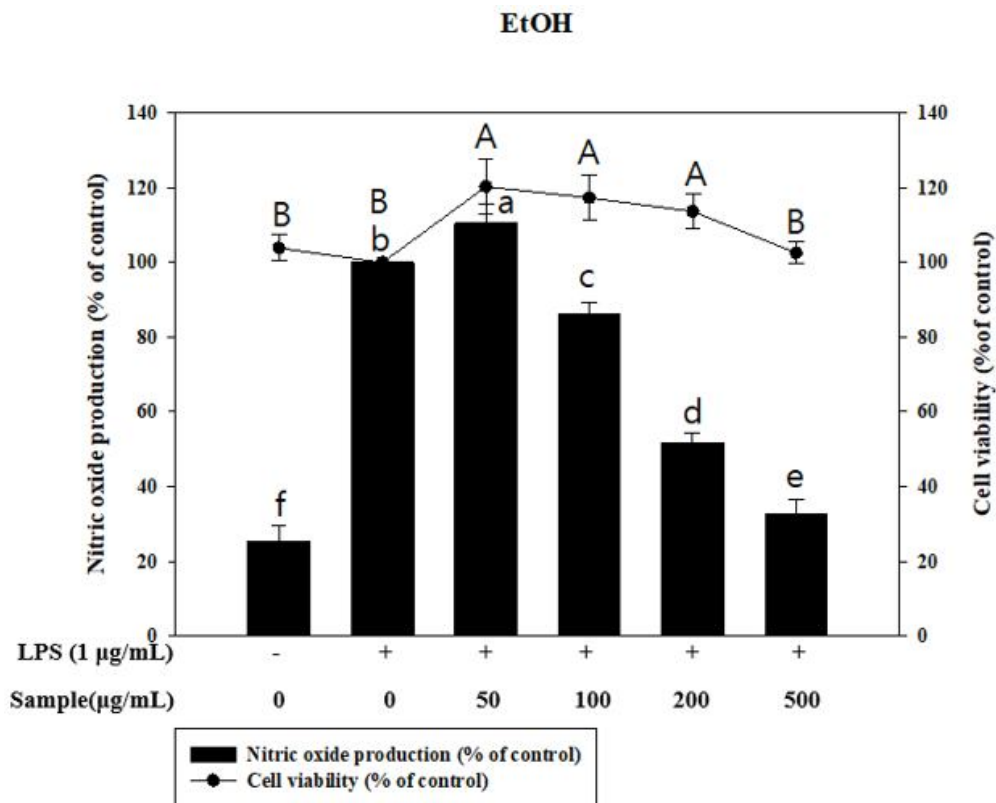


Figure 2. Effect of EtOH extract on cell viability and nitric oxide production in LPS-stimulated RAW 264.7 cells. Raw 264.7 cell were incubated with 50, 100, 200 and 500 $\mu\text{g/mL}$ of EtOH extract for 1 h, and then incubated with LPS (1 $\mu\text{g/mL}$) for 24 h. The data expressed as a mean \pm SD ($n = 4$). Symbols or bars having the same letter are not significantly different at the 0.05 level. Uppercase letters show difference between symbols, while lowercase letters show difference between bars

HPLC

Since the extracts of *H. radicata* have shown some effects, HPLC analysis was expected to detect a certain level of natural products. However, only 1-Trans-Cinnamic

acid was detected in the detection of phenolic compounds using 12 commonly used standards (Fig. 3). This suggests that the substances showing the function of the above results are slightly different from those of other plants, and *H. radicata* extracts are likely to contain new natural products rather than general ones. This shows that it is possible to obtain unusual natural products through a detailed analysis of this species in the future.

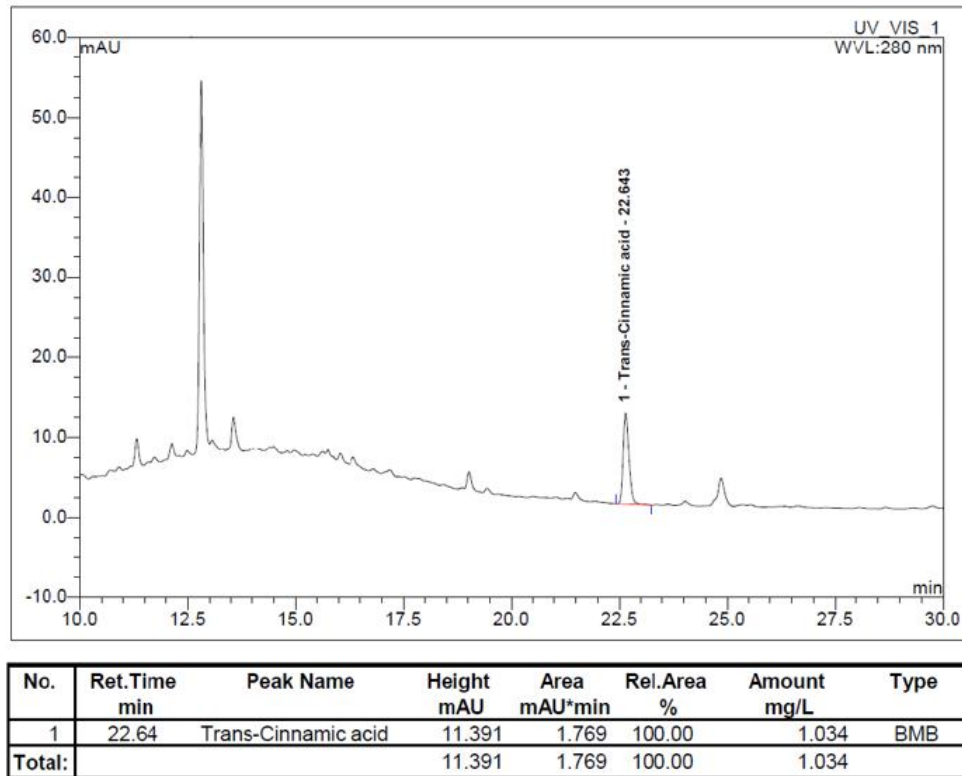


Figure 3. High performance liquid chromatography (HPLC) result of HW extract

Conclusion

H. radicata has been reported as an invasive alien species that has been degrading ecosystem functions as a result of environmental damage, resulting in the extinction of native species and ultimately ecosystem diversity. However, despite the fact that it has been designated as a dangerous species, there is no effective way to prevent it from spreading. In Jeju Island, frequent mowing is used for environmental management of *H. radicata*, but still the species are dominating the island. It implies that we need a better engineering solution of management of *H. radicata*. Therefore, this study aims to contribute to the utilization of invasive alien species and resource management, and to some extent to prevent diffusion, by exploring the possibility of using *H. radicata*, an invasive alien species already introduced in Korea. All results show that *H. radicata* can be used for natural antioxidants and anti-inflammatory effects. Further researches could find correlation between environmental factors (soil, climate, species composition etc.) and medicinal effects of *H. radicata* and molecular reactions such as expression of Nuclear factor-kappa B. When the researches on effect of *H. radicata* are discovered more, the utilization of this species will be increased and the environmentally friendly

public participation management will be possible due to the increase of the collection. As some medicinal or gardening herbs such as *Panax ginseng* (Park and Park, 2007), *Hanabusaya asiatica* (Park et al., 2013), *Saccolabium japonicum* (Jung et al., 2012) are endangered because it is being overharvested (Sangwon and Seonyeong, 2005), same effects can help to reduce *H. radicata* by increased usage. As harvesting wild vegetables are the common act in local (Hwang, 1991), this management mechanism is worthy to study. Therefore, we believed that it can be contributed to the prevention of diffusion of *H. radicata* to some degree when functions of *H. radicata* are discovered and be known to the public. In addition, it is meaningful that we have attempted to find an ecological approach (management through utilization) through utilization methods of alien species that has been spread widely in Korea.

REFERENCES

- [1] Blois, M. S. (1958): Antioxidant determinations by the use of a stable free radical. – *Nature* 181: 1199.
- [2] Bradford, M. M. (1976): A rapid and sensitive method for the quantitation of microgram quantities of protein utilizing the principle of protein-dye binding. – *Analytical Biochemistry* 72: 248-254.
- [3] Grassmann, J., Hippeli, S., Elstner, E. F. (2002): Plant's defence and its benefits for animals and medicine: role of phenolics and terpenoids in avoiding oxygen stress. – *Plant Physiology and Biochemistry* 40: 471-478.
- [4] Griess, P. (1879): Bemerkungen zu der Abhandlung der HH. Weselsky und Benedikt „Ueber einige Azoverbindungen“. – *Berichte der deutschen chemischen Gesellschaft* 12: 426-428.
- [5] Hwang, E. H. (1991): A survey on availability of wild vegetables. – *The Korean Society of Food Science and Nutrition* 20: 440-446.
- [6] Hyun, J. O., Na, H. R., Kim, Y., Han, B. (2018): Floristic study of Aphaedo Island in Shinan-gun, Jeollanam-do, Korea. – *Korean Journal of Plant Taxonomy* 48: 65-99.
- [7] Jaramillo, M. E., Gonz, L., Cornejo, M., Dorantes, L., Gutierrez, G. F., Hernandez, H. (2003): Effect of thermal treatment on the antioxidant activity and content of carotenoids and phenolic compounds of cactus pear cladodes (*Opuntia ficus-indica*). – *Food Science and Technology International* 9: 271-278.
- [8] Jung, J., Lee, H., Jo, Y., Lee, B. (2012): Genetic diversity for restoration of *Dendrobium moniliforme* (L.) Sw. and *Saccolabium japonicum* Makino (Orchidaceae). – *Korean Society of Forest Science* 2012: 1112-1113.
- [9] Khalaf, N. A., Shakya, A. K., Alothman, A., Elagbar, Z., Farah, H. (2008): Antioxidant activity of some common plants. – *Turkish Journal of Biology* 32: 51-55.
- [10] Kim, C., Koh, J., Kang, Y., Moon, M., Lim, E., Kim, H. (2006): Scheme to classify invasive alien plants for natural ecosystem management in Jeju Island. – *Korean Society of Forest Science* 2006: 154-156.
- [11] Ko, H., Eom, T., Song, S., Jo, G., Kim, J. (2017): Tyrosinase and alpha-glucosidase inhibitory activities and antioxidant effects of extracts from different parts of *Hypochaeris radicata*. – *Korean Journal of Medicinal Crop Science* 25(3): 139-145.
- [12] Li, W., Luo, J., Tian, X., Chow, W. S., Sun, Z., Zhang, T., Peng, S., Peng, C. (2015): A new strategy for controlling invasive weeds: selecting valuable native plants to defeat them. – *Scientific Reports* 5: 11004.
- [13] Maema, L. P., Potgieter, M., Mahlo, S. M. (2016): Invasive alien plant species used for the treatment of various diseases in Limpopo Province, South Africa. – *African Journal of Traditional, Complementary and Alternative Medicines* 13: 223-231.

- [14] Park, H., Park, A. (2007): Research on mountain ginseng. – The Korean Society of Ginseng 2007: 311-320.
- [15] Park, S., Kim, H., Chang, J. (2013): Assessing Red List categories to a Korean endangered species based on IUCN criteria. *Hanabusaya asiatica* (Nakai) Nakai. – Korean J. Pl. Taxon. 43: 128-138.
- [16] Peskin, A. V., Winterbourn, C. C. (2000): A microtiter plate assay for superoxide dismutase using a water-soluble tetrazolium salt (WST-1). – *Clinica Chimica Acta* 293: 157-166.
- [17] Rafat, A., Philip, K., Muniandy, S. (2010): Antioxidant potential and phenolic content of ethanolic extract of selected Malaysian plants. – *Research Journal of Biotechnology* 5: 1.
- [18] Ryu, T. B., Kim, M. J., Lee, C. W., Kim, D. K., Choi, D. H., Lee, H., Jeong, H. R., Lee, D. H., Kim, N. Y. (2017): Distribution characteristic of invasive alien plants in Jeju Island. – *Journal of Ecology and Environment* 41: 24.
- [19] Samways, M. J., Caldwell, P., Osborn, R. (1996): Ground-living invertebrate assemblages in native, planted and invasive vegetation in South Africa. – *Agriculture, Ecosystems & Environment* 59: 19-32.
- [20] Sangwon, B., Seonyeong, A. (2005): A study on the evaluation method of endangered animals and plants species in the wild. – *Korea Environment Institute* 2005: 1-350.
- [21] Scalbert, A., Manach, C., Morand, C., Rmsy, C., Jim, L. (2005): Dietary polyphenols and the prevention of diseases. – *Critical Reviews in Food Science and Nutrition* 45: 287-306.
- [22] Senguttuvan, J., Paulsamy, S., Karthika, K. (2014): Phytochemical analysis and evaluation of leaf and root parts of the medicinal herb, *Hypochoeris radicata* L. for in vitro antioxidant activities. – *Asian Pacific Journal of Tropical Biomedicine* 4: S359-S367.
- [23] Song, U., Shin, M., Lee, G., Roh, J., Kim, Y., Lee, E. J. (2013): Functional analysis of TiO₂ nanoparticle toxicity in three plant species. – *Biological Trace Element Research* 155: 93-103.
- [24] Yang, E. J., Ham, Y. M., Lee, W. J., Lee, N. H., Hyun, C. G. (2013): Anti-inflammatory effects of apo-9'-fucoxanthinone from the brown alga, *Sargassum muticum*. – *DARU Journal of Pharmaceutical Sciences* 21: 62.
- [25] Zhu, K. X., Lian, C. X., Guo, X. N., Peng, W., Zhou, H. M. (2011): Antioxidant activities and total phenolic contents of various extracts from defatted wheat germ. – *Food Chemistry* 126: 1122-1126.

DOES LIVELIHOOD VULNERABILITY INDEX JUSTIFY THE SOCIO-ECONOMIC STATUS OF MOUNTAINOUS COMMUNITY? A CASE STUDY OF POST-EARTHQUAKE ECOLOGICAL ADAPTATION OF BALAKOT POPULATION

SHAHZAD, L.^{1,2} – TAHIR, A.¹ – SHARIF, F.² – HAYYAT, M. U.² – GHANI, N.¹ – FARHAN, M.² – DOGAR, S. S.³

¹*Environmental Science Department, Lahore College for Women University, Lahore, Pakistan (e-mail/phone: arifatahir@gmail.com/+92-333-458-9622; nadiaghani2@yahoo.com/+92-315-422-4226)*

²*Sustainable Development Study Center, Government College University, Lahore, Pakistan (e-mail/phone: faizasharif@gcu.edu.pk/+92-331-447-1118; umerenv@yahoo.com/+92-321-403-2300; dr.muhammadfarhan@gcu.edu.pk/+92-321-412-2078)*

³*National Agricultural Research Center (NARC), Islamabad, Pakistan (e-mail/phone: salaar.saeed@gmail.com/+92-324-432-7567)*

**Corresponding author*

e-mail: lailashahzad@gcu.edu.pk; phone: +92-322-787-8517

(Received 1st Feb 2019; accepted 29th Mar 2019)

Abstract. Hindu Kush Himalayan is facing greater threat from socio-economic and climatic transitions. The current study has assessed livelihood vulnerability due to climatic variability of natural resource dependent mountainous communities. The northern side of Pakistan is expected to bear severe impacts due to its distinct topography, land use and climate change. Based on primary data collected from four villages complemented with secondary climatic data, livelihood vulnerability was evaluated through a composite indicator as livelihood vulnerability index (LVI) and LVI-IPCC. GIS mapping was carried out to assess land use change in the area. The comparative analysis of Tehsil Balakot showed that UC Balakot was more vulnerable with a LVI score of 0.41 than UC Kawai 0.35. The results of in-depth analysis of differential vulnerability showed that households in UC Balakot had the low adaptive capacity and higher exposure to natural disasters. Developmental planners and policy makers should use such indices to assess root causes of vulnerability and specify community needs in policy making.

Keywords: *climate change, natural disaster, differential vulnerability, adaptive capacity, land use change*

Introduction

Rural people living on mountains are “vulnerable” to natural calamities and they need to adapt to climatic changes for their survival and better livelihood opportunities (Macchi, 2011; Gentle and Maraseni, 2012). The fifth assessment report of Intergovernmental Panel on Climate Change (IPCC) states that the climate change is one of the biggest challenges of the 21st century that will bring about unexpected extreme events throughout the world ranging from polar regions to the tropics, islands, developed as well as developing countries (Hijioka et al., 2014). The Himalayas are of prime significance for Pakistan and as known to be the water towers. The ongoing climate change is showing negative impacts on the mountainous life by affecting water volumes, biodiversity, increasing natural hazards, ecosystem structure and function (Basharat et al., 2016; Sarwar et al., 2016). Sustainability of life in the mountainous

regions is under extreme pressure due to higher dependence on natural resources and prevailing poverty (de Sherbinin, 2008).

Although, Pakistan has a very little contribution to the global climate change by greenhouse gases emissions but local climate change is becoming visible from the frequency and intensity of natural disasters affecting livelihoods of the rural communities. Pakistan faces a natural disaster almost every year and is now well-thought-out as one of the most vulnerable and highly effected country by changing climate in South Asia (IPCC, 2012; Shah et al., 2017). According to German-watch global climate risk index measured for a period of 1997 to 2016, Pakistan was on number seven among the world's vulnerable countries those faces most economic losses due to climatic changes (Ali and Erenstein, 2016; Abid et al., 2016). Factors that contribute to Pakistan's vulnerability profile are distinct geography, demographic trends, socioeconomic factors, and lack of adaptive capacity along with the perpetuating vicious cycle of poverty (Ainuddin et al., 2013; Elalem et al., 2015). Pakistan is among one of the countries with the least adaptive capacity due to the existence of a high level of poverty and lack of physical as well as financial resources (Chaudhury et al., 2016; Shah et al., 2018). Himalayan part of Pakistan is predominantly facing higher threats from changing climate and specific ecosystems are under significant pressure of loss in its services. In a recent study, people's perception of climate change has reported in terms of reduction in forest ecosystem services. In such marginalized communities, local ecosystems like forest and water provide multiple services, which will either diminished or reduced in quantity or quality (Shahzad et al., 2018). These ecosystems services are lifeline of local communities and in face of changing climate, livelihood and its related opportunities will be threatened (Shahzad et al., 2019).

IPCC defines vulnerability as a term which corresponds more to exposure and sensitivity of a system, place and people, and adaptation based on the wellbeing's resources (IPCC, 2001a, b, 2007). Vulnerability assessment is a study of conditions and process resulting from physical, social, economic and environmental factors that increase the susceptibility of a community to the impacts of hazards (Gerlitz et al., 2016). Different methods and indices have been explained through vulnerability assessment to examine the interactions between social and ecological systems, non-linear feedbacks, spatial and temporal variation, human and their physical, social surroundings. Their application includes the measurement of trends in poverty, human development, food security, vulnerability and bio-diversity (Kotzee and Reyers, 2016). Vulnerability assessments can be conducted according to a range of approaches from descriptive to quantitative (Choe et al., 2017).

Livelihood Vulnerability Index (LVI) is used to analyze the vulnerability of domestic farming to climate change (Hahn et al., 2009). LVI is widely used in different parts of the world by many scientists to understand the specific vulnerability related to water, food, health and others sectors (Alam et al., 2017; Houg et al., 2018; Zhang et al., 2018). LVI is used to assess climate change vulnerability in coastal and inland communities of Mabote and Moma Districts of Mozambique, Africa (Hahn et al., 2009). It is widely used to understand climate based vulnerability of wetland-dependent communities (Shah et al., 2013) and rural riverine households (Alam et al., 2017) of Trinidad and Tobago islands and Bangladesh, respectively. Then LVI was used to indicate vulnerability in flood affected households of Bhagalpur Bihar, India (Madhuri et al., 2014). Gentle et al. (2014) assessed differential impacts of climate change based on distinct well beings of the communities in the Lamjung district of Nepal. The study

coupled LVI with participatory well-beings ranking. In agriculture sector, LVI was used to analyze the impact of climate change on agro-livestock smallholders in Gandaki River Basin of Nepal (Panthi et al., 2015) and Northwest Vietnam (Houng et al., 2018) identified livelihood cycle and vulnerability in the rural riverine households of Bangladesh using LVI. However, most recently Zhang et al. (2018) examined the vulnerability of communities to climatic changes using LVI in the Gannan Plateau, which is one of most environmentally sensitive region of China. Such studies identified the root causes of vulnerability in different communities and helped locals in developing adaptations to identified vulnerable sectors. Gerlitz et al. (2016) used the multidimensional livelihood vulnerability index in the Hindu Kush Himalayan (HKH) region to examine livelihood vulnerability due to socio-economic and climatic changes.

However, there are very few reports available about the rural mountainous communities and no such study was undertaken to calculate the livelihood adaptations by using LVI after earthquake, 2005 in Balakot region. The current study has explored the livelihood vulnerability by accounting household adaptations and climate exposure of rural mountainous communities in Tehsil Balakot, Pakistan by using the Livelihood vulnerability index (LVI). The paper investigates potential factors of vulnerability based on community's exposure, sensitivity and adaptive capacity. It also aimed to assess land use changes in the region and its consequences on the livelihood of the rural people.

Materials and methods

Study area

Tehsil Balakot is a sub division of District Mansehra, Khyber Pukhton khawa (KPK) Province of Pakistan with an expected population of 22894 persons distributed in four main villages in almost 2857 households according to Mansehra District Plan Balakot (UNDP, 2007). It is geographically located at 34°33N and 73°20E and encompasses an area of about 740 km². The mountainous region has an average elevation of 500 to 5000 m asl with dense pine forest and River Kunhar flowing throughout (Somroo et al., 2012). Geologically this area comes under Hazara-Kashmir Syntax (HKS), which is circumscribed by the Main Boundary Thrust (MBT) (Sarwar et al., 2016). On the basis of seismological and structural data of 1904 to 2007, Bagh to Balakot has the most critical fault line of 120 km long (Mona, 2014). This makes the whole region highly susceptible to natural disasters, including earthquakes, landslides and avalanches (Baig, 2006; Kumar et al., 2006). The area was severely affected by the Kashmir Earthquake in 2005 which destroyed about 80 to 90% of the houses and resulted in huge death toll (Halvorson and Hamilton, 2007; Munir and Mirza, 2007). Loss of agricultural land had further enhanced their economic loses (Somroo et al., 2010). Rural people of Balakot are facing livelihood stress due to higher dependence on natural resources of the mountainous region which is already environmentally sensitive (Soomro et al., 2012). The rural community heavily relies on the forest and water resources of the area for subsistence livelihood. As a result, there is a higher threat of ecosystem changes and degradation which will amplify human vulnerabilities (Qasim et al., 2010). Forest cover has reduced due to the requirement of fuelwood and clearing the land to cultivate (UNDP Mansehra District 2007). Most of the people are cultivating seasonal vegetables on steep slopes of mountains. The region is a popular tourist destination of northern Pakistan which has many pros and cons for rural people. This condition has provided a rationale to assess that how the livelihood of the vulnerable rural people of Balakot will

be further influenced by the changing climate. The map of study area is shown in *Figure 1*.

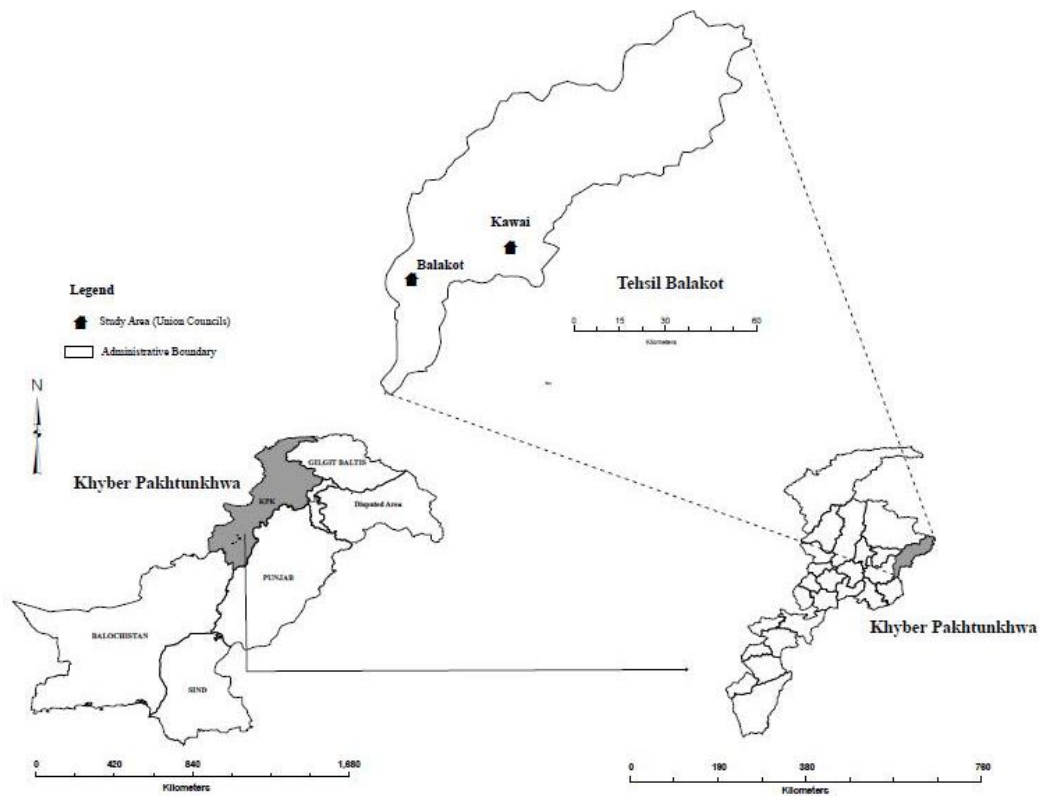


Figure 1. Map of Tehsil Balakot, District Mansehra, KPK Province-Pakistan indicating surveyed Union Council Balakot and Kawai

Study population

For the current study, households were the unit of observation to assess vulnerability based on the climatic and socio-ecological changes. The reason to choose such community is their dependence on the respective area's natural resources; so it becomes easy to assess their resilience or status of vulnerability (Shah et al., 2017). On the basis of these facts, two villages were surveyed from each UC to gather desired data. Taking 95% of confidence level, ± 10 interval, a minimum sample size of 96 households was calculated. Keeping this in consideration, a total of 200 households were surveyed, where hundred 100 were chosen from each of two villages in Tehsil Balakot (Shahzad et al., 2018). The first site is Union council Balakot where most of households are close to river Kunhar and on the foothills. This area has sufficient human settlements living in higher vulnerability due to multi-hazards scenario of flood, earthquake and landslides. Second site Union Council Kawai was on the mid hill slopes near cultivated and forested lands, but far from water body. This area has usual landslides resultantly erosion and weathering are common phenomenon (Ullah et al., 2017).

Methods used

A mixed method approach was used to gather data based on interpretivist pragmatism which merges quantitative methods to qualitative methods dealing with

individuals and their interactions in the society. Two extensive field visits were carried out, first in April 2017 and secondly in October 2017. In primary data collection, qualitative data was gathered through the participant's observations and focus group discussions (FGDs) (N = 10). A field survey to get household level records (n = 200) was also done which provided the quantitative data. Secondary data was taken from the union councils of Balakot and Kawai. Climate data consisting of temperatures and precipitation of Balakot and Kaghan stations was taken for the period of 1988 to 2017, accounting 30 years span. This data was provided by Meteorological Department Pakistan (PMD) and used to measure climatic variability and natural disaster's exposure. Along with LVI, land use maps were generated for the Tehsil to plot the change over the period of 20 years. For mapping land use change, remote sensed data of LANDSAT 5 and LANDSAT 7 were taken with path 150 and row 36. The spatial resolution of images used was 30 m. Images of month of May 1990, 1995, 2010 and 2015 were taken for determining the variability. Images of year 2000 and 2005 were not accessible.

Details of each of method are explained under specific heading:

Participants' observation

In the study, participant's observation as a technique of qualitative research method was used to record the day to day activities and connection within communities (Fine, 2003; Stacy, 2004). This helped the in getting a better picture of community's culture and livelihood setting by observing how the people in the area live their life.

Focus group discussions

After acquiring the brief picture of local community, focus group discussions were carried out with the locals. A total of 10 groups were carried out, 5 in each village which facilitated in mapping the livelihood assets and threats due to changing climatic conditions. Male and female population was requested to be part of the discussions to have a representative approach in the study design.

Household survey

In addition to above methods, 200 households were visited door to door to get livelihood data using a questionnaire.

Livelihood vulnerability index

Two approaches were used to assess livelihood vulnerability: LVI and LVI-IPCC on the gathered data. The livelihood vulnerability index was established on the descriptive information generated by the field survey which was based on set of indicators. These sub components were coupled into eight major components and three factors of vulnerability in both UCs (*Table A1* in the *Appendix*).

Approach I – LVI: The eight major components of vulnerability were inquired using survey questions as livelihood indicators. The eight components calculated at household level were socio-demographic profile (SDP), livelihood strategies (LS), social network (SN), health (H), food (F), water (W), natural disaster (ND) and climatic variability (CV). Each of these major components had different questions; seven indicator questions were placed for LS, six for H, five for F, four for ND, SN, W, SDP and three

questions for CV. Therefore, a total of 37 indicator questions were described in column three of *Table A1*. Each major component of LVI was measured through four steps: (1) Compute the questionnaire data of sub-component and transform into percentage, ratio and index. (2) Unit standardization of each sub-component (Sullivan et al., 2002) (3) Calculate the average of each standardized score to get the final value for each main component. (4) Weighed the averages of all major components to obtain the LVI value. This procedure confirms the equal contribution of main components to generate the overall LVI. The scale of LVI calculated from this approach ranges from 0 (minimum) to 0.5 (maximum) as described by Hahn et al. (2009).

The formula is shown as *Equation 1*:

$$Index_s = \frac{S_s - s_{min}}{s_{max} - s_{min}} \quad (Eq.1)$$

where s_s = original sub-component for each of the site,
 s_{min} = minimum value for each sub-component,
 s_{max} = maximum value for each sub-component.

After obtaining values of sub-components, average of each sub-component was calculated using *Equation 2*:

$$M_s = \frac{\sum_{i=1}^n index\ s_{s_i}}{n} \quad (Eq.2)$$

where M_s = one of the eight major components for study site,
 $index\ s_{s_i}$ = subcomponent, n = number of subcomponents in each major component.

The above values were calculated for each of the eight components and LVI was calculated using the formula mentioned as *Equation 3* and elaborated in *Equation 4*:

$$LVI_s = \frac{\sum_{i=1}^8 W_{M_i} M_s}{\sum_{i=1}^8 W_{M_i}} \quad (Eq.3)$$

Equation 3 can also be elaborated as:

$$LVI_s = \frac{W_{SDP} SDP_s + W_{LS} LS_s + W_{SN} SN_s + W_H H_s + W_F F_s + W_W W_s + W_{CV} W_s + W_{ND} W_s}{W_{SDP} + W_{LS} + W_{SN} + W_H + W_F + W_W + W_{CV} + W_{ND}} \quad (Eq.4)$$

where SDP represents socio-demographic profile for each UC, LS is livelihood strategies, SN is social networking, H is for health, W for water, CV is climatic variability and ND is natural disasters.

Approach II – LVI-IPCC: Livelihood vulnerability based on the IPCC definition was also quantified which is the measurement of exposure, sensitivity and adaptive capacity (represented in *Equation 5*). According to the framework, exposure represented by “e” is ranking of exposure to any natural hazards/disaster which rural community has faced in last 5 years. Whereas “s” is for sensitivity and “a” is for adaptive capacity measured for household. Adaptive capacity is based on the scores of socio-demographic, livelihood strategies and social networks. Exposure is grouped in natural disasters and climatic variability. However Sensitivity is calculated by taking the scores of health, food and water. The LVI-IPCC scale ranges from -1 (minimum) to +1 (maximum).

$$LVI - IPCC_s = (e_s + a_s) \times s_s \quad (\text{Eq.5})$$

Land-use change mapping

To obtain information of land use changes in Tehsil Balakot, remote sensing data was interpreted to produce maps of these years; 1990, 1995, 2010 and 2015. Landsat 7 Enhanced thematic Mapper Plus (ETM+) and Landsat 5 Thematic Mapper (TM) were used from United State Geological Survey (USGS). The interpretation was done using Erdas imagine software through supervised maximum likelihood classification, also used Google Earth Engine and ArcGIS for further processing on classified rasters. Final output maps were designed by using ArcGIS 10.5. Six major classes of land use were described and shown in *Table 4*. Changes in time periods were calculated for each land use class between a final year V2 and an initial year, V1 as shown in *Equation 6*.

$$\text{Percentage Change} = (V_1 - V_2/V_1) \times 100 \quad (\text{Eq.6})$$

Results

Livelihood vulnerability index in Tehsil Balakot

Household level of vulnerability was calculated at both study sites (*Table A1; Fig. 2*). It was found that both areas were vulnerable to the changing climate, however; LVI values were higher for UC Balakot (0.43) than UC Kawai (0.33). This indicated that riverbank communities were more vulnerable than people living on slopes. The major differences in the sub-component scores were of natural disasters accounting 0.52 for Kawai and 0.78 for Balakot. Balakot community was exposed to higher hazards due to floods and landslides. Climatic variability was similar in both study areas due to having similar meteorological data of Tehsil Balakot. However, health status of the respondents was not much different in both UCs having a major component score of 0.45 (Balakot) and 0.46 (Kawai). Both areas had no household gas supply for cooking, therefore using woods, leaf litter and other biomass fuels to cook and heat the homes. In terms of food availability, households had less storage of seed in Balakot (0.07) which is an adaptation in time of crises. Many households had no crop diversity; they were sowing same crops over time which indicates lower adaptations in changing time. The maximum score of food was shown in Kawai (0.34) relative to Balakot (0.24). Most of the households had higher dependency on natural water sources in Kawai (0.66) rather than Balakot (0.42). In assessing the status of water accessibility in households, Balakot had higher LVI value (0.49) as compared to Kawai (0.45). Socio-demographically Balakot had shown poor statistics with an index value of 0.4 as compared to Kawai (0.28). In UC Balakot, villages are highly vulnerable, due to low income and education having an average score of LVI 0.41.

After calculating and summarizing LVI for both union councils, a spider diagram (*Fig. 2a*) was developed to indicate value of major components and resulting vulnerabilities. In both study areas, exposure to natural disasters had comparatively higher score than other components.

Calculating LVI-IPCC

The three major components of vulnerability were calculated from eight major components. Adaptive capacity index consist of socio demographic profile, livelihood

strategies and social networks in a community. Sensitivity index is composed of health, food and water related issues. In exposure index only natural disasters and climatic variability is considered. For LVI-IPCC approach, +1 indicates most vulnerable and -1 is for least vulnerable. The contributing factor value for IPCC-LVI approach is 0 for low contributing factor value and 0.6 for high contributing factor value. Results of LVI-IPCC have suggested that the community of Tehsil Balakot has higher exposure level. UC Kawai has comparatively low exposure to natural hazards and climatic variability than UC Balakot. Overall both communities had shown very low adaptive capacity, therefore highly vulnerable to environmental and social changes in the study area. There are three categories to recognize the vulnerability status as shown in *Table 1*.

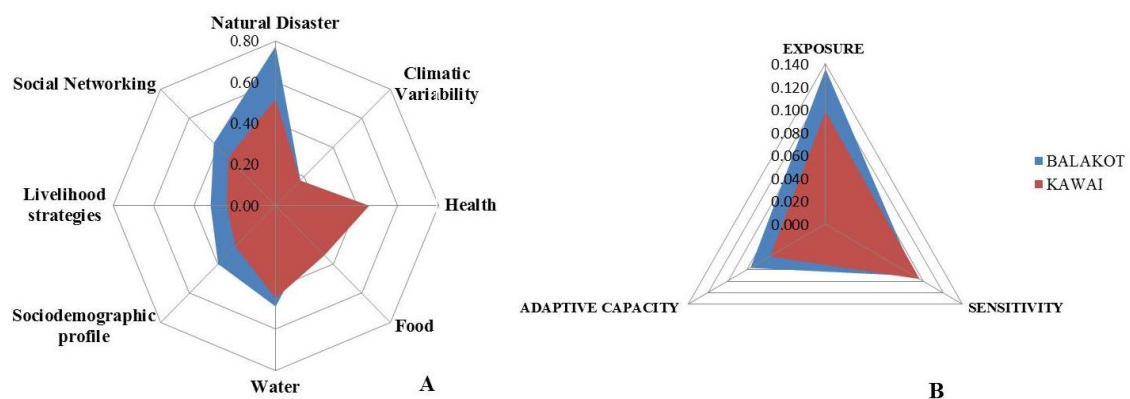


Figure 2. a Spider diagram indicating major component scores of LVI. b Vulnerability triangular sketch showing scores of LVI-IPCC in Tehsil Balakot

Table 1. Status of vulnerability based on IPCC-LVI (a = adaptive capacity; e = exposure and s = sensitivity)

LVI-IPCC categories	UC Balakot	UC Kawai
Adaptive Capacity > (Exposure + Sensitivity) = <i>Less Vulnerable</i>	$a < (e + s)$	$a < (e + s)$
Adaptive Capacity = (Exposure + Sensitivity) = <i>Moderately Vulnerable</i>	$0.077 < (0.091 + 0.136)$	$0.057 < (0.096 + 0.099)$
Adaptive Capacity < (Exposure + Sensitivity) = <i>Highly Vulnerable</i>	$0.077 < 0.227$	$0.057 < 0.195$

Vulnerability triangular diagram was developed from the scores of LVI-IPCC (*Fig. 2b*). It ranges from 0 to 0.14 which showed that UC Kawai was more sensitive to climatic and livelihood changes with less adaptive capacities however UC Balakot has higher level of exposure. An in-depth analysis showed Balakot has geographically more prone to natural disasters and as a result community has learnt some adaptations due to facing losses. An overall impact analysis indicated (*Table 2*) that low adaptive capacity was due to poor social status coupled with low social support. Sensitivity was influenced by the primary factors of water and health related issues whereas exposure was significantly due to presence of nature hazards already established in study area.

Table 2. LVI and LVI-IPCC based on contributing factors and vulnerability scores for Tehsil Balakot

Contributing factors	Major components	No. of sub components	Balakot		Kawai	
			Major components values	Contributing factor values	Major components values	Contributing factor values
Adaptive capacity	Social demographic	4	0.40	0.077	0.28	0.057
	Livelihood strategies	7	0.32		0.24	
	Social networks	4	0.43		0.33	
Sensitivity	Health issues	6	0.45	0.091	0.46	0.096
	Food related	5	0.24		0.34	
	Water issues	4	0.49		0.45	
Exposure	Natural disasters	4	0.78	0.136	0.52	0.099
	Climatic variability	3	0.172		0.172	
LVI (0 minimum to 0.5 maximum)			0.41		0.35	
LVI-IPCC (-1 minimum to +1 maximum)			0.0054		0.0040	

Mapping land use change and its effect on livelihood

Tehsil Balakot has been affected by changing in its land use scenarios which was shared by most of the households during in-depth interview. Many were of view that availability of fresh and clean water has reduced along with reduced forest cover. Results revealed (*Table 3; Fig. 3*) that there was significantly increase in the settlements in year 2015 than 1990. A drop in population from 1995 to 2010 was due to a higher death toll in earthquake of 2005. It was documented that 90% households suffered two or more than two deaths in this disaster (Qasim et al., 2010). Forest cover was significantly reduced from 1990s to 1995 and 2010. An increase in forest cover in 2015 was due to a provincial program namely Billion Tree Tsunami Project (BTTP) which was an afforestation effort in line with international Bonn Challenge (WWF, 2017.). Pakistan promised to restore six million hectares of degraded forest land by year 2020 according to this commitment. Another greater change reported by locals in their FGD was conversion of forest land into cultivation. Vegetation in the map and tabular data represents all type of cultivation carried out in the study area. Tehsil Balakot has higher production of maize and wheat, rice production comes in third place with many seasonal vegetables. Agriculture has been a substantial livelihood strategy in this region. It can be seen from the land use mapping that agriculture has got momentous increase which will affect climate and livelihood in positive and negative too. Barren land in the region has increased also which was majorly due to drying of river body. On the hand, ice and snow has reduced too which was supported by aged people during FGD that glacier' melting is amplified in the region coupled with flooding and resulting landslides. Water bodies including rivers, springs and lakes have significantly reduced in its volume affecting agriculture, fishing, livestock rearing and related livelihood activities.

Discussion

The outcome of the study in Tehsil Balakot revealed that all four villages in both UCs were highly vulnerable based on LVI and LVI-IPCC approaches. In the first glance, the study suggests that there was a less difference in the vulnerability scenario of two areas. However a closer look reveals that there were much more differences.

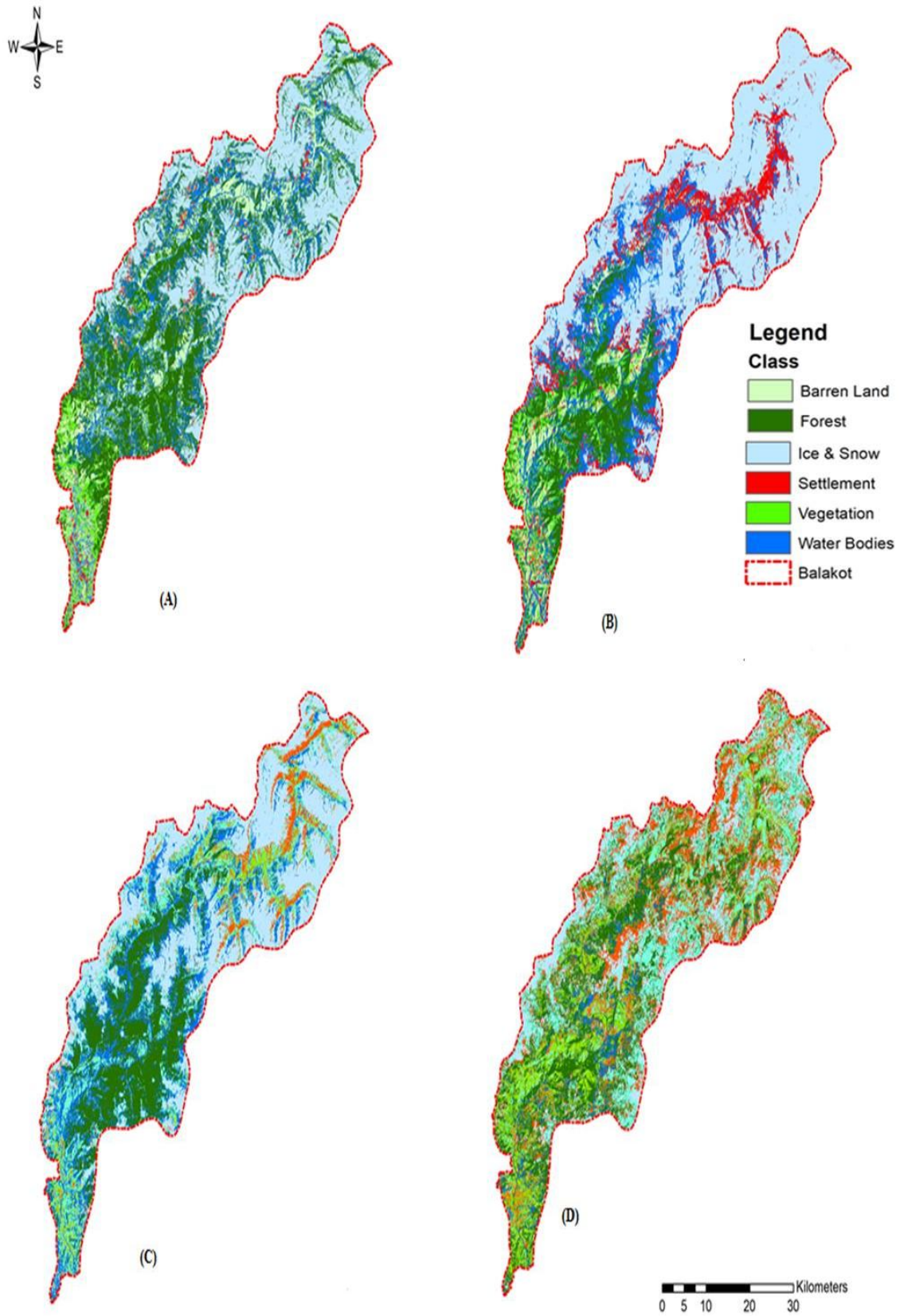


Figure 3. Land use changes reported in Tehsil Balakot for the period of 1990 (a), 1995 (b), 2010 (c) and 2015 (d)

Table 3. Land- use classes in Tehsil Balakot and change in land use reported from 1990 to 2015

Land use classes	Description in the study area	Land use (% response)				Percentage change			
		1990	1995	2010	2015	1990-1995	1995-2010	2010-2015	Overall 1990-2015
Forest	All type of forests where trees growing in patches and canopies	30.05	12.56	19.24	24.67	-58.81	+53.34	+28.08	-17.90
Settlement	Continuous and discontinuous buildings where people living	1.64	10.45	5.67	18.26	+537.19	- 45.74	+ 222.04	+1013.41
Vegetation (agriculture)	Regularly ploughed land for irrigated crops or growing rain-fed crops	4.54	5.75	6.08	18.26	+26.65	+5.73	+200.32	+302.20
Barren land	Land with eroded soil and top surface soil with no vegetation and no settlements	14.98	5.71	16.3	21.07	-61.88	+185.46	+29.26	+40.65
Ice & snow	Area covered with ice and snow continuously or for a part of time in a year	31.82	46.55	32.54	16.91	+46.29	- 30.09	- 48.03	- 46.85
Water bodies	Water courses like rivers and streams, lakes and ponds	16.97	19.15	20.19	5.09	+12.84	+5.43	-74.78	-70.05

+ indicates increase in certain activity whereas a minus (-) indicates decrease

Livelihood vulnerability status in Tehsil Balakot

The overall analysis has shown that UC Balakot had higher dependence ratio per household with more female headed households than UC Kawai which make their low socio-demographic profile. In addition to this, UC Balakot has low education and less income in most of the households. Most households had shown less or no livelihood diversification that showed their dependence on single source of income which was on-farm activities in most villages. Poverty and vulnerability are thoroughly linked; poor households are characterized as more vulnerable (Isabel and Buchenrieder, 2010). Many studies have reported similar findings (Adu et al., 2018; Sujakhu et al., 2018; Huong et al., 2018) where poverty is leading to vulnerability in most parts of the world. In addition, literature has strongly supported the idea of livelihood diversification leads to community resilience (Rahut et al., 2014; Gautam and Andersen, 2016). Most of the households involved in farming had less or no crop diversification as an adaptation technique. UC Balakot had many households involved in nature-based tourism; ranging from running huts for tourists to selling day to day items. This area is a popular tourist destination which has resulted in unstable construction of motels and huts on the riverbank as well as hill slopes. Social networking is taken as an adaptation strategy in rural livelihood (Sujakhu et al., 2018) as it enhanced community linkages and a support system. The livelihood was under stress due to low adaptive capacity which has indicated the people had low socio-demographic profiles with poor social networking. In addition to this, people had less livelihood adaptations in both areas. Similar finding were reported by an earlier study done by Gerlitz et al. (2016) in Hindu Kush Himalayan (HKH) where the community was identified more vulnerable due to low adaptive capacity and higher exposure to climatic and socio-economic factors. Surveys in this mountainous region has shown that the majority of households observed changes in their environment, precipitation and monthly temperatures; further it was reported that these changes will be adverse in next few years (Colom and Pradhan, 2013; Zaheer and Colom, 2013; Gambhir and Kumar, 2013; Tse-ring et al., 2010). In a similar study

conducted by Wang et al. (2016) uneven seasonal precipitation distribution was also reported in this region which wills undesirably effects the agriculture and livestock production. Literature reported less rainfall and extreme weather array in this region of Hindukush Himalayan which has provided environmental and socio-economic shocks to the livelihood of marginalized communities (Akhtar et al., 2008; Gerlitz et al., 2015; Alam, 2017). Reduction in water springs and change in water quality was reported by the people during their focus group discussion. This was severely affecting agriculture productivity as well as food security of rural farmers.

However the regional Himalayan are experiencing similar conditions but different sensitivities also due to different types of income, education household characteristics, and way of livelihood diversification. For instance, in Gannan Plateau, located in the east of the Qinghai-Tibet Plateau, which is highly environmental sensitive region of china showed higher exposure scenarios than sensitivity (Zhang et al., 2018). In another in-depth study, comparative analysis among, India, Nepal and Pakistan; multidimensional vulnerability index showed higher exposure to changing environmental and socio-economic status. Access to basic faculties was highlighted as an additional burden on population of this region (Gerlitz et al., 2016). In riverbank erosion-affected riparian regions of Bnagladesh (Chauhali and Nagarpur), LVI accounted food, water and health issues causing higher vulnerability. Poverty is reasoned as main source of higher exposure to extreme conditions (Alam et al., 2017). However In Ghana Africa, it was reported that livelihood based on climate regulated water resources was highly vulnerable due to low adaptive capacity then exposure and sensitivities. Most municipalities in the Brong-Ahafo region were involved in maize farming and it was indicated that change in water availability was considered as main livelihood threat (Adu et al., 2018). In another study conducted by Jianchu et al. (2007) in context of melting Himalayan showed that mountain people have lived with extreme conditions but more effecting is the pace and magnitude of changing climate. And other contribution in higher community's vulnerability is lack of scientific investigation. Therefore more and more scientific studies coupled with indigenou knowledge are needed to make poor locals of Himalayan more resilient.

Land use changes and livelihood analysis

Field survey with local people and remote sensed data has established the fact that land use change has influenced the socio-economic and livelihood conditions in the region. The data of last five years has seen vivacious effects on forest, agriculture and water resources. In HKH region the environmental changes were reported earlier in 1970s; which included higher deforestation, burgeoning population growth, glacier melting, soil erosion and low lying flooding (Sterling, 1976; World Bank, 1979; Karan and Iijima, 1985; Schickhoff, 1995). Hence with poor evidences and empirical studies, an in-depth livelihood analysis was not possible. The current study therefore provided ground data to support the limited works. The land use change data has long-established fact that agriculture and water bodies were significantly reduced whereas settlements due to growing population had amplified (Khurshid et al., 2016). Higher population will subsequently put higher pressure on natural resources which in turn elevates poverty. This vicious cycle was reported already in Bangladesh, India, Nepal and other neighboring countries (Gentle et al., 2014; Aryal et al., 2016). In the study area, settlements have increased 10-folds since 1990; after 2010 a rapid increase in population was seen which was may be due to higher tourism demand linked to this

area. Better road infrastructure was one of facilitation which has developed access to off-routes. Many people travel to this part of country around the year, which has resulted in environmental degradation. Water resources of HKH are critical for Pakistan as an agricultural economy, the water bodies are reduced and snow and ice are melting; this will have cascading effects. HKH are known as water towers for Pakistan and drying water bodies will threaten country's socioeconomic growth as well. Further, increase in global warming and climate change will likely effect the hydrological cycle.

Agriculture productivity and livelihood of rural mountainous communities heavily depend upon water availability (Sullivan, 2002; Khattak et al., 2011; Yang and Yang, 2014; Aryal et al., 2018). In current scenario, local people are converting more and more forest land into cultivation but in near future with less water available, food insecurity will result. The drying water bodies were extending barren lands in the region (Jainachu et al., 2007; Mahmood et al., 2016). Reduction in forest size and cover was already described by the locals for higher need of fuel wood (Khan, 1970; Gentle and Maraseni, 2012; Aryal et al., 2017). These forests are lifeline to rural community; rapid deforestation will expose local people to more natural hazards and warming also. Many plants and animal species have already moved from these temperate zones as reported by local people during the field surveys. Tehsil Balakot is a famous tourism area in northern Pakistan; which will be severely affected due to loss of forest and water bodies. These land use changes in the HKH region will have long term effects on the livelihood of rural people.

In terms of changes mapped over Himalayan region, many similar studies showed change in land use and related phenomenon. Sharma et al. (2007) carried out land use change mapping in western Himalayan, State of Himachal Pradesh, India indicating two-folded increase in population growth and reduced forest cover. Another change was in form of introduction of profitable crops other than wheat and maize in the region. In a recent study in Garhwal Himalayan region (Batar et al., 2017), vulnerability to life of locals due to higher deforestation and forest fragmentation was reported. The major land-use change was accounted to fuel-wood consumption and other anthropogenic activities. The study has described fast decline in the forest cover which will be higher threat to locals in form of natural hazards. However a study conducted in Himalayan region of Nepal showed transitions in land use change from forest to agriculture and shrubs and agriculture to forested land (Chapagain et al., 2018). It was also reported that beginning of community forest was considered a main driver behind the increase in forest cover in the region, followed by shortage of labor and development of infrastructure. Another study in the landscape of Abaya-Chamo Basin (ACB), southern Ethiopia, the main changes observed were rapid reduction in shrubland and grassland (33.13%), and massive increase in arable land (Yohannes et al., 2018). Rapid population growth was also seen in the region resulting in higher pressure on natural resources.

Overall the higher vulnerability in the different parts of world was due to risk factors related to poverty, poor basic life facilities and low adaptive capacity. Most of the populations had been exposed to climate related threats and thus have vulnerable livelihoods. On the other hand, land use change poses additional burden in all regions of world because of growing population, reduced forest cover and increased arable land (Gentle et al., 2014; Gerlitz et al., 2016; Yohannes et al., 2018; Adu et al., 2018).

Conclusion

People in Tehsil Balakot are vulnerable due to their poor social and environmental conditions. The current study highlighted vulnerability at a household level using acknowledged method. Surveys in this region showed that the majority of households had already observed the change in environment and climatic conditions. Local people had higher exposure to changes but low adaptive capacity to cope it. This condition has made them highly susceptible to bear lose. Land use analysis has also indicated alteration in agriculture and water availability which will negatively affect the rural livelihood. There are few empirical studies using indices to identify root causes of vulnerability across different sectors. The study offers an assessment approach which can be replicated for regional and national level studies to know the causes of susceptibility to natural disasters. Realistic studies are needed to highlight exposure, sensitive and adaptive capacity of rural people to enhance their resilience and adaptations to change. This can help decision makers and planners to address the challenge which is biggest in 21st century.

REFERENCES

- [1] Abid, M., Schilling, J., Scheffran, J., Zulfiqar, F. (2016): Climate change vulnerability, adaptation and risk perceptions at farm level in Punjab, Pakistan. – *Science of the Total Environment* 547: 447-460.
- [2] Adu, D. T., Kuwomu, J. K. M., Somuah, H. A., Sasaki, N. (2018): Application of livelihood vulnerability index in assessing smallholder maize farming households' vulnerability to climate change in Brong-Ahafo region of Ghana. – *Kasetsart Journal of Social Sciences* 39: 22-32.
- [3] Ainuddin, S., Aldrich, D. P., Routray, J. K., Ainuddin, S., Achkazai, A. (2013): The need for local involvement: decentralization of disaster management institutions in Baluchistan, Pakistan. – *International Journal of Disaster Risk Reduction* 6: 50-58.
- [4] Akhtar, M., Ahmad, N., Booij, M. J. (2008): The impact of climate change on the water resources of Hindukush–Karakorum–Himalaya region under different glacier coverage scenarios. – *Journal of Hydrology* 355: 148-163.
- [5] Alam, G. M. M. (2017): Livelihood cycle and vulnerability of rural households to climate change and hazards in Bangladesh. – *Environmental Management* 59: 777-791.
- [6] Ali, A., Erenstein, O. (2016): Assessing farmer use of climate change adaptation practices and impacts on food security and poverty in Pakistan. – *Climate Risk Management* 16: 183-194.
- [7] Aryal, S., Cockfield, G., Maraseni, T. N. (2016): Perceived changes in climatic variables and impacts on the transhumance system in the Himalayas. – *Climate and Development* 8(5): 1-12.
- [8] Aryal, S., Cockfield, G., Maraseni, T. N. (2017): Globalisation and traditional social-ecological systems: understanding impacts of tourism and labour migration to the transhumance systems in the Himalayas. – *Environmental Development*. <http://dx.doi.org/10.1016>.
- [9] Aryal, S., Panthi, J., Dhakal, Y. R., Gaire, N. P., Karki, K., Joshi, N. R. (2018): Historically evolved practices of the Himalayan transhumant pastoralists and their implications for climate change adaptation. – *International Journal of Global Warming* 14(3): 356-371.
- [10] Baig, M. S. (2006): Active Faulting and Earthquake Deformation in Hazara–Kashmir Syntaxis, Azad Kashmir, Northwest Himalaya. – In: Kausar, A. B., Karim, T., Kham, T. (eds.) *International Conference on 8 October 2005 Earthquake in Pakistan: Its*

- Implications and Hazard Mitigation. January 18-19, 2006, Islamabad, Pakistan, Extended Abstract, pp. 27-28.
- [11] Basharat, M., Shah, H. R., Arab, N. H. (2016): Landslide susceptibility mapping using GIS and weighted overlay method: a case study from NW Himalayas. – *Pakistan Journal of Geosciences* 9: 292.
- [12] Batar, A. K., Watanabe, T. Kumar, A. (2017): Assessment of land-use/land-cover change and forest fragmentation in the Garhwal Himalayan region of India. – *Environments* 4(34). <http://doi:10.3390/environments4020034>.
- [13] Chaudhury, A. S., Ventresca, M. J., Thornton, T. F., Helfgott, A., Sova, C., Baral, P., Ligthart, J. (2016): Emerging meta-organisations and adaptation to global climate change: Evidence from implementing adaptation in Nepal, Pakistan and Ghana. – *Global Environmental Change* 38: 243-257.
- [14] Chapagain, P. S., Rai, M. K., Paudel, B. (2018): Land use land cover change and its pathways in Sidin VDC, Panchthar district, Nepal. – *The Geographical Journal of Nepal* 11: 77-94.
- [15] Choe, H., Thorne, J. H., Hijmans, R., Kim, J., Kwon, H., Seo, C. (2017): Meta-corridor solutions for climate-vulnerable plant species groups in South Korea. – *Journal of Applied Ecology* 54(6): 1742-1754.
- [16] Colom, A., Pradhan, S. (2013): Nepal - How the people of Nepal live with Climate Change and What Communication Can Do. – BBC Media Action, London, UK.
- [17] de Sherbinin, A., VanWey, L. K., McSweeney, K., Aggarwal, R., Barbieri, A., Henry, S., Hunter, L. M., Twine, W., Walker, R. (2008): Rural household demographics, livelihoods and the environment. – *Global Environmental Change* 18(1): 38-53.
- [18] Elalem, S., Pal, I. (2015): Mapping the vulnerability hotspots over Hindu-Kush Himalaya region to flooding disasters. – *Weather and Climate Extremes* 8: 46-58.
- [19] Fine, G. A. (2003): Towards a peopled ethnography developing theory from group life. – *Ethnography* 4(1): 41-60.
- [20] Gambhir, V., Kumar, P. (2013): India - How The People of India Live with Climate Change and What Communication Can Do. – BBC Media Action, London, UK.
- [21] Gautam, Y., Andersen, P. (2016): Rural livelihood diversification and household well-being: Insights from Humla, Nepal. – *Journal of Rural Studies* 44: 239-249.
- [22] Gentle, P., Maraseni, T. N. (2012): Climate change, poverty and livelihoods: adaptation practices by rural mountain communities in Nepal. – *Environmental Science and Policy* 21: 24-34.
- [23] Gentle, P., Thwaites, R., Race, D., Alexander, K. (2014): Differential impacts of climate change on communities in the middle hills region of Nepal. – *Natural Hazards*. <http://doi.10.1007/s11069-014-1218-0>.
- [24] Gerlitz, J. Y., Banerjee, S., Brooks, N., Hunzai, K., Macchi, M. (2015): Vulnerability and Adaptive Capacity Assessment: An Approach to Measure Vulnerability and Adaptation to Climate Change. – In: Leal Filho, W. (ed.) *Handbook of Climate Change Adaptation*. Springer, Berlin/Heidelberg, pp. 151-176.
- [25] Gerlitz, J. Y., Macchi, M., Brooks, N., Pandey, R., Banerjee, S., Jha, S. K. (2016): The multidimensional livelihood vulnerability index - an instrument to measure livelihood vulnerability to change in the Hindu Kush Himalayas. – *Climate and Development* 9(2): 124-140.
- [26] Hahn, M. B., Riederer, A. M., Foster, S. O. (2009): the livelihood vulnerability index: a pragmatic approach to assessing risks from climate variability and change - a case study in Mozambique. – *Global Environmental Change* 19(1): 74-88.
- [27] Halvorson, S. J., Hamilton, J. P. (2007): Vulnerability and the erosion of seismic culture in mountainous Central Asia. – *Mountain Research and Development* 27(4): 322-330.
- [28] Hijioka, Y., Lin, E., Pereira, J. J., Corlett, R. T., Cui, X., Insarov, G. E., Lasco, R. D., Lindgren, E., Surjan, A. (2014): Asia. – In: *Climate Change 2014: Impacts, Adaptation, and Vulnerability. Part B: Regional Aspects. Contribution of Working Group II to the*

- Fifth Assessment Report of the Intergovernmental Panel on Climate Change. Cambridge University Press, Cambridge, UK and New York, pp. 1327-1370.
- [29] Huong, N. T. L., Shunbo, Y., Shah, F. (2018): Assessing household livelihood vulnerability to climate change: the case of Northwest Vietnam. – *Human and Ecological Risk Assessment: An International Journal*. <https://doi.org/10.1080/10807039.2018.1460801>.
- [30] IPCC (2001a): *Climate Change 2001. The Scientific Basis*. Intergovernmental Panel on Climate Change. – Cambridge University Press, Cambridge, UK.
- [31] IPCC (2001b): *Climate change 2001. Impacts, Adaptation and Vulnerability*. Intergovernmental Panel on Climate Change. – Cambridge University Press, Cambridge, UK.
- [32] IPCC (2007): *Climate Change 2007. The Physical Science Basis*. Contribution of Working Group I to the Fourth Assessment Report of the Intergovernmental Panel on Climate Change. – Cambridge University Press, Cambridge, UK.
- [33] IPCC (2012): *Managing the Risks of Extreme Events and Disasters to Advance Climate Change Adaptation. A Special Report of Working Groups I and II of the Intergovernmental Panel on Climate Change*. – Cambridge University Press, Cambridge, UK, and New York.
- [34] Isabel, F., Buchenrieder, G. (2010): Risk management of vulnerable rural households in southeast Asia. – 9th European IFSA Symposium, 4-7 July 2010, Vienna (Austria).
- [35] Jianchu, X., Shrestha, A., Vaidya, R., Eriksson, M. Hewitt, K. (2007): *The Melting Himalayas. Regional Challenges and Local Impacts of Climate Change on Mountain Ecosystems and Livelihoods*. – Technical Paper. International Centre for International Mountain Development (ICIMOD) Kathmandu, Nepal.
- [36] Kamwi, J. M., Chirwa, P. W. C., Manda, S. O. M., Graz, P. F. (2015): Livelihoods, land use and land cover change in the Zambezi Region, Namibia. – *Population and Environment* 37(2): 207-230.
- [37] Karan, P. P., Lijima, S. (1985): Environmental stress in the Himalaya. – *Geographical Review* 75: 71-92.
- [38] Khan, M. A. (1970): *Working Plan of the Upper Kaghan Guzara Forests 1967-68 to 1976-77*. – Govt. of West Pakistan, Peshawar.
- [39] Khattak, M. S., Babel, M. S., Sharif, M. (2011): Hydro-meteorological trends in the upper Indus river basin in Pakistan. – *Climate Research* 46: 103-119.
- [40] Khurshid, M., Nafees, M., Rahim, I., Rashid, W. (2016): Impacts of agriculture land use changes on mobile pastoral system in Naran valley of Western Himalayan Northern Pakistan. – *Sarhad Journal of Agriculture* 32(4): 282-288.
- [41] Kotzee, I., Reyers, B. (2016): Piloting a social-ecological index for measuring flood resilience: a composite index approach. – *Ecological Indicators* 60: 45-53.
- [42] Kumar, K. V., Martha, T. R., Roy, P. S. (2006): Mapping damage in the Jammu and Kashmir caused by the 8 October 2005 Mw 7.3 earthquake from the Cartosat-1 and Resourcesat-1 imagery. – *International Journal of Remote Sensing* 27: 4449-4459.
- [43] Macchi, M. (2011): *Framework for Climate-based Climate Vulnerability and Capacity Assessment in Mountain Areas*. – International Centre for Integrated Mountain Development (ICIMOD), Kathmandu, Nepal.
- [44] Madhuri, M., Tewari, H. R., Bhowmick, P. K. (2014): Livelihood vulnerability index analysis: An approach to study vulnerability in the context of Bihar. – *Jamba Journal of Disaster Risk Studies* 6(1): 127-140.
- [45] Mahmood, R., Jia, S., Babel, M. S. (2016): Potential impacts of climate change on water resources in the Kunhar River Basin, Pakistan. – *Water* 8(1): 23. doi: 10.3390/w8010023.
- [46] Mona, L. (2014): Seismic hazard assessment of District Mansehra, Khyber Pakhtoonkhawa, Pakistan. – *Acta Geologica Sinica* 88(4): 1157-1168.

- [47] Munir, M. H., Mirza, K. (2007): Stratigraphic aspect of recent earthquake occurred along the balakot-bagh fault, north-west Himalayas, Pakistan. – *Geological Bulletin of Punjab University* 42: 25-36.
- [48] Panthi, J., Aryal, S., Dahal, P., Bhandari, P., Krakauer, N. Y., Pandey, V. P. (2015): Livelihood vulnerability approach to assessing climate change impacts on mixed agro-livestock smallholders around the Gandaki River Basin in Nepal. – *Regional Environmental Change*. DOI: 10.1007/s10113-015-0833-y.
- [49] Qasim, M., Alam, M., Khan, B., Ahmad, E. (2010): Earthquake induced forest damages in Balakot, Palas Valley, Muzaffarabad and Bagh areas of north west frontier province and Azad Jammu and Kashmir Regions. – *World Applied Sciences Journal* 8: 912-913.
- [50] Rahut, D. B., Ali, A., Kassie, M. P., Marenya, P., Basnet, C. (2014): Rural livelihood diversification strategies in Nepal. – *Poverty Public Policy* 6(3): 259-281.
- [51] Sarwar, F., Iqbal, S., Qaisar, M., Rehman, A., Akhtar, F., Raza, S. M. (2016): Earthquake statistics and earthquake research studies in Pakistan. – *Open Journal of Earthquake Research* 5: 97-104.
- [52] Schickhoff, U. (1995): Himalayan forest-cover changes in historical perspective: A case study in the kaghan valley, northern Pakistan. – *Mountain Research and Development* 15(1): 3-18.
- [53] Shah, A. A., Ye, J., Abid, M., Ullah, R. (2017): Determinants of flood risk mitigation strategies at household level: a case of Khyber districts of Pakhtunkhwa (KP) province, Pakistan. – *Natural Hazards* 88(1): 415-430.
- [54] Shah, A. A., Ye, J., Abid, M., Khan, J., Amir, S. M. (2018): Flood hazards: household vulnerability and resilience in disaster-prone of Khyber Pakhtunkhwa province, Pakistan. – *Natural Hazards* <https://doi.org/10.1007/s11069-018-3293-0>.
- [55] Shah, K. U., Dulal, H. B., Johnson, C. Baptiste, A. (2013): Understanding livelihood vulnerability to climate change: applying the livelihood vulnerability index in Trinidad and Tobago. – *Geoforum* 47: 125-137.
- [56] Shahzad, L., Tahir, A., Sharif, F. (2018): Understanding the community's perception of climate change and adaptations in the Mid Hills of Pakistan. – *Biologia (Pakistan)* 64(II): 197-209.
- [57] Shahzad, L., Tahir, A., Sharif, A. Haq, I. U., Mukhtar, H. (2019): Assessing the impacts of changing climate on forest ecosystem services and livelihood of Balakot mountainous communities. – *Pakistan Journal of Botany* 51(4). DOI: [http://dx.doi.org/10.30848/PJB2019-4\(1\)](http://dx.doi.org/10.30848/PJB2019-4(1)).
- [58] Sharma, R. K., Sankhayan, P. L., Hofstad, O., Singh, R. (2007): Land use changes in the western Himalayan region - a study at watershed level in the state of Himachal Pradesh, India. – *International Journal of Ecology and Environmental Sciences* 33(2-3): 197-206.
- [59] Soomro, A. S., Rajput, A. Q. K., Solangi, S. H. (2010): The study of change after occurrence of earthquake induced landslide disaster in 2005 in Balakot, Pakistan. – *Mehran University Research Journal of Engineering & Technology* 31(3): 461-468.
- [60] Soomro, A. S., Abbasi, H. U., Memon, A. G., Samo, S. R. (2012): A conceptual model for identifying landslide risk: a case study Balakot, Pakistan. – *Sindh University Research Journal* 44: 203-208.
- [61] Stacy, H. J. (2004): Building connections in qualitative research. Carolyn Ellis and Art Bochner in conversation with Stacy Holman Jones. – *Forum Qualitative Sozialforschung/Forum: Qualitative Social Research (On-line Journal)* 5(3): Art.28.
- [62] Sterling, C., 1976: Nepal. – *Atlantic Monthly* (Oct) 238(4): 14-25.
- [63] Sujakhu, N., Ranjitkar, M., Niraula, S., Asad, R. R., Nizami, A., Schmidt-Vogt, A. D., Xu, J. (2018): Determinants of livelihood vulnerability in farming communities in two sites in the Asian Highlands. – *Water International* 43(2): 165-182.
- [64] Sullivan, C. (2002): Calculating a water poverty index. – *World Development* 30: 1195-1210.

- [65] Tse-ring, K., Sharma, E., Chettri, N., Shrestha, A. (2010): Climate Change Vulnerability of Mountain Ecosystems in the Eastern Himalayas-Climatic Change Impact and Vulnerability in the Eastern Himalayas. Synthesis Report. – ICIMOD, Kathmandu.
- [66] Ullah, R., Shivakoti, G. P., Ali, G. (2015): Factors affecting farmers’ risk attitude and risk perceptions: The case of Khyber Pakhtunkhwa, Pakistan. – International Journal of Disaster Risk Reduction 13: 151-157.
- [67] Ullah, W., Takaaki, N., Muhammad, N., Rahman, Z., Muhammad, A. (2017): Understanding climate change vulnerability, adaptation and risk perceptions at household level in Khyber Pakhtunkhwa, Pakistan. – International Journal of Climate Change Strategies and Management. doi.org/10.1108/IJCCSM-02-2017-0038.
- [68] UNDP (2007): Building Enabling Governance and Institutions for Earthquake Response (BEGIN-ER): Mansehra District Disaster Risk Management Plan. – United Nations Development Programme, Govt. of Pakistan.
- [69] Wang, Y. R., Zhao, X. Y., Zhang, Q., Luo, L. (2016): Farmers’ climate change adaptation strategies in an ecologically vulnerable alpine region: a case of Gannan Plateau. – Geographical Research 37: 2392-2402.
- [70] World Bank (1979): Nepal: Development Performance and Prospects - A World Bank Country Study. – South Asia Regional Office, World Bank, Washington, DC.
- [71] WWF (2017): Third Party Monitoring of Billion Trees Afforestation Project in Khyber Pakhtunkhwa. – WWF, Pakistan.
- [72] Yang, W., Yang, Z. F. (2014): Evaluation of sustainable environmental flows based on the valuation of ecosystem services: a case study for the Baiyangdian Wetland, China. – Journal of Environmental Informatics 24: 90-100.
- [73] Yohannes, A. W., Cotter, M., Kelboro, G., Dessalegn, W. (2018): Land use and land cover changes and their effects on the landscape of Abaya-Chamo Basin, Southern Ethiopia. – Land 7: 2.
- [74] Zaheer, K., Colom, A. (2013): Pakistan - How the People of India live with Climate Change and what Communication Can Do. – BBC Media Action, London, UK.
- [75] Zhang, Q., Xueyan, Z., Haiping, T. (2018): Vulnerability of communities to climate change - application of the livelihood vulnerability index to an environmentally sensitive region of China. – Climate and Development <https://doi.org/10.1080/17565529.2018.1442808>.

APPENDIX

Table A1. Summary of LVI scores for UC Kawai and UC Balakot

Vulnerability components	Major components	Indicators (questions inquired)	Units	BALAKOT		KAWAI		Max. value	Min. value
				Actual value	Standardized value	Actual value	Standardized value		
Exposure	Natural disasters	Number of hazards/natural disasters faced in the last 5 years	Range/count (0-5)	4.4	0.8	2.8	0.27	5	2
		Family members did not get any warning of natural disasters	Percentage	100	1	100	1.00	100	0
		Death/Injury in your household due to natural disaster	Percentage	52.5	0.525	24.5	0.25	100	0
		Damage to physical properties and loss of agriculture land as a consequence of natural disasters	Percentage	77.5	0.775	56.7	0.57	100	0
				0.78		0.52			

Climate variability	Mean standard deviation of monthly average of average maximum daily temperature	Celsius	12.8	0.052	12.8	0.052	34.7	11.6	
	Mean standard deviation of monthly average of average minimum daily temperature	Celsius	6.9	0.197	6.9	0.197	20.8	3.5	
	Mean standard deviation of monthly average precipitation	mm	116	0.266	116	0.266	324.4	40.3	
				0.172		0.172			
Sensitivity	Health	Average time to reach basic health facility	Min	20.5	0.24	33.6	0.44	70	5
		Affordability of basic health services	Percentage	32	0.32	29.5	0.30	100	0
		Household with chronic ill members	Percentage	22	0.22	18	0.18	100	0
		Household members missing school or work due to illness (in last 2 weeks)	Percentage	11	0.11	9	0.09	100	0
		Household having toilet in use	Percentage	83.5	0.84	77.8	0.78	100	0
		Household using wood	Percentage	98.6	0.99	95.4	0.95	100	0
					0.45		0.46		
	Food	Food sufficiency (household has food storage for six month)	Percentage	24.4	0.24	39.2	0.39	100	0
		Average crop diversity	1/no.of crops	0.18	0.29	0.21	0.36	0.5	0.05
		Housing dependency on fishing/hunting for food	Percentage	39.5	0.40	35.6	0.36	100	0
		Household primarily dependent on self-farmed food	Percentage	22.5	0.23	34.4	0.34	100	0
		Household saving seeds	Percentage	6.8	0.07	23.5	0.24	100	0
					0.24		0.34		
	Water	Dependency of household on natural water sources	Percentage	42	0.42	66	0.66	100	0
		Average days without a water supply per month	Days	8.55	0.71	6.71	0.34	10	5
		Household without pipe borne water	Percentage	49	0.49	55	0.55	100	0
		Consistency of drinking water supply	Percentage	32	0.32	25	0.25	100	0
					0.49		0.45		
Adaptive capacity	Socio-demo	Dependency ratio per household	Ratio	2.44	0.44	1.56	0.25	5	0.4
		Households with a head who is a female	Percentage	26	0.26	18	0.18	100	0
		Households having access to radio, telephone or television	Percentage	66	0.66	48	0.48	100	0
		Head of household never joined any school/college etc.	Percentage	23	0.23	19	0.19	100	0
					0.40		0.28		
	Livelihood strategies	Any member of household working outside the Tehsil for spontaneous work	Percentage	54	0.54	41	0.41	100	0
		Any family member involved in local tourism for their livelihood	Percentage	22	0.22	4	0.04	100	0
		Household's dependence upon fishing and hunting for their day to day life	Percentage	21	0.21	16	0.16	100	0
		Crop cultivation as a main source of income	Percentage	48	0.48	54	0.54	100	0
		Agricultural livelihood diversification in a household	1/no.of livelihoods	0.24	0.00	0.22	0.00	100	0

	Household having livelihood without any contribution of crops cultivation	Percentage	42	0.42	34	0.34	100	0
	Household having no direct water supply facilities to produce crops	Percentage	36	0.36	21	0.21	100	0
				0.32		0.24		
Social networks	Household having social support in terms of getting and providing help	Ratio	1.51	0.36	1.22	0.29	4	0.1
	Family members in household can borrow money from a certain social group	Ratio	1.01	0.34	0.89	0.26	2	0.5
	Is there any private money lender in your community to borrow money from?	Percentage	20	0.20	12	0.12	100	0
	Have you or any family member in household has ever seek help from any government office (last 12 months)?	Percentage	82	0.82	65	0.65	100	0
				0.43		0.33		

PHYSICO-CHEMICAL DIVERSITY AND MICROBIAL BURDEN IN FOUR DATES PALM (*PHOENIX DACTYLIFERA* L.) FRUIT VARIETIES GROWN IN AGRO-CLIMATIC CONDITION OF TURBAT, BALOCHISTAN-PAKISTAN

ASLAM, A.¹ – LEGHARI, S. K.^{1*} – ASRAR, M.¹ – SAEED, S.¹ – SHAFI, M.² – SIDDIQI, M. F.⁴ –
SUMALANI, M. A.¹ – MAHAM, F.¹ – MERRI, A. A.³

¹Department of Botany, University of Balochistan, Quetta 87300, Pakistan
(phone: +92-81-921-1264)

²Faculty of Pharmacy, University of Balochistan, Quetta 87300, Pakistan

³Department of Statistics, University of Balochistan, Quetta 87300, Pakistan

⁴Department of Botany, University of Karachi, Sindh 75270, Pakistan

*Corresponding author

e-mail: saadbotany@yahoo.com, drsaadullahleghari@gmail.com

(Received 1st Feb 2019; accepted 8th Apr 2019)

Abstract. The aim of this study was to measure the quality indices (physico-chemical and microbial assessment) of four popular date palm fruits (*Phoenix dactylifera* L.) varieties (Begamjangi, Haleeni, Dashtri and Peshnah) grown in ecologically same agro climatic condition of Turbat Balochistan, Pakistan. Different date palm characteristics including; harvesting time, color and taste of fruits, diversity in fruit, stone weight, length and diameter, variation in chemical composition, sugar, minerals and amino acids contents were recorded by standard methods. Results indicated that there was slightly to highly significant variations among the investigated parameters in different cultivars. Further that microbial burden (cfu/g) on four fruit sizes classes (large, small, medium and mixed) in three fruit processing techniques (unpressed-unpitted, pressed-pitted and unpressed-pitted date fruits) were examined. The results revealed that the different date varieties showed different load of microbial infections. On the basis of all investigated parameters the fruit performance index (FPI) and valuation classes were calculated. The consequences indicated that the Begamjangi score highest grade point (6) and stood in excellent class, followed by Haleeni with grade point 4.0 and categorized in good class. Other two date cultivars Dashtri and Peshnah score 2.0 & 1.0 grade points and classified into poor and very poor group of date palm fruits, respectively.

Keywords: date cultivars, productivity, sugar and mineral contents, bacterial infection, fruit performance index (FPI), fruit size classes

Introduction

The date fruit (*Phoenix dactylifera* L.) is an important food product and extensively cultivated all over the world for its edible fruits. It is a monocotyledonous belongs to the family Arecaceae. Mostly cultivated in semi-arid regions of the world (Ashraf and Hamidi-Esfahani, 2011). Fruit is highly nutritious with delicious taste and a basic part of human diet (Vayalil, 2002). Date fruit is constituted high percentage of carbohydrates (glucose and fructose), proteins, vitamins, fats, dietary fibers, minerals and low amount of starch. Their Chemical composition depends on cultivar type, fruit developmental stage and agro-climatic conditions (Al-farsi et al., 2005; Al-farsi and Lee, 2008; Safi et al., 2009; Baliga et al., 2011). Pakistan is well known for its date industry with annual production of 70 thousand tons (Anonymous, 2012), contributing 10.3% of total world's

production. Aseel, Dhakki, Begumjungi and Koharba are amongst the most important native date palm varieties. Many other local cultivars are also grown in different agro-ecological zones of Pakistan (Iqbal et al., 2016). The farmers have denominated the cultivars on the basis of shape and color of the fruits or the presence of specific locations (Ahmed et al., 2011). The date palm is selected for cultivation on the basis of better fruit quality and post-harvest life. Based on the botanic interpretation, there are about 244 cultivars in Morocco, 250 in Tunisia, 370 in Iraq, 400 in Iran (Zaid and de Wet, 2002), 400 in Sudan (Osman, 1984), 325 in Pakistan (Botes and Zaid, 2002; Jamil et al., 2010). About 5000 different date palm cultivars are known to present worldwide (Jaradat and Zaid, 2004).

Quality standards of dates must include chemical, physical and sensory attributes. Date varieties significantly vary in terms of their chemical composition. The variation in chemical composition affects the structural, sensory and textural properties of fruits (Rahman and Al-Farsi, 2005). The function of sensory analysis is to provide measurements that are accurate, precise, and valid (Piggott, 1995) and variation in sensory attributes is due to the genetic differences and variable growth conditions. There is a considerable diversity within date palm cultivars. Although, accurate characterization of cultivars need a huge set of morphological as well as biochemical and molecular (isozymes) markers. Moreover, vegetative characteristics, phenotypic diversity and phylogenetic relationship are important to evaluate date palm ecotypes (Haider et al., 2015). This significant plants are endangered through hereditary corrosion, change of agrarian land, irritant and infections. Numerous investigations have emphasized this concern (Zehdi et al., 2005, 2012). Hammadi et al. (2009) and Ahmed et al. (2011) used phenotypic data to classify dissimilar date palm cultivars. Wills et al. (1998) stated that, with respect to consumers, the important quality criteria of a product are appearance (including color, size, and shape, condition and absence of defects), mouth feel or texture, flavor, and nutritional value. So due to the importance of date fruits a number of countries have formulated and applied date standards at the national level both for locally produced and imported dates. So there are many date standards that include both local and international specifications. They contributed to the ease of global trade for dates. However, the standards do not emphasize some important quality parameters of these fruits.

There are no extensive studies on the quality indices and standards for the most abundant and commercially important date palm fruits (Begamjangi, Haleeni, Dashtri and Peshnah) in Turbat Balochistan, Pakistan. Therefore, this study is designed to assess the physico-chemical and microbial estimation of four popular and important date cultivars.

Materials and methods

Plant material and samples collection

Fruit samples were collected from four date palm varieties from same ecological conditions in regional date field of Turbat, Balochistan. These date cultivars were Begamjangi, Haleeni, Dashtri and Peshnah. Study was based on fruit physiochemical characters. Analysis were carried out on 40 randomly selected trees (10 from each cultivar). A total of 20.0 kg of fruit samples from ten randomly selected trees of each cultivar were collected separately at maturity stage (August to September) during 2018. Samples were cleaned, washed and packaged in polyethylene bags inside 20 kg cartons,

and preserved in a refrigerator at 5°C until experimental tests were performed. Typical morphological image of the experimental cultivars are shown in *Fig. 1*. Further that on the basis of harvesting time the date palm varieties were classified in to early, mid and late variety (*Table 1*).



Figure 1. Picture of investigated dry date palm varieties

Table 1. Indication of harvesting time, fruit color, and taste in four date palm varieties

Date Variety	Parameters			
	Harvesting time	Type	Fruit colour	Taste
Begamjangi	20 th August – 20 th September	Med verity	Light yellow	Delicious
Haleeni	After 20 th September	Late verity	Yellow	Tasteful
Dashtri	20 th August – 20 th September	Med verity	Dark brown	Slightly tasty
Peshnah	20 th July-20 th August	Early verity	Light yellow	Poor taste

Physiochemical character study

Fruit and stone weight was assessed by analytical balance and calculated as a mean of randomly designated 30 mature fruits from each cultivar as used by Lemine et al. (2014). Fruit and stones length and breadth were noted by using complete numerical microelectronic Vernier-caliper as the method used by Mughal et al. (2018). Fruit moisture/water contents were measured by dehydrating 5 g date pulp in vacuum oven for 24 hr at 70°C by using the following formula: % water = [(initial weight- dry weight) × 100]/initial weight] (Leghari et al., 2017). Fruit color was measured by color difference meter and the measurements were performed on 10 individual randomly selected fruits from each cultivar (a total of 120 fruits) with three replicate (Aleid et al., 2014). Entire nitrogen was measured by the Kjeldahl method as described by AOAC (1995) and protein was expressed as the overall factor 6.25 (Laurey, 1997). The entire lipid contents were determined through the methods as described by Folch et al. (1957). Water activity was determined in a water activity meter (Rotronic) and ash level was measured from the differences after warming softened date sample in an oven at 600°C for 8 h. Electrical conductivity (EC) was noted from dry sieved sample. 20 g dry date sample was stimulated by 50 ml distilled water and left-hand to equilibrate for 40 min and then filter the mixture. The EC of each variety sample was measured by using the electrical conductivity meter (Crison Basic 30+EC-Meter, 08323 Alella-Bacrelona made in EU). Sugars contents from soaked date pulp samples were measured with water at 85°C and it was computed through the 3,5-dinitrosalicylic acid technique as described by Laurey (1997). Overall sugar (Sucrose, glucose, and fructose) contents were noted by high performance liquid chromatography (HPLC) according to the methods of AOAC (1995). Date samples were spiked by several mixtures of average

sugars (1-5 ppm) to display retrieval and the sugar content was intended from highest area of measurement according to the method of Langemeier and Rogers (1995). Minerals (calcium, phosphorus, potassium, sodium and magnesium) contents were determined through atomic absorption spectrophotometer and expressed by mg/100 g dw. Different obtainable amino acids (proline, glycine, histidine, valine, leucine, serine, methionine, isoleucine, tyrosine, phenylalanine, lysine and alanine) were examined through the technique as described by Laurey (1997). Date fruit samples were hydrolysis by vapors HCl and standard for 20 hr at 110°C. After that the date samples were extracted on poly-vinylidene difluoride with 100 µL of 40% aceto-nitrile and 0.5% trifluoroacetic acid for three times. The excerpts were then dehydrated entirely in a Rapidity Vac earlier re-suspension in sample buffer. After that the samples and standards were examined in a Beckman system 6300 (Laurey, 1997). Different amino acids were articulated in to mg/100 g dw. Total acidity was measured by using 10 ml of fruit juice which were titrated against 0.1 M sodium hydroxide solution by the utilization of phenolphthalein as an indicator (AOAC, 1995). Total acidity was calculated according the following formula: Volume NaOH (ml) × 0.1 M × 0.067 and expressed as malic acid content. The pH measurement was done by calibrated digital pH meter (CyberScan 510 USA).

Classification of fruits into fruit size classes

Fruits were classified into four size classes including; large, small, medium and mixed were arranged according to the fruits weight (g). Fruit size classes were calculated by the following formula: large= weight>x gram; medium= x gram>weight>y gram; and small= weight<y gram. For four fruit size classes (large, small, medium and mixed) and three fruit processing methods (unpressed-unpitted, pressed-pitted and unpressed-pitted) a 4 × 3 factorial treatment strategy was acquired. Where the term “pressed” mentions to dates that were compacted into layers through mechanical force and unpressed refers to dates that were packed without powered presser or density. Pressing of entire dates was made with packing in a flexible sealed. The term “pitted” used to date palm fruits whose seeds/stones were removed. In order to remove the pit a sharp knife was used for pitting of whole dates and the date fruits were cut from end to end. As per outcome, there were 12 samples from each date variety and a total number of 36 samples. Microbial burden was measured in the study through Coliform, Moulds and Yeast and total bacterial counts.

Microbial burden study

Pour plate method was used to count the aerobic mesophilic bacteria on plate count agar dishes. These plates were incubated for 3 days at 35°C. From the sample, the counts were expressed as colony forming units per gram (cfu/g). Fruit samples were aseptically destoned by utilizing sterilized pincers and microbial burden was calculated for the skin. Skin samples were weighed 10 g into sterilized stomacher bags and 90 ml of sterilized peptone water. For homogenization of mixture a stomacher was used for 50 seconds and aliquots (1.0 or 0.1 ml) plated out in duplicate as 10-fold dilutions in peptone water. The pour plate/overlay method was used to count the coliforms on Vilet Red Bile Agar (VRBA). The plates were incubated for 48 hours at 35°C. The round, purple-red colonies (0.5-2 mm diameter) surrounded by purple-red haloes on VRBA plates were counted as coliforms. Spread plate method was used to culture the yeasts and moulds on

potato dextrose agar. Yeasts plates were incubated for 3 days at 35°C and for moulds it was incubated 5-7 days at 25-30°C (Atlas, 2004; Abekhti et al., 2013).

Fruit Quality Assessment

Fully ripened fruits were harvested from four selected varieties and dried until a constant weight was reached (moisture content 12 to 25%). Fruit weight, stone weight, reducing sugar, over all minerals, moisture %/water activity and microbial burden hardy were determined according to the standard methods as described above in this research methodology. Acidity, Taste and flavor of fruit was tested by a panel of six experienced judges (one from food department, two date farmers, two Ph.D. Professor from botany department university of Balochistan Quetta and other one from agriculture department) from and values/scales were given from 1-5/1-10 (Leghari et al., 2019). 10 fruits from each varieties were randomly selected for taste and flavor for each expert/judges.

Fruit performance index (FPI) through fruit quality and valuation Classes

For the date fruit performance index (*FPI*) the methods described by Prajapati and Tripathi (2008) and Leghari et al. (2019) was used. *FPI* values were calculated by combining the different fruit quality parameters (fruit weight, stone weight, taste of fruit, acidity, reducing sugar, over all minerals, moisture %/water activity and microbial burden hardy) of four date palm varieties based on character grading (+ or -) fixed to the plant.

Statistical analysis

Statistical analysis of data collected during the course of each trial was performed by analysis of variance (ANOVA) to determine the interaction effects among the main factors using SPSS software version 16.0 and for the comparison between the means of treatments duncans multiple-range test ($P=0.05$) was used (Steel and Torrie, 1980).

Results and discussion

Results shown in *Table 1* indicated that Begumjangi was designated med variety with light yellow fruit color and delicious taste. Haleeni was noted late variety with yellow fruit color and tasteful. Dashtri was found med variety with Dark brown fruit color and slightly tasty. Peshnah was found early variety with light yellow fruit color and poor taste. The variation in harvesting time, fruit color and taste in different date varieties was also noted previously (Abekhti et al., 2013; Aleid et al., 2014). They reported a great differences in date fruits color from different date varieties of Saudi Arabia.

Productivity variation in date varieties

Results in *Table 2* indicated statistically significant variation in average weight, length and breadth of fruits and stone in four date palm varieties grown in agro climatic condition of Turbat. Fruit and stone weight, length and breadth is directly related to productivity of a cultivar. In this study the average weight, length and breadth were noted from the ranged 2.75 - 8.57 g/fruit, 2.7 - 3.1 cm/fruit & 1.3 - 1.9 cm/fruit, respectively. Haleeni showed maximum average fruit weight and Dashtari minimum and the highest length of fruit was noted for Begamjangi and lowest for Dashtari. The

uppermost fruit breadth was presented by Begamjangi and lowermost by Haleeni. The average weight and length of stone were ranged 0.54 - 0.66 g/fruit fw and 1.7 - 1.9 g/fruit fw, respectively, while stone breadth was noted same (0.7 g/fruit fw) in all investigated varieties. The extreme average weight and length of stone was found in Dashtari and Peshnah and least in Haleeni and Dashtri, respectively. Variation in these parameters were also observed by Ragab et al. (2011). They reported differences in fruit weight at different stages in diverse variety. Variation in these parameters in diverse varieties led to the variation in total yield.

Table 2. Diversity in average weight, length and diameter of fruits and stones in four date palm varieties

Date palm variety	Parameters						P value
	Fruit weight	Stone weight	Fruit length	Stone length	Fruit breadth	Stone breadth	
Begamjangi	6.87 ^{ab}	0.60 ^{ab}	3.1 ^a	1.8 ^a	1.9 ^a	0.7 ^a	0.031
Haleeni	8.57 ^a	0.54 ^b	2.9 ^a	1.8 ^a	1.3 ^b	0.7 ^a	0.021
Dashtri	2.75 ^b	0.66 ^a	2.7 ^a	1.7 ^a	1.5 ^{ab}	0.7 ^a	0.022
Peshnah	4.00 ^{ab}	0.64 ^b	2.8 ^a	1.9 ^a	1.5 ^{ab}	0.7 ^a	0.031
P value	0.036	0.002	0.457	0.468	0.034	1.00	

Each value is the mean of 30 replicates, Different letters in the same column and row indicate statistically significant differences (significance level $P = 0.05$)

Diversity in Chemical composition of date varieties

Consequences displays slightly to highly significant diversity in various chemicals (Moisture, Protein, Lipid, Ash contents and Water activity) composition in four date palm fruits varieties. Results indicated that the moisture contents in four investigated date palm fruits varieties was in ranged between 15.4 - 24.3% and the highest moisture content was found in Peshnah fruits and lowest in Begumjangi. Protein and lipid contents were in between 2.15 - 3.24 g/100g dw, 0.13 - 0.54 g/100g dw, respectively. The uppermost protein and lipid content were showed by Begumjangi fruits and minimum by Dashtari and Peshnah, respectively. The ash contents and water activity in all investigated date varieties were recorded in the range of 1.23 - 3.52 g/100g dw and 0.421 - 0.675 aw, respectively. The highest ash contents were originate by Begumjangi, whereas lowest by Peshnah and Water activity was exhibited highest in Peshnah and lowest in Begumjangi (Table 3). The outcomes of this study are analogous to other researchers as they testified before (Elleuch et al., 2008; Assirey, 2015), through approximately variances associated to date cultivar and agro-climatic and environmental circumstances (Myhara et al., 1999; Biglari et al., 2009). It has been also described earlier that the dates are not a decent basis of protein (Al-Hooti et al., 1997).

Sugar contents in date fruits

The sucrose, glucose, fructose, Reducing sugar contents and ratio between glucose and fructose were found from ranged 2.00 - 4.24, 35.5 - 48.5, 27.0 - 35.5, 62.5 - 84.0 and 1.31 - 1.37 g/100g dw, respectively in four different date varieties. The maximum glucose, fructose, reducing sugar and ratio between glucose and fructose was shown by Begumjangi and minimum Peshnah. Highest content of sucrose was noted in Peshnah and lowest in Begumjangi fruits (Table 4). Similar observation was also noted by Assirey (2015). Richness in reducing sugars (glucose and fructose) is being significantly decrease its sucrose content (Elleuch et al., 2008; Besbes et al., 2009). Statistical

analysis exhibited that sucrose, glucose and reducing sugar were found slightly significant different between the four examine date varieties, while fructose content and ratio between glucose and fructose were non-significant between four date varieties (Table 4). Non-significant variation in these parameters were also reported by Assirey (2015) between Ajwa, Shalaby, Suqaey, Sukkari, Burni, Mabroom and Anabarah and between Khodari and Safawy.

Table 3. Diversity of chemical composition in four different date palm fruits

Variables	Date Varieties				P value
	Begamjangi	Haleeni	Dashtri	Peshnah	
Fruit moisture (%)	15.4 ^b	18.3 ^b	23.3 ^a	24.3 ^a	0.035
Protein (g/100 g dw)	3.24 ^a	2.16 ^b	2.15 ^b	2.54 ^b	0.044
Lipid (g/100 g dw)	0.54 ^a	0.51 ^a	0.34 ^b	0.13 ^c	0.000
Ash (g/100 g dw)	3.52 ^a	2.01 ^{ab}	2.35 ^{ab}	1.23 ^b	0.025
Water activity (aw)	0.421 ^b	0.503 ^{ab}	0.622 ^a	0.675 ^a	0.044

Each value is the mean of three replicate, different letters in the same column indicate statistically significant differences (significance level $P = 0.05$)

Table 4. Sugar contents in four different date palm fruits varieties

Variables	Date palm varieties				P value
	Begam Jangi	Haleeni	Dashtri	Peshnah	
Sucrose (g/100g dw)	2.00 ^b	2.75 ^b	3.45 ^{ab}	4.24 ^a	0.013
Glucose (g/100g dw)	48.5 ^a	43.6 ^{ab}	40.7 ^{ab}	35.5 ^b	0.024
Fructose (g/100g dw)	35.5 ^a	33.4 ^{ab}	30.2 ^{ab}	27.0 ^b	0.042
Reducing sugar (g/100g dw)	84 ^a	77 ^{ab}	70.9 ^{ab}	62.5 ^b	0.010
Glu/Fru (g/100g dw)	1.37 ^a	1.31 ^a	1.35 ^a	1.31 ^a	0.145
P value	0.000	0.004	0.007	0.002	

Each value is the mean of five replicate, different letters in the same column and raw indicate statistically significant differences (significance level $P = 0.05$)

It is authenticated that dates are vital bases of sugar. In present investigation the overall total sugar was recorded from the ranged of 66.74 - 86 g/100g dw in four date palm varieties. The maximum content was noted in Begumjangi, which followed by Haleeni (79.75 g/100g dw), Dashtari (74.35 g/100g dw) and minimum was found in Peshnah fruit. Statistical analysis indicated that there was significant variation in total sugar contents among four investigated date varieties (Fig. 2). The variation in total sugar by different cultivar were also noted by other authors. Elleuch et al. (2008) and Besbes et al. (2009) reported variation in total sugar contents (81.6 - 88.4%, 72.8 - 79.1% and 72.8 - 79.1% and 78.3 - 87.6%), in different date varieties. Contrary to this, Non-significant variation in total sugar was reported by Assirey (2015) between Khodari, Anabarah, Sukkari, Suqaey and Burni and between Ajwa, Shalaby, Safawy and Labanah.

Mineral diversity in date fruits varieties

The mean contents of calcium, phosphorous, potassium, sodium and magnesium were found in ranged from 120 - 180, 12.5 - 25.02, 276 - 450.5, 4.6 - 7.05 and 55.4 - 120.4 mg/100g dw, respectively. The maximum calcium, phosphorus, potassium, sodium and magnesium were recorded in Begumjangi and minimum in Peshnah fruits.

Statistical analysis indicated that calcium, potassium, sodium and magnesium were found slightly to highly significant different in four investigated date palm varieties, while phosphorus showed non-significant variation (Table 5). The mean contents of overall minerals was found in the ranged 156.7 - 93.7 mg/100g. The highest overall minerals contents was recorded in Begumjangi which followed by Haleeni (130.144 mg/100 g) then Dashtri (108.1 mg/100 g) and least in Peshnah (Fig. 2). Variation in mineral contents in different date cultivar were also reported by Ragab et al. (2011) and Assirey (2015). They found differences in mineral contents between different date varieties such as; Khodari, Anabarah, Sukkari, Suqaey and Burni and between Ajwa, Shalaby, Safawy and Labanah. The consequences of our study supported by authors of numerous other investigation. They indicated that date fruits had appropriate level of different minerals (calcium, potassium and phosphorus) which are essential for human bodies (Sawaya et al., 1983; Gasim, 1994). The differences in minerals especially; magnesium and sodium contents might be clarified by the influences such as variety, soil types and environmental conditions.

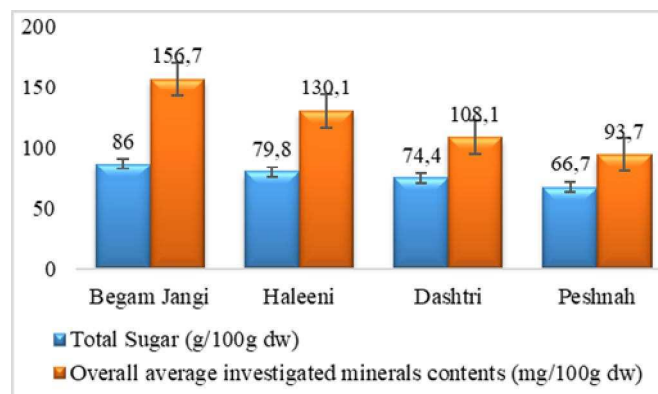


Figure 2. Total Sugar contents (g/100g dw) and Overall Mineral contents (mg/100g dw) in four different date palm fruits varieties

Table 5. Mineral composition in four different date palm fruits varieties

Minerals variables	Date varieties				P value
	Begamjangi	Haleeni	Dashtri	Peshnah	
Calcium (mg/100g dw)	180.4 ^b	150.2 ^b	142.0 ^b	120 ^b	0.002
Phosphorus (mg/100g dw)	25.02 ^c	19.3 ^c	15.8 ^c	12.5 ^c	0.004
Potassium (mg/100g dw)	450.5 ^a	370 ^a	310 ^a	276 ^a	0.037
Sodium (mg/100g dw)	7.05 ^d	6.22 ^d	6.03 ^d	4.6 ^d	0.018
Magnesium (mg/100g dw)	120.4 ^b	105 ^b	66.6 ^b	55.4 ^b	0.000
P value	0.002	0.000	0.000	0.000	

Each value is the mean of five replicate, different letters in the same column and different rows indicates statistically significant differences at significance level $P = 0.05$

Amino Acids Contents

Calculated mean values of proline, glycine, histidine, valine, leucine, serine, methionine, isoleucine, tyrosine, phenylalanine, lysine and alanine in investigated varieties were found ranged between 73 - 114, 89 - 93, 25 - 10, 60 - 77, 51 - 86, 54 - 62, 10 - 25, 35 - 48, 10 - 20, 46 - 55, 44 - 70 and 75 - 86 mg/100 g dw, respectively. The

maximum histidine, leucine, methionine, isoleucine, tyrosine and lysine were shown by Begumjangi and minimum by Peshnah fruits. Glycine and alanine were found highest in Haleeni and lowest in Begumjangi and Peshnah fruits, respectively. However, Peshnah showed uppermost values of serine, phenylalanine, proline and valine and lowermost showed by Haleeni and Begumjangi respectively (Table 6). The aspartic acid and overall average amino acid contents were recorded in ranged 105 - 165 and 22.7 - 56.7 mg/100g in four investigated date palm varieties.

Table 6. Amino Acids Contents (mg/100 g dw) in four different date palm fruits varieties

Amino acids variables	Date Variety				P value
	Begumjangi	Haleeni	Dashtri	Peshnah	
Proline	73 ^b	82 ^b	94 ^{ab}	114 ^a	0.027
Glycine	89 ^a	93 ^a	90 ^a	92 ^a	0.056
Histidine	25 ^a	18 ^{ab}	14 ^b	10 ^b	0.031
Valine	60 ^b	70 ^{ab}	75 ^a	77 ^a	0.078
Leucine	86 ^a	76 ^{ab}	60 ^{ab}	51 ^b	0.013
Serine	58 ^a	54 ^b	60 ^a	62 ^a	0.104
Methionine	25 ^a	23 ^a	16 ^b	10 ^b	0.034
Isoleucine	48 ^a	43 ^{ab}	40 ^b	35 ^b	0.031
Tyrosine	20 ^a	16 ^{ab}	12 ^b	10 ^b	0.022
Phenylalanine	50 ^{ab}	46 ^b	53 ^a	55 ^a	0.033
Lysine	70 ^a	62 ^a	57 ^{ab}	44 ^b	0.027
Alanine	76 ^b	86 ^a	80 ^a	75 ^b	0.024
P value	0.041	0.041	0.028	0.034	

Each value is the mean of three replicate, different letters in the same column and raw indicate statistically significant differences (significance level $P = 0.05$)

The highest aspartic acid and over average amino acids were found in Begumjangi and lowest in Dashtri (Fig. 3). Statistical analysis ($p=0.05$) showed that proline, leucine, methionine, histidine, isoleucine, tyrosine, lysine, phenylalanine and alanine were noted slightly to highly significant different between the four investigated date palm varieties, but glycine serine, valine, exhibited non-significant variation. Similar observation was reported by Assirey (2015). They found variations in amino acid contents in different date varieties. Further that a normal level of amino acids is essential for human and it cannot be form in human body and it can be provided by diet (Al-Farsi et al., 2005).

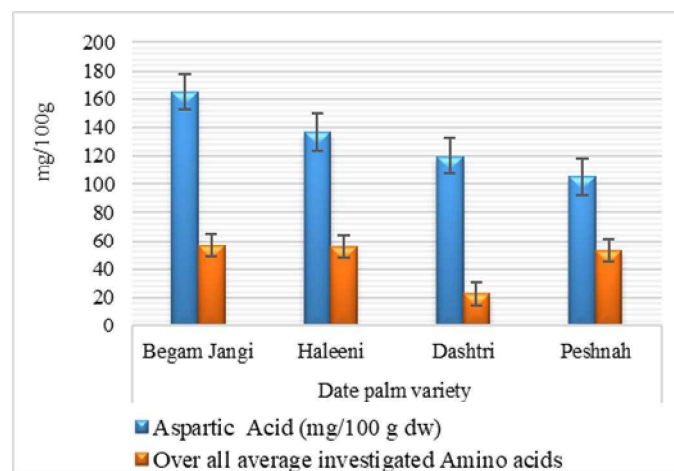


Figure 3. Aspartic Acid and Overall Ave. investigated Amino acids in date palm fruits

Fruit extract pH and total acidity

Total acidity and pH in four date palm fruit varieties are shown in Fig. 4. The pH and total acidity in four observed date palm varieties were noted in ranged between 4.8 - 5.7 and 2.2 – 4.0 mg/100 g dw, respectively. The maximum pH and total acidity were found in Begumjangi and Peshnah, while minimum in Dashtri and Begumjangi juice respectively. The similar trend was observed by Reynes et al. (1994) in 21 date varieties from Tunisia.

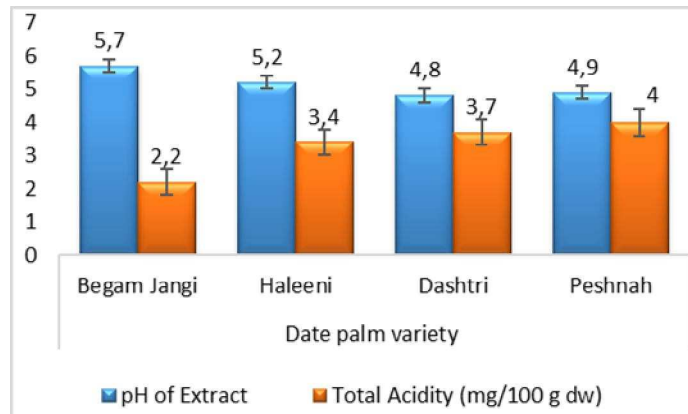


Figure 4. pH and Total Acidity date palm fruits

Microbial Burden (cfu/g)

Earlier investigation of microbial burden on examined date palm fruits varieties, the fruits were classified in to four size classes. The consequences of classification revealed that in large, medium, small and mixed size classes the number of fruits were in ranged of 38 - 84, 45 - 125, 69 - 167 and 48 - 127, respectively. In all fruit size classes (large, medium, small and mixed) the maximum number of fruits were noted for Peshnah, followed by Dashtri, and Begamjangi and minimum was noted for Haleeni (Fig. 5). Variation in fruit size classes were also absorbed by Aleid (2014).

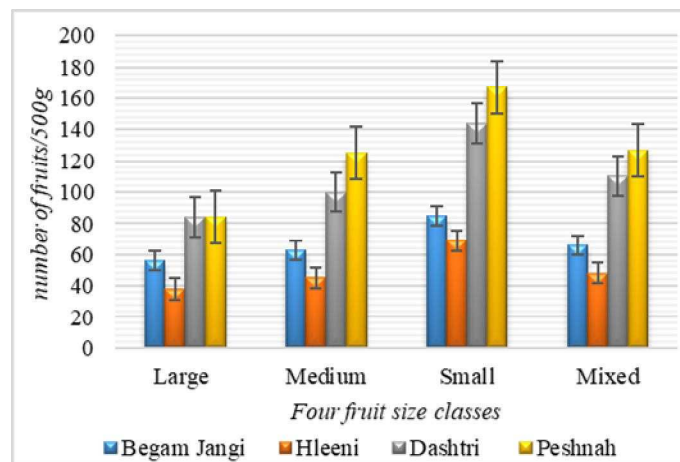


Figure 5. Classification of date palm fruits in to four size classes according to the number of fruits/500g

Microbial Burden (cfu/g) in un-pressed un- pitted dates fruits

The results of un-pressed un- pitted dates fruits exhibited that in Begumjangi the microbial load (coliform VRBA, Moulds and yeast and Mesophilic aerobic bacteria) were found in the ranged 0.0 - 0.0, 2.4 - 46.3 and 25.4 - 196.3 cfu/g in four different fruit size classes, respectively. In Begumjangi the maximum microbial load was found by mesophilic aerobic bacteria, followed by moulds and yeast and minimum by Coliform VRBA. *P* value indicated that different microbial organisms put highly significant different burden, similarly different fruit size classes showed highly significant variation in loads of Moulds and yeast and mesophilic aerobic bacteria but non-significant load of Coliform VRBA (Table 7). On Haleeni fruit the microbial i.e. Coliform VRBA, Moulds and yeast and Mesophilic aerobic Bacteria, load was recorded in between 0.0 - 3.4, 400.3 - 905.3 and 48.0 - 375.0 cfu/g for four fruit size classes (large, medium, small and mixed), respectively (Table 7). Statistical analysis indicated that there was highly significant variation between the fruit size classes as well as among the investigated microbial organisms at $p=0.05$ significant level (Table 7).

Table 7. Microbial Burden (cfu/g) in un-pressed un- pitted dates of four local varieties of date palm

Date variety	Fruit Size classes	Microbial variable			P value
		Coliform VRBA	Moulds and yeast	Mesophilic aerobic bacteria	
Begumjangi	Large	0.0 ^b	2.4 ^b	25.4 ^b	0.000
	Medium	0.0 ^b	5.3 ^b	75.2 ^{ab}	0.000
	Small	0.0 ^b	46.3 ^a	196.3 ^a	0.000
	Mixed	0.0 ^b	20.37 ^a	102.66 ^{ab}	0.007
	P value	7.078	0.000	0.007	
Haleeni	Large	0.0 ^b	400.3 ^b	48.0 ^c	0.000
	Medium	0.0 ^b	662.0 ^{ab}	106.0 ^b	0.000
	Small	3.4 ^a	905.3 ^a	375.0 ^a	0.000
	Mixed	1.13 ^b	655.87 ^{ab}	176.33 ^b	0.000
	P value	0.000	0.000	0.005	
Dashtri	Large	0.0 ^b	28.0 ^{ab}	112 ^c	0.000
	Medium	0.0 ^b	16.4 ^b	345 ^b	0.000
	Small	2.1 ^b	53.2 ^a	712 ^a	0.000
	Mixed	0.7 ^a	32.53 ^a	389.67 ^b	0.000
	P value	0.157	0.003	0.000	
Peshnah	Large	0.0 ^c	684.0 ^a	900.0 ^b	0.000
	Medium	5.0 ^b	423.8 ^b	1200.0 ^{ab}	0.000
	Small	53.7 ^a	100.2 ^c	1607 ^a	0.017
	Mixed	19.57 ^b	402.67 ^b	1235.67 ^{ab}	0.000
	P value	0.000	0.0234	0.000	

Each value is the mean of four replicate, different letters in the same column and row indicate statistically significant differences (significance level $P = 0.05$)

In Dashtri fruit the Coliform VRBA, Moulds and yeast and Mesophilic aerobic Bacterial loads were found in the ranged of 0.0 - 2.1, 16.4 - 53.2 and 112 - 712 cfu/g in four fruit size classes, respectively. *P* value indicated that the coliform VRBA was found non-significantly different between the classes and other two microbial organism was recorded with highly significant variation between the fruit size classes (Table 7).

Microbial (Coliform VRBA, Moulds and yeast and Mesophilic aerobic Bacteria) burden on Peshnah date palm fruits were from the ranged 0.0 - 53.7, 100.2 - 684.0 and 900.0 - 1600.7 cfu/g, in large, medium, small and mixed fruit size classes respectively.

The maximum load of Coliform VRBA was noted in small size class and minimum in large size class, but Moulds and yeast burden was noted highest in large and minimum on small size class. Mesophilic aerobic Bacteria was found highest in small size class which followed by mixed class and lowest in large size class (Table 7). Statistical analysis indicated that there was highly to slightly significant variation in response to microbial load between different date cultivar and fruit size classes at $P=0.05$ significant level (Table 7) in un-pRESSED un-pitted dates fruits. Among the classes overall investigated microbial load on four cultivar, was recorded highest burden for small fruit size class, followed by mixed and minimum was noted for large fruit size class (Fig. 6).

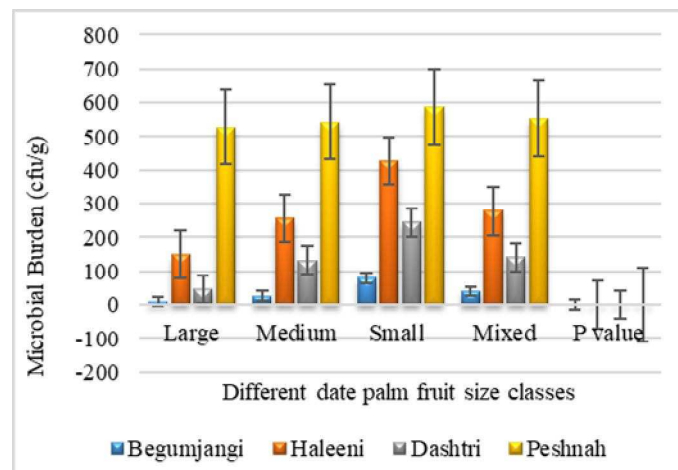


Figure 6. Overall Microbial Burden (cfu/g) in un-pRESSED-un pitted date palm varieties

Microbial burden (cfu/g) in pressed-un pitted dates

Microbial load in pressed-un pitted date fruit of Begumjangi was ranged between 100.0 - 296.0, 1660 - 2800 and 14.0 - 222 cfu/g for the Coliform VRBA, Moulds and yeast and Mesophilic aerobic Bacteria in different fruit size classes, respectively. On Haleeni fruit microbial load was recorded in between 22.0 - 56.7, 542.0 - 5000 and 180 - 500 cfu/g for the Coliform VRBA, Moulds and yeast and Mesophilic aerobic Bacteria in different fruits size classes, respectively and for Dashtri fruit it was found in range between 25.0 - 500.0, 1200.0 - 7807 and 387 - 1000.0 cfu/g for Coliform VRBA, Moulds/yeast and Mesophilic aerobic Bacteria in different fruits size class, respectively. Microbial burden on Peshnah fruit was noted in ranged between 74 - 433, 678 - 7000.0 and 400 - 1300 cfu/g for the Coliform VRBA, Moulds and yeast and Mesophilic aerobic Bacteria in different fruit size classes, respectively. The maximum microbial loads for all four cultivar were found in small size class, which followed by mixed and medium class and minimum was in large size class. Similarly Over all investigated microbial burden was noted in small size class which followed by mixed then medium and lowest was found for large size class. Statistically analysis indicated that there was highly significant variation among microbial infection in all fruit size classes but individual microbe showed slightly to non-significant variation between the classes (Table 8 and Fig. 7). Aleid (2014) reported that the small-sized fruits of Sukkary cultivar showed significantly ($P \leq 0.05$) higher counts for mesophilic aerobic bacteria and mould and yeasts than the larger or medium-sized fruits. In this investigation among the examined

varieties Begumjangi was found hardest to microbial burden and peshnah was noted softened. Similar observation was also reported by Aleid (2014) during study of Microbial loads and physicochemical characteristics of fruits from four Saudi date palm tree cultivars: Conformity with Applicable Date Standards. Nussinovitch et al. (1989) found colony counts of soft dates in the order of 10^4 cfu/g lactic acid bacteria. Aidoo et al. (1996) found bacteria, coliforms and moulds to be pollutants of dates (Tamr) bought from the stores with in greater Glasgow.

Table 8. Microbial burden (cfu/g) in pressed-un pitted dates of four local date palm varieties

Date variety	Fruit size classes	Microbial variable			P value
		Coliform VRBA	Moulds and yeast	Mesophilic aerobic bacteria	
Begumjangi	Large	100.0 ^c	1660 ^c	14.0 ^c	0.00
	Medium	150.0 ^b	2047 ^b	107 ^b	0.00
	Small	296.0 ^a	2800 ^a	222 ^a	0.00
	Mixed	182.0 ^b	2169 ^b	114.33 ^b	0.01
	P value	0.031	0.075	0.045	
Haleeni	Large	22.0 ^b	542.0 ^d	180 ^c	0.00
	Medium	34.2 ^{ab}	1086.0 ^b	323 ^b	0.00
	Small	56.7 ^a	5000 ^a	500 ^a	0.00
	Mixed	37.63 ^{ab}	2209.33 ^c	334.33 ^b	0.00
	P value	0.027	0.000	0.040	
Dashtri	Large	25.0 ^c	5630 ^a	387 ^c	0.00
	Medium	150.0 ^b	7807 ^a	543 ^b	0.00
	Small	500.0 ^a	1200.0 ^b	1000.0 ^a	0.00
	Mixed	225 ^a	4879 ^a	643.33 ^b	0.00
	P value	0.002	0.007	0.023	
Peshnah	Large	74 ^d	678 ^c	400 ^c	0.00
	Medium	158 ^c	7000.0 ^a	570 ^b	0.00
	Small	433 ^a	10750 ^a	1300 ^a	0.00
	Mixed	221.67 ^b	6142.67 ^b	756.67 ^b	0.00
	P value	0.006	0.000	0.000	

Each value is the mean of four replicate, different letters in the same column and raw indicate statistically significant differences (significance level $P = 0.05$)

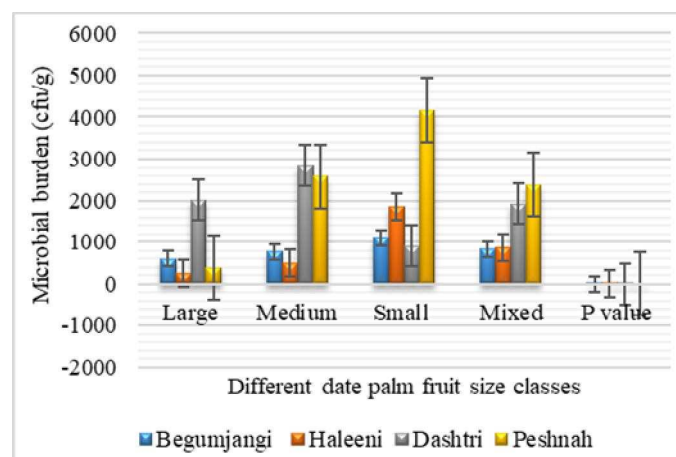


Figure 7. Over all microbial burden (cfu/g) in pressed-un pitted date palm varieties. In

Figures 2-7. bars on graphs showed standard error and statistically significant differences are at significance level $P = 0.05$.

Kader (2007) reported that the microbial spoilage of dates (Tamar) can be caused by yeasts, moulds and bacteria. Abu-Zinada and Ali (1982) reported fungi contamination of different date (Tamar) varieties. Further that the dates contamination with microbial are eaten without further processing may represent a health risk for consumers, and therefore a food safety problem (Brandl, 2006; Hamilton et al., 2006; Tyler and Triplett, 2008). According to the Public Health Laboratory Services (PHLS, 1992, 1996) the Khalas, Sugai and Anbara dates showed unacceptable levels of coliform bacteria.

Fruit Quality Assessment (FQA)

Fruit Quality Assessment (FQA) through fruit performance index (FPI) and valuation classes indicated that the Begamjangi score highest grade point (6) and stand in excellent classes, which followed by Haleeni (4 grade point) with good class and other two dates cultivars Dashtri and Peshnah score 2.0 and 1.0 grade points and classified into poor and very poor category, respectively (Tables 9 and 10).

Table 9. Standard of grade point for fruit quality of date palm [references: Prajapati and Tripathi (2008); Govindaraju et al. (2012); Leghari et al. (2019)]

Valuation classes	Scoring percentage	Grade point
Not recommended	30	0
Very poor	31-40	1
Poor	41-50	2
Moderate	51-60	3
Good	61-70	4
Very good	71-80	5
Excellent	81-90	6
Best	91-100	7

Table 10. Fruit Quality Assessment through fruit performance index (FPI) and valuation classes

Quality Variables	Values/Scale	Date Palm Varieties			
		Begamjangi	Haleeni	Dashtri	Peshnah
Fruit weight	1-5	++++	+++++	++	+++
Stone weight	1-5	++++	+++++	+++	++
Taste and flavor of fruits	1-5	+++++	++++	+++	++
Acidity	1-5	++++	+++	++	+
Reducing Sugar	1-5	+++++	++++	+++	++
Overall Minerals	1-5	++++	+++	++	+
Moisture/ Water activity	1-10	+++++++	+++++	++++	+++
Microbial burden hardy	1-10	+++++++	++++	+++++	++
Obtain Plus/50	50	43	34	24	16
Score %age		86	68	48	32
Grade point		6	4	2	1
Valuation Classes		Excellent	Good	Poor	Very poor

Conclusion

From the facts cited in this study it could be established that some significant performance characteristics were determined in the investigated dates palm fruits of Turbat, the results provide new information needed to adapt excellent dates standard for cultivation. A proportional examination of microbiological quality and physiochemical

properties at the farm level, as well as a complete examination of current guidelines on date quality, are obligatory in order to review the significant quality criteria of date fruit standards. Moreover valuation of the investigated fruit performance or quality index is important for the dates of local area. The present study also concluded that the date variety Begamjangi and Haleeni due to their highest grade point and good financial worth are expected to be a decent performers and might be suggested for the cultivation.

REFERENCES

- [1] Abekhti, A., Zarour, K., Boulal, A., Benmechernene, Z., Kihal, M. (2013): Evaluation of Microbiological Quality of the Date Fruit Product “*Btana*” Produced in Adrar South Algeria. – *Journal of Microbiology Research* 3(5): 163-170.
- [2] Abu-Zinada, A. H., Ali, M. I. (1982): Fungi associated with dates in Saudi Arabia. – *Journal of Food Protection* 45(9): 842-844.
- [3] Ahmed, M. V. O. M., Bouna, Z. E. O., Lemine, F. M. M., Djeh, T. K. O., Mokhtar, T., Salem, A. O. M. (2011): Use of multivariate analysis to assess phenotypic diversity of date palm (*Phoenix dactylifera* L.) cultivars. – *Scientia Horticulturae* 127(3): 367-371.
- [4] Aidoo, K. E., Tester, R. F., Morrison, J. E., MacFarlane, D. (1996): The Composition and Microbial Quality of Pre- Packed Dates Purchased in Greater Glasgow. – *International Journal of Food Science & Technology* 31(5): 433-438.
- [5] Aleid, S. M., Hassan, B. H., Almaiman, S. A., Al-Kahtani, S. H., Ismail, S. M. (2014): Microbial loads and physicochemical characteristics of fruits from four Saudi date palm tree cultivars: conformity with applicable date standards. – *Food and Nutrition Sciences* 5(04): 316-327.
- [6] Al-Farsi, M., Alasalvar, C., Morris, A., Baron, M., Shahidi, F. (2005): Compositional and sensory characteristics of three native sun-dried date (*Phoenix dactylifera* L.) varieties grown in Oman. – *Journal of agricultural and food chemistry* 53(19): 7586-7591.
- [7] Al-Farsi, M. A., Lee, C. Y. (2008): Nutritional and functional properties of dates: a review. – *Critical reviews in food science and nutrition* 48(10): 877-887.
- [8] Al-Hooti, S., Sidhu, J. S., Qabazard, H. (1997): Physicochemical characteristics of five date fruit cultivars grown in the United Arab Emirates. – *Plant Foods for Human Nutrition* 50(2): 101-113.
- [9] Anonymous. (2012): Food and Agriculture Organization (FAO). Retrieved 15th March 2014. – from <http://faostat.fao.org/site/567/default.aspx#ancor>.
- [10] AOAC. (1990): Official methods of analysis. – Association of Official Analytical Chemists.
- [11] AOAC. (1995): Official Methods of Analysis. – 15th Edition, Association of Official Analytical Chemists, Washington DC.
- [12] Ashraf, Z., Hamidi-Esfahani, Z. (2011): Date and Date Processing: A Review. – *Food Reviews International* 27: 101-133.
- [13] Assirey, E. A. R. (2015): Nutritional composition of fruit of 10 date palm (*Phoenix dactylifera* L.) cultivars grown in Saudi Arabia. – *Journal of Taibah University for science* 9(1): 75-79.
- [14] Atlas, R. M. (2004): Handbook of Microbiological Media. – 3rd Edition, CRC Press, Boca Raton, 2051 p. <http://dx.doi.org/10.1201/9781420039726>.
- [15] Baliga, M. S., Baliga, B. R. V., Kandathil, S. M., Bhat, H. P., Vayalil, P. K. (2011): A review of the chemistry and pharmacology of the date fruits (*Phoenix dactylifera* L.). – *Food research international* 44(7): 1812-1822.
- [16] Besbes, S., Drira, L., Blecker, C., Deroanne, C., Attia, H. (2009): Adding value to hard date (*Phoenix dactylifera* L.): compositional, functional and sensory characteristics of date jam. – *Food chemistry* 112(2): 406-411.

- [17] Biglari, F., AlKarkhi, A. F., Easa, A. M. (2009): Cluster analysis of antioxidant compounds in dates (*Phoenix dactylifera*): Effect of long-term cold storage. – Food chemistry 112(4): 998-1001.
- [18] Botes, A., Zaid, A. (2002): Date production support program. – FAO plant production and protection paper, 156, Rev. 1. FAO United Nations, Rome, Italy.
- [19] Brandl, M. T. (2006): Fitness of human enteric pathogens on plants and implications for food safety. – Annu. Rev. Phytopathol 44: 367-392.
- [20] Elleuch, M., Besbes, S., Roiseux, O., Blecker, C., Deroanne, C., Drira, N. E., Attia, H. (2008): Date flesh: Chemical composition and characteristics of the dietary fiber. – Food chemistry 111(3): 676-682.
- [21] Folch, J., Lees, M., Sloane Stanley, G. H. (1957): A simple method for the isolation and purification of total lipids from animal tissues. – J. boil. Chem. 226(1): 497-509.
- [22] Gasim, A. A. A. (1994): Changes in sugar quality and mineral elements during fruit development in five date palm cultivars in Al-Madinah Al-Munawwarah. – Journal of King Abdul Aziz University, Science 6: 29-36.
- [23] Govindaraju, M., Ganeshkumar, R. S., Muthukumar, V. R., Visvanathan, P. (2012): Identification and evaluation of air-pollution-tolerant plants around lignite-based thermal power station for greenbelt development. – Environmental Science and Pollution Research 19(4): 1210-1223.
- [24] Haider, M. S., Khan, I. A., Jaskani, M. J., Naqvi, S. A., Hameed, M., Azam, M., Khan, A. A., Pintaud, J. C. (2015): Assessment of morphological attributes of Date palm accessions of diverse agro-ecological origin. – Pak. J. Bot. 47(3): 1143-1151.
- [25] Hamilton, A. J., Stagnitti, F., Premier, R., Boland, A. M., Hale, G. (2006): Quantitative microbial risk assessment models for consumption of raw vegetables irrigated with reclaimed water. – Appl. Environ. Microbiol 72(5): 3284-3290.
- [26] Hammadi, H., Mokhtar, R., Mokhtar, E., Ali, F. (2009): New approach for the morphological identification of date palm (*Phoenix dactylifera* L.) cultivars from Tunisia. – Pak. J. Bot. 41(6): 2771-2681.
- [27] Iqbal, M., Rahman, U. U., Niamatullah, M., Khan, S. M., Akhtar, A. (2016): Periodic growth and development of fruits of different date cultivars grown under the agro-climatic conditions of DI Khan. – Pakistan Journal of Science (Pakistan) 64(3): 259-264.
- [28] Jamil, M. S., Nadeem, R., Hanif, M. A., Ali, M. A., Akhtar, K. (2010): Proximate composition and mineral profile of eight different unstudied date (*Phoenix dactylifera* L.) varieties from Pakistan. – African Journal of Biotechnology 9(22): 3252-3259.
- [29] Jaradat, A. A., Zaid, A. (2004): Quality traits of date palm fruits in a center of origin and center of diversity. – Journal of Food Agriculture and Environment 2: 208-217.
- [30] Kader, A. A. (2007): Recommendation for Maintaining Post-harvest Quality. – University of California, Davis, <http://postharvest.ucdavis.edu/produce/fruit/dates.shtm>.
- [31] Langemeier, J. M., Rogers, D. E. (1995): Rapid method for sugar analysis of doughs and baked products. – Cereal chemistry (USA) 72: 349-351.
- [32] Laurey, S. (1997): Protein structure core facility. – Omaha, NE, 68: 198-4525.
- [33] Leghari, S. K., Asrar, M., Muhammad, A., Rahman, S., Ilahi, Z. (2017): Impact of Air Pollution Caused By Fire Smoke on Yield and Nutritional Value of Pleurotus (*Flabellatus*) Djamor, R-22. – Pak. J. Bot 49(SI): 279-282.
- [34] Leghari, S. K., Akbar, A., Qasim, S., Ullah, S., Asrar, M., Rohail, H., Ahmed, S., Mehmood, K., Ali, I. (2019): Estimating Anticipated Performance Index and Air Pollution Tolerance Index of Some Trees and Ornamental Plant Species for the Construction of Green Belts. – Polish Journal of Environmental Studies 28(3): 1759-1769.
- [35] Lemine, F. M. M., Samb, A., Zein-el-Abidine, O. B., Ahmed, M. V. O. M., Djeh, T. K. O., Boukhary, A. O. M. S. O. (2014): Assessment of physicochemical diversity in fruit of Mauritanian date palm (*Phoenix dactylifera* L.) cultivars. – African Journal of Agricultural Research 9(28): 2167-2176.

- [36] Mughal, S. A., Leghari, S. K., Achakzai, A. K. K., Asrar, M., Ismail, Ponya, Z., Rehman, S. R., Sadiq, N. (2018): Effects of road side pollution on physio-morphology of apple (*Malus pumila* Miller.) at District Kalat Balochistan, Pakistan. – International Journal of Biosciences 12(6): 334-345.
- [37] Myhara, R. M., Karkalas, J., Taylor, M. S. (1999): Determination of the mineral compositions of some selected oil-bearing seeds and kernels using inductively coupled plasma atomic emission spectrometry (ICP-AES). – Grasas Aceites 57: 211-218.
- [38] Nussinovitch, A., Rosen, B., Salik, H., Kopelman, I. J. (1989): Effect of Heating Media on the Microbiology and Shelf Life of Heat Pasteurized Soft Dates, Lebensmittel-Wissenschaftund. – Technologie 22(5): 245-247.
- [39] Osman, A. M. A. (1984): The performance of date palms in the Sudan. – Acta Hort 143: 231-237.
- [40] Piggott, J. R. (1995): Design Questions in Sensory and Consumer Science. – Food Quality and Preference 6(4): 217-220.
- [41] Prajapati, S. K., Tripathi, B. D. (2008): Anticipated Performance Index of some tree species considered for green belt development in and around an urban area: A case study of Varanasi city, India. – Journal of environmental management 88(4): 1343-1349.
- [42] Public Health Laboratory Services (PHLS). (1992): Provisional Microbiological Guidelines for Some Ready-to-Eat Foods Sampled at Point of Sale, Notes for PHLS Food Examiners. – PHLS Microbiology Digest 9: 98-99.
- [43] Public Health Laboratory Services (PHLS). (1996): Microbiological Guidelines for Some Ready-to-Eat Foods Sampled at the Point of Sale: An Expert Opinion from the PHLS. – PHLS Microbiology Digest 13: 41-43.
- [44] Ragab, W. S., Ramadan, B. R., Sorour, M. A., Naglaa, A. (2011): Physical and Chemical Changes In Fruits of Three Dates Palm (*Phoenix Dactylifera* L.) Grown In South Valley Egypt. – Journal of Food and Dairy Sci., Mansoura Univ. 2(11): 605-615.
- [45] Rahman, M. S., Al-Farsi, S. A. (2005): Instrumental Texture Profile Analysis (TPA) of Date Flesh as a Function of Moisture Content. – Journal of Food Engineering 66(4): 505-511.
- [46] Reynes, M., Bouabibi, H., Piombo, G., Risterucci, A. M. (1994): Characterization of the principal varieties of dates cultivated in the area of Djejrjd in Tunisia. – Fruits 49: 289-298.
- [47] Safi, E. B., El Arem, A., Issaoui, M., Hammami, M., Achour, L. (2009): Phenolic content and antioxidant activity of four date palm (*Phoenix dactylifera* L.) fruit varieties grown in Tunisia. – International journal of food science & technology 44(11): 2314-2319.
- [48] Sawaya, W. N., Miski, A. M., Khalil, J. K., Khatchadourian, H. A., Mashadi, A. S. (1983): Physical and chemical characterisation of the major date varieties grown in Saudi Arabia: I. Morphological measurements, proximate and mineral analyses. – Date Palm Journal 2: 1-25.
- [49] Steel, R. G., Torrie, J. H. (1980): Principles and Procedures of Statistics. A Biometrical Approach. – 2nd ed., McGraw-Hill, New York.
- [50] Tyler, H. L., Triplett, E. W. (2008): Plants as a Habitat for Beneficial and/or Human Pathogenic Bacteria. – Annual Review of Phytopathology 46: 53-63.
- [51] Vayalil, P. K. (2002): Antioxidant and antimutagenic properties of aqueous extract of date fruit (*Phoenix dactylifera* L. Arecaceae). – Journal of Agricultural and Food Chemistry 50(3): 610-617.
- [52] Wills, R., McGlasson, B., Graham, D., Joyce, D. (1998): Post Harvest: An Introduction to the Physiology and Handling of Fruits, Vegetables and Ornamentals. – 4th Edition, University of New South Wales Press Ltd, Australia, 262 p.
- [53] Zaid, A., de Wet, P. F. (2002): Origin, geographical distribution and nutritional values of date palm. – In: Zaid, A. (ed.) Date palm cultivation. Rev. Ed. Plant production and protection paper 156. Food and Agriculture Organization of the United Nations, Rome, pp 29-44.

- [54] Zehdi, S., Trifi, M., Billote, N., Marrakchi, M., Pintaud, J. C. (2005): Genetic diversity of Tunisian date palms (*Phoenix dactylifera* L.) revealed by nuclear microsatellite polymorphism. – *Hereditas* 141(3): 278-287.
- [55] Zehdi, S., Cherif, E., Rhouma, S., Santoni, S., Hannachi, A. S., Pintaud, J. C. (2012): Molecular polymorphism and genetic relationships in date palm (*Phoenix dactylifera* L.): The utility of nuclear microsatellite markers. – *Sci. Hortic.* 148: 255-263.

MASH BEAN [*Vigna mungo* (L.) HEPPER] GERMPLASM EVALUATION AT DIFFERENT ECOLOGICAL CONDITIONS OF PAKISTAN

QAYYUM, A.^{1*} – IQBAL, J.^{2,3} – BARBANTI, L.⁴ – SHER, A.^{5*} – SHABBIR, G.² – RABBANI, G.³ – RAFIQ, M. K.⁶ – TAREEN, M. N.⁷ – TAREEN, M. J.⁷ – AMIN, B. A. Z.⁸

¹*Department of Agronomy, The University of Haripur, 22620, Pakistan*

²*Department of Plant Breeding and Genetics, Pir Mehr Ali Shah-Arid Agriculture University Rawalpindi, 46300, Pakistan*

³*Pulses Program, Barani Agriculture Research Institute, Chakwal, 48800, Pakistan*

⁴*Department of Agricultural and Food Sciences, University of Bologna, 40127, Italy*

⁵*College of Agriculture, Bahauddin Zakariya University, Bahadur Campus Layyah, 31200, Pakistan*

⁶*School of Geosciences, The University of Edinburgh, EH3 9FF, United Kingdom*

⁷*Agriculture Research Institute, Sariat, Quetta, Pakistan*

⁸*Department of Environmental Sciences, COMSATS University Islamabad, Abbottabad Campus, 22060, Pakistan*

**Corresponding authors*

e-mail: aqayyum@uoh.edu.pk; ahmad.sher@bzu.edu.pk

(Received 1st Feb 2019; accepted 8th Mar 2019)

Abstract. Mash bean [*Vigna mungo* (L.) Hepper], is the third largest pulse crop in Pakistan. Nine advanced breeding lines were compared with two commercial varieties, in order to investigate their potential prior to release as cultivated varieties. A field experiment was conducted in three environments in Punjab, Pakistan, during the 2014 kharif (wet) season. Developmental, morphological and yield traits included time to reach 90% maturity, plant height, the number of branches, grain yield (GY) and its components. GY varied between 778 kg ha⁻¹ (cv. Mash Arooj) and 1005 kg ha⁻¹ (line 11CM-709) in the eleven genotypes, and between 438 and 1667 kg ha⁻¹ in the three environments. The lowland environment (Piplan) was the highest yielding, despite significant water deficit. In each genotype average yield across the three environments, plotted against the regression slope of specific yield vs. average yield in each environment, allowed yield potential and stability to be shown. As a result, five breeding lines exhibited a remarkable yield potential in exchange for low stability, i.e. modest suitability for low yielding environments. The remaining lines yielded as the two commercial varieties with a higher stability across environments. These are good premises for mash bean wider diffusion in the surveyed area.

Keywords: *mash bean, black gram, genotypes, plant traits, yield potential, yield stability*

Introduction

Mash bean [*Vigna mungo* (L.) Hepper], black gram, is an important legume crop widely grown in Asia and has great value as food, fodder and green manure. In addition to improving the soil fertility, it is a cheap source of protein for direct human consumption. It has a close relationship with human being due to high and easily digestible protein content (20.8–30.5%) and carbohydrate (56.5–63.7%) on dry weight

basis (Sharma et al., 2012). Thus, it has a great potential to improve protein deficiency in human beings by providing a low cost protein. Mash bean not only fixes free atmospheric N₂, but also enriches the soil with nitrogen for the growth of succeeding crops (Sen, 1996). This crop can be successfully grown on marginal lands where other crops perform poorly (Ghafoor et al., 2003).

By establishing the International Year of Pulses in 2016, the FAO has shown renewed interest in these crops as components of the diets in many countries (Sharma, 2014). This is supported by their annual increase rate that, based on the cited source, has resulted slightly higher than that of cereals (1.84% vs. 1.82% over the past two decades).

Despite these premises, worldwide yield of mash bean including Pakistan is very poor. In Pakistan it is the least researched crop among pulses despite its high nutritive and economic value, due to which its area of cultivation and production have both gradually decreased. In Pakistan during 2016-17, mash bean was grown over an area of 17 thousand hectares with a total production of 7 thousand tonnes. However, it is estimated that mash bean is the major food legume grown in Pakistan during the summer season after gram and mung bean: it occupies 1.5% of total pulses area contributing 1.4% to total pulses production (GOP, 2017). Though it is grown all over the country, Punjab is the major mash bean producing province. The productivity of mash bean in the country has remained quite low as compared to other grain legumes (GOP, 2017).

Mash bean is mainly grown as a pulse crop, although sometimes it is used as a green manure to improve soil fertility. Mash bean is a short-duration crop that requires less water as compared to other summer crops and thus qualifies as a suitable candidate for rainfed areas. Successful cultivation in rainfed areas can give significant economic benefits to farmers (Singh et al., 2015). Like other legumes, mash bean also possesses the ability to establish a symbiotic relationship with the nitrogen fixing soil bacteria generally known as “rhizobia”, which is a term used for a broad range of microsymbionts from α - and β -*Proteobacteria* that establish symbiosis with leguminous plants for biological nitrogen fixation. Mash bean can fix approximately 37–83 kg ha⁻¹ of nitrogen through this symbiotic association (Mohammad et al., 2010).

The performance of any character is a combined result of the genotype, the environment and the interaction between genotype (G) and environment (E). It is necessary to research on yield stability and G × E interactions to improve consistency in performance across diverse environments and years (Blanche et al., 2009). Significant genotype and environment interactions occur when the responses of two genotypes to different levels of environmental stress are variable. An efficient genotype must remain consistent in different years and environmental conditions (Hill, 1975). Better understanding of the G × E interactions and stability in crops is generally used as a decision tool, particularly at the final stage of variety development process, to generate essential information on pattern of adaptation in breeding lines, screen new varieties for release, and determine the recommendation domains for released varieties (Yan and Kang, 2003).

Based on these premises, the main objectives of the present study were to identify more high-yielding, stable and promising lines and areas where mash bean lines would be adapted. The novelty of this research is that promising lines, having desirable plant traits and high yield stability, could be introduced as released varieties.

Material and Methods

Plant materials, environments and experimental conditions

Mash bean germplasm comprising nine advanced breeding lines (11CM-707, 11CM-705, 11CM-709, 11CM-701, 11CM-703, 11CM-706, 11CM-710, 11CM-702, 11CM-704) and two commercial varieties commonly cultivated among farmers (Chakwal Mash and Mash Arooj) was evaluated over three environments in the framework of Barani Agricultural Research Stations: Chakwal (32°55'49"N 72°51'20"E, 525 m asl), Piplan (32°17'12"N 71°21'59"E, 198 m asl) and Fateh Jang (33°33'57"N 72°38'57"E, 514 m asl) in Punjab province, Pakistan, during 2014 (*Figure 1*).

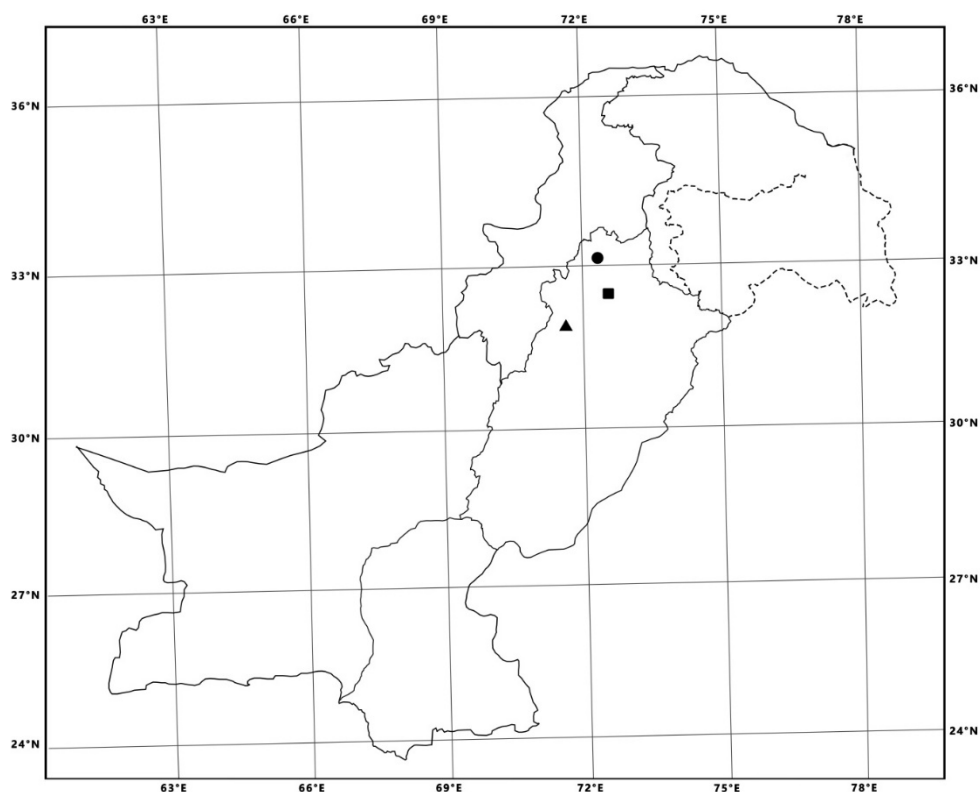


Figure 1. Mash bean germplasm evaluation at Barani Agricultural Research Stations: Chakwal (▲), Piplan (●) and Fateh Jang (■) in Punjab province, Pakistan

The experiment was laid out in a Randomized Complete Block Design (RCBD) at three replicates, with a net plot size of 4.8 m² (4 × 1.2 m). Preceding crop, in the frame of the National Coordinated Pulses Program, was groundnut at all three environments. The fields were supplied with a recommended dose of Di-Ammonium Phosphate (DAP) fertilizer (50 kg ha⁻¹) before preparation of seed bed. Seeds of mash bean were sown with hand drill and planted at a depth of 3-4 cm. Row width was 30 cm, while plant to plant distance was kept at 10 cm by means of over-seeding and subsequent thinning of seedlings. The crop was sown on July 22 and harvested on October 10, 2014, at all three environments. Hand weeding was carried out, and all recommended cultural practices were followed to maintain a healthy crop stand. Irrigation was not applied.

Weather during the experiment (minimum and maximum temperature, precipitation and relative humidity) was daily monitored at the three environments' meteorological

stations. Based on this, reference evapo-transpiration (ET_0) was calculated with the Hargreaves equation (Hargreaves and Samani, 1985). The thermal sum of average daily temperatures above 10°C was also calculated, and expressed as growing degree days (GDD) from sowing to harvest. GDD are a measure of heat accumulation commonly used to predict plant development, and rate genotype behaviour across time and space.

Crop monitoring

The following traits pertaining to plant development and morphology were specifically monitored during the experiment: seedling emergence, days to reach the beginning of the reproductive stage (50% flowering) and final senescence (90% maturity), plant height and the number of primary branches.

At maturity, five plants from each plot were randomly selected and the number of pods per plant and seeds per pod were counted. The grain was then harvested from the whole plot surface (4.8 m^2), weighted, and a sample was oven dried (48 hours at 105°C). Based on this, grain yield per hectare adjusted at 12% moisture was determined. Finally, the thousand-seed weight that is the third yield component was determined, based on pods per plant and seeds per pod that are the other two yield components, and grain yield.

Data analysis

Morphological, developmental and yield data were submitted to a combined ANOVA for the sources Genotypes (G), Environments (E), and their interaction ($G \times E$), using R-program 3.2.1 (R Development Core Team 2012). Student Newman-Keuls (SNK) test at $P \leq 0.05$ was used to separate data of significant ANOVA sources.

Pearson's correlation (r) between crop traits was assessed to evaluate the degree of inter-relationship. Additionally, the relative importance of yield components on grain yield was assessed through the Lindeman, Merenda and Gold's (LMG) method (Lindeman et al., 1980).

Lastly, yield data representation according to Eberhart and Russel (1966) was used to highlight each genotype's average yield vs. yield stability among experimental environments.

Results

Meteorological conditions

The experiment was conducted during the kharif (wet) season in 2014. The amount of precipitation greatly differed among the three environments: 390, 169 and 852 mm were received during mash bean cultivation in Chakwal, Piplan and Fateh Jang, respectively. Differences were also shown in average temperature: 27.4 , 31.5 and 28.2°C at the three respective environments. Thus, Piplan that has a lower elevation appeared a drier and warmer environment than Chakwal and Fateh Jang. The thermal sum cumulated steadily from sowing to harvest in all environments (*Figure 2*). However, Piplan diverged from the other two environments, achieving a final 1744 GDD vs. an average 1444 GDD of the combined Chakwal and Fateh Jang.

The balance between water supply (precipitation) and demand (ET_0) showed very different patterns (*Figure 2*). Chakwal remained slightly above the break-even line for most of the time. Piplan portrayed increasing water deficit up to -264 mm at harvest.

Lastly, Fateh Jang featured much more P than ET_0 , resulting in a considerable gain (+477 mm).

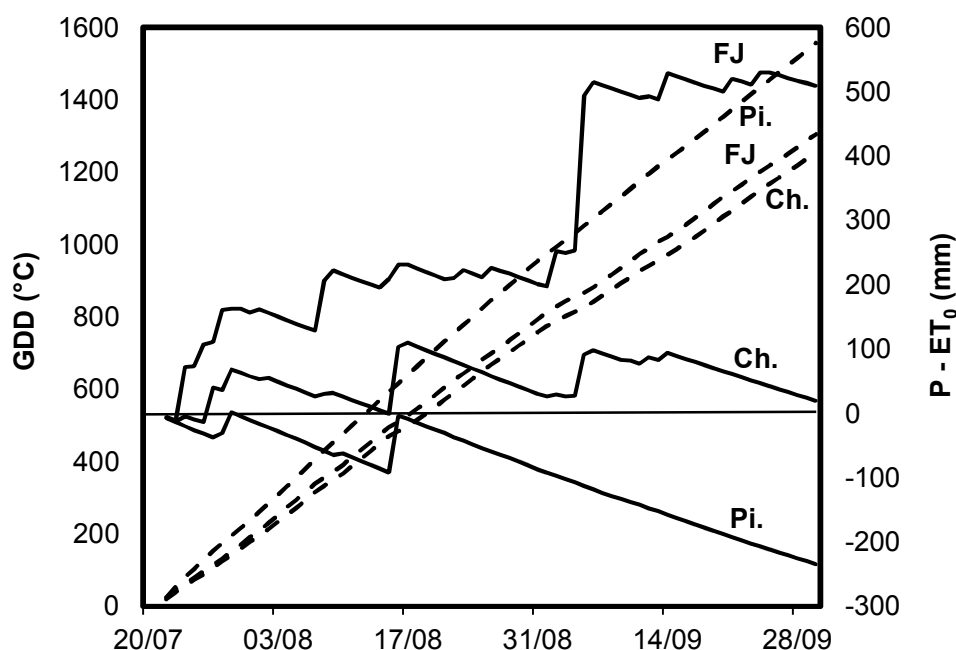


Figure 2. Cumulated growth degree days (GDD) (dashed lines) and precipitation minus reference evapo-traspiration ($P - ET_0$) (solid lines) from seeding to harvesting in the three environments. Ch., Chakwal; Pi., Piplan; FJ, Fateh Jang. The horizontal line indicates the break-even in the balance between precipitation and evapotranspiration

Plant development and morphology

Seedling emergence was very high (average, 92.6%); no ANOVA source (G, E, $G \times E$) significantly influenced this trait (Table 1). The eleven genotypes exhibited a modest difference in earliness at 50% flowering (Table 1): only 11CM-703 was significantly earlier than the rest of genotypes by an approximate six days. An average 48 days was needed to achieve 50% flowering in the three environments, corresponding to 969 GDD.

A stronger differentiation was shown at 90% maturity (Table 1): 11CM-704 was the earliest genotype at par with 11CM-707, 11CM-703 and 11CM-710. 11CM-706 and 11CM-702 were the latest, and the other five genotypes were statistically undifferentiated between the two groups. Slight differences to achieve 90% maturity were also shown among the three environments. An average 78 days was needed, corresponding to 1515 GDD.

Plant height varied between 37.9 and 44.4 cm among the eleven genotypes (Table 1): 11CM-701, 11CM-702 and Mash Arooj were the shortest genotypes; Chakwal Mash was the tallest, while the other seven genotypes were intermediate. Among the three environments, Piplan featured much taller plants (average, +35%) than Chakwal and Fateh Jang.

In contrast to this, the number of primary branches was undifferentiated (Table 1). An average 1.88 branches per plant was recorded, with minor differences among genotypes and environments.

Table 1. Plant development and morphology of eleven genotypes grown at the three environments

Source	Seedling emergence (%)	Days to 50% flowering	Days to 90% maturity	Plant height (cm)	Primary branches
Genotypes (G)					
11CM-707	93.1	48.9 a	78.0 b	40.7 ab	1.86
11CM-705	92.7	49.1 a	78.5 ab	40.7 ab	1.91
11CM-709	92.5	50.9 a	78.3 ab	40.5 ab	1.86
11CM-701	92.1	46.6 a	78.7 ab	38.9 b	1.86
11CM-703	92.4	43.0 b	78.0 b	40.0 ab	1.97
11CM-706	92.2	48.1 a	79.2 a	39.7 ab	1.84
11CM-710	92.3	50.1 a	78.0 b	40.5 ab	1.82
11CM-702	93.2	48.2 a	79.3 a	39.1 b	1.88
11CM-704	92.7	49.4 a	77.9 b	40.2 ab	1.86
Chakwal Mash	92.7	47.0 a	79.0 ab	44.4 a	1.93
Mash Arooj	92.9	47.2 a	78.3 ab	37.9 b	1.86
<i>P</i>	0.9554 ns	0.0001**	0.0465*	0.0304*	0.9828 ns
Environments (E)					
Chakwal	92.6	47.4	78.0 b	35.7 b	1.83
Piplan	92.6	48.1	77.7 b	48.6 a	1.95
Fateh Jang	92.5	48.6	79.7 a	36.4 b	1.86
<i>P</i>	0.9451 ns	0.2251 ns	0.0001**	0.0001**	0.1272 ns
G × E					
<i>P</i>	0.8308 ns	0.1365 ns	0.0016**	0.0054**	0.7745 ns
C.V. (%)	1.8	5.7	1.4	8.2	13.0

ns, * and ** mean non-significant, significant at $P \leq 0.05$ and $P \leq 0.01$, respectively. Different letters indicate statistical differences at $P \leq 0.05$ (SNK test)

Yield and yield components

The number of pods per plant varied in genotypes between 17.1 (Mash Arooj) and 21.8 (average of 11CM-707, 11CM-705, 11CM-709, 11CM-701, 11CM-703, 11CM-706 and Chakwal Mash) (Table 2). The remaining three genotypes were intermediate (average, 19.0). The three environments exhibited a much higher variation in this trait: Piplan exhibited a more than double data (32.1) than the combined Chakwal and Fateh Jang (average, 14.9).

Compared to this, the number of seeds per pod did not significantly vary among genotypes, whereas modest but significant differences were shown among environments (Table 2): also in this case Piplan displayed a certain advantage over Chakwal and Fateh Jang.

The thousand-seed weight varied among genotypes from a minimum of 17.6 g (11CM-705) to a maximum of 22.5 g (11CM-703), although ANOVA was significant only at $P < 0.10$ (Table 2). Stronger differences were evidenced among the three environments: Piplan exhibited a ca. 40% higher data than Fateh Jang, which in turn passed Chakwal by ca. 20%.

Grain yield significantly varied among genotypes (Table 2). It ranged from less than 800 kg ha⁻¹ (Mash Arooj) to more than 1000 kg ha⁻¹ (11CM-709). The remaining genotypes were quite evenly distributed in this range. Much stronger differences were shown among environments: Chakwal and Fateh Jang averaged 485 kg ha⁻¹, whereas Piplan achieved ca. 3.5 times as much.

The significant $G \times E$ interaction (*Table 2*) suggests a different behaviour of the eleven genotypes in the three environments, despite analogous grain yield variation in the single environments (C.V. between 13.9% and 16.4%; not shown).

Table 2. Grain yield and yield components of eleven genotypes grown at the three environments

Source	Pods per plant	Seeds per pod	Thousand seed weight (g)	Grain yield (kg ha ⁻¹)
Genotypes (G)				
11CM-707	21.5 a	6.31	20.2	826 cd
11CM-705	22.0 a	6.44	17.6	801 d
11CM-709	22.8 a	6.37	20.5	1005 a
11CM-701	22.1 a	6.37	20.1	944 ab
11CM-703	21.2 a	6.31	22.5	954 ab
11CM-706	21.5 a	6.40	19.7	921 abc
11CM-710	19.0 ab	6.44	21.5	921 abc
11CM-702	18.7 ab	6.37	21.7	873 bcd
11CM-704	19.3 ab	6.40	20.2	831 cd
Chakwal Mash	21.6 a	6.42	18.1	817 cd
Mash Arooj	17.1 b	6.40	21.7	778 d
<i>P</i>	0.0006**	0.7684 ns	0.0676 ns	0.0001**
Environments (E)				
Chakwal	15.0 b	6.35 b	15.6 c	438 c
Piplan	32.1 a	6.46 a	26.6 a	1667 a
Fateh Jang	14.8 b	6.35 b	18.8 b	532 b
<i>P</i>	0.0001**	0.0127*	0.0001**	0.0001**
G × E				
<i>P</i>	0.0008**	0.7012 ns	0.0001**	0.0001**
C.V. (%)	13.6	2.6	16.3	9.3

ns, * and ** mean non-significant, significant at $P \leq 0.05$ and $P \leq 0.01$, respectively. Different letters indicate statistical differences at $P \leq 0.05$ (SNK test)

Data representation according to Eberhart and Russel (1966) allows these differences to be interpreted based on the two factors average yield in the three environments, and regression slope of genotype yield vs. average yield in each environment (*Figure 3*). In practice, almost all genotypes fall in the first and the third quadrant, i.e. all genotypes belong to either high producing under favourable conditions types (first quadrant), or low producing but suited for unfavourable conditions types (third quadrant).

However, in the former group 11CM-703 could be seen a better genotype than 11CM-709 despite lower average yield, thanks to a higher suitability for unfavourable conditions (regression slope closer to 1). In fact, 11CM-703 attained a relative yield > 100.0 in all three environments, whereas 11CM-709 attained a relative yield > 100.0 only in two environments (data not shown).

At the opposite end, 11CM-705 and Mash Arooj appeared to be intrinsically suited for unfavourable conditions (regression slope below 0.9), but did not achieve a relative yield > 100.0 in any of the three environments. Compared to them, 11CM-707 had a similar regression slope, i.e. good suitability for unfavourable conditions, but achieved a relative yield > 100.0 in the two low yielding environments (Chakwal and Fateh Jang) (data not shown).

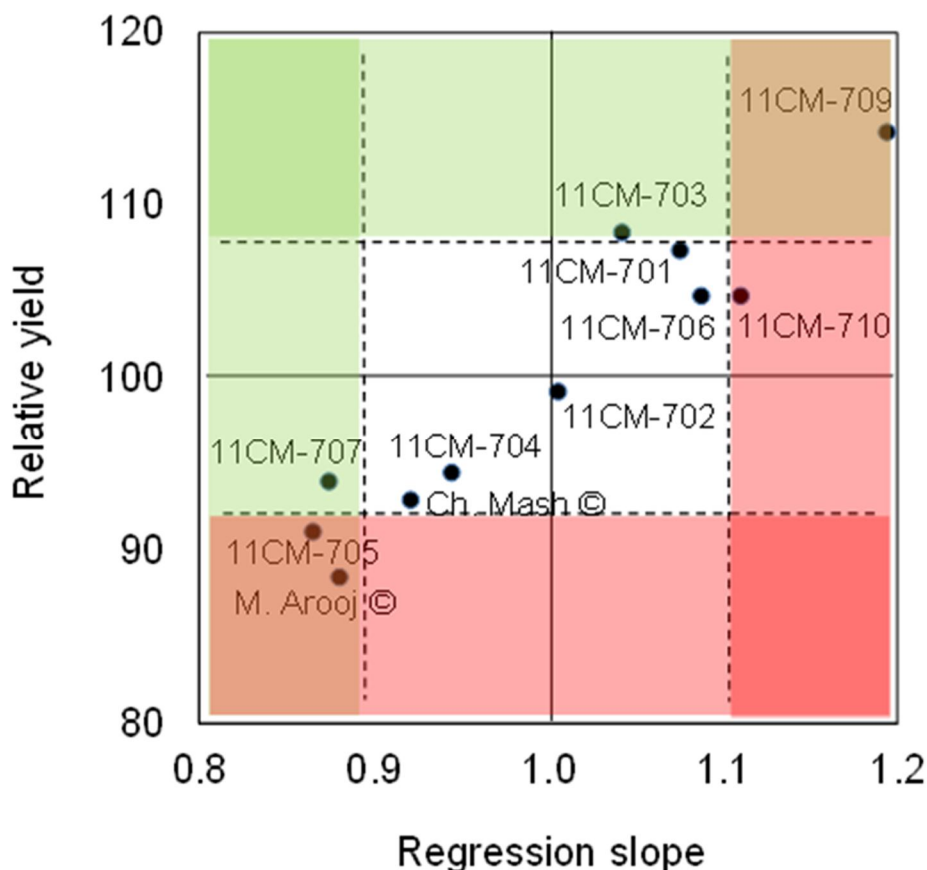


Figure 3. Slope of the regression between genotype yield and average yield in the three environments ($1 = \text{average}$), and relative yield across the three environments ($100 = \text{average}$). Vertical and horizontal dashed lines indicate \pm standard deviation for the two respective traits. Beyond dashed lines, green and red colour indicate favourable and unfavourable conditions, respectively. Based on this, the four quadrants indicate high yield and low stability (top right); low yield and stability (bottom right); low yield and high stability (bottom left); high yield and stability (top left)

Relationships among developmental, morphological and yield traits

The table of correlations involving all investigated traits displays several inter-relations (Table 3). Seedling emergence was not related to any other trait, which is consistent with the low variation observed for this trait (Table 1). The time to 50% flowering was not related to any other trait, either, whereas the time to 90% maturity was adversely related to plant height, the number of pods per plant and final yield. Plant height was directly related to the number of primary branches, the three yield components and, especially ($r = 0.86^{**}$), final yield.

The three yield components were generally inter-related, and unsurprisingly well related to yield. However, the relative importance of yield components through the LMG method (Figure 4) indicated pods per plant and thousand-seed weight as prominent components (respective weights, 49% and 39%), compared to seeds per pod weighing a residual 12%. This is consistent with the different influence exerted by the investigated factors on the three yield components (Table 2).

Table 3. Pearson's correlations between developmental, morphological and yield traits

	Emergence	D50F	D90M	Height	Branches	Pods	Seeds	TSW
D50F	0.17							
D90M	-0.01	0.10						
Height	0.17	0.09	-0.42*					
Branches	0.12	-0.05	-0.29	0.56**				
Pods	0.13	0.00	-0.39*	0.91**	0.47**			
Seeds	0.11	0.11	-0.09	0.54**	0.15	0.60**		
TSW	-0.08	-0.01	-0.25	0.59**	0.20	0.57**	0.18	
GY	0.05	0.02	-0.38*	0.86**	0.38*	0.93**	0.51**	0.83**

Emergence, seedling emergence; D50F, days to 50% flowering; D90M, days to 90% maturity; Height, plant height; Branches, primary branches; Pods, pods per plant; Seeds, seeds per pod; TSW, thousand-seed weight; GY, grain yield. * and ** indicate r values significant at $P \leq 0.05$ and $P \leq 0.01$, respectively (n = 33)

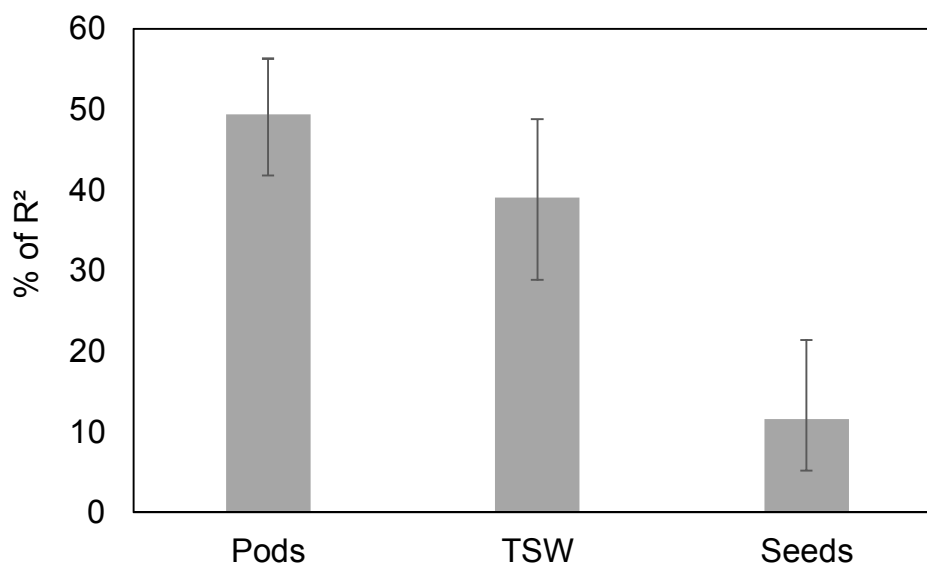


Figure 4. Relative importance of the three yield components on grain yield (LMG method). Total R² (99.1%) is normalized to sum 100%. Bars indicate 95% confidence intervals. Pods, pods per plant; TSW, thousand seed weight; Seeds, seeds per pod

Discussion

Increased interest in pulses is stemming research worldwide. New mash bean cultivars are being released to replace old genotypes in the quest for higher and more consistent yields in both traditional (Khaimichho et al., 2014; Sartaj and Anwar, 2015; Mbeyagala et al., 2016) and new cropping areas (Pekşen et al., 2015). The appraisal of yield related attributes and yield stability across environments is of crucial importance in development and introduction of improved varieties.

Several works addressed the genetic control of quantitative traits associated with yield in mash bean genotypes (Khaimichho et al., 2014; Hemavathy et al., 2015; Mbeyagala et al., 2016). Only in one work (Mbeyagala et al., 2016) this process involved a multi-location experiment as in our case. In the cited paper, a two-year test in six locations served to assess genotype yield and stability across environments, as well as each environment's discriminative ability and representativeness. In our case, the significant

G × E interaction stimulated the assessment of genotype suitability for low vs. high yielding environments through Eberhart and Russel's (1966) approach: the wide range in average yield between Chakwal and Fateh Jang, on one side, and Piplan, on the other side (Table 2), facilitated the accomplishment of this task. Additional years are, nevertheless, needed to better state a location's characteristic or rate its value as testing environment, as also Mbeyagala et al. (2016) cautioned.

The procedure described allowed the eleven genotypes to be discriminated based on two equally important attributes as yield potential and stability. Five out of nine advanced breeding lines fell in the first quadrant (Figure 3), i.e. they expressed a competitive edge over the two commercial varieties (third quadrant), although at the expenses of stability. Another new line fell very close to the centre of the graph, indicating well balanced yield vs. stability. The remaining three new lines fell in the third quadrant, yet expressed some advantage over the two commercial varieties in either attribute. It results that the nine breeding lines possess in general ameliorated characteristics with respect to the two varieties they are intended to replace. However, no clear advantage in any morphological trait (Table 1) or yield component (Table 2) can be seen between the nine lines combined, on one side, and the two varieties combined, on the other side. It may be evinced, therefore, that the breeding programme targeted a general better efficiency in plant processes, more than a specific plant type associated with higher yield. It is noticed, incidentally, that the plant traits best related to yield in this experiment (Table 3) are almost the same evidenced in other works (Khaimichho et al., 2014; Hemavathy et al., 2015).

Lastly, mash bean is mostly grown in the sub-tropics during the summer, kharif (wet) season, although cultivation under winter, dry (rabi) conditions is also reported (Kumar and Kumar, 2016). Mash bean sensitivity to the drought (Baroowa et al., 2016) and especially heat stress (Kaur et al., 2015; Solai et al., 2015) is generally acknowledged. Flowering and the reproductive stage are indicated as the most critical period, during which time temperatures above 40°C adversely affect yield. In our experiment, this threshold was briefly passed after sowing only in the lowland environment (Piplan). This site also featured a sizeable water deficit (Figure 2) cumulating in the most sensitive reproductive stage (Baroowa et al., 2016). However, this circumstance did not hamper growth (Table 1) and the achievement of a high yield potential in this specific environment (Table 2). These points to factors other than water deficit as main drivers for mash bean yield in the three surveyed environments.

Conclusions

Eleven genotypes of mash bean comprising two commercial varieties and nine advanced breeding lines, tested in three environments in Punjab, Pakistan, have portrayed a remarkable variation in plant development and morphology, as well as grain yield and yield components. This provides enough scope for significant improvement of plant traits through selection.

Five new lines have exhibited higher yield potential under favourable conditions, reaching up to 1000 kg ha⁻¹ yield that is a level seldom echoed in the literature. Three other lines have shown a yield potential similar to that of commercial varieties, in exchange for which the new lines have featured a slightly higher yield stability.

The present work demonstrates, in accordance with other literary sources, that there is ample space for improvement of the mash bean crop in view of a wider diffusion in the sub-tropical to temperate areas of the world.

The research on mash bean is committed to further breeding effort aimed at obtaining more genotypes, and multi-location testing in view of releasing new improved varieties.

Compliance with Ethical Standards. There is no potential conflict of interests and authors confirm that the field studies did not involve endangered or protected species.

REFERENCES

- [1] Baroowa, B., Gogoi, N., Farooq, M. (2016): Changes in physiological, biochemical and antioxidant enzyme activities of green gram (*Vigna radiata* L.) genotypes under drought. – *Acta Physiologiae Plantarum* 38(9): 219. <https://doi.org/10.1007/s11738-016-2230-7>.
- [2] Blanche, S. B., Utomo, H. S., Wenefrida, I., Myers, G. O. (2009): Genotype×environment interactions of hybrid and varietal rice cultivars for grain yield and milling quality. – *Crop Science* 49(6): 2011-2018.
- [3] Eberhart, S. A., Russel, W. A. (1966): Stability parameters for comparing varieties. – *Crop Science* 6: 36-40.
- [4] Ghafoor, A., Ahmad, Z., Qayyum, A. (2003): Black gram (*Vigna mungo* L. Hepper) germplasm catalogue. – Plant Genetic Resources Programme, PARC/JICA, Islamabad, Pakistan, pp. 75-80.
- [5] GOP (Government of Pakistan). (2017): Economic survey of Pakistan. – Economic Advisory Wing, Finance Division, Islamabad.
- [6] Hargreaves, G. H., Samani, Z. A. (1985): Reference crop evapotranspiration from temperature. – *Applied Engineering in Agriculture* 1: 96-99.
- [7] Hemavathy, A. T., Shunmugavalli, N., Anand, G. (2015): Genetic variability, correlation and path co-efficient studies on yield and its components in mungbean [*Vigna radiata* (L.) Wilczek]. – *Legume Research* 38(4): 442-446.
- [8] Hill, J. (1975): Genotype × environment interactions: A challenge to plant breeding. – *Journal of Agricultural Science* 85(3): 477-493.
- [9] Kaur, R., Bains, T. S., Bindumadhava, H., Nayyar, H. (2015): Responses of mungbean (*Vigna radiata* L.) genotypes to heat stress: effects on reproductive biology, leaf function and yield traits. – *Scientia Horticulturae* 197: 527-541.
- [10] Khaimichho, E. B., Hijam, L., Sarkar, K. K., Mukherjee, S. (2014): Genetic control and character association estimates of yield and yield attributing traits in some mungbean genotypes. – *Journal of Crop and Weed* 10(2): 82-88.
- [11] Kumar, S. T., Kumar, P. A. (2016): Effect of tillage and nutrient-management practices on yield, economics and soil health in rice (*Oryza sativa*)-greengram (*Vigna radiata*) cropping system under rainfed condition of Odisha. – *Indian Journal of Agronomy* 61(2): 148-153.
- [12] Lindeman, H. G., Merenda, P. E., Gold, R. Z. (1980): Introduction to bivariate and multivariate analysis. – Scott Foresman, Glenview, IL, USA.
- [13] Mbeyagala, E. K., Amayo, R., Obuo, J. E. P. (2016): Adaptation of introduced mungbean genotypes in Uganda. – *African Crop Science Journal* 24(2): 155-166.
- [14] Mohammad, W., Shehzadi, S., Shah, S. M., Shah, Z. (2010): Effect of tillage and crop residues management on mungbean (*Vigna radiata* (L.) Wilczek) crop yield, nitrogen fixation and water use efficiency in rain fed areas. – *Pakistan Journal of Botany* 42: 1781-1789.
- [15] Pekşen, E., Toker, C., Ceylan, F. O., Farooq, T. A. M. (2015): Determination of promising high yielded mungbean (*Vigna radiata* (L.) Wilczek) genotypes under middle Black Sea Region of Turkey. – *Anadolu Journal of Agricultural Sciences* 30(2): 169-175.

- [16] RDCT (R Development Core Team). (2012): R: A language and environment for statistical computing. – R Foundation for Statistical Computing, Vienna. <http://cran.r-project.org/>.
- [17] Sartaj, K., Anwar, M. T. (2015): Status of pulses in Pakistan. – RAP Publication (2015/05): 117-129.
- [18] Sen, S. (1996): Economic Botany. – New Central Book Agency (Pvt.) Ltd. Calcutta, India, 42-43 pp.
- [19] Sharma, P., Sekhon, H. S., Bains, T. S. (2012): Performance and growth analysis in Mash bean genotypes. – World Journal of Agricultural Sciences 8(3): 303-308.
- [20] Sharma, A. (2014): Current trends in pulse crops production: an overview. – Economic Affairs 59: 569-578.
- [21] Singh, G., Kumar, D., Sharma, P. (2015): Effect of organics, biofertilizers and crop residue application on soil microbial activity in rice-wheat and rice-wheat mungbean cropping systems in the Indo-Gangetic Plains. – Cogent Geoscience 1: 1085296. <https://doi.org/10.1080/23312041.2015.1085296>.
- [22] Solai, M. A. P., Vijayalakshmi, C., Basu, P. S. (2015): Effect of high temperature on flowering pattern, pollen germination and pod setting in green gram (*Vigna radiata* (L.) Wilczek). – The International Journal of Plant Reproductive Biology 7(1): 59-66.
- [23] Yan, W. K., Kang, M. S. (2003): GGE biplot analysis: A graphical tool for breeders, geneticists and agronomists. – Boca Raton, USA: CRC Press.

HISTOPATHOLOGICAL CHANGES AND BACTERIOLOGICAL SURVEY OF INTERNAL ORGANS IN THE ASPECT OF THE INDIVIDUAL CONDITION OF A HARE (*LEPUS EUROPAEUS* PALL.)

RATAJ, B.¹ – FLIS, M.^{1*} – PIÓRKOWSKI, J.²

¹*Department of Zoology, Ecology and Wildlife Management, Faculty of Biology, Animal Sciences and Bioeconomy, University of Life Sciences in Lublin, 20-950 Lublin, Poland*

²*Department of Pathomorphology and Forensic Veterinary Medicine, University of Life Sciences in Lublin, ul. Głęboka 30, 20-612 Lublin, Poland*

**Corresponding author*

e-mail: marian.flis@up.lublin.pl

(Received 1st Feb 2019 ; accepted 29th Mar 2019)

Abstract. The analysis of bacteriological changes in hare internal organs has been performed in the paper. The assessment was made with regards to the individual condition of animals. Anatomical and pathological changes were found in 80% of the hare from the obtained sample. These occurred regardless of the age and gender of animals and were mostly inflammatory infiltrates and necrosis in the testes of males as well as inflammatory infiltrates of the liver and emphysema found in both males and females. There was also an increase in flora of two bacterial strains in hares internal organs. The *Nocardia* strain was found in the testes of two individuals, whereas the *Providencia rustigianii* strain was found, at various severity levels, in the liver, kidneys, lungs and heart of males and females, regardless of their age. Isolated strain of *Providencia rustigianii* proved to be resistant to three antibiotics, while *Nocardia* strain to one of the antibiotics used. The analyses carried out indicate that in addition to population and ecological factors resulting from environmental changes, a number of pathogenic agents, including the presence of bacteria that have not been described in this animal species, are a significant factor limiting the reproductive potential of the population. Therefore, disturbances of physiological processes having a diverse etiological background can lead to numerous anatomical and pathological changes, and thus increase susceptibility to diseases and falls of animals, and at the same time, deepen the ongoing regress of this species population. Not without significance is the fact that the described changes were found regardless of the gender and age of animals.

Keywords: *brown hare, body mass, population structure, bacterial diseases, diseases changes, Lublin Upland*

Introduction

Almost since the end of the 1970s, both in Poland and many European countries, a downward trend of the hare population has been observed (Burel and Baudry, 1990; Flis, 2009, 2016; Frylestam, 1980; Schmidt et al., 2004; Wibbelt and Frölich, 2005; Nasiadka and Dziedzic, 2014). In our country, in many cases, the level of spring density is currently lower compared to the volume of acquisition in the 1960s and 70s of the twentieth century. In the 1970s, the average population density in our country remained at the level of about 50 individuals per 100 ha of the field areas of hunting grounds (Pielowski, 1976, 1979). At the beginning of the 21st century, the average level of hare density in the country varied in individual regions and was within the range of 5-9 individuals/100 ha (Dziedzic et al., 2002; Wasilewski, 2007; Flis, 2009, 2016). However, there are still areas where density of the population is so high that the species

is still regularly hunted (Dziedzic et al., 2002; Flis, 2009, 2015, 2016; Nasiadka and Dziedzic, 2014).

Despite the fact that there is no possibility of indicating a clear cause of the persistent population trend, usually the most frequent changes are those in agrocenoses constituting the basic areas of this species. Intensification of agriculture significantly influences the simplification of agrocenosis structures, which in turn leads to a significant decrease in the heterogeneity of these environments. This entails the shrinking of optimal hare habitats (Lewandowski and Nowakowski, 1993; Panek and Kamieniarz, 1999; Schmidt et al., 2004; Kryński et al., 2007; Petrovan, 2011; Kamieniarz et al., 2013; Schai-Braun et al., 2015; Panek, 2018). Another, not less important, element that directly affects the dynamics of the number of hares is predation. The use of oral treatments for immunization of free-living foxes eliminated one of the basic factors limiting the population, which in turn increased the impact of this species on small animals (Demirbas, 2015; Gołdyn, et al., 2003; Goszczyński and Wasilewski, 1992; Panek et al., 2006; Wasilewski, 2007; Flis et al., 2017, 2018). Hušek et al. (2015) a high rate of fox predation targeting hares depending on the habitat and reported that hare males tend to fall as a prey. Therefore, an extremely important element in hare population management as a monomorphic species is knowledge of the individual condition and population structures that have a direct impact on the reproductive potential of the population (Méres et al., 2016; Misiorowska et al., 2014; Pintur et al., 2006). The impact of hare population, and thus local density indices, on the impact of synanthropic predation is also significant (Flis, 2013; Nasiadka and Dziedzic, 2014).

Another elements that directly affect survival, and thus the size of the population are numerous disease entities found in this species. Coccidiosis and other parasitic diseases are the basic mention. Nevertheless, bacterial and viral diseases, such as brucellosis and European Brown Hare Syndrome – EBHS – and many other slightly less common ones also exert quite considerable impact (Gavier-Widén and Mörner, 1991; Duff et al., 1994; Pikula et al., 2004; Wibbelt and Frölich, 2005; Frölich and Lavazza, 2008; Dubinský et al., 2010; Decors et al., 2011; Chroust et al., 2012; Kornaś et al., 2014; Flis et al., 2016).

The aim of the study was the assessment of histopathological changes and bacteriological analysis of internal organs as well as individual condition in the population of European hare originating from the region where hunting acquiring is still taking place.

Materials and methods

Characteristics of the research area

The research was conducted in two hunting districts with a total area of 13,600 ha, the forest cover of which is 25.2%. They are located in the western part of the Lublin region, in the mesoregion of Kotlina Chodelska and the northern part of Wzniesienia Urzędowskie, in Poland (*Fig. 1*). This region is characterized by the presence of fertile soils of the chernozem type on the loess ground (Kondracki, 2000). Despite fairly fertile soils, it is distinguished by significant fragmentation of agricultural crops, and thus large heterogeneity of field environments. Field crops are dominated by plants with high soil requirements, with particular reference to orchards and plantations of perennial soft fruits, mainly raspberries and currants. In the agricultural landscape, there are numerous

wastelands as well as small wooded enclaves and forest complexes (Witek, 1991). Heterogeneity evaluation of the natural environment of agrocenoses in the area of research, performed according to the method proposed by Schrödel (1991) showed an average size of individual fields at the level of 0.95 ha, while the average distance between landscape elements ranged from 0.5 to 0.7 km. In turn, the relative length of contour lines in agrocenoses having significant impact on the functioning of small game population, despite the variation in individual regions of the study area, was on average at 0.1–0.2 km/km². All described elements determine quite significant mosaicism of field environments, creating almost optimal conditions for living and functioning of the hare population (Pielowski, 1979; Nasiadka and Dziedzic, 2014).



Figure 1. Location of the research area

Material for research

As part of the research, hares obtained in collective hunts during the hunting season 2017/18 have been weighed and their gender and age have been determined. The whole material consisted of 20 hares obtained first during two hunts, which is representative of the sample. Due to minimizing the amount of shooting in recent years and the fact that in accordance with the law, holder of the hunting district is the owner of hunting grounds, it was not possible to collect larger number of hare for study. In total, 9 males and 11 females were assessed, of which the share of young and adult hares was half.

Methods and measurements

All shot-off hares were weighed directly in the field. Weighing was carried out to the nearest 0.1 kg. Also in the field, their gender and age were assessed. Gender assessments were made based on the appearance of secondary sexual characteristics.

The age of hare was also determined directly in the field on the basis of the palpation assessment of the occurrence or disappearance of the Stroh mark (cartilaginous elbow base cap). Such an assessment allows the division of hares into young (up to 1 year old) and adult (over 1 year old) (Stroh, 1931; Pielowski, 1979).

Histopathological and bacteriological material

Lung, liver, kidneys and testes sections in males were taken from all acquired hares for histopathological and bacteriological examinations. Sectional examination performed under the field conditions and material collection for bacteriological examination required the use of a transport set containing rods to collect swabs from pre-isolated organs. Material for histopathological analysis was fixed in 4% formalin, and then dehydrated and embedded in paraffin. The 4 µm thick sections were stained with hematoxylin and eosin (HE). A bacteriological analysis of the collected samples was also carried out.

Laboratory preparations

Different propagating and differentiating media were used to identify individual species of microorganisms. The solid substrate was agar with the addition of 5% sheep blood to breed aerobic microorganisms and possible determination of hemolysis. Sugar broth was used as a liquid substrate to reproduce aerobic bacteria. Other substrates were also used, including Chapman, Mac Conkey and Sabouard medium to identify any organ mycoses that occur. The study also applied a medium with cetrimid to identify microorganisms of the *Pseudomonas* genus and D-coccosel medium to identify fecal bacteria. Further identification of individual bacteria types was carried out with the BioMerieux bio-chemical tests (Analytical Profile Index). The control of substrates fertility was carried out using reference strains. After determining the bacterial strain, the growth rate of bacterial flora was assessed using the criterion of low (+), intensive (++) and very intense (+++) growth. Although it is a simplified method, it allowed preliminary assessment of the health status of the hare, and most of all it revealed the type of bacterial environmental threats. An analysis of the sensitivity of isolated bacterial strains to 8 commonly used antibiotics was also carried out applying the criterion of subdivision into sensitive, medium sensitive and resistant ones. The following antibiotics were used for the analyzes in doses: Enrofloxacin ENR – 5 µg, Amoxicillin/clavulanic acid AMC – 30 µg, Gentamycin CN – 10 µg, Penicillin G P – 10 µg, Oxytetracycline OT – 30 µg, Trimethoprim/sulphamethoxazole SXT – 25 µg (trimetoprim- 1.25 µg+sulfametoksazof 23.75 µg), Marbofloksacin MAR – 5 µg, Tylozyna TY – 30 µg.

Results

Characteristics of the structure and individual quality of the population

The conducted research shows that the average body weight of three young males was 3.9 kg, and 7 young females 3.7 kg (*Table 1*). In adults, the body weight was uniform. The average value of this feature of 6 males and 4 females was at the level of 4.7 kg. The overall value of the gender index was at 1:1.2 in favor of females. The reproductive success rate defined as the ratio of the number of young hares that survived till the hunting season per 1 adult female was high and amounted to 2.5.

Table 1. Body mass and results of bacteriological analysis as well as histopathological changes in internal organs of acquired hares

No.	Individuals characterization			Organs covered by the analysis				
	Gender	Age	Body weight (kg)	Testes	Liver	Kidneys	Lungs	Heart
1	♀	Young	4.0	x	Small inflammatory infiltrations	x	x	x
2	♀	Adult	4.6	x	x	x	Emphysema	x
3	♂	Adult	4.7	Small inflammatory infiltrations	x	x	x	x
4	♂	Young	3.5	x	x	x	x	x
5	♀	Young	3.9	x	x	x	x	x
6	♀	Adult	4.7	x	Medium inflammatory infiltrations	x	x	x
7	♂	Adult	4.5	x	x	Low (+) growth of <i>Providencia rustigianii</i>	Intensive (++) growth of <i>Providencia rustigianii</i>	Intensive (++) growth of <i>Providencia rustigianii</i>
8	♂	Adult	4.4	Necrosis Very intense (+++) growth of <i>Nocardia</i>	Intensive inflammatory infiltrations	Glomerulonephritis low (+) growth of <i>Providencia rustigianii</i>	Intensive (++) growth of <i>Providencia rustigianii</i>	Intensive (++) growth of <i>Providencia rustigianii</i>
9	♀	Adult	4.7	x	Small inflammatory infiltrations	x	Emphysema	x
10	♀	Young	4.0	x	Low (+) growth of <i>Providencia rustigianii</i>	x	x	x
11	♂	Young	4.0	x	x	x	Low (+) growth of <i>Providencia rustigianii</i>	x
12	♀	Adult	4.8	x	x	Glomerulonephritis low (+) growth of <i>Providencia rustigianii</i>	x	x
13	♂	Adult	4.6	Necrosis Intensive inflammatory infiltrations	x	x	x	x
14	♂	Adult	4.9	x	x	x	x	x
15	♂	Young	4.2	Medium inflammatory infiltrations Low (+) growth of <i>Nocardia</i>	x	Low (+) growth of <i>Providencia rustigianii</i>	Emphysema	x
16	♀	Young	3.2	x	x	x	Emphysema low (+) growth of <i>Providencia rustigianii</i>	x
17	♀	Young	3.6	x	Small inflammatory infiltrations	x	x	x
18	♂	Adult	5.1	Necrosis	x	Low (+) growth of <i>Providencia rustigianii</i>	x	x
19	♀	Young	3.7	x	x	x	x	x
20	♀	Young	3.6	x	Small inflammatory infiltrations	x	x	x

Anatomical and pathological analysis

Performed anatomical-pathological analyses of testicles showed that in the examined sample, extensive areas of necrosis were found in three adult males. In the central parts of the necrotic areas, there were numerous foci indicating the progressive process of calcification (*Fig. 2*). In addition, in the testes of two young and one adult males, inflammatory infiltrates of varying intensity were found. Numerous purulent infiltrates

contained neutrophil granulocytes, giant cells, fibroblasts and histiocytes. Glandular epithelial atrophy and progressive fibrosis around the glandular tissue were found, which was caused by an ongoing inflammatory process with irreversible effects. Anatomical-pathological changes of liver were found in 6 individuals, which were manifested by a partial lack of individual cells in a radiative manner within some of the hepatic lobes (Fig. 3). There were numerous focal inflammatory infiltrates between the hepatic lobes. Small inflammatory infiltrates occurred in 3 young females and one adult. One adult female showed medium inflammatory infiltrates, while in one adult male - intense inflammatory infiltrates. Analysis of kidneys from shot hares showed numerous inflammatory infiltrations within the glomerulus of the vessels with partial or complete closure of the kidney tubules (Fig. 4). This indicates the occurrence of glomerulonephritis. This condition was found in one adult male and one young female. Among the analyzed sample, one young and two adult females as well as one young male were diagnosed with emphysema with characteristic foci of congestion and inter-vesicular tissue hyperplasia (Fig. 5). Analysis of samples taken from myocardial muscles did not show any anatomical-pathological changes.

Bacteriological analysis

The results of bacteriological analysis of the testes revealed two cases of *Nocardia* bacteria. One young male showed a fairly low (+) growth, and in one adult male a very intense (+++) growth of this bacterium. In turn, in the liver of 1 young female, quite low growth (+) of *Providencia rustigianii* was found. Analysis of kidneys of the acquired individuals showed that 5 of them revealed quite low (+) growth of *Providencia rustigianii*. This condition occurred in one young and three adult males and one adult female. In samples taken from lungs, 2 adult males revealed very intense (++) growth, while in a young male and adult female, quite low growth (+) of *Providencia rustigianii*. In the collected heart tissue samples, two adult males showed a significant very intense growth (++) of *Providencia rustigianii*.

Resistance to antibiotics

As part of the study, the *in vitro* sensitivity assessment of isolated bacterial strains to antibiotics was performed (Table 2). The isolated strain of *Providencia rustigianii* turned out to be resistant to three antibiotics used, moderately sensitive to one and sensitive to another four antibiotics. In turn, the isolated *Nocardia* strain was sensitive to seven of the eight antibiotics used and resistant only to one of them.

Table 2. Sensitivity of isolated bacterial strains to antibiotics

Antibiotic used	Type of bacterial strain	
	<i>Providencia rustigianii</i>	<i>Nocardia</i>
Tylozyna TY30	O	W
Amoxicillin/clavulanic acid AMC 30	O	W
Gentamycin CN10	W	W
Penicillin G P10	O	W
Sulphamethoxazol/Trimethoprim SXT25	ŚW	O
Marbofloksacin MAR5	W	W
Oxytetracycline OT3	W	W
Enrofloxacin ENR5	W	W

W - sensitive; ŚW - moderately sensitive; O - resistant

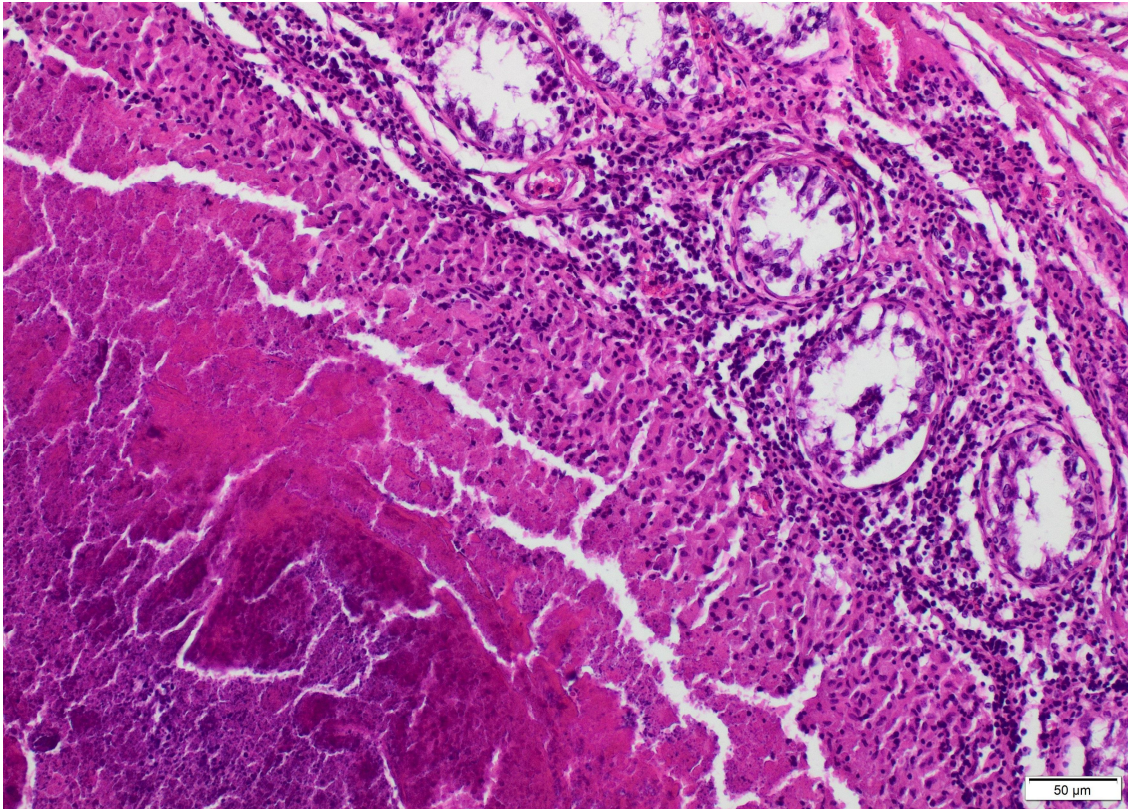


Figure 2. Numerous necrotic areas in the testes of males

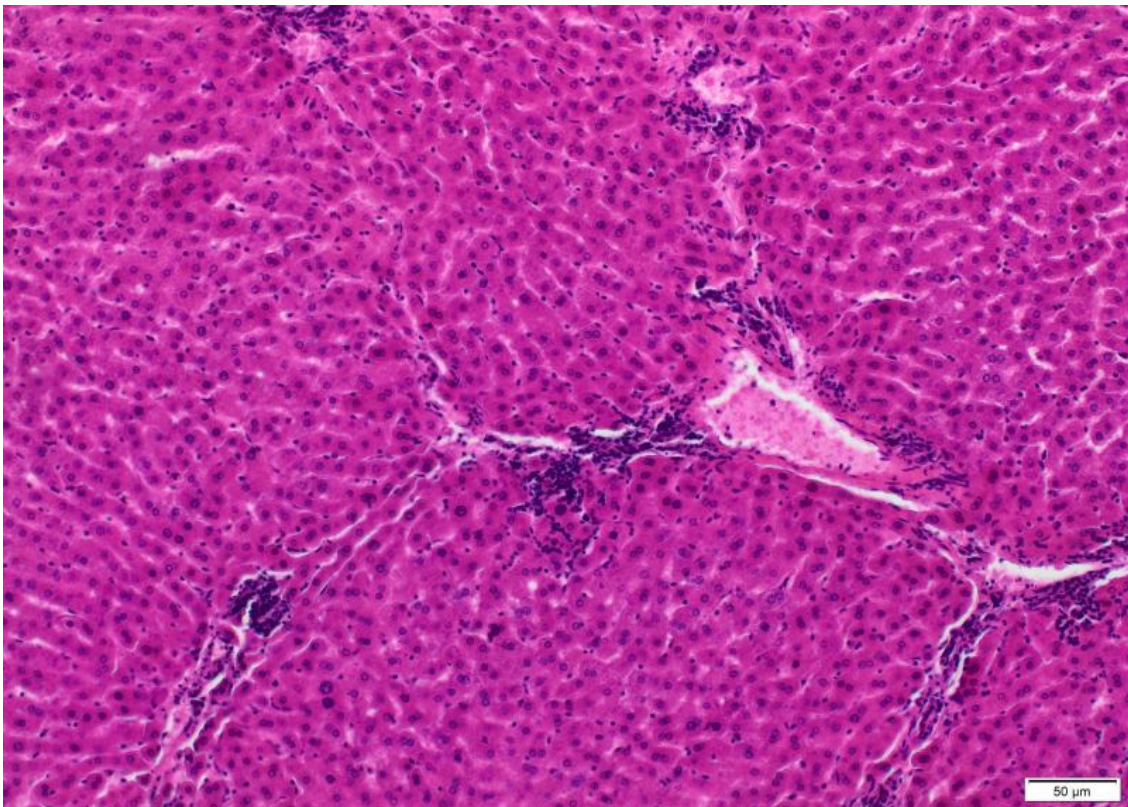


Figure 3. Focal inflammatory infiltrates between the hepatic lobes

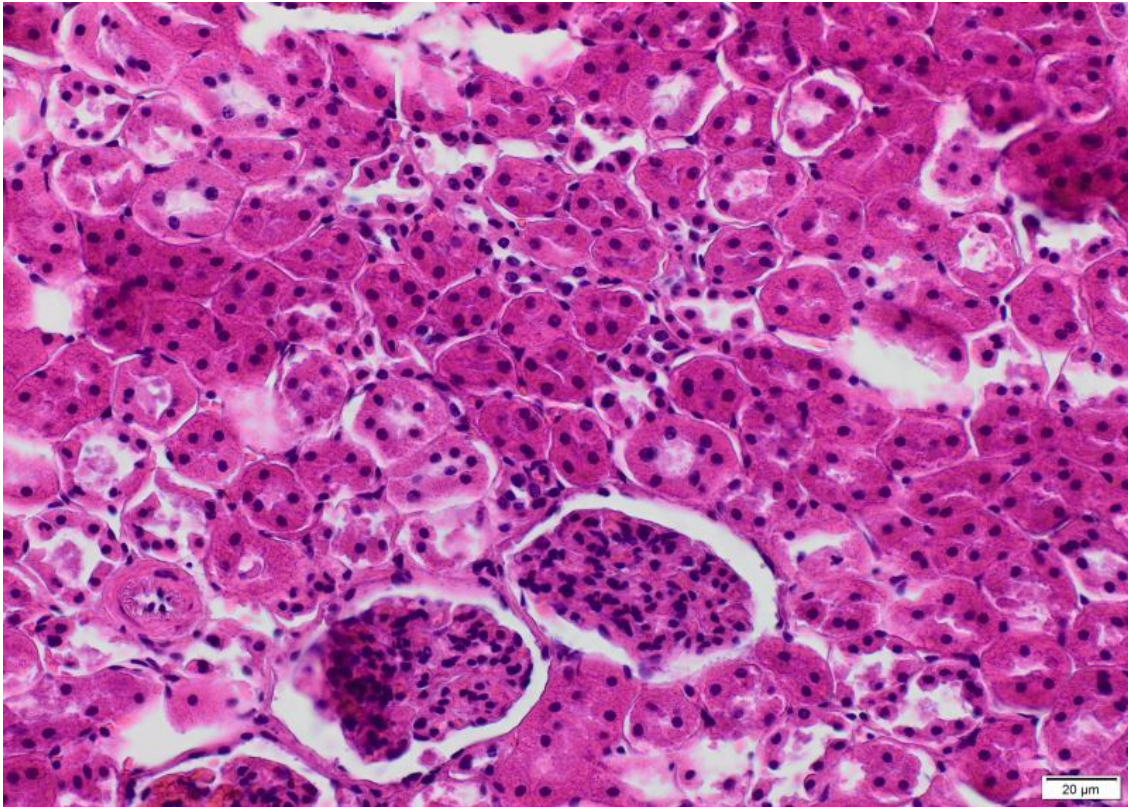


Figure 4. *Glomerulonephritis with partial or complete renal tubular closure*

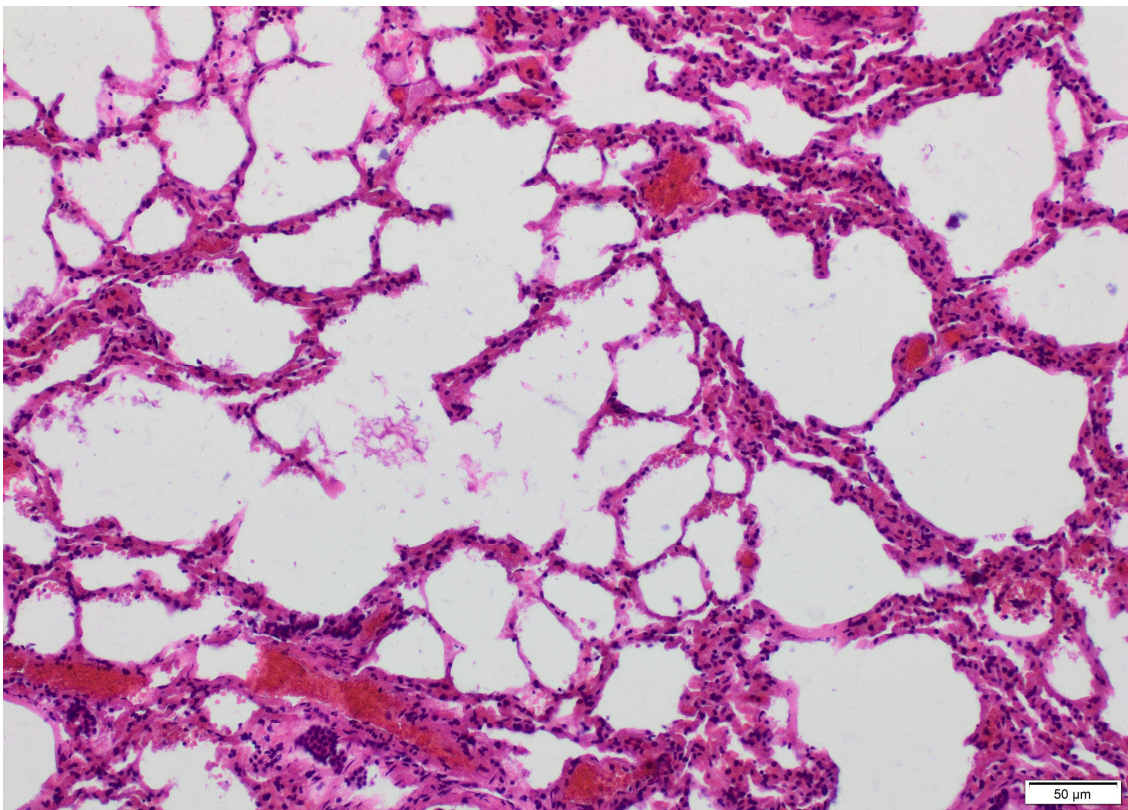


Figure 5. *Numerous foci of congestion and inter-follicular tissue growth, indicating*

Discussion

The analysis of population parameters based on a sample of 20 individuals indicates that the values of body weight, being an expression of the individual condition, in significant way do not differ from those reported by Flis (2015). Obtained body mass values slightly exceed those given by Dziejczak et al. (1998) from Lublin Upland and Podlasie region in the mid-1990s. These results are higher than those from research conducted in areas of the highest population size of this species in our country during the hunting season 2009/2010 (Misirowska et al., 2014). The presented results are characterized by much higher body weight values than those in Croatia in the 2004/2005 hunting season, reported by Pintura et al. (2006), as well as in Hungary in both age and gender groups (Farkas et al., 2016). In turn, the obtained gender structure is similar to both the research conducted by Flis (2015), and that reported by Misirowska et al. (2014).

The reservoir of bacteria from the genus *Providencia* are insects, and most of all, houseflies, from which *Providencia alcalifaciens*, *Providencia rettgerii* and *Providencia stuarti* were isolated. The species of *Providencia rettgerii* was isolated from *Helaemyia petrolei* fly larvae found in oil-bearing areas. Bacteria of the genus *Providencia rettgerii* are found as an indispensable element of natural flora of crocodiles, frogs, vipers, as well as snakes, and in particular of python and boa snakes. In addition, the occurrence of *Providencia rettgerii* was found in roundworms, sea lions and seals. Quite rarely, this species is isolated from birds (falcons, bustards). As a rule, they were found in dogs, cats, guinea pigs, as well as in cattle and sheep as part of the natural flora of the gastrointestinal tract and quite often they are referred to as intestinal bacteria. It should be mentioned that the bacteria of *Providencia* genus also cause many diseases. Attention is being paid to *Providencia alcalifaciens* during dog diarrhea and *Providencia rettgerii* causing generalized infections and meningitis, especially in crocodiles up to the age of 3 years. There have also been reports of this type of oral inflammation cases in seals and snakes. These bacteria have never aroused so much interest among the bacteria of the *Enterobacteriaceae* family. This was mainly due to their reduced pathogenicity. Currently, they are beginning to play an increasingly important role as pathogens that cause urinary and digestive tract infections. Up to date, there have been no reports of their presence in hare; however, it is possible that their strong uropathogenic properties confirmed in histopathological studies in mice and monkeys may also have an impact on hare mortality (Janda and Abbot, 2006; O'Hara Mohr et al., 2000).

Nocardia belong to aerobic bacteria. Their natural reservoir is water, soil, vegetation and sewage systems. Infection in animals is quite rare, mainly in tropical countries. These bacteria can be transmitted by castor bean tick. Among animals, they were found in cattle, and the symptoms are dermatitis, pneumonia, mastitis and diarrhea. They were also found in dogs and cats, where lesions were found mainly in lungs and pleural cavity. Infection with these bacteria occurs mainly by inhalation or also by damaged skin. In the skin form, inflammation of regional lymph nodes and nodular lymphangitis are mainly observed. Inhaled form affects the lung and pleura and takes the form of inflammatory granulomas, very similar to those caused by closely related *Actinomyces* bacteria. Due to the fact that so far there have been no reports of their presence on hare, it is difficult to indicate their impact on the health status of this species population. Nevertheless, their numerous occurrences in the testes of two males indicate that they

can affect the reproductive processes (Tropiło et al., 1996; Gliński and Chełmiński, 2014; Katkiewicz, 2017; Wiciński et al., 2018).

Conclusions

1. The individual quality expressed as body weight in both young and adult hares is high, and the obtained values of this feature definitely exceed those from other parts of the country, as well as in some European countries. In turn, the balanced gender structure, with a slight majority of females, indicates that this population has developing characteristics, which should favorably affect the dynamics of its size in subsequent years.
2. In the examined sample, only 20% of hares did not reveal any lesions, and this concerned 3 young and one adult. In the rest of the sample, anatomical-pathological changes were found. They occurred regardless of the age and gender of animals. These were inflammatory infiltrates and necrosis in the testes of males as well as inflammatory infiltrates of the liver and emphysema found in both males and females.
3. There was also a growth in bacterial flora of two strains in the hare's internal organs. The *Nocardia* strain was found in the testes of two individuals, whereas the strain of *Providencia rustigianii* was found to vary in severity in the liver, kidneys, lungs and heart of males and females, regardless of their age. These strains have not yet been described in this species. Therefore, it is advisable to carry out further research in this respect, because described bacteria affecting the reproduction processes may be one of the factors contributing to the ongoing regression of this species population.
4. Performed antibiograms indicate that the isolated strain of *Providencia rustigianii* proved to be resistant to three antibiotics, while *Nocardia* strain to one of the antibiotics used.
5. The analyses carried out indicate that in addition to population and ecological factors resulting from environmental changes, numerous pathogenic factors are significant in limiting the reproductive potential of the population. Thus, disturbances of physiological processes having a diverse etiological background can lead to numerous anatomical and pathological changes, and thus increase susceptibility to diseases and falls of animals.
6. Considering the fact that the individual condition and parameters of the population covered by the research are high, it is necessary to conduct further comprehensive research, mainly in the direction of diseases of diverse etiological background. Research should cover larger areas with different densities, and in particular, if possible, concentrate on low-density areas. Such a comprehensive assessment should help to identify environmental hazards for the hare population and to develop directions for actions to reduce the adverse downward trend.

REFERENCES

- [1] Burel, F., Baudry, J. (1990): Structural dynamic of hedgerow network landscape in Brittany, France. – *Landscape Ecology* 4(4): 197-210.

- [2] Chroust, K., Vodnansky, M., Pikula, J. (2012): Parasite load of European brown hares in Austria and Czech Republic. – *Veterinarni Medicina* 57(10): 551-558.
- [3] Dubinský, P., Vasilková, Z., Hurníková, Z., Miterpáková, M., Slamečka, J., Jurčík, R. (2010): Parasitic infections of the European brown hare (*Lepus europaeus* Pallas, 1778) in south-western Slovakia. – *Helmintologia* 47(4): 219-225.
- [4] Duff, J. P., Chasey, D., Munro, R., Wooldridge, M. (1994): European brown hare syndrome in England. – *Veterinary Record* 134(26): 669-673.
- [5] Decors, A., Lesage, C., Jourdain, E., Giraud, P., Houbron, P., Vanhem, P., Madani, N. (2011): Outbreak of tularemia in brown hares (*Lepus europaeus*) in France, January to March 2011. – *Euro Surveillance* 16(28): pii: 19913.
- [6] Demirbas, Y. (2015): Density of European hare and red fox in different habitats of Kirikkale Province (Central Anatolia), with a low level in hare number and an expected correlation in spring. – *Acta Zoologica Bulgarica* 67(4): 515-520.
- [7] Dziedzic, R., Flis, M., Olszak, K., Wójcik, M., Beeger, S. (1998): Hare body weight in the Lublin Upland and Podlasie. – *Annales UMCS XVI(35, EE): 261-267.*
- [8] Dziedzic, R., Kamieniarz, R., Majer-Dziedzic, B., Wójcik, M., Beeger, S., Flis, M., Olszak, K., Żontała, M. (2002): The reasons for the decline of the gray hare population in Poland. (Original in Polish - Przyczyny spadku populacji zająca szaraka w Polsce). – Wyd. Ministerstwo Środowiska, Fundacja Ekonomistów Środowiska i Zasobów Naturalnych, Warszawa.
- [9] Farkas, P., Kusza, S., Majzinger, I. (2016): Analysis of some population parameters of the brown hare (*Lepus europaeus* Pallas, 1758) in two hunting areas on the Hungarian great plain. – *Lucrări Științifice* 18(1): 71-74.
- [10] Flis, M. (2009): Temporal variability of concentrations and habitat preferences of hares under the conditions of a hunting district, in the years 1998-2008. – *Roczniki Naukowe Polskiego Towarzystwa Zootechnicznego* 5(1): 139-147.
- [11] Flis, M. (2013): Synanthropic predators as an environmental threat. – *Annales UMCS Sectio EE XXXI(1): 1-9.*
- [12] Flis, M. (2015): Diversity of age, gender, and body mass of hares living in low density in the Lublin Upland. – *Sylvan* 159(7): 579-585.
- [13] Flis, M. (2016): Variability of density and habitat preferences of brown hare in hunting district located in the Lublin Upland. – *Sylvan* 16(10): 829-836.
- [14] Flis, M., Nozdryn-Płotnicki Z, Wrona, Z., Piórkowski, J. (2016): Granulomatous inflammation of the genital system in male hare (*Lepus europaeus* Pall. 1778) - A case report. – *Życie Weterynaryjne* 91(8): 579-581.
- [15] Flis, M., Grela, E. R., Gugala, D. (2017): Occurrence of rabies in Poland in 2011-2015 in relation to the free-living fox population. – *Medycyna Weterynaryjna* 73(1): 43-47.
- [16] Flis, M., Grela, E. R., Gugala, D. (2018): Effectiveness of oral immunization of free-living foxes in reducing rabies in Poland in 2011-2015. – *Medycyna Weterynaryjna* 74(3): 203-208.
- [17] Frölich, K., Lavazza, A. (2008): European Brown Hare Syndrome. – In: Alves, P. C., Ferrand, N., Hackländer, K. (eds.) *Lagomorph Biology*. Springer, Berlin, Heidelberg, pp. 253-261.
- [18] Frylestam, B. (1980): Reproduction in the European hare in southern Sweden. – *Ecography* 3(1): 74-80.
- [19] Gavier-Widén, D., Mörner, T. (1991): Epidemiology and diagnosis of the European brown hare syndrome in Scandinavian countries: a review. – *Review Science Technology* 10(2): 453-458.
- [20] Gliński, Z., Chelmiński, A. (2014): Actinomyces infections in humans and animals. – *Życie Weterynaryjne* 89(6): 499-504.
- [21] Gołdyn, B., Hromada, M., Surmacki, A., Tryjanowski, P. (2003): Habitat use and diet of the red fox *Vulpes vulpes* in an agricultural landscape in Poland. – *Zeitschrift für Jagdwissenschaft* 49: 191-200.

- [22] Goszczyński, J., Wasilewski, M. (1992): Predation of foxes on a hare population in central Poland. – *Acta Theriologica* 37(4): 329-338.
- [23] Hušek, J., Panek, M., Tryjanowski, P. (2015): Predation risk drives habitat-specific sex ratio in a monomorphic species, the brown hare (*Lepus europaeus*). – *Ethology* 121(6): 593-600.
- [24] Janda, J. M., Abbot, S. L. (2006): *The Enterobacteriaceae*. – ASM Press, Washington, pp. 279-299.
- [25] Kamieniarz, P., Voigt, U., Panek, M., Strauss, E., Niewęglowski, H. (2013): The effect of landscape structure on the distribution of brown hare *Lepus europaeus* in farmlands of Germany and Poland. – *Acta Theriologica* 58(1): 39-46.
- [26] Katkiewicz, M. (2017): Nocardiosis - rare disease of humans and animals. A histopathological study. – *Życie Weterynaryjne* 92(9): 675-677.
- [27] Kondracki, J. (2000): *Regional Geography of Poland*. (Original in Polish - *Geografia Regionalna Polski*). – PWN, Warszawa.
- [28] Kryński, A., Chudzińska-Popek, M., Majdecka, T. (2007): The environment of modern agrocenoses and the situation of a hare of a gray hare. (Original in Polish - *Środowisko współczesnych agrocenoz a sytuacja zająca szaraka*). – *Nauka łowiectwu. Cz. 2. Zającowi na ratunek*. Wyd. Samorząd Województwa Mazowieckiego, Warszawa, pp. 110-113.
- [29] Kornaś, S., Wierzbowska, I., Wajdzik, M., Kowal, J., Basiaga, M., Nosal, P. (2014): Endoparasites of European Brown Hare (*Lepus europaeus*) from Southern Poland based on necropsy. – *Annals of Animal Science* 14(2): 297-306.
- [30] Lewandowski, K., Nowakowski, J. (1993): Spatial distribution of brown hare *Lepus europaeus* in habitats of various types of agriculture. – *Acta Theriologica* 38(4): 435-442.
- [31] Méres, J., Ostrihoň, M., Slamečka, M., Kaštier, J. (2016): Population structure of brown hare (*Lepus europaeus*): a case study in selected areas of Nitra region [2013]. – *Acta Facultatis Forestalis Zvolen* 55(suppl. 1).
- [32] Misiórowska, M., Ludwisiak, Ł., Nasiadka, P. (2014): Population parameters of brown hare (*Lepus europaeus*, L.) in regions of the species highest density in Poland. – *Sylvan* 158(12): 901-910.
- [33] Nasiadka, P., Dziedzic, R. (2014): Handbook of best practices for the protection of partridges and hares. (Original in Polish - *Podręcznik najlepszych praktyk ochrony kuropatwy i zająca*). – *Dla różnorodności biologicznej. Centrum Koordynacji Projektów Środowiskowych*, Warszawa, pp. 66-118.
- [34] O'Hara Mohr, C., Brenner, F. W., Miller, J. M. (2000): Classification, identification, and clinical significance of *Proteus*, *Providencia* and *Morganella*. – *Clinical Microbiology Reviews* 13(4): 534-546.
- [35] Panek, M. (2018): Habitat factors associated with the decline in brown hare abundance in Poland in the beginning of the 21st century. – *Ecological Indicators* 85: 915-920.
- [36] Panek, M., Kamieniarz, R. (1999): Relationships between density of brown hare *Lepus europaeus* and landscape structure in Poland in the years 1981–1995. – *Acta Theriologica* 44: 67-75.
- [37] Panek, M., Kamieniarz, R., Bresiński, W. (2006): The effect of experimental removal of red foxes *Vulpes vulpes* on spring density of brown hares *Lepus europaeus* in western Poland. – *Acta Theriologica* 51: 187-193.
- [38] Petrovan, S. O. (2011): *The Landscape Ecology of Brown Hares and European Rabbits in Pastures in the North East of England*. – Biological Sciences, University of Hull, Kingston upon Hull, pp. 5-184.
- [39] Pielowski, Z. (1976): On the Present State and Perspectives of the European Hare Breeding in Poland. – In: Pucek, Z., Pielowski, Z. (eds.). *Ecology and Management of European Hare Populations*. PWRiL, Warszawa, pp. 25-27.
- [40] Pielowski, Z. (1979): *Hare. Natural-Hunting Monography*. (Original in Polish - *Zajac. Monografia przyrodniczo-łowiecka*). – PWRiL, Warszawa.

- [41] Pikula, J., Beklova, M., Holesovska, Z., Treml, F. (2004): Ecology of european brown hare and distribution of natural foci of tularemia in the Czech Republik. – Acta Veterinaria Brno 73(2): 267-273.
- [42] Pintur, K., Popović, N., Alegro, A., Severin, K., Slavica, A., Kolić, E. (2006): Selected indicators of brown hare (*Lepus europaeus* Pallas, 1778) population dynamics in northwestern Croatia. – Veterinarski Arhiv 76: 199-209.
- [43] Schai-Braun, S. C., Reichlin, T. S., Ruf, T., Klansek, E., Tataruch, F., Arnold, W., Hackländer, K. (2015): The European hare (*Lepus europaeus*): A picky herbivore searching for plant parts rich in fat. – PLoS One 10(7): e0134278.
- [44] Schmidt, N. M., Asferg, T., Forchhammer, M. C. (2004): Long-term patterns in European brown hare population dynamics in Denmark: effects of agriculture, predation and climate. – BMC Ecology 4: 1-7.
- [45] Schrödl, G. (1991): Ein Stichprobenverfahren zur Biotopcharakterisierung Niederwildgebieten. – Beiträge zur Jagd und Wildforschung XVII: 93-98.
- [46] Stroh, G. (1931): Zwei sichere Altersmerkmale beim Hasen. – Berliner Tierärztl. Wschr 47: 180-181.
- [47] Tropiło, J., Katkiewicz, M., Podsiadło, B. (1996): Nocardiosis in slaughter cattle imported to Poland. – Medycyna Weterynaryjna 52: 106-109.
- [48] Wasilewski, M. (2007): Predation and Small Animals. (Original in Polish - Drapieżnictwo a zwierzyna drobna). – In: Nauka łowiectwu. Cz. 1. Kryzys zwierzyny drobnej i sposoby przeciwdziałania. Wyd. Samorząd Województwa Mazowieckiego, Warszawa, pp. 34-38.
- [49] Wibbelt, G., Frölich, K. (2005): Infectious diseases in European brown hare (*Lepus europaeus*). – Wildlife Biology Practice 1(1): 86-93.
- [50] Wiciński, M., Leis, K., Węclewicz, M. M., Malinowski, B., Żak, J., Grzešek, E., Grzešek, G. (2018): Nocardia spp. - characteristics, pathogenicity, treatment. – Postępy Mikrobiologii 57(1): 68-76.
- [51] Witek, T. (1991): Natural Conditions of Agricultural Production: Province Lublin. (Original in Polish - Warunki przyrodnicze produkcji rolnej: woj. lubelskie). – IUNiG, Puławy.

SUITABILITY EVALUATION OF SHALLOW NET CAGE CULTURE BASED ON INTERACTION MATRIX – A CASE STUDY OF XINCUN LAGOON, HAINAN, CHINA

FANG, X.^{1,2} – LI, X. Y.¹ – HAO, C. L.¹ – ZHANG, D. R.¹ – WANG, J. C.¹ – ZHANG, Y. F.^{1*}

¹*Second Institute of Oceanography, Ministry of Natural Resources
36 BaochubeiLu Rd., Hangzhou 310012, P. R. China
(phone: +86-571-8196-3336; fax: +86-571-8805-4750)*

²*School of Geography and Ocean Science, Nanjing University
No.163 Xianlin Rd., Qixia District, Nanjing, Jiangsu 210093, P. R. China*

**Corresponding author
e-mail: fangx@sio.org.cn*

(Received 2nd Feb 2019; accepted 21st Mar 2019)

Abstract. Shallow water cage culture is the main marine activity of Xincun Lagoon, Hainan. However, the continuous growth of aquaculture activities not only aggravates the deterioration of the ecological environment of Lagoon, but also affects the healthy development of mariculture. Suitability analysis on net cage mariculture can reduce the pressure of marine ecological environment, increase the yield of aquaculture and alleviate the conflict between different marine activities to a certain extent. However, the interaction of various factors affecting the suitability evaluation of mariculture constitutes a complex system, and the traditional method of weight determination cannot fit the actual situation well. For this reason, this paper attempts to introduce the interaction matrix of rock engineering systems (RES) to evaluate the weight of each index. At the same time, a multi-criteria decision analysis (MCDA) model based on GIS is established. Finally, a continuous graph of the suitability change of shallow sea cage culture in Xincun Lagoon is obtained. The results show that (1) the entrance area of Lagoon is the most suitable area for cage culture in shallow water; (2) the evaluation results are in agreement with the actual situation and previous studies, and the weight determination method is reasonable and feasible.

Keywords: *mariculture, suitability analysis, rock engineering systems, GIS, multivariate analysis, ecosystem approach*

Introduction

Shallow sea cage culture is the main production activity of Xincun Lagoon, Hainan. However, the continuous growth of aquaculture activities not only aggravates the deterioration of Lagoon ecological environment, but also affects the healthy development of mariculture (Yin et al., 2018). In 2016 and 2017, widespread cage-cultured fish deaths occurred continuously in Xincun Lagoon. After field investigations, the main reason was found to be that the fish were hypoxic due to the high density of fish cultures, and the excessive feed also caused eutrophication of the water body. A recent study showed that the amount of TN and TP discharged from cage culture in shallow water accounts for more than 50% of the total discharge of all marine activities (Fang et al., 2018).

With China's attention to eco-environmental protection, the State Oceanic Administration proposed the Blue Bay Remediation Action Plan to restore the ecological environment quality in the Gulf region. Some researches of FAO also show that the ecosystem approach to aquaculture (EAA) and spatial planning are both important tools for sustainable aquaculture (FAO, 2015). Therefore, it is necessary to

formulate scientific aquaculture planning to reduce the pressure of aquaculture activities on the ecosystem of Xincun Lagoon, to improve the production of mariculture, and to alleviate the conflict between different marine activities. In view of the above objectives, this paper evaluates the suitability of shallow sea cage culture by taking Lagoon as an example, selecting appropriate parameters, using interaction matrix to calculate the weight and combining with Geographic Information System (GIS) to do multi-criteria decision analysis.

Since the end of the 1980s, the academia has begun to study the site selection of aquaculture and guide the actual management of government departments (Parker et al., 1998). For example, when Joaquin (2011) chose the aquaculture area for oysters in the Caribbean Sea, they used multi-factor evaluation method and analytic hierarchy process to calculate the weight of each index and obtain the result of suitability evaluation by combining four kinds of indicators including the internal environment of sea area, the external environment of sea area, the transportation convenience and the social and economic conditions. Dapuetto et al. (2015) proposed the spatial multi-criteria evaluation (SMCE) method to determine the area suitable for offshore medium-sized fish farms in Liguria, Italy. The result shows that the SMCE method has good practical significance. Yin et al. (2018) established a high-resolution hydrodynamic model to increase the availability of data, selected environmental and socio-economic indicators and used Multi-Criteria Decision Analysis (MCDA) to determine the suitable aquaculture sites in the coastal areas of Menai Strait.

Considering the complexity of mariculture suitability indicators, this study intends to use interaction matrix to determine the weight of indicators. This method was first proposed by Hudson (1989) to study the problem of rock engineering system (RES). Then it was developed with Mazzoccola to make it more suitable for the application of soft science (Mazzoccola and Hudson, 1996). The basic idea is to treat rock engineering as a complete system. The interaction matrix is constructed by enumerating the variables related to the system, and the interaction between variables is quantitatively evaluated by matrix coding. This method considers not only the influence of each parameter on the system, but also the contribution of the interaction between parameters to the whole system. Compared to other methods, such as Analytic Hierarchy Process, it is more suitable for solving the complex problems of interaction and coupling among various factors (Wu et al., 2011). Subsequently, this method was applied to many disciplines, such as ecosystem assessment (Velasco et al., 2006) and gas spontaneous combustion (Zhou et al., 2017), and so on.

Preparation

Conceptual framework

In this paper, taking Xincun Lagoon as an example and referring to the current research situation in related fields at home and abroad, we select appropriate indicators according to local conditions. Considering the interlaced relationship between indicators, it is difficult for the general method of determining indicators, such as analytic hierarchy process, to reflect the relative importance of indicators perfectly. In this paper, the concept of interaction matrix is introduced and the weight values of indicators are calculated. The spatial distribution of the results of each index is quantified by using the Geographic Information System (GIS) method. Then, the multi-criteria decision

analysis method is used to perform linear superposition in ArcGIS software. Finally, the spatial distribution map of the suitability of shallow sea cage culture is obtained.

Study region and area

Xincun Lagoon (N18°22'-18°47', E109°45'-110°08') is located in the southeast part of Xincun Town, Lingshui County, Hainan Province, China, as shown in *Fig. 1*. Its East-West width is 5.1 km, its north-south length is 4.5 km, and its area is 24 km². It is a medium-sized sand bar-tidal inlet-lake system, and its ebb-flow tidal delta is relatively developed. According to the analysis of remote sensing images, the area of Lagoon decreased by 1.69 km² in the 25 years from 1988 to 2013. There are many marine activities around the Lagoon, including use of the sea areas for tourism, town, land aquaculture pond and shallow sea cage culture, among which the pollutants discharged from shallow sea cage culture account for more than 50%. To this end, the local government has formulated the Beach planning of aquaculture waters in Lingshui Li Autonomous County (2018-2030), which sets a ceiling on the area of cage culture, but does not make recommendations on specific suitable areas for aquaculture.

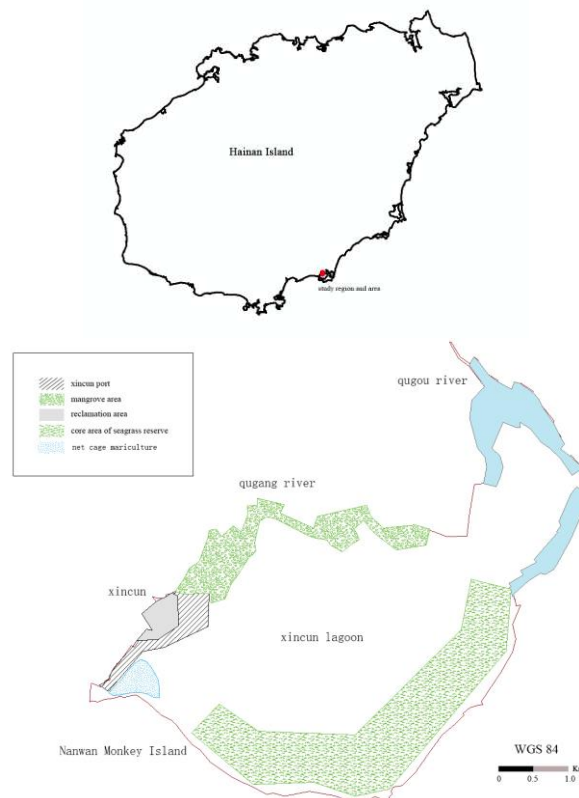


Figure 1. Map of study region and area

Methods

Index selection

The rationality of index selection is the basis of determining the rationality of the results of suitability analysis of shallow sea cage culture. In this paper, indicators are chosen according to the following three principles, including (a) reducing the maritime

conflicts in other human activities in the region, (b) reducing the pressure on Xincun Lagoon ecosystem caused by aquaculture activities and (c) improving the yield and efficiency of mariculture as much as possible. Specific indicators are explained as follows:

(1) The relations with protected areas. According to the requirements of the Planning of seagrass bed special protection area in New Village port, the Seagrass Bed Reserve is divided into general area and core area. The core area requires prohibition of all human activities, which is a prohibitive index. Other areas of the reserve belong to compatible fisheries and aquaculture, as shown in *Fig. 2*.

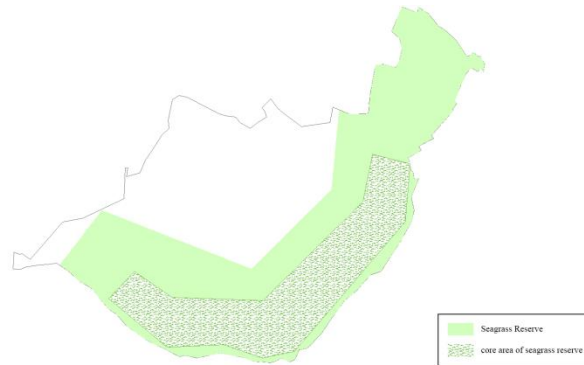


Figure 2. Scope of Seagrass Bed Reserve

(2) The water depth condition. The cage culture needs certain water depth conditions. According to the survey, the local cage depth is about 1.5 m. Thus, if the water is too shallow, the cage culture will not work properly.

(3) The hydrodynamic conditions. The self-purification ability of water body is the main factor to ensure that no major environmental problems occur in aquaculture. In this paper, the semi-exchange ability of water body is selected as the hydrodynamic evaluation index. The stronger the semi-exchange ability of water body is, the better the hydrodynamic conditions are, so it is more suitable for aquaculture activities. The semi-exchange ability of water body is shown in *Fig. 3*.

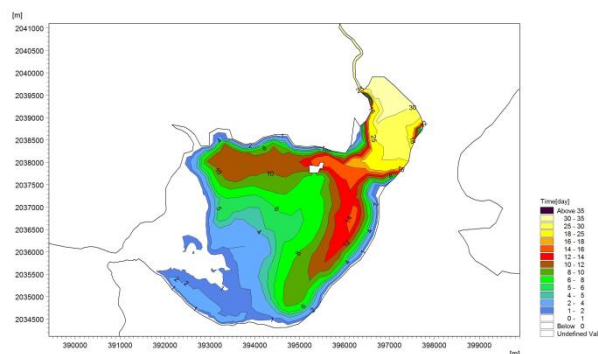


Figure 3. Semi-exchange time of water body

(4) Dissolved oxygen content. Considering the phenomenon of fish death caused by hypoxia in the history of Lagoon, dissolved oxygen content was selected as an index to

determine the suitability of mariculture in this paper. The higher dissolved oxygen content, the more suitable for aquaculture activities.

(5) Water environment quality. The quality of water environment is one of the important factors to decide whether it is suitable for aquaculture. Good water environment can effectively improve the yield of aquaculture. In this paper, eutrophication index is selected to represent the water environment quality. The higher the degree of eutrophication, the worse the water environment quality.

(6) Terrigenous pollution intensity. There are many human activities around the study area, and a large number of pollutants are discharged directly from the land to the sea. Therefore, the direct discharging area should be kept away from as far as possible to avoid the influence of pollutants on aquaculture.

(7) Wind and wave condition. Because of the small size of shallow sea cages and the weak ability to withstand wind and wave, the areas with smaller wind and wave should be selected for aquaculture.

Determination of index weight values

This study used the interaction matrix method to calculate the index weight value. Taking the 3*3 matrix as shown in *Table 1* as an example, all the main factors related to the problem listed on the main diagonal of the square matrix (i. e. A→C), and their state variables possess conceptual attributes. Spaces on the non-diagonal lines of the matrix are assigned a value which can be obtained through the numerical analysis, empirical judgment or experimental research to describe the degree of interaction between the two parameters. The interaction matrix shows asymmetry, such as the effect of A on B can be different from the effect of B on A. Analysis and assignment of influences in a strict clockwise direction after the matrix is established.

Table 1. Basic principles of rock engineering systems

A	The effect of A on B	The effect of A on C
The effect of B on A	B	The effect of B on C
The effect of C on A	The effect of C on B	C

When the interaction matrix is built and encoded, the coded values of the matrix rows and columns are added to determine the degree of interaction of each variable in the system, as shown in *Eq.1*. The sum of each row represents the effect of the parameters on the main diagonal of the row on the system, while the sum of each column refers to the effect of the system on the parameters on the main diagonal of the column. The higher the degree of interaction is, the greater the importance of this parameter in the system plays, so the interaction matrix can be used to determine the weight of each relevant parameter in the studied system. The weight of the parameter k_i can be calculated by from *Eq.2* to *Eq.4*:

$$V = \begin{pmatrix} V_{11} & V_{12} & \dots & V_{1j} & \dots & V_{1m} \\ V_{21} & V_{22} & \dots & V_{2j} & \dots & V_{2m} \\ \dots & \dots & \dots & \dots & \dots & \dots \\ V_{i1} & V_{i2} & \dots & V_{ij} & \dots & V_{im} \\ \dots & \dots & \dots & \dots & \dots & \dots \\ V_{m1} & V_{m2} & \dots & V_{mj} & \dots & V_{mm} \end{pmatrix} \quad (\text{Eq.1})$$

$$k_i = \frac{S_R(i) + S_C(i)}{2 \sum_{i=1}^n V_{ij}}, (i = 1, 2, \dots, m) \quad (\text{Eq.2})$$

$$S_R(i) = \sum_{i=1}^m V_{ij}, (i = 1, 2, \dots, m) \quad (\text{Eq.3})$$

$$S_C(i) = \sum_{j=1}^m V_{ij}, (i = 1, 2, \dots, m) \quad (\text{Eq.4})$$

where, in Formula (3) and (4), V_{ij} is the influence degree of parameter i on parameter j ; $S_R(i)$ and $S_C(i)$ represent the sum of the elements of each row, and column respectively in the multi-factor interaction matrix. The sum of each row represents the effect of the influence factor in the main diagonal line of the row, and the effect of the factor on the whole system by affecting other influence factors; the sum of each column refers to the effect of the influence factor in the main diagonal line of the column, and the effect of the factor affected by other factors on the entire system.

Weighted stacking

The comprehensive index of suitability evaluation can be calculated by the following weighted model:

$$S = \sum_{i=1}^n B_i W_i \quad (\text{Eq.5})$$

where, S is the comprehensive evaluation index of suitability of net cage mariculture in the shallow sea; B_i refers to the score of the i th evaluation factor (which is dimensionless); W_i denotes the weight of the i th evaluation factor; n refers to the number of factors in the evaluation.

Results

Index space quantization

The spatial distributions of each index on ArcGIS are displayed in *Fig. 4* to *Fig. 10*.

(1) Relationships to the conservation area

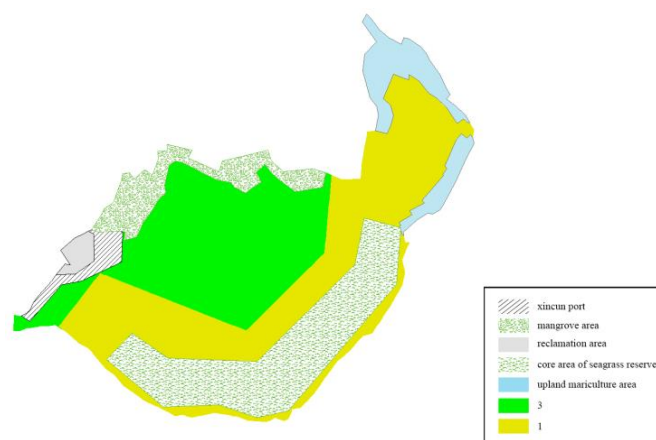


Figure 4. The spatial distributions of “relationships to the conservation area” on ArcGIS

(2) Hydrodynamic conditions

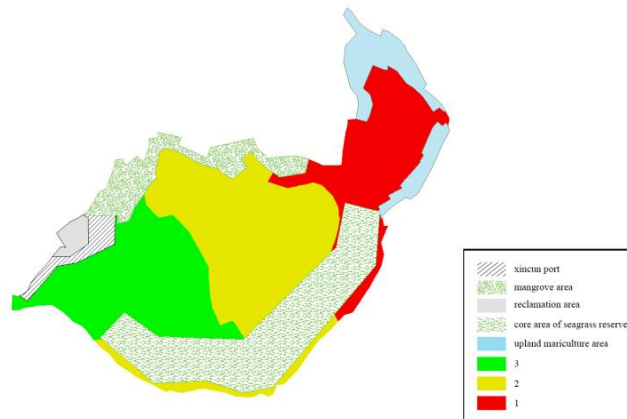


Figure 5. The spatial distributions of “hydrodynamic conditions” on ArcGIS

(3) Land-based pollution intensity

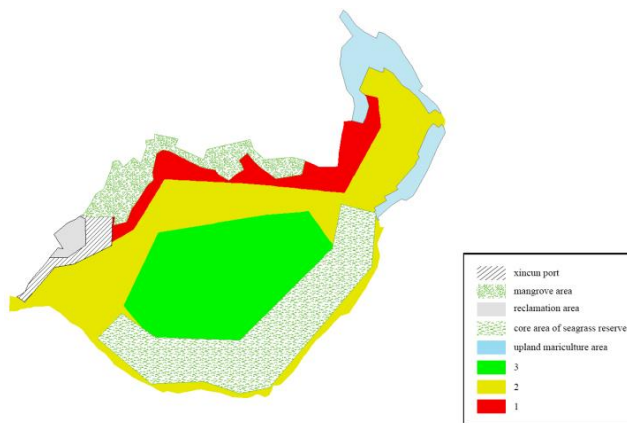


Figure 6. The spatial distributions of “land-based pollution intensity” on ArcGIS

(4) Suitability of water depth

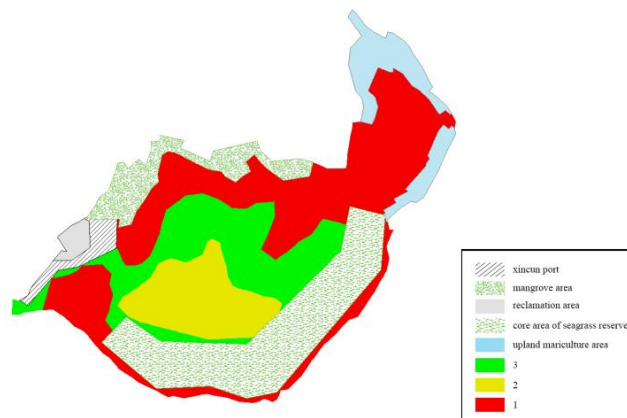


Figure 7. The spatial distributions of “suitability of water depth” on ArcGIS

(5) Water environmental quality

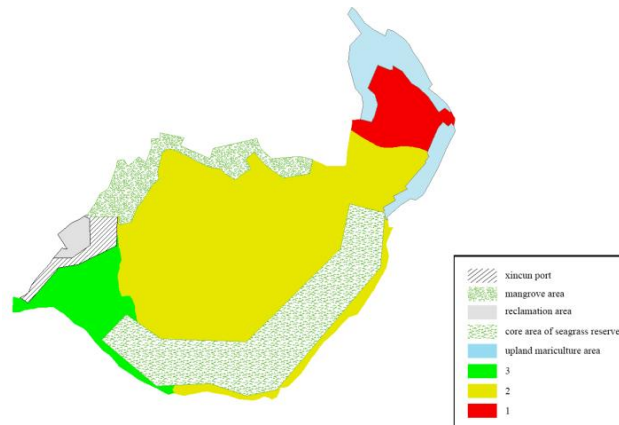


Figure 8. The spatial distributions of “water environmental quality” on ArcGIS

(6) Dissolved oxygen content

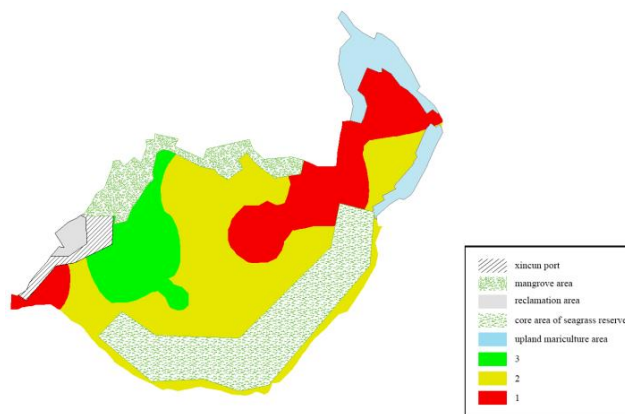


Figure 9. The spatial distributions of “dissolved oxygen content” on ArcGIS

(7) Status of flows and waves

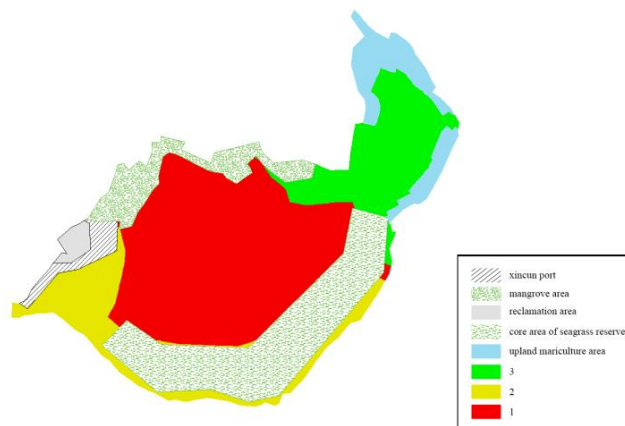


Figure 10. The spatial distributions of “status of flows and waves” on ArcGIS

Calculation of indices

According to the previous steps, the interaction matrix of suitability of net cage mariculture in the shallow sea was constructed, as shown in *Table 2*. The degrees of influence between the evaluation indices were divided into 5 levels, represented by the four dimensionless values 0 to 4 respectively: 0 means no effect; 1 indicates weak influence; 2 refers to big influence; 3 represents strong influence; 4 means extremely strong influence.

Table 2. Values of influence degrees of influence factors and their interactions

(1)1	0	3	0	3	2	0
3	(2)3	0	0	3	2	0
3	0	(3)2	0	3	3	0
0	2	0	(4)1	1	0	2
2	0	0	0	(5)2	2	0
2	0	0	0	1	(6)3	0
0	3	0	0	2	2	(7)2

The interaction matrix V of the suitability evaluation factors of net cage mariculture in the shallow sea is as follows:

$$V = \begin{pmatrix} 1 & 0 & 3 & 0 & 3 & 2 & 0 \\ 3 & 3 & 0 & 0 & 3 & 2 & 0 \\ 3 & 0 & 2 & 0 & 3 & 3 & 0 \\ 0 & 2 & 0 & 1 & 1 & 0 & 2 \\ 2 & 0 & 0 & 0 & 2 & 2 & 0 \\ 2 & 0 & 0 & 0 & 1 & 3 & 0 \\ 0 & 3 & 0 & 0 & 2 & 2 & 2 \end{pmatrix}$$

Based on *Eq.2* to *Eq.4*, the weights W_i of these seven influence factors can be calculated.

The weight of relationships to the conservation area W_1 was calculated as 0.1724, the hydrodynamic conditions W_2 as 0.1639, the land-based pollution intensity W_3 as 0.1379, the suitability of water depth W_4 as 0.0603, the water environmental quality W_5 as 0.1810, the dissolved oxygen content W_6 as 0.1724, and the status of flows and waves W_7 as 0.1121.

C, the sum of the row values, and E, the sum of the column values, C+E represents the value of interaction strength of each principal factor. The larger the value is, the stronger the importance of the parameter is; C-E indicates the dominance of each principal factor. C-E is greater than 0, indicating that the parameter is dominant, while C-E is less than 0, implying that the parameter is dependent. The detailed relationships are displayed in *Table 3*.

Table 3. Relationship parameters between C and E

Relationship of C and E	V_1	V_2	V_3	V_4	V_5	V_6	V_7
C	9	11	11	6	6	6	9
E	11	8	5	1	15	14	4
C+E	20	19	16	7	21	20	13
C-E	-2	3	6	5	-9	-8	5

Implementation of weighted stacking on ArcGIS

On the basis of the calculation according to Eq.5 by using ArcGIS10.0 and the spatial quantitative analysis, the spatial distribution of the suitability of mariculture in the shallow sea on ArcGIS can be obtained (Fig. 11). It can be seen that the most suitable area for net cage mariculture in the shallow sea is located at the mouth of the gate, accounting for about 10.00% of the total sea area, while the most unsuitable area for net cage mariculture in the shallow sea stands in the secondary bay, covering approximately 13.04% of the total sea area.

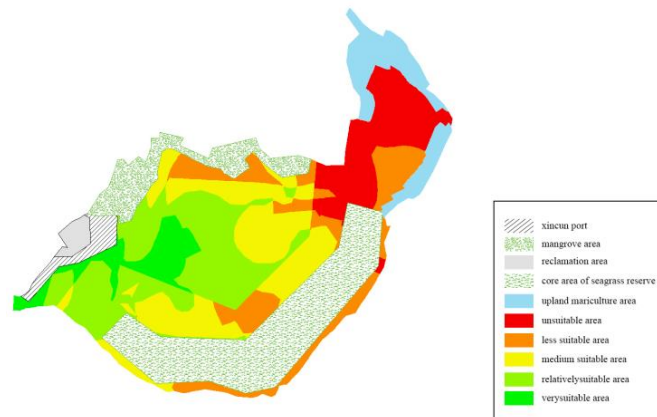


Figure 11. The spatial distributions of suitability of mariculture in the shallow sea on ArcGIS

Conclusions

On the above research, it can be determined that the areas suitable for shallow sea net cage mariculture in the Xincun Lagoon are mainly located at Area of 1, 2 and 3 (Fig. 12). However, this paper did not take into account factors such as social economy and transportation services in selecting the indicators. Unlike other cage cultures, farmers in the region live in shelters built by cages on the water. Therefore, the site selection should also consider the convenience of transportation to surrounding towns. For the spatial distance, Area 1 demonstrates as the most suitable one, and in fact, it is more conforming with the current farming situation.

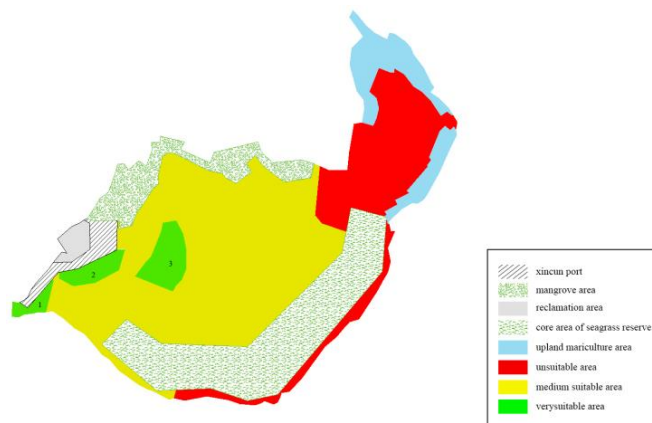


Figure 12. The simplified distribution of suitable area for mariculture in the shallow sea

This paper can clarify the suitable area for net cage mariculture in the shallow sea, but the accumulation of a large number of cages will cause changes in hydrodynamic conditions in the surrounding waters, as well as pollutants. Thus, further research is required to determine the division and layout of the cages to minimize the pressure on the ecosystem in the lagoon.

The interaction matrix can consider the interactions between the factors and calculate the affiliation of the factors. The results show that hydrodynamic conditions, the land-based pollution intensity, the suitability of water depth, and the status of water flows and waves are the dominant parameters, all of which are the driving factors for system changes. Although the conclusions of this study are highly credible, the dynamic changes of the indicators are not taken into account in the calculation process. In the future research work, the changes of the dominating parameters should be focused on and adjusted at any time.

Acknowledgements. This work was supported by Scientific Research Fund of the Second Institute of Oceanography, MNR, grant No. JG1917.

REFERENCES

- [1] Dapueto, G., Massa, F., Costa, S., Cimoli, L., Olivari, E., Chiantore, M., Federici, B., Povero, P. (2015): A spatial multi-criteria evaluation for site selection of offshore marine fish farm in the Ligurian sea, Italy. – *Ocean & Coastal Management* 116: 64-77.
- [2] Fang, X., Hao, C. L., Cheng, C. G., Ni, W., Wang, J. C., Zhang, Y. F. (2018): Pressure analysis and spatial quantitative assessment of impact of human activities on Lagoon ecosystem: a case study in Xincun and Li'an Lagoons, Hainan, China. – *Applied Ecology And Environmental Research* 16(5): 6253-6266.
- [3] FAO. (2015): *Aquaculture Zoning, Site Selection and Area Management under the Ecosystem Approach to Aquaculture*. – Policy brief.
- [4] Hudson, J. A. (1989): *Rock mechanics principle in engineering practice*. – CIRIA Ground Engineering Report: Underground Construction.
- [5] Joaquin, B. (2011): *A Single-Use Site Selection Technique, Using GIS, for Aquaculture Planning: Choosing Locations for Mangrove Oyster Raft Culture in Margarita Island, Venezuela*. – Site Selection Technique for Aquaculture Planning.
- [6] Mazzoccola, D. F., Hudson, J. A. (1996): A comprehensive method of rock mass characterization for indicating natural slope instability. – *Quarterly Journal of Engineering Geology and Hydrogeology* 29(1): 37-56.
- [7] Parker, M. R., Beal, B. F., Congleton Jr, W. R., Pearce, B. R., Morin, L. (1998): Utilization of GIS and GPS for shellfish grow out site selection. – *J. Shellfish Res.* 17: 1491-1495.
- [8] Velasco, H. R., Ayub, J. J., Belli, M., Sansone, U. (2006): Interaction matrices as a first step toward a general model of radionuclide cycling: application to the ¹³⁷Cs behavior in a grassland ecosystem. – *Journal of Radioanalytical and Nuclear Chemistry* 268: 503-509.
- [9] Wu, H. G., Ma, H. M., Zhang, H. L. (2011): Evaluation of subgrade stability of mountainous highway exhibition based on interaction matrix. – *Chinese Journal of Geotechnical Engineering* 33(S1): 209-213.
- [10] Yin, S., Takeshige, A., Miyake, Y., Kimura, S. (2018): Selection of suitable coastal aquaculture sites using multi-criteria decision analysis in Menai Strait, UK. – *Ocean & Coastal Management* 165: 268-279.
- [11] Zhou, Q., Herrera, J., Hidalgo, A. (2017): Development of a quantitative assessment approach for the coal and gas outbursts in coal mines using rock engineering systems. – *International Journal of Mining Reclamation & Environment*, DOI:10.1080/17480930.2017.1326077.

ADOPTION OF SUSTAINABLE INTENSIFICATION PRACTICES AND ITS EFFECT ON SMALLHOLDERS' FOOD SECURITY IN ETHIOPIA

ASERES, M. E.¹ – LIU, A.^{2*} – MWALUPASO, G. E.¹

¹*College of Economics and Management, Nanjing Agricultural University
No. 1 Weigang, Nanjing 210095, China*

²*China Center for Food Security Studies, Nanjing Agricultural University, Nanjing,
No. 1 Weigang, Nanjing 210095, China
(e-mail: A. M. Eshetie – aseresm@yahoo.com, G. E. Mwalupaso – rinscod@gmail.com)*

**Corresponding author
e-mail: liuaj@njau.edu.cn; phone: +86-25-8439-6037*

(Received 3rd Feb 2019 ; accepted 29th Mar 2019)

Abstract. Sustainable intensification practice (SIP) facilitates increased and sustained productivity of the limited and existing farmland with less pressure on the environment. Currently, there is a myriad of literature on the effect of SIP on food security. However, unlike previous studies, this study examines the effect of the adoption of multiple sustainable intensification practices on the improvement of food security among smallholder farmers in Ethiopia. Three basic conservation techniques, Agronomic (A), Biological (B) and Physical (P), are analyzed after derivation from 13 implemented soil and water conservation (SWC) practices using principal component analysis (PCA). The result of the multinomial endogenous switching regression (MNESR) shows that SIP adopters have a 55% higher food security, have 51% more access to clean water and sanitation, and consume at least one more dietary food item daily than non SIP adopters. A complete ($A_1B_1P_1$) and combined ($A_0B_1P_1$ and $A_1B_1P_0$) package had the highest food security status as compared to other combination strategies, while single technology users gain the least benefit. Our findings strongly promote the adoption of a complete or combined SIP package in agriculture to leverage the full benefits associated with food security.

Keywords: *land degradation, packages, environmental protection, SWC, impact*

Introduction

In African dryland agriculture, food security and livelihood of rural households are highly dependent on crop production and livestock farming, which are sensitive to climate-related impacts leading to deforestation and land degradation (Asfaw and Neka, 2017; Kassie et al., 2013; Nkomoki et al., 2018; Wolka et al., 2018). In Sub-Saharan Africa, those whose livelihood and income depend on the most vulnerable agriculture are adversely affected by climate change (Kim et al., 2018). By 2030, the fraction of population living in poverty is expected to reach 122 million (FAO, 2016). Particularly for Ethiopia, the population is expected to reach 160 million by 2050, which is linked to a sizable increase in agricultural production (Josephson et al., 2014). Increasing productivity will be achieved via extensification (expanding farming area) or by intensification (applying technologies in existing areas) (Anderson and Elisabeth, 2015).

Even though food deficiency and income are linked to farm size, 87% of farming households' in Ethiopia own less than two hectares of cropping land (Anderson and Elisabeth, 2015). Therefore, increasing productivity and securing food demand are prior objectives for adopting new household practice decisions. Rapid population growth and low levels of technology- adopting societies, could contribute to achieving productivity

increment at the expense of significant environmental risk through cropland expansion (Kassie et al., 2013). *Figure 1* presents the trade-off between forest share and arable land expansion due to rural population growth.

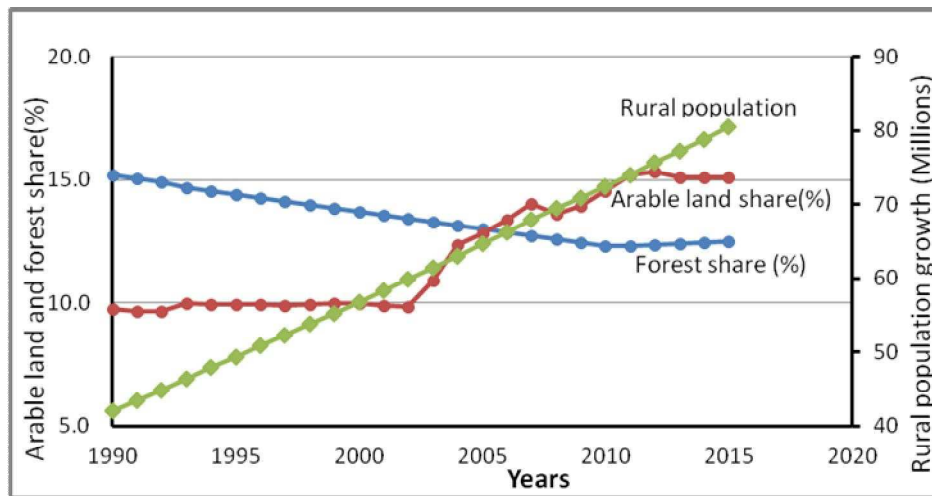


Figure 1. Rural population growth and land use trend in Ethiopia (1990-2015). (Source: WBdataset, 2018)

Food security and poverty reduction for subsistence farmer strongly correlate with environmental degradation by exploitation of land, forest, and water resources (Abdul-Rahim et al., 2018; Dejene, 2003). In this context, Ethiopia adopted a Sustainable Intensification Practice (SIP) approach as a new scientific arena for connecting environment and agriculture, which is considered a policy approach for achieving two goals simultaneously (Kassie et al., 2013).

The SIP approach could potentially achieve both economic improvement and environmental protection by maintaining soil fertility and produce higher output in existing cropping areas with less environmental pressure (Kassie et al., 2015a; Kim et al., 2018; Nkomoki et al., 2018). Adopting this strategy improved soil quality and reduced deforestation via climate change mitigation, thereby improving households' nutritional food intake, reducing months of food deficits, as well as food insecurity and poverty (Abdul-Rahim et al., 2018; Kassie et al., 2013, 2015a, b; Nkomoki et al., 2018).

In Ethiopia, farmers adopt different SWC technologies at a given time. Particularly in our chosen study area, more than half of the sampled households (51.04%) used 4-8 practices in a production season. Considering a single technology's effect on food security analysis will lead to a biased estimation. A review of 160 original field studies by Branca et al. (2013) confirms that isolating the impact of a single practice on productivity or food security is intricate. The author explained that a combined SIP package comprised of agronomy, agroforestry, water harvesting, and conservation techniques contributes to increased yield, as well as reduced soil loss and erosion. Similar studies in Ethiopia (e.g., Coulibaly et al., 2017; Asfaw and Neka, 2017; Wolka et al., 2018) showed similar results. More specifically, Amare et al. (2014) found that in northern Ethiopia, farmers increased their yield by 7% and reduced soil loss by 68%, by adopting integrated soil bund and grass strips.

Notwithstanding their benefits, land degradation and soil erosion remain very complex and convoluted problems in Ethiopia. A recent SWC government campaign

mainly focused on the participatory community watershed area conservation and to a much lesser extent on individual plot-farm management. Moreover, SIP package combination and structure technical design are not well understood by farmers.

The objectives of this study are twofold: First, to assess factors that influence the SIP choice by smallholder farmers. Second, estimating the effect of SIP adoption and package choice among adopters on households' food security. We found significant food security improvement for households that practiced complete packages. Also, our study showed better performance in nutritional food consumption and food security status in households that adopted combined agro-biological and biophysical packages compared to those that adopted a single package.

Our paper contributes to the existing literature in four aspects. First, most SIP studies focus on the use of a single practice and related adoption constraints (Branca et al., 2013). However, this paper attempts to link the adoption factors and their impact by considering the many SIPs choice strategy, which is important for development agents focusing on SIP adoption strategies. Second, to the best of our knowledge, the related literature in Ethiopia considered the impact of SIP estimation either in the context of general adoption or package choice approach separately. In this study, we analyzed both cases and found a comprehensive and consistent result. Third, we considered three food security measurement indicators at the same instance which helps to address the dimensions of food availability, access, and utilization, resulting in a robust and consistent estimation. Finally, we employed a systematic model combination where Principal Component Analysis (PCA) was used for variable reduction without losing information from data, while the MNESR model was used to avoid endogeneity and self-selection bias.

Materials and methods

Description of the study area

This study was conducted in Benishangul Gumuz National Regional State (BG) in Ethiopia (Fig. 2). It is located in the western part of the country and has three administrative provinces and 21 districts. The Blue Nile River divides the region into two main parts, the northern part Metekel province, and southern part Assosa and Kemashi provinces. The region is endowed with water sources such as Beles, Dhidhsa, Dinder and Dabus rivers all of which are a tributary of Abay (Blue Nile) river. From the total estimated area to about 5,069,900 ha of the region, the arable land accounts about 911,877 ha and 24.4% of this land has potential for irrigation (Emana, 2010; Teklemariam et al., 2016); and forest land is estimated to be 3,963,750 ha (WBISPP, 2005).

The three major agro-climatic zones of the region are (i) low land or Kola (about 75% of the region), (ii) Midland or Woynadega (accounts 24%), and (iii) Highland or Dega agro-climatic zone about 1% of the region (Teklemariam et al., 2016). The mean annual rainfall of the region is between 860 and 1275 mm, and the temperature varies with a daily maximum of 20-25 °C in the rainy season and rises to 35-40 °C in the dry season.

According to 2007 CSA (Central Statistics Agency) population census report, the region had a total population of 670,847 with 3% annual growth rate which is higher than the national growth rate of 2.6% per annum. Field crops including maize, sorghum, finger millet, okra, soybean, haricot bean, sesame, and groundnut are majorly produced

in seven districts of the study area. The region recently experienced environmental degradation resulting to severe soil erosion, long dry season, erratic rainfall, and loss of soil fertility. Migration and resettlement programmes is the main cause of deforestation and cropland expansion. For example, in Sirba Abay district, between 1987 and 1998, the cultivable land expanded by 100% and between 1998 and 2007, the expansion was tripled (300%). Petteri Vuorinen (2016) in four districts confirmed that 74% of the forest were cleared due to cropland expansion, whereas 11% was done for fuelwood/charcoal as an income source, and 6% attributed for investment purpose. This evidently indicates that agricultural land expansion effect takes a lion-share for environmental degradation that is aimed to increase productivity and smallholders food provision (Petteri Vuorinen, 2016).

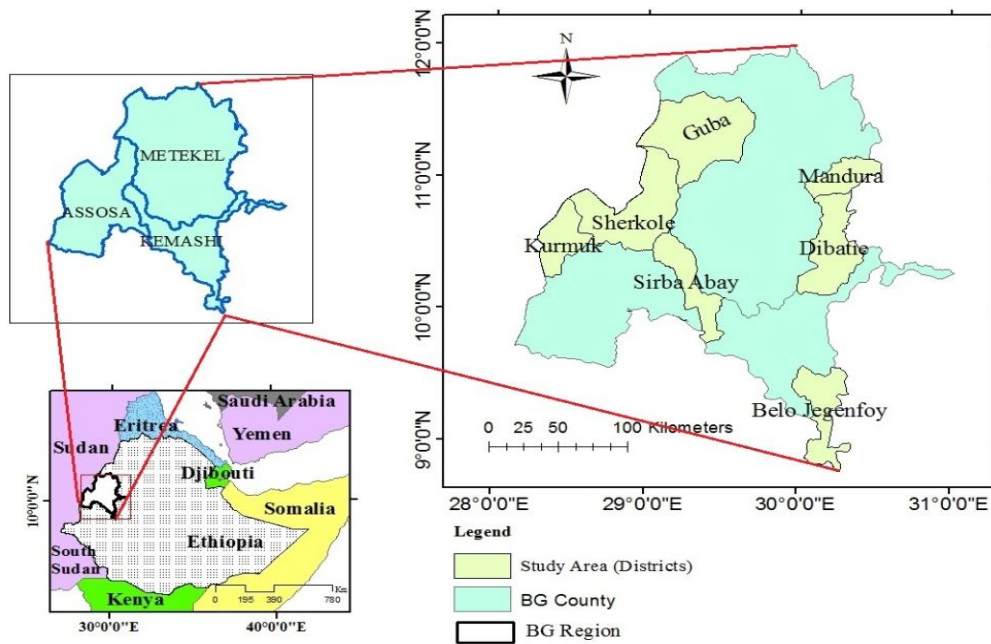


Figure 2. Study area location

Data source

We employed a two-stage sampling technique to select respondents. In the first stage, 7 out of 21 districts were purposively selected. The selection was based on regional government, development of stakeholders intervention, and strong SWC campaign. Population size within the seven districts accounted for 27% (179,313) of the total regional population (Emana, 2010). Furthermore, people from neighboring regions also migrated to this area as seasonal and contract farming actors.

In stage two, 30 peasant associations (PAs) from all seven districts were purposively selected. During PA (village) selection, the landscape condition, soil quality, vegetation cover, erosion incidence; SWC practice, farming trends, and experience; and area productivity were taken into consideration. Finally, a simple random sampling technique was employed to select 909 respondents (heads of household) from the PAs (Table 1). Trained enumerators interviewed the sampled household heads using a pre-tested and structured questionnaire with supervision of the extension officer.

Prior to conducting the farmer interviews, various key informants and focus group discussions were held on institutional (56 agriculture office experts at a different level), community, and district levels (132 model farmers and community elders). Data on household SIP adoption and food security impact estimation were collected in 2016 using a one-year recall questionnaire. We consider two reference periods of different production seasons: For SIP adoption, the reference period was March 2014 to February 2015, whereas for food security and production, information was gathered from March 2015 to February 2016.

Table 1. Sampled household heads by district and adoption frequency ($N = 909$)

No.	Districts	Adopters		Non-adopters		Pooled sampled	
		Frequency	%	Frequency	%	Frequency	%
1	Belojiganfoy	86	11.21	24	16.90	110	12.1
2	Debati	56	7.30	3	2.11	59	6.49
3	Guba	19	2.48	14	9.86	33	3.63
4	Kurmuk	90	11.73	13	9.15	103	11.33
5	Mandura	247	32.20	25	17.61	272	29.92
6	Sherkole	246	32.07	21	14.79	267	29.37
7	Sirbabay	23	3.00	42	29.58	65	7.15
	Total	767	84.4%	142	15.6%	909	100.00

Variable description

Food security measurement

Measuring food (in)security is quite complex, where household behaviors and dimension aspect should be considered. Food security entails multiple aspects, and it is therefore not easy to capture the full range of dimensions relating to food availability, access, and safety of a household or individual from a single measurement (Mabiso et al., 2014). Again, there is no a separate best measurement metric; and using multiple indicators is recommended by Maxwell et al. (2014) and Mabiso et al. (2014).

In this paper, we estimated household food security status using three different indicators as described below. These multiple indicators provide robust estimation for the evaluation's consistency and comparability purposes. *Table 2* presents the definition and summary statistics for all variables.

Dependent variables

1. Household dietary diversity score (HDDS)

Household dietary diversity (HDD) is used to compute a household's access to nutritional food and energy intake within 24-hours consumption recall period (Ecker, 2018; Maxwell et al., 2014; McDonald et al., 2015; Moroda et al., 2018; Pérez-Escamilla et al., 2017). The number of consumable food groups range from 0 to 12 point scale. In this study, they include cereals; and pulse; vegetable with tuber; root and tubers; leafy vegetable; fruits, egg; meat, poultry; fish; milk and milk products; honey and sugar; and oil and condiments. All the food groups have equal value of one, and the total score value is calculated as a whole food list consumed by the family during the last 24 h.

2. Self-assessed measures of food security (SAFS)

Self-assessment of a household on their food security status examines the change in food availability (shortage or surplus) during the past 12 months (January to December 2016). SAFS used to measure the household's access to enough food. Since SAFS estimation is subjective and constructed from a single question, one might expect this indicator to be less reliable. However, Shiferaw et al. (2014) and Maxwell et al. (2014) from Ethiopia applied it as an indicator to estimate food security. The response was recorded as 1 if the household had no food shortage throughout the year and, zero otherwise.

3. Access to water availability, sanitation, and hygiene (WASH)

The food security outcome is not only determined by food-related constraints of a household, but also by non-food causes that affect its status. WASH is used to estimate the food utilization dimension of food security as an additional parameter. Pinstrup-Andersen (2009) and Moroda et al. (2018) suggested a consideration of the non-food factors like access to clean water and sanitation factors. The households' self-response is recorded as a dummy variable 1 if HH had access to WASH, and 0 otherwise.

Key independent variables

Sustainable intensification practice (SIP) adoption and package choice

To maximize productivity through improving and conserving soil and water resource, farmers are more likely to practice multiple SWC techniques (Kassie et al., 2013). Thirteen SWC practices were reduced and categorized into three main groups Agronomic (A), Biological (B) and Physical (P) conservation practices. We define SIP adoption as a dummy, where 1 denotes a household that practiced at least one of the three categories, and 0 otherwise.

On the other hand, three SIP categories generate six probability combinations (*Table 5*). The first SIP choice was adopting a complete SIP- $A_1B_1P_1$ (Agronomic-Biological-Physical) package. However, not all farmers practice full SWC techniques, except for innovative and model farmers who may implement many practices at once in a single production season. Adopting a complete package has short-term benefits such as augmented productivity, income, and fodder (Amare et al., 2014; Wolka et al., 2018). The second SIP choice was the $A_1B_1P_0$ (Agronomic-Biological) package that required less technical skill and knowledge. For example, multipurpose trees and grass strips integrated with agronomic practice aided in nutrient recycling for crops, soil fertility improvement, and water-holding capacity enhancement. The third SIP choice considered was the $A_0B_1P_1$ (biophysical) package, which was adopted mainly to support physical structures with grass strips.

Farmers are less likely to practice physical structure alone due to area share from cropping and the higher frequency of repairs. Amare et al. (2014) confirm that the combined bio-physical technique has a substantial effect on runoff reduction and soil loss compared to other treatments.

The fourth SIP choice was the $A_1B_0P_1$ (Agronomic-Physical) combination. Farmers built physical structures when the plot area was gentle or sloppy to minimize the run-off velocity and conserve soil and water. The fifth SIP single package choice was the $A_0B_1P_0$ (Biological) conservation method, which has a dual benefit of conserving and

recycling soil nutrients and generating income from plants (fodder, fuelwood, and wood product). Our final consideration was the agronomic practice choice $A_1B_0P_0$. Usually, it is assumed that farmers practice at least one measure of the soil fertility improvement techniques as a coping strategy to reduce production risk.

Table 2. Variable definition and descriptive statistics

Variables	Description	Mean	Std dev
Outcome variable			
HDD	Household dietary diversity score	5.81	2.25
Food secure (SAFS)	Does HH have enough food in the last year? (yes = 1)	0.53	0.50
Water & sanit access	Household water and sanitation accessibility (yes = 1)	0.47	0.50
Intervention variable			
SIPs adoption (dummy)	Head of HH who adopt sustainable intensification practice (1 = adopter)	0.84	0.37
A0B0P0	Head of HH who do not adopt any SIP practice	0.16	
A0B0P1	Head of HH who adopts physical structure package	0.01	
A0B1P1	Head of HH who adopts a biophysical package	0.12	
A1B1P1	Head of HH who adopts all SIPs package	0.37	
A1B1P0	Head of HH who adopts an agro-biological package	0.15	
A1B0P0	Head of HH who adopts the agronomic practice	0.06	
A0B1P0	Head of HH who adopts the biological practice	0.04	
A1B0P1	Head of HH who adopts the agro-physical practice	0.11	
Explanatory variable			
HH education	Household head have formal education (yes = 1)	0.72	
Gender	Sex of the head of a household (1 = male)	0.85	
Family size (AEU)	Family size in adult equivalent unit (AEU)	6.26	2.63
Cropping area	Household owned Farm size (ha)	1.89	0.91
Livestock asset (TLU)	livestock asset in tropical livestock unit (TLU)	2.16	2.90
Crop income	Annual household crop income in ETB	16069.11	16538.38
Off-farm participate	household participated in off-farm income activity	0.56	
Extension access	Household have access to extension service	0.72	0.45
Market access	Household have access to input & output market	0.65	0.48
Main road access	household who have road access (yes = 1)	0.70	0.46
Access to credit	1 = if a household has access to credit service	0.44	
Group membership	1 = if the household is a member of a rural social network	0.61	0.49
HH trained on SWC	1 = if HH trained on soil and water conservation	0.64	
HH trained on SNRM	1 = if HH trained on sustainable natural resource management	0.60	
Total		909	

Table 4 presents the identified SIP measures and their grouping categories. We consider agronomic package adoption (A_1), if a household head practices at least two techniques from an agronomic; for Biological (B_1) at least one from the biological method; and if HH adopts at least one from four structural measures, we assign as physical practice adopter (P_1). Finally, the causal effect of SIP adoption on food security

was estimated in overall (SIP adoption dummy) and unconditional probabilities (six possible combinations) method.

The choice of the explanatory variable was based on related smallholders SIP adoption decision and economic welfare effect study literature and presented in *Table 2* (Amare et al., 2014; Kassie et al., 2013, 2015a, b; Kpadonou et al., 2017; Nkomoki et al., 2018; Wekesa et al., 2018).

Econometrics approach

In many developing countries including Ethiopia, input and output market imperfection and high seasonality are common constraints for smallholder farmers. Also, high fluctuation and volatility nature of food and agricultural input price strongly correlates to the availability of food. Therefore, the adoption intensity and willingness to invest for newly introduced practice is dependent on net benefit gained from the process. The farm household adjusts adoption behavior for readily available technologies by looking for the opportunity. If the utility from a new method is higher than the conventional system, a farmer will decide to adopt. Farmers want to maximize their income by choosing the optimal combination of SIP package.

Unlike experimental studies, the selection of adoption and non-adoption in cross-sectional survey research was not randomized, and observable and unobservable characteristics profoundly influence the decisions. It implies that farmers in the research area were not equally exposed to the new technology. In causal effect analysis, both controlled and treatment groups must have similar behaviors to avoid a biased estimation. As a result, we employed a new two-stage selection-bias correction approach of the multinomial endogenous switching regression (MNLESR) (Bourguignon et al., 2007) to determine the real effects of farmers choice of SIP package and the outcome equation. Use of MNLESR model has a triple advantages. First, it helps to address biasness that arises from the unobservable variable. Second, the model allows getting consistent and efficient estimates of the adoption process with reasonable correction for the outcome equation. Third, it assists in computing the impacts of both separate and combined practice simultaneously (Abdulai and Huffman, 2014; Coulibaly et al., 2017; Kassie et al., 2015b; Wekesa et al., 2018).

Multinomial adoption selection model (MNL)

In the first stage, we used a multinomial logit model (MLM) to examine the factors that affect a farmers SIP packages choice. Farmers have six mutually exclusive (P) alternative SIP strategies and will adapt by comparing its effect to maximize their utility. Consider I_{ij}^* is a latent variable that represents the j th farmers behavior in practicing SIP combinations i ($i = 1, \dots, 6$) and expressed as follows (Eq. 1):

$$I_{ij}^* = X_{ij} \beta_j + \varepsilon_{ij} \quad (\text{Eq.1})$$

where X_{ij} captures vector observed exogenous variable (household characteristics, farm, and asset characteristics, institutional features, and knowledge and extension access variable), while ε_{ij} are the error term from an observed characteristics.

From available mutually exclusive SIP p combinations of packages, a farmer will choose the SIPs combination if:

$$I = \begin{cases} 1 & \text{if } I_{ij}^* > \max_{p \neq 1} (I_{pj}^*) \text{ or } \omega_{1j} < 0 \\ \vdots \\ i & \text{if } I_{ij}^* > \max_{p \neq i} (I_{pj}^*) \text{ or } \omega_{ij} < 0 \end{cases} \quad \text{for all } p \neq i. \quad (\text{Eq.2})$$

According to Equation 2, the *j*th will adopt *i*th package to maximize utility, if

$$\max_{p \neq i} (I_{pj}^* - I_{ij}^*) < 0.$$

Since we are assuming ε_{ij} as the error term from an observed characteristics and to be identically Gumbel distributed and independent, Equation 2 leads to the multinomial logit model of the probability that farmers will choose combinations (*p**ij*) as shown in Equation 3:

$$p_{ij} = \text{pr}(\omega_{ij} < 0 | X_{ij}) = \frac{\exp(X_{ij} \beta_j)}{\sum_{p \neq 1} \exp(X_{ij} \beta_p)} \quad (\text{Eq.3})$$

Multinomial endogenous switching regression estimation

Following similar impact studies of Abdulai and Huffman (2014), Kassie et al. (2015b), Coulibaly et al. (2017) and Wekesa et al. (2018), we applied a multinomial endogenous switching regression model which is developed by Lee (1982) to estimate the SIP adoption causal effect.

An endogenous switching regression model of a selection bias correction framework used to estimate the farmers SIP adoption impact of each strategy on household food security through multiple indicators. The $A_0 B_0 P_0$ SIPs package was taken as the base category (non-responsive) and denoted as $i = 1$ and the adopter practiced at least one from remaining SIP ($i = 2, 3, 4, 5, 6$) combination package. The food security status implication for each regime is described as Equation 4:

$$\begin{cases} \text{Regime 1: } \Omega_{i1} = \alpha_1 + v_{i1} & \text{if } i = 1 \\ \vdots \\ \text{Regime } i: \Omega_{ij} = \alpha_j + v_{ij} & \text{if } i = j \end{cases} \quad (i = 2, 3, 4, 5, 6) \quad (\text{Eq.4})$$

where Ω_{ij} denoted the *j*th farmers food security status in regime *i* combination, α_i is for the set of exogenous variable (household characteristics, farm, and asset characteristics, institutional features, and knowledge and extension access variable) and the error term denoted by v_{ij} that capture the uncertainty and distributed with $E(v_{ij}) = 0$ and $\text{var}(v_{ij}) = \sigma_j^2$. If the error term v_{ij} and ε_{ij} are not independent a consistent estimation of α_j requires to avoid biased and the inclusion of the selection correction term of alternative choice in Equation 4. Then based on Bourguignon et al. (2007) suggestion we can estimate v_{ij} and ε_{ij} consistently with Equation 4 by MESR model developed by Lee (1982) and specified as in Equation 5:

$$\left\{ \begin{array}{l} \text{Regime 1: } \Omega_{i1} = {}_i\alpha_1 + \sigma_{11} + e_{i1} \quad \text{if } i = 1 \\ \vdots \\ \text{Regime } i: \Omega_{ij} = {}_i\alpha_j + \sigma_{jj} + e_{ij} \quad \text{if } i = j, \end{array} \right. \quad (\text{Eq.5})$$

where e_{ij} is the error term and σ_j is also the covariance between e 's and v 's, while f_j is the inverse Mills ratio from the estimated probabilities.

Following (Di Falco et al., 2011), ESR can be used to examine the average treatment effect on the treated (ATT) and by comparing the expected outcome of the food security status of adopters with and without adoption of SIP combination packages in the actual and counterfactual scenario presented and defined in Equation 6:

$$ATT = E(\Omega_{ij}|i = j) - E(\Omega_{i1}|i = j) = {}_i(\alpha_j - \alpha_1) + i(\sigma_j - \sigma_1) \quad (\text{Eq.6})$$

Results and discussion

Descriptive statistics

A household intensity of SIP adoption estimation

Under dry land economy, as in the case of Ethiopia, farmers adopt multiple SWC technologies aimed at increasing productivity and reducing the risk of food deficiency (Kpadonou et al., 2017). Table 3 presents the households' SIP adoption intensity, which ranges from zero to eleven SWC measures. Households are selective, and have different SIP adoption intensities (Wolka et al., 2018). While some farmers practice up to 11 SWC techniques, 15.62% (142 HHs) do not implement any of the 13 practices. However, from the sampled heads of HHs, 84.38% adopted at least one sustainable intensification technology in their cropping area.

Table 3. Heads of households adoption intensity on SIP package

Number of practice	Frequency	Adopters (%)	Cumulative
Heads of HHs who did not practice any SIP (0)	142	15.62	15.62
Heads of HHs who practice 1	29	3.19	18.81
2	48	5.28	24.09
3	128	14.08	38.17
4	119	13.09	51.27
5	125	13.75	65.02
6	91	10.01	75.03
7	74	8.14	83.17
8	55	6.05	89.22
9	51	5.61	94.83
10	32	3.52	98.35
11	15	1.65	100.00
12	0.00	0.00	100.00
13	0.00	0.00	100.00
Total	909	100.00	

More than half of the sampled households (51.04%) used 4-8 practices, 22.55% used 1-3 practices and a few (10.78%) used >8 SIP technologies. The adoption intensity descriptive results showed that in the study area, most households experienced at least one practice from each SWC category (Agronomic, Biological and Physical measures), and entirely adopted more than three technologies.

SIP variable reduction and grouping strategy

Table 4 presents the reduced form of linear combination loadings estimation results from multiple on-farm level SIP practices. Following suggestions by Goswami et al. (2012) and Chatterjee et al. (2015), the orthogonal rotation was executed on principal components, and four principal components with eigenvalue > 1 were considered. From the overall data variability, 61.03% is explained by four components. The first component (hereafter called agronomic practice) had a positive effect on loadings and explained 20.11% of the variance from total PC variability.

Principal components 2-4 accounted for 15.6, 14.04, and 11.29% of the loadings, respectively. The second principal component group is hereafter named as biological practice. In this study, the third most determinant component group was associated with a farmers participation in physical structure practices. The fourth principal component included one physical element (employing check dum) and an agronomic element (strip mulching) which was inconsistent with SWC groupings (Abdul-Rahim et al., 2018). We, therefore, excluded component 4 to harmonize SIP groupings. Whether component 4 affects the impact analysis requires further investigation. Therefore, for this study, three component loading variables had more importance in explaining SIP adoption and variance of effect analysis. According to Kaiser (1958), an average communality above 0.60 is the minimum criteria for PCA analysis, which was met in our study 61.03%. This shows that our PCA estimation is a good fit, with good data quality.

Table 4. Rotated components loading (greater than 0.3)

Strategy	Comp1	Comp2	Comp3	Comp4	Unexplained
Apply soil bund			0.6265		0.3095
Apply check dam				0.3059	0.5784
Use cut-off drain			0.4449		0.4649
Apply micro-basin			0.4630		0.396
Use organic fertilizer	0.5229				0.3014
Use conservation agriculture	0.3048				0.4779
Apply crop rotation	0.5039				0.3812
Apply shifting cultivation	0.5162				0.2835
Apply strip mulching				0.4356	0.4537
Apply terrace			0.7316		0.3113
Planting grass strips		0.3992			0.5036
A forestation of fields		0.6271			0.2917
Apply agroforestry		0.5243			0.3125
Eigenvalue	2.6148	2.0270	1.8248	1.4678	
Eigenvalues % contribution	20.11	15.59	14.04	11.29	
Cumulative %	20.11	35.71	49.74	61.03	

Comp1 denotes agronomic practices (A), Comp2 for biological (B) and Comp3 for physical (P)

A household probability for SIP choice description

After considering varimax rotation from high factor loadings, household choice to different SIP packages (combinations) was estimated. *Table 5* presents the different possible combination of packages chosen by households referring to non-adopters $A_0B_0P_0$ (15.62%) as a base. The study discussed six out of eight SIP probabilities.

Table 5. *Alternative sustainable intensification practices (SIPs) package probabilities*

Choice (ith)	Combination	A = agronomic		B = biological		P = physical		Frequency	Percentage
		A ₁	A ₀	B ₁	B ₀	P ₁	P ₀		
1	A ₀ B ₀ P ₀		✓		✓		✓	142	15.62
2	A ₀ B ₀ P ₁		✓		✓	✓		6	0.70
3	A ₀ B ₁ P ₁		✓	✓		✓		111	12.20
4	A ₁ B ₁ P ₁	✓		✓		✓		336	36.96
5	A ₁ B ₁ P ₀	✓		✓			✓	132	14.52
6	A ₁ B ₀ P ₀	✓			✓		✓	50	5.50
7	A ₀ B ₁ P ₀		✓	✓			✓	32	3.50
8	A ₁ B ₀ P ₁	✓			✓	✓		100	11.00
Total								909	100

A₁ = agronomic users, A₀ = non-users of agronomic and others have a similar interpretation

The farmer had a chance to choose from the set of six mutually exclusive combinations during a production season. Approximately 14.52% of the farmers applied Agro-Biological methods (A₁B₁P₀), while 12.2% applied the biophysical conservation package (A₀B₁P₁).

Other farmers used packages A₁B₀P₁, A₁B₀P₀, and A₀B₁P₀. Overall the majority of the farmers (37%) applied a complete SIP package (A₁B₁P₁). This observation concurs with other studies such as (Kipkoech Anderson et al., 2015; Wekesa et al., 2018).

Empirical result

Determinants of SIP adoption choices

The objective of this study dwelt on the SIP adoption constraints and their impact on households' food security. In the first stage, we used the Multinomial logit (MNL) model to describe SIP packages adoption decision and possible constraints by considering non SIP users (A₀B₀P₀) as the base. The result of this estimation is essential for identifying factors that affect SIP package combination adoption and suggesting possible adoption constraints to development partners and policymakers. A unit change in an explanatory variable and its variation on the probability of particular choices was estimated by the MNL marginal effect model and is reported in *Table 6*. The Wald test estimation result of the regression coefficient was jointly equal to zero (Wald χ^2 (91) = 918.10; $p = 0.000$). Farmers who only adopted the physical structure were not discussed due to the mundane representation of this group. The marginal effect estimation result confirmed that the explanatory variable coefficients varied substantially across the alternative packages.

Among the household characteristics, male household heads positively associated with agronomic (A₁B₀P₀) and biological (A₀B₁P₀), but negatively associated with labor-intensive Agro-Physical (A₁B₀P₁) packages. The results were in agreement with data

from Asfaw and Neka (2017) and Tiwari et al. (2008). However, having the formal education of a household head reduced the probability of adopting agronomic ($A_1B_0P_0$) practice by 4.6%. This could be due to the fact that education is necessary for adopting the knowledge-intensive physical structure compared to the agronomic practice. Kpadonou et al. (2017) also observed a negative correlation between formal education and mulching and sustainable agricultural practices (SAP) adoption.

Table 6. Marginal effect based on SIP choice

Variables	$A_1B_1P_0$ dy/dx	$A_0B_1P_1$ dy/dx	$A_1B_1P_1$ dy/dx	$A_1B_0P_0$ dy/dx	$A_0B_1P_0$ dy/dx	$A_1B_0P_1$ dy/dx
Gender	0.0408	-0.0510	0.0292	0.0452**	0.0264*	-0.1086**
	0.0387	0.0491	0.0568	0.0197	0.0156	0.0468
HH education	-0.0103	0.0216	0.0256	-0.0464*	0.0035	0.0386
	0.0367	0.0385	0.0482	0.0273	0.0176	0.0278
Family size	-0.0037	0.0096	-0.0062	-0.0037	-0.0006	-0.0028
	0.0065	0.0072	0.0086	0.0046	0.0036	0.0059
Cropping area	-0.0088	-0.0245	0.0302	-0.0007	-0.0064	0.0402***
	0.02	0.0224	0.0253	0.0127	0.0101	0.0156
Log-crop-Inc	-0.1204***	-0.0829***	0.4342***	-0.0473***	-0.0454***	-0.0827***
	0.0242	0.0264	0.0339	0.0154	0.0117	0.0193
Off-farm partici	0.0187	0.0610*	0.0286	0.0049	0.0036	-0.1445***
	0.0335	0.0356	0.0444	0.0207	0.0162	0.0305
Exten-access	0.0721**	-0.0160	0.0411	-0.0153	-0.0008	-0.0365
	0.0345	0.0436	0.0546	0.0252	0.0180	0.0335
Market access	-0.002	0.0366	0.0104	-0.0423	-0.0110	0.0140
	0.0368	0.0388	0.0502	0.0264	0.0184	0.0294
Road access	0.0016	0.0401	-0.0696	-0.0007	-0.0119	0.0959***
	0.0386	0.0399	0.0525	0.0227	0.0194	0.0253
Credit access	0.2218***	-0.0608*	-0.0264	-0.0459**	-0.0123	-0.0318
	0.0350	0.0335	0.0410	0.0213	0.0157	0.0247
G- membership	0.0704**	-0.0563*	0.1456***	-0.0347**	-0.0091	0.0107
	0.0335	0.0367	0.0413	0.0233	0.0174	0.0258
SWC_trained	-0.0643*	-0.0093	0.1185**	-0.0128	-0.0478**	0.0910***
	0.0376	0.0404	0.0469	0.0235	0.0230	0.0264
SNRM_train	0.0091	0.0210	0.1575***	-0.0504**	0.0194	-0.1334***
	0.0346	0.0375	0.0448	0.0254	0.0160	0.0324
Number of Obs.		909				
Wald ch ² (91)		918.10***				
Pseudo R2		0.2884				
Log pseudo likelihood		-1132.645				

***, **, and * indicate significance level at 1%, 5%, and 10%, and ($A_0B_0P_0$) is stand for base category ($i = 1$) in the MNL

An increase in a household's plot size by one unit, increased the likelihood of practicing the $A_1B_0P_1$ package by 4%. Large farm owners were closer to perceiving soil

erosion problems and thus highly adopt physical conservation measures (Anim, 1999; Fikru, 2009; Mekuriaw et al., 2018; Moges and Taye, 2017; Nkomoki et al., 2018; Wekesa et al., 2018). Crop income is another important variable (a proxy of household food security status) for SIP adoption. A unit change in the amount of income is associated with a higher likelihood of adopting complete SIP packages ($A_1B_1P_1$) by 43.42%, at 1% significance level. However, it was also negatively associated with other combinations. The change in productivity due to SWC practices, especially from the physical structure, has a long-term effect. Wolka et al. (2018) confirmed that short-term low benefit from conservation practices demotivates farmers' interest in adopting the introduced SWC measures. Household off-farm participation was positively associated with ($A_0B_1P_1$), while negatively associated with the Agronomic-Physical combination ($A_1B_0P_1$). Since building physical structures is a labor-intensive practice, a household that frequently engages in off-farm employment wants to combine physical structures with others like a tree and supportive grass structures.

Information has played a vital role in driving farmers participation in the plot-level sustainable intensification decision process. The more a farmer has contact with agricultural extension workers, the higher the probability of adopting the $A_1B_1P_0$. Moreover, farmers' access to SWC, and SNRM related training showed positive association, and statistically significant with complete package ($A_1B_1P_1$) and Agro-Physical ($A_1B_0P_1$) choices. In essence, building a physical conservation structure demands technical skill and knowledge-intensive with regard to structure depth, width, and length design (Wolka et al., 2018). Similarly, main road access positively influenced SIP usage by farmers, and increased the probability of applying Agro-Physical measures ($A_1B_0P_1$) by 9.6%.

The rural network farmer members were 7 and 14.6% more likely to adopt $A_1B_1P_0$ and $A_1B_1P_1$ practices, respectively. This estimation result was consistent with a report by Kassie et al. (2013). Similarly, HH heads with access to credit were more likely to practice the Agro-Biological measures ($A_1B_1P_0$), but less likely to apply Bio-Physical ($A_0B_1P_1$) and Agronomic ($A_1B_0P_0$) practices. The farmers preferred to expend borrowed money on other short respond business. Nkomoki et al. (2018) and Kpadonou et al. (2017) concurred with the negative influence of credit on SAP adoption.

Impacts of SIPs adoption on smallholder food security

In this section we used a joint analysis framework of SIP adoption average treatment effect on household food security in two ways. First, we compared the overall adoption effect between adopter and non-adopter groups. Second, we estimated a separate analysis of six SIP package choices' effect on the outcome variable to gain a better understanding of package combination.

Overall SIP adoption impact on food security

Table 7 illustrates the causal effect estimation result of SIP adoption on smallholders' food security. We compared changes in food security status among SIP adopters under the actual case and counterfactual (if not adopt) any SIP technology. ATT and ATU in table represent the average treatment effect on the treated and untreated conditions, respectively. ATE Diff column explains the net effect change on the outcome variable. It is calculated by controlling for the effect of several covariates,

and the selection bias stemming problem, which comes from unobserved and observed conditions.

All food security indicator results showed that SIP adoption had a positive and significant effect, and adopters highly benefited compared to their counterparts in ranges of 1% significance level. SIP adopters were 55% more food secure, had 51% higher access to clean water and sanitation, and consumed at least one more dietary food item daily compared to non SIP adopters. Particularly, for nutritional dietary food access estimation (HDD), adoption would be advantageous and significant for both adopters and non-adopters, although adopter households would benefit the most. The majority of SIP adopters were better-off and exhibited higher dietary food intake compared to non SIP adopters. Likewise, adopting SIP technology ensured the household food availability (SAFS) throughout the year and improve the utilization of pure water and sanitation (WASH) facilities. Weight change was in agreement with results described by Coulibaly et al. (2017) and Kassie et al. (2015b).

In line with our result, other scholars have independently confirmed the positive effect of SIP adoption on the crop productivity and smallholders food security improvement. Kassie et al. (2015b) observed maize productivity increment following SIP adoption in Malawi, and Wekesa et al. (2018) investigated the positive association of Climate Smart Agriculture (CSA) and food security in Kenya. Similarly, Nkomoki et al. (2018) conducted a study on Sustainable Agricultural Practice (SAP) and food security in Zambia; where as Wolka et al. (2018) and Adgo et al. (2013) demonstrated that SAP and SWC adoption positively contributed to crop productivity and food security improvement for smallholders in Ethiopia.

Table 7. *ATET of SIPs intervention on food security: endogenous switching regression estimation*

Treatment effect	Outcome variable	SIP decision stage		ATE Diff
		Adopters	Non-adopters	
ATT	HDD	6.86	5.62	1.24(0.068) ^{***}
ATU	HDD	4.23	3.74	0.49(0.080) ^{***}
ATT	SAFS	0.62	0.07	0.55(0.025) ^{***}
ATU	SAFS	0.16	0.55	-0.39(0.023) ^{***}
ATT	WASH	0.55	0.04	0.51(0.026) ^{***}
ATU	WASH	0.15	0.57	-0.41(0.015) ^{***}

Outcome variable spearman correlation matrix

	HDD	SAFS	WASH
HDD	1.000		
SAFS	0.492 ^{***}	1.000	
WASH	0.602 ^{***}	0.981 ^{***}	1.000

Standard errors in parentheses and ^{***}, ^{**}, and ^{*} indicate significance level at 1%, 5%, and 10%

Specific SIP package choice average treatment effect on food security

Table 8 presents the treatment effect of food security indicators (HDD, SAFS, and WASH) from each combination of SIP choice under actual and counterfactual cases. A household that practices A₁B₁P₁ packages benefits from dietary food consumption and has pure water access under the actual and counterfactual condition. Agro-Biological

package $A_1B_1P_0$ users would be better off to adopt, because HDD and SAFS measures had a significant ATT value at 1% significance level. Biophysical ($A_0B_1P_1$) strategies integration also had a significant and positive contribution to food security through HDD and WASH improvements. The households that practiced the agro-physical structure combination ($A_1B_0P_1$) were better off in the non-usage (ATU) scenarios suggesting that the household had other better combination available.

The appropriateness of SIP technologies practiced by a farmer was of profound importance in the context of changes in food security status. Overall, average effect estimation confirmed that a household that practiced $A_1B_1P_0$, $A_1B_1P_1$, and $A_0B_1P_1$ packages substantially improved its food security status compared to its counterparts. In contrast, $A_0B_1P_0$, $A_1B_0P_0$ and $A_1B_0P_1$ package usage had less contribution to reducing food insecurity compared to other strategies, while better than a scenario had they not adopted. The above comparison shows that mutually inclusive multiple SIP adoptions had a substantial impact on food security improvement compared to practicing individual agronomic or physical structure packages (Kpadonou et al., 2017)

Planting multi-purpose trees with physical structure would increase crop productivity through recycling soil nutrients as well as benefit farmers through generating diversified income. The benefits include forage for the animal (Amare et al., 2014), fruits, fuelwood, and immediate income (Mbow et al., 2014). Our findings on combined SIP adoption benefit were in accordance with other findings from Ethiopia reported by Sinore et al. (2018) and Wolka et al. (2018) from the south, Mekuriaw et al. (2018) and Amare et al. (2014) and Asfaw and Neka (2017) from the north.

Table 8. The average treatment effect of sustainable intensification practice choice on food security: Endogenous switching regression estimation

Treatment effect	SIP choice	HDD		ATE Diff	SAFS		ATE Diff	WASH		ATE Diff
		To participate	Not to participate		To participate	Not to participate		To participate	Not to participate	
ATT	$A_1B_1P_1$	7.46(0.06)	5.31(0.05)	2.15(0.08)***	0.75(0.01)	0.36(0.01)	0.38(0.02)***	0.67(0.00)	0.63(0.00)	0.04(0.00)***
ATU		6.65(0.06)	5.91(0.04)	0.74(0.07)**	0.75(0.01)	0.41(0.01)	0.34(0.01)**	0.41(0.00)	0.42(0.00)	-0.01(0.00)
ATT	$A_1B_1P_0$	6.83(0.07)	5.26(0.05)	1.57(0.12)***	0.38(0.01)	0.04(0.01)	0.34(0.02)***	0.36(0.00)	0.38(0.02)	-0.02(0.01)
ATU		5.15(0.06)	5.66(0.04)	-0.50(0.11)	0.43(0.01)	0.42(0.01)	0.01(0.02)*	0.44(0.03)	0.46(0.00)	-0.02(0.02)
ATT	$A_0B_1P_1$	6.13(0.06)	5.06(0.04)	1.07(0.09)***	0.41(0.02)	0.38(0.01)	0.03(0.02)**	0.33(0.00)	0.28(0.02)	0.05(0.00)***
ATU		4.42(0.07)	5.02(0.04)	-0.60(0.11)	0.47(0.00)	0.48(0.05)	-0.01(0.02)	0.14(0.03)	0.59(0.00)	-0.44(0.02)
ATT	$A_1B_0P_1$	5.09(0.08)	5.08(0.04)	0.01(0.06)	0.54(0.03)	0.53(0.01)	0.01(0.03)	0.48(0.03)	0.36(0.01)	0.12(0.03)***
ATU		6.17(0.12)	5.89(0.05)	0.28(0.14)**	0.56(0.03)	0.46(0.01)	0.11(0.03)***	0.57(0.05)	0.56(0.00)	0.01(0.02)
ATT	$A_1B_0P_0$	5.65(0.06)	5.91(0.04)	0.26(0.05)***	0.29(0.02)	0.31(0.01)	-0.20(0.01)	0.38(0.01)	0.36(0.02)	0.02(0.02)
ATU		4.03(0.03)	4.41(0.04)	-0.38(0.10)	0.60(0.04)	0.34(0.01)	0.24(0.03)***	0.23(0.02)	0.27(0.01)	0.04(0.01)*
ATT	$A_0B_1P_0$	5.31(0.07)	5.68(0.05)	-0.37(0.12)**	0.21(0.05)	0.25(0.01)	-0.04(0.02)	0.41(0.00)	0.42(0.00)	-0.01(0.00)
ATU		5.43(0.06)	5.52(0.04)	-0.09(0.10)	0.64(0.04)	0.37(0.01)	0.27(0.03)***	0.53(0.00)	0.47(0.00)	0.06(0.01)**

Standard errors in parentheses and ***, **, and * indicate significance level at 1%, 5%, and 10%, and ($A_0B_0P_0$) is stand for base category ($i = 1$) as non-adopters from alternative packages

Conclusion and policy implication

Sustainable agricultural discourse comprises food security and SIP, which focus on increasing productivity and improving environmental protection. In Ethiopia, where frequent drought, poverty, and food shortages occur, environmental degradation represents a severe challenge. Therefore, SIP adoption must be considered as a policy approach, due to the fact that farmers in low-income countries are highly dependent on agriculture to increase farm productivity and reduce food deficiency risks.

In this study, we investigated the factors that influence the adoption of SIP and their impact on food security using cross-sectional data from 909 farm households in Ethiopia. The study addresses three dimensions of food security- availability, access, and utilization. Principal component analysis (PCA) was employed first for variable reduction. Afterwards, we applied a two-stage multinomial endogenous switching regression model to obtain consistent and efficient estimates. Our study reveals that SIP adoption is positively correlated with households' food security. Adopting at least one SIPs package had a positive effect on food security improvement compared to not adopting a practice. Ultimately, households that adopt all three packages ($A_1B_1P_1$) are the best in all three food security dimensions. Combining of the physical structure with biological measures ($A_0B_1P_1$), and integrating agronomic with biological measures ($A_1B_1P_0$) proved to be the best strategies besides complete SIP adoption.

Furthermore, the findings reveal that a male-headed household is positively associated with the use of Agro-Biological ($A_1B_1P_0$), than labor-intensive Agro-Physical ($A_1B_0P_1$) package. Again, formal education is required for adopting knowledge-intensive physical structures much more so than for agronomic practices, although large farm size owner households are more likely to practice the Agro-Physical ($A_1B_0P_1$) package. A proxy crop income variable significantly determined complete package adoption, and a unit change income improved the ($A_1B_1P_1$) adoption by 43.42%. A household off-farm participation increases adoption of the Biophysical ($A_0B_1P_1$) package by 6%. Other information and training related variables such as farmers contact to extension worker, training participation on SWC and SNRM, access to roads and farmers' participation in the rural network are positively associated with biophysical and agro-biological adoption compared to the agro-physical and individual package.

Therefore, our findings strongly indicate that SIP adoption has the potential to reduce food insecurities and poverty among smallholder farmers in fixed cropping areas. Regarding SIP adoption campaign and sensitization program for development partners and government, we recommend the adoption of SIP combinations such as Bio-Physical ($A_0B_1P_1$), and Agro-Biological ($A_1B_1P_0$) for integration as a priority policy approach, in addition to the complete package ($A_1B_1P_1$).

Finally, our study is not without limitations, with time being the major limitation in that we used a single round survey of one-year response, which might affect the quality of our impact analysis. Exclusion of plot-level SIP and agro-ecological information is another limitation. However, the sample size, number of outcome variable used, and models applied for consistency and robustness can minimize these limitation effects. Other follow-up studies are needed to support our findings in other settings, with better long-period data and methodologies to validate the analysis.

Acknowledgements. The authors acknowledge the research fund sponsorship by “Social Science Foundation for Universities in Jiangsu, China, grant number 2017ZDIXM096”, “National Social Science Foundation, China, grant number 13&zdzd160” and “the Priority Academic Program Development of Jiangsu Higher Education Institutions (PAPD) Project”. Also, we thank the reviewers for the useful reviews which have significantly improved the quality of the paper.

REFERENCES

- [1] Abdul-Rahim, A., Sun, C., Noraida, A. (2018): The impact of soil and water conservation on agricultural economic growth and rural poverty reduction in China. – *Sustainability* 10(12): 4444.
- [2] Abdulai, A., Huffman, W. (2014): The adoption and impact of soil and water conservation technology: an endogenous switching regression application. – *Land Economics* 90(1): 26-43.
- [3] Adgo, E., Teshome, A., Mati, B. (2013): Impacts of long-term soil and water conservation on agricultural productivity: the case of Anjenie watershed, Ethiopia. – *Agricultural Water Management* 117: 55-61.
- [4] Amare, T., Zegeye, A. D., Yitafaru, B., Steenhuis, T. S., Hurni, H., Zeleke, G. (2014): Combined effect of soil bund with biological soil and water conservation measures in the northwestern Ethiopian highlands. – *Ecohydrology & Hydrobiology* 14(3): 192-199.
- [5] Anderson, S., Elisabeth, F. (2015): USAID Office of Food for Peace Food Security Country Framework for Ethiopia FY 2016–FY 2020. – Food Economy Group, Washington, DC.
- [6] Anim, F. D. (1999): A note on the adoption of soil conservation measures in the Northern Province of South Africa. – *Journal of Agricultural Economics* 50(2): 336-345.
- [7] Asfaw, D., Neka, M. (2017): Factors affecting adoption of soil and water conservation practices: the case of Wereillu Woreda (District), South Wollo Zone, Amhara Region, Ethiopia. – *International Soil and Water Conservation Research* 5(4): 273-279.
- [8] Bourguignon, F., Fournier, M., Gurgand, M. (2007): Selection bias corrections based on the multinomial logit model: Monte Carlo comparisons. – *Journal of Economic Surveys* 21(1): 174-205.
- [9] Branca, G., Lipper, L., McCarthy, N., Jolejole, M. C. (2013): Food security, climate change, and sustainable land management. A review. – *Agronomy for Sustainable Development* 33(4): 635-650.
- [10] Chatterjee, S., Goswami, R., Bandopadhyay, P. (2015): Methodology of identification and characterization of farming systems in irrigated agriculture: case study in west Bengal State of India. – *Journal of Agricultural Science and Technology* 17(5): 1127-1140.
- [11] Coulibaly, J. Y., Chiputwa, B., Nakelse, T., Kundhlande, G. (2017): Adoption of agroforestry and the impact on household food security among farmers in Malawi. – *Agricultural Systems* 155: 52-69.
- [12] Dejene, A. (2003): Integrated natural resources management to enhance food security. – The case for community-based approaches in Ethiopia. Environment and natural resources working paper 16.
- [13] Di Falco, S., Veronesi, M., Yesuf, M. (2011): Does adaptation to climate change provide food security? A micro-perspective from Ethiopia. – *American Journal of Agricultural Economics* 93(3): 829-846.
- [14] Ecker, O. (2018): Agricultural transformation and food and nutrition security in Ghana: Does farm production diversity (still) matter for household dietary diversity? – *Food Policy* 79: 271-282.
- [15] Emana, B. (2010): Market Assessment and Value Chain Analysis in Benishangul Gumuz Regional State, Ethiopia. – SID-Consult-Support Integrated Development, Addis Ababa, Ethiopia.
- [16] FAO (2016): The State of Food and Agriculture–Climate Change, Agriculture and Food Security. – Food and Agriculture Organization of the United Nations, Rome.
- [17] Fikru, A. (2009): Assessment of adoption of soil and water conservation practice in Koga watershed, highlands of Ethiopia. – Unpublished Master Thesis. Cornell University, Faculty of Graduate School, Cornell.

- [18] Goswami, R., Biswas, M. S., Basu, D. (2012): Validation of participatory farming situation identification: a case of rainfed rice cultivation in selected area of West Bengal, India. – *Indian Journal of Traditional Knowledge* 11(3): 471-479.
- [19] Josephson, A. L., Ricker-Gilbert, J., Florax, R. J. (2014): How does population density influence agricultural intensification and productivity? Evidence from Ethiopia. – *Food Policy* 48: 142-152.
- [20] Kaiser, H. F. (1958): The varimax criterion for analytic rotation in factor analysis. – *Psychometrika* 23(3): 187-200.
- [21] Kassie, M., Jaleta, M., Shiferaw, B., Mmbando, F., Mekuria, M. (2013): Adoption of interrelated sustainable agricultural practices in smallholder systems: evidence from rural Tanzania. – *Technological Forecasting and Social Change* 80(3): 525-540.
- [22] Kassie, M., Teklewold, H., Jaleta, M., Marennya, P., Erenstein, O. (2015a): Understanding the adoption of a portfolio of sustainable intensification practices in eastern and southern Africa. – *Land Use Policy* 42: 400-411.
- [23] Kassie, M., Teklewold, H., Marennya, P., Jaleta, M., Erenstein, O. (2015b): Production risks and food security under alternative technology choices in Malawi: application of a multinomial endogenous switching regression. – *Journal of Agricultural Economics* 66(3): 640-659.
- [24] Kim, J., Park, H., Chun, J., Li, S. (2018): Adaptation strategies under climate change for sustainable agricultural productivity in Cambodia. – *Sustainability* 10(12): 4537.
- [25] Kipkoech Anderson, K., Emmanuel, T., Bangali Solomon, F. (2015): State of Knowledge on CSA in Africa. Case Studies from Ethiopia, Kenya and Uganda. – Forum for Agricultural Research in Africa, Accra, Ghana ISBN.
- [26] Kpadonou, R. A. B., Owiyo, T., Barbier, B., Denton, F., Rutabingwa, F., Kiema, A. (2017): Advancing climate-smart-agriculture in developing drylands: joint analysis of the adoption of multiple on-farm soil and water conservation technologies in West African Sahel. – *Land Use Policy* 61: 196-207.
- [27] Lee, L.-F. (1982): Some approaches to the correction of selectivity bias. – *The Review of Economic Studies* 49(3): 355-372.
- [28] Mabiso, A., Cunguara, B., Benfica, R. (2014): Food (in)security and its drivers: insights from trends and opportunities in rural Mozambique. – *Food Security* 6(5): 649-670.
- [29] Maxwell, D., Vaitla, B., Coates, J. (2014): How do indicators of household food insecurity measure up? An empirical comparison from Ethiopia. – *Food Policy* 47: 107-116.
- [30] Mbow, C., Van Noordwijk, M., Luedeling, E., Neufeldt, H., Minang, P. A., Kowero, G. (2014): Agroforestry solutions to address food security and climate change challenges in Africa. – *Current Opinion in Environmental Sustainability* 6: 61-67.
- [31] McDonald, C. M., McLean, J., Kroeun, H., Talukder, A., Lynd, L. D., Green, T. J. (2015): Correlates of household food insecurity and low dietary diversity in rural Cambodia. – *Asia Pacific Journal of Clinical nutrition* 24(4): 720-730.
- [32] Mekuriaw, A., Heinemann, A., Zeleke, G., Hurni, H. (2018): Factors influencing the adoption of physical soil and water conservation practices in the Ethiopian highlands. – *International Soil and Water Conservation Research* 6(1): 23-30.
- [33] Moges, D. M., Taye, A. A. (2017): Determinants of farmers' perception to invest in soil and water conservation technologies in the North-Western Highlands of Ethiopia. – *International Soil and Water Conservation Research* 5(1): 56-61.
- [34] Moroda, G. T., Tolossa, D., Semie, N. (2018): Food insecurity of rural households in Boset district of Ethiopia: a suite of indicators analysis. – *Agriculture & Food Security* 7(1): 65.
- [35] Nkomoki, W., Bavorová, M., Banout, J. (2018): Adoption of sustainable agricultural practices and food security threats: effects of land tenure in Zambia. – *Land Use Policy* 78: 532-538.

- [36] Pérez-Escamilla, R., Gubert, M. B., Rogers, B., Hromi-Fiedler, A. (2017): Food security measurement and governance: assessment of the usefulness of diverse food insecurity indicators for policy makers. – *Global Food Security* 14: 96-104.
- [37] Petteri Vuorinen, M. T., Jorn Laxen (2016): Study of causes of deforestation and forest degradation in Ethiopia and the identification and prioritization of strategic options to address those final reports. – Ministry of Environment, Forest and Climate Change, The Federal Democratic Republic of Ethiopia, Addis Ababa.
- [38] Pinstrup-Andersen, P. (2009): Food security: definition and measurement. – *Food Security* 1(1): 5-7.
- [39] Shiferaw, B., Kassie, M., Jaleta, M., Yirga, C. (2014): Adoption of improved wheat varieties and impacts on household food security in Ethiopia. – *Food Policy* 44: 272-284.
- [40] Sinore, T., Kissi, E., Aticho, A. (2018): The effects of biological soil conservation practices and community perception toward these practices in the Lemo District of Southern Ethiopia. – *International Soil and Water Conservation Research* 6(2): 123-130.
- [41] Teklemariam, D., Azadi, H., Nyssen, J., Haile, M., Witlox, F. (2016): How sustainable is transnational farmland acquisition in Ethiopia? Lessons learned from the Benishangul-Gumuz Region. – *Sustainability* 8(3): 213.
- [42] Tiwari, K. R., Sitaula, B. K., Nyborg, I. L., Paudel, G. S. (2008): Determinants of farmers' adoption of improved soil conservation technology in a middle mountain watershed of central Nepal. – *Environmental Management* 42(2): 210-222.
- [43] WB Dataset (2018): Agriculture & Rural Development. – World Bank. <https://data.worldbank.org/indicator>. 12 December 2018.
- [44] WBISPP (2005): A national strategy plan for the biomass sector. Available online: <https://www.coursehero.com/file/32669878/ddfd-midtermreportdoc/>, The Federal Democratic Republic of Ethiopia, REDD+ Secretariat, Ministry of Environment and Forest Addis Ababa, Ethiopia (Accessed on 25 January, 2019).
- [45] Wekesa, B. M., Ayuya, O. I., Lagat, J. K. (2018): Effect of climate-smart agricultural practices on household food security in smallholder production systems: micro-level evidence from Kenya. – *Agriculture & Food Security* 7(1): 80.
- [46] Wolka, K., Sterk, G., Biazin, B., Negash, M. (2018): Benefits, limitations and sustainability of soil and water conservation structures in Omo-Gibe basin, Southwest Ethiopia. – *Land Use Policy* 73: 1-10.

COMBINING GIS, FUZZY LOGIC, AND AHP MODELS FOR SOLID WASTE DISPOSAL SITE SELECTION IN NASIRIYAH, IRAQ

ABDULHASAN, M. J.¹ – HANAFIAH, M. M.^{1*} – SATCHET, M. S.² – ABDULAALI, H. S.³ – TORIMAN, M. E.⁴ – AL-RAAD, A. A.^{1,5}

¹*Center for Earth Sciences and Environment, Faculty of Science and Technology, Universiti Kebangsaan Malaysia, 43600 Bangi, Selangor, Malaysia*

²*Civil Engineering Department, University of Thi-Qar, Nasiriyah, Iraq*

³*Department of Architecture, Faculty of Engineering and Built Environment, Universiti Kebangsaan Malaysia, 43600 UKM Bangi, Selangor, Malaysia*

⁴*School of Social, Development and Environmental Studies, Faculty of Social Sciences and Humanities, Universiti Kebangsaan Malaysia, 43600 Bangi Selangor, Malaysia*

⁵*Department of Biology, College of Science, Al-Muthanna University, Al-Muthanna Governorate, Iraq*

**Corresponding author*

e-mail: mhmarlia@ukm.edu.my; phone: +60-3-8921-5865; fax: +60-3-8925-3357

(Received 3rd Feb 2019; accepted 8th Apr 2019)

Abstract. Finding locations suitable for disposal of solid waste is one of the fundamental challenges facing municipal cities and environmental stability. The present study aims to identify the most suitable solid waste disposal site using Geographic Information System (GIS), remote sensing, and the multi criteria decision-making (MCDM) technique. In addition, the study compares the proposed method for suitability with the traditional analytic hierarchy process (AHP) approach. A new validation approach was applied to evaluate the accuracy of the AHP and Fuzzy logic methods based on the selected solid waste locations. Remote sensing data (ASTER GDEM) and field/reference maps were used to derive 12 conditioning factors required to produce a suitable location for solid waste disposal. The result shows that the accuracy of AHP, based on the consistency index (CI), is acceptable (greater than 0.1). However, Fuzzy logic was shown to be more accurate than AHP. The total surface areas of suitable locations based on AHP and Fuzzy models are 4.4 km² and 13.35 km², respectively. This study showed that AHP, Fuzzy logic and GIS can be integrated for waste management decision issues related to site selection to reduce negative effects on the environment and inhabitants.

Keywords: *waste management, landfill site selection, remote sensing, multi-criteria decision analysis*

Introduction

Selection of landfill locations for solid waste (SW) is determined by waste management operations based on multiple factors, including the geographic formation of a region. The decision for this selection is vested in governmental authorities (Hanine et al., 2016). Location selection for solid waste landfills is crucial for every region due to the cost implications, difficulty of reversal, and long-term commitment required (Gorsevski et al., 2012; Liu et al., 2014). Finding suitable location for landfills is also very challenging due to various factors, such as increasing waste quantities, population growth, environmental and public health risk factors, and decreasing land availability for waste disposal (Srivastava and Nema, 2012). Therefore, geographic information should not be the only criteria for site selection, however, flexibility to accommodate future changes should also be considered in regional policies. In determining solid waste disposal landfill sites, environmentally friendly and financially sound

selection is a challenge. Selecting a suitable landfill location involves a considerable array of points, criteria, and verification of a given set of limitations to ultimately provide an optimal solution.

The analytic hierarchy process (AHP) method is one of the most commonly used methods for multi-criteria decision-making (MCDM) (Beskese et al., 2015; Moeinaddini et al., 2010). It is capable of solving complex decision-making problems across various fields (Saaty et al., 2000; Uyan, 2013; Tavares et al., 2011). It is also used to determine the consistency of weightings for criteria by constructing a matrix for pairwise comparisons. This combination provides an appropriate language to manage imprecision criteria and integrate qualitative analysis with quantitative factors.

Even though many researches have proposed the use of Fuzzy multi-criteria decision-making methods, very few have applied the combined use of these methods for the selection of suitable landfill location. Torabi-Kaveh et al. (2016) proposed a combination of Geographic Information System (GIS) with a Fuzzy analytical hierarchy process (FAHP) to determine suitable locations for landfill site in Iranshahr, Iran. Chabuk et al. (2017) combined GIS analysis and MCDM for selecting landfill locations in Al-Hashimiyah Qadhaa, Babylon, Iraq. Foroughian and Eslami (2015) presented a study using GIS and AHP indicators for identification of solid waste disposal landfill sites in the city of Susa. Various techniques have been utilized for selecting landfill locations (Gbanie et al., 2013; Khorram et al., 2015; El Baba et al., 2015; Rathore et al., 2016). These authors determined that a combined evaluation using MCDM methods in landfill location selection is imperative. This is due to the fact that relative advantages of several methods depend on the characteristics of the problem domain.

The present study aims to determine a suitable disposal site using Fuzzy logic approach and justify the approach by comparing with traditional AHP approach, which is used for determination of suitable waste disposal sites in Nasiriyah, Iraq. Currently, there is only one available landfill site in Nasiriyah and it does not meet the relevant scientific and environmental standards. The main objective of this paper is to propose the best method for identification of solid waste disposal sites that is suitable for Nasiriyah, Iraq, and fulfills environmental and scientific criteria.

Materials and methods

The map layers were prepared using GIS and cover the most important 12 criteria in the study area. The landfill site selection model is illustrated in *Figure 1*. The raster maps of selected criteria were prepared and the final map of landfill siting was produced in the GIS software. Each raster map for the selected criteria was divided into categories, with each category is given appropriate weight. The final map of landfill siting was determined using GIS single output map algebra. The methodology and framework adopted in this study is presented in *Figure 1*.

Study area

This research was conducted in Nasiriyah, Iraq. The Governorate of Thiqr is located to the south of Iraq at the intersection of longitude 31° 01' E to 31° 08' E and latitude 46° 08' N to 46° 18' N. The city of Nasiriyah is the administrative center of the governorate and is 380 km to the south of Baghdad and 214 km to the north of Basra City. The total area is 12,900 km², equivalent to 5,160,000 acres. The desert land area covers 6.7% of the governorate and has a population of about 1.99 million. This population is expected to grow significantly over the next decade as a result of significant economic and security improvements. It is also home

to the largest marshlands of Iraq, with an area of 1,048,600 acres, which is 3.1% of the total area of Iraq. *Figure 2* shows the map of the area.

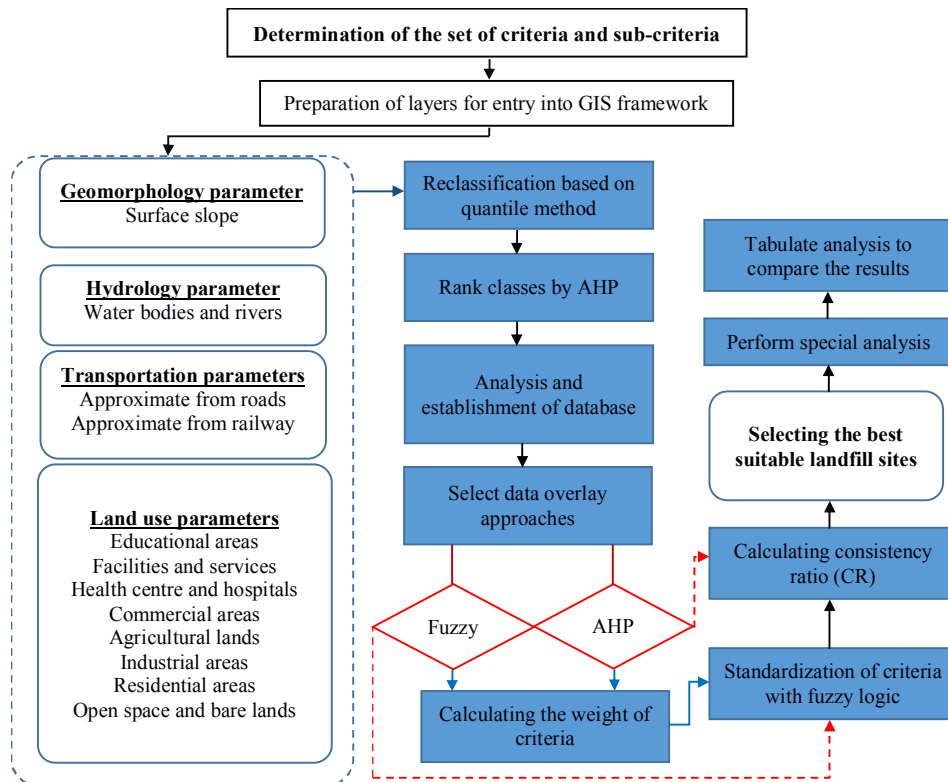


Figure 1. Conceptual framework of the present study

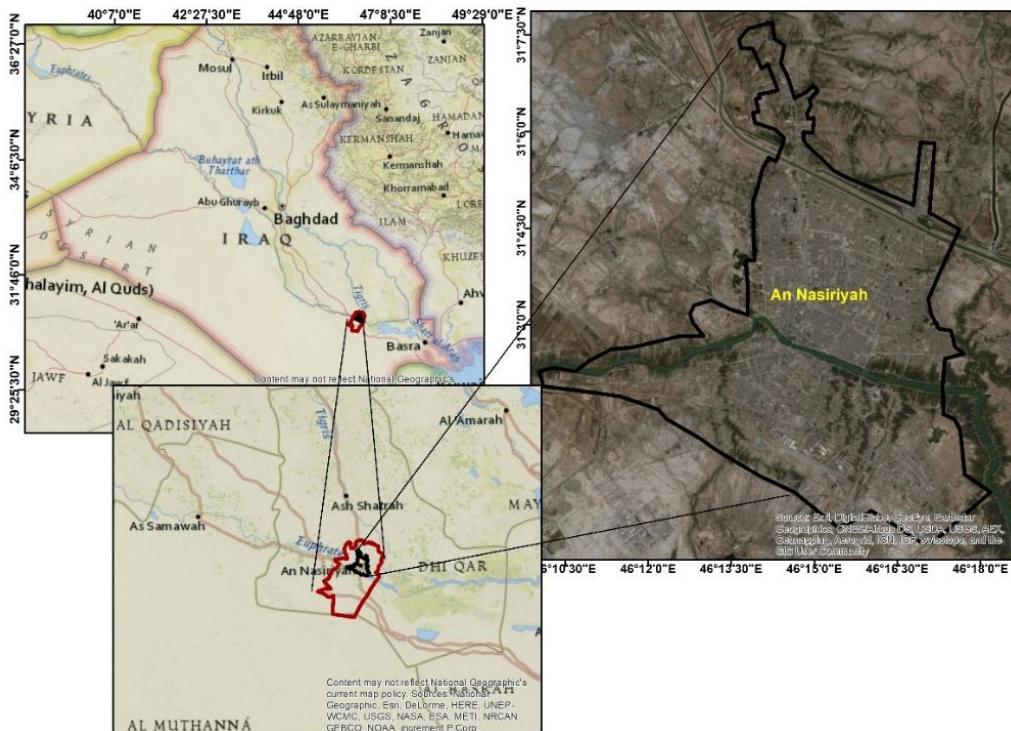


Figure 2. Map of the study area

Suitability criteria

In this study, 12 criteria were derived from 4 main criteria to determine suitable areas for solid waste disposal sites; these criteria were slope, distance from bodies of water, distance from roads, distance from railways, distance from open space, distance from agricultural lands, distance from health centers and hospitals, distance from residential areas, distance from commercial areas, distance from industrial areas, distance from facilities, and distance from educational areas, as shown in *Table A1* in the *Appendix* and *Figure 3*.

Analytic hierarchy process

Due to its simplicity and robustness in finding weights and combining heterogeneous data, AHP has been applied for MCDM, conflict management, total quality management, suitability analysis, resource allocation, design, and engineering (Jiang and Eastman, 2000; Vaidya and Kumar, 2006; Gorsevski et al., 2006; Şener et al., 2010; Vasiljević et al., 2012). In addition, it has been applied in many practical applications across fields, including site selection (Abdullahi et al., 2014). The various factors considered are not of equal importance in the determination of a potential solid waste site, therefore, the importance of each parameter was identified. In terms of the suitability of a solid waste site, hydrological formation has more importance in weight than distance from railways. Therefore, a weighted linear combination (WLC) was used in this study, in line with Drobne and Liseć (2009) and Kritikos and Davies (2011). It can be considered a hybrid of qualitative and quantitative techniques (Ayalew et al., 2004).

Determination of weights

The MCDM module was used for the weight-selecting criteria (Drobne and Liseć, 2009). A pairwise comparison referred to as the analytic hierarchy process developed by Saaty (1980) was used in this study. This method includes the comparison of each factor against every other factor in pairs (Chang et al., 1996). The weights of criteria in Saaty's technique were computed by applying the main eigenvector of the square reciprocal matrix of the pairwise comparisons between the two factors (Drobne and Liseć, 2009). The pairwise comparison evaluates the two criteria against each other to determine the most important criteria for a given objective.

Estimating consistency of pairwise comparisons

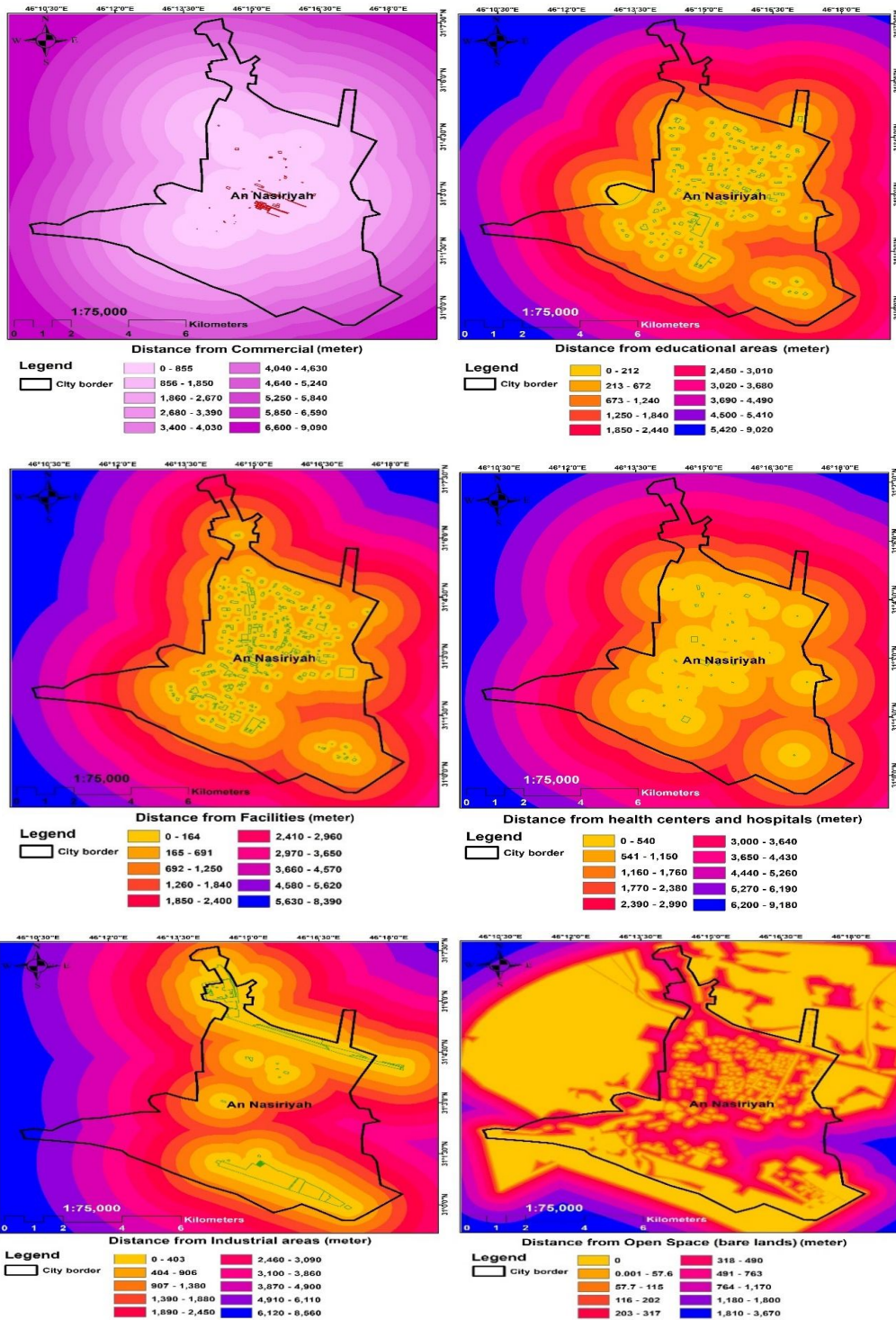
The accuracy of pairwise comparisons was evaluated by calculating the consistency ratio (CR), which is the ratio of the consistency index (CI) and the randomness index (RI). CR was used to estimate the relative weightings of all criteria on a consistency ratio in which values under 10% are considered acceptable. Otherwise, the consistency ratio allows for reevaluation of comparisons. *Table A2* shows the RI developed by Saaty et al. (1977), based on the order of the matrix according to the number of criteria. *Equations 1* and *2* show the consistency ratio and consistency index, respectively.

$$CR = \frac{CI}{RI} \quad (\text{Eq.1})$$

CI is calculated using Equation 2:

$$CI = \frac{\lambda_{max} - n}{n - 1} \quad (Eq.2)$$

where: λ_{max} = (Weight1*S1 + Weight2*S2 + Weight3*S3+.....) and n = number of criteria.



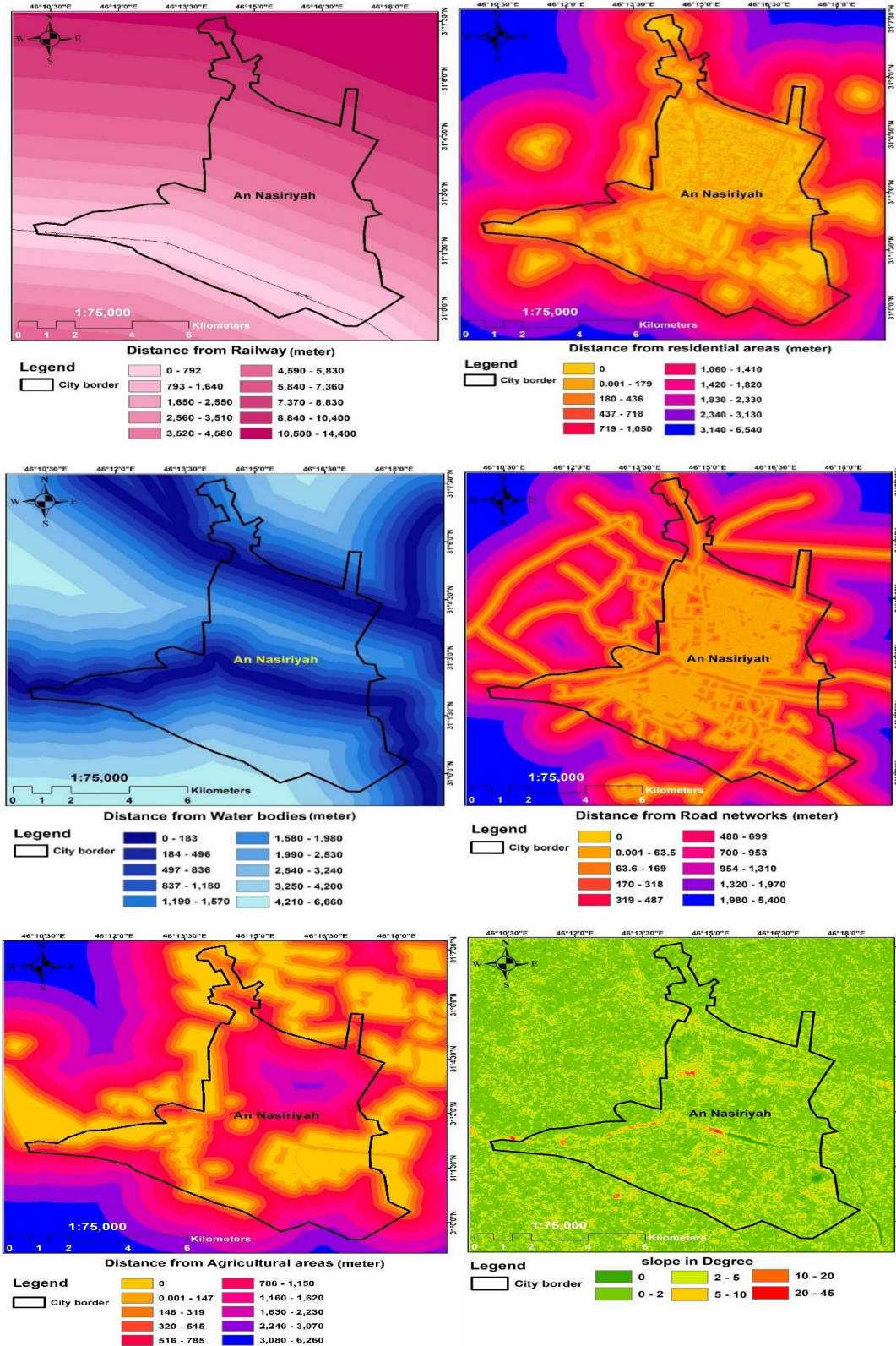


Figure 3. Suitability indexes in the current study; slope, distance from water bodies, distance from roads, distance from railways, distance from open space, distance from health centres and hospitals, distance from commercial areas, distance from agricultural lands and distance from industrial areas

Application of the fuzzy logic model

In a Fuzzy approach, suitability of land is mapped by pixels of causal factor layers. Pixel values are numeric and range from 0 to 1, from not suitable to very suitable. Pixel values must be within the range of 0 to 1, although there is no practical constraint on the choice of the values. Values can be chosen to reflect the degree of membership of a set based on subjective judgment (Amato et al., 2018) or can be derived by various functions representing reality (Eastman et al., 2003). In this study, linear functions were used to represent the reality function. Fuzzy logic is preferred for land suitability evaluation due to its ability to estimate land use suitability on a continuous scale, which helps to cope with vagueness and uncertainty (Elaalem et al., 2012). Site suitability application using Fuzzy logic comprises three steps, as shown below:

Step 1: Normalization or standardization of land characteristics using fuzzy set models

Fuzzy logic helps the user to determine the likelihood that a site is suitable or unsuitable. This step assigns values from 0 to 1, with 0 being not likely or unsuitable and 1 being most likely or suitable (Elaalem et al., 2012). Thus, the higher Fuzzy value implies the ideal of the site. When assigning Fuzzy values, four types of membership need to be understood to choose the best fits of the analysis criteria. There are four types of membership function in Fuzzy systems: linear, small, large and Gaussian. In this study, the linear membership function was used to normalize the parameters, due to its dependence on input parameters. If the input parameters seem chaotic, similar to a time series, the Gaussian type of membership function would be suggested, otherwise, the linear type is recommended (Qiu et al., 2014). High Fuzzy membership is assigned to large or small values, and Fuzzy membership decreases at a constant rate. A triangular membership function is specified by three parameters {a, b, c} as shown in *Equation 3* (Önüt and Soner, 2008):

$$\text{Triangulation}(x; a, b, c) = \begin{cases} 0, & x \leq a \\ \frac{(x - a)}{(b - a)}, & a \leq x \leq b \\ \frac{(c - x)}{(c - b)}, & b \leq x \leq c \\ 0, & c \leq x \end{cases} \quad (\text{Eq.3})$$

Step 2: Generation of the criteria map layers

Fuzzy logic offers an alternative scaling approach, using linguistic variables to represent quantitative and qualitative criteria (Sreedevi et al., 2016). For quantitative criteria, such as return on resources, representation by a linguistic variable requires the definition of term sets, such as “very low,” “low,” “medium,” “high,” and “very high”. In this study, linear membership function was used to normalize the parameters because it depends on input parameters. The linear membership function is suggested if the input parameter is not chaotic (Elaalem et al., 2012). This step assigns values from 0 to 1, with 0 being not likely or unsuitable and 1 being most likely or suitable. The range between 0 and 1 for membership function corresponds to the intensity of importance of each criterion, which is obtained from the literature and experts’ opinions.

Step 3: Generation of the overall land suitability map layers

Once the appropriate Fuzzy membership value for data criteria is assigned, several reclassified surfaces showing values from 0 to 1 are generated (Klir and Yuan, 1995), and subsequently, the Fuzzy logic model is applied. This step is similar to weighted site selection, which is a site selection method that allows users to rank raster cells and assign a relative importance value to each layer so that different reclassified surfaces can be compared to each other. In order to complete this step, one of several Fuzzy overlay types must be chosen. In this study, the “AND” Fuzzy overlay type was used due to its ability to determine the best values in finding locations that meet all criteria (Qiu et al., 2014).

Results and discussion

Classification of criteria

Each criterion was classified into 10 classes based on the quantile model, except for slope, which was classified into six classes using GIS software. The results showed that variation in each class affects the rank of the class. In some criteria, values were close to the target and thus achieved a higher rank. For some other criteria, values far from the target were considered an advantage and given high weight. For instance, low-distance classes of the open space criteria are more suitable for waste landfill, while far-distance classes in education are more suitable for solid waste landfill allocation. Some criteria prioritize the middle classes; for example, landfill sites should be located neither too close nor too far from residential areas.

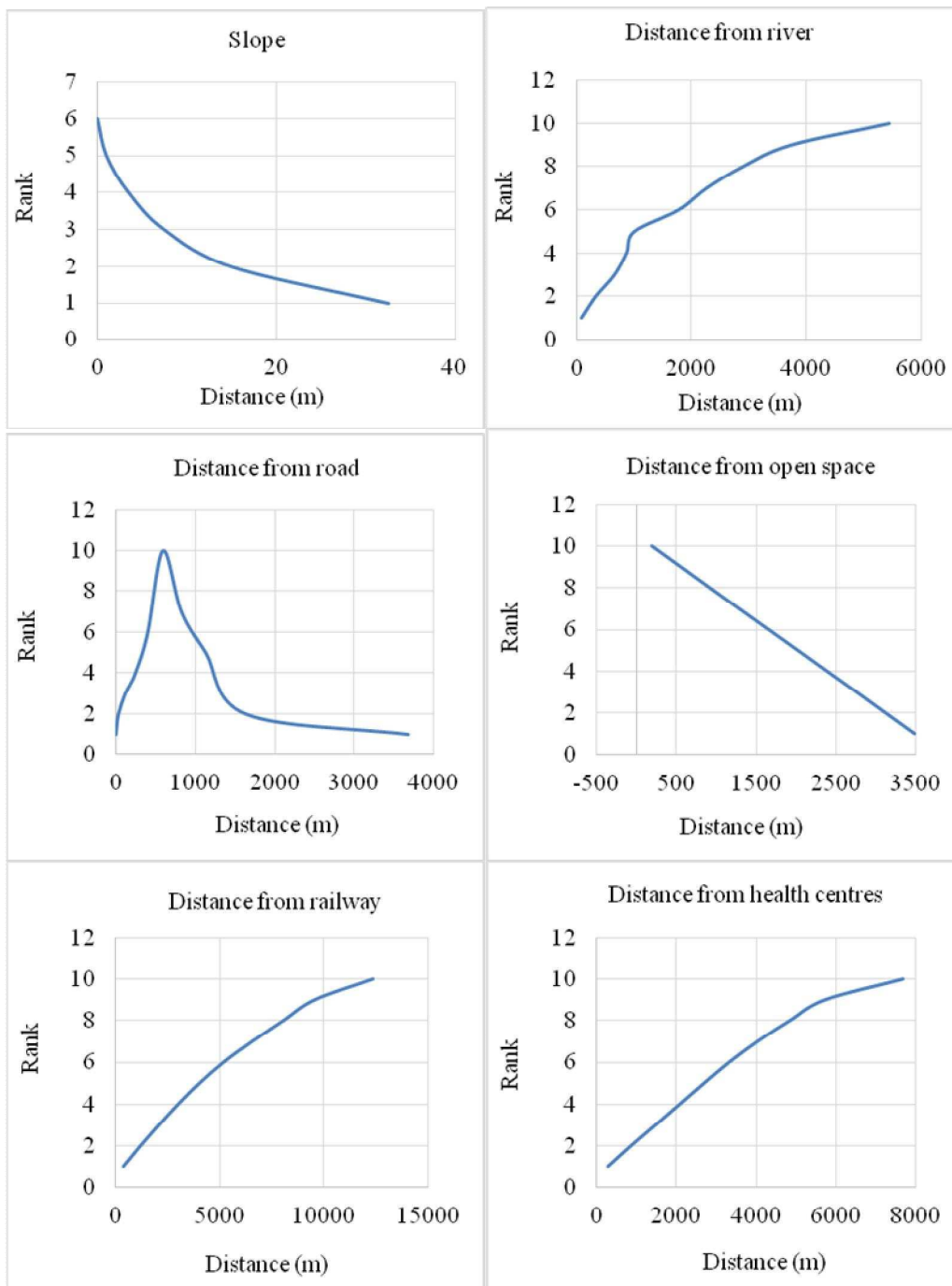
Figure 4 illustrates the weight variation in slope, distance from bodies of water, distance from roads, distance from railways, distance from open space, distance from agricultural lands, distance from health centers and hospitals, distance from residential areas, distance from commercial areas, distance from industrial areas, distance from facilities, and distance from educational areas. An indirect linear relationship between the average of each class and its ranking was found for slope indicates that flat areas are weighted higher than steep fields for landfill site selection.

A direct linear relationship was obtained for other criteria. The farther the distance from rivers, the higher the rank for landfill suitability, as shown in *Figure 4*. Greater distance from hospitals or health centers, roads, railways, agricultural lands, public facilities, educational areas, and commercial centers equates to a higher rank and suitability for landfill. For residential areas, the logarithmic relationship shows that distances too close or too far (greater than 3 km) from residential areas receive a lower rank and are thus unsuitable for solid waste disposal. This is because if the distance is too close, the landfill can infect the inhabitants with diseases or odors, while placing dump sites too far away from the source of the waste is uneconomical and time-consuming. *Figure 4* also shows that the class too close or far from industrial areas, mostly out of the city, showed a lower rank for solid waste landfill.

Table A3 shows the classification and rank for 12 criteria based on the quantile method using GIS software. Six classes of slope show that a 0 degree angle of steepness achieved the highest rank using the AHP model, implying that these are the most suitable classes for landfill use. Inversely, the lowest classes are those with a 45 degree angle of steepness; these are ranked as 1. Ten classes of distance from the river indicated that the class at an average of 91 meters away from the river had the lowest

rank using the AHP model, thus is least suitable for landfill. Inversely, the most suitable class is ranked with 9, which is 3,721 m away from water bodies.

Table A3 also shows that the class at an average of 593 m away from roads achieved the highest rank of suitability for landfills, using the AHP model, while the lowest suitable classes, ranked number 1, recorded the closest and farthest distance classes from the road (0 and 3,684 m). The highest suitable class that attained rank number 10 indicating the greatest distance from the railways (12,393 m) and from railway. For agricultural, commercial and residential areas, the highest suitable class gained ranking number 10 at distance of 7,688 m away from health centers, 2,730 m away from residential areas and 7,839 m away from commercial areas, respectively.



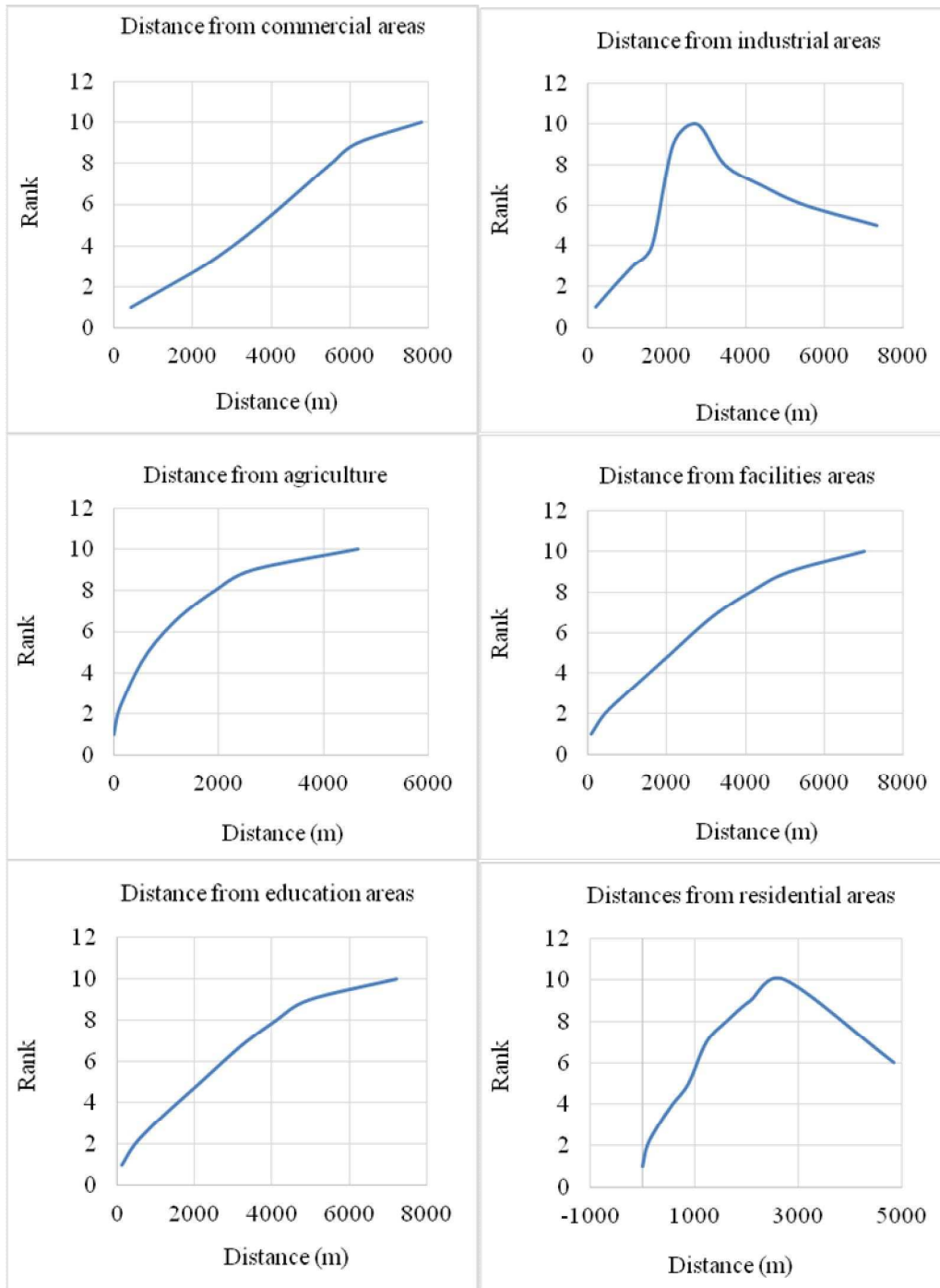


Figure 4. Weight variation in: slope, distance from river, distance from roads, distance from railways, distance from open space, distance from agricultural lands, distance from health centres and hospitals, distance from residential areas, distance from commercial areas, distance from industrial areas, distance from facilities areas and distance from education areas

Table A3 also shows that the highest suitable class for industrial areas and facilities ranked number 10, representing an average distance from industrial areas of 2,770 m and from the facilities of 7,007 m, respectively. The highest suitable class for education areas obtained ranking number 10, which is the farthest distance from educational

facilities (7,216 m). The soil stratification is not significantly contributed to the site selection as the study area has mostly covered by one soil type. In addition, due to the impervious surface of the study area, pollution might not be possible to deeply penetrate through the soil surface to groundwater. In contrary, there is a high chance to affect the surface water bodies.

Selection of suitable sites for solid waste using the AHP model

Questionnaires were prepared based on expert’s response regarding to the most significant factors in the selection of suitable sites for a solid waste landfill in the study area. After the preparation of the conditioning factors using GIS, the weights of each factor were calculated using the geometric mean method to determine the final weight of each factor. Then, the factors were reclassified based on their weights and prepared using a raster calculator to generate a suitability map, which describes the suitable locations for solid waste landfill. The result of the pairwise comparison matrix obtained from questionnaires for the 12 criteria is shown in *Table 1*.

Table 1. Pairwise comparison matrix extracted from questionnaires for 12 criteria

Pairwise comparison matrix	Solid waste landfill selection											
	Res	Open	Road	Ind	Agri	Edu	Health	Faci	Com	Slope	Rail	WB
Residential	1	2	4	3	5	8	7	7	9	9	8	6
Open space	1/2	1	3	3	4	6	6	5	8	8	8	4
Road	1/4	1/3	1	1/2	2	5	4	3	6	7	6	2
Industrial	1/3	1/3	2	1	1	4	3	3	5	5	6	2
Agricultural	1/5	1/4	1/2	1	1	3	2	2	5	5	5	1
Educational	1/8	1/6	1/5	1/4	1/3	1	1/3	1/3	2	3	4	1/4
Health	1/7	1/6	1/4	1/3	1/2	3	1	1	4	6	5	1
Facilities	1/7	1/5	1/3	1/3	1/2	3	1	1	3	5	4	1/5
Commercial	1/9	1/8	1/6	1/5	1/5	1/2	1/4	1/3	1	2	2	1/6
Slope	1/9	1/8	1/7	1/5	1/5	1/3	1/6	1/5	1/2	1	1/2	1/7
Railway	1/8	1/8	1/6	1/6	1/5	1/4	1/5	1/4	1/2	2	1	1/9
River	1/6	1/4	1/2	1/2	1	4	1	5	6	7	9	1

*Res = Residential, Open = Open Space, Ind = Industrial, Agri = Agricultural, Edu = Educational, Faci = Facilities, Com = Commercial, Rail = Railway, WB = Water Bodies

The pairwise comparison matrix shown in *Table 1* was assembled from the input of 13 different experts in the field of environmental and waste management. The results were summarized based on the average of the distributed questionnaires. *Table 2* shows the weight of each criteria in percentage and their ranks from the most to the least important criteria. It was deduced that proximity to residential areas was the most important criteria in solid waste selection. The second most important parameter was observed to be proximity to open space followed by distance from roads and industrial facilities. Inversely, the slope and distance from railways were determined to be the least important criteria in terms of landfill selection.

Table 2. Weightage for criteria in percentage

Criteria	AHP-Weightage (%)
Residential	26.36
Open Space	19.63
Road	10.35
Industrial	10.13
Agricultural	7.19
Educational	2.97
Health	5.29
Facilities	4.58
commercial	1.97
Slope	1.40
Railway	1.63
River	8.50

The accuracy of AHP is within acceptable limits, as the CI (0.128) is greater than 0.1. In addition, Lambda value of 13.41 and the Randomness Index (RI) with 1.54 were observed to show high accuracy based on the CI. The CI/RI ratio is 0.083 implying that the experts assigned the weight of each criterion logically, and the prioritization of the criteria was consistent. *Figure 5* is a suitability map produced using the AHP model that shows the suitable areas in green and non-suitable areas in gray. It was observed that suitable areas were almost distributed across the entire study area. However, most suitable areas were found outside the city, mostly toward to the west and south of the study area. The overall area of very highly suitable lands for solid waste was found to be about 1.66 km². Therefore, field visits are required to identify the final location of the solid waste landfill. The suitability map produced in GIS using AHP model shows that suitable sites are not clustered in one single area, but distributed over different locations within the study area. This indicates that some of the conditioning factors have a huge influence on the selection process for suitable sites and were distributed across the study area.

Suitable areas were determined using the AHP model and were mostly found far from urban areas, and no suitable area was observed around the city borders. These sites require further investigation to determine the possibility of constructing a solid waste disposal field.

Selection of suitable sites for solid waste using the fuzzy model

The suitability map produced using the Fuzzy model is presented in *Figure 5*. The map shows suitable and unsuitable locations in the study area, identified based on 12 factors for solid waste disposal. The map shows that most suitable areas are located in the middle and in the north part of the study area. On the other hand, the southern part of the study area was observed to have no identified suitable site for solid waste, thus, should be ignored in the field visit. The overall surface area of suitable land is estimated to be 13.35 km². The suitability map produced using the Fuzzy model shows the spatial distribution of the suitable areas and their patterns in the study area. It can be observed that most of the suitable areas are clustered into groups and are not randomly scattered in different directions. This indicates that the suitable areas identified are homogenous

and share similar characteristics with each other. This is very important for decision makers, as it makes final selection easier and more accurate. Decision makers can use this method to easily identify suitable areas for constructing solid waste landfill sites in a particular area.

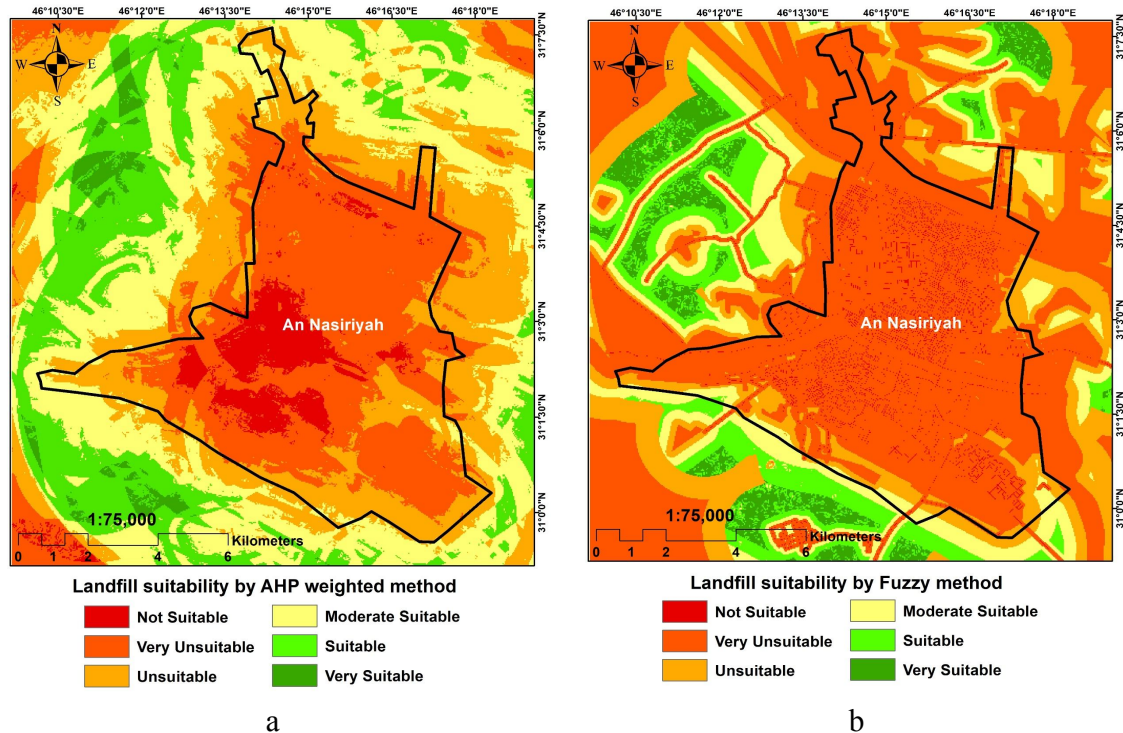


Figure 5. Map produced using a) AHP model and b) fuzzy model

It is imperative to compare the results of the AHP and Fuzzy models to identify their similarities and possible differences. The comparison between the maps produced by these models showed that the AHP maps identified the suitable areas as scattered regions, while the Fuzzy model generated a map with clustered suitable areas. It was observed that the AHP map located suitable areas in almost all parts of the study area, while the Fuzzy map identified suitable areas at the middle and northern parts of the study area. In terms of the surface area of suitable lands identified, the AHP model indicated 4.14 km² area as highly suitable, while the Fuzzy model identified 13.35 km² as highly suitable for solid waste landfill. *Figure 6* illustrates the percentage of landfill suitability based on the AHP and Fuzzy Models with 2% and 5% for very suitable areas.

Table 3 shows the results of the AHP model in terms of very suitable landfill areas, 4.14 km², and very unsuitable areas, 60.6 km². The Fuzzy model obtained 13.35 km² for very suitable areas and 131.56 km² for very unsuitable areas (*Table 3*). In addition, the Fuzzy model showed more areas considered very suitable compared to the AHP model, which could be due to the mathematical nature of the Fuzzy algorithm. The common areas identified by both methods showed the most suitable lands for waste disposal landfills, far away from residential areas and close to bare lands. Traditional AHP approach is more simplistic and robust while Fuzzy logic approach help in coping with vagueness and uncertainty of determining site suitability. The results further display that

the AHP maps identified the suitable areas as scattered regions, while the Fuzzy model generated a map with clustered suitable areas.

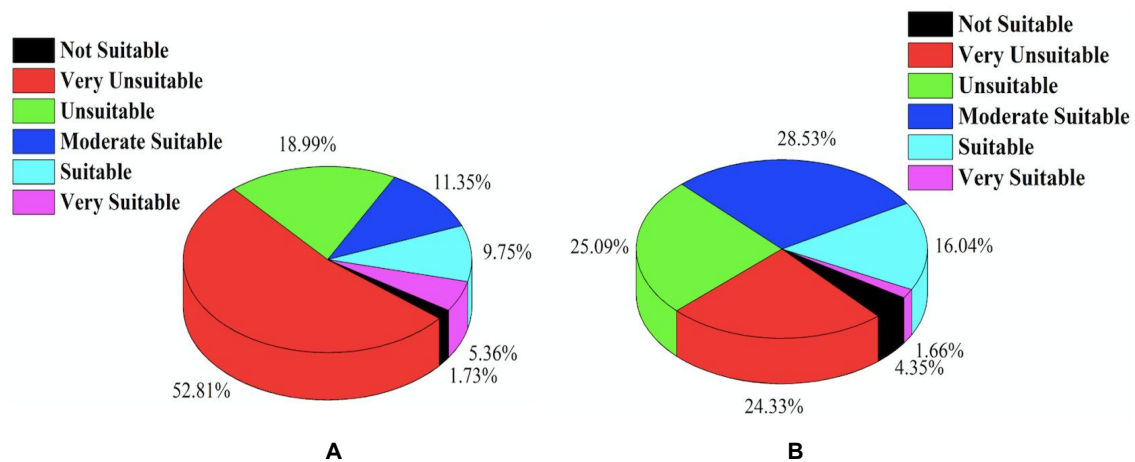


Figure 6. Percentage of landfill suitability A) fuzzy model and B) AHP model

Table 3. The results of AHP and fuzzy models

Suitability class	Cell count		Area (m ²)		Area (km ²)		Percentage (%)	
	AHP	Fuzzy	AHP	Fuzzy	AHP	Fuzzy	AHP	Fuzzy
Not suitable	12036	4790	10832400	4311000	10.83	4.31	4.35	1.73
Very unsuitable	67332	146178	60598800	131560200	60.60	131.56	24.33	52.81
Unsuitable	69456	52570	62510400	47313000	62.51	47.31	25.09	18.99
Moderate suitable	78969	31411	71072100	28269900	71.07	28.27	28.53	11.35
Suitable	44389	26997	39950100	24297300	39.95	24.30	16.04	9.75
Very suitable	4600	14836	4140000	13352400	4.14	13.35	1.66	5.36
Total area	276782	276782	249103800	249103800	249.10	249.10	100	100

However, a field visit is required to confirm the final location for the landfill site in order to take into account other factors that were excluded in the model, such as the population and other environmental changes. There may be some changes to the sites that may not be favorable for the intended purposes. Therefore, a field investigation was conducted to further assess the reliability of the proposed methodology. A handheld GPS device (GeoExplorer 6000) was used to determine the location of the sites. Figure 7 shows the location of the most suitable sites obtained during field investigation. The information acquired from field measurements allow for the assessment of the precision and reliability of the produced suitable areas for waste disposal landfill.

Several studies have been conducted for the site selection and disposal of the solid wastes by applying multi-criteria decision analysis (MCDA) using GIS as shown in Table 4. However, in this work shown Fuzzy logic was more accurate than AHP. The most significant physical parameters were derived and then ranked according to their contribution to landfill. This model is a first attempt in our study area. We optimized knowledge driven method by data driven approach in order to minimize the spatial errors.



Figure 7. The most suitable sites identified during field investigation (A: $31^{\circ} 3' 32.81''N$, $46^{\circ} 13' 41.20''E$; B: $31^{\circ} 0' 27.49''N$, $46^{\circ} 11' 5.09''E$)

Table 4. The comparison of technique of landfill site selection

Study area	Technique	Criteria	References
Mexico	MCDM and GIS	Social, economic and environmental criteria, proximity cost consideration	Delgado et al. (2008)
Northern Italy	MCDM, simple additive weighting	Social, economic and environmental criteria	Geneletti (2010)
Karaj, Iran	GIS, cluster analysis, AHP	Social, economic and environmental criteria	Moeinaddini et al. (2010)
Iran	AHP for weights, GIS, simple additive weighting	Social, economic and environmental criteria	Eskandari et al. (2012)
Macedonia	MCDM: AHP and ordered weighted average	Economic and environmental criteria	Gorsevski et al. (2012)
Turkey	AHP for weights	Social, economic and environmental criteria	Yildirim (2012)
Iraq	MCDM and GIS	Social, economic and environmental criteria	Mohammad Ali Al-Anbari (2014)
Morocco	MCDM, GIS and remote sensing	Social, economic and environmental criteria	Abdelhakim El Maguiri (2016)
			Zeinhom El Alfy (2018)
Mansoura city, Egypt	MCDM, GIS, AHP	Social, economic and environmental criteria	Zeinhom El Alfy (2018)
Nasiriyah city, Iraq	MCDM, GIS and Fuzzy logic, AHP	Social, economic and environmental criteria	Present study

Conclusion

In this study, 12 criteria were used in an overlaying analysis of potential areas with GIS to identify a suitable landfill site in Nasiriyah, Iraq. A combination of GIS, AHP and Fuzzy logic models were used in this study; layers such as slope, distance from bodies of water, distance from roads, distance from railways, distance from open space, distance from agricultural lands, distance from health centers and hospitals, distance

from residential areas, distance from commercial areas, distance from industrial areas, distance from facilities, and distance from educational areas were considered. The criteria weightings were derived from the AHP method by constructing a matrix of pairwise comparisons between criteria.

This study found the areas identified by both methods as most suitable, which were observed to be outside of the city boundary, mostly to the west and south of the study area and met the requirements of environmental, economic and residential factors. The common areas identified in both methods showed the most suitable lands for waste disposal landfill with an appropriate distance from residential areas and open space. Therefore, the result showed that a combination of GIS, AHP and Fuzzy models using multi-scientific and environmental criteria could be used to develop an effective and efficient methodology for selecting suitable landfill sites in Nasiriyah, Iraq. It can be concluded that the methodology applied in the present study is capable in locating the suitable landfill site in Nasiriyah city, thus future study should be carried out as well at other provinces in Iraq. It is recommended that future study should consider other important parameters such as soil type, soil layer stratification, levels and movements of the groundwater, etc. These parameters need to be studied in detail and field work analysis needs to be conducted for providing accurate and comprehensive study.

Acknowledgements. Marlia M. Hanafiah was supported by the Universiti Kebangsaan Malaysia (DIP-2017-006) and the Ministry of Education Malaysia (FRGS/1/2018/WAB05/UKM/02/2).

REFERENCES

- [1] Abdullahi, S., Mahmud, A. R. B., Pradhan, B. (2014): Spatial modelling of site suitability assessment for hospitals using geographical information system-based multicriteria approach at Qazvin city, Iran. – *Geocarto International* 29(2): 164-184.
- [2] Al-Anbari, M. A., Al-Ansari, N., Jasim, H. K. (2014): GIS and multicriteria decision analysis for landfill site selection in AL-HashimiyahQadaa. – *Natural Science* 6(5): 282-304.
- [3] Amato, F., Tonini, M., Murgante, B., Kanevski, M. (2018): Fuzzy definition of rural urban interface: an application based on land use change scenarios in Portugal. – *Environmental Modelling & Software* 104: 171-187.
- [4] Ayalew, L., Yamagishi, H., Ugawa, N. (2004): Landslide susceptibility mapping using GIS-based weighted linear combination, the case in Tsugawa area of Agano River, Niigata Prefecture, Japan. – *Landslides* 1: 73-81.
- [5] Beskese, A., Demir, H. H., Ozcan, H. K., Okten, H. E. (2015): Landfill site selection using Fuzzy AHP and Fuzzy TOPSIS: a case study for Istanbul. – *Environmental Earth Sciences* 73(7): 3513-3521.
- [6] Chabuk, A., Al-Ansari, N., Hussain, H. M., Knutsson, S., Pusch, R., Laue, J. (2017): Combining GIS applications and method of multi-criteria decision-making (AHP) for landfill siting in Al-Hashimiyah Qadhaa, Babylon, Iraq. – *Sustainability* 9(11): 1932.
- [7] Delgado, O. B., Mendoza, M., Granados, E. L., Geneletti, D. (2008): Analysis of land suitability for the siting of inter-municipal landfills in the Cuitzeo Lake Basin, Mexico. – *Waste Management* 28(7): 1137-1146.
- [8] Drobne, S., Lisec, A. (2009): Multi-attribute decision analysis in GIS: weighted linear combination and ordered weighted averaging. – *Informatica* 33: 459-474.
- [9] Eastman, J. R. (2003): *IDRISI Kilimanjaro: guide to GIS and image processing*. – Idrisi Production, Clark University.

- [10] El Alfy, Z., Elhadary, R., Elashry, A. (2010): Integrating GIS and MCDM to deal with landfill site selection. – *International Journal of Engineering & Technology* 10(6): 32-42.
- [11] El Baba, M., Kayastha, P., De Smedt, F. (2015): Landfill site selection using multi-criteria evaluation in the GIS interface: a case study from the Gaza Strip, Palestine. – *Arabian Journal of Geosciences* 8(9): 7499-7513.
- [12] El Maguiri, A., Kissi, B., Idrissi, L., Souabi, S. (2016): Landfill site selection using GIS, remote sensing and multicriteria decision analysis: case of the city of Mohammedia, Morocco. – *Bulletin of Engineering Geology and the Environment* 75(3): 1301-1309.
- [13] Eskandari, M., Homaei, M., Mahmodi, S. (2012): An integrated multi criteria approach for landfill siting in a conflicting environmental, economical and socio-cultural area. – *Waste Management* 32(8): 1528-1538.
- [14] Foroughian, A., Eslami, H. (2015): Application of AHP and GIS for landfill site selection (A case study: city of Susa). – *Journal of Scientific Research and Development* 2(5): 129-134.
- [15] Gbanie, S. P., Tengbe, P. B., Momoh, J. S., Medo, J., Kabba, V. T. S. (2013): Modelling landfill location using geographic information systems (GIS) and multi-criteria decision analysis (MCDA): case study Bo, Southern Sierra Leone. – *Applied Geography* 36: 3-12.
- [16] Geneletti, D. (2010): Combining stakeholder analysis and spatial multicriteria evaluation to select and rank inert landfill sites. – *Waste Management* 30(2): 328-337.
- [17] Gorsevski, P. V., Jankowski, P., Gessler, P. E. (2006): An heuristic approach for mapping landslide hazard by integrating fuzzy logic with analytic hierarchy process. – *Control and Cybernetics* 35: 121-146.
- [18] Gorsevski, P. V., Donevska, K. R., Mitrovski, C. D., Frizado, J. P. (2012): Integrating multi-criteria evaluation techniques with geographic information systems for landfill site selection: a case study using ordered weighted average. – *Waste Management* 32(2): 287-296.
- [19] Hanine, M., Boutkhoul, O., Tikniouine, A., Agouti, T. (2016): Comparison of fuzzy AHP and Fuzzy TODIM methods for landfill location selection. – *SpringerPlus* 5: 501.
- [20] Jiang, H., Eastman, J. R. (2000): Application of fuzzy measures in multi-criteria evaluation in GIS. – *International Journal of Geographical Information Science* 14(2): 173-184.
- [21] Khorram, A., Yousefi, M., Alavi, S. A., Farsi, J. (2015): Convenient landfill site selection by using fuzzy logic and geographic information systems: A case study in Bardaskan, East of Iran. – *Health Scope* 4(1): e19383.
- [22] Kritikos, T. R., Davies, T. R. (2011): GIS-based multi-criteria decision analysis for landslide susceptibility mapping at northern Evia, Greece [GIS-basierte multikriterielle Entscheidungsanalysen zur Kartierung von Massenverlagerungspotenzialen im nördlichen Evia, Griechenland]. – *Zeitschrift der Deutschen Gesellschaft für Geowissenschaften* 162(4): 421-434.
- [23] Liu, H. C., You, J. X., Fan, X. J., Chen, Y. Z. (2014): Site selection in waste management by the VIKOR method using linguistic assessment. – *Applied Soft Computing* 21: 453-461.
- [24] Sredevi, R. P., Vimala, V., Rameswari, P., Sateesh, S. (2016): an application of fuzzy logic and DEA in agriculture sector. – *International Journal of Engineering Science* 6(5): 4876-4878.
- [25] Moeinaddini, M., Khorasani, N., Danehkar, A., Darvishsefat, A. A. (2010): Siting MSW landfill using weighted linear combination and analytical hierarchy process (AHP) methodology in GIS environment (case study: Karaj). – *Waste Management* 30(5): 912-920.
- [26] Qiu, F., Chastain, B., Zhou, Y., Zhang, C., Sridharan, H. (2014): Modeling land suitability/capability using fuzzy evaluation. – *GeoJournal* 79(2): 167-182.
- [27] Önüt, S., Soner, S. (2008): Transshipment site selection using the AHP and TOPSIS approaches under fuzzy environment. – *Waste Management* 28(9): 1552-1559.

- [28] Rathore, S., Ahmad, S. R., Shirazi, S. A. (2016): Use of the suitability model to identify landfill sites in Lahore-Pakistan. – *Journal of Basic and Applied Sciences* 12: 103-108.
- [29] Saaty, T. L. (1977): A scaling method for priorities in hierarchical structures. – *Journal of Mathematical Psychology* 15(3): 234-281.
- [30] Saaty, T. L. (1980): *The Analytic Hierarchy Process: Planning, Priority Setting, Resources Allocation*. – McGraw Hill, New York.
- [31] Saaty, T. L. (2000): *Fundamentals of Decision Making and Priority Theory*. – McGraw Hill, New York.
- [32] Şener, Ş., Şener, E., Nas, B., Karagüzel, R. (2010): Combining AHP with GIS for landfill site selection: a case study in the Lake Beyşehir catchment area (Konya, Turkey). – *Waste Management* 30(11): 2037-2046.
- [33] Srivastava, A. K. Nema, A. K. (2012): Fuzzy parametric programming model for multi-objective integrated solid waste management under uncertainty. – *Expert Systems with Applications* 39(5): 4657-4678.
- [34] Tavares, G., Zsigraiová, Z., Semiao, V. (2011): Multi-criteria GIS-based siting of an incineration plant for municipal solid waste. – *Waste Management* 31(9-10): 1960-1972.
- [35] Torabi-Kaveh, M., Babazadeh, R., Mohammadi, S. D., Zaresefat, M. (2016): Landfill site selection using combination of GIS and Fuzzy AHP, a case study: Iranshahr, Iran. – *Waste Management & Research* 34(5): 438-448.
- [36] Uyan, M. (2014): MSW landfill site selection by combining AHP with GIS for Konya, Turkey. – *Environmental Earth Sciences* 71(4): 1629-1639.
- [37] Vaidya, O. S., Kumar, S. (2006): Analytic hierarchy process: an overview of applications. – *European Journal of Operational Research* 169(1): 1-29.
- [38] Vasiljević, T. Z., Srdjević, Z., Bajčetić, R., Miloradov, M. V. (2012): GIS and the analytic hierarchy process for regional landfill site selection in transitional countries: a case study from Serbia. – *Environmental Management* 49(2): 445-458.
- [39] Yildirim, V. (2012): Application of raster-based GIS techniques in the siting of landfills in Trabzon Province, Turkey: a case study. – *Waste Management & Research* 30(9): 949-960.

APPENDIX

Table A1. Sub-criteria factors extracted from main criteria

Main criteria	Sub-criteria
G) Geomorphology parameter	G1) Slope
H) Hydrology	H1) Distance from water bodies
T) Transporting parameters	T1) Distance from railway T2) Distance from road
L) Land use parameters	L1) Distance from educational areas L2) Distance from facilities and services L3) Distance from health centres and hospitals L4) Distance from commercial areas L5) Distance from agricultural areas L6) Distance from industrial areas L7) Distance from residential areas L8) Distance from open space

Table A2. Fundamental scale of AHP multi criteria decision making

Fundamental scale (row v column)	
Extremely less important	1/9
	1/8
Very strongly less important	1/7
	1/6
Strongly less important	1/5
	1/4
Moderately less important	1/3
	1/2
Equal importance	1
	2
Moderately more important	3
	4
Strongly more important	5
	6
Very strongly more important	7
	8
Extremely more important	9

Table A3. Sub-classes and rank of slope, distance from river, distance from roads, distance from railways, distance from open space, distance from agricultural lands, distance from health centres and hospitals, distance from residential areas, distance from commercial areas, distance from industrial areas, distance from facilities areas and distance from education areas

Slope			
From (degree)	To (degree)	Average (degree)	Rank
0	0	0	6
0	2	1	5
2	5	3.5	4
5	10	7.5	3
10	20	15	2
20	45	32.5	1

River (meter)			
From (meter)	To (meter)	Average (meter)	Rank
0	183	91	1
183	496	339	2
496	836	666	3
836	1175	871	4
1175	1567	1005	5
1567	1985	1776	6
1985	2533	2259	7
2533	3238	2885	8
3238	4204	3721	9
4204	6659	5431	10

Distance from the road			
From (meter)	To (meter)	Average (meter)	Rank
0	0	0	1
0	64	32	2
64	169	116	3
169	318	243	4
318	487	402	6
487	699	593	10
699	953	826	7
953	1313	1133	5
1313	1969	1641	2
1969	5398	3684	1

Distance from the railway			
From (meter)	To (meter)	Average (meter)	Rank
0	792	396	1
792	1641	1217	2
1641	2546	2094	3
2546	3508	3027	4
3508	4584	4046	5
4584	5829	5206	6
5829	7356	6592	7
7356	8828	8092	8
8828	10356	9592	9
10356	14430	12393	10

Distance from open space (bare land)			
From (meter)	To (meter)	Average (meter)	Rank
0	367	184	10
367	735	551	9
735	1102	918	8
1102	1469	1286	7
1469	1837	1653	6
1837	2204	2020	5
2204	2571	2387	4
2571	2938	2755	3
2938	3306	3122	2
3306	3673	3489	1

Distance from health			
From (meter)	To (meter)	Average (meter)	Rank
0	540	270	1
540	1152	846	2
1152	1764	1458	3
1764	2377	2071	4
2377	2989	2683	5
2989	3637	3313	6
3637	4429	4033	7
4429	5257	4843	8

5257	6194	5725	9
6194	9182	7688	10
Distance from commercial			
From (meter)	To (meter)	Average (meter)	Rank
0	855	428	1
855	1853	1354	2
1853	2672	2263	3
2672	3385	3029	4
3385	4026	3706	5
4026	4632	4329	6
4632	5238	4935	7
5238	5844	5541	8
5844	6592	6218	9
6592	9086	7839	10
Distance from agriculture			
From (meter)	To (meter)	Average (meter)	Rank
0	0	0	1
0	147	74	2
147	319	233	3
319	515	417	4
515	785	650	5
785	1154	969	6
1154	1620	1387	7
1620	2233	1927	8
2233	3068	2651	9
3068	6259	4663	10
Residential			
From (meter)	To (meter)	Average (meter)	Rank
0	0	0	1
0	179	90	2
179	436	308	3
436	718	577	4
718	1051	884	5
1051	1410	1230	7
1410	1820	1615	8
1820	2332	2076	9
2332	3127	2730	10
3127	6536	4831	6
Industrial			
From (meter)	To (meter)	Average (meter)	Rank
0	403	201	1
403	906	655	2
906	1376	1141	3
1376	1880	1628	4
1880	2451	2165	9
2451	3089	2770	10

3089	3861	3475	8
3861	4902	4381	7
4902	6110	5506	6
6110	8561	7336	5
Facilities			
From (meter)	To (meter)	Average (meter)	Rank
0	164	82	1
164	691	428	2
691	1250	970	3
1250	1842	1546	4
1842	2401	2122	5
2401	2960	2681	6
2960	3651	3306	7
3651	4572	4112	8
4572	5625	5099	9
5625	8388	7007	10
Distance from educational			
From (meter)	To (meter)	Average (meter)	Rank
0	212	106	1
212	672	442	2
672	1238	955	3
1238	1839	1539	4
1839	2441	2140	5
2441	3006	2724	6
3006	3679	3342	7
3679	4492	4085	8
4492	5412	4952	9
5412	9019	7216	10

THE CHANGE OF SOME HEAVY METAL CONCENTRATIONS IN SCOTCH PINE (*PINUS SYLVESTRIS*) DEPENDING ON TRAFFIC DENSITY, ORGANELLE AND WASHING

ARICAK, B.¹ – CETIN, M.^{2*} – ERDEM, R.³ – SEVIK, H.⁴ – COMETEN, H.⁵

¹*Department of Forest Engineering, Faculty of Forestry, Kastamonu University, Kastamonu, Turkey*
(phone: +90-366-280-1744; fax: +90-366-215-2316)

²*Department of Landscape Architecture, Faculty of Engineering and Architecture, Kastamonu University, Kastamonu, Turkey*

³*Department of Forestry, Arac Rafet Vergili Vocational School, Kastamonu University, Kastamonu, Turkey*
(phone: +90-366-280-1744; fax: +90-366-215-2316)

⁴*Department of Environmental Engineering, Faculty of Engineering and Architecture, Kastamonu University, Kastamonu, Turkey*
(phone: +90-366-280-2921; fax: +90-366-280-2900)

⁵*Programs of Forest Engineering, Institute of Science, Kastamonu University, Kastamonu, Turkey*
(phone: +90-366-280-1744; fax: +90-366-215-2316)

**Corresponding author*

e-mail: mcerin@kastamonu.edu.tr; phone: +90-366-280-2920; fax: +90-366-280-2900

(Received 6th Feb 2019; accepted 8th Apr 2019)

Abstract. Increasing population and industrialization have caused air pollution and air pollution in some cities has increased to such an extent that it has started to threaten human health and has become one of the most important agenda topics of our day. Many pollutants arise in cities due to exhaust gases, car wheels, vehicles and vehicle wear. Heavy metals are one of the most infamous pollutants, because they can remain in nature for a long time without degradation and the amount of heavy metal concentration in the environment is constantly increasing. Heavy metals also tend to bioaccumulate. Therefore, the determination of heavy metal concentration is of great importance in terms of identifying risk regions and risk levels. Determination of heavy metal concentrations in plants is important both for determining plants' ability to remove heavy metals from the air and thus to improve air quality, as well as for monitoring air quality. Bio-indicators are the most important indicators of the change in the concentration of heavy metal in the atmosphere. This study aims to determine the usability potential of Scotch Pine (*Pinus sylvestris*) in monitoring the traffic related heavy metal concentration. For this purpose, samples of Scotch Pine individuals were collected from one of the busiest highways of Turkey, at the route of Ankara-Istanbul, from refuges, at roadsides and at distances of 3 m, 10 m, 30 m, 50 m and 100 m from the roadside, some of the branch and needle samples were washed and the change of Cu, Pb and Cd concentrations on these samples was determined. As a result of the study, the change of the concentrations of these heavy metals depending on distance to the road, organelle and washing conditions all seem to indicate that the Scotch Pine is a good bio-monitor which could be used especially to monitor the change of Cd concentration.

Keywords: *bioaccumulate, bio-monitor, highway, plant, pollution, Cd concentration*

Introduction

In addition to the rising population of the world, the increasing population density in city centers has brought various problems with it (Cetin and Sevik, 2016a, b; Gülgün et al., 2014; Cetin et al., 2017a, b, 2018a, b, c, d). This process causes destruction of nature, pollution of air, water and soil, and deterioration of the ecological balance (Mutlu, 2016; Mutlu et al., 2016; Kaya et al., 2018). This process brings many problems with it, but one of the biggest problems is the pollution of environment and especially air (Sevik et al., 2018). Air pollution has become such a big problem that approximately 30 million people die every year due to air pollution related reasons (Cetin et al., 2018).

Air pollution can be defined as the existence of one or more contaminants in the air in amounts and durations which could be harmful to humans, animals and plant life and commercial or personal properties and environmental quality (Cetin et al., 2018).

While there are many components responsible for air pollution, heavy metals are one of the more significant among them. Heavy metals do not deteriorate and disappear in nature.

There are various methods that are used to determine the air pollution. Direct measurement of air pollution via these methods requires both expensive measuring instruments and has a higher risk of contamination compared to bioindicators. Plants have many environmental, social and economic contributions to the environment in which we live, one of which is their use as a bio-indicator in the detection and monitoring of air pollution (Gülgün et al., 2015; Cetin et al., 2018b). Using bioindicators is one of the most effective methods of determining air pollution.

This method is inexpensive and easy to provide, as well as its ability to provide more accurate data on the periodic change of heavy metal concentration. Therefore, many studies have been conducted to determine the change of heavy metal concentrations via bioindicators (Sevik et al., 2018; Turkyilmaz et al., 2018b).

However, different heavy metals can accumulate at different levels in the organelles of the plants. Therefore, it is very important to determine the accumulation level of each heavy metal in each organelle to enable the usage of the right organelle of the right plant as biomonitors in order to get more reliable results from the studies. In this study, it was aimed to determine the change of some heavy metals concentrations depending on the plant organelles and the distance to the road with heavy traffic in Scotch Pines (*Pinus sylvestris*).

Materials and methods

Materials

The study was conducted on the samples collected from the Scotch Pines from the roadside on the Ankara-İstanbul highway between Kaynaşlı province of Düzce city and Bolu city. The highway that was chosen as the case of this study is one of the busiest highways in Turkey. Samples were especially taken from the closest branches to the road. The Scotch Pine individuals were selected on a specific direction on the highway between Kaynaşlı district of Düzce province and Bolu province from the refuge, roadside and at 3 m, 10 m, 30 m, 50 m and 100 m distances. The half-meter length of branch samples collected from the road side parts of seven Scotch Pines constitute the materials of this study (*Table 1*). The samples used in the study were collected in the last week of September following the end of the vegetation season of 2018.

Table 1. The exact locations of sampling indicated by GPS coordinates

Distance (m)	Coordinates DMS (degrees, minutes, seconds)	
	Latitude N	Longitude E
0	40°46'32.225"	31°19'41.524"
1	40°46'45.450"	31°19'25.086"
3	40°46'48.105"	31°19'53.024"
10	40°47'09.660"	31°18'22.076"
30	40°47'36.155"	31°18'39.323"
50	40°48'07.464"	31°17'23.096"
100	40°48'23.124"	31°17'15.233"

Determination of heavy metal concentrations

Samples brought to the laboratory were firstly divided into groups and some of the samples were washed. The samples were then separated into organelles and the bark of the wood was peeled; and washed needles, unwashed needles, washed bark, unwashed bark and wood samples were obtained. The samples were labeled and kept for 15 days until they got air dried. Air dried samples were taken into glass containers and dried in drying oven at 50 °C for one week.

The dried samples were pulverized by a steel blender in the laboratory. The pulverized samples were made to weigh 2 g each in 10 ml concentrated HNO₃ at room temperature for 1 day in the fume cupboard, and then boiled at 180 °C for 1 h. 20 ml of distilled water were added to the prepared solutions and the solution was filtered through a 45-µm filter paper. The prepared solutions were numbered in order to prevent any mix-ups and prepared for analysis. In the solutions obtained from the filtrate; heavy metal analysis was performed with the GBC Integra XL ICSDS-270 ICP-OES (Inductively Coupled Plasma Optical Emission Spectrometer) device (Sevik et al., 2018; Turkyilmaz et al., 2018b).

Statistical analysis

The obtained data were evaluated with the help of SPSS package program, variance analysis was applied to the data and homogeneous groups were obtained by applying the Duncan test to the values having at least 95% confidence level differences statistically. The obtained data is simplified and tabulated and interpreted (Sevik et al., 2018; Turkyilmaz et al., 2018b).

Results

The change in Cu concentration due to organelle and distance to the traffic source was determined separately and F value and significance level obtained by variance analysis and homogeneous groups resulting from Duncan test are shown in *Table 2*.

As the result of the variance analysis, it was determined that the change of Cu concentration was significant at a 99.9% confidence level for all factors. When the change of Cu concentration due to distance was examined, no significant change was observed. For example, in the unwashed bark samples, some of the lowest and the

highest values were obtained at the farthest distance from the road. A similar situation is also noticeable in wood samples. The lowest and the highest values of the wood samples were also obtained at the farthest distance to the road.

Table 2. The change of Cu (ppm) concentration depending on organelle and on distance from the road

Distance (m)	Needle		Bark		Wood (ppm)	Value (ppm)
	Washed (ppm)	Unwashed (ppm)	Washed (ppm)	Unwashed (ppm)		
0	1642.8 Ce	783.7 Ac	1274.6 Bc	6094.9 Df	6461.1 Eg	3615.463***
1	786.5 Bb	220.4 Aa	2956.5 De	1620.2 Cc	128.7 Aa	897.041***
3	1034.6 Bc	559.3 Ab	1295.5 Cc	1020.1 Bb	2728.2 Dd	294.611***
10	1909.5 Cg	1124.9 Ad	1686.0 Bd	1880.3 Cd	3170.6 De	193.553***
30	1787.9 Df	1572.0 Ce	503.1 ABa	332.0 Aa	561.2 Bb	127.001***
50	1418.0 Dd	1482.4 De	712.5 Bb	194.3 Aa	834.8 Cc	203.899***
100	550.2 Aa	1805.6 Cf	1321.8 Bc	2759.7 De	5296.4 Ef	1390.201***
	237.794***	174.617***	209.164***	1024.679***	3880.312***	

*Significant at 0.05 level; **significant at 0.01 level; ***significant at 0.001 level

The letters a, b, c, etc. means according to Duncan test results; show that the group is located. It is statistically different from the values contained in different groups, starting with the letter a, the numerical value grows

Capital letters in rows; lower case letters show groupings in columns. For example, the concentration of Cu in the washed needle is also as the distance of the fifth; C is in the third homogeneous group

When examining the change of Cu concentration depending on the organelles; it is noteworthy that the concentration amounts in wood samples were considerably high. It was observed that the amount of the Cu concentration in wood samples were higher than the values obtained from the other organelles.

The change in Pb concentration due to organelle and distance to the traffic source was determined separately and F value and significance level obtained by variance analysis and homogeneous groups resulting from Duncan test are shown in *Table 3*.

When the results of the analysis of variance in Pb are examined, it is noteworthy that Pb concentration in wood does not differ statistically significant at least at 95% confidence level depending on distance. Apart from this, it can be said that the change of Pb concentration due to distance is statistically meaningless. However, when the change of Pb concentration is examined depending on organelle, it is observed that all values obtained from the wood samples are quite low and all the values obtained from the wood samples are in the first two homogenous groups that were formed as the result of Duncan test. Furthermore, it was observed that the values obtained from needles were lower than the values obtained from the bark samples, while the values of washed samples were also lower than the values of unwashed samples.

The change in Cd concentration due to organelle and distance to the traffic source was determined separately and F value and significance level obtained by variance analysis and homogeneous groups resulting from Duncan test are shown in *Table 4*.

As the result of the variance analysis, it was determined that the change of Cd concentration was significant at a 99.9% confidence level for all factors. When the

change of Cd concentration due to distance was examined, it was seen that Cd concentration decreases generally as the distance increases.

Table 3. The change of Pb (ppm) concentration depending on organelle and distance

Distance (m)	Needle		Bark		Wood	Value (ppm)
	Washed (ppm)	Unwashed (ppm)	Washed (ppm)	Unwashed (ppm)	Unwashed (ppm)	
0	267.9 Abc	337.1 Ab	1246.2 Bb	1304.1 Bbc	361.6 A	41.008***
1	93.6 Aa	765.6 Ccd	1592.2 Dc	1766.1 Dd	421.7 B	122.962***
3	371.4 Ac	1042.4 Be	1110.1 Bb	1023.0 Ba	273.1 A	22.517***
10	258.2 Abc	458.5 Ab	2131.8 Dd	1778.7 Cd	404.7 A	82.814***
30	150.1 Aab	74.3 Aa	947.6 Cb	1070.8 Cab	581.6 B	39.022***
50	321.2 Ac	656.2 Bc	1089.1 Cb	1196.7 Cab	371.2 A	33.357***
100	219.4 Aabc	942.3 Cde	395.2 Aa	1455.2 Dc	581.2 B	70.513***
	3.936*	31.334***	27.357***	15.223***	2.096ns	

*Significant at 0.05 level; **significant at 0.01 level; ***significant at 0.001 level

The letters a, b, c, etc. means according to Duncan test results; show that the group is located. It is statistically different from the values contained in different groups, starting with the letter a, the numerical value grows

Capital letters in rows; lower case letters show groupings in columns. For example, the concentration of Cu in the washed needle is also as the distance of the fifth; C is in the third homogeneous group

Table 4. The change of Cd (ppm) concentration depending on organelle and distance

Distance (m)	Needle		Bark		Wood	Value (ppm)
	Washed (ppm)	Unwashed (ppm)	Washed (ppm)	Unwashed (ppm)	Unwashed (ppm)	
0	40.8 Ac	65.9 Ac	172.4 Ce	157.0 BCc	138.8 Bb	36.731***
1	14.7 Aa	32.8 Bab	81.5 Cc	69.9 Ca	45.4 Ba	35.040***
3	25.9 Ab	41.1 Bb	80.6 Dc	53.9 Ca	43.2 Ba	95.119***
10	17.3 Aa	25.0 Aa	114.0 Cd	95.0 Cb	46.0 Ba	45.881***
30	19.0 Aa	25.2 Aa	73.6 Dbc	50.9 Ca	39.9 Ba	31.902***
50	26.6 Ab	26.0 Aa	61.4 Cab	57.5 Ca	40.4 Ba	103.357***
100	19.3 Aa	36.4 Bab	46.9 Ca	65.2 Da	39.5 BCa	27.582***
	30.335***	14.796***	49.714***	24.435***	58.942***	

*Significant at 0.05 level; **significant at 0.01 level; ***significant at 0.001 level

The letters a, b, c, etc. means according to Duncan test results; show that the group is located. It is statistically different from the values contained in different groups, starting with the letter a, the numerical value grows

Capital letters in rows; lower case letters show groupings in columns. For example, the concentration of Cu in the washed needle is also as the distance of the fifth; C is in the third homogeneous group

When the change of Cd concentration depending on the organelles was examined, it was determined that the lowest values were obtained from the needle samples, the highest values were obtained from bark samples, and the values obtained from wood samples were higher than the values of needle samples while lower than the values of bark samples. Apart from that, the Cd concentration amount calculated in unwashed

needle samples were generally higher than the washed needle samples, and the Cd concentration amount calculated in washed bark samples were higher than the unwashed bark samples.

In addition, the Cd concentrations obtained from the unwashed samples in the hands are generally higher than the washed samples and the Cd concentrations in the washed samples are higher than the Cd concentrations obtained in the washed samples.

Discussion

Plants are often used as biomonitors in monitoring the heavy metal concentration. Some of the species that are used as biomonitors of traffic related air pollution are; *Aesculus hippocastanum* (Anicic et al., 2011), *Elaeagnus angustifolia* (Aksoy and Şahin, 1999), *Robinia pseudoacacia* (Celik et al., 2005), *Tilia* sp. (Tomasevic and Anicic, 2010), *Quercus ilex* (Gratani et al., 2008) and some other species (Ozturk and Bozdogan, 2015; Mossi, 2018).

Cu, one of the heavy metals that were evaluated within the scope of this study is quite an important element for plant organisms due to its involvement in enzyme activation, carbohydrate and lipid metabolism (Asri and Sönmez, 2006). It has been determined that copper plays an important role in physiological events such as photosynthesis, respiration, carbohydrate degradation, nitrogen use and storage, cell wall metabolism, and that it regulates xylem permeability, controls the production of DNA and RNA and plays an important role in resistance mechanism against diseases. In case of copper deficiency, it is stated that plant growth stopped (Okcu et al., 2009).

Although plant species need different amounts of it, copper is a highly toxic metal. Some effects of copper poisoning include tissue damage, deterioration of roots and darkening of plant color. Other effects of copper poisoning are, loss of ion as a result of deterioration of membrane permeability in the stem cells and disruption of photosynthesis process as a result of DNA damage (Okcu et al., 2009). Acute copper intoxication may cause abdominal pain, nausea, vomiting and diarrhea in humans (Asri and Sönmez, 2006). While taking low amounts of copper ions may cause liver cirrhosis, Wilson's disease, systemic rheumatic diseases, kidney diseases; taking high amounts of copper ions may cause blood cancer (Mossi, 2018). Therefore, many studies have been conducted to determine Cu concentration in plants and to correlate with traffic density (Turkyilmaz et al., 2018a, b).

Turkyilmaz et al. (2018c) stated that Cu concentration amount in plant organelles differ depending on traffic density and that while they calculated the Cu concentration at 69.615 ppb in areas with none-traffic, it was 71.096 ppb in areas with low dense traffic and it reached up to 110.441 ppb level in areas with heavy traffic. Suzuki et al. (2009) determined that the concentration of Cu could reach up to 22.22 mg kg⁻¹ in the leaves of *Rhododendron pulchrum* in Okayama, Japan; while Demirayak et al. (2011) reported that Cu concentration was averagely at 35 ppm level in the leaves of *M. grandiflora* in Samsun city. Li et al. (2007) stated that the amount of Cu concentration in *Sophora japonica* L. leaves were higher in the individual trees on roadside than the ones in the parks.

Sawidis et al. (2011) determined that the Cu concentration in *Pinus nigra* leaves in the control group was calculated at 3.182 µg/g in Salzburg; 3.263 µg/g in Belgrade; and 2.432 µg/g in Thessaloniki; while it increased up to 4.875 µg/g in Salzburg; 25.391 µg/g in Belgrade and 16.486 µg/g in Thessaloniki in contaminated regions.

Erdem (2018) in his study on different species that the Cu concentration between 0.16 and 24.66 ppm and depending on the intensity of the traffic varies depending on a high level of values, for example, *Ailanthus altissima* in the areas of heavy traffic in the Cu concentration of the determined concentration of Cu in areas where the approximately 80 times. Pınar (2019) in his study of five species on the Cu concentration of 3 ppm to 286.5 ppm ranged between the highest value of the traffic is concentrated in the linden seeds.

Cu concentration in wood samples was higher than in the other organelles. This result is generally consistent with the literature. Cu concentration varies in different species, depending on species and organelles (Mossi, 2018; Turkyilmaz et al., 2018d).

In his study of four different types, Erdem (2018) states that the Cu concentration changes significantly on the basis of the organelle. In some species, the highest values are determined on the leaf and in some species on the branches and seeds. Similar results were obtained by Özel (2019) and Pınar (2019). Pb is one of the other heavy metals that were evaluated within this study. Pb concentration is of great importance among the other heavy metals. Pb, which is a widely used element in industrial and agricultural activities, is a heavy metal that is emitted to the atmosphere as a metal or compound and in each case has toxic properties. Pb is one of the heavy metals that cause the most damage to the ecological system by human activities (Mossi, 2018). Therefore, a large number of studies have been performed on the change of Pb due to traffic density (Lei et al., 2015; Assirey et al., 2015; Galal et al., 2015).

In the study, it was determined that the values obtained in the wood samples were quite low, and the values obtained from the needle samples were lower than the values obtained from the bark samples and the values obtained from the washed samples were lower than the values obtained from the unwashed samples. Mossi (2018) found similar results in different studies; he determined that the lowest values of Pb concentrations were obtained from washed samples while the highest values were calculated in the unwashed samples in areas with heavy traffic.

Pb with more than the normal levels can be found in the foods of animal and vegetable origin that are grown in areas close to the city centers and industrial regions (França et al., 2017; Mossi, 2018). In addition, lead-containing gasoline is an important source (Okcu et al., 2009). Therefore, there are numerous studies documenting the relationship between Pb and traffic density (Qing et al., 2015; Begum et al., 2017).

Erdem (2018) stated that different types of Pb concentrations vary significantly depending on the traffic density, whereas the average Pb concentration in areas where there is no traffic is 346 ppb is 635 ppb in areas with low traffic and 1782 ppb in high traffic areas. Pınar (2019) stated that Pb concentration increased with traffic density and this level was quite high in some organelles.

There are many studies on the change of Pb in organelle and species. In studies, it is stated that Pb changes significantly on organelle basis. For example, Akarsu (2019) stated that the Pb concentration in *Cedrus arizonica* wood was 1619 ppb and this value increased to 5902 ppb in the outer shell. Ozel (2019) indicates that the concentration of Pb in the mulberry shells in the areas where there is no traffic is increased to 2630 ppb in the leaves. The same figures in the areas where traffic is 5352 ppb in the shell, 11582 ppb level in the leaf (Ozel, 2019).

Pb is one of the most studied elements due to the properties of this element. Numerous studies have been conducted on many species to be used as the biomonitor of Pb. Some of the studies that were aimed to determine the change of Pb concentration in

different species depending on traffic density are; Aksoy and Şahin (1999) *Elaeagnus angustifolia*, Tam et al. (1987) *Bauhinia variegata*, Çelik et al. (2005) *Robinia pseudoacacia*, Demirayak et al. (2011) *M. grandiflora* and *A. Cyanophylla*, Tanushree et al. (2011) *Alstonia scholaris*, *Ficus bengalensis*, *Morus alba*, and *Polyalthia longifolia*, Sawidis et al. (2011) *Platanus orientalis* (Ozel et al., 2015), *Pinus nigra*, Li et al. (2007) *Sophora japonica*.

Another heavy metal that has been mostly studied is Cd. Cd is a highly toxic metal that comes to the fore with a variety of usage areas and with its role in the environmental pollution. The carcinogen effect of Cd in human body was identified in 1976 and it was classified as Type 1 carcinogen by IARC (International Agency for Cancer Research) in 1993 (Boğa, 2007). Cd is an element that is toxic for both humans and animals as well as plants (Asri and Sönmez, 2006; Boğa, 2007). Not only is it toxic for the human body even at very low doses, but it also has a long biological half-life.

In addition to industrial activities, cadmium is spread through phosphorous fertilizers used in agriculture, sewage wastes in residential areas and atmospheric deposits. It is estimated that 0.2-1.0 mg/m² of Cd is added annually in the soils of the roadsides in areas with heavy traffic (Asri and Sönmez, 2006). In our study, it was determined that Cd concentration decreased as the distance to the road increased. In addition, the lowest values were obtained in needles while the highest values were obtained in bark samples.

The results of the study revealed that the amount of Cd changed depending on both traffic density and organelle. In a large number of studies, it was determined that the concentration of Cd varies according to plant species, traffic density and plant organelle (Mossi, et al., 2018; Turkyilmaz et al., 2018e). Ozel (2019) Cd concentration, depending on the type, organelle and traffic density, Akarsu (2019) *Cedrus arizonica* facing the road in the average Cd concentration of wood at 157 ppb level of this value is 2601 ppb level in the outer shell.

In this study, the possibility of using pine as a biomonitor to determine the heavy metal pollution in the air was investigated. It is stated in the studies that it can be used as biomonitor in determining the heavy metal pollution of traffic origin of pine in different areas (Turkyilmaz et al., 2018b). In order for a species to be used as a biomonitor for monitoring heavy metal pollution, it must first be able to collect heavy metals within that species (Bat et al., 1999). Plants that can collect heavy metals in the air can also remove heavy metals from the air. Therefore, they can clean the air in terms of heavy metal. Therefore, the plants that can collect heavy metals within the body can also contribute to the cleaning of the heavy metal. This situation was also expressed in other studies (Saleh, 2018; Mossi, 2018; Erdem, 2018). In this study, it was determined that pine can collect some heavy metals within its structure. Therefore, in the environment where yellow pine is grown, it will help to remove heavy metals from the air and contribute to the cleaning of air pollution.

Conclusions

Expanding green areas is one of the most effective methods among the solution proposals to tackle air pollution. In many studies, it has been proved that green areas and the plants used in these areas reduce all kinds of air pollution in different ways (Cetin and Sevik, 2016a, b; Cetin et al., 2017).

Although a large number of plant species have been the subject of studies to date, these studies are not yet sufficient. There is no information about the potential of many

plant species to accumulate heavy metals. However, it has been reported in numerous studies that there are great differences between the heavy metal deposition potentials of plant species. Therefore, it is necessary to use the species that are not examined yet in similar studies and to identify the plants that will be more effective in monitoring and reducing the heavy metal pollution. Therefore, it is suggested to keep similar studies going by diversifying the studied plant species.

In the selection of the plants used in urban centers, their visual qualities are generally prioritized and their functional uses are made to be of secondary importance. However, in order to use the plants in a proper manner; it is vital to determine the more effective species to perform the desired function and the selection of the species in such areas should be made accordingly. Scotch pine is a tree species that can be used for forestation of the urban areas especially due to being an evergreen species as well as being extremely resistant to cold climates. Also, as it has low needs for maintenance, soil and water tree, it is a valuable landscape plant. It is determined that it is also a good biomonitor especially for the monitoring of Cd pollution.

Within the scope of the study, measurements have only been conducted on needles, branches and wood samples of the tree. However, former studies have proved that the heavy metal concentration in different organelles of the plants such as root, fruit, etc. can be higher. Therefore, the low concentration in the needles, branches and wood samples of a tree may not mean that the plant does not accumulate heavy metals as the plant may have a significant amount of heavy metal concentration in its other organelles. The inclusion of other organelles of the plants in the studies to be carried out in this field may provide important results.

REFERENCES

- [1] Aksoy, A., Sahin, U. (1999): *Elaeagnus angustifolia* L. as a biomonitor of heavy metal pollution. – Turkish Journal of Botany 23: 83-87.
- [2] Akarsu, H. (2019): Determination of heavy metal accumulation in atmosphere by being aid of annual rings. – Master Thesis, Kastamonu University, Graduate School of Natural and Applied Sciences Department of Sustainable Agriculture and Natural Plant Resources, Kastamonu, Turkey.
- [3] Anicic, M., Spasic, T., Tomasevic, M., Rajsic, S., and Tasic, M. (2011): Trace elements accumulation and temporal trends in leaves of urban deciduous trees (*Aesculus hippocastanum* and *Tilia* spp.). – Ecological Indicators 11: 824-830.
- [4] Asri, F. Ö., Sönmez, S. (2006): Ağır metal toksisitesinin bitki metabolizması üzerine etkileri. – Derim, Batı Akdeniz Tarımsal Enstitüsü, Dergisi 23(2): 36-45.
- [5] Assirey, E., Al-Qodah, Z., Al-Ahmadi, M. (2015): Impact of traffic density on roadside pollution by some heavy metal ions in Madinah city, Kingdom of Saudi Arabia. – Asian Journal of Chemistry 27(10): 3770-3776.
- [6] Bat, L., Gündoğdu, A., Öztürk, M. (1999): Heavy Metals. – SDU Eğirdir Su Ürünleri Fak. Derg. 1998-1999, pp. 166-175
- [7] Begum, H. A., Hamayun, M., Zaman, K., Shinwari, Z. K., Hussain, A. N. W. A. R. (2017): Heavy metal analysis in frequently consumable medicinal plants of Khyber Paktunkhwa, Pakistan. – Pak. J. Bot 49(3): 1155-1160.
- [8] Boğa, A. (2007): Ağır Metallerin Özellikleri ve Etki Yolları. – Çukurova Üniversitesi Tıp Fakültesi, Fizyoloji Anabilim Dalı, Adana 16: 218.
- [9] Celik, A., Kartal, A. A., Kaska, Y. (2005): Determining the heavy metal pollution in Denizli (Turkey) by using *Ro-binia pseudo-acacia* L. – Environment International 31: 105-112.

- [10] Cetin, M., Sevik, H. (2016a): Measuring the impact of selected plants on indoor CO₂ concentrations. – Polish Journal of Environmental Studies 25(3): 973-979.
- [11] Cetin, M., Sevik, H. (2016b): Change of air quality in Kastamonu City in terms of particulate matter and CO₂ amount. – Oxidation Communications 39(4-II): 3394-3401.
- [12] Cetin M, Sevik H, Isinkaralar, K. (2017a): Changes in the particulate matter and CO₂ concentrations based on the time and weather conditions: the case of Kastamonu. – Oxidation Communications 40(1-II): 477-485.
- [13] Cetin, M., Sevik, H., Saat, A. (2017b): Indoor air quality: the samples of Safranbolu Bulak Mencilis cave. – Fresenius Environmental Bulletin 26(10): 5965-5970.
- [14] Cetin, M., Onac, A. K., Sevik, H., Canturk, U., Akpinar, H. (2018a): Chronicles and geoheritage of the ancient Roman city of Pompeiopolis: a landscape plan. – Arabian Journal of Geosciences 11: 798. DOI: 10.1007/s12517-018-4170-6.
- [15] Cetin, M., Kalayci Onac, A., Sevik, H., Sen, B. (2018b): Temporal and regional change of some air pollution parameters in Bursa. – Air Quality, Atmosphere & Health. DOI: <https://doi.org/10.1007/s11869-018-00657-6>.
- [16] Cetin, M., Sevik, H., Yigit, N. (2018c): Climate type-related changes in the leaf micromorphological characters of certain landscape plants. – Environmental Monitoring and Assessment 190: 404. <https://doi.org/10.1007/s10661-018-6783-3>.
- [17] Cetin, M., Sevik, H., Yigit, N., Ozel, H. B., Aricak, B., Varol, T. (2018d): The variable of leaf micromorphological characters on grown in distinct climate conditions in some landscape plants. – Fresenius Environmental Bulletin 27(5): 3206-3211.
- [18] Demirayak, A., Kutbay, H. G., Kilic, D., Bilgin, A., Huseyinova, R. (2011): Heavy metal accumulation in some natural and exotic plants in Samsun City. – Ekoloji 20(79): 1-11.
- [19] Erdem, T. (2018): the change of heavy metal concentrations in some plants due to species, organelles and traffic densities. – Master Thesis, Kastamonu University Institute of Science Department of Forest Engineering, Kastamonu, Turkey.
- [20] França, F. C., Albuerque, A. M., Almeida, A. C., Silveira, P. B., Crescêncio Filho, A., Hazin, C. A., Honorato, E. V. (2017): Heavy metals deposited in the culture of lettuce (*Lactuca sativa* L.) by the influence of vehicular traffic in Pernambuco, Brazil. – Food Chemistry 215: 171-176.
- [21] Galal, T. M., Shehata, H. S. (2015): Bioaccumulation and translocation of heavy metals by *Plantago major* L. grown in contaminated soils under the effect of traffic pollution. – Ecological Indicators 48: 244-251.
- [22] Gratani, L., Crescente, M. F., Varone, L. (2008): Long-term monitoring of metal pollution by urban trees. – Atmospheric Environment 42: 8273-8277.
- [23] Gülgün, B., Güney, M., A., Aktaş, E., Yazici, K. (2014): Role of Landscape Architect in Interdisciplinary Planing of Sustainable Cities. – Journal of Environmental Protection and Ecology 15(4): 1877-1880.
- [24] Gülgün, B., Yazici, K., Dursun, Ş., Balık, G. (2015): Forest plantation and alternative utilization of some cultivated plants in Turkey. – 15th Scientific Geoconference, Albena/Bulgaria. SGEM 1: 377-383. DOI: 10.5593/SGEM2015/B51/S20.049.
- [25] Kaya, L. G., Kaynakci-Elinc, Z., Yucedag, C., Cetin, M. (2018): Environmental outdoor plant preferences: a practical approach for choosing outdoor plants in urban or suburban residential areas in Antalya, Turkey. – Fresenius Environmental Bulletin 27(12): 7945-7952.
- [26] Lei, J., Hasi, E., Sun, Y. (2015): Assessing the Influence of Different Road Traffic on Heavy Metal Accumulation in Rural Roadside Surface Soils of the Eastern Ordos Plateau Grassland in China. – In: Scholz, M. (ed.) Water Resources and Environment. CRC Press, Boca Raton, FL, pp. 247-252.
- [27] Li, F. R., Kang, L. F., Gao, X. Q., Hua, W., Yang, F. W., Hei, W. L. (2007): Traffic-related heavy metal accumulation in soils and plants in Northwest China. – Soil & Sediment Contamination 16(5): 473-484.

- [28] Mossi, M. M. M. (2018): Determination of heavy metal accumulation in some shrub formed landscape plants. – Ph.D. Thesis, Kastamonu University, Institute of Science Department of Forest Engineering, Kastamonu, Turkey.
- [29] Mutlu, E. (2016): The effects of lead-induced toxicity on metabolic biomarkers in common carp (*Cyprinus carpio* L.). – *Fresenius Environ Bull* 25(5): 1419-1427.
- [30] Mutlu, E., Demir, T., Yanik, T., Anca Sutan, N. (2016): Determination of environmentally relevant water quality parameters in Serefiye Dam-Turkey. – *Fresenius Environ Bull* 25(12): 5812-5818.
- [31] Okcu, M., Tozlu, E., Kumlay, A. M., Pehlivan, M. (2009): Ağır Metallerin Bitkiler Üzerine Etkileri. – *Alinteri Dergisi* 17: 14-26.
- [32] Özel, S. (2019): The variation of heavy metal accumulation in some fruit tree organelles due to traffic density. – Master Thesis, Kastamonu University, Graduate School of Natural and Applied Sciences Department of Sustainable Agriculture and Natural Plant Resources, Kastamonu, Turkey.
- [33] Ozel, H. B., Ozel, H. U., Varol, T. (2015): Using leaves of oriental plane (*Platanus orientalis* L.) to determine the effects of heavy metal pollution caused by vehicles. – *Pol. J. Environ. Stud.* 24(6): 2569.
- [34] Ozturk, S., Bozdogan, E. (2015): The contribution of urban road trees on improving the air quality in an urban area. – *Fresenius Environmental Bulletin* 24(5): 1-9.
- [35] Qing, X., Yutong, Z., Shenggao, L. (2015): Assessment of heavy metal pollution and human health risk in urban soils of steel industrial city (Anshan), Liaoning, Northeast China. – *Ecotoxicology and Environmental Safety* 120: 377-385.
- [36] Pinar, B. (2019): The variation of heavy metal accumulation in some landscape plants due to traffic density. – Master Thesis, Kastamonu University, Graduate School of Natural and Applied Sciences Department of Sustainable Agriculture and Natural Plant Resources, Kastamonu, Turkey.
- [37] Sawidis, T., Breuste, J., Mitrovic, M., Pavlovic, P., Tsigaridas, K. (2011): Trees as bioindicator of heavy metal pollution in three European cities. – *Environmental Pollution* 159: 3560-3570.
- [38] Saleh, E. A. A. (2018): Determination of heavy metal accumulation in some landscape plants. – Ph.D. Thesis, Kastamonu University Institute of Science Department of Forest Engineering, Kastamonu, Turkey.
- [39] Sevik, H., Ozel, H. B., Cetin, M., Özel, H. U., Erdem, T. (2018): Determination of changes in heavy metal accumulation depending on plant species, plant organism, and traffic density in some landscape plants. – *Air Quality, Atmosphere & Health*. <https://doi.org/10.1007/s11869-018-0641-x>.
- [40] Suzuki, K., Yabuki, T., Ono, Y. (2009): Roadside *Rhododendron pulchrum* leaves as bioindicators of heavy metal pollution in traffic areas of Okayama. – *Japan, Environ Monit Assess* 149: 133-141.
- [41] Tam, N. F. Y., Liu, W. K., Wang, M. H., Wong, Y. S. (1987): Heavy metal pollution in roadside, urban parks and gardens in Hong Kong. – *Sci. Toplam Environ.* 59: 325-328.
- [42] Tanushree, B., Chakraborty, S., Bhumik, F., Piyal, B. (2011): Heavy metal concentrations in street and leaf deposited dust in Anand City, India. – *Research Journal of Chemical Sciences* 1(5): 61-66.
- [43] Turkyilmaz, A., Sevik, H., Isinkaralar K, Cetin M (2018a) Use of tree rings as a bioindicator to observe atmospheric heavy metal deposition. – *Environmental Science and Pollution Research*. DOI: 10.1007/s11356-018-3962-2.
- [44] Turkyilmaz, A., Sevik, H., Cetin, M. (2018b): The use of perennial needles as bio-monitors for recently accumulated heavy metals. – *Landsc Ecol Eng* 14(1): 115-120. <https://doi.org/10.1007/s11355-017-0335-9>.
- [45] Turkyilmaz, A., Sevik, H., Cetin, M. Saleh, EAA. (2018c): Changing of heavy metal accumulation dependent on traffic density in some landscape plants. – *Polish Journal of Environmental Studies* 27(5): 2277-2284.

- [46] Turkyilmaz, A., Cetin, M., Sevik, H., Isinkaralar, K., Saleh, E. A. A. (2018d): Variation of heavy metal accumulation in certain landscaping plants due to traffic density. – Environment, Development and Sustainability. DOI: <https://doi.org/10.1007/s10668-018-0296-7>.
- [47] Turkyilmaz, A., Sevik, H., Isinkaralar, K., Cetin, M. (2018e): Using Acer platanoides annual rings to monitor the amount of heavy metals accumulated in air. – Environ Monit Assess 190: 578. <https://doi.org/10.1007/s10661-018-6956-0>.

SPATIOTEMPORAL ASSESSMENT AND VALUATION OF PROVISIONING ECOSYSTEM SERVICES OF PAKISTAN

SHEDAYI, A. A.^{1,2,3} – XU, M.^{1,4*} – GONALEZ-REDIN, J.⁵ – HAGIST, S. C. N.⁶ – ASLAM, S.⁷ –
KHAN, N.⁸

¹*Key Laboratory of Ecosystem Network Observation and Modelling, Institute of Geographic Sciences and Natural Resources Research, Chinese Academy of Sciences
Beijing 100101, China*

²*University of Chinese Academy of Sciences, Beijing 100049, China
(arshadbio@kiu.edu.pk)*

³*Department of Biological Sciences, Karakoram International University
Gilgit 15100, Pakistan*

⁴*Department of Ecology, Evolution, and Natural Resources, Grant F. Walton Center for Remote Sensing & Spatial Analysis, School of Environmental and Biological Sciences
Rutgers University 14 College Farm Road New Brunswick, NJ 08901-8551, USA*

⁵*The James Hutton Institute Craigiebuckler, Aberdeen, AB15 8QH Scotland, UK*

⁶*Freeman Spogli Institute for International Studies, Stanford University
Stanford, CA 94305-6055, USA*

⁷*MOE Key Laboratory for Biodiversity Science and Ecological Engineering
College of Life Sciences, Beijing Normal University, Beijing, China*

⁸*Department of Botany, University of Malakand, Lower Dir, Khyber Pakhtunkhwa 18800,
Pakistan*

**Corresponding author*

e-mail: mingxu@crssa.rutgers.edu

(Received 7th Feb 2019; accepted 10th Apr 2019)

Abstract. Developing countries are often beset by poverty and hunger. While provisioning ecosystem services (Prov.ES) are essential for eradication of these issues, they are being rapidly depleted due to climate change and anthropogenic impacts. However, their depletion has not been accounted for in sustainable use policy. Taking Pakistan as a case study, this research focuses on assessing and evaluating the dynamics of Prov.ES. It evaluates the contribution of Prov.ES to poverty reduction using key indicators over different spatiotemporal scales. Among provisioning services, livestock's contribution was the highest, followed by agricultural products, while fisheries and forests contributed the least. Prov.ES were shown to be important to Pakistan's economy. Product analysis revealed that livestock was the most contributing service (53%), followed by agriculture (44%), while fisheries and forests contributed to a smaller extent ($\leq 2\%$). Livestock products, major crops, marine fish products, and medicinal plants are the main contributors in those respective fields. Our results showed a net present value of 569 US\$/ha/year, which is very close to the median value of the 16 previous studies analyzed. Incorporating natural resource conservation into sustainable development policies, with a focus on the impacts of climate change and the increasing human population, is essential.

Keywords: *conservation, food security, human well-being, poverty reduction, valuation*

Introduction

Poverty, hunger, and food, water and energy security are key issues in the contemporary developing world (Hanjra and Qureshi, 2010). In 2013, 10.7% of the world's population was estimated to live on less than US\$1.90 a day (World Bank, 2016). The increasing human population and the resulting degradation of natural resources and climate change are the main causes of drought and poverty (Kraus, 2016). The effects of climate change on ecosystem service processes and flows are apparent (Wood et al., 2018), particularly in the developing world (Lam et al., 2016). The impacts of climate change need to be considered in policymaking for sustainable natural resource use and development (Halsnæs et al., 2014). People in developing countries rely on the provisioning ecosystem services (Prov.ES) for their livelihoods (Khan, 2012), for example, food, water, wood, and NTFPs (non-timber forest products) (MEA, 2005a).

ES functions and drivers are interlinked (Butler, 2006). The sources of Prov.ES, such as crops, livestock, fishery, and forestry, are influenced by other ES and processes (TEEB, 2010a). Food security and hunger have become serious issues in developing countries owing to exponential population growth (Rosegrant et al., 2014), resulting in malnutrition, especially among women and children (MEA, 2005b). The demand for food and food prices will increase as a result of population growth, climate change, and income growth (Rosegrant et al., 2014). Therefore, it is important to protect natural resources and increase production in all sectors linked to human livelihoods. Currently, agroecosystems cover about 40% of the terrestrial landform and provide humans with various Prov.ES, such as food, forage, bioenergy, and pharmaceuticals (Power, 2010). Furthermore, agroecosystems also support other types of regulating, supporting, and cultural ES, such as pest control, soil retention, nutrient cycling, flood control, water quality, carbon storage, climate and disease regulation, beauty, education, recreation, and tourism (Power, 2010). Livestock is widely recognized and valued as a source of food, income, employment, nutrients, and risk insurance. It directly supports 600 million poor smallholders in developing countries, contributing 17% of kilocalorie and 33% of protein consumption globally (Théwis, 2012). Both cropping and livestock husbandry offer many opportunities for sustainability by raising productivity and increasing resource use efficiency (Herrero et al., 2010). Forests provide different ES, including timber, fuelwood, medicines, and other NTFPs (Hlaing et al., 2017), and are home to 1.6 billion people around the globe (IUCN, 2012). Land clearing and deforestation cause floods, local climate change, and contamination of water (Tariq, 2015). The global fisheries sector supports 10–12% of the world population but climate change is predicted to reduce fisheries production by 35% by 2050 (Lam et al., 2016).

Many people in Pakistan depend on agriculture, it contributed 20.9% to GDP in 2014–2015 and 26.0% in 1997–1998 (Chandio et al., 2016). More than 43.5% of the rural population are engaged in this sector (Ahmed and Javed, 2018). Livestock, forestry, and fisheries account for 56.3%, 2.0%, and 2.1% (Chandio et al., 2015) of the agricultural industry, respectively. More than 8.0 million rural families are engaged in raising livestock, which plays an important role in poverty reduction improving socioeconomic conditions (Chandio et al., 2015). Pakistan has 4.8% forest cover area, but 60% of urban and 90% of the rural population depend on fuelwood as their primary source of energy (FAO_UN, 2010). Both inland and marine fish in Pakistan are a source of food (Nazir et al., 2015). Fisheries are important in the economies of developing countries. Pakistan's total coastline covers an area of approximately 300,270 km², where the fisheries and

fishing industry are source of employment, income, and food, as well as a substantial amount of foreign exchange via exports (FAO-UN, 2016a).

The monetary value of ES has recently gained attention (Lienhoop et al., 2015). Market price-based valuation of ES is considered a valid method of estimating the contribution of Prov.ES to human wellbeing, especially in poverty reduction (Daw et al., 2016). In this work, a market price-based approach is used to assess and value the products of Prov.ES. Discounting on the net present value (NPV) of ES is used to explore the future values of ES regarding their sustainable use, policy framework, and intergenerational benefits (Sterner and Kyriakopoulou, 2012). The selection of discount rates depends on the type of ES and future impacts affecting their delivery and flow, such as climate change. Previous studies on ES discount rates reported mean values of 1–12% (Dutton et al., 2015). Most researchers suggest low discount rates since we cannot assume that there will be an abundance of natural resources available in the future (TEEB, 2010b).

Despite their importance, natural resources are being depleted by anthropogenic and climate change impacts; some studies have been undertaken, but still, there is a gap in linking ecosystem services with poverty reduction and informing policymakers for sustainable development through conservation and management. Based on the current level of natural resource degradation in Pakistan, the aims of this research were to: (i) conduct a spatiotemporal assessment and valuation of Prov.ES in Pakistan, (ii) assess the role of the major indicators in poverty reduction and livelihood, (iii) determine the status of the national ES versus other countries; and (iv) assess NPV based on different time horizons and discount rates. The findings of this study will be useful for informing policymaking bodies.

Materials and Methods

Study Area

Pakistan (803,940 km²) is a predominantly mountainous and desertous country located at 23°37' North and 61°76' east in South Asia at the junction of Central Asia and the Middle East. The highest point is the mountain K2 (8,616.3 m), in the north, and the lowest point is the Arabian Sea (0 m). The 2017 population was 207,774,520, with a growth rate of 2.40%. Pakistan has four provinces (Punjab, Sindh, Khyber Pakhtunkhwa, and Baluchistan) and administers Azad Jammu and Kashmir (AJK) and Gilgit-Baltistan (unofficial province) (*Figure 1*). Pakistan can be divided into five major topographic areas, including mountains, deserts, plateaus, salt ranges, and plains. Pakistan has four seasons, and the temperature varies both seasonally and regionally; the southern part has a hot and dry climate, while the northwest has a temperate climate and the northern part is arctic. Temperatures range from -22°C in winter in the north to 50°C in summer in the south. The precipitation is 1500–2000 mm and 100–200 mm across north and south Pakistan, respectively (Sarfaraz et al., 2014).

Agriculture is the backbone of Pakistan, contributing 21% to the GDP, 43.5% to the livelihood of rural communities, and 43.5% of employment opportunities (GoP, 2013). Livestock is an important sub-sector of agriculture, accounting for 56.3% of this sector and 11.8% of national GDP (Khan et al., 2015). The area covered by natural forests is small (4.2% of the total area), contributing only 2% to the agriculture sector and 0.44% to GDP (FAO_UN, 2010). Fisheries are a potential income generation source in Pakistan, but its growth rate in 2013–2014 was only 0.87% (Altaf et al., 2015). Pakistan has the potential to increase its supply of Prov.ES, which will not only help generate income but

also assist poor people because poverty is linked with the provision of natural resources (Irfan, 2007).

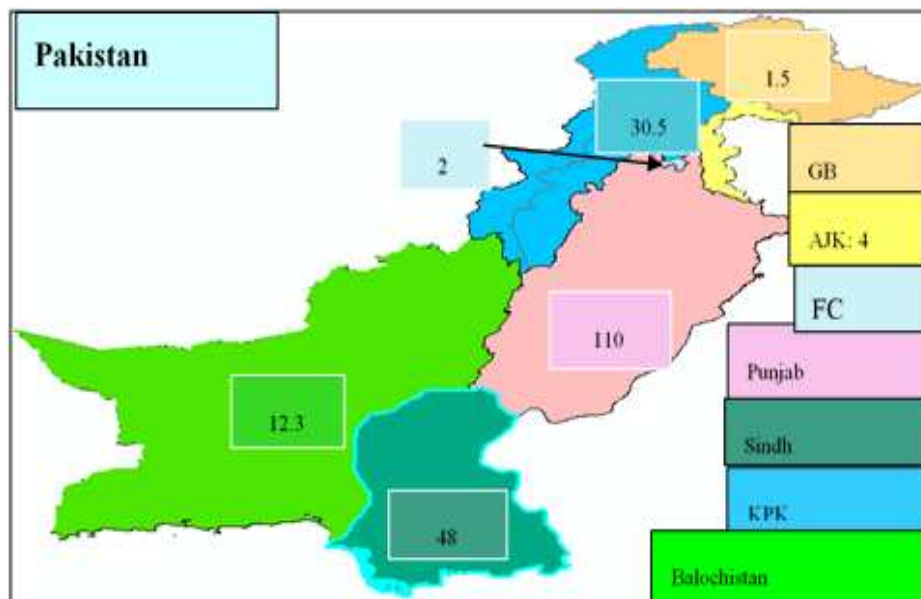


Figure 1. Map of Pakistan showing the administrative units and population in millions from the 2017 census (Abbreviations: GB (Gilgit-Baltistan), AJK (Azad Jammu & Kashmir, FC (Federal capital), KPK (Khyber Pukhtunkhwa)

Methods

Data for crops, livestock, and forestry were obtained from the respective government departments and the Pakistan Bureau of Statistics (PBS, 2015); relevant data for agriculture and forestry included area cover, quantity, and market prices. All data was obtained for the five-year period from 2011 to 2015, except for forestry data which was only available for the years 2009 to 2013 and the distribution of livestock by province which was based on 2011 and 2012 (PBS, 2017). The required data was extracted and analyzed for evaluation purpose.

The number of livestock, quantity produced, and market price were considered for livestock, and quantity and market price for fisheries. The market price method was used for direct use values for provisioning products, as in previous studies (Grădinaru, 2013; Siwar et al., 2016). Crops were classified as food crops, cash crops, pulses, and edible oilseeds, and were valued based on major and minor food crops. Major food crops included wheat, maize, rice, sugarcane, cotton, and their byproducts, while minor food crops included vegetables, fruits, condiments, oilseeds, and green fodder. Livestock was divided into major livestock and poultry. Forestry was divided into two main types: major forestry products such as timber and fuelwood and NTFPs; NTFPs is used throughout this research for all products except timber, fuelwood, wildlife, and bushmeat. The estimated value of each Prov.ES product was based on both spatial (by province, marine and inland) and temporal scales for 2011 to 2015 (Table 1). ANOVA was also used to describe the significance of variables for the ecosystem assets such as crop, livestock, forestry and fisheries.

Table 1. Provisioning ecosystem services assessed in this study

*ESS asset	Sub-type	*Prov.ES type	Value	Method	Time period
Crops	Major and minor crops, fruits, vegetables	Food, trade	Use value	Market price	2011–2015
Livestock	Goats, sheep, cattle, poultry	Food, decoration, trade, manure	Use value	Market price	2011–2015
Forestry	Timber, fuelwood, *NTFPs	Construction, heating, medicine, food, agriculture, tools	Use value	Market price	2011–2015
Fisheries	Marine and freshwater	Food, trade	Use value	Market price	2011–2015

*ESS: ecosystem service, *Prov.ES: provisioning ecosystem service, *NTFPs: non timber forest products

The annual average of the five-year data was calculated to get the gross total value. The NPV, also known as net total value (NTV), for all the environmental assets was calculated using *Equation (1)*.

$$NPV = TGV - IC \quad (\text{Eq.1})$$

where TGV = total gross value total value and IC = input cost. The ICs vary by environmental asset in agriculture and include seeds, fertilizers, water, electricity, tube wells, mechanization, and labor.

Discount rates of 0.74%, 6%, and 11.26% were applied to the NPV for time horizons of 35 (2050), 85 (2080), and 105 (2120) years to predict future NPV values using *Equation (2)*. A regression model with a 95% confidence interval was used to find the demand curve trend between the quantities and the values.

In Pakistan, the average interest/discount rate for 1992–2017 was 11.26% and the current (2016, 2017) discount rate is 6%. A discount rate of 0.74% was chosen as most scholars recommend a low discount rate to enhance intergenerational benefits. The future NPV was calculated using *Equation (2)* (Griffin, 2006).

$$NPV = \sum_{t=0}^T \frac{NB_t}{(1+r)^t} = C_0 + \frac{NB_{t1}}{(1+r)^t} + \frac{NB_{t2}}{(1+r)^t} + \frac{NB_{t3}}{(1+r)^t} + \quad (\text{Eq.2})$$

where t = time period (years); T = planning horizon; NB_t = net benefits in period t; and r = discount rate.

The mean, median, standard error, standard deviation, and other statistical parameters were calculated for the NTV (NPV) and the NPV for 35 (2050), 70 (2080), and 100 (2020) year time horizons.

Our NPV was also compared with those from 16 previous similar studies performed worldwide. The studies were identified by searching for the keywords provisioning ecosystem service, valuation ecosystem service, and valuation of natural resources in the EVRI, Science Direct, and PubMed databases. After screening these articles/reports, based on the keywords, 16 were selected for comparison. Many of the studies did not report the total or unit value, so we calculated the values from these articles and converted all results to USD per hectare, which enabled comparison by mean, median, sum, standard deviation (SD), and maximum and minimum values.

Results

Crops

The total area dedicated to crops in Pakistan is 17,769,000 ha, of which Punjab accounts for the greatest portion and Baluchistan the smallest. Cereals make up the greatest area, followed by fodder, whereas pulses, vegetables, and fruits are grown on merely 13% of the total area. During the period 2011–2015, an annual average of 19,392,000 ha was cultivated, with food crops making up the largest area followed by cash crops, whereas pulses and edible oilseeds covered only a small area. The mean was 16% over the five-year period (*Appendix A*). On average, 92,638,000 tons of agriculture commodities were produced annual over the five-year period (2011-2015), of which fodder production was the highest followed by cereals. The average cultivated crop production was 114,353,000 tons, among which food and cash crops contributed the most. In the study period, the lowest and highest production rates were in 2013 and 2014, respectively. Overall, production was highest in Punjab and lowest in Baluchistan (*Figure 2*). The production of crops at spatial scale were found non-significantly different in the provinces in and ANOVA test with F value 2.7766 and P value 0.0751 (at $P > 0.05$), while the production of crop commodities found a significantly different from each other with F value of 523.710 and P value 3.55E-16.

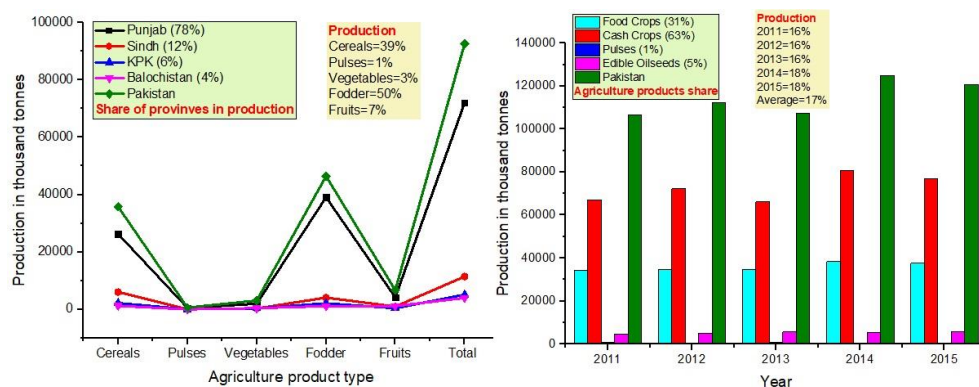


Figure 2. Agricultural production by province for 2011–2015 (KPK: Khyber Pukhtunkhwa)

The five-year average TGV, IC, and NPV for major crops and byproducts were 2,454,808, 552,581, and 1,902,227 million PKR, respectively. Wheat had the highest average NPV followed by cotton, while maize was the lowest. Crops had a higher NPV value (86%) than the byproducts (14%). The mean NPVs for the major crops and byproducts for 2011–2015 showed a statistically non-significant difference (p -value = 0.97825). The TGV, IC, and NPV values for minor crops and other agriculture products were found to be 950,199, 121,156 and 829,043 million PKR, respectively, with fruits the highest and pulses the lowest value. The NPV for the given period was found to be highest in 2015 and lowest in 2012, with an overall non-significant difference (p -value = 0.98144) in means (*Figure 3*). The NPV of the byproducts was 341,295 million PKR in which major crops contributed the more (85%) as compared to the minor crops (15%), over all wheat contributes the highest (55%).

The NPV for crops products consists of the value of the major crops, minor crops and byproducts was estimated to be 2,731,270 million PKR, of which the major crops (62%) and minor crops (28%) contributed more than the byproducts (10%) (*Figure 4*).

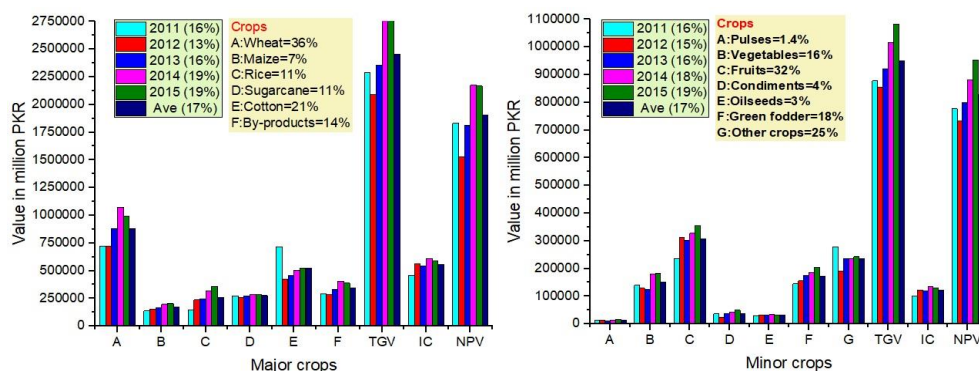


Figure 3. Agriculture product type and value for 2011–2015. TC = total cost, BPs = byproducts, TGV = total gross value, IC = input cost, NPV = net total value

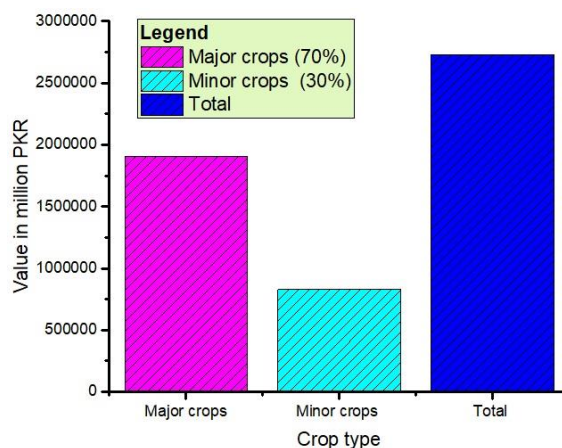


Figure 4. Total value of agriculture products 2011-2015

Livestock

The total livestock population was 219,147,000 in 2006, with the highest proportion in Punjab followed by KPK and Sindh. Excluding poultry, goats contributed the most (38%) followed by cattle, buffalo, and sheep. An increasing trend was observed in the number of livestock from 2011 to 2015 (*Figure 5*), but it was not significant with F value 0.0167 and p-value = 0.99904. From the five-year average total milk production, buffalo produced the most followed by cows. The total milk production for the study period tended to increase, although no significant difference (F-value 0.0064, p-value = 0.9991) was found. The five-year average meat production was 3,387,000 tonnes, with beef contributing the most followed by poultry and mutton, and an increasing trend was observed (*Figure 6*) It also showed a non-significantly different value (F-0.0484, p-value 0.9957).

Hide and skin production totaled 65,128,000 with goat the highest, followed by fancy and sheep. Egg, gut, and casings production totaled 80,384,000, of which guts contributed the most and eggs the least (*Appendix B*). Production of skin and hide from different animals showed significantly different values (F-value 1220.864, p-value 4.69E-28). There were 3,228,000 tonnes of other products, with dung, bones, offal, and urine being

the main contributions (81%) (Appendix C). These products had also significantly different (F-Value 1012.288, p-value 2.84E-44) production for the 5 years' period.

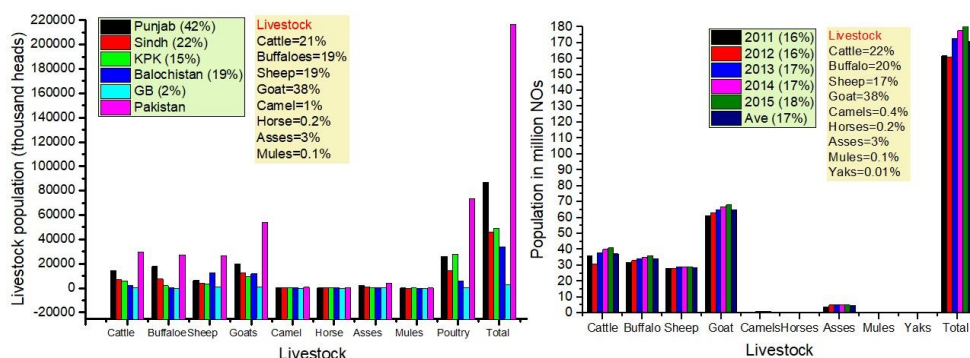


Figure 5. Livestock type and population

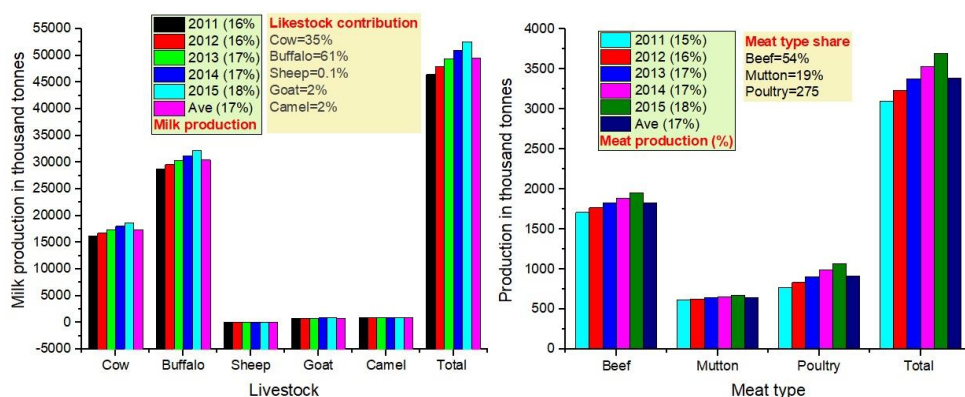


Figure 6. Milk and meat type and production for 2011–2015

The five-year average value of livestock was 3,242,691 million PKR, of which livestock products were highest and natural growth and regeneration were lowest. Among the products, the value of milk was the highest while wool and hair contributed the least. The analysis showed an increasing but not significant trend (p-value = 0.99343) (Figure 7).

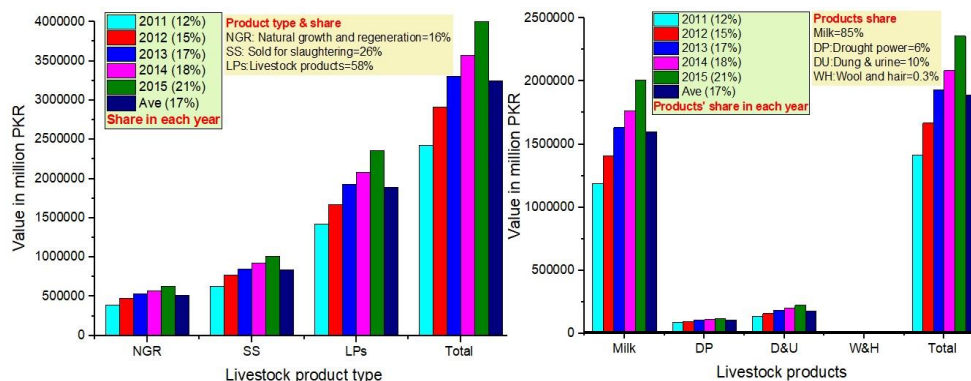


Figure 7. Livestock product type and value for 2011–2015

Similarly, the average value of poultry products was 288,559 million PKR. Farmed chickens contributed the most followed by eggs. The TGV, IC, and NPV were 3,545,051, 634,885 and 2,910,166 million PKR, respectively. Livestock products contributed the most followed by animals sold and slaughtered while poultry products contributed only 8%. Sub-categories showed a generally increasing, but not significant (p -value = 0.945072), trend (Figure 8).

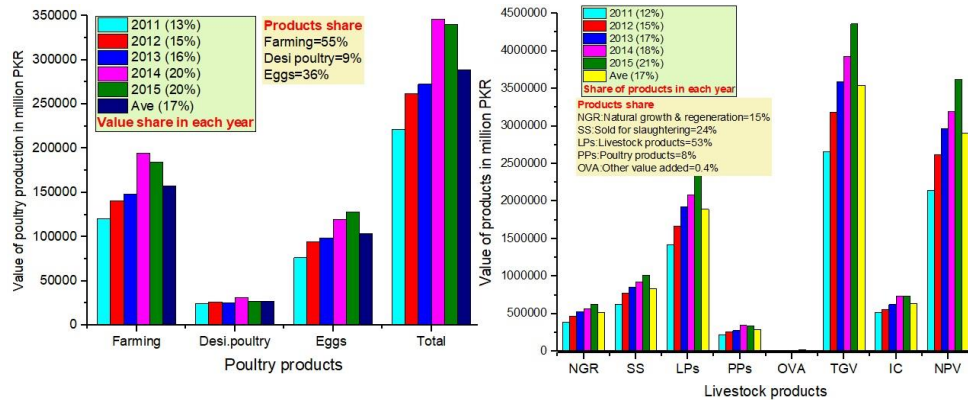


Figure 8. Value of poultry and overall livestock products for 2011–2015

Forestry

The total forest cover area in Pakistan is 11,032 thousand hectares, of which 60% and 40% is protected and unprotected, respectively. Punjab and Gilgit-Baltistan have the highest forest coverage (Appendix D, Fig. 4). The five-year average major forestry products were estimated to be 462 thousand cubic meters, and there was an increasing trend from 2009 to 2013. Firewood production was higher than timber production. These products had non significantly different values (F-value 2.3566, p -value 0.1632). There were estimated to be 147,478 tonnes of NTFPs, while others were produced in very low quantities. Production levels remained consistent over the study period (Figure 9). The five-year mean TGV of the NTFPs was 12,184 million PKR. The NPV was 10,472 million PKR, with medicinal plants contributing the most and vegetables the least. There was an increasing trend in the value of NTFPs from 2011 to 2015 (Figure 10).

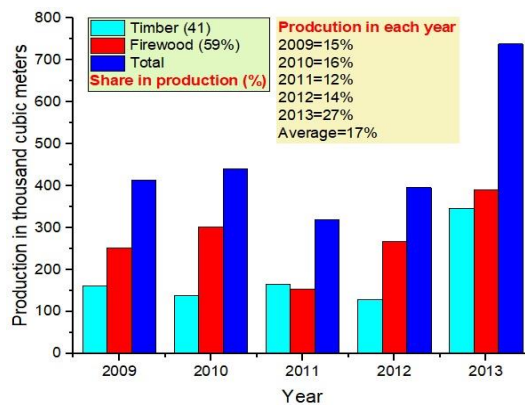


Figure 9. Major forest products for 2011–2015

The five-year mean TGV and NPV of major forest products was estimated to be 1,757 and 1,732 million PKR respectively, in which timber contributed the most as compared to the firewood. An increasing trend in the value of the major forest products was observed from 2011 to 2015; that is, the highest value was in 2015 and the lowest was in 2011 (*Figure 11*). Overall, the NPV of forests was found to be 12,204 million PKR. In which NTFPs products contributed the most, while timber and fuelwood contributed the least. An increasing trend in the value of forestry products was observed from 2011 to 2015 (*Figure 11*).

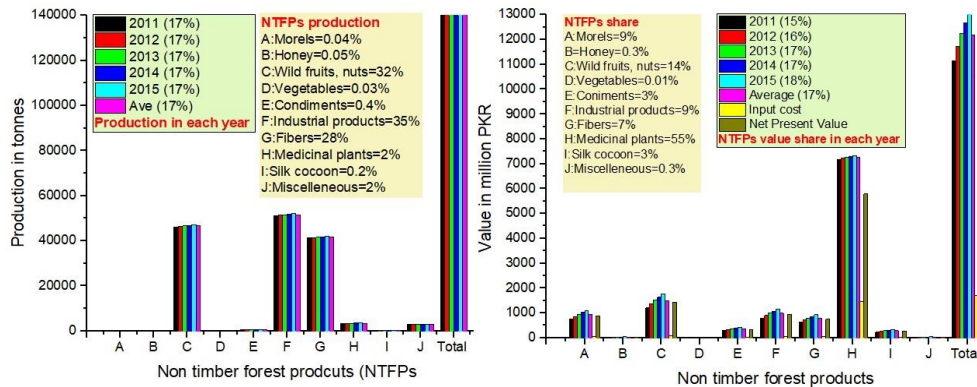


Figure 10. Minor/Non-timber forest product types and values for 2011–2015

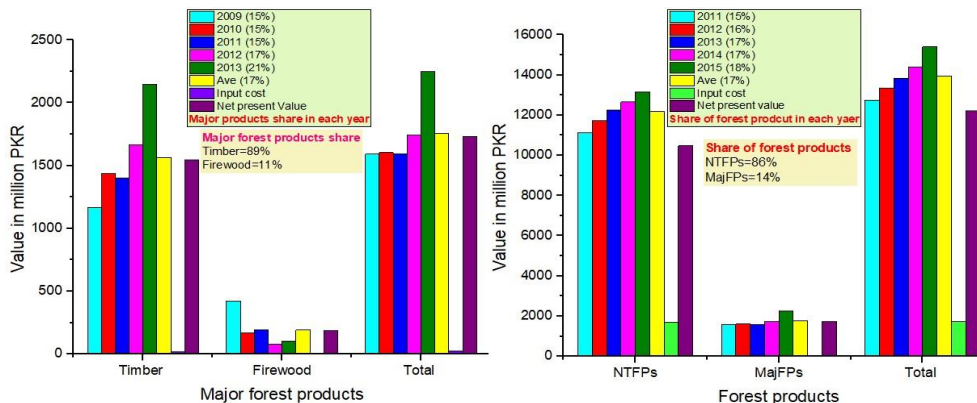


Figure 11. Value of the major forest products (MajFPs) and net total value of forest products (NTFPs: non timber forest products)

Fisheries

In Pakistan, the five-year mean total freshwater fish production was 238 thousand tonnes. There was an increasing trend from 2011 to 2015, freshwater fish production was highest in Sindh followed by Punjab, while there was no inland fish production in the Baluchistan province (*Figure 12*). The average annual marine fish production for the five-year period was 492 thousand tonnes, and again an increasing trend for fish production was found from 2011 to 2015. Sindh and Baluchistan were the only marine fish-producing provinces, accounting for 70% and 30% of production, respectively (*Figure 12*). The average total fish production in Pakistan was 730 thousand

tonnes per year with an increasing trend from 2011 to 2015. There was an average 67% and 33% of fish production per year from marine and freshwater respectively. Province-wise, fish production was highest in Sindh (66%) followed by Baluchistan (20%), while KPK contributed the least (1%) (Figure 13). The spatial distribution of the total fish production was significantly different among the provinces with F-value 17136.97 and P-value 2.93E-28, while the temporal distribution of the fish production was not different for the period 2010-2015 with F-value 0.000614 and p-value 0.9999.

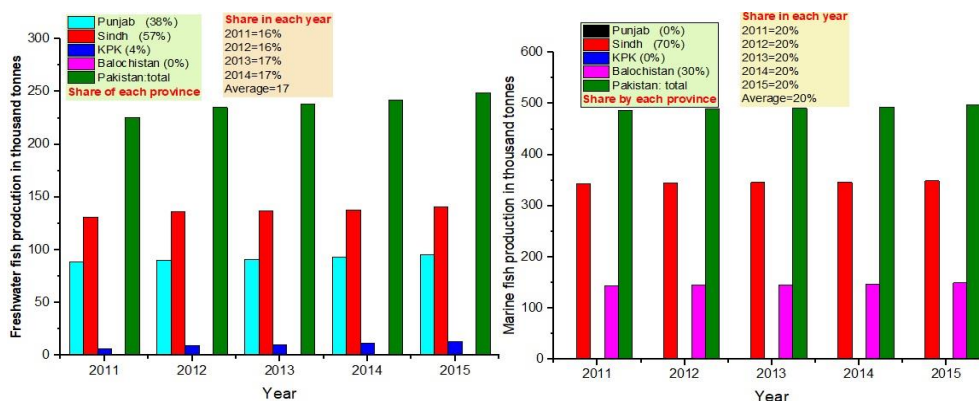


Figure 12. Freshwater and marine fish production by province for 2011–2015 (KPK: Khyber Pukhtunkhwa)

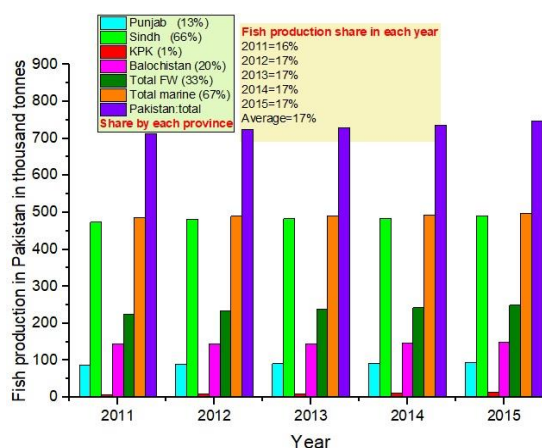


Figure 13. Total fish production by province for 2011–2015 (KPK: Khyber Pukhtunkhwa, FW: freshwater)

The five-year average TGV for freshwater fish was 51,755 million PKR, while the NPV was 41,404 million PKR. During the study period, the proportion of the freshwater value ranged from 12% to 21%, with the highest in 2015 and the lowest in 2011. Sindh contributed the most followed by Punjab (Figure 14). The average TGV of marine fish for the five-year period was 106,603 million PKR (17%) and the NPV was 85,283 million PKR. The marine fish value was highest in 2015 (20%) and lowest in 2013 (13%). The average NPV for marine fish in Punjab and KPK was zero, while Sindh contributed the most (70%) followed by Baluchistan (30%) (Figure 14).

The five-year average TGV of fish production in Pakistan was found to be 158358 million PKR and the NPV was 126686 million PKR. The total market value of fish showed an increasing trend from 2011 to 2015. As a whole, marine fish value contributed higher (67%) than the freshwater fish value (33%). By province, Sindh contributed the most (66%) followed by Punjab (13%), while KPK contributed the least (1%) (Figure 15).

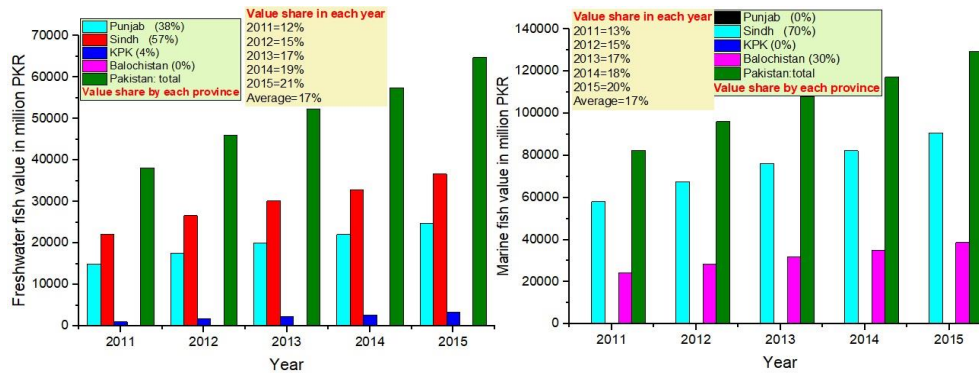


Figure 14. Value of freshwater and marine fish by province for 2011–2015 (KPK: Khyber Pukhtunkhwa)

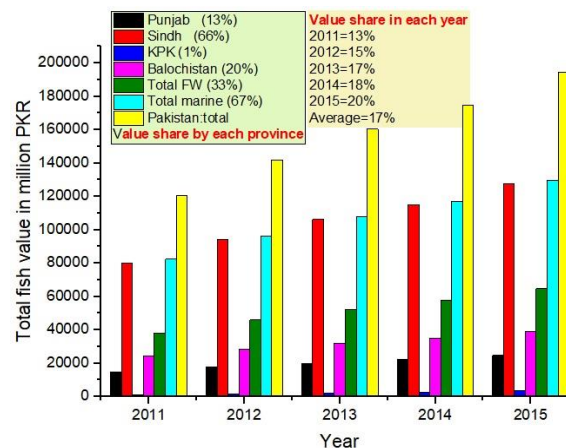


Figure 15. Total fish value by province for 2011–2015 (KPK: Khyber Pukhtunkhwa, FW: freshwater)

NPV and discounting for Provisioning Ecosystem Services

The mean NPV of provisioning services was estimated to be 5,471,304 million PKR for the period 2011-2015. The NPV for crop, livestock, forest, and fisheries was 2,390,715 (44%), 2,910,166 (53%), 35,105 (1%) and 135,318 (2%), million PKR respectively (Figure 16). Discounting rates of 0.74%, 6%, and 11.26% were applied to the NPVs for time horizons of 35, 70 and 105 years. The results clearly show that NPVs decreased with increasing discount rate and increasing time horizon as was expected. Results also shown for mean, SD, minimum and maximum values (Table 2).

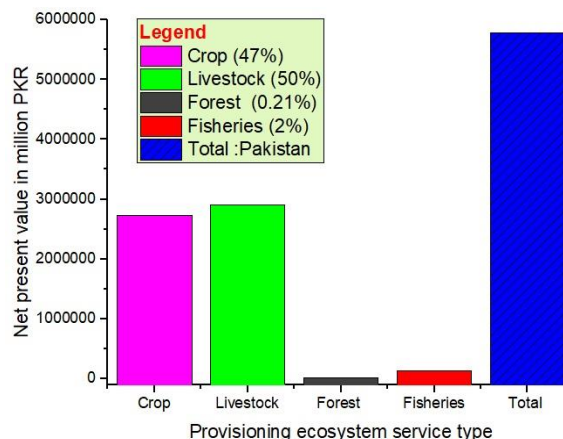


Figure 16. Total value of provisioning ecosystem services

Table 2. Discount rates for different time horizons (value in PKR)

ESS asset	Current	35 years (2050)			70 years (2085)			105 years (2120)		
		Type	*NPV	0.74%	6%	11.26%	0.74%	6%	11.26%	0.74%
Agriculture	2390715	1846969	311044	57103	1426893	40469	1364	1102360	5265	33
Livestock	2910166	2248276	378628	69511	1736927	49261	1660	1341879	6409	40
Forest	35105	27121	4567	838	20952	594	20	16187	77	0.5
Fisheries	135318	104541	17606	3232	80764	2291	77	62395	298	2
Statistics										
Sum	5471304	4226907	711845	130684	3265537	92615	3121	2522821	12050	74.56
Mean	1367826	1056727	177961	32671	816384	23154	780	630705	3012	18.64
Standard error	748350	578145	97364	17875	446651	12668	427	345065	1648	10.20
Median	1263017	975755	164325	30168	753829	21380	721	582378	2782	17.21
*SD	1496700	1156290	194729	35749	893303	25335	854	690129	3296	20.40
Minimum	35105	27121	4567	838	20952	594	20	16187	77	0.48
Maximum	2910166	2248276	378628	69511	1736927	49261	1660	1341879	6409	39.66
Conf. level (95%)	2381584	1839915	309857	56885	1421444	40314	1359	1098150	5245	32.45

*NPV: Net present value, *SD: Standard deviation

Comparison with Other Studies

The Prov.ES values obtained in this work were compared with the results from 16 previous studies from around the world. The previous studies showed a sum of 96,985 USD/ha/y, mean 6062, SD 13731, median 666, minimum 7, and maximum 53736 USD/ha/y. While our results showed a value of 569 USD/ha/y, which is very close to the median value of the previous studies (Figure 17). Our results were consistent with many of the previous studies (Jenerette et al., 2005; Huxham et al., 2008; Paletto et al., 2008; Häyhä et al., 2015), although some of them presented very high values, ranging from 2,142 to 53,736 USD/ha/y (Chiabai et al., 2008; Wang et al., 2008; Martín-López et al., 2008; Chang et al., 2008; Molnar et al., 2008; Li et al., 2008), while others presented much lower values compared to our results (Fang et al., 2009; Voora and Barg, 2008; Hussain et al., 2008; de Groot et al., 2008; Dupras et al., 2008; Valatin and Starling, 2008).

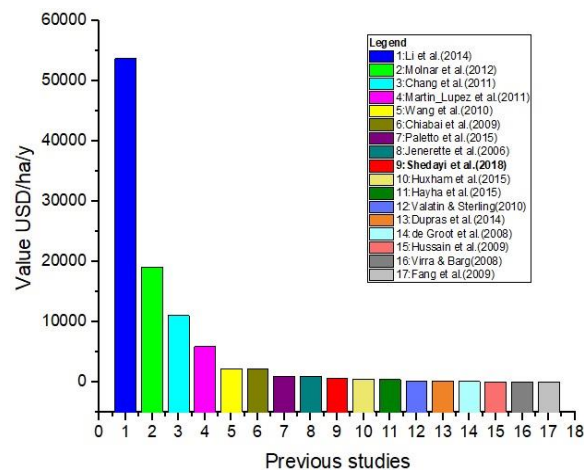


Figure 17. Comparison with previous studies

Discussion

Crops

Agriculture is a dominant land management technique globally, and agricultural ecosystems cover nearly 40% of the terrestrial surface on Earth (FAO, 2015a). In our case study, the products of agricultural ES were evaluated using standard market analysis. Valuing the Prov.ES that are derived from agriculture was relatively straightforward since agricultural commodities are traded in local, regional, or global markets (Power, 2010).

Agriculture is the backbone of Pakistan's economy, contributing 21% to the national GDP, and 43.5% of the labor force is engaged in agriculture (Chandio et al., 2015). Furthermore, it plays a vital role in ensuring food security, generating economic growth, reducing poverty, and the transformation towards industrialization. The major crops cultivated in Pakistan are wheat, rice, cotton, and sugarcane, which attribute for 29% of overall agriculture, while minor crops, e.g. oilseeds, potato and pulses, contribute 6% of GDP (PBS, 2015).

Owing to the demand from the increasing human and livestock populations, fodder is grown in large parts of the country, followed by cereal crops. These provide the basic requirements of humans and livestock. Cereal production requires a lot of resources and labor while fodder crops can be grown with little effort as compared to the food crops. Secondly, the demand for food of livestock is high, which is why in Pakistan fodder crops had the highest production followed by cereals, while the production of fruits, vegetables, and pulses is relatively low. Punjab had the highest production of crops, followed by Sindh, KPK, and Baluchistan, mainly because Punjab covers a larger area than the other provinces. Cash crops showed the highest production, followed by food crops, while edible oil seeds and pulses were produced at low levels because people prefer to grow crops that are more profitable. Statistically a non-significant increasing trend of agriculture production was observed from 2011 to 2015 because people have realized that they need to produce more to meet the demand from the increasing population.

Overall, in the agriculture sector, major crops contributed the most to NPV, followed by minor crops. There was a non-significantly increasing trend for both the major crop and overall NPV of agriculture products. This is because of the higher demand for the

major crops as compared to the minor crops, and secondly, in most parts of the country, the climatic conditions are more suitable for the major crops than the minor crops.

The agriculture sector showed positive growth of 2.9% in 2015 compared to the previous years (2013 and 2014) (GoP, 2014). This is because of the improvement in the agricultural practices in Pakistan. The production of the agriculture commodities found significantly different from each other. In the agriculture sector, wheat was found to contribute the most served in the income followed by cotton, while other crops such as rice, sugarcane, and maize contributed very little. This is because Pakistan has favorable climatic and soil conditions for wheat growth and secondly the demand for wheat consumption is much higher than that for other crops because wheat foods are popular among the Pakistani people owing to their nutritional value; wheat is served in all three daily meals. It is grown in all the provinces and across a wide range of altitudes. Pakistan ranks fourth and third worldwide among cotton-growing and -consuming countries (PBS, 2015) because the climatic and edaphic conditions in Pakistan are suitable for growing cotton. The other crops include bajra, jowar, gram, barley, rapeseed and mustard, and tobacco. Pulses include masoor, mong, chana, and mash. Besides these, potatoes, onions and chilies are also grown to meet the requirements of the country at the local level.

Agricultural crops are not only important for their value as food for human beings, but also as a source of food for livestock. In many developing countries, some crops, such as maize, wheat, sorghum, and millet, are dual purpose: their grain provides food for humans and their residues are used as feed for livestock. In mixed crop–livestock systems, the value of the crop residues is sometimes as much as that of the grain itself owing to the importance of the residue as a feed for livestock, particularly in the dry season. In mixed agriculture systems, there are always tradeoffs; for example, people obtain milk products from the buffaloes and cows while and at the same time achieving high grain production by manuring their fields using cow or buffalo wastes.

This has increased the demand for dual-purpose crops with relatively high-quality crop residues, and burgeoning fodder markets have developed around cities such as Hyderabad in India (Blummel and Rao, 2006). The cropping–livestock mixed farming system is considered to be more beneficial than a single system. Mixed agro-pastoral systems produce close to 50% of the world's cereals and most of the staples consumed by poor people (Herrero et al., 2010). Depending on their structure and management, agroecosystems also contribute a number of other globally important ecosystem services (MEA, 2005a), such as supporting biodiversity and enhancing carbon sequestration (Power, 2010).

Livestock

Livestock production makes a large contribution to the GDP of developing countries. It is an essential activity that contributes multiple services, such as fertility of land, maintenance of biodiversity, food security, and cultural and rural vitality (Ryschawy et al., 2017). Sustainable farming based on environmental conditions is essential for the livelihood of people in developing counties (Herrero et al., 2009). Livestock contributed 11.8% of the country's GDP and 56.3% of the agriculture sector share of GDP in Pakistan (PBS, 2015). In the livestock sector, the average number of animals was 285 million with a non-significantly increasing trend during the period 2011-2015, of which goat contributed the most followed by cattle, buffalo, and sheep. People prefer to keep goats because they are easily handled and provide manifold benefits compared to other livestock. Goats provide meat, milk, hair, and manure. Most people in Pakistan prefer

goat meat to fulfil their protein requirements that is also expensive in the market as compared to lamb and beef. People prefer to rear livestock that provide multiple benefits over livestock that provide only one benefit and are expensive to keep, such as asses, poultry, camels, horses, mules, and yaks. Punjab province has the highest population of livestock. Punjab is the most populated province so has more livestock. Milk production from buffaloes was highest followed by cows because these animals are large so produce more milk than smaller animals. In meat production, beef contributed the most followed by poultry and mutton owing to the size and number of animals. The production of livestock product was found non-significantly increasing from 2011-2015, while the production of skin, hide and other products from different animals was found significantly different. The average NPV for livestock was in a non-significantly increasing trend over the five years studied. Livestock-products contributed more to the NPV compared to animals slaughtered or kept live. Overall, milk was the dominant livestock product because people use milk on a daily basis and thus prefer to keep livestock that produce milk. Milk is used for various purposes, such as making tea, yogurt, lassy, and cheese, while meat is used less frequently, which is why milk makes a bigger contribution to NPV compared to the other products.

The economic benefits obtained from livestock are greater than those from the agricultural cropping system. Agro-pastoral and pastoral systems cover 45% of Earth's usable surface (Reid et al., 2008) and supply 24% of global meat production (Steinfeld et al., 2006). Projections show that in the next three decades 30% more grass will be required to meet the global demand for meat and milk and that improved management and use of fertilizers in parts of the world will be necessary to meet this increased demand (Herrero et al., 2009). Mixed agro-pastoral systems generate the bulk of livestock products in the developing world, that is, 75% of the milk and 60% of the meat, and employ many millions of people in farms, formal and informal markets, processing plants, and other parts of long value chains (Herrero et al., 2010).

Forestry

Forests play a significant role in any country's wellbeing and economy (Economics for the Environment, 2011). According to the FAO, the area coverage of the world's forests was 3,999 million ha in 2015, a decrease from 4,128 ha in 1990; forestry cover fell from 31.6% to 30.6% during this period. This change resulted from an increasing deforestation trend, especially in developing countries (FAO-UN, 2016b). Forest components, such as timber, fuelwood, and NTFPs, are important to the livelihood of people in developing countries (TEEB, 2009). In Pakistan, there are more protected forests than unprotected forests. Punjab and Gilgit-Baltistan have the biggest share of the total forest area followed by KPK. A non-significantly increasing trend in the production of major forest products was observed owing to increased plantation sizes in some parts, especially in KPK. Fuelwood production was greater than timber production. More NTFPs, including industrial products, wild fruits and nuts, and fibers, were produced than other NTFPs, such as medicinal plants, condiments, silk cocoons, honey, morels, and vegetables. In the NTV of forest products, NTFPs contribute the biggest share while other products, like timber and fuelwood, contributed very little to the NPV. There was an increasing trend of the NPV over the five-year period, because of the increased production and increasing market value each year. Timber made a higher contribution to the NPV than fuelwood because of its greater market value. Among the NTFPs, the medicinal

plants' share of the NPV was much higher than for the other products. In addition, forest departments earn a substantial amount of revenue from forests.

Most of the population of Pakistan lives in rural areas, depending on natural resources for their livelihoods. In addition, there are many industries that depend on forest products, such as timber, processed wood and paper, rubber, and fruits. Forests provide essential services for rural agricultural communities, such as fuel, fodder, game, fruits, building materials, medicines, and herbs. A large number of livestock in rural communities, as well as wildlife, also depend on the forest ecosystem for their survival. Forests are blessings that help humans in many ways both in good times and in times of difficulty (Mitchell et al., 2014).

NTFPs play a very important role in the livelihoods of the people in the study area. They are a source of income for poor rural population (Ingram and Bongers, 2009) and provide job opportunities and sources of livelihood to a large number of people (Pandey et al., 2016). In addition, NTFPs are also an important source of foreign exchange; morels, for example, are exported entirely by local grocers (Wahlén, 2017). Honey production from beekeeping is an important source of income as well as being nutritious and having medical applications. In Pakistan, around 15,000 people are involved in beekeeping. Good quality honey production can be increased by modern beekeeping techniques with the introduction of European bees. Other wild NTFPs, including wild fruits, nuts, vegetables, condiments, wild pomegranate seeds, and caraway, are produced in small quantities and consumed locally (FAO, 2015b).

Pakistan has a diverse environment and hosts a large variety of medicinal plants. These medicinal plants are used locally for the treatment of various diseases as well as being sold commercially. Pakistan is gifted with tremendous natural resources and plants have long been used to cure different human and animal diseases (Shedayi et al., 2014, 2016). Thanks to their life-saving properties, medicinal plants are the most expensive among the NTFPs, and they contribute the biggest share of income. Industrial products, such as resin, vegetable tanning, bhabar grass, Sabai grass, babul bark, dwarf palm leaves (Mazri), and silk cocoons, are collected and used in various large and small industries for the synthesis of a range of products (FAO, 1994).

Conservation of forests is important not only because they provide provisioning services to the locals but also for the sociocultural and regulating services they provide to a wide range of people. Developmental activities have both merits and demerits for forest ecosystems; for example, road construction provides easy access to tourists, but it destroys the forests and their natural systems.

Fisheries

According to the Food and Agriculture Organization of the United Nations, feeding more than 9.7 billion people by 2050 the context of climate change impacts, financial uncertainty, and growing competition for food owing to an exponential population growth trend, especially in developing countries, is one of the greatest challenges to face. The annual per capita fish consumption has grown from 5.2 kg in 1961 to 18.8 kg in 2013 in developing countries, while it has increased from 3.5 to 7.6 kg in low-income countries (FAO-UN, 2016a). Pakistan has an arid climate, but it has great potential for small-scale inland fish farming for local consumption as well for earning foreign exchange through exports (Nazir et al., 2016). The long coastline of 1,050 km in Pakistan provides the best opportunity for marine fishing in an area of approximately 300,270 sq. km. Pakistan's fishing grounds are highly rich in marine life with a vast variety of species having

commercial value, both for domestic consumption as well as for export. More than one million people depend on the fisheries profession, and they are mainly settled in villages along the coastline (Nazir et al., 2015).

Spatial distribution of fish production was found significantly different among the provinces, while there was a non-significantly increasing trend of fish production at temporal scale. The fisheries and fishing industry are growing in Pakistan, both inland and marine. Marine fish contributes more to the NPV compared to freshwater fish farming. Most fish production is found in the Sindh province, followed by Punjab and Baluchistan. There was an increasing trend over the five-year period of study with an average of 30% in this period because the demand for food increases with increasing population size. The population of Pakistan is increasing with an annual growth rate of 2.6% (Raza and Siddiqui, 2014). There are 760 fish species in total across fresh and marine waters, of which 200 species are economically important; approximately 71% of the fish production in Pakistan is exported (Nazir et al., 2015). Pakistan's contribution to world fish production is 0.30%, which is the lowest in the world market and can be improved by adopting modern techniques (FAO- Fisheries and Aquaculture Department, 2017).

The average annual catch was almost 600,000 tonnes (Nazir et al., 2015) of which most are exported, as noted earlier. Besides exporting fish products, fish is an important source of food for the people of Pakistan, especially those living in Sindh. Seafood is also exported to other provinces, such as from Karachi to Punjab and KPK.

The seafood export rate in Pakistan increased by 49.82 million USD in 2013–2014 as compared to 2012–2013 (Shah et al., 2018) an estimated increase of 12.25% in term of quantity (Nazir et al., 2015). Pakistan exports 60 million seafood products to China and Vietnam. Other markets for Pakistani seafood include Thailand, Saudi Arabia, Malaysia, Bangladesh, Egypt, Hong Kong, Japan, Kuwait, South Korea, and the UAE. (Nazir et al., 2015). Pakistan has a good market for fish products. Inland fish farming is increasing in many provinces to fulfil the demand for protein. The majority of marine fish production is exported to other countries for income generation, and production and export can be increased further by using the latest equipment and techniques.

Climate change and discounting

The world is facing impacts from climate change in the form of global warming, floods, rising sea levels, and drought. Poor people, who depend on natural resources for their livelihood, suffer the most from climate change. Climate change is predicted to have a severe impact on natural resources in the future. This will disturb the processes, functions, and services of ecosystems (Soudzilovskaia et al., 2013). It is important to include climate change impacts in policymaking frameworks (Hermwille et al., 2017). It is thus necessary to estimate the future values for ecosystem services based on current NPVs by employing discount rates on different time horizons. We, therefore, applied three different discount rates (0.74%, 6%, and 11.26%) on three time horizons (2050, 2085, and 2120). With the increasing discount rates and time horizons, the values decreased accordingly. These estimated NPVs for the different time horizons and discount rates will help policymaking bodies, conservation organizations, and researchers assess the impacts of climate change. Discounting is important for the sustainable use of natural resources and development (Gowdy et al., 2010).

Comparison with other studies

Our results were consistent with those of some previous studies, especially with those focused on food (meat and fisheries), wood (timber and fuelwood), and water for irrigation, similar to how we focused on food (agriculture, fisheries, and livestock), wood (timber and fuelwood), and medicinal plants. Those studies that showed high values of provisioning ES, focused on wetland production, freshwater for drinking, and agriculture products. The studies that reported low values of provisioning ES had focused on hydropower, irrigation, and food provision. The variation in the values of providing ecosystem services is attributed to the geographic, ecological, and climatic factors, which vary from country to country. Our results for the provisioning ecosystem services showed reasonable homogeneity with the results of other studies. However, the previous studies did not link Prov.ES to poverty and food, water, and energy security. In addition, policy recommendations were merely discussed and highlighted. We recommend conducting studies linking Prov.ES with poverty reduction, focusing on major drivers of the services.

Conclusions

Provisioning services provide tremendous benefits to people's livelihoods, including food, water, fiber, medicine, energy, and many others. These services are directly taken from nature in various forms, via crops, vegetables, fruits, livestock, forests, and fisheries. More than 60% of the population of Pakistan lives in rural areas, where people depend on natural resources to fulfil their living requirements. Pakistan's natural resources are being depleted by overexploitation, impacts of climate change, and poor management systems. Among the provisioning services, livestock's contribution was the highest followed by agricultural products, while fisheries and forests contributed the least. This situation is alarming for the forestry sector: only 4% of the total land area of Pakistan is covered by forests, which is why its contribution as a provisioning ecosystem services is very low. Poor forest cover leads to other environmental consequences, such as floods and landslides, which cause major destruction and loss to infrastructure, crops, livestock, and human lives, resulting in mass migration to other areas from 2003 to 2014. Livestock is the major contributor in the ecosystem services, but livestock depend on other ecosystems, such as grassland, forests, and agriculture. Forests also provide habitats for many of the rare, threatened, and endangered species in Pakistan. The rapidly accelerating rate of forest depletion is leading to the extinction of some animals from the wild while others have migrated to more suitable areas in neighboring countries. Forests, peatlands, and pastures act as carbon sinks. Land use degradation causes carbon release into the atmosphere, adding to the global atmospheric carbon, which is the main cause of climate change and global warming. All ecosystem services are interlinked with several tradeoffs. Being an agricultural country, Pakistan needs to improve its agricultural system as most of the people in urban and rural areas depend on agricultural products, while a mixed agriculture system is practiced in most parts of the country. Pakistan needs to enhance the quantity and quality of its crop production for both domestic consumption and exporting as a source of income generation. Sustainable agro-forestry and agro-pastoral systems are suitable for Pakistan with the introduction of the latest technology and biological control methods, instead of traditional farming or high doses of synthetic fertilizers. Pakistan has the potential to increase its fish production for domestic and export purposes by improving management systems and reducing freshwater and marine pollution. It is

suggested that policies relating to Prov.ES should be reframed for better management, conservation, and utilization purposes. Funds need to be allocated to the research sector, especially universities, to frame policies based on research and on-the-ground realities, keeping the consequences of depleting natural resources in focus in the future.

Acknowledgements. The authors are thankful to the respective organizations for providing the data. "This study was supported by the National Key Research and Development Program of China (2018YFA0606500) and the GEF "Qinghai Biodiversity Conservation Project" (Y55M1200AL).

Conflicts of Interests. We declare no conflict of interests.

REFERENCES

- [1] Ahmed, V., Javed, A. (2018): National Study on Agriculture Investment in Pakistan. – A working paper.
- [2] Altaf, M., Javid, A., Khan, A. M., Hussain, A., Umair, M., Ali, Z. (2015): The status of fish diversity of River Chenab , Pakistan. – *The Journal of Animal & Plant Sciences* 25(3): 564-569.
- [3] Blummel, M., Rao, P. P. (2006): Economic Value of Sorghum Stover Traded as Fodder for Urban and Peri-urban Dairy Production in Hyderabad, India. – *International Sorghum and Millets Newsletter* 47(Table 2): 97-100.
- [4] Chandio, A. A., Yuansheng, J., Rahman, T., Khan, M. N., Guangshun, X., Zhi, Z. (2015): Analysis of agricultural subsectors contribution growth rate in the agriculture GDP growth rate of Pakistan. – *International Journal of Humanities and Social Science Invention* 4(8): 101-105.
- [5] Chandio, A. A., Yuansheng, J., Magsi, H. (2016): Agricultural Sub-Sectors Performance: An Analysis of Sector-Wise Share in Agriculture GDP of Pakistan. – *International Journal of Economics and Finance* 8(2): 156.
- [6] Chang, J., Wu, X., Liu, A., Wang, Y., Xu, B., Yang, W., Meyerson, L. A., Gu, B., Peng, C., Ge, Y. (2008): Assessment of net ecosystem services of plastic greenhouse vegetable cultivation in China. – *Ecological Economics journal* 70: 740-748.
- [7] Chiabai, A., Traversi, C. M., Ding, H., Markandya, A., Nunes, P. L. D. (2009): Economic Valuation of Forest Ecosystem Serices: Methodology and Monetary Estimates. – *Nota di Lavoro* 12: 1-34.
- [8] Daw, T. M., Hicks, C. C., Brown, K., Chaigneau, T., Januchowski-hartley, F. A., Cheung, W. W. L. (2016): Elasticity in ecosystem services : exploring the variable relationship between ecosystems and human well-being. – *Ecology and Society* 21(2).
- [9] de Groot, R., Finlayson, M., Verschuuren, B., Ypma, O., Zylstra, M. (2008): Integrated assessment of wetland services and values as a tool to analyse policy trade-offs and management options: A case study in the Daly and Mary River catchments, northern Australia. – Darwin NT 0801 Australia.
- [10] Dupras, J., Alam, M., Revéret, J.-P. (2008): Economic value of Greater Montreal's non-market ecosystem services in a land use management and planning perspective. – Vol. 001. Darwin NT 0801 Australia.
- [11] Dutton, L. R., Rister, M. E., Lacewell, R. D., Sturdivant, A. W. (2015): A Review of Discounting Natural Resources: Technical Report. – Texas Water Resources Institute, 1-25. Texas Water Resources Institute.
- [12] Economics for the Environment (2011): Scoping Study on Valuing Ecosystem Services of Forests Across Great Britain Final Report. – Vol. 44.
- [13] FAO (1994): Non-Wood Forest Products in Asia. – Food and Agriculture Organization of

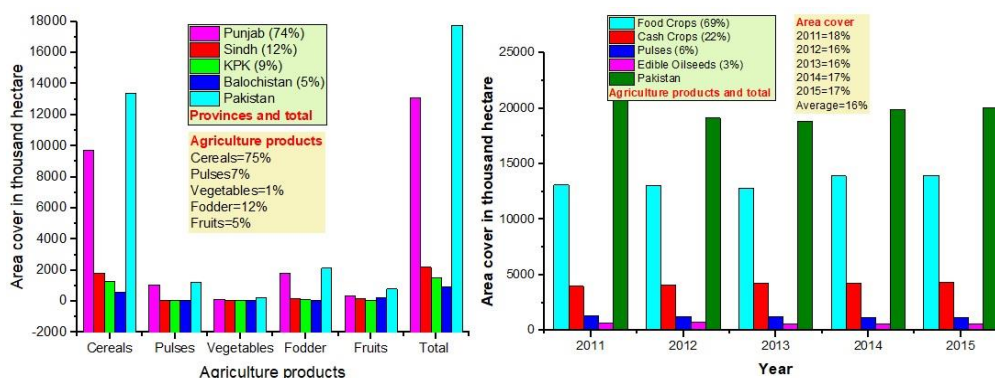
- the United Nations Rome.
- [14] FAO_UN (2010): Pakistan Forestry outlook study. Asia-Pacific forestry sector outlook study II. – Ministry of Environment, GoP and FAO-UN.
- [15] FAO (2015a): FAO Statistical Pocketbook 2015. – Food and Agriculture Organization of the United Nations. doi:978-92-5-108802-9.
- [16] FAO (2015b): Bee products : providing nutrition and generating income - Honeybees, beekeeping and bee products in our daily lives Collection of contributions received. – FAO-UN.
- [17] FAO-UN (2016a): The State of World Fisheries and Aquaculture: Contributing to Food Security and Nutrition for All.
- [18] FAO-UN (2016b): Global Forest Resources Assessment 2015: How are the world’s forests changing. – (Second Edi.). Food and Agriculture Organization of the United Nations Rome.
- [19] FAO- Fisheries., Aquaculture Department (2017): FIGIS. – Time-series query on : Production.
- [20] GoP (2013): Chapter 8 Agriculture and Food Security: Annual Plan Government of Pakistan. – In-Annual Plan 2013-2014.
- [21] GoP (2014): Pakistan Economic Survey. – Pakistan Economic Survey, 2013-14: 23-41. doi:10.1038/479299e.
- [22] Gowdy, J., Howarth, R. B., Tisdell, C., Hepburn, C., Mäler, K.-G., Hansjürgens, B. (2010): Discounting, ethics, and options for maintaining biodiversity and ecosystem integrity. – *The Economics of Ecosystems and Biodiversity: The Ecological and Economic Foundations* (March): 257-283. doi:10.4324/9781849775489.
- [23] Grădinaru, G. (2013): Methods and Techniques For Quantifying the Value Of Ecosystem Services. – *Revista Română de Statistică* 61(5): 29-44.
- [24] Griffin, R. C. (ed.) (2006): *Water Resource Economics. The Analysis of Scarcity, Policies, and Projects* (XV.). – London: The MIT Press, Cambridge.
- [25] Halsnæs, K., Garg, A., Christensen, J., Føyn, H. Y., Karavai, M., Rovere, E. La, Bramley, M., Zhu, X., Mitchell, C., Roy, J., Tanaka, K., Katayama, H., Mena, C., Obioh, I., Bashmakov, I. (2014): Climate change mitigation policy paradigms—national objectives and alignments. – *Mitigation and Adaptation Strategies for Global Change* 19(1): 1-27.
- [26] Hanjra, M. A., Qureshi, M. E. (2010): Global water crisis and future food security in an era of climate change. – *Food Policy* 35(5): 365-377.
- [27] Häyhä, T., Paolo, P., Paletto, A., Fath, B. D. (2015): Assessing , valuing , and mapping ecosystem services in Alpine forests. – *Ecosystem Services* 14: 12-23.
- [28] Hermwille, L., Obergassel, W., Ott, H. E., Beuermann, C. (2017): UNFCCC before and after Paris – what’s necessary for an effective climate regime? – *Climate Policy* 17(2): 150-170.
- [29] Herrero, M., Thornton, P. K., Gerber, P., Reid, R. S. (2009): Livestock, livelihoods and the environment: understanding the trade-offs. – *Current Opinion in Environmental Sustainability* 1(2): 111-120.
- [30] Herrero, M., Thornton, P. K., Notenbaert, A. M., Wood, S., Msangi, S., Freeman, H. A., Bossio, D., Dixon, J., Peters, M., Steeg, J., van de Lynam, J., Rao, P. P., Macmillan, S., Gerard, B., McDermott, J., Seré, C., Rosegran, M. (2010): Smart Investments in Sustainable Food Production: Revising Mixed Crop-Livestock Systems. – *Science* 327: 822-825.
- [31] Hlaing, Z. C., Kamiyama, C., Saito, O. (2017): Interaction between Rural People’s Basic Needs and Forest Products : A Case Study of the Katha District of Myanmar. – *International Journal of Forestry Research* 2017: 18.
- [32] Hussain, S. S., Winrow-Giffin, A., Moran, D., Robinson, L. A., Fofana, A., Paramor, O. A. L., Frid, C. L. J. (2008): An ex ante ecological economic assessment of the bene fits arising from marine protected areas designation in the UK. – *Ecological Economics* 69: 94.

- [33] Huxham, M., Emerton, L., Kairo, J., Munyi, F., Abdirizak, H., Muriuki, T., Nunan, F., Briers, R. A. (2008): Applying Climate Compatible Development and economic valuation to coastal management: A case study of Kenya's mangrove forests. – *Journal of Environmental Management* 157: 94.
- [34] Ingram, V., Bongers, G. (2009): Valuation of Non-Timber Forest Product Chains in the Congo Basin: a methodology for valuation.
- [35] Irfan, M. (2007): Poverty and Natural Resource Management in Pakistan. – *The Pakistan Development Review* 46(4): 691-708.
- [36] IUCN (2012): Facts and figures on Forests. ICUN factsheet about Forests. – <https://www.iucn.org/content/facts-and-figures-forests>. IUCN.
- [37] Jenerette, G. D., Marussich, W. A., Newell, J. P. (2005): Linking ecological footprints with ecosystem valuation in the provisioning of urban freshwater. – *Ecological Economics* 59.
- [38] Khan, S. R. (2012): Linking Conservation with Sustainable Mountain Livelihoods: A Case Study of Northern Pakistan. – (August): 385.
- [39] Khan, K., Khan, G., Zahri, M., Altaf, M. (2015): Role of Livestock in Poverty Reduction : A Case Study of District. – *Lasbela, U. J.Sci. Technl.*: 153-156.
- [40] Kraus, D. (2016): Greenhouse gas emissions and global warming potential of traditional and diversified tropical rice rotation systems. – *Glob. Chang. Biol.* 22(1): 432-448. doi:10.1111/gcb.13099.
- [41] Lam, V. W. Y., Cheung, W. W. L., Reygondeau, G., Rashid Sumaila, U. (2016): Projected change in global fisheries revenues under climate change. – *Scientific Reports* 6: 6-13.
- [42] Li, X., Yub, X., Jiang, L., Li, W., Liu, Y., Hou, X. (2008): How important are the wetlands in the middle-lower Yangtze River region: An ecosystem service valuation approach. – *Ecosystem Services* 10: 94.
- [43] Lienhoop, N., Bartkowski, B., Hansjrgens, B. (2015): Informing biodiversity policy: The role of economic valuation, deliberative institutions and deliberative monetary valuation. – *Environmental Science and Policy* 54: 522-532.
- [44] Martín-López, B., García-Llorente, M., Palomo, I., Montes, C. (2008): The conservation against development paradigm in protected areas : Valuation of ecosystem services in the Doñana social – ecological system (southwestern Spain). – *Ecological Economics* 70(8): 94.
- [45] McMichael, A., Scholes, R., Hefny, M. (2005): Linking ecosystem services and human well-being. – *Millenium Ecosystem Assessment Series, 4*. Island Press, Washington DC, USA.
- [46] MEA (2005a): Ecosystems and human well-being. – *World Resources Institute (Vol. 5)*. ISLAND PRESS.
- [47] MEA (2005b): Ecosystems and Human Well-being: Health Synthesis. – *A millennium Ecosystem Assessment Publication*, p 64. WHO Publication.
- [48] Mitchell, M. G. E., Bennett, E. M., Gonzalez, A. (2014): Forest fragments modulate the provision of multiple ecosystem services. – *Journal of Applied Ecology* 51(4): 909-918.
- [49] Molnar, M., Kocian, M., Batker, D. (2008): Valuing the Aquatic Benefits of British Columbia's Lower Mainland: Nearshore Natural Capital Valuation. A working paper. – *David Suzuki Foundation and Earth Economics* p 94. Darwin NT 0801 Australia.
- [50] Nazir, K., Yongtong, M., Ali, M., Hussain, K., Mohsin, M. (2015): A Preliminary Study on Fisheries Economy of Pakistan : Plan of Actions for Fisheries Management in Pakistan. – *Canadian Journal of Basic and Applied Sciences* 03(January): 7-17.
- [51] Nazir, K., Yongtong, M., Hussain, K., Kalhor, M. A., Kartika, S., Mohsin, M. (2016): A Study on the Assessment of Fisheries Resources in Pakistan and its Potential to Support Marine Economy. – *Indian Journal of Geo-Marine Sciences* 45(9): 1181-1187.
- [52] Paletto, A., Geitner, C., Grilli, G., Hastik, R., Pastorella, F., Garcia, L. R. (2008): Mapping the value of ecosystem services: A case study from the Austrian Alps. – *Annals of Forest*

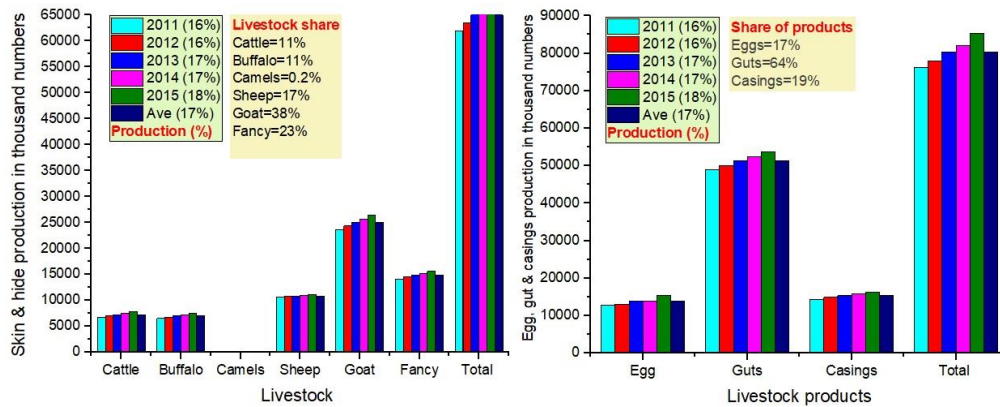
- Research 58(1): 94.
- [53] Pandey, A. K., Tripathi, Y. C., Kumar, A. (2016): Non Timber Forest Products (NTFPs) for Sustained Livelihood: Challenges and Strategies. – *Research Journal of Forestry* 10(1): 1-7.
- [54] PBS (Pakistan Bureau of Statistics) (2015): Pakistan Bureau of Statistics Government of Pakistan ISLAMABAD.
- [55] PBS (Pakistan Bureau of Statistics) (2015): Economic survey of Pakistan. – Year Book; p 150.
- [56] PBS (Pakistan Bureau of Statistics) (2017): Agriculture Statistics of Pakistan 2010-11. – Annual report by Pakistan Bureau of Statistics.
- [57] Power, A. G. (2010): Ecosystem services and agriculture: tradeoffs and synergies. – *Philosophical Transactions of the Royal Society B: Biological Sciences* 365(1554): 2959-2971.
- [58] Raza, J., Siddiqui, W. (2014): Determinants of Agricultural Output in Pakistan: A Johansen co-integration approach. – *Academic Research International* 5(4): 30-46.
- [59] Reid, R. S., Galvin, K. A., Kruska, R. S. (2008): Global significance of extensive grazing lands and pastoral societies: An introduction. – In-*Fragmentation in Semi-Arid and Arid Landscapes: Consequences for Human and Natural Systems*. doi:10.1007/978-1-4020-4906-4-1.
- [60] Rosegrant, M. W., Koo, J., Cenacchi, N., Ringler, C., Robertson, R., Fisher, M., Cox, C., Garrett, K., Perez, N. D., Sabbagh, P. (2014): Food security in a world of natural resource scarcity: Role of agricultural technologies. – IFPRI Book. doi:10.2499/9780896298477.
- [61] Ryschawy, J., Disenhaus, C., Bertrand, S., Allaire, G., Aznar, O., Plantureux, S., Josien, E., Guinot, C., Lasseur, J., Perrot, C., Tchakerian, E., Aubert, C., Tichit, M. (2017): Assessing multiple goods and services derived from livestock farming on a nation-wide gradient. – *Animal* (May): 1-12. doi:10.1017/S1751731117000829.
- [62] Sarfaraz, S., Hasan Arsalan, M., Fatima, H. (2014): Regionalizing the Climate of Pakistan Using Köppen Classification System. – *Pakistan Geographical Review* 69(2): 111-132.
- [63] Shah, S. B. H., Mu, Y., Abbas, G., Pavase, T. R., Mohsin, M., Malik, A., Ali, M., Noman, M., Soomro, M. A. (2018): An economic analysis of the fisheries sector of Pakistan (1950-2017): Challenges , opportunities and development strategies. – *International Journal of Fisheries and Aquatic Studies* 6(2): 515-524.
- [64] Shedayi, A. A., Xu, M., Gulraiz, B. (2014): Traditional medicinal uses of plants in Gilgit-Baltistan, Pakistan. – *Journal of Medicinal Plants Research* 8(30): 992-1004.
- [65] Shedayi, A. A., Xu, M., Hussain, F., Sadia, S., Naseer, I., Bano, S. (2016): Threatened plant resources: Distribution and ecosystem services in the world's high elevation park of the karakoram ranges. – *Pakistan Journal of Botany* 48(3): 999-1012.
- [66] Siwar, C., Chinade, A. A., Ismail, S. M., Isahak, A. (2016): Economic valuation of soil carbon sequestration services in Malaysia's forest sector: A review of possible approaches. – *Journal of Sustainability Science and Management* 11(1): 14-28.
- [67] Soudzilovskaia, N. A., Elumeeva, T. G., Onipchenko, V. G., Shidakov, I. I., Salpagarova, F. S., Khubiev, A. B., Tekeev, D. K., Cornelissen, J. H. C. (2013): Functional traits predict relationship between plant abundance dynamic and long-term climate warming. – *Proceedings of the National Academy of Sciences* 110(45): 18180-18184.
- [68] Steinfeld, H., Gerber, P., Wassenaar, T., Castel, V., Rosales, M., De Haan, C. (2006): *Livestock's Long Shadow: Environmental Issues and Options*. – FAO ftp://ftp.fao.org/docrep/fao/010/A0701E/A0701E00.pdf:1-377. doi:10.1007/s10666-008-9149-3.
- [69] Sterner, T., Kyriakopoulou, E. (2012): (The Economics of) Discounting: Unbalanced Growth, Uncertainty, and Spatial Considerations. – *Annual Reviews of Resources Economics* 4: 285-402.

- [70] Tariq, M. (2015): An Overview of Deforestation Causes and Its Environmental Hazards in Khyber Pukhtunkhwa. – Journal of Natural Sciences Research 5(1): 52-58.
- [71] TEEB (2009): The Economics of Ecosystems and Biodiversity (TEEB) for National and International Policy Makers. – In-The Economics of Ecosystems and Biodiversity (TEEB). doi:10.1016/j.ecolecon.2009.11.019.
- [72] TEEB (2010a): The Economics of Ecosystems & Biodiversity. – TEEB report.
- [73] TEEB (2010b): The Economics of Ecosystem and Biodiversity for local and regional policy makers. – EEB report. UNEP.
- [74] Théwis, A. (2012): Prospects for Livestock Production in the Next Future. – Bulletin UASVM Animal Science and Biotechnologies 69: 1-11.
- [75] Valatin, G., Starling, J. (2008): Valuation of ecosystem services from Woodlands. – UK NEA Economic Analysis Report: 94.
- [76] Voora, V., Barg, S. (2008): Pimachiowin Aki World Heritage Project Area Ecosystem Services Valuation Assessment. – International Institute for Sustainable Development, Winnipeg, Manitoba Canada (Vol. 1). Darwin NT 0801 Australia.
- [77] Wahlén, C. B. (2017): Opportunities for making the invisible visible: Towards an improved understanding of the economic contributions of NTFPs. – Forest Policy and Economics 84: 11-19.
- [78] Wang, X., Chen, W., Zhang, L., Jin, D., Lu, C. (2008): Estimating the ecosystem service losses from proposed land reclamation projects: A case study in Xiamen. – Ecological Economics 69(12): 94.
- [79] Wang, G., Fang, Q., Zhanga, L., Chen, W., Chen, Z., Hong, H. (2009): Estuarine, Coastal and Shelf Science Valuing the effects of hydropower development on watershed ecosystem services: Case studies in the Jiulong River Watershed, Fujian Province, China. – Estuarine, Coastal and Shelf Science 86(3): 94.
- [80] Wood, S. L. R., Jones, S. K., Johnson, J. A., Brauman, K. A., Chaplin-kramer, R., Fremier, A., Girvetz, E., Gordon, L. J., Kappel, C. V, Mandle, L., Mulligan, M., Farrell, P. O., Smith, W. K., Willemen, L., Zhang, W., Declerck, F. A. (2018): Distilling the role of ecosystem services in the Sustainable Development Goals. – Ecosystem Services 29: 70-82.
- [81] World Bank (2016): Poverty Overview. – World Bank. Accessed: www.worldbank.org/en/topic/poverty/overview.

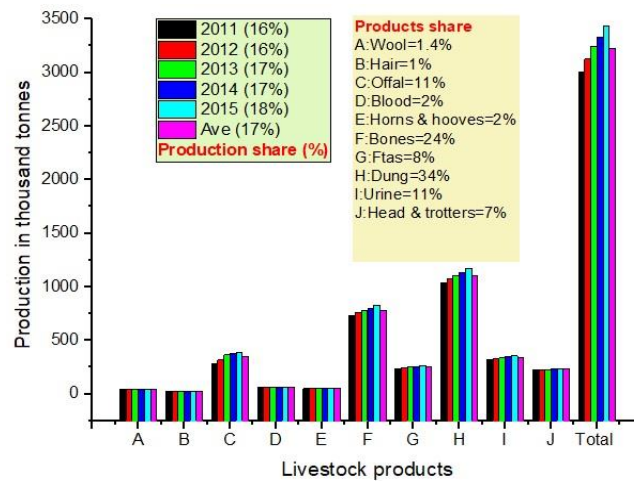
APPENDICES



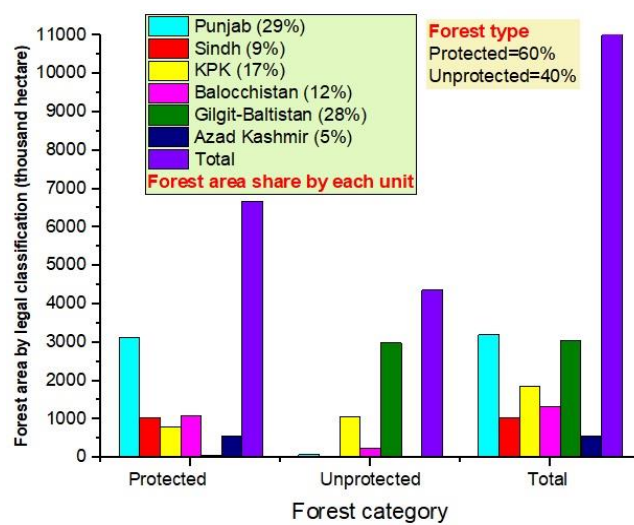
Appendix A. Area cover of agriculture products by province from 2011 to 2015. (KPK: Khyber Pukhtunkhwa)



Appendix B. Skin and hide, eggs, guts, and casings production from 2011 to 2015



Appendix C. Other livestock products from 2011 to 2015



Appendix D. Forest category, area cover, and distribution by province. (KPK: Khyber Pukhtunkhwa)

ANALYSIS OF CLIMATE VARIABILITY AND ITS RELATIONS TO VEGETATION DYNAMICS IN TOGO, WESTERN AFRICA FROM 1984 TO 2017

FANDJINO, K.^{1,2} – ZHANG, K. B.^{1*} – FOLEGA, F.² – MUKETE, B.³ – YANG, X. H.^{4*} – WALA, K.² – AKPAGANA, K.²

¹*School of Soil and Water Conservation, Beijing Forestry University, 35 Qinghua East Road, Haidian District, Beijing 100083, China
(e-mail: fandnew@yahoo.fr – F. K., ctccd@126.com–Z.K.B)*

²*Laboratoire de Botanique et d'Ecologie Végétale, Université de Lome, BP 1515, Lome, Togo
(e-mail: ffolegamez@live.fr – F. F., kpwala@yahoo.fr – W. K., koffi2100@gmail.com – A. K.)*

³*Department of Forest Management, Beijing Forestry University, 35 Qinghua East Road, Haidian District, 100083 Beijing, China
(e-mail: munasawa@gmail.com–M.B)*

⁴*Institute of Desertification Studies, Chinese Academy of Forestry, P. O. Box 35, Yiheyuanhou, Haidian District, Beijing 100091, China
(e-mail: yangxh@caf.ac.cn–Y.X)*

**Corresponding authors
e-mail: ctccd@126.com, yangxh@caf.ac.cn*

(Received 8th Feb 2019 ; accepted 29th Mar 2019)

Abstract. Vegetation, climate and anthropogenic factors in the country of Togo are thought to mutually correlate, however, the degrees to which they correlate remains unclear. This study examined and analyzed patterns of climate variability and how these patterns have influenced vegetation cover dynamics in Togo. Based on data collected from eight meteorological stations, the global climate monitor and European Space Agency, this study analyzed existing trends and relationships between vegetation cover, climate and Normalized Difference Vegetation Index (NDVI) using Mann Kendall non-parametric test, ANOVA and p-value tests. The results showed that (1) rainfall correlated strongly with NDVI (p-value < 0.00001), (2) evapotranspiration was influenced by annual temperatures in the eight sampled meteorological stations across the country (p-values < 0.0001), (3) evapotranspiration and rainfall were negatively correlated, (4) annual NDVI changes can be used to monitor annual rainfalls, (5) Anthropogenic disturbances, such as deforestation from uncontrolled tree logging, farming and low household income, can be quoted among the limiting factors of vegetation cover.

Keywords: *greenness drivers, remote sensing, NDVI, sustainable forest management, plant seasonality*

Introduction

From 1990 to 2015, the total forest coverage in Togo decreased from 12.59 to 3.46% showing a loss of 9.13% as estimated by the United Nations Food and Agricultural Organization. Studies have shown many significant interchanges occurring between climate, vegetation and human activities, for example, interactions have been found between the soil and atmosphere (Zhang et al., 2011), and vegetation is thought to respond to climate changes through temperature and rainfall variations, and obviously or subtly by seasonal changes (Weiss et al., 2004.; Cui and Shi, 2010.; Meng et al., 2011).

Various studies have analyzed vegetation indices to understand the impacts of climate on vegetation cover, showing that rainfall regimes correlate strongly with Normalized Difference Vegetation Index (NDVI) (Martiny et al., 2006; Capodici et al., 2008), green biomass estimation (Rosental et al., 1985; Prince et al., 1991; Julien, 2014) and as vegetation photosynthetic activity indicator (Gausman et al., 1985; Gilabert et al., 1985). Even early satellite data from the 1970's were used to monitor vegetation and climate patterns conditions for management purposes (Rouse et al., 1974). Some research findings showed that an increase of temperature could potentially change the ecosystem composition of the vegetation cover (Serreze et al., 2000). Other studies have shown broad results that NDVI and rainfall correlated effectively (Kendall et al., 1975; Nicholson et al., 1994; Richard et al., 1998; Foody et al., 2003; Ma et al., 2006). For instance, the influence of temperature on NDVI was significant only during the early and the late growing season, while NDVI correlated with rainfall within the growing season (Wang et al., 2012). However, NDVI time series were not strongly correlated with climate variations at global scale, even if rainfall was reported to have the capacity to limit vegetation growth in semi-arid areas (Schultz, 1995; Ichii et al., 2002).

Literature review

Dominated by the Sahel's arid and semi-arid climatic conditions, West Africa reported obvious climatic changes by the early and late drought period (1970 and 1980), shown by decadal increases of the temperature and a decrease of rainfall (Biasutti et al., 2009). These findings have been consistent in Togo, with climate changes being assessed through slight increases of temperature and irregular rainfall regimes (Adjoussi, et al., 2000). Climate change in the area is also projected to continue exacerbating weather and climate conditions the future decades (IPCC, 2013).

Moreover, many other studies addressing climate change showed that in West Africa, and especially in Togo, temperatures have been increasing steadily each year from 0.4 to 1.6 °C, depending on the ecoregions in Togo (Badameli et al., 2015). Estimates of green vegetation dynamics in West Africa, especially in the North mountainous region of Togo, have revealed that since 1987 vegetation has been declining, and socio-economic factors were thought to be the main dynamic factors of this decrease (FAO, 2017). Togo was quoted as having some of the highest deforestation rates in the world, with a deforestation rate of 4.5% from 2002 to 2005 and 5.75% from 2005 to 2010 (FAO, 2006; Biasutti et al., 2009). These deforestation rates are due to supplying firewood as main source of energy for 90% of the household energy needs (Fontodji et al., 2007; Gazull et al., 2009; Koku et al., 2009). Other factors for vegetation degradation include agricultural pressure, animal husbandry and bush fires (Traore et al., 1998)

Within the past decades, most of the studies related to vegetation in Togo were analyzed at the local level for vegetation management strategies or plant species inventory. This is the first study to explore climatic variations and the drivers between climate variations and vegetation at two scales from local to national level. The current study bridge gaps in the research about Togo by putting together climate and vegetation variations using NDVI, temperature, rainfall and potential evapotranspiration (PET) data to clarify the relationship of vegetation and climate changes under a tropical climate conditions.

Materials and methods

Study area

Togo (6°06'N; 11°08'N; 0°09'W and 1°49'W), a West African country, covers a total area of 56,600 km² and is bordered by the Atlantic Ocean, Benin, Ghana, and Burkina-Fasso to the South, East, West and North respectively. With 61% urban population and 229 persons/km² of density, his total population was 7,965,055 persons in 2017 according to the United Nation for Food and Agriculture Organization (FAO). This population has quadrupled from 1960 to 2010, since gaining independence, with 60% under the age of 25 years. Togo's tropical climate is characterised by two main regimes from the south to the north. The Guinean regime comprises two rainy seasons and two dry seasons with an annual rainfall from 1000 to 1600 mm while the Sudanese regime in the North has only one short rainy season and one long dry season with an annual rainfall of 850-1400 mm (Badameli et al., 2015) and an annual average temperature around 27.8 °C. The country has rich vegetation with more than 4000 plant species, mainly from the forest species as discovered recently (Brunei et al., 1984; Akpagana et al., 1994; Kouami et al., 2009). Unfortunately, this rich flora is threatened by anthropogenic activities which depend on forest resources for fire wood energy and charcoal (Folega et al., 2011). The soils of Togo are diverse and include ferralitic soils, vertisols, tropical ferruginous soils, although mainly dominated by poorly developed soils (Folega et al., 2015). The hydrology of Togo comprises three southern rivers including Mono (450 km) the longest, Zio (176 km) Haho (140 km) and lagoons, Togoville, Lomé and Aneho lagoons. In the northern part the Oti basin, there is the only one river watering the vegetations. The climate of Togo is under the influence of two high-pressure air masses, Harmattan and Monsoon, whose encounter produces an Inter-Tropical Front (FIT) that determines the seasons by its fluctuation. In terms of botany, Togo comprises five ecofloristic areas (Ern et al., 1979; Kokou et al., 2009) which combine ecological, floristic and physiognomic patterns, including Sudanese savannas in the northern plains, dry savannahs and forests covering the northern mountains, Guinean woodland savannahs in the central plains, dense semi-deciduous forests in the southern section in the Mont's of Togo, and mosaics (savannahs, forest relics and fallow forests) in the coastal plains of southern Togo. Land use cover is estimated at 67.4% of agricultural land, 45.2% of arable land, 3.8% of permanent crops, 18.4% of permanent pasture and of forest 4.9% others estimates to 27.7% in 2011.

Data collection

Meteorological data and NDVI

Data were downloaded from eight meteorological stations located in various ecofloristic regions of the country (*Fig. 1*). The meteorological stations are found in open air environments free from shade. These meteorological stations include Lomé (6°9'56"N, 1°15'16.24"E), Tabligbo (6°34'59"N, 1°30'00"E), Atakpamé (7°31'37"N, 1°7'36"E), Kouma konda (6°95'N, 0°58'E), Mango (10.37°N/0.47°E), Sokodé (8.98°N/1.15°E), Kara (9.55°N/1.17°E), Dapaong (10.87°N/0.25°E) from 1984 to 2017. The NDVI annual time series data were available from the European Space agency at the resolution of 500 m completed from the MODIS website for the years 1992 and 1993 at the same resolution. The annual evapotranspiration data were freely available in the global climate monitoring website. The Normalized Difference Vegetation Index

(NDVI) ranged from (-)1 to (+)1. It can be extremely negative for water surfaces, zero for barren areas or rocks, sands or snow and highly positive for healthy vegetation including grassland, shrub land, temperate and tropical rainforest (Tucker et al., 1979; Tarpley et al., 1984; Gausman et al., 1985; Goward et al., 1985; Rosental., 1985; Sellers et al., 1985; Townshend et al., 1985; Bartlett et al., 1988; Wilson et al., 2002).

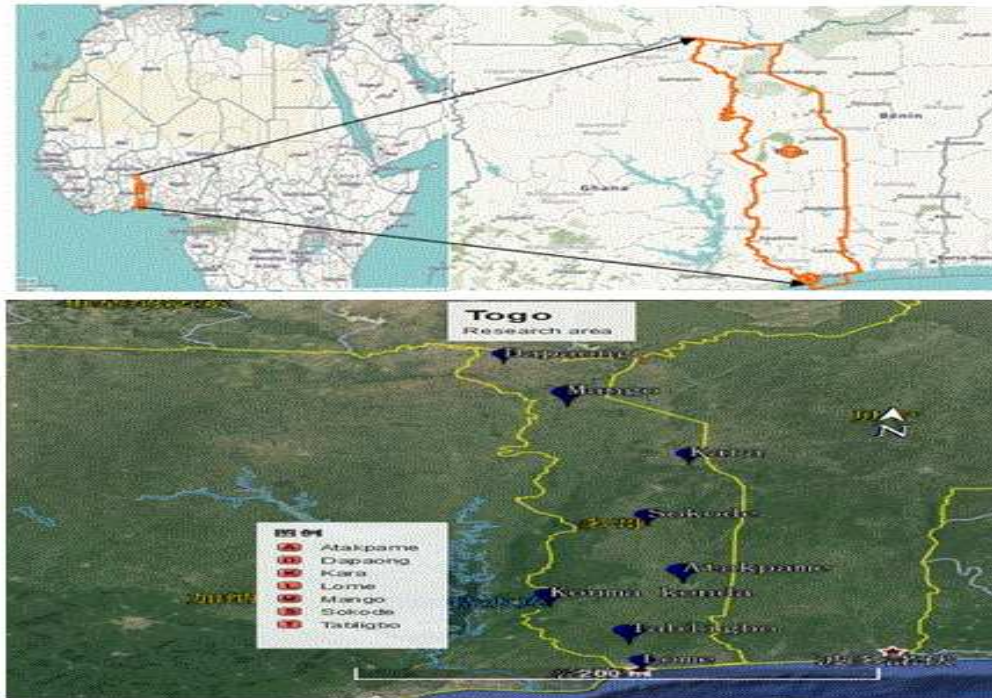


Figure 1. Location map of the study area

Statistical analyses

Regression analysis

All collected data were analyzed by regression (*Eq. 1*) method with SPSS software to determine the relationship between dependent and independent variables. Thus, the dependent variables were regressed on the independents in order to determine if their relation was significant and how much the confidence of the dependents explain the independents. The p -value < 0.05 represents statistically a significant relationship to 95% of confidence interval (Kleinbaum et al., 1998; Mbatu et al., 2006; Mukete et al., 2018).

$$y = ax + b \quad (\text{Eq.1})$$

where y is the dependent variable and x the independent variable.

Non parametric test of Mann Kendall (MK)

Non-parametric analysis known as Mann Kendall (MK) was performed using the following steps: the observed data in year Y_j and Y_i respectively differ and the sign ($Y_j - Y_i$) equals to 1, -1 or 0 with $j > i$. The test statistic, S , was then calculated (*Eq. 2*).

$$S = \sum_{i=1}^{n-1} \sum_{j=i+1}^n \text{Sign}(y_j - y_i) \quad (\text{Eq.2})$$

When S is a larger positive integer, the values measured later tend to be larger than earlier values and an upward trend is indicated. When S is a larger negative number, later values tend to be smaller than earlier values and a downward trend is indicated. When the absolute value of S is small, no trend is indicated. The test static τ was calculated (Eq. 3).

$$\tau = \frac{S}{n(n-1)/2} \quad (\text{Eq.3})$$

τ has a range from -1 to +1 and is analogous to the correlation coefficient in regression analysis. The null hypothesis of no trend is rejected when S and τ are significantly different from zero. If a significant trend is found, the rate of change can be calculated using the Sen slope estimator (Eq. 4).

$$\beta = \text{median}\left(\frac{y_j - y_i}{x_j - x_i}\right) \quad (\text{Eq.4})$$

For all $i < j$ and $I = 1, 2, \dots, n-1$ and $j = 2, 3, \dots, n$; in order words, computing the slope for all pairs of data that were used to compute S. The median of those slopes is the Sen slope estimator. For Mann et al. (1945), the S statistic is roughly in the norms if and only if the time interval is greater than eight. When there is no tie between the values of the data, see Equations 5 and 6.

$$E(s) = 0 \quad (\text{Eq.5})$$

$$\text{Var}(S) = \frac{n(n-1)(2n+5)}{18} = \sigma \quad (\text{Eq.6})$$

The standard test statistic Z is calculated by the following formula:

$$\begin{aligned} Z &= \frac{S - 1}{\sqrt{\text{Var}(s)}} \text{ For } S \geq 0 \\ Z &= 0 \text{ For } S = 0 \\ Z &= \frac{S + 1}{\sqrt{\text{Var}(s)}} \text{ For } S \leq 0 \end{aligned} \quad (\text{Eq.7})$$

When there is no trend or a null hypothesis, Z evolves with mean zero. A positive Z value indicates an upward trend value while a negative value indicates a downward trend. The p-value of a Mann-Kendall S can then be determined using the normal cumulative distribution function (Eq. 8; Blain, 2013; Helsel et al., 1992).

$$p = 2[1 - \phi(|z|)] \quad (\text{Eq.8})$$

where $\Phi(p)$ describes the cumulative distribution function of a standard normal variate.

Results

Climate variability and vegetation dynamics

The NDVI analysis showed variations in vegetation cover throughout the country, (Fig. 2), and correlation analysis performed also showed climatic factors to correlate with NDVI, (Figs. 9-10). Observing the correlation between NDVI and temperature at the national level.

NDVI, temperature, rainfall and evapotranspiration changes at local level

The annual time series of temperature, rainfall, evapotranspiration and NDVI in Togo at national level from 1984 to 2017 (Fig. 2), shows obvious changes in each parameter during these three last decades in Togo. Temperatures is increasing continuously especially from 1990 in the country. The NDVI and mean rainfall are changing in the same way so that an uptrend year of rainfall corresponds to an uptrend year of NDVI. The temperature and the evapotranspiration both changed at certain time period in the opposite directions especially from 1990 till 2017.

From the analysis we can conclude NDVI and rainfall correlate strongly and positively, similarly with mean annual temperature and evapotranspiration, while the annual rainfall and evapotranspiration correlate negatively (Fig. 3). It can be seen also that, there is no correlation between mean NDVI and mean annual temperature under the tropical climate condition that prevails in the research area.

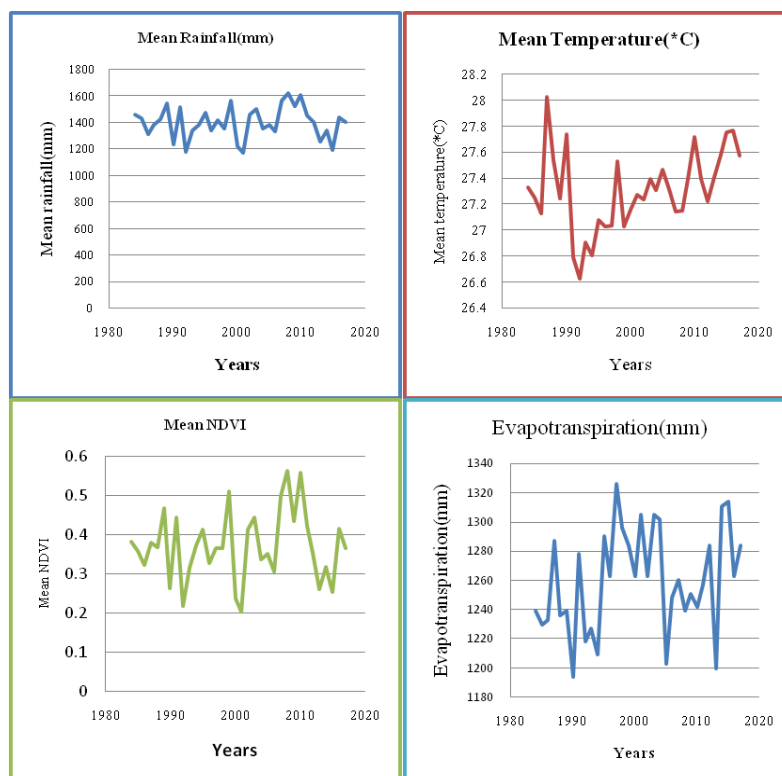


Figure 2. Annual time series changes of mean NDVI, rainfall (mm), evapotranspiration (mm) and temperature (°C) at national scale in Togo during 1984-2017

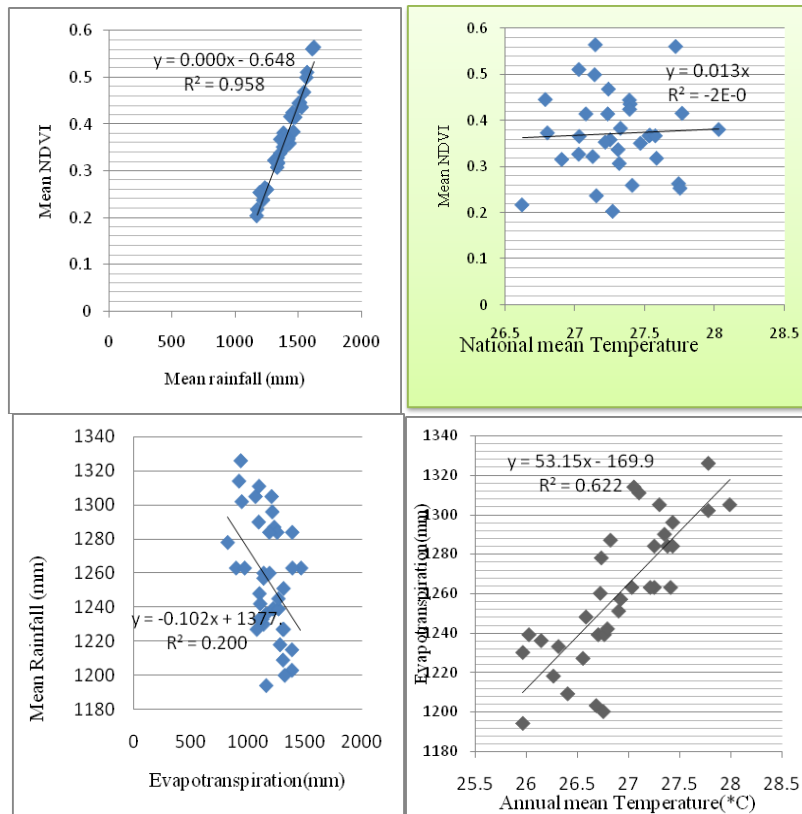


Figure 3. Cross-analysis relationship between mean NDVI, evapotranspiration, temperature (°C), rainfall at national scale in Togo from 1984 to 2017

National level forest area changes in Togo from FAO survey (Fig. 4)

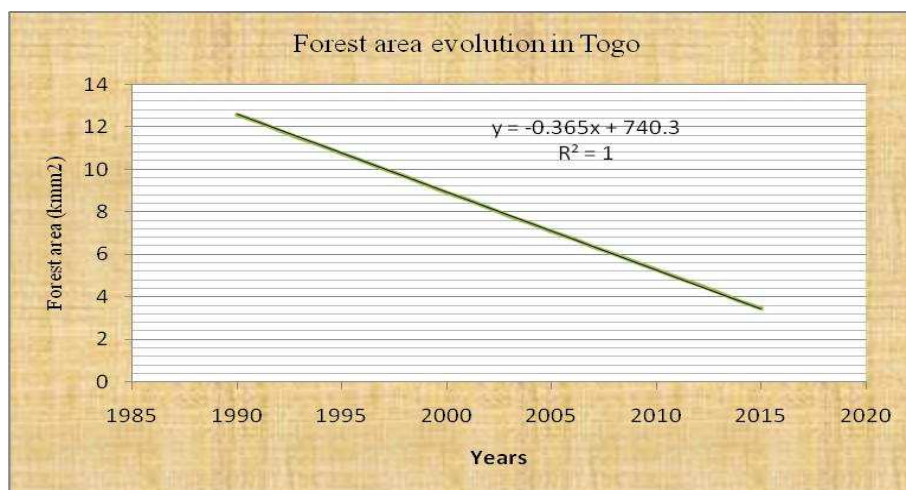


Figure 4. Togolese forest area changes from 1990

Local scale climate variability and vegetation dynamics

The relationship between climate variability and vegetation cover was performed at local scale for all the eight sampled meteorological stations (Figs. 5-10).

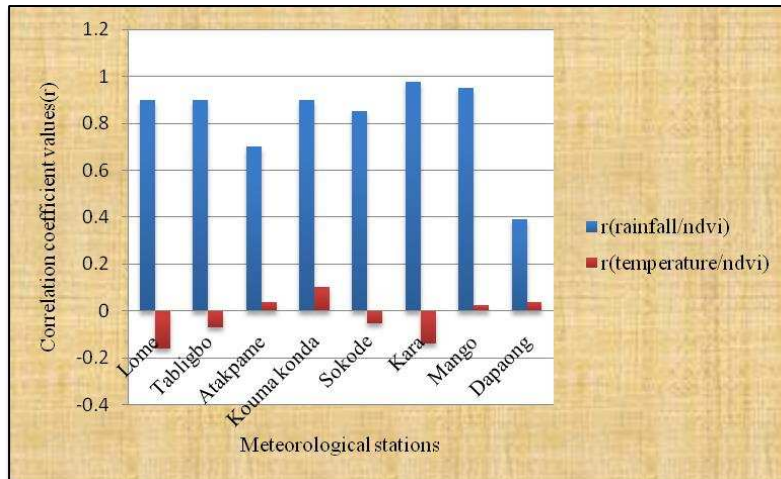
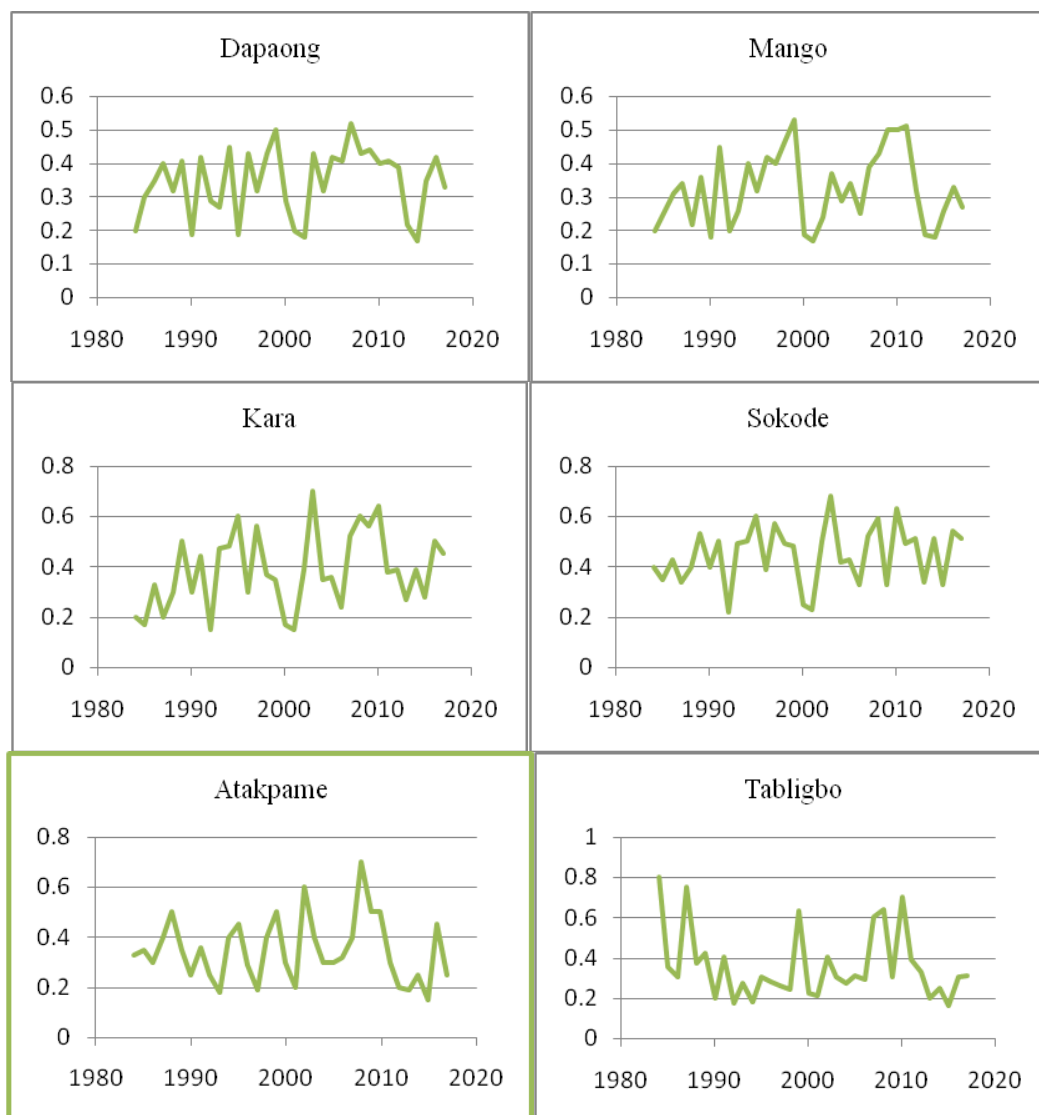


Figure 5. Correlation coefficient analysis between NDVI/ rainfall and NDVI/temperature for the entire study area in the eight meteorological stations from the South subtropical Guinean climate to the North tropical Sudanese climate during the 33 years of observation



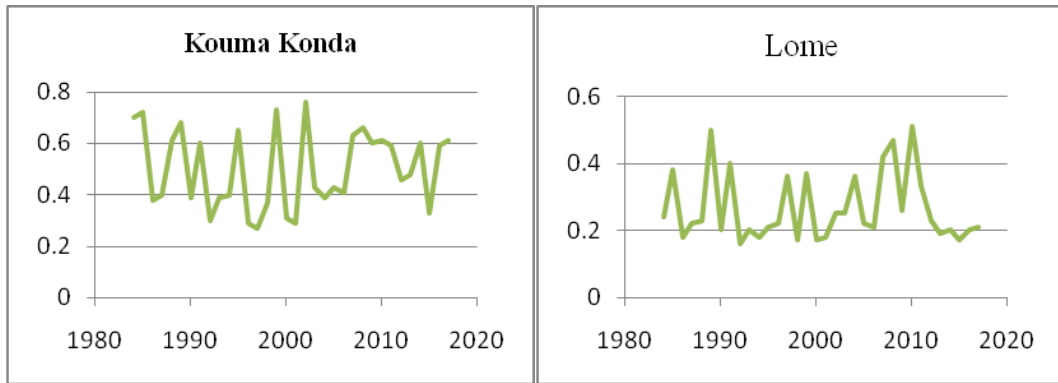
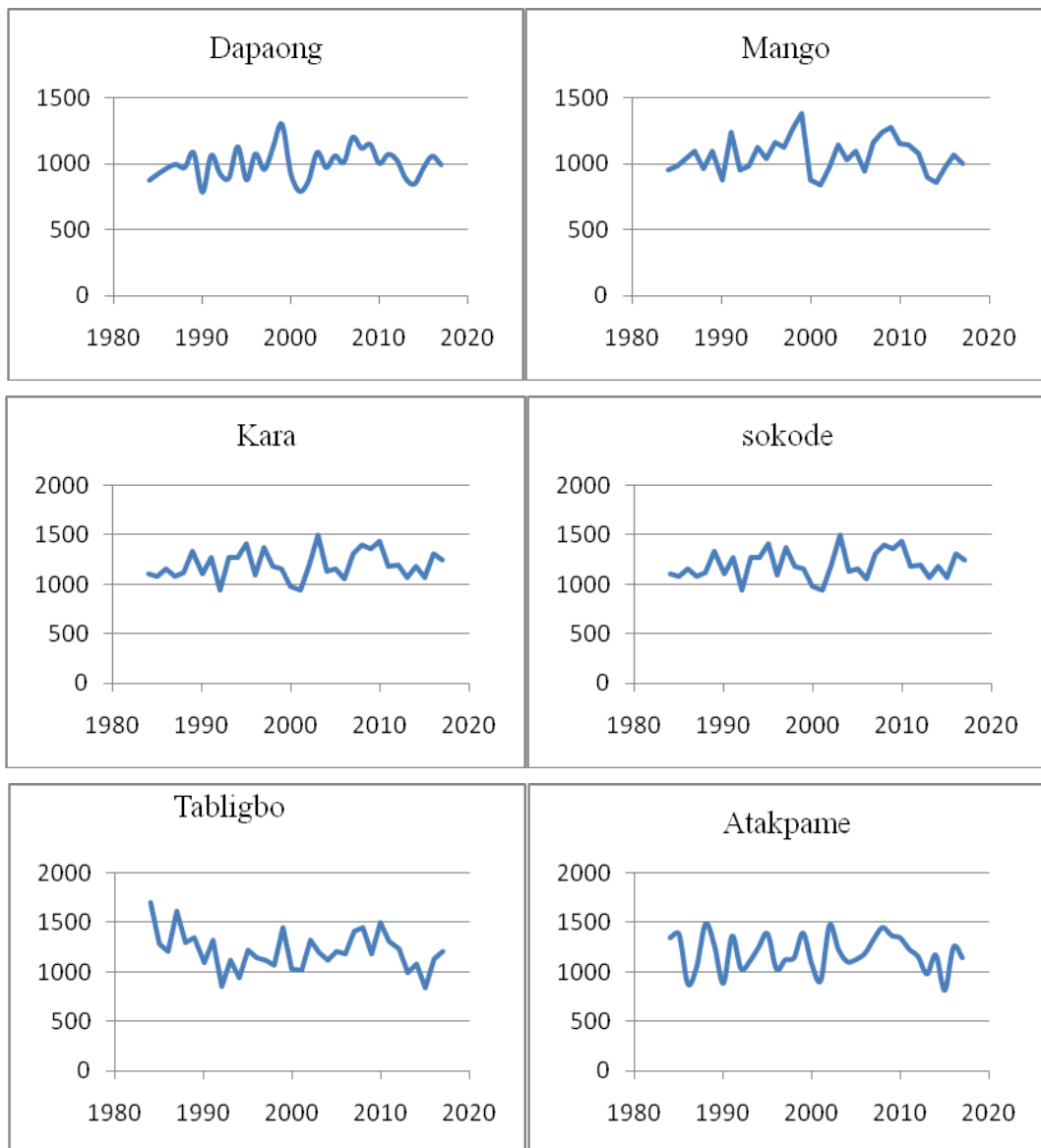


Figure 6. Annual changes in NDVI for the eight sampled meteorological stations in Togo during 1984-2017



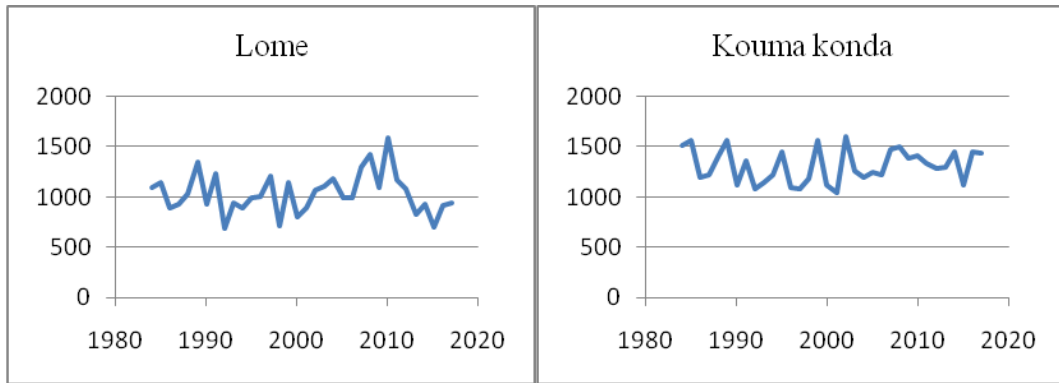
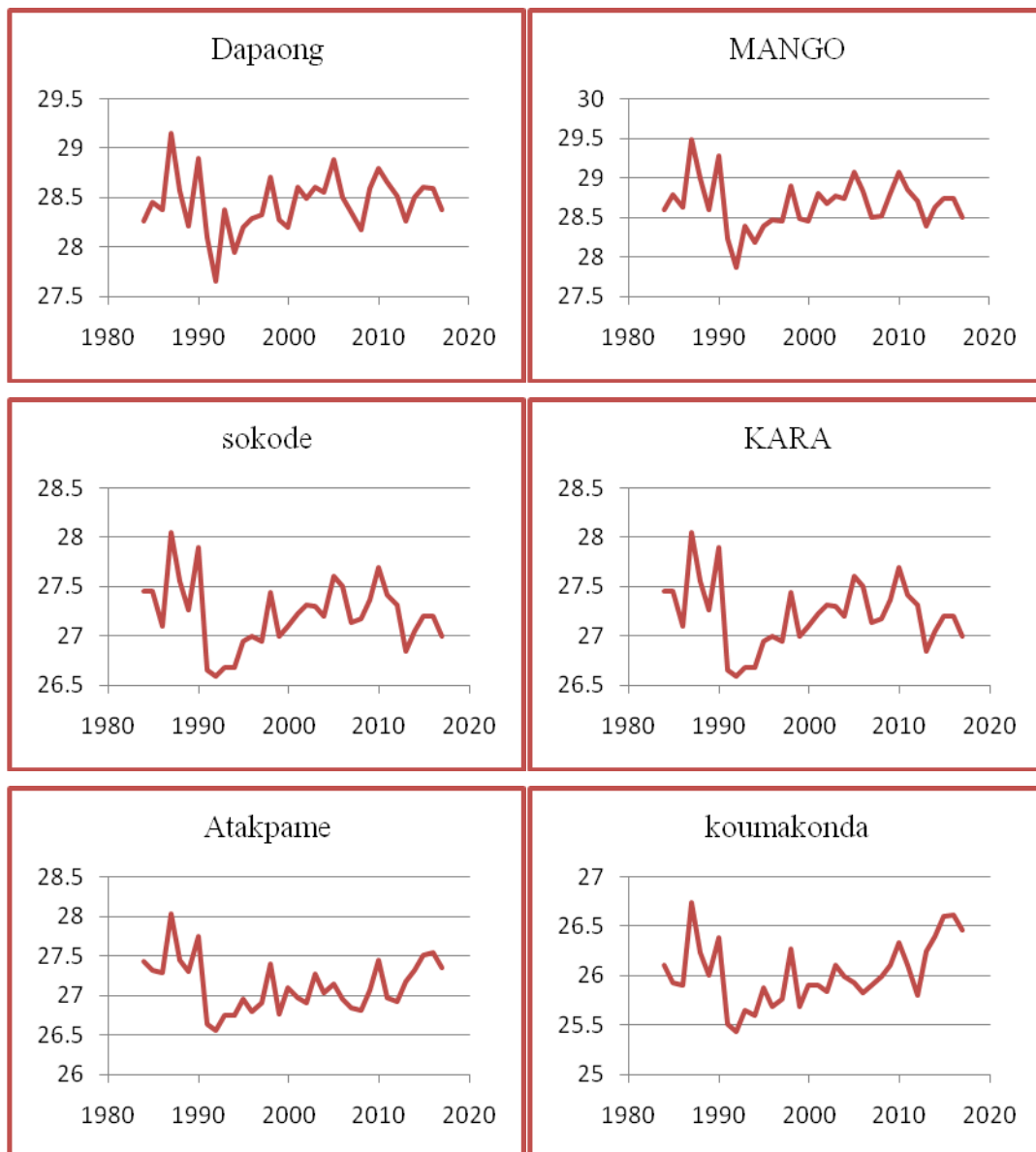


Figure 7. Annual of rainfall (mm) in the eight sampled meteorological stations in Togo during 1984-2017



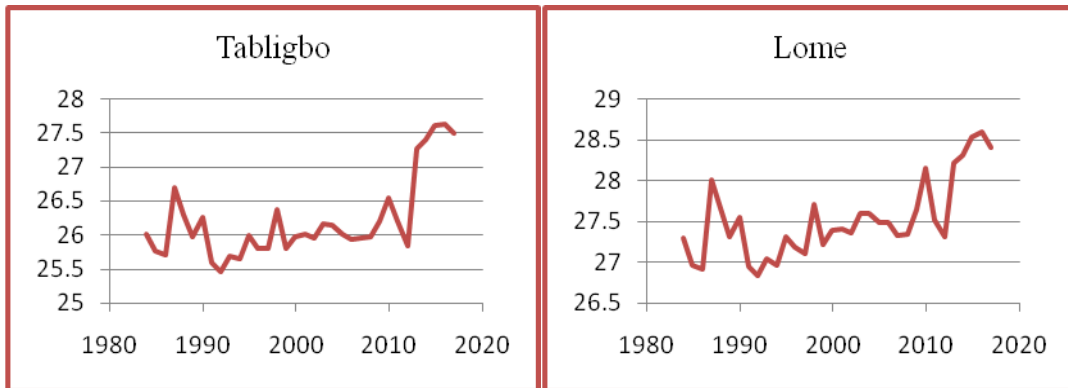
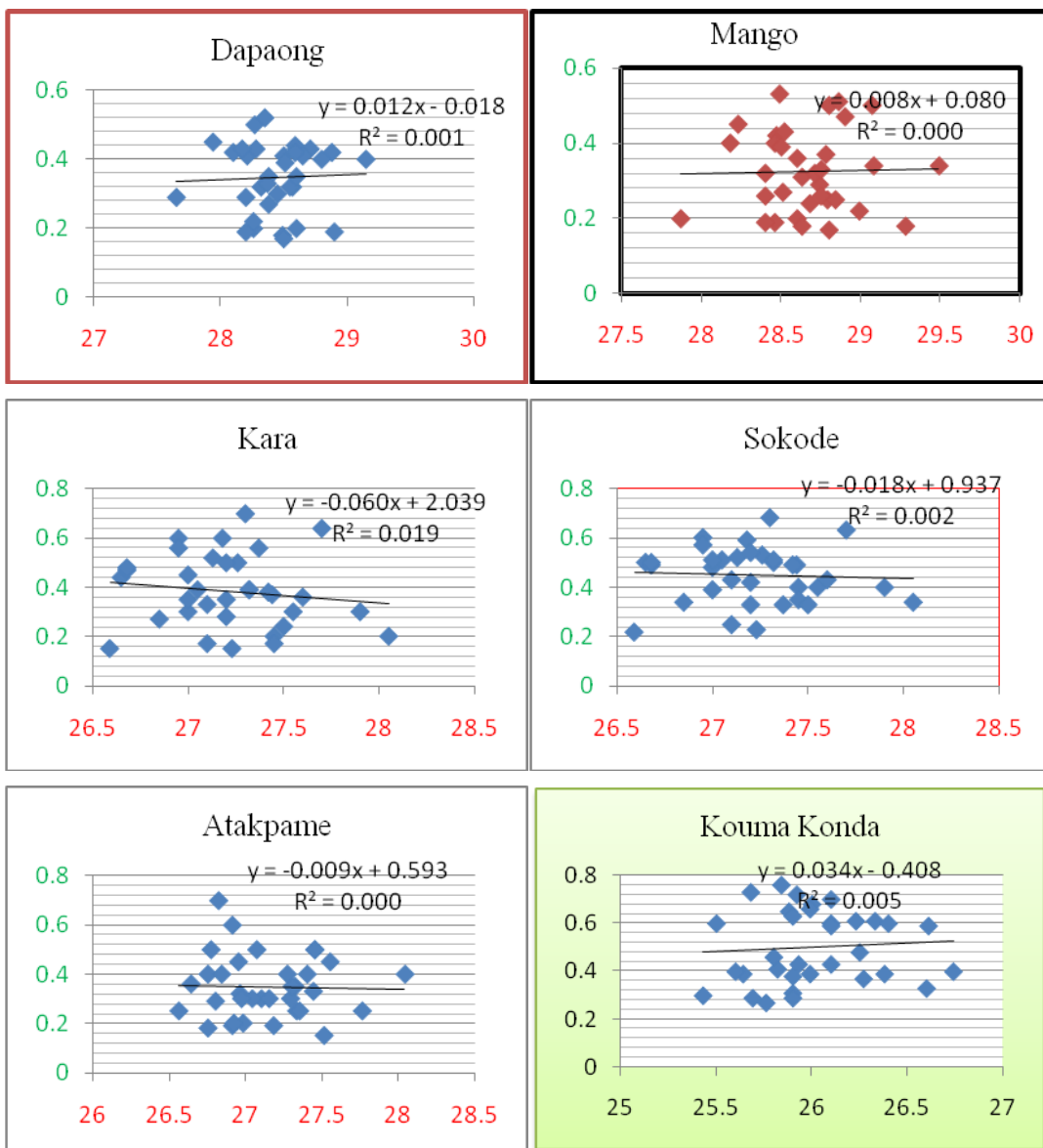


Figure 8. Time series of annual temperature ($^{\circ}\text{C}$) variations in eight meteorological stations

Regression analysis at local level



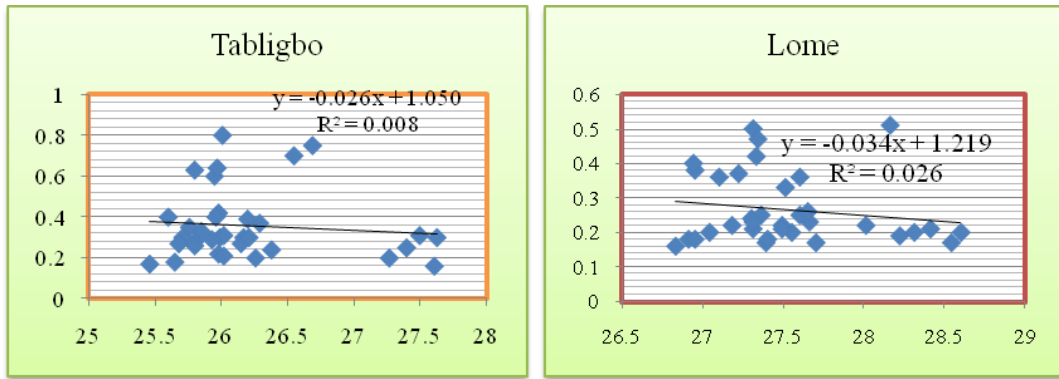
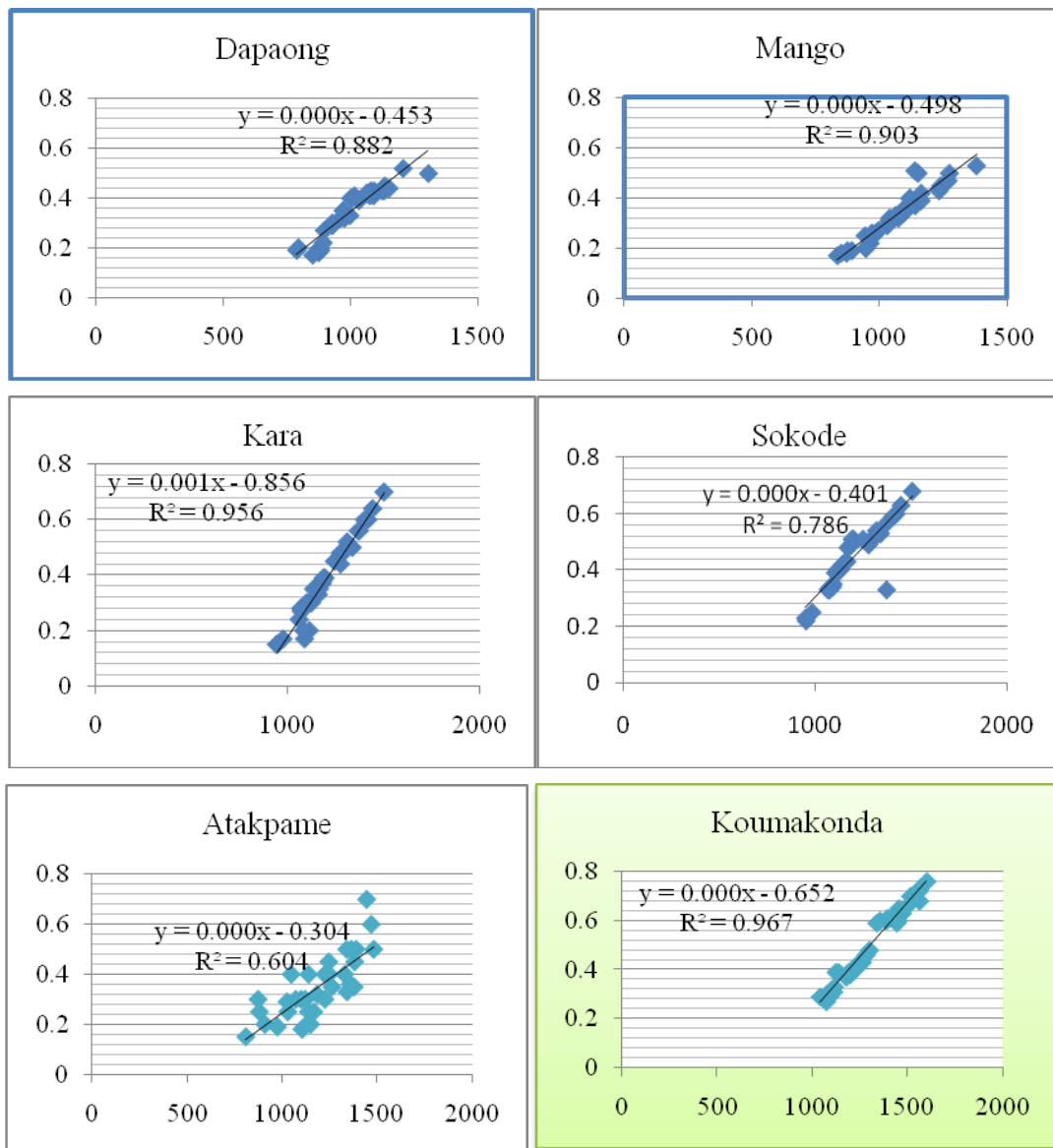


Figure 9. Annual changes in NDVI, temperature (°C) for the eight sampled meteorological stations in Togo during 1984-2017



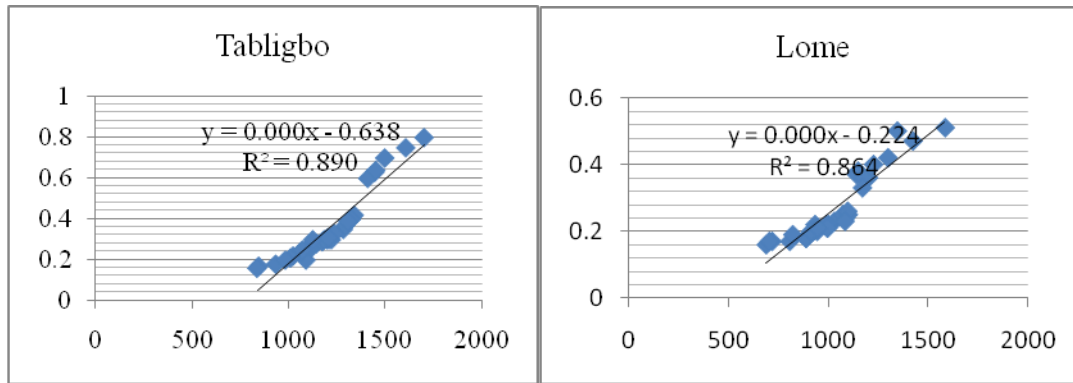


Figure 10. Annual changes in NDVI, rainfall (mm) for the eight sampled meteorological stations in Togo during 1984-2017

Through the regressions analysis between temperature and NDVI in one hand and between NDVI and annual rainfall at local scale in the eight sampled meteorological stations areas, several observation can be seen from 1984 to 2017

Under the Guinean subequatorial climate including Lome, Tabligbo, Kouma konda and Atakpame meteorological stations

- At Lome area, the relationship between NDVI and rainfall was significant at $p < 0.05$. The Kendall coefficient between NDVI and rainfall was 0.912 with a Pearson coefficient of 0.92 (Table 1; Figs. 9 and 10).
- In the Tabligbo area, the correlation between NDVI and rainfall is significant at $p < 0.05$. The Kendall coefficient between NDVI and rainfall is 0.944 and the Pearson coefficient is also 0.94 (Figs. 9 and 10).
- For the Kouma konda area, the correlation between NDVI and rainfall is significant at $p < 0.05$. The Kendall coefficient between NDVI and rainfall is 0.92 while the Pearson coefficient is 0.98 (Fig. 9).
- For the Atakpame area, NDVI changes according to rainfall more than temperature (Figs. 9 and 10). The Kendal's coefficient is -0.104 between temperature and rainfall and 0.625 between NDVI and rainfall and 0.028 between temperature and NDVI.
- In the Sokode area, the relationship between NDVI and rainfall is significant at $p < 0.05$. The Kendall coefficient between NDVI and precipitation is 0.845 while the Pearson coefficient is 0.88 (Table 1; Figs. 9 and 10).

Under the Tropical Sudanese climate including Dapaong, Mango, Kara and Sokode meteorological stations

- At Sokode station, NDVI was found to correlate strongly with NDVI with a p-value less than 0.00001 and statistic Z equal to 4.26489. The Pearson coefficient and the Kendall's were 0.85 and 0.88 respectively. But the temperature did not correlate strongly with the NDVI with a p-value less than 0.05. The correlation coefficient for temperature and NDVI were -0.101 for Kendall's and -0.05404108 for Pearson's.

- For the Kara area, the only significant relationship was between NDVI and rainfall ($p < 0.05$). The Kendall coefficient between NDVI and rainfall is 0.913 while the Pearson coefficient is 0.97 (Figs. 9 and 10).

Table 1. Annual correlation coefficient and two-tailed significance test values (p) between NDVI, rainfall, and temperature at local level during the last three decades (1984-2017) in the eight sampled areas in Togo

Station	Annual rainfall/NDVI				Annual temperature/NDVI			
	p-value	z	MK	Pearson's	z	MK	Pearson's	p-value
Lome	<0.00001	4.26489	0.92	0.9	0.35843	-0.102	-0.1621578	0.360009
Tabligbo	<0.00001	4.26489	0.94	0.9	0.51924	-0.011	-0.0692178	0.698202
Atakpame	<0.00001	4.26489	0.66	0.7	0.97054	0.028	0.03732365	0.834111
Koumakongda	<0.00001	4.26489	0.92	0.9	0.17585	0.071	0.10106936	0.569794
Sokode	<0.00001	4.26489	0.88	0.85	0.71162	-0.101	-0.0540411	0.76165
Kara	<0.00001	4.26489	0.913	0.977	0.1516	0.34	-0.1379442	0.439751
Mango	<0.00001	4.26489	0.9	0.95	1.23214	-0.004	0.02444853	0.891052
Dapaong	<0.00001	4.26489	0.896	0.39	0.97054	0.027	0.03732365	0.834111

In the Mango region, the only significant relationship also is that between NDVI and rainfall which is significant at $p < 0.05$. The Kendall coefficient between NDVI and rainfall is 0.92 while the Pearson coefficient is 0.98 (Fig. 9 and 10).

At Dapaong, the sole statistical relationship was between NDVI and rainfall, and was significant at $p < 0.05$. The Kendall coefficient between NDVI and rainfall is 0.896 while the Pearson coefficient is 0.94 (Fig. 9 and 10).

In addition, both at local and national scale the climatic parameters showed obvious changes for annual temperatures and annual rainfalls. At national level, the general trend of temperature is increasing since 1990. Before this upward trend, there has a slight decrease from 1984 to 1990 (Fig. 2). This observation is the same at local scale as the entire national trend of temperature (Fig. 4).

For the annual rainfall, the general trend at national level showed as constant trend ($y = 0.611x + 176.8$, $R^2 = 0.002$) (Fig. 2) with slight changes. It decreases from 1948 to 2000 and increases from 2000 to 2010 before dropping till 2015 and started increasing from 2015 to 2017. The general trend of rainfall is the same at national level for annual mean NDVI while at local level, NDVI showed different trends at each meteorological station areas.

In Dapaong, the general trend of NDVI is increasing (Dapaong annual rainfall = $0.001x - 2.776$ $R^2 = 0.024$; Fig. 4) with maximum values in 1999 and 2007 and minimums in 1990, 1995 and 2014 mainly.

In the Mango area, NDVI increased from 1984-1990 and then decreased from 1990-2000 and then increased again from 2000-2010 before decreasing from 2010 to 2017 (Mango annual rainfall = $0.001x - 2.456$ $R^2 = 0.016$; Fig. 4).

In the Kara area, the general trend of ndvi showed an increase (Kara annual ndvi mean = $0.004x - 8.987$, $R^2 = 0.098$ (Fig. 4). It peaked down in 1990, 2000, 2005 and 2015 mainly with maximums in 1989, 1995, 2003 and 2010 mainly.

At Sokode, the NDVI showed a general upward trend during these last three decades from 1984 with a regression equation from Fig. 4 (Sokode annual NDVI = $0.002x -$

4.005, $R^2 = 0.038$). Maximums were observed in the years 1989, 1995, 1997, 2003, 2008 and 2010 mainly.

At Atakpame, the general trend of NDVI is decreasing ($y = -0.0001x + 1.493$, $R^2 = 0.002$). At Kouma Konda, the NDVI trend is increasing slightly (*Fig. 4*) ($y = 0.000x - 1.026$, $R^2 = 0.002$) with maximums in 1985, 1989, 1995, 2002 and 2008 mainly and minimums in 1986, 1990, 1992, 1996, 2000, 2004, 2012 and 2015 mainly.

At Tabligbo it can be seen that the general trend of NDVI is decreasing ($y = -0.002x + 6.120$).

Lome station showed that the uptrend years of the annual temperature were different from that of rainfall and NDVI. Plots revealed changes in average NDVI between the eight sampled meteorological stations and their surroundings for NDVI, temperature and rainfall from 1984 to 2017 in Togo for chlorophyllous vegetation (green plants) (*Figs. 5-7*). There was a remarkable increase in (year) at (area name). All annual uptrend of NDVI can be interpreted as a vegetation growing.

Discussion

NDVI and climatic variability analysis at national level

The inter-annual variation of temperature trend at the national level has been increasing since 1984 in Togo. This increase of temperature has been already found by some previous studies related to climate change (Badameli et al., 2015). At the same time, the general trend of annual evapotranspiration is being increasing, these two factors correlated strongly (*Figs. 9-10*).

In addition, NDVI, which reflects chlorophyll (green plant material), correlated remarkably with rainfall at national level. These two findings showed a couple of factors which correlate one another: (NDVI, rainfall), and (temperature, evapotranspiration) while an increase of annual rainfall decreases the evapotranspiration (*Figs. 2-3*). This last observation can be explained by the decrease of temperature by rainfall which caused the evapotranspiration to decrease.

In other studies, an obvious impact of climatic factors on annual NDVI trends was shown, and differences can exist among the chlorophyll of plant species responding to the climate changes (Gang et al., 2016).

NDVI and climatic variability analysis at local level

All of the eight selected meteorological stations showed that a correlation between rainfall and NDVI was significant (*Figs. 9-10*) with a p-value < 0.00001 . The correlation coefficients both of Pearson and Kendall are highly positive and near 1 with a statistic $Z = 4.26489$. Except for KARA area where both the coefficient of Kendall is high and above 0.3 (*Fig. 10*) between NDVI and temperature and above 0.8 between NDVI and rainfall (*Fig. 10*). Between temperature and NDVI, the correlation is not significant (*Fig. 9-10*). These findings implied that NDVI which reflects the vegetation activity becomes rainfall dependent in the research area. This statement confirms the fact that green plants depend on water for their photosynthesis activities as all these findings are consistent with some of the previous studies related to the topic of rainfall and NDVI correlation (Malo et al., 1990). In addition, the NDVI is known not only to correlate well with rainfall, and also can be used as a useful tool to monitor rainfall under different climatic conditions (Di et al., 1994).

Other studies found that water availability is a limiting factor of green plant activity especially in carbon sequestration and photosynthesis activities (Gang et al., 2016). It has been found that, evapotranspiration can be used as a tool to measure the chlorophyll of green plants, with the capacity to influence rainfall, for instance, in the research area, the evapotranspiration correlates strongly with temperature (*Fig. 3*). An increase in temperature accelerates the evapotranspiration both by plants (transpiration) and rivers or soil (evaporation) explaining the positive correlation between annual mean temperature and evapotranspiration during these last three decades in Togo. These findings were consistent to the one found previously by (Shouichi et al., 1979) who reported that, between soil and vegetation there is the transfer of energy due to consumption of net radiation by green plants through photosynthesis, which will be used for evapotranspiration. Some other previous findings recognized the relationship between evapotranspiration and temperature due to solar radiation and chlorophyllous plant requirements for their several biosynthesis functions (Chapman et al., 1972; Julian et al., 1973; Wickham et al., 1978). In fact, not only the solar radiation (sunshine) but also temperature and rainfall (water availability) impacts deeply green plants photosynthetic activities under any climatic conditions (Gang et al., 2016).

This study showed that, the general trend of annual temperature is obviously increasing since 1990 in Togo. This upward trend could probably explained by global climate changes in the West Africa and the whole world. Many other studies confirmed this findings (IPCC, 2007) stressing the need to survey the influence of climatic factors especially temperature on vegetation.

Many other studies are of the opinion that the increase of annual temperature influences vegetation growth (Rustad, 2001). This statement is contrary to the observations made during our research in Togo where the upward trend of temperature does not correlate with the vegetation (NDVI) growth. Thus, the climatic factors are not the only factors to influence chlorophyllous plants growth.

Socio-economic drivers of NDVI and climatic inter annual changes

Any changes of NDVI reflects directly the variation of green plant covers, an indicator of chlorophyll or plants activity (photosynthesis and evapotranspiration) (Tucker et al., 1979). Therefore, the decrease of NDVI at national level from 1990 can be due to uncontrolled tree logging during the political events as bad implementation and understanding of democratization which put more pressure on the protected areas especially on forestland. From this year, the half part the Togolese national protected areas has been spoilt away putting the country on the list of highest rate of deforestation countries (Blaser J., 201) with a deforestation rate reported at 4.5% each year in 2000 (*Fig. 4*). Thus, the anthropogenic pressure on vegetation can be also justified by domestic energy needs as the population is increasing sharply, as their household energy use relies mainly on firewood and charcoal, and also for traditional medicinal use (Wala et al., 2005; Folega, 2011). Natural gas energy can be promoted and subsidized by the national leaders and reinforcements can be required in woodland, forest and natural protected areas management for more stringent restrictions for sustainability in nature conservation and green recovery.

In other perspectives, the high dependency of the majority of households on plant resources and farming related activities are also explained by the low income of the population in developing countries and the general conditions of poverty related resource use (Mukete, 2016). Therefore, the unceasing decrease of the forestlands in

Togo is due to anthropogenic pressure, especially in rural areas to the detriment of the forest and green vegetation in Togo.

Conclusions

During these last three decades in Togo from 1984 to 2017, the annual temperature, rainfall, evapotranspiration and NVDI obviously changed. A correlation analysis based on the annual time series data of temperature, rainfall, NDVI and evapotranspiration showed that, (1) rainfall correlated strongly with NDVI which reflect the chlorophyllous plants activities both at local and national scale. (2) evapotranspiration was influenced by annual temperatures all over the country in the eight sampled meteorological stations while (3) evapotranspiration and rainfall correlated negatively. (4) annual NDVI changes can be used to monitor annual rainfalls. (5) anthropogenic activities such as deforestation by uncontrolled tree logging, farming and low household income were the main contributing factors in addition to climate change. Among the high deforestation countries in the world, the Togo a national leaders would mitigate this challenge by promoting alternative energy sources to replace firewood for households, especially natural gas and reinforcements to be implemented in the current resources managements plans by participative management for sustainable development in Togo. The national level of climatic variations measurements and their impacts on some main species in the study areas is encouraged in next research projects to clarify the specific influence of climate change on each plant species.

Acknowledgements. This research was funded by the International Science & Technology cooperation Programme of China (2015DFR31130) and the National Natural Science Foundation of China (31670715; 41471029; 41371500). We are also grateful to the Chinese and Togolese Government for the cooperation scholarship and to my Supervisors and to Eve Bohnett for their generous help in the field investigation and English improvement during this research.

Conflict of interests. The authors declare that there is no conflict of interests regarding this paper.

REFERENCES

- [1] Adjoussi, P. (2000): Changement climatique global: évaluation de l'évolution des paramètres climatiques au Togo. – Mémoire de maîtrise, Département de Géographie, Université de Lomé.
- [2] Akpagana, K., Guelly, A. K. (1994): Nouvelles especes d'Angiospermes pour IA flore du Togo. – Acta Bot. Gallica 141(6/7): 781-787.
- [3] Badameli, A., Bubreuil, V. V. (2010): Diagnostic of climatic changes in Togo through temperature evolution from 1961 to 2010. – XXVIIIe Colloque de l'Association Internationale de Climatologie, Liège 2015.
- [4] Bartlett, D. S., Hardisky, M. A., Johnson, R. W., Gross, M. F., Klemas, V., Hartman, J. M. (1988): Continental scale variability in vegetation reflectance and its relationship to canopy morphology. – International Journal of Remote Sensing 9: 1223-1241.
- [5] Biasutti, M., Sobel, A. (2009): Delayed Sahel rainfall and global seasonal cycle in a warmer climate. – Geophysical Research Letters 36(L23): 707.
- [6] Blain, G. C. (2013): The modified Mann-Kendall test: on the performance of three variance correction approaches. – *Bragantia*, Campinas 72(4): 416-425.

- [7] Blaser, J., Sarre, A., Poore, D. et al. (2011): Status of Tropical Forest Management 2011. – ITTO Technical Series No 38. International Tropical Timber Organization, Yokohama, Japan. http://www.itto.int/news_releases/id=2663 (accessed on 28 February 2013).
- [8] Brunei, J. F., Scholz, H., Hiepko, P. (1984): Flore analytique du Togo. Phanerogames. – GTZ, Eschorn.
- [9] Capodici, F. G., Ciraolo, G., Loggia, L., Liuzzo, L. V., Noto, M. T. (2008): Time Series Analysis of Climate and Vegetation Variables in the Oreto Watershed (Sicily, Italy). – *European Water* 23/24: 133-145.
- [10] Chapman, A. L., Kininmonth, W. R. (1972): Water balance model for rain-grown, lowland rice in northern Australia. – *Agric. Meteorol.* 10: 65-82.
- [11] Chuai, X. W., Huang, X. J., Wang, W. J., Bao, G. (2013): NDVI, temperature and precipitation changes and their relationships with different vegetation types during 1998-2007 in Inner Mongolia, China. – *International Journal of Climatology* 33: 1696-1706.
- [12] Cui, L. Shi, J. (2010): Temporal and spatial response of vegetation NDVI to temperature and precipitation in eastern China. – *Journal of Geographical Sciences* 20(2): 163-176.
- [13] Di, L., Rundquist C., Luoheng, H. (1994): Modelling relationships between NDVI and precipitation during vegetative growth cycles. – *International Journal of Remote Sensing* 15(10): 2121-2136.
- [14] Ern, H. (1979): Die Vegetation Togo. Gliederung, Gefährdung, Erhaltung. – *Wildenowia* 9(2): 295-312.
- [15] FAO (2006, 2017): <http://www.fao.org/home/fr/>. – FAO, Rome.
- [16] Folega, F., Zhang, C. Y., Samake, G., Wala, K., Batawila, K., Zhao, X. H., Akpagana, K. (2011): Evaluation of agroforestry species in potential fallows of areas gazetted as protected areas in north-Togo. – *Afr J Agric Res* 6(12): 2828-2834.
- [17] Folega, F., Woegan, Y., Marra, D. (2015): Long term evaluation of green vegetation cover dynamic in the Atakora mountain chain (Togo) and its relation to carbon sequestration in West Africa. – *Journal of Mountain Science* 12(4):921-934
- [18] Fontodji, K. J. (2007): Impact de la production du charbon de bois sur les propriétés du sol et la biodiversité au Togo. – Mémoire de DEA, Université de Lomé, Togo.
- [19] Foody, G. M. (2003): Geographical weighting as a further refinement to regression modelling: an example focused on the NDVI-rainfall relationship. – *Remote Sensing of Environment* 88: 283-293.
- [20] Fu, G., Li, S.W., Sun, W., Shen, Z. X. (2016): Relationships between vegetation carbon use efficiency and climatic factors on the Tibetan Plateau. – *Canadian Journal of Remote Sensing*. 42:16-26.
- [21] Gausman, H. W. (1985): Plant Leaf Optical Properties in Visible and Near-Infrared Light. – Graduate Studies #29, Texas Tech University, Lubbock, TX.
- [22] Gazull, L. (2009): Bassin d’approvisionnement en bois-énergie de la ville de Bamako. Une approche par un modèle d’interaction spatiale. – Thèse de Doctorat, Université de Paris.
- [23] Gilabert, M., Gonzalez-Piqueras, J., Garcia-Haro, F. J. (2002): A generalized soil-adjusted vegetation index. – *Remote Sensing of Environment* 82: 303-310.
- [24] Goward, S. N., Tucker, C. J., Dye, D. G. (1985): North American vegetation patterns observed with the NOAA-7 advanced very high resolution radiometer. – *Vegetatio* 64: 3-14.
- [25] Helsel, D. R., Hirsch, R. M. (1992): Statistical Methods in Water Resources. – Elsevier, New York.
- [26] Ichii, K. A., Kawabata, Y. (2002): Global correlation analysis for NDVI and climatic variables and NDVI trends: 1982-1990. – *International Journal of Remote Sensing* 23(18): 3873-3878.
- [27] IPCC (2007): Climate Change 2007. The Physical Science Basis. – In: Solomon, S., Qin, D., Manning, M., Chen, Z., Marquis, M., Averyt, K. B., Tignor, M., Miller, H. L. (eds.) Contribution of Working Group I to the Fourth Assessment Report of the

- Intergovernmental Panel on Climate Change. Cambridge University Press Cambridge, UK and New York, USA.
- [28] IPCC (2013): Climate Change 2013. The Physical Science Basis. – In: Plattner, G.-K., Tignor M., Allen S. K., Boschung J., Nauels A., Xia Y., Bex V., Midgley P. M. (eds.) Contribution of Working Group I to the Fifth Assessment Report of the Intergovernmental Panel on Climate Change. Cambridge University Press, Cambridge, UK, New York, USA.
- [29] Julian, S. I. (1973): Water Management Innovations in the National Irrigation Administration. – In: Water Management in Philippine Irrigation Systems: Research and Operations. The International Rice Research Institute, Los Banos, Philippines, pp. 97-112.
- [30] Julien, M. (2014): Estimation de la biomasse de canne par modélisation et télédétection, Application à la Réunion. Océanographie. – Université de la Réunion, France.
- [31] Kendall, M. G. (1975): Rank Correlation Methods. – Charles Griffin, London, UK.
- [32] Kleinbaum, G., Kupper, L., Muller, K. (1998): Applied Regression Analysis and Other Multivariate Methods. – Duxbury Press, Toronto, pp.111-119.
- [33] Kokou, K., Guy, C., Koffi, A. (1999): Analyse floristique des îlots forestiers du sud du Togo. – Acta Botanica Gallica 146(2): 139-144.
- [34] Kokou, K., Nuto, K., Atsri, H. (2009): Impact of charcoal production on woody plant species in West Africa: a case study in Togo. – Scientific Research and Essay 4(8): 881-893.
- [35] Ma, M. G., Veroustraete, F. (2006): Interannual variability of vegetation cover in the Chinese Heihe River Basin and its relation to meteorological parameters. – International Journal of Remote Sensing 27: 3473-3486.
- [36] Malo, A. R., Nicholson, S. E. (1990): A study of rainfall and vegetation dynamics in the African Sahel using normalized differenced vegetation index. – Journal of Arid Environments 19: 1-24.
- [37] Mann, H. B. (1945): Nonparametric tests against trend. – Econometrica 13(3): 245-259.
- [38] Martiny, N., Camberlin, P., Richard, Y., Phillippon, N. (2006): Compared regimes of NDVI and rainfall in semi-arid regions of Africa. – International Journal of Remote Sensing 27(23-24): 5201-5223.
- [39] Mbatu, R. (2006): Forest policy, forest loss and land use cover change in Cameroon. – PhD Thesis, Oklahoma State University, Stillwater, USA.
- [40] Meng, M., Ni, J., Zong, M. J. (2011): Impacts of changes in climate variability on regional vegetation in China: NDVI-based analysis from 1982 to 2000. – Ecological Research 26: 421-428.
- [41] Mukete, B., Sun, Y., Zama, E., Achem, B., Mukete, T., Ndolo, L., Lonje, B. (2016): Environmental degradation in conflict and post-conflict regions. – International Journal of Environmental Protection and Policy 4(6): 187-195.
- [42] Mukete, B., Sun, Y., Etongo, D., Sajjad, S., Abdul, M. (2018): Assessing the drivers of land use change in the Rumpi hills forest protected area, Cameroon. – Journal of Sustainable Forestry. 37:592-618.
- [43] Nicholson, S. E., Farrar, T. J. (1994): The influence of soil type on the relationships between NDVI, rainfall and soil moisture in semiarid Botswana. I. NDVI response to rainfall. – Remote Sensing of Environment 50: 107-120.
- [44] Prince, S. D. (1991): Satellite remote sensing of primary production: comparison of results for Sahelian grassland 1981-1998. – International Journal of Remote Sensing 12: 1301-1311.
- [45] Richard, Y., Pocard, I. (1998): A statistical study of NDVI sensitivity to seasonal and interannual rainfall variations in Southern Africa. – International Journal of Remote Sensing 19(15): 2907-2920.

- [46] Rosental, W. D., Blanchard, B. J., Blanchard, A. J. (1985): Visible infrared microwave agriculture classification, biomass, and plant height algorithms. – *IEEE Transactions on Geoscience and Remote Sensing* (2):84-90.
- [47] Rouse, J. W., Hass, R. H., Schell, J. A., Deering, D. W., Harlan, J. C. (1974): Monitoring the Vernal Advancement and Retro Gradation (green wave effect) of Natural Vegetation. – NASA/GSFC Type 111 Final Report, Greenbelt, MD.
- [48] Rustad, L. E., Campbell, J. L., Marion, G. M., Norby, R. J., Mitchell, M. J., Hartley, A. E., Cornelissen, J. H. C., Gurevitch, J., *GCTE News* (2001): A meta-analysis of the response of soil respiration, net nitrogen mineralization, and aboveground plant growth to experimental ecosystem warming. – *Oecologia* 126(4): 543-562.
- [49] Schultz, P. A., Halpert, M. S. (1995): Global analysis of the relationships among a vegetation index, precipitation, and land surface temperature. – *International Journal of Remote Sensing* 16: 2755-2777.
- [50] Sellers, P. J. (1985): Canopy reflectance, photosynthesis, and transpiration. – *Int J Remote Sens* 6: 1335-1372.
- [51] Serreze, M. C., Walsh, J. E., Chapin III, F. S., Osterkamp T., Dyurgerov M., Romanovsky V., Oechel W. C., Morison J., Zhang T., Barry R. G. (2000): Observational evidence of recent change in the northern high-latitude environment. – *Climatic Change* 46: 159-207.
- [52] Shouichi, Y. (1979): A simple evapotranspiration model of a paddy field in tropical Asia. – *Soil Science and Plant Nutrition* 25(1): 81-91.
- [53] Tao, S., Dawson, R. W. (2002): Relations between AVHRR NDVI and eco-climatic parameters in China. – *International Journal of Remote Sensing* 23: 989-999.
- [54] Tarpley, J. D., Schneider, S. R., Money, R. L. (1984): Global vegetation indices from the NOAA-7 meteorological satellite. – *Journal of Climate and Applied Meteorology* 23: 491-494.
- [55] Townshend, J. R. G., Goff, T. E., Tucker, C. J. (1985): Multi-temporal dimensionality of images of normalized difference vegetation index at continental scales. – *IEEE Transactions on Geoscience and Remote Sensing* 23: 888-895.
- [56] Traore, S. A., Madsen, S. (1998): Quelques caractéristiques de la régénération naturelle des espèces ligneuses du Parc National du Niokolo Koba (Sénégal oriental). *Végétation et biodiversité au Sahel*. – *AAU Report* 39: 275-288.
- [57] Tucker, C. J. (1979): Red and photographic infrared linear combinations for monitoring vegetation. – *Remote Sens Environ* 8: 127-150.
- [58] Wala, K., Sinsin, B., Guely, A. K., Kokou, K., Akpagana, K. (2005): Typology and structure of parkland in the prefecture of Doufelgou (Togo). – *Sécheresse* 16(3): 209-216.
- [59] Wang, J., Price, K. P., Rich, P. M. (2001): Spatial patterns of NDVI in response to precipitation and temperature in the central Great Plains. – *International Journal of Remote Sensing* 22(18): 3827-3844.
- [60] Wang, S. P., Duan, J. C., Xu, G. P., Wang, Y. F., Zhang, Z. H., Rui, Y. C., Luo, C. Y., Xu, B., Zhu, X. X., Chang, X. F., Cui, X. Y., Niu, H. S., Zhao, X. Q., Wang, W. Y. (2012): Effects of warming and grazing on soil N availability, species composition, and ANPP in an alpine meadow. – *Ecology* 93(11): 2365-2376.
- [61] Weiss, J. L., Gutzler, D. S., Coonrod, J., Dahm, C. N. (2004): Seasonal and inter-annual relationships between vegetation and climate in central New Mexico, USA. – *Journal of Arid Environments* 57(4): 507-534.
- [62] Wickham, T. H., Sen, L. N. (1978): Water Management for Lowland Rice: Water Requirements and Yield Response. – In: *Soils and Rice*. International Rice Research Institute, Los Banos, Philippines.
- [63] Wilson, E. F., Sader, S. A. (2002): Detection of forest type using multiple dates of Landsat TM imagery. – *Remote Sens Environ* 80: 385-396.

- [64] Zhang, G. L., Xu, X. L., Zhou, C. P., Zhang, H. B., Ouyang, H. (2011): Responses of grassland vegetation to climatic variations on different temporal scales in Hulun Buir Grassland in the past 30 years. – *Journal of Geographical Sciences* 21(4): 634-650.

INTEGRATION OF HUMIC ACID WITH NITROGEN YIELDS AN AUXILIARY IMPACT ON PHYSIOLOGICAL TRAITS, GROWTH AND YIELD OF MAIZE (*Zea mays* L.) VARIETIES

KHAN, S. A.¹ – KHAN, S. U.¹ – QAYYUM, A.^{1*} – GURMANI, A. R.² – KHAN, A.¹ – KHAN, S. M.³ – AHMED, W.³ – MEHMOOD, A.² – AMIN, B. A. Z.⁴

¹*Department of Agronomy, The University of Haripur, 22620 Pakistan*

²*Department of Soil Science, The University of Haripur, 22620 Pakistan*

³*Department of Horticulture, The University of Haripur, 22620 Pakistan*

⁴*Department of Environmental Sciences, COMSATS University Islamabad, Abbottabad Campus, 22060 Pakistan*

**Corresponding author*

e-mail: qayyum2811@gmail.com, aqayyum@uoh.edu.pk

(Received 10th Feb 2019; accepted 8th Apr 2019)

Abstract. A field experiments was conducted to investigate the soil application of humic acid and nitrogen levels at Agricultural Research Station, Swabi, Pakistan during 2014. Experimental soil was deficient in organic matter (0.52%) and total nitrogen (0.029%). Effect of humic acid and nitrogen levels on plant height, leaves plant⁻¹, leaf area plant⁻¹, leaf area index, grain yield, total N uptake, net assimilation rate as well as nitrate reductase activity in leaves were determined using maize variety Jalal and Iqbal. Four levels of humic acid (0, 0.6, 1.2 and 1.8 kg ha⁻¹) and two levels of nitrogen (0 and 120 kg ha⁻¹) were applied in soil along with basal fertilization of phosphorus and potassium. Nitrogen concentrations and uptake were determined from the grain and stover. All the applied levels of humic acid significantly enhanced growth and yield attributes of both maize varieties in the presence of nitrogen. However, application of 1.2 and 1.8 kg ha⁻¹ were only effective to increase growth and yield attributes in the absence of nitrogen. Soil application of nitrogen significantly increased growth and yield of both maize varieties; however, it was significantly lower than all the soil applied HA levels with nitrogen. Maize variety Iqbal showed significantly higher NR activity in leaves, net assimilation rate, grain yield and harvest index than Jalal. Nitrogen concentration and uptake were significantly augmented with increasing level of humic acid in grain and stover. However, maximum total N uptake was recorded with the application of 1.8 kg ha⁻¹ HA+N in maize variety Iqbal. Among different applied HA levels, maximum grain yield was obtained from the soil application of 1.8 kg HA ha⁻¹ with nitrogen in both varieties. Therefore, 1.8 kg ha⁻¹ HA along with 120 kg N ha⁻¹ in maize variety Iqbal could be recommended for higher grain yield in calcareous N deficient soil conditions.

Keywords: *grain yield, leaf area index, net assimilation rate, humic acid, nitrogen levels*

Introduction

Maize is considered a major crop in Pakistan, as it occupy third most important position after wheat and rice in terms of area and grain yield (Government of Pakistan, 2016). Maize is cultivated for fodder and grain in various tropical, subtropical and temperate areas of the world; including Pakistan. Due to rapid increase in human population, horizontal increase in maize area is not possible. Therefore, the only way to increase maize productivity lies in increasing yield of existing maize genotypes through various integrated nutrient management practices (Grassini et al., 2011). Pakistani soils are mostly calcareous, alkaline and deficient in organic matter (Azam et al., 2001). Nutrients deficiencies prevail in the soil due to insufficient and poor

nutrient management which adversely affect the yield of crops and fertility of the soil with the course of time (Afzal and Ahmad, 2009). Different management practices are applied to enhance and sustain soil fertility. For example, production of field crops had been successfully improved with the application of farm yard manure, green manure, composting and application of some organic fertilizers. Nitrogen has main role in various physiological, biochemical processes and yield traits of maize (Amanullah, 2016; Maheswari et al., 2017). Nitrogen application improves growth rate of the plants with greater leaf expansion, reduced senescence and higher dry matter accumulation (Rizwan et al., 2003). It performs a crucial role in crop production as it contributes significantly to the yield and yield components of maize crop (Sharifi and Taghizadeh, 2009). However, its scarcity is regarded as one of the major yield retarding factors because it is prone to a number of losses.

Humic acid is an organically charged bio-stimulant (Moghadam et al., 2015) made by the bacterial and chemical processes in the soil. It is an essential part of organic matter that improves physical, biological and chemical properties of the soil, for example water holding capacity, nutrient availability, soil penetrability and soil structure (Nardi et al., 2002; Khan et al., 2013). It increases organic matter, organic carbon and water retention which ultimately augment fertilizer retention in the soil (Dong et al., 2006). It has the potential to enhance various physiological and biochemical process within the plant; for example, chlorophyll, net assimilation rate, carbohydrate, leaf area and roots development (Turkmen et al., 2004; Khan et al., 2013; Traversa et al., 2014). It can diminish nitrogen losses by stimulating soil exchangeable ammonium (NH_4^+) and available nitrate (NO_3^-) which leads towards higher nitrogen retention in the soil and uptake by the plants (Mohd et al., 2009). Therefore, adequate application of humic substances in the soil has capability to increase the availability of macro (N, P, K and Ca) and micro nutrients (Fe, Zn and Mn) as well as their uptake in the plants (Saruhan et al., 2011; Daur and Bakhshwain, 2013; Khan et al., 2013). It is important to identify maize varieties which have the ability to produce higher grain yield under the cropping systems practiced by the small land holder farmers, as very little effort has been made in this regard (Tolessa et al., 2007). Sustainable crop production depends on the continuous renewal of soil fertility through a balance between N demand and supply in cropping systems (Yousaf et al., 2016). There seems to be a synergistic relationship between humic acid and N as it has a crucial role on the fate of organic nitrogen in the soil, N cycling, distribution and its availability to the plants (Dong et al., 2009).

Soil of arid and semi-arid region having low precipitation and high evapotranspiration resulted in lower organic matter, nutrient deficiencies and high pH. The beneficial effect of humic acid and nitrogen in various plant species has been well reported; however, specific effect of different levels of HA with and without nitrogen in maize has yet to be explored. In addition, we will determine the potential of humic acid to trigger net assimilation rate, nitrate reductase activity, total nitrogen uptake and grain yield in two different maize varieties under field conditions.

Materials and methods

Experimental site

The study was conducted at experimental field located at 34° 7' 12 N and 72° 28' 12 E in Agricultural Research Station Swabi, Pakistan. The climate of the experimental site is sub-tropical, semi-arid, hot and continental with 568 mm annual rainfall on average basis. The average temperature of 40°C was recorded in the summer season, while the lower level of

temperature was 25°C in the same season. Average maximum temperature during the winter months was 18.4°C while the minimum temperature was 4°C.

Experimental procedure

Before starting the experiment, soil samples were collected from 0-30 cm depth at different locations of the field to determine the physico-chemical properties of soil. Soil was air dried, grinded and passed through 2 mm sieve to remove clods and materials other than soil. Soil characteristics were silt loam textural class with pH 7.8, electrical conductivity 0.20 dS m⁻¹, organic matter 0.52%, total nitrogen 0.029%, available phosphorous 5.72 mg kg⁻¹, potassium 118 mg kg⁻¹, zinc 2.30 mg kg⁻¹, copper 2.70 mg kg⁻¹, iron 2.41 mg kg⁻¹ and manganese 97 mg kg⁻¹. Field experiment was conducted during the summer 2014 in a randomized complete block design with split plot arrangement having three replications. Factorial experiment comprised of two maize varieties Jalal and Iqbal in the main plot, while the treatments of humic acids and N levels were allotted to the subplots. The area of each subplot was 4.9 m x 3 m (14.7 m²). Manual method of sowing was used for planting with plant to plant distance of 20 cm and row to row distance of 70 cm. Detail of treatments is given in *Table 1*. The Humic harvest, USA was purchased from market and used in the research study at 2000 ppm (2 g humic acid liter⁻¹) solution from the matured dried stems and empty heads of sunflower after seed removal. Basal fertilizer of P and K was applied at 100 and 60 kg ha⁻¹ in the form of single super phosphate and sulphate of potash. Soil was prepared well for sowing of maize varieties with the help of primary and secondary tillage. The required N levels were applied to the subplots of maize varieties in two split applications (17 days-after-sowing (DAS) and 35 DAS. Humic acid was applied to maize varieties 14 DAS in a single application. Weeds were controlled by the application of Primextra 400 mL (Atrazine 223 g/L + Metolachlor 277 g L⁻¹) weedicide before pre-emergence. Five irrigations were applied to the crop at knee stage (grand growth stage), pre-tasseling, silking, dough stage and seed fill stage with the help of canal water. Various cultural practices were done all over the growing period.

Table 1. Detail of treatments is given below

Treatments	Detail
T1	Control (without HA and N)
T2	Soil application of 0.6 kg HA + 0 kg N ha ⁻¹
T3	Soil application of 1.2 kg HA + 0 kg N ha ⁻¹
T4	Soil application of 1.8 kg HA + 0 kg N ha ⁻¹
T5	Soil application of 0 kg HA + 120 kg N ha ⁻¹
T6	Soil application of 0.6 kg HA + 120 kg N ha ⁻¹
T7	Soil application of 1.2 kg HA + 120 kg N ha ⁻¹
T8	Soil application of 1.8 kg HA + 120 kg N ha ⁻¹

The data on plant height, leaves plant⁻¹ at silking, leaf area plant⁻¹ at silking, leaf area index (LAI) at silking, nitrate reductase (NR) activity in leaves at 30 DAS, net assimilation rate (NAR) at 30-75 DAS, ears m⁻², ears plant⁻¹, ear length (cm), thousand grain weight (g), grain yield (kg ha⁻¹), stover yield (kg ha⁻¹), harvest index (%), grain N concentration (%), stover N concentration (%), grain N uptake (kg ha⁻¹), stover N uptake (kg ha⁻¹) and total N uptake (kg ha⁻¹) were determined. For determining plant height, five maize plants were selected randomly at silking from each subplot and the average length was measured from ground level to the top of tassel by using a measuring tape. Likewise,

at silking five maize plants were taken at random from each subplot, leaves counted and the average calculated. The leaf area (cm^2) plant^{-1} was measured by multiplying average leaf area with number of leaves plant^{-1} and the LAI was calculated by digital hand held laser leaf area meter (CI-203 Bio- Science, USA). The enzyme nitrate reductase (NR EC 1.7.1.1) activity in leaves was measured from fresh plant tissues of three top leaves at 30 DAS and expressed as unit per mg protein (Lewis et al., 1982). One unit equivalents to the production of 1 μmol of NO_2 per minute at 25°C . Net assimilation rate (30-75 DAS) was determined by dividing the total dry matter of plants by their leaf area duration (Beadle, 1993). It was expressed as $\text{g m}^{-2} \text{day}^{-1}$.

The number of ears m^{-2} was calculated by dividing the number of ears by row length (m) x r-r distance x number of rows. The number of ears plant^{-1} was recorded by dividing the numbers of ears by the number of ears in each subplot. For ear length of maize varieties, after harvesting and dehusking, the length of five ears was recorded and averaged. At crop maturity, the two central rows were harvested manually. All the plots of the crop were bundled separately, labeled properly and brought to the threshing room. The 1000-grain weight, stover yield and grain yield were estimated with electrical balance. Likewise, the harvest index (HI) was recorded by dividing the grain yield by biological yield and then multiplying by 100. The grain and stover N concentration (%) was calculated by the Bremner and Mulvaney (1982) method, which is known as Kjeldahl method. The grain and stover N uptake (kg ha^{-1}) were measured by multiplying the grain and stover N concentration (%) with grain and stover yield (kg ha^{-1}) respectively and then dividing by 100. Furthermore, the total N uptake was calculated by adding the grain N uptake and stover N uptake.

Statistical analysis

Data were statistically analyzed using the analysis of variance using the method described by Steel et al. (1997), and means between treatments was compared by least significant difference ($P \leq 0.05$). All the parameters mean values were expressed as mean value with standard error (SE).

Results

Plant height (cm)

Plant height of both maize varieties were significantly increased with the combined effect of all the applied levels of humic acid with N; however, alone application of humic acid was only significant in 1.8 kg ha^{-1} in both varieties. The sole application of N substantially increased plant height of both varieties, however, it was significantly lower than the application of 1.2 and 1.8 kg HA with N (Table 2). Plant height increase due to the application of 1.2 and $1.8 \text{ kg HA ha}^{-1}$ with N was statistically at par with each other. Maximum plant height was recorded with the application of $1.8 \text{ kg HA ha}^{-1}$ with N; while the minimum was achieved with control plants in both maize varieties. Plant height of maize variety Jalal was significantly higher than Iqbal.

Leaves plant⁻¹

The sole application of 1.2 and $1.8 \text{ kg HA ha}^{-1}$ significantly enhanced the number of leaves plant^{-1} , however, any increase due to individual application of $0.6 \text{ Kg HA ha}^{-1}$ was statistically not different as compared to control in both maize varieties (Table 2). The alone effect of 1.2

and 1.8 kg HA ha⁻¹ was statistically at par with each other in terms of number of leaves plant⁻¹. Individual application of N and all the combined applications of HA with N significantly increased number of leaves plant⁻¹ in both the maize varieties. The maximum number of leaves plant⁻¹ was observed with the combined application of 1.8 kg HA ha⁻¹ + N which was at par with 1.2 kg HA ha⁻¹ + N. Higher number of leaves plant⁻¹ were recorded in maize variety Jalal as compared to Iqbal.

Table 2. Effect of different levels of humic acid in the absence and presence of nitrogen on plant height (cm) and leaves plant⁻¹ of maize variety Jalal and Iqbal

Treatments	Plant height (cm)		Leaves plant ⁻¹	
	Jalal	Iqbal	Jalal	Iqbal
Control (0 kg HA + 0 kg N ha ⁻¹)	197.8±0.92 de	177.0±0.44 i	11.56±0.04 f	10.74±0.04 i
0.6 kg HA + 0 kg N ha ⁻¹	199.3±0.87 d	178.8±0.28 hi	11.72±0.05 ef	10.79±0.04 hi
1.2 kg HA + 0 kg N ha ⁻¹	201.0±1.05 cd	180.3±0.86 hi	11.87±0.02 de	10.96±0.04 gh
1.8 kg HA + 0 kg N ha ⁻¹	202.6±1.19 c	181.7±0.80 h	11.99±0.04 d	11.06±0.04 g
0 kg HA + 120 kg N ha ⁻¹	207.8±0.52 b	190.1±0.23 g	12.45±0.04 c	11.57±0.02 f
0.6 kg HA + 120 kg N ha ⁻¹	209.2±0.41 b	192.0±0.36 fg	12.62±0.04 bc	11.74±0.04 ef
1.2 kg HA + 120 kg N ha ⁻¹	210.9±0.40 ab	193.2±0.28 fg	12.83±0.04 ab	11.81±0.05 de
1.8 kg HA + 120 kg N ha ⁻¹	213.3±0.45 a	194.80±0.38 ef	12.98±0.07 a	11.97±0.04 d
Means	205.2 a	186.0 b	12.25 a	11.33 b

Mean followed by same letters in a column do not differ significantly at P ≤ 0.05

Leaf area (cm²) plant⁻¹

Leaf area index was significantly improved with all the applied levels of humic acid, except 0.6 Kg HA ha⁻¹ in the absence of N in both maize varieties. (Table 3). The alone impact of 1.2 and 1.8 kg HA ha⁻¹ on leaf area plant⁻¹ of both maize varieties were statistically same with each other. However, the effect of alone application of humic acid on leaf area plant⁻¹ was lower than sole use of N. The integrated application of all the HA levels with N significantly accelerated the leaf area plant⁻¹ in both maize varieties. Maximum leaf area plant⁻¹ was recorded with 1.8 Kg ha⁻¹ HA+N in maize variety Jalal, while the minimum was recorded with control plants in Iqbal.

Leaf area index (LAI)

All the levels of applied humic acid in the absence and presence of nitrogen and alone application of nitrogen improved leaf area index in both maize varieties (Table 3). However, in the absence of nitrogen, 1.8 kg ha⁻¹ humic acid significantly enhanced leaf area index in both varieties. The leaf area index increase due to the individual application of HA at 0.6 and 1.2 kg HA ha⁻¹ was at par with each other in either maize variety. The combined use of 1.8 kg HA ha⁻¹ + N resulted in maximum leaf area index which was at par with 1.2 kg HA ha⁻¹ + N in both varieties. Maize variety Jalal exhibited higher leaf area index as compared to Iqbal. Lower leaf area index was recorded in control plots of humic acid and N.

Nitrate reductase activity in leaves (unit mg⁻¹ protein)

Nitrate reductase (NR) activity in leaves was significantly accelerated with the increasing level of humic acid in the absence and presence of nitrogen in both maize varieties (Table 4). The sole impact of 1.2 and 1.8 kg HA ha⁻¹ on NR activity of maize

varieties was statistically at par with each other. Although, the alone application of N significantly increased NR activity; however, the magnitude of increase was higher under the combined use of humic acid and nitrogen. Moreover, highest NR activity was observed at 1.8 kg HA ha⁻¹ + N while the lowest was recorded with control plants in both varieties. The impact of 1.8 kg HA ha⁻¹ + N on NR activity was at par with 1.2 kg HA ha⁻¹ + N in each variety. The average mean of Iqbal superseded the mean of Jalal variety.

Table 3. Effect of different levels of humic acid in the absence and presence of nitrogen on leaf area plant⁻¹ and leaf area index (LAI) of maize variety Jalal and Iqbal

Treatments	Leaf area (cm ²) plant ⁻¹		Leaf area index (LAI)	
	Jalal	Iqbal	Jalal	Iqbal
Control (0 kg HA + 0 kg N ha ⁻¹)	4469±38.55 gh	3959±28.30 k	3.16±0.01 f	2.76±0.03 h
0.6 kg HA + 0 kg N ha ⁻¹	4596±9.45 efg	4064±40.48 jk	3.18±0.03 ef	2.80±0.02 gh
1.2 kg HA + 0 kg N ha ⁻¹	4697±31.39 de	4194±39.61 ij	3.25±0.02 de	2.83±0.01 gh
1.8 kg HA + 0 kg N ha ⁻¹	4827±24.26 d	4265±27.17 i	3.28±0.01 d	2.86±0.01 g
0 kg HA + 120 kg N ha ⁻¹	5122±49.69 c	4418±33.03 h	3.56±0.01 c	3.11±0.01 f
0.6 kg HA + 120 kg N ha ⁻¹	5279±30.15 b	4541±25.71 fgh	3.66±0.02 b	3.18±0.01 ef
1.2 kg HA + 120 kg N ha ⁻¹	5390±27.02 ab	4643±28.04 ef	3.75±0.02 ab	3.24±0.01 de
1.8 kg HA + 120 kg N ha ⁻¹	5499±33.87 a	4729±28.06 de	3.82±0.02 a	3.30±0.02 d
Means	4985 a	4352 b	3.46 a	3.01 b

Mean followed by same letters in a column do not differ significantly at P ≤ 0.05

Table 4. Effect of different levels of humic acid in the absence and presence of nitrogen on nitrate reductase activity in leaves and net assimilation rate of maize variety Jalal and Iqbal

Treatments	Nitrate reductase activity in leaves (30 DAS)		Net assimilation rate (30-75 DAS)	
	Jalal	Iqbal	Jalal	Iqbal
Control (0 kg HA + 0 kg N ha ⁻¹)	0.17±0.01 i	0.19±0.01 i	8.34±0.03 l	10.30±0.06 g
0.6 kg HA + 0 kg N ha ⁻¹	0.24±0.01 h	0.27±0.01 gh	8.50±0.07 k	10.38±0.02 fg
1.2 kg HA + 0 kg N ha ⁻¹	0.27±0.01 gh	0.31±0.02 f	8.66±0.08 j	10.52±0.02 ef
1.8 kg HA + 0 kg N ha ⁻¹	0.29±0.01 fg	0.33±0.01 ef	8.79±0.02 j	10.65±0.02 e
0 kg HA + 120 kg N ha ⁻¹	0.32±0.01 f	0.37±0.01 d	9.45±0.05 i	11.69±0.02 d
0.6 kg HA + 120 kg N ha ⁻¹	0.37 ± 0.01 de	0.42±0.01 c	9.54±0.05 hi	11.85±0.02 c
1.2 kg HA + 120 kg N ha ⁻¹	0.41±0.01 bc	0.46±0.01 ab	9.71±0.03 fg	12.03±0.04 b
1.8 kg HA + 120 kg N ha ⁻¹	0.45±0.01 b	0.50±0.01 a	9.76±0.04 f	12.23±0.02 a
Means	0.32 b	0.36 a	9.09 b	11.21 a

Mean followed by same letters in a column do not differ significantly at P ≤ 0.05

Net assimilation rate (g m⁻² day) (30-75 DAS)

Increasing level of applied humic acid significantly improved net assimilation rate (NAR) respectively in the absence and presence of nitrogen, except individual application of humic acid at 0.6 kg ha⁻¹ in both varieties (Table 4). Each variety showed similar net assimilation rate due to the individual application of 1.2 and 1.8 kg HA ha⁻¹. The application of 1.8 kg HA ha⁻¹ along with N showed highest net assimilation rate in both varieties. Maize variety Iqbal exhibited higher NAR than Jalal. Net assimilation rate increase due to the application of humic acid at 1.2 kg ha⁻¹ and 1.8 kg ha⁻¹ along with nitrogen was statistically at par with each other in maize variety Jalal. Likewise, net assimilation rate increase due to the alone application of nitrogen and 0.6 kg ha⁻¹ HA+N was statistically at par with each other in Jalal.

Ears m⁻²

Both of the maize varieties showed a significant response for the number of ears m⁻² against the applied levels of humic acid in the presence and absence of N, except the sole application of humic acid at 0.6 kg ha⁻¹. The alone application of N had a significant impact on the number of ears m⁻² in both maize varieties (*Table 5*). Individual application of humic acid at 1.2 and 1.8 kg ha⁻¹ on ears m⁻² was statistically at par with each other in both the maize varieties. The highest number of ears m⁻² was observed at 1.8 kg HA ha⁻¹ + N in both varieties. The effect of 1.8 kg HA ha⁻¹ + N was statistically at par with 1.2 kg HA ha⁻¹ in Jalal regarding the number of ears m⁻². The lowest number of ears m⁻² was recorded in the control plots of Jalal, while the highest was achieved with Iqbal.

Table 5. Effect of different levels of humic acid in the absence and presence of nitrogen on ears m² and ears plant⁻¹ of maize variety Jalal and Iqbal

Treatments	Ears m ²		Ears plant ⁻¹	
	Jalal	Iqbal	Jalal	Iqbal
Control (0 kg HA + 0 kg N ha ⁻¹)	5.26±0.02 h	5.47±0.01 fg	0.76±0.01 j	0.78±0.01 ij
0.6 kg HA + 0 kg N ha ⁻¹	5.31±0.02 hi	5.53±0.02 ef	0.78±0.01 hj	0.80±0.01 ghi
1.2 kg HA + 0 kg N ha ⁻¹	5.38±0.01 gh	5.65±0.01 de	0.79±0.01 hi	0.82±0.01 fg
1.8 kg HA + 0 kg N ha ⁻¹	5.46±0.02 fg	5.70±0.02 d	0.82±0.01 g	0.85±0.01 e
0 kg HA + 120 kg N ha ⁻¹	5.75±0.05 d	5.95±0.04 c	0.86±0.01 de	0.89±0.01 cd
0.6 kg HA + 120 kg N ha ⁻¹	5.98±0.03 c	6.11±0.01 b	0.88±0.01 d	0.91±0.01 c
1.2 kg HA + 120 kg N ha ⁻¹	6.04±0.03 bc	6.16±0.03 b	0.91±0.01 bc	0.94±0.01 ab
1.8 kg HA + 120 kg N ha ⁻¹	6.15±0.04 b	6.33±0.03 a	0.94±0.01 ab	0.97±0.01 a
Means	5.67 b	5.86 a	0.84 b	0.87 a

Mean followed by same letters in a column do not differ significantly at P ≤ 0.05

Ears plant⁻¹

The application of humic acid in the presence and absence of N, as well as the alone application of N significantly influenced the number of ears plant⁻¹ in both the maize varieties of Jalal and Iqbal. However, the alone application of 0.6 kg HA ha⁻¹ did not cause any significant increase in the number of ears plant⁻¹ (*Table 5*). The sole application of humic acid at 1.8 kg HA ha⁻¹ produced the highest number of ears plant⁻¹. Though the sole application of N enhanced the ear bearing capacity of maize varieties, but the maximum number of ears plant⁻¹ was recorded with 1.8 kg HA ha⁻¹ + N. The minimum number of ears plant⁻¹ was observed in the control plots. The higher number of ears plant⁻¹ was measured in Iqbal variety of maize as compared with Jalal.

Ear length (cm)

The ear length of both maize varieties exhibited a significant response to the sole application of N as well as all the applied levels of humic acid with and without N, except the alone application of humic acid at 0.6 kg ha⁻¹ (*Table 5*). The alone impact of 1.2 and 1.8 kg HA ha⁻¹ on ear length of maize variety Jalal was statistically at par with each other. The maximum ear length was recorded with the combined use of 1.8 kg HA ha⁻¹ + N, although the sole use of N also had a significant impact on the bulk of increase in each variety. The effect 1.8 HA ha⁻¹ + N and 1.2 kg HA ha⁻¹ + N on ear length of each variety was statistically at par with each other in both varieties. The minimum ear length was measured in control plots of both varieties. The mean average of ear length of Iqbal was significantly higher than Jalal variety of maize.

Thousand grain weight (g)

The individual application of humic acid and N as well as their integrations had a substantial influence on thousand grain weight of maize variety Jalal and Iqbal (Table 6). Under the sole application of humic acid, the plots treated with 1.8 kg HA ha⁻¹ produced highest thousand grain weight in both maize varieties. The individual effect of 0.6 and 1.2 kg HA ha⁻¹ was statistically at par with each other in both varieties. The highest thousand grain weight was recorded in plots supplied with 1.8 kg HA ha⁻¹ + N in Iqbal while the lowest was recorded in control plots of Jalal. Furthermore, the plots treated with sole N and 0.6 kg HA ha⁻¹ + N produced the same thousand grain weight in Jalal.

Table 6. Effect of different levels of humic acid in the absence and presence of nitrogen on ear length (cm) and thousand grain weight (g) of maize variety Jalal and Iqbal

Treatments	Ear length (cm)		Thousand grain weight (g)	
	Jalal	Iqbal	Jalal	Iqbal
Control (0 kg HA + 0 kg N ha ⁻¹)	14.30±0.04 k	15.22±0.03 i	179.9±0.95 k	192.6±0.47 gh
0.6 kg HA + 0 kg N ha ⁻¹	14.46±0.05 jk	15.37±0.04 hi	183.4±0.32 j	195.5±0.55 ef
1.2 kg HA + 0 kg N ha ⁻¹	14.70±0.04 i	15.56±0.02 gh	185.2±0.23 j	197.3±0.49 de
1.8 kg HA + 0 kg N ha ⁻¹	14.90±0.01 hi	15.82±0.03 ef	187.5±0.38 i	199.7±0.38 d
0 kg HA + 120 kg N ha ⁻¹	15.84±0.04 g	17.14±0.04 d	191.8±1.04 h	204.1±0.94 c
0.6 kg HA + 120 kg N ha ⁻¹	16.07±0.01 f	17.36±0.03 c	194.3±0.75 fg	206.5±0.42 c
1.2 kg HA + 120 kg N ha ⁻¹	16.31±0.03 de	17.65±0.07 ab	197.1±0.55 e	209.4±0.60 b
1.8 kg HA + 120 kg N ha ⁻¹	16.51±0.03 d	17.76±0.05 a	199.4±0.51 d	212.9±0.97 a
Means	15.39 b	16.48 a	189.8 b	202.2 a

Mean followed by same letters in a column do not differ significantly at P ≤ 0.05

Grain yield (kg ha⁻¹)

The grain yield of both varieties was substantially enhanced with the increasing levels of humic acid, nitrogen as well as their combined application (Table 7). Under the alone application of humic acid, 1.8 kg HA ha⁻¹ resulted in higher grain yield in each variety. The application of humic acid at 1.8 kg ha⁻¹ with N, produced the plants with the highest grain yield in both the maize varieties. The impact of 1.8 HA ha⁻¹ + N and 1.2 kg HA ha⁻¹ + N on grain yield of both varieties was statistically at par with each other. The highest grain yield was achieved in plots of Iqbal treated with 1.8 kg HA ha⁻¹ + N while the lowest was recorded in control plots of Jalal.

Table 7. Effect of different levels of humic acid in the absence and presence of nitrogen on grain yield (kg ha⁻¹) and stover yield (kg ha⁻¹) of maize variety Jalal and Iqbal

Treatments	Grain yield (kg ha ⁻¹)		Stover yield (kg ha ⁻¹)	
	Jalal	Iqbal	Jalal	Iqbal
Control (0 kg HA + 0 kg N ha ⁻¹)	2540±21.65 l	2937±7.88 k	7648±23.41 h	6847±47.94 j
0.6 kg HA + 0 kg N ha ⁻¹	3066±4.37 j	3209±20.43 i	8298±21.73 e	7031±42.04 i
1.2 kg HA + 0 kg N ha ⁻¹	3224±20.46 i	3328±31.12 h	8485±37.29 e	7084±71.96 i
1.8 kg HA + 0 kg N ha ⁻¹	3385±14.97 h	3517±23.81 g	8751±53.13 d	7303±17.36 h
0 kg HA + 120 kg N ha ⁻¹	3942±19.19 f	4064±32.32 e	9115±43.37 c	7605±44.55 g
0.6 kg HA + 120 kg N ha ⁻¹	4192±27.22 d	4312±23.38 c	9367±15.13 b	7778±33.74 fg
1.2 kg HA + 120 kg N ha ⁻¹	4465±31.65 b	4564±19.40 b	9542±23.07 ab	7851±22.98 ef
1.8 kg HA + 120 kg N ha ⁻¹	4742±9.53 a	4817±17.95 a	9623±62.44 a	8012±25.10 e
Means	3694 b	3844 a	8854 a	7439 b

Mean followed by same letters in a column do not differ significantly at P ≤ 0.05

Stover yield (kg ha⁻¹)

Stover yield of both maize varieties were significantly increased with the combined application of humic acid + N as well as under the alone application of humic acid and N (Table 7). The alone effect of 0.6 and 1.2 kg HA ha⁻¹ on stover yield of both varieties was statistically at par with each other. Though the sole application of N improved stover yield of maize varieties but the maximum response was observed at 1.8 kg HA ha⁻¹ + N which was at par with 1.2 kg HA ha⁻¹ + N. The Jalal variety of maize exhibited highest stover yield than Iqbal. In Iqbal variety of maize, the individual effect of N was similar with the combined effect of 0.6 kg HA ha⁻¹ + N.

Harvest index (%)

The integration of humic acid and nitrogen as well as their alone applications considerably affected the harvest index of both maize varieties. The individual effect of 0.6 and 1.2 kg HA ha⁻¹ on harvest index was statistically at par with 1.8 kg HA ha⁻¹ in both varieties (Table 8). Maximum harvest index was recorded at 1.8 kg HA ha⁻¹ + N in each variety of maize. However, the impact of 1.8 kg HA ha⁻¹ + N was similar with 1.2 kg HA ha⁻¹ + N in both the varieties. Moreover, in Jalal variety of maize the integrated impact of 0.6 kg HA ha⁻¹ + N were found to be at par with individual application of N in terms of harvest index. The Iqbal variety of maize exhibited higher harvest index than Jalal.

Table 8. Effect of different levels of humic acid in the absence and presence of nitrogen on harvest index (%) and grain N concentration (%) of maize variety Jalal and Iqbal

Treatments	Harvest index (%)		Grain N concentration (%)	
	Jalal	Iqbal	Jalal	Iqbal
Control (0 kg HA + 0 kg N ha ⁻¹)	24.93±0.14 j	29.72±0.18 h	1.27±0.01 j	1.31±0.02 i
0.6 kg HA + 0 kg N ha ⁻¹	26.97±0.06 i	31.34±0.19 ef	1.32±0.01 i	1.36±0.01 h
1.2 kg HA + 0 kg N ha ⁻¹	27.53±0.16 i	31.97±0.42 de	1.40±0.01 g	1.42±0.01 fg
1.8 kg HA + 0 kg N ha ⁻¹	27.88±0.20 i	32.49±0.10 cde	1.43±0.01 efg	1.46±0.01 def
0 kg HA + 120 kg N ha ⁻¹	30.19±0.10 gh	34.82±0.20 c	1.44±0.01 efg	1.47±0.01 cde
0.6 kg HA + 120 kg N ha ⁻¹	30.92±0.15 fg	35.67±0.04 b	1.47±0.01 cd	1.50±0.01 bc
1.2 kg HA + 120 kg N ha ⁻¹	31.89±0.11 de	36.76±0.05 a	1.48±0.01 cd	1.53±0.01 b
1.8 kg HA + 120 kg N ha ⁻¹	33.01±0.19 c	37.55±0.05 a	1.53±0.01 b	1.57±0.01 a
Means	29.16 b	33.79 a	1.41 b	1.45 a

Mean followed by same letters in a column do not differ significantly at $P \leq 0.05$

Grain N concentration (%)

The response of maize varieties Jalal and Iqbal for grain N concentration was found to be significant against all the applied levels of humic acid, nitrogen and their combination. However, the effect of sole application of 1.2 and 1.8 kg HA ha⁻¹ on grain N concentration was statistically at par with each other in both the varieties (Table 8). Likewise, the impact of alone application of N and 1.8 kg HA ha⁻¹ on grain N concentration was statistically not different from each other in either of the maize variety. In both varieties, the combined application of 1.8 kg HA ha⁻¹ + N produced the plants with the highest grain N concentration. Furthermore, the grain N concentration of maize variety Iqbal were higher than Jalal. The control plots of maize varieties resulted in lower grain N concentration.

Stover N concentration (%)

The different application levels of humic acid in the absence and presence of nitrogen as well as the sole application of N substantially enhanced the stover N concentration of maize varieties Jalal and Iqbal, except the alone application of humic acid at 0.6 kg ha⁻¹ (Table 9). Humic acid application at 1.8 kg HA ha⁻¹ produced the highest stover N concentration in both varieties which was at par with 1.2 kg HA ha⁻¹ and the individual application of N. Although, the alone N accelerated the grain N concentration of both varieties but the maximum N concentration was recorded at 1.8 kg HA ha⁻¹ + N which was statistically at par with 1.2 kg HA ha⁻¹ + N. The higher stover N concentration was observed in the maize variety Jalal as compared to Iqbal. The plants of control plots were studied to be lower in the stover N concentration in both the maize varieties.

Table 9. Effect of different levels of humic acid in the absence and presence of nitrogen on stover N concentration (%) and grain N uptake (kg ha⁻¹) of maize variety Jalal and Iqbal

Treatments	Stover N concentration (%)		Grain N uptake (kg ha ⁻¹)	
	Jalal	Iqbal	Jalal	Iqbal
0 kg HA + 0 kg N ha ⁻¹	0.24±0.01 j	0.27±0.01 hij	32.30±0.20 l	38.87±0.16 k
0.6 kg HA + 0 kg N ha ⁻¹	0.26±0.01 ij	0.29±0.01 fg-i	40.42±0.25 k	43.49±0.46 j
1.2 kg HA + 0 kg N ha ⁻¹	0.28±0.01 ghi	0.31±0.01 de-g	45.26±0.20 ij	47.15±0.34 hi
1.8 kg HA + 0 kg N ha ⁻¹	0.30±0.01 ef-h	0.33±0.01 cde	48.52±0.39 h	51.23±0.56 g
0 kg HA + 120 kg N ha ⁻¹	0.31±0.01 def	0.35±0.01 bc	56.59±0.51 f	59.72±0.45 e
0.6 kg HA + 120 kg N ha ⁻¹	0.33±0.01 cd	0.37±0.01 b	61.43±0.65 e	64.66±0.72 d
1.2 kg HA + 120 kg N ha ⁻¹	0.35±0.01 bc	0.41±0.01 a	66.22±0.73 d	69.79±0.32 c
1.8 kg HA + 120 kg N ha ⁻¹	0.37±0.01 b	0.44±0.02 a	72.55±0.31 b	75.73±0.54 a
Means	0.30 b	0.35 a	52.91 b	56.33 a

Mean followed by same letters in a column do not differ significantly at P ≤ 0.05

Grain N uptake (kg ha⁻¹)

In both the maize varieties the grain N uptake were significantly affected by the alone application of humic acid, nitrogen as well as their integration (Table 9). Although the sole use of N fertilizer enhanced the grain N uptake of each variety, but the maximum N uptake was observed at 1.8 kg HA ha⁻¹ + N. The minimum grain uptake of maize varieties was observed in the control plots of humic acid and nitrogen. The plants of Iqbal variety showed the highest grain N uptake when they were compared with the maize plants of Jalal variety.

Stover N uptake (kg ha⁻¹)

The sole application of N as well as the applied levels of humic acid in combination with N and without N substantially influenced the stover N uptake of both maize varieties, except at 0.6 kg ha⁻¹ in Iqbal (Table 10). However, under the alone application of humic acid, 1.8 kg HA ha⁻¹ resulted in higher stover N uptake which was statistically at par with 1.2 kg HA ha⁻¹ in both varieties. The sole use of N significantly increased the stover N uptake in both maize varieties. Moreover, the integrated application of 1.8 kg HA ha⁻¹ + N produced the highest stover N uptake in both varieties which was statistically at par with 1.2 kg HA ha⁻¹ + N. The higher average mean of stover N uptake was recorded in the maize variety Jalal than Iqbal.

Total N uptake (kg ha⁻¹)

The total N uptake of both maize varieties had significant response to the alone application of N as well as applied levels of humic acid in the presence and absence of N (Table 10). As far as the sole application of humic acid is concerned, 1.8 kg HA ha⁻¹ resulted in maximum uptake of N in both the varieties. Likewise, the alone application of N increased the total N uptake in both maize varieties but the maximum response was observed under the combined application at 1.8 kg HA ha⁻¹ + N. The total N uptake was lower in control plots of humic acid and N as compared with other treatments. The Iqbal variety of maize exhibited higher total N uptake than Jalal.

Table 10. Effect of different levels of humic acid in the absence and presence of nitrogen on stover N uptake (kg ha⁻¹) and total N uptake (kg ha⁻¹) of maize variety Jalal and Iqbal

Treatments	Stover N uptake (kg ha ⁻¹)		Total N uptake (kg ha ⁻¹)	
	Jalal	Iqbal	Jalal	Iqbal
0 kg HA + 0 kg N ha ⁻¹	18.35±0.38 k	18.49±0.46 k	50.65±0.23 i	57.36±0.62 h
0.6 kg HA + 0 kg N ha ⁻¹	21.58±0.45 ij	20.39±0.52 jk	62.00±0.49 g	63.88±0.59 g
1.2 kg HA + 0 kg N ha ⁻¹	23.76±0.43 hi	21.96±0.49 ij	69.02±0.53 f	69.11±0.25 f
1.8 kg HA + 0 kg N ha ⁻¹	25.96±0.60 gh	23.86±0.55 ghi	74.48±0.55 e	75.09±1.01 e
0 kg HA + 120 kg N ha ⁻¹	28.56±0.84 ef	26.36±0.60 f	85.15±1.33 d	86.09±1.05 d
0.6 kg HA + 120 kg N ha ⁻¹	31.22±0.83 cd	29.04±0.80 de	92.65±1.42 c	93.70±1.41 c
1.2 kg HA + 120 kg N ha ⁻¹	34.03±0.86 ab	32.19±0.54 bc	100.25±1.38 b	101.98±0.64 b
1.8 kg HA + 120 kg N ha ⁻¹	35.60±0.50 a	34.25±0.36 ab	108.15±0.80 a	110.99±0.77 a
Means	27.38 a	25.82 b	80.27 b	82.29 a

Mean followed by same letters in a column do not differ significantly at P ≤ 0.05

Discussion

The application of humic acid and N caused significant increase in the plant height and leaf growth of both maize varieties. Maximum plant height, leaves plant⁻¹, leaf area plant⁻¹ and leaf area index was recorded in the Jalal variety of maize at 1.8 kg HA ha⁻¹. The beneficial effect of humic acid on crop growth, number of leaves plant⁻¹, leaf growth and its expansion in maize and other species has been reported by a number of plant researchers (Atiyeh et al., 2002; Daur and Bakhshwain, 2013). The possible explanation is the higher number of sinks produced, uptake of nutrients, and increased plant biomass due to humic acid application (El-Mekser et al., 2014). Likewise, the experimental plots treated with N fertilizer showed maximum plant height, number of leaves plant⁻¹, leaf area plant⁻¹ and leaf area index in maize varieties Jalal and Iqbal. The stimulatory impact of N on plant height and leaf growth has been studied by many researchers (Onasanya et al., 2009; Inamullah et al., 2011; Kolari et al., 2014). The underlying reason is that N is an integral constituent of chlorophyll tissues of plant (Rizwan et al., 2003) which accelerated vegetative growth of the crop (Gokmen et al., 2001), leaf production and its size (Jasemi et al., 2013).

The nitrate reductase (NR) activity of leaves and net assimilation rate of both maize varieties significantly enhanced with the integration of humic acid and N. Higher NR activity of leaves and net assimilation rate was recorded in Iqbal as compared to Jalal variety of maize. The plants supplied with 1.8 kg HA ha⁻¹ produced higher nitrate reductase (NR) activity and net assimilation rate. These findings are supported by Vaccaro et al. (2015) and Azeem et al. (2015) who found an acceleration in the NR activity and net assimilation rate of maize when they treated it with 5 mg of humic acid

liter⁻¹ of water and 1.5 kg HA ha⁻¹, respectively. The possible explanation is the optimum nutrients availability, H⁺-ATPase synthesis (Canellas et al., 2013), and increased root length that in turn made better use of the available nutrients (Motaghi and Nejad, 2014). Similarly, the N nutrient activated the NR activity of leaves and net assimilation rate of both maize varieties against control plots of N. As a result of higher N concentrations in the soil, higher nitrate accumulation occurred within the leaves of maize (Soleymani and Shahrajabian, 2013) with the activation of NR activity in leaves. It is because NR activity seemed to be directly related to nitrate or N availability within the plants (Vincentz et al., 1993; Cazetta et al., 2004). Habib et al. (2016) has also reported an increase in the net assimilation rate of maize due to N application. It is due to the beneficial effect of N on maize as it is a nitro positive crop (Gokmen et al., 2001) and responds well to N application under favourable soil moisture conditions. It is because humic acid has a crucial role in mineral nutrition and moisture retention capacity of the soil (Celik et al., 2011).

The integration of humic acid with N substantially increased the number of ears m⁻² and ears plant⁻¹ in maize varieties Jalal and Iqbal. The higher ear density was measured in Iqbal variety of maize at 1.8 kg HA ha⁻¹. These results are in line with the findings of Iqbal (2014) who reported maximum productive tillers in wheat crop, treated with humic acid as compared to control. It could be due to the rapid penetration of humic acid in the plant cells, direct effect on chlorophyll content, acceleration of respiration, activation of growth enzymes, and indirectly through improved biological, physical and chemical conditions of the soil (Rajpar et al., 2011). The experimental application of N fertilizer increased the number of ears in maize varieties. The increase in number of ears with inorganic N fertilizer has been demonstrated by many researchers in maize crop (Hago and Sawi, 1995; Inamullah et al., 2011). The hidden reason is the provision of N nutrient in proper amount at reproductive growth stage of the crop (Shah et al., 2009) which accelerated the rate of photosynthesis (Kolari et al., 2014) and ear bearing capacity of maize crop (Bashir et al., 2012).

The ear length, thousand grain weight, grain yield, stover yield and harvest index of both maize varieties significantly increased with the application of humic acid and N. The Iqbal variety of maize produced maximum ear length, thousand grain weight, grain yield and harvest with the application of 1.8 kg HA ha⁻¹ while the Jalal showed higher magnitude of stover yield with the same dose of humic acid. Various studies have shown the significant impact of humic acid on yield, yield components, stover yield and harvest index of maize crop (Ghorbani et al., 2010; Mohana et al., 2015). The reason is that humic acid creates an improvement in the physico-chemical properties of soil, and increased biomass production then occurs as a result of acceleration in plant biochemistry, physiology and productivity (Canellas and Olivares, 2014). Furthermore, N application accelerated the yield, yield components, stover yield and harvest index of maize varieties Jalal and Iqbal as compared to control plots of N (Sharifi and Taghizadeh, 2009). It is because N is a major plant nutrient and yield deciding factor for maize crop production (Manzoor et al., 2006) as it forms an integral component of protein and amino acids in the plants (Bakht et al., 2007). It enhanced nutrients uptake, assimilate production (Cirilo et al., 2009) and translocation of photosynthates from source to sink (Jena et al., 2015) which positively contributed to the increase in yield components of maize crop (Kaur et al., 2012).

The grain and stover N concentration of both maize varieties as well as their N uptake (grain N uptake, stover N uptake and total N uptake) considerably improved with the

integration of humic acid and nitrogen. The plants of Iqbal variety treated with 1.8 kg HA ha⁻¹ showed higher grain and stover N concentration, grain N uptake and total N uptake. A number of plant researchers has described the significant impact of humic acid on enhancing the grain and stover N concentration of maize crop as well as its N uptake (Celik et al., 2010; Anees et al., 2016; Niaz et al., 2016). It is due to the stimulatory effect of humic acid on physical (Varanini et al., 1995), chemical and biological properties of soil (Khattak, 2004), nutrients concentrations, their availability, and transportation to the growing parts of maize plants (Celik et al., 2011). It is highly involved in the hormonal activities and enzymatic reactions within the plants (Nardi et al., 2002) and is responsible for the reduction and assimilation of N nutrient (Vaccaro et al., 2015). It provides particular bioactive molecules to the cell membranes of plants roots for N uptake (Canellas and Olivares, 2014). Likewise, higher N concentration, and N uptake were studied in the grain and stover of maize varieties Jalal and Iqbal with the use of N fertilizer because maize crop is an aggressive utilizer of available plant nutrients (Ayoola and Makinde, 2009). The possible explanation could be the increase in total N of soil, residual N of soil (Yang et al., 2007), mineralization of soil organic N (Li et al., 2003), amino acid formation (Almodares et al., 2009), an acceleration in physiological and bio-chemical processes of the plants (Rawal and Kuligod, 2014) that promoted N concentration and N uptake of maize varieties. These findings are supported by El-Hassan et al. (2014), Biswas and Ma (2014) and Niaz et al. (2016) who reported an increase in the grain and stover N concentration, and total N uptake of maize crop with applications of N fertilizer.

Conclusion

It was concluded that 1.8 kg HA ha⁻¹ + 120 kg N ha⁻¹ resulted in maximum plant height, leaves plant⁻¹, leaf area plant⁻¹, leaf area index, NR activity in leaves, net assimilation rate, ears m⁻², ears plant⁻¹, ear length, thousand grain weight, grain yield, stover yield, harvest index, grain N concentration, stover N concentration, grain N uptake, stover N uptake and total N uptake of maize varieties. However, the maize variety Iqbal out yielded than Jalal under the applied levels of humic acid with nitrogen. Therefore, against the sole use of inorganic N, the local growers should use integration of 1.8 kg HA ha⁻¹ + 120 kg N ha⁻¹ along with maize variety Iqbal for obtaining higher yield of maize crop under the local environmental conditions. With this combination, it will be possible for local growers to accelerate the growth, physiology and yield of maize varieties with acceleration in the uptake of N nutrient which is often a limiting factor for crop production under the local semi-arid conditions. However, further research is needed to investigate the impact of higher levels of humic acids in integration with N on maize yield under the local agro-ecology.

Acknowledgements. The author and co-authors acknowledge Cereal Crops Research Institute, Pirsabak, Nowshera for providing seed material and technical help for conducting maize research experiments.

REFERENCES

- [1] Abrol, Y. P., Adhya, T. K., Aneja, V. P., Raghuram, N., Pathak, H., Kulshrestha, U., Sharma, C., Singh, B. (eds.) (2017): *The Indian Nitrogen Assessment: Sources of Reactive Nitrogen, Environmental and Climate Effects, Management Options, and Policies.* – Elsevier.

- [2] Abu-Grab, O. S., El-Kady, F. A., Darwich, A. A. (1997): Response of some maize cultivars to nitrogen fertilization under North and Middle Delta conditions. – *Ann. of Agric. Sc., Moshtohor, Egypt.* 35: 1-14.
- [3] Afzal, N., Ahmad, S. (2009): Agricultural input use efficiency in Pakistan-key issues and reform areas. – *Managing Natural Resources for Sustaining Future Agriculture Research Briefings* 1: 1-12.
- [4] Almodares, A., Hadi, M. R. (2009): Bioethanol production from sweet sorghum. – *Afr. J. Agric. Res.* 4: 772-780.
- [5] Amandeep, K., Seema, B., Gill, G. K., Mahesh, K. (2012): Effect of nitrogen fertilizers on radiation use efficiency, crop growth and yield in some maize (*Zea mays* L.) genotypes. – *Maydica* 57: 75-82.
- [6] Amanullah. (2016): Rate and timing of nitrogen application influence partial factor productivity and agronomic NUE of maize (*Zea mays* L.) planted at low and high densities on calcareous soil in North West Pakistan. – *J. Plant Nutr.* 39: 683-690.
- [7] Atiyeh, R. M., Lee, S., Edwards, C. A., Arancon, N. Q., Metzger, J. D. (2002): The influence of humic acids derived from earthworm-processed organic wastes on plant growth. – *Bioresource Technol.* 84: 7-14.
- [8] Ayoola, O. T., Makinde, E. A. (2009): Maize growth, yield and soil nutrient changes with N-enriched organic fertilizers. – *Afr. J. Food Agric. Nutr. Dev.* 9: 580-592.
- [9] Azam, F., Iqbal, M. M., Inayatullah, C., Malik, K. A. (2001): Technologies for sustainable agriculture. – Nuclear Institute for Agriculture and Biology, Faisalabad; p. 144.
- [10] Azeem, K., Shah, S., Ahmad, N., Shah, S. T., Khan, F., Arafat, Y., Naz, F., Azeem, I., Ilyas, M. (2015): Physiological indices, biomass and economic yield of maize influenced by humic acid and nitrogen levels. – *Basic Res. J. Agric. Sci. Rev.* 4: 158-163.
- [11] Bakht, J., Siddique, M. F., Shafi, M., Akbar, H., Tariq, M., Khan, N., Zubair, M., Yousef, M. (2007): Effect of planting methods and nitrogen levels on the yield and yield components of maize. – *Sarhad J. Agric.* 23: 253-259.
- [12] Bashir, N., Malik, S. A., Mahmood, S., Mahmood-ul-Hassan, Athar, H. R., Athar, M. (2012): Influence of urea application on growth, yield and mineral uptake in two corn (*Zea mays* L.) cultivars. – *Afr. J. Biotechnol.* 11: 10494-10503.
- [13] Beadle, C. L. (1993): Growth analysis. In photosynthesis and production in a changing environment. – Springer Dordrecht; p. 36-46.
- [14] Biswas, D. K., Ma, B. L. (2016): Effect of nitrogen rate and fertilizer nitrogen source on physiology, yield, grain quality, and nitrogen use efficiency in corn. – *Canadian J. Plant Sci.* 96: 392-403.
- [15] Bremner, J. M., Mulvaney, C. S. (1982): Nitrogen-total. Methods of soil analysis. Part 2. – Chemical and microbiological properties; p. 595-624.
- [16] Camara, K. M., Payne, W. A., Rasmussen, P. E. (2003): Long-term effects of tillage, nitrogen, and rainfall on winter wheat yields in the Pacific Northwest. – *Agron. J.* 95: 828-835.
- [17] Canellas, L. P., Balmori, D. M., Médici, L. O., Aguiar, N. O., Campostrini, E., Rosa, R. C., Façanha, A. R., Olivares, F. L. (2013): A combination of humic substances and herbaspirillum seropedicae inoculation enhances the growth of maize (*Zea mays* L.). – *Plant Soil.* 366: 119-132.
- [18] Canellas, L. P., Olivares, F. L. (2014): Physiological responses to humic substances as plant growth promoter. – *Chem. Biol. Technol. Agric.* 1:3.
- [19] Cazetta, J. O., Villela, L. C. V. (2004): Nitrate reductase activity in leaves and stems of tanner grass (*Brachiaria radicans* Napper). – *Sci. Agric.* 61: 640-648.
- [20] Celik, H., Katkat, A. V., Aşik, B. B., Turan, M. A. (2010): Effects of humus on growth and nutrient uptake of maize under saline and calcareous soil conditions. – *Agric.* 97: 15-22.
- [21] Celik, H., Katkat, A. V., Aşik, B. B., Turan, M. A. (2011): Effect of foliar-applied humic acid to dry weight and mineral nutrient uptake of maize under calcareous soil conditions. – *Commun. Soil Sci. Plant Anal.* 42: 29-38.

- [22] Cirilo, A. G., Dardanelli, J., Balzarini, M., Andrade, F. H., Cantarero, M., Luque, S., Pedrol, H. M. (2009): Morphophysiological traits associated with maize adaptations to environments differing in nitrogen availability. – *Field Crop Res.* 113: 116-124.
- [23] Daur, I., Bakhshwain, A. A. (2013): Effect of humic acid on growth and quality of maize fodder production. – *Pak. J. Bot.* 45: 21-25.
- [24] Derby, N. E., Casey, F. X. M., Knighton, R. E., Steel, D. D. (2004): Midseason nitrogen fertility management for corn based on weather and yield prediction. – *Agron. J.* 96: 494-501.
- [25] Dong, H., Zhang, G., Jiang, H., Yu, B., Chapman, L. R., Lucas, C. R., Fields, M. W. (2006): Microbial diversity in sediments of saline Qinghai Lake, China: linking geochemical controls to microbial ecology. – *Microb. Ecol.* 51: 65-82.
- [26] Dong, L., Cordova-Kreylos, A. L., Yang, J., Yuan, H., Scow, K. M. (2009): Humic acids buffer the effects of urea on soil ammonia oxidizers and potential nitrification. – *Soil Biol. Biochem.* 41: 1612-1621.
- [27] El-Hassan, W. H. A., Hafez, E. M., Ghareib, A. A. A., Freeg, M. R., Seleiman, M. F. (2014): Impact of nitrogen fertilization and irrigation on water utilization efficiency, N accumulation, growth and yields of *Zea mays* L. – *J. Food, Agric. Environ.* 12: 217-222.
- [28] El-Mekser, H., Mohamed, Z. E. O. M., Ali, M. A. M. (2014): Influence of humic acid and some micronutrients on yellow corn yield and quality. – *World Appl. Sci. J.* 32: 1-11.
- [29] Ghorbani, S., Khazaei, H. R., Kafi, M., Bannayan, A. M. (2010): Effect of humic acid application with irrigation water on yield and yield components of corn (*Zea mays* L.). – *J. Agroecol.* 2: 111-118.
- [30] Gokmen, S. O., Sencar, O., Sakin, M. A. (2001): Response of popcorn (*Zea mays* L. everta) to nitrogen rates and plant densities. – *Turk. J. Agric. For.* 25: 15-23.
- [31] Government of Pakistan. (2016): Pakistan Economic Survey 2014-15. – Finance division, Economic Advisor's Wing, Islamabad, Pakistan; p. 26.
- [32] Grassini, P., Thorburn, J., Burr, C., Cassman, K. G. (2011): High-yield irrigated maize in the Western U.S. Corn Belt: I. On-farm yield, yield potential, and impact of agronomic practices. – *Field Crops Res.* 120: 142-150.
- [33] Habib, M. D., Asif, M., Aziz, M., Ali, A., Ashraf, M., Mahmood, A., Javaid, M. M. (2016): Growth performance of spring maize and soil fertility status as influenced by nutrient sources. – *Int. J. Agric. Appl. Sci.* 4: 35-41.
- [34] Hago, T. E. M., Sawi, S. M. A. (1995): The effects of nitrogen and phosphorus on yield and yield components of maize (*Zea mays* L.) under irrigation. – *J. Agric. Sci.* 3: 22-31.
- [35] Iqbal, B. (2016): Response of wheat crop to humic acid and nitrogen levels. – *EC Agric.* 3: 558-565.
- [36] Jasemi, M., Darab, F., Naser, R. (2013): Effect of planting date and nitrogen fertilizer application on grain yield and yield components in maize. – *Am-Eurasian J. Agric. Environ. Sci.* 13: 914-919.
- [37] Jena, N., Vani, K. P., Rao, V. P., Sankar, A. S. (2015): Effect of nitrogen and phosphorus fertilizers on growth and yield of quality protein maize (QPM). – *Int. J. Sci. Res.* 4: 1839-1840.
- [38] Kaur, A. (2012): Physiological basis of nitrogen use efficiency in maize at various rates of applied nitrogen. – Ph.D. dissertation, Punjab Agricultural University, Ludhiana.
- [39] Khan, H. Z., Iqbal, S., Akbar, N., Saleem, M. F., Iqbal, A. (2013): Integrated management of different nitrogen sources for maize production. – *Pak. J. Agric. Sci.* 50: 55-61.
- [40] Khattak, M. K. (2004): Influence of various tillage practices on yield of wheat-maize under clay loam soil condition. – *Sarhad J. Agric.* 20: 429-443.
- [41] Kolari, F., Bazregar, A., Bakhtiari, S. (2014): Phenology, growth aspects and yield of maize affected by defoliation rate and applying nitrogen and vermicompost. – *Indian J. Fundamental Appl. Life Sci.* 4: 61-71.

- [42] Lewis, O. A. M., James, D. M., Hewitt, E. J. (1982): Nitrogen assimilation in barley (*Hordeum vulgare* L.) in response to nitrate and ammonium nutrition. – *Ann. Bot.* 49: 39-49.
- [43] Li, H., Han, Y., Cai, Z. (2003): Nitrogen mineralization in paddy soils of the Taihu region of China under anaerobic conditions: dynamics and model fitting. – *Geoderma* 115: 161-175.
- [44] Maheswari, M., Murthy, A. N. G., Shanker, A. K. (2017): Nitrogen nutrition in crops and its importance in crop quality. – In: *The Indian nitrogen assessment: sources of reactive nitrogen, environmental and climate effects, management options, and policies*; p. 175.
- [45] Moghadam, H. T., Khamene, M. K., Zahedi, H. (2015): Effect of humic acid foliar application on growth and quantity of corn in irrigation withholding at different growth stages. – *Maydica* 59: 124-128.
- [46] Mohana, A. A., Suleiman, M. M., Khedr, W. S. (2015): Effect of humic acid and rates of nitrogen fertilizer on yield and yield components of corn (*Zea mays* L.). – *Jordan Journal of Agricultural Sciences* 11: 229-241.
- [47] Mohd, T., Osumanu, H. A., Nik, M. (2009): Effect of mixing urea with humic acid and acid sulphate soil on ammonia loss, exchangeable ammonium and available nitrate. – *Am. J. Environ. Sci.* 5: 588-591.
- [48] Motaghi, S., Nejad, T. S. (2014): The effect of different levels of humic acid and potassium fertilizer on physiological indices of growth. – *Int. J. Biosci.* 5: 99-105.
- [49] Nardi, S., Pizzeghello, D., Muscolo, A., Vianello, A. (2002): Physiological effects of humic substances on higher plants. – *Soil Biol. Biochem.* 34: 1527-1536.
- [50] Niaz, A., Yaseen, M., Shakar, M., Sultana, S., Ehsan, M., Nazarat, A. (2016): Maize production and nitrogen use efficiency in response to nitrogen application with and without humic acid. – *J. Anim Plant Sci.* 26: 1641-1651.
- [51] Onasanya, R. O., Aiyelari, O. P., Onasanya, A., Oikeh, S., Nwilene, F. E., Oyelakin, O. O. (2009): Growth and yield response of maize (*Zea mays* L.) to different rates of nitrogen and phosphorus fertilizers in southern Nigeria. – *World J. Agric. Sci.* 5: 400-407.
- [52] Rajpar, I., Bhatti, M. B., Zia-ul-Hassan, Shah, A. N., Tunio, S. D. (2011): Humic acid improves growth, yield and oil content of *Brassica campestris* L. – *Pak. J. Agric. Agricul. Eng. Vet. Sci.* 27: 125-133.
- [53] Rawal, R., Kuligod, V. B. (2014): Influence of graded doses of nitrogen on nutrient uptake and grain yield of maize (*Zea mays* L.) under varying levels of soil salinity. – *Karnataka J. Agric. Sci.* 27: 22-24.
- [54] Rizwan, M., Maqsood, M., Rafiq, M., Saeed, M., Ali, A. (2003): Maize (*Zea mays* L.) response to split application of nitrogen. – *Int. J. Agric. Biol.* 5: 19-21.
- [55] Saruhan, V., Kusvuran, A., Kokten, K. (2011): The effect of different replications of humic acid fertilization on yield performances of common vetch (*Vicia sativa* L.). – *Afr. J. Biotechnol.* 10: 5587-5592.
- [56] Shah, S. T. H., Zamir, M. S. I., Waseem, M., Ali, A., Tahir, M., Khalid, W. B. (2009): Growth and yield response of maize (*Zea mays* L.) to organic and inorganic sources of nitrogen. – *Pak. J. Life Soc. Sci.* 7: 108-111.
- [57] Sharifi, R. S., Taghizadeh, R. (2009): Response of maize (*Zea mays* L.) cultivars to different levels of nitrogen fertilizer. – *J. Food, Agri. Environ.* 7: 518-521.
- [58] Soleymani, A., Shahrajabian, M. H. (2012): The effects of nitrogen fertilizer on ash, nitrate, organic carbon, protein and total yield of forage maize in semi-arid region of Iran. – *Res. on Crops* 13: 1030-1034.
- [59] Steel, R. G. D., Torrie, J. H. (1997): *Principles and procedures of statistics*. – 2nd ed. McGraw Hill Book Company, Inc: New York.
- [60] Tolessa, D., Du Preez, C. C., Ceronio, G. M. (2007): Comparison of maize genotypes for grain yield, nitrogen uptake and use efficiency in western Ethiopia. – *S. Afr. J. Plant Soil* 24: 70-76.

- [61] Traversa, A., Loffredo, E., Gattullo, C. E., Palazzo, A. J., Bashore, T. L., Senesi, N. (2014): Comparative evaluation of compost humic acids and their effects on the germination of switchgrass (*Panicum vigatum* L.). – J. Soil Sediment 14: 432-440.
- [62] Turkmen, O., Dursun, A., Turan, M., Erdinc, C. (2004): Calcium and humic acid affect seed germination, growth, and nutrient content of tomato (*Lycopersicon esculentum* L.) seedlings under saline soil conditions. – Acta Agriculturae Scandinavica 54: 168-174.
- [63] Vaccaro, S., Ertani, A., Nebbioso, A., Muscolo, A., Quaggiotti, S., Piccolo, A., Nardi, S. (2015): Humic substances stimulate maize nitrogen assimilation and amino acid metabolism at physiological and molecular level. – Chem. Biol. Technol. Agric. 2:5.
- [64] Varanini, Z., Pinton, R., Behnke, H. D., Luttge, U., Esser, K., Kadereit, J. W., Runge, M. (1995): Humic substances and plant nutrition. Progress in Botany: Structural botany, physiology, genetics and taxonomy. – Geobotany 56: 97-117.
- [65] Vincentz, M., Moureaux, T., Leydecker, M. T., Vaucheret, H., Caboche, M. (1993): Regulation of nitrate and nitrite reductase expression in *Nicotiana plumbaginifolia* leaves by nitrogen and carbon metabolites. – Plant J. 3: 315.
- [66] Yang, J. Y., Huffman, E. C., De Jong, R., Kirkwood, V., MacDonald, K. B., Drury, C. F. (2007): Residual soil nitrogen in soil landscapes of Canada as affected by land use practices and agricultural policy scenarios. – Land Use Policy 24: 89-99.
- [67] Yousaf, M., Li, X., Zhang, Z., Ren, T., Cong, R., Ata-Ul-Karim, S. T., Fahad, S., Shah, A. N., Lu, J. (2016): Nitrogen fertilizer management for enhancing crop productivity and nitrogen use efficiency in rice-oil seed rape rotation system in china. – Front. Plant Sci. 7:1496.

APPROACHES REGARDING ENVIRONMENTAL KUZNETS CURVE IN THE EUROPEAN UNION FROM THE PERSPECTIVE OF SUSTAINABLE DEVELOPMENT

PANAIT, M.* – VOICA, M. C. – RĂDULESCU, I.

*Petroleum-Gas University of Ploiesti
Blvd. Bucuresti, No. 39, 100680 Ploiesti, Prahova, Romania*

**Corresponding author
e-mail: mirela.matei@upg-ploiesti.ro; phone: +40-727-733-622*

(Received 11th Feb 2019 ; accepted 8th Apr 2019)

Abstract. The paper investigates the relation between environmental degradation and economic development. The authors focused on the situation specific to the EU-28 Member States for the timeframe 1960-2014. The study used the variables CO₂ emissions, GDP per capita, imports of goods and services, exports of goods and services and energy use. The research has been divided in three distinct stages. The first stage consisted in data collection and management by analysing the existence of the unit root and determining the level at which the data is stationary. The second stage consisted in the testing Granger Causality relations between the variables for 2-5 lags. The third stage consisted in the estimation of a regression equation of the environmental Kuznets curve type. The results demonstrate the applicability of environmental Kuznets curve for the EU-28 Member States. These results can be used for design of industrial policies of these states, considering these states sustainable development goals. The public authorities are aware of the importance of environmental protection and of the correlation between environment and the economy development. The authors consider that the results of this article are an useful instrument to establish the macroeconomic policies while considering the perspective of sustainable development.

Keywords: *environment, economic development, CO₂ emissions, energy, imports, exports*

Introduction

The Kuznets Curve has extended its applicability from the social field to the environmental field. We are witnessing the promotion of new concepts, such as the environmental Kuznets (EKC) curve or the forest transition curve (Kuznets, 1955). Simon Kuznets launched a hypothesis in the 1950s on the existence of a relationship between the level of development of a country and the income of the population. As the level of development of a country increases, in the first stage, there is a deepening of the inequality between the population incomes, as the investment opportunities are capitalized by the persons with important capital, and the migration from the villages to the cities of cheap labor force keeps the salaries at a reduced level. The mechanization of agriculture and industrialization generate international migration and a reduction in the rural population. Increasing the level of development ultimately generates revenue growth, thus recording a negative relationship between income inequality and economic development. For this reason, the Kuznets curve is shaped as a U curve.

In the first stage of industrialization, environmental issues were not a main concern either for authorities or for citizens, as everyone was focused to income (profit-making) and increasing the number of jobs. Also, the small number of strict regulations on environmental protection and, after that, the costs of protective measures, contributed to some secondary concerns and measuring of business development and diversification to environment preservation. The pressure on the environment is very high during

industrialization, as industrial production increases are based on excessive consumption of resources and increased pollution (Marcu et al., 2016). As the level of development of a state increases, authorities, citizens and companies become more aware of the impact of their activities on the environment; environmental protection rules and regulations are strictly enforced and adhered to, and investments are made to protect the environment. In addition, factors such as income elasticity to environmental quality and changes in the composition of consumption and production (Selden and Song, 1994; Bo, 2011) have led to a decrease in pollution. Moving to a higher level of industrialization reduces environmental pressure, measured with various instruments such as pollution levels, emissions flows, resource depletion. Therefore, the pressure on the environment grows faster than the incomes in the first stages of development. The pressure will slow down as a country develops (Dinda, 2004).

The specialists concerns about the relationship between the environment and economic growth have been generated by the intensification, in the last decade of environmental degradation, with major economic, social and political implications; this has generated a change in the behaviour of companies and public institutions that have tried to identify solutions to the development of this problem (Al-Mulali et al., 2015b; Popescu et al., 2016; Andrei et al., 2017; Cristea and Dobrota, 2017). Sustainable development and corporate social responsibility are concepts accepted and promoted by authorities, companies, consumers, portfolio investors, universities, financial institutions, etc. (Ciutacu et al., 2005; Zaman, 2005; Vasile and Balan, 2008; Anghelache, 2011; Ene, 2011; Nica, 2015; Andrei et al., 2014; Sima and Georgiana, 2014; Voica et al., 2015; Ene et al., 2017; Popescu et al., 2017).

The Kuznets Curve, which was initially used for demonstrating the relation between the level of development of a country and the income of its population, has had its applicability extended, from the social field to the environmental field; we are witnessing the promotion of new concepts, such as the environmental Kuznets (EKC) curve or the forest transition curve (Kuznets, 1955).

In international scientific literature, the Kuznets curve environmental analysis was conducted, in a first phase, by researchers such as Grossman and Krueger (1991), then the issue entered into the areas of concern of international financial institutions such as the World Bank, which dedicated the 1992 report to the relationship between economic development and the environment. The 1992 report of the World Bank presents the links between the environment and economic development and draws attention to the importance of integrating environmental aspects into public policies promoted by the authorities in view of the negative environmental impacts on the quality of life, productivity and further development of a country (World Bank, 1992). Although it does not use the environmental Kuznets curve term, this report called “Development and the Environment”, considers that “As incomes rise, the demand for improvements in environmental quality will increase, as will the resources available for investment”. The dedication of the EKC term came a few years later, when Panayiotou (1993) named the inverted U-shaped relationship as environmental Kuznets curve (EKC).

We consider that our paper contributes to the debate on environmental degradation by estimating an EKC for the EU member states CO₂ emissions over the period 1960-2014. The major contribution of this paper is the analysis of the relationship between CO₂ emissions and the level of development of the states in the European Union. We consider that CO₂ emissions is a relevant indicator in the research of the EKC as they

alone are responsible for almost 60% of all greenhouse gas emissions. As we will present in the literature review section, studies made by other researchers have focused on other groups of countries and do not target the period we are considering. Our analysis was done on two levels. The first step consisted in carrying out a causal analysis of variables using the Granger causality test, and the second level consisted in identifying a regression equation based on the Kuznets theory (1955) applied to the medium-economic relationship. A series of researchers (Panayotou et al., 1999; Cole et al., 1997; Scmalensee et al., 1998) has demonstrated that the theory is valid for greenhouse gas emissions by using “environmental Kuznets curves” (EKC) term.

The novelty of our research lies in the fact that the analysis is done at the level of the 28 countries in the EU and for a period of more than 50 years. Using and interpreting data for the period 1960-2014, allows the authors to capture several stages of development specific to the EU countries, which contributes to a better substantiation of the obtained results.

The objective of this article is to determine the impact of economic development on the environment in the 28 EU countries for the period 1960-2014. This article aims to examine the potential for convergence in the environmental policy field of the 28 EU member states, on the assumption that they represent a specific, easily identifiable model in the environmental field, namely in the field of reducing the environmental impact. Environmental taxation and other (internal) variables imply some specific behavior in the field of environmental economics and political sector, but EU countries form a functional model with specificities that can be translated into the case of other states. In this case, we consider the possibility of substantiating a European environmental and ecological model

Even if the EU member states have gradually joined to this construction over several decades, we believe that we can have an aggregated approach of these states taking in consideration aspects like geographic proximity, the existence of European values that can be traced back to history and the obligation of fulfilling certain criteria for EU membership. Therefore, economic and political convergence is ensured at the moment a state enters the EU, thus ensuring a certain level of economic development, political and ideological harmonization.

The expansion of the EU after the fall of the communist era was a normal phenomenon, despite a period of rupture of the former Central and Eastern European countries by the capitalist system. The accession of the former communist countries was progressively achieved, as they have met the criteria imposed by the European Treaties and have proved consistency with European values by having the status of associated countries in the EU. Even though the current EU member states have had different political regimes in the past, they have undergone an intense economic development and industrialization process with negative impact on the environment. The classification and grouping of states in a model, depending on the previous political situation, influences to a relatively insignificant degree the behaviour in the field of environmental policy. Reducing sectoral environmental disparities across the 28 EU states requires a holistic analysis of these in terms of the specificities of countries where reality variables are insignificant in the model under analysis.

The novelty of our study is to select the sum of countries, i.e. the EU countries, for which there have not been too many studies on this issue, as we will present in the literature review section, but also in the selection of variables for 1990-2014. The accession of the countries to the EU has had an impact not only on the legislative

system, but to a large extent to the intra-community trade that have been dynamized, which is why we analyzed the imports and exports as variables. In addition, they contribute to increased production, with direct effects on the environment.

Review of literature

This section is dedicated to the literature review of the main researches regarding the implications of economic development on the environment. The link between the environment and economic development was analyzed a few decades before the EKC concept was crystallized through the famous IPAT equation ($I = PAT$), which established a relationship between Impact (e.g., pollution, or natural resource use) to Population, Affluence often proxied with per capita income, and Technology (Ehrlich and Holdren, 1971; Commoner, 1972).

The Growth Limit Report, developed by Dennis Meadows of the Massachusetts Institute of Technology for the Club of Rome, is a work that draws attention to the link between economic growth and environmental pollution (Carson, 2010; Bo, 2011). So, the concerns in this area are old, but the first reference work for the EKC is the study by Grossman and Krueger in 1991 that analyzed the environmental impact of North American Free Trade Agreement. Therefore, trade/ development economists have a major influence on promoting the concept of environmental Kuznets curve in the context of an international trade agreement rather than environmental/resource economists in a pollution control context (Carson, 2010). These American economists (Grossman and Krueger, 1991) analyzed the influence of the policy promoting trade and foreign investments on pollution and the rate of depletion of natural resources.

Liberalization of trade and capital flows generates:

- Increased economic activity with direct implications on the pollution (scale effect).
- Increasing the country's specialization in accordance with the comparative advantage, which will contribute to the increase of production in those sectors where the costs of pollution abatement are relatively low, and the resources will be directed to those industries that use them intensively (composition effect).
- Transfer of new technology from foreign investors and more stringent environmental protection standards by public authorities as the level of development of the host country increases (technique effect).

This first study (Grossman and Krueger, 1991) has demonstrated the link in the form of EKC between the income and sulphur dioxide (SO_2), suspended particle matter (SPM) as environmental pollutants. Other studies have also considered other pollutants that reflect air quality such as nitrogen oxide, carbon monoxide or CO_2 (Selden and Song, 1994).

The environmental Kuznets curve has generated numerous debates in the literature, and it has been accepted by most specialists who have tried to measure its parameters and determine the income/inhabitant from which the level of pollution trend changes, as well as the shape of this curve considering various factors of influence. The regressions have indicated different income per capita as the inflection point for Kuznets environmental curves depends on the variables considered (Grossman and Krueger, 1991; Stern et al., 1996; Dasgupta et al., 2002). In addition, a change in the shape of the

Kuznets curve has been observed in the sense that it is flattened downward due to the influence of factors such as economic liberalization, improvement and transparency of information, environmental protection and pollution prevention regulations from developing countries conditions based on the actions taken internationally (Dasgupta et al., 2002). So, the shape of the EKC is influenced by certain factors. In addition to the factors presented above, other researchers insist on specific elements of influence such as Inward elasticity of environmental quality demand, scale, technological and compositional effects, international trade (Dinda, 2004), but also liberalization and financial development, institutional quality (Tamazian and Rao, 2010), political and civil liberties (Shafik and Bandyopadhyay, 1992; Torras and Boyce, 1998).

The impact of economic development on the environment has been analyzed through EKC across different countries or groups of countries, with results underestimating in some cases the EKC hypothesis, as follows:

- Shahbaz et al. (2013) conducted an empirical analysis based on the 1970-2010 annual data for Turkey based on CO₂ emissions and economic growth, taking in consideration the candidate status of this country to the EU. The main conclusion of the article is that an inverted U-shaped relationship is found between economic growth and CO₂ emissions.
- Esteve and Tamarit (2012) confirmed the non-linearity of the link between per capita CO₂ and per capita income for Spain over the period 1857-2007;
- Al-Mulali et al. (2015b) demonstrated, based on data from 1987 to 2011, that the EKC hypothesis does not exist for Vietnam because GDP and pollution have a positive relationship in the short and long run.
- Apergis and Ozturk (2015) test the environmental Kuznets curve (EKC) hypothesis for some Asian countries using data for the period 1990-2011; the main indicators used are CO₂ emissions, GDP per capita, population density, land, industry shares in GDP. The result of this study was the presence of an inverted U-shape association between emissions and income per capita for 14 Asian countries.
- Li et al. (2016) used data for 28 provinces of China from 1996 to 2012 and demonstrated that the Environmental Kuznets Curve (EKC) hypothesis is verified for some of the pollutant emissions (carbon dioxide, waste water and waste solid emissions).
- Al-Mulali, Tang and Ozturk (2015a) made a study and explored the impact of economic growth (GDP), renewable energy (RE) and financial development (FD) on CO₂ emissions (CO₂); the sample was composed by Latin America and Caribbean countries and data were collected for the period 1980-2010. The conclusion was that CO₂ emission, GDP growth, renewable energy consumption and financial development are cointegrated and an inverted U-shaped relationship between GDP growth and CO₂ emission exists.
- Cristea and Dobrota (2017) analyzed the CO₂ emissions, greenhouse gas emissions (GGE), the renewable energy consumption (REC) and the consumption of biofuel (BC) in Romania in relation with the intensity of energy in economy (IEE) and the population number (PN). The authors underlined “the need to adopt Green Energy Economy in Romania, in relation to the economic activity and demographic changes...focusing mainly on energy technologies with low-carbon”.

According to our knowledge, the issue of economic development's impact on the environment at EU level has not been the subject of many scientific researches published in the mainstream in recent years. In international scientific literature, we have identified several studies published in ISI-indexed journals, the results of which are presented below.

Thus, Wawrzyniak (2018) has tested the environmental Kuznets curve in European Union countries and his econometric study was based on data for EU-28 countries in years 1990-2013. This study focuses on the impact of energy consumption, foreign direct investment, trade openness and GDP on CO₂ emissions in EU states. The conclusion was that for these countries an inverted U-shaped relationship between CO₂ emissions per capita and GDP per capita is observed.

Kasperowicz (2015) was interested in the study of the relationship between economic growth and CO₂ emissions for 18 EU Member States from 1995 to 2012. The analysis was based on the ECM estimation, the panel cointegration test and EGLS estimator for some European countries (including some former communist countries) and demonstrated that the long-term relationship between GDP and CO₂ emissions is negative.

Armeanu et al. (2018) have explored the link between environmental pollution and economic growth in EU-28 countries; the results of the analysis confirm the EKC hypothesis in the case of emissions of sulphur oxides and emissions of nonmethane volatile organic compounds

Sterpu et al. (2018) analyzes the relationship of economic growth and energy consumption on greenhouse gas emissions for a panel of 28 countries of the European Union in the period 1990-2016. They used four macroeconomic indicators: Gross Domestic Product (GDP), Gross Inland Energy Consumption (GIC), Renewable Energy Consumption (REC), and Greenhouse Gas Emissions (GHG), in order to statistically test the EKC hypothesis. The results of the study demonstrate a non-conclusive evidence for the EKC hypothesis.

Lapinskienė et al. (2017) conducted a scientific research based on the expanded EKC model to estimate the relationship between GHG and GDP and additional factors such as energy consumption, energy taxes and R & D. The panel used is formed by twenty EU countries, including three Baltic States, and the data are for the period 1995-2014. The main conclusion of the article is the presence of the inverse U-shaped relationship for these EU countries.

Materials and methods

In order to evaluate the relationship between CO₂ emissions and the economic development, we have analyzed the following variables: CO₂ emissions (metric tons per capita), GDP per capita (constant 2010 US\$), imports of goods and services (constant 2010 US\$), exports of goods and services (constant 2010 US\$) and energy use (kg of oil equivalent per capita). The research was applied for the European Union - 28 Member States. The database used for collecting the data was the World Bank, for the 1960-2014 period. For the analysis, we have opted for the World Bank database to avoid the lack of data for certain countries and the inconsistency of the data series.

First, we will make a short presentation of the average evolution for the independent variables at the EU level. We must acknowledge that different countries joined the EU at different times and so many factors influenced each country's independent variables.

We will start by analyzing the evolution of CO₂ per capita emissions. World Bank uses this definition: carbon dioxide emissions are those stemming from the burning of fossil fuels and the manufacture of cement. They include carbon dioxide produced during consumption of solid, liquid, and gas fuels and gas flaring. The source of the data is Carbon Dioxide Information Analysis Center, Environmental Sciences Division, Oak Ridge National Laboratory, Tennessee, United States.

As we can see in *Figure 1*, the CO₂ emissions per capita started to decrease after reaching the peak of 10 metric tons per capita in 1979. Since that moment, the trend was downward. By following that trend, we can pinpoint major events in the evolution of the European countries, like 1989-1990 fall of the communism in the Eastern European member states, 1997 signing of Kyoto protocol, 2008 triggering of international financial crisis. All these events had a favourable impact on the evolution of CO₂ emissions. Another important aspect is that the EU member states are reducing their CO₂ per capita emissions, closing on the 1960 level.

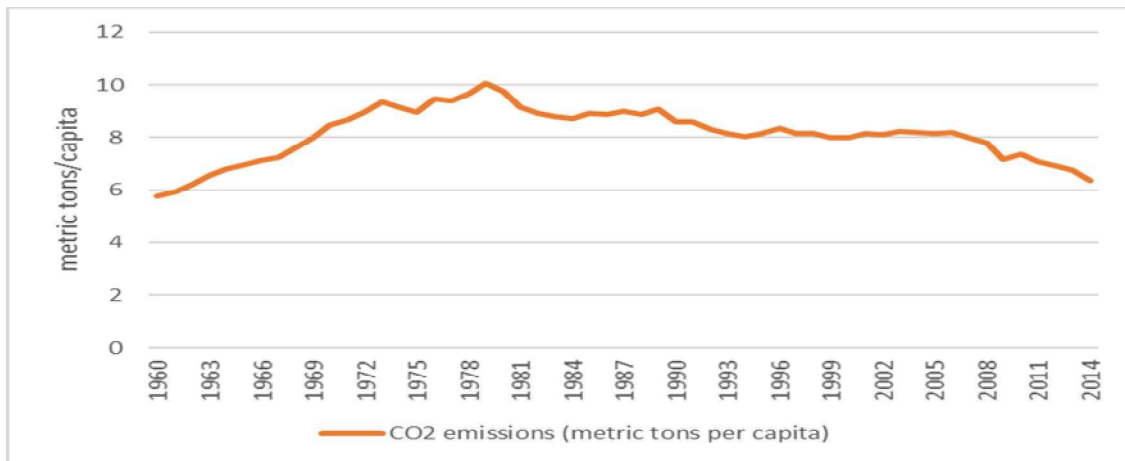


Figure 1. EU-28 average CO₂ emissions (metric tons per capita) for the period 1960-2014. (Source: World Bank)

The second variable is GDP per capita. GDP per capita is gross domestic product divided by midyear population. According to World Bank, GDP is the sum of gross value added by all resident producers in the economy plus any product taxes and minus any subsidies not included in the value of the products. It is calculated without making deductions for depreciation of fabricated assets or for depletion and degradation of natural resources. Data is in constant 2010 U.S. dollars.

The third variable is represented by exports. According to the World Bank, exports of goods and services represent the value of all goods and other market services provided to the rest of the world. They include the value of merchandise, freight, insurance, transport, travel, royalties, license fees, and other services, such as communication, construction, financial, information, business, personal, and government services. They exclude compensation of employees and investment income (formerly called factor services) and transfer payments. Data is in constant 2010 U.S. dollars.

The fourth variable is represented by imports. According to the World Bank, imports of goods and services represent the value of all goods and other market services

received from the rest of the world. They include the value of merchandise, freight, insurance, transport, travel, royalties, license fees, and other services, such as communication, construction, financial, information, business, personal, and government services. They exclude compensation of employees and investment income (formerly called factor services) and transfer payments. Data are in constant 2010 U.S. dollars.

The data for these three variables is obtained from World Bank national accounts data, and OECD National Accounts data files.

In *Figure 2* we can observe the evolution of the three variables. The most relevant observation is that the imports have a higher increase than the exports. This trend became more obvious after the 1990. This can be explained by the fact that the former communist countries started their transition to the open market. The GDP/capita had a steady trend in the analyzed period and, only after the financial crisis of 2008, the ascending trend of GDP/capita slowed down. Like in the case of GDP/capita, imports and exports also have been influenced by the financial crisis.

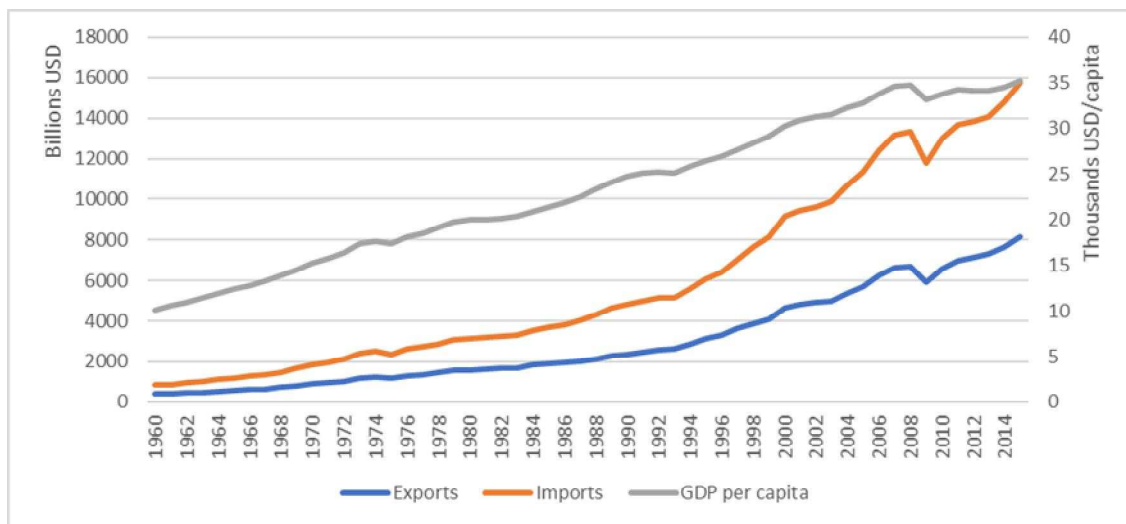


Figure 2. EU-28 average GDP/capita, exports and imports for the period 1960-2014 (constant US \$ 2010). (Source: World Bank)

The fifth variable presented in *Figure 3* is energy use. According to the World Bank, energy use refers to use of primary energy before transformation to other end-use fuels, which is equal to indigenous production plus imports and stock changes, minus exports and fuels supplied to ships and aircraft engaged in international transport. The source of the data is IEA Statistics © OECD/IEA 2014.

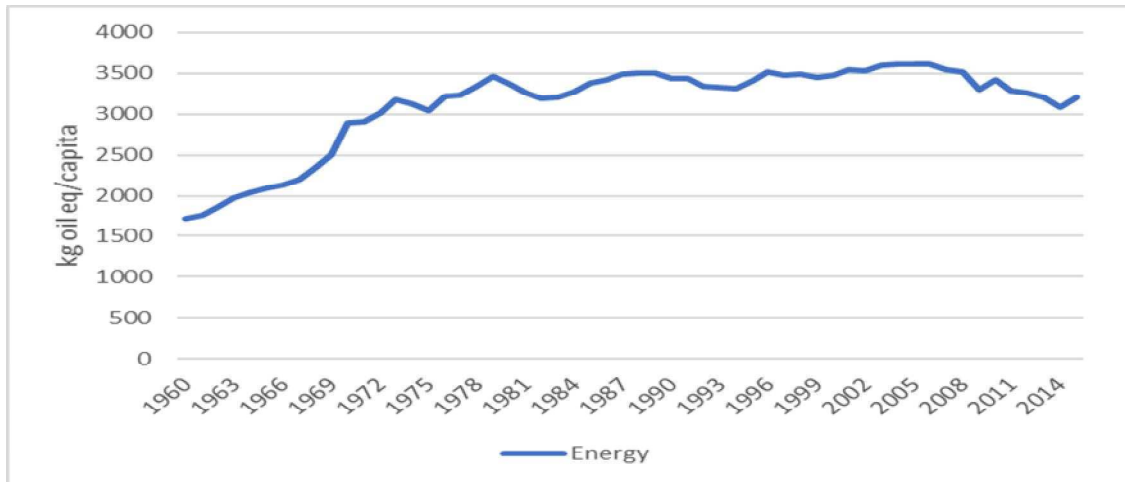


Figure 3. EU-28 average energy use (kg of oil equivalent per capita) for the period 1960-2014. (Source: World Bank)

The energy use in the analyzed period showed an ascending trend until 1979, and after that the evolution was constant until 2008, when the trend changed direction.

The research has been divided in three distinct stages. The first stage consisted in data collection and treatment by analyzing the existence of the unit root and determining the level at which the data is stationary. The second stage consisted in the testing of Granger Causality relations between the variables for 2-5 lags. The third stage consisted in the estimation of a regression equation of the environmental Kuznets curve type.

Unit root was tested using Levin et al. (2002) (LLC) test, ADF Fisher-type test, Im, Pesaran and Shin (2003) W-stat and PP Fisher-type test (Choi, 2001; Maddala, 1999). For a better understanding of these tests forward we provide a review of them (Kuzume, 2005).

Levin et al. (2002) tested the null hypothesis $H_0: \delta = 0$ compared with the alternative hypothesis $H_0: \delta < 0$, using:

$$\Delta q_{i,t} = \alpha_{mi} d_{mt} + \delta q_{i,t-1} + \sum_{k=1}^p \gamma_k \Delta q_{i,t-k} + \epsilon_{i,t} \quad (\text{Eq.1})$$

where d_{mt} denotes the determinant parts and $\epsilon_{i,t}$ is considered to be independent distributed among I and t , with $i = 1, \dots, N$ and $t = 1, \dots, T$. Immediately after the normalized interference and the correspondent of the pseudo ratio t of cumulated OLS estimations of δ in Equation 1 are properly normalized, the convergence at a standard limit of normal distribution is achieved as $N \rightarrow \infty, T \rightarrow \infty$ so that $\sqrt{N}/T \rightarrow 0$.

Im et al. (2003) test is built on the estimation (Eq. 1) but changing δ with δ_i . The null hypothesis is $H_0: \delta = 0 \forall_i$, while the alternative hypothesis is $H_1: \delta < 0 \ i = 1 \dots N_1; \delta_i = 0, \ i = N_1 + 1, \dots, N$. So, the null hypothesis is rejected if the is a subset (N_1) of stationary data. First test is the standardized group-mean Lagrange Multiplier (LM) bar test statistic

$$\psi_{LM} = \frac{\sqrt{N} [LM - N^{-1} \sum_{i=1}^N E(LM_i)]}{\sqrt{N^{-1} \sum_{i=1}^N Var(LM_i)}} \quad (\text{Eq.2})$$

with $\overline{LM} = N^{-1} \sum_{i=1}^N LM_i$, where LM_i denotes the individual LM tests for testing $\delta_i = 0$ in Equation 1, and $E(LM_i)$ and $Var(LM_i)$ are achieved through Monte Carlo simulation.

The next test is the standardized group mean t bar test statistic $\psi_{\bar{t}}$, with a similar expression like Equation 2, replacing \overline{LM} and LM_i with \bar{t} and t_i .

We defined $\bar{t} = N^{-1} \sum_{i=1}^N t_i$, where t_i denotes the individual pseudo t ratio for testing $\delta_i = 0$ in Equation 2, and $E(t_i)$ and $Var(t_i)$ are computed using the Monte Carlo simulation. In Im et al. (2003), because $N \rightarrow \infty$, $T \rightarrow \infty$ and $N/T \rightarrow k$, both statistic tests for distribution limitation are standard normal.

Fisher-ADF and Fisher-PP test are an alternative approach to test for unit root in panel data that uses the results of Fisher (1932) in testing for combined p values of the individual test of unit root, as they were propose by Maddala and Wu (1999) and Choi (2001).

If π_i is the p value of any individual unit root test for transversal section i , then, under the nullity of unit root for every transversal section N , we have the asymptotic result:

$$-2 \sum_{i=1}^N \log(\pi_i) \rightarrow \chi_{2N}^2 \quad (\text{Eq.3})$$

Choi (2001) proves that:

$$Z = \frac{1}{\sqrt{N}} \sum_{i=1}^N \Phi^{-1}(\pi_i) \rightarrow N(0,1) \quad (\text{Eq.4})$$

where Φ^{-1} is the inverse of the standard normal distributed cumulative function.

For the unit root tests, we used Schwarz info criterion, Newey-Vest automatic band width selection and Bartlett kernel.

In order to test the causality relation between the variables, we start from the Granger (1969) Hypothesis that asked how much of the variable y may be deduced from the past values of y and then asked if by adding the past values of x he can obtain a better approximation of y . A variable y is Granger caused by x when x improves the predictive capacity of y , or when the past coefficients of variable x are statistically significant. We must acknowledge that a two-way causality is a frequent case when x Granger causes y and y Granger causes x .

In order to apply a Granger causality, test we must specify the lag length l . Usually it is better to use more lags in order to get the relevant information form the past. In our study we tested the Granger causality relation between the variables for 2, 3, 4, and 5.

After establishing the lag length, we will estimate a bivariate regression of the form:

$$y_t = \alpha_0 + \alpha_1 y_{t+1} + \dots + \alpha_l y_{t-l} + \beta_1 x_{t+1} + \dots + \beta_l x_{t-l} + \varepsilon_t \quad (\text{Eq.5})$$

$$x_t = \alpha_0 + \alpha_1 x_{t+1} + \dots + \alpha_l x_{t-l} + \beta_1 y_{t+1} + \dots + \beta_l y_{t-l} + \mu_t \quad (\text{Eq.6})$$

for each possible pair of (x,y) series of the group. F-statistic reported values are the Wald statistics for the consolidated hypotheses:

$$\beta_1 = \beta_2 = \dots = \beta_l = 0 \quad (\text{Eq.7})$$

for each equation, the null hypothesis is that x does not Granger cause y in the first regression and y does not Granger cause x in the second regression.

In order to estimate the regression equation, we started from the linear regression using the OLS method with panel data of the form:

$$Y_{it} = f(X_{it}, \beta) + \delta_i + \gamma_t + \epsilon_{it} \quad (\text{Eq.8})$$

This specific case implies a conditional mean linear specification so that we achieve:

$$Y_{it} = \alpha + X'_{it}\beta + \delta_i + \gamma_t + \epsilon_{it} \quad (\text{Eq.9})$$

where Y_{it} is the dependent variable, X_{it} is a regressor vector k and ϵ_{it} error terms for $i = 1, 2, \dots, M$ transversal units, observed for the dated periods $t = 1, 2, \dots, T$. α is the general constant of the model while δ_i and γ_t represents the effects specific to transversal section or time period.

By introducing the variables specific to our study and of EKC conditions in Equation 9 we achieve a regression of the form:

$$\ln CO_2 = \beta_0 + \beta_1 \ln GDP + \beta_2 \ln GDP^2 + \beta_3 \ln ENERGY + \beta_4 \ln EXP + \beta_5 \ln IMP + \epsilon \quad (\text{Eq.10})$$

where: CO_2 – CO_2 emissions (metric tons per capita), GDP – GDP per capita (constant 2010 US\$), $ENERGY$ – Energy use (kg of oil equivalent per capita), IMP – Imports of goods and services (constant 2010 US\$), EXP – Exports of goods and services (constant 2010 US\$), $\beta_0, \beta_1, \beta_2, \beta_3, \beta_4, \beta_5$ – regression coefficients, ϵ – estimation error.

Results and discussions

Unit root tests

In this part, we present the summary statistics for each variable in *Table 1* and we have tested the variables for unit root in order to find the correct level at which the data has achieved stationarity. Because we are working with monetary units, first, we will apply logarithms to the variables and after will proceed with the unit root tests. For unit root testing we use Augmented Dickey–Fuller Fisher Chi-square test, Phillips–Perron Fischer Chi-square test, Im, Pesaran and Shin W-stat test and Levin, Lin & Chu t^* test. Probabilities for Fisher tests are computed using an asymptotic Chi-square distribution. All other tests assume asymptotic normality. The results of the unit root test are presented in *Table 2*.

As we can see in *Table 2*, the CO_2 emissions (CO_2) are not stationary at level so we proceed to 1st difference in order to achieve a stationary series. In the case of GDP per capita (GDP), energy use ($ENERGY$), imports of goods and services (IMP) and

exports of goods and services (EXP) they are stationary at level so there is no need for the first difference in their case. After the unit root testing we can proceed to the next steps of pair wise Granger causality tests and estimating the regression equation.

Table 1. Summary statistics

Variable	CO2	GDP	ENERGY	IMP	EXP
Mean	8.568981	24186.28	3350.261	1.15E+11	1.17E+11
Median	8.342206	24596.83	3449.615	1.05E+11	1.11E+11
Maximum	10.61663	31640.55	3817.867	2.43E+11	2.61E+11
Minimum	6.536127	13653.27	2188.12	2.12E+10	2.07E+10
Std. Dev.	1.010208	4735.476	423.3341	6.47E+10	6.79E+10
Skewness	0.076213	-0.49537	-1.43333	0.518412	0.536285
Kurtosis	2.193371	2.49813	4.007721	2.330016	2.397456

Table 2. Unit root tests results

Variable	Test	Level		1 st difference	
		Statistic	Prob	Statistic	Prob
CO2	ADF Fischer Chi-square	42.5443	0.9076	630.455	0.0000
	PP Fischer Chi-square	55.2986	0.5014	634.417	0.0000
	Im, Pesaran and Shin W-stat	-0.55240	0.2903	-25.3097	0.0000
	Levin, Lin & Chu t*	-0.74218	0.2290	-32.9086	0.0000
GDP	ADF Fischer Chi-square	140.743	0.0000	-	-
	PP Fischer Chi-square	131.884	0.0000	-	-
	Im, Pesaran and Shin W-stat	-7.15187	0.0000	-	-
	Levin, Lin & Chu t*	-12.5479	0.0000	-	-
ENERGY	ADF Fischer Chi-square	266.800	0.0000	-	-
	PP Fischer Chi-square	266.800	0.0000	-	-
	Im, Pesaran and Shin W-stat	-12.7320	0.0000	-	-
	Levin, Lin & Chu t*	-16.0019	0.0000	-	-
IMP	ADF Fischer Chi-square	115.479	0.0000	-	-
	PP Fischer Chi-square	95.6684	0.0008	-	-
	Im, Pesaran and Shin W-stat	-5.79535	0.0000	-	-
	Levin, Lin & Chu t*	-13.1799	0.0000	-	-
EXP	ADF Fischer Chi-square	106.632	0.0001	-	-
	PP Fischer Chi-square	92.0854	0.0017	-	-
	Im, Pesaran and Shin W-stat	-5.28681	0.0000	-	-
	Levin, Lin & Chu t*	-12.9788	0.0000	-	-

Granger causality test

As we already explained, the pair wise Granger causality test consists in determining if a variable y is Granger-caused by x when x improves the prediction of y , or when the coefficients of the lagged x are statistically significant. We must acknowledge that a two-way causation is a frequent case in which x Granger causes y and y Granger

causes. In *Table 3* we have the results of the pair wise Granger causality tests for our variables for a lag range from 2 to 5.

By analyzing the data from *Table 3* we observe that between the pairs of variables there are two-way Granger causality of a high level of statistical significance at a level of 1%. Another interesting thing observed is that the significance tends to be lower only for a smaller number of lags and as we past lag three all pairs have a two-way Granger causality significance lower than 1%, which is a logic evolution as time must pass before the evolution from one variable fully affect the evolution of the other variables.

Table 3. Pair wise Granger causality tests

Pair	Lags	2	3	4	5
	Null hypothesis	F-statistic	F-statistic	F-statistic	F-statistic
GDP-CO2	GDP does not Granger Cause CO2	139.360***	140.541***	108.515***	106.431***
	CO2 does not Granger Cause GDP	2.28528*	13.0574***	15.5907***	13.6148***
EXP-CO2	EXP does not Granger Cause CO2	174.258***	182.581***	138.809***	110.860***
	CO ₂ does not Granger Cause EXP	5.80083***	5.77247***	3.62445***	3.52626***
ENERGY-CO2	ENERGY does not Granger Cause CO2	273.439***	178.078***	154.679***	136.132***
	CO2 does not Granger Cause ENERGY	97.6253***	84.7030***	91.0687***	79.1074***
IMP-CO2	IMP does not Granger Cause CO ₂	165.690***	163.380***	130.129***	105.108***
	CO ₂ does not Granger Cause IMP	10.3148***	10.8472***	5.12759***	13.2843***
EXP-GDP	EXP does not Granger Cause GDP	87.9991***	79.5266***	68.5079***	55.7066***
	GDP does not Granger Cause EXP	84.2777***	76.2382***	66.7145***	62.2858***
ENERGY-GDP	ENERGY does not Granger Cause GDP	4.19931**	3.02615**	27.7061***	22.5724***
	GDP does not Granger Cause ENERGY	3.68748**	22.9844***	18.3863***	28.0118***
IMP-GDP	IMP does not Granger Cause GDP	75.7645***	78.0957***	60.0087***	47.0374***
	GDP does not Granger Cause IMP	91.3735***	72.4171***	56.2888***	44.1893***
ENERGY-EXP	ENERGY does not Granger Cause EXP	70.3780***	54.6008***	50.6015***	49.6728***
	EXP does not Granger Cause ENERGY	23.7478***	59.7225***	51.9012***	67.0064***
IMP-EXP	IMP does not Granger Cause EXP	7.70112***	6.59588***	16.1623***	43.6035***
	EXP does not Granger Cause IMP	28.8718***	26.1496***	31.4193***	40.9379***
IMP-ENERGY	IMP does not Granger Cause ENERGY	17.1906***	36.4039***	31.1759***	33.6088***

	ENERGY does not Granger Cause IMP	88.8461***	68.0739***	62.9387***	66.0642***
--	--------------------------------------	-------------------	-------------------	-------------------	-------------------

*significance at 10%; **significance at 5%; ***significance at 1%

As we can observe from the data presented in *Table 3*, the CO₂ has two-way relations with the independent variables from the study. These relations have been explained in previous studies (Pirlogea and Cicea, 2012; Allen, 2012; Su and Ang, 2016; López, et al., 2013) and our results provide similar conclusions. The CO₂ emissions have always been linked to the level of development, quantified by the GDP per capita. As a country reaches a higher level of development, its technological endowment changes from high pollution generating machinery, to environmentally friendly ones. This happens through the change of policy towards CO₂ emissions. The increase of GDP is linked with intensified activity on the international market quantified in our study by the imports and exports. Our results support this link, as the growth of CO₂ emissions is generated by the industrial production and other sectors growth. This growth generates, on one hand, a need for raw materials and intermediate goods, which takes the form of imports, and, on the other hand, the need to sell the produced goods to new markets which takes the form of exports. Another problem that must be acknowledged in respect to the international trade is the shift of CO₂ emissions from one country to another through imports and exports. As a country reaches a higher level of development and the pressure regarding the CO₂ emissions from policymakers, NGOs or other forms increases, there is the possibility to import the goods whose production generates high levels of CO₂ emissions. In this case, we have only a false reduction of CO₂ emissions, as the quantity of CO₂ emissions is shifted from the importing country to the exporting one, usually a developing country where there is a lower pressure regarding the CO₂ emissions and a higher demand for development. The link between CO₂ and energy consumption is one of the easiest to explain as the production of energy generates the largest amount of CO₂ apart from the energy produced from renewable sources, but even here the topic is under debate.

Environmental Kuznets curves for EU

We chose the EU for our study because the EU took a lot of steps toward reducing the CO₂ emissions and it has a proactive approach on the climate change issue that troubles the world leaders' minds. In this stage, we are going use the EKC model to estimate an equation with the CO₂ emissions as the dependent variable, and GDP/capita, energy consumption, imports and exports, as the independent variables. Previous studies (Apergis and Ozturk, 2015; Li et al., 2016; Al-Mulali et al., 2015a) added different variables to the model in order to better estimate the evolution of the dependent variable. For our estimation, we used the panel least squares method with a sample of 53 periods, between 1961 and 2013 and 28 cross-sections for each of the Member States, resulting a number 1484 observations.

In *Table 4* we have presented the results for the regression coefficients and forward the regression equation will be of the form:

$$\ln CO_2 = 35.89 - 7.42 \ln GDP + 0.36 \ln GDP^2 + 0.27 \ln ENERGY - 0.17 \ln EXP + 0.18 \ln IMP \quad (\text{Eq.11})$$

Our regression equation has an R-square value of 0.30 which means the model can explain only a part of the evolution of the CO₂, and a value of 1.94 for the Durbin-Watson test. The values of the coefficients provide us important information regarding the influence of each independent variable on the CO₂ evolution.

Table 4. EKC regression coefficients

Variable	Coefficient	Std. error	t-statistic	Prob.
C	35.88499	3.068164	11.69592	0.0000
GDP	-7.420802	0.635589	-11.67548	0.0000
GDP ²	0.360973	0.031047	11.62684	0.0000
ENERGY	0.266519	0.022969	11.60349	0.0000
EXP	-0.174257	0.026417	-6.596447	0.0000
IMP	0.176767	0.028129	6.284131	0.0000

According to EKC, the coefficient of GDP should be positive, while the coefficient of GDP² should be negative. In our results, we observe that the coefficients do not have the same signs as the EKC and the sign of GDP is negative while the sign of GDP² is positive.

The plus sign of the per capita energy consumption coefficient confirms that as the energy consumption increases, the CO₂ emission will follow a similar trend, fact discovered in previous studies (Du et al., 2012; Shahbaz et al., 2012; Jalil and Mahmud, 2009; Saboori and Sulaiman, 2013; Andrei et al., 2017). The CO₂ emissions have always been in relation with the energy consumption as its production generates a high percentage of the total amount of greenhouse gas emissions. The only way to reduce the emissions generated from energy production is the technological conversion to renewable sources and the general adoption of clean technologies. The main problem of renewable energy is that they also have an impact on the environment as the materials and the production process of the renewable sources power plants generates greenhouse gases. Also, they impact the environment by affecting the landscape and in some cases negatively impacting the food production by converting the land used for food production to land used for energy plants in the case of biomass, biogas and biodiesel.

The exports have a negative impact on CO₂ emissions. There can be many explanations about this relation and this depends on the level of development of each country, the structure of the industrial endowment. As an example, we can say that the exports may have a negative impact on CO₂ emissions in the case of a country which exports raw materials or low fabrication ones. Also, a country could execute only some operations of the supply chain with a low level of emissions, and then export them to continue production in countries with a less strict regulation on environment.

In the case of imports, the same examples are available but from the opposed side as importing raw materials and executing the high CO₂ emitting activities from the production chain of goods.

We must acknowledge that the model has its limitations and even Kuznets had his caveats regarding the original model mainly regarding the fragility of the data and even if the data turned out to be valid, it pertained to an extremely limited period and to exceptional historical experiences (Fogel, 1987).

Starting from this statement, we further stress that there were gaps in the availability of data, especially in the case of former communist countries. Also, there is a development gap between the older members of the EU and the newcomers which generated real convergence problem acknowledge by the EU and which was discussed on many occasions. Although the problem is well known, little has been done to reduce the gap and many times we found ourselves talking about a two speed European Union or a center-periphery relation between groups of member states.

Conclusions

The sample of countries chosen for this analysis was based on several considerations. The EU countries are characterized by high growth rates, and commercial and financial liberalization has a bivalent impact on the environment. On the one hand, the accession of Central and Eastern European countries can lead to a significant increase in the production of domestic companies and the attraction of important foreign capital flows, which can have a negative impact on the environment. On the other hand, environmental protection is a constant preoccupation of the European authorities, and the accession to the EU supposes the transposition of the European directives in the national legislation (Marcu et al., 2015). The liberalization of trade flows between Member States is an important factor of economic development (fact emphasized in the very first article dedicated to the EKC), which has a strong impact on the environment.

More and more specialists have drawn attention to the modification of the EKC in terms of its flattening, given that the environmental protection regulations adopted in the developed countries have been rapidly copied by the authorities in the developing countries. In addition, international efforts by institutions such as the United Nations or the OECD have had their effects, and their concerns about environmental protection, sustainable development and corporate social responsibility have been promoted both in developed countries and in developing countries. The levers by which the negative impact of economic activity on the environment can be limited have also multiplied. For example, the Kyoto Protocol of the United Nations Framework Convention on Climate Change was signed in 1997 (and entered into force in February 2005) and the parties committed to reducing greenhouse gas (GHG) emissions in line with specific targets. It is the first step towards a truly global emission reduction regime. In addition, the principles of sustainable development or social responsibility are followed by companies, financial institutions and portfolio investors.

The free movement of capital in the EU has generated robust financial flows in new member countries from both EU-developed companies and companies from other host countries that wanted to have fast access to the entire European market. Transferred technology has not always been last generation and environment friendly, which is why the impact of foreign direct investment on the environment in the host country, in some cases, may be negative.

The presence of large European financial groups in the new member states also determines the development of local financial markets, as well as the promotion of sustainable financing techniques for local companies. More and more banks are concerned not only with the economic impact of the investment projects they finance, but also with the environmental impact, which is why the financing of green investments is a reality in these countries as well.

The results of the study show us that the EU countries followed the Kuznets environmental curve; however, the multitude of levels of development may interfere with the end conclusion. The EU has its core problems regarding the real convergence of the new member states, fact highlighted by the latest talks about a two-speed union.

The data used for the study has some gaps in the case of the former communist countries data from before 1990, when these countries started the transition towards democracy. Also, in some of these countries, the reduction of CO₂ emissions was the result of industrial activity reduction generated by the restructuring or closing of entire facilities.

Based on these limitations of the study, we further intend to expand the research and try a deeper analysis of the EU member states by using a grouping analysis to observe the evolution of variables for countries in different stages of development.

REFERENCES

- [1] Al-Mulali, U., Tang, C. F., Ozturk, I. (2015a): Estimating the environment Kuznets curve hypothesis: evidence from Latin America and the Caribbean countries. – *Renewable and Sustainable Energy Reviews* 50: 918-924.
- [2] Al-Mulali, U., Saboori, B., Ozturk, I. (2015b): Investigating the environmental Kuznets curve hypothesis in Vietnam. – *Energy Policy* 76: 123-131.
- [3] Allen, R. C. (2012): Backward into the future: the shift to coal and implications for the next energy transition. – *Energy Policy* 50: 17-23.
- [4] Andrei, J., Panait, M., Ene, C. (2014): Environmental protection between social responsibility, green investments and cultural values. – *Proceedings of the 3rd International Conference Competitiveness of Agro-Food and Environmental Economy, Bucharest, 7-12 November*, pp. 179-187.
- [5] Andrei, J., Mieila, M., Popescu, G., Nica, E., Cristina, M. (2016): The impact and determinants of environmental taxation on economic growth communities in Romania. – *Energies* 9(11): 902.
- [6] Andrei, J. V., Mieila, M., Panait, M. (2017): The impact and determinants of the energy paradigm on economic growth in European Union. – *PloS One* 12(3).
- [7] Anghelache, C. (2011): Management of the environmental risk—an economic-social priority. – *Theoretical and Applied Economics* 3(3): 117-130.
- [8] Apergis, N., Ozturk, I. (2015): Testing environmental Kuznets curve hypothesis in Asian countries. – *Ecological Indicators* 52: 16-22.
- [9] Armeanu, D., Vintilă, G., Andrei, J. V., Gherghina, Ș. C., Drăgoi, M. C., Teodor, C. (2018): Exploring the link between environmental pollution and economic growth in EU-28 countries: is there an environmental Kuznets curve? – *PloS One* 13(5).
- [10] Bo, S. (2011): A literature survey on environmental Kuznets curve. – *Energy Procedia* 5: 1322-1325.
- [11] Carson, R. T. (2010): The environmental Kuznets curve: seeking empirical regularity and theoretical structure. – *Review of Environmental Economics and Policy* 4(1): 3-23.
- [12] Choi, I. (2001): Unit root tests for panel data. – *Journal of International Money and Finance* 20(2): 249-272.
- [13] Commoner, B. (1972): *The Environmental Cost of Economic Growth. Population, Resources and the Environment*. – Government Printing Office, Washington, DC, pp. 339-63.
- [14] Ciutacu, C., Chivu, L., Preda, D. (2005): The social responsibility of the company - a challenge for the contemporary world. – *The Romanian Economics Magazine* 2: 79.
- [15] Cole, M. A., Rayner, A. J., Bates, J. M. (1997): The environmental Kuznets curve: an empirical analysis. – *Environment and Development Economics* 2(4): 401-416.

- [16] Cristea, M., Dobrota, C. E. (2017): Green energy for sustainable development in Romania's economy. – *Revista de Chimie* 68(6): 1473-1478.
- [17] Dasgupta, S., Laplante, B., Wang, H., Wheeler, D. (2002): Confronting the environmental Kuznets curve. – *The Journal of Economic Perspectives* 16(1): 147-168.
- [18] Dinda, S. (2004): Environmental Kuznets curve hypothesis: a survey. – *Ecological Economics* 49(4): 431-455.
- [19] Du, L., Wei, C., Cai, S. (2012): Economic development and carbon dioxide emissions in China: provincial panel data analysis. – *China Econ. Rev.* 23: 371-384.
- [20] Ene, C. (2011): Pesticides pollution of food-risks and implications for consumer protection. – *The USV Annals of Economics and Public Administration* 10(1): 46-55.
- [21] Ene, C., Voica, M. C., Panait, M. (2017): Green Investments and Food Security: Opportunities and Future. – In: Mieila, M. (ed.) *Measuring Sustainable Development and Green Investments in Contemporary Economies*. IGI Global, Pennsylvania, USA, pp. 163-200.
- [22] Ehrlich, P. R., Holdren, J. P. (1971): Impact of Population Growth. – *Science* 171: 1212-1217.
- [23] Esteve, V., Tamarit, C. (2012): Threshold cointegration and nonlinear adjustment between CO₂ and income: the environmental Kuznets curve in Spain, 1857-2007. – *Energy Economics* 34(6): 2148-2156.
- [24] Fisher, R. A. (1932): *Statistical Methods for Research Workers*. 4th Ed. – Oliver & Boyd, Edinburgh.
- [25] Fogel, R. W. (1987): *Some Notes on the Scientific Methods of Simon Kuznets*. – National Bureau of Economic Research, Cambridge, MA.
- [26] Granger, C. (1969): Investigating causal relations by econometric models and cross-spectral Methods. – *Econometrica* 37(3): 424-438.
- [27] Grossman, G. M., Krueger, A. B. (1991): Environmental Impacts of a North American Free Trade Agreement. – NBER Working Paper No. 3914.
- [28] Im, K. S., Pesaran, M. H., Shin, Y. (2003): Testing for unit roots in heterogeneous panels. – *Journal of Econometrics* 115(1): 53-74.
- [29] Jalil, A., Mahmud, S. F. (2009): Environment Kuznets curve for CO₂ emissions: A cointegration analysis for China. – *Energy Policy* 37: 5167-5172.
- [30] Kasperowicz, R. (2015): Economic growth and CO₂ emissions: the ECM analysis. – *Journal of International Studies* 8(3): 91-98.
- [31] Kuzume, T. (2005): Intra-national and International PPP between cities of Japan and South Korea: Empirical evidence using panel unit root and panel cointegration tests. – Paper presented at the 64th Annual Meeting of the Japan Society of International Economics, Ritsumeikan University.
- [32] Kuznets, S. (1955): Economic growth and income inequality. – *American Economic Review* 45(1): 1-28.
- [33] Lapinskienė, G., Peleckis, K., Slavinskaitė, N. (2017): Energy consumption, economic growth and greenhouse gas emissions in the European Union countries. – *Journal of Business Economics and Management* 18(6): 1082-1097.
- [34] Levin, A., Lin, C.-F., James Chu, C.-S. (2002): Unit root tests in panel data: asymptotic and finite-sample properties. – *Journal of Econometrics* 108(1): 1-24.
- [35] Li, T., Wang, Y., Zhao, D. (2016): Environmental Kuznets curve in China: new evidence from dynamic panel analysis. – *Energy Policy* 91: 138-147.
- [36] López, L. A., Arce, G., Zafrilla, J. E. (2013): Parcelling virtual carbon in the pollution haven hypothesis. – *Energy Economics* 39: 177-186.
- [37] Maddala, G. S., Wu, S. (1999): A comparative study of unit root tests with panel data and a new simple test. – *Oxford Bulletin of Economics and Statistics* 61: 631-652.
- [38] Marcu, N., Meghisan, G. M., Cristea, M. (2015): Environmental protection and mobile telecommunications services marketing strategies. – *Proceedings of the Romanian Academy, Series B* 17(1): 57-63.

- [39] Marcu, N., Cristea, M., Meghisan, G. M., Dascalu, D., Nasta, L. N. (2016): Impact of certain sectors of the economy on the chemical pollution of atmosphere in Romania. – *Revista de Chimie* 67(6): 1195-1199.
- [40] Nica, E. (2015): Public administration as a tool of sustainable development. – *Journal of Self-Governance and Management Economics* 3(4): 30-36.
- [41] Panayotou, T. (1993): Empirical Tests and Policy Analysis of Environmental Degradation at Different Stages of Economic Development (No. 992927783402676). – International Labour Organization, Geneva.
- [42] Panayotou T., Sachs J., Peterson, A. (1999): Developing Countries and Control of Climate Change: A Theoretical Perspective and Policy Implications. – CAER II Discussion Paper 45.
- [43] Pirlogea, C., Cicea, C. (2012): Econometric perspective of the energy consumption and economic growth relation in European Union. – *Renewable and Sustainable Energy Reviews* 6(8): 5718-5726.
- [44] Popescu, G. H., Comanescu, M., Dinca, Z. (2016): Economic growth and energy utilization in China. – *Economics, Management and Financial Markets* 11(2): 94.
- [45] Popescu, G. H., Sima, V., Nica, E., Gheorghe, I. G. (2017): Measuring sustainable competitiveness in contemporary economies—insights from European economy. – *Sustainability* 9(7): 1230.
- [46] Saboori, B., Sulaiman, J. (2013): CO₂ emissions, energy consumption and economic growth in association of Southeast Asian Nations (ASEAN) countries: a cointegration approach. – *Energy* 55: 813-822.
- [47] Schmalensee, R., Stoker, T. M, Judson, R. A. (1998): World carbon dioxide emissions: 1950–2050. – *The Review of Economics and Statistics* 80(1): 15-17.
- [48] Selden, T. M., Song, D. (1994): Environmental quality and development: is there a Kuznets curve for air pollution emissions? – *Journal of Environmental Economics and management* 27(2): 147-162.
- [49] Shafik, N., Bandyopadhyay, S. (1992): Economic Growth and Environmental Quality: Time-Series and Cross-Country Evidence (Vol. 904). – World Bank Publications, Washington, DC.
- [50] Shahbaz, M., Lean, H. H., Shabbir, M. S. (2012): Environmental Kuznets curve hypothesis in Pakistan: cointegration and Granger causality. – *Renewable and Sustainable Energy Reviews* 16: 2947-2953.
- [51] Shahbaz, M., Ozturk, I., Afza, T., Ali, A. (2013): Revisiting the environmental Kuznets curve in a global economy. – *Renewable and Sustainable Energy Reviews* 25: 494-502.
- [52] Sima, V., Georgiana, G. I. (2014): Analyze of environmental performance in Romania based on environmental performance index. – *Annals-Economy Series* 3: 101-104.
- [53] Stern, D. I., Common, M. S., Barbier, E. B. (1996): Economic growth and environmental degradation: the environmental Kuznets curve and sustainable development. – *World Development* 24(7): 1151-1160.
- [54] Sterpu, M., Soava, G., Mehedintu, A. (2018): Impact of Economic Growth and Energy Consumption on Greenhouse Gas Emissions: Testing Environmental Curves Hypotheses on EU Countries. – *Sustainability* 10(9): 3327.
- [55] Su, B., Ang, B. W. (2016): Input–output analysis of CO emissions embodied in trade: Competitive versus non-competitive imports. – *Energy Policy* 56: 83-87.
- [56] Tamazian, A., Rao, B. B. (2010): Do economic, financial and institutional developments matter for environmental degradation? Evidence from transitional economies. – *Energy Economics* 32(1): 137-145.
- [57] Torras, M., Boyce, J. K. (1998): Income, inequality, and pollution: a reassessment of the environmental Kuznets curve. – *Ecological economics* 25(2): 147-160.
- [58] Vasile, V., Balan, M. (2008): Impact of greenhouse effect gases on climatic changes. measurement indicators and forecast models. – *Annales Universitatis Apulensis Series Oeconomica* 2(10).

- [59] Voica, M. C., Panait, M., Radulescu, I. (2015): Green Investments–Between Necessity, Fiscal Constraints and Profit. – *Procedia Economics and Finance* 22: 72-79.
- [60] Wawrzyniak, D. (2018): Testing environmental Kuznets curve in European Union countries. – *Ekonomista* 3: 318-334.
- [61] World Bank (1992): *World Development Report 1992: Development and the Environment*. – Oxford University Press, New York.
- [62] Zaman, G. (2005): The social-economic implications of the climate changes in Romania. – *Romanian Journal of Economics* 21(2): 116-134.

EFFECT OF ENVIRONMENTAL POLLUTION WITH TETRACYCLINE AND CADMIUM ON CHLOROPHYLL CONTENT IN SPINACH (*SPINACIA OLERACEA* L.) LEAVES SUBJECTED TO COLD STORAGE

RYDZYŃSKI, D.^{1,2} – PIOTROWICZ-CIEŚLAK, A. I.^{1*} – GRAJEK, H.² – BOROWSKA, E. J.³

¹*Department of Plant Physiology, Genetics and Biotechnology, Faculty of Biology and Biotechnology, University of Warmia and Mazury in Olsztyn, Oczapowskiego 1A, 10-718 Olsztyn, Poland*

²*Department of Physics and Biophysics, Faculty of Food Science, University of Warmia and Mazury in Olsztyn, Oczapowskiego 4, 10-719 Olsztyn, Poland*

³*Department of Food Plant Chemistry and Processing, Faculty of Food Science, University of Warmia and Mazury in Olsztyn, Plac Cieszyński 1, 10-957 Olsztyn, Poland*

**Corresponding author
e-mail: acieslak@uwm.edu.pl*

(Received 11th Feb 2019; accepted 8th Apr 2019)

Abstract. This paper analysed chlorophyll degradation in spinach leaves from plants affected by cadmium and tetracycline soil contamination, stored for 32 weeks at $t = -18\text{ }^{\circ}\text{C}$. The first-order reaction kinetics were determined for chlorophyll degradation. In plants growing on soil containing tetracycline and cadmium, two ranges of chlorophyll degradation occur: 1 – a slow degradation, during storage for up to 20 weeks, occurring at constant degradation rate, $k = 0.00594 \pm 0.00029\text{ week}^{-1}$ for tetracycline and $k = 0.00761 \pm 0.00026\text{ week}^{-1}$ for cadmium, and 2 – a fast degradation, occurring later, with constant $k = 0.04484 \pm 0.00137\text{ week}^{-1}$ and $k = 0.06777 \pm 0.00171\text{ week}^{-1}$ for tetracycline and cadmium, respectively. Those two ranges were not observed for spinach growing without contamination ($k = 0.00679 \pm 0.00027\text{ week}^{-1}$). Chlorophyll degradation occurred eight times faster for tetracycline and ten times faster for cadmium. After 32 weeks of storage 19.4% and 13.6% of chlorophyll were left in small leaves affected by tetracycline and cadmium, respectively. In spinach leaves of harvesting maturity (50-days-old, large leaves), lower values of rate constants were found for range 2, amounting for dose (90 mg/kg soil) to $k = 0.02945 \pm 0.00151\text{ week}^{-1}$ (for tetracycline) and $k = 0.03511 \pm 0.00124\text{ week}^{-1}$ (for cadmium) and 50% chlorophyll was left after 32 weeks. Chlorophyll degradation degree depends on soil contamination, leaf size and time of exposure to contaminants.

Keywords: *chlorophyll content, chlorophyll degradation, absorption and fluorescence spectra, degradation rate, storage of spinach*

Introduction

The spinach is a popular vegetable due to its taste and sensory values. Spinach leaf chemical composition is also significant, including the high level of vitamin (C, E), folic acid, polyphenols, β -carotene, mineral component and dietary fibre, as well as strong antioxidant properties related to the high chlorophyll content (Jaworska, 2005; Lisiewska et al., 2009; Xie et al., 2013). A drawback of spinach is its short shelf life in a chilled state. After being subject to minimum processing, spinach packed in perforated bags remains fit for consumption for eight days when stored in the refrigerator at $8\text{ }^{\circ}\text{C}$ (Kou et al., 2014). For this reason, spinach leaves are very often purchased by consumers in a frozen form (Jaworska and Kmiecik, 2000). Freezing is one of the most

frequently applied food storage methods. Despite undeniable usefulness of spinach storage at freezing temperatures, such treatments also have negative effects on food quality. Freezing involves physical changes, such as re-crystallization of ice and moisture migration, resulting in a decrease in weight and nutrient content, as well as changes in the product texture (Van Buggenhout et al., 2006; Pukszta and Palich, 2007). In the freezing process, chemical changes also take place, which can result in a change in taste or colour (Lisiewska et al., 2009). The colour is of great importance, since it is one of main factors considered by consumers purchasing fruit and vegetables. Orange and yellow colour of vegetables is, to a significant extent, caused by carotenoids, while green is related to the presence of chlorophyll (Sánchez et al., 2014). The change of the green colour in frozen products is related to degradation of chlorophyll content in plants (Koca et al., 2007). Chlorophyll degradation occurs not only when leaves are being frozen, but also in plants growing in a contaminated environment (Bartha et al., 2010; Kong et al., 2007). The main environmental contaminants include heavy metals and antibiotics, which have also been emphasized recently as cropland contaminating factors (Zhang et al., 2016). Progressive contamination results in increasing the content of antibiotics and heavy metals in soils and surface water (Azeez et al., 2009; Kim and Carlson, 2007; Nicholson et al., 2003). Contamination of arable soils in Poland with cadmium exceeded 90.87 mg/kg in 2000 (IUNG, 2017). Both heavy metals and antibiotics are taken up by plants from soil (Pan and Chu, 2017). After taking up, they are transported to the above-ground parts, including leaves, where they disturb the process of photosynthesis. The plant's response to environmental contamination caused by heavy metals has been quite well explored. It is known that heavy metals replace a magnesium atom in chlorophyll, creating chlorophyll-metal bonds (Küpper et al., 2000, 2001). Chlorophyll and metal complexes, even if they occur in low amounts in relation to pure chlorophyll, can entirely inhibit the process of photosynthesis (Küpper et al., 1996). Metals with high toxicity towards plants include cadmium (Smeets et al., 2005; Mishra et al., 2006), this toxicity mainly results from changes occurring in the process of photosynthesis and changes in the structure and the content of photosynthetic dyes (Kummerova et al., 2006; López-Millán et al., 2009). Just like heavy metals, antibiotics also reduce the chlorophyll content in plants, thus reducing the process of photosynthesis (D'Abrosca et al., 2008; Li et al., 2011; Liu et al., 2013).

The effect of plant contamination with heavy metals or antibiotics on chlorophyll concentration in leaves intended for freezing has not yet been examined. The aim of this study was to determine changes in chlorophyll concentration during the storage of spinach containing cadmium and tetracycline. Additionally, the contents of tetracycline and cadmium, as soil pollutants, were analysed for any effect on the quality of frozen raw material.

Material and methods

Materials

The research material consisted of spinach (*Spinacia oleracea* L.) plants, Matador cultivar. The seeds were sown to the soil in 300 ml pots. After 20 or 40 days of plant growth, aqueous solutions of cadmium sulphate (Cd) and tetracycline (TC) at concentrations of 3, 45 and 90 mg/kg soil were added to the pots. Due to the fact that soil pollution in Poland exceeds 90 mg/kg of cadmium, the same concentrations for cadmium and tetracycline were used for comparison. Additionally, we applied to

smaller doses for large leaves – 3 and 45 mg/kg. After ten days as of adding metal and antibiotics to the soil, the leaves were cut, washed with water and prepared for freezing.

The spinach was frozen in two variants:

1. Small leaves (SL) – with a surface area of $10 \pm 0.5 \text{ cm}^2$, growing for 30 days, of which 10 days on the soil containing TC and Cd in the dose of 90 mg/kg soil.
2. Large leaves (BL) – with a surface area of $55 \pm 2 \text{ cm}^2$, growing for 50 days (harvesting maturity of leaves) of which 10 days on the soil containing with TC and Cd in the dose of 3, 45 and 90 mg kg soil.

BL and SL leaves were homogenized and stored in the freezer at $-18 \text{ }^\circ\text{C}$ for 32 weeks. The temperature was additionally monitored with a thermometer located in the freezer. Samples from the freezer were collected at one week intervals. Analyses were performed in five replications. Leaves from plants growing on soil not contaminated with cadmium or tetracycline were used as control. The leaves were stored in parallel with the plant material from contaminated soil.

Chlorophyll extraction

Chlorophyll was extracted from spinach leaves (300 mg) with 5 ml of methanol (Rydzynski et al., 2017). The obtained homogenate was centrifuged at room temperature at 4,000 RPM. The extract was then 5-fold diluted and used for spectrophotometric and fluorometric analyses. All extraction procedures were conducted in cold temperatures and dim light.

Absorption and fluorescence spectra

The absorption and fluorescence spectra of solutions were measured using, respectively, the Carry 5000 UV-Visible Spectrophotometer (Varian, Inc) and a Cary Eclipse Fluorescence Spectrophotometer (Varian, Inc) with right-angle geometry. The fluorescence spectra were measured at excitation wavelength $\lambda_{\text{exc}} = 650 \text{ nm}$. Chlorophyll concentrations were calculated, based on Lambert-Beer law, on the basis of the known molar extinction coefficient of chlorophyll in methanol, which is $\varepsilon = 66600 \text{ M}^{-1} \text{ cm}^{-1}$ in the first chlorophyll absorption band maximum (Seely and Jensen, 1965).

Results and discussion

Chlorophyll is not only an indispensable plant dye, but has also been proven to be an important compound for the human body, with favourable antihyperglycemic and antihyperlipidemic properties (Patar et al., 2016). Chlorophyll also demonstrates antioxidant effects, eliminates free radicals and shows a positive effect in cancer treatment (Gore et al., 2017). Therefore, reduction of the chlorophyll content in the human diet is highly undesirable.

It was proven (Rydzynski et al., 2017) that plants growing on soils contaminated with antibiotics feature a high decrease in chlorophyll. Therefore, the consumption quality of plants growing on such soils is impaired. The present study examined the process of chlorophyll degradation in plants growing on soil contaminated with antibiotics and heavy metal (cadmium), during the storage of such leaves at $t = -18 \text{ }^\circ\text{C}$ for 32 weeks.

Figure 1A and A' present changes in the absorption and fluorescence spectra of chlorophyll extracted from spinach grown on soil without (control) the content of tetracycline or cadmium and stored at $t = -18^{\circ}\text{C}$ for 32 weeks. During the storage, absorption decreased from $A_1 = 1.122$ to $A_{32} = 0.874$. Chlorophyll concentration was reduced from the value of $C_0 = 8.42 \times 10^{-5}$ M to $C_{32} = 6.56 \times 10^{-5}$ M. Chlorophyll concentration decreased by 22%, which is in agreement with the results obtained by Dermesonluoglu et al. (2015) in the storage of frozen spinach at -18°C .

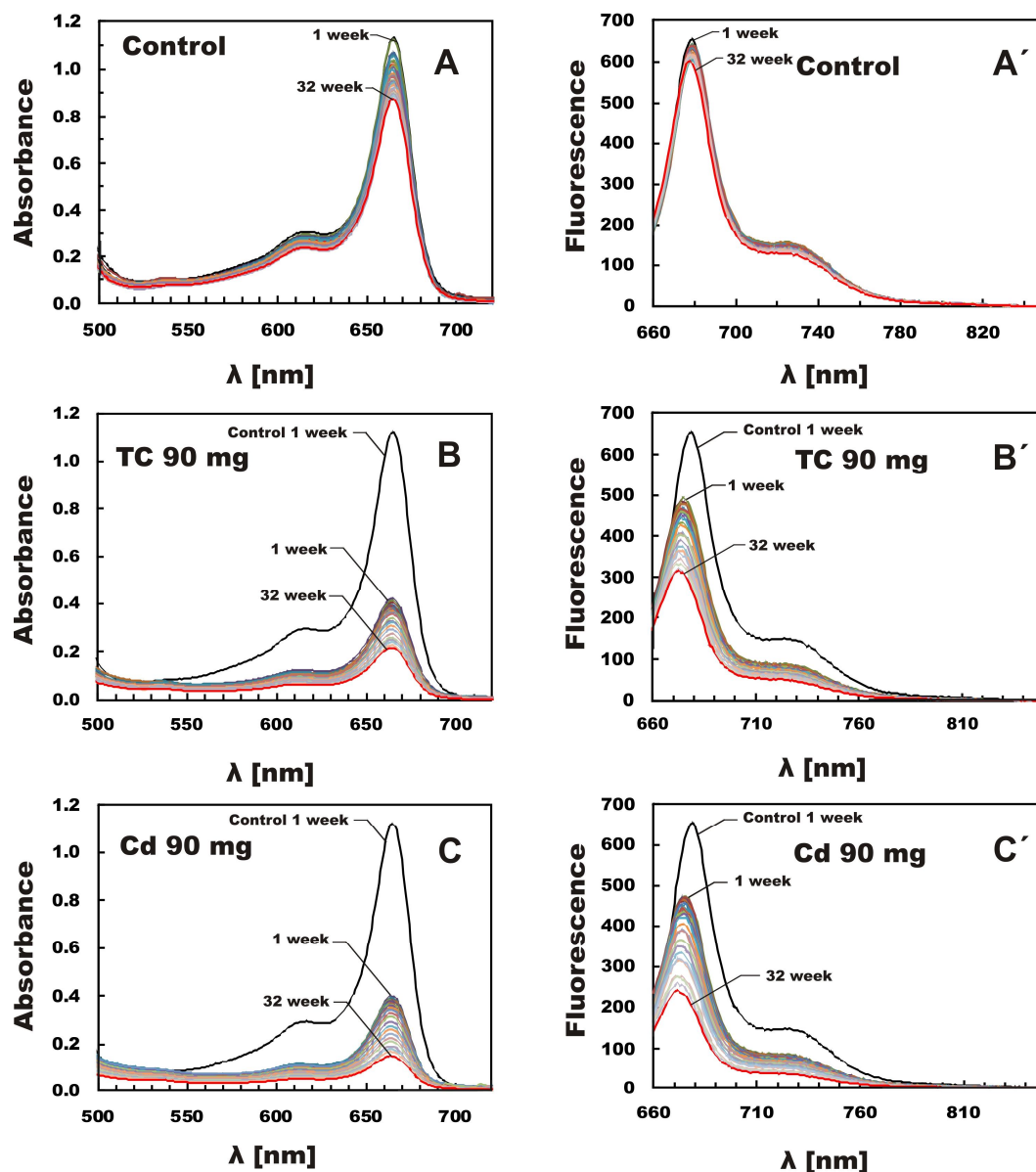


Figure 1. Absorption (A, B, C) and fluorescence (A', B', C') spectra for chlorophyll extracted from stored (small) spinach leaves growing on soil: A, A' - without contamination (control); B, B' - containing 90 mg tetracycline (TC); C, C' - containing 90 mg cadmium (Cd) per kg soil

Figure 1B, B', C and C' present, respectively, the absorption and fluorescence spectra of chlorophyll obtained from spinach plants growing on soil containing TC and

Cd, and stored at $t = -18^{\circ}\text{C}$ for 32 weeks. In these figures, the chlorophyll absorption and fluorescence spectrum for spinach without TC and Cd treatment (control) was added.

As *Figure 1B* shows, the absorption of chlorophyll extracted from plant leaves growing for 10 days in soil containing TC (90 mg/kg) decreased by 64% in relation to the control sample (from the value of $A = 1.12$ to $A = 0.407$) and *Figure 1C* demonstrates that for cadmium treatment (90 mg/kg), a decrease of 65% was observed (to the value of $A = 0.394$). The decrease observed occurred in leaves growing on contaminated soil, even before spinach leaves underwent the freezing process. The leaves growing on soil contaminated with TC and Cd, containing less chlorophyll, were then subject to the freezing process, as a result of which, as can be seen in *Figure 1B* and *C*, a further decrease in chlorophyll took place: absorption was reduced from $A_1 = 0.407$ to $A_{32} = 0.217$ (a further decrease in chlorophyll concentration to the value of $C_{32} = 1.63 \times 10^{-5}\text{M}$) for TC, and to the value of $A_{32} = 0.152$ (a decrease in concentration to the value of $C_{32} = 1.14 \times 10^{-5}\text{M}$) for Cd. After 32 weeks of storage, 19.4% chlorophyll content remained in TC contaminated leaves and 13.6% in Cd contaminated leaves.

It can be clearly seen that during the low temperature storage of spinach leaves grown on soil contaminated with TC and Cd, a further process of chlorophyll degradation took place. In the fluorescence spectra (*Fig. 1B'* and *C'*) major changes are observed – a large decrease in fluorescence concentration, particularly for samples containing cadmium. The fluorescence spectrum clearly shifted towards shorter wavelengths by 6 nm at TC contamination, and by 8 nm at Cd contamination, which clearly proves the formation of chlorophyll degradation products. A high decrease in absorbance between the control sample and the first week of freezing for spinach containing TC or Cd results from chlorophyll degradation in the plant under the effect of tetracycline and cadmium, while a further decrease in chlorophyll content was caused by the storage process.

Figure 2 presents the relation between chlorophyll concentration in spinach leaves (SL) and the time of storage at $t = -18^{\circ}\text{C}$. These figures present the values of chlorophyll concentration for five independent samples of spinach leaves in the function of storage time. Statistical data of these changes is shown in *Table A1* in the *Appendix*. For spinach grown on soil contaminated with antibiotic and metal, two ranges of chlorophyll degradation can be distinguished: the first range of slow degradation up to week 20, and the second range, of the so-called faster degradation. King et al. (2001) also observed a two-range course of chlorophyll degradation rate, but during dehydration by freeze-drying at -5°C , -20°C , -30°C and 45°C . At the beginning, for 6 days of the process, they observed fast Chl degradation, followed by slow degradation. Those two ranges were recorded for blanched spinach, particularly at -5°C and -30°C . In the current study, two ranges of chlorophyll degradation were not observed for spinach growing on uncontaminated soil (control).

On the basis of concentrations obtained, the kinetics of chlorophyll degradation during spinach storage time was examined. As provided in the literature (Koca et al., 2007; Dermesonluoglu et al., 2015; Steet and Tong, 1996) in the examined cases, total chlorophyll loss in vegetables during various technological processes was described by 1st order reaction kinetics.

The concentration of chlorophyll as a function of time at a constant temperature for a first-order degradation kinetics model is:

$$C = C_0 e^{-kt} \quad (\text{Eq. 1})$$

where C is the chlorophyll concentration at any time t , C_0 is the initial concentration, and k is the first-order constant estimated by slope of the linearized plot of $\ln C$ vs t .

Chlorophyll degradation reactions during spinach storage for 32 weeks at low temperature $t = -18^\circ\text{C}$ were described by 1st order kinetics (Fig. 3). The $\ln C$ function linearly described the dependence of chlorophyll concentration decrease in the time of leaf storage at $t = -18^\circ\text{C}$ in both ranges for contaminated spinach, and in one range for uncontaminated spinach.

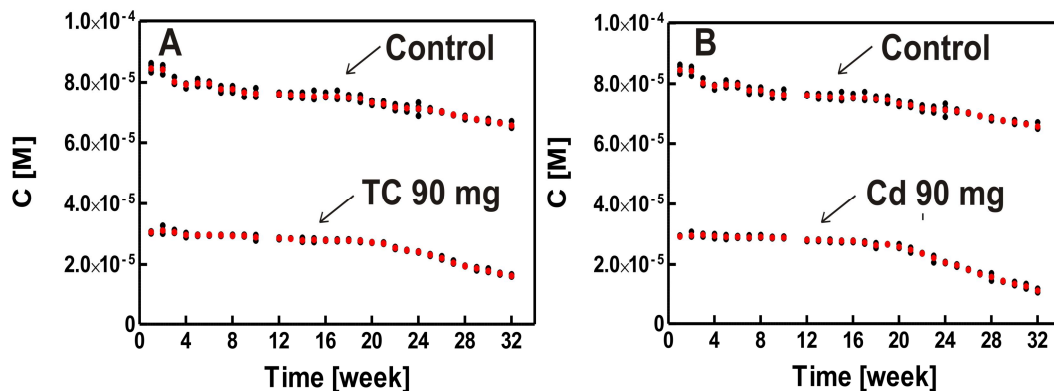


Figure 2. Relation between chlorophyll concentration ($C[M]$) in small spinach leaves and storage time. A – plants growing with TC (90 mg/kg soil), B - with Cd (90 mg/kg soil). The results were given for 5 independent measurements, the average value is shown in red. Data provided for 5 samples (●a, ●b, ●c, ●d, ●e, ●av – average for five samples) during 32 weeks of storage at $t = -18^\circ\text{C}$. The time dependence of chlorophyll concentration on leaf storage time has also been drawn for control (without contamination).

Figure 3 presents the linear adjustment of $\ln C$ relation to spinach storage time. In frozen spinach, grown on uncontaminated soil, the chlorophyll degradation reaction occurred at a rate constant of $k = 0.00679 \pm 0.00027 \text{ week}^{-1}$ ($R^2 = 0.958$). On the other hand, in spinach with TC, $k = 0.00594 \pm 0.00029 \text{ week}^{-1}$ ($R^2 = 0.966$) in the slow degradation range, the process occurred faster in the second range, with constant $k = 0.04484 \pm 0.00137 \text{ week}^{-1}$ ($R^2 = 0.989$). For cadmium, k constants were higher and amounted to $k = 0.00761 \pm 0.00026 \text{ week}^{-1}$ ($R^2 = 0.982$) in the first range, and in the second – $k = 0.06777 \pm 0.00171 \text{ week}^{-1}$ ($R^2 = 0.993$). The value of the constant describing chlorophyll degradation rate in leaves growing without contamination (antibiotics and Cd) in this study corresponds to the values obtained by other authors. Dermesonluoglu et al. (2015) observed a 25% decrease in chlorophyll content after 36 weeks of storage at -18°C . The value of the first-order chlorophyll degradation constant they obtained, converted into the same units, is equal, within the margin of error, to the rate constant k obtained for uncontaminated spinach in the current study.

Some authors suggest that during spinach storage, chlorophyll is decomposed to pheophytin. After three weeks of spinach storage at 8°C , pheophytin becomes the main chlorophyll degradation product (López-Ayerra et al., 1998). Moharram and Rofael (1993) and Symons (1994) suggest that during storage at low temperatures, chlorophyll is also degraded to pheophytin. Kidmose et al. (2002) indicate that during freezing,

storage and thermal treatment, chlorophyll is converted or degraded to pheophytin, pheophorbide, pyropheophytin and pyropheophorbide. Niedzielski and Mokrosinska (1990) indicate that before low temperature storage of leaves, their blanching is recommended, as this process causes denaturation of the protein complex, which reduces chlorophyll content loss.

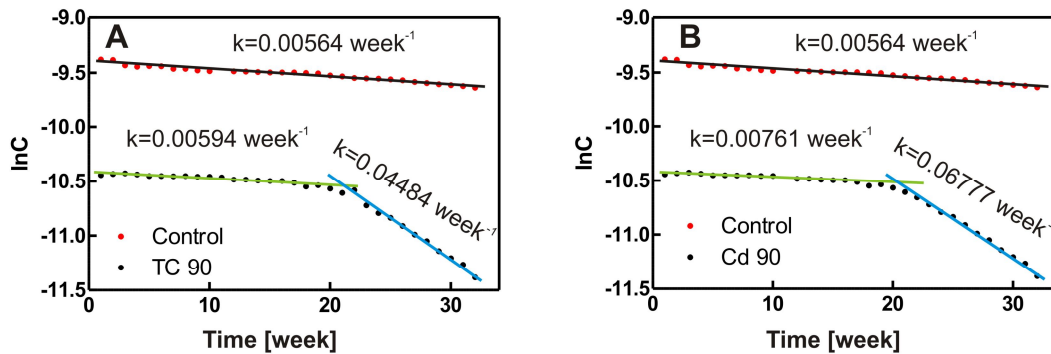


Figure 3. Relation between concentration of chlorophyll extracted from plants growing with antibiotics (A) or cadmium (B) (90 mg/kg soil) and leaf storage time at $t = -18\text{ }^{\circ}\text{C}$. Dotted points – experimental data, line – obtained from the linear regression based on the experimental data. The following equation was applied: $C = C_0 e^{-kt}$

In our paper we postulated that the two-range chlorophyll degradation observed in the current study results from the fact that chlorophyll subject to the freezing process is quite quickly degraded in plants growing for 10 days on TC and Cd contaminated soil and, afterwards, during the storage of such spinach, degradation occurred slower in the first period, with further strong chlorophyll degradation taking place only after 20 weeks of freezing, as a result of which after 32 weeks, only 19.4% and 13.6% chlorophyll was remain in plants contaminated with TC and Cd, respectively. However, for freezing leaves growing without antibiotics or Cd, it was observed that after 32 weeks (in control spinach), 78% chlorophyll was left. Therefore, 22% chlorophyll degradation occurred (Fig. 2).

When freezing spinach leaves at $t = -18\text{ }^{\circ}\text{C}$, Dermesonluoglu et al. (2015) observed a similar course of degradation as we observed for uncontaminated spinach. On the other hand, King et al. (2001) observed freeze-drying of dehydrated spinach at various temperatures (from $-5\text{ }^{\circ}\text{C}$ to $-45\text{ }^{\circ}\text{C}$) and found very fast chlorophyll degradation at the beginning, within six weeks, followed by slow degradation. After twelve weeks, chlorophyll degradation reached 45% at $t = -20\text{ }^{\circ}\text{C}$. Even faster chlorophyll degradation in comparison to spinach occurs in turnip greens (*Brasica rapa* var. *rapa* L.). During 28-day storage at $-30\text{ }^{\circ}\text{C}$, chlorophyll a is 40% degraded and chlorophyll b is 44% degraded (Martínez et al., 2013). An interesting result of chlorophyll degradation was obtained by Grzeszczuk et al. (2007) for New Zealand spinach stored at $t = -25\text{ }^{\circ}\text{C}$. Changes in chlorophyll content during storage are completely different. Grzeszczuk et al. (2007) observed an initial growth in chlorophyll content in New Zealand spinach in the first three months of storage, and only between month 3 and 6 of storage at about $-26\text{ }^{\circ}\text{C}$, a decrease in chlorophyll content takes place. On the other hand, in dill frozen at $-20\text{ }^{\circ}\text{C}$, Lisiewska et al. (2004) observed a slow decrease in chlorophyll content up to about week 24, after which chlorophyll degradation was accelerated, similar to

contaminated spinach leaves examined in the our current research. As it can be concluded from the data quoted above, depending on the plants, chlorophyll degradation during storage at low temperature can have various courses.

Our study also examined the process of chlorophyll degradation in harvest-ready, large, developed spinach leaves. Such spinach (growing for 50 days, of which 10 days with 3, 45 and 90 mg TC and Cd per kg soil) was subject to the freezing process and stored at $t = -18\text{ }^{\circ}\text{C}$ for 32 days. The absorption spectra of chlorophyll extracted every week from those leaves are presented in *Figure 4*. As shown in *Figure 4*, the decrease in chlorophyll absorption during the storage of harvest-mature leaves contaminated with TC was slower in the first weeks. For three doses of TC and Cd, for 3, 45, 90 mg/kg soil, absorbance decreased after 32 weeks to the following values: $A_3 = 0.724$, $A_{45} = 0.637$, $A_{90} = 0.500$ for TC, and for Cd treatment: $A_3 = 0.714$, $A_{45} = 0.583$, $A_{90} = 0.498$ It can be noted that chlorophyll degradation was only slightly lower after Cd application.

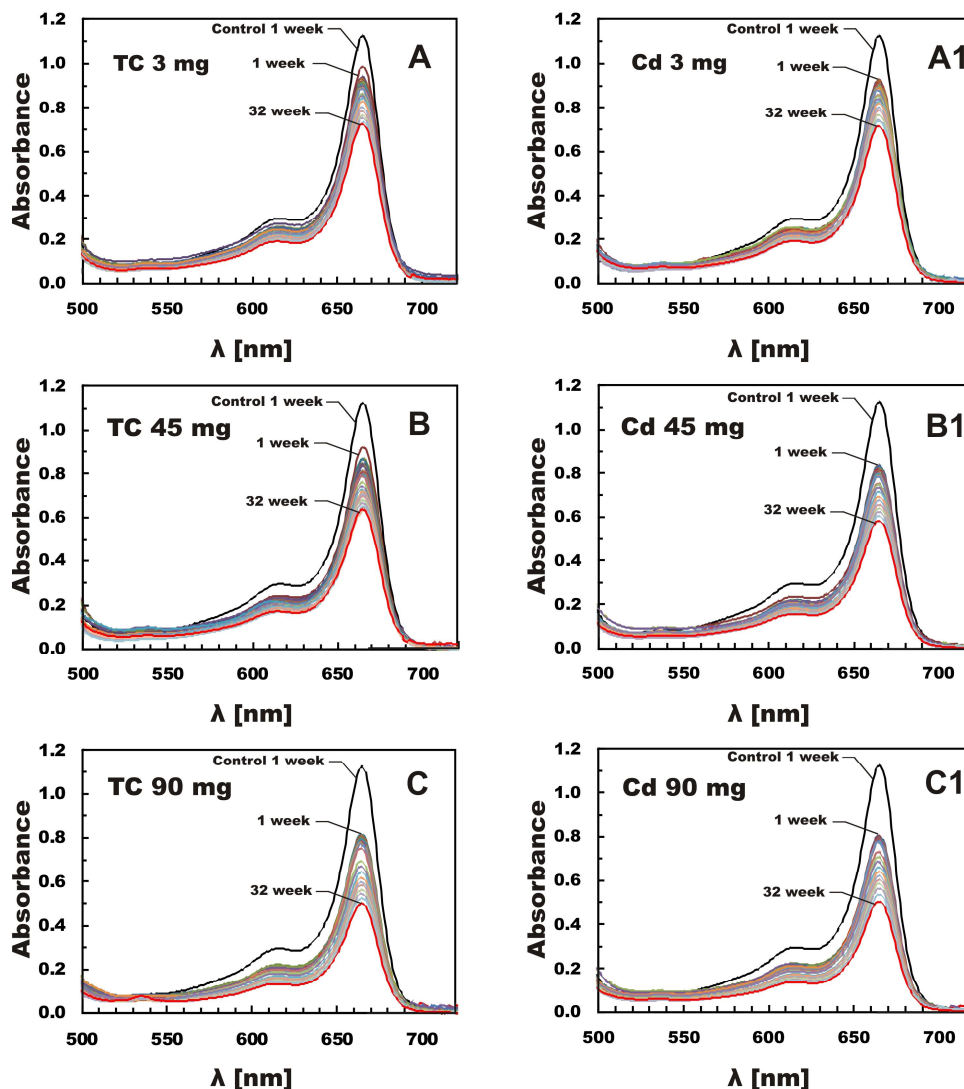


Figure 4. Absorption spectra for chlorophyll extracted from fully developed spinach leaves growing on soil contaminated with tetracycline and cadmium at the dose of: 3 mg/kg soil (A - tetracycline, A1 - cadmium), 45 mg/kg soil (B - tetracycline, B1 - cadmium) and 90 mg/kg soil (C - tetracycline, C1 - cadmium)

Figure 5 presents storage time dependence of chlorophyll concentration in subsequent weeks of its storage at $t = -18\text{ }^{\circ}\text{C}$ for developed spinach leaves. Statistical data of these changes is shown in Table A2. The percentage content of chlorophyll remaining in spinach after 32 weeks of freezing in relation to the control sample, in which chlorophyll concentration was $C_0 = 8.42 \times 10^{-5}\text{ M}$ (chlorophyll concentration in leaves uncontaminated with TC and Cd), depending on the dose and was amounted for TC: 64.49% (3 mg) and 56.65% (45 mg), 44.42% (90 mg) and for Cd: 63.68% (3 mg), 51.90% (45 mg) and 44.54% (90 mg). The results show that chlorophyll degradation is lower in large, developed leaves, which were subject to the antibiotic and metal treatment only after their development. Undoubtedly, degradation would have taken a completely different course if the plants had grown on the contaminated soil for 50 days. The results clearly indicate that in developed spinach leaves, degradation is also a two-stage process.

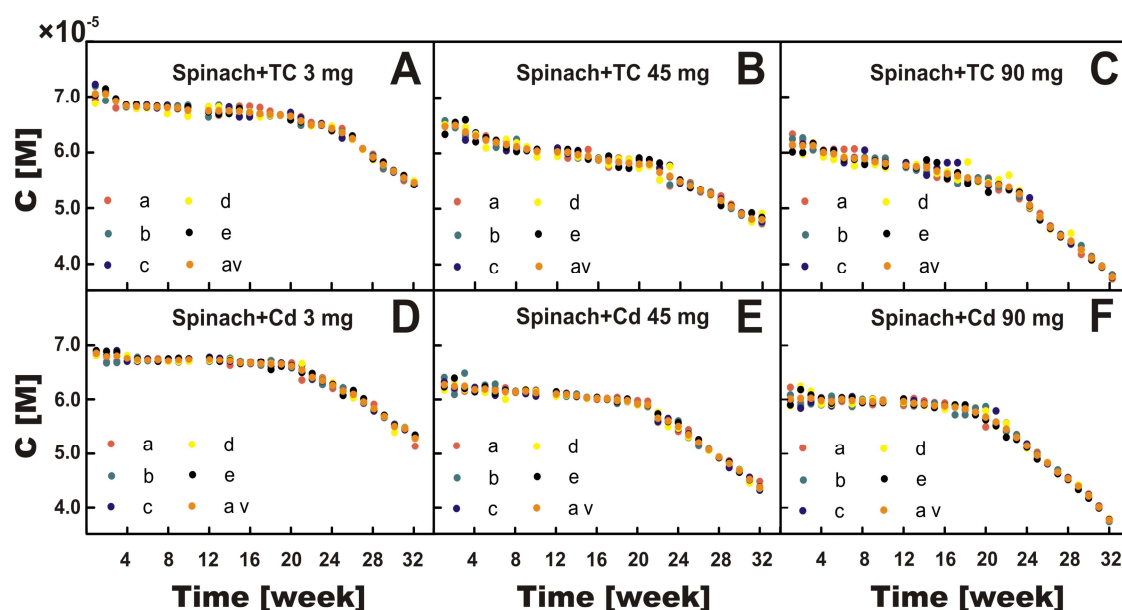


Figure 5. Relation between chlorophyll concentration ($C[M]$) in large spinach leaves and storage time. Panel A, B, C – plants growing with tetracycline (3, 45 and 90 mg/kg soil), Panel D, E, F - with cadmium (3, 45 and 90 mg/kg soil). The results were given for 5 independent measurements, the average value is shown in red. Data provided for 5 samples (● a, ● b, ● c, ● d, ● e, ● av – average for five samples) during 32 weeks of storage at $t = -18\text{ }^{\circ}\text{C}$

Table 1 shows degradation rate constants for 50-day spinach contaminated with TC and Cd. As shown in the table, chlorophyll degradation rate constants depend on the TC and Cd dose, which indicates that Cd is more toxic in the second range, while degradation occurs faster in plants growing on soil contaminated with Cd. In the first range, degradation rate constants did not differ much, and varied from $k = 0.00168 \pm 0.00006\text{ week}^{-1}$ to $k = 0.00550 \pm 0.00019\text{ week}^{-1}$ for TC, and from $k = 0.00134 \pm 0.00014\text{ week}^{-1}$ to $k = 0.002217 \pm 0.00017\text{ week}^{-1}$ for Cd. In the second range, the values of k were 10 times higher (Tab.1) and took significantly higher values for Cd. It is also worth emphasizing that degradation rate constants k for Cd in the first range are lower than for TC. This probably results from the fact that plants have an efficient cadmium resistance mechanism. Metal transporters can play a significant role in

controlling plant tolerance to Cd (Rui et al., 2018). It was also demonstrated that plants more readily take up tetracycline from soil than cadmium (Rydzynski et al., 2018).

Table 1. Values of the reaction chlorophyll degradation rate constant k for harvest-ready spinach

Harvesting maturity of leaves	I range			II range			
	mg/kg soli	k [week ⁻¹]	Storage time	R ²	k [week ⁻¹]	Storage time	R ²
TC 3	0.00168 ± 0.00006		From 3 to 19 weeks	0.985	0.01551 ± 0.00117	From 20 to 31 weeks	0.951
TC 45	0.00456 ± 0.00015		From 5 to 21 weeks	0.985	0.01811 ± 0.00054	From 21 to 31 weeks	0.992
TC 90	0.00550 ± 0.00019		From 4 to 19 weeks	0.986	0.02945 ± 0.00151	From 19 to 31 weeks	0.983
mg/kg soil	k [week ⁻¹]		R ²	k [week ⁻¹]		R ²	
Cd3	0.00134 ± 0.00014		From 1 to 20 weeks	0.840	0.01855 ± 0.00079	From 21 to 32 weeks	0.982
Cd 45	0.00272 ± 0.00011		From 1 to 21 weeks	0.971	0.02613 ± 0.00070	From 21 to 32 weeks	0.993
Cd 90	0.002217 ± 0.00020		From 1 to 19 weeks	0.947	0.03511 ± 0.00124 0.03421 ± 0.00123	From 22 to 32 weeks From 21 to 32 weeks	0.987 0.987

Conclusion

The research demonstrated that the degree of chlorophyll degradation depends on the soil contamination degree, the leaf size and the time for which the plant grew on contaminated soil. At the same time, cadmium toxicity is higher despite the plants taking it up in smaller amounts, since chlorophyll degradation is higher in the presence of Cd than TC. To preserve the highest consumption quality of spinach leaves (high chlorophyll content), the leaves intended for freezing should be large and should grow on soil free of any contamination. We recommend storing spinach leaves at -18 °C for not longer than 20 weeks. In addition to the analysis of chlorophyll quality, the studies of stored leaves from spinach grown on contaminated soils will be carried out in the immediate future to consider biologically active substances such as vitamins, carotenes, xanthophylls that have a significant impact on the biological value of the vegetable raw material.

REFERENCES

- [1] Azeez, J. O., Adekunle, I. O., Atiku, O. O., Akande, K. B., Jamiu-Azeez, S. O. (2009): Effect of nine years of animal waste deposition on profile distribution of heavy metals in Abeokuta, south-western Nigeria and its implication for environmental quality. – *Waste Management* 29(9): 2582–2586.
- [2] Bartha, B., Huber, C., Harpaintner, R., Schröder, P. (2010): Effects of acetaminophen in *Brassica juncea* L. Czern.: investigation of uptake, translocation, detoxification, and the induced defense pathways. – *Environmental Science and Pollution Research* 17(9): 1553–1562.
- [3] D'Abrosca, B., Fiorentino, A., Izzo, A., Cefarelli, G., Pascarella, M. T., Uzzo, P., Monaco, P. (2008): Phytotoxicity evaluation of five pharmaceutical pollutants detected in surface water on germination and growth of cultivated and spontaneous plants. – *Journal of Environmental Science and Health Part A* 43(3): 285–294.

- [4] Dermesonluoglu, E., Katsaros, G., Tsevdou, M., Giannakourou, M., Taoukis, P. (2015): Kinetic study of quality indices and shelf life modelling of frozen spinach under dynamic conditions of the cold chain. – *Journal of Food Engineering* 148: 13–23.
- [5] Gore, R. D., Palaskar, S. J., Bartake, A. R. (2017): Wheatgrass: green blood can help to fight cancer. – *Journal of Clinical and Diagnostic Research* 11(6): ZC40–ZC42.
- [6] Grzeszczuk, M., Jadczyk, D., Podsiadło, C. (2007): The effect of blanching, freezing and freeze-storage on changes of some chemical compounds content in New Zealand spinach. – *Vegetable Crops Research Bulletin* 2(66): 95–103.
- [7] IUNG (2017): Monitoring Chemizmu Gleb Ornych Polski (in Polish). – https://www.gios.gov.pl/chemizm_gleb/index.php?mod=wyniki&cz=G.
- [8] Jaworska, G. (2005): Nitrates, nitrites, and oxalates in products of spinach and New Zealand spinach: effect of technological measures and storage time on the level of nitrates, nitrites, and oxalates in frozen and canned products of spinach and New Zealand spinach. – *Food Chemistry* 93: 395–401.
- [9] Jaworska, G., Kmiecik, W. (2000): Comparison of the nutritive value of frozen spinach and New Zealand spinach. – *Polish Journal of Food and Nutrition Sciences* 50(4): 79–84.
- [10] Kidmose, U., Edelenbos, M., Nørbæk, R., Christensen, L. P. (2002): Colour Stability in Vegetables. – In: MacDougall, D. B. (ed.) *Colour in Food: Improving*. CRC Press LLC, Boca Raton, pp. 179–232.
- [11] Kim, S. C., Carlson, K. (2007): Temporal and spatial trends in the occurrence of human and veterinary antibiotics in aqueous and river sediment matrices. – *Environmental Science & Technology* 41(1): 50–57.
- [12] King, V. A. E., Liu, C. F., Liu, Y. J. (2001): Chlorophyll stability in spinach dehydrated by freeze-drying and controlled low-temperature vacuum dehydration. – *Food Research International* 34(2-3): 167–175.
- [13] Koca, N., Karadeniz, F., Burdurlu, H. S. (2007): Effect of pH on chlorophyll degradation and colour loss in blanched green peas. – *Food Chemistry* 100: 609–615.
- [14] Kong, W. D., Zhu, Y. G., Liang, Y. C., Zhang, J., Smith, F. A., Yang, M. (2007): Uptake of oxytetracycline and its phytotoxicity to alfalfa (*Medicago sativa* L.). – *Environmental Pollution* 147(1): 187–193.
- [15] Kou, L., Luo, Y., Park, E., Turner, E. R., Barczak, A., Jurick, W. M. (2014): Temperature abuse timing affects the rate of quality deterioration of commercially packaged ready-to-eat baby spinach. Part I: sensory analysis and selected quality attributes. – *Postharvest Biology and Technology* 91: 96–103.
- [16] Kummerova, M., Bartak, M., Dubova, J., Triska, J., Zubrova, E., Zezulka, S. (2006): Inhibitory effect of fluoranthene on photosynthetic processes in lichens detected by chlorophyll fluorescence. – *Ecotoxicology* 15: 121–131.
- [17] Küpper, H., Lombi, E., Zhao, F. J., Wieshammer, G., McGrath, S. P. (1996): Cellular compartmentation of nickel in the hyperaccumulators *Alyssum lesbiacum*, *Alyssum bertolonii* and *Thlaspi goesingense*. – *Journal of Experimental Botany* 52(365): 2291–2300.
- [18] Küpper, H., Lombi, E., Zhao, F. J., McGrath, S. P. (2000): Cellular compartmentation of cadmium and zinc in relation to other elements in the hyperaccumulator *Arabidopsis halleri*. – *Planta* 212: 75–84.
- [19] Küpper, H., Küpper, F., Spiller, M. (2001): Environmental relevance of heavy metal substituted chlorophylls using the example of water plants. – *Journal of Experimental Botany* 47: 259–266.
- [20] Li, Z. J., Xie, X. Y., Zhang, S. Q., Liang, Y. C. (2011): Negative effects of oxytetracycline on wheat (*Triticum aestivum* L.) growth, root activity, photosynthesis, and chlorophyll contents. – *Agricultural Sciences in China* 10(10): 1545–1553.
- [21] Lisiewska, Z., Kmiecik, W., Słupski, J. (2004): Contents of chlorophylls and carotenoids in frozen dill: effect of usable part and pre-treatment on the content of chlorophylls and

- carotenoids in frozen dill (*Anethum graveolens* L.), depending on the time and temperature of storage. – Food Chemistry 84: 511–518.
- [22] Lisiewska, Z., Gebczynski, P., Bernas, E., Kmiecik, W. (2009): Retention of mineral constituents in frozen leafy vegetables prepared for consumption. – Journal of Food Composition and Analysis 22: 218–223.
- [23] Liu, L., Liu, Y. H., Liu, C. X., Wang, Z., Dong, J., Zhu, G. F., Huang, X. (2013): Potential effect and accumulation of veterinary antibiotics in *Phragmites australis* under hydroponic conditions. – Ecological Engineering 53: 138–143.
- [24] López-Ayerra, B., Murcia, A. M., Garcia-Carmona, F. (1998): Lipid peroxidation and chlorophyll levels in spinach during refrigerated storage and after industrial processing. – Food Chemistry 61: 113–118.
- [25] López-Millán, A. F., Morales, F., Gogorcena, Y., Abadía, A., Abadía, J. (2009): Metabolic responses in iron deficient tomato plants. – Journal of Plant Physiology 166(4): 375–384.
- [26] Martínez, S., Pérez, N., Carballo, J., Franco, I. (2013): Effect of blanching methods and frozen storage on some quality parameters of turnip greens (“grelos”). – LWT - Food Science and Technology 51(1): 383–392.
- [27] Mishra, S., Srivastava, S., Tripathi, R. D., Govindarajan, R., Kuriakose, S. V., Prasad, M. N. V. (2006): Phytochelatin synthesis and response of antioxidants during cadmium stress in *Bacopa monnieri* L. – Journal of Plant Physiology and Biochemistry 44: 25–37.
- [28] Moharram, Y. G., Rofael, S. D. (1993): Shelf Life of Frozen Vegetables. – In: Charalambous, G. (ed.) Shelf Life Studies of Foods and Beverages. Elsevier Science Publishers BV, Amsterdam.
- [29] Nicholson, F. A., Smith, S. R., Alloway, B. J., Carlton-Smith, C., Chambers, B. J. (2003): An inventory of heavy metals inputs to agricultural soils in England and Wales. – Science of the Total Environment 311(1–3): 205–219.
- [30] Niedzielski, Z., Mokrosińska, K. (1990): Wpływ mrożenia gazami skroplonymi na jakość przechowywanej kapusty brukselskiej. – Zeszyty Nauk Politechniki Łódzkiej, seria Technol Chem Spoż 47: 119–125 (English summary).
- [31] Pan, M., Chu, L. M. (2017): Fate of antibiotics in soil and their uptake by edible crops. – Science of the Total Environment 599–600: 500–512.
- [32] Patar, A. K., Bhan, S., Syiem, D. (2016): Effect of chlorophyllin, an semi-synthetic chlorophyll molecule on hyperglycemia and hyperlipidemia in streptozotocin induced diabetic mice. – International Journal of Pharmacy and Pharmaceutical Sciences 8: 293–296.
- [33] Puksza, T., Palich, P. (2007): The effect of freezing conditions of strawberry storage on the level of thawing drip loss. – Acta Agrophysica 9: 203–208.
- [34] Rui, H., Zhang, X., Shinwari, K. I., Zheng, L., Shen, Z. (2018): Comparative transcriptomic analysis of two *Vicia sativa* L. varieties with contrasting responses to cadmium stress reveals the important role of metal transporters in cadmium tolerance. – Plant Soil 423(1-2): 41–255.
- [35] Rydzyński, D., Piotrowicz-Cieślak, A. I., Grajek, H., Michalczyk, D. J. (2017): Instability of chlorophyll in yellow lupin seedlings grown in soil contaminated with ciprofloxacin and tetracycline. – Chemosphere 184: 62–73.
- [36] Rydzyński, D., Piotrowicz-Cieślak, A. I., Grajek, H., Michalczyk, D. J. (2018): Different ways of chlorophyll degradation by tetracycline and cadmium in spinach (*Spinacia oleracea* L.) leaves. – International Journal of Environmental Science and Technology DOI: 10.1007/s13762-018-2142-8.
- [37] Sánchez, C., Baranda, A. B., Martínez de Marañón, I. (2014): The effect of high pressure and high temperature processing on carotenoids and chlorophylls content in some vegetables. – Food Chemistry 163: 37–45.
- [38] Seely, G. R., Jensen, R. G. (1965): Effect of solvent on the spectra of chlorophyll. – Spectrochimica Acta 21(10): 1835–1845.

- [39] Smeets, K., Cuypers, A., Lambrechts, A., Semane, B., Hoet, P., Laerve, A. V., Vangronsveld, J. (2005): Induction of oxidative stress and antioxidative mechanisms in *Phaseolus vulgaris* after Cd application. – Journal of Plant Physiology and Biochemistry 43: 437–444.
- [40] Steet, J. A. Tong, C. H. (1996): Degradation of green color and chlorophylls in peas by colorimetry and HPLC. – Journal of Food Science 61(5): 924–928.
- [41] Symons, H. (1994): Frozen Foods. – In: Man, C. M. D., Jones, A. A. (eds.) Shelf Life Evaluation of Foods. Blackie Academic Professional. London.
- [42] Van Buggenhout, S., Lille, M., Messagie, I., Van Loey, A., Autio, K., Hendrickx, M. (2006): Impact of pretreatment and freezing conditions on the microstructure of frozen carrots: qualification and relation to texture loss. – European Food Research and Technology 222: 43–553.
- [43] Xie, J., Zhu, J., Lin, Y. (2013): Effect of vacuum pre-cooling on quality changes of spinach during cold storage. – Advanced Materials Research. 641–642(1): 886–889.
- [44] Zhang, H., Zhou, Y., Huang, Y., Wu, L., Liu, X., Luo, Y. (2016): Residues and risks of veterinary antibiotics in protected vegetable soils following application of different manures. – Chemosphere 152: 229–237.

APPENDIX

Table A1. Statistical analysis of chlorophyll content in small leaves of plants grown in soil contaminated with tetracycline or cadmium (means \pm SD; different lowercase letters denote significantly different results across storage periods, different capital letters denote significant differences across contaminant doses; $NIR \leq 0.01$)

t (week)	Control C (M) $\times 10^{-5}$	Tetracycline C (M) $\times 10^{-5}$	Cadmium C (M) $\times 10^{-5}$
	0 mg	90 mg	90 mg
1	8.45 \pm 0.14 ^{aA}	3.05 \pm 0.03 ^{aB}	2.92 \pm 0.02 ^{aB}
2	8.42 \pm 0.11 ^{aA}	3.10 \pm 0.11 ^{aB}	2.95 \pm 0.07 ^{aB}
3	8.02 \pm 0.10 ^{aA}	3.05 \pm 0.04 ^{aB}	2.97 \pm 0.05 ^{aB}
4	7.93 \pm 0.07 ^{aA}	2.96 \pm 0.05 ^{aB}	2.94 \pm 0.06 ^{aB}
5	7.97 \pm 0.10 ^{aA}	2.95 \pm 0.02 ^{aB}	2.90 \pm 0.06 ^{aB}
6	7.96 \pm 0.05 ^{aA}	2.96 \pm 0.01 ^{aB}	2.90 \pm 0.03 ^{aB}
7	7.78 \pm 0.10 ^{bA}	2.95 \pm 0.02 ^{aB}	2.89 \pm 0.04 ^{aB}
8	7.78 \pm 0.09 ^{bA}	2.94 \pm 0.02 ^{aB}	2.90 \pm 0.04 ^{aB}
9	7.66 \pm 0.09 ^{bA}	2.94 \pm 0.02 ^{aB}	2.88 \pm 0.02 ^{aB}
10	7.62 \pm 0.12 ^{bA}	2.89 \pm 0.07 ^{aB}	2.88 \pm 0.03 ^{aB}
11	7.62 \pm 0.12 ^{bA}	2.86 \pm 0.05 ^{aB}	2.88 \pm 0.03 ^{aB}
12	7.61 \pm 0.04 ^{bA}	2.85 \pm 0.02 ^{aB}	2.80 \pm 0.02 ^{aB}
13	7.58 \pm 0.08 ^{bA}	2.84 \pm 0.00 ^{aB}	2.80 \pm 0.03 ^{aB}
14	7.55 \pm 0.08 ^{bA}	2.79 \pm 0.05 ^{aB}	2.78 \pm 0.03 ^{aB}
15	7.53 \pm 0.12 ^{bA}	2.80 \pm 0.05 ^{aB}	2.77 \pm 0.03 ^{aB}
16	7.53 \pm 0.07 ^{bA}	2.79 \pm 0.01 ^{aB}	2.77 \pm 0.02 ^{aB}
17	7.53 \pm 0.11 ^{bA}	2.79 \pm 0.03 ^{aB}	2.72 \pm 0.03 ^{aB}
18	7.49 \pm 0.06 ^{cA}	2.79 \pm 0.02 ^{aB}	2.63 \pm 0.07 ^{aB}
19	7.46 \pm 0.10 ^{cA}	2.77 \pm 0.02 ^{aB}	2.66 \pm 0.01 ^{aB}
20	7.32 \pm 0.08 ^{cA}	2.72 \pm 0.01 ^{aB}	2.58 \pm 0.05 ^{aB}
21	7.27 \pm 0.06 ^{cA}	2.69 \pm 0.02 ^{bB}	2.48 \pm 0.06 ^{bB}

22	7.16±0.09 ^{cA}	2.54±0.03 ^{bB}	2.54±0.04 ^{bB}
23	7.13±0.09 ^{cA}	2.46±0.01 ^{cB}	2.21±0.09 ^{bB}
24	7.11±0.16 ^{cA}	2.41±0.01 ^{dB}	2.06±0.02 ^{cC}
25	7.07±0.04 ^{cA}	2.31±0.03 ^{eB}	1.97±0.04 ^{cC}
26	7.01±0.01 ^{dA}	2.20±0.04 ^{eB}	1.83±0.02 ^{cC}
27	6.91±0.01 ^{dA}	2.05±0.04 ^{eB}	1.69±0.02 ^{dC}
28	6.84±0.06 ^{dA}	1.95±0.01 ^{eB}	1.59±0.09 ^{dC}
29	6.76±0.01 ^{dA}	1.87±0.05 ^{bB}	1.45±0.02 ^{dC}
30	6.71±0.06 ^{dA}	1.79±0.06 ^{bB}	1.36±0.06 ^{dC}
31	6.65±0.01 ^{dA}	1.70±0.03 ^{bB}	1.28±0.07 ^{dC}
32	6.56±0.08 ^{cA}	1.63±0.04 ^{bB}	1.14±0.06 ^{dC}

Table A2. Statistical analysis of chlorophyll content in mature leaves of plants grown in soil contaminated with tetracycline or cadmium (means ± SD; different lowercase letters denote significantly different results across storage periods, different capital letters denote significant differences across contaminant doses; NIR ≤ 0.01)

t (week)	Tetracycline C (M) × 10 ⁻⁵			Cadmium C (M) × 10 ⁻⁵		
	3 mg	45 mg	90 mg	3 mg	45 mg	90 mg
1	7.04±0.16 ^{aA}	6.45±0.08 ^{aB}	6.12±0.13 ^{aB}	6.92±0.04 ^{aA}	6.26±0.09 ^{aB}	6.00±0.14 ^{aB}
2	7.04±0.08 ^{aA}	6.47±0.03 ^{aB}	6.10±0.13 ^{aB}	6.86±0.11 ^{aA}	6.23±0.12 ^{aB}	6.01±0.18 ^{aB}
3	6.90±0.07 ^{aA}	6.35±0.15 ^{aB}	6.10±0.06 ^{aB}	6.87±0.11 ^{aA}	6.23±0.13 ^{aB}	6.01±0.10 ^{aB}
4	6.81±0.02 ^{aA}	6.28±0.06 ^{aB}	5.98±0.05 ^{aB}	6.82±0.04 ^{aA}	6.17±0.04 ^{aB}	5.97±0.06 ^{aB}
5	6.80±0.03 ^{aA}	6.21±0.08 ^{aB}	5.96±0.09 ^{aB}	6.80±0.04 ^{aA}	6.18±0.06 ^{aB}	5.95±0.08 ^{aB}
6	6.70±0.03 ^{aA}	6.17±0.06 ^{aB}	5.89±0.09 ^{aB}	6.79±0.02 ^{aA}	6.15±0.08 ^{aB}	5.99±0.03 ^{aB}
7	6.79±0.02 ^{aA}	6.13±0.08 ^{aB}	5.88±0.11 ^{aB}	6.79±0.02 ^{aA}	6.13±0.08 ^{aB}	5.97±0.09 ^{aB}
8	6.77±0.06 ^{aA}	6.09±0.09 ^{aB}	5.87±0.10 ^{aB}	6.78±0.03 ^{aA}	6.13±0.01 ^{aB}	5.96±0.02 ^{aB}
9	6.77±0.02 ^{aA}	6.05±0.03 ^{aB}	5.82±0.05 ^{aB}	6.79±0.04 ^{aA}	6.14±0.04 ^{aB}	5.95±0.04 ^{aB}
10	6.73±0.10 ^{aA}	6.01±0.06 ^{bB}	5.79±0.07 ^{aB}	6.80±0.03 ^{aA}	6.11±0.04 ^{aB}	5.95±0.02 ^{aB}
11	6.73±0.11 ^{aA}	6.01±0.06 ^{bB}	5.78±0.07 ^{aB}	6.80±0.03 ^{aA}	6.10±0.04 ^{aB}	5.95±0.01 ^{aB}
12	6.72±0.07 ^{aA}	6.00±0.05 ^{bB}	5.75±0.03 ^{aB}	6.80±0.04 ^{aA}	6.09±0.03 ^{aB}	5.95±0.05 ^{aB}
13	6.72±0.08 ^{aA}	5.99±0.07 ^{bB}	5.73±0.04 ^{aB}	6.79±0.03 ^{aA}	6.08±0.02 ^{aB}	5.92±0.06 ^{aB}
14	6.72±0.06 ^{aA}	5.95±0.07 ^{cB}	5.71±0.11 ^{aB}	6.78±0.05 ^{aA}	6.06±0.02 ^{aB}	5.91±0.03 ^{aB}
15	6.71±0.09 ^{aA}	5.92±0.07 ^{cB}	5.65±0.10 ^{aB}	6.74±0.02 ^{aA}	6.02±0.01 ^{aB}	5.88±0.04 ^{aB}
16	6.60±0.07 ^{aA}	5.86±0.01 ^{cB}	5.60±0.14 ^{bB}	6.73±0.02 ^{aA}	6.01±0.01 ^{aB}	5.87±0.04 ^{aB}
17	6.67±0.07 ^{aA}	5.84±0.09 ^{cB}	5.57±0.15 ^{bB}	6.72±0.03 ^{aA}	6.00±0.01 ^{aB}	5.85±0.08 ^{aB}
18	6.66±0.03 ^{aA}	5.82±0.09 ^{cB}	5.53±0.16 ^{bB}	6.71±0.08 ^{aA}	5.97±0.04 ^{aB}	5.82±0.07 ^{aB}
19	6.64±0.01 ^{aA}	5.80±0.09 ^{cB}	5.49±0.03 ^{cB}	6.71±0.03 ^{aA}	5.97±0.02 ^{aB}	5.76±0.06 ^{aB}
20	6.62±0.05 ^{aA}	5.78±0.09 ^{cB}	5.42±0.11 ^{cB}	6.67±0.03 ^{aA}	5.91±0.03 ^{aB}	5.67±0.15 ^{aB}
21	6.54±0.06 ^{aA}	5.78±0.05 ^{cB}	5.40±0.08 ^{cB}	6.60±0.12 ^{aA}	5.89±0.04 ^{aB}	5.58±0.11 ^{aB}
22	6.47±0.02 ^{bA}	5.64±0.14 ^{cB}	5.36±0.14 ^{dB}	6.47±0.04 ^{bA}	5.65±0.09 ^{bB}	5.45±0.11 ^{bB}
23	6.47±0.01 ^{bA}	5.57±0.18 ^{cB}	5.23±0.07 ^{dB}	6.41±0.04 ^{bA}	5.60±0.06 ^{bB}	5.30±0.04 ^{bB}
24	6.39±0.04 ^{bA}	5.47±0.03 ^{cB}	5.03±0.08 ^{cC}	6.32±0.04 ^{bA}	5.50±0.08 ^{cB}	5.14±0.04 ^{cB}
25	6.32±0.06 ^{aA}	5.39±0.04 ^{dB}	4.82±0.04 ^{cC}	6.22±0.06 ^{bA}	5.35±0.06 ^{cB}	4.96±0.05 ^{cB}
26	6.23±0.03 ^{bA}	5.31±0.03 ^{dB}	4.64±0.02 ^{cC}	6.16±0.06 ^{bA}	5.20±0.05 ^{dB}	4.82±0.02 ^{cB}
27	6.05±0.01 ^{bA}	5.24±0.02 ^{dB}	4.49±0.02 ^{IC}	6.02±0.03 ^{cA}	5.07±0.01 ^{dB}	4.65±0.03 ^{cB}

28	5.89±0.04 ^{bA}	5.12±0.06 ^{dB}	4.39±0.08 ^{aC}	5.90±0.05 ^{cA}	4.93±0.01 ^{dB}	4.53±0.02 ^{cC}
29	5.75±0.06 ^{cA}	5.01±0.03 ^{eB}	4.24±0.05 ^{fC}	5.76±0.02 ^{cA}	4.81±0.06 ^{dB}	4.39±0.04 ^{cC}
30	5.64±0.01 ^{bA}	4.88±0.02 ^{eB}	4.09±0.03 ^{fC}	5.58±0.06 ^{dA}	4.68±0.02 ^{eB}	4.21±0.03 ^{cC}
31	5.52±0.03 ^{bA}	4.79±0.06 ^{eB}	3.94±0.01 ^{gC}	5.54±0.02 ^{dA}	4.52±0.05 ^{eB}	4.01±0.02 ^{dC}
32	5.43±0.03 ^{cA}	4.78±0.07 ^{eB}	3.74±0.03 ^{gC}	5.36±0.09 ^{eA}	4.37±0.06 ^{eB}	3.77±0.02 ^{eC}

INFLUENCE OF X DIRECTION MOTION OF THE SUSPENSION POINT AND RIGID BODY SWING ON THE DISPLACEMENT OF A STEEL CATENARY RISER UNDER WAVE ACTION

ZHU, B.^{1*} – HUANG, W. P.¹ – YAO, X. L.¹ – LIU, J.²

¹*Shangdong Province Key Laboratory of Ocean Engineering, Ocean University of China, Qingdao 266071, China*

²*Institute of Civil Engineering, Agriculture University of Qingdao, Qingdao 266009, China*

**Corresponding author*

e-mail: beiji_dongjie@qq.com; phone: +86-176-8574-3056

(Received 12th Feb 2019; accepted 10th Apr 2019)

Abstract. The response and force effect of rigid body swing (RBS) on transverse flow direction is not negligible. Based on slender beam model, wave action (WA), RBS model and in-line movement of suspension point (TSM) are simulated. And structural response effect of RBS is simulated and estimated. The simulation and evaluation display that in terms of overall motion pattern, response in xy plane develops gradually from a narrow swing in x direction to a narrow swing in y direction. It is important to consider a particular location conservation of energy in three directions with water depth. As water depth increases, displacement and main frequency decrease. The decrease amplitude is strongest or most severe in top suspension region. For the spectrum analysis, the response main frequency and wave frequency are very close, and the motion is a forced motion. As water depth increases, the main frequency first increases then decreases. The trend is similarly to corresponding response change and contrary to energy or amplitude of xy plane change. As the energy decreases and then increases in xy plane, the z direction increase of RBS presents the opposite change in three directions. The effect of RBS on structural response can reach 20% after simulation. The effect of RBS is different from that of WA and TSM, which decreases with depth increase. And RBS is positively correlated to vector diameter S. It is expected that analysis and study may provide some advice for simulation of SCR and its RBS.

Keywords: SCR, rigid body swing, wave action, platform motion, spectrum analysis

Introduction

Steel catenary riser (SCR) is one of important facility for oil exploitation. It has recently been researched extensively and in-depth on the dynamic and vibration characteristics. And in particular the phenomenon of RBS is important and affected in the deep-sea environment. It is due to the waves, currents and other large range of loads, and it has attracted the attention.

The phenomenon of RBS is a large range and whole rotation from moving suspension point in top region to touch down point (TDP) in the seabed region. This paper focuses on the influence that WA and TSM are in the same in-line (x) direction. And RBS is in cross flow (z) direction. These motions are mutually perpendicular in the plane. A simulation was realized on the basis of Cable3D (Bai, 2009; Chen, 2002). Liu (2013), Liu and Huang (2014a, 2014b, 2013) proposed and simulated the phenomenon of RBS. And the simulation was on the basis of vibration theory of large-deflection beam and RBS model. Liu and Huang (2014c) compare analysis of coupling between RBS and bending vibration to that without RBS. They concluded that RBS has a relatively great impact on transverse flow direction response. Yao et al. (2018) did the model analysis of RBS and then carried out the spectral analysis. And he believed

experiment could prove the existence of RBS and give the frequency formula. Yao et al. (2017) simulated RBS phenomenon coupling the vortex-induced vibration model. And he proposed a RBS model considering vortex-induced vibration. Lin and Wang (2019) adopted DVM code in 2 dimensions for riser VIV analysis. Kim and O'Reilly (2019) provided a research on the dynamic, stability and vibration of riser with Kirchhoff's theory. Lotsberg (2019) did an overview of fatigue design standards. Wu et al. (2019) provided a relatively reliable combined IL and CF load model. Yamamoto and Morooka (2019) carried out simulation for riser and platform with nonlinear models. Guan et al. (2019) obtained understanding of the mechanics of scour such as steel catenary riser without currents and waves. He et al. (2019) adopted beam bending model of large deformation characteristics and estimated the critical factors for flexible riser. Numkam et al. (2019) researched the drilling muds which display liquid and solid flow characteristics. Zhao and Van der Heijden (2019) solved the wave equation that governs the prebulking torsion dynamics and boundary conditions. Wang and Pei (2019) applied a structural strain model to determine elastic characteristic of pipe core and pseudo parameters of stress.

RBS is a kind of rotation, which has rotation axis, angular velocity, angular acceleration, etc. It is different from the physical quantities such as vibration velocity and mode of bending vibration. And RBS is a rotation movement normal to bending vibration plane of riser. In the article, the effect of RBS on riser response is simulated and analyzed. And the effect of in-line (x) direction TSM and WA are studied.

The purpose of the study is in order to better discuss the RBS effect on cross flow displacement. Discussion includes the following viewpoints.

1. The RBS's effect on cross flow response cannot be ignored. And it is indispensable to pay more attention to long-term load terms and need more efforts for simulation and check.
2. Structural RBS is an inherent phenomenon of structures. And the calculation program explains RBS more from influence of WA and suspension movements.
3. The analysis of three-dimensional motion and energy conservation is very important for RBS analysis.
4. In particular, it is essential to understand characteristics of RBS when external energy of system decreases, vibration intensity of structure increases. Especially for wave reduction in this paper, RBS response increases.
5. When wave and natural vibration are in the same direction, the response is similar to that of shallow water. From top to bottom, the dominant influence of natural vibration on the structure is constantly enhanced.
6. The contribution of different loads to structural response can be calculated from frequency amplitude.

Study methods

SCR beam model considering large deformation

Basic equations

Vibration control equation (Liu, 2013) of steel catenary riser is *Equation 1*:

$$M\ddot{r} + Br^{(4)} - (\lambda r')' = q \quad (\text{Eq.1})$$

M – mass matrix, q – load matrix and λ – Lagrange operator.

SCR RBS model

Figure 1 shows RBS model. Point A is the connection location of wellhead. Point B is TDP. Top suspension point (TSP) is Point O. ω is rotation axis vector of ODB. S is vector from rotation axis to point C (Liu and Huang, 2013; Liang et al., 2016; Du, 2016; Yao et al., 2018).

According to kinetic moment theorem, the equation is:

$$(m + m_a)s^2\ddot{a}_r + c_a s^2\dot{a}_r + mgc_1sa_r = q_z\sqrt{s_1^2 + s_2^2} + q_xc_2s_3 \quad (\text{Eq.2})$$

m , m_a – mass and additional mass, c_a – coefficient for additional damping. q_x , q_z – distribution load of environment, \ddot{a}_r , \dot{a}_r , a_r – angular acceleration, velocity and displacement.

Node location:

Node 10th, $x=-15.8273$ m, $y=-54.1376$ m.

Node 80th, $x=-163.2674$ m, $y=-467.0530$ m.

Node140th, $x=-343.3629$ m, $y=-796.3470$ m.

Node200th, $x=-616.8364$ m, $y=-1049.0293$ m.

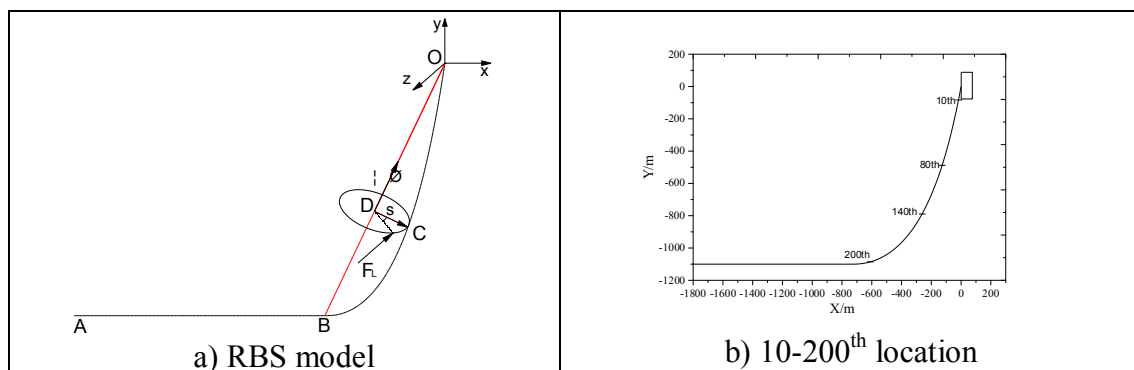


Figure 1. SCR RBS system

Wave force simulation model

Morison formula for wave force is Equation 3:

$$f_H = \frac{1}{2}C_D\rho A(u_x - \dot{x})|u_x - \dot{x}| + C_M\rho\frac{\pi D^2}{4}\frac{\partial u_x}{\partial t} - C_m\rho\frac{\pi D^2}{4}\ddot{x} \quad (\text{Eq.3})$$

In the formula, A – projected area, ρ – density of seawater, C_m – coefficient of additional mass, C_M – coefficient of mass, C_D – coefficient of drag force, u_x – water horizontal velocity, \dot{x} – cylinder horizontal velocity.

Adding Equations 2 and 3 to Equation 1, we can get:

$$M\ddot{r} + Br^{(4)} - (\lambda r')' = q + mg - (m + m_a)\ddot{r}_r - c_a\dot{r}_r + f_H + Q_x \quad (\text{Eq.4})$$

SCR movement boundary conditions

Fixed constraints are adopted for wellhead and TSP of SCR. And TSM affects riser's whole movement. During simulation and analysis, the motion in the in-line (x) direction is added into a calculation input file. And the effect of RBS is superimposed through a load term. Then variation characteristics of the structural amplitude and frequency are studied under WA, RBS. and TSM.

SCR seabed boundary conditions

In addition to both ends fixed constraints of SCR, there are also constraints during streamline and seabed coupling interaction. It includes normal elastic and plastic support, seabed suction, tangential friction and resistance of grooves (Liu, 2013; Liu and Huang, 2014a; Yang, 2014; Zhou et al., 2017). Seabed normal constraints are simulated by spring and spring-damping system during the static and dynamic analysis. Since this part is not the focus of paper, it is not expanded in detail.

Results and discussion

Response numerical simulation of RBS under linear TSM and WA

RBS (Liu and Huang, 2014a) is an important part of SCR response study. Simulation superimposed x direction WA and TSM (Du, 2016) is rarely recorded in domestic and foreign literature. This section expects to analyze and summarize simulation characteristics under action of RBS, WA and TSM. It is expected to obtain some new understandings of RBS under influence of complex motion.

In this part, Cable3D and Cable3D_Vswing newly developed program (Yao et al., 2018) are adopted during numerical simulation respectively. The program of Cable3D_Vswing has a promotion of original program through Qforce subroutine. It couples and improves vortex-induced vibration, RBS and load model. It also considers the fact that wave and structure move relative to each other.

Cable3D calculates the structure's response of x direction WA and TSM without taking into account the action of water flow and its fluid-solid coupling. Cable3D_Vswing is adopted to simulate response under effect of WA, TSM and RBS. The difference is whether RBS is taken into account during simulation.

In this paper, SCR works at a depth of 1100 m and is subjected to a pretension of 2100 KN. Other specific SCR parameters are shown in *Table 1*. The parameters of linear wave height is 3.5 m, and cycle is 8.60 s. WA Frequency is 0.11622 Hz and it is relative to x axis for 6.67°.

Table 1. SCR key parameters. (Yao et al., 2018)

Parameters	Values	Parameters	Values
Fluid density in the riser (kg.m ⁻³)	865	Elasticity Modulus (Gpa)	207
SCR material density (kg.m ⁻³)	7850	Coefficient of Lift force	0.7
Seawater density (kg.m ⁻³)	1025	Coefficient of drag force	1.2
Outer diameter (m)	0.355	Quality factor	1.0
Inner diameter (m)	0.305	Hydrodynamic parameter (m)	0.355

Coordinate system: X (in-line flow), Y (heave or vertical) and Z (cross flow). This paper applies TSM of the SCR to simulate floating platform response. *Table 2* shows TSM parameters under different conditions.

Table 2. Motion parameters of different conditions. (Yao et al., 2018)

Conditions	Direction	Amplitude /m	Period /s	Frequency /Hz	Cab	Csw
1	x	3.00	10.8	0.093	√	√
2	x	2.00	9.90	0.101	√	√
3	x	1.00	9.00	0.111	√	√

Three-dimensional response diagram of particle displacement of the structure

The structure is subjected to WA, TSM and RBS. The node 10th-200th displacement of riser could be got through simulation. 10th-200th node displacements have been plotted for three-dimensional view with no RBS and with RBS in *Figure 2*. And an xy plan with RBS and no RBS is in *Figure 3*.

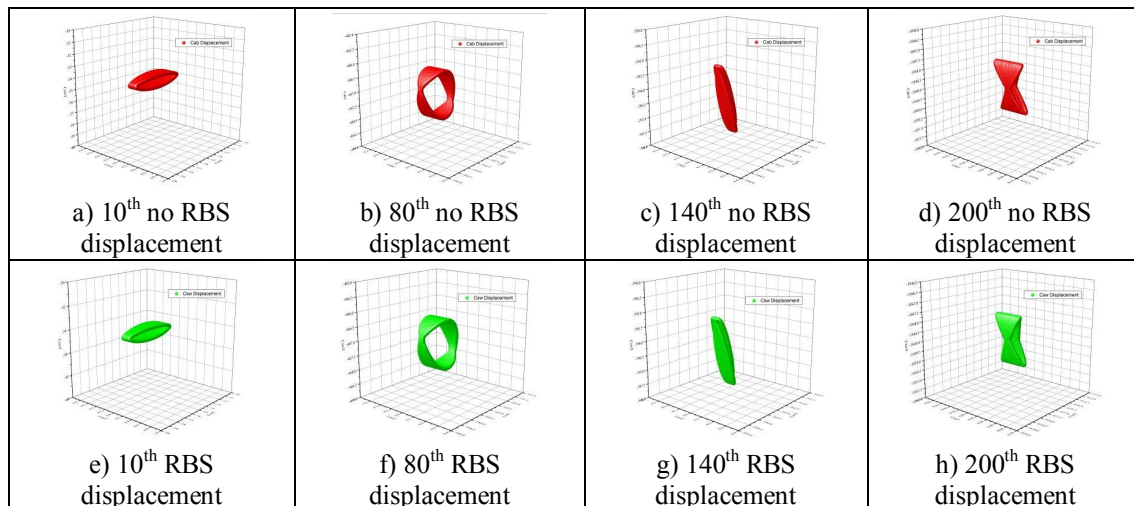


Figure 2. 10-200th displacement response of RBS and no RBS

In terms of transverse comparison, *Figure 2* is a three-dimensional graph of response with or without RBS under TSM and WA. There is no obvious difference between two groups of graphs in morphology or overall graph. It indicates that effect of RBS is weak, which can be proved by graph with or no RBS in xy plane in *Figure 3*. The xy plane is the projection of structural response on the plane with x-direction (in-line) and y-direction (vertical) axis. There is no important difference between two graphs in plane with in-line direction and heave direction axis. It means that there is no significant difference in the response of the bending plane of the SCR. And the effect of RBS on this plane is feeble. It can be acknowledged from a perspective of orthogonality of RBS and bending vibration. And RBS is planar motions perpendicular to bending vibrations. There is no obvious difference in the xy plane. However, the difference in z direction is the difference of the amplitude and curve form of the structural response. And graph and text are described in detail in the following chapters and are not expanded here.

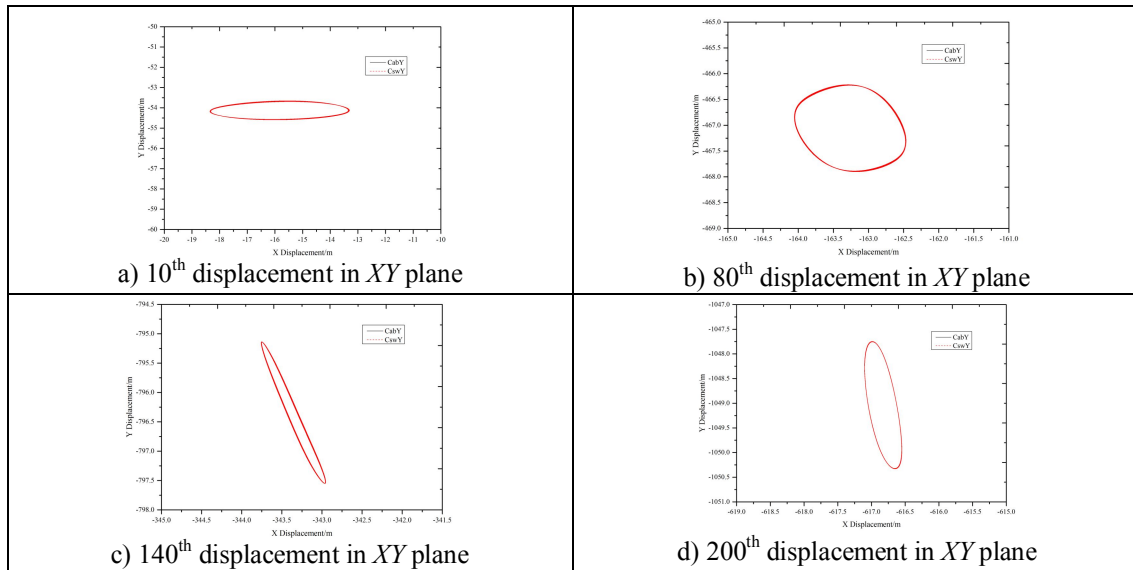


Figure 3. 10-200th displacement of RBS and no RBS in XY plane

For a longitudinal comparison, *Figure 2* corresponds to node 10th-200th displacement responses, respectively. It is more appropriate to understand *Figure 2* from the two-dimensional plane in *Figure 3*. With the increase of water depth, response on xy plane changed from a narrower swing in x direction to a narrower oscillation in y direction. The specific forms of swing are: the oscillation of 10th is a narrow range of swing in x direction. The oscillation of 80th is a wide range of oscillation about 40° deflection x direction. The oscillation of 140th is a narrow range of oscillation around 70° deflection x direction. The oscillation of 200th is a narrow range of oscillation around 80° deflection x direction.

For vibration amplitude, vibration gradually reduces. The maximum displacement of 10th, 80th, 140th and 200th are 2.523235 m, 0.911102346 m, 1.270945958 m and 1.315001323 m. It means that structural response or the energy of the xy plane goes down and then goes up. After RBS is superimposed, structural response and motion in xy plane increases slightly. *Table 3* shows the detailed parameters.

Table 3. Amplitude and Angle of XY plane oscillation for condition 1

Node	<i>AmpCab</i> (m)	<i>AmpCsw</i> (m)	<i>Amp</i> difference rate	<i>AngCab</i> (°)	<i>AngCsw</i> (°)	<i>Ang</i> difference rate
10	2.52323500	2.52324300	0.000%	0.91561700	0.9127021	-0.318%
80	0.911102346	0.911394511	0.032%	-40.149901	-41.391644	3.093%
140	1.270945958	1.270957523	0.001%	-72.166466	-72.166832	0.001%
200	1.315001323	1.315305591	0.023%	-81.537765	-81.537482	0.000%

With depth increase, movement of structure in xy plane vibrates from the narrow amplitude oscillation in x direction gradually to the narrow amplitude oscillation in y direction. The amplitude oscillation of upper node decreases to a maximum near top suspension region 10th-80th. As water depth increases, amplitude of y-direction swing

gradually increases, and the structural response or energy of xy plane decreases first and then rises.

The study above helps understand response of SCR structural particles at different positions from a space angle.

Analysis of transverse direction of SCR response under linear TSM, RBS and WA.

For riser, the above displacement research in xy plane is response in the SCR pipe body plane. This chapter mainly focuses on the response of z direction (transverse flow).

The displacement and its frequency in transverse direction is simulated from perspective normal to xy plane, which is non-negligible part of three-dimensional analysis. It is an important problem for structural vibration system study.

Cross flow response of structure including response caused by vortex-induced vibration (VIV), transverse direction action, RBS and so on is worth studying.

Compared with structural response caused by bending vibration and vortex-induced vibration, the response study of RBS in transverse direction is relatively few. This chapter focuses on the response characteristics in the transverse direction under linear WA, linear TSM and RBS.

Figure 4 shows the displacement of node 10-200th in condition 1.

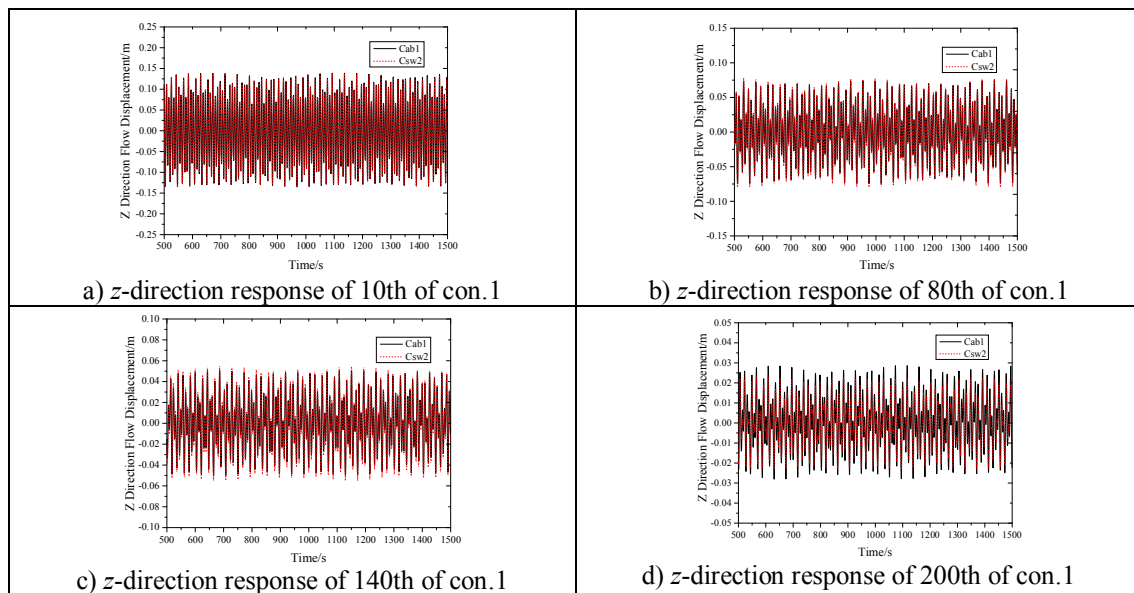


Figure 4. The transverse-direction response of 10th-200th of riser of con.1

Figure 4 shows simulation results of con.1, respectively, and results of node 10th-200th are random sequences. The maximum of response are 0.13922 m, 0.07491 m, 0.0509 m and 0.0286 m, and minimum of response are -0.13483 m, -0.07496 m, -0.05014 m and -0.02802 m. Standard deviation of fluctuation are 0.07544, 0.03754, 0.02523 and 0.01304. It shows that with node number increase, that is, the region away from top suspension point or water depth increase, cross flow response of riser is weakened. And Figure 6 shows it is under the action of WA and TSM. Not considering

action of current, the WA on the structure and TSM both weaken with the depth increase, and then response weakens.

Under WA and TSM coupling RBS model, results of node 10th-200th are still random sequences. The maximum of the response are 0.1383 m, 0.0782 m, 0.0550 m, and 0.0237 m. And minimum of response are -0.1350 m, -0.08003 m, -0.0551 m and -0.0237 m. The standard deviation of fluctuation are 0.07534, 0.03959, 0.02733, 0.01143. It can be seen that as distance of region away from the top suspension point increases, transverse flow response of structure is weakened. *Figure 6* shows the response under WA, TSM and RBS. It is noteworthy that when RBS is superimposed, response trend is equivalent to that only under WA and TSM. And effect of RBS on the riser does not exceed that of WA and TSM.

RBS influence with WA and TSM is briefly regarded as a linear overlay or superposition. Node 10-200th have a maximum increase of -0.69%, 4.35%, 8.02% and -17.48%. The minimum increases by 0.14%, 6.76%, 9.79% and -15.45%. With increase of water depth, RBS effect first augments and then reduces. That is, the trend is positively related to S which is RBS vector diameter, as shown in *Figure 1*. And this change is related to response of xy plane or the trend that energy decreasing and then increasing. It can be explained in terms of the total energy conservation of the structure. Other conditions have similar trends, as shown in *Figures 5-6* and *Tables 4-6*.

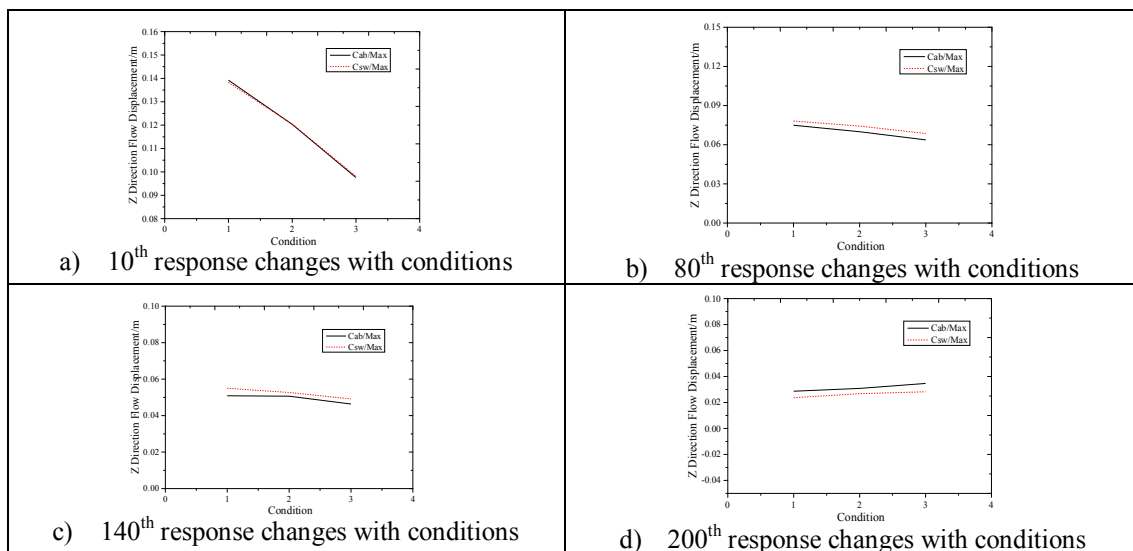
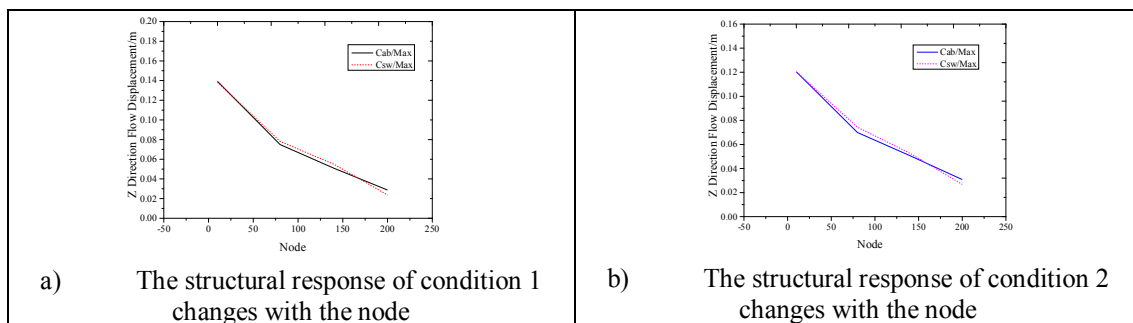


Figure 5. The structural response of 10th-200th changes with the conditions



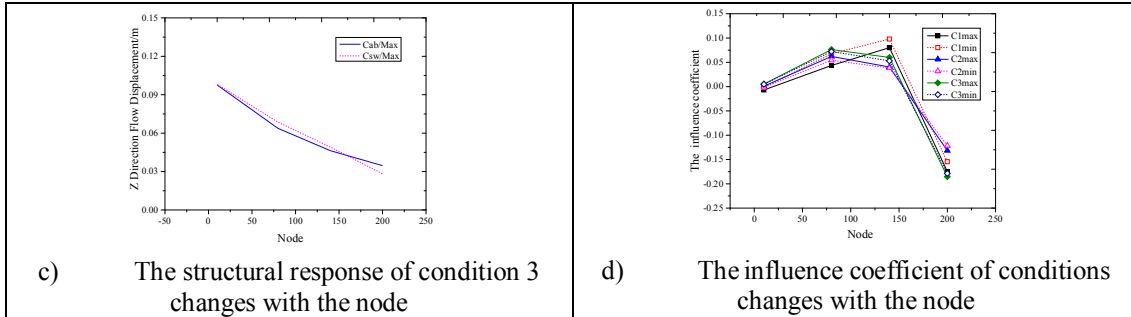


Figure 6. The structural response of condition changes with the node

Table 4. The z direction maximum, minimum and equilibrium position of node displacement of each condition

Cdt	Node	Cab_{rmax} (m)	Csw_{rmax} (m)	Inc_{rmax}	Cab_{rmin} (m)	Csw_{rmin} (m)	Inc_{rmin}	Cab_{rmean} (m)	Csw_{rmean} (m)
1	10 th	0.13922	0.13826	-0.69%	-0.13483	-0.13502	0.14%	4.28518e-4	-3.21780e-4
1	80 th	0.07491	0.07817	4.35%	-0.07496	-0.08003	6.76%	2.43481e-4	-4.59409e-4
1	140 th	0.0509	0.05498	8.02%	-0.05014	-0.05505	9.79%	2.97209e-4	-3.32327e-4
1	200 th	0.02866	0.02365	-17.48%	-0.02802	-0.02369	-15.45%	2.96427e-4	-2.06679e-4
2	10 th	0.12032	0.12043	0.09%	-0.11648	-0.11631	-0.15%	1.32305E-4	5.31018E-4
2	80 th	0.06994	0.07429	6.22%	-0.07190	-0.0758	5.42%	-9.64794E-5	2.39313E-4
2	140 th	0.05065	0.05269	4.03%	-0.05185	-0.05383	3.82%	-6.27087E-5	2.25175E-4
2	200 th	0.03085	0.02679	-13.16%	-0.03057	-0.02686	-12.14%	-3.37246E-5	2.19485E-4
3	10 th	0.0976	0.09811	0.52%	-0.09532	-0.09579	0.49%	7.800820E-5	5.39977E-4
3	80 th	0.06373	0.06859	7.63%	-0.06609	-0.07087	7.23%	-2.96270E-5	3.63584E-4
3	140 th	0.04637	0.04915	6.00%	-0.04812	-0.05067	5.30%	-3.91931E-5	2.84196E-4
3	200 th	0.03464	0.02822	-18.53%	-0.03573	-0.02935	-17.86%	-9.64304E-6	2.50152E-4

Table 5. z direction fluctuation standard deviation reduction and maximum normalized coefficient of each condition

Cdt	Node	Cab_{rstd}	Rdt_{rcab}	Csw_{rstd}	Rdt_{rcsw}	Cab_{rmax}	Nml_{rmax}	Csw_{rmax}	Nml_{rmin}
1	10 th	0.07544	50.24%	0.07534	47.45%	0.13922	1.00	0.13826	1.00
1	80 th	0.03754	16.32%	0.03959	16.27%	0.12032	0.86	0.12043	0.87
1	140 th	0.02523	16.16%	0.02733	21.10%	0.0976	0.70	0.09811	0.71
1	200 th	0.01304	17.29%	0.01143	15.17%	0.07491	1.00	0.07817	1.00
2	10 th	0.06803	46.38%	0.06808	42.60%	0.06994	0.93	0.07429	0.95
2	80 th	0.03648	15.21%	0.03908	17.19%	0.06373	0.85	0.06859	0.88
2	140 th	0.02613	16.10%	0.02738	21.81%	0.0509	1.00	0.05498	1.00
2	200 th	0.01518	22.31%	0.01253	18.40%	0.05065	1.00	0.05269	0.96
3	10 th	0.06039	38.05%	0.06079	33.90%	0.04637	0.91	0.04915	0.89
3	80 th	0.03741	20.77%	0.04018	22.57%	0.02866	1.00	0.02365	1.00
3	140 th	0.02487	13.51%	0.02646	22.77%	0.03085	1.08	0.02679	1.13
3	200 th	0.01671	27.67%	0.01262	20.76%	0.03464	1.21	0.02822	1.19

Cab represents the motion response under WA and TSM. Csw is a superposition of the motion of WA, TSM and RBS

Table 6. Calculation of reduction of each node response compared to condition 1

<i>Cdt</i>	Node	Cab_{rmax} (m)	Rdt_{rmax}	Csw_{rmax} (m)	Rdt_{rmax}	Cab_{rmin} (m)	Rdt_{rmin}	Csw_{rmin} (m)	Rdt_{rmin}
1	10 th	0.13922	46.19%	0.13826	43.46%	-0.13483	44.40%	-0.13502	40.73%
1	80 th	0.07491	17.25%	0.07817	16.77%	-0.07496	18.41%	-0.08003	18.50%
1	140 th	0.0509	15.97%	0.05498	22.66%	-0.05014	16.41%	-0.05505	23.23%
1	200 th	0.02866	20.59%	0.02365	17.11%	-0.02802	20.78%	-0.02369	17.55%
2	10 th	0.12032	41.87%	0.12043	38.31%	-0.11648	38.27%	-0.11631	34.83%
2	80 th	0.06994	16.03%	0.07429	17.94%	-0.0719	17.21%	-0.0758	18.89%
2	140 th	0.05065	16.46%	0.05269	21.51%	-0.05185	18.27%	-0.05383	23.19%
2	200 th	0.03085	25.64%	0.02679	22.25%	-0.03057	26.24%	-0.02686	23.09%
3	10 th	0.0976	34.70%	0.09811	30.09%	-0.09532	30.67%	-0.09579	26.02%
3	80 th	0.06373	17.79%	0.06859	19.81%	-0.06609	18.85%	-0.07087	21.09%
3	140 th	0.04637	12.02%	0.04915	21.33%	-0.04812	13.00%	-0.05067	22.26%
3	200 th	0.03464	35.49%	0.02822	28.76%	-0.03573	37.48%	-0.02935	30.64%

With the increase of nodes, the attenuation of maximum for node 10th, 80th, 140th and 200th are 46.19%, 17.25%, 15.97% and 20.59%. The attenuation of minimum are 44.40%, 18.41%, 16.41% and 20.78%. And the attenuation of standard deviation are 50.24%, 16.32%, 16.16% and 17.29%. With water depth increase, maximum, minimum and standard deviation of structure attenuate the most in top suspension point region, followed by touch down point region. The structural response decays to zero gradually, and attenuation amplitude in the intermediate region of riser is small. It is related to decrease of WA and TSM on the structure, with increase of depth. SCR is gradually close to the seabed, and finally presents as the submarine streamline section. The structure is subject to the reaction force of seabed support, which is more obvious in the bottom contact area. In middle region, TSM is related to the attenuation of WA and increasing of RBS, and the reduction shows a small attenuation.

With the increase of conditions, the attenuation of node 10th maximum are 46.19%, 41.87%, and 34.70%. The attenuation of minimum are 44.40%, 38.27% and 30.67%. The attenuation of standard deviation are 50.24%, 46.38% and 38.05%. As the condition increases, the attenuation of maximum, minimum and standard deviation gradually decreases. And the structural attenuation is more affected by the amplitude of condition of TSM as shown in *Table 2*, showing a positive correlation.

The rest of the nodes are shown in *Tables 5-6*. It is noteworthy that after RBS superimposed, the attenuation tendency of response is equivalent to that only under WA and TSM. And the effect of RBS on riser does not exceed that of WA and TSM.

Node response of 10-200th are compared in *Figures 5-6*. With motion amplitude decrease, each node response decreases or increases in different location. On the whole, the hanging point 10th have a more obvious decrease with conditions, and the response have an increase near the touch down point. The maximum influence coefficient of structure is about 20%, as shown in *Figure 6* and *Table 4*.

Spectrum analysis

For z-response, spectrum analysis can transform the random signal in time domain into the signal in the frequency domain. Spectrum analysis can obtain main frequency

of structure. It shows that there is a large value at a certain frequency point, and there is a maximum at one or more frequencies. By extracting maximum, this chapter mainly analyzes it:

1. Relative attenuation with the increase of water depth;
2. Increase or decrease of frequency caused by RBS;
3. The variation characteristics of structural displacement response frequency with the TSM frequency.

Through spectrum analysis, displacement spectrum responses of 10th, 80th, 140th and 200th are obtained, as shown in *Figure 7*.

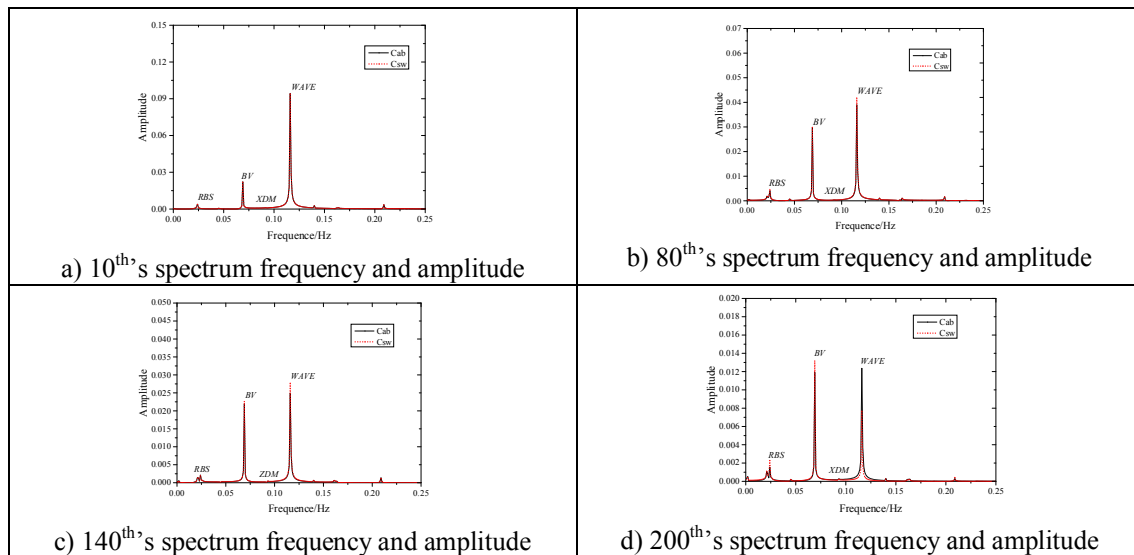


Figure 7. 10-200th's spectrum amplitude of con.1

Figure 7 shows displacement spectrum response of condition 1's node 10-200th. The x value is 0.115988 Hz, which is very close to WA frequency 0.11622 Hz. It could be considered that the structure's frequency is the same as that of the applied external load, and it is a forced motion.

For y value (spectral amplitude), as the node increases, amplitude values of each node are shown in *Table 7*. Spectrum response of 10th, 80th, 140th and 200th are 0.094425, 0.039063, 0.025002 and 0.012396. The amplitude of node is decreasing, indicating that maximum energy point of structure is decreasing, as shown in *Table 7*. This point can be proved from response of z-direction displacement of the structure, as shown in *Table 4*. For *Table 7*, it is similar to the corresponding change of displacement in terms of main frequency first increasing and then decreasing with increase of node. In contrast to change of energy or amplitude in xy plane, main frequency and displacement in z direction can be explained from energy conservation in three directions. With the decrease in the xy plane before the increase, the z direction displacement due to RBS in the 3d direction presents an opposite change, as shown in *Table 4*.

From the calculation of the same node in different conditions, the values of node 10th in condition 1-3 without RBS are 0.094425 m, 0.086288 m and 0.077539 m. And considering the RBS, the values are 0.094317 m, 0.086327 m and 0.078034 m. Relatively speaking, the difference between the RBS and non-RBS are -0.11%, 0.05%

and 0.64%. It indicates that main frequency of the structure increases or decreases after the RBS is applied. The maximum influence for 10th is 0.64%. At nodes 80th, 140th and 200th, the main frequency of the structure increases by 8.17%, 11.27% and -37.71%. It indicates that when RBS applied, main frequency of riser changes. It increases above 140th or in non-touch down area, and decreases in touch down area, as shown in *Tables 7-8*.

Table 7. The maximum value table of non-RBS and RBS spectrum

<i>Cdt</i>	Node	<i>Xr</i> (Hz)	<i>Cab/Yr</i>	<i>Rdt_{rcab}</i>	<i>Xr</i> (Hz)	<i>Csw/Yr</i>	<i>Rdt_{rcsw}</i>
1	10 th	0.115988	0.094425	58.63%	0.115988	0.094317	55.52%
1	80 th	0.115988	0.039063	14.89%	0.115988	0.041956	14.99%
1	140 th	0.115988	0.025002	13.35%	0.115988	0.027820	21.31%
1	200 th	0.115988	0.012396	13.13%	0.115988	0.007721	8.19%
2	10 th	0.115988	0.086288	51.42%	0.115988	0.086327	47.48%
2	80 th	0.115988	0.041916	15.99%	0.115988	0.045341	17.64%
2	140 th	0.115988	0.028117	13.18%	0.115988	0.030113	21.88%
2	200 th	0.115988	0.016743	19.40%	0.115988	0.011225	13.00%
3	10 th	0.115988	0.077539	39.19%	0.115988	0.078034	35.16%
3	80 th	0.115988	0.047149	22.04%	0.115988	0.050597	23.30%
3	140 th	0.115988	0.030059	13.88%	0.115988	0.032412	23.62%
3	200 th	0.115988	0.019296	24.89%	0.115988	0.013983	17.92%

Table 8. The spectrum analysis and normalized table of nodes under different conditions

<i>Cdt</i>	Node	<i>Xr</i> (Hz)	<i>Cab/Yr</i>	<i>Csw/Yr</i>	<i>Incr</i>	<i>Cdtr</i>	Node	<i>Nml_{rmax}</i>	<i>Nml_{rmin}</i>
1	10 th	0.115988	0.094425	0.094317	-0.11%	1	10 th	1.00	1.00
1	80 th	0.115988	0.039063	0.041956	7.41%	2	10 th	0.91	0.92
1	140 th	0.115988	0.025002	0.027820	11.27%	3	10 th	0.82	0.83
1	200 th	0.115988	0.012396	0.007721	-37.71%	1	80 th	1.00	1.00
2	10 th	0.115988	0.086288	0.086327	0.05%	2	80 th	1.07	1.08
2	80 th	0.115988	0.041916	0.045341	8.17%	3	80 th	1.21	1.21
2	140 th	0.115988	0.028117	0.030113	7.10%	1	140 th	1.00	1.00
2	200 th	0.115988	0.016743	0.011225	-32.96%	2	140 th	1.12	1.08
3	10 th	0.115988	0.077539	0.078034	0.64%	3	140 th	1.20	1.17
3	80 th	0.115988	0.047149	0.050597	7.31%	1	200 th	1.00	1.00
3	140 th	0.115988	0.030059	0.032412	7.83%	2	200 th	1.35	1.45
3	200 th	0.115988	0.019296	0.013983	-27.53%	3	200 th	1.56	1.81

At the same time, with the increase of conditions, the main frequency of 10th decreases. The other nodes show an increase of main frequency, with an increase of 80% in the bottom touch down area. The energy goes down at 10th, and the amplitude goes down, while it goes up in other areas, with amplitude shown in *Table 8*. After the normalized operation, coefficient in touch down point without RBS are 1.00, 1.35 and 1.56. And the coefficient superposed RBS are 1.00, 1.45 and 1.81. The coefficients of the two groups differ greatly, and the differences in other conditions are not significant.

In addition, it indicates that Z direction response of each position or node is proportional to the frequency of load applied. There is a certain resonance between loads and the response increases.

It is worth that *Table 9* gives some data of wave main frequency influence. *Figure 8* shows the effect of RBS on spectrum amplitude of different loads of the structure. These data can make some judgments about the effects of different loads. From 10th to 200th, the wave main frequency has an influence of 77.62%, 53.31%, 50.32%, and 47.35%. With the increase of water depth, the influence gradually decreases. RBS increases the spectral analysis amplitude of structural RBS, bending vibration, TSM and WA. The RBS increases response of riser to different degrees. It is worth noting that the bottom contact point is 200th. And RBS reduces both WA response and TSM response, as shown in *Figure 8*. To some extent, WA and TSM reduce oscillation of RBS at bottom TDP. It is similar to decrease of riser displacement in *Table 4*. In a word, spectrum analysis is of great significance for structural response interpretation.

Table 9. The spectrum analysis and normalized table of nodes under different conditions

Conditions		RBR/x (Hz)	RBR/y	BV/x (Hz)	BV/y	XDM/x (Hz)	XDM/y	WAVE/x (Hz)	WAVE/y	WAVE influence
Theoretical (Yao et al., 2018)		0.0290	/	0.0640	/	0.0930	/	0.1162	/	
10 th	Cab	0.0240	0.0041	0.0690	0.0223	0.0930	8.1679E-4	0.1160	0.0944	77.62%
	Csw	0.0240	0.0041	0.0690	0.0222	0.0930	8.0093E-4	0.1160	0.0943	77.68%
80 th	Cab	0.0240	0.0041	0.0690	0.0298	0.0930	3.4824E-4	0.1160	0.0391	53.31%
	Csw	0.0240	0.0047	0.0690	0.0300	0.0930	3.7593E-4	0.1160	0.0420	54.49%
140 th	Cab	0.0240	0.0022	0.0690	0.0220	0.0930	4.8580E-4	0.1160	0.0250	50.32%
	Csw	0.0240	0.0021	0.0690	0.0227	0.0930	5.2845E-4	0.1160	0.0278	52.33%
200 th	Cab	0.0240	0.0016	0.0690	0.0119	0.0930	2.9034E-4	0.1160	0.0124	47.35%
	Csw	0.0240	0.0023	0.0690	0.0132	0.0930	2.5167E-4	0.1160	0.0077	32.83%

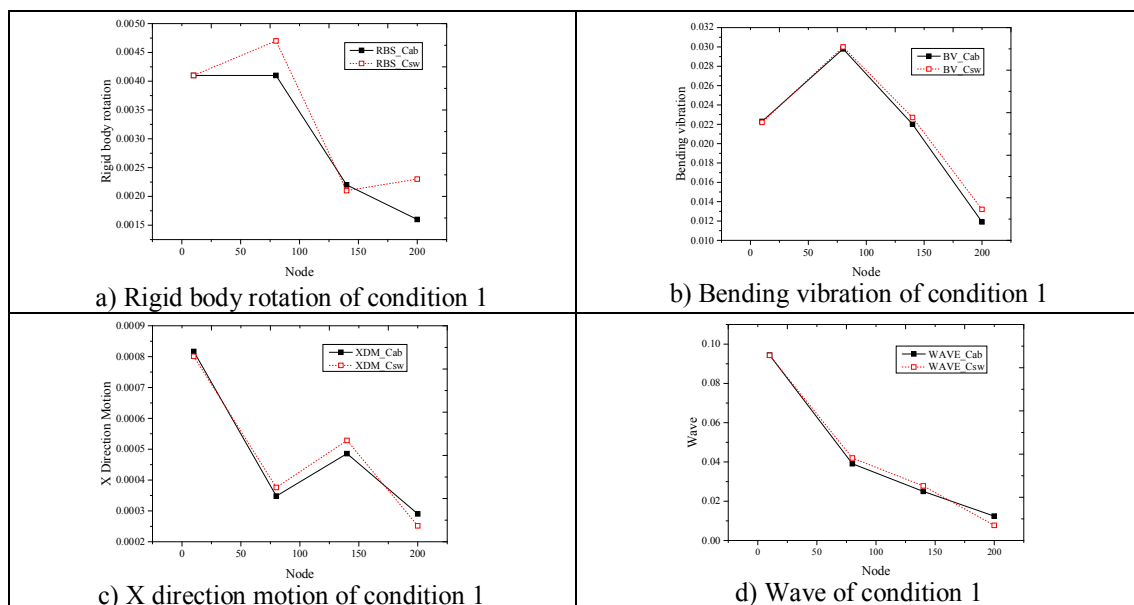


Figure 8. The effects of RBS on the amplitude of load frequency spectrum along water depth of condition 1

Conclusion

It is a relatively important problem to simulate the transverse response of riser under RBS. The swing is around the rotating axis with TSP and TDP under WA. In this paper, without considering current, the relatively complicated response of riser coupled RBS is studied. And response is influenced by linear WA and TSM on the structure.

From a perspective of the overall motion pattern, response on the xy plane has developed from a narrow range swing in x direction to a narrow range oscillation in y direction. Under the WA, response of riser reduces gradually with depth. When coupling x direction TSM, phenomenon that response decreases when water depth increases still persists. In terms of variation in the depth direction of the structure, with increase of water depth, displacement decreases. And attenuation range is more intense in the top suspension region, while attenuation is weak in bottom region.

From the frequency of structure, it can be considered that the response of structure is the same as that of external load, and the response is forced motion. In terms of the conditions, as the node increases or the water depth increases, the main frequency first increases and then decreases, which is similar to the change of the structural response. In contrast to the change of energy or amplitude of response in the xy plane, it can be explained from the energy conservation of the structure in three directions of the node. As the response in the xy plane decreases first and then increases, the z direction response of RBS presents an opposite change.

After RBS is applied to structure, the main frequency increases above 140th or in the non-touch down area, and decreases in the touch down area. And the z-direction response of structure is inversely proportional to frequency increase of load applied and proportional to amplitude reduction.

Recommendations for future studies include the following points:

1) For the load term of the structural vibration equation, it is also necessary to consider the internal flow, isolated wave, etc. And multiple coupling calculation is needed to expand the program development and response calculation range.

2) To be specific, in this paper, linear wave is adopted, and more random wave check is required. Fluid-solid coupling phenomenon also needs to be taken into consideration. And it is suggested to adopt wake oscillator programming for the further calculation.

3) It is necessary to study response from a three-dimensional perspective, and spatial response characteristics cannot be easily ignored.

4) This paper considers contribution of load to response from the perspective of frequency amplitude. And it needs more detailed and accurate calculation from the contribution of load response.

5) In this paper, the number of conditions is few and it is suggested to search for more conditions to evaluate the effect of RBS by a safety ratio.

6) In this paper, there is also a deficiency in analytical calculation of structural vibration. It is suggested to increase the analytical solution of RBS, such as multi-load vibration matrix for verification, which may further increase the solution speed.

For analysis in Cable3D, the prospects are slightly better. It is expected that work of this paper could give some simulation advice for RBS research.

Acknowledgements. Thanks to all the help. And the work is supported by National natural science foundation of China (Number: 51239008, 51739010, 51679223, 51409232) and Natural science foundation of SHANGDONG province (ZR2016GM06). Thanks to National high-tech research and

development program (863) (2013AA09A218) and National Science and Technology Major Project (2011ZX05026-005-003). Thanks to professor ZHANG Jun researching in Texas A&M United States.

REFERENCES

- [1] Bai, X. L. (2009): A study on Method for Nonlinear Analysis of Deepwater SCR Based on Inertial Coupling. – Ocean University of China, Qingdao.
- [2] Bai, X. L., Huang, W. P., Murilo, A. V., Yang, C. F., Duan, M. L. (2015): Riser-soil interaction model effects on the dynamic behavior of a steel catenary riser. – Marine Structures 41: 53-76.
- [3] Chang, S., Huang, W. P., Yang, C. F. (2017): The influence of nonlinear seabed on the dynamic response and fatigue damage of SCR at TDZ. – The Ocean Engineering 35(2): 67-82.
- [4] Chen, X. H. (2002): Studies on Dynamic Interaction between Deep-Water Floating Structures and Their Mooring/Tendon Systems. – Texas A&M University, College Station.
- [5] Du, J. F. (2016): Investigation on Dynamic Response Characteristics and Fatigue Assessment Damage Methods for Mooring Lines of Semi-Submersible Platforms. – Ocean University of China, Qingdao.
- [6] Guan, D., Hsieh, S. C., Chiew, Y. M., Low, Y. M. (2019): Experimental study of scour around a forced vibrating pipeline in quiescent water. – Coastal Engineering 143: 1-11.
- [7] He, Y. Y., Vaz, M. A., Caire, M. (2019): An inverse problem methodology for multiple parameter estimation in bend stiffeners. – Applied Ocean Research 83: 37-47.
- [8] Kim, H. T., O'Reilly, O. M. (2019): Instability of catenary-type flexible risers conveying fluid in subsea environments. – Ocean Engineering 173: 98-115.
- [9] Liang, N., Huang, W. P., Yang, C. F. (2016): Study on method of interaction between steel catenary riser and nonlinear seabed. – Ocean Engineering 34(1): 40-49.
- [10] Lin, K., Wang, J. S. (2019): Numerical simulation of vortex-induced vibration of long flexible risers using a SDVM-FEM coupled method. – Ocean Engineering: 468-486.
- [11] Liu, J. (2013): Study of Out-of-Plane Motion of SCRs with Rigid Swing. – Ocean University of China, Qingdao.
- [12] Liu, J., Huang, W. P. (2013): A Nonlinear vortex induced vibration model of marine risers. – Journal of Ocean University of China 12(1): 32-36.
- [13] Liu, J., Huang, W. P. (2014a): The coupling VIV analysis of SCRs with rigid swing. – Journal of Ocean University of China 14: 645-650.
- [14] Liu, J., Huang, W. P. (2014b): Fluid-structure interaction analysis for VIV of steel catenary risers. – Journal of Vibration and Shock 33(3): 41-45.
- [15] Liu, J., Huang, W. P. (2014c): Analysis of out-of-plane motion of SCRS with rigid rotation. – Engineering Mechanics 31(2): 53-57.
- [16] Lotsberg, I. (2019): Development of fatigue design standards for marine structures. – Journal of Offshore Mechanics and Arctic Engineering 141(3). DOI: 10.1115/OMAE2017-62516.
- [17] Numkam, G. L., Akbari, B. (2019): Effect of surfactant chemistry on drilling mud performance. – Journal of Petroleum Science and Engineering. DOI: 10.1016/j.petrol.2018.11.075.
- [18] Wang, W., Pei, X. J. (2019): An analytical structural strain method for steel umbilical in low cycle fatigue. – Journal of Offshore Mechanics and Arctic Engineering 141(1). DOI: 10.1115/1.4040721.
- [19] Wu, J., Lekkala, M. R., Ong, M. C., Passano, E., Voie, P. E. (2019): Prediction of combined inline and crossflow vortex-induced vibrations response of deepwater risers. – Journal of Offshore Mechanics and Arctic Engineering 141(4). DOI: 10.1115/1.4042072.

- [20] Yamamoto, M., Morooka, C. K. (2019): Feedback control system for blow-out preventer positioning. – *Applied Ocean Research* 82: 362-369.
- [21] Yang, C. F. (2014): Study on Nonlinear Interaction between SCR and Seabed. – Ocean University of China, Qingdao.
- [22] Yao, X. L., Huang, W. P., Liu, J., Luo, K. H. (2017): Study on the Coupling of Rigid swing and vortex-induced vibration of steel catenary risers. – *Ship & Ocean Engineering* 46: 191-197.
- [23] Yao, X. L., Huang, W. P., Chang, S., Liu, J., Fu, X. P. (2018): Modal analysis and test verification for out-of-plane vortex induced vibration of a SCR. – *Journal of Vibration and Shock* 37(13): 78-84.
- [24] Zhao, X. W., van der Heijden, G. H. M. (2019): Dynamic torsional buckling: prebuckling waves and delayed instability. – *Journal of Petroleum Science and Engineering* 69: 1309-1320.
- [25] Zhou, Y., Yang, C. F., Huang, W. P. (2017): Dynamic response analysis of steel catenary riser based on nonlinear stiffness of seabed. – *Journal of Harbin Engineering University* 38(3): 356-362.

EFFECT OF ENTERPRISE DEVELOPMENT SUPPORT PROGRAM ON MARKET PARTICIPATION AND PROFIT EFFICIENCY OF INDIGENOUS VEGETABLE PRODUCTION IN SOUTH AFRICA

MPHAFI, K.¹ – OYEKALE, A. S.^{2*} – NDOU, P.¹

¹*Agricultural Research Council (ARC), Pretoria, South Africa*

²*Department of Agricultural Economics and Extension, North-West University
Mafikeng Campus, Mmabatho 2735, South Africa*

**Corresponding author*

e-mail: asoyekale@gmail.com; phone: +27-787-144-271

(Received 13th Feb 2019; accepted 10th Apr 2019)

Abstract. African indigenous vegetables (AIVs) play a very significant role in food security of poor households. However, some AIVs are still underutilised in many African countries. The aim of this study was to analyse the effect of farm support program on market participation and profitability of AIV production in South Africa. Data were collected from 86 AIV farmers from South Africa. Probit regression and Stochastic Frontier efficiency analyses were employed for data analyses. The results revealed that infrastructure support assisted farmers to improve participation in markets. In addition, engagement in growing spinach and amaranth vegetables, farm income, gender, cooperative membership and access to EDSP significantly increased the probability of participating in informal markets ($p < 0.05$). Also, the determinants of indigenous vegetable farmers' profit were seed input, land area cultivated, interactions of fertilizer with fertilizer, seed with seed and fertiliser with seed. Profit efficiency was significantly influenced by farm distance, road conditions and access to EDSP. It was concluded that EDSP enhanced farmers' access to informal markets and profit efficiency.

Keywords: *farm support program, informal market, profit efficiency, African indigenous vegetables, South Africa*

Introduction

African indigenous vegetables (AIVs) play a very significant role in promoting food security for under-privileged households in many African countries (Weinberger and Msuya, 2004). Their importance is underscored as prime facilitators of food security and sources of essential nutrients (Muhanji et al., 2011). Food and Agriculture Organisation (FAO) (2010) noted that as primary sources of food for many people, AIVs are not only associated with provision of vital energy and micronutrients in the diets of isolated communities (Grivetti and Ogle, 2000), but also constitute part of the conglomeration of African indigenous or traditional medicinal plants (Spring, 2015). Some investment opportunities for promoting availability of AIVs have been embarked upon by some African farmers given the growing knowledge of their nutritive values.

However, in sub-Saharan Africa, the potential benefits of AIVs have been overlooked over time due to negligence by consumers (FAO, 2005; Yang and Kedin, 2009). In some developing countries, including South Africa, AIVs hold excellent potentials to improve nutrition and increase households' dietary diversity (Lotter et al., 2014). A study by the World Bank (2010) found that despite the nutritional significance of vegetables, malnutrition remains a problem with stunting greatly affecting children and pregnant women (Fanzo et al., 2013). Inadequate consumption of vegetables is

resulting in Vitamin A deficiency in about 43.6% of children and 46% of pregnant women (Shisana et al., 2014).

In South Africa, there has been a shift towards non-indigenous food by the majority of the population. This has been driven by urbanization and wrong perception of nutritional worth of indigenous food and vegetables (Talení and Goduka, 2013). Therefore, the government of South Africa has taken some policy measures for promoting production, consumption and marketing of AIVs. The Farmers' Support Program (FSP) was introduced in the mid-1980s and financed by the Development Bank of Southern Africa (DBSA) with the aim of supporting all sub-sectors of agronomy and horticulture agricultural systems. The aim of FSP was to promote structural changes to ensure agricultural commercialisation through the provision of comprehensive agricultural support services and incentives to existing farmers (PSPPD, 2010). In order to support government's efforts, some non-parastatal organisations such as the Agricultural Research Council (ARC) embarked on agricultural programs that are aimed at promoting vegetable production and marketing. ARC's programs are aimed at smallholding crop production, agro-processing, food technology and agricultural commercialisation, among others.

There is dearth of studies on the marketing and significance of AIVs in South Africa. Chetty (2013) conducted a study on the dietary analysis of South African indigenous vegetables and traditional food. The findings did not account for the marketing aspect of vegetable production. Mavengahama et al. (2013) analysed the contributions of indigenous vegetables to food security and nutrition across selected communities in South Africa. They pointed out the significance of indigenous vegetables on households' nutritional status given its high composition of micronutrients.

Many smallholder farmers can benefit from agricultural markets. Markelova et al. (2009) conducted a study on the challenges and constraints faced by smallholder farmers in market participation. The study did not cover the issue of farm profits obtained from participating in agricultural markets. It only focused on identifying barriers and innovations to alleviating constraints and challenges. Another study conducted by Maponya et al. (2015) examined the determinants of participation in agricultural markets in the Eastern Cape province of South Africa. Despite the numerous policies and studies regarding vegetables and their significance to human life, the study of vegetable marketing and profitability in South Africa has not been properly researched. It is, therefore, imperative to examine the effect of enterprise development support program on market participation and profitability of indigenous vegetable farmers in South Africa.

Different studies have identified the factors that limit farmers' production and marketing of vegetables. Okoruwa et al. (2009) identified farm size, access to credit facilities, transportation costs and contact with extension agents as the factors that affect market participation. Randela et al. (2008) reported that age, literacy level, ability to speak English, ownership of transport, access to market information, distance to market, dependency ratio and land size have significant influence on market participation. These constraints constitute the greatest barrier to smallholding agriculture, in terms of having access to high value markets (Vink and Kirsten, 2000). The aim of this study is therefore to analyse how enterprise development support affects marketing and profitability of indigenous vegetable production in South Africa.

Materials and Methods

Sampling methods

The study was conducted in Limpopo, Mpumalanga, Eastern Cape and KwaZulu-Natal provinces of South Africa. These provinces are involved in agricultural projects that support the promotion and cultivation of AIVs on commercial basis. The respondents were therefore drawn from those farmers that are growing AIVs namely Amaranth, Spinach and Mustard.

Data were collected with structured questionnaire largely comprising of close-ended questions. Eighty six (86) of AIV farmers were interviewed comprising 41 ARC beneficiaries and 45 non-ARC beneficiaries. The survey was conducted with the assistance of agricultural extension officers from the Department of Agriculture. The questionnaire requested information on demographic and household characteristics of respondents such as age, gender, education and marital status, farm specific characteristics, remittances, form of assistance as well as other major challenges to AIV marketing.

Market Participation Modelling

Probit model was used to model determinants of market participation. This is a type of regression where the dependent variable can only take two values (Yes coded as 1 and No coded as 0). The model estimates the probability that an observation with certain characteristics will fall into a specific category. The model can be specified as follows:

$$P_i^* = \beta X_i + \mu_i \quad (\text{Eq.1})$$

which determines the value of participation by

$$P_i = \begin{cases} 1 & \text{if } P_i^* > 0 \\ 0 & \text{if } P_i^* \leq 0 \end{cases} \quad (\text{Eq.2})$$

where P_i^* = latent continuous index measuring market participation for the i th farmer. β is a vector of estimated parameters. X_i is a vector of factors which affect participation which are planted mustard (yes =1, 0 otherwise), planted spinach (yes =1, 0 otherwise), planted amaranth (yes =1, 0 otherwise), market price per kg (Rand), farm revenue (Rand), distance to markets (km), condition of roads (bad road =1, 0 otherwise), land area used (hectares), gender (female = 1, 0 otherwise), age of farmers (years), marital status of farmers (married = 1, 0 otherwise), formal education (yes =1, 0 otherwise), household size, member of cooperative (yes =1, 0 otherwise), farming experience (years), extension support (yes =1, 0 otherwise), market linkage (yes =1, 0 otherwise) EDSP farmers (yes =1, 0 otherwise). μ_i is the random error term.

Profitability of AIVs modelling

The profit function was specified as:

$$\pi(x) = R(x) - C(x) = 0 \quad (\text{Eq.3})$$

where:

$\pi(x)$ = profit from AIV production

$R(x)$ = total revenue for sale of AIV

$C(x)$ = Cost of associated vegetable farming.

The profit function was estimated with Trans log profit function model as:

$$\ln \pi' = \alpha_0 + \alpha_1 \ln f_i + \alpha_2 \ln lb_i + \alpha_3 \ln S_i + \alpha_4 \ln t_i + \alpha_5 \ln ld_i + \alpha_6 \ln lb_i^2 + \alpha_7 \ln ld_i^2 + \alpha_8 \ln f_i^2 + \alpha_9 \ln S_i^2 + \alpha_{10} f_i * S_i + \alpha_{10} lb_i * f_i + z_i + k_i \quad (\text{Eq.4})$$

where: In = natural log

π' = normalised profit

α_0 = constant parameter

f_i = fertiliser, lb_i = labour, S_i = seed, t_i = transport, $\ln lb_i^2$ = labour*labour, $\ln ld_i^2$ = land*land, $\ln f_i^2$ = fertiliser*fertiliser, $\ln S_i^2$ = Seed*seed, $f_i * S_i$ = fertiliser*seed, $lb_i * f_i$ = labour*fertiliser and z_i = random error term and k_i is the inefficiency error term.

The profit inefficiency model is specified as:

$$k_i = \delta + \sum_{k=1}^{14} G_{ik} + m_i \quad (\text{Eq.5})$$

where planted spinach (yes =1, 0 otherwise), planted amaranth (yes =1, 0 otherwise), market price per kg (Rand), distance to markets (km), condition of roads (bad road =1, 0 otherwise), gender (female = 1, 0 otherwise), age of farmers (years), marital status of farmers (married = 1, 0 otherwise), formal education (yes =1, 0 otherwise), household size, non-farm income (Rand), member of cooperative (yes =1, 0 otherwise), farming experience (years), extension support (yes =1, 0 otherwise), market linkage (yes =1, 0 otherwise) EDSP farmers (yes =1, 0 otherwise). μ_i is the random error term.

Results and Discussions

Socio-economic and demographic characteristics of vegetable farmers

The results in *Table 1* show the socioeconomic characteristics of AIV farmers who were being categorized into EDSP beneficiaries and non EDSP beneficiaries. The results show that 51% of the farmers that were supported by EDSP were female, while most of the non-EDSP farmers were male. Similar results had been reported by Ozkan et al. (2000) who found that production of vegetables was associated with female. On the contrary, Mumbi et al. (2006) found that male farmers were taking the lead in the production and marketing of vegetables.

The results in *Table 1* further revealed that 59% of the farmers that were supported by EDSP were more than 40 years old. Some farmers are involved in AIV production as a livelihood strategy for promoting households' nutrition and incomes. The age of AIV farmers as well as their years of farming experience are essential in agricultural market participation (Ramoroka, 2012). In both categories of farmers, those who were married formed a larger proportion than those who were not married. The results are in agreement with those reported by Baba et al. (2010) who found that married farmers participated more in vegetable farming in order to support their families.

Household size could play an important role in farming as it can be an important source of family labour. About 41% of the respondents who received support from the Agricultural Research Council (EDSP) had a family size of 4-6 members; an indication that family labour was still a common practice among farmers in order to reduce the cost of hiring labour. Non-EDSP farmers had household sizes of 1-3 members. In South Africa, the average household size is 3.4 members (Stats SA, 2010).

More than half of EDSP farmers (54%) had secondary education. Masuku and Xaba (2013) highlighted the importance of education in farming and maintained that it enables farmers to adopt change and innovation faster than the uneducated. An average of 62% of the farmers from EDSP and non-EDSP had farm size of three hectares, while 25% had ten hectares and more. Land plays an important role in the production of vegetables because it grants farmers an opportunity to expand their farming enterprises. According to Mumbi et al. (2006), the bigger the size of the farm, the higher the yield and the better the chances of the farmer participating in the markets. The average number of years of farming experience was 8 years. Over 30% of EDSP farmers had substantial farming experience, while non-EDSP farmers had 15 years or more. Farmers with adequate experience are reported by Osmani and Hossain (2015) to participate in the markets better than those who do not have any farming experience.

Table 1. Socio-economic and demographic characteristics of vegetable farmers

Variable	EDSP		Non EDSP	
	Frequency	Percentage	Frequency	Percentage
	N= 41	%	N= 45	%
Gender				
Male	20	48.78	26	58
Female	21	51.22	19	42
Age				
10-20	1	2	11	24
21-40	16	39	17	38
≥ 41	24	59	17	38
Marital status				
Married	36	88	31	69
Not married	5	12	14	31
Household size				
1-3	11	27	20	44
4-6	17	41	17	38
≥7	13	32	8	18
Education				
Primary	12	29	5	11
Secondary	22	54	30	67
Tertiary	2	5	5	11
No formal education	5	12	5	11
Farm size				
0.5-5 ha	25	61	28	62
5-10 ha	5	12	7	16
≥ 10	11	27	10	22
Distance to markets				
0-5 km	8	19	4	9
6-20 km	15	37	5	56
20-38 km	18	44	16	36
Road conditions				

Good	14	34	20	44
Bad	27	66	25	56

Source: Field survey, 2016

Determinants of Market Participation

The results in *Table 2* are for econometric modeling of determinants of AIV farmers' participation in informal markets. The results show that revenue, condition of roads, gender and market linkage had negative relationship with market participation, while growing of Spinach, growing of Amaranths, membership of cooperative and being EDSP farmers showed positive statistically significant relationship ($p < 0.05$). Growing of Amaranth was statistically significant at 5% level, while growing of Spinach was statistically significant at 1% level. Thus, involvement of farmers in growing Spinach or Amaranths increased the probability of participating in informal markets ($p < 0.05$). However, the results of the marginal effect show that the three indigenous vegetables (mustard, spinach and amaranth) produced by farmers were statistically significant and had a positive relation to informal participation in markets. The results imply that growing of each of these vegetables increased the probability of farmers' participation in informal markets.

Table 2. *Probit regression estimate and marginal effect of the determinants of informal market participation*

Variables	Probit regression		Marginal effect	
	Coefficient	P z	Coefficient	P z
Planted mustard	1.0760	0.136	3628837	0.07*
Planted spinach	3.6483	0.005***	0.7618	0.000***
Planted amaranth	3.0860	0.038**	0.8008	0.000***
Market price	-0.2142	0.13	-0.0835	0.125
Revenue	-0.0002	0.027**	-0.0008	0.3
Distance to markets	-0.0049	0.189	-0.0019	0.181
Condition of roads	-2.4623	0.003**	-0.7813	0.000***
Land use	-0.8773	0.161	-0.3419	0.161
Gender	-1.1476	0.038**	-0.4213	0.19
Age	-0.0087	0.697	-0.0034	0.696
Marital status	-0.5947	0.283	-0.2205	0.246
Education	0.4361	0.574	0.1609	0.541
Household size	0.0487	0.571	0.0190	0.571
Membership of cooperative	2.7590	0.019**	0.8192	0.000***
Farming experience	0.0341	0.124	0.0133	0.122
Extension support	-0.1274	0.816	-0.0492	0.814
Market linkage	-4.5535	0.003***	-0.9531	0.000***
EDSP farmers	2.8226	0.013**	0.8290	0.000***
Constant term	1.9099	0.254		
Number of observations	86			
LR chi 2(19)	59.73			
Prob > chi2	0.000			
Pseudo R2	0.5108			
Log likelihood	-28.6034			

Source: Field survey, 2016

Hint: *** $p < 0.001$; ** $p < 0.05$; * $p < 0.1$; CI = Confidence Interval

Increase in farm revenue will decrease the probability of participating in informal markets as farmers will produce more and target formal markets to sell their farm

produce. This is in agreement with results reported by Moyo (2010), Montshwe et al. (2005) and Magingxa et al. (2005) that an increase in revenue increases participation in formal markets. Similarly, the parameter of condition of roads showed statistical significance with negative sign. According to Hlomendlini (2015), condition of roads influences participation in informal markets negatively. However, as the condition of the roads improves, participation will improve. The negative relationship implies that the probability of participating in informal market decreased by -0.781 when the condition of the road networks is bad. The same results were reported by Ramoroka (2012) who pointed out that the condition of roads is one of the fundamental factors that enables farmers to deliver their produce to the markets.

The age of farmers showed a negative relationship with participation in markets but was statistically significant at 5% level. This implies that as a farmer grows older, the probability of participating in informal markets also decreases. Arega and Manyong (2007) argued that participation in both formal and informal markets decreases with age because older people consider farming as a way of life rather than business. They are also reluctant to adopt new technologies in farming due to production uncertainties. In this study, a positive and statistically significant relationship between membership of cooperative and market participation was found at 5% level of significance. Similarly, being an EDSP farmer showed a positive relationship with participation in markets. This is in agreement with results obtained by Sikwela and Mushunye (2013) who found that farmers who received supports performed better in the agricultural food chains. The results of market linkage showed a statistical significance to participation in informal markets ($p < 0.01$). As reported by Rios et al. (2009), farmers who are linked to the market participate better and tend to stay longer for better profits.

AIVs Profitability Analysis

Increasing profitability is the major production goal of farmers. Various factors affect the level of profit and hence determine the growth potential of farm business. This section provides the results of some of the factors that influence profitability of vegetable farmers. Variables that are assumed to have an impact are then interacted to determine which combinations best influence profitability of farmers positively.

The results in *Table 3* show that the coefficient of seed is with negative sign and is statistically significant at 10%. This implies that a 1% increase in seed will result in a decrease in AIVs profit by 0.2985%. Rachmina et al. (2014) maintained that an increase in seed seldom results in an increase in yields. On the contrary, transportation cost has positive and significant impact on profit with a parameter of 0.2772 ($p < 0.01$). Therefore, increase in transportation cost by 1% increases profits from AIV cultivation by 0.2772%. According to Mérel et al. (2006), high cost of transportation affects profitability of farm business. The results further showed that the parameter of land is statistically significant ($p < 0.01$). This parameter indicates that a 1% increase in land areas cultivated would decrease profit from AIV cultivation by 0.007%.

Some of the variables were further interacted in order to determine their interactive impacts on AIV profitability. Interaction of labour with itself shows a negative relationship to AIV profit level but statistically significant ($p < 0.01$). This implies that multiplication of currently engaged labour in AIV production will reduce profit. This may occur through increase in labour cost and reduction in the level of output due to excessive intensification. Feroz et al. (2009) found that labour plays an important role in

farm profitability. According to Sikwela and Mushunye (2013), most of the sampled farmers made use of their household members as labour in order to increase profit.

Multiplication of the quantity of fertiliser shows a statistically significant ($p < 0.01$) negative relationship with profit realized from AIV production. The results imply that if the amount of fertiliser used in AIV production increases, outputs and profit will decrease. On the contrary, other researchers such as Pender and Gebremedhin (2008), Murthy et al. (2009), and Tilman et al. (2002) found that an increase in fertiliser resulted in increase in profitability. However, multiplication of quality of seeds shows a positive relationship that is statistically significant with profit ($p < 0.01$). This result is in accordance with that of Abu and Asemer (2011). The parameter of interacting fertiliser with seed shows negative relationship with profit. This implies that interaction of these inputs will decrease profit. However, a positive and statistically significant parameter was estimated with interaction of labour and fertiliser ($p < 0.01$). This result implies that an increase in both labour and fertiliser will increase profit.

Table 3. Translog profit function modelling of AIV Production

Parameters	Coefficient	P z	95% Confidence Interval.	
Log fertiliser	.5065765	0.221	-.3050489	1.318202
Log labour	.2403793	0.333	-.2457891	.7265477
Log seed	-.2985276	0.069	-.6204112	.0233559
Log transport	.2771733	0.001	.1175209	.4368258
Log land	-.0069876	0.000	-.0103408	-.0036343
Log labour*labour	-.1424943	0.009	-.2497931	-.0351956
Log land*land	-.0001865	0.612	-.0009064	.0005335
Log fertiliser*fertiliser	-.0997815	0.021	-.1843299	-.015233
Log seed*seed	.1717867	0.000	.0924892	.2510842
Log fertiliser*seed	-.1114082	0.007	-.1930228	-.0297935
Log labour*fertiliser	.1891201	0.003	.0629148	.3153254
Constant	4.522231	0.000	2.844452	6.20001
Number of observations	86			
Wald chi 2(13)	146.10			
Log likelihood	-114.93155			
Prob> chi2	0.000			

Hint: *** $p < 0.001$; ** $p < 0.05$; * $p < 0.1$; CI = Confidence Interval

Determinants of AIV Profit Inefficiency

From the results that are presented in *Table 4*, distance to the market shows a negative effect on profit inefficiency with a coefficient of -0.988 ($p < 0.05$). This result implies that as market distance increases, profit inefficiency decreases. Renkow et al. (2004) had reported similar results. The objective of the condition of roads is to maintain and increase frequency to markets which is important in profit making. It is the major means of transporting agricultural produce from the farms to the markets. In this study, it is revealed that the condition of roads has a positive and significant effect on inefficiency of profit. Thus, inefficiency increased among farmers that had access to bad roads. Ogunniyi (2011) also reported that profit efficiency was affected by the condition roads. This result is also supported by research conducted by Rachmina et al. (2014). With the rapid transformation of marketing systems, traditional marketing channels are being replaced by coordinated links between farmers, processors and retailers. The results of this study show that support on market linkage has a positive and statistically

significant effect on profit inefficiency. This result is a pointer to inadequate access that AIV farmers are having to formal markets. Presently, majority of them only sold at some informally organized markets. However, Morgan et al. (2009) found that market linkage improves the efficiency of farm profit.

Table 4. Analysis of profit inefficiency of profitability of indigenous vegetable farmers

Inefficiency	Coefficient	P z	95% Confidence Interval	
Planted mustard	-28.91409	0.986	-3246.414	3188.585
Planted spinach	-2.013768	0.297	-5.796296	1.76876
Planted amaranth	4.458002	0.107	-.9656879	9.881692
Market price	.3412082	0.158	-.1329746	.815391
Distance	-.0988926	0.024	-.1846088	-.0131765
Road condition	4.122046	0.044	.109334	8.134758
Gender	1.495443	0.193	-.7555125	3.746399
Age	.0486561	0.387	-.061485	.1587971
Marital status	-1.37785	0.405	-4.61795	1.862249
Education	-1.432988	0.487	-5.470397	2.604421
Household size	.3318576	0.248	-.2310566	.8947719
Non-farm income	.2661136	0.867	-2.855204	3.387432
Membership of cooperative	2.358589	0.108	-.5166361	5.233814
Farming experience	-.0727185	0.182	-.1794658	.0340287
Extension support	2.534668	0.177	-1.145015	6.214351
Market linkage	6.845036	0.066	-.46571	14.15578
EDSP farmers	-4.718239	0.187	-11.72866	2.292181
Constant term	-11.68467	0.055	-23.62724	.2579025
Number of obs	86			
Wald chi 2(13)	146.10			
Log likelihood	-114.93155			
Prob> chi2	0.000			

Hint: ***p < 0.001; ** p < 0.05; * p < 0.1; CI = Confidence Interval

Conclusion

The aim of this study was to examine the effects of enterprise development support program on market participation and profit efficiency of AIV farmers. The results have indicated that the support program enhanced access to informal markets by AIV farmers. This suggests that the program had been able to facilitate marketing of AIV although such linkages are yet to explore some more lucrative formal markets. It was also found that the condition of road influenced access to market and profit inefficiency. These results are reemphasizing the importance of adequate maintenance of feeder roads to the villages on market participation and production efficiency. There should be adequate efforts from government to properly link farmers in some interior villages to urban markets through adequate maintenance and construction of more roads.

REFERENCES

- [1] Abu, O., Asembler, D. J. (2011): Opportunities for smallholder Spinach farmers in Nigeria: a Profit efficiency analysis. – Journal of Economics 2(2): 75-79.
- [2] Arega, A. D., Manyong, V. M. (2007): The effect of education on agricultural productivity under traditional & improved technology in Northern Nigeria: An endogenous switching regression analysis. – Empirical Economics 32(1): 141-159.

- [3] Baba, S. H., Zargar, B. A., Ganaie, S. A., Yousuf, S., Sehr, H. (2010): Gender participation in vegetable cultivation in Kashmir valley. – *Indian Res. J. Ext. Edu* 10(2): 66-69.
- [4] Chetty, J. M. (2013): Dietary analysis of South African indigenous vegetables and traditional food assumptions made by nutritionists and the impact on public health outcomes. – Doctoral dissertation, University of Cape Town.
- [5] Fanzo, J., Heywood, V., Hunter, D. (2013): Overview of agricultural biodiversity & its contribution to nutrition & health. – *Diversifying Food and Diets: Using Agricultural Biodiversity to Improve Nutrition & Health*: 35-67.
- [6] Feroz, A. N. M., Rashid, M. H. A., Hossain, M. (2009): Profitability analysis of Bagda farming in some selected areas of Satkhira district. – *Journal of Progress. Agric.* 20(1-2): 221-229.
- [7] Food and Agriculture Organisation (FAO). (2005): Marketing Extension guide: Horticultural marketing. – Retrieved from www.fao.org/3/a-a0185e.pdf. Retrieved on 13th August, 2015. p 1-43.
- [8] Food and Agriculture Organisation (FAO). (2010): Sustainable pathways: Smallholders and family farmers?. – Retrieved from www.fao.org/.../sustainability_pathways/.../Factsheet on 13 August, 2015.
- [9] Grivetti, L. E., Ogle, B. M. (2000): Value of Traditional Food in Meeting Macro- and Micronutrient Needs: The Wild Plant Connection. – *Nutrition Research Reviews* 13(1): 31-46.
- [10] Hlomendlini, P. H. (2015): Key factors influencing smallholder market participation in the former homelands of South Africa: case study of the Eastern Cape. – Doctoral dissertation, Stellenbosch: Stellenbosch University.
- [11] Lotter, D. W., Marshall, M. I., Weller, S., Mugish, A. (2014): African indigenous & traditional vegetables in Tanzania: production, post-harvest management and marketing. – *African Crop Science Journal* 22(3): 181-189.
- [12] Magingxa, L. L., Alemu, Z., Van Schalkwyk, H. D. (2005): Factors that influencing market access for smallholder irrigators in South Africa. – A paper presented at the 43rd Annual AEASA conference in Polokwane, Limpopo, September, 21-23, 2005.
- [13] Maponya, P., Venter, S. L., Modise, D., Van Den Heever, E., Kekana, V. (2015): Determinants of Agricultural Market Participation in the Sarah Baartman District, Eastern Cape of South Africa. – *Journal of Human Ecology* 50(1): 1-9.
- [14] Markelova, H., Meinzen-Dick, R., Hellin, J., Dohrn, S. (2009): Collective action for smallholder market access. – *Food policy* 34(1): 1-7.
- [15] Masuku, M. B., Xaba, B. (2013): Factors Affecting the Productivity & Profitability of Vegetables Production in Swaziland. – *Journal of Agricultural Studies* 1(2): 37-52.
- [16] Mavengahama, S., McLachlan, M., De Clercq, W. (2013): The role of wild vegetable species in household food security in maize subsistence cropping systems. – *Journal of food Science* 5(2): 227-233.
- [17] Mérel, P. R., Sexton, R. J., Suzuki, A. (2006): Transportation cost and market power of middlemen: A spatial analysis of agricultural commodity markets in developing countries. – Available at SSRN: <https://ssrn.com/abstract=944167> or <http://dx.doi.org/10.2139/ssrn.944167>.
- [18] Montshwe, B. D., Jooste, A., Alemu, Y. G. (2005): An Econometric Analysis of Determinants of Market Participation within the South African Small-Scale Cattle Sub Sector. – A paper presented at the 43rd AEASA conference, Limpopo Polokwane, September 21-23, 2005.
- [19] Morgan, N. A., Slotegraaf, R. J., Vorhies, D. W. (2009): Linking marketing capabilities with profit growth. – *International Journal of Research in Marketing* 26(4): 284-293.
- [20] Moyo, T. (2010): Determinants of participation of smallholder farmers in the marketing of small grains and strategies for improving their participation in the Limpopo River Basin of Zimbabwe. – Doctoral dissertation, University of Pretoria.

- [21] Muhanji, G., Roothaert, R. L., Webo, C., Stanley, M. (2011): African indigenous vegetable enterprises and market access for small-scale farmers in East Africa. – *International Journal of Agricultural Sustainability* 9(1): 194-202.
- [22] Mumbi, K., Karanja, N., Njenga, M., Kamore, M., Achieng, C., Ngeli, P. (2006): Investigative Market Research: Viable Market Opportunities & Threats for Urban & Peri-Urban Farmers. – Farm Concern International, Urban Harvest & International Potato Centre, Nairobi.
- [23] Murthy, D. S., Sudha, M., Hegde, M. R., Dakshinamoorthy, V. (2009): Technical efficiency & its determinants in tomato production in Karnataka, India: Data Envelopment Analysis (DEA) Approach. – *Agricultural Economics Research Review* 22(2): 215-224.
- [24] Ogunniyi, L. T. (2011): Profit efficiency among maize producers in Oyo State, Nigeria. – *ARPN J. Agric. Boi. Sci.* 61(11): 11-17.
- [25] Okoruwa, V. O., Akindeinde, A. O., Salimonu, K. K. (2009): Relative economic efficiency of farms in rice production: A profit function approach in North Central Nigeria. – *Tropical & Subtropical Agroecosystems* 10(2): 279-286.
- [26] Okoye, B. C., Abass, A., Bachwenkizi, B., Asumugha, G., Alenkhe, B., Ranaivoson, R., Randrianarivelo, R., Rabemanantsoa, N., Ralimanana, I. (2016): Effect of transaction costs on market participation among smallholder cassava farmers in Central Madagascar. – *Cogent Economics & Finance* 4(1): 1143597.
- [27] Osmani, A. G., Hossain, E. (2015): Market participation decision of smallholder farmers & its determinants in Bangladesh. – *EkonomikaPoljoprivrede* 62(1): 163.
- [28] Ozkan, B., Ediz, D., Ceyhan, V., Goldey, P. (2000): Women's role in the vegetable farming systems in Antalya, Turkey: a gender analysis of labour participation & decision-making in the agricultural sector. – In XIVth International Symposium on Horticultural Economics 536: 419-438.
- [29] Pender, J., Gebremedhin, B. (2008): Determinants of agricultural management practices & impacts on crop production & household income in the highlands of Tigray, Ethiopia. – *Journal of African Economies* 17(3): 395-450.
- [30] PSPPD. (2011): Program to Support Pro-Poor Policy Development in South Africa. – Retrieved from [www. presidency.gov.za/.../Program%20to%20Support%20Pro-Poor%20Policy%20..](http://www.presidency.gov.za/.../Program%20to%20Support%20Pro-Poor%20Policy%20..) Retrieved on 20th June 2016.
- [31] Rachmina, D., Daryonto, A., Tambunan, M. (2014): Impact of infrastructure on profit efficiency of vegetable farming in west Java. – Online paper retrieved 19/05/2015. *J. ISSAAS* 20(1): 77-92.
- [32] Ramoroka, K. H. (2012): Participation and utilisation of formal vegetable markets by smallholder farmers in Limpopo: A tobit II approach. – Doctoral dissertation, University of Limpopo (Turffloop Campus).
- [33] Randela, R., Alemu, Z. G., Groenewald, J. A. (2008): Factors enhancing market participation by small-scale farmers. – *Agrekon* 47(4): 451-469.
- [34] Renkow, M., Hallstrom, D. G., Karanja, D. D. (2004): Rural infrastructure, transactions costs and market participation in Kenya. – *Journal of Development Economics* 73(1): 349-367.
- [35] Rios, A. R., Shively, G. E., Masters, W. A. (2009): Farm productivity and household market participation: Evidence from LSMS data. – In International Association of Agricultural Economists Conference, August, Beijing.
- [36] Shisana, O., Labadarios, D., Rehle, T., Simbayi, L., Zuma, K., Dhansay, A., Reddy, P., Parker, W., Hoosain, E., Naidoo, P., Hongoro, C. (2014): The South African National Health and Nutrition Examination Survey, 2012: SANHANES-1: the health and nutritional status of the nation. – HSRC press.
- [37] Sikwela, M. M., Mushunye, A. (2013): The impact of farmer support Programs on household income & sustainability in smallholder production: A case study of the Eastern

- Cape & Kwazulu Natal farmers', South Africa. – African Journal of Agricultural Research E 8(21): 2502-2511. <http://www.academicjournals.org/AJAR>.
- [38] Spring, A. (2015): Haiti: Final Country Report. – Arlington, VA: Strengthening Partnerships, Results, and Innovations in Nutrition Globally (SPRING) project.
- [39] Taleni, V., Goduka, N. (2013): Creating Spaces for Indigenous Research Around Eziko for Strengthening Sustainable Livelihoods within Rural Contexts. – East London-South Africa, p.205.
- [40] Tilman, D., Cassman, K. G., Matson, P. A., Naylor, R., Polasky, S. (2002): Agricultural sustainability and intensive production practices. – Nature 418(6898): 671-677.
- [41] Vink, N., Kirsten, J. F. (2000): Market Development & Smallholder Farmers. A Selective Literature Survey. – Agricultural Economics Research, Policy & Practice in Southern Africa.
- [42] Weinberger, K., Msuya, J. M. (2004): Indigenous vegetables in Tanzania: significance & prospects (Vol. 600). – AVRDC-WorldVegetableCentre.
- [43] World Bank (2010): Agriculture & Rural Development. Retrieved from data.worldbank.org/topic/agriculture-&-rural-development.
- [44] Xaba, B. G., Masuku, M. B. (2012): Factors affecting the choice of marketing channel by vegetable farmers in Swaziland. – Sustainable Agriculture Research 2.1: 112.
- [45] Yang, R. Y., Keding, G. B. (2009): Nutritional contributions of important African indigenous vegetables. African indigenous vegetables in urban agriculture. – Earthscan, London, pp. 105-144.

NUMERICAL SIMULATION OF HYDROLOGICAL AND HYDRODYNAMIC RESPONSES TO CHANNEL EROSION IN CHINA'S LARGEST FRESHWATER LAKE

LIANG, D.¹ – LU, J. Z.^{1*} – CHEN, X. L.^{1,2} – ZHANG, L.¹

¹*State Key Laboratory of Information Engineering in Surveying, Mapping and Remote Sensing, Wuhan University, 129 Luoyu Road, Wuhan 430079, China*

²*Key Laboratory of Poyang Lake Wetland and Watershed Research, Ministry of Education, Jiangxi Normal University, Nanchang 330022, China*

**Corresponding author*

e-mail: lujzhong@whu.edu.cn; phone: +86-27-6877-8755

(Received 14th Feb 2019; accepted 8th Apr 2019)

Abstract. Topography determines the nature of hydrodynamic processes and its changes potentially affect the water quantity and quality. This study assessed the spatiotemporal impacts of topography changes on hydrological and hydrodynamic characteristics of China's largest freshwater lake, Poyang Lake. Results from simulation of different channel erosion intensities indicated that topography changes induced hydrological and hydrodynamic variations with spatiotemporal heterogeneity. Water levels in the lake decreased and the effect was enhanced with stronger erosion intensities. The decrease in water level was significant during the dry period, but negligible during the wet period. Water levels decreased by an average of 0.90-1.1 m in the northern channel during the dry period, and 0.27 m and 0.20 m in the central and eastern lakes during the rising and recession periods. The changing water level further affected the distribution of water with the effect of gathering water to the channel from nearby areas. Moreover, channel erosion altered the lake-river interactions. During the dry period, outflow discharges increased as the channel conveyance capacity increased by 25-136%. In contrast, during the wet period, outflow discharges decreased as the inflow regulation volume increased by $3.8-8.2 \times 10^8$ m³. Particularly, backflow frequency and volume increased during the flooding period of the Yangtze River. In addition, the dry period in Poyang Lake was extended, and the frequency of low-water events increased significantly. This study demonstrated the spatiotemporal impacts of topographical changes on hydrodynamic processes in Poyang Lake, therefore providing a better understanding of variations in water regimes and lake-river interactions.

Keywords: *topography changes, hydrological and hydrodynamic impacts, numeric model, eco-hydrology, Poyang Lake*

Introduction

Topography has a fundamental control on the flow of water in gravity-driven shallow waters. It has a strong influence on the hydrological and hydrodynamic characteristics of water systems, and is closely related to water quantity and quality (Oliveira et al., 2006; Rinaldi et al., 2008; Malhadas et al., 2009; Mosley, 2015). Changes in topography affect flow patterns and material transportation, and these variations, in turn, alter the topographic evolution. Erosion and sedimentation processes occur frequently through interaction between water and suspended matters (Yang et al., 2007). As water usually contains suspended matters, such as mud, sand, salt, and floating algae, suspended particles contained in the flow can be deposited and attach to the surface of the bed or the bank of the watercourse. Thus depositional processes may increase the bottom surface and make the cross section of the waterway narrower. Conversely, the erosion process entrains particles from the bottom surface into the water and scours the bed and

sidewalls, making the watercourse deeper and wider. Under the combined effects of deposition and erosion, underwater topography usually changes slowly. Therefore, topography is regarded to be stable over short timescales and deformation is often neglected in studies of hydrological and hydrodynamic processes. However, disasters such as landslides, earthquakes, and debris flows, as well as human activities, such as dredging, lake infilling, and dam construction, can change topography in a short amount of time. The bottom may be raised or lowered, or the watercourse may be broken up, blocked, or diverted. Thus the spatial characteristics may change significantly. As an influential factor to hydrodynamic processes, topography changes have a substantial impact on water flow, water distribution, and material transportation, affecting the availability of water consumption for living organisms, agriculture and industry, as well as for ecological processes.

Poyang Lake, the largest freshwater lake in China, is one of the few existing lakes connected to the Yangtze River. The lake has a complex underwater topography (Feng et al., 2011) influenced by erosion and deposition processes. Moreover, human activities in Poyang Lake, including lake reclamation, reservoir construction and sand mining, induced significant changes (Min, 2000; Lai et al., 2014). Studies have indicated that active sand dredging in Poyang Lake after the enactment of a sand mining ban in Yangtze River in 2001 have altered the lake to an erosional system (Lai et al., 2014; Li et al., 2014). Monitoring the sand-dredging activities in Poyang Lake through remote sensing imagery was used to estimate the location and extent of decrease in elevation (Leeuw et al., 2010; Li et al., 2014). Further comparison of DEMs extracted from remote sensing images and in situ bathymetry measurements showed that the outflow channel was deeper and wider than before (Cui et al., 2009; Feng et al., 2011; Lai et al., 2014; Qi et al., 2014; Wu et al., 2015; Yao et al., 2018). Using the bathymetry data acquired in 1998 and 2010, Wu et al. (2015) found that the bottom elevation decreased 3.7 m on average in the outflow channel of the lake and 2 m on average in the inflow channel of the western branch of Ganjiang from 1998 to 2010, respectively. These studies traced topography changes using multiple methods, and provided the foundation for further studies on the impact of topography changes on hydrodynamic processes in the lake.

In recent years, serious problems, such as severe drought, the earlier arrival of the dry period, and wetland recession, have attracted wide attentions. Topographical changes across Poyang Lake are considered a critical element impacting the hydrology and hydrodynamic characteristics of the lake. Empirical analysis based on observations were used to show the correlation between channel deformation and hydrological and hydrodynamic fluctuations. Gao et al. (2014) analyzed and examined water discharges and sediment load data of Poyang Lake. The study deduced that a deepened channel increased the outflow and sediment flowing from the lake. Moreover, the river-lake interaction was potentially altered by channel morphological changes. Lai et al. (2014) estimated the lake conveyance capacity using outflow discharge and water level observations and deduced that the discharge ability of the lake increased during the dry period. The study demonstrated that the decreasing channel elevation influenced the abnormal low water levels during the winter dry season. These studies, based on observations and empirical analysis, suggested a link between channel erosion and hydrological and hydrodynamic changes in Poyang Lake. However, the impact of channel erosion cannot be fully explained by physical processes. Yao et al. (2018) quantified the impact of bathymetric changes on the lake's water level using a

hydrodynamic model. The influence on hydrological and hydrodynamic characteristics, such as water distribution and lake-river interaction, were not considered. It is necessary to assess the spatiotemporal influence of channel erosion through a physically based hydrodynamic model to better understand the hydrological, hydrodynamic, and ecological changes in the lake.

In this study, we aim to assess the spatiotemporal hydrological and hydrodynamic responses to channel erosion in Poyang Lake using a numeric method. A hydrodynamic model is constructed to reveal the flow characteristics. The established model is used for simulating the streamflow processes with different channel erosion intensities. The spatiotemporal impacts of topography changes on hydrological and hydrodynamic characteristics, including the lake water level, water distribution, lake-river interaction, and the wet-dry characteristics, are assessed. This study shows the spatiotemporal impact of topography change on water regime fluctuations and water quality changes in a shallow water system. The simulation supports analysis of spatiotemporal variations of hydrological and hydrodynamic characteristics, which will assist analysis of the driving forces related to water shortage problems, as well as terrestrial and aquatic environment dynamics. Therefore, more effective measures can be taken to solve problems in water supply shortages and water pollution.

Materials and methods

Study area and dataset

Poyang Lake is located in the middle section of the Yangtze River. The lake has a complex topography with shallow floodplain areas separated and alternating with deeper channels. The elevation of the lake bottom decreases markedly from south to north. The local annual precipitation around Poyang Lake fluctuates by approximately 1620 mm, and it changes dramatically affected by the subtropical humid monsoon climate. Water regimes and hydrodynamic characteristics of Poyang Lake show spatiotemporal heterogeneity. In the wet season period, usually from April to September, water level at Duchang (the representative gauge in Poyang Lake) rises to more than 12.8 m (Min and Zhan, 2012) and the inundation area expands to more than 3000 km² (Feng et al., 2012a), covering most of the lake extent. In the dry period, usually from October to March, the inundation area can shrink to less than 1000 km², and the lake assumes a river-like shape. The difference in water surface elevation from south to north can be more than 5 m in the dry period, whereas there is little difference during the wet period. Consequently, the flow velocity in the dry period is much faster than in the wet period. As a throughput type lake, Poyang Lake usually regulates water from five main rivers in the catchment, including the Xiushui, Ganjiang, Fuhe, Xinjiang, and Raohe (*Fig. 1*), and drains into the Yangtze River through the Hukou outlet. During flooding periods however, high water level in the Yangtze River, usually from July to September, may lead to backflow into the lake as well. The lake-river interactions exert a profound impact on the hydrological and hydrodynamic characteristics of Poyang Lake.

Three types of data were used in this study, including in situ measurements and products of the bottom elevation, daily water level and discharge data from the gauge stations, and satellite remote sensing images. Underwater terrain data was acquired in 1998 by the Changjiang Water Resources Commission of China. Changes in channel elevation between 1998 and 2010 were provided by the Jiangxi Administration of

Surveying, Mapping and Geoinformation (<http://www.jxcehui.gov.cn>). The bottom elevation data was processed to generate bathymetry for our numeric model. Time series of daily station discharge and water level data over the study period (January 1, 2001 to December 31, 2002) were collected from the Jiangxi Bureau Hydrology Department (<http://www.jxsw.cn/>). Upstream discharge data were collected from seven gauging stations (Qiujin, Wanjiabu, Waizhou, Lijiadu, Meigang, Hushan, and Dufengkeng) on the five main rivers in the catchment. Among them, Qiujin and Wanjiabu measure discharge from the Xiushui, Waizhou for Ganjiang, Lijiadu for Fuhe, Meigang for Xinjiang, and Hushan and Dufengkeng for Raohe (Fig. 1). Downstream discharge data at Hukou, which monitors the lake-river interaction, was collected. Water level data from six hydrological stations (Hukou, Xingzi, Duchang, Tangyin, Longkou, Kangshan) across Poyang Lake were collected to document the water regime of the lake. Besides, the 40-year (from 1970 to 2009) time series daily water level data at Duchang and Hukou were collected to analyze the water regime changes. A Landsat ETM+ image acquired on August 12, 2010 when a large flood occurred in Poyang Lake, was obtained from the USGS (<https://glovis.usgs.gov/>) to extract the extent of the water boundary.

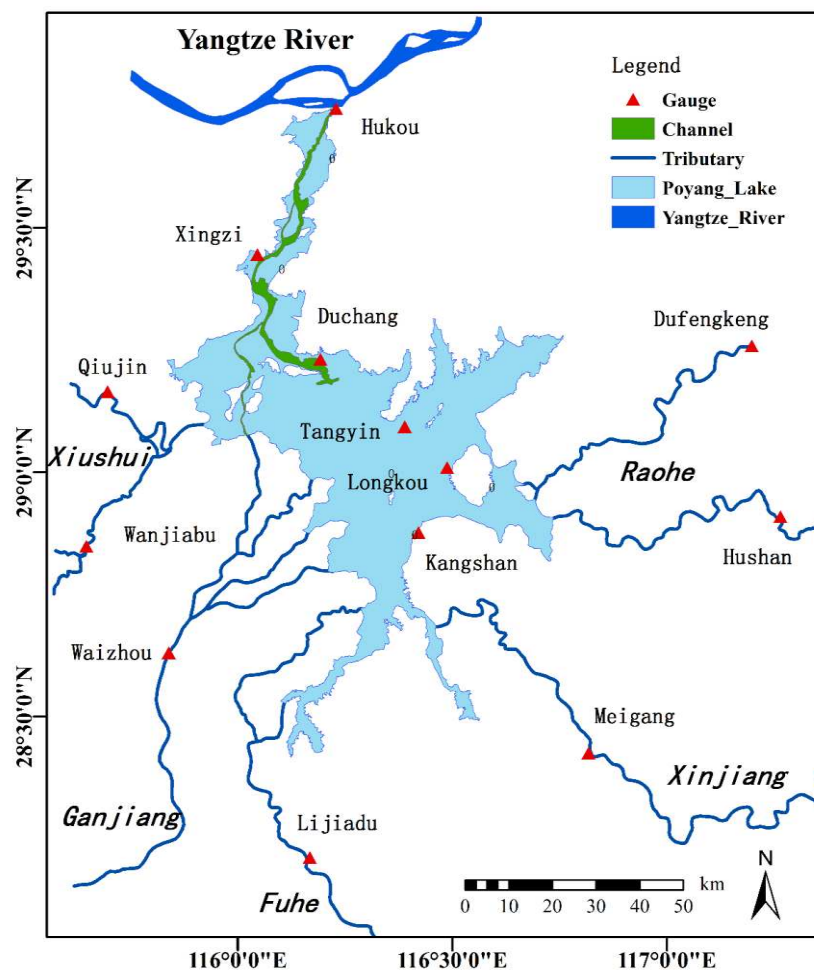


Figure 1. Location of Poyang Lake and gauging stations. The lake inflow sources consist of five main tributaries: Xiushui, Ganjiang, Fuhe, Xinjiang, and Raohe. Water flow into the lake and run south-to-north through the channel into the Yangtze River at Hukou. Gauging stations on the tributaries and hydrological stations in the lake are marked as red triangles

Methodology

Hydrodynamic model of Poyang Lake

In this study, a hydrodynamic model of Poyang Lake was established based on Delft3D-Flow, which is a module of the open source software Deltares (Delft Hydraulics, 2014). The software was developed to investigate hydrodynamics, sediment transport and water quality for fluvial, estuarine and coastal environments. As vertical currents could be neglected in Poyang Lake (Li et al., 2014; Zhang et al., 2015), a 2D free-surface model was constructed. The numerical program has been widely used to reveal hydrodynamic processes and transport phenomena in shallow waters.

Delft-Flow calculates multidimensional hydrodynamics based on the Navier Stokes equations, which consist of the continuity equation and the momentum equations. In an orthogonal coordinate system, the depth-averaged continuity and momentum equations are described as follows (Eqs. 1-3):

Continuity equation:

$$\frac{\partial \zeta}{\partial t} + \frac{1}{\sqrt{G_{\xi\xi}G_{\eta\eta}}} \frac{\partial[(d+\zeta)U\sqrt{G_{\eta\eta}}]}{\partial \xi} + \frac{1}{\sqrt{G_{\xi\xi}G_{\eta\eta}}} \frac{\partial[(d+\zeta)V\sqrt{G_{\xi\xi}}]}{\partial \eta} = (d+\zeta)q \quad (\text{Eq.1})$$

Momentum equations:

$$\begin{aligned} \frac{\partial u}{\partial t} + \frac{u}{\sqrt{G_{\xi\xi}}} \frac{\partial u}{\partial \xi} + \frac{v}{\sqrt{G_{\eta\eta}}} \frac{\partial u}{\partial \eta} + \frac{\omega}{d+\zeta} \frac{\partial u}{\partial \sigma} - \frac{v^2}{\sqrt{G_{\xi\xi}G_{\eta\eta}}} \frac{\partial \sqrt{G_{\eta\eta}}}{\partial \xi} + \frac{uv}{\sqrt{G_{\xi\xi}G_{\eta\eta}}} \frac{\partial \sqrt{G_{\xi\xi}}}{\partial \eta} - fv \\ = -\frac{1}{\rho\sqrt{G_{\xi\xi}}} P_{\xi} + F_{\xi} + \frac{1}{(d+\zeta)^2} \frac{\partial}{\partial \sigma} (v_v \frac{\partial u}{\partial \sigma}) \end{aligned} \quad (\text{Eq.2})$$

$$\begin{aligned} \frac{\partial v}{\partial t} + \frac{u}{\sqrt{G_{\xi\xi}}} \frac{\partial v}{\partial \xi} + \frac{v}{\sqrt{G_{\eta\eta}}} \frac{\partial v}{\partial \eta} + \frac{\omega}{d+\zeta} \frac{\partial v}{\partial \sigma} - \frac{u^2}{\sqrt{G_{\xi\xi}G_{\eta\eta}}} \frac{\partial \sqrt{G_{\xi\xi}}}{\partial \eta} + \frac{uv}{\sqrt{G_{\xi\xi}G_{\eta\eta}}} \frac{\partial \sqrt{G_{\eta\eta}}}{\partial \xi} + fu \\ = -\frac{1}{\rho\sqrt{G_{\eta\eta}}} P_{\eta} + F_{\eta} + \frac{1}{(d+\zeta)^2} \frac{\partial}{\partial \sigma} (v_v \frac{\partial v}{\partial \sigma}) \end{aligned} \quad (\text{Eq.3})$$

where ξ , η are the horizontal curvilinear coordinates and σ is the scaled vertical coordinate; $G_{\xi\xi}$ and $G_{\eta\eta}$ are the coefficients to transform curvilinear to rectangular coordinates; ζ represents water level above the reference plane, and d represents water depth below the reference plane; (u, v) represent the flow velocity and (U, V) represent the depth-averaged flow velocity of the ξ - and η -direction, respectively; q represents the contributions of source and sink terms per unit area; ω represents the vertical velocity in the adapting σ -coordinate; v_v represent the vertical eddy viscosity coefficient; f represents the Coriolis coefficient; P_{ξ} and P_{η} represent the pressure gradients; F_{ξ} and F_{η} represent the unbalance of horizontal Reynold's stresses; ρ represents the density of water.

The set of partial differential equations were solved by an implicit finite difference method on a staggered grid. To get a good solution from the hydrodynamic model, we should specified a set of model inputs, which can be divided into four data groups

including model domain and time parameters, boundary conditions, initial conditions, and physical parameters. Model domain is usually defined by the computational grid and bathymetry. The time parameters contain the simulation runtime and computation steps. In the numeric model, the inflow and outflow boundary conditions are often used to restrict the computation, and the initial hydrodynamic state of the computation domain are used to launch the model. Physical parameters contain physical constants, such as water density, and calibration factors, such as bottom roughness.

To obtain the maximum water boundary for model calculation, a Landsat image acquired on August 12, 2010 was employed when a large flood occurred and the entire lake was covered by water (Zhang et al., 2015). Disconnected segments separated by islands and artificial structures were removed. Rectangle model grids were generated based on the maximum water boundary with a resolution of 300 m. The bottom topography data was processed to fit the coordinate system in Delft3D and interpolated into the model grid points. The run time of the simulation extended from January 1, 2001 to December 31, 2002, covering both complete wet and dry periods. The computation time step was set as 1 minute to meet the Courant-Friedrichs-Lewy (CFL) condition, which is related to model stability and accuracy (Delft Hydraulics, 2014). To simulate the dramatically and rapidly changing inundation extent in Poyang Lake, a drying and flooding algorithm was used in our study. Grids were removed from the computation domain when grids became dry as the water fell. Conversely, grids were added to the computation domain when grids became wet as the water rose.

Boundary conditions at the inflow and outflow were specified to restrict the computation. The upper open boundary was prescribed as the daily inflow discharges of Poyang Lake. As there is an ungauged area of 19,867 km² between the gauging stations of the five main inflow rivers and Poyang Lake (Zhang et al., 2014; Li et al., 2014; Zhang et al., 2017), daily total inflow discharges were calculated from the gauged discharges by using a simple water balance model put forward by Zhang et al. (2014). The lower open boundary of the model was prescribed as the daily water level at Hukou. Initial conditions were obtained by interpolating the measured water levels from the gauge stations in Poyang Lake.

After establishing the hydrodynamic model, the calibration and validation process were performed to make the model suitable for use. In this study, initial parameter values of the constructed hydrodynamic model were defined based on literature values (Zhang et al., 2015; Li et al., 2016; Qi et al., 2016) and recommended values in the Delft3D user manual (Delft Hydraulics, 2014). A trial-and-error method was used to adjust the critical parameters (Zhang et al., 2015), including bottom roughness, eddy viscosity, and threshold depth for drying and flooding, to optimal values by comparing simulated results with station observations. Daily water levels at the five hydrological stations in the lake (Xingzi, Duchang, Tangyin, Longkou, and Kangshan) and discharge data at Hukou station in 2001 was employed for model calibration and data in 2002 was used for model validation. Statistical indices, including the coefficient of determination (R^2), the Nash-Sutcliffe Efficiency coefficient (NSE), and percent bias (PBIAS), were calculated for evaluating the performance of the model (Moriassi et al., 2007).

Channel erosion simulation

To evaluate the impact of bottom deformation on hydrodynamic characteristics of rivers and lakes, the deformation area and intensity should be estimated firstly. *Figure 2a* shows the bottom elevation of Poyang Lake in 1998 and *Figure 2b* shows the

elevation change from 1998 to 2010. The remarkable decrease in channel elevation was the main feature of topographical changes in Poyang Lake during this period. The bottom elevation in the main channel and the inflow channel of the western branch of Ganjiang (as shown in *Fig. 1*) decreased by an average of 4.0 m and 2.1 m, respectively. In our experiment, channel erosion in these areas was considered. Four scenarios, including slight, moderate, serious and severe intensity, were set to simulate different intensities of channel erosion in the lake. The severe channel erosion was set as the loss in channel bottom elevation from 1998 to 2010 by average of 4.0 m. The bottom elevation after slight, moderate and serious intensity of channel were obtained by interpolation, with an average of 1.0 m, 2.0 m, and 3.0 m decrease in the main channel. Bottom topography was processed and re-interpolated to hydrodynamic model grid points. In order to distinguish the impact of channel erosion on the hydrological and hydrodynamic characteristics in Poyang Lake, the same model configurations, except for bathymetry data, were used for simulations in all four scenarios.

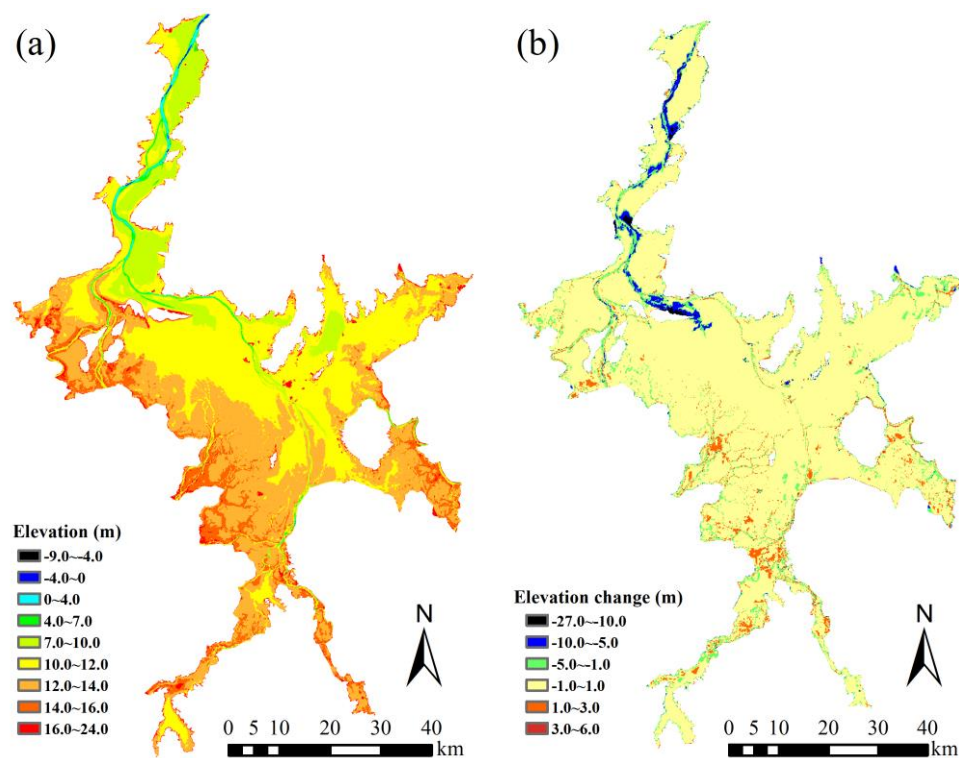


Figure 2. *a* The bottom elevation of Poyang Lake acquired in 1998. *b* Topography changes from 1998 to 2010

Results

Observed changes of water regime

Figure 3 shows the variations of the averages of daily water levels from 2000 to 2009 at Duchang and Hukou, compared to the 40-year (from 1970 to 2009) average conditions. Water levels in Poyang Lake were generally lower during the 2000s. Compared to the 40-year average, mean water level during the 2000s decreased approximately 0.68 m and 0.55 m at Duchang and Hukou, respectively. And the dry

period in the lake during the 2000s became approximately 40-day longer. The results indicated that Poyang Lake experienced a more severe dry condition in the 2000s.

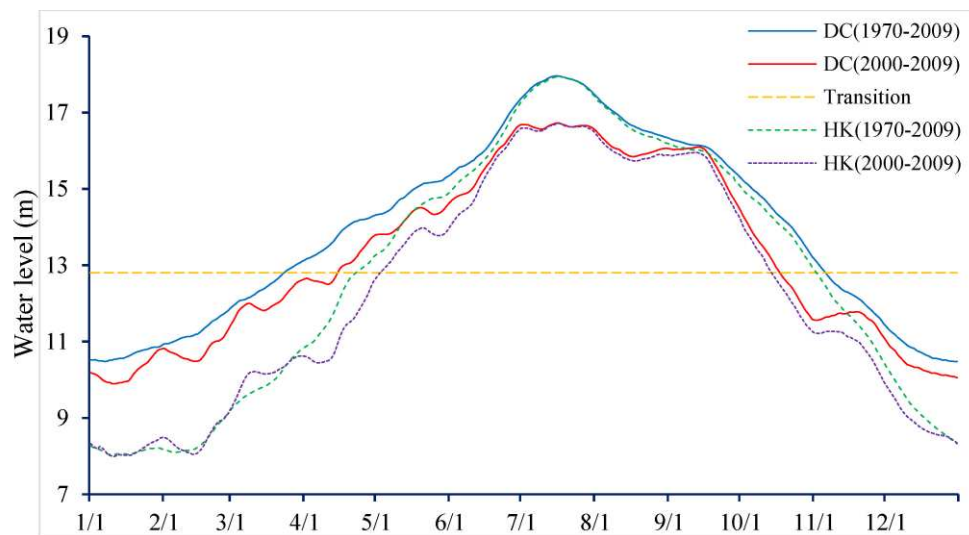


Figure 3. Daily mean water level variations of the 2000s compared to the averages from 1970 to 2009 at Duchang (DC) and Hukou (HK). The “Transition” water level represents the transition water level of the wet and dry periods at Duchang in Poyang Lake

Hydrodynamic model evaluation

Parameters of the hydrodynamic model were calibrated by comparing the simulated water levels and discharges to the measurements in 2001. After many tests by repeatedly refining the critical parameters, the Manning roughness was set to be $0.020 \text{ s/m}^{1/3}$ for the channel and $0.030 \text{ s/m}^{1/3}$ for floodplain area according to the terrain features. Eddy viscosity was set to $1 \text{ m}^2/\text{s}$ and the threshold depth for drying and flooding was set to 0.10 m. The calibrated model was validated based on a comparison between simulation results and observations in 2002. Statistic indices were calculated to evaluate model performance (Table 1). Simulated water levels and outflow discharges were compared to station observations over the calibration and validation period, as shown in Figure 4. Results show that the hydrodynamic model is capable of capturing the dynamic changes of Poyang Lake. Simulated water levels are consistent with observations from the five hydrological stations (Xingzi, Duchang, Tangyin, Longkou and Kangshan) from north to south of the lake in both the calibration and validation periods. The R^2 and NSE of Xingzi, Duchang, Tangyin, Longkou and Kangshan gauging stations are all higher than 0.95 and 0.93, respectively, which indicate that most of the variance in the measured data could be explained by the model and the simulated results fit the observations well. The PBIAS values vary from -0.72% to 0.76%, which suggests no significant overestimation or underestimation in the model. In particular, the significant overestimation of water levels during the dry period caused by bathymetry errors (Lai et al., 2011) was eliminated. The results indicate that the hydrodynamic model is able to reproduce the rapid water level changes over wet and dry periods, as well as the remarkable spatial variation. The associated R^2 and NSE of simulated discharge at Hukou station are all larger than 0.9 and the PBIAS during calibration and validation are 5.78% and 1.18% respectively, which suggests an

acceptable level of accuracy for the discharge simulation. Generally, the calibrated and validated hydrodynamic model employed in this study has the capability to simulate the hydrological and hydrodynamic characteristics of Poyang Lake. Thus, it provides the possibility of reproducing and predicting of hydrodynamics of the lake.

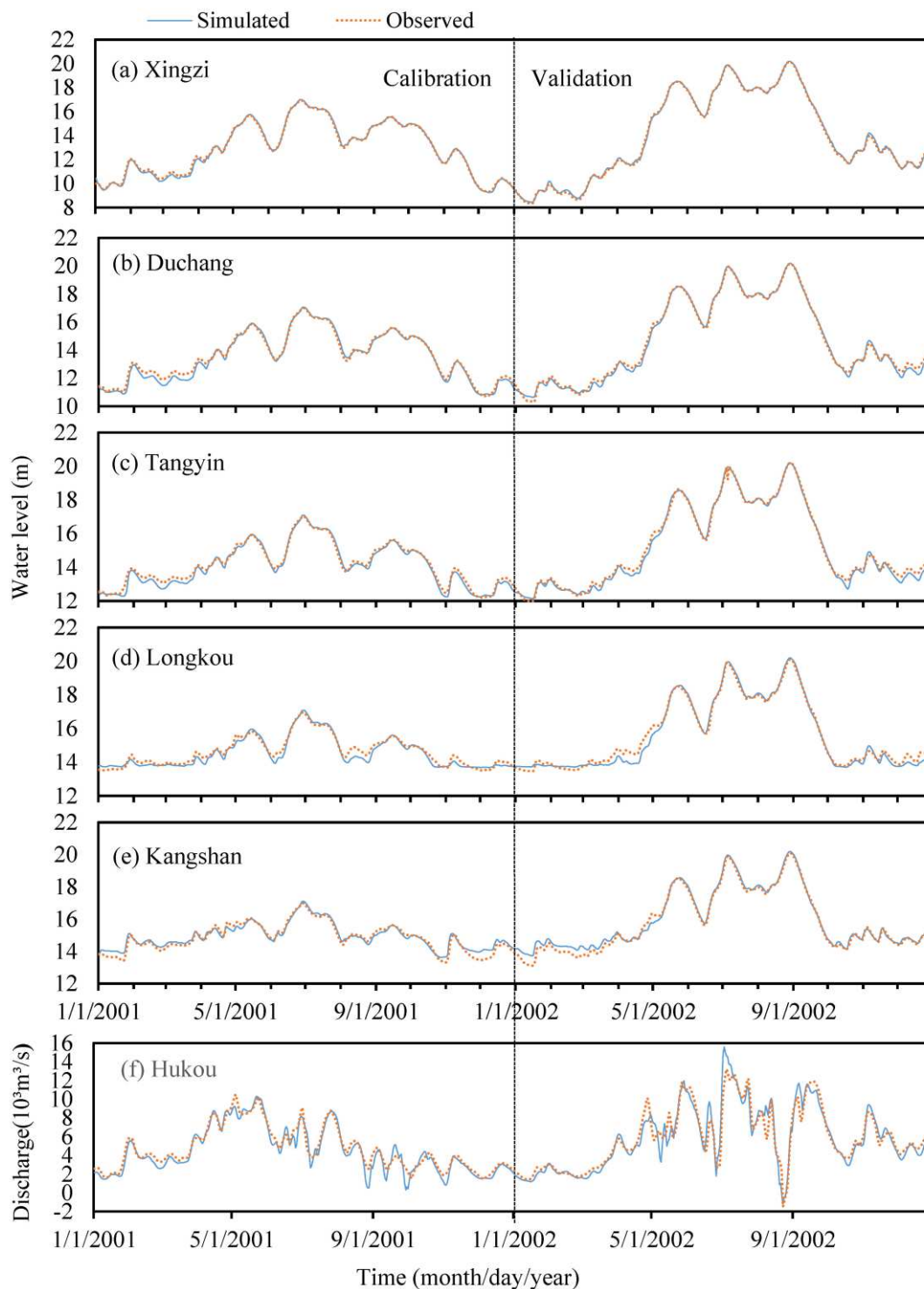


Figure 4. Comparison of simulated (solid line) water levels at **a** Xingzi, **b** Duchang, **c** Tangyin, **d** Longkou, **e** Kangshan and outflow discharges at **f** Hukou and hydrological station measurements (dotted line) in Poyang Lake during the model calibration and validation periods

Table 1. Quantitative assessment of hydrodynamic model performance for daily water level and discharge during the calibration and validation periods

	Indices	Water level					Discharge Hukou
		Xingzi	Duchang	Tangyin	Longkou	Kangshan	
Calibration period (2001)	R ²	0.998	0.993	0.989	0.954	0.952	0.936
	NSE	0.997	0.986	0.977	0.936	0.936	0.909
	PBIAS	0.16%	0.68%	0.76%	0.65%	-0.44%	5.78%
Validation period (2002)	R ²	0.999	0.997	0.996	0.988	0.989	0.922
	NSE	0.999	0.996	0.994	0.984	0.985	0.910
	PBIAS	-0.27%	0.40%	0.52%	0.51%	-0.72%	1.18%

Water levels influenced by channel erosion

The simulated daily water levels under different channel erosion intensities at the five stations were compared to the conditions before channel erosion. *Figure 5* indicates that water levels in Poyang Lake became lower after channel erosion. An increased reduction in water levels occurred at the five stations as the channel became deeper. However, the impact of channel erosion on water levels is spatially and temporally heterogeneous. The extent of water level decline varies over time and space.

Table 2 shows the changes of mean water level at the five gauging stations under different channel erosion intensities. Mean water level reductions during the simulation period all increased with downcutting depth, nonlinearly. Water levels at Duchang station decreased the most after channel erosion, followed by Xingzi, Tangyin, Longkou, and Kangshan. Under severe channel erosion conditions, mean water levels at Duchang and Xingzi decreased by 0.551 m and 0.422 m, respectively. Meanwhile, mean water level decreased by approximately 0.1 m at Tangyin and less than 0.1 m at Longkou and Kangshan.

Table 2. Changes of mean water level (unit: m) under different channel erosion intensities (slight, moderate, serious, severe intensity) compared to the original scenario at five hydrological stations in Poyang Lake during the simulation period

	Xingzi	Duchang	Tangyin	Longkou	Kangshan
Slight	-0.183	-0.229	-0.049	-0.025	-0.021
Moderate	-0.301	-0.401	-0.075	-0.040	-0.025
Serious	-0.378	-0.501	-0.091	-0.050	-0.034
Severe	-0.422	-0.551	-0.101	-0.057	-0.041

Moreover, spatial differences in channel erosion impact on water level leads to changes in water surface slope. Generally, the water surface elevation decreases from south to north in Poyang Lake and the water head from Kangshang to Hukou can be more than 7 m during the dry period. Water level declines caused by channel erosion increased gradually from Kangshan, through Longkou to Tangyin, and reached a maximum at Duchang (*Table 2*). Therefore, the water surface slope increased significantly from Kangshan to Duchang. Under severe channel erosion conditions, the mean water head between Kangshan and Duchang increases by approximately 0.5 m

and the maximum increase reaches approximately 1.4 m. However, due to the blocking effect of the Yangtze River, the impact of channel erosion on water levels decreased from Duchang to the north end of the lake. In particular, water level at Hukou are thought to be determined by the Yangtze River (Cai et al., 2015), thus the impact of channel erosion can be neglected. The water surface gradient from Duchang to Hukou declined after channel erosion. The water head decreased by an average of 0.6 m under severe channel erosion condition.

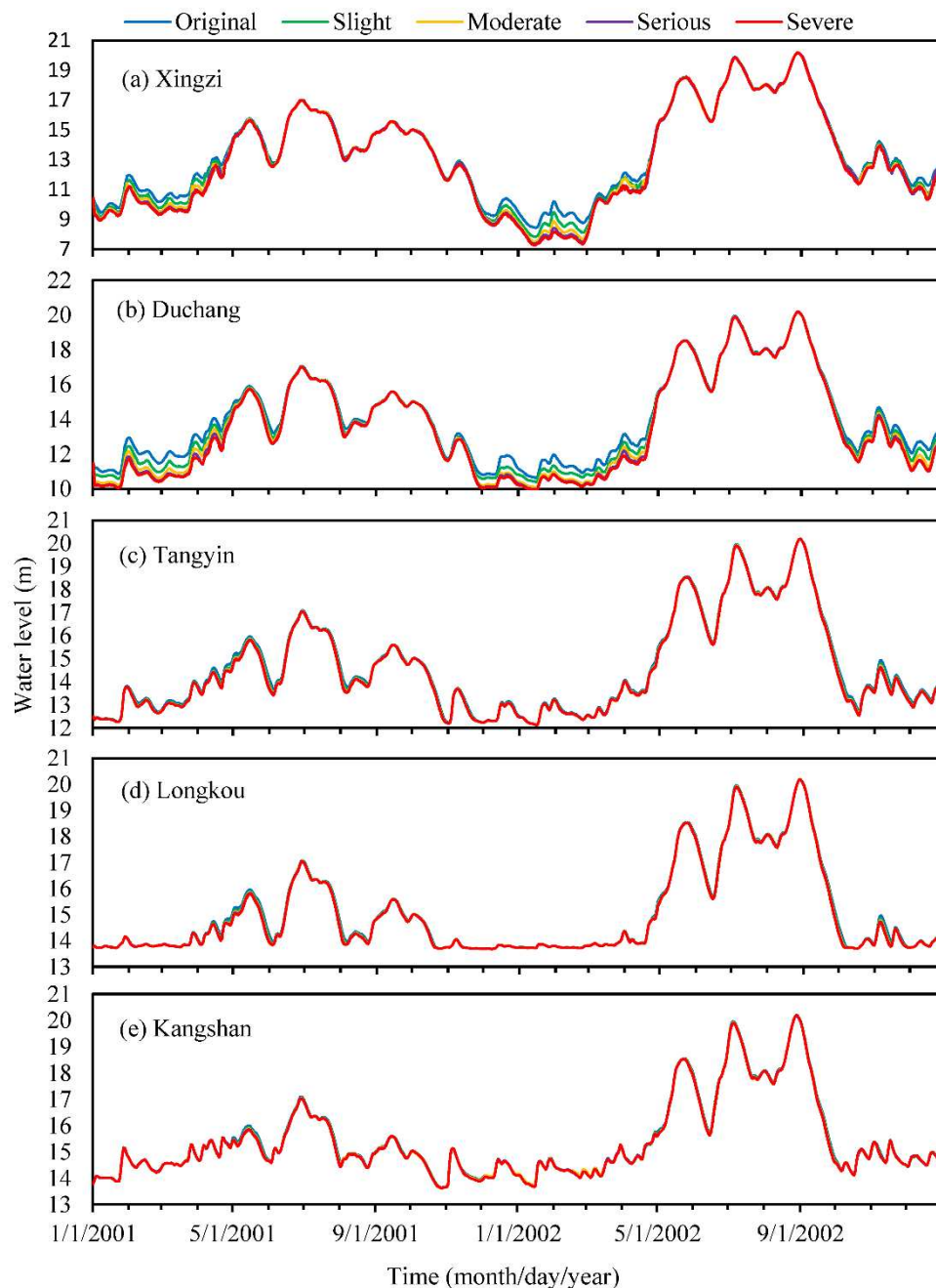


Figure 5. Comparison of the simulated water levels under different channel erosion intensities (slight, moderate, serious, severe intensity) with the water levels before channel erosion (original) at **a** Xingzi, **b** Duchang, **c** Tangyin, **d** Longkou, **e** Kangshan. Water levels at the five gauging stations all decreased after channel erosion

Furthermore, the decrease in water level at the five stations influenced by channel erosion were not temporally identical. *Figure 6* shows the amplitude of decrease in monthly average water levels under severe channel erosion conditions. In general, water levels in the dry period were more sensitive to channel erosion than in the wet period. During the dry period, the water level in the northern channel was most affected. The water levels at Xingzi and Duchang decreased significantly, by an average of 0.90 m and 1.1 m. Monthly average water levels at Xingzi and Duchang all reduced more than 0.52 m and 0.70 m, respectively. The maximum daily water level reduction in Xingzi and Duchang station occurred on January 31, 2002, and March 30, 2001, reaching 2.05 m and 1.37 m, respectively. During the rising and receding water periods, water levels at Xingzi and Duchang decreased an average of 0.40 m and 0.61 m. Water levels in the central and eastern part of the lake decreased by an average of 0.27 m and 0.20 m at Tangyin and Longkou, respectively. The maximum water level reductions at Tangyin and Longkou all occurred in May 2001, reaching 0.46 m, and 0.37 m, respectively. During the wet period, water level changes were all less than 0.1 m.

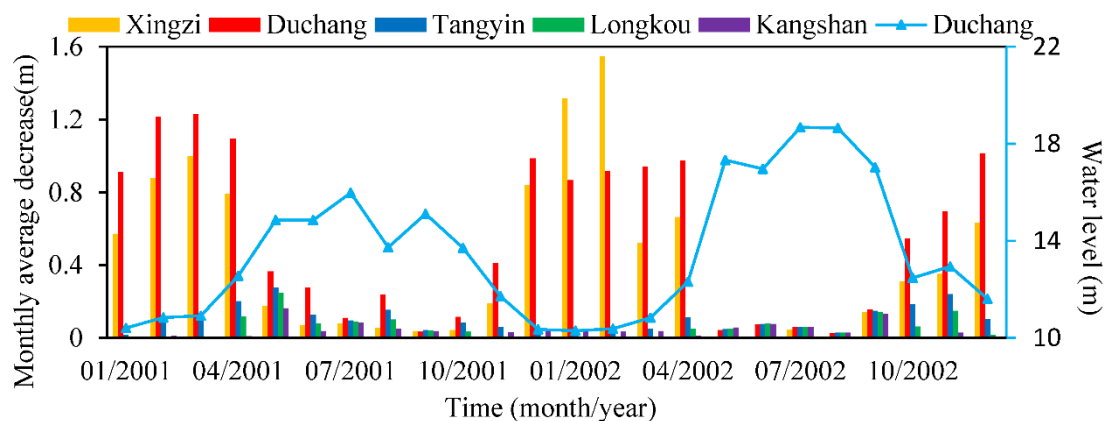


Figure 6. Decrease in monthly average water level (marked as bars) at Xingzi, Duchang, Tangyin, Longkou and Kangshan under severe channel erosion conditions. Decrease of water level caused by channel erosion was more significant in the dry period when water level in the lake (marked as dots with solid line, Duchang) is low

Channel erosion impact on water distribution in the lake

An additional study was performed on the effect of water distribution in Poyang Lake, which was represented by water depth changes after channel erosion. *Figure 7* shows the water depth changes after a severe intensity of erosion during a low water period, rising water period, high water period, and receding water period in 2001. Although water levels in the channel from Duchang to Hukou decreased, the water depth in the channel increased by 2.0 m to 4.0 m over the whole year. Similarly, the water depth in the northern branch inflow channel of Ganjiang increased by 0.5 m to 1.0 m. However, the influence of water depth on the floodplain areas changed in the different periods. During the low water period, the water depth in the floodplain between Xingzi and Duchang decreased by 1.0 to 2.0 m. In addition, the water depth in the middle of the lake decreased by 0.1 to 0.5 m. During the rising water period, the water depth decreased by 0.5 to 1.0 m in the central lake area, and 0.1 to 0.5 m in the eastern floodplain. During the high water period, the impact of water depth on the

floodplain area was negligible. During the receding water period, the water depth decreased by 0.1 to 0.5 m in the central and eastern part of the lake. Changing water depths in Poyang Lake indicated that channel erosion redistributed water in the lake, namely, water in the middle and eastern floodplain and areas nearby the channel drained to the outflow channel.

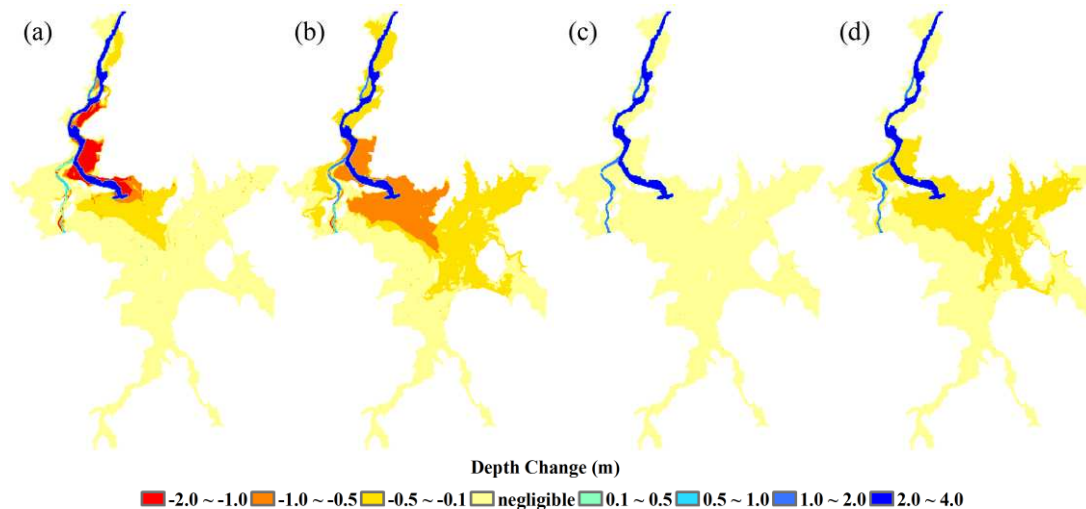


Figure 7. Water depth changes under severe channel erosion conditions on **a** March 30, 2001, during low water period, **b** May 30, 2001, during rising water period, **c** June 29, 2001, during high water period, and **d** October 17, 2001, during the receding water period

Impact of channel erosion on lake-river interactions

Simulated daily discharge at Hukou under different channel erosion intensities were compared with the outflow before channel erosion. The results in *Table 3* show that channel erosion increased the total outflow discharge to the Yangtze River from the Poyang Lake slightly during the simulation period. Although the channel's morphological changes influence on the outflow discharge was not as great as the inflow volumes and the outlet water level variations, the temporally heterogeneous influence changed lake-river interactions. The results indicate that outflow discharges increased in the dry period, but tended to decrease in the wet period. The impact on outflow discharge enhanced due to stronger channel erosion intensities. Topographical changes altered the lake volume and hydraulic condition of the lake, thereby changing the lake's discharge ability and regulation capacity. As erosion decreased the bottom elevation, the lake volume in the four scenarios with different intensities of channel erosion increased by $1.3 \times 10^8 \text{ m}^3$, $2.6 \times 10^8 \text{ m}^3$, $3.9 \times 10^8 \text{ m}^3$, and $5.2 \times 10^8 \text{ m}^3$, respectively. The increasing storage capacity of the lake might decrease the outflow discharge since the lake was able to hold more water. However, variations in the channel bottom topography elevation increased the wetted cross-sectional area and the hydraulic gradient. These two different processes induced a considerable variation in lake-river interaction.

During the dry period, the lake outflow into the Yangtze River increased with channel downcutting depth. During this period, inflow water flow ran through the channel in the lake and drained into the Yangtze River due to the large difference in water level between the southern and the northern part of the lake (an average of 4.5 m

from Kangshan to Hukou) and the weak blocking effect of the Yangtze River. Channel erosion increased the wetted cross-sectional area and the hydraulic radius of the lake outflow channel, thus increasing the lake conveyance capacity, which represents the essential discharge ability of an open lake outflow channel (Lai et al., 2014). The results in *Figure 8* show that Poyang Lake's outflow channel conveyance capacity increased with different intensities of channel erosion. The average lake conveyance capacity before channel erosion was approximately $2290 \text{ m}^{2.5}/\text{s}$, and for the four channel erosion scenarios in this study it increased by 25.0%, 58.7%, 99.4%, and 135.8%, respectively. The increasing conveyance capacity implies that water flows more easily from the channel into the Yangtze River. A larger increase in the outflow channel conveyance capacity occurred during the low water period of Hukou. For example it increased by 260% at a level of 7.2 m, which has the potential to intensify the drought during this period. Moreover, significant decrease in water levels in the northern watercourse caused by channel erosion increased the water surface slope during the dry period, accelerating the water flow into the channel, and increasing the total outflow discharge.

Table 3. Relative change rate of outflow discharge at Hukou station compared to that before channel erosion after slight, moderate, serious, severe intensity of channel erosion

	Dry period	Wet period	All
Slight	0.38%	-0.01%	0.05%
Moderate	0.76%	-0.06%	0.08%
Serious	1.02%	-0.09%	0.10%
Severe	1.20%	-0.11%	0.11%

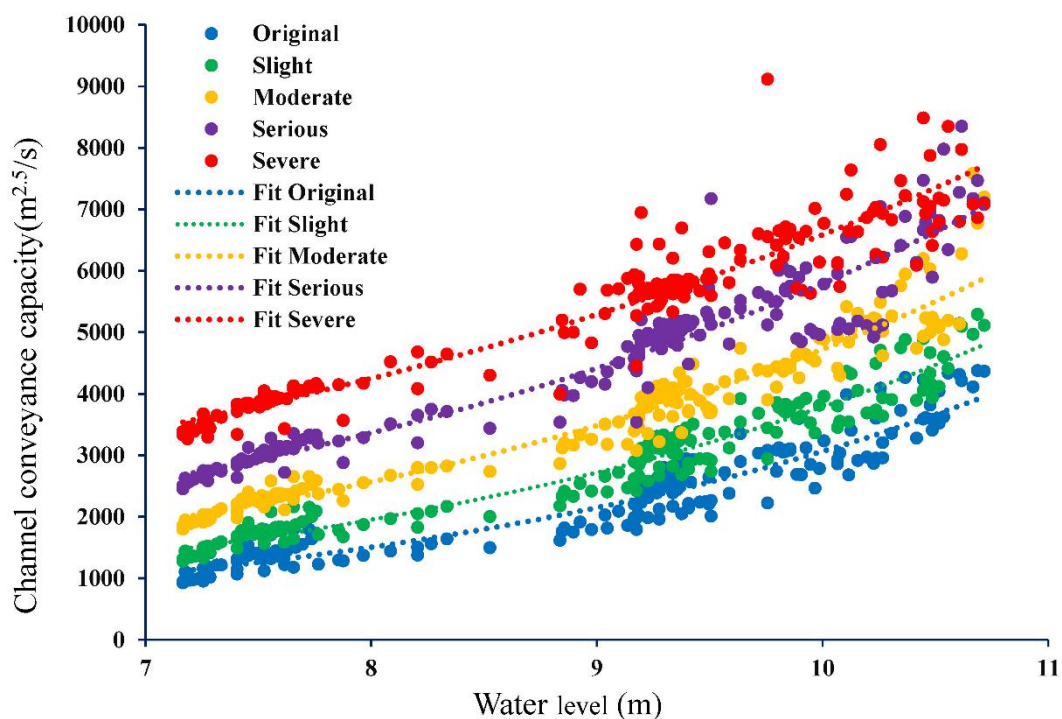


Figure 8. The impact of channel erosion on the relationship between the lake conveyance capacity and Hukou water level during the low water period

During the wet period, outflow discharge tended to decrease. During this period, the water head between the southern upstream and the northern downstream in Poyang Lake decreased dramatically (an average of 1.0 m from Kangshan to Hukou). Simultaneously, higher water levels in the Yangtze River significantly enhanced the blocking effect to Poyang Lake outflow. The changing hydraulic conditions and lake volume caused by channel morphological variations altered the regulation process, thereby affecting the river-lake interaction and outflow discharge. A quantitative analysis of the lake's water balance can be expressed as *Equation 4*:

$$\Delta V = I - Q \quad (\text{Eq.4})$$

where Q is the outflow at Hukou, I is the inflow of Poyang Lake, and ΔV is the change in lake water storage (positive for volume increase). *Figure 9a* shows a good-fit linear relationship between the lake volume (V) and water level (Z) during high water period. Therefore, the change in lake water storage can be represented as a curve differential coefficient (*Eq. 5*).

$$\Delta V = \Delta f(Z) / \Delta Z \quad (\text{Eq.5})$$

The relationship between lake water storage and water levels before channel erosion and after severe channel erosion is shown in *Figure 9b*, which indicates that channel erosion altered the lake volume change rate. In the four channel erosion scenarios, the change in lake volume caused by per meter variation in water level at Hukou increased $1.7 \times 10^7 \text{ m}^3$, $2.8 \times 10^7 \text{ m}^3$, $3.6 \times 10^7 \text{ m}^3$, and $4.1 \times 10^7 \text{ m}^3$, respectively. During the high water period, the lake pondage of inflows (Huang, 2011) increased by $3.8 \times 10^8 \text{ m}^3$, $5.8 \times 10^8 \text{ m}^3$, $7.3 \times 10^8 \text{ m}^3$, and $8.2 \times 10^8 \text{ m}^3$, respectively. Thereby, outflow discharge to the Yangtze River decreased.

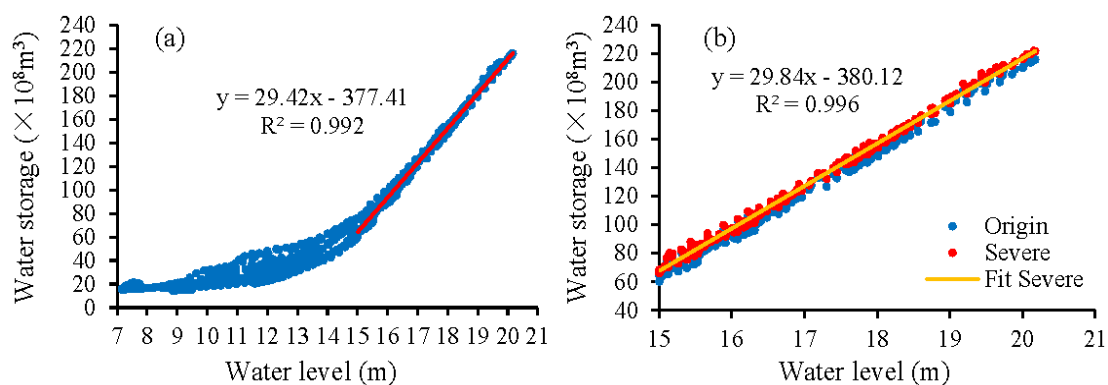


Figure 9. a Relationship between water storage in Poyang Lake and water level at Hukou, and there is a good-fit linear relationship during high water period. **b** The changing relationship between the lake water storage and Hukou water level under severe channel erosion condition during high water period

Furthermore, a larger storage capacity and lower water levels in the lake theoretically increased the backflow frequency and volume from the Yangtze River towards Poyang Lake (Gao et al., 2014). During the simulation period, backflow occurred from August

23 to August 26, 2002, and the volume of backflow was approximately $3.2 \times 10^8 \text{ m}^3$. In our four different intensities of channel erosion scenarios, the backflow volume increased to $3.3 \times 10^8 \text{ m}^3$, $4.5 \times 10^8 \text{ m}^3$, $4.6 \times 10^8 \text{ m}^3$, and $5.1 \times 10^8 \text{ m}^3$, respectively. The backflow occurred 3 days in advance under severe channel erosion conditions. Therefore, channel erosion has a significant influence on the water exchange between the Yangtze River and Poyang Lake.

Changes of wet-dry characteristics

Poyang Lake shows significant seasonal variations, alternating between wet and dry periods. Using six decades (1952-2011) of observed water level data from Duchang station, the representative hydrological station of Poyang Lake, Min and Zhan (2012) divided the dry period into five low-water level statuses, including a general low-water level ($11.8 \text{ m} < H \leq 12.8 \text{ m}$), a moderate low-water level ($10.8 \text{ m} < H \leq 11.8 \text{ m}$), a serious low-water level ($9.8 \text{ m} < H \leq 10.8 \text{ m}$), a severe low-water level ($8.8 \text{ m} < H \leq 9.8 \text{ m}$) and an extreme low-water level ($H \leq 8.8 \text{ m}$). The wet-dry characteristics are closely associated with water supply, irrigation and shipping. During the simulation period, water level at Duchang station varied from 9.90 m to 20.12 m, encompassing the low-water level status except for severe and extreme low-water level.

Figure 10 shows the alteration of wet and dry periods in Poyang Lake during 2001 and 2002. The results imply that channel downcutting made the dry period start earlier and end later, resulting in a longer dry period and an emergence of lower water levels. As bottom erosion increased the outflow channel conveyance capacity and the hydraulic slope from the channel to the floodplain area, the transitional process from dry to wet slowed down. The date the dry period ended in 2001 and 2002 was delayed 6 to 27 days under different channel erosion intensities. Generally, the time delay increased with the channel erosion depth. The effect in drier years was more significant as less water supply was available to supplement the water loss in the lake. Moreover, the results indicate an earlier arrival of the dry period due to larger bottom slope that accelerated water drainage to the channel. The date the dry period started in 2001 and 2002 advanced 1 to 5 days. The two effects of channel erosion on wet-dry characteristics extended the dry period time in Poyang Lake.

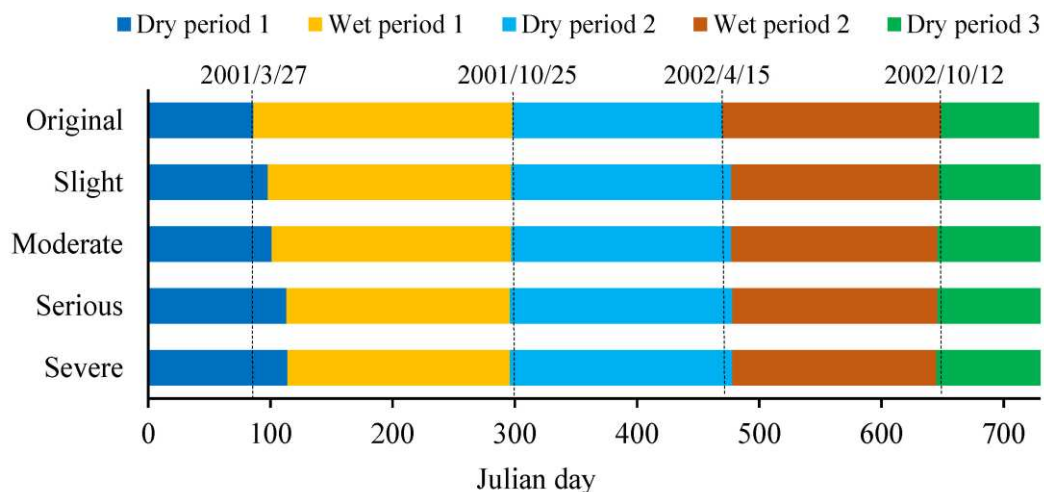


Figure 10. Comparison of the distribution of wet and dry periods in 2001 and 2002 without or under different channel erosion intensities

Furthermore, days of general low-water level (T1 in Fig. 11), moderate low-water level (T2 in Fig. 11) and serious low-water level (T3 in Fig. 11) displayed on an upward trend with an increase in the channel erosion intensity. Cumulative days of general low-water level increased 15%, 22%, 28%, and 32%, respectively under slight, moderate, serious, and severe channel erosion conditions. In addition, moderate low-water level days increased 47%, 63%, 81% and 92%, respectively. In particular, days of serious low-water level were 5.2 to 14.6 times that before channel downcutting. The results under severe channel erosion show that the frequency of serious low-water level increased dramatically from 1.5 to 23.6%. Additionally, the lowest water levels over the runtime decreased 0.23 m, 0.54 m, 0.68 m, and 0.73 m. Extreme low water level may occur as the bottom elevation of the channel decreases.

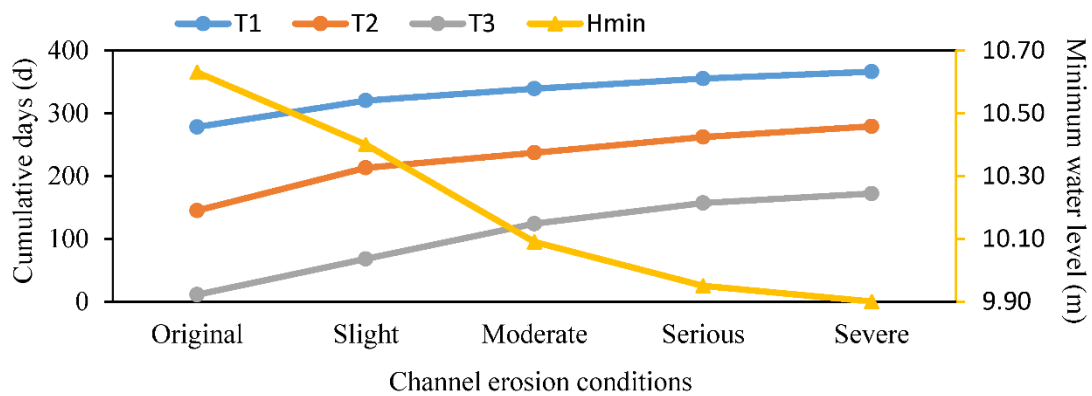


Figure 11. Cumulative days of low-water level and lowest water level under different channel erosion conditions. T1, T2, and T3 represent cumulative days of general low water level, moderate low water level, and serious low water level during the simulation period. H_{min} is the minimum water level occurred at Duchang station

Discussion

A long-term examination of lake water levels conducted by Min and Zhan (2012) and trend testing of lake water levels conducted by Zhang et al. (2014) showed that water levels of Poyang Lake were significantly lower during the 2000s. In addition to the influence of variations in Yangtze River water regime, local catchment precipitation, lake inflow runoff (Hu et al., 2007; Zhang et al., 2012; Feng et al., 2012b; Liu et al., 2013), the changes in bottom topography were identified as one of the influential factors (Lai et al., 2014; Yao et al., 2018). Our study further investigated the spatiotemporal impact of channel erosion on the hydrological and hydrodynamic characteristics. The results of this work agreed with the previous studies, which suggested that decreases in channel elevation lead to lower water levels in the lake during the dry period. An assessment of the lake water level variations indicated significant spatiotemporal heterogeneity in channel erosion impact. Water surface elevation during the dry period near the channel decreased most and water levels in the middle of the lake near Duchang and the floodplain area in the eastern and southern part of the lake were evidently affected. In contrast, water levels during the wet period were almost unaffected. Thus the influences of topography changes on specific low-water regimes in the lake needs further evaluation combined with the spatiotemporal characteristics of the events. The results from the simulation of different channel erosion intensities

showed that the reduction of water levels increased with the downcutting depth of the watercourse. Lower water levels, especially during the dry period, potentially caused great water intake difficulties for industry, agriculture and living organisms. With the influence of both climate changes and human activities, dramatic changes in water regime and hydro-environment have occurred in many shallow waters (Ma et al., 2010; Feng et al., 2012; Gosling et al., 2016; Lu et al., 2019; Zhou et al., 2019). Topography changes were often ignored in water balance analysis, as much effort was expended on the changes of inflow volume and outflow boundary conditions. However, topography changes can also induced significant variations in hydrological and hydrodynamic processes. Thus consideration of topography changes and their impacts promote understanding of the water regime fluctuation and assist management of water resources.

Erosion in the outflow channel influenced water exchanges between the Yangtze River and Poyang Lake. The results in this study suggest that outflow discharge during the dry period was larger after channel erosion, which agreed with the analysis of Lai et al. (2014). The increase in outflow discharge from Poyang Lake enhanced the emptying effects (Zhang et al., 2012), which may lead to a drier lake environment. Moreover, larger outflow discharge increased the sediment load from the lake, which in turn decreased the bottom of the lake basin. Gao (2014) investigated the sand budget between Poyang Lake and Yangtze River and stressed that sediment load from the lake over the low-water period increased by 10.08 Mt during the 2003-2010 owing the outflow discharge increase. Our study further analyzed the impact of channel erosion on lake-river interactions during the high water period, which was not considered in previous studies. The results indicated that channel erosion increased the regulation capacity of Poyang Lake during the wet period, therefore increasing the pondage volume of inflows. The increase in regulation capacity of Poyang Lake reduced outflow discharges into the Yangtze River during the flooding period and it reduced the flood pressure of downstream. In addition, channel erosion facilitated backflow from the Yangtze River to Poyang Lake. The increase of backflow frequency and volume altered the exchange of suspended sediments and nutrients between Poyang Lake and the Yangtze River, which further affected ecological processes. Cui (2009) estimated the spatiotemporal effects of backflow on the water clarity in Poyang Lake by satellite images. As the river water contains a higher concentration of sediment, the increase of backflow would result in decline of water clarity in the northern and central lake. The changing lake-river interaction has a vitally important influence on water regimes in Poyang Lake, as well as the hydro-environment.

Further studies on changes of the wet-dry characteristics indicated that channel erosion may have a substantial influence on vegetation and ecosystems. An extension of the dry period would affect vegetation growth since water is a critical factor for vegetation growth. Moreover, as the water demand for growth varies for different vegetation, changes in the growth environment may also alter the competitive advantage of different species, causing related ecological and environmental problems. Wu (2017) found that the early arrival of dry period caused the expanding of *Phalaris* to mudflat zone in Poyang Lake after 2000. Longer duration and lower water levels of the dry period resulted in sharp decrease of lake grass land and increase of woodland and reed (Yang et al., 2016). Additionally, long dry periods are not beneficial to water self-purification, and increases the risk of water pollution. Ni (2015) examined the effects of hydrological conditions on organic phosphorus and found that the prolonged dry period

caused a longer exposed time of sediments and resulted in a higher concentration of organic phosphorus. Therefore, variations in hydrological and hydrodynamic processes induced by topography changes deserve attention for maintaining reasonable conditions for the hydro-environment.

Conclusions

This study assessed the spatiotemporal impacts induced by topography changes, specifically channel erosion, on hydrological and hydrodynamic characteristics in China's largest freshwater lake, Poyang Lake. A hydrodynamic model was used to simulate hydrodynamic processes under different erosion intensities. The spatiotemporal impacts of channel erosion on water levels, water distribution, lake-river interactions, and wet-dry characteristics were assessed. The results show that channel erosion induced variations in hydrological and hydrodynamic characteristics in Poyang Lake with spatiotemporal heterogeneity. The channel erosion caused lower water levels in the lake, and the reduction in water level was enhanced due to stronger erosion intensity. The decrease in water level was significant during the dry period, whereas it was negligible during the wet period. The topographical changes affected water levels the most in the northern channel with an average water level decrease of 0.9-1.1 m during the dry period. Water levels in the central and eastern part of the lake decreased by an average of 0.27 m and 0.20 m, respectively, during the rising water and receding water period. In contrast, the water level decreased an average of ≤ 0.1 m in the southern lake. Moreover, the water surface slope changed and further influenced the distribution of water by gathering water to the channel from nearby floodplain areas. Furthermore, the topographic changes affected the exchange of water between Poyang Lake and the Yangtze River, as well as interactions between Poyang Lake and inflow tributaries. During the dry period, the channel conveyance capacity increased by 25-136%, resulting in a larger outflow discharge into the Yangtze River. In contrast, during the wet period, the regulation capacity increased the pondage volume of inflows by $3.8\text{-}8.2 \times 10^8 \text{ m}^3$, decreasing outflow discharges. In particular, the backflow frequency and volume from the Yangtze River to Poyang Lake increased after channel erosion during the flooding period of the Yangtze River. Additionally, the hydrological and hydrodynamic changes increased the duration of the dry period of Poyang Lake and significantly increased the frequency of the low water regime events. The decreased minimum water level in the lake indicated that Poyang Lake faced more serious drought conditions after channel erosion.

Results in this study indicate that topographic changes have substantial impacts on flow patterns and material transportation in shallow waters such as Poyang Lake. Hydrological and hydrodynamic changes, resulting in water shortage and ecological problems in shallow water, are not only associated with inflow water regime and outflow conditions, but also significantly influenced by topographic changes. Bathymetry monitoring would provide fundamental data for assessment of topographic variations caused by natural factors and human activities, which supports further studies on the hydrological and environmental impacts induced by topography changes. Extensive sand mining is a critical cause of channel erosion in Poyang Lake. The lower water level and extended dry period, in turn, aggravates scour of the channel bottom. Thus, supervision of human activities such as sand dredging in the lake is necessary. The numerical simulation method provided in this study to analyze hydrological and

hydrodynamic changes can be extended to other rivers or lake basins, where significant topographic changes such as erosion and deposition occur. Further study should investigate the impacts of topography changes on water quality and eco-hydrological environment, coupling the water quality models and ecological models. Reproduction and prediction with numeric models can inform quantitative assessment of the impacts of topography deformation, supporting analysis of water resource and management decisions of the watershed.

Acknowledgements. This work was funded by the National Key Research and Development Program (2017YFB0504103), the National Natural Science Funding of China (NSFC) (41331174), the Open Foundation of Jiangxi Engineering Research Center of Water Engineering Safety and Resources Efficient Utilization (OF201601), the Fundamental Research Funds for the Central Universities (2042018kf0220) and the LIESMARS Special Research Funding. We would thank the Delft Hydro-Morphodynamics for providing open source code of Delft3D-Flow.

REFERENCES

- [1] Cai, X., Gan, W., Ji, W., Zhao, X., Wang, X., Chen, X. (2017): Optimizing remote sensing-based level–area modeling of large lake wetlands: case study of Poyang Lake. – *IEEE Journal of Selected Topics in Applied Earth Observations and Remote Sensing* 8(2): 471-479.
- [2] Cui, L., Wu, G., Liu, Y. (2009): Monitoring the impact of backflow and dredging on water clarity using MODIS images of Poyang Lake, China. – *Hydrological Processes* 23(2): 342-350.
- [3] Delft Hydraulics (2014): *Delft3d-Flow User Manual: Simulation of Multi-Dimensional Hydrodynamic Flows and Transport Phenomena, Including Sediments*. – Deltares, Delft, The Netherlands, pp.1-683.
- [4] Feng, L., Hu, C., Chen, X., Li, R., Tian, L., Murch, B. (2011): MODIS observations of the bottom topography and its inter-annual variability of Poyang Lake. – *Remote Sensing of Environment* 115(10): 2729-2741.
- [5] Feng, L., Hu, C., Chen, X., Cai, X., Tian, L., Gan, W. (2012a): Assessment of inundation changes of Poyang Lake using MODIS observations between 2000 and 2010. – *Remote Sensing of Environment* 121(2): 80-92.
- [6] Feng, L., Hu, C., Chen, X. (2012b): Satellites capture the drought severity around China's largest freshwater lake. – *IEEE Journal of Selected Topics in Applied Earth Observations and Remote Sensing* 5(4): 1266-1271.
- [7] Gao, J., Jia, J., Kettner, A. J., Xing, F., Wang, Y. P., Xu, X. N., Yang, Y., Zou, X., Gao, S., Qi, S., Liao, F. (2014): Changes in water and sediment exchange between the Changjiang River and Poyang Lake under natural and anthropogenic conditions, China. – *Science of the Total Environment* 481(1): 542-553.
- [8] Gosling, S. N., Arnell, N. W. (2016): A global assessment of the impact of climate change on water scarcity. – *Climate Change* 134: 371-385.
- [9] Hu, Q., Feng, S., Guo, H., Chen, G., Jiang, T. (2007): Interactions of the Yangtze River flow and hydrologic processes of the Poyang Lake, China. – *Journal of Hydrology* 347(1): 90-100.
- [10] Huang, S. Y. (2011): *Research on Poyang Lake's pondage action under extreme flood encountering*. – Master Thesis, Nanjing University, Nanjing.
- [11] Lai, X., Jiang, J., Huang, Q., Xu, L. (2011): Two-dimensional numerical simulation of hydrodynamic and pollutant transport for lake Poyang. – *Journal of Lake Science* 23(6): 893-902.

- [12] Lai, X., Shankman, D., Huber, C., Yesou, H., Huang, Q., Jiang, J. (2014): Sand mining and increasing Poyang Lake's discharge ability: a reassessment of causes for lake decline in China. – *Journal of Hydrology* 519: 1698-1706.
- [13] Leeuw, J. D., Shankman, D., Wu, G., Boer, W. F., Burnham, J., He, Q., Yesou, H., Xiao, J. (2010): Strategic assessment of the magnitude and impacts of sand mining in Poyang Lake, China. – *Regional Environmental Change* 10(2): 95-102.
- [14] Li, H., Chen, X., Lu, J., Zhang, P., Qi, H. D., Chen, L. (2016): Numerical simulation of suspended sediment concentration in Lake Poyang during flood season considering dredging activities. – *Journal of Lake Science* 28(2): 421-431.
- [15] Li, J., Tian, L., Chen, X., Li, X., Huang, J., Lu, J., Feng, L. (2014): Remote-sensing monitoring for spatiotemporal dynamics of sand dredging activities at Poyang Lake in China. – *International Journal of Remote Sensing* 35(16): 6004-6022.
- [16] Li, Y., Zhang, Q., Yao, J., Werner, A. D., Li, X. (2014): Hydrodynamic and Hydrological modeling of Poyang Lake catchment system in China. – *Journal of Hydrologic Engineering* 19(3): 607-616.
- [17] Liu, Y., Wu, G., Zhao, X. (2013): Recent declines in China's largest freshwater lake: trend or regime shift? – *Environmental Research Letters* 8(1): 14010-14019.
- [18] Lu, J., Zhang, L., Cui, X., Zhang, P., Chen, X., Sauvage, S., Sanchez, J. M. (2019): Assessing the climate forecast system reanalysis weather data driven hydrological model for the Yangtze River Basin in China. – *Applied Ecology and Environmental Research* 17: 3615-3632.
- [19] Ma, R., Duan, H., Hu, C., Feng, X., Li, A., Ju, W., Jiang, J., Yang, G. (2010): A half-century of changes in China's lakes: Global warming or human influence? – *Geophysical Research Letters* 37: L24106.
- [20] Malhadas, M. S., Silva, A., Leitao, P. C., Neves, R. (2009): Effect of the bathymetric changes on the hydrodynamic and residence time in Obidos Lagoon (Portugal). – *Journal of Coastal Research* 2009: 549-553.
- [21] Min, Q. (2000): Changes of morphology and water regime in Poyang Lake over the recent 50 years and its relation to reclamation. – *Advances in Water Science* 11(1): 76-81.
- [22] Min, Q., Zhan, L. (2012): Characteristics of low-water level changes in Lake Poyang during 1952-2011. – *Journal of Lake Science* 24(5): 675-678.
- [23] Moriasi, D. N., Arnold, J. G., Van Liew, M. W., Bingner, R. L., Harmel, R. D., Veith, T. L. (2007): Model evaluation guidelines for systematic quantification of accuracy in watershed simulations. – *Transactions of the ASABE* 50(3): 885-900.
- [24] Mosley, L. M. (2015): Drought impacts on the water quality of freshwater systems, review and integration. – *Earth-Science Reviews* 140(3): 203-214.
- [25] Ni, Z., Wang, S., Zhnag, L., Wu, Z. (2015): Role of hydrological conditions on organic phosphorus forms and their availability in sediments from Poyang Lake, China. – *Environmental Science and Pollution Research* 22: 10116-10129.
- [26] Oliveira, A., Fortunato, A., Rego, J. (2006): Effect of morphological changes on the hydrodynamics and flushing properties of the Obidos lagoon (Portugal). – *Continental Shelf Research* 26: 917-942.
- [27] Qi, H., Lu, J., Chen, X., Sauvage, S., Sanchez-Pérez, J. M. (2016): Water age prediction and its potential impacts on water quality using a hydrodynamic model for Poyang Lake, China. – *Environmental Science and Pollution Research* 23(13): 13327-13341.
- [28] Qi, S., Zhang, X., Wang, D., Zhu, J., Fang, C. (2014): Study on morphologic change in Poyang Lake basin caused by sand dredging using multi-temporal Landsat images and DEMs. – *The International Archives of the Photogrammetry, Remote Sensing and Spatial Information Science*, Volume XL-1, 2014. ISPRS Technical Commission I Symposium, 17-20 November 2014, Denver, Colorado, USA.
- [29] Rinaldi, M., Mengoni, B., Luppo, L., Darby, S. E., Mosselman, E. (2008): Numerical simulation of hydrodynamics and bank erosion in a river bend. – *Water Resource Research* 44: W09428.

- [30] Wu, G., Liu, Y., Fan, X. (2015): Bottom topography change patterns of the Lake Poyang and their influence mechanisms in recent 30 years. – *Journal of Lake Science* 27(6): 1168-1176.
- [31] Wu, H., Zeng, G., Liang, J., Chen, J., Xu, J., Dai, J., Sang, L., Li, X., Ye, S. (2017): Response of landscapr pattern of China's two largest freshwater lakes to early dry season after the impoundment of Three-Gorges Dam. – *International Journal of Applied Earth Observation and Geoinformation* 56(2017): 36-43.
- [32] Yang, G., Zhang, Q., Wan, R., Lai, X., Jiang, X., Li, L., Dai, H., Lei, G., Chen, J., Lu, Y. (2016): Lake hydrology, water quality and ecology impacts of altered river-lake interactions: advances in research on the middle Yangtze River. – *Hydrology Research* 47(S1): 1-7.
- [33] Yang, S., Zhang, J., Dai, S., Li, M., Xu, X. J. (2007): Effect of deposition and erosion within the main river channel and large lakes on sediment delivery to the estuary of the Yangtze River. – *Journal of Geophysical Research Earth Surface* 112: F022005.
- [34] Yao, J., Zhang, Q., Ye, X., Zhang, D., Bai, P. (2018): Quantifying the impact of bathymetric changes on the hydrological regimes in a large floodplain lake: Poyang Lake. – *Journal of Hydrology* 561: 711-723.
- [35] Zhang, L., Lu, J., Chen, X., Liang, D., Fu, X., Sauvage, S., Perz, J. S. (2017): Stream flow simulation and verification in ungauged zones by coupling hydrological hydrodynamic models: a case study of the Poyang Lake ungauged zone. – *Hydrology and Earth System Science* 21(11): 5847-5861.
- [36] Zhang, P., Lu, J., Feng, L., Chen, X., Zhang, L., Xiao, X., Zhang, L., Xiao, X., Liu, H. (2015): Hydrodynamic and inundation modeling of China's largest freshwater lake aided by remote sensing data. – *Remote Sensing* 7(4): 4858-4879.
- [37] Zhang, Q., Li, Y., Wang, Y., Werner, A. D., Xin, P., Jiang, T., Barry, D. A. (2012): Has the three-gorges dam made the Poyang Lake wetlands wetter and drier? – *Geophysical Research Letters* 39: L20402.1-L20402.7.
- [38] Zhang, Q., Ye, X., Werner, A. D., Li, Y., Yao, J., Li, X., Xu, C. (2014): An investigation of enhanced recessions in Poyang Lake: comparison of Yangtze River and local catchment impacts. – *Journal of Hydrology* 517: 425-434.
- [39] Zhou, C. W., Yang, R., Yu, L. F., Zhang, Y., Yan, L. B. (2019): Hydrological and ecological effects of climate change in Caohai watershed based on SWAT model. – *Applied Ecology and Environmental Research* 17: 161-172.

MULTIRESIDUE ANALYSIS OF OVER 233 PESTICIDES IN CUCUMBER AND GRAPEFRUIT SAMPLES USING A QuEChERS AND GAS CHROMATOGRAPHY-TANDEM MASS SPECTROMETRY-BASED METHOD

HEPSAĞ, F.

*Korkut Ata University, School of Applied Sciences, Department of Food Technology
Kadirli Campus, 80750 Osmaniye, Turkey*

*ORCID ID: 0000-0002-3688-4106; e-mail: fatmahepsag@osmaniye.edu.tr
phone: +90-328-888-0090; fax: +90-328-888-0091*

(Received 15th Feb 2019; accepted 8th Apr 2019)

Abstract. This report describes the 233 pesticide residue in cucumber and grapefruit sold in Turkey. In total, 680 fruit and vegetable samples were analyzed by liquid chromatography connected to tandem mass spectrometry (LC-MS / MS) with the device in which gas chromatography to mass spectrometry (GC-MS) units work together. In cucumber, limit of detection (LOD) varied from 0.17 $\mu\text{g kg}^{-1}$ to 11.8 $\mu\text{g kg}^{-1}$ and the limit of quantifications (LOQ) varied from 0.42 $\mu\text{g kg}^{-1}$ to 39.35 $\mu\text{g kg}^{-1}$; whereas for grapefruit, LOD, and LOQ values varied from 0.13 $\mu\text{g kg}^{-1}$ to 11.80 $\mu\text{g kg}^{-1}$, 0.42 $\mu\text{g kg}^{-1}$, and 39.35 $\mu\text{g kg}^{-1}$, respectively. Recoveries obtained for each pesticide in both matrices ranged between 77.87% and 104.15%. Relative standard deviation (RSD) values calculated were > 20% (24.32%) for clofentazine in cucumber at 20.0 mg kg^{-1} and (21.36%) for propyzamide, (29.11%) for fludioxonil grapefruit at 100 $\mu\text{g kg}^{-1}$. For the other compounds, at both concentration levels evaluated in cucumber and grapefruit, the RSD values were < 20%. The extended measurement uncertainty for individual pesticides ranged from 0.208 to 0.434. In general, 11.6% of cucumbers and 13.8% of grapefruits contained at least one detectable residue, but levels were below the EU legal limits.

Keywords: *QuEChERS, GS-MS, LC-MS / MS, pesticide, grapefruit, cucumber*

Introduction

Pesticide is used in all kinds of chemical substances and preparations used in agricultural researches and applications. The pesticide may be a chemical agent, a biological agent such as a virus or a bacterium, an antimicrobial, a disinfectant or any other vehicle. Although the use of pesticides may have some benefits, it can cause problems for humans and other living things due to their potential toxicity. Such as pesticides, some of which include biopreparations, insect and plant growth regulators, pheromones (hormone-bearing) and other attractants, feed-blockers, repellents (insect repellents), traps, plant activators, preparations used in the treatment of physiological diseases (Epstein and Zhang, 2014).

Turkey is the 4th largest fresh fruit and vegetable producers in the world. As of 2015, about 37% of the total production of the citrus group consisting of lemon, orange, mandarin and grapefruit (3.7 million tons) and cucumber (100 thousand tons) accounted for approximately 2.8% of exports. Almost all of the total value of exported fresh fruits and vegetables has entered the EU, Russian Federation, Ukraine and Iraqi markets (TUIK, 2015; FAO, 2015).

In food, the permissible residual limit values are as low as in parts per million (ppm) and in parts per billion (ppb). Therefore, it is accepted that the most effective approach in pesticide residue analysis is multiresidue analyzes. In recent years, many different methods have been successfully used in the detection of pesticide residues in

foods, especially fruits and vegetables. In order to use these methods gas chromatography (GC), liquid chromatography (LC), coupled to mass selective detectors (MS), many new sample preparation techniques and extraction methods have been developed. Many sample preparation techniques for the detection of many pesticides used in vegetables and fruits, including solid-phase extraction (SPE) (Campone et al., 2018; Chan et al., 2018), solid-phase microextraction (SPME) (Li et al., 2019; Dong et al., 2019), accelerated solvent extraction (ASE) (Su et al., 2018; Stachniuk, 2018), supercritical fluid extraction (SFE) (Alvarez et al., 2019; Khan et al., 2018), matrix solid-phase dispersion (MSPD) (Liu et al., 2018; Jiang et al., 2018), microwave-assisted extraction (MAE) (Du et al., 2018; Wang et al., 2018), membrane extraction (Salemi et al., 2019), gel permeation chromatography (GPC) (Zhu et al., 2019), and QuEChERS (quick, easy, cheap, effective, rugged and safe) method (Tankiewicz, 2019), have been used. Within these techniques, QuEChERS has become more preferred in recent years, because it reduces the use of solvents in accordance with the 'green chemistry' principles, and provides a simple, inexpensive, fast and reliable result.

In this study, 205 pesticides of different classes, which are suitable for LC-MS/MS analysis, and 28 pesticides for GC-MS analysis, were discussed. In our country, pesticide use is still indispensable within the framework of integrated pest management principles. Selected pesticides, widely used in the production stages of fruits and vegetables in Turkey. Some of the selected pesticides may cause acute and chronic diseases due to their toxicity (Kumar et al., 2018).

In Turkey, along with concepts such as food security, have been a lot of studies in a very food production due to the increased use of pesticides. For example, tomatoes (Cengiz et al., 2018), baby foods (Kilic et al., 2018), oranges (Golge and Kabak, 2015), fish products (Polat et al., 2018), apricots (Ersoy et al., 2018), olive oil (Razzaghi et al., 2018) and milk (Yıldırım et al., 2018). However, there are very little data about the presence and levels of pesticide residues in cucumber and grapefruit consumed in Turkey.

This report aims to determine multi-residue pesticides in cucumber and grapefruits consumed in Turkey, monitor the compliance of the fruit and vegetables with the legal limits for target pesticide residues. In this context, the validated analytical method based on gas chromatography to mass spectrometry (GS-MS) and liquid chromatography coupled with tandem mass spectrometry (LC-MS/MS) was applied to 680 samples for a total of 233 pesticides for the periods 2015–2017.

Material and Method

Sample collection

A total of 680 fruit and vegetable samples, including 330 cucumber and grapefruits 350 samples, were obtained from three provinces of Turkey, namely Hatay, İskenderun, Adana, Mersin and Antalya. Approximately 2 kg of cucumber and grapefruit samples were supplied from bazaar, supermarkets (2015–2017). The vegetables were transported quickly to the laboratory, chopped and homogenised with a home food processor (Robot Coupe model R10, Turkey). The chopped samples were then stored at -18°C until sample preparation step.

Reagents and chemicals

Standards of pesticides detected in GC-MS were supplied from ChemService (West Chester, PA, USA) and Standards of pesticides detected in LC-MS/MS from Sigma – Aldrich (St. Louis, MO, USA). All standards were of $\geq 98\%$ purity. Stock solution of multistandard mixture at a concentration of 10 mg L^{-1} for each substance was dissolved in acetonitrile and kept at -18°C in the dark. This solution was used for preparation of matrix-matched calibration standards at concentrations varying from 0.1 to $100 \text{ }\mu\text{g kg}^{-1}$ and for spiking the QuEChERS extracts in validation study.

Acetone, acetonitrile and methanol (GS-MS and LC-MS/MS grade), Isooctane, cyclohexane, ethyl acetate, magnesium sulphate, sodium acetate, glacial acetic acid, formic acid and ammonium formate (purity $\geq 99.9\%$) were supplied from Sigma – Aldrich (Stenheim, Germany). Helium (purity $\geq 99.9\%$) was supplied by Praxair (Colima, Mexico). Ultrapure water of $18.2 \text{ M}\Omega$ was purchased using a Milli Q water purification system (Milford, MA, USA). The primary-secondary amine (PSA) was supplied from Supelco (Darmstadt, Germany).

Sample preparation

Pesticide residues were extracted from cucumber and grapefruit samples using QuEChERS protocol according to AOAC official method (AOAC, 2007) with some changes. Cucumber representing high water content product groups, grapefruit with high acid and high water content groups were selected as samples for this study. These vegetable and fruit were selected because of their economic importance in export. Fifteen grams of homogenised sample was placed in to a 50 mL polypropylene tube, then 15 mL methanol-acetic acid (99:1, v/v), 6 g MgSO_4 and 1.5 g sodium acetate were added. The mixture was shaken vigorously by vortex mixer (Vortex Jr. Mixer from American Scientific Products, catalog no. S82251-1) for 1 min and centrifuged (Eppendorf 022628225 5804R Centrifuge with A-2-DWP-Plate, Germany) for 2 min at 2000 rpm. Later, 8 mL of the upper methanol phase was added in a 15 mL polypropylene tube containing 900 mg of MgSO_4 and 150 mg of PSA. The mixture was vortexed for 1 min, followed by centrifugation for 2 min at 2000 rpm. For each sample, 200 μL was injected into GS-MS and LC-MS / MS.

For GC-MS, 0.010, 0.025, 0.05, 0.1, 0.2, 0.5 and 1 ppm prepared standards were given to the device and the corresponding area and retention time were determined. Calibration curve is obtained by plotting the area graph against concentration. For LC-MS/MS, 0.005, 0.010, 0.020, 0.040, 0.080 and 0.160 ppm prepared standards were delivered to the device and the area corresponding to these concentrations and retention time were determined. The fortified samples were released to equilibrate for 80 minutes before treatment. Blank samples were also prepared according this procedure.

GC-MS conditions

Analyses were carried out with a Agilent GC-MS, 5975C inert MSD Series gas chromatograph equipped with an MS detector. The system was equipped with capillary column (Rtx-440 GC). Oven start temperature was set at 110°C , increased to 250°C at a rate of $35^\circ\text{C}/\text{min}$, increased again at a rate of $40^\circ\text{C}/\text{min}$ to 280°C , this temperature was kept for 3 minutes. The total run time was 5.5 minutes. One mL of sample was injected in split mode (2:1). The injector temperature was set at 250°C .

The helium carrier gas flow was 1.1 mL/min. The mass spectrometer was operated in electron impact ionization mode at 70 eV of collision energy with 2 minute solvent delay to prevent damage to the filament of the ion source. The temperature of the ion source, manifold, and transfer line was set at 250°C, 40°C, and 280°C, respectively. For qualitative analysis a full scan from 75 mass/charge (m/z) to 280 mass/charge (m/z) was applied. For quantitative pesticide analysis preferred ion monitoring (SIM) mode was used.

LC-MSMS conditions

Analyses were carried out with a ThermoQuest Surveyor MS Pump and autosampler. Chromatographic separation was carried out on a Waters C18 analytical column Phenomenex LUNA 5 µm C18 150 x 2 mm from Phenomenex (Torrance, CA, USA). The system was controlled by Xcalibur Home Page, Version 1.2 software. The column temperature was set at 40°C. The solvent systems used were (A) 0.1% acetic acid and 10 mM ammonium acetate in water and (B) 0.1% acetic acid and 10 mM ammonium acetate in 95:5 CH₃CN:Water. A flow rate of 200 µL min⁻¹ and an injection volume of 10 µL were applied.

The MS was operated using a Negative Ion Electrospray – with metal needle option. The metal needle was connected with a zero dead volume union to the fused silica capillary delivering the mobile phase to the ESI source. Device parameters optimized for MS are as follows. Precursor ion (m/z): 321, product ions (m/z): 257, 194, 176, 152, spray voltage: 1.5 kV, collision voltage: 26 V, source offset voltage: 5 V, electron multiplier voltage: 1.27 kV, capillary temperature: 350 C, N₂ sheath gas: 80 arbitrary units, N₂ auxiliary gas: 35 psi, collision gas: Ar.

Method validation

The proposed method was validated following the European SANTE/11945/2015 Guideline (European Commission, 2015). The established GC-MS and LCMS-MS method were validated in terms of its linearity, limit of detection (LOD), limit of quantification (LOQ), selectivity and recovery. Linearity was evaluated by constructing calibration curves with standard solutions.

Limit of detection (LOD), limit of quantification (LOQ)

For detection limit of detection (LOD) and limit of quantification (LOQ) operation; In GC-MS, 20 µg kg⁻¹ kg and LC-MS/MS 10 µg kg⁻¹ recovery was performed. 205 pesticides were injected 10 times with the LC-MS/MS device and 28 pesticide GC-MS devices. The LOD values and LOQ values were calculated according to the following formula: LOD = 3s, LOQ = 10s, s: Standard deviation.

Linear measurement range

In order to determine the linear measurement range; Standards for 10 different concentrations (5, 10, 20, 40, 80, 160 µg kg⁻¹) for LC-MS / MS, 7 different concentrations for GC-MS (10, 25, 50, 100, 200, 500, 1000 µg kg⁻¹) prepared, injected into devices and calibration graphs are drawn.

Precision

Repeatability

For repeatability study; A total of 40 recovery studies were performed by 4 analysts for GC-MS at a concentration of 20 $\mu\text{g kg}^{-1}$ and 100 $\mu\text{g kg}^{-1}$, for LC-MS/MS at concentrations of 10 $\mu\text{g kg}^{-1}$ and 100 $\mu\text{g kg}^{-1}$, each with 5 replicates.

For repeatability control, RSD% values were calculated for each person and for each concentration separately. For each individual and for each concentration, the RSD values were calculated from the mean (\bar{x}) and standard deviation (s) of the measured concentrations, separately. Then the RSD_{pool} values were calculated and the repeatability control was performed: $\text{RSD} = \frac{s}{\bar{x}} \cdot 100$

Reproducibility

Intra-laboratory reproducibility study; 20 $\mu\text{g kg}^{-1}$ and 100 $\mu\text{g kg}^{-1}$ for GC-MS, LC-MS/MS at concentrations of 10 $\mu\text{g kg}^{-1}$ and 100 $\mu\text{g kg}^{-1}$, by 4 analysts for each at five different times, recovery work, was carried out. For each concentration, RSD_{WR} values were calculated and reproducibility checked.

Accuracy

Reality study for accuracy was done with recovery. For the reality parameter; A total of 40 recovery studies were carried out by 4 analysts at concentrations of 20 $\mu\text{g kg}^{-1}$ and 100 $\mu\text{g kg}^{-1}$ for GC-MS 10 $\mu\text{g kg}^{-1}$ and 100 $\mu\text{g kg}^{-1}$ for LC-MS/MS each. For reality control, all recovery values must be in the range of 70-120%.

Percentage recovery (%R) values were calculated for each individual, each concentration and each repetition. $\%R = \frac{(C2-C1)}{C3} \cdot 100$, C1: Measured sample concentration (blank), C2: Measured, spike made sample concentration (blank+spike), C3: Spike made concentration.

Uncertainty assessment

The standard uncertainty (u_x) from reality is equal to the standard deviation ($S_{\bar{x}}$) of the mean, if the unit average recovery value (\bar{R}) is not significantly different from 1. t test deđer was applied to determine if the unit mean recovery value was significantly different from 1.

- If $t < t_{\text{table}}$, then the reality standard uncertainty (u_x) is equal to the, mean deviation ($S_{\bar{x}}$) of the mean.
- If $t \geq t_{\text{table}}$, the elevated standard uncertainty (u_i) value should be calculated.

$$u_i = \sqrt{(|1 - \bar{R}|/k)^2 + (u_x)^2} \quad (\text{Eq.1})$$

where

k: Scope factor (k = 2, for 95% confidence interval)

\bar{R} : Unit average recovery value.

$$\bar{R} = \frac{\% \bar{R}}{100} \quad (\text{Eq.2})$$

$$S_{\bar{x}} = \frac{s}{\sqrt{n}} \quad (\text{Eq.3})$$

$$t = \frac{|1 - R|}{S_{\bar{x}}} \quad (\text{Eq.4})$$

where

$S_{\bar{x}}$: Standard deviation of mean

s: Standard deviation

n: Total concentrations and total number of repetitions for all contacts.

In cucumber and grapefruit, the standard uncertainty from reality and the relative standard uncertainty were calculated using the *Equations 1, 2, 3 and 4*.

$$RSD_{pool} = \sqrt{\frac{(n_1-1) \times RSD_1^2 + (n_2-1) \times RSD_2^2 + \dots + (n_n-1) \times RSD_n^2}{(n_1-1) + (n_2-1) + \dots + (n_n-1)}} \quad (\text{Eq.5})$$

In cucumber and grapefruit, relative standard uncertainty from repeatability was calculated using *Equation 5*.

$$RSD_{WR(pool)} = \sqrt{\frac{(n_1-1) \times RSD_{WR1}^2 + (n_2-1) \times RSD_{WR2}^2}{(n_1-1) + (n_2-1)}} \quad (\text{Eq.6})$$

In cucumber and grapefruit, standard uncertainty from reproducibility was calculated using *Equation 6*. Relative standard uncertainty values are used in the total combined uncertainty calculation; however, since the relative standard deviation values are already used in the reproducibility calculations as in the reproducibility uncertainty calculations, the calculated standard uncertainty value is also equal to the relative standard uncertainty value.

Results and discussion

Method validation and application

Selectivity was evaluated by checking the presence of coextracted interferences in the chromatograms from blank samples. Hence, chromatograms of blank and fortified (100 µg/kg) samples of cucumber and grapefruit were compared (*Figure 1*). The presence of matrix interferences were interpreted by monitoring the SIM chromatograms for each pesticide at the retention time window expected for each compound. It can be observed that there are no extracted matrix interferences for the determination of the pesticides studied in both fruits; therefore this method can be considered as selective.

The matrix compatible standard calibration curves showed smooth linearity over a concentration range of 20- 100 µg kg⁻¹. As shown in *Figure 2*, correlation coefficients were > 0.98. The values of Limits of detection (LOD) ranged from 0.17 to 11.8 µg kg⁻¹ and Limits of quantification (LOQ) ranged from 0.42 to 39.35 µg kg⁻¹ in cucumber, whereas for grapefruit, LOD, and LOQ values varied from 0.13 µg kg⁻¹ to 11.80 µg kg⁻¹, 0.42 µg kg⁻¹, and 39.47 µg kg⁻¹, respectively.

The baseline (basal signal) in blank samples at the time window in which each pesticide is expected is different due to the quantification being made using different

ions. Therefore, the LOD and LOQ calculation are different for each compound. With these results it can be concluded that the method has good sensibility for cucumber and grapefruit fruits because LOD and LOQ values of all pesticides are <0.50 mg / kg. The LOQ were well below the maximum residue levels (MRL) established by European Union for regulated pesticide residues both in cucumber and grapefruit, except for methylparathion, malathion and diazinon.

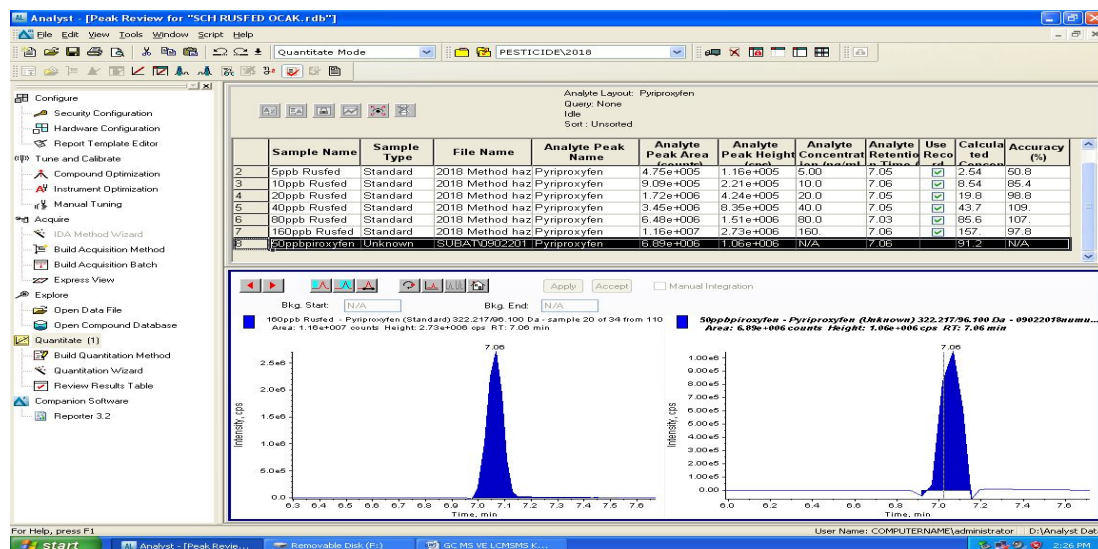


Figure 1. Chromatograms (SIM mode) obtained for pyriproxyfen injection of blank and fortified samples of cucumber and grapefruit for checking matrix interferences. Pesticide concentration was $100\mu\text{g/L}$

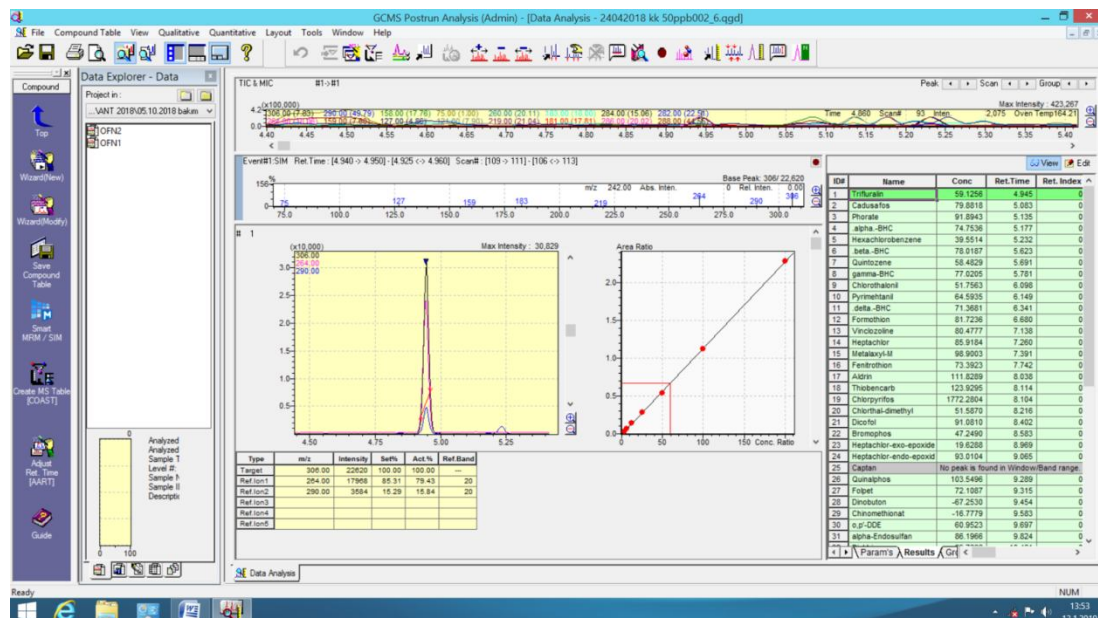


Figure 2. Chromatograms (SIM mode) obtained for trifluralin injection of blank and fortified samples of cucumber and grapefruit for checking matrix interferences. Pesticide concentration was $100\mu\text{g/L}$

The recovery values correspond to the lowest and highest concentration of the linear range. The recovery results are as shown in *Table 1*. Recoveries obtained for each pesticide in both matrices ranged between 77.87% and 104.15%. Thus, the recovery data is in the range of values required by the SANTE Guidelines, which recommends a recovery rate of 70-120% (European Commission, 2015).

Precision was expressed as relative standard deviation (RSD) and evaluated in different days (see *Table 1*). For this purpose, 20 $\mu\text{g kg}^{-1}$ and 100 $\mu\text{g kg}^{-1}$ for GC-MS, LC-MS / MS at concentrations of 10 $\mu\text{g kg}^{-1}$ and 100 $\mu\text{g kg}^{-1}$, by four analysts for each at five different times, recovery work, was carried out. Relative standard deviation (RSD) values calculated were > 20% (24.32%) for clofentazine in cucumber at 20.0 mg kg^{-1} and (21.36%) for propyzamide, (29.11%) for fludioxonil grapefruit at 100 $\mu\text{g kg}^{-1}$. For the other compounds, at both concentration levels evaluated in cucumber and grapefruit, the RSD values were < 20%. The RSD values obtained are considered satisfactory according to the European SANTE Guideline (European Commission, 2015).

Pesticide analysis in commercial fruit and vegetable samples

The validated analytical method was used to analyse 233 pesticide residues in cucumber and grapefruit samples collected from bazaar, supermarkets in four provinces of Turkey. In our monitoring program, a total of 680 vegetable samples, including 75 cucumbers and 110 grapefruits in 2015, 90 cucumbers and 120 grapefruits in 2016, and 165 cucumbers and 120 grapefruits in 2017, were analysed. Of the 680 fruit and vegetable samples, 11.6% (35 samples) of cucumbers and 13.8% (39 samples) of grapefruits contained at least one detectable residue, but levels were below the EU MRL. There were 1 acaricide, 3 insecticides and 5 fungicides in cucumbers, while 4 insecticides and 4 fungicides were detected in grapefruit samples.

While 27 cucumber samples gave positive results, multiple pesticide residues were found in 8 samples, corresponding to 2.4% of the total samples. Clofentezine was the most frequently detected pesticide measured in cucumber with a percentage occurrence value of 4.4%, and in concentrations ranging from 0.021 to 0.042 mg kg^{-1} . This insecticide is an acaricide used in various products (fruit crops, leafy vegetables, some fruiting vegetables, citrus fruits, pome fruits, grapes, cotton etc.) against red spider species. Acaricides in this group are contact effective. They also have a gastric venom effect (European Commission, 2008; Van Leeuwen et al., 2010).

The fungicide propyzamide was the second most abundant pesticide (199 out of 330 samples) in cucumbers, with levels ranging from 0.002 to 0.009 mg kg^{-1} . Propyzamide, effectively controls a wide range of herbicides in several agricultural crops, including hard-shelled fruits, in grape fruits, and tree nuts. It has a chronic toxic effect (European Commission, 2008; Tian et al., 2018).

The fungicide propamocarb was the third most abundant pesticide (230 out of 330 samples) in cucumbers, with levels ranging from 0.022 to 0.032 mg kg^{-1} . Propamocarb, which belongs to the class of carbamate, is used in cucumber against mildew. Does not have toxic effects (FAO, 2012; Bhat et al., 2018).

Azinphosethyl was detected individually in 6 cucumber samples (1.8%) in concentrations between 0.013 and 0.016 mg kg^{-1} . It has a protective and therapeutic properties. Alternaria, Botrytis, Pythium, Rhizoctonia, Venturia and many other diseases are widely used as a fungicide. It has no acute and chronic effects (Polyiem et al., 2018).

Table 1. LOD, LOQ study results for GC-MS and LC-MS / MS

Pesticides	Cucumber						Grapefruit					
	LOD	LOQ	Precision		Recovery		LOD	LOQ	Precision		Recovery	
			RSD (%)		(%)				RSD (%)		(%)	
			20	100	20	100			10	100	10	100
(µg/kg)						(µg/kg)						
Trifluralin	8.08	26.94	7.45	8.65	101.91	88.39	1.04	19.26	9.15	12.54	101.91	87.45
Chlorothalonil	4.78	15.94	8.65	7.23	100.96	85.72	2.03	17.28	9.12	14.56	94.87	100.69
Formothion	6.37	21.25	9.21	6.14	96.5	88.88	2.96	17.14	10.12	17.85	95.67	91.24
Vinclozolin	5.76	19.2	11.45	8.74	104.15	91.82	2.38	10.89	15.14	19.63	104.15	96.78
Fenitrothion	8.27	27.58	10.54	9.65	100.6	88.4	4.99	5.98	14.12	15.36	100.6	85.92
Dicofol	5.66	18.87	9.65	7.32	103.01	92.15	3.85	10.66	11.1	19.36	103.01	88.41
Captan	7.31	24.38	13.65	7.65	102.61	83.91	4.53	10.14	13.1	18.36	102.61	90.69
Folpet	6.8	22.67	18.65	6.84	93.95	88.28	3.65	8.52	10.21	10.15	95.62	87.3
Qinomethionate	10.15	33.83	11.32	6.45	99.51	91.2	3.97	5.03	10.14	17.32	93.73	103.21
Dinobuton	11.8	39.35	9.32	6.21	98.75	89.45	5.26	15.42	9.85	18.36	94.54	92.38
Endosulfan A	7.56	25.2	8.65	7.52	99.77	88.52	3.64	6.89	7.65	11.1	99.77	99.56
Endosulfan B	7.38	24.61	7.45	6.36	101.08	89.17	2.99	3.48	12.69	11.2	101.08	91.18
Bromopropylate	7.49	24.96	14.12	15.36	102.61	78.55	4.77	6.77	11.36	10.21	102.61	88.69
Tetradifon	6.88	22.93	15.36	19.36	102.27	89.25	2.57	9.86	10.87	9.65	102.27	93.87
Alfa-Cypermethrin a	7.38	24.58	18.69	11.36	102.82	90.64	3.76	7.93	10.96	8.65	102.82	86.17
Alfa-Cypermethrin b	7.2	24.02	14.65	10.15	97.51	91.77	4.71	16.63	10.23	9.67	92.82	99.31
alpha.-BHC	3.96	13.19	15.21	17.32	98.26	91.28	3.02	12.82	10.65	8.63	98.99	97.52
delta.-BHC	5.94	19.79	17.45	18.36	99.6	88	2.46	15.11	11.23	8.65	99.6	90.54
Heptachlor	7.2	23.99	18.21	11.1	101.72	80.22	4.83	12.16	12.32	9.45	101.72	90.64
2,4-DDE	4.45	14.85	19.32	11.2	101.45	83.73	5.13	13.23	11.56	14.65	101.45	100.53
Dieldrin	4.24	14.13	18.65	10.54	98.88	83.67	5.54	17.53	11.45	19.32	98.88	90.56
4,4-DDE	5.78	19.26	15.32	14.32	101.79	94.44	3.76	12.14	10.65	18.65	101.79	89.22
2,4-DDD	4.8	16.01	11.35	12.36	99.8	88.56	4.32	9.97	9.63	15.32	99.8	93.71
Endrin	3.49	11.64	9.14	10.23	102.21	93.36	6.01	15.89	7.23	11.35	102.21	99.19
Chlorfenapylyl	5.82	19.4	8.54	17.36	100.93	90.78	4.44	8.56	9.63	9.14	100.93	93.53
4,4-DDD	4.84	16.12	11.21	14.65	102.11	95.72	4.88	12.54	10.25	8.54	102.11	99.48
Ethion	8.6	28.67	12.41	13.85	101.54	87.48	3.07	15.69	14.52	11.21	101.54	91.5
DDT	6.69	22.31	16.74	14.87	102.37	91.95	4.75	10.05	11.52	12.41	102.37	98.37
Abamectin	4.07	13.56	18.69	14.23	87.45	89.17	4.12	8.21	10.65	16.74	88.39	92.89
Acetamiprid	4.32	14.41	17.21	16.65	100.69	91.6	2.87	16.09	10.65	18.69	85.72	90.59
Acetochlor	4.2	14.01	11.32	18.98	91.24	88.53	2.42	17.09	11.23	17.21	88.88	91.85
Acrinathrin	4.75	15.82	8.14	9.47	96.78	89.55	0.49	18.45	11.25	14.32	91.82	90.79
Alachlor	5.04	16.79	7.65	8.31	85.92	89.36	3.01	12.54	10.87	12.63	88.4	91.43
Amitraz	3.23	10.75	10.14	7.54	88.41	86.21	5.85	14.41	9.63	14.36	92.15	90.31
Atrazine	2.43	8.1	14.65	7.98	90.69	93.05	3.26	20.03	8.35	12.31	83.91	94.33
Azinphos methyl	5.01	16.68	14.12	7.47	87.3	89.89	2.4	14.81	8.65	11.32	88.28	90.22
Azoxystrobin	6.17	20.58	11.25	6.32	103.21	89.93	4.97	16.27	7.65	10.63	91.2	104.09
Bensulfuron-Methyl	0.13	0.42	17.32	14.36	92.38	95.37	4.14	10.24	8.32	9.36	89.45	94.94
Bentazone	3.09	10.3	18.36	12.31	99.56	90.67	4.42	15.84	9.63	9.56	88.52	91.4
Beta-Cyfluthrin	3.39	11.3	11.1	11.32	91.18	91.11	3.51	13.73	12.54	8.36	89.17	89.6

Pesticides	Cucumber						Grapefruit					
	LOD	LOQ	Precision		Recovery		LOD	LOQ	Precision		Recovery	
			RSD (%)		(%)				RSD (%)		(%)	
			20	100	20	100			10	100	10	100
(µg/kg)						(µg/kg)						
Bifenthrin	2.09	6.96	11.2	10.63	88.69	86.67	5.55	9.57	14.56	9.1	78.55	98.32
Boscalid	4.23	14.1	10.21	9.36	93.87	88.36	5.94	8.08	17.85	9.89	89.25	92.43
Bromoxynil	2.68	8.92	9.65	9.56	86.17	87.84	3.3	1.63	19.63	8.63	90.64	87.48
Bromuconazole	4.18	13.92	8.65	8.36	99.31	90.22	4.69	10.02	15.36	9.52	91.77	92.72
Bupirimate	5.81	19.37	9.67	9.1	97.52	87.81	3.6	19.5	19.36	9.38	91.28	87.53
Buprofezine	3.56	11.87	8.63	9.89	90.54	88.94	4.66	10.86	11.36	10.54	88	89.81
Carbaryl	1.8	5.99	8.65	14.65	90.64	88	5.16	8.45	18.65	11.52	80.22	86.85
Carbendazim	1.24	4.12	9.45	12.32	100.53	93.49	4.08	16.56	11.32	7.65	83.73	83.68
Carbofuran	2.33	7.76	14.65	17.14	90.56	90.44	4.13	13.8	9.32	12.69	83.67	94.06
Carbosulfan	3.65	12.16	17.23	11.65	89.22	87.56	5.98	14.75	8.65	11.36	94.44	91.79
Carboxin	2.43	8.11	15.21	12.31	93.71	84.98	1.34	11.69	7.45	10.87	88.56	91.78
Carfentrazone-Ethyl	4.49	14.97	14.32	11.32	99.19	89.06	3.32	18.51	14.12	10.96	93.36	99.05
Chlofentazine	4.58	15.28	24.32	10.63	93.53	95.76	1.27	19.81	15.36	10.23	90.78	92.5
Chlorfluozuron	2.83	9.44	14.36	9.36	99.48	87.17	1.64	11.01	18.69	10.65	95.72	84.8
Chloridazon	4.01	13.37	12.31	9.56	91.5	96.47	4.34	15.65	14.65	11.23	87.48	95.69
Chlormequat chloride	0.65	2.17	11.32	8.36	98.37	92.06	4.99	12.14	15.21	12.32	91.95	102.17
Chlorpham	4.95	16.51	10.63	9.1	92.89	96.36	3.29	15.54	17.45	11.56	89.17	92.83
Chlorpyrifos ethyl	5.11	17.02	9.36	9.89	90.59	92.62	1.48	17.19	18.21	11.45	91.6	95.66
Chlorpyrifos Methyl	5.82	19.41	9.56	8.63	91.85	86.75	3.46	13.59	19.32	9.45	88.53	88.12
Chlorsulfuron	4.9	16.33	8.36	9.52	90.79	88.56	1.27	13.77	18.65	14.65	89.55	90.98
Clethodim	2.76	9.2	9.1	10.65	91.43	89.94	4.77	19.93	15.32	17.23	89.36	90.15
Clodinafop-Propargyl	4.97	16.57	9.89	8.36	90.31	86.66	1.28	4.47	11.35	15.21	86.21	93.05
Clothianidin	2.74	9.12	8.63	9.1	94.33	92.59	5.93	11.07	9.14	14.32	93.05	98.78
Cyclanilide	4.61	15.36	9.52	9.89	90.22	91.03	4.48	4.23	8.54	12.63	89.89	95.08
Cycloate	3.73	12.44	9.38	8.63	104.09	90.99	4.99	5.46	11.21	14.36	89.93	90.12
Cyhalofop-butyl	3.01	10.03	10.54	9.52	94.94	97.87	4.38	14.48	12.41	12.31	95.37	90.62
Cymoxanil	0.52	1.72	11.52	9.38	91.4	85.36	5.99	16.63	10.63	11.32	90.67	90.67
Cypermethrin	2.17	7.22	10.45	10.54	89.6	82.92	5.89	10.95	9.36	5.12	91.11	88.33
Cyproconazole	5.36	17.85	10.78	11.52	98.32	86.39	6.36	4.93	9.56	4.12	86.67	87.89
Cyprodinil	4.67	15.57	11.65	7.65	92.43	89.93	2.38	11.53	8.36	6.18	88.36	90.05
Dazomet	1.09	3.62	5.65	12.69	87.48	88.64	4.55	4.23	9.17	6.45	87.84	99.29
Deltamethrin	3.95	13.16	6.85	14.36	92.72	88.57	4.03	15.91	9.89	8.12	90.22	96.14
Diafenthiuron	3.4	11.32	7.65	12.31	87.53	86.73	4.22	4.28	8.63	9.15	87.81	94.59
Diazinon	3.46	11.53	8.41	11.32	89.81	85.88	6.06	19.77	9.52	9.12	88.94	95.27
Dicamba	3.51	11.71	8.69	10.63	86.85	88.28	2.13	14.95	9.38	10.12	88	96.27
Dichlofluanid	2.08	6.94	7.36	9.36	83.68	88.85	4.97	16.62	10.54	15.14	93.49	89.8
Dichlorvos	3.21	10.71	8.65	9.56	94.06	93.14	4.81	14.59	11.52	14.12	90.44	100.03
Diclofop Methyl	2.7	8.99	9.36	8.36	91.79	88.32	5.55	19.97	14.32	11.1	87.56	94.38
Diethofencarb	3.67	12.23	11.52	9.1	91.78	93.82	4.28	19.64	12.63	13.1	84.98	97.31
Difenoconazole	4.05	13.49	10.54	9.89	99.05	92.41	3.96	21.21	14.36	14.12	89.06	93.77
Diflubenzuron	3.53	11.78	11.57	14.65	92.5	91.96	5.7	7.92	12.31	17.52	95.76	94.41

Pesticides	Cucumber						Grapefruit					
	LOD	LOQ	Precision		Recovery		LOD	LOQ	Precision		Recovery	
			RSD (%)		%				RSD (%)		%	
			20	100	20	100			10	100	10	100
(µg/kg)						(µg/kg)						
Dimethenamid	4.68	15.6	12.65	12.32	84.8	93.18	4.37	15.17	11.32	10.32	87.17	92.01
Dimethoate	3.02	10.05	13.25	15.32	95.69	90.99	5.82	13.43	10.63	9.32	96.47	90.12
Dimethomorph	4.6	15.35	14.32	10.11	102.17	91.82	0.17	14.08	9.36	10.65	92.06	98.19
Diniconazole	4.83	16.11	14.58	11.21	92.83	83.81	5.17	20.19	9.56	11.25	96.36	86.9
Dinocap	3.06	10.2	12.69	12.32	95.66	88.55	4.21	7.12	8.36	10.87	92.62	95.16
Dioxathion	5.62	18.73	11.36	15.36	88.12	94.05	6.02	16.57	9.14	9.63	86.75	90.98
Diphenamid	3.88	12.93	10.87	19.36	90.98	92.6	5.82	16.05	9.89	8.35	88.56	100.65
Dithianon	3.19	10.63	10.96	21.36	90.15	95.55	5.75	18.48	8.63	8.65	89.94	91.63
Diuron	3.49	11.64	10.23	18.65	93.05	84.51	5.22	14.26	9.52	7.65	86.66	91.9
Epoxiconazole	6.3	20.99	10.65	11.32	98.78	91.54	4.57	13.21	9.38	8.32	92.59	96.78
EPTC	4.33	14.42	11.23	9.32	95.08	86.61	4.99	19.01	10.54	9.63	91.03	91.34
Esfenvalerate	2.96	9.86	12.32	8.65	90.12	85.69	0.55	14.56	11.52	12.54	90.99	83.28
Ethalfuralin	3.7	12.33	11.56	7.45	90.62	82.77	1.25	19.41	9.45	14.56	97.87	92.14
Ethiofencarb	1.4	4.67	11.45	14.12	90.67	84.53	2.33	0.56	8.65	17.85	85.36	90.38
Ethofumasate	4.21	14.03	10.65	9.32	88.33	89.26	4.82	17.23	7.23	9.74	82.92	99.63
Ethoprophos	4.26	14.21	9.63	10.63	87.89	88.09	2.64	14.02	6.14	10.11	86.39	93.6
Etofenprox	5.78	19.26	7.23	17.01	90.05	90.08	0.66	20.06	8.74	15.14	89.93	86.83
Etozazole	5.18	17.28	9.63	10.32	99.29	85.11	3.29	19.4	9.65	14.12	88.64	96.2
Famoxadone	5.14	17.14	10.25	11.21	96.14	93.47	5.79	19.16	7.32	13.12	88.57	92.24
Fenamidone	3.27	10.89	14.52	15.56	94.59	92.45	5.25	17.39	7.65	19.11	86.73	96.87
Fenamiphos (sum)	1.79	5.98	11.52	9.45	95.27	91.03	3.91	15.24	6.84	18.14	85.88	97.06
Fenarimol	3.2	10.66	10.65	14.65	96.27	86.62	1.69	16.63	6.45	17.14	88.28	93.21
Fenazaquin	3.04	10.14	10.65	17.23	89.8	92.99	3.55	1.82	6.21	12.11	88.85	94.41
Fenbuconazole	2.56	8.52	11.23	15.21	100.03	89.33	5.82	4.18	7.52	9.52	93.14	88.87
Fenoxaprop-P-Ethyl	1.51	5.03	11.25	14.32	94.38	78.75	4.73	7.75	6.36	8.32	88.32	89.11
Fenoxycarb	4.63	15.42	10.87	12.63	97.31	85.39	2.56	16.08	7.65	11.45	93.82	86.91
Fenpropathrin	2.07	6.89	9.63	14.36	93.77	89.51	1.57	8.79	12.69	10.65	92.41	87.7
Fenpyroximate	1.04	3.48	8.35	12.31	94.41	90.84	0.7	2.21	11.36	9.63	91.96	82.97
Fenthion	2.03	6.77	8.65	11.32	92.01	85.23	0.27	10.96	10.87	7.23	93.18	86.94
Fenvalerate	2.96	9.86	7.65	15.65	90.12	90.35	2.73	19.29	10.96	9.63	90.99	93.64
Fipronil	2.38	7.93	8.32	18.69	98.19	90.9	4.12	17.51	10.23	9.52	91.82	85.09
Fluazifop-P-Butyl	4.99	16.63	9.63	14.36	86.9	89.68	3.21	13.02	10.65	10.74	83.81	101.63
Fluazinam	3.85	12.82	12.54	7.65	95.16	85.02	3.4	5.62	11.23	11.74	88.55	92.88
Fludioxynil	4.53	15.11	14.56	6.84	90.98	91.03	1.75	11.82	12.32	29.11	94.05	93.48
Flufenoxuron	3.65	12.16	17.85	6.45	100.65	94.58	3.24	19.41	11.56	17.85	92.6	94.7
Flurasulam	3.97	13.23	19.63	6.21	91.63	92.08	3.59	15.77	11.45	19.21	95.55	92.49
Flurochloridone	5.26	17.53	15.36	7.52	91.9	83.14	0.55	8.53	8.65	8.65	84.51	90.09
Flusilazole	3.64	12.14	19.36	19.36	96.78	98.84	0.51	5.22	10.45	7.65	91.54	93.67
Flutriafol	2.99	9.97	18.36	19.36	91.34	91.02	0.79	2.35	11.74	8.32	86.61	96.84
Foramsulfuron	4.77	15.89	17.15	18.65	83.28	85.58	3.6	0.91	9.65	9.63	85.69	90.22
Formatanate	2.57	8.56	19.56	11.32	92.14	77.87	4.76	9.09	10.65	12.54	82.77	83.83
Fosthiazate	3.76	12.54	18.65	9.32	90.38	82.08	3.99	13.72	11.63	14.56	84.53	91.1

Pesticides	Cucumber						Grapefruit					
	LOD	LOQ	Precision		Recovery		LOD	LOQ	Precision		Recovery	
			RSD (%)		(%)				RSD (%)		(%)	
			20	100	20	100			10	100	10	100
(µg/kg)						(µg/kg)						
Furathiocarb	4.71	15.69	17.65	8.65	99.63	82.96	3.19	10.68	12.36	17.85	89.26	90.53
Giberellic acid	3.02	10.05	14.36	7.45	93.6	94.33	4.39	11.33	10.54	19.63	88.09	91.53
Halfenprox	2.46	8.21	17.89	14.12	86.83	95.57	8.08	5.83	11.57	15.36	90.08	100.83
Haloxyfop-2-Etoxyethyl	4.83	16.09	17.25	15.36	96.2	86.59	4.78	10.8	12.65	19.36	85.11	91.07
Haloxyfop-P-Methyl	5.13	17.09	14.56	14.36	92.24	87.72	6.37	11.98	13.25	12.36	93.47	90.46
Hexaconazole	5.54	18.45	14.85	21.36	96.87	89.58	5.76	1.84	14.32	10.15	92.45	82.71
Hexaflumuron	3.76	12.54	12.65	11.32	97.06	87.05	8.27	1.7	14.58	15.36	91.03	90.08
Hexythiazox	4.32	14.41	15.23	11.25	93.21	91.54	5.66	2.64	10.32	14.36	86.62	90.99
Imazalil	6.01	20.03	12.14	14.32	94.41	87.12	7.31	11.99	10.74	11.36	92.99	91.16
Imazamox	4.44	14.81	18.23	12.36	88.87	86.71	6.8	15.87	11.35	11.32	89.33	87.18
Imazapic	4.88	16.27	15.65	11.17	89.11	89.99	10.15	13.31	12.65	11.25	78.75	88.97
Imazapyr	3.07	10.24	18.56	10.12	86.91	86.63	11.8	10.65	16.74	29.11	85.39	99.31
Imazethapyr	4.75	15.84	14.89	11.14	87.7	85.85	7.56	14.63	17.96	12.36	89.51	90.05
Imidacloprid	4.12	13.73	9.63	18.69	82.97	92.52	7.38	26.94	11.85	11.17	90.84	91.09
Iodosulfuron-Methyl	2.87	9.57	6.52	12.32	86.94	85.14	7.49	15.94	14.96	10.12	85.23	86.93
Ioxynil	2.42	8.08	5.36	11.41	93.64	83.96	6.88	21.25	18.74	11.14	90.35	86.71
Iprodione	0.49	1.63	6.89	17.24	85.09	86.97	7.38	19.2	15.65	13.36	90.9	87.3
Isoxaflutole	3.01	10.02	8.47	9.63	101.63	94.06	7.2	27.58	16.32	14.63	89.68	91.93
Kresoxim methyl	5.85	19.5	8.45	8.47	92.88	88.11	3.96	18.87	15.32	15.32	85.02	86.56
Lambda Cyhalothrin	3.26	10.86	7.23	7.85	93.48	85.43	5.94	24.38	14.85	17.45	91.03	95.71
Lenacil	2.4	8.12	9.62	8.24	94.7	90.01	7.2	22.67	17.85	14.11	94.58	91.53
Lufenuron	4.97	16.56	7.21	7.65	92.49	90.03	4.45	33.83	9.32	9.45	92.08	92.44
Malathion	4.14	13.8	8.24	14.85	90.09	93.99	4.24	39.35	6.21	14.65	83.14	93.37
MCPA	4.42	14.75	9.65	17.85	93.67	85.93	5.78	25.2	8.32	17.23	98.84	88.68
Mecoprop	3.51	11.69	8.21	9.32	96.84	87.24	4.8	24.61	8.14	15.21	91.02	96.15
Mefenpyr-diethyl	5.55	18.51	9.32	6.21	90.22	82.44	3.49	24.96	9.12	14.32	85.58	90.69
Mesosulfuron methyl	5.94	19.81	10.65	8.32	83.83	84.01	5.82	22.93	8.14	12.63	77.87	91.93
Mesotrione	3.3	11.01	11.45	8.14	91.1	86.82	4.84	24.58	5.12	14.36	82.08	89.28
Metalaxyl	4.69	15.65	18.63	9.12	90.53	91.51	8.6	24.02	4.12	12.31	82.96	96.41
Metamitron	3.6	12	14.85	14.54	91.53	94.7	6.69	13.19	6.18	11.32	94.33	98.44
Metconazole	4.66	15.54	15.65	13.65	100.83	91.65	4.07	19.79	6.45	9.74	95.57	92.27
Methidathion	5.16	17.19	12.32	14.52	91.07	87.26	4.32	23.99	8.12	4.65	86.59	92.02
Methomyl	4.08	13.59	14.15	18.65	90.46	85.96	4.2	14.85	9.15	6.18	87.72	89.77
Methoxyfenozide	4.13	13.77	14.78	14.65	82.71	89.59	4.75	14.13	9.12	6.45	89.58	96.25
Metolachlor	5.98	19.93	14.56	17.96	90.08	94.47	5.04	19.26	10.12	8.12	87.05	93.4
Metribuzin	1.34	4.47	18.45	11.85	90.99	86.83	3.23	16.01	15.14	9.15	91.54	90.22
Metsulfuron-methyl	3.32	11.07	14.52	14.96	91.16	91.52	2.43	11.64	14.12	9.12	87.12	96.98
Monocrotophos	1.27	4.23	12.54	18.74	87.18	87.68	5.01	19.4	11.1	10.12	86.71	96.66
Monolinuron	1.64	5.46	16.52	15.65	88.97	83.56	6.17	16.12	13.1	15.14	89.99	99.51
Myclobutanil	4.34	14.48	18.25	16.32	99.31	93.36	0.13	28.67	17.23	14.12	86.63	93.42
Nicosulfuron	4.99	16.63	14.65	15.32	90.05	84.52	3.09	22.31	15.21	11.1	85.85	97.25

Pesticides	Cucumber						Grapefruit					
	LOD	LOQ	Precision		Recovery		LOD	LOQ	Precision		Recovery	
			RSD (%)		%				RSD (%)		%	
			20	100	20	100			10	100	10	100
(µg/kg)						(µg/kg)						
Novaluron	3.29	10.95	14.32	14.85	91.09	88.19	3.39	13.56	14.32	13.1	92.52	96.79
Omethoate	1.48	4.93	13.21	17.85	86.93	87.11	2.09	14.41	12.63	10.21	85.14	90.71
Oxadixyl	3.46	11.53	15.36	9.32	86.71	87.44	4.23	14.01	14.36	10.14	83.96	98.12
Oxamyl	1.27	4.23	14.36	6.21	87.3	86.5	2.68	15.82	12.31	9.85	86.97	91.6
Oxyflourfen	4.77	15.91	11.36	8.32	91.93	83.48	4.18	16.79	11.32	15.17	94.06	99.08
Parathion Methyl	1.28	4.28	11.32	8.14	86.56	93.11	5.81	10.75	9.65	11.12	88.11	86.35
Penconazole	5.93	19.77	11.25	9.12	95.71	83.77	3.56	8.1	10.32	12.23	85.43	96.45
Pendimethalin	4.48	14.95	24.32	8.14	91.53	90.2	1.8	16.68	11.85	18.32	90.01	92.42
Permethrin	4.99	16.62	12.36	14.12	92.44	92.26	1.24	20.58	14.65	14.36	90.03	90.57
Phenmedipham	4.38	14.59	11.17	11.12	93.37	92.3	2.33	0.42	17.64	9.15	93.99	90.06
Phenthoate	5.99	19.97	10.12	10.12	88.68	95.18	3.65	10.3	8.65	9.12	85.93	85.16
Phosalone	5.89	19.64	11.14	18.26	96.15	85.34	2.43	11.3	7.65	10.32	87.24	93.31
Phosmet	6.36	21.21	15.36	17.32	90.69	84.19	4.49	6.96	8.32	11.25	82.44	93.71
Pirimicarb	2.38	7.92	18.36	14.32	91.93	93.02	4.58	14.1	9.63	10.87	84.01	86.76
Pirimiphos methyl	4.55	15.17	12.35	18.65	89.28	88.01	2.83	8.92	12.54	9.63	86.82	89.6
Prochloraz	4.03	13.43	14.36	12.74	96.41	90.23	4.01	13.92	14.56	8.35	91.51	102.06
Procymidone	4.22	14.08	17.96	9.12	98.44	87.9	0.65	19.37	17.85	8.65	94.7	95.94
Profenofos	6.06	20.19	11.85	10.11	92.27	91.11	4.95	11.87	19.63	7.65	91.65	100.07
Profoxydim (Clefoxydim)	2.13	7.12	14.96	17.85	92.02	88.23	5.11	5.99	15.36	8.32	87.26	86.06
Prometryn	4.97	16.57	18.74	19.63	89.77	93.85	5.82	4.12	19.36	9.63	85.96	94.31
Propaquizafop	4.81	16.05	15.65	15.36	96.25	87.19	4.9	7.76	17.36	12.54	89.59	92.67
Propargite	5.55	18.48	16.32	19.36	93.4	96.29	2.76	12.16	16.15	14.56	94.47	100.31
Propazine	4.28	14.26	15.32	21.36	90.22	84.29	4.97	8.11	15.17	17.85	86.83	92.13
Propoxycarbazono	3.96	13.21	14.85	10.12	96.98	87.32	2.74	14.97	11.12	39.47	91.52	96.42
Propyconazole	5.7	19.01	17.85	14.25	96.66	84.74	4.61	15.28	12.23	17.96	87.68	87.28
Propyzamide	4.37	14.56	21.36	9.15	99.51	89.42	3.73	9.44	18.32	11.85	83.56	86.31
Prothopos	5.82	19.41	6.21	9.12	93.42	89.52	3.01	13.37	14.36	14.96	93.36	99.09
Pymetrozine	0.17	0.56	8.32	10.12	97.25	85.74	0.52	2.17	9.15	18.74	84.52	92.48
Pyraclostrobin	5.17	17.23	8.14	15.14	96.79	83.32	2.17	16.51	9.12	15.65	88.19	85.9
Pyraflufen-Ethyl	4.21	14.02	9.12	14.12	90.71	92.91	5.36	17.02	6.45	16.32	87.11	82.99
Pyrazophos	6.02	20.06	8.14	11.1	98.12	88.05	4.67	19.41	8.12	15.32	87.44	98.77
Pyridaben	5.82	19.4	10.12	13.1	91.6	90.89	1.09	16.33	9.15	14.85	86.5	98.8
Pyridaphention	5.75	19.16	10.11	10.21	99.08	96.07	3.95	9.2	9.12	17.85	83.48	97.12
Pyridate	5.22	17.39	14.32	10.14	86.35	91.46	3.4	16.57	10.12	9.32	93.11	94.68
Pyriproxyfen	4.57	15.24	10.34	9.85	96.45	86.32	3.46	9.12	15.14	6.21	83.77	85
Quizalofop-P-Ethyl	4.99	16.63	15.32	9.85	92.42	89.45	3.51	15.36	14.12	8.32	90.2	96.72
Rimsulfuron	0.55	1.82	9.98	10.25	90.57	89.54	2.08	12.44	11.1	8.14	92.26	90.67
Sethoxydim	1.25	4.18	8.32	11.14	90.06	91.31	3.21	10.03	13.1	9.12	92.3	90.39
Simozine	2.33	7.75	7.23	14.25	85.16	90.57	2.7	1.72	10.21	8.14	95.18	95.14
Spirodiclofen	4.82	16.08	8.23	18.21	93.31	92.29	3.67	7.22	10.14	10.21	85.34	95.23
Spiroxamine	2.64	8.79	6.12	14.32	93.71	99.81	4.05	17.85	9.85	10.14	84.19	94.61

Pesticides	Cucumber						Grapefruit					
	LOD	LOQ	Precision		Recovery		LOD	LOQ	Precision		Recovery	
			RSD (%)		%				RSD (%)		%	
			20	100	20	100			10	100	10	100
(µg/kg)						(µg/kg)						
Sulfosulfuron	0.66	2.21	14.23	14.32	86.76	101.91	3.53	15.57	8.45	9.85	93.02	101.91
Tau-Fluvalinate	3.29	10.96	15.21	19.32	89.6	94.87	4.68	3.62	10.11	10.12	88.01	100.96
Tebuconazole	5.79	19.29	14.23	10.12	102.06	95.67	3.02	13.16	14.65	14.12	90.23	96.5
Tebufozide	5.25	17.51	9.14	15.14	95.94	104.15	4.6	11.32	17.65	15.17	87.9	104.15
Teflubenzuron	3.91	13.02	8.14	14.12	100.07	100.6	4.83	11.53	12.11	11.52	91.11	100.6
Tepraloxymid	1.69	5.62	7.56	11.1	86.06	103.01	3.06	11.71	17.15	10.54	88.23	103.01
Terbutylazine	3.55	11.82	8.14	13.1	94.31	102.61	5.62	6.94	19.12	11.57	93.85	102.61
Terbutryn	5.82	19.41	8.65	10.21	92.67	95.62	3.88	10.71	13.25	12.65	87.19	93.95
Tetraconazole	4.73	15.77	7.12	10.14	100.31	93.73	3.19	8.99	10.11	13.25	96.29	99.51
Thiabendazole	2.56	8.53	8.45	9.85	92.13	94.54	3.49	12.23	9.85	14.32	84.29	98.75
Thiacloprid	1.57	5.22	8.69	10.12	96.42	99.77	6.3	13.49	8.63	14.58	87.32	99.77
Thiamethoxam	0.70	2.35	6.25	14.12	87.28	101.08	4.33	11.78	7.98	12.69	84.74	101.08
Thifensulfuron-methyl	0.27	0.91	5.12	15.17	86.31	102.61	2.96	15.6	7.63	11.36	89.42	102.61
Thiohanate methyl	2.73	9.09	4.12	11.12	99.09	102.27	3.7	10.05	7.52	10.87	89.52	102.27
Thiometon	4.12	13.72	6.18	12.23	92.48	102.82	1.4	15.35	9.41	9.15	85.74	102.82
Tolyfluanid	3.21	10.68	6.45	18.32	85.9	92.82	4.21	16.11	7.45	8.32	83.32	97.51
Tralkoxydim	3.4	11.33	8.12	14.36	82.99	98.99	4.26	10.2	11.25	9.74	92.91	98.26
Triadimefon	1.75	5.83	9.15	9.15	98.77	99.6	5.78	18.73	10.87	6.32	88.05	99.6
Triadimenol	3.24	10.8	9.12	9.12	98.8	101.72	5.18	12.93	9.63	7.14	90.89	101.72
Triallate	3.59	11.98	10.12	10.12	97.12	101.45	5.14	10.63	8.35	6.32	96.07	101.45
Triasulfuron	0.55	1.84	15.14	15.14	94.68	98.88	3.27	11.64	8.65	7.52	91.46	98.88
Tribenuron-Methyl	0.51	1.7	14.12	14.12	85	101.79	1.79	20.99	7.65	10.21	86.32	101.79
Trichlorfon	0.79	2.64	11.1	11.1	96.72	99.8	3.2	14.42	8.32	10.14	89.45	99.8
Trifloxystrobin	3.6	11.99	13.1	13.1	90.67	102.21	3.04	9.86	9.63	9.85	89.54	102.21
Triflumizole	4.76	15.87	10.21	10.21	90.39	100.93	2.56	12.33	12.54	10.12	91.31	100.93
Triflumuron	3.99	13.31	10.14	10.14	95.14	102.11	1.51	4.67	14.56	14.12	90.57	102.11
Triticonazole	3.19	10.65	9.85	9.85	95.23	101.54	4.63	14.03	17.85	15.17	92.29	101.54
2,4-D Acid	4.39	14.63	7.65	11.23	94.61	102.37	2.07	14.21	14.12	9.12	99.81	102.37

LOD: limit of detection (µg/kg); LOQ: limit of quantification (µg/kg)

Calculated at 20 µg/kg and 100 µg/kg in fortified cucumber matrix

Calculated at 10 µg/kg and 100 µg/kg in fortified grapefruit matrix

The fungicides metalxyl and procymidone were found in 4 cucumber samples at levels varying from 0.011 to 0.039 mg kg⁻¹ and from 0.014 to 0.033 mg kg⁻¹, respectively. The insecticide chlorpyrifos was detectable only in 1 cucumber samples, with a mean concentration of 0.037 mg kg⁻¹. Similarly, two cucumber samples were found to contain iprodione, Carbendazim, which is an authorised neonicotinoid insecticide. The concentrations of iprodione, carbendazim in positive samples were from 0.022 to 0.029 mg kg⁻¹ and from 0.014 to 0.032 mg kg⁻¹, respectively.

The results show that grapefruits had slightly higher frequencies (13.8%) of pesticide residues than cucumber samples (11.6%), but the number of residues was less. Of the

233 target analytes monitored, only 9 pesticide residues were found in grapefruits at concentrations varying from 0.002 to 0.042 mg kg⁻¹; none above the MRL. Multiple residues in grapefruits were found in 3.5% of the samples. While 15 grapefruit samples contained two residues of pesticides, only 2 samples were contaminated with three pesticide residues.

The fungicide fludioxonil was the most prominent pesticide found in grapefruit samples, with a frequency of 9.1%, and with levels ranging from 0.019 to 0.041 mg kg⁻¹. Fludioxonil, which belongs to the class of phenylpyrrole, is used to control a broad spectrum of plant diseases in various vegetables. The acute toxicity of fludioxonil is low. Fludioxonil did not have carcinogenic potential (FAO, 2012).

Imazalil was the second most commonly found pesticide in grapefruits with 4.7% of the samples. The results obtained from the second and third year showed that 7 samples contained imazalil at levels varying from 0.017 to 0.102 mg kg⁻¹, and from 0.021 to 0.109 mg kg⁻¹, respectively. In the first year, 4 samples had this residue at concentrations ranging from 0.016 to 0.032 mg kg⁻¹.

Thiabendazol was detected in 7 samples at levels ranging from 0.014 to 0.081 mg kg⁻¹, of which 5 samples contained simultaneously the fungicide quinophos. Thiabendazol, belongs to the class of benzimidazole. It is a systemic fungicide used in citrus fruits such as orange, lemon and grapefruit against *Penicillium digitatum*.

The insecticide carbaryl was present in 4 grapefruit samples, with a mean concentration of 0.028 mg kg⁻¹. Carbaryl belongs to the class of carbamate. It is a pesticide and plant growth regulator used in citrus fruits such as orange, lemon, grapefruit.

Uncertainty assessment

The results of method uncertainty assessment considering six sources are presented in *Table 2*. For cucumber samples the overall contributions to U_c of the method of the uncertainties associated with U_1 (standard solution preparation), U_2 (calibration curve preparation), U_3 (sample preparation treatment), U_4 (precision), and U_5 (accuracy/bias) ranged from 5.3% to 10.6% and U_6 (linear least square fitting) ranged from 85.6% to 93.1%. In the same way, for grapefruit, the overall contributions of the uncertainties associated with U_1 , U_2 , U_3 , U_4 , and U_5 varied from 5.1% to 11.8% and U_6 ranged from 87.8% to 95.1%. In the light of these results, the uncertainty associated with u_6 presents the highest contribution for all the pesticides under study in cucumber and grapefruit.

As can be seen in *Table 2*, U_c values at 95% confidence level for cucumber ranged from 12.3% to 18.7% and for grapefruit from 15.6% to 23.6%. U_c values of all pesticides detected in cucumber samples generally offer lower values than grapefruit. For all target analytes, the U_c was within the criteria specified in the SANTE Guideline (less than 50%). These results are similar to those reported for methods using GC-MS, LCMS-MS and the QuEChERS procedure. For example, Walorczyk (2014) reported U_c values ranging from 7.0% to 53.0% for samples of black currant, where the majority of pesticides had a uncertainty of <30.0%. In addition, da Silva Sousa et al. (2018) reported U_c values from 7.9% to 36.1% for melon samples. At first glance, the results of this method are high, but the uncertainty acceptance criteria according to the European SANTE / 11945/2015 guideline European Commission (2015) is the time when the value is 50.0%. Although it is recommended to use the internal standard to minimize uncertainties, the proposed method indicated that expanded uncertainties are not necessary.

Table 2. Method uncertainties estimated for different sources and, combined (U_c) and expanded (U_e) uncertainty

Pesticide	Cucumber										Grapefruit									
	U_1	U_2	U_i^a (mg/kg (%))		U_5	U_6	U_c	U_e^b	$U_e(\%)$		U_1	U_2	U_i^a (mg/kg (%))		U_5	U_6	U_c	U_e^b	$U_e(\%)$	
			U_3	U_4									U_3	U_4						
				(mg/kg)			(mg/kg)							(mg/kg)				(mg/kg)		
Trifluralin	0.044 (2.3)	0.036 (1.0)	0.031 (0.9)	0.023 (0.7)	0.039 (1.8)	0.301 (92.1)	0.313	0.618	15.6		0.044 (2.3)	0.036 (1.0)	0.031 (0.9)	0.050 (1.7)	0.064 (2.8)	0.350 (88.4)	0.384	0.765	15.7	
Chlorothalonil	0.044 (2.1)	0.036 (0.9)	0.031 (0.8)	0.072 (4.3)	0.032 (1.5)	0.317 (89.5)	0.311	0.662	15.8		0.044 (2.1)	0.036 (0.9)	0.031 (0.8)	0.034 (1.2)	0.044 (1.7)	0.318 (87.8)	0.382	0.665	16.4	
Formothion	0.044 (2.0)	0.036 (1.2)	0.031 (1.5)	0.008 (4.2)	0.054 (2.6)	0.245 (90.4)	0.320	0.665	16.2		0.044 (2.0)	0.036 (1.2)	0.031 (1.5)	0.076 (2.2)	0.068 (1.6)	0.333 (92.1)	0.381	0.654	18.3	
Vinclozolin	0.044 (3.2)	0.036 (1.1)	0.031 (1.6)	0.007 (4.1)	0.048 (2.2)	0.298 (88.7)	0.254	0.514	16.3		0.044 (3.2)	0.036 (1.1)	0.031 (1.6)	0.071 (4.4)	0.060 (3.5)	0.368 (91.2)	0.504	0.774	19.5	
Fenitrothion	0.044 (3.5)	0.036 (1.5)	0.031 (1.0)	0.009 (3.9)	0.038 (1.8)	0.332 (85.6)	0.256	0.512	15.6		0.044 (3.5)	0.036 (1.5)	0.031 (1.0)	0.097 (6.3)	0.071 (3.4)	0.495 (95.1)	0.501	0.771	15.6	
Dicofol	0.044 (1.9)	0.036 (1.6)	0.031 (1.1)	0.070 (3.7)	0.039 (1.8)	0.312 (92.4)	0.245	0.628	12.6		0.044 (1.9)	0.036 (1.6)	0.031 (1.1)	0.096 (5.4)	0.062 (2.6)	0.452 (94.1)	0.359	0.659	16.2	
Captan	0.044 (2.0)	0.036 (1.7)	0.031 (1.4)	0.066 (0.2)	0.041 (2.1)	0.298 (89.7)	0.287	0.624	12.8		0.044 (2.0)	0.036 (1.7)	0.031 (1.4)	0.071 (2.1)	0.045 (1.6)	0.413 (92.1)	0.385	0.662	19.6	
Folpet	0.044 (3.4)	0.036 (1.2)	0.031 (1.3)	0.052 (0.1)	0.068 (3.5)	0.291 (93.1)	0.298	0.701	12.9		0.044 (3.4)	0.036 (1.2)	0.031 (1.3)	0.033 (1.5)	0.061 (3.2)	0.402 (90.8)	0.504	0.652	20.3	
Qinomethionate	0.044 (3.3)	0.036 (1.4)	0.031 (0.9)	0.054 (0.6)	0.071 (3.9)	0.335 (95.4)	0.301	0.704	12.7		0.044 (3.3)	0.036 (1.4)	0.031 (0.9)	0.051 (1.9)	0.070 (3.3)	0.350 (88.4)	0.501	1.014	21.6	
Dinobuton	0.044 (3.2)	0.036 (1.5)	0.031 (1.1)	0.051 (0.7)	0.065 (4.1)	0.301 (92.1)	0.305	0.517	12.8		0.044 (3.2)	0.036 (1.5)	0.031 (1.1)	0.076 (2.2)	0.064 (2.8)	0.318 (87.8)	0.328	0.665	23.4	
Endosulfan A	0.044 (3.1)	0.036 (1.2)	0.031 (1.4)	0.041 (0.5)	0.070 (3.6)	0.317 (89.5)	0.321	0.514	13.1		0.044 (3.1)	0.036 (1.2)	0.031 (1.4)	0.071 (4.4)	0.044 (1.7)	0.333 (92.1)	0.329	1.011	21.8	
Endosulfan B	0.044 (2.1)	0.036 (1.3)	0.031 (1.3)	0.040 (0.6)	0.068 (4.2)	0.245 (90.4)	0.315	0.548	13.6		0.044 (2.1)	0.036 (1.3)	0.031 (1.3)	0.097 (6.3)	0.068 (1.6)	0.368 (91.2)	0.385	0.774	22.8	
Bromopropylate	0.044 (3.5)	0.036 (1.0)	0.031 (0.9)	0.043 (0.2)	0.039 (1.8)	0.298 (88.7)	0.311	0.621	13.8		0.044 (3.5)	0.036 (1.0)	0.031 (0.9)	0.096 (5.4)	0.060 (3.5)	0.495 (95.1)	0.384	0.776	21.8	
Tetradifon	0.044 (3.3)	0.036 (0.9)	0.031 (0.7)	0.054 (0.4)	0.048 (2.2)	0.332 (85.6)	0.314	0.514	13.9		0.044 (3.3)	0.036 (0.9)	0.031 (0.7)	0.071 (2.1)	0.071 (3.4)	0.452 (94.1)	0.391	0.778	23.6	
Alfa-Cypermethrin a	0.044 (2.3)	0.036 (1.2)	0.031 (0.8)	0.071 (0.3)	0.038 (1.8)	0.312 (92.4)	0.317	0.665	14.6		0.044 (2.3)	0.036 (1.2)	0.031 (0.8)	0.033 (1.5)	0.062 (2.6)	0.413 (92.1)	0.398	0.662	20.8	
Alfa-Cypermethrin b	0.044 (2.1)	0.036 (1.1)	0.031 (0.9)	0.041 (0.5)	0.039 (1.8)	0.298 (89.7)	0.298	0.541	15.8		0.044 (2.1)	0.036 (1.1)	0.031 (0.9)	0.051 (1.9)	0.045 (1.6)	0.402 (90.8)	0.387	1.010	19.6	
alpha.-BHC	0.044 (2.0)	0.036 (1.5)	0.031 (1.0)	0.040 (0.6)	0.041 (2.1)	0.291 (93.1)	0.289	0.526	14.9		0.044 (2.0)	0.036 (1.5)	0.031 (1.0)	0.076 (2.2)	0.061 (3.2)	0.350 (88.4)	0.384	0.669	18.9	
delta.-BHC	0.044 (3.2)	0.036 (1.6)	0.031 (1.1)	0.043 (0.2)	0.068 (3.5)	0.331 (91.7)	0.287	0.668	15.6		0.044 (3.2)	0.036 (1.6)	0.031 (1.1)	0.071 (4.4)	0.070 (3.3)	0.318 (87.8)	0.385	0.771	17.6	
Heptachlor	0.044 (3.5)	0.036 (1.7)	0.031 (1.4)	0.054 (0.4)	0.032 (1.5)	0.301 (92.1)	0.269	0.662	16.9		0.044 (3.5)	0.036 (1.7)	0.031 (1.4)	0.097 (6.3)	0.064 (2.8)	0.333 (92.1)	0.381	0.778	15.9	
2,4-DDE	0.044 (1.9)	0.036 (1.4)	0.031 (1.3)	0.071 (0.3)	0.039 (1.8)	0.317 (89.5)	0.278	0.669	16.8		0.044 (1.9)	0.036 (1.4)	0.031 (1.3)	0.096 (5.4)	0.044 (1.7)	0.368 (91.2)	0.329	0.668	16.3	

Pesticide	Cucumber									Grapefruit									
	U ₁	U ₂	U _i ^a (mg/kg (%))			U ₆	U _c	U _e ^b	U _e (%)		U ₁	U ₂	U _i ^a (mg/kg (%))			U ₆	U _c	U _e ^b	U _e (%)
			U ₃	U ₄	U ₅								U ₃	U ₄	U ₅				
(mg/kg)									(mg/kg)										
Dieldrin	0.044 (2.0)	0.036 (1.5)	0.031 (0.9)	0.072 (4.3)	0.045 (2.7)	0.245 (90.4)	0.259	0.554	14.3	0.044 (2.0)	0.036 (1.5)	0.031 (0.9)	0.071 (2.1)	0.068 (1.6)	0.495 (95.1)	0.501	0.669	15.9	
4,4-DDE	0.044 (3.4)	0.036 (1.2)	0.031 (0.7)	0.008 (4.2)	0.065 (2.6)	0.298 (88.7)	0.314	0.552	15.9	0.044 (3.4)	0.036 (1.2)	0.031 (0.7)	0.033 (1.5)	0.060 (3.5)	0.452 (94.1)	0.384	0.765	18.6	
2,4-DDD	0.044 (3.3)	0.036 (1.3)	0.031 (0.8)	0.007 (4.1)	0.048 (2.2)	0.332 (85.6)	0.315	0.661	17.6	0.044 (3.3)	0.036 (1.3)	0.031 (0.8)	0.051 (1.9)	0.071 (3.4)	0.413 (92.1)	0.382	0.665	18.7	
Endrin	0.044 (3.2)	0.036 (1.0)	0.031 (0.9)	0.009 (3.9)	0.038 (1.8)	0.312 (92.4)	0.347	0.618	18.6	0.044 (3.2)	0.036 (1.0)	0.031 (0.9)	0.097 (6.3)	0.062 (2.6)	0.402 (90.8)	0.381	0.654	16.9	
Chlorfenapyl	0.044 (3.1)	0.036 (0.8)	0.031 (1.0)	0.070 (3.7)	0.039 (1.8)	0.291 (93.1)	0.325	0.662	17.8	0.044 (3.1)	0.036 (0.8)	0.031 (1.0)	0.096 (5.4)	0.045 (1.6)	0.350 (88.4)	0.504	0.774	18.3	
4,4-DDD	0.044 (2.1)	0.036 (1.0)	0.031 (1.1)	0.066 (0.2)	0.041 (2.1)	0.330 (94.5)	0.287	0.665	17.6	0.044 (2.1)	0.036 (1.0)	0.031 (1.1)	0.071 (2.1)	0.061 (3.2)	0.318 (87.8)	0.501	0.771	16.9	
Ethion	0.044 (3.4)	0.036 (0.9)	0.031 (1.4)	0.052 (0.1)	0.068 (3.5)	0.296 (95.2)	0.298	0.514	15.9	0.044 (3.4)	0.036 (0.9)	0.031 (1.4)	0.033 (1.5)	0.070 (3.3)	0.333 (92.1)	0.359	0.659	18.1	
DDT	0.044 (1.9)	0.036 (1.2)	0.031 (1.3)	0.054 (0.6)	0.052 (3.4)	0.332 (85.6)	0.301	0.512	18.1	0.044 (1.9)	0.036 (1.2)	0.031 (1.3)	0.051 (1.9)	0.064 (2.8)	0.368 (91.2)	0.385	0.662	18.6	
Abamectin	0.044 (2.1)	0.036 (1.1)	0.031 (0.9)	0.051 (0.7)	0.037 (1.7)	0.301 (92.1)	0.305	0.628	17.6	0.044 (2.1)	0.036 (1.1)	0.031 (0.9)	0.076 (2.2)	0.044 (1.7)	0.495 (95.1)	0.504	0.652	17.8	
Acetamiprid	0.044 (2.3)	0.036 (1.5)	0.031 (1.1)	0.041 (0.5)	0.045 (1.8)	0.317 (89.5)	0.321	0.624	15.9	0.044 (2.3)	0.036 (1.5)	0.031 (1.1)	0.071 (4.4)	0.068 (1.6)	0.452 (94.1)	0.501	1.014	17.3	
Acetochlor	0.044 (2.0)	0.036 (1.6)	0.031 (1.4)	0.040 (0.6)	0.065 (2.6)	0.245 (90.4)	0.315	0.701	14.3	0.044 (2.0)	0.036 (1.6)	0.031 (1.4)	0.097 (6.3)	0.060 (3.5)	0.413 (92.1)	0.328	0.665	19.6	
Acrinathrin	0.044 (3.4)	0.036 (1.7)	0.031 (1.3)	0.043 (0.2)	0.048 (2.2)	0.298 (88.7)	0.311	0.704	13.6	0.044 (3.4)	0.036 (1.7)	0.031 (1.3)	0.096 (5.4)	0.071 (3.4)	0.402 (90.8)	0.329	1.011	20.5	
Alachlor	0.044 (3.3)	0.036 (1.4)	0.031 (0.9)	0.054 (0.4)	0.062 (2.1)	0.332 (85.6)	0.314	0.517	13.5	0.044 (3.3)	0.036 (1.4)	0.031 (0.9)	0.071 (2.1)	0.062 (2.6)	0.350 (88.4)	0.385	0.774	21.5	
Amitraz	0.044 (3.2)	0.036 (1.5)	0.031 (0.7)	0.071 (0.3)	0.039 (1.8)	0.312 (92.4)	0.317	0.514	18.1	0.044 (3.2)	0.036 (1.5)	0.031 (0.7)	0.033 (1.5)	0.045 (1.6)	0.318 (87.8)	0.384	0.776	22.5	
Atrazine	0.044 (3.1)	0.036 (1.2)	0.031 (0.8)	0.041 (0.5)	0.065 (2.6)	0.298 (89.7)	0.298	0.548	14.5	0.044 (3.1)	0.036 (1.2)	0.031 (0.8)	0.051 (1.9)	0.061 (3.2)	0.333 (92.1)	0.507	0.669	21.7	
Azinphos methyl	0.044 (2.1)	0.036 (1.3)	0.031 (0.9)	0.040 (0.6)	0.048 (2.2)	0.291 (93.1)	0.298	0.664	16.5	0.044 (2.1)	0.036 (1.3)	0.031 (0.9)	0.076 (2.2)	0.070 (3.3)	0.368 (91.2)	0.504	0.771	22.9	
Azoxystrobin	0.044 (2.1)	0.036 (1.0)	0.031 (1.0)	0.043 (0.2)	0.048 (2.2)	0.332 (85.6)	0.337	0.663	15.7	0.044 (2.1)	0.036 (1.0)	0.031 (1.0)	0.071 (4.4)	0.064 (2.8)	0.495 (95.1)	0.394	0.778	21.7	
Bensulfuron-Methyl	0.044 (2.0)	0.036 (0.8)	0.031 (1.1)	0.054 (0.4)	0.038 (1.8)	0.301 (92.1)	0.315	0.559	14.9	0.044 (2.0)	0.036 (0.8)	0.031 (1.1)	0.097 (6.3)	0.044 (1.7)	0.452 (94.1)	0.392	0.668	20.6	
Bentazone	0.044 (3.2)	0.036 (0.9)	0.031 (1.4)	0.071 (0.3)	0.039 (1.8)	0.317 (89.5)	0.347	0.557	17.6	0.044 (3.2)	0.036 (0.9)	0.031 (1.4)	0.096 (5.4)	0.068 (1.6)	0.413 (92.1)	0.389	0.669	15.7	
Beta-Cyfluthrin	0.044 (3.5)	0.036 (1.0)	0.031 (1.3)	0.041 (0.5)	0.041 (2.1)	0.245 (90.4)	0.325	0.621	18.1	0.044 (3.5)	0.036 (1.0)	0.031 (1.3)	0.071 (2.1)	0.060 (3.5)	0.402 (90.8)	0.374	1.015	16.4	
Bifenthrin	0.044 (1.9)	0.036 (0.9)	0.031 (0.9)	0.040 (0.6)	0.068 (3.5)	0.298 (88.7)	0.289	0.514	16.9	0.044 (1.9)	0.036 (0.9)	0.031 (0.9)	0.033 (1.5)	0.071 (3.4)	0.350 (88.4)	0.365	1.016	18.3	

Pesticide	Cucumber									Grapefruit								
	U ₁	U ₂	U _i ^a (mg/kg (%))			U ₆	U _c	U _e ^b	U _e (%)	U ₁	U ₂	U _i ^a (mg/kg (%))			U ₆	U _c	U _e ^b	U _e (%)
			U ₃	U ₄	U ₅							U ₃	U ₄	U ₅				
(mg/kg)									(mg/kg)									
Boscalid	0.044 (2.0)	0.036 (1.2)	0.031 (0.7)	0.043 (0.2)	0.065 (2.6)	0.332 (85.6)	0.287	0.665	18.2	0.044 (2.0)	0.036 (1.2)	0.031 (0.7)	0.051 (1.9)	0.062 (2.6)	0.318 (87.8)	0.361	0.887	19.5
Bromoxynil	0.044 (3.4)	0.036 (1.1)	0.031 (0.8)	0.054 (0.4)	0.048 (2.2)	0.312 (92.4)	0.269	0.541	14.3	0.044 (3.4)	0.036 (1.1)	0.031 (0.8)	0.076 (2.2)	0.045 (1.6)	0.333 (92.1)	0.368	0.778	15.6
Bromuconazole	0.044 (3.3)	0.036 (1.5)	0.031 (0.9)	0.071 (0.3)	0.062 (2.1)	0.298 (89.7)	0.278	0.526	15.1	0.044 (3.3)	0.036 (1.5)	0.031 (0.9)	0.071 (4.4)	0.061 (3.2)	0.368 (91.2)	0.501	0.779	16.2
Bupirimate	0.044 (3.2)	0.036 (1.6)	0.031 (1.0)	0.008 (4.2)	0.045 (1.8)	0.291 (93.1)	0.259	0.668	18.3	0.044 (3.2)	0.036 (1.6)	0.031 (1.0)	0.097 (6.3)	0.070 (3.3)	0.495 (95.1)	0.500	0.765	19.6
Buprofezine	0.044 (3.1)	0.036 (1.7)	0.031 (1.4)	0.007 (4.1)	0.048 (2.2)	0.332 (85.6)	0.335	0.662	14.6	0.044 (3.1)	0.036 (1.7)	0.031 (1.4)	0.096 (5.4)	0.064 (2.8)	0.452 (94.1)	0.384	0.669	20.3
Carbaryl	0.044 (2.1)	0.036 (1.4)	0.031 (1.3)	0.009 (3.9)	0.038 (1.8)	0.301 (92.1)	0.287	0.669	17.6	0.044 (2.1)	0.036 (1.4)	0.031 (1.3)	0.071 (2.1)	0.044 (1.7)	0.413 (92.1)	0.382	0.765	21.6
Carbendazim	0.044 (2.3)	0.036 (1.5)	0.031 (0.9)	0.070 (3.7)	0.039 (1.8)	0.317 (89.5)	0.298	0.665	15.9	0.044 (2.3)	0.036 (1.5)	0.031 (0.9)	0.033 (1.5)	0.068 (1.6)	0.402 (90.8)	0.381	0.665	23.4
Carbofuran	0.044 (2.1)	0.036 (1.2)	0.031 (1.1)	0.066 (0.2)	0.041 (2.1)	0.245 (90.4)	0.301	0.514	17.6	0.044 (2.1)	0.036 (1.2)	0.031 (1.1)	0.051 (1.9)	0.060 (3.5)	0.350 (88.4)	0.504	0.654	21.8
Carbosulfan	0.044 (1.9)	0.036 (1.3)	0.031 (1.4)	0.052 (0.1)	0.068 (3.5)	0.298 (88.7)	0.305	0.512	18.6	0.044 (1.9)	0.036 (1.3)	0.031 (1.4)	0.034 (1.2)	0.071 (3.4)	0.318 (87.8)	0.501	0.774	22.8
Carboxin	0.044 (2.3)	0.036 (1.0)	0.031 (1.3)	0.054 (0.6)	0.052 (3.4)	0.291 (93.1)	0.321	0.628	17.8	0.044 (2.3)	0.036 (1.0)	0.031 (1.3)	0.076 (2.2)	0.062 (2.6)	0.333 (92.1)	0.359	0.771	21.8
Carfentrazone-Ethyl	0.044 (2.3)	0.036 (0.9)	0.031 (0.9)	0.051 (0.7)	0.037 (1.7)	0.338 (89.6)	0.315	0.624	17.6	0.044 (2.3)	0.036 (0.9)	0.031 (0.9)	0.071 (4.4)	0.045 (1.6)	0.368 (91.2)	0.385	0.659	23.6
Chlofentazine	0.044 (2.1)	0.036 (1.0)	0.031 (0.7)	0.041 (0.5)	0.045 (1.8)	0.332 (85.6)	0.311	0.701	15.9	0.044 (2.1)	0.036 (1.0)	0.031 (0.7)	0.097 (6.3)	0.061 (3.2)	0.495 (95.1)	0.504	0.662	20.8
Chlorfluozuron	0.044 (2.0)	0.036 (0.9)	0.031 (0.8)	0.040 (0.6)	0.062 (2.1)	0.312 (92.4)	0.314	0.704	18.1	0.044 (2.0)	0.036 (0.9)	0.031 (0.8)	0.096 (5.4)	0.070 (3.3)	0.452 (94.1)	0.501	0.652	19.6
Chloridazon	0.044 (3.2)	0.036 (1.2)	0.031 (0.9)	0.043 (0.2)	0.039 (1.8)	0.298 (89.7)	0.317	0.517	17.6	0.044 (3.2)	0.036 (1.2)	0.031 (0.9)	0.071 (2.1)	0.064 (2.8)	0.413 (92.1)	0.328	1.014	18.9
Chlormequat chloride	0.044 (3.5)	0.036 (1.1)	0.031 (1.0)	0.054 (0.4)	0.065 (2.6)	0.301 (92.1)	0.298	0.514	15.9	0.044 (3.5)	0.036 (1.1)	0.031 (1.0)	0.033 (1.5)	0.044 (1.7)	0.402 (90.8)	0.329	0.665	17.6
Chlorpham	0.044 (1.9)	0.036 (1.5)	0.031 (1.6)	0.071 (0.3)	0.048 (2.2)	0.317 (89.5)	0.331	0.548	14.9	0.044 (1.9)	0.036 (1.5)	0.031 (1.6)	0.051 (1.9)	0.068 (1.6)	0.350 (88.4)	0.385	1.011	15.9
Chlorpyrifos ethyl	0.044 (2.0)	0.036 (1.6)	0.031 (1.0)	0.041 (0.5)	0.045 (1.8)	0.245 (90.4)	0.289	0.514	17.5	0.044 (2.0)	0.036 (1.6)	0.031 (1.0)	0.076 (2.2)	0.060 (3.5)	0.318 (87.8)	0.384	0.774	19.8
Chlorpyrifos Methyl	0.044 (3.4)	0.036 (1.7)	0.031 (1.1)	0.040 (0.6)	0.048 (2.2)	0.298 (88.7)	0.287	0.665	15.3	0.044 (3.4)	0.036 (1.7)	0.031 (1.1)	0.071 (4.4)	0.071 (3.4)	0.333 (92.1)	0.394	0.776	18.7
Chlorsulfuron	0.044 (3.3)	0.036 (1.4)	0.031 (1.4)	0.043 (0.2)	0.038 (1.8)	0.291 (93.1)	0.269	0.541	16.1	0.044 (3.3)	0.036 (1.4)	0.031 (1.4)	0.097 (6.3)	0.062 (2.6)	0.368 (91.2)	0.392	0.669	19.3
Clethodim	0.044 (3.2)	0.036 (1.5)	0.031 (1.3)	0.054 (0.4)	0.039 (1.8)	0.298 (89.7)	0.278	0.526	14.7	0.044 (3.2)	0.036 (1.5)	0.031 (1.3)	0.096 (5.4)	0.045 (1.6)	0.495 (95.1)	0.389	0.771	17.6

Pesticide	Cucumber									Grapefruit								
	U _i ^a (mg/kg (%))									U _i ^a (mg/kg (%))								
	U ₁	U ₂	U ₃	U ₄	U ₅	U ₆	U _c	U _e ^b	U _e (%)	U ₁	U ₂	U ₃	U ₄	U ₅	U ₆	U _c	U _e ^b	U _e (%)
(mg/kg)									(mg/kg)									
Clodinafop-Propargyl	0.044 (3.1)	0.036 (1.2)	0.031 (0.9)	0.071 (0.3)	0.041 (2.1)	0.332 (85.6)	0.259	0.668	15.2	0.044 (3.1)	0.036 (1.2)	0.031 (0.9)	0.071 (2.1)	0.061 (3.2)	0.452 (94.1)	0.374	0.778	20.1
Clothianidin	0.044 (2.1)	0.036 (1.3)	0.031 (1.1)	0.008 (4.2)	0.068 (3.5)	0.312 (92.4)	0.332	0.662	12.5	0.044 (2.1)	0.036 (1.3)	0.031 (1.1)	0.033 (1.5)	0.070 (3.3)	0.413 (92.1)	0.365	0.668	21.5
Cyclanilide	0.044 (2.3)	0.036 (1.0)	0.031 (1.4)	0.007 (4.1)	0.065 (2.6)	0.298 (89.7)	0.287	0.669	13.6	0.044 (2.3)	0.036 (1.0)	0.031 (1.4)	0.051 (1.9)	0.064 (2.8)	0.402 (90.8)	0.361	0.669	23.4
Cycloate	0.044 (2.1)	0.036 (0.8)	0.031 (1.3)	0.009 (3.9)	0.048 (2.2)	0.301 (92.1)	0.298	0.665	18.1	0.044 (2.1)	0.036 (0.8)	0.031 (1.3)	0.034 (1.2)	0.044 (1.7)	0.350 (88.4)	0.368	0.664	20.9
Cyhalofop-butyl	0.044 (1.9)	0.036 (0.9)	0.031 (0.9)	0.070 (3.7)	0.039 (1.8)	0.317 (89.5)	0.301	0.514	14.8	0.044 (1.9)	0.036 (0.9)	0.031 (0.9)	0.076 (2.2)	0.068 (1.6)	0.318 (87.8)	0.498	0.774	21.7
Cymoxanil	0.044 (3.2)	0.036 (1.0)	0.031 (0.7)	0.066 (0.2)	0.062 (2.1)	0.245 (90.4)	0.305	0.512	17.5	0.044 (3.2)	0.036 (1.0)	0.031 (0.7)	0.071 (4.4)	0.060 (3.5)	0.333 (92.1)	0.465	0.778	19.8
Cypermethrin	0.044 (3.1)	0.036 (0.9)	0.031 (0.8)	0.052 (0.1)	0.048 (2.2)	0.298 (88.7)	0.321	0.628	17.6	0.044 (3.1)	0.036 (0.9)	0.031 (0.8)	0.097 (6.3)	0.071 (3.4)	0.368 (91.2)	0.395	0.779	19.5
Cyproconazole	0.044 (2.8)	0.036 (1.2)	0.031 (0.9)	0.054 (0.6)	0.038 (1.8)	0.337 (92.6)	0.315	0.624	12.5	0.044 (2.8)	0.036 (1.2)	0.031 (0.9)	0.096 (5.4)	0.062 (2.6)	0.495 (95.1)	0.401	1.010	19.1
Cyprodinil	0.044 (2.0)	0.036 (1.1)	0.031 (1.0)	0.051 (0.7)	0.039 (1.8)	0.298 (89.7)	0.311	0.701	14.8	0.044 (2.0)	0.036 (1.1)	0.031 (1.0)	0.071 (2.1)	0.045 (1.6)	0.452 (94.1)	0.425	1.011	18.7
Dazomet	0.044 (3.4)	0.036 (1.5)	0.031 (1.1)	0.041 (0.5)	0.041 (2.1)	0.332 (85.6)	0.314	0.704	17.9	0.044 (3.4)	0.036 (1.5)	0.031 (1.1)	0.033 (1.5)	0.061 (3.2)	0.413 (92.1)	0.384	0.998	19.3
Deltamethrin	0.044 (3.3)	0.036 (1.6)	0.031 (1.4)	0.040 (0.6)	0.068 (3.5)	0.312 (92.4)	0.317	0.517	18.6	0.044 (3.3)	0.036 (1.6)	0.031 (1.4)	0.051 (1.9)	0.070 (3.3)	0.402 (90.8)	0.382	0.884	16.4
Diafenthiuron	0.044 (3.2)	0.036 (1.7)	0.031 (1.3)	0.043 (0.2)	0.039 (1.8)	0.298 (89.7)	0.298	0.514	16.5	0.044 (3.2)	0.036 (1.7)	0.031 (1.3)	0.076 (2.2)	0.064 (2.8)	0.350 (88.4)	0.381	0.765	19.1
Diazinon	0.044 (3.1)	0.036 (1.4)	0.031 (0.9)	0.054 (0.4)	0.065 (2.6)	0.301 (92.1)	0.289	0.548	15.4	0.044 (3.1)	0.036 (1.4)	0.031 (0.9)	0.071 (4.4)	0.044 (1.7)	0.318 (87.8)	0.504	0.665	18.4
Dicamba	0.044 (2.1)	0.036 (1.5)	0.031 (0.7)	0.071 (0.3)	0.048 (2.2)	0.317 (89.5)	0.287	0.612	15.8	0.044 (2.1)	0.036 (1.5)	0.031 (0.7)	0.097 (6.3)	0.068 (1.6)	0.333 (92.1)	0.501	0.654	19.6
Dichlofluanid	0.044 (2.1)	0.036 (1.2)	0.031 (0.8)	0.041 (0.5)	0.048 (2.2)	0.245 (90.4)	0.269	0.514	15.9	0.044 (2.1)	0.036 (1.2)	0.031 (0.8)	0.096 (5.4)	0.060 (3.5)	0.368 (91.2)	0.359	0.774	18.9
Dichlorvos	0.044 (2.0)	0.036 (1.3)	0.031 (0.9)	0.040 (0.6)	0.038 (1.8)	0.298 (88.7)	0.278	0.665	17.6	0.044 (2.0)	0.036 (1.3)	0.031 (0.9)	0.071 (2.1)	0.071 (3.4)	0.495 (95.1)	0.385	0.771	15.8
Diclofop Methyl	0.044 (3.2)	0.036 (1.0)	0.031 (1.0)	0.043 (0.2)	0.039 (1.8)	0.332 (85.6)	0.259	0.541	18.6	0.044 (3.2)	0.036 (1.0)	0.031 (1.0)	0.033 (1.5)	0.062 (2.6)	0.452 (94.1)	0.504	0.659	19.6
Diethofencarb	0.044 (3.5)	0.036 (1.6)	0.031 (1.4)	0.054 (0.4)	0.041 (2.1)	0.312 (92.4)	0.315	0.526	17.8	0.044 (3.5)	0.036 (1.6)	0.031 (1.4)	0.051 (1.9)	0.045 (1.6)	0.413 (92.1)	0.501	0.662	20.1
Difenoconazole	0.044 (1.9)	0.036 (1.5)	0.031 (1.3)	0.071 (0.3)	0.068 (3.5)	0.298 (89.7)	0.347	0.668	17.6	0.044 (1.9)	0.036 (1.5)	0.031 (1.3)	0.034 (1.2)	0.061 (3.2)	0.402 (90.8)	0.328	0.652	15.7
Difflubenzuron	0.044 (3.2)	0.036 (1.0)	0.031 (0.9)	0.007 (4.1)	0.065 (2.6)	0.291 (93.1)	0.325	0.662	15.9	0.044 (3.2)	0.036 (1.0)	0.031 (0.9)	0.076 (2.2)	0.070 (3.3)	0.350 (88.4)	0.329	1.014	16.4
Dimethenamid	0.044 (3.1)	0.036 (0.9)	0.031 (1.1)	0.009 (3.9)	0.048 (2.2)	0.337 (92.6)	0.333	0.669	18.1	0.044 (3.1)	0.036 (0.9)	0.031 (1.1)	0.071 (4.4)	0.064 (2.8)	0.318 (87.8)	0.385	0.665	18.3

Pesticide	Cucumber									Grapefruit									
	U ₁	U ₂	U _i ^a (mg/kg (%))			U ₆	U _c	U _e ^b	U _e (%)		U ₁	U ₂	U _i ^a (mg/kg (%))			U ₆	U _c	U _e ^b	U _e (%)
			U ₃	U ₄	U ₅								U ₃	U ₄	U ₅				
(mg/kg)									(mg/kg)										
Dimethoate	0.044 (2.8)	0.036 (1.2)	0.031 (1.4)	0.070 (3.7)	0.039 (1.8)	0.298 (89.7)	0.287	0.618	17.6	0.044 (2.8)	0.036 (1.2)	0.031 (1.4)	0.097 (6.3)	0.044 (1.7)	0.333 (92.1)	0.384	1.011	19.5	
Dimethomorph	0.044 (3.4)	0.036 (1.1)	0.031 (1.3)	0.066 (0.2)	0.062 (2.1)	0.301 (92.1)	0.298	0.662	15.9	0.044 (3.4)	0.036 (1.1)	0.031 (1.3)	0.096 (5.4)	0.068 (1.6)	0.368 (91.2)	0.394	0.774	15.6	
Diniconazole	0.044 (3.3)	0.036 (1.5)	0.031 (0.9)	0.052 (0.1)	0.045 (1.8)	0.317 (89.5)	0.301	0.665	15.6	0.044 (3.3)	0.036 (1.5)	0.031 (0.9)	0.071 (2.1)	0.060 (3.5)	0.495 (95.1)	0.392	0.776	16.2	
Dinocap	0.044 (3.2)	0.036 (1.6)	0.031 (0.7)	0.054 (0.6)	0.048 (2.2)	0.245 (90.4)	0.305	0.514	15.8	0.044 (3.2)	0.036 (1.6)	0.031 (0.7)	0.033 (1.5)	0.071 (3.4)	0.452 (94.1)	0.389	0.669	19.6	
Dioxathion	0.044 (3.1)	0.036 (1.7)	0.031 (0.8)	0.051 (0.7)	0.038 (1.8)	0.298 (88.7)	0.321	0.512	17.4	0.044 (3.1)	0.036 (1.7)	0.031 (0.8)	0.051 (1.9)	0.062 (2.6)	0.413 (92.1)	0.374	0.771	20.3	
Diphenamid	0.044 (2.1)	0.036 (1.4)	0.031 (0.9)	0.041 (0.5)	0.039 (1.8)	0.332 (85.6)	0.315	0.628	16.5	0.044 (2.1)	0.036 (1.4)	0.031 (0.9)	0.076 (2.2)	0.045 (1.6)	0.402 (90.8)	0.365	0.778	21.6	
Dithianon	0.044 (2.3)	0.036 (1.5)	0.031 (1.0)	0.040 (0.6)	0.041 (2.1)	0.312 (92.4)	0.311	0.624	13.4	0.044 (2.3)	0.036 (1.5)	0.031 (1.0)	0.071 (4.4)	0.061 (3.2)	0.350 (88.4)	0.361	0.668	23.4	
Diuron	0.044 (2.1)	0.036 (1.2)	0.031 (1.5)	0.043 (0.2)	0.068 (3.5)	0.298 (89.7)	0.314	0.701	15.2	0.044 (2.1)	0.036 (1.2)	0.031 (1.5)	0.097 (6.3)	0.070 (3.3)	0.318 (87.8)	0.368	0.669	21.8	
Epoxyconazole	0.044 (2.0)	0.036 (1.3)	0.031 (1.6)	0.054 (0.4)	0.052 (3.4)	0.337 (92.6)	0.317	0.704	14.2	0.044 (2.0)	0.036 (1.3)	0.031 (1.6)	0.096 (5.4)	0.064 (2.8)	0.333 (92.1)	0.432	0.774	22.8	
EPTC	0.044 (3.2)	0.036 (1.0)	0.031 (1.0)	0.071 (0.3)	0.037 (1.7)	0.332 (87.4)	0.298	0.517	18.1	0.044 (3.2)	0.036 (1.0)	0.031 (1.0)	0.071 (2.1)	0.044 (1.7)	0.368 (91.2)	0.425	0.885	21.8	
Esfenvalerate	0.044 (3.5)	0.036 (1.4)	0.031 (1.1)	0.041 (0.5)	0.045 (1.8)	0.301 (92.1)	0.289	0.514	15.4	0.044 (3.5)	0.036 (1.4)	0.031 (1.1)	0.033 (1.5)	0.068 (1.6)	0.495 (95.1)	0.421	0.668	23.6	
Ethalfuralin	0.044 (1.9)	0.036 (1.0)	0.031 (1.4)	0.040 (0.6)	0.065 (2.6)	0.317 (89.5)	0.287	0.548	16.4	0.044 (1.9)	0.036 (1.0)	0.031 (1.4)	0.051 (1.9)	0.060 (3.5)	0.452 (94.1)	0.384	0.662	20.8	
Ethiofencarb	0.044 (2.0)	0.036 (0.9)	0.031 (1.3)	0.043 (0.2)	0.048 (2.2)	0.245 (90.4)	0.269	0.621	15.9	0.044 (2.0)	0.036 (0.9)	0.031 (1.3)	0.050 (1.7)	0.071 (3.4)	0.413 (92.1)	0.382	0.775	19.6	
Ethofumasate	0.044 (3.4)	0.036 (1.2)	0.031 (0.9)	0.054 (0.4)	0.062 (2.1)	0.298 (88.7)	0.278	0.514	17.6	0.044 (3.4)	0.036 (1.2)	0.031 (0.9)	0.034 (1.2)	0.062 (2.6)	0.402 (90.8)	0.381	0.771	18.9	
Ethoprophos	0.044 (3.3)	0.036 (1.1)	0.031 (1.1)	0.071 (0.3)	0.039 (1.8)	0.291 (93.1)	0.259	0.665	18.6	0.044 (3.3)	0.036 (1.1)	0.031 (1.1)	0.076 (2.2)	0.045 (1.6)	0.350 (88.4)	0.504	0.770	17.6	
Etofenprox	0.044 (3.2)	0.036 (1.5)	0.031 (1.4)	0.023 (0.7)	0.065 (2.6)	0.298 (89.7)	0.287	0.541	17.8	0.044 (3.2)	0.036 (1.5)	0.031 (1.4)	0.071 (4.4)	0.061 (3.2)	0.318 (87.8)	0.501	0.776	15.9	
Etoxazole	0.044 (3.1)	0.036 (1.6)	0.031 (1.3)	0.072 (4.3)	0.048 (2.2)	0.337 (92.6)	0.298	0.526	17.6	0.044 (3.1)	0.036 (1.6)	0.031 (1.3)	0.097 (6.3)	0.070 (3.3)	0.333 (92.1)	0.359	0.778	20.1	
Famoxadone	0.044 (2.1)	0.036 (1.7)	0.031 (0.9)	0.008 (4.2)	0.048 (2.2)	0.298 (89.7)	0.301	0.668	15.9	0.044 (2.1)	0.036 (1.7)	0.031 (0.9)	0.096 (5.4)	0.064 (2.8)	0.368 (91.2)	0.385	0.776	21.8	
Fenamidon	0.044 (3.2)	0.036 (1.4)	0.031 (0.7)	0.007 (4.1)	0.038 (1.8)	0.332 (85.6)	0.305	0.662	18.1	0.044 (3.2)	0.036 (1.4)	0.031 (0.7)	0.071 (2.1)	0.044 (1.7)	0.495 (95.1)	0.504	0.765	22.6	
Fenamiphos (sum)	0.044 (3.1)	0.036 (1.5)	0.031 (0.8)	0.009 (3.9)	0.039 (1.8)	0.312 (92.4)	0.321	0.669	17.6	0.044 (3.1)	0.036 (1.5)	0.031 (0.8)	0.033 (1.5)	0.068 (1.6)	0.452 (94.1)	0.501	0.665	19.3	
Fenarimol	0.044 (2.8)	0.036 (1.2)	0.031 (0.9)	0.070 (3.7)	0.041 (2.1)	0.298 (89.7)	0.315	0.662	15.9	0.044 (2.8)	0.036 (1.2)	0.031 (0.9)	0.051 (1.9)	0.060 (3.5)	0.413 (92.1)	0.328	0.654	18.9	
Fenazaquin	0.044 (3.1)	0.036 (1.3)	0.031 (1.0)	0.066 (0.2)	0.068 (3.5)	0.301 (92.1)	0.311	0.665	16.5	0.044 (3.1)	0.036 (1.3)	0.031 (1.0)	0.076 (2.2)	0.071 (3.4)	0.402 (90.8)	0.329	0.774	15.6	

Pesticide	Cucumber									Grapefruit									
	U ₁	U ₂	U _i ^a (mg/kg (%))			U ₆	U _c	U _e ^b	U _e (%)		U ₁	U ₂	U _i ^a (mg/kg (%))			U ₆	U _c	U _e ^b	U _e (%)
			U ₃	U ₄	U ₅								U ₃	U ₄	U ₅				
(mg/kg)									(mg/kg)										
Fenbuconazole	0.044 (3.3)	0.036 (1.0)	0.031 (1.1)	0.052 (0.1)	0.039 (1.8)	0.317 (89.5)	0.314	0.514	15.3	0.044 (3.3)	0.036 (1.0)	0.031 (1.1)	0.071 (4.4)	0.062 (2.6)	0.350 (88.4)	0.385	0.771	16.2	
Fenoxaprop-P-Ethyl	0.044 (2.3)	0.036 (0.9)	0.031 (1.4)	0.054 (0.6)	0.065 (2.6)	0.245 (90.4)	0.317	0.512	15.9	0.044 (2.3)	0.036 (0.9)	0.031 (1.4)	0.097 (6.3)	0.045 (1.6)	0.318 (87.8)	0.384	0.659	19.6	
Fenoxycarb	0.044 (2.1)	0.036 (0.8)	0.031 (1.3)	0.051 (0.7)	0.048 (2.2)	0.298 (88.7)	0.298	0.628	14.8	0.044 (2.1)	0.036 (0.8)	0.031 (1.3)	0.096 (5.4)	0.061 (3.2)	0.333 (92.1)	0.394	0.662	20.3	
Fenpropathrin	0.044 (2.0)	0.036 (1.6)	0.031 (0.9)	0.041 (0.5)	0.048 (2.2)	0.291 (93.1)	0.335	0.624	18.1	0.044 (2.0)	0.036 (1.6)	0.031 (0.9)	0.071 (2.1)	0.070 (3.3)	0.368 (91.2)	0.392	0.652	21.6	
Fenpyroximate	0.044 (3.2)	0.036 (1.0)	0.031 (0.7)	0.040 (0.6)	0.038 (1.8)	0.298 (89.7)	0.289	0.701	16.9	0.044 (3.2)	0.036 (1.0)	0.031 (0.7)	0.033 (1.5)	0.064 (2.8)	0.495 (95.1)	0.389	1.014	18.9	
Fenthion	0.044 (3.5)	0.036 (0.9)	0.031 (0.8)	0.043 (0.2)	0.039 (1.8)	0.285 (91.1)	0.287	0.704	15.8	0.044 (3.5)	0.036 (0.9)	0.031 (0.8)	0.051 (1.9)	0.044 (1.7)	0.452 (94.1)	0.374	0.665	17.8	
Fenvalerate	0.044 (1.9)	0.036 (1.2)	0.031 (0.9)	0.054 (0.4)	0.041 (2.1)	0.331 (92.2)	0.269	0.517	17.5	0.044 (1.9)	0.036 (1.2)	0.031 (0.9)	0.076 (2.2)	0.068 (1.6)	0.413 (92.1)	0.365	1.011	16.9	
Fipronil	0.044 (2.0)	0.036 (1.1)	0.031 (1.0)	0.071 (0.3)	0.068 (3.5)	0.337 (92.6)	0.278	0.514	15.8	0.044 (2.0)	0.036 (1.1)	0.031 (1.0)	0.071 (4.4)	0.060 (3.5)	0.402 (90.8)	0.361	0.774	20.1	
Fluazifop-P-Butyl	0.044 (3.4)	0.036 (1.5)	0.031 (1.4)	0.041 (0.5)	0.062 (2.1)	0.298 (89.7)	0.259	0.548	16.4	0.044 (3.4)	0.036 (1.5)	0.031 (1.4)	0.097 (6.3)	0.071 (3.4)	0.350 (88.4)	0.368	0.776	23.4	
Fluazinam	0.044 (3.3)	0.036 (1.6)	0.031 (1.3)	0.040 (0.6)	0.039 (1.8)	0.291 (93.1)	0.315	0.587	15.8	0.044 (3.3)	0.036 (1.6)	0.031 (1.3)	0.096 (5.4)	0.062 (2.6)	0.318 (87.8)	0.401	0.669	20.4	
Fludioxynil	0.044 (3.2)	0.036 (1.7)	0.031 (0.9)	0.043 (0.2)	0.045 (1.8)	0.332 (85.6)	0.347	0.514	15.9	0.044 (3.2)	0.036 (1.7)	0.031 (0.9)	0.071 (2.1)	0.045 (1.6)	0.333 (92.1)	0.384	0.771	21.8	
Flufenoxuron	0.044 (3.1)	0.036 (1.4)	0.031 (1.1)	0.054 (0.4)	0.048 (2.2)	0.312 (92.4)	0.325	0.665	18.1	0.044 (3.1)	0.036 (1.4)	0.031 (1.1)	0.033 (1.5)	0.061 (3.2)	0.368 (91.2)	0.382	0.778	19.8	
Flurasulam	0.044 (2.1)	0.036 (1.5)	0.031 (1.4)	0.071 (0.3)	0.038 (1.8)	0.298 (89.7)	0.287	0.541	15.9	0.044 (2.1)	0.036 (1.5)	0.031 (1.4)	0.051 (1.9)	0.070 (3.3)	0.495 (95.1)	0.381	0.668	18.9	
Flurochloridone	0.044 (3.2)	0.036 (1.2)	0.031 (1.3)	0.008 (4.2)	0.039 (1.8)	0.301 (92.1)	0.298	0.526	17.6	0.044 (3.2)	0.036 (1.2)	0.031 (1.3)	0.096 (5.4)	0.064 (2.8)	0.452 (94.1)	0.504	0.669	15.7	
Flusilazole	0.044 (3.1)	0.036 (1.3)	0.031 (0.9)	0.007 (4.1)	0.041 (2.1)	0.317 (89.5)	0.301	0.668	18.6	0.044 (3.1)	0.036 (1.3)	0.031 (0.9)	0.071 (2.1)	0.044 (1.7)	0.413 (92.1)	0.501	0.770	16.4	
Flutriafol	0.044 (2.8)	0.036 (1.0)	0.031 (0.7)	0.009 (3.9)	0.068 (3.5)	0.245 (90.4)	0.305	0.662	17.8	0.044 (2.8)	0.036 (1.0)	0.031 (0.7)	0.033 (1.5)	0.068 (1.6)	0.402 (90.8)	0.359	0.776	18.3	
Foramsulfuron	0.044 (2.3)	0.036 (0.9)	0.031 (0.8)	0.070 (3.7)	0.039 (1.8)	0.298 (88.7)	0.321	0.669	17.6	0.044 (2.3)	0.036 (0.9)	0.031 (0.8)	0.051 (1.9)	0.060 (3.5)	0.350 (88.4)	0.385	0.778	19.5	
Formatanate	0.044 (2.1)	0.036 (0.8)	0.031 (0.9)	0.066 (0.2)	0.065 (2.6)	0.285 (91.1)	0.315	0.665	15.9	0.044 (2.1)	0.036 (0.8)	0.031 (0.9)	0.076 (2.2)	0.071 (3.4)	0.318 (87.8)	0.504	0.776	15.6	
Fosthiazate	0.044 (2.0)	0.036 (1.6)	0.031 (1.0)	0.052 (0.1)	0.048 (2.2)	0.337 (92.6)	0.311	0.663	18.1	0.044 (2.0)	0.036 (1.6)	0.031 (1.0)	0.071 (4.4)	0.062 (2.6)	0.333 (92.1)	0.501	0.765	16.2	
Furathiocarb	0.044 (3.2)	0.036 (1.0)	0.031 (0.9)	0.054 (0.6)	0.048 (2.2)	0.298 (89.7)	0.314	0.664	17.6	0.044 (3.2)	0.036 (1.0)	0.031 (0.9)	0.097 (6.3)	0.045 (1.6)	0.368 (91.2)	0.328	0.998	19.6	
Giberellic acid	0.044 (3.5)	0.036 (0.9)	0.031 (0.8)	0.051 (0.7)	0.038 (1.8)	0.332 (85.6)	0.317	0.521	15.9	0.044 (3.5)	0.036 (0.9)	0.031 (0.8)	0.096 (5.4)	0.061 (3.2)	0.495 (95.1)	0.329	0.884	20.3	

Pesticide	Cucumber									Grapefruit								
	U ₁	U ₂	U _i ^a (mg/kg (%))			U ₆	U _c	U _e ^b	U _e (%)	U ₁	U ₂	U _i ^a (mg/kg (%))			U ₆	U _c	U _e ^b	U _e (%)
			U ₃	U ₄	U ₅							U ₃	U ₄	U ₅				
(mg/kg)									(mg/kg)									
Halfenprox	0.044 (1.9)	0.036 (0.8)	0.031 (1.5)	0.041 (0.5)	0.039 (1.8)	0.312 (92.4)	0.298	0.547	18.4	0.044 (1.9)	0.036 (0.8)	0.031 (1.5)	0.071 (2.1)	0.070 (3.3)	0.452 (94.1)	0.385	0.771	21.6
Haloxypop-2-Etoxyethyl	0.044 (2.0)	0.036 (1.6)	0.031 (1.6)	0.040 (0.6)	0.041 (2.1)	0.298 (89.7)	0.337	0.618	15.2	0.044 (2.0)	0.036 (1.6)	0.031 (1.6)	0.033 (1.5)	0.064 (2.8)	0.413 (92.1)	0.384	0.665	23.4
Haloxypop-P-Methyl	0.044 (3.4)	0.036 (0.9)	0.031 (1.0)	0.043 (0.2)	0.068 (3.5)	0.301 (92.1)	0.289	0.662	16.5	0.044 (3.4)	0.036 (0.9)	0.031 (1.0)	0.051 (1.9)	0.044 (1.7)	0.402 (90.8)	0.394	0.882	21.8
Hexaconazole	0.044 (3.3)	0.036 (1.2)	0.031 (1.1)	0.054 (0.4)	0.062 (2.1)	0.317 (89.5)	0.287	0.665	16.9	0.044 (3.3)	0.036 (1.2)	0.031 (1.1)	0.076 (2.2)	0.068 (1.6)	0.350 (88.4)	0.392	0.962	22.8
Hexaflumuron	0.044 (3.2)	0.036 (1.1)	0.031 (1.4)	0.071 (0.3)	0.045 (1.8)	0.245 (90.4)	0.269	0.514	16.3	0.044 (3.2)	0.036 (1.1)	0.031 (1.4)	0.071 (4.4)	0.060 (3.5)	0.318 (87.8)	0.389	1.012	21.8
Hexythiazox	0.044 (3.1)	0.036 (1.5)	0.031 (1.3)	0.041 (0.5)	0.039 (1.8)	0.298 (88.7)	0.278	0.512	16.1	0.044 (3.1)	0.036 (1.5)	0.031 (1.3)	0.097 (6.3)	0.071 (3.4)	0.333 (92.1)	0.374	0.669	23.6
Imazalil	0.044 (2.1)	0.036 (1.6)	0.031 (0.9)	0.040 (0.6)	0.065 (2.6)	0.291 (93.1)	0.259	0.628	15.9	0.044 (2.1)	0.036 (1.6)	0.031 (0.9)	0.096 (5.4)	0.062 (2.6)	0.368 (91.2)	0.365	0.771	20.8
Imazamox	0.044 (3.2)	0.036 (1.7)	0.031 (1.1)	0.043 (0.2)	0.048 (2.2)	0.285 (91.1)	0.339	0.624	17.5	0.044 (3.2)	0.036 (1.7)	0.031 (1.1)	0.071 (2.1)	0.045 (1.6)	0.495 (95.1)	0.361	0.778	19.6
Imazapic	0.044 (3.1)	0.036 (1.4)	0.031 (1.4)	0.054 (0.4)	0.048 (2.2)	0.331 (92.2)	0.341	0.701	15.4	0.044 (3.1)	0.036 (1.4)	0.031 (1.4)	0.033 (1.5)	0.061 (3.2)	0.452 (94.1)	0.368	0.668	18.9
Imazapyr	0.044 (2.8)	0.036 (1.5)	0.031 (1.3)	0.071 (0.3)	0.038 (1.8)	0.337 (92.6)	0.287	0.704	16.4	0.044 (2.8)	0.036 (1.5)	0.031 (1.3)	0.051 (1.9)	0.070 (3.3)	0.413 (92.1)	0.382	0.669	17.6
Imazethapyr	0.044 (2.7)	0.036 (1.2)	0.031 (0.9)	0.072 (4.3)	0.039 (1.8)	0.298 (89.7)	0.298	0.517	15.7	0.044 (2.7)	0.036 (1.2)	0.031 (0.9)	0.097 (6.3)	0.064 (2.8)	0.402 (90.8)	0.381	0.770	15.9
Imidacloprid	0.044 (2.5)	0.036 (1.3)	0.031 (0.7)	0.008 (4.2)	0.041 (2.1)	0.291 (93.1)	0.301	0.514	15.9	0.044 (2.5)	0.036 (1.3)	0.031 (0.7)	0.096 (5.4)	0.044 (1.7)	0.350 (88.4)	0.504	0.776	19.8
Iodosulfuron-Methyl	0.044 (2.3)	0.036 (1.0)	0.031 (0.8)	0.007 (4.1)	0.068 (3.5)	0.332 (85.6)	0.305	0.548	17.6	0.044 (2.3)	0.036 (1.0)	0.031 (0.8)	0.071 (2.1)	0.068 (1.6)	0.318 (87.8)	0.501	0.778	18.6
Ioxynil	0.044 (2.1)	0.036 (1.3)	0.031 (0.9)	0.009 (3.9)	0.065 (2.6)	0.312 (92.4)	0.321	0.587	18.6	0.044 (2.1)	0.036 (1.3)	0.031 (0.9)	0.033 (1.5)	0.060 (3.5)	0.333 (92.1)	0.359	0.776	23.6
Iprodione	0.044 (2.0)	0.036 (1.0)	0.031 (1.0)	0.070 (3.7)	0.048 (2.2)	0.298 (89.7)	0.315	0.514	17.8	0.044 (2.0)	0.036 (1.0)	0.031 (1.0)	0.051 (1.9)	0.071 (3.4)	0.368 (91.2)	0.385	0.765	20.8
Isoxaflutole	0.044 (3.2)	0.036 (0.9)	0.031 (1.1)	0.066 (0.2)	0.039 (1.8)	0.301 (92.1)	0.311	0.665	17.6	0.044 (3.2)	0.036 (0.9)	0.031 (1.1)	0.076 (2.2)	0.062 (2.6)	0.495 (95.1)	0.504	0.765	19.6
Kresoxim methyl	0.044 (3.5)	0.036 (1.3)	0.031 (1.4)	0.052 (0.1)	0.052 (3.4)	0.317 (89.5)	0.314	0.541	15.9	0.044 (3.5)	0.036 (1.3)	0.031 (1.4)	0.071 (4.4)	0.045 (1.6)	0.452 (94.1)	0.501	0.665	18.9
Lambda Cyhalothrin	0.044 (1.9)	0.036 (1.0)	0.031 (1.3)	0.054 (0.6)	0.037 (1.7)	0.245 (90.4)	0.317	0.526	18.1	0.044 (1.9)	0.036 (1.0)	0.031 (1.3)	0.097 (6.3)	0.061 (3.2)	0.413 (92.1)	0.328	0.654	17.6
Lenacil	0.044 (2.0)	0.036 (0.9)	0.031 (0.9)	0.051 (0.7)	0.045 (1.8)	0.298 (88.7)	0.298	0.668	17.6	0.044 (2.0)	0.036 (0.9)	0.031 (0.9)	0.096 (5.4)	0.070 (3.3)	0.402 (90.8)	0.329	0.774	15.9
Lufenuron	0.044 (3.4)	0.036 (0.8)	0.031 (0.7)	0.041 (0.5)	0.062 (2.1)	0.291 (93.1)	0.324	0.662	15.9	0.044 (3.4)	0.036 (0.8)	0.031 (0.7)	0.071 (2.1)	0.064 (2.8)	0.350 (88.4)	0.385	0.771	19.8

Pesticide	Cucumber									Grapefruit								
	U ₁	U ₂	U _i ^a (mg/kg (%))			U ₆	U _c	U _e ^b	U _e (%)	U ₁	U ₂	U _i ^a (mg/kg (%))			U ₆	U _c	U _e ^b	U _e (%)
			U ₃	U ₄	U ₅							U ₃	U ₄	U ₅				
(mg/kg)									(mg/kg)									
Malathion	0.044 (3.3)	0.036 (1.6)	0.031 (0.8)	0.040 (0.6)	0.048 (2.2)	0.337 (92.6)	0.289	0.669	14.6	0.044 (3.3)	0.036 (1.6)	0.031 (0.8)	0.033 (1.5)	0.044 (1.7)	0.318 (87.8)	0.384	0.659	20.1
MCPA	0.044 (3.2)	0.036 (1.2)	0.031 (0.9)	0.043 (0.2)	0.038 (1.8)	0.285 (91.1)	0.287	0.662	15.6	0.044 (3.2)	0.036 (1.2)	0.031 (0.9)	0.051 (1.9)	0.068 (1.6)	0.333 (92.1)	0.394	0.662	20.8
Mecoprop	0.044 (3.1)	0.036 (1.1)	0.031 (1.0)	0.054 (0.4)	0.039 (1.8)	0.329 (93.3)	0.269	0.547	12.3	0.044 (3.1)	0.036 (1.1)	0.031 (1.0)	0.076 (2.2)	0.060 (3.5)	0.368 (91.2)	0.392	0.652	22.8
Mefenpyr-diethyl	0.044 (2.1)	0.036 (1.5)	0.031 (1.0)	0.071 (0.3)	0.041 (2.1)	0.331 (92.2)	0.278	0.521	14.8	0.044 (2.1)	0.036 (1.5)	0.031 (1.0)	0.071 (4.4)	0.071 (3.4)	0.495 (95.1)	0.389	1.014	22.7
Mesosulfuron methyl	0.044 (3.2)	0.036 (1.6)	0.031 (1.1)	0.041 (0.5)	0.068 (3.5)	0.285 (91.1)	0.259	0.562	15.4	0.044 (3.2)	0.036 (1.6)	0.031 (1.1)	0.097 (6.3)	0.062 (2.6)	0.452 (94.1)	0.374	0.665	21.6
Mesotrione	0.044 (3.1)	0.036 (1.7)	0.031 (1.4)	0.040 (0.6)	0.039 (1.8)	0.337 (92.6)	0.321	0.574	14.6	0.044 (3.1)	0.036 (1.7)	0.031 (1.4)	0.096 (5.4)	0.045 (1.6)	0.413 (92.1)	0.365	1.011	20.4
Metalaxyl	0.044 (2.8)	0.036 (1.4)	0.031 (1.3)	0.043 (0.2)	0.052 (3.4)	0.298 (89.7)	0.287	0.618	14.5	0.044 (2.8)	0.036 (1.4)	0.031 (1.3)	0.071 (2.1)	0.061 (3.2)	0.402 (90.8)	0.361	0.774	19.8
Metamitron	0.044 (2.1)	0.036 (1.5)	0.031 (0.9)	0.054 (0.4)	0.037 (1.7)	0.332 (85.6)	0.298	0.662	17.2	0.044 (2.1)	0.036 (1.5)	0.031 (0.9)	0.033 (1.5)	0.070 (3.3)	0.350 (88.4)	0.368	0.776	15.7
Metconazole	0.044 (2.0)	0.036 (1.2)	0.031 (1.1)	0.071 (0.3)	0.045 (1.8)	0.312 (92.4)	0.301	0.665	17.1	0.044 (2.0)	0.036 (1.2)	0.031 (1.1)	0.051 (1.9)	0.064 (2.8)	0.318 (87.8)	0.501	0.669	16.4
Methidathion	0.044 (3.2)	0.036 (1.3)	0.031 (1.4)	0.008 (4.2)	0.048 (2.2)	0.298 (89.7)	0.305	0.514	15.6	0.044 (3.2)	0.036 (1.3)	0.031 (1.4)	0.096 (5.4)	0.044 (1.7)	0.333 (92.1)	0.425	0.771	18.3
Methomyl	0.044 (3.5)	0.036 (1.0)	0.031 (1.3)	0.007 (4.1)	0.038 (1.8)	0.301 (92.1)	0.321	0.512	18.1	0.044 (3.5)	0.036 (1.0)	0.031 (1.3)	0.071 (2.1)	0.068 (1.6)	0.368 (91.2)	0.384	0.778	19.5
Methoxyfenozide	0.044 (1.9)	0.036 (1.3)	0.031 (0.9)	0.009 (3.9)	0.039 (1.8)	0.317 (89.5)	0.315	0.628	16.4	0.044 (1.9)	0.036 (1.3)	0.031 (0.9)	0.033 (1.5)	0.060 (3.5)	0.495 (95.1)	0.382	0.668	15.6
Metolachlor	0.044 (2.2)	0.036 (1.0)	0.031 (0.7)	0.070 (3.7)	0.041 (2.1)	0.245 (90.4)	0.311	0.624	15.3	0.044 (2.2)	0.036 (1.0)	0.031 (0.7)	0.051 (1.9)	0.071 (3.4)	0.452 (94.1)	0.381	0.669	16.2
Metribuzin	0.044 (2.0)	0.036 (0.9)	0.031 (0.8)	0.066 (0.2)	0.068 (3.5)	0.298 (88.7)	0.314	0.701	15.8	0.044 (2.0)	0.036 (0.9)	0.031 (0.8)	0.076 (2.2)	0.062 (2.6)	0.413 (92.1)	0.504	0.770	19.6
Metsulfuron-methyl	0.044 (3.4)	0.036 (0.8)	0.031 (0.9)	0.052 (0.1)	0.065 (2.6)	0.291 (93.1)	0.317	0.704	15.9	0.044 (3.4)	0.036 (0.8)	0.031 (0.9)	0.071 (4.4)	0.045 (1.6)	0.402 (90.8)	0.501	0.776	20.3
Monocrotophos	0.044 (3.3)	0.036 (1.6)	0.031 (1.0)	0.054 (0.6)	0.048 (2.2)	0.285 (91.1)	0.298	0.517	17.6	0.044 (3.3)	0.036 (1.6)	0.031 (1.0)	0.097 (6.3)	0.061 (3.2)	0.350 (88.4)	0.359	0.778	21.6
Monolinuron	0.044 (3.2)	0.036 (0.9)	0.031 (1.1)	0.051 (0.7)	0.039 (1.8)	0.337 (92.6)	0.297	0.514	18.6	0.044 (3.2)	0.036 (0.9)	0.031 (1.1)	0.096 (5.4)	0.070 (3.3)	0.318 (87.8)	0.385	0.776	23.4
Myclobutanil	0.044 (3.1)	0.036 (1.2)	0.031 (1.4)	0.041 (0.5)	0.062 (2.1)	0.298 (89.7)	0.299	0.548	17.8	0.044 (3.1)	0.036 (1.2)	0.031 (1.4)	0.071 (2.1)	0.064 (2.8)	0.333 (92.1)	0.504	0.765	21.8
Nicosulfuron	0.044 (2.1)	0.036 (1.1)	0.031 (1.3)	0.040 (0.6)	0.045 (1.8)	0.332 (85.6)	0.289	0.514	17.6	0.044 (2.1)	0.036 (1.1)	0.031 (1.3)	0.033 (1.5)	0.044 (1.7)	0.368 (91.2)	0.501	1.011	22.8
Novaluron	0.044 (2.3)	0.036 (1.5)	0.031 (0.9)	0.043 (0.2)	0.048 (2.2)	0.312 (92.4)	0.287	0.665	15.9	0.044 (2.3)	0.036 (1.5)	0.031 (0.9)	0.051 (1.9)	0.068 (1.6)	0.495 (95.1)	0.328	0.994	21.8

Pesticide	Cucumber									Grapefruit								
	U ₁	U ₂	U _i ^a (mg/kg (%))			U ₆	U _c	U _e ^b	U _e (%)	U ₁	U ₂	U _i ^a (mg/kg (%))			U ₆	U _c	U _e ^b	U _e (%)
			U ₃	U ₄	U ₅							U ₃	U ₄	U ₅				
(mg/kg)									(mg/kg)									
Omethoate	0.044 (2.1)	0.036 (1.6)	0.031 (0.7)	0.054 (0.4)	0.038 (1.8)	0.298 (89.7)	0.269	0.541	18.1	0.044 (2.1)	0.036 (1.6)	0.031 (0.7)	0.076 (2.2)	0.060 (3.5)	0.452 (94.1)	0.329	0.886	23.6
Oxadixyl	0.044 (1.9)	0.036 (1.7)	0.031 (0.8)	0.071 (0.3)	0.039 (1.8)	0.301 (92.1)	0.278	0.526	17.6	0.044 (1.9)	0.036 (1.7)	0.031 (0.8)	0.071 (4.4)	0.071 (3.4)	0.413 (92.1)	0.385	0.887	20.8
Oxamyl	0.044 (3.2)	0.036 (1.4)	0.031 (0.9)	0.041 (0.5)	0.041 (2.1)	0.317 (89.5)	0.259	0.668	15.9	0.044 (3.2)	0.036 (1.4)	0.031 (0.9)	0.097 (6.3)	0.062 (2.6)	0.402 (90.8)	0.384	0.885	19.6
Oxyflourfen	0.044 (3.1)	0.036 (1.5)	0.031 (1.0)	0.040 (0.6)	0.068 (3.5)	0.245 (90.4)	0.317	0.662	16.3	0.044 (3.1)	0.036 (1.5)	0.031 (1.0)	0.096 (5.4)	0.045 (1.6)	0.350 (88.4)	0.394	0.881	18.9
Parathion Methyl	0.044 (2.8)	0.036 (1.2)	0.031 (1.4)	0.043 (0.2)	0.052 (3.4)	0.298 (88.7)	0.287	0.669	15.6	0.044 (2.8)	0.036 (1.2)	0.031 (1.4)	0.071 (2.1)	0.061 (3.2)	0.318 (87.8)	0.392	0.669	17.6
Penconazole	0.044 (2.1)	0.036 (1.3)	0.031 (1.3)	0.054 (0.4)	0.037 (1.7)	0.332 (85.6)	0.298	0.618	16.3	0.044 (2.1)	0.036 (1.3)	0.031 (1.3)	0.033 (1.5)	0.070 (3.3)	0.333 (92.1)	0.389	0.771	15.9
Pendimethalin	0.044 (2.0)	0.036 (1.0)	0.031 (0.9)	0.071 (0.3)	0.045 (1.8)	0.312 (92.4)	0.301	0.662	15.6	0.044 (2.0)	0.036 (1.0)	0.031 (0.9)	0.051 (1.9)	0.064 (2.8)	0.368 (91.2)	0.374	0.778	18.3
Permethrin	0.044 (3.2)	0.036 (1.0)	0.031 (1.1)	0.023 (0.7)	0.065 (2.6)	0.298 (89.7)	0.305	0.665	18.1	0.044 (3.2)	0.036 (1.0)	0.031 (1.1)	0.096 (5.4)	0.044 (1.7)	0.495 (95.1)	0.365	0.668	17.5
Phenmedipham	0.044 (3.5)	0.036 (0.9)	0.031 (1.4)	0.072 (4.3)	0.048 (2.2)	0.291 (93.1)	0.321	0.514	14.5	0.044 (3.5)	0.036 (0.9)	0.031 (1.4)	0.071 (2.1)	0.068 (1.6)	0.452 (94.1)	0.361	0.669	17.3
Phenthoate	0.044 (1.9)	0.036 (1.2)	0.031 (1.3)	0.008 (4.2)	0.062 (2.1)	0.285 (91.1)	0.315	0.512	16.2	0.044 (1.9)	0.036 (1.2)	0.031 (1.3)	0.033 (1.5)	0.060 (3.5)	0.413 (92.1)	0.368	0.770	17.2
Phosalone	0.044 (2.0)	0.036 (1.1)	0.031 (0.9)	0.007 (4.1)	0.039 (1.8)	0.329 (93.3)	0.311	0.628	18.2	0.044 (2.0)	0.036 (1.1)	0.031 (0.9)	0.051 (1.9)	0.071 (3.4)	0.402 (90.8)	0.441	0.776	19.6
Phosmet	0.044 (3.4)	0.036 (1.5)	0.031 (0.7)	0.009 (3.9)	0.065 (2.6)	0.337 (92.6)	0.314	0.624	14.3	0.044 (3.4)	0.036 (1.5)	0.031 (0.7)	0.076 (2.2)	0.062 (2.6)	0.350 (88.4)	0.445	0.778	15.6
Pirimicarb	0.044 (3.3)	0.036 (1.6)	0.031 (0.8)	0.070 (3.7)	0.048 (2.2)	0.298 (89.7)	0.317	0.701	16.9	0.044 (3.3)	0.036 (1.6)	0.031 (0.8)	0.071 (4.4)	0.045 (1.6)	0.318 (87.8)	0.384	0.776	16.2
Pirimiphos methyl	0.044 (3.2)	0.036 (1.7)	0.031 (0.9)	0.066 (0.2)	0.048 (2.2)	0.301 (92.1)	0.298	0.704	14.8	0.044 (3.2)	0.036 (1.7)	0.031 (0.9)	0.097 (6.3)	0.061 (3.2)	0.333 (92.1)	0.382	0.765	19.6
Prochloraz	0.044 (3.1)	0.036 (1.4)	0.031 (1.0)	0.052 (0.1)	0.038 (1.8)	0.317 (89.5)	0.315	0.517	15.9	0.044 (3.1)	0.036 (1.4)	0.031 (1.0)	0.096 (5.4)	0.070 (3.3)	0.368 (91.2)	0.381	0.765	20.3
Procymidone	0.044 (2.1)	0.036 (1.5)	0.031 (0.8)	0.054 (0.6)	0.039 (1.8)	0.245 (90.4)	0.347	0.514	17.6	0.044 (2.1)	0.036 (1.5)	0.031 (0.8)	0.071 (2.1)	0.064 (2.8)	0.495 (95.1)	0.504	0.665	21.6
Profenofos	0.044 (2.3)	0.036 (1.2)	0.031 (1.5)	0.051 (0.7)	0.041 (2.1)	0.298 (88.7)	0.325	0.548	18.6	0.044 (2.3)	0.036 (1.2)	0.031 (1.5)	0.033 (1.5)	0.044 (1.7)	0.452 (94.1)	0.501	0.654	20.8
Profoxydim (Clefoxydim)	0.044 (2.1)	0.036 (1.3)	0.031 (1.6)	0.041 (0.5)	0.068 (3.5)	0.332 (85.6)	0.298	0.587	17.8	0.044 (2.1)	0.036 (1.3)	0.031 (1.6)	0.051 (1.9)	0.068 (1.6)	0.413 (92.1)	0.359	0.774	19.6
Prometryn	0.044 (1.9)	0.036 (1.0)	0.031 (1.0)	0.040 (0.6)	0.045 (1.7)	0.312 (92.4)	0.289	0.514	17.6	0.044 (1.9)	0.036 (1.0)	0.031 (1.0)	0.076 (2.2)	0.060 (3.5)	0.402 (90.8)	0.385	0.771	17.6
Propaquizafop	0.044 (3.2)	0.036 (1.3)	0.031 (1.1)	0.043 (0.2)	0.039 (1.8)	0.298 (89.7)	0.287	0.665	15.9	0.044 (3.2)	0.036 (1.3)	0.031 (1.1)	0.071 (4.4)	0.071 (3.4)	0.350 (88.4)	0.504	0.659	18.2
Propargite	0.044 (3.1)	0.036 (1.0)	0.031 (1.4)	0.054 (0.4)	0.052 (3.4)	0.291 (93.1)	0.269	0.541	18.1	0.044 (3.1)	0.036 (1.0)	0.031 (1.4)	0.097 (6.3)	0.062 (2.6)	0.318 (87.8)	0.501	0.662	17.1

Pesticide	Cucumber									Grapefruit								
	U_i^a (mg/kg (%))									U_i^a (mg/kg (%))								
	U_1	U_2	U_3	U_4	U_5	U_6	U_c	U_e^b	$U_e(\%)$	U_1	U_2	U_3	U_4	U_5	U_6	U_c	U_e^b	$U_e(\%)$
		(mg/kg)						(mg/kg)				(mg/kg)					(mg/kg)	
Propazine	0.044 (2.8)	0.036 (0.9)	0.031 (1.3)	0.071 (0.3)	0.037 (1.7)	0.285 (91.1)	0.278	0.526	17.6	0.044 (2.8)	0.036 (0.9)	0.031 (1.3)	0.096 (5.4)	0.045 (1.6)	0.333 (92.1)	0.328	0.652	18.7
Propoxycarbazon	0.044 (2.1)	0.036 (0.8)	0.031 (0.9)	0.041 (0.5)	0.045 (1.8)	0.337 (92.6)	0.259	0.668	15.9	0.044 (2.1)	0.036 (0.8)	0.031 (0.9)	0.071 (2.1)	0.061 (3.2)	0.368 (91.2)	0.329	1.014	18.8
Propyconazole	0.044 (2.0)	0.036 (1.6)	0.031 (1.1)	0.040 (0.6)	0.048 (2.2)	0.298 (89.7)	0.315	0.662	18.5	0.044 (2.0)	0.036 (1.6)	0.031 (1.1)	0.033 (1.5)	0.070 (3.3)	0.495 (95.1)	0.385	0.665	16.4
Propyzamide	0.044 (3.2)	0.036 (1.2)	0.031 (1.4)	0.043 (0.2)	0.038 (1.8)	0.301 (92.1)	0.347	0.669	14.5	0.044 (3.2)	0.036 (1.2)	0.031 (1.4)	0.051 (1.9)	0.064 (2.8)	0.452 (94.1)	0.384	1.011	18.3
Prothopos	0.044 (3.5)	0.036 (1.1)	0.031 (1.3)	0.054 (0.4)	0.039 (1.8)	0.317 (89.5)	0.325	0.514	16.9	0.044 (3.5)	0.036 (1.1)	0.031 (1.3)	0.071 (4.4)	0.044 (1.7)	0.413 (92.1)	0.394	0.774	19.5
Pymetrozine	0.044 (1.9)	0.036 (1.5)	0.031 (0.9)	0.071 (0.3)	0.041 (2.1)	0.245 (90.4)	0.317	0.618	15.6	0.044 (1.9)	0.036 (1.5)	0.031 (0.9)	0.097 (6.3)	0.068 (1.6)	0.402 (90.8)	0.392	0.776	15.6
Pyraclostrobin	0.044 (2.0)	0.036 (1.6)	0.031 (0.7)	0.008 (4.2)	0.068 (3.5)	0.298 (88.7)	0.315	0.662	18.2	0.044 (2.0)	0.036 (1.6)	0.031 (0.7)	0.096 (5.4)	0.060 (3.5)	0.350 (88.4)	0.389	0.669	16.2
Pyraflufen-Ethyl	0.044 (3.4)	0.036 (1.7)	0.031 (0.8)	0.007 (4.1)	0.052 (3.4)	0.332 (85.6)	0.347	0.665	17.6	0.044 (3.4)	0.036 (1.7)	0.031 (0.8)	0.071 (2.1)	0.071 (3.4)	0.318 (87.8)	0.374	0.771	19.6
Pyrazophos	0.044 (3.3)	0.036 (1.4)	0.031 (0.9)	0.009 (3.9)	0.037 (1.7)	0.312 (92.4)	0.325	0.514	13.6	0.044 (3.3)	0.036 (1.4)	0.031 (0.9)	0.033 (1.5)	0.062 (2.6)	0.333 (92.1)	0.365	0.778	20.3
Pyridaben	0.044 (3.2)	0.036 (1.5)	0.031 (1.0)	0.070 (3.7)	0.045 (1.8)	0.298 (89.7)	0.287	0.512	15.2	0.044 (3.2)	0.036 (1.5)	0.031 (1.0)	0.051 (1.9)	0.045 (1.6)	0.368 (91.2)	0.361	0.668	21.6
Pyridaphention	0.044 (3.1)	0.036 (1.2)	0.031 (1.1)	0.066 (0.2)	0.065 (2.8)	0.291 (93.1)	0.298	0.628	14.6	0.044 (3.1)	0.036 (1.2)	0.031 (1.1)	0.076 (2.2)	0.061 (3.2)	0.495 (95.1)	0.368	0.669	23.4
Pyridate	0.044 (2.1)	0.036 (1.3)	0.031 (1.4)	0.052 (0.1)	0.039 (1.8)	0.285 (91.1)	0.301	0.624	12.5	0.044 (2.1)	0.036 (1.3)	0.031 (1.4)	0.071 (4.4)	0.070 (3.3)	0.452 (94.1)	0.384	0.770	21.8
Pyriproxyfen	0.044 (2.3)	0.036 (1.0)	0.031 (1.3)	0.054 (0.6)	0.065 (2.6)	0.337 (92.6)	0.305	0.701	13.6	0.044 (2.3)	0.036 (1.0)	0.031 (1.3)	0.097 (6.3)	0.064 (2.8)	0.413 (92.1)	0.382	0.776	22.8
Quizalofop-P-Ethyl	0.044 (2.1)	0.036 (1.3)	0.031 (0.9)	0.051 (0.7)	0.048 (2.2)	0.298 (89.7)	0.321	0.704	14.8	0.044 (2.1)	0.036 (1.3)	0.031 (0.9)	0.096 (5.4)	0.044 (1.7)	0.402 (90.8)	0.381	0.778	21.8
Rimsulfuron	0.044 (1.9)	0.036 (1.0)	0.031 (0.7)	0.041 (0.5)	0.048 (2.2)	0.301 (92.1)	0.315	0.517	15.9	0.044 (1.9)	0.036 (1.0)	0.031 (0.7)	0.071 (2.1)	0.068 (1.6)	0.350 (88.4)	0.504	0.776	23.6
Sethoxydim	0.044 (3.2)	0.036 (0.9)	0.031 (0.8)	0.040 (0.6)	0.038 (1.8)	0.317 (89.5)	0.311	0.514	17.6	0.044 (3.2)	0.036 (0.9)	0.031 (0.8)	0.033 (1.5)	0.060 (3.5)	0.318 (87.8)	0.501	0.765	20.8
Simozine	0.044 (3.1)	0.036 (0.8)	0.031 (0.9)	0.043 (0.2)	0.039 (1.8)	0.245 (90.4)	0.314	0.548	18.6	0.044 (3.1)	0.036 (0.8)	0.031 (0.9)	0.051 (1.9)	0.071 (3.4)	0.333 (92.1)	0.359	0.884	19.6
Spirodiclofen	0.044 (2.8)	0.036 (1.6)	0.031 (1.0)	0.054 (0.4)	0.041 (2.1)	0.298 (88.7)	0.317	0.514	15.6	0.044 (2.8)	0.036 (1.6)	0.031 (1.0)	0.076 (2.2)	0.062 (2.6)	0.368 (91.2)	0.385	0.765	18.9
Spiroxamine	0.044 (2.3)	0.036 (1.1)	0.031 (0.8)	0.071 (0.3)	0.068 (3.5)	0.332 (85.6)	0.298	0.665	15.2	0.044 (2.3)	0.036 (1.1)	0.031 (0.8)	0.071 (4.4)	0.045 (1.6)	0.495 (95.1)	0.504	0.665	17.6
Sulfosulfuron	0.044 (2.1)	0.036 (1.5)	0.031 (1.5)	0.041 (0.5)	0.070 (3.4)	0.312 (92.4)	0.315	0.541	17.8	0.044 (2.1)	0.036 (1.5)	0.031 (1.5)	0.097 (6.3)	0.061 (3.2)	0.452 (94.1)	0.501	0.654	15.9
Tau-Fluvalinate	0.044 (2.0)	0.036 (1.6)	0.031 (1.6)	0.040 (0.6)	0.039 (1.8)	0.298 (89.7)	0.347	0.526	17.9	0.044 (2.0)	0.036 (1.6)	0.031 (1.6)	0.096 (5.4)	0.070 (3.3)	0.413 (92.1)	0.328	0.774	20.6

Pesticide	Cucumber									Grapefruit								
	U ₁	U ₂	U _i ^a (mg/kg (%))			U ₆	U _c	U _e ^b	U _e (%)	U ₁	U ₂	U _i ^a (mg/kg (%))			U ₆	U _c	U _e ^b	U _e (%)
			U ₃	U ₄	U ₅							U ₃	U ₄	U ₅				
(mg/kg)									(mg/kg)									
Tebuconazole	0.044 (3.2)	0.036 (1.7)	0.031 (1.0)	0.043 (0.2)	0.052 (3.4)	0.291 (93.1)	0.325	0.668	12.3	0.044 (3.2)	0.036 (1.7)	0.031 (1.0)	0.071 (2.1)	0.064 (2.8)	0.402 (90.8)	0.329	0.771	22.3
Tebufenozide	0.044 (3.5)	0.036 (1.4)	0.031 (1.1)	0.054 (0.4)	0.037 (1.7)	0.337 (92.6)	0.314	0.662	15.6	0.044 (3.5)	0.036 (1.4)	0.031 (1.1)	0.033 (1.5)	0.044 (1.7)	0.350 (88.4)	0.385	0.659	22.9
Teflubenzuron	0.044 (1.9)	0.036 (1.5)	0.031 (1.4)	0.071 (0.3)	0.045 (1.8)	0.298 (89.7)	0.289	0.669	14.3	0.044 (1.9)	0.036 (1.5)	0.031 (1.4)	0.051 (1.9)	0.068 (1.6)	0.318 (87.8)	0.384	0.662	21.8
Tepraloxymid	0.044 (2.0)	0.036 (1.2)	0.031 (1.3)	0.041 (0.5)	0.048 (2.2)	0.301 (92.1)	0.287	0.662	15.6	0.044 (2.0)	0.036 (1.2)	0.031 (1.3)	0.076 (2.2)	0.060 (3.5)	0.333 (92.1)	0.394	0.652	15.6
Terbutylazine	0.044 (3.4)	0.036 (1.3)	0.031 (0.9)	0.040 (0.6)	0.038 (1.8)	0.317 (89.5)	0.269	0.665	18.5	0.044 (3.4)	0.036 (1.3)	0.031 (0.9)	0.071 (4.4)	0.071 (3.4)	0.368 (91.2)	0.392	1.014	16.2
Terbutryn	0.044 (3.3)	0.036 (1.0)	0.031 (0.7)	0.043 (0.2)	0.039 (1.8)	0.245 (90.4)	0.278	0.514	14.3	0.044 (3.3)	0.036 (1.0)	0.031 (0.7)	0.097 (6.3)	0.062 (2.6)	0.495 (95.1)	0.389	0.665	19.6
Tetraconazole	0.044 (3.2)	0.036 (1.3)	0.031 (0.8)	0.054 (0.4)	0.041 (2.1)	0.298 (88.7)	0.259	0.512	15.2	0.044 (3.2)	0.036 (1.3)	0.031 (0.8)	0.096 (5.4)	0.045 (1.6)	0.452 (94.1)	0.374	1.011	20.3
Thiabendazole	0.044 (3.1)	0.036 (1.0)	0.031 (0.9)	0.071 (0.3)	0.068 (3.5)	0.289 (88.9)	0.311	0.628	15.6	0.044 (3.1)	0.036 (1.0)	0.031 (0.9)	0.071 (2.1)	0.061 (3.2)	0.413 (92.1)	0.365	0.774	21.6
Thiacloprid	0.044 (2.1)	0.036 (0.9)	0.031 (1.0)	0.007 (4.1)	0.052 (3.4)	0.288 (96.5)	0.287	0.624	18.1	0.044 (2.1)	0.036 (0.9)	0.031 (1.0)	0.033 (1.5)	0.070 (3.3)	0.402 (90.8)	0.361	0.776	19.5
Thiamethoxam	0.044 (2.3)	0.036 (0.8)	0.031 (1.1)	0.009 (3.9)	0.037 (1.7)	0.291 (93.1)	0.298	0.701	14.5	0.044 (2.3)	0.036 (0.8)	0.031 (1.1)	0.051 (1.9)	0.064 (2.8)	0.350 (88.4)	0.368	0.669	18.2
Thifensulfuron-methyl	0.044 (2.1)	0.036 (1.6)	0.031 (1.4)	0.070 (3.7)	0.045 (1.8)	0.332 (85.6)	0.301	0.704	16.7	0.044 (2.1)	0.036 (1.6)	0.031 (1.4)	0.076 (2.2)	0.044 (1.7)	0.318 (87.8)	0.381	0.771	18.1
Thiohanate methyl	0.044 (1.9)	0.036 (1.1)	0.031 (1.3)	0.066 (0.2)	0.072 (41)	0.312 (92.4)	0.305	0.517	16.9	0.044 (1.9)	0.036 (1.1)	0.031 (1.3)	0.071 (4.4)	0.068 (1.6)	0.333 (92.1)	0.504	0.778	17.3
Thiometon	0.044 (3.2)	0.036 (1.5)	0.031 (0.9)	0.052 (0.1)	0.039 (1.8)	0.298 (89.7)	0.321	0.514	17.6	0.044 (3.2)	0.036 (1.5)	0.031 (0.9)	0.097 (6.3)	0.060 (3.5)	0.368 (91.2)	0.501	0.668	17.1
Tolyfluanid	0.044 (3.1)	0.036 (1.6)	0.031 (0.7)	0.054 (0.6)	0.052 (3.4)	0.332 (94.6)	0.315	0.548	17.2	0.044 (3.1)	0.036 (1.6)	0.031 (0.7)	0.096 (5.4)	0.071 (3.4)	0.495 (95.1)	0.359	0.669	15.7
Tralkoxydim	0.044 (2.8)	0.036 (1.7)	0.031 (0.8)	0.051 (0.7)	0.037 (1.7)	0.301 (92.1)	0.311	0.623	15.9	0.044 (2.8)	0.036 (1.7)	0.031 (0.8)	0.071 (2.1)	0.062 (2.6)	0.452 (94.1)	0.385	0.765	16.4
Triadimefon	0.044 (2.4)	0.036 (1.4)	0.031 (0.9)	0.041 (0.5)	0.045 (1.8)	0.317 (89.5)	0.314	0.654	14.8	0.044 (2.4)	0.036 (1.4)	0.031 (0.9)	0.033 (1.5)	0.045 (1.6)	0.413 (92.1)	0.504	0.665	18.3
Triadimenol	0.044 (3.1)	0.036 (1.5)	0.031 (0.8)	0.040 (0.6)	0.074 (3.8)	0.245 (90.4)	0.317	0.681	15.9	0.044 (3.1)	0.036 (1.5)	0.031 (0.8)	0.051 (1.9)	0.061 (3.2)	0.402 (90.8)	0.501	0.654	19.5
Triallate	0.044 (2.3)	0.036 (1.2)	0.031 (1.5)	0.043 (0.2)	0.048 (2.2)	0.298 (88.7)	0.298	0.618	17.6	0.044 (2.3)	0.036 (1.2)	0.031 (1.5)	0.034 (1.2)	0.070 (3.3)	0.350 (88.4)	0.328	0.774	15.6
Triasulfuron	0.044 (2.1)	0.036 (1.3)	0.031 (1.6)	0.054 (0.4)	0.038 (1.8)	0.335 (95.6)	0.301	0.662	18.6	0.044 (2.1)	0.036 (1.3)	0.031 (1.6)	0.076 (2.2)	0.064 (2.8)	0.318 (87.8)	0.329	0.771	16.2
Tribenuron-Methyl	0.044 (2.0)	0.036 (1.0)	0.031 (1.0)	0.071 (0.3)	0.039 (1.8)	0.332 (85.6)	0.308	0.665	17.8	0.044 (2.0)	0.036 (1.0)	0.031 (1.0)	0.071 (4.4)	0.044 (1.7)	0.333 (92.1)	0.385	0.659	19.6
Trichlorfon	0.044 (3.2)	0.036 (1.0)	0.031 (1.1)	0.008 (4.2)	0.041 (2.1)	0.312 (92.4)	0.296	0.514	17.6	0.044 (3.2)	0.036 (1.0)	0.031 (1.1)	0.097 (6.3)	0.068 (1.6)	0.368 (91.2)	0.384	0.662	20.3

Pesticide	Cucumber									Grapefruit								
	U ₁	U ₂	U ₃ ^a (mg/kg (%))	U ₄	U ₅	U ₆	U _c	U _e ^b	U _c (%)	U ₁	U ₂	U ₃ ^a (mg/kg (%))	U ₄	U ₅	U ₆	U _c	U _e ^b	U _c (%)
Trifloxystrobin	0.044 (3.5)	0.036 (0.9)	0.031 (1.4)	0.007 (4.1)	0.068 (3.5)	0.298 (89.7)	0.289	0.512	15.9	0.044 (3.5)	0.036 (0.9)	0.031 (1.4)	0.096 (5.4)	0.060 (3.5)	0.495 (95.1)	0.394	0.652	21.6
Triflumizole	0.044 (1.9)	0.036 (1.2)	0.031 (1.3)	0.009 (3.9)	0.039 (1.8)	0.301 (92.1)	0.287	0.628	18.1	0.044 (1.9)	0.036 (1.2)	0.031 (1.3)	0.071 (2.1)	0.071 (3.4)	0.452 (94.1)	0.392	1.014	23.4
Triflumuron	0.044 (2.3)	0.036 (1.1)	0.031 (0.9)	0.070 (3.7)	0.052 (3.4)	0.317 (89.5)	0.269	0.624	17.6	0.044 (2.3)	0.036 (1.1)	0.031 (0.9)	0.033 (1.5)	0.062 (2.6)	0.413 (92.1)	0.389	0.665	21.8
Triticonazole	0.044 (2.1)	0.036 (1.5)	0.031 (1.5)	0.066 (0.2)	0.037 (1.7)	0.245 (90.4)	0.278	0.701	15.9	0.044 (2.1)	0.036 (1.5)	0.031 (1.5)	0.051 (1.9)	0.045 (1.6)	0.402 (90.8)	0.374	1.011	22.8
2.4 D Acid	0.044 (1.9)	0.036 (1.6)	0.031 (0.8)	0.052 (0.1)	0.045 (1.8)	0.298 (88.7)	0.259	0.704	18.7	0.044 (1.9)	0.036 (1.6)	0.031 (0.8)	0.071 (4.4)	0.061 (3.2)	0.452 (94.1)	0.365	0.774	21.8

U_i^a are the contributions of each uncertainty source to U_c of the method.

U_e^b is the expanded uncertainty for a 4 mg/kg estimated for a level of confidence of 95%

Conclusions

In this paper, an analytical method for the separation of 233 pesticide in cucumber and grapefruits using QuEChERS method and GC-MS, LC-MS/MS is presented. The validation data showed satisfactory performance of analytical method, in terms of specificity, sensitivity, linearity, recovery, precision and U_e according to the European SANTE/11945/2015 Guideline. One or multiple pesticide residues were detected in 11.6% of cucumber and 13.8% of grapefruit samples, but the levels were below the EU MRLs. The residues found in cucumbers and grapefruits were belonging to the group of fungicides, insecticides, herbicide, acaricide and plant growth regulator. The most frequently detected residues in cucumber samples were Clofentezine (4.4%), propyzamide (3.96), propamocarb (3.03), Azinphosethyl (1.8), metalxyl, procymidone, chlorpyrifos and Carbendazim. However, the fungicide propamocarb (8.8%) was the most common residue in cucumbers, followed by propyzamide (6.3%) and Clofentezine (2%). The fungicide fludioxonil was the most prominent pesticide found in grapefruit samples, with a frequency of 9.1%. Imazalil was the second most commonly found pesticide in grapefruits with 4.7% of the samples, followed by Thiabendazol, quinophos and carbaryl. The proposed method was also found to be suitable for different kinds of fruits.

REFERENCES

- [1] Alvarez, M. V., Cabred, S., Ramirez, C. L., Fanovich, M. A. (2019): Valorization of an agroindustrial soybean residue by supercritical fluid extraction of phytochemical compounds. – *The Journal of Supercritical Fluids* 143: 90-96.
- [2] AOAC International (Association of Official Analytical Chemists). (2007): Pesticide Residues in Foods by Acetonitrile Extraction and Partitioning with Magnesium Sulphate. – AOAC Official method 2007.01.
- [3] Bakırcı, G. T., Acay, D. B. Y., Bakırcı, F., Ötleş, S. (2014): Pesticide residues in fruits and vegetables from the Aegean region, Turkey. – *Food Chem.* 160: 379-392.
- [4] Bhat, J. A., Rashid, R., Dar, W. A., Bhat, R. A. (2018): Efficacy of Different Fungicides for the Management of Downy Mildew of Cucumber Grown Under Low Plastic Tunnel. – *Int. J. Pure App. Biosc.* 6(2): 884-890.
- [5] Campone, L., Piccinelli, A. L., Celano, R., Pagano, I., Russo, M., Rastrelli, L. (2018): Rapid and automated on-line solid phase extraction HPLC–MS/MS with peak focusing for the determination of ochratoxin A in wine samples. – *Food chemistry* 244: 128-135.
- [6] Cengiz, M. F., Başlar, M., Basancelebi, O., Kılıçlı, M. (2018): Reduction of pesticide residues from tomatoes by low intensity electrical current and ultrasound applications. – *Food chemistry* 267: 60-66.
- [7] Chan, K. K., Hamid, M. S. B., Webster, R. D. (2018): Quantification of capsaicinoids in chillies by solid-phase extraction coupled with voltammetry. – *Food Chemistry* 265: 152-158.
- [8] da Silva Sousa, J., de Castro, R. C., de Albuquerque Andrade, G., Lima, C. G., Lima, L. K., Milhome, M. A. L., do Nascimento, R. F. (2013): Evaluation of an analytical methodology using QuEChERS and GC-SQ/MS for the investigation of the level of pesticide residues in Brazilian melons. – *Food Chem.* 141: 2675e81.
- [9] Dong, H., Xian, Y., Xiao, K., Wu, Y., Zhu, L., He, J. (2019): Development and comparison of single-step solid phase extraction and QuEChERS clean-up for the analysis of 7 mycotoxins in fruits and vegetables during storage by UHPLC-MS/MS. – *Food Chemistry* 274: 471-479.

- [10] Du, L. J., Chu, C., Warner, E., Wang, Q. Y., Hu, Y. H., Chai, K. J., Cao, J., Peng, L. Q., Chen, Y. B., Yang, J., Zhang, Q. D. (2018): Rapid microwave-assisted dispersive micro-solid phase extraction of mycotoxins in food using zirconia nanoparticles. – *Journal of Chromatography A* 1561: 1-12.
- [11] Epstein, L., Zhang, M. (2014): The impact of integrated pest management programs on pesticide use in California, USA. – In: Peshin, R., Pimentel, D. (eds.) *Integrated pest management: experiences with implementation, global overview*. Netherlands 4: 173-200.
- [12] Ersoy, N., Tekinarslan, O., Ozgür, E. A., Göktas, U. (2018): Determination of Pesticide Residues in Apricot (*Prunus armeniaca* L.) Grown at Good Agricultural Practices (GAPs) by LC-MS/MS and GC-MS. – *Erwerbs-Obstbau* 60: 349-358.
- [13] European Commission. (2008): Review Report for the Active Substance Boscalid. – SANCO 3919/2007-rev.5. Finalised in the Standing Committee on the Food Chain and Animal Health at its Meeting on 22 January 2008 in View of the Inclusion of Boscalid in Annex I of Directive 91/414/EEC.
- [14] European Commission. (2015): Guidance Document on Analytical Quality Control and Method Validation Procedures for Pesticides Residues Analysis in Food and Feed. – Document No. SANTE/11945/2015 European Commission Directorate-General for Health and Food Safety. Available from: http://ec.europa.eu/food/plant/doc/plant_pesticides_mrl_guidelines_wrkdoc_11945_en.pdf (cited 2017 Jul 25).
- [15] FAO. (2012): FAO specifications and Evaluations for Agricultural Pesticides. – Propamocarb, pp. 42. Available from: <http://www.fao.org/agriculture/crops/core-themes/theme/pests/jmps/en/> (cited 2018 Jul 23).
- [16] FAO. (2015): FAO statistical databases and data sets. – Available from: <http://faostat.fao.org> (cited 2018 Jan. 23).
- [17] Golge, O., Kabak, B. (2015): Determination of 115 pesticide residues in oranges by high-performance liquid chromatography–triple-quadrupole mass spectrometry in combination with QuEChERS. – *Journal of Food Composition and Analysis* 41: 86-97.
- [18] Golge, O., Hepsag, F., Kabak, B. (2018): Health risk assessment of selected pesticide residues in green pepper and cucumber. – *Food and Chemical Toxicology* 121: 51-64.
- [19] Jiang, Z., Cao, X., Li, H., Zhang, C., El-Aty, A. M. A., Jeong, J. H., Shao, Y., Shao, H., Jin, M., Jin, F., Wang, J. (2018): Rapid analysis of tristyrylphenol ethoxylates in cucumber-field system using supercritical fluid chromatography-tandem mass spectrometry. – *Food Chemistry* 266: 119-125.
- [20] Khan, Z., Kamble, N., Bhongale, A., Girme, M., Chauhan, V. B., Banerjee, K. (2018): Analysis of pesticide residues in tuber crops using pressurised liquid extraction and gas chromatography-tandem mass spectrometry. – *Food Chemistry* 241: 250-257.
- [21] Kilic, S., Tongur, T., Kilic, M., ErKaymaz, T. (2018): Determination of Some Endocrine-Disrupting Metals and Organochlorinated Pesticide Residues in Baby Food and Infant Formula in Turkish Markets. – *Food Analytical Methods* 11: 3352-3361.
- [22] Kumar, M., Chand, R., Shah, K. (2018): Mycotoxins and Pesticides: Toxicity and Applications in Food and Feed. – *Microbial Biotechnology* 2: 207-252.
- [23] Li, G. J., Wu, H. J., Wang, Y., Hung, W. L., Rouseff, R. L. (2019): Determination of citrus juice coumarins, furanocoumarins and methoxylated flavones using solid phase extraction and HPLC with photodiode array and fluorescence detection. – *Food Chemistry* 271: 29-38.
- [24] Liu, W., Quan, J., Hu, Z. (2018): Detection of Organophosphorus Pesticides in Wheat by Ionic Liquid-Based Dispersive Liquid-Liquid Microextraction Combined with HPLC. – *Journal of analytical methods in chemistry*. <https://doi.org/10.1155/2018/8916393>.
- [25] Polat, A., Polat, S., Simsek, A., Kurt, T. T., Ozyurt, G. (2018): Pesticide residues in muscles of some marine fish species and seaweeds of Iskenderun Bay (Northeastern Mediterranean), Turkey. – *Environmental Science and Pollution Research* 25: 3756-3764.

- [26] Polyiem, W., Naksen, W., Prapamontol, T. (2018): Gas chromatographic-flame photometric detection of organophosphate pesticide residues and its application in real vegetable and fruit samples from Chiang. – *Chiang Mai J. Sci.* 45(4): 1933-1943.
- [27] Razzaghi, N., Ziarati, P., Rastegar, H., Shoeibi, S., Amirahmadi, M., Conti, G. O., Ferrante, M., Fakhri, Y., Khaneghah, A. M. (2018): The concentration and probabilistic health risk assessment of pesticide residues in commercially available olive oils in Iran. – *Food Chem. Toxicol.* 120: 32-40.
- [28] Salemi, A., Khaleghifar, N., Mirikaram, N. (2019): Optimization and comparison of membrane-protected micro-solid-phase extraction coupled with dispersive liquid-liquid microextraction for organochlorine pesticides using three different sorbents. – *Microchemical Journal* 144: 215-220.
- [29] Stachniuk, A. L. C. (2018): MS/MS determination of pesticide residues in fruits and vegetables. – *Bioactive Molecules in Food* 14: 1-26.
- [30] Su, M., Jia, L., Wu, X., Sun, H. (2018): Residue investigation of some phenylureas and tebuthiuron herbicides in vegetables by ultra performance liquid chromatography coupled with integrated selective accelerated solvent extraction–clean up in situ. – *Journal of the Science of Food and Agriculture* 98: 4845-4853.
- [31] Tankiewicz, M. (2019): Determination of Selected Priority Pesticides in High Water Fruits and Vegetables by Modified QuEChERS and GC-ECD with GC-MS/MS Confirmation. – *Molecules* 24: 417.
- [32] Tian, Z., Wang, Z., Han, X., Wang, N., Wang, R. (2018): Study on the interaction between cannabidiol and DNA using acridine orange as a fluorescence probe. – *Journal of Molecular Recognition* 31: 2682.
- [33] TÜİK (Turkish Statistical Institute). (2015): The summary of agricultural statistics. – Available from: <http://tuik.gov.tr> (cited 2018 June 17).
- [34] Van Leeuwen, T., Vontas, J., Tsagkarakou, A., Dermauw, W., Tirry, L. (2010): Acaricide resistance mechanisms in the two-spotted spider mite *Tetranychus urticae* and other important Acari: a review. – *Insect biochemistry and molecular biology* 40(8): 563-572.
- [35] Walorczyk, S. (2014): Validation and use of a QuEChERS - based gas chromatographic tandem mass spectrometric method for multiresidue pesticide analysis in blackcurrants including studies of matrix effects and estimation of measurement uncertainty. – *Talanta* 120: 106-113.
- [36] Wang, K., Xie, X., Zhang, Y., Huang, Y., Zhou, S., Zhang, W., Lin, Y., Fan, H. (2018): Combination of microwave-assisted extraction and ultrasonic-assisted dispersive liquid-liquid microextraction for separation and enrichment of pyrethroids. – *Food chemistry* 240: 1233-1242.
- [37] Yıldırım, E., Macun, H. C., Yaçınkaya, İ., Kocasarı, F. Ş., Ekici, H. (2018): Survey of aflatoxin residue in feed and milk samples in Kırıkkale province, Turkey. – *Ankara Üniversitesi Veteriner Fakültesi Dergisi* 65: 99-204.
- [38] Zhu, B., Xu, X., Luo, J., Jin, S., Chen, W., Liu, Z., Tian, C. (2019): Simultaneous determination of 131 pesticides in tea by on-line GPC-GC-MS/MS using graphitized multi-walled carbon nanotubes as dispersive solid phase. – *Food chemistry* 276: 202-208.

ARTIFICIAL NEURAL NETWORK MODELING FOR ANNUAL PEAK FLOWS: A CASE STUDY

AHMAD, I.^{1,2*} – ALMANJAHIE, IBRAHIM M.¹ – HAMEEDULLAH² – CHIKR-ELMEZOUAR, Z.¹ – LAKSACI, A.¹

¹*Department of Mathematics, College of Science, King Khalid University, 61413 Abha, Kingdom of Saudi Arabia*

²*Department of Mathematics and Statistics, Faculty of Basic and Applied Sciences, International Islamic University, 44000 Islamabad, Pakistan*

**Corresponding author
e-mail: Ishfaq.ahmad@iiu.edu.pk*

(Received 15th Feb 2019; accepted 8th Apr 2019)

Abstract. The data of annual peak flows in river system is not straight forward but rather complex function of hydrology and geography of the area. In such composite situations, models based on soft computing approaches such Artificial Neural Network (ANN) may increase understanding of the hidden hydrological processes. The primary objective of this study is to determine the best approach among Traditional Artificial Neural Network (T-ANN) and Wavelet Artificial Neural Network (W-ANN) using Annual Peak flows data of Mangla site on River Jhelum, Pakistan. The results reveal the better performance of W-ANN approach under db2 scheme. Further, to justify the authenticity of W-ANN we compared it with the frequency analysis by fitting best probability distribution and non-parametric kernel density estimation (KDE) using Gaussian kernel approach for the same data. Results reveal that probability distribution modeling approach by fitting the Generalized Logistic (GLO) distribution being the most suitable model provides comparable results with W-ANN-db2 approach but outperforms than non-parametric KDE. Overall, the performance of W-ANN-db2 is better in the present study. The findings of the study are useful for better policy implications in water resources management.

Keywords: *flood frequency analysis, water resources management, probability models, kernel density estimation, non-parametric*

Introduction

We are living in the age where we have more awareness than ever about the environmental events around us, including the brittleness of ecosystems, the incompatible needs of human culture, and the complications of geologic records. Scientists are looking for, to create, upgrade, and revise the theories and mathematical models of the Earth's dynamics at an unprecedented rate. Rather than traditional modeling techniques, the Artificial Neural Network (ANN) methodology has the prospective aspects to see the problems in a simpler and more modular form. For sustainable development of the societies it is an urgent need to make predictions with more accuracy of different environmental events including floods, earthquakes, droughts, air pollution, wind gusts and others. Since last few years ANN are widely applied in different fields such as Image Processing, Signal Processing, power systems, medical studies, pattern recognition and hydrology among others (for example, see Rabuñal, 2005; Aziz et al., 2016; Jimeno-Sáez et al., 2017; Kumar et al., 2015; Rahman et al., 2018; Requena et al., 2018 among others). ANN modeling has the capability of learning from the data. They can be proved as time saving for development of the models and especially useful for nonlinear and complicated processes which cannot be modeled through traditional methods. Streamflow forecasting is a challenging task for

water resources engineers and managers. Reliable forecasts of streamflows make an efficient operation of water resources systems within legal, political, technical and economical priorities. A forecasting system that considers all important spatial and temporal variation of the whole streamflow regime, delivers a good basis for appropriate control and management of the water resources system.

The principle parameters for flood forecasts are scale and frequency of events. Since the annual peak flows can be used to give flood forecasts. Statistical studies in view of probabilistic methods can be embraced to tell about the probability and frequency of peak flows that cause flooding. The principal parameters for flood forecasts in probabilistic approach are frequency and magnitude of events (for example see Ahmad et al., 2015; Rahman et al., 2013; Drissia et al., 2019; Cassalho et al., 2019; Mostofi et al., 2019). Mostly, the Hydrologic time series are autocorrelated. However annual precipitation and peak flows are generally uncorrelated (Salas et al., 1993). Rarely, substantial autocorrelation might be the result of trends as well as movements in the time series (Salas et al., 1988). There is lot of current literature which discusses about aspects related to flood occasions (Agarwal et al. 2005; Rahimi and Abbaspour, 2011; Guresen et al., 2011.) Peak flows in the stream or waterway is a composite capacity of hydrology of the area and land designs in a given stream basin or waterway being considered as are hard to evaluate precisely. Generally the models which use streamflow data along with many other hydrologic and climatic factors for example precipitation, temperature, and snow water in a completely statistical or stochastic manners are black-box type models (see for example Hipel and MeLeod, 1994).

In the current study, we have applied ANN and W-ANN models to only one variable that is peak flows of Mangla site and compared the results of W-ANN (being the better one) with probability distribution modeling approach and Non-Parametric KDE approach. ANN modeling for peak flows has been performed in some studies (see for example Harinarayan et al., 2015).

Materials and methods

Study area and data collection

The annual peak flows data of Mangla site situated at River Jhelam, Pakistan is being retrieved from Water and Power Development Authority (WAPDA) and Federal Flood Commission of Pakistan. The data used in this study (annual peak flows) have been recorded during monsoon season in Pakistan (from July to September). Monsoon is the peak season of rainfalls and peak flows in Pakistan. The river system of Pakistan begins from the snow-covered Himalayan and the Karakoram series. There are mainly five rivers mostly located in the province of Punjab. These rivers are Sutlej, Ravi, Jhelum, Indus and Chenab. River Jhelum originates from south eastern part of Kashmir and its width is approximately 774 km and it meets with Chenab River at Trimmu. Jhelum also passes through Srinagar before entering Pakistan. Number of barrages and dams have been constructed on River Jhelum. One of them is Mangla dam constructed in 1967. It has a stowage dimensions of approximately 5.9 million acre-feet.

Artificial neural network (ANN)

ANN approach is based on function of the human brain and nervous system. ANNs trace the associations between two types of factors, i.e. inputs and outputs of a task by

interlinks of nodes that activate and operate through connecting weights using different functions called “training samples”, and in the result we can determine the procedures and relationship between the inputs and outputs. The processing of every neuron is performed in dual steps, in first step, the weighted summation of the inputs is brought and in second they are trailed by the importance of activation function (Bishop, 1995).

Artificial Neural Network are commonly applied by using electrical mechanisms or by imitation on a computer system. They are categorized by the designs of networks amongst the nodes (named as architecture), the procedures of defining weights on the networks (called their learning procedure), the activation function, and the number of layers (single layer, bilayer, and multilayer). When overall signals of a network move in only one direction, the ANN is known as Feed-Forward Network (FFN), otherwise they are known as Recurrent Networks. Generally, the artificial neural networks used in hydrological models are Feed-Forward Multilayer Perceptron’s (FFMLPs), which include three layers, and employ monotonic activation functions in all layers. Their weights are generally found by organized training using back-propagation process. The performance and learning capability of artificial neural network depend upon the fitness of its architecture which is needed to be pre-specified more precisely, the number and configuration of its hidden nodes see for example (Hertz, 2018; Denis, 2009).

Composite non-linear problems such as time series data prediction can be solved through ANN being non-linear mathematical model. Multilayer Perceptron (MLP) is the type of Artificial Neural Network which is used to adjust the connection weights. MLP comprises three layers: input layer; hidden layer; and output layer. MLP has only one input and output layer but more than one hidden layer. Each of these layers comprises nodes. These nodes are associated to each other. Input layer can contain that number of nodes while output layer, must have only one node to get output. It is up to user selection how to use hidden layer. There must be an additional dummy neuron as bias node in input layer. Bias node acts as one of the players in the network. The activation function is used to calculate the arriving value and gives the value in output layer for the actual computational process occurrence. Input layer applies linear transfer function. However, a sigmoid function is normally used in hidden and output layer. Following the activation function, we can determine the connection weight by data training. The procedure for the adjustment of weight begins in the output layer and carries backward to the input layer. Until the performance of target is obtained the process of feed-forward and back propagation algorithm continues. The weights of the values are determined when the data training process is completed. Following this, a single feed forward computation is employed. Results are then assessed by conducting performance measures between actual and predicted values (for detail see for example Bishop, 1995; Singh et al., 2004).

This study used Levenberg Marquardt (LM) procedure to streamline the biases and weights in the system. LM procedure is more effective and quicker than the traditional gradient descent procedure (Huang et al., 2015; Kisi and Shiri, 2011). *Figure 1* shows the Multilayer Perceptron with three layers as stated before.

The *Figure 1* shows a three-layer feed forward ANN. The first layer, called the input layer, comprises I nodes and connected with the input variables. This layer performs no computation but is used to distribute I inputs into the network. The last layer is connected to the output variables, and called the output layer. This layer consists of K output nodes. One or more layers of processing units that have no direct relation to the outside variable and are located between the input and output layers are called hidden

layers. An MLP may have many hidden layers. However, only one hidden layer is considered in *Figure 1*. This layer consists of J hidden nodes. In each layer, the processing elements are called nodes or neurons. Each of these neurons connected to all the neurons of adjoining layers. The parameters linked with these connections are known as weights. Information used by the network to solve a problem is represented by weights. Generally, all connections are ‘feed forward’ that allow information to transfer from an earlier layer to the next consecutive layer. The neurons in a layer are not interconnected, and neurons in non-adjointing layers are also not connected, however, for recurrent neural networks this is not the case (Zurada, 1992).

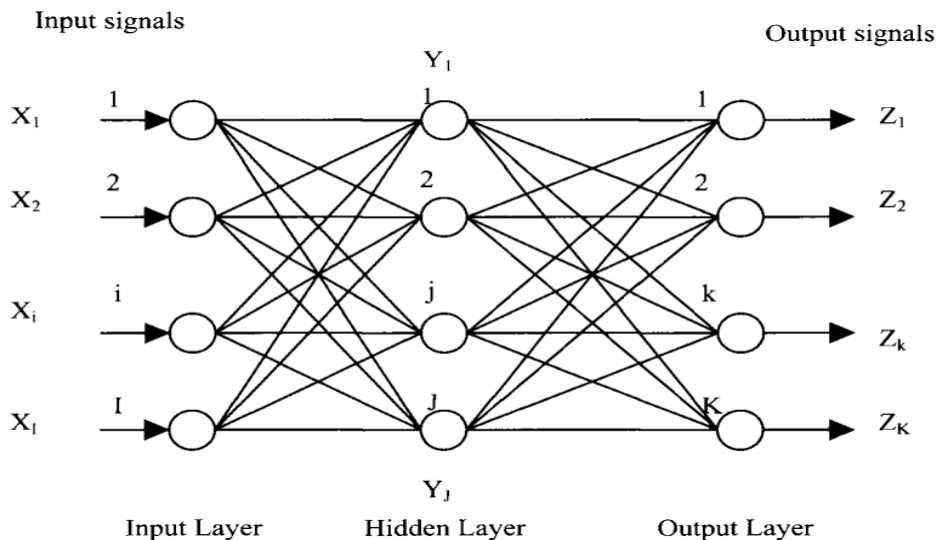


Figure 1. Multilayer perceptron with three layers artificial neural network model

The architecture of a typical neuron is shown in the *Figure 2*. Every hidden neuron j gets total I arriving signals (X_i , i.e. $X_1, X_2, \dots, X_i, \dots, X_I$) from any neuron i in the preceding layer (for instance, from Input layer to hidden layer). Connected with every arriving signal (X_i), a weight (W_{ij}) is connected between layer i and j . The effective arriving signal (net_j) to neuron j is the sum of weights of all the arriving signals as follows in *Equation 1*:

$$net_j = \sum_{i=1}^I W_{ij} X_i \quad (\text{Eq.1})$$

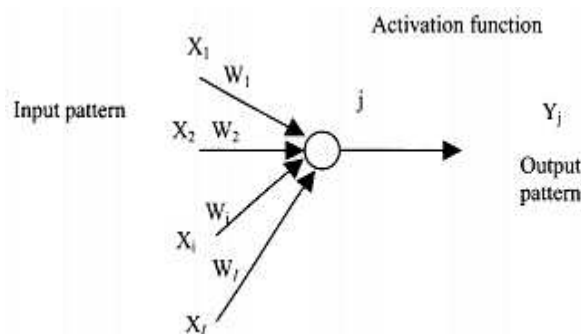


Figure 2. The architecture of a typical neuron

This effective arriving signal (net_j) passes over a non-linear activation function (also called a transfer function or threshold function) that produces the outgoing signal which is called activation or activity level (Y_j) of the neuron. Usually, a neuron sends its activation as a signal to several other neurons. It is pertinent to note that at one time only one signal can be sent by a neuron, though that signal is programmed to numerous other neurons simultaneously.

Delta learning rule for feed-forward multilayer perceptron

The delta learning rule is also called the LMS (Least Mean Square) error back propagation training algorithm. In the feed forward propagation training Input patterns are entered sequentially. If a pattern is entered and its classification or association comes out to be inaccurate, the value of LMS error is minimized through the adjustment of the synaptic weights as well as the thresholds. Therefore, the purpose of this algorithm is to adjust the synaptic weights w_{ij} ($i = 1, \dots, I$) and w_{jk} ($j = 1, \dots, J$), which connect input to hidden layer, and then hidden to output layer respectively. In the result, it will assure the minimization of the error function $\{E_k\}$ given in Equation 2. The instantaneous estimate of the mean-square error calculated at the output layer is defined as follows (Derks, 1995; Mukerji, 2009):

$$E_k = \frac{1}{2} (z_k - t_k)^2 \quad (\text{Eq.2})$$

where z_k the output from output layer and t_k is the target value. The outgoing signal (z_k) is a function of the activation as follows (Eq. 3):

$$z_k = f(net_k) \quad (\text{Eq.3})$$

The effective incoming signal net_k , comprising weighted sum signals from the hidden layer (y_j) and calculated as follows (Eq. 4):

$$net_k = \sum_{j=1}^J w_{jk} y_j \quad (\text{Eq.4})$$

The outgoing signal (y_j) is the result of the incoming signal net_j , being passed through the activation function, which is not necessarily the same as that for z_k , is given as follows (Eq. 5):

$$y_j = f(net_j) \quad (\text{Eq.5})$$

Again, the effective incoming signal net_j , comprising weighted sum signals from input layer (x_i) is calculated as Equation 6:

$$net_j = \sum_{i=1}^I w_{ij} x_i \quad (\text{Eq.6})$$

The derivative of the error functions with respect to w_{jk} , can be expressed after applying the chain rule, as follows in Equation 7:

$$\frac{\partial E_k}{\partial w_{jk}} = \frac{\partial E_k}{\partial Z_k} \frac{\partial Z_k}{\partial net_k} \frac{\partial net_k}{\partial w_{jk}} \quad (\text{Eq.7})$$

Finally, the updated weights are given in *Equation 8*:

$$w_{ij} = w_{ij} + \Delta w_{ij} \quad (\text{Eq.8})$$

Activation function

Artificial neural network is a procedure to sum the product of the connected weights, the input signals, and produce an output or activation transfer function. The activation function is the specific function for the input units. The nodes of a specific layer get the equivalent type of activation function. Generally, in every case a non-linear activation transfer function is used. There are several activation transfer functions employed in ANNs, but in this study we will focus on unipolar binary function or sigmoid function (S).

The unipolar binary function or sigmoid function (S)

The sigmoid function, as implemented by Hall and Minns (1996) and Dawson and Wilby (2001) is defined as in *Equation 9*:

$$S(\text{net}_j) = \frac{1}{1 + \exp(-\lambda \text{net}_j)} \quad (\text{Eq.9})$$

where $\lambda > 0$ in above sigmoid function. λ is in proportion to the nodes defining the steepness of the function, which in general is set equal to one. The term λnet_j , will lies between $(-\infty$ and $+\infty)$, whereas $S(\text{net}_j)$ will lies between (0 and 1).

Wavelet analysis

Two primary types of wavelet transforms are commonly used i.e. continuous wavelet transform (CWT) and Discrete Wavelet Transform (DWT). The CWT works with functions defined over the whole real axis while the DWT deals with functions defined over a range of integers. Wavelets are mathematical processes which represent a time-scale of the time series and their relationships to analyze time series when the data is non-stationary. Wavelet analysis is helpful in the long-time intervals where the frequency information's are low and also in the short time intervals where the frequency information is high.

Wavelet is a small wave function denoted by the notation $\psi(\cdot)$. The range of a wavelet mother function ($\psi(\cdot)$) lies between $-\infty$ and ∞ , and it must fulfill the following given properties:

The value of the integral of $\psi(\cdot)$ is always equal to zero as shown in *Equation 10*:

$$\int_{-\infty}^{+\infty} \Psi(u) du = 0 \quad (\text{Eq.10})$$

The integral of the square of $\psi(\cdot)$ is unity as in *Equation 11*:

$$\int_{-\infty}^{+\infty} \Psi^2(u) du = 1 \quad (\text{Eq.11})$$

Admissibility Condition of $\Psi(f)$ is given in *Equation 12*:

$$C_{\Psi}(t) = \int_0^{\infty} \Psi^* \frac{[\Psi(f)]^2}{f} df \quad \text{satisfies} \quad 0 < C_{\Psi} < \infty \quad (\text{Eq.12})$$

Haar created a wavelet function in 1910 (*Fig. 3*), named Haar wavelet function (Ogden, 2012) and considered one of the oldest wavelet functions, given in *Equation 13*:

$$\Psi^{(H)}(u) = \begin{cases} +1 & \text{if } 0 \leq u < \frac{1}{2} \\ -1 & \text{if } \frac{1}{2} \leq u < 1 \\ 0 & \text{else} \end{cases} \quad (\text{Eq.13})$$

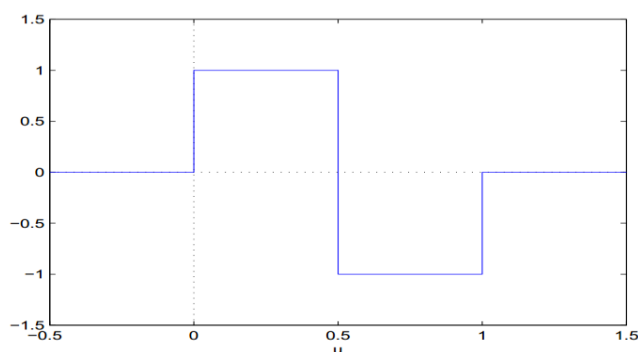


Figure 3. The Haar wavelet function

It is a discrete wavelet and looks like a step function. Harr wavelet and Daubechies (db) are the same. Daubechies family wavelets are written as dbN, where N stands for the order of Daubechies family. There is more flexibility in wavelet analysis due to which we can choose a specific Wavelet for matching the type of function under analysis.

The function $\psi(\cdot)$ is the mother wavelet and a double wavelet index family can be constructed by *Equation 14*:

$$\Psi_{\lambda,t}(u) = \frac{1}{\sqrt{\lambda}} \Psi\left(\frac{u-t}{\lambda}\right) \quad (\text{Eq.14})$$

where $\lambda > 0$ and t is finite.

The standardization on the right-hand side of *Equation 14* is:

$$\|\Psi_{\lambda,t}\| = \|\Psi\| \quad \text{for all } \lambda, t.$$

Functions are considered linear combination where the information is secure and make no losses to those functions which are in discrete form or as an integral in the continuous form of the selected wavelet family.

Wavelet-ANN conjunction model for flood events prediction

The wavelet analysis is connected to the Artificial Neural Network approach for annual peak flows prediction in this research, also depicted in *Figure 4*. First of all, the

observe annual peak flows time series, Q were decayed into several multi-frequencies time series including details (high frequency, low scale), such as, $Q_{D1}(t)$; $Q_{D2}(t)$; $Q_{Di}(t)$, and approximate (high scale, low frequency) such as, $Q_{Da}(t)$ by DWT. The symbol D_i shows the Wavelet-ANN Model for Flood prediction, level i decayed details time series and a denote approximation time series.

However, the decayed $Q(t)$ time series were used as inputs to ANN model. The original data of time series in the next step, $Q(t + 1)$ is output of the Wavelet-ANN conjunctural model. The graphical representation of above methodology is shown in *Figure 4*.

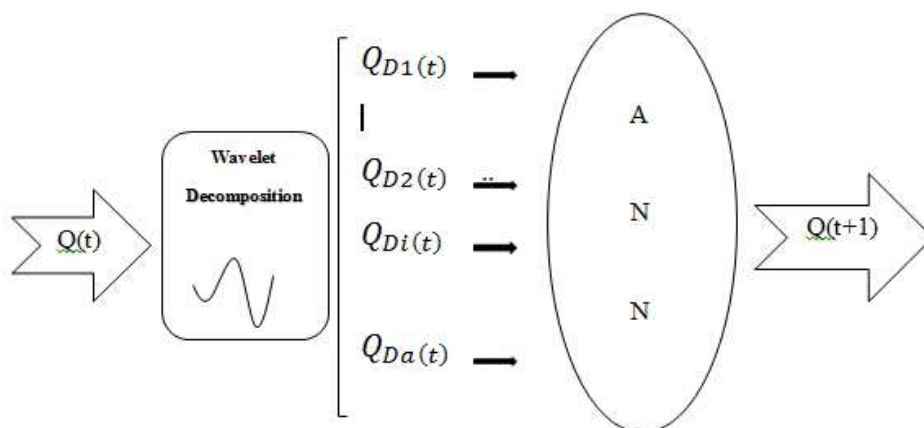


Figure 4. Schematic diagram of wavelet-ANN conjunction model

Criteria for the evaluation of a model

To evaluate the consistency of the models, it is compulsory to check the capabilities of ANN in both training and testing period (see for example Beven, 2011). Several statistical techniques are generally used for this purpose. Some of the evaluations measures are given below, which will be used in this study.

Pearson correlation coefficient (R)

Correlation coefficient (R) designates the direction of the linear association among two variables (i.e., model input and output values). The R coefficient is achieved by dividing the co-variance of the two random variables by the multiplication of their standard deviations. The R is given by the formula given in *Equation 15*:

$$R = \frac{\sum_{i=1}^n (Y_{mi} - \hat{Y}_{mi})(Y_{ci} - \hat{Y}_{ci})}{\sqrt{\sum_{i=1}^n (Y_{mi} - \hat{Y}_{mi})^2 \sum_{i=1}^n (Y_{ci} - \hat{Y}_{ci})^2}} \quad (\text{Eq.15})$$

where Y_{mi} indicate the observed values and Y_{ci} indicate the model or predicted values of annual peak flows at particular site at time i ., \hat{Y}_{mi} and \hat{Y}_{ci} are the average values of Y_{mi} and Y_{ci} respectively.

If the association is +1 then there is a perfect positive linear relationship between actual and estimated values while a value of -1 refers to perfect negative linear relationship between them. If R comes with 0 value, then it indicates no linear relationship between them.

Root mean square error (RMSE)

The positive square root of the mean/average of the square of all the errors. RMSE measures the spread/ variation of these residuals. RMSE is a commonly used measure to see the variances between the predicted values and estimated values with a range from 0 to ∞ . When $Y_{mi} = Y_{ci}$, then $RMSE = 0$, which implies that the model is perfectly fitted. The smaller RMSE shows that the model is best fitted. The formula of RMSE is given by Equation 16:

$$RMSE = \sqrt{\frac{1}{n} \sum_{i=1}^n (Y_{mi} - Y_{ci})^2} \quad (\text{Eq.16})$$

Mean absolute error (MAE)

MAE calculates the average size of the errors, without caring about the direction of the error. It is average of absolute differences between predicted and estimated values. The minimum value of MAE indicates that the model is best fitted. The formula of MAE is shown as given in Equation 17:

$$MAE = \frac{1}{n} \sum_{j=1}^n |Y_{mi} - Y_{ci}| \quad (\text{Eq.17})$$

Nash-Sutcliffe coefficient

To evaluate the prediction of a hydrological model this co-efficient is frequently used. It is proposed by Nash-Sutcliffe coefficient in 1970. The Nash-Sutcliffe coefficient E is defined by Equation 18:

$$E = 1 - \frac{\sum_{i=1}^n (Y_{mi} - Y_{ci})^2}{\sum_{i=1}^n (Y_{mi} - \bar{Y}_{mi})^2} \quad (\text{Eq.18})$$

The range of E lies between $-\infty$ and 1. A value of $E = 1$ indicates the perfect match among observed and predicted values while a value of 0 implies that the predictions of model are as correct as the average of the actual data. However the value of $-\infty < E < 0$ arises in case of week prediction. For more details see Grossmann (2010).

Index of agreement (IOA)

The term Index of Agreement established by Willmott (2012) as a standard quantity to evaluate the prediction error of a model and it lies between 0 and 1. The value of $IOA = 1$ shows an accurate prediction while of 0 shows no agreement at all. It is defined as in Equation 19:

$$IOA = 1 - \frac{\sum_{i=1}^n (Y_{mi} - Y_{ci})^2}{\sum_{i=1}^n (|Y_{mi} - \bar{Y}_{mi}| + |Y_{ci} - \bar{Y}_{ci}|)^2} \quad (\text{Eq.19})$$

Non-parametric kernel density estimation

We also consider non-parametric kernel density estimation (KDE) approach for comparison with ANN approach. In Statistics, KDE is a well-known nonparametric method, which is used to estimate the probability density estimation (PDF) of a random variable. KDE is a principal data smoothing issue where decisions about the population are made, on the basis of finite data sample. Cross validation (CV) smoothing technique

being more efficient is used in this study to estimate the smoothing parameter of the nonparametric KDE for annual peak stream flows of Mangla site. By using the estimates of smoothing parameters we estimate the nonparametric kernel density using Gaussian kernel (for details see Shabri, 2002; Lall, 1995; Silverman, 2018; Gramacki, 2018). Let Y be a random variable with PDF. The PDF f provides the actual behavior of the distribution of Y . The probability density function for a certain range is as follows in Equation 20:

$$\int_a^b f(y)dy \quad \forall a < b \quad (\text{Eq.20})$$

For parametric approach, it is always necessary to check the all fundamental assumptions but in non-parametric KDE, we move towards the assumption free estimation methodology.

Let K denotes the kernel function which holds the following condition given in Equation 21:

$$\int_{-\infty}^{+\infty} K(y) = 1 \quad (\text{Eq.21})$$

The kernel estimator can be defined as in Equation 22:

$$\hat{f}(y) = \frac{1}{nh} \sum_{i=1}^n K\left(\frac{y - Y_i}{h}\right) \quad (\text{Eq.22})$$

where h denotes the smoothing parameter or bandwidth or window width. The kernel estimator is the sum of bumps placed at the sample values. Further, kernel function K and bandwidth h determine the shape of the bumps and width for the kernel estimator, respectively. In NP kernel density estimation, calculation of smoothing parameter h is crucial. If the value of h is too small then used kernel estimator leads to larger variance and smaller bias. The value of smoothing parameter or bandwidth h has to be selected optimally. We have opted Cross Validation (CV) method in this study.

At site flood frequency analysis by fitting appropriate probability model

For fitting probability model to peak flows (*at-site flood frequency analysis*), we considered method of L-moments for estimation of parameters of different probability models and also for different goodness of fit tests. Method of L-moments is considered as more robust in the presence of extreme observations. After fulfilment of the basic assumptions of randomness, stationarity, independence and homogeneity through different statistical tests, the next step is to choose the best fit probability distribution among the most commonly used probability models in hydrology such as generalized Logistic (GLO), Generalized Extreme Value (GEV), Generalized Pareto (GPA), Pearson Type 3 (PE3), an Generalize Normal (GNO) (for example see Ahmad et al., 2015; Rahman et al., 2013; Drissia, 2019; Cassalho et al., 2019; Mostofi, et al., 2019). The best model is selected on the basis of different goodness of fit tests such as Anderson Darling (AD) test, Kolmogrove-Smirknove (KS) and L-moments ratio

diagram (LMRD). After finding the best models, the next step is to find the results in the form of Pearson correlation coefficient, Root Mean Square Error (RMSE), Mean Absolute Error (MAE), Nash-Sutcliffe coefficient and Index of Agreement (IOA) for observed and predicted values and then compare these results with other techniques.

Results and discussions

Data exploration

The annual peak flows data of Mangla site located at River Jhelum, Pakistan was retrieved from WAPDA and federal flood commission of Pakistan. The peak flows normally occur in monsoon season of Pakistan i.e. from July to September. The basic statistics of the data used in this research is given in *Table 1*.

Table 1. Basic information about all of the sites used in the study

Number of observations	Mean (Cusecs)	Standard deviation (Cusecs)	Coefficient of skewness	Coefficient of variation	Latitude	Longitude	Elevation
$n = 54$	132480	136390	4.2402	1.0295	33.15	73.65	14902.7

Table 1 shows that there are total 54 values of peak flows for Mangla site. Each value represents the maximum value in the whole year. The data of peak flows at Mangla site is positively skewed with the coefficient of skewness as 4.2402. The mean of time series is 132480 cusecs. First estimate of first L-moment is equal to mean of the data. The standard deviation of the data is little bit higher than its mean i.e. 136390 cusecs. The coefficient of variation for this time series is 1.0295.

ANN and W-ANN modeling

Annual peak flows for 54 years (1960-2013) of Mangla site on River Jhelum in Pakistan are used for the performance evaluation of Artificial Neural Network (ANN) and Wavelet-ANN Conjunctural model (W-ANN). Eighty percent annual peak flows (1960-2002) are used for training ANN and Wavelet-ANN conjunctural model. The remaining twenty percent data (2003-2013) are used for testing the trained model,

By using the Discreet Wavelet-transform (DWT-Haar wavelet level 1), the approximation and details sub-signals are obtained from the temporal characteristics of of annual peak observed annual peak flows, which are considered as the inputs for W-ANN model. The output for W-ANN model is the original peak flows in the present time step (*Fig. 5*). In the previous step, original values flows are input and in the present time step the values of annual peak flows are used as output to the T-ANN model. In this way, for both models the output is same.

The approximation and detail sub-signals of the annual peak flows series by using DWT db1 (Haar wavelet level 1) are shown in *Figure 6a* and *b*. The approximation and detail sub-signals for DWT db2 (Haar wavelet level 2) are shown in *Figure 7a* and *b*. In this study, two W-ANN models are introduced for comparing purpose such as db1 and db2 respectively. Utilizing db1 transform as inputs for the first W-ANN model and db2 transform as inputs for the second W-ANN model.

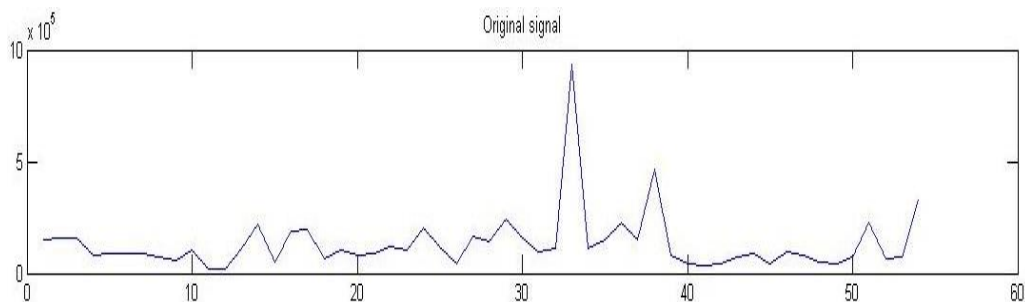


Figure 5. Plot of Annual peak flows (Cusecs) at Mangla site

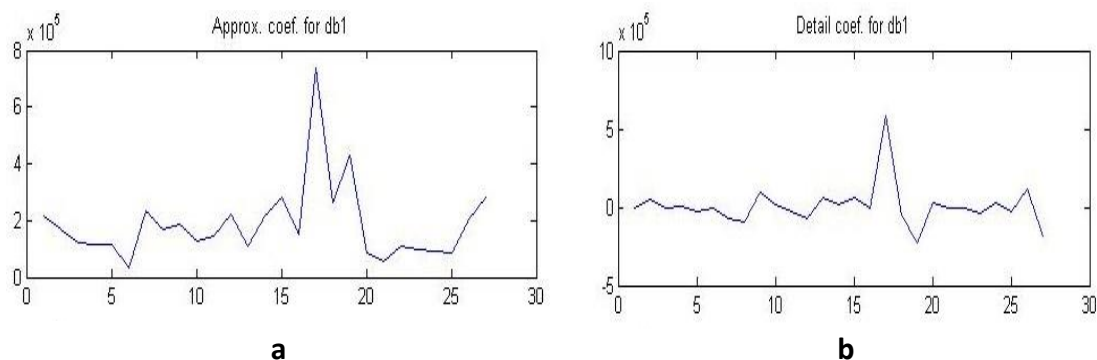


Figure 6. a Approximation sub-signal of peak flows by DWT db1 at Mangla site. **b** Detail sub-signal of peak flows by DWT db1 at Mangla site

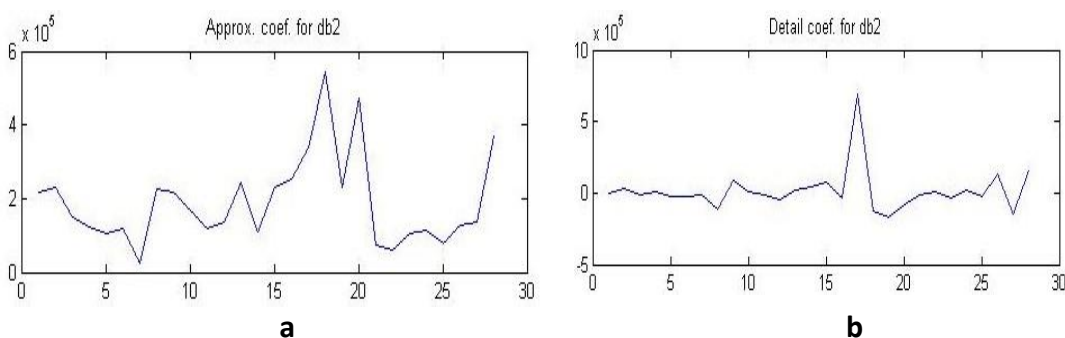


Figure 7. a Approximation sub-signal of peak flows (cusecs) by DWT db2 at Mangla site. **b** Detail sub-signal of peak flows (cusecs) by DWT db2 at Mangla site

By using the methodology shown in *Figure 4*, the (W-ANN) conjunctional model is used here. Back propagation neural network training algorithm is executed on MATLAB platform. Internal parameters used are, momentum coefficient = 0.5 and number of iterations = 1000 to obtain the ideal architecture. Furthermore, ideal combinations of activation functions in both hidden and output layers are obtained with sigmoid function. In this study we consider two input, two hidden, and one output node (2-2-1) for W-ANN conjunctional model and one input, two hidden, and one output nodes (1-2-1) for T-ANN model. The performance of both models W-ANN-db1 (2-2-1) and T-ANN model (1-2-1) for one step ahead forecasting is compared in *Table 2*.

Table 2. Training and testing errors for T-ANN and W-ANN-db1

Models	Evaluation Measures					
	Training/testing	R	RMSE (Cusecs)	E	IOA	MAE (Cusecs)
W-ANN (2-2-1)	Training	0.6394	1.63E+04	0.4914	0.8965	1.83E+04
	Testing	0.5631	3.85E+04	0.3085	0.7382	2.96E+04
T-ANN (1-2-1)	Training	0.4963	2.13E+04	0.2168	0.7317	1.96E+04
	Testing	0.4891	4.26E+04	0.0938	0.5861	3.05E+04

Table 2 shows the performance of W-ANN and T-ANN model in both phases training and testing by using various statistical evaluations measures. W-ANN-db1 (2-2-1) and T-ANN (1-2-1) are chosen as best models among class of other W-ANN and T-ANN models. From Table 2, it is observed that prediction for testing data is not good as compared to the training data using evaluation measures for W-ANN-db1 and T-ANN. From Table 2, the R (0.6394 and 0.5631) for training and testing data of W-ANN-db1 model is greater than the R (0.4963 and 0.4891) for training and testing data respectively of T-ANN model. The RMSE of W-ANN-db1 model for training and testing are (1.63E+04 and 3.85E+04) which is less than the RMSE (2.13E+04 and 4.26E+04) of T-ANN model for training and testing data respectively. Nash-Sutcliffe coefficient E (0.4914 and 0.3085) and Index of Agreement IOA (0.8965 and 0.7382) of W-ANN-db1 model for both training and testing data are also greater than the corresponding E (0.2168 and 0.0938) and IOA (0.7317 and 0.5861) of T-ANN model for training and testing data respectively. The MAE (1.83E+04 and 2.96E+04) for training and testing data of W-ANN-db1 model are less than the MAE (1.96E+04 and 3.05E+04) for training and testing data of T-ANN model respectively. Therefore, due to goodness of fit tests (R, RMSE, E, IOA, & MAE) W-ANN conjunctive model (db1) with two input, two hidden, and one output nodes i.e. W-ANN-db1 (2-2-1) is selected as best performing model as compare T-ANN i.e. T-ANN (1-2-1).

Also, Figure 8, given below compares the actual and predicted peak flows in result of T-ANN (1-2-1) model. Peak flows in the start were accurately forecasted while at the end these flows were not showing harmony with each other. Figure 9 compares the actual flows and predicted peak flows in the result of W-ANN-db1 (2-2-1) model. Peak flows were forecasted in a better way at different parts as compared to previous T-ANN model.

Results are further improved when approximation and detail sub-signal of the annual peak flows are obtained using DWT at db2 (Haar wavelet level 2) as presented in Table 3. Results are improved with W-ANN-db2 (2-2-1) model as compared to W-ANN-db1 (2-2-1). Table 3, shows the results of R, RMSE, E, IOA and MAE for T-ANN (1-2-1) and W-ANN-db2 (2-2-1) model for Mangla site.

Table 3 shows the results of W-ANN-db2 model for Mangla site which clearly shows that the R is improved from 0.6394 to 0.7984 for training data and from 0.4963 to 0.6108 for testing data. The value RMSE are reduced from 1.63E+04 to 1.21E+04 for training and from 3.85E+04 to 2.99E+04 for testing data. The statistical measure Nash-Sutcliffe coefficient E is also improved from 0.4914 to 0.6362 and from 0.3085 to 0.4158 for training and testing data respectively. Similarly, the term Index of Agreement (IOA) is improved from 0.8965 to 0.9135 and from 0.7382 to 0.7916 for

training and testing data respectively. MAE are reduced from 1.83E+04 to 1.04E+04 and from 2.96E+04 to 2.11E+04 for training and testing data respectively. It could be observed from *Table 3* that the performance of W-ANN-db2 model is better than the W-ANN-db1 model for Mangla station.

Table 3. Training and testing errors for T-ANN and W-ANN-db2

Models	Evaluation measures					
	Training/ Testing	R	RMSE (Cusecs)	E	IOA	MAE (Cusecs)
W-ANN (2-2-1)	Training	0.7984	1.21E+04	0.6362	0.9135	1.04E+04
	Testing	0.6108	2.99E+04	0.4158	0.7916	2.11E+04
T-ANN (1-2-1)	Training	0.4963	2.13E+04	0.2168	0.7317	1.96E+0R
	Testing	0.4891	4.26E+04	0.0938	0.5861	3.05E+04

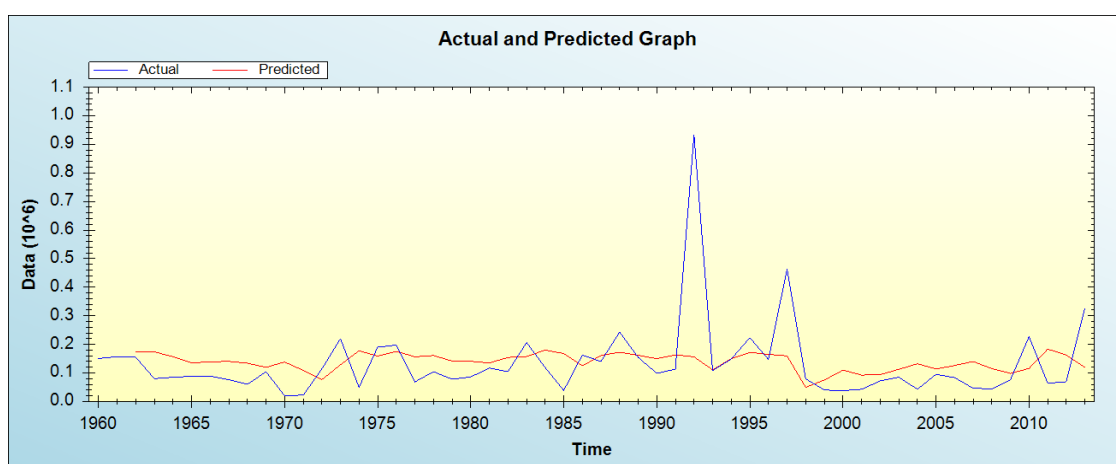


Figure 8. Graph of observed and predicted flows (cusecs) using T-ANN-db1(1-2-1) for Mangla site

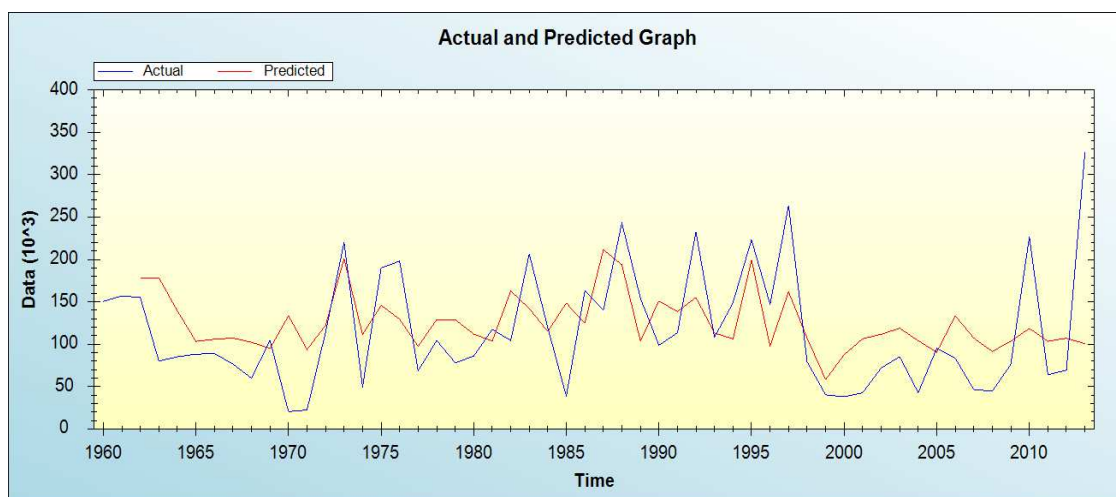


Figure 9. Graph of observed and predicted flows (cusecs) using W-ANN-db1(2-2-1) for Mangla site

Figure 10 compares the actual and predicted peak flows from W-ANN-db2 model. Peak flows at different stages were accurately forecasted. It can be seen that the W-ANN-db1 model was not suitable model for forecasting purpose in the present study. On the other side, W-ANN-db2 model provides closer estimates of predicted values to the corresponding observed peak flows for a lead-time of 1 year.

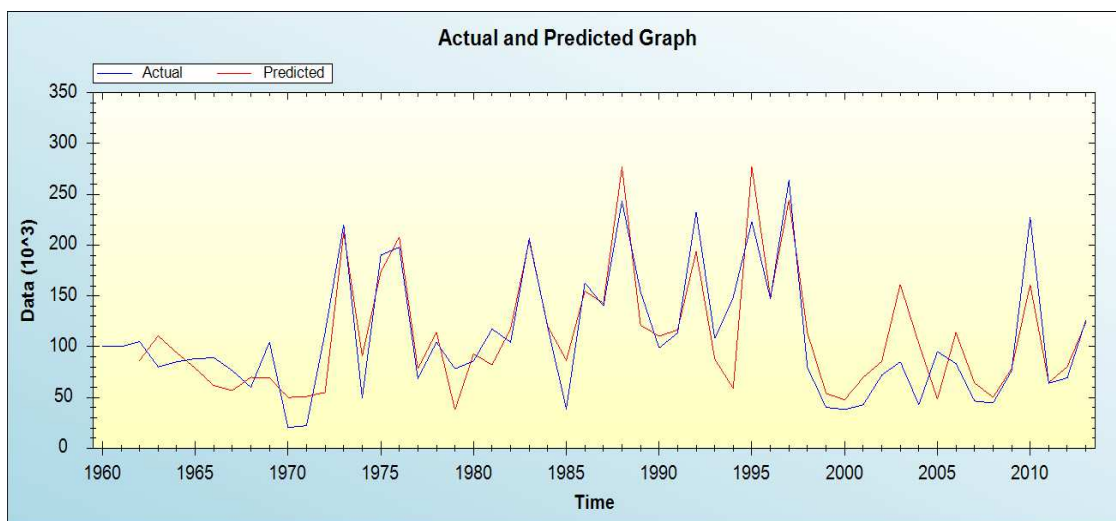


Figure 10. Graph of observed and predicted flows (cusecs) using W-ANN-db2(2-2-1) for Mangla site

Probability distribution modeling and kernel density estimation of annual peak flows

There are four basic assumptions of a time series which must be checked before any further probability distribution modeling in statistical hydrology. These assumptions are randomness, stationarity, independence, and homogeneity. These assumptions are of great importance, without them the results are not accurate and may affect the policy implications. We tested these assumptions with the help of different tests such as Mann Kendall's test for trend detection and Mann-Whitney test for homogeneity with respect to location parameters, and for independence we applied the Lag1 correlation test. One sample runs test is also applied for detection of randomness in the present study.

Table 4 shows that all of the fundamental assumptions are fulfilled and we can say that the time series of peak flows is suitable for further analysis. In the next step, we will find best suitable model among GLO, GPA, GEV, GNO and PE3. We used different goodness of fit tests such as Anderson – Darling (AD), Kolmogrove-Smirknove (KS) test and L-moments ratio diagram (LMRD). For estimation of parameters of these distributions we used method of linear moments (L-moments) because of its outperformance in the presence of extreme observations. From KS and AD test, GLO got first rank and declared as the most suitable probability model for peak flows of Mangla site. The same data has also been used in Ahmad et al. (2015). LMRD is a visual inspection for selecting the most appropriate probability model among class of different probability models. It is a graph of theoretical L-moments ratio of skewness and kurtosis of different probability models. This ratio is represented by a curve in the case of three parameters distribution. The sample ratio of these L-moments ratios using the data of Mangla site is shown with “+” sign. The closeness of this “+” to

any distribution's curve will identify the suitability of that probability model for a particular data. This LMRD, in the present case, also suggest that GLO distribution is the most suitable model for Peak flows of Mangla site see *Figure 10*. The result of LMRD and other goodness fit tests show the same result. After selection of the most suitable model, the next step is find different evaluation measures such as R, RMSE, IOA, MAE for comparison purposes with other approaches. The results are given in *Table 5*.

Table 4. Results of different assumption for annual peak flows (cusecs) at Mangla site

Assumption of stationarity		Assumption of homogeneity		Assumption of independence		Assumption of randomness	
Test statistic	P-value	Test statistic	P-value	Test statistic	P-value	Test statistic	P-value
-0.154	0.238	69	0.074	0.236	0.174	14	1

Table 5. Results of various evaluation measures through probability distribution modeling and kernel density estimation

Models	Evaluation measures				
	R	RMSE (cusecs)	E	IOA	MAE (cusecs)
Probability distribution modeling	0.9401	1.94E+04	0.3513	0.8661	1.55E+04
Kernel density estimation	0.7415	3.8E+04	0.5035	0.5940	5.01E+04

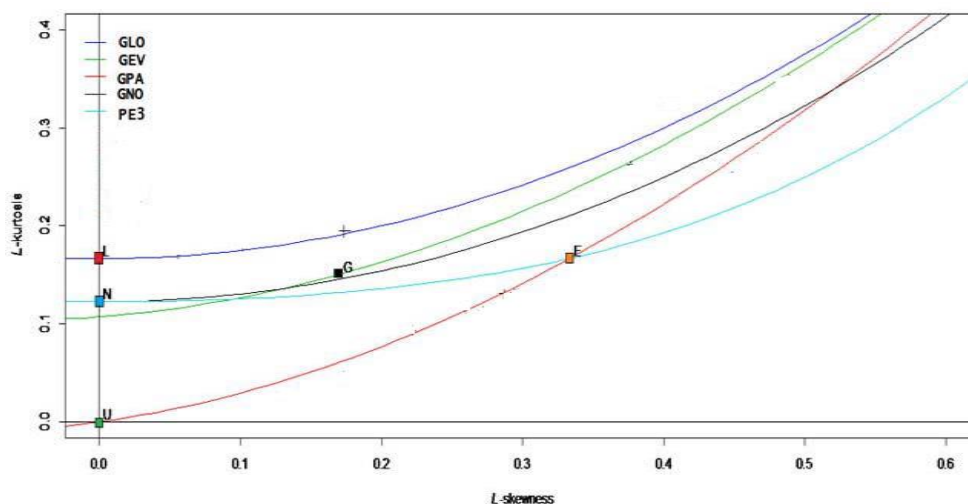


Figure 10. L-moments ratio diagram for Mangla site

For KDE, we use Gaussian kernel and cross validation technique for estimation of smoothing parameter. The choice of kernel is not important as compared to choice of smoothing parameter. In KDE, there is no need to check the assumptions of data like probability distribution modeling. The results of KDE are also presented in *Table 5*.

Results show that probability distribution modeling approach is providing comparable results with W-ANN-db2 model, but outperforms than KDE. Overall the performance of W-ANN-db2 model is better than all other approaches discussed in this study for peak flows of Mangla site.

The results of non-parametric KDE are also presented in the *Table 5*, which are not so promising as W-ANN-db2 and Probability distribution modeling approach. Over all, the W-ANN-db2 approach outperforms than T-ANN, probability modeling and KDE.

Conclusion

In this study the annual peak flows series measured in cusecs at Mangla site situated on the river Jhelum, Pakistan with length of 54 years has been considered for identification of the most suitable modeling approach among T-ANN, W-ANN, Probability distribution modeling and non-parametric KDE. In the light of statistical evaluation criteria, it can be seen that W-ANN model under db1 gave more accurate forecasting results than the T-ANN model. The results further are improved by fitting the W-ANN conjunctive models under db2 scheme. Further to check the authenticity of W-ANN-db2 model, we compared it with probability distribution modeling approach by fitting GLO probability model being the most suitable model and KDE approach using Gaussian kernel approach. The comparison reveals that, probability distribution modeling approach gives us comparable results as of W-ANN-db2 model. The results of KDE are not as promising as of W-ANN and probability distribution modeling approach. Overall, comparison among four approaches, we notice that W-ANN-db2 model outperformed in this study. These results are useful in water resources management such as construction of different hydrological structures.

Acknowledgements. Authors are very grateful to deanship of scientific research at King Khalid University, Abha, Saudi Arabia for the financial support through General Research Program under project number GRP-133-40.

REFERENCES

- [1] Agarwal, A., Singh, R. D., Mishra, S. K., Bhunya, P. K. (2005): ANN-based sediment yield models for Vamsadhara River basin (India). – *Water Sa* 31(1): 85-100.
- [2] Ahmad, I., Fawad, M., Mahmood, I. (2015): At-site flood frequency analysis of annual maximum stream flows in Pakistan using robust estimation methods. – *Polish Journal of Environmental Studies* 24(6): 11-20.
- [3] Aziz, K., Rahman, A., Shamseldin, A. (2016): Development of Artificial Intelligence Based Regional Flood Estimation Techniques for Eastern Australia. – In: Shanmuganathan, S., Samarasinghe, S. (eds.) *Artificial Neural Network Modelling*. Springer, Cham.
- [4] Beven, K. J. (2011): *Rainfall-Runoff Modelling: The Primer*. – John Wiley & Sons, Lancaster, UK.
- [5] Bishop, C. M. (1996): *Neural Networks for Pattern Recognition*. – Oxford University Press, New York.
- [6] Cassalho, F., Beskow, S., de Mello, C. R., de Moura, M. M., de Oliveira, L. F., de Aguiar, M. S. (2019): Artificial intelligence for identifying hydrologically homogeneous regions: A state-of-the-art regional flood frequency analysis. – *Hydrological Processes*. <https://doi.org/10.1002/hyp.13388>.

- [7] Dawson, C. W., Wilby, R. L. (2001): Hydrological modelling using artificial neural networks. – *Progress in Physical Geography* 25(1): 80-108.
- [8] Denis, C., Assis, W. O., Coelho, A. D. (2009): Sorting tomatoes for industrial processing through of computer vision system based on neural networks. – COBEM 2009– International Congress of Mechanical Engineering, Gramado, RS.
- [9] Derks, E. P. P. A., Pastor, M. S., Buydens, L. M. C. (1995): Robustness analysis of radial base function and multi-layered feed-forward neural network models. – *Chemometrics and Intelligent Laboratory Systems* 28(1): 49-60.
- [10] Drissia, T. K., Jothiprakash, V., Anitha, A. B. (2019): Flood frequency analysis using L moments: a comparison between at-site and regional approach. – *Water Resources Management* 2019: 1-25.
- [11] Gramacki, A. (2018): Nonparametric Kernel Density Estimation and Its Computational Aspects. – Springer International Publishing, New York.
- [12] Grossmann, I. E., Guillén-Gosálbez, G. (2010): Scope for the application of mathematical programming techniques in the synthesis and planning of sustainable processes. – *Computers & Chemical Engineering* 34(9): 1365-1376.
- [13] Guresen, E., Kayakutlu, G., Daim, T. U. (2011): Using artificial neural network models in stock market index prediction. – *Expert Systems with Applications* 38(8): 10389-10397.
- [14] Hertz, J. A. (2018): Introduction to the Theory of Neural Computation. – CRC Press, Boca Raton, FL.
- [15] Hipel, K. W., McLeod, A. I. (1994): Time Series Modelling of Water Resources and Environmental Systems. (Vol. 45). – Elsevier, Amsterdam.
- [16] Huang, G., Huang, G. B., Song, S., You, K. (2015): Trends in extreme learning machines: A review. – *Neural Networks* 61(1): 32-48.
- [17] Jimeno-Sáez, P., Senent-Aparicio, J., Pérez-Sánchez, J., Pulido-Velazquez, D., Cecilia, J. (2017): Estimation of instantaneous peak flow using machine-learning models and empirical formula in peninsular Spain. – *Water* 9(5): 347-359.
- [18] Khosrow-Pour, M. (ed.) (2006): Dictionary of Information Science and Technology. (Vol. 1). – IGI Global, Hershey, Pennsylvania.
- [19] Kisi, O., Shiri, J. (2011): Precipitation forecasting using wavelet-genetic programming and wavelet-neuro-fuzzy conjunction models. – *Water Resources Management* 25(13): 3135-3152.
- [20] Kumar, R., Goel, N. K., Chatterjee, C., Nayak, P. C. (2015): Regional flood frequency analysis using soft computing techniques. – *Water Resources Management* 29(6): 1965-1978.
- [21] Lall, U. (1995): Recent advances in nonparametric function estimation. Hydrologic applications. – *Reviews of Geophysics* 33(S2): 1093-1102.
- [22] Maidment, D. R. (1993): Handbook of Hydrology. – McGraw-Hill, New York.
- [23] Minns, A. W., Hall, M. J. (1996): Artificial neural networks as rainfall-runoff models. – *Hydrological Sciences Journal* 41(3): 399-417.
- [24] Mostofi Zadeh, S., Durocher, M., Burn, D. H., Ashkar, F. (2019): Pooled flood frequency analysis: a comparison based on peaks-over-threshold and annual maximum series. – *Hydrological Sciences Journal*. <https://doi.org/10.1080/02626667.2019.1577556>.
- [25] Mukerji, A., Chatterjee, C., Raghuvanshi, N. S. (2009): Flood forecasting using ANN, neuro-fuzzy, and neuro-GA models. – *Journal of Hydrologic Engineering* 14(6): 647-652.
- [26] Ogden, T. (2012): Essential Wavelets for Statistical Applications and Data Analysis. – Springer Science & Business Media, New York.
- [27] Rahimi-Ajdadi, F., Abbaspour-Gilandeh, Y. (2011): Artificial neural network and stepwise multiple range regression methods for prediction of tractor fuel consumption. – *Measurement* 44(10): 2104-2111.
- [28] Rahman, A. S., Rahman, A., Zaman, M. A., Haddad, K., Ahsan, A., Imteaz, M. (2013): A study on selection of probability distributions for at-site flood frequency analysis in Australia. – *Natural Hazards* 69(3): 1803-1813.

- [29] Rahman, A., Charron, C., Ouarda, T. B., Chebana, F. (2018): Development of regional flood frequency analysis techniques using generalized additive models for Australia. – *Stochastic Environmental Research and Risk Assessment* 32(1): 123-139.
- [30] Requena, A. I., Ouarda, T. B., Chebana, F.(2018): Low-flow frequency analysis at ungauged sites based on regionally estimated streamflows. – *Journal of Hydrology* 563: 523-532.
- [31] Salas, J. D. (1980): *Applied Modeling of Hydrologic Time Series*. – Water Resources Publication, Littleton.
- [32] Shabri, A. (2002): Nonparametric kernel estimation of annual maximum stream flow quantiles. – *Matematika* 18(1): 99-107.
- [33] Silverman, B. W. (2018): *Density Estimation for Statistics and Data Analysis*. – Routledge, Boca Raton, FL.
- [34] Singh, R. M., Datta, B., Jain, A. (2004): Identification of unknown groundwater pollution sources using artificial neural networks. – *Journal of Water Resources Planning and Management* 130(6): 506-514.
- [35] Tiwari, H., Rai, S. P., Sharma, N., Kumar, D. (2015): Computational approaches for annual maximum river flow series. – *Ain Shams Engineering Journal*. DOI: 10.1016/j.asej.2015.07.016.
- [36] Willmott, C. J., Robeson, S. M., Matsuura, K. (2012): A refined index of model performance. – *International Journal of Climatology* 32(13): 2088-2094.
- [37] Zurada, J. M., Malinowski, A., Usui, S. (1997): Perturbation method for deleting redundant inputs of perceptron networks. – *Neurocomputing* 14(2): 177-193.

A COMPARISON OF QUADRATIC REGRESSION AND ARTIFICIAL NEURAL NETWORKS FOR THE ESTIMATION OF QUANTILES AT UNGAUGED SITES IN REGIONAL FREQUENCY ANALYSIS

KHAN, M. S. R.^{1*} – HUSSAIN, Z.² – AHMAD, I.^{3,1}

¹*Department of Mathematics and Statistics, International Islamic University
H-10 Islamabad, Pakistan*

²*Research Center for Modeling and Simulation (RCMS), National University of Sciences and
Technology (NUST), H-12 campus Islamabad, Pakistan*

³*Department of Mathematics, College of Sciences, King Khalid University, 61413 Abha, Saudi
Arabia*

*Corresponding author

e-mail: shafiqnaizi@gmail.com (phone: +92-334-760-3022)

(Received 16th Feb 2019; accepted 29th Mar 2019)

Abstract. The study illustrates application of Regional Flood Frequency Analysis (RFFA) using Annual Maximum Peak Flows (AMPF) of eleven gauging sites of various streams of Khyber-Pakhtunkhwa, Pakistan. Assumptions associated to recorded data at various sites have been validated through various statistical tests. The discordancy measure indicates that there is no discordant site in the cluster of eleven sites. Heterogeneity measure based on l-moments confirms that the group of eleven sites is definitely homogeneous. Criterion of $|Z - Dist|$ statistic and L-moment ratio diagram show that Generalized Pareto (GPA) distribution is the best fitted regional distribution of the study region. Regional flood quantiles for various return periods have been estimated using the quantile function of GPA distribution. Artificial Neural Networks (ANN) and Quadratic Regression (QR) model with robust estimation method have been used for the estimation of quantiles at ungauged sites. Model evaluation criteria's (error comparison of predicted values) suggested that estimated quantiles through ANN are accurate relative to quadratic regression. Historical comparison shows that the quantiles estimated through index flood method and ANN are closely related to the highest recorded values of AMPF at each corresponding site for shorter as well as longer return periods.

Keywords: *analyzing extremes of floods, L-moments, regional frequency analysis, Khyber-Pakhtunkhwa, Pakistan, machine learning, non-linear regression*

Abbreviations: AMPF, Annual Maximum Peak flows; RFFA, Regional Flood Frequency Analysis; KPK, Khyber Pakhtunkhwa; AARF, Average Annual Rainfall; ARMS, Average Rainfall in Monsoon; long, Longitude; lat, Latitude; ele, Elevation; QR, Quadratic Regression; ANN, Artificial Neural Networks; RMSE, Root Mean Square Error; MAPE, Mean Absolute Percentage Error; MAE, Mean Absolute Error; GPA, Generalized Pareto Distribution; GLO, Generalized Logistic Distribution; GNO, Generalized Normal Distribution; GEV, Generalized Extreme Value Distribution; PE3, Pearson Type Three Distribution; l_1 , First sample L-moment

Introduction

Reliable estimation of extreme hydrological events is needed for designing and building of hydrological structures on stream channels. These structures are important to provide protection against floods and to regulate the supply of available water. Various approaches including at-site and regional are in practice for flood frequency analysis in different parts of the world. However, regional approach has advantageous results relative to at-site analysis. For instance, the estimated flood quantiles can be

interpolated and/or extrapolated to obtain estimates for the poorly gauged or ungauged sites of the study area. The most commonly used techniques for the estimation of quantiles at ungauged sites include the regression techniques, rational method, ANN, etc. The current study has adopted RFFA using index flood method based on L-moments coupled with QR with robust estimation method and ANN, to estimate flood quantiles at gauged and ungauged or poorly gauged sites, emphasizing the complete justifications related to the regression modeling and comparison with the historical record to investigate the practical validity of the resultant estimates.

Pakistan, with integrated river basins, has a long history of floods since 1947 (from the year of its independence). Twenty-four major floods have occurred in the country from 1947 to 2016, resultantly, the country has suffered direct economic loss of about 38.171 million USD (Government of Pakistan, 2016). Secondly, Pakistan, being a developing country with agriculture sector as a major contributor to its gross domestic product (GDP) requires effective planning and management, based on reliable estimates, for optimum utilization of the available water resources. Agriculture sector contributes about 24 percent in the GDP of Pakistan (Pakistan Bureau of Statistics, 2018). Thirdly, Pakistan's major rivers originate in India and Jammu & Kashmir (a disputed territory between India and Pakistan), and flows from north to south in the country. Due to the Indus Waters Treaty signed in 1960 between India and Pakistan for the division of major rivers of Indus river basins, and the lack of planning and development of the hydrological structures (dams and barrages) on the major rivers (Jhelum, Chenab and Indus), Pakistan is facing problems of shortage of water every year. This crisis will become even worst in future (Development Advocate Pakistan, 2017), as officials are forecasting severe crises of usable water by the year 2025. Therefore, planning, management and efficient utilization of available water resources, especially small rivers and stream flows of north-western areas of Pakistan, which originates in Pakistan, using standard methods of analysis is a primary need of time. The current study has focused, for the first time (to the best of author's knowledge), on various sites of the area of Khyber Pakhtunkhwa (KPK) (an important province in the north-west region of the country) to perform RFFA.

RFFA basically involves two principle steps, (1) identification of regions having similar site characteristics and (2) development of forecast equations for the estimation of flood quantiles at gauged and ungauged sites. RFFA has widely been used all over the world (including the neighboring countries of Pakistan) for the estimation of extreme events. For example; in Canada, (Glaves and Waylen, 1997; Pokhrel, 2002; Requena et al., 2017); in India, (Kumar et al., 2003a,b; Kumar and Chatterjee, 2006; Alam et al., 2016); in China, (Jingyi and Hall, 2004; Yang et al., 2010); in Iran, (Modarres, 2008; Malekinezhad and Zare-Garizi, 2014); in Turkey, (Saf, 2009; Aydoğan et al., 2016); in Italy, (Noto and La Loggia, 2009) and many more. In RFFA, several methods are in practice including regression techniques, rational methods, ANNs, etc. for the development of forecast equations to estimate flood quantiles at ungauged sites. Few details of the adopted methods in published studies are illustrated in the following sections.

Regression techniques have been used by various published studies for the estimation of quantiles at ungauged sites (Griffis and Stedinger, 2007; Hailegeorgis and Alfredsen, 2017), but very few of them have illustrated the complete theoretical and statistical justifications of the developed models. Moreover, scarce literature is available analyzing the nonlinear relationships of the site characteristics with observed AMPF of

gauged sites. Importantly, the relationship between hydrological and physio-meteorological variables is usually categorized as strongly nonlinear (Sivakumar and Singh, 2012). Nonlinear relationships may provide more accurate estimates of flood quantiles at ungauged sites as compared to linear relationships (Ouali et al., 2017). Secondly, due to the existence of outliers in the observed AMPF and availability of fewer values for analysis, the Ordinary Least Squares (OLS) estimation method may no longer be feasible. This problem requires robust methods for the estimation. In the current study, a quadratic term of the most influential site characteristic as independent variable has been introduced in the model along with a robust method for the estimation of the proposed model.

ANN is a nonparametric calculating and modeling approach stimulated by the biological operative of the human brain (Rumelhart et al., 1985). This method has significant advantages over other estimation techniques including regression analyses (Liu et al., 2009; Landi et al., 2010). One major advantage of ANN is their capacity to identify the complex nonlinear relationships and there is no need to express such relationship in mathematical form as the data itself recognizes the model form through use of artificial intelligence (Hjelmfelt and Wang, 1996). ANN approach coupled with RFFA can provide more accurate estimates of flood quantiles for ungauged sites relative to regression models (Dawson et al., 2006; Shu and Ouarda, 2007; Aziz et al., 2014; Anilan et al., 2016). Therefore, adopting recent trends in statistical hydrology, ANN has been used, for the first time in Pakistan, for the estimation of flood quantiles at ungauged sites.

Since, one of the emphases of this study is the identification of optimum method coupled with RFFA to obtain quantiles for ungauged sites. Therefore, the estimates through QR and ANN have been compared using Root Mean Square Error (RMSE), Mean Absolute Percentage Error (MAPE) and Mean Absolute Error (MAE) of predicted values from both the methods of estimation. Moreover, a comparison with the historical flood information has been done to investigate the practical validity of the provided estimates through different methods.

Keeping in view the aforementioned details, major objectives of the study are:

- Estimation of flood quantiles using RFFA based on L-moments for the gauged sites of important streams of KPK with complete justifications of the adopted procedure through various statistical tests.
- Estimating quadratic regression model with robust method of estimation for the estimation of quantiles at ungauged sites.
- Introduction of ANN for the estimation of quantiles for ungauged sites of the study area.
- Comparison of the estimates obtained through various procedures of estimation for ungauged sites using statistical measures along with historical information to identify the optimum method to be used in RFFA for the estimation of quantiles at ungauged sites.

Study area and data utilized

The KPK region, having various small rivers and stream flows, is the second source of river water in Pakistan. KPK has 101,741 km² area with steep geography and a population of about 35.53 million (as per population censuses of 2017 by the Government of Pakistan). The terrain of KPK consists of mountainous in the north, sub mountainous and lands surrounded by hills to the south. Due to steep geography and mountain land

of KPK the heavy rainfall usually turns into flash flooding affecting the whole of KPK (Pakistan Meteorological Department, 2012). Southern KPK is the most populated area of the province, and due to its downstream location, it has been affected badly due to heavy floods in 1992 and 2010 (Hashmi et al., 2012). Therefore, preventive measures against these natural disasters are a popular demand of the people of KPK which requires quantification of the frequency associated to these floods. Moreover, KPK has an identified potential of hydro-electricity of about 18698 Mega Watt, as reported in a study on Hydel Potential in Pakistan by National Electric Power Regulatory Authority (NEPRA), Pakistan (NEPRA, 2018). None of the published studies so far has used L-moment based RFFA for flood quantiles estimation at various sites of KPK. Few published studies in Pakistan related to statistical hydrology include (Muhammad and Afreen, 2007; Hussain and Pasha, 2009; Hussain, 2011; Ahmad et al., 2015; Ahmad et al., 2016; Batool, 2017; Hussain, 2017; Hussain et al., 2017 etc.). These studies have focused on the areas of Punjab and Sindh only (the two provinces of Pakistan). Other studies including (Shahzadi et al., 2013; Khan et al., 2017) performed rainfall frequency analysis considering few areas of KPK and Sindh.

The current study has performed RFFA using AMPF in cusecs of eleven gauging sites situated in the southern KPK. The data has been provided by the Provincial Irrigation Department of KPK. *Fig. 1* illustrates the geographical information of the sites used for the analyses. The details of these sites and their respective site characteristics, such as, Latitude (lat), Longitude (long), Elevation (ele), Average Annual Rainfall (AARF) and Average Rainfall in Monsoon (ARMS) are given in *Table 1*. Few missing observations have been found in the observed data series of the sites, Wazir Ghari, Chinkar, Bara Tarnab, Khuderzai, Jundi Utmanzai, Lund Khwar East, Jundi Tangi, and Swat Ningolai. The percentage of these missing observations is available in *Table 1*. These missing observations have been replaced by the average value of observed AMPF of the corresponding site.

Table 1. Site characteristics of eleven sites of Khyber-Pakhtunkhwa, Pakistan

S. No.	Site Name	Latitude (North)	Longitude (East)	Elevation (meters)	AARF (mm)	ARMS (mm)	Percentage of missing observations
1	Kalpani Deheri	33.9931	71.7461	303	559	255	0
2	Wazir Ghari	33.9845	71.7749	303	400	119	6
3	Chinkar	34.014	71.754	301	400	119	7
4	Bara Tarnab	34.0168	71.7037	305	400	119	7
5	Khuderzai	34.0121	71.7743	300	532	240	3
6	Jundi Utmanzai	34.0094	71.8328	294	460	170	16
7	Lund Khwar East	34.0060	71.9777	285	559	255	14
8	Kalpani Saidabad	34.0516	71.5282	314	559	255	0
9	Jundi Tangi	34.2826	71.6828	335	460	170	12
10	Swat Ningolai	33.9043	71.5584	379	400	328	6
11	Bara Kohat Road	33.8638	71.5635	413	400	119	0

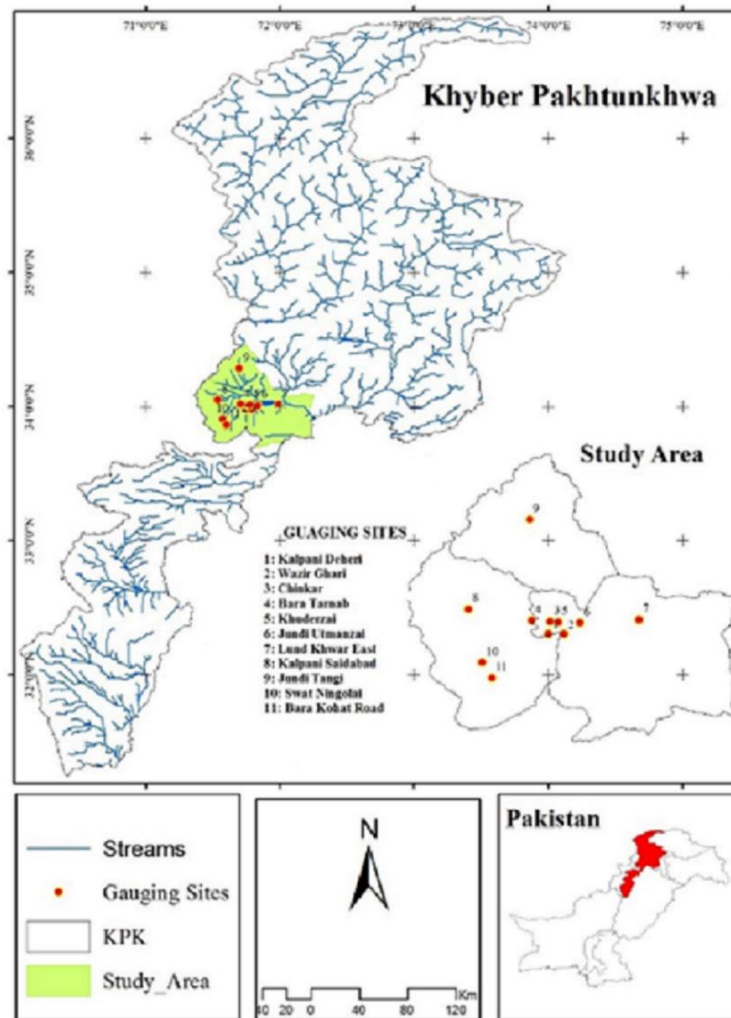


Figure 1. Study area and geographical locations of eleven gauging sites of Khyber-Pakhtunkhwa, Pakistan

Methodology

Index Flood Method

This study has adopted L-moments based RFFA, described in details in (Hosking and Wallis, 1997). RFFA is based on certain assumptions related to the observed data series, for instance, the data series is random, stationary and identically distributed etc. These assumptions have been validated using various statistical tests. The first step afterwards is to check whether there exists a discordant site, using D_i measure, in a group of available sites. The formula of D_i is:

$$D_i = \frac{1}{3} N(u_i - \bar{u})^T S^{-1} (u_i - \bar{u}), i = 1, 2, 3 \dots N \quad (\text{Eq.1})$$

$$S = \sum_{i=1}^N (u_i - \bar{u}) (u_i - \bar{u})^T$$

where u_i is the vector of sample L-moments ratios of site i , \bar{u} is its mean and N is the total number of sites. A site is discordant if its D_i value is greater than the critical value. These critical values are provided in (Hosking and Wallis, 1997).

Next important step in RFFA is the identification of homogeneous region. Homogeneity of the identified region can be checked using regional heterogeneity measure H , for which the formula is:

$$H = \frac{V - \mu_v}{\sigma_v} \quad (\text{Eq.2})$$

where $V = \left[\frac{\sum_{i=1}^N n_i (\tau^i - \tau^R)^2}{\sum_{i=1}^N n_i} \right]^{\frac{1}{2}}$ and μ_v is mean and σ_v is standard deviation of computed inter-site variation figured through simulations using Kappa distribution.

For a region to be declared as statistically homogeneous, the calculated value of H should be less than one. After the identification of homogeneous region, the next obvious step is to check the goodness of fit of the candidate distribution(s) using L-moment ration diagram (a graph of sample L-skewness Vs sample L-kurtosis of the sites) and $Z - Dist$ statistic. The formula for $Z - Dist$ statistic is:

$$Z - Dist = \frac{\tau_4^{Dist} - \tau_4^R + \beta_4}{\sigma_4} \quad (\text{Eq.3})$$

where τ_4^{Dist} is the L-kurtosis of fitted candidate regional distribution, τ_4^R is the regional L-kurtosis, σ_4 is standard deviation and β_4 is the bias of τ_4^R obtained through simulations. A distribution having minimum $|Z - Dist|$ value can be considered as the best fitted regional probability distribution.

Parameters of best fitted regional distribution can be estimated through method of L-moments and regional quantiles for various return periods can be estimated using the quantile function of the fitted regional distribution. Using the estimated regional quantiles, at-site quantiles can be estimated using:

$$\hat{Q}_i(F) = l_1^{(i)} \hat{q}(F) \quad (\text{Eq.4})$$

where $\hat{Q}_i(F)$ is the estimated quantile of site i , $l_1^{(i)}$ is the first sample L-moment of site i and $\hat{q}(F)$ is the estimated regional quantile for any return period.

Operational configuration of ANN

For ungauged quantiles estimation QR and ANN have been used. ANN consist of input layer, hidden layers, neurons in each layer, activation function and output layer. Among the various methods of ANN, multilayer feed forward network has been selected for the current study. Back propagation method has been used for the training of ANN which may also be referred as Back Propagation Neural Networks (BPNN). BPNN is a popular tool and dominates for predictions of river flow at different points and well suited to various types of hydrological modelling especially for non-linear regression operations (Maier and Dandy, 2000; Abrahart et al., 2004). Structure of threelayer feed forward network has been dispalyed in *Fig. 2*.

In Fig. 2 circles represents neurons in the layers of ANN structure and arrow lines for connections between neurons in each layer. Weight function has been used as connection parameter and every input of neurons is multiplied by a weight and then the values are pooled to produce one output value. This value is usually produced with certain bias and then operated by activation function. Therefore, output of each neuron stated as below:

$$Z_j = f(X (T_i - b_j)) \quad (\text{Eq.5})$$

where X is the input vector in the first layer and T_i is the weight vector. Its order of weights leading to the neurons given as:

$$T_{mj} = (t_{1j} \dots t_{ij} \dots t_{nj})$$

where $j = 1, 2, \dots, n$ and $m =$ number of neurons, $t_{ij} =$ joining weight from the i neuron in the earlier layer to the current neuron.

The output of neuron j is Z_j and obtained by the inner product of the function defined in Equation 5 where b_j represent the value of bias associated with neuron j .

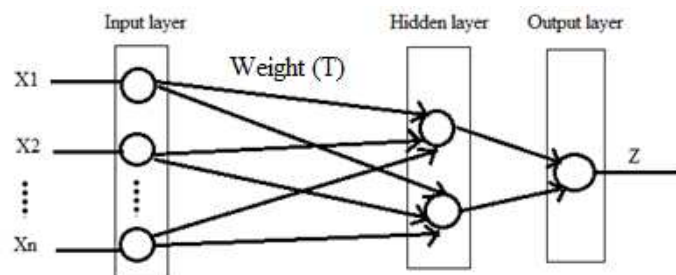


Figure 2. The Configuration of Artificial Neural Networks

The main purpose of training ANN with a data set (input and output) is to adjust the weights to minimize the errors between ANN outputs and the desired outputs. Before training of any neural network, data is scaled using z-normalization, minimum-maximum scale, etc. For the present study minimum-maximum scale has been used to scale the data into the interval $[0, 1]$, and randomly splitting the data into training and testing set. Most commonly known activation functions for neural networks are logistic function, hyperbolic tangent function, bipolar function, scaled arctan function, and arctan function. Shamseldin et al. (2002) states that logistic function performs well relative to other activation function for river flow forecasting. Therefore, logistic function has been used as activation function for hidden and output layers. Number of hidden layers and neurons in each layer has been selected by using trial and error method.

Results and discussion

RFFA is based on few critical assumptions related to the observed data series at each site. For instance, the recorded data at different sites is random, independent and identically distributed as well as free of the step changes and trend. There are various methods available in the literature for the validation of these assumptions. For the current

study, Run test for randomness (Bradley, 1968), Wald-Wolfowitz test for independence and stationary (Wald and Wolfowitz, 1943), Rank-sum test for homogeneity (Hirsch et al., 1992), have been used and the results are given in *Table 2*. All these tests have been performed using 5% level of significance. The results of *Table 2* show that the recorded data of eleven gauging sites fulfill all the critical assumptions related to RFFA, therefore, can be used for further analysis.

Table 2. Calculated values of non-parametric test statistics and their corresponding p-values for the validation of assumptions related to the observed data series at various sites

S.No.	Site name		Rank-Sum	Run Test	Wald-Wolfowitz
1	Kalpani Deheri	Test statistics	0.739	0.459	-0.955
		P-value	0.4599	0.6459	0.3392
2	Wazir Ghari	Test statistics	-0.132	0.574	-0.678
		P-value	0.8950	0.5656	0.4975
3	Chinkar	Test statistics	1.126	-1.201	0.309
		P-value	0.2602	0.2298	0.7573
4	Bara Tarnab	Test statistics	-1.659	-1.858	1.251
		P-value	0.0971	0.0631	0.2109
5	Khuderzai	Test statistics	0.955	-1.274	0.268
		P-value	0.3396	0.2026	0.7887
6	Jundi Utmanzai	Test statistics	0.578	-0.481	1.851
		P-value	0.5633	0.6305	0.0641
7	Lund Khwar East	Test statistics	-1.44	-1.155	0.109
		P-value	0.1499	0.2479	0.9131
8	Kalpani Saidabad	Test statistics	-1.008	-1.797	0.765
		P-value	0.3135	0.0723	0.4443
9	Jundi Tangi	Test statistics	-1.49	1.436	1.182
		P-value	0.1362	0.1510	0.2372
10	Swat Ningolai	Test statistics	1.864	-0.371	1.758
		P-value	0.0623	0.7106	0.0787
11	Bara Kohat Road	Test statistics	-1.171	-0.542	-0.083
		P-value	0.2416	0.5878	0.9339

Discordancy measure

The calculated values of D_i using *Equation 1* for eleven sites along with corresponding descriptive statistics in terms of L-moments have been illustrated in *Table 3*. The results show that the values of D_i for each site are less than the critical value i.e. 2.64 (as proposed by Hosking and Wallis (1997) for eleven sites). Therefore, there is no discordant site in the set of eleven gauging sites.

Descriptive statistics given in *Table 3* show that Wazir Ghari, Chinkar and Lund Khwar East have smaller magnitude of AMPF while Bara Tarnab, Kalpani Saidabad and Swat Ningolai have relatively larger magnitude of AMPF in the region. Sample L-moments ratios L-CV (t_1), L-skewness (t_3) and L-kurtosis (t_4) for the sites Jundi Utmanzai and Jundi Tangi are very high. This shows that there exists high variations in the observed data series at these sites. Moreover, the shape of the distribution associated

to AMPF at these sites is positively skewed with high kurtosis. The sample L-moments ratios for all the sites, in general, show that the observed data series have high variations, positive skewness and high kurtosis. Moreover, the values of L-skewness are smaller than L-CV while values of L-kurtosis are relatively less than L-skewness for almost all the sites. The site Bara Tarnab have the value of L-skewness greater than L-CV. This high variation within the AMPF may be due to the uncontrolled/natural flow of the stream associated to this site and mountainous and steep geography of the region. An important point is that the flow of the streams in the study region heavily depends on rainfall and the pattern of rainfall in the basin area is irregular. The reason of this high variation within the AMPF has been observed due the presence of outliers, may be due to storm rainfalls in the basin area, especially during monsoon season (from June and August).

Table 3. L-moments based descriptive statistics and values of discordancy measures

S. No.	Site name	n_i	l_1	t	t_3	t_4	D_i
1	Kalpani Deheri	21	2856.61	0.6276	0.4218	0.0894	0.97
2	Wazir Ghari	32	426.47	0.6457	0.5864	0.4113	0.28
3	Chinkar	28	922.27	0.7141	0.6098	0.4117	0.28
4	Bara Tarnab	30	11884.18	0.6480	0.7284	0.6424	2.24
5	Khuderzai	33	1758.37	0.6765	0.5319	0.3616	1.98
6	Jundi Utmanzai	25	2052.57	0.8038	0.7232	0.5031	1.06
7	Lund Khwar East	28	484.08	0.5903	0.4183	0.1166	0.88
8	Kalpani Saidabad	33	9408.82	0.6699	0.5780	0.2949	1.05
9	Jundi Tangi	42	1104.65	0.8156	0.8131	0.6705	1.30
10	Swat Ningolai	33	8933.68	0.6163	0.5349	0.3515	0.53
11	Bara Kohat Road	34	1453.00	0.7243	0.5959	0.3249	0.43

Note: " n_i " is the number of observations at each site, " l_1 " is the first sample l-moment, " t " is the sample L-CV, " t_3 " is the sample L-skewness, " t_4 " is the sample L-kurtosis and " D_i " is the discordancy measure

Regional heterogeneity measure

Initially, the group of eleven sites has been considered as a single region for the analysis. The reason being these sites are geographically contiguous; therefore, their climate conditions, and topography (the variables affecting the flow behavior of the sites under study) may be similar to each other. For the calculations of H , the simulations have been performed using four parameters Kappa distribution. Large number of simulations, i.e. 1000, have been performed to calculate the values of μ_v and σ_v . The calculated value of H by using Equation 2 is 0.09; therefore, the region consisting of eleven sites is homogeneous and suitable for further analysis.

Fitting of regional probability distribution

After the formation of homogeneous region, the next important step is to identify the best fitted regional probability distribution that accurately defines the observed AMPF within the homogeneous region. Graphical/informal method (L-moment ratio diagram) and formal method ($|Z - Dist|$ statistic) have been used for the selection of best fitted regional distribution for the recorded data series. L-moment ratio diagram is presented in

Fig. 3, in which sample L-skewness has been plotted against the values of sample L-kurtosis. From Fig. 3, it has been observed that the regional average value of sample L-skewness and L-kurtosis lies closer to the theoretical curves of Generalized Normal (GNO) and GPA distributions suggesting their appropriateness as regional distribution. Moreover, the tendency of sample L-skewness and L-kurtosis of all the sites is closer to the theoretical curve of GPA distribution.

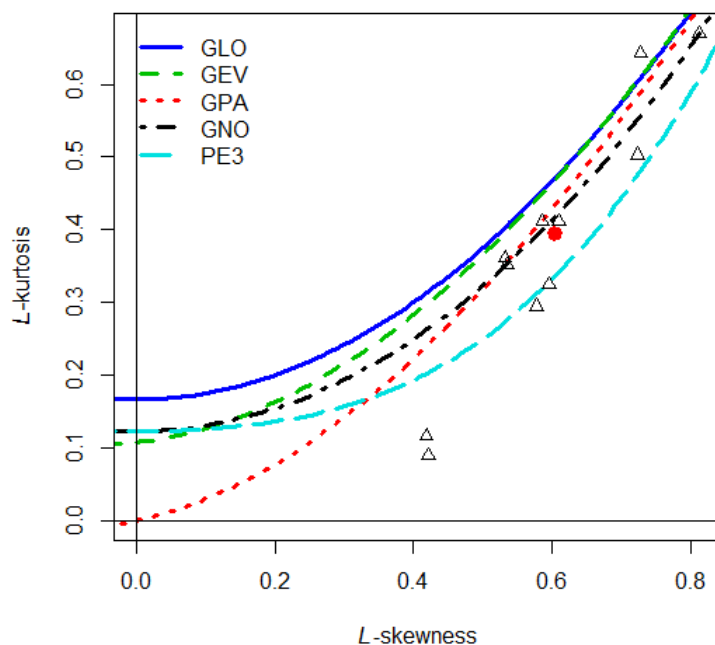


Figure 3. L-moment ratio diagram. Note: (●) represents the average value of L-skewness & L-kurtosis of the region, (Δ) denotes the values of sample L-skewness & L-kurtosis of each site in the region

Calculated values of $|Z - Dist|$ statistic, using Equation 3, for each candidate distributions i.e. Generalized Extreme Value (GEV), Generalized Logistic (GLO), Pearson type-3 (PE3), GNO and GPA have been given in Table 4. Four distributions; GNO, GPA, GEV, and GLO fulfill the criteria for best fitted regional distributions, that is, having value of $|Z - Dist| \leq 1.64$. Among these distributions, GPA distribution has minimum value of $|Z - Dist|$ statistic. Therefore, based on the results of L-moment ratio diagram and $|Z - Dist|$ statistic, GPA distribution has been selected as the best fitted distribution for the region under study.

Table 4. Values of $|Z - Dist|$ statistic for each candidate regional distribution

GLO	GEV	GNO	PE3	GPA
0.46	0.39	0.70	2.45	0.34

Note: Generalized Pareto (GPA), Generalized Logistic (GLO), Generalized Normal (GNO), Generalized Exterem Value (GEV), Pearson type-3 (PE3)

Estimation of regional probability distribution and quantiles

The parameters of GPA distribution have been estimated using method of L-moments. Dimensionless regional quantiles have been estimated using the quantile function of GPA distribution. The estimated parameters and quantiles for different return periods of GPA distribution are given in *Table 5*. The estimated regional quantiles show increasing trend, as usual, for shorter as well as longer return periods.

Table 5. Estimated parameters of Generalized Pareto (GPA) distribution and regional quantiles for various return periods

Distribution	Estimated Parameters			Regional quantiles for various return periods in years				
	ϵ	α	k	10	20	100	500	1000
GPA	-0.0282	0.5064	-0.5075	2.184	3.538	9.303	22.351	32.207

In RFFA, for a homogeneous region, the selected regional distribution is considered as parent distribution for various sites of the region. The estimated at-site quantiles using *Equation 4* for various return periods are given in *Table 6*. The results show that the estimated quantiles at site Wazir Ghari for 100 years return period is 3967 cusecs which is the lowest as compared to other sites in the region. The highest of the estimated quantile for 100 years return period is at site Bara Tarnab as 110560 cusecs. The estimated quantiles at various sites for smaller to larger return periods, i.e. 10, 20, 100, 500 and 1000 years are greater than the average AMPF of their corresponding sites.

Table 6. Estimated quantiles for each site obtained using index flood method, i.e. Eq. 4, for various return periods

S. No.	Sites	Quantiles for various return periods in years				
		10	20	100	500	1000
1	Kalpani Deheri	6239	10106	26575	63849	92002
2	Wazir Ghari	931	1508	3967	9532	13735
3	Chinkar	2014	3262	8579	20614	29703
4	Bara Tarnab	25958	42043	110560	265627	382753
5	Khuderzai	3840	6220	16358	39302	56631
6	Jundi Utmanzai	4483	7261	19095	45878	66107
7	Lund Khwar East	1057	1712	4503	10820	15590
8	Kalpani Saidabad	20551	33286	87531	210299	303029
9	Jundi Tangi	2412	3908	10276	24690	35577
10	Swat Ningolai	19513	31605	83110	199679	287727
11	Bara Kohat Road	3173	5140	13517	32476	46796

Quantiles for ungauged sites

For the current study, quadratic regression and ANN have been used to develop a functional relationship between l_1 (mean of observed AMPF at given sites) and their corresponding available site characteristics within the homogeneous region. This functional relationship will provide the estimates of at-site mean (for ungauged sites) within the homogeneous region for the estimation of T-years flood quantiles.

Quadratic regression analysis

This section describes the development of QR model using the most suitable site characteristic as an explanatory variable (to predict $l_1^{(i)}$, for site i). The details are: *Table 7* provides the correlation matrix, between l_1 and the available site characteristics along with corresponding p-values to check the significance of the respective correlation coefficients.

Table 7. Values of the correlation coefficients between site characteristics along with their corresponding p-values for testing the significance of correlation coefficients

Variables		l_1	Latitude	Longitude	Elevation	AARF	ARMS
l_1	r	1	-0.1245	-0.5486	0.1324	-0.0952	0.2656
	(P-value)	(0)	(0.7153)	(0.0805)	(0.7032)	(0.7807)	(0.4299)
Latitude	r	-0.1245	1	0.1377	-0.3690	0.2385	-0.0942
	(P-value)	(0.7153)	(0)	(0.6864)	(0.2641)	(0.4800)	(0.7829)
Longitude	r	-0.5486	0.1377	1	-0.7252	0.2912	-0.0919
	P-value	(0.0805)	(0.6864)	(0)	(0.0116)	(0.3850)	(0.7881)
Elevation	r	0.1324	-0.3690	-0.7252	1	-0.4633	0.0185
	P-value	(0.7032)	(0.2641)	(0.0116)	(0)	(0.1512)	(0.9569)
AARF	r	-0.0952	0.2385	0.2912	-0.4633	1	0.5850
	P-value	(0.7807)	(0.4800)	(0.3850)	(0.1512)	(0)	(0.0587)
ARMS	r	0.2656	-0.0942	-0.0919	0.0185	0.5850	1
	P-value	(0.4299)	(0.7829)	(0.7881)	(0.9569)	(0.0587)	(0)

Note: “ r ” is the correlation coefficient

The results show that the correlations between l_1 and the available site characteristics are statistically insignificant at 5% level of significance; hence there does not exist significant linear relationship between l_1 and the available site characteristics. Therefore, simple/multiple linear regression model (using linear form of available site characteristic(s)) would not be appropriate to predict the values of l_1 . The next obvious choice is the use of quadratic forms of the pertinent site characteristic(s) among available to predict the average value of l_1 for ungauged sites. To select the best independent variable for inclusion in the regression model with linear and quadratic form, following details have been considered. Results of *Table 7* show that the correlation between l_1 and longitude is the highest relative to all other sites characteristics but the problem is that longitude and latitude are imaginary lines on earth glob to identify the geographical location of any site. These site characteristics may be negligible if additional site characteristics are available (Hussain, 2017). The next obvious choice of variable having highest correlation with l_1 as compared to other available site characteristics is ARMS. Therefore, it has been considered as an explanatory variable in the model. Moreover, *Table 8* provides the percentage of occurrence of observed AMPF at different sites during various seasons of a year which shows that a large percentage of values of AMPF have been observed in the monsoon season (from June to August). Therefore, ARMS can be considered as the most influential variable having relatively direct and strong relationship with the observed AMPF in the study region. Based on the aforementioned details, it is

appropriate to use quadratic form of ARMS as explanatory variable in the regression model. Scatter plot of l_1 and ARMS is illustrated in Fig. 4 in which a nonlinear relationship between the variables is obvious.

Table 8. Percentage (%) of frequency of AMPF (Annual Maximum Peak Flows) in four seasons at each site

S. No.	Site name	n_i	Monsoon (%)	Autumn (%)	Winter (%)	Spring (%)
1	Kalpani Deheri	21	85.7	4.7	0.0	9.5
2	Wazir Ghari	32	46.8	12.5	12.5	21.8
3	Chinkar	28	64.2	7.1	10.7	10.7
4	Bara Tarnab	30	56.6	3.3	3.3	30.0
5	Khuderzai	33	51.5	12.1	9.1	24.2
6	Jundi Utmanzai	25	80.0	0.0	0.0	4.0
7	Lund Khwar East	28	64.2	17.8	0.0	3.5
8	Kalpani Saidabad	33	84.8	12.1	3.0	0.0
9	Jundi Tangi	42	69.04	9.5	0.0	9.5
10	Swat Ningolai	33	81.0	10.0	0.0	3.0
11	Bara Kohat Road	34	83.0	5.0	0.0	12.0

Note: The time period for Monsoon is from June to August, autumn is from September to November, winter is from December to February and spring is from March to May

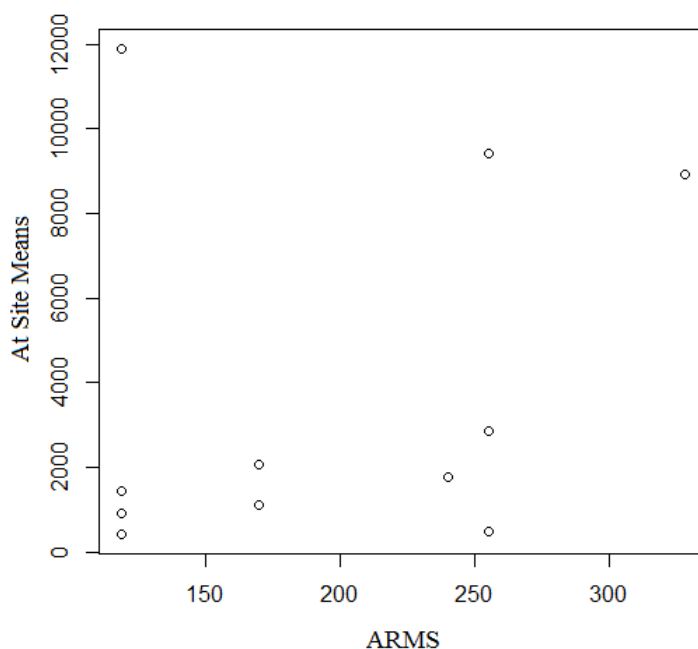


Figure 4. Scatter plot between l_1 (first sample l -moment of observed annual maximum peak flows) and ARMS (Average rainfall in monsoon)

Few observations in the data series do not follow the usual pattern of the data and create high scatter in the data. In classical linear regression modeling, such observations

(outliers) create problems of estimation and in such a situation it is very difficult to fulfill the critical assumptions of classical linear regression (normality and constant variance of the error term).

Therefore, robust estimation methods are obvious choice. For the current study, due to the existence of high scatter in the observed data series and the dependent variable is the mean of extreme values, M-estimation method (Huber, 1973) with covariance type Huber type-III as weight function has been used to estimate the developed regression model. M-estimation technique does not rely on the normality assumption of error term and is more resistant to outliers (Stuart, 2011). M-estimates are consistent, asymptotically unbiased and normally distributed (Chen and Wu, 1989; Hengjian, 1997; Ivanov and Orlovs, 2008; Ruckstuhl, 2014). Thus the fitted regression model based on the aforementioned details is.

$$\hat{l}_1 = 9220.21 - 104.20 ARMS + 0.3107 (ARMS)^2 \quad (\text{Eq.6})$$

Values of the coefficients, standard errors of estimates, t-calculated (to validate the statistical significance of the provided coefficients) and their corresponding p-values are given in *Table 9*.

Table 9. Estimated values of the fitted regression model, coefficients and their corresponding standard errors (S.E.), t-values and P-values

S. No.	Independent variables	Coefficients	S.E.	t-value	P-value
1	ARMS	-104.20	32.01	-3.2554	0.001
2	(ARMS) ²	0.3107	0.0719	4.3186	0.000

Note: ARMS (Average rainfall in monsoon)

The results show that the coefficients of the fitted regression model in *Equation 6* are highly significant at 5% level of significance. Quadratic term of the model have positive impact on flood flows when rainfall during monsoon season is increased from its average value. Value of the adjusted R_w^2 is 0.89 for the fitted model. Diagnostics plots of fitted vs residuals and residual vs leverage are given in *Fig. 5* and *Fig. 6*, respectively.

These plots show that high residuals are observed for the 4th site (Bara Tarnab) and 8th site (Kalpani Saidabad) observations. These high residuals lies on the cook's distance limit. Diagnostics plots also show that the 10th observation (the site Swat Ningolai) has deviated largely from other plotted points, as its predicted value is very large and much closer to its observed average AMPF. Therefore, these observations don't have any undue influence on the estimated values. These details reveal that the developed regression model is statistically sound; however, another desirable is the practical validity of the model, which has been provided in second last section.

Artificial neural networks

Five input and one output variables have been used for the prediction of the dependent variable (average value of the observed AMPF at various sites (l_i)). Site characteristics, such as, "lat", "long", "ele", "AARF" and "ARMS" have been used as input variables of ANN model. The variable l_i has been used as the dependent variable of the model. Functional relationship of the dependent and independent variables is given as

$$f(l_1) = g(\text{lat}, \text{long}, \text{ele}, \text{AARF}, \text{ARMS}) \quad (\text{Eq.7})$$

Two hidden layers, with four neurons in first layer and two in second layer, have been used to perform the algorithm. The graphical representation of the fitted model using the relationship of Equation 7 with the weights on each connection and bias has been illustrated in Fig. 7.

Predicted values of the dependent variable (l_1 of gauged site) have been provided in Table 10. Table 10 also includes the estimated values of l_1 using QR analysis. The results show that ANN algorithm closely estimates l_1 for the gauged sites (Kalpani Deheri, Bara Tarnab, Khuderzai, Kalpani Saidabad, Jundi Tangi, Swat Ningolai and Bara Kohat Road) using available site characteristics as independent variables. ANN and QR model over estimate the values of l_1 for the sites (Wazir Ghari, Chinkar and Lund Khwar East) having smaller magnitude of AMPF. QR model under estimates l_1 for the sites (Jundi Utmanzai, Kalpani Saidabad and Jundi Tangi) having large value of L-CV. The site Bara Tarnab have the larger magnitude of AMPF and its l-skewness is greater than L-CV QR model also under estimates its value. QR model provide reliable estimate of the values of l_1 for the sites (Kalpani Deheri, Khuderzai, Swat Ningolai and Bara Kohat Road). Similar results have been reported by (Dawson et al., 2006) showing the under and over estimation of floods at few gauged and ungauged sites for 10, 20 and 30 years return periods through multiple linear regression analysis and ANN. They proposed that this problem may be related to the accuracy and availability of the relevant site characteristics.

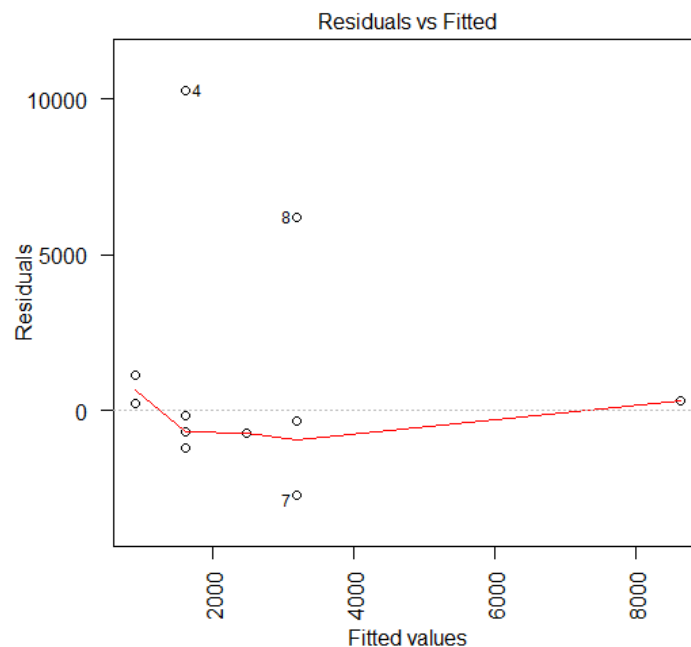


Figure 5. Plot of fitted values of dependent variable, (first sample l-moment of annual maximum peak flows (l_1)) and residuals of the fitted regression model in Equation 6

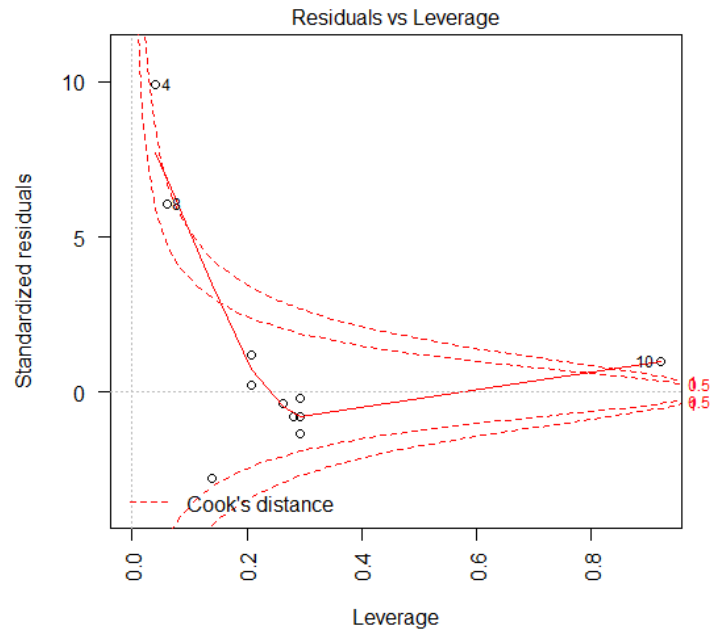


Figure 6. Diagnostic plot of fitted regression model (Equation 6)

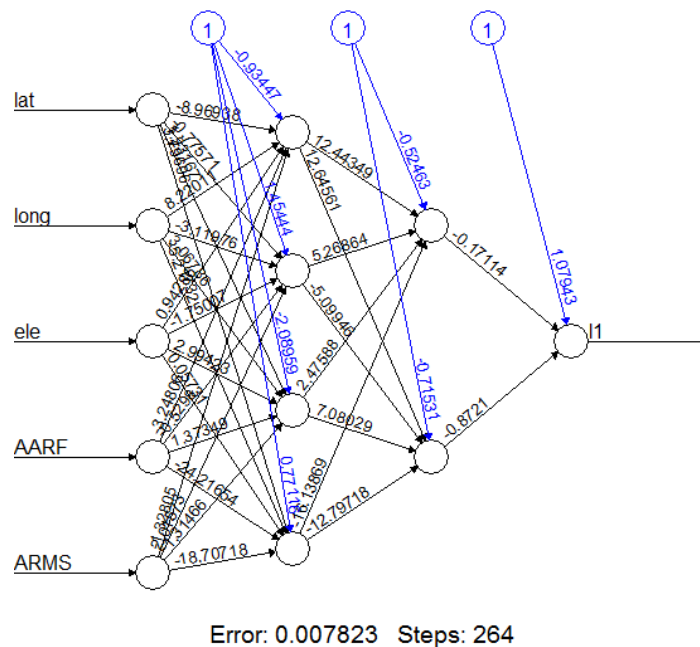


Figure 7. Graphical representation of artificial neural networks (ANN) procedure adopted for the area under study to show the convergence of the model

The performance of the QR model is not effective for the gauge site having smaller and larger magnitude of AMPF and for those sites also that show very high variation in the data set. As compared to QR model ANN estimates are more reliable and accurate accept the sites have smaller magnitude of AMPF. In Fig. 8, fitted values of dependent variable have been plotted against the observed values of the dependent variable. All the values predicted through ANN lie on the straight line relative to the predicted values

through QR. Therefore, the observed and the predicted values of the dependent variable through ANN are quite close to each other, especially, for the sites having larger magnitude of AMPF.

Table 10. Estimated values of l_1 of gauged sites through artificial neural networks (ANN) and quadratic regression (QR)

S.No.	Site name	l_1 (observed)	l_1 (fitted) using QR	l_1 (fitted) using ANN
1	Kalpani Deheri	2856.61	2854.886	2697.19
2	Wazir Ghari	426.47	1220.572	845.78
3	Chinkar	922.27	1220.572	1306.46
4	Bara Tarnab	11884.18	1220.572	11651.88
5	Khuderzai	1758.37	2110.622	1880.46
6	Jundi Utmanzai	2052.57	486.3447	842.53
7	Lund Khwar East	484.08	2854.886	841.43
8	Kalpani Saidabad	9408.82	2854.886	9587.09
9	Jundi Tangi	1104.65	486.3447	1199.7
10	Swat Ningolai	8933.68	8473.219	8874.14
11	Bara Kohat Road	1453	1220.572	1461.24

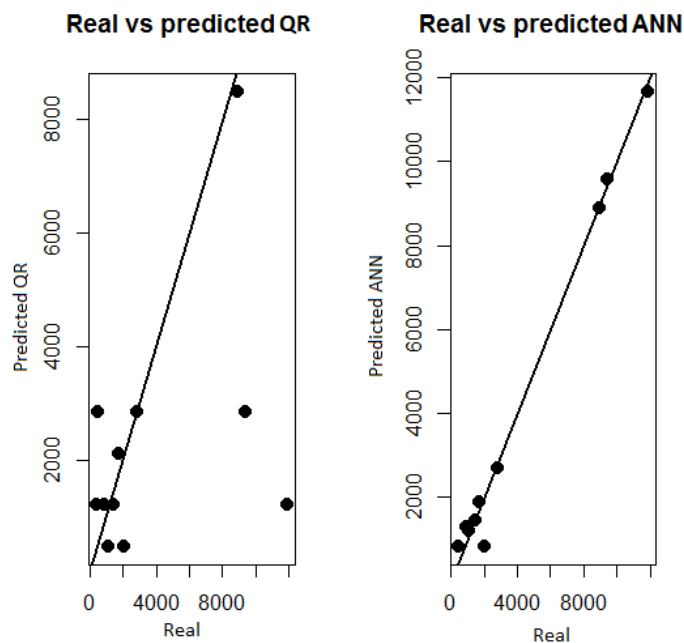


Figure 8. Comparison of fitted values of site statistic l_1 (first sample l -moment of annual maximum peak flows) through artificial neural networks (ANN) and quadratic regression (QR)

Assessment analysis

The two estimation methods (ANN and QR) have been used for T-year flood quantiles estimation at ungauged sites within the homogeneous region. The development of these two methods is theoretically justified in the study, still an assessment analysis is requisite to check the relative accuracy of estimates of the T-year flood quantiles for gauged, poorly

gauged and ungauged sites. To do so, RMSE, MAPE and MAE have been calculated using the information of *Table 10* (observed and fitted values of each site of the homogeneous region) and the results are given in *Table 11*. Their corresponding formulas are:

$$RMSE = \sqrt{\frac{\sum_{i=1}^n (i_i - \hat{i}_i)^2}{n}} \quad (\text{Eq.8})$$

$$MAPE = \left(\frac{1}{n} \sum_{i=1}^n \frac{|i_i - \hat{i}_i|}{|i_i|} \right) \times 100 \quad (\text{Eq.9})$$

$$MAE = \frac{\sum_{i=1}^n |i_i - \hat{i}_i|}{n} \quad (\text{Eq.10})$$

The results of *Table 11* show that the estimates through ANN are more accurate than QR as values of RMSE, MAPE and MAE calculated by using *Equation 8*, *Equation 9* and *Equation 10* respectively are relatively low. Therefore ANN can be preferred over QR to predict the flood quantiles for ungauged and poorly gauged sites of the study region.

Table 11. Assessment measures for validation of the estimates through Artificial Neural Networks (ANN) and Quadratic Regression (QR)

	RMSE	MAPE	MAE
ANN	432.12	27.17%	293.25
QR	3887.42	94.65%	2173.83

Note: Root Mean Square Error (RMSE), Mean Absolute Percentage Error (MAPE), Mean Absolute Error (MAE)

Cross validation of estimated quantiles

The estimates of quantiles for various return periods through RFFA for gauged and ungauged sites are statistically sound but their practical validation is still requisite. A comparison of quantiles estimates obtained using index flood method, QR model and ANN for 10, 20 and 100 year return periods with highest values of observed/historic AMPF (first, second and third as per their order of magnitude along with their year of occurrence) at various sites, has been illustrated in *Table 12*. Due to high variation in the observed AMPF of each site three highest values are selected for the historic comparison of predicted quantiles.

A flood of 2010 has been considered as one of the worst in Pakistan's history (Government of Pakistan, 2016). The current study region is one of the affected areas of this heavy flood. There are four sites Chinkar, Jundi Utmanzai, Kalpani Saidabad and Bara Kohat Road where the highest values of the series of AMPF has been observed in 2010 (as shown in *Table 12*). For these sites, the predicted quantiles for 100 year return period using index flood method for gauged sites and through ANN for ungauged sites are quite close to the highest observed AMPF for 2010. At site Jundi Tangi, second highest value of AMPF has been observed in 2010 and similar magnitude of flood has been predicted for 100 year return period through index flood and ANN. For the site Lund Khwar East, third highest value of AMPF has been observed in 2010 and same magnitude

of flood has been predicated for 20 year return period through index flood and 10 year return period for ANN. Similar trends of the observed and predicted values are obvious from the results of *Table 12*. This shows the accuracy and reliability in the predictive ability of the adopted procedure.

Table 12. Cross validation of the estimated flood quantiles through index flood method, Quadratic Regression (QR) model and Artificial Neural Networks (ANN)

S.No	Site name	Highest values of observed AMPF (year)			Estimated quantiles through index flood			Estimated quantiles through QR			Estimated quantiles through ANN		
		1 st Highest	2 nd Highest	3 rd Highest	10	20	100	10	20	100	10	20	100
1	Kalpani Deheri	10845 (1995)	9380 (1997)	7915(1988)	6239	10106	26575	6236	10100	26559	5891	9542	25092
2	Wazir Ghari	3080 (1998)	2784 (1982)	849 (1994)	931	1508	3967	2666	4318	11355	1847	2992	7868
3	Chinkar	7500 (2010)	5625 (2011)	1387(2008)	2014	3262	8579	2666	4318	11355	2854	4622	12154
4	Bara Tarnab	159100 (2013)	20300(2005)	16912(1991)	25958	42043	110559	2666	4318	11355	25451	41222	108399
5	Khuderzai	13952 (1984)	9000 (1997)	5000 (1985)	3840	6220	16358	4610	7467	19635	4107	6653	17494
6	Jundi Utmanzai	19433 (2010)	11360(2008)	6465 (2011)	4483	7261	19095	1062	1720	4524	1840	2981	7838
7	Lund Khwar East	1891 (1997)	1735 (2006)	1546 (2010)	1057	1712	4503	6235	10100	26559	1838	2977	7828
8	Kalpani Saidabad	52912 (2010)	44321(2013)	39259(2015)	20551	33286	87531	6235	10100	26559	20941	33917	89190
9	Jundi Tangi	18679 (2008)	8382 (2010)	5837 (2007)	2412	3908	10276	1062	1720	4524	2621	4244	11161
10	Swat Ningolai	52098 (2016)	44870(2013)	28403(2014)	19513	31605	83110	18508	29976	78827	19384	31395	82557
11	Bara Kohat Road	11698 (2010)	5688 (1991)	5120 (1997)	3173	5140	13517	2666	4318	11355	3192	5170	13594

The results of *Table 12* show that the estimates, obtained using index flood method, are quite close to the historical values of AMPF at all most all of the sites. The results, obtained using QR model (for ungauged sites), have also been compared with the highest observed values of gauged sites. The comparison reveals that the estimates are comparable for the sites Kalpani Deheri, Wazir Ghari, Chinkar, Khuderzai, Swat Ningolai and Bara Kohat Road for smaller return periods with in the span of data. Significant deviations in the estimates have been observed for the sites Bara Tarnab, Jundi Utmanzai, Lund Khwar East, Kalpani Saidabad and Jundi Tangi for the smaller and longer return periods. The performance of QR estimates for the sites having large magnitude of observed AMPF has been observed as less efficient (sites Bara Tarnab and Kalpani Saidabad).

Estimates obtained through ANN are closed to the highest values of observed/historic AMPF of each site. Moreover, for the sites having large magnitude of observed AMPF, the results of ANN have been observed very close to the highest historical values of AMPF for smaller as well as longer return periods. Based on the historical comparison, ANN can be considered as more reliable relative to QR method to estimate quantiles for ungauged sites for smaller as well as larger return periods.

Summary, findings and conclusions

For a developing state with agro centered economy and facing problems of water shortage along with high variations in the stream flows, the importance of precise flood estimates becomes vast, especially for the small streams and rivers which originates with in the country. Some of the conclusions and key findings of the study are given below:

- i. Few critical assumptions associated to the observed data series at various sites for RFFA has been tested and validated through various statistical tests. The results have revealed that the observed data at each site is random, independent, homogeneous and free of regular trends. Moreover, the results of the discordancy measure have shown that none of the site is discordant in the set of eleven gauging sites.
- ii. Descriptive statistics have shown that there exist high variations, skewness and kurtosis in the observed AMPF of eleven gauging sites. However, the values of L-kurtosis are relatively smaller than the L-skewness. One possible reason of these variations is the irregular patterns of the monsoon rainfall, as flood flows in Pakistan depend mostly on the heavy monsoon rainfall. Similar findings have been reported by (Hussain, 2017) for the sites of major rivers of Punjab, Pakistan.
- iii. The geographical locations of eleven sites reveal that the sites are geographically contiguous; therefore, it may be possible that they belong to the similar cluster with respect to their site characteristics. Formal heterogeneity measure, based on 1000 simulations assuming four parameters kappa distribution as regional probability distribution, confirms that the cluster of eleven sites is definitely homogeneous. GPA distribution has been identified as suitable regional distribution for the region under study. Regional quantiles have been estimated using quantile function of the GPA distribution. Estimated flood quantiles for 10 years return period or more at all sites are greater than the average value of observed AMPF of the respective sites.
- iv. For flood quantiles estimation at ungauged sites, QR with robust estimation method and ANN have been used to develop a functional relationship between l_I (mean of observed AMPF) of each site and their respective available site characteristics. The results show that the estimates using ANN are accurate and reliable as compared to QR analysis especially for longer return periods.
- v. To assess the practical validity of the provided estimates, for various return periods, through L-moments based RFFA using index flood method, ANN and QR, a comparison has been illustrated using first, second and third highest values of the recorded AMPF at eleven gauging sites. The estimates of RFFA are closer to the recorded highest values of AMPF at all sites for different return periods. Moreover, the estimates obtained through ANN (though comparison has been provided for gauged sites only) are also very close to the highest historic values of AMPF of each corresponding site for different return periods. Therefore, ANN would be a preferred approach as compared to QR for flood quantiles estimation at ungauged sites (especially for longer return periods) within the homogeneous region.

The study contributes in terms of promoting non-linear relationship of the most influential site characteristic with the observed AMPF with robust estimation method emphasizing the complete justifications related to the estimation procedure of the regression modeling. Moreover, the introduction of ANN to obtain flood quantiles for

ungauged sites in Pakistan and comparison with the historical record to investigate the practical validity of the resultant estimates. The results of this study not only provide assistance to the officials dealing with flood risks management but will also be useful for management of agriculture water and design capacity of existing and proposed hydrologic structures in the study region. For instance, a proposed project of the provincial government of KPK is the site Bara Dam (an ungauged site of the study area).

Acknowledgements. Authors are very grateful to the Higher Education Commission, Pakistan for financial support under the project number: 5790/Federal/NRPU/R&D/HEC/2016. We are very grateful to the editor of the journal and anonymous reviewers for their constructive comments to improve the quality of the paper. We are also thankful to the Irrigation Department of Khyber Pakhtunkhwa for providing flood data for the study.

REFERENCES

- [1] Abrahart, R., Kneale, P. E. See LM (eds.) (2004): Neural networks for hydrological modeling. – CRC Press.
- [2] Ahmad, I., Fawad, M., Mahmood, I. (2015): At-Site Flood Frequency Analysis of Annual Maximum Stream Flows in Pakistan Using Robust Estimation Methods. – Polish Journal of Environmental Studies 24(6): 2345-2353.
- [3] Ahmad, I., Fawad, M., Akbar, M., Abbas, A., Zafar, H. (2016): Regional Frequency Analysis of Annual Peak Flows in Pakistan Using Linear Combination of Order Statistics. – Polish Journal of Environmental Studies 25(6): 2255-2264.
- [4] Alam, J., Muzzammil, M., Khan, M. K. (2016): Regional flood frequency analysis: comparison of L-moment and conventional approaches for an Indian catchment. – ISH Journal of Hydraulic Engineering 22(3): 247-253.
- [5] Anilan, T., Satilmis, U., Kankal, M., Yuksek, O. (2016): Application of Artificial Neural Networks and regression analysis to L-moments based regional frequency analysis in the Eastern Black Sea Basin, Turkey. – KSCE Journal of Civil Engineering 20(5): 2082-2092.
- [6] Aydoğan, D., Kankal, M., Önsoy, H. (2016): Regional flood frequency analysis for Çoruh Basin of Turkey with L-moments approach. – Journal of Flood Risk Management 9(1): 69-86.
- [7] Aziz, K., Rahman, A., Fang, G., Shrestha, S. (2014): Application of artificial neural networks in regional flood frequency analysis: a case study for Australia. – Stochastic environmental research and risk assessment 28(3): 541-554.
- [8] Batool, Z. (2017): Flood Frequency Analysis of Stream Flow in Pakistan Using L-Moments and TL-Moments. – International Journal of Advance Research, Ideas and Innovations in Technology 3(4): 136-142.
- [9] Bradley, J. V. (1968): Distribution-free statistical tests. – No. 04; QA278. 8, B7.
- [10] Dawson, C. W., Abrahart, R. J., Shamseldin, A. Y., Wilby, R. L. (2006): Flood estimation at ungauged sites using artificial neural networks. – Journal of hydrology 319(1-4): 391-409.
- [11] Development Advocate Pakistan (2017): Water Security in Pakistan: Issues and Challenges 3(4). http://www.pk.undp.org/content/pakistan/en/home/library/hiv_aids/development-advocate-pakistan--volume-3--issue-4.html.
- [12] Graves, R., Waylen, P. R. (1997): Regional flood frequency analysis in southern Ontario using L-moments. – The Canadian Geographer/Le Géographe canadien 41(2): 178-193.
- [13] Government of Pakistan (2016): Annual flood report 2016. – Ministry of Water and Power, Office of the Chief Engineer Advisor and Chairman, Federal Flood Commission, Islamabad

<http://www.ffc.gov.pk/download/AFR/Annual%20Flood%20Report%202016.pdf>.
(Accessed June 2018).

- [14] Griffis, V. W., Stedinger, J. R. (2007): The use of GLS regression in regional hydrologic analyses. – *Journal of Hydrology* 344(1-2): 82-95.
- [15] Hailegeorgis, T. T., Alfretdsen, K. (2017): Regional flood frequency analysis and prediction in ungauged basins including estimation of major uncertainties for mid-Norway. – *Journal of Hydrology: Regional Studies* 9: 104-126.
- [16] Hashmi, H. N., Siddiqui, Q. T. M., Ghumman, A. R., Kamal, M. A. (2012): A critical analysis of 2010 floods in Pakistan. – *African Journal of Agricultural Research* 7(7): 1054-1067.
- [17] Hirsch, R. M., Helsel, D. R., Cohn, T. A., Gilroy, E. J. (1992): Statistical analysis of hydrologic data. – In: Maidment, D. R. (ed.) *Handbook of Hydrology*, Chapter 17. McGraw-Hill, New York.
- [18] Hjelmfelt, A. T., Wang, M. (1996): Predicting runoff using artificial neural networks. – In *Proceedings of the International Conference on Hydrology and Water Resources*, New Delhi, India, December 1993, Springer, Dordrecht: 233-244.
- [19] Hosking, J. R. M., Wallis, J. R. (1997): *Regional frequency analysis: an approach based on L-moments*. – Cambridge University Press.
- [20] Hussain, Z., Pasha G. R. (2009): Regional flood frequency analysis of the seven sites of Punjab, Pakistan, using L-moments. – *Water resources management* 23(10): 1917-1933.
- [21] Hussain, Z. (2011): Application of the regional flood frequency analysis to the upper and lower basins of the Indus River, Pakistan. – *Water resources management* 25(11): 2797-2822.
- [22] Hussain, Z. (2017): Estimation of flood quantiles at gauged and ungauged sites of the four major rivers of Punjab, Pakistan. – *Natural hazards* 86(1): 107-123.
- [23] Hussain, Z., Shahzad, M. N., Abbas, K. (2017): Application of regional rainfall frequency analysis on seven sites of Sindh, Pakistan. – *KSCE Journal of Civil Engineering* 21(5) 1812-1819.
- [24] Jingyi, Z., Hall, M. J. (2004): Regional flood frequency analysis for the Gan-Ming River basin in China. – *Journal of hydrology* 296(1): 98-117.
- [25] Khan, S. A., Hussain, I., Hussain, T., Faisal, M., Muhammad, Y. S., Mohamd Shoukry, A. (2017): Regional Frequency Analysis of Extremes Precipitation Using L-Moments and Partial L-Moments. – *Advances in Meteorology*.
- [26] Kumar, R., Chatterjee, C., Panigrihy, N., Patwary, B. C., Singh, R. D. (2003a): Development of regional flood formulae using L-moments for gauged and ungauged catchments of North Brahmaputra river system. – *Journal of the Institution of Engineers India Civil Engineering Division* 84: 57-63.
- [27] Kumar, R., Chatterjee, C., Kumar, S., Lohani, A. K., Singh, R. D. (2003b): Development of regional flood frequency relationships using L-moments for Middle Ganga Plains Subzone 1 (f) of India. – *Water Resources Management* 17(4): 243-257.
- [28] Kumar, R., Chatterjee, C. (2006): Closure to “Regional Flood Frequency Analysis Using L-Moments for North Brahmaputra Region of India”. – *Journal of Hydrologic Engineering* 11(4): 380-382.
- [29] Landi, A., Piaggi, P., Laurino, M., Menicucci, D. (2010): Artificial neural networks for nonlinear regression and classification. – In *Intelligent Systems Design and Applications (ISDA)*, 10th International Conference IEEE: 115-120.
- [30] Liu, D., Yuan, Y., Liao, S. (2009): Artificial neural network vs. nonlinear regression for gold content estimation in pyrometallurgy. – *Expert Systems with Applications* 36(7): 10397-10400.
- [31] Maier, H. R., Dandy, G. C. (2000): Neural networks for the prediction and forecasting of water resources variables: a review of modelling issues and applications. – *Environmental modelling & software* 15(1): 101-124.

- [32] Malekinezhad, H., Zare-Garizi, A. (2014): Regional frequency analysis of daily rainfall extremes using L-moments approach. – *Atmosfera* 27(4): 411-427.
- [33] Modarres, R. (2008): Regional frequency distribution type of low flow in North of Iran by L-moments. – *Water Resources Management* 22(7): 823-841.
- [34] Muhammad, F., Afreen, S. (2007): Modeling annual maximum peak flows at various dams and barrages in Pakistan. – *Journal of Hydrology and Hydromechanics* 55(1): 43-53.
- [35] National Electric Power Regulatory Authority (NEPRA) (2018): Hydel Potential in Pakistan. – <http://www.nepra.org.pk/Policies/Hydel%20Potential%20in%20Pakistan.pdf>.
- [36] Noto, L. V., La Loggia, G. (2009): Use of L-moments approach for regional flood frequency analysis in Sicily, Italy. – *Water resources management* 23(11): 2207-2229.
- [37] Ouali, D., Chebana, F., Ouarda, T. B. (2017): Fully nonlinear statistical and machine-learning approaches for hydrological frequency estimation at ungauged sites. – *Journal of Advances in Modeling Earth Systems* 9(2): 1292-1306.
- [38] Pakistan Bureau of Statistics (2018). <http://www.pbs.gov.pk/content/agriculture-statistics>.
- [39] Pakistan Meteorological Department (2012): The implementation of diagnostic study for 2010 flood and extreme moon soon rains 2011 in Pakistan under sustainable development through peace building, governance and economic recovery in KP and support landslide IDPs in Hunza Nagar and Gilgit district when UNDP serves as implementing partner. – http://www.pmd.gov.pk/reports/flood_diagnostic_2010_2011.pdf. (Accessed June 2018).
- [40] Pokhrel, J. (2002): Regional flood frequency analysis for the island of Newfoundland, Canada using L-Moments. – Doctoral dissertation, Memorial University of Newfoundland.
- [41] Requena, A. I., Ouarda T. B., Chebana, F. (2017): Flood Frequency Analysis at Ungauged Sites Based on Regionally Estimated Stream flows. – *Journal of Hydrometeorology* 18(9): 2521-2539.
- [42] Rumelhart, D. E., Hinton, G. E., Williams, R. J. (1985): Learning internal representations by error propagation (No. ICS-8506). – California Univ San Diego La Jolla Inst for Cognitive Science.
- [43] Saf, B. (2009): Regional flood frequency analysis using L-moments for the West Mediterranean region of Turkey. – *Water Resources Management* 23(3): 531-551.
- [44] Shahzadi, A., Akhter, A. S., Saf, B. (2013): Regional frequency analysis of annual maximum rainfall in monsoon region of Pakistan using L-moments. – *Pakistan Journal of Statistics and Operation Research* 9(1): 111-136.
- [45] Shamseldin, A. Y., Nasr, A. E., O'Connor, K. M. (2002): Comparison of different forms of the multi-layer feed-forward neural network method used for river flow forecast combination. – *Hydrology and earth system sciences* 6(4): 671-684.
- [46] Shu, C., Ouarda, T. B. M. J. (2007): Flood frequency analysis at ungauged sites using artificial neural networks in canonical correlation analysis physiographic space. – *Water Resources Research* 43(7).
- [47] Sivakumar, B., Singh, V. P. (2012): Hydrologic system complexity and nonlinear dynamic concepts for a catchment classification framework. – *Hydrology and Earth System Sciences* 16(11): 4119-4131.
- [48] Wald, A., Wolfowitz, J. (1943): An exact test for randomness in the non-parametric case based on serial correlation. – *The Annals of Mathematical Statistics* 14(4): 378-388.
- [49] Yang, T., Xu, C. Y., Shao, Q. X., Chen, X. (2010): Regional flood frequency and spatial patterns analysis in the Pearl River Delta region using L-moments approach. – *Stochastic Environmental Research and Risk Assessment* 24(2): 165-182.

PHYTOCHEMICAL SCREENING, TOTAL PHENOLIC AND FLAVONOIDS CONTENTS AND ANTIOXIDANT ACTIVITIES OF *CITRULLUS COLOCYNTHIS* L. AND *CANNABIS SATIVA* L.

AHMED, M.¹ – JI, M.^{1*} – QIN, P.¹ – GU, Z.¹ – LIU, Y.¹ – SIKANDAR, A.¹ – IQBAL, M. F.² – JAVEED, A.²

¹College of Plant Protection, Shenyang Agricultural University No. 120 Dongling Road, Shenyang, 110866 Liaoning, China

²College of Biosciences and Biotechnology, Shenyang Agricultural University No. 120 Dongling Road, Shenyang, 110866 Liaoning, China

*Corresponding author

e-mail: jimingshan@163.com; phone: +86-24-8848-7148; fax: +86-24-8834-2315

(Received 16th Feb 2019 ; accepted 8th Apr 2019)

Abstract. *Citrullus colocynthis* L. and *Cannabis sativa* L. are well known herbs for their curative value and farming applications. Thus, extraction was performed to examine yield, total phenolic, flavonoids content and antioxidant activities for farming exertions. Qualitative analyses were conducted to scrutinize alkaloids, glycosides, terpenoids, flavonoids, flavones, steroids, tannins, phenols, saponins and quantitative analysis for total phenolic and flavonoids content was assessed by Folin-Ciocalteu and aluminium chloride colourimetric method respectively, while antioxidant activities was assessed by using 1, 1-Diphenyl-1-picrylhydrazyl. Results showed that distilled water afforded the maximum extract yield followed by methanol and ethanol thus, coefficient of determination (R^2) of extract yield present a positive correlation compared to root mean square error (RMSE). Phytoconstituents except terpenoids from *C. sativa* and *C. colocynthis* leaves were reported while, in contrast, steroids, tannins and phenols were absent in *C. colocynthis* roots. The methanol derived maximum phenolic contents from *C. sativa* and *C. colocynthis* leaves were 36.42 and 37.69 mg gallic acid equivalent GAE/g respectively. However, total flavonoids registered from *C. sativa* leaves and *C. colocynthis* leaves and roots were 59.03, 50.58 and 43.32 mg quercetin equivalent QE/g respectively. Interestingly, *C. colocynthis* leaves produced the highest flavonoids 119.63 mg QE/g using ethyl acetate extract. DPPH inhibition (%) was high in acetone 55.57, hexane 45.98 and distilled water 35.5% from *C. sativa*, *C. colocynthis* leaves and roots respectively. Our findings suggest that studied plants contain phytochemicals, reasonable quantity of phenol and flavonoids content confer to the potential antioxidant activity responsible for insecticidal properties as safer alternatives of synthetic pesticides.

Keywords: solvent extraction, biochemical analysis, DPPH inhibition %, insecticidal agents

Introduction

Plants are a God-given treasure to human beings; they produce a variety of secondary metabolites, i.e., alkaloids, flavonoids, steroids, glycosides, terpenoids, tannins, saponins, quinine and phenols (Jung et al., 2009) and have the best curative potential of pharmaceutical medicines, biocides and biopesticides (Edeoga et al., 2005; Wells et al., 2009). Plant-produced phytochemicals perform distinctive functions in agriculture, veterinary, and pharmaceutical industries (Vasu et al., 2009).

Several plants are used as herbal medicines and in agriculture farming, including *Citrullus colocynthis* and *Cannabis sativa*. *C. colocynthis*, locally known as Tumba, is viny herbaceous plant that grows in desert or sandy soils, inhabitant to North Africa and is scattered in northern Africa, eastward Sahara, Morocco, Egypt, Sudan, Iran, Afghanistan, Pakistan, India and other tropical areas (Dane et al., 2007; Pravin et al., 2013). It belongs to the family Cucurbitaceae has, gained attention as a natural botanical

insecticide; its insecticidal activity has been evaluated against several insect pests' species (Soam et al., 2013). Moreover, extract obtained by dichloromethane from *C. Colocynthis* showed 98.4% mortality against *Culex quinquefasciatus* at 100 ppm concentration and LC₅₀ and LC₉₀ value were 19.26 ppm and 84.84 ppm respectively after 24 h of exposure period (Arivoli et al., 2015). Dimetry et al., (2007) documented that *C. colocynthis* formulations are effective biopesticides against stored grain pest like adults of *Callosobruchus maculatus*. Similarly, aqueous extract from various parts of this plant extensively reduced the population of *Rhopalosiphum padi* (Asiry, 2015). The ethanolic extract from *C. colocynthis* exhibited the insecticidal effect against *Aphis craccivora* and this insecticidal potential is due to the presence of alkaloids, glycosides and saponins (Torkey et al., 2009). It has antifeedants, deterrent, growth-regulating and infertility properties against insects (Seenivasan et al., 2004) and familiar in the traditional medicine and used as purgative, anti-inflammatory, cathartic and pain relieving properties (Mehrzadi et al., 2016; Memon et al., 2003; Shi et al., 2014)

Cannabis is another paramount annual weedy and dioecious plant belongs to family Cannabaceae. Historically, it appears to have been cultivated in Northern China since 4000 BC (Mabberley, 2008). *Cannabis* is used as a pest repellent and has been grown as a companion crop to kill several insects, fungi, weeds and nematodes. Its extracts have the ability to repel or kill insects, mites, and microorganisms and can be used as allelochemicals. *Cannabis* leaves have great potential against pests (McPartland, 1997) and these insecticidal properties of plants can be found in their secondary metabolites. For example, crude extract from *Chenopodium ficifolium* and *Jatropha curcas* exhibits aphicidal activity, and alkaloids from *Corydalis turtschaninovii* tubers and *Macleaya cordata* seeds harbour insecticidal potential (Abdoul Habou et al., 2011; Le Dang et al., 2010; Park et al., 2011; Rashid et al., 2013). The essential oil of *Cannabis* has demonstrated antimicrobial activity (Nissen et al., 2010; Novak et al., 2001) while, essential oil from Nepalese origin of *C. sativa* was evaluated for cytotoxic, larvicidal and insecticidal activity, and was found as relatively non-toxic (Satyal and Setzer, 2014).

The main bioactive components i.e. flavonoids, alkaloids, terpenoids and phenols from plant origin show strong insecticidal activity. Benelli et al. (2018) reported that essential oil obtained from fresh inflorescence of *C. sativa* dominated by monoterpenes and sesquiterpenes showed strong toxic effects against *M. domestica* at the rate of 43.3 µg/adult and *M. persicae* with LC₅₀ of 3.5 ml/l, moderately toxic against *S. littoralis* larvae at the rate of 152.3 µg/larva while least toxic against *C. quinquefasciatus* larvae with LC₅₀ of 252.5 ml/l. It contains pesticidal properties however, tetrahydrocannabinol (THC) is the prime constituent and sixty six other cannabinoids are reported including cannabidiol (CBD) and cannabinol (CBN) showing different effects (Fusar-Poli et al., 2009). Moreover, Pellati et al. (2018) analyzed the bioactive components from inflorescences of *C. sativa* (hemp) by means of innovative HPLC and GC methods coupled with GC-MS and GC-FID. Analysis showed the abundance of cannabidiol (CBD) and Cannabidiolic acid (CBDA) while, β-caryophyllene and β-myrcene were the major terpenes.

Plants are also a source of cheap antioxidant substitutes; they have the ability to scavenge free radicals, avoid the reaction transmission and hence prevent humans from their damage (Moure et al., 2001). Phenolic compounds, flavonoids and terpenes collected from natural plant resources have potential free radical scavenger activity (Mathew and Abraham, 2006) and are omnipresent groups of plant secondary metabolites (Singh et al., 2007).

The phytochemical extraction mechanism is important for obtaining better extract yield both qualitatively and quantitatively and scientists have studied the importance of *C. colocynthis* and *C. sativa* as a medicinal, insecticidal and antibacterial agent, but existing knowledge and research presented by different authors is limited to use of few solvents for extraction, extract properties as well as qualitative, quantitative analysis and antioxidants properties are not properly investigated in such a comprehensive way. Although, selected plants belong to different families and also harvested from different locations but it is worth noted that selected plants are potential source of phytochemicals and antioxidants responsible for insecticidal activities. Thus, at present extensive studies have been conducted on qualitative and quantitative extract estimations to identify different phytochemicals responsible for insecticidal potential and to determine the best extraction solvent with maximum phenolic and flavonoid contents and antioxidant activities using seven different solvents from *C. sativa* (leaves) and *C. colocynthis* (leaves and roots) collected from China and Pakistan respectively over the years 2017-2018.

Materials and methods

Plant material collection

Citrullus colocynthis (Colocynth), locally known as Tumba, and *Cannabis indica* formerly called as *Cannabis sativa* sub-species *indica* (Hemp) were the study plants. Young leaves and roots of Colocynthis were collected from (Bahawalnagar) a desert area of Punjab Province, Pakistan from March-April 2018 (Fig. 1a and 1b), while hemp leaves were collected from different locations of Shenyang, Liaoning Province, China from August-September 2017 (Fig. 1c). In total ten samples of each plant were collected belongs to same area and same species. Collected samples of colocynthis and hemp were then mixed together separately to obtain bulk volume of each plant. Botanical identification of colocynthis as *C. colocynthis* was performed at Department of Botany Pir Mehar Ali Shah Arid Agriculture University Rawalpindi (PMAS, AAUR) Pakistan, while hemp was identified as *C. sativa* by Professor Ji Mingshan, Department of Pesticides Science, College of Plant Protection, Shenyang Agriculture University, Shenyang Liaoning China.

Sample preparation

Leaves and roots were washed, dried under shade at room temperature, crushed into a fine powder by using an electric blender, sieved through 100 µm mesh and finally 1 kg of each plant sample was obtained and stored in airtight glass jars at 4°C.

Solvent extraction

Different solvents were selected with varying polarity level to extract crude material by cold extraction method which was simple, easy and safe for elution of bioactive compounds along with pigments (Handa et al., 2008). For each solvent extraction of each bulk plant material, 100 g of powdered sample was taken in a 1000 ml conical flask separately and extracted with 400 ml of respective solvent (Mondal, 2015). Extraction was performed at room temperature for 72 h (Mojab et al., 2010; Senguttuvan et al., 2014). The extraction process was repeated thrice to ensure that all polar and non-polar materials were eluted completely (Waiganjo et al., 2013). Filtered the contents, and

concentrated to reduce the volume on a rotary evaporator (Buchi Switzerland R-210). The concentrated filtrate was dried in a fume cupboard at 25°C. Solvent-free extract was placed in a stoppered glass bottle and stored at 4°C for further use. The physical properties of each extract (colour, stickiness and appearance) were recorded visually.



Figure 1. *a C. colocynthis* plant. *b C. colocynthis* (roots). *c C. sativa* plant

Aqueous extraction

A total of 100 g powdered plant samples was extracted at room temperature with 400 ml of distilled water for 72 h. The rest of the procedure was same as for solvent extraction.

Calculation of extract yield (g)

The extract yield was calculated for each solvent from the respective plant material and stored at 4°C for further studies.

Model validations

The relationship was used to develop the model for yield and for the comparison of coefficient of determination (R^2) values with root mean square error (RMSE). The coefficient of determination R^2 and RMSE represent the standard deviation of the residuals (prediction errors). Residuals are the measures that how the values are far from the regression lines where the data points were. This measure also told us how condensed the data were around the line of best fitness and model validity (Hossain et al., 2017). Performance of the model in the crude extract yield was evaluated by using RMSE. In the experiment with observations 'n', RMSE was calculated by identity *Equation 1* (Debaeke et al., 1997).

$$\text{RMSE} = \sqrt{1/n \times \sum_{j=1}^n ((\text{Yield}_{\text{meas}} - \text{Yield}_{\text{stim}})^2)} \quad (\text{Eq.1})$$

Qualitative phytochemical analysis

Phytochemical screening tests were performed to evaluate the presence or absence of phytoconstituents in *C. colocynthis* and *C. sativa* extracts using standard methods.

Test for alkaloids

For the estimation of alkaloids, 0.5 ml of each solvent extract was allowed to dry and 2 ml of 2% hydrochloric acid (HCl) was added to the residue in the test tube for 15 min in a water bath at 100°C. After cooling, the mixture was filtered and divided into two equal portions. A few drops of Mayer's reagent were added to one portion, while a few drops of Dragendoff's reagent were added to the other portion. Turbidity or the presence of a yellow precipitate confirm the presence of alkaloids (Siddiqui and Ali, 1997).

Test for glycosides

The presence of glycosides was evaluated by adding 2 ml distilled water and 2 ml 5% ferric chloride (FeCl_3) into 2 ml extract. The mixture was heated for 15 min in a water bath and then allowed to cool. Next, 1 ml benzene was added to the mixture and subjected to settle for 1 min after shaking. Next, 4 to 5 drops of concentrated ammonia (NH_3) was added. A pink or red colour indicates the presence of glycosides (Siddiqui and Ali, 1997; Siddiqui et al., 2009; Sofowora, 1993).

Test for terpenoids and steroids

The presence of terpenoids and steroids was determined by a previously described method (Kantamreddi and Lakshmi; Siddiqui and Ali, 1997) with slight modifications. Briefly, 0.5 g of solvent-free extract was added in 2 ml chloroform and then filtered. The filtrate was placed on ice; addition of 2 ml of acetic acid and then a few drops of concentrated sulfuric acid (H_2SO_4) was carefully applied to the inner sides of the test tubes. The emergence of a pink or pinkish brown colour/ring indicates the terpenoids existence, while a blue or bluish green colour for steroids presence and the combination of pink and blue/bluish green colours confirmed the presence of both terpenoids and steroids.

Test for flavonoids and flavones

Two millilitres of diluted sodium hydroxide (NaOH) was added to the 3 ml extract solution, which turned the solution into a yellow colour. The solution was treated with 1 ml 5N hydrochloric acid (HCl), which turned the solution colourless, indicate flavonoids, and an orange colour indicate flavones (Siddiqui and Ali, 1997; Siddiqui et al., 2009; Sofowora, 1993).

Test for tannins

For the estimation of tannins, 1 ml distilled water and ferric chloride ($FeCl_3$) 1-2 drops were added to 0.5 ml plant extract. The appearance of a blue and green/black colour indicates gallic and catecholic tannin, respectively (Iyengar, 1995).

Test for phenols

To detect phenols, 1 ml of extract solution was added to 2 ml distilled water and a few drops of 10% ferric chloride ($FeCl_3$). The appearance of a green or blue colour is the indication of phenols presence. Next, 0.50 g of plant extract was added and allowed to dissolve in distilled water and then 3 ml of 10% lead acetate was added. The presence of phenolic compounds was confirmed by the appearance of white precipitation (Trease et al., 2003).

Test for saponins

One gram of solvent-free extract was diluted with 20 ml of distilled water and shaken vigorously. The formation of a foam layer (1 cm) indicates the presence of saponins (Siddiqui and Ali, 1997).

Quantitative phytochemical analysis

Determination of total phenolic content (TPC)

The total phenols present in the crude extract of *C. colocynthis* and *C. sativa* was calculated by the Folin-Ciocalteu reagent method, with slight modifications. Briefly, 1 ml plant extract (1 mgml⁻¹ of solvent) was added to 2.5 ml of 10% Folin-Ciocalteu reagent (1:1) and 2 ml of 2% sodium carbonate (Na_2CO_3). The consequential mixture was allowed to stand for incubation for 15 min at room temperature in the dark. The solution was then transferred to a 96-well ELISA plate to measure the absorbance at 765 nm using an absorbance microplate reader (SpectraMax 190, manufactured in

China; designed in USA). All test calculations were carried out in triplicate. A standard calibration curve was constructed using gallic acid (1 mgml⁻¹). The results were calculated from the standard curve obtained by using different concentrations of gallic acid (1, 0.50, 0.25, 0.10, 0.05, 0.02, 0.01 and 0 mgml⁻¹) and are expressed as gallic acid equivalent (GAE) mgg⁻¹ of extracted compounds (Aiyegoro and Okoh, 2010).

Determination of total flavonoid content (TFC)

The amount of total flavonoids in the crude extract of *C. colocynthis* and *C. sativa* was estimated by a colourimetric method using aluminium trichloride (AlCl₃) and sodium hydroxide (NaOH). Briefly, 1 ml of extract (1 mgml⁻¹ of solvent) was added to 3 ml methanol, 0.2 ml 10% aluminium chloride, 0.2 ml 1M potassium acetate (CH₃COOK) and 5.6 ml distilled water. The resulting mixture was incubated at room temperature in the dark for 30 min. The assay was performed at 420 nm in a 96-well ELISA plate. Quercetin was used as the standard (1 mgml⁻¹) and a standard curve was obtained using different concentrations of quercetin (1, 0.50, 0.25, 0.10, 0.05, 0.02, 0.01 and 0 mgml⁻¹). Results are expressed as quercetin equivalent (QE) mgg⁻¹ of extracted compounds (Aiyegoro and Okoh, 2010). All test determinations were carried out in triplicate.

Determination of DPPH radical scavenging activity

The antioxidant activities of crude extracts of *C. colocynthis* and *C. sativa* were measured on the basis of the scavenging activities of the stable 1,1-diphenyl-1-picrylhydrazyl (DPPH) radical (Yu et al., 2003). Briefly, 0.5 ml of each respective extract was added to a sample cavity containing 3.5 ml of freshly prepared methanol solution of DPPH (0.004 g100ml⁻¹). The mixture was subjected to incubation for 30 min at room temperature in the darkness and absorbance was calculated at 517 nm. The percent inhibition of DPPH (I %) was calculated from the decrease of absorbance by *Equation 2*. A lower absorbance value represents higher free radical scavenging activity (Zhao et al., 2008).

$$I\% = \frac{A_{\text{blank}} - A_{\text{sample}}}{A_{\text{blank}}} \times 100 \quad (\text{Eq.2})$$

Whereas A_{blank} = absorbance of control; A_{sample} = absorbance of samples.

Statistical analysis

Data were analysed statistically by one-way analysis of variance (ANOVA) in Duncan's multiple range test (DMRT) and values are represented as the mean±standard deviation, with P = 0.05 indicating a significant difference. Analyses were conducted by using SPSS 13.0 (Inc.) software while graph was constructed by sigma Plot software.

Results

Potential solvent for extraction

Extraction was performed on *C. colocynthis* leaves and roots and on *C. sativa* leaves using different solvents and distilled water. Extract yields (g) was calculated and

presented in *Figure 2* while extract properties were described in *Table 1*. *Figure 2* and *Table 1* showed that using distilled water, *C. sativa* leaves produced a significant yield (11.688 g), with the physical properties of dark brown colour, non sticky and dry solid, followed by methanol (9.412 g), black shiny, more sticky, and ethanol (6.296 g), blackish and shiny.

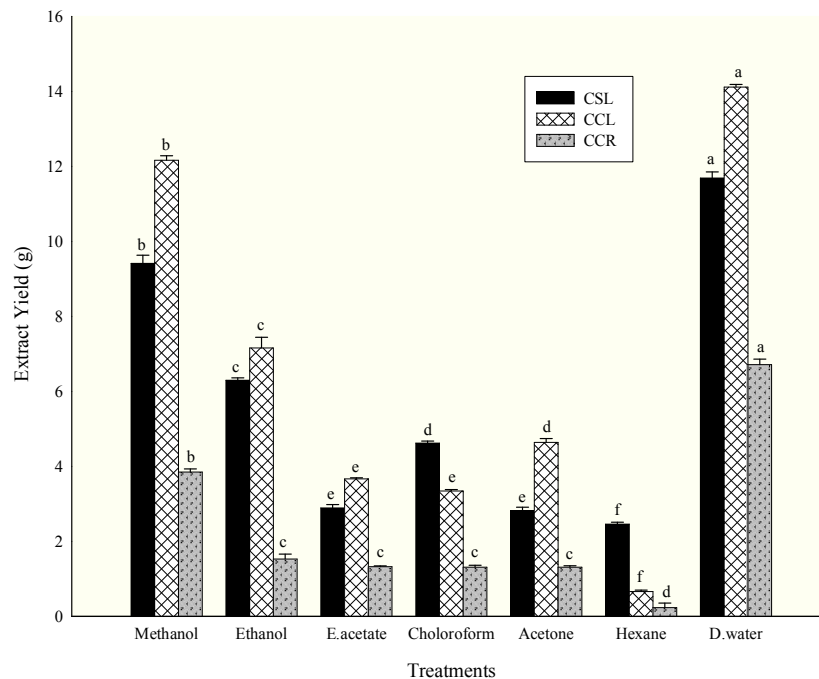


Figure 2. Extract yield (g) of *C. sativa* leaves (CSL) and *C. colocynthis* leaves (CCL) and roots (CCR) by using different solvents. Highest yield produced by D. water and methanol while lower yield produced by hexane from CCL, CSL and CCR respectively. Data corresponding to treatments labelled with different letters are significantly different (Duncan's multiple range test DMRT at $P \leq 0.05$); the error bars represent standard of the means

Table 1. Properties of CSL, CCL and CCR crude extract

Solvents extract	CSL			CCL			CCR		
	Colour	Stickiness	Appearance	Colour	Stickiness	Appearance	Colour	Stickiness	Appearance
Methanol	Black, shiny	More sticky	Slowly flowable	Greenish black, shiny	Sticky	Oily, flowable	Brown	Non-sticky	Semi solid, non-oily
Ethanol	Blackish, shiny	More sticky	Slowly flowable	Brownish black, shiny	Sticky	Oily, flowable	Yellowish brown	Non-sticky	Dry, waxy
E. acetate	Blackish	Sticky	Oily, flowable	Blackish	Sticky	Oily	Dark brown	Less sticky	Dry, non-oily
Chloroform	Brownish black	Less sticky	Less oily, non-flowable	Black, Shiny	Less sticky	Less oily, non-flowable	Brown	Less sticky	Semi-solid, non-flowable
Acetone	Brownish black	sticky	Oily, flowable	Greenish black	Sticky	Oily	Yellow	Non-sticky	Dry, Non-flowable
Hexane	Yellowish	Less sticky	Non-oily, non flowable	Yellowish brown	Less sticky	Non-oily, non flowable	Light yellow	Non-sticky	Semi-solid, non-flowable
Distilled water	Dark brown	Non-sticky	Dry solid	Dark brown	Less sticky	Less oily	Brown	Less sticky	Dry, non-flowable

CSL (*C. sativa* leaves), CCL (*C. colocynthis* leaves), CCR (*C. colocynthis* roots)

C. colocynthis leaves produced significant yield (14.115 g) using distilled water, with the physical properties of dark brown colour, less sticky followed by methanol (12.161 g), greenish shiny black and sticky, and ethanol (7.158 g), brownish black shiny and sticky.

C. colocynthis roots recorded a significantly high yield by distilled water (6.712 g), with the physical properties of dark brown colour and less sticky, followed by methanol (3.848 g), with the physical properties of greenish black, oily and ethanol (1.528 g), yellowish brown and waxy. However, the yields recorded by ethyl acetate (1.324 g), chloroform and acetone (1.312 g) were non significant ($P > 0.05$) to each other but differed significantly compared with all other treatments.

Model validation

The model validation performance for extract yield in response to *C. sativa* leaves and *C. colocynthis* leaves and roots is listed in Table 2. The *C. sativa* leaves extract exerted significant ($P < 0.001$) effects on the aqueous extract compared to all other treatments. The extract yield revealed that R^2 values of *C. sativa* using methanol, ethanol, ethyl acetate, chloroform, acetone, hexane and distilled water were 0.99, 0.93, 0.92, 0.87, 0.87, 0.93 and 0.82 respectively showed better performances compared to RMSE. Data on the extract yield for *colocynthis* leaves were statistically analysed and recorded as significant ($P < 0.05$) when obtained by methanol, with R^2 values of 0.99, 0.80, 0.98, 0.99, 0.81, 0.99 and 0.91. These extract yields for *C. colocynthis* roots were highly significant ($P < 0.01$) when obtained by distilled water and methanol compared to all other treatments. However, R^2 values of *C. colocynthis* roots 0.89, 0.84, 0.95, 0.94, 0.99, 0.94 and 0.92 showed the best curvature and best fit to the obtained data.

Table 2. Regression model for phytochemical screening of cumulative extract yield

Solvent extract	CSL		CCL		CCR	
	R^2	RMSE	R^2	RMSE	R^2	RMSE
Methanol	0.99	0.045266	0.99	0.0041231	0.89	0.0360786
Ethanol	0.93	0.588661	0.79	0.2680105	0.84	0.0989949
Ethyl acetate	0.92	0.075688	0.97	0.0245221	0.95	0.0070711
Chloroform	0.87	0.009556	0.99	0.0311127	0.94	0.0141421
Acetone	0.87	0.024042	0.81	0.1209201	0.99	0.0023804
Hexane	0.93	0.024338	0.99	0.0028284	0.94	0.1075546
Distilled water	0.82	0.308299	0.91	0.0268886	0.92	0.0287171

R^2 (Correlation coefficient), RMSE (Root mean square error), CSL (*C. sativa* leaves); CCL (*C. colocynthis* leaves); CCR (*C. colocynthis* roots)

Qualitative phytochemical analysis

Tests for phytochemical screening were conducted to determine the presence of bioactive compounds, namely, alkaloids, glycosides, terpenoids, flavonoids, flavones, steroids, tannins, phenols and saponins from *C. colocynthis* and *C. sativa* (Tables 3, 4 and 5). However the confirmation of a bioactive compound was referred as high presence (++) on strong resemblance; moderate presence (+) on medium or weak and (-) with no resemblance, appearance or change of colour of the reactive solution. The detection of alkaloids in the solvent extract was confirmed by turbidity or the emergence of a yellow

precipitate. The glycosides presence was confirmed by the appearance of a red or pink colouration in the reaction mixture. Positive results for terpenoids were confirmed by *C. colocynthis* roots, with the appearance of a pink or pinkish brown colour. Flavonoids and flavones were recorded by the transformation of the mixture from yellow to colourless and orange, respectively. The presence of tannins was confirmed by the appearance of a blue colour for gallic tannin and green/black for catecholic tannin. Blue or green colour in the reaction mixture indicated the presence of phenols while, foaming character in extract solution is important for the confirmation of saponins.

Phytochemical analysis indicated a high presence of steroids in chloroform and hexane extracts and a moderate presence in most other solvent extracts from *C. sativa* leaves except for distilled water extract (Table 3). Terpenoids were absent in all extracts. Alkaloids were absent in ethyl acetate, chloroform and distilled water extracts, while glycosides were present in all of these extracts except for hexane. Moreover, flavonoids were highly present in methanol and ethanol but moderately present in acetone and hexane. Flavones were present in acetone, as well as hexane and distilled water extracts. Saponins were present in chloroform, hexane and Distilled water extracts. However, gallic tannins were absent in all extracts, while catecholic tannins were absent in acetone, hexane and distilled water extracts. Phytochemical screening showed that phenols were present in methanol, ethyl acetate, ethanol and distilled water extracts.

Table 3. Qualitative phytochemical screening of *C. sativa* leaves crude extract

Solvents extract	Alkaloids	Glycosides	Terpenoids	Steroids	Flavonoids	Flavones	Tannins		Phenols	Saponins
							Catecholic	Gallic		
Methanol	+	-	-	+	++	-	+	-	+	-
Ethanol	+	-	-	+	++	-	+	-	+	-
Ethyl acetate	-	+	-	+	-	-	+	-	+	-
Chloroform	-	+	-	++	-	-	-	-	-	+
Acetone	+	-	-	+	+	+	+	-	-	-
Hexane	+	+	-	++	+	+	-	-	-	+
Distilled water	-	-	-	-	-	+	-	-	+	+

++high presence, +moderate presence, -absence

Table 4. Qualitative phytochemical screening of *C. colocynthis* leaves crude extract

Solvents extract	Alkaloids	Glycosides	Terpenoids	Steroids	Flavonoids	Flavones	Tannins		Phenols	Saponins
							Catecholic	Gallic		
Methanol	+	-	-	+	++	-	+	-	++	-
Ethanol	-	+	-	+	++	-	+	-	+	-
Ethyl acetate	-	+	-	+	++	+	-	++	++	-
Chloroform	-	++	-	+	+	+	-	-	-	-
Acetone	-	-	-	+	-	-	+	-	+	-
Hexane	-	++	-	+	+	+	-	-	-	-
distilled water	-	-	-	-	-	-	-	-	+	+

++high presence, +moderate presence, -absence

Table 5. Qualitative phytochemical screening of *C. colocynthis* roots crude extract

Solvents extract	Alkaloids	Glycosides	Terpenoids	Steroids	Flavonoids	Flavones	Tannins		Phenols	Saponins
							Catecholic	Gallic		
Methanol	-	-	-	-	++	+	-	-	-	+
Ethanol	-	-	++	-	++	+	-	-	-	-
Ethyl Acetate	-	-	+	-	+	-	-	-	-	+
Chloroform	-	-	+	-	+	-	-	-	-	-
Acetone	+	-	+	-	+	-	-	-	-	-
Hexane	-	-	-	-	+	-	-	-	-	-
Distilled water	-	+	-	-	-	-	-	-	-	+

++high presence, +moderate presence, -absence

C. colocynthis leaves showed a moderate presence of phenols by methanol, ethanol, ethyl acetate, acetone and distilled water but an absence in other extracts. However, a high glycoside presence was recorded by chloroform and hexane, with a moderate presence by ethanol and ethyl acetate (Table 4). Alkaloids were absent in all extracts except for methanol. Terpenoids were absent in all extracts. A high presence of flavonoids was recorded in methanol, ethanol and ethyl acetate, while a moderate presence of flavonoids was recorded in chloroform and hexane extracts. Flavones were present in ethyl acetate, chloroform and hexane extracts. Steroids were present in all extracts except for distilled water. Tannins were present in methanol, ethanol, ethyl acetate and acetone extracts, while saponins were present only in distilled water extract.

As shown in (Table 5), the phytochemical analysis of *C. colocynthis* roots demonstrated the presence of glycosides and alkaloid in distilled water and acetone extract, respectively. Steroids, tannins and phenols were absent in all extracts. However, terpenoids showed a high presence in ethanol and a moderate presence in ethyl acetate, chloroform and acetone extracts but an absence in methanol and distilled water. Although the presence of flavonoids was recorded in all extracts except for distilled water extract, flavones were recorded by methanol and ethanol only. The presence of saponins was recorded by methanol, ethyl acetate and distilled water extract.

Quantitative analysis

Total phenolic content (TPC)

The total phenolic contents of various extracts from *C. colocynthis* leaves and roots and *C. sativa* leaves varied slightly. The maximum and minimum phenolic contents from *C. sativa* leaves were recorded by methanol and distilled water (36.42 ± 1.905 and 29.98 ± 0.56 mg gallic acid equivalent GAE/g, respectively). However, minimum phenols recorded by ethyl acetate and ethanol were (12.16 ± 0.977 and 2.70 ± 0.109 mg GAE/g) respectively while other solvents recorded negative phenols (Table 6). Methanol and distilled water extracts from *C. colocynthis* leaves showed a higher phenolic content of 37.69 ± 0.35 and 37.25 ± 0.83 mg GAE/g, respectively, followed by acetone, ethanol and ethyl acetate (24.08 ± 1.78 , 22.82 ± 0.37 and 5.73 ± 0.56 mg GAE/g, respectively). However, *C. colocynthis* roots showed negative results for phenols.

Table 6. Total phenolic content (TPC) from CSL, CCL and CCR

Solvents extract	Total phenolic contents mg GAE/g		
	CSL	CCL	CCR
Methanol	36.42±1.905 ^a	37.69±0.35 ^a	-
Ethanol	2.70±0.109 ^d	22.82±0.37 ^b	-
Ethyl acetate	12.16±0.977 ^c	5.73±0.561 ^c	-
Chloroform	-	-	-
Acetone	-	24.08±1.78 ^b	-
Hexane	-	-	-
Distilled water	29.98±0.56 ^b	37.25±0.83 ^a	-

Results are presented as the mean values ± standard deviation. Same letters within a column indicate that mean values are not significantly different ($P > 0.05$) according to Duncan's multiple range test; CSL (*C. sativa* leaves); CCL (*C. colocynthis* leaves); CCR (*C. colocynthis* roots)

Total flavonoid content (TFC)

The total flavonoid content was high in the methanol and ethanol extracts of *C. sativa* leaves (59.03±1.31 and 56.00±1.85 mg quercetin equivalent QE/g, respectively), followed by hexane and acetone (17.35±0.43 and 12.08±0.62 mg QE/g, respectively) (Table 7). Thus, ethyl acetate extract from *C. colocynthis* leaves produced the highest flavonoid content (119.63 mg QE/g), followed by ethanol, methanol and hexane (54.84±0.90, 50.58±0.85 and 22.7±1.14 mg QE/g, respectively). However, the lowest flavonoid content was detected by chloroform (1.73±0.09 mg QE/g). The total flavonoid content of *C. colocynthis* roots by methanol and ethanol was the highest (43.32±0.33 and 42.34±0.23 mg QE/g, respectively), followed by ethyl acetate and acetone (28.93 and 8.86 mg QE/g, respectively). Chloroform and hexane extracts showed the lowest flavonoid content (2.23±0.18 and 1.23±0.09 mg QE/g, respectively).

Table 7. Total flavonoids content (TFC) from CSL, CCL and CCR

Solvents extract	Total flavonoid contents mg QE/g		
	CSL	CCL	CCR
Methanol	59.03±1.312 ^a	50.58±0.85 ^c	43.32±0.33 ^a
Ethanol	56.001±1.85 ^b	54.84±0.9 ^b	42.34±0.235 ^b
Ethyl acetate	-	119.63±0.31 ^a	28.93±0.19 ^c
Chloroform	-	1.7318±0.09 ^e	2.233±0.182 ^e
Acetone	12.086±0.62 ^d	-	8.863±0.154 ^d
Hexane	17.35±0.43 ^c	22.7±1.14 ^d	1.2343±0.094 ^f
Distilled water	-	-	-

Results are presented as the mean values ± standard deviation. Same letters within a column indicate that mean values are not significantly different ($P > 0.05$) according to Duncan's multiple range test; CSL (*C. sativa* leaves); CCL (*C. colocynthis* leaves); CCR (*C. colocynthis* roots)

DPPH radical scavenging activity

DDPH is a stable and free radical which is easily dissolved in methanol showed characteristics colour absorption at 517 nm using spectrophotometer. Free radicals are scavenged by antioxidant molecules due to donation of hydrogen molecules and the colour of DPPH assay solution changed to light yellow colour causing reduction of absorbance. To determine free radical scavenging activity, the DPPH radicals are widely used. Data on the 1,1-Diphenyl-1-picrylhydrazyl (DPPH) scavenging activity of free radical of *C. sativa* leaves and *C. colocynthis* leaves and roots are presented in (Table 8).

Table 8. DPPH radical scavenging activity from CSL, CCL and CCR

Solvents extract	DPPH Inhibition (%)		
	CSL	CCL	CCR
Methanol	49.5±0.7 ^b	30.65±1.07 ^e	23.63±0.68 ^f
Ethanol	54.1±0.2 ^a	36.52±0.62 ^c	33.83±0.351 ^b
Ethyl acetate	46±1 ^c	27.66±1.53 ^f	27.65±0.01 ^e
Chloroform	40.6±0.8 ^d	29.64±0.05 ^e	30.69±0.8 ^c
Acetone	55.57±1.2 ^a	33.5±0.51 ^d	30.97±0.98 ^c
Hexane	41.7±0.5 ^d	45.98±0.14 ^a	29.12±0.7 ^d
Distilled water	34.2±1.1 ^e	39.8±0.21 ^b	35.5±0.16 ^a

Results are presented as the mean values ± standard deviation. Same letters within a column indicate that mean values are not significantly different ($P > 0.05$) according to Duncan's multiple range test; CSL (*C. sativa* leaves); CCL (*C. colocynthis* leaves); CCR (*C. colocynthis* roots)

For *C. sativa* leaves, DPPH inhibition (%) by distilled water and acetone ranged from 34.2±1.10 to 55.57±1.20%. For *C. colocynthis* leaves, the DPPH inhibition (%) of chloroform and hexane extract ranged from 29.64±0.05 to 45.98±0.14%. However, the DPPH scavenging activity of *C. colocynthis* roots for methanol and distilled water ranged from 23.63±0.68 to 35.5±0.16%. It was also noted that all extracts of *C. sativa* and *C. colocynthis* showed varying levels of DPPH radical scavenging activity.

Discussion

The comparative extraction of crude extracts from *C. colocynthis* and *C. sativa* demonstrated that using methanol as an extraction solvent resulted in the maximum extract yield followed by ethanol, chloroform, ethyl acetate, acetone and hexane. However, using distilled water instead of organic solvent produced the maximum yield. Our results are consistent with (Awang et al., 2016; Markom et al., 2007; Pin et al. 2009) who reported that the highest extract yield was obtained by using water for extraction from *M. malabathricum* leaves, *Phyllanthus niruri* and *Piper betel*. Among the polarity-based solvents, methanol produced the maximum yield, followed by ethanol. Similar results were demonstrated by (Dhawan and Gupta, 2017; Paulsamy and Jeeshna, 2011) that methanol produced the maximum extract yield from *Datura metel* and *H. radicata* leaves.

The extract yield revealed that R^2 relationship of *C. sativa* ranging from 0.82-0.99 for distilled water and methanol have strong positive correlation compared to RMSE 0.308-

0.045 which showed better performance of model fitness. The trendline regression R^2 for *C. colocynthis* leaves were 0.99 for methanol, chloroform and hexane showed strong correlation while for *C. colocynthis* roots 0.99 by acetone recorded the best curvature and fitness of the model with recorded data.

The extraction of secondary metabolites highly depends on the extraction technique, solvent used and the chemical properties of the compounds. The analysis of *C. Sativa* leaf extracts showed the presence of alkaloids, glycosides, steroids, flavonoids, flavones, tannins, phenols and saponins and the absence of terpenoids. Relevant results were presented by Audu et al. (2014), who reported the presence of phytochemicals except for saponins and phenols in the leaves and roots of *C. sativa*. Various bioactive compounds such as flavonoids, alkaloids, glycosides, carbohydrates and essential oils have been documented previously from *C. colocynthis* by Wasylikowa and Van der Veen (2004). These isolated compounds like Flavonoids, isovitexin, isosaponarin and isoorientin 3'-O-methyl ether are revealed as significant antioxidants (Kumar et al., 2008). The results described by Najafi et al. (2010) on the phytochemical constituents from *C. colocynthis* leaves showed the presence of alkaloids, glycosides, tannins, flavonoids and saponins, consistent with our results. However, the results from our study are strongly correlated with Uma and Sekar (2014), who reported the presence of secondary metabolites in *C. colocynthis* leaves and roots. Singh (2010) reported the presence of bioactive compounds but no saponins or anthraquinones were reported from *C. colocynthis* roots.

C. colocynthis contains mostly flavonoids, while *Ziziphus spina-christi* contains the highest phenolic content (Tawfik et al., 2015). Phenols are biologically active compounds that are potent antioxidants with free radical scavenging behaviour. Haniyeh et al. (2016) reported that phenolic and flavonoid contents from the methanol extract of *C. Colocynthis* leaves were 79.78 and 45.46 μgml^{-1} , respectively. Similar findings were also observed herein, with phenolic and flavonoid contents of 37.69 and 50.58 mgg^{-1} , respectively. However, phenols were absent in all extracts of *C. colocynthis* roots. Moreover, Rizvi et al. (2018) reported the presence of polyphenol content from *C. colocynthis* leaves using different polarity solvent, methanol, ethyl acetate, chloroform, hexane and distilled water 74.34, 55.16, 56.32, 67.61 and 86.6 mg100g^{-1} respectively which is relevant to our findings for phenol content from *C. colocynthis* leaves. Maximum phenol and flavonoids content recorded by methanol from *C. sativa* 36.42 and 59.03 mgg^{-1} are consistent with Abd-Alla and Haggag (2013) who reported total phenol and flavonoid contents of 9.62 mgg^{-1} and 1.9 mgg^{-1} , respectively, with 14.5% antioxidant activity from the leaf extract of *C. sativa*.

The results from different studies have revealed that phenols, flavonoid content and antioxidant properties differ in different parts of *C. colocynthis*. Plants are an active source of valuable chemicals and other bioactive compounds that contain pesticidal activity against numerous insect pests (Koul and Walia, 2009). Salama and Al Rabiah (2015) reported the presence of phenol, flavonoid and antioxidant activities from twenty medicinal plants, with maximum phenol and flavonoid contents of 224.49 $\text{mg}/100\text{ g}$ and 126.24 mg100g^{-1} , respectively, from *C. colocynthis* (seeds). However, the inhibition percent in the ethanol extracts of roots and leaves was 56.8-67.2% and 5.97-6.42 μgml^{-1} , respectively. Among the ethanol extracts, leaves had the highest free radical inhibition activity in *C. colocynthis* ($\text{IC}_{50} = 2.97, 67.2\%$) (Hussain et al., 2013). Our findings also demonstrated that inhibition (%) in the ethanolic extract from leaves and roots was 36.52 and 33.83%, respectively. However, there are variations in antioxidants contained

by *C. sativa* and *C. colocynthis* among different solvents extract. Additionally, Eddouks et al. (2002) reported that methanolic extract of *C. colocynthis* seed exhibited highest inhibition 79.4 and 72.4% by using 1, 1-diphenyl-2-picrylhydrazyl (DPPH). Rathanavel and Arasu (2014) documented that Colocynth contains several phytoconstituents, such as flavonoids, alkaloids, glycosides, tannins saponins, carbohydrates and essential oils responsible for insecticidal activities.

Results from phytochemical analysis of *C. sativa* and *C. colocynthis* are characterized by the presence of various phytochemicals along with phenols, flavonoids content and antioxidant activity. However, data on previous studies for extraction and comparing the extract yield using different solvent, qualitative and quantitative analysis, antioxidant activity and use of bioactive compounds as alternative of synthetic chemicals from these plants is limited. Also synthetic agents in present era liberate maximum residues in environment and naturally grown population which is burning issue in current agro-ecosystem. So the study was conducted to examine extract yields using seven different solvents by solvent extraction method, to observe physical properties of extract, scrutinize bioactive compounds and to quantify total phenol, flavonoids contents and to asses' antioxidant activities by DPPH radical scavenging from crude extracts of study plants. Also solvents extract from *C. colocynthis* roots, yield calculation and physical properties were studied for the first time in such a comprehensive way.

Conclusion

The results demonstrated that crude extracts obtained by using different solvents from *C. colocynthis* and *C. sativa* possess biological compounds, such as terpenoids, glycosides, alkaloids, flavonoids, flavones, steroids, tannins, phenols and saponins. Owing to extraction, distilled water afforded the maximum yield followed by methanol with high phenol and flavonoid content. Hence, the studied plants are a rich source of phytocompounds, conferring them interesting antioxidant activity and supporting their use as potential insecticidal agents which are safe for environment and biodiversity. However, comprehensive research is needed to identify additional solvents and techniques for the extraction, isolation, purification and identification of active ingredient responsible for insecticidal activities.

Acknowledgements. The financial support provided by National Key Research & Development Programme of China (2016YFD0200500).

Conflict of interests. The authors have declared no conflict of interests.

REFERENCES

- [1] Abd-Alla, M., Haggag, W. M. (2013): Use of some plant essential oils as post-harvest botanical fungicides in the management of anthracnose disease of mango fruits (*Mangifera indica* L.) caused by *Colletotrichum gloeosporioides* (penz). – International Journal of Agriculture and Forestry 3: 1-6.
- [2] Abdoul Habou, Z., Haougui, A., Mergeai, G., Haubruge, E., Toudou, A., Verheggen, F. (2011): Insecticidal effect of *Jatropha curcas* oil on the aphid *Aphis fabae* (Hemiptera: Aphididae) and on the main insect pests associated with cowpeas (*Vigna unguiculata*) in Niger. – Tropicicultura 29: 225-229.

- [3] Aiyegoro, O. A., Okoh, A. I. (2010): Preliminary phytochemical screening and in vitro antioxidant activities of the aqueous extract of *Helichrysum longifolium* DC. – *BMC Complementary and Alternative Medicine* 10: 21.
- [4] Asiry, K. A. (2015): Aphidicidal activity of different aqueous extracts of bitter apple *Citrullus colocynthis* (L.) against the bird cherry-oat aphid, *Rhopalosiphum padi* (L.) (Homoptera: Aphididae) under laboratory conditions. – *J. Anim. Plant. Sci.* 25: 456-462.
- [5] Audu, B. S., Ofojekwu, P. C., Ujah, A., Ajima, M. N. (2014): Phytochemical, proximate composition, amino acid profile and characterization of Marijuana (*Cannabis sativa* L.). – *J Phytopharm* 3: 35-43.
- [6] Awang, M. A., Aziz, R., Sarmidi, M. R., Abdullah, L. C., Yong, P. K., Musa, N. F. (2016): Comparison of different solvents on the extraction of *Melastoma malabathricum* leaves using Soxhlet extraction method. – *Der Pharmacia Lettre* 8: 153-157.
- [7] Benelli, G., Pavela, R., Petrelli, R., Cappellacci, L., Santini, G., Fiorini, D., Sut, S., Dall'Acqua, S., Canale, A., Maggi, F. (2018): The essential oil from industrial hemp (*Cannabis sativa* L.) by-products as an effective tool for insect pest management in organic crops. – *Industrial Crops and Products* 122: 308-315.
- [8] Dane, F., Liu, J., Zhang, C. (2007): Phylogeography of the bitter apple, *Citrullus colocynthis*. – *Genetic Resources and Crop Evolution* 54: 327-336.
- [9] Debaeke, P., Caussanel, J. P., Kiniry, J. R., Kafiz, B., Mondragon, G. (1997): Modelling crop: weed interactions in wheat with ALMANAC. – *Weed Research* 37: 325-341.
- [10] Dhawan, D., Gupta, J. (2017): Comparison of different solvents for phytochemical extraction potential from *Datura metel* plant leaves. – *International Journal of Biological Chemistry* 11: 17-22.
- [11] Dimetry, N. Z., El-Gengaihi, S., El-Salam, A. A. (2007): Protection of stored cowpea from *Callosobruchus maculatus* (F.) attack by some plant extract formulations in different storage sacks. – *Herba Polonica* 53: 71-84.
- [12] Eddouks, M., Maghrani, M., Lemhadri, A., Ouahidi, M.-L., Jouad, H. (2002): Ethnopharmacological survey of medicinal plants used for the treatment of diabetes mellitus, hypertension and cardiac diseases in the south-east region of Morocco (Tafilalet). – *Journal of Ethnopharmacology* 82: 97-103.
- [13] Edeoga, H. O., Okwu, D. E., Mbaebie, B. O. (2005): Phytochemical constituents of some Nigerian medicinal plants. – *African Journal of Biotechnology* 4: 685-688.
- [14] Fusar-Poli, P., Crippa, J. A., Bhattacharyya, S., Borgwardt, S. J., Allen, P., Martin-Santos, R., Seal, M., Surguladze, S. A., O'Carroll, C., Atakan, Z. (2009): Distinct effects of Δ^9 -tetrahydrocannabinol and cannabidiol on neural activation during emotional processing. – *Archives of General Psychiatry* 66: 95-105.
- [15] Handa, S., Khanuja, S., Longo, G., Rakesh, D. (2008): Extraction Technologies for Medicinal and Aromatic Plants. – *Earth, Environmental and Marine Sciences and Technologies, International Centre for Science and High Technology, Trieste.*
- [16] Haniyeh, R., Hamzeh, A., Ahmad, G. (2016): Antioxidant properties and flavonoids-phenolic content of *Citrullus colocynthis* (L.) schrad growing in Khuzestan, Iran. – *Bimonthly Journal of Hormozgan University of Medical Sciences* 20: 33-38.
- [17] Torkey, H.M., Abou-Yousef, H.M., Abdel Azeiz, A.Z., Hoda, Farid, E.A. (2009): Insecticidal effect of cucurbitacin E glycoside isolated from *Citrullus colocynthis* against *Aphis craccivora*. – *Australian Journal of Basic and Applied Sciences* 3: 4060-4066.
- [18] Hossain, S. A. A. M., Wang, L., Chen, T., Li, Z. (2017): Leaf area index assessment for tomato and cucumber growing period under different water treatments. – *Plant, Soil and Environment* 63: 461-467.
- [19] Hussain, A. I., Rathore, H. A., Sattar, M. Z. A., Chatha, S. A. S., ud din Ahmad, F., Ahmad, A., Johns, E. J. (2013): Phenolic profile and antioxidant activity of various extracts from *Citrullus colocynthis* (L.) from the Pakistani flora. – *Industrial Crops and Products* 45: 416-422.

- [20] Iyengar, M. A., 1995: Study of Crude Drugs. 8th Ed. – Manipal Power Press, Manipal, India.
- [21] Arivoli, S., Raveen, R., Samuel, T. (2015): Larvicidal activity of *Citrullus colocynthis* (L.) Schrad (Cucurbitaceae) isolated fractions against *Aedes aegypti* (L.), *Anopheles stephensi* (L.) and *Culex quinquefasciatus* say (Diptera: Culicidae). – Indian Journal of Applied Research 5: 97-101.
- [22] Jung, H. W., Tschaplinski, T. J., Wang, L., Glazebrook, J., Greenberg, J. T. (2009): Priming in systemic plant immunity. – Science 324: 89-91.
- [23] Kantamreddi, V. S. S. N., Lakshmi, Y. N., Kasapu, V. V. V. S. (2010): Preliminary phytochemical analysis of some important indian plant species. – International Journal of Pharma and Bio Sciences 1: B-358 ref.12.
- [24] Koul, O., Walia, S. (2009): Comparing impacts of plant extracts and pure allelochemicals and implications for pest control. – CAB Reviews: Perspectives in Agriculture, Veterinary Science, Nutrition and Natural Resources 4: 1-30.
- [25] Kumar, S., Kumar, D., Saroha, K., Singh, N., Vashishta, B. (2008): Antioxidant and free radical scavenging potential of *Citrullus colocynthis* (L.) Schrad. methanolic fruit extract. – Acta Pharmaceutica 58: 215-220.
- [26] Le Dang, Q., Lee, G. Y., Choi, Y. H., Choi, G. J., Jang, K. S., Park, M. S., Soh, H. S., Han, Y. H., Lim, C. H., Kim, J.-C. (2010): Insecticidal activities of crude extracts and phospholipids from *Chenopodium ficifolium* against melon and cotton aphid, *Aphis gossypii*. – Crop Protection 29: 1124-1129.
- [27] Mabberley, D. (2008): Mabberley's Plant Book. 3rd Ed. – Cambridge University Press, Cambridge.
- [28] Markom, M., Hasan, M., Daud, W. R. W., Singh, H., Jahim, J. M. (2007): Extraction of hydrolysable tannins from *Phyllanthus niruri* Linn.: Effects of solvents and extraction methods. – Separation and Purification Technology 52: 487-496.
- [29] Mathew, S., Abraham, T. E. (2006): In vitro antioxidant activity and scavenging effects of *Cinnamomum verum* leaf extract assayed by different methodologies. – Food and Chemical Toxicology 44: 198-206.
- [30] McPartland, J. M. (1997): Cannabis as repellent and pesticide. – Journal of the International Hemp Association 4: 89-94.
- [31] Mehrzadi, S., Shojaii, A., Pur, S. A., Motevalian, M. (2016): Anticonvulsant activity of hydroalcoholic extract of *Citrullus colocynthis* fruit: involvement of benzodiazepine and opioid receptors. – Journal of Evidence-Based Complementary & Alternative Medicine 21: NP31-NP35.
- [32] Memon, U., Brohi, A. H., Ahmed, S. W., Azhar, I., Bano, H. (2003): Antibacterial screening of *Citrullus colocynthis*. – Pakistan journal of pharmaceutical sciences 16: 1-6.
- [33] Mojab, F., Kamalinejad, M., Ghaderi, N., Vahidipour, H. R. (2010): Phytochemical screening of some species of Iranian plants. – Iranian Journal of Pharmaceutical Research: 77-82.
- [34] Mondal, K. K. (2015): Potential investigation of anti-inflammatory activity and phytochemical investigations of ethanolic extract of *Glycosmis pentaphylla* Leaves. – American Journal of Biomedical Research 3: 6-8.
- [35] Moure, A., Cruz, J. M., Franco, D., Domínguez, J. M., Sineiro, J., Domínguez, H., Núñez, M. a. J., Parajó, J. C. (2001): Natural antioxidants from residual sources. – Food Chemistry 72: 145-171.
- [36] Najafi, S., Sanadgol, N., Nejad, B. S., Beiragi, M. A., Sanadgol, E. (2010): Phytochemical screening and antibacterial activity of *Citrullus colocynthis* (Linn.) Schrad against *Staphylococcus aureus*. – Journal of Medicinal Plants Research 4: 2321-2325.
- [37] Nissen, L., Zatta, A., Stefanini, I., Grandi, S., Sgorbati, B., Biavati, B., Monti, A. (2010): Characterization and antimicrobial activity of essential oils of industrial hemp varieties (*Cannabis sativa* L.). – Fitoterapia 81: 413-419.

- [38] Novak, J., Zitterl-Eglseer, K., Deans, S. G., Franz, C. M. (2001): Essential oils of different cultivars of *Cannabis sativa* L. and their antimicrobial activity. – *Flavour and Fragrance Journal* 16: 259-262.
- [39] Park, H.-J., Baek, M.-Y., Cho, J.-G., Seo, K.-H., Lee, G.-Y., Moon, S.-J., Ahn, E.-M., Baek, N.-I. (2011): Insecticidal alkaloids on aphids from *Corydalis turtschaninowii* tubers. – *Journal of the Korean Society for Applied Biological Chemistry* 54: 345-352.
- [40] Paulsamy, S., Jeeshna, M. V. (2011): Preliminary phytochemistry and antimicrobial studies of an endangered medicinal herb *Exacum bicolor* Roxb. – *Res J Pharm Biol Chem Sci* 2: 447-457.
- [41] Pellati, F., Brighenti, V., Sperlea, J., Marchetti, L., Bertelli, D., Benvenuti, S. (2018): New methods for the comprehensive analysis of bioactive compounds in *Cannabis sativa* L. (hemp). – *Molecules* 23: 2639.
- [42] Pin, K. Y., Chuah, T. G., Rashih, A. A., Law, C. L., Rasadah, M. A., Choong, T. S. Y. (2009): Drying of betel leaves (*Piper betle* L.): Quality and drying kinetics. – *Drying Technology* 27: 149-155.
- [43] Pravin, B., Tushar, D., Vijay, P., Kishanchnad, K. (2013): Review on *Citrullus colocynthis*. – *Int. J. Res. Pharm. Chem* 3: 46-53.
- [44] Rashid, T., Chen, J., McLeod, P. (2013): Toxicity of newly isolated piperidine alkaloids from the red imported fire ant, *Solenopsis invicta* Buren, against the green peach aphid, *Myzus persicae* (Sulzer). – *Advances in Entomology* 1: 20.
- [45] Rathanavel, C., Arasu, P. T. (2014): Antioxidant activity, phenol and flavonoid contents of some selected Indian medicinal plants. – *Int. J. Curr. Microbiol. App. Sci* 3: 830-838.
- [46] Rizvi, T. S., Mabood, F., Ali, L., Al-Broumi, M., Al Rabani, H. K. M., Hussain, J., Jabeen, F., Manzoor, S., Al-Harrasi, A. (2018): Application of NIR spectroscopy coupled with PLS regression for quantification of total polyphenol contents from the fruit and aerial parts of *Citrullus colocynthis*. – *Phytochemical Analysis* 29: 16-22.
- [47] Salama, H. M., Al Rabiah, H. K. (2015): Physiological effects of allelopathic activity of *Citrullus colocynthis* on *Vicia faba* and *Hordeum vulgare*. – *European Journal of Biological Research* 5: 25-35.
- [48] Satyal, P., Setzer, W. N. (2014): Chemotyping and determination of antimicrobial, insecticidal, and cytotoxic properties of wild-grown *Cannabis sativa* from Nepal. – *Journal of Medicinally Active Plants* 3: 9-16.
- [49] Seenivasan, S. P., Jayakumar, M., Raja, N., Ignacimuthu, S. (2004): Effect of bitter apple, *Citrullus colocynthis* (L.) Schrad seed extracts against pulse beetle, *Callosobruchus maculatus* Fab. (Coleoptera: Bruchidae). – *Entomon-Trivandrum* 29: 81-84.
- [50] Senguttuvan, J., Paulsamy, S., Karthika, K. (2014): Phytochemical analysis and evaluation of leaf and root parts of the medicinal herb, *Hypochoeris radicata* L. for in vitro antioxidant activities. – *Asian Pacific Journal of Tropical Biomedicine* 4: S359-S367.
- [51] Shi, C., Karim, S., Wang, C., Zhao, M., Murtaza, G. (2014): A review on antidiabetic activity of *Citrullus colocynthis* Schrad. – *Acta Pol Pharm* 71: 363-367.
- [52] Siddiqui, A. A., Ali, M., 1997. *Practical Pharmaceutical Chemistry*. – CBS Publishers & Distributors., Delhi.
- [53] Siddiqui, S., Verma, A., Rather, A. A., Jabeen, F., Meghvansi, M. K. (2009): Preliminary phytochemicals analysis of some important medicinal and aromatic plants. – *Advances in Biological Research* 3: 188-195.
- [54] Singh, R., Singh, S., Kumar, S., Arora, S. (2007): Evaluation of antioxidant potential of ethyl acetate extract/fractions of *Acacia auriculiformis* A. Cunn. – *Food and Chemical Toxicology* 45: 1216-1223.
- [55] Singh, S. (2010): Phytochemical investigation of *Sonchus oleraceus* leaves and *Citrullus colocynthis* root. – *Journal of Herbal Medicine and Toxicology* 4: 159-162.

- [56] Soam, P. S., Singh, T., Vijayvergia, R. (2013): *Citrullus colocynthis* (LINN.) and *luffa acutangula* (L.) roxb, schrad. source of bioinsecticides and their contribution in managing climate change. – IJABPT 4: 7-9.
- [57] Sofowora, A. (1993): *Medicinal Plants and Traditional Medicine in Africa*. – Spectrum Books, Ibadan, Nigeria.
- [58] Tawfik, K., Al-Barazi, M., Bashir, M., Al-Marzouq, W., Al-Soufi, R., Kharsa, H. (2015): A comparative study of antioxidant activities of ziziphus and colocynth from Saudi Arabia deserts and proposed pharmaceutical products. – *International Research Journal of Pharmaceutical and Applied Sciences* 5: 08-13.
- [59] Trease, G. E., Evans, W. C. (2003): *Pharmacognosy*. – Saunders, London, pp. 479-480.
- [60] Uma, C., Sekar, K. G. (2014): Phytochemical analysis of a folklore medicinal plant *Citrullus colocynthis* L (bitter apple). – *Journal of Pharmacognosy and Phytochemistry* 2.
- [61] Vasu, S. S., Davidson, D. F., Hong, Z., Vasudevan, V., Hanson, R. K. (2009): n-Dodecane oxidation at high-pressures: measurements of ignition delay times and OH concentration time-histories. – *Proceedings of the Combustion Institute* 32: 173-180.
- [62] Waiganjo, N., Ochanda, H., Yole, D. (2013): Phytochemical analysis of the selected five plant extracts. – *Chemistry and Materials Research* 3: 12-17.
- [63] Wasylkowa, K., Van der Veen, M. (2004): An archaeobotanical contribution to the history of watermelon, *Citrullus lanatus* (Thunb.) Matsum. & Nakai (syn. *C. vulgaris* Schrad.). – *Vegetation History and Archaeobotany* 13: 213-217.
- [64] Wells, J. B., Christiansen, M. H., Race, D. S., Acheson, D. J., MacDonald, M. C. (2009): Experience and sentence processing: statistical learning and relative clause comprehension. – *Cognitive Psychology* 58: 250-271.
- [65] Yu, L., Perret, J., Harris, M., Wilson, J., Haley, S. (2003): Antioxidant properties of bran extracts from “Akron” wheat grown at different locations. – *Journal of Agricultural and Food Chemistry* 51: 1566-1570.
- [66] Zhao, H., Fan, W., Dong, J., Lu, J., Chen, J., Shan, L., Lin, Y., Kong, W. (2008): Evaluation of antioxidant activities and total phenolic contents of typical malting barley varieties. – *Food Chemistry* 107: 296-304.

STUDY OF REMOBILIZATION OF WINTER BREAD WHEAT (*TRITICUM AESTIVUM* L.) UNDER RAINFED CONDITIONS

JAHANGIROV, A. A.¹ – ALLAHVERDIYEV, T. I.^{2,3*} – TALAI, J. M.² – HUSEYNOVA, I. M.³

¹*Gobustan Experimental Station of Research Institute of Crop Husbandry
Gobustan AZ 3700, Azerbaijan*

²*Research Institute of Crop Husbandry, Ministry of Agriculture of the Republic of Azerbaijan
Pirshagy village, Sovkhoz 2, Baku AZ 1098, Azerbaijan*

³*Institute of Molecular Biology and Biotechnology, Azerbaijan National Academy of Sciences
2A Matbuat Avenue, Baku AZ 1073, Azerbaijan*

**Corresponding author*

e-mail: tofig_1968@mail.ru; phone: +994-50-463-1989

(Received 17th Feb 2019; accepted 8th Apr 2019)

Abstract. Remobilization coefficient of 21 winter bread wheat genotypes has been studied under rainfed conditions during two growing seasons with contrasting climate of Mountainous Shirvan district of Azerbaijan Republic. Remobilization coefficient was found to be higher in the year of drought compared to the year with normal precipitation. Remobilization coefficient of short and medium height genotypes was higher than that of tall genotypes, which indicates a negative correlation between plant height and remobilization coefficient. However, this correlation was not observed in the year with severe drought stress.

Keywords: *bread wheat, remobilization coefficient, drought, plant height, grain yield*

Introduction

As all living organisms, plants are also exposed to the effects of adverse environmental factors. Under the influence of these factors, stress or state of the “tension”, providing the universal protective reaction during growth, is created. The existence of the “echeloned defense” system provides a necessary tolerance for plant organisms and it is a main condition for the protection of species. Currently, intensive efforts have been made for studying stress mechanisms at molecular-genetic and cellular levels (Mwadzingeni et al., 2016; Gupta et al., 2017). Response of plants to stresses changes depending on plant species and genotype, duration and intensity of water deficiency, plant age and growth phase, plant organ and cell type, and at last cell compartmentalization (Zhu, 2002; Rampino et al., 2006). A high ability of the plant to change its metabolism according to the environment leads to a high reaction norm for this plant, which is a distinctive trait for tolerant plant varieties (Moussa and Abdel-Aziz, 2008).

Various stresses cause a decline in the productivity of agricultural plants. Considering the possibility of future difficulties in the meet of the demand of population in food products, one of the main tasks is developing new productive and tolerant varieties using genotypes tolerant to stress factors-adverse soil and climatic conditions, drought, high temperature, salinity etc. (Aliyev, 2012). Water restriction is main factor that limiting plant growth.

Wheat (*Triticum aestivum* L.) is one of the main crops in human nutrition. Adverse biotic and abiotic stresses negatively affect the productivity of wheat, do not allow the realization of genetic potential (Allahverdiyev et al., 2018). The forming of winter wheat yield depends on the factors affecting plants during a long vegetation period. Annual precipitation and air temperature are very important ecological factors affecting plant productivity. From this point of view developing drought tolerant varieties is of great importance. Therefore, new methods considering physiological properties of plants are to be used along with classical methods.

The process of remobilization has also a great role in the formation of grain yield of wheat plants under drought. Remobilization is a process of the use of compounds, which had been synthesized prior to the reproductive phase and preserved as resources in the stem, at the stages of grain formation and grain filling. Kalayci et al. (1998) argued that remobilization in wheat genotypes is of great importance only when drought is imposed at the grain filling stage. According to Blum and Pnuel (1998) remobilization has no effect on productivity when drought stress is imposed at the tillering stage, plants are not exposed to stress at the grain filling stage and productivity is about 1.78 ton/ha. Yang et al. (2002) reported high variation among genotypes for relative contribution of photosynthesis and stem reserves in wheat grain yield under the heat stress condition. Some genotypes tolerated the heat stress by preserving the stable photosynthesis and some others via the stem reserves. During grain filling, most of assimilates translocated to grains are provided by current photosynthesis in flag, penultimate leaves and spike (Arduini et al., 2006). A substantial part of grain dry matter can originate from remobilization of assimilates accumulated until anthesis and deposited temporarily in different vegetative parts of plants (Dordas, 2012).

Some authors showed that remobilization was more important during ear filling in cases of weakened photosynthesis, when soluble carbohydrates accumulated earlier in stem were transported to grain, because more carbohydrates were accumulated in tall and thick stems (Reynolds et al., 1999).

It was also shown that as leaf yellowing and plant drying processes proceed very fast at high temperatures, because of the short period between the start of yellowing and maturing, less dry matter can be accumulated in grain by remobilization (Zamani et al., 2014). Thus, the study of remobilization is suggested to be very important for developing wheat genotypes with more stable productivity under drought conditions. The presented research is devoted to the study of remobilization in winter wheat under dry rainfed conditions.

Materials and methods

Plant material and growth conditions

The present studies were performed in the field of Gobustan Experimental Station, Research Institute of Crop Husbandry, Azerbaijan. Twelve winter bread wheat varieties and nine stable lines selected for rainfed regions were used in the experiments. The experiments were conducted during the 2012-2013 and 2013-2014 growing seasons under dry rainfed conditions of Mountainous Shirvan district. Each genotype was grown in 1 m² areas with three replications according to randomized block design. Sowing was done at an average density 400 seeds × m⁻². The cultivated area is at an altitude of 780 m above sea level and it is light chestnut type, medium carbonate soil. According to the

perennial data, the amount of annual atmospheric precipitation in the region is 350-400 mm. Precipitation occurs mainly during autumn-winter periods.

Treatment

Sprinkling was performed with 4% magnesium chlorate ($Mg(ClO_3)_2$) on 20-25 days after earing in order to dry green parts of the plant. Prior to the sprinkling ear samples were taken. Two days after the sprinkling, plants began to dry. After the complete maturation, samples were taken from unsprinkled area for control and 10 ears were taken from the sprinkled area. The ear samples were kept at 85 °C for 24 h in the dryer, then grains were detached from ears, weighed and the weight of one grain was calculated. Coefficient of remobilization was calculated according to the formula (Kalayci et al., 1998): $CR = (WGS - WGB) / (CW - WGB) \times 100\%$, where: CR – coefficient of remobilization, WGS – weight of one grain from the sprinkled area (mg), WGB – weight of one grain before sprinkling (mg), CW – weight of one grain from the control area (mg).

Statistical analyses were performed by SPSS 16 software.

Results and discussion

The monthly rainfall and average temperatures during the wheat vegetation period (September-June) for the two growing seasons and average perennial (1984-2014) shown in *Table 1* were provided by the Gobustan Hydrometeorological Station. As seen in the table amount of the precipitation during the 2012-2013 growing season was 337.7 mm, and during the 2013-2014 growing season it significantly decreased to 222.3 mm. Air temperature also varied during the years of the study. Thus, in 2012-2013 air temperature was in average perennial limits, but in the spring months of the 2013-2014 growing season air temperature was above average perennial values. The mentioned changes in weather conditions affected the remobilization process in winter bread wheat.

Table 1. Weather conditions during the two growing seasons and average perennial

Months	2012-2013		2013-2014		Average perennial	
	Precipitation (mm)	Average temp. (°C)	Precipitation (mm)	Average temp. (°C)	Precipitation (mm)	Average temp. (°C)
September	23.1	18.0	52.0	19.5	31.0	17.1
October	24.1	14.9	23.2	11.2	45.0	11.2
November	21.6	7.8	11.7	7.2	36.0	6.0
December	28.7	2.2	18.3	-0.7	30.0	1.7
January	27.5	1.0	20.1	0.03	26.0	-0.2
February	48.2	3.2	12.5	-0.23	35.0	0.1
March	28.9	6.2	37.4	4.9	42.0	3.1
April	40.2	9.7	19.8	10.7	47.0	9.2
May	75.2	15.7	23.2	19.5	47.0	14.9
June	20.2	20.9	4.1	21.1	40.0	19.5
Total	337.7		222.3		379.0	
Average		9.96		9.32		8.3

The remobilization coefficient of the studied genotypes is presented in *Table 2*. As seen in the table in 2013 the average remobilization coefficient of all studied genotypes was 13.2%. In 2014 this value significantly increased to 21.4%. Low values of the remobilization coefficient in the 2012-2013 and high values in the 2013-2014 growing seasons are attributed to favorable and unfavorable weather conditions of these years, respectively.

Table 2. Coefficient of remobilization (%) of the studied genotypes

Number	Genotypes	Years		Average
		2013	2014	
1	Bezostaya 1	8.7	22.5	15.6
2	Gyzyl bugda	7.3	23.3	15.3
3	Sheki 1	9.2	23.6	16.4
4	Sonmez	8.5	25.8	17.2
5	Aran	15.1	20.2	17.7
6	Vostorg	17.0	25.7	21.4
7	Murov 2	17.1	27.8	22.5
8	Gobustan	11.2	21.4	16.3
9	Tale 38	13.9	19.3	16.6
10	Fatime	12.2	10.9	11.6
11	Gyrmyzy gul 1	17.3	28.7	23.0
12	Zirve 85	14.5	19.2	16.9
13	7WON-SA № 465	13.9	15.1	14.5
14	FERRIGINEUM 2/19	13.5	15.9	14.7
15	11 IWWYT № 20	14.6	20.2	17.4
16	12 IWWYT № 6	14.3	23.1	18.7
17	12 IWWYT № 8	14.3	15.2	14.8
18	12 IWWYT № 9	11.6	16.3	14.0
19	12 IWWYT № 17	11.3	30.4	20.9
20	7 WON-SA № 477	16.3	20.3	18.3
21	4 th FEFWSN № 50	15.1	25.5	20.3
Average		13.2	21.4	17.3

In 2013 the remobilization coefficients of the Gyrmyzy gul 1, Murov 2, Vostorg and Aran varieties were found to be higher compared with other studied varieties. This may be due to the late maturation of the varieties, except Murov 2, thus, the ear filling stage of these varieties occurred under high temperature and drought period. There were also reports on late maturing varieties, which remobilization coefficients were higher due to drought and high temperature (Chekich, 2007). Higher remobilization coefficient of Murov 2 compared with other genotypes is probably related to individual biological properties of this genotype. It should be noted that the remobilization coefficients of the Vostorg and Gyrmyzy gul 1 varieties were also higher in 2014. There were reports on the existence of a positive correlation between productivity and remobilization coefficient during drought years (Kalayci et al., 1998; Chekich, 2007). However, we did not observe a significant relation between the remobilization coefficient and

productivity during favorable 2013 year and unfavorable 2014 drought year. We suggest that remobilization was not very important for the productivity under favorable weather conditions of 2013.

In 2014 remobilization coefficient increased in all genotypes because of severe drought and temperature stress. However, the period between the beginning of leaf yellowing and maturing was very short and other factors appeared to be more important for productivity than remobilization. As a result, in spite of the higher remobilization coefficient during the drought year, there was no correlation between productivity and remobilization coefficient. Moreover, different remobilization coefficients were found for the genotypes during the unfavorable year with higher values for Sonmez, Vostorg, Murov 2, Gyrgyz gul 1 and 12thIWWYT№17. There was no significant relation between grain yield and water soluble carbohydrate remobilization under heat stress during grain filling (Zamani et al., 2014). Grain yield exhibited a low positive correlation with water soluble carbohydrates at anthesis under water stress (Del Pozo et al., 2016).

In 2012-2013 growing season we detected a negative correlation (*Fig. 1*) between the remobilization coefficient and plant height with $R^2 = 0.38^{**}$ (reliability within 0.01), while there was no correlation between the remobilization coefficient and the length of peduncle. However, in 2014 we observed the absence of the correlation between remobilization coefficient and both mentioned parameters, which could be attributed to severe drought and high temperatures.

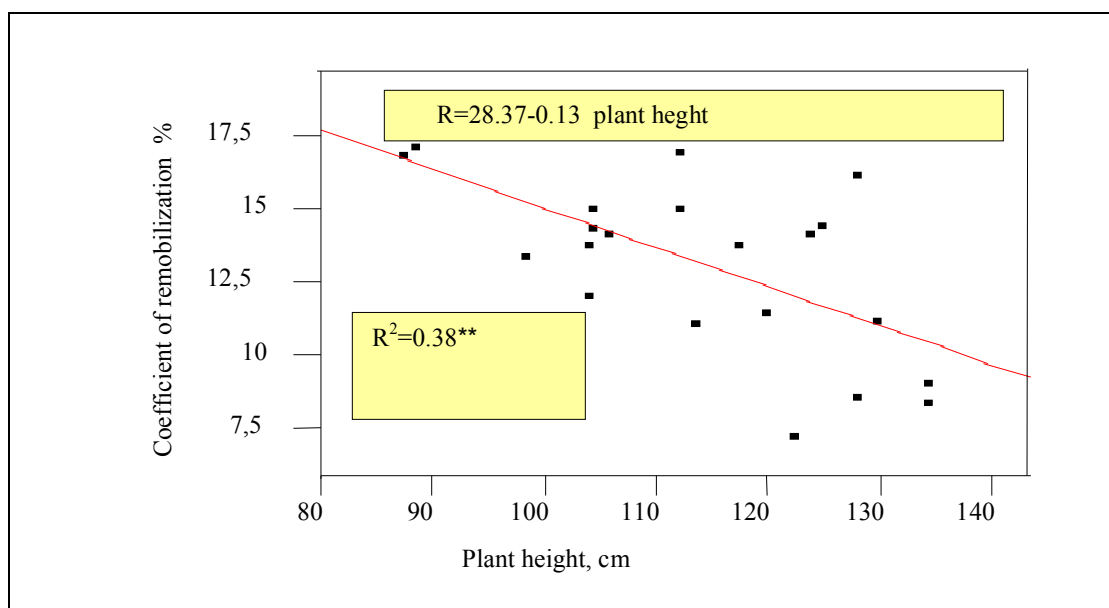


Figure 1. Interrelation between the plant height and remobilization coefficient in the 2012-2013 growing season

We suggest that the reason of the low values of remobilization coefficient for the varieties Bezostaya 1, Gyrgyz bugda, Shaki 1 and Sonmez is the tallness of these varieties. As assimilates should pass very long distance to be transported to grain.

The high values of the remobilization coefficient in the Gyrgyz gul 1, Vostorg and other genotypes can be attributed to their late maturation and short stature. Analogical

results were obtained in the previous experiments conducted with radioactive C atoms (Jahangirov, 1987).

Conclusion

Thus, the study of remobilization in winter bread wheat genotypes under dry rainfed conditions of Mountainous Shirvan region showed that this parameter was dependent on weather conditions and individual biological properties of the genotypes. Remobilization coefficient was found to be higher during drought years. It was also established that remobilization coefficient was higher in short and medium-height genotypes compared with tall genotypes, which indicate a negative correlation between the remobilization coefficient and plant height.

Acknowledgments. Authors are thankful to Gobustan Hydrometeorological Station for providing information on annual and perennial precipitation and temperature.

REFERENCES

- [1] Aliyev, J. A. (2012): Photosynthesis, photorespiration and productivity of wheat and soybean genotypes. – *Physiol. Plantarum* 145: 369-383.
- [2] Allahverdiyev, T., Jahangirov, A., Talai, J., Huseynova, I. (2018): Dry matter remobilization, yield and yield components of durum (*Triticum durum* Desf.) and bread (*Triticum aestivum* L.) wheat genotypes under drought stress. – *Pak. J. Bot.* 50: 1745-1751.
- [3] Arduini, I., Masoni, A., Ercoli, L., Mariotti, M. (2006): Grain yield, and dry matter and nitrogen accumulation and remobilization durum wheat as affected by variety and seeding rate. – *Eur. J. Agron.* 25: 309-318.
- [4] Blum, A., Pnuel, Y. (1998): Physiological attributes associated with drought resistance of wheat cultivars in a Mediterranean environment. – *Australian Journal of Agricultural Research* 41: 799-810.
- [5] Chekich, C. (2007): Investigation of the physiological parameters which may be the criteria of selection for the reproduction of drought resistant wheat (*Triticum aestivum* L.). – PhD Thesis, Ankara (in Turkish).
- [6] Del Pozo, A., Yanez, A., Matus, I. A., Tapia, G., Castillo, D., Sanches-Jardon, L., Araus, J. L. (2016): Physiological traits associated with wheat yield potential and performance under water-stress in a Mediterranean environment. – *Front. Plant Sci.* <https://doi.org/10.3389/fpls.2016.00987>.
- [7] Dordas, C. (2012): Variation in dry matter and nitrogen accumulation and remobilization in barley as affected by fertilization, cultivar, and source-sink relations. – *Eur. J. Agron.* 37: 31-42.
- [8] Gupta, P. K., Balyan, H. S., Gahlaut, V. (2017): QTL analysis for drought tolerance in wheat: present status and future possibilities. – *Agronomy* 7: 1-21.
- [9] Jahangirov, A. A. (1987): Products of photosynthesis and peculiarities their utilization in wheat plants with various grain yield. – PhD Thesis in Biology, Baku.
- [10] Kalayci, M., Ozbek, V., Chekich, C., Ekiz, H., Keser, M., Altay, F. (1998): Determination of drought resistant wheat genotypes in Central Anatolia conditions and development of morphological and physiological parameters. – Final Report of Tübitak Research Project, Eskişehir (in Turkish).
- [11] Moussa, H. R., Abdel-Aziz, S. M. (2008): Comparative response of drought tolerant and drought sensitive maize genotypes to water stress. – *Australian J. Crop Science* 1: 31-36.

- [12] Mwadzingeni, L., Shimelis, H, Dube, E., Laing, M. D., Tsilo, T. J. (2016): Breeding wheat for drought tolerance: progress and technologies. – Journal of Integrative Agriculture 15: 935-943.
- [13] Rampino, P., Pataleo, S., Gerardi, C., Perotta, C. (2006): Drought stress responses in wheat: physiological and molecular analysis of resistant and sensitive genotypes. – Plant Cell Environment 29: 2143-2152.
- [14] Reynolds, M. P., Skovmand, B., Trethowan, R., Pfeiffer, W. (1999): Evaluating a Conceptual Model for Drought Tolerance. – In: Ribaut, J.-M., Poland, D. (eds.) Molecular Approaches for the Genetic Improvement of Cereals for Stable Production in Water-Limited Environments. A Strategic Planning Workshop Held at CIMMYT. CIMMYT, Mexico, El Batan, DF.
- [15] Yang, J., Sears, R. G., Gill, B. S., Paulsen, G. M. (2002): Genetic differences in utilization of assimilate sources during maturation of wheat under chronic heat and heat shock stresses. – Euphytica 125: 179-188.
- [16] Zamani, M. M., Nabpour, M. Meskarbashee, M. (2014): Stem water-soluble carbohydrate remobilization in wheat under heat stress during the grain filling. – Int. J. Agric. Biology 16: 401-405.
- [17] Zhu, J. K. (2002): Salt and drought stress signal transduction in plants. – Annu. Rev. Plant Biology 53: 247-273.

FOREST FIRES IN IZMIR REGIONAL DIRECTORATE OF FORESTRY

KUCUKOSMANOGLU, A.¹ – UZMEZ, İ.²

¹*Faculty of Forestry, Istanbul University-Cerrahpasa, Istanbul, Turkey*

²*General Directorate of Forestry, Ankara, Turkey*

**Corresponding author
e-mail: aliko@istanbul.edu.tr*

(Received 19th Feb 2019; accepted 10th Apr 2019)

Abstract. One of the major problems in many countries is the forest fires. Forest fires are the source of the most of the problems of fire protection organization in every year. Why does Turkey still have too many forest fires? And how do we eliminate forest fires? We are trying to approach this problem under our country conditions, and explain that how we are able to eliminate the forest fires in Izmir Forest Directorate. Forest fires stands out especially in the provinces of forests under the influence of the Mediterranean climate in Turkey. However, the forest directorate that are at risk in terms of both burning areas and fire numbers in these provinces are Mugla, Antalya and Izmir. For this reason, this study was carried out in Izmir Regional Directorate of Forestry between the years 2006-2015, one of the regional directorates that are always at risk.

Keywords: *Izmir, forest fire, forest directorate, burnt area, forest conservation*

Introduction

Forest fires are one of the important factors that jeopardize the continuity of forests in various parts of the world, especially in developed countries. Forest fires do not only damage timber and other forest products, they also harm ecosystem services, such as conserving the top soil etc. They destroy the habitats of forest biota and bring death to all sort of creatures. Even if the burned land is restored and reforested, forest fire change environmental conditions in forest (Mol et al., 1997). According to the recent fire statistics (from 1988 to 2016) in Turkey, the annual average number of forest fire is 2114 and that of burned forested area is 10615 ha (Goltas et al., 2017a).

Today, the importance of forest fires has increased due to global warming. Especially in the European continent, countries in the Mediterranean climate zone with low humidity and high temperature values are under the threat of forest fires with global warming. This situation is a top problem in terms of the sustainability of forests. Because of heat waves and drought, risk of forest fire, fire intensity, number of fire, fire frequency and burning area is expected to increase (Goltas et al., 2017b).

A large proportion of Turkey lies within the Mediterranean climate zone, which is characterized by hot and arid summer seasons, followed by warm and mild winters. Similar to many countries in the Mediterranean basin, Turkey is a country, which is prone to forest fires, which are frequently encountered phenomena due to climatic conditions (Mol and Kucukosmanoglu, 1998). In Turkey, about 35% of total forested areas are sensitive to forest fires at first-degree, 23% at second-degree, and 22% at third-degree (Bilgili and Kucuk, 2001).

Therefore they should be considered as usual events. Unfortunately, forest fires are rarely a result of natural causes such as the lightning. Forest fires are mostly human

induced events (Demir et al., 2009). Manager of the fire fighting team should comprehend the behavior of fire and customize a tailor made fire fighting strategy (Ayberk, et al., 2010).

The aim of this study is to make a detailed assessment of forest fires in general Turkey and in particular İzmir benefiting from fire reports, fire statistics, forest inventories and management plans. Results of the study will contribute to fire protection and fire suppression activity in both Turkey and Izmir Forest Directorate.

Materials and methods

The forest fires statistics occurred in Turkey between the years of 2006-2015 were evaluated in various aspects. In this study; Causes of forest fires, distribution in the field (hectare), the numerical distribution to the regional directories and the number of forest fires and total burned area in İzmir Regional Directorate of Forestry has investigated. Among the State forest Enterprises of regional Directorates; Bayındır, Bergama, İzmir, Menderes, Akhisar, Demirci, Gördes and Manisa are particularly considered. The main data of these directorates are sorted by years and calculated one by one in order to create systematic schemes. Moreover to reveal accurate investigation over these numbers, their 10 years total and 10 years average values are conceived and examined. For the investigation of forest fires in 10-year period; forest inventory and forest management plans obtained from İzmir Regional Directorate of Forestry in Izmir region has taken into consideration. In this way, the fire sensitivity of the Izmir Regional Directorate of Forestry has been tried to determine.

Study area

Surrounded by the Mediterranean, the Black Sea, the Sea of Marmara and the Aegean Sea; Turkey has 97% of its land area in Asia and 3% in Europe. It also has 8333 km of coastline and related to its geographical position, properties such as climate, relief and location have caused the formation of different geographical regions within the boundaries of the country (Demir et al., 2009).

Izmir regional directorate of forestry, which includes a large part of the Aegean region, is located within the territorial boundaries of Izmir and Manisa provinces. It is surrounded by Balıkesir in the north, Denizli and Kutahya in the east, Muğla Forest Regional Directorates in the south and Aegean Sea in the west. The geographical location of the Izmir Forest Directorate is located between the northern longitude of $39^{\circ}35'38''$ – $37^{\circ}52'30''$ and eastern latitudes of $26^{\circ}11'42''$ – $28^{\circ}52'28''$ (Fig. 1).

Under the influence of the Mediterranean climate, the plant species determined by this climate are located in İzmir. For many years, a wide variety of plant species have been destroyed due to grazing, breeding, smuggling, fire and insect damages. Especially in these areas where main tree species were damaged, drought resistant forest species were included. Main forest species are *Pinus brutia* and *Pinus nigra* in Izmir. Additionally there are many other tree species like *Pinus pinea*, *Quercus* sp., *Castanea* sp., *Juglans* sp., *Fagus* sp. in Izmir forests. General area of Izmir Forest Directorate is 2,509,336 ha and 39% of this area is forest lands. This value is calculated by creating relevant pie-chart, that presents damaged forests (22%), efficient forests (17%) and non-forest area (61%). 417,910 ha efficient forests, 557,095 ha damaged forest in Izmir Forest Directorate (Uzmez, 2011) (Fig. 2).

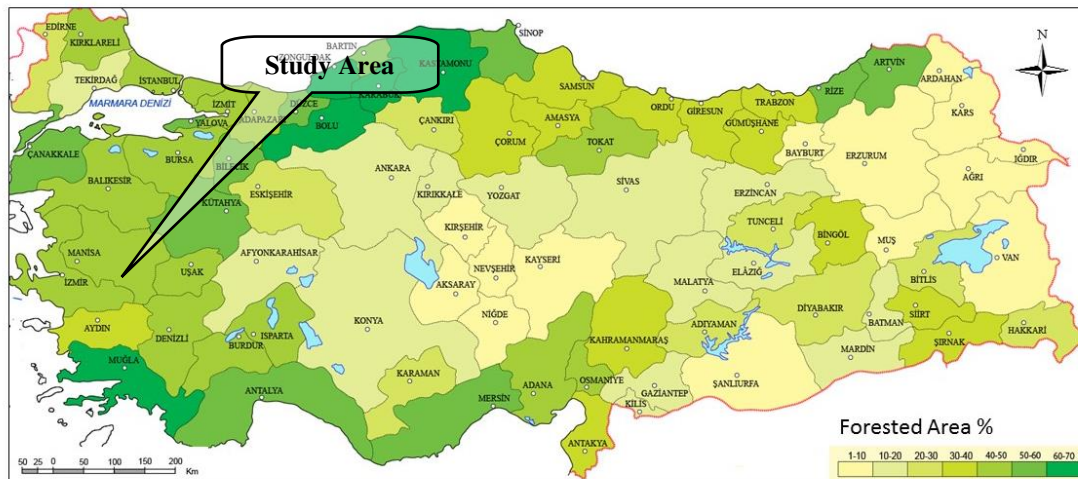


Figure 1. The location of the study area in Turkey

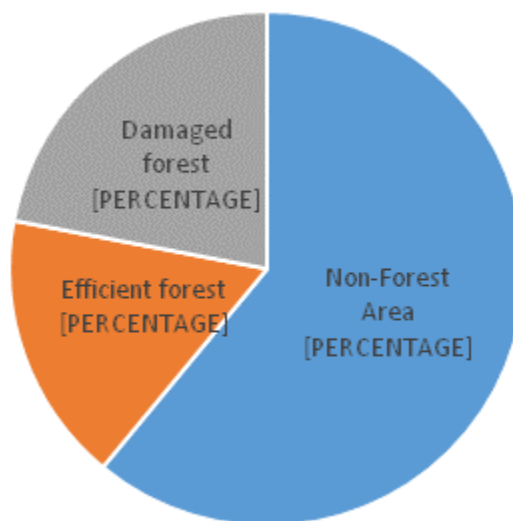


Figure 2. Forest status in İzmir Forest Directorate

Results

Different factors influencing forest fire danger

Many factors such as weather conditions, forest vegetation and fire season influence the forest fire danger (Noble et al., 1980). For instance, some weather conditions such as high air temperature, low relative humidity and dry winds reduce the moisture contents of flammable materials. In Mediterranean region the wind of South, South East and South West are oceanic origin, and so they bring more humidity. As a result, the fire danger is less. But the wind of North, North East and North West origin, bring dry air masses, because they are Central Anatolian origin. So, this situation created severe fire seasons (Mol and Kucukosmanoglu, 1998).

Forest vegetation also has a great influence on the damage of the forest fires. Most of the forest fires in Turkey occur in pine forest (49%) At the same time it is difficult to

prepare a fire season list for different parts of Turkey, because of various climatic conditions and forest fuels. But we frequently notice almost two characteristic types of fire season. Short fire season, this is well illustrated in Black-Sea and Marmara regions. In Black-Sea region July-August, and in Marmara region June-August are the peak points. Long fire season, Mediterranean and Aegean regions are typical examples. It continues about 5-8 months, but some part of these regions has year-long fire season (Demir et al., 2009).

Forest fire statistics in Turkey

The major destructive factor in Turkish forests is forest fires. Large or small, high severity or low severity they have had a profound influences on forests and wildlands. Especially the Mediterranean area has very suitable combustion and spreading factors. Forest fires cause great damage especially in Mediterranean, Aegean and Marmara regions. Forest fires not only cause the destruction of forest resources, but also destroy the balance of the ecological system. The coastal band, which starts from Hatay in particular from the Mediterranean and the Aegean coastal regions to Istanbul, constitutes the most risky area in terms of fires. In this region, the first sensitive area of fire is 7,182,051 ha, the second sensitive area to the fire is 5,091,788 ha. According to this, 12 million ha of the forests corresponding to approximately 60% of our forests are located in areas sensitive to fire (Uzmez, 2011) (Fig. 3).

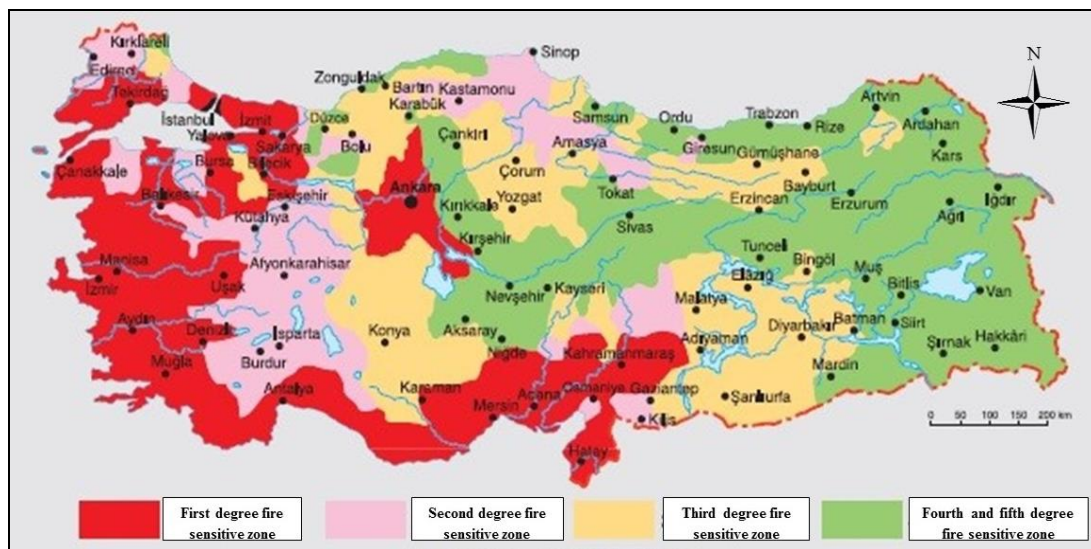


Figure 3. Sensitive regions of Turkey against to forest fire

Considering the causes of forest fires, which emerged in Turkey between the years 2006-2015, their numbers and area distributions are shown in *Table 1*. With the examination of *Table 1*, it is possible the state that among the period of 2006-2015; the year 2013 reached the highest level in terms of the number of forest fires (16.1%), yet the year 2008 reached highest value relating to amount of burnt area (33.4%). The reason of why the year 2013 has the highest number of fire, is explained by the social events such as communal violence occurred in Turkey during 2013. It is also emerged that, with respect to amount of burnt area, the year 2008 has the highest value. This situation can be explained with the fact that the temperatures of 2008 were 0.5-2.4 °C

higher than the average seasonal normals (1971-2000) as shown in *Figure 4*. This also causes the increase in number and burnt areas by means of forest fire. Moreover, it is obvious that our findings are supported by Kucuk and Saglam (2004).



Figure 4. Average monthly temperatures of 1971-2000 and 2008 (MGM, 2017)

In Turkey, the main causes of the forest fires are human being (99%) and lightning (1%) (Mol and Kucukosmanoglu, 1998). According to Demir et al. (2009), forest fires have many causes in Turkey, such as; human activities (smoking, negligence, carelessness, accidents, deliberate fire setting etc.), shortage of basic equipment for fire fighting, climate and weather variation (lightning etc.) and unknown reasons.

Among the causes of forest fires, four main subjects; Intentional, Negligence-Accident, Natural (Lightning) and Unknown are particularly chosen and their values by years calculated in detail. In *Table 1*, it is important to point out that during the year 2008; number value of Intentional is 18.1%, field value of Negligence-Accident is 43.7% and field value of Natural (Lightning) is 29.8%. Furthermore, during the year 2013; it is possible to find out that by 24.4% in terms of number value and by 30.7% in terms of field value, Unknown has reached its highest values. During the examination period (2006-2015), within the range of these causes, in respect to number value Intentional and in accordance to its field value, Negligence-Accident comes forward.

For this reason, regarding the protection of forests from fires; more emphasis should be put on to the issues of public awareness and education. These findings and suggestions of ours are also validated by related work of Ryan (2012).

Detailed examination through *Table 2* makes possible to reveal total forest fires within the mentioned years, in terms of number and area. For the year 2008, number value of fires generated from Intentional causes calculated as 1.6% and for the year 2007 field value is found as 1.9%. In addition to this, it is revealed through *Table 2* that in 2013 number value of Negligence-Accident obtained as 6.1% and in 2008 field value as 29.5%. In 2007, number value of Natural (Lightning) is obtained as 1.7% and in 2008 field value as 0.8%. Finally, in 2013 with respect to number value of Unknown as 7.8% and field value as 6.5%; all of these mentioned years have reached their highest rates

within *Table 2*. It seems clear that, likewise in *Table 1*, the year 2008 and the year 2013 comes forward in also *Table 2*. On the other hand, within mentioned decade when the total causes of forest fires are examined; it is seen that the Negligence-Accident has the first place concerning both number value (46.1%) and area value (67.6%). This finding shows that, fires are mostly caused by negligence and accident, rather than natural or unknown ones among the reasons of forest fires. For this reason, in order to protect forests from fire before the fire starts, precautions such as; fire safety roads, firebreaks, transportation roads, silvicultural measures, arrangement of flammable materials etc. are should be given priority and they should be practiced accurately.

In our work, *Tables 3* and *4* show the field distribution of forest fires with respect to regional forest directorates. *Table 3* reveals the field distribution, while *Table 4* shows the numerical distribution.

As it is understood by generating and analyzing *Tables 3* and *4*, related to the regional forest directorates and field distribution of forest fires in terms of number and field (hectare) between the years 2006 and 2015 it is seen that numerical findings of Izmir, Antalya and Mugla reach the highest rates. Therefore it is possible to state that forest fires are mainly concentrated upon these three regions in Turkey. As being sensitive to forest fires; this is one of the reasons why Izmir is selected as our study subject.

It is also seen that our findings regarding to these observations are supported by the research that carried out by Mol and Kucukosmanoglu (1997) and Kucuk and Unal (2011).

Forest fire statistics in İzmir

In Izmir there are many factors that destroy the forests. Among these destruction factors besides grazing, smuggling, insect damages and breeding, fire is the most dangerous one which especially harms plant species. All these mentioned factors are effective in Izmir Regional Directorate of Forestry that located in the west of Turkey as our study area.

Akyuz and Kucukosmanoglu (1997) especially draw attention to the fact that fire is the most important reason leading to destruction of forest resources in Izmir.

Izmir Regional Directorate of Forestry has the total area of 248986 ha. Approximately 968078 ha that constitutes the 39% of this area is covered with forests (GDF, 2016). Bayındır, Bergama, Izmir, Menderes, Akhisar, Demirci, Gördes, and Manisa are the names of the eight enterprises that Izmir Regional Directorate of Forestry contains. Between the years 2006-2015, number distribution of forest fires with respect to these State Forest Enterprises are stated and analyzed in *Table 5*. Within this 10 years period, calculations carried out in *Table 5* expose that total fire number is 2333 and average fire number is 233. Also it is indicated in *Table 6* that amount of burnt area is 7963 ha and the average amount of burnt area is calculated as 796 ha during this 10 years. As can be understood through the detailed investigation of *Tables 5* and *6*, Izmir Forest Enterprise steps forward with highest values in respect to area and number, concerning the forest fires. This situation reveals similar results that forest fires reach the highest values of both number and field value, as we obtained from the examination of Izmir Regional Directorate of Forestry (*Tables 3* and *4*). These relevant findings indicate that Izmir Region has a sensitive status concerning the forest fires. Therefore; during the fire seasons, it is a necessity to take all the required precautions against fires in Izmir.

Table 1. Forest fires in Turkey between 2006 and 2015

Year	Numbers of forest fires		Amount of burnt area		Causes of forest fires															
					Intentional				Negligence-accident				Natural (lightning)				Unknown			
	Number	Number %	Field (ha)	Field (%)	Number	Number %	Field (ha)	Field (%)	Number	Number %	Field (ha)	Field (%)	Number	Number %	Field (ha)	Field (%)	Number	Number %	Field (ha)	Field (%)
2006	2227	9.6	7762	8.7	166	8	206	2.7	1315	12.2	5873	9.8	330	10.9	543	23.2	416	5.6	1139	6
2007	2829	12.1	11664	13.1	292	14	1705	22.3	1642	15.3	7994	13.3	407	13.4	243	10.4	488	6.5	1722	9.1
2008	2135	9.2	29749	33.4	377	18.1	797	10.4	1018	9.5	26283	43.7	330	10.9	699	29.8	410	5.5	1970	10.4
2009	1793	7.7	4679	5.3	231	11.1	792	10.3	884	8.2	3082	5.1	333	11	105	4.5	345	4.6	700	3.7
2010	1861	8.0	3317	3.7	146	7	526	6.9	861	8	1851	3.1	281	9.3	69	2.9	573	7.7	871	4.6
2011	1954	8.4	3612	4.1	153	7.3	283	3.7	1067	9.9	2368	3.9	130	4.3	39	1.7	604	8.1	922	4.9
2012	2450	10.5	10454	11.7	197	9.4	1615	21.1	936	8.7	5780	9.6	373	12.3	334	14.3	944	12.7	2725	14.4
2013	3755	16.1	11456	12.9	260	12.5	1478	19.3	1419	13.2	4051	6.7	258	8.5	138	5.9	1818	24.4	5789	30.7
2014	2149	9.2	3117	3.5	127	6.1	85	1.1	801	7.5	1682	2.8	328	10.8	77	3.3	893	12	1273	6.7
2015	2150	9.2	3219	3.6	138	6.6	167	2.2	794	7.4	1198	2	257	8.5	95	4.1	961	12.9	1759	9.3
Total	23303	100	89029	100	2087	100	7654	100	10737	100	60162	100	3027	100	2342	100	7452	100	18870	100

Table 2. Evaluation of the total forest fires in terms of number and area between the years 2006 and 2015

Year	Numbers of forest fires		Amount of burnt area		Causes of forest fires															
					Intentional				Negligence-accident				Natural (lightning)				Unknown			
	Number	Field (ha)	Number	Number %	Field (ha)	Field (%)	Number	Number %	Field (ha)	Field (%)	Number	Number %	Field (ha)	Field (%)	Number	Number %	Field (ha)	Field (%)		
2006	2227	7762	166	0.7	206	0.2	1315	5.6	5873	6.6	330	1.4	543	0.6	416	1.8	1139	1.3		
2007	2829	11664	292	1.3	1705	1.9	1642	7	7994	9	407	1.7	243	0.3	488	2.1	1722	1.9		
2008	2135	29749	377	1.6	797	0.9	1018	4.4	26283	29.5	330	1.4	699	0.8	410	1.8	1970	2.2		
2009	1793	4679	231	1	792	0.9	884	3.8	3082	3.5	333	1.4	105	0.1	345	1.5	700	0.8		
2010	1861	3317	146	0.6	526	0.6	861	3.7	1851	2.1	281	1.2	69	0.1	573	2.5	871	1		
2011	1954	3612	153	0.7	283	0.3	1067	4.6	2368	2.7	130	0.6	39	0.1	604	2.6	922	1		
2012	2450	10454	197	0.8	1615	1.8	936	4	5780	6.5	373	1.6	334	0.4	944	4.1	2725	3.1		
2013	3755	11456	260	1.1	1478	1.7	1419	6.1	4051	4.6	258	1.1	138	0.2	1818	7.8	5789	6.5		
2014	2149	3117	127	0.5	85	0.1	801	3.4	1682	1.9	328	1.4	77	0.1	893	3.8	1273	1.4		
2015	2150	3219	138	0.6	167	0.2	794	3.4	1198	1.3	257	1.1	95	0.1	961	4.1	1759	2		
Total	23303	89029	2087	9	7654	8.6	10737	46.1	60162	67.6	3027	13	2342	2.6	7452	32	18870	21.2		

Table 3. The distribution of the field (ha) to the regional directorates of forest fires between 2006 and 2015

Regional directorates of forestry	2006		2007		2008		2009		2010		2011		2012		2013		2014		2015	
	Field (ha)	Field (%)	Field (ha)	Field (%)	Field (ha)	Field (%)	Field (ha)	Field (%)	Field (ha)	Field (%)	Field (ha)	Field (%)	Field (ha)	Field (%)	Field (ha)	Field (%)	Field (ha)	Field (%)	Field (ha)	Field (%)
Adana	443	5.7	704	6	415	1.4	183	3.9	237	7.1	222	6.1	916	8.8	875	7.6	145	4.6	402	12.5
Amasya	93	1.2	413	3.5	46	0.2	85	1.8	306	9.2	158	4.4	139	1.3	280	2.4	201	6.4	119	3.7
Ankara	314	4	80	0.7	63	0.2	65	1.4	43	1.3	165	4.6	158	1.5	177	1.5	36	1.2	15	0.5
Antalya	515	6.6	2093	17.9	17026	57.2	469	10	503	15.2	92	2.5	653	6.2	1312	11.5	234	7.5	197	6.1
Artvin	7	0.1	6	0.1	34	0.1	-	0	42	1.3	20	0.6	7	0.1	20	0.2	9	0.3	5	0.2
Balikesir	302	3.9	543	4.7	1974	6.6	328	7	64	1.9	421	11.7	658	6.3	2350	20.5	33	1.1	39	1.2
Bolu	284	3.7	80	0.7	29	0.1	12	0.3	85	2.6	83	2.3	65	0.6	77	0.7	14	0.4	51	1.6
Bursa	159	2	386	3.3	54	0.2	452	9.7	108	3.3	121	3.4	343	3.3	532	4.6	40	1.3	263	8.2
Denizli	61	0.8	369	3.2	71	0.2	88	1.9	91	2.7	116	3.2	235	2.2	122	1.1	80	2.6	34	1.1
Elazığ	104	1.3	338	2.9	859	2.9	210	4.5	235	7.1	73	2	20	0.2	53	0.5	63	2	71	2.2
Erzurum	65	0.8	28	0.2	14	0	-	0	-	0	40	1.1	66	0.6	55	0.5	9	0.3	83	2.6
Eskişehir	66	0.9	107	0.9	24	0.1	70	1.5	46	1.4	54	1.5	105	1	155	1.4	22	0.7	5	0.2
Giresun	10	0.1	33	0.3	51	0.2	11	0.2	106	3.2	27	0.7	32	0.3	91	0.8	89	2.9	74	2.3
Isparta	49	0.6	55	0.5	61	0.2	38	0.8	130	3.9	127	3.5	297	2.8	97	0.8	61	2	54	1.7
İstanbul	67	0.9	263	2.3	96	0.3	90	1.9	8	0.2	67	1.9	107	1	77	0.7	18	0.6	41	1.3
İzmir	579	7.5	963	8.3	1790	6	1603	34.3	502	15.1	733	20.3	474	4.5	862	7.5	270	8.7	153	4.8
K. Maraş	45	0.6	949	8.1	710	2.4	78	1.7	162	4.9	204	5.7	3669	35.1	1579	13.8	160	5.1	184	5.7
Kastamonu	166	2.1	311	2.7	83	0.3	26	0.6	48	1.4	40	1.1	205	2	77	0.7	46	1.5	30	0.9
Kayseri	-	0	-	0	-	0	-	0	-	0	161	4.5	51	0.5	203	1.8	69	2.2	41	1.3
Konya	132	1.7	42	0.4	17	0.1	88	1.9	106	3.2	78	2.2	85	0.8	182	1.6	49	1.6	64	2
Kütahya	574	7.4	581	5	15	0.1	25	0.5	11	0.3	14	0.4	183	1.8	72	0.6	52	1.7	6	0.2
Mersin	29	0.4	1053	9	5080	17.1	80	1.7	105	3.2	114	3.2	505	4.8	509	4.4	79	2.5	282	8.8
Muğla	3416	44	1531	13.1	665	2.2	260	5.6	160	4.8	165	4.6	242	2.3	972	8.5	724	23.2	184	5.7
Sakarya	170	2.2	321	2.8	192	0.6	358	7.7	87	2.6	106	2.9	99	0.9	117	1	28	0.9	34	1.1
Şanlıurfa	-	0	-	0	-	0	-	0	-	0	45	1.2	89	0.9	387	3.4	302	9.7	536	16.7
Trabzon	10	0.1	40	0.3	324	1.1	46	1	61	1.8	73	2	39	0.4	166	1.4	268	8.6	141	4.4
Zonguldak	101	1.3	373	3.2	56	0.2	14	0.3	71	2.1	91	2.5	1013	9.7	57	0.5	19	0.6	111	3.4
Total	7761	100	11662	100	29749	100	4679	100	3317	100	3610	100	10455	100	11456	100	3120	100	3219	100

Table 4. Numerical distribution (number) to the regional directorates of forest fires between 2006 and 2015

Regional directorates of forestry	2006		2007		2008		2009		2010		2011		2012		2013		2014		2015	
	Number	%	Number	%	Number	%	Number	%	Number	%	Number	%	Number	%	Number	%	Number	%	Number	%
Adana	105	4.7	123	4.3	107	5	83	4.6	84	4.5	88	4.5	101	4.1	173	4.6	81	3.8	176	8.2
Amasya	116	5.2	165	5.8	63	3	74	4.1	104	5.6	93	4.8	95	3.9	144	3.8	84	3.9	60	2.8
Ankara	76	3.4	95	3.4	38	1.8	84	4.7	57	3.1	73	3.7	113	4.6	233	6.2	46	2.1	43	2
Antalya	240	10.8	265	9.4	212	9.9	144	8	125	6.7	152	7.8	214	8.7	321	8.5	169	7.9	189	8.8
Artvin	5	0.2	8	0.3	8	0.4	-	0	17	0.9	5	0.3	3	0.1	7	0.2	6	0.3	5	0.2
Balıkesir	105	4.7	122	4.3	80	3.7	90	5	57	3.1	79	4	73	3	96	2.6	72	3.4	68	3.2
Bolu	57	2.6	61	2.2	45	2.1	18	1	30	1.6	32	1.6	40	1.6	57	1.5	26	1.2	24	1.1
Bursa	82	3.7	94	3.3	97	4.5	105	5.9	53	2.8	72	3.7	81	3.3	118	3.1	64	3	43	2
Denizli	128	5.7	154	5.4	90	4.2	79	4.4	72	3.9	76	3.9	68	2.8	146	3.9	47	2.2	41	1.9
Elazığ	27	1.2	56	2	77	3.6	45	2.5	47	2.5	14	0.7	4	0.2	72	1.9	79	3.7	84	3.9
Erzurum	26	1.2	8	0.3	8	0.4	2	0.1	1	0.1	7	0.4	16	0.7	21	0.6	5	0.2	17	0.8
Eskişehir	43	1.9	59	2.1	42	2	51	2.8	44	2.4	32	1.6	38	1.6	79	2.1	21	1	12	0.6
Giresun	11	0.5	19	0.7	27	1.3	9	0.5	60	3.2	16	0.8	30	1.2	40	1.1	46	2.1	43	2
Isparta	47	2.1	53	1.9	69	3.2	76	4.2	78	4.2	56	2.9	105	4.3	120	3.2	70	3.3	74	3.4
İstanbul	151	6.8	186	6.6	136	6.4	115	6.4	42	2.3	172	8.8	228	9.3	271	7.2	108	5	153	7.1
İzmir	179	8	256	9	151	7.1	183	10.2	216	11.6	197	10.1	269	11	344	9.2	284	13.2	265	12.3
K. Maraş	71	3.2	100	3.5	64	3	79	4.4	119	6.4	78	4	132	5.4	262	7	155	7.2	170	7.9
Kastamonu	97	4.4	169	6	67	3.1	39	2.2	48	2.6	63	3.2	120	4.9	146	3.9	88	4.1	57	2.7
Kayseri	-	0	-	0	-	0	-	0	-	0	54	2.8	16	0.7	69	1.8	27	1.3	26	1.2
Konya	42	1.9	37	1.3	30	1.4	36	2	51	2.7	32	1.6	50	2	91	2.4	31	1.4	29	1.3
Kütahya	46	2.1	63	2.2	48	2.2	55	3.1	34	1.8	41	2.1	54	2.2	90	2.4	55	2.6	33	1.5
Mersin	50	2.2	128	4.5	93	4.4	60	3.3	90	4.8	98	5	75	3.1	155	4.1	91	4.2	80	3.7
Muğla	326	14.6	415	14.7	348	16.3	252	14.1	309	16.6	267	13.7	383	15.6	395	10.5	320	14.9	254	11.8
Sakarya	57	2.6	80	2.8	98	4.6	74	4.1	54	2.9	58	3	56	2.3	78	2.1	33	1.5	46	2.1
Şanlıurfa	-	0	-	0	-	0	-	0	-	0	21	1.1	23	0.9	101	2.7	66	3.1	89	4.1
Trabzon	3	0.1	5	0.2	26	1.2	9	0.5	25	1.3	21	1.1	6	0.2	41	1.1	29	1.3	22	1
Zonguldak	137	6.2	108	3.8	111	5.2	30	1.7	44	2.4	57	2.9	57	2.3	85	2.3	46	2.1	47	2.2
Total	2227	100	2829	100	2135	100	1792	100	1861	100	1954	100	2450	100	3755	100	2149	100	2150	100

Table 5. Distribution of forest fire numbers to the State Forest Enterprises in the İzmir Regional Directorates between 2006 and 2015

State Forest Enterprise	2006		2007		2008		2009		2010		2011		2012		2013		2014		2015		10 years total		10-year average	
	Number	%	Number	%	Number	%	Number	%	Number	%	Number	%	Number	%	Number	%	Number	%	Number	%	Number	%	Number	%
Bayındır	24	13.4	26	10.2	15	9.9	30	16.4	13	6.2	25	13	29	10.9	24	7	18	6.3	28	10.6	232	9.9	23	9.9
Bergama	19	10.6	17	6.6	23	15.1	21	11.5	19	9	26	13.5	44	16.5	45	13	19	6.7	44	16.6	277	11.9	28	12
İzmir	53	29.6	56	21.9	33	21.7	48	26.2	71	33.8	71	36.8	54	20.3	85	24.6	85	29.9	73	27.5	629	27	63	27
Menderes		0.0		0		0		0		0		0	32	12	53	15.4	37	13	32	12.1	154	6.6	39	16.7
Akhisar	31	17.3	55	21.5	42	27.6	28	15.3	46	21.9	32	16.6	49	18.4	67	19.4	43	15.1	53	20	446	19.1	45	19.3
Demirci	12	6.7	30	11.7	8	5.3	17	9.3	16	7.6	7	3.6	15	5.6	19	5.5	22	7.7	6	2.3	152	6.5	15	6.4
Gördes	13	7.3	19	7.4	4	2.6	1	0.5	11	5.2	2	1	10	3.8	5	1.4	17	6	7	2.6	89	3.8	9	3.9
Manisa	27	15.1	53	20.7	27	17.8	38	20.8	34	16.2	30	15.5	33	12.4	47	13.6	43	15.1	22	8.3	354	15.2	35	15
Total	179	100	256	100	152	100	183	100	210	100	193	100	266	100	345	100	284	100	265	100	2333	100	233	100

Table 6. Amount of burnt area (ha) to the State Forest Enterprises in the İzmir Regional Directorates between 2006-2015

State Forest Enterprise	2006		2007		2008		2009		2010		2011		2012		2013		2014		2015		10 years total		10-year average	
	Field (ha)	%	Field (ha)	%	Field (ha)	%	Field (ha)	%	Field (ha)	%	Field (ha)	%	Field (ha)	%	Field (ha)	%	Field (ha)	%	Field (ha)	%	Field (ha)	%	Field (ha)	%
Bayındır	418	72.3	28	2.9	63	3.5	48	3	6	1.2	22	3	19	3.8	8	0.9	22	8.1	8	5.3	642	8.1	64	8
Bergama	30	5.25	130	13.5	23	1.3	12	0.7	398	80.4	148	20.3	76	15.4	22	2.6	4	1.5	15	9.9	859	10.8	86	10.8
İzmir	71	12.3	468	48.6	1513	84.5	1457	89.7	40	8.1	439	6.3	100	20.2	215	24.9	64	23.6	39	25.7	4407	55.3	441	55.4
Menderes	-	0	-	0	-	0	-	0	-	0	-	0	94	19	57	6.6	26	9.6	11	7.2	188	2.4	47	5.9
Akhisar	23	4	36	3.7	94	5.2	21	1.3	13	2.6	65	8.9	37	7.5	58	6.7	111	41	62	40.8	520	6.5	52	6.5
Demirci	18	3.1	15	1.6	31	1.7	23	1.4	17	3.4	14	1.9	40	8.1	25	2.9	20	7.4	1	0.7	205	2.6	21	2.6
Gördes	5	0.9	13	1.3	50	2.8	3	0.2	6	1.2	1	0.1	4	0.8	3	0.3	7	2.6	1	0.7	93	1.2	9	1.1
Manisa	13	2.2	273	28.3	17	0.9	60	3.7	15	3	39	5.4	125	25.3	472	54.8	18	6.6	15	9.9	1048	13.2	105	13.2
Total	578	100	963	100	1791	100	1625	100	495	100	728	100	495	100	862	100	271	100	152	100	7963	100	796	100

Turkish Forest Organization and present activities against fires

Ministry of Agriculture and Forestry of Turkey and the Turkish General Directorate of Forestry have the main responsibility over the fire prevention and forest protection. All the organizational framework is set up in accordance with the Turkish Constitution (Dated 07.11.1982, Nr.2709, Section 169) and Turkish Forest Law (Dated 08.09.1956, Nr.6831, Section 68-76) besides relevant rules and regulations. The General Directorate of Forestry contains primary departments of fire control and forest protection.

General Directorate of the Turkish Forestry has three main sections which are: Forest Protection, Control of Forest Pests and Prevention and Control of Forest Fires. Especially, the section of Prevention and Control of Forest Fires is charged to prevent forest fires by means of the Regional forest directorates, forest enterprises and forest rangers. Fire suppression activities are realized by different kind of tools, equipment, man and machine powers and also sometimes by aerial supports which can be summarized as: fire attack crews, fire personnel, fire boss, fire lookouts, power chain saws, bulldozers, tractors, lorries, water trucks, pick-ups, off-road cars, water reservoirs, UHF and FM communication radios, telescopes, different masks, fire resistant clothes, chemical retardants, planes and helicopters. Furthermore; meteorological data is taken from the weather stations. Meantime various firebreaks, fuelbreaks, fire lookout roads and telephone lines are also constructed (Mol and Kucukosmanoglu, 1998).

Discussion and conclusion

Forest fires are one of the major problems in many countries. As we know, in context of location and climate properties; during fire seasons the environmental effects of drought, low rates of relative humidity and wind occur in Mediterranean, Aegean and Marmara Regions of Turkey. Due to these reasons; as being located at Aegean Region, Izmir Regional Directorate of Forestry is also at remarkable risk. However regarding the forest protection and fire prevention, there is no doubt that much development has been achieved in Turkey. Within the results of our study, fires are mostly caused by negligence and accident, rather than natural or unknown ones among the reasons of forest fires. During the examination period (2006-2015), within the range of these causes, in respect to number value Intentional and in accordance to its field value, Negligence-Accident comes forward.

For this reason, regarding the protection of forests from fires; more emphasis should be put on to the issues of public awareness and education. Between the years 2006 and 2015, it is seen that numerical findings of Izmir, Antalya and Muğla reach the highest rates. Therefore it is possible to state that forest fires are mainly concentrated upon these three regions in Turkey. Izmir Forest Enterprise steps forward with highest values in respect to area and number, concerning with forest fires.

There are 603 forest villages in İzmir. It is emphasized that the socio-economic level of the people which are living in or near the forest, is highly below the standard of living. According to statistical data, 343.513 forest villagers live there (GDF, 2016). The average income of forest villagers is \$250 per month, mainly from forestry work and farming. Forest villagers regularly clear fields from forest land for subsistence farming. So, these villagers would like to use the forest without limitation for their survival. This brought out the forest-human activities relationship. Furthermore, this helps to explain why the three causes of forest fires are negligence, carelessness and accidents, unknown reasons, and deliberate fire setting.

Demir et al. (2019) stated that however, with the fast-growing economy in Turkey, the present situation of forest fire protection is becoming severe. The main causes are that technical forest fire protection work has failed to keep up with social development and that regulation and management systems for forest fire protection are falling behind the present state of social development. Therefore, more effective regulations and rules should be set up soon, and a strategy should be developed in Turkey to carry out timely forest fire research work so as to cope with the new challenges of forest fire hazards in the future.

Boazountas et al. (2005) stated that most of the Mediterranean region suffers from extensive forest fires, and in some cases socioeconomic factors are key determinants in wildfire causality classification. Determinants are those components within the forestry environment that help explain the intensity and spread of wildfires. The module developed here incorporates five factors representing forestry profitability, demographic pressure, social tension, forestry culture, and organizational thinking. These factors are sufficient to explain the increase or decrease of fire risk. These factors can be modelled by considering variables which describe the behaviour of the socioeconomic fire risk (local permanent population, tourists, domestic animals, houses, type and height of vegetation) and constructing transformation functions that will determine the final value of fire risk.

Ayberk et al. (2010) has similar results as our research and stated that fire is a natural element and plays an important role in the natural dynamics of the forest ecosystems. However, fire can be a very destructive force. According to the establishment of new and modern fire prevention and suppression techniques, the number of fires and burning area will be getting decreased. Adverse burning conditions will occur in the future as they have been in the past. The important measures to be taken are firstly to keep away the fire from the forests and secondly to suppress the fire immediately and effectively as it is still at the beginning stage. The sooner a fire is detected and reported, the larger the initial attack force and the quicker it arrives at the fire, the more likely the fire will be contained at a small size. This could be realized by effective protective measures and well-trained fire fighting teams using appropriate high technology and equipment.

Therefore, all relevant findings in our study indicate that Izmir Region has a sensitive status concerning the forest fires. Therefore; during the fire seasons in Izmir, it is a necessity to take all the required measures against fires. Also, fire suppression activities in Izmir should be carried out by different kind of tools, equipment, man and machine powers and aerial supports such as fire attack crews, fire personnel, off-road cars, water reservoirs, UHF and FM communication radios, fire resistant clothes, planes and helicopters, etc. Due to the fact that Izmir Regional Directorate of Forestry where the forest fires are frequently occurred has a long fire season (5-8 months), flammable material reduction and road cleaning works in forests should be performed. Izmir Regional Directorate of Forestry is one of the most dangerous forest region directorate compared to other directorates in terms of both number of fires and burnt area. For this reason, in context of forest fires all essential precautions should be taken and applied carefully.

Acknowledgements. Authors would like to thank to Turkish General Directorate of Forestry and Izmir Directorate of Forestry.

REFERENCES

- [1] Akyuz, Y. F., Kucukosmanoglu, A. (1996): Studies on fire-damaged area in Turkey for GIS Application. – XVIII ISPRS-Congress, International Society for Photogrammetry and Remote Sensing, Austria, 12-18 July, pp.45-49.
- [2] Akyuz, Y. F., Kucukosmanoglu, A. (1997): Application of GIS for fire-damaged area in Izmir. – Proceedings of the XI World Forestry Congress, Turkey, 13-22 October, Vol. 1.
- [3] Ayberk, H., Kucukosmanoglu, A., Cebeci, H. H. (2010): The structure and importance of fire suppressing organizations in Turkey. – Scientific Research and Essays 5: 456-460.
- [4] Boazountas, M., Kallidromitou, D., Kassomenos, P. A., Passas, N. (2005): Forest fire risk analysis. – Human and Ecological Risk Assessment 11(3): 617-626.
- [5] Bilgili, E., Kucuk, O. (2001): The importance of fire fuel in determination of fire sensitivity degrees. – 1st National Forestry Congress of Foresters Association of Turkey, 19-20 March, Turkey.
- [6] Demir, M., Kucukosmanoglu, A., Hasdemir, M., Ozturk, T., Acar, H. (2009): Assessment of forest roads and firebreaks in Turkey. – African Journal of Biotechnology 18: 4553-4561.
- [7] GDF (2016): Turkish General Directorate of Forestry. – <https://www.ogm.gov.tr/ekutuphane/Sayfalar/Istatistikler> Forestry Statistics.
- [8] Goltas, M., Demirel, T., Caglayan, I. (2017a): Visibility analysis of fire watchtowers using GIS. A case study in Dalaman State Forest Enterprise. – European Journal of Forest Engineering 3(2): 66-71.
- [9] Goltas, M., Kucuk, O., Ayberk, H., Akkuzu, E. (2017b): Global Climate Change and Forest Fires. – In: Fakir, H. (ed.) International Symposium on New Horizons in Forestry. Proceedings & Abstracts Book. Süleyman Demirel University, Isparta-Turkey.
- [10] Kucuk, O., Saglam, B. (2004): Forest Fires and Fire Weather. – Kastamonu University, Journal of Forestry Faculty, Kastamonu 4(2): 220-230.
- [11] Kucuk, O., Unal, S. (2011): Determination of fire sensitivity degree: a case study in Taşköprü State Forest Enterprise. – Artvin Çoruh University, Journal of Forestry Faculty 6(1): 28-34.
- [12] Kucukosmanoglu, A. (1987): Classification of the Forest Fires and the Causes of Occurrence and Spread of Large Forest Fires in Turkey. – The Publication of General Directorate of Forestry, Ankara.
- [13] MGM (2017): Turkish General Directorate of Meteorology. – <https://www.mgm.gov.tr/>.
- [14] Mol, T., Kucukosmanoglu, A. (1998): Forest fires in Turkey. – Journal of Faculty of Forestry İstanbul University 48: 53-59.
- [15] Mol, T., Kucukosmanoglu, A., Bilgili, E. (1997): Forest fires in global environment and changing attitudes toward fire. – Proceedings of the XI World Forestry Congress, Turkey, 13-22 October, Vol. 1, pp. 214-222.
- [16] Noble, I. R., Gill, A. M., Bary, G. A. V. (1980): McArthur's fire-danger meters expressed as equations. – Australian Journal of Ecology 5(2): 201-203.
- [17] Ryan, R. L. (2012): The influence of landscape preference and environmental education on public attitudes toward wildfire management in the Northeast Pine barrens (USA). – Landscape and Urban Planning 107(1): 55-68.
- [18] Uzmez, I. (2011): Forest Fire Control Activities and Their Efficiency in Turkey (A Case of Study of Izmir Forest Directorate). – Istanbul University Institute of Graduate Studies in Sciences, Istanbul.

AN OVERVIEW OF ENHANCING DROUGHT TOLERANCE IN COTTON THROUGH MANIPULATING STRESS RESISTANCE GENES

HAFEEZ, M. N.¹ – AHMAD, S.² – MAMOON-UR-RASHID, M.³ – ALI, A.^{1,4} – SALMAN, S.⁵ – BAKHSH, A.⁶ – MAHPARA, S.⁶ – KAMARAN, S.⁶ – RAMZAN, I.⁵ – WASEEM, M.⁷ – ALI, Q.^{1,8*} – RASHID, B.¹

¹*Centre of Excellence in Molecular Biology, University of the Punjab Lahore, Lahore, Pakistan*

²*Institute of Agricultural Sciences, University of the Punjab Lahore, Lahore, Pakistan*

³*Department of Entomology, Faculty of Agriculture, Gomal University, Dera Ismail Khan, Pakistan*

⁴*1-FB. Genetics, Four Brothers Group, Lahore- Pakistan*

⁵*Department of Plant Breeding and Genetics, Gomal University, Dera Ismail Khan, Pakistan*

⁶*Department of Plant Breeding and Genetics, Ghazi University, Dera Ghazi Khan, Pakistan*

⁷*Department of Agronomy, Faculty Agriculture, Lasbela University of Agriculture, Water and Marine Science, Uthal, Lasbela, Pakistan*

⁸*Institute of Molecular Biology and Biotechnology, University of Lahore, Lahore, Pakistan*

**Corresponding author
e-mail: saim1692@gmail.com*

(Received 20th Feb 2019; accepted 8th Apr 2019)

Abstract. Drought stress affects the normal growth of plant by influencing Physiological, morphological molecular and biochemical traits at cellular level. It is a polygenic trait, controlled by multiple genes, which makes its manipulation difficult by genetic engineering. It seems drought could be major threat in future to high yield of cotton in Pakistan as well around the globe because it is spontaneous and cannot be controlled with manuring and skilled agricultural practices. Gene manipulation could be a solution of this threat by producing transgenic cotton plants. As it is polygenic trait, so, understanding about cellular mechanism of drought tolerance is crucial to impart tolerance by controlling gene expression under stressed conditions. Universal Stress Proteins (USP) genes have already been identified in drought stressed leaves of *Gossypium arboreum* which make this variety of cotton a rich source of stress tolerance genes. USP genes could be manipulated for drought tolerant transgenic cotton with high yielding as well and it is most important family of proteins in this regard. This family encompasses a conserved group of proteins that has been reported in different organisms which are activating under various abiotic stress conditions. USP is also a regulatory protein; its activity can be increased by manipulating its interactions.
Keywords: *Gossypium arboreum*, polygenic traits, drought stress, universal stress proteins, transgenic

Introduction

Unfavorable environmental conditions usually inhibit the normal plant growth. There are several abiotic factors, which interrupt the bumper growth of crops, among them drought is worth to be mentioned (Farooq et al., 2009). Drought means loss of water either at elevated or normal temperature. It triggers biochemical and physiological modifications at cellular level, among them loss of turgor pressure, changes in

membrane fluidity, membrane composition, solute concentration, protein-lipid and protein-protein interactions are need to be studied. Plants respond to drought stress at physiological level as well as at molecular level. They activate diverse set of metabolic activities to defend themselves against drought stress and initiate their struggle to be survived at the onset of this extreme unfavorable condition (Fahramand et al., 2014). At genetic level, multiple genes are involved, which are responsible to initiate the defense system of plants. Hence, involvement of multiple genes makes it complex to control the drought resistivity of plants by using genetic engineering. However, different studies like transcriptomics, proteomics and expression of genes have identified the activation and regulation of several stress-related genes at cellular level. It has been observed that expression level of different genes in plants is changed under the spell of drought stress (Ribas et al., 2006).

Plants' responses against stresses are mounted and co-ordinated by two types of signaling pathways namely ABA-independent and ABA-dependent pathways. The products of these genes are classified as regulatory and functional proteins which are responsible to activate stress related pathways (Shinozaki and Yamaguchi-Shinozaki, 2007). Functional and regulatory proteins include enzymes for biosynthesis of osmolyte, water channel proteins, LEA-proteins, chaperones, detoxicating enzymes, proteinases, transcription factors, phospholipases and protein kinases. These functional and regulatory proteins are playing their role to regulate signal transduction mechanism and stress related gene expression (Sivamani et al., 2000). The interaction studies of the genes responsible for plants' biological processes are important to comprehend the mechanism of abiotic stresses in plants. Plants express a multitude of proteins containing USP domains. An analysis of different plant taxa shows that a plant contains an average of 200 different USP domain containing proteins (Maqbool et al., 2009; Isokpehi et al., 2011). Two genes have been identified in cotton which encodes USP proteins named GUSP1 and GUSP2 (Maqbool et al., 2009; Fahramand et al., 2014). These genes are up-regulated during drought stress. Studies conducted on the role of USP in tomato shows that USP activates two gene clusters. One cluster produces LHCB (light harvesting chlorophyll a and b binding proteins) and reduction in aperture of stomata aperture while second cluster produces osmo-protective compounds, i.e. proline. Furthermore, USP is also shown to interact with annexin proteins but the details about how actually the USP performs its functions are still to be elucidated (Loukehaich et al., 2012; Fahramand et al., 2014).

It has been observed that plants respond increasing osmo-protectant production, detoxification of ROS, biosynthesis of chlorophyll, increasing water uptake and stabilizing its proteins (Hayano-Kanashiro et al., 2009), all these processes are triggered by several genes. It is obvious from the previous studies that manipulation of drought responsive genes and maintenance of cellular components has remained as major target of attempts to produce plants having enhanced drought tolerance. Cotton (*Gossypium* spp.), is genetically diverse plant, it has four domesticated species. *G. arboreum* has many remarkable benefits over *G. hirsutum*, it has considerable resistance against biotic and abiotic stresses especially drought stress which makes it priceless gene pool to improve future cotton cultivars (Mehetre et al., 2003; Huang and Liu, 2006; Liu et al., 2006). Several stress proteins and soluble sugars have been reported to act as protectants during cell dehydration in many plants (Kosmas et al., 2006; Padmalatha et al., 2012). The universal stress protein (USP) is one of the most important family of protein for this purpose. USP is a cytoplasmic protein present in bacteria; its expression

is enhanced, when cellular viability is challenged by drought spell and other abiotic stresses (Sousa and McKay, 2001; Maqbool et al., 2009; Zahur et al., 2009). The USP super family encompasses a conserved and ancient group of proteins that are present in archaea, bacteria, fungi, plants and flies (Kvint et al., 2003). *E. coli* contains six USP proteins (USPa, USPb, USPc, USPd, USPe, USPf), which are sub divided into two sub-groups on the basis of their sequence similarity (Gustavsson and Nyström, 2002). It has been reported the presence of USP-genes in different organisms, where they are playing role in response to heat shock, cold shock, DNA management, metabolic control (Persson et al., 2007; Isokpehi et al., 2011; He et al., 2012; Mbah et al., 2013). Furthermore, USP is a regulatory unit protein; its activity can be increased by manipulating its interactions.

This review will cover the role of drought tolerance related gene in plants and their effect on cellular mechanism in response to drought stress (Maqbool et al., 2009; Zahur et al., 2009). A comprehensive screening of Universal Stress Protein gene-2 will enhance our basic knowledge about key metabolic pathways relating to drought and open ways for future engineering of drought stress tolerance. The functional and cellular characterization of USP genes would be investigated to ascertain its potential role in drought stress tolerance mechanism in plants especially in cotton. Understanding the mechanism of interaction of universal stress protein genes and its role in drought tolerance will enable us to breed economically important cotton varieties which are adapted to drought stress. The review will cover the major metabolic pathways in connection with drought tolerance, which will be helpful in providing direction for future metabolic engineering for drought-stress tolerance.

What is abiotic stress?

Negative influence of non living things of environment on living things in an ecosystem is called abiotic stress (Degenkolbe et al., 2009; Ali et al., 2013, 2017). The common stressors are easiest to identify, but some other are less recognizable stress factors which are affecting environment constantly (Kogan et al., 2013). Extreme temperature, drought, salinity, wildfire and sporadic floods are well known abiotic stresses in our ecosystem for plants. Hence, Scarcity of water resources, environmental pollution, salinity, intensified erosional problems are marked in the beginning of 21st century. All these offer abiotic stress to the plant growth, which is the limiting factor in crop yield around the world (Ali et al., 2014, 2016; Wang et al., 2003). Roots are first line of defense against any type of abiotic stress in plants, if soil is healthy, porous, well aerated and contain all essential nutrients then survival rate of plant is automatically increased. Furthermore, abiotic stress not only limits the crop productivity, (Jaleel et al., 2009) but also distribution of plants. Drought stress is major threat among abiotic stresses, which has drastic affects on yield and growth of plants. Drought is a metrological phenomenon which can be defined as a depletion of moisture to the economic injury level, because of prolong period of meager rain fall (Kramer, 1979).

Effects of extreme water deficiency on plant growth

Water deficiency results in loss of turgor pressure and osmotic stress in plants (Mansoor et al., 2003). The osmotic stress results in reduction of plant height, decrease in root length, yellowing of leaves because of reduction in chlorophyll content and

overall growth rate of plant is reduced. Deficiency in nutrient distribution is another negative effect of drought stress. Reduction in water uptake from the soil to roots also results in slow entry of essential minerals such as nitrate, phosphorus, calcium and potassium into plant and in turn growth rate is ultimately reduced (Zhu et al., 2000). Secondary effect of water deficiency is oxidative stress because of the accumulation of excessive ROS (Reactive Oxygen Species) like hydroxyl radicals, hydrogen peroxide and superoxide anions. Usually ROS are found to be involved in normal metabolic reactions of cells, however, when plants are growing under water deficient environment, the amount of ROS increases to protect the cells from oxidative injuries (Altaf-Khan et

al., 2002). The exogenous use of 2,2-diphenyl-1-picrylhydrazyl, 3,3'-diaminobenzidine

and methyl viologen in *Arabidopsis thaliana* indicated that there was an over accumulation of reactive oxygen species under drought and oxidative stress conditions (Nakabayashi et al., 2014). The *dry2/seqe1-5* (*Arabidopsis* drought

hypersensitive/squalene epoxidase 1-5) mutant was found to produce antioxidants as far

as the RHD2 NADPH oxidase was de-localized under drought stress conditions and

caused the formation of reactive oxygen species (Pose et al., 2009). Similarly, water deficiency results in the reduction of root and shoot length and their fresh and dry biomass, therefore roots and shoots may become thinner or thicker (Ashraf and Foolad, 2007). Studies have been revealed that water deficiency is a chief limiting aspect at initial stages of plant growth. Both cell elongation and cell division are severely affected by the drought stress (Bhatt and Rao, 2005; Koroleva et al., 2005; Shao et al., 2008). Various physiological and biochemical processes like ion uptake, respiration, photosynthesis, nutrient metabolism and translocation are severely affected by the reduction in plant growth as a result of drought stress. Similarly studies of Farooq et al. (2009) observed changes in chlorophyll a and b because of drought stress. All cash crops are affected by drought stress among them rice as a submerged crop is more susceptible to the drought stress (Jaleel et al., 2009). Another effect of water deficiency is reduction in the stem length (Specht et al., 2001). Similarly, 25% reduction in plant height was observed in water stressed citrus seedlings (Wu et al., 2008). Significant reduction in the stem length of potato plant was also reported under drought stress (Heuer and Nadler, 1998). The height of other plants like, *Petroselinum crispum* (Jaleel et al., 2007), *Abelmoschus esculentus* (Manivannan et al., 2007), and *Vigna unguiculata* (Petropoulos et al., 2008) were reported to be decreased. In short, effects of drought stress are characterized by diminished water potential, reduction of total water content, loss of turgor pressure, closing of stomata and reduction of cell division along with cell elongation.

Drought stress and cotton yield

G. arboreum is diploid and possesses several desired characteristics (resistance to diseases and insect pests and tolerance to drought and salinity), while *G. hirsutum* are lacking these characters but it has high crop yield and fiber quality. *G. arboreum* provides space to cultivate it in semiarid and arid regions with minimum farming inputs. Besides this, it is also considered a vital gene pool source because of its distinctive qualities for improvement of other cotton cultivars via genetic engineering. Cost of irrigated cotton production is increasing continuously because of ground water supplies are decreasing in Pakistan; it forces to select drought tolerant cultivars as well as other agricultural commodities. Drought stress at very early stage affected the expansion of leaves in cotton and roots are less sensitive as compared to shoot growth (Malik and Srivastava, 1979; Quisenberry et al., 1985). It was found under drought stress leaf expansion was inhibited which results in decrease in utilization of energy and carbon finally result larger portion of assimilates are translocated to plant roots. Hence, characteristics plant roots can be used as important indicator to drought stress.

The consequence of drought stress on total yield of cotton depends upon severity and timing of drought spell. Krieg (1983) reported that crop yield was decreased under drought stress because of reduction in size and number of leaves and decrease in photosynthetic activity. It has also been observed that initiation of square to first flowering stage is the most susceptible development stage affected by water deficiency. The peak flowering stage was the more susceptible to drought stress which results in heavy losses to crop yield (Golldack et al., 2014). Cotton seeds yield was also decreased because of reduction in total number of bolls per plant under drought stress (Hamada, 2000) and also affected quality of lint in several ways, particularly fiber elongation; maturity and length was reported (Krieg, 1983).

Sensitivity of cotton plant to drought stress

Cotton plant is sensitive to drought stress during boll development and flowering stage (Turner, 1981; Isokpehi et al., 2011). The pollen tube formation in cotton is extremely sensitive to drought stress (Burke et al., 1985; Kawakami et al., 2010). There are several stages of flowering and boll formation in cotton because of perennial growth pattern so, the uncertainty has exists owing to conflicting reports about the sensitive stage of development to water deficiency (Gazanchian et al., 2007). The early flowering period in cotton, according to Umbeck (1987), is sensitive to drought stress while Vereyken et al. (2001) reported that peak flowering stages is more susceptible to drought stress which results in yield reduction of cotton. The production of fructans in phospholipids initiated under drought stress condition of plant cells (Vierling and Kimpel, 1992). Cotton bolls appear to be less sensitive to drought stress than the leaves since they are significantly resistant to water loss and are considered essentially non-transpiring (Quisenberry et al., 1985; Kawakami et al., 2010). A number of researchers however, have reported that limited supply of water during boll development can result in significantly lower yields (Koroleva et al., 2005). In support of these observations, (Quisenberry et al., 1985) it was observed that if drought stress occurs during the first fourteen days after anthesis (on set of flowering), young bolls generally abscise (fall off). Chaves et al., conducted growth chamber experiments where bract and capsule wall water potential of 5-, 20-, and 30-day old bolls was monitored along with leaf water potential under a moderate and a severe drought stress regime. They reported that

mild drought stress had no effect on bract and capsule wall water potentials while leaf water potentials were significantly decreased (Chaves et al., 2009).

A similar pattern was observed under severe drought stress conditions with the exception of the dark respiration rates of the capsule wall that were significantly decreased under drought stress conditions. Bayely et al. (1992) reported that the inverted water potential gradient that was observed for the petals was also present in 20-day after anthesis (on set of flowering) bolls. Water and osmotic potential of bracts and subtending to the bolls leaves compared to the bolls. This was attributed to the xylem connections of the fruits being immature and, hence non-functional, until three weeks post anthesis (on set of flowering), and it was concluded that since the water potential gradient is directed from the fruits to the leaves, the main entrance of water in cotton bolls is through the phloem (Vierling and Kimpel, 1992).

Response of plants to drought stress

Morphological and physiological responses of plants

It is reported that drought stress has drastic affects on plant growth while influencing various biochemical, morphological and physiological reactions, like photosynthesis, fluorescence of chlorophyll, stomatal conductance, ion uptake, respiration, translocation, nutrient metabolism, promoters of growth, carbohydrates, proline and malondialdehyde (MDA) contents and cellular integrity, (Jaleel et al., 2008; Shao et al., 2008; Farooq et al., 2009; Filippou et al., 2011). Susceptibility of crops to various environmental stresses frequently changes with growth stages of plant and requirements for best possible and development growth (Specht et al., 2001). In soybean shoot length and dry biomass was decreased under drought stress (Kawakami et al., 2010). Almost 25% decrease in the length of citrus seedlings observed (Wu et al., 2008) under drought stress. In potato, shoot length of plant was considerably affected because of drought stress (Heuer and Nadler, 1998), *Vigna unguiculata* (Manivannan et al., 2007) and *Abelmoschus esculentus* (Jaleel et al., 2008). Water uptake is also observed to be reduced under deficiency of which results in the decrease of water contents and elongation of cell is also inhibited because of decrease in turgor pressure.

Leaf water potential

Water potential is a potential energy of water per unit volume relative to pure water. It means to quantify the tendency of water to move from one place to another because of osmosis, gravity and mechanical pressure. Relative water potential is useful to understand the water movement within plants. The measurement of leaf water potential is a reliable indicator of drought stress (Farooq et al., 2009; Fahramand et al., 2014). Morgan (1984) revealed in a study that plants of drought tolerant cotton variety, *G. arboreum* have more number of cells and stomata per unit of leaf relative to the plants of drought intolerant cotton variety, *G. hirsutum*. Ackerson (1981) described while comparing 7 drought resistance and drought prone varieties of cotton that drought resistant varieties have minimum leaf water potential and have ability to maintain turgor at lower relative water potential than that of drought prone cotton plants. Because of turgor maintenance, photosynthesis continues in drought tolerant plants while drought intolerant plants are failed in doing so. Photosynthesis in drought tolerant varieties

remain at maximum level because chloroplast of fully turgid leaves contain numerous starch granules and has minimum damage to thylakoid membrane structures. So, Quisenberry and McMichael (1991) used the leaf turgidity for the selection of drought tolerant cotton plants.

Relative water content (RWC)

Water content and moisture content is quantity of water contained in soil, rocks, ceramics, fruits and in different tissues of the plants. Relative water content is used in wide range of scientific and technical area. Along with other indicators relative water content can also be used for the identification of drought resistant plants. It has been observed that the older leaves of *Gossypium arboreum* have relatively low water potential than that of younger leaves. It was further found that older leaves absorb relatively less water than that of younger one which results in the higher relative water content (Knipling, 1967). Similarly, it has been reported that progressive decline in RWC is because of drought stress in plants especially in *Gossypium hirsutum* (Ferreira et al., 1979). In another experiment Assaad and Signer found a positive relationship between RWC and leaf water content. They also co-relate it with genotype of cotton plants especially desi cotton. However, when the stress is disappeared, RWC progressively recovered within 48 h (Assaad and Signer, 1992).

Cell membrane permeability

Cell membrane is a biological membrane that separates the interior of cell from outside environment. It is a selectively permeable membrane which controls the movement of ions, organic molecules and other important substances (Choffnes et al., 2001). Its basic function is to protect the cell. Various other biochemical reactions are taking place on the interior surface of the cell membrane so, its stability is imperative for all metabolic reactions of the cell. Both biotic and abiotic stresses affect the stability of cell membrane (Kramer, 1979). Cell membrane stability is influenced by age of the plant, growing season, development of stage, degree of hardening, type of tissue culture and plant species. However, it is observed injury to plasma membrane because of drought stress in maize plants is much less severe in developing leaves as compared to mature leaves (Nath et al., 2005). It was also measured an increase in the saturated fatty acid under stress (Singh et al., 2015), which alleviates the melting point of plasma membrane and in turn reduce the stress tolerance in plant. Somerville and Browse, revealed that total lipid content of leaves in the membrane of Arabidopsis plant, growing under high temperature are decreased up to 1/2 and ratio of the unsaturated to saturated fatty acid is also decreased up to 1/3 of the normal temperature. It must be noted, here, that some species cannot co-relate with the degree of lipid saturation (Somerville and Browse, 1991). It was concluded that other factors for membrane stability are also involved along with the fluctuation in temperature. The relationship between the cell membrane stability and crop yield under drought condition may vary from plant to plant (Tanou et al., 2012). For example Showler, described such kind of relationship in few plants especially in sorghum (Showler, 2002). However, before Showler, Martin et al., were failed in defining such kind of relationship in soya bean plants. In short, it can be said that the major cause of yield suppression under drought stress is still obscure and deserve further experimentation (Martin et al., 1993).

Biochemical response of plants under drought stress

Proline content

Proline is an essential amino acid, which is biosynthetically derived from the glutamate. It is a major osmoregulant in plant tissues under drought conditions. Proline is produced in larger amount as compared to the normal conditions (Alamillo et al., 1995). It is considered as a compatible solute as well as osmo-protectant, which protects the plant tissues by producing stress responsive protein comparative analysis between CIM-496 *G. hirsutum* and FDH-786-*G. arboreum* (Khedr et al., 2003) in plants of *G. arboreum*. Kumar and his coworkers revealed that when water potential becomes the amount of osmolytes which are imperative for osmoregulation, allows additional water from environment. This helps in minimizing the immediate effect of drought stress (Kumar et al., 2003). Similarly, Unyayer and his coworkers, while studying the characteristics of *Helianthus annuus* under drought condition observed a strong correlation between proline content and water deficiency (Ünyayar et al., 2004).

In another experiment the over production of proline in transgenic tobacco was reported, which resulted in increase in biomass of roots (Quisenberry et al., 1985). Similarly, Zhu and his colleagues performed experiment on transgenic rice plants, the conclusion showed that drought stress condition causes the decrease in biomass (Zhu et al., 1998). Other scientists around the world like in sorghum (Yadav et al., 2005), bell pepper (Nath et al., 2005), *Gossypium hirsutum* (Massacci et al., 2008), wheat (Hamada, 2000) and in *Catharanthus roseus* (Jaleel et al., 2009) found that amount of proline content increased under drought stress condition.

Chlorophyll content

Chlorophyll is a green pigment present in chloroplast of all green plants and tissues. It is essential for photosynthesis which has ability to absorb light energy and responsible for the carbohydrate metabolism. By measuring the chlorophyll content of a plant tissue, a reliable estimate of photosynthetic rate in green tissues of a plant can be gaged (Ackerson, 1981; Ali et al., 2017; Mahmood et al., 2017). Various studies by different scientists revealed that photosynthetic activity is decreased under drought stress. To prove this notion, Arnon and Whatley, performed experiment on *G. barbadense*, *G. arboreum*, *G. herbaceum* and *G. hirsutum*. It was also found that chlorophyll content, soluble sugar content and photosynthetic ratio is higher in *G. barbadense*, which is followed by *G. arboreum*, *G. herbaceum* and significantly by *G. hirsutum* (Arnon and Whatley, 1949). Krasichkova and his colleagues observed that rate of photosynthetic activity and chlorophyll content is higher in high yielding cotton varieties (Krasichkova et al., 1989). It is observed that total chlorophyll content in *G. arboreum* is decreased with decreasing the soil water potential (Kvint et al., 2003). Similarly, it was also found that content of the chlorophyll b is higher as compared to the chlorophyll a content in various cotton genotypes in drought condition (Burke et al., 1985). Kar and his colleagues while performing experiment on various lines of *G. hirsutum* plants; they maintained that chlorophyll b has affinity to clear weather condition. They also concluded that moisture deficit condition affects the total chlorophyll as well as proline content in *G. hirsutum* (Kar et al., 2001).

Antioxidant enzymes

Antioxidant enzymes in plant tissues, i.e. super oxide dismutase, catalases, glutathione, peroxidase and methadone reductase. An antioxidant is a molecule that inhibits the oxidation of other molecules. Oxidation is a metabolic reaction in which free radicals are produced. In turn these can start chain reactions which can damage or death to the cell. Antioxidant terminates these chain reactions by removing free radicals intermediates and inhibits other oxidation reactions (Wanner and Junttila, 1999). So, antioxidants are reducing agents. Drought stress in addition to dehydration also induces oxidative stress such as generation of active oxygen species (ROS) including super oxide radical (O^{2-}), nasent oxygen (O), hydrogen peroxide (H_2O_2), hydroxyl ion ($OH\cdot$). Their production is injurious to the cell (Nepomuceno et al., 1998). Xu and his colleagues revealed that antioxidant species cause the auto-catalytic oxidation of membrane lipids and pigments then leading to the loss of membrane semi permeability and modification in its functions. Among antioxidant species superoxide radical (O^{2-}) is regularly synthesized in a chloroplast and mitochondria (Xu et al., 2006). However, some of its quantity is also produced in micro-bodies. The quenching of super oxide radical by super oxide dismutase (SOD) results in production of hydrogen peroxide (H_2O_2). However, both O^{2-} and H_2O_2 are not toxic to the cell as $OH\cdot$ is injurious to cell, which is formed by the combination of O^{2-} and H_2O_2 in the presence of trace amount of Fe^{2+} and Fe^{3+} (Monk et al., 1989). The O^{2-} can damage chlorophyll, protein, DNA, lipid and other important micro-molecules. Thus affect the plant metabolism and limit the crop yields. Sairam and Tyagi, found that plants have, developed a series of both enzymatic and non-enzymatic detoxification systems to counteract activated oxygen species (AOS), thereby protecting the cells from oxidative damage (Sairam and Tyagi, 2004). Similarly, it was also found by Kosmidou and his colleagues that various physiological and metabolic reactions have been affected by the over expression of super oxide dismutase (SOD) (Voloudakis et al., 2002).

Molecular response of plants to drought stress

The molecular details of a plant's response against stresses are complicated. These involve receptors, transcription factors, genes, noncoding RNAs, ions, and enzymes etc. Despite of the variability the plant response against a stress condition begins with the perception of the signal by specific receptors. Plants perceive dehydration by one of the following two mechanisms (Chaves et al., 2003). Through changes in osmotic potential; the membrane protein AtHK1 (Histidine Kinase 1) senses the change in osmotic potential produced inside the cell, while EcHKT1 works in the similar for sensing changes in extracellular environment. Through changes in membrane texture; the dehydration results in interaction of cationic and anionic amphiphilic substances which changes the membrane texture which is sensed by membranes proteins like OpuA. The above mentioned proteins initiate a series of signaling events. These involve many molecular respondents. Urao and his colleagues identified three phospho-relay intermediates (ATHP1-3) and four response regulators (ATRR1 -4). These molecules are supposed to play role in post perception events; however, their function is not yet clear (Urao et al., 2000). Post perception events are shown to include phosphorylation and dephosphorylation of phosphatases and changes in cytoplasmic Calcium concentration (Luan, 1998). These events then result in activation of various signaling cascades. These relative unclear cascades divide dehydration response in to branching one that involves ABA and the other which works independent of ABA. ABA

dependent responses are major cellular responses against stress. Two enzymes of ABA biosynthesis have been shown to respond to the cellular perception of stress namely these enzymes are Zeaxanthin epoxidase (ZEP) and 9-cis-epoxycarotenoid dioxygenase (NCED) (Qin and Zeevaart, 1999; Taylor et al., 2000). Stomata closure, maintenance of root growth and restricted leaf expansion are some of the many consequences of ABA activities in different organs of the plants. ABA mediated signaling cascades that make the mentioned things to happen were reviewed (Bray, 2002). ABA independent pathways are of limited importance for stress response. Mostly these involve genes which have conserved dehydration response element (DRE) in their promoters (Luan, 1998).

Cotton responds to stresses by bringing a large number of changes in its morphology and physiology. Tracking these changes down to molecular level leads to the conclusion that the basic framework of cotton response is similar to other plants but for the large part the specific effectors used by cotton are unique to this plant. ABA mediated responses remain an important part of cotton cells' response to osmotic stress; however, osmotin is shown to be a very important downstream target of ABA in cotton. This protein has binding sites of several TFs in its promoter and has capability to interact with different proteins hence working as a hub in molecular response to osmotic stress (Wilkinson et al., 1995). Trehalose 6 phosphate synthase gene is believed to be important in stress signal transduction suggesting that Trehalose 6 phosphate has a vital role as a secondary messenger in cotton (Kosmas et al., 2006). ABA mediated responses, for the large part, work by the involvement of calcium. In stressed cotton cells calcium based activities are mostly driven by calmodulins. Owing to the importance of calmodulins cotton produce a specific heat shock protein named Heat Shock Protein Calmodulin Binding (HSPCB). This protein has the duty to bind with calmodulin and keep it active so that it is able to play its role efficiently (Voloudakis et al., 2002).

Contribution of genetic engineering to drought tolerance

Drought tolerant genes have been identified while investigating the molecular mechanisms of plants response to drought stress. These genes were isolated and characterized by transferring them into drought prone plant species. This approach in some cases has been found successful to increase agronomic performance and crop yield. A good example of this success story is transgenic wheat expressing HVA1 gene from barley, encoding late embryogenesis abundant (LEA) proteins. Results showed that the HVA1 protein confers a significant protection from drought stress (Bahieldin et al., 2015). Aquaporins mediate symplastic water transportation in plants could be a limiting factor for growth under unfavorable environmental conditions. Differential expression of these genes during plant development that encode for aquaporins has been observed to be associated with various physiological processes. Such processes include opening and closing of stomata, cell elongation, cell division and organ movement (Berriman et al., 2009). The SITIP-2 gene coding aquaporin protein was found predominantly effective to improve drought stress tolerance in tomato plants (Hajheidari et al., 2005). Another successful gene is OsNAC10, introduced in rice plants under the control of GOS2 constitutive promoter and RCc3 root-specific promoter (Tang and Page, 2013).

Gene cloning and expression

Gene cloning and expression makes it possible to transfer biological properties from one organism to another. This exciting field of research owes its spectacular development to emergence of tools for DNA manipulation, enhancements and extensions in the existing knowledge, novel ways that investigators are using to apply the available technologies and finally the rapid pace with which research is being carried out in this field. The idea of transferring a gene between organisms was first conceived and materialized in the decade of 1970. Phages have the ability to transfer portions of DNA between bacteria through generalized or specialized transduction mechanisms. It was reported in early 1970s that some linear phage DNAs contain sticky ends on their terminals and that in some abnormal conditions a linear phage DNA may be separated into two or more pieces while retaining the sticky in their original positions. In their first effort to attach two DNA fragments investigators used TdT, an enzyme which adds poly A or poly T tails to 3' blunt ends, and DNA ligase. A small part of bacterial DNA was isolated and it was treated with TdT similarly two fragments of phage DNA were treated with complementary TdT and finally these three fragments were ligated with DNA ligase. This experiment resulted in the creation of a circular phage DNA containing a bacterial DNA fragment in it. The hence produced circular phage DNA was found to be the target of restriction enzyme EcoRI which was observed to cut this circular DNA on one place and make it linear. In final step this EcoRI cut linear phage DNA was ligated with a similarly prepared phage DNA containing antibiotic resistance gene (Berg and Mertz, 2010).

Universal stress protein (USP)

A protein that contains a USP domain (a characteristic USP structure) is referred to as a universal stress protein (USP). A USP may contain one or more USP domains a fact that allows USPs to perform a board range of functions (Isokpehi et al., 2011). USP gene was first discovered in bacteria via 2D gel electrophoresis and was named as C-13.5 based on its migration during 2D experiment. Later studies recognized these proteins as part of all stress and starvation stimulus known at that time and thus these were renamed as Universal Stress Proteins (Kvint et al., 2003). USP genes are involved in wide range of metabolic activities. These have been described to play role in bacterial virulence, heat shock, cold shock, DNA management and metabolic control (Persson et al., 2007; Loukehaich et al., 2012). In most cases the mechanisms of functions performed by USPs are still undiscovered but for a few functions some information is gathered about the mechanisms. When a plant is subjected to water stress, ABA level is increased which resulted in expression of USP genes. This is consistent with the finding that USPs can bind with transcription factors (Gury et al., 2009). One of the two activated gene clusters produces LHCB (Light Harvesting Chlorophyll a/b Binding) proteins. LHCB keeps the chloroplasts intact and reduces the stomatal aperture to preserve water during water stress. The second gene cluster produces some osmo-protective solutes, e.g. proline which protects the cells from harmful effects of ROSs (Loukehaich et al., 2012). In water stress USP is believed to interact with Annexin protein but the details about how actually the USP performs its functions are still to be elucidated.

E coli responds to salt stress by producing an ion transporter called (KdpFABC) which transports the extra salt ions out of the bacterial cell. The production of this

transporter comes after induction of its gene with a complex of KdpD and KdpE. This complex is only formed when KdpE is phosphorylated. In excess ions KdpE phosphorylation is inhibited. Here USP comes to play its part such as USP phosphorylates the KdpE and then hold it with KdpD forming the complex which induces the production of KdpFABC (Heermann et al., 2009). Another similar mechanism is also described in *Halomonas elongate*. Here the USP instead of inducing the expression of transporter binds itself with the transporter named TeaABC making it active. The study on *H. elongate* TeaABC and USP interaction stresses on the assertion that ATP binding USP does not play any role in transcription regulation (Huang et al., 2012). Owing to their importance several studies have been conducted to find out the structure of USPs. These investigations reveal that the structure of USP remains similar in different organisms. A USP contains an ATP binding motif at its N-terminal while the C-terminal region takes different forms depending upon the context of the protein. In many proteins the C-terminal region also binds with an ATP molecule making USP capable of binding with two ATPs at a time (Gonzali et al., 2015). The N-terminal ATP binding motif in various USPs have high % of glycine amino acids which allow USP-proteins to attach with ATP molecules (Drumm et al., 2009).

Plant transformation

Conventional breeding methods were slow and laborious; to beat these limitations plant transformation methods were developed for the production of genetically engineered plants. Through transformation gene of interest can be introduced into plants without altering their vital characters. Plant transformation method is the set of events used to introduce a fragment of DNA, having specific trait, into host plant. By utilizing this method plants are engineered to produce new varieties with desirable traits. It can be achieved either by *Agrobacterium tumefaciens*-mediated transformation or by gold particle bombardment. In the first method plant cells are infected with pathogenic *Agrobacterium tumefaciens* bacterium possessing the desired gene. In the later procedure gene gun is used for the gene coded bombardment of particles. Both of these methods are extensively used in research applications (Somerville and Browse, 1991; Tinland, 1996; Tzfira et al., 2004).

Agrobacterium-mediated transformation

Agrobacterium tumefaciens-mediated transformation is leading technology used for production of transgenic plants. The genus *Agrobacterium* has been classified into various species because of its disease symptomology and host range (Otten et al., 1984). *A. tumefaciens*, naturally present in soil, it penetrates in plants at wound sites and initiates the formation of tumor, disease commonly known as crown gall (Smith and Townsend, 1907). The crown gall disease has been observed because of the transfer of T-DNA (transfer DNA) from tumor-inducing (Ti) plasmid from *A. tumefaciens* to plant cells (Zaenen et al., 1974) and integrated into plant genome (Chilton and Que, 2003). Two genetic elements are required for transfer of T DNA to plants. The first element is 25 bp direct repeats defining and flanking region of T-DNA border sequence (Zambryski et al., 1983). The second element virulence genes (*vir*) encoded by the Ti-Plasmid in a region present outside of the T-DNA region. The *vir* genes encode a set of proteins responsible for the excision, transfer and integration of the T-DNA into the plant genome. In plant transformation, use of T-DNA process is because of three facts.

Firstly, the tumor is formed that resulted from integration of T-DNA and its subsequent expression Secondly, the T-DNA genes do not play role during their transfer process, they are only transcribed inside plant cells. Thirdly, any gene of interest placed between T-DNA borders can be transferred to plant cell.

Cellular localization of gene expression

Eukaryotic cell organelles are membrane bounded there for various cellular activities are restricted to specific well defined organelle inside the cell. These cell organelles have been studied via cell fractionation method and by analyzing samples of fixed tissues. Information about localization of sub-cellular protein is first footstep towards understanding its function (Kokkiralala et al., 2010) and this process direct the retention and transportation of protein complexes into tissue specific location. It is imperative to understand complex metabolic processes in various plant tissues such as fruits, roots stem and leaves. To study the metabolism in abundant plant tissues is comparatively easy, because the whole tissue can be used as the sample while, less abundant plant tissues are difficult to be used as sample because their basic metabolic reactions are masked by more abundant plant tissues (Carrigan et al., 2011). It is also difficult in case of plants to understand the specific function of single protein due to the presence of multi gene families. So, it is imperative to compare among different patterns of multi gene families at sub-cellular level (Hanson and Köhler, 2001).

The cellular location of different regulatory proteins and enzymes in plant cells during different stages of development, under diverse environmental circumstances is indicated its functional pathway. Mostly, prediction models of bioinformatics are used for location of different proteins. Moreover, localization of several plant proteins has been found at numerous cellular regions (Small et al., 1998). Green fluorescent protein is green light emitting protein, when it is excited with lower wavelength light. Light emitting proteins also know as fluorescent proteins (FPs), they are classified as brand range family of fluorescent proteins and GFP-proteins belong to this family. Now GFPs are being used in various applications of molecular biology (Zhang et al., 2002). Common use of fluorescent protein has one main advantage of its normal light emitting process with involvement of any enzyme or substrate (Ei-Shemy et al., 2009).

Green fluorescent proteins (GFPs)

Green fluorescent protein is a green light emitting protein, when it is excited with lower wavelength light. Now GFPs are being used in various applications of molecular biology (Zhang et al., 2002). Common use of fluorescent protein has one main advantage of its normal light emitting process with involvement of any enzyme or substrate (Ei-Shemy et al., 2009). The 238 amino acids long GFP has a tightly closed structure which is found to be conserved in all different types of FPs characterized so far. Truncation studies show that about 7 amino acids from C- terminal and only the first methionine from N-terminal can be removed without abolishing the GFP function. This signifies that most of the structure of GFP is important for development and maintenance of fluorescence. GFPs (like all FPs) consist of 11 beta sheets, small alpha helices and some irregular peptides. The beta sheets come together and form a rigid structure which is known as "Beta Barrel". The beta sheets in a barrel are connected with each other through small helices and flexible proline rich peptides. In addition an

alpha helix is present in the center of the beta barrel. This helix contains a highly conserved sequence of three amino acids which come together and form the structure which is responsible for the production of fluorescence (Khedr et al., 2003). The structure thus formed is termed as chromophore (sometimes as fluorophore). The location of chromophore in GFP is very important for its function. The beta barrel has polar amino acids branching out towards the chromophore and hold water molecules hence producing an environment for chromophore to exhibit fluorescence. In addition the barrel also protects the chromophore from the outside environment (Zhang et al., 2002; Foolad, 2004). The native GFP which was isolated from *Aequorea Victoria* is found to be of just a little usage. Research carried out on GFP resulted in modification of native GFP to produce a broad range of derivatives which can be used more readily in the molecular biology applications. These new derivatives of GFP have some properties to make them suitable. The modifications introduced in GFPs along with the resultant properties can be categorized into following categories:

The modification made in the chromophore sequence result in the production of different coloured GFP derivatives. Such changes in the sequence produce different energy states of chromophore as compare to the native, which are capable of emitting light of different wavelengths (producing colours other than green). By using same mechanism, the chromophore modifications can also alter the excitation wavelength of the native GFP hence producing derivatives which absorb different wavelengths while producing same colour (Foolad, 2004). This kind of shift is especially helpful in fine tuning the GFP for the fluorescence detection system present in place. In addition, change in chromophore sequence also is shown to be associated with increased emission of a particular wavelength, i.e. increased luminescence (Berriman et al., 2009).

Site directed mutagenesis

Point mutation or site directed mutagenesis has been used to ascertain the function of unknown gene; this technique causes alteration at specific point in the sequence of a gene. This is also known as oligonucleotide directed mutagenesis. Point mutations can be randomly inserted in the whole sequence of gene at multiple locations or it can be specifically integrated at predetermined location by site directed mutagenesis (Sturm, 2009). It can be carried out both in-vivo and in-vitro. Model organisms are used in case of in-vivo while plasmid constructs are used in case of later. To ascertain the importance of amino acids and their function in protein structure, site directed mutagenesis has been used extensively (Kunkel et al., 1991; Ishii et al., 1998). It can be utilized to study protein function and structural relationship, protein binding sites, active sites present in enzymes, gene characterization and protein-protein interaction.

To alter the sequence of gene of interest, synthetic oligonucleotides are extensively used in research. Numerous protocols have been used and for this purpose while PCR-mediated site directed mutagenesis was found efficient most common method (Saiki et al., 1985). For this purpose two complementary mutagenic primers (40 bp long) with mutated nucleotide in its center are designed by using online software (Zhang et al., 2015). Laible and Boonrod carried out site directed mutagenesis of whole plasmid by using non-PCR thermo cycling reaction. This technique was used to produce mutated enzyme to wipe out its enzymatic activity to utilize as experimental model (Laible and Boonrod, 2009). Dipetarudin protease is potent inhibitor of thrombin it inhibits the

normal function of trypsin and plasmin (Lopez-Molina et al., 2002). When single amino

acid (Arginine-10) was replaced by histidine then mutant form, dipetarud in R10H, had lost its activity to inhibit plasmin and trypsin as compared to wild type. In the beginning, artificial oligonucleotides were being used for the rectification of site directed mutagenesis in β -globin gene which causes sickle cell anemia (Saiki et al., 1985). Rectification of sickle cell anemia was a turning point in commercializing this technology (Saiki et al., 1985; Zhang et al., 1995; Beetham et al., 1999; Zhu et al., 2000).

Initially, site directed mutagenesis was used in tobacco and corn, model species. Point mutation in acetohydroxy acid synthase I and III genes, at specific sites made them resistant against herbicide both in corn and tobacco (Zhang et al., 2015). Endo and his colleagues mutated acetolactate Synthase (ALS) gene of rice at specific point by using site directed mutagenesis and developed resistance against bispyribac herbicide. They reported that change in two amino acids separately in two different clones causes tolerance in bispyribac herbicide. These two amino acids are Serine and Tryptophan which replaced with Isoleucine and Leucine respectively (Endo et al., 2007). However, if both amino acids will change at a time then it confers bispyribac herbicide resistance to plant. This technique has broad range of applications because it can create several mutations, insertions and deletions. This can also be used for the characterization of unknown genes responsible for fatal diseases. Now commercial kits are easily available which makes it faster, reliable and efficient (Carrigan et al., 2011). This technique has been utilized for the customization of various crops for introduction of desired traits and for increase per capita yield.

Conclusion

In view of above discussion it can be concluded that drought stress affects morphological, physiological, biochemical and molecular traits of cotton plants which became the major cause of yield reduction. Drought stress is an important threat among abiotic stresses, which has drastic effects on normal growth of plants. It is considered as a major reason for low productivity of cotton in Pakistan and the situation could worsen in the future because of depleting irrigation capacity. Drought stress is natural and spontaneous; it cannot be controlled with either synthetic chemicals or skilled agricultural practices. Modern view about control of drought stress is the production of transgenic crops having tolerance towards drought stress. Drought tolerance mechanism is controlled by multiple genes, so, manipulation of one or two drought stress related genes could not be much effective. It is a need of the hour to understand the cellular mechanism of drought tolerance for future engineering of tolerant plants. USP genes have been identified in one variety of cotton which could be manipulated for drought tolerant transgenic cotton plants with high yielding as well. Several soluble sugars and stress proteins have been reported to act as protectants under drought stress and universal stress protein (USP) is the most important family of proteins in this regard. This family encompasses a conserved and ancient group of proteins that are present and has been reported in different organisms including cotton, where they are playing a role in response to heat

shock, cold shock, DNA management, metabolic control. Furthermore, USP is a regulatory unit protein; its activity can be increased by manipulating its interactions.

Author contribution statement. MNH wrote the initial draft of manuscript. MNH and QA edited the manuscript and made minor corrections. QA made final editing and corrections in manuscript to make it in its final version to be published. All of the authors have proof-read the manuscript before submission. The final approval for publication was given by BR.

Conflict of interests. The authors declared that there is no conflict of interests for the manuscript.

REFERENCES

- [1] Ackerson, R. C. (1981): Osmoregulation in cotton in response to water stress ii. Leaf carbohydrate status in relation to osmotic adjustment. – *Plant Physiology* 67(3): 489-493.
- [2] Alamillo, J., Almoquera, C., Bartels, D., Jordano, J. (1995): Constitutive expression of small heat shock proteins in vegetative tissues of the resurrection plant *craterostigma plantagineum*. – *Plant Molecular Biology* 29(5): 1093-1099.
- [3] Ali, F., Ahsan, M., Ali, Q., Kanwal, N. (2017): Phenotypic stability of zea mays grain yield and its attributing traits under drought stress. – *Frontiers in Plant Science* 8: 1397.
- [4] Ali, Q., Ahsan, M., Ali, F., Aslam, M., Khan, N. H., Munzoor, M., Mustafa, H. S. B., Muhammad, S. (2013): Heritability, heterosis and heterobeltiosis studies for morphological traits of maize (*Zea mays* L.) seedlings. – *Advancements in Life Sciences* 1(1) 52-63.
- [5] Ali, Q., Ali, A., Ahsan, M., Ali, S., Khan, N. H., Muhammad, S., Abbas, H. G., Nasir, I. A., Husnain, T. (2014): Line × Tester analysis for morpho-physiological traits of *Zea mays* L. seedlings. – *Advancements in Life Sciences* 1(4): 242-253.
- [6] Ali, Q., Ahsan, M., Malook, S., Kanwal, N., Ali, F., Ali, A., Ahmed, W., Ishfaq, M., Saleem, M. (2016): Screening for drought tolerance: comparison of maize hybrids under water deficit condition. – *Advancements in Life Sciences* 3(2): 51-58.
- [7] Altaf-Khan, M., Myers, G., Stewart, J. (2002): Molecular Markers, Genomics and Cotton Improvement. – In: Kang, M. S. (ed.) *Crop Improvement Challenges in the Twenty First Century*. CRC, Boca Raton, FL, pp. 253-284.
- [8] Arnon, D. I., Whatley, F. (1949): Is chloride a coenzyme of photosynthesis? – *Science* 110(2865): 554-556.
- [9] Ashraf, M., Foolad, M. (2007): Roles of glycine betaine and proline in improving plant abiotic stress resistance. – *Environmental and Experimental Botany* 59(2): 206-216.
- [10] Assaad, F. F., Signer, E. R. (1992): Somatic and germinal recombination of a direct repeat in arabidopsis. – *Genetics* 132(2): 553-566.
- [11] Bahieldin, A., Atef, A., Shokry, A. M., Al-Karim, S., Al, S. G. Attas, Gadallah, N. O., Edris, S., Al-Kordy, M. A., Omer, A. M. S., Sabir, J. S. (2015): Structural identification of putative usps in catharanthus roseus. – *Comptes Rendus Biologies* 338(10): 643-649.
- [12] Bayley, C., Trolinder, N., Ray, C., Morgan, M., Quisenberry, J., Ow, D. (1992): Engineering 2, 4-d resistance into cotton. – *Theoretical and Applied Genetics* 83(5): 645-649.
- [13] Beetham, P. R., Kipp, P. B., Sawycky, X. L., Arntzen, C. J., May, G. D. (1999): A tool for functional plant genomics: Chimeric rna/DNA oligonucleotides cause in vivo gene-specific mutations. – *Proceedings of the National Academy of Sciences* 96(15): 8774-8778.
- [14] Berg, P., Mertz, J. E. (2010): Personal reflections on the origins and emergence of recombinant DNA technology. – *Genetics* 184(1): 9-17.

- [15] Berriman, M., Haas, B. J., LoVerde, P. T., Wilson, R. A., Dillon, G. P., Cerqueira, G. C., Mashiyama, S. T., Al-Lazikani, B., Andrade, L. F., Ashton, P. D. (2009): The genome of the blood fluke schistosoma mansoni. – *Nature* 460(7253): 352-358.
- [16] Bhatt, R., Rao, N. S. (2005): Influence of pod load on response of okra to water stress. – *Indian Journal of Plant Physiology* 10(1): 54.
- [17] Bray, E. (2002): Abscisic acid regulation of gene expression during water deficit stress in the era of the arabidopsis genome. – *Plant, Cell and Environment* 25(2): 153-161.
- [18] Burke, J. J., Hatfield, J. L., Klein, R. R., Mullet, J. E. (1985): Accumulation of heat shock proteins in field-grown cotton. – *Plant Physiology* 78(2): 394-398.
- [19] Carrigan, P. E., Ballar, P., Tuzmen, S. (2011): Site-directed mutagenesis. – *Disease Gene Identification: Methods and Protocols*: 107-124.
- [20] Chaves, M. M., Maroco, J. P., Pereira, J. S. (2003): Understanding plant responses to drought—from genes to the whole plant. – *Functional Plant Biology* 30(3): 239-264.
- [21] Chaves, M. M., Flexas, J., Pinheiro, C. (2009): Photosynthesis under drought and salt stress: Regulation mechanisms from whole plant to cell. – *Annals of Botany* 103(4): 551-560.
- [22] Chilton, M.-D. M., Que, Q. (2003): Targeted integration of t-DNA into the tobacco genome at double-stranded breaks: New insights on the mechanism of t-DNA integration. – *Plant Physiology* 133(3): 956-965.
- [23] Choffnes, D., Philip, R., Vodkin, L. (2001): A transgenic locus in soybean exhibits a high level of recombination. – *In Vitro Cellular & Developmental Biology-Plant* 37(6): 756-762.
- [24] Degenkolbe, T., Do, P. T., Zuther, E., Repsilber, D., Walther, D., Hinch, D. K., Köhl, K. I. (2009): Expression profiling of rice cultivars differing in their tolerance to long-term drought stress. – *Plant Molecular Biology* 69(1-2): 133-153.
- [25] Drumm, J. E., Mi, K., Bilder, P., Sun, M., Lim, J., Bielefeldt-Ohmann, H., Basaraba, R., So, M., Zhu, G., Tufariello, J. M. (2009): Mycobacterium tuberculosis universal stress protein rv2623 regulates bacillary growth by atp-binding: Requirement for establishing chronic persistent infection. – *PLoS Pathogens* 5(5): e1000460.
- [26] Ei-Shemy, H. A., Khalafalla, M. M., Ishimoto, M. (2009): The role of green fluorescent protein (gfp) in transgenic plants to reduce gene silencing phenomena. – *Current Issues in Molecular Biology* 11(1): I21.
- [27] Endo, M., Osakabe, K., Ono, K., Handa, H., Shimizu, T., Toki, S. (2007): Molecular breeding of a novel herbicide-tolerant rice by gene targeting. – *The Plant Journal* 52(1): 157-166.
- [28] Fahramand, M., Mahmood, M., Keykha, A., Noori, M., Rigi, K. (2014): Influence of abiotic stress on proline, photosynthetic enzymes and growth. – *Int Res J Appl Basic Sci* 8(3): 257-265.
- [29] Farooq, M., Wahid, A., Kobayashi, N., Fujita, D., Basra, S. (2009): Plant drought stress: Effects, mechanisms and management. – *Agronomy for Sustainable Development* 29(1): 185-212.
- [30] Ferreira, L. G., De Souza, J. G., Prisco, J. T. (1979): Effects of water deficit on proline accumulation and growth of two cotton genotypes of different drought resistances. – *Zeitschrift für Pflanzenphysiologie* 93(3): 189-199.
- [31] Filippou, P., Antoniou, C., Fotopoulos, V. (2011): Effect of drought and rewatering on the cellular status and antioxidant response of Medicago truncatula plants. – *Plant Signaling & Behavior* 6(2): 270-277.
- [32] Foolad, M. (2004): Recent advances in genetics of salt tolerance in tomato. – *Plant Cell, Tissue and Organ Culture* 76(2): 101-119.
- [33] Gazanchian, A., Hajheidari, M., Sima, N. K., Salekdeh, G. H. (2007): Proteome response of elymus elongatum to severe water stress and recovery. – *Journal of Experimental Botany* 58(2): 291-300.

- [34] Gollmack, D., Li, C., Mohan, H., Probst, N. (2014): Tolerance to drought and salt stress in plants: Unraveling the signaling networks. – *Frontiers in Plant Science* 5.
- [35] Gonzali, S., Loreti, E., Cardarelli, F., Novi, G., Parlanti, S., Pucciariello, C., Bassolino, L., Banti, V., Licausi, F., Perata, P. (2015): Universal stress protein hrul1 mediates ros homeostasis under anoxia. – *Nature Plants* 1: 15151.
- [36] Gury, J., Seraut, H., Tran, N. P., Barthelmebs, L., Weidmann, S., Gervais, P., Cavin, J.-F. (2009): Inactivation of *padr*, the repressor of the phenolic acid stress response, by molecular interaction with *usp1*, a universal stress protein from *lactobacillus plantarum*, in *escherichia coli*. – *Applied and Environmental Microbiology* 75(16): 5273-5283.
- [37] Gustavsson, N., Nyström, T. (2002): The universal stress protein paralogues of *escherichia coli* are co-ordinately regulated and co-operate in the defence against DNA damage. – *Molecular Microbiology* 43(1): 107-117.
- [38] Hajheidari, M., Abdollahian-Noghabi, M., Askari, H., Heidari, M., Sadeghian, S. Y., Ober, E. S., Salekdeh, G. H. (2005): Proteome analysis of sugar beet leaves under drought stress. – *Proteomics* 5(4): 950-960.
- [39] Hamada, A. (2000): Amelioration of drought stress by ascorbic acid, thiamin or aspirin in wheat plants. – *Indian Journal of Plant Physiology* 5(4): 358-364.
- [40] Hanson, M. R., Köhler, R. H. (2001): Gfp imaging: Methodology and application to investigate cellular compartmentation in plants. – *Journal of Experimental Botany* 52(356): 529-539.
- [41] Hayano-Kanashiro, C., Calderón-Vázquez, C., Ibarra-Laclette, E., Herrera-Estrella, L., Simpson, J. (2009): Analysis of gene expression and physiological responses in three mexican maize landraces under drought stress and recovery irrigation. – *PLoS One* 4(10): e7531.
- [42] He, R., Kim, M.-J., Nelson, W., Balbuena, T. S., Kim, R., Kramer, R., Crow, J. A., May, G. D., Thelen, J. J., Soderlund, C. A. (2012): Next-generation sequencing-based transcriptomic and proteomic analysis of the common reed, *phragmites australis* (poaceae), reveals genes involved in invasiveness and rhizome specificity. – *American Journal of Botany* 99(2): 232-247.
- [43] Heermann, R., Weber, A., Mayer, B., Ott, M., Hauser, E., Gabriel, G., Pirch, T., Jung, K. (2009): The universal stress protein *uspC* scaffolds the *kdpD/kdpE* signaling cascade of *escherichia coli* under salt stress. – *Journal of Molecular Biology* 386(1): 134-148.
- [44] Heuer, B., Nadler, A. (1998): Physiological response of potato plants to soil salinity and water deficit. – *Plant Science* 137(1): 43-51.
- [45] Huang, B., Liu, J.-Y. (2006): A cotton dehydration responsive element binding protein functions as a transcriptional repressor of *dre*-mediated gene expression. – *Biochemical and Biophysical Research Communications* 343(4): 1023-1031.
- [46] Huang, G.-T., Ma, S.-L., Bai, L.-P., Zhang, L., Ma, H., Jia, P., Liu, J., Zhong, M., Guo, Z.-F. (2012): Signal transduction during cold, salt, and drought stresses in plants. – *Molecular Biology Reports* 39(2): 969-987.
- [47] Ishii, T. M., Zerr, P., Xia, X.-M., Bond, C. T., Maylie, J., Adelman, J. P. (1998): Site-directed mutagenesis. – *Methods in Enzymology* 293: 53-71.
- [48] Isokpehi, R. D., Mahmud, O., Mbah, A. N., Simmons, S. S., Avelar, L., Rajnarayanan, R. V., Udensi, U. K., Ayensu, W. K., Cohly, H. H., Brown, S. D. (2011): Developmental regulation of genes encoding universal stress proteins in *Schistosoma mansoni*. – *Gene Regulation and Systems Biology* 5: 61.
- [49] Jaleel, C. A., Manivannan, P., Sankar, B., Kishorekumar, A., Gopi, R., Somasundaram, R., Panneerselvam, R. (2007): Water deficit stress mitigation by calcium chloride in *catharanthus roseus*: Effects on oxidative stress, proline metabolism and indole alkaloid accumulation. – *Colloids and Surfaces B: Biointerfaces* 60(1): 110-116.
- [50] Jaleel, C. A., Sankar, B., Murali, P., Gomathinayagam, M., Lakshmanan, G., Panneerselvam, R. (2008): Water deficit stress effects on reactive oxygen metabolism in

- Catharanthus roseus*; impacts on ajmalicine accumulation. – *Colloids and Surfaces B: Biointerfaces* 62(1): 105-111.
- [51] Jaleel, C. A., Manivannan, P., Wahid, A., Farooq, M., Al-Juburi, H. J., Somasundaram, R., Panneerselvam, R. (2009): Drought stress in plants: a review on morphological characteristics and pigments composition. – *Int J Agric Biol* 11(1): 100-105.
- [52] Kar, M., Patro, B., Sahoo, C., Patel, S. (2001): Response of hybrid cotton to moisture stress. – *Indian Journal of Plant Physiology* 6(4): 427-430.
- [53] Kawakami, E. M., Oosterhuis, D. M., Snider, J. L. (2010): Physiological effects of 1-methylcyclopropene on well-watered and water-stressed cotton plants. – *Journal of Plant Growth Regulation* 29(3): 280-288.
- [54] Khedr, A. A. H., M. A. Abbas, Wahid, A. A. A., Quick, W. P., Abogadallah, G. M. (2003): Proline induces the expression of salt stress-responsive proteins and may improve the adaptation of *pancratium maritimum* L. To salt stress. – *Journal of Experimental Botany* 54(392): 2553-2562.
- [55] Knipling, E. B. (1967): Effect of leaf aging on water deficit—water potential relationships of dogwood leaves growing in two environments. – *Physiologia Plantarum* 20(1): 65-72.
- [56] Kogan, F., Adamenko, T., Guo, W. (2013): Global and regional drought dynamics in the climate warming era. – *Remote Sensing Letters* 4(4): 364-372.
- [57] Kokkiralala, V. R., Yonggang, P., Abbagani, S., Zhu, Z., Umate, P. (2010): Subcellular localization of proteins of *Oryza sativa* L. In the model tobacco and tomato plants. – *Plant Signaling and Behavior* 5(11): 1336-1341.
- [58] Koroleva, O. A., Tomlinson, M. L., Leader, D., Shaw, P., Doonan, J. H. (2005): High-throughput protein localization in arabidopsis using agrobacterium-mediated transient expression of GFP-ORF fusions. – *The Plant Journal* 41(1): 162-174.
- [59] Kosmas, S. A., Argyrokastritis, A., Loukas, M. G., Eliopoulos, E., Tsakas, S., Kaltsikes, P. J. (2006): Isolation and characterization of drought-related trehalose 6-phosphate-synthase gene from cultivated cotton (*Gossypium hirsutum* L.). – *Planta* 223(2): 329-339.
- [60] Kramer, P. J. K. (1979): *Physiology of Woody Plants*. – Academic Press, New York.
- [61] Krasichkova, G., Asoeva, L., Giller, Y., Singinov, B. (1989): Photosynthetic system of *g. Barbadanse* at the early stages of development. – *Doklady Vsesovuznoi Ordena Trudovogo Krasnogo Znameni Akademii Sel Skokhozya Istvennykh Nauk Imen VI Lemina* 12: 9-11.
- [62] Krieg, D. R. (1983): Photosynthetic activity during stress. – *Agricultural Water Management* 7(1-3): 249-263.
- [63] Kumar, S. G., Reddy, A. M., Sudhakar, C. (2003): NaCl effects on proline metabolism in two high yielding genotypes of mulberry (*Morus alba* L.) with contrasting salt tolerance. – *Plant Science* 165(6): 1245-1251.
- [64] Kunkel, T. A., Bebenek, K., McClary, J. (1991): Efficient site-directed mutagenesis using uracil-containing DNA. – *Methods in Enzymology* 204: 125-139.
- [65] Kvint, K., Nachin, L., Diez, A., Nyström, T. (2003): The bacterial universal stress protein: Function and regulation. – *Current Opinion in Microbiology* 6(2): 140-145.
- [66] Laible, M., Boonrod, K. (2009): Homemade site directed mutagenesis of whole plasmids. – *Journal of Visualized Experiments: JoVE*(27).
- [67] Liu, D., Guo, X., Lin, Z., Nie, Y., Zhang, X. (2006): Genetic diversity of asian cotton (*Gossypium arboreum* L.) in china evaluated by microsatellite analysis. – *Genetic Resources and Crop Evolution* 53(6): 1145-1152.
- [68] Lopez-Molina, L., Mongrand, S., McLachlin, D. T., Chait, B. T., Chua, N. H. (2002): *Abi5* acts downstream of *abi3* to execute an *aba*-dependent growth arrest during germination. – *The Plant Journal* 32(3): 317-328.
- [69] Loukehaich, R., Wang, T., Ouyang, B., Ziaf, K., Li, H., Zhang, J., Lu, Y., Ye, Z. (2012): Spusp, an annexin-interacting universal stress protein, enhances drought tolerance in tomato. – *Journal of Experimental Botany* 63(15): 5593-5606.

- [70] Luan, S. (1998): Protein phosphatases and signaling cascades in higher plants. – *Trends in Plant Science* 3(7): 271-275.
- [71] Mahmood, A., Haider, M. S., Ali, Q., Nasir, I. A. (2017): Multivariate analysis to assess abscisic acid content association with different physiological and plant growth related traits of petunia. – *Acta Agriculturae Slovenica* 109(2): 175-186.
- [72] Malik, C. P., Srivastava, A. K. (1979): *Text Book of Plant Physiology*. – Kalyani Publishers, New Dehli, pp. 3-41.
- [73] Manivannan, P., Jaleel, C. A., Sankar, B., Kishorekumar, A., Somasundaram, R., Lakshmanan, G. A., Panneerselvam, R. (2007): Growth, biochemical modifications and proline metabolism in *Helianthus annuus* L. As induced by drought stress. – *Colloids and Surfaces B: Biointerfaces* 59(2): 141-149.
- [74] Mansoor, S., Amin, I., Iram, S., Hussain, M., Zafar, Y., Malik, K., Briddon, R. (2003): Breakdown of resistance in cotton to cotton leaf curl disease in pakistan. – *Plant Pathology* 52(6): 784-784.
- [75] Maqbool, A., Zahur, M., Husnain, T., Riazuddin, S. (2009): *Gusp1* and *gusp2*, two drought-responsive genes in *Gossypium arboreum* have homology to universal stress proteins. – *Plant Molecular Biology Reporter* 27(1): 109-114.
- [76] Martin, M., Miceli, F., Morgan, J., Scalet, M., Zerbi, G. (1993): Synthesis of osmotically active substances in winter wheat leaves as related to drought resistance of different genotypes. – *Journal of Agronomy and Crop Science* 171(3): 176-184.
- [77] Massacci, A., Nabiev, S., Pietrosanti, L., Nematov, S., Chernikova, T., Thor, K., Leipner, J. (2008): Response of the photosynthetic apparatus of cotton (*Gossypium hirsutum*) to the onset of drought stress under field conditions studied by gas-exchange analysis and chlorophyll fluorescence imaging. – *Plant Physiology and Biochemistry* 46(2): 189-195.
- [78] Mbah, A. N., Mahmud, O., Awofolu, O. R., Isokpehi, R. D. (2013): Inferences on the biochemical and environmental regulation of universal stress proteins from schistosomiasis parasites. – *Advances and Applications in Bioinformatics and Chemistry: AABC* 6: 15.
- [79] Mehetre, S., Aher, A., Gawande, V., Patil, V., Mokate, A. (2003): Induced polyploidy in *Gossypium*: A tool to overcome interspecific incompatibility of cultivated tetraploid and diploid cottons. – *Current Science* 84(12): 1510-1512.
- [80] Monk, L. S., Fagerstedt, K. V., Crawford R. M. (1989): Oxygen toxicity and superoxide dismutase as an antioxidant in physiological stress. – *Physiologia Plantarum* 76(3): 456-459.
- [81] Morgan, J. M. (1984): Osmoregulation and water stress in higher plants. – *Annual Review of Plant Physiology* 35(1): 299-319.
- [82] Nakabayashi, R., Yonekura, Sakakibara, K., Urano, K., Suzuki, M., Yamada, Y., Nishizawa, T., Matsuda, F., Kojima, M., Sakakibara, H., Shinozaki, K., Michael, A. J. (2014): Enhancement of oxidative and drought tolerance in *Arabidopsis* by overaccumulation of antioxidant flavonoids. – *The Plant Journal* 77(3), pp.367-379.
- [83] Nath, A. K., Kumari, S., Sharma, D. (2005): In vitro selection and characterization of water stress tolerant cultures of bell pepper. – *Indian Journal of Plant Physiology* 10(1): 14-19.
- [84] Nepomuceno, A., Oosterhuis, D., Stewart, J. (1998): Physiological responses of cotton leaves and roots to water deficit induced by polyethylene glycol. – *Environmental and Experimental Botany* 40(1): 29-41.
- [85] Otten, L., De, H. Greve, Leemans, J., Hain, R., Hooykaas, P., Schell, J. (1984): Restoration of virulence of vir region mutants of *Agrobacterium tumefaciens* strain b6s3 by coinfection with normal and mutant *Agrobacterium* strains. – *Molecular and General Genetics* MGG 195(1-2): 159-163.
- [86] Padmalatha, V. K., Dhandapani, G., Kanakachari, M., Kumar, S., Dass, A., Patil, D. P., Rajamani, V., Kumar, K., Pathak, R., Rawat, B. (2012): Genome-wide transcriptomic analysis of cotton under drought stress reveal significant down-regulation of genes and

- pathways involved in fibre elongation and up-regulation of defense responsive genes. – *Plant Molecular Biology* 78(3): 223-246.
- [87] Persson, Ö., Valadi, Å., Nyström, T., Farewell, A. (2007): Metabolic control of the *Escherichia coli* universal stress protein response through fructose-6-phosphate. – *Molecular Microbiology* 65(4): 968-978.
- [88] Petropoulos, S., Daferera, D., Polissiou, M., Passam, H. (2008): The effect of water deficit stress on the growth, yield and composition of essential oils of parsley. – *Scientia Horticulturae* 115(4): 393-397.
- [89] Posé, D., Castanedo, I., Borsani, O., Nieto, B., Rosado, A., Taconnat, L., Ferrer, A., Dolan, L., Valpuesta, V., Botella, M. A. (2009): Identification of the *Arabidopsis* *dry2/sqe1-5* mutant reveals a central role for sterols in drought tolerance and regulation of reactive oxygen species. – *The Plant Journal* 59(1): 63-76.
- [90] Qin, X., Zeevaert, J. A. (1999): The 9-cis-epoxycarotenoid cleavage reaction is the key regulatory step of abscisic acid biosynthesis in water-stressed bean. – *Proceedings of the National Academy of Sciences* 96(26): 15354-15361.
- [91] Quisenberry, J., McMichael, B. (1991): Genetic variation among cotton germplasm for water-use efficiency. – *Environmental and Experimental Botany* 31(4): 453-460.
- [92] Quisenberry, J., Wendt, C., Berlin, J., McMichael, B. (1985): Potential for using leaf turgidity to select drought tolerance in cotton. – *Crop Science* 25(2): 294-299.
- [93] Ribas, A. F., Pereira, L. F. P., Vieira, L. G. E. (2006): Genetic transformation of coffee. – *Brazilian Journal of Plant Physiology* 18(1): 83-94.
- [94] Saiki, R. K., Scharf, S., Faloona, F., Mullis, K. B., Horn, G. T., Erlich, H. A., Arnheim, N. (1985): Enzymatic amplification of β -globin genomic sequences and restriction site analysis for diagnosis of sickle cell anemia. – *Science* 230(4732): 1350-1354.
- [95] Sairam, R., Tyagi, A. 2004. Physiological and molecular biology of salinity stress tolerance in deficient and cultivated genotypes of chickpea. – *Plant Growth Regul* 57(10).
- [96] Shao, H.-B., Chu, L.-Y., Jaleel, C. A., Zhao, C.-X. (2008): Water-deficit stress-induced anatomical changes in higher plants. – *Comptes Rendus Biologies* 331(3): 215-225.
- [97] Shinozaki, K., Yamaguchi-Shinozaki, K. (2007): Gene networks involved in drought stress response and tolerance. – *Journal of Experimental Botany* 58(2): 221-227.
- [98] Showler, A. T. 2002. Effects of water deficit stress, shade, weed competition, and kaolin particle film on selected foliar free amino acid accumulations in cotton, *Gossypium hirsutum* (L.). – *Journal of Chemical Ecology* 28(3): 631-651.
- [99] Singh, R., Pandey, N., Naskar, J., Shirke, P. A. (2015): Physiological performance and differential expression profiling of genes associated with drought tolerance in contrasting varieties of two *Gossypium* species. – *Protoplasma* 252(2): 423-438.
- [100] Sivamani, E., Bahieldin, A., Wraith, J. M., Al-Niemi, T., Dyer, W. E., Ho, T.-H. D., Qu, R. (2000): Improved biomass productivity and water use efficiency under water deficit conditions in transgenic wheat constitutively expressing the barley *hva1* gene. – *Plant Science* 155(1): 1-9.
- [101] Small, I., Wintz, H., Akashi, K., Mireau, H. (1998): Two birds with one stone: Genes that encode products targeted to two or more compartments. – *Plant Molecular Biology* 38(1): 265-277.
- [102] Smith, E. F., Townsend, C. O. (1907): A plant-tumor of bacterial origin. – *Science* 25(643): 671-673.
- [103] Somerville, C., Browse, J. (1991): Plant lipids: Metabolism, mutants, and membranes. – *Science* 252(5002): 80-87.
- [104] Sousa, M. C., McKay, D. B. (2001): Structure of the universal stress protein of *Haemophilus influenzae*. – *Structure* 9(12): 1135-1141.
- [105] Specht, J., Chase, K., Macrander, M., Graef, G., Chung, J., Markwell, J., Germann, M., Orf, J., Lark, K. (2001): Soybean response to water. – *Crop Science* 41(2): 493-509.
- [106] Sturm, R. A. (2009): Molecular genetics of human pigmentation diversity. – *Human Molecular Genetics* 18(R1): R9-R17.

- [107] Tang, W., Page, M. (2013): Overexpression of the arabidopsis *atem6* gene enhances salt tolerance in transgenic rice cell lines. – *Plant Cell, Tissue and Organ Culture (PCTOC)* 114(3): 339-350.
- [108] Tanou, G., Filippou, P., Belghazi, M., Job, D., Diamantidis, G., Fotopoulos, V., Molassiotis, A. (2012): Oxidative and nitrosative□based signaling and associated post□translational modifications orchestrate the acclimation of citrus plants to salinity stress. – *The Plant Journal* 72(4): 585-599.
- [109] Taylor, B. I., Burbidge, A., Thompson, A. J. (2000): Control of abscisic acid synthesis. – *Journal of Experimental Botany* 51(350): 1563-1574.
- [110] Tinland, B. (1996): The integration of t-DNA into plant genomes. – *Trends in Plant Science* 1(6): 178-184.
- [111] Turner, N. C. (1981): Techniques and experimental approaches for the measurement of plant water status. – *Plant and Soil* 58(1): 339-366.
- [112] Tzfira, T., Li, J., Lacroix, B., Citovsky, V. (2004): Agrobacterium t-DNA integration: Molecules and models. – *Trends in Genetics* 20(8): 375-383.
- [113] Umbeck, P., Johnson, G., Barton, K., Swain, W. (1987): Genetically transformed cotton (*Gossypium hirsutum* L.) plants. – *Nature Biotechnology* 5(3): 263-266.
- [114] Ünyayar, S., Keleş, Y., Ünal, E. (2004): Proline and aba levels in two sunflower genotypes subjected to water stress. – *Bulg. J. Plant Physiol.* 30: 34-47.
- [115] Urao, T., Miyata, S., Yamaguchi-Shinozaki, K., Shinozaki, K. (2000): Possible his to asp phosphorelay signaling in an arabidopsis two□component system. – *Febs Letters* 478(3): 227-232.
- [116] Vereyken, I. J., Chupin, V., Demel, R. A., Smeekens, S. C., De Kruijff, B. (2001): Fructans insert between the headgroups of phospholipids. – *Biochimica et Biophysica Acta (BBA)-Biomembranes* 1510(1): 307-320.
- [117] Vierling, E., Kimpel, J. A. (1992): Plant responses to environmental stress. – *Current Opinion in Biotechnology* 3(2): 164-170.
- [118] Voloudakis, A. E., Kosmas, S. A., Tsakas, S., Eliopoulos, E., Loukas, M., Kosmidou, K. (2002): Expression of selected drought-related genes and physiological response of greek cotton varieties. – *Functional Plant Biology* 29(10): 1237-1245.
- [119] Wang, W., Vinocur, B., Altman, A. (2003): Plant responses to drought, salinity and extreme temperatures: Towards genetic engineering for stress tolerance. – *Planta* 218(1): 1-14.
- [120] Wanner, L. A., Junttila, O. (1999): Cold-induced freezing tolerance in arabidopsis. – *Plant Physiology* 120(2): 391-400.
- [121] Wilkinson, J. Q., Lanahan, M. B., Conner, T. W., Klee, H. J. (1995): Identification of mrnas with enhanced expression in ripening strawberry fruit using polymerase chain reaction differential display. – *Plant Molecular Biology* 27(6): 1097-1108.
- [122] Wu, Q.-S., Xia, R.-X., Zou, Y.-N. (2008): Improved soil structure and citrus growth after inoculation with three arbuscular mycorrhizal fungi under drought stress. – *European Journal of Soil Biology* 44(1): 122-128.
- [123] Xu, S., Li, J., Zhang, X., Wei, H., Cui, L. (2006): Effects of heat acclimation pretreatment on changes of membrane lipid peroxidation, antioxidant metabolites, and ultrastructure of chloroplasts in two cool-season turfgrass species under heat stress. – *Environmental and Experimental Botany* 56(3): 274-285.
- [124] Yadav, S., Lakshmi, N. J., Maheswari, M., Vanaja, M., Venkateswarlu, B. (2005): Influence of water deficit at vegetative, anthesis and grain filling stages on water relation and grain yield in sorghum. – *Indian Journal of Plant Physiology* 10(1): 20.
- [125] Zaenen, I., Van Larebeke, N., Teuchy, H., Van, M. Montagu, Schell, J. (1974): Supercoiled circular DNA in crown-gall inducing agrobacterium strains. – *Journal of Molecular Biology* 86(1): 109-117.
- [126] Zahur, M., Maqbool, A., Irfan, M., Barozai, M. Y. K., Qaiser, U., Rashid, B., Husnain, T., Riazuddin, S. (2009): Functional analysis of cotton small heat shock protein promoter

- region in response to abiotic stresses in tobacco using agrobacterium-mediated transient assay. – *Molecular Biology Reports* 36(7): 1915-1921.
- [127] Zambryski, P., Joos, H., Genetello, C., Leemans, J., Van Montagu, M., Schell, J. (1983): Ti plasmid vector for the introduction of DNA into plant cells without alteration of their normal regeneration capacity. – *The EMBO Journal* 2(12): 2143.
- [128] Zhang, C.-S., Lu, Q., Verma, D. P. S. (1995): Removal of feedback inhibition of δ -pyrroline-5-carboxylate synthetase, a bifunctional enzyme catalyzing the first two steps of proline biosynthesis in plants. – *Journal of Biological Chemistry* 270(35): 20491-20496.
- [129] Zhang, F., Puchta, H., Thomson, J. G. (2015): *Advances in New Technology for Targeted Modification of Plant Genomes*. – Springer, New York.
- [130] Zhang, J., Campbell, R. E., Ting, A. Y., Tsien, R. Y. (2002): Creating new fluorescent probes for cell biology. – *Nature Reviews Molecular Cell Biology* 3(12): 906-918.
- [131] Zhu, B., Su, J., Chang, M., Verma, D. P. S., Fan, Y.-L., Wu, R. (1998): Overexpression of a δ 1-pyrroline-5-carboxylate synthetase gene and analysis of tolerance to water-and salt-stress in transgenic rice. – *Plant Science* 139(1): 41-48.
- [132] Zhu, T., Mettenburg, K., Peterson, D. J., Tagliani, L., Baszczyński, C. L. (2000): Engineering herbicide-resistant maize using chimeric rna/DNA oligonucleotides. – *Nature Biotechnology* 18(5): 555-558.

THE COMPARATIVE ANALYSIS ON THE OVERVIEW OF HAIR GOAT BREEDINGS TO SUSTAINABLE FOREST RESOURCES MANAGEMENT

KASIKCI, D.^{1*} – TURKOGLU, T.² – BEKIROGLU, S.³ – OZMIS, M.⁴ – TOLUNAY, A.⁴

¹*Department of Animal Science, Faculty of Agriculture, Isparta University of Applied Sciences, 32260 Isparta, Turkey*

²*Department of Forestry, Koycegiz Vocational School, Mugla Sitki Kocman University, Mugla, Turkey*

³*Department of Forest Engineering, Faculty of Forestry, Istanbul University, Istanbul, Turkey*

⁴*Department of Forest Engineering, Faculty of Forestry, Isparta University of Applied Sciences, 32260 Isparta, Turkey*

**Corresponding author*

e-mail: duygukasikci@isparta.edu.tr; phone: +90-246-211-8584; fax: +90-246-211-8696

(Received 22nd Feb 2019; accepted 10th Apr 2019)

Abstract. Goat breedings in Turkey is a traditional profession dating back centuries which is carried out in and around forests of rural regions. The purpose of this study was to determine the factors with an impact on sustainable natural resource management based on the opinions of goat breeders and to put forth the contributions that may be provided to establish a sustainable management. The study will contribute to establishing a sustainable goat breeding system in Turkey as well as the management of sustainable forest resources. In this scope, the study was carried out in two different areas in the Mediterranean region of Turkey where goat breeding is widespread. The opinions of goat breeders on demographics, socioeconomic, hair goat breeding and sustainable forest resources management were acquired via survey method and used as the primary data of the study. Descriptive statistics such as frequency, percentage and crosstab values along with Mann-Whitney U Test, Chi-Square Test of Independence and Multivariate Linear Regression Analysis were used as the method. It was determined based on the study results that grazing in forest area is the most important problem for goat breeders and various other problems were also observed related to cooperation with the forest administration. It was observed that goat breeding is carried out via traditional methods by families that are above middle age. The findings indicate that the number of goat breeders decrease as a result of increasing age due to interventions for preventing damages given to trees in the forest by goats during grazing, decrease in the education level and the duration of experience in this profession.

Keywords: *traditional goat breeding, sustainability, goat-grazing damages*

Introduction

People in rural areas have used their natural resources (agricultural areas, forests, pastures, water sources, etc.) by way of implementing the methods they have learned from their ancestors. These methods of production have been criticized and abandoned with the advent of methods aimed at cheaper mass production in agriculture. However, there is increasing concern with regard to the implications of the widely used modern production methods such as environmental pollution and prevention of the sustainability of ecosystems etc. Therefore, traditional land use methods which do not pollute the environment and which prevent loss of soil were re-evaluated and combined under the concept of agroforestry (Gholz, 1986; Ocak et al., 2007; Tolunay et al., 2002).

There is an increasing interest in sustainable agriculture defined as the preservation and management of the natural resources for meeting the demands of current and future generations at the highest possible level (Schmincke, 1995; Heitschmidt et al., 1987, 1993; Semerci and Çelik, 2016). Sustainable agriculture is a system used for the production of organic substances that does not pollute the agriculture, soil and water resources with pollutants, that minimizes energy consumption while protecting animal species and the environment (Ocak et al., 2010). Because sustainability with regard to the use of natural resources has gained significant importance due to increasing population and energy demand. In this context, goats bred at high elevations have unique skills in using pastures, rangelands and crop residue as well as the side products in the ecosystem and to transform these into food. Thanks to these skills, it is easier to feed the goats that have adapted to high elevation areas. Based on this knowledge, local people living at areas of high elevation have earned their living for centuries by breeding animals by using such traditional methods (Aldezabal and Garin, 2000; Ainalis and Tsiouvaras, 2004; Ainalis et al., 2006; Zarovali et al., 2007).

It is known that traditional land use methods are mostly applied by rural populations in underdeveloped or developing countries. Because majority of these people live far away from modern education opportunities and acquire their knowledge on earning a living and life in general from the information passed down to them by their ancestors. In addition, the importance given to traditional production methods has increased in our day resulting in increased support to such methods. In this scope, traditional goat and hair goat breeding that makes use of mountainous and unfertile rangelands in marginal lands of rural areas are among the activities that stand out (Ocak et al., 2007). Of these, hair goat breeding attracts attention as a form of cultural life in addition to being a unique economical production system (Güney and Darcan, 2005). The relation between socioeconomic, cultural, and recreational needs of the pastoral people and goat breeding is an undeniable reality (Kıvrak, 2014; Bekiroğlu et al., 2016).

The hair goat breeding areas in Europe are located within the borders where certain tree and shrub species considered among Mediterranean scrub vegetation are distributed. It has been determined that Kermes oak (*Qercus coccifera* L.) and Holm oak (*Qercus ilex* L.) species the leaves of which are preferred by hair goats can be found frequently in these areas (Ainalis et al., 2006; Zarovali et al., 2007; Tolunay et al., 2002; Tolunay et al., 2009; Tasligil and Sahin, 2010). Thus, it is accepted that the hair goat population living areas in the Mediterranean region overlap with the areas where these two tree species are naturally distributed. However, grazing bans have been imposed for hair goat owners in state forests where these two tree species are distributed since it is indicated that the goats damage the trees of the forests. Moreover, hair goat breeding villagers have been forced to put an end to their adopted cultural ways of life. Therefore, the hair goat population in the Mediterranean Region has declined drastically (Ince et al., 2009; Ince, 2010; Güney and Darcan, 2005). In addition, the tendency for natural and organic nutrition has increased in recent years resulting in an increased demand in products produced in completely natural environments (Morand-Fehr et al., 2004; Boyazoglu et al., 2005). In line with this tendency, natural products obtained from animals raised at high elevations have started to be preferred more by consumers. Because it has been proven scientifically that the cholesterol and protein values of these animal products (meat, milk, fat, cheese etc.) are superior in comparison with those obtained from other environments of production (Koyuncu and Tuncel, 2010; Laugesen et al., 2003). Indeed, the plant diversity of meadows and rangelands at high elevations is

higher in comparison with others and the plants that grow on these areas have higher nutritive values. Moreover, industrial activities decrease with increasing elevation resulting in less environmental pollution in such areas. In conclusion, natural environments at high elevation that are not damaged by people have recently started to become centers of attraction as quality grazing areas for animal breeding. As a result, hair goats that have provided natural products such as wool, milk, meat, horn to the breeding local public started to gain importance as a popular economic commodity and the relationship between hair goat-ecosystem has been subject to re-evaluations. Recent scientific studies have shown that hair goats are not actually enemies of the forest as was considered previously but are animals that support the sustainability of the current ecosystem. As a result of this development, countries in the Mediterranean Region are trying to develop traditional goat breeding systems at the distribution areas of especially the Kermes oak (*Qercus coccifera* L.) and Holm oak (*Qercus ilex* L.) species (Aldezabal and Garin, 2000; Ainalis and Tsiouvaras, 2004; Ainalis et al., 2006; Zarovali et al., 2007).

Turkey is one of the countries where the rural population carries out hair goat breeding traditionally and culturally. It is known that hair goat breeding is carried out for thousands of years on a wide geographical area stretching out in south and southeastern Turkey. The hair goat population was decreased in this country by applying the “Hair goat Action Plan” on the basis of the opinion that hair goats are among the animals that harm forests the most thereby resulting in the narrowing down of areas where these animals are bred. However, there is still a certain rural population that insists on sustaining the traditional way of life based on a breeding despite all the imposed sanctions. Isparta is one of the cities where majority of this rural population lives (Fig. 2). However, hair goat breeders in the city of Isparta have not yet started to benefit from the positive atmosphere resulting from the increased organic nutrition demand and the global importance given to traditional methods of production. In addition, the breeding of hair goats adopted to these areas dates back centuries in Mediterranean forest ecosystems and is receiving continuously increasing support for the as one of the most successful methods of organic animal breeding (Ince and Karaca, 2009; Ince et al., 2009; Koknaroglu et al., 2007; Basullu and Tolunay, 2010).

The aim of this study was to determine the opinions of breeders at two study areas that have similar demographic, socioeconomic and geographical conditions in the Isparta region on the improvement of sustainable forest resources, rangeland management and the ecosystem conditions in the region. Factors that impact the sustainability of natural resources were determined based on the opinions of goat breeders living on both study areas in the rural region after which the contributions that can be made for a sustainable management were indicated.

Materials and methods

Study area

Merkez and Sutculer districts in the province of Isparta located in the Mediterranean Region of Turkey were selected as the study area (Fig. 1). Because, the city of Isparta is one of the most important cities with regard to traditional hair goat breeding.

The study area is a mountainous region with high elevation (the average elevation of Merkez is 1068 m, and the average elevation of Sutculer is 991 m). This is a unique region where air pressure, oxygen amount and climate conditions differ. Therefore, it

has an impact on all living population in this region. Hair goat breeding is an important means of living that provides income and food safety for the villagers in this region.

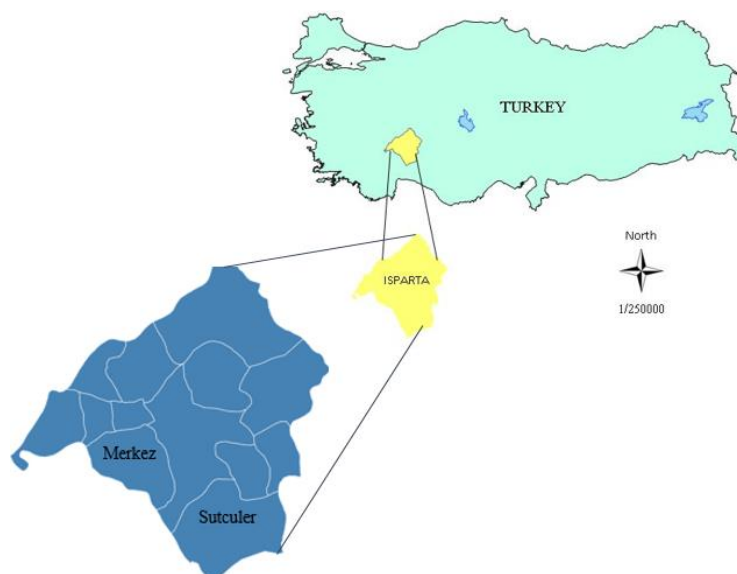


Figure 1. Map of the study area

Materials

The survey form prepared for obtaining the opinions of goat breeders on sustainable forest resources management was used for data acquisition. The survey form was comprised of 3 questions on the demographic characteristics of goat breeders, 4 questions on their socioeconomic characteristics, 10 questions on hair goat breeding and 13 questions on sustainable forest resource (forest-rangeland) management. The dependent and independent variables of the study are given in *Table 1*. There were a total of 180 and 144 goat breeders in the first and second study areas respectively and face to face interviews were carried out with 71 (40%) of the breeders in the first study area and 97 (67%) in the second study area. This sample group is considered as sufficient at a confidence interval of 10% (Karaasar, 2012; Sample Size Calculator; 2018). The survey was applied during March–August 2018 on randomly selected hair goat breeders aged above 18. The study variables generated based on the survey questions are given in *Table 1*.

Methods

Descriptive statistics such as frequency, percentage and crosstab values were used as the method of this study along with Mann-Whitney U Test, Chi-Square Test of Independence and Multivariate Linear Regression Analysis. The demographic-socioeconomic characteristics of Sutculer and Isparta districts breeders as well as their characteristics related with hair goat breeding-sustainable forest management were indicated via frequency and percentage values. Crosstab results were calculated for the “Age” and “Marital Status” characteristics as well as the variables of “Grazing penalty from the Forest Administration”, “Cooperation with the Forest Administration” and “Quitting the breeding profession”.

Table 1. The survey questions

Variables			Marked options
	Definition	Symbol	
Demographic	Age (year)	X1	a) 18-30, b) 31-42, c) 43-55, d) 56-70
	Marital status	X2	a) Single, b) Married, c) Widowed
	Education	X3	a) Not Literate, b) Literate, c) Elementary school, d) Secondary school, e) High school, f) University
Socio-economic	Shepherd time (year)	X4	a) <5, b) 6-10, c) 11-15, d) 16-20, e) >20
	Traditionally shepherd	X5	a) Yes, b) No
	Get help from family other	X6	a) Yes, b) No
	Other sources of income	X7	a) Yes, b) No
Hair goat breeding	The new generation willing to be a shepherd	X8	a) Yes, b) No, c) Undecided
	Having grazing penalty	X9	a) Yes, b) No
	Altitude of pasturage (m)	X10	a) 0-500, b) 501-800, c) 801-1200, d) >1200
	Favorite plants of hair goats	X11*	a) Bush, b) Annual plants grown in forest, c) Fresh exiles of pine trees
	Goat breeds supported by state	X12*	a) Hair goats, b) Honamli, c) Kilis, d) Tiftik, e) Others
	Grazing areas	X13*	a) Any place in the county, b) Rangelands, c) Forest areas, d) Highlands
	Ownership of grazing land	X14	a) Forest land, b) I own the land, c) I know the landowner, d) I do not know the landowner
	Is the village pasture mismanaged	X15	a) Yes, b) No, c) Undecided
	Foreign shepherds should be allowed grazing	X16	a) Yes, b) No, c) Undecided
	The most important problem of the shepherds	X17	a) Grazing, b) Low income c) Animal sale, d) Living condition
Characteristics related to sustainable natural resource management	Collaborating with the forest administration	X18	a) Yes, b) No, c) Undecided, d) Other
	Request from the Forest Administration	X19	a) Creating pastures, b) Forgiving crimes, c) Ensuring trust, d) Other
	Prevention of damage to trees	X20	a) Yes, b) No, c) Somewhat, d) Not interested
	Prevention of damage to sapling	X21	a) Yes, b) No, c) Somewhat, d) Not interested
	Easily overcome fences in forests by animals	X22	a) Yes, b) No, c) Undecided
	Barbed wires in forests damage animals	X23	a) Yes, b) No, c) Undecided
	Characteristics of the grazing area to be requested from the forest administration	X24	a) Only me, b) Only give to 2-3 shepherds, c) Let grazing permission be given everyone, d) It does not matter
	Pasture problem of forest area	X25	a) Yes, b) No, c) Undecided
	Quitting shepherd profession	X26	a) Yes, b) No, c) Seldom, d) Undecided
	To want their children to be a shepherd	X27	a) Yes, b) May be, c) If they cannot find other jobs, d) Certainly not
	Raising children's awareness about forest conversation	X28	a) Yes, b) No, c) Undecided
	To planting saplings on forest land	X29	a) Yes, b) No, c) Undecided
	To warn people who damage forests	X30	a) Yes, b) No, c) Undecided

*Multiple options were marked

Mann-Whitney U Test was used for determining whether there are differences in opinion between the breeders of the two selected districts with regard to the study variables (Table 1). Chi-Square Test of Independence was used for determining if there is any relationship between the demographic-socioeconomic characteristics and hair goat breeding-sustainable natural resource management characteristics for the two districts. In addition, Multivariate Linear Regression Analysis was applied for predicting the variables of “Cooperation with the forest administration (X18)”, “Expelling tree-harming animals from the forest (X20)”, “Expelling shoot-harming animals from the forest (X21)”, “Desiring the children to be breeders (X27)”, “quitting the breeding profession (X26)” and “Warning people who can harm the forest (X30)”. These analyses were carried out via IBM SPSS 22.0 package software and the reliability level during these statistical tests was accepted as 95%.

Results and discussion

Opinions of goat breeders on demographics, socioeconomics and hair goat breeding and sustainable natural resource management

Figures 2, 3, 4 and 5 provide an overview on the descriptive statistics related with the demographic, socioeconomic and hair goat breeding and sustainable natural resource management characteristics of breeders in Sutculer and Merkez districts.

As can be seen when the demographic characteristics of the Sutculer and Merkez districts breeders are examined that their age interval is 43-55 for 37% of the breeders in Sutculer and 36% in Merkez districts (Fig. 2). About 30% of all breeders in both study areas were above the age of 55. It is observed that the desire of the new generation to work as breeders was slightly higher in the Sutculer district (51%) in comparison with Merkez district (Fig. 2). Goat breeding is not a preferred profession among the young population in Turkey (Guney and Darcan, 2001). Hence, the concept of “Herd Manager” was tried to be integrated instead of the term “breeder” but to no avail. Recently, goat breeders in Turkey employ breeders from foreign countries such as Afghanistan, Pakistan and Syria (Tolunay et al., 2018).

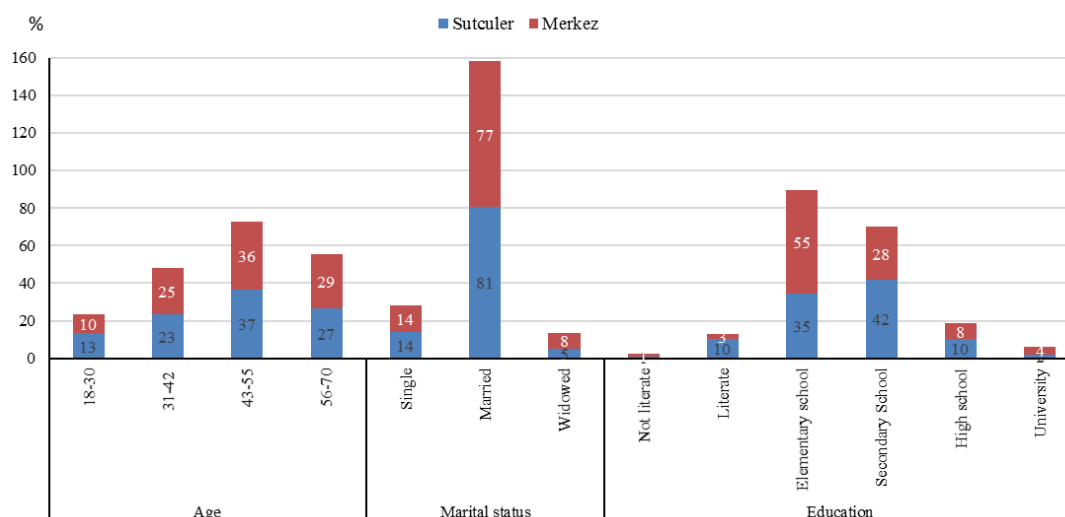


Figure 2. Demographic characteristics of the samples

It was observed that 81% of the goat breeders who participated in the study were married, while this ratio for the Merkez district was 77%. Of the breeders in both study areas, 84-93% continues this profession together with their family members (Fig. 2). Goat breeding in Turkey is a family profession (Arac and Daskiran, 2010). If we consider the levels of education, 55% in Merkez district were primary school graduates, whereas 42% in Sutculer district were secondary school graduates. The education level of goat breeders is generally low. The reasons for this can be indicated as nomadic life in rural areas, the distance of rangelands to areas of settlement as well as the fact that breeding is a full time profession (Ince et al., 2009).

Of the breeders, 73% in Sutculer and 59% in Merkez districts have been working in this profession for over 20 years. It was indicated by 96% of the breeders in Sutculer district, and 89% in Merkez district that they are continuing this profession based on traditional methods (Fig. 3). Traditional breeding is a unique form of breeding that is mostly based on methods passed down from earlier generations for which a style specific to the related region is adopted with positive impacts on the economy and handcrafts by way of different animal based products. It is of significant importance since these primeval traditions reflect the socio-cultural and economical lives of the local public.

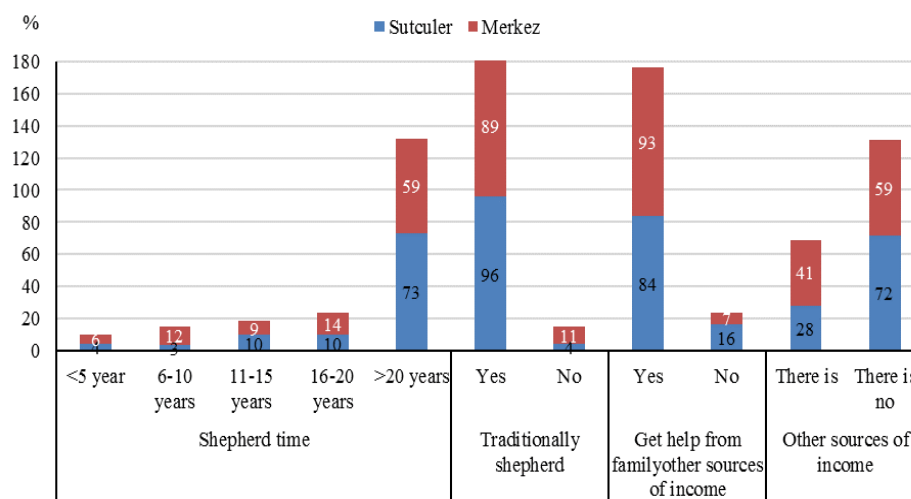


Figure 3. Socio-economics characteristics of the samples

When examined with regard to hair goat breeding characteristics, the most important problems that breeders face were grazing in Merkez district (39%) and low income in Sutculer district (55%). Grazing permit to foreign breeders was 83% in Merkez and 63% in Sutculer (Fig. 4). Hair goat breeding in Turkey is completely based on Forests and Forest rangelands. Other animal breeding activities either cannot be carried out in these areas due to environmental conditions or they can be carried out at minimum levels. Forests are legally allocated areas for hair goat breeding. However, “Grazing Regulation” has prohibited the grazing of hair goats in forests. The Forest Administration has filed lawsuits against individuals grazing hair goats in state forests based on the provisions of this regulation. Individuals convicted by judicial authorities were subject to fines and prison terms. Rangeland issue is still waiting to be solved as the most important problem of goat breeders (Tolunay et al., 2015).

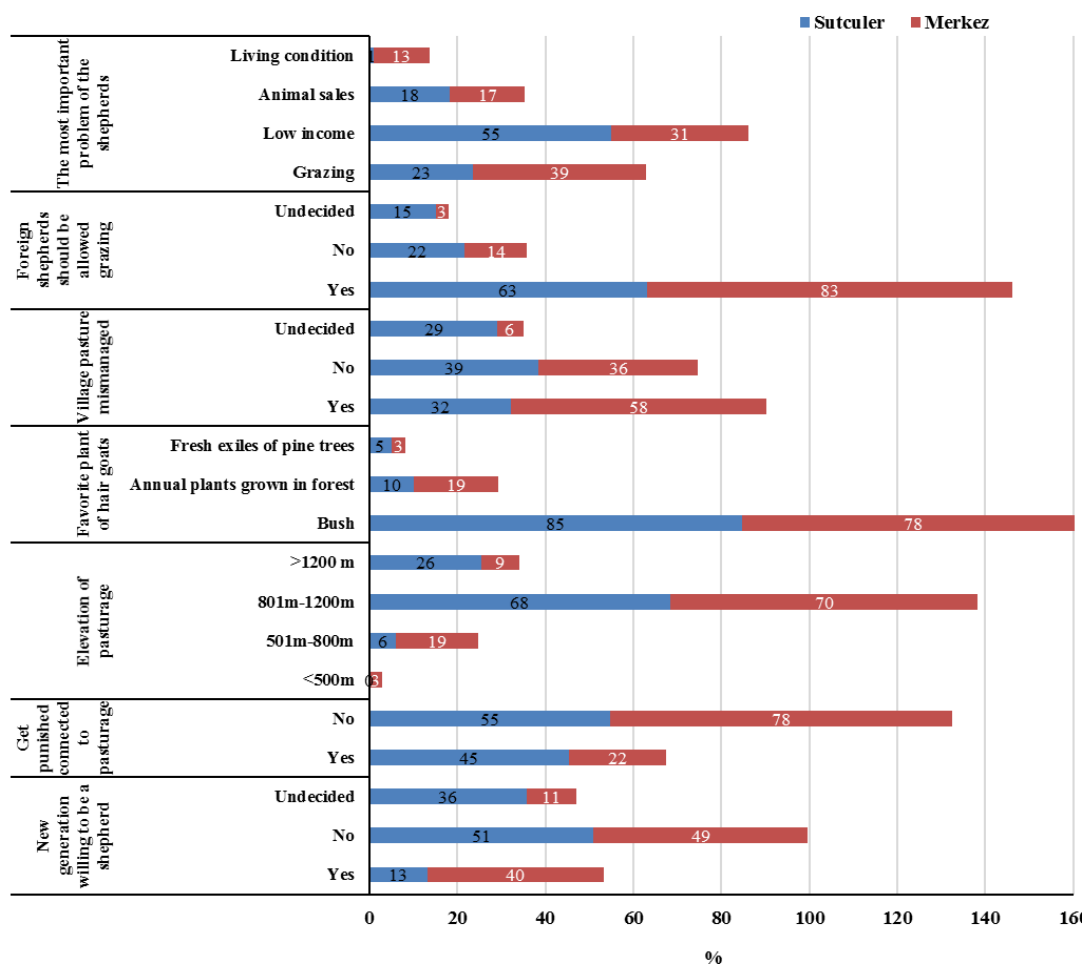


Figure 4. Characteristics related to hair goat breeding of samples

The fact that rangelands in Turkey are small and fragmented results in overgrazing pressure. Rangeland and Grazing are still issues waiting to be solved due to reasons such as the lack of planned grazing, excessive damages due to off-season grazing and overgrazing, failure to protect the rangeland borders, infrastructure problems of Rangeland Management Associations, general decisions on Grazing Period (Kaşıkcı et al., 2016).

Of the breeders, 58% are of the opinion that village headmen in Sutculer implement erroneous management with regard to rangelands. This ratio is 32% in Merkez District and is lower. Kermes oak and other shrubbery making up the Mediterranean scrubs were indicated in both groups as food preferred by the goats (85%, 78%). The goats are grazed at elevations ranging between 801-1200 m in both groups. Especially in the Sutculer District, 55% of the breeders were fined by the Forest Administration. Goat breeds of Turkey have been supported by Ministry of Agriculture and Forestry in Turkey. In the study areas, 65% of goat breedings are supported by the state for hair goat breeding, 17% of the others are for Honamli goat, 14% for Kilis goat and 4% of the other breeds. Goats are grazed in 35% mountain areas (around of forest areas), 30% in pastures, 24% in highlands and 11% in other fields.

It attracts attention that there both groups are sensitive with regard to warning those who harm the forests. It is striking that the children of breeders in both groups are

conscious with regard to the protection of forests. A very little portion of the breeders want their children to be breeders. Of the breeders, 79% in Sutculer district and 64% in Merkez district indicated the need for new grazing areas. 75% of the breeders stated that there is no pasture in forest areas or around the forest (Fig. 5). It is also understood that the breeders are sensitive with regard to the prevention of harming the trees.

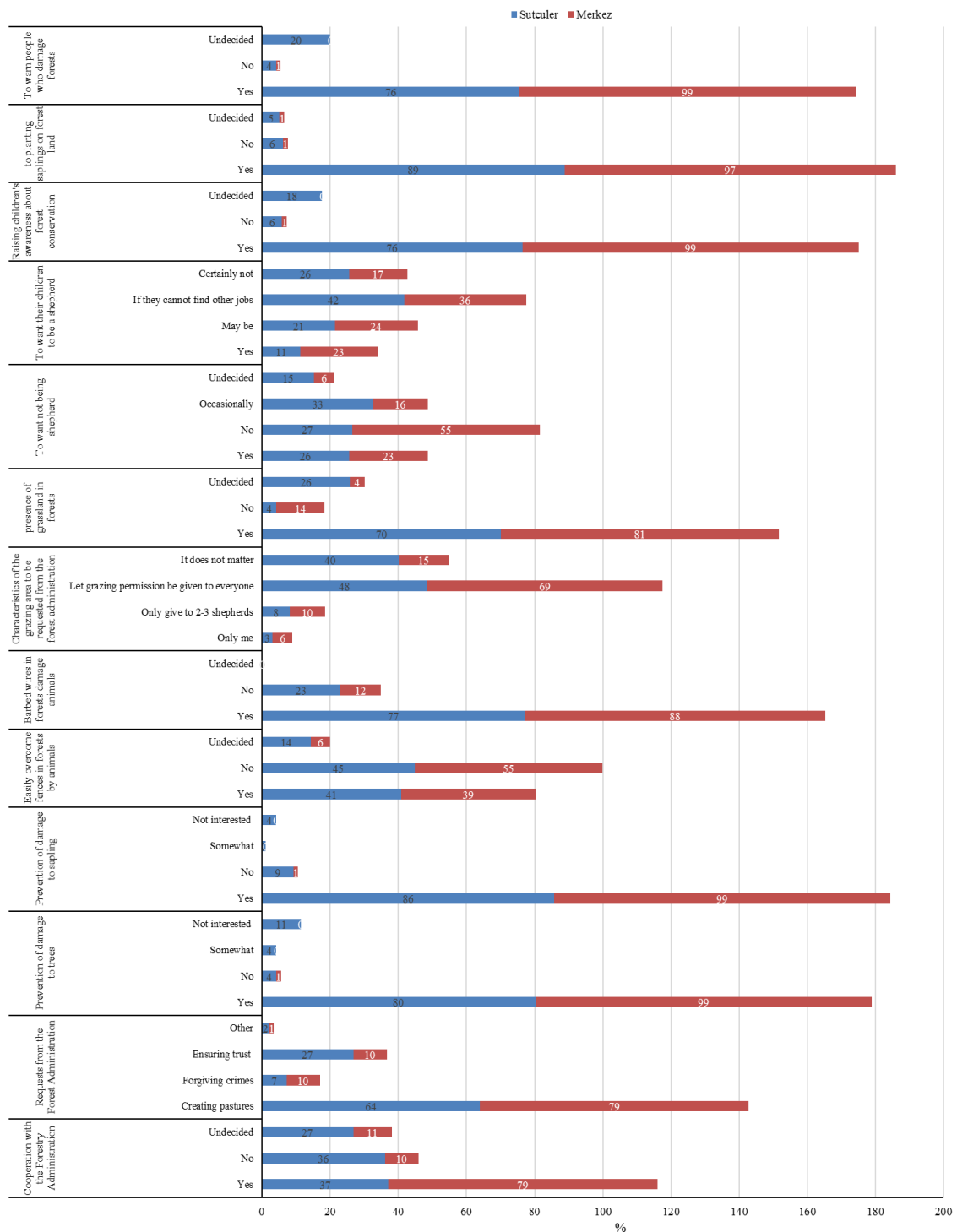


Figure 5. Characteristics related to sustainable natural resource management of samples

Examination of the impacts of the age and marital status of goat breeders on the management of sustainable forest resources

Crosstab results were calculated for the relation between the “Age” and “Marital status” characteristics of breeders in Sutculer and Isparta and the variables of “Grazing penalty from the Forest Administration”, “Cooperation with the Forest Administration” and “Quitting the breeding profession” (Tables 2 and 3).

Table 2. Cross tabulation results of Sutculer district

		Having grazing penalty		Total	Collaborating with the forest administration			Total	Quitting shepherd profession				Total	
		Yes	No		Yes	No	Undecided		Yes	No	Seldom	Undecided		
Age	18-30	Count	7	6	13	3	6	4	13	6	1	4	2	13
		% within X _i	15.9%	11.3%	13.4%	8.3%	17.1%	15.4%	13.4%	24.0%	3.8%	12.5%	13.3%	13.3%
	31-42	Count	11	12	23	7	11	5	23	6	8	6	3	23
		% within X _i	25.0%	22.6%	23.7%	19.4%	31.4%	19.2%	23.7%	24.0%	30.8%	18.8%	20.0%	23.5%
	43-55	Count	15	20	35	15	11	10	36	8	11	11	6	36
	% within X _i	34.1%	37.7%	36.1%	41.7%	31.4%	38.5%	37.1%	32.0%	42.3%	34.4%	40.0%	36.7%	
	56-70	Count	11	15	26	11	7	7	25	5	6	11	4	26
	% within X _i	25.0%	28.3%	26.8%	30.6%	20.0%	26.9%	25.8%	20.0%	23.1%	34.4%	26.7%	26.5%	
	Total	Count	44	53	97	36	35	26	97	25	26	32	15	98
	% within X _i	100.0%	100.0%	100.0%	100.0%	100.0%	100.0%	100.0%	100.0%	100.0%	100.0%	100.0%	100.0%	100.0%
Marital status	Single	Count	8	6	14	4	7	3	14	6	1	5	2	14
		% within X _i	18.2%	11.3%	14.4%	11.1%	20.0%	11.5%	14.4%	24.0%	3.8%	15.6%	13.3%	14.3%
	Married	Count	33	45	78	30	26	22	78	18	23	26	12	79
		% within X _i	75.0%	84.9%	80.4%	83.3%	74.3%	84.6%	80.4%	72.0%	88.5%	81.3%	80.0%	80.6%
	Other	Count	3	2	5	2	2	1	5	1	2	1	1	5
	% within X _i	6.8%	3.8%	5.2%	5.6%	5.7%	3.8%	5.2%	4.0%	7.7%	3.1%	6.7%	5.1%	
	Total	Count	44	53	97	36	35	26	97	25	26	32	15	98
	% within X _i	100.0%	100.0%	100.0%	100.0%	100.0%	100.0%	100.0%	100.0%	100.0%	100.0%	100.0%	100.0%	100.0%

X_i: having grazing penalty, collaborating with the forest administration, quitting shepherd profession

Table 3. Cross tabulation results of Merkez district

		Having grazing penalty		Total	Collaborating with the forest administration				Total	Quitting shepherd profession				Total	
		Yes	No		Yes	No	Undecided	Other		Yes	No	Seldom	Undecided		
Age	18-30	Count	1	6	7	5	1	1	0	7	2	4	1	0	7
		% within X _i	6.7%	11.3%	10.0%	9.1%	14.3%	14.3%	.0%	10.0%	12.5%	10.5%	9.1%	.0%	10.1%
	31-42	Count	6	11	17	14	3	0	0	17	4	6	5	1	16
		% within X _i	40.0%	20.8%	24.3%	25.5%	42.9%	.0%	.0%	24.3%	25.0%	15.8%	45.5%	25.0%	23.2%
	43-55	Count	5	19	25	20	1	3	1	25	6	12	4	3	25
	% within X _i	33.3%	35.8%	35.7%	36.4%	14.3%	42.9%	100%	35.7%	37.5%	31.6%	36.4%	75.0%	36.2%	
	56-70	Count	3	17	21	16	2	3	0	21	4	16	1	0	21
	% within X _i	20.0%	32.1%	30%	29.1%	28.6%	42.9%	.0%	30%	25.0%	42.1%	9.1%	.0%	30.4%	
	Total	Count	15	53	70	55	7	7	1	70	16	38	11	4	69
	% within X _i	100%	100%	100%	100%	100%	100%	100%	100%	100%	100%	100%	100%	100%	
Marital status	Single	Count	1	8	9	8	1	1	0	10	3	3	3	0	9
		% within X _i	7.7%	16.3%	14.1%	16.0%	14.3%	14.3%	.0%	15.4%	20.0%	8.6%	33.3%	.0%	14.3%
	Married	Count	12	41	55	42	6	6	1	55	12	32	6	4	54
	% within X _i	92.3%	83.7%	85.9%	84.0%	85.7%	85.7%	100%	84.6%	80.0%	91.4%	66.7%	100%	85.7%	
	Total	Count	13	49	64	50	7	7	1	65	15	35	9	4	63
	% within X _i	100%	100%	100%	100%	100%	100%	100%	100%	100.0%	100%	100%	100%	100%	

X_i: having grazing penalty, collaborating with the forest administration, quitting shepherd profession

It was observed in the Sutculer district study area that the goat breeders in the age interval of 43-55 received more grazing penalties in comparison with the other age groups, that they are more inclined towards cooperation with the forest administration and that they do not want to quit this profession. It was also determined that the married goat breeders who continue this profession as a family received more grazing penalties in comparison with others but that they are always more inclined towards communication and cooperation with the forest administration. It was found that the individuals in this group do not want to quit the goat breeding profession.

Whereas it was observed in the Merkez district study area that goat breeders in the age interval of 31-42 received more grazing penalties and that they are not inclined towards cooperation with the forest administration. Some of the breeders in this age group stated that they are planning to quit this profession. It was also observed in this study area that the married goat breeders and those who continue this profession with their families were subject to more grazing penalties in comparison with others, that their levels of cooperation with the forest administration were low and that they do not want to quit this profession.

Differences in the opinions of goat breeders in the two study areas

Table 4 presents the Mann Whitney U test results indicating the differences in opinion of the breeders in both districts with regard to the study variables. There are certain differences between the perspectives of Sutculer and Merkez district breeders regarding hair goat breeding and sustainable natural resource management. In other words, the Mann Whitney U Test (*Table 4*) results indicate that 15 out of the 30 opinions obtained from Sutculer and Merkez district breeders differ. Of these, the desire of the new generation to continue the breeding profession for hair goat breeding was higher in the Sutculer district in comparison with the Merkez district. The breeders in Sutculer district suffer more due to grazing penalties. The average grazing elevation for hair goats in Sutculer district was higher in comparison with the Merkez district. It is a common opinion in Sutculer district that the village headmen implement erroneous management applications with regard to the rangelands. While foreign breeders receive more grazing permits in the Merkez district, but this ratio is quite low in Sutculer district. It was observed with regard to the perspective on the management of sustainable natural resources that the capacity to cooperate with the forest administration is quite high in the Merkez district and that the goat breeders are more conscious in the Merkez district in preventing the harms given to trees and young saplings.

Goat breeders in the Merkez district study area request new grazing areas with higher quality from the forest administration. Therefore, it is necessary to provide new grazing areas especially in shrubberies. The goat breeders generally have a tendency to quit the breeding profession, however rural conditions do not present them with job opportunities other than agriculture and ovine breeding. In general, they do not want their children to continue this profession. The breeders in the Merkez district stated that they try to raise the awareness of their children for protecting the forests and nature. They stated that they plant various tree saplings from time to time at certain locations. The goat breeders in the Merkez district indicated that they warn the people harming the forests for a sustainable nature.

According to the Chi-Square Test of Independence, the variables from among the X1, X2; X3, X4, X5, X6 and X7 variables for the breeders in Sutculer and Merkez

districts and other study variables for which there are statistically significant relationships are presented in *Tables 5* and *6*.

A statistically significant relationship was determined between the age parameter of the goat breeders in the Merkez district and their children continuing the breeding profession. Elderly breeders indicated that they do not want the new generation to continue this profession. Grazing was determined as a significant problem in this area as well. The environmental awareness of individuals who continue this profession as a tradition increases with increasing levels of education. Those who continue this profession as a family have more requests from the forest administration with regard to the conditions at the grazing areas. Those who have an additional income from professions other than goat breeding want to continue this profession at areas of lower elevation.

Table 4. Results of Mann Whitney U test

Variables	Mann-Whitney U Value	Asymp. Sig. (2-tailed)	Variables	Mann-Whitney U Value	Asymp. Sig. (2-tailed)
X1	3250.00	0.55	X16*	2561.00	0.00 ^a
X2	2930.00	0.51	X17	3313.50	0.57
X3	3251.50	0.44	X18*	2067.50	0.00 ^a
X4	2606.50	0.05	X19	3134.50	0.23
X5	2827.00	0.12	X20*	2785.50	0.00 ^a
X6	3037.00	0.08	X21*	3028.50	0.00 ^a
X7	2449.50	0.10	X22	3342.00	0.63
X8*	2118.00	0.00 ^a	X23	2476.00	0.08
X9*	2529.50	0.00 ^a	X24*	2451.50	0.00 ^a
X10*	2487.50	0.00 ^a	X25*	2891.50	0.03 ^a
X11	2893.50	0.22	X26*	2743.00	0.03 ^a
X12	62.00	0.02	X27*	2792.00	0.03 ^a
X13	12.00	1.00	X28*	2277.50	0.00 ^a
X14	7.00	0.89	X29*	3187.00	0.04 ^a
X15*	2199.50	0.00 ^a	X30*	2683.50	0.00 ^a

^aAsymp. Sig. (2-tailed) p < 0.05

*H₀ is rejected (shepherds in Merkez and Sutculer districts belong to the same community)

Table 5. Merkez district's chi-square independence test result

		X8	X10	X17	X18	X19	X21	X23	X25	X26	X27	X29
X1	Chi-Square Value	17.8	17.2	11.01	6.98	20.1	9.27	3.10	17.9	10.6	20.1	36.8
	Exact Sig. (2-sided)	0.02 ^a	0.14	0.54	0.84	0.08	0.12	0.54	0.02 ^a	0.54	0.04 ^a	0.56
X2	Chi-Square Value	6.78	5.99	16.49	1.98	1.42	6.18	0.14	8.16	6.25	10.71	6.45
	Exact Sig. (2-sided)	0.13	4.40	0.01 ^a	0.92	1.00	0.22	1.00	0.10	0.37	0.08	0.40
X3	Chi-Square Value	7.02	14.5	10.7	12.68	10.66	71.0	2.37	24.9	29.04	18.8	45.9
	Exact Sig. (2-sided)	0.72	0.41	0.82	0.46	0.53	0.01 ^a	0.67	0.53	0.04 ^a	0.18	0.03 ^a
X4	Chi-Square Value	21.48	8.06	13.51	10.78	17.6	7.36	18.34	17.88	11.00	12.05	25.86
	Exact Sig. (2-sided)	0.00 ^a	0.78	0.33	0.53	0.17	0.27	0.00 ^a	0.03 ^a	0.53	0.46	0.01 ^a
X5	Chi-Square Value	3.79	4.95	1.48	11.3	8.40	0.12	4.14	9.61	2.03	9.11	8.41
	Exact Sig. (2-sided)	0.14	0.15	0.79	0.03 ^a	0.14	1.00	0.10	0.03 ^a	0.61	0.02 ^a	0.10
X6	Chi-Square Value	0.21	1.79	6.51	1.89	8.40	0.70	0.74	0.49	0.83	2.96	1.46
	Exact Sig. (2-sided)	0.93	0.66	0.10	0.73	0.01 ^a	1.00	0.43	0.85	0.83	0.42	0.40
X7	Chi-Square Value	1.10	12.97	2.82	6.33	6.05	0.079	0.63	3.36	4.60	8.11	13.04
	Exact Sig. (2-sided)	0.66	0.01 ^a	0.48	0.12	0.12	1.00	0.41	0.22	0.14	0.06	0.14

^aExact Sig. (2-sided) p < 0.0; H₀ is rejected

Table 6. Sutculer district's chi-square independence test result

		X9	X10	X11	X15	X16	X17	X18	X20	X21	X22	X25	X26	X27	X29
X1	Chi-Square Value	0.62	7.30	6.25	15.79	15.26	4.80	3.81	2.17	7.65	7.37	4.36	6.62	13.16	5.84
	Exact Sig. (2-sided)	0.89	0.29	0.40	0.14	0.17 ^a	0.99	0.70	0.99	0.56	0.29	0.64	0.69	0.15	0.44
X2	Chi-Square Value	1.51	7.80	10.22	17.76	4.02	4.25	1.56	12.19	35.25	9.73	1.10	4.83	10.83	7.26
	Exact Sig. (2-sided)	0.47	0.92	0.051	0.00 ^a	0.39	0.70	0.85	0.07	0.00 ^a	0.04 ^a	0.94	0.59	0.85	0.11
X3	Chi-Square Value	12.85	39.08	11.34	12.09	12.01	16.91	8.40	28.69	17.95	12.32	8.55	14.57	21.57	6.68
	Exact Sig. (2-sided)	0.03 ^a	0.00 ^a	0.33	0.26	0.22	0.47	0.64	0.09	0.23	0.25	0.48	0.50	0.10	0.59
X4	Chi-Square Value	0.23	25.97	15.34	25.69	10.75	16.15	10.94	37.33	23.42	12.65	6.27	15.58	21.43	6.73
	Exact Sig. (2-sided)	1.00	0.05	0.85	0.00 ^a	0.20	0.40	0.19	0.00 ^a	0.11	0.11	0.57	0.20	0.04 ^a	0.49
X5	Chi-Square Value	1.45	13.45	17.99	2.69	7.02	12.86	7.47	16.37	7.85	0.70	21.61	4.09	8.70	3.35
	Exact Sig. (2-sided)	0.32	0.02 ^a	0.00 ^a	0.38	0.04 ^a	0.00 ^a	0.01 ^a	0.01 ^a	0.09	0.85	0.00 ^a	0.25	0.02 ^a	0.21
X6	Chi-Square Value	5.38	3.15	2.00	1.48	0.42	4.84	1.28	2.68	4.07	1.31	0.52	10.53	5.53	1.69
	Exact Sig. (2-sided)	0.02 ^a	0.2	0.34	0.47	0.88	0.31	0.55	0.47	0.25	0.53	0.81	0.01 ^a	0.14	0.60
X7	Chi-Square Value	0.54	17.17	15.82	7.87	3.11	3.62	2.08	37.82	38.03	8.41	3.42	2.55	10.99	11.86
	Exact Sig. (2-sided)	0.58	0.00 ^a	0.00 ^a	0.02 ^a	0.24	0.43	0.37	0.00 ^a	0.00 ^a	0.01 ^a	0.22	0.46	0.01 ^a	0.01 ^a

^aExact Sig. (2-sided) p < 0.0, H₀ is rejected

Young goat breeders in Sutculer district are of the opinion that the village rangelands are managed erroneously and do not approve of the grazing permits provided for their own regions to breeders from other districts. It was determined that goat breeders with lower education levels are subject to more grazing penalties. Breeders involved in this profession for shorter periods of time are of the opinion that the village rangelands are managed erroneously. It was observed that goat breeders with means of income other than goat breeding graze their goats at lower elevations, follow up state aids and display more sensitive behaviors towards the environment.

The variables with a statistically significant relation between them are indicated in bold in *Tables 5 and 6*.

The results for the Sutculer district Multivariate Linear Regression Analysis carried out via Stepwise method are presented in *Table 7*. However, the R² levels were calculated to be very low (below 30%) in the Merkez district Multivariate Linear Regression Analysis carried out via stepwise method and hence the acquired results were not tabulated.

Table 7. Multivariate regression analysis result of Sutculer district

Dep. variables	Model	R ²	Anova		Constant		Dependent variables									
			F	Sig.	Beta	Sig.	X1		X3		X4		X6		X7	
							Beta	Sig.	Beta	Sig.	Beta	Sig.	Beta	Sig.	Beta	Sig.
X18	1	0.10	5.61	0.02	0.88	0.00									0.36	0.02
	2	0.20	6.19	0.00	0.34	0.00	0.17	0.01							0.38	0.01
X20	1	0.08	4.54	0.03	0.68	0.00						0.46	0.03			
X21	1	0.16	10.49	0.00	1.24	0.00			-0.08	0.00						
	2	0.44	20.02	0.00	1.69	0.00			-0.11	0.00	-0.067	0.00				
	3	0.49	16.26	0.00	1.75	0.00	-0.05	0.00	-0.11	0.00	-0.050	0.00				
X26	1	0.09	5.84	0.19	1.24	0.00							1.08	0.019		
X27	1	0.24	16.05	0.00	0.75	0.00							0.25	0.00		
X30	1	0.19	12.05	0.00									0.20	0.00		

The specificity coefficient (R^2) level in regression models that explain the change in the dependent variables of the Sutculer district in a statistically significant manner was calculated as 44-49% for the X21 dependent variable and as lower than 25% for the other dependent variables. Hence, only the regression equalities for the “Expelling tree-harming animals from the forest” dependent variable can be used for estimation. Therefore, there is a need for other variables to estimate the related dependent variables for the Sutculer and Merkez districts breeders.

Conclusions

It was observed upon evaluating the results related with the general characteristics of goat breeding businesses that the breeders are generally above middle age and that they do not want their children to continue this profession. The education levels of current goat breeders were determined to be quite low. In light of these findings, it can be estimated that traditional goat breeding profession will decrease at a rapid rate in the coming years. The most important problem of goat breeders was determined to be grazing issue and a solution for this problem should be developed in cooperation with the forest administration. Of the goat breeders, 21% in the first study area and 45% in the second study area were subject to fines due to unauthorized grazing in forest resource areas. This is an important finding of the study and it can be stated that goat breeders make certain violations with regard to sustainable forest resources management due to the grazing problem they face. Hence, the cooperation between goat breeders and forest administrators should be increased to provide solutions to this issue.

It was determined that the interventions by goat breeders in the Sutculer district for preventing the goats from harming the trees in the forest during grazing decreased with increasing age, decreasing education level and the duration of experience in this profession (*Table 7*).

According to the study results, the two rural settlement areas are not similar with regard to characteristics related to demographic-socioeconomic and hair goat breeding as well as sustainable management of forests even though they are located in the same geographical region. Therefore, it is not sufficient to only consider geographical area similarity when determining the precautions for preventing breeders from harming the forests or in other words the precautions for enabling them to contribute to the sustainable management of forests. In addition, it was observed that especially age, education level and the duration of experience in breeding are variables that should be taken into consideration with regard to precautions for increasing the participation of breeders in the sustainable management of forest resources.

Acknowledgments. This study was supported by the Turkish Scientific and Technical Research Council of Turkey (TUBITAK) (Project No: 117O549). The authors extend their gratitude to the TUBITAK.

Conflict of interests. The authors declare that there is no conflict of interests regarding the publication of this paper.

REFERENCES

- [1] Ainalis, A. B., Tsiouvaras, C. N. (2004): Forage production of woody fodder species and herbaceous vegetation in a silvopastoral system in Northern Greece. – *Agroforestry Systems*, 42: 1-11.
- [2] Ainalis, A. B., Tsiouvaras, C. N., Nastis, A. S. (2006): Effect of summer grazing on forage quality of woody and herbaceous species in a silvopastoral system in Northern Greece. – *Journal of Arid Environment* 67: 90-99.
- [3] Aldezabal, A., Garin, I. (2000): Browsing preference of feral goats (*Capra hircus* L.) in a Mediterranean mountain scrubland. – *Journal of Arid Environment* 44: 133-142.
- [4] Arac, B., Daskiran, I. (2010): Diyarbakır ili keçicilik işletmelerinin yapısal özellikleri (Structural Characteristics of Goats in Diyarbakir Province). – *Journal of Tekirdag Agricultural Faculty* 3(7).
- [5] Bassullu, C., Tolunay, A. (2010): Analysis on traditional homegarden involving animals practices and its importance classification of usage purposes in rural areas of Isparta region of Turkey. – *Asian Journal of Animal Veterinary Advances* 5: 450-464.
- [6] Bekiroğlu, S., Özdemir, M., Özyürek, E., Arslan, A. (2016): Opportunities to enhance contribution of model forests in the sustainable forest resources management (example from Yalova Model Forest). – *Journal of Environmental Management* 181(1): 701-709.
- [7] Boyazoglu, J., Hatziminaoglou, I., Morand-Fehr, P. (2005): The role of the goat in society: past, present and perspectives for the future. – *Small Ruminant Research* 60: 13-23. <https://doi.org/10.1016/j.smallrumres.2005.06.003>.
- [8] FAO (1991): The State of Food and Agriculture 1991. – FAO Agriculture Series, no. 24, Rome.
- [9] Gholz, H. L. (1986): Canopy Development and Dynamics in Relation to Primary Production. – In: Fujimori, T., Whitehead, D. (eds.) *Crown and Canopy Structure in Relation to Productivity*. Proc. Int. Workshop, October 1985, Ibraki, Japan, pp. 224-242.
- [10] Guney, O., Darcan, N. (2001): Süt keçiciliğinde ileri tekniklerin uygulanabilirliği için gerekli koşullar (Necessary conditions for applicability of advanced techniques in goat milk production). – Goat Cultivation Panel in Canakkale Province, 12 June, Canakkale, Turkey.
- [11] Guney, O., Darcan, N. (2005): Akdeniz kuşağında keçi yetiştiriciliğinin yapısal durumu ve gelişme perspektifleri (The structural status and development perspectives of goat cultivation in the Mediterranean Zone). – International Symposium on Forest, Goat, Erosion and Tourism, 12-13 April 2005, Adana, Turkey.
- [12] Heitschmidt, R. K., Taylor, C. A. (1993): Livestock Production. – In: Heitschmidt, R. K., Stuth, J. W. (eds.) *Grazing Management: An Ecological Perspective*. Timber Press, Portland, OR, pp. 161-177.
- [13] Heitschmidt, R. K., Dowhower, S. L., Walker, J. W. (1987): Some effects of rotational grazing treatment on quantity and quality of available forage and amount of ground litter. – *J. Range Manage.* 40: 318-321.
- [14] Ince, D. (2010): Reproduction performance of Saanen goats raised under extensive conditions. – *African Journal of Biotechnology* 9(48): 8253-8256.
- [15] Ince, D., Karaca, O. (2009): Effects of oestrus synchronization and various doses of PMSG administration in Chios×Kivircik (F1) sheep on reproductive performances. – *Journal of Animal Veterinary Advances* 8: 1948-1952.
- [16] Ince, D., Koknaroglu, H., Toker, M. T. (2009): Sustainability suggestions for goat husbandry in Isparta, Turkey. – *Macedonian Journal of Animal Science* 2(2): 133-138.
- [17] Karasar, N. (2012): *Scientific Research Method: Concepts, Principles, Techniques*. – Nobel Press, Ankara.
- [18] Kasikci, D. (2016): Grazing in forests. – Isparta Province Pasture Workshop, 09-10 March 2016, Isparta, Turkey.

- [19] Kıvrak, R. (2014): Walking Turks Nomadics (Yürüyen Türkler Yörükler). – Ege reklam basım sanatları San. Tic. Ltd., Şti. İzmir.
- [20] Koknaroglu, H., Ali, A., Ekinci, K. Morrival, D. G., Hoffman, M. P. (2007): Cultural energy analysis of lamb production in the feedlot or on pasture and in the feedlot. – Journal of Sustainable Agriculture 30: 95-108.
- [21] Koyuncu, M., Tuncel, E. (2010): Keçinin Önemi ve Yörük Kültüründeki Yeri (Importance of goat and its place in nomadic culture). – Uludağ University Agricultural Faculty, Zootechnology Department, National Congress on Goat Cultivation, Bursa, Turkey.
- [22] Laugesen, M., Elliot, R. (2003): Ischaemic heart disease, Type 1 diabetes, and cow milk A1 β -casein. – New Zealand Medical Journal 116(1168): U295.
- [23] Morand-Fehr, P., Boutomet, J. P., Devendra, C., Dubeuf, J. P., Haeinlein, G. F. W., Holst, P., Mowlem, L., Capote, J. (2004): Strategy for goat farming in the 21st century. – Small Ruminant Research 51: 175-183.
- [24] Sample Size Calculator (2018): <https://www.surveysystem.com/sscalc.htm>.
- [25] Schmincke, K. H. (1995): Forest industries: crucial for overall socio-economic development. – Unasylva-No.182-FAO 50th anniversary. <http://www.fao.org/3/v6585e/v6585e00.htm#Contents>.
- [26] Semerci, A., Çelik, A. D. (2016): Türkiye’de küçükbaş hayvan yetiştiriciliğinin genel durumu. (Small Ruminant Breeding in Turkey). – Mustafa Kemal Üniversitesi Ziraat Fakültesi Dergisi 21(2): 182-196.
- [27] Ocak, S., Torun, O., Guney, O. (2007): A novel method of analyzing rearing system on lamb growth and farm profitability. – African Journal of Agricultural Research 6: 495-499.
- [28] Ocak, S., Davran, M., Guney, O. (2010): Small ruminant production in turkey: highlighting in goat production. – Tropical Animal Health and Production 42(2): 155-159.
- [29] Tasligil, N., Sahin, G. (2010): Türkiye’de Keçi Yetiştiriciliğinin Coğrafi Dağılımı (Geographical Distribution of Goat Breeding in Turkey). – Ulusal Keçicilik Kongresi (National Congress on Goat Cultivation, 24-26 June, Çanakkale, Turkey).
- [30] Tolunay, A., Alkan, H., Korkmaz, M. (2002): Batı Akdeniz Bölgesi’nin Agroforestry (Tarımsal Ormancılık) Üretim Potansiyeli (Agroforestry (Agricultural Forestry) Production Potential in the Western Mediterranean Region). – Office for Research Projects Management, University of Suleyman Demirel. Project No: 275, Isparta, Turkey.
- [31] Tolunay, A., Ayhan, V., Adiyaman, E., Akyol, A., Ince, D. (2009): Herbage growth and fodder yield characteristics of kermes oak (*Quercus coccifera* L.) in a vegetation period. – Journal of Animal and Veterinary Advances 8(2): 290-294.
- [32] Tolunay, A., Babalik, A., Yavuz, M., Akyol, A., Kasikci, D., Adiyaman, E. (2015): Keçi Orman Çelişkisinde Son Durum: Ne Yapıldı? Ne Yapılıyor? Ne Yapılmalı? (Contradiction between Goat and Forest: What was done? What is being done? What should be done?) – Orman ve Av Dergisi (Journal of Forest and Hunt) 6(2): 24-29.
- [33] Tolunay, A., Ince, D., Daskiran, I., Turkoglu, T., Ozmis, M. (2018): Role of Goat Breeding in Reducing Rural Poverty in the Western Mediterranean Region of Turkey. – 1st International Symposium on Silvopastoral Systems and Nomadic Societies in Mediterranean Countries, 22-24 October 2018, Isparta, Turkey.
- [34] Zarovali, M. P., Yiakoulaki, M. D., Papanastasis, V. P. (2007): Effects of shrub encroachment on herbage production and nutritive value in semi-arid Mediterranean grasslands. – Grassland Forage Science 62: 355-363.

MODELING OF DAM RESERVOIR VOLUME USING GENERALIZED REGRESSION NEURAL NETWORK, SUPPORT VECTOR MACHINES AND M5 DECISION TREE MODELS

ÜNEŞ, F.* – DEMIRCI, M. – TAŞAR, B. – KAYA, Y. Z. – VARÇIN, H.

*Hydraulics Division, Civil Engineering Department, Iskenderun Technical University
31040 İskenderun, Hatay, Turkey*

**Corresponding author*

e-mail: fatih.unes@iste.edu.tr; phone: +90-326-613-5600(2806)

(Received 22nd Feb 2019; accepted 29th Mar 2019)

Abstract. Dam reservoir capacity estimation is an important issue for operation, design and safety assessments of dam structures. In this study, the reservoir capacity of the Stony Brook dam in the USA was estimated by Generalized Regression Neural Network (GRNN), Support Vector Machines (SVM) and M5 Tree Model (M5T) methods with using 3726 data taken from United States Geological Survey Institute (USGS) for 2012-2015 years. Listed soft computing techniques give opportunities to researchers working on non-linear problems. Based on the non-linear approach, models are generated by using precipitation, flow, temperature hydrological parameters. The models were compared with each other according to the three statistical criteria, namely, mean absolute error (MAE), root mean square error (RMSE), and determination coefficient. As a result of the study, it is seen that Support Vector Machines (SVM) models have better performance in predicting dam reservoir level than the other used soft computing models.

Keywords: *estimation, reservoir management, soft computing techniques, neural network, statistical approach*

Introduction

Control of the water volume in the reservoir is achieved by accumulating and distributing water at the right time. There may be loss of life and property due to non-timely measures and water-related problems such as flood planning and management, design and operation of the hydraulic structures, navigation in the dam reservoirs, water supply for municipalities and industries, irrigation and drainage, flood damage reduction and water quantity modeling in the reservoir. That is why a proper dam reservoir management is a requirement not only in terms of fresh water supply, but also to prevent potential damages. One of the basic requirements for managing the dam reservoir in the most effective way is to determine the reservoir water volume, estimations the elevations and outflows in this volume. There are so many direct or indirect effects on reservoir levels changes. These effects can be listed as influences of atmospheric, natural, social and environmental conditions. Subdivisions of listed effects are seasonal climate changes and global warming, topography of watershed, fresh water demand, water distribution etc. Each of these effects has different impact on reservoir volume fluctuations and it needs to be considered for analyzes.

Artificial Intelligence methods are called black box models and in recent years they are frequently used in hydraulic and water structures planning because of the prediction abilities of these methods on non-linear problems (Demirci and Baltacı, 2013; Demirci et al., 2015a, 2015b, 2019; Kaya et al., 2018; Tasar et al., 2017, 2018). Artificial Neural Networks (ANN) is one of these models. Artificial Neural Networks are able to solve

complex problems successfully due to their ability to learn and generalize (Ergezer et al., 2003). The foundations of the first modeling of artificial neural networks were laid in an article by McCulloch and Pitts (1943). They modeled simple artificial nerves on electrical circuits. Nowadays, there are many studies on the application of ANN to various cases frequently experienced in water resources. The ANN approach has been shown to represent the precipitation-flow relationship well (Mason et al., 1996; Minns and Hall, 1996; Fernando and Jayawardena, 1998). Turhan (2012) modeled the precipitation-flow relationship of the Seyhan Basin with the ANN method. Unes (2010a) predicted dam reservoir level by artificial neural network. Unes (2010b) also predicted density flow plunging depth in dam reservoir using artificial neural network. Chitsaz et al. (2016) used different estimation techniques for river flow forecasting and compared the results of generalized regression neural network (GRNN), multi-layer perceptron (MLP), adaptive neuro-fuzzy inference system (ANFIS) with each other. The result illustrated that MLP outperformed ANFIS and GRNN. Demirci et al. (2018) predicted dam reservoir volume using adaptive neuro-fuzzy inference system (ANFIS). Yin et al. (2016) compared abilities of different GRNN models such as rotated general regression neural network (RGRNN), feed-forward error back-propagation (FFBP) for river flow forecasting, models are created for semi arid region in China and results clarify that the combined RGRNN model has better performance on river flow forecasting. Unes et al. (2017) predicted dam reservoir volume using adaptive neuro fuzzy approach (ANFIS).

Support Vector Machines (SVM) are machine learning algorithms developed by Vapnik and other researchers (Vapnik, 1995; Cortes and Vapnik, 1995; Vapnik et al., 1997). This approach was originally developed as a way of interpreting sensor data and includes a two-tier structure. The first layer is a weightless nonlinear nucleus on the support vectors containing the input variable series, and the second is a weighted sum of core outputs. Once support vectors and appropriate core filters have been applied, the performance of SVM can be much better than the one of the other soft computing technique ANN in many cases. Many studies have been done for the learning of possible solving performance of SVM in hydrological problems. Dibike et al. (2001) investigated SVM performance for rainfall-runoff modeling and compared to ANN models. Bray and Han (2004) underlined the difficulty in determining a suitable model structure and related parameters for precipitation modeling. Chen et al. (2010) used SVMs to predict daily rainfall in the Hanjiang basin. The SVM technique has recently been effective in solving forestry problems (Nieto et al., 2012), in determining solar rays (Antonanzas et al., 2015) and predicting daily rainfall-runoff (Hosseini and Mahjouri, 2016). Recently, SVMs have been widely used to predict rainfall-runoff and water reservoirs. (flood and stream flow (Yu et al, 2006), atmospheric temperature (Radhika and Shashi, 2009), lake water levels (Khan and Coulibaly, 2006; Asefa et al., 2005; Khalil et al., 2006). Unes al. (2013) estimated dam reservoir level using artificial neural (ANN) network and support vector machines (SVM). M5T is one of the algorithms of decision trees. Decision trees, classification and regression can be applied to problems, effective, non-parametric, is a method that requires intensive calculation (Rao et al, 2007) The application of decision trees in hydrology is limited; only a part of published articles were used to estimate the dam reservoir capacity. Bhattacharya and Solomatine (2005) and Solomatine and Xue (2004) proved that M5T was very effective technique in the prediction rainfall-runoff. Goyal et al. (2013) applied ANN, fuzzy logic and decision tree models (M5T) for the development of reservoir operating rules.

Sattari et al. (2013) used M5T for Turkey, Ankara, Sohi River to investigate the potential of daily stream flow. Esmailzadeh et al. (2017) studied performance evaluation of ANNs and an M5T model tree in Sattarkhan Reservoir inflow prediction.

Aim of this study is to estimate the reservoir capacity of the Stony Brook dam in Massachusetts, USA. By using temperature, precipitation and flow data, the reservoir capacity was estimated with GRNN, SVM and M5T models and the models were compared with each other.

Materials and methods

Study area

In this study, dam reservoir volume was estimated by using the temperature, precipitation and flow data obtained from the United States Geological Survey (USGS). The Stony Brook dam reservoir in the USA was selected as application area (*Fig. 1*). (USGS station no: 01104480). The Stony Brook dam is located in Middlesex County, Massachusetts with $42^{\circ} 35' 46.3''$ (42.5962°) latitude and $71^{\circ} 26' 18.7''$ (71.4385°) longitude. Drainage area of dam reservoir is 70.7 km^2 . Stony Brook Reservoir reaches a height of 21 m; the deepest point is about 9.15 m, roughly $1.608 \cdot 10^6 \text{ m}^3$ of water at full capacity. Stony Brook is relatively small compared to the large basin and is much faster than other dams. Ekstrem air-temperatures were recorded as maximum, 36.5°C , and minimum, -23.3°C for all the dam catchment area. Stony Brook dam catchment's climate is classified as warm and temperate. Stony brook catchment has a significant amount of rainfall during the year. The average annual temperature is 11.3°C in Stony brook. About 1025 mm of precipitation falls annually. 3726 daily data for five years were used between 2012-2017 years.

Daily air average temperature, precipitation, river inflow, lag time reservoir volume are taken as inputs and reservoir volume as output of the models. The temperature, precipitation, flow and past reservoir volume (time, $t-1$) of the Stony Brook dam were taken as input. 2126 of 3726 data were used for the training; remaining 1600 data were utilized for the test. Probable volumes in the next times are generated by the Generalized Regression Neural Network (GRNN), Support Vector Machines (SVM) and M5 Tree Model (M5T) artificial techniques. Reliability of the model results are examined with error parameters as root mean square error, mean absolute error, and coefficient of determination (R^2) between model volume estimations and observed reservoir volumes.

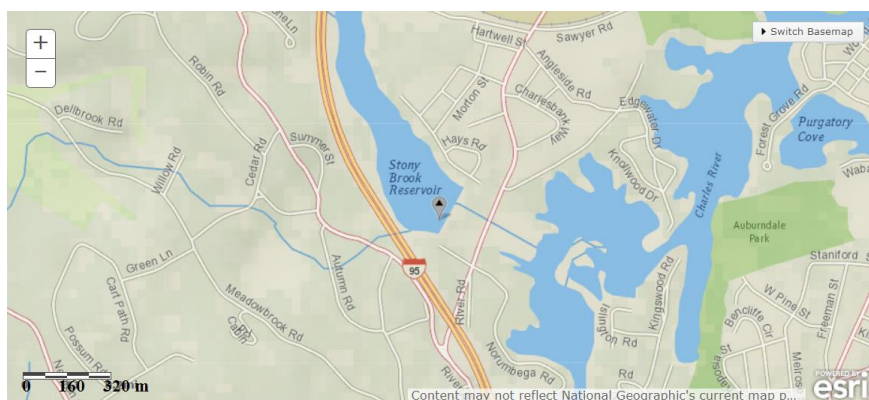


Figure 1. Overview of Stony Brook Dam (USGS)

Methods

In this study 3726 day precipitation, flow and temperature data of the observation station were used in the Stony Brook Reservoir volume prediction. The results of Generalized Neural Network (GRNN), Support Vector Machines (SVM) and M5 Tree Model (M5T) are given as follows. The root mean square error (RMSE), mean absolute error (MAE), and the determination coefficients (R^2) were calculated for each model. The results were also used to compare the performance of the model estimation and observation data. RMSE and MAE are determined as follows in *Equations 1* and *2*, respectively:

$$\text{RMSE} = \sqrt{\frac{1}{N} \sum_{i=1}^N (Y_{i\text{observed}} - Y_{i\text{prediction}})^2} \quad (\text{Eq.1})$$

$$\text{MAE} = \frac{1}{N} \sum_{i=1}^N |Y_{i\text{observed}} - Y_{i\text{prediction}}| \quad (\text{Eq.2})$$

where N is the data number and Y_i is the reservoir volume data. Determination coefficient (R^2), root mean square error (RMSE) and absolute mean error (MAE) were calculated for the performance evaluation of GRNN, SVM and M5T models.

Support vector machines (SVM)

Support vector (SVM) is machine-learning approach in data-driven research fields which founded by Cortes and Vapnik (1995). SVM is basically used to best distinguish between two data classes. For this purpose decision limits or hyper planes are determined. In a non-linear dataset, SVM cannot draw a linear hyper plane. Therefore, the kernel numbers are used. The Kernel method greatly improves machine learning in nonlinear data. In the kernel method, the SVM estimator (y) process can be expressed as in *Equation 3*:

$$y = (K_{xi} \cdot W_{jk}) + b \quad (\text{Eq.3})$$

In *Equation 3*, b is the bias term of the SVM network, and W_{jk} is called the weight vector. K_{xi} is a non-linear function that maps input vectors to a high-dimensional property field. The structure of the SVM model with three layers used in this study is given in *Figure 2*. The output value for this example SVM model is equal to the sum of the three products in the inputs and the independent combinations of Lagrange multipliers. Nonlinear nuclear functions used in this study are radial based kernel function and poly kernel functions.

Support vector machines with radial base functions (SVM-RBF)

Lagrange multipliers show the importance of training data sets for output data. The non-linear radial-based kernel function (Hsu et al., 2003) is shown in the *Equation 4*:

$$K_{xi} = e^{-\gamma \|p_i - y_i\|^2} \quad \gamma > 0 \quad \text{and} \quad i = 1, 2, 3, \dots, n \quad (\text{Eq.4})$$

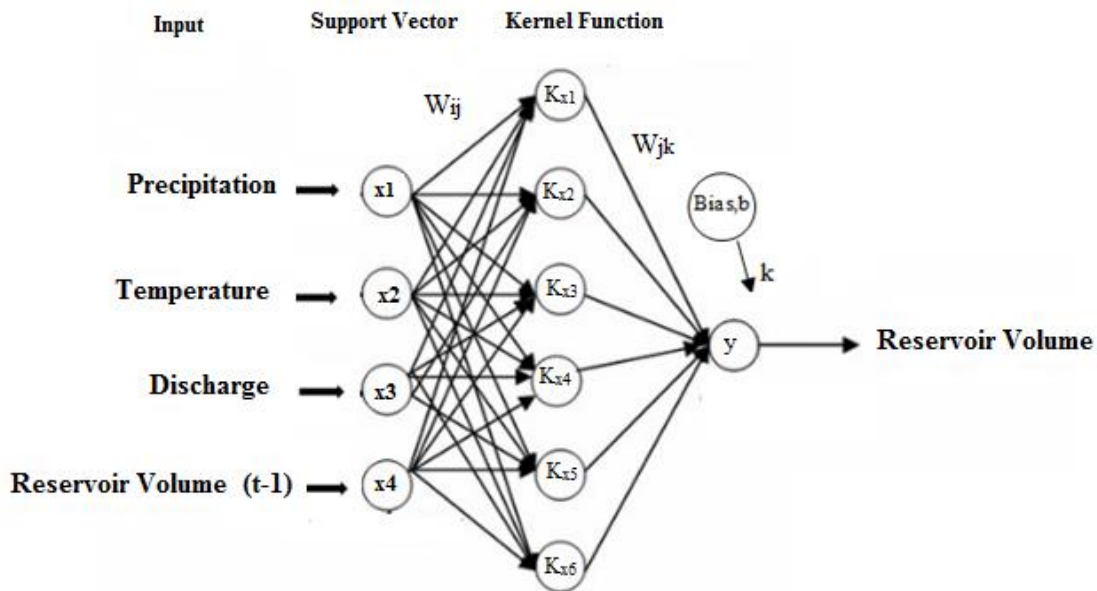


Figure 2. Structure of SVM-1 model used in this study

Support vector machines with poly kernel (SVM-PK)

Poly kernel function (Hsu et al, 2003) is shown by the Equation 5:

$$K_{xi} = (p \cdot y + c)^d \quad i = 1, 2, 3, \dots, n \quad (\text{Eq.5})$$

M5 decision tree method (M5T)

A decision tree is a logical model shown as a binary (two-way split) tree that shows how the value of a dependent variable can be estimated by using the values of the argument set. There are basically two types of decision trees:

- (1) Classification trees are the most common and a symbolic class used to estimate the value of a numerical attribute.
- (2) Used to predict regression trees (Witten and Frank (2005).

If each leaf in the tree contains a linear regression model used to estimate the target variable in that leaf, then it is called a model tree.

The M5 decision tree algorithm was originally developed by Quinlan (1992). A detailed description of this technique can be found in Witten and Frank (2005). A brief description of this technique is as follows. The M5 algorithm creates a regression sequence by iteratively dividing the sample space using tests on a single attribute that maximizes the variance in the target space. Mathematical formula to calculate standard deviation reduction (SDR) can be written as in Equation 6:

$$SDR = sd(T) - \sum I \frac{T_i}{T} I \quad sdIT_i \quad (\text{Eq.6})$$

where T represents a group of samples reaching the node; T_i represents a subset of samples that are the result of the potential cluster; and sd represents the standard deviation. After the tree is enlarged, a linear multiple regression is created for each

internal node using all the attributes associated with that node and the tests in the subtest of that node. Each sub-tree is then taken into account in pruning to overcome the problem of pruning. Pruning occurs when the estimated error for the linear model at the root of a child tree is less than or equal to the expected error for the child tree. Finally, smoothing is used to compensate for sharp discontinuities between adjacent linear models in the leaves of the pruning tree.

Generalized regression neural network (GRNN)

The GRNN architecture (Specht, 1991) includes the radial basic function (RBF) method. Any optional function between input and output vectors is derived directly from training data. GRNN is based on nonlinear regression theory for function estimation. The training set consists of x input values, each of which has a corresponding value of y output. This regression method estimates the y value.

GRNN estimates any function between input and output vectors using the training data. As the training set expands, the prediction error is reduced to zero. GRNN is used for estimation of continuous variables, just like standard regression techniques. *Figure 3* shows the Generalized Regression Neural Network model used in the present study.

Function classification with GRNN is done by using *Equations 7 and 8*:

$$K(x, x_k) = e^{-d_k/2\sigma^2} \quad (\text{Eq.7})$$

$$d_k = (x - x_k)^T * (x - x_k) \quad (\text{Eq.8})$$

where d_k is the squared Euclidean distance between the training samples x_k and the input x

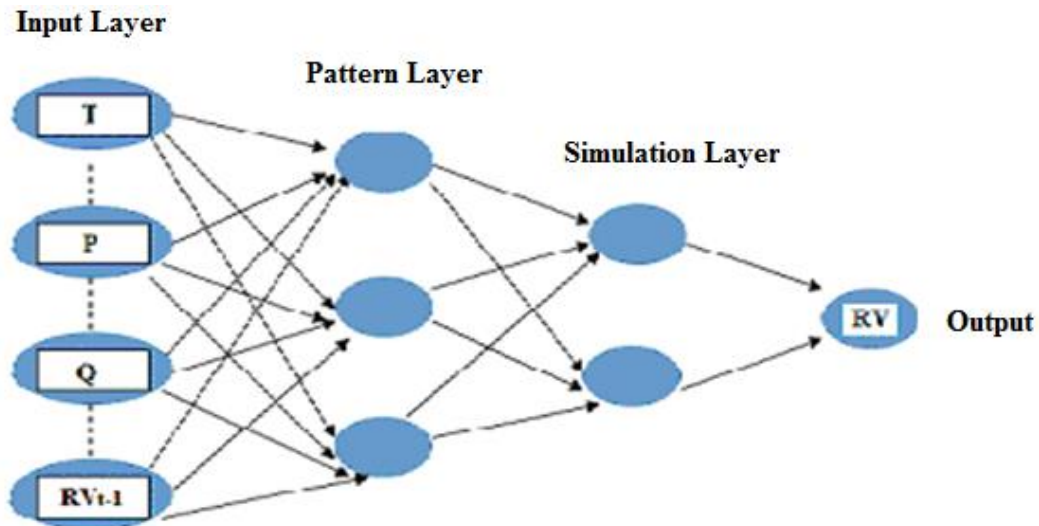


Figure 3. Structure of GRNN1 model used in this study

In GRNN1 model, Average temperature (T), Precipitation (P), Flow (Q), 1 lagged day reservoir volume (RVt-1) were taken as input and reservoir volume (RV) was predicted as output.

Results and discussion

The results were used to compare the performance of the model estimation and the observation data. The comparison of RMSE, MAE and R^2 parameters obtained from the test data is shown in *Table 1*.

Table 1. Performance comparison of models

Methods	Method inputs	RMSE	MAE	R^2
GRNN1	T_t, Q_t, P_t, RV_{t-1}	41.5001	27.1486	0.8636
GRNN2	$T_t, Q_t, P_t, P_{t-1}, RV_{t-1}$	37.1542	25.0508	0.8935
GRNN3	$T_t, Q_t, Q_{t-1}, P_t, P_{t-1}, RV_{t-1}$	36.9193	24.7788	<u>0.8951</u>
M5T 1	T_t, Q_t, P_t, RV_{t-1}	25.0649	16.9725	0.9465
M5T 2	$T_t, Q_t, P_t, P_{t-1}, RV_{t-1}$	22.4109	14.9732	0.9577
M5T 3	$T_t, Q_t, Q_{t-1}, P_t, P_{t-1}, RV_{t-1}$	22.1890	14.9199	<u>0.9584</u>
SVM RBF1	T_t, Q_t, P_t, RV_{t-1}	24.0233	15.5659	0.9523
SVM RBF2	$T_t, Q_t, P_t, P_{t-1}, RV_{t-1}$	22.2190	14.7506	0.9591
SVM RBF3	$T_t, Q_t, Q_{t-1}, P_t, P_{t-1}, RV_{t-1}$	21.8718	14.4796	<u>0.9605</u>
SVM PK1	T_t, Q_t, P_t, RV_{t-1}	23.9572	15.2520	0.9536
SVM PK2	$T_t, Q_t, P_t, P_{t-1}, RV_{t-1}$	22.1670	14.4932	0.9605
SVM PK3	$T_t, Q_t, Q_{t-1}, P_t, P_{t-1}, RV_{t-1}$	21.8393	14.2555	<u>0.9617</u>

RMSE: root mean square error, MAE: mean absolute error, R^2 : determination coefficient

In this study, Mean Air Temperature (T_t), Flow (Q_t), the lagged time Flow (Q_{t-1}), Mean Precipitation (P_t), the lagged time Precipitation (P_{t-1}) and the lagged time Reservoir Storage (RV_{t-1}) were used to reservoir storage capacity prediction.

The temperature, precipitation, flow and lagged time reservoir volume of the Stony Brook dam were taken as input. 2126 of 3726 data were used for the training; remaining 1600 data were applied for the test. The results obtained by the model were compared with the measured values. Obtained results of these studies are given in *Table 1*.

Predictions were made by using Generalized Neural Network (GRNN), Support Vector Machines with basic radial functions (SVM-RBF), Support Vector Machines with poly kernel (SVM-PK) and Decision Tree Methods (M5T). Three evaluations were made in all three models. Estimation results of the models were compared according to R^2 (Determination Factor), Mean Absolute Error (MAE) and Root Mean Square Error (RMSE) criteria.

In GRNN1, SVM RBF1, SVM PK1 and M5T 1 models, average temperature (T), Precipitation (P), Flow (Q), 1 lagged day reservoir volume (RV_{t-1}) were taken as input, In GRNN2, SVM RBF2, SVM PK2 and M5T 2 models, average temperature (T), Precipitation (P), Flow (Q), 1 lagged day Precipitation (P_{t-1}) and 1 lagged day reservoir volume (V_{t-1}) were taken as input In GRNN3, SVM RBF3, SVM PK3 and M5T 3 models, average temperature (T), Precipitation (P), Flow (Q), 1 lagged day Flow (Q_{t-1}), 1 lagged day Precipitation (P_{t-1}) and 1 lagged day reservoir volume (V_{t-1}) were taken as input.

Scatter and distribution graphs showing the relationships of the three models with the real data are shown in *Figure 4* for GRNN, *Figure 5* for M5T, *Figure 6* for SVM PK and *Figure 7* for SVM RBF.

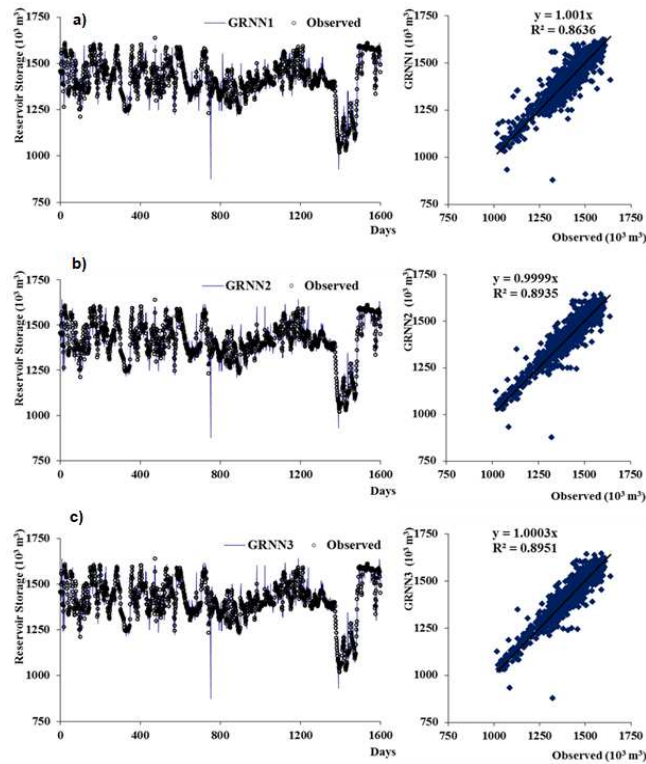


Figure 4. Observed and GRNN distribution-scatter chart for dam reservoir volume test data *a* GRNN1, *b* GRNN2, *c* GRNN3

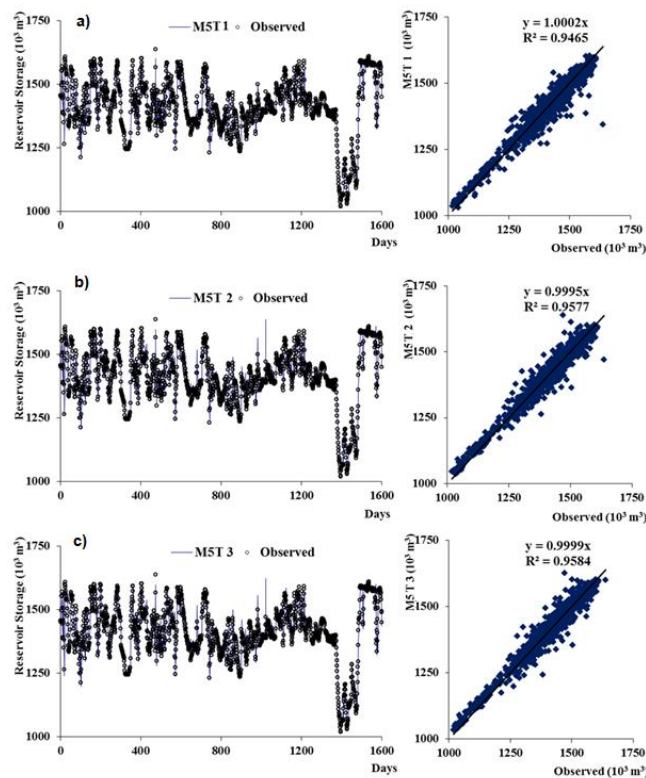


Figure 5. Observed and M5T distribution-scatter chart for dam reservoir volume test data *a* M5T 1, *b* M5T 2, *c* M5T 3

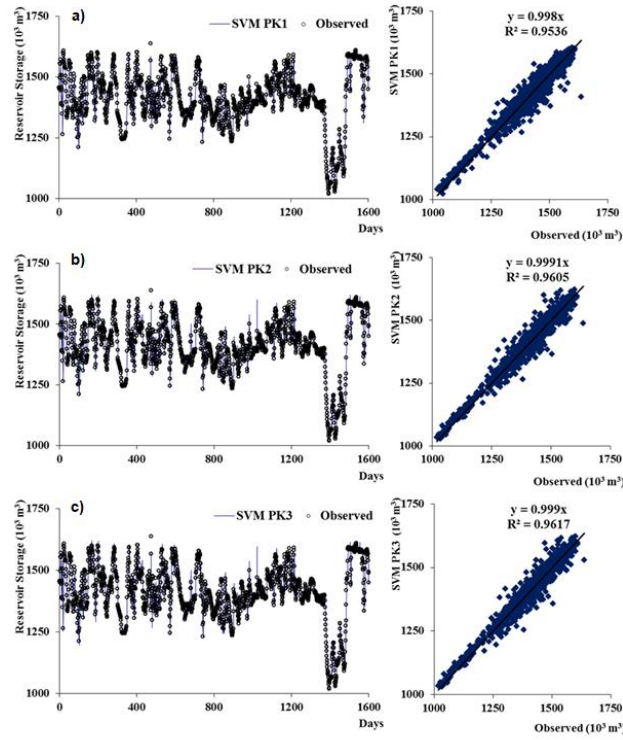


Figure 6. Observed and SVM-PK distribution-scatter chart for dam reservoir volume test data
 a SVM PK1, b SVM PK2, c SVM PK3

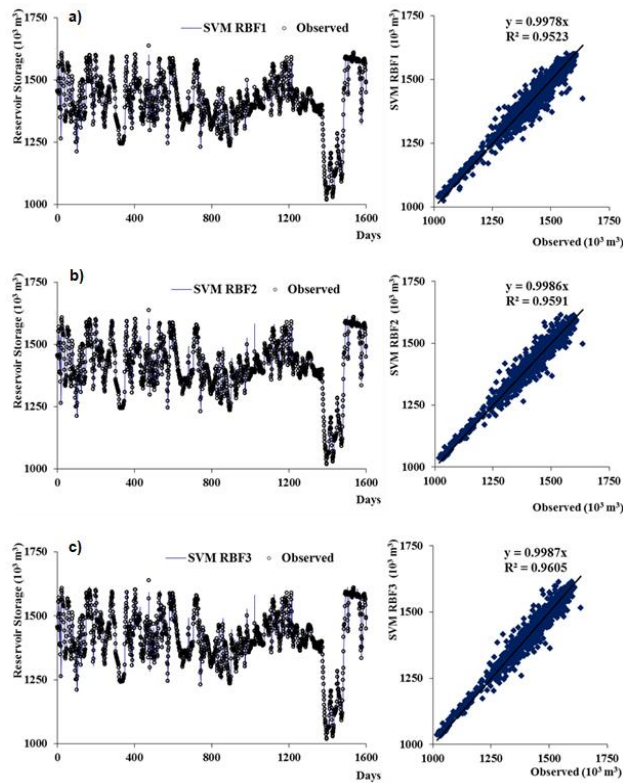


Figure 7. Observed and SVM-PK distribution-scatter chart for dam reservoir volume test data
 a SVM RBF1, b SVM RBF2, c SVM RBF3

The performance of GRNN model is presented graphically in *Figure 4*. If the distribution and scatter graphs are examined, there is a good relationship between the estimated and observed values. When we looked at the RMSE, MAE and R^2 (21.8718, 14.4796, 0.9605) shown in *Table 1*, compared to other models, GRNN models showed the worst performance.

Data for 3726 days were evaluated for M5T models and the results were defined as follows. The distribution and scatter graphs of the M5T models are shown in *Figure 5*. When the distribution and scatter patterns are examined, the estimated values are close to the actual values. When we look at the benchmark values of RMSE, MAE and R^2 (22.1890, 14.9199, 0.9584) shown in *Table 1*, the M5T 3 model result are better than the other M5T models. Generally M5T model results showed better performance than GRNN models but showed better a little bit worst performance compared with SVM models.

In *Figure 6*, when the SVM RBF models are considered, it is seen that the determination coefficient is high and dam reservoir volume estimations are close to the actual values. The SVM RBF3 model showed low error, high correlation and better performance than other SVM RBF models according to the criteria of RMSE, MAE and R^2 (21.8718, 14.4796, 0.9605) as shown in *Table 1*.

For SVM PK models, the distribution and scatter plots are shown in *Figure 7*. When the scatter graphs were analyzed for the test data, SVM PK model results showed a better performance than SVM RBF models. The SVM PK3 model estimates are close to the actual values. In the SVM PK3 model with the highest coefficient of determination, $R^2 = 0.9617$. The SVM PK3 model gave best results than the other SVM PK, SVM RBF, GRNN and M5T models according to the criteria of RMSE, MAE and R^2 (21.8393, 14.2555, 0.9617)

Conclusion

In this study, Stony Brook dam reservoir volumes estimated by using Support Vector Machines with Radial Base Functions (SVM-RBF), Support Vector Machines with Poly Kernel (SVM-PK), Generalized Regression Neural Network (GRNN) and M5 Decision Tree (M5T). Precipitation, temperature, discharge parameters were applied as input to the models. The results were compared to the actual results and the relationship between the models was examined. As a result of the study in this paper it is possible to derive the following conclusions.

Different combinations of inputs parameters were used for each model. As it is expected, the model which use the all four suggested parameters as input has better performance than the other combinations in SVM, GRNN and M5T models.

Comparing all models, SVM-PK models have better performance in predicting dam reservoir volume. The SVM PK-3 model provides the best performance according to the low amount of error (RMSE, MAE) ratios and high coefficient of determination (R^2). In all models, GRNN models showed the worst performance in the prediction reservoir dam volume. SVM model performances are preferably better than M5T models. It is possible to state that However, comparisons indicate that Support Vector Machines model solutions can provide a tighter fit to the observed data. It was seen that SVM-PK method had less error than the SVM-RBF method.

The ANN correctly adapts to the changing input conditions, such as irrigation policy changes in this example. This is quite important since similar sudden changes can be

observed on the related time series within the reservoir operation management studies. The advantages of applied soft computing techniques in this study over past conventional methods in the prediction of reservoir volume can be explained by saying that soft computing techniques structure includes the non-linear dynamics of the problem in the whole data set.

The monthly reservoir volume estimations obtained results based on this study can be quite informative for the determination of flood planning and management, the hydroelectric energy computations, design and operation of the hydraulic structures, navigation in the dam reservoirs, water supply for municipalities and industries, irrigation and drainage, flood damage reduction and water quantity modeling in the reservoir.

Acknowledgements. The data used in this study were downloaded from the web server of the USGS. The authors wishes to thank the staff of the USGS who are associated with data observation, processing, and management of USGS websites.

REFERENCES

- [1] Antonanzas, J., Urraca, R., Martinez-de-Pison, F. J., Antonanzas-Torres, F. (2015): Solar irradiation mapping with exogenous data from support vector regression machines estimations. – *Energy Conversion and Management* 100: 380-390.
- [2] Asefa, T., Kemblowski, M., Lall, U., Urroz, G. (2005): Support vector machines for nonlinear state space reconstruction: application to the Great Salt Lake time series. – *Water Resources Research* 41(12). DOI: 10.1029/2004WR003785.
- [3] Bhattacharya, B., Solomatine, D. P. (2005): Neural networks and M5 model trees in modelling water level–discharge relationship. – *Neurocomputing* 63: 381-396.
- [4] Bray, M., Han, D. (2004): Identification of support vector machines for runoff modelling. – *Journal of Hydroinformatics* 6(4): 265-280.
- [5] Chitsaz, N., Azarnivand, A., Araghinejad, S. (2016): Pre-processing of data-driven river flow forecasting models by singular value decomposition (SVD) technique. – *Hydrol Sci J* 61(12): 2164-2178.
- [6] Chen, H., Guo, J., Xiong, W., Guo, S., Xu, C. Y. (2010): Downscaling GCMs using the Smooth Support Vector Machine method to predict daily precipitation in the Hanjiang Basin. – *Advances in Atmospheric Sciences* 27(2): 274-284.
- [7] Cortes, C., Vapnik, V. (1995): Machine learning. – *Support Vector Networks* 20: 273-297.
- [8] Demirci, M., Baltaci, A. (2013): Prediction of suspended sediment in river using fuzzy logic and multilinear regression approaches. – *Neural Computing and Applications* 23(1): 145-151.
- [9] Demirci, M., Unes, F., Saydemir, S. (2015a): Suspended Sediment Estimation Using an Artificial Intelligence Approach. – In: Heininger, P., Cullmann, P. (eds.) *Sediment Matters*. Springer, Switzerland, pp. 83-95.
- [10] Demirci, M., Unes, F., Aköz, M. S. (2015b): Prediction of cross-shore sandbar volumes using neural network approach. – *Journal of Marine Science and Technology* 20(1): 171-179.
- [11] Demirci, M., Unes, F., Kaya, Y. Z., Tasar, B., Varcin, H. (2018): Modeling of dam reservoir volume using adaptive neuro fuzzy method. – *Conference Aerul si Apa. Componente ale Mediului*, pp. 145-152. DOI: 10.24193/AWC2018_18.
- [12] Demirci, M., Unes, F., Körlü, S. (2019): Monthly groundwater level modeling of Reyhanli region in Turkey using artificial intelligence techniques. – *Applied Ecology and*

- Environmental Research 17(2): 2651-2663. DOI: http://dx.doi.org/10.15666/aeer/1702_26512663.
- [13] Dibike, Y. B., Velickov, S., Solomatine, D., Abbott, M. B. (2001): Model induction with support vector machines: introduction and applications. – *Journal of Computing in Civil Engineering* 15(3): 208-216.
- [14] Ergezer, H., Dikmen, M., Özdemir, E. (2003): Yapay sinir ağları ve tanıma sistemleri. – *PiVOLKA* 2(6): 14-17.
- [15] Esmaeilzadeh, B., Sattari, M. T., Samadianfard, S. (2017): Performance evaluation of ANNs and an M5 model tree in Sattarkhan Reservoir inflow prediction. – *ISH Journal of Hydraulic Engineering* 23(3): 283-292.
- [16] Fernando, D. A. K., Jayawardena, A. W. (1998): Runoff forecasting using RBF networks with OLS algorithm. – *Journal of Hydrologic Engineering* 3(3): 203-209.
- [17] Goyal, M. K., Ojha, C. S. P., Singh, R. D., Swamee, P. K., Nema, R. K. (2013): Application of ANN, fuzzy logic and decision tree algorithms for the development of reservoir operating rules. – *Water Resources Management* 27(3): 911-925.
- [18] Hosseini, S. M., Mahjouri, N. (2016): Integrating support vector regression and a geomorphologic artificial neural network for daily rainfall-runoff modeling. – *Applied Soft Computing* 38: 329-345.
- [19] Hsu, C. W., Chang, C. C. Lin, C. J. (2003): A Practical Guide to Support Vector Classification. – Tech. Report, Dept Computer Sci. & Info. Engng, National Taiwan University, Taiwan, China.
- [20] Kaya, Y. Z., Üneş, F., Demirci, M., Taşar, B., Varçin, H. (2018): Groundwater level prediction using artificial neural network and M5 tree models. – *Conference Aerul si Apa. Componente ale Mediului*, pp. 195-201. DOI: 10.24193/AWC2018_23.
- [21] Khalil, A. F., McKee, M., Kembrowski, M., Asefa, T., Bastidas, L. (2006): Multiobjective analysis of chaotic dynamic systems with sparse learning machines. – *Advances in Water Resources* 29(1): 72-88.
- [22] Khan, M. S., Coulibaly, P. (2006): Application of support vector machine in lake water level prediction. – *Journal of Hydrologic Engineering* 11(3): 199-205.
- [23] Mason, J. C., Price, R. K., Tem'Me, A. (1996): A neural network model of rainfall-runoff using radial basis functions. – *Journal of Hydraulic Research* 34(4): 537-548.
- [24] McCulloch, W. S., Pitts, W. (1943): A logical calculus of the ideas immanent in nervous activity. – *The Bulletin of Mathematical Biophysics* 5(4): 115-133.
- [25] Minns, A. W., Hall, M. J. (1996): Artificial neural networks as rainfall-runoff models. – *Hydrological Sciences Journal* 41(3): 399-417.
- [26] Nieto, P. G., Torres, J. M., Fernández, M. A., Galán, C. O. (2012): Support vector machines and neural networks used to evaluate paper manufactured using *Eucalyptus globulus*. – *Applied Mathematical Modelling* 36(12): 6137-6145.
- [27] Quinlan, J. R. (1992): Learning with continuous classes. – *5th Australian Joint Conference on Artificial Intelligence* 92: 343-348.
- [28] Radhika, Y., Shashi, M. (2009): Atmospheric temperature prediction using support vector machines. – *International Journal of Computer Theory and Engineering* 1(1): 55.
- [29] Rao, M., Fan, G., Thomas, J., Cherian, G., Chudiwale, V., Awawdeh, M. (2007): A web-based GIS decision support system for managing and planning USDA's conservation reserve program (CRP). – *Environmental Modelling & Software* 22(9): 1270-1280.
- [30] Sattari, M. T., Pal, M., Apaydin, H., Ozturk, F. (2013): M5 model tree application in daily river flow forecasting in Sohu Stream, Turkey. – *Water Resources* 40(3): 233-242.
- [31] Solomatine, D. P., Xue, Y. (2004): M5 model trees and neural networks: application to flood forecasting in the upper reach of the Huai River in China. – *Journal of Hydrologic Engineering* 9(6): 491-501.
- [32] Specht, D. F. (1991): A general regression neural network. – *IEEE Transactions on Neural Networks* 2(6): 568-576.

- [33] Tasar, B., Kaya, Y. Z., Varçin, H., Unes, F., Demirci, M. (2017): Forecasting of suspended sediment in rivers using artificial neural networks approach. – *International Journal of Advanced Engineering Research and Science* 4(12): 79-84.
- [34] Tasar, B., Unes, F., Demirci, M., Kaya, Y. Z. (2018): Yapay sinir ağları yöntemi kullanılarak buharlaşma miktarı tahmini. – *DÜMF Mühendislik Dergisi* 9(1): 543-551.
- [35] Turhan, E. (2012): Seyhan Havzası'nın Yağış. – Akış İlişkisinin Yapay Sinir Ağları Yöntemi ile Modellenmesi, Yüksek Lisans Tezi, Adana.
- [36] Unes, F. (2010a), Dam reservoir level modeling by neural network approach: a case study. – *Neural Network World* 4(10): 461.
- [37] Unes, F. (2010b): Prediction of density flow plunging depth in dam reservoirs: an artificial neural network approach. – *Clean–Soil, Air, Water* 38(3): 296-308.
- [38] Unes, F., Yildirim, S., Cigizoglu, H. K., Coskun, H. (2013): Estimation of dam reservoir volume fluctuations using artificial neural network and support vector regression. – *Journal of Engineering Research* 1(3): 53-74.
- [39] Unes, F., Gumuscan, F. G., Demirci, M. (2017): Prediction of dam reservoir volume fluctuations using adaptive neuro fuzzy approach. – *EJENS* 2(1): 144-148.
- [40] USGS.gov | Science for a changing world. – <https://www.usgs.gov/>.
- [41] Vapnik, V. (1995): *The Nature of Statistical Learning Theory*. – Springer, New York.
- [42] Vapnik, V., Golowich, S., Smola, A. (1997): *Support Vector Method for Function Approximation, Regression Estimation, and Signal Processing*. – In: Jordan, M. I. et al. (eds.) *Advances in Neural Information Processing Systems*. MIT Press, Cambridge, MA, pp. 281-287.
- [43] Witten, I. H., Frank, E. (2005): *Data Mining: Practical Machine Learning Tools and Techniques with Java Implementations*. – Morgan Kaufmann, San Francisco, CA.
- [44] Yin S, Tang D, Jin X, Chen W, Pu N (2016): A combined rotated general regression neural network method for river flow forecasting. – *Hydrol Sci J* 61(4): 669-682.
- [45] Yu, P. S., Chen, S. T., Chang, I. F. (2006): Support vector regression for real-time flood stage forecasting. – *Journal of Hydrology* 328(3-4): 704-716.

STUDY OF MORPHOLOGICAL AND QUALITATIVE PLANT TRAITS AGAINST THE INFESTATION OF *Chilo infuscatellus* L. (PYRALIDAE, LEPIDOPETRA)

AHMAD, S.^{1*} – ALAM, M. W.¹ – MAJEED, S.² – BILAL, M.¹ – SHAFIQ, M.¹ – KHURSHID, M.³ – SARWAR, M.¹ – SHAFEEQ, T.¹ – SALMAN, S.⁴ – ALI, Q.^{5*}

¹*Institute of Agricultural Sciences, University of the Punjab Lahore, Lahore, Pakistan*

²*Department of Entomology, University of Agriculture Faisalabad, Pakistan*

³*Institute of Biochemistry and Biotechnology, University of the Punjab Lahore, Lahore, Pakistan*

⁴*Department of Plant Breeding and Genetics, Gomal University, Dera Ismail Khan, Pakistan*

⁵*Institute of Molecular Biology and Biotechnology, University of Lahore, Lahore, Punjab, Pakistan*

*Corresponding authors

e-mail: shahbaz.iags@pu.edu.pk, saim1692@gmail.com

(Received 22nd Feb 2019 ; accepted 8th Apr 2019)

Abstract. The *Chilo infuscatellus* (Pyralidae, Lepidoptera; Snellen) caused significant losses in production and quality of sugarcane in Pakistan. The deficiency of easily discrete morphological and quantitative characters makes it remarkable to identify these characters in pest management. Present study; investigates the impact of morphological and quality traits of pest infestation during different stages of plant growth. Results revealed that varieties US-312, 1491, 718, 133 and CPF-246 performed better in terms of brix, POL, CSS, fiber, recovery, carbohydrates, moisture and fat contents percentage. Correlation values of different varieties in terms of qualitative factors were positive and significant. All plants traits in terms of qualitative factors including plant girth (cm), leaf area (cm), leaf sheath hairiness (cm²) and leaf thickness (mm) showed positive and had highly significant correlation with pest infestation. The coefficient of determination value $R^2 = 0.821$ was obtained by computing brix, fiber contents, POL and CCS factors mutually from multivariate regression models. It was concluded, that morphological and qualitative plant factors could be helpful for management of sugarcane shoot borer.

Keywords: *Lepidopteran pest, management, plants, shoot borer, sugarcane*

Introduction

Sugarcane (*Saccharum officinarum*) is a perennial, tropical and subtropical crop cultivated in various regions of the world (Kfir et al., 2002). It is grown between tropical and sub-tropical climate (North latitude = 350C and South latitude = 350C) around the world. In Pakistan, sugarcane is a cash as well as industrial crop and grown on an area of 1217 thousand hectares with 73.6 million tons' annual production (Anonymous, 2016-17). The Pakistan sugar industry is second largest industry of the country after textile having GDP of 0.7% (Anonymous, 2016-17). Being a cash crop, it provides a huge quantity of raw material to sugar industry. In Pakistan, the average sugarcane yield is much lower than the other growing countries of the world (Kumarasinghe, 1999). There are many factors which are responsible for low sugarcane yield of sugarcane but most important factors are pests, in which borers are most damaging. Among borers, sugarcane shoot borer (Lepidoptera: Crambidae) is considered as the most damaging and injurious

pest of sugarcane that resulted in reduced quality and quantity of cane sugar (Zia et al., 2007; Sabir et al., 2014). The molecular study was described to identify *C. infuscatellus* through PCR by using barcode region CO1 sequence between the sugarcane shoot borer and four other species of sugarcane. A 285bp fragment was effectively amplified from all stages of different geographical population (Wang et al., 2017). It has been reported that sugarcane yield had been decreased from 20.78% to 57.9% in most parts of the world including Pakistan (Anwar et al., 2004). The injured plants attacked by this pest produce dead hearts during growing season before till the formation of canes and such plants do not grow further (Shahid et al., 2007). Yield losses could be minimized by planting some resistant varieties i.e. (R570) instead of susceptible i.e. (R579) (Goebel et al., 1999). Knowing the morphological and qualitative plant factors are helpful to examined the relationship between pest infestations (Khaliq et al., 2005). Therefore, objective of the present study was to find out the impact of morphological and quality traits of sugarcane against the pest infestations.

Materials and Methods

The experiment was conducted field area of University of Agriculture, Faisalabad-Pakistan under randomized complete block design (RCBD). The climate is very hot in summer up to 45°C while winter, it is cold up to 22°C. The average rainfall is very low as compared to other areas of Punjab. After the preliminary screening, nine sugarcane varieties including US-676, US-133, US-312, SPF-234, US-1491, US-824, CPF-246, US-718 and CPF-237 were selected.

The plot size was kept 5×10 m² and the experiment was repeated thrice. There were five rows in each plot for each variety. Middle three rows were selected for recording the data during preliminary screening. All the recommended agronomic practices (hoeing, earthing up, balance use of fertilizer and irrigations) were applied. The observations were taken at weekly intervals. The number of total internodes and infested internodes were counted separately from each cane and the borer infestation percentage was calculated by the following formula.

$$\text{Borer Infestation (\%)} = \frac{\text{Number of Infested Internodes}}{\text{Number of total Internodes}} \times 100 \quad (\text{Eq.1})$$

Morphological Factors

Leaf thickness

Five plants were selected randomly from each block. The leaves were cut from the upper, middle and lower part of the plant and measured in (mm) to determine the leaf thickness with help of a binocular microscope (Made by Omax).

Leaf Area

Ten plants from each block were selected randomly. Three leaves one from top, middle and bottom portion of the sugarcane was taken and measured in (cm). Leaf area was measured with help of LI-30000, a portable leaf area meter.

Leaf Sheath Hairiness

Five canes were selected randomly from each block. Each leaf sheath was examined from three different places by a phase contrast stereo microscope (Made by Euromax). The number of hairs was counted in one (cm²).

Stalk Girth

For stalk girth, 10 cane samples from each block were randomly selected from three different places upper, middle and lower from each the sugarcane sample was selected for stalk girth. The stalk girth was measured with help of ordinary measured (cm) using a measuring tape.

Qualitative Factors

Analysis of Sugar Cane

Analysis of cane includes brix%, POL%, CCS% and fiber% was determined. On the basis of these qualitative factors, the maturity of a cane variety was decided. When a cane variety attains brix (20%), POL (18%) and purity (80%) in any month from October to March, it was considered matured.

Juice Extraction

The representative cane sample consists of 8-10 numbers of canes which were passed through cane crusher to get juice. The extracted juice was collected into a plastic bucket.

Brix (%)

For the brix determination juice 400-500 ml was taken. The Brix was recorded through brix hydrometer (Made by Yuyao Hjiyi Electronics) calibrated at 200°C. When temperature of juice was above 200°C, then a correction factor was added (47) into brix reading, if the temperature was below 20°C, then correction factor was subtracted. Hydrometer was dip to down the movement into cylinder after 25 minutes, after that juice temperature was come at room temperature.

POL (%)

Two hundred ml of extracted juice was placed into a flask and 5g basic lead acetate was added and shaken well. The juice was filtered into a volumetric flask through a filter paper and injected into 200 mm polarimeter tube to record the POL reading. The POL reading was the measurement of the angle of rotation of dextrorotatory substances. Polarity worked on the principle that under certain standard conditions i.e. standard tube length, standard solution concentration and standard room temperature when a polarized light was passed through that sugar solution, then substances present rotate light at a definite angle. The measurement of that angle of rotation was POL reading. Calculations were done by following the formula of Payne (1968).

Commercial Cane Sugarcane (CCS)

The commercial cane sugar percentage (CCS%) was calculated by using following formula (Meade and Chen, 1977).

$$\text{CCS \%} = \{\text{Sucrose \%} - (\text{Brix \%} - \text{Sucrose \%}) \times 0.4\} \times 0.74 \quad (\text{Eq.2})$$

where, 0.4 = multiplication factor, 0.74 = crusher factor.

Fiber Contents

Fiber contents were determined by collecting 12 canes, top internodes of three canes, and middle portion internodes of next three canes while lower internodes of remaining three canes were cut, separated, mixed and fed to the Jaffco cutter grinder (Jeffress Engineering). This instrument was not only cuts and grinds but also minces the internodes. 500 g sample of this grinded bagasse was weighed and pressed less than 2000 pound per square inches on a hydraulic press for two minutes. The fresh fiber cake was then prepared and weighed and dried in oven for 12 hours at 1000°C. Percentage fiber was calculated using following formula (Payne, 1968).

$$\text{Percent fiber} = \frac{\text{Weight of dried sample}}{\text{Weight of sample (gram)}} \times 100 \quad (\text{Eq.3})$$

Sugar Recovery

It was calculated by multiplying CCS with a constant factor 0.94. Actually, to convert brown sugar into white sugar; 6% white sugar was also lost, therefore, a constant factor used. Sugar recovery was calculated with the following formula (Mathur, 1981).

$$\text{Recovery} = \text{B.H.E.} \times \text{B.H.R.} \times \text{POL\% juice} \times \text{Juice extraction 0.94} \quad (\text{Eq.4})$$

where

- B.H .E = Boiling House Efficiency
- B.H.R. = Boiling House Recovery i.e. B.H.R. = S (J-M)

J (S-M), here

- S = Sucrose purity
- J = Juice purity
- M = Molasses purity

Weight of sample + wt. lost during preparation.

Fat Contents

Fat was determined by taking 50 grams of crushed, oven dried sample in thimble plugged with cotton using n-hexane as solvent in a Soxhlet apparatus (Made by Corning Life Sciences) and heating the flask containing solvent. The fat extraction in Soxhlet was done by adjusting 3 drops of n-hexane per second till complete drawing of fat from sample. Then the content of the receiving flask was transferred to a pre weighed Petri dish and dried till to constant weight was obtained. Fat calculated with help of following formula (AOAC, 1996):

$$\text{Fat (\%)} = \frac{\text{Weight of fat in sample (gram)}}{\text{Weight of sample (gram)}} \times 100 \quad (\text{Eq.5})$$

Moisture Content

For the determination of moisture, 50% sample from each variety was taken in petri dishes dried in hot air oven at 70°C for 24 hours, till constant weight. The moisture contents were calculated by the formula:

$$\text{Moisture}(\%) = \frac{\text{Moisture losses}}{\text{Weight of original sample}} \times 100 \quad (\text{Eq.6})$$

Moisture losses = Weight of original sample – Weight of oven dried sample.

Carbohydrates

Carbohydrate contents were determined by following formula:

$$\text{Carbohydrate} (\%) = 100 - \text{crude protein} + \text{fats}\% + \text{crude fiber} + \text{ashes} \quad (\text{Eq.7})$$

Statistical analysis

The data were analysed by analysis of variance (ANOVA) and means were compared by the Tukey's HSD test ($P \leq 0.05$) using software Statistix 8.1.

Results

Role of Physico-Morphic Factors on the Shoot Borer Infestation

The maximum leaf sheath hairiness (102 cm²) was recorded in CPF-246 and variety SPF-234 showed minimum leaf sheath hairiness (53 cm²). The maximum leaf thickness (0.660 mm) was found in variety CPF-246 while the variety CPF-237 showed minimum leaf thickness (0.583 mm). The maximum plant girth (5.4 cm²) in variety US-824 and the variety CPF-246 showed minimum plant girth (4.37 cm²) (*Table 1*). It is evident from the results (*Table 2*) that plant girth, leaf area, leaf sheath hairiness and leaf thickness showed highly significant correlation with pest infestation with r-value 0.139, 0.181, 0.287 and 0.381, respectively. Plant girth contributes 2% while leaf area contributes 6%. The contribution of leaf sheath hairiness and leaf thickness was 35.6% in fluctuating the pest infestation. The analysis of variance exhibited that all varieties were highly significant in terms of plant girth and leaf area showed significant impact on the pest infestation while leaf sheath hairiness and leaf thickness were important factors which showed maximum per unit change in population fluctuation of the pest. The maximum leaf area 466 cm² recorded in variety SPF-234 and the variety US-824 showed minimum leaf area (318 cm²) (*Table 3*).

Role of Qualitative Factors on the Shoot Borer Infestation

The data regarding qualitative factors were subjected to mean performance, correlation coefficient values and multiple linear regression models to find out the impact of these factors on the infestation. The maximum percentage of brix was recorded in variety US-312 (23.43%) and the variety SPF-234 showed minimum percentage of 18.46%. The POL percentage in US-312 was higher (20.93%) while SPF-234 showed minimum POL percentage (15.27%). The variety US-718 showed maximum (15.84%) of CCS while variety SPF-234 showed minimum percentage of CCS (11.08%). The maximum fiber

contents were found in US-676 (13.68%) while US-1491 showed minimum percentage of fiber contents (11.99%). The sugar recovery (11.74% and 11.52%) was maximum in US-312 and US-718, respectively while the variety SPF-234 showed minimum percentage of recovery (8.12%) (Table 4).

It is evident from the results (Table 2) that Brix and POL percentage showed significant correlation with pest infestation with r-values 0.650 and 0.683, respectively while the fiber and CCS also showed positive and significant correlation with shoot borer infestation with r-values 0.291 and 0.643, respectively. From the results it is concluded that that brix and POL were the important factors which showed significant effect on the infestation. Similarly, fiber contents contributed minimum (8.5%) towards the infestation while the brix contributed 44.6%. The POL contribution was recorded 58.5% when POL was added (Table 5). The 100 R² value was reached to 61.4% when all the factors computed together. From these results it is concluded that fiber contents showed negligible impact while other qualitative factors showed maximum per unit change in population fluctuation of the pest infestation.

Table 1. Comparison of means for the data regarding plant girth, leaf thickness, leaf sheath hairiness and leaf area in various chosen varieties of sugarcane

Varieties	Plant Girth (cm)	Leaf Thickness (mm)	Leaf Sheath Hairiness (cm ²)	Leaf Area (cm ²)
US-676	5.13±0.035B	0.627±0.007BC	63.02±2.76D	461.84±1.85A
US-133	4.73±0.052CD	0.617±0.012CD	82.54±1.32C	337.84±3.55F
US-312	5.23±0.052AB	0.617±0.012CD	76.66±2.00C	359.11±1.34E
SPF-234	4.56±0.205CDE	0.597±0.009DE	53.42±2.65E	466.57±1.14A
US-1491	5.43±0.145AB	0.637±0.003ABC	95.25±1.74B	382.99±1.82D
US-824	5.47±0.085A	0.647±0.009AB	77.76±1.75C	318.50±3.45G
CPF-246	4.37±0.059E	0.660±0.006A	102.42±1.11A	414.99±1.27B
US-718	4.78±0.074C	0.613±0.003CD	81.57±1.89C	394.45±1.97C
CPF-237	4.44±0.067DE	0.583±0.003E	95.73±0.69B	323.31±2.43G

In a column, means with different letters are statistically significant as determined by Tukey HSD test at P≤0.05

Table 2. Correlation between Infestation and Various Sugars Physico-Morphic and Qualitative Factors

Factors	Correlation (r)
Fiber	0.291*
Brix	0.650*
POL	0.683*
CCS	0.643*
Recovery	0.547*
Carbohydrate	0.288*
Fat	0.095*
Moisture	0.239*
Plant Girth	0.139**
Leaf Area	0.181**
Leaf sheath hairiness	0.287**
Leaf Thickness	0.381**

*=Significant at P≤0.05 **=highly Significant at P≤0.05

Table 3. Regression analysis for Physico-Morphic plant factors

Regression Equation	R ²
$Y = 16.2 - 0.188 X_1$	0.020
$Y = 17.4 - 0.248 X_1 - 0.00223 X_2$	0.066
$Y = 22.1 - 0.510 X_1 - 0.00621 X_2 - 0.0240 X_3$	0.356
$Y = 22.0 - 0.520 X_1 - 0.00629 X_2 - 0.0244 X_3 + 0.3 X_4$	0.356

Y = Infestation, X₁ = Plant Girth, X₂ = Leaf Area, X₃ = Leaf sheath hairiness, X₄ = Leaf Thickness, R² = Coefficient of Determination

Table 4. Comparison of means for the data regarding Brix, Pol, Ccs, Fiber, Recovery, Fat, Moisture contents and Carbohydrate in various chosen varieties of sugarcane

Varieties	Brix (%)	POL (%)	CCS%	Fiber (%)	Recovery (%)	Fat (%)	Moisture Content (%)	Carbohydrates (%)
US-676	21.04±0.48	18.00±0.07 ^D	13.18±0.17 ^E	13.68±0.08 ^A	10.16±0.18 ^C	2.16±0.009 ^{AB}	78.35±0.037 ^{CD}	49.55±0.11 ^D
US-133	22.50±0.28	19.83±0.38 ^{AB}	14.99±0.34 ^{ABC}	12.74±0.10 ^B	11.15±0.16 ^B	1.99±0.024 ^D	78.04±0.042 ^E	52.57±0.19 ^A
US-312	23.43±0.47	20.93±0.34 ^A	15.66±0.37 ^A	13.47±0.14 ^A	11.74±0.13 ^A	2.12±0.027 ^{BC}	78.65±0.137 ^A	49.46±0.11 ^D
SPF-234	18.46±0.75	15.27±0.30 ^E	11.08±0.26 ^F	12.59±0.16 ^B	8.12±0.12 ^D	2.20±0.022 ^A	78.60±0.023 ^{AB}	50.32±0.16 ^C
US-1491	23.06±0.10	20.16±0.43 ^{AB}	15.30±0.53 ^{AB}	11.99±0.05 ^C	11.29±0.14 ^{AB}	1.99±0.024 ^D	78.32±0.055 ^{CD}	47.57±0.22 ^F
US-824	21.41±0.74	18.50±0.34 ^{CD}	13.66±0.17 ^{DE}	12.64±0.07 ^B	10.05±0.14 ^C	2.17±0.020 ^{AB}	78.51±0.018 ^{ABC}	48.42±0.24 ^E
CPF-246	22.68±0.34	19.93±0.51 ^{AB}	14.17±0.64 ^{CDE}	13.60±0.10 ^A	10.55±0.29 ^C	2.06±0.023 ^{CD}	78.37±0.035 ^{CD}	51.12±0.40 ^B
US-718	23.33±0.27	20.92±0.31 ^A	15.84±0.28 ^A	13.45±0.06 ^A	11.52±0.16 ^{AB}	2.18±0.009 ^B	78.42±0.025 ^{BCD}	50.32±0.09 ^C
CPF-237	22.34±0.65	19.34±0.44 ^{BC}	14.31±0.27 ^{BCD}	13.52±0.22 ^A	10.42±0.14 ^C	2.00±0.023 ^D	78.26±0.020 ^D	52.34±0.09 ^A

± (SE) = Standard error

Table 5. Regression analysis for sugar Qualitative factors

Regression Equation	R ²
$Y = 18.9 - 0.275 X_1$	0.085
$Y = 22.1 - 0.147 X_1 - 0.223 X_2$	0.446
$Y = 13.4 - 0.073 X_1 + 1.33 X_2 - 1.38 X_3$	0.585
$Y = 11.6 + 0.056 X_1 + 1.52 X_2 - 1.91 X_3 + 0.434 X_4$	0.614
$Y = 12.3 + 0.061 X_1 + 1.64 X_2 - 1.97 X_3 + 0.454 X_4 + 0.195 X_5$	0.632
$Y = 11.3 + 0.073 X_1 + 1.87 X_2 - 1.99 X_3 + 0.488 X_4 + 0.123 X_5 + 0.074 X_6$	0.657
$Y = 13.2 + 0.086 X_1 + 2.11 X_2 - 2.09 X_3 + 0.668 X_4 + 0.1373 X_5 + 0.086 X_6$	0.682
$Y = 12.5 + 0.098 X_1 + 2.43 X_2 - 2.89 X_3 + 0.712 X_4 + 0.1421 X_5 + 0.121 X_6 + 0.253 X_7$	0.713

Y = Infestation (%), X₁ = Fiber, X₂ = Brix, X₃ = POL, X₄ = Commercial Cane Sugar (CCS), X₅ = Recovery, X₆ = Fat, X₆ = Moisture, X₇ = Carbohydrate, R² = Coefficient of Determination

Discussion

The performance of all varieties in terms of morphological plant factors like plant girth, leaf area, leaf sheath hairiness and leaf thickness showed highly significant interaction towards the borer infestation. The present findings are comparable with those of Khliq et al. (2005) who reported that leaf thickness, cane girth and leaf area showed positive and significant correlation with borer infestation. Significant differences were documented among all the trait for recovery. The maximum recovery was exhibited by the trait US-718 whereas the lowest was observed for the trait SPF-234. Similar results were also reported by earlier research of Sarwar et al. (2011). Khan et al. (2004) reported

that there was no relation between plant girth and shoot borer infestation. Cornelissen and Fernandes (2001) described that the absorption of sugars in leaves affects the area of leaf damaged by herbivores in *Bauhinia brevipes*. The accessibility of plants increases with the quantity of reducing sugars, and resistance increases with organic acids according to Comes (1916). The quantity of reducing sugars, affected by insects which increased the vegetable tissues, as a result caused reduction in the organic acids. Correlation among morphological characters may reproduce biological processes that are of considerable evolutionary interest, correlation can be the result of functional, genetic and physiological or developmental characters (Mehmood et al., 2000; Ali et al., 2013, 2014, 2016).

The results are similar in with Baloch et al. (2005) reported that factors like fiber, brix, POL and CCS showed significant variations and reduced the damage. Brix and POL percentage showed significant correlation with pest infestation, while fiber contents and CCS showed significant correlation with infestation. The qualitative parameters after brix% and POL% in (Table 5) showed significant differences among the brix% and POL%. The lowest brix% was recorded for SPF-234 whereas highest was displayed by US-312. The maximum POL% was showed by US-312 and US-318 whereas the minimum POL% was showed by US-676. These results are in contrary with the findings of Panhwar et al. (2004). The present results are similar with those of Khan et al. (2004) who reported that there is positive relation between brix and shoot borer infestation. The present findings are partially comparable with those of Gupta and Singh (1997) who reported that brix, POL, fiber contents and CCS are affected by the borer infestation. Chang and Wang (1995) reported that sugar contents, brix and sugar purity are heavily affected by sugarcane borer. The CCS, POL% and brix contents showed significant effect on the borer infestation Khaliq et al. (2005).

Conclusion

It was concluded from present study that varieties US-312, 1491, 718, 133 and CPF-246 could be used to minimize the losses caused by shoot borer pest infestation and all these varieties showed significant qualitative and quantitative interaction towards *Chilo infuscatellus*.

Acknowledgements. The authors are thankful for financial support provided by Department of Entomology, University of Agriculture Faisalabad and Higher Education Commission of Pakistan.

REFERENCES

- [1] Ali, Q., Ahsan, M., Ali, F., Aslam, M., Khan, N. H., Munzoor, M., Mustafa, H. S. B., Muhammad, S. (2013): Heritability, heterosis and heterobeltiosis studies for morphological traits of maize (*Zea mays* L.) seedlings. – *Advancements in Life sciences* 1(1): 52-63.
- [2] Ali, Q., Ali, A., Waseem, M., Muzaffar, A., Ahmad, S., Ali, S., Awan, M., Samiullah, T., Nasir, I., Tayyab, H. (2014): Correlation analysis for morpho-physiological traits of maize (*Zea mays* L.). – *Life Science Journal* 11: 9-13.
- [3] Ali, Q., Ahsan, M., Malook, S., Kanwal, N., Ali, F., Ali, A., Ahmed, W., Ishfaq, M., Saleem, M. (2016): Screening for drought tolerance: comparison of maize hybrids under water deficit condition. – *Advancements in Life Sciences* 3(2): 51-58.
- [4] Anonymous (2016-17): Economic Survey of Pakistan. – Govt. Pak. Eco. Advisory Wing, Finance Div. Islamabad.

- [5] Anwar, M. S., Ali, H. W., Ahmad, A., Chatta, A. A. (2004): Integrated management of sugarcane insects. – Journal of Pakistan Sugarcane 19(6): 28-31.
- [6] AOAC. (1996): Methods of Analyses. – 15th Association of Official Analytical Chemistry, Arlington, VA.: 40-50, 237-238.
- [7] Baloch, F. M., Soomro, N. A., Usmanikhail, M. U., Tunio, G. S., Baloch, L. M. (2005): Growth and yield behaviour of different sugarcane varieties under agro ecological conditions of lower Sindh. – Journal of Pakistan Sugarcane 4(3): 287-291.
- [8] Chang, Y. S., Wang, K. R. (1995): Statistical analysis of the effect of sugarcane borer damage on cane juice quality. – Report of Taiwan Sugar Research Institute 149(06): 1-12.
- [9] Comes, O. (1916): La Profilaxia en Patologia Vegetal, Reale Institutd, Incoraggiamentdi Napoli, Naples. – Biology and Agriculture 9(102): 173.
- [10] Cornelissen, T., Fernandes, G. W. (2001): Defense, growth, and nutrient allocation in the tropical shrub *Bauhinia brevipes* (Leguminosae). – Australian Ecology 26: 246-253.
- [11] Goebel, F. R. (1999): Biocontrol of *Chilo sacchariphagus* (Lepidoptera: Crambidae) a key pest of sugarcane: Lessons from the past and future prospects. – Unité de Lutte Biologique and 400 Route des Chappes, 06410 Sophia Antipolis, France.
- [12] Goettel, M. S. (1999): Directory of Microbial Control Products and Services, Division on microbial Control. – Society for Invertebrate Pathology, Division on Microbial Control, Gainesville, USA, 81.
- [13] Gupta, M. K., Singh, S. N. (1997): Qualitative losses in sugarcane by plassy borer and top borer damage. – Indian Sugar 47(4): 275-277.
- [14] Kfir, R., Overholt, W. A., Khan, Z. R., Polaszek, A. (2002): Biology and management of economically important lepidopteron cereal stem Borers in Africa. – Annuals Reviews of Entomology 47(26): 701-31.
- [15] Khaliq, M. A., Ashfaq, M., Ali, A. (2005): Chemical plant factors affecting resistance in sugarcane against *Scirpophaga nivella*. – Journal of Pakistan Science and Technology 27(2): 67-71.
- [16] Khan, I. A. (2004): Performance of promising sugarcane clone for yield and quality traits in different ecological zones of Sindh. – Pakistan Journal of Botany 4(1): 92-95.
- [17] Kumarasinghe, N. C. (1999): Insect fauna associated with sugarcane plantations in Srilanka Division of Pest Management. – Sugarcane Research Institute, Uda Walawe, Srilanka.
- [18] Mahmood, T., Nazir, M. S., Ashfaq, M., Chodhery, N. A. (2000): Correlation in sugarcane. – Journal of Agriculture Research 28: 359-63.
- [19] Meade, G. P., Chen, J. C. P. (1977): Cane Sugar Hand Book (10th). – Wiley Inter Science, John Wiley and Sons, New York, PP. 947.
- [20] Panhwar, R. N., Keerio, H. K., Keerio, A. R. (2004): Evaluation of sugarcane genotypes for yield and yield contributing traits under thatta conditions. – Pakistan Journal of Agricultural Research 18(1): 34-36.
- [21] Payne, J. H. (1968): Sugarcane factory analytical control. – Elsevier pub. Co. Amsterdam, London, New York.
- [22] Sarwar, M. A., Fiaz, A. N., Hussain, S., Chattha, A. A. (2011): Evaluation of approved sugarcane varieties through hydraulic press method. – International Journal of Agriculture and Applied Sciences 3(1): 14-17.
- [23] Shahid, M. R. (2007): Effectiveness of *Trichogramma chilonis* (ishii) (Hymenoptera: Trichogrammatidae) against sugarcane stem borer (*Chilo infuscatellus* Snellen) (Lepidoptera: Pyralidae). – Pakistan Journal of Entomology 29(2): 141-146.
- [24] Wang, J., Wang, W., Rong, W., Zheng, H., Gao, G. (2017): Molecular Detection of *Chilo infuscatellus*. – Journal of Insect Science 17(05): 102.
- [25] Zia, H. A. (2007): Bio control of insect pests of sugarcane (*Saccharum* sp). – Journal of Pakistan Sugarcane 22(5): 13-22.

CHEMICAL ANALYSIS AND ENVIRONMENTAL IMPACT OF HEAVY METALS IN SOIL OF WADI JAZAN AREA, SOUTHWEST OF SAUDI ARABIA

AL-BOGHDADY, A. A.^{1,2*} – HASSANEIN, K. M. A.^{3,4}

¹*Deanship of Academic Development, Jazan University, Jazan, Saudi Arabia*

²*Department of Geology, Faculty of Science, Minufiya University, Minufiya, Egypt*

³*Deanship of Scientific Research, Jazan University, Jazan, Saudi Arabia*

⁴*Department of Pathology and Clinical Pathology, Faculty of Veterinary Medicine, Assiut University, Assiut, Egypt*

**Corresponding author
e-mail: a_h_boghdady@yahoo.com*

(Received 22nd Feb 2019; accepted 10th Apr 2019)

Abstract. A few investigations have been done on characterizing heavy metals at Jazan district, mostly done as analyses of heavy metals associated with water, sediments and shrimps. The current study was carried out mainly to evaluate and characterize heavy metals concentrations in soils of the main Wadi Jazan and its tributaries in order to determine its environmental impacts. The heavy metals were measured by using ICP-MS. Results indicate that soil of Wadi Jazan area has different concentrations of heavy metals; some of them have economic importance such as Au, Ag and U, some other considered useful for the environment (Such as Cu, Se and Zn) and others are harmful for the environment (Such as Cd, Pb, and others). The most extremely soil pollution at Wadi Jazan is by Cd, where all analyzed samples have higher concentration than the maximum permissible concentration by the World Health Organization. Heavy metals concentrations along Wadi Jazan indicate that the most polluted area is located around Abu Arish City. The current investigation conclude that there are a direct effect of the harmful heavy metals on plants, terrestrial animals, fishes and marine organisms and human; due to the ability of these heavy metals to reach and entered the food chain, and hence causes different types of harmful effects and diseases. Present study refers also to the suitability of some recent techniques for soil remediation at Wadi Jazan, such as engineering remediation (Replacement of contaminated soil, soil removal, soil isolation and adsorption) and bioremediation (Phytoremediation).

Keywords: *environment, metals pollution, health risk assessment, sediments, Saudi Arabia*

Introduction

Minerals and rocks are important role in our lives due to their many benefits for humans, especially as they intervene in every industrial, agricultural and economic needs (Mart, 2014). The extent of nations and peoples progress is measured by its ability to find out what their lands contain from metals and rocks of economic value and also minerals and rocks which have a harmful impact on the environment and its components (Uluturhan et al., 2011). Soil pollution by heavy metals is considered one of the hot topics all over the world due to its direct and indirect impact on human health. The main objective of the current work is to analyze and characterize heavy metals in soil of Wadi Jazan, in addition the determination of its environmental impacts.

The most harmful minerals to the environment are arsenic, asbestos, cadmium, lead, mercury, manganese, antimony, zinc, barium, beryllium, bismuth, bromine,

chlorine, thallium and uranium. Recently it is approved that the aluminum is considered as a highly toxic metal (El Tahlawy, 2007). Most of these minerals present in the rocks and nature in very small amounts and for a long time, but as a result of erosion, decomposition and transportation of the exposed rocks by rains, flood, winds and others, as well as the extraction of these metals and their use in the industry led to many environmental and health problems that were not known before (Nadia et al., 2009). Usually these health problems arise due to these heavy metals replace other metals found in the body and perform important role in the organic function. For example, cadmium replaces zinc and lead eliminates calcium anywhere, and when concentrated cadmium or lead in the bone or tissue happens, it becomes difficult to get rid of them and they cannot be able to carry out the operations which were carried out by the original elements. This of course leads to a lot of diseases and health complications (Campbell, 2015).

Human activities at the Red Sea coastal area of Saudi Arabia have been increases during the last three decades causing different types of contaminants including heavy metals (Nadia et al., 2009). A comparative study on the concentrations of heavy metals in sediments and fish at Jazan - Saudi Arabia reported a higher percentage of heavy metals than those at the city of Beech for industrial activities and wastewater. The weathering of rocks and flash floods through valleys carry heavy metals such as Ni and Cr to coastal areas, leading to increase pollution with heavy metals (Alhababy, 2016).

Golam and Fahad (2017) have been studied the concentration of heavy metals at Jazan, Saudi Arabia, Red Sea coast within water, sediments and white shrimp. They indicated that heavy metals concentration is higher in water than those in sediments and white leg shrimp. Al Bratty et al. (2017) in their study of determining trace metals in drinking water sources at Jazan Area, Saudi Arabia, stated that trace and major elements were found to be below the standard guideline values, except for uranium in some tap water samples.

Alzahrani et al. (2018) assessed the heavy metals in grey mangrove (*Avicennia marina*) and its associated sediments at the Red Sea coast, Saudi Arabia. They stated that mangrove can accumulate heavy metals, notably Cr and Pb. Also sediments within mangrove areas ranged from moderately to heavily contaminate with Cd at Al-Haridhah area, and moderately contaminated with Cd at South Jeddah, Rabigh, Duba, and Jazan waste water treatment station.

Current research identifies types of heavy metals in Wadi Jazan and their concentrations in order to determine their impact on the environment and its natural components. This will cause pollution of not only the Wadi Jazan land, but the tributaries leading from it and the Red Sea coast beyond. The work will also discuss how to avoid the harmful effects of these minerals and rocks on the environment; as well as the economic importance of some analyzed heavy metals.

Materials and methods

The area of study and sampling

The study area was visited several times to conduct field studies, monitor and photograph observations and field relations. Collection and numbering of samples representing the soil and rocks and plotting their places on the topographical map of the study area by using GPS instrument have been done. In each station, a pit of 40 cm

depth was made and the sample taken at three levels. Level one at the ground surface while level two at depth of 20 cm and level three at depth of 40 cm. The three parts of the sample were mixed in one sample representing the location of the station (*Fig. 1*).



Figure 1. Field photographs clarifying sampling pits and GPS usage for determining sample location attitudes

16 samples were selected for the chemical analysis (Due to the limitation in financial coast which specify for chemical analyses). The chemical analysis carried out for about 25 heavy and rare earths elements which include Li, Be, Al, V, Cr, Mn, Fe, Co, Ni, Cu, Zn, Ga, As, Se, Rb, Sr, Ag, Cd, Sn, Cs, Ba, Au, Tl, Pb and U to identify heavy metals and their concentrations in ppm. The analyzed heavy metals divided into certain groups according to the periodic table of elements. These groups include: Basic metals (Such as Al, Ga, Tl and Pb); transition metals (Such as V, Cr, Mn, Fe, Co, Ni, Cu, Zn, Ag, Cd, and Au); alkali metals (Such as Li, Rb and Cs); alkaline earth metals (Such as Be, Se and Ba); semi-metals as As; basic metal as Sn; nonmetallic as Se; and actinides as U. It is clear that the transition heavy metals represent the main bulk of analyzed metals.

The analyses have been done at King Khalid University, Department of Chemistry-Saudi Arabia by using Inductively Coupled Plasma-Mass Spectrometer (ICP-MS). Argon 99.999% - AH and ICP/ICP-MS standard solution of the 25 analysed elements were used. Microwave Digestion System (Anton Par Multiwave ECO) and (Hydrofluoric, Nitric and Hydrochloric acids and Cyclohexanone ACS reagent 99.0%) were used. Where all vessels have been cleaned with deionized water and 1% HNO₃. 0.2 g has been taken from each sample. The following acids (Reagents) were added to each sample: 1 ml of HF (Conc.), 1.5 ml of HNO₃ (Conc.) and 4.5 ml of HCl (Conc.). Then all samples have been digested using the following conditions: Power (800 W), total time (60 min) and temperature (240 °C). Each sample was repeated 3 times. Blank sample was prepared and spike sample as well. The end result of each metal analysis is considered the mean parameter of the three measured values of the same metal in each sample. Standard Deviation was also measured at every time from the three analysed values of each metal, and then the standard deviation mean was calculated for each metal analysis.

Geographical and geological setting

The studied Wadi Jazan area is located at the south west corner of Saudi Arabia on Red Sea coast. Investigated samples were collected during the field work at academic year 2017/2018, in addition some geological and geomorphological characters of the investigated area have been observed. *Figure 2* shows the satellite image of the investigated area around Wadi Jazan, and the location of the analyzed samples. It is clear from the map that Wadi Jazan up streams came from slightly mountainous areas and the main Wadi Jazan and its delta (downstream) are going towards the Red Sea coast at Jazan City.

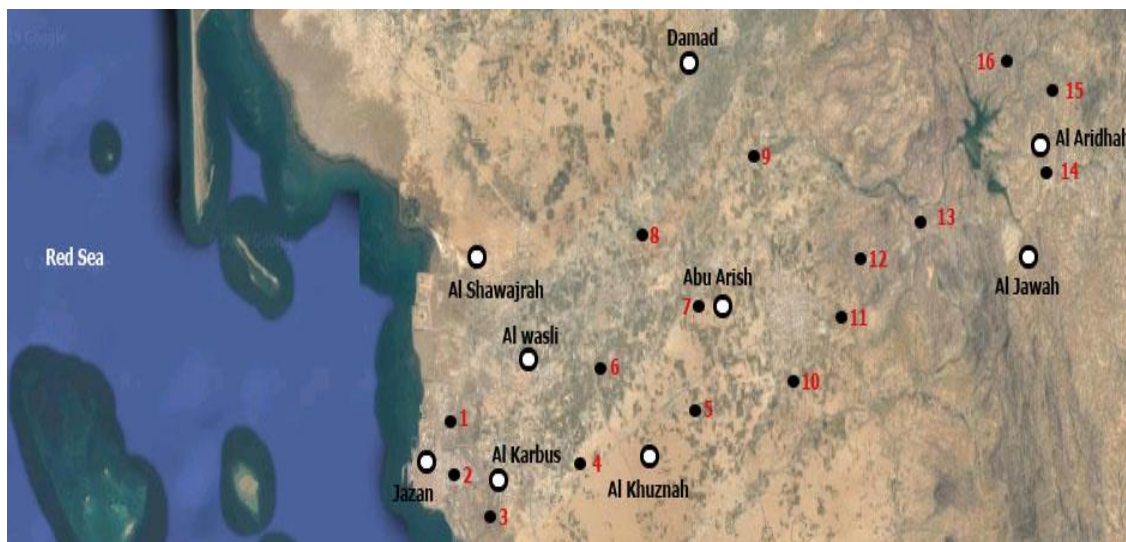


Figure 2. *Satellite image map of Wadi Jazan area, its tributaries, main cities (o) and locations of the analyzed samples (●)*

The investigated area mostly covered by alluvial and compact sediments of recent ages. In some areas near by the Wadi Jazan Dam Lake a volcanic lava flow rocks are present. Upon going further to the east, nearby Al Ardah, mountainous regions are stand up. To the west of Wadi Jazan Dam Lake, alluvial derived sediments are overlying the lava flow rocks. On the ground surface of this area it is observed the presence of rounded pebbles of different composition, shale and andesite flakes and quartz grains. At Wadi Sabiya and its tributaries there are a floodplain sediments of lower relief than its surrounded landscape rocks. These floodplain sediments were covered or capped by a lava flow rocks due to volcanic eruptions (Dabbagh, 1984).

One of the most important field observation at the study area is the presence of wadi floodplain sediments located under the lava flows of volcanic eruption which have been dated locally to 0.8 ± 0.3 mya, K/Ar age dating method (Dabbagh, 1984). There is a possibility to found in Wadi Jazan and its tributaries stratified old relics distributed at different places (Deves et al., 2013). A large numbers of old runes and relics were recovered on the surface of the lava flow on both sides of some tributaries of Wadi Jazan and commonly seen at the base of the quarry sections and represent different historical periods (Inglis, 2014).

Results

Data analysis

Chemical analyses have been done for 16 selected samples from Wadi Jazan area. The selection based on homogenous geographic distribution of samples at Wadi Jazan area and taking in consideration the field observations and surface features examination of mineral grains by using hand lens (10 X magnification). The chemical analyses have been done at King Khalid University, Department of Chemistry-Saudi Arabia by using Inductively Coupled Plasma-Mass Spectrometer (ICP-MS). 25 heavy metals were analyzed in each sample and *Table 1a* shows the chemical analyses of these heavy metals.

In general *Table 1a* delineated that there is richness in the concentration of heavy metals at Wadi Jazan area, in addition to the presence of some concentrations of precious metals such as gold and silver, and the presence of uranium as a radioactive mineral. *Table 1b* provides more comparison between the concentration of analyzed heavy metals in all investigated samples and locations. It shows the average range and the means of analyzed heavy metals concentrations at Wadi Jazan, in addition to the richest areas by heavy metal concentration. For examples: Cadmium (Cd) has an average concentration of 8.98 – 32.97 mg/kg and 20.97 mg/kg as a mean; the richest area is of sample no. 7. Nickel (Ni) ranges from 11.94 to 85.38 mg/kg with average of 48.66 mg/kg, and the richest area is of sample no. 11. Copper (Cu) occurs in-between 12.73 to 132.97 mg/kg and its mean is 72.85 mg/kg; the richest area is of sample No. 15. Lead (Pb) ranges from 6.79 to 32.03 mg/kg with a mean of 19.41 mg/kg; sample no. 7 is considered the richest area. Chromium (Cr) has a range of 23.3 – 131.15 mg/kg and 77.22 mg/kg as a mean; sample no. 16 is the richest area. For uranium (U), the range in-between 0.45 to 23.25 mg/kg and the mean is 11.85 mg/kg while area no. 7 is considered the richest area by uranium. From the data presented in *Table 1b*, it seems that sample no. 7 is the richest sample, of the studied 16 samples, by 9 different heavy metals (Pb, Rb, Sr, As, Se, Tl, Ag, Au and U). This of course will put a great attention on this location at Wadi Jazan (Around Abu Arish City) which will consider as the most polluted area by some harmful heavy metals such as Pb and U. Area of sample no. 11 (also nearby Abu Arish City) is also considered the second polluted locality as it is the richest area by 5 types of heavy metals (Ni, Co, Mn, Be and Ga). One of the most important observation is the more concentrations of heavy metals in areas located mainly nearby the Wadi Jazan upstream (Samples no. 11, 12, 14, 15, and 16), and heavy metal concentrations slightly became lower in areas nearby Wadi Jazan downstream (Samples no 1, 2, 3, 4, 5 and 6). This may explain that the main source of Wadi Jazan heavy metals might be the weathered sedimentary and volcanic rocks that mainly located at Wadi Jazan upstream tributaries. Rains and floods leached these heavy metals and transfer them along through Wadi Jazan to the Red Sea coast. Except the location of samples no 7 and 11 (Around Abu Arish City), which may have additional sources of heavy metals due to human activities in this area (agriculture and industries). *Figure 3* represents histograms for some heavy metals, such as Al, Be, Li and Cr, to show the variation in its concentrations along all analyzed samples.

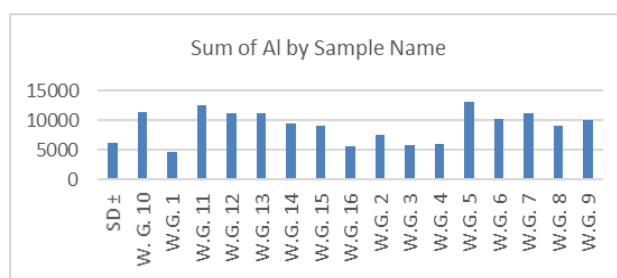
Comparing current data with world permissible levels, general heavy metals characteristics background and the impact of heavy metal contamination of soils will help to understand the impact of heavy metal contamination of soil at Wadi Jazan.

Table 1a. Chemical analyses (mg/kg or ppm) of heavy and rare earth metals of the studied samples (W.G. = Wadi Jazan, SD = standard deviation)

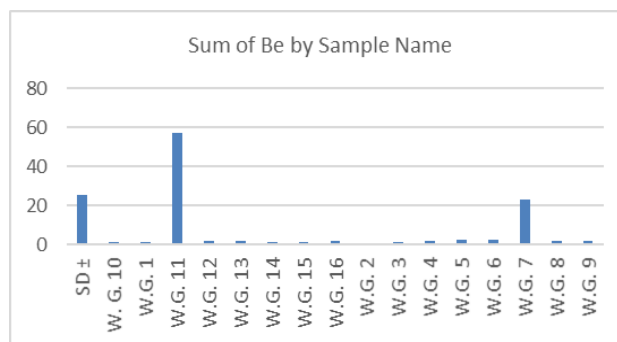
Sample No	Li	Be	Al	V	Cr	Mn	Fe	Co	Ni	Cu	Zn	Ga	As	Se	Rb	Sr	Ag	Cd	Sn	Cs	Ba	Au	Tl	Pb	U
W.G. 1	6.65	1.11	4580.06	74.23	79.7	413.84	18197.38	7086.99	38.17	30.06	71.79	39.28	4.36	1.76	6.62	214.82	19.57	11.25	1.76	0.26	967.33	0.59	226.54	14.92	0.88
SD ±	1.81	1.21	105.86	0.64	1.64	2.27	75.75	73.07	1.12	0.42	1.46	0.41	0.13	0.15	0.31	6.17	0.77	0.23	0.14	0.03	27.98	0.08	1.02	0.97	0.03
W.G. 2	4.77	0.59	7456.47	80.42	38.09	461.39	16479.68	6806.88	12.77	19.46	52.59	33.66	3.2	1.72	4.37	84.46	11.27	11.92	1.36	0.43	582.31	0.47	475.88	11.11	0.56
SD ±	0.59	0.88	233.38	0.21	1.24	6.88	435.57	33.97	0.39	0.41	13.04	0.59	0.95	0.18	0.19	3.85	1.12	0.32	0.05	0.01	31.69	0.06	4.93	0.11	0.01
W.G. 3	3.67	1.17	5834.61	74.18	23.3	368.85	11877.4	5367.14	11.94	14.26	41.43	23.15	3.64	1.75	6.8	123.12	6.41	12.04	1.46	0.43	754.71	0.37	283.61	11.89	0.68
SD ±	1.25	0.74	930.38	1.18	0.6	7.18	21.71	32.99	0.24	0.21	0.95	0.37	0.06	0.12	0.45	4.74	0.43	0.49	0.07	0.04	15.33	0.07	7.61	0.14	0.01
W.G. 4	3.31	1.62	5942.86	110.33	90.01	668.12	27814.62	13194.14	64.46	39.74	66.05	27.03	3.27	1.62	3.08	131.85	13.73	11.66	1.73	0.44	542.65	2.25	642.69	16.58	0.68
SD ±	0.52	1.08	110.56	0.77	1.5	3.93	121.64	1221.91	1.5	0.38	1.88	0.35	0.03	0.15	0.26	6.33	0.25	0.48	0.06	0.02	10.52	0.04	7.75	0.22	0.02
W.G. 5	7.25	2.34	13149.02	98.86	47.76	509.77	29187.03	15578.13	15.63	27	39.26	35.43	3.83	2.22	6.88	101.45	10.64	11.49	1.84	0.42	1347.52	1.33	779.38	16.42	0.76
SD ±	1.35	0.65	597.27	0.94	0.35	8.21	137.2	641.61	0.54	0.42	1.13	0.99	0.13	0.2	0.39	0.46	0.6	0.36	0.1	0.02	24.71	0.13	25.98	0.15	0.02
W.G. 6	5.77	2.37	10174.13	103.23	57.94	597.88	24053.7	10770.64	17.41	12.73	55.89	30.62	4.27	1.73	6.35	75.4	5.21	11.07	1.71	0.61	2444.49	1.37	348.07	9.3	0.97
SD ±	2.37	1.16	890.4	1.23	1.05	11.82	128.98	738.03	0.39	0.26	0.32	1.25	0.17	0.16	0.23	1.63	0.31	0.25	0.09	0.03	177.12	0.1	0.04	0.11	0.42
W.G. 7	29.82	22.93	11249.09	144.59	95.31	686.71	21311.04	11786.54	52.54	56.23	102.18	64.95	25.92	23.75	26.93	96.14	46.41	32.97	2.05	21.57	727.09	2053.01	982.08	32.03	23.25
SD ±	5.05	3.68	189.78	1.03	1.52	9.05	267.42	599.55	1.36	0.71	2.69	0.42	0.11	0.12	0.5	1.48	0.47	0.18	0.12	0.01	13.17	0.09	15.28	0.15	0.03
W.G. 8	4.21	1.72	9121.44	112.2	56.23	505.18	23005.42	9454.87	22.86	26.64	63.48	63.46	6.02	2.86	4.78	79.74	9.93	10.57	1.82	0.46	771.51	0.8	441.75	9.12	0.81
SD ±	1.95	2.29	279.53	1.61	1.93	9.3	124.97	37.67	0.49	0.99	1.21	0.89	0.09	0.22	0.14	1.59	0.07	0.19	0.09	0.02	54.61	0.09	12.14	0.1	0.02
W.G. 9	7.42	1.98	10044.48	95.48	65.05	505.46	20.8	8.99	18.32	23.12	61.72	69.63	3.18	2.23	4.5	70.11	2.41	8.98	1.83	0.26	650.81	0.87	115.62	10.35	0.89
SD ±	2.24	1.92	72.37	2.02	1.36	4.53	81.95	43.15	0.51	0.6	0.6	1.24	0.07	0.21	0.43	4.01	0.15	0.15	0.12	0.02	24.58	0.11	2.12	0.25	0.01
W.G. 10	5.74	1.15	11418.38	86.15	52.88	462.14	18432.85	7512.95	21.77	23.97	69.29	69.63	2.57	1.87	5.59	55.92	4.16	11.64	1.67	0.33	597.16	0.54	628.85	13.61	1.44
SD ±	1.79	0.83	490.24	1.26	2.13	3.3	141.44	167.18	0.27	0.31	2.11	0.96	0.07	0.23	0.26	3.62	0.26	0.54	0.24	0.02	14.76	0.06	51.12	0.15	0.05
W.G. 11	8.07	57.24	12449.26	183.57	106.22	811.58	39325.02	15434.45	85.38	60.2	104.34	89.19	5.35	2.93	4.34	53.92	6.7	11.35	2.63	0.45	1253.98	0.59	503.8	16.66	1.09
SD ±	4.26	2.69	294.63	2.35	2.52	15.14	182.95	562.81	2.16	1.2	1.88	1.74	0.15	0.16	0.07	1.36	0.32	0.22	0.19	0.02	31.64	0.08	26.58	0.32	0.05
W.G. 12	5.8	1.75	11262.12	149.12	87.35	729.78	47601.44	12278.77	33.61	48.09	91.99	47.38	6.55	4.54	2.94	9.05	41.15	10.13	1.75	0.47	1000.97	1	732.01	12.82	0.55
SD ±	3.42	1.78	334.2	3.47	1.02	28.18	333.72	153.45	0.63	1.33	1.64	1.72	0.24	0.32	0.24	1.06	0.72	0.62	0.06	0.04	42.92	0.06	64.33	0.24	0.04
W.G. 13	7.36	1.44	11235.5	85.55	38.37	355.59	16755.41	8412.82	11.69	23.85	61.16	36.27	2.68	1.97	13.31	67.29	8.98	11.37	2.05	2.23	1007.6	0.66	139.93	12.05	0.45
SD ±	4.18	1.3	1374.81	1.59	0.48	14.76	112.57	99.89	0.38	0.54	1.14	0.97	0.09	0.22	0.19	1.02	0.7	0.77	0.19	0.06	31.5	0.07	0.03	0.15	0.01
W.G. 14	46.64	1.41	9467.42	97.93	52.62	573.49	25821.97	8179.59	16.3	49.47	64.66	35.45	2.35	1.95	26.68	69.89	6.68	11.72	1.62	6.95	698.73	3.14	488.15	11.27	0.61
SD ±	5.3	1.89	89.06	2.23	1.57	4.99	44.66	176.63	0.73	0.63	1.22	1.48	0.17	0.28	2.03	2.23	0.44	0.39	0.07	0.11	35.49	0.19	11.54	0.23	0.03
W.G. 15	6.83	0.91	9018.99	97.09	34.34	704.53	22440.49	8299.29	18.04	132.97	112.34	44.23	3.54	2.2	10.4	54.74	3.37	11.34	1.78	1.52	999.39	0.88	218.6	9.51	0.6
SD ±	3.05	1.46	165.76	1.02	0.77	8.53	139.4	371.66	0.51	3.12	1.76	1.31	0.07	0.19	0.77	2.02	0.07	0.3	0.25	0.06	40.63	0.08	4.93	0.09	0.04
W.G. 16	7.68	1.91	5665.41	169.89	131.15	763.04	40590.34	15241.46	84.77	73.92	81.76	47.4	7.46	3.79	0.92	15.29	8.03	10.02	2.8	0.4	146.44	0.53	708	6.79	1.3
SD ±	2.97	1.61	102.37	1.4	2.33	14.46	2224.39	120.53	0.97	1.06	1.5	1.46	0.18	0.27	0.1	0.6	0.05	0.06	0.21	0.01	37.87	0.05	0.01	0.2	0.05

Table 1b. Comparison between range, mean and the richest concentrations of analyzed heavy metals at Wadi Jazan

Heavy metal (mg/kg)	Range at Wadi Jazan (mg/kg)	Mean at Wadi Jazan (mg/kg)	The richest area (Sample No.)
Li	3.67 – 46.64	24.15	14
Be	0.59 – 57.24	28.91	11
Al	4580.06 – 13149.02	8864.54	5
V	74.18 – 169.89	122.03	16
Cr	23.3 – 131.15	77.22	16
Mn	355.59 – 811.58	583.58	11
Fe	20.8 – 47601.44	23811.12	12
Co	8.99 – 15434.45	7721.72	11
Ni	11.94 – 85.38	48.66	11
Cu	12.73 – 132.97	72.85	15
Zn	39.26 – 112.34	75.80	15
Ga	23.15 – 89.19	56.17	11
As	2.35 – 25.92	14.13	7
Se	1.62 – 23.75	12.68	7
Rb	0.92 – 26.93	13.92	7
Sr	15.29 – 214.82	115.05	1
Ag	2.41 – 46.41	24.41	7
Cd	8.98 – 32.97	20.97	7
Sn	1.36 – 2.80	2.08	16
Cs	0.26 – 6.95	3.61	14
Ba	146.44 – 2444.49	1295.46	6
Au	0.37 – 2053.01	1026.69	7
Tl	115.62 – 982.08	548.85	7
Pb	6.79 – 32.03	19.41	7
U	0.45 – 23.25	11.85	7



a



b

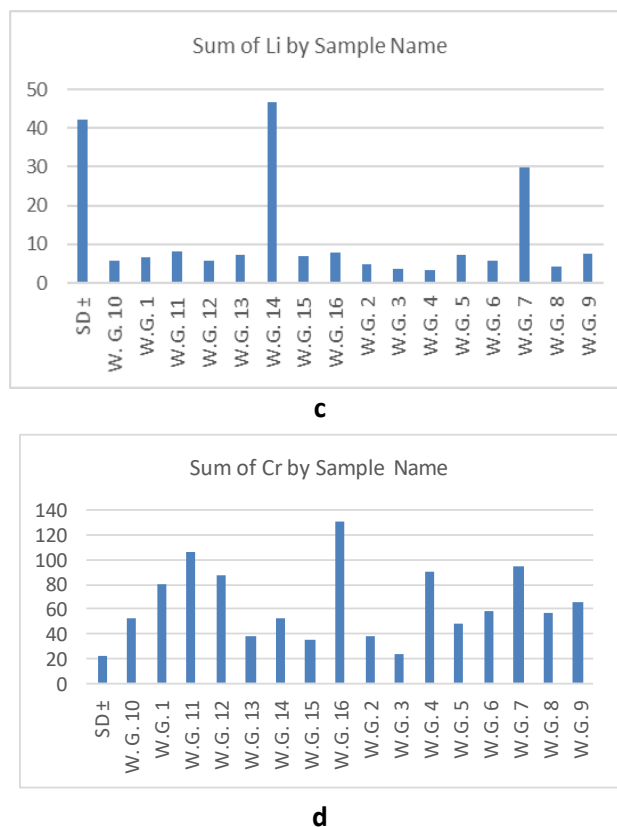


Figure 3. Histograms showing the concentrations of some selected heavy metals at different locations of the analyzed samples at the study area: (a) Shows that sample no 5 is the richest in Al, (b) Delineates that sample no. 11 is the richest in Be, (c) Shows that sample no. 14 considered the richest in Li, while (d) Indicate that sample no 16 is the richest in Cr

Worldwide characteristics of heavy metal contamination of soils

1. **Wide distribution:** Economy and society development makes heavy metal contamination a serious threat to every country. In the world's top ten environmental events, two events have related to heavy metal contamination (Yang and Sun, 2009).
2. **Strong concealment:** As a result of colorless and odorless of heavy metal contamination, so it is difficult to be noticed. Nevertheless, when environmental conditions have changed heavy metals in the soil may be activated and cause serious ecological damage. So heavy metal contamination is usually chemical time bombs (Wood, 1974).
3. **Difficulty of treatment:** Air and water pollution problems can be solved by dilution and self-purification after controlling the sources of pollution. However, it is difficult to apply these techniques to get soils improved. Some soils contaminated by heavy metals could take one or two hundred years to be remediated (Wood, 1974). Therefore, remediation of heavy metal contamination in soils is expensively and the remediation cycle is relatively long.
4. **Complex heavy metal contamination:** Soil contamination in the past was mainly caused by a single heavy metal. However, in recent years more cases

are found to be caused by a variety of heavy metals that led to compose contamination by heavy metal complexes (Zhou, 1995).

Common sources of heavy metals

Heavy metals in soils have different sources which include atmospheric deposition, sewage irrigation, industrial solid waste, mining activities, use of pesticides and fertilizers (Zhang et al., 2011).

1. Atmosphere to soils pathway: Heavy metals in the atmosphere are mainly from gas and dust produced by energy, transport, metallurgy and production of construction materials. The amount of heavy metals which went into the soil through natural deposition and raining sedimentation are related to the level of development of heavy industry, the city's population density, land utilization and traffic level. Soil contamination became to be heavier as closing to the city (Chen, 2002).
2. Sewage to soils pathway: Heavy metals are brought to the soil by irrigative sewage and are fixed in the soil in different ways. It causes heavy metals (Hg, Cd, Pb, Cr, etc.) to continually accumulate in the soil year by year.
3. Solid wastes to soils pathway: Mining and industrial solid waste contamination is the most common. When these wastes are piled or governed, heavy metals move easily due to the facilitation of sunlight, raining and washing leading to spread to the surrounding water and soils (Ding, 2000).
4. Agricultural supplies to soils pathway: Fertilizers, pesticides and mulch are important agricultural inputs for agricultural production (Zhang and Zhang, 2007; Zhang et al., 2011). Heavy metals are the most reported pollutants in fertilizers and the long time using of these products has resulted in the heavy metal contamination of soils (Arao et al., 2010).

Results compared with international permissible contamination

The maximum permissible heavy metal concentration in soil designated by the world health organization (WHO) is tabulated in *Table 2*.

Table 2. Maximum allowed concentration limits of some toxic metals in soil (mg/kg or ppm). (WHO, 1996)

Toxic metal	WHO maximum allowed limits (ppm)
Nickel (Ni)	80
Copper (Cu)	30
Cadmium (Cd)	3
Chromium (Cr)	100
Lead (Pb)	100
Zinc (Zn)	300

When comparing analyzed data of heavy metals in Wadi Jazan soils (*Table 1*) with those of WHO (1996) which presented in (*Table 2*) we found that: For Ni, only samples 11 and 16 are highly polluted and toxic by Ni. Samples 4, 7, 11, 12, 14, 15 and 16 at Wadi Jazan are highly polluted by Cu. For Cr only samples 11 and 16 are the most toxic, while for Pb and Zn all analyzed samples at Wadi Jazan are not polluted. The

most extremely soil pollution at Wadi Jazan is by Cd, where all analyzed samples have higher concentration than the maximum permissible concentration by WHO. One of the most important observations from this comparison is the high toxicity of samples 11 and 16 by different heavy metals that should be taken in consideration for its environmental impact.

Table 3 presents the results of some trace and heavy metals concentration levels (Range and mean) in soils of Wadi Jazan, compared with international standard permissible levels in mg/kg (Hong, et al., 2014).

Table 3. Mean concentration of investigated Wadi Jazan heavy metals compared to international standard limits of heavy metals in soil in mg/kg (Hong et al., 2014). EU = European Union Standard, USA = United State of America Standard, UK = United Kingdom standard

Heavy metal (mg/kg)	Range at Wadi Jazan	Mean at Wadi Jazan	EU standard (mg/kg)	UK standard (mg/kg)	USA standard (mg/kg)
Fe	20.8 - 47601.44	23811.12	-	-	-
Zn	39.26 – 104.34	71.8	300	200	200 - 300
Mn	355.59 – 811.58	583.58	-	-	-
Cu	12.73 – 132.97	72.85	140	63	80 – 200
Cd	8.98 – 32.97	20.97	3	1.4	3
Cr	34.34 – 131.15	82.74	180	6.4	400
Pb	6.79 - 32.03	19.41	300	70	300

The compared results indicate significant variation in heavy metal levels in Wadi Jazan soil with respect to international levels. At all sites higher concentrations of Cd were observed than those compared world permissible Cd concentration. However concentrations of Wadi Jazan Zn, Cu, Cr and Pb heavy metals are lower than the compared international levels.

Heavy metals are specified into three classes of hazard according to (Vodyanitskii, 2016): The first (high-hazard) class includes As, Cd, Hg, Se, Pb, and Zn; the second (medium-hazard) class contains B, Co, Ni, Mo, Cu, Sb, and Cr; and the third (low-hazard) class encompasses Ba, V, W, Mn, and Sr. So it is possible to generalize that the total contamination will apparently be more hazardous in the case when the most toxic elements belonging to the first group are accumulated in soils rather than the low-toxic elements of the third group. Our analyzed data on Table 1 indicates the presence of the three hazard classes of heavy metals, which led to take the environmental impact of these heavy metals concentration at Wadi Jazan very seriously now.

Discussion

Living organisms require various amounts of heavy metals such as iron, cobalt, copper, manganese, molybdenum, zinc and selenium. Where the consumption of these minerals is necessary and important to activate the metabolism of the body of these organisms. However, the consumption of large amounts (high concentrations) is harmful and even toxic and results in so-called heavy metal poisoning (Bolzan, 2014). Minerals account for 45% of the human body's weight, and most are concentrated in the skeleton. The dangerous of heavy metals comes from their bioaccumulation within the

human body faster than their degradation through the metabolism or output. The impact of heavy metals is due to the large distribution of biological agents among the various environmental components (water, air, soil) as well as among the components of the food chain. For example, rainwater works to dissolve rocks and raw minerals that are transported to currents and rivers to be distributed among the various environmental components and are bio concentration among organisms and then reach the food chain (Bharti, 2012).

Concentration of heavy metals, whether high or low, depends on several things (Jiwan et al., 2011) including: 1- If these minerals are found in water (Water pollution), their concentration is controlled by temperature, salinity, water waves, density, and the presence of coral reefs. 2- If these minerals are found in the air (Air pollution), they depend on air components in the environment such as carbon dioxide, nitrogen dioxide, temperature, and humidity. 3- If these minerals are present in the soil (Soil pollution), there are several factors that lead to increased concentration (Soil pollution), the presence of binding elements such as zinc to connect cadmium, as well as bacterial and biological groups, and concentration of organic gases such as methane and ethane. 4- If these minerals exist in living organisms (Pollution in living organisms), they are controlled by many factors such as: the movement of enzymes and the type of the organism. Some organisms have found quick absorption of contaminants due to the presence of help factors, and some animals reject heavy elements and contaminants due to the presence of other help factors as well. 5- It has also been scientifically proven that the concentration of minerals in different environments depends on the type of the pollutant and the state of the pollutant (gas, liquid, or solid).

Impact of heavy metal contamination of soils

1. Impact on soil microorganisms and enzymatic activity

Soil pollution can be caused by various pollutants, but heavy metals (Specially Cu, Ni, Cd, Zn, Cr and Pb) considered the main source (Hinojosa et al., 2004). Soil content from organic matter, clay minerals and P^H value have a direct influence on the effects of heavy metals on the soil biochemical characteristics of organisms (Speira et al., 1999). The toxic effect of heavy metals on soil organisms is to disrupt their biological processes, reduce their activity and their numbers. Some heavy metals cause disturbances on the enzyme activities and their chemical effects in the soil by different ways. Cd has more toxic effect to enzymes than Pb due to its higher ability for movements and lower adhesion with soil granules (Karaca et al., 2010). Our investigated samples at Wadi Jazan (*Table 1*) proved the presence of some heavy metals by considerable concentrations that caused soil pollution of Wadi Jazan area. These metals are mostly represented by Cu, Ni, Cd, Zn, Cr and Pb. On the other hand, one of the most important harmful mineral on the soil and all environments is U, which all our analyzed samples indicate its appearance in all over Wadi Jazan soil.

2. Impact on the plants

Plants growth has a physiological relationship with metals content of soil. Some heavy metals as As, Cd, Hg, Pb and Se are not provide any known physiological role in plants, but Co, Cu, Fe, Mn, Mo, Ni and Zn are considered a required metals for normal plants growth and activation of its metabolism processes. When the concentration of these elements increased over the suitable needed amount of plants growth, they

become poisoning for plants and its final products (Rascio and Izzo, 2011). According to plant species and its ability for absorbing metals, the accumulation of heavy metals in plants occurs (Khan et al., 2008). In Florida, it was found that if the copper content in soil was more than 50 mg/ kg, it would affect citrus seedlings; if soil copper content reached 200 mg/ kg, wheat would wither (Zhang et al., 1989). This mean that soil of samples 15 (Cu = 132 mg/kg) and 16 (Cu = 73 mg/kg) at wadi Jazan are considered the worst places that have direct poisonous impact on plants. Plants absorption of heavy metals and subsequently its entering to the food chain is consider a harmful effect to animals and human health (Sprynskyy et al., 2007). Heavy metals absorption by plants roots is the main reason of heavy metals entrance to the food chain (Jordao et al., 2006). Presence of high concentrations of some heavy metals in Wadi Jazan area (*Table 1*) such as Cd, Zn, Cr, Mn, Cu, Ni, Pb, U and others may indicate that the growing plants, vegetation and trees at Wadi Jazan could have the chance for pollution by these heavy metals. Further future studies are needed to characterize the effect of high concentrations of some heavy metals in soil of Wadi Jazan area on plants, and to see to what extent these heavy metals were entered to the food chain.

3. Impact on the animals and fish

Terrestrial animals are mostly growing by consumption of water and plants during their daily life. High concentrations of heavy metals at Wadi Jazan soil and ground (*Table 1*) may cause the entrance of these heavy metals to the ground water and plants, hence the transfer to the food chain of animals. Of course these heavy metals cause danger effect on animal health and their growing. Not only this, but also will accumulated in the tissues of these animals and will transfer to human during the food chain.

In aquatic environment heavy metals are toxic even though when they present by small amounts. Heavy metals stand strongly against bacterial alteration and remain always in the marine (Woo et al., 2008). Heavy metals in aquatic environment commonly associated with small particles which precipitated with sediments. Recent surface sediments is considered the main tank of different minerals including heavy ones. Upon accumulation of heavy metals in aquatic microorganisms then fish, the transportation of these heavy metals to higher classes food chain is possible. Humans and other carnivores which represent the food chain top obtained their heavy metals indirectly from marine environments through the food. Fish consider the main factor for transferring heavy metals to higher classes food chain (Ayandiran et al., 2009). Taking into consideration the presence of different types of heavy metals at Wadi Jazan soil and its tributaries (*Table 1*). There is ability of rain water and runoff to transfer these heavy metals to the ground water and the Red Sea aquatic environment.

4. Impact on humans

The transportation of heavy metals from soil to plants, pastoral animals and fish, especially soil of high concentration in heavy metals led to human's health risk. Also taking into consideration the implications of food-chain that contaminated by heavy metals, it is intrinsic to conclude that food-chain considered the main route for humans exposure. Of course when heavy metals are not metabolized by human body they will accumulate in soft tissues causing different diseases. For example, Cd is a toxic heavy metal and has 8.65 specific gravity which is considered greater than water nearly by 8

times. The liver, kidneys, lungs, bones and brain are the main target organs for Cd toxicity (Sobha et al., 2007). Cd may damage the metabolism of calcium, which will cause calcium deficiency and result in cartilage disease and bone fractures, etc. Agency for Toxic Substances Management Committee has listed Cd as the sixth most toxic substance that damages human health. Also the toxic clinical characteristics of Zn mainly referred as vomiting, diarrhea, bloody urine, liver and kidney failure and anemia (Duruibe et al., 2007). Despite Cu is considered as an essential element for mammalian nutrition where it is activate electrons movements between enzymes, but when they exposed to high Cu levels a number of harmful health problems could be happened (Stern et al., 2007). Pb affects and damages many of the body organs and systems, such as kidney, liver, reproductive system, nervous system, urinary system, immune system and the basic physiological processes of cells and gene expression. Ni is tumor promoting factor, whose carcinogenesis effect has attracted global concerns. Workers who are in close contact with the nickel powder are more likely to suffer from respiratory cancer, and the content of Ni in the environment is positively correlated with nasopharyngeal carcinoma (Chen, 2011).

According to the previous discussion and explanation about the effect of heavy metals on human, it is possible to reflect to what extent the presence and concentrations of heavy metals (*Table 1*) at Wadi Jazan area have a direct effect on the health of human populations and the environment in general. The source of these heavy metals at Wadi Jazan is most probably the different types of igneous and sedimentary rocks that located at the upper streams of the Wadi. The product of weathering processes of these rocks led to the release of their heavy metals content, and as a result of water runoff along the different wadi tributaries these heavy metals transfer to everywhere at Wadi Jazan and coastal areas. It could be some other additional sources such as industrial activities and the used compost in agriculture activities along the wadi.

From an economic point of view, *Table 1* shows the presence of some economic minerals such as Au, Ag, U, Li and other rare earth elements. In the future the precious metals such as Au and Ag should be evaluated by further studies at Wadi Jazan area, it could be present by economical values. U and Li are very important minerals (strategic minerals) which could be used in different industries. The present study refers preliminary to its presence, of course it need further detailed studies for make full evaluation and prediction of its reserve at Wadi Jazan area. Other occurred rare earth elements participate in different high tech industries and need further investigations as it wasn't the target of this research.

As a result of heavy metals accumulation in food chains and its harmful effect to living organisms a demand was increased around the world to technology of heavy metals separation and purification. Heavy metals can reach to water bodies due to agricultural runoff, industrial activities and applications. There are different technologies that can be used for heavy metals removal from water. These remediation technologies include: Precipitation and coagulation, ion exchange, membrane filtration, bioremediation, heterogeneous photo catalysts and adsorption (Gautam et al., 2015).

Remediation of heavy metal contaminated soils

1. Engineering remediation

Engineering remediation refers to using physical or chemical methods to control heavy metal contamination of soils.

a) Replacement of contaminated soil, soil removal and soil isolation:

Replacement of contaminated soil means adding large amount of clean soil to cover on the surface of the contaminated soil. Soil removal refers to remove the contaminated soil and renew it with the clean soil. Soil isolation means that to isolate the contaminated soil from the uncontaminated soil, but to completely remedy it still needs other auxiliary engineering measures (Zheng et al., 2002). All of these methods will cost large amount of manpower and material resources, so they can only be applied to small area of soils.

b) Electro kinetic remediation:

Soil electro kinetic remediation is a new economically effective technology. The principle is that the DC-voltage is applied to form the electric field gradient on both sides of the electrolytic tank which contains the contaminated soil. Through the way of electro-migration, electric seepage or electrophoresis, and thus reduce the contamination. The method performs well in the soil with low permeability (Hanson et al., 1992).

c) Soil leaching:

Soil leaching is to wash the heavy metal contaminated soil with specific reagents and thus remove the heavy metal complex and soluble ions adsorbed on the solid phase particles. By using this method, heavy metals are separated from the soil, and heavy metals are then recycled from extracting solution.

d) Adsorption:

Adsorption method is based on the fact that almost all heavy metal ions can be fixed and adsorbed by clay mineral (bentonite, zeolite, etc.), a steel slag, furnace slag, etc. (Wang and Zhou, 2004).

The most suitable techniques for Wadi Jazan are replacement of contaminated soil, soil removal, soil isolation and adsorption because of the small area of soils that have metal toxicity, and also due to the presence of some local resources (Such as used bentonite clay mineral in adsorption technique).

2. *Bioremediation*

a) Phytoremediation:

Using plants and their coexisting microbial system to remove heavy metals is a new technology. The key of the method is to find the suitable plants with strong ability for heavy metal accumulation and tolerance. Now more than 400 species of such plants have been found in the world, and most of them belong to Cruciferae, including the genus Brassica, Alyssums, and Thlaspi (Xin et al., 2003).

b) Microbial remediation:

Microbial remediation refers to using some microorganisms to perform the absorption, precipitation, oxidation and reduction of heavy metals in the soil. Siegel et al. (1986) found that fungi could secrete amino acids, organic acids and other

metabolites to dissolve heavy metals and the mineral containing heavy metals. Fred et al. (2001) reported that the fungi, *Gomus intraradices*, may improve the tolerance and absorption of sunflower to Cr.

c) Animal remediation:

Some animals living in the soil (maggots, earthworms, etc.) can take heavy metals in the soil. Wang et al. (2007) proved that when the concentration of Cu was low in the soil, the activities and secretion of earthworms could promote the absorption of Cu by ryegrass.

Phytoremediation technique could be considered most more effective to use at Wadi Jazan due to the suitability of the environmental conditions at Wadi Jazan for growing some plants which used in removing heavy metals depending on its microbial system (Such as Cruciferae, including the genus Brassica, Alyssums, and Thlaspi).

Conclusion

Sediments of Wadi Jazan area contaminated by different types of heavy metals and by different concentrations. These metals include Li, Be, Al, V, Cr, Mn, Fe, Co, Ni, Cu, Zn, Ga, As, Se, Rb, Sr, Ag, Cd, Sn, Cs, Ba, Au, Tl, Pb and U. Investigated heavy metals has a direct and indirect harmful environmental impact on soil, plants, terrestrial animals, aquatic environment and human health. Comparing analyzed heavy metals with those permissible by WHO indicate that: For Ni, only samples 11 and 16 are highly polluted and toxic by Ni. Samples 4, 7, 11, 12, 14, 15 and 16 at Wadi Jazan are highly polluted by Cu. For Cr only samples 11 and 16 are the most toxic, while for Pb and Zn all analyzed samples at Wadi Jazan are not polluted. The most extremely soil pollution at Wadi Jazan is by Cd, where all analyzed samples have higher concentration than the maximum permissible concentration by WHO. One of the most important observations is the high toxicity of samples 11 and 16 by different heavy metals that should be taken in consideration for its intensive environmental impact.

Heavy metals concentrations along Wadi Jazan indicate that the most polluted area is located around Abu Arish City. The main source of Wadi Jazan heavy metals might be the weathered sedimentary and igneous rocks that located at Wadi Jazan upstream tributaries. Rains and floods leached these heavy metals and transfer them along through Wadi Jazan to the Red Sea coast. Except the location of Abu Arish City which may have additional sources of heavy metals due to human activities in agriculture and industries.

The present study concluded the suitability of some recent techniques for soil remediation at Wadi Jazan, such as engineering remediation (Replacement of contaminated soil, soil removal, soil isolation and adsorption) and bioremediation (Phytoremediation). Selected techniques of engineering remediation are considered the most suitable ones for Wadi Jazan because of the small area of soils that have metal toxicity, and also due to the presence of some local resources (Such as used bentonite mineral in adsorption technique). Phytoremediation technique can also use due to the suitability of the environmental conditions at Wadi Jazan for growing some plants that used in removing heavy metals depending on its microbial system (Such as Cruciferae, including the genus Brassica, Alyssums, and Thlaspi).

Current investigation also clarify that some studied heavy metals have economic importance usage (Such as Au, Ag and U), and need further evaluations in the future.

Acknowledgements. The authors are greatly indebted and thankful the Deanship of Scientific Research, Jazan University for the financial supports of this research proposal no (JUP8/000252). Many thanks also are extended to Dr. Eid Brima, King Khalid University - Chemistry Department for doing the chemical analyses.

REFERENCES

- [1] Al Bratty, M., Arbab, I. A., Alhazmi, H. A., Attafi, I. M., Al-Rajab, A. J. (2017): Icp-MS determination of trace metals in drinking water sources in Jazan Area, Saudi Arabia. – *Current World Environment* 12(1): 06-16.
- [2] Al Zahrani, D. A., Selim, E. M., El-Sherbiny, M. M. (2018): Ecological assessment of heavy metals in the grey mangrove (*Avicennia marina*) and associated sediments along the Red Sea coast of Saudi Arabia. – *Oceanologia* 60: 513-526.
- [3] Alhababy, A. M. (2016): Comparative study on concentration of heavy metals in sediments and fish, Jazan Area, Saudi Arabia. – *Journal Biol Chem Research* 33(2): 828-835.
- [4] Arao, T., Ishikawa, S., Murakami, I. M. (2010): Heavy metal contamination of agricultural soil and counter measures in Japan. – *Paddy and Water Environment* 8(3): 247-257.
- [5] Ayandiran, T. A., Fawole, O. O., Adewoye, S. O., Ogundiran, M. A. (2009): Bioconcentration of metals in the body muscle and gut of *Clarias gariepinus* exposed to sublethal concentrations of soap and detergent effluent. – *Journal of Cell and Animal Biology* 3(8): 113-118.
- [6] Bharti, P. K. (2012): *Heavy Metals in Environment*. – Lambert Academic Publishing, Germany.
- [7] Bolzan, B. D. (2014): Effect of heavy metals on living organisms. – *World Scientific News* 5: 26-34.
- [8] Campbell, J. D. (2015): Minerals and disease. – *J Orthomol Med* 1995(3-4): 177-188.
- [9] Chen, H. M. (2002): *Behaviors and Environmental Quality of Chemical Substances in the Soil*. – Science Press, Beijing, China.
- [10] Chen, Y. F. (2011): Review of the research on heavy metal contamination of China's city soil and its treatment method. – *China Population, Resources and Environment* 21(3): 536-539.
- [11] Dabbagh, A., Emmermann, R., Hötzl, H. H., Jado, A. R., Lippolt, H. J., Kollman, W., Moser, H., Rauert, W., Zotl, J. G. (1984): The Development of Tihamat Asir during the Quaternary. – In: Jado, A. R., Zotl, J. G. (eds.) *Quaternary Period in Saudi Arabia Volume 2: Sedimentological, Hydrogeological, Hydrochemical, Geomorphological, Geochronological and Climatological Investigations in Western Saudi Arabia*. Springer-Verlag, Vienna, pp. 150-73.
- [12] Deves, M. H., Inglis, R. H., Meredith-Williams, M. G., Al Ghamdi, S., Alsharekh, A., Bailey, G. (2013): Palaeolithic survey in southwest Saudi Arabia: methodology and Preliminary results. – *Adumatu* 27: 7-30.
- [13] Ding, Y. (2000): The management of polluted soils by heavy metal. – *Environment and Development* 15(2): 25-28.
- [14] Duruibe, J. O., Ogwuegbu, M. O.C, Ekwurugwu, J. N. (2007): Heavy metal pollution and human biotoxic effects. – *International Journal of Physical Sciences* 2(5): 112-118.
- [15] Fred, T., Davies, J., Jeffrey, D. P. et al. (2001): Mycorrhizal fungi enhance accumulation and tolerance of chromium in sunflower (*Helianthus annuus*). – *Journal of Plant Physiology* 158: 777-786.
- [16] El Tahlawy, M. R. (2007): Harmful minerals and rocks to the environment. – *Assuit Journal of Environmental Studies*, in Arabic, 31: 101-117.

- [17] Gautam, R. K., Sharma, S. K., Mahiyab, S., Chattopadhyaya, M. C. (2015): Contamination of Heavy Metals in Aquatic Media: Transport, Toxicity and Technologies for Remediation. – In: Sharma, S. (ed.) Heavy Metals in Water: Presence, Removal and Safety. The Royal Society of Chemistry, Burlington House, UK, pp. 1-24.
- [18] Golam, M. M., Fahad, A. A. (2017): Environmental contamination and assessment of heavy metals in water, sediments and shrimp of Red Sea coast of Jazan, Saudi Arabia. – *Journal of Aquatic Pollution and Toxicology* 1(1): 1: 5.
- [19] Hanson, A., David, T., Sabatin, A. (1992): Transport and Remediation of Subsurface Contaminants. – American Chemical Society, Washington, DC, pp. 108-120.
- [20] Hinojosa, M. B., Carreira, J. A., Ruiz, R. G., Dick, R. P. (2004): Soil moisture pre-treatment effects on enzyme activities as indicators of heavy metal contaminated and reclaimed soils. – *Soil Biology & Biochemistry* 36: 1559-1568.
- [21] Hong, A. H., Law, P. L., Onni, S. S. (2014): Environmental burden of heavy metal contamination levels in soil from sewage irrigation area of Geriyo Catchment, Nigeria. – *Civil and Environmental Research* 6(10): 118-124.
- [22] Inglis, R. H., Sinclair, A., Shuttleworth, A., Alsharekh, A., Al Ghamdi, S., Deves, M., Meredith-Williams, M. G., Bailey, G. N. (2014): Investigating the palaeolithic landscapes and archaeology of the Jazan and Asir Regions, Southwest Saudi Arabia. – *Proceedings of the Seminar for Arabian Studies* 44: 193-212.
- [23] Jiwan, S., Ajay, S. K. (2011): Effects of heavy metals on soil, plants, human health and aquatic life. – *International Journal of Research in Chemistry and Environment* 1(2): 15-21.
- [24] Jordao, C. P., Nascentes, C. C., Cecon, P. R., Fontes, R. L.F, Pereira, J. L. (2006): Heavy metal availability in soil amended with composted urban solid wastes. – *Environmental Monitoring and Assessment* 112: 309-326.
- [25] Karaca, A. Cetin, S. C., Turgay, O. C., Kizilkaya, R. (2010): Effects of Heavy Metals on Soil Enzyme Activities. – In: Sherameti, I., Varma, A. (ed.) *Soil Heavy Metals (Soil Biology)*. Springer, Heidelberg, pp. 237-265.
- [26] Khan, S., Cao, Q., Zheng, Y. M., Huang, Y. Z., Zhu, Y. G. (2008): Health risks of heavy metals in contaminated soils and food crops irrigated with wastewater in Beijing, China. – *Environmental Pollution* 152: 686-692.
- [27] Mart, V. B. (2014): *Minerals in Your Life*. – Euro Geoscience, Brussels.
- [28] Nadia, B. E., Anwar, A. E., Alaa, R. M., Bandr, A. A. (2009): Metal pollution records in core sediments of some Red Sea coastal areas, Kingdom of Saudi Arabia. – *Environ Monit Assess* 155: 509-526.
- [29] Rascio, N., Izzo, F. N. (2011): Heavy metal hyper accumulating plants: how and why do they do it? And what makes them so interesting? – *Plant Science* 180: 169-181.
- [30] Siegel, S. M., Keller, P. et al. (1986): *Metal Speciation*. – Kluwer Academic Publishers, Chicago, USA.
- [31] Sobha, K., Poornima, A., Harini, P., Veeraiah, K. A. (2007): Study on biochemical changes in the fresh water fish, catla catla (hamilton) exposed to the heavy metal toxicant cadmium chloride. – *Kathmandu University Journal of Science, Engineering and Technology* 1(4): 1-11.
- [32] Speira, T. W., Kettlesb, H. A., Percivalc, H. J., Parshotam, A. (1999): Is soil acidification the cause of biochemical responses when soils are amended with heavy metal salts? – *Soil Biology and Biochemistry* 31: 1953-1961.
- [33] Sprynskyy, M., Kosobucki, P., Kowalkowski, T., Buszewsk, B. (2007): Influence of clinoptilolite rock on chemical speciation of selected heavy metals in sewage sludge. – *Journal of Hazardous Materials* 149: 310-316.
- [34] Stern, B. R., Solioz, M., Krewski, D., Aggett, P., Aw, T. C., Baker, S., Crump, K., Dourson, M., Haber, L., Hertzberg, R., Keen, C., Meek, B., Rudenko, L., Schoeny, R., Slob, W., Starr, T. (2007): Copper and human health: biochemistry, genetics, and

- strategies for modeling dose response relationships. – *Journal of Toxicology and Environmental Health* 10: 157-222.
- [35] Uluturhan, E., Kontas, A., Can, E. (2011): Sediment concentrations of heavy metals in the Homa Lagoon (Eastern Aegean Sea): assessment of contamination and ecological risks. – *Mar Poll Bull* 62: 1989-1997.
- [36] Vodyanitskii, Y. N. (2016): Standards for the contents of heavy metals in soils of some states. – *Annals of Agrarian Science* 14: 257-263.
- [37] Wang, D. D., Li, H. X., Hu, F. G. et al. (2007): Role of earthworm-straw interactions on phytoremediation of Cu contaminated soil by ryegrass. – *Acta Ecologica Sinica* 27(4): 1292-1299.
- [38] Wang, X., Zhou, Q. X. (2004): The ecological process, effect and remediation of heavy metals contaminated soil. – *Ecologic Science* 23(3): 278-281.
- [39] WHO (1996): World Health Organization Report. – WHO, Geneva.
- [40] Woo, S., Yum, S., Park, H. S., Lee, T. K., Ryu, J. C. (2008): Effects of heavy metals on antioxidants and stress-responsive gene expression in Javanese medaka (*Oryzias javanicus*). – *Comparative Biochemistry and Physiology* 149: 289-299.
- [41] Wood, J. M. (1974): Biological cycles for toxic elements in the environment. – *Science* 183: 1049-1052.
- [42] Xin, Q. G., Pan, W. B., Zhang, T. P. (2003): On phytoremediation of heavy metal contaminated soils. – *Ecologic Science* 22(3): 275-279.
- [43] Yang, Y. B., Sun, L. B. (2009): Status and control countermeasures of heavy metal pollution in urban soil. – *Environmental Protection Science* 35(4): 79-81.
- [44] Zhang, W. J., Zhang, X. Y. (2007): A forecast analysis on fertilizers consumption worldwide. – *Environmental Monitoring and Assessment* 133: 427-434.
- [45] Zhang, W. J., Jiang, F. B., Ou, J. F. (2011): Global pesticide consumption and pollution: with China as a focus. – *Proceedings of the International Academy of Ecology and Environmental Sciences* 1(2): 125-144.
- [46] Zhang, Z. J., Lu, Q. F., Fang, F. (1989): Effect of mercury on the growth and physiological function of wheat seedlings. – *Chinese Journal of Environmental Science* 10(4): 10-13.
- [47] Zheng, X. S., L. U., A. H., Gao, X. (2002): Contamination of heavy metals in soil present situation and method. – *Soils and Environmental Sciences* 11(1): 79-54.
- [48] Zhou, Q. X. (1995): *Ecology of Compound Pollution*. – China Environmental Science Press, Beijing.

CLIMATE CHANGE PERCEPTION AND ADAPTATION IN NIGERIA'S GUINEA SAVANNA: EMPIRICAL EVIDENCE FROM FARMERS IN NASARAWA STATE, NIGERIA

TARFA, P. Y.¹ – AYUBA, H. K.² – ONYENEKE, R. U.^{3*} – IDRIS, N.² – NWAJUBA, C. A.⁴ – IGBERI, C. O.³

¹*Department of Climate Change, Federal Ministry of Environment, Abuja, Nigeria*

²*Department of Geography, Nasarawa State University, Keffi, Nigeria*

³*Department of Agriculture (Agricultural Economics and Extension Programme)
Alex Ekwueme Federal University Ndufu-Alike, Ebonyi State, Nigeria*

⁴*Department of Educational Foundations
Alex Ekwueme Federal University Ndufu-Alike, Ebonyi State, Nigeria*

**Corresponding author*

e-mail: robertonyeneke@yahoo.com, robert.onyeneke@funai.edu.ng

(Received 23rd Feb 2019; accepted 10th Apr 2019)

Abstract. Nigeria's guinea savanna produces the bulk of the food consumed in the country and climate change is adversely affecting agriculture in the area. Farmers in the area respond differently to climate change based on their perception. Yet, studies that systematically link farmers' perception on climate change to scientific data from meteorological stations are rare in Nigeria's guinea savanna. Much rarer are studies that consider the simultaneity in the adaptation decisions of the farmers. This study therefore aimed at analysing farmers' perception in comparison with meteorological data and the determinants of adaptation efforts of crop farmers in the areas with data from Nasarawa State of Nigeria. To achieve this aim, the study combined time-series data on climatic variables obtained from a weather station and cross-sectional data from 160 smallholder farmers selected from the area. The study applied descriptive statistics, trend analysis, and multivariate probit model in analysing data collected. The study showed reduction in volume of rainfall and significant increase in surface temperature with the farmers having firm perception of these changes. The farmers responded to the changes in temperature and rainfall by choosing adaptation strategies such as use of improved crop varieties, soil and water conservation, tree planting, changing dates of sowing and tillage options, irrigation, diversifying their means of livelihood, and farmland management. Interestingly, these strategies were complementary and farmers' socioeconomic and institutional characteristics significantly determined adaptation in the area. Therefore, considering farmers' socioeconomic characteristics and improving the institutions will help in future and planned adaptation efforts of governments.

Keywords: *crop farmers, climate risk management, determinants, multivariate probit model*

Introduction

Climate change, which can be described at various scales – regional, national, or global – is a non-random change in the average weather conditions of a place overtime (Adejuwon, 2004; BNRCC, 2007; Nigerian Meteorological Agency, 2017). Empirical evidence confirms that the Earth has experienced a significant rise in temperature – between 0.65°C and 1.06°C – over the past 100 years (IPCC, 2013, 2014). The warming is real and significant but has varied across time and space with greenhouse gases, emanating from anthropogenic activities, being the major cause (Crosson, 1997; IPCC, 2014).

Climate change can retard/impede efforts being made by nations to achieve the sustainable development goals. The region that will suffer most of the impacts of climate change is Africa because it is the most vulnerable among other regions of the world and has the lowest capacity to adapt (Niang et al., 2014). Niang et al. (2014) documented dramatic and widespread evidence of global warming and other climate changes. Some of these impacts include threats to global food supply citing a decrease of up to 2 percent each decade in yields of staple crops like maize, wheat and rice; freshwater and marine species; ecosystem shift and species extinction; negative impact on agriculture; migration and security; heat waves, flood; shortage of water resources; destruction of homes and infrastructure; increased food insecurity; and violent conflict that lead to the destruction of infrastructure, livelihood opportunities and natural resources. Scientific evidence suggests that climate change may decline the output of major staple crops - wheat, maize, and rice (Niang et al., 2014; Olsson et al., 2014; Magrin et al., 2014; Hijioka et al., 2014; IPCC, 2015).

In Africa, the African Union adopted an African Climate Change Strategy in 2011, while, in the West African sub-region, ECOWAS has developed and adopted Climate Change Policy and Strategy Plan (2011). These policy documents provide priority actions in the region, which shape national climate change policies and strategies in member countries. The present research has been informed by the global, regional and national commitments and obligations.

In Nigeria's guinea savanna, the frequency and severity of heat waves, drought and intense rainfall is increasing and this is changing the vulnerability and exposure of economic sectors, livelihoods, people and assets. Agriculture is perhaps the most sensitive of all the sectors as most of the farmers depend on rain-fed agriculture. Reduced growing seasons and higher temperatures will affect agriculture (IPCC, 2007; Babatunde et al., 2011; Federal Ministry of Environment, 2014).

The guinea savanna area of Nigeria is known as the 'food basket' of Nigeria. Therefore, climate change will increase the challenge of food insecurity, compound or worsen the degree of seasonal hunger that pervades in many parts of Nigeria, especially Nasarawa State (Babatunde et al., 2011; DCC, 2013, 2014; Ethan, 2015). Dry-spell occurring any time during the growing season often exposes crops to moisture stress, hence farmers usually face problems of both too much and little moisture (Babatunde et al., 2011; Osabo et al., 2014). These have brought about changes in the way smallholder farmers make decision to adapt to their environment (Ajetomobi et al., 2010).

Lazkano et al. (2016) describe adaptation as any activity that reduces climate change-induced damages. The literature captures well some adaptation practices used by farmers in different parts of Nigeria. These include use of improved crop varieties, conservation practices, planting different crops, farmland management, agroforestry and irrigation (NEST and Woodley, 2011; BNRCC, 2011; Women Farmers Advancement Network, 2014; Onyeneke et al., 2017). Even though there are several studies on crop production and climate change (NEST, 2011; BNRCC, 2011; NEST and Woodley, 2011; Onyeneke et al., 2012; Falaki et al., 2013; Ezeaku et al., 2014; Ibrahim et al., 2014; Women Farmers Advancement Network, 2014; Odiana and Ibrahim, 2015; Tihamiyu et al., 2015; Tsojon, 2017), still little is known regarding the farmers' perceptions and adaptations in smallholder agricultural production systems in Nasarawa State in Nigeria's guinea savanna. In spite of the efforts of researchers in documenting climate risk management measures in agriculture in Nigeria, there is scanty empirical evidence on the determinants of the choice of adaptation strategies

used by crop farmers in Nigeria. Furthermore, farmers by nature adopt multiple strategies to manage climate risks and such decisions are made simultaneously. Much rarer are research works accounting for the possibility of simultaneously or sequentially adopting multiple climate change adaptation strategies by farmers in Nigeria in particular and sub-Saharan Africa at large. Previous studies on climate change adaptation of farmers in sub-Saharan Africa mainly treated adaptation strategies singly without considering the joint and simultaneous adaptation decisions of farmers. Our study filled this gap in research by analysing the determinants of sequential adoption of climate risk management of farmers. Understanding farmers' perception, adaptation strategies and the complementarity or substitutability of the chosen strategies and their determinants is important for the determination of the effectiveness of farmers' adaptation efforts. Such knowledge will enhance policies and programmes directed towards enhancing the resilience of the agricultural sector of Nasarawa State and Nigeria. This study therefore aims to assess climate change perception and adaptation practices of farmers in Nasarawa State, Nigeria. In specific terms, the study:

- i) described crop farmers' socioeconomic characteristics in Nasarawa State;
- ii) compared trend of climatic data from the meteorological station with farmers' perception on the changes observed;
- iii) identified and classified farmers' chosen adaptation strategies to deal with climate change; and
- iv) analysed the effect of farmers' characteristics on adaptation choices.

Materials and Methods

Study Area

Nasarawa State is located in north-central Nigeria (*Figure 1*). The State lies within the guinea savanna and has a tropical climate. Two major seasons characterise the State – the rainy and dry seasons. The vegetation of Nasarawa is characterised by tall grasses and scattered trees. The population of Nasarawa State is 1,863,275 persons (National Population Commission, 2006). The State has thirteen (13) Local Government Areas namely. The inhabitants of the State depend mainly on agriculture with the production of varieties of cash crops throughout the year.

Sampling Technique

In selecting respondents for this study, the researchers employed purposive and random sampling methods. Firstly, two Local Government Areas (LGAs), Lafia and Toto LGAs, from the thirteen (13) Local Government Areas of Nasarawa State (*Figure 1*), that have high concentration of smallholder farmers and visible impacts of climate change LGAs, were selected. Since Lafia and Toto LGAs have high concentration of smallholder farmers and are affected by climate change, the researchers focused on these LGAs and randomly selected four communities in each of the LGAs. Finally, the researchers selected twenty (20) farmers randomly without replacement in each selected community making the sample size of the study 160 farmers. The sampling frames were provided by the extension agents working in the selected communities. Subjective judgment of ten officials of the Ministries of Agriculture and Environment in the State revealed that about 12 percent of farmers in the LGAs have been adversely affected by climate change hazards. The researchers

used this proportion with a z-value of 1.96 for 95% confidence level and 5% error margin to compute the final sample size which gave about 161 farmers. The formula for calculating the final sample size is given in *Equation 1* as:

$$n = p(1 - p) (z/E)^2 \quad (\text{Eq.1})$$

where:

n = Final sample size;

p = Proportion farmers adversely affected by climate change (12% or 0.12);

z = Z-value at 95% confidence level (1.96);

E = error margin (5% or 0.05).

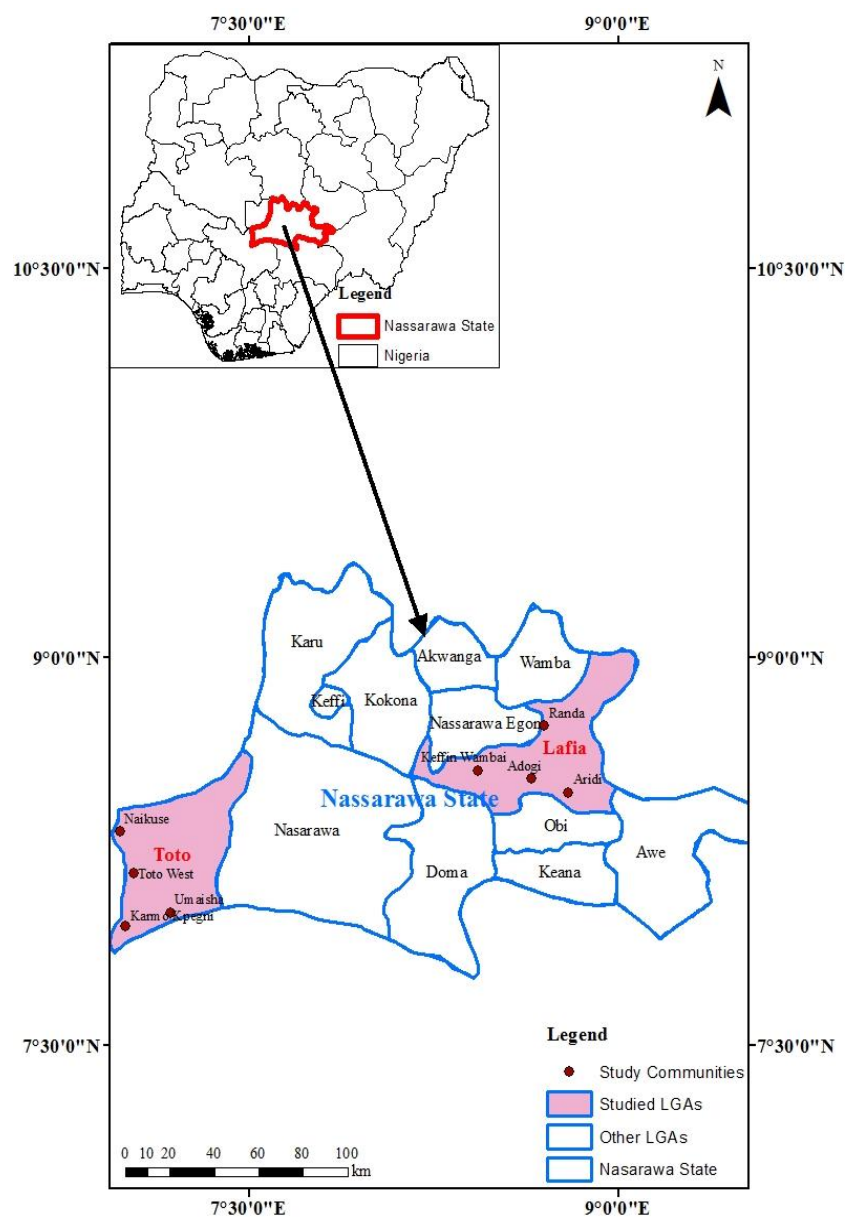


Figure 1. Nasarawa State showing the two selected Local Government Areas and Study Communities

Types and Sources of Data

The study collected primary and secondary data. Interview schedule developed by the researchers was used to collect primary data from the farmers. The information contained in the interview schedule consisted of household characteristics of the farmers, institutional factors, perception, and adaptation measures. The researchers hired eight enumerators to assist in data collection in the eight communities. That is one enumerator per community. In order to ensure uniform and accurate data collection by all enumerators, one-day training was held for the enumerators. The researchers supervised the data collection as the study progressed. The survey was conducted between January and June 2014. The secondary data collected included climatic data such as annual temperature means, and annual aggregate rainfall. The climatic data were annual time-series data obtained in 2014 from the Nigerian Meteorological Agency for at least a period of thirty years. Due to data availability, the temperature data covered a period of thirty-three years (1981 – 2013) while rainfall covered a period of fifty-three years (1961 – 2013).

Method of Data Analysis

Descriptive statistics, trend analysis and multivariate probit analysis were statistical tools adopted for data analysis. Specific objectives i and iii were achieved with descriptive statistics. To compare farmers' perception on climate change and scientific data from meteorological station, a trend analysis was used to present the change observed in climate variables in the area and then link that to the anecdotal accounts from the farmers to check whether there is convergence or divergence. Many researchers have applied this method to model climate change trend and people's perception (Vedwan and Rhoades, 2001; Maddison, 2006; Gbetibouo, 2009). Multivariate probit regression was used to analyse the determinants of climate change adaptation decisions of farmers.

Multivariate Probit Model (MVP)

Multivariate probit technique was used to determine the interdependency of the adaptation practices and the socioeconomic factors influencing adaptation decisions. Lin et al. (2005) used similar model in their study. The adaptation practices are nominal variables and the researchers constructed a dichotomous dependent variable to capture whether such practice was adopted by a farmer or not. If a farmer used such practice, the researchers coded it as one and coded 0 for farmers who did not use such practice, and this makes the dependent variables binary taking only two values – 0 or 1 – (Gujarati, 1995; Greene, 2003). The study adopted the multivariate probit approach to model the factors influencing adaptation decisions of the farmers. An important advantage of the multivariate probit (MVP) framework is its strength in modeling the simultaneous or sequential decisions farmers make in climate risk management and this informed the choice of the MVP for this study. Farmers usually make complementary or substitutive decisions in choosing climate risk management strategies and the multivariate probit model makes interpretation of such simultaneous adaptation decisions possible and less difficult. The study has a set of eight binary dependent variables representing adaptation choices made by farmers, Y_1, \dots, Y_8 such that:

$$Y_i = 1 \text{ if } \beta_i X' + \varepsilon_i > 0 \quad (\text{Eq.2})$$

and

$$Y_i = 0 \text{ if } \beta_i X' + \varepsilon_i \leq 0, i = 1, 2, \dots, 8 \quad (\text{Eq.3})$$

where

$i = 1, 2, \dots, 8$ are the chosen climate risk management practices/adaptation options; X represents the vector of the predictors; β_i is the parameter estimates of the predictors; and ε_i , random error vectors having a zero mean, unitary standard deviation, and an 8×8 correlation matrix. *Equations 2 and 3* represent the multivariate probit framework of this study.

Dependent variables of the MVP

The adaptation strategies identified in this study as dependent variables are planting improved varieties of crops, portfolio diversification, soil and water conservation practices, adjusting the time of planting, changing soil tillage options, tree planting, irrigation, and farmland management. These are defined as follows:

1. Use of improved crop varieties: The adaptation options in this category are use of short gestation crops, use of flood tolerant crop, planting drought-tolerant crops, cultivating disease/pest-resistant crop cultivars, and planting different varieties of crops. These strategies have been documented as climate-resilient practices in the agricultural sector in sub-Saharan Africa (Napier, 1991; Nhemachena and Hassan, 2007; Yegbemey et al., 2014; Wondimagegn and Lemma, 2016; Mulwa et al., 2017). Any farmer who adopted at least fifty percent of the options under this category was considered an adopter of improved crop varieties and was coded 1 while any farmer who adopted less than fifty percent of the options under this category was coded 0.

2. Portfolio diversification: Piya et al. (2012), Gbetibouo (2009) and Deressa et al. (2008) classified portfolio diversification as an important climate risk management measure. The adaptation options in this category include diversifying from agriculture to non-agricultural activities, crop farming to livestock farming and mixed farming. Any farmer who adopted at least fifty percent of the options under this category was considered an adopter of portfolio diversification and was coded 1 while any farmer who adopted less than fifty percent of the options under this category was coded 0.

3. Soil and water conservation practices: These are very important measures in managing climate change because they aid in maintaining soil fertility, increasing yield and improving resilience. The adaptation options here include terracing, mulching, planting of cover crops, crop rotation and water harvesting. Any farmer who adopted at least fifty percent of the options under this category was considered an adopter of soil and water conservation practices and was coded 1 while any farmer who adopted less than fifty percent of the options under this category was coded 0.

4. Adjusting planting dates: This is a straightforward farm-level climate change adaptation strategy in Nigeria. The options here cover adjusting planting dates and shortening the length of growing period. Any farmer who adopted at least fifty percent of the options under this category was considered an adopter of adjusting planting dates and was coded 1 while any farmer who adopted less than fifty percent of the options under this category was coded 0.

5. Changing tillage operations: Changing tillage operations is also very important in climate change adaptation management in Nigeria. This involves planting on mounds and/or ridges. Any farmer who adopted this option/category was considered an adopter

of changing tillage operations and was coded 1 while any farmer who adopted less than fifty percent of the options under this category was coded 0.

6. Planting trees: This covers tree planting on the farms for protection against scorching of crops. Any farmer who adopted this option/category was considered an adopter of planting trees on farms and was coded 1 while any farmer who did not adopt it was considered non-adopter and was coded 0.

7. Irrigation: This category includes irrigation and drainage. Any farmer who adopted at least fifty percent of the options under this category was considered an adopter of irrigation and was coded 1 while any farmer who adopted less than fifty percent of the options under this category was coded 0.

8. Farmland management: This involves adjustments in land use and land management. The main option here is changing land area cultivated. Any farmer who adopted this option/category was considered an adopter of farmland management and was coded 1 while any farmer who did not adopt it was considered non-adopter and was coded 0.

Independent variables of the MVP

The independent variables are:

X₁= Education of household head (years spent in school)

X₂= Age of household head (years)

X₃= Household size (number of persons)

X₄= Income (Naira)

X₅= Livestock ownership (number owned)

X₆= Extension contact

X₇= Farming experience (years)

X₈= Availability of credit (Naira)

X₉= Farm size (hectares)

X₁₀= Distance to markets (kilometres)

X₁₁= Distance to water sources (minutes)

X₁₂= Disposed to take crop farming risks (Dummy variable; yes = 1, no = 0)

X₁₃= Membership to farmer groups (Dummy variable; 1=member or 0 =not member)

Results and Discussion

Farmers' Characteristics

Table 1 presents the demographic characteristics of the farmers. Analysing the demographic properties of farmers is very important in understanding the type of farmers studied, which has implications on the adaptive capacity, choice and degree of climate resilient agricultural practices chosen and implemented. *Table 1* showed that the farmers' average age was 45.66 years which is an indication that they are mainly young adults. Younger farmers are more experimental and productive than older farmers and would be more disposed to adopt strategies that build their resilience than their older counterparts. This result is not far from the findings of other researchers in different parts of Nigeria. Onyegbula and Oladeji (2017) noted that the average age of rice farmers in three rice-producing States in Nigeria was 45.3 years while Ifeanyi-Obi et al. (2017) averred that the average age of cocoyam farmers in Southeast Nigeria was 51

years. Also, similar findings abound in other parts of Africa. For example, Mulwa et al. (2017), in their study on farmers' response to climate risks in Malawi, found that the average of the farmers was 50 years, Feleke et al. (2016) recorded an average age of 43.4 years among Ethiopian farmers while Nhemachena et al. (2014) found the average age of Southern African farmers to be 47.41 years.

Table 1. Socio-economic characteristics of the farmers (n = 160)

Variable	Frequency	Percentage	Average
Age (Years)			
Less than 40	50	31.25	45.66 years
41-50	70	43.75	
51-60	22	13.75	
Above 61	18	11.25	
Total	160	100.00	
Sex			
Female	3	1.88	
Male	157	98.12	
Total	160	100.00	
Marital Status			
Married	150	93.75	
Single	6	3.75	
Widowed	3	1.88	
Divorced	1	0.62	
Total	160	100.00	
Educational level (Years)			
No Formal Education (0)	23	14.38	10.1 years
Primary Education (1-6)	34	21.25	
Secondary Education (7-12)	48	30.00	
Tertiary Education (12-18)	53	33.12	
Total	160	100.00	
Farm size (Ha)			
0.1-1.9	94	58.75	4.31Ha
1.91-2.9	44	27.50	
2.91-5	22	13.75	
Total	160	100.00	
Household size (Number of Persons)			
1-5	34	21.25	10 persons
6-10	70	43.75	
11-15	56	35.00	
Total	160	100.00	

Majority (98.12%) of the farmers were males. Thus, male-headed households are predominantly involved in agriculture in the area than the female-headed households. This may be connected to ownership of agricultural production resources in the area as men have more access to the resources than females, and hence will adapt more readily to climate change than females. Mulwa et al. (2017), Wondimagegn and Lemma (2016), Asfaw and Admassie (2004), Tenge et al. (2004) documented male dominance in agriculture across sub-Saharan Africa. The majority of the farmers (93.75%) were married with both partners alive which is similar to the percentage (92.00%) recorded by Ifeanyi-Obi et al. (2017) among farmers in Southeast Nigeria. In many rural

agricultural communities, husbands, wives and children work in the farm which usually compensates farm labour needs of the household and increases agricultural production.

The level of education of farmers showed that majority of the farmers (85%) received a formal education suggesting that the farmers are literates. Similar level of literacy was recorded by Okpe and Aye (2015) among farmers in Makurdi, Benue State of Nigeria. With this level of education, farmers in the area would be readily disposed to adopting strategies that will help them manage climate change. The result of household size indicates that the farmers have large families with an average of 10 persons per family. The farmers were smallholders because they operated an average farm size of 4.31 ha. This may support or discourage adaptation depending on the farm management options and decisions pursued by the farm household.

Comparison between Farmers' Perception of Climate Change and Meteorological Station's Recorded Data

The study also analysed trend of climate data recorded for a long period. The trends in recorded climate data were then linked to farmers' perception of the changes. Climatic variables (temperature and rainfall) were explained to smallholder farmers using their knowledge of local weather conditions and the researchers sought their perception on changes in the climatic variables for at least for the past twenty years.

Temperature

Perception on changes in temperature is classified into three categories- "decreased", "unchanged" and "increased" (Table 2). The result indicates that most farmers (76.25%) perceived that long-term temperature is increasing.

Table 2. Farmers perception on change in temperature (n = 160)

Perception	Frequency	Percentage
Decreased	23	14.38
Unchanged	15	9.38
Increased	122	76.25
Total	160	100.0

Temperature data from the weather station showed an increasing and statistically significant trend and correlation with time (Figure 2). Time is therefore, a major determinant of temperature changes observed in Nasarawa State. This confirms that global warming is real and significant in Nasarawa State. Babatunde et al. (2011) and Anuforum (2010) reported significant and steady increase in the temperature of the savanna region of Nigeria where Nasarawa is located. Scientists in different parts of Africa and Asia have documented similar evidence. For example, Fosu-Mensah et al. (2010), Akponikpe et al. (2010), Nwajiuba and Onyeneke (2010), Acquah-de Graft and Onumah (2011), Enete and Onyekuru (2011), Acquah-de Graft (2011), Fosu-Mensah et al. (2012), Falaki et al. (2013), Umeh and Chukwu (2015), Biola et al. (2015), Olujobi (2015), Nkwusi et al. (2015), Ndamani and Watanabe (2016), and Ehiakpor et al. (2016) documented evidence of increasing temperature across different countries in West Africa. Maddison (2006), Kurukulasuriya and Mendelson (2006), Nyanga et al. (2011), Mandleni and Anim (2011), Gandure et al. (2013), Hitayezu et al. (2017) recorded steady increase in surface and atmospheric temperature across Southern Africa while in

East Africa, Gbegbelegbe et al. (2018), Mkonda and He (2017), Mutunga et al. (2017), Kebede and Gizachew (2017), Mwalusepo et al. (2015) found that most agroecological zones in East Africa are experiencing rising temperature. Shrestha (2014) recorded changing temperature in Nepal.

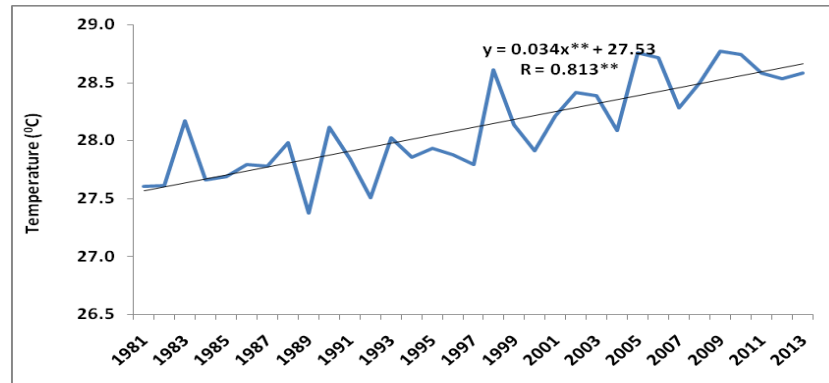


Figure 2. Trend of average temperature in Nasarawa State from 1981 to 2013. Nb: ** Significant at 1% level of probability

There is convergence in temperature data from the meteorological station and anecdotal accounts from the local crop farmers. Consequently, farmers' perception of climate change through observation of temperature increase could affect the climate change adaptation decisions they make. This corroborates the findings of Rakgase and Norris (2015), Ugwoke et al. (2012), Onumadu and Okore (2012), Nwosu et al. (2014) in Nigeria; Boansia et al. (2017) in Ghana and Burkina Faso; Ogalleh et al. (2012), Mwalusepo et al. (2015), Mutunga et al. (2017) in Kenya; and Jiri et al. (2015) in Zimbabwe. These scientists showed that farmers perceived increasing temperature in their respective study areas.

Aggregate Rainfall Volume

Most of the farmers (77.50%) averred that rainfall in the area is reducing in aggregate volume (*Table 3*).

Table 3. Farmers' perception on change in total rainfall volume (n = 160)

Perception	Frequency	Percentage
Decreased	124	77.50
Unchanged	2	1.25
Increased	34	21.25
Total	160	100.0

The result of the trend analysis on volume of rainfall in the area shows a high inter-annual variability in volume of rainfall which also resulted in a negative and very low correlation between rainfall volume and time (*Figure 3*). The result implies that aggregate rainfall volume shows a slight but insignificant reduction while surface temperature is getting hotter in Nasarawa State. If this trend continues Nasarawa and the Guinea Savanna may experience increasing challenges of climate change in the nearest future. This may aggravate the risks of floods and droughts as observed by Babatunde et

al. (2011) and Anuforom (2010). Farmers' perceptions on aggregate volume of rainfall in other savanna regions across Africa recorded declining aggregate rainfall volume and change in the pattern of rainfall (Maddison, 2006; Nhemachema and Hassan, 2007; Yesuf et al., 2008; Mandleni and Amin, 2011; Sofoluwe et al., 2011; Fosu-Mensah et al., 2012; Tessema et al., 2013; Olujobi, 2015; Mwalusepo et al., 2015; Ehiakpor et al., 2016; Ndamani and Watanabe, 2016; Hitayezu et al., 2017; Mkonda and He, 2017; Mutunga et al., 2017; Kebede and Gizachew, 2017; Boansia et al., 2017; Gbegbelegbe et al., 2018).

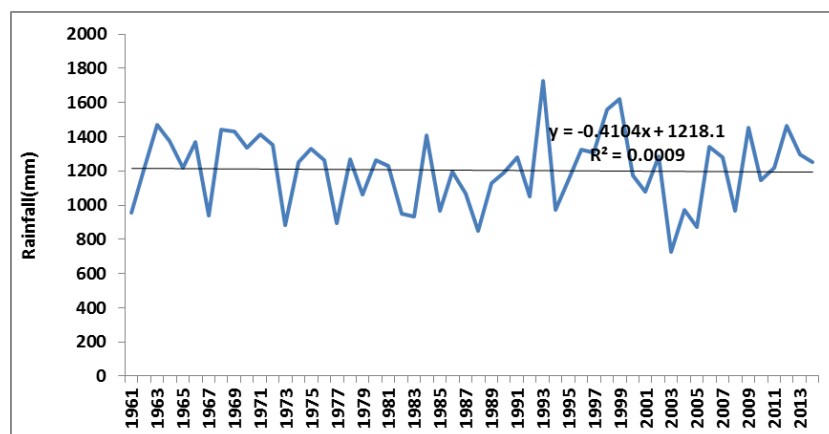


Figure 3. Trend of total annual rainfall in Nasarawa State from 1961 to 2013

Adaptation Strategies

The various climate change adaptation measures farmers adopt were classified into eight broad categories as shown in *Table 4* and they include cultivating improved crop varieties, portfolio diversification, practicing soil and water conservation, adjusting time of sowing, changing tillage operations, planting trees, irrigation, and farmland management. These are considered important climate change adaptation strategies in Nigeria (BNRCC, 2011; Okpe and Age, 2015; Onyegbula and Oladeji, 2017; Onyeneke, 2018).

Crop diversification – cultivating different crops – was adopted by majority of the farmers (95.00%). The dominant practice under crop diversification is intercropping of sorghum, maize with sweet potatoes and cowpea or melon (Agboire, 2017). This option is not expensive to practice and farmers have various crops at their disposal to plant. This may be the reason for greater adoption of this option. Furthermore, Bradshaw et al. (2004), Smit and Wandel (2006), Speranza (2006) noted that planting different crop varieties is an important farm-level climate change adaptation strategy. The increasing unpredictable nature of Africa's climate predisposes farmers to risk and shock associated with climate change, hence, makes them to grow different crop varieties. Planting short gestation crop varieties was also commonly practiced by farmers (73.75%) in the area. Farmers living in low rainfall and warm climates switch to short gestation crop varieties in managing climate risks (Wondimagegn and Lemma, 2016).

Mixed farming was the commonly used (68.75%) practice under portfolio diversification by the farmers followed by diversifying from farm to non-farm livelihood activities. Mixed farming is not new to farmers in the area. Farmers who *ab initio* combined livestock production and crop production are gradually intensifying

on crop production only because of increasing scarcity of fodder for livestock like cattle, sheep and goat. Farmers in the area whose animals are affected seriously by climate change are resorting to only crop production, especially farmers living in the low-lying plains of the area. This may be connected to the fact that, some farm household members who rear livestock in the area move around in search of pasture, and the rangelands in the State are becoming drier, thereby making fodder unavailable for the farmers and their livestock. Instead of the continuous search of pasture everywhere and the resultant conflicts that follow, the original livestock farmers are now settling near watersheds and low-lying plains where water is almost available all year round, and are cultivating crops and grasses in such areas in order to survive. Another related practice is farmland management which 78.13% of the farmers adopted. This was not far from the adoption level of farmland management reported in the study of Onyeneke et al. (2018).

Table 4. Distribution of farmers according to climate change adaptation strategies adopted (n = 160)

Adaptation Strategy	Frequency	Percentage
1. Use of improved varieties		
Use of short gestation crops	118	73.75
Use of flood tolerant crop	93	58.13
Use of drought tolerant crops	91	56.88
Use of disease/pest resistant varieties	94	58.75
Planting different varieties of crops	152	95.00
2. Portfolio diversification		
Diversifying from farm to non-farm activities	109	68.13
Changing from crop farming to livestock farming	106	66.25
Mixed farming	110	68.75
3. Soil and water conservation		
Terracing	77	48.13
Mulching	112	70.00
Planting of cover crops	112	70.00
Crop rotation	113	70.63
Water harvesting	99	61.88
4. Changing planting dates		
Adjusting planting dates	126	78.75
Shortening the length of growing period	122	76.25
5. Changing tillage operations		
Planting on mounds and planting on ridges	126	78.75
6. Planting Trees		
Planting Trees	112	70.00
7. Irrigation and drainage		
Irrigation/watering	70	43.75
Drainage	79	49.38
8. Farmland management		
Changing land area cultivated	125	78.13

The commonly practised conservation strategies were crop rotation, cover cropping and mulching. Mulching was practised due to its benefit in soil moisture conservation and soil fertility management which often increases farmers' yield. These are similar to

the reasons adduced by Agele et al. (2000) and Onyeneke (2016a) for the high adoption rates of mulching in their research works. The reasons for embarking on cover cropping lies in the fact that cover crops suppress weeds, conserve soil moisture, and add nutrient to the soil. These are in line with the explanations given by Sanginga and Woomeer (2009), Olaitan and Omomia (2006) and Egbule et al. (2012). Crop rotation is also a common adaptation strategy by farmers in the area and the probable reason for its adoption by about 70.63% of the farmers is because it enhances production, controls pest and diseases, conserves soil moisture and is less expensive. Sorghum, maize and soybean are very important crops cultivated by many farmers in the State and a very important crop rotation practice in the State observed in the course of data collection of this study was planting of *Striga* suppressive soybean varieties in rotation with sorghum and maize.

Furthermore, about 79.00% of the farming households reported that because of the erratic rainfall pattern in the area, they now change the time of planting to match the current distribution and pattern of rainfall. Also, 76.25% of the farmers reported that the growing periods have been shortened. This is now a common practice that farmers across sub-Saharan Africa use in managing vagaries of rainfall that characterise the region. Tadross and Hewitson (2005) have documented the frequency at which farmers change the time of planting in Zimbabwe.

Changing tillage operations was another common (78.75%) practice because of its characteristic benefit of controlling farm erosion and soil moisture conservation. It can also contribute to soil carbon sequestration (Niggli et al., 2009).

Also, 70.00% of the farmers opted for planting trees on farms to serve as shade and help in protecting crops from scorching and controlling farm erosion. Farmers also opted for this strategy because it contributes to mitigation of carbon and increases their income through sales of the products of the trees planted. This can also be considered as a climate-smart agricultural practice because it brings “triple wins” of increased productivity and adaptation (reducing/eliminating scorching of crops and fertilizes the soil), serving as a sink for carbon dioxide (mitigation of carbon) and increased income and ecosystem resilience (resilience) (Nwajiuba et al., 2015; Fadina and Barjolle, 2018).

Terracing (48.13%) was not common in the area and may be as a result of constraining factors such as high labour requirement, frequent inspection, large expanse of farmland needed, and the huge construction material required (Igbokwe, 1996). Also, irrigation (43.75%) and drainage (49.38%) were not commonly practiced by the farmers, perhaps because these options are capital intensive.

The researchers classified the adaptation options into eight broad categories. For categories having more than one specific adaptation option, the authors summed such adaptation options and divided by the number of specific adaptation practices identified/mentioned under such category as presented in *Table 4*. The quotient was further converted to percentage by multiplying by 100 and any farmer with a percentage score of 50 and above was considered as an adopter of such category while those with a percentage score of less than 50 were considered as non-adopters. These categories were used as the dependent variables in the multivariate probit model of this study reported in *Table 8*.

The result in *Table 5* indicates that the level of adoption of the different categories of climate change adaptation was quite high. Adjusting planting dates and changing tillage operations were the most common in the list of the categories of climate change adaptation while irrigation and drainage was the least common.

Table 5. Distribution of farmers according to adaptation categories adopted ($n = 160$)

Adaptation Category	Frequency	Percentage
Improved varieties	103	64.40
Portfolio diversification	103	64.40
Soil and water conservation	110	68.80
Changing planting dates	133	83.10
Changing tillage operations	126	78.80
Planting trees on farms	112	70.00
Irrigation and drainage	90	56.30
Farmland management	125	78.10

The number of adaptation categories adopted by the farmers was presented in *Table 6*. It could be deduced from the table that in managing climate risks farmers adopted various adaptation strategies. The average number of strategies adopted by the farmers was approximately 6 reflecting the adoption of multiple strategies by farmers in climate risk management. Therefore, farmers' decision in climate risk management in the Guinea savanna is simultaneous and the choice is not mutually exclusive. Hence, analysis of the determinants of farmers' adaptation decisions should account for the simultaneity in the choice of climate risk management strategies. This informed the choice of the multivariate probit regression which models the sequential decisions farmers make in climate change adaptation.

Table 6. Distribution of farmers according to number of adaptation categories adopted ($n = 160$)

Adaptation Category	Frequency	Percentage
One	23	14.38
Two	3	1.88
Three	4	2.50
Four	17	10.63
Five	17	10.63
Six	20	12.50
Seven	20	12.50
Eight	56	35.00
Total	160	100.00
Average	5.64	

Factors determining Choice of Adaptation Category

The multivariate probit model results on the factors determining choices of adaptation options are presented in *Tables 7 and 8*. The model is very fit considering the significance of the likelihood ratio result ($\text{Chi}^2 = 202.68$, $p < 0.01$) (*Table 8*). This led to the rejection of the hypothesis of independence of the random errors of the different adaptation models and acceptance of the alternative hypothesis of interdependence of the adaptation practices.

The test of complementarity and/or substitutability of the adaptation measures was done using the pairwise coefficients of the multivariate probit result and is presented in *Table 7*. Two adaptation measures are considered to be complementary when the pairwise coefficient is positive while they are substitutes when the resultant pairwise coefficient has a negative sign. The analysis yielded positive correlations across all the pairs of adaptation categories in this study except between adjusting planting dates and

changing tillage operations, which yielded a negative but insignificant correlation. This implies that the strategies were mainly interdependent and complementary.

The analysis indicated that there was positive and significant interdependence between household decisions to cultivate improved crop varieties and conserving the soil, cultivating improved crop varieties and portfolio diversification, adjusting planting dates and cultivation of improved crop varieties, planting improved crop varieties and trees on farms, farmland management and cultivating improved crop varieties, planting improved crop varieties and changing tillage operations and irrigation with cultivation of improved crops. The model results also suggested that there was positive and significant interdependence between household decisions to adopt use of irrigation and farmland management, irrigation and soil conservation, use of irrigation and portfolio diversification, adjusting planting dates and portfolio diversification, portfolio diversification and farmland management, portfolio diversification and planting trees on farms, portfolio diversification and changing tillage operations, soil conservation and changing tillage operations, soil conservation and adjusting planting dates, soil conservation and planting trees on farms, and portfolio diversification and soil conservation. It also suggested that there was positive and significant interdependence between household decisions to adopt use of planting trees on farm and adjusting planting date, planting trees on farms and changing tillage operations, and using improved varieties of crops and adjusting planting date.

Table 7. Correlation coefficients of the adaptation categories (from the MVP) (n=160)

Adaptation Category	Improved varieties	Portfolio diversification	Soil and water conservation	Changing planting dates	Changing tillage operations	Planting trees	Irrigation and drainage	Farmland management
Improved varieties	1.000							
Portfolio diversification	0.346**	1.000						
Soil and water conservation	0.428**	0.343**	1.000					
Changing planting dates	0.606**	0.431**	0.632**	1.000				
Changing tillage operations	0.060	0.092	0.210**	-0.071	1.000			
Planting trees	0.424**	0.310**	0.677**	0.688**	0.127	1.000		
Irrigation and drainage	0.475**	0.475**	0.465**	0.376**	0.281**	0.467**	1.000	
Farmland management	0.427**	0.522**	0.654**	0.650**	0.021	0.577**	0.356**	1.000

**p < 0.01

The result of the parameter estimates of the multivariate probit model is presented in Table 8. Education significantly increased adaptation to climate change through cultivating improved crop varieties, soil conservation, adjusting planting dates, planting of trees, irrigation and farmland management. More educated farmers understand and appreciate the benefits associated with cultivating improved crop varieties, soil conservation, adjusting planting dates, planting of trees, irrigation and farmland management and possess higher managerial ability in farm businesses than the less educated ones. This result is in consonance with the research findings of Onyeneke (2016b) and Nhemachena and Hassan (2007).

Table 8. Multivariate probit estimates of the determinants of farmers' adaptation options to climate change in Nasarawa State (n = 160)

Variable	Use of improved varieties	Portfolio Diversification	Soil Conservation	Adjusting planting dates	Change Tillage Operations	Planting Trees	Irrigation	Farmland management
Education	0.008 (2.44)**	0.0003 (0.27)	0.016 (2.29)**	0.007 (2.23)**	0.003 (0.54)	0.008 (1.80)*	0.011 (1.69)*	0.014 (1.97)***
Age	-0.008 (-2.08)**	-0.010 (-1.65)*	0.005 (2.55)**	-0.001 (-2.31)**	0.00006 (0.70)	0.006 (1.87)*	-0.015 (-2.88)***	-0.002 (-0.40)
Household size	0.008 (1.29)	-0.001 (-0.10)	0.018 (2.53)**	-0.006 (-1.94)*	0.011 (1.68)*	0.015 (2.55)**	0.019 (2.12)**	-0.007 (-3.49)***
Income	5.43e-07 (2.46)**	4.10e-07 (1.68)*	9.69e-07 (1.44)	7.05e-08 (0.34)	1.22e-06 (2.01)**	6.59e-07 (1.44)	1.06e-06 (2.50)**	1.91e-07 (0.42)
Livestock ownership	0.0018 (2.24)**	0.010 (3.11)***	0.003 (1.98)*	0.004 (2.39)**	0.001 (2.77)***	0.005 (3.25)***	0.007 (3.17)***	0.005 (2.58)**
Extension Contact	0.076 (2.92)***	0.025 (1.64)*	0.018 (2.15)**	0.017 (2.34)**	0.057 (2.07)**	0.015 (1.51)	0.013 (1.76)*	0.029 (1.85)*
Farming experience	0.005 (1.74)*	0.018 (3.33)***	0.009 (2.74)***	0.001 (3.84)***	0.004 (1.34)	0.005 (1.81)*	0.019 (4.16)***	0.004 (2.66)***
Credit	1.11e-06 (2.10)**	3.87e-07 (2.43)**	1.06e-07 (0.18)	3.99e-07 (1.25)	5.47e-08 (0.10)	1.19e-06 (1.69)*	7.32e-07 (1.71)*	5.14e-07 (0.88)
Farm size	0.019 (1.98)*	-0.003 (-0.20)	0.00001 (2.19)**	0.008 (1.89)*	0.011 (1.19)	0.005 (0.52)	0.009 (1.88)*	0.007 (1.71)*
Distance to market	-0.017 (-3.79)***	-0.002 (-2.51)**	-0.014 (-2.92)***	0.002 (0.96)	-0.002 (-1.65)*	-0.011 (-2.87)***	-0.018 (-3.42)***	0.0063 (1.52)
Distance to water source	-0.003 (-2.24)**	-0.003 (-1.41)	-0.0006 (-1.76)*	-0.0005 (-0.87)	-0.0001 (-0.11)	-0.0001 (-0.15)	-0.0008 (-0.67)	-0.004 (-2.85)***
Risk orientation	0.007 (1.83)*	0.170 (1.70)*	0.169 (2.37)**	0.182 (3.23)***	0.061 (1.73)*	0.213 (3.29)***	0.147 (1.77)*	0.295 (3.54)***
Member of farmer group	0.016 (1.68)*	-0.071 (-0.66)	0.021 (0.34)	0.005 (0.20)	-0.061 (-1.04)	-0.045 (-0.85)	0.165 (2.21)**	-0.053 (-0.80)
Likelihood Chi square	202.68***							

Note: values in parenthesis are z-values

*** Significant at 1% level, ** Significant at 5% level

Age and adoption of improved crop varieties, portfolio diversification, irrigation and adjusting planting dates yielded significant negative associations while age and soil and water conservation and planting trees yielded positive relationship. The effect of age on soil and water conservation as well as planting trees on farms were surprising in the light of the theory of adoption of technologies. One key reason for this surprising result could be that soil and water conservation practices identified in this study as well as tree planting on farms are relatively old practices in the Guinea savanna and the older farmers are better positioned to adopt such strategies than their younger counterparts because they understand and appreciate the benefits more. The effect of age and climate change adaptation is well captured by research results (Boansi et al., 2017; Gbetibouo, 2009; Deressa et al., 2008).

Farmers' household size significantly increased the likelihood of using soil conservation, changing tillage operations (digging ridges and mounds), planting trees and irrigation. These strategies require additional labour from the farmer, which the household members can provide. Teklewold et al. (2006) also found household size significant in determining the adoption of poultry technologies. However, household size diminished the probability of uptake of adjusting planting dates and farmland management. As the land area cultivated by each farmer reduces, the farm labour needed by such farmers also reduces which in turn frees some members of the family to pursue other income-generating activities (Tizale, 2007).

Income increased the probability of adoption of improved crop varieties, portfolio diversification, changing tillage operations and irrigation. Adaptation to climate change needs financial capital and information and wealthier farmers would adapt more readily than their poorer counterparts (CIMMYT, 1993; Franzel, 1999; Knowler and Bradshaw, 2007; Kassie, 2017).

Livestock ownership significantly increased uptake of all the options. Livestock is an asset to the farmer and could be sold anytime to purchase other farm inputs needed by farmers and could be responsible for the positive and significant impact recorded across all the adaptation options. Moreover, livestock dungs and dropping are used in soil fertility management. Tizale (2007) documented the benefits of livestock in storing wealth and maintaining soil fertility.

Government extension services significantly increased adoption of all the strategies. Most of the practices are an integral part of the packages disseminated to farmers across Nigeria by extension agents. This may be related to the positive and significant impact of extension services on all the climate change adaptation strategies. This confirms the increasing role of extension in climate risk management which supports better and effective agricultural management decisions (Gbetibouo, 2009; Umar et al., 2014; Duniya and Rekwot, 2015). Tripathi and Mishra (2017) and Mulwa et al. (2017) noted that extension services help farmers in adopting climate change management strategies.

Another important determinant of climate change adaptation strategies is experience (Gbetibouo, 2009) and it significantly increased the adoption of improved crop varieties, portfolio diversification, soil and water conservation practices, adjusting planting dates, planting trees, irrigation, and farmland management. Fadina and Barjolle (2018) also found that experience increased uptake of climate change adaptation strategies in Southern Benin.

Credit access enhanced adoption of improved crop varieties, portfolio diversification, irrigation and planting trees. Availability of credit reduces financial challenges of farmers and allows them to buy agrochemicals, seedlings and other inputs. Access to

credit enhances the adoption of climate change adaptation strategies (Nhemachena and Hassan, 2007). In rural El Salvador, Saín and Barreto (1996) found access to credit to have positive impact on adoption of soil conservation technology while Hansen et al. (1987) reported same result in the Dominican Republic. In Rondônia area of Brazil in South America, Caviglia-Harris (2002) noted that credit is a significant predictor of adoption of sustainable agricultural practices.

Farm size significantly increased uptake of improved crop varieties, soil conservation practices, adjusting planting dates, and irrigation and farmland management. Most of the climate change adaptation measures are optimally practised in large farms because farmers who have large farm sizes at their disposal and are more likely to adopt soil conservation techniques, irrigation, farmland management for the purpose of increasing soil fertility and efficiency of their farms (Negash, 2013; Erhabor and Ahmadu, 2013; Wondimagegn and Lemma, 2016) and improved crop varieties for incremental yield.

There was a negative and significant relationship between distance to the market and the uptake of improved crop varieties, portfolio diversification, soil conservation practices, changing tillage operations, planting trees, and irrigation. Nearness and availability of input in the market facilitate the adoption and intensive use of adaptation technologies. Also, transportation cost of agricultural inputs increases with market distance which may discourage farmers from purchasing agricultural inputs and selling their outputs too (Ulimwengu et al., 2009; Kiprono and Matsumoto, 2014).

Distance to water source also emerged as a significant predictor climate change adaptation choices of the farmers. This variable was inversely related to the likelihood of adopting improved crop varieties, soil conservation practices, and farmland management. The distance from the water source to the home and farm of the farmer negatively impacts on the quality and volume of water used for farm and domestic consumption.

Risk orientation demonstrated positive and significant association on adoption of all the climate risk management strategies - improved crop varieties, portfolio diversification, soil and water conservation, adjusting planting dates, changing tillage options, planting trees on farms, irrigation, and farmland management. Adaptation to climate change requires adoption of technology which involves risk-taking and farmers who are willing to take the risk of experimenting the technologies will adapt more readily to climate risks. Farmers who are more disposed to risk-taking were significantly more likely to increase the adoption of improved crop varieties, portfolio diversification, soil and water conservation, adjusting planting dates, changing tillage operations, planting trees, irrigation, and farmland management than their counterparts who are less risk-oriented.

Membership of farmer groups positively impacted the adoption of improved crop varieties and irrigation. Farmers get information about innovations from their associations. Membership to such groups increased the uptake of improved crop varieties and irrigation. Targeting farmers who are members of farmer groups will be important in increasing farmers' adaptive capacity. This result is in line with Mulwa et al. (2017) finding in Malawi. They found that membership of farmer groups significantly increased the adoption of disease/pest-tolerant crop varieties in Malawi.

Conclusion

The research matched perception survey with scientific data from meteorological agency. We distinguished scientific data and local peoples' accounts of climate change and matched both datasets to find convergence or divergence and see to what extent perceptions data reflects true empirical reality. Farmers' perception reflects empirical reality and they have adopted some strategies to respond to the observed vagaries in climate.

There is interrelationship in the adaptation strategies employed by the smallholder farmers. Most farming households used improved crop varieties (especially growing different varieties of crops and those with short gestation period), portfolio diversification (especially practicing mixed farming and diversifying to non-farm activities), soil and water conservation (crop rotation, mulching, cover cropping and water harvesting), adjusting planting dates, and changing tillage operations. Demographic and farm characteristics and institutions determined climate change management decisions.

Scientific data and farmers' experience point to changing patterns of temperature and rainfall in the region. Therefore, adaptation measures need to focus more on these climate elements to reduce the impact on farmers by boosting access to the livelihood assets. Support to farmers should strengthen their capacity and ability to cultivate improved crop varieties, adopt portfolio diversification, practice water and soil conservation, and use irrigation. Strengthening public extension services and credit institutions such as microfinance and commercial banks as well as cooperative societies should be the priority of government if climate risk management in agricultural production must be achieved. This will support the achievement of food security and poverty reduction objectives of the Nigerian government. Local responses and the adaptive capacity of the farmers cannot be enough but they are very important in shaping government and development partners' planned adaptation interventions. The adaptation practices identified should be integrated into governments' overall strategies and policies.

Conflict of Interests. The authors declared that they have no conflict of interests.

REFERENCES

- [1] Acquah-de Graft, H. (2011): Farmers' perception and adaptation to climate change: A willingness to pay analysis. – *Journal of Sustainable Development in Africa* 13(5): 150-161.
- [2] Acquah-de Graft, H., Onumah, E. E. (2011): Farmers' perception and adaptation to climate change: an estimation of willingness to pay. – *Agris-on-line Papers in Economics and Informatics* 3(4): 31-39.
- [3] Adejuwon, S. A. (2004): Impacts of Climate Variability and Climate Change on Crop Yield in Nigeria. – Lead Paper Presented at the Stakeholders' Workshop on Assessment of Impacts and Adaptation to Climate Change, Conference Center, Obafemi Awolowo University, Ile-Ife 20-21 September, 2004.
- [4] Agboire, S. (2017): Research and Development Activities of the National Cereals Research Institute Badeggi in Promoting a Shift to Climate Smart Agriculture in Nigeria. – A Paper presented at the National Stakeholders Workshop on Building Resilience to

- Climate Change among smallholders in Nigeria holding at Postgraduate School Auditorium, Abeokuta; October 19th -20th, 2017.
- [5] Agele, S. O., Iremiren, G. O., Ojeniye, S. O. (2000): Effects of Tillage and Mulching on the Growth, Development and Yield of Late-Season Tomato (*Lycopersicon esculentum* L.) in the Humid South of Nigeria. – *Journal of Agricultural Science* 134(1): 55-59. <https://doi.org/10.1017/S0021859699007273>.
- [6] Ajetomobi, J. O., Abiodun, A., Hassan, R. (2010): Economic Impact of Climate Change on Irrigated Rice Agriculture in Nigeria. – Contributed Paper presented at the Joint 3rd African Association of Agricultural Economists (AAAE) and 48th Agricultural Economists Association of South Africa (AEASA) Conference, Cape Town, South Africa, September 19-23, 2010. <http://ageconsearch.tind.io/bitstream/95778/1/19.%20Climate%20change%20Nigerian%20rice.pdf>. Accessed 29th April, 2017.
- [7] Akponikpe, P., Johnston, P., Agbossou, E. K. (2010): Farmers' perceptions of climate change and adaptation strategies in sub-Saharan West Africa. – 2nd International Conference on Climate, Sustainability and Development in Arid Regions, Fartaleza-Ceara, Brazil.
- [8] Anuforum, A. C. (2010): Demonstration and Assessment of Climate Change in Nigeria and Development of Adaptation Strategies in the key Socio-economic Sectors: Meteorological Approach. – Paper presented at the National Stakeholders Workshop on Developing National Adaptation Strategies and Plan of Action for Nigeria, held on 22nd, March, Abuja, Nigeria.
- [9] Asfaw, A., Admassie, A. (2004): The Role of Education on the Adoption of Chemical Fertilizer under different Socioeconomic Environments in Ethiopia. – *Agricultural Economics* 30(3): 215-228. <https://doi.org/10.1111/j.1574-0862.2004.tb00190.x>.
- [10] Babatunde, J. A., Salami, A. T., Tadross, M. (2011): Climate Change Scenarios for Nigeria: Understanding Biophysical Impacts. – Climate Systems Analysis Group, Cape Town, for Building Nigeria's Response to Climate Change Project. Ibadan, Nigeria: Nigerian Environmental Study/Action Team (NEST).
- [11] Biola, K. B., Villamor, G. B., Agodzo, S. K., Odai, S. N. (2015): Heterogeneous farm household perceptions about climate change: a case study of a semi-arid region of Ghana. – *The International Journal of Climate Change: Impacts and Responses* 7(3): 67-79.
- [12] Boansia, D., Tamboa, J. A., Müller, M. (2017): Analysis of farmers' adaptation to weather extremes in West African Sudan Savanna. – *Weather and Climate Extremes* 16: 1-13. <http://dx.doi.org/10.1016/j.wace.2017.03.001>.
- [13] Bradshaw, B., Dolan, H., Smit, B. (2004): Farm-level adaptation to climatic variability and change: Crop diversification in the Canadian prairies. – *Climatic Change* 67: 119-141. <https://doi.org/10.1007/s10584-004-0710-z>.
- [14] Building Nigeria's Response to Climate Change (BNRCC) (2007): Background to Building Nigeria's Response to Climate Change Project. – www.nestinteractive.org, www.nigeriaclimatechange.org. Accessed 20th June, 2009.
- [15] Building Nigeria's Response to Climate Change (BNRCC) (2011): National Adaptation Strategy and Plan of Action on Climate Change for Nigeria (NASPA-CCN).
- [16] Caviglia-Harris, J. (2002): Sustainable Agricultural Practices in Rondônia, Brazil: Do Local Farmer Organizations Impact Adoption Rates? – Department of Economics and Finance, Salisbury University.
- [17] CIMMYT (International Maize and Wheat Improvement Center) (1993): The Adoption of Agricultural Technology: A Guide for Survey Design. – Economics Program. Mexico City, Mexico.
- [18] Crosson, P. (1997): Impacts of Climate Change on Agriculture. – Climate Issues Brief No.4. Washington D.C., Resources for the Future.
- [19] Department of Climate Change (2013): National Policy on Climate Change, Department of Climate Change of the Federal Ministry of Environment, Abuja, Nigeria.

- [20] Department of Climate Change (2014): National Strategic Roadmap for Responding to Climate Change in Nigeria, Department of Climate Change of the Federal Ministry of Environment, Abuja, Nigeria
- [21] Deressa, T., Hassan, R., Ringler, C., Alemu, T., Yesuf, M. (2008): Analysis of the determinants of farmers' choice of adaptation methods and perceptions of climate change in the Nile basin of Ethiopia. – IFPRI Discussion Papers No. 798, International Food Policy Research Institute, Washington DC.
- [22] Duniya, K. P., Rekwot, G. Z. (2015): Determinants of Poverty among Groundnut Farming Households in Jigawa State, Nigeria. – Asian Journal of Agricultural Extension, Economics and Sociology 4(3): 224-230.
- [23] Egbule, C. L., Agwu, A. E., Nwadike, F. U. (2012): Climate change adaptive strategies used by arable crop farmers in Umuahia North Local Government Area (LGA) of Abia State, Nigeria. – Proceedings of the 17th Annual National Conference of Agricultural Extension Society of Nigeria (AESON) held at the Princess Alexandra Unity Hall, University of Nigeria, Nsukka, Enugu State, Nigeria from the 11st – 14th March, 2012.
- [24] Ehiakpor, D. S., Danso-Abbeam, G., Baah, J. E. (2016): Cocoa farmer's perception on climate variability and its effects on adaptation strategies in the Suaman district of western region, Ghana. – Cogent Food & Agriculture 2, <http://dx.doi.org/10.1080/23311932.2016.1210557>.
- [25] Enete, A., Onyekuru, A. (2011): Challenges of agricultural adaptation to climate change: empirical evidence from South-east Nigeria. – Tropicultura 29(4): 243-49.
- [26] Erhabor, P. O., Ahmadu, J. (2013): Technical Efficiency of Small-Scale Rice Farmers in Nigeria. – Research and Reviews: Journal of Agriculture and Allied Sciences 2(3): 14-22.
- [27] Ethan, S. (2015): Impact of climate change on agriculture and food security in Nigeria: challenges and adaptation. – Global Advanced Research Journal of Medicinal Plant 3(1): 001-009.
- [28] Ezeaku, I. E., Okechukwu, E. C., Aba, C. (2014): Climate Change Effects on Maize (*Zea mays*) Production in Nigeria and Strategies for Mitigation. – Asian Journal of Science and Technology 5(12): 862-871.
- [29] Fadina, A. M. R., Barjolle, D. (2018): Farmers' Adaptation Strategies to Climate Change and their Implications in the Zou Department of South Benin. – Environments 5(1): 15. doi:10.3390/environments5010015.
- [30] Falaki, A. A., Akangbe, J. A., Ayinde, O. E. (2013): Analysis of Climate Change and Rural Farmers' Perception in North Central Nigeria. – Journal of Human Ecology 43(2): 133-140. <https://doi.org/10.1080/09709274.2013.11906619>.
- [31] Federal Ministry of Environment (2014): Nigeria's Second National Communication under the United Nations Framework Convention on Climate Change, Federal Republic of Nigeria. – <http://unfccc.int/resource/docs/natc/nganc2.pdf>. Accessed 4th May, 2014.
- [32] Feleke, F. B., Berhe, M., Gebru, G., Hoag, D. (2016): Determinants of adaptation choices to climate change by sheep and goat farmers in Northern Ethiopia: the case of Southern and Central Tigray, Ethiopia. – SpringerPlus (2016) 5:1692. DOI 10.1186/s40064-016-3042-3.
- [33] Fosu-Mensah, B., Vlek, P., Manschadi, M. (2010): Farmers' perceptions and adaptations to climate change: a case study of sekyedumase district in Ghana. – A Contributed paper presented at World Food Systems Conference in Tropentag, Zurich: 14th -16th September, 2010.
- [34] Fosu-Mensah, B., Vlek, P., MacCarthy, D. (2012): Farmers' perception and adaptation to climate change: A case study of Sekyedumase district in Ghana. – Environment, Development and Sustainability 14(4): 495-505. <https://doi.org/10.1007/s10668-012-9339-7>.
- [35] Franzel, S. (1999): Socioeconomic Factors affecting the Adoption Potential of Improved Tree Fallows in Africa. – Agroforestry Systems 47(1-3): 305-321. <https://doi.org/10.1023/A:1006292119954>.

- [36] Gandure, S., Walker, S., Botha, J. J. (2013): Farmers' perceptions of adaptation to climate change and water in a South African rural community. – *Environment Development* 5: 39-53. <http://dx.doi.org/10.1016/j.endev.2012.11.004>.
- [37] Gbегbelegbe, S., Serem, J., Stirling, C., Kyazze, F., Radeny, M., Misiko, M., Tongruksawattana, S., Nafula, L., Gakii, M., Sonder, K. (2018): Smallholder farmers in eastern Africa and climate change: a review of risks and adaptation options with implications for future adaptation programmes. – *Climate and Development* 10(4): 289-306. <https://doi.org/10.1080/17565529.2017.1374236>.
- [38] Gbetibouo, G. A. (2009): Understanding Farmers' Perception and Adaptations to Climate Change and Variability: The Case of the Limpopo Basin, South Africa. – International Food Policy Research Institute (IFPRI) Discussion Paper 00849, February 2009. Environment and Production Technology Division, IFPRI.
- [39] Greene, W. H. (2003): *Econometric Analysis*, 5th edition. – Prentice Hall, Upper Saddle River, New Jersey.
- [40] Gujarati, D. N. (1995): *Basic Econometrics*, 3rd edition. – McGraw-Hill, Inc., New York.
- [41] Hansen, D., Erbaugh, J., Napier, T. (1987): Factors Related to Adoption of Soil Conservation Practices in the Dominican Republic. – *Journal of Soil and Water Conservation* 42: 367-369.
- [42] Hijioka, Y., Lin, E., Pereira, J. J., Corlett, R. T., Cui, X., Insarov, G. E., Lasco, R. D., Lindgren, E., Surjan, A. (2014): Asia. – In: Barros, V. R., Field, C. B., Dokken, D. J., Mastrandrea, M. D., Mach, K. J., Bilir, T. E., Chatterjee, M., Ebi, K. L., Estrada, Y. O., Genova, R. C., Girma, B., Kissel, E. S., Levy, A. N., MacCracken, S., Mastrandrea, P. R., White, L. L. (eds.) *Climate Change 2014: Impacts, Adaptation, and Vulnerability. Part B: Regional Aspects. Contribution of Working Group II to the Fifth Assessment Report of the Intergovernmental Panel on Climate Change*. Cambridge University Press, Cambridge, United Kingdom and New York, NY, USA, pp. 1327-1370.
- [43] Hitayezu, P., Wale, E., Ortmann, G. (2017): Assessing farmers' perceptions about climate change: A double-hurdle approach. – *Climate Risk Management* 17: 123-138. <http://dx.doi.org/10.1016/j.crm.2017.07.001>.
- [44] Ibrahim, K., Shamsudin, M. N., Yacob, R., Radam, A. (2014): Economic Impact of Climate Change on Maize Production in Northern Nigeria. – *Trends in Applied Sciences Research* 9: 522-533. <https://doi.org/10.3923/tasr.2014.522.533>.
- [45] Ifeanyi-Obi, C. C., Togun, A. O., Lamboll, R., Adesope, O. M., Arokoyu, S. B. (2017): Challenges faced by cocoyam farmers in adapting to climate change in Southeast Nigeria. – *Climate Risk Management* 17: 155-164. <https://doi.org/10.1016/j.crm.2017.04.002>.
- [46] Igbokwe, E. M. (1996): A Soil and Water Conservation System under Threat: A Visit to Maku, Nigeria. – In: Scoones, I. R., Toulmin, I. C. (eds) *Sustaining the Soil - Indigenous soil and Water Conservation in Africa*, Earthscan Publication, London.
- [47] Intergovernmental Panel on Climate Change (IPCC) (2007): *Climate Change 2007: Impacts, Adaptation and Vulnerability*. – In: Parry, M. L., Canziani, O. F., Palutikof, J. P., van der Linden, P. J., Hanson, C. E. (eds.) *Contribution of Working Group II to the Fourth Assessment Report of the Intergovernmental Panel on Climate Change*. Cambridge University Press, Cambridge, UK. <https://www.ipcc.ch/pdf/assessment-report/ar4/wg2/ar4-wg2-intro.pdf>. Accessed April 29th, 2017.
- [48] Intergovernmental Panel on Climate Change IPCC (2013): Summary for Policymakers. – In: Stocker, T. F., Qin, D., Plattner, G.-K., Tignor, M., Allen, S. K., Boschung, J., Nauels, A., Xia, Y., Bex, V., Midgley, P. M. (eds.) *Climate Change 2013: The Physical Science Basis. Contribution of Working Group I to the Fifth Assessment Report of the Intergovernmental Panel on Climate Change*. Cambridge University Press, Cambridge, United Kingdom and New York, NY, USA. http://www.ipcc.ch/pdf/assessment-report/ar5/wg1/WG1AR5_SPM_FINAL.pdf. Accessed 4th May, 2017.
- [49] Intergovernmental Panel on Climate Change IPCC (2014): *Climate Change 2014: Synthesis Report*. – In: Core Writing Team, Pachauri, R. K., Meyer, L. A. (eds.)

- Contribution of Working Groups I, II and III to the Fifth Assessment Report of the Intergovernmental Panel on Climate Change. IPCC, Geneva, Switzerland.
- [50] Intergovernmental Panel on Climate Change IPCC (2015): Meeting Report of the Intergovernmental Panel on Climate Change Expert Meeting on Climate Change, Food, and Agriculture. – In: Mastrandrea, M. D., Mach, K. J., Barros, V. R., Bilir, T. E., Dokken, D. J., Edenhofer, O., Field, C. B., Hiraishi, T., Kadner, S., Krug, T., Minx, J. C., PichsMadruga, R., Plattner, G.-K., Qin, D., Sokona, Y., Stocker, T. F., Tignor, M. (eds.) World Meteorological Organization, Geneva, Switzerland. https://www.ipcc.ch/pdf/supporting-material/Food-EM_MeetingReport_FINAL.pdf. Accessed 4th May, 2017.
- [51] Jiri, O., Mafongoya, P., Chivenge, P. (2015): Smallholder farmer perceptions on climate change and variability: a predisposition for their subsequent adaptation strategies. – *Journal of Earth Science and Climate Change* 6(5): 1-7. <https://doi.org/10.4172/2157-7617.1000277>.
- [52] Kassie, G. W. (2017): Agroforestry and farm income diversification: synergy or trade-off? The case of Ethiopia. – *Environmental Systems Research* 6:8. <https://doi.org/10.1186/s40068-017-0085-6>.
- [53] Kebede, W., Gizachew, Z. (2017): Understanding Farmers' Perception on Climate Change and Adaptation Strategies in Kareth Watershed, Omo-gibe Basin, Ethiopia. – *Asian Journal of Earth Sciences* 10: 22-32. <https://doi.org/10.3923/ajes.2017.22.32>.
- [54] Kiprono, P., Matsumoto, T. (2014): Roads and farming: The effect of infrastructure improvement on agricultural input use, farm productivity and market participation in Kenya. – Paper Presented at Center for Study of African Economies Conference, St. Catherine's College, Oxford, 23rd-25th March, 2014.
- [55] Knowler, D., Bradshaw, B. (2007): Farmers' Adoption of Conservation Agriculture: A Review and Synthesis of Recent Research. – *Food Policy* 32(1): 25-48. <https://doi.org/10.1007/s10584-004-0710-z>.
- [56] Kurukulasuriya, P., Mendelsohn, R. (2006): Crop selection: adapting to climate change in Africa. – Centre for Environmental Economics and Policy in Africa (CEEPA), University of Pretoria, Pretoria, South Africa.
- [57] Lazkano, I., Marrouch, W., Nkuiya, B. (2016): Adaptation to Climate Change: How Does Heterogeneity in Adaptation Costs affect Climate Coalitions? – *Environment and Development Economics* 21: 812-838. <https://doi.org/10.1017/S1355770X16000097>.
- [58] Lin, C-T. J., Jensen, K. L., Yen, S. T. (2005): Awareness of foodborne pathogens among US consumers. – *Food Quality and Preference* 16(5): 401-412. <https://doi.org/10.1016/j.foodqual.2004.07.001>.
- [59] Maddison, D. (2006): The Perception of and Adaptation to Climate Change in Africa. – CEEPA. Discussion Paper No.10. Centre for Environmental Economics and Policy in Africa. Pretoria, South Africa: University of Pretoria.
- [60] Magrin, G. O., Marengo, J. A., Boulanger, J.-P., Buckeridge, M. S., Castellanos, E., Poveda, G., Scarano, F. R., Vicuña, S. (2014): Central and South America. – In: Barros, V. R., Field, C. B., Dokken, D. J., Mastrandrea, M. D., Mach, K. J., Bilir, T. E., Chatterjee, M., Ebi, K. L., Estrada, Y. O., Genova, R. C., Girma, B., Kissel, E. S., Levy, A. N., MacCracken, S., Mastrandrea, P. R., White, L. L. (eds.) *Climate Change 2014: Impacts, Adaptation, and Vulnerability. Part B: Regional Aspects. Contribution of Working Group II to the Fifth Assessment Report of the Intergovernmental Panel on Climate Change*. Cambridge University Press, Cambridge, United Kingdom and New York, NY, USA, pp. 1499-1566.
- [61] Mandleni, B., Anim, F. (2011): Perceptions of Cattle and Sheep Framers on Climate Change and Adaptations in the Eastern Cape Province of South Africa. – *Journal of Human Ecology* 34(2): 107-112. <https://doi.org/10.1080/09709274.2011.11906375>.

- [62] Mkonda, M. Y., He, X. (2017): Are Rainfall and Temperature Really Changing? Farmer's Perceptions, Meteorological Data, and Policy Implications in the Tanzanian Semi-Arid Zone. – *Sustainability* 9: 1412. <https://doi.org/10.3390/su9081412>.
- [63] Mulwa, C., Marenya, P., Rahut, D. B., Kassie, M. (2017): Response to climate risks among smallholder farmers in Malawi: A multivariate probit assessment of the role of information, household demographics, and farm characteristics. – *Climate Risk Management* 16: 208-221. <https://doi.org/10.1016/j.crm.2017.01.002>.
- [64] Mutunga, E. J., Ndungu, C. K., Muendo, P. (2017): Smallholder Farmers' Perceptions and Adaptations to Climate Change and Variability in Kitui County, Kenya. – *Journal of Earth Science & Climatic Change* 8: 389. <https://doi.org/10.4172/2157-7617.1000389>.
- [65] Mwalusepo, S., Massawe, E. S., Affognon, H., Okuku, G. O., Kingori, S., Mburu, P. D. M., Ong'amo, G. O., Muchugu, E., Calatayud, P., Landmann, T., Muli, E., Raina, S. K., Johansson, T., Ru, B. P. L. (2015): Smallholder Farmers' Perspectives on Climatic Variability and Adaptation Strategies in East Africa: The Case of Mount Kilimanjaro in Tanzania, Taita and Machakos Hills in Kenya. – *Journal of Earth Science & Climatic Change* 6: 313. doi:10.4172/2157-7617.1000313.
- [66] Napier, T. (1991): Factors Affecting Acceptance and Continued Use of Soil Conservation Practices in Developing Societies: A Diffusion Perspective. – *Agriculture, Ecosystems and Environment* 36: 127-140. [https://doi.org/10.1016/0167-8809\(91\)90010-U](https://doi.org/10.1016/0167-8809(91)90010-U).
- [67] National Population Commission (NPC) (2006): Provisional of State and Local Government Totals of the 2006 Population Census of the Federal Republic of Nigeria. – <http://www.nigerianstat.gov.ng>. Accessed 23rd April 2011.
- [68] Ndamani, F., Watanabe, T. (2016): Determinants of farmers' adaptation to climate change: a micro-level analysis in Ghana. – *Scientia Agricola* 73(3): 201-208. <http://dx.doi.org/10.1590/0103-9016-2015-0163>.
- [69] Negash, M. (2013): Determinants of farmers' preference for adaptation strategies to climate change: evidence from north Shoa zone of Amhara region Ethiopia. – MPRA Paper No. 48753.
- [70] Nhemachena, C., Hassan, R. (2007): Micro-level Analysis of Farmers' Adaptation to climate change in Southern Africa. – International Food Policy Research Institute (IFPRI), Discussion Paper 714.
- [71] Nhemachena, C., Hassan, R., Chakwizira, J. (2014): Analysis of determinants of farm-level adaptation measures to climate change in Southern Africa. – *Journal of Development and Agricultural Economics* 6(5): 232-241. <http://dx.doi.org/10.5897/JDAE12.0441>.
- [72] Niang, I., Ruppel, O. C., Abdrabo, M. A., Essel, A., Lennard, C., Padgham, J., Urquhart, P. (2014): Africa. – In: Barros, V. R., Field, C. B., Dokken, D. J., Mastrandrea, M. D., Mach, K. J., Bilir, T. E., Chatterjee, M., Ebi, K. L., Estrada, Y. O., Genova, R. C., Girma, B., Kissel, E. S., Levy, A. N., MacCracken, S., Mastrandrea, P. R., White, L. L. (eds.) *Climate Change 2014: Impacts, Adaptation, and Vulnerability. Part B: Regional Aspects. Contribution of Working Group II to the Fifth Assessment Report of the Intergovernmental Panel on Climate Change* Cambridge University Press, Cambridge, United Kingdom and New York, NY, USA, pp. 1199-1265. https://www.ipcc.ch/pdf/assessment-report/ar5/wg2/WGIIAR5-Chap22_FINAL.pdf. Accessed 29th April, 2017.
- [73] Nigerian Environmental Study Action Team (NEST) (2011): Reports of Research Projects on Impacts and Adaptation. Building Nigeria's Response to Climate Change (BNRCC). – Ibadan, Nigeria: Nigerian Environmental Study/Action Team (NEST).
- [74] Nigerian Environmental Study Action Team NEST, Woodley, E. (2011): Reports of Pilot Projects in Community-based Adaptation - Climate Change in Nigeria. – Building Nigeria's Response to Climate Change (BNRCC). Ibadan, Nigeria. Nigerian Environmental Study/Action Team (NEST).

- [75] Nigerian Meteorological Agency (2017): 2017 Seasonal Rainfall Prediction. – Nigerian Meteorological Agency, Abuja.
- [76] Niggli, U., Fließbach, A., Hepperly, P., Scialabba, N. (2009): Low Greenhouse Gas Agriculture: Mitigation and Adaptation Potential of Sustainable Farming Systems. – FAO, April 2009, Revised Version 2 – 2009. <http://orprints.org/15690/1/niggli-et-al-2009-lowgreenhouse.pdf>. Accessed 29th April, 2017.
- [77] Nkwusi, G., Adeaga, S., Ayejuyo, S., Annuk, A. (2015): Climate change; farmers' awareness, perceptions and responses in Lagos State. – *Applied Ecology and Environmental Sciences* 3(4): 95-99.
- [78] Nwajiuba, C., Onyeneke, R. (2010): Economic Effects of Climate on the Agriculture of sub-Saharan Africa: Lessons from Nigeria. – Proceedings of the 10th Global Conference on Business and Economics, St. Hugh's College, Oxford University, June 28-29, 2010.
- [79] Nwajiuba, C., Tambi, E. N., Bangali, S. (2015): State of Knowledge on CSA in Africa: Case Studies from Nigeria, Cameroon and Democratic Republic of Congo. – Forum for Agricultural Research in Africa, Accra, Ghana.
- [80] Nwosu, C. S., Onyeneke, R. U., Joshua, B. N., Mmagu, C. J., Nwaodu, K. T. (2014): Perception on and Adaptation to Climate Change by Farming Households in Etim Ekpo Local Government Area of Akwa Ibom State, Nigeria. – Proceedings the 14th Annual National Conference of the Nigerian Association of Agricultural Economists, Federal University of Technology, Akure, 24th – 27th February, 2014.
- [81] Nyanga, P., Johnsen, F., Aune, J., Kahinda, T. (2011): Smallholder farmers' perceptions of climate change and conservation agriculture: evidence from Zambia. – *Journal of Sustainable Development* 4(4): 73-85. <http://dx.doi.org/10.5539/jsd.v4n4p73>.
- [82] Odiana, S., Ibrahim, A. (2015): An Assessment of the evidence of Climate change in Bauchi, Nigeria. – *Journal of Applied Sciences and Environmental Management* 19(3): 375-381. <https://doi.org/10.4314/jasem.v19i3.5>.
- [83] Ogalleh, S. A., Christian, R., Vogl, C. R., Eitzinger, J., Hauser, M. (2012): Local perceptions and responses to climate change and variability: The case of Laikipia District, Kenya. – *Sustainability* 4: 3302-3325. <https://doi.org/10.3390/su4123302>.
- [84] Okpe, B. E., Aye, G. C. (2015): Adaptation to Climate Change by Farmers in Makurdi, Nigeria. – *Journal of Agriculture and Ecology Research International* 2(1): 46-57. <http://dx.doi.org/10.9734/JAERI/2015/12169>.
- [85] Olaitan, S. O., Omomia, O. A. (2006): Round-up Agricultural Science: A Complete Guide. – Longman Nigerian PLC, Lagos.
- [86] Olsson, L., Opondo, M., Tschakert, P., Agrawal, A., Eriksen, S. H., Ma, S., Perch, L. N., Zakieldean, S. A. (2014): Livelihoods and poverty. – In: Field, C. B., Barros, V. R., Dokken, D. J., Mach, K. J., Mastrandrea, M. D., Bilir, T. E., Chatterjee, M., Ebi, K. L., Estrada, Y. O., Genova, R. C., Girma, B., Kissel, E. S., Levy, A. N., MacCracken, S., Mastrandrea, P. R., White, L. L. (eds.) *Climate Change 2014: Impacts, Adaptation, and Vulnerability. Part A: Global and Sectoral Aspects. Contribution of Working Group II to the Fifth Assessment Report of the Intergovernmental Panel on Climate Change*. Cambridge University Press, Cambridge, United Kingdom and New York, NY, USA.
- [87] Olujobi, O. J. (2015): Perception and adaptation strategies of agroforestry farmers to climate change in Ekiti State. – *American Journal of Human Ecology* 4(1): 1-8.
- [88] Onumadu, F. N., Okore, H. O. (2012): Assessment of the effects of climate change and its adaptation measures on agricultural production in Arochukwu Local Government Area, Abia State. – *International Journal of Applied Research and Technology* 1(2): 260-269.
- [89] Onyegbula, C. B., Oladeji, J. O. (2017): Utilization of climate change adaptation strategies among rice farmers in three states of Nigeria. – *Journal of Agricultural Extension and Rural Development* 9(10): 223-229. <http://dx.doi.org/10.5897/JAERD2017.0895>.
- [90] Onyeneke, R. U., Iruo, F. A., Ogoko, I. M. (2012): Micro-level Analysis of Determinants of Farmers' Adaptation Measures to Climate Change in the Niger Delta Region of

- Nigeria: Lessons from Bayelsa State. – *Nigerian Journal of Agricultural Economics* 3(1): 9-18.
- [91] Onyeneke, R. U. (2016a): Effects of Livelihood Strategies on Sustainable Land Management Practices among Arable Crop Farmers in Imo State, Nigeria. – *Nigerian Journal of Agriculture, Food and Environment* 12(3): 230-235.
- [92] Onyeneke, R. U. (2016b): Effects and Coping Measures of the 2012 Flood among Farming Households in Oguta Local Government Area of Imo State, Nigeria. – *Nigerian Journal of Agriculture, Food and Environment* 12(3): 225-229.
- [93] Onyeneke, R. U., Mmagu, C. J., Aligbe, J. O. (2017): Crop Farmers' Understanding of Climate Change and Adaptation Practices in southeast Nigeria. – *World Review of Science, Technology and Sustainable Development* 13(4): 299-318. <https://doi.org/10.1504/WRSTSD.2017.10010650>.
- [94] Onyeneke, R. U. (2018): Challenges of Adaptation to Climate Change by Farmers Anambra State, Nigeria. – *International Journal of BioSciences, Agriculture and Technology* 9(1): 1-7.
- [95] Onyeneke, R. U., Igberi, C. O., Uwadoka, C. O., Aligbe, J. O. (2018): Status of climate-smart agriculture in southeast Nigeria. – *GeoJournal* 83(2): 333-346. <https://doi.org/10.1007/s10708-017-9773-z>.
- [96] Osabo, P., Bello, D., Agwale, A. O., Zaknayiba, D. B., Sunday, D. P. (2014): Analysis of Climate Impacts on Crop Production in Savannah Region of Nigeria. – *Production Agriculture and Technology* 10(2): 91-102.
- [97] Piya, L., Maharjan, K. L., Joshi, N. P. (2012): Comparison of Adaptive Capacity and Adaptation Practices in Response to Climate Change and Extremes among the Chepang Households in Rural Mid-Hills of Nepal. – *Journal of International Development and Cooperation* 18(4): 55-75.
- [98] Raghase, M. A., Norris, D. (2015): Determinants of livestock farmers' perception of future droughts and adoption of mitigating plans. – *International Journal of Climate Change Strategies and Management* 7(2): 191-205. <https://doi.org/10.1108/IJCCSM-01-2014-0011>.
- [99] Saín, G., Barreto, H. J. (1996): The Adoption of Soil Conservation Technology in El Salvador: Linking Productivity and Conservation. – *Journal of Soil and Water Conservation* 51: 313-321.
- [100] Sanginga, N., Woomer, P. L. (2009): Integrated Soil Fertility Management Practices in Africa: Principles, Practices and Developmental Processes. – Tropical Soil Biology and Fertility Institute of the International Centre for Tropical Agriculture, Nairobi, Kenya.
- [101] Shrestha, S. L. (2014): Climate Change Resilience and Vulnerability of Farmers in Nepal. – Doctoral Dissertation, Graduate School for International Development and Cooperation, Hiroshima University.
- [102] Smit, B., Wandel, J. (2006): Adaptation, adaptive capacity and vulnerability. – *Global Environmental Change* 16(3): 282-292. <https://doi.org/10.1016/j.gloenvcha.2006.03.008>.
- [103] Sofoluwe, N. A., Tijani, A. A., Baruwa, O. I. (2011): Farmers' perception and adaptation to climate change in Osun State Nigeria. – *African Journal of Agricultural Research* 6(20): 4789-4794.
- [104] Speranza, C. I. (2006): Drought Vulnerability and Risk in Agro-Pastoral Areas – An Integrative Approach and Its Application in Kenya. – Centre for Development and Environment-CDE, Bern.
- [105] Tadross, M. A., Hewitson, B. C. (2005): The interannual variability of the onset of the maize growing season over South Africa and Zimbabwe. – *Journal of Climate* 18(16): 3356-3372. <https://doi.org/10.1175/JCLI3423.1>.
- [106] Teklewold, H., Dadi, L., Yami, A., Dana, N. (2006): Determinants of adoption of poultry technology: A double-hurdle approach. – *Livestock Research for Rural Development* 18(3). Retrieved March 26, 2018, from <http://www.lrrd.org/lrrd18/3/tek118040.htm>.

- [107] Tenge, A. J., De Graaff, J., Hella, J. P. (2004): Social and Economic Factors affecting the Adoption of Soil and Water Conservation in West Usambara Highlands, Tanzania. – *Land Degradation and Development* 15(2): 99-114. <https://doi.org/10.1002/ldr.606>.
- [108] Tessema, Y. A., Aweke, C. S., Endris, G. S. (2013): Understanding the process of adaptation to climate change by small-holder farmers: the case of east Hararghe Zone, Ethiopia. – *Agricultural and Food Economics* 1(13): 1-17. <https://doi.org/10.1186/2193-7532-1-13>.
- [109] Tihamiyu, S. A., Eze, J. N., Yusuf, T. M., Maji, A. T., Bakare, S. O. (2015): Rainfall Variability and Its Effect on Yield of Rice in Nigeria. – *International Letters of Natural Sciences* 49: 63-68. <https://doi.org/10.18052/www.scipress.com/ILNS.49.63>.
- [110] Tizale, C. Y. (2007): The dynamics of soil degradation and incentives for optimal management in the Central Highlands of Ethiopia. – PhD thesis. Faculty of Natural and Agricultural Sciences, University of Pretoria; Pretoria, South Africa.
- [111] Tripathi, A., Mishra, A. K. (2017): Knowledge and passive adaptation to climate change: An example from Indian farmers. – *Climate Risk Management* 16: 195-207.
- [112] Tsojon, J. D. (2017): Impact of Climate Change on Agricultural Production by Farmers in Taraba State, Nigeria. – *International Journal of Entrepreneurial Development, Education and Science Research* 4(1): 178-190.
- [113] Ugwoke, F. O., Nnadi, F. N., Anaeto, C. F., Aja, O. O., Nwakwasi, R. N. (2012): Crop farmers' perception of and adaptation to climate change in Orlu Agricultural Zone of Imo State, Nigeria. – *Journal of Agricultural Extension* 16(2): 212-223.
- [114] Ulimwengu, J., Funes, J., Headey, D., You, L. (2009): Paving the way for development: The impact of road infrastructure on agricultural production and household wealth in the Democratic Republic of Congo. – Paper presented at the 2009 Annual Meeting of the Agricultural and Applied Economics Association, Milwaukee, Wisconsin, July 26–28.
- [115] Umar, S., Musa, M. W., Kamsang, L. (2014): Determinants of Adoption of Improved Maize Varieties among Resource-Poor Households in Kano and Katsina States, Nigeria. – *Journal of Agricultural Extension* 18(2): 196-205. <https://doi.org/10.4314/jae.v18i2.20>.
- [116] Umeh, G. N., Chukwu, V. A. (2015): Farmers' perception and adaptive initiative to the effect of climate change on food production in Abakaliki Local Government Area of Ebonyi State, Nigeria. – *International Journal of Science and Research* 4(12): 417-422.
- [117] Vedwan, N., Rhoades, R. (2001): Climate change in the Western Himalayas of India: A study of local perception and response. – *Climate Research* 9: 109-117. <https://doi.org/10.3354/cr019109>.
- [118] Women Farmers Advancement Network (2014): Report of Focus Groups Discussions (FGD) Conducted With Farmers in Eight Villages from Four Northern States of Nigeria on Adaptation to Climate Change and Radio Listening Habits. – Report submitted to African Radio Drama Association. <http://www.ardaradio.net/wp-content/uploads/2014/03/WOFAN-FGD-report-FINAL.pdf>. Accessed 4th May, 2017.
- [119] Wondimagegn, T., Lemma, S. (2016): Climate change perception and choice of adaptation strategies: Empirical evidence from smallholder farmers in east Ethiopia. – *International Journal of Climate Change Strategies and Management* 8(2): 253-270. <https://doi.org/10.1108/IJCCSM-01-2014-0017>.
- [120] Yegbemey, R. N., Yabi, J. A., Aihounon, G. D. B., Kokoye, S. E. H. (2014): Economic valuation of maize farming profitability under climate change adaptation in Benin, West Africa. – *International Journal of Agricultural Resources Governance and Ecology* 10(3): 269-280. <https://doi.org/10.1504/IJARGE.2014.064006>.
- [121] Yesuf, M., Di Falco, S., Deressa, T., Ringler, C., Kohlin, G. (2008): The impact of climate change and adaptation on food production in low-income countries: evidence from the Nile Basin, Ethiopia. – International Food Policy Research Institute Discussion (IFPRI) Paper No. 00828. Environment and Production Technology Division, IFPRI, Washington D.C.

SALICYLIC ACID EFFECT ON CADMIUM-INDUCED ACCUMULATION OF MINERAL CONTENT IN LEAVES OF PISTACHIO SPECIES FROM TURKEY: AN ANALYSIS COUPLED WITH CHEMOMETRICS AND MULTIPLE REGRESSION ANALYSIS

CETINKAYA, H.^{1*} – KULAK, M.^{2,3}

¹*Department of Horticulture, Faculty of Agriculture, Kilis 7 Aralik University, Kilis, Turkey*

²*Department of Nursing, Yusuf Serefoglu Faculty of Health, Kilis 7 Aralik University, Kilis, Turkey*

³*Advanced Technology Application and Research Center, Kilis 7 Aralik University, Kilis, Turkey*

**Corresponding author*

e-mail: hcetinkaya67@gmail.com; phone: +90-348-814-2666/7214

(Received 24th Feb 2019; accepted 10th Apr 2019)

Abstract. Cadmium (Cd) is highly toxic and causes detrimental effects on plants but the adverse effects of Cd can be alleviated by exogenous applications. Hence, in the current study, the possible alleviative roles of salicylic acid (SA) on accumulation of Cd were investigated in leaves of pistachio species. Mineral accumulation variations in leaves were tested by analysis of variance (ANOVA) followed by multiple comparison test of Duncan using SPSS and chemometric analysis. For the present study, two-year old pistachio species (*Pistacia vera*, *Pistacia khinjuk*, *Pistacia terebinthus*) were exposed to the combination Cd (50 and 100 μ M) from root and SA (0.5 μ M) with foliar applications. Accordingly, both SA treatment and Cd had significant effects on accumulation of minerals but SA acid was found to have a little alleviative effect on accumulation Cd. Of the investigated elements, P (2.151 fold-change; $p < 0.001$) and Cu (4.702 fold-change; $p < 0.001$) were significant and highly variable over-accumulated elements. According to the principal component analysis (PCA), the multivariate data processing for elements allowing for a large group of diverse data samples was explained in 23.95% and 22.61% as the first and second principal components (PC₁ and PC₂). Two components extracted were describing approximately 46.55% of the common variance.

Keywords: *macro and micro element, cadmium stress, foliar salicylic acid application, environmental health, Pistacia vera, Pistacia khinjuk, Pistacia terebinthus*

Introduction

Expansion of agricultural areas, increment of soil pollutants, chemical fertilizers, uses of wastewater in agriculture and industrialization have led to pollution of agricultural lands. Although heavy metals are not essential elements for plants, they are transported from soil to the plant and subsequently pose a threat to the health of other livings through food chain. Of those heavy metals, Cd as a non-essential element to plants is a highly toxic and persistent environmental poison for plants and animals (di Toppi and Gabbrielli, 1999).

Cd accumulation causes structural, physiological and biochemical changes in plants (Khan et al., 2007; Feng et al., 2010). Disruption of the water balance of the plant by affecting stomatal movements, degradation of carbohydrate and interruption of photosynthesis mechanisms are of the consequences after Cd uptake. Accordingly,

decrease in yield has been deemed to be associated with Cd accumulation (Mobin et al., 2007; Hossain et al., 2010; Shie et al., 2010). Cd hinders many cellular functions and inhibits essential activities through complex formation with proteins. Albeit those cytoplasmic toxicity mechanisms are similar in all organisms, different plant species and their varieties, populations and genotypes exhibit a wide range of plasticity in response to the Cd accumulation (McGrath et al., 2001). We should note that even sensitive or tolerant species also vary considerably for their responses against Cd.

As a response to unfavorable conditions, signal molecules are synthesized and subsequently activate a range of signal transduction pathways in complex plant system. Furthermore, the plausible protective roles of some signal molecules are known in helping plant to cope with the stress (Ganesan and Thomas, 2001). Calcium, jasmonic, ethylene and ethylene and salicylic acid are of the identified signaling molecules (El Tayeb and Ahmed, 2010). Of the identified molecules, the protective roles of salicylic acid (SA) as a defense signal transducer or messenger under stress conditions has been well-reported (Raskin, 1992; Klessig and Malamy, 1994; Ganesan and Thomas, 2001). SA is a hormone-like and phenolic structured molecule modulating and regulating biochemical, physiological and molecular processes of the plants and then favors plant growth and development. It is worthy to note that SA should not be narrowly discussed as an endogenous molecule but also defined, described and discussed as a potent molecule vital to plant systems once used an exogenous regulator under optimal conditions including optimal concentration, mode of applications, appropriate application time etc. for plants (Kulak, 2018). In many studies with different agricultural crops, the role of exogenous SA application has been well-documented in regulation of physiological processes in plants, such as stomatal closure, ion uptake and transport, membrane permeability, and photosynthesis and growth under stress conditions (Shakirova and Bezrukova, 1997; Mishra and Choudhuri, 1999; Pa'l et al., 2002; Sakhabutdinova et al., 2003; Shakirova et al., 2003; Bhupinder and Usha, 2003). However, there are a few studies on the salicylic acid and cadmium interaction for fruit trees.

For the horticultural plant and crops, rootstocks are of the essential and fundamental issues. In this context, they have been screened and used for propagating temperate fruit trees more than 2000 years due to their influence on scion vigor, cropping, fruit quality, climatic adaptability, and susceptibility to pests and diseases (Webster, 1995; Acar et al., 2017a). In the studies reported by (Acar et al., 2017a, 2017b), the distribution and rootstocks of pistachio have been well-documented, informing that *Pistacia* genus (Anacardiaceae family) consists of at least eleven species. Of those species, *P. mexicana* and *P. texana* are of USA and Mexico originated. The other species are mainly distributed within the Mediterranean region, Western and Central Asia and the Middle East (Esmail-Pour, 2001). Turkey is of the important pistachio producer and suppliers in the world and possesses many wild species of pistachio nut. Of those species, *P. vera*, *P. terebinthus*, *P. khinjuk*, *P. atlantica*, *P. mutica*, *P. palaestina* and *P. lentiscus* exhibit distribution in different regions of Turkey. The main pistachio rootstock used in Turkey is *P. vera*, and followed by *P. khinjuk*, *P. terebinthus* and *P. atlantica* (Acar et al., 2017b).

Of the environmental factors, heavy metals are well-documented to possess potentially deleterious effects on fruit quality of the plants and subsequently on human health. The response of the grafted plants against stress conditions owing to the nutrient status and the presence of heavy metals in the root environment may differ than that of self-rooted plants and may be dependent on the rootstock genotype (Savvas et al., 2010, 2011). As

highlighted by Savvas et al. (2011), appropriate rootstocks selection may be significant step for restriction of heavy metal accumulation in the aerial parts of the plants.

In this context, we monitored the nutritional status of three rootstocks namely, *P. vera*, *P. terebinthus* and *P. khinjuk* in response to cadmium treatments by addition of foliar salicylic treatments. Along with the study, the results were analyzed using chemometrics and multiple regression analysis in order to discriminate and identify the differences between pistachio rootstocks.

Material and Methods

Plant material, growth conditions, salicylic acid and Cd application

In the study, 2-year old seedlings of *Pistacia vera*, *Pistacia terebinthus* and *Pistacia khinjuk* pistachio species were used. The experiment was carried out in greenhouses of Kilis 7 Aralık University Agricultural Application and Research Center (Turkey). Experiments were conducted in a greenhouse with a 14 h photoperiod. Mean temperature and relative humidity were 26-30°C during day and 16-20°C at night, 60% respectively. The experiments were performed with the replicates including ten pistachio seedlings for each replicate. The physical and chemical properties of experimental soil were as follows: pH (8.15; alkali); water saturation (clay loam); calcium carbonate (CaCO₃) content (47.49%; very calcareous); total salt (0.016%; low salt), phosphorus (P₂O₅) (4.12 kg/ha; low); organic matter (2.11%; medium). For the experimental group, pistachio seedlings were regularly root-irrigated with two different concentration of cadmium alone (Cd₁:50 µM; Cd₂:100 µM) for three weeks. Furthermore, the seedlings were foliar sprayed with addition of 0.5 µM salicylic acid once. After 3-week experimental period, leaves of seedlings were harvested and lyophilized for analysis.

Experimental design

The experimental groups with their abbreviations were represented as follows:

T-C: *Pistacia terebinthus* (T)-Control

T+SA: *Pistacia terebinthus* (T)+Salicylic acid (SA)

T+Cd₁: *Pistacia terebinthus* (T)+Cadmium:50 µM (Cd₁)

T+Cd₂: *Pistacia terebinthus* (T)+Cadmium:100 µM (Cd₂)

T+Cd₁+SA: *Pistacia terebinthus* (T)+Cadmium:50 µM (Cd₁) +Salicylic acid (SA)

T+Cd₂+SA: *Pistacia terebinthus* (T)+Cadmium:100 µM (Cd₂) +Salicylic acid (SA)

K+C: *Pistacia khinjuk* (K)-Control

K+SA: *Pistacia khinjuk* (K)+Salicylic acid (SA)

K+Cd₁: *Pistacia khinjuk* (K)+Cadmium:50 µM (Cd₁)

K+Cd₂: *Pistacia khinjuk* (K)+Cadmium:100 µM (Cd₂)

K+Cd₁+SA: *Pistacia khinjuk* (K)+Cadmium:50 µM (Cd₁)+Salicylic acid (SA)

K+Cd₂+SA: *Pistacia khinjuk* (K)+Cadmium:100 µM (Cd₂) +Salicylic acid (SA)

V+C: *Pistacia vera* (V)-Control

V+SA: *Pistacia vera* (V)+Salicylic acid (SA)

V+SA: *Pistacia vera* (V)+Salicylic acid (SA)

V+Cd₁: *Pistacia vera* (V)+Cadmium:50 µM (Cd₁)

V+Cd₂: *Pistacia vera* (V)+Cadmium:100 µM (Cd₂)

V+Cd₁+SA: *Pistacia vera* (V)+Cadmium:50 µM (Cd₁) +Salicylic acid (SA)

V+Cd₂+SA: *Pistacia vera* (V)+Cadmium:100 µM (Cd₂) +Salicylic acid (SA)

Preparation of plant samples for mineral content

First of all, the plant samples were cleaned and washed by deionized water, later air dried. Pre-dried samples were de-moisturized at 70°C for 48 h in an oven and ground for chemical analysis. 0.2 g of ground samples was placed into burning cup, 5 ml HNO₃ 65% (Merck, Darmstadt, Germany) and 2 ml H₂O₂ 30% (Merck, Darmstadt, Germany) were added immediately. After incinerating in a HP-500CEM MARS 5 microwave (crop. Mathews NC, USA) at 200°C, the solution was cooled at room temperature for 45 minutes. The extracts were passed through a filter paper and the filtrates were collected by high-deionized water in a 20 ml of polyethylene bottles and kept at 4°C in laboratory for ICP-AES analysis. Each sample was analyzed in triplicate. Phosphorus (P) and nitrogen (N) content were determined by vanadomolybdate method (Chapman and Pratt, 1961) and modified Kjeldahl method (Kacar and Inal, 2008) while K, Ca, Mg, S, P, Fe, Zn, Mo, Mn and Cu were ascertained by Inductively coupled plasma-optical emission spectrometry (ICP-OES). For all analytical works, distilled-deionized water was used. All the glassware and polyethylene bottles were attentively leached with 2-4% HCl and rinsed through deionized water for three times. Merck standards (R1 and R2 groups) were used as analytical reagent grade chemicals.

Statistical analysis

Three replications were used for each treatment. Data were expressed as mean. The means were compared using the one-way ANOVA followed by Duncan's multiple range tests. The differences between individual means were considered to be significant at $p < 0.05$. Moreover, a principal component analysis (PCA) was performed in order to discriminate between pistachio species exposed to the different treatments on the basis of the macro and micro elements identified along with the study. Also, correlation coefficients were calculated on the basis of the elements at different plant species in order to determine whether correlation coefficients among elements are the same or not. All analyses were performed using XLSTAT and SPSS.

Results

To assess the plausible roles of salicylic acid in reducing cadmium toxicity in *P. terebinthus* (T), *P. khinjuk* (K) and *P. vera* (V) plants, the macro and micro elements and protein contents were investigated in pistachio seedlings foliar treated with 0.5 μM SA under 50 (Cd₁) and 100 (Cd₂) μM conditions, respectively.

The results of the study were analyzed using one-way variance analysis (*Tables 1-2*), multiple linear regression analysis (*Tables 3-13*), correlation analysis (*Tables 14-16*) and principal component analysis (*Figs. 1-4*) in order to define, discriminate and clarify the differences between the rootstocks of pistachio.

Nitrogen (N) content

Cadmium (Cd) and salicylic acid separately caused a decrease of N in leaves of *P. terebinthus* but N content increased by the combination of cadmium concentrations with salicylic acid. However, the effects of Cd₂⁺ and Cd₂+SA were only significant ($p=0.000$ and $p=0.004$, respectively) according to the multiple linear regression analysis. As a result of multiple linear regression analysis, which is thought to have an effect on the accumulation of N, the variables including SA, Cd₁⁺, Cd₁+SA, Cd₂⁺ and

Cd₂+SA exhibited significant effects ($R^2=0.897$, $p<0.005$). Moreover, Cd₁+ ($p=0.000$), Cd₂+ ($p=0.000$) treatments, SA ($p=0.000$), Cd₁+SA ($p=0.000$) and Cd₂+SA ($p=0.000$) decreased N content in *P. khinjuk*. The significant effects of applications were also exhibited with the regression analysis ($R^2=0.955$, $p<0.005$). For *P. vera*, SA alone ($p=0.146$) and its interaction with Cd₁+ ($p=0.006$) and Cd₂+ ($p=0.315$) caused a decline in leaf N content. Regression analysis exhibited non-significant effect of applications together ($R^2=0.614$, $p<0.005$) (Table 3). Singh and Usha (2003) reported a decline in the nitrogen content in leaves of wheat seedlings treated with salicylic acid.

Phosphorus (P) content

A quantitatively increment in leaf P content of *P. terebinthus* was observed with all treatments. However, the effects of SA ($p=0.000$) and Cd₂+SA ($p=0.001$) were deemed as significant according to the multiple linear regression analysis. However, a quantitatively decline in leaf P content of *P. khinjuk* was recorded under SA+ ($p=0.146$), Cd₁+SA ($p=0.006$) Cd₂+SA ($p=0.315$), suggesting the adverse influence of SA on P content for *P. khinjuk*. The similar results regarding P content were observed for *P. vera* in response to treatments (Table 4). In the study by Wang et al. (2011), SA alone increased the P concentration whereas Pb decreased the concentration. 50 μ M Pb-induced decrease was improved by the addition of 10 μ M SA.

Potassium (K) content

Augmented and significant changes were recorded except SA alone treatment, of which effects were not significant ($p=0.421$) for K content of *P. terebinthus*. For *P. khinjuk*, all treatments adversely affected the K content in leaves. Of the treatments, SA+ ($p=0.884$) and Cd₁+ ($p=0.356$) caused decreases in K content for *P. vera* but the changes were not significant. The interaction of SA and Cd₁+ increased the content ($p=0.011$). Interestingly, whereas Cd₂+ significantly increased the content, Cd₂+ SA interaction did not cause a significant change ($p=0.259$), proposing the influence of SA on the activities of cadmium treatments (Table 5).

The treatments of excessive Mn, salicylic acid and both did not significantly affect K content in leaves (Shi and Zhu, 2008).

Calcium (Ca) content

Attenuated changes were observed with the treatments except SA+, of which effect was not significant ($p=0.136$). Interaction of Cd₁+SA decreased Ca content ($p=0.000$) whereas Cd₂+SA caused an increase in Ca content ($p=0.011$) for *P. terebinthus*. We noted the decreases in Ca content in leaves of *P. khinjuk* under all treatments except Cd₂+SA, which was not significant ($p=0.346$). The quantitatively attenuated changes were significant for other treatments, whereas SA coupled with Cd₁+ decreased the content; SA suppressed the attenuated change in Ca content by Cd₂+.

The similar responses against treatments were observed by *P. vera*. SA improved quantitatively the adverse effects of Cd₁+ and Cd₂+ treatments ($p=0.201$ and $p=0.570$, respectively) (Table 6). In the study by Shi and Zhu (2008), salicylic acid increased Ca content and excessive Mn decreased the content but the addition of SA significantly increased Ca concentration under excess Mn condition. Furthermore, Pb treatments and SA alone treatment induced an increase in Ca concentration whereas addition of SA significantly decreased under Pb condition (Wang et al., 2011).

Table 1. Macro element contents in leaves of pistachio species under different treatments

Groups	N	Change (%)	P	Change (%)	K	Change (%)	Ca	Change (%)	Mg	Change (%)	Protein	Change (%)
T-C	1.77fgh	0.00	2.07de	0.00	0.58gh	0.00	1.51a	0.00	0.22de	0.00	10.96ef	0.00
T+SA	1.74hg	-1.69	4.5a	117.39	0.52h	-10.3	1.61a	6.62	0.32abc	45.45	10.78ef	-1.64
T+Cd1	1.70ih	-3.95	2.09de	0.97	0.82be	41.38	1.06def	-29.80	0.16ef	-27.27	10.60f	-3.28
T+Cd2	1.51j	-14.69	2.24de	8.21	0.78cf	34.48	1.08cf	-28.48	0.17ef	-22.73	9.38h	-14.42
T+Cd1+SA	1.78fgh	0.56	2.23de	7.73	0.9bc	55.17	1def	-33.77	0.26bcd	18.18	11.12de	1.46
T+Cd2+SA	1.92de	8.47	3.45b	66.67	0.94b	62.07	1.3b	-13.91	0.2def	-9.09	12.00c	9.49
K+C	2.07b	0.00	2.38de	0.00	1.07a	0.00	1.16bcd	0.00	0.22de	0.00	12.84b	0.00
K+SA	1.46j	-29.47	2.03de	-14.71	0.94b	-12.1	0.92fgh	-20.69	0.17ef	-22.73	9.03h	-29.67
K+Cd1	1.62i	-21.74	3.2bc	34.45	1.17a	9.35	0.95eh	-18.10	0.13f	-40.91	10.08g	-21.50
K+Cd2	1.84def	-11.11	2.55cd	7.14	0.93b	-13.1	0.8gh	-31.03	0.18def	-18.18	11.48d	-10.59
K+Cd1+SA	1.75fgh	-15.46	1.64e	-31.09	0.66fg	-38.3	0.82gh	-29.31	0.13f	-40.91	10.95ef	-14.72
K+Cd2+SA	1.83efg	-11.59	2.14de	-10.08	0.87bcd	-18.69	1.23bc	6.03	0.23de	4.55	11.47d	-10.67
V+C	1.96c	0.00	1.82de	0.00	0.74def	0.00	1.11cde	0.00	0.25cde	0.00	12.18c	0.00
V+SA	1.63i	-16.84	2.11de	15.93	0.73ef	-1.35	1.48a	33.33	0.37a	48.00	10.08g	-17.24
V+Cd1	1.93d	-1.53	2.15de	18.13	0.69efg	-6.76	0.79h	-28.83	0.22de	-12.00	12.00c	-1.48
V+Cd2	2.82a	43.88	1.89de	3.85	0.93b	25.68	0.96efg	-13.51	0.22de	-12.00	17.60a	44.50
V+Cd1+SA	1.92de	-2.04	2.23de	22.53	0.9bc	21.62	1.0def	-9.91	0.26bcd	4.00	12.00c	-1.48
V+Cd2+SA	1.94c	-1.02	3.34b	83.52	0.81be	9.46	1.06def	-4.50	0.34ab	36.00	12.17c	-0.08

Table 2. Micro element contents in leaves of pistachio species under different treatments

Groups	Zn	Change (%)	Mn	Change (%)	Cu	Change (%)	Fe	Change (%)	Cd	Change (%)
T-C	11.66ad	0.00	1.61fg	0.00	0.21e	0.00	46.6cde	0.00	0.31d	0.00
T+SA	5.22dh	-55.23	1.47g	-8.70	1.12ae	433.33	42.2ed	-9.44	0.30d	-3.23
T+Cd1	0.67h	-94.25	4.48cde	178.26	0.91cde	333.33	55.36be	18.80	0.41ab	32.26
T+Cd2	0.61gh	-94.77	4.9cde	204.35	1.09be	419.05	59.7bcd	28.11	0.41ab	32.26
T+Cd1+SA	3.19fgh	-72.64	3.85dg	139.13	1.33ad	533.33	46.4cde	-0.43	0.46a	48.39
T+Cd2+SA	8.68bf	-25.56	2.45efg	52.17	0.35de	66.67	72.7ab	56.01	0.39bc	25.81
K+C	16.59a	0.00	4.76cde	0.00	1.12ae	0.00	66.2b	0.00	0.3d	0.00
K+SA	13.9ab	-16.21	4.1c-f	-13.87	1.37ad	22.32	69.37b	4.79	0.4ab	33.33
K+Cd1	10.82ae	-34.78	6.48bc	36.13	1.82abc	62.50	61.6bc	-6.95	0.34cd	13.33
K+Cd2	7.6bg	-54.19	2.73efg	-42.65	0.91cde	-18.75	64.27b	-2.92	0.41ab	36.67
K+Cd1+SA	11.66ad	-29.72	5.7cd	19.75	1.19ae	6.25	85.4a	29.00	0.3d	0.00
K+Cd2+SA	12.18abc	-26.58	4.17cde	-12.39	2.03ab	81.25	61.2bc	-7.55	0.40ab	33.33
V+C	4.45eh	0.00	1.47g	0.00	1.47abc	0.00	59.6bcd	0.00	0.42ab	0.00
V+SA	5.99ch	34.61	14.56a	890.48	1.89abc	28.57	45.73cde	-23.27	0.40ab	-4.76
V+Cd1	4.38eh	-1.57	3.33dg	126.53	1.82abc	23.81	39.8e	-33.22	0.41ab	-2.38
V+Cd2	9.87be	121.80	3.15efg	114.29	2.14a	45.58	43.6ed	-26.85	0.40ab	-4.76
V+Cd1+SA	3.19fgh	-28.31	3.85dg	161.90	1.33ad	-9.52	46.4cde	-22.15	0.38bc	-9.52
V+Cd2+SA	7.63bg	71.46	8.02b	445.58	0.95cde	-35.37	56.2be	-5.70	0.42ab	0.00

Table 3. N contents in leaves of pistachio species under different treatments

N	<i>P. terebinthus</i>			<i>P. khinjuk</i>			<i>P. vera</i>		
	B	Mean Dif.	Sig.	B	Mean Dif.	Sig.	B	Mean Dif.	Sig.
(Constant)	1.768		.000	2.070		.000	1.964		.000
SA+	-.028	.03000	.511	-.610	.61000	.000	-.336	.33000	.000
Cd ₁ +	-.066	.07000	.137	-.452	.45000	.000	-.038	.03000	.376
Cd ₂ +	-.262	.26000	.000	-.228	.23000	.000	.858	-.86000	.000
Cd ₁ +SA	.008	-.01000	.850	-.322	.32000	.000	-.048	.04000	.268
Cd ₂ +SA	.148	-.15000	.004	-.238	.24000	.000	-.020	.02000	.637
R ²		.897			.955			.988	

Table 4. P contents in leaves of pistachio species under different treatments

P	<i>P. terebinthus</i>			<i>P. khinjuk</i>			<i>P. vera</i>		
	B	Mean Dif.	Sig.	B	Mean Dif.	Sig.	B	Mean Dif.	Sig.
(Constant)	2.070		.000	2.380		.000	1.821		.000
SA+	2.428	-2.430	.000	-.347	.34667	.146	.289	-.2900	.482
Cd ₁ +	.018	-.0166	.956	.820	-.8200	.003	.324	-.3266	.432
Cd ₂ +	.166	-.1666	.609	.174	-.1700	.452	.074	-.0733	.856
Cd ₁ +SA	.158	-.1600	.627	-.743	.7400	.006	.407	-.4100	.328
Cd ₂ +SA	1.383	-1.380	.001	-.234	.2333	.315	1.514	-1.516	.003
R ²		.893			.825			.614	

Table 5. K contents in leaves of pistachio species under different treatments

K	<i>P. terebinthus</i>			<i>P. khinjuk</i>			<i>P. vera</i>		
	B	Mean Dif.	Sig.	B	Mean Dif.	Sig.	B	Mean Dif.	Sig.
(Constant)	.581		.000	1.070		.000	.745		.000
SA+	-.057	.05667	.421	-.133	.1333	.024	-.008	.00667	.884
Cd ₁ +	.243	-.2433	.004	.103	-.1000	.069	-.050	.05000	.356
Cd ₂ +	.196	-.2000	.015	-.145	.1400	.016	.183	-.18333	.005
Cd ₁ +SA	.322	-.3233	.001	-.407	.4100	.000	.158	-.16000	.011
Cd ₂ +SA	.357	-.3600	.000	-.200	.2000	.002	.062	-.06667	.259
R ²		.836			.906			.731	

Table 6. Ca contents in leaves of pistachio species under different treatments

Ca	<i>P. terebinthus</i>			<i>P. khinjuk</i>			<i>P. vera</i>		
	B	Mean Dif.	Sig.	B	Mean Dif.	Sig.	B	Mean Dif.	Sig.
(Constant)	1.509		.000	1.160		.000	1.110		.000
SA+	.109	-.1066	.136	-.238	.23667	.005	.370	-.36667	.001
Cd ₁ +	-.449	.45000	.137	-.211	.21000	.010	-.321	.32000	.002
Cd ₂ +	-.430	.43000	.000	-.356	.35667	.000	-.151	.15000	.085
Cd ₁ +SA	-.508	.50667	.000	-.340	.33667	.000	-.109	.10667	.201
Cd ₂ +SA	-.205	.20667	.011	.068	-.0700	.346	-.047	.04667	.570
R ²		.923			.842			.873	

Magnesium (Mg) content

Mg content decreased with Cd₁+ (p=0.101) and Cd₂+ (p=0.101) treatments but the content was quantitatively but not significantly improved with SA+ (p=0.016) alone or interaction with Cd₁+ (p=0.285) and Cd₂+ (p=0.579) in *P. terebinthus*. All treatments

except Cd₂+SA (p=0.767) caused significantly decreases in Mg content in *P. khinjuk*. Treatments including SA+ (p=0.029), Cd₁+SA (p=0.762) and Cd₂+SA (p=0.089) improved the Mg content whereas Cd₁+ (p=0.603) and Cd₂+ (p=0.582) decreased the content of Mg in *P. vera* (Table 7). For the case in cucumber (Shi and Zhu, 2008), the treatment SA did not significantly influence the Mg concentration but excess Mn significantly decreased the Mg concentration in leaf tissues. After, addition of SA significantly improved the concentration.

Table 7. Mg contents in leaves of pistachio species under different treatments

Mg	<i>P. terebinthus</i>			<i>P. khinjuk</i>			<i>P. vera</i>		
	B	Mean Dif.	Sig.	B	Mean Dif.	Sig.	B	Mean Dif.	Sig.
(Constant)	.224		.000	.224		.000	.247		.000
SA+	.096	-.09667	.016	-.054	.05333	.000	.124	-.12333	.029
Cd ₁ +	-.061	.06000	.101	-.092	.09000	.000	-.027	.02667	.603
Cd ₂ +	-.050	.05000	.168	-.044	.04333	.001	-.028	.02667	.582
Cd ₁ +SA	.038	-.04000	.285	-.094	.09333	.000	.016	-.01667	.762
Cd ₂ +SA	-.020	.02000	.579	.003	-.00333	.767	.093	-.09333	.089
R ²	.711			.938			.577		

Iron (Fe) content

SA+ alone (p=0.524) and its interaction with Cd₁ (Cd₁+SA; p=0.976) treatments decreased Fe content whereas Cd₁+ (p=0.221) and Cd₂+ (p=0.078) increased the content. The interaction of SA with higher concentration of cadmium (Cd₂+) approximately doubled the content in *P. terebinthus* (p=0.002). Interestingly, *P. khinjuk* exhibited converse responses against treatments in comparison with *P. terebinthus*. Herewith, SA+ (p=0.713) and Cd₁+SA (p=0.040) increased Fe content whereas Cd₁+ and Cd₂+ caused quantitatively but non-significant changes (p=0.590 and p=0.818, respectively). On the other hand, treatments including SA+ (p=0.072, Cd₁+ (p=0.015) and Cd₂+ (p=0.042) adversely affected Fe content but the adverse effects of Cd₁+ and Cd₂+ treatments were quantitatively but non-significant improved with SA+ (p=0.085 and p=0.636, respectively) *P. vera*. According to the multiple linear regression analysis, treatments were not significant for *P. khinjuk* and *P. vera* (R²=0.494, p>0.05; R²=0.499, p>0.05, respectively) (Table 8). Of the heavy metals, excess treatment of Mn and SA diminished Fe concentration in leaves of cucumber. However, addition of SA aggravated the decline in leaves (Shi and Zhu, 2008). Pb alone significantly increased the Fe concentration in comparison with control whereas SA caused a decline in the concentration. With the addition of SA, a statistically significant decrease was observed in the plants grown under Pb (Wang et al., 2011).

Table 8. Fe contents in leaves of pistachio species under different treatments

Fe	<i>P. terebinthus</i>			<i>P. khinjuk</i>			<i>P. vera</i>		
	B	Mean Dif.	Sig.	B	Mean Dif.	Sig.	B	Mean Dif.	Sig.
(Constant)	46.62		.000	66.22		.000	59.57		.000
SA+	-4.445	4.4000	.524	3.150	-3.1666	.713	-13.8	13.8666	.072
Cd ₁ +	8.750	-8.7666	.221	-4.62	4.6000	.590	-19.7	19.8000	.015
Cd ₂ +	13.06	-13.100	.078	-1.96	1.9333	.818	-15.9	16.0000	.042
Cd ₁ +SA	-.210	.20000	.976	19.18	-19.200	.040	-13.1	13.2000	.085
Cd ₂ +SA	26.11	-26.100	.002	-5.04	5.0000	.557	-3.39	3.40000	.636
R ²	.698			.494 (p>.05)			.499 (p>.05)		

Copper (Cu) content

A quantitatively but non-significant change was recorded for Cu content under all treatments in *P. terebinthus* ($R^2=0.488$, $p>0.05$) but we should note that Cd₁+SA increased the content once compared to SA+ and Cd₁+ whereas Cd₂+SA decreased the content in comparison with SA+ and Cd₂+. Cu contents were positively influenced with the SA+ but Cd₁+ and Cd₂+. However, the adverse effects of Cd₁+ and Cd₂+ were improved with the foliar application of SA+ for *P. khinjuk*.

Interestingly, SA+, Cd₁+ and Cd₂+ increased the content but foliar application of SA to the plants exposed to the Cd₁+ and Cd₂+ diminished the content in *P. vera* (Table 9). Shi and Zhu (2008) reported that SA treatment did not significantly change the Cu concentration and excess Mn treatment significantly decreased the concentration. However, addition of SA did not cause any changes in the concentration. The concentration of Cu decreased significantly in leaves of *Vallisneria natans* by SA treatment. Pb treatment did not cause significant changes on the concentration but addition of 100 µM SA significantly decreased the concentration (Wang et al., 2011).

Table 9. Cu contents in leaves of pistachio species under different treatments

Cu	<i>P. terebinthus</i>			<i>P. khinjuk</i>			<i>P. vera</i>		
	B	Mean Dif.	Sig.	B	Mean Dif.	Sig.	B	Mean Dif.	Sig.
(Constant)	.210		.496	1.120		.015	1.470		.000
SA+	.910	-.91000	.052	.245	-.24666	.670	.420	-.42000	.090
Cd ₁ +	.700	-.70000	.124	.700	-.70000	.235	.350	-.35000	.151
Cd ₂ +	.875	-.87666	.061	-.210	.21000	.714	.665	-.66667	.013
Cd ₁ +SA	1.120	-1.1200	.021	.070	-.07000	.903	-.140	.140000	.551
Cd ₂ +SA	.140	-.14000	.746	.910	-.91000	.130	-.525	.523333	.040
R ²	.488; $p>.05$.332 ($p>.05$)			.750		

Zinc (Zn) content

Zn content was significantly decreased with all treatments except Cd₂+SA ($p=0.147$) but the adverse effects of Cd₁+ and Cd₂+ was improved by foliar application of SA ($p=0.001$ and $p=0.147$). The most hazardous effects on Zn content was more pronounced under Cd₁+ and Cd₂+ for *P. terebinthus*. The similar responses in accumulation of Zn against treatments were also recorded for *P. khinjuk*. On the other hand, SA+ and Cd₂+ caused increases in Zn and Cd₁+ decreased the content. The contents in plants exposed to Cd₁+ and Cd₂+ were still decreased with foliar application of SA. We should state that the quantitative changes were not significant ($R^2=0.381$, $p>0.05$) for *P. vera* (Table 10). The Zn concentration leaves was significantly diminished with the excess Mn treatment but the decrease was alleviated by SA addition under excess Mn treatment in cucumber. Furthermore, SA alone treatment itself did not significantly change the Zn concentration (Shi and Zhu, 2008). Pb treatment did not significantly affect the Zn concentration. SA alone induced a decrease in the concentration (Wang et al., 2011).

Manganese (Mn) content

Mn content was adversely affected with foliar application of SA. Cadmium treatments (Cd₁+; $p=0.001$ and Cd₂+; $p=0.000$) increased Mn content but the effects of treatments were suppressed with SA (Cd₁+SA; $p=0.006$ and Cd₂+SA; $p=0.230$) for

P. terebinthus. SA+ and Cd₂ + decreased the content whereas the lower cadmium treatment (Cd₁+) increased the content. However, SA+ treatment caused a decrease in Mn content in plants exposed to Cd₁+ treatment and vice-verse for the plants under Cd₂+ treatment for *P. khinjuk*. All treatments positively influenced Mn content in *P. vera* (Table 11). Of the heavy metals, treatments with 50 µM Pb induced significant decrease of Mn and SA alone did not exhibit significant effects on Mn concentration. However, the decrease was alleviated by SA addition in *Vallisneria natans* under Pb treatment (Wang et al., 2011).

Table 10. Zn contents in leaves of pistachio species under different treatments

Zn	<i>P. terebinthus</i>			<i>P. khinjuk</i>			<i>P. vera</i>		
	B	Mean Dif.	Sig.	B	Mean Dif.	Sig.	B	Mean Dif.	Sig.
(Constant)	11.65		.000	16.59		.000	4.445		.050
SA+	-6.440	6.4400	.006	-2.69	2.6933	.463	1.540	-1.5400	.602
Cd ₁ +	-10.99	10.990	.000	-5.77	5.7733	.130	-.070	.07000	.981
Cd ₂ +	-10.04	10.046	.000	-8.99	8.9933	.026	5.425	-5.4233	.084
Cd ₁ +SA	-8.470	8.4700	.001	-4.93	4.9333	.191	-1.26	1.26000	.669
Cd ₂ +SA	-2.975	2.9766	.147	-4.41	4.4100	.239	3.185	-3.1833	.290
R ²	.805			.375 (p>.05)			.381 (p>.05)		

Table 11. Mn contents in leaves of pistachio species under different treatments

Mn	<i>P. terebinthus</i>			<i>P. khinjuk</i>			<i>P. vera</i>		
	B	Mean Dif.	Sig.	B	Mean Dif.	Sig.	B	Mean Dif.	Sig.
(Constant)	1.610		.005	4.760		.000	1.470		.223
SA+	-.140	.14000	.837	-.665	.66500	.323	13.09	-13.090	.000
Cd ₁ +	2.870	-2.8700	.001	1.715	-1.7150	.021	1.855	-1.8550	.273
Cd ₂ +	3.290	-3.2900	.000	-2.03	2.0300	.008	1.680	-1.6800	.319
Cd ₁ +SA	2.240	-2.2400	.006	.945	-.94500	.169	2.380	-2.3800	.167
Cd ₂ +SA	.840	-.8400	.230	-.595	.59500	.374	6.545	-6.5450	.002
R ²	.806			.777			.882		

Cadmium (Cd) content

Cd content in leaves significantly decreased with SA alone (p=0.001), Cd₁+ (p=0.002) whereas the content was not significantly influenced with Cd₂+ (p=1.000), Cd₁+SA (p=0.072) and Cd₂+SA (p=0.446) for *P. terebinthus*. For *P. khinjuk*, SA+ (p=0.002), Cd₁+ (p=0.141), Cd₂+ (p=0.001) and Cd₂+SA (p=0.002) induced an increase in Cd content in leaves. However, Cd₁+SA did not significantly affect the content (p=1.000). Interestingly, all treatments quantitatively but non-significantly influenced the Cd content in leaves of *P. vera* (Table 12). The root samples of maize (*Zea mays*) treated with SA contained less Cd than in the plants treated with Cd alone. However, the highest Cd content in the leaves was found in SA+Cd plants (Gondor et al., 2016) but SA+Cd₁ or SA+Cd₂ did not exhibit any significant effects regarding Cd content in leaves of three *Pistacia* species herein.

Protein content

Protein content decreased with SA+(p=0.451) Cd₁+ (p=0.140) and Cd₂+ (p=0.000) but the content in plants under Cd₁+ and Cd₂+ treatments coupled with foliar applications of SA increased for *P. terebinthus*. All treatments reduced the protein

content in *P. khinjuk*. SA+ increased content when applied with Cd₁+ in comparison to the single treatment of Cd₁+ (Cd₁+SA; p=0.000) but SA+ did not cause quantitatively changes when applied with Cd₂+ in comparison to the single treatment of Cd₂+ (Cd₂+SA; p=0.000) in *P. khinjuk*. On the other hand, all treatments except Cd₂+ decreased the protein content in *P. vera*. SA+ did not cause quantitatively changes when applied with Cd₁+ in comparison to the single treatment of Cd₁+ but brought about significant changes when applied with Cd₂+ in comparison to the single treatment of Cd₂+. Cd₂+ significantly increased the content but the interaction of Cd₂+SA decreased the content (p=0.965) (Table 13).

Salarizadeh et al. (2016) reporting that the excessive copper decreased the protein content in the pistachio plant but the adverse effects were improved with the addition of SA. The decrease in protein content has been attributed to the toxic effects of heavy metals and their reaction with the SH-groups which subsequently causes protein denaturation (Fuhrer, 1982). Furthermore, the protein content along with the decline in nitrogen content was observed in leaves of wheat seedlings treated with salicylic acid (Singh and Usha, 2003).

Table 12. Cd contents in leaves of pistachio species under different treatments

Cd	<i>P. terebinthus</i>			<i>P. khinjuk</i>			<i>P. vera</i>		
	B	Mean Dif.	Sig.	B	Mean Dif.	Sig.	B	Mean Dif.	Sig.
(Constant)	.410		.000	.300		.000	.420		.000
SA+	-.110	.1100	.001	.100	-.100	.002	-.020	.0200	.446
Cd ₁ +	-.100	.1000	.002	.040	-.040	.141	-.010	.0100	.701
Cd ₂ +	.000	.0000	1.00	.110	-.110	.001	-.020	.0200	.446
Cd ₁ +SA	.050	-.0500	.072	-1.035E-16	.000	1.00	-.040	.0400	.141
Cd ₂ +SA	-.020	.0200	.446	.100	-.100	.002	-8.614E-2	0.000	1.00
R ²	.835			.775			.229 (p>.05)		

Table 13. Protein contents in leaves of pistachio species under different treatments

Protein	<i>P. terebinthus</i>			<i>P. khinjuk</i>			<i>P. vera</i>		
	B	Mean Dif.	Sig.	B	Mean Dif.	Sig.	B	Mean Dif.	Sig.
(Constant)	10.95		.000	12.84		.000	12.18		.000
SA+	-.175	.18000	.451	-3.81	3.8100	.000	-2.10	2.1000	.000
Cd ₁ +	-.355	.35667	.140	-2.76	2.7633	.000	-.180	.17667	.438
Cd ₂ +	-1.580	1.5833	.000	-1.36	1.3633	.000	5.420	-5.4233	.000
Cd ₁ +SA	.165	-.16000	.477	-1.89	1.8900	.000	-.185	.18000	.426
Cd ₂ +SA	1.040	-1.0400	.001	-1.37	1.3700	.000	-.010	.01000	.965
R ²	.923			.966			.991		

Correlations

Herewith correlation analysis, it was aimed to determine whether the coefficient and directions of correlation vary with the pistachio species or not. Hence, correlation analyses for pistachio species were separately performed. Accordingly, correlation coefficients between elements of pistachio species leaves were given in Tables 14-16. According to the correlation matrix of the elements in leaves of *P. terebinthus*, there were negative correlations between N and Mn (r= -0.606), N and Cu (r= -0.489), N and Cd (r= -0.124), P and K (r= -0.345), P and Mn (r= -0.345), P and Fe (r= -0.042), P and Fe (r= -0.042), P and Cd (r= -0.519), K and Ca (r= -0.796), K and Mg (r= -0.517), K

and Zn ($r = -0.313$), Ca and Mn ($r = -0.931$), Ca and Cu ($r = -0.459$), Ca and Fe ($r = -0.316$), Ca and Cd ($r = -0.966$), Mg and Mn ($r = -0.657$), Mg and Fe ($r = -0.656$), Mg and Cd ($r = -0.441$), Zn and Mn ($r = -0.845$), Zn and Cu ($r = -0.816$), Zn and Fe ($r = -0.001$), Zn and Cd ($r = -0.612$), Cu and Fe ($r = -0.393$). The remained correlation coefficients were positive for *P. terebinthus* (Table 14).

Table 14. Correlation for *P. terebinthus*

Variables	N	P	K	Ca	Mg	Zn	Mn	Cu	Fe	Cd	Protein
N	1										
P	0.343	1									
K	0.224	-0.345	1								
Ca	0.314	0.650	-0.796	1							
Mg	0.297	0.684	-0.517	0.583	1						
Zn	0.663	0.201	-0.313	0.705	0.265	1					
Mn	-0.606	-0.345	0.605	-0.931	-0.657	-0.845	1				
Cu	-0.489	0.065	0.092	-0.459	0.300	-0.816	0.511	1			
Fe	0.195	-0.042	0.691	-0.316	-0.656	-0.001	0.294	-0.393	1		
Cd	-0.124	-0.519	0.883	-0.966	-0.441	-0.612	0.826	0.463	0.355	1	
Protein	0.999	0.326	0.270	0.270	0.272	0.633	-0.567	-0.471	0.223	-0.077	1

According to the correlation matrix of the elements in leaves of *P. khinjuk*, there were negative correlations between N and P ($r = -0.009$), N and Mn ($r = -0.186$), N and Cu ($r = -0.288$), N and Fe ($r = -0.108$), N and Cd ($r = -0.380$), P and Mg ($r = -0.120$), P and Zn ($r = -0.266$), P and Fe ($r = -0.733$), K and Fe ($r = -0.766$), Ca and Fe ($r = -0.502$), Ca and Cd ($r = -0.044$), Mg and Mn ($r = -0.561$), Mg and Fe ($r = -0.505$), Zn and Cd ($r = -0.472$), Mn and Cd ($r = -0.717$), Cu and Fe ($r = -0.426$), Fe and Cd ($r = -0.520$). The remained correlation coefficients were positive for *P. khinjuk* (Table 15).

Table 15. Correlations for *P. khinjuk*

Variables	N	P	K	Ca	Mg	Zn	Mn	Cu	Fe	Cd	Protein
N	1										
P	-0.009	1									
K	0.029	0.884	1								
Ca	0.447	0.051	0.294	1							
Mg	0.594	-0.120	0.112	0.786	1						
Zn	0.217	-0.266	0.171	0.613	0.391	1					
Mn	-0.186	0.202	0.168	0.047	-0.561	0.267	1				
Cu	-0.288	0.242	0.211	0.568	0.111	0.076	0.411	1			
Fe	-0.108	-0.733	-0.766	-0.502	-0.505	0.082	0.269	-0.426	1		
Cd	-0.380	0.090	0.024	-0.044	0.287	-0.472	-0.717	0.184	-0.520	1	
Protein	0.999	-0.019	0.003	0.445	0.589	0.192	-0.185	-0.272	-0.101	-0.371	1

According to the correlation matrix of the elements in leaves of *P. vera*, there were negative correlations between N and P ($r = -0.254$), N and Ca ($r = -0.466$), N and Mg ($r = -0.611$), N and Mn ($r = -0.513$), N and Fe ($r = -0.202$), N and Cd ($r = -0.068$), P and Ca ($r = -0.026$), P and Cu ($r = -0.755$), K and Ca ($r = -0.193$), K and Mg ($r = -0.229$), K and Mn ($r = -0.253$), K and Fe ($r = -0.076$), K and Cd ($r = -0.554$), Ca and Cd ($r = -0.040$), Mg and Cu ($r = -0.358$), Zn and Fe ($r = -0.038$), Mn and Fe ($r = -0.090$), Cu and Fe ($r =$

-0.677), Cu and Cd ($r = -0.244$). The remained correlation coefficients were positive for *P. vera* (Table 16).

Considering all correlation coefficients, Cd negatively correlated with N, Ca and protein content in leaves for all three-pistachio species. We should note that those correlations might differ than that of the other tissues of the plants as a consequence of allocation, transport or sequestration of the elements in order to cope with the exogenous treatments.

Table 16. Correlations for *P. vera*

Variables	N	P	K	Ca	Mg	Zn	Mn	Cu	Fe	Cd	Protein
N	1										
P	-0.254	1									
K	0.679	0.032	1								
Ca	-0.466	-0.026	-0.193	1							
Mg	-0.611	0.534	-0.229	0.819	1						
Zn	0.699	0.186	0.423	0.049	0.080	1					
Mn	-0.513	0.321	-0.253	0.809	0.909	0.158	1				
Cu	0.441	-0.755	0.000	0.036	-0.358	0.305	0.020	1			
Fe	-0.202	0.315	-0.076	0.267	0.304	-0.038	-0.090	-0.677	1		
Cd	-0.068	0.295	-0.554	-0.040	0.104	0.235	-0.070	-0.244	0.566	1	
Protein	1.000	-0.236	0.687	-0.472	-0.607	0.700	-0.515	0.424	-0.195	-0.068	1

Principal component analysis (PCA)

The discrimination can be evaluated from the principal component analysis scores plot between pistachio species using identified macro and micro elements as shown in Figs. 1-4. This pair of graphs is a biplot, i.e., macro and micro elements were more expressed in pistachio species leaf samples in the same area of the graph. The experimental groups in each group represent a similar response regarding with element contents, discriminating the experimental group behaviors in response to the treatments. Along with the present study, we discriminated the groups using the macro and micro elements measured. We herein performed four principal component analysis to visualize and discriminate each experimental group (PCA-1: *P. terebinthus*; PCA-2: *P. khinjuk*; PCA-3: *P. vera*; PCA-4: *P. terebinthus*, *P. khinjuk* and *P. vera*). In this context, it was aimed to determine whether the element changes were species or treatment dependent. For *P. terebinthus* (T-C, T+SA, T+Cd₁, T+Cd₂, T+Cd₁+SA, T+Cd₂+SA), the two principal components accounted for 76.66% of total variance, whereas the first axis and second axis explained 49.396% and 26.70% of total variance (Fig. 1). Experimental groups were well-defined and discriminated, suggesting that addition of the SA did not affect the element content of *P. terebinthus* against Cd₁ treatment but significant changes were recorded with the addition of SA to *P. terebinthus* the grown under Cd₂ conditions.

For *P. khinjuk* (K-C, K+SA, K+Cd₁, K+Cd₂, K+Cd₁+SA, K+Cd₂+SA), the two principal components accounted for 58.18% of total variance, whereas the first axis and second axis explained 31.98% and 26.19% of total variance (Fig. 2). Experimental groups were well-defined and discriminated from control group (K-C), proposing the responsive structure of *P. khinjuk* against any external stimuli. With addition of SA, the adverse effects of Cd₂ were alleviated.

species and exogenous treatments, proposing all species exhibited different mechanisms in accumulation, transport or sequestration of the elements. Along with the visualization provided by principal component analysis, K, Zn and Fe for *P. khinjuk*, Cu, Cd, N, Mn, and Mg for *P. vera*, Mn, Ca and P for *P. terebinthus* were more pronounced (Fig. 4).

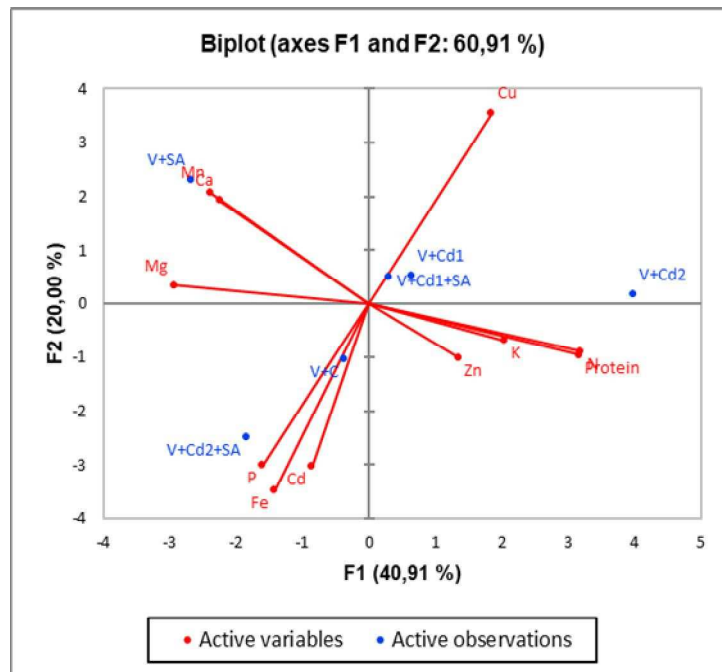


Figure 3. Principal component analysis for *P. vera*

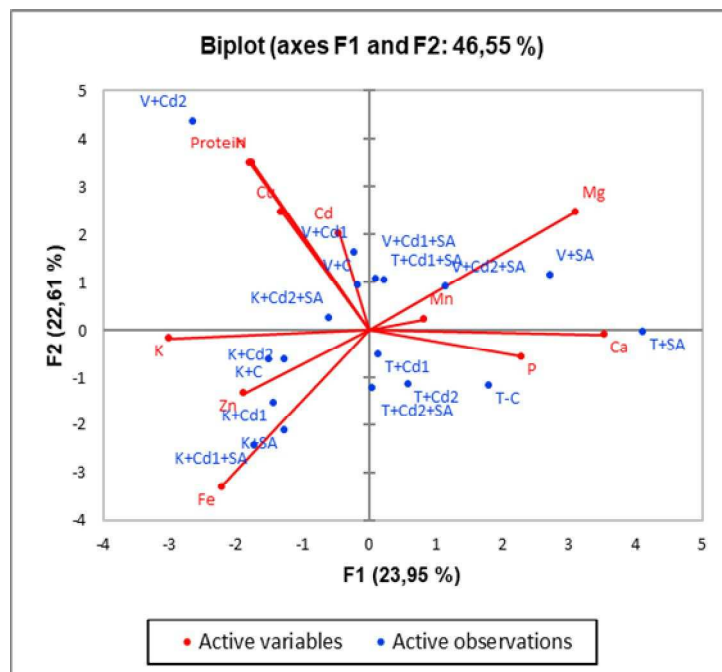


Figure 4. Principal component analysis for three pistachio species exposed to the different treatments

Prominent and over accumulated elements

Of the examined elements, P and Cu concentrations increased 2.151 and 4.702 times by applications of the cadmium and salicylic acid to pistachio species (Table 17, Figs. 5-6).

Table 17. Over-accumulation of P and Cu under various treatments in different pistachio species

Element	Mean (2)	Mean (1)	Log-ratio	Fold change	p	FDR
P	0.6478	0.315	0.3328	2.151	0.0001	0.001
Cu	-0.0225	-0.6723	0.6723	4.702	0.0003	0.0017

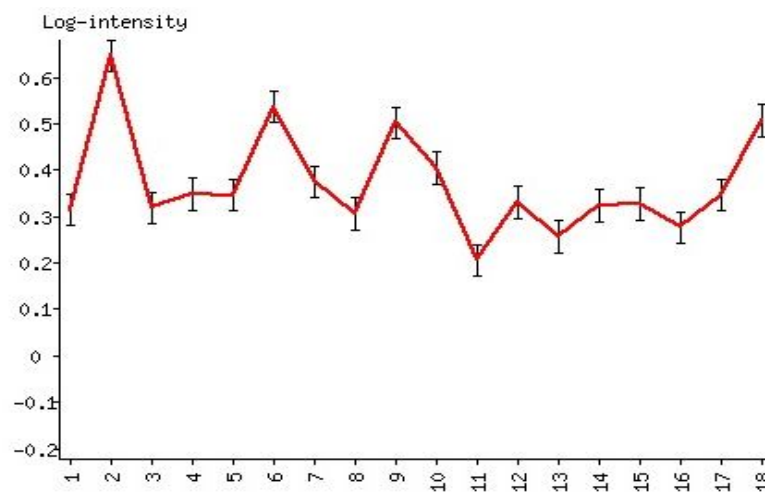


Figure 5. Mean log-intensity for P under various treatments in different pistachio species
1: T-C; 2: T+SA; 3: T+Cd₁; 4: T+Cd₂; 5: T+Cd₁+SA; 6: T+Cd₂+SA; 7: K+C; 8: K+SA; 9: K+Cd₁; 10: K+Cd₂; 11: K+Cd₁+SA; 12: K+Cd₂+SA; 13: V+C; 14: V+SA; 15: V+Cd₁; 16: V+Cd₂; 17: V+Cd₁+SA; 18: V+Cd₂+SA

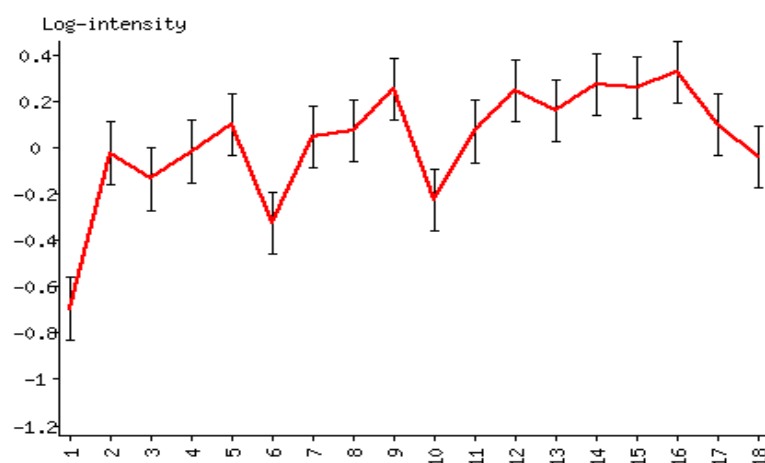


Figure 6. Mean log-intensity for Cu under various treatments in different pistachio species
1: T-C; 2: T+SA; 3: T+Cd₁; 4: T+Cd₂; 5: T+Cd₁+SA; 6: T+Cd₂+SA; 7: K+C; 8: K+SA; 9: K+Cd₁; 10: K+Cd₂; 11: K+Cd₁+SA; 12: K+Cd₂+SA; 13: V+C; 14: V+SA; 15: V+Cd₁; 16: V+Cd₂; 17: V+Cd₁+SA; 18: V+Cd₂+SA

Phosphorus (P), as phosphate (PO_4^{3-}), is a complementary component of important compounds that form plant cells, including sugar-phosphates and phospholipids that form the plant membrane as intermediates in respiration and photosynthesis. Since it is an important part of DNA and RNA molecules, it has been reported that phosphor-specific genes are necessary in the expression mechanism and may be involved in the regulation of enzyme reactions as part of proteins (Dordas, 2009). In addition, phosphorus, as an element of ATP, helps transform energy in many biochemical events (Sieprawska et al., 2014). In the case of arid regions or any disruption in the roots of the plant, the phosphate content decreases in the tissues of the plant. Due to this decrease, the rate of photosynthesis per unit in leaves is also significantly affected. It was reported that the decrease in leaf growth and photosynthetic ratio due to phosphorus may be related to permeability of stomata and ribulose 1,5 biphosphate carboxylase regeneration capacity (Brooks, 1986).

Of the microelements, copper (Cu) plays significant roles in regulation of photosynthesis, respiration, antioxidant activity, cell wall metabolism and hormone perception. Furthermore, Cu is a cofactor of various enzymes such as copper/zinc superoxide dismutase (Cu/ZnSOD), cytochrome-c oxidase (Pilon et al., 2006).

Discussion

Exogenous SA applications have been determined to increase the development and photosynthetic efficiency in plants such as *Oryza sativa* (Chen et al., 2007), *Zea mays* (Krantev et al., 2008), *Phaseolus vulgaris* (Zengin, 2014) which have been exposed to various heavy metals. It has also been shown to be effective on antioxidant mechanism by lowering membrane lipid peroxidation (Chen et al., 2007; Zengin, 2014). Moreover, SA application regulates various metabolic processes in plants, encourages the production of osmolyte and secondary metabolites, adjusts the nutrient status and protects the plant under abiotic stress conditions (Khan et al., 2015). SA triggered high production coupled with high concentration of photosynthetic pigments, photosynthetic activities and higher antioxidant enzymes in plants exposed to Cd stress (Zhang et al., 2015). As a regulatory role of SA, Studies have shown that SA applications are an important elicitor that regulates photosynthesis, photosystem II, photosynthetic pigments and enzyme activities in plants under metal stress and controls the formation of H_2O_2 and gives endurance by controlling the formation of H_2O_2 (Al-Whaibi et al., 2012; Noriega et al., 2012; Belkadhi et al., 2014; Zhang et al., 2015).

Furthermore, SA has a role in alleviating heavy metal toxicity (Shi and Zhu, 2008; Zhou et al., 2009; Wang et al., 2013). In addition, it has been determined that SA acts as a regulator in the increase of antioxidant enzymes and in the absorption and distribution of nutrients by reducing the Mn transport from the roots to the shoot (Sheng et al., 2015).

Of the studies carried out on the accumulation of nutrients, the content of elements exhibited different responses. Application of SA in salt stressed plants caused a decrease in K, Ca and P content (El-Tayeb, 2005). However, exogenous SA treatments in wheat caused increases in P, K, Ca and Mg contents (Aldesuquy et al., 2012; Hassanein et al., 2012; Loutfy et al., 2012).

Along with the current study, the effect of salicylic acid treatments on the element content of pistachio species was different. According to the results, SA application increased P, Ca, Mg and Cu content and decreased N content in *Pistacia terebinthus*.

While Fe content increased in *Pistacia khinjuk*, the other elements decreased. In *Pistacia vera*, P, Ca, Mg, Zn, Mn, Cu content increased.

50 μM cadmium (Cd_1) reduced the content of most elements. As a result of Cd_1 treatment, *Pistacia terebinthus* has increased K, Mn, Cu, Fe and Cd uptake while other elements and protein have decreased or remained at the same level. While P, Mn, Cu and Cd accumulation increased, N, Ca, Mg, Zn, Fe and protein decreased in *Pistacia khinjuk*. P, Mn, and Cu content increased while N, K, Ca, Mg and Fe content decreased in *Pistacia vera*.

Three pistachio species exhibited different responses against 100 μM cadmium (Cd_2) treatment. As a result of treatment, K, Mn, Cu, Fe and Cd content increased while N, Ca, Mg, Zn, and protein decreased in *Pistacia terebinthus*. P content exhibited an increase whereas other element and protein content decreased in *Pistacia khinjuk*. In *Pistacia vera*, N, K, Zn, Mn, Cu and protein content increased while Ca, Mg and Fe content decreased.

Pistachio species exhibited different responses concerned with the concentration of element under 50 μM with addition of SA (Cd_1+SA). As a result of the treatment, the concentration of K, Mg, Mn, Cu, protein and Cd increased in *P. terebinthus*. In *P. khinjuk*, Mn and Fe concentration increased whereas other elements concentration and protein content decreased. Furthermore, K, Mg, Mn and protein content increased while N, Ca, Zn, Cu, Fe and Cd concentration decreased in *P. vera*.

Herewith the correlation analysis, pistachio species exhibited different behaviors regarding with correlations for their element contents, which might be deemed as consequences of uptake and accumulation in response to the exogenous treatments.

Conclusion

To sum up, pistachio species exhibited different responses with respect to the content of elements and proteins in their leaf tissues under cadmium and salicylic acid treatments. Also, species responded differently against cadmium concentrations and salicylic acid. Generally, the changes in content of elements were more pronounced by 100 μM Cd treatment. Although the response of the species was different, addition of SA positively affected the element and protein content. While cadmium and salicylic acid affected the content of elements in the leaf, the effect of salicylic acid on cadmium was not significant.

Differences concerned with element content and responses against foliar SA among cultivars were revealed and discriminated via chemometric techniques. Also, possible active roles of P and Cu against Cd and SA applications were also determined for pistachio species. By applications of the cadmium and salicylic acid to pistachio species, leaves' P content 2.151 times and leaves' Cu content 4.702 times were increased, suggesting the forthcoming studies to be concentrated on the exogenous applications of P or Cu in order to improve the responses of pistachio species against Cd stress.

Furthermore, these results might be considered to be significant in terms of the selection and use of rootstocks of pistachio species by considering the different reactions regarding with the element and protein content. Subsequently, the element-mediated or induced growth parameters might also be considered under unfavorable environmental conditions.

Acknowledgements. This study was supported by Scientific Research Foundation Unit of Kilis 7 Aralik University with the code 2013/01/MAP/03.

REFERENCES

- [1] Acar, I., Kafkas, S., Kapchina-Toteva, V., Ercisli, S. (2017a): Effect of rootstock on fat content and fatty acid composition of immature pistachio kernels. – *Comptes rendus de l'Académie Bulgare des Sciences* 70(7): 1049-1056.
- [2] Acar, I., Yasar, H., Ercisli, S. (2017b): Effects of dormancy-breaking treatments on seed germination and seedling growth of *Pistacia khinjuk* Stocks using as rootstock for pistachio trees. – *Journal of Applied Botany and Food Quality* 90: 191-196.
- [3] Aldesuquy, H. S., Abbas, M. A., Abo-Hamed, S. A., Elhakem, A. H., Alsokari, S. S. (2012): Glycine betaine and salicylic acid induced modification in productivity of two different cultivars of wheat grown under water stress. – *Journal of Stress Physiology and Biochemistry* 8(2): 72-89.
- [4] Al-Whaibi, M. H., Siddiqui, M. H., Basalah, M. O. (2012): Salicylic acid and calcium-induced protection of wheat against salinity. – *Protoplasma* 249: 769-778.
- [5] Belkadhi, A., DeHaro, A., Obregon, S., Chaïbi, W., Djebali, W. (2014): Positive effects of salicylic acid pretreatment on the composition of flaxplastidial membrane lipids under cadmium stress. – *Environmental Science and Pollution Research* 22: 1457-1467.
- [6] Bhupinder, S., Usha, K. (2003): Salicylic acid induced physiological and biochemical changes in wheat seedlings under water stress. – *Plant Growth Regulation* 39: 137-41.
- [7] Brooks, A. (1986): Effects of phosphorus nutrition on ribulose-1, 5-bisphosphate carboxylase activation, photosynthetic quantum yield and amounts of some Calvin-cycle metabolites in spinach leaves. – *Functional Plant Biology* 13(2): 221-237.
- [8] Chapman, H. D., Pratt, P. F. (1961): *Methods of Analysis for Soils, Plants and Waters*. – University of California, Division of Agricultural Sciences, USA.
- [9] Chen, J., Zhu, C., Li, L., Sun, Z., Pan, X. (2007): Effects of exogenous salicylic acid on growth and H₂O₂-metabolizing enzymes in rice seedlings under lead stress. – *Journal of Environmental Science* 19: 44-49.
- [10] di Toppi, L. S., Gabbrielli, R. (1999): Response to Cadmium in Higher Plants. – *Environmental and Experimental Botany* 41(2): 105-130.
- [11] Dordas, C. (2009): Dry matter, nitrogen and phosphorus accumulation, partitioning and remobilization as affected by N and P fertilization and source-sink relations. – *European Journal of Agronomy* 30(2): 129-139.
- [12] El-Tayeb, M. A. (2005): Response of barley grains to the interactive effect of salinity and salicylic acid. – *Plant Growth Regulation* 45(3): 215-224.
- [13] El-Tayeb, M. A., Ahmed, N. L. (2010): Response of wheat cultivars to drought and salicylic acid. – *American-Eurasian Journal of Agronomy* 3(1): 1-7.
- [14] Esmail-Pour, A. (2001): Distribution, use and conservation of pistachio in Iran. In *Toward a Comprehensive Documentation and Use of Pistacia Genetic Diversity in Central and West Asia, North Africa and Europe*. – Report of the IPGRI Workshop: 16-26.
- [15] Feng, J., Shi, Q., Wang, X., Wei, M., Yang, F., Xu, H. (2010): Silicon Supplementation Ameliorated the Inhibition of Photosynthesis and Nitrate Metabolism by Cadmium (Cd) Toxicity in *Cucumis sativus* L. – *Scientia Horticulturae* 123(4): 521-530.
- [16] Fuhrer, J. (1982): Early effects of excess cadmium uptake in *Phaseolus vulgaris*. – *Plant Cell and Environment* 5: 263-270.
- [17] Ganesan, V., Thomas, G. (2001): Salicylic acid response in rice: influence of salicylic acid on H₂O₂ accumulation and oxidative stress. – *Plant Science* 160(6): 1095-1106.

- [18] Gondor, O. K., Pál, M., Darkó, É., Janda, T., Szalai, G. (2016): Salicylic acid and sodium salicylate alleviate cadmium toxicity to different extents in maize (*Zea mays* L.). – PloS ONE 11(8): 1-18.
- [19] Hassanein, R. A., Abdelkader, A. F., Ali, H., Amin, A. A. E. S., Mohammed Rashad, E. S. (2012): Grain-priming and foliar pretreatment enhanced stress defense in wheat (*Triticum aestivum* var. Gimaza 9) plants cultivated in drought land. – Australian Journal of Crop Science 6(1): 121-129.
- [20] Hossain, M. A., Hasanuzzaman, M., Fujita, M. (2010): Up Regulation of Antioxidant and Glyoxalase Systems by Exogenous Glycinebetaine and Proline in Mung Bean Confer Tolerance to Cadmium Stress. – Physiology and Molecular Biology of Plants 16(3): 259-272.
- [21] Kacar, B., Inal, A. (2008): Plant Analysis. – Nobel Press, (Bitki Analizleri. Nobel Yayınları) Ankara.
- [22] Khan, N. A., Singh, S., Nazar, R. (2007): Activities of Antioxidative Enzymes, Sulphur Assimilation, Photosynthetic Activity and Growth of Wheat (*Triticum aestivum*) Cultivars Differing in Yield Potential under Cadmium Stress. – Journal of Agronomy and Crop Science 193(6): 435-444.
- [23] Khan, M. I. R., Fatma, M., Per, T. S., Anjum, N. A., Khan, N. A. (2015): Salicylic acid-induced abiotic stress tolerance and underlying mechanisms in plants. – Frontiers in Plant Science 6: 1-17.
- [24] Klessig, D. F., Malamy, J. (1994): The salicylic acid signal in plants. – Plant Molecular Biology 26(5): 1439-1458.
- [25] Krantev, A., Yordanova, R., Janda, T., Szalai, G., Popova, L. (2008): Treatment with salicylic acid decreases the effect of cadmium on photosynthesis in maize plants. – Journal of Plant Physiology 165: 920-931.
- [26] Kulak, M. (2018): A bibliometric review of research trends in salicylic acid uses in agricultural and biological sciences: where have been studies directed? – Scientific Papers. Series A. Agronomy LXI(1): 296-303.
- [27] Loutfy, N., El-Tayeb, M. A., Hassanen, A. M., Moustafa, M. F., Sakuma, Y., Inouhe, M. (2012): Changes in the water status and osmotic solute contents in response to drought and salicylic acid treatments in four different cultivars of wheat (*Triticum aestivum*). – Journal of Plant Research 125(1): 173-184.
- [28] McGrath, S. P., Zhao, F. J., Lombi, E. (2001): Plant and rhizosphere processes involved in phytoremediation of metal-contaminated soils. – Plant and Soil 232(1-2): 207-214.
- [29] Mishra, A., Choudhuri, M. A. (1999): Effects of salicylic acid on heavy metal-induced membrane deterioration mediated by lipoxygenase in rice. – Biologia Plantarum 42(3): 409-415.
- [30] Mobin, M., Khan, N. A. (2007): Photosynthetic Activity, Pigment Composition and Antioxidative Response of Two Mustard (*Brassica juncea*) Cultivars Differing in Photosynthetic Capacity Subjected to Cadmium Stress. – Journal of Plant Physiology 164(5): 601-610.
- [31] Noriega, G., Caggiano, E., Lecube, M. L., Santa Cruz, D., Batlle, A., Tomaro, M., Balestrasse, K. B. (2012): The role of salicylic acid in the prevention of oxidative stress elicited by cadmium in soybean plants. – Biometals 25(6): 1155-1165.
- [32] Pál, M. (2002): Effect of salicylic acid during heavy metal stress. – Acta Biologica Szegediensis 46(3-4): 119-120.
- [33] Pilon, M., Abdel-Ghany, S. E., Cohu, C. M., Gogolin, K. A., Ye, H. (2006): Copper cofactor delivery in plant cells. – Current Opinion in Plant Biology 9(3): 256-263.
- [34] Raskin, I. (1992): Role of salicylic acid in plants. – Annual Review of Plant Biology 43(1): 439-463.
- [35] Sakhabutdinova, A. R., Fatkhutdinova, D. R., Bezrukova, M. V., Shakirova, F. M. (2003): Salicylic acid prevents the damaging action of stress factors on wheat plants. – Bulgarian Journal of Plant Physiology 21: 314-319.

- [36] Salarizadeh, M. R., Saeidisar, S., Abbaspour, H., Hokmabadi, H. (2016): The Effects of Spermine and Salicylic Acid on Pistachio (*Pistacia vera* L.) Cultivars (Badami and Qazvini) under Copper Stress. – Journal of Nuts 7(2): 89-99.
- [37] Savvas, D., Colla, G., Roupshael, Y., Schwarz, D. (2010): Amelioration of heavy metal and nutrient stress in fruit vegetables by grafting. – Scientia Horticulturae 127: 156-161.
- [38] Savvas, D., Ntatsi, G., Moiras, N., Tsakalidis, A., Ropokis, A., Liopa-Tsakalidi, A. (2011): Impact of grafting and rootstock on the responses of cucumber to heavy metal stress. – In V Balkan Symposium on Vegetables and Potatoes 960: 49-56.
- [39] Shakirova, F. M., Bezrukova, M. V. (1997): Induction of wheat resistance against environmental salinization by indolylacetic acid. – Izvestiya Akademii Nauk Seriya Biologicheskaya 2: 149-153.
- [40] Shakirova, F. M., Sakhabutdinova, A. R., Bezrukova, M. V., Fatkhutdinova, R. A., Fatkhutdinova, D. R. (2003): Changes in the hormonal status of wheat seedlings induced by salicylic acid and salinity. – Plant Science 164(3): 317-322.
- [41] Sheng, H., Zeng, J., Yan, F., Wang, X., Wang, Y., Kang, H., Fan, X., Sha, L., Zhang, H., Zhou, Y. (2015): Effect of exogenous salicylic acid on manganese toxicity, mineral nutrients translocation and antioxidative system in polish wheat (*Triticum polonicum* L.). – Acta Physiologiae Plantarum 37(2): 1-11.
- [42] Shi, Q., Zhu, Z. (2008): Effects of exogenous salicylic acid on manganese toxicity, element contents and antioxidative system in cucumber. – Environmental and Experimental Botany 63: 317-326.
- [43] Shi, G., Liu, C., Cai, Q., Liu, Q., Hou, C. (2010): Cadmium accumulation and tolerance of two safflower cultivars in relation to photosynthesis and antioxidative enzymes. – Bulletin of Environmental Contamination and Toxicology 85(3): 256-263.
- [44] Sieprawska, A., Filek, M., Walas, S., Tobiasz, A., Mrowiec, H., Miszalski, Z. (2014): Does micro-and macroelement content differentiate grains of sensitive and tolerant wheat varieties? – Acta Physiologiae Plantarum 36(11): 3095-3100.
- [45] Singh, B., Usha, K. (2003): Salicylic acid induced physiological and biochemical changes in wheat seedlings under water stress. – Plant Growth Regulation 39(2): 137-141.
- [46] Wang, C., Zhang, S., Wang, P., Hou, J., Qian, J., Ao, Y., Li, L. (2011): Salicylic acid involved in the regulation of nutrient elements uptake and oxidative stress in *Vallisneria natans* (Lour.) Hara under Pb stress. – Chemosphere 84(1): 136-142.
- [47] Wang, Q., Liang, X., Dong, Y., Xu, L., Zhang, X., Kong, J., Liu, S. (2013): Effects of exogenous salicylic acid and nitric oxide on physiological characteristics of perennial ryegrass under cadmium stress. – Journal of Plant Growth Regulators 32: 721-731.
- [48] Webster, A. D. (1995): Rootstock and interstock effects on deciduous fruit tree vigour, precocity, and yield productivity. – New Zealand Journal of Crop and Horticultural Science 23: 373-382.
- [49] Zengin, F. (2014): Exogenous treatment with salicylic acid alleviating copper toxicity in bean seedlings. – Proceedings of the National Academy of Sciences, India Section B: Biological Sciences 84(3): 749-755.
- [50] Zhang, Y., Xu, S., Yang, S., Chen, Y. (2015): Salicylic acid alleviates cadmium-induced inhibition of growth and photosynthesis through up regulating antioxidant defense system in two melon cultivars (*Cucumis melo* L.). – Protoplasma 252(3): 911-924.
- [51] Zhou, Z. S., Guo, K., Elbaz, A. A., Yang, Z. M. (2009): Salicylic acid alleviates mercury toxicity by preventing oxidative stress in roots of *Medicago sativa*. – Environmental and Experimental Botany 65: 27-34.

THE PRESENCE OF PATHOGENIC BACTERIA IN TRADITIONAL CHEESE SOLD IN LOCAL MARKET IN HATAY PROVINCE, TURKEY

UNAL TURHAN, E.

*Osmaniye Korkut Ata University, Kadirli Applied Sciences School, Food Technology
Department*

TR-80760 Osmaniye, Turkey

(e-mail: emelunalturhan@gmail.com; phone: +90-0-328-888-0090; fax: +90-0-328-0091)

(Received 24th Feb 2019; accepted 11th Apr 2019)

Abstract. Contamination of cheese by foodborne pathogens may pose a risk for human health. Especially, microbiological quality of cheese sold in local market and produced on a small scale is generally lower than industrial production. The aim of the present research was to investigate the presence of pathogenic bacteria such as coagulase positive staphylococci, *Escherichia coli*, *Listeria monocytogenes* and *Salmonella* spp. in twenty white cheese samples from local market on a small scale in the province of Hatay, Turkey. In this study, none of cheese samples contained *L. monocytogenes* and *Salmonella* spp. while *E. coli* and coagulase positive staphylococci were detected in cheese samples. The higher prevalence of coagulase positive staphylococci (100%) than *E. coli* (65%) were detected in cheese samples, but contamination levels of *E. coli* (mean 4.05 log cfu/g) were found higher than coagulase positive staphylococci (mean 2.47 log cfu/g) in terms of viable cell counts of pathogenic bacteria in cheese samples. The present results indicated that traditional cheeses manufactured in Hatay province were generally satisfactory microbiological safety according to Turkish Food Safety Criteria. As a result, the presence of pathogenic bacteria in traditional cheese from Hatay region could cause outbreaks affecting public health and reduce positive impression on traditional cheeses which have potential for geographical indication.

Keywords: *small scale food producers, Turkish food codex, microbiological criteria, dairy products, contamination*

Introduction

Cheese is fermented dairy product known as a safe and nutritious food with high protein and dietary calcium contents. Cheese is often consumed due to these beneficial impacts on human health, favorable sensorial and nutritional properties (Mikulec and Jovanovic, 2005; Kurşun et al., 2008; Choi et al., 2016). In Turkey, cheese is produced by both traditional methods (manual handling and unmechanized) and industrial methods (production based on mechanization). The production and consumption of domestic natural or traditional cheese in the world is rising year by year. Traditional cheeses which have distinctive taste and odor are produced on a small scale by using raw milk in mostly east, southeast region of Turkey (Hayaloğlu et al., 2002; Ozer et al., 2004; Jorgensen et al., 2005). East, south east and south of Turkey are famous for quite high summer temperatures, for example Hatay. Hatay is one of the cities where food products are frequently sold in open market places or local market on a small scale due to traditional habits (Cokal et al., 2012).

Turkish traditional white cheese is usually produced under unmechanized or artisanal conditions and is handled at various stages of manufacture. Thus, various types of microorganisms may enter the cheese during manufacture and subsequent handling (Hayaloglu et al., 2002). As a result of climate and improper hygiene conditions, white cheese producer on a small scale of Turkey often encounter with contamination risk of pathogens. In particular traditional cheese sold local market have low hygienic quality

(Ozer et al., 2004; Başkaya et al., 2006; Uraz et al., 2008). Four bacterial pathogens including *Listeria monocytogenes*, *Salmonella* spp., *Staphylococcus aureus* and pathogenic *Escherichia coli* are the predominant microorganisms that caused outbreaks as result of contaminated traditional cheese (Motarjemi et al., 2002; Hudson et al., 2003). *Salmonella* spp. is gram negative gastroenteritis-inducing pathogens and the majority of *Salmonella* cases are foodborne (Donnelly et al., 2018). The primary source of *Salmonella* spp. is humans and animals as carrier (mostly their feces). Animal products are among the most common foodstuffs of *Salmonella*. The main foods as source of *Salmonella* are meat, milk and eggs and their products and also inadequately heat treated food products (Akkaya and Alişarlı, 2006). In many reports, the outbreaks of *Salmonella* were associated with raw milk cheese (Donnelly, 2018). *Staphylococcus aureus* as coagulase positive staphylococci plays an important role on human health due to the production of thermo-stable enterotoxins that causes foodborne illness. Particularly, in the dairy industry *S. aureus* is mostly pathogen as it can induce foodborne intoxications through dairy products including cheeses (Donnelly, 2018). *S. aureus* is usually transmitted to food by personnel (hands, coughing, sneezing, etc.). Milk and milk products are the main foods that cause poisoning from *S. aureus* (Pacheco and Galindo, 2010). *L. monocytogenes* is gram positive facultative anaerobic foodborne pathogen and one of the most dangerous pathogens in food industry. It is usually found in soil, surface waters, sewage, plants, faeces and animal feed. Diseases from *L. monocytogenes* are more rare than others, but their effect is more severe and even fatal (Chavant et al., 2002; Pacheco and Galindo, 2010). Human listeriosis outbreaks are often associated with ready-to-eat food products including cheese. Several outbreaks and sporadic cases of disease associated with the consumption of pasteurized milk, cheeses made from unpasteurized milk, and other dairy products in USA and Europe in the past decade (Esho et al., 2013). *L. monocytogenes* contamination was mostly found in raw milk (Esho et al., 2013). *Escherichia coli* is gram negative, *Enterobacteriaceae* family of *Escherichia* genus dependent, facultative anaerob, mostly moving, non-spore, rod-shaped bacteria. *E. coli* infection may cause foodborne diseases such as diarrhea, hemorrhagic colitis, and hemolytic uremic syndrome. According to epidemiological findings, *E. coli* epidemic is generally seen as a result of cucumber, carrot and lettuce consumption (Almosoud et al., 2015). *E. coli* are known as indicator organisms of fecal contamination during cheese processing (IDF, 2016).

Today, foodborne diseases related to cheese consumption are common problems in many countries. Microbial contamination in traditional cheese as the main potential risk factor is increasingly growing and has detrimental effects on public health (Belli et al., 2013). High pathogen risk in milk and dairy products originates from cow itself, inefficient animal health control, insufficient training of farmers, dairy raw milk used unpasteurized for the production, processing environment and employees about milk hygiene, utensils, post processing, retail process collection, transport and weakness in the cold chain during production processes and storage (Telli et al., 2012; Cokal et al., 2012; Belli et al., 2013). Especially traditional cheeses produced from raw milk (unpasteurized) pose a risk due to its pathogenic contents (Atasoy et al., 2003). Microbial safety of cheese is dependent on good manufacturing practices. Cheese producers have to comply with hygienic practices to ensure safety (Donnelly, 2018). Considering that traditional cheese is mostly made from raw milk, the application of food safety policy are essential in order to avoid microbial spoilage of milk, especially in local small scale dairy processing plants (Belli et al., 2013). The World Health Organization requires that small scale dairy

processing plants in the developing countries urgently comply with the Codex Alimentarius principles (WHO, 2007). Hazard Analysis of Critical Control Points (HACCP) and Good Manufacturing Practices (GMP) are also recommended for the small production units (Belli et al., 2013).

There are limited studies based on microbial safety of traditional cheese in the province of Hatay. The present study was aimed to evaluate hygienic quality and safety of traditional cheese from local market on a small scale in Hatay province, Turkey.

Material and Methods

Samples and indicator microorganisms

In this study, totally 20 cheese samples were collected from small scaled local market in Hatay province, Turkey (*Figure 1 and Figure 2*). For all identification tests, pathogenic bacteria including *Escherichia coli* ATCC-35150, *Salmonella* spp., *Listeria monocytogenes* ATCC7644 (Remel-USA) and *Staphylococcus aureus* ATCC-25923 was used as indicator organisms for the aim of positive control. Pathogen bacteria were grown in BHI (Merck, Germany) and stocked at -20°C in BHI supplemented with 20% (v/v) glycerol.



Figure 1. Traditional cheese collected from local market on a small scale in Hatay province

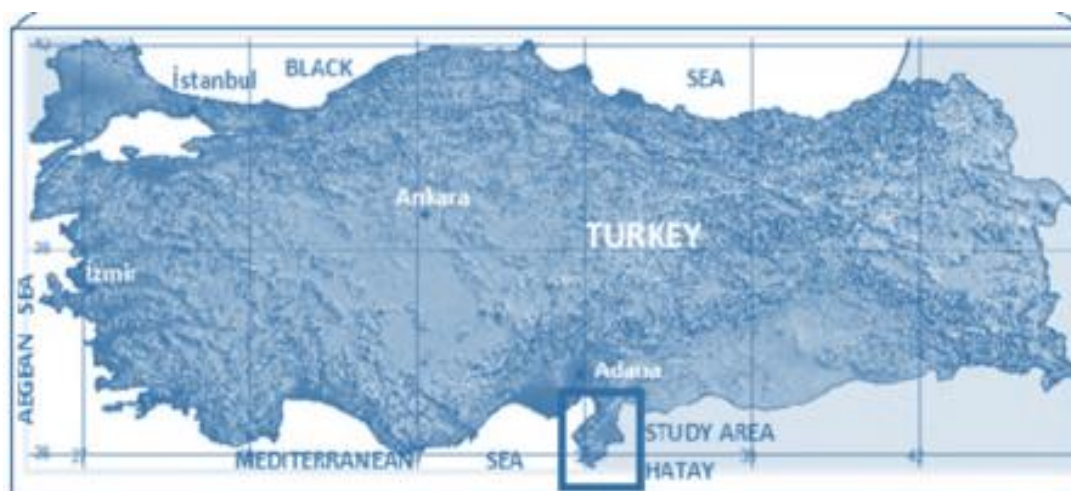


Figure 2. Hatay province of Turkey (Demirkesen, 2012)

The preparation of samples for microbiological analysis

The homogenates of cheese samples were prepared by aseptically removing 25 g of cheese into sterile filter-stomaching bags (Isolab). A 225 mL of buffered peptone water was also added into the stomaching bags containing the samples and homogeneously mixed in stomacher (Bagmixer-interscience, France) twice for 1 min. The sample homogenates were serially diluted with buffered peptone water.

Isolation and enumeration of microorganisms

The isolation of pathogenic bacteria in cheese samples was performed according to the reference methods of EN/ISO 6888 for coagulase positive staphylococci, EN/ISO 11290-1 for *L. monocytogenes* and EN/ISO 6579 for *Salmonella* spp. and EN/ISO 16649 for *E. coli* (Halkman, 2005; Turkish Food Codex, 2011).

For *E. coli* enumeration, decimal serial dilutions of the homogenate were plated in duplicate on TBX agar (Merck) plates. After incubation of plates at 44°C for 18-24 hours, the blue green colonies were counted as *E. coli*.

For coagulase positive staphylococci (*S. aureus* and other species) enumeration, decimal serial dilutions of the homogenate were plated in duplicate on Baird parker-RPF agar (Oxoid) plates. After at 37°C, for 24 hours, typical black and bright colonies were counted as coagulase positive staphylococci.

For the isolation of *Salmonella* spp., homogenate of cheese samples in erlenmeyer flask were incubated at 35-37°C for 16-20 hours. Then, 10 mL homogenate were added to RVS broth (Oxoid) as selective pre-enrichment medium and incubated at 42-43°C for 24 hours. Afterthat, inocula from the pre-enrichment medium were streaked in duplicate onto Brilliant Green agar plates (Oxoid). After incubation of plates at 37°C for 24 hours, typical *Salmonella* colonies reproduced or not on the selective agar plates.

For the isolation of *L. monocytogenes*, 25 g of each sample was taken aseptically and homogenized in 225 mL Fraser broth (Oxoid) using a stomacher (Bagmixer-interscience, France) for 1 min and incubated at 30°C for 48 hours. Then, inocula from the enrichment culture were streaked in duplicate onto each of two selective agars, Oxford agar (Oxoid) and PALCAM agar (Oxoid). After incubation of both selective plates at 35-37°C for 48 h, typical *Listeria* colonies reproduced or not on the selective agar plates.

Results

To assess microbiological safety of traditional cheese in Hatay province, a total of 20 cheese samples were collected from local market on a small scale in Hatay. *Table 1* represented the presence of pathogenic bacteria in traditional cheese samples from local markets on a small scale in Hatay. Additionally, viable cell counts of these pathogens which are present in these cheese were given in *Figure 3*. In this study, while *E. coli* (n=13) and coagulase positive staphylococci (n=20) were isolated in cheese samples, *Salmonella* spp. and *L. monocytogenes* were not isolated from any cheese samples. 45% of coagulase positive staphylococci exceeded the acceptable levels in Turkish Food Safety Criteria. However, since the Turkish Food Safety Criteria does not include any limitation on the number of *E. coli* that is allowed to be present in the white cheese, no comment could be made for *E. coli* levels in the present study.

Table 1. The presence of pathogenic bacteria in cheese from milk

Microorganism	n	m	Mean (log cfu/g)	Std. Dev	Max (log cfu/g)	Min (log cfu/g)
<i>E. coli</i>	13	UD	4.05	1.03	5.67	1.91
Coagulase positive staphylococci	20	9	2.47	1.32	4.69	1
<i>L. monocytogenes</i>	NF	NF	NF	NF	NF	NF
<i>Salmonella</i> spp.	NF	NF	NF	NF	NF	NF

n: The number of samples containing pathogens, m: The number of samples containing pathogens at unacceptable level according to Turkish Food Safety criteria, NF: not found, UD: undefined in Turkish Food Safety criteria for white cheese samples

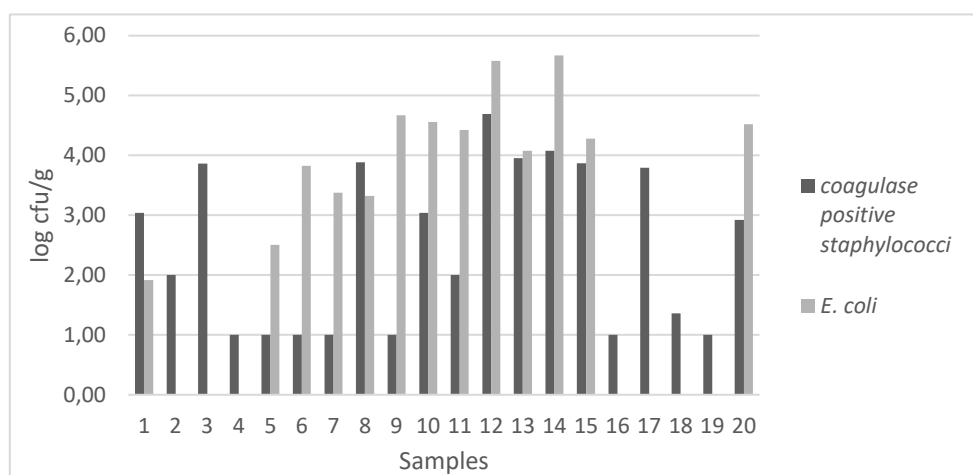


Figure 3. Viable cell counts of pathogens which are present in traditional cheese

Discussion

Farmhouse or small scale production of traditional cheeses was associated with higher microbiological risk. Food safety was seen as a critical factor in the production of such cheese types. Various small-scale production of raw milk products has performed in the world (Obrien et al., 2009). However, there is some concern that such foods may pose a risk of pathogenic bacterial food poisoning to consumers (Jorgensen et al., 2005). Similarly, in Turkey traditional cheeses were obtained with small scale production and sold in local markets. Traditional handmade cheese in Hatay, mostly reach to local market without retaining ripening duration or without providing cold chain. Thus, these cheeses are susceptible to the development of pathogenic bacteria.

In brief, as known, cheese produced with unpasteurized milk may result in foodborne outbreaks. On this sense, food industry which purposes microbiological safety prefers the use of pasteurized milk for the production of cheese. However, sensorial properties of cheeses from unpasteurized milk and pasteurized milk are different from each other and according to consumer demands both type cheese were also sold on the market. Therefore the achievement of microbiological safety in traditional cheese is essential during processing including manual handling, molding and ripening. Additionally, concentration of brine solution, storage conditions, ingredients, cheese composition and packaging etc. play an important role on microbial charge of cheese. The safety of traditional cheese

could particularly ensure with microbial risk assessments based on ripening duration, water activity and storage conditions (Choi et al., 2016).

L. monocytogenes, *S. aureus*, *E. coli* and *Salmonella* spp. are well-recognized foodborne bacterial pathogens. Traditional cheese from raw milk could support the growth of such foodborne pathogens. Therefore, there is concern for microbiological safety of domestically produced traditional cheeses (Esho et al., 2013). If pathogens are present in raw milk, they can be present throughout a cheese. Raw milk or contaminated milk was seen as the source of *L. monocytogenes*, however the primary route of *Listeria* contamination of dairy products results from environmental contamination during processing (Donnelly, 2018). Various reports detected its presence in milk and cheese (Akkaya and Alişarlı, 2006). In addition to this, traditional cheeses are at risk of containing pathogenic bacteria due to post-processing contamination that can occur during manufacture, as well as during ripening and washing, or at retail (Donnelly, 2018). The incidence of high *E. coli* and *S. aureus* count in food is considered as indicator for poor hygienic condition in production process (Obrien et al., 2009; Samouris et al., 2011; Esho et al., 2013).

The result of this study showed that 65% and 100% of cheese samples contains *E. coli* and coagulase positive staphylococci, respectively. The presence of *E. coli* and coagulase positive staphylococci showed that microbiological quality of traditional white cheese samples was generally poor because of inadequate hygienic conditions during production (Hayaloğlu et al., 2002; Ozer et al., 2004; Telli et al., 2012; Belli et al., 2013). In general while the presence of *S. aureus*, *L. monocytogenes* and *Salmonella* spp. in cheese stemmed from raw milk, the presence of *E. coli* associated with inappropriate or hygienic conditions (Torkar et al., 2006; Obrien et al., 2009; Pacheco and Galindo, 2010; Yücel and Anıl, 2011). According to microbiological criteria linked to food safety policy in Turkey, while the presence of *L. monocytogenes* and *Salmonella* spp. are not allowed in cheese, the presence of coagulase positive staphylococci are limited between 2 and 3 log cfu/g (Turkish Food Codex, 2011). Similarly, microbiological criteria prepared by European commission associated with food safety and hygiene referred the same limits with regard to *L. monocytogenes*, *Salmonella* spp. and coagulase positive staphylococci in cheese. Our results about the presence of *L. monocytogenes* and *Salmonella* spp. in cheese samples comply with microbiological criteria. However, the amount of coagulase positive staphylococci isolated from some cheese samples used in this study has exceed the limit values. As seen in *Figure 3*, higher amounts of coagulase positive staphylococci than microbiological criteria were found as 4.69 and 4.68 log cfu/g in samples 12 and 14. Although microbiological criteria for *L. monocytogenes*, *Salmonella* spp. and coagulase positive staphylococci in cheese are described by Turkish Food Safety criteria and European Commission microbiological criteria, *E. coli* are not specified. In case of using unpasteurized raw milk, producers must process products under equivalent temperature condition (63°C for 30 min) to eliminate the risk of pathogenic bacteria. Thus, *E. coli* are not expected to exist due to the heating process in the production of traditional cheese. Additionally, postproduction contamination, poor hygienic practices and equipment are the challenging factors in cheese-related foodborne illness (Esho et al., 2013). As shown in *Table 1*, traditional white cheese in Hatay province contained detectable numbers of coagulase positive staphylococci between 1 and 4.69 log cfu/g and *E. coli* between 1.91 and 5.67 log cfu/g. Similar to our results, according to the previous reports based on Turkish traditional white cheese, *E. coli* and *S. aureus* amounts in white cheese were between 0.60-5.15 log cfu/g and 1.30-1.70 log cfu/g, respectively, whereas *Salmonella*

spp. and *L. monocytogenes* were generally not present from the cheese samples (Hayaloğlu et al., 2002).

The presence of *Staphylococcus aureus*, *Salmonella* spp. and *L. monocytogenes* were mostly found during the cheese making process in small-scale raw milk cheese production. The main reason for such contamination is considered as the use of raw milk (Jorgensen et al., 2005; Kaynar et al., 2005; Jakobsen et al., 2011; Esho et al., 2013; Rola et al., 2016). *E. coli* are one of indicators of fecal contamination during cheese processing. Especially, cheese produced from unpasteurised milk (raw) can contain *E. coli*. Because *E. coli* is seen as a hygiene indicator for raw milk cheese, a manufacturer need to attempt to implement an appropriate HACCP plan. (Samouris et al., 2011; IDF, 2016). *E. coli* and *S. aureus* are the dominant pathogenic microflora in traditional cheese (Ozer et al., 2004). Previous studies were usually referred *E. coli* and *S. aureus* as the main contamination sources of cheeses whereas contamination of cheese by *Salmonella* spp. and *L. monocytogenes* stated as very few or none (Torkar et al., 2006; Obiren et al., 2009; Pacheco and Galindo, 2010). The presence of *L. monocytogenes* and *Salmonella* spp. in traditional cheese samples was highly rare and generally at rate of between 1 and 3% or none (Kara, 1999; Kaynar et al., 2005; Torkar et al., 2006; Keskin et al., 2006; Jakobsen et al., 2011; Telli et al., 2012; Esho et al., 2013). The present results confirmed this literature information.

S. aureus is common in milk and milk products and could cause intoxications with its toxins during processing (Ünlütürk, 2003). In international literature information, coagulase positive staphylococci were isolated on farms with small scale production of saw milk cheeses in Poland and their concentrations were ranged from approximately 0.5 to 7.5 log cfu/g (Rola et al., 2016). For example, Jorgensen et al. (2005) detected the presence of *S. aureus* in raw milk cheese with small scale production at levels of 3 log cfu/g. On the other hand, *E. coli* amounts of cheese made with raw milk were ranged from 0.46 to 5.38 log cfu/g (Samouris et al., 2011).

In previous studies based on microbiological quality of white cheese in Turkey, the presence of *S. aureus* and *E. coli* were found about between 40% and 100% and their amounts were varied from 1 and 6 log cfu/g. For instance, Torkar et al. (2006) investigated the occurrence of pathogenic bacteria in cheese produced at small dairy processing plants. Accordingly, all tested samples contained coagulase staphylococci (approximately 4 log cfu/g) and *E. coli* (approximately 6 log cfu/g) whereas *Salmonella* spp. and *L. monocytogenes* were not detected. Ozer et al (2004) reported that at the end of the 90-day storage period (at different brine concentration) in white Urfa cheese samples, *S. aureus* and *E. coli* were respectively found at level of between 3 and 4 log cfu/g and 0 and 3.5 log cfu/g however, *Salmonella* spp. could not detected. As seen, up to 90 days *S. aureus* and *E. coli* protected their viability. Our result also supported the hypothesis that the presence of *E. coli* and coagulase positive staphylococci in traditional cheese produced from raw milk in local market is possible. Additionally, Cokal et al (2012) reported that while contamination levels of *L. monocytogenes*, *E. coli* and *S. aureus* in Turkish traditional cheese samples were found 5%, 43% and 100%, respectively, none of food samples contained *Salmonella* spp. In accordance with this, the highest pathogen contamination arisen from coagulase positive staphylococci and followed *E. coli*. In the present study none of 20 samples had the presence of *L. monocytogenes* and *Salmonella* spp., however it does not mean that *L. monocytogenes* is not present in the whole cheese samples sold in Hatay. If more cheese samples were collected in Hatay, the prediction of pathogen contamination levels could be increased.

Keskin et al. (2006) investigated microbiological quality of the white cheese sold on street markets. The presence of 86% *E. coli* and 66% *S. aureus* were detected and were not present *Salmonella* spp. and *L. monocytogenes*. Başkaya et al. (2006) determined approximately 2 log cfu/g *E. coli* and *S. aureus* in civil cheese (another Turkish traditional cheese). Bilge and Karaboz (2005) detected the presence of *Staphylococcus aureus* (about 2-3 log cfu/) in some white cheese marketed in Izmir. Our results are in accordance with these previous reports.

To improve the food safety in small-scale cheese production, producers should be increasingly aware of the importance of some pre-requisites and process control points. As process control in cheese production, producers could focus on the quality of milk, regular cleaning of equipment and facilities, optimal concentrations of brine and processing factors such as time, pH and temperature. To reveal strengths and weaknesses of small scale cheese production, survey including questions such as personnel, education, dairy premises, utensils, production volume, hygiene barriers, control measures, water supply, pasteurization conditions and procedures for handling starter cultures should be implemented to producers (Rosengren et al., 2012; Damico et al., 2017). For example, by food safety authority of Ireland, a workbook has been produced to assist farmhouse cheesemakers meet their legal obligation to develop and implement a food safety management system based on the principles of HACCP (Hazard Analysis and Critical Control Point), also referred to as HACCP-based procedures. This workbook provides a controlled approach by describing and recording each step during individual operations in cheesemaking, from raw material production/purchasing through to the storage and dispatch of cheese (Food Safety Authority of Ireland, 2019). On this sense, small scale cheese producers need to develop and implement HACCP plan based on their specific productions (Zhao et al., 2003; Hof et al., 2008). HACCP system as one of the most important systems in quality assurance programs is a plant-specific and product-specific quality system. The application of HACCP plan in small-scale cheese plant could ensure the food safety via the identification of microbiological hazards (Nasr et al., 2017).

Conclusion

The present study concluded that the microbiological quality and hygienic status of traditional cheese analyzed in this study were mainly favorable. Most of traditional cheese samples analyzed in this paper complied with the microbiological criteria notifications on food safety by Turkish government. In Turkey, cheese is automatically produced in industrial plants with large food factories or traditionally on a small scale in local markets. Handmade cheeses with raw milk could have deficiencies from utensils, staff and other unstable processing conditions in terms of hygienic quality. In particular, raw milk constitutes the critical control point in the production process of traditional cheeses. Pathogen risk is inevitable in cheeses manufactured from low microbial quality milk. As a matter of fact such contaminated cheese could result in the outbreaks of foodborne pathogens including *L. monocytogenes*, *Salmonella* spp., *E. coli* and *S. aureus*. Policies on food safety and protection have focused on ensuring food safety in conventional products. On this sense, for the sustainability of traditional cheeses, microbial safety must be ensured with a HACCP or other food safety plan in manufacturing field and producers should focus on the hygienic conditions during milking and cheese processing.

REFERENCES

- [1] Akkaya, L., Alişarlı, M. (2006): Afyonkarahisar’da tüketime sunulan peynirlerde *Listeria monocytogenes* ve *Salmonella* spp. varlığının belirlenmesi (An investigation on the presence of *Listeria monocytogenes* and *Salmonella* spp. in retail cheeses consumed in Afyonkarahisar province, Turkey). – YYÜ Vet Fak Derg 17(1-2): 87-91.
- [2] Almasoud, A., Hettiarachchy, N., Rayaprolu, S., Horax, R., Eswaranandam, S. (2015): Electrostatic spraying of organic acids on biofilms formed by *E. coli* O157:H7 and *Salmonella Typhimurium* on fresh produce. – Food Research International 78: 27-33.
- [3] Atasoy, F. E., Türkoğlu, H., Ozer, B. H. (2003): Şanlıurfa ilinde üretilen ve satışı sunulan süt, yoğurt ve urfa peynirlerinin bazı mikrobiyolojik özellikleri (Some microbiological properties of raw milk, yogurt and fresh Urfa cheese produced and sold in Sanliurfa province). – J. Agric Fac. HR. U. 7(3-4): 77-83.
- [4] Başkaya, R., Atasever, M., Çakmak, Ö., Yıldız, A. (2006): Civil peynirinin mikrobiyolojik nitelikleri (Microbiological properties of civil cheese). – J Fac. Vet. Med. istanbul Univ. 32(2): 87-94.
- [5] Belli, P., Cantafora, A. F. A., Stella, S., Barbieri, S., Crimella, C. (2013): Microbiological survey of milk and dairy products from a small scale dairy processing unit in Maroua (Cameroon). – Food Control 32: 366-370.
- [6] Bilge, F., Karaboz, İ. (2005): İzmir’de piyasada açıkta satışı sunulan bazı gıdaların *Staphylococcus aureus* ve enterotoksinleri bakımından incelenmesi (Investigation of some foodstuffs marketed in Izmir in terms of *Staphylococcus aureus* and enterotoxins). – OrLab On-Line Mikrobiyoloji Dergisi 3(6): 1-6.
- [7] Chavant, P., Martinie, B., Meylheuc, T., Fontaine, M. N. B., Hebraud, M. (2002): *Listeria monocytogenes* LO28: Surface physicochemical properties and ability to form biofilms at different temperatures and growth phases. – Applied and Environmental Microbiology 68(2): 728-737.
- [8] Choi, K. H., Lee, H., Lee, S., Kim, S., Yoon, Y. (2016): Cheese microbial risk assessments — a review. – Asian Australas. J. Anim. Sci. 29(3): 307-314.
- [9] Cokal, Y., Dagdelen, A., Cenet, O., Gunsen, U. (2012): Presence of *L. monocytogenes* and some bacterial pathogens in two Turkish traditional foods, Mihalic cheese and Hosmerim dessert. – Food Control 26: 337-340.
- [10] Damico, D. J. (2017): Recommendations and outcomes from the first artisan cheese food safety forum. – Food Protection Trends 37(5): 332-339.
- [11] Demirkesen, A. C. (2012): Multi-risk interpretation of natural hazards for settlements of the Hatay province in the east Mediterranean region, Turkey using SRTM DEM. – Environmental Earth Sciences 65(6): 1-13.
- [12] Donnelly, C. (2018): Review of controls for pathogen risks in scottish artisan cheeses made from unpasteurised milk. – Food Standards Scotland 134p.
- [13] Esho, F. K., Enkhtuya, B., Kusumota, A., Kawamoto, K. (2013): Microbial assesment and prevelance of foodborne pathogens in natural cheeses in Japan. – Hindawi Publishing Corporation, Biomed Research International 6p.
- [14] Food Safety Authority of Ireland. (2019): HACCP/Food safety workbook for farmhouse cheesemakers. – <https://www.fsai.ie>.
- [15] Halkman, K. (2005): Merck Gıda Mikrobiyolojisi Uygulamaları (Merck Food Microbiology Practices). – Başak Matbaacılık Limited Şti., Ankara, Türkiye, 358s.
- [16] Hayaloğlu, A. A., Guven, M., Fox, P. F. (2002): Microbiological, biochemical and technological properties of Turkish White cheese ‘Beyaz Peynir’. – International Dairy Journal 12: 635-648.
- [17] Hofi, M. E., Tanboly, E. S. E., Ismail, A. (2008): Implementation of the hazard analysis critical control point (haccp) system to uf white cheese production line. – Internet Journal of Food Safety 10: 1-8.

- [18] Hudson, A., Wong, T., Lake, R. (2003): Pasteurisation of dairy products: times, temperatures and evidence for control of pathogens. – Institute of Environmental Science & Research Limited, Christchurch Science Centre, Food Safety Authority 55p.
- [19] IDF Factsheet. (2016): International dairy federation. – www.fil.idf.org.
- [20] Jakobsen, R. A., Heggebo, R., Sunde, E. B., Skjervheim, M. (2011): *Staphylococcus aureus* and *Listeria monocytogenes* in Norwegian raw milk cheese production. – Food Microbiology 28: 492-496.
- [21] Jorgensen, H. J., Mork, T., Rorvik, L. M. (2005): The occurrence of *Staphylococcus aureus* on a farm with small-scale production of raw milk cheese. – J. Dairy Sci. 88: 3810-3817.
- [22] Kara, A. A. (1999): Erzurum piyasasından temin edilen beyaz ve civil peynirlerden, *Listeria* türlerinin izolasyon ve identifikasyonu (Investigation on the isolation and identification of the *Listeria* species in the white and civil cheeses purchased from Erzurum region). – Tr. J. of Biology 23: 331-337.
- [23] Kaynar, Z., Kaynar, P., Koçak, C. (2005): Ankara piyasasında tüketime sunulan beyaz peynirlerin hijyenik kalitelerinin belirlenmesi üzerine bir araştırma (A research on hygienic quality of pickled white cheeses in Ankara market). – Türk Hij Den Biyol Der 62: 1-10.
- [24] Keskin, Y., Özyaral, O., Başkaya, R., Susur, M. A. (2006): Investigation of microbiological quality of the white cheese sold on street markets. – Türk Mikrobiyol Cem Derg 36(1): 9-19.
- [25] Kurşun, Ö., Kırdar, S. S., Kale, A. S. A., Güner, A. (2008): Burdur'da tüketime sunulan beyaz salamura peynirlerin mikrobiyolojik kalitesinin belirlenmesi (The determination of microbiological quality of white brine cheese consumed in Burdur). – Türkiye 10. Gıda Kongresi, 21-23 Mayıs Erzurum, 817-820.
- [26] Mikulec, D. P., Jovanovic, L. (2005): Microbiological study of fresh white cheese (a serbian craft variety). – Applied Ecology and Environmental Research 4(1): 129-134.
- [27] Motarjemi, Y. (2002): Impact of small scale fermentation technology on food safety in developing countries. – International Journal of Food Microbiology 75: 213-229.
- [28] Nasr, N. F., Gizawy, S. E., Zahra, M. K. (2017): Application of quality assurance programs in small dairy plants. – Journal of Nutritional Health & Food Engineering 7(1): 214-220.
- [29] O'Brien, M., Hunt, K., McSweeney, S., Jordan, K. (2009): Occurrence of food borne pathogens in Irish farm house cheese. – Food Microbiology 26: 910-914.
- [30] Ozer, H. B., Uraz, G., Yilmaz, E. B., Atasoy, A. F. (2004): The effects of brine concentration and scalding on survival of some pathogens in urfa cheese: a traditional white-brined turkish cheese. – International Journal of Food Science and Technology -39: 727-735.
- [31] Pacheco, F. P., Galindo, A. B. (2010): Microbial safety of raw milk cheeses traditionally made at a pH below 4.7 and with other hurdles limiting pathogens growth. – In: Mendez Vilas, A. (ed.) FORMATEX, Current Research, technology and Education Topics in Applied Microbiology and Microbial Biotechnology, p: 1205-1216.
- [32] Rola, J. G., Czubkowska, A., Dzirba, W. K., Osek, J. (2016): Occurrence of *Staphylococcus aureus* on farms with small scale production of raw milk cheeses in Poland. – Toxins 8(62): 1-9.
- [33] Rosengren, A. (2012): Microbiological food safety of cheese produced in swedish small-scale dairies. – Swedish University of Agricultural Sciences, Faculty of Natural Resources and Agricultural Sciences, Department of Microbiology, Uppsala, Licentiate Thesis, 60p.
- [34] Samouris, G., Zdragas, A., Vafeas, G., Belibasaki, S. (2011): Survival of pathogens in "Graviera Kritis" cheese made with raw and pasteurized milk. – Journal of the Hellenic Veterinary Medical Society 62(3): 205-21.
- [35] Telli, N. (2012): *Listeria monocytogenes*'in salamura beyaz peynir üretim hattında kontaminasyon kaynaklarının belirlenmesi ve PFGE metodu ile genotiplendirilmesi (Detection of contamination sources of *Listeria monocytogenes* in pickled white cheese production process line and genotyping with PFGE method). – Selçuk Üniversitesi Sağlık Bilimleri Enstitüsü (Selcuk University Health Sciences Institute), Besin Hijyeni ve

- Teknolojisi Anabilim Dalı (Food hygiene and technology department), Doktora Tezi (PhD Thesis), 120p.
- [36] Torkar, K. G., Teger, S. G. (2006): The presence of some pathogen micro organisms, yeasts and moulds in cheese samples produced at small dairy-processing plants. – *Acta agriculturae Slovenica* 88(1): 37-51.
- [37] Turkish Food Codex. (2011): Mikrobiyolojik Kriterler Tebliği (Communiqué on microbiological criteria). – Ek-1:Gıda Güvenilirliği Kriterleri (Annex-1: Food safety criteria), 17 p.
- [38] Uraz, G., Coşkun, S., Ozer, B. (2008): Microflora and pathogen bacteria (*Salmonella*, *Klebsiella*, *Yersinia*, *Pseudomonas*, *Aeromonas*, *Esherichia coli*, *Staphylococcus aureus*) in Urfa cheese (a traditional white brined turkish cheese). – *Pakistan Journal of Nutrition* 7(5): 630-635.
- [39] Ünlütürk, A. (2003): Süt ve süt ürünlerinde mikrobiyolojik bozulmalar ve muhafaza yöntemleri (Microbiological spoilage and preservation methods in dairy products). – In: Ünlütürk, A., Turantaş, F. (eds.) *Gıda Mikrobiyolojisi (Food Microbiology)*, p: 287-306 3. Baskı, Metesan Basım Matbaacılık, Bornova-İZMİR.
- [40] WHO. (2012): World Health Organization, General information related to microbiological risks in food. – <http://www.who.int/foodsafety/micro/general/en/index.html> Accessed on 19.07.12.
- [41] Yücel, N., Anıl, Y. (2011): Çiğ süt ve peynir örneklerinden *Staphylococcus aureus* ve koagülaz negatif staflokokların identifikasyonu ve antibiyotik duyarlılığı (Identification and antimicrobial susceptibility of *Staphylococcus aureus* and coagulase negative Staphylococci isolated from raw milk and cheese samples). – *Türk Hijyen ve Deneysel Biyoloji Dergisi* 68(2): 73-78.
- [42] Zhao, M. (2003): The design of haccp plan for a small-scale cheese plant. – The Graduate School, University of Wisconsin-Stout, Food and Nutritional Sciences, Master of Science Degree, 46p.

ASSESSING DYNAMICS IN THE VALUE OF ECOSYSTEM SERVICES IN RESPONSE TO LAND COVER/LAND USE CHANGES IN ETHIOPIA, EAST AFRICAN RIFT SYSTEM

NEGUSSIE, W.^{1,2} – WU, W.^{1,3*} – ALEMAYEHU, A.^{1,2} – YIRSAW, E.⁴

¹*College of Land Management, Nanjing Agricultural University, Nanjing 210095, China
(e-mail: wube14@yahoo.com, asferaalem2011@yahoo.com)*

²*Department of Natural Resources Management, Assosa ATVET College, Assosa 242, Ethiopia*

³*National and Joint Local Engineering Research Center for Rural Land Resources Use and Consolidation, Nanjing 210095, China*

⁴*Department of Natural Resources Management, Dilla University, Dilla, Ethiopia
(e-mail: eshetu.yirsaw@yahoo.com)*

**Corresponding author*

e-mail: ww@njau.edu.cn; phone: +86-137-7065-1675

(Received 25th Feb 2019; accepted 10th Apr 2019)

Abstract. Ecosystem services (ES) are essential to human well-being. Assessing dynamics of ES is crucial to shaping the concept of sustainable development and creating public understanding of the status of ES. This study proposes to quantify the change in ES value in response to Land cover/land use (LCLU) changes over the past 33 years in the Rift Valley Lakes Region of Ethiopia. A combined approach of LCLU classification and modified ES value coefficients was employed for quantifying the ES value. Results revealed that approximately USD196.04 ×10⁶ (12.4%) of ES value was lost during the study period. Although cropland experienced a dramatic expansion, the total gain in ES value of the cropland was too small to balance out the overall loss. A continuous reduction in values of specific ES functions has also occurred except for food production, biological control, and pollination service function over the last three decades, indicating an apparent deterioration of the fragile Rift Valley ecosystem. Hence, to enhance the continuous supply of ES and economic development, an integrated approach to managing land and water resources is recommended. Moreover, payment for ES is also a potential remedy for ES loss at the regional and local scale.

Keywords: *combined approach, benefit transfer, modified coefficient, East Africa Rift system, average ecosystem service value, loss, water bodies, woodland, cropland*

Introduction

Ecosystem services (ES) are essential to human welfare (Xu and Ding, 2018; Costanza et al., 2014; Braat and de Groot, 2012; MEA, 2005). These include regulating, provisioning, supporting, and cultural services (MEA, 2005; Costanza et al., 1997). The amount and quality of ES depend on the types of ecosystem and their status (Tolessa et al., 2017a; MEA, 2005). Each ecosystem provides distinct services that could not be substituted with another (Gashaw et al., 2018). ES are closely related with land cover/land uses (LCLU), and they alter across time and space (Xu and Ding, 2018; Schirpke et al., 2017; Tolessa et al., 2017a; Costanza et al., 2014). Land cover/land use change (LCLUC) is altering the amount and quality of ES provided by ecosystems. LCLUC is an essential landscape process (Schröter et al., 2005; Daily, 1997) designed by the interaction between the social-economical activities of human beings and the natural environment (Chang et al., 2018).

Changes in LCLU may lead to differences in the value of ES (Locatelli et al., 2017; Polasky et al., 2011; Hu et al., 2008; Kreuter et al., 2001). It may raise the value of some services while reducing that of others, which affects the capability of the biological system to sustain human needs, indicating ecological deterioration (Polasky et al., 2011), or may cause conversely (Kindu et al., 2016). For example, studies show that the transformation of forest land to cropland increases food production while reduces the regulating services provided by the forest land (Fedele et al., 2018; Rodríguez et al., 2006; Foley et al., 2005). However, a recent land development activity in marginal grassland have effected in the conversion of ES from provisioning to regulating services as a result of natural reforestation processes (Schirpke et al., 2017; Vigl et al., 2016). Thus, the study of ES value changes caused by the change in LCLU has implications (Chen et al., 2015) through creating public awareness of the continuing LCLU dynamics and is vital to indicate the vulnerability of each ES (Cabral et al., 2016).

Monetization of ES has been promoted by numerous as a model strategy to create public alertness, provide evidence for consultations with decision makers, flag up the opportunity costs of rehabilitation and/or restoration, and assist in payments for ES (Alarcon et al., 2016; Baveye et al., 2013; de Groot et al., 2012; Nelson et al., 2009; Costanza et al., 1997). Recognising and quantifying the influence of LCLUCs on global, regional, and local ES is a practical approach to evaluating the costs and benefits to the environment and supporting sustainable land management decisions (Xu and Ding, 2018; Song and Deng, 2017; Liang et al., 2017). It also assists with devising a land use planning framework suitable for sustaining the health and sustainability of land resources (Bartkowski, 2017; Cabral et al., 2016; Jacobs et al., 2016).

The results of many studies that estimated ES value in response to LCLUC were location specific. For example, some studies reveal an overall increase in ES value (Temesgen et al., 2018; Wang et al., 2014; Sawut et al., 2013) while others confirm the opposite, i.e. a decreasing trend (Gashaw et al., 2018; Leh et al., 2013; Tolessa et al., 2017a); whereas, globally, the total net loss due to LCLUC has been estimated at USD 20.2 trillion/ year between 1997 and 2011 (Costanza et al., 2014). However, estimation of ES value change at a regional scale from the global study is challenging; in fact, a regional study of a country often results in a different yield due to various approaches and classifications. Moreover, the prevailing ES valuation in response to LCLUC is not comprehensive across the whole world due to the lack of inclusion of vast ecological regions and services (Tadesse et al., 2014; Satz et al., 2013; de Bello et al., 2010); its applicability to different regions leads to improper valuation of ES (Wang et al., 2015). Even though a number of recent works have quantified and mapped ES (e.g. Leh et al., 2013; Egoh et al., 2009; Nelson et al., 2009), despite some efforts (by Arowolo et al., 2018; Niquisse and Cabral, 2018; Gashaw et al., 2018; Temesgen et al., 2018; Tolessa et al., 2017a; Kindu et al., 2016), such studies are lacking in other regions of Africa (Leh et al., 2013; Seppelt et al., 2011) that serve as a source of the world's biodiversity.

Many regions of Africa are facing rapid and profound transformation economically, socially, and environmentally a transformation that is already endangering the long-standing conservation of its substantial natural heritage and biodiversity (Mwampamba et al., 2016). Hence, the ongoing deterioration of ecosystems occurs in many regions of the continent at the expense of the well-being

of the coming generations (Kubiszewski et al., 2017; de Groot et al., 2012); this is particularly true for Ethiopia, which lost approximately 17.7% of its overall terrestrial ES values due to LCLUC (Sutton et al., 2016).

In Ethiopia, LCLUC is a common and ever-present phenomenon because agricultural activities mainly dominate rural landscapes, affecting ES (Tolessa et al., 2017a). Integrating LCLU and an ES value dataset can assist in detecting the areas highly susceptible to change in ES at the landscape scale and provide an avenue for land management opportunities in the future. Moreover, research works carried out on LCLUC in the country mainly focuses on the driving factors and the LCLU dynamics (Meshesha et al., 2012; Tsegaye et al., 2010; Reid et al., 2000). However, the consequence of LCLUC on a wide-range of ES is rarely attempted. Currently, there has been no estimation of the impacts of such changes at a regional scale, just a few efforts made to evaluate ES in response to LCLUC at the local scale (Gashaw et al., 2018; Temesgen et al., 2018; Tolessa et al., 2017a; Kindu et al., 2016).

The study area, the Rift Valley Lakes Region (RVLR) of Ethiopia, is situated in the Eastern part of the African Rift System, and consists of lakes, streams and wetlands with unique hydro-ecological characteristics (Jansen et al., 2007; Hengsdijk and Jansen, 2006), and a wide range of landscapes with high biodiversity. It is the largest freshwater ecosystem in the nation with considerable social, economic and ecological significance. However, the RVLR is one of the most environmentally susceptible areas in Ethiopia. Being a landlocked basin, relatively little intervention in the water and land resources can have substantial consequences for ecosystems goods and services, and weaken the potential sustainable use of the region (Ayenew, 2004; Legesse et al., 2004).

Therefore, recognising the influences of LCLUC on ES value in the study region is vital to increasing public understanding and indicating the proper land use policy direction. Previous studies emphasised potential LCLUC, although the majority were carried-out at a local scale and described the LCLUC qualitatively. The consequences of the existing LCLU and land degradation are huge, including declining crop and livestock production and exacerbated food shortages in the area (Meshesha et al., 2012). Hence, the objective of this study was 1) to characterise changes in LCLU over the last three decades and 2) to quantify and map the ES value alteration in response to LCLUC using a modified ES value coefficient in the RVLR of Ethiopia from 1986 to 2018.

This study estimates changes of ES in response to LCLUC using a conservative ES coefficient modified by (Kindu et al., 2016) using benefit transfer approach. Kindu et al. (2016) developed modified conservative value coefficients through a review of the previous studies, and dataset available from the Economics of Ecosystems and Biodiversity (TEEB) database. This value coefficient is assumed to be suitable for the RVLR of Ethiopia, which is a developing region with a rapidly growing population (Legesse et al., 2004), abundant livestock (Meshesha et al., 2012) and a vulnerable ecosystem, and for other areas with a similar landscape setting.

This paper has five sections: The first section is the introduction of the study. The second section gives a concise description of the study area, introduces methods to assess LCLUC, quantifies ES change in response to LCLUC, and statistical analysis. The third and fourth sections give the results and discussion, respectively, and the fifth section concludes and provides some future recommendations.

Materials and methods

Study area

The RVL of Ethiopia ($38^{\circ}11'$ to $39^{\circ}9'$ E and $6^{\circ}55'$ to $8^{\circ}29'$ N) (Fig. 1), is located in the Eastern part of the Great African Rift system, with an altitude ranging from 1,384 m at the valley floor to more than 3,040 m asl at the escarpment (Fig. 1). The region where the study conducted includes eight administrative districts and two town districts with a total area of about 0.81 million ha (Table 6) and a projected population for 2017 of 2.1 million (CSA, 2013). The national GDP per capita was about USD233.82 in 1986 and USD706.76 in 2016 (WorldBank, 2019). The study region is characterised by rift valley lakes, namely Ziway, Langano, Shalla, Abiyata, Hawasa Lakes and Koka. Lake Ziway is one of the centres for agricultural development in the country (Hengsdijk and Jansen, 2006); Lake Abyata and Lake Shalla are important nature reserves, integrating the Abyata-Shala Lakes National Park, primarily established for aquatic bird protection (de Francisco et al., 2008; Hengsdijk and Jansen, 2006), which is currently heavily invaded by human and cattle populations (Scholten, 2007). Lake Hawasa, situated at the high elevation in the central main Ethiopian Rift Valley, is one of the essential bird sanctuaries in the country and is significant source of tourism income (Wondrade et al., 2014; Ayenew and Gebreegziabher, 2006). Lake Koka (artificial) is the second oldest hydro-power dam in the country. It provides multiple services besides hydropower (Gebretsadik, 2016). The study area also covers another sanctuary established for protecting Swayne's hartebeest (*Alcelaphus buselaphus swaynei*) which is called Sinkele sanctuary, located in the southwest of the study area (Nishizaki, 2004). The climate is arid to semi-arid (Scholten, 2007), but varies markedly with altitude (Jansen et al., 2007), with an annual precipitation of about 600 mm. About 70% of the rainfall is received from July to September.

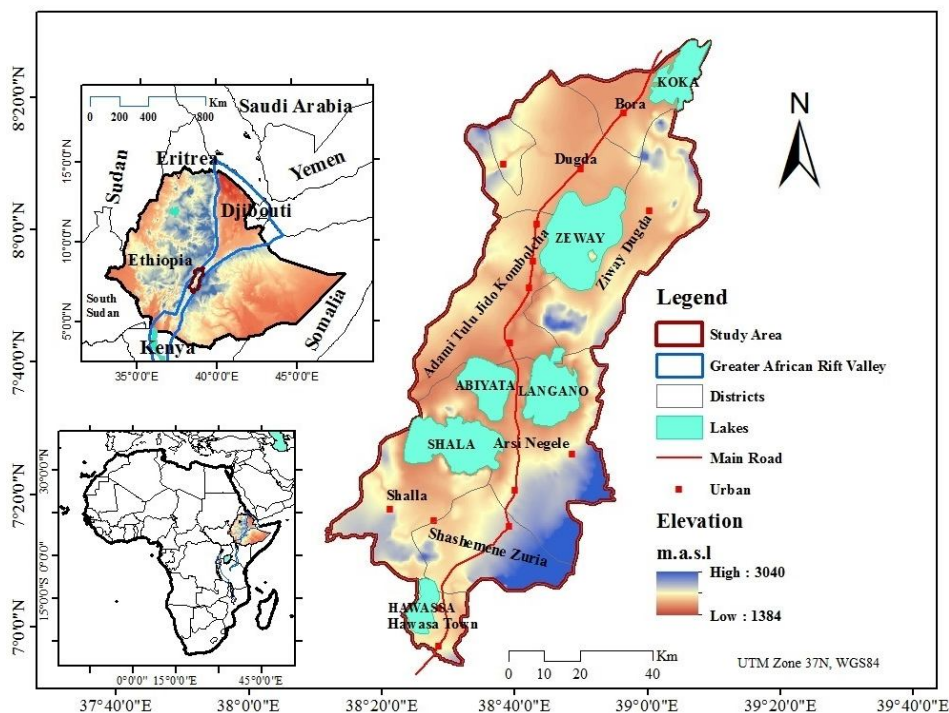


Figure 1. Location of the study area: RVL of Ethiopia, East African Rift system

Methods

The methods followed were an analysis of remotely-sensed data to detect LCLUCs and to estimate economic values for ES in response to LCLUC using a modified ES value coefficient.

Data processing and LCLUC detection

The LCLU datasets were derived from multi-spectral Landsat imageries (Landsat-5 Thematic Mapper (TM) 1986, Landsat-7 Enhanced Thematic Mapper Plus (ETM+) 2000, and Landsat-8 Operational Land Imager (OLI) 2018 with 30 m resolution (USGS, 2018). Two Landsat imageries were needed to get complete coverage of the study region. Therefore, a total of six imageries were acquired free of charge from the USGS (United States Geological Survey) Center for Earth Resources Observation and Science (EROS). Detailed characteristics of the remote sensing data (i.e. Landsat imageries) are tabulated in *Table 1*.

Table 1. Description of remote sensing data used in the study

Year	Sensors	Path and row	Resolution	Date of acquisition	Source
1986	Landsat-5 Thematic Mapper (TM)	168/054, 168/055	30 m	21 Jan, 1986	USGS, 2018
2000	Landsat-7 Enhanced Thematic Mapper Plus (ETM+)	168/054, 168/055	30 m	29 Feb, 2000	USGS, 2018
2018	Landsat-8 Operational Land Imager (OLI)	168/054, 168/055	30 m	13 Jan, 2018	USGS, 2018

Each of the acquired imageries was clear and nearly free of clouds. Imageries were pre-processed in ERDAS Imagine 2015 software (Hexagon Geospatial, Alabama, USA) for geometric corrections, geo-referencing, mosaicking and sub-setting of the images (Lin et al., 2018; Gashaw et al., 2017; Mosammam et al., 2017; Gebrehiwot et al., 2014; Schulz et al., 2010; Teferi et al., 2010). All of Landsat imageries were geo-rectified to UTM/WGS84, zone 37 N coordinates using 1:250,000 topographic maps and 20 GPS (global positioning system) points gathered during field observation using Garmin eTrex handheld instrument. Each of the pre-processed imageries was classified using a hybrid classification method that integrates both the supervised and unsupervised classification techniques (Gashaw et al., 2017; Gebrehiwot et al., 2014; Teferi et al., 2010). The unsupervised techniques utilizing Iterative Self-Organizing Data Analysis (ISODATA) grouping (Boakye et al., 2008) were employed as a starting point for collecting GPS points as ground truth points. Using signature editors (spectral signatures) of the unsupervised categories, a pixel-based supervised classification technique with the Maximum Likelihood algorithm (MLC) (Gebrehiwot et al., 2014) was conducted using GPS points collected. The GPS points (i.e., 80 from each LCLU class) were gathered for classifying LCLU classes of the year 2018. A brief description of the identified LCLU classes in the RVLRL of Ethiopia is given in *Table 2*. Reference data from topographic maps (scale: 1:50,000 and 1:250,000) obtained from the Ethiopia Mapping Agency, Google Earth, raw images, focus group discussions, and researchers' experience of the area were also used for the classification of the 1986 and 2000

images. Moreover, geo-linking Google Earth with ERDAS Imagine 2015 software was employed for classification. ERDAS Imagine 2015 software was employed for classification purposes.

Table 2. A brief description of LCLU classes identified in the RVLR of Ethiopia

LCLU classes	Brief descriptions
Cropland	Land used for rain-fed and irrigated cropping (small plot to large scale)
Bare land	Non-vegetated areas dominated by rock outcrops, eroded and degraded land
Forest land	Land dominated by plantation and natural forest
Grassland	Grass & herb cover with scattered trees and shrubs
Marsh	Includes: river beds, intermittent ponds and marshy areas with shallow water and permanent reed vegetation
Urban/built-up	Land mainly towns dominated by permanent residential areas of varied patterns and scale occupied by backyards, compounds, individual houses, and industries
Water body	open water, lakes (Abiyata, Shalla, Ziway, Langano, and Koka), ponds, rivers and streams
Woodland	Woody acacia dominated areas, and trees outside forest

Lastly, to confirm the quality and usability of each of the classified imageries, classification accuracy was computed from the error matrix. The error matrix compares the information obtained by sample LCLU sites with that provided by the classified image. It is also used to calculate the user's, producer's and overall accuracies (Congalton, 1991). About 85 random points were generated for each LCLU class using a stratified random sampling approach for better accuracy assessment (Congalton, 1991). The reference sample points for the 1986 and 2000 images were collected from the respective historical Google Earth images (i.e., January 1986 and February 2000). A similar technique was conducted by Gashaw et al. (2017).

Accuracy classification assessments were performed for classified imageries of 1986, 2000 and 2018. Accordingly, the results of imagery classification showed that the overall accuracies were higher than 80%, and the Kappa coefficients were found to be higher than 0.77 (Table 3). This clarified that the results of image classification were satisfactory for further analysis.

Table 3. Accuracy assessment of the 1986, 2000, and 2018 classified images

LCLU class	Classification accuracy					
	1986		2000		2018	
	Producer's	User's	Producer's	User's	Producer's	User's
Cropland	81.48	81.48	81.82	90	77.27	85
Bare Land	84.62	88	85.42	80.39	85.42	80.39
Urban/built-up	87.1	72.97	86.96	80	89.19	89.19
Forest land	76.92	80	73.68	82.35	72.22	81.25
Grassland	67.86	86.36	86.67	96.3	86.36	95
Marsh areas	85.71	73.68	80.43	75.51	80.43	74
Water body	80	96	83.33	89.29	79.31	88.46
Woodland	85.29	85.29	84	95.45	80.77	95.45
Overall accuracy (%)	80.05		81.82		80.37	
Kappa statistics	0.77		0.77		0.74	

Finally, the classified images were exported to ArcGIS 10.2 software (Esri, California, USA) for further spatial analysis and ES value spatial distribution mapping. The percentage of dynamics of LCLUC were computed using the following equation:

$$\Delta L = \frac{A_2 - A_1}{A_1} \times 100 \quad (\text{Eq.1})$$

where ΔL is the LCLUC proportion, and A_2 and A_1 are final and initial area cover of the LCLU classes.

Estimation of ES values

Many scholars have used a range of methods to estimate ES value since 1970 (Zhang et al., 2015). Costanza et al. (1997) categorised the global biosphere into sixteen types of ecosystem and seventeen types of service functions and estimated their ES value. Although Costanza's method is criticised for its uncertainties (Braat and de Groot, 2012; Kreuter et al., 2001), it served as the basis for further progress in the development and use of monetary valuation studies (Braat and de Groot, 2012). Referring to Costanza's parameter, Xie et al. (2003) provided the equivalent weighting factors of ES per hectare of terrestrial ecosystems and used these factors to adjust the value coefficient for the ecosystems of China. Although Xie et al.'s (2003) approach to quantifying ES value is also criticised for its uncertainties, it is still broadly applied for its feasibility, particularly in data-scarce areas (Lin et al., 2018). The ES value coefficient was also modified by Van der Ploeg and De Groot (2010) for 11 biomes based on Costanza et al.'s (1997) estimates, which are very general and could not represent the regional context.

Moreover, an additional estimation of global ecosystems was undertaken by de Groot et al. (2012) and Costanza et al. (2014). Their estimates were also criticised for overemphasising some ES (Tolessa et al., 2017a). Hence, referring to the existing dataset of TEEB, compiled by the international Ecosystem Service Partnership (ESP-www.es-partnership.org), as well as the ES value coefficients of Costanza et al. (1997), and dataset from peer-reviewed included in (de Groot et al., 2012), other related research and expert knowledge of the study landscape conditions, Kindu et al. (2016) has modified the ES value coefficients for nine biomes for the Ethiopian case. A summary of LCLU categories and corresponding ES coefficients is provided in *Table 4*. We associated the eight LCLU classes in the RVLR of Ethiopia (*Table 5*) with the biomes identified by Kindu et al. (2016), and the closest equivalent biome was used as a proxy. Cropland was used as a substitute for cropland, grass/rangelands for grasslands, tropical forest for forest land and woodland, lakes/rivers for a water body and marsh areas, desert for bare land, and urban for urban/built-up.

In this study, we rely upon a more conservative ES coefficient using the benefit transfer approach, which provides a means to estimate values (both the market and the non-market components) of various ES by transferring information of the existing valuation research from a similar location (Costanza et al., 1997; Kubiszewski et al., 2017). It is the approach most often used to estimate the economic value of ES when time, funding, information accessibility or other difficulties prevent the usage of primary studies (Kreuter et al., 2001; Rolfe et al., 2015; Temesgen et al., 2018; Wilson and Hoehn, 2006). This approach has been used in numerous studies for instance, (Costanza et al., 1997; Kramer et al., 1997; Kubiszewski et al., 2013; Liu et al., 2010;

Temesgen et al., 2018; Torras, 2000) to quantify the worth of ES. Although, there are some weaknesses to this approach such as the context sensitivity of value estimates the accuracy will noticeably improve as the extent, richness, and detail of the information increases (Troy and Wilson, 2006; Wilson and Hoehn, 2006).

Table 4. Details of modified annual value coefficient for ESs of individual LCLU classes (Kindu et al., 2016)

ESs	LCLU classes /biome (USD ha ⁻¹ yr ⁻¹)							
	Cropland	Bare Land	Urban/built-up	Forest land	Grassland	Marsh areas	Water body	Woodland
Water supply	0	0	0	8	0	2117	2117	8
Food production	187.56	0	0	32	117.45	41	41	32
Raw material	0	0	0	51.24	0	0	0	51.24
Genetic resources	0	0	0	41	0	0	0	41
Water regulation	0	0	0	6	3	5445	5445	6
Water treatment	0	0	0	136	87	431.5	431.5	136
Erosion control	0	0	0	245	29	0	0	245
Climate regulation	0	0	0	223	0	0	0	223
Biological control	24	0	0	0	23	0	0	0
Gas regulation	0	0	0	13.68	7	0	0	13.68
Disturbance regulation	0	0	0	5	0	0	0	5
Nutrient cycling	0	0	0	184.4	0	0	0	184.4
Pollination	14	0	0	7.27	25	0	0	7.27
Soil formation	0	0	0	10	1	0	0	10
Habitat/refugia	0	0	0	17.3	0	0	0	17.3
Recreation	0	0	0	4.8	0.8	69	69	4.8
Cultural	0	0	0	2	0	0	0	2
Total ES value	225.56	0	0	986.69	293.25	8103.5	8103.5	986.69

Table 5. Summary of LCLU categories and corresponding ES coefficients based on modified estimates (Kindu et al., 2016)

LCLU Type	Equivalent biome	Modified value coefficient (USD ha ⁻¹ yr ⁻¹)
Cropland	Cropland	225.56
Bare land	Desert	0
Forest land	Tropical Forest	986.69
Grassland	Grass/rangelands	293.25
Marsh areas	Lakes/rivers	8103.5
Urban/built-up	Urban	0
Water body	Lakes/rivers	8103.5
Woodland	Tropical Forest	986.69

The ES value of each LCLU category, their corresponding service function and the total ES values for 1986, 2000 and 2018 were calculated using *Equations 2, 4, and 3*, respectively, as considered by (Temesgen et al., 2018; Hu et al., 2008; Li et al., 2007). The modified annual value coefficients that were used for this study are presented in *Tables 4 and 5*.

$$ES\ Value_k = A_k \times VC_k \quad (Eq.2)$$

$$ES\ Value = \sum(A_k \times VC_k) \quad (Eq.3)$$

$$ES\ Value_f = \sum(A_k \times VC_{kf}) \quad (Eq.4)$$

where $ES\ value_k$ ES value and $ES\ value_f$ denotes the ES value of the LCLU category “k”, the total ES value, and the value of ES function category “f”, respectively. A_k is the area (ha) for LCLU category k; VC_k is the value coefficient (USD ha⁻¹ yr⁻¹) for LCLU category k; and VC_{kf} is the value coefficient (USD ha⁻¹yr⁻¹) for LCLU category k with ES function category “f”.

Estimation of the average ES values of the study area was undertaken using Equation 5, following the method employed in (Gashaw et al., 2018). The average ES value was calculated by dividing the total ES value by the area of the study region:

$$ES\ Value_{av} = \frac{ES\ Value_t}{Area_t} \quad (Eq.5)$$

where $ES\ value_{av}$ is the average ES value of the study region (USD ha⁻¹ yr⁻¹) during the specific year, $ES\ value_t$ is the total ES value in that particular year, and Area is the area coverage of the study region.

Statistical analysis

To analyse the relationship between LCLUC, dynamics in ES value, and socioeconomic shift (i.e., GDP, population), one-way analysis of variance (ANOVA) was conducted. Moreover, to quantitatively scrutinise the relationship between LCLUC, and hence provide more information for this work, the analyses were carried out using IBM SPSS Statistics Version 20. By carefully examining whether the detected changes were significant or not, and the interaction effects of the variables, it was decided that nonlinear regression models were suitable and thus were adopted.

Results

Land cover/land use change (1986–2018)

The area coverage of LCLU classes (Table 6; Fig. 3) extracted as a result of the classification indicated that grassland, cropland, woodland, water bodies, forest land, bare land, urban/built-up and marsh areas were the dominant LCLU classes in the study period. The dominant LCLU classes that declined progressively over the study period were woodland, water bodies, grassland, forest land, and marsh areas. However, the highest decline was observed for woodland, which declined from 20.96% of the total area in 1986 to 16.75% in 2000 (i.e., declined by 20.09%), and then declined to 11.52% in 2018 (i.e., declined by 31.24%). The overall decrement of woodland was 45.05% between 1986 and 2018. Forest land decreased from 3.65% in 1986 to 2.52% in 2018. Marsh areas also decreased from 2.28% in 1986 to 1.80% in 2018. Grassland decreased from 26.77% in 1986 to 25.46% in 2018. Water bodies decreased from 17.21% in 1986 to 15.72% in 2018. During the last three decades (1986–2018), woodland, water bodies, forest land, marsh areas, and grassland all decreased, while cropland increased

continually and remarkably from 25.89% of the total land in 1986 to 37.21% in 2018. The aggregate area of bare land and urban/built-up, which constituted the smallest proportion of the study area (3.25%) in 1986 speed up its expansion to 3.65% in 2000 and further to 5.78% in 2018. On the other hand, a higher percent increment was indicated for urban/built-up by 34.79% from 1986 to 2000 and by 191.68%, from 2000 to 2018. The overall increment for urban/built-up was 293.14%. The higher increment for urban/built-up does not mean a more extensive area covered by urban/built; instead, it refers to the proportional increment observed during the study period. Moreover, cropland and bare land increased by 43.72% and 50.10% from 1986 to 2018, respectively.

Table 6. LCLU classes with their areas and changes (1986–2018)

LCLU Classes	LCLU area coverage						LCLUC between periods (Δ L)		
	1986		2000		2018		1986–2000	2000–2018	1986–2018
	Area (ha)	%	Area (ha)	%	Area (ha)	%		%	%
Cropland	209659.05	25.89	252820.35	31.22	301319.55	37.21	20.59	19.18	43.72
Bare land	23320.98	2.88	25538.76	3.15	35005.41	4.32	9.51	37.07	50.10
Urban/built-up	2997.63	0.37	4040.37	0.50	11784.87	1.46	34.79	191.68	293.14
Forest land	29549.34	3.65	26504.37	3.27	20368.35	2.52	-10.3	-23.15	-31.07
Grassland	216746.73	26.77	213019.29	26.31	206178.66	25.46	-1.72	-3.21	-4.88
Marsh areas	18495.27	2.28	17054.91	2.11	14577.21	1.80	-7.79	-14.53	-21.18
Water body	139326.84	17.21	135205.47	16.70	127309.95	15.72	-2.96	-5.84	-8.62
Woodland	169704.81	20.96	135617.13	16.75	93256.65	11.52	-20.09	-31.24	-45.05
Total	809800.65	100	809800.65	100	809800.65	100			

ES value dynamics (1986–2018)

The value of ES for each LCLU class and the total ES value for 1986, 2000 and 2018 were estimated with the modified ES value coefficients (Table 5) and the area covered by each LCLU class in the RVLRL of Ethiopia (Table 6). The finding indicated that the total ES value of the region was USD 1586.37×10^6 in 1986, USD 1513.3×10^6 in 2000 and USD 1390.32×10^6 in 2018 (Tables 7 and 8). The total ES value showed a reduction of about USD 196.04×10^6 from 1986 to 2018 (Tables 7 and 8; Fig. 2 and 3), mainly due to the decreased areas of water bodies, woodland, marsh areas, and forest land. Even though the ES value of cropland increased, such increments were so small as to counterbalance the decreases in ES value of water bodies, woodland, marsh areas, and forest land.

Due to the highest value coefficient of water bodies (Table 4), they produce the highest ES value compared to the rest of the LCLU categories. Next to water bodies, woodland also produces a high ES value during 1986 because of its large area, which covered 20.96% of the studied region (Tables 6 and 7). The value coefficient of the marsh areas was also similar to that of the water body, and it produces the second highest ES value in 2000 and 2018 followed by woodland. The sub-total ES value of water body, woodland and marsh covered more than 89.32% of the total value (Tables 7 and 8). Even though the value coefficient of the forest land was similar to that of woodland, because forest land covered a small area in the study region, it contributed to low ES value. The ES value for cropland and grassland is also low owing to the low ES

value coefficient (Table 7). Thus, the water body, woodland, and marsh LCLU categories were significant contributors to the ES value in the RVLRL of Ethiopia in the last three decades (Fig. 3).

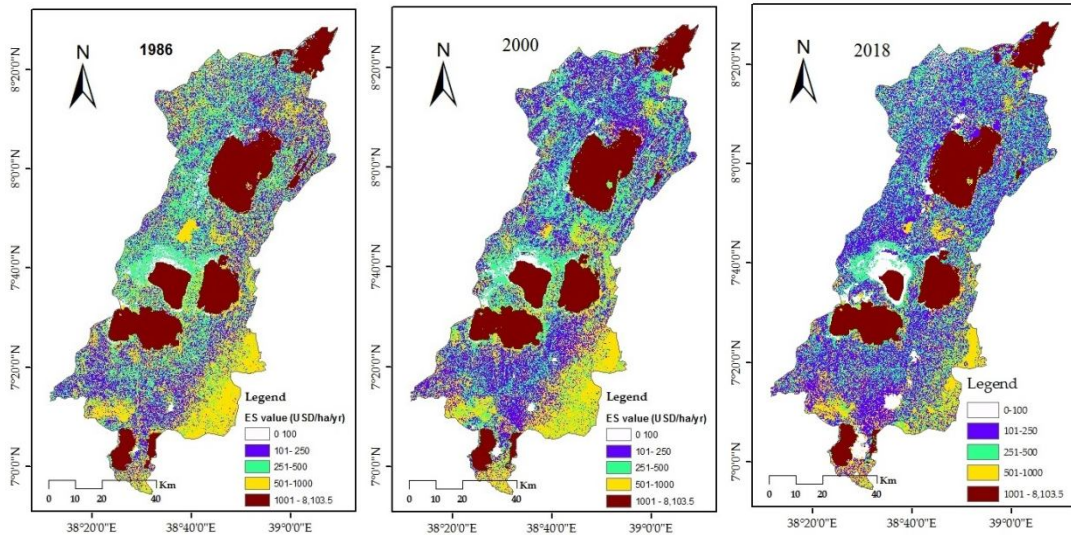


Figure 2. Spatial distribution of ES value in the RVLRL of Ethiopia in 1986, 2000 and 2018 using modified estimates adopted from (Kindu et al., 2016)

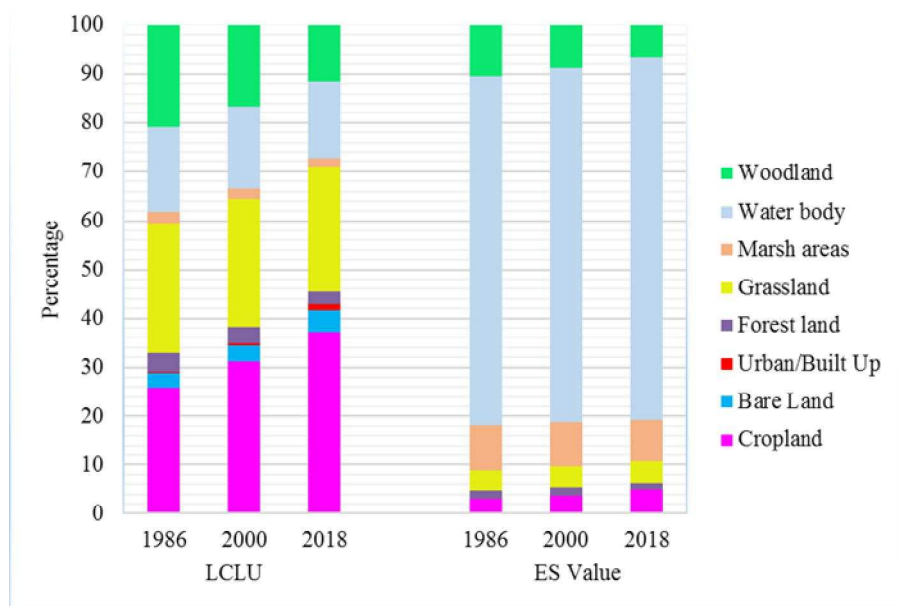


Figure 3. Proportions of LCLU (%) and ES value (%) for 1986, 2000 and 2018 in the RVLRL of Ethiopia

Table 8 estimates an annual value of 17 ES. Concerning their contribution to the overall ES value, individual ES value functions were ranked from 1 to 17 (Table 8). The top six individual ES value functions were predominantly from the ES category of regulating (water regulation, water treatment, erosion control, climate regulation),

provisioning (water supply and food production) for the study period (*Table 8*). Their combined contribution represented about USD 1488.11×10^6 , 1426.50×10^6 , and 1319.12×10^6 in 1986, 2000 and 2018, respectively. The combined contribution of other ES functions of each ES category, i.e. supporting (nutrient cycling, pollination, habitat/refugia and soil formation), regulating (biological control, gas regulation and disturbance regulation), provisioning (genetic resources), and cultural services (recreation and cultural), were about USD 98.25×10^6 (6.19%), USD 86.8×10^6 (5.74%), USD 71.21×10^6 (5.12%) in 1986, 2000 and 2018, respectively. This order of contribution by ES categories remained unchanged over the three study periods.

Table 7. Total ES values estimated for each LCLU categories and changes from 1986 to 2018 in the study area

LCLU Classes	ES value (USD million)					
	1986	2000	2018	1986–2000	2000–2018	1986–2018
Cropland	47.29	57.03	67.97	9.74	10.94	20.67
Bare Land	0.00	0.00	0.00	0.00	0.00	0.00
Urban/built-up	0.00	0.00	0.00	0.00	0.00	0.00
Forest land	29.16	26.15	20.10	-3.00	-6.05	-9.06
Grassland	63.56	62.47	60.46	-1.09	-2.01	-3.10
Marsh areas	149.88	138.20	118.13	-11.67	-20.08	-31.75
Water body	1129.04	1095.64	1031.66	-33.40	-63.98	-97.38
Woodland	167.45	133.81	92.02	-33.63	-41.80	-75.43

In general, the total regulatory services contributed to more than two-thirds (about 67%) of ES value, followed by provisioning (approximately 27%), supporting (approximately 2.48%), and cultural services (approximately 0.78%) (*Table 8*). During the period 1986–2000, the ES values of supporting services declined more rapidly than any other ES (-14.62%), followed by cultural (-5.23%) and regulating services (-5.10%).

The contribution of water regulation service to overall ES value was higher than 54% (the highest value), and cultural service was about 0.02% (the lowest value) (*Table 8*). The aggregate contributions of water regulation, water supply, water treatment, and food production, were more than 87% of the total ES value. During those three decades, the contribution of water regulation, water supply, and water treatment decreased, while the contribution of food production increased.

The change rate of each ecosystem functions was computed and the loss in ES value was observed in service functions of water regulation (USD 87.31×10^6), water supply (USD 34.42×10^6), erosion control (USD 21.29×10^6), water treatment (USD 19.44×10^6), climate regulation (USD 19.10×10^6), nutrient cycling (USD 15.79×10^6), raw materials (USD 4.39×10^6), and genetic resources (USD 3.51×10^6), while the gains observed in ES values were in food production (USD 12.59×10^6), biological control (USD 1.96×10^6) and pollination (USD 0.4×10^6). The aggregate contribution of food production, biological control, and pollination was less than 9%. The finding also indicated that dramatic expansion of cropland in the study landscape results in a consistent increment in the food production service function, though the increment was not drastic.

Table 8. Estimated value of ES function (ES value_t in USD million per year)

ES	ES value _{t1986}		ES value _{t2000}		ES value _{t2018}		Overall change	Rank
		%		%		%		
Provisioning services								
Water supply	335.70	21.16	323.63	21.39	301.28	21.67	-34.42	2
Food production	77.63	4.89	83.87	5.54	90.18	6.49	12.56	4
Raw material	10.21	0.64	8.31	0.55	5.82	0.42	-4.39	11
Genetic resources	8.17	0.51	6.65	0.44	4.66	0.34	-3.51	12
Regulating services								
Water regulation	861.19	54.29	830.67	54.89	773.88	55.66	-87.31	1
Water treatment	114.06	7.19	106.28	7.02	94.61	6.81	-19.44	3
Erosion control	55.10	3.47	45.90	3.03	33.82	2.43	-21.29	5
Climate regulation	44.43	2.80	36.15	2.39	25.34	1.82	-19.10	6
Biological control	10.02	0.63	10.97	0.72	11.97	0.86	1.96	9
Gas regulation	4.24	0.27	3.71	0.25	3.00	0.22	-1.25	13
Disturbance regulation	1.00	0.06	0.81	0.05	0.57	0.04	-0.43	16
Supporting services								
Nutrient cycling	36.74	2.32	29.90	1.98	20.95	1.51	-15.79	7
Pollination	9.80	0.62	10.04	0.66	10.20	0.73	0.40	10
Soil formation	2.21	0.14	1.83	0.12	1.34	0.10	-0.87	15
Habitat/refugia	3.45	0.22	2.80	0.19	1.97	0.14	-1.48	14
Cultural services								
Recreation	12.02	0.76	11.45	0.76	10.50	0.76	-1.52	8
Cultural	0.40	0.03	0.32	0.02	0.23	0.02	-0.17	17
Total ES value	1586.37	100	1513.30	100	1390.32	100	-196.04	

Variations of ES value in response to LCLUC and socioeconomic drivers

Figure 4 indicates a negative non-linear relationship ES value per capita and GDP per capita. Regional GDP per capita in constant year-1986 prices increased by 69.5%, from USD 233.82 in 1986 to USD 767.56 in 2018. At the same time, Regional ES value per capita reduced by 76.97%, from USD 2706.86 in 1986 to USD 623.45 in 2018. Moreover, Figure 5 indicates a polynomial decline in the ratio of total ES value to total GDP from 1986 to 2018.

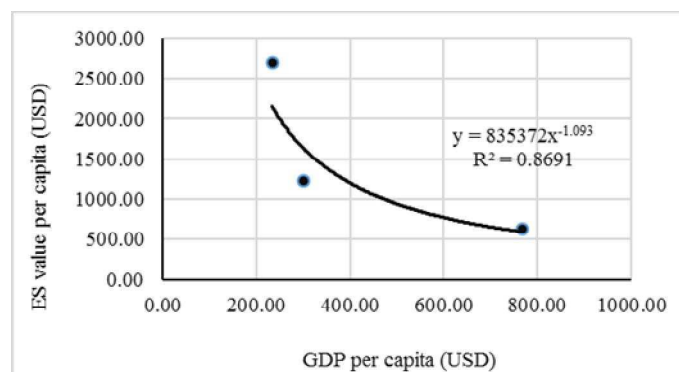


Figure 4. The relationship between ES value per capita and GDP per capita from 1986 to 2018

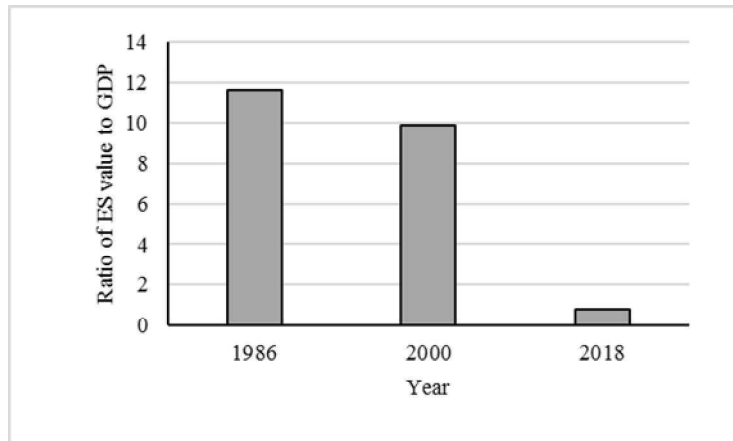


Figure 5. Changes in the ratio of total ES value to total GDP from 1986 to 2018

Additionally, both *Figures 4* and *5* indicate that rapid economic growth had a significantly negative impact on regional ESs. Similar to *Figure 2*, *Figures 6*, *7* and *8* indicate the ongoing trend of reduction in ES value per capita and total ES value with significant demographic growth and continual expansion of built-up land, cropland and bare land.

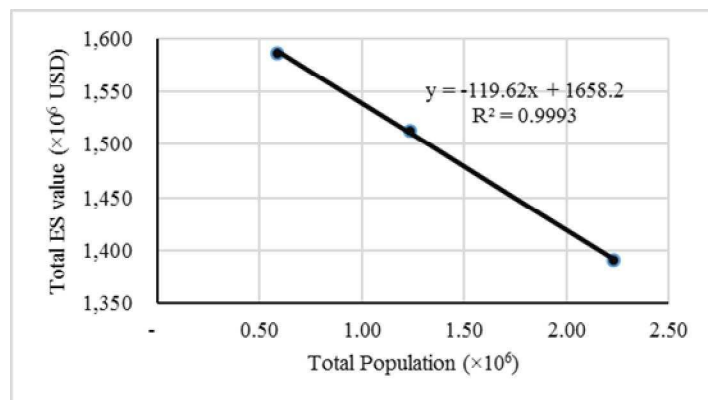


Figure 6. The relationship between total ES value and total regional population from 1986 to 2018

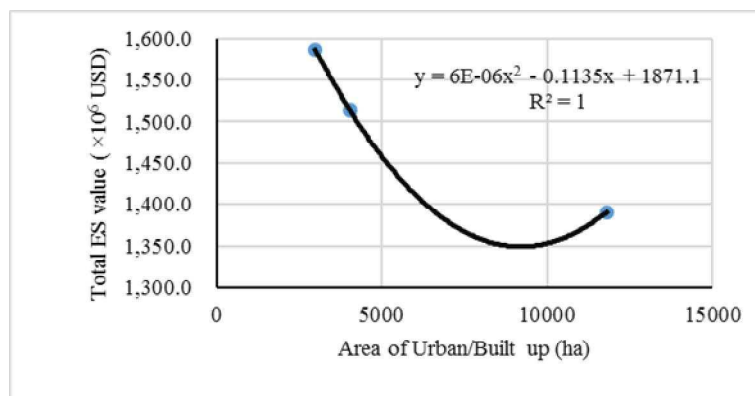


Figure 7. The relationship between ES value and area of urban/built-up from 1986 to 2018

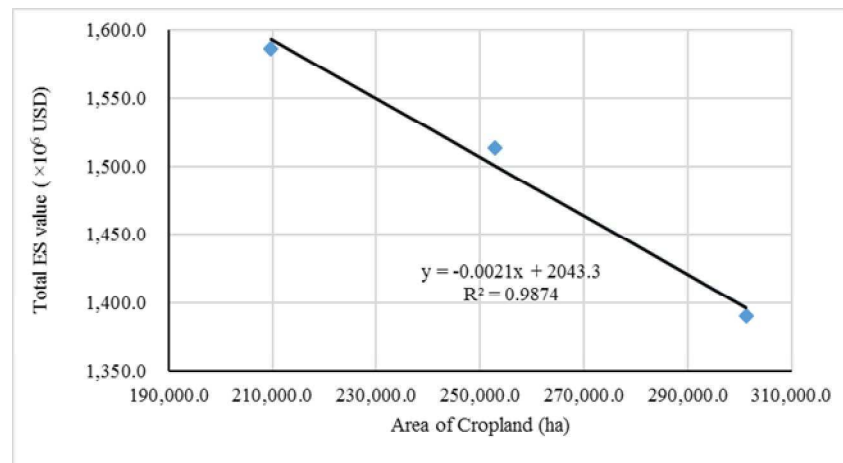


Figure 8. The relationship between total ES value and the area of cropland from 1986 to 2018

Discussion

Dynamics of LCLU and ES value change

In general, the area coverage of woodland, forest land, grassland, marsh areas, and water bodies consistently declined in varying proportions in the study period. The declines in these LCLU classes were mainly because of the conversion of the areas to cropland. The finding indicated that LCLUC is consistent with the results of previous research conducted in Ethiopia. For instance, the decline in woodland and the increase in cropland were also observed in Ziway-shalla basin (Bekele et al., 2018), Arsi-Negele district (Molla, 2015; Garedeu et al., 2009), Munessa–Shashemene landscapes (Kindu et al., 2013), Central Rift Valley (Meshesha et al., 2012) in 1973–2010, 1973–2006, 1973–2006 and 1973–2012, respectively. Moreover, Kindu et al. (2013) and Meshesha et al. (2012) also reported a decrease in water bodies and forest land.

The loss of ES value in the RVLRL of Ethiopia is predominantly due to the decreased areas of the water body, woodland, marsh areas, and forest land categories. According to *Table 6* and *Figure 3*, there was a significant rise in the area of cropland over the other LCLU categories from 209,659.05 ha in 1986 to 301,319.55 ha in 2018. Remarkably, this increment exceeds the extent of land that changed from cropland to other LCLU types. The increment in the area of cropland increased the value of ES over the study period, but such increments were so small as to counterbalance the decreases in the total ES value in water bodies, woodland and forest land.

The trend of changes in ES value conforms with other studies in Ethiopia and elsewhere. For instance, in the Munessa–Shashemene landscapes, Kindu et al. (2016) reported a decline in ES value from 1973 to 2013. Gashaw et al. (2018) estimated a massive loss of ES value of about 21.7% from 1986 to 2015 as a result of the altered forest, shrubland and grassland ecosystems in Andessa watershed, Ethiopia. Tolessa et al. (2017a) point out a cumulative decline of ES value of 40.7% from 1973 to 2015 in Chilimo Forest, Ethiopia, which was attributed to a reduction in forest cover. Another study by Tolessa et al. (2017b) also revealed an overall loss of 68% of ES value from 1973 to 2014 in Toke Kutaye district, Ethiopia, was mainly as a result of the loss of forest cover. A study mapping and quantifying ES in West Africa also reported an overall decline in ES value during 2000–2009 (Leh et al., 2013). Similarly, in Pingbian

County, China (Li et al., 2007) revealed a 19.4% decline of ES value during 1973–2004. San Antonio, Texas, (Kreuter et al., 2001) also reported a general decline of ES value of about USD 6×10^6 during 1976–1991. All these findings are in line with our finding that the dynamics of LCLU have resulted in a significant decline of ES value. On the other hand, an increase in ES values has been reported by studies in Ethiopia and elsewhere. For example, there were increases in the value of ES in Gedeo-Abay, Ethiopia (Temesgen et al., 2018), Ningxia, China (Wang et al., 2014), and Chengdu, China (Li et al., 2018) of 14.2% during 1986–2015, 22.7% during 2000–2010, and 75.46% during 2000–2015, respectively.

Specifically, the results of the study showed that the predominant types of LCLU by which the ES value in RVLRL were water body, marsh areas, and woodland, which contributed over 89% of the total values. For water bodies, the ES value accounted for 74.2% of the total value in 2018, which related to the high ES value coefficient in water bodies. According to Zhou et al. (2017), water bodies and wetlands were significant contributors to ES value, which covers more than 60% of the total, in Denqing, China during 1995–2015. The ES value of water bodies in the study region was high during the study period; however, its ES value was declining due to the degradation of the water environment, especially weak protection and rehabilitation of Feeder rivers, and water conservation in the study region. Bekele et al. (2018) noted the occurrence of severe lake water degradation in the region such as accelerated retreat of Lake Ziway and Lake Abiyata, drying /reduction of Rivers and Stream volumes (e.g., Bulbula River), huge water abstraction for irrigation (Raventós Vilalta, 2010; Legesse and Ayenew, 2006), and water pollution from the chemical intensified farming. The most apparent effect of water abstraction for trona or soda ash production during the last three decades, has been decline in the water level at Lake Abiyata (Legesse and Ayenew, 2006) and reduced about 50% of the area between 1973 and 2006 (Hengsdijk et al., 2009), which could forms as terminal lake of the closed Central Rift valley basin (Getnet et al., 2014).

The projected dynamics by Jansen et al. (2007) and Raventós Vilalta (2010) indicated that Lake Abiyata and Lake Ziway would continue to lose more than 10% of their area coverage until 2034. Studies also projected that Lake Abiyata would dry up within the coming five decades (Seyoum et al., 2015; Temesgen et al., 2013; Jansen et al., 2007). In line with this, unless rehabilitation and restoration actions are taken, the adjacent Lake Ziway also faces a similar fate of drying shortly (Bekele et al., 2018; Jansen et al., 2007) since it is an open lake connected to Lake Abiyata through Bulbula River. The lowering in the discharge of the Feeder River and the declining of the water level of Ziway Lake are owing to the development of recently irrigated land (Scholten, 2007). According to Jansen et al. (2007), Lake Ziway has declined by about 0.5 m since 2002 that is equivalent to a loss of approximately 200×10^6 cubic meters of water. Similarly, Lake Cheleka whose area coverage was 11.3 km² in 1973, was gone entirely in the year 2011, changed into swamp and mud flats, while Lake Hawasa showed an increment from 91.9 km² in 1973 to 95.2 km² in 2011, which is a rise of about 3.3 km² between 1973 and 2011 (Wondrade et al., 2014). However, early research works showed a relatively broad area cover estimates inclusive of Lake Cheleka. For example, 150 km² (Zanon, 1942 cited in Ayenew and Gebreegziabher, 2006). Moreover, a study by Bewketu (2010) revealed a decline in Lake Langanos' water level. This, in turn, constitutes a significant threat to biodiversity loss, especially fish and bird species besides a significant loss to ES value at large.

Therefore, protecting those LCLU classes that have high ES values is crucial for formulating a sustainable land use/cover policy, since this high ES value will help to maintain a sense of balance between ecosystem health and economic development in the future (Sawut et al., 2013). Similarly, Tianhong et al. (2010) suggested that land use planning should focus on LCLU classes with the highest ES value including water bodies, wetlands, and woodland.

The decline in the average ES value of the study region over the study period is because of the decline in water bodies, woodland, marsh areas and forest land and the expansion of cropland and urban/built-up areas. The calculated average ES value of the RVLRL is higher than in other studies such as in Kashgar Region, (Mamat et al., 2018), Andassa watershed (Gashaw et al., 2018), Gedeo–Abaya landscape (Temesgen et al., 2018), Munessa–Shashemene landscape (Kindu et al., 2016), Chillimo Forest (Tolessa et al., 2017a), Toke Kutaye district (Tolessa et al., 2017b), and Menglun (Hu et al., 2008) (Table 9). The high average ES value of the RVLRL could be attributed to the size of the water body, which cover more than 15% of the study region during the study period and high ES value coefficient for the water body. However, studies such as Wang et al. (2015) conducted in Nenjiang River Basin, Heilongjiang Province, Northeast China have shown higher average ES value as compared with our findings. If our study had employed the coefficient developed by Costanza et al. (1997) for a similar LCLU/biome (i.e. 8498 for water bodies, 2008 for woodland, 14,785 for marsh areas, 244 for grassland, 2008 for forest land and 92 for cropland) the overall ES value of the RVLRL would have been USD1929.73 in 1986, USD1801.91 in 2000, and USD1603.59 in 2018. Subsequently, the average ES value of the study region would have slightly increased to USD2383 in 1986, USD2225 in 2000, and USD1980 in 2018. Moreover, considering the coefficients developed by Temesgen et al. (2018) for similar biomes (i.e. 3226.8 for water bodies, 897 for woodland, 2856.1 for marsh areas, 355.5 for grassland, 1093.2 for forest land and 169.2 for cropland) the overall ES value of the RVLRL would have been USD 799.46 in 1986, USD754.12 in 2000, and USD682.64 in 2018. Subsequently, the average ES value of the study region would have dropped to USD987.2 in 1986, USD931.2 in 2000, and USD843.0 in 2018.

The reduction of most ES value functions during the study period is highly related to the decline in water bodies, marsh areas, woodland, and grassland. In line with this finding, a decline in the aquatic regions, grassland, and woodland between 2003 and 2013 period in Manas River Basin, China has caused a drop in the value of gas regulation, climate regulation and various types of ES value functions (Wang et al., 2017).

In this research, the consistent increase in food production, biological control, and pollination services over the study period is undoubtedly attributed to the expansion of cropland. The cropland category gained areas, which is negatively affecting the overall ES value for the study region. In the future, cropland area and the associated ES value will likely increase because of the increased need for food production to meet the growing population (WorldBank, 2019). These dynamics hurt the ES offered by other LCLU categories such as water bodies, woodland, marsh areas, grassland, and forest land. For example, the conversion of woodland and forest land to cropland is a negative factor affecting the provision of several ES, such as erosion control, which is a severe problem in the study region. It is evident that LCLU dynamics in Ethiopia has resulted in severe soil erosion and land deterioration, which in turn threaten food security and cause economic and social problems across the country (Zeleeke and Hurni, 2001). On

the other hand, loss of vegetation cover and deforestation induce erosion, and the deposition of nutrients and sediment accounts for the eutrophication in Lake Abiyata, which is already killing fish and other aquatic organisms inhabiting (Ayenew, 2007).

Table 9. The estimated average ES value of the selected studies and own estimation that was calculated using Equation 4 with the available data from the respective studies

Study location	Area	Year	ES value (USD × 10 ⁶)	Average ES value of the land (USD ha ⁻¹ yr ⁻¹)	Reference
Kashgar Region, Northwest China	11,350,200	1985	10,845.3	955.5	Mamat et al. (2018)
		2005	10,291.7	906.7	
		2015	10,127.3	892.3	
Andassa watershed, Upper Blue Nile basin, Ethiopia	58,760	1985	26.83	457	Gashaw et al. (2018)
		2000	22.58	384	
		2015	21	357	
Gedeo_Abaya landscape, Southeastern rift escarpment of Ethiopia	184,794.4	1986	129	698	Temesgen et al. (2018)
		2000	145	785	
		2015	147.3	797	
Toke Kutaye district, West Shewa zone of Oromia National Regional State, Central highlands of Ethiopia	72,697.2	1984	33.93	467	Tolessa et al. (2017b)
		2000	28.22	388	
		2014	16.71	230	
Munessa–Shashemene landscape, Central highlands of Ethiopia	103,675	1986	118.5	1143	Kindu et al. (2016)
		2000	114.8	1107	
		2012	111.1	1072	
Chillimo Forest, Dendi district of Oromia National Regional State, Ethiopia	7687.26	1986	7.66	996	Tolessa et al. (2017a)
		2001	6.4	833	
		2015	5.37	699	
Menglun, Xishuangbanna, Southwest China	33,488.34	1988	41.2	1230	Hu et al. (2008)
		2006	29.773	889	
Nenjiang River Basin, Heilongjiang Province, Northeast China	29,420,000	1980	99,940	3397	Wang et al. (2015)
		2005	97,510	3314	
Rift Valley Lakes Region, Ethiopia	809,800.65	1986	1586.37	1959	Own data
		2000	1513.3	1869	
		2018	1390.32	1717	

Woodland and forest land provide services such as raw materials, food production, gas regulation, water regulation, water treatment, and recreation. However, this study confirmed the massive conversion of these LCLU categories to cropland during the study period. According to Arndt et al. (2011), the most common farming system in Ethiopia is small-scale subsistence rain-fed farming, which accounts for 90% of the country's agricultural output. Farming in the country was characterised with a low level of productivity due to a lack of production technologies, weak extension services, low use of improved seed, and minimal application of pesticides and fertilisers (Deressa, 2007). Consequently, to increase agricultural production, small farms expand their growing area by converting other LCLU categories to cropland. Similar to this finding,

the increment in the intensity of cultivated land was attributed to the decline in the woodland and forest land categories between 1973 and 2006 in the Central Rift Valley, Ethiopia (Meshesha et al., 2012). A study by Kibret et al. (2016) also revealed that agricultural land is expanding to the maximum suitable size, even to the peripheral land, thus endangering biodiversity. Also, the conversion of marsh areas to cropland is a negative factor regarding the provision of several ES, such as water regulation, water supply, water treatment, and recreation services, which is a prevalent problem in the RVL. Therefore, changing the widely employed traditional farming system through the improved farming technologies would play an important role in intensifying the productivity of the cropland thereby increasing agricultural production rather than converting other LCLUC classes to cropland.

Limitation of the study

The method of employing LCLUC in estimating ES value for the period 1986–2018 includes various sources of limitation. The primary constraint of this research is related to the accuracy of the LCLU classification. The LCLU classification of 1986, 2000, and 2018 was attained with an overall accuracy of 80.05%, 81.82% and 80.37%, and kappa coefficient of 0.77, 0.76, and 0.74 (Table 3), respectively. Although the classification result meets the standard requirement (kappa coefficient higher than 0.70) (Monserud, 1990), there are still some limitations that are associated with the classification. There are also limitations from the adopted benefit transfer approach, such as considering all biomes/LCLU classes as a similar unit and using the same ES value coefficient derived from another site as an average unit value. This approach presumes the sameness of ESs values within the whole biomes/LCLU classes (Arowolo et al., 2018). Although there are drawbacks, this approach is often the only or the best option available for policy analysts and resource managers when time, information accessibility, or other difficulties prevent the usage of primary studies. Furthermore, funding limitations for gathering the primary data in developing countries such as Ethiopia often make benefit transfer is the sole feasible option.

Moreover, numerous studies used the coefficient of sensitivity approach to check the reliability of the ES value estimations, and mostly the value coefficients of ES value were corrected by $\pm 50\%$, (e.g. Hu et al., 2008; Temesgen et al., 2018; Tolessa et al., 2017a; Yirsaw et al., 2017). Nevertheless, employing this approach to test the reliability of evaluation results is disapproved of since the value of the coefficient of sensitivity is often less than 1 even when the values of the coefficients of sensitivity were corrected by $\pm 25\%$, which implies incorrectly robust coefficients (Aschonitis et al., 2016). Thus, this study did not conduct a coefficient of sensitivity analysis to check the validity of the estimation with another approach. Hence, another reliable approach that accounts the uncertainty needs to be considered. However, this study will contribute to the development of scientific literature on a similar topic to scrutinise how ES value is altering in response to the existing LCLUC.

Research of this kind is limited in many regions of Africa, which has resulted in a lack of information for decision making procedure about resource conservation and sustainable utilisation. It could also be used in data-short areas of developing regions with a similar landscape. Therefore, the findings of this study will offer regional-scale information to be added to global values for decision-making procedures. Besides the local level estimation, this study also emphasises the importance of regional-level and

country-level ES value estimation based on expert knowledge of the region for better estimation of the LCLU/biome.

Conclusions

This study provides estimations of the ES value alteration in response to the dynamics of LCLU in the Rift Valley Lakes region of Ethiopia. The dynamics of LCLU over the past 33 years have resulted in a decline in the specific and overall ES value. Our estimation of the ES value alteration in response to LCLUC has indicated an overall reduction of approximately USD 5.77×10^6 per year, or a total loss of about 12.4% over the last 33 years. These changes are mostly associated with the decreased areas of the water body, woodland, marsh areas, forest land, and grassland categories. However, cropland has experienced a dramatic expansion by 43.72% during the study period. The estimation of lost ES value is about 9.5 times larger than the whole value of cropland in the study area. Water bodies, woodland and marsh areas were the three major contributors to the ES value in the RVLR of Ethiopia, contributing more than 89.32% of the overall ES value in 2018, indicating that these LCLU classes play an essential role in the ES of the study area.

LCLUC in the RVLR of Ethiopia affects the supply of ES, including water regulation, water supply, water treatment, and food production, erosion control, climate regulation, nutrient cycling, recreation, raw material, genetic resources, gas regulation, habitat/refugia, soil formation, disturbance regulation, and cultural service function. However, as a result of the dramatic expansion of cropland, the worth of food production, biological control, and pollination service function has invariably increased, though not drastically, over the study period. Except for these three ES functions, all other values have been decreasing continuously over the last three decades, indicating the deterioration of the fragile Rift Valley ecosystem.

In this research, the loss of ES value in RVLR was attributed to the dynamics of LCLU, which can impede the ability of the ecosystem to offer sustainable ES, possibly causing a long-term deterioration of the natural environment quality. In other words, these changes signify severe environmental repercussions for the fragile RVLR ecosystem. To enhance the continuous supply of ES, management should focus on LCLU classes with the highest ES values. Moreover, a nation-wide food security strategy of boosting crop production should work towards sustainable agricultural intensification rather than expanding cropland at the expense of the other LCLU classes. Hence, to improve the continuous supply of ES and economic development, an integrated approach to managing land and water resources needs to be considered. Furthermore, designing and operating a payment scheme for ES at the regional and local is also a potential remedy for ES loss. Moreover, quantitative assessment of ES value at local and regional scales should be considered as a conservation strategy to encourage resource conservation and utilisation.

Acknowledgements. The authors are pleased to acknowledge the financial support from the National Natural Sciences Foundation of China (Fund No. 41571176). The first author thanks Chinese Government Scholarship Council (CSC) for granting scholarship.

Conflict of interests. The authors declare no conflict of interests.

REFERENCES

- [1] Alarcon, G., Antônio dos Santos de Freitas, L., Oliveira da Fountoura, G., Ximenes de Macedo, C., Casarin Ribeiro, D. (2016): The challenges of implementing a legal framework for Payment for Ecosystem Services in Santa Catarina, Brazil. – *Natureza & conservação revista brasileira de conservação da natureza* 14(2). DOI: 10.1016/j.ncon.2016.05.003.
- [2] Arndt, C., Robinson, S., Willenbockel, D. (2011): Ethiopia's growth prospects in a changing climate: A stochastic general equilibrium approach. – *Global Environmental Change* 21(2): 701-710.
- [3] Arowolo, A. O., Deng, X., Olatunji, O. A., Obayelu, A. E. (2018): Assessing changes in the value of ecosystem services in response to land-use/land-cover dynamics in Nigeria. – *Science of the Total Environment* 636: 597-609.
- [4] Aschonitis, V., Gaglio, M., Castaldelli, G., Fano, E. (2016): Criticism on elasticity-sensitivity coefficient for assessing the robustness and sensitivity of ecosystem services values. – *Ecosystem Services* 20: 66-68.
- [5] Ayenew, T. (2004): Environmental implications of changes in the levels of lakes in the Ethiopian Rift since 1970. – *Regional Environmental Change* 4(4): 192-204. DOI: 10.1007/s10113-004-0083-x.
- [6] Ayenew, T. (2007): Water management problems in the Ethiopian rift: challenges for development. – *Journal of African Earth Sciences* 48(2-3): 222-236.
- [7] Ayenew, T., Gebreegziabher, Y. (2006): Application of a spreadsheet hydrological model for computing the long-term water balance of Lake Awassa, Ethiopia. – *Hydrological Sciences Journal* 51(3): 418-431.
- [8] Bartkowski, B. (2017): Are diverse ecosystems more valuable? Economic value of biodiversity as result of uncertainty and spatial interactions in ecosystem service provision. – *Ecosystem Services* 24: 50-57.
- [9] Baveye, P., Baveye, J., Gowdy, J. (2013): Monetary valuation of ecosystem services: it matters to get the timeline right. – *Ecological Economics* 95: 231-235. DOI: 10.1016/j.ecolecon.2013.09.009.
- [10] Bekele, B., Wu, W., Legesse, A., Temesgen, H., Yirsaw, E. (2018): Socio-environmental impacts of land use/cover change in Ethiopian central rift valley lakes region, East Africa. – *Applied Ecology and Environmental Research* 16(5): 6607-6632. DOI: 10.15666/aeer/1605_66076632.
- [11] Bewketu, K. (2010): Hydrodynamics of selected Ethiopian Rift Lakes. – Unpublished MSc Thesis, Addis Ababa University, Ethiopia. [http://etdaau.edu.et/dspace/bitstream/123456789/2767/1/Kassaye% 20Bewketu pdf](http://etdaau.edu.et/dspace/bitstream/123456789/2767/1/Kassaye%20Bewketu.pdf).
- [12] Boakye, E., Odai, S., Adjei, K., Annor, F. (2008): Landsat images for assessment of the impact of land use and land cover changes on the Barekese catchment in Ghana. – *European Journal of Scientific Research* 22(2): 269-278.
- [13] Braat, L. C., de Groot, R. (2012): The ecosystem services agenda: bridging the worlds of natural science and economics, conservation and development, and public and private policy. – *Ecosystem Services* 1(1): 4-15.
- [14] Cabral, P., Feger, C., Levrel, H., Chambolle, M., Basque, D. (2016): Assessing the impact of land-cover changes on ecosystem services: a first step toward integrative planning in Bordeaux, France. – *Ecosystem Services* 22: 318-327.
- [15] Chang, Y., Hou, K., Li, X., Zhang, Y., Chen, P. (2018): Review of land use and land cover change research progress. – *IOP Conference Series: Earth and Environmental Science* 113(1): 012087.
- [16] Chen, M., Lu, Y., Ling, L., Wan, Y., Luo, Z., Huang, H. (2015): Drivers of changes in ecosystem service values in Ganjiang upstream watershed. – *Land Use Policy* 47: 247-252.

- [17] Congalton, R. G. (1991): A review of assessing the accuracy of classifications of remotely sensed data. – *Remote Sensing of Environment* 37(1): 35-46.
- [18] Costanza, R., d’Arge, R., De Groot, R., Farber, S., Grasso, M., Hannon, B., Limburg, K., Naeem, S., O’neill, R. V., Paruelo, J. (1997): The value of the world’s ecosystem services and natural capital. – *Nature* 387(6630): 253-260.
- [19] Costanza, R., de Groot, R., Sutton, P., van der Ploeg, S., Anderson, S. J., Kubiszewski, I., Farber, S., Turner, R. K. (2014): Changes in the global value of ecosystem services. – *Global Environmental Change* 26: 152-158.
- [20] CSA (2013): Population Projection of Ethiopia for All Regions at Wereda Level from 2014-2017. – Central Statistical Agency, Ethiopia.
- [21] Daily, G. C. (1997): *Nature’s Services: Societal Dependence on Natural Ecosystems*. – Islands Press, Washington, DC.
- [22] de Bello, F., Lavorel, S., Díaz, S., Harrington, R., Cornelissen, J. H. C., Bardgett, R. D., Berg, M. P., Cipriotti, P., Feld, C. K., Hering, D., Martins da Silva, P., Potts, S. G., Sandin, L., Sousa, J. P., Storkey, J., Wardle, D. A., Harrison, P. A. (2010): Towards an assessment of multiple ecosystem processes and services via functional traits. – *Biodiversity and Conservation* 19(10): 2873-2893. DOI: 10.1007/s10531-010-9850-9.
- [23] de Francisco, J. C. R., Hellegers, I. P., Hengsdijk, H., Weikard, H. P. (2008): Preconditions for a Payment for Environmental Services establishment at Central Rift Valley, Ethiopia. – Environmental Economics and Natural Resources Group, Department of Environmental Sciences, Wageningen University.
- [24] de Groot, R., Brander, L., van der Ploeg, S., Costanza, R., Bernard, F., Braat, L., Christie, M., Crossman, N., Ghermandi, A., Hein, L., Hussain, S., Kumar, P., McVittie, A., Portela, R., Rodriguez, L. C., ten Brink, P., van Beukering, P. (2012): Global estimates of the value of ecosystems and their services in monetary units. – *Ecosystem Services* 1(1): 50-61. DOI: <https://doi.org/10.1016/j.ecoser.2012.07.005>.
- [25] Deressa, T. T. (2007): Measuring the economic impact of climate change on Ethiopian agriculture. – World Bank Policy Research Working Paper No. 4342.
- [26] Egoh, B., Reyers, B., Rouget, M., Bode, M., Richardson, D. M. (2009): Spatial congruence between biodiversity and ecosystem services in South Africa. – *Biological Conservation* 142(3): 553-562. DOI: <https://doi.org/10.1016/j.biocon.2008.11.009>.
- [27] Fedele, G., Locatelli, B., Djoudi, H., Colloff, M. J. (2018): Reducing risks by transforming landscapes: Cross-scale effects of land-use changes on ecosystem services. – *PloS One* 13(4): e0195895.
- [28] Foley, J. A., DeFries, R., Asner, G. P., Barford, C., Bonan, G., Carpenter, S. R., Chapin, F. S., Coe, M. T., Daily, G. C., Gibbs, H. K. (2005): Global consequences of land use. – *Science* 309(5734): 570-574.
- [29] Garedew, E., Sandewall, M., Söderberg, U., Campbell, B. M. (2009): Land-use and land-cover dynamics in the Central Rift Valley of Ethiopia. – *Environmental Management* 44(4): 683-694.
- [30] Gashaw, T., Tulu, T., Argaw, M., Worqlul, A. W. (2017): Evaluation and prediction of land use/land cover changes in the Andassa watershed, Blue Nile Basin, Ethiopia. – *Environmental Systems Research* 6(1): 17.
- [31] Gashaw, T., Tulu, T., Argaw, M., Worqlul, A. W., Tolessa, T., Kindu, M. (2018): Estimating the impacts of land use/land cover changes on Ecosystem Service Values: The case of the Andassa watershed in the Upper Blue Nile basin of Ethiopia. – *Ecosystem Services* 31: 219-228.
- [32] Gebrehiwot, S. G., Bewket, W., Gärdenäs, A. I., Bishop, K. (2014): Forest cover change over four decades in the Blue Nile Basin, Ethiopia: comparison of three watersheds. – *Regional Environmental Change* 14(1): 253-266.
- [33] Gebretsadik, H. Y. (2016): Towards an optimal integrated reservoir system management for the Awash River Basin, Ethiopia. – *Proceedings of the International Association of Hydrological Sciences* 373: 215.

- [34] Getnet, M., Hengsdijk, H., van Ittersum, M. (2014): Disentangling the impacts of climate change, land use change and irrigation on the Central Rift Valley water system of Ethiopia. – *Agricultural Water Management* 137: 104-115.
- [35] Hengsdijk, H., Jansen, H. (2006): *Agricultural Development in the Central Ethiopian Rift Valley: A Desk-Study on Water-Related Issues and Knowledge to Support a Policy Dialogue*. – Plant Research International B.V., Wageningen.
- [36] Hengsdijk, H., Groot, A., van Driel, L., Jembere, K., van Uum, J., Boone, P. (2009): Towards a sustainable future of the western shoreline of Lake Ziway. – *Participatory Land Use Plan Development Workshop, Ziway, December 1-4, 2008*. Plant Research International.
- [37] Hu, H., Liu, W., Cao, M. (2008): Impact of land use and land cover changes on ecosystem services in Menglung, Xishuangbanna, Southwest China. – *Environmental Monitoring and Assessment* 146(1): 147-156.
- [38] Jacobs, S., Dendoncker, N., Martín-López, B., Barton, D. N., Gomez-Baggethun, E., Boeraeve, F., McGrath, F. L., Vierikko, K., Geneletti, D., Sevecke, K. J. (2016): A new valuation school: Integrating diverse values of nature in resource and land use decisions. – *Ecosystem Services* 22: 213-220.
- [39] Jansen, H., Hengsdijk, H., Legesse, D., Ayenew, T., Hellegers, P., Spliethoff, P. (2007): *Land and Water Resources Assessment in the Ethiopian Central Rift Valley*. – Project: Ecosystems for Water, Food And Economic Development in the Ethiopian Central Rift Valley, Alterra.
- [40] Kibret, K. S., Marohn, C., Cadisch, G. (2016): Assessment of land use and land cover change in South Central Ethiopia during four decades based on integrated analysis of multi-temporal images and geospatial vector data. – *Remote Sensing Applications: Society and Environment* 3: 1-19.
- [41] Kindu, M., Schneider, T., Teketay, D., Knoke, T. (2013): Land use/land cover change analysis using object-based classification approach in Munessa-Shashemene landscape of the Ethiopian highlands. – *Remote Sensing* 5(5): 2411-2435. DOI: doi.org/10.3390/rs5052411.
- [42] Kindu, M., Schneider, T., Teketay, D., Knoke, T. (2016): Changes of ecosystem service values in response to land use/land cover dynamics in Munessa–Shashemene landscape of the Ethiopian highlands. – *Science of the Total Environment* 547: 137-147. DOI: <https://doi.org/10.1016/j.scitotenv.2015.12.127>.
- [43] Kramer, R. A., Richter, D. D., Pattanayak, S., Sharma, N. P. (1997): Ecological and Economic Analysis of Watershed Protection in Eastern Madagascar. – *Journal of Environmental Management* 49(3): 277-295. DOI: <https://doi.org/10.1006/jema.1995.0085>.
- [44] Kreuter, U. P., Harris, H. G., Matlock, M. D., Lacey, R. E. (2001): Change in ecosystem service values in the San Antonio area, Texas. – *Ecological Economics* 39(3): 333-346. DOI: [https://doi.org/10.1016/S0921-8009\(01\)00250-6](https://doi.org/10.1016/S0921-8009(01)00250-6).
- [45] Kubiszewski, I., Costanza, R., Anderson, S., Sutton, P. (2017): The future value of ecosystem services: global scenarios and national implications. – *Ecosystem Services* 26: 289-301.
- [46] Kubiszewski, I., Costanza, R., Dorji, L., Thoennes, P., Tshering, K. (2013): An initial estimate of the value of ecosystem services in Bhutan. – *Ecosystem Services* 3: e11-e21.
- [47] Legesse, D., Ayenew, T. (2006): Effect of improper water and land resource utilization on the central Main Ethiopian Rift lakes. – *Quaternary International* 148(1): 8-18.
- [48] Legesse, D., Vallet-Coulomb, C., Gasse, F. (2004): Analysis of the hydrological response of a tropical terminal lake, Lake Abiyata (Main Ethiopian Rift Valley) to changes in climate and human activities. – *Hydrological Processes* 18(3): 487-504. DOI: [10.1002/hyp.1334](https://doi.org/10.1002/hyp.1334).

- [49] Leh, M. D., Matlock, M. D., Cummings, E. C., Nalley, L. L. (2013): Quantifying and mapping multiple ecosystem services change in West Africa. – *Agriculture, Ecosystems & Environment* 165: 6-18. DOI: 10.1016/j.agee.2012.12.001.
- [50] Li, R.-Q., Dong, M., Cui, J.-Y., Zhang, L.-L., Cui, Q.-G., He, W.-M. (2007): Quantification of the impact of land-use changes on ecosystem services: a case study in Pingbian County, China. – *Environmental Monitoring and Assessment* 128(1): 503-510. DOI: 10.1007/s10661-006-9344-0.
- [51] Li, Y., Zhan, J., Liu, Y., Zhang, F., Zhang, M. (2018): Response of ecosystem services to land use and cover change: a case study in Chengdu City. – *Resources, Conservation and Recycling* 132: 291-300.
- [52] Liang, J., Zhong, M., Zeng, G., Chen, G., Hua, S., Li, X., Yuan, Y., Wu, H., Gao, X. (2017): Risk management for optimal land use planning integrating ecosystem services values: A case study in Changsha, Middle China. – *Science of the Total Environment* 579: 1675-1682.
- [53] Lin, X., Xu, M., Cao, C., P Singh, R., Chen, W., Ju, H. (2018): Land-use/land-cover changes and their influence on the ecosystem in Chengdu city, China during the period of 1992–2018. – *Sustainability* 10(10): 3580.
- [54] Liu, S., Costanza, R., Troy, A., D’Aagostino, J., Mates, W. (2010): Valuing New Jersey’s ecosystem services and natural capital: a spatially explicit benefit transfer approach. – *Environmental Management* 45(6): 1271-1285. DOI: 10.1007/s00267-010-9483-5.
- [55] Locatelli, B., Lavorel, S., Sloan, S., Tappeiner, U., Geneletti, D. (2017): Characteristic trajectories of ecosystem services in mountains. – *Frontiers in Ecology and the Environment* 15(3): 150-159.
- [56] Mamat, A., Halik, Ü., Rouzi, A. (2018): Variations of ecosystem service value in response to land-use change in the Kashgar Region, Northwest China. – *Sustainability* 10(1): 200.
- [57] MEA (2005): *Ecosystems and Human Well-Being*. – Island Press, Washington DC.
- [58] Meshesha, D. T., Tsunekawa, A., Tsubo, M. (2012): Continuing land degradation: cause-effect in Ethiopia’s Central Rift Valley. – *Land Degradation & Development* 23(2): 130-143. DOI: 10.1002/ldr.1061.
- [59] Molla, M. B. (2015): Land use/land cover dynamics in the Central Rift Valley region of Ethiopia: case of Arsi Negele District. – *African Journal of Agricultural Research* 10(5): 434-449.
- [60] Monserud, R. (1990): *Methods for Comparing Global Vegetation Maps*. – Report WP-90-40. IIASA, Laxenburg.
- [61] Mosammam, H. M., Nia, J. T., Khani, H., Teymouri, A., Kazemi, M. (2017): Monitoring land use change and measuring urban sprawl based on its spatial forms: the case of Qom city. – *The Egyptian Journal of Remote Sensing and Space Science* 20(1): 103-116.
- [62] Mwampamba, T. H., Abrams, R. W., Awoyemi, S., Babalola, F. D., Borokini, T. I., Egoh, B., Rguibi Idrissi, H., Koussa, T., Nganje, M., O’Leary, J. (2016): The implications of globalization for conservation in Africa. – *African Journal of Ecology* 54(2): 133-135.
- [63] Nelson, E., Mendoza, G., Regetz, J., Polasky, S., Tallis, H., Cameron, D., Chan, K., Daily, G. C., Goldstein, J., Kareiva, P. M. (2009): Modeling multiple ecosystem services, biodiversity conservation, commodity production, and tradeoffs at landscape scales. – *Frontiers in Ecology and the Environment* 7(1): 4-11.
- [64] Niquisse, S., Cabral, P. (2018): Assessment of changes in ecosystem service monetary values in Mozambique. – *Environmental Development* 25: 12-22.
- [65] Nishizaki, N. (2004): Resisting imposed wildlife conservation: Arssi Oromo and the Senkelle Swayne’s Hartebeest sanctuary, Ethiopia. – *African Study Monographs* 25(2): 61-77.
- [66] Polasky, S., Nelson, E., Pennington, D., Johnson, K. A. (2011): The impact of land-use change on ecosystem services, biodiversity and returns to landowners: a case study in the state of Minnesota. – *Environmental and Resource Economics* 48(2): 219-242.

- [67] Raventós Vilalta, E. (2010): Water resources management in the Central Rift Valley in Ethiopia. – MSc Thesis. Universitat Politècnica Catalunya, Spain.
- [68] Reid, R. S., Kruska, R. L., Muthui, N., Taye, A., Wotton, S., Wilson, C. J., Mulatu, W. (2000): Land-use and land-cover dynamics in response to changes in climatic, biological and socio-political forces: the case of southwestern Ethiopia. – *Landscape Ecology* 15(4): 339-355.
- [69] Rodríguez, J. P., Beard Jr, T. D., Bennett, E. M., Cumming, G. S., Cork, S. J., Agard, J., Dobson, A. P., Peterson, G. D. (2006): Trade-offs across space, time, and ecosystem services. – *Ecology and Society* 11(1).
- [70] Rolfe, J., Johnston, R. J., Rosenberger, R. S., Brouwer, R. (2015): Introduction: Benefit Transfer of Environmental and Resource Values. – In: Johnston, R. J., Rolfe, J., Rosenberger, R. S., Brouwer, R. (eds.) *Benefit Transfer of Environmental and Resource Values: A Guide for Researchers and Practitioners*. Springer Netherlands, Dordrecht, pp. 3-17. DOI: 10.1007/978-94-017-9930-0_1.
- [71] Satz, D., Gould, R. K., Chan, K. M., Guerry, A., Norton, B., Satterfield, T., Halpern, B. S., Levine, J., Woodside, U., Hannahs, N. (2013): The challenges of incorporating cultural ecosystem services into environmental assessment. – *Ambio* 42(6): 675-684.
- [72] Sawut, M., Eziz, M., Tiyyip, T. (2013): The effects of land-use change on ecosystem service value of desert oasis: a case study in Ugan-Kuqa River Delta Oasis, China. – *Canadian Journal of Soil Science* 93(1): 99-108.
- [73] Schirpke, U., Kohler, M., Leitinger, G., Fontana, V., Tasser, E., Tappeiner, U. (2017): Future impacts of changing land-use and climate on ecosystem services of mountain grassland and their resilience. – *Ecosystem Services* 26: 79-94.
- [74] Scholten, W. (2007): Agricultural development and water use in the Central Rift Valley of Ethiopia: a rapid appraisal. – Internship Report, University of Twente, The Netherlands.
- [75] Schröter, D., Cramer, W., Leemans, R., Prentice, I. C., Araújo, M. B., Arnell, N. W., Bondeau, A., Bugmann, H., Carter, T. R., Gracia, C. A. (2005): Ecosystem service supply and vulnerability to global change in Europe. – *Science* 310(5752): 1333-1337.
- [76] Schulz, J. J., Cayuela, L., Echeverria, C., Salas, J., Rey Benayas, J. M. (2010): Monitoring land cover change of the dryland forest landscape of Central Chile (1975–2008). – *Applied Geography* 30(3): 436-447. DOI: <https://doi.org/10.1016/j.apgeog.2009.12.003>.
- [77] Seppelt, R., Dormann, C. F., Eppink, F. V., Lautenbach, S., Schmidt, S. (2011): A quantitative review of ecosystem service studies: approaches, shortcomings and the road ahead. – *Journal of applied Ecology* 48(3): 630-636. DOI: 10.1111/j.1365-2664.2010.01952.x.
- [78] Seyoum, W. M., Milewski, A. M., Durham, M. C. (2015): Understanding the relative impacts of natural processes and human activities on the hydrology of the Central Rift Valley lakes, East Africa. – *Hydrological processes* 29(19): 4312-4324.
- [79] Song, W., Deng, X. (2017): Land-use/land-cover change and ecosystem service provision in China. – *Science of the Total Environment* 576: 705-719.
- [80] Sutton, P. C., Anderson, S. J., Costanza, R., Kubiszewski, I. (2016): The ecological economics of land degradation: Impacts on ecosystem service values. – *Ecological Economics* 129: 182-192.
- [81] Tadesse, G., Zavaleta, E., Shennan, C., Fitzsimmons, M. (2014): Local ecosystem service use and assessment vary with socio-ecological conditions: a case of native coffee-forests in southwestern Ethiopia. – *Human Ecology* 42(6): 873-883. DOI: 10.1007/s10745-014-9704-2.
- [82] Teferi, E., Uhlenbrook, S., Bewket, W., Wenninger, J., Simane, B. (2010): The use of remote sensing to quantify wetland loss in the Choke Mountain range, Upper Blue Nile basin, Ethiopia. – *Hydrology and Earth System Sciences* 14(12): 2415-2428.

- [83] Temesgen, H., Nyssen, J., Zenebe, A., Haregeweyn, N., Kindu, M., Lemenih, M., Haile, M. (2013): Ecological succession and land use changes in a lake retreat area (Main Ethiopian Rift Valley). – *Journal of Arid Environments* 91(4): 53-60.
- [84] Temesgen, H., Wu, W., Shi, X., Yirsaw, E., Bekele, B., Kindu, M. (2018): Variation in ecosystem service values in an agroforestry dominated landscape in Ethiopia: implications for land use and conservation policy. – *Sustainability* 10(4): 1126.
- [85] Tianhong, L., Wenkai, L., Zhenghan, Q. (2010): Variations in ecosystem service value in response to land use changes in Shenzhen. – *Ecological Economics* 69(7): 1427-1435.
- [86] Tolessa, T., Senbeta, F., Abebe, T. (2017a): The impact of land use/land cover change on ecosystem services in the central highlands of Ethiopia. – *Ecosystem Services* 26(2): 111-123. DOI: 10.1080/14728028.2016.1221780.
- [87] Tolessa, T., Senbeta, F., Abebe, T. (2017b): Land use/land cover analysis and ecosystem services valuation in the central highlands of Ethiopia. – *Forests, Trees and Livelihoods* 26(2): 111-123.
- [88] Torras, M. (2000): The total economic value of Amazonian deforestation, 1978–1993. – *Ecological Economics* 33(2): 283-297.
- [89] Troy, A., Wilson, M. A. (2006): Mapping ecosystem services: practical challenges and opportunities in linking GIS and value transfer. – *Ecological Economics* 60(2): 435-449. DOI: <https://doi.org/10.1016/j.ecolecon.2006.04.007>.
- [90] Tsegaye, D., Moe, S. R., Vedeld, P., Aynekulu, E. (2010): Land-use/cover dynamics in Northern Afar rangelands, Ethiopia. – *Agriculture, Ecosystems & Environment* 139(1-2): 174-180.
- [91] USGS (2018): Earth Explorer. – <http://earthexplorer.usgs.gov/> (accessed 26.03.18).
- [92] Van der Ploeg, S., De Groot, R. (2010): The TEEB Valuation Database—a Searchable Database of 1310 Estimates of Monetary Values of Ecosystem Services. – Foundation for Sustainable Development, Wageningen, The Netherlands.
- [93] Vigl, L. E., Schirpke, U., Tasser, E., Tappeiner, U. (2016): Linking long-term landscape dynamics to the multiple interactions among ecosystem services in the European Alps. – *Landscape Ecology* 31(9): 1903-1918.
- [94] Wang, X., Dong, X., Liu, H., Wei, H., Fan, W., Lu, N., Xu, Z., Ren, J., Xing, K. (2017): Linking land use change, ecosystem services and human well-being: a case study of the Manas River Basin of Xinjiang, China. – *Ecosystem Services* 27: 113-123.
- [95] Wang, Y., Gao, J., Wang, J., Qiu, J. (2014): Value assessment of ecosystem services in nature reserves in Ningxia, China: A response to ecological restoration. – *PloS One* 9(2): e89174.
- [96] Wang, Z., Wang, Z., Zhang, B., Lu, C., Ren, C. (2015): Impact of land use/land cover changes on ecosystem services in the Nenjiang River Basin, Northeast China. – *Ecological Processes* 4(1): 11. DOI: 10.1186/s13717-015-0036-y.
- [97] Wilson, M. A., Hoehn, J. P. (2006): Valuing environmental goods and services using benefit transfer: The state-of-the art and science. – *Ecological Economics* 60(2): 335-342. DOI: <https://doi.org/10.1016/j.ecolecon.2006.08.015>.
- [98] Wondrade, N., Dick, Ø. B., Tveite, H. (2014): GIS based mapping of land cover changes utilizing multi-temporal remotely sensed image data in Lake Hawassa Watershed, Ethiopia. – *Environmental Monitoring and Assessment* 186(3): 1765-1780.
- [99] WorldBank (2019): <https://data.worldbank.org/country/ethiopia>. – WorldBank, Washington, DC.
- [100] Xie, G.-D., Lu, C.-X., Leng, Y.-F., Zheng, D., Li, S. (2003): Ecological assets valuation of the Tibetan Plateau. – *Journal of Natural Resources* 18(2): 189-196. DOI: 10.1002/ldr.2575.
- [101] Xu, D., Ding, X. (2018): Assessing the impact of desertification dynamics on regional ecosystem service value in North China from 1981 to 2010. – *Ecosystem Services* 30: 172-180.

- [102] Yirsaw, E., Wu, W., Shi, X., Temesgen, H., Bekele, B. (2017): Land use/land cover change modeling and the prediction of subsequent changes in ecosystem service values in a coastal area of China, the Su-Xi-Chang Region. – Sustainability 9(7): 1204.
- [103] Zeleke, G., Hurni, H. (2001): Implications of land use and land cover dynamics for mountain resource degradation in the Northwestern Ethiopian highlands. – Mountain Research and Development 21(2): 184-191.
- [104] Zhang, Z., Gao, J., Gao, Y. (2015): The influences of land use changes on the value of ecosystem services in Chaohu Lake Basin, China. – Environmental Earth Sciences 74(1): 385-395.
- [105] Zhou, J., Sun, L., Zang, S., Wang, K., Zhao, J., Li, Z., Liu, X., Liu, X. (2017): Effects of the land use change on ecosystem service value. – Global Journal of Environmental Science and Management 3(2): 121-130.

COMPARATIVE ALLELOPATHIC ACTIVITY OF *RHAZYA STRICTA*, *PINUS ROXBURGHII*, *CARICA PAPAYA* AND *LANTANA CAMARA* AGAINST NOXIOUS WEEDS

ANWAR, T.^{1*} – ILYAS, N.¹ – QURESHI, R.¹ – QURESHI, H.^{1,2} – GILANI, N.³ – KHAN, S.⁴ – KHAN, S. A.⁵ – FATIMAH, H.⁶ – WASEEM, M.⁶ – MAHMOOD, R. T.⁷ – MAQSOOD, M.¹

¹Department of Botany, Pir Mehr Ali Shah Arid Agriculture University, Murree Road, Shamsabad, Rawalpindi-46300, Punjab, Pakistan

²Department of Botany, Government Post Graduate College (Women) Sub-Campus, University of Gujrat, Satellite Town, Rawalpindi-46300, Punjab, Pakistan

³Department of Zoology, Pir Mehr Ali Shah Arid Agriculture University, Murree Road, Shamsabad, Rawalpindi-46300, Punjab, Pakistan

⁴Department of Environmental Science, Gomal University, Dera Ismail Khan-29050, Khyber Pakhtunkhwa, Pakistan

⁵Department of Earth and Environmental Science, Bahria University, Islamabad Campus, Shangrilla Road, Sector E-8, Islamabad-44000, Pakistan

⁶Department of Biology, Allama Iqbal Open University, H-8, Islamabad-44000, Pakistan

⁷Department of Biotechnology, Mirpur University of Science and Technology, Mirpur-10250, Azad Jammu & Kashmir, Pakistan

*Corresponding author

e-mail: drtauseefanwar@hotmail.com; phone: +92-33-3686-0562

(Received 27th Feb 2019; accepted 10th Apr 2019)

Abstract. ‘Yield maximization’ is the last word of modern agriculture for food security of ever-increasing population of the world. Maximizing world’s agricultural efficiency depends largely on controlling pests and diseases. Although, demand for insecticides and fungicides by successful breeding for resistant cultivars has reduced, use of herbicides is still increasing globally. Application of heavy doses of herbicides is directly/indirectly causing negative impact on quality of produce, human health and environment. Allelopathic weeds and their allelochemicals have wide application prospects in increasing crop production, plant protection and biological control. This study was aimed at evaluating allelopathic activity of methanol extracts of *Rhazya stricta* (Harmal), *Pinus roxburghii* (Chir-Pine), *Carica papaya* (Papaw) and *Lantana camara* (Wild-sage) against selected weeds viz. *Phalaris minor* (Canary grass), *Avena fatua* (Wild oat), *Chenopodium album* (Goosefoot), *Euphorbia helioscopia* (Sun-spurge) and *Rumex dentatus* (Knotweed) on filter paper, soil and agar at 100%, 75%, 50% and 0% concentration. Germination percentage (%), radicle length (cm) and plumule length (cm) were parameters to assess allelopathic potential. The STATISTIX 9 software was used to analyse data. Based on results, it was concluded that methanolic extract of *R. stricta*, *P. roxburghii*, *C. papaya* and *L. camara* possess potential inhibitory effects amongst which *L. camara* showed most prominent inhibitory effects towards selected weeds. The germination and growth inhibition effects were found in order *L. camara*>*P. roxburghii*>*C. papaya*>*R. stricta*. Detailed field study is recommended to establish allelopathic potential of these species to be utilized as phytoherbicide.

Keywords: third generation herbicides, ecofriendly weed management, bioassay screening, polar phytochemicals, seedling growth inhibition

Introduction

Agriculture is the backbone of Pakistan's economy. This sector gave 20.9% of the Gross Domestic Product (GDP) for the fiscal year 2014-15. Moreover, agriculture is a source of income for 43.5% of the village population of the country. Food security depends upon a sustainable agricultural production and higher levels of yield. It may also enable the agricultural sector less vulnerable to the threat of climate change (Shah et al., 2016).

Wheat (*Triticum aestivum* L.), is one of the most important cereal crops of the world. Its role is quite important in the provision of human nutrition. It has been shown that wheat farmers are offering very little time and attention to the weed management practices, consequently, 15 to 25% wheat grain losses occur. Weeds are causing annual damage of about 10% in agricultural yields globally (Cavero et al., 2011). In Pakistan, weeds cause 45% loss in wheat production (Anwar et al., 2016).

In Pakistan, however, annual economic loss, due to weeds in agricultural production is estimated around 18.2 billion dollars. Including, 3-6 billion dollars spent on weeds control methods. There are around 30 different weed species generally found in the wheat crop, becoming the sources of losses. As the smaller farmers lack related tact and necessary resources, it becomes quite impossible to remove these weeds from the cultivated field. Weed harms most of the crops and grain. Moreover, it remains as a perennial problem in Pakistan's agriculture sector (Mubarik et al., 2015). Weeds are growing with cultivated crops and compete with crop for light, moisture, other vital elements of nutrition and space. The referred result cause low quality and less production of crops with raised costs of production. According to an estimate, grain produce in Pakistan can be enhanced by up to 41% if weeds are managed properly. The controlling of weeds through traditional methods is time consuming, weather hinged and exhibit more labour cost. While modern weed control techniques have not been up to the mark in solving this problem (Arafat et al., 2015).

Synthetic chemicals are in wider use for controlling weeds. These chemicals may enhance crop production, but concurrently these may have a negative effect on the environment as well as upon human health. In addition to these, the heading up of synthetic herbicides resistant weeds is another major area of concern. Excessive use of herbicides for controlling weeds during the last few years is becoming one of the noteworthy ecological and environmental threats for the world. Herbicide remnants in crops, soil and underground water, which cause an evolution of various resistant weed biotypes and linked health threats, are some of the huge dangers that scientists are facing these days in devising various weed management techniques. Due to the negative effect of using synthetic chemicals, one may highly be in demand the new classes of chemicals, especially, biodegradable products such as those originating from plants, which have the potential of being developed as herbicides (Aryakia et al., 2015). This guides us forward for searching new weed management strategies, which may be cost effective, easy and eco-friendly.

Allelopathy is a natural and eco-friendly technique. This strategy might be one of the very efficient tools for weed management and thereby increasing crop production (Kamran et al., 2017). An Austrian Professor Hans Molisch first used the term allelopathy in 1937. He got it from two Greek roots: allelon (of each other) and pathos (to suffer). It can be translated as the harmful effect of one organism upon any other. In the beginning, allelopathy referred to both killing and favorable interactions between

any species. However, lately allelopathy is being used for only harmful plant interactions, rather for the both.

In 1996, the International Allelopathy Society defined allelopathy in the following words “The science that studies any process involving secondary metabolites produced by plants, micro-organisms, viruses, and fungi that influence growth and development of agricultural and biological systems” (Kong et al., 2006). Natural herbicides obtained from allelopathic plants can help in reducing usage of synthetic herbicides for weed control that will cause less pollution as well as alleviate human health concerns. The most commonly available allelochemicals are cinnamic and benzoic acids, alkaloids, flavonoids, phenolics, glucosionates and various terpenes (Khan et al., 2014).

Keeping all this in view, the present study was performed for evaluating *Rhazya stricta* (Harmal), *Lantana camara* (Wild-sage), *Carica papaya* (Papaw) and *Pinus roxburghii* (Chir-Pine), for their allelopathic activity against major weeds viz. *Phalaris minor* (Canary grass), *Avena fatua* (Wild oat), *Chenopodium album* (Goosefoot), *Euphorbia helioscopia* (Sun-spurge) and *Rumex dentatus* (Knotweed) of wheat (*Triticum aestivum*).

Materials and methods

Allelopathic potential of leaves of selected plants viz., *R. stricta*, *P. roxburghii*, *C. papaya* and *L. camara* was evaluated. Fresh leaves (~50 g) for each species were collected (73°02' E longitude and 33°36' N latitude) during March-April 2018 (Fig. 1). Collected plant material was washed under running tap water and dried at 30 °C in laboratory that was crushed using heavy duty blender to make fine powder (mesh size 2 mm) and preserved in air tight plastic zip lock bags (Ramsumair et al., 2014; Anwar et al., 2016). Seeds of test weeds viz. *Phalaris minor*, *Avena fatua*, *Chenopodium album*, *Euphorbia helioscopia* and *Rumex dentatus* were procured from the Barani Agricultural Research Institute (BARI), Pakistan. Seeds were surface sterilized by 2% solution of Sodium hypochlorite (NaOCl) (Biljana and Kragujevac, 2015).

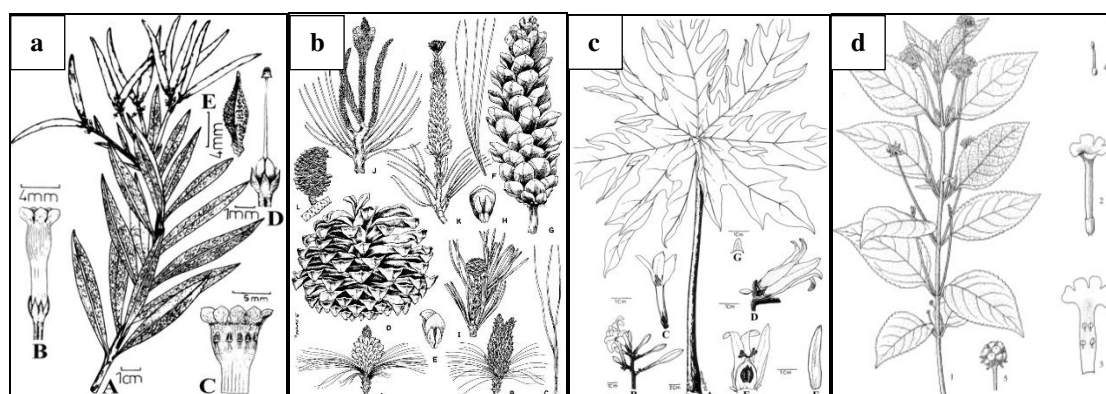


Figure 1. Illustrations of plants studied for their phytotoxic activity (a) *Rhazya stricta*, (b) *Pinus roxburghii*, (c) *Carica papaya* (d): *Lantana camara* (Pakistan eflora; <http://www.efloras.org/flora>)

Dried leaf powder of each plant species (40 g) was soaked in 400 ml methanol and agitated for 24 h (25 °C) at 160 rpm on orbital shaker. The filtrate was obtained through

Whatman filter paper No. 1. The final volume of filtrate was adjusted to 400 ml that gave 10% methanol extract as stock solution. Three concentrations i.e. T1 (100%), T2 (75%), T3 (50%) while T4 (0%) were further prepared.

Bioassays were carried out using soil and filter paper as medium. An aliquot (15 ml) of extract for each of three concentrations was added on 25 g soil per petri dish while 5 ml extract on filter paper per petri dish. Ten seeds of weed test species were used per petri dish. Each treatment was replicated three times. The petri dishes were wrapped with aluminium foil and incubated in growth chamber (NTS Model MI-25S set at 28 °C) for 15 days.

The germination percentage (%), lengths of radicle and plumule (cm) were calculated by comparing with control (Maharjan et al., 2007; Anwar et al., 2017). The statistical analysis was carried out using STATISTIX 9 and means were separated by Fisher's protected LSD test (Nekonom et al., 2014).

Results and discussion

Allelopathic potential of R. stricta

The results obtained in indicated that *R. stricta* methanolic extract significantly inhibited germination of *C. album* (42%) followed by *P. minor* (41%) and *R. dentatus* (37%) on filter paper, whereas, no significant effect on germination of *A. fatua* and *E. helioscopia* showing resistance against extract. Similarly, *R. stricta* methanolic extract on soil significantly suppressed seed germination of *C. album* (47%) followed by *P. minor* (43%) and *R. dentatus* (42%). Maximum (95%) germination was observed for *A. fatua* and *E. helioscopia*. It was recognized that minimum germination was noted for *C. album* i.e. 68% and 53% on filter paper and soil, respectively. The results revealed that germination reduction for *C. album*, *P. minor* and *R. dentatus* was concentration dependent (Fig. 2a).

The statistical data revealed that *R. stricta* methanolic extract significantly inhibited radical length of *R. dentatus* (45%) and *A. fatua* (44%) on filter paper, whereas, no significant effect was noted for *P. minor*, *E. helioscopia* and *C. album* showing resistance against extract. Similarly, the applications of extract into soil significantly suppressed radical length of *R. dentatus* (51%) and *A. fatua* (50%) as compared to control. The maximum (96%) radical length was observed for *P. minor*, *E. helioscopia* and *C. album*. The final data concluded that minimum radical length was noted for *R. dentatus* i.e. 55% and 49% on filter paper and soil, respectively (Fig. 2b).

Analysis of the data revealed that *R. stricta* methanolic extract significantly suppressed the plumule length of *A. fatua* (33%) and *R. dentatus* (28%) as compared control on filter paper. Interestingly, there was no significant effect on plumule elongation of *P. minor*, *E. helioscopia* and *C. album*. Likewise, *R. stricta* methanolic extract significantly inhibited plumule length of *A. fatua* (55%) and *R. dentatus* (34%) in soil. The statistical figures also proposed that maximum plumule length (96%) was noted for *P. minor*, *E. helioscopia* and *C. album* (Fig. 2c).

The plumule, radicle length and germination of cowpea and rice were significantly reduced with increasing concentration of *R. stricta* leaf extract (Jadhar and Gayanar, 1992). Moreover, inhibitory potential of different plants had pointedly checked seedling growth and seed germination of different crops and weed (Lisanetwork and Michelson, 1993; Khan et al., 2004) and their results exposed that extract of *R. stricta* inhibited plumule length of weed species. Similar results were also explained by Tefera, 2002 and

Siddiqui et al., 2009. They noticed a suppressive effect on plumule length and seed germination. These findings were in accordance to Kaul and Bansal (2002) who stated that *R. stricta* leaf extract reduced growth of weeds species. Likewise, Maciel et al. (2003) also observed the same findings. The differences in germination response of tested species were expected and agree with those of Patil (1994) who reported variations in germination response of various field crops in the presence of *R. stricta* leaf extract. Some current revisions demonstrate the allelopathic potential of *Parthenium hysterophorus* (Tawaha and Turk, 2003), *Brassica nigra* (Singh et al., 2003) and *Raphanus raphanistrum* (Batish et al., 2002). All these revisions designate the production of allelochemicals during the preparation of extract. Likewise, results had been noted by Norsworthy (2003) while studying the inhibitory potential of different plants. They noticed that the leaf extracts had been more allelopathic in nature. The current results agree with the earlier findings described by Bora et al. (1999) who noticed the suppressive potential of *R. stricta* extract.

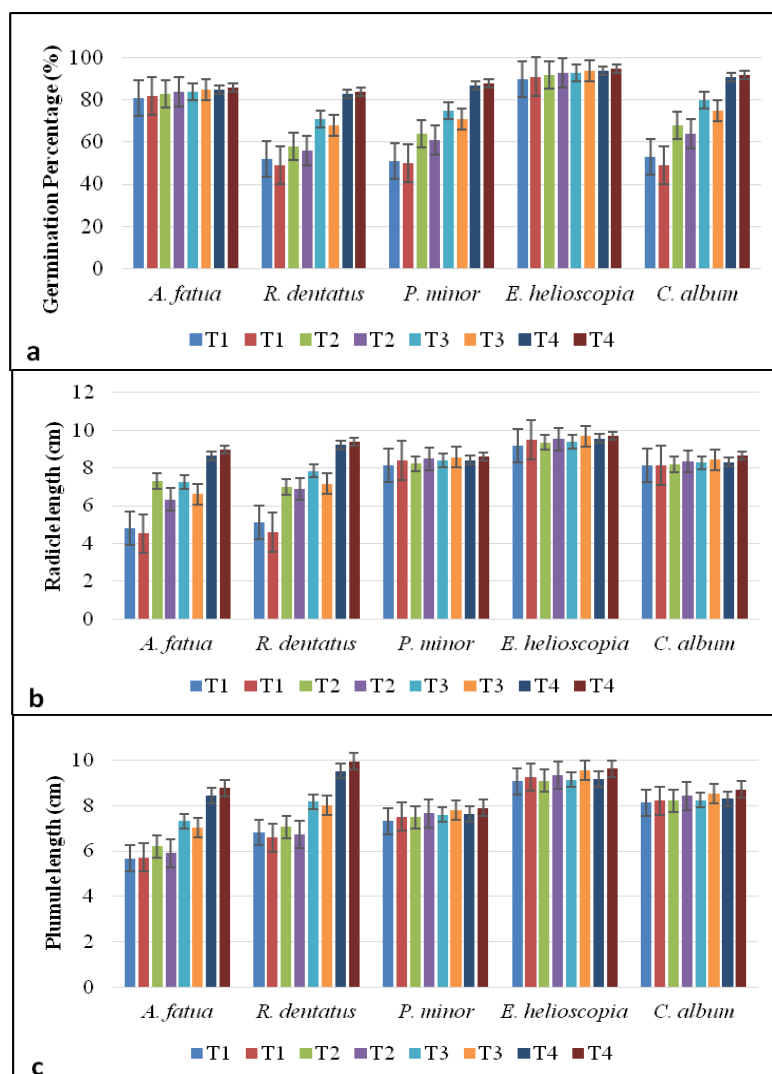


Figure 2. Allelopathic potential of *R. stricta* methanol extract on (a) germination (%), (b) radicle length (cm) and (c) plumule length (cm) against weed test species on filter paper (FP) and soil (S) where; T₁ (100%), T₂ (75%), T₃ (50%) and T₄ (control)

I

Allelopathic potential of *L. camara*

The statistical data exposed that *L. camara* methanolic extract significantly inhibited germination of *R. dentatus* (68%), *A. fatua* (66%), *E. helioscopia* (63%) and *P. minor* (62%) on filter paper, whereas, no significant effect on germination of *C. album* showing resistance against extract. Similarly, *L. camara* methanolic extract on soil significantly suppressed seed germination of *A. fatua* (76%), *E. helioscopia* (73%), *R. dentatus* (70%) and *P. minor* (69%). It was noted that maximum (95%) germination was observed for *C. album*. In the present study, it was recognized that minimum germination percentage was noted for *R. dentatus* (32%) followed by *A. fatua* (24%) on filter paper and soil, respectively. The results revealed that germination reduction of the *R. dentatus*, *A. fatua*, *E. helioscopia* and *P. minor* were concentration dependent (Fig. 3a).

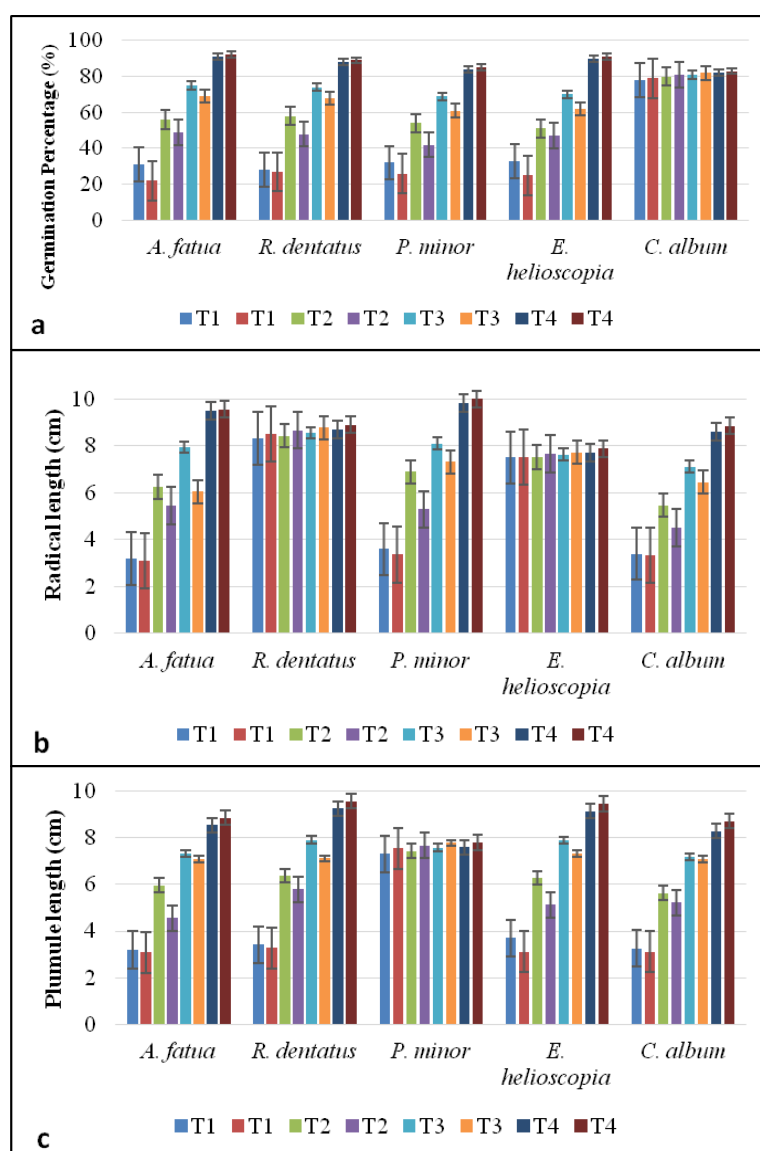


Figure 3. Allelopathic potential of *L. camara* methanol extract on (a) germination (%), (b) radicle length (cm) and (c) plumule length (cm) against weed test species on filter paper (FP) and soil (S) where; T₁ (100%), T₂ (75%), T₃ (50%) and T₄ (control)

The results obtained in the study indicated that *L. camara* methanolic extract significantly inhibited radical length of *C. album* (40%), *P. minor* (37%) and *A. fatua* (34%) on filter paper, whereas, no significant effect was noted for *R. dentatus* and *E. helioscopia* showing resistance against extract. Similarly, the applications of extract into soil significantly suppressed radical length of *A. fatua* (68%), *P. minor* (66%) and *E. helioscopia* (63%) as compared to control. The maximum (96%) radical length was observed for *R. dentatus* and *E. helioscopia*. The final data concluded that minimum radical length was noted for *C. album* (60%) and *A. fatua* (32%) on filter paper and soil, respectively (Fig. 3b).

The data obtained exhibited that *L. camara* methanolic extract significantly suppressed the plumule length of *R. dentatus* (63%), *A. fatua* (62%), *C. album* (60%) and *E. helioscopia* (61%) as compared control on filter paper. Interestingly, there was no significant effect on plumule elongation of *P. minor*. Likewise, *L. camara* methanolic extract significantly inhibited plumule length of *E. helioscopia* (67%), *R. dentatus* (66%), *A. fatua* (65%) and *C. album* (64%) in soil. The statistical data concluded that minimum plumule length was noted for *R. dentatus* (37%) and *E. helioscopia* (33%) on filter paper and soil, respectively. The statistical figures also proposed that maximum plumule length (96%) was noted for *P. minor* (Fig. 3c).

The results revealed that maximum germination was observed for *C. album*. The results further revealed that minimum germination was noted for *R. dentatus* and *A. fatua* showed being most susceptible to *L. camara* methanolic extract on filter paper and soil respectively. The data suggested that the maximum radical length was observed for *R. dentatus* and *E. helioscopia* showed most tolerance to allelopathic *L. camara* methanolic extract. The results indicated that minimum radical length was noticed for *A. fatua*. The study indicated that maximum plumule length was measured for *P. minor*. However, the lowermost plumule length was noticed for *R. dentatus* and *E. helioscopia* on filter paper and soil respectively. Mishra (2015) stated similar results that growth inhibitory effect of plants was concentration dependent. These results stated that *L. camara* has allelopathic effect on *Lepidium sativum* germination and growth. Ahmed et al. (2007) described the inhibitory potential of *L. camara* in different crops. Mishra (2012) stated that *L. camara* extract checked *Parthenium hysterophorus* seed germination demonstrating that the presence of inhibitory phytochemicals. Oudhia (2000) noticed germination of *Melilotus alba* was significant inhibited by extract of *L. camara*.

Allelopathic potential of C. papaya

The data illustrated that *C. papaya* methanolic extract significantly inhibited germination of *P. minor* (41%), *E. helioscopia* (37%) and *A. fatua* (36%) on filter paper, whereas, no significant effect on germination of *R. dentatus* and *C. album* showing resistance against extract. Similarly, *C. papaya* methanolic extract on soil significantly suppressed seed germination of *E. helioscopia* (50%), *P. minor* (45%) and *A. fatua* (41%). It was noted that maximum (95%) germination percentage was observed for *R. dentatus* and *C. album*. In the present study, it was recognized that minimum germination was noted for *P. minor* (59%) and *E. helioscopia* (50%) on filter paper and soil, respectively. The results revealed that germination reduction of the *P. minor*, *E. helioscopia* and *A. fatua* were concentration dependent (Fig. 4a).

The data revealed that *C. papaya* methanolic extract significantly inhibited radical length of *P. minor* (47%), *R. dentatus* (45%) and *A. fatua* (42%) on filter paper,

whereas, no significant effect was noted for *C. album* and *E. helioscopia* showing resistance against extract. Similarly, the applications of extract into soil significantly suppressed radical length of *R. dentatus* (50%), *P. minor* (49%) and *A. fatua* (46%) as compared to control. The maximum (96%) radical length was observed for *C. album* and *E. Helioscopia* (Fig. 4b).

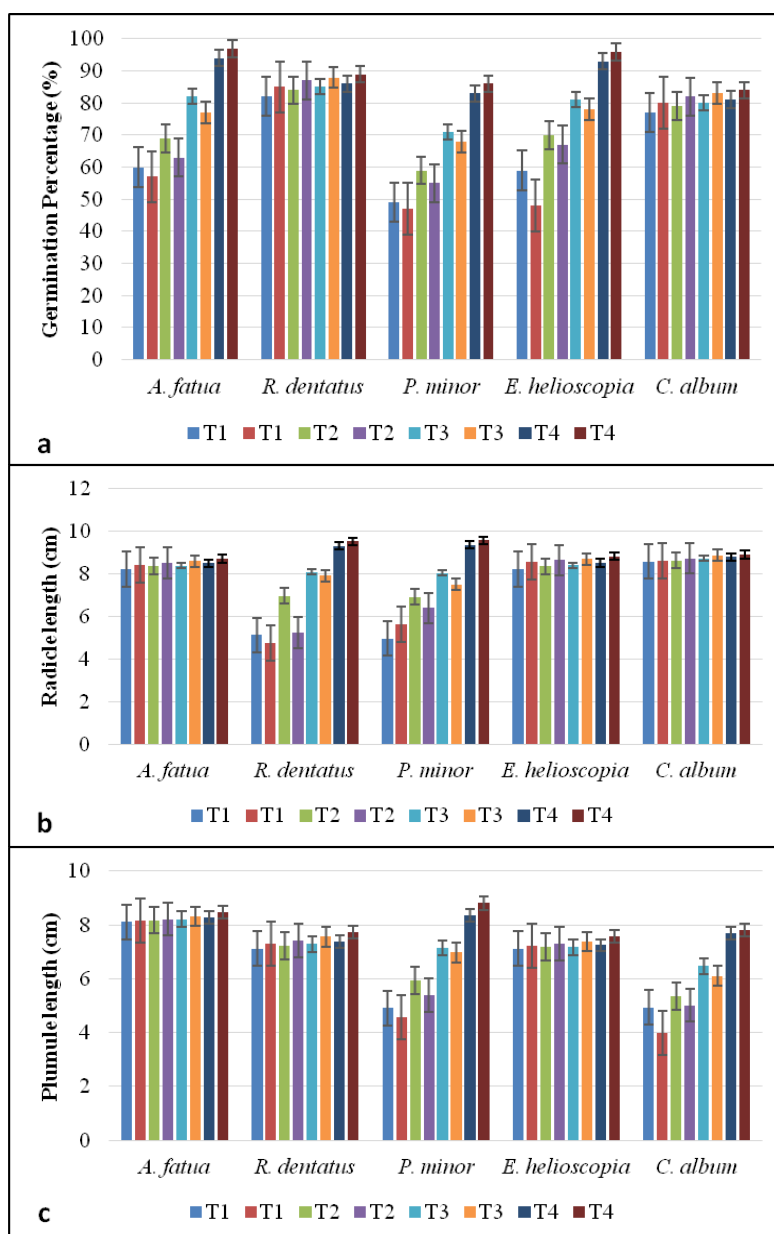


Figure 4. Allelopathic potential of *C. papaya* methanol extract on (a) germination (%), (b) radicle length (cm) and (c) plumule length (cm) against weed test species on filter paper (FP) and soil (S) where; T₁ (100%), T₂ (75%), T₃ (50%) and T₄ (control)

The data obtained exhibited that *C. papaya* methanolic extract significantly suppressed the plumule length of *P. minor* (41%) and *C. album* (36%) as compared to control on filter paper. Interestingly, there was no significant effect on plumule elongation of *A. fatua*, *R. dentatus* and *E. helioscopia*. Likewise, *C. papaya* methanolic

extract significantly inhibited plumule length of *C. album* (49%) and *P. minor* (48%) in soil. The statistical data concluded that minimum plumule length was noted for *P. minor* (59%) and *C. album* (51%) on filter paper and soil, respectively. The statistical figures also proposed that maximum plumule length (96%) was noted for *A. fatua*, *R. dentatus* and *E. helioscopia* (Fig. 4c).

The data also suggested that the maximum germination was observed for *R. dentatus* and *C. album*. The statistical results recommended that minimum germination percentage was noted for *P. minor* and *E. helioscopia* on filter paper and soil respectively. The highest radical length inhibition was measured for *C. album* and *E. helioscopia*. The statistical data concluded that maximum plumule length was measured for *A. fatua*, *R. dentatus* and *E. helioscopia*. The statistical results of the data showed that lowermost plumule length was noticed for *C. album* and *P. minor* on soil and filter paper respectively. Likewise, observations were also reported by Turk and Tawaha (2003) showing negative germination effects by *C. papaya* extract of on *Avena fatua*. According to observations of Bajwa et al. (2013) different types of plant extracts were observed to be completely inhibitory on germination of *A. fatua*. Likewise, finding was also reported by Oudhi (2001) and Maharjan et al. (2007).

Allelopathic potential of *P. roxburghii*

P. roxburghii methanolic extract on filter paper showed significant inhibitory activity on seed germination of *C. album* (49%) and *A. fatua* (46%), respectively as compared to control. Likewise, *P. roxburghii* methanolic extract on soil exhibited the highest degree of inhibition germination for *C. album* (52%) and *A. fatua* (49%) respectively as compared to control. The statistical data also suggested that there was no significant effect on germination percentage of *P. minor*, *R. dentatus* and *E. helioscopia*. The maximum (98%) germination was observed for *P. minor*, *R. dentatus* and *E. helioscopia*. The statistics recommended that allelopathic inhibitory effect was concentration dependent for *C. album* and *A. fatua* (Fig. 5a).

The data revealed that the highest radical length inhibition activity exhibited by *R. dentatus* (47%) followed by *C. album* (43%) in *P. roxburghii* methanolic extract on filter paper. Likewise, methanolic extract on soil caused significant radical length reduction of *R. dentatus* and *C. album* measuring 50% and 48%, respectively as compared to control, while *P. minor*, *E. helioscopia* and *A. fatua* remained unaffected. The maximum radical length was noted for *P. minor*, *E. helioscopia* and *A. fatua* (98%). The results also illustrated that minimum radical length was noted for *R. dentatus* i.e. 53% and 50% on filter paper and soil, respectively. The results revealed that allelopathic inhibitory effect was concentration dependent for *R. dentatus* and *C. album* (Fig. 5b).

P. roxburghii methanolic extract on filter paper significantly inhibited plumule length of *R. dentatus* (46%) and *A. fatua* (42%). Likewise, the highest degree of inhibition in plumule length was measured for *R. dentatus* (49%) and *A. fatua* (45%) in methanolic extract applied into soil. The data further suggested that there was no significant effect on germination of *P. minor*, *E. helioscopia* and *C. album*. The statistical results recommended that highest plumule length (98%) was exhibited by *P. minor*, *E. helioscopia* and *C. album*. The results further indicated that minimum plumule length noticed for *R. dentatus* i.e. 54% and 51% on filter paper and soil, respectively. The statistics also recommended that allelopathic inhibitory effect was concentration dependent for *R. dentatus* and *A. fatua* (Fig. 5c).

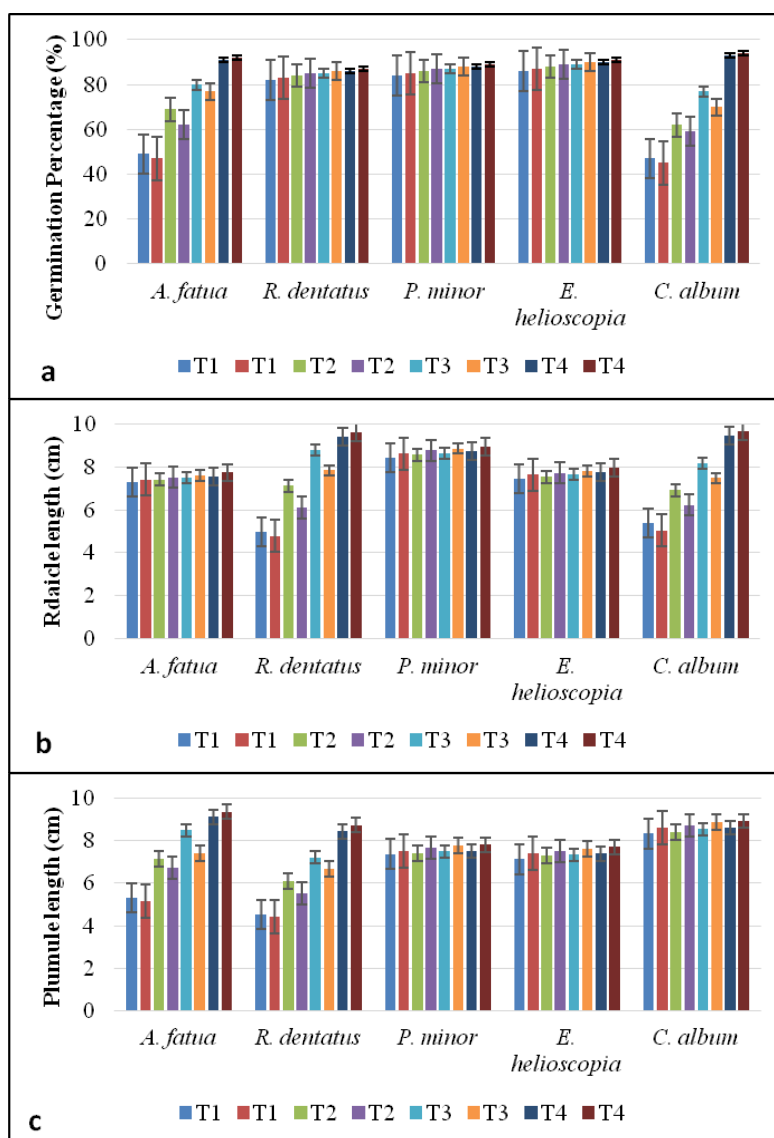


Figure 5. Allelopathic potential of *P. roxburghii* methanol extract on (a) germination (%), (b) radicle length (cm) and (c) plumule length (cm) against weed test species on filter paper (FP) and soil (S) where; T₁ (100%), T₂ (75%), T₃ (50%) and T₄ (control)

It was revealed that maximum germination was observed for *P. minor*, *R. dentatus* and *E. helioscopia*. The results recommended that the maximum radical length was noted for *P. minor*, *E. helioscopia* and *A. fatua*. The results illustrated that minimum radical length was noted for *R. dentatus*. It was observed that *P. minor*, *E. helioscopia* and *C. album* exhibited highest activity for plumule length. The results further indicated that minimum plumule length noticed for *R. dentatus*. The black pine was shown to inhibit the growth of *Phalaris canariensis*, *Trifolium campestre* and *Sinapis arvensis* seeds (Amri et al., 2013). Different pinene isomers exhibited allelopathic potential against *Zea mays* seed germination (Areco et al., 2014). The leaf methanolic extract from *P. nigra* suppressed the seed germination of perennial ryegrass and tall fescue (Robert, 1986; Terzi et al., 2013). Valera-Burgos et al. (2012) noticed inhibitory

potential of *Pinus pinea* needles extract on seedling growth and seed germination of three Mediterranean shrub species.

Some recent studies indicating the phytotoxic/allelopathic effect of weeds include *Raphanus raphanistrum* (Ali, 2016), *Brassica napus* (Rodriguez et al., 2016), *Ageratum conyzoides* (Kumar et al., 2018) and *Parthenium hysterophorus* (Saranya et al., 2019). All these studies indicate the release of phototoxic chemicals. Based on this, studies were further extended to explore the impact of selected species, as they possessed greater phytotoxicity on the emergence and growth of weed plants in wheat crop.

Conclusions

Experiments showed that methanolic extracts of selected plants at higher concentrations reduce the seed germination, radicle and plumule length of weeds associated with the wheat crop. Results provided evidence about herbicidal potential of tested plant species viz. *L. camara*, *P. roxburghii*, *C. Papaya* and *R. stricta* against weeds of wheat crop (*Avena fatua*, *Phalaris minor*, *Chenopodium album* and *Rumex dentatus*). Further work is recommended to appraise the potential inhibitory effects of allelochemicals from these plants.

REFERENCES

- [1] Ali, K. A. (2016): Allelopathic potential of radish (*Raphanus sativus* L.) on germination and growth of some crop and weed plants. – Int. J. Biosci. 9: 394-403.
- [2] Ahmed, R., Uddin, M. B., Khan, M. A., Mukul, S. A., Hossain, M. K. (2007): Allelopathic effects of *Lantana camara* on germination and growth behavior of some agricultural crops in Bangladesh. – J. For. Res. 18: 301-304.
- [3] Amri, I., Hamrouni, L., Hanana, M., Gargouri, S., Fezzani, T., Jamoussi, B. (2013): Chemical composition, physico-chemical properties, antifungal and herbicidal activities of *Pinus halepensis* Miller essential oils. – Biol. Agric. Hortic. 29: 91-106.
- [4] Anwar, T., Khalid, S., Saeed, M., Mazhar, R., Qureshi, H., Rashid, M. (2016): Allelopathic interference of leaf powder and aqueous extracts of hostile weed: *Parthenium hysterophorus* (Asteraceae). – Sci. Int. 4: 86-93.
- [5] Anwar, T., Khalid, S., Panni, M. K., Qureshi, H., Rashid, M. (2017): Allelopathic effect of *Euphorbia helioscopia* on *Avena fatua*, *Rumex dentatus*, *Helianthus annuus*, *Zea mays* and *Triticum aestivum*. – Pak. J. Weed Sci. Res. 23: 165-177.
- [6] Arafat, Y., Khalid, S., Lin, W., Fang, C., Sadia, S., Ali, N., Azeem, S. J. (2015): Allelopathic evaluation of selected plants extract against broad and narrow leaves weeds and their associated crops. – Acad. J. Agric. Res. 3: 226-234.
- [7] Areco, V. A., Figueroa, S., Cosa, M. T., Dambolena, J. S., Zygadlo, J. A., Zunino, M. P. (2014): Effect of pinene isomers on germination and growth of maize. – Biochem. Syst. Ecol. 55: 27-33.
- [8] Aryakia, E., Naghavi, M. R., Farahmand, Z., Fazeli, S. A. H. S. (2015): Evaluating allelopathic effects of some plant species in tissue culture media as an accurate method for selection of tolerant plant and screening of bioherbicides. – J. Agr. Sci. Tech. 17: 1011-1023.
- [9] Bajwa, A. H., Khalid, S., Sadia, S., Nabeel, M., Nafees, W. (2013): Influence of combinations of allelopathic water extracts of different plants on wheat and wild oat. – Pak. J. Weed Sci. Res. 19: 157-166.

- [10] Batish, D. R., Singh, H. P., Kohli, R. K., Saxena, D. B., Kaur, S. (2002): Allelopathic effect of *parthenium* against two weedy species, *Avena fatua* and *Bidens pilosa*. – Environ. Exp. Bot. 47: 149-155.
- [11] Biljana, M. B., Kragujevac, D. Z. J. (2015): Allelopathic relations of selected cereal and vegetable species during seed germination and seedling growth. – J. Sci. 37: 135-142.
- [12] Bora, I. P., Singh, J., Borthakur, R., Bora, E. (1999): Allelopathic effect of leaf extracts of *Acacia auriculiformis* on seed germination of some agricultural crops. – Annl. For. 7: 143-146.
- [13] Cavero, J., Zaragoza, C., Cirujeda, A., Anzalone, A., Faci, J. M., Blanco, O. (2011): Selectivity and weed control efficacy of some herbicides applied to sprinkler irrigated rice (*Oryza sativa* L.). – Spanish J. Agric. Res. 9: 597-605.
- [14] Jadhav, B. B., Gayanar, D. G. (1992): Allelopathic effects of *Acacia auriculiformis* on germination of rice and cowpea. – Ind. J. Plant Physiol. 1: 86-89.
- [15] Kamran, M., Raza, A., Ali, Q., Ali, H. H., Chattha, M. S. (2017): Investigating the influence of fertilizer and allelopathic water extracts on maize and associated weeds. – Pak. J. Weed Sci. Res. 23: 361-378.
- [16] Kaul, S., Bansal, G. L. (2002): Allelopathic effect of *Ageratina adenophora* on growth and development of *Lantana camara*. – Ind. J. Plant Physiol. 7: 195-197.
- [17] Khan, I., Ali, Z., Khan, M. I., Hussain, Z., Khan, I. A., Waqas, M., Khan, R., Khan, S. (2014): Allelopathic effects of some weeds on chickpea crop. – Pak. J. Weed Sci. Res. 20: 207-211.
- [18] Khan, M. A., Marwat, K. B., Hassan, G., (2004): Allelopathic potential of some multipurpose trees species (MPTS) on the wheat and some of its associated weeds. – Int. J. Biol. Biotechnol. 1: 275-278.
- [19] Kong, C. H., Li, H. B., Hu, F., Xu, X. H., Wang, P. (2006): Allelochemicals released by rice roots and residues in soil. – Plant Soil 288: 47-56.
- [20] Lisanewok, N., Michelen, A. (1993): Allelopathy in agro forestry systems. The effects of leaf extracts of eucalyptus species on three crops. – Agro-Forestry Syst. 21: 63-74.
- [21] Maciel, C. D. G., Correa, M. R., Alves, E., Negrisoni, E., Velini, E. D., Rodrigues, J. D., Ono, E. O., Boaro, C. S. F. (2003): Influence of *Brachiaria decumbens* straw management on the initial development of soybean (*Glycine max*) and peanut-brav (*Euphorbia heterophylla*). – Plant Weed 21(3): 635-637.
- [22] Maharjan, S., Shrestha, B. B., Jha, P. K. (2007): Allelopathic effects of aqueous extract of *Parthenium hysterophorus* L. on seed germination and seedling growth of some cultivated and wild herbaceous species. – Sci. World 5: 35-39.
- [23] Mishra, A. (2012): Allelopathic interaction of *Lantana camara* leaf of extract on growth of *Parthenium hysterophorus* in seedling stage. – Int. J. Plant Sci. 7: 259-262.
- [24] Mishra, A. (2015): Review; Allelopathic properties of *Lantana camara*. – Int. Res. J. Basic Clin. Stud. 3: 13-28.
- [25] Mubarik, S., Khan, K., Memon, R. A., Shaheen, G., Hashmatulla. (2015): Allelopathic effects of important weeds on germination and growth of maize (*Zea mays* L.). – Pak. J. Weed Sci. Res. 21: 181-180.
- [26] Nekonam, M. S., Kraimmojeni, H., Sharifnabi, B., Razmjoo, J., Amini, H., Bahrami, F. (2014): Assessment of some medicinal plants for their allelopathic potential against redroot pigweed (*Amaranthus retroflexus*). – J. Plant Prot. Res. 54: 90-95.
- [27] Norsworthy, J. K. (2003): Allelopathic potential of wild radish (*Raphanus raphanistrum*). – Weed Technol. 17: 307-313.
- [28] Oudhi, P. A. (2001): Germination and seedling vigour of wheat as affected by allelopathy of some obnoxious weeds. – Agric. Sci. Digest. 21: 275-276.
- [29] Oudhia, P. (2000): Allelopathic effects of some obnoxious weeds on germination of *Melilotus alba*. – Legume Res. 22: 133-134.
- [30] Patil, B. P. (1994): Effects of *Glyricidia maculate* L. extracts on field crops. – Allelopathy J. 1: 118-120.

- [31] Ramsumair, A., Mlambo, V., Lallo, C. H. O. (2014): Effect of drying method on the chemical composition of leaves from four tropical tree species. – Trop. Agric. (Trinidad) 91: 179-186.
- [32] Robert, J. (1986): Allelopathic potential of coniferous species to old-field weeds in Eastern Quebec. – For. Sci. 32: 112-118.
- [33] Rodriguez, D., Casagrande, G., Carmona-Galindo, V. D. (2016): Effects of black mustard allelopathy on the fitness and life history strategies of buffalo gourd in southern California. – Bios 87(3): 98-103.
- [34] Saranya, M., Rangaraj, T., Ragavan, T., Amutha, R. (2019): Allelopathic Potential of *Parthenium hysterophorus* and *Tridax procumbens* aqueous leaf extracts on weed control and growth of Blackgram (*Vigna mungo* L.). – Int. J. Agric. Sci. 11: 7697-7700.
- [35] Shah, S. H., Khan, E. A., Shah, H., Ahmed, N., Khan, J., Sadozai, G. U. (2016): Allelopathic sorghum water extract helps to improve yield of sunflower (*Helianthus annuus* L.) – Pak. J. Bot. 48: 1197-1202.
- [36] Siddiqui, S., Meghvansi, M. K., Yadav, K., Yadav, R., Wani, F. A., Ahmad, A. (2009): Efficacy of aqueous extracts of five arable trees on the seed germination of *Pisum sativum* L. var. VRP-6 and KPM-522. – Botany Res. Int. 2: 30-35.
- [37] Singh, H. P., Batish, D. R., Pandher, J. K., Kohli, R. K. (2003): Assessment of allelopathic properties of *Parthenium hysterophorus* residues. – Agric. Ecosyst. Environ. 95: 537-541.
- [38] Tawaha, A. M., Turk, M. A. (2003): Allelopathic effects of black mustard (*Brassica nigra*) on germination and growth of wild barley (*Hordeum sponataneum*). – J. Agron. Crop Sci. 189: 298-303.
- [39] Tefera, T. (2002): Allelopathic effects of *Parthenium hysterophorus* extracts on seed germination and seedling growth of *Eragrostis tef* (Zucc.) Trotter. – J. Agron. Crop Sci. 188: 306-310.
- [40] Terzi, I., Kocacaliskan, I., Demir, Y. (2013): Allelopathic effects of some tree leaf extracts on seed germination and seedling growth of turf grasses. – J. Environ. Prot. Ecol. 14: 1236-1243.
- [41] Turk, M. A., Tawaha, A. M. (2003): Allelopathic Effect of Black Mustard (*Brassica nigra* L.) on the germination and growth of wild oat (*Avena fatua* L.). – Crop Prot. 22: 673-677.
- [42] Valera-Burgos, J., Diaz-Barradas, M. C., Zunzunegui, M. (2012): Effects of *Pinus pinea* Litter on seed germination and seedling performance of three Mediterranean shrub species. – Plant Growth Regul. 66: 285-292.

MINERAL COMPOSITION OF HERBY CHEESE PRODUCED FROM RAW AND PASTEURIZED MILK

KÖSE, Ş.* – OCAK, E.

Department of Food Engineering, Faculty of Engineering, Van Yuzuncu Yil University, 65080 Van, Turkey

**Corresponding author*

e-mail: senolkose28@gmail.com; phone: +90-432-225-1024; fax: 90-432-225-1730

(Received 27th Feb 2019; accepted 10th Apr 2019)

Abstract. In this study, the effects of sirmo (*Allium vineale* L.), mendi (*Chaerophyllum macropodium* Boiss.) and siyabo (*Ferula rigidula* DC.) on mineral compositions of herby cheese produced from raw and pasteurized milk in brine and vacuum package during 90 days ripening were determined. Macroelements (Ca, Mg, Na, K) and micro elements (Fe, Zn, Mn) concentration of herby cheese samples were examined by Inductively Coupled Plasma-Optical Emission Spectrometer (ICP-OES). It was determined that the mineral concentration was changed from highest to lowest Na>Ca>K>Mg>Zn>Fe>Mn in the herby cheese. The highest mean concentration of Na was found in Sirmo added cheeses manufactured from raw milk in brine on the second day of ripening and the lowest mean concentration of Mn was found in Sirmo added cheeses produced from pasteurized milk in brine at the end of 90 days. Na, Ca, K, Mg, Zn, Fe and Mn content of cheeses in brine and vacuum package decreased during ripening period.

Keywords: *herbs, mineral content, ripening period, packaging type*

Introduction

Herby cheese is one of the most popular cheeses traditionally produced from raw sheep's milk in the Eastern and South eastern region of Turkey (Tarakci and Temiz, 2009) particularly around Van province. If sheep milk is not available, sheep milk can be mixed with goat and cow milk for cheese production (Tarakci et al., 2004). Herby cheese variety has a salty taste, semi hard texture and is produced in small families (Andic et al., 2010, 2015; Tuncturk et al., 2014) between May and June (Tarakci and Temiz, 2009). It has been traditionally produced more than 200 years in Van and Eastern region of Turkey (Tarakci and Akyuz, 2009). But nowadays the cheeses are also manufactured commercially using pasteurized milk, starter culture in some dairies (in Van or other parts of Turkey). Almost 12 kinds of herbs are used for the production of Herby cheese. However, the most preferred herbs are sirmo (*Allium vineale* L.), mendi (*Chaerophyllum macropodium* Boiss.) and siyabo (*Ferula rigidula* DC.) (Kose, 2015). The herbs ensure the cheese its characteristic aroma/flavour and appearance, but also prolong the shelf-life of cheese (Hayaloglu and Fox, 2008).

There are many macro and micro minerals in milk and dairy products. These minerals are very important both in terms of nutritional physiology and physical stability of the cows and the catalytic effects of milk and dairy products (Ocak and Kose, 2015). The mineral content of cheese sample depends on various factors such as feeding, genetic, lactation period, geographical area of milk production, environmental conditions, lack of a standart technique in cheese production and possible contamination from the equipment during the cheese production (Altun and Kose, 2016).

There are many studies related to mineral content of herby cheese. The concentration of cheese samples were found by Tarakci and Kucukoner (2008) as 313.7, 552.6, 2606, 12.70 mg/100 g for Ca, P, Na, Mg, respectively. Heavy metals (ppm) were determined as 41.79, 33.99, 6.25, 2.05 mg/kg for Fe, Zn, Cu and Mn, respectively. Tarakci et al. (2005) determined the mineral contents of herby cheese samples (mg/100 g) as 289.49, 499.54, 2798.61, 3.20, 31.93, 46.07, 5.95 for Ca, P, Na, Mg, Zn, Fe and Cu, respectively. The same study, Mn, Cr, Co, Cd and Ni concentrations (ppm) were determined as 2.18, 0.23, 0.29, 0.22 and 0.19, respectively. Ocak and Kose (2015) determined Ca, K, Mg, Cu, Mn, Fe and Zn content of 26 Herby cheese samples obtained from retail markets in Van. They determined the concentration ranges in the cheese samples as 268.7-678.7, 84.6-163.2, 26.3-80.8, mg/100 g, 0.38-2.23, 8.13-25.94, 0.29-2.60, 3.14-29.25 mg/kg for Ca, K, Mg, Mn, Zn, Cu and Fe, respectively. Sagun et al. (2005) determined mineral contents of herby cheeses during ripening (90 days). It was determined that Ca, Mg, Fe, Zn, Mn, Ni and Cr contents decreased ($P < 0.05$), the Na content of cheeses increased ($P < 0.05$).

Many studies were performed to determine mineral contents of herby cheese samples but there is no study focusing on the effect of packaging, ripening and different herbs on macro and micro element accumulations in herby cheese. Therefore, the purpose of this investigation was to determine the effect of packaging, ripening and different herbs on the mineral content of herby cheese produced from raw and pasteurized milk during ripening.

Materials and methods

Production of herby cheese

Two different manufacturing methods were applied for production of herby cheese samples.

In the first method, milk and herbs were not pasteurized and the starter culture was not used. The pickled forms of the most preferred three local herbs such as Sirmo (*Allium vineale* L.), Mendi (*Chaerophyllum macropodum* Boiss.) and Siyabo (*Ferula rigidula* DC.) were separately and mixed used for cheese production. The raw milk is filtered through a cloth filter and heated to 32 °C and is then coagulated by using commercial rennet (Mayasan company, İstanbul, Turkey) for 1 h. After coagulation, the curd is cut into small cubes. The curd partly drained and divided into 5 groups (A1 control group, A2 sirmo-added groups, A3 mendi-added groups, A4 siyabo-added groups, A5 sirmo, mendi and siyabo mixture added groups). Then the pickled herbs were added at levels of 2 kg to the curd obtained from 100 kg of milk. The mixture of curd and herbs were pressed with a heavy object for 3 h and then cut into blocks (7 × 7 × 2 cm). The cheese blocks were placed in glass jars which are salted with 14% brine and held 12 h. At the end of this time, some of cheeses were continue to ripened in glass jars which were salted with 14% brine concentration, a portion of cheese were vacuum packed in plastic bags and were ripened at 4 °C for 90 days.

In the second method, the raw milk was filtered and pasteurized at 65 °C for 30 min. Then milk was cooled to 32 °C, CaCl₂ and starter culture (*Streptococcus thermophilus*, *Lactococcus lactis* subsp. *lactis* and *Lactococcus lactis* subsp. *cremoris*) were added at the ratios of 0.02 and 1.5%, respectively. Then, milk was

coagulated with rennet enzyme. After coagulation, the curd was cut into small pieces. The curd partly drained and divided into 5 groups as in the first method (B1 control group, B2 sirimo-added groups, B3 mendi-added groups, B4 siyabo-added groups, B5 sirimo, mendi and siyabo mixture added groups). The pasteurized herbs (at 95 °C for 5 min) were added into the curd and mixed well. Then the mixture of curd and herbs were pressed for 3 h to remove the whey sufficiently and the curd was cut into the blocks (7 × 7 × 2 cm). The cheese blocks were placed in glass jars which were salted with 14% brine and held 12 h. At the end of this time, some of cheeses were continue to ripened in glass jars which were salted with 14% brine concentration, a portion of cheeses were vacuum packaged in plastic bags and were ripened at 4 °C for 90 days. Mineral compositions of samples were analyzed 2, 30, 60, 90 days of storage at 4 °C. Each assay was performed in triplicate.

Mineral analysis

The cheese samples were burned by using dry ashing method in a ash furnace at 550 °C for 16 h. Before the samples were put in the ash furnace, they were dried in the oven at 105 °C for 1 h (IDF, 1992). The ash was dissolved with 5 ml nitric acid (1 N HNO₃) on heating plate and were filtered using (Whatman no: 41) filter paper. Then the solution was diluted with 1 N HNO₃ and completed in 50 ml with 1 N HNO₃. The concentrations of Ca, Mg, K, Na, Zn, Fe and Mn of the samples were measured by Inductively Coupled Plasma-Optical Emission Spectrometer (ICP-OES) (Thermo Scientific ICAP 6300 DUO, England) at 317.93, 279.55, 766.49, 588.99, 213.86, 259.94, and 257.61 respectively. Also, blank samples were prepared for use in calculations.

Statistical analysis

Concentrations of cheese samples were recorded as means± standard deviation of triplicate measurements. In the analysis of the data, SPSS (V.20) package program was used. A general linear model (GLM) analysis was used to determine the differences between the groups and the Duncan multiple comparison test was used to determine differences among the three groups. Also, for comparison of two independent groups, t test was used.

Results and discussion

The mineral content of herby cheese manufactured from raw and pasteurized milk in vacuum and brine are given *Tables 1-7*.

Calcium

The calcium concentration of vacuum and brine herby cheese samples varied from 2362.47-4820.35 mg/kg. Our results were accordance with findings of Ocak and Kose (2015), Mendil (2006) and higher than the values of determined by Ozlu et al. (2012).

As seen *Table 1*, the calcium content of cheese samples decreased from the 2th until 90 th days. The Ca loss of cheeses in brine were higher than in vacuum packaged, due to salt uptake from brine during the ripening period. Transport of Na⁺ and Cl⁻ ions from brine into the cheese, as a consequence of the osmotic pressure

difference between the brine and the moisture of the cheese. Depending on the amount of lactose and minerals in it, moisture of cheese has a certain osmotic pressure. The osmotic pressure of the brine is higher due to the excess of salt. For this reason, the pressure difference between the brine and cheese causes diffusion. When a moulded cheese is placed in brine, diffusions of Na⁺ and Cl⁻ ions from brine into the cheese and diffusions of H₂O, lactose, serum protein, various mineral substances such as Ca, Mg, K, P from cheese into the brine until the osmotic pressure between both phases is equalized. The amount of water lost is about twice the amount of salt obtained. For this reason, the weight of cheese decreases during the storage period (Gider, 2006). As long as the ripening period is long, transport of Na⁺ and Cl⁻ ions from brine into the cheese increases with very rapid salt uptake in the beginning but decreases during the storage periods (Guinee and Fox, 1986). Similarly, in our study the Ca concentrations of the herby cheeses in brine rapidly decreased from the 2nd until the 30th day of storage but the loss of Ca has decreased from the 30th until the 90th days. The reason for this explained by the some researchers as a reduction of NaCl concentration difference between brine and cheese moisture (Guinee and Fox, 1986; Gider, 2006).

Table 1. The effects of Sirmo, Mendi and Siyabo on Ca concentrations of herby cheese produced from pasteurized and raw milk in brine and vacuum package during ripening

Packaging type	Storage time	Treatment				
		A1	A2	A3	A4	A5
Brine	2	4650.72±161.53 ^{bAB}	4184.15±170.48 ^{cAB}	4532.91±259.5 ^{bAB}	4820.35±407.42 ^{bB}	4066.94±181.56 ^{cA}
	30	3556.06±83.64 ^{aAB#α}	3635.36±73.11 ^{bAB#}	3570.58±141.42 ^{aAB#}	3152.73±0.28 ^{aA#}	3783.52±392.8b ^{cB}
	60	3314.44±186.85 ^{aA#}	3570.53±114.2 ^{abA}	3280.50±0.71 ^{aA}	3399.15±131.61 ^{aA}	3399.96±119.32 ^{bA}
	90	3242.70±181.08 ^{aB#}	3209.54±189.66 ^{aB#}	3265.66±225.17 ^{aB}	3204.24±91.51 ^{aB}	2588.47±100.07 ^{aA#}
Vacuum	2	4650.72±161.53 ^{aB}	4184.15±170.48 ^{bAB}	4532.91±259.5 ^{bAB}	4820.35±407.42 ^{bB}	4066.94±181.56 ^{aA}
	30	4525.97±179.03 ^{aBC}	4114.33±7.21 ^{abAα}	4456.70±0.00 ^{bBα}	4726.87±0.00 ^{bC}	3929.99±16.67 ^{abAα}
	60	4384.07±97.56 ^{aA}	4068.84±11.31 ^{abB}	4216.63±141.42 ^{abBC}	4329.94±12.73 ^{abC}	3834.68±22.63 ^{abAα}
	90	4226.46±166.78 ^{aBα}	3886.58±35.54 ^{aA}	3810.42±14.14 ^{aA}	3968.64±2.83 ^{aAα}	3788.74±0.14 ^{aA}
		B1	B2	B3	B4	B5
Brine	2	4502.60±407.15 ^{bA}	4365.97±564.35 ^{cA}	4285.91±482.4 ^{bA}	4384.37±296.76 ^{cA}	4271.32±54.28 ^{cA}
	30	3058.23±14.14 ^{aA#}	3523.21±32.82 ^{bcC#}	3188.32±64.86 ^{aAB#}	3369.00±141.42 ^{bB}	3252.86±141.42 ^{bAB}
	60	2910.64±141.03 ^{aA}	3448.22±31.19 ^{bC#}	3057.73±132.72 ^{aAB}	3055.33±70.71 ^{abAB#}	3225.56±141.42 ^{bB}
	90	2942.95±2.83 ^{aB}	2362.47±282.84 ^{aA#}	2833.74±4.24 ^{aB}	2876.38±18.74 ^{aB#}	2855.01±141.42 ^{aB#}
Vacuum	2	4502.60±407.15 ^{cA}	4365.97±564.35 ^{aA}	4285.91±482.4 ^{aA}	4384.37±296.76 ^{aA}	4271.32±54.28 ^{bA}
	30	4179.68±77.32 ^{bcA}	4256.25±0.00 ^{aA}	4127.20±24.37 ^{aA}	4224.23±349.78 ^{aA}	4204.50±0.28 ^{bA}
	60	3739.81±0.14 ^{abA}	4142.80±2.83 ^{aD}	3915.40±21.21 ^{aB}	3985.59±7.07 ^{aC}	4189.15±12.73 ^{bE}
	90	3200.25±238.5 ^{aA}	4116.04±203.92 ^{aB}	3895.31±2.83 ^{aB}	3853.78±4.24 ^{aB}	3963.99±40.9 ^{aB}

Data values are expressed as means±standard deviation. Values in the same column followed by a different letters (a-c) are significantly different ($P < 0.05$). Values in the same row followed by a different letters (A-C) are significantly different ($P < 0.05$). Values in the same column showed different letter (α) between different treatments in the same day and package ($P < 0.05$). Values in the same column showed different letter (#) between different packages in the same day and package ($P < 0.05$).

A1: control cheese manufactured from raw milk, A2: sirmo-added cheese manufactured from raw milk, A3: mendi-added cheese manufactured from raw milk, A4: siyabo-added cheese manufactured from raw milk, A5: sirmo, mendi and siyabo mixture added cheese manufactured from raw milk, B1: control cheese manufactured from pasteurized milk, B2: sirmo-added cheese manufactured from pasteurized milk B3: mendi-added cheese manufactured from pasteurized milk, B4: siyabo-added cheese manufactured from pasteurized milk, B5: sirmo, mendi and siyabo mixture added cheese manufactured from pasteurized milk

Magnesium

It was determined that the magnesium content of samples ranged from 114.79-282.30 mg/kg. Therefore, the level of magnesium in the vacuum cheeses were higher than in brine cheeses. These results were agreement with findings obtained by Cetinkaya et al. (2016) as 111.20-214 mg/kg for Camibogazı and Ozlu et al. (2012) as 65.83-210.09 mg/kg for Kasar cheese but higher than the value determined by Kirdar et al. (2013) as 49.62 mg/kg for Akçakatik and Kirdar et al. (2015) as 72.6 to 88.9 for Kargı Tulum cheese.

The magnesium concentration of herby cheese decreased throughout the storage period similar to that Ca content. The possible reason for this situation, 70% of the Mg is in soluble form (Ocak and Kose, 2015) so transport of Mg from cheese into the brine until the osmotic pressure between brine and cheese phase is equalized during the storage period.

At the end of the ripening period, Siyabo added herby cheese (A4 and B4) in vacuum packaged had higher Mg values. This is probably due to the high Mg content of Siyabo in comparison to Sirmo and Mendi and loss of Mg in brine cheeses were higher than vacuum packaged.

Table 2. The effects of Sirmo, Mendi and Siyabo on Mg concentrations of herby cheese produced from pasteurized and raw milk in brine and vacuum package during ripening

Packaging type	Storage time	Treatment				
		A1	A2	A3	A4	A5
Brine	2	282.30±0.94 ^{cC}	250.81±8.3 ^{cAB}	268.49±7.54 ^{cBC}	280.80±21.01 ^{bBC}	226.08±10.71 ^{cA}
	30	157.84±7.21 ^{bA#}	165.45±3.13 ^{bA#}	166.85±2.44 ^{bA}	152.74±3.68 ^{aA}	172.62±16.38 ^{bA}
	60	141.58±4.84 ^{aA#}	148.16±6.35 ^{bAB#}	142.99±1.85 ^{aAB#}	153.79±4.64 ^{aB#}	149.14±3.45 ^{abAB#}
	90	137.35±0.49 ^{aAB#}	123.30±10.65 ^{aA}	139.62±7.94 ^{aAB}	140.02±2.97 ^{aB#}	126.51±1.35 ^{aAB}
Vacuum	2	282.30±0.94 ^{cC}	250.81±8.3 ^{bAB}	268.49±7.54 ^{bBC}	280.80±21.01 ^{bBC}	226.08±10.71 ^{aA}
	30	216.65±8.85 ^{bA}	241.66±13.08 ^{bA}	244.16±36.23 ^{bA}	241.94±27 ^{abA}	220.96±3.15 ^{aA}
	60	203.93±1.07 ^{abB}	207.00±1.46 ^{aB}	186.47±2.83 ^{aA}	203.93±9.02 ^{aB}	207.90±7.52 ^{aB}
	90	191.35±2.79 ^{aA}	197.06±0.33 ^{aA}	178.28±0.81 ^{aA}	197.67±7.18 ^{aA}	193.57±20.6 ^{aA}
		B1	B2	B3	B4	B5
Brine	2	251.56±26.04 ^{bA}	252.58±33.79 ^{bA}	246.22±24.08 ^{bA}	238.89±6.82 ^{cA}	239.63±4.74 ^{cA}
	30	161.33±5.54 ^{aC#}	162.02±1.54 ^{aC}	152.00±0.44 ^{aB}	163.62±0.43 ^{bC}	142.27±3.75 ^{bA#}
	60	140.78±10.85 ^{aAB}	151.76±1.08 ^{abB#}	137.21±3.03 ^{aAB#}	135.41±6.88 ^{aA#}	137.10±2.16 ^{abAB#}
	90	135.72±0.33 ^{aA}	114.79±40.06 ^{aA}	130.97±0.98 ^{aA}	134.35±1.85 ^{aA}	128.72±2.31 ^{aA#}
Vacuum	2	251.56±26.04 ^{bA}	252.58±33.79 ^{aA}	246.22±24.08 ^{cA}	238.89±6.82 ^{bA}	239.63±4.74 ^{bA}
	30	217.14±2.32 ^{abA}	244.17±26.86 ^{aA}	238.67±10.67 ^{bcA}	219.90±7.94 ^{abA}	218.36±11.14 ^{aA}
	60	192.20±5.33 ^{aA}	211.66±1.81 ^{aB}	203.66±7.95 ^{abAB}	211.87±2.64 ^{aB}	211.70±1.82 ^{aB}
	90	184.31±15.04 ^{aA}	188.74±21.67 ^{aA}	193.05±10.34 ^{aA}	203.33±13.92 ^{aA}	203.28±6.34 ^{aA}

Data values are expressed as means±standard deviation. Values in the same column followed by a different letters (a-c) are significantly different ($P < 0.05$). Values in the same row followed by a different letters (A-C) are significantly different ($P < 0.05$). Values in the same column showed different letter (α) between different treatments in the same day and package ($P < 0.05$). Values in the same column showed different letter (#) between different packages in the same day and package ($P < 0.05$).

A1: control cheese manufactured from raw milk, A2: sirmo-added cheese manufactured from raw milk, A3: mendi-added cheese manufactured from raw milk, A4: siyabo-added cheese manufactured from raw milk, A5: sirmo, mendi and siyabo mixture added cheese manufactured from raw milk, B1: control cheese manufactured from pasteurized milk, B2: sirmo-added cheese manufactured from pasteurized milk B3: mendi-added cheese manufactured from pasteurized milk, B4: siyabo-added cheese manufactured from pasteurized milk, B5: sirmo, mendi and siyabo mixture added cheese manufactured from pasteurized milk

Sodium

The 2005 Dietary Guidelines for Americans recommends that healthy adults limit consumption of sodium 2300 mg/d (5.84 g of NaCl or about 1 teaspoon of table salt) and hypertensive patients and the older adults should not take more than 1500 mg of sodium per day (Agarwal et al., 2011). The main source of sodium in diet is NaCl, most of salt comes from commercial food in the improved countries. Sodium is important for regulation of blood and osmotic pressure, transport of water into and out of cells and transmission of nerve cell impulses (Cruz et al., 2011). However, excess intake of Na causes high blood pressure and other chronic diseases (Felicio et al., 2013). Another symptom that may be caused by high intake of sodium is the interference in bioavailability of calcium due to the increase in the renal excretion of this mineral. According to predictive equations, it is believed that urinary excretion of calcium will increase by 30-40 mg, for each 2 g of sodium consumed. However, if the intake of sodium is below 2.4 g per day, there will be no negative effect on the bones (Cruz et al., 2011).

Table 3. The effects of Sirmo, Mendi and Siyabo on Na concentrations of herby cheese produced from pasteurized and raw milk in brine and vacuum package during ripening

Packaging Storage type time		Treatment				
		A1	A2	A3	A4	A5
Brine	2	9294.33±37.50 ^{aAB}	10063.22±97.13 ^{cB}	9760.38±801.6 ^{bB}	8988.52±458.28 ^{aAB}	8544.34±156.38 ^{aA}
	30	8893.50±496.39 ^{aA}	9191.56±276.77 ^{bA}	9357.64±210.07 ^{abA}	8174.47±1069.8 ^{aA}	8304.72±216.93 ^{aA}
	60	8459.21±257.28 ^{aA}	8378.36±7.91 ^{aA}	8277.06±128.85 ^{abA}	7992.04±484.57 ^{aA}	8091.53±13.73 ^{aA}
	90	7695.82±1064.04 ^{aA}	8177.62±50.2 ^{aA}	7936.84±841.97 ^{aA}	7438.06±62.95 ^{aA}	7411.54±1143.34 ^{aA}
Vacuum	2	9294.33±37.50 ^{aAB}	10063.22±97.13 ^{cB}	9760.38±801.6 ^{cB}	8988.52±458.28 ^{bAB}	8544.34±156.38 ^{bA}
	30	8312.71±688.16 ^{bA}	9301.38±207.3 ^{cA}	8323.66±1090.16 ^{bc} _A	8111.66±478.75 ^{bA}	7678.90±251.44 ^{bA}
	60	7059.16±342.85 ^{aAB}	7779.52±252.12 ^{bB}	7151.20±653.1 ^{abAB}	7464.23±639.8 ^{abAB}	6239.40±513.97 ^{aA}
	90	6182.13±415.69 ^{aA}	6955.23±301.85 ^{aA}	5954.15±188.08 ^{aAa}	5800.43±1235.84 ^a _A	5719.61±581.63 ^{aA}
		B1	B2	B3	B4	B5
Brine	2	8498.95±983.67 ^{aA}	8603.88±1441.57 ^{aA}	9474.39±277.38 ^{bA}	9236.33±208.12 ^{cA}	9028.79±612.69 ^{aA}
	30	8633.91±51.39 ^{abB}	8499.30±132.67 ^{abB}	7855.82±351.88 ^{aA}	8738.28±53.74 ^{bB}	8561.86±151.17 ^{abB}
	60	8499.70±412.14 ^{abB}	8352.02±276.7 ^{aAB}	7760.03±293.9 ^{aA}	7832.21±2.53 ^{aAB}	8114.84±12.18 ^{aAB}
	90	8279.66±238.89 ^{aA}	6533.16±1312.67 ^{aA}	7352.96±2.83 ^{aA}	7402.20±282.84 ^{aA}	7491.24±1378.04 ^{aA}
Vacuum	2	8498.95±983.67 ^{aA}	8603.88±1441.57 ^{aA}	9474.39±277.38 ^{bA}	9236.33±208.12 ^{dA}	9028.79±612.69 ^{bA}
	30	8104.64±30.11 ^{aA}	8531.79±734.49 ^{aA}	7866.53±315.04 ^{aA}	8401.65±225.07 ^{cA}	7631.18±93.44 ^{aA}
	60	8342.28±533.16 ^{abA}	7340.69±573.69 ^{aA}	7299.02±438.74 ^{aA}	7470.44±195.13 ^{bA}	7393.15±439.59 ^{aA}
	90	7689.56±11.77 ^{aC}	6902.22±202.43 ^{abB}	7344.09±234.14 ^{abBC}	6139.72±363.35 ^{aA}	7193.61±296.89 ^{abC}

Data values are expressed as means±standard deviation. Values in the same column followed by a different letter (a-c) are significantly different ($P < 0.05$). Values in the same row followed by a different letter (A-C) are significantly different ($P < 0.05$). Values in the same column showed different letter (α) between different treatments in the same day and package ($P < 0.05$). Values in the same column showed different letter (#) between different packages in the same day and package ($P < 0.05$).

A1: control cheese manufactured from raw milk, A2: sirmo-added cheese manufactured from raw milk, A3: mendi-added cheese manufactured from raw milk, A4: siyabo-added cheese manufactured from raw milk, A5: sirmo, mendi and siyabo mixture added cheese manufactured from raw milk, B1: control cheese manufactured from pasteurized milk, B2: sirmo-added cheese manufactured from pasteurized milk B3: mendi-added cheese manufactured from pasteurized milk, B4: siyabo-added cheese manufactured from pasteurized milk, B5: sirmo, mendi and siyabo mixture added cheese manufactured from pasteurized milk

The sodium content of cheese samples ranged from 5719.61 to 10063.22 mg/kg. It has been exhibited that the sodium levels suggested for a healthy person can be met by consuming about 250 g of Herby cheese. Sodium in herby cheese is due to milk naturally contain some sodium as well as due to added salt and pickled herbs. Our results were similar with findings obtained by Cetinkaya et al. (2016) as 4852.5-10520 mg/kg for Camiboğazi, by Holland et al. (1995) as 700 mg/100 g for Brie cheese, lower than the value determined by Tarakci and Kucukoner (2008) as 2606 mg/100 g for herby cheese and higher than the value determined by Holland et al. (1995) as 380 mg/100 g for Cottage cheese, by Felicio et al. (2013) as 574.5, 473.4, 588.8 mg/100 g for Mozzarella, Minas and Prato cheeses, respectively.

Potassium

The metabolism of water is affected and myoneural activities are stimulated by Na as well as K, in the human body. According to nutritional recommendations, the sufficient Na and K proportion in diet must be of 0.6 for adults and 0.5 for children (Cruz et al., 2011).

Table 4. The effects of Sirmo, Mendi and Siyabo on K concentrations of herby cheese produced from pasteurized and raw milk in brine and vacuum package during ripening

Packaging type	Storage time	Treatment				
		A1	A2	A3	A4	A5
Brine	2	1124.98±152.2 ^{bb}	890.48±30.02 ^{baB}	1059.20±271.59 ^{bb}	992.24±31.94 ^{cAB}	642.36±44.39 ^{cA}
	30	474.88±58.23 ^{aA}	475.31±107.91 ^{aA}	410.84±3.1 ^{aAα}	450.57±0.71 ^{ba#α}	483.70±64.63 ^{bA}
	60	422.42±21.23 ^{aA}	384.14±5.66 ^{aA}	390.02±7.79 ^{aAα}	447.76±18.59 ^{abA#}	444.56±64.2 ^{abA}
	90	384.69±5.66 ^{aA#}	367.78±94.54 ^{aA}	309.00±107.08 ^{aA}	396.60±4.24 ^{aA#}	321.25±51.88 ^{aA}
Vacuum	2	1124.98±152.2 ^{bb}	890.48±30.02 ^{cAB}	1059.20±271.59 ^{bb}	992.24±31.94 ^{cAB}	642.36±44.39 ^{aA}
	30	570.76±48.91 ^{aA}	626.63±2.88 ^{ba}	587.25±116.72 ^{aA}	642.82±4.03 ^{ba}	628.33±11.53 ^{aA}
	60	555.95±40.22 ^{aA}	622.50±36.34 ^{ba}	497.59±98.92 ^{aA}	625.46±0.32 ^{abA}	611.76±7.07 ^{aA}
	90	499.50±4.84 ^{aAB}	418.10±87.89 ^{aA}	504.98±40.13 ^{aAB}	581.95±11.4 ^{ab}	605.94±1.41 ^{aBa}
		B1	B2	B3	B4	B5
Brine	2	758.55±85.55 ^{ba}	914.23±159.64 ^{ba}	791.87±90.63 ^{ba}	650.45±87.45 ^{ba}	799.25±14.14 ^{aA}
	30	466.96±16.55 ^{aAB#}	435.83±75.24 ^{aA}	486.75±4.95 ^{aAB}	510.83±4.17 ^{aAB}	535.39±21.09 ^{bb}
	60	373.15±123.6 ^{aA}	390.57±44.53 ^{aA}	445.62±7.07 ^{aA}	478.45±42.56 ^{aA}	508.18±32.36 ^{ba}
	90	351.61±1.41 ^{aA}	323.87±104.81 ^{aA}	416.09±29.32 ^{aA}	387.75±7.71 ^{aA}	364.35±8.61 ^{aA#}
Vacuum	2	758.55±85.55 ^{ba}	914.23±159.64 ^{ba}	791.87±90.63 ^{cA}	650.45±87.45 ^{ba}	799.25±14.14 ^{ba}
	30	579.43±6.72 ^{aA}	594.53±86.59 ^{aA}	716.41±54.22 ^{bcA}	612.98±36.8 ^{abA}	591.21±66.76 ^{aA}
	60	554.07±27.89 ^{aA}	555.28±1.9 ^{aA}	547.57±53.44 ^{abA}	563.62±39.39 ^{abA}	553.08±35.54 ^{aA}
	90	515.10±70.92 ^{aA}	419.22±67.96 ^{aA}	525.52±46.95 ^{aA}	476.80±53.76 ^{aA}	507.70±3.54 ^{aA}

Data values are expressed as means±standard deviation. Values in the same column followed by a different letters (a-c) are significantly different ($P < 0.05$). Values in the same row followed by a different letters (A-C) are significantly different ($P < 0.05$). Values in the same column showed different letter (α) between different treatments in the same day and package ($P < 0.05$). Values in the same column showed different letter (#) between different packages in the same day and package ($P < 0.05$).

A1: control cheese manufactured from raw milk, A2: sirmo-added cheese manufactured from raw milk, A3: mendi-added cheese manufactured from raw milk, A4: siyabo-added cheese manufactured from raw milk, A5: sirmo, mendi and siyabo mixture added cheese manufactured from raw milk, B1: control cheese manufactured from pasteurized milk, B2: sirmo-added cheese manufactured from pasteurized milk B3: mendi-added cheese manufactured from pasteurized milk, B4: siyabo-added cheese manufactured from pasteurized milk, B5: sirmo, mendi and siyabo mixture added cheese manufactured from pasteurized milk

As seen in *Table 4*, the K values of herby cheese samples were significantly decreased during the ripening period. The K values of brine cheeses were determined lower than vacuum packaged cheeses at the end of the storage periods. The possible reason for this situation, the cheese that was ripened in a brine had a higher salt content than the cheese ripened in vacuum packaging. In general, as the salt content increases, the acidity decreases and the pH value increases in the cheese (Kose, 2015; Almenara et al., 2007). The final average values were lower than those described by Ocak and Kose (2015) and similar with findings obtained by Mendil (2006) for herby cheeses and by Murtaza et al. (2014) for cheddar cheese.

Iron

Iron is an essential trace element is incorporated as a catalyst in various metabolic reactions. It is a component of hemoglobin, myoglobin, cytochrome and other proteins and plays an important role in the transport, storage and use of oxygen. Milk and dairy products are insufficient source in terms of Fe for human nutrition (Zamberlin et al., 2012). Its deficiency causes anaemia, decrease in immunity and alteration in mental development (Gaucheron, 2000).

Table 5. The effects of Sirmo, Mendi and Siyabo on Fe concentrations of herby cheese produced from pasteurized and raw milk in brine and vacuum package during ripening

Packaging type	Storage time	Treatment				
		A1	A2	A3	A4	A5
Brine	2	6.59±0.13 ^{bCα}	5.00±0.20 ^{aB}	4.08±0.1 ^{aAα}	4.19±0.43 ^{aA}	6.04±0.06 ^{bCα}
	30	5.33±1 ^{abA}	4.89±0.31 ^{aA}	3.76±0.29 ^{aA}	4.11±0.02 ^{aA}	4.89±1.05 ^{abA}
	60	4.26±1.44 ^{abA}	4.10±1.05 ^{aA}	3.70±0.71 ^{aA}	3.66±0.66 ^{aA}	4.29±0.73 ^{abA}
	90	3.28±0.5 ^{aA}	3.52±0.54 ^{aA}	3.42±0.74 ^{aA}	3.28±0.06 ^{aA}	3.06±0.25 ^{aA}
Vacuum	2	6.59±0.13 ^{dC}	5.00±0.2 ^{bB}	4.08±0.1 ^{bA}	4.19±0.43 ^{bA}	6.04±0.06 ^{cC}
	30	4.75±0.07 ^{cDα}	4.44±0.33 ^{aCD}	3.78±0.04 ^{abA}	3.84±0.13 ^{abAB}	4.26±0.08 ^{bBC}
	60	3.79±0.12 ^{bB}	4.37±0.07 ^{aC}	3.61±0.07 ^{abAB}	3.49±0.19 ^{abAB}	3.42±0.06 ^{aA}
	90	3.19±0.29 ^{aA}	4.27±0.1 ^{aB}	3.44±0.33 ^{aAB}	3.30±0.35 ^{aA}	3.06±0.49 ^{aA}
		B1	B2	B3	B4	B5
Brine	2	4.39±0.34 ^{cA}	4.89±0.06 ^{bAB}	5.54±0.08 ^{dAB}	5.63±0.95 ^{bB}	5.26±0.13 ^{bAB}
	30	4.11±0.08 ^{bcA#}	4.70±0.28 ^{bBC}	4.51±0.01 ^{cABC}	4.47±0.28 ^{abAB}	5.05±0.19 ^{bC}
	60	3.83±0.09 ^{bB}	4.13±0.14 ^{aC}	3.80±0.1 ^{bB}	3.48±0.11 ^{aA}	3.72±0.03 ^{aAB}
	90	3.16±0.02 ^{aA}	3.84±0.07 ^{aA}	3.03±0.43 ^{aA}	3.46±0.19 ^{aA}	3.61±0.49 ^{aA}
Vacuum	2	4.39±0.34 ^{cA}	4.89±0.06 ^{aAB}	5.54±0.08 ^{cAB}	5.63±0.95 ^{bB}	5.26±0.13 ^{bAB}
	30	3.51±0.06 ^{abA}	3.99±0.75 ^{aA}	4.45±0.13 ^{bA}	4.02±0.45 ^{aA}	4.50±0.35 ^{abA}
	60	3.79±0.04 ^{bcA}	3.78±1.32 ^{aA}	3.40±0.06 ^{aA}	3.43±0.29 ^{aA}	3.67±0.37 ^{aA}
	90	3.06±0.27 ^{aA}	3.65±0.4 ^{aA}	2.97±0.27 ^{aA}	3.29±0.07 ^{aA}	3.51±0.54 ^{aA}

Data values are expressed as means±standard deviation. Values in the same column followed by a different letters (a-c) are significantly different ($P < 0.05$). Values in the same row followed by a different letters (A-C) are significantly different ($P < 0.05$). Values in the same column showed different letter (α) between different treatments in the same day and package ($P < 0.05$). Values in the same column showed different letter (#) between different packages in the same day and package ($P < 0.05$).

A1: control cheese manufactured from raw milk, A2: sirmo-added cheese manufactured from raw milk, A3: mendi-added cheese manufactured from raw milk, A4: siyabo-added cheese manufactured from raw milk, A5: sirmo, mendi and siyabo mixture added cheese manufactured from raw milk, B1: control cheese manufactured from pasteurized milk, B2: sirmo-added cheese manufactured from pasteurized milk B3: mendi-added cheese manufactured from pasteurized milk, B4: siyabo-added cheese manufactured from pasteurized milk, B5: sirmo, mendi and siyabo mixture added cheese manufactured from pasteurized milk

Zinc

Zinc is an essential mineral that is very nutritionally for human and deficiency creates significant implications for human health. The deficiency of Zn results in a wide spectrum. Its clinical effects depending on age, stage of development and deficiencies of related metals (Bakircioglu et al., 2011). The maximum tolerable daily intake of Zn is 60 mg (FAO/WHO, 1999, 1999). In this study, the content of Zn for herby cheeses in brine and vacuum packages were lower than the WHO's values.

Table 6. The effects of Sirmo, Mendi and Siyabo on Zn concentrations of herby cheese produced from pasteurized and raw milk in brine and vacuum package during ripening

Packaging type	Storage time	Treatment				
		A1	A2	A3	A4	A5
Brine	2	16.65±0.86 ^{aB}	14.63±0.13 ^{bAB}	14.87±0.08 ^{bAB}	16.67±1.34 ^{cB}	14.12±1.32 ^{bA}
	30	16.03±0.87 ^{aB}	14.50±0.24 ^{bAB}	14.76±0.27 ^{bAB}	15.67±0.95 ^{bcB}	13.91±0.17 ^{bA}
	60	14.95±0.23 ^{aB}	14.16±0.52 ^{abAB}	14.25±0.66 ^{abAB}	13.48±0.42 ^{abA#}	13.24±0.01 ^{abA}
	90	13.71±2.58 ^{aA}	13.63±0.16 ^{aA}	13.49±0.13 ^{aA}	11.36±0.08 ^{aA#}	11.28±0.88 ^{aA}
Vacuum	2	16.65±0.86 ^{aB}	14.63±0.13 ^{aB}	14.87±0.08 ^{aB}	16.67±1.34 ^{aB}	14.12±1.32 ^{aA}
	30	16.36±0.5 ^{aB}	14.45±0.19 ^{aA}	14.42±0.62 ^{aA}	16.02±0.84 ^{aB}	13.94±0.07 ^{aA}
	60	16.05±0.31 ^{aC}	14.16±0.13 ^{aB}	13.87±0.19 ^{aB}	15.89±0.28 ^{aC}	13.42±0.33 ^{aA}
	90	15.79±0.34 ^{aCα}	13.93±0.65 ^{aB}	13.69±0.59 ^{aB}	14.59±0.16 ^{aB}	13.04±0.05 ^{aA}
		B1	B2	B3	B4	B5
Brine	2	15.61±1.84 ^{aA}	14.75±2.09 ^{aA}	15.65±1.69 ^{bA}	16.59±1.99 ^{aA}	16.58±0.19 ^{bA}
	30	14.22±3.1 ^{aA}	15.00±0.53 ^{aA}	14.68±0.95 ^{abA}	15.11±4.08 ^{aA}	15.32±1.94 ^{abA}
	60	13.54±1.61 ^{aA}	14.92±0.86 ^{aA}	14.47±0.86 ^{abA}	14.93±0.04 ^{aA}	13.87±1.02 ^{abA}
	90	12.36±0.96 ^{aAB}	13.99±0.28 ^{aB}	12.20±0.28 ^{aA#}	13.31±0.41 ^{aAB#}	12.22±0.96 ^{aAB}
Vacuum	2	15.61±1.84 ^{aA}	14.75±2.09 ^{aA}	15.65±1.69 ^{aA}	16.59±1.99 ^{aA}	16.58±0.19 ^{aA}
	30	15.53±1.38 ^{aA}	14.54±0.07 ^{aA}	15.50±0.31 ^{aA}	16.41±0.49 ^{aA}	16.16±0.80 ^{aA}
	60	15.25±0.19 ^{aA}	14.34±0.15 ^{aA}	15.35±0.76 ^{aA}	15.80±0.84 ^{aA}	15.25±1.10 ^{aA}
	90	12.96±0.34 ^{aA}	14.13±0.37 ^{aB}	15.36±0.05 ^{aC}	15.09±0.34 ^{aC}	14.93±0.31 ^{aC}

Data values are expressed as means±standard deviation. Values in the same column followed by a different letters (a-c) are significantly different ($P < 0.05$). Values in the same row followed by a different letters (A-C) are significantly different ($P < 0.05$). Values in the same column showed different letter (α) between different treatments in the same day and package ($P < 0.05$). Values in the same column showed different letter (#) between different packages in the same day and package ($P < 0.05$)

A1: control cheese manufactured from raw milk, A2: sirmo-added cheese manufactured from raw milk, A3: mendi-added cheese manufactured from raw milk, A4: siyabo-added cheese manufactured from raw milk, A5: sirmo, mendi and siyabo mixture added cheese manufactured from raw milk, B1: control cheese manufactured from pasteurized milk, B2: sirmo-added cheese manufactured from pasteurized milk B3: mendi-added cheese manufactured from pasteurized milk, B4: siyabo-added cheese manufactured from pasteurized milk, B5: sirmo, mendi and siyabo mixture added cheese manufactured from pasteurized milk

The Zn concentration of herby cheeses produced from raw and pasteurized milk changed from 11.28 to 16.67, 12.96 to 16.59 mg/kg, respectively. It has been found that the Zn concentration of cheese produced from both pasteurized and raw milk decreased during the storage period. But, at the end of the storage periods, the Zn content of brine cheeses were found lower than vacuum packaged cheeses. When the findings are compared with the literature, our results were lower than the value determined by Oksuztepe et al. (2013) as 20.50 mg/kg for white cheese, by Isleten et al. (2007) as 2.12-8.19 mg/100 g for Ezine cheese, by Cichoscki et al. (2002) as 29.21-36.60 mg/kg

for Prato cheese, by Altun and Kose (2016) as 22.70 to 65.37 for Kelle cheese, by Bilandzic et al. (2015) as 46 mg/kg for semi hard fat cheese consumed in Croatia.

Manganese

The Institute of Medicine suggests that intake of Mn should not exceed the tolerable daily maximum limit of 11 mg/day (National Research Council, 1989). In this study, Mn concentrations of cheese samples changed from 0.70 to 0.26 mg/kg. The content of Mn for Herby cheese samples in brine and vacuum packages were lower than the National Research Council.

Table 7. The effects of Sirmo, Mendi and Siyabo on Mn concentrations of herby cheese produced from pasteurized and raw milk in brine and vacuum package during ripening

Packaging time	Storage type	Treatment				
		A1	A2	A3	A4	A5
Brine	2	0.52±0.11 ^{ba}	0.70±0.08 ^{bb}	0.46±0.06 ^{aA}	0.59±0.04 ^{cAB}	0.43±0.01 ^{aA}
	30	0.50±0.03 ^{abA}	0.46±0.01 ^{aA}	0.39±0.16 ^{aA}	0.38±0.01 ^{ba}	0.39±0.01 ^{aA}
	60	0.37±0.04 ^{abA}	0.37±0.01 ^{aA}	0.35±0.01 ^{aAα}	0.34±0.01 ^{abA}	0.38±0.02 ^{aA}
	90	0.34±0.04 ^{aA}	0.33±0.03 ^{aA}	0.33±0.00 ^{aA}	0.31±0.00 ^{aA}	0.33±0.13 ^{aA}
Vacuum	2	0.52±0.11 ^{ba}	0.70±0.08 ^{bb}	0.46±0.06 ^{ba}	0.59±0.04 ^{baB}	0.43±0.01 ^{ba}
	30	0.37±0.01 ^{abA}	0.46±0.04 ^{abA}	0.44±0.05 ^{baB}	0.51±0.06 ^{bb}	0.40±0.02 ^{baB}
	60	0.36±0.04 ^{abA}	0.40±0.07 ^{aA}	0.30±0.01 ^{aA}	0.39±0.01 ^{aA}	0.36±0.03 ^{abA}
	90	0.34±0.01 ^{aAB}	0.38±0.01 ^{aBα}	0.31±0.01 ^{aA}	0.37±0.01 ^{aB}	0.30±0.03 ^{aA}
		B1	B2	B3	B4	B5
Brine	2	0.42±0.05 ^{aA}	0.42±0.06 ^{ba}	0.51±0.11 ^{ba}	0.55±0.02 ^{ba}	0.46±0.08 ^{aA}
	30	0.39±0.00 ^{aA}	0.36±0.04 ^{abA}	0.31±0.01 ^{aA}	0.35±0.11 ^{abA}	0.42±0.13 ^{aA}
	60	0.35±0.02 ^{aAB}	0.36±0.01 ^{abB}	0.31±0.01 ^{aA}	0.33±0.01 ^{abAB}	0.34±0.02 ^{aAB}
	90	0.33±0.05 ^{aA}	0.26±0.00 ^{aA}	0.30±0.06 ^{aA}	0.28±0.10 ^{aA}	0.35±0.01 ^{aA}
Vacuum	2	0.42±0.05 ^{aA}	0.42±0.06 ^{aA}	0.51±0.11 ^{aA}	0.55±0.02 ^{ba}	0.46±0.08 ^{aA}
	30	0.39±0.01 ^{aAB}	0.38±0.01 ^{abA}	0.40±0.02 ^{aAB}	0.40±0.03 ^{aAB}	0.44±0.02 ^{aB}
	60	0.34±0.01 ^{aA}	0.36±0.02 ^{abA}	0.37±0.03 ^{aA}	0.38±0.01 ^{aA}	0.39±0.05 ^{aA}
	90	0.32±0.05 ^{aA}	0.30±0.01 ^{aA}	0.34±0.06 ^{aA}	0.38±0.04 ^{aA}	0.38±0.01 ^{aA}

Data values are expressed as means±standard deviation. Values in the same column followed by a different letters (a-c) are significantly different ($P < 0.05$). Values in the same row followed by a different letters (A-C) are significantly different ($P < 0.05$). Values in the same column showed different letter (α) between different treatments in the same day and package ($P < 0.05$). Values in the same column showed different letter (β) between different packages in the same day and package ($P < 0.05$).

A1: control cheese manufactured from raw milk, A2: sirmo-added cheese manufactured from raw milk, A3: mendi-added cheese manufactured from raw milk, A4: siyabo-added cheese manufactured from raw milk, A5: sirmo, mendi and siyabo mixture added cheese manufactured from raw milk, B1: control cheese manufactured from pasteurized milk, B2: sirmo-added cheese manufactured from pasteurized milk B3: mendi-added cheese manufactured from pasteurized milk, B4: siyabo-added cheese manufactured from pasteurized milk, B5: sirmo, mendi and siyabo mixture added cheese manufactured from pasteurized milk

Decrease in the Mn concentrations of pasteurized and raw milk herby cheeses were determined during the ripening period. The possible decrease in pH can induce this situation. In general, Mn are linked to the insoluble fraction of casein micelle of milk in a ratio of 95% (Cichoski et al., 2002). However, as the pH in cheese decreases during ripening, migration of Mn towards the soluble fraction is monitored (Macedo and Malcata, 1997). As a result, the loss of Mn content occurs in brine or vacuum packaged

samples. Our results showed similar behaviour with findings obtained by Cichoski et al. (2002) as 0.36 to 0.26 mg/kg for Prato cheese, were higher than the value determined by Kirdar et al. (2015) as 0.11 to 0.19 µg/g for Kargi Tulum Cheese and were lower than the value determined by Macedo and Malcata (1997) as 1.17 to 1.40 mg/kg for Serra cheese.

Conclusions

As a result, Na, Ca, K, Mg, Zn, Fe and Mn content of cheese samples were influenced by herbs, packaging, ripening and heat treatment. It was observed that ripening has the most pronounced effect on studied variables. The concentrations of minerals in cheese samples decreased and the changes of ratios of mineral compounds were different during storage period. The vacuum packaged cheeses were found to have a higher mineral content than the cheeses stored in brine at the end of 90 days. Because of the mineral loss of cheeses in brine were higher than in vacuum packaged due to diffusions of mineral substances from cheese into the brine during maturation. This investigation is first study comparing herbs species, packaging type and ripening period on the mineral content of herby cheeses produced from pasteurized and raw milk. Therefore, further investigations are needed to determine the influence of various factors on the mineral compositions of herby cheeses.

REFERENCES

- [1] Agarwal, S., McCoy, D., Graves, V., Gerard, P. D., Clark, S. (2011): Sodium content in retail Cheddar, Mozzarella and process cheeses varies considerably in the United States. – *Journal of Dairy Science* 94: 1605-1615.
- [2] Almenara, F., Alvarez, S., Darias, J., Rodriguez, E., Diaz, C., Fresno, M. (2007): Effect of the ripening in the mineral composition of the cheese made with Majorera goat's milk. – *Archivos de Zootecnia* 56(1): 667-671.
- [3] Altun, I., Kose, S. (2016): Determination of some properties of traditional Kelle cheese. – *Yuzuncu Yil University Journal of Agricultural Sciences* 26(4): 642-647 (in Turkish).
- [4] Andic, S., Gencelep, H., Kose, S. (2010): Determination of biogenic amines in Herby cheese. – *International Journal of Food Properties* 13: 1300-1314.
- [5] Andic, S., Tuncurk, Y., Javidipour, I., Gencelep, H. (2015): Effect of different herbs on biogenic amine contents and some characteristics of herby cheese. – *Gıda* 40(1): 1-8.
- [6] Bakircioglu, D., Bakircioglu Kurtulus, Y., Ucar, G. (2011): Determination of some traces metal levels in cheese samples packaged in plastic and tin containers by ICP-OES after dry, wet and microwave digestion. – *Food and Chemical Toxicology* 49: 202-207.
- [7] Bilandzic, N., Sedak, M., Dokic', M., Bozic, D., Vrbic, A. (2015): Content of macro and microelements and evaluation of the intake of different dairy products consumed in Croatia. – *Journal of Food Composition and Analysis* 40: 143-147.
- [8] Cichoski, A. J., Valduga, E., Valduga, A. T., Tornadijo, M. E., Fresno, J. M. (2002): Characterization of Prato cheese, a Brazilian semi-hard cow variety: evolution of physico-chemical parameters and mineral composition during ripening. – *Food Control* 13: 329-336.
- [9] Cruz, A. G., Faria, J. A. F., Pollonio, M. A. R., Bolini, H. M. A., Celeghini, R. M. S., Granato, D., Shah, N. P. (2011): Cheeses with reduced content: Effects on functionality, public health benefits and sensory properties. – *Trends in Food Science & Technology* 22: 276-291.

- [10] Cetinkaya, A., Akbaba, G. B., Ozcakmak, S., Gulbaz, G. (2016): Mineral and heavy metal content in Cami Bogazi cheese on sale in Trabzon, Turkey. – *Gıda* 41(5): 317-321 (in Turkish).
- [11] FAO/WHO (1999): Joint FAO/WHO foods standards programme. Expert committee on the food additives, summary and conclusions. – 53rd Meeting, June 1-10. FAO, Rome.
- [12] Gaucheron, F. (2000): Iron fortification in dairy industry. – *Trends in Food Science-Technology* 11: 403-409.
- [13] Gider, K. (2006): Determination of Some Factors that Affects Salt Immigration in White Cheese. – Selcuk University Graduate School of Natural and Applied Sciences Department of Food Engineering, Konya.
- [14] Guinee, T. P., Fox, P. F. (1986): Transport of sodium chloride and water in Romano cheese slices during brining. – *Food Chemistry* 19: 49-64.
- [15] Hayaloglu, A. A., Fox, P. F. (2008): Cheeses of Turkey: 3. Varieties containing herbs or spices. – *Dairy Science and Technology* 88: 245-256.
- [16] Felicio, T. L., Esmerino, E. A., Cruz, A. G., Nogueira, L. C., Raices, R. S. L., Deliza, R., Bolini, H. M. A., Pollonio, M. A. R. (2013): Cheese. What is its contribution to the sodium intake of Brazilians? – *Appetite* 66: 84-88.
- [17] Holland, B., Welch, A. A., Unwin, I. D., Buss, D. H., Paul, A. A., Southgate, D. A. T. (1995): *The Composition of Foods*. 5th Ed. – Royal Society of Chemistry and Ministry of Agriculture, Fisheries and Food, London.
- [18] IDF (International Dairy Federation). (1992): Trace Elements in Milk and Milk Products. – *Bulletin of the International Dairy Federation*, No: 278, Brussels.
- [19] Isleten, M., Uysal-Pala, C., Karagul-Yuceer, Y. (2007): Mineral content of Ezine cheese. – *The Journal of Food* 32(4): 173-179 (in Turkish).
- [20] Kirdar, S. S., Ocak, E., Kose, S. (2013): Mineral and trace metal levels of Akcakatik cheese collected from Mediterranean region-Turkey. – *Asian Journal of Chemistry* 25: 1643-1646. DOI: 10.14233/ajchem.2013.13611.
- [21] Kirdar, S. S., Kose, S., Gun, I., Ocak, E., Kursun, O. (2015): Do consumption of Kargı Tulum cheese meet daily requirements for minerals and trace elements? *Mljekarstvo* 65(3): 203-209.
- [22] Kose, S. – (2015): The effect of some herbs added to herby cheese on antimicrobial properties, antioxidant capacity and phenolic compounds of cheese. – PhD Thesis. Yuzuncu Yil University Department of Food Engineering, Van (in Turkish).
- [23] Kose, S., Ocak, E. (2015): Determination of some characteristic properties of traditional Surk cheese. – *Academic Food Journal* 13(2): 135-139 (in Turkish).
- [24] Macedo, A. C., Malcata, F. X. (1997): Changes of mineral concentrations in Serra cheese during ripening and throughout the cheesemaking season. – *Journal of the Science of Food and Agriculture* 74: 409-415.
- [25] Mendil, D. (2006): Mineral and trace metal levels in some cheese collected from Turkey. – *Food Chemistry* 96: 532-537.
- [26] Murtaza, M. A., Huma, N., Sameen, A., Saeed, M., Murtaza, M. S. (2014): Minerals and lactic acid contents in buffalo milk cheddar cheese; a comparison with cow. – *Journal of Food and Nutrition Research* 2(8): 465-468.
- [27] National Research Council (1989): *Recommended Dietary Allowances*. 10th ed. – National Academic Press, Washington, DC.
- [28] Ocak, E., Kose, S. (2015): Production of Van Herby cheese and Its mineral content. – *The Journal of Food* 40(6): 343-348 (in Turkish).
- [29] Ozlu, H., Aydemir-Atasever, M., Urcar, S., Atasever, M. (2012): Mineral contents and heavy metal contamination in Kashar cheeses consumed in Erzurum province, Turkey. – *Journal of the Faculty of Veterinary Medicine, Kafkas University* 18(2): 205-208 (in Turkish).

- [30] Oksuztepe, G., Karatepe, P., Ozcelik, M., Incili, G. K. (2013): Mineral substances and heavy metal contents in Tulum cheese and fresh White cheese. – *Firat University Health Sciences Veterinary Journal* 27(2): 93-97 (in Turkish).
- [31] Sagun, E., Tarakci, Z., Sancak, H., Durmaz, H. (2005): Change of mineral content in pickled Herby cheese during ripening. – *Van Veterinary Journal* 16(1): 21-25 (in Turkish).
- [32] Tarakci, Z., Akyuz, N. (2009): Effects of packaging materials and filling methods on selected characteristics of Otlu (Herby) cheese. – *International Journal of Food Properties* 12(3): 496-511. DOI: 10.1080/10942910701813941.
- [33] Tarakci, Z., Kucukoner, E. (2008): Comparison of basic nutrients, mineral and heavy metal contents of herby dairy products. – *International Journal of Food Science and Technology* 43: 216-219.
- [34] Tarakci, Z., Temiz, H. (2009): A review of the chemical, biochemical and antimicrobial aspects of Turkish Otlu (herby) cheese. – *International Journal of Dairy Technology* 62(3): 354-360.
- [35] Tarakci, Z., Coskun, H., Tuncturk, Y. (2004): Some properties of fresh and ripened herby cheese, a traditional variety produced in Turkey. – *Food Technology and Biotechnology* 42(1): 47-50.
- [36] Tarakci, Z., Sancak, H., Durmaz, H., Kilicel, F. (2005): Mineral substances and heavy metal contents of herby cheeses. – *Van Health Sciences Journal* 8: 18-23 (in Turkish).
- [37] Tuncturk, Y., Ocak, E., Kose, S. (2014): Changes in chemical and physical properties and proteolysis of Van herby (otlu) cheese during ripening. – *The Journal of Food* 39(3): 163-170 (in Turkish).
- [38] Yuzbasi, N., Sezgin, E., Yildirim, M., Yildirim, Z. (2003): Survey of lead, cadmium, iron, copper and zinc in Kashar cheese. – *Food Additives and Contaminants* 20: 464-469. DOI: 10.1080/0265203031000094654.
- [39] Zamberlin, S., Antunac, N., Havranek, J., Samaržija, D. (2012): Mineral elements in milk and dairy products. – *Mljekarstvo* 62(2): 111-125.

THE EFFECT OF THE TYPES OF FOLIAR FEEDING ON FRESH AND DRY WINTER RAPE MASS (*BRASSICA NAPUS* L.)

SIKORSKA, A.¹ – GUGAŁA, M.^{2*} – ZARZECKA, K.²

¹*Department of Agriculture, State Higher Vocational School in Ciechanów
ul. Narutowicza 9, 06-400 Ciechanów, Poland
(e-mail: anna.sikorska@pwszciechanow.edu.pl)*

²*Department of Agrotechnology, Siedlce University of Natural Sciences and Humanities
ul. Prusa 14, 08-110 Siedlce, Poland
(e-mail: kzarzecka@uph.edu.pl)*

**Corresponding author
e-mail: gugala@uph.edu.pl*

(Received 28th Feb 2019; accepted 10th Apr 2019)

Abstract. The field experiment was carried out in 2016-2019 at the Agricultural Experimental Station - Zawady belonging to the University of Natural Sciences and Humanities in Siedlce. The experiment was established in a random split-plot system in three repetitions. The surface of one plot was 21 m². The examined factors were I - three varieties of winter rape: Monolit (population variety), PX115 (hybrid variety restored with a semi-dwarf growth type), PT248 (hybrid variety restored with a traditional growth type). II - four types of foliar feeding: 1. control object (without foliar feeding and biostimulator were sprayed with distilled water), 2. biostimulator Aminoplant, 3. Foliar fertilizer Siarkomag + foliar fertilizer Bormax, 4. Foliar fertilizer Siarkomag + foliar fertilizer Bormax + biostimulator Aminoplant. The aim of the study was to determine the effect of foliar feeding on the growth of fresh and dry mass of plants (leaf rosette, root) of three winter rape varieties. On the basis of the conducted research, it was found that autumn foliar feeding of plants significantly increased the fresh and dry weight of the rosette and the root system in comparison to the control variant. The highest growth of plant weight and root system was recorded on object 4, which proves that the biostimulator applied with foliar fertilizers had a positive effect on the uptake and accumulation of micro and macro-elements provided with foliar fertilizers. The Monolit population variety was distinguished by the largest green and dry mass of the rosette and root system. In the growing season 2018-2019 characterized by very hot and dry autumn, the largest fresh and dry mass of plants (rosettes and root system) was found.

Keywords: *morphotype, leaf rosette, root, foliar fertilization, biostimulator, amino acids*

Introduction

Insufficient feeding of plants leads to the disturbances of basic physiological processes, which adversely affects the growth and development of plants, contributing as a consequence to a decrease in yields (Kocot and Grenda, 2004). Sienkiewicz-Cholewa and Kieloch (2015) and Jankowski et al. (2016b) they emphasize that during the growing season some nutrients can be delivered directly on the plant leaves.

Foliar feeding of plants supplying, in addition to the necessary nutrients, biostimulator compounds, is more and more often treated as permanent elements of the proper agrotechnology of many crop plants. According to Harris et al. (2018) the foliar application is the fastest method of providing nutrients for plants.

Szewczuk (2003) and Kocoń (2009) in their research emphasized the beneficial effect of foliar nutrition in winter plants in the period of autumn growing season.

The macro and microelements provided at the time influence the accumulation of sugars in plant cells, which is associated with the hardening of plants and increased

resistance to wintering conditions (Szewczuk and Sugier, 2009). Noreen et al. (2018) and Yakhin et al. (2017) they stated that plants well fed with essential nutrients have greater tolerance to environmental stress.

According to Jankowski et al. (2016a) and White et al. (2015) foliar fertilization is an alternative method of providing macro-elements, it can be used only to reverse the effects of nutritional deficiencies and can serve as the main technique of fertilization only to provide plants with the required micronutrients.

Kocira et al. (2016) and Złotek and Wójcik (2014) biostimulators and agents containing micronutrient additives are safe to use and do not exhibit any destructive effects on the environment.

The study assumes the hypothesis that the use of foliar fertilizers and biostimulators may affect the growth of fresh and dry mass of plants (rosettes, root system). The aim of the research was to determine the effect of foliar nutrition on the growth of fresh and dry mass of the aboveground part of the rosette and fresh and dry mass of the root system of three varieties of winter rape.

Materials and methods

Experimental and agronomic management

The field experiment was carried out in 2016-2019 at the Agricultural Experimental Station Zawady (52°03'N and 22°33'E) belonging to the University of Natural Sciences and Humanities in Siedlce. The experiment was established in a random split-plot system in three repetitions. The surface of one plot was 21 m².

The following factors were studied in the experiment:

Factor I - three varieties of rape:

1. Monolit (population variety)
2. PT 248 (hybrid variety restored with a traditional growth type)
3. PX 115 (hybrid variety restored with a semi-dwarf growth type)

Factor II - four types of foliar feeding:

1. Control object - without using foliar feeding and a biostimulator were sprayed with distilled water
2. Biostimulator Aminoplant (N_{total} - 8.5%): I term - in autumn in the 4-6 leaf phase (BBCH 14-16) at a dose of 1.0 dm³·ha⁻¹
3. Foliar fertilizer Siarkomag (MgO - 5%. SO_{3total} - 85%. SO_{3soluble} in water - 10%) + foliar fertilizer Bormax (B - 11%): I term - in autumn in the 4-6 leaf phase (BBCH 14-16) at a dose of 2.0 dm³·ha⁻¹ + 0.5 dm³·ha⁻¹
4. Foliar fertilizer Siarkomag + foliar fertilizer Bormax + biostimulator Aminoplant: I term - in autumn in the 4-6 leaf phase (BBCH 14-16) at a dose of 2.0 dm³·ha⁻¹ + 0.5 dm³·ha⁻¹ + 1.0 dm³·ha⁻¹

The forecrop for winter rape in particular years of the research was spring wheat (1st year of research), winter triticale (2nd year of research), winter triticale (3rd year of research). The experiment was carried out on soil classified in the order of soils with clay translocation, type – Luvisols, subtype - Albic Luvisols (WBR FAO 2014). This soil was classified as IVa bonitation class soil, of very good rye complex for agricultural use. During the years of the experiment, soil pH (in 1n KCl) was slightly acidic, ranging from 5.68 to 5.75. The soil was characterized by a low total content of nitrogen (on

average $0.85 \text{ g}\cdot\text{kg}^{-1}$), phosphorus (on average $0.44 \text{ g}\cdot\text{kg}^{-1}$), potassium (on average $0.65 \text{ g}\cdot\text{kg}^{-1}$) and calcium (on average $0.83 \text{ g}\cdot\text{kg}^{-1}$) and the medium content of magnesium (on average $0.42 \text{ g}\cdot\text{kg}^{-1}$) and sulphur (on average $0.13 \text{ g}\cdot\text{kg}^{-1}$). It demonstrated low content of available phosphorus forms (on average from 75 to $80 \text{ mg}\cdot\text{kg}^{-1}$) and medium content of available forms of potassium (on average from 200 to $205 \text{ mg}\cdot\text{kg}^{-1}$) and magnesium (on average from 59 to $61 \text{ mg}\cdot\text{kg}^{-1}$).

After forecrop harvest, a set of post-harvest procedures was carried out using the ploughing aggregate + open cage roller, and then two weeks after the first procedure, pre-sow ploughing at the depth of 20.0 cm was carried out, using a ring roller at the same time. To prepare the soil for sowing and to mix fertilizers, a complex soil tillage unit was used. Before sowing, phosphorus-potassium fertilization was applied at the dose of $40 \text{ kg P}\cdot\text{ha}^{-1}$ and $110 \text{ kg K}\cdot\text{ha}^{-1}$ and the first dose of $40 \text{ kg N}\cdot\text{ha}^{-1}$. Fertilization was applied in the form of Lubofos at the dose of 600 kg . Fertilizing doses were supplemented with $55.9 \text{ kg}\cdot\text{ha}^{-1}$ of ammonium nitrate ($19 \text{ kg N}\cdot\text{ha}^{-1}$), $29.6 \text{ kg}\cdot\text{ha}^{-1}$ triple superphosphate ($13.6 \text{ kg P}\cdot\text{ha}^{-1}$) and $29 \text{ kg}\cdot\text{ha}^{-1}$ potassium salt ($17.9 \text{ kg K}\cdot\text{ha}^{-1}$). The second dose of nitrogen in the amount of $100 \text{ kg}\cdot\text{ha}^{-1}$ was applied in spring, before vegetation started (BBCH 28-30) applying ammonium nitrate at the dose of $255.5 \text{ kg}\cdot\text{ha}^{-1}$ ($86.9 \text{ kg N}\cdot\text{ha}^{-1}$) and ammonium sulphate at the dose of $62.5 \text{ kg}\cdot\text{ha}^{-1}$. The third dose of ammonium $60 \text{ kg}\cdot\text{ha}^{-1}$ was applied at the inflorescence emergence (BBCH 50) by applying ammonium nitrate at the dose of $176.5 \text{ kg}\cdot\text{ha}^{-1}$ ($60 \text{ kg N}\cdot\text{ha}^{-1}$).

Winter rapeseed sowing was made at spacing between rows of 22.5 cm , assuming the sow of $60 \text{ pcs}\cdot\text{m}^{-2}$. Sowing was made at the optimal time recommended for this region (in 2016 - on 12 August, 2017 - on 14 August, and in 2018 - on 13 August).

Chemical protection against weeds, diseases and pests was applied in accordance with the recommendations of good agricultural practice.

Immediately before the inhibition of the autumn vegetation the following biometric characteristics were identified on the randomly selected sample of 20 plants:

- Fresh mass of the aboveground part of 1 rosette (g)
- Dry mass of the aboveground part of 1 rosette (g)
- Fresh mass of the root system of 1 plant (g)
- Dry mass of the root system of 1 plant (g)

In all years of conducting experiments, plant samples were collected in the 16-19 BBCH phase, in the second decade of October.

The method of determining air dry matter in fresh plant material consisted in drying the sample to air-dry state in a natural way, and then at a temperature not exceeding $105 \text{ }^{\circ}\text{C}$ for 3 h.

Statistical analysis

The results of the study were statistically analysed with the use of the analysis of variance. The significance of variation sources was tested with the “F” Fischer-Snedecor test and the assessment of significance at the significance level of $p = 0.05$ between compared means with Tukey’s range test.

Weather conditions

In autumn, varied weather conditions prevailed in the analysed vegetation seasons (Table 1). In the first year of research, autumn was quite dry ($K = 1.30$). The period

from August to October was characterized by a smaller average of 11.3 mm of rainfall compared to the average of that period from 1996-2010, while the average air temperature was similar to the long-term period of 13.3 °C. In the growing season of 2017-2018 based on the calculated Sielianinow coefficient (Skowera, 2014), it was found that autumn was quite wet ($K = 1.76$). The sum of precipitation from August to October was higher by an average of 61.9 mm compared to the average for many years, and the average air temperature was higher by 0.5 °C. In the last year of research, autumn was very dry ($K = 0.68$). The sum of precipitation from August to October was lower by 51.2 mm compared to the long-term, and the average air temperature was higher on average by 2.1 °C compared to many years.

Table 1. Characteristics of weather conditions in the years 2016-2019 (Zawady Meteorological Station, Poland)

Months	Rainfalls (mm)				Air temperature (°C)			
	Multiyear sum	Monthly sum			Multiyear mean	Monthly mean		
		1996-2010	2016-2017	2017-2018		2018-2019	1996-2010	2016-2017
VIII	59.9	31.7	54.7	24.5	18.5	18.0	18.4	20.6
IX	42.3	13.6	80.6	27.4	13.5	14.9	13.9	15.9
X	24.2	69.8	53.0	23.3	7.9	7.0	9.0	9.6
XI	20.2	19.5	21.3	9.8	4.0	2.4	4.1	7.9
XII	18.6	22.5	15.8	9.0	-0.1	0.0	2.7	0.3
I	19.0	0.4	10.1	7.9	-3.2	-6.6	-0.7	-3.0
Mean	184.2	157.5	235.5	101.9	12.1	5.9	7.9	8.5

Sielianinows hydrothermic coefficients*			
	2016-2017	2017-2018	2018-2019
VIII	0.61	1.00	0.40
IX	0.28	1.92	0.71
X	3.02	2.36	0.94
Mean	1.30	1.76	0.68

*Index value (Skowera, 2014): extremely dry $k \leq 0.4$, very dry $0.4 < k \leq 0.7$, dry $0.7 < k \leq 1.0$, rather dry $1.0 < k \leq 1.3$, optimal $1.3 < k \leq 1.6$, rather humid $1.6 < k \leq 2.0$, humid $2.0 < k \leq 2.5$, very humid $2.5 < k \leq 3.0$, extremely humid $k > 3.0$

Results and discussion

On the basis of the conducted research, it was found that the applied foliar nutrition significantly influenced the increase of fresh and dry mass of the aboveground part of the rosette and root system in comparison to the control variant (Tables 2, 4, 6 and 7). This is consistent with the results of Gawrońska et al. (2008) and Sikorska et al. (2017). The authors after using biostimulators Asahi SL, Tytanit and Silvit noted an increase in the value of these features compared to the control object. Albayrak and Camas (2005), Soheir et al. (2012) and Aisha et al. (2014) under the influence of stimulation with humic acids received a greater fresh and dry mass of the aboveground part of the rosette and root system in comparison of the object on which no fertilization was applied. Similarly, Krawczyk and Skoczyński (2008) showed a beneficial effect of the foliar fertilizer Route on the fresh and dry mass of the root system. In own studies, the largest increase in plant mass and root system was noted on object 4, where the foliar fertilizer Siarkomag. Bormax and biostimulator Aminoplant were used. This proves that the applied biostimulator positively influenced the uptake and accumulation of micro and macro-elements provided with foliar fertilizers. In our own research, the genetic factor

significantly affected the fresh and dry mass of aboveground part of the rosette and root system. The highest values of the discussed features were found in the Monolit population variety, while the lowest in the restored hybrid with a semi-dwarf growth type (PX 115) (Tables 2, 4, 6 and 7). This is in line with the results of studies by Kotecki et al. (2007) and Sikorska et al. (2017). These authors also recorded the largest fresh and dry mass of the aboveground part of the rosette and root system in the Monolit population variety, while the smallest in the semi-dwarf PR44D06. Similarly, Wielebski and Wójtowicz (2018) showed that the hybrid morphotype with a semi-dwarf growth type PR45D03 was characterized by a smaller fresh mass compared to the varieties with a traditional type of growth: hybrid Poznaniak and population Starter. Jankowski and Budzyński (2007) and Wielebski (2007) came to different conclusions, who showed that hybrid forms produced a rosette with a larger fresh and dry mass of 1 plant and the root system. The largest fresh and dry mass of the above-ground of 1 rosette and the root system was noted in the last year of research, in which autumn was very dry and warm, while the lowest in the fairly humid vegetation season 2017-2018 (Tables 2, 4, 6 and 7). In turn, in earlier studies by Sikorska et al. (2017), the highest values of the discussed features were demonstrated in the season characterized by heavy rainfall in August and alternate rainfall in September and higher than the average air temperature in September and October, while the lowest in the season in which strong drought occurred in August and the first two decades of September.

Table 2. Green matter of one plant (g) depending on factors of experience

Cultivars	Years			Types of foliar feeding				Mean
				Objects				
	2016-2017	2017-2018	2018-2019	1.	2.	3.	4.	
				Control variant	Biostimulator Aminoplant	Foliar fertilizer Siarkomag + foliar fertilizer Bormax	Foliar fertilizer Siarkomag + foliar fertilizer Bormax + biostimulator Aminoplant	
Monolit	34.708	27.542	41.033	32.533	32.833	35.733	36.611	34.428 a
PT 248	31.650	25.458	35.800	29.322	29.933	31.600	33.022	30.969 b
PX 115	27.083	23.075	32.508	25.811	26.467	28.256	29.689	27.556 c
Mean	31.147 a	25.358 b	36.447 c	29.222 a	29.744 b	31.863 c	33.107 d	-

LSD_{0.05} for: years - 0.460; cultivars - 0.460; types of foliar feeding - 0.331; interaction: years x cultivars - 0.796; cultivars x types of foliar feeding - 0.522

The statistical calculations showed the interaction of years and studied varieties with the fresh and dry matter of the aboveground part of 1 rosette and the root system, which means that varieties reacted to the humidity and thermal conditions differently in the years of research (Tables 2, 4, 6 and 7). Based on the conducted studies, the interaction of varieties and types of foliar feeding was found, which means that varieties reacted differently to the types of foliar feeding (Tables 2 and 4). The fresh and dry mass of the above ground part of 1 rosette of the Monolit variety after the application of the Aminoplant biostimulator containing amino acids was the same as in the control object. In all studied varieties, the highest increase in fresh and dry matter was recorded as a result of the application of the Aminoplant biostimulator with foliar fertilizers Siarkomag and Bormax. The impact of biostimulators and foliar fertilizers on the fresh and dry mass of the aboveground part of 1 rosette was determined by the climatic

conditions prevailing in the years of research (Tables 3 and 5). In autumn in the growing seasons 2017-2018 and 2018-2019, the fresh mass of aboveground part of rosette after the application of the Aminoplant biostimulator was the same as in the control object, while the dry mass of the aboveground part after using the bioregulator with the amino acid was the same as in the control object only in the last growing season.

Table 3. Green matter of one plant (g) depending on the years and types of foliar feeding

Years	Types of foliar feeding				Mean
	Objects				
	1.	2.	3.	4.	
	Control variant	Biostimulator Aminoplant	Foliar fertilizer Siarkomag + foliar fertilizer Bormax	Foliar fertilizer Siarkomag + foliar fertilizer Bormax + biostimulator Aminoplant	
2016-2017	29.611 a	30.189 d	31.944 g	32.844 j	31.147
2017-2018	23.356 b	23.867 b	26.367 h	27.844 k	25.358
2018-2019	34.700 c	35.178 c	37.278 i	38.633 l	36.447
Mean	29.222	29.744	31.863	33.107	-

LSD_{0.05} for: years - 0.460; types of foliar feeding - 0.331; interaction: years x types of foliar feeding - 0.522

Table 4. Dry matter of one plant (g) depending on factors of experience

Cultivars	Years			Types of foliar feeding				Mean
				Objects				
	1.	2.	3.	4.				
	2016-2017	2017-2018	2018-2019	Control variant	Biostimulator Aminoplant	Foliar fertilizer Siarkomag + foliar fertilizer Bormax	Foliar fertilizer Siarkomag + foliar fertilizer Bormax + biostimulator Aminoplant	
Monolit	7.633	6.058	9.075	7.144	7.222	7.889	8.100	7.589 a
PT 248	6.958	5.600	7.867	6.433	6.556	6.956	7.289	6.808 b
PX 115	5.950	5.067	7.208	5.711	5.844	6.211	6.533	6.075 c
Mean	6.847 a	5.575 b	8.050 c	6.430 a	6.541 b	7.019 c	7.307 d	-

LSD_{0.05} for: years - 0.097; cultivars - 0.097; types of foliar feeding - 0.065; interaction: years x cultivars - 0.169; cultivars x types of foliar feeding - 0.102

Table 5. Dry matter of one plant (g) depending on the years and types of foliar feeding

Years	Types of foliar feeding				Mean
	Objects				
	1.	2.	3.	4.	
	Control variant	Biostimulator Aminoplant	Foliar fertilizer Siarkomag + foliar fertilizer Bormax	Foliar fertilizer Siarkomag + foliar fertilizer Bormax + biostimulator Aminoplant	
2016-2017	6.500 a	6.644 d	7.022 f	7.222 i	6.847
2017-2018	5.133 b	5.244 e	5.789 g	6.133 j	5.575
2018-2019	7.656 c	7.733 c	8.244 h	8.567 k	8.050
Mean	6.430	6.541	7.019	7.307	-

LSD_{0.05} for: years - 0.097; types of foliar feeding - 0.065; interaction: years x types of foliar feeding - 0.102

Table 6. Green matter of the root system of one plant (g) depending on factors of experience

Cultivars	Years			Types of foliar feeding				Mean
				Objects				
	2016-2017	2017-2018	2018-2019	1.	2.	3.	4.	
				Control variant	Biostimulator Aminoplant	Foliar fertilizer Siarkomag + foliar fertilizer Bormax	Foliar fertilizer Siarkomag + foliar fertilizer Bormax + biostimulator Aminoplant	
Monolit	8.975	7.433	11.483	8.744	8.933	9.578	9.933	9.297 a
PT 248	8.367	6.875	10.025	7.956	8.089	8.600	9.044	8.422 b
PX 115	8.275	6.225	9.100	7.356	7.511	8.078	8.522	7.867 c
Mean	8.539 a	6.844 b	10.203 c	8.019 a	8.178 b	8.752 c	9.167 d	-

LSD_{0.05} for: years - 0.116; cultivars - 0.116; types of foliar feeding - 0.088; interaction: years x cultivars - 0.201; cultivars x types of foliar feeding - n.s.

Table 7. Dry matter of the root system of one plant (g) depending on factors of experience

Cultivars	Years			Types of foliar feeding				Mean
				Objects				
	2016-2017	2017-2018	2018-2019	1.	2.	3.	4.	
				Control variant	Biostimulator Aminoplant	Foliar fertilizer Siarkomag + foliar fertilizer Bormax	Foliar fertilizer Siarkomag + foliar fertilizer Bormax + biostimulator Aminoplant	
Monolit	2.075	1.925	2.975	2.189	2.233	2.378	2.500	2.325 a
PT 248	1.900	1.825	2.617	1.989	2.056	2.156	2.256	2.114 b
PX 115	1.883	1.792	2.400	1.900	1.956	2.078	2.167	2.025 c
Mean	1.953 a	1.847 b	2.664 c	2.026 a	2.082 b	2.204 c	2.307 d	-

LSD_{0.05} for: years - 0.041; cultivars - 0.041; types of foliar feeding - 0.04; Interaction: years x cultivars - 0.07; cultivars x types of foliar feeding - n.s.

Conclusions

1. Autumn foliar feeding of plants significantly increased the fresh and dry mass of the rosette and root system in comparison to the control variant. The highest growth of plant weight and root system was noted on object 4. Biostimulator applied with foliar fertilizers had a positive effect on the uptake and accumulation of micro and macro-elements provided with foliar fertilizers.
2. Spraying plants of the Monolit variety only with the Aminoplant amino acid meant that dry and fresh mass of the aboveground part of 1 plant was at a similar level as in the control object.
3. From the compared morphotypes, the Monolit population variety was characterized by the largest green and dry mass of the rosette and root system, whereas the smallest hybrid variety with a semi-dwarf growth-type PX 115.
4. The largest fresh and dry mass of the aboveground part of rosette and root system was obtained in the warmest and driest autumn period.

Acknowledgements. The research was carried out under the research project No. 363/S/13, financed from a science grant by the Ministry of Science and Higher Education.

REFERENCES

- [1] Aisha, H., Ali. Shafeek, M. R., Mahmoud, R., Asmaa, R., El- Desuki, M. (2014): Effect of various levels of organic fertilizer and humic acid on the growth and roots quality of turnip plants (*Brassica rapa*). – Current Science International 3(1): 7-14.
- [2] Albayrak, S., Camas, N. (2005): Effects of different levels and application times of humic acid on root and leaf yield components of forage turnip (*Brassica rapa* L.). – J. Agronomy 4(2): 130-133.
- [3] Gawrońska, H., Przybysz, A., Szalacha, E., Słowiński, A. (2008): Physiological and Molecular Mode of Action of Asahi SL Biostimulator under Optimal and Stress Conditions. – In: Gawronska, H. (ed.) Biostimulators in Modern Agriculture. General Aspects. Wieś Jutra, Warsaw, pp. 54-76.
- [4] Harris, K. D. Vanajah, T. Puvanitha, S. (2018): Effect of foliar application of boron and magnesium on growth and yield of green chilli (*Capsicum annum* L.). – J. Agr. Sci-Cambridge 12(1): 26-33.
- [5] Jankowski, K. J., Budzyński, W. (2007): Reaction of various winter rape cultivation forms to date and sowing density I. Autumn growth and development and wintering of plants. – Rośliny Oleiste - Oilseed Crops 28(2): 177-194 (in Polish).
- [6] Jankowski, K. J., Hulanicki, P. S., Krzebietke, S., Żarczyński, P., Hulanicki, P., Sokólski, M. (2016a): Yield and quality of winter oilseed rape in response to different systems of foliar fertilization. – J. Elem. 21(4): 1017-1027. DOI: 10.5601/ jelem.2016.21.1.1108.
- [7] Jankowski, K. J., Sokólski, M., Dubis, B., Krzebietke, S., Żarczyński, P., Hulanicki, P., Hulanicki, P. S. (2016b): Yield and quality of winter oilseed rape (*Brassica napus* L.) seeds in response to foliar application of boron. – Agricultural and Food Sci. 25: 164-176.
- [8] Kocira, A., Świeca, M., Kocira, S., Złotek, U., Jakubczyk, A. (2016): Enhancement of yield, nutritional and nutraceutical properties of two common bean cultivars following the application of seaweed extract (*Ecklonia maxima*). – Saudi J. Biol. Sci. 25(3): 563-571. doi.org/10.1016/j.sjbs.2016.01.039.
- [9] Kocoń, A. (2009): Foliar top dressing efficiency of winter wheat and rape of chosen fertilizers inoptimal fertilization and soil moisture conditions. – Annales UMCS, s. E. 64(2): 23-28 (in Polish).
- [10] Kocoń, A., Grenda, A. (2004): The influence of Titanite on photosynthesis, yield and nutrient uptake by rape plants. – Zesz. Probl. Post. Nauk Roln. 502(1): 49-64 (in Polish).
- [11] Kotecki, A., Malarz, W., Kozak, M., Pogorzelec, A. (2007): The effect of plants' location in a canopy on the growth and yield of rape hybrids and population cultivars. Part I. Plant morphology and seed yields. – Zesz. Nauk. Uniwersytetu Przyrodniczego we Wrocławiu, Rolnictwo XC(553): 7-39 (in Polish).
- [12] Krawczyk, R., Skoczyński, J. (2008): Winter Survival and Yield of Oilseed Rape Depending on Sowing Date and Application of Micronutrient Preparation Route® Acting as a Growth Stimulator. – In: Dąbrowski, Z. T. (ed.) Monographs Series: Biostimulators in Modern Agriculture: Field Crops. Editorial House Wieś Jutra, Warsaw, pp. 33-40.
- [13] Noreen, S., Fatima, Z., Ahmad, S., Athar, H. R., Ashraf, M. (2018): Plant Nutrients and Abiotic Stress Tolerance. – In: Hasanuzzaman, M., Fujita, M., Oku, H., Nahar, K., Hawrylak-Nowak, B. (eds.) Plant Nutrients and Abiotic Stress Tolerance. Springer, Singapore.
- [14] Sienkiewicz-Cholewa, U., Kieloch, R. (2015): Effect of sulphur and micronutrients fertilization on yield and fat content in winter rape seeds (*Brassica napus* L.). – Plant, Soil and Environ. 61: 164-170.
- [15] Sikorska, A., Gugąła, M., Zarzecka, K., Kapela, K., Mystkowska, I. (2017): The impact of agrotechnical factors on fresh and dry matter of oilseed rape (*Brassica napus* L.). – J. Ecol. Eng. 18(3): 174-179.
- [16] Skowera, B. (2014): Changes of hydrothermal conditions in the Polish area (1971–2010). – Fragm. Agron. 31(2): 74-87 (in Polish).

- [17] Soheir, E. El-Sherbeny, Hendawy, S. F., Youssef, A. A., Naguib, N. Y., Hussein, M. S. (2012): Response of turnip (*Brassica rapa*) plants to Minerals or Organic Fertilizers treatments. – J. Appl. Sci. Res. 8(2): 628-634.
- [18] Szewczuk, Cz. (2003): Effect of application of chosen foliar fertilizers on winter hardiness and seed yields of winter rape. – Acta Agroph. 85: 289-295 (in Polish).
- [19] Szewczuk, Cz., Sugier, D. (2009): General characteristics and types of foliar fertilizers offered on the Polish market. – Annales UMCS. s. E. LXIV(1): 29-36 (in Polish).
- [20] White, C. A., Roques, S. E., Berry, P. M. (2015): Effects of foliar-applied nitrogen fertilizer on oilseed rape (*Brassica napus*). – J. Agri. Sci. 153(1): 42-51.
- [21] Wielebski, F. (2007): Response of different types of winter oilseed rape varieties to various plant density in the field I. Seed yield and its components. – Rośliny Oleiste - Oilseed Crops 28(2): 209-226 (in Polish).
- [22] Wielebski, F., Wójtowicz, M. (2018): Effect of date and density of sowing and weather conditions on growth in the autumn and winter survival of winter oilseed rape morphotypes with traditional and semidraft type of growth. – Fragn. Agron. 35(2): 133-145 (in Polish).
- [23] World Reference Base for Soil Resources (2014): International Soil Classification System for Naming Soils and Creating Legends for Soil. Field Experiment. – FAO, WorldSoil Resources Reports, 106, Rome. <http://www.fao.org>.
- [24] Yakhin, O. I., Lubyantsev, A. A., Yakhin, I. A., Brown, P. H. (2017): Biostimulants in plant science: a global perspective. – Front. Plant Sci. 7: 2049. DOI: 10.3389/fpls.2016.02049.
- [25] Złotek, U., Wójcik, W. (2014): Effect of arachidonic acid elicitation on lettuce resistance towards *Botrytis cinerea*. – Sci. Hortic. 179: 16-20.

EXPRESSION AND BIOINFORMATIC ANALYSIS OF *ANTPS1* GENE IN NAKED OATS (*AVENA NUDA* L.)

LIU, W.^{1*} – WANG, R.¹ – ZHOU, F.¹ – LIU, J.¹ – LIU, R.¹ – LIU, L.¹ – LI, F.¹ – LI, G.² – TIAN, H.² – ZHANG, Y.¹ – ZHANG, D.¹

¹*Applied Biotechnology Institute, Shanxi Datong University, Datong, Shanxi 037009, China*

²*High Latitude Crops Institute to Shanxi Academy of Agriculture Sciences, Datong, Shanxi 037009, China*

*Corresponding author

e-mail: 15035246759@163.com

(Received 6th Mar 2019; accepted 2nd Apr 2019)

Abstract. Ongoing climate change has led to more extreme global temperature variations, and coupled with other environmental issues such as soil salinization, these changes pose serious challenges to future farming efforts. As such, it is vitally important both to identify crops able to resist temperature and salt stress and to explore the underlying molecular mechanisms governing such resistance in order to facilitate the selective production of crops with superior resistance traits able to persist in an increasingly harsh global environment. To that end, in this study, PCR was used to isolate the *AnTPS1* gene, which encodes trehalose 6-phosphate synthases (TPS). Real-time PCR was used to detect the expression of the gene in different tissues and under low temperature. We used a bioinformatics approach to assess key characteristics of the *AnTPS1* gene, determining its physicochemical properties, signal peptides, transmembrane structural domains, hydrophilicity, hydrophobicity, secondary structures, modules, and tertiary structures. We isolated an important abiotic stress resistance gene *AnTPS1* in naked oats. Real-time quantitative PCR analysis showed *AnTPS1* to be expressed in different tissues of naked oats, and we found that low temperature stress was sufficient to induce the upregulation of this gene. We determined that the protein encoded by *AnTPS1* gene is a soluble hydrophobic protein composed of 326 amino acids, containing signal peptides and transmembrane structures. The protein does not feature crimp spirals, instead featuring α -helices and irregular crimps are the main secondary structure elements. Together, these results provide an important biochemical foundation for the study of *AnTPS1* as a putative cold-resistance gene in naked oats, and may offer valuable insights necessary for enabling selective production of temperature-resistant crops suitable for growth in previously untenable locations.

Keywords: *naked oats, AnTPS1, gene, bioinformatics, trehalose 6-phosphate synthase (TPS), cold stress*

Introduction

Constant global climate change and rapid population increase pose significant challenges for securing a sufficient global food supply (Tai et al., 2014). There is a vital need to breed key staple crops that are able to resist abiotic stressors such as drought

conditions, extreme cold, and highly saline soil stress (Flowers, 2004; Hu and Xiong, 2014). It is thus critically important that crops with ideal resistance traits be identified, and that the molecular mechanisms governing their resistance behaviors be fully elucidated to allow for the selective production of resistant crops capable of meeting future global food production needs.

Naked oat (*Avena nuda* L.), also known as oil wheat, jade wheat, and bell wheat, is a member of the family of Gramineae, genus *Hordeum*, of Chinese origin (Zhou et al., 2016). Naked oats are a cold-tolerant crop, withstanding temperatures as low as -2 to -4°C in the seedling and tillering growth stages (Liu et al., 2013). Naked oats are additionally a quick-growing, drought-resistant, and saline-alkali-resistant species. Given these key resistance characteristics, naked oats are well-suited for growth in harsh environments, and are primarily distributed in northern China and in the arid and semi-arid areas of northwest China (Ma et al., 2013). Naked oats are high in nutritional value, being rich in eight necessary amino acids, various trace elements, abundant linoleic acid, dietary fiber, and other important nutritional compounds (Wang et al., 2017). The levels of vitamin E and B in naked oats are similarly high, and the levels of protein and fat in the seeds are higher than in most food crops (Lin et al., 2011). Naked oats are primarily harvested and used for human consumption, medicine, and feeding poultry. The optimal resistance characteristics of this strain to environmental stressors make it ideal in harsh environments. Characterizing the specific molecular mechanisms underlying these resistance traits therefore offers a unique opportunity to facilitate the selective breeding or modification of strains of oats and other crops in order to allow them to better grow in non-permissive environments.

Trehalose is an important sugar molecule that is known to be vital for plant resistance to abiotic stress (Oide and Inui, 2017). Trehalose can prevent the transition of a cellular phospholipid bilayer from a liquid crystal state to the solid state, thus stabilizing proteins and other macromolecules within the bilayer and thereby enhancing the resistance of plant cells to various forms of abiotic stress (van Dijken et al., 2004). The synthesis of trehalose is catalyzed by TPS and trehalose-6-phosphate phosphatase (TPP), with the former being the rate-limiting enzyme for its production (Xu et al., 2017). The introduction of fusion genes for TPS and TPP from *Escherichia coli* and yeast into transgenic tobacco, potato, rice and *Arabidopsis* plants has been found to increase resistance to abiotic stress such as drought tolerance among these transgenic plants (Delorge et al., 2015). These studies thus indicate the TPS gene plays an important role in enhancing plant stress resistance, making it an important target of research aimed at improving the resistance characteristics of crops. This has led to extensive efforts to better understand the role of trehalose in the context of abiotic stress resistance, and as such TPS gene sequences have been isolated and validated from herbaceous plants such as *Arabidopsis thaliana* in recent years (Xu et al., 2017). Whether particular species of plants possess unique TPS genes with potentially advantageous properties remains to be determined, and at present there are no reports on the characteristics of TPS in naked

oats. As such, in the present study we used a bioinformatics approach to assess the properties of the *AnTPS1* gene in naked oats, exploring its physicochemical properties, signal peptides, transmembrane structural domains, hydrophilicity, hydrophobicity, secondary structures, modules, and tertiary structures. Through these efforts, this study aimed to provide a theoretical basis both for improving naked oats yield and quality, and to more broadly produce information that may be of value for the selective production of crops with advantageous abiotic stress resistant traits.

Materials and methods

Materials and cold treatment

Naked oats cultivar Jinyan 17 was used in this study. Seeds were sterilized through incubation for 1 min in 75% ethanol, and thoroughly being washed with sterile water. The seeds were germinated in soil in pots at 20°C under long-day conditions (16 h of cool white fluorescent light, photon flux of 70 $\mu\text{mol m}^{-2} \text{s}^{-1}$). 50 Seedlings at the four-leaf stage were subjected to cold stress. 50 Seedlings in the control group were grown at 20°C continuously. To induce cold stress, seedlings were transferred to an artificial climate box at 4°C under the same light and photoperiodic conditions. The leaves were then treated with cold temperature at 4°C for 0 h, 1 h, 3 h, 6 h, 12 h, 24 h (Indeok, 2016). This stressor procedure was conducted in triplicate.

AnTPS1 gene expression analysis

Total RNA was extracted from plants using the RNA Plant Plus Reagent Kit (Tiangen Biochemical Technology Co., Ltd.) and was reverse transcribed into cDNA using the FastQuant RT Kit. The cDNA of *AnTPS1* was amplified by PCR and sequenced. The primer sequences were: AnTPS1-F1 (5'- CATCACGCTGCTCTCTCTAC -3') and AnTPS1-R1 (5'- GAGGTCCGACACTTGCGTT -3'). The relative expression of *AnTPS1* was then detected by real-time fluorescent quantitative PCR (Guo et al., 2015; Reem et al., 2017). The cDNA derived from root, stem, and leaves of plants exposed to temperature stress treatment were used for all qPCR reactions. The primer sequences for *AnTPS1* were: AnTPS1-F2 (5'- TCCTATGCTGTGTCCCAATC -3') and AnTPS1-R2 (5'- CAGACCAGTGAACAATAGGG -3'). *Actin* served as an internal reference gene; the primer sequences for actin were: Actin-F (5' TATTGCTTTCTCCTGCTGTC-3') and Actin-R (5'-CTATGTATCCTGGTATTGCG-3'). The qPCR reaction was conducted under the following conditions: pre-denaturation at 95°C for 3 min; denaturation at 94°C for 30 s, annealing at 60°C for 30 s, extension at 72°C for 30 s, 30 cycles. A melting curve was then constructed via the system default procedure. All samples were run in triplicate.

Biological information analysis of AnTPS1

A comprehensive bioinformatics analysis was conducted using tools including the NCBI, PDB, and ExPASy databases and further online ones (*Table 1*) (Lu et al., 2018), in order to predict and analyze characteristics such as conserved domains, the physicochemical properties of the primary structure, signal peptides, transmembrane structural domains, subcellular localization, hydrophilicity and hydrophobicity, secondary structure, modules, and tertiary structures (Mao et al., 2018). Briefly, bioinformatics tools were used as follows: CD Search was used for conservative domain prediction; the ExPASy Protparam tool was used to predict the physicochemical properties of the encoded protein; the ExPASy ProtScale tool was used for hydrophobicity/hydrophilicity predictions; SignalP4.1 Server was used for signal peptide predictions; TMHMM Server v.2.0 was used for predicting transmembrane regions; SOSUI was used to predict protein solubility; SOMPA was used for secondary structure predictions; CILS was used for crimp spiral analyses; SWISS-MODEL was used for tertiary structure modeling.

Table 1. Web tools for predicting protein structure and function

Application website	Website	Website usage
BLAST	https://blast.ncbi.nlm.nih.gov/Blast.cgi	Sequence download
CD search	http://www.ncbi.nlm.nih.gov/Structure/cdd/wrpsb.cgi	Conservative domain prediction
Protparam	http://www.expasy.org/tools/protparam.html	Physicochemical properties prediction
SignalP4.1Server	http://www.cbs.dtu.dk/services/SignalP	Signal peptide prediction
TMHMM Server v. 2.0	http://www.cbs.dtu.dk/services/TMHMM/	Transmembrane region prediction
SOSUI	http://harrier.nagahama-i-bio.ac.jp/sosui/sosui_submit.htm	Soluble protein prediction
ProtScale	http://ca.expasy.org/tools/protscale.html	Hydrophobic and hydrophilic prediction
SOMPA	https://npsa-prabi.ibcp.fr/cgi-bin/npsa_automat.pl?page=npsa_sopma.html	Secondary structure prediction
COILS	http://www.ch.embnet.org/software/COILS_form.html	Crimp spiral analysis
SWISS-MODEL	https://www.swissmodel.expasy.org/	Tertiary structure modeling
3DLigandSite	http://www.sbg.bio.ic.ac.uk/~3dligandsite/	Ligand binding site prediction

Results and analysis

Expression analysis of the AnTPS1 gene

The cDNA of *AnTPS1* was amplified by PCR (Fig. 1) and then sequenced (Fig. 2). To assess the expression and relevance *AnTPS1* to cold stress in naked oats, we used real-time qPCR to assess its expression within various parts of the naked oats plant. Results showed the *AnTPS1* gene to be most abundantly expressed in the leaves of naked oats, with lower levels in stems, and limited expression in roots (Fig. 3). Under low temperature cold stress conditions, the expression of *AnTPS1* changed significantly. The gene expression was significantly increased at 3 h and 6 h. After 6 h, the expression level reached its maximum – roughly twice that of the control plants - and then decreased significantly (Fig. 4).

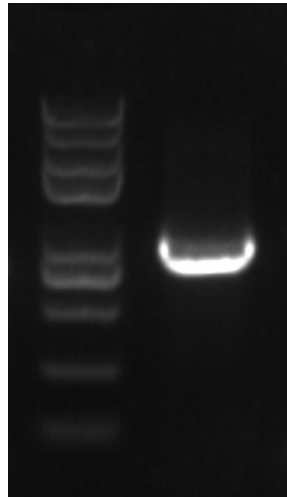


Figure 1. The *AnTPS1* fragment amplified by PCR

1	ATGGAGAAAT	CCTGTCCAGC	AGCCACCGCC	GGCCTAGGAG	AGGAACTCTT	CATGCCAGCA
61	TGGGCTCCTA	TGCTGTGTCC	CAATCCCAGG	CGAGCACGGA	AGGAGCCGTT	AAGCACGATG
121	TCGTTGACA	GGGACTACTC	GTTCCGAATG	AGTACCCTCT	GGTCGTGGAG	GATCCATCTG
181	TGCCTTTTTT	TTGAGCTTGT	TTCTGCATA	ATTCTACCAT	TCAGATGGAT	GTCCGATCGC
241	TTTGCCCCCA	GCAGATCAAT	CGGAGAACCA	CGCCCGAACT	TGTCTTTGAG	CTTCTTTGAA
301	GATGACCGCG	GTTACATGGA	TTATCCTTTT	CGGAAGAGGA	CTCCCGAGTA	TGTTGAAAGA
361	ATTGCTTGGA	GTGAATGGAT	GATGCTTCTT	ATTTTTGTGA	TGGTGAAGG	CTGGTACATG
421	ATCAAGGATG	CATGCTGGAT	CGAGGATGCC	TGGTCAACTG	CTATTATGTT	TTGTCTTAT
481	ATTCTTCAGG	GGCGTCTGAA	GCACATCAAA	AGCCATATTT	TCGGAAAACC	AAGGATGGTT
541	CCGACGGAAA	CAATTGCGGC	TTTTGGTTCT	TCTTCAACTG	GCAGTGGTCG	CTTTATAATG
601	GACTCTGGTG	CCACTTCACA	TTTTGTTGGT	AATGCCAGTA	TGCTGCAGGA	CATCATATAT
661	TTTCCTCTTG	AGCAGCGTCA	GCTTGTACC	TTAGCAGATG	GCTTCTGTCT	TCCCATGTGC
721	GGCATTGGCA	CCCTATTGTT	CACTGGTCTG	AGCGAGTGTG	GGAGCTATAC	TCGGTCTTAC
781	AGAGTCCCCA	ATGTCCGCTA	CGTGCGTGGC	CTTGCGATGA	ACGTGATATC	TGTCGGCCAG
841	CTTGACAATG	AGCATGGCTT	GTGCAGCGCC	TTCCACAGCG	AGAAATGCGA	GATTATGGCT
901	GACAGAACCG	TCATTGGGCA	AGCTGTTCTT	GTGAACCGCT	TGTACGAGGT	GGTCTACCTC
961	CATGTCCAC	GAGTGTGTA	G			

Figure 2. Sequence of the *AnTPS1* gene

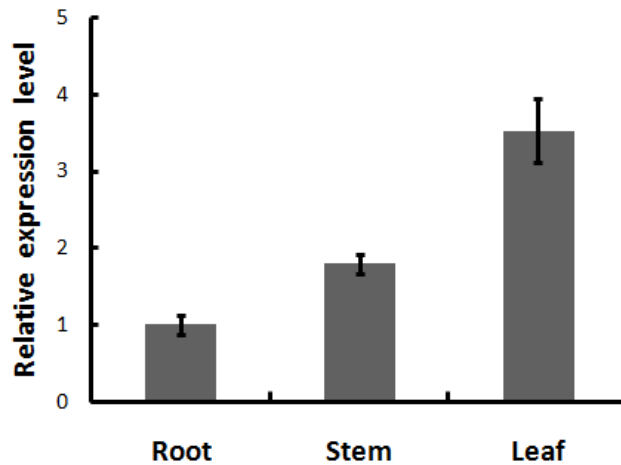


Figure 3. Relative expression levels of *AnTPS1* in different tissues

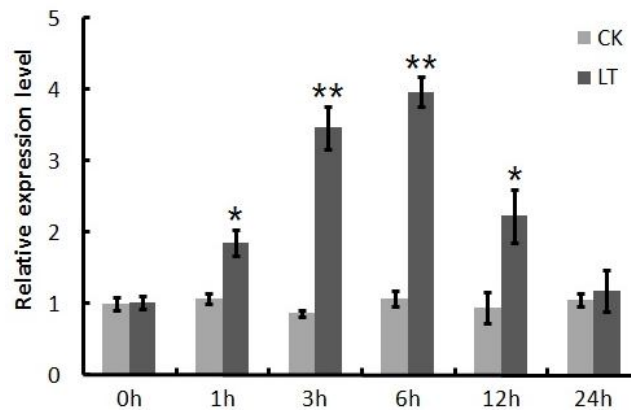


Figure 4. Relative expression levels of *AnTPS1* at different times under low temperature treatment. Note: CK represents control, LT represents low temperature treatment

Analysis of AnTPS1 primary structure and physicochemical properties

We predicted and analyzed the amino acid composition and physicochemical properties of *AnTPS1*, which encodes TPS, using the ProtParam tool available from ExPASy. We found *AnTPS1* to encode a 326 amino acid protein enriched in serine and leucine (8.6% each), and with a low glutamine content (1.8%). The protein formula for *AnTPS1* was $C_{1694}H_{2592}N_{448}O_{458}S_{28}$, with 5220 total atoms and a relative molecular weight of 37459.62 Da. The total number of negatively charged amino acid residues (Asp and Glu) and positively charged amino acid residues (Arg and Lys) were 32 and 34, respectively. The theoretical isoelectric point (pI) of this protein was 7.99, leaning towards alkalinity. The extinction coefficients at 280 nm for this protein were $68005 \text{ M}^{-1} \cdot \text{cm}^{-1}$ when assuming all cysteine residues were from cysteine, and

67380 M⁻¹·cm⁻¹ when assuming none were. Based on an N-terminal methionine, the estimated half-lives of this protein in mammalian reticular cells (*in vitro*), yeast (*in vivo*), and colibacillus (*in vivo*) were 30 hours, more than 20 hours, and more than 10 hours, respectively. The instability coefficient was 82.55, classifying AnTPS1 as an unstable protein. The fat coefficient of AnTPS1 was 51.90. The total average of hydrophilicity of this protein was 0.052, classifying *AnTPS1* as a hydrophobic protein.

AnTPS1 protein signal peptide, transmembrane domain, and hydrophilicity predictions

Through the measurement of protein shearing sites, signal peptide predictions can categorize the functional domains of proteins and determine their likely subcellular localization. An assessment of AnTPS1 using the SignalP4.1Server yielded a cleavage site score (C-score) of 0.168, a synthetic shearing site score (Y-score) of 0.167, and a signal peptide score (S-score) of 0.248 (Fig. 5). These results were consistent with AnTPS1 being a secretory protein containing a signal peptide, suggesting that the resultant TPS protein may be involved with transmembrane transport within cells.

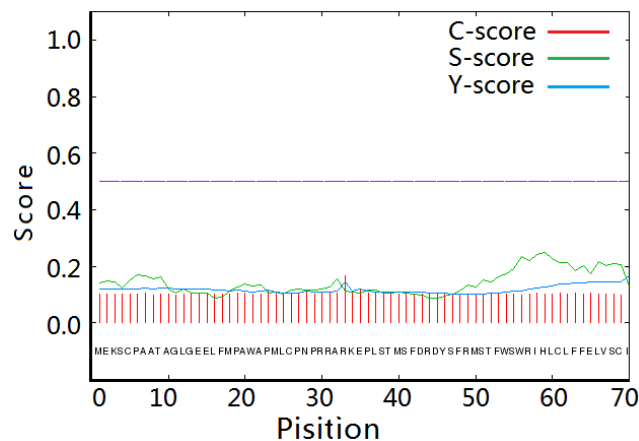


Figure 5. Signal peptide analysis of the *AnTPS1* protein by SignalP 4.1

Membrane proteins may have extracellular, transmembrane and intracellular domains (Fraihat et al., 2018; Radwan et al., 2018; Saeed et al., 2018; Rajagopalan et al., 2018). Transmembrane regions generally are α -helical structures with hydrophobic amino acids embedded in the cytoplasmic membrane. A transmembrane structure analysis of the *AnTPS1* protein using the TMHMM Server v2.0 revealed that the encoded protein has a transmembrane helix (TMH) with a TMH value of 57.31 (Fig. 6). The value of the non-transmembrane helical region (ExpAA) of this protein was 6.41447, consistent with it being transmembrane protein. The probability of the N-terminal domain of the protein locating inside the membrane was 0.2999, and this sequence is typically located outside the membrane, further suggesting that the protein encoded by *AnTPS1* is a

transmembrane protein. An analysis of the solubility of the *AnTPS1*-encoded protein via SOSUI revealed that this protein was a membrane protein with two transmembrane helices and a total length of 326 amino acids – slightly longer than the initial prediction. This protein was predicted to be soluble, with an average hydrophobicity of 0.037160.

Amino acid hydrophilicity is the primary force driving protein folding, and it can thus help in the evaluation of secondary structural features such as transmembrane helices and amino acid surface distributions within a given protein (Woldesemayat et al., 2017). The hydrophilicity of the naked oats *AnTPS1* amino acid sequence was predicted using the ExPASy ProtScale tool (Fig. 7), revealing the 131st amino acid in the peptide chain to be the most hydrophobic, with a positive score of 3.222; while amino acids 31 and 32 were the most hydrophilic, with a negative score of -2.867. Figure 4 illustrates that the N-terminal domain of this protein is negative (hydrophilic), while the C-terminal domain is positive (hydrophobic), with fewer hydrophilic amino acids in the overall peptide chain than hydrophobic ones. This suggests *AnTPS1* is a soluble hydrophobic protein.

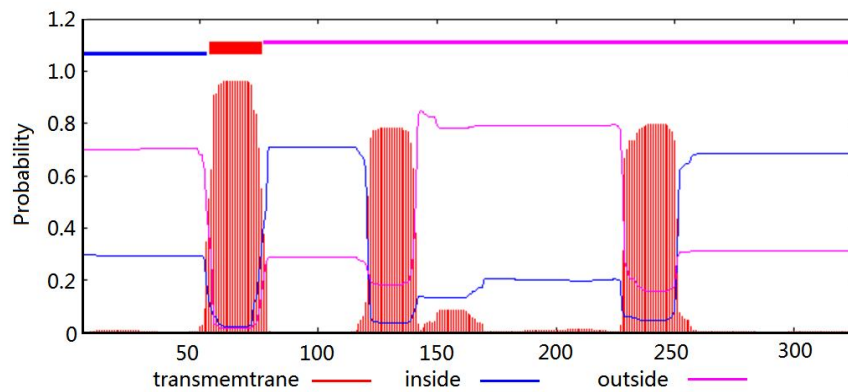


Figure 6. Transmembrane analysis of the *AnTPS1* protein by TMHMM

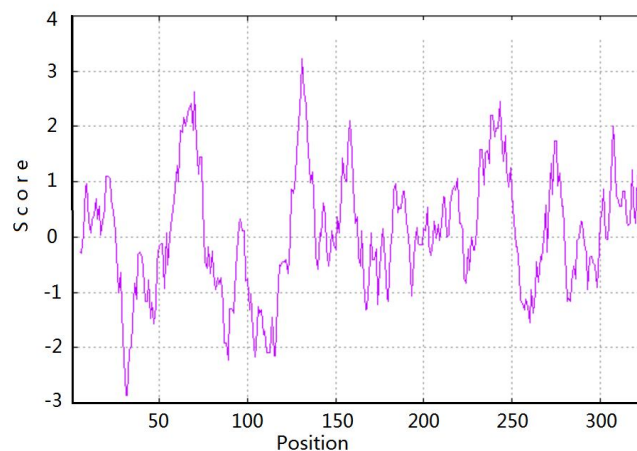


Figure 7. Prediction of hydrophilicity of the *AnTPS1* protein by ProtScale

Prediction and analysis of AnTPS1 protein secondary structure and modules

The secondary structure of the AnTPS1 protein was assessed using the SOMPA online prediction program, which predicted 113 amino acid residues in the protein to be, accounting for 34.66% of the overall peptide chain. In total, 63 amino acid residues had an extended chain structure (19.33% of the overall peptide chain), 29 amino acid residues had a β -rotation structure (8.90% of the overall peptide chain), and 121 amino acid residues had an irregular curl structure (37.12% of the overall peptide chain) (Fig. 8). The α -helix and irregular crimp were the main structural components of the AnTPS1 protein, contributing to its structural stability (Geourjon and Deléage, 1995). The PredictProtein tool was used to predict the presence of disulfide bonds, none of which were predicted to reside within the resultant protein. Functional sites were analyzed using the PROSITE tool, identifying 11 phosphorylation sites, 2 glycosylation sites, and 5 acylation sites.

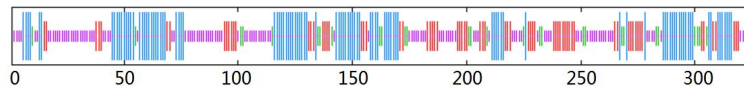


Figure 8. Analysis of the secondary structure of the AnTPS1 protein by SOMPA. Note: blue represents α -helical, red represents extended strand, green represents β -rotation, purple represents irregular curl

AnTPS1 protein tertiary structure modeling and binding site prediction

SWISS-MODEL was utilized for homology modeling of this predicted protein (using PyMOL view) (Fig. 9), while a Ramachandran evaluation in MolProbity software was employed to evaluate the tertiary structure of the AnTPS1-encoded protein as previously described (Liu et al., 2017). Modeling by the SWISS-MODEL server is based on the A chain of PDB ID 3d79.1, with a sequence consistency value of 20.41%. Ramachandran plot-based evaluation determined that 93.64% (103/126) of amino acid sites are located in the favored region, while 100% (126/126) are located in the permitted region, indicating that the tertiary structure model is accurate and reliable.



Figure 9. Tertiary structure of the AnTPS1 protein predicted by SWISS-MODEL

Discussion

Trehalose is a stress metabolite, only accumulating in plants under conditions of stress such as drought, extreme temperatures, and high salinity (Chary et al., 2008). The accumulation of trehalose enhances the protection of proteins, enzymes, and cell membranes, preserving cellular and organismal viability. Trehalose is degraded when the noxious environmental conditions subside (Lunn et al., 2014). The TPS gene is essential for the synthesis of trehalose in plants. Introduction of the exogenous TPS allows for the synthesis of trehalose 6-phosphate (T6P), which is dephosphorylated to form trehalose by a wide range of non-specific phosphatases, making TPS the rate-limiting enzyme for trehalose accumulation (Cai et al., 2009).

TPS is important for glycometabolism, embryonic development, and the response to abiotic stress, making it essential for overall crop development. The TPS gene family has been evaluated structurally, functionally and evolutionarily in rice, *Arabidopsis thaliana*, poplar, and cotton (Tang et al., 2018). However, similar studies have not been conducted to date in naked oats, despite the notable hardiness of this species and its effective stress resistance, making it an important species in which to study such a key abiotic stress resistance gene. Bioinformatics allow for the detailed prediction and analysis of predicted proteins encoded by particular gene sequences, offering potential insights into the structure and function thereof. Our assessment of the peptide sequence of the *AnTPS1*-encoded protein revealed the ORF to encode for 326 amino acids without multiple domains. The N-terminal TPS (T6P synthase) domain catalyzes the production of T6P using glucose-6-phosphate and UDP-glucose as substrates, whereas the C-terminal TPP domain dephosphorylates T6P, generating trehalose (Matsuda et al., 2015). The protein formula of *AnTPS1* is C1694H2592N448O458S28, with a relative molecular weight of 37459.62 Da and a predicted isoelectric point (pI) of 5.75. The protein is positively charged and leans towards alkalinity. It is a soluble hydrophobic protein containing a signal peptide and transmembrane helix. The α -helix and irregular crimp are the main structural components of the *AnTPS1* protein. In a previous study by Tang et al. (2018) in *N. lugens*, three TPS genes were cloned, and their protein secondary structures contained similar components to those identified in the present study, with α -helices, β -sheets, and random coils. We further verified that the *AnTPS1* protein had a signal peptide, consistent with the results of the transmembrane structure analysis. Subcellular localization revealed the *AnTPS1* protein to be potentially located in the cytoplasm, which is consistent with a finding by Xu et al. (2017) which revealed that the majority of TPS in *Solanum tuberosum* may be located in the cytoplasm, with only limited quantities located in the plasma membrane or nucleus. This variation in localization may be dynamic, potentially having a relationship with stress response behavior, although further microscopy-based studies would be needed to verify this hypothesis. The localization of a given protein is closely related to its functional involvement. In assessing the functional domains of the protein encoded by *AnTPS1*, we

identified 11 phosphorylation sites, 2 glycosylation sites and 5 acylation sites without crimp helix domain in the protein. Together, these predictive bioinformatics analyses confirmed that the protein encoded by *AnTPSI* is consistent with other published TPS protein sequences and structures, suggesting that such structural homology is likely accompanied by functional homology as well in the context of stress responses.

Analysis of the expression of *AnTPSI* in different tissues of naked oats revealed that this gene is expressed at the highest level in leaves and at the lowest level in roots. This differential expression may be due to differences in developmental differentiation, spatial location, function, metabolic activity, and environmental conditions among these different organs and tissues (Jin et al., 2016). We found that the *AnTPSI* gene was up-regulated by cold temperature stress, indicating it to have an expression pattern consistent with the abiotic stress response to cold and potentially to other factors as well. Thus, *AnTPSI* may play a role in the resistance of naked oats to low temperature stress, as has been found in other studies. Indeed, transgenic plants expressing TPS have increased tolerance to stress (Mu et al., 2016). In *Arabidopsis* plants, transgenic TPS expression was shown to substantially increase resistance to extreme stress without disrupting normal cellular morphology (Miranda et al., 2007). Despite these promising results, some authors have raised concerns that trehalose expression may be advantageous under stress conditions, but may become deleterious over time, making plants more susceptible to certain plant pathogens and potentially altering growth kinetics (Fernandez et al., 2010). Interestingly, we found that the expression of *AnTPSI* increased substantially under cold stress conditions, before declining at later time points, potentially suggesting that the *AnTPSI* gene from naked oats may be regulated in an optimal fashion that allows it to be acutely expressed as a part of the early stress response, before decreasing expression levels over time to reduce potential adverse outcomes of prolonged expression. Selective expression of comparably regulated proteins in other crops could feasibly offer optimal resistance characteristics without disrupting normal morphology, although more work will be needed to confirm such a hypothesis. In naked oats, the intermediate metabolite T6P catalyzed by the TPS domain may participate in the response to cold stress by acting as signaling molecule, or by catalyzing the production of trehalose which is important for the osmotic regulation of naked oats in response to abiotic stress.

There are limitations to the present study that should be considered. For one, the bioinformatics-based predictive approaches are by their very nature uncertain. While all tools were used as intended, inherent uncertainties in the resultant predicted *AnTPSI* protein structure and localization can result in apparent inconsistencies in its characteristics. Further molecular approaches will be needed to therefore validate its subcellular localization and expression patterns, and to determine whether its localization changes depending on the functional context. In addition, while our *in vivo* assessment of *AnTPSI* expression revealed patterns of expression consistent with a stress response, formal knockout experiments will be needed to fully validate the role of

this gene in abiotic stress responses in naked oats. Given that naked oats are well-adapted to growth under adverse conditions, and that we observed time-dependent expression of this trehalose-producing gene in response to stress, it is possible that further study of the optimal regulation and expression patterns of this gene will yield further fundamental insights into optimal stress resistance strategies suitable for improving global crop yields.

Conclusion

Ongoing environmental changes and a rapidly increasing global population both necessitate the growth of selectively bred or transgenic crops capable of withstanding serious environmental stress conditions. In this study, we analyzed the expression and bioinformatics analysis of *AnTPSI* gene. *AnTPSI* was upregulated by low temperature. The expression of *AnTPSI* in naked oats represents an important step towards understanding the molecular mechanisms governing the responses of plants to abiotic stressors. While further study will be necessary to validate these results using genetic modifications and molecular imaging approaches, this work represents an important step towards the production of robust and resistant plant species.

Contributions. Wenying Liu and Feng Li conceived and designed the study. Rui Liu, Lizhen Liu, and Yongfang Zhang performed the experiments. Gang Li and Hongxian Tian provided the seeds. Wenying Liu and Jianxia Liu wrote the paper. Runmei Wang, Feng Zhou, and Dongxu Zhang reviewed and edited the manuscript. All authors read and approved the manuscript.

Acknowledgements. This work is supported by Basic research project of Shanxi Province (2015021149); Datong agricultural key research and development project (2017082).

REFERENCES

- [1] Cai, Z., Peng, G., Cao, Y., Liu, Y., Jin, K., Xia, Y. (2009): Trehalose-6-phosphate synthase 1 from *Metarhizium anisopliae*: clone, expression and properties of the recombinant. – *Journal of Bioscience and Bioengineering* 107(5): 499-505.
- [2] Chary, S. N., Hicks, G. R., Choi, Y. G., Carter, D., Raikhel, N. V. (2008): Trehalose-6-phosphate synthase/phosphatase regulates cell shape and plant architecture in *Arabidopsis*. – *Plant physiology* 146(1): 97-107.
- [3] Delorge, I., Figueroa, C. M., Feil, R., Lunn, J. E., Van Dijck, P. (2015): Trehalose-6-phosphate synthase 1 is not the only active TPS in *Arabidopsis thaliana*. – *Biochemical Journal* 466(2): 283-290.
- [4] Fernandez, O., Béthencourt, L., Quero, A., Sangwan, R. S., Clément, C. (2010): Trehalose and plant stress responses: friend or foe? – *Trends Plant Science* 15(7): 409-417.

- [5] Flowers, T. J. (2004): Improving crop salt tolerance. – *Journal of Experimental Botany* 55(396): 307-319.
- [6] Fraihat, A., Alatrash, L., Abbasi, R., Abu-Irmaileh, B., Hamed, S., Mohammad, M., Abu-Rish, E., Bustanji, Y. (2018): Inhibitory effects of methanol extracts of selected plants on the proliferation of two human melanoma cell lines. – *Tropical Journal of Pharmaceutical Research* 17(8): 1645-1650.
- [7] Geourjon, C., Deléage, G. (1995): SOPMA: significant improvements in protein secondary structure prediction by consensus prediction from multiple alignments. – *Bioinformatics* 11(6): 681-684.
- [8] Guo, Q., Hao, Y. J., Li, Y., Zhang, Y. J., Ren, S., Si, F. L., Chen, B. (2015): Gene cloning, characterization and expression and enzymatic activities related to trehalose metabolism during diapause of the onion maggot *Delia antiqua* (Diptera: Anthomyiidae). – *Gene* 565(1): 106-115.
- [9] Hu, H., Xiong, L. (2014): Genetic engineering and breeding of drought-resistant crops. – *Annual Review of Plant Biology* 65: 715-741.
- [10] Hussain, R. M., Ali, M., Feng, X., Li, X. (2017): The essence of NAC gene family to the cultivation of drought-resistant soybean (*Glycine max* L. Merr.) cultivars. – *BMC Plant Biology* 17: 55.
- [11] Hwang, I., Manoharan, R. K., Kang, J. G., Chung, M. Y., Kim, Y. W., Nou, I. S. (2016): Genome-Wide Identification and Characterization of bZIP Transcription Factors in *Brassica oleracea* under Cold Stress. – *Biomed Research International* 2016: 4376598.
- [12] Jin, Q., Hu, X., Li, X., Wang, B., Wang, Y., Jiang, H., Mattson, N., Xu, Y. (2016): Genome-wide identification and evolution analysis of trehalose-6-phosphate synthase gene family in *Nelumbo nucifera*. – *Frontiers in Plant Science* 7: 1445.
- [13] Lin, W. J., Wu, G. F., Li, C. H., Wang, Y., Zhou, S. M. (2011): Effects of cultivar and environment on nutritional quality of Chinese naked oats. – *Acta Agronomica Sinica* 37: 1087-1092.
- [14] Liu, W., Yu, K., He, T., Li, F., Zhang, D., Liu, J. (2013): The low temperature induced physiological responses of *Avena nuda* L., a cold-tolerant plant species. – *The Scientific World Journal* 2013(6): 658793.
- [15] Liu, J., Gao, F., Ren, J., Lu, X., Ren, G., Wang, R. (2017): A novel AP2/ERF transcription factor CR1 regulates the accumulation of vindoline and serpentine in *Catharanthus roseus*. – *Frontiers in Plant Science* 8: 2082.
- [16] Lu, Z., Liang, Y. L., Wang, J. (2018): Bioinformatic Analysis of 4-Hydroxyphenylpyruvate Dioxygenase in *Coptis japonica*. – *Genomics and Applied Biology* 37(04): 1604-1613.
- [17] Lunn, J. E., Delorge, I., Figueroa, C. M., Van Dijck, P. (2014): Trehalose metabolism in plants. – *The Plant Journal* 79(4): 544-567.
- [18] Ma, X., Gu, J., Zhang, Z., Jing, L., Xu, M., Dai, X., Jiang, Y., Li, Y., Bao, L., Cai, X., Ding, Y., Wang, J., Li, Y., Li, Y. (2013): Effects of *Avena nuda* L. on metabolic control and cardiovascular disease risk among Chinese patients with diabetes and meeting metabolic

- syndrome criteria: secondary analysis of a randomized clinical trial. – *European Journal of Clinical Nutrition* 67(12): 1291-1297.
- [19] Mao, Y., Zhao, Q., Yin, S., Ding, X., Wang, H. (2018): Genome-wide expression profiling and bioinformatics analysis of deregulated genes in human gastric cancer tissue after gastroscopy. – *Asia-Pacific Journal of Clinical Oncology* 14: 29-36.
- [20] Matsuda, H., Yamada, T., Yoshida, M., Nishimura, T. (2015): Flies without trehalose. – *Journal of Biological Chemistry* 290: 1244-1255.
- [21] Miranda, J. A., Avonce, N., Suárez, R., Thevelein, J. M., Van Dijck, P., Iturriaga, G. (2007): A bifunctional TPS-TPP enzyme from yeast confers tolerance to multiple and extreme abiotic-stress conditions in transgenic *Arabidopsis*. – *Planta* 226: 1411-1421.
- [22] Mu, M., Lu, X. K., Wang, J. J., Wang, D. L., Yin, Z. J., Wang, S., Fan, W. L., Ye, W. W. (2016): Genome-wide Identification and analysis of the stress-resistance function of the TPS (Trehalose-6-Phosphate Synthase) gene family in cotton. – *BMC Genetics* 17(1): 54.
- [23] Oide, S., Inui, M. (2017): Trehalose acts as a uridine 5'-diphosphoglucose-competitive inhibitor of trehalose 6-phosphate synthase in *Corynebacterium glutamicum*. – *FEBS Journal* 284(24): 4298-4313.
- [24] Radwan, A. M., Reyad, N. F., Donia, A. M., Ganaie, M. A. (2018): Comparative studies on the effect of environmental pollution on secondary metabolite contents and genotoxicity of two plants in Asir area, Saudi Arabia. – *Tropical Journal of Pharmaceutical Research* 17(8): 1599-1605.
- [25] Rajagopalan, U., Samarakoon, S. R., Tennekoon, K. H., Malavige, N., de Silva, E. D. (2018): Screening of five Sri Lankan endemic plants for anti-cancer effects on breast cancer stem cells isolated from MCF-7 and MDA-MB-231 cell lines. – *Tropical Journal of Pharmaceutical Research* 17(9): 1825-1832.
- [26] Saeed, M. A. A., Memon, A. H., Hamil, M. S. R., Beh, H. K., Saghir, S. A. M., Kaur, G., Sadikun, A., Ismail, Z. (2018): Toxicity evaluation of standardized and nanoliposomal extracts of *Labisia pumila* whole plant (Blume, Myrsinaceae) in Sprague Dawley rats. – *Tropical Journal of Pharmaceutical Research* 17(8): 1557-1564.
- [27] Tai, A. P. K., Martin, M. V., Heald, C. L. (2014): Threat to future global food security from climate change and ozone air pollution. – *Nature Climate Change* 4(9): 817-821.
- [28] Tang, B., Wang, S., Wang, S. G., Wang, H. J., Zhang, J. Y., Cui, S. Y. (2018): Invertebrate trehalose-6-phosphate synthase gene: genetic architecture, biochemistry, physiological function, and potential applications. – *Frontiers in Physiology* 9: 30.
- [29] van Dijken, A. J., Schluepmann, H., Smeekens, S. C. (2004): *Arabidopsis* trehalose-6-phosphate synthase 1 is essential for normal vegetative growth and transition to flowering. – *Plant physiology* 135(2): 969-977.
- [30] Wang, T., Du Y. L., He, J., Turner, N. C., Wang, B. R., Zhang, C., Cui, T., Li, F. M. (2017): Recently-released genotypes of naked oat (*Avena nuda* L.) out-yield early releases under water-limited conditions by greater reproductive allocation and desiccation tolerance. – *Field Crops Research* 204: 169-179.

- [31] Woldesemayat, A. A., Van Heusden, P., Ndimba, B. K., Christoffels, A. (2017): An integrated and comparative approach towards identification, characterization and functional annotation of candidate genes for drought tolerance in sorghum (*Sorghum bicolor* (L.) Moench). – *BMC Genetics* 18(1): 119.
- [32] Xu, Y., Wang, Y., Mattson, N., Yang, L., Jin, Q. (2017): Genome-wide analysis of the *Solanum tuberosum* (potato) trehalose-6-phosphate synthase (TPS) gene family: evolution and differential expression during development and stress. – *BMC Genomics* 18: 926.
- [33] Zhou, X., Lin, W., Tong, L., Liu, X., Zhong, K., Liu, L., Wang, L., Zhou, S. (2016): Hypolipidaemic effects of oat flakes and β -glucans derived from four Chinese naked oat (*Avena nuda*) cultivars in Wistar-Lewis rats. – *Journal of the Science of Food and Agriculture* 96(2): 644-649.